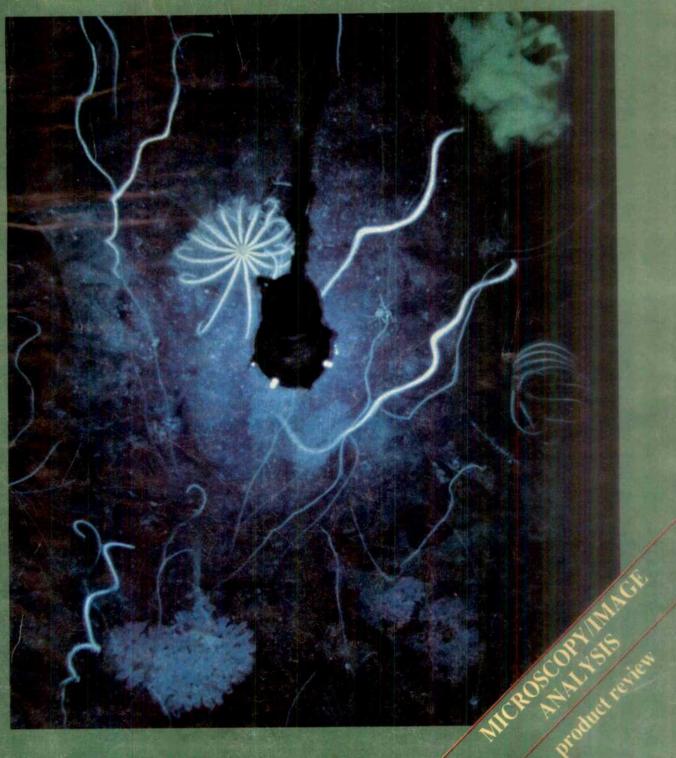
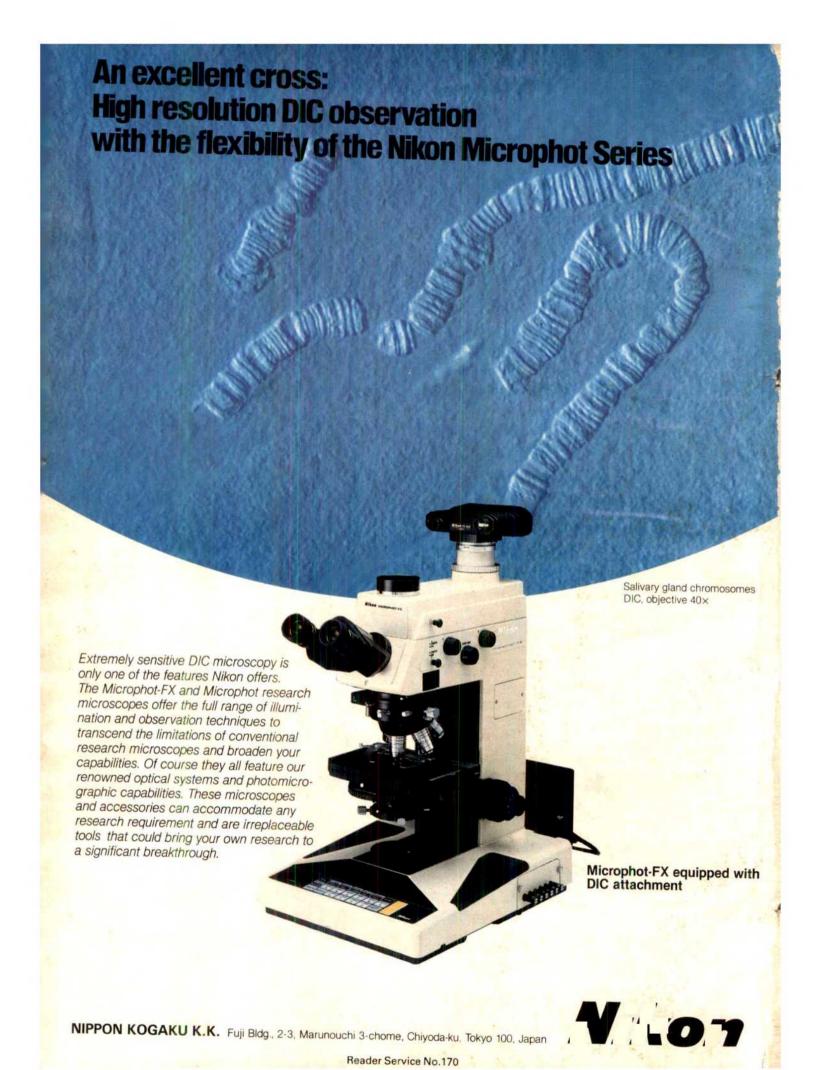
1021111C INTERNATIONAL WEEKLY JOURNAL OF SCIENCE

Volume 322 No.6074 3-9 July 1986 £1.90

OCEAN-FLOOR ECOLOGY





AUTHOR INDEX-

CUR-HOG856-313-RP440

Author Index for Volume 322

July — August 1986

Issue no.	Issue date	Pagination
6074	3 July	1-96
6075	10 July	97-194
6076	17 July	195-292
6077	24 July	293-392
6078	31 July	393-484
6079	7 August	485-580
6080	14 August	581-670
6081	21 August	671-758
6082	28 August	759-854

Abe, Y. See under Matsui, T., 322, 526

ns, R.J. Propulsion of organelles isolated from along actin filaments by myosin-I (with Pollard, T D) Letter to re, **322,** 754

Adler, K. Editor, The Encyclopaedia of Reptiles and Amphibians, Book review by Crothers, J. 322, 416

Agnew, W.S. Neurochemistry; Lessons from large molecules, News and views, 322, 770

ayo, J B. Nuclear magnetic resonance imaging of a single cell (with Blackband, S J, Schoeniger, J, Mattingly, M A, Hintermann, M) Letter to Nature, 322, 190 Akhtar, D. See under Rajasekharan, K., 322, 528

Aksu, A.E. See under Macko, S.A., 322, 730

Aktories, K. Botulinum C2 toxin ADP-ribosylates actin (with Bariann, M. Ohishi, I., Tsuyama, S., Jakobs, K.H., Habermann, E.) Letter to Nature, 322, 390

Albert, V.R. See under Nelson, C., 322, 557

Alexander, W. See under Neison, C., 322, 337

Alexander, B. See under Smith, R. A., 322, 722

Alexandropoulos, N. G. Chernobyl fallout on loannina, Greece (with Alexandropoulos, E., Kotsis, K. T. Theodoridou, I.) Scientific correspondence, 322, 779

Alexandropoulos, T. See under Alexandropoulos, N. G., 322, 779

Alexandropoulos, K. See under Varotsos, P., 322, 120

Allaby, M. Editor, The Oxford Dictionary of Natural History, Book review by Fitter, A. 322, 23

Allen, J R L. Book review of Coastal and estuarine sediment dynamics (by Dyer, K.R.) 322, 318

Alley, R.B. See under Blankenship, D.D., 322, 54

Deformation of till beneath ice stream B, West Australia (with Blankenship, D D, Bentley, C R, Rooney, S T) Letter to Nature, 322, 57

Aloisi, M. See under Salviati, G., 322, 637

Alpert, J.C. See under Stolarski, R.S., 322, 808 See under Stolarski R.S. 322, 808

rt, S. See under Lacey, M., 322, 609

Alt, F W. Antibody diversity; New mechanism revealed, News and views, 322, 772

See under Bank, L., 322, 179

ier, R. See under Kachar, B., 322, 365

Alurkar, S.K. Radio observations of PKS2314+03 during occultation by comet Halley (with Bhonsle, R V, Sharma, A K) Letter to iture, **322**, 439

brose, S H. See under Giles, E., 322, 21

Anagasstopoulos, D. See under Alexandropoulos, N.G., 322, 779

Anderson, A. Biotechnology: UNIDO centre taking shape, News,

Strategic Defense Initiative: Britain wins first big contracts, News,

UK science: Save British Science takes off, News, 322, 9

Nature conservation; Too many of the wrong trees?, News, 322,

ation technology: Where next for Alvey?, News, 322, 105 Energy: Power from the Severn waters, News, 322, 202 Getting tough on doctorates, News, 322, 298

UK universities: Research gradings stir emotions, News, 322, 299 UK research grants: Research board pleads for more, News, 322,

New career for Sydney Brenner, News, 322, 397

High-technology trade: Anger over supercomputer veto, News,

Inventors' rewards, News, 322, 487

Plant research: Success breeds privatization, News, 322, 491 Timber trade: A little hope for tropical forests, News, 322, 493 UK Universities; Government yields just a little, News, 322, 764 on, D M. See under Binder, B J., 322, 659

derson, J.A. Neural models: Networks for fun and profit, News

Anderson, R.M. Rabies control: Vaccination of wildlife reservoirs. News and views, 322, 304

Andrews, J. Book review of The Sparrowhawk (by Newton, 1,) 322,

bault, L. P. See under Pakull, M.W., 322, 511

Angel, J R P. A space telescope for infrared spectroscopy of Earthlike planets (with Cheng, A Y S, Woolf, N J) Letter to Nature, 322, 341

Aota, S-i. See under Ohyama, K., 322, 572

Appleby, J.F. See under Diner, D.J., 322, 436

Appleby, P.G. See under Jones, G.D., 322, 313

Argenbright, L. W. See under Doherty, J.B., 322, 192
Argyle, B. RGO move OK (with Jenkins, C. Jones, D. Laing, R. Marsh, T. Martin, B. Murdin, P. Pettini, M. Schild, H. Taylo

K, Terlevich, R, Tritton, K, Wall, J) Correspondence, 322, 402 Arp, H. Recent discoveries of a supermass in the Universe, Scientific correspondence, 322, 316

Ashe, B M. See under Doherty, J B., 322, 192

Ashmore, J F. Ionic basis of membrane potential in outer hair cells of guinea pig cochlea (with Meech, R W) Letter to Nature, 322, 368

Ashtekar, A. Book review of Spinors and space-time. Vol. 2 Spinor and twistor methods in space-time geometry (by Penrose, R. Rindler, W.) 322, 318

orth, A. Disease gene relationship seen (with Shephard, E.A., Phillips, J R) Scientific correspondence, 322, 599 ich, I. See under Forsyth, D A., 322, 349

Atkins, PW. Book review of The unfinished Universe (by Young, L. B.) 322, 122 Atkinson, D.E. Frequency of dizygotic twinning, Scientific corres-

pondence, 322, 780

Attileid, J.P. Structure determination of a CrPO₄ from powder synchrotron X-ray data (with Sleight, A.W., Cheetham, A.K.) Letter tò Nature, 322, 620

Aubert, C. See under Hauser, S.L., 322, 176

Auer, H E. The mechanism of activation of porcine pepsinogen (with

Glick, D M) Matters arising, 322, 664

Awad, J. See under Festenstein, H., 322, 64 Axon, D.J. See under Bailey, J., 322, 150

Bachner, R L. See under Royer-Pokora, B., 322, 32 Bailey, J. Infrared polarimetry of the nucleus of Centaurus A: the nearest blazar? (with Sparks, W B, Hough, J H, Axon, D J) Letter to Nature, 322, 150

Bains, W. Legal problems of Huntington's chorea tests, Scier correspondence, 322, 20

Baker, DG. Visual observation of lightning propagation (with Baker-Blocker, A) Scientific correspondence, 322, 215

Baker, E.T. See under Cowen, J.P., 322, 169
Baker-Blocker, A. See under Baker, D.G., 322, 215

Balmain, A. See under Quintanilla, M., 322, 78 ore, D. See under Weinberger, J., 322, 846

Bank, I. A functional T3 molecule associated with a novel heterodia er on the surface of immature human thymocytes (with De-Phinho, R A, Brenner, M B, Cassimeris, J, Alt, F W, Chess, L) Letter to Nature, 322, 179

Barnt, C. See under Laros, J G., 322, 152

Barker, P.L. See under Doherty, J.B., 322, 192
Barkew, D.J. Continuous flow and discontinuous protein antigenic determinants (with Edwards, M.S. Thornton, J.M.) Letter to Nature, 322, 747

unn, M. See under Aktories, K., 322, 390

Barnes, G L. Archaeology: Japanese agricultural beginnings, News and views, 322, 595

Barnett, J A. The stability of biological nomenclature: yeasts, Scien-

tific correspondence, 322, 599

rrett, D. See under Wasielewski, M.R., 322, 570

Bartelmie, R.J. See under Duncan, R.A., 322, 534 Barthelmie, R.J. See under Davies, T.D., 322, 359

Bartlett, P. See under Cohen, J., 322, 465

za, R. See under Langmuit, C.H., 322, 422

Battarbee, R.W. See under Jones, V.1., 322, 157

Bauer, F W. See under Micr. P.D., 322, 504

Baxter, C S. High-resolution lattice imaging reveals a 'phase trans tion' in Cu/NiPd multilayers (with Stobbe, W.M.) Letter to Nature, 322, 814

ardsley, T. US research: Campus bonanza from the military, News, 322, 4

Scraping the barrel, News, 322, 4

Others have problems too, News, 322, 99

US nutritional research: Your grant is what you eat, News, 322, 104 Genetic engineering: Hepatitis vaccinewins approval. News. 322,

Biotechnology: Regulations please nobody, News, 322, 398 Science Digest dies, News, 322, 401

US budget: Winners and losers worry about Gramm-Radman News, 322, 487

Technology journals: Time to learn Japanese, News, 322, 486 NASA: US space station heads for deep freeze, News, 322, 583

Guatemala accused of political killings, News, 322, S88 Hubble space telescope: Every delay has a silver lining, News, 322,

Weight problems, News, 322, 589

See under Palca, J., 322, 761

Space station; Taming the last lawless frontier, News, \$22,764

Bechtold, R. Directional electron transfer in rathenum-modified horse heart cytochrome c (with Kuehn, C. Lepre, C. Isied, § S) Letter to Nature, 322, 286

cke, M. See under Preisinger, A., 322, 794

See under Preisinger, A., 322, 794

cher, A. See under Squire, J., 322, 555

Begelman, M C. Cooling flows in ellipticals and the nature of radia galaxies, Letter to Nature, 322, 614

Behike, M A. Alternative splicing of murine T cell recepts. β-chain transcripts (with Loh, D Y) Letter to Nature, 322, 379

Bellugi, U. See under Damasio, A., 322, 363

nt, J W. Expression of human adenosine deaminuse in marine haematopoietic progenitor cells following retrovirui transfer (with Henkel-Tigges, J., Chang, S.M.W., Wager-Smith, K., Kellems, R.E. Dick, J.E., Magli, M.C., Phillips, R.A., Bernstein, A. Caskey, C.T.) Letter to Nature, 322, 385

der, J.F. See under Langmuir, C.H., 322, 422 Bender, TP. See under Dmitrovsky, E., 322, 748

Bentley, C B. See under Blankenship, D D., 322, 54 Bentley, C.R. See under Alley, R.B., 322, 57

Berland, J-P. Breeders' rights and patenting life forms (with Lewontin, R) Commentary, 322, 785

an, T. GAP protest over South Africa. Correspondence, 322. 402

n, A. See under Belmont, J.W., 322, 385

Berry, R J. What to believe about miracles, Commentary, 322, 321

Berry-Lowe, S. See under Schön, A., 322, 281

Bertaux, J.L. See under Morcels, G., 322, 90 chart, B. See under Jenni, 1... 322, 173

isle, RV. See under Alurkar, SK., 322, 439

chi, U. A new term in the global carbon balance (with Musi. L. Picardi, M. Piovano, E) Scientific correspondence, 322, 19

ia, E. See under Salviati, G., 322, 637

Bidaux, P. See under Drogue, C., 322, 361

Billon-Galland, M A. See under Lefevre, R., 322, 817

```
Binder. B J. Green light-mediated photomorphogenesis in a dinof-
    lagellate resting cyst (with Anderson, D M) Letter to Nature,
    322, 659
```

d, A P. See under Brown, W R A., 322, 477

Bird, R J. Is cannibalism all in the mind?, Scientific correspondence, 322, 20

Blackband, S.J. See under Aguayo, J.B., 322, 190

Blackett, N.M. Diversity of haematopoietic stem cell prowth from a uniform population of cells (with Necas, E, Frindel, E) Matters arising, 322, 289

nt. JE. See under Moreels, G., 322, 90

recombinant vaccination of the fox against rables using a live recombinant vaccinia virus (with Kieny, M.P. Lathe, R. Lecocq, JP, Pastoret, PP, Soulebot, JP, Desmettre, P) Letter to Nature 322, 373

ik, JL. See under Desjardins, C., 322, 172

bin. D D. Seismic measurements reveal a saturated norous layer beneath an active Antarctic ice stream (with Bentley, CB, Rooney, ST, Alley, RB) Letter to Nature, 322, 54 See under Alley, R.B., 322, 57

ne R. P. See under Moulin R 1 322 450

m, J. Geomagnetic reversals: Evidence for asymmetry and fluctuation. News and views. 322, 13

etti, E.A. Characteristics of Chernobyl radioactivity in Tennes see (with Brantley, J N) Scientific correspondence, 322, 313
sey, R J. See under Doherty, J B., 322, 192

lott, M H P. See under Ussami, N., 322, 629

ger, H. Hopping Conduction in Solids, Book review by Rosseins

eret, L. See under Dejean, A., 322, 70

sa, G S. Geophysics: A paradigm shift in glaciology?, News and views, 322, 18

rke, J.B. Editor, Lindow Man: The Body in the Bog, Book review Molleson, T. 322, 602

rae, WRP, Henderson Island (with David, ACF) Correspond ence, 322, 302

Brable, M. See under Hauser St. 322, 176

mmer, W. J. Editor, Cloning Vectors: A Laboratory Manual, Book review by Harris, T. 322, 603 atley, J. N. See under Bondietti, E. A., 322, 313

eur, G. See under Keating, G M., 322, 43

Bray, W. Book review of American Archaeology Past and Future: A Celebration of the Society for American Archaeology 1935-1985 (Metizer, D J, Fowler, D D, Sabloff, J A editors) 322, 784

ok, J. AGS vindicated (with Dunsmuir, P. Lindemann, J. Suslow, T. Warren, G) Correspondence, 322, 494

er, M B. Identification of a putative second T-cell receptor (with McClean, J, Dialynas, DP, Strominger, JL, Smith, JA, Owen, FL, SeidmanSeidman, JG, Ip, S, Rosen, F, Krangel, M S) Article, 322, 145

See under Bank, I., 322, 179

combe, P. See under Davies, T.D., 322, 359

on. F H. See under Designdins, C. 322, 172

Brookfield, JFY. See under Jeffreys, A.J., 322, 290 Brooks, R.R. See under Lichte, F.E., 322, 816

othwell, D. Editor, Lindow Man: The Body in the Bog, Book review by Molleson, T. 322, 602

own, F.H. See under Walker, A., 322, 517

Brown, K. See under Ouintanilla, M., 322, 78 wn, T. See under McCall, M., 322, 661

wa, W R A. Long-range restriction site mapping of mammalian genomic DNA (with Bird, A P) Letter to Nature, 322, 477

mell, W E. See under Kachar, B., 322, 365 ming, K A. Meteorology: European collaboration on dynamic

atmospheric fronts (with Hoskins, B J, Jonas, P R, Thorpe, A J) News and views, 322, 114

wastein, M. J. Book review of Neurobiology of Vasopressin (Ganten, D, Pfaff, D editors) 322, 25

Book review of Vasopressin (Schrier, R W editor) 322, 25

Brunet, J-F. The inducible cytotoxic T-lymphocyte-associated gene transcript CTLA-1 sequence and gene localization to mouse chromosome 14 (with Dosseto, M, Denizot, F, Mattei, M-G, Clark, W R, Haqqi, T M, Ferrier, P, Nabholz, M, Schmitt-Verhulst, A-M, Luciani, M-F, Golstein, P) Letter to Nature,

Brvce, M. Chiral chemistry; Asymmetric epoxidation gives organic ists a hand, News and views, 322, 776

Bryskin, V V. Hopping Conduction in Solids, Book review by Ros seinsky, D.R. 322, 220

ton, A. Sequences similar to the I transposable element in volved in I-R hybrid dysgenesis in D. melanogaster occur in other Drosophila species (with Simonelig, M, Vaury, C, Croza-tier, M) Letter to Nature, 322, 650

rke, B F. Detection of planetary systems and the search for evidence of life, Letter to Nature, 322, 340

Burks, JS. See under Hauser, SL., 322, 176

Burne, J.F. See under Cohen, J., 322, 465

Cairns, P. Intermolecular binding of xanthan gum and carob gum (with Miles, M J, Morris, V J) Letter to Nature, 322, 89

ack, R. Nitrogen fixation: A role for vanadium at last, News and views, 322, 312

mpbell, K. See under Sodroski, J., 322, 470

Canton, M. See under Squire, J., 322, 555 Carlson, T A. Apparent eukaryotic origin of glutamine synthetase II from the bacterium Bradyrhizobium jap K) Letter to Nature, 322, 568 onicum (with Chelm, B

Case, M. Physiology: Chloride ions and cystic fibrosis, News and views, 322, 407

Case, T J. Editor, Community Ecology, Book review by Townsend,

Caskey, CT. See under Craigen, W J., 322, 273 See under Belmont, J.W., 322, 385

Cussell, P. See under Festenstein, H., 322, 64

Cassimeris, J. See under Bank 1, 322, 179

Custellucci, V F. See under Goelet, P., 322, 419

Casu, B. Controversial glycosaminoglycan conformations (with Choay, J. Ferro, D R. Gatti, G. Jacquinet, J -C, Petitou, M. Provasoli, A. Ragazzi, M. Sinay, P. Torri, G) Scientific correspondence, 322, 215

Cech, TR. See under Garriga, G., 322, 86

Cervetto, L. See under McNaughton, P A. 322, 261

Chadelle, J.P. See under Valladas, H., 322, 452 Chakrabarti, S. See under Chin. V T 322, 441

Chambon, G. See under Laros, J G., 322, 152

Chandler, G O. See under Doherty, J B., 322, 192 Chang, S M W. See under Belmont, J W., 322, 385

Chang, Z. See under Ohvama, K., 322, 572

Chantler, PD. Muscle contraction: Through thick and thin, News and viewe, 322, 498

Charles, S W. See under van Wonterghem, J., 322, 622

Chase, C.G. See under Norman, S.E., 322, 450

Chau, C Y. See under Hard, T M., 322, 617

Cheetham, A K. See under Attfield, J P., 322, 620

Chelm, B K. See under Carlson, T A., 322, 568 Cheng, A Y S. See under Angel, J R P., 322, 341

Cheng, Y. The Geology of China, Book review by Sengor, A M C ..

Chess, L. See under Bank, L., 322, 179

Chiu, Y T. Imaging the outflow of ionospheric ions into the magne tosphere (with Robinson, R.M., Swenson, G.R., Chakrabarti, S. Evans, DS) Letter to Nature, 322, 441

Chony, J. See under Casu, B., 322, 215

Chamet, S. Soviet computers, Correspondence, 322, 204

Church, T M. See under Cutter, G A., 322, 720

Churchwell, E.B. See under Hollis, J.M., 322, 524

Clairemidi, J. See under Moreels, G., 322, 90 Clark, W.R. See under Brunet, J.F., 322, 268

Clarke, R. J. Transform Coding of Images, Book review by Hawkes, P 322, 787

Clegg, J.B. See under Wainscoat, J.S., 322, 21

Coakley, A.J. See under Mountford, P.J., 322, 600

Coan, E.J. See under Herron, C E., 322, 265 Coffey, D.S. See under Nelson, W.G., 322, 187

Cohen, J. Retinal ganglion cells lose response to laminin with maturation (with Burne, J.F., Winter, J., Bartlett, P) Letter to Nature, 322, 465

Cole, F.S. See under Royer-Pokora, B., 322, 32

Coley, P.D. See under Salo, J., 322, 254 Colin, C. See under Weisberg, R.H., 322, 240

Collett, G. See under Heaton, THE., 322, 822 Collingridge, GL. See under Herron, CE., 322, 265

Collins, E. Laboratory safety: Just how hot is Harvard?, News, 322, 7 Concar, D. See under Williams, R J P., 322, 213

Connerney, JEP. See under Desch, M.D., 322, 42

Cooper, D.N. See under Schmidtke, J., 322, 119

Cooper, W. Book review of The Red and the Blue: Intelligence, Treason and the Universities (by Sinclair, A.) 322, 217 witts, R. Plant viruses: New threats to crops from changing farming

practices, News and views, 322, 594

Cowen, J.P. Bacterial scavenging of Mn and Fe in a mid- to far-field hydrothermal particle plume (with Massoth, G.J., Baker, E.T) Letter to Nature, 322, 169

Cox, G. The origins of chloroplasts in eukaryotes. Scientific correspondence, 322, 412

Craigen, W J. Expression of peptide chain release factor 2 requires high-efficiency frameshift (with Caskey, CT) Letter to Nature, 322, 273

Crawley, M J. Book review of Ecological Knowledge and Environmental Problem-Solving: Concepts and Case Studies (by Committee on the Applications of Ecological Theory to EnvironmentalProblems.) 322, 219

shaw, EB III. See under Nelson, C., 322, 557

Crompton, R. W. Aussie disclaimer, Correspondence, 322, 107 rs, J. Book review of The Encyclopaedia of Reptiles and

Amphibians (Halliday, T, Adler, K editors) 322, 416 Book review of The Encyclopaedia of Insects (O'Toole, C editor) 322. 416

wn, D A. Planetology: Sulphur and volcanism on Io (with Greeley, R) News and views, 322, 593 regatier, M. See under Bucheton, A., 322, 650

Curautte, J.T. See under Royer-Pokora, B., 322, 32 Curran, T. See under Morgan, J.L., 322, 552

sh, S. See under Festenstein, H., 322, 64

Cutler, D J. Observation of terrestrial orbital motion using the mic-ray Compton-Getting effect (with Groom, DE) Letter to Nature, 322, 434

Cutter, G. A. Selenium in western Atlantic precipitation (with Church, T.M.) Letter to Nature, 322, 720

ahlgren, M E. See under Doherty, J B., 322, 192

masto, A. Sign language aphasia during left-hemisphere Amytal injection (with Bellugi, U., Damasio, H., Poizner, H., Van Gilder, S.) Letter to Nature, 322, 363

Damasio, H. See under Damasio, A., 322, 363 Dangl, J. See under Kleinfield, R., 322, 843

David, A C F. See under Bourne, W R P., 322, 302
Davies, T D. Acidity of Scottish rainfall influenced by climatic change (with Kelly, PM, Brimblecombe, P, Farmer, G, Barthelmie, R I) Letter to Nature, 322, 359

ison, W. Sewage sludge as an acidity filter for groundwater-fed lakes, Letter to Nature, 322, 820

Dawkins, M S. Book review of Laboratory Animal Husbandry: Ethology, Welfare and Experimental Variables (by Fox, M.W.) 322, 782

Dayton, P K. See under Genin, A., 322, 59

De Lucia, F.C. See under Hollis, J.M., 322, 524

De Rudder, A. See under Keating, G.M., 322, 43 de The, G. See under Hauser, S.L., 322, 176

de Vries, RRP. See under Ottenhoff, THM., 322, 462

Dejean, A. Hepatitis B virus DNA integration a sequence homolo-gous to v-erb-A and steroid receptor genes in a hepatocellular carcinoma (with Bougueleret, L. Grzeschik, K-H, Tiollais, P) Letter to Nature, 322, 70

on, E. Palaeoanthropology: Human phylogeny revised again, News and views, 322, 496

ning, D. Infrared helioseismology: detection of the chromospheric mode (with Glenar, D.A., Käufl, H.U., Hill, A.A., Espenak, F.) Letter to Nature, 322, 232

izat, F. See under Brunet LF 322, 768

DePhinho, R A. See under Bank, L., 322, 179

Desch, M.D. The rotation period of Uranus (with Connerney, J.E.P., Kaiser, M.L.) Letter to Nature, 322, 42

Desjardins, C. Genetic selection for reproductive photoresponsiveness in deer mice (with Bronson, F H, Blank, J L) Letter to Nature, 322, 172

ettre, P. See under Blancou, J., 322, 373

Devés, R. Academic oppression in Chile (with Galanti, N, Valenzuela, C. Vivaldi, E A) Correspondence, 322, 494

rey, R J. Binary pulsar with a very small mass function (with Maguire, CM, Rawley, LA, Stokes, GH, Taylor, JH) Letter to

di Paoli, P. Italian biotechnology: New initiative is called for, News, 322. 8

Dialynas, D.P. See under Brenner, M.B., 322, 145

See under Overtermous, T., 322, 184

Diamond, J. Editor, Community Ecology, Book review by Town-send, C. 322, 507

ond, J M. Animal behaviour; How great white sharks, sabretoothed cats and soldiers kill, News and views, 322, 773

Dick, JE. See under Belmont, JW., 322, 385

Dickson, D. Book review of Scientists and journalists: Reporting science as news (Friedman, S M, Dunwoody, S, Rogers, C L editors) 322, 317

dorf, M. The mystery of declining tooth decay, Commentary, 322 125

DiLella, A.G. Tight linkage between a splicing mutation and a specific DNA haplotype in phenylketonuria (with Marvit, J, Lidsky, A S, Güttler, F, Woo, S L C) Article, 322, 799

Diner, D J. Prospecting for planets in circumstellar dust: sifting the evidence from \$ Pictoris (with Appleby, J F) Letter to Nature,

Dixon, R. Book review of The Biochemistry and Physiology of Plant Disease (by Goodman, R N, Király, Z, Wood, K R.) 322, 604 trovsky, E. Expression of a transfected human c-myc oncoger inhibits differentiation of a mouse erythroleukaemia cell line (with Kuehl, W M, Hollis, G F, Kirsch, I R. Bender, T P, Segal, S) Letter to Nature, 322, 748

erty, J B. Cephalosporin antibiotics can be modified to inhibit human leukocyte elastase (with Ashe, B M. Argenbright, L W. Barker, P L., Bonney, R J., Chandler, G O., Dahlgren, M E., Dorn, C P Jr, Finke, P E, Firestone, R A, Fletcher, D, Hag-mann, W K, Mumford, Mumford, R, O'Grady, L, Maycock, A L, Pisano, J M, Shah, S K, Thompson, K R, Zimmerman, M) Letter to Nature, 322, 192

Dorn, CP Jr. See under Doherty, JB., 322, 192

seto, M. See under Brunet, I-F. 322, 268

over, G A. See under Tautz, D., 322, 652

Dragovan, M. See under Stark, A.A., 322, 805 See under Stark, A.A., 322, 805

Drake, M.J. See under Jones, J.H., 322, 221 Drogue, C. Simultaneous outflow of fresh water and inflow of sea

water in a coastal spring (with Bidaux, P) Letter to Nature, 322, 361

Dubois-Daleq, M. See under Kristensson, K., 322, 544

Dubowitz, V. X;autosome translocations in females with Duchenne or Becker muscular dystrophy, Matters arising, 322, 291

hala. C S. See under Kristensson, K., 322, 544

can, R A. Plume versus lithospheric sources for melts at Ua Pou, Marquesas Islands (with McCulloch, M.T., Barsczus, H.G., Nelson, DR) Letter to Nature, 322, 534

smuir, P. See under Bredbrook, J., 322, 494

Dunwoody, S. Editor, Scientists and journalists: Reporting science as news, Book review by Dickson, D. 322, 317 Nessy, J C. See under Labeyrie, L.D., 322, 701

Duprat, J. See under Labevrie, L.D., 322, 701 Dyer, KR. Coastal and estuarine sediment dynamics, Book review by

Allen, J R L. 322, 318 Endy, R.R. See under Robson, R.L., 322, 388

Eder, G. See under Preisinger, A., 322, 794
See under Preisinger, A., 322, 794

Edwards, G.R. Archaean geology; Hungry komatiites and indigesti-ble zircons (with Nisbet, E.G.) News and views, 322, 771

Edwards. J G. Pesticide regulation, Correspondence, 322, 768 Edwards, M S. See under Barlow, D J., 322, 747

Efstathiou, G. Computational cosmology: Galactic haloes need computers, News and views, 322, 311

Eichmann, K. See under Hochgeschwender, U., 322, 376
Ellers, M. Binding of a specific ligand inhibits import of a purified precursor protein into mitochondria (with Schatz, G) Article, 322, 228

Eisinger, J. Book review of The Lead Debate: The Environ

```
AUTHOR INDEX-
                                                                                     Gauthier, L. See under Payette, S., 322, 724
     Toxicology and Child Health 322, 601
                                                                                     Gee, R W. Screwworm fly, Correspondence, 322, 106
Efferink, D.G. See under Ottenhoff, T.H.M., 322, 462.
Elinson, R.P. See under Kao, K.R., 322, 371
                                                                                     Gehrmann, P. See under Reth, M., 322, 840
Geneste, J M. See under Valladas, H., 322, 452
   dier, JA. Natural selection in the wild, Book review by Jones, JS.
                                                                                     Genin, A. Corals on seamount peaks provide evidence of current
     122, 124
                                                                                           acceleration over deep-sea topography (with Dayton, P K, Lonsdale, P F, Spiess, F N) Letter to Nature, 322, 59
Enger-Valle, B E. Editor, Cloning Vectors: A Laboratory Man
      Book review by Harris, T. 322, 603
                                                                                           ach, D.C. Mantle heterogeneity beneath the Nazca plate: San
Felix and Juan Fernandez islands (with Hart, S.R., Morales, V.W.
 Epplen, J.T. See under Hochgeschwender, U., 322, 376
Erickson, W.C. See under Kassim, N.E., 322, 522
Erwin, J. Monkeyed about, Correspondence, 322, 204
                                                                                           J. Palacios, C) Letter to Nature, 322, 165
        k, F. See under Deming, D., 322, 232
                                                                                            sin, R N. See under Kroczek, R A., 322, 181
                                                                                     Gletz, R D. See under Spencer, C A., 322, 279
        don, R. See under Alexandropoulos, N.G., 322, 779
Evans, DS. See under Chiu, YT., 322, 441
                                                                                     Giles, E. Are we all out of Africa? (with Ambrose, S H) Scientific
                                                                                           correspondence, 322, 21
Evans, R.M. See under Nelson, C., 322, 557
Fabian, A C. Astronomy: First X-ray-ionized nebula, News and
                                                                                            ore, G. The chemical evolution of the Galaxy (with Wyse, R.F.
                                                                                           G) Letter to Nature, 322, 806
views, 322, 496
Fakley, D. Book review of Verification: How Much is Enough? (by
                                                                                        The chemical evolution of the Galaxy (with Wyse, RFG) Letter to
      Krass, A S.) 322, 218
                                                                                           Nature, 322, 806
                                                                                            ir, D A. See under Deming, D., 322, 232
Fan, X. See under Modlin, R.L., 322, 459
                                                                                     Glick, D.M. See under Auer, H.E., 322, 664
Goddard, A.D. See under Squire, J., 322, 555
Farmer, G. See under Davies, TD., 322, 359
Feldmann, R.M. The stability of zoological nomenclature, Scientific
                                                                                     Goelet, P. The long and the short of long-term memory-a molecular framework (with Castellucci, V F, Schacher, S, Kandel, E R)
     correspondence, 322, 120
Fellgett, PB. A threat to medical progress, Correspondence, 322, 204
Fellous, M. See under Israel, A., 322, 743
                                                                                           Review article, 322, 419
                                                                                     Goff, S.C. See under Royer-Pokora, B., 322, 32
Fenimore, E.E. See under Laros, J.G., 322, 152
Ferrier, P. See under Brunet, J-F., 322, 268
                                                                                          oshev, M. See under Moreels, G., 322, 90
osheva, Ts. See under Moreels, G., 322, 90
Ferrill. A. The Origins of War From the Stone Age to Alexander the
      Great, Book review by McNeill, W H. 322, 416
                                                                                      Gob, W.C. See under Sodroski, J., 322, 470
Ferro, D.R. See under Caso, B., 322, 215
                                                                                     Goldfarb, DS. Synthetic peptides as nuclear localization signals (with
                                                                                           Gariépy, J., Schoolnik, G., Kornberg, R.D.) Letter to Nature,
 Fersht, A.R. Quantitative analysis of structure-activity relatio
      in engineered proteins by linear free-energy relationships (with
                                                                                           322, 641
      Leatherbarrow, R.J., Wells, T.N.C.) Letter to Nature, 322, 284
                                                                                           tein, P. See under Brunet, J-F., 322, 268
     enstein, H. New HLA DNA polymorphisms associated with autoimmune diseases (with Awad, J. Hitman, G. A., Cutbrush,
                                                                                          odfeliow, P.N. Duchenne muscular dystrophy: Collaboration and
progress, News and views, 322, 12
       S, Groves, A V, Cassell, P, Ollier, W, Sachs, J A) Letter to
                                                                                                 w, W D. Earth sciences: Anoxic o
                                                                                           carbon isotope trends, News and views, 322, 116
      Nature. 322, 64
     amour immunology: MHC antigens and malignancy (with Garrido, F) News and views, 322, 502
                                                                                               m, R N. The Biochemistry and Physiology of Plant Disease,
                                                                                           Book review by Dixon, R. 322, 604
 Festow, M.C. See under Moreels, G., 322, 90
                                                                                             un, R. See under Rajasekharan, K., 322, 528
 Fex, J. See under Kachar, B., 322, 365
Fikani, M.M. See under Laros, J.G., 322, 152
                                                                                     Gorski, J. Polymorphism of human la antigens: gene conversion between two DR \beta loci results in a new HLA-D/DR specificity
 Filippenko, A.V. See under Sargent, W.L.W., 322, 40
Finke, P.E. See under Doherty, J.B., 322, 192
                                                                                     (with Mach, B) Letter to Nature, 322, 67
Gott, JR III. See under Stark, A A., 322, 805
 Finney, J.L. See under Savage, H.F.J., 322, 717
Firestone, R.A. See under Doherty, J.B., 322, 192
                                                                                        See under Stark, A.A., 322, 805
                                                                                      Gough, S. See under Schön, A., 322, 281
 Fischer, J. See under Woods, J.D., 322, 446
                                                                                     Grant, S. Normal maturation involves systematic changes in b
 Fischer, K.M. Thermal and mechanical constraints on the lithosphere
                                                                                           lar visual connections in Xenopus laevis (with Keating, M J)
      beneath the Marquesas swell (with McNutt, M. A., Shure, L.)

Letter to Nature, 322, 733
                                                                                           Letter to Nature, 322, 258
                                                                                     Grass, F. See under Preisinger, A., 322, 794
See under Preisinger, A., 322, 794
Gratz, A.J. See under Preisinger, A., 322, 794
See under Preisinger, A., 322, 794
 Fitter, A. Book review of The Oxford Dictionary of Natural History
 (Allaby, M editor) 322, 23
Fleet, I R. See under Mountford, P J., 322, 600
                                                                                     Gratzer, W. Book review of Diamond Dealers and Feather Mer-
chants: Tales from the Sciences (by Klotz, I M.) 322, 781
 Fletcher, D. See under Doherty, J.B., 322, 192
 Fleury, B.E. Darwin's vellow rain. Correspondence, 322, 767
 Forsyth, DA. Crustal structure of the northern Alpha Ridge beneath
                                                                                     Gray, J. Molecular botany: Wonders of chloroplast DNA, News and
      the Arctic Ocean (with Asudeh, I. Green, A.G. Jackson, H.R.)
                                                                                           views, 322, 501
       Letter to Nature, 322, 349
                                                                                      Greeley, R. See under Crown, D A., 322, 593
 Forsyth, P.D. See under Jones, G.D. 322, 313
                                                                                     Green, A.G. See under Forsyth, D.A., 322, 349
Grenier, I. See under Payette, S., 322, 724
 Fournier, A. See under Israel, A., 322, 743
 Fowler, D D. Editor, American Archaeology Past and Future: A
                                                                                     Gribbin, J. In Search of the Big Bang: Quant
      Celebration of the Society for American Archaeology 1935-
                                                                                           ogy, Book review by Silk, J. 322, 505
 1985, Book review by Bray, W. 322, 784
Fowler, V.M. Cytoskeleton, New views of the red cell network, News
                                                                                     Griffith, J. DNA loops induced by cooperative binding of lambda repressor (with Hochschild, A. Ptashne, M) Letter to Nature,
and views, 322, 777

Fox, M W. Laboratory Animal Husbandry: Ethology, Welfare and
                                                                                            322, 750
                                                                                     Griffiths, E.C. Thyrotrophin-releasing hormone: New applications in
      Experimental Variables, Book review by Dawkins, M S. 322,
                                                                                           the clinic, News and views, 322, 212
      782
                                                                                     Griffiths, J.F. Novel experimental investigation of spontaneous igni-
                                                                                           tion of gaseous hydrocarbons (with Nimmo, W) Letter to Na-
 Franco, R. See under Nelson, C., 322, 557
 Frazier, K. Editor, Science Confronts the Paranormal. Book review
                                                                                            ture 322, 46
      by Hansel, CE M. 322, 505
                                                                                            m. D E. See under Cutler, D J., 322, 434
 Frerichs, G N. Ulcerative rhabdovirus in fish in South-East Asia
                                                                                           sberg, R K. The genetic control and consequences of kin recogni-
      (with Millar, S.D., Roberts, R.J.) Scientific correspondence, 322,
                                                                                           tion by the larvae of a colonial marine invertebrate (with Quinn,
                                                                                           JF) Letter to Nature, 322, 456
 Fried, M. See under Williams, T., 322, 275
                                                                                      Groves, A V. See under Festenstein, H., 322, 64
 Friedman, S.M. Editor, Scientists and journalists: Reporting science
                                                                                          ass, P. A system of nomenclature for murine ho
      as news, Book review by Dickson, D. 322, 317
                                                                                           Kessel, M) Scientific correspondence, 322, 780
 Friend, R. H. Solid-state physics: New semiconducting polymers,
News and views, 322, 308
                                                                                      Grzeschik, K-H. See under Dejean, A., 322, 70
                                                                                      Gumbiner, B. See under van Meer, G., 322, 639
Gunter, K.C. See under Kroczek, R.A., 322, 181
 Frindel, E. See under Blackett, N.M., 322, 289
                                                                                     Gusella, J.F. See under Scizinger, B.R., 322, 644
Gust, D. See under Wasielewski, M.R., 322, 570
 Fruchter, A.S. See under Segelstein, D.J., 322, 714
 Fryer, G. Ecology: Lunar cycles in lake plankton, News and views,
       322, 306
                                                                                      Güttler, F. See under DiLella, A.G., 322, 799
 Fukuzawa, H. See under Ohyama, K., 322, 572
                                                                                      Hause, A.T. Pathogenesis of lentivirus infections, Review article, 322.
 Galini, N. See under Devés, R., 322, 494
Gallie, B.L. See under Squire, J., 322, 555
                                                                                      Habermann, E. See under Aktories, K., 322, 390
                                                                                     Hagmann, W K. See under Doherty, J B., 322, 192
Häkkinen, I. See under Salo, J., 322, 254
 Galloway, J. Protein structure: Kinky variations of collagen, News
      and views, 322, 497
 Ganten, D. Editor, Neurobiology of Vasopressin, Book review by
Brownstein, M.J. 322, 25
                                                                                      Halliday, T. Editor, The Encyclopaedia of Reptiles and Amphibians,
                                                                                           Book review by Crothers, J. 322, 416
 Garcia, J. V. Synergism between immunoglobulin enhancers and
promoters (with thi Bich-Thuy, L., Stafford, J., Queen, C) Letter
                                                                                              er, C. Glaciology; Frozen news on hot events, News and views,
                                                                                           322, 778
       to Nature, 322, 383
                                                                                             m, M. See under Mountford, P.J., 322, 600
```

Article, 322, 137

Happle, R. See under Micr, P.D., 322, 504 Haqqi, T.M. See under Brunet, J-F., 322, 268

Garlépy, J. See under Goldfarb, D.S., 322, 641

TR) Letter to Nature, 322, 86

Garzoli, S.L. See under Katz, E.J., 322, 245 Gatti, G. See under Casu, B., 322, 215 Gaudichet, A. See under Lefèvre, R., 322, 817

Garrido, F. See under Festenstein, H., 322, 502

Garriga, G. Mechanism of recognition of the 5' splice site in self-splicing group I introns (with Lambowitz, A.M., Inoue, T., Cech,

```
Hard, T.M. Dimmal cycle of tropospheric OH (with Chau, C.Y.
                                                                                           Mehrabzadeh, A.A., Pan, W.H., O'Brien, R.J.) Letter to Nature,
                                                                                           322 617
                                                                                     Hardwick, R C. Linkage between the nation states, Scientific corres-
                                                                                           pondence, 322, 20
                                                                                     Hardy, R.R. See under Kleinfield, R. 322, 843
                                                                                     Harlharan, P. Optical interferometry, Book review by Heavens, O.S.
                                                                                           322 414
                                                                                     Harnad, S. Book review of A Difficult Balance: Editorial Peer
                                                                                           Review in Medicine (by Lock, S.) 322, 24
                                                                                     Harris, J M. See under Walker, A., 322, 517
                                                                                     Harris, J. M. See trader Watter, A., 545, 517

Harris, T. Book review of Cloning Vectors: A Laboratory Manual
(Pouwels, P. H., Enger-Valk, B. E., Brammer, W. J. editors) 322.
                                                                                          rison, E. Kelvin on an old, celebrated hypothesis. Comm
                                                                                           rison, S.C. Gene regulation: Fingers and DNA half-turns, News
                                                                                           and views, 322, 597
                                                                                      Hart, S.R. See under Gerlach, D.C., 322, 165
                                                                                      Harvey, P.H. See under Read. A.F., 322, 408
                                                                                              orn, R. Biochemistry: New role for transfer RNA, News and
                                                                                           views 322: 208
                                                                                              ne, W A. See under Sodroski, J., 322, 470
                                                                                      Hastenrath, S. See under Lamb, P.J., 322, 238
                                                                                                d, K. See under Kristoffersen, Y., 322, 538
                                                                                          seer, S.L. Analysis of human T-lymphotropic virus sequences in
multiple sclerosis tISSUE (with Aubert, C. Burks, J.S. Kerr, C.
                                                                                           Lyon-Caen, O, de The, G, Brahic, M) Letter to Nature, 322, 176
                                                                                     Hawkes, P.W. Book review of Transform Coding of Images (bu
                                                                                           Clarke, R J.) 322, 782
                                                                                        Book review of Image analysis: Principles & practice 322, 122
                                                                                        wkesworth, C J. Evidence from the Parana of south Brazil for a
                                                                                           continental contribution to Dupal basalts (with Mantovani, MS M, , Taylor, P N, Palacz, Z) Letter to Nature, 322, 356
                                                                                         wkins, M. See under Robson, R L., 322, 388
uzard, C. A QSO with redshift 3.8 found on a UK Schmidt tele-
                                                                                            scope IIIa-F prism plate (with McMahon, R.G. Sargent, W.L.W).
                                                                                           Letter to Nature, 322, 38
                                                                                        See under Sargent, W L. W., 322, 40
                                                                                     Heap, R.B. See under Mountford, P.J., 322, 600
Heaton, T.H.E. Climatic influence on the isotopic composition of
                                                                                           bone nitrogen (with Vogel, J.C., von la Chevallerie, G. Collett,
                                                                                           G) Letter to Nature, 322, 822
                                                                                            ens. OS. Book review of Optical interferometry (by Haribaran,
                                                                                           P.) 322, 414
                                                                                      Hellig, J S. Diversity of murine gamma genes and expression in fetal
                                                                                           and adult T lymphocytes (with Tonesawa, S) Letter to Nature,
                                                                                           322, 836
                                                                                           drickson, W. Physical Methods for Inorganic Biochemistry,
                                                                                           Book review by Thomson, A J. 322, 506
                                                                                        enin, C. See under Hisard, P., 322, 243
tenkel-Tieges, J. See under Belmont, J.W., 322, 385
                                                                                      Herbst, E. See under Hollis, J M., 322, 524
                                                                                          rero-Bervera, E. Non-axisymmetric behavious of Olduvai and
                                                                                           Jaramillo polarity transitions recorded in north-central Pacific
                                                                                           deep-sea sediments (with Theyer, F) Letter to Nature, 322, 189
                                                                                           ron, C E. Frequency-dependent involvement of NMDA recep-
                                                                                          tors in the hippocampus: a novel synaptic mechanism (with Lester, R A J, Coan, E J, Collingridge, G L) Lener to Nature,
                                                                                           322, 265
                                                                                                erg, L. A. See under Kleinfield, R., 322, 843
                                                                                     Hill, A A. See under Deming, D., 322, 232
Hill, A V S. See under Wainscoat, J S., 322, 21
                                                                                      Hill, W G. DNA fingerprint analysis in immigration test-cases, Mat-
                                                                                           ters arising, 322, 290
                                                                                          termann, M. See under Aguayo, J B., 322, 190
                                                                                      Himma, Y. See under Ishida, T., 322, 504
                                                                                        Irano, S. Japanese education, Correspondence, 322, 402
                                                                                     Hisard, P. Oceanic conditions in the tropical Atlantic during 1983 and 1984 (with Henin, C. Houghton, R. Piton, B. Rusi, P.
                                                                                           Letter to Nature, 322, 243
                                                                                        See under Katz, E.J., 322, 245
                                                                                     Hitman, G.A. See under Festenstein, H., 322, 64
Hachgeschwender, U. Preferential expression of a defined T-cell.
                                                                                           receptor β-chain gene in hapten-specific cytotoxic T-cell closs
                                                                                           (with Weltzien, H.U. Eichmann, K. Wallace, R.B. Ecoles, J.T.
                                                                                            Letter to Nature, 322, 376
                                                                                      Hochschild, A. See under Griffith, J., 322, 750
                                                                                      Hodgetts, R.B. See under Spencer, C.A., 322, 279
                                                                                      Hekkvo. N. Anti-darwinism in Japan, Correspondence, 322, 107
                                                                                           in, GF. See under Dmitrovsky, E., 322, 748
                                                                                     Hollis, J.M. An interstellar line coincident with the P(2,1) transition of hydronium (H<sub>3</sub>O<sup>+</sup>) (with Churchwell, E.B., Herbst, E. De
                                                                                           Lucia, FC) Letter to Nature, 322, 524
nes, KV. See under Kristensson, K., 322, 544
                                                                                     Holzbecher, J. See under Lichte, F.E., 322, 816
Hongzhen, W. The Geology of China, Book review by Sengor, A.M.
                                                                                           C. 322, 507
                                                                                      Horel, J.D. Atmospheric conditions in the Atlantic sector during 1983
                                                                                                1984 (with Kousky, V E, Kagano, M T) Letter to N
                                                                                           322, 248
                                                                                           ins, BJ. See under Browning, KA., 322, 114
Hanahan, D. See under Lacey, M., 322, 609
Hanan, B B. Pb isotope evidence in the South Atlantic for migrating
                                                                                      Hough, J.H. See under Bailey, J., 322, 150
                                                                                                m, R. See under Hisard, P., 322, 243
      ridge-hotspot interactions (with Kingsley, R H, Schilling, J-G)
                                                                                      Howie, A. Reply: Motions of the images of asoms, Scientific corres-
                                                                                           pondence, 322, 19
     sel, C E M. Book review of Science Confronts the Paranormal (Frazier, K editor) 322, 505

    Hoyle, F. The case for life as a cosmic phenomenon (with Wickramasinghe, N C) Commentary, 322, 509
    Humphrey, J. The World of Science and the Rule of Law. Book
```

review by Maddox, J. 322, 783

```
ster, T. Cancer: Cell growth control mechanisms, News and
       views, 322, 14
der, W N. See under McCall, M., 322, 661
 Huppert, H E. Fluid mechanics: G.I. Taylor and his influence, News
        and views 322, 500
 Hurley, K. See under Laros, J G., 322, 152
 Ikeda, T. See under Noda, M., 322, 826
Imoto, K. See under Mishina, M., 322, 90
 Inokuchi, H. See under Ohyama, K., 322, 572
 Inoue, T. See under Garriga, G., 322, 86
Ip, S. See under Brenner, MB., 322, 145
         to, P. See under Labevrie 1 D 322, 701
 leving, M. Book review of Skeletal Muscle. Handbook of Microsco-
     pic Anatomy, Vol.2, Part 6 (by Schmalbruch, H.) 322, 415

ove, N. N. Reply: Diversity of haematopoietic stem cell growth
       from a uniform population of cells (with Magli, M.C., Odart-chenko, N) Matters arising, 322, 289
fishida, T. The origin of Japanese HTLV-I (with Hinuma, Y) Scien-
tific correspondence, 322, 504
Isled, S S. See under Bechtold, R., 322, 286
Israel, A. Interferon response sequence potentiates activity of an enhancer in the promoter region of a mouse H-2 gene (with Kimura, A. Fournier, A. Fellous, M., Kourilsky, P) Letter to
       ickis, M. Product review: Imaging cells with acoustic micros-
       copy, Miscellany, 322, 91
Jackson, H R. See under Forsyth, D A., 322, 349
      seen, M. J. Hydrocarbon shows and petroleum source rocks in sediments as old as 1.7x10<sup>9</sup> years (with Powell, T.G., Summons,
       R E, Sweet, I P) Letter to Nature, 322, 727
            t, J.-C. See under Casu. B., 322, 215
Jakobs, K.H. See under Aktories, K., 322, 390

James, G. Physical Methods for Inorganic Biochemistry, Book re-
```

ses, M N G. Reply: The mechanism of activation of porcine pepsinogen (with Sielecki, A R) Maners arising, 322, 664 sraman, K S. Eucalyptus clean-up, News, 322, 102 India: Space programme uncertainty, News, 322, 198

Jeffreys, A J. Reply: DNA fingerprinting analysis in immigration test-cases (with Brookfield, J F Y, Semeonoff, R) Matters arising 322, 290

the, S.A. A class of narrow-band-gap semiconducting polymers. Letter to Nature, 322, 345 ins, C. See under Argyle, B., 322, 402

Jenni, L. Hybrid formation between African trypanosomes during cyclical transmission (with Marti, S, Schweizer, J, Betschart, B, Le Page, R W F, Wells, J M, Tait, A, Paindavoine, P, Pays, E, Steinert, M) Letter to Nature, 322, 173

ngs, W H. Product review: The laboratory networking dilemma, Miscellany, 322, 665

view by Thomson, A J. 322, 506

nas, PR. See under Browning, KA., 322, 114
nes, D. See under Argyle, B., 322, 402
nes, G. D. Observation of ^{110m}Ag in Chernobyl fallout (with Forsyth, P.D. Appleby, P.G.) Scientific correspondence, 322, 313 s, J.H. Geochemical constraints on core formation in the Earth (with Drake, M.J) Review article, 322, 221

s, JS. Book review of Natural selection in the wild (by Endler, J

A.) 322, 124 Mankind's genetic bottleneck (with Rouhani, S) Scientific correspondence, 322, 599

s, P D. Global temperature variations between 1861 and 1984 (with Wigley, TML, Wright, PB) Article, 322, 430

s, R V. Book review of A life in science (by Mott, N.) 322, 121 s, V J. Lake acidification and the land-use hypothesis: a m post-glacial analogue (with Stevenson, A C, Battarbee, R W) Letter to Nature, 322, 157

B. J.L. See under Valladas, H., 322, 452

Kachar, B. Electrokinetic shape changes of cochlear outer hair cells (with Brownell, W E, Altschuler, R, Fex, J) Letter to Nature, 322, 365

Kagano, M T. See under Horel, J D., 322, 248 Kaiser, M L. See under Desch, M D., 322, 42 Kalijola, R. See under Salo, J., 322, 254 Kampf, U. See under Karpas, A., 322, 177 Kandel, E.R. See under Goelet, P., 322, 419 Kane, S.R. See under Laros, J.G., 322, 152

para, C G. See under Schön, A., 322, 281

Kao, K R. Lithium-induced respecification of pattern in Xenopus luevis embryos (with Masiu, Y, Elinson, R P) Letter to Nature, 322, 371

er, G D. See under Ussami, N., 322, 629

Karpas, A. Lack of evidence for involvement of known human retro viruses in multiple sclerosis (with Kämpf, U, Siden, A, Koch, M. Poser, S) Letter to Nature, 322, 177

Kaasim, N E. Steep-spectrum radio lobes near the galactic centre (with LaRosa, T N, Erickson, W C) Letter to Nature, 322, 522
 Kato, H. See under Modlin, R L., 322, 459
 Kato, T. See under Ohtani, E., 322, 352
 Katz, E J. Annual change of sea surface slope along the Equator of the control of the contr

the Atlantic Oceanin 1983 and 1984 (with Hisard, P, Verstraete, J-M, Garzoli, S L) Letter to Nature, 322, 245

Käuft, H U. See under Deming, D., 322, 232

Kay, R W. Aleutian terranes from Nd isotopes (with Rubenstone, J L, Kay, SM) Article, 322, 605

Kay, S M. See under Kay, R W., 322, 605

Keating, G.M. Detection of stratospheric HNO₃ and NO₂ response to short-term solar ultraviolet variability (with Nicholson, J.III. Brasseur, G. De Rudder, A. Schmailzl, U. Pitts, M) Letter to

Keating, M J. See under Grant, S., 322, 258

Keny, R. Help for Africa, Correspondence, 322, 767 erling, T. A. Product review: Vibrational CD of biopolymers, Miscellany, 322, 851 Kellems, R E. See under Belmont, J W., 322, 385

Kelly, P M. See under Davies, T D., 322, 359

Kendrick-Jones, J. See under Reinach, F.C., 322, 80 Kennard, O. See under McCall, M., 322, 661 Kerr, C. See under Hauser, S L., 322, 176

haw, A P. Climatic change and Aboriginal burning in north-east Australia during the last two glacial/interglacial cycles, Letter to Nature, 322, 47

Kessel, M. See under Gruss, P., 322, 780

Kieny, M.P. See under Blancou, 1., 322, 373
Kijima, T. A new type of host compound consisting of a-zirconium phosphate and an aminated cyclodextrin (with Matsui, Y) Letter to Nature, 322, 533

orth, PD. Adrian Edmund Gill (1937-1986), News and views. 322, 410

ara, A. See under Israel, A., 322, 743

King, R C. How to abbreviate recombinant genes, Scientific correspondence, 322, 780

Kingland, S.E. Modeling Nature. Episodes in the History of Population Ecology, Book review by Lawton, J H. 322, 603

Kingsley, R.H. See under Hanan, B.B., 322, 137 Király, Z. The Biochemistry and Physiology of Plant Disease, Book review by Dixon, R. 322, 604

Kirsch, I R. See under Dmitrovsky, E., 322, 748

Kitcher, P. Book review of Neurophilosophy: Toward a Unified Science of the Mind-Brain (by Smith Churchland, P.) 322, 413

Kintser, PR. See under Ottenhoff, THM., 322, 462

Klebesadel, R. W. See under Laros, J.G., 322, 152 Kleinfield, R. Recombination between an expressed in lin heavy-chain gene and a germline variable gene segment in a Ly 1* B-cell lymphoma (with Hardy, R R, Tarlinton, D, Dangl J, Herzenberg, L A, Weigert, M) Letter to Nature, 322, 843

Klempner, M S. See under Pollack, C., 322, 834 Kline, P. Models of man, Correspondence, 322, 767

Klotz, I M. Diamond Dealers and Feather Merchants: Tales from the Sciences, Book review by Gratzer, W. 322, 781

mpp, S. See under Schultz, J E., 322, 271

Ko, K W. See under Tung, K-K., 322, 811

Ko, M K W. See under Tung, K-K., 322, 811

Koch, C.J W. See under van Wonterghem, J., 322, 622

Koch, M. See under Karpas, A., 322, 177

Koenderink, J. See under Rogers, B., 322, 62 Kohchi, T. See under Ohyama, K., 322, 572

Koff, W J. Speaking up, Correspondence, 322, 106
Korn, A P. Motions of the images of atoms, Scientific correspondence, 322, 19
Kornberg, R D. See under Rothman, J E., 322, 209

See under Goldfarb, D S., 322, 641

Kotsis, K.T. See under Alexandropoulos, N.G., 322, 779

Kourlisky, P. See under Israel, A., 322, 743 Kousky, V E. See under Horel, J D., 322, 248 Krangel, M S. See under Brenner, M B., 322, 145

Krasnopolsky, V A. See under Morcels, G., 322, 90
Krass, A S. Verification: How Much is Enough?, Book review by Fakley, D. 322, 218

Krawczak, M. See under Schmidtke, J., 322, 119 Kreil, G. See under Kuhn, A., 322, 335

Kristensson, K. Increased levels of myelin basic protein transcripts gene in virus-induced demyelination (with Holmes, K V. Duchala, C S, Zeller, N K, Lazzarini, R A, Dubois-Dalcq, M)
Letter to Nature, 322, 544

Kristoffersen, Y. Geophysical evidence for the East Antarctic plate boundary in the Weddell Sea (with Haugland, K) Letter to Nature, 322, 538

Kroczek, R A. Thy-1 functions as a signal transduction molecule in T lymphocytes and transfected B lymphocytes (with Gunter, K C, Germain, R N, Shevach, E M) Letter to Nature, 322, 181

Kroto, H W. What's in a name?, Correspondence, 322, 766

Krueger, A.J. See under Stolarski, R.S., 322, 808

der Stolarski, R.S., 322, 808

Krupp, G. See under Schön, A., 322, 281 Krysko, A.A. See under Moreels, G., 322, 90

Kuehl, W.M. See under Dmitrovsky, E., 322, 748

in, C. See under Bechtold, R., 322, 286

Kuhn, A. The cytoplasmic carboxy terminus of M13 procoat is required for the membrane insertion of its central domain (with Wickner, W. Kreil, G) Article, 322, 335

Kukowska, J. See under Prochownik, EV., 322, 848 Kunkel, L. M. See under Royer-Pokora, B., 322, 32

Kunkel, L. M and co-authors. Analysis of deletions in DNA from patients with Becker and Duchenne muscular dystrophy, Letter to Nature, 322, 73 o, M. See under Noda, M., 322, 826

Kurt, V G. See under Laros, J G., 322, 152

Labeyrie, L.D. Melting history of Antarctica during the past 60,000 years (with Pichon, J.J., Labracherie, M., Ippolito, P., Duprat, J., Duplessy, J.C.) Article, 322, 701

Laberacherle, M. See under Labeyrie, L. D., 322, 701

Lacey, M. Bovine papillomavirus genome elicits skin tumours in transgenic mice (with Alpert, S, Hanahan, D) Article, 322, 609

Labodynsky, R. See under Preisinger, A., 322, 794

See under Preisinger, A., 322, 794
sing, R. See under Argyle, B., 322, 402

Laj, C. See under Valet, J.P., 322, 27

Lamb, P J. Interannual variability of rainfall in the tropical Atlantic (with Peppler, R A, Hastenrath, S) Letter to Nature, 322, 238 showitz, A M. See under Garriga, G., 322, 86

Langmuir, C H. Petrological and tectonic segmentation of the East Pacific Rise, 530'-1430'N (with Bender, J F, Batiza, R) Article, 322 422

324, 442
Laros, J G. The soft μ-ray burst GB790107 (with Fenimore, E E, Fikani, M M, Klebesadel, R W, Barat, C, Chambon, G, Hurley, K, Niel, M, Vedrenne, G, Kane, SR, Kurt, VG, Mersov, GA, Zenchenko, VM) Letter to Nature, 322, 152

LaRosa, T N. See under Kassim, N E., 322, 522

snitzki, I. Dame Honor Fell FRS (1900-1986), News and views, 322 214

Lathe, R. See under Blancou, J., 322, 373

Lawton, J H. Book review of Modeling Nature. Episodes in the History of Population Ecology (by Kingland, SE,) 322, 603 Lazaridou, M. See under Varotsos, P., 322, 120

Lazzarini, R A. See under Kristensson K 322 544

Le Page, R W F. See under Jenni, L., 322, 173

Lenkey, R E. See under Walker, A., 322, 517 Leatherbarrow, R.J. See under Fersht, A.R., 322, 284

Lecocq, J.P. See under Biancou, J., 322, 373

Lee, C-S. The Banda-Celebes-Sulu basin: a trapped piece of

Cretaceous-Eocene oceanic crust? (with McCabe, R) Letter to Nature, 322, 51 Lefèvre, R. Silicate microspherules intercepted in the plume of Etna

volcano (with Gaudichet, A. Billon-Galland, M A) Letter to Nature, 322, 817

Leg 106 shipboard scientific party. Ocean Drilling Program: Palaeoc-limatic linkage between high and low latitudes, News and views, 322, 211

Lepre, C. See under Bechtold, R., 322, 286

Lester, R A J. See under Herron, C E., 322, 265

Levine, M A. See under Weinstock, R S. 322, 635

vontin, R. See under Berland, J-P., 322, 785

Lichte, F E. New method for the measurement of osmium isotopes applied to a New Zealand Cretaceous/Tertiary boundary shale (with Wilson, S M, Brooks, R R, Reeves, R D, Holzbecher, J, Ryan, DE) Letter to Nature, 322, 816

Liddell, P A. See under Wasielewski, M R., 322, 570 Lidsky, A S. See under DiLella, A G., 322, 799

Liedtke, C M. See under Welsh, M J., 322, 467

Lindemann, J. See under Bredbrook, J., 322, 494

Lira, S A. See under Nelson, C., 322, 557

 Liu, L.F. See under Nelson, W.G., 322, 187
 Livermore, R.A. Late Palaeozoic to early Mesozoic evolution of Pangaea (with Smith, A.G., Vine, F.J.) Letter to Nature, 322, 162
 Lock, S. A Difficult Balance: Editorial Peer Review in Medicine, Book review by Harnad, S. 322, 24

Lodish, H F. See under Mueckler, M., 322, 549 Loh, DY. See under Behike, MA., 322, 379 Lonsdale, PF. See under Genin, A., 322, 59

Luciani, M-F. See under Brunet, J-F., 322, 268

Lyon-Caen, O. See under Hauser, S L., 322, 176 Mach, B. See under Gorski, J., 322, 67

Macko, S A. Amino acid epimerization in planktonic foraminifera suggests slow sedimentation rates for Alpha Ridge, Arctic Ocean (with Aksu, A E) Letter to Nature, 322, 730

MacLeod, A R. See under Reinach, F.C., 322, 648

Maddox, J. Scientific American: Unwanted fly in merger ointment. News. 322, 99

Looking for gravitational errors, News and views, 322, 109 Test ban made more respectable, News and views, 322, 205 Gentle warning on fractal fashions, News and views, 322, 303

Catching atoms in beams of light, News and views, 322, 403 New ways with quasi-crystals, News and views, 322, 495 What happens on Cygnus X-3?, News and views, 322, 591

New ways with interatomic forces, News and views, 322, 769 Book review of The World of Science and the Rule of Law (by

Ziman, J., Sieghart, P., Humphrey, J., 322, 783
Chernobyl report; Drama of human perversity, News, 322, 763
Magli, M.C. See under Belmont, J.W., 322, 385
See under Iscove, N.N., 322, 289

Maguire, C.M. See under Dewey, R.J., 322, 712 Mäkinen, Y. See under Salo, J., 322, 254

Mallard, J. Nuclear magnetic resonance: First sight of a single cell, News and views, 322, 116

Manning, J.E. See under Peterson, D.S., 322, 566
Mantovani, M.S.M. See under Hawkesworth, C.J., 322, 356

Marks, J. See under Walsh, J.B., 322, 590 Marsh, T. See under Argyle, B., 322, 402

Marshall, J C. Cognitive neurophysiology: Signs of language in the brain, News and views, 322, 307

Martens, C L. See under Moore, K W., 322, 484

Marti, S. See under Jenni, L., 322, 173 Martin, B. See under Argyle, B., 322, 402

Martuza, R.L. See under Seizinger, B.R., 322, 644 Marvit, J. See under DiLella, A.G., 322, 799 Masiu, Y. See under Kao, K.R., 322, 371

Masson, D. See under Tschopp, J., 322, 831

Massoth, G.J. See under Cowen, J.P., 322, 169 Matsubara, H. See under Wakabayashi, S., 322, 481

Matsui, T. Impact-induced atmospheres and oceans on Earth and Venus (with Abe, Y) Letter to Nature, 322, 526

Matsul, Y. See under Kijima, T., 322, 533 Mattei, M-G. See under Brunet, J-F., 322, 268

Mattingly, M.A. See under Aguayo, J.B., 322, 190
Mattioli, G.S. Upper mantle oxygen fugacity recorded by spinel Iherzolites (with Wood, B I) Letter to Nature, 322, 626 faunsell, J H R. See under Schiller, P H., 322, 824

Mauritsch, H J. See under Preisinger, A., 322, 794

See under Preisinger, A., 322, 794 May, JW. Length growth in fission yeast cells measured by two novel

ques (with Mitchison, J.M.) Letter to Nature, 322, 752 Maycock, A L. See under Doherty, J B., 322, 192 McCabe, R. See under Lee, C-S., 322, 51 McCall, M. The crystal structure of d(GGATGGGAG) forms an essential part of the binding site for transcription factor HIA (with Brown, T, Hunter, W N, Kennard, O) Letter to Nature. McClena, J. See under Brenner, MB., 322, 145 McClerke, RA: Science and faith, News, 322, 590 McClerke, MT, See under Duncan, RA, 322, 534 McGowan, C. A putative ancestor for the swordfish-like ichthyosaut Eurhinosaurus, Letter to Nature, 322, 454 McMahon, R G. See under Hazard, C., 322, 38 See under Sargent, W.L.W., 322, 40

McNaughton, P.A. Measurement of intracellular free calcium con centration in salamander rods (with Cervetto, L. Nunn, B Letter to Nature, 322, 261

McNeill, W.H. Book review of The Origins of War From the Stene
Age to Alexander the Great (by Ferrill, A.) 322, 416

McNett, M.A. See under Fischer, K.M., 322, 733

McNett, M.A. See under Fischer, K.M., 322, 733 McPeters, R D. See under Stolarski, R S., 322, 808 See under Stolarski, R.S., 322, 808 dev, Z A. Roman Khesin-Lur'e, Correspondence, 322, 108 Meech, R. W. See under Ashmore, J.F., 322, 368 Mehra, V. See under Modlin, R L., 322, 459 Mehra, V. See under Modun, R. L., 322, 617
Mehrabzadeh, A. A. See under Hard, T. M., 322, 617
Mellars, P. Archaeology: A new chronology for the French Mounterian period, News and views, 322, 410 Mersov, G.A. See under Laros, J.G., 322, 152 Methfessel, C. See under Mishina, M., 322, 90
Methger, D.J. Editor, American Archaeology Past and Future: A Celebration of the Society for American Archaeology 1935-1985. Book review by Bray, W. 322, 784 Meyers, N. Israeli science: Medical schools seek US students, News, 322, 584 Mier, P.D. Phosphoinositol more than skin deep (with Bauer, F W Happie, R) Scientific correspondence, 322, 504
Miles, M J. See under Cairns, P., 322, 89 Millar, S D. See under Frerichs, G N., 322, 216 Miller, R W. See under Robson, R L., 322, 388 sina, M. Erratum: Molecular distinction between fetal and adult forms of muscle acetylcholine receptor (with Takai, T, Imoto, K. Noda, M. Takahashi, T. Numa, S. Methfessel, C. Sakmann, B) Letter to Nature, 322, 90 Mitchison, J.M. See under May, J.W., 322, 752 Miyata, T. Repty: Homology between IgH-binding factor and retro-virus genes (with Toh, H, Ono, M) Matters arising, 322, 484 Mizuochi, T. See under Rosenberg, A S., 322, 829

Modile, R L. Genetically restricted suppressor T-cell clones derived from lepromatous leprosy lesions (with Kato, H, Mehra, V, Nelson, E E, Xue-dong, F, Rea, T H, Pattengale, P K, Bloom, BR) Letter to Nature, 322, 459 T. Book review of Lindow Man: The Body in the Bog (Stead, I M, Bourke, J B, Brothwell, D editors) 322, 602 Queensland, Australia, Letter to Nature, 322, 736 see, A.P. See under Royer-Pokora, B., 322, 32 re, K W. Homology between IgE-binding factor and retrovirus nes (with Martens, C L) Matters arising, 322, 484 Moore, P.D. Book review of Studies on Plant Demography: A Festschrift for John L Harper (White, J editor) 322, 320 Book review of The population structure of vegetation. Handbook of vegetation science, Vol. 3. (White, J editor) 322, 320

Moore, T.A. See under Wasielewski, M.R., 322, 570 Morales, V.W.J. See under Gerlach, D.C., 322, 165 Moreels, G. Corrigendum: Near-ultraviolet and visible spectropho tometry of comet Halley from Vega 2 (with Gogoshev, M, Krasnopolsky, V A, Clairemidi, J, Vincent, M, Parisot, J P, Bertaux, J. L., Blamont, J. E., Festou, M. C., Gogosheva, Ts., Sargiochev, S., Palasov, K., Moroz, V.I., Krysko, A. A., Vanysek, V) Letter to Nature, 322, 90 Morgan, J.I. Role of ion flux in the control of c-fos expression (with Curran, T) Letter to Nature, 322, 552 Morez, VI. See under Moreels, G., 322, 90 Morris, V J. See under Cairns, P., 322, 89

Merup, S. See under van Wonterghem, J., 322, 622

Mumford, See under Doherty, J.B., 322, 192 Mumford, R. See under Doherty, J.B., 322, 192

Murdin, P. See under Argyle, B., 322, 402
Murre, C. See under Quertermous, T., 322, 184
Musi, L. See under Bianchi, U., 322, 19
Nabholz, M. See under Brunet, J-F., 322, 268

s. E. See under Blackett, N M., 322, 289

Nagai, K. See under Reinach, F.C., 322, 80 Naval, J. Spanish universities, Corresponder

cose transporter into microsomes requires phospho

122 308 322, 557 102 Moses, A M. See under Weinstock, R S., 322, 635 Mott, N. A life in science, Book review by Jones, R V. 322, 121 ntiford, P. J. Transfer of radioiodide to milk and its inhibition (with Coakley, A. J. Fleet, I. R. Hamon, M. Heap, R. B.)
Scientific correspondence, 322, 600 sckler, M. Post-translational insertion of a fragment of the glubond cleavage (with Lodish, H.F.) Letter to Nature, 322, 549
Mues, G.E. See under Munn, T.Z., 322, 314 ms, T.Z. Human lipocortis similar to ras gene products (with Mues, G.I) Scientific correspondence, 322, 314

alcedharan, K. See under Rajasekharan, K., 322, 528 Neffe, J. West German space research: Hermes causes sacking and cabinet unrest, News, 322, 3

AUTHOR INDEX-Space antiques hedge against inflation. News, 322, 297 German universities, News, 322, 197
The deutschmarks that count, News, 322, 199 US space: Shuttle faces more delay, News, 322, 301 Human genome: No consensus on sequence (with Swinbanks, D) West Germany: Terror against technology, News, 322, 202 News. 322. 397 West German nuclear power: The fast breeder is stumbling, News, US-Japan trade: No easy end to chip war (with Swinbanks, D) News. 322, 400 Terrorists strike again, News, 322, 400 US-Japan trade: Truce agreed in chip war. News. 322, 489 Soviet/West German cooperation agreed, News, 322, 488
Nelson, C. Discrete cis-active genomic sequences dictate pituitary US-Soviet exchange: Relations thaw in the far north, News, 322, cell type-specific expression of rat prolactin and growth hor-US space: Continuing problems all round, News, 322, 492 mone genes (with Crenshaw, E B III, Franco, R, Lira, S A, New telescopes: Shining mirrors at Apache Point, News, 322, 483. Environmental pollution: Pushing for a new clean-up law, News, Albert, V R. Evans, R M, Rosenfeld, M G) Letter to Nature, Nelson, D.R. See under Duncan, R.A., 322, 534 Computer models: Cooperation on new molecules, News, 322, 586 elson, E E. See under Modlin, R L., 322, 459 Doing things the all-American way, News, 322, 587 son, W G. Newly replicated DNA is associated with DNA Research donations: Tax bill provides fewer breaks for US edia topoisomerase II in cultured rat prostatic adenoca tion (with Beardsley, T) News, 322, 761 (with Liu, L.F., Coffey, D.S) Letter to Nature, 322, 187 Private money for AIDS research, News, 322, 763 urger, P E. See under Royer-Pokora, B., 322, 32 nan, P A. See under Stolarski, R S., 322, 808 US Defence; Congress takes a moderate line, News, 322, 765. mer, T.N. Influence of the Atlantic, Pacific and Indian Oceans on Sahel rainfall, Letter to Nature, 322, 251 See under Stolarski, RS., 322, 808 ark, P. AIDS: Depressing news from Paris, News, 322, 6 Pan, WH. See under Hard, TM., 322, 617 Vane back to basics, News, 322, 102 Book review of Mobilizing Against AIDS: The Unfinished Story of a Virus (by Nichols, E K.,) 322, 220 Parlant 1 P See under Morcels, G., 322, 90 Parker, M A. See under Sinclair, R., 322, 531 Parsons, A. Espresso coffee emporia take note. Scientific corres-AIDS: Confused ethics of blood testing, News, 322, 296 pondence, 322, 316 Newton, I. The Sparrowhawk, Book review by Andrews, J. 322, 508 Pastoret, P P. See under Blancou, J., 322, 373
Pattengale, P K. See under Modlin, R L., 322, 459 Newton, M E. X chromosomes and dosage compensation, Scientific correspondence, 322, 19 Payette, S. Dating ice-wedge growth in subarctic peatlands following deforestation (with Gauthier, L. Grenier, 1) Letter in Nature, ols, E. K. Mobilizing Against AIDS: The Unfinished Story of a Virus, Book review by Newmark, P. 322, 220 322, 724 n, J III. See under Keating, G M., 322, 43 Pays, E. See under Jenni, L., 322, 173 Niel, M. See under Laros, J.G., 322, 152 Niemelii, P. See under Salo, J., 322, 254 Pearson, B. Environmentalism, Correspondence, 322, 108 Pearson, R. Will industry support higher education?. Employment, ching, E. European research priorities, Correspo 322, 96 rose, R. Spinors and space-time. Vol. 2 Spinor and twister methods in space-time geometry. Book review by Ashtekar, A. , W. See under Griffiths, J F., 322, 46 Nishet, E.G. Origin of life: RNA and hot-water springs, News and views, 322, 206 Peppler, R A. See under Lamb, P 1., 322, 238 See under Edwards, G.R., 322, 771 Perner, D. Atmospheric chemistry: Hunting tropospheric OH ions.

News and views, 322, 595 Noda, M. Expression of functional sodium channels from cloned cDNA (with Ikeda, T. Suzuki, H. Takeshima, H. Takahashi, T. Perutz, M.F. A bacterial haemoglobin. News and views, 322, 305 Kuno, M. Numa. S) Letter to Nature, 322, 826 eterson, D.S. Cloming of a major surface-antigen of Trypanoscina cruzi and identification of a nonapeptide repeat (with Wrights-man, R.A., Manning, J.E.) Letter to Nature, 322, 566 See under Mishina, M., 322, 90 Nomicos, K. See under Varotsos, P., 322, 120 a, SE. Uplift of the shores of the western Mediterranean due Petitou, M. See under Casu, B., 322, 215 to Messinian desiccation and flexural isostasy (with Chase, CG) Petrac, E. See under Reth, M., 322, 840 Letter to Nature, 322, 450 Pettini, M. See under Argyle, B., 322, 402 th. G. Pattern formation: Descartes and the fruitfly, News and Platt, D. Editor, Neurobiology of Vasopressin. Book review by views, 322, 404 Brownstein, M.J. 322, 25 a, S. See under Noda, M., 322, 826 Philander, S G H. Unusual conditions in the tropical Atlantic Ocean Numa, S. See under Noda, N., 322, 90 Numa, B.J. See under McNaughton, P.A., 322, 261 O'Brien, R.J. See under Hard, T.M., 322, 617 in 1984, Letter to Nature, 322, 236
Phillips, I.R. See under Ashworth, A., 322, 599 Phillips, P. Archaeology: Towards a scientific approach, News and O'Grady, L. See under Doherty, J B., 322, 192 O'Riordan, M C. Prehistoric protection, Correspon views, 322, 112 dence, 322, 106 Phillips, R A. See under Belmont, J W., 322, 385 O'Toole, C. Editor, The Encyclopaedia of Insects, Book review by See under Squire, J., 322, 555
Picardi, M. See under Bianchi, U., 322, 19 Crothers, J. 322, 416 Odartchenko, N. See under Iscove, N N., 322, 289 Pichon, J J. See under Labeyrie, L D., 322, 701 Ohishi, I. See under Aktories, K., 322, 390 Pinker, S. Editor, Visual Cognition. Book review by Sutherland, S. Ohtani, E. Melting of a model chondritic mantle to 20 GPa (with 322, 415 Kato, T. Sawamoto, H) Letter to Nature, 322, 352 Pinkerton, J M M. Book review of Memoirs of a Computer Pioneer Ohyama, K. Chloroplast gene organization deduced from complete (by Wilkes, M.) 322, 26 sequence of liverwort Marchantia polymorpha chloroplast DNA (with Fukuzawa, H, Kohchi, T, Shirai, H, Sano, T, Sano, R See under Bianchi, U., 322, 19 S, Umesono, K, Shiki, Y, Takeuchi, M, Chang, Z, Aota, S-i, Inokuchi, H, Ozeki, H) Letter to Nature, 322, 572 Pisano, J M. See under Doberty, J B., 322, 192 Piton, B. See under Hisard, P., 322, 243 Pitts, M. See under Keating, G M., 322, 43 Offer, W. See under Festenstein, H., 322, 64 Pohl, T. See under Schultz, J E., 322, 271
Poizner, H. See under Damasio, A., 322, 363 Onken, R. See under Woods, J.D., 322, 446 Ono, M. See under Miyata, T., 322, 484 Pollack, C. Probing the phagolysosomal environment of human mac-rophages with a Ca²⁺-responsive operon fusion in Yersinia pre-Orkin, S. H. See under Royer-Pokora, B., 322, 32
Osaki, S. Physical Methods for Inorganic Biochemistry, Book review tis (with Straley, S.C., Klempner, M.S.) Letter to Natiste, 322, 834.

Pollard, T.D. See under Adams, R.J., 322, 754 by Thomson, A J. 322, 506 Pologe, G. A chromosomal rearrangement in a P. falcipiarum histidine-rich protein gene is associated with the knobless phenotype (with Ravetch, J V) Letter to Nature, 322, 474

Porter, R. Book review of Franklin of Philadelphia (by Wright, E.) 322, 23 Ostriker, J P. Effect of gravitational lenses on the microwave background, and 1146+111B,C (with Vishniac, ET) Letter to Nature, 322, 804 Effect of gravitational lenses on the microwave background, and 1146+111B,C (with Vishniac, ET) Letter to Nature, 322, 804

nhoff, T H M. Cloned suppressor T cells from a lepromatous Poser, S. See under Karpas, A., 322, 177
Postgate, J.R. See under Robson, R.L., 322, 388 leprosy patient suppress Mycobacterium leprae reactive helper Tcells (with Elferink, D.G. Klatser, P.R., de Vries, R.R.P.) Letter Poulain, D.A. See under Theodosis, D.T., 322, 738
Pouwels, P.H. Editor, Cloning Vectors: A Laboratory Manual. Book to Nature, 322, 462 Owen, F L. See under Brenner, M B., 322, 145 review by Harris, T. 322, 603

Powell, T G. See under Jackson, M J., 322, 727 Ozeki, H. See under Ohyama, K., 322, 572 Paindavoine, P. See under Jenni, L., 322, 173 Prats, M. Lateral proton conduction at lipid-water interfaces and its implications for the chemiosmotic-coupling hypothesis (with Teissie, J. Tocanne, 3-F) Letter to Nature, 332, 756 kull, M W. Detection of an X-ray-ionized nebula around the black hole candidate binary LMC X-1 (with Angebault, LP) Article, Preisinger, A. The Cretaceous/Tertiary boundary in the Gossu Palacies, C. See under Gerlach, D.C., 322, 165 Basin, Austria (with Zobetz, E. Gratz, A. J. Labodynsky, R. Becke, M. Mauritsch, H. J. Eder, G. Grass, F. Rögl, F. Strad-Palacz, Z. See under Hawkesworth, C.J., 322, 356 Palasov, K. See under Morcels, G., 322, 90 ner, H. Surenian, R.) Article, 322, 794

The Cretaceous/Tertiary boundary in the Gossau Basso. Austria Palca, J. High-energy physics: Supercollider in the balance, News, 322, 5 (with Zobetz, E. Gratz, A J. Lahodynsky, R. Becke, M. Mauritsch, H J. Eder, G. Grass, F. Rögl, F. Stradaer, H. US space: Air Force moves on launchers, News, 322, 8 Ocean satellites: Topex launch comes closer, News, 322, 9
AIDS: New centres for clinical trials, News, 322, 100 Surenian, R) Article, 322, 794 hownik, E V. Deregulated expression of compc by marine erythroleukaemia cells prevents differentiation (with Kirkowska, I) Letter to Nature, 322, 848 See under Walgate, R., 322, 101 AIDS: US wins round in patent row, News, 322, 200 Patent law: Boost for Canadian drug research, News, 322, 201
US education: Liberal colleges ask for more, News, 322, 203
US and Pakistan: Agreement on technology. News, 322, 295 udfoot, N J. Transcriptional interference and termination be-

tween duplicated a globin gene constructs suggests a novel

mechanism for gene regulation, Letter to Nature, 322, 562

Prulja, G J M. Nuclear factor III, a novel sequence-specific DNAbinding protein from HeLa cells stimulating adenovirus DNA replication (with van Drie), W. van der Vliet, P.C.) Letter to Nature, 322, 656

shoe, M. See under Griffith, J., 322, 750

Gene regulation by proteins acting nearby and at a distance, Review article, 322, 697

Puhakka, M. See under Salo, 1. 322, 254

Puigdomenech, P. Spain: More university reforms needed, News. 322, 198

en, C. See under Garcia, J V., 322, 383

nous, T. Human T-cell # genes contain N segments and have marked junctional variability (with Strauss, W. Murre, C. Dialynas, DP, Strominger, JL, Seidman, JG) Letter to Nature, 122 184

, JF. See under Grosberg, RK., 322, 456

itan, P J. Primordial density fluctuations and the structure of galactic haloes (with Salmon, J K, Zurek, W H) Article, 322, 329

nilla, M. Carcinogen-specific mutation and amplification of Ha-ras during mouse skin carcinogenesis (with Brown, K, Ramsden, M, Balmain, A) Letter to Nature, 322, 78

ann, M. More bright ideas (with Schwartzentruber, K) Corres ndence, 322, 302

ezri, M. See under Casu B 322, 215

sekharan, K. The quasi-crystalline phase in the Mg-Al-Zn system (with Akhtar, D. Gopalan, R. Muraleedharan, K.) Letter to ure, 322, 528

rasad, M.P. See under Sarolia A 322, 119 en, M. See under Quintanilla, M., 322, 78

Rao, R. Indian science: Making the numbers count, News, 322, 98 Ariane ride for Indian satellite, News, 322, 587

vetch, J V. See under Pologe, G., 322, 474 Rawley, L. A. See under Dewey, R.J., 322, 712

under Segelstein, D.J., 322, 714

Ren, TH. See under Modlin, R.L., 322, 459

Read, A F. Population biology: Genetic management in zoos (with Harvey, PH) News and views, 322, 408

Reed, R K. Effects of surface heat flux during the 1972 and 1982 El Nino epidsodes, Letter to Nature, 322, 449

eves, R.D. See under Lichte, F.E., 322, 816

sach, F.C. Site-directed mutagenesis of the regulatory light-chain Ca^{2+}/Mg^{2+} binding site and its role in hybrid myosins (with Nagai, K, Kendrick-Jones, J) Letter to Nature, 322, 80

Tissue-specific expression of the human tropomyo volved in the generation of the trk oncogene (with MacLeod, A R) Letter to Nature, 322, 648

Reth, M. A novel VH to VHDJH joining mechanism in heavy-chainnegative (null) pre-B cells results in heavy-chain production (with Gehrmann, P. Petrac, E. Wiese, P) Letter to Nature, 322,

Rich, V. Falkland Islands: Opinions divided on penguin deaths. News, 322, 4

Young Hungarian academics protest, News, 322, 104 Chinese science: Legal protection for scientists, News, 322, 105

Eureka: Soviets feel left out of Europe, News, 322, 200

Chernobyl: Inquest continues on nuclear power, News, 322, 203 Soviet inquiry: Chernobyl accident is blamed on human er News, 322, 295

More dead penguins, News, 322, 296

Chinese science: Back to your work units, News, 322, 297

Academician's Berlin arrest riddle, News, 322, 298

Transplant donor held up by red tape, News, 322, 490 Seismic monitoring: Station goes with a bang, News, 322, 587

Chernobyl accident: Reactor design not perfect, News, 322, 588 Chernobyl accident; Fallout pattern puzzles Poles, News, 322, 765 Richardson, S. H. Latter-day origin of diamonds of eclogitic para-genesis, Letter to Nature, 322, 623

rdson, TH. See under Robson, RL., 322, 388

sidler, W. Spinors and space-time. Vol. 2 Spinor and twistor thods in space-time geometry, Book review by Ashtekar, A.

gwood, A E. Terrestrial origin of the Moon, Review article, 322, 323

erts, R.J. See under Frerichs, G.N., 322, 216

Robertson, H D. Biochemistry Clues about RNA enzymes, News and views, 322, 17

rtson, M. The proper study of mankind, News and views, 322, 11 Immunology: T-cell receptor: gamma gene product surfaces, News

and views, 322, 110 inson, R.M. See under Chiu, Y.T., 322, 441

son, R.L. The alternative nitrogenase of Azotobacter chroococ-cum is a vanadium enzyme (with Eady, R.R., Richardson, T.H., Miller, RW, Hawkins, M, Postgate, JR) Letter to Nature, 322,

riguez, F. See under Theodosis, DT., 322, 738

Rodriguez, J. M. See under Tung, K-K., 322, 811

See under Tung, K-K., 322, 811

Rogers, B. Monocular aniseikonia: a motion parallax analogue of the

disparity-inducedeffect (with Koenderink, J) Letter to Nature, 322, 62

rs, C L. Editor, Scientists and journalists: Reporting science as news, Book review by Dickson, D. 322, 317

Rogi, F. See under Preisinger, A., 322, 794 See under Preisinger, A., 322, 794

Rooney, ST. See under Blankenship, DD., 322, 54 See under Alley, RB., 322, 57

Rosen, C. See under Sodroski, J., 322, 470 Rosen, F. See under Brenner, M.B., 322, 145

esherg, A.S. Analysis of T-cell subsets in rejection of K^b mutant skin allografts differing at class I MHC (with Mizuochi, T. Singer, A) Letter to Nature, 322, 829

senfeld, M G. See under Nelson, C., 322, 557
sseinsky, D R. Book review of Hopping Conduction in Solids (by Böttger, H, Bryskin, V V.) 322, 220 siter, A. Evolutionary 'classics' may self-destruct, Scientific cor-

respondence, 322, 315

Roth, J S. The origins of the Earth's oceans, Scientific correspond-

Rothman, JE. Cell biology: An unfolding story of protein translocation (with Kornberg, RD) News and views, 322, 209 uhani, S. See under Jones, J.S., 322, 599

Roy, R. See under Yarborough, W A., 322, 347

Royer-Pokora, B. Cloning the gene for an inherited human disorder - chronic granulomatous disease - on the basis of its chromosomal location (with Kunkel, L.M., Monaco, A.P., Goff, S.C. Newburger, P.E. Bachner, R.L. Cole, F.S. Curnutte, J.T. Orkin, S H) Article, 322, 32

Rust, P. See under Hisard, P., 322, 243

stone, J L. See under Kay, R W., 322, 605

Rupke, N A. Book review of Climatic change and world affairs. revised edition. (by Tickell, C.) 322, 319

Ryun, D.E. See under Lichte, F.E., 322, 816

I, J A. Editor, American Archaeology Past and Future: A Celebration of the Society for American Archaeology 1935-1985, Book review by Bray, W. 322, 784

Sachs, J A. See under Festenstein, H., 322, 64

Sakintvala, J. Tumour necrosis factor a stimulates resorption and inhibits synthesis of proteoglycan in cartilage, Letter to Nature, 322, 547

unn, B. See under Mishina, M., 322, 90

Salmon, J.K. See under Quinn, P.J., 322, 329

Salo, J. River dynamics and the diversity of Amazon lowland forest (with Kalliola, R. Häkkinen, I. Mäkinen, Y. Niemelä, P. hakka, M. Coley, PD) Letter to Nature, 322, 254

Salt, T E. Mediation of thalamic sensory input by both NMDA receptors and non-NMDA receptors, Letter to Nature, 322, 263

Salviati, G. Synthesis of fast myosin induced by fast ectopic innervation of rat soleus muscle is restricted to the ectopic endolate region (with Biasia, E. Aloisi, M) Letter to Nature, 322, 637

dell, I.H. See under Schiller P.H. 322, 874 Sander, L.M. Fractal growth processes, Review article, 322, 789

Fractal growth processes, Review article, 322, 789 ano, S. See under Ohyama, K., 322, 572

Sano, T. See under Ohyama, K., 322, 572 Sargent, W.L. W. See under Hazard, C., 322, 38

ectrum of a QSO with redshift 3.8 (with Filippenko, A V. Steidel, C.C., Hazard, C., McMahon, R.G.) Letter to Nature, 322.

Sargiochev, S. See under Moreels, G., 322, 90

srma, A. Parapsychology, Correspondence, 322, 494

Saunders, PAH. Environmentalism, Correspondence, 322, 108 Savage, HFJ. Repulsive regularities of water structure in ices and crystalline hydrates (with Finney, J.L.) Letter to Nature, 322, 717 amoto, H. See under Ohtani, E., 322, 352

Scarfe, C M. Melting of garnet peridotite to 13 GPa and the early history of the upper mantle (with Takahashi, E) Letter to Nature, 322, 354

Schacher, S. See under Goelet, P., 322, 419

Schaefer, M. See under Sprent, J., 322, 541

Schutz, G. See under Filers M. 322, 228

Schild, H. See under Argyle, B., 322, 402

Schiller, P.H. Functions of the ON and OFF channels of the visual system (with Sandell, J.H. Maunsell, J.H.R.) Letter to Nature, 322 824

lling, J-G. See under Hanan, B B., 322, 137

Schmaltel, U. See under Keating, G M., 322, 43

Schmalbruch, H. Skeletal Muscle, Handbook of Microscopic Anatomy, Vol.2, Part 6, Book review by Irving, M. 322, 415

midtke, J. Human gene cloning: the storm before the lull? (with Krawczak, M, Cooper, D N) Scientific correspondence, 322,

ist, A-M. See under Brunet, J-F., 322, 268

Schoeberl, M.R. See under Stolarski, R.S., 322, 808 See under Stolarski, R.S., 322, 808

Schoeniger, J. See under Aguayo, J B., 322, 190 Schön, A. The RNA required in the first step of chlorophyll biosynthesis is a chloroplast glutamate tRNA (with Krupp, G, Gough, S, Berry-Lowe, S, Kannangara, C G, Söll, D) Letter to Nature, 322, 281

Schoolnik, G. See under Goldfarb, D.S., 322, 641 Schrier, R. W. Editor, Vasopressin, Book review by Brownstein, M.J.

322, 25

altz, J E. Voltage-gated Ca2+ entry into Param intraciliary increase in cyclic GMP (with Pohl, T. Klumpp, S) Letter to Nature, 322, 271

Schweitzentruber, K. See under Ragan, M., 322, 302 Schweitzer, J. See under Jenni, L., 322, 173

Scott, E.L. History of chemistry: Carl Scheele (1742-1786) and the scovery of oxygen, News and views, 322, 305

Sears, D. Meteorites: Window on the early Solar System. News and views, 322, 309

Segal, S. See under Dmitrovsky, E., 322, 748 Segelstein, D J. New millisecond pulsar in a binary system (with

Rawley, L. A. Stinebring, D. R. Fruchter, A. S. Taylor, J. H. Letter to Nature, 322, 714

ian, J.G. See under Quertermous, T., 322, 184 Seidman Seidman, J G. See under Brenner, M B., 322, 145
Seip, H M. Palaeoecology: Surface water acidification, News and

. iews. 322, 118.

inger, B R. Loss of genes on chromosome 22 in tumorigenesis of hi/man acoustic neuroma Letter to Nature, 322, 644 uroma (with Martuza, R L, Guselia, J F)

od. J. Why not move RGO to Manchester?, Correspondence. wojod, J. V 322, 106

noff, R. See under Jeffreys, A.J., 322, 290

Sengor, AMC. Book review of The Geology of China (by Zunyi, Y, Yuqi, C, Hongzhen, W.) 322, 507

Shap, S K. See under Doherty, J B., 322, 192

Shannon, I L. See under Wyborny, L. E., 322, 21

Sherma, A.K. See under Alurkar, S.K., 322, 439

Sharp, P A. See under Weinberger, J., 322, 846

Spephard, E A. See under Ashworth, A., 322, 599

Shevach, E.M. See under Kroczek, R.A., 322, 181

Saiki, Y. See under Ohyama, K., 322, 572 Shirni, H. See under Ohyama, K., 322, 572

Shure, L. See under Fischer, K M., 322, 733

Siden, A. See under Karpas, A., 322, 177 Sieghart, P. The World of Science and the Rule of Law, Book review by Maddox, J. 322, 783 Sielecki, A.R. See under James, M.N.G., 322, 664

SER, J. Cosmology: What makes nearby galactic clusters all move as one?. News and views. 322, 207

Book review of In Search of the Big Bang: Quantum Physics and

Cosmology (by Gribbin, J.) 322, 505 Silvertooth, E. W. Special relativity, News, 322, 590

Simonelig, M. See under Bucheton, A., 322, 650 Simons, K. See under van Meer, G., 322, 639

Sinay, P. See under Casu, B., 322, 215

Sinclair, A. The Red and the Blue: Intelligence, Treason and the Universities, Book review by Cooper, W. 322, 217

Sinclair, R. High-resolution transmission electron microscopy of silicon re-growth at controlled elevated temperatures (with Parker,

M A) Letter to Nature, 322, 531 ger, A. See under Rosenberg, A S., 322, 829

Sleight, A.W. See under Attfield, J.P., 322, 620

th, A G. See under Livermore, R A., 322, 162

ith, JA. See under Brenner, M B., 322, 145

Smith, P.J. Book review of Continuum theories in solid Earth physics (Teisseyre, Reditor) 322, 123

ith. R A. Correlations between stream sulphate and regional SO2 emissions (with Alexander, R.B) Letter to Nature, 322, 722

aith Churchtand, P. Neurophilosophy: Toward a Unified Science of the Mind-Brain, Book review by Kitcher, P. 322, 413 brooki, J. Role of the HTLV-III/LAV envelope in syncytium

formation and cytopathicity (with Goh, W C, Rosen, C, Campbell, K, Haseltine, W A) Letter to Nature, 322, 470

Soll, D. See under Schön, A., 322, 281 mon, F. Microtubule assembly in the axon, Scientific correspond-

ence, 322, 599 ett, C P. Secular change in solar activity derived from ancient varves and the sunspot index (with Trebisky, T J) Letter to

lebot, J.P. See under Blancon, L. 322, 373

Sparks, W B. See under Bailey, J., 322, 150

neer, C.A. Overlapping transcription units in the dopa decarboxy-lase region of *Drosophila* (with Gietz, R.D., Hodgetts, R.B.) Letter to Nature, 322, 279

icer, M. Problems of Africa, Correspondence, 322, 10

Spiegel, A.M. See under Weinstock, R.S., 322, 635 Spiess, F.N. See under Genin, A., 322, 59

rent, J. Capacity of purified Lyt-2+ T cells to mount primary proliferative and cytotoxic responses to Ia' tumour cells (with Schaefer, M) Letter to Nature, 322, 541

ulre, J. Tumour induction by the retinoblastoma mutation is inde-pendent of N-myc expression (with Goddard, A.D., Canton, M. Becker, A. Phillips, R.A. Gallie, B.L.) Letter to Nature, 322, 555

Stachel, S E. Generation of single-stranded T-DNA transfer from Agrobacterium tumefaciencs to plant cells (with Timmerman, B. Zambryski, P) Article, 322, 706

Stafford, J. See under Garcia, J V., 322, 383

Stanley, K. K. See under Tschopp, J., 322, 831 Stark, A. A. Observations of the cosmic background radiation near the double quasar 1146+111B,C (with Dragovan, M, Wilson, R W. Gott, J R III) Letter to Nature, 322, 805

Observations of the cosmic background radiation near the double quasar 1146+111B,C (with Dragovan, M., Wilson, R.W., Gott. J.

R III) Letter to Nature, 322, 805 ad, I M. Editor, Lindow Man: The Body in the Bog, Book review

by Molleson, T. 322, 602 eidel, C.C. See under Sargent, W.L.W., 322, 40

Steinert, M. See under Jenni, L., 322, 173 Stevens, C.F. Neurotransmission: Are there two functional classes of

glutamate receptors?, News and views, 322, 210 Stevenson, A C. See under Jones, V J., 322, 157

Stewart, I. Geometry: Exotic structures on four-space. News and views, 322, 310

ebring, D.R. See under Segelstein, D.J., 322, 714

Stobbs, W.M. See under Baxter, C.S., 322, 814

Stokes, G.H. See under Dewey, R.J., 322, 712 Stolarski, R S. Nimbus 7 satellite measurements of the springtime Antarctic ozone decrease (with Krueger, A J. Schoeberl, M R. McPeters, R D, Newman, P A, Alpert, J C) Letter to Nature,

Nimbus 7 satellite measurements of the springtime Antarctic ozone decrease (with Krueger, A.J., Schoeberl, M.R., McPeters, R D, Newman, P A, Alpert, J C) Letter to Nature, 322, 808

ers, R.B. Periodicity of the Earth's magnetic reversals. Letter to Nature, 322, 444

11. See under Preisinger, A., 322, 794 See under Preisinger, A., 322, 794 322, 762

Straley, S.C. See under Pollack, C., 322, 834 Strauss, W. See under Quertermous, T., 322, 184 Strominger, J.L. See under Brenner, M.B., 322, 145 See under Quertermous, T., 322, 184 Sugita, S. See under Tsukada, M., 322, 632 ns, R.E. See under Jackson, M.J., 322, 727 Surenian, R. See under Preisinger, A., 322, 794 der Preisinger, A., 322, 794 alia. A. Immunotoxins to combat AIDS (with Ramprasad, M. P.) Scientific correspondence, 322, 119 ow, T. See under Bredbrook, J., 322, 494 Sutherland, S. Book review of Visual Cognition (Pinker, S edil Suzuki, H. See under Noda, M., 322, 826 Swain, M V. Shape memory behaviour in partially stabilized zirconia ceramics, Letter to Nature, 322, 234 eet, I.P. See under Jackson, M.J., 322, 727 Swenson, GR. See under Chiu, YT., 322, 441 inbanks, D. Japan's islands coming home, News, 322, 6 Animal welfare: Laboratory animals unprotected, News, 322, 163 Space vehicles: A short flight for Japan's shuttle, News, 322, 201 Japan: Islanders put environment first, News, 322, 296
Atomic power: No nuclear doubts for Japan, News, 322, 399 See under Palca, J., 322, 400 See under Palca 1 322, 397 Made in Japan label on launchers, News, 322, 488 More ocean dives, News, 322, 493 Japanese space plans go ahead, News, 322, 583 Strategic Defense Initiative: Japan ready to participate, News, 322, Return of tamarins proves expensive, News, 322, 586 Japan's sunset export industry, News, 322, 588 Japanese space science: Joint project for solar maximum, News, dale, N.V. Neurophysiology; Parallel channels and redu mechanisms in visual cortex, News and views, 322, 775 Sze, N.D. See under Tung, K-K., 322, 811 See under Tung, K-K., 322, 811 Szestak, J W. Enzymatic activity of the conserved core of a group I self-splicing intron, Letter to Nature, 322, 83 Taam, R E. See under van den Heuvel, E P J., 322, 153 Tait, A. See under Jenni, L., 322, 173 Takahashi, E. See under Scarfe, C.M., 322, 354 Takahashi, T. See under Noda, M., 322, 826 See under Mishina, M., 322, 90 Takai, T. See under Mishina, M., 322, 90 Takemoto, S. Application of laser holographic techniques to investigate crustal deformations, Letter to Nature, 322, 49 Takeshima, H. See under Noda, M., 322, 826 Takeuchi, M. See under Ohyama, K., 322, 572 Tarlinton, D. See under Kleinfield, R., 322, 843 Tautz, D. Cryptic simplicity in DNA is a major source of genetic variation (with Trick, M. Dover, G.A.) Letter to Nature, 322, 652
Taylor, J.H. See under Dewey, R.J., 322, 712
See under Segelstein, D.J., 322, 714 Taylor, K. See under Argyle, B., 322, 402 Taylor, P.N. See under Hawkesworth, C.J., 322, 356 Teisseyre, R. Editor, Continuum theories in solid Earth physics, Book review by Smith, P.J. 322, 123 Teissie, 1. See under Prats, M., 322, 756 Terlevich, R. See under Argyle, B., 322, 402 Thein, S.L. See under Wainscoat, J.S., 322, 21
Theodoridou, L. See under Alexandropoulos, N.G., 322, 779 Throdosis, D. T. Oxytocin induces morphological plasticity in the adult hypothalamo-neurohypophysial system (with Mongagnese, C. Rodriguez, F. Vincent, J-D. Poulain, D A) Letter to Nature, 322, 738 Theyer, F. See under Herrero-Bervera, E., 322, 159 thi Bich-Thuy, L. See under Garcia, J V., 322, 383 s, J M. Catalysis: Designing porous solids, News and views, 322, 500 mas, N. An explanation of the east-west asymmetry of lo's sodium cloud, Letter to Nature, 322, 343
Thompson, K.R. See under Doberty, J.B., 322, 192 mson, A J. Book review of Physical Methods for Inorganic Biochemistry (by Wright, J., Hendrickson, W., Osaki, S., James, G.) 322, 506 Thornton, J.M. See under Barlow, D.J., 322, 747 Thorpe, A.J. See under Browning, K.A., 322, 114.
Tickell, C. Chimatic change and world affairs, revised edition., Book review by Rupke, NA. 322, 319

merman, B. See under Stachel, S.E., 322, 706

Tiollais, P. See under Dejean, A., 322, 70 Tocanne, L.E. See under Prats. M. 322, 756 Toh, H. See under Miyata. T., 322, 484

Tonegawa, S. See under Heilig, J S., 322, 836 Torri, G. See under Casu, B., 322, 215 Townsend, C. Book review of Community I

Trebisky, T.J. See under Sonett. C.P., 322, 615

Tritton, K. See under Argyle, B., 322, 402
Tschopp, J. Structural/functional similarity between proteins in-

Tsukada, M. Oldest primitive agriculture and vegetational environments in Japan (with Sugita, S, Tsukada, Y) Letter to Nature,

volved in complement- and cytotoxic T-lymphocyte-mediated cytolysis (with Masson, D. Stanley, K.K.) Letter to Nature, 322,

Case, T J editors) 322, 507

Trick, M. See under Tautz, D., 322, 652

322, 632 kada, Y. See under Tsukada, M., 322, 632 Tsuvama, S. See under Aktories, K., 322, 390

olka, P. See under Valet, J-P., 322, 27 Tung, K-K. Are Antarctic ozone variations a manifestation of dynamics or chemistry? (with Ko, M K W, Rodriguez, J M, Sze, N D) Letter to Nature, 322, 811 Are Antarctic ozone variations a manifestation of dynamics or chemistry? (with Ko, K W, Rodriguez, J M, Sze, N D) Letter to Nature 377 811 Turok, N. Particle physics: Particles and the Universe, News views, 322, 111 Tyrer, M. Invertebrate neurobiology: Catching up with peptides, News and views, 322, 596 Umesono, K. See under Ohyama, K., 322, 572 Ussami, N. Crustal detachment during South Atlantic rifting and formation of Tucano-Gabon basin system (with Karner, G D. Bott, MHP) Letter to Nature, 322, 629 Uzveh.L. Law and genetic testing, Correspondence, 322, 767 ela, C. See under Devés, R., 322, 494 Valet, J. P. High-resolution sedimentary record of a geom reversal (with Laj, C, Tucholka, P) Article, 322, 27 Valladas, H. Thermoluminescence dating of Le Moustier (Dor-dogne, France) (with Geneste, J M, Joron, J L, Chadelle, J P) Letter to Nature, 322, 452 den Henvel, E.P.J. Evidence for an asymptotic lower limit to the surface dipole magnetic field strengths of neutron stars (with van Paradijs, J A, Taam, R E) Letter to Nature, 322, 153 ler Vilet, P.C. See under Pruijn, G.J.M., 322, 656 van Driel, W. See under Pruijn, G J M., 322, 656 Van Gilder, J. See under Damasio, A., 322, 363 van Meer, G. The tight junction does not allow lipid molecules to diffuse from one epithelial cell to the next (with Gumbiner, B, Simons, K) Letter to Nature, 322, 639 van Paradijs, J. A. See under van den Heuvel, E.P.J., 322, 153 Van Valen, L. M. Speciation and our own species, Scientific correspondence, 322, 412 Wonterghem, J. Formation of ultra-fine amorphous alloy particles by reduction in aqueous solution (with Mørup, S, Koch, CJ W, Charles, S W, Wells, S) Letter to Nature, 322, 622 Vanysek, V. See under Moreels, G., 322, 90 Varotsos, P. Earthquake prediction and electric signals (with Alexopoulos, K. Nomicos, K. Lazaridou, M) Scientific correspondence, 322, 120 Vaury, C. See under Bucheton, A., 322, 650 Vedrenne, G. See under Laros, J.G., 322, 152 enkatakrishnan, P. Inhibition of convective collapse of solar magnetic flux tubes by radiative diffusion. Letter to Nature. 322. Ventura, V. Science and faith, Correspondence, 322, 768 Verstracte, J-M. See under Katz, E.J., 322, 245 Vickerman, K. Parasitology: Clandestine sex in trypanosomes, News and views, 322, 112 Vilenkin, A. Looking for cos nic strings, Letter to Na Vincent, J-D. See under Theodosis, D.T., 322, 738 Vincent, M. See under Morecls, G., 322, 90 Vine, F J. See under Livermore, R A., 322, 162 nc, ET. See under Ostriker, JP., 322, 804 See under Ostriker, J.P., 322, 804 Vivaidi, E.A. See under Devés, R., 322, 494 Vogel, J.C. See under Heaton, T.H.E., 322, 822 von la Chevallerie, G. See under Heaton, T.H.E., 322, 822 Wager-Smith, K. See under Belmont, J.W., 322, 385
Wainscoat, J.S. Are we all out of Africa?: Reply (with Hill, A.V.S. Thein, S L., Clegg, J B) Scientific corresponding ndence, 322, 21 Wakahayashi, S. Primary sequence of a dimeric bacterial haemoglobin from Vitreoscilla (with Matsubara, H, Webster, DA) Letter to Nature, 322, 481 Walgate, R. Hermes limps on to ESA's agenda, News, 322, 3 European cooperation: Eureka gets down to business, News, 322, French science: Legal niceties end an era, News, 322, 8 Galactic strings are stable, News and views, 322, 17 Space vehicles: British HOTOL closes in on French Hermes, News. 322, 98 OECD report: Sweden nun er one for research, News, 322, 100 Launch vehicles: France and US explain failures (with Palca, J) News. 322, 101 Eiffel in orbit. News, 322, 103 European research: Framework programme poses political questions, News, 322, 197 s: Confusion over European rules, News, Engineered organ 322, 297 OECD indicators: Science statistics prove slippery, News, 322, 298 Now it's save French science!, News, 322, 301 French budget: Bleak prospect for researchers, News, 322, 400

European nuclear power: Muddle over safety measures, News,

European biotechnology: Parliament giving up alcohol, News, 322, 490

European Commission: Framework to be scaled down, News, 322,

Particle physics: Where now with superstrings?, News and views,

European agriculture: Politics before scientific advice, News, 322,

lker, A. 2.5-Myr Australopithecus boisei from west of Lake Turkana, Kenya (with Leakey, R E, Harris, J M, Brown, F H) Article, 322, 517

322, 488

322, 592

Wall, J. See under Argyle, B., 322, 402

nity Ecology (Diamond, J.

Wallace, R.B. See under Hochgeschwender, U., 322, 376 Walsh, J B. Sequencing the human genome (with Marks, 1) Correspondence, 322, 590 Walton, P. SDI: UK scientists should take care, News, 322, 300 UK star wars consortium launched, News, 322, 3(8) Wang, H. The Geology of China, Book review by Sengor. A.M.C., 322, 507 Warming, B. Condoms in Japan, Correspondence, 322, 10 Warren, G. See under Bredbrook, J., 322, 494 Wasielewski, M R. Ultrafast caretenoid to pheophorbide energy transfer in a biomimetic model for antenna function in pla synthesis (with Liddell, P.A., Barrett, D., Moore, T.A., Gust, D) Letter to Nature, 322, 570 Webster, D A. See under Wakabayashi, S., 322, 481 Weigert, M. See under Kleinfield, R., 322, 843 Weinberger, J. Distinct factors bind to apparently homologous ences in the immunoglobulin heavy-chain enhancer (with Balti-more, D, Sharp, PA) Letter to Nature, 322, 846 Weinreich Haste, H. Belief in miracles, Correspondence, 322, 766
Weinstock, R S. Olfactory dysfunction in humans with deficient
guanine nucleotide-binding protein (with Wright, H.N. Spieges, A.M., Levine, M.A., Moses, A.M.) Letter to Nature, 322, 635 Weisberg, R.H. Equatorial Atlantic Ocean temperature and current variations during 1983 and 1984 (with Colin. C) Letter to Nature, 322, 240 Wells, J M. See under Jenni, L., 322, 173 Wells, S. See under van Wonterghem, J., 322, 622 Wells, TNC. See under Forsht, AR., 322, 284 Weish, M.J. Chloride and potassium channels in cystic fibrosis airway epithelia (with Liedtke, C.M.) Letter to Nature, 322, 467 Weltzien, H.U. See under Hochgeschwender, U., 322, 376 White, J. Editor, Studies on Plant Demography: A Festachrift fire John L Harper, Book review by Moore, P.D. 322, 320 Editor, The population structure of vegetation. Handbook of vegetation science, Vol. 3., Book review by Moore, P.D. 332, 320 Wickner, W. See under Kuhn, A., 322, 335 Wicknemasinghe, N.C. See under Hoyle, F., 322, 509 Wiese, P. See under Reth, M., 322, 840 Wieley, T.M.L. See under Jones, P.D., 322, 430 Wilkes, M. Memoirs of a Computer Pioneer. Book review by Pinker. ton. J M M. 322, 26 Williams, R J P. Biological chemistry: Long-range electron transfer (with Concar, D) News and views, 322, 213 iams, T. A mouse locus at which transcription from both DNA strands produces mRNAs complementary at their 3' ends (with Fried, M) Letter to Nature, 322, 275 n, R. Risk analysis, Corresponde once. 322, 768 Wilson, R. W. See under Stark, A.A., 322, 805 See under Stark, A.A., 322, 805 Wilson, S.M. See under Lichte, F.E., 322, 816 Winter, J. See under Cohen, J., 322, 465 Woo, S.L.C. See under Dillella, A.G., 322, 799 Wood, B.J. See under Mattioli, G.S., 322, 626 Wood, K.R. The Biochemistry and Physiology of Plant Disease, Book review by Dixon, R. 322, 604 ds, J D. Thermohaline intrusions created isopycnically at oceanic fronts are inclined to isopvensls (with Onken, R. Fischer, J) Letter to Nature, 322, 446 Woolf, N.J. See under Angel, J.R.P., 322, 341
Worton, R.G. Reply: X;autosome translocations in females with Duchenne or Becker muscular dystrophy. Matters arising, 322. Wright, E. Franklin of Philadelphia. Book review by Porter, R. 322, Wright, H N. See under Weinstock, R S., 322, 635 Wright, J. Physical Methods for Inorganic Biochemistry. Book review by Thomson, A.J. 322, 506 Wright, K. National Science Foundation: Grant applications go paperless, News, 322, 102 US technology: Making rivals work together, News, 322, 199 Wright, P.B. See under Jones, P.D., 322, 430 Wrightsman, R.A. See under Peterson, D.S., 322, 566
Wyborny, L.E. Is Classic Coca-Coca the real thing? (with Shanson, 3) L) Scientific correspondence, 322, 21 Wyse, R F G. See under Gilmore, G., 322, 806 See under Gilmore, G., 322, 806 Yang, Z. The Geology of China. Book review by Sengor, A M. C., 322, 507 Yarborough, W A. Extraordinary effects of mortar-and-postis grieding on microstructure of sintered alumina gel (with Roy, R) Letter to Nature, 322, 347 Yellen, J E. Anthropology; The longest human record. News and views, 322, 774 Voung, L. B. The unfinished Universe. Book review by Atkins, P.W.

Zambryski, P. See under Stachel, S.E., 322, 706

Zeller, N.K. See under Kristensson, K., 322, 544

Maddox, J. 322, 783

Zenchenko, V M. See under Laros, J G., 322, 152 Zenger, D H. Darwin, Lyell and gradualism, Correspon

Zimmerman, M. See under Doherty, J.B., 322, 192 Zobetz, E. See under Preisinger, A., 322, 794

See under Preisinger, A., 322, 794
Zurek, W H. See under Quinn, P J., 322, 329

m, J. The World of Science and the Rule of Law. Book review by

CONVENIENT-INFORMATIVE-TIMELY-PROVOCATIVE

FOUR DYNAMITE REASONS WHY YOU SHOULD SUBSCRIBE TO BIO/TECHNOLOGY NOW . . .

You'll save time. Because you don't have time to read every journal in the field. **BIO/TECHNOLOGY** is written and edited to give you all the information you need in ONE convenient source. BIO/TECH-NOLOGY is the only journal to give you news. Features. Original research. Product evaluations. Industrial applications, Job openings, Book and product reviews. And more, If it's important to your work. you'll find it between the covers of BIO/TECHNOLOGY.

You'll learn new ways to im-**L** prove your on-the-job skills and run a more successful operation. Each month BIO/TECH-NOLOGY gives you the scoop on invaluable start-up information...the latest instrumentation...marketing breakthroughs . . . funding sources...new technologies... patents and licences...profiles on how others are avoiding the pitfalls and reaping the rewards. In fact, just one practical tip from BIO/-TECHNOLOGY can be worth many times the cost of your subscription.



You'll be up-to-date on all major industry developments. With correspondents all over the world, BIO/TECHNOLOGY delivers the inside story on who's doing what, where. You'll get the latest word on changing government regulations and tax law, and how they affect your work.

Plus you'll read original research papers by bench scientists, engineers, and biologists that will help keep you in the forefront of every new discovery worth knowing about.

You'll get new ideas you can put to use immediately.BIO/-TECHNOLOGY lets you rub elbows with eminent scientists, tour new facilities and learn how new processes work in every field from genetic engineering to molecular biology. Each month, BIO/TECHNOLOGY helps spark ideas for your own research, for new industrial applications and for getting along in the increasingly competitive financial arena.

If you're not already subscribing to BIO/TECHNOLOGY, don't delay the moment any longer - return the coupon below and we will send you twelve issues. You risk nothing. If for any reason BIO/TECHNOLOGY doesn't live up to your highest expectations, just let us know and you'll receive a full refund on all unmailed copies. Remember too, that your subscription may be tax deductible.

TO START RECEIVING YOUR SUBSCRIPTION, FILL OUT THE COUPON BELOW AND RETURN WITH PAYMENT TO:

U.S.A.: BIO/TECHNOLOGY Subscription Order Dept., P.O. Box 1543 Neptune, New Jersey 07754-1543 U.S.A. To speed up your subscription in the U.S.A., call toll free	ENGLAND: BIO/TECHNOLOGY Subscription Order Dept., Macmillan Journals, Ltd Brunel Road, Houndmills, Basingstoke Hampshire RG21 2XS, England		
□ YES! Please send me one year of BIO/TECHNOLOGY (12 issues). I understand that I may cancel my subscription at any time and receive a full refund on all unmailed issues. □ U.S.A\$59.00* □ Australia-A\$130** □ U.K£70** □ Elsewhere-U.S.\$112**	☐ My payment is enclosed at the price checked. ☐ Please charge my credit card account: ☐ American Express ☐ Mastercard ☐ Visa Card No.:		
Japan Publications Trading Company Ltd 2-1 Sarugaku-cho 1-chome Chiyoda-ku, Tokyo, Japan Tel: (03) 292 3755	Company: Address: City/State/Postal Code:		
Note: *Represents 24% off Basic Subscription Price of U.S. \$78.00 **All other prices quoted are "Air Speed"	Country:		

innaralo adiminara ensaler sensilivity

Zeta-Probe membranes exhibit the unique quality of binding DNA in alkaline solution. There's no need for pre-transfer denaturation and neutralization steps. Eliminating these steps results in significantly improved resolution!

In conventional Southern blotting, pre-transfer neutralization can lead to partial renaturation. Alkaline transfer insures that DNA is bound and quantitatively fixed in a denatured state. This eliminates another step-post-transfer UV fixation. Because base fixed DNA is more hybridizable than UVfixed DNA, detection sensitivity is greater.

Successful alkaline Southern blotting is strongly dependent upon using the proper nylon-based blotting membrane. Zeta-Probe membranes are the perfect choice. They are well characterized quaternary amine-derivatized nylon membranes, widely used for nucleic acid blotting.

- 1. Reed, K.C., & Mann, D.A. (1986) Nuc. Acids Res. 13, 7207-7221.
- 2. Gross, D.S., Huang, S., & Gerrard, W.T. (1985) J. Mol. Biol. 183, 251-265.
- 3. Gatti, R.A., Concannon, P., & Salser, W. (1984) Biotechniques 2, 148-155.
- Bodkin, D.K. & Knudson, D.L. (1985) J. Virological Methods 10, 45-52.
- 5. Sealey, P.G., Whittaker, P.A., & Southern, E.M. (1985) Nuc. Acids Res. 13, 1905-1923.

- and tragateria in small as 10 bases? Prytotidize Southern blots up to 6 times? Paybridge Morthern blots up to 6 times? Ow protocols eliminate background on Zeia-Probe membranes
- High sensitivity for single copy detection?
 Bind native DNA¹
- Electrophoretically blot nucleic acids in low ionic strength buffers 1,2,4

For more basic facts on alkaline Southern blotting. and other applications of Zeta-Probe membranes, ask for Bulletin 1110.

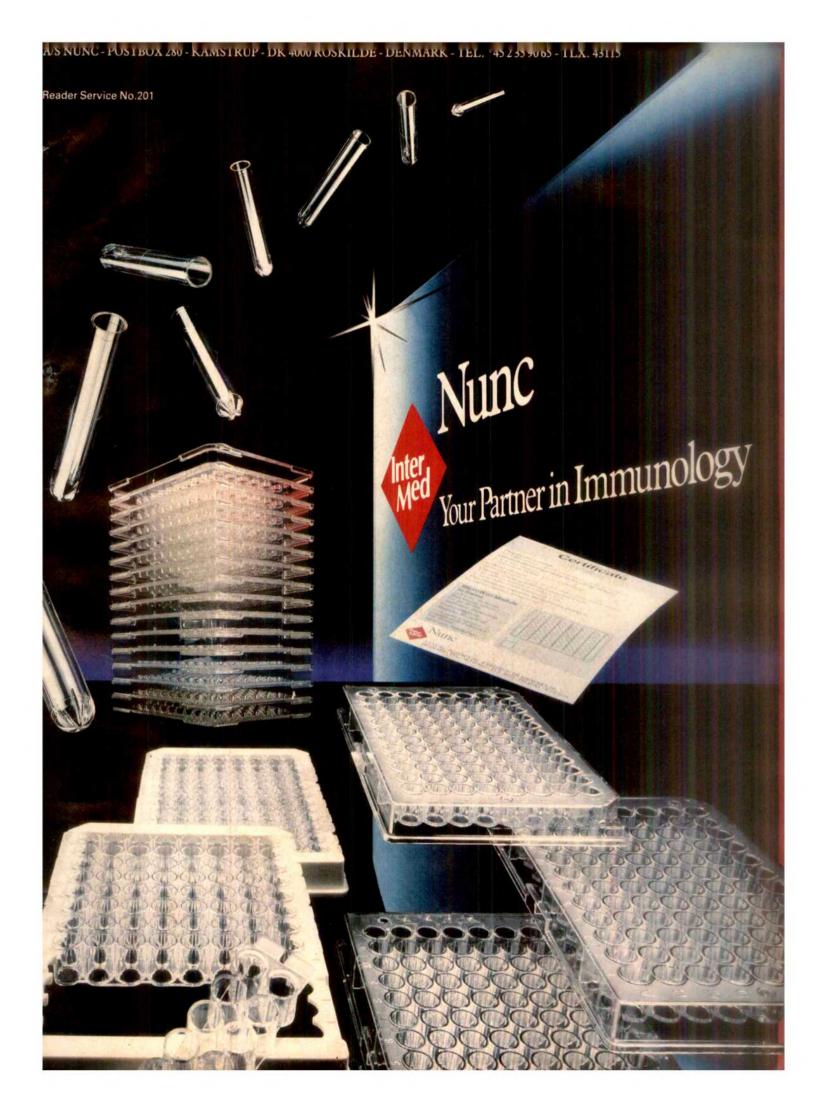
Compare membranes: ZETA-PROBE* Nitrocellulose Nitrocellulose ZETA-PROBE* - 9.4 kb - 2.0 14 haur exposure 4 hour exposure 1 hour exposure Room temperature -70°C -70°C No intensifying screen Intensifying screen Intensitying screen Data provided by Dr. Ken C. Reed Australian National University, Canberra



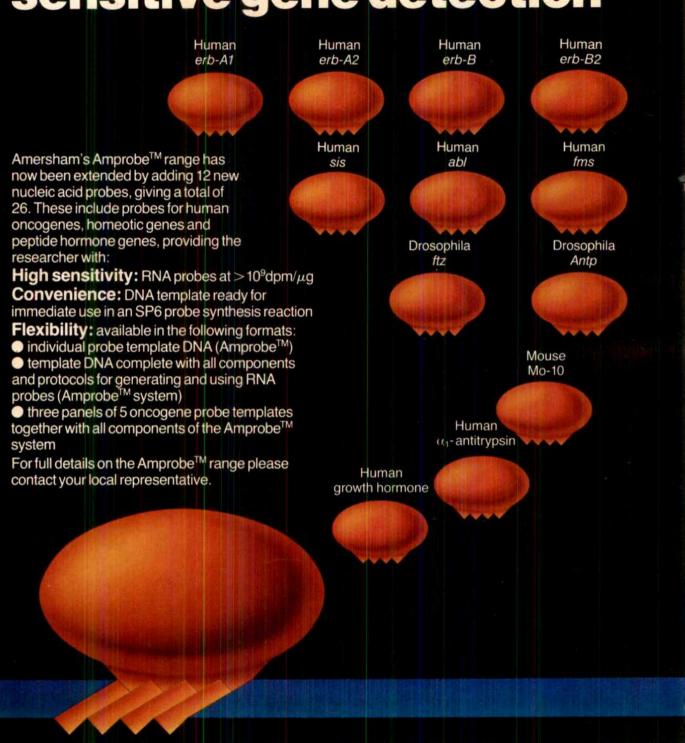
Chemical Division

1414 Harbour Way South Richmond, CA 94804 (415) 232-7000 800-4-BIO-RAD

Also in Rockville Centre, NY; Hornsby, Australia; Vienna, Austria; Mississauga, Canada; Watford, England; Munich, Germany; Milan, Italy; Tokyo, Japan; Utrecht, The Netherlands; and Glattbrugg, Switzerland.



The Amprobe™ range now offers more choice in sensitive gene detection



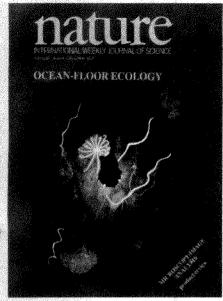
Amersham International plc

Amersham Place Little Chalfont Buckinghamshire England HP7 9NA telephone Little Chalfont (02404) 4444 telex 838818 ACTIVL G



nature

NATURE VOL. 322 3 JULY 1986



A close-up of corals, sponges and other suspension feeders on the Jasper Scamount — a 3.5-km-high extinct volcatio built on the Pacific floor at a depth of 4.200 m some 550 km southwest of San Diego, California. Little is known about deep-scamount faunabut on page 59 of this issue the rich coral community of Jasper Scamount is described. Analysis of populations of deep-sea suspension feeders could provide a measure of the average physical conditions at deep hard-bottom sites. The cover photo was taken by the Deep Tow instrument of Scripps Institution of Oceanography. In the centre is the 16-cm-diameter strobe.

OPINION	
Compromise on arms control?	1
Research democracy	
Eureka discovered	2
NEWS	
West German space research	3
Hermes limps onto ESA's agenda	
Biotechnology	
US research	4
Scraping the barrel	
Falkland Islands	
Strategic Defense Initiative	5
High-energy physics	
AIDS	6
Japan's islands coming home	
European cooperation	7
Laboratory safety	
French science	8
Italian biotechnology	
US space	
UK science	9
Ocean satellites	
CORRESPONDENCE-	
Were Darwin and Lyall	10

NEWS AND VIEWS

The proper study of mankind

Miranda Robertson

Duchenne muscular dystrophy:		ARTICLES	
Collaboration and progress			
Peter N Goodfellow	12	High-resolution sedimentary	
Geomagnetic reversals: Evidence for		record of a geomagnetic	
asymmetry and fluctuation		reversal	
Jeremy Bloxham	13	J-P Valet, C Laj	فقائق
Cell growth control mechanisms		& PTucholka	27
Tony Hunter	14	Cloning the gene for an inherited	en-mare en la
Clues about RNA enzymes		human disorder — chronic	
HD Robertson	16	granulomatous disease — on the	
Galactic strings are stable		basis of its chromosomal location	
Robert Walgate	17	B Royer-Pokora, L M Kunkel.	
A paradigm shift in glaciology?		A P Monaco, S C Goff.	- 9
G S Boulton	18	PE Newburger, R L Baehner,	
-SCIENTIFIC CORRESPONDENCE	_	FS Cole, JT Curnutte	
A new term in the global		& S H Orkin	32
carbon balance		LETTERS TO NATURE	an management
U Bianchi, L Musi,			
M Picardi & E Piovano	19	A QSO with redshift 3.8 found	
X chromosomes and dosage		on a UK Schmidt telescope	
compensation		IIIa-F prism plate	
MENewton	19	C Hazard, R G McMahon	
Motions of the images of atoms		& W L W Sargent	38
A P Korn			- or trapeled (
Reply: A Howie	19	Spectrum of a QSO with	
Legal problems of Huntington's		redshift 3.8	
chorea tests		W L W Sargent, A V Filippenko.	
W Bains	20	C C Steidel, C Hazard	4 44
Is cannibalism all in the mind?		& R G McMahon	40
RJBird	20	The actual according of Hanney	n in Parameter of
Linkage between the nation states		The rotation period of Uranus	
R C Hardwick	20	MD Desch, JEP Connerney & ML Kaiser	42
Is Classic Coca-Cola		& M L Kaiser	·
the real thing?		Detection of stratospheric HNO,	
LE Wyborny & IL Shannon	21	and NO, response to short-term	
Are we all out of Africa?		solar ultraviolet variability	
E Giles & S H Ambrose		G M Keating, J Nicholson III,	
Reply: J S Wainscoat,		G Brasseur, A De Rudder,	
A V S Hill, S L Thein		U Schmailzi & M Pitts	43
& JB Clegg	21		e and produced and a sign
40. 40-		Novel experimental investigation	
BOOK REVIEWS		of spontaneous ignition of	
Franklin of Philadelphia		gaseous hydrocarbons	
by E Wright		J F Griffiths	
Roy Porter	23	& W Nimmo	46
The Oxford Dictionary of			
Natural History	-	Climatic change and Aboriginal	
M Allaby, ed.		burning in north-east Australia	
Alastair Fitter		during the last two	-75
A Difficult Balance: Editorial		glacial/interglacial cycles	di digina
Peer Review in Medicine		A P Kershaw	47
by S Lock		Application of laser holographic	an managagan)
Stevan Harnad	24	techniques to investigate crustal	
Neurobiology of Vasopressin		deformations	
D Ganten and D Pfaff, eds		S Takemoto	49
and Vasopressin		ample operation and all the second and the second a	-46754)
R W Schrier, ed.		The Banda - Celebes - Sulu basin:	
Michael J Brownstein	25	a trapped piece of	
Memoirs of a Computer Pioneer		Cretaceous - Eocene oceanic crust?	
by M Wilkes		C-S Lee & R McCabe	51
J M M Pinkerton	26	Contents continued over	rleaf
		· · · · · · · · · · · · · · · · · · ·	

Nature* (ISSN 0028-0836) is published weekly on Thursday, except the last week in December, by Macmillan Journals Ltd and includes the Annual Index (mailed in February). Annual subscription for USA and Canada US \$240. USA and Canadian orders to: Nature, Subscription Dept, PO Box 1501, Neptune, NJ 07753, USA. Other orders to Nature, Brunel Road, Basingstoke, Hants & G22 2XS, UK. Second class postage paid at New York, NY 10012 and additional mailing offices. Authorization to photocopy material for internal or personal use, or internal or personal use, of internal or internal or personal use, of internal or personal use, of internal or internal or personal use, of internal or intern



New from Beckman

The Most Advanced Robot To Enter The Laboratory

The Biomek™ 1000 Automated Laboratory Workstation. It's a new concept in laboratory automation, and it's changing the way researchers spend their time.

Ideal for immunoassays such as ELISA, hybridoma screening and selection, or other bioassays, Biomek takes over all liquid handling steps. Pipetting, diluting, dispensing, plate washing, even photometry can be completed at this single workstation.

Fast

With Biomek™ 1000, plate-

 With the Biomek™ 1000 Automated Laboratory Workstation, you can use the labware you're accustomed to.

Complex procedures, from pipetting through photometry, can be performed at this single workstation. based enzyme immunoassays, from sample transfer to OD measurement, can take just 12 minutes, excluding incubations. And a tenfold, 96-tube serial dilution and transfer, with tip changes, can be completed in just over 3 minutes.

Flexible

With Biomek™ 1000, you're not restricted to a manufacturer-supplied program. Biomek does your work the way you want it done. A proprietary assay language lets you easily program methods from simple to complex. And you can use labware you're accustomed to: multiwell plates,

cryovials, tubes, or our new modular reservoirs.

As cost and labor savings become more critical to the research lab, the demand grows for instruments that speed research and stretch research dollars. Biomek 1000 does both.

To find out more, call toll-free (800) 742-2345, or write to Beckman Instruments, Inc., Spinco Division, 1050 Page Mill Rd., Palo Alto, CA 94304. Offices in major cities worldwide.

BECKMAN

Reader Service No.281

NATURE'S GUIDE TO HOW BRITAIN RUNS ITS SCIENCE

Nature's practical and useful wallchart has now been thoroughly updated. It provides a complete survey of the administration of British science, showing the functions, key personnel and finance of

- Government departments
- Public and independent bodies
- Research councils

Easily carried to meetings or hung as a wall poster for permanent reference, the new Nature wallchart is an ideal source of reference.

Prices: £4.75 (UK) US\$8.50 (USA/ Canada) £5.75 (All other countries) Airmail despatch BUY YOURS NOW!

From our offices in Basingstoke

Annual Subscription Pri	ices	
UK & Irish Republic		£104
USA & Canada		US\$240
Australia, NZ &		
S. Africa	Airspeed	£150
	Airmail	£190
Continental Europe	Airspeed	£125
India	Airspeed	£120
	Airmail	£190
Japan	Airspeed	Y90000
Rest of World	Surface	£120
	Airmail	£180
Orders (with remittance) to:	

USA & Canada UK & Rest of World Subscription Dept PO Box 1501 Circulation Dept Brunel Road Neptune NJ 07753 Basingstoke Hants RG212XS, UK Tel: 0256 29242

(The addresses of Nature's editorial offices are shown facing the first editorial page)

Japanese subscription enquiries to: Japan Publications Trading Company Ltd 2-1 Sarugaku-cho 1-chome Chiyoda-ku, Tokyo, Japan Tel: (03) 292 3755

Personal subscription rates: These are available in

some countries to subscribers paying by personal cheque or credit card. Details from:
USA & Canada UK & Europe Felicity Parker 65 Bleecker Street Nature New York NY 10012, USA 4 Little Essex Street London WC2R 3LF, UK Fel: (212) 477-9600

Back issues; UK, £2.50; USA & Canada, US\$6.00 (surface), US\$9.00 (air); Rest of World, £3.00 (surface), £4.00 (air)

Rinders

Single binders: UK. £5.25; USA & Canada \$11.50; Rest of World, £7.75. Set of four: UK. £15.00; USA & Canada \$32.00; Rest of World, £22.00

Annual indexes (1971-1985) UK, £5.00 each; Rest of World, \$10.00

Nature First Issue Facsimile

UK, £2.00; Rest of World (surface), \$3.00; (air) \$4.00

Nature in microform

Vrite to University Microfilms International. 300 North Zeeb Road. Ann Arbor. MI 48106, USA

Seismic measurements reveal	
a saturated porous layer	
beneath an active	
Antarctic ice stream	
D D Blankenship, C R Bentley,	
ST Rooney & RB Alley	

Deformation of till beneath ice stream B, West Antarctica R B Alley, D D Blankenship, CR Bentley & ST Rooney

Corals on seamount peaks provide evidence of current acceleration over deep-sea topography A Genin, P K Dayton,

PF Lonsdale & FN Spiess

Monocular aniseikonia: a motion parallax analogue of the disparity-induced effect B Rogers & J Koenderink

New HLA DNA polymorphisms associated with autoimmune diseases

H Festenstein, J Awad, G A Hitman, S Cutbush, A V Groves, P Cassell, W Ollier & J A Sachs

Polymorphism of human Ia antigens: gene conversion between two DR β loci results in a new **HLA-D/DR** specificity J Gorski & B Mach

Hepatitis B virus DNA integration in a sequence homologous to v-erb-A and steroid receptor genes in a hepatocellular carcinoma A Dejean, L Bougueleret, K-H Grzeschik & P Tiollais

Analysis of deletions in DNA from patients with Becker and **Duchenne muscular dystrophy** L.M Kunkel and co-authors

Carcinogen-specific mutation and amplification of Ha-ras during mouse skin carcinogenesis M Quintanilla, K Brown, M Ramsden & A Balmain 78

Site-directed mutagenesis of the regulatory light-chain Ca2+ /Mg2+ binding site and its role in hybrid myosins

F C Reinach, K Nagai & J Kendrick-Jones

Enzymatic activity of the conserved core of a group I self-splicing intron

J W Szostak

Mechanism of recognition of the 5' splice site in self-splicing group I introns

G Garriga, A M Lambowitz, T Inoue & TR Cech

Intermolecular binding of xanthan gum and carob gum P Cairns, M J Miles & V J Morris

Erratum...page 90 Molecular distinction between fetal and adult forms of muscle acetylcholine receptor M Mishina, T Takai, K Imoto, M Noda, T Takahashi.

54

57

59

62

64

67

70

73

80

83

86

Corrigendum...page 90 Near-ultraviolet and visible spectrophotometry of comet Halley from Vega 2 G Moreels, M Gogoshev. V A Krasnopolsky, J Clairemidi, M Vincent, J P Parisot, J L Bertaux. J E Blamont, M C Festou Ts Gogosheva, S Sargiochev, K Palasov, V I Moroz, A A Krysko & V Vanysek

S Numa, C Methfessel

& B Sakmann

-PRODUCT REVIEW

Imaging cells with acoustic microscopy M Issouckis Setting the stage for microscopy

92

EMPLOYMENT

Will industry support higher education? R Pearson

MISCELLANY

100 years ago

12

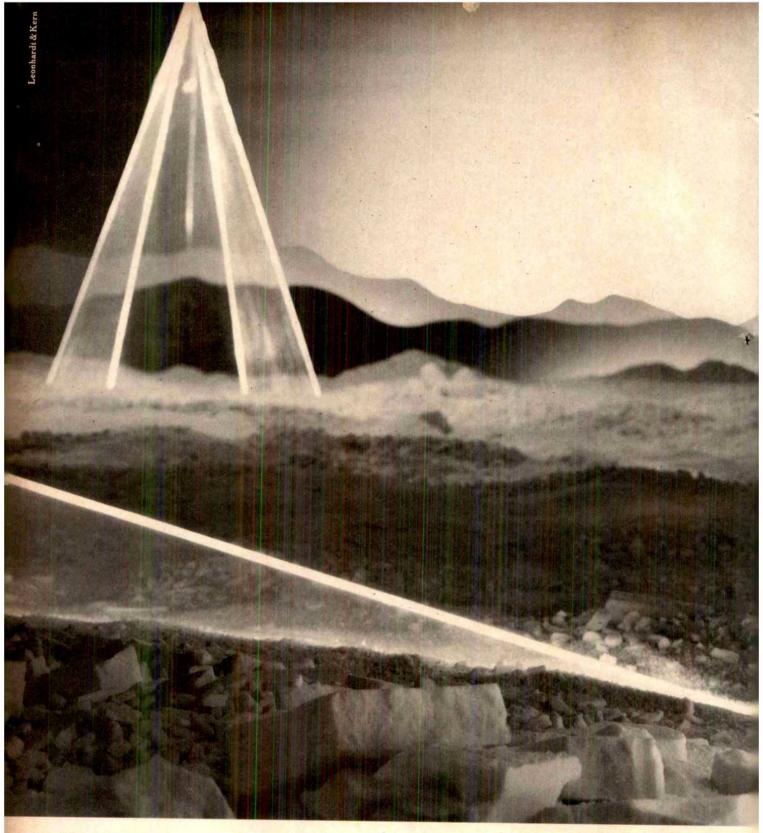
-NATURE CLASSIFIED

Professional appointments — Research posts — Studentships Fellowships — Conferences Courses — Seminars — Symposia:

Back Pages

Next week in Nature:

- Centaurus A the nearest blazar^o
- Lake acidification
- Magnetic reversals
- Pangaea's Mesozoic evolution.
- Bacterial metal scavengers
- Second T-cell receptor?
- Mystery of declining tooth decay
- Search for viruses in multiple sclerosis
- Lentivirus infections reviewed
- Immunotoxins against AIDS
- Genetic exchange in trypanosomes
- NMR image of single cell



THE DAWN OF A NEW Z

Whenever Zeiss has turned its hand to the very fundamentals of microscopy, microscopy has changed.

In 1846 and the years following, the reputation of the Carl Zeiss workshop was established, based upon microscopes of unparalleled mechanical precision, optical quality and reliability.

In 1866 Ernst Abbe, working with Zeiss, formulated his "Theory of Image Formation in the Microscope", which made possible the series production of high-quality microscopes.

In ensuing decades, Zeiss has pioneered many of the major advances in microscope production and technique.

Now in 1986, a further chapter in the history of Zeiss Microscopy begins: Zeiss presents microscopes with entirely pay infinity corrected

nature

NATURE VOL. 322 3 JULY 1986

Compromise on arms control?

Recent noises from the United States and the Soviet Union suggest that the prospect of a deal on arms control may be more immediate than it has seemed.

More than usual confusion seems to mark the ending a week ago of the latest session of the bilateral talks on arms control at Geneva. On the face of things, President Reagan's declaration that the United States would not necessarily be bound by the SALT II agreement on strategic arms from the autumn of this year made the prospect of an agreement at Geneva less easily attainable than since the negotiations began. Yet Mr Mikhail Gorbachev, the general secretary of the Soviet Communist Party, appears to have sent Mr Reagan a conciliatory letter. coinciding with the summer break at Geneva, whose effect is to suggest that compromise is within the bounds of possibility on the control of weapons of intermediate range in Europe. What is going on? Were the Soviet Union's fierce reactions to Mr Reagan's announcement mere bluff? Or has the Soviet Union been told privately that it is Mr Reagan who was bluffing, and that his threat that SALT II might be abandoned was directed not so much at Moscow as at the hard-liners in Washington?

Enough has now leaked out about the conduct of the Geneva negotiations to sustain a degree of nervous optimism. Mr Gorbachev's message bears on one stumbling block: how to legislate for the complete banning of intermediate-range missiles (SS20 Soviet missiles and the Pershing II and cruise missiles deployed in Europe by the United States) while recognizing that SS20s could be quickly moved from Asia, that the British and French nuclear forces exist and that both sides also have a large number of shorter-range weapons which, if the major Soviet and US missiles were withdrawn, would acquire a strategic significance they now lack? Both sides at Geneva appear to have been captivated by the notion that it would be simplest to do away with all missiles of intermediate range (which, Mr Reagan's "zero option" of 1982, is progress in itself). Mr Gorbachev's suggestion now that compromise is possible suggests the possibility of an agreement on the basis of a sharply reduced but nonzero intermediate force. Few would complain at that.

Much less has been said about progress at Geneva on strategic arms. It would help, of course, if the two sides were merely to agree to limit strategic weapons to the numbers allowed under SALT II (a gigantic 5,000 warheads each) and were to take the opportunity to tidy up the treaty, making it acceptable to the US Congress, but that will not satisfy the aspirations of the rest of the world, while even the negotiators at Geneva appear to think that would be a prize not worth having (which, again, is progress of a kind). The best bet is that a fifty per cent reduction of warheads is attainable now; Mr Gorbachev made an important mark earlier this year with his declaration that even such an agreement could be only an interim measure, a prelude to further more substantial reductions of nuclear arms. The paradox is that, if that principle were accepted by both sides, the degree of reduction agreed in the next few months would be less important, and so would be more easily attained.

The third item on the agenda at Geneva is the most taxing, and that most likely to prevent an agreement being reached: to what extent will the devotion of the US administration to the Strategic Defense Initiative (SDI) stick in the throat of the Soviet Union? Here too, Mr Gorbachev has been making conciliatory noises: if research means only laboratory research, all

well and good. But then, Mr Gorbachev continues (as in his latest letter to Mr Reagan) why should not both sides reaffirm their adherence to the Anti-Ballistic Missile Treaty, undertaking that they will not quit the treaty for, say, 15 years? This position represents a Soviet retreat from the fierce declarations from Moscow in 1983, suggesting that merely toying with the idea of a defence against ballistic missiles was an act of aggression. But it seems improbable that Mr Gorbachev's moderation of the past few weeks suggest he will to let SDI go ahead full tilt.

Fortunately, even here constructive compromises should be possible. First, Mr Gorbachev probably knows as well as anybody of the reluctance of the US Congress to give the project the huge sums of money it has been asking for, implying that decisions about the deployment of SDI will not take place until long after the promised decision time in the early 1990s. Second. it is also well known that there has to be a general election in the United States two years from now, and that a new president (Mr Reagan cannot stand for a third term), whatever his or her political stripe, may not set as much store by the benefits of SDL Finally, however meagre the outlook for this ambitious project. there is no obvious reason why the most likely outcome of this system, an efficient system of early warning based on infrared detectors, should not be welcomed by both sides. That is one sense in which Mr Gorbachev's suggestion that both sides should reaffirm the ABM treaty for 15 years is already a useful compromise. It requires from the United States only that degree of restraint likely to be forced on it by the technological difficulties of this ambitious project and by the increasing scepticism of the US Congress; if the two sides can make some kind of agreement this year, Congress will be even less willing to spend, with the result that the dangerous features of SDI will wither away

So much for the carrots; Mr Gorbachev's stick is the threat that he will not attend a second summit meeting unless there is something substantial about which to agree. Once the summer is over, and the campaign for the mid-term elections has begun, there will be powerful forces in the United States pushing the administration towards some lasting achievement on the international front. To fail to have a summit meeting will seem, or be made to seem, a black mark in the first week in November. Not for the first time, Mr Reagan may find that his natural (and evidently deeply felt) suspicion of arms control agreements will have to be forsaken in the face of the general feeling that there is no more laudable goal. This is the turnabout forced on him during the first year of his administration six years ago.

Research democracy

Moving Greenwich to Cambridge is not the end of the world, but users' voices need to be heard.

How should grant-making agencies manage their relations with those parts of the research community that rely on them for support? That is the question most urgently prompted by the decision of the British Science and Engineering Research Council (SERC) last week that the Royal Greenwich Observatory (RGO) should be moved to Cambridge rather than to

Edinburgh or Manchester.

The decision itself is impeccable, and properly within SERC's gift. SERC decided early in the year that a move was necessary, largely on the grounds that RGO had become a somewhat self-preoccupied institution that would benefit from stronger links with British universities. The managerial case for combining RGO with the Royal Observatory, Edinburgh, SERC's first preference, has been talked down by the British community of astronomers, while the more daring option, that of moving to Manchester, seems to have been abandoned out of deference to those among the RGO staff who believe that life north of the River Trent would be uncomfortable, a little like living in a foreign country. The result is that Cambridge will become both the administrative and academic centre of British astronomy. (Those now working at Edinburgh will increasingly think themselves marooned.)

This prospect is not necessarily bad; Cambridge is an excellent place. SERC also deserves some credit for having made a decision, a decision of any kind. But it has had to do so in the face of a torrent of complaints. Having pulled off this one triumph, SERC should resolve that it will not allow itself to be alienated a second time from those whose interests it exists to foster. This moral needs to be learned elsewhere as well.

Nobody doubts that SERC has the interests of British astronomers at heart. Over the past few years, it has been exceedingly generous towards them. There is now a prospect that British astronomers will have access to optical observing equipment, in the Canary Islands and in Hawaii, relatively more modern than they have enjoyed since, in the eighteenth century, Herschel made his name as a builder of telescopes. So why do British astronomers bite the hand that feeds them so well? Because they have a sense that SERC, acknowledged to be generous, is nevertheless acting high-handedly. It is not so much a benefactor as a nanny who "knows best". Why else does it not publish the two reports on the future of RGO (and Edinburgh) which apparently failed to come to an acceptable conclusion (in the eyes of SERC).

The remedy should be obvious. SERC should devise means by which its constituents can make their needs felt. Traditionally, SERC has delegated this task to the Space, Astronomy and Radio Board, formally taken as representative of astronomers because, in due course, most people of distinction pop up amongst its membership. But this is no longer an acceptable way of dealing with major decisions about the development of new instruments, telescopes in particular. Instead, there should be a committee whose members are not bound by secrecy and which is not forever having to measure its claims on resources by the calculation that rebuffs will diminish its authority in the competition for dwindling resources. Far better that there should be an open independent committee representing astronomers and their interests to which all working astronomers would have access, and able to ask for projects that are occasionally turned down. This is how high-energy physics is dealt with in the United States (see Nature 321, 636; 1986). The system does not rid highenergy physics of frustration, but is makes decisions intelligible.

How would such a system work in Britain, where restraints on public discussion seem all too natural? As things are the best lightning conductor for the opinions of the users of SERC's generously equipped new observatories would be a committee organized by the Royal Society or on some other independent base whose job would be the definition and repeated redefinition of researchers' needs. It would remain for SERC to decide how its facilities should be managed, which is its proper function. While about the job of setting up this mechanism, the research councils should also pay attention to the needs of other disgruntled parts of the research enterprise, the geophysicists, for example. The principle, which applies generally, is that users' needs are not merely useful planning information for managers, but are the only basis on which a sensible programme can be designed.

Eureka discovered

The ministerial meeting of the Eureka project has said all the right things. Does it mean them?

THE European Eureka project, conceived by President François Mitterrand of France as a counter to what seemed the technological threat to Europe of the Strategic Defense Initiative, seems to have taken on a life of its own. The British government, for one, seems to have been converted from scepticism to enthusiasm, at least to judge from the speech at the opening of the third ministerial conference, in London this week, by the British Prime Minister, Mrs Margaret Thatcher. The British government seems to have been persuaded by the experience of the past eighteen months that the Eureka project has not flowered into yet another trans-national bureaucracy in Europe, that there is no danger that it will become a vehicle for other peoples' chauvinism and that it may even be a useful vehicle for urging on faltering Europe some of the policies from which it has consistently shied over recent years. That is more than a little to be grateful for.

Yet Eureka remains a project whose success so far are intangible, and whose promise is hard to pin down. Mrs Thatcher this week repeated the old adage that Britain is strong on discovery and weak in their application. She went on to complain at the tendency of technical people in Europe to disparage the application of good ideas, and to urge that people should pay more attention to the design of products suited to their intended markets. The difficulty with this familiar homily is that, now, it is out of date. Technical people all over Europe would give their eye teeth for the opportunity to design marketable products. They know that nations that fail on that score become impoverished remarkably quickly. The impediments to European prosperity are now more probably structural than psychological.

Structural? When much of Europe is linked together in a community called popularly a "common market"? How can that be? Because the common market is in no real way a common market in the ordinary sense, but rather a loose gathering of ten European nations provided with common (and often irksome) services by a central bureaucracy, with a general understanding that they may discriminate against each other's goods and services only by bureaucratic means and, to the extent that they are united, drawn together by their mutual suspicion of each other as traders. The unexpected success of Eureka, which functions by facilitating but not financing collaborative projects involving European companies and universities on technical projects, is that it has helped in several subtle ways to exorcise this long-standing suspicion.

So where will Eureka lead? Mrs Thatcher was right to insist this week that Eureka by itself is insufficient, and that something has to be done to make the common market genuinely common. But how? Governments' own xenophobia in public purchasing is an obvious place to start (as she said), but governments have been more willing to applaud the abstract principle than to change their own ways. That is why Eureka's well-wishers must also hope to build on the psychological changes now well under way in the informal European community, that in which people enjoy crossing frontiers without formality. One of the missing ingredients of Mrs Thatcher's speech this week was the recognition of the importance of the educational system, and especially of European universities, in providing the cultural cement that will, given encouragement, turn into economic cement as well. For, when everything has been said about the need that Europe should be more conscious of markets in Europe and elsewhere, it remains the case that Europe is dangerously short of the skills needed to carry out that task. Eureka may be working well so far, but its further success will only serve to draw attention to the urgent need for a coordinated system of higher education and research. This will be a great opportunity, but will at first be seen as a threat to national integrity.

West German space research

Hermes causes sacking and cabinet unrest

Hamburg

A ROW over the West German space programme has resulted in the sacking of the head of the Department for Space Affairs. Aeronautics and Traffic Research. Wolfgang Finke, a Social Democrat, was removed from the post he has held for 13 years by the Minister of Research and Technology, Heinz Riesenhuber, a Christian Democrat, last week.

The two have disagreed over almost everything: Riesenhuber accused Finke of not having done enough for the ocean research programme; Finke in turn opposed his boss's decision to cut traffic research. But the crucial point of their disagreement reflects a political quarrel within the coalition cabinet over West German participation in European space programmes and, in particular, over participation in the French Hermes space shuttle project.

Like some ministers, Finke has fought for "stronger engagement for an independent European space potential that represents our political importance, our economic capacity, and technical knowledge".

Riesenhuber, however, is against a European space adventure. He has already agreed to cooperate in the construction of the Ariane 5 rocket, under French management, and to join with the United States to build the space station Columbus, at a cost for West Germany of DM 4 million. But two years ago he rejected France's offer of a share in the development of Hermes because of doubts over costs.

The French estimate of a total cost of DM 6,600 million was referred to as "total nonsense" by the minister, who considers that the worldwide satellite system necessary for the control and supervision of the space shuttle will alone cost at least DM 6,600 million. And he is very much aware of the words of Gerhard Stoltenberg, Minister of Finance, who announced to the cabinet in June last year that there was to be no money for Hermes or similar big projects. Before he is willing to reconsider his position, Riesenhuber wants a more realistic calculation of the likely costs.

On the other hand, Chancellor Helmut Kohl, another Christian Democrat, supports cooperation with France in general, and Foreign Minister Hans-Dietrich Genscher, of the Free Democrats, is urging his colleagues to back Hermes. The two—among others—have been influenced by a report published last week by the Research Institute for Foreign Policy, in which support is demanded for both

Hermes and a European space station. One of the authors of the paper is none other than fired Wolfgang Finke. It appears that Finke had told Kohl that he had his chief's support for the report — without the latter's knowledge. Riesenhuber thus had no choice but to sack him.

On balance there remains lukewarm support for the Hermes project within the cabinet. But questions over real costs and the extent of French domination of the project will need to be answered before any real commitment is forthcoming.

Jürgen Neffe

Hermes limps on to ESA's agenda

WEST Germany gave a grudging commitment last week to go ahead with "preparatory studies" for a possible European space shuttle, Hermes, despite the sacking of the official responsible for coordinating Germany's space policy (see above).

However, the agreement last week by all 13 member states of the European Space Agency (ESA) that Hermes, so far only a French project, should be thus "Europeanized", falls far short of a total commitment to build a shuttle.

No money has yet been committed, but in three months, at the October meeting in Paris of the ESA council, states will be expected to make a declaration of what share they will take of a 48-million-ECU (European Currency Unit) nine-month detailed analysis of the real costs, benefits and likely technical problems of building Hermes

ESA officials believe that the commitments made in October to this £32-million preparatory programme should be a "good indication" of likely future national involvement in the full construction of the space plane. However, a spokesman for the West German research ministry, BMFT, took time off from a European technology conference in London on Monday to say that German estimates of the true cost of Hermes were "five to six times" the £1,500 million or so suggested by the French. Moreover, the spokesman said, the German research minister, Heinz Reisenhuber, had told his British opposite number, Geoffrey Pattie, that Germany backed the British alternative project, "Hotol", a project for a horizontal take-off, partly air-breathing space-plane. "Hermes is old technology", the spokesman said. "Hotol is the future". Robert Walgate

Biotechnology

UNIDO centre taking shape

An international biotechnology centre for the developing countries came a step closer to realization last week with the appointment of its first director. Professor Irwin Gunsalus, emeritus professor at the University of Illinois, was chosen to head the International Centre for Genetic Engineering and Biotechnology (ICGEB) at a meeting organized by the United Nations Industrial Development Organization (UNIDO).

Five years have passed since the idea of a centre to bring the benefits of biotechnology to the developing countries was first proposed. During that time, many scientists, recognizing that there is a void in knowledge of molecular genetics and recombinant DNA technology in these countries, have given the centre their blessing. Now, UNIDO has provided funding to employ Gunsalus for three years, during which time he will recruit the scientists and technical staff needed to make the centre operational. He will also have to try to raise funds for the centre, which is not expected to be easy.

Italy has so far been generous in supporting the scheme and one of the centre's two branches is planned for Trieste. The other is to go to New Delhi. Rapid progress is unlikely, for almost all of the 37 countries that have signed up to support the centre are from the developing regions of Africa, South America, the Caribbean and Asia and are not easily able to provide money. The major industrial European countries, the United States and Japan have yet to support the centre and may well not do so until they have a chance of seeing how successful it will be.

Control of the centre is intended to remain within the developing countries so they can be confident that it is not just a route by which their best researchers can vanish to the advanced nations. Indeed, it is hoped that the flow will be in the opposite direction, with researchers from the advanced nations taking visiting fellowships at the centre. It is planned that each will have a staff of 30 scientists, 20 post-doctoral students and 40 technicians. Many of the staff will be on 2-3 year appointments.

Running the pair of institutes is not going to be easy. In theory, with the developing countries' heavy dependence on agriculture, biotechnology should bring enormous benefits. But much basic research on tropical agriculture remains to be done and the institutes will need to stimulate such research, at the same time fighting off demands for rapid returns on investment.

Alun Anderson

Campus bonanza from the military

Washington

US SECRETARY of Defense Caspar Weinberger last week announced the first round of winners in a \$110 million bonanza designed to improve universities' military research capabilities. The University Research Initiative (URI) will support 86 research projects at 70 institutions with awards ranging in value between \$170,000 and \$3 million.

The projects supported cover a wide spectrum. Most are intended to bring together small groups of researchers from different disciplines. But funds will also be set aside for instrumentation and for fellowships designed to encourage exchanges between universities and other institutions, especially the Department of Defense (DoD)'s own laboratories. Awards are conditional upon the successful conclusion of negotiations between DoD and the institutions.

The universities' enthusiastic response to URI seems to suggest that sensitivity on campus to military research has all but vanished. According to Dr Ronald Kerber, deputy under secretary of defence for research and advanced technology, most of the 963 URI research proposals received were of strikingly high quality. Kerber sees the large number of proposals received — worth nearly \$6,000 million in funds - as confirming universities' willingness to conduct basic research of possible military interest. Kerber said there had been no evidence of boycotts by academics opposed to the growth in the defence research budget.

Awards are typically in the \$1 million—\$2 million range, less than the \$4 million originally expected. That, Kerber explains, was partly to prevent faculty from "building empires". A single faculty member can be well supported with about \$200,000, so the average group will be of between five and ten researchers. Several awards will go to consortia of two or more universities.

Awards were made on the basis of competitive review by DoD scientists, helped by some outside consultants. As expected, most go to materials science and electronics.

Composite materials and electronic control dominate; there is also special emphasis on artificial intelligence, robotics, biotechnology, oceanography, hydrodynamics and biological structures. The awards, lasting 3–5 years, will be made through the Army Research Office, the Office of Naval Research, the Air Force Office of Scientific Research and the Defense Advanced Projects Research Agency.

The awards are still conditional upon availability of funds in DoD's budget for

fiscal year 1987, but Congress has so far strongly supported URI, providing funds beyond those requested. The first URI round comes out of 1986 and 1987 funds; the next round will not be until 1988. All URI projects will be unclassified, and Kerber expects them to remain so.

Tim Beardsley

Scraping the barrel

Washington

IRONICALLY, on the day that US Secretary of Defense Caspar Weinberger announced the first competitive awards to be made under DoD's new University Research Initiative, the Senate finally gave in to pressure from the House of Representatives to divert \$55.6 million of DoD funds to unreviewed research and construction projects at nine named universities and colleges.

The funds are provided in amendments to an emergency DoD money bill. Ten such "pork-barrel" projects were approved at the end of last year. But as they had not been subjected to peer review, they were opposed by DoD itself, which prefers to make research awards by competitive merit review (see *Nature* 321, 549; 1986).

Several of the universities provided for in the DoD bill employed influential lobbying and public relations companies in Washington to make their case to wavering congressmen. Their task was made easier because federal support for university facilities is generally agreed to be inadequate, and politicians like to be seen appearing to benefit education in their home states.

Two attempts were made in the Senate to block the disputed projects, but the Senate finally voted 56-42 last Thursday to accept a House version of the bill that reinstated nine pork-barrel projects. The Senate Appropriations Committee's report notes, however, that the Senate does not intend to support similar unreviewed projects in future.

The original ten pork-barrel projects in the DoD appropriation bill were reduced to nine last December when Frank Rhodes, president of Cornell University, refused to accept \$10 million that Congress had earmarked for computer research there, unless the project was approved by merit review.

The universities due to benefit from Congress's generosity are: Wichita State (\$5 million); Nevada (\$3.5 million); Oklahoma State (\$1 million); Iowa State (\$6.5 million); Rochester Institute of Technology (\$11.1 million); Syracuse (\$12 million); Northeastern (\$13.5 million); Oregon Graduate Center (\$1 million); and Kansas (\$2 million).

Falkland Islands

Opinions divided on penguin deaths

"NUCLEAR cargo" from the four British ships sunk during the Falklands conflict is polluting the South Atlantic, according to Soviet officials in Buenos Aires. At a press conference called last week to condemn President Reagan's unilateral repudiation of the SALT II agreement, the Soviet representatives claimed that the British military presence in the Falklands was a major threat to world peace, and that "the Argentines now have their own Chernobyl in the Atlantic".

This allegation was said to be based on research by the Buenos Aires correspondent of the Moscow weekly Literaturnarya Gazeta, Mr Vladimir Vesenskii, and on the Spanish newspaper Cambio 16. Vesenskii, the only civilian on the threeman Soviet panel, claimed that all four ships had had nuclear weapons on board and that HMS Sheffield, after being damaged by Argentine bombs, had been sunk by the British themselves "because of the danger of contamination". Vesenskii implied that contamination from these alleged bombs was responsible for the recent appearance of larger numbers of dead penguins "on the Malvinas beaches". Quoting an unnamed Argentine legislator, Vesenskii said that the "outer casings of the nuclear bombs were designed for dry places, not the ocean".

Asked if the Soviet Union had any information proving that there are now nuclear bombs on the Falklands, the Soviet chargé d'affaires Viktor Tkachenko said simply that the Soviet Union and Argentina were "greatly concerned" about the building of a British military base on the islands, and called for Argentine–Soviet military relations to be strengthened at the "non-strategic level".

• Vera Rich
• Results from UK laboratories seem to show that the penguin death-rate, in fact, is considerably worse than Vesenskii implied. He spoke of "tens" of dead penguins being washed up. In fact, from mid-February, elevated death rates of rock-hopper penguins, and, to a lesser extent, gentoo penguins, began to be observed, and on 25 May, more than 3,000 dead rockhoppers were counted in a single rookery on New Island (off West Falk-land).

Three batches of specimens have been spent to the United Kingdom, to the laboratories of the Ministry of Agriculture, Fisheries and Food (MAFF). Preliminary reports indicate that the birds died of starvation. Some appear to have suffered from puffinosis, a viral disease affecting sea-birds, and some show elevated lead levels in liver and kidneys.

Strategic Defense Initiative

Britain wins first big contracts

Britain has become the first foreign country to win a substantial contract for research in the US Strategic Defense Initiative (SDI). On Tuesday last week, George Younger, the Secretary of State for Defence, and Caspar Weinberger, his opposite number in the United States, signed a \$10 million letter of offer and acceptance in Washington. A further \$4.3 million contract goes to the United Kingdom Atomic Energy Authority's Culham Laboratory.

The contracts come at a time when there had been increasing criticism of British failure to obtain funds for research in the SDI programme. As Britain was the first country to back the US "star wars" project and to agree to cooperate on research and development, there were hopes that major contracts would be won —£1,000 million was announced as a possible figure last year by the then Secretary of State for Defence, Michael Heseltine. But there is now little hope that expenditure in Britain will come anywhere near this target.

The \$10 million contract is for a theoretical research study, expected to last 22 months, of the systems "necessary for the integrated defence of Europe". At present, that means the study will give a British view of the defence of Europe; at a later date, European allies may be added to the project. The contract has been put out to tender.

Culham Laboratory's contract is to cover research on neutral-beam particle systems. Neutral-beam weapons could form part of the first layer of an SDI system, shooting down ballistic missiles from space-based platforms. The Culham group, headed by Dr Tom Green, has already built up an international reputation for neutral-beam research. In collaboration with a French group, it designed the neutral-beam injectors for the Joint European Torus (JET) which sits alongside the Culham laboratories. The injectors fire intense beams of very energetic hydrogen and deuterium atoms into the tokamak to help heat up the plasma inside it. To generate the beam, positively-charged ions are accelerated electrostatically: they are subsequently neutralized in a gas cell, as charged particles would not be able to penetrate the intense magnetic field confining the plasma. Neutral beams are also essential for a space-based weapon as charged particles would be sent off course by the Earth's magnetic field. But for SDI application, where very high-energy beams are needed, negatively charged ions will be accelerated and an electron stripped off them before firing - it is here that the Culham group will have to develop new technology.

Any application for neutral beams as weapons is, of course, a long way off. Much basic research remains to be done. But if the present work, to extend over a three-year period, is successful, further SDI contracts may come along. The Culham group has already proved itself to be imaginative in finding research contracts; since the JET work drew to a close it has carried out research on semiconductor ion implantation, tokamak plasma beam diagnostics and ion thruster engines for keeping geostationary satellites on station.

Other SDI projects are rumoured to be in the pipeline for British research groups. The United States is interested in work on electromagnetic guns carried out at the

Royal Armament Research and Development Establishment and it is likely that a contract will be signed in the coming months.

Electromagnetic guns come in two varieties. In a rail gun two rails are bridged by an armature behind a metal protectile. When a current of several million amps is applied the expanding current loop fires the projectile.

Other electromagnetic guns are more similar to a linear induction motor, a series of switched coils induces a current in the projectile to fire it.

Either way velocities in the tens of kilo metres per second can be achieved – a standard army rifle bullet goes at less than a kilometre a second. The aim is for velocities of 50–100 km per sec tor electromagnetic guns which might be based in space or on land.

Alun Anderson

High-energy physics

Supercollider in the balance

Washington

ELEVEN US senators have signed a letter to President Reagan urging him to give his personal support to the Superconducting Supercollider (SSC), the 40 TeV proton-proton collider now at the design stage. Without strong White House support, the senators say the project "cannot go forward".

Already there are rumblings in Congress that the Challenger accident and the Gramm-Rudman deficit reduction act will make it hard to find the \$3,010 million needed to build SSC. The Department of Energy (DoE) steadfastly maintains that it has not decided SSC's future, but construction delays seem likely, and it is just possible that the project may be cancelled.

Senators Barry Goldwater and Dennis DeConcini, both Republicans from Arizona, organized the letter to President Reagan. While the letter describes SSC as "a very important national science project", the senators also find SSC attractive for the 7,000–8,000 jobs and millions of construction dollars it will bring to the state where it is built.

In testimony last week before the Senate Committee on Energy and Natural Resources, Alvin Trivelpiece, director of DoE's Office of Energy Research, called technical progress on SSC "excellent". But Trivelpiece said DoE is still weighing its options. A decision must be made soon so that the department's budget can reach the White House by September. Members of Congress in both the House and Senate feel a full-scale start for SSC in the 1988 budget is unlikely.

The House Appropriations Committee last month removed from the DoE budget request \$20 million that was to be used for continued development of SSC. While the committee's action must still be approved

by the full House, and later by the Senate, it was a signal that Congress is not interested in seeing more money put into SSC until its future is determined.

In May, DoE completed a favourable review of the conceptual design of SSC. The review described the \$3,010 million budget proposed for SSC as "credible and consistent with the scope of the project" The report also called the six-and-a-half-year construction schedule feasible, and said SSC will meet the requirements of high-energy physics "well into the next century".

But SSC's timing may be bad. William Graham still awaits confirmation by the Senate as director of the White House Office of Science and Technology Policy (OSTP). Until he comes on board as director, nobody at OSTP is anxious to carry the torch for such an ambitious project. The retirement of Hugh Loweth from the Office of Management and Budget, after 13 years as head of the Energy and Science Division, may also influence reception of the budget.

Senator Daniel Evans (Republican. Washington), a member of the Senate Energy and Natural Resources Committee, has declined to sign the Goldwater-De Concini letter because he feels it would be irresponsible to commit funds to SSC when Congress is trying desperately to reduce the budget deficit. But he does have a modest proposal for DoE. Evans wants DoE to offer SSC as a "carrot" to the state it chooses for the site of the first deep geological repository for high-level nuclear waste. The three states chosen by DoE as final candidates for the waste storage site, Washington, Texas and Nevada, have so far been less than enthusiastic. All three have gone to court to try to block DoE's plans. Joseph Palca

Depressing news from Paris

Paris

Tin: razzmatazz of last week's international conference on acquired immune deficiency syndrome (AIDS) in Paris was tempered by gloomy facts and figures. Unless some effective form of therapy is found, 179,000 people in the United States will die of AIDS in the next five years; no doubts remain about the heterosexual transmission of the AIDS virus; at least half the members of several groups of intravenous drug users are now infected; the virus evolves as rapidly as the influenza virus; and it already has an alarming hold in some cities in central Africa.

There are still doubts about the validity of some of the African statistics, but those, from Kinshasa, capital of Zaire, are copious and reliable. Of a group of prostitutes, 27 per cent have been infected by the virus as have 6.5 per cent of all the patients in hospital. In Rwanda, the equivalent fig-

Japan's islands coming home

Tokyo

FOR years, the Japanese government has been doggedly trying to get the Soviet Union to return four small islands off the coast of Hokkaido seized in the closing days of the Second World War. Now a new survey shows that some of the islands will return quite soon — geologically speaking, that is.

The islands of Etorofu, Kunashiri, Shikotan and the Habomai group — the "northern territories" — were home to 16,000 Japanese before the Soviet invasion took their troops to an island within 5 km of the shores of Hokkaido in 1945. The continuing occupation is an endless source of friction between the two countries and has prevented Japan from concluding a post-war peace treaty with the Soviet Union, with all the trade benefits that might bring. But it seems the islands are creeping home at the rate of some 2 metres every 80 years.

The figures come from a resurvey of Hokkaido by the mapping division of the Geographical Survey Institute of the Ministry of Construction. A laser range-finder has revealed crustal movement that has occurred since an earlier triangulation survey carried out between 1908 and 1916. Throughout most of Hokkaido, net movement has been of the order of only a few centimetres or tens of centimetres. The two closest islands, the Habomais and Shikotan, are moving very much faster. If things continue as they are, they should collide with the mainland in about one million David Swinbanks vears.

ures are 88 per cent and 18 per cent, with 28 per cent recorded in pregnancy. With similar figures from other countries that border on Zaire, it is clear the virus is very well established and will continue to spread from mother to child and, most importantly, by heterosexual intercourse. That accounts for the approximately equal distribution of infection between the sexes in central Africa, whereas in developed countries male homosexuals still account for about 70 per cent of cases.

In western Africa the situation is less clear and, in many ways, more interesting. There is little, if any, evidence of the presence of HTLV-III/LAV, the standard A1DS virus, but increasing evidence of the distantly related HTLV-IV and LAV-2 viruses. It remains uncertain whether these are two names for the same virus. HTLV-IV was identified in Senegalese prostitutes whose health seems unaffected by the virus. As many as half the prostitutes in one unidentified (for political reasons) country in the region have been infected with HTLV-IV, with 38, 7 and 0 per cent in three nearby countries.

So far, not a single case of AIDS has been recorded in an HTLV-IV infected person, according to Max Essex of Harvard University. On the other hand, LAV-2 has now been isolated by the Pasteur Institute team led by Luc Montagnier from 8 AIDS or pre-AIDS patients from Guinea Bissau, Senegal and Cape Verde Islands, but its prevalence in prostitutes, or in general, is not yet known. There seems to be little prospect of an immediate exchange of material between Essex and Montagnier or, therefore, of establishing the precise relationship of the two viruses.

Hope remains that once the west African and monkey viruses have all been molecularly cloned and compared with HTLV-III/LAV, there will be a clear indication of which DNA sequences are responsible for pathogenicity and might form the best vaccines. Meanwhile, there is steady progress towards trials, perhaps later this year, of whether chimpanzees immunized with vaccinia virus engineered to contain the envelope gene of HTLV-III/LAV will be protected against infection with the virus.

There are, however, distinctly mixed views on the likely success of such a trial without (or even with) refinement of the envelope gene. Furthermore, there is emerging evidence of the rapid evolution of the virus within individuals. Thus Beatrice Hahn of the University of Alabama reported that consecutive isolates of the virus from individual patients had distinctive genetic maps, and comparable differences between the virus from infected blood donors and their recipients were

described by A. Srinivasan of the Centers for Disease Control in Atlanta. Probably both the direct evolution of the virus under pressure to escape the immune system and the emergence of different viruses from a mixed infecting population are involved. The chances of effective vaccination against such a moving target may be slim, as in the case of influenza virus.

For want of anything better as an advance in AIDS therapy, attention (certainly press attention) focused on the partial reconstitution of immune function in one AIDS patient given a bone marrow transplant from his healthy identical twin along with transfers of peripheral lymphocytes both before and after the transplant. But two other identical twins did not respond to the same form of treatment. Anthony Fauci, of the National Institutes of Health, intends to pursue such treatment, assessing the value of transplantation from matched siblings, the frequency of lymphocyte transfers and the value of simultaneous therapy with antivirals.

Little progress with antivirals was reported, although the first results of a double-blind placebo trial of azidothymidine are due this summer. Samuel Broder, of the National Cancer Institute in Maryland, who is persisting with the trial in the face of considerable pressure from some quarters simply to give the drug to all patients, is quietly optimistic about the outcome, particularly as the drug gains access at potentially therapeutic levels to the brain where it may reverse the loss of cognitive functions caused by the virus. Burroughs Wellcome, which makes azidothymidine, has exhausted the world supply of thymidine, from which it is made, but has plans to overcome this problem if the drug is shown to be valuable.

Without effective therapy, progression from infection to disease is not inevitable, but the cumulative incidence of AIDS in some well-studied cohorts of homosexuals is now around 30 per cent and showing no signs of decreasing with time. Moreover, Bob Redfield, of the Walter Reed Army Institute of Research in Washington, reported that 90 per cent of a series of patients who could be classified as belonging to one of 5 stages that precede full-blown AIDS progressed by at least one stage within 18–36 months.

Without an effective vaccine, the only means of prevention is to avoid intimate sexual contact with infected people, and to avoid their blood or blood products. There are clear signs that some homosexual communities have effectively taken this advice to heart. But it is less certain that drug users are doing so. In the worst reported case, 76 per cent of a group of Italian drug takers are now infected, compared with 6 per cent in 1980. In some groups fewer than 10 per cent are yet infected, but the reason for these differences is still unclear.

Peter Newmark

European cooperation

Eureka gets down to business

EUREKA, the long-heralded but somewhat formless European programme of industrial cooperation on high-technology products, came a little more into shape on Monday, with the ministerial conference in London that marked the end of Britain's six-month secretaryship of the programme and the approval of over 60 new projects costing some 2,000 million ECU (£1,300 million).

Industry, it seems, is beginning to take Eureka seriously as a means of developing products -- such as metal-working carbon dioxide lasers and advanced road vehicle guidance and communications systems that can take a slice not only of Europe's market of 400 million consumers but also of the 120 million in Japan and the 240 million in the United States. Governments are involved because they can use their political weight to help remove trade barriers and develop common standards. Already five or six of the projects approved on Monday involve requests for additional political support of that kind, British officials say.

Monday's meeting, opened with evident enthusiasm by British Prime Minister Margaret Thatcher, approved a fivefold increase in the number of Eureka projects since the last ministerial conference in November, and established a significantly tiny secretariat of seven civil servants in appropriately - Archimedes' Street in Brussels. The significance of the size of secretariat was that governments are determined not to create "another bureaucracy" but merely a clearing house for projects proposed by industry itself.

Research is not a problem. Europe's research laboratories "burst with talent and imagination", said Mrs Thatcher, but the old continent fell down in turning this into market success. To change that, Eureka is encouraging companies to share development. But Eureka "was not a source of funds" said Thatcher (this despite the efforts by some smaller countries and Italy to establish a central European funding system for the programme). Rather, Eureka seems set to develop with governments providing support only for their national companies within particular cooperations, a system which will clearly favour the larger countries.

The British government is setting aside no new money for Eureka, but, according to technology minister Geoffrey Pattie, it will find some £10 million a year from within the Department of Trade and Industry's "Support for Innovation" scheme to back the British companies in 28 Eureka projects. These projects, including company and other national support, will account for some £750 million of new technology development over the next | internal memorandum by its office of in- | legal".

five years or so, Pattie indicated. But onethird of the Eureka projects involving Britain have no government support at all. said Pattie. West German government support is said to be on a similar scale. Italian research minister Luigi Granelli said on Monday that he "guaranteed" that every high quality proposal will get government support, but put no scale to funding which must finally pass a sceptical ministry of finance. Italian foreign minister Andreotti also hinted that Italian companies must beef up their proposals: there is no point in getting involved in Eureka "merely as a matter of prestige", he said. Meanwhile, the backing for Eureka in France, where the project originated 18 months ago, remains strong politically but uncertain financially, in a country which recently slashed its research and technology spending. Other countries, a total of 19 in all, including Iceland which joined on Monday, plan backing in proportion to the interest of their national companies.

Monday's meeting promised clarifica-

tion of one long-standing issue, the relationship of Eureka to the European Commission's own international research and development programme. According to Pattie, who for the next six months, which mark Britain's presidency of the European Council of Ministers, will chair the council of research ministers controlling the Commissions's programme, "it is quite clear there will be a linkage between certain Eureka projects and the Commission's programme". According to Research Commissioner Karl-Heinz Naries. the programmes can be complementary because the Commission's programmes are pre-competitive and Eureka's clearly competitive.

'A senior commission official at the meeting said there could still be "considerable differences" in arranging cooperation between Eureka and Commission programmes, however. For example, the two large environmental projects (EURO-MAR on sea pollution and EUROTRAC on tracing air pollution) included in Eureka on West Germany's insistence overlap strongly with Commission research and are not aimed at winning markets.

Robert Walgate

Laboratory safety

Just how hot is Harvard?

Boston, Massachusetts

HAVE the mistakes in the management of radioactive materials, for which Harvard University last month received a \$2,500 fine from the Nuclear Regulatory Commission (NRC) been corrected? Harvard vice-president Robert Scott says they have. But graduate students in the medical research area have a different tale to tell. Left unresolved, according to the students, all of whom were unwilling to be named, is the pervasive mishandling of radioactive materials stemming from short cuts taken because of research pressure and inadequate training.

"Safety regulations are often perceived as a waste of time, standing in the way of a Nobel prize", said one student. The risks of this approach are high — a laboratory stripped of its NRC licence loses its research edge as well as its personnel - yet a fear of a loss of prestige could cause management to look the other way. Dr Warren Wacker, director of Harvard's University Health Services, denies such blinkering at Harvard. Using radioactivity is a privilege, he said, and he would brook "no nonsense and no pressure" in its management. As proof, he pointed to the three well-known laboratories in microbiology and AIDS (acquired immune deficiency syndrome) research that have just lost their licences for such infractions as inadequate cleaning of a spill.

NRC fined Harvard, according to an

spection and enforcement, less because of the twelve specific incidents cited than for "lack of effective management control and oversight" of radioactivity. As a result, the violations that occurred were of particular concern to NRC because "they could have resulted in unnecessary radiation exposure to individuals".

By law, NRC can fine nuclear power plants up to \$100,000 per infraction per day, but academic institutions only \$5,000. On a severity scale of 1-5. Harvard's infractions were rated as 3, for which the highest fine is \$2,500. Harvard has been warned about a number of other incidents, but they were not deemed serious enough to warrant a fine.

NRC, savs Wacker, is cracking down on universities and Harvard, which is paying its fine without appeal, is not resisting. The salaries of two additional radiation health safety engineers will come from grants, not overhead. Other elements in Wacker's "model" programme will be continued — including surprise visits by Harvard's radiation service and immediate cancellations of licences for any serious infractions.

Radioactive materials are used on a daily basis in many medical research departments, amounting to "a couple of millicuries a week". Still, claims Wacker, "the highest level of radioactivity at Harvard is probably in the geology department in uranium ores, which are perfectly **Elizabeth Collins** French science

Legal niceties end an era

French scientists were on the streets of Paris last week demonstrating against what placards described at the "strangling" of public research by a government that has cut ten per cent from its 1986 research budget, hitting research harder than any other field of government spending. After five heady years of strong support for science in France, laboratory staff and university lecturers are shocked, and were issuing posters last week claiming that French research was "in a coma".

One of the latest and most extraordinary blows, however, is not of the government's making. The Conseil d'État, effectively the French supreme court, has ruled that a body which for three years had made all the appointments and promotions in France's premier research council, the Centre National de la Recherche Scientifique (CNRS), was illegally elected.

This extraordinary decision, made on the basis of a legal technicality, to disestablish and annul the "Comité National" of CNRS, in theory invalidates all decisions taken by that body since 1983, thus affecting many of the academic scientists and technicians in France. In practice, the decision may play into the government's hands, as its science advisers have long felt that the Comité National is too dominated by trades union interests. Paradoxically, it was a union that first made the legal complaint to the Conseil d'État back in 1983, over an election which had been designed to reduce union power.

Now, the ministry of research and the council of ministers will have the freedom to define a completely new election procedure at just the moment they would have desired — after a change of government from the political left to the right.

Appointments and promotions made by the Comité National since 1983 are thought likely to stand. But young researchers who recently attended interview boards arranged by the Comité and have been offered places in CNRS are less lucky. Some 375 of the 500 affected will be offered one-year temporary posts instead—to be reviewed next year when a new Comité is in place—and the others will fall by the wayside. This represents a 25 per cent reduction in the scientific recruitment rate projected by the previous government.

Robert Walgate

Italian biotechnology

New initiative is called for

Rome

ITALY needs to spend a million million lire (£420 million) on a massive biotechnology programme over the next five years, according to a new report from the Italian National Committee for Biotechnologies. That, says Minister of Research Luigi Granelli, will give the government a tool to make Italy competitive in previously neglected sectors such as chemicals and agriculture.

Four areas are earmarked for funds: fundamental research in public centres and universities including three special projects from the Consiglio Nazionale della Ricerca (CNR), the national research council (25 per cent of funds), national research involving both scientific bodies and industry (40 per cent), the finance of research societies and stimulation of industrial activity (25 per cent) and training of researchers (10 per cent).

Established in July 1985 by Granelli, the committee includes 14 representatives from universities and public research centres and eight from industry. Coordinated by Professor Arturo Falaschi, director of the CNR Institute of Genetic Engineering in Pavia, the report looks largely at the short term. In countries such as the United States and Japan, says the report, basic research in biotechnology is

strongly supported by government, with private investment strong in biomedicine in the United States and in agriculture in Japan. In Europe, adds the report, the United Kingdom leads in biotechnology, but good state-financed programmes have been launched elsewhere.

Italy has good scientists, says Professor Luigi Rossi Bernardi, CNR president, as well as a good research tradition at the Institute of Molecular Biology. And there is the new International Centre for Genetic Engineering and Biotechnology in Trieste (see p.3). But this is not enough for Italy to catch up with other nations.

The biomedical field, says the report, is likely to yield returns in the short term, while agriculture, the food industry and fine chemicals have good medium-term prospects. So the report suggests doubling in five years the number of researchers in biotechnology in public centres such as CNR and ENEA (the national centre for alternative energy), as well as in the universities and health ministry, rather than in industry.

To coordinate the programme, it is suggested that either the present committee should be institutionalized or a National Institute of Biotechnology should be set up like that for nuclear physics.

Paola di Paoli

US space

Air Force moves on launchers

Washington

The US Air Force has announced plans to build at least twelve medium launch vehicles (MLVs) as an alternative to the space shuttle for launching military payloads. In seeking the new rocket, the Air Force has indicated it wants potential suppliers to develop a commercial version of the rocket to compete with Europe's Ariane for commercial payloads.

The new rocket will be able to launch 10,000-lb payloads into low Earth orbit, and 2,200-lb payloads into a 10,000-mile high circular orbit. The Air Force intends to use the new rocket primarily to launch its Navstar satellites, part of a new Global Positioning System under development.

Air Force interest in a complementary commercial vehicle may seem odd, but building a launch vehicle with commercial applications would have the obvious benefit of spreading development costs. Air Force Secretary Edward C. Aldridge has consistently shown concern for the viability of the US space programme, according to space policy consultant Christopher Roberts, and by providing a steady customer, the Air Force can go a long way towards assuring the success of a commercial launcher. John Pike of the Federation of American Scientists takes a more cynical view, believing that the new MLV results from an "unholy alliance" between the Air Force and the rocket manufacturers. As Pike sees it, the Air Force gains more positions for uniformed officers in its space command, and the manufacturers get to crank up their production lines.

Money for starting the procurement process of the new MLVs was in the urgent supplement appropriations bill passed by Congress last week. Also in the appropriations bill were funds for an additional 13 Titan 34D7 rockets, the workhorse of the Titan series. With the new orders, Martin Marietta, the manufacturer of the Titan 34D7, will be in a position to compete with Ariane-4, due to launch next year, should the company decide to enter the commercial launch arena.

In a related development, the National Aeronautics and Space Administration (NASA) announced last week that it was offering Indonesia the opportunity to launch its Palapa communications satellite aboard a Delta rocket. The Palapa satellite had been scheduled to fly on the shuttle last month. If Indonesia accepts, NASA will have to build one more Delta to meet its launch commitments. But NASA denies that the new Delta would mark NASA return to expendable launch vehicles.

Joseph Palca

UK science

Save British Science takes off

An extra £100 million pounds a year is the minimum needed to "save British science" according to the new pressure group of the same name. The figure comes in the first major effort by Save British Science (SBS) to win influence in Parliament: the presentation of evidence to the House of Lords Select Committee on Science and Technology

The SBS campaign was born last January with a half-page advertisement in The Times newspaper protesting against the underfunding of UK scientific research. At that time, it was not a formal organization, but the response the advertisement provoked made it seem worthwhile to become so. More than 2,500 scientists have already contributed financially. From last week, SBS is a formally constituted body and will start to collect membership fees from individual scientists and students and from societies and companies. Its aims are to "communicate to the public, parliament and the government a proper appreciation of the economic and cultural benefits of scientists' research . . . ". A London office is being opened.

Individual members of SBS have argued their case with the recently departed Secretary of State for Education and Science, Sir Keith Joseph, and have urged scientists to write to their Members of Parliament, but the evidence to the House of Lords is their first major move.

The House of Lords select committee has just finished taking evidence on the state of British science - SBS actually squeezed in just after the deadline. The committee is expected to send a report to the Secretary of State or to call for a debate in the House of Lords on the state of science, perhaps in the next session.

SBS's evidence is not an overall analysis of British science but a collection of reallife stories from scientists depicting the difficulties they face. Taken as a whole, it should depress their lordships: libraries where core international journals can no longer be afforded, electron microscopes and other vital equipment without funds to keep them in use, talented postdoctoral students who vanish abroad, equipment that ceased to be up to date a decade ago, time wasted on an endless struggle to obtain funds, and out of work young researchers who carry on as "DHSS fellows" (living on social security payments).

A case is made that the damage extends to research with clear economic potential. Experts in high growth areas such as electronics are packing up and going abroad where they will help to train the next generation of foreign competitors. The fear is expressed that once Britain falls too far | (ERS-1) will carry altimetry instruments. | NASA projects.

behind, it will become impossible to catch up again and there will be nothing to offer in international exchange and collaboration. Evidence is given that Britain is already regarded as not being a serious partner in European ventures.

For Save British Science, the remedy lies in tackling the "alphas", grant proposals given the highest priority rating. In the past, these would have received automatic support. Now, around threequarters are funded to about two-thirds of the sum requested, but full amounts are rarely asked for as there is so little chance of success. Adequate support for all alpha-graded proposals plus the basic infrastructure needed for them would cost an extra £100 million a year.

That money would still, however, be

little more than a stopgap. What SBS wants is a coherent scientific policy that would raise the low level of investment in research by UK industry in comparison with other nations and establish a "new sharing of responsibilities between government, higher education and industry

The future success of SBS's own campaign must depend on its forming close links with industry. The only argument that is likely to carry real weight with the government is that basic research is essential if there is to be applied research that benefits British industry

So far, SBS's support has come almost entirely from academics, implying that the two constituencies of industrial and university researchers are far apart. In the future there will be efforts to recruit industrial support, beginning with companies that have links to universities and those dependent on high technology.

Alun Anderson

Ocean satellites

Topex launch comes closer

Washington

Congress has given the National Aeronautics and Space Administration (NASA) a green light to seek final design proposals for the Topex/Poseidon satellite. A joint project with the French space agency (CNES), Topex/Poseidon will provide the most accurate data on ocean surface topography ever recorded.

Topex/Poseidon is scheduled for launch in 1991 aboard the French rocket launcher Ariane. Three companies are in the running for the final contract to build the satellite: Fairchild Industries, RCA and Rockwell International have all completed design proposals, and will now provide a final design to NASA by the end of September. In addition to approving selection of the hardware, Congress is allowing NASA to solicit proposals from potential users of the satellite. According to the agreement with CNES, the French will review scientific proposals from most of Europe and Africa, while NASA will judge proposals from the rest of the world.

One of the primary beneficiaries of the ocean topography data will be the World Ocean Circulation Experiment (WOCE). Carefully calibrated altimetry data from Topex/Poseidon will provide an acccurate picture of ocean currents. Because Topex/ Poseidon has a design life of three years and will carry enough fuel to last two years longer - oceanographers expect to build up a picture of variations in ocean currents as well as their steady-state behaviour.

Both Japan and the European Space Agency (ESA) also have plans for complementary satellites. Japan's Marine Observations Satellite (MOS-1) and ESA's Earth Remote Sensing Satellite Having several satellites in orbit concurrently will provide useful cross checks on their data, says Worth Nowlin of Texas A&M University, co-chairman of the US WOCE scientific steering committee Nowlin also says the accuracy of Topex Poseidon data will help to validate less precise measures from the other satellites Another advantage of Topex/Poseidon will be its orbit. At 63.1 degrees inclination and 1,334-km altitude, Topex Poseidon will pass over the same point on Earth once every ten days. Using a laser tracking system, NASA and CNI-S will be able to calibrate the satellite's altimeters regularly. In addition, because it will not be launched into a Sun-synchronous orbit. Topex/Poseidon will provide data on solar tides that typically confound ocean current measurements.

Topex/Poseidon fits nicely into the scheme of coordinated Earth observations foreseen by the Earth System Sciences Committee in its report to NASA released last week (see Nature 321, 801: 1986). The committee has endorsed the Geopotential Research Mission (GRM) as a sequel to Topex/Poseidon, GRM will provide detailed measurements of the Earth's gravitational field, giving an absolute reference point for sea-surface heights measured by Topex/Poseidon.

Money for the final design stage of Topex/Poseidon has already been allocated to NASA, but Congress must still approve funds for full-scale development Until the Reagan administration says how it plans to balance manned and unmanned missions in the wake of the Challenger accident. Congress is likely to postpone definite decisions about support for Joseph Palca

CORRESPONDENCE-

Darwin, Lyell and gradualism

Sir-In an elegant essay, Rhodes' convincingly demonstrated that Darwin was not a strict gradualist — that he was, in fact, a pluralist and his views overlapped what over the past decade or so has been hailed as a new theory, "punctuated equilibria". According to Rhodes, Darwin recognized a component of stasis, a tenet of punctuated equilibria, and repudiated the gradualistic aspect of evenness in transformation but "...whether it was 'slow' depends on our definition of speed"; slowness is not synonymous with gradualism. Darwin, Rhodes correctly points out, clearly appreciated the significance of local, periodic speciation and its representation in the fossil record. Although rapidity of speciation is associated with punctuation, Rhodes argues that this rapidity might well be encompassed within the "gradualism" of Darwin; whether "gradual" or "rapid" becomes a matter of definition.

Recently, Dawkins2, in his review of a book Time Frames: The Rethinking of Darwinian Evolution and the Theory of Punctuated Equilibria by one of the originators of the theory, Niles Eldredge, substantiates many of the claims of Rhodes. Although the fervent punctuationists have stressed the revolutionary and anti-darwinian aspects of the concept, Dawkins states that "it lies firmly within the neo-darwinian synthesis". Darwin emphasized the term "gradual" in his campaign against creationism; in such a context, explains Dawkins, gradualism is practically synonymous with evolution itself. "The punctuationists deluded themselves that they were saying something revolutionary. And it was all due to a simple verbal misunderstanding: a confusion of two senses of the word 'gradual'."

In a very recent defence of "lyellian uniformitarianism", I4 have, by referring to Lyell's original works, demonstrated that he certainly appreciated episodicity, both past and present, and clearly incorporated that concept in his use of 'gradual". In a parallel situation (and with some overlap) to Darwin's combat with creationists in the palaeontological and biological realm, Lyell was waging an intense philosophical battle against the catastrophists, a still very vociferous and influential group in the 1830s when his early editions were written. In comparison with this antagonistic philosophy, which emphasized truly cataclysmic events beyond our present knowledge, Lyell's uniformitarianism seemed gradualistic, and was - relatively speaking; he used "gradual" in a broader sense than most have realized. One quotation from the first edition of his Principles of Geology describing the episodic uplift of a faultbounded mountain range serves as a representative statement of his concept of "gradual": "We know that one earthquake may raise the coast of Chili for a hundred miles to the average height of about five feet. A repetition of two thousand shocks of equal violence might produce a mountain chain one hundred miles long and ten thousand feet high. Now, should only one of these convulsions happen in a century, it would be consistent with the order of events experienced by the Chilians from the earliest times5 "

In another recent review, Cloud6 criticized authors who labelled Lyell a gradualist, advising them to review original sources. Cloud has suggested (personal communication), correctly I feel, that Lyell's sense of gradual and uniform was with regard to the "long average". Although he frequently used the word uniformity, it seems clear from content that what he had in mind was far from simple gradualism.

I think that both Darwin and Lyell have been rather seriously misjudged with regard to their use of "gradual". For more than a century, it seems we have cast aspersions on their gradualism without appreciating the context of their times and, apparently, frequently without carefully consulting the original sources.

DONALD H. ZENGER

Department of Geology, Pomona College, Claremont, California 91711, USA

- Rhodes, F.H.T. Nature 305, 269-272 (1983)
- Dawkins, R. Nature 316, 683-684 (1985).
- Eldredge, N. Time Frames: The Rethinking of Darwinian Evolution and the Theory of Punctuated Equilibria (Simon and Schuster, New York, 1985).

 Zenger, D.H. J. Geol. Ed. 34, 10–13 (1986).
- Lyell, C. Principles of Geology Vol. 1 (John Murray. London, 1830).
- 6. Cloud, P. Bull. Am. Ass. Petr. Geol. 69, 138-139 (1985).

Problems of Africa

SIR-I have often wished that your Opinion and News columns showed more awareness of the Third World's worsening problems; but if your editorial "Who will pity Africa?" (Nature 321, 548; 1986) is the best you can do, it might be better to remain silent. In one column of pontification you reveal a remarkable ignorance of Africa's history and economy, and even of recent events in the continent.

You say that Uganda, once a kind of paradise, "has now settled for inter-tribal violence and the chaos that follows". Apart from the fact that Britain fostered tribal rivalries in colonial days by recognizing the Kabaka of Buganda as ruler, and then backed two disastrous leaders (Obote, Amin and Obote again) who deepened these divisions, you seem to have missed the news earlier this year that Uganda now has a widely popular president (Musevini) who offers real hope of reconciliation.

Your reference to Nigeria having "squandered" its oil wealth is also somewhat misplaced, in view of the fact that Britain's oil boom appears to have financed nothing more tangible than tax cuts for the better-off. Would you call this a good example?

Worse than all of this, however, is your failure to comment on the external factors, particularly falling commodity prices, that lie at the heart of Africa's crisis. For example, Tanzania spends 60 per cent of its external earnings on oil, and while 1 tonne of tea paid for 60 barrels of oil in 1972, by 1980 it bought only $4\frac{1}{2}$ barrels. In the same period, the amount of coffee needed to pay for a lorry rose from 5 to 28 tonnes. This is the "free market" over which Africa has no control.

There has been no shortage of "good ideas" on what to do next, but Western governments have found most of them deeply unpalatable. Instead of joining Mr Schulz in lecturing Africans on their improvidence, you could start by asking why Britain and the United States have so far failed to contribute to the special programme for sub-Saharan Africa set up by the International Fund for Agricultural Development.

MICHAEL SPENCER

34 Bayham Road, Sevenoaks, Kent TN13 3XE, UK

Condoms in Japan

SIR-Legalization of the contraceptive pill seems to be regarded as an entirely positive development1. The cautiousness of the Japanese authorities has, however, contributed greatly to the wide popularity of the condom, which is more frequently used than any other form of contraception.

The low incidence of acquired immune deficiency syndrome (AIDS) in Japan and the relaxed attitude towards the possible spread of the disease among the general population, as well as the low incidence of infertility caused by salpingitis', may be explained in part by the widespread use of the condom.

Rather than Japan copying Western habits of contraception, it would be better for those in the West to attempt to understand (and possibly copy) the cultural patterns that make this simple contraceptive acceptable to Japanese men and women rather than being considered unnatural and unwelcome.

Bo Warming

Sperm-Help Foundation, Bjelkes Alle 46, DK-2200 Copenhagen N, Denmark

1. Nature 317, 760 (1985)

- Coleman, S. Family Planning in Japanese Society (Princeton University Press, 1983).
- 3. Nature 318, 306 (1985).

The proper study of mankind

Molecular biology has made the human genome accessible to laboratory investigation. But does that mean that the sequence of the human genome would be worth the effort?

There is no scientific reason for studying man. Thus one of the 120 speakers at this year's Cold Spring Harbor Symposium on the molecular biology of *Homo sapiens* from 28 May to 4 June. The issue arises because, as the programme was designed to demonstrate, there are now few fundamental questions in biology that cannot be explored using human genes and human cells.

This in itself is scarcely sufficient reason for overlooking the rather obvious shortcomings of man as an object of investigation. But there is one reason, just the same: the human species alone preserves its rare defective variants. Mouse mothers, whose matings are manipulable and whose generation times are manageable, tend to eat offspring that seem not quite right before they have grown large enough to be investigated, and thus destroy the rich mine of information that medical genetics has made available in man.

If we accept that man's sole unique contribution is his genetic diseases, the content of the Cold Spring Harbor Symposium has some interesting reflections to offer in the light of the debate, discussed in *Nature* (321, 371; 1986) and formally tabled at the symposium, on whether to launch into the gargantuan exercise of sequencing the entire human genome.

There have been two outstanding contributions of medical genetics to science. One is the analysis of mutant haemoglobins; the other is the remarkable achievement of Michael Brown and Joseph Goldstein (University of Texas, Dallas) who uncovered the cellular and molecular basis of the hypercholesterolaemia that predisposes to heart disease (see *Nature* 317, 569; 1985), the essence of which was reviewed by Goldstein at Cold Spring Harbor.

Cholesterol is cleared from the blood-stream in the form of a lipid – protein complex (LDL) that binds to a specific receptor (the LDL receptor) on the surface of cells, whence it is internalized by endocytosis and released to provide the substrate for the synthesis of cell membranes and steroid hormones, as appropriate. If the receptor-mediated internalization fails for any reason, the cholesterol builds up in the bloodstream, atherosclerotic plaques develop and heart disease ensues. By investigation of precisely why internalization does fail in individuals with familial hypercholesterolaemia, Brown

and Goldstein have built up a picture of the cellular and, more recently, the molecular biology of receptor-mediated endocytosis which has provided fundamental insights into these processes as well as clarifying the mechanism of atherosclerosis.

This has been possible only because Brown and Goldstein worked up to the molecular biology from classical genetics via biochemistry. More characteristic of latter-day triumphs were the papers presented by Louis Kunkel (Boston Children's Hospital) and Stuart Orkin (Harvard Medical School), both published in this issue of *Nature* (pp 73 and 32). They have arrived directly at the genes responsible for two human genetic diseases without engaging with the intervening biochemistry.

Kunkel and his collaborators have succeeded in forging a path to the gene for Duchenne muscular dystrophy (DMD); Orkin and his colleagues have identified, cloned and sequenced the gene for X-linked chronic granulomatous disease (CGD). Neither group is any the wiser about the molecular or cellular mechanisms of the disease.

From this point of view, DMD and CGD present problems of a different order. DMD is a programmed wasting disease of muscle whose mechanism and site of action are wholly unknown, whereas CGD is an immune deficiency known to be consequent upon a defect in the oxidase system in phagocytic cells. Peter Goodfellow explains in an article on p. 12 the route by which Kunkel and his collaborators have arrived at a region of 20,000 base pairs comprising possibly no more than a part of the DMD gene, and what this implies for the daunting prospect of identifying the gene product or products. The problem here, and much of the excitement, is that there is so little idea what to look for.

The CGD gene is much more tractable. Starting with genetic linkage analysis using polymorphic DNA probes, Orkin and co-workers identified a sequence that is transcribed specifically in normal phagocyte but not in the phagocytic cells of three of their four CGD patients. The fourth patient produced a transcript containing a small deletion that presumably abrogates the production of a functional protein. Whether the transcript encodes one of a number of known but poorly characterized components of the oxidase system, or some so far unknown enzyme,

may require some ingenuity, as well as some biochemistry, to discover.

The substantial challenge now facing Orkin and Kunkel and their collaborators is in no sense a reflection on the quality of the work or the validity of their approach. But it is an inevitable consequence of approaching the DNA directly, and thus has a direct bearing on the desirability of sequencing the rest of the human genome

In the discussion on that topic at the symposium, Paul Berg (Stanford) set out the issues—is it feasible, who will pay and is it worth it? Walter Gilbert (Harvard) seraphically chalked up the tally—three thousand million bases at 10° bases per year equals 30,000 person-years or, at the current rate of $2 \times 10^{\circ}$ bases per year, but allowing for the 6 million already sequenced, 1,000-1,500 years to finish all of it; at a going rate of \$1.00 a base

Nobody seems to doubt that it is feasible; nor that with improvements in technology it can be done in perhaps a century or less. The question is whether it is worthwhile. There is a general conviction that, even with funding from the US Department of Energy (see *Nature* 321, 371; 1986), the project would be bound to divert resources from other areas of research. In return, it is argued, it will encourage innovative technology and provide an information resource that would nourish other areas.

But technical innovations are already occurring with impressive momentum: and as an information resource, the sequence of the human genome is an extremely doubtful asset. If the skill and ingenuity of modern biology are already stretched to interpret sequences of known importance, such as those of the DMD and CGD genes, what possible use could be made of more sequences? Moreover, it is believed that roughly half the human genome is nonsense and repetition; and those who argue that there may be meaning in the nonsense and function in the repeats are not likely to prove their point by sequencing it all.

The difficulty is the same for all attempts to answer biological problems by reading DNA: unless you have a very good idea how to phrase the question, the sequence is not going to give you the answer. Blind sequencing at the expense of good ideas would, in the words of David Botstein, be for biologists to "indenture [themselves] to mindlessness".

Miranda Robertson

Duchenne muscular dystrophy

Collaboration and progress

from Peter N. Goodfellow

PROGRESS in science often reflects the Hegelian dialectic between collaboration and competition. Collaboration allows the most efficient use of resources and competition can generate original approaches to solving problems. Geneticists, molecular biologists and clinicians studying Duchenne muscular dystrophy (DMD) have demonstrated both originality and a willingness to collaborate. The scale of that collaboration can be estimated from the 75 co-signatories to the paper' on page 73 of this issue.

DMD, a devastating X-linked genetic disease afflicting one in every 4,000 newborn boys, is characterized by progressive muscle wasting that is fatal during the second or third decade of life. The apparently simple X-linked mode of inheritance makes DMD a model system for the application of the techniques of molecular genetics. For any genetic disease of unknown actiology the strategy is the same (see ref. 2): pinpoint the location of the defective gene; starting from neighbouring reference points 'walk' to the gene by isolating overlapping DNA sequences; and deduce the nature of the disease from. the sequence of the gene and the gene alterations found in disease sufferers. For DMD the gene has been localized and chromosomal walks have begun. Unfortunately, nature has a habit of putting new twists into the theoretical constructs of scientists. New results reviewed at the recent Cold Spring Harbor Symposium (see page 11) and described by L. Kunkel and collaborators' suggest that DMD gene identification and description will prove difficult: either the gene is very large or the region is very complex.

Three different paths have led to the chromosomal position of the DMD gene. The first followed from the discovery of rare female DMD patients resulting from chromosomal translocations between one X chromosome and an autosome. In each case the breakpoint on the autosome varies but the breakpoint on the X chromosome is similar^{3,4}. In normal females one of the two X chromosomes is inactivated to avoid gene-dosage problems. What happens in the DMD females is that the normal X chromosome is inactivated, and DMD results because the breakpoint on the translocated X chromosome disrupts the DMD gene. The second path follows from classical mendelian genetics and involves the identification of sequences genetically linked to the DMD gene'. The third path followed from the discovery of a boy with DMD who had a deletion of DNA from within the short

arm of the X chromosomes⁶. None of the paths was well signposted and there was potential for straying. But the fact that all three paths led to the same point within Xp21 on the short arm of the X chromosome provided overwhelming evidence that this was the chromosomal position of the *DMD* gene⁷.

The next step was to isolate the DNA sequences within the region Xp21 that correspond to the disease gene. Unfortunately, this region contains about 10⁷ base pairs (bp) of DNA and the closest DNA sequences used as genetic markers were at least 10 per cent recombination away from the DMD gene. If it is assumed that 1 per cent recombination corresponds to about 106 bp, walking the 107 bp to the disease locus would be a daunting task. In the near future, the new technologies of chromosome jumping and hopping may ameliorate the worst aspects of chromosome walking (see the recent News and Views article2 by Peter Little). But the groups of L. Kunkel (Boston) and R. Worton (Toronto) decided not to wait for the future.

The short-cut taken by Kunkel and colleagues was to develop and exploit an accelerated hybridization technique which enabled them to clone, by subtraction, sequences defined by chromosomal deletions^{8,9}. That taken by Worton and colleagues was to clone the sequences at the breakpoint present on the X chromosome of a female DMD patient¹⁰. One of

the sequences described by Kunkel and collaborators is deleted from between 5 and 10 per cent of all DMD patients. In several other human genes about 10 per cent of mutations causing disease are caused by small deletions within the gene (for example, HPRT; ref.11). By analogy with these genes it was thought that the sequence DXS164 was derived from within the DMD gene. It was therefore very disappointing to learn that 5 per cent recombination occurs between DXS164 and the DMD gene; that is, if DXS164 is part of the disease gene it would not be expected to recombine with the disease phenotype at a detectable frequency. Another disappointment was the discovery that the sequence XJ-1.1 isolated by Worton et al. from the X-chromosome translocation breakpoint also recombines with the DMD gene at about 5 per cent despite the fact that some patients had deletions which included both XJ-1.1 and DXS164. Perhaps these observations were not totally unexpected — careful cytogenetic observation had suggested that not all the X-chromosome breakpoints associated with DMD were precisely in the same position4 and chromosomal translocations may cause deleterious effects over large areas.

In an attempt to regain the path leading directly to the DMD defect, Kunkel et al. describe in this issue the cloning of 140,000 bp of DNA around the DXS164 locus and the use of the isolated sequences to analyse DNA from 57 DMD patients with deletions. As the authors point out, ascertainment of the deletions may be biased because more patients have been screened with the original DXS164 probes than have been screened with probes from

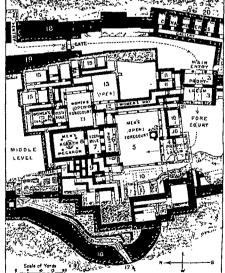
100 years ago

The recent discoveries at Tiryns

THE excavations, made during the last two years at Tiryns, by Dr. Schliemann and Dr. Dörpfeld, have thrown new light on what has been hitherto an almost unknown period of Greek history when Hellenic civilisation had not yet emerged from its Oriental cradle, nor developed its highly cultured systems of social and political government.

The literature of Greece has made us familiar with the later times, when the individual was for the most part merged in the State, and when the wealth and artistic skill of each city was devoted to public uses, such as the Council-chamber, the Agora, or the stately temples of the gods, rather than to the luxury of any one person.

But at Tiryns a very different picture is presented to us: we see a single autocratic chieftain, ruling in a sort of feudal state, and occupying a magnificent palace, surrounded by the humbler dwellings of his circle of retainers; while, instead of the utmost resources of the architect, the sculptor, and the painter being lavished on the shrine of the presiding diety, a mere open-air altar is dedicated to the



PLIN OF THE PALACE MEASURED BY DR. DÖRFFELD.
god, and it is the chieftain's house which is
decked out with the splendours of gilt bronze,
marble sculpture, and painted walls.
From Nature 34, 218; 8 July, 1886.

other parts of Xp21. Most of the deletions have removed the whole 140,000 bp of the expanded DXS164 region. One deletion of 40,000 bp is completely contained within the DXS164 region and most of the other deletions overlap each other in the DXS164 region. However, five deletions within DXS164 show no region of overlap. The breakpoints in the latter deletions may be separated by up to 80,000 bp of DNA. The only obvious conclusion is that the deletions are large, a conclusion supported by the deletion of the flanking markers and, occasionally, adjacent disease loci. These deletions are quite unlike the small deletions associated with mutations at other disease genes, although a similar spectrum of large deletions on the Y chromosome has been associated with the generation of XY females12.

Conclusions about the nature of the DMD gene must remain speculative and are based on two plausible, but unproven, assumptions. The first is that the deletions are simple and not part of complex rearrangements, which can be tested. The second assumption is that the deletions, when present, are responsible for the disease and are not merely markers for the disease. Accepting these limitations, the simplest interpretation is that either the DMD gene is large or mutation in several different genes in the same region can cause the disease. The deletion data are consistent with a single large gene of 100,000-200,000 bp — no larger than the factor 8C gene¹³. Less consistent with this view is the apparent variable position of the *DMD* locus as defined by the recombination and deletion studies with respect to the DXS164 locus. To accommodate these results either one or several genes need to be spread over a distance as large as several million base pairs. Alternatively, recombination rates in this region may be greatly elevated. Neither possibility is without precedent: the bithorax gene of Drosophila is greater than 100,000 bp, the same fraction of the human gene would represent 2,000,000 bp; and in human male meiosis the pseudoautosomal region shows a 10-fold elevation in recombination.

A more radical explanation of the results acknowledges the variable order of DMD with respect to DXS164. If a polymorphism exists in the human population for inversion of a few million base pairs in the Xp21 region, several of the observed phenomena could be explained. Regions of inversion would lead to different gene orders in different families. Recombination outside the inversion followed by a second abnormal and rare (10⁻³) recombination event within the inversion (perhaps between ubiquitous and inverted repeat sequences) would result in the generation of large deletions. This model predicts the concomitant generation of duplications and the observed high frequency of mutation at the DMD locus. A disadvantage 1 of the model is that it requires the new assumption of an inversion present in the population at high frequency. Molecular analysis of deletions of the gene encoding the LDL receptor demonstrates repeat sequences flanking the breakpoints within the gene (D. Russel, Dallas). However, Kunkel et al. have not seen a similar preponderance of repeats associated with breakpoints in DMD.

Several groups are attempting to resolve these questions by constructing restriction maps of the Xp21 region of the X chromosome using pulse-field gradient gel electrophoresis (K. Davies, Oxford; P. Pearson, Leiden; see ref. 2). But even more pressing is the need to find transcribed sequences within the DXS164 region. Several strategies are possible, but the most straightforward is to screen messenger RNA isolated from adult muscle with probes derived from the expanded DXS164 region. Another approach is to screen for conserved sequences between man and mouse. Using this method Kunkel et al. find potential exons within the DXS164 locus which are also X-linked in the mouse and Worton and collaborators find conserved exons near XJ-1.1 []

- Kunkel, L.M. et al. Nature 321, 73 (1986)
- Little, P. Nature News and Views 321 558 (1986)
- Lindenbaum, R.H. et al. J. med. Genet. 16, 384 (1979) Boyd, Y. & Bucke, V.J. Clin. Genet. 29, 108 (1986)
- Davies, K. et al. Nucleic Acids Res. 11, 2303 (19-3)
- Francke, U. et al. Am. J. hum Genet 37 250 (1985) Craig, I.W. & Goodfellow, P.N. Lab Invest 54 241 (1986)
- Kunkel, L.M. et al Proc. natn Acad Sci USA 82 4778 (1985).
- Monaco, A.P. et al. Nature 316, 842 (1985)

- Nay, P.N. et al. Nature 318, 672 (1985)
 Ray, P.N. et al. Nature 318, 672 (1985)
 Yang, T.P. et al. Nature 310, 412 (1984)
 Vergnaud, G. et al. Am. J. hum. Genet 38, 109 (1986)
 Gitschier et al. Nature 312, 326 (1984)

Peter N. Goodfellow is in the Laboratory of Human Molecular Genetics at the Imperial Cancer Research Fund, Lincoln's Inn Fields, London WC2A 3PX, UK.

Geomagnetic reversals

Evidence for asymmetry and fluctuation

from Jeremy Bloxham

FIELD reversals, occurring roughly every million years, are the most dramatic of the wide range of phenomena exhibited by Earth's magnetic field. And the next reversal on Earth may not be so far away: if the current rate of decay of Earth's dipole component is maintained it will vanish in less than 2,000 years' time. Reversals are studied using palaeomagnetic techniques to recover the remanent magnetization of lavas and sediments; in recent years, attention has focused on obtaining reliable records spanning actual reversals, in order to build up a description of the field in transition. Two papers in this issue^{1,2} present such records obtained from sedi-

Most previous work has concentrated on using lavas to study the field in transition. From these studies a picture, albeit rather blurred, has begun to emerge as to how the field reverses, and it has been possible to draw some tentative conclusions about the working of the dynamo during a reversal.

First came the recognition that the reversing field is non-dipolar³. The more interesting issue of whether the field is axisymmetric is still undecided: the evidence tends to suggest that reversals are initially axisymmetric, but may become nonaxisymmetric as the reversal progresses. Hide suggested that reversals are initiated if the field becomes axisymmetric, since axisymmetric fields cannot be maintained by dynamo action and must decay diffusively. However, it appears that reversals are not entirely diffusive; instead. fluid motions in the core actively contribute to the reversal process. This viewpoint is supported by the observation of Prévot et al. of very rapid variations in the field during reversals, variations with characteristic times very much shorter than appropriate diffusive timescales. Other work has indicated that reversals take place in two distinct phases'; in the first phase an intermediate state is reached from which either the reversal is completed, or the field returns to its original polarity.

On page 27 of this issue Valet et al. report results obtained from marine clavs from western Crete. They find evidence of short-term variations in the field, the amplitude of which seem to increase during the reversal. They also find evidence of an intermediate state. Now that studies based on both lavas and sediments have indicated some of the same characteristics of reversals, the evidence that such characteristics are real is greatly strengthened. In a forthcoming issue, Herrero-Bervera and Theyer² will report on four transition records obtained from deep-sea sediments from the north central Pacific Ocean. They find evidence that the transition field is non-axisymmetric and that it is characterized by quite rapid fluctuations. They also consider which of the two common phenomenological models of the reversal process is favoured by their data. The

flooding model, whereby the reversal is believed to be initiated in some region of the core and subsequently spreads, or floods, throughout the core, seems to be favoured over the standing model, whereby the dipole reverses while most of the non-dipole field is unaffected.

Valet et al.'s results also indicate the presence of longer-term variations, of between 2,000 and 4,500 years periodicity. Sediments are a very good way of detecting such long-term variations, although it is hard to pinpoint their precise period because of uncertainties in the sedimentation rate. Interestingly, these variations appear to be unaffected by the reversal. They claim that this observation has some relevance for the validity of the frozenflux approximation.

The frozen-flux approximation which has recently become the object of renewed controversy - consists of neglecting the effects of magnetic diffusion in the core so that the secular variation is considered as being due entirely to the advection of magnetic field lines by the fluid motions in the core. The application of the frozen-flux approximation to reversals — a process with rather longer timescale than is normally believed appropriate for the approximation — was first considered by Gubbins and Roberts8, who presented simple examples of frozen-flux reversals, and showed that axisymmetric, frozen-flux reversals are impossible. Valet et al. refer to the recent extension to the frozen-flux theory of the secular variation made by LeMouël", who showed that the force balance at the top of the core is likely to be geotrophic. This imposes strong constraints on the flow at the core-mantle boundary and, in particular crossequatorial flow is not permitted, a condition which makes geostrophic frozen-flux reversals very hard, if not impossible, to

LeMouël also showed that with geostrophy and frozen-flux the dipole component of the field has no effect on the secular variation: Valet et al.'s observation that certain aspects of the secular variation, namely the long-term variations, are preserved through a reversal tends to support LeMouël's results. Moreover, they claim that this suggests that only the internal parts of the core are involved in the mechanism of a reversal. Herein lies a problem: for not only are geostrophic frozen-flux reversals very hard to effect, but if the reversal process is effectively frozen-flux then the uppermost part of the core must be involved in the process otherwise the reversed field originating deeper in the core would never be able to permeate the perfectly conducting fluid overlying it.

Alternative explanations of the persistence of these long-term variations are available. A wide variety of types of oscillatory behaviour are possible in the

core, from relatively simple hydrodynamic waves to fully nonlinear dynamo oscillations. Hide considered free hydrodynamic oscillations, the period of which depend on the Earth's rotation rate and the strength of the toroidal field in the core. Of these the former is certainly constant to a very good approximation through a reversal and the latter may not necessarily change greatly. The period of Hide's fundamental mode of oscillation, with the assumption of a toroidal field strength of 100 µT, is 2,900 years.

The study of reversals seems to be typical of other branches of geophysics: as the available observations have improved, so the complexity of the process has become apparent. However, the two papers in this issue do reinforce the picture of fluiddriven reversals, characterized by a Cambridge, Massachusetts 02138, USA.

metastable intermediate field configuration, that has been emerging over the last few years. Perhaps now the ball is back in the court of the dynamo theorists to explain the observations, but given the highly nonlinear nature of the dynamo problem, such a prospect seems rather dim.

- Valet, J.-P., Laj, C. & Tucholka, P. Nature 322, 27 (1986).
 Herrero-Bervera, E. & Theyer, F. Nature (in the press).
 Hillhouse, J. & Cox. A. Earth planet. Sci. Lett. 29, 51
- Hide, R. Nature 293, 728 (1981).
 Prévot, M., Mankinen, E.A., Grommé, C.S. & Coe, R. Nature 316, 230 (1985).

- Shaw, J. Geophys. J. R. astr. Soc. 40, 345 (1970).
 Hoffman, K.A. Nature 320, 228 (1986).
 Gubbins, D. & Roberts, N. Geophys. J. R. astr. Soc. 73,
- LeMouël, J.-L. Nature 311, 734 (1984).
- 10. Hide, R. Phil. Trans. R. Soc. A259, 615 (1966).

Jeremy Bloxham is at the Department of Earth

Cancer

Cell growth control mechanisms

from Tony Hunter

Understanding the cellular basis of cancer means being able to describe the biochemistry of the regulated pathways between cell surface and nucleus that control cell growth. Two concurrent recent symposia* on the activation and inhibition of oncogenic proliferation provided much new information on the balance of regulatory influences that constrain the growth of normal cells and fail in cancer.

On the basis of a simple observation made some 15 years ago, Henry Harris inferred the existence of 'tumour suppressor genes': if cells from two highly malignant tumour lines are hybridized, the resultant hybrid is usually non-malignant. This implies that many oncogenic mutations involve the loss of function (that is, that they are recessive). More recently, evidence for such recessive mutations in human tumours has emerged from studies of hereditary predisposition to cancers such as retinoblastoma and Wilms' tumour, which are characterized by the loss of a specific region of both copies of chromosome 13 or 11, respectively. These observations imply that the missing region contains a suppressor gene, and have no doubt helped to stimulate the recent resurgence of interest in suppressor genes, which three groups have been reinvestigating at the molecular level.

E.J. Stanbridge (University of California, Irvine), for example, reported on the occasional tumorigenic segregants that arise from hybrids between normal human fibroblasts and tumorigenic HeLa cells, which are generally non-tumorigenic. A common feature of these segregants is the

*Growth Factors, Tumour Promoters and Cancer Genes and Interferons as Cell Growth Inhibitors. UCLA Symposia held at Steamboat Springs. Colorado, 6-13 April 1986.

loss of a single copy of chromosome 11 or 14, and, by using restriction fragment length polymorphisms, Stanbridge has been able to establish that in 5 out of 6 cases the normal fibroblast chromosome 11 has been lost. The introduction of a normal human chromosome 11 (marked with a drug-resistance gene) by mini-cell fusion into HeLa cells suppressed their tumorigenicity, implying the presence of a suppressor gene on chromosome 11. Hybrids of human keratinocytes with HeLa cells, which are of epithelial origin, are also non-tumorigenic, but in this case the tumorigenic segregants have lost chromosome 1 or 4. This suggests that cells of different embryonic lineages express different suppressor genes.

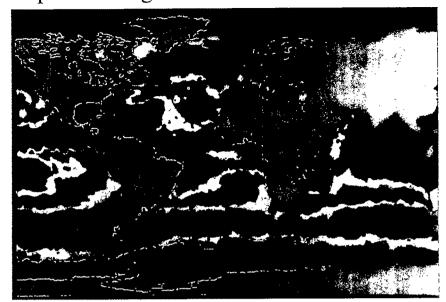
How do suppressor genes work? Experiments with transfected cells show that they can act to nullify the effects of exogenously added oncogenes. J.C. Barrett (National Institute of Environmental Health Science, Research Triangle Park), for example, has isolated tumorigenic Syrian hamster embryo (SHE) cells following co-transfection with the v-Ha-ras and v-myc genes and finds that such tumour cells nonrandomly lose one copy of chromosome 15. Fusion of these cells with normal SHE cells suppresses the tumorigenic phenotype, but the level of p21" is not decreased. (The occasional retransformant generated from such hybrids had again lost chromosome 15.) Similarly, normal hamster fibroblasts (CHEF) can suppress the phenotype of CHEF cells transformed with the EJ-Ha-ras oncogene on fusion, while expression of p21^m remains undiminished (R. Sager, Dana-Farber Cancer Institute, Boston). The transformed cells characteristically lack

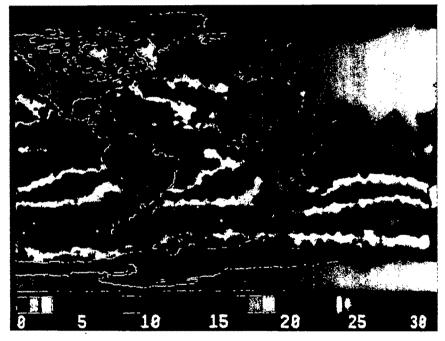
part of chromosome 3, which would be restored in the hybrids. This suggests that there is a suppressor gene on hamster chromosome 3.

One obvious area of interest is the identification of natural inhibitors of growth. It now seems that both interferon and transforming growth factor (TGF- β) may fulfil this function. Moreover, it is becoming clear that many growth factors induce the expression of a β -type interferon, presumably providing an inhibitory feedback loop to prevent runaway proliferation. Tumour necrosis factor (TNF), which paradoxically is cytotoxic to many human tumour cells while being a growth factor for normal human fibroblasts, induces interferon- β_2 (IFN- β_2) Vilcek, New York University Medical Center). Anti-IFN- β antibodies increase the growth-stimulatory effect of TNF, implying that the IFN- β_2 acts as a growth inhibitor. Platelet-derived growth factor induces delayed IFN-β, expression in quiescent mouse 3T3 cells (C.J. Stiles, Dana-Farber Cancer Institute). TGF-β, which like TNF has a dual stimulatory/ inhibitory nature depending on the target cell, induces IFN- β in fibroblasts for which $TGF-\beta$ is mitogenic, but not in epithelial cells for which it is a growth inhibitor (H.L. Moses, Vanderbilt University). Perhaps significantly, the induced IFN- β , is not an interferon which is classically involved in the antiviral response, but one with a rather poor antiviral activity, possibly because its natural function is in growth control. Haematopoietic cells stimulated with mitogens also conform to this pattern. For instance IFN-y is induced in T cells by the experimental mitogen phytohaemagglutinin (PHA) and in macrophages by the natural mitogen CSF-1.

A major signpost to pathways of tumorigenesis is provided by the evidence that one class of oncogenes is derived from the genes encoding the receptors for growth factors with protein-tyrosine kinase activities. In this connection, the most exciting result was the report of the activating mutation in the neu oncogene (C.I. Bargmann, Massachusetts Institute of Technology). The product of the neu oncogene, which is present in a series of ethylnitrosourea (ENU)-induced rat neuroblastomas, is a protein-tyrosine kinase, closely related to the epidermal growth factor (EGF) receptor, that is presumed to be a growth factor receptor, although no ligand has yet been identified. The activating event is a point mutation converting a valine to a glutamic acid in the transmembrane domain. Strikingly, the same mutation in the neu gene occurs in four independent tumour lines. As with other oncogene products of this type, it is assumed that the activated neu protein has constitutive, rather than ligand-regulated, protein kinase activity, although this re-

Tropical changes at the sea surface





Satellite measured sea surface temperatures (°C) show that on 28th June 1983 (bottom) the eastern tropical Pacific was unusually warm (during El Niño) while the eastern tropical Atlantic was cold. A year later (top) the sea surface temperature patterns in the two regions were reversed. Papers describing and interpreting the unusual conditions in the tropical Atlantic over this period will appear in *Nature* on 17th July. (Photograph from R. Legeckis, National Earth Satellite Service and O. Brown, University of Miami).

mains to be proven. If so, this clearly suggests that the transmembrane domain is much more important in transmembrane signalling by growth factor receptors than heretofore ceded.

How exactly the activation of proteintyrosine kinases contributes to tumorigenesis has not been established. There is, however, some evidence linking their activities to the phosphatidylinositol (PI) cycle system that is known to be activated by mitogenic signals. These signals are believed to stimulate a GTP-dependent phospholipase C in the cell membrane, leading in turn to the production of inositol trisphosphate and diacylglycerol, which activates protein kinase C. an effector on this mitogenic pathway.

It now seems there may be several ways for transforming proteins to accelerate PI turnover and the consequent activation of protein kinase C and Ca²⁻ release. C.J. Sherr (St Jude's Children's Hospital, Memphis), using a new *in vitro* assay for the membrane-associated phospholipase C, finds a GTP-dependent increase in activity in mink cells transformed by either *v-fes* or *v-fms*, both of which encode pro-

tein-tyrosine kinases. This implies that either the phospholipase itself or one of its regulatory factors may be phosphorylated and stimulated by the protein-tyrosine kinase in question. Cells transformed by v-ras, which does not encode a proteintyrosine kinase, also display increased phospholipase C activity, presumably by a different mechanism. By contrast, polyoma virus transformation may stimulate one of the PI kinases, possibly through direct phosphorylation by the activated form of pp60° found in association with the viral middle-T antigen (L.C. Cantley, Tufts University). This lipid kinase activity has been partially purified, which should allow the necessary biochemistry to be done.

The effector end of the cycle was addressed by two groups who reported the isolation of complementary DNA clones for protein kinase C using brain RNA as a source of messenger RNA. Evidence for a second closely related protein, which was differentially expressed, emerged from the cloning, suggesting that protein kinase C is a family of enzymes rather than a single-entity. This has obvious implications for understanding the regulation of protein kinase C by its natural regulators, Ca2+ and diacylglycerol, and by tumour promoters acting through the diacylglycerol binding site. The predicted structure of the enzyme is largely as anticipated, with the protein kinase domain near its carboxy-terminal end, but provides no clues to the nature and location of the Ca2+, phospholipid and tumour promoter/diacylglycerol binding sites. These will have to be defined by molecular manipulations of the cDNA clones.

To complete the circle, there is now evidence suggesting that some of the substrates of protein-tyrosine kinases are inhibitors of phospholipid turnover. Of two purified phospholipase A, inhibitors from human placenta (Barbara Wallner, Biogen Research Corporation), one seems to be identical to the known phospholipase A, inhibitor lipocortin, which in turn is probably the same as the EGF receptor protein-tyrosine kinase substrate p35 — at least to judge from a comparison of the lipocortin cDNA with the partial aminoterminal sequence of p35 (S. Cohen, Vanderbilt University). Moreover, the sequence of the second placental inhibitor (Wallner) reveals it to be the major retroviral protein-tyrosine kinase substrate p36 (my own work and R.L. Erikson, Harvard University); and there proves to be more than 50 per cent amino-acid sequence identity between lipocortin/p35 and p36, suggesting that there is a family of such proteins.

The ultimate target of most plasma membrane signalling systems is the nucleus. The *myc* and *fos* genes, which have been shown to be rapidly activated in quiescent fibroblasts by various mitogenic

stimuli, received the most attention. The mechanism of induction of the c-fos gene in PC12 cells (a pheochromocytoma cell line able to differentiate into cells with neuronal properties in response to nerve growth factor, NGF) has been studied in detail by T. Curran (Roche Institute of Molecular Biology) and E. Ziff (New York University Medical Center). There seem to be at least two induction pathways: first, NGF and fibroblast growth factor induce expression of the c-fos gene, possibly in part through the activation of protein kinase C; and second, opening of a voltage-dependent Ca2+ channel and an increase in intracellular Ca2+ may activate a calmodulin-dependent enzyme.

Except for their localization to the nucleus, there has been a paucity of clues as to the functions of the myc and fos proteins. The independent observations by R. Watt (Smith Kline and French Laboratories) and J.M. Bishop (University of California, San Francisco), which show that c-myc proteins co-localize with snRPs in the nucleus by immunofluorescence staining, is intriguing and suggests that the c-myc protein may have a role in RNA processing. The c-myc and c-myb proteins have previously been found to bind to DNA, albeit without displaying any sequence specificity. A fraction of the fos protein from induced PC12 cells will bind DNA (Curran), and the N-myc gene product (a phosphoprotein of relative molecular mass 65,000-68,000) can do the same thing (Bishop). Perhaps the DNA binding activity of all these proteins means that they can also interact with RNA and are involved in RNA processing.

Attempts to analyse the function of the

nuclear oncoproteins by genetic means has been frustrated by the apparent absence of these genes from genetically tractable organisms such as yeast and *Drosophila*. The characterization of a putative N-myc gene in *Drosophila* by M.E. Lambert (Cold Spring Harbor) may make it possible to carry out the critical experiments to test its function.

The work of A. Balmain (reported on page 78 of this issue) provides a nice example of how one can do molecular biology with the whole animal. Analysis of ras gene mutations occurring in papillomas and squamous cell carcinomas, induced by treatment of mouse skin with an ordered combination of an initiating carcinogen and a tumour promoter, shows that the different types of point mutation in the oncogenically activated c-Ha-ras genes detected by transfection correlate well with those known to be caused by the initiating carcinogen. In this model of the initiation, promotion and progression events in carcinogenesis, mutation of the c-Ha-ras gene appears to be an early, initiating event, and can be mimicked by infection with Harvey murine sarcoma virus or by application of v-Ha-ras DNA to the skin followed by TPA (a caution to those who work with cloned oncogenes and TPA without gloves). Progression from a papilloma to a full-blown carcinoma is commonly associated with amplification or homozygotization of the mutant ras allele and presumably other events, such as loss of suppressor genes.

Tony Hunter is in the Molecular Biology and Virology Laboratory at the Salk Institute, La Jolla, California 92037, USA.

Biochemistry

Clues about RNA enzymes

from H.D. Robertson

THREE recent papers in *Nature*, one published in May¹ and two published on pages 83 and 86 of this issue²³, present a preview of coming attractions in the study of multiple structural requirements for RNA catalysis. One emerging theme is the dynamic nature of potential RNA active sites, in which the same bases may need to undergo several kinds of secondary and tertiary structural interactions during the reaction.

The ribosomal RNA precursor from *Tetrahymena* has been shown to be capable of self-catalysed cleavage by Cech and his colleagues (ref. 4; see the *News and Views* article⁵ by F. Westheimer). Predictions by Davies *et al.*⁶ suggested a role for certain elements of secondary structure in the processing of the *Tetrahymena* rRNA precursor and other RNAs with Group I introns.

In their new work, Waring et al. point to the importance of a short helix involving the 5' (upstream) splice site of the Tetrahymena rRNA precursor. They used a series of carefully selected mutants in two non-contiguous 9-nucleotide-long regions of the Tetrahymena rRNA precursors: one region includes the 5' splice site; the other, the internal guide sequence (IGS), is part of the intron. These data support the idea that nine Watson-Crick base pairs (bp) form between these two segments to produce a helix which spans the 5' splice site. Waring et al. report. that single or double mutations which interrupt the pairing of this stem block cleavage at the 5' splice site. Compensatory mutations, designed to restore base pairing, lead to cleavage at the correct site. However, in one striking example, a simple transversion of two consecutive

base pairs from one strand to the other reduced the rate of RNA cleavage nearly 100-fold. The authors conclude that the RNA-RNA helix is necessary, but not sufficient, for effective 5' splicing and comment that it is very unlikely that the energy differences between two such closely related 9-bp stems could account for the observed rate differences. Instead. they suggest that "the sequence of (these segments) may play a role in positioning the helix via tertiary interactions between exposed groups on bases in (this) and other parts of the RNA catalyst"

The detailed crystal structures of various model DNA helices support this idea and indicate future directions for experimentation. In addition, the exact role of the 9bp Watson-Crick seondary structure needs to be investigated in more detail, using techniques similar to those of Waring et al. to generate mutations which give aberrant cleavage, rather than no cleavage. Although a helix may help to define the splice site, precision may be conferred by other structural features, with the base pairs needed for stability.

The two papers in this issue address additional aspects of 5' splice-site specifications in Group I introns. One of these', by Garriga, Lambowitz, Inoue and Cech. takes advantage of a previous finding' that certain RNA-catalysed reactions involving the 5' splice site of the Tetrahmyena rRNA precursor can occur in trans. For example, when the dinucleotide CU is incubated with the rRNA precursor in the absence of a guanosine cofactor, normal cleavage at the 5' splice site is not observed; however, the dinucleotide becomes attached to the 3' (downstream) exon at the exact 3' splice site. From this work and the studies of Waring et al.', it appears that the 5' exon remains bound to the IGS even after cleavage at the 5' splice site and that the IGS then positions the 3' splice site for cleavage. Thus, the interaction which forms the 9-bp stem may normally hold the 5' exon in position to attack the 3' splice site, but when cleavage at the 5' splice site (...CU,) is blocked, the dinucleotide CU temporarily disrupts the structure around the 5' splice site and cleaves, adding itself to the 3' exon. This explanation for the effect of CU has been tested by Garriga et al.3.

The authors took a second Group I intron, which has a different sequence in the helix spanning the 5' splice site. In agreement with earlier predictions of Davies et al.", the sequence in the Neurospora mitochondrial cytochrome b intron 1 messenger RNA (CUGGGU, in-stead of the CUCUCU of Tetrahymena) has a complementary region in a segment analogous to the IGS of Tetrahymena. Garriga et al. show that CU promotes cleavage of the Neurospora mRNA precursor to give a 3' exon with GU attached to its 5' end. CU is inactive in this assay. Interestingly,

Galactic strings are stable

Loops of cosmic string may be the seeds of galaxies, as many astrophysicists have suggested, but are they stable and do they last long enough to set galactic formation going? Two theorists from Imperial College, London, have just addressed this key issue, and found that the answer is ves (Copeland, E.J. & Turok, N. Phys. Letts. B 173, 129; 1986).

Initially the strings emerge from the mesh of vortices presumed present after the "phase transition" or "condensation" that takes place when the universe cools through the grand unification temperature - a temperature above which the strong, weak and electromagnetic forces behave as if they had equal strength. The galactic loops are chopped off the mesh about 108 seconds (3 years) after the Big Bang. But the seeding of galactic matter cannot take place before the Universe passes the state of equal matter and radiation density some 10" seconds (3,000 years) later.

Thus the cosmic loops of self-gravitating string, weighing 1,000 tonnes per Fermi (10^{-13} cm) , must last 3,000 years — or the stringy explanation of galactic formation will not work.

Basically, Copeland and Turok set out to show that a complete "seed" loop, which should weigh in at about one-hundredth of a galatic mass and be 30 parsecs long at the seeding time, will not intersect itself on a 3,000-year timescale. Other studies have shown that self-intersecting loops cut themselves in two to form smaller loops, and if this process continued over a timescale short compared with 3,000 years there would be no loops left of the right size to seed galaxies.

In fact, the spectrum of loops that Copeland and Turok start with at 10' seconds has already ironed out simple twisting (as when an elastic band is twisted into a figure eight); the loops they begin with are those left after all initial motions that lead to self intersection have done their work. For the problem in hand, it is necessary to consider perturbations of the remaining strings caused by gravitational effects — reaching sufficiently large amplitudes to cause selfintersection. In principle, cusps can form, for example, that will bite off small loops. Copeland and Turok's calculations show that these effects are negligible over a 3,000-year period, however, so the galactic loops remain effectively stable.

Do the loops remain in present galaxies? No. They steadily shrink, losing mass as gravitational waves, until they vanish in a puff of super-heavy bosons. Looking out into the Universe from our present vantage point, this process was occurring at a redshift of around 100. The furthest known objects are something over a redshift of 3. However, the larger and so longer-lived loops that are postulated to cause the formation of galactic clusters should still be around. They should be hiding in the clusters with lengths of a few kiloparsecs, and masses of the order of that of a galaxy. Robert Walgate

adding trinucleotides to these reactions gives less clear results, leading the authors to point out that "...although Watson-Crick base pairing with the intron binding sites may be an important determinant of the trans-splicing reaction, additional interactions must also contribute to determining the extent of reaction with trinucleotides. Base stacking or non-Watson-Crick hydrogen bonding might allow certain trinucleotides to interact with the normal binding site. Alternatively, the trinucleotide might interact with other, at present unidentified binding sites within the intron". Again we have here base-pairing rules as part of the explanation but additional structural elements are invoked.

In the other paper in this issue' J.W. Szostak synthesized in vitro a 'core' of the rRNA intron containing about 250 internal bases but neither of the splice junctions nor either of the two 9-nucleotide RNA segments whose base pairing I have described here as an important element in cleavage at the 5' splice site. Both these segments are present in a second 'substrate' molecule, a 119-base-long RNA which contains the last 32 nucleotides of the 5' exon and the first 62 nucleotides of the intron, and thus spans the 5' splice site. Neither core enzyme nor substrate RNA is capable of self-cleavage, but gel electrophoresis shows that the core cleaves the substrate accurately to give the expected 5' end of the intron sequence. The interactions between the two molecules studied by Szostak cannot be stabilized by Watson-Crick structural interactions involving the IGS.

Furthermore, Szostak finds optimal cleavage under conditions quite different from those originally characterized by Cech and colleagues' for the self-catalysed splicing of the intact Tetrahymena rRNA precursor. Remarkably, the optimal temperature is 58°C. Szostak concludes "it is likely that the structure of the enzyme is stabilized by numerous tertiary interactions, and that the enzyme in turn stabilizes the structure of the substrate.

- 1. Waring, R.B., Towner, P., Minter, S.J. & Davies, R.W. Nature 321, 133 (1986)
- Szostak, J.W. Nature 322, 83 (1986) Garriga, G., Lambowitz, A.M., Inoue T. & Cryb. J. R. Nature 322, 86 (1986). Kruger, K. et al. Cell 31, 147 (1982)
- Westheimer, F. Nature News and Views 319, 534 (1986)
 Davies, R.W. et al. Nature 300, 719 (1982)
- 7. Inoue, T. et al. Cell. 43, 431 (1985)

H.D. Robertson is in the Laboratory of Genetics at Rockefeller University, 1230 York Avenue, New York 10021, USA.

Geophysics

A paradigm shift in glaciology?

from G.S. Boulton

Two papers on pages 54 and 57 of this | suggest that part of the west Antarctic ice sheet is underlain by a thin layer of deforming water-soaked sediment. In such areas, the rheological properties of the sediment must largely control the dynamic behaviour of the ice sheet. Until now, most models of glacier flow have assumed that the ice moves over a rigid surface, although this was clearly not true for the great mid-latitude ice sheets of the Quaternary era which flowed over strongly deformed and predominantly soft sediment beds. Perhaps we must now revise our view of the sub-glacial processes which control modern ice-sheet flow, and use the new geophysical data that have been gathered from Antarctica to improve our reconstructions of the Quaternary ice sheets.

The great naturalists of the eighteenth and nineteenth centuries established the fact of glacier movement and observed both internal flow and basal sliding. They were impressed by the erosive power of the debris-studded soles of glaciers, which ground over bedrock to produce smoothed and striated surfaces. Similar surfaces in the mid-latitude lowlands of Europe and North America were thought to support the glacial theory, which asserted that in the recent past these areas had been covered by glaciers of continental scale, similar to the modern ice sheets of Greenland and Antarctica.

Subsequent discussions about glacierbed processes during the early years of this century concentrated on the erosion of rock beds in alpine and highland regions, as the only direct observations of the glacier/bed interface were in natural cavities on the lee-side of bedrock protuberances3. Soft sediment-floored glaciers do not permit such observations as sediment is readily squeezed into incipient subglacial cavities. Thus, it is not surprising that sliding over a rigid bed provided the first quantitative analyses of the processes of basal decollement of glaciers1.5, and that glacier movement was generally viewed as consisting of only two possible components, internal flow and basal sliding. As late as 1979, the symposium of the Glaciological Society on glacier beds was subtitled 'the Ice-Rock Interface', as if the two were synonymous.

Such a paradigm should have been quite implausible to geologists; that it survived so long is an indication of how little note the glaciological community took of the views of geologists. A representative measure of the relative importance of different basal processes has until now been accessible only by the study of the exposed beds of the last mid-latitude ice sheets in Europe and North America (where more than 80 per cent of the surface is overlain by soft deformable sediments) and in the areas exposed by recent retreat of valley glaciers, where sediment beds also predominate. A model in which a glacier slides over a smooth, passive, rigid surface seems quite inappropriate for most of these areas. The existence of widespread glacially induced deformation structures in these sediments has long been known6; such structures are now being more widely recognized, and are often associated with drumlins⁷ (streamlined sediment hills produced beneath glaciers). Recent experiments demonstrate that even relatively coarse-grained subglacial sediments deform readily beneath a glacier and may play a dominant role in glacier movement⁸. It has been further argued that such a mechanism controlled the behaviour of mid-latitude Quaternary ice sheets, with a soft, easily deforming sedimentary substratum permitting high glacier velocities for relatively low driving stresses; rapid responses to changing climate; and fast volumetric growth and decay facilitated by rapid changes in the extent of the ice sheets.

The modern ice sheets of Antarctica and Greenland are thought to be quite different: large, sluggish masses moving by internal flow with fast ice streams radiating through them" and discharge (in Antarctica) up to 90 per cent of the mass flux, although they comprise only 13 per cent of the ice-sheet perimeter. It is assumed that sliding over bedrock occurs beneath these ice streams with a lubricating water layer that decouples the glacier from its bed, thereby reducing friction and permitting fast, low-stress sliding". A predominantly rock bed could result from progressive stripping of pre-existing sediment during the 15 million years of continuous ice-sheet residence on the Antarctic continent.

The recent exciting results from Antarctica reported in this issue1.2 suggest that this picture may not be correct. The results are particularly important in demonstrating the relationship between a possibly drumlinized subglacial sediment stratum and a fast ice stream, and illustrate a geophysical technique that could establish the distribution of their physical properties and their relationship to icesheet dynamics on a wide scale.

Two important implications should be explored: first, that Pleistocene drumlin fields reflect widespread deformation of

soft subglacial sediments, offer little frictional resistance to ice movement and are therefore geological reflections of former fast ice streams; and, second, that soft subglacial sediments are important in regulating the response of the modern Antarctic ice sheet to climate and sealevel changes, a matter of concern even in the short-term future¹³. They may also be important in glacier-surging behaviour.

To explore the implications of subglacial sediment deformation for ice-sheet behaviour we need to understand more about the rapid but sustained deformation of sediments at very low effective stresses. in which dilation is important. Sadly, although such processes are widespread in gravitational flows of many types, adequate flow laws have not been developed and the small strains in most conventional geotechnical experiments make these experiments an inappropriate basis for such laws. Strain rates are strongly affected by water content, so the behaviour of the interstitial water system is of critical importance.

The subglacial zone is different from the decollement zone in most other gravityflow systems, such as gliding nappes and mud flows, in that the glacier sole is a water source, the glacier is an acquiclude and the subglacial water escape pathways are long. Thus, high pore-water pressures need not be transient but can be sustained in a steady state.

The fundamental conceptual difference between analyses of fast low-stress glacier movement over rigid or deformable surfaces is that whereas in the former the surface can be regarded as passive (although it may be temporarily changed by the thickening of a subglacial water film), the strong interaction in the latter requires a coupled analysis of both ice and sediment deformation. Moreover, in coupling the form and structure of the bed with the dynamics of the glacier, such analyses might help to unify glaciology and glacial geology, to the benefit of both disciplines, in a way which until now has been sadly lacking.

- 1. Blankenship, D.D., Rooney, S.T., Bentley, C.R. & Alley, R.B. Nature 322, 54 (1986).

 2. Alley, R.B., Blankenship, D.D., Bentley, S.T. & Rooney.
- S.T. Nature 322, 57 (1986). Carol, H. J. Glaciol. 2, 57 (1947).
- Weertman, J. J. Glaciol. 21, 33 (1957)
- Lilboutry, L. Ann. Geophys. 15, 250 (1959).
 Slater, G. Proc. Geol. Ass. 37, 392 (1926).
 Stanford, S.D. & Mickelson, D.M. J. Glaciol. 109, 220
- Boulton, G.S. & Jones, A.S. J. Glaciol. 90, 29 (1979).
- Boulton, G.S., Smith, G.D., Jones, A.S. & Newsome, J. J. gcol. Soc. Lond. 142, 447 (1985).
- Rose, K.E. J. Glaciol. 108, 99 (1985).

 McIntyre, N.F. J. Glaciol. 108, 99 (1985).
- Glaciers. Ice Sheets and Sea Level: Effects of a CO2 Induced Climatic Change (US Department of Energy, Washington

G.S. Boulton is a Reader in Environmental Sciences at the University of East Anglia, Norwich, UK, and Professor of Physical Geology at the University of Amsterdam, Spui 21, 1012 WX Amsterdam, The Netherlands.

A new term in the global carbon balance

Sir-The yearly carbon balance is unbalanced: man-made emissions of carbon dioxide into atmosphere, through combustion of fossil fuels and deforestation, are not fully accounted for by ocean adsorption and measured increase of CO, in the atmosphere. Man can operate powerful disturbances on ecosystems; we will show he can also operate powerful segregation of carbon through a multiplicity of actions which altogether we propose to call "stock and waste" segregation.

Confining ourselves to the most recent estimates of anthropogenic emissions of carbon into the atmosphere, we have a flow of 5.2 gigatons (1015g) carbon per year coming from fossil fuel combustion1 and a flow from deforestation estimated either to be $0.9-2.5\times10^{15}$ g C yr ¹ (ref.2) or $1.6\pm0.8\times10^{15}$ g Cyr ⁻¹ (ref.3). The classical sinks for this total C flow, ocean adsorption (maximum rate 2.5×1015 g Cyr-1) and increase of CO₂ in the atmosphere (measured rate of 2.3×10¹⁵ g C yr⁻¹) are evidently not large enough to accommodate for emissions. We therefore need one or more new carbon sinks.

While revision of older mechanisms is going on and new mechanisms await better understanding and quantification3, we wish to draw attention to a new carbon segregation path whose existence seems to us beyond any doubt.

The fundamental starting point is to recognize that each of the 4,000 million people in the world, within their social and economic structure, is entitled to the possession or use of an array of commodites and services, each having a material base and therefore a carbon content. The ensemble of these posessions, which in developed countries covers an impressive variety of objects, is what we call stock.

In societies recording a continued increase in the standard of living after correction for population growth, stock increases every year.

The carbon content of the global annual increase of stock is a sink that needs evaluation. But commodities and services do not last for ever. Goods must be renewed and new products displace older ones. This creates an enormous flow of materials — the flow of waste.

Whenever waste is not somehow "recycled" but, as in landfilling or dumping, essentially subtracted from natural cycles, its carbon content is segregated for many years. This represents the waste component of our stock and waste segregation mechanism.

Our group is still working on the quantitative evaluation of the stock and waste mechanism in terms of the amounts of carbon that are segregated every year. We can, however, give some preliminary results which show that stock and waste must be taken into account as a term in a correct carbon balance of the world.

As an example of stock increase, we took into consideration the Food and Agricultural Organization4 data on wood production in 1982, during which the wood and pulp and paper industries dealt with 0.7×10^{15} g of carbon. Looking at final uses of this carbon⁵, at least 0.45×10¹⁵g C yr⁻¹ are accumulating in the stock, whereas the rest enters the flow of waste.

Considering the waste contribution to the carbon sink, we note that despite the fact that we are the only producers, our knowledge of global waste production is very uncertain.

Recent data on 10 European countries with a population of 270 million people show that total waste reaches a value of 2 gigatons per year (W. Ganapini, personal communication); a very conservative extrapolation gives a value of at least 7 gigatons for the world.

Heating values for wastes are in the range 800-3,000 kcal kg⁻¹ (ref. 6); an average value of 1,200 kcal kg⁻¹ gives, according to the correlation shown by Tillman⁵, a content of 10% of carbon; assuming that 50% of this waste is subtracted from any substantial oxidation, waste is responsible for the segregation of an impressive amount of carbon, at least 0.35×10^{15} g C yr⁻¹.

Thus the evaluation of just a few terms of the stock and waste mechanism already shows its importance: anthropogenic contribution to carbon subtraction ranks of some 1015g every year. Carbon balance must be accordingly modified.

Umberto Bianchi Luigi Musi Marina Picardi Eugenio Piovano

Institute of Industrial Chemistry, University of Genoa, C.so Europa 30, 16132 Genoa, Italy

- 1. Woodwell, G.M. et al. Science 222, 1081 (1983).
- Houghton, R.A. et al. Nature 316, 617 (1985).
 Bolin, B. The Greenhouse Effect, Climatic Change and Ecosystems (Wiley, Chichester, in the press).
- Production Yearbook, FAO (Rome) 1982.
- Tillman, D.A. Wood as an Energy Resource (Academic, London, 1978).
- 6. Cassitto, L. & Magnani, P. Ambiente e Sicurezze, 44 (Nov-

X chromosomes and dosage compensation

Sir-The contention of Chandra^{1,2} that the primary function of X-chromosome inactivation is one of sex determination rather than dosage compensation is difficult to justify for more reasons than those considered by Lyon3. When examined in the context of the homomorphic sex chromosomes of diploid dioecy and in relation to the X and Y of haploid dioccy, the thesis is untenable.

Sex determination which depended solely on differential inactivation in one or other of a pair of homologues must be recognized as environmental or phenotypic. There is therefore no reason to suppose that alleles related to secondary sexspecific characters would accumulate preferentially in either homologue, for each chromosome could play the role of an X or Y in different individuals. Genetic fixation of sex determination is thus an essential precursor to the evolution of heteromorphic sex chromosomes in an XX/XY or ZŽ/ZW system, and the same is true of the haploid X/Y system of bryophytes'

In many mosses and liverworts there are reports of homomorphic sex chromosomes where the Y of male plants differs from the X of females only in the greater extent of its heterochromatin which, there is evidence to suggest', is facultative. It has been seen in terms of more extensive gene inactivation of secondary female characters in the Y than of male characters borne by the X, characters which it is hypothesized are thus located as a consequence of an earlier monoecious condition45. If sex-determining factors were not chromosomally fixed, both of these homologues would be variously phenotypic X or Y chromosomes. Evolution of heteromorphic X and Y chromosomes, as seen in many families and genera, would not then have followed. Instead, limited but equal erosion of the X and Y would be an expected consequence if crossing-over were excluded from lengths of chromosomes bearing secondary sexual characters', whereas no significant erosion would occur in the absence of chiasma localization.

M.E. Newton

Department of Botany, University of Manchester. Manchester M13 9PL, UK

- 1. Chandra, H.S. Proc. natn. Acad. Sci. U.S. A. 82 6947 6949 (1985).
- Chandra, H.S. Nature 319, 18 (1986)
- Cuandra, P.S., Nature 319, 18 (1986)
 Lyon, M.F. Nature 320, 313 (1986)
 Newton, M.E. in The Experimental Biology of Breef bytes (eds. Dyer, A.F. & Duckett, J.G.) 65, 96 (Academic London, 1984).
- Newton, M.E. Bull, Br. bryol. Soc 45 9 (1935)
- 6. Newton, M.E. in New Manual of Bryology Vol. 1 (ed. Schuster, R.M.) 117-148 (Hattor) Botanical Laboratory Nichinan-shi 1983)
- 7. Bull, J.J. A. Nat. 112, 245-250 (1978)

Motions of the images of atoms

SIR-Howie might have missed an alternative explanation for motions of atom images under the electron microscope in his article "Coulomb explosions in metals" (Nature 320, 684; 1986). The observations made by the groups whose work he reports consist of apparent movement of atoms or columns in gold microcrystals when imaged in the electron

microscope using the rather high electron flux rates required for high resolution. Undoubtedly, there must exist fiendishly high electric field gradients on a highly local level caused by electron-atom collision-induced ionization, and they might be responsible for some positional instabilities of the atoms.

However, one should also consider the effect these charges in the specimen might have on the trajectories of subsequent incoming electrons. They would most certainly distort the optics on a local level. Furthermore, as the charges build up and dissipate — by whatever mechanism(s) the fluctuating local electric fields cause fluctuating local distortions in the microscope's optics (A.P.K. Ultramicroscopy 7, 351-370; 1982). The net result would be somewhat like looking at a photograph lying (face up) on the bottom of a pool of water whose surface is inundated by random ripples. Is it the painting that is undergoing 'convulsions', or is it just its image?

ALEX P. KORN

Biochemistry Department, Weizmann Institute of Science, 76100 Rehovot, Israel

Howie REPLIES-Specimen charging effects certainly can disrupt the imaging process in the electron microscope, giving rise for example to sudden and large image displacements. It seems unlikely, however, that this can account for the majority of the observed apparent changes of structure, particularly changes from single 'crystal to multiple twin and back again.

A. Howie

Department of Physics, Cavendish Laboratory, Madingley Road, Cambridge CB3 0HE, UK

Legal problems of **Huntington's chorea tests**

SIR—Recent correspondence on the ethics of using a recombinant DNA probe to diagnose Huntington's chorea has not mentioned counsellors' potential legal obligation to provide such a test, regardless of their personal ethical judgement. That the G8 probe does not provide accurate diagnosis is irrelevant here, as all medical diagnoses provide only evidence for disease states, not proof of them. An established genetic screen, fetal karyotyping to detect Downs syndrome, can give good evidence that a fetus is normal, but can also give false negatives for a mosaic fetus1 or for one carrying a Downscausing translocation2, as well as through sampling or laboratory errors. Counselling about the test for at-risk mothers includes mention of these risks, as will analagous counselling for the G8 probe³.

The expectation that mothers over 35 years old will receive fetal karyotyping, with attendant counselling, has recently

acquired a legal standing, with the award of £35,000 damages to Mrs Ayten Yagiz, who sued the City and Hackney Health Authority after giving birth to a Downs syndrome daughter when she claimed not to have been offered fetal karyotyping4. This would appear to establish a precedent for saying that doctors have a legal liability to provide established genetic tests for at-risk mothers. At 40 years old, Mrs Yagiz daughter's risk of Downs was \approx 1% (ref. 5), far less than that facing most parents seeking counselling for Huntington's chorea, cystic fibrosis or other inherited diseases for which cloned probes are becoming available. Other analagous cases are currently awaiting trial. Once cloned probes join fetal karyotyping as an established genetic screen, genetic counsellors may find they have an obligation to use them beyond their present research facilities' ability to do so. This may be a constraint on putting such probes into clinical use.

WILLIAM BAINS

Department of Biochemistry University of Bath, Claverton Down, Bath BA27AY, UK

- 1. Stern, C. Genetic Mosaics and other Essays, 68-69 (Harvard
- University Press, Boston, 1969).

 2. Fraser Roberts, J.A. An Introduction to Medical Genetics, 182-187 (Oxford University Press, 1973).
 Watt, D.C., Lindenbaum, R.H., Jonasson, J.A. &
- Edwards, J.H. et al. Nature 320, 21–22 (1986).
 4. Illman, J. Daily Mail 7 November 1985.
- Cavalli-Sforza, L.L. & Bodmer, W.F. The Genetics of Human Populations, 101 (Freeman, London, 1971).

Is cannibalism all in the mind?

SIR—Behrensmeyer et al. 1 show that trampling of bones in sand can produce marks mimicking cutmarks made by flake tools. They comment that the evidence for meat-eating among early hominids is called into question by this finding.

Putative cutmarks on human bones found at various historical sites, notably at Knossos², have been used to advance the hypothesis that cannibalism was practised in these cultures. The finding of Behrensmeyer et al. raises the possibility that this hypothesis, too, is unfounded and strengthens Arens's contention that apparent evidence for ritual human cannibalism is in fact a psychological phenomenon of anthropologists rather than a dietary phenomenon of 'barbaric' civilizations.

R.J. BIRD

School of Behavioural Science, Newcastle-upon-Tyne Polytechnic, Northumberland Road, Newcastle-upon-Tyne NE1 8ST, UK

- Behrensmeyer, A.K., Gordon, K.D. & Yanagi, G.T. Nature 319, 768-771 (1986). Warren P. in Proceedings of the Swedish Institute in Athens, Stockholm (eds Hagg, R. & Marinatos, N.)
- 3. Arens, W. The Man-eating Myth: Anthropology and Anthropophagy (Oxford University Press, New York

Linkage between the nation states

Sir-The 'self-thinning' rule of plant ecology^{1,2} states that as communities of plants mature, increases in the mean mass per individual plant (W) tend to be accompanied by decreases in the number of plants per unit area (N), and in particular

 $\log W = A + B \log N$

where A and B are constants. If B took the value -1 then decreases in N due to selfthinning would be exactly matched by increases in W and the mass of standing crop per unit area (=W.N) would be constant (= A). In practice^{3,4}, B tends to take values close to -3/2, so that

 $\log W = A - 3/2 \log N$

Hence

 $\log W = 3\log(W.N) - 2A$

and the standing crop increases with W. Denness⁵ suggests that the '-3/2 rule' applies to the distribution of size and density between the states of Europe; and hence he argues that if the total population is to expand the number of nation states in a given area must decrease. The evidence rests on a log-log graph in which W was equated with nation size (population) and N with 1/(national area) (that is, with number of nations per unit area)6. The graph resembled a scatter plot, but the addition of a grid of lines of slope -3/2yielded some apparently meaningful associations between nations6. I suggest that any resemblance with the -3/2 rule' of plant ecology is fortuitous.

The figures for population density of

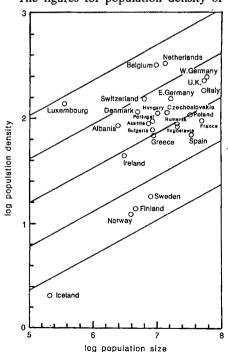


Fig. 1 A plot of log₁₀ population density (people per km²) against log 10 population size (people per nation). The added lines have a slope 1/3.

different nations conceal substantial fluctuations; in cities the number of people per square kilometre may be greater than in rural areas by several orders of magnitude. It seems reasonable to suppose that bigger nations will support bigger conurbations than small, and that hence the mean population density for a large nation may be greater than for smaller ones. If this were so, then nations of similar character might fall into alignment on a graph of log population density on log nation size (Fig.1). They would also give apparently meaningful alignments in graphs of log nation size (W) on log area (= 1/N) (ref. 6). In particular, if the slope of the graph of log population density (=W.N) on log nation size (=W) is approximately 1/3, then the slope of the graph of log nation size (W) on log area (=1/N) will be approximately 3/2; but this does not mean that people obey the same 'laws' of nature as plants. The alignments, I suggest, are attributable to the factors that control the aggregation of people in cities and not to any inherent tendency for the nation states within a continent to undergo 'self-thinning'.

RICHARD C. HARDWICK National Vegetable Research Station, Wellesbourne, Warwick CV35 9EF, UK

- 1. Tadaki, Y. & Shidei, T. Nippon Rin Gakkaishi 41, 341-349
- Yoda, K., Kira, T., Ogawa, H. & Hozumi, K. J. Inst. Polytech. Osaka City Univ. 14, 107-129 (1963).
 Gorham, E. Nature 279, 148-150 (1979).
- Westoby, M. Adv. Ecol. Res. 14, 167-225 (1984).
- Denness, B. Nature 320, 491 (1986).
- Hayton, A. F. Nature 310, 178 (1984).

Is Classic Coca-Cola the real thing?

SIR-During 1985, the Coca-Cola Company discontinued production of its "old" Cola-Cola soft drink and introduced the New Coca-Cola. In response to public demand for the "old" Coke, the Coca-Cola Company began marketing the Classic Coca-Cola. Consumer complaints about difference in taste between the Classic and "old" version were supported by claims from both the Sugar Association, Inc. and Newsweek that the Coca-Cola Company had discontinued the use

of sucrose (table sugar) in 1984. Since the Classic Coca-Cola container bears the words "Original Formula" and the major ingredient other than carbonated water in both the Classic and the New Coca-Cola is "high fructose corn syrup and/or sucrose", while that of "old" Coca-Cola was "sugar", we determined the sugar content of the newly introduced drinks to compare them with our previous analyses of "old" Coca-Cola.

Sugar analyses, using a gas-liquid chromatographic procedure3, confirm claims12 that neither Classic nor New Coca-Cola contain sucrose, whereas in 1983 we found that "old" Coca-Cola contained 4.7% sucrose (Table 1). There was also no sucrose in what we refer to as "transition" Coke since it was produced just prior to the introduction of the New Coca-Cola on 23 April 1985. Total sugar content of "transition", Classic and "old" Coca-Cola was very similar, but the new version contains about 10% more total sugars than any of the others.

As noted above, the Coca-Cola labels now read "high fructose corn syrup and/or sucrose", thus eliminating the use of the word "sugar". Recently the cereal industry made a similar move by eliminating the word "sugar" from the name of cereals and from its advertising even though the product and the sugar content remained unchanged4. Why discontinue the use of the word "sugar" which most consumers understand to be table sugar? Because health conscious consumers often associate sugar with obesity, diabetes mellitus, heart disease and dental caries5

Sucrose (table sugar) has long been considered the mortal enemy of the teeth by virtue of the amount ingested and its pattern of use6. What impact upon dental health should one expect from the replacement of sucrose with fructose and glucose in soft drinks? Such an assessment is impossible at the present time because there are no definitive studies which demonstrate clearly the contribution of sucrose, fructose, or glucose in soft drinks to incidence of dental caries.

If sucrose is the arch criminal of dental caries as has been claimed, one might expect a decrease in the incidence of

Table 1 Sugar analysis of Coca-Cola by gas-liquid chromatography

			Sugar content (%)				
Product (code)	Date of production	Date of analysis	Fructose	Glucose	Sucrose	Total	
"Old" (032483289)	24 Mar. '83	12 Apr. '83	3.3±0.1	2.9±0.3	4.7±0.3	10.9	
"Transition" (no code)	Early 1985 before 23 Apr. '85	13 Sept. '85	6.3±0.1	4.5±0.1	0	10.8	
New Coca-Cola (061485189)	14 June '85	13 Sept. '85	7.0±0.1	4.9±0.1	0	11.9	
Classic Coca-Cola (K8H22)	22 Aug. '85	13 Sept. '85	6.3±0.1	4.6±0.1	0	10.9	

Sugar contents are mean ± standard deviation of triplicate determinations.

dental caries due to the elimination of sucrose from the soft drinks. However, if fructose and glucose are as cariogenic as sucrose in soft drinks, one might expect an increase in the incidence of dental caries due to an increased amount of total sugar as seen in the New Coca-Cola. What effect, if any, the changes will have on consumer demand and/or health remains to be seen.

This work was supported by Veterans Administration Research Service We thank R.W. Christensen and H.V. Nguyen for technical assistance and D.M. Larson for secretarial assistance.

> LEIGH E. WYBORNY IRA L. SHANNON

Oral Disease Research Laboratory, Veterans Administration Medical Center. Houston, Texas 77211, USA

Department of Biochemistry. University of Texas Dental Branch, Houston, Texas 77225, USA

- 1. The Sugar Association, Inc. The Houston Post "B 115 August, 1985). Newsweek, 54-55 (26 August, 1985)
- Li, B. W. & Schuhmann, P.J. J. Food Sci. 45, 138-141
- Liebman, B. Nutr. Action 12, 10-11 (Jul'Aug 1985)
- Shannon, I.L. Brand Name Guide to Sugar (Nelson Ha') Chicago, 1977).
- Shannon, I.L. Amer. Chirop. 1, 54-57 (1974)
- 7. Newburn, E. Odont. Rev. 18, 373-386 (1967)

Are we all out of Africa?

SIR-Additional information on world population distributions of human marker genes, such as that provided by Wainscoat et al. for five closely linked polymorphic restriction enzyme sites in the β -globin gene cluster, is always welcome. One must agree, on the basis of the restriction enzyme evidence provided, that there is a clear distinction between African and Eurasian populations, an opinion in accord with at least some other genetic studies. While Wainscoat et al. are nominally cautious about a second proposition, stating that their data are "consistent with" the notion that anatomically modern man (Homo sapiens sapiens) arose in Africa and subsequently spread to Eurasia and the Americas, it is difficult to deny that their results will be taken as "new evidence that the origin of modern man lies in Africa"2.

frica"². R 440 A close scrutiny of this new evidence is especially important because of its potential value when the prime archaeological rationale for asserting great antiquity for South African H. s. sapiens at Klasies River Mouth and Border Cave is not conclusive^{3,4}, has been challenged⁵, and the H. s. sapiens status of the Omo specimens from Ethiopia has been questioned.

On the basis of a sample perhaps more limited than the authors concede. Wainscoat et al. note that three haplotypes (the specific sequence of appearance [+] or absence [-] of the five sites along one chromosome), namely (+---), (-+-++) and (-++-+), are common in Eurasia, while a fourth, (---+), is common in Africa and absent elsewhere. A punctuationalist evolutionary explanation is advanced: that a 'small' founder population of H. s sapiens migrated from Africa to Eurasia, losing the characteristic African haplotype (----+) en route to Eurasia by genetic drift. Present-day 'new' haplotypes, that is, other than the four common haplotypes assumed to "predate the racial divergence", may in most instances "be derived from the four common ones by single crossovers".

Forty years ago Fisher⁷ first applied the crossover hypothesis in human genetics to the rhesus (Rh) blood group system, suggesting less common Rh types "are maintained [our italics] by such occasional cross-overs" of the more common types in the British population. Wainscoat et al. propose a similar origin for haplotypes (+--++) and (-++++) in Melanesia and Polynesia, presumably from (+---) and (-+-++) for the former and (-+-++) and (-++-+) for the latter. Since the Eurasian recombinants' frequencies are 2.0% and 1.1%, while the putative parental frequencies are 65.6%, 19.8% and 6.7%, the explanation has distinguished precedent. But in Africa, which Wainscoat et al. do not discuss, using analogous logic, (-+--+) should be a recombinant form of the common haplotypes (-+-++) and (-++-+). Curiously, this recombinant's frequency in Africa is 19.7%; the frequencies of the presumptive parental types in Africa are 9.8% and 1.6%. In fact, the recombinant's frequency in Africa is the same as the frequency of the second most common haplotype, (-+-++), in Eurasia.

We are certain that Wainscoat et al. would agree that their data are limited and interpretations preliminary. Nevertheless, we believe that unwarranted credence accrues to the sequence of events they outline, however hedged, when it is presented simply as the loss of one haplotype in a founder population's move from Africa to Eurasia. It ignores the need to interpret the 20% frequency of an apparent recombinant form in Africa, and the ostensible reduction of all three common haplotypes in Africa: to 4.9% (+----), 9.8% (-+-++) and 1.6% (-++-+) from the current Eurasian frequencies 65.6%, 19.8% and 6.7%, respectively. Jones and Rouhani' in their imaginative "Out of Africa" scenario see no need to explain how, for example, the common haplotypes (+---), (-+-++) and (-++-+) went from 75% in their proposed "ancestral African populations" to their current combined frequency in Africa of 16.4%.

Our view is not that the data are incom-

patible with the proposition that H, s, sapiens evolved in Africa and moved to Eurasia, but that they do not provide any evidence for that, and are, in fact, equally compatible with the position that H. s. sapiens originated in Eurasia and migrated to Africa, or perhaps other alternatives. It could be argued that in Africa not only (-+--+) but also the common haplotype (---+) are recombinants: Wainscoat et al. suggest that (---+) in Papua New Guinea may have arisen through recombination, even though it could not be by a single crossover between any of the three common Eurasian haplotypes. If so, one might ask whether the African population, characterized (80%) by thus possibly recombinant forms, is more likely to be ancestral or derived. We believe the genetic data provided by Wainscoat et al. are at the very least a tossup in terms of African or Eurasian H. s. sapiens origins, and that the genetic distance analysis presented in their Fig. 1 dendrogram, an analytical approach notorious for its pitfalls8, speaks basically to what is not at issue, namely that the Eurasian and African frequencies are very different

It should not be forgotten, as Antonarakis et al.9 note, that while the mechanism for producing nonrandom association of DNA sequences located in the region of the β -globin gene cluster is unknown, possible explanations include selection pressure for specific DNA sequences within the region. Selection and migration may be a better model for the observed data than reconstructions based on an assumption of drift and migration alone. with direction of migration emerging from, rather than imposed on, such a study.

> EUGENE GILES STANLEY H. AMBROSE

Department of Anthropology, University of Illinois, Urbana, Illinois 61801, **USA**

- Wainscoat, J.S. et al. Nature 319, 491-493 (1986).
- Jones, J.S. & Rouhani, S. Nature 319, 449 450 (1986).
 Rightmire, G.P. Curr. Anthrop. 20, 25 35 (1979).
- Howell, F.C. in *The Origins of Modern Humans* (eds Smith, F.H. & Spencer, F.) xiii-xxii (Liss, New York,
- 5. Binford, L.R. Curr. Anthrop. 27, 57-62 (1986).
- Wolpoff, M.H. Paleoanthropology (Knopf, New York,
- 7. Fisher, R.A. & Race, R.R. Nature 157, 48-49 (1946). Morton, N.E. & Lalouel, J.M. Am. J. hum. Genet. 25,
- 422-432 (1973). Antonarakis, S.E., Boehm, C.D., Giardina, P.J.V. & Kazazian, H.H. Proc. natn. Acad. Sci. U.S.A. 79, 137-141
- Hiorns, R.W. & Harrison, G.A. Man 12, 438-445 (1977).

WAINSCOAT ET AL. REPLY—We agree that data on β-globin gene haplotypes¹ should be analysed in relation to their evolutionary implications for human populations. Giles and Ambrose do not question our conclusion that there is a major division of human populations into African and Eurasian groups, but they raise the im-

portant issues as to which haplotypes and indeed which populations are ancestral. We believe that a small number of common haplotypes predated the racial divergence and that many of the rare haplotypes have since arisen by crossovers between them. Giles and Ambrose emphasize the fact that the second most common haplotype in Africa (-+--+) could result from recombination between two haplotypes (-+-++) and (-++-+) which, although common in Eurasia, are relatively uncommon in Africa. It is, however, also possible that this African haplotype (-+--+) is derived from the most common African haplotype (---+) by a single point mutation rather than by recombination. Fortunately, these questions may be answered by sequence analysis of the haplotypes as demonstrated by the elegant study of the 'R' and 'T' haplotypes in a segment of the β-globin gene cluster2.

Of course, the data on the B-haplotypes taken by themselves do not prove an African origin for modern man. Nevertheless, this hypothesis is consistent not only with fossil evidence³, but also with the available molecular data. The two lines of evidence that are emerging from DNA analysis of human populations are, firstly, genetic distance analyses, based on allele and haplotype frequencies, which show a distinct African lineage^{1,4}, and second, data indicating a greater nucleotide sequence diversity at particular loci in African populations^{4.5}. Our β -haplotype data and more recent population data on a a-globin haplotypes⁶ both suggest greater diversity in African populations, making an African origin for man more likely than one in Eurasia.

These observations are preliminary and will require confirmation by analysis of other world populations and investigation of many other loci. Nevertheless, if they are corroborated, it would be very difficult to postulate that Eurasian populations were ancestral to African populations. Much more likely, as Giles and Ambrose put it, "Out of Africa".

J.S. WAINSCOAT A.V.S. HILL S.L.THEIN J.B. CLEGG

Department of Haematology and MRC Molecular Haematology Unit, John Radcliffe Hospital, Oxford OX3 9DU,

- 1. Wainscoat, J.S. et al. Nature 319, 419-493 (1986).
- Maeda, N., Bliska, J.B. & Smithies, O. Proc. natn. Acad. Sci. U.S.A. 80, 5012-5014 (1983).
- Sci. U.S.A. 80, 5012-5014 (1983).
 Stringer, C. in Honind Evolution (ed. Foley, R.) 55-83 (Academic, New York, 1984).
 Johnson, M.J., Wallace, D.C., Ferris, S.D., Rattazzi, M.C. & Cavalli-Sforza, L.L. J. molec. Evol. 19, 255-271 (1983).
 Chakravarti, A., Phillips, J.A., Mellits, K.H., Buetow, K.H. & Seeburg, P.H. Proc. natn. Acad. Sci. U.S.A. 81, 6085-6089 (1984).
- 6. Higgs, D.R. et al. Proc. natn. Acad. Sci. U.S.A. (in the

Behind the bifocals

Roy Porter

Franklin of Philadelphia. By Esmond Wright. Harvard University Press:1986. Pp. 404. \$25, £21.25.

Benjamin Franklin is safely installed in one of the most prominent niches in science's pantheon. An early dabbler in experiments, the Philadelphia printer had put electrostatics on a new footing by the time he was forty. He advanced the theory that electricity constituted a single fluid, explained the conservation of charge, and introduced the concepts of plus and minus, positive and negative. But harnessing that terrifying force was no less vital to him than understanding it. Through demonstrating by experiment that lightning was electrical, Franklin was able to pioneer the lightning conductor (though George III stubbornly refused to employ the gadget of the Yankee rebel). And by explaining the charges of the Leyden Jar, he anticipated times when electricity would constructively lie at man's service (he himself tried shock treatment in cases of paralysis, but doubted the lasting efficacy of electrotherapy). As thumbnail sketches go, it is accurate enough to see Franklin as the founder of modern electrical science.

Yet he was also a scientific all-rounder with a ready gift for invention. He studied the Gulf Stream, developed bifocal glasses, rationalized spelling and fireplace design, and even improved the rocking-horse (how like his English contemporary Erasmus Darwin!). A jack-of-all-trades, it was his rare good fortune to be master of many.

But Franklin was never more than a part-time scientist. And it is the achievement of Esmond Wright's polished biography that, recognizing that Franklin's scientific career has already been fully analysed, he has concentrated on painting a rounded portrait of all the facets of this supremely versatile and talented man. Franklin as business-man, journalist, raconteur, politician, diplomat, sage, architect of American independence and man of the world: all are here. Not least, we see Franklin as author and embodiment of the American dream. His is an extraordinary tale of self-help and hard work leading to success.

Born in 1706 of poor immigrant stock, Franklin trained as a printer; publishing led to writing, and Franklin soon won himself renown as the author of *Poor Richard's Almanac*, full of wise saws for getting on ("Early to bed, early to rise..."). By mid-life he was wealthy enough to retire from business. Ever energetic, he threw himself into public

affairs. Prominent in founding the American Philosophical Society and what was to become the University of Pennsylvania, he was elected to the colony's assembly in 1746. Soon he found himself sent to England, in effect as ambassador for the Colonies, at precisely the moment when relations between them and Westminster were going sour.

The canny Franklin was all for compromise not confrontation. In any case, he was profoundly Anglophile, envisaging America's greatness lying within a glorious global British Empire. But it was not to be. Extreme counsels prevailed on both sides of the Atlantic, Parliament became intransigent and Franklin found himself forced to abandon pragmatism for patriotism. Becoming the elder statesman of the War of Independence, he ensured that France entered the war on the rebels' side, helping to tip the balance. He was sure of American victory, for there was no hold-

ing back progress. New Worlders were ambitious, no-nonsense and free from the fossilized forms of the Old. Combining realism and optimism, Franklin nailed his colours to the mast of the future.

Scientific biographers all too often forget that their subjects are flesh and blood creatures, with lives outside the laboratory. Franklin certainly was, with his eve for women, a taste for old madeira and an unquenchable thirst for life. Above all. Wright shows how science and politics were inextricably linked in Franklin's outlooks and career. Natural science was the technique of improving man's material lot; politics the art of social progress. "O that moral science were in as fair a way of improvement", lamented Franklin. "that men would cease to be wolves to one another, and that human beings would at length learn what they now improperly call humanity".

Amen. Ben Franklin was full of such maxims, no less wise for being homely. Anyone wishing to penetrate behind the bifocals, into the urbane mind of the first and greatest of the Yankee scientists, cannot do better than to sample this feast of a biography.

Roy Porter is at the Wellcome Institute for the History of Medicine, 183 Euston Road. London NWI 2BP, UK.

Only natural?

Alastair Fitter

The Oxford Dictionary of Natural History. Edited by Michael Allaby. Oxford University Press:1986. Pp.688. £20, \$29.95.

The two essentials of a good dictionary are comprehensive coverage of its subject, and accurate and up-to-date definition of terms. The editor of *The Oxford Dictionary of Natural History* (who, incidentally, has only edited it, and not provided definitions) states that it takes in the "earth sciences, atmospheric sciences, genetics, cell structure and function, biochemistry, parasitology and other disciplines". Curiously missing from this list is ecology, once described as scientific natural history.

The natural history component is in fact supplied by copious and extensive references to taxa of living organisms, complete (apparently, and I found no exceptions) down to family level and with many genera and species of greater than average interest included as well. These entries make up at least half of the total, and they will, I suspect, be of great value both to professional biologists and to the book's intended audience: students and amateur naturalists. I know of no equivalent compilation with coverage ranging through

bacteria to fungi, plants and animals, and both the choice of taxa and the comments in each entry seem appropriate.

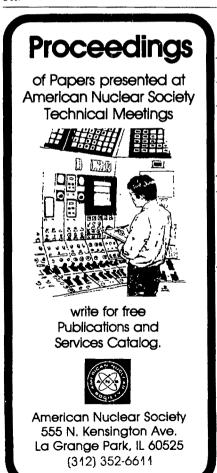
But the list of disciplines included, with biochemistry and cell structure and function among them, worries me. How many amateur naturalists want to know about the sliding-filament theory of muscle contraction? And, curiously, though many enzymes have entries to themselves, those that might interest naturalists, such as esterases (for their importance in electrophoretic studies) and ribulose bisphosphate carboxylase (the commonest protein in the world) do not appear. Surely natural history is not concerned with mechanisms at the infra-organismic level, and biochemistry and cell biology are out of place in a book such as this. Conversely, the word "history" is used here in the Aristotelian sense, a general account of natural phenomena; so it is right that the earth and atmospheric sciences should be represented.

What, then, of the details? Here I can only turn to the areas I know best. Generally, the definitions seem good, though I would quibble with some (for example those of *fitness*, *polyploidy* and *red light*), and others seem a little dated (under *succession* no mention is made of concepts such as facilitation). But in a book of over 12,000 entries it is pointless to pick out one or two individual definitions. More disturbing is the absence of some terms:

mimicry (unless you look up Müllerian), CAM (though C, photosynthesis is in), Red Queen, the MacArthur-Wilson. hypothesis (though island biogeography makes it). Clements (though Gleason gets a mention). There is in this a certain lack of consistency. Some entire fields seem simply to have been overlooked: for example, a whole suite of terms in common use in the study of plant-breeding systems (geitonogamy, gynodioecy, incompatibility) are undefined, at least in this sense. Similarly the coverage of statistical terms is poor and uneven: correlation appears, but analysis of variance, chi-squared, degrees of freedom, regression and t-test do not.

It is surprising that a dictionary of natural history should seem weakest in its coverage of ecology and evolution, but perhaps this is because ecology, though rich in jargon, has yet to develop a stable vocabulary. I doubt whether this dictionary will enable amateur naturalists to understand the American Naturalist, but it contains a wealth of useful taxonomic, geological (in the broad sense) and atmospheric information. Hidden away in it, too, are some real gems: apparently you do get blue moons, particularly in China!

Alastair Fitter is a Lecturer in the Department of Biology, University of York, York YOI 5DD, UK.



Policing the paper chase

Stevan Harnad

A Difficult Balance: Editorial Peer Review in Medicine. By Stephen Lock. Nuffield Provincial Hospitals Trust, London: 1985. Pp. 172.*

How grave a problem is peer review? The answer is likely to depend on which of the following propositions one judges to be closer to the truth: (i) most of the scientific research that appears in print is significant and essential to the progress of science; (ii) most of it is neither significant nor essential. There is evidence in favour of both propositions. Most papers have minimal content and are rarely or never cited or built upon. On the other hand, it is not clear that high-quality work could be done in a less permissive atmosphere; so, the wheat may always be proportional to the chaff.

Propositions (i) and (ii) have very different implications for the problem of peer review. If most published work is significant, then it is critical what one accepts and rejects for publication, and how: the consequences of the two types of errors, false negatives (failures to accept important papers) and false positives (failures to reject wrong or trivial papers), loom large. If, instead, most published work is insignificant (which is equivalent to saying that most work is published), then the repercussions of the two types of errors diminish considerably.

What is peer review? In his welldocumented and informative survey of editorial procedures in the biomedical sciences, Stephen Lock, editor of the British Medical Journal, indicates that it is the relatively recent practice of having work formally (and usually anonymously) evaluated by fellow-scientists. Publication and funding decisions are then made on the basis of the recommendations of these "referees". But whereas the institutionalization of the practice may be recent, it seems apparent that human judgement (not necessarily on the part of peers) has always entered into publication and funding decisions, even in the good old days when just about all research was published and funded.

The funding situation has unfortunately become much more competitive (and perhaps here a more serious problem is developing), but it is still true that just about everything is being published. The

only question is where. Peer review seems to serve to channel the higher quality work towards the more prestigious and widely read journals: in effect, it serves as a selective filter for the beleaguered reader who must keep up with the glut of literature.

Why is there a literature glut? Lock indicates that the emphasis placed on publication-counts in decisions about appointments, promotion and even funding has favoured the strategy of publishing as much as possible, in minimal increments. He sees it as an urgent problem — though not strictly one of peer review - to stem this swelling tide of superfluous publication, perhaps by permitting individuals to publish only five articles per year. This suggestion is not as capricious as it may sound, and would certainly be one way of improving the ratio of quality to quantity in the literature. An intermediate measure would be to place more emphasis on citation-counts than on publicationcounts. Unfortunately, however, both of these are merely black-box, quantitative criteria.

Peer review looks into the black box. but how discerning is it? False positives are easier to identify than false negatives, and Lock surveys some of the prominent cases of error and fraud that have found their way into print. Yet their proportion seems low, probably because science is cumulative and self-corrective, and one cannot build much on a defective foundation (although Lock does give an alarming example of an over-hasty clinical application of a false toxicological report, which had serious consequences for public health). Proposition (ii) — that most published work is inconsequential - suggests another reason why false positives may not represent such a critical problem.

But even proposition (ii) implies that false *negatives* may be a problem. A conservative tendency (and perhaps a regression towards the average) in collective endeavours puts disproportionate innovativeness at something of a disadvantage among peers, and this is most likely to occur at the high end of the spectrum of significance. Yet quackery and dilettantism need to be filtered out too, and most articles do benefit from the revision they have undergone through peer scrutiny.

False positives and negatives are optimization problems, and Lock offers many useful ideas for investigating and improving the peer-review system. One wonders, however, about the generality and representativeness of conclusions based largely on the biomedical and social sciences. The picture may be quite different in the physical sciences and mathematics (which have lower rejection rates and perhaps different evaluative criteria), and may even vary with whether research is experimental or theoretical, pure or

^{*} Available in Europe from STM Distribution Ltd, Enterprise House, Ashford Road, Ashford, Middlesex TW15 1XB, UK, and in North America from ISI Press, Philadelphia. Price is £9, \$24.95.

applied, specialized or interdisciplinary.

Nevertheless, Lock's survey and recommendations are welcome. They include a suggestion that in special cases it would be useful to complement closed peer review with the publication of open peer commentary. I cannot but second this, particularly as 39 of the 281 items in Lock's reference list come from a controversial peer-review study that appeared in the peer-commentary journal I edit — a study whose themes, Lock writes, "run through this monograph as a leit-motiv. almost as obsessionally (to mix my metaphors) as the Suez canal ran through Lady Eden's drawing room during the 1956 Suez crisis".

There is an interesting parallel between beliefs about "the peer review system" and beliefs about "the scientific method". Those who favour proposition (i) tend to worry about biases and conspiracies that could impede the ideal march of progress. Those, like myself, who lean towards (ii), feel that it's more a matter of trying to reduce inefficiencies in vet another very human domain of endeavour.

Stevan Harnad is Editor of The Behavioral and Brain Sciences, 20 Nassau Street, Princeton, New Jersey 08542, USA.

Hormonal activity

Michael J. Brownstein

Neurobiology of Vasopressin. Edited by D. Ganten and D. Pfaff. Springer-Verlag: 1985. Pp.203. DM 98.

Vasopressin. Edited by Robert W. Schrier. Raven:1985. Pp.577. \$104.50.

THE history of research on vasopressin goes back almost a hundred years, to 1895, when Oliver and Schafer showed that mammalian pituitary extracts had pressor (blood-pressure-elevating activity). Three years later Howell demonstrated that the factor responsible resided in the posterior or neural lobe of the gland. Subsequently, Dale found that neural lobe extracts possessed oxytocic activity (that is, they contracted uterine smooth muscle) and von den Velden showed that these extracts could inhibit diuresis as well. In the course of the next 20 years it was established that the oxytocic and pressor-antidiuretic effects were mediated by separate factors, oxytocin and vasopressin, respectively. These were finally purified, characterized and chemically synthesized by du Vigneaud and his colleagues in the 1950s.

Early workers found it difficult to believe that the posterior pituitary could elaborate hormones. Cytologically it is very different from most glands. The revolutionary discovery by Bargmann and Scharrer in 1951 that the neural lobe is part of a neurosecretory system resolved this problem. The vasopressin in the neural lobe is actually in axons and nerve terminals provided by hypothalamic neurones: vasopressin is released from these nerve terminals into blood vessels to act on its peripheral targets.

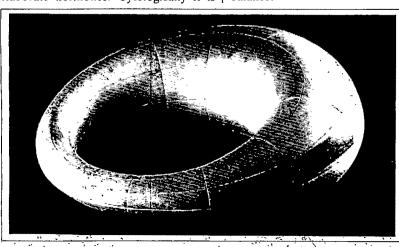
Neurobiology of Vasopressin, the fourth book in a series on current topics in neuroendocrinology, contains five chapters contributed by a total of nine authors. It nicely outlines the research work on vasopressin of the past decade, a period during which many other neuropeptides have come under careful scrutiny. The amino-acid sequence of the vasopressin precursor is now known and its gene has been characterized. Cells that make it have been visualized immunocytochemically. (Many of these lie outside the nuclei that project to the posterior pituitary and seem to be involved in central regulation of autonomic function; surprisingly, some vasopressin-positive cells are present in peripheral tissues such as the adrenal and ovaries.) Steps are being taken towards understanding how vasopressin's synthesis is regulated, and how the afferent inputs to the cells that manufacture it control its production and release in response to changes in water balance.

In spite of the fact that vasopressin's name derives from its effects on blood vessels, these effects are only seen at high dose levels and its cardiovascular effects attracted little interest for many years. This is no longer the case. It is now understood that vasopressin's vasoconstrictor effects are masked by some of its other actions: facilitation of the inhibitory actions of baroreceptive pathways on sympathetic vasomotor activity, and depression of renin secretion. Appropriately, therefore, a large part of Vasopressin, the second book reviewed here, is given over to descriptions of the hormone's interactions with central and peripheral baroreceptor systems and regional vascular beds. Also included are sections devoted to the cellular action of vasopressin, vasopressin antagonists, osmoregulation of drinking and vasopressin secretion, neural control of vasopressin release, and the role of vasopressin in producing pathological states.

While many of the individual chapters are very good, the overall organization of the book leaves something to be desired. Those new to the field would have profited from introductory descriptions of vasopressin's structure, biosynthesis, site of production and release, actions and receptors. It is only in the context of this background information that subsequent chapters, which deal with intricate physiological and pharmacological experiments, can be appreciated.

For this reason, I would suggest that readers should tackle Neurobiology of Vasopressin before attempting to digest its larger sister volume; in particular, the chapters on volume and cardiovascular regulation in Ganten and Pfaff's book will provide helpful overviews for those attempting to get their bearings on the vasopressin literature. Both books are worth studying, and that neither of them is quite up to date might be seen as a plus point; work on vasopressin is moving along very quickly.

Michael J. Brownstein is in the Laboratory of Cell Biology, National Institute of Mental Health, Bethesda, Maryland 20205, USA.



ONE of the pleasanter branches of nineteenth-century mathematics was the study of curves and surfaces in space. In order to examine and communicate their properties, geometers built three-dimensional models which frequently possess that interplay of simplicity and complexity, of order and chaos, which characterizes the best abstract art.

The illustration shows one of the "cyclides of Dupin", a class of surfaces whose lines of curvature are all circles or straight lines. Photographs of 132 such models, with mathematical commentary, have been collected into a two-volume work, Mathematical Models, edited by Gerd Fischer and published by Vieweg, Wiesbaden, FRG, as part of their two-hundredth anniversary celebrations. In Britain, the books are distributed by Wiley; in the United States, by International Publishing Services, PO Box 230, Accord, Massachusetts 02018.

David Singmaster

FLAMMARION MÉDECINE-SCIENCES

Jean-françois BACH IMMUNOLOGIE

immunologie

J.F. BACH et Ph. LESAVRE

De façon claire, directe et très illustrée, les principales connaissances modernes de l'immunologie fondamentale et de l'immunopathologie.

1981, broché, 328 p., 198 fig., 185.00 FF.

de la biologie à la dinique , de la biologie û | jossa-4 a dinique, de la biologie à la divique, de la biologie à la dinique, de la biologie à la dinique dinique, de la biologie à la dinique dinique dinique, de la biologie à la dinique, de la dinique, de la biologie à la dinique, de la dinique,

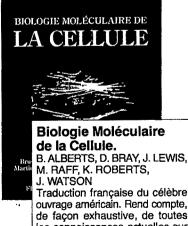
immunologie

es biologie à la chique. de la biologie à la chique.

Immunologie - J.F. BACH

3° édition de ce livre de référence totalement réécrit. La source la plus actuelle et la plus complète des connaissances en immunologie.

1986, relié, 1100 p., 370 illustr. 697,00 FF.



de façon exhaustive, de toutes les connaissances actuelles sur la Cellule à un niveau très approfondi.

1986, 1300 illustr. en 2 coul.,

1986, 1300 illustr. en 2 coul., édition brochée: 620,00 FF, édition reliée: 695,00 FF.

4, rue Casimir-Delavigne 75006 PARIS

Men and machines remembered

J.M.M. Pinkerton

Memoirs of a Computer Pioneer. By Maurice Wilkes. MIT Press:1985. Pp.240. \$19.95, £19.95.

ELECTRONIC computing and communications technologies are of indisputable social and economic importance. To anyone in the field, and many outside it, the history of their development recorded by one of the innovators must be of the greatest interest. Professor Wilkes's book, part of a historical series published by MIT Press, is therefore likely to find a large and receptive audience.

About half of the book deals with the author's family background, his education, his radio research at the Cavendish Laboratory before the war under J.A. Ratcliffe and at the Mathematical Laboratory in Cambridge, and his varied wartime activities as a government radar scientist. All this experience was in fact invaluable, not only because many of the electronic techniques used for radar were readily adapted to the design of early computers, but because Wilkes had become familiar with problems and methods of computation for which computers were suitable.

A fascinating chapter describes the conception, planning and successful construction of EDSAC 1 in the Mathematical Laboratory in the years 1946 to 1949. Wilkes records this in such straightforward terms as almost to belittle the achievement. He carefully acknowledges where due his indebtedness to others for inspiration — to John von Neumann; to speakers on the course at the Moore School of the University of Pennsylvania in 1946, when a variety of techniques were proposed to build a working computer; to the Eckert-Mauchly report proposing a design for EDVAC; and, especially, to Douglas Hartree.

As the series editors say in their foreword, Wilkes aimed not merely to build a machine that would work, but also to investigate programming as an art and an intellectual process applicable to problems, for example in physics, whose numerical solution called for extended computation. While scientists at Cambridge were using the differential analysers, originally developed by Hartree at Manchester and already installed in Wilkes's laboratory, it was anticipated that EDSAC would be faster and better in all respects. With Wheeler and Gill, Wilkes was the first to write subroutines and incorporate them in programs, and a library of subroutines was quickly assembled for programmers' use. Even before EDSAC was finished, much thought had been given to feeding decimal numbers in and out; for scientific work, the simple paper tape and teleprinter combination adopted was reasonably well matched to EDSAC's arithmetic speed.

Remarkably soon after EDSAC successfully ran programs, Wilkes started to teach others how to develop them, very much in the tradition of the Cavendish Laboratory. Ratcliffe, whose guidance in his earlier career Wilkes acknowledges, used to say that no research was complete until it had been taught, not just published. The course first given in 1950, was the basis of the first book on programming ever to appear - The Preparation of Programs for an Electronic Digital Computer, with Special Reference to the EDSAC and the Use of a Library of Subroutines (Addison-Wesley, 1951), which was re-printed by Tomash and MIT Press in 1982.

After starting an informal computing service, based on EDSAC, for the whole University, Wilkes began to design EDSAC2. This was to be a parallel machine retaining the ultrasonic memory, though in the event core memories were invented in time. A major innovation was microprogramming, a concept Wilkes first described in 1951 and which, of course, has since had a profound influence on computer design.

In the book Wilkes refers to the key contribution he made in the early 1950s to the LEO project (Lyons Electronic Office, the first computer built specifically for clerical work) and later, obliquely, to his present job with Digital Equipment Corporation. But he says little about the guidance he gave as Director of the Cambridge Computer Laboratory until he moved to the United States in 1980, not only to his students but to anyone else who asked for it, as many did.

The book concludes with chapters on more recent developments on both sides of the Atlantic, with many of which Wilkes was involved (for example use of capabilities and the Cambridge Ring LAN). In sum, this is a straightforward personal account, clearly and readably told; it represents a notable contribution to the early history of ideas and practice in digital computing, as they have evolved throughout the world.

J.M.M. Pinkerton, formerly Manager, Strategic Requirements, with ICL, now runs an information-technology consultancy, McLean Pinkerton Associates, 2 Sandown Road, Esher, Surrey K109TU, UK.

• Recently published by Morgan Kaufmann is Machine Learning: An Artificial Intelligence Approach, Vol.II, edited by Ryszard S. Michalski, Jaime G. Carbonell and Tom M. Mitchell. Distributor is W.H. Freeman, price is \$39.95, £39.95. The previous volume was reviewed by Margaret Boden in Nature 308, 89 (1984).

High-resolution sedimentary record of a geomagnetic reversal

J.-P. Valet, C. Laj & P. Tucholka

Centre des Faibles Radioactivités, Laboratoire mixte CNRS-CEA, Avenue de la Terrasse, Parc du CNRS, 91190 Gif sur Yvette, France

A detailed study of a geomagnetic reversal shows that during the transition the geomagnetic field undergoes both short-and long-term fluctuations. The first are thought to be linked to the reversal process; the second are present with the same time constants both before and during—the reversal. This suggests that the secular variation, at least in its longer-period terms, is not affected by the reversal of the main field. This feature has important consequences for the validity of the frezen-flux approximation.

SEVERAL recent publications have demonstrated that palaeomagnetic studies of reversals may contribute to a better understanding of the mechanisms of the geodynamo. For example, a comparison of the trajectories of the virtual geomagnetic pole (VGP) during the Brunhes-Matuyama transition, as seen from two different sites¹, has led to the conclusion that the geomagnetic field shows a predominantly non-dipole behaviour during a reversal. Other studies have demonstrated that, although axisymmetrical terms certainly play a key role in the morphology of the transitional field, large non-zonal terms are also present²⁻⁴. Various models for reversals have been proposed to account for these observed features^{5,6}.

With a few exceptions⁷⁻⁹, however, the published records are not sufficiently accurate to provide detailed information about the precise geomagnetic variations occurring during a reversal, often because of a lack of intermediate directions, or because of bad stratigraphic control of the different samples. Here we describe the results obtained from a reversal recorded in a sequence of Tortonian marine clays near the village of Skouloudhiana in the Khania province of western Crete. We have already described^{10,11} some of the main characteristics of the different reversals recorded in this section and in another nearby section at Potamida. Here we consider only the upper reversal in Skouloudhiana (KS 06 in the previous work), which has been studied in great detail. About 100 additional transitional palaeomagnetic directions have been obtained and the results analysed with suitable mathematical techniques.

Geological setting and sampling

The section at Skouloudhiana comprises 54 m of homogeneous blue-grey marine clays. In the sampled portion of the section, which is well-exposed, there is no evidence of faults or slumped beds. The bedding plane is very nearly horizontal, so no tilt correction has been applied to the results. Previous biostratigraphic results have established that the section belongs to the Upper Tortonian stage¹², and correlation with the geomagnetic polarity timescale¹² gives an age of 5.87 Myr for the upper R-N (reverse- to normal-polarity) sixth reversal (upper part of epoch 6).

In a dense sampling programme during two field trips, 295 cores (6-15 cm long) were collected over a stratigraphic height of 4.7 m, comprising the entire transition zone and also levels outside the zone. The cores were cut in the field into 22-mm samples.

Very careful attention was paid to the determination of the exact stratigraphic position of the samples. Stratigraphic reference levels were marked every ~20 cm on the surface of the section, and the position of each core was measured with respect to these levels. Measurements of core positions with respect to different reference levels yielded identical results to within 0.5 cm: this value was then taken as an estimate of the error. Precise stratigraphic marks and photographic records have

allowed us to correlate the stratigraphic position of cores drilled during the second field trip with those obtained during the first, with almost the same accuracy. The final stratigraphic position of the different samples obtained from the cores was calculated using a computer program which took into account the usual orientation parameters of the cores, their stratigraphic position, and even the width of the diamond saw used to cut the samples.

The result of the sampling programme was an almost continuous stratigraphic succession with several specimens at each horizon, so that different experiments could be performed on samples from the same stratigraphic level.

Sedimentology and magnetic mineralogy

Although the good magnetic properties of the clays of the Skouloudhiana section had already been established¹², further analyses were made in the stratigraphic interval corresponding

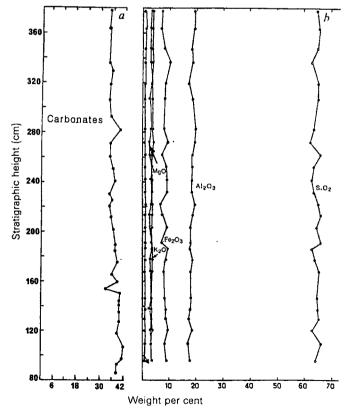


Fig. 1 Evolution of characteristic sedimentary parameters as a function of stratigraphic height. a, Variations of the carbonate fraction expressed in percent of the total weight; b, variations of the major elements expressed in weight per cent of the residual carbonate-free fraction.

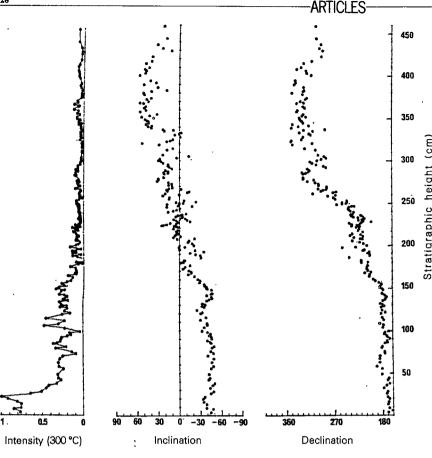


Fig. 2 Records of the intensity (after heating at 300 °C), declination and inclination, plotted against stratigraphic height. The results have been averaged for 10 pairs of samples separated by less than 0.5 cm.

to KS 06. Particular attention was paid to those parameters whose possible variation with stratigraphic height could be an indication of large perturbations or changes in the sedimentary regime.

At 34 levels regularly spaced over the KS 06 interval, X-ray diffraction analyses show the mineralogy to be dominated by detrital quartz, clay minerals and some feldspar, in addition to the carbonate fraction. Illite, kaolinite and chlorite have been identified as the main components of the clay fraction. Both the nature and the relative abundances of the different minerals are quite constant throughout the sampled interval. The carbonate content (Fig. 1a) shows no significant deviation from a mean value of 37 ± 2.5 wt%. Furthermore, the relative abundances of major elements (Fig. 1b) in the decarbonated fraction, determined by microprobe analysis, are also remarkably constant over the KS 06 transition zone.

The nature of the magnetic minerals was investigated by combining measurements of the IRM (isothermal remanent magnetization) acquired step-wise in fields up to 1.5 tesla (T) and of the low-field magnetic susceptibility x. The results obtained on a series of 40 samples regularly spaced over the sampled zone indicate that $90\pm4\%$ of the saturation IRM (SIRM) is acquired in a field of 0.2 T. Successive alternating-field or thermal demagnetizations show that the median destructive field of the SIRM is 25 mT and that >95% of it is lost by heating at 580 °C, complete removal being obtained between 580 and 630 °C. There are no significant differences in the low-field susceptibility of the samples, indicating that the concentration of magnetic minerals does not vary appreciably over the transition zone. Moreover, the $\chi/SIRM$ ratios are grouped around the value 4×10^{-5} m A⁻¹, typical of fine-grained magnetite ^{13,14}. All of these experiments indicate that the remanent magnetization of the clays in the KS 06 transition zone is mainly carried by magnetite, with a mineral of higher coercivity, presumably haematite, also present in very small amounts.

These magnetic minerals proved to be stable during heating. Indeed, the low-field magnetic susceptibility measured at each

step of the thermal demagnetization shows only moderate changes (up to a factor of 3) in the interval between 450 and 550 °C.

Measurements of the anistropy of magnetic susceptibility in a series of samples distributed over the transition zone show that the magnetic fabric of the sediment is characterized by an oblate ellipsoid with a very weak magnetic lineation (1.015). The axes of minimum susceptibility K_{\min} are very close to the vertical while those of maximum susceptibility K_{\max} are horizontal and their directions are largely scattered in the foliation plane. These results are a good indication of sedimentation in rather calm water; distortion of the results by bottom currents, if any, is certainly very limited.

All of the experiments carried out in the mineralogy and sedimentatology of the samples section provide evidence of a uniform, undisturbed sedimentary environment. We are well aware that this evidence does not constitute absolute proof of a constant sedimentation rate during the entire interval of sediment deposition. However, the fact that none of the measured parameters shows significant time variation makes this hypothesis very reasonable, and we can rule out the possibility of any major changes in the sedimentation rate.

Transitional palaeomagnetic directions

Measurements were made partly with a Digico spinner magnetometer and partly with a LETI cryogenic magnetometer. Both alternating-field and thermal demagnetization were used on pilot samples. The results obtained by thermal demagnetization were systematically more consistent than those obtained with the alternating field; for this reason, thermal demagnetization was used throughout, with steps of 40-50 °C from 100 °C to the highest temperature at which the measurements could still be made with sufficient accuracy.

The final palaeomagnetic directions were determined from demagnetization plots by hand-fitting a straight line through at least the last 4-5 points. Two secondary components have been identified. The first one is completely removed at $\sim 100-150$ °C.

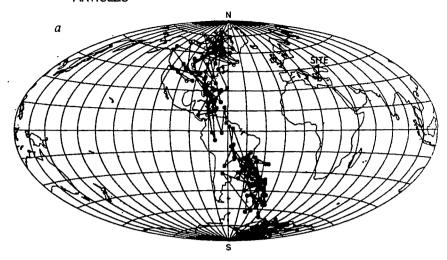
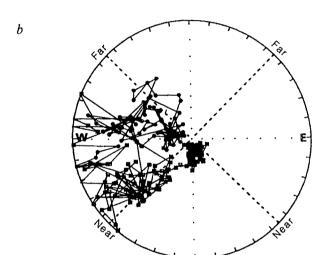


Fig. 3 a, VGP path relative to the KS 06 transition calculated from the results in Fig. 2 and plotted in the planisphere centred at 300 °E (83° west from the site longitude). b, Polar stereographic projection of the 'rotated directions' $\frac{D'}{I'}$



The second one, clearly observed in reverse- and intermediate-polarity samples, with a direction similar to that of the present geomagnetic field, is probably of viscous origin and is removed at 200-300 °C. No other unstable components have been found up to the highest temperatures, so that the final palaeomagnetic directions could be determined with a good overall accuracy (only 11 out of 245 demagnetized samples did not yield a stable direction and were rejected).

Figure 2 shows the results obtained after demagnetization, in the form of a detailed record of inclination (I) and declination (D) as a function of stratigraphic height. Each point corresponds to the result obtained on a single sample, except for 10 pairs of samples whose stratigraphic height was found to differ by less than 0.5 cm. Because this difference is less than the estimated accuracy of the measurement of the stratigraphic position, the results from these 10 pairs were averaged, and only one point is reported for each of them; the mean dispersion of the averaged directions is 11° .

The inclination values measured on samples from outside the transition zone are shallower by $\sim 10^{\circ}$ than the value of 54.5° expected at the site latitude, assuming an axial geocentric dipole field. This inclination anomaly has been frequently observed in similar sediments from throughout the Hellenic Arc¹⁵. Although no definite conclusions have been reached concerning its origin, an overall analysis of the results from many sections suggests that compaction of the sediments is a plausible cause.

The duration of the transition can be estimated by considering the stratigraphic height relative to the transitional directions and assuming a regular accumulation rate. The boundaries of the transition, defined as where the directional changes exceed the amplitude of the field variations before and after the transition, show that the stratigraphic height occupied by intermediate directions is 1.80 m. This value is twice as large as for records of the same transition in the adjacent sections Potamida 1 and 4, although the lengths of the polarity zones deduced from magnetostratigraphic results^{12,16} are the same in the three sections. We therefore conclude that the sedimentation rate during this reversal was higher than the mean value for the whole section and, moreover, that the deposition was roughly twice as fast in Skouloudhiana as in Potamida at that time. The average sedimentation rate determined by Langereis^{12,16} for western Crete is ~4 cm per 1,000 yr. Using a value twice as large for the KS 06 reversal in Skouloudhiana we obtain a duration of the reversal of ~20,000 yr. Estimates of the transition duration from directional changes^{18,19} range from 2,000 to 10,000 yr.

Discussion

Figure 3 presents the results in the alternative forms of the VGP path (Fig. 3a) and the 'rotated directions' 20 D', I' (Fig. 3b); the two representations yield very similar results. The record is characterized by a considerable number of intermediate directions—more than 120 VGP positions between 60 °S and 60° N. A very detailed record has thus been obtained and it is possible to observe some characteristics of the reversal. Some of them, previously mentioned elsewhere 11,12 , will not be discussed here, and we will concentrate mainly on the detailed variations of the transition field.

Before proceeding, it is important to examine whether the

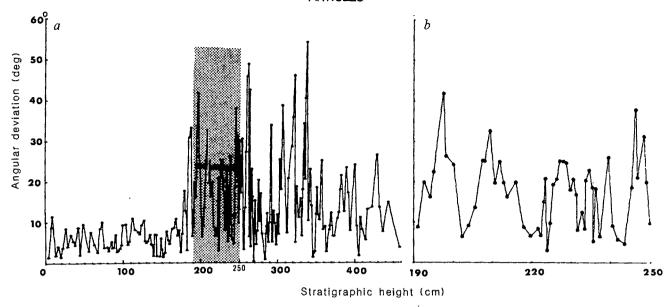


Fig. 4 a, Engular deviations between the successive magnetization vectors as a function of stratigraphic height. The shaded part of the plot is enlarged in b, to show that some of the fluctuations include several successive points.

sediment of KS 06 is adapted to this kind of study. It is well known that in a newly deposited sediment, some grains can remain free to rotate inside water-filled voids after deposition, so that a range of blocking times will be associated with each horizon within the sample, thus introducing additional spread into the magnetic record (a phenomenon known as post-detrital remanent magnetization, PDRM). Experiments using laboratory-deposited sediments^{20,21} have shown that this process depends on the type of sediment. Following preliminary work by Salloway²², the results of a model simulating the remanence acquisition in a sediment column deposited during a reversal show that a very long acquisition delay eliminates any rapid field fluctuation. Consequently, any fluctuation superimposed on a VGP trajectory is representative of a real geomagnetic field variation and a reasonable estimate of the depth of smoothing introduced by the PDRM process can be deduced from the length of the oscillations.

The results obtained on KS 06 show the presence of oscillations in the geomagnetic record, which in addition to their physical significance prove that the smoothing due to PDRM is very limited. Two types of oscillations are observed, with different time constants.

Rapid fluctuations. Fluctuations occur on a very short timescale, and a plot of the angular deviation between two successive vectors as a function of stratigraphic height (Fig. 4a) shows a significant increase of the fluctuation amplitude during the transition. Similar fluctuations are frequent in most sedimentary records of reversals and have usually been implicitly assumed to represent an overall random noise, although no thorough investigation of their origin has been performed. In the case of KS 06 several features indicate that no factor, other than the geomagnetic field itself, can account for the amplitude of the observed fluctuations.

First of all, note that several fluctuations are characterized by several successive points (Fig. 4b), and thus cannot be entirely related to random errors. The instrumental error in the measurements does not exceed 5° for the least magnetized samples, and the demagnetization diagrams are of a generally good quality. Thus, variations as large as $40-60^{\circ}$ cannot be explained by inaccuracies in the measurements or in the determination of the final palaeomagnetic directions. Fluctuations can also be induced by errors in the stratigraphic positions of the samples. However, this error is too small $(0.5 \, \text{cm})$ to account for the amplitude of the observed fluctuations. Finally, Merrill and

McElhinny²³ have pointed out that "a secondary component acquired in the relatively high fields in non-transitional times can produce a large spurious direction when vectorially added to a primary direction acquired in a relatively weak transition field". Poor magnetic cleaning could thus result in fluctuations not related to the reversal process. If this were the case, however, the vector differences between the palaeomagnetic directions of successive samples should be predominantly aligned with the direction of the dipole field at the site (or its opposite for secondary components acquired in a reverse field). A stereographic plot of these vector differences, shown in Fig. 5, shows no evidence of such a grouping, indicating that secondary components certainly play no major role in the observed fluctuations.

Thus we think that at least a significant part of these fluctuations represent very rapid variations of the geomagnetic field, and therefore there has been negligible smoothing due to PDRM. Of course, we do not rule out the effects of the previously mentioned parameters, it would not be reasonable to attribute a quantitative value to the amplitude of the fluctuations; neither do we propose a time constant, because of the averaging introduced by the stratigraphic height covered by each sample.

In their interpretation of the volcanic record of the Steens Mountain reversal, Prevot and co-workers^{3,8} suggested that the large directional jumps could reflect an increase in the level of turbulence within the Earth's liquid core during reversals. The significant increase in the amplitude of the variations observed in the KS 06 record could also reflect such an increase in turbulence.

Long-term variations. Fluctuations also occur on a considerably longer timescale, but are masked by the high-frequency fluctuations, so that a smoothing of the data was necessary to reveal them. Three independent smoothing methods have been used, involving running averages with gaussian windows, and polynomial and cubic spline approximations. The results in Fig. 6A, obtained after smoothing by cubic splines with 27 knots, are virtually identical to the results of the other smoothing procedures. The directional variations display a succession of regular oscillations, which provide additional proof that the PDRM is extremely limited.

These slow fluctuations are thus truly representative of geomagnetic changes, and therefore merit further consideration. It can be seen in the declination and inclination (Fig. 2), and in the angular variations in Fig. 6A (curve a), that three well-defined oscillations occurred before the transition, with identical

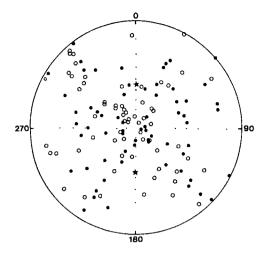


Fig. 5 Stereographic projection of the vector differences between the successive transitional directions. The normal and reverse dipole field directions at the site are represented by asterisks. Symbols, positive inclinations; open symbols, negative inclinations.

wavelengths suggesting a periodicity between 2,000 and 4,500 yr by comparison with the duration of the transition. These values are in the same range as the periodicities which are commonly reported for the non-dipolar field variations obtained from high-deposition-rate lake records during the past 15,000 yr (ref. 24). Variations with similar time constants persist during the transition, and a more quantitative picture is shown by the curve in Fig. 6B, obtained by substracting from Fig. 6Aa the monotonic angular changes of the reversal (Fig. 6Ab). The results show a very regular succession of oscillations, and the increasing amplitude of these fluctuations during the transition is consistent with the fact that the dipole field intensity decreases. Some characteristics of the non-dipolar geomagnetic field are thus not affected by the polarity change.

Reversal dynamics. The samples are almost equally spaced in stratigraphic height, and the previously described experiments have shown that there is no reason to suspect major changes in the sedimentation rate. In spite of this, it can be seen that the variations (curve b) obtained in Fig. 6A after subtracting the oscillaring part (Fig. 6b) are not strictly monotonic. This feature is also apparent from the VGP path (Fig. 3a), in which the successive positions of the VGPs are not equally distributed along the trajectory. This inhomogeneous distribution reflects the fact that the reversal did not occur at constant speed. After a quick passage of the pole through the high southern latitudes there is a quiet episode in the mid-southern latitudes, after which the equatorial zone is crossed rather quickly. It can therefore be suggested that during this reversal the least stable 'state' of the field corresponds to the middle of the transition (when the field intensity is very weak^{25,26}). Unfortunately, the number of detailed geomagnetic records is too limited (or the time sequence is too often poorly defined or interrupted) to compare the dynamical characteristics of KS 06 with other distinct reversals. It seems, however, that the VGP path configuration is similar to that associated with an R-N reversal recorded from the Chugwater Triassic formation²⁷, but differs from that reported by Liddicoat⁹ for the Gauss-Matuyama reversal from Searles Valley. There is, of course, no reason why all reversals should be characterized by the same dynamical structure.

Finally, it can be seen in Fig. 6a that the end of the record is characterized by a movement of the VGPs towards equatorial latitudes, which probably reflects a geomagnetic excursion occurring after the revesal itself. Excursions occurring before or after a transition have been observed in some records and

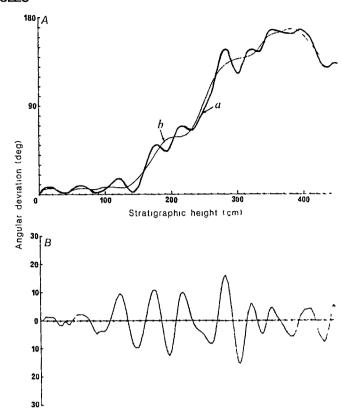


Fig. 6 A, Angular deviations from the pre-reversal direction plotted against stratigraphic height: a, after smoothing by cubic splines with 27 knots; b, after smoothing with 15 knots. B, Periodic oscillations obtained by subtracting curve b from curve a in a.

they could be related to the decrease or recovery phases of the dipole field. However, it is not always easy to distinguish, as in the case of the Steens Mountain reversal record²⁸⁻³⁰, to what extent these excursions are connected to the reversal. The configuration of transitional and excursional VGPs of KS 06 along the same longitudinal band (see Fig. 2) suggests a similarity of the mechanisms for both and, in this case, this observation can also be reconciled with Hoffman's suggestion³¹ that excursions are aborted reversals.

Conclusion

The high time-resolution of this record, which is less than a few hundred years, has allowed us to observe some detailed characteristics of the transitional field. Apart from the dynamical apsect of the reversal, which could be different for each reversal, the most important result is the presence of two types of geomagnetic field variations during the transition. Very fast fluctuations seem to be directly related to the reversal process and, as has been previously suggested², they could result from an increase of turbulence in the Earth's core during the transition. On another timescale, this record has shown the persistence of long-term variations of the non-dipole field during the transition. The non-dipole field, at least in its longer-term components (of the order of 10³ yr), has not been affected by the reversal of the main field.

This last feature has some bearing on the validity of the frozen-flux approximation. Le Mouël³² has shown that an outer-core geostrophic flow accounts for the observed temporal variations of the main field (secular variation), that is, for the different time constants of its dipolar and nondipolar parts. Indeed, this motion involves the two parts of the field in a different way and the axial dipolar component is not re-engaged in the process that builds up the secular variation. Assuming furthermore that the frozen flux approximation holds for time

spans of thousands of years, Le Mouël has demonstrated that the non-dipole field cannot disappear during the process of a geomagnetic reversal. On the other hand, Bloxham and Gubbins³³ have found evidence for flux diffusion in the South Atlantic region and have tentatively concluded that the frozenflux hypothesis can be rejected with 95% confidence. However, as pointed out by the authors themselves, this conclusion depends critically on error estimates for the field at the coremantle boundary which are difficult to assess, so that at present it cannot be considered as definitely established.

In this respect the observed continuity of the secular variation during the KS 06 reversal is to our best knowledge the first experimental evidence supporting Le Mouël's theoretical results.

Moreover, the fact that the processes leading to the observed secular variation would persist unchanged during a reversal suggests that only the internal part of the core would be involved in the mechanism of reversal.

We thank Dr C. Langereis and Dr H. Zijderveld for many helpful discussions and comments; C. Jehanno for supplying the microprobe analyses; L. De Seze for help in the mathematical treatment by cubic splines; and C. Kissel and S. Sen for help in sampling. The director of the Institute of Geology and Mining Research (IGME) at Athens kindly provided the necessary permits. This work was partly supported by the French CNRS ATP Géologie et Géophysique des Océans and CNRS-INSU ATP-Noyau, This is CFR contribution no. 761.

- Received 3 February; accepted 7 May 1986.

 1. Hillbouse, J. W. & Cox, A. Earth planet. Sci. Lett. 29, 51-64 (1976).
- Williams, I. & Fuller, M. J. geophys. Res. 87, 9408-9418 (1982).
- Yrivot, M., Mankinen, E. A., Grommé, C. S. & Coe, R. S. Nature 316, 230-234 (1985).
 Theyer, F., Hertero-Bervera, E. & Hsu, U. J. geophys. Res. 90, 1963-1982 (1985).
 Hoffman, K. A. Earth. planet. Sci. Lett. 44, 7-17 (1979).
 Kaiser, A. D. & Verosub, K. L. Geophys. Res. Lett. 12, 777-780 (1985).
 Clement, B. M. & Kent, D. V. J. geophys. Res. 89, 1049-1055 (1984).
 Prévot M. Mapking, F. A. Co. P. S. & Grommé, C. J. Legabre, Beauting, E. A. Co.

- 8. Prévot, M., Mankinen, E. A., Coe, R. S. & Grommé, C. S. J. geophys. Res. 90, 10417-10448
- Liddicoat, J. C. Phil. Trans. R. Soc. A306, 121-128 (1982).
 Valet, J.-P., Laj, C. & Langereis, C. G. Nature 304, 330-332 (1983).
 Valet, J.-P. & Laj, C. Nature 311, 552-555 (1984).
- 12. Langereis, C. G., Zachariasse, W. J. & Zijderveld, J. D. A. Mar. Micropaleont. 8, 261-282 (1983-84). 13. Harstra, R. L. Geophys. J.R. astr. Soc. 71, 477-495 (1982).

- Dankers, P. H. M. thesis, State Univ. Utrecht (1978).
 Laj, C., Jamet, M., Sorel, D. & Valente, J.-P. Tectonophysics 86, 45-67 (1982).
- 16. Langereis, C. G. thesis, State Univ. Utrecht (1984).

- 17. Jacobs, J. A. Reversals of the Earth's Magnetic Field (Hilger, Bristol, 1984).
- Hoffman, K. A. Rev. Geophys. Space Phys. 21, 614-620 (1983).
 Hoffman, K. A. J. geophys. Res. 89, 6285-6292 (1984).

- Tucker, P. Geophys. J.R. astr. Soc. 63, 149-163 (1980).
 Tucker, P. in Geomagnetism of Baked Clays and Recent Sediments (eds Creer, K. M., Tucholka, P. & Barton, C. E.) 3 (Elsevier, Amsterdam, 1983).

 22. Salloway, J. C. thesis, Univ. Edinburgh (1983).

 23. Merrill, R. T. & McElhinny, M. W. (eds) The Earth's Magnetic Field (Academic, London,

- 24. Creer, K. M. & Tucholka, P. Phil. Trans. R. Soc. A306, 87-102 (1982).
- Valet, J.-P. & Laj, C. Earth planet. Sci. Lett. 54, 53-63 (1981). Valet, J.-P. thesis, Univ. Paris XI (1985).
- Herrero-Bervera, E. & Helsley, C. E. J. geophys. Res. 88, 3506-3522 (1983).
 Valet, J.-P., Laj, C. & Tucholka, P. Nature 316, 217-218 (1985).
- Grommé, C. S., Mankinen, E. A., Prévot, M. & Coe, R. S. Nature 318, 487 (1985).
 Valet, J.-P., Laj, C. & Tucholka, P. Nature 318, 487-488 (1985).
- 31. Hoffman, K. A. Nature 294, 67-68 (1981)
- 32. Le Mouël, J.-L. Nature 311, 734-735 (1984).
- 33. Bloxham, J. & Gubbins, D. Geophys. J.R. astr. Soc. 84, 139-152 (1986).

Cloning the gene for an inherited human disorder—chronic granulomatous disease—on the basis of its chromosomal location

Brigitte Royer-Pokora*, Louis M. Kunkel*, Anthony P. Monaco*, Sabra C. Goff*, Peter E. Newburger*, Robert L. Baehner*, F. Sessions Cole\$, John T. Curnutte & Stuart H. Orkin*1#

- * Division of Hematology-Oncology, The Children's Hospital, Dana-Farber Cancer Institute, Department of Pediatrics, † Division of Genetics, The Children's Hospital, Department of Pediatrics and the Program in Neuroscience, § Division of Cell Biology, The Children's Hospital, Department of Pediatrics, Harvard Medical School, Boston, Massachusetts 02115, USA
- ‡ Division of Pediatric Hematology, Department of Pediatrics, University of Massachusetts Medical School, Worcester, Massachusetts 01605, USA Division of Pediatric Hematology, Department of Pediatrics, University of Michigan Medical School, Ann Arbor, Michigan 48109, USA ⁹ Howard Hughes Medical Institute, Children's Hospital, Boston, Massachusetts 02115, USA

The gene that is abnormal in the X-linked form of the phagocytic disorder chronic granulomatous disease has been cloned without reference to a specific protein by relying on its chromosomal map position. The transcript of the gene is expressed in the phagocytic lineage of haematopoietic cells and is absent or structurally abnormal in four patients with the disorder. The nucleotide sequence of complementary DNA clones predicts a polypeptide of at least 468 amino acids with no homology to proteins described previously.

MANY inherited disorders in man result from mutations in genes whose protein products are as yet unknown. For some disorders specific proteins may be suspected as candidates for the primary gene products, whereas in other situations no biochemical clues exist. Molecular cloning offers an approach to the analysis of disease gene loci which, in principle, may be executed without specific information regarding the nature of the proteins involved. The use of genetic linkage to establish the location of a disease gene within the chromosome complement has generally been considered an initial step in this analysis1. Major diseases

of unknown aetiology such as Duchenne muscular dystrophy (DMD), Huntington's disease and cystic fibrosis, have been the focus of intensive study from this perspective²⁻⁷. It has been anticipated that extended genomic cloning⁸, coupled with searches for transcribed regions, will provide a means of defining each disease locus in precise genetic terms. Here we describe the successful application of this general strategy to the identification and characterization of the gene involved in chronic granulomatous disease (CGD), an X-chromosome-linked disorder of phagocytic cells. Affected individuals have greatly impaired host defences against infection with a wide variety of microorganisms⁹. In contrast to the normal situation, phagocytes

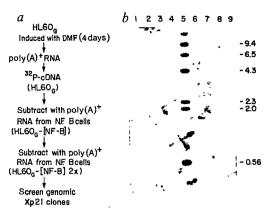


Fig. 1 Detection of a transcribed region of Xp21. a, Strategy for the preparation of an enriched cDNA probe. Granulocytic HL60 cells (HL60_G) were used as a source of mRNA and total $^{32}\text{P-cDNA}$. Sequences in common between HL60_G and the B-cell line of patient N.F. were removed by the method of Davis 32 . b, Southern blot hybridization 33 of the enriched cDNA probe with EcoRI+HindIII-digested DNAs of bacteriophage derived from Xp21. Bacteriophage clone designations: lane 1, 469-7A2; 2, 378-40A1; 3, 378-29A1; 4, 378-19A1; 6, 379A6; 7, 379 π ; 8, 55 π ; 9, 145-A1. These bacteriophage correspond to clones hybridizing with the pERT clones 469, 378, 379, 55 and 145 (ref. 15). Lane 5, HindIII-digested λ DNA as a marker. Hybridization to fragments of 2.5 and 3.3 kb was observed for the samples in lanes 6 and 7. These clones overlapped the same genomic region. Bands of greater size, visible in lane 6, are due to slightly incomplete digestion of phage 379-A6 DNA and not additional hybridizing fragments, as verified by subsequent direct analysis of the phage with cloned cDNA (not shown).

Methods. a, Total poly(A)⁺ RNA was prepared from HL60_G cells as described elsewhere^{20, 32}P-labelled cDNA was synthesized using random primers and AMV (avian myeloblastosis virus) reverse transcriptase³² (specific activity of 1 × 10⁸ c.p.m. μg⁻¹). cDNA was depleted of template RNA by base hydrolysis and hybridized in 0.5 M sodium phosphate buffer, 0.1% SDS, 5 mM EDTA in sealed glass capillaries at 69 °C to a R₀t of 2,700 with a 20-fold excess of poly(A)⁺ RNA prepared from cultured B cells of patient N.F. Single-stranded cDNA was isolated in 0.12 M sodium phosphate on hydroxyapatite at 60 °C and rehybridized to N.F. poly(A)⁺ RNA as described above³². b, Single-stranded cDNA (1× 10⁶ c.p.m.) from the second hydroxyapatite step was hybridized with the digested phage DNAs on a GeneScreen filter in a 1.0-ml solution containing 1 M NaCl, 2× Denhardt's solution, 10% dextran sulphate, 1% SDS, 0.2 M sodium phosphate, 50 μg ml⁻¹ salmon sperm DNA, 50 μg ml⁻¹ oligo(dA)₁₈ for 60 h at 68 °C. The filter was washed in 1×SSC, 1% SDS, and 0.5×SSC, 1% SDS at the same temperature. Autoradiographic exposure was for 10 days with an intensifying screen.

(granulocytes, monocytes and eosinophils) isolated from the blood of CGD patients fail to generate superoxide and activated oxygen derivatives on ingestion of microbes. The precise lesion in the membrane-associated NADPH-oxidase system of these cells is unknown. Cell complementation¹⁰ and family studies⁹ have defined X-linked and autosomal recessive varieties of the disorder. In most families the disease is transmitted as an Xlinked trait. Over the past two decades several proteins, including an unusual b-type cytochrome¹¹ and a flavoprotein¹², have been considered as potential candidates for the primary products of CGD loci, but difficulties in solubilizing membrane-associated components have impeded biochemical characterization of the oxidase system. A consistent finding in the X-linked variety, however, is the absence of the haem spectrum derived from cytochrome b^{11} . Given the potential complexity of the oxidase system and the possible requirement for assembly of several components into an enzymatically active unit, this recognized deficiency in the cytochrome b spectrum may be secondary to the primary genetic abnormality.

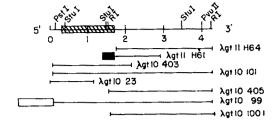


Fig. 2 cDNA clones spanning the 379-encoded RNA. Granulocytic HL60 cDNA libraries were constructed in λ gt11 and λ gt10 using procedures described elsewhere 18-20. Initial screening with a subclone from the 379-A6 bacteriophage yielded λ gt11 H64 and H61. The latter contained a segment absent from other overlapping clones (indicated by the solid box) and thought to represent intron sequences. Repeated screenings with additional cDNA subfragments of the λ gt10 library yielded cDNAs spanning the entire mRNA, representative examples of which are shown. The open box at the 5' end of clone 99 contained sequences unrelated to the 379 transcript. The cross-hatched box represents the major open reading frame of the mRNA, as defined by DNA sequence analysis (Fig. 6a).

In view of the problems inherent in conventional biochemical analysis, we have adopted a genetic approach to define the molecular basis of the X-linked form of CGD as a means of delineating at least one critical protein of the oxidase system.

General strategy

Four discrete steps are involved in our analysis: (1) The position of the CGD gene on the X chromosome (X-CGD) was mapped by both deletion and formal linkage analysis, described recently¹³. (2) Messenger RNA transcripts derived from the assigned chromosomal region were sought. (3) The relevance of one specific mRNA transcript to the disorder was investigated by studying affected patients. (4) The protein product encoded by the X-CGD gene was predicted from isolated complementary DNA clones. Taken together, the results provide persuasive genetic evidence that we have identified the X-CGD gene and characterized its mRNA transcript.

Expressed Xp21 sequences

From the study of two patients (B.B. and N.F.) with interstitial deletions of Xp21 and from linkage of X-CGD with two Xp21 DNA markers (p745 and pERT 84), the CGD locus has been assigned to Xp21.1 (refs 13-15, 42). This delimits the X-CGD locus to ~0.1% of the genome, or perhaps 3,000 kilobases (kb) of DNA. As part of chromosome walking experiments originally aimed at characterizing the DMD locus, a series of bacteriophage clones derived from seven regions of Xp21 that were absent from the DNA of patient B.B. were obtained 3.15, using pERT clones 55, 84, 87, 145, 378, 379 and 469 as probes (L.M.K. and A.P.M., unpublished data). (These bacteriophage clones span at most 10% of the DNA deleted in patient B.B.) In this manner, approximately 250 kb of Xp21 DNA was isolated

The experiment outlined in Fig. 1a was performed to search for regions of these bacteriophage clones that are transcribed in phagocytic cells. Briefly, a Southern blot filter bearing restriction enzyme-digested bacteriophage DNAs was hybridized with a radioactive cDNA probe enriched for sequences expressed in phagocytic cells. As a source likely to contain transcripts of the CGD gene, we chose cultured human HL60 leukaemic cells¹⁶ treated with dimethylformamide (DMF) for 4-7 days. Such treatment induces the NADPH-oxidase system together with most other components of granulocytic differentiation¹⁷. To remove constitutive transcripts, but not sequences derived from Xp21, HL60-cell-induced cDNA was enriched for Xp21 transcripts by subtractive hybridization twice with RNA from an Epstein-Barr virus (EBV)-transformed B-cell line of the

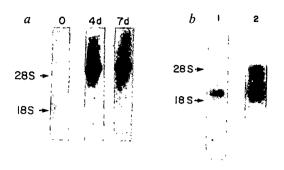


Fig. 3 Expression of 379 RNA in HL60 cells and monocytes. a, Total cell RNA (10 μ g) isolated from uninduced (0) or dimethyl sulphoxide (DMSO)-induced (either 4 days or 7 days) human leukaemic HL60 cells was analysed with a fragment of 379 cDNA derived from the 3'-untranslated region. The uninduced cells are undifferentiated HL60 cells prepared by centrifugal elutriation¹⁷. b, Poly(A)⁺ mRNA (~1 μ g) from human hepatoma cells (HepG2; lane 1) or from cultured human monocytes (lane 2) was similarly examined using the 379 probe plus phosphoglycerate kinase (PGK) cDNA. The latter detects a 2-kb mRNA species in all somatic cells³⁴.

Methods. RNA was prepared by guanidine-HCl precipitation and phenol extraction (a) or by centrifugation through CsCl₂ following solubilization with guanidine isothiocyanate³⁵ (b). Samples were electrophoresed in 1% agarose formaldehyde gels³⁶, transferred to nitrocellulose, and hybridized with a 1.8-kb Bg/II-Bg/II restriction enzyme fragment of H64 cDNA (see Fig. 5a) labelled by random priming³⁷. 28S and 18S denote the migration of ribosomal RNAs. In b, the filter was simultaneously hybridized with labelled insert prepared from the cDNA clone PGK-7e³⁴.

CGD/DMD patient N.F. (Fig. 1a). The subtracted radiolabelled cDNA, representative of \sim 500 individual mRNA sequences, was hybridized to a Southern blot of the Xp21 bacteriophage clones (Fig. 1b). Two overlapping clones, designated 379-A6 and 379- π , showed hybridization.

Isolation of cDNA clones

The results shown in Fig. 1b indicated that the bacteriophage clones originally isolated with pERT 379 contained sequences ultimately represented in the mRNA of induced HL60 cells. To locate the transcribed segment(s), non-repetitive DNA fragments of the 379-A6 insert were used as hybridization probes to Northern blots of the HL60 RNA used to generate the enriched cDNA. A probe consisting of three fragments (0.45, 0.5 and 1.8 kb) arising from a HindIII/BglII digest of a 5-kb HindIII fragment (designated 379-10) detected a 5-kb mRNA transcript (see below). cDNA clones corresponding to this mRNA species were isolated from 4-day-induced HL60 cDNA libraries constructed in bacteriophage λ gt10 and λ gt11 (refs 18-20) (Fig. 2). Repeated screening yielded cDNA clones spanning the entire mRNA transcript. Based on the frequency with which clones were obtained from the cDNA libraries, the abundance of the specific RNA in DMF-induced HL60 cells was ~0.02-0.05%. For purposes of discussion these are referred to as 379 cDNA and 379 RNA. Cloned cDNA was used to examine (1) the tissue distribution of the RNA, (2) its structure and expression in X-CGD, and (3) the nature of its predicted protein sequence.

Tissue distribution

The 379 cDNA detects a 5-kb RNA that is markedly induced in HL60 cells during granulocytic differentiation stimulated by DMF treatment (Fig. 3a). This RNA was also induced on treatment with either the tumour promoter TPA (12-O-tetradecanoyl phorbol-13-acetate) or vitamin D₃, agents that promote monocytic differentiation of HL60 cells in culture²¹. Moreover, the transcript was abundant in cultured normal human monocyte RNA (Fig. 3b) and absent from the hepatoma line HepG2

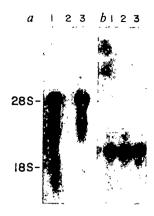


Fig. 4 Absence of 379 RNA from X-CGD monocytes. Total cell RNA (5 μ g) prepared from the cultured monocytes of two X-CGD patients (lanes 1 and 2) and from a normal individual (lane 3) was examined for 379 sequences (a) or PGK sequences (b). In addition to the patient whose sample is shown in lane 2, two unrelated patients also had monocytes that were negative for 379 RNA. Peripheral blood monocytes were isolated and cultured as described previously³⁸. Other methods were as given in Fig. 3 legend.

(Fig. 3b) as well as from total kidney, fibroblasts and HeLa cells (not shown). A low level of the transcript was detected in normal EBV-transformed B-cell lines (not shown), which have been reported to exhibit low levels of oxidase activity²².

As the RNA transcript encoded by 379 sequences appeared to be a marker for the phagocytic lineage (granulocytes and monocytes) based on our limited survey of different cell types, it represented a suitable candidate for the product of the X-CGD locus.

Relevance of 379 transcript

Given that the X-CGD locus was mapped to ~0.1% of the genome, as many as 20 transcripts derived from this region might exist in an average cell (containing perhaps 10,000-20,000 mRNA species). This estimate does not take into account possible variation in the fraction of DNA transcribed in different regions of the genome. The finding of an Xp21 phagocyte-specific RNA cannot, by itself, be interpreted as strong evidence that it encodes the X-CGD product. To determine more specifically the potential relevance of the transcript to the disease, we analysed material from classical X-linked CGD patients by hybridization with the putative X-CGD cDNA. If the transcript were derived from the relevant disease gene locus, quantitative and/or qualitative RNA or DNA alterations would be anticipated in these genetic variants.

We first analysed RNA isolated from cultured human monocytes of both normal and CGD origin. Only CGD patients with the X-linked variety were examined. Their clinical and family histories were consistent with this classification, as were negative phagocyte NBT tests9 and the absence of the cytochrome b spectrum. Figure 4 shows the monocyte RNA analysis of two such patients: in one patient (lane 2) no 379-specific RNA was detectable; in the other patient (lane 1) 379 RNA was apparently normal in size and abundance. Integrity of RNA samples was confirmed by hybridization with a constitutively expressed sequence (phosphoglycerate kinase) derived from a different X-chromosomal region (Fig. 4b). Monocyte RNA of two additional X-CGD patients examined also lacked 379specific RNA (not shown). In the RNA-negative CGD patients, Southern blot analysis with cDNA probes spanning the entire gene revealed no DNA deletions or rearrangements (not shown). These genetic variants provide strong initial support for the relevance of the 379 transcript to the disease. Although unlikely, these findings might be explained by abnormal regulation of

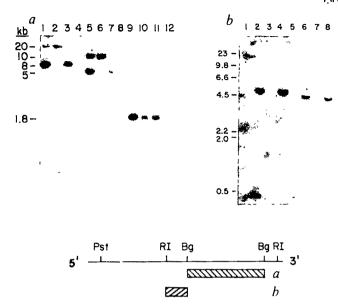


Fig. 5 Partial gene deletion in an X-CGD patient. Total cellular DNAs (5 μg per lane) were digested with BamHI (a, lanes 1-4), HindIII (a, 5-8; b, 1-4) or BgIII (a, 9-12; b, 5-8), electrophoresed, and hybridized with the regions of the 379 cDNA indicated at the bottom of the figure. a, DNAs from mother of patient J.W. (lanes 1, 5, 9), X-CGD patient J.W. (lanes 2, 6, 10) and Xp21 deletion patient N.F. ¹³ affected with CGD and DMD (lanes 4, 8, 12). Lanes 3, 7, 11, normal DNA. b, DNAs from patient J.W. (lanes 1, 5), mother of J.W. (lanes 2, 6) and patient N.F. (lanes 3, 7). Lanes 4, 8, normal DNA.

the 379 transcript due to a defect in a trans-acting factor produced by the authentic X-CGD locus.

Conclusive evidence regarding the role of the 379 transcript, though, was provided by an analysis of patient J.W. whose monocyte RNA appeared grossly normal in abundance and structure (Fig. 4a, lane 1). Analysis of DNA from patient J.W. with the 3' half of the cDNA revealed a DNA alteration on digestion with some (for example, HindIII and BamHI), but not all (for example, Bg/II), restriction enzymes (Fig. 5a, lanes 2, 6, 10). The patient's mother was heterozygous for this alteration (lanes 1, 5), consistent with her assignment as an obligate carrier. Various subregions of the full-length cDNA were used as probes to define the nature of the DNA alteration in J.W. Use of a 0.3-kb segment encompassing the middle of the cDNA revealed an interstitial deletion in the DNA (Fig. 5b, lanes 1, 5) and monocyte RNA (not shown). Most of the region between the central EcoRI and BglII restriction sites of the cDNA was absent. Sequences 3' to the deleted segment were present in both the DNA and monocyte RNA (not shown). Although the precise boundaries of the interstitial deletion have yet to be defined, it overlaps the 3' terminus of the large open reading frame (ORF) of the cDNA (see Fig. 2 and below). The failure of cDNA probes to hybridize with the DNA of the CGD/DMD patient N.F. established that the transcribed sequences were derived from Xp21 (Fig. 5a, lanes 4, 8, 12).

Thus, the 379-encoded transcript was abnormal in abundance or structure in the monocytes of all four classical X-linked CGD patients examined. These observations provide conclusive evidence that the transcript defines the product of the X-CGD locus. Therefore, we refer to it henceforth as the X-CGD RNA.

Analysis of genomic DNAs of 17 additional, independent X-CGD patients with the 3' half of the cDNA revealed no detectable DNA deletions or alterations (not shown).

Sequence of X-CGD cDNA

cDNA clones spanning the 379-encoded RNA are shown in Fig. 2. The transcriptional orientation of the mRNA was estab-

lished by hybridization of single-stranded SP6 RNA transcripts²³ to Northern blots (not shown). DNA sequences of cDNA clones were obtained from both strands either from restriction enzyme fragments subcloned into M13 vectors²⁴ or by progressive deletions as described by Dale *et al.*²⁵; the assembled sequence is shown in Fig. 6a.

Although the estimated size of the RNA transcript from Northern blot analysis is nearly 5 kb, two findings indicate that the 4.27 kb of cDNA sequence that we have obtained encompasses the entire mRNA. First, the 3' terminus is defined by clone 100.1 which contained a short oligo(dA) tract. Second, primer extension analysis revealed an extended product corresponding to the most 5' extent of clone 23 (Fig. 6b). Although we cannot exclude the presence of a strong stop for reverse transcriptase, the failure to observe cDNAs with additional 5' sequences probably indicates that the true 5' terminus of the mRNA has been recognized. Genomic studies that are in progress should assign the precise transcription initiation site(s).

A single large open reading frame, extending from potential initiator ATGs at nucleotide 208 or 322 to a termination codon (TAA) at 1,726-1,728, is present. Additional ATGs, each followed closely by an in-frame termination codon, are located at positions 35 and 113. As the ATG at position 208 is in the same translational frame as that located at position 322, we cannot unambiguously assign the initiation codon. However, given that the ATG at 322 closely resembles the consensus sequence for functional initiator codons defined by Kozak²⁶, whereas that at 208 does not, it is highly likely that the former would be used for translation initiation in vivo. Whether the upstream ATGs have a role in regulating production of the X-CGD-encoded protein is unknown.

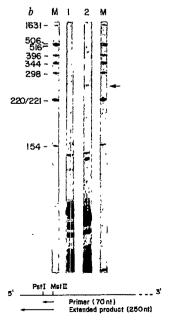
The 3'-untranslated region of the mRNA is 2.5 kb long. Although we have not analysed in detail the organization of the CGD gene in genomic DNA, comparison of the 379 bacteriophage subclones and cDNA clones indicated that the entire 3'-untranslated region is represented in a signal exon, which also contains a small coding segment 3' to the central EcoR1 site of the cDNA. A putative polyadenylation signal (ATTAAA) occurs 14 nucleotides before the poly(A) tract of clone 100.1. Several more typical potential polyadenylation signals (AATAAA)²⁷ are found elsewhere in the cDNA sequence but do not appear to be utilized in mRNA processing. A notable feature of the 3'-untranslated region is the presence of T₂₁ (nucleotides 4,018-4,028), followed 19 nucleotides in the 3' direction by TTTATT (nucleotides 4,057-4,062). On the complemetary strand this organization [AATAAA-19 nucleotides-A₂₁] resembles the 3' end of a processed transcript²⁵ ²⁹. It is possible that a processed sequence integrated at the 3' end of the CGD gene. As the genomic DNA encoding this region has the identical sequence (not shown), this novel organization in the transcript is not the result of a cloning artefact.

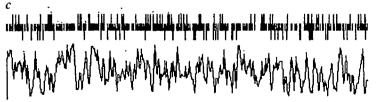
The open reading frame extending from position 322 to 1,726 predicts a primary translation product of 468 amino acids (Fig. 6) with an estimated relative molecular mass (M_r) of 54,000 (54K). If the atypical initiator ATG at position 208 were used, a polypeptide with an additional 38 amino acids at the N-terminus would result. Four potential N-linked glycosylation sites of the canonical form Asn-X-(Thr/Ser) are present. The calculated pI of the predicted protein is 9.5. Figure 6c shows the distribution of charged residues and a hydropathicity profile of the predicted protein. One extensive hydrophobic segment is evident; this spans amino acids 65-92. Screening of the GENBANK and protein database revealed no significant homology of the cDNA or of its predicted protein to known sequences.

Conclusions

Based on genetic linkage data, chromosome walking within a defined region, and hybridization with an enriched cDNA probe, we have identified and characterized the genetic locus for an

CTTCCTCTGCACCATCGGGGAACTGGGCTGTGAATGAGGGGCTCTCCATTTTGCTATTCTGGTTTGGCTGGGGTTGAACGTCTTCCTCTTTGTCTGGTATTACCGGGTTTATGATATT 120 CCACCTAAGTTCTTTTACACAAGAAACTTCTTGGGTCAGCACTGGCCAGGGGCCCTGGCAGCCCTGCACCTCCAATTTCAACTGCATCTCTATTCTCTTGCCAGTCTGTAATTCG CTGTCCTTCCTCAGGGGTTCCAGTGCTGCTCCAACAAGAGTTCGAAGACAACTGGACAGGAATCTCACCTTTCATAAA<u>ATG</u>GTGGCATGGATGATTGCACTTCACTCTGCGATTCAC 600 720 840 960 GGGTTCAAAATGGAAGTGGGACAATACATTTTTGTCAAGTGCCCAAAGGTGTCCAAGCTGGAGTGGCACCCTTTTACACTGACATCCGCCCTTGAGGAAGACTTCTTTAGTATCCATATC 1080 260 270 280 290 .
CGCATCGTTGGGGACTGGACAGAGGGGCTGTTCAATGCTTGGCACTTGCAGAAGCAGGAGTTTCAAGATGCGTGGAAACTACCTAAGATAGCGGTTGATGGGCCCTTTGGCACTGCCAGT 1680 1800 aataccccciccttaaaaaiggacaaaaagaaactataaigtaaatggttitcccttaaaggaatgtcaaiggattgtttgatagtgataagttacatitacatitaigg 1920 GAGCACTTTTACAAACATTÄTTTCATTTTTTCCTCTCAGTAATGTCAGTGGAAGTTAGGGAAAGATTCTTGGACTCAÄTTTTAGAATCAAAAGGGAAÁGGATCAAAAGGTTCAGTAAC 2040 TTCCCTAAGATTATGAAACTOTGACCAGATCTAGCCCATCTTACTCCAGGTTTGATACTCTTTCCACAATACTGAGCTGCCTCAGAATCCTCAAAAATCAGTTTTTTATATTCCCCCAAAAGA 2160 agaaggaaaccaaggagtagctatatatattictacttigtgicattititigccatcattattatcatactgaaggaaattitccagatcattaggacataatacatgttgagagggatctcaa 2280 catcattrácactgroctiggcagagagóggatactcaágtaágtttróttaaatgaatgaattjagaaccacacaatgecaagátagaattaaittaaagccttaaaccaaaatt ·ceágctagcccttatgaatattgaácttaggaáttgtgacaaátatgtatctgatatggtcatttgttttaáátaacacccácccttattttccgtaaatacacacaaaá egcatetgtgtgactratggtttatttgtrtatatateregeerteatertertaraarregergaaceergaarcaraaartetetataergagagateraatterege 3480 3600 agtatgåactggagagggtacctcagttataaggagtctgagaatattggccctttctaacctatgtgcataattaaaccagcttcatttgttgctccgagagtgt rctateteaaareractaggtatatgaaggaggatetgeectgtgtgttategggagataaaaaaatgagtataagaggtgettgtcattataaaggtte ttateteteaagecaeeagetgecagecageagageagetgeeagetgeeagettetttitititititittageaettagtatitagea<mark>ettati</mark>aaeagetaetetaagaat 4080 GATGAAGCATTGTTTTAATCTTAAGACTATGAAGGTTTTTCTTAGTTCTTCTGCTTTTGCAATTTTGAAATTTGAATATTTGCAGGGCTTTGTATGTGAATAATTCTAGCGGGG 4200





inherited human disorder (chronic granulomatous disease) without reference to a specific protein product. The derivation of the 379 RNA transcript from Xp21, its high-level expression in the phagocytic lineage, and its derangement in patients with classical X-linked CGD provide the elements of the formal argument that the appropriate locus has been recognized.

Several aspects which contributed to the success of the transcript search are relevant to its potential application to other disorders. (1) Although only ~10% of Xp21 was represented in bacteriophage clones isolated with pERT clones¹⁵, a portion of the X-CGD gene (notably its 3'-untranslated region) was fortuitously present in the collection. (2) The 3'-untranslated region of 2.5 kb provided a large, uninterrupted exon for hybridization with the enriched cDNA probe. Although almost any transcribed segments would, in principle, be detectable by hybridization of subtracted cDNA with cloned genomic DNAs. the strength of the observed signal will be greater for larger exons. (3) Previous knowledge of cells expressing the phagocytic oxidase system suggested a convenient source for the isolation of RNA used in preparation of the enriched probe. Specifically, the abundance of the 379-encoded RNA transcript in DMFtreated HL60 cells is appreciable (on the order of 0.02-0.05%). (4) The availability of an EBV-transformed cell line from patient N.F. with a deletion through the entire Xp21 region permitted removal of most constitutive transcripts from the enriched cDNA without depletion of Xp21 sequences. The extent to which our strategy may be applied to the isolation of transcripts for other disorders for which a chromosomal map position is established may well depend on these factors.

Although the oxidase system of phagocytes has been studied by conventional biochemical analyses for two decades, no clear view of the components involved or the specific protein abnormalities manifest in the major functional deficiency seen in CGD has emerged. Recently,, the findings of Segal and colleagues

Fig. 6 (Left) DNA sequence of the X-CGD cDNA (a), primer extension analysis (b) and charge distribution and hydropathicity profile of predicted X-CGD protein (c). a, Bacteriophage cDNA inserts were cloned in M13 derivatives²⁴ for sequence analysis by the methods of Sanger *et al.*³⁹ and Dale *et al.*²⁵. All regions were sequenced on both DNA strands. Clones from which sequences were derived are shown in Fig. 2. H64 and H61 were sequenced in their entirety. The initial 0.1-kb displayed was assembled from clones 23, 101, 403 and 99. The 2 kb spanning the open reading frame was derived from clone 99. Overlaps with the 5' regions of H64, H61 and 405 were examined. Based on this, and restriction mapping of genomic DNA, the intron sequences at the 5' end of H61 were identified. The extreme 3'-terminal sequences were obtained from clone 100.1. The first four ATGs in the sequence are underlined, with the predicted initiator codon double-underlined. The presumed processed cDNA sequence near the 3' end of the transcript is boxed. Canonical N-glycosylation sites are underscored with broken lines, and the presumptive poly(A) addition signal (ATTAAA) is overlined. b, The position of the 5' terminus of the X-CGD mRNA was assigned by primer extension analysis. A 70-nucleotide (nt) end-labelled primer was hybridized with yeast transfer RNA (10 µg, lane 1) or total monocyte (20 µg, lane 2) and extended with reverse transcriptase. Lanes labelled M, marker DNA. The observed product of 250 nt corresponds precisely to the 5' extent of clone 23 (see Fig. 2). Use of a synthetic 30-mer primer (nucleotides 80-110) confirmed the position of the extended product and suggested, in addition, the existence of three possible mRNA start sites within about 10 nucleotides (not shown). c, Distribution of charged residues and the hydropathicity profile of the predicted X-CGD protein. +, H and - refer to cationic (Arg, His, Lys), hydrophobic (Ala, Ile, Met, Trp, Val, Phe, Pro, Leu) and anionic (Glu, Ser, Tyr, Asp, Thr) amino acids, respectively. In the hydrophobicity profile, shown at the bottom, upward deflections indicate hydrophobic regions. Methods. b, The indicated 70-nt MstII-PstI restriction fragment was 5'-end-labelled with $[\gamma^{-32}P]$ ATP using polynucleotide kinase⁴⁰ hvbridized with RNA, and extended with AMV reverse transcriptase using methods described previously⁴¹. Reaction products were phenolextracted, ethanol-precipitated and separated in an 8% urea/acrylamide gel. Marker DNAs were pBR322 digested with Hinfl. Autoradiography was performed overnight with an intensifying screen.

have implicated an unusual b-type cytochrome in the oxidase system 11,30,31. As such, it represented a plausible candidate for the protein mutated in the X-linked form of CGD^{11,30,31}. Our results, however, argue against this conclusion. First, the aminoacid composition of the protein predicted by our sequence does not resemble that reported for purified cytochrome b^{30} . Second, the predicted protein encoded by the 379 RNA does not show significant homology to previously sequenced cytochromes of several origins. No evidence for a haem-binding region was evident from analysis of the predicted protein. Third, although its spectrum is absent in CGD granulocytes, the proposed cytochrome b protein has been reported to be present in extracts of neutrophils from affected individuals31. This finding is not in accord with the apparently frequent observation of RNA-negative X-CGD patients. Whether the predicted protein is related to the flavoprotein found in phagocytes¹² must await further biochemical characterization of the latter.

We propose that the 379-encoded protein, which we designate the X-CGD protein, is an essential component of the oxidase system of the phagocyte and probably interacts with other proteins to form an active complex. Among those components that may interact with the X-CGD protein are the membrane-associated cytochrome b and a flavoprotein. Spectral abnormalities of cytochrome b in CGD phagocytes are probably secondary to the absence (or abnormal structure) of the predicted X-CGD protein.

Characterization of the X-CGD protein in vivo and examination of proteins with which it associates should help to elucidate the organization and function of the oxidase system of the phagocyte. Analysis of the predicted sequence of the X-CGD protein has provided few clues, as yet, to the nature of the protein itself. The protein has an estimated M_r of a minimum 54K, and is probably basic. Modification at the four potential N-linked glycosylation sites may alter the apparent size of the observed protein in vivo. One marked hydrophobic region noted above (amino acids 65-92) may represent a transmembrane segment. Finally, the interstitial deletion found in patient J.W. may serve to locate an important functional domain at the carboxy-terminus of the protein, as the deletion is predicted to remove the last 50 amino acids (distal to the EcoRI site at nucleotide 1,571). Further characterization of the X-CGD protein and delineation of its functional domains will ultimately require the introduction and expression of the cDNA in phagocytic cells of X-CGD patients.

We thank Dr Temple Smith of the Dana-Farber Cancer Institute for assistance and advice in computer analysis of the sequence and Dr Mark Davis for advice on subtractive hybridization. S.H.O. is an Investigator of the Howard Hughes Medical Institute. P.E.N. was supported by NIH grant CA38325, by the Socha Memorial Fund for CGD research, and by an Established Investigatorship of the American Heart Association with funds contributed in part by its Massachusetts affiliate. This work was also supported in part by grants from the Muscular Dystrophy Association to L.M.K. and from the NIH to J.T.C. (AI-21320) and S.H.O. (HD18661).

Received 17 May; accepted 21 May 1986.

- 1. Botstein, D., White, R. L., Skolnick, M. & Davis, R. W. Am. J. hum. Genet. 32, 314-331 (1980)
- Davies, K. E. et al. Nucleic Acids Res. 11, 2303-2312 (1983). Monaco, A. P. et al. Nature 316, 842-845 (1985).
- Knowlton, R. G. et al. Nature 318, 380-382 (1985).
- White, R. et al. Nature 318, 382-384 (1985).
- Wainwright, B. J. et al. Nature 318, 384-385 (1985).
- Gusella, J. F. et al. Nature 306, 234-238 (1983).
- Collins, F. & Weissman, S. Proc. natn. Acad. Sci. U.S.A. 81, 6812-6818 (1984).

- Tauber, A. I., Borregaard, N., Simons, E. & Wright, J. Medicine 62, 286-309 (1983)
 Weening, R. S. et al. J. clin. Invest. 75, 915-920 (1985).
 Segal, A. W. et al. New Engl. J. Med. 308, 245-251 (1983).
 Markert, M., Glass, G. A. & Babior, B. M. Proc. natn. Acad. Sci. U.S.A. 82, 3144-3148 (1985)
- Baeliner, R. L. et al. Proc. natn. Acad. Sci. U.S.A. 83, 3398-3401 (1986)
 Francke, U. et al. Am. J. hum. Genet. 37, 250-267 (1985).
- 15. Kunkel, L. M. et al. Proc. natn. Acad. Sci. U.S.A. 82, 4778-4782 (1985).
- 16. Collins, S. J., Ruscetti, F. W., Gallagher, R. E. & Gallo, R. C. Proc. natn. Acad. Sci. I'S.A. 75, 2458-2462 (1978). 17. Newburger, P. E. et al. J. blol. Chem. 259, 3771-3776 (1984).
- 18. Young, R. A. & Davis, R. W. Proc. natn. Acad. Sci. U.S.A. 80, 1194-1198 (1983)

- 19. Gubler, U & Hoffman, B. J. Gene 25, 263-279 (1983).
- Ginsburg, D. et al. Science 228, 1401-1406 (1985).
 Rovera, G., Santoli, D. & Damsky, C. Proc. natn. Acad. Sci. U.S.A. 76, 2779-2783 (1979).
- Volkman, D. J., Buescher, E. S., Gallin, J. I. & Fauci, A. S. J. Immun. 133, 3006-3009 (1984). Melton, D. A. et al. Nucleic Acids Res. 12, 7035-7056 (1984).
- Messing, J. Meth. Enzym. 101, 20-78 (1983).
 Dale, R. M. K., McClure, B. A. & Houchins, J. P. Plasmid 13, 31-40 (1985).
- Kozak, M Nucleic Acids Res. 12, 857-872 (1984).
- Proudfoot, N. J. & Brownless, G. G. Nature 263, 211-214 (1976)
- Nishioka, Y, Leder, A. & Leder, P. Proc. natn. Acad. Sci. U.S.A. 77, 2806-2809 (1980).
- Sharp, P. A. Nature 301, 471-472 (1983). Harper, A. M., Chaplin, M. F. & Segal, A. W. Biochem. J. 227, 783-788 (1985).
- Segal, A. W. Lancet i, 1378-1382 (1985)
- 32. Davis, M. Proc. natn Acad. Set. U.S.A. 81, 2194-2198 (1984).

- 33. Southern, E. M. J. molec. Biol. 98, 503-517 (1975).
- 34. Michelson, A. M., Markham, A. F. & Orkin, S. H. Proc. natn. Acad. Sci. U.S.A. 80, 472-476
- 35. Chirwin, J. M., Przygyla, A. E., MacDonald, R. J. & Rutter, W. J. Biochemistry 18, 5294-5298
- 36. Maniatis, T., Fritsch, E. & Sambrook, J. Molecular Cloning: a Laboratory Manual (Cold Spring Harbor Laboratory, New York, 1982).
- 37. Feinberg, A. P. & Vogelstein, B. Analyt. Biochem. 132, 6-13 (1983)
- 38. Strunk, R. C., Whitehead, A. S. & Cole, F. S. J. clin Invest. 76, 985-990 (1985)
- Sanger, F., Nicklen, S. & Coulson, A. R. Proc. natn. Acad. Sci. U.S.A. 74, 5463-5467
- 40. Maxam, A. M. & Gilbert, W. Meth. Enzym. 65, 499-580 (1980).
- 41. Treisman, R., Proudfoot, N. J., Shander, M. & Maniatis, T. Cell 29, 903-911 (1982). 42. Francke, U. Cytogenet. Cell Genet. 38, 298-307 (1984).

-----LETTERS TO NATURE

A QSO with redshift 3.8 found on a UK Schmidt telescope IIIa-F prism plate

C. Hazard*†, R. G. McMahon*† & W. L. W. Sargent‡

- * Department of Physics and Astronomy, University of Pittsburgh, Pittsburgh, Pennsylvania 15260, USA
- † Institute of Astronomy, University of Cambridge, Madingley Road, Cambridge CB3 0HA, UK
- ‡ Palomar Observatory, California Institute of Technology, Pasadena, California 91125, USA

High-redshift QSOs (quasi-stellar objects) are important because of the information they provide on the early history and evolution of the Universe: the brighter ones are particularly valuable as probes of the intervening material. During the past 20 years much effort has been devoted to trying to discover QSOs at redshifts z > 3.5, but progress has been so slow that it has been suggested that there is a cutoff in the QSO distribution at $z \approx 3.5$ (ref. 1). However, we have already demonstrated²⁻⁴ how unfiltered UK Schmidt telescope (UKST) IIIa-F low-dispersion objective prism plates can be used successfully in such searches up to at least $z \approx 3.7$ (ref. 3). We report here the use of this technique to discover a QSO, 1208 + 1011, with a redshift z = 3.80. The highest redshift previously known was that of the radio-selected QSO, PKS2000-330 with z = 3.78 (ref. 5). In two UKST fields we have now discovered six QSOs with redshifts between 3.3 and 3.8, of which four have $z \ge 3.50$; including PKS2000-330, only four other QSOs with $z \ge 3.50$ are known over the whole sky^{5-7,10}. Our success up to z = 3.8 indicates that redshifts >4 could soon be attained.

Up to $z \approx 3.3$, searches for high-z QSOs by their Ly- α + N V emission are best carried out on IIIa-J prism plates, which have a red cutoff to their spectral response at ~5,200 Å. The IIIa-F plates, with a corresponding limit at 6,800 Å, extend the range above z = 3.3 to a possible maximum of z = 4.6. However, to avoid confusion with cool stars our searches on these plates have been restricted to the interval $3.3 \le z \le 3.9$. With this restriction and using auxiliary IIIa-D and IIIa-J prism and direct J and R or I plates to check the spectral features and colours of the IIIa-F-selected objects we have shown how high-redshift QSOs can be selected with complete reliability^{2,3}. For these prime selections we require that the reality of the emission line in the IIIa-F spectrum be confirmed by the presence of a corresponding emission line in the Ha-D spectrum and that its identification with Ly- α + N V be confirmed by the detection of O VI emission on the Illa-J spectrum. We also look for a fall in the continuum level going from red to blue across Ly- α + N v and check for, but do not demand, a cutoff near the Lyman limit. When these conditions are met, the selections are no longer candidate high-redshift QSOs but certain QSOs with redshifts within about ± 0.05 of those measured from the prism spectra; the accurate redshifts now available for our other high-z selections have allowed us to correct a slight systematic bias of +0.03 in our earlier prism redshifts. These prime selections are necessarily restricted to bright QSOs with strong O VI as well

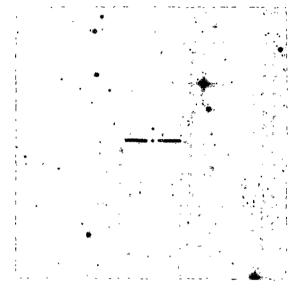


Fig. 1 Finding chart of 1208 + 1011, 8 × 8 arc min reproduced from a direct IIIa-J UKST plate (courtesy of the UKST unit). North is up, and east is to the left.

as strong Ly- α + N v emission and including 1208+1011 we have so far found only five objects²⁻⁴ which could confidently be classified as QSOs with $z \ge 3.3$ from the prism data alone; a sixth, the broad absorption line (BAL) QSO 0105-2634 with z = 3.50, appeared a certain QSO from the prism data but was relegated to the 'candidate' category because of its unusual colours⁴. As among the numerous IIIa-F selected candidates there may be high-z OSOs with weak O VI, and because we are still refining our selection criteria, we have not confined our follow-up slit spectroscopy to the certain selections. However,

Table 1 Measured wavelengths of emission lines, with corresponding redshifts

Emulsion	Feature	Wavelength* (Å)	Identification	Redshift*
IIIa-F IIa-D IIIa-J‡	Emission Emission Emission	5,860±50 ~5,950† 4,980±80	Ly-α + N v Ly-α + N v O vi	3.82 ± 0.04 ~3.89 3.82 ± 0.08
			Adopted redshift	3.82 ± 0.04

^{*} The errors are maximum errors. The calibration curve for the IIIa-F spectra was normalized using Ly- α + N v in QSOs of known redshift, assuming the wavelength of the blend to be 1,216 Å. It automatically takes into account the N v contribution unless it differs markedly from the average.

‡ The IIIa-J spectrum dispersion is perpendicular to that of the IIIa-F spectrum, and is thus not confused with the nearby star.

[†] Ly- α + N v is too close to the red limit of the IIa-D spectrum to be accurately measured. The quoted wavelength is based on measurements relative to nearby stars.

Table 2 Seven OSOs with	$\tau \ge 3.3$ visible on the 0053 -	-2803 and 1204+1129 IIIa-F prism plates

	Positi (Epoch 1				Equivalent width	
Name*	RA	Dec.	$m_{ m R}^{\dagger}$	M_R ‡	$Ly-\alpha+Nv$	$Z_{ m em}$
0042 - 2627	00 h 42 min 06.22 s	-26° 27′ 42.9″	17.0	-29.3	50	3.30§
DHM0054-284	00 53 59.8	$-28\ 24\ 45$	17.8	-28.7	60	3.61
0055 2659	00 55 32.46	-25 29 26.0	17.1	-29.5	15	3.67
0105-2634	01 05 48.19	-26 34 20.2	17.3	-29.2	50 (BAL)	3.50
1159+1223	11 59 14.23	+12 23 11.9	17.5	-29.0	150	3.51
1208 + 1011	12 08 23.73	+10 11 07.9	17.5	-29.2	46	3.80
1209+0919	12 09 01.66	+09 19 04.0	18.5	-27.8	120	3.31

* All except the colour-selected DHM0056-2847 were discovered in the present programme.

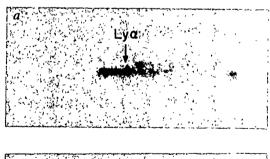
§ This is lower than the previously quoted z = 3.4, which was a provisional estimate made at the telescope.

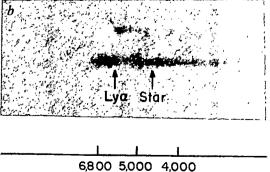
of \sim 20 'candidates' all but the BAL QSO0105 - 2634 have turned out to be galactic stars.

Until recently we possessed only one set of high-quality prism plates, centred on (RA, dec.) = $(00 \text{ h} 53 \text{ min}, -28^{\circ}03')$, and on which we found³ the z = 3.67 QSO 0055-2659. The z = 3.51OSO 1159+1223 had been found earlier² on a set of lowerquality plates, centred on (12 h 04 min, 11°29'), but it is an exceptional object with the observed equivalent width of Ly- α + N $v \approx 700$ Å. The QSO 1208+1011 was found on a new highquality IIIa-F plate of this latter region taken at an exposure of 20 min and with a limiting magnitude $m_R \approx 19$. On it, 1159 + 1223 is much more prominent than on the earlier discovery plate on which 1208+1011 is not even recognizable as a OSO. The IIIa-F spectra of both 1159 + 1223 and 1208 + 1011 from the new plate, which are reproduced in Fig. 1, with Ly- α + N v indicated in each case, show clearly the higher redshift of 1208+1011. The sharp drop in the continuum level, going from red to blue across Ly- α + N v and which is particularly prominent in 1208 + 1011, is a characteristic of high-z QSOs and in itself a valuable selection criterion. The lower visibility of the emission line in 1208+1011 shows that it has a significantly smaller observed equivalent width than the 700 Å of the emission line in 1159+ 1223. The emission line is also visible on the IIa-D spectrum, but too close to the plate's red limit to permit an accurate wavelength measurement. Its identification with Ly- α + N V was confirmed by the IIIa-J spectrum, which shows a second emission line at the expected position of Ovi. This IIIa-J spectrum, with dispersion perpendicular to that of the IIIa-F spectrum, and therefore not confused by the nearby star, also shows a highly unusual continuum distribution, with a steep decrease in level at ~4,250 Å, below which wavelength it continues faintly before disappearing at ~3,700 Å. The decrease in continuum level is ~150 Å to the blue of the Lyman limit at the emission line redshift, but relatively few QSOs show strong absorption at the Lyman limit.

Table 1 lists the measured wavelengths of the emission lines and the corresponding redshifts. The calibration curve used for the IIIa-F plate was normalized using the Ly- α + N v emission in other OSOs of known redshift. The wavelength of the Ly- α + Nv blend was assumed to be 1,216 Å, but the method of calibration automatically takes into account the N v contribution unless it differs markedly from the average. The redshifts calculated from Ly- α + N v and O vI are in such excellent agreement as to remove any doubt about the line identifications or our adopted redshift of 3.82 ± 0.04. These quoted errors are maximum errors, giving a minimum possible redshift for 1208+ 1011 of 3.78, equal to that of PKS2000 - 3305. However, a careful comparison of the IIIa-F spectrum of 1208+1011 with those of 1159+1223, DHM0054-284 and 0059-2659, all with redshifts >3.5 (refs 2, 3, 7), showed that a redshift as low as 3.78 was highly improbable. The QSO 1208+1011 was therefore selected as our highest priority object for further study, and a slit spectrum was obtained using the 5-m Hale telescope on Mount Palomar, which gives an accurate redshift of $z = 3.803 \pm 0.005$ (see ref. 8).

1208+1011 is the sixth QSO with z>3.3 to be selected from the 0053-2803 and 1204+1129 low-dispersion IIIa-F prism plates and for which slit spectra are now available. The data on all six objects are summarized in Table 2, together with those for the z = 3.61 QSO DHM0054 – 2847, which is also recognizable on the 0053-2803 plate. Their rest-frame equivalent widths, W_{λ} , of Ly- α + N v are consistent with the spread of W_{λ} in a sample of IIIa-J-selected QSOs having 2.6 < z < 3.3, with four lying towards the lower limit ($W_1 \approx 50$) of this distribution. This lower limit is not an inherent observational limit but reflects only that the preliminary surveys with both IIIa-J and IIIa-F plates concentrated on strong-emission-line objects. Other than the objects in Table 2, only eight QSOs with z>3.3 are known^{10,11}. If attention is restricted to the higher-redshift objects, the potential of the IIIa-F surveys becomes even more striking. It lists five QSOs with $z \ge 3.50$ visible in two UKST fields with a useful area of ~60 deg². There are only three other QSOs known above this redshift over the whole sky.





Wavelength (Å)

Fig. 2 IIIa-F prism spectra of the z = 3.51 QSO 1159 + 1223 (a) and of 1208 + 1011 (b) showing clearly the higher redshift (z = 3.80) of the latter object. The spectrum to the immediate right of 1208 + 1011 is that of a galactic star. (Courtesy of the UKST unit.)

[†] The magnitude of the BAL 0105 - 2636 has been corrected for heavy absorption in the R pass-band. Magnitudes are accurate to ±0.5 mag.

[‡] Calculated for $q_0 = 0.5$, $H_0 = 50 \text{ km s}^{-1} \text{ Mpc}^{-1}$ and assuming a continuum spectra index of -0.5.

The significance of 1208 + 1011 is not so much its high redshift but that it is the third QSO with z>3.3 to be found on the 1204+1129 plate. This effectively eliminates the possibility that the high density of such QSOs on the 0053 – 2802 plate³ represented only a violent statistical fluctuation or was indicative of QSO clustering. With the results from the two plates we have now established not only that QSOs with z>3.5 exist in relatively large numbers but that they may be found on unfiltered IIIa-F objective prism plates at a rate of $\sim 0.1 \text{ deg}^{-2}$ for 3.5 < z < 3.8and $m_R \le 18$. A remarkable feature is that this relatively high density is for objects with absolute magnitudes $M_R \leq -28.5$ (calculated for deceleration parameter $q_0 = 0.5$, Hubble constant $H_0 = 50 \text{ km s}^{-1} \text{ Mpc}^{-1}$ and a continuum spectral index of -0.5). At z = 2.25 similar QSOs would have apparent magnitudes $B \le$ 17.5, but the observed surface density for $B \le 17.5$ in the redshift interval 2.0 < z < 2.5 is only 0.01 deg^{-2} (ref. 12). The interval 2.0 < z < 2.5 corresponds to a co-moving volume twice that of the interval 3.5 < z < 3.8, so that, even allowing for uncertainties in the magnitude estimates, our incomplete observations imply a strong increase in the co-moving density of the brightest QSOs with increasing redshift. Our success in finding bright OSOs with z > 3.5 contrasts with the reported null detections in deep surveys over areas of 1-5 deg² for QSOs with 3.5 < z < 4.7 and $m_{\rm R} \le 21$ (refs 1, 13, 14). The results of these deep surveys appear incompatible with our observations unless the increasing density of QSOs with $M_R < -28.5$ is accompanied by a decrease in the co-moving density of lower-luminosity QSOs with $-28.5 < M_{\rm R} <$ -26, the lower limit of $M_R < -26$ corresponding to $m_R \le 21$ at z = 3.5. This implies a transition from the steep QSO luminosity function found at lower redshifts¹² to one that is relatively flat above z = 3.5 or perhaps even one where the number of QSOs per magnitude interval decreases at lower luminosities. For an unchanged flat luminosity function and constant co-moving density above z = 3.5 our observations would imply 1 QSO deg with $m_R < 21$ in the redshift range 3.5 < z < 4.7.

Above $z \approx 4.2$, Ly- α + N v will lie so close to the red limits of the low-dispersion IIIa-F prism spectra that it will be very difficult to distinguish it from the enhancement in the continuum level produced by the decreased prism dispersion which is a feature of most low-dispersion IIIa-F prism spectra and particularly those of cool stars. However, there now appears to be no problem in detecting it up to $z \approx 4.2$ because we have already seen C IV at $\lambda = 6,200 \text{ Å}$ in QSOs with $z \approx 3$. The problem in redshift range is that above $z \approx 3.9$, Ly- α passes beyond the red limit of the IIa-D emulsion and O VI moves close to the red limit of the IIIa-J emulsion so that the auxiliary plates no longer provide a useful check on the selections. Typically, our searches yield about 30 candidates per plate with 3.9 < z < 4.2. Assuming that the properties and surface density of QSOs in the redshift range do not differ significantly from those in the range 3.5 < z <3.9, we would expect only one or two of these to be genuine QSOs. About 20 candidates will need to be studied spectroscopically to give a reasonable chance of finding one QSO with z > 3.9. However, with modern instrumentation this is not a particularly formidable task, requiring about one night's observing. Also, our experience with IIIa-J prism plates has shown that the results of follow-up slit spectroscopy soon allows a refinement of the selection procedures so that the number of candidates per plate should be reduced significantly. The discovery of OSOs with z>4 would now appear to require only an adequate number of high-quality UKST prism plates and time to follow up the candidates on large telescopes. As we have already noted³, for rare objects with a flat luminosity function, the large area which can be covered by Schmidt plates in such surveys is a more significant consideration than their relatively bright limiting magnitude. Our results so far have demonstrated that these surveys can be more productive than deep surveys over small areas of sky.

We thank UKST for their help and plate material, without which our studies would not have been possible.

Received 27 February; accepted 29 April 1986.

- Osmer, P. S. Astrophys. J. 253, 28-37 (1982). Hazard, C. et al. Mon. Not. R. astr. Soc. 211, 45P-50P (1984). Hazard, C. & McMahon, R. G. Nature 134, 238-240 (1985).
- Hazard, C., McMahon, R. G. & Morton, D. C. Mon Mot. R. astr. Soc. (submitted). Peterson, B., Savage, L. A., Jauncey, D. L. & Wright, A. E. Astrophys. J. 260, L27-L29 (1983).

- Yampler, E. J., Robinson, I. B., Baldwin, J. A. & Burbidge, E. M. Nature 243, 336-337 (1973).
 Shanks, T., Fong, R. & Boyle, B. J. Nature 303, 156-158 (1983).
 Sargent, W. L. W., Filippenko, A. V., Steidel, C., Hazard, C. & McMahon, R. G. Nature 322, 40-42 (1986).
- 9. Hazard, C., Morton, D. C., McMahon, R. C., Sargent, W. L. W. & Terlevich, R. Mon. Not.
- R. astr. Soc. (in the press).

 10. Dunlop, J. S. et al. Nature 319, 564-567 (1986).
- Veron-Cetty, M.-P. & Veron, P. A Catalogue of Quasars and Active Nuclei (Eur. Southern Observ. scient. Rep. No. 4, 1985).
 Weedman, D. Astrophys. J. Suppl. Ser. 57-532 (1985).
 Koo, D. C. in Proc. 24th Liège. int. Astrophys. Colloq. (ed. Swings, J. P.) (University of
- Liège, 1984).
- 14. Schneider, D., Schmidt, M. & Gunn, J. Bull. Am. astr. Soc. 16, 488 (1984).

Spectrum of a QSO with redshift 3.8

Wallace L. W. Sargent*, Alexei V. Filippenko†, Charles C. Steidel*, Cyril Hazard‡ & Richard G. McMahon‡§

- * Palomar Observatory, California Institute of Technology, Pasadena, California 91125, USA
- † Department of Astronomy, University of California, Berkeley, California 94720, USA
- ‡ Department of Physics and Astronomy, University of Pittsburgh, Pittsburgh, Pennsylvania 15260, USA
- § Institute of Astronomy, University of Cambridge, Madingley Road, Cambridge CB3 0HA, UK

Hazard et al. have described the circumstances leading to the identification of a quasi-stellar object (QSO) (1208+1011) with $z = 3.82 \pm 0.04$. Here we present a moderate-resolution optical spectrum of this object. Its precise redshift, $z = 3.803 \pm 0.005$, is the highest ever recorded.

The data were obtained on 13 January 1986 UT with the double spectrograph² at the Cassegrain focus of the 5.08-m Hale telescope at Palomar Observatory. A slit of width 2 arc s was aligned along the parallactic angle corresponding to the approximate midpoint of the 4,000-s exposure. Observations were made through clouds whose extinction was visually estimated to be ~1 mag. The average air mass (density) was ~1.11. A dichroic filter directly behind the slit reflected blue light ($\lambda \le 5,500 \text{ Å}$) to one camera and transmitted red light to the other. The detector on the blue side was the '2D-Frutti' photon counting system devised by Shectman³. When used with a grating with 600 grooves mm⁻¹ and blazed at 3,780 Å in first order, this arrangement gives spectra covering the range 3,200-5,600 Å at a resolution of ~6 Å. The detector on the red side of the spectrograph was a Texas Instruments 800×800 CCD (charge-coupled device). A grating with 158 grooves mm⁻¹ blazed at 7,560 Å in first order produced a resolution of ~18 Å over the range 5,400-10,200 Å.

Calibrations were performed in the usual manner⁴, and fluxes were derived with the standard stars^{5,6} GD-248 (for the blue spectrum) and BD+26°2606 (for the red). Some uncertainty is present in the continuum shape of the QSO between ~5,100 and 5,500 Å due to the low signal-to-noise ratio in this region of the spectrum of GD-248. The two individual spectra were combined to yield one complete scan over the wavelength range 3,200-10,200 Å, as shown in Fig. 1. Although clouds affected the QSO observations, data for BD+26°2606 were obtained in similar conditions, and the absolute flux scale is probably accurate to within $\sim \pm 0.6$ mag (1σ) .

Figure 1 confirms that 1208+1011 is indeed a QSO of high redshift. Prominent, broad emission lines of Lyman- β + O VI, Ly- α + N v, Si Iv + O Iv], C Iv, and Al III + C III] are present.

c, λ _{vac} (Å)	Observed \[\lambda_{\text{air}} \text{ of } \] peak (\lambda)	z (peak)*	$R(\lambda)/F(C \text{ iv})^{\dagger}$	Observed W(Å)‡
β,1,025.7 π,1,033.8	<u> </u>	3.810	0.46	53
α,1,215.7 v,1,240.1	5,873 5,946	3.832 \ 3.796 \	2.29	220
11,1,260.4	6,090	3.83	0.13	12

Table 1 Measurements of emission lines, 1208+1011

Line, λ _{vac} (Å)	Observed λ_{air} of peak (Å)	z (neak)*	$R(\lambda)/F(C \text{ IV})^{\dagger}$	Observed W(Å)‡
	P**** (-1)	- (P+)	()/ - (/)	(/.
Ly-β,1,025.7		}	0.46	53
O v1,1,033.8	4,971	3.810 ∫		
Ly- α ,1,215.7	5,873	3.832	2,29	220
N v,1,240.1	5,946	3.796 {		
Si 11,1,260.4	6,090	3.83	0.13	12
O 1,1,303.5	6,300	3.82	0.07	6
Si 11,1,307.6	0,300	3.62	0.07	U
?,1,342§	6,442		0.08	7
Si 1v,1,396.8	6,732	3.804	0.28	27
O IV],1,402.5	0,/32	3.804	0.28	21
C iv,1,549.1	7,437	3.802	1.00	107
He 11,1,640.4	7,850	3.79		<5¶
Al 111,1,858 #	8,950	3.82	0.27	35
C 111],1,908.7	9,170	3.806	0.35	47
?,2,080§	9,990		0.36	50

^{*} Assumptions: Ly- β negligible compared to O VI; λ (O I+Si II)= 1,306 Å; $\lambda(\text{Si IV} + \text{O IV}) = 1,401.6 \text{ Å}$; Si III] 1,892 Å negligible compared to Al III 1,858 Å.

† Flux of C IV 1,549 Å = 1.77×10^{-14} erg s⁻¹ cm⁻². Galactic extinction $A_{\rm v} \approx 0.0$ mag.

‡ Observed equivalent width. Divide by 1+z=4.803 to get W in OSO rest frame.

§ Derived from z = 3.803 and the observed λ ; exact identity unknown.

|| Very approximate wavelength and redshift. ¶ Upper limit; line not detected with certainty.

Possibly contaminated by Si III] 1,892 Å and Fe II 1,860 Å.

The velocity widths of Ly- α and C IV are \sim 6,000 km s⁻¹ (full width at half-maximum) and ~18,500 km s⁻¹ (full width at zero-intensity). There is a sharp decrease in the continuum flux blueward of the Ly- α emission. This is undoubtedly due to the Ly- α absorption-line 'forest' which is so typical of distant QSOs⁷⁻⁹, and the spectrum consequently appears quite red.

Table 1 lists the observed emission lines, together with their strengths, equivalent widths, wavelengths, and redshifts. The relative intensities of strong lines are uncertain by $\sim \pm 15\%$, primarily because of difficulties in defining the continuum. Weak lines obviously have larger errors. Regions containing several closely-spaced emission lines (for example, that between Ly- α and Si IV+O IV]) exhibit a deceptively high continuum due to the blending of the line wings, so the quoted fluxes are lower limits. Extinction produced by our Galaxy is negligible at the latitude of 1208 + 1011 ($b \approx 70^{\circ}$).

A redshift of $z = 3.803 \pm 0.005$ is derived from a weighted average of the apparent peaks of CIV 1,549.1 Å, {Si IV+ O IV] 1,401.6 Å (ref. 10) and C III] 1,908.7 Å. Ly- α is not used in the average, because its blue side is eroded by numerous absorption lines. O VI is also severely affected. Although Table 1 lists several weak emission lines, they are excluded from the average because of large uncertainties in their measured wavelengths.

If redshifts are of cosmological origin, as is generally assumed, 1208+1011 is now the most distant known object in the Universe; PKS2000-330, the previous champion¹¹, has z= 3.78 ± 0.01. Like many other high-redshift QSOs, 1208 + 1011 is exceedingly luminous: we find $m(6.960 \text{ Å}) \approx 17.8$, comparable to that of PKS2000 – 330. If the Hubble constant $H_0 = 50 \text{ km s}^{-1}$ Mpc^{-1} , this corresponds to an absolute magnitude M = -30.8(for deceleration parameter $q_0 = 0$) or $M \approx -28.5$ (for $q_0 = 1$) at a rest wavelength of 1,450 Å.

With the exception of He II 1,640 Å, which is unusually weak and may even be absent, the relative strengths of emission lines in 1208+1011 are similar to those observed in many QSOs¹². Although the Ly- α /C IV ratio is slightly lower than normal, the observed flux of Ly- α is decreased by the forest of absorption lines on the blue side of the profile. High-resolution spectra are needed to quantify the effect of these lines. The C III]/C IV ratio is also fairly small, but part of the CIII] flux may have been incorrectly attributed to Al III 1,858 Å. The equivalent width (W_0) of C IV 1.549 Å in the OSO's rest frame is 22.3 Å, lower than the average value $(35\pm25 \text{ Å})$ found by Baldwin¹² in a sample of high-redshift QSOs. Given the uncertainty in the measured magnitude of 1208 + 1011, however, this W_0 (C IV) is quite consistent with the correlation he discovered¹³ between $W_0(C \text{ IV})$ and the continuum luminosity at

 $(1+z)1,450 \text{ Å}: \log L_{\text{cont}} = 33.34 - 1.57 \log W_0 \text{ (for } q_0 = 1).$ Note that a broad emission line appears to be present at a rest wavelength of ~2,080 Å. This feature has previously been seen in the spectra of some QSOs¹⁴⁻¹⁶, but its exact identity remains unknown. One possibility is permitted Fe II, as suggested by Arp¹⁵.

The continuum in the range 3,200-5,600 Å undulates in a peculiar manner. It is possible that the strong feature around 4,050 Å represents the Lyman limit of absorbing clouds at z = 3.44, but the deep, rather broad dips near 5,500 Å, 4,560 Å, and 4,410 Å are more consistent with Ly- α , Ly- β , and Ly- γ absorption (respectively) at $z \approx 3.53$. Better spectra are needed to confirm this, as well as to investigate the properties of the Ly- α forest. Unlike the case of PKS2000-330, continuum radiation is visible all the way down to the atmospheric ozone cutoff at ~3200 Å. This precludes the presence of very optically thick

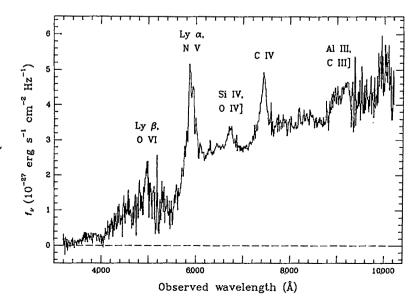


Fig. 1 Spectrum of 1208+1011, obtained with the Palomar Hale telescope on 13 January 1986 UT. A point13 convenient continuum reference $m(6,960 \text{ A})\sim 17.8$, but the flux scale is only approximate (±0.6 mag). Prominent features are marked. The blue spectrum ($\lambda \le 5,800 \text{ Å}$) is affected by numerous Ly- α absorption lines. Incomplete removal of atmospheric absorption and emission lines produces narrow spikes in some places (such as the O2 band at ~6,860 and 7,600 Å).

clouds in the range $2.5 \le z \le 3.8$ along the line of sight to 1208 +1011. At wavelength longer than ~6,000 Å, the observed continuum can roughly be described by a power law, $f_{\nu} \propto \nu^{-1}$.

We thank J. Henning, C. Price, S. Staples and D. Tennant for assistance at Palomar Observatory. This research was supported by NSF grant AST84-16704 (W.L.W.S.) and by the Miller Institute for Basic Research in Science (A.V.F.).

Received 18 February; accepted 9 May 1986.

- 1. Hazard, C., McMahon, R. G & Sargent, W. L. W. Nature 322, 38-40 (1986).
- Oke, J. B. & Gunn, J. E. Publs astr. Soc. Pacif. 94, 586-594 (1982).
 Shectman, S. A. in Annual Report of the Director, Mt Wilson and Las Campanas Observatories,
- 676-677 (Carnegie Institution of Washington, 1982).
 Filippenko, A. V. & Sargent, W. L. W. Astrophys. J. Suppl. Ser. 57, 503-522 (1985).

- Filippenko, A. V. & Sargent, W. L. W. Astrophys. J. Suppl. Ser. 51, 303-522 (1983). Filippenko, A. V. & Greenstein, J. L. Publs astr. Soc. Pacif. 96, 530-536 (1984). Oke, J. B. & Gunn, J. E. Astrophys. J. 266, 713-717 (1983). Lynds, C. R. Astrophys. J. 164, L73-L78 (1971). Young, P. J., Sargent, W. L. W., Boksenberg, A., Carswell, R. F. & Whelan, J. A. J. Astrophys. J. 208, 203, 103 (1972).
- 9. Sargent, W. L. W., Young, P. J., Boksenberg, A. & Tytler, D. Astrophys. J. Suppl. Ser. 42, 41-81 (1980).
- Young, P., Sargent, W. L. W. & Boksenberg, A. Astrophys. J. 252, 10-31 (1982).
 Peterson, B. A., Savage, A. Jauncey, D. L. & Wright, A. E. Astrophys. J. 260, L27-L29 (1982).
- 12. Baldwin, J. A. in Active Galactic Nuclei (eds Hazard, C. & Mitton. S.) 51-78 (Cambridge University Press, 1979).
- Baldwin, J. A. Astrophys. J. 214, 679-684 (1977).
 Phillips, M. M. & Hawley, S. A. Publs astr. Soc. Pacif. 90, 650-651 (1978).
 Arp, H. Astrophys. J. 283, 59-63 (1984).
- 16. Ulrich, M. H. & Perryman, M. A. C. Mon. Not. R. astr. Soc. 220, 429 (1986).

The rotation period of Uranus

M. D. Desch, J. E. P. Connerney & M. L. Kaiser

Laboratory for Extraterrestrial Physics, Goddard Space Flight Center, Greenbelt, Maryland 20771, USA

The recent fly-by of Uranus by the Voyager 2 spacecraft provided a singular opportunity to measure one of the fundamental but poorly known physical properties of the planet, its intrinsic rotation period. Earth-based photometric and spectroscopic estimates of the 'atmospheric' period vary greatly, with values ranging from ~12 to 24 h (refs 1-4); estimates of the period based on the dynamical flattening of a rotating body range from ~15 to 17 h (refs 5, 6). Here we use the Voyager planetary radioastronomy⁷ and magnetometer⁸ observations at Uranus to derive a period of 17.24 ± 0.01 h. The greatly improved precision of this measurement provides useful constraints on models of the planet's internal structure.

The Voyager 2 radioastronomy data provide only an indirect determination of the rotation period, because we must make the commonly accepted assumption that the periodic nature of the emission is closely related to the intrinsic rotation of the planet. In order to minimize possible measurement bias due to unknown variations in beaming of the radiation with uranographic latitude, we restricted the analysis interval to post-encounter observations, when the spacecraft latitude changed by only a few degrees. This yielded a total data span of 42 planetary rotations, from 16:00 (spacecraft time) on 25 January to 20:00 on 24 February 1986, when we observed the last detectable emission from Uranus.

This is an extremely short interval compared with the nearly 600 rotations used to determine Saturn's period9. However, the discovery⁷ by Voyager of a highly repetitive emission feature has permitted a far more precise determination than would have been possible for Saturn using an equivalent span of data. The clock-like character of this feature is apparent in total energy plots (Fig. 1), in which the radio-wave energy is derived from an integration over the frequency band from 40 to 800 kHz. The highly periodic radiation drop-outs are evident as decreases of 2-3 orders of magnitude in the total radiated power.

To obtain an initial estimate of the rotation period, the data were Fourier-analysed, following correction of the observation

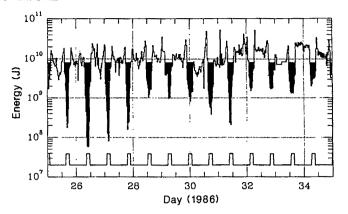


Fig. 1 Energy emitted by the Uranus radio source as a function of time for 10 days (14 rotations). For clarity, the emission dropouts are shaded. An artificial 17.24-h clock is shown as a square wave pulse in the bottom of the figure. The highly periodic nature of the emission drop-outs is evident from a comparison of the timing of the event minima with the timing of the 17.24-h clock.

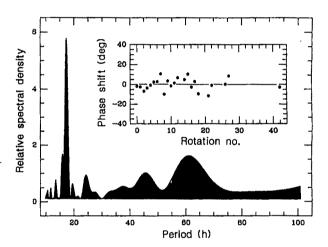


Fig. 2 Power spectral analysis of the Uranus radio-energy data of Fig. 1. The primary spectral peak is between 17.0 and 17.5 h. A linear least-squares fit to the midpoints of the emission drop-outs measured over 42 Uranus rotations is shown in the inset. When the midpoints are plotted in an arbitrary longitude system that rotates with a period of 17.24 h, the result is zero average phase shift, representing no long-term drift of the events with time. The maximum deviation of individual points from the least-squares line is ~±12°, corresponding to events leading or lagging a perfect clock by ±35 min.

times for spacecraft motion and differential light travel time. Figure 2 shows the resulting power spectral density as a function of period. There is only one significant peak in the power spectrum, corresponding to the Uranus rotation period, at $17.25 \pm 0.25 \text{ h}.$

This determination was improved by performing a linear least-squares fit to the midpoint times of the emission drop-outs. The procedure was very similar to that used to derive Saturn's rotation period⁹. By computing the phase of each midpoint in an arbitrary longitude system, the period and hence the phase shift of each point was adjusted until negligible long-term drift (zero least-squares slope) of the events with time was achieved (see Fig. 2 inset). This yielded a rotation period of 17.239 ± 0.006 h.

A second source of error in determining the period from the radioastronomy data arises from the fact that the midpoints were non-randomly distributed about the best-fit line (see Fig. 2 inset). This systematic variation introduced an additional uncer-

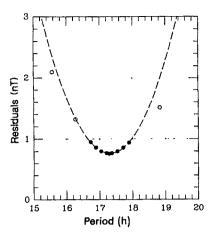


Fig. 3 Root-mean-square residual error between the best-fitting magnetic field model and the observations, as a function of assumed rotation period. The minimum r.m.s. error was obtained for a rotation period of 17.29 h. The parabolic least-squares line, shown by the dashed curve, is fit to the filled points.

tainty in the period measurement of ±0.003 h. The final determination from the radioastronomy data is, therefore, 17.239 ± 0.009 h.

The magnetic field data provide a direct measure of the rotation period of the planet's interior, where the field is generated. The data used in this study spanned the interval from 15:00 to 21:00 (spacecraft time) on 24 January 1986. During this time Voyager 2 traversed the innermost magnetosphere, passing from a radial distance of 8 $R_{\rm U}$ (the planet radius $R_{\rm U}$ = 25,600 km) at 40° S latitude, through closest approach (4.2 R_U), to a radial distance of $8 R_U$ at 78° N latitude. The maximum observed magnetic field, measured just before closest approach, was 413 nT. Without accurate knowledge of the planet's rotation period, the location of the spacecraft in the reference frame rotating with Uranus is unknown, making global magnetic field determinations difficult. In order to determine the rotation period, spherical harmonic analyses were performed with the rotation period treated as a free parameter. For each assumed period, ranging from 15.5 to 18.8 h, the best-fitting I2E1 (dipole plus quadrupole internal field plus uniform external field) model was found.

Figure 3 shows the root-mean-square (r.m.s.) residual between the best-fitting models and the observations as a function of assumed period. The best fit was obtained for a rotation period of 17.29 h, for which the r.m.s. error was 0.76 nT. We believe that this residual error is largely due to that part of the external fields (for example, fields due to the magnetopause and magnetotail currents) not well approximated by a uniform field. Figure 3 also shows a parabolic least-squares fit to the points having r.m.s. error <1 nT; the uncertainty in the parabola coefficients yields an uncertainty of $\pm 0.05 \, h$ in the rotation period.

The I2E1 model is the simplest spherical harmonic model for which an acceptable fit to the observations is obtained. Centred dipole models fit poorly (r.m.s. error >7.8 nT) for all assumed rotation periods. An offset, tilted dipole representation of the field, presented in ref. 8, has an associated r.m.s. error of 2.4 nT. More complex (for example, octupole) models can be considered only in part using generalized inverse methods¹⁰, because of the limited observations. An examination of the impact of increasing model complexity on the deduced rotation rate suggests an uncertainty several times that obtained assuming an I2E1 model, or $\sim \pm 0.2$ h. The best direct estimate of the rotation period is then $17.29 \pm 0.2 \text{ h}$.

The two period determinations made here are entirely independent and self-consistent. Combining the two periods yields a weighted mean value of $P = 17.24 \pm 0.01$ h. As no further

spacecraft observations of Uranus are planned at this time, we believe that this value is not likely to be improved upon in the foreseeable future.

The 17.24-h rotation period has important consequences for studies of atmospheric dynamics¹² and the internal structure and composition of Uranus. Inferences regarding the internal structure can be drawn from the relationship between the observed planetary oblateness, rotation period and gravitational moment (J_2) . The latter two are now known with great precision, constraining plausible models of the interior. Several 2- and 3-layer models, incorporating a 'rock' core, 'ice' mantle and gaseous outer envelope, have been considered 13,14 for Uranus. A model (U4, ref. 14) containing a rocky core of ~6.6 Earth masses (M_{\oplus}) and an outer envelope with ~3.7 M_{\ominus} H₂-H gas and 4.4 M_{\oplus} ice is most consistent with the rotation period reported here.

We thank our colleagues on the Voyager magnetometer investigation, led by principal investigator N. Ness; our colleagues on the Voyager planetary radioastronomy investigation, led by J. Warwick; and the data processing and display staff of the Laboratory for Extraterrestrial Physics, GSFC, under the direction of W. Mish, for support during the intensive Uranus encounter.

Received 23 April; accepted 16 May 1986.

- 1. Brown, R. A., Goody, R. Astrophys. J. 235, 1066-1070 (1980).
- Trauger, J. T., Roessier, F. L. & Munch, G. Astrophys. J. 219, 1070-1083 (1978). Trafton, L. Icarus 32, 402-412 (1977).
- Munch, G. & Hippelein, H. Astr. Astrophys. 81, 189-197 (1979).
 Elliot, J. L. et al. Astr. J. 86, 444-455 (1981).
- 6. Goody, R. in Uranus and the Outer Planets (ed. Hunt, G.) (Cambridge University Press.
- Warwick, J. W. et al. Science (in the press).
- Ness, N. F. et al. Science (in the press).
 Desch, M. D. & Kaiser, M. L. Geophys. Res. Lett. 8, 253-256 (1981).
- Connerney, J. E. P. J. geophys. Res. 86, 7679-7693 (1981). 11. Stone, P. H. Icarus 24, 292-298 (1975).
- Smith, B. et al. Science (in the press).
- Hubbard, W. B. & MacFarlane, J. J. geophys. Res. 85, 225-234 (1980).
 Podolak, M. & Reynolds, R. T. Icarus 46, 40-50 (1981).

Detection of stratospheric HNO₃ and NO₂ response to short-term solar ultraviolet variability

G. M. Keating*, J. Nicholson III†, G. Brasseur‡, A. De Rudder‡, U. Schmailzl§ & M. Pitts||

- * Atmospheric Sciences Division, NASA Langley Research Center, Hampton, Virginia 23665-5225, USA
- † Vigyan Research Associates, Hampton, Virginia 23666, USA
- ‡ Institut d'Aéronomie Spatiale, 1180 Brussels, Belgium
- § Max Planck Institute for Chemistry, 6500 Mainz, FRG
- SASC Technologies, Hampton, Virginia 23666, USA

Variations in the solar ultraviolet irradiance with a period equal to or approximately one-half of the rotation period of the Sun (27 days) are currently observed by satellite monitoring. These variations have typical peak-to-peak amplitudes of ~3% between 170 and 208 nm and <1.5% at longer wavelengths. Detection of the response of stratospheric species to solar ultraviolet variability is crucial for understanding the photochemical behaviour of the middle atmosphere. Understanding the natural variations of the stratosphere is also a prerequisite for isolating possible anthropogenic effects; up to now most work has concerned stratospheric ozone¹⁻⁸. Recent analysis⁵ of measurements by the Nimbus 7 satellite's LIMS (limb infrared monitor of the stratosphere) and SBUV (solar backscatter ultraviolet) experiments has established very high correlations between ozone mixing ratios (detrended and corrected for temperature effects) and short-term variations in 205-nm solar radiation. A similar approach is used here to detect

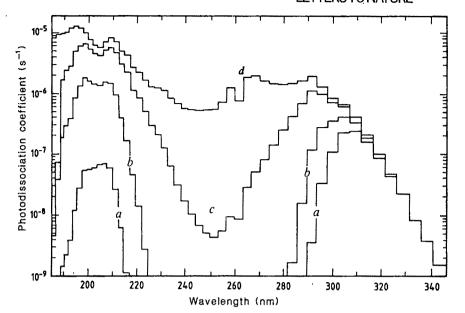


Fig. 1 Spectral distribution between 185 and 345 nm of the photodissociation coefficient of nitric acid for selected altitudes: a, 20 km; b, 30 km; c, 40 km; d, top of the atmosphere. The calculation assumes an overhead Sun (from ref. 16).

a relation between LIMS measurements of HNO₃^{9,10} and NO₂¹¹ and the SBUV measurements of short-term variations in 205-nm radiation¹². Observations show that the response of HNO₃ is much stronger than, but in the opposite sense to the ozone response, and that the NO₂ response is in the opposite sense to the HNO₃ response. This is the first detection of such a response for species other than ozone. Model calculations are in fair agreement with observed short-term variations and predict large variations in HNO₃ over the 11-vr solar cycle.

Nitrous oxide (N₂O) is the major source of odd nitrogen $(N + NO + NO_2 + NO_3 + 2N_2O_5 + HNO_3 + HO_2 + HO_2NO_2 +$ ClONO₂) in the stratosphere. It is formed in the soil by bacterial action and transported into the middle atmosphere, where it is destroyed by photodissociation or by reaction with the electronically excited oxygen atom O(1D). Nitric oxide (NO), which is produced by the reaction of N₂O with O(¹D), is converted to nitrogen dioxide (NO₂) essentially through reaction with ozone, but also by reaction with ClO, HO₂ or CH₃O₂. The NO₂ molecule reacts rapidly during the day to form NO either by reaction with O or by photolysis. During the night a significant amount of NO₂ reacts with O₃ to produce NO₃, which, in turn, is converted into N₂O₅ by reaction with NO₂. After sunrise the N₂O₅ concentration decreases continuously as solar ultraviolet radiation (primarily above 300 nm) photodissociates the molecule, replenishing NO_2 . The behaviour of NO_2 is also affected by chlorine compounds, as ClONO2 is formed by the three-body reaction of ClO and NO2. The ClONO2 is partly destroyed during the day by photodissociation or reaction with O or OH. Nitric acid is formed by the three-body reaction

$$NO_2 + OH \xrightarrow{M} HNO_3$$
 (1)

The HNO₃ molecule is relatively stable in the lower stratosphere and is therefore subject to a variety of transport processes leading, for example, to large mixing ratios at high latitudes. The loss processes for HNO₃ are

$$HNO_3 + h\nu \rightarrow OH + NO_2$$
 (2)

and

$$HNO_3 + OH \rightarrow NO_3 + H_2O \tag{3}$$

The sensitivity of HNO₃ to change in the solar ultraviolet output is predicted by a one-dimensional time-dependent chemical-radiative model^{13,14}. The short-term spectral variability⁵ of the solar irradiance is applied in the model in accord with the solar data of Heath *et al.*¹². The average solar ultraviolet irradiances adopted in the model are based on ref. 15, and we assume a sinusoidal variation of the solar ultraviolet output.

At 10 mbar, the model predicts a reduction of 0.4% in HNO₃ for a 1% increase in solar radiation at 205 nm, with a response time of less than 1 day. This strong response to short-term solar ultraviolet variations can be understood by referring to Fig. 1 (see ref. 16), in which the photodissociation frequency of HNO₃ at different altitudes is shown as a function of wavelength for overhead Sun conditions. The decrease of photodissociation with decreasing altitude for wavelengths centred on 250 nm is due to increasing ozone absorption. The sharp decrease below 200 nm is due to absorption in the molecular oxygen Schuman-Runge bands. The net effect of solar absorption by stratospheric O₃ and O₂ results in an enhancement of the effects of solar variability near 200 nm on the photodissociation of HNO₃.

The detection of the HNO₃ response to ultraviolet variations can be expected only in regions of the atmosphere where the chemical lifetime is short compared with the transport lifetime. and significantly shorter than the period of the solar oscillation. A calculation based on the model of Crutzen and Schmailzl12 shows that the chemical lifetime of HNO3 increases with decreasing altitude and, at a given level, increases with latitude, particularly in winter. At 10 mbar near equinox, for example, the HNO₃ lifetime is enhanced by 40% going from 0 to 40° latitude, while at 20 mbar it is enhanced by 60% over the same latitudinal range. In winter, the variation of the lifetime at a given altitude is larger than in other seasons. At 10 mbar, for example, the lifetime increases by more than 300% between 0 and 40° latitude. Therefore, data from near the winter solstice and high-latitude data (latitudes > 40°) were removed from the LIMS data set. Moreover, the width of the latitudinal region about the Equator from which data were used was decreased at lower altitudes ($\pm 40^{\circ}$ at 10 mbar and $\pm 20^{\circ}$ at 20 mbar), to reduce dynamical effects. By this method, the data examined were limited to those from atmospheric regions where the photochemical lifetime of HNO₃ is calculated to be less than 2 days.

Finally, to remove any possible bias, the measurements were detrended relative to a running mean, averaged over a period slightly longer than the solar oscillation period characteristic of the interval investigated (similar to the approach used for the ozone data by Keating et al.⁵). No significant HNO₃-temperature relation was predicted or observed at this level, so no correction was made. At 10 mbar, Fig. 2 shows the resulting relation between the ultraviolet ratio $(\bar{I}_{205} - \bar{I}_{205})/\bar{I}_{205}$ and the dayside HNO₃ ratio (HNO₃-HNO)/HNO₃, where I_{205} is the 5-day running mean of the 205-nm solar radiation, \bar{I}_{205} is the 19-day running mean of I_{205} , HNO₃ is the 5-day running mean of the nitric acid volume mixing ratio averaged zonally and averaged between +40° and -40° latitude, and $\bar{H}\bar{N}\bar{O}_3$ is the

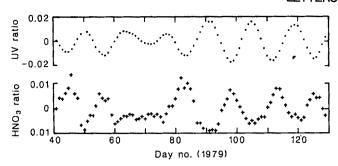


Fig. 2 Relation between dayside nitric acid ratio $[(HNO_3 - \overline{HNO_3})/\overline{HNO_3}]$ at 10 mbar (+) and 205-nm solar irradiance (UV) ratio $[(I_{205} - \overline{I}_{205})/\overline{I}_{205}]$ (\bullet) between days 40 and 130 of 1979. The correlation coefficient between the two parameters is r = -0.78.

19-day running mean of HNO3. Clearly, HNO3 is negatively correlated with the approximate 13.5-day solar ultraviolet oscillation. The correlation coefficient between the two parameters shown in Fig. 2 is -0.78. This correlation with the 205-nm solar irradiance is significantly higher than the correlation (-0.38) with the emission from the Sun at 10.7 cm (the classical 10.7-cm solar index). This is to be expected because, as indicated previously, the 205-nm radiation is very efficient in photodissociating HNO₃ throughout the stratosphere. The regression coefficient (sensitivity) for the 10-mbar dayside HNO ratio against the ultraviolet ratio is -0.44 ± 0.07 (2 σ uncertainty). In order to determine the lag time between the solar variability and the nitric acid response, the correlation coefficient between the two parameters was determined as a function of positive and negative lag (days). The resulting relationship is shown in Fig. 3: the maximum correlation occurs for a lag of 0 ± 1 days.

The 0.44% reduction in HNO₃ at 10 mbar can be compared with the variation of ozone at the same level. At low latitudes, the ozone response is calculated to be an increase of 0.17% for a 1% increase in 205-nm radiation, with a response time of 4 days (ref. 5). Observations indicate an increase in O_3 of $0.16 \pm 0.05\%$ for a 1% increase in 205-nm radiation, and a response time of 2 ± 1 days (ref. 5). Thus, the HNO₃ has an even stronger short-term response to solar ultraviolet variability than has ozone, and in the opposite sense.

It is difficult to study HNO₃ at higher altitudes because of the sharp decrease in concentration with altitude, but a similar study can be performed at 20 mbar over a smaller latitudinal interval (±20°) to minimize dynamical effects. Table 1 summarizes the results reported here and compares the model prediction (sensitivity (S) of HNO₃, expressed in per cent change, to a 1% increase in the solar 205-nm irradiance and the calculated time lag of the response) to the corresponding values derived from the LIMS data. The statistical analysis has been performed using the combined day and night data, the day data, and the night data, respectively. As the model provides 24-h averaged values, only the results provided by the combined day and night data should be compared with the calculated sensitivities. As expected, the correlation coefficient (r) is higher for the daytime observations than for the night-time. A solar effect is, nevertheless, still visible in the night data, because the signature of the daytime photochemistry is essentially frozen during the night

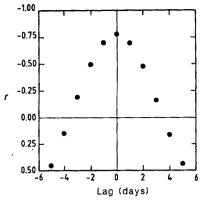


Fig. 3 Correlation coefficient between the nitric acid ratios and the 205-nm solar irradiance ratios in Fig. 2 for different time lags between these two quantities.

and is degraded principally by dynamics. The theoretical sensitivities calculated for the 13.5- and 27-day periods are in good agreement at 10 mbar with the value obtained from the data analysis, but are smaller than the observation at 20 mbar. One should, however, recall that the model provides globally-averaged sensitivities, whereas the data used for the 20 mbar analysis proceed from observations confined to the tropics, where sensitivities should be higher.

Because the photodissociation of HNO₃ leads to the formation of nitrogen oxides, there should also be a solar effect on the NO₂ mixing ratio. The LIMS NO₂ data, averaged in the same way as the HNO₃ data, show a rapid response time (less than 1 day) and positive correlation with the solar irradiance. At 10 mbar, an increase in combined day and night NO₂ of $0.22 \pm 0.12\%$ is found, for a 1% increase in the 205-nm solar irradiance. The model^{13,14} provides a corresponding increase of 0.15% in NO₂ for the 24-h average conditions. The observed NO₂ sensitivity on the dayside is larger ($+0.36 \pm 0.15\%$).

The variation in the nitric acid concentration in the stratosphere over the 11-yr solar cycle can be estimated by calculating the HNO₃/ultraviolet sensitivity from a steady-state version of the model and by scaling the amplitude of the 205-nm solar forcing to the assumed 11-yr variation. If a $10\pm5\%$ increase is adopted for the 205-nm solar irradiance (based on a number of studies, including a regression analysis between detrended 205-nm and 10.7-cm solar irradiance over a period of 4 yr), the resulting long-term variation in the HNO₃ mixing ratio is estimated to be $-10\pm5\%$ at 10 mbar and $-5\pm2\%$ at 20 mbar. The sensitivity of the HNO₃ concentration to the solar ultraviolet irradiance is thus significantly increased for this longer-period oscillation. Such a large variation may be detectable in long-term measurements of HNO₃.

The detection of a solar signal in the LIMS HNO₃ and NO₂ variations provides a new test of the validity of currently assumed photochemistry in the stratosphere. Indeed, the HNO₃ response to short-term solar variability depends on several simultaneous photochemical processes, including the sensitivity of the HNO₃ photodissociation rate to the solar radiation near 200 nm and the sensitivity of HNO₃ production to variations in NO₂ and OH. These latter parameters are modulated through O₃ and N₂O variations caused by solar ultraviolet changes. The

Toble 1	Response of HNO.	to 205 nm	color variability

Pressure		odel iction	Combined day and night		Day		Night			
(mbar)	•	27 days	S	r	S	r	S	r	Δ lat	
10	-0.37	-0.42	-0.42 ± 0.07	-0.74	-0.44 ± 0.07	-0.78	-0.42 ± 0.12	-0.58	±40^	
20	-0.13	-0.15	-0.29 ± 0.08	-0.57	-0.35 ± 0.09	-0.59	-0.25 ± 0.13	-0.34	±20° >	

Sensitivity, $S = \frac{(\text{HNO}_3 - \overline{\text{HNO}_3})/\overline{\text{HNO}_3}}{(I_{205} - \overline{I}_{205})/\overline{I}_{205}}$; correlation coefficient, r. Time lag at both altitudes: 0.5 ± 0.5 days (model) and 0 ± 1.0 days (data analysis).

observed amplitude and phase of the responses at 10 mbar of HNO₃ and NO₂ to solar ultraviolet variability are in fair accord with predicted responses based on the currently accepted chemical scheme¹⁸ used in the model. The results also imply large variations of HNO3 over the 11-yr solar cycle, which should significantly affect other chemical species, including ozone. Indeed, increased solar activity can result in increased conversion of HNO3 into active NOx, which in turn can affect the ozone balance.

We thank J. M. Russell III for providing data on HNO₃, NO₂ and temperature from the Nimbus 7 LIMS experiment in November 1983, D. F. Heath for providing 205-nm solar spectral irradiance values from the Nimbus 7 SBUV experiment in August 1984, and J. E. Nealy for photochemical calculations. Some of this work was accomplished under NASA contract NAS1-15785 and CMA contract 83-468.

Received 18 February; accepted 11 March 1986.

- 1. Keating, G. M. Sol. Phys. 74, 321-347 (1981).
- Chandra, S. J. geophys. Res. 89, 1373-1379 (1984).
 Hood, L. L. J. geophys. Res. 89, 9557-9568 (1984).
- Gille, J. C., Smythe, C. M. & Heath, D. F. Science 225, 315-317 (1984).
- Keating, G. M., Brasseur, G. P., Nicholson III, J. Y. & De Rudder, A. Geophys. Res. Lett. 12, 449-452 (1985).
- 6. Heath, D. F. & Schlesinger, B. M. in Atmospheric Ozone (eds Zerefos, C. S. & Ghazi, A.) (Reidel, Dordrecht, 1985).
- 7. Hood, L. L. J. geophys. Res. 91, 5264-5276 (1986). 8. Chandra, S. J. geophys. Res. 91, 2719-2734 (1986).

- Chandra, S. J. geophys. Res. 91, 2719-2734 (1986).
 Gille, J. C. et al. J. geophys. Res. 89, 5179-5190 (1984).
 Russell III, J. M. Adv. Space Res. 4, (4), 107-116 (1984).
 Russell III, J. M. et al. J. geophys. Res. 89, 5099-5107 (1984).
 Heath, D. F., Donnelly, F. F. & Merrill, R. G. NOAA tech. Rep. No. ERL 424-ARL7 (1983).
 Brasseur, G., De Rudder, A., Keating, G. M. & Pitts, M. J. geophys. Res. (submitted).
 Brasseur, G., De Rudder, A. & Roucour, A. in Proc. int. Conf. Environmental Pollution, 839-910 (University of Thessalonika, 1982).
- Res. 86, 7343-7362 (1981).
- 15. Brasseur, G. & Simon, P. C. J. geophys. 16. Biaumé, F. J. Photochem. 2, 139-149 (1973).
- 17. Crutzen, P. & Schmailzl, U. Planet. Space Sci. 31, 1009-1032 (1983).
- 18. Demore, W. B. et al. Jet Propulsion Lab. Publ. No. 85-37 (1985).

Novel experimental investigation of spontaneous ignition of gaseous hydrocarbons

J. F. Griffiths & W. Nimmo

Department of Physical Chemistry, The University, Leeds LS2 9JT, UK

Studies of spontaneous ignition of gases under rapid compression 1-3 are directed mainly towards understanding 'knock' in sparkignition engines and the duration of ignition delays in diesels. The relevance to engine combustion lies in the ability to investigate the effects of fuel structure on the development of spontaneous ignition (arising either in different isomers of a hydrocarbon or due to reaction of mixtures of different hydrocarbons), while avoiding complicating practical features such as droplet evaporation, induction and exhaust of the charge, reciprocating piston motion and cycle-to-cycle variations. We report here a novel development, in which a variable-speed impeller in the combustion chamber of a rapid compression apparatus is used, first, to bring about spatial uniformity of temperature and concentration throughout the ignition delay period and, second, to enhance the rate of heat dissipation by successive increases in the speed of rotation. We show that, at given conditions for rapid compression, spontaneous ignition ceases to be possible beyond a limiting rotor

The single-shot rapid compression machine⁴ is operated at a compression ratio ($V_{\text{initial}}/V_{\text{final}}$) of 10.6:1 and at a combustion chamber temperature (T_a) of 293 K. During operation the piston

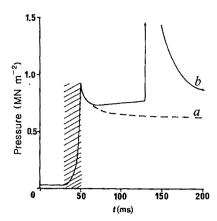


Fig. 1 Pressure-time records for non-reactive (a) and reactive (b) compositions compressed rapidly under identical conditions in the absence of mechanical stirring. Ignition occurs after a delay of 80 ms from the time when rapid piston motion ceases. The shaded area represents the interval during which rapid piston motion takes placed. The zero of time is selected by the microcomputer control system.

travels 23.2 cm from its initial position in ~22 ms and on completion of its stroke has compressed the pre-loaded (33.0 kN m pre-mixed gaseous reactants into a squat cylindrical chamber of volume 31.9 cm³ and depth 1.92 cm. End-of-compression pressures are ~0.9 MN m⁻² (~9 atm) yielding, at the moment the piston stops, gas temperatures (T_c) of 775 K in the present study. A virtually ideal adiabatic compression is achieved, and so this temperature is determined by the relationship $T_c/T_a = (V_i/V_t)^{\gamma-1} = (P_t/P_i)^{\gamma-1/\gamma}$, where γ is the ratio of the principal specific heats of the reactant mixture. Our choice of initial composition, 0.03 $nC_4H_{10}+0.20 O_2+0.77$ Ar, is governed by the desire to achieve the highest possible initial temperature, using the present mechanical system, in reactants that mimic 'typical' hydrocarbon-air mixtures in engines. Thus a stoichiometric proportion of fuel to oxygen is used, but the nitrogen is substituted by argon so as to augment γ as far as possible. The highest value for γ is that of the monatomic gases ($\gamma = 5/3$), but only in this limit is γ independent of temperature. In practice, for mixtures of gases, γ is derived at the compression temperature by an iterative procedure using a second-order polynomial representing the molar heat capacity as a function of temperature for each component of the system.

Butane, in its isomeric n- and iso-forms, is the simplest hydrocarbon with which the effect of structural change on the spontaneous ignition behaviour of hydrocarbons can be investigated. Its gaseous state is preserved throughout the course of compression. This report concerns only n-butane.

Pressure changes that take place during compression, and afterwards in the closed, constant-volume chamber, are measured by a pressure transducer and recorded digitally. Because there is no significant loss of material by leakage and because the reactant is in sufficiently great dilution that only a very small change in the number of moles of material occurs during reaction, any pressure change measured during the postcompression period reflects a temperature change. Thus, in non-reactive compositions (Fig. 1, curve a) the gas temperature (and thus pressure) falls from its maximum at the end of piston travel due to heat loss to the walls. The pressure record can be used to calculate a mean gas temperature when heat transfer occurs only by residual gas motion due to the preceding piston motion. When vigorous mechanical stirring is introduced, the measured pressure is directly proportional to the spatially uniform gas temperature. Quantitative interpretations of heat release and dissipation rates may then follow³.

Curve b in Fig. 1 is the pressure record obtained, in the absence of stirring, in a reactive composition of the same heat

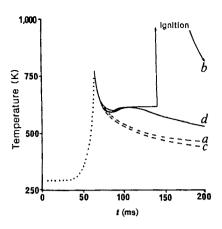


Fig. 2 Temperature-time records for non-reactive and reactive compositions following rapid compression with different rotor speeds. The dotted line represents the temperature change during the mechanical compression stroke. a, Non-reactive, stirring rate $850 \pm 50 \text{ r.p.m.}$; b, reactive, stirring rate $850 \pm 50 \text{ r.p.m.}$; c, nonreactive, stirring rate 1,100 ± 50 r.p.m.; d, reactive, stirring rate $1,100 \pm 50 \text{ r.p.m.}$

capacity as that associated with curve a. When piston motion ceases, the two curves at first show an identical cooling rate: the initial rate exceeds 3×10^4 K s⁻¹. The separation of curve b from curve a at 10 ms after compression shows that heat is being released from the exothermic oxidation of butane at a sufficient rate to augment the gas temperature. The mean temperature corresponds to 610 K at this time. During the next 70 ms the temperature increases monotonically (by ~50 K): thermal feedback is taking place. There is a critical transition to ignition 80 ms after rapid piston motion ceases, due not only to the enhanced reaction rate caused by the rising temperature but also to chain branching by means of organic peroxides formed as molecular intermediates during the ignition delay period⁵. Photographic records of the development of ignition in the chamber have been published elsewhere⁶.

Figure 2 shows temperature-time records derived from pressure histories obtained under the effect of mechanical stirring. The dashed curves (Fig. 2a, c) are from the cooling of a nonreactive composition when the rotor speed is raised from 850 (±50) to 1,100 (±50) revolutions per minute. An enhanced cooling rate is discerned after 10 ms into the post-compression period, once the initially dominant gas movement caused by rapid piston motion has subsided sufficiently. The corresponding records from reactive compositions at the respective rotor speeds are shown as solid curves (Fig. 2b, d). There is a failure of spontaneous ignition at the higher rotor speed (curve d) even though exothermic oxidation has taken place. Ignition has failed in this case because the heat release rate, which rises to a maximum and then begins to wane as the primary reactant concentration falls, is unable to maintain the gas temperature. The heat release rate diminishes to zero at 80 ms after compression (W.N., unpublished data). At marginally supercritical conditions (curve b), the heat release also falls virtually to zero just before hot ignition takes place, but as a consequence of the lower heat dissipation rate, the reactant temperature remains higher and chain branching becomes effective, giving rise to chain-thermal criticality⁷.

We thank SERC, EEC and UKAEA for financial support.

Received 20 February; accepted 18 April 1986.

- 1. Martinengo, A. & Homann, K. H. Oxidation and Combustion Reviews Vol. 2 (ed. Tipper,
- C. F. H.) 207-256 (Elsevier, Amsterdam, 1967). Fish, A., Haskell, W. W. & Reed, I. A. Proc. R. Soc. A313, 261-297 (1969).
- Griffiths, J. F. & Hasko, S. M. Proc. R. Soc. A393, 371 (1984).
 Beeley, P., Griffiths, J. F. & Gray, P. Combust. Flame 39, 255-268; 269-282 (1980).
- Griffiths, J. F. Adv. chem. Phys. 64, 203-303 (1986). Griffiths, J. F. & Nimmo, W. Combust. Flame 60, 215-218 (1985).
- 7. Gray, B. F. Trans Faraday Soc. 65, 1623-1613 (1969).

Climatic change and Aboriginal burning in north-east Australia during the last two glacial/interglacial cycles

A. P. Kershaw

Department of Geography, Monash University, Clayton, Victoria. Australia 3168

Long palynological records from continental deposits may be divided into two categories: detailed sequences seldom extending back much further than the most recent interglacial 1-3, and more generalized or discontinuous sequences which cover all or a substantial part of the Quaternary⁴⁻⁶. I present here a record which is unusual in that it provides, in some detail, changes through a period considered to embrace the last two glacial/interglacial cycles. It provides the opportunity to compare the results of climatically-induced changes at corresponding stages within the two cycles and also to assess the impact of Aboriginal people on the vegetation. People have been present in Australia for the past 40,090 years⁷ and possibly as long ago as the last interglacial period⁸, but are unlikely to have been present before this.

The record presented here is an extension of that described previously from Lynch's Crater on the Atherton Tableland⁹⁻¹². Figure 1 shows selected results, including percentages of major gymnosperm and angiosperm big-tree taxa derived from rainforest, and the most common canopy tree taxa from open sclerophyll vegetation, together with a summary of the relative proportions of all pollen from these three groups. Six major zones are recognized, of which the top four have been described previously¹¹. Zones G, E and A are dominated by pollen from rain-forest angiosperms, zones F and D contain high percentages of the rain-forest gymnosperms Araucaria and Podocarpus together with a substantial sclerophyll component, and zone B is dominated by the sclerophyll taxa. Zone C is transitional between rain-forest and sclerophyll-dominated periods. A timescale has been determined for the past 40,000 yr from radiocarbon dates and estimated beyond this time by applying known rates of accumulation of similar sediments from sites within the region to sections of the core, taking into account the degree of sediment compaction¹³.

A large degree of vegetation variation can be explained as a response to climatic change, particularly precipitation. Very high values for rain-forest angiosperms in zones G, E and A indicate domination by complex rain-forest existing in high rainfall conditions. Slightly higher gymnosperm values and higher percentages of Elaeocarpus relative to Cunoniaceae in subzone E1 than in zone A and subzones G2 and E3 suggest that precipitation did not reach equivalent levels, while generally higher sclerophyll and rain-forest gymnosperm percentages in subzones G1 and E2 indicate that effective precipitation was lower still.

Sharp reductions in precipitation are suggested at the beginning of zones F and D by substantial rises in sclerophyll taxa, particularly Casuarina, and the gymnosperm Araucaria. Subzone D2 can be separated on the basis of a higher rain-forest angiosperm component and a peak in Elaeocarpus, which signify slightly wetter conditions. The increases in sclerophyll taxa through zone C and their predominance in zone B are difficult to interpret in climatic terms, but precipitation was certainly no higher than in the period represented by zone D.

The best-estimate precipitation curve in Fig. 1 is based on information derived from modern pollen samples10 and on the known ecology of individual plant taxa and vegetation types. A more cautious precipitation estimate is shown as a range calculated mainly from bioclimatic analyses¹⁴ undertaken on an extensive Australian rain-forest data set15. The range is one standard deviation from the mean annual precipitation calculated for the most likely predominant structural vegetation type 16

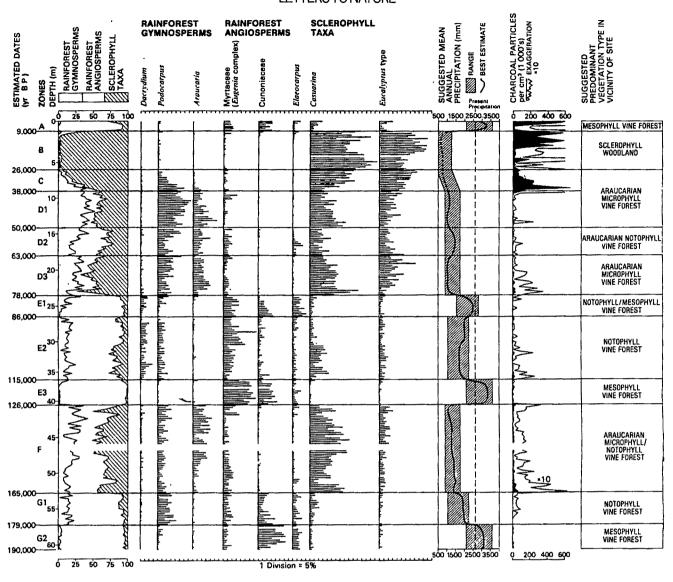


Fig. 1 Selected attributes of pollen diagram from Lynch's Crater. The frequencies of pollen of all taxa are shown as percentages of the dry-land-plant pollen total.

surrounding the pollen site during the period represented by each zone.

A comparison of the precipitation curve with that from the deep-sea core V28-238¹⁷ (Fig. 2) reinforces the suggestion from analyses of the more recent part of the record that precipitation changes within this area have been largely controlled by global changes in sea level and/or sea surface temperatures¹⁸.

Despite the strong climatic control of vegetation variation, there are some features of the record which cannot be explained by climate alone. One example is the inconsistent performance of Eugenia complex, particularly within the high-precipitation 'interglacial' periods represented by zones G2, E3 and A. This is at least partly related to the inclusion in the taxon of several different species with various ecological requirements and differential pollen production and dispersal capabilities. This is a common problem of palynology in areas dominated by highly diverse communities. A second feature is the attainment of somewhat different percentages by taxa and taxon groups in corresponding phases of the two identified cycles. This applies most obviously to the attainment of higher levels of gymnosperms within the penultimate glacial. The preferred explanation here relates to the general infilling of the lake basin and its effects on pollen influx. With the extension of swamp over the lake basin, it is probable that the inwash pollen component, likely to have been dominated by lake-edge angiosperms with poor aerial pollen dispersal, would have been reduced. This would have effectively increased the proportions of wind-dispersed, more regional pollen such as that from the gymnosperms.

The most important difference between the two cycles is the almost total replacement of rain-forest by sclerophyll vegetation towards the end of the most recent dry period. It was originally proposed that a change in climate could not alone have brought about this change because of the potential of 'drier' rain-forest to survive mean annual precipitation levels as low as 600 mm on basaltic soils such as those surrounding the site, and because of the extinction of *Dacrydium* and perhaps other taxa which must have been equipped to survive the vicissitudes of Quaternary climates^{9,10}. Instead, an increase in burning, most probably due to the activities of Aboriginal people, was proposed as the most likely cause. Subsequently, charcoal analyses on the core sediment indicating a sharp increase in burning about 38,000 yr ago (see Fig. 1) gave some support to this interpretation⁸.

The evidence presented here, that sclerophyll vegetation did not totally replace rain-forest during the penultimate 'dry glacial' period in contrast to the last 'glacial', is strong support for a

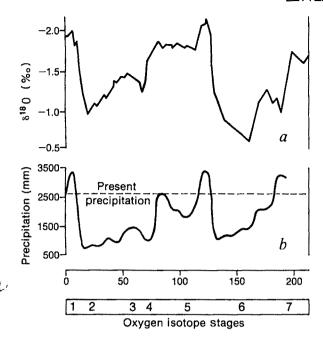


Fig. 2 Comparison of the precipitation curve derived from Lynch's Crater (b) with the oxygen isotope curve from deep-sea core V28-238 (a). Oxygen isotope stages from ref. 17.

recent increase in burning. Furthermore, the nature of the change from araucarian vine forest to sclerophyll vegetation can be shown to be different from other major changes in the record for which a climatic cause is invoked. Most changes from one zone to another are abrupt, and span perhaps only a few hundred years. Small charcoal peaks accompanying many of these changes suggest a role for fire in facilitating the climatically controlled transition from one vegetation state to another, as has been proposed for vegetation changes elsewhere 19-21. By contrast, the change to sclerophyll vegetation is gradual, taking as long as the period represented by zone C, perhaps ~12,000 yr. It is best explained as a gradual replacement of fire-sensitive rain-forest by fire-promoting sclerophylls under a regime of frequent burning of the sclerophyll vegetation.

I thank C. Shaw, L. Head, S. Matiske, R. Phelps, I. Sluiter, G. Werren and Professor B. Thom for help with drilling, and the Australian Research Grants Scheme for finance.

Received 3 February; accepted 4 April 1986.

- 1. Adam, D. P. & West, G. J. Science 219, 168-170 (1983).
- Hauser, C. J. Quat. Res. 16, 293-321 (1981). Woillard, G. M. Quat. Res. 9, 1-21 (1978).
- Honghiemstra, H. Vegetational and Climatic History of the High Plain of Bogota, Colombia (Cramer, Lichtenstein, 1984).
 Singh, G., Opdyke, N. D. & Bowler, J. M. J. geol. Soc. Aust. 28, 435-452 (1981).

- Fuji, N. & Horie, S. Proc. Jap. Acad. 4, 500-504 (1972).
 Pearce, R. H. & Barbetti, M. Archaeol. phys. Anthropol. Oceania 16, 173-178 (1981). Pearce, R. H. & Barbetti, M. Archaeol, phys. Aninropol. Oceania 16, 173-178 (1981).
 Singh, G., Kershaw, A. P. & Clark, R. in Fire and Australian Biota (eds Gill, A. M., Groves, R. A. & Noble, I. R.) 23-54 (Australian Academy of Sciences, Canberra, 1981).
 Kershaw, A. P. Nature 251, 222-223 (1974).
 Kershaw, A. P. New Phytol. 77, 469-498 (1976).

- Kershaw, A. P. New Phytol. 71, 469-498 [1916].
 Kershaw, A. P. Neure 272, 159-161 (1978).
 Kershaw, A. P. New Phytol. 94, 669-682 (1984).
 Kershaw, A. P. Proc. Fourth int. Palynol. Conf., Lucknow 3, 28-35 (Birbal Sahni Institute of Palaeobotany, Lucknow, 1980).
- Nix, H. A. in National Rainforest Study Report (eds Werren, G. L. & Kershaw, A. P.)
 421-425 (Geography Dept. Monash University, Clayton, 1984).
- Webb, L. J., Tracey, J. G. & Williams, W. T. Aust. J. Ecol. 9, 169-198 (1984).
 Webb, L. J. Aust. Plants 9, 349-363 (1978).
- 17. Shackleton, J. J. & Opdyke, N. D. Quat. Res. 3, 39-55 (1973).
- 18. Kershaw, A. P. in Quaternary Studies (eds Suggate, R. P. & Creswell, M. M.) 181-187

- Kersnaw, A. P. in Quaternary Studies (eds Suggate, K. P. & Creswell, M. M.) 181-187 (Royal Society of New Zealand, Wellington, 1975).
 Green, D. G. J. Biogeog. 9, 29-40 (1982).
 Hooley, A. D., Southern W. & Kershaw, A. P. J. Biogeog. 7, 349-362 (1980).
 Walker, D. in The Plant Community as a Working Mechanism (ed. Newman, E. I.) 27-43 (1980). (Blackwell, Oxford, 1982).

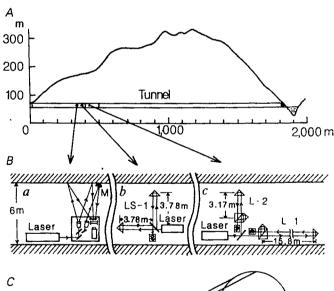
Application of laser holographic techniques to investigate crustal deformations

Shuzo Takemoto

Disaster Prevention Research Institute, Kyoto University, Kyoto, 611 Japan

Laser holographic techniques can be used to detect small deformations of three-dimensional objects, of the order of the wavelength of the laser light. We report the use of laser holography to measure the crustal deformation in a deep tunnel at Amagase, Kyoto, Japan. A recording system consisting of a helium-neon gas laser and associated optical elements was installed in the observation tunnel in 1984. Using this sytem, holograms of a section of the tunnel wall ~2 m in diameter are directly recorded on photographic plates. When the reconstructed image of a hologram is superposed on the current ('real-time') image of the tunnel wall, many interference fringes can be seen through the developed photographic plate. The fringe displacement, formed by the deformation of the tunnel, is continuously monitored with a video camera and a video-cassette recorder. The measured fringe displacement in the interference pattern is consistent with strain changes obtained from extensometers which have been installed in the same tunnel.

Observations of crustal deformation have been commonly made with extensometers by continuously measuring the relative displacement between two piers fixed into the bedrock. The



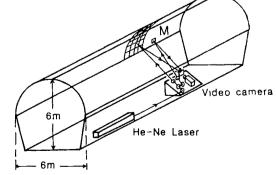


Fig. 1 A, Topographic profile of the Amagase tunnel. B, Arrangement of the laser holography system and laser extensometers installed in the tunnel. C, Isometric view of the laser holography system, comprising a He-Ne laser, optical mirrors and lenses, a photographic plate and a video camera.

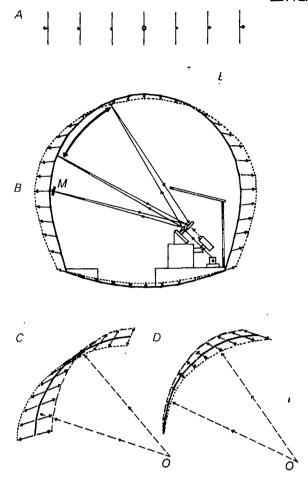


Fig. 2 Tunnel deformation calculated with the two-dimensional finite element method. A, Uniform strains in the absence of the tunnel due to a uniaxial tensile stress. B, Displacements around the horseshoe-shaped tunnel caused by the tensile stress which would produce uniform strains in the absence of the tunnel. C, Displacements of the tunnel wall relative to point O, where optical elements, except the reference mirror (M), are fixed. Dotted line, displacements due to tensile stress; dashed line, displacement due to compressive stress. D, Displacements of the tunnel wall relative to point M. Dotted and dashed lines as in C.

early developments of these instruments were due to Benioff¹, Ozawa² and Takada³. Their extensometers, using length standards of fused quartz tubes or super-invar bars, have been installed in many observatories for investigating secular strains, tidal strains and low-frequency seismic waves. Extensometers of this type, however, suffer from the disadvantages inherent in length standards of solid material, that is, deformation of the length standards themselves and frictional forces between length standards and their supports. In contrast, laser extensometers are free from these disadvantages because they are capable of detecting linear strains without using length standards of solid material. Various instruments have been developed by a number of groups in the past two decades⁴⁻¹¹. In addition, unlike conventional extensometric methods, which can detect only onedimensional linear strains, the holographic method can detect two- or three-dimensional strain patterns.

Laser holography has been used to measure tunnel deformation at the Amagase Crustal Movement Observatory since 1984. A laser holographic recording system was installed 320 m from the entrance of a disused tunnel of length 1,830 m. The section of the tunnel has a horseshoe shape, with a diameter of ~ 6 m. The observation site is ~ 130 m below the surface. The annual variation of air temperature at the observation site is ~ 0.2 °C

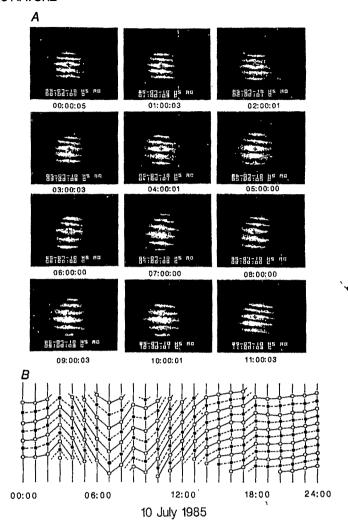


Fig. 3 A, Examples from 10 July 1985 of interference fringes superposed on the holographic image of the tunnel wall, on which the standard mark '+', has been drawn with black paint. B, Hourly plots of fringe displacements measured along the vertical line (~1 m) passing through the standard mark '+'. Open and filled circles represent bright and dark fringes, respectively. The plots are inverted (upside-down), for convenince of comparison with Fig. 4.

and its daily variation is <0.05 °C. The amplitude of microtremor measured in the tunnel does not exceed 20 nm s⁻¹ at \sim 0.1-10 Hz. These quiet circumstances allow us to obtain clear holograms of objects having a dimension of \sim 1 m. Figure 1 shows the arrangement of the holographic recording system together with three laser extensometers (L-1, L-2, LS-1) which have been installed in the same tunnel.

The holographic recording system consists of a helium-neon gas laser with an emission power of 50 mW, optical mirrors and lenses, a video camera and a video-cassette recorder. Optical elements, with the exception of a reference mirror, are fixed with magnetic holders to a massive steel plate (60 × 90 cm) which is fastened to a concrete base on the floor. The reference mirror ('M' in Fig. 1c) is attached to the tunnel wall with anchor bolts. The laser source is set on another concrete base and covered by polystyrene boards. A coherent light beam emitted from the laser source is split into two beams at the surface of the beam splitter, which deflects ~5% of the light beam and transmits the remaining portion. The former is used as a reference wave and the latter illuminates an area of the tunnel wall ~2 m in diameter. Two waves, reflected from the reference mirror and the tunnel wall, respectively, are superposed on a photographic plate (Agfa 10E75) measuring 6.5×9 cm. After an exposure of

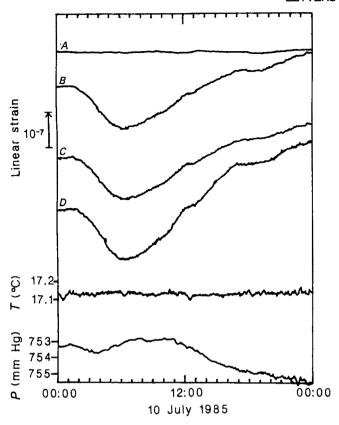


Fig. 4 Strain changes observed with laser extensometers installed in the Amagase tunnel [A, (L-1); B, (L-2); C, ((L-2)-(L-1)); D, (LS-1)], together with thermometric and barometric records on 10 July 1985.

~1-3 min, the photographic plate is developed and fixed. The developed plate is used as the original hologram, and is carefully reset in the position at which the hologram was taken. By again illuminating the plate with the same reference wave, the holographic image of the tunnel wall is reconstructed. In this procedure, the plate is slightly inclined from the original position. A number of dark and bright lines ('fringes') over the object image can then be seen on the hologram: these are caused by the interference of two waves; one reconstructed from the hologram and the other scattered directly by the tunnel wall. The movements of these interference fringes enable us to estimate the tunnel deformation.

We now calculate strain changes in a long tunnel which is assumed to be driven in an infinite, homogeneous, isotropic, elastic medium. Because the change in strain components along the tunnel axis can be assumed to be negligibly small compared with that across the tunnel, calculations are made with the two-dimensional finite element technique under the plane-strain condition. Results of the calculations are illustrated in Fig. 2B-D. Figure 2B shows displacements around the tunnel due to the uniaxial tensile stress which would produce uniform strains (Fig. 2A) in the absence of the tunnel; Fig. 2C and D show displacements of the tunnel wall relative to the points 'O' and 'M', respectively. Fringe displacements in the interference pattern at the Amagase tunnel are predicted from these figures. If the developed photographic plate is adjusted to produce interference fringes parallel to the direction of tunnel axis, upward and downward displacements of fringes and changes in their width should be observed: the former correspond to the mean displacement of the tunnel wall relative to point O and the latter correspond to the tilt of the tunnel wall relative to point M.

Figure 3 shows examples of fringe patterns recorded with the video-cassette recorder, together with hourly plots of their position on 10 July 1985. The drift of the fringe indicates an initial

upward trend, reversing at 03:00 and again at 07:00. The fringe width is narrowest at 03:00 and widest at 07:00.

The holographic results may be compared with the strain changes measured by laser extensometers.

Figure 4A and B are the linear strains measured by laser extensometers L-1 and L-2, with a frequency-stabilized laser source and mutually perpendicular evacuated light paths. As shown in Fig. 1B, L-1 is oriented along the tunnel and L-2 across the tunnel. The curve in Fig. 4C shows the difference between these two components of linear strain ((L-2)-(L-1)). The curve in Fig. 4D shows the strain measured by a new type of laser extensometer¹⁰ which has a simple, unstabilized laser source and two light paths of equal length, and detects the difference between two axial linear strains. (LS-1) is thus equivalent to (L-2) – (L-1). The strain change along the tunnel (L-1) is smaller by an order of magnitude than that across the tunnel, (L-2): this is explained by the cavity effect¹². Therefore, (L-2) - (L-1) and (LS-1) are nearly equal to (L-2), which has a maximum at 02:00 and a minimum at 07:00 on 10 July.

The trends of the strain changes observed with extensometers are consistent with those of the fringe displacements in the interference pattern shown in Fig. 3B. Thus, the fringe displacements observed with the laser holographic method are indicative of the tunnel deformation caused by tectonic and tidal stresses. In addition, the change of the fringe width is probably related to the tilt of the tunnel wall. This method is likely to prove useful in the observation of crustal deformation.

I thank Drs Torao Tanaka, Yoshimasa Kobayashi and Kojiro Irikura for critical reading of the manuscript.

Received 31 December 1985; accepted 12 March 1986.

- Benioff, H. Bull, seism. Soc. Am. 25, 283-309 (1935).
- Ozawa, I. Bull. Disast. Prev. Res. Inst. Kyoto Univ. 6, 2-35 (1957). Takada, M. Bull. Disast. Prev. Res. Inst., Kyoto Univ. 8, 1-27 (1959).
- Van Veen, H. J., Savino, J. & Alsop, L. E. J. geophys. Res. 71, 5478-5479 (1966). Vali, V. & Bostrom, R. C. Rev. scient. Instrum. 39, 1304-1306 (1969).

- Vall, Y. & Dostolin, N. C. Rete steeln. Institute, 39, 1904-1904 (1907). Berger, J. & Lovberg, R. H. Rev. scient. Instrum. 40, 1569-1575 (1969). Levine, J. & Hall, J. L. J. geophys. Res. 77, 2595-2609 (1972). Goulty, N. R., King, G. C. P. & Wallard, A. J. Geophys. J.R. astr. Soc. 39, 269-282 (1974).
- 9. Takemoto, S. Bull. Disast. Prev. Res. Inst., Kyoto Univ. 29, 65-81 (1979).
 10. Takemoto, S. & Kobayashi, T. Ann. Disast. Prev. Res. Inst., Kyoto Univ. 25, 31-39 (1982).
- 11. Alyoshin, V. A., Dubrov, M. N. & Yakovlev, A. P. Dokl. Akad. Nauk SSSR 253, 1343-1346
- 12. Takemoto, S. Bull. Disast. Prev. Res. Inst., Kyoto Univ. 31, 211-237 (1981).

The Banda-Celebes-Sulu basin: a trapped piece of Cretaceous—Eocene oceanic crust?

Chao-Shing Lee* & Robert McCabe

Geodynamics Research Program and Department of Geophyics, Texas A&M University, College Station, Texas 77843, USA * Present address: Bureau of Mineral Resources, Geology and Geophysics, Canberra ACT 2601, Australia

The Banda, Celebes and Sulu basins are poorly understood marginal seas located at the junction of the Eurasian, Indian-Australian and Pacific-Philippine Sea plates. The incompleteness of the data sets, the complex geology of the surrounding islands and the late Cenozoic evolution involving subduction, rifting, transform faulting and island arc collision have complicated tectonic interpretation of the region. The Banda basin is underlain by oceanic crust¹⁻³. Bowin et al.² and Lapouille et al.³ have suggested that it is a trapped oceanic basin which was once continuous with the late Jurassic Argo Abyssal Plain off north-west Australia. Similarly, the Celebes and Sulu basins are also underlain by oceanic crust⁴⁻⁶. On the basis of newly identified magnetic reversal ages (Fig. 1), heat-flow data and on-land geological studies, we

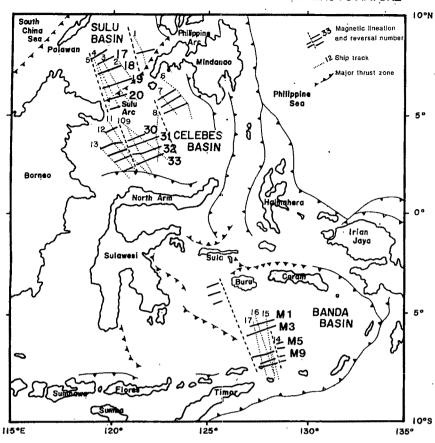


Fig. 1 Tectonic structure and magnetic anomalies in the Banda, Celebes and Sulu basins. Dotted lines are the ship tracks used for magnetic correlation in Figs 2-4. (The timescale used in this and succeeding figures is from refs 7 and 8.) These data are compiled from the global marine geophysical data set. The data sources are the Lamont-Doherty Geological Observatory (profiles 2, 4-6, 9-14 and 16), the Scripps Institute of Oceanography (1, 3, 7, 8 and 15) and the Woods Hole Oceanographic Institution (17). The tectonic structures are revised from Hamilton 16.

suggest that the Celebes and Sulu seas may have been continuous with the Banda basin. This Cretaceous-Eocene basin has been dissected into its present configuration by Tertiary tectonic processes

Re-analyses of the existing marine geophysical data suggest that the magnetic lineations in the Banda, Celebes and Sulu basins have similar trends, of about N70 °E, N60 °E and N55 °E, respectively. Although the incomplete data sets from each individual basin do not allow magnetic ages to be determined confidently, we believe that a combined analysis of the magnetic anomalies from all three basins does permit a tentative best fit to the geomagnetic reversal model^{7,8}. Our assignments are: (1) anomalies M1-M11 (111-123 Myr BP) in the Banda basin at a half-spreading rate of \sim 2.9 cm yr⁻¹; (2) anomalies 30-33 (65-72 Myr) in the Celebes basin at a half-spreading rate of ~3.9 cm yr⁻¹; and (3) anomalies 17-20 (41-47 Myr) in the Sulu basin at 4.2 cm yr⁻¹ (Figs 2-4). The magnetic anomalies in each of these three basins become younger toward the north. Similar north-east-trending late Jurassic anomalies have also been identified in the Argo Abyssal Plain⁹. These observations suggest that the Banda-Celebes-Sulu ocean basins were once part of a continuous basin, probably a northern extension of the eastern Indian Ocean¹⁰

Recent seismic reflection and side-scan sonar studies in the Banda Sea^{11,12} have shown that the central portion of this basin is composed of prominent north-east-trending ridges and faults. Dredge data, collected in coordination with these geophysical studies, suggest that these ridges represent slivers of a continental margin. The presence of these structural features in the central portion of the Banda Sea suggests that the basin may have a complex tectonic history and is presently dissected into two or more smaller basins. This complication aside, both our model and that of Lapouille et al.³ for the Banda basin suggest that the entire basin is early Cretaceous in age and becomes progressively younger to the north.

Heat-flow data from the three basins are qualitatively consistent with our assigned magnetic ages: the averaged heat-flow

data fit the Parsons and Sclater¹³ heat flow versus age curve for an oceanic basin. Thus, the Banda basin² is characterized by low heat-flow values, averaging 1.09 h.f.u. (1 h.f.u. = 1 μ cal cm⁻² s⁻¹ = 41.87 mW m⁻²), the Celebes basin^{6,14} by intermediate heat flow, averaging 1.38 h.f.u., and the Sulu basin¹⁴ by high heat flow; averaging 1.67 h.f.u. The fact that the heat-flow data show a good fit to the Parsons and Sclater curve also suggests that these basins are probably underlain by normal oceanic crust. (Heat flow in back-arc basins does not usually fit the global heat flow versus age curve¹⁵ this well.) The bathymetric data from the three basins also show a crude age-dependence, the Banda basin being the deepest and the basins to the north becoming progressively shallower.

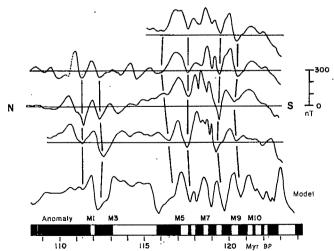


Fig. 2 Correlations of magnetic profiles with the geomagnetic timescale in the Banda basin. (The timescale used in this and succeeding figures is from refs 7 and 8.) The model is a phase-shifted synthetic magnetic profile with $\theta = -15^{\circ}$ where θ is the phase shift angle (see Schouten and McCamy³⁰).

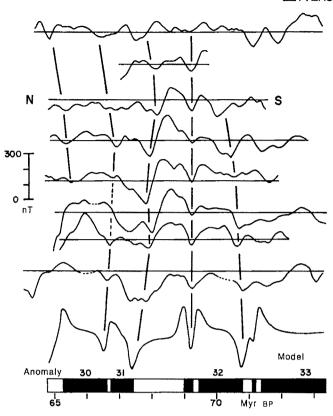


Fig. 3 Correlation of magnetic profiles with the phase-shifted synthetic model ($\theta = -330^{\circ}$) in the Celebes basin.

The region is complicated by numerous landmasses that divide this old oceanic basin into the present configuration of marginal seas (Fig. 1). We argue that each of these landmasses either arrived at its present location by late Tertiary tectonic movements or has been constructed in place upon this older oceanic basement. Below we briefly discuss the origin of these landmasses.

The Philippine Arc, a complex mixture of early Cretaceous to Recent island arc fragments and ophiolites¹⁶⁻¹⁹, appears to have been welded together in early to middle Tertiary time. Palaeomagnetic studies^{20,21} in the central Philippines show that this island arc has undergone motions that are consistent with the clockwise rotation of the Philippine Sea plate²². This suggests that the Philippines were located far to the south-east during the middle Tertiary. Northern Palawan is a microcontinent, composed of Palaeozoic rocks, which rifted away from southern China and translated southward during the Oligocene to Miocene opening of the South China Sea^{16,23,24}. The limited data for the Sulu Arc suggest that these islands are a late Neogene volcanic arc which developed in response to the southward subduction of the Sulu Basin¹⁶. Although the age of the island arc ophiolite is unknown, radiolarian cherts from eastern Borneo yield a late Cretaceous to Eocene age²⁵. This age is consistent with the suggestion that the basement is composed of pieces of the hypothesized Banda-Celebes-Sulu ocean basin.

Eastern Sulawesi is characterized by an ophiolite and mélange belt faulted against a metamorphosed sequence of marine strata¹⁶. Western Sulawesi, including the east-west-trending North Arm, is composed of folded sequences of Mesozoic and Tertiary metamorphic rocks, Cenozoic platform deposits and arc-derived volcanic and sedimentary rocks²⁶. Western Sulawesi probably rifted away from eastern Borneo during the middle Tertiary¹⁶. It has been suggested that the Neogene arc of the North Arm, a north-facing arc system, results from a change in subduction polarity and a clockwise rotation of the active arc16,27. Although Sulawesi now divides the Celebes and Banda

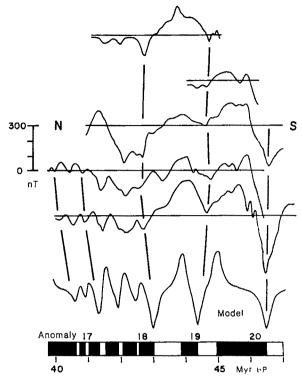


Fig. 4 Correlation of magnetic profiles with the phase-shifted synthetic model ($\theta = -270^{\circ}$) in the Sulu basin.

basins, we suggest that the separation of these two basins occurred during the Tertiary.

The islands of the north Banda basin, including Sula, Buru and Ceram, are composed of mélanges and continental rocks16. Stratigraphic models indicate that these islands were rifted continental fragments detached from Irian Jaya in the late Cenozoic and transported westward by strike-slip faulting28. Most of the south Banda basin islands are Neogene volcanic features developed in response to late Tertiary subduction around the Banda basin¹⁶. Timor is believed to be made up of portions of the foundered Australian crust incorporated into the upper plate during the Cenozoic 16,29. Before this Neogene tectonics, our model suggests that this ocean and Australia were part of the same plate.

Based on marine geophysical data we propose that the Banda, Celebes and Sulu basins formed a continuous ocean basin during Cretaceous to early Tertiary times. This hypothesis is supported by the fact that the various islands which currently fragment this older basin either arrived at their present location by middle to late Tertiary tectonic movements or were built in place by Neogene subduction. The trapped portions of old oceanic crust were further reduced in size by Neogene subduction beneath the Banda Arc, the North Arm of Sulawesi and the Sulu archinelago.

We thank Tom Hilde, Robin Lighty, Jay Cole and Chris Pigram for their comments and reviews. The research was supported by the United States Department of Energy, the Center of Energy and Mineral Resources at Texas A&M University and the Amoco Production Company. This is Texas A&M Geodynamics Program Contribution No. 49.

Received 21 March; accepted 8 April 1986.

- Purdy, G. M. & Detrick, R. S. J. geophys. Res. 83, 2247-2257 (1978).
- Bowin, C. O. et al. Bull. Am. Ass. Petrol. Geol. 64, 868-915 (1980).

- Lapouille, A. et al. Tectonophysics (in the press).

 Murauchi, S. et al. J. geophys. Res. 78, 3437-3447 (1973).

 Mascle, A. & Biscarrat, P. A. Mem. Am. Ass. Petrol. Geol. 29, 373-381 (1979).

 - Weissel, J. K. Monogr. Am. geophys. Un. 23, 37-47 (1980). Larson, R. L. & Hilde, T. W. C. J. geophys. Res. 80, 2586-2594 (1975)
- LaBrecque, J. L. et al. Geology 5, 330-335 (1977).
 Veevers, J. J. et al. Earth planet. Sci. Lett. 72, 415-426 (1985)

- 10. Hilde, T. W. C. et al. Tectonophysics 38, 145-165 (1977).
- Schwartz, D., Gill, J. B. & Silver, E. A., EOS 64, 872 (1983).
 Silver, E. A., Gill, J. B., Schwartz, D., Prasetyo, H. & Duncan, R. A. Geology 13, 687-691 (1985). 13. Parsons, B. & Sclater, J. G. J. geophys, Res. 82, 803-827 (1977).

- Sclater, J. G. et al. J. geophys. Res. 81, 309-318 (1976).
 Watanabe, T. et al. Maurice Ewing Ser. Am. geophys. Un. 1, 137-161 (1977).
- 16. Hamilton, W. Prof. Pap. U.S. geol. Surv. No. 1078, 1-345 (1979).
- 17. Karig, D. E. Tectonics 2, 211-236 (1983).
- McCabe, R. et al. Circum-Pacific Coun. Energy Miner. Res. 1, 421-436 (1985).
- 19. Hawkins, J. W. et al. Circum-Pacific Coun. Energy Miner. Res. 1, 437-463 (1985).
- 20. Hsu, I. thesis, Washington Univ. (1972).
- McCabe, R. Tectonics (in the press).
 Louden, K. J. geophys. Res. 82, 2989-3002 (1977).
- Taylor, B. & Hayes, D. E. Monogr. Am. geophys. Un. 27, 23-56 (1983).
- Holloway, N. H. Bull. Am. Ass. petrol. Geol. 66, 1355-1383 (1981).
 Haile, N. S. & Wang, N. P. Mem. Malay. geol. Surv. 16, 1-199 (1965).
- Sukamoto, R. & Simandjuntak, T. O. Bull. geol. Res. Dev. Cent. 7, 1-12 (1983). Silver, E. A. et al. J. geophys. Res. 83, 1681-1691 (1983).
- Visser, W. A. & Hermes, J. J. Verh. K. Ned. Geol. mijnb. Geroot 20, 1-265 (1962).
 Audley-Charles, M. G. Geol. Mag. 102, 267-272 (1968).
- 30. Schouten, H. & McCamy, K. J. geophys. Res. 77, 7089-7099 (1972).

Seismic measurements reveal a saturated porous layer beneath an active Antarctic ice stream

D. D. Blankenship, C. R. Bentley, S. T. Rooney & R. B. Alley

Geophysical and Polar Research Center, University of Wisconsin-Madison, 1215 West Dayton Street, Madison, Wisconsin 53706, USA

Seismic reflection studies recently conducted on ice stream B, part of the marine ice sheet of West Antarctica, show a metres-thick layer immediately beneath the ice in which both compressional (P) and shear (S) wave speeds are very low. These low wave speeds imply that the material in the layer is highly porous and is saturated with water at a high pore pressure. From this, and from arguments presented in an accompanying paper to the effect that the layer would be too weak to support the shear stress exerted by the overlying ice, we conclude that the layer is deforming and that the ice stream probably moves principally by such deformation.

For the past decade, the stability of marine ice sheets (ice sheets grounded below sea level) has stood as a fundamental unsolved problem in glaciology. In particular, the West Antarctic ice sheet has been of concern because of the possibility that it might shrink rapidly in response to climatic warming, thus raising sea level by ~5 m. But no understanding of the dynamics of the West Antarctic ice sheet is possible until the processes and interactions that govern the development and movement of ice streams, by far the most active parts of the ice sheet, are understood.

Consequently, a major program was initiated in 1983 to study the West Antarctic ice streams that feed into the Ross Ice Shelf and their interaction with that ice shelf. One aspect of this program is a concentrated geophysical study at a site on ice stream B (Fig. 1), aimed at learning more about the nature of the contact zone between the ice stream and its bed, because in this zone lies the crucial determinant of ice movement. Glaciologists agree that water lubrication must be an important factor in allowing ice streams to move so rapidly despite small driving stresses (small surface slopes), but just how the water effects the rapid sliding—whether it acts through the mechanism of a thin, approximately uniform sheet, through channels incised in the underside of the ice, or through some other mechanism—is

The field survey during the first season of the program (1983-84) comprised seismic recordings at ~300 sites along three lines at angles of 60° to one another, over an area of $\sim 10 \text{ km}^2$. Geophone spreads were generally ~720 m long, with 30-m geophone spacings. All three components of motion were recorded so as to yield both P-wave and S-wave arrivals. Shots ranging

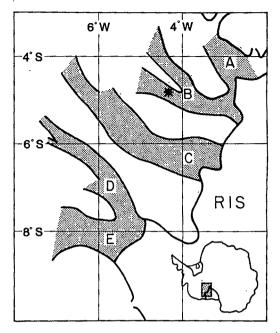


Fig. 1 Location map of ice streams along the Siple Coast of West Antarctica. An index map of Antarctica is in the lower right-hand corner. RIS, Ross Ice Shelf. Stippled areas are ice streams; the measurement site on ice stream B is marked by an asterisk. Standard grid coordinates are shown: in this rectangular system, 0° of longitude lies along the Greenwich meridian; and 0° of latitude passes through the South Pole.

in size from 0.15 to 0.45 kg were fired in shot holes ~20 m deep at spread centres and at various distances up to 4 km from the ends of the spreads. All the data were recorded on a digital recording system which was designed and built at the Geophysical and Polar Research Center. The system has a dynamic range of 84 dB and, for these experiments, sampled each of 24 channels at 0.4-ms intervals.

The existence of two reflectors near the base of the ice is seen very clearly in the seismogram of Fig. 2. In this example, the second echo is actually stronger than the first. The entire doubleecho pattern is repeated 21 ms later in secondary ('ghost') seismic waves that have travelled upward from the shot to be reflected first from the surface of the glacier and then from the bed. All of the travel times in Fig. 2 have been reduced for 'normal move-out', so that reflections from a flat, level surface

Table 1 Porosities calculated by comparing v_p as measured on ice stream B with laboratory measurements

Sample	f (kHz)	$\frac{\Delta v_{\rm p}}{({ m m~s}^{-1})}$	Porosity	Ref.
Sand	1,000	100	0.38 ± 0.10	11
Variety of marine	•			
sediments	200	35	0.45 ± 0.18	12
Clayey silt	400	10	0.38 ± 0.10	13
Shallow water				
clayey silt	400	10	0.39 ± 0.09	13
Lake Erie sediments	330	0	0.41 ± 0.13	14
Artificial sands	250	100	0.33 ± 0.07	15
	Unweigh	ted mean	0.39 ± 0.06	

f is the frequency in the laboratory measurements, and Δv_p is the velocity correction relative to low frequency. Error figures on porosities correspond to a velocity uncertainty of ±120 m s⁻¹, compounded, in an r.m.s. sense, of the uncertainty in measured velocity of $\pm 100 \text{ m s}^{-1}$, and assumed uncertainty in Δv_p of $\pm 50 \text{ m s}^{-1}$, and a characteristic r.m.s. scatter in the laboratory data of $\pm 40 \text{ m s}^{-1}$. We use an unweighted mean because we view all of the standard deviations as equally valid estimates of a single value applicable to all the measurements.

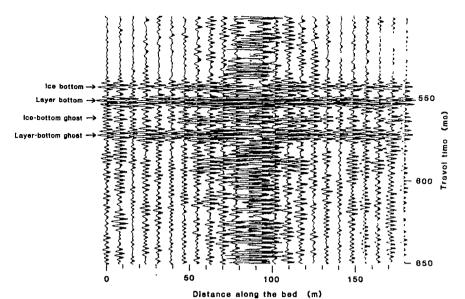


Fig. 2 Seismogram showing ice-bottom, layerbottom, and ghost echoes, as marked. All traces have been adjusted for 'normal move-out'.

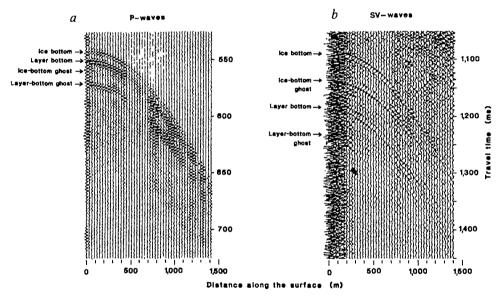


Fig. 3 Sequences of seismograms depicting 'wide-angle' (oblique) reflections. Not corrected for normal move-out. a, P-wave reflections; b, SV-wave reflections.

will appear at the same time regardless of the different horizontal distances between the shot and the various geophones.

The seismogram of Fig. 2, which was recorded along a direction parallel to the ice movement, depicts two level, coherent, reflecting surfaces separated by a travel-time difference (δt) of 10 ms. At a P-wave speed (v_p) in the layer of 1,600 m s⁻¹, that value of δt corresponds to a layer 8 m thick.

The wave speed in the layer was determined by means of 'wide-angle' (oblique) reflections over the section shown in Fig. 2. (The change in the travel-time difference between the two reflections as the shot and detectors are moved symmetrically outwards from the centre in opposite directions is a measure of the wave speed between the two reflectors.) The wide-angle profile (Fig. 3a) reveals that there is little change in the reflection-time difference between the two reflectors, which means that v_p in the layer is low compared with v_p in the ice (3,830 m s⁻¹). Thus, we are not seeing a basal layer within the ice. Numerical inversion of the wide-angle travel times yielded $v_p = 1,600 \pm 100 \,\mathrm{m \, s^{-1}}$ in the layer. This precision was made possible by the large signal-to-noise ratio and the high frequency of the echoes, which permitted a timing precision of 0.2 ms. The inversion procedure fully considers the dip of both the top and bottom of the layer as well as the ray bending caused by the vertically inhomogeneous velocity structure near the surface of the ice stream.

S-wave reflections from the upper and lower surfaces of the layer were recorded also (Fig. 3b), but with a δt that is 11 times as great as that for P-waves. This indicates an S-wave speed (v_s) of only $150\pm10~{\rm m~s^{-1}}$ in the layer. In the Earth, v_s values this low are found only in very porous material under low effective (differential) pressure (the difference between the overburden pressure, which tends to force the grains more tightly together and thus increase the rigidity of the solid framework of the sediment, and the pore-water pressure, which tends to weaken the contact between the grains). Beneath ice stream B this must mean a saturated sediment, in which the weight of the thousand metres of overlying ice is supported principally by the pore fluid

Along the direction of ice movement the subglacial reflecting horizons are clearly parallel to the ice bottom (Fig. 4a). The occurrence of more than one reflector suggests some stratification within the layer; the indicated strata are all nearly flat in the upstream-downstream direction. Transverse to the ice movement, however, there is much less continuity in the subglacial reflectors, and several sloping features appear (Fig. 4b). Most striking is the hump, occurring at ~ 0.8 km along the profile, that seems to rise near, or even to, the base of the ice. Since no deeper reflectors can be seen, it appears that

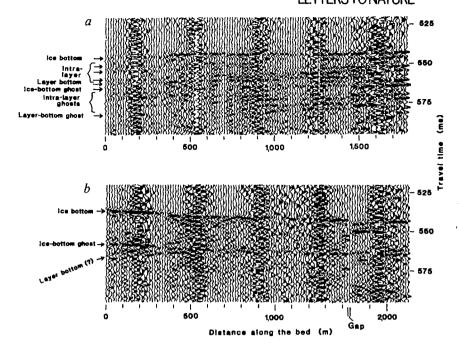


Fig. 4 Seismic reflection sections, each comprising five individual seismograms. Corrected for normal move-out. a, Section parallel to direction of ice movement; b, section transverse to ice movement.

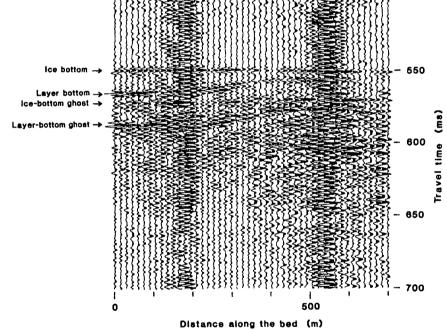


Fig. 5 Seismic reflection section transverse to ice movement, comprising two individual seismograms. Corrected for normal move-out.

locally, the layer nearly or entirely pinches out. Another section transverse to the ice stream (Fig. 5) shows a coherent layer-bottom reflection across the entire 0.8 km with a clear topographic relief of 8 m (10 ms). The maximum layer thickness on this section is 12 m (15 ms). From the available data we estimate an average thickness of 5 or 6 m.

The picture that emerges from the longitudinal and transverse sections is one of ridges and valleys in the basal surface of the sub-glacial layer, trending parallel to the axis of the ice stream. The alignment of these features along the direction of movement suggests that they are formed by erosion. It is significant to our model of a deforming bed¹ that there is no reflection of the ridges and troughs in the glacial/sub-glacial interface.

In a porous, saturated sediment, v_p depends primarily on the porosity n (and therefore the density), whereas v_s is most sensitive to the effective pressure ΔP . We can therefore estimate both n and ΔP using the v_p and v_s we have observed for the layer. Because $v_s \ll v_p$, both the rigidity and the incompressibility of the sedimentary frame are small compared with the bulk incom-

pressibility, κ , which then can be expressed simply as $\kappa = [(1-n)\beta_s + n\beta_w]^{-1}$, wherein β_s and β_w are the compressibilities of the sedimentary particles and the water, respectively. For a typical rock particle, we take $\beta_s = 2.6 \times 10^{-11} \,\mathrm{m}^2 \,\mathrm{N}^{-1}$, and for fresh water at $0 \,^{\circ}\mathrm{C}$, $\beta_w = 5.0 \times 10^{-10} \,\mathrm{m}^2 \,\mathrm{N}^{-1}$. From the seismic measurements, on the other hand, $\kappa = \rho v_p^2$, where the bulk sediment density $\rho = (1-n)\rho_s + n\rho_w$; ρ_s is the density of the sedimentary particles and ρ_w is the density of fresh water. We take $\rho_s = 2.6 \times 10^3 \,\mathrm{kg} \,\mathrm{m}^{-3}$ and $\rho_w = 10^3 \,\mathrm{kg} \,\mathrm{m}^{-3}$. Equating the two expressions for κ , we obtain $n = 0.365 \pm 0.075$ for $v_p = 1.600 \pm 100 \,\mathrm{m} \,\mathrm{s}^{-1}$.

Comparisons can also be made with laboratory and in situ measurements of v_p versus n in saturated sediments, but two corrections are needed. First, because most of the published values of v_p refer to sediments saturated with sea water and are corrected approximately to standard laboratory temperature and pressure, we must add a correction of $100 \, \mathrm{m \ s^{-1}}$ (ref. 7) to our measured velocity, which refers to fresh water at $0 \, ^{\circ}\mathrm{C}$ and a glaciostatic pressure of $9 \, \mathrm{MPa}$.

Table 2 Effective pressures (ΔP) calculated by comparing v_s as measured on ice stream B with laboratory measurements

Sample	ΔP (kPa)	Ref.
Artificial sand	40 ± 5	15
Silt	60 ± 5	16
Silty clay	30 ± 5	16
Potter's clay	120 ± 5	16
Marine silt-clays	70 ± 50	17*
Angular-grained material	15 ± 5	17†
Sands	25	18
Clays and silts	60	18
Unweighted mean	50±40	

Error figures for ΔP correspond directly to a velocity uncertainty of ±10 m s⁻¹ except in the case of the marine silt-clays¹⁷, for which a range of observed curves was taken into account. In calculating the standard error estimate for the mean, we have assumed a standard deviation of ± 50 kPa in ΔP for each sample.

* From Fig. 2 in ref. 17, using the supplementary relation: depth= $\Delta P/(\rho-\rho_{\rm w})g$, where g is the acceleration of gravity.

† From equation (6) in ref. 17.

Second, most laboratory measurements are made at frequencies between 100 kHz and 1 MHz, whereas our seismic frequencies are only ~ 400 Hz. Standard Biot theory^{8,9} with n = 0.4 (to be justified below) leads to a limiting high-frequency wave speed that is ~100 m s⁻¹ higher than the low-frequency speed. We have, therefore, added to our field measurements approximate frequency-effect corrections (Δv_p in Table 1) calculated according to standard theory¹⁰. These corrections are in approximate agreement with those measured for 1 MHz for various sediments, but because Δv_p depends on permeabilities in the sediment samples that had to be estimted, we assume an uncertainty in Δv_p of ± 50 m s⁻¹. Fuller details will be given elsewhere.

The porosities obtained from these comparisons show considerable scatter (Table 1) but are in satisfactory agreement with the value calculated above by linearly combining compressibilities and densities. It therefore seems safe to conclude that n in the sub-glacial layer is close to 0.4, although probably a bit less. That is is close to 0.4 and not 0.3 or less is significant, as it strongly suggests that the sub-glacial material is dilated and deforming1.

From v_p and ρ in the layer we can calculate that the acoustic impedance of the sediment is close to that of the ice. This explains how the echo from the bottom of the sediment could be stronger than that from the base of the ice. Echo amplitudes vary widely over the survey area, however; they will be considered in detail elsewhere.

The other quantity we wish to estimate is ΔP , since it is critical to the shear strength of the medium. The best measure of ΔP is v_s , because in an unconsolidated sediment v_s depends principally on the intergranular friction, and therefore on the intergranular pressure. Again, comparison with several experimental values leads to a considerable uncertainty (Table 2); nevertheless, all estimates of ΔP lie in the range 15-120 kPa. We adopt the mean value of 50 ± 40 kPa for ΔP in the sub-glacial layer.

We conclude that at least at one location, an active Antarctic ice stream is underlain by a layer of saturated sediment ranging in thickness from zero or nearly zero to at least 12 m, with an average of 5 or 6 m. The layer varies much less in thickness parallel to the direction of ice movement than normal to it; because its upper surface is planar, this gives the impression of a series of longitudinal grooves in the substrate beneath the layer. The low seismic wave speeds in the layer indicate that the material has a porosity of ~0.4 and is saturated with water at a pore pressure only ~50 kPa less than the glaciostatic pressure (9 MPa). Because these characteristics imply that the subglacial material is very weak¹, we believe that the sub-glacial layer is deforming and eroding the stationary surface below, and that it is deformation within the layer rather than deformation in the ice or basal sliding that is the principal component of ice-stream movement.

The field program is a cooperative effort among investigators from the University of Wisconsin, the Ohio State University, NASA and the University of Chicago. We thank B. R. Weertman, J. E. Nyquist, R. Flanders, S. Shabtaie, D. G. Schultz, K. C. Taylor, Jr and J. Dallman for help with field work, L. A. Powell. B. D. Karsh, R. B. Abernathy, W. L. Unger, and Weertman for engineering assistance, and A. N. Mares and S. H. Smith for manuscript and figure preparation. Financial support was provided by NSF under grants DPP81-20322 and DPP84-12404. This is contribution number 447 of the University of Wisconsin-Madison, Geophysical and Polar Research Center.

Received 23 December 1985; accepted 15 April 1986.

- Alley, R. B., Blankenship, D. D., Bentley, C. R. & Rooney, S. T. Nature 322, 57-59 (1986).
- Iken, A. J. Glaciel 27, 407-421 (1981).
- Weertman, J. & Birchfield, G. E. Ann. Glaciol. 3, 316-320 (1982) Bindschadler, R. J. Glaciol. 29, 3-19 (1983).
- Iken, A., Rothlisberger, H., Flotron, A. & Haeberli, W. J. Glaciol. 29, 28-47 (1983). Kamb. B. et al. Science 227, 469-479 (1985).
- Clay, C. S. & Medwin, H. Acoustical Oceanography: Principles and Applications (Wiley, New York, 1977). Biot, M. A. J. acoust. Soc. Am. 28, 168-191 (1956).
- 9. Hamdi, F. A. I. & Taylor Smith, D. Geophys. Prospect. 30, 622-640 (1982) 10. Geertsma, J. & Smith, D. C. Geophysics 26, 169-181 (1961).
- Hamdi, F. A. I. & Taylor Smith, D. Geophys. Prospect. 29, 715-729 (1981).
 Hamilton, E. L. J. geophys. Res. 75, 4423-4445 (1970).
- 13. Anderson, R. S. in Physics of Sound in Marine Sediments (ed Hampton, L., 481 518 (Plenum, New York, 1974). Morgan, N. A. Geophysics 34, 529-545 (1969).
- 15. Schultheiss, P. J. in Acoustics and the Sea Bed (ed. Pace, N. G.) 19-27 (Bath University Press, 1983).
- Schultheiss, P. J. Marine Geotechnol. 4, 343-367 (1981).
 Hamilton, E. L. Geophysics 41, 985-996 (1976).
- 18. Ohta, V. & Goto, N. Earthq. Engng struct. Dyn. 6, 167-187 (1978).

Deformation of till beneath ice stream B, West Antarctica

R. B. Alley, D. D. Blankenship, C. R. Bentley & S. T. Rooney

Geophysical and Polar Research Center, University of Wisconsin-Madison, 1215 West Dayton Street, Madison, Wisconsin 53706, USA

The behaviour and possible instability of the West Antarctic ice sheet depend fundamentally on the dynamics of the large ice streams which drain it. Model calculations show that most icestream velocity arises at the bed1,2, and radar sounding has shown the bed to be wet³, but the basal boundary condition is not well understood. Seismic evidence from the Upstream B camp (UpB) on the Siple Coast of West Antarctica4 shows that the ice stream there rests on a layer of unconsolidated sediment averaging 5 or 6 m thick, in which the water pressure is only ~50 kPa less than the overburden pressure. Because this thin layer occurs well inland beneath an active ice sheet and rests on a surface showing flutes characteristic of glacial erosion⁵, we presume that it is glacial till. We propose here that deformation within the till is the primary mechanism by which the ice stream moves, and we discuss implications of this hypothesis.

Three distinct lines of evidence relating to till porosity, force balance, and water balance indicate that the till at UpB is deforming; we present each of these here. First, lodged basal till has a porosity of ≤30%, whereas deformation of till causes dilation and porosity of ~40% (refs 6-8). The seismically determined porosity of ~40% for till at UpB⁴ is consistent with active deformation but too high for lodged till.

Second, we estimate that the basal shear stress is about twice the strength of till at UpB, so that the till should be deforming.

The strength of till can be estimated from measured properties of deforming till, collected by Boulton and co-workers⁶⁻⁹ beneath Breidamerkurjökull in Iceland. Briefly, Boulton found that the basal-ice velocity of Breidamerkurjökull arises largely from deformation of a dilated till layer of 40% porosity, that large stress concentrations occur locally during deformation, and that the dilated structure collapses and till strength increases by a factor of 1.6-4 if the strain rate is too low.

Because of the large stress concentrations in deforming till. ice-stream flow would dilate and deform lodged, low-porosity till if the average basal shear stress, τ , exceeded the strength of dilated till, τ_d . This is because, if the till at UpB were lodged, then the basal-ice velocity would arise from sliding across a water layer that reduced ice-bed contact to local patches. Weertman¹⁰ has shown that total ice-bed contact area would have to be reduced greatly to allow sliding at ice-stream velocities, so that the local shear stress in patches of contact would significantly exceed 4τ . However, the strength of lodged till is $<4\tau_d$ (refs 6-8), so that local mobilization of till would occur for $\tau \ge \tau_{\rm d}$. The stress concentrations caused by deformation would then mobilize adjacent, lodged till to form a continuous deforming layer that would thicken to intersect bedrock or until the strain rate became too small to generate stress concentrations large enough to mobilize more till. (Till would also be mobilized locally for some range of $\tau < \tau_d$, but the average basal shear stress would not be large enough in such conditions to deform a continuous layer of till.)

Boulton⁹ argues that till obeys a Coulomb-type failure criterion, so we let $\tau_d = \Delta P \tan \phi_d$, where ΔP is the excess of overburden pressure over water pressure and tan ϕ_d is the internal friction. (We have set cohesion to zero in the failure criterion, in accordance with the observations of Engelhardt et al.11 and because we expect dilation of till to disrupt the short-range electrostatic forces between clay particles that cause the cohesion in saturated, lodged till.) Till is deforming at Breidamerkurjökull, so τ must be $\geq \tau_d$ there. Using measured ΔP (ref. 7) and basal shear stress calculated from the geometry of Breidamerkurjökull9, we estimate from the Coulomb failure criterion that tan $\phi_d \le 0.15$. (Direct measurements of recently deformed till at Breidamerkurjökull⁶⁻⁸ using a shear box give values of tan ϕ_d equal to or slightly larger than that reported here, but laboratory shear tests consistently overestimate the strength of materials undergoing slow, large-scale deformation¹².) At UpB, $\Delta P =$ 50 ± 40 kPa (ref. 4); if internal friction of till is similar at UpB and Breidamerkurjökull, then $\tau_d \leq 8 \pm 6$ kPa at UpB.

The driving stress for ice flow at UpB is ~ 19 kPa, calculated from the familiar formula: driving stress = ρgh tan α , where the ice density $\rho = 920$ kg m⁻³; the gravitational acceleration g = 9.8 m s⁻²; the ice thickness h = 1,050 m, and the surface slope tan $\alpha = 0.002$ (ref. 13). The driving stress is resisted by gradients in stretching stress and by side drag as well as by the basal drag, τ , but a force-balance calculation for the ice stream by Whillans indicates that basal drag is the major resistive force. We have reached the same conclusion independently, and estimate that $\sim 95\%$ of the driving stress is balanced by basal drag at UpB, so that $\tau \approx 18$ kPa. This is more than twice the best estimated value of τ_d at UpB, so we expect till deformation to be occurring there.

The third argument for till deformation comes from a water-balance calculation. As noted above, if till is not deforming then ice-stream velocity must arise from sliding of ice over a rigid substrate lubricated by water. Weertman¹⁰ estimates that fast sliding requires a water film of thickness $d \approx 5$ mm or greater. At the head of an ice stream fed by a catchment area of length $L \approx 400$ km and width $F \approx 4$ times as wide as the ice stream¹³, the existence of fast sliding requires production averaged over the catchment area of a thickness of water per unit time, λ , given by¹⁰: $\lambda = d^3 \rho g \tan \alpha (12 \eta L F)^{-1}$, where $\rho g \tan \alpha$ is the pressure gradient driving water flow in the ice stream (assuming bed slope is of the same magnitude as surface slope or smaller¹³)

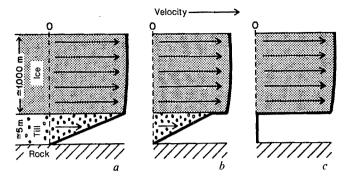


Fig. 1 Possible models for an ice-stream bed. a, Till deformation only; our model for UpB. b, Till deformation plus basal sliding; our model for near the grounding line of line stream B. c, Basal sliding only; not realized on ice stream B.

and $\eta = 1.8 \times 10^{-3}$ Pa s is the viscosity of water¹⁰. The minimum water production for fast sliding is then $\lambda = 2 \text{ mm yr}^{-1}$. We consider this much water production to be unlikely because: (1) the Byrd borehole, in the catchment area of ice stream D. showed that net basal freezing rather than melting occurs over some distance up-glacier of the borehole¹⁵, and the catchment of ice stream B is sufficiently similar to that of ice stream D in surface mass balance, surface topography, bed topography and ice thickness13 that we expect net basal freezing in parts of the ice-stream-B catchment; (2) in numerical experiments, Budd et al. 16 were able to generate a melt rate of 2 mm yr⁻¹ for most of the catchment only by increasing the geothermal heat flow by 50% above the value they expected based on the geology of West Antarctica; their expected value has been confirmed by measurements in the Byrd Station borehole^{17,18}; and (3) ice stream B and its catchment are underlain by ≥1 km of sedimentary rock^{19,20} that may have sufficient permeability²¹ to drain a significant amount of water. The amount of water available to lubricate sliding would be reduced further if some water flowed in channels rather than in a Weertman film²². It is thus unlikely that enough water is supplied to the ice stream to allow high velocities near its head by sliding. (Note, however, that water generated beneath the ice stream may form a film at the ice-till interface²³, so that both till deformation and water-lubricated sliding may be important near the grounding line (Fig. 1).)

The above arguments show that most ice-stream velocity arises from till deformation, and we now use this result to show that the entire thickness of till at UpB is deforming. As noted above, stress concentrations in active till increase with increasing strain rate, $\dot{\varepsilon}$. If $\dot{\varepsilon}$ were to exceed $\dot{\varepsilon}_b$ the minimum strain rate required to cause stress concentrations large enough to mobilize lodged till, then active till would mobilize subjacent, lodged till until the strain rate was reduced to $\dot{\varepsilon}_l$ or until till activation reached bedrock. We thus expect $\dot{\varepsilon} = \dot{\varepsilon}_l$ if active till overlies lodged till and $\dot{\varepsilon} \ge \dot{\varepsilon}_l$ if active till reaches bedrock. The average simple strain rate in till is u/h_b , where u is the velocity of the till at its upper surface and h_b is the thickness of the active layer. At Breidamerkurjökull⁹, where active till overlies lodged till, $u = 16 \text{ m yr}^{-1}$, $h_b = 0.5 \text{ m}$ and $\dot{\varepsilon} = 32 \text{ yr}^{-1} = \dot{\varepsilon}_l$. At Blue Glacier¹¹, where active till reaches bedrock, $u = 4 \text{ m yr}^{-1}$, $h_b = 0.1 \text{ m}$ and $\dot{\varepsilon} \simeq 40 \text{ yr}^{-1} \ge \dot{\varepsilon}_h$ At UpB, for little slip between ice and till, $u \simeq 450 \text{ m yr}^{-1}$ (ref. 24) and $h_b \simeq 6 \text{ m}$, so $\dot{\varepsilon} \simeq 75 \text{ yr}^{-1}$. As this is much greater than $\dot{\varepsilon}_l$ at Blue Glacier and Breidamerkurjökull, and there is no reason for \dot{e}_i to be grossly different at UpB, we conclude that the entire thickness of till at UpB is deforming.

Given that the entire thickness of till at UpB is deforming, we can now calculate the fluxes of till and water beneath UpB and the generation rates in the catchment area required to sustain these fluxes if they are steady-state values. Water moves by advection with till and by conduction through till. From Darcy's law, the conductive flow velocity is $u_c = k/\eta (dP/dx)$ where

 $k = \text{till permeability} \approx 1.6 \times 10^{-13} \,\text{m}^2(\text{ ref. 7}), \, \eta$ -dynamic viscosity of water = 1.8×10^{-3} Pa s, and (dP/dx) = pressure gradient from weight of ice = $\rho g \tan \alpha \approx 18 \text{ Pa m}^{-1}$ (again assuming that bed slope is of the same magnitude as surface slope or smaller¹³). The flow velocity, u_c , is then $1.6 \times 10^{-9} \,\mathrm{m \, s^{-1}} \simeq 0.05 \,\mathrm{m \, yr^{-1}}$. The depth-averaged advective flow velocity, \bar{u}_a , is given by $\bar{u}_a = \bar{u}n$, where \bar{u} is the depth-averaged velocity of bulk till and n = 0.4 is the till porosity⁴. For no-slip boundaries and any reasonable till rheology (such as linearviscous, power-law creep with finite exponent, or Bingham substance) velocity will vary almost linearly from 450 m yr⁻¹ at the ice-till interface²⁴ to zero at the till-bedrock interface, so $\bar{u} = 225 \text{ m yr}^{-1}$ and $\bar{u}_a = 90 \text{ m yr}^{-1}$. This is more than three orders of magnitude larger than the conductive velocity, so essentially all the water flow is advective.

The total water flux per unit width of ice stream is $h_h \bar{u}_a w$, where $h_b \approx 6$ m is the till thickness and w is the ice-stream width. In steady state, this flux corresponds to an average watergeneration rate of thickness λ over an area $(FL+L_2)w$, where $L_2 \simeq 100 \, \text{km}$ is the length of the ice stream above UpB, $L \simeq$ 400 km is the length of the catchment area, and $F \approx 4$ is the width of the catchment area feeding unit width of the ice stream¹³. Then $\lambda = h_b \bar{u}_a (LF + L_2)^{-1} \approx 0.3 \text{ mm} \text{ yr}^{-1}$. This is almost an order of magnitude less than the 2 mm yr⁻¹ melt rate needed for Weertman sliding at the head of the ice stream, and is consistent with our knowledge of water generation in the catchment area. The average erosion rate of rock can be obtained from the same calculation by replacing porosity, n, by rock fraction, 1-n, and is $\sim 0.5 \text{ mm yr}^{-1}$.

We thus hypothesize that the velocity of ice stream B near UpB arises largely from deformation of a sub-glacial till layer (Fig. 1). This hypothesis suggests several corollaries, which include: (1) the basal boundary condition for ice-stream flow depends on the constitutive relation for till; (2) the till flux beneath UpB is equivalent to steady-state erosion of ~0.5 mm yr⁻¹ of rock over the catchment area and the upstream part of the ice stream; (3) this till flux requires deposition of morainal banks or 'till deltas' at the grounding line; recent mapping of the grounding line²⁵ is consistent with the existence of such deltas; (4) the fluted nature of the till-rock interface at UpB may be a characteristic erosional consequence of deforming till²⁶; and (5) variations in till thickness over flutes may cause fluctuations in basal drag that affect ice-stream flow, with higher drag over bedrock ridges and lower drag over troughs. Our work also suggests the possibility that other ice streams and other wet-based regions of ice sheets²⁷ may rest on till. We are conducting further field work and analysis to test these hypotheses.

This work was supported in part by NSF under grants DPP-8120322 and DPP-8412404. We thank I. M. Whillans for helpful comments on the manuscript, and A. N. Mares and S. H. Smith for manuscript and figure preparation. This is contribution number 448 of the Geophysical and Polar Research Center, University of Wisconsin-Madison.

Received 24 December 1985; accepted 21 April 1986.

- Alley, R. B. Inst. Polar Stud. Rep. No. 84 (The Ohio State University, 1984).
- Budd, W. F., Jenssen, D. & Smith, I. N. Ann. Glaciol. 5, 29-36 (1984).

 Robin, G. de Q., Swithinbank, C. W. M. & Smith, B. M. E. IASH Publ. 86, 97-115 (1970).
- Gravenor, G. S. & Paul, M. A. G. H. S. M. S. J. S. M. S. M.

- Weertman, J. Can. J. Earth Sci. 6, 929-939 (1969).
 Engelhardt, H. F., Harrison, W. D. & Kamb, B. J. Glaciol. 20, 469-508 (1978).
- Walker, B. F. in In-situ Testing for Geotechnical Investigations (ed. Ervin, M. C.) 65-72 (Balkema, Rotterdam, 1983).
- (Balkema, Rotterdam, 1983).
 Drewry, D. J. (ed.) Antarctica: Glaciological and Geophysical Folio (Scott Polar Research Institute, Cambridge, 1983).
 Whillans, I. M. Proc. Int. Workshop, Stability of West Antarctic Ice Sheet and Sea Level (Reidel, Dordrecht, in the press).
 Gow, A. J., Epstein, S. & Sheehy, W. J. Glaciol. 89, 185-192 (1979).
 Budd, W. F., Jenssen, D. & Radok, U. ANARE Interim Rep. Ser. A(IV) (Glaciology) No. 170 (1971).

- 120 (1971).

- 17. Gow, A. J., Ueda, H. T. & Garfield, D. E. Science 161, 1011-1013 (1958) 18. Rose, K. E. J. Glaciol. 24, 63-74 (1979).
- 19. Bentley, C. R. & Clough, J. W. in Antarctic Geology and Geophysics (ed. Adie, R. J.) 683-691 (Universitetsforlaget, Oslo, 1972).
- Rooney, S. T., Blankenship, D. D. & Bentley, C. R. in Proc. 6th Gondwana Symp. (American Geophysical Union, in the press).
- 21. Freeze, R. A. & Cherry, J. A. Groundwater (Prentice-Hall, New Jersey, 1979) 22. Bindschadler, R. A. J. Glaciol. 29, 3-19 (1983).

- Weertman, J. & Birchfeld, G. E. Ann. Glaciol. 3, 316-320 (1982).
 Vornberger, P. O. & Whillans, I. M. Ann. Glaciol. 7, (in the press)
 Shabtale, S. & Bentley, C. R. Ann. Glaciol. 8 (in the press).
 Also see MacClintock, P. & Dreimanis, A. Am. J. Sci. 262, 133-142 (1964).
- 27. Oswald, G. K. A. & Robin, G. de Q. Nature 245, 251-254 (1973)

Corals on seamount peaks provide evidence of current acceleration over deep-sea topography

Amatzia Genin, Paul K. Dayton, Peter F. Lonsdale & Fred N. Spiess

Scripps Institution of Oceanography, University of California, San Diego, La Jolla, California 92093, USA

Geological and physical studies of seamounts have suggested the existence of distinct deep-sea habitats, characterized by exposed rocky bottom and a unique current regime 1-9. However, few biological data have been collected for deep seamounts 10-12. Here we present some of the first quantitative observations of hard-bottom (non-hydrothermal) fauna in the deep sea. These observations show that black corals (antipatharians) and horny corals (gorgonians) present on the slopes of a multi-peaked seamount are more abundant near peaks, compared with mid-slope sites at corresponding depths. On narrow peaks corals are most abundant on the crest, whereas on wide peaks, coral densities are highest at the edge of the crest. The abundance of corals also increases on knobs and pinnacles. Physical models and observations2.4-9,13-15, together with our direct measurements, suggest that the seamount topography affects the local current regime. Corals appear to benefit from flow acceleration, and some of their patterns of distribution can be explained by current conditions. These results suggest that suspension feeders have some potential as indicators of prevailing currents at deep hard-bottom sites.

We made our observations on Jasper Seamount, which is an extinct volcano 3.5 km high 30 km in diameter, built on the 4,200-m-deep abyssal Pacific floor, about 550 km south-west of San Diego, California. It has a multi-peaked summit area (Fig. 1) with two of the peaks rising higher than 600 m depth. Most of the summit area consists of bare basaltic rock, with thin pockets of sediment in some depressions between the peaks. A rich and diverse fauna, dominated by sedentary suspension feeders such as sponges, black corals, horny corals, anemones and tunicates, was discovered in our photographic survey of the seamount. The most common species on the upper slopes of the seamount is the spiral black coral, Stichopathes sp., which occupies rocky substrata at depths from 550 m to 1,150 m, where it sometimes forms 'forests' with densities of up to 20 colonies per m². In areas partially covered with sediment, Stichopathes is found only on protruding rocks; it is absent in areas with 100% sediment cover. Along its upper range, the Stichopathes zone overlaps a rich sponge zone. Gorgonians and branched antipatharians are the dominant taxa on the rocky bottom at depths below the Stichopathes zone. However, coral densities at these greater depths are much lower than in the Stichopathes zone.

Variations of coral abundances, at any depth, are associated with the local topography, on three different scales:

(1) Over the entire seamount, Stichopathes densities are significantly higher near peaks than at mid-slope sites at corresponding depths (Fig. 2). For example, the average Stichopathes

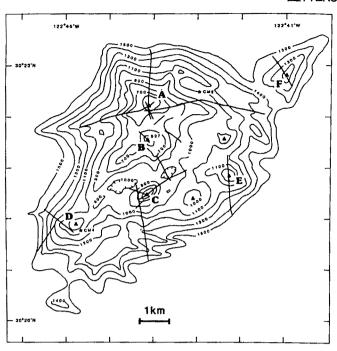


Fig. 1 The summit of Jasper Seamount, showing bathymetry, designated peak names, locations of current-meter moorings (*), and photographic transect lines (heavy black lines). Contours are in metres. Photographs were taken by the Deep-Tow instrument package²⁰ at ~10-m intervals. The camera-to-bottom distance was recorded when each photograph was taken, allowing computation of areas and animal densities.

density near peak C, between 700 and 750 m depth, is about 15 colonies per m² (Fig. 3), which is about three times the mean density of the species on slopes at the same depth interval (Fig. 2). Similarly, densities of gorgonians near peak F, at a depth of 1,170-1,250 m (Fig. 3), are more than five times higher than at the same depth interval on the slopes.

(2) On the peaks, the species exhibit two distribution patterns: on wide peaks (diameter > 1 km), with a flat or gradually sloping top, highest densities are found along the perimeter of the top, and lower densities on the top itself (Fig. 3, peaks A and F); on narrow, tapering peaks, highest densities are found on the crests (Fig. 3, peak C).

(3) On a smaller scale, *Stichopathes* exhibits increased abundances on knobs and pinnacles. For example, a sharp increase in density is found on the small knobs at 1.4 km and 3.9 km along the transect across peak A (Fig. 3).

Why are corals more abundant near peaks? We assume that concentrations of food and larvae in waters impinging on the seamount are independent of the local topography, that is, the average concentrations of food and larvae in waters impinging on a peak and on a slope at the same depth are similar. However, fluxes of food and larvae could vary at different sites due to topographic effects on water flow. Within a certain range of current speed, areas of flow acceleration are expected to be favourable for recruitment and growth of passive suspension feeders; this may be attributed to either the 'settlement pathway'. in which a site is colonized by relatively more recruits simply because more water, and hence more larvae, are flowing by per unit of time, or the 'feeding pathway', in which an increase of water flow past suspension feeders results in increased feeding and growth rates 16-18. This may also be critical for the survival of small recruits. Both pathways can lead to long-term integration of current conditions by the animals.

There are two lines of evidence for intensified water flow near peaks, where the abundance of corals is relatively high. First, our direct current measurements on Jasper Seamount (Fig. 4), although short-term and limited to two stations, showed that the mean total speed near a peak was about twice the mean speed at the same depth but on a mid-slope site. Second, observations on other seamounts^{9,13-15} have demonstrated hydrographic conditions near the summit which differ from those along the slopes, because the upwelling requires acceleration over the top of the seamounts.

The distribution of corals on wide peaks can be explained by predictions of physical theory. When water is upwelled above wide topography, vortex lines are compressed and anticyclonic motion is induced, because of conservation of potential vorticity^{4,5}. The resulting flow-field is a combination of the velocity induced by this anticyclonic component and the free-stream velocity. Thus, looking downstream, flow acceleration occurs on the left side of the topographic feature (in the Northern Hemisphere) and deceleration above the centre and right side of the peak^{3,4,7}. As this theory has been developed for a uniform and steady flow, the validity of the model for strong tidal currents (see, for example, Fig. 4) is less certain. A possible effect of the tide would be a switch of the anticyclonic acceleration-deceleration zones. The overall mean velocity pattern would therefore comprise alternating periods of acceleration on the peak's edges and recurrent deceleration trend over the centre. This postulated velocity pattern is consistent with the lower densities of corals observed at the centre of the wide peaks of Jasper Seamount (Fig. 3). Furthermore, the combination of tidal fluctuations and a general southward flow in the vicinity of the seamount (Fig. 4; ref. 19) could result in a stronger average acceleration on the eastern side of the seamount; this could explain why Stichopathes is about twice as dense on the eastern edge of the main seamount peak as on the western edge (Fig. 3, peak A).

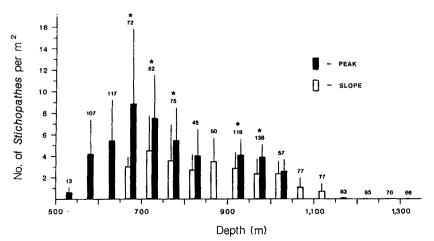


Fig. 2 Densities of Stichopathes (mean \pm s.d.) at different depth intervals on Jasper Seamount. The photographs were divided into those near peaks (solid bars) and those >150 m below a peak (open bars). Only photographs which exhibited <10% sediment cover were included in the computation. Stars indicate the intervals in which the mean nearpeak density is significantly higher than the mean mid-slope density (P<0.001, Mann-Whitney Utest). The number of photographs taken at each depth interval is indicated above the corresponding bar.

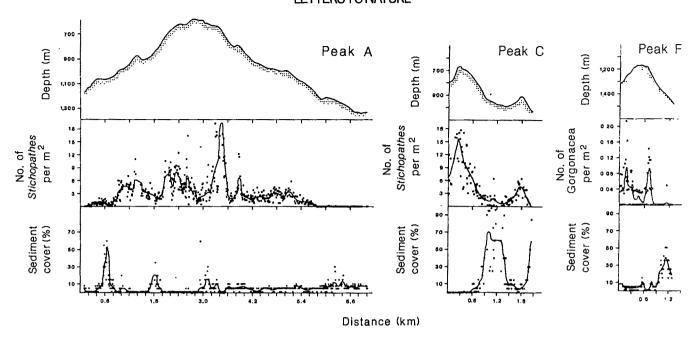


Fig. 3 Bathymetry, animal densities and sediment cover in transects across peaks A. C and F. Each dot indicates the animal density or sediment cover in a single photograph. Solid lines indicate 9-point running means. The transects are from west to east across peaks A and C, and from south-east to north-west across peak F. Sediment cover, which can have a deleterious effect on suspension feeders^{21,22}, cannot explain why corals are more abundant near peaks and on pinnacles. For example, the distribution pattern exhibited by Stichopathes close to peak C occurs along the initial 600 m of the transect, which is sediment-free. Similarly, distinct changes in gorgonian densities near peak F occur in an area where the sediment cover is low and nearly uniform. Overall, the correlation between sediment cover and Stichopathes density between 527 and 1,150 m depth is low but significantly different from zero (Kendall rank correlation = -0.2, P < 0.01, n = 1,359).

Fig. 4 (Right) Current velocity and progressive vector diagram of records taken near peak D (CM 4) and at a mid-slope site east of peak A (CM 2), both at a depth of ~1,000 m. Dots on the progressive vector diagram of CM 4 indicate 24-h intervals. The mean current speed (15min averages) was significantly higher (P < 0.001, Student's t-test) near the peak (4.9 cm s⁻¹) than at the mid-slope site (2.7 cm s⁻¹). Measurements were made with two SIO-Model 6 Savonius rotor current meters, deployed at 46 m above the bottom. Spectral analysis of these records indicates that the kinetic energy of internal waves near a critical frequency (0.5 cycles h⁻¹), in which internal waves are reflected parallel to the topographic slope^{8,23,24}, is negligible compared with the energetically dominant diurnal frequency. Such reflection, when present, may intensify water flow over seamounts and slopes8.

We conclude that the current regime is a key factor in determining community structure on the deep hard-bottom areas of Jasper Seamount, where suspension feeders are more abundant at sites of flow acceleration.

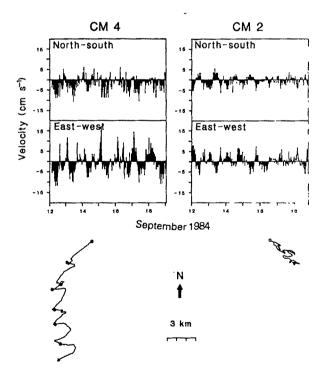
We thank D. Boegman, R. Elder, D. Genin, R. Knox, M. Linzer, A. Neori and M. Olsson for technical assistance, and C. Eriksen, J. Barry, L. Fogiel, D. Genin, R. Hessler, T. Klinger, R. Knox, M. Mullin, L. Mullineaux, K. Smith, M. Tegner and W. Wakefield for discussions and comments on the manuscript. This research was supported by NSF grant OCE 85-10057, ONR contracts N00014-79-C-0472 and N00014-82-K-0147, and by a grant from The Scripps Industrial Association.

Received 14 February; accepted 7 May 1986.

- Lonsdaie, P., Normark, W. R. & Newman, W. A. Bull. geol. Soc. Am. 83, 289-315 (1972).
 Hogg, N. G. J. Fluid Mech. 58, 517-537 (1973).
- 3. Roberts, D. G., Hogg, N. G., Bishop, D. G. & Flewellen, C. G. Deep-Sea Res. 21, 175-184
- 4. Huppert, H. E. J. Fluid Mech. 67, 397-412 (1975).

- Huppert, H. E. & Bryan, K. Deep Sea Res. 23, 655-679 (1976).
 Owens, W. B. & Hogg, N. G. Deep Sea Res. 27, 1029-1045 (1980).
 Gould, W. J., Hendry, R. & Huppert, H. E. Deep-Sea Res. 28, 409-440 (1981).
 Ericksen, C. J. geophys. Res. 87, 525-538 (1982).
 Roden, G. I. & Taft, B. A. J. geophys. Res. 90, 839-856 (1985).

- 10. Pratt, R. M. in Deep-Sea Photography (ed. Hersey, J. B.) 145-158 (Johns Hopkins University Press, Baltimore, 1967).



- 11. Raymore, P. A. Pacif. Sci. 36, 15-34 (1982).

- Grigg, R. W. Mar. Ecol. 5, 57-74 (1984).
 Genin, A. & Boehlert, G. W. J. mar. Res. 43, 907-924 (1985).
 Genin, A., Boehlert, G. W. & Lonsdale, P. F. Eos 65, 969 (1984).
- Fukasawa, M. & Nagata, Y. J. oceanogr. Soc. Japan. 34, 41-49 (1978).
 Sebens, K. P. Proc. natn. Acad. Sci. U.S.A. 81, 5473-5477 (1984).

- Pequegnat, W. E. Ecology 45, 272-283 (1964).
 Grigg, R. W. & Maragos, J. E. Ecology 55, 387-395 (1974).
 Reid, J. L. Jr Intermediate Waters of the Pacific Ocean (Johns Hopkins University Press, Baltimore, 1965).
- Spiess, F. N. & Tyce, R. C. Scripps Instn. Oceanogr. Ref. 73-74 (1973)
 Sara, M. & Vacclet, T. Traite de Zool. 3, 462-576 (1973).
 Loya, Y. Bull. mar. Sci. 26, 450-466 (1976).
 Wunsch, C. J. Fluid Mech. 35, 131-144 (1969).

- Cacchione, D. & Wunsch, C. J. Fluid Mech. 66, 223-239 (1974).

Monocular aniseikonia: a motion parallax analogue of the disparity-induced effect

Brian Rogers

Department of Experimental Psychology, University of Oxford, South Parks Road, Oxford OX1 3UD, UK

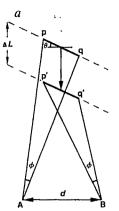
Jan Koenderink

Department of Medical Physics, University of Utrecht, The Netherlands

Mayhew and Longuet-Higgins have recently outlined a computational model of binocular depth perception¹ in which the small vertical disparities between the two eyes' views of a three-dimensional scene are used to determine the 'viewing parameters' of fixation distance (d) and the angle of asymmetric convergence of the eyes (g) (refs 2, 3). The d/g hypothesis, as it has been called⁴, correctly predicts that a fronto-parallel surface, viewed with a vertically magnifying lens over one eye, should appear to be rotated in depth about a vertical axis^{1,3-5}. We report here a comparable illusion for surfaces specified by monocular motion parallax information, which can be explained more simply by considering the differential invariants of the optic flow field. In addition, our observations suggest that the disparity-induced effect is not a 'whole field' phenomenon nor one limited to small magnification differences between the eyes^{1,4}.

The vertical magnification of one eye's image of a binocularlyviewed surface produces the impression of a surface rotated about a vertical axis through the fixation point. This effect was called the 'induced effect' by Ogle⁶ because he believed that horizontal disparities were 'induced' into the neural representations by a compensatory isotropic scaling mechanism acting to minimize the vertical size differences caused by eccentric fixation. Since horizontal disparities are affected by both the magnitude of any depth differences and the degree of eccentric fixation (g), the zero horizontal disparities in an induced effect stimulus have to be 'corrected' so that the relative distance and the slant of a surface can be perceived correctly. However, it appears that Ogle did not appreciate the more general significance that vertical disparities at other retinal locations apart from the vertical meridian provide a potential source of information about distance to the fixation point, as well as the angle of eccentric convergence. The mathematical proof for this has been independently provided by Gillam and Lawergren⁷ and Mayhew and Longuet-Higgins¹⁻³. In both cases, the induced effect is seen as a necessary consequence of a stereoscopic system which uses vertical disparities to determine the viewing system parameters.

As yet, there is little evidence that presence of vertical disparities in a stereogram actually gives a subjective impression of eccentric convergence but, as several authors have pointed out, this might be due to the presence of conflicting oculomotor information^{1,7}. However, the magnitude and the direction of the induced effect are both consistent with the d/g hypothesis³. Mayhew and Longuet-Higgins also argue the case for the induced effect being a global or 'whole field' phenomenon, since there could only be a single estimate of eccentric fixation angle and therefore only a single 'correction' would be applied to the horizontal disparities in the surrounding area^{1,4}. As additional evidence for their theory, they note that the magnitude of the induced effect does not increase when the vertical size difference is greater than about 4-6% 1.6. This would be predicted by their hypothesis since larger differences in size would imply impossibly large angles of asymmetric convergence^{1,7}. Both claims are examined in this paper.



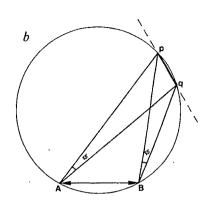


Fig. 1 In a, pq represents part of a surface slanting at an angle θ to the frontoparallel plane, which moves forward to p'q' at the same time as a monocular observer moves from A to B. It can be shown that the horizontal angle subtended at the eye ϕ will remain constant when $\tan \theta = \Delta L/d$. In contrast, since the surface is closer at B than A, the vertical angle subtended will increase. In b, the horizontal angle subtended again remains constant and the vertical angle subtended increases when the monocular observer moves from A to B towards an eccentrically placed slanting surface pq. The two situations differ only by an eccentric rotation of the lines of sight.

The disparity-induced effect can be perceived when one eye's image of a binocularly-viewed scene is magnified vertically. The motion parallax analogue of this illusion-monocular aniseikonia-was created by continuously magnifying and minifying the image projected to a single viewing eye during side-to-side movements of the observer's head8. The instantaneous monocular images of the scene at the end points of the lateral head movement necessarily correspond to the two simultaneous binocular views of the same scene when a meridional magnifying lens is placed over one eye. For all the observations reported in this paper, the image transformations for both the parallax and disparity-induced effects were effected electronically, rather than by optical means. The images consisted of either a single random dot pattern, or a pair of random dot patterns viewed independently by the two eyes, each subtending a 20°×20° visual angle. The disparity-induced effect was produced by increasing the vertical gain slightly on one oscilloscope and decreasing it slightly on the other. The horizontal widths of the patterns remained identical. To produce the parallaxinduced effect, the vertical gain of a single, monocularly-viewed oscilloscope was modulated according to the position of the observer's head. Thus the vertical size of the dot pattern was maximal at one end of travel and minimal at the opposite end of travel. Observers were asked to report the perceived orientation and shape of the random dot surfaces in the different experimental conditions.

With binocular viewing of the disparity-induced surface, our results replicate those of previous studies^{3,6,7}. Observers reported that the surface appeared to be slanting in depth with the right-hand side apparently closer than the left, when the right eye's image was vertically magnified, and vice versa for magnification of the left eye's image. Increasing the difference in vertical magnification between the two eyes increased the angle of perceived slant, as found previously.

With monocular viewing of the parallax-induced surface, a similar pattern of results was obtained. Observers reported that the surface appeared to be slanting in depth with the right-hand side closer than the left when the monocular image was progressively magnified with head movement to the right and vice versa. Again, the angle of perceived slant increased with an increase in the extent of vertical magnification/minification (for a constant head movement). In both the disparity-induced effect and its parallax analogue, the apparently slanting surfaces were

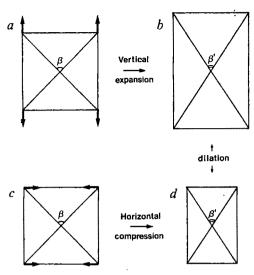


Fig. 2 The vertical expansion of the square pattern segment from a to b will produce the same amount of local and global deformation (as indicated by the change in the orientation difference between the diagonals $\beta \rightarrow \beta'$) as the horizontal compression of the same pattern segment from c to d. The transformed patterns, b and d, are related by a uniform or isotropic expansion.

always perceived as lying directly in front of the observer, rather than eccentrically to one side. In the case of the parallax-induced effect, the slanting surface was also perceived to approach and recede along a median path as the image expanded and contracted. This percept is entirely consistent with the geometry of the transformation, since the image of a slanting surface which approached an observer as he moved laterally towards the "closer" side, would indeed expand vertically, but remain of constant width (Fig. 1a).

The interpretation chosen by the visual system is, however, not the only one consistent with the image transformation. In fact, there are an infinite number of possible solutions (unlike the disparity-induced effect which has only one solution). For example, a surface positioned eccentrically and slanting with respect to the direction of gaze, would also generate an image whose vertical size increased and decreased with head movements whilst its horizontal size remained constant (Fig. 1b). This particular solution lies behind the explanation proposed by Mayhew and Longuet-Higgins to account for the disparityinduced effect¹. The fact that observers do not experience this perceptual outcome suggests that, for the parallax system, a vertical size change which accompanies a horizontal head movement is interpreted as a motion in depth rather than resulting from eccentric fixation.

Two additional sets of observations were made for the disparity- and parallax-induced effects. First, as mentioned above, the d/g hypothesis predicts that the induced effect should be 'whole field' phenomenon, since it seems unlikely that the visual system could entertain different, and therefore contradictory, estimates of the angle of eccentric convergence at the same time. Empirical evidence for the 'whole field' characteristic of the effect comes from the observation that an embedded region which is magnified in one eye's view does not appear to be slanted with respect to the surround^{1,5,9}. However, the perception of opposite induced effects in neighbouring spatial regions is possible in both the classical induced effect and the parallax analogue reported here. For example, if the images of the left and right halves of the random dot pattern seen by the right eye are minified and magnified respectively (with respect to the images seen by the left eye), subjects report that the left half of the pattern appears to be slanting closer to the left and the right half slanting closer to the right. According to the d/g hypothesis this could only be possible if the vertical disparities in the left half field were interpreted as indicating asymmetric convergence to the right, and in the right half field as indicating asymmetric convergence to the left. A comparable 'double' induced effect was also obtained for surfaces specified by motion parallax

The second piece of evidence cited in favour of the d/ghypothesis is that the induced effect does not increase with vertical magnifications greater than 4-6% 3,6. Indeed, this prediction was used by Frisby⁴ to discount Westheimer's finding that sensitivity to vertical disparities is much poorer than for horizontal disparities¹⁰. However, we have found that the apparent slant of induced effect surfaces does still increase monotonically right up to a 50% magnification difference, when induced effects specifying opposite slants are alternated every few seconds. At the 57-cm viewing distance used in the present experiments, the maximum possible magnification difference which could result from asymmetric convergence would be less than 7%.

Our proposed explanation of the parallax-induced effect is based on the use of differential invariants to describe the optic flow field¹¹⁻¹³. As Koenderink has shown, the slant of a surface is uniquely specified by the amount of deformation or shear in the flow field, if the extent of observer motion is known. Clearly, the vertical expansion of a monocular image, which underlies the parallax-induced effect, will produce the same degree of deformation in the flow field as a horizontal contraction of the same image (Fig. 2). Hence, the same surface slant is specified. What remains after the deformation component has been extracted is a simple divergence term which is positive in the first case and negative in the second. In the parallax-induced effect, the divergence term is clearly not ignored but instead is responsible for the apparent approach and recession of the slanted surface noted earlier.

Could the proposed explanation also account for the disparity-induced effect? Given that both the mathematical analyses of disparity and parallax transformations¹⁴ and their perceptual characteristics are so similar 15,16, it is tempting to speculate that the perceived surface slants seen in the disparity-induced effect are the result of having a visual system which uses the amount of deformation between the two binocular images as an indicator of surface slant¹⁷. If this were the case, then the visual system would be left to account for the isotropic size difference between the eyes (the divergence component). The human visual system may have evolved to use this as an indicator of eccentric fixation or it may simply be ignored. Hence, our explanation of the induced effect also allows for the angle of eccentric fixation to be recovered from the disparity field, but differs from the Mayhew and Longuet-Higgins interpretation in that this does not have to be done, even implicitly. According to the d/g hypothesis, vertical disparities are used to signal the angle of asymmetric convergence which is then used to scale horizontal disparities. The fact that vertical disparities do not appear to give the impression of asymmetric convergence, together with the other characteristics of the induced effects reported here, suggests that our proposed explanation may be more parsimonious.

This work was supported by the SERC (UK) and the Dutch Organisation for the Advancement of Pure Research (ZWO).

Received 27 January; accepted 13 April 1986.

- 1. Mayhew, J. E. W. & Longuet-Higgins, H. C. Nature 297, 376-379 (1982).
- Longuet-Higgins, H. C. Perception 11, 377-386 (1982). Mayhew, J. E. W. Perception 11, 387-403 (1982).
- 4. Frisby, J. Nature 307, 592-593 (1984).
- Prisby, J. Padure 301, 592-393 (1984).
 Stenton, S. P., Frisby, J. P. & Mayhew, J. E. W. Nature 309, 622-623 (1984)
 Ogle, K. N. Researches in Binocular Vision (Saunders, Philadelphia, 1950).
 Gillam, B. & Lawetgren, B. Percept. Psychophys. 24, 121-130 (1983).

- Rogers, B. J. & Graham, M. E. Perception 8, 125-134 (1979). Mayhew, J. E. W. & Frisby, J. P. Vision Res. 22, 1225-1228 (1982).
- 10. Westheimer, G. Nature 307, 632-634 (1984).
- Koenderink, J. J. & van Doom, A. J. Optica Acta 22, 773-791 (1975).
 Koenderink, J. J. Brain Mechanisms and Spatial Vision (eds Ingle, D., Jeannerod, M. & Lee, D.) 31-58 (Nijhof, Amsterdam, 1985).
- Koenderink, J. J. Vision Res. 26, 161-179 (1986).
 Longuet-Higgins, H. C. Nature 293, 133-134 (1981).
- 15. Rogers, B. J. & Graham, M. E. Vision Res. 22, 261-270 (1982).
- 16. Rogers. B. J. & Graham, M. E. Science 221, 1409-1411 (1983) 17. Koenderink, J. J. & van Doorn, A. J. Biol. Cybernet. 21, 29-35 (1976)

New HLA DNA polymorphisms associated with autoimmune diseases

H. Festenstein*, J. Awad*, G. A. Hitman†, S. Cutbush*, A. V. Groves*, P. Cassell‡, W. Ollier* & J. A. Sachs*‡

Certain class II determinants of the human histocompatibility locus antigens (HLA) have been implicated in the aetiology of several autoimmune diseases, including rheumatoid arthritis (RA) and insulin-dependent diabetes mellitus (IDDM). HLA-Dw4 was the first HLA determinant found to be significantly increased in RA patients compared with controls¹, while Dw4 and Dw3 were found to be significantly increased in IDDM patients^{2,3}. When the HLA-DR system was defined, RA patients were found to have an increased frequency of DR4 and IDDM patients an increased incidence of both DR4 and DR3 (ref. 4) compared with controls. As the HLA-Dw specificities are narrower than the serologically defined DR specificities, it was of specific interest to the present study that Dw4, Dw10, Dw13, Dw14, Dw15 and DKT2 are included in DR4 (ref. 5). We describe here new restriction fragment length polymorphisms (RFLPs) and, together with the newly described serologically defined DQ specificity TA10 (ref. 6), test their prevalence and associations in controls and diseased patients. We find that the newly characterized DNA bands are present at a much higher frequency in RA and IDDM patients than in controls. These findings may lead to a greater understanding of the pathogenesis of such diseases.

The HLA class II region is considered to consist of five α -chain genes and eight β -chain genes; these are encoded in three subregions, HLA-DP, -DQ and -DR. The DR subregion contains one α -chain gene and three or four polymorphic β -chain genes, while the DP and DQ subregions each have two α - and two β -chain genes, all of which are polymorphic. The class II molecules encoded by these genes are transmembrane dimers consisting of an α - and a β -chain. Certain alleles of the HLA-DR series are in strong positive linkage disequilibrium with alleles of the DQ series (reviewed in ref. 7). The genetic basis of the DW determinants, determined by homozygous typing cells (HTCs) in mixed lymphocyte culture, remains controversial. It is our view that these determinants are encoded in the HLA-DR subregion but are not identical to the specificities of the DR segregant series 8,9 .

We first investigated the DR4 RFLP, using as reference DNA panels of HTCs covering all the Dw specificities. The DNA was digested with TaqI, PvuII, PstI and EcoRI, electrophoresed on

agarose gels, and the gels were then blotted onto nitrocellulose filters and hybridized with DR β , DQ β and DQ α probes. Out of 11 DR4⁺ HTCs tested, 3 were Dw4, 1 was Dw10, 2 each were Dw13, Dw14 and Dw15 and 1 was DKT2 (Table 1).

No differences were seen in the Southern blot patterns obtained after hybridization with the DR β probe (not shown). However, after TaqI digestion followed by hydridization with the DQ α probe, which detects DX and DQ genes^{10,11}, we observed clear differences in the Southern blot bands. This probably represents the $DX\alpha$ polymorphism first described by Hui et al. 12 and confirmed by others 13. Taq I digestion showed the DX α polymorphism to consist of 2.1-kilobase (kb) ('upper' = U) and 1.9-kb ('lower' = L) fragments; U and L correspond to the 2.2- and 2.1-kb bands described by Nepom et al.14 Two consanguineous DR4/Dw4 HTCs tested show different patterns; MCF contains the L fragment while BM14 contains the U fragment. All the other HTCs have one or other of these fragments; the two Dw13 HTCs also have different DX α RFLPs (Fig. 1). In addition, BM14 and MCF give different DQα RFLPs using PvuII (8 and 7.5 kb respectively, not shown); these probably also represent the DX α polymorphism, and we have now used this to investigate HLA associations in IDDM and RA. Our results suggest that DQ differences do not correlate with Dw definitions. Figures 2 and 3 show Southern blot patterns öbtained using the DQβ probe and EcoRI, PstI, PvuII and TaqI to digest the DNA. Two patterns, which we have called Ω and ϕ (see Table 1), were seen among the HTCs; when they are compared using BM14 (Ω) and MCF (ϕ) (Fig. 2), both of which are DR4/Dw4, the bands which distinguish most clearly between the two patterns are of 12 kb (Ω) and 4.4 kb (ϕ) using PstI, and 19 kb (Ω) and 13 kb (ϕ) using EcoRI, while with PvuII a 2.6-kb band is absent in Ω and present in ϕ . The patterns obtained on TaaI digestion (Fig. 3) are more complex, consisting of bands of 2.0, 2.3 and 2.5 kb for Ω and of 1.8, 1.95, 2.2, 2.4 and 2.6 kb for ϕ . The two DR4/Dw13 HTCs show different DOB RFLPs, as do the two DR4/Dw4 HTCs (Fig. 3). These results support our earlier findings that the DQ types detected using alloantisera do not materially affect HLA-Dw assignment and that the same Dw specificity can occur in cells that differ for HLA-DQ (ref. 15).

We next performed serological and monoclonal antibody studies of the DR4 cells using the FLEGG alloantiserum¹⁶ and the A10-83 monoclonal antibody (Maeda, 9w790) in a standard microcytotoxicity test. These reagents define a specificity designated TA10 (ref. 6) which splits DQw3 into DQw3.1 and DQw3.2 (see ref. 14) and which is associated with DR5-DQw3 and a subset of DR4. One of the two DR4/Dw4 HTCs was TA10-positive (MCF, ϕ) and the other (BM14, Ω) was TA10-negative (Table 1). The two DR4/Dw13 HTCs also had disparate TA10 typings. Table 2 shows the frequency of TA10 positivity in the DR4⁺, DR5⁻ controls. Positivity for the TA10 subtype of DQw3 coincides with the DQ $\beta\phi$ pattern in the small number of DR4⁺

Table 1 DR4+ homozygous typing used in the present study

		I able I	71C4 11O11102	Jeous typing	used in the	prosent staay				
									RFLP	
				HLA				naubinous anno ann ann ann ann ann ann ann ann an	DQB	
Name (source)	Α	В	Cw	Dw	DR	DQw	TA10	DX	Ω or ϕ	DQBT6
MCF (Local)	2/-	62/ -	3/-	4/-	4/ —	3/-	+	L	$\boldsymbol{\phi}$	+
BM14 (Ferrara, Bergamo)	3/-	7/-	?	4/-	4/	3/-	-	U	Ω	+
19W4(ER) (Dupont, New York)	2/-	44/ —	5/-	4/ —	4/	3/-	NT	NT	φ	NT
110W10(FS) (Dupont, New York)	26/-	38/ —	?	10/ —	4/	3/-	NT	NT	Ω	+
FLE (Local)	2/ —	63/	7/	13/ -	4/	3/-	-	υ	Ω	+
JHA (Local)	31/	51/ —	-/-	13/ -	4/	3/-	+	L	φ	+
MT (Bashir, Sydney)	31/-	60/ —	3/	14/ —	4/-	3/-	NT	U	Ω	+
KY (Bashir, Sydney)	31/-	60/ -	3/	14/-	4/	3/	NT	U	Ω	+
EbWa (Kashiwagi, Kanagawa)	24/ -	54/ —	1/-	15/-	4/-	Blank	NT	L	Ω	+
KT9 (Kashiwagi, Kanagawa)	11/24	40/ -	1/3	15/	4/-	Blank	NT	NT	Ω	+
KT13 (Kashiwagi)	24/31	7/51	-/-	DKT2	4/-	?	NT	NT	Ω	+

^{*} Department of Immunology, † Medical Unit and ‡ Bone and Joint Research Unit, London Hospital Medical College, Turner Street, London E1 2AD, UK

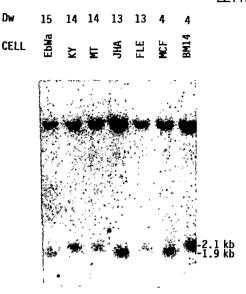


Fig. 1 DNA of homozygous DR4 cells digested with TaqI and probed with DQ α . The figure shows the DX α 'U' band at 2.1 kb and the 'L' band at 1.9 kb. The cell lines MCF, JHA and EbWa have the L band, whereas BM14, FLE, MT and KY have the U band.

Methods. Genomic DNA was either extracted from Epstein-Barr virustransformed cell lines derived from the HTCs shown in Table 1, or from peripheral blood lymphocytes from patients and controls. DNA (10 μ g) was digested for 16 h with EcoRI, PoulI or PstI at 37 °C, or with TaqI at 65 °C (enzymes from Boehringer Mannheim). The resulting DNA fragments were separated on 0.5% agarose gels by electrophoresis at 30 V for 18-20 h and then transferred 30 to nitrocellulose filters (Schleicher & Schuell). Fragments of HindIII-digested λ DNA were used as molecular size markers. The DNA probes used were labelled with $[\alpha^{32}P]dATP$ and $[\alpha^{32}P]dTTP$ (NEN) by nick-translation³¹. Before hybridization, the nitrocellulose filters were incubated for 2 h at 65 °C in 0.45 M NaCl/45 mM trisodium citrate (pH 7.0) and 10× Denhardt's reagent. The filters were then hybridized with the ³²P-labelled heat-denatured probe in 0.45 M NaCl/45 mM trisodium citrate (pH 7.0)/10× Denhardt's reagent/10% sodium dextran sulphate and 500 μg denatured salmon sperm DNA per ml of hybridization mix. After 16 h at 65 °C the filters were washed three times at 65 °C for 15 min each with 0.45 M NaCl/45 mM trisodium citrate (pH 7.0)/0.1% sodium dextran sulphate, three times at 65 °C for 15 min each with 0.15 M NaCl/15 mM trisodium citrate (pH 7.0)/0.1% sodium dextran sulphate, and three times at 65 °C for 15 min each with 50 mM NaCl/5 mM trisodium citrate (pH 7.0)/0.1% sodium dextran sulphate. The labelled fragments were then detected by exposing Kodak XAR-5 film with intensifying screens to the radioactive filters at -70 °C for 2-3 days.

HTCs. This was confirmed by Nepom et al.¹⁷ using a larger panel and may correspond to the DQR4 (Ω) and DQR5 (ϕ) patterns described by Cohen-Haguenauer et al.¹⁸. Although the TA10/DQ $\beta\phi$ association is not absolute in heterozygous individuals, as TA10 is included within DQ $\beta\phi$, it may define a DQ $\beta\phi$ subtype (Table 3). TA10 positivity is also associated with B44 in our DR4⁺ panel.

As all these new polymorphisms are associated with each other and with specific HLA determinants, we were able to construct three series of associated alleles, or preferential allelic associations (PAAs); one was based on the B8/DR3 haplotype, one on the DR4/B44 haplotype and one on the DR4/Bw62 haplotype, which includes alleles not only of the newly described RFLPs (see below) but also of TA10.

Disease associations were thus investigated in two ways. First, the incidence of the newly described polymorphisms was compared directly in patients and control subjects— $DX\alpha U$ and L; $DQ\beta\phi$ and Ω ; and $DQ\beta T6$ and TA10 positivity and negativity. $DQ\beta T6$ was defined by a 6-kb fragment obtained with the $DQ\beta$ probe following TaqI digestion and was present in all the DR4 HTCs (Fig. 3) but was absent in some of the DR4⁺ patients and controls.

In diabetics who type as DR4, the positive associations between diabetes and certain RFLPs compared with those of control subjects are as follows: DX α U, 92% versus 46%; DQB β Ω , 81%, 46%; DQ β T6, 81%, 24%; and Bw62, 39%,

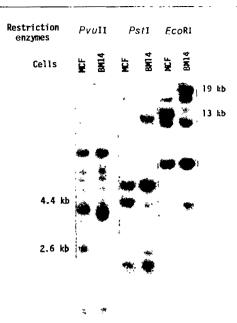


Fig. 2 DNA from HTCs BM14 and MCF (DR4, Dw4) hybridized with a $DQ\beta$ probe. The figure shows the distinguishing features between the $DQ\beta\Omega$ pattern (BM14) and the DQ $\beta\phi$ pattern (MCF). EcoR1 digestion gives a 19-kb (Ω) and a 13-kb (ϕ) band, PstI a 12-kb (Ω) and a 44-kb (ϕ) band. and with Poull a 2.6-kb band is present in the ϕ pattern and absent in the Ω pattern. When DNA from DR4 individuals is digested with Pst1, the 12 5and 4.4-kb bands are used to distinguish Ω from ϕ . However, other DR types also give one or other of these bands; for example, DR1 has a 4 4-kb band, DR2 and DR6 give a 12.5-kb band. It is therefore possible to designate the DR4 to Ω or ϕ by eliminating a band associated with the other haploty pe For example, a DR1, DR4 patient displayed both the 12.5 and 4 4-kb bands By eliminating the 4.4-kb band associated with the DR1 it is possible to assign the DR4 to the Ω type. On this basis all individuals with DR1, DR2 or DR6 showing both bands were classified as Ω or & There was one DR4, DR7 patient and two controls not classified due to clear polymorphism in the DR7. Also amongst the controls was one DR4, DR11 which was not classified due to insufficient data on this group, and a DR3, DR4 due to possible polymorphism here also.

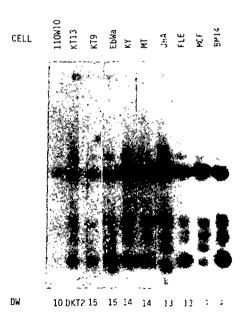


Fig. 3 DNA from HTCs BM14 and MCF (DR4, Dw4) hybridized with a DQ β probe. The distinguishing features between IOQ β Ω and ϕ patterns with Taq1 are 2.0-, 2.3- and 2.5-kb bands with Ω (BM14) and 1.8-, 1.95., 2.2-, 2.4- and 2.6-kb bands with the ϕ (MCF) pattern. Note that the 6-kb band is present in all the DR4 cell lines. All cells give the Ω pattern except for MCF and JHA.

Table 2 Frequencies in DR4⁺ controls, RA and IDDM patients, of DX α and DQ β RFLPs, TA10 and HLA-Bw62 and HLA-B44

RFLP	Controls (%)	RA patients (%)	IDDM patients (%)
DXαU	13/28 (46.4)	15/29 (51.7)	47/51 (92.2)
DXαL	21/28 (75.0)	21/29 (72.4)	24/51% (47.1)
$DQ\beta\Omega^*$	12/26 (46.1)	1	29/36 (80.5)
$DQB\Omega \uparrow$	6/24 (25.0)	16/30 (53.0)§	, , , , , ,
DQβφ*	21/26 (80.8)		12/27# (44.0)
$DQB\Omega t$	19/24 (79.0)	18/30 (60.0)	,,
$DQ\beta\phi T6$	7/29 (24.1)	18/34§ (52.9)	29/36 (80.5)
Serological specificities			
TA10‡	10/24 (41.7)	13/27 (48.1)	4/15 (26.7)
Bw62	5/30 (16.7)	10/32 (31.2)	18/46¶ (39.1)
B44	13/30 (43.3)	13/32 (40.6)	8/469 (17.4)

Significance of differences in frequencies was tested by Haldane's modification²⁸ of Woolf's method²⁹. P values are not corrected for the number of tests.

17%; while negative ones are with DX α L, 47% versus 75%; DQ $\beta\phi$, 44%, 81%; B44, 17%, 43%; and TA10, 27%, 42%. In DR3⁺ diabetics there is also a strong association with DX α U (Table 2).

In rheumatoid arthritis patients, there were no significant differences in the DX α U and DX α L frequencies in DR4⁺ patients and control subjects, although associations were found with DQ $\beta\Omega$ (53% compared with 25%), DQ β T6 (53%, 24%) and Bw62 (31%, 17%) (Table 2).

We next investigated HLA haplotypes that might be potential disease markers by testing the associations between the newly described RFLPs, the serologically detectable DQ-like determinant TA10 and established antigens of the DR, DQ, Dw and HLA-B segregant series in the IDDM and RA patients. Although additional DR4⁻ IDDM patients and controls were used in this analysis, the total control group does not constitute a random panel, having a preponderance of DR3⁺ and DR4⁺ individuals. The significant associations (Table 3) are DX α U with DQ β α , DX α L with DQ β α , TA10 with DQ β α and TA10 with B44; DX α U with DR3; DQ β T6 with DR4 and DQ β T6 with DR1. However, the significance of these associations varied in the three groups tested (control subjects, RA and IDDM patients). The constructs of the three PAAs are based on the significant associations indicated above and shown in Table 2; they are:

```
PAA 1. DX\alpha U \cdots DQB\Omega \cdots
```

The DX α U/DQ $\beta\Omega$ or DX α L/DQ $\beta\phi$ association was present in all the HTCs except EbWa, Dw15 (Table 1).

Our main aim was to try to identify specific molecules or haplotypes likely to be directly involved in the pathogenesis of RA and IDDM. The striking association (>92%) of DX α U with IDDM may be attributable to the high prevalence of the combinations of PAA 1 and PAA 2 which have previously been marked by DR3 and DR4 antigens, both of which are associated with $DX\alpha U$ and are present at a high frequency in $IDDM^{32}$. It is already known that individuals heterozygous for DR3 and DR4 run a higher risk of developing IDDM than do those who are either DR3 or DR4 homozygous¹⁹. The DX α U allele in itself may thus be a risk factor for IDDM. Our studies also indicate that the Bw62/DR4 haplotype is important in both IDDM and RA. The RA patients used in our study did not show as marked an increase in the DQ $\beta\Omega$ component that is part of PAA 2 as did the controls, even though increased frequencies of the Bw62/DR4 haplotype have been reported in RA patients with severe disease^{20,21}. Our RA patients, although fulfilling the clinical criteria for RA, were not selected for severe

Table 3 Associations between RFLPs and serological specificities in controls, RA and IDDM patients

RFLP versus RFLP						
DQα versus DQβ	n	++	+-	-+		P
$DX\alpha U$ versus $DQ\beta\Omega^*$ in:						
Controls	23	6	7	0	10	0.017
RA patients	28	14	5	1	8	0.003
IDDM patients	32	19	8	2	3	0.21
$DX\alpha L$ versus $DQ\beta\phi^*$ in:						
Controls	23	18	2	0	3	0.0056
RA patients	30	17	6	0	7	0.0008
RFLP versus class II antigens						
DQβ						
$DQ\beta\phi$ versus TA10* in:						
Controls	16	8	5	0	3	0.10
RA patients	21	9	2	2	8	0.007
DOBT6 versus DR4† in:						
Controls	44	8	4	21	11	0.62
RA patients	62	23	10	19	10	0.47
IDDM patients	46	28	1	7	10	< 0.00005
DQβT6 versus DR1† in:						
Controls	36	5	3	0	28	0.00015
RA patients	62	19	14	0	29	1.9×10^{-7}
IDDM patients	46	4	25	1	16	0.38
DQαU						
DXαU versus DR3† in:						
Controls	48	17	9	1	21	<00005
IDDM patients	68	41	21	1	5	0.03
RA patients	30	1	18	1	10	0.61
Class I versus class II						
B44 versus TA10 in						
DR4 controls	24	8	3	3	10	0.02

P values were computed using Fisher's exact test.

disease, and greater increases in $DQ\beta\Omega$ and $DX\alpha U$ might thus be expected in patients with severe disease. There was no difference in the frequency of TA10 in the RA patients compared with the controls, but its frequency was reduced in IDDM patients, as found by Tait et al.²².

We have also found an increase in the frequency of $DQ\beta\Omega$ in IDDM patients. However, Cohen-Haguenauer et al. 18 reported that, compared with DR-matched controls, IDDM patients showed a decrease in a TaqI, $DQ\beta$, 2.1-kb fragment, which may correspond to our $DQ\beta\Omega$ pattern in PAA 2. This difference may be due to heterogeneity between the populations studied.

The increase in the frequency of the DQ β T6 RFLP in the RA and IDDM patients seems to be a novel finding, whereas the increases in DX α U and DQ $\beta\Omega$ in the IDDM patients represent extensions of known susceptibility axes. In IDDM patients the $DQ\beta T6$ fragment is found at a very high frequency, together with DR4 and DQ $\beta\Omega$ (Table 3); these associations are not apparent in the controls and hence it is not certain whether they represent true associations or combined increases of separate elements in the IDDM patients. The DQ β T6 RFLP does not show preferential association with Bw62 in the DR4⁺ IDDM patients (7/8 of the Bw62⁺ patients and 15/19 of the Bw62⁻ patients have the DQ β T6 fragment). As the frequency of the DQ\beta T6 RFLP is also increased in the RA patients compared with the controls, it could be a new common susceptibility marker in these disorders. Our data also indicate a highly significant association between DQ β T6 and DR1, especially in RA. patients (Table 3); this may have some bearing on the reported increased frequency of DR1 in British²³, Indian²⁴ and Jewish²⁵ RA patients. Interestingly 'MC1', a specificity common to DR1 and DR4, has been described²⁶ and a monoclonal antibody recognizing this specificity has been produced which reacts with cells from more than 90% of RA patients (R. Winchester, personal communication).

Although it is not known whether the $DX\alpha U$ and L, $DQ\beta\Omega$ and ϕ $DB\beta T6$ fragments encode functional HLA class II molecules, we can postulate that these RFLPs may encode class II molecules associated with the pathogenesis of IDDM and RA. Alternatively, they may be in linkage disequilibrium with

^{*} Assignments of DQ β in IDDM patients and control subjects were based solely on TaqI RFLPs, that is, 2 kb for Ω and 1.9 kb for ϕ .

[†] Assignments based on PstI, as described in Fig. 2 legend.

DR4+, DR5 individuals were tested for TA10.

 $^{||}P<0.0005; \#P<0.01; \PP<0.05; \SP=0.06.$

^{*} DR4⁺ individuals; † all individuals.

some other, more relevant, genes in the PAAs concerned. We consider that there is not a single gene and/or gene product of each of the PAAs involved, but that several different genes or molecules, possessing complementary functions with hierarchical as well as additive effects, are implicated. Hybrid DQ molecules²⁷, trans combinations of DQ α chains from one PAA and DQB chains from another PAA, may also be relevant, particularly with regard to IDDM susceptibility. These findings provide a basis for investigating the putative HLA class II molecules potentially encoded by genes associated with the DO RFLPs described here.

We thank Dr P. Petersen (DNA probes), Drs G. B. Ferrara, B. Dupont, H. Bashir and N. Kashiwagi (homozygous typing cells) and Dr H. Maeda (monoclonal antibody) for reagents used in this study. Patient material was provided by Professor H. Currey and Dr J. P. Monson of the London Hospital. Financial support was provided by the Arthritis and Rheumatism Council (S.C., W.O.), the Multiple Sclerosis Society (J.A., A.V.G.), MRC (H.F.) and the Wellcome Trust (J.A.S., P.C.). We thank Joanna Lee for help in the preparation of this manuscript.

Received 7 February; accepted 26 March 1986.

- 1. Stastny, P. Tissue Antigens 4, 571-579 (1974).
- 2. Thomsen, M. et al. Transplantn Rev. 22, 120-147 (1985).

- Sachs, J. A., Cudworth, A. G., Jaraquemada, D., Gorsuch, A. N. & Festenstein, H. Diabetologia 18, 41-43 (1980).
- Batchelor, J. R. & Morris, P. J. in Histocompatibility Testing 1977 (eds Bodmer, W. F. et al.) 205-258 (Munksgaard, Copenhagen, 1977).
- 5. Jaraquemada, D. et al. in Histocompatibility Testing 1984 (eds Albert, E. D. et al.) 270-273
- (Springer, Berlin, 1984).

 6. Maeda, H. Tissue Antigens 23, 163-170 (1984).
- Miscus, H. Hssue Antigens 23, 163-170 (1964).
 Giles, R. C. & Capra, J. D. Tissue Antigens 25, 57-68 (1985).
 Jaraquemada, D., Okoye, R. C., Ollier, W., Awad, J. & Festenstein, H. in Histocompatibility Testing 1984 (eds Albert, E. D. et al.) 472-473 (Springer, Berlin, 1984).
 Sachs, J. A., Jaraquemada, J. & Festenstein, H. Tissue Antigens 17, 43-56 (1981).
- Auffray, C., Kuo, J., Demars, R. & Strominger, J. L. Nature 304, 174-177 (1983).
 Trowsdale, J. et al. Proc. natn. Acad. Sci. U.S.A. 80, 1972-1976 (1983).
- 12. Hui, K. M. et al. in Histocompatibility Testing 1984 (eds Albert, E. D. et al.) 590-594
- (Springer, Berlin, 1984).

 13. Spielman, R. S., Lee, J., Bodmer, W. F., Bodmer, J. G. & Trowsdale, J. Proc. natn. Acad. Sci. U.S.A. 81, 3461-3465 (1984).
- 14. Nepom, B. S. et al. J. exp. Med. (in the press).
 15. Jaraquemada, D. et al. Hun. Immun. (in the press).
 16. Navarrete, C. thesis, Univ. London (1985).

- Kim, S. J. et al. Proc. natn. Acad. Sci. U.S.A. (in the press).
 Cohen-Haguenauer, O. et al. Proc. natn. Acad. Sci. U.S.A. 82, 3335-3339 (1985).
- Svejgaard, A., Platz, P. & Ryder, L. P. Immun. Rev. 70, 193-218 (1983).
 Ollier, W. et al. Tissue Antigens 24, 279-291 (1984).
- 21. Jaraquemada, D. et al. Ann. rheum. Dis. (in the press)
- 22. Tait, B. D. et al. Tissue Antigens 24, 228-233 (1984).

- Grennan, D. M., Sanders, P. A., Dyer, P. A. & Harris, R. Ann. Rheum. (in the press).
 Nichol, F. E. & Woodrow, J. C. Lancet 1, 220-221 (1981).
 Schiff, B., Mizrachi, Y., Orgad, S., Yaron, J. & Gazit, E. Ann. rheum. Dis. 41, 403 (1982).
- Duquesnoy, R. J., Marrari, M., Hackbarth, S. & Zeevi, A. Hum. Immun. 10, 165-176 (1984).
 Charron, D. J., Lotteau, V. & Turmel, P. Nature 312, 157-159 (1984).
 Haldane, J. B. S. Ann. hum. Genet. 20, 309-311 (1955).
 Woolf, B. Ann. hum. Genet. 19, 251-253 (1955).

- 30. Southern, E. M. J. molec. Biol. 98, 503-517 (1975)
- 31. Rigby, P. W. J., Dickmann, M., Rhodes, C. & Berg, P. J. molec. Biol. 113, 237-251 (1977). 32. Hitman, G. A. et al. Immunogenetics 23, 47-51 (1986).

Polymorphism of human Ia antigens: gene conversion between two DR β loci results in a new HLA-D/DR specificity

Jack Gorski & Bernard Mach

Department of Microbiology, University of Geneva Medical School, 1211 Geneva 4, Switzerland

The polymorphic HLA-DR β -chains are encoded within the human major histocompatibility complex (MHC) by multiple loci resulting from gene duplications. Certain DR haplotypes can be grouped into families based on shared structural factors. We have studied the molecular basis of HLA-DR polymorphism within such a group which includes the haplotypes DR3, DR5 and DRw6. Molecular mapping of the DR β -chain region allows true allelic comparisons of the two expressed DR β -chain loci, $DR\beta I$ and $DR\beta III$. At the more polymorphic locus, $DR\beta I$, the allelic differences are clustered and may result from gene conversion events over very short distances. The gene encoding the HLA-DR3/Dw3 specificity has been generated by a gene conversion involving the $DR\beta I$ and the DRBIII loci of the HLA-DRw6/Dw18 haplotype, as recipient and donor gene, respectively. Based on which allele is found at DRBIII, the less polymorphic locus, two groups of haplotypes can be defined: DRw52a and DRw52b. The generation of HLA-DR polymorphism within the DRw52 supertypic group can thus be accounted for by a succession of gene duplication, divergence and gene conversion.

The polymorphism of class II molecules is responsible for the restriction of T-cell activation by antigen-presenting cells. The polymorphic regions of the class II molecules are therefore implicated in interactions with both the T-cell receptor and with antigen. Since some alleles are more efficient at presenting certain antigens than others, class II genes are also referred to as immune response genes (reviewed in refs 1 and 2). The class II products of the human MHC (the HLA complex) include the HLA-DR, DQ and DP antigens³. HLA-DR molecules are the predominant class II products on the cell surface, and the polymorphism is associated with the β -chain. The polymorphic regions of the DR β -chains are located predominantly at the N-terminal of the mature polypeptide chain⁴, corresponding to the first structural domain. The DR subregion contains multiple highly homologous β -chain loci⁵⁻⁷ but only one α -chain

locus ⁸⁻¹⁰. In the DR3 and DRw6 haplotypes, the three β -chain loci have been linked on a molecular map¹¹. The DRβII locus is a pseudogene without a first domain exon and the two expressed loci, βI and βIII , are the result of a recent duplication11.

The serologically identified DR specificities can be grouped on the basis of their reactivity with supertypic sera¹². The haplotypes within such a supertypic group have similar Southern blot patterns^{13,14} and, within the supertypic group DRw52, restriction maps of genomic clones are very similar¹¹. This implies a common evolutionary origin of the haplotypes within a supertypic group. Based on the structural similarity of the HLA-DR β -chain region of these haplotypes, individual DR B-chain genes can now be assigned to specific loci and true allelic comparisons made.

The nucleotide sequences of the polymorphic first domains of the two active loci (βI and βIII) of the DR3, DRw6a and DRw6b haplotypes were determined. The sequence of a DR5 βI locus¹⁵ is added to the comparison. The allelic sequences for each locus (Fig. 1a and b) are presented in relation to a consensus sequence. It is evident that locus $DR\beta I$ (a) is more polymorphic than $DR\beta III$ (b) as all the $DR\beta I$ sequences are different. Within the locus $DR\beta I$ there is a clearcut clustering of the nucleotide differences around position 185-205 (the 'hypervariable region'). This is in contrast with DR β -chain sequence comparisons made in a nonallelic manner and across supertypic groups, where a different pattern of variation is observed. This can be seen when the consensus sequences of the two loci are compared (Fig. 1c). An additional region of variability is seen from base pair (bp) 15 to 22.

The nature of the polymorphic differences at the βI locus was explored in detail. It was observed that the sequence of the DR\$I locus of HLA-DR3 can be generated by exchanging two short segments of DNA from the βI and the βIII loci of the haplotype DRw6a (Fig. 2a). Given the phenomenon of positive interference for multiple double recombination events, it is more likely that a single gene conversion with interrupted repair¹⁶ accounts for the structure of the DR3 BI locus. A schema of the conversion event is shown in Fig. 2b, where the DRw6a βIII locus acts as donor and the DRw6a BI locus as recipient, resulting in the sequence of the DR3 gene. As expected with such a mechanism, the βIII locus of HLA-DR3 is identical to that of HLA-DRw6a.



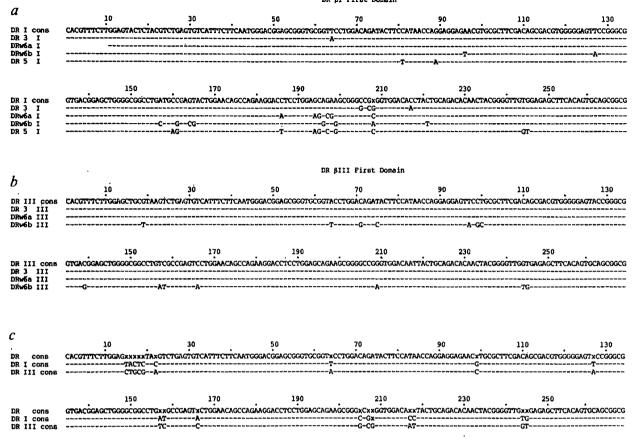


Fig. 1 Sequence of the DR β-chain first domain of the DR3 haplotype, two DRw6 haplotypes and a published DR5 haplotype¹⁵. a, βI locus; b, βIII locus. The consensus sequence (cons) is the base found at that position in at least two of the sequences. c, Comparison of locus I and locus III sequence differences by aligning the consensus sequences for each locus and deriving a DRβ consensus. Regions where βI and βIII differ from each other and which may influence locus-specific conformation of the protein product are easily visualized.

Methods. Sequences were obtained from subclones of the first domain exon of previously described cosmid and phage genomic clones^{6,11}, by both the chemical²³ and dideoxy²⁴ methods, as well as from cDNA clones⁵. DR3 sequences are from a cosmid library of the consanguineous typing cell line AVL; DRw6a sequences are derived from a cosmid library and cDNA library of the consanguinous homozygous typing cell line HHK; DRw6b sequences are from a Charon 30 phage library of a DR4, DRw6 line. The DRw6 genes were identified by Southern blot comparisons with DRw6 and DR4 genomic DNAs (see ref. 25 for an example). The cDNA-derived sequence of DRw6b βIII⁵ as well as a phage-derived sequence²⁵ have been published previously.

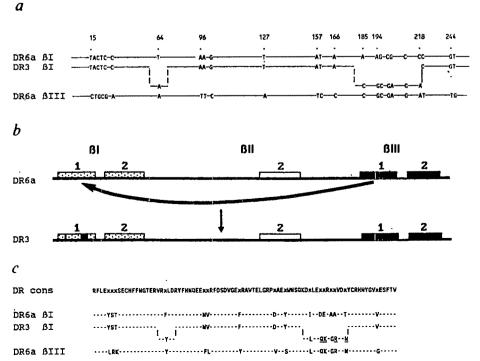


Fig. 2 Intrachromosomal gene conversion between two DRw6 β-chain loci genes. a, The first-domain sequences of the two DR6a loci are aligned with the sequence of the DR3 βI locus. A solid line indicates identical sequences. Relevant nucleotide positions are shown to facilitate comparison with the sequence in Fig. 1. Because of the uncertainty in the limits of the conversion event, dotted lines are used to indicate cross-over points. b, Schematic representation of genes participating in the conversion event; c, aminoacid sequence of the first domains of the DR3 β I and DRw6a β I and β III chains showing the block of amino acids transferred by the conversion event. Non-conservative aminoacid changes in the DR3 BI chain are underlined. The consensus approach is used to aid visualization of amino-acid differences between the βI and βIII loci. The block of amino acids transferred must interact with these differences in the generation of the novel epitope.

The replacement of this short segment of DNA of the DRw6 βI locus (Fig. 2) has given rise to a gene encoding a different serological and T-cell specificity. The B-cell lines AVL (DR3, 3) and HHK (DRw6, w6), from which these genes have been cloned, have distinct serological reactivities, and alloreactive T-cell proliferation assays distinguish these lines as Dw3 and Dw18, respectively¹⁷. The transfer of the block of amino acids from the DR β III-chain to the DR β I-chain (Fig. 2c) results in the loss of two negatively charged amino acids and a gain of two positively charged residues. The introduction of this region into the context of the βI locus must result in a novel conformation which gives rise to the DR3/Dw3 specificity. DR3 is a common haplotype which is associated with an increased risk for certain diseases.

Upon further analysis of the highly polymorphic region of the $DR\beta I$ locus, an example of a possible interchromosomal

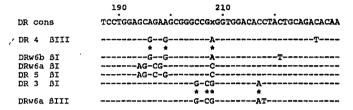
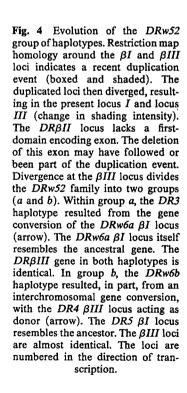


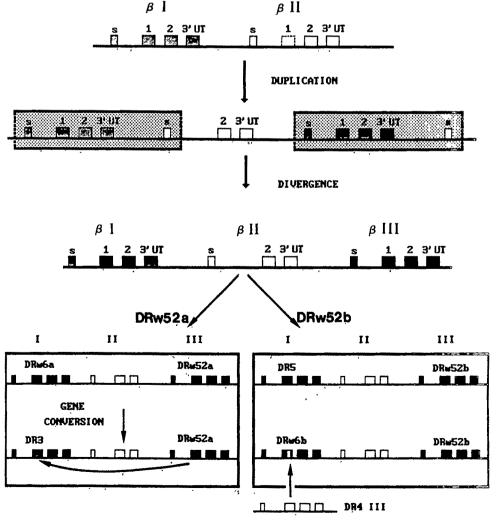
Fig. 3 An example of a possible interchromosomal gene conversion between distantly related haplotypes. The asterisks mark positions common to the DR6b βI- and DR4 βIII-chains. The DR3 conversion event is also marked. The DR4 βIII sequence is derived from a Charon 30 phage library of the DR4, DRw6 cell line mentioned previously.

gene conversion event was observed (Fig. 3). This region, which is similar in $DRw6a\ \beta I$ and $DR5\ \beta I$, is very different in the βI locus of DRw6b. Surprisingly, it is identical to the same region in the βIII locus of DR4, a haplotype from a distantly related supertypic group, DRw53. It is thus likely that the $DRw6b\ \beta I$ locus has resulted from a gene conversion between an ancestral gene similar to $DRw6b\ \beta I$ as recipient and the βIII locus of the DR4 haplotype which acted as donor.

This region of high allelic polymorphism, where we observe examples of gene conversion, is the same as that involved in the I-E to I-A conversion event giving rise to the $I-A^{bm12}$ mutation in mice¹⁸⁻²⁰. Furthermore, a micropolymorphism reported in the DR4 haplotype in this same DNA segment²¹, correlating with changes in alloreactive T-cell recognition, can be attributed to a gene conversion of the DR4 βII locus, with the DR4 βIII locus acting as donor. An interesting observation is that in all these cases the donor locus is 3' of the target locus with respect to the direction of transcription. Together, these results suggest a conversion hotspot responsible for this hypervariable region. The presence of this hotspot implies either that conversion occurs here preferentially for physical reasons or that conversion is random but selection has favoured those events occurring in this region.

Concerning the less polymorphic $DR\beta III$ locus, nucleotide sequence comparison defines two groups of haplotypes, DRw52a and DRw52b, whose $DR\beta III$ loci differ by 11 bp. The first group, DRw52a, includes some DR3 and some DRw6 haplotypes (Fig. 1b). The second group, DRw52b, includes other DR3 and DRw6 haplotypes (Fig. 1b and unpublished results) as well as DR5 (B. Schwartz, personal communication). Hybridization with appropriately chosen oligonucleotides has





allowed us to type unknown individuals as DRw52a or DRw52b (ref. 22 and unpublished) in a sizeable number of normal and diseased individuals. This form of analysis can be of considerable use in phylogenetic studies of human populations.

Taken together, these results can account for the evolution of the DR genes in the DRw52 supertypic group (Fig. 4). The ancestral features of this family are the relatively recent duplication of the βI locus and the silencing of the βII locus by deletion of the first domain encoding exon¹¹. The duplicated $DR\beta I$ loci then diverged into βI and βIII . Further divergence resulted in a branching into two lineages (DRw52a and DRw52b) based on common alleles at the less polymorphic locus, DRβIII. In the DRw52a group, the DRw6a haplotype gave rise to the DR3 specificity by the gene conversion described here. The DRw6b haplotype was probably involved in an interchromosomal gene conversion with the DR4 BIII locus acting as donor.

This analysis provides a framework for assigning serological specificities to the products of the different loci of the DRw52 haplotypes. Allelic differences in the product of the DR\$III locus split DRw52 into a and b. It has already been shown that this locus encodes the DRw52 specificity for the case of the DRw6b haplotype²⁵. We propose that the distinct epitopes DRw52a and DRw52b (Fig. 4) will correspond to serological and T-cell specificities. In addition to the product of locus DRBIII, each haplotype obviously also expresses the product of their βI locus, which determines the fine DR specificity.

The data described here represent an example of relatively rapid evolution of a multigene family in which the loci appear to diverge at different rates following a duplication event. The time of divergence may be estimated by analysing this group of haplotypes in other geographical (non-European) groups whose migratory patterns are known.

The divergence in this gene family is generated in part by gene conversion. Since this mechanism can involve the transfer of preselected epitopes, the resulting additional polymorphism is frequently maintained in the population. Therefore, even if gene conversion is a relatively rare event, it can play a major role in the generation of polymorphism by producing functionally effective variants. It is generally thought that this polymorphism confers a selective advantage to a population in terms of its ability to cope with various pathogens. A genetic system with multiple loci undergoing conversion events could regenerate polymorphism in populations which have undergone bottlenecks due to migration or adverse environmental factors.

We thank Chantal Mattmann and Madeleine Zufferey for technical assistance, Dr B. Schwartz for providing sequence data for DR5 prior to publication and Dr J. J. van Rood for comments on the manuscript. This work was supported by a grant from the Swiss National Fund for Scientific Research.

Note added in proof: From a recent analysis of micropolymorphism of HLA-DR4 (ref. 26), we propose that one DR4βI allele, Dw10, has arisen by a gene conversion, with DRw6aβI acting as donor.

Received 17 January; accepted 4 April 1986.

- Schwartz, R. A. Rev. Immun. 3, 237-261 (1985).
- Nagy, Z. et al. Immun. Rev. 60, 61-83 (1981).
 Kaufman, J. et al. Cell 36, 1-13 (1984).
- Kaufman, J. F. & Strominger, J. L. Nature 297, 694-697 (1982).
 Long, E. O. et al. EMBO J. 2, 389-394 (1983).

- Gorski, J. et al. in UCLA Symp. 18, 47-56 (1984). Speis, T. et al. Proc. natn. Acad. Sci. U.S.A. 82, 5165-5169 (1985).
- Lee, J., Trowsdale, J. & Bodmer, W. F. Proc. natn. Acad. Sci. U.S.A. 79, 545-549 (1982).
 Korman, A. et al. Proc. natn. Acad. Sci. U.S.A. 79, 1844-1848 (1982).
- Wake, C. et al. Proc. natn. Acad. Sci. U.S.A. 79, 6979-6983 (1982).
 Rollini, P., Mach, B. & Gorski, J. Proc. natn. Acad. Sci. U.S.A. 82, 7197-7201 (1985).
- 12. Tanigaki, N. & Tosi, R. Immun. Rev. 66, 5-37 (1982).
 13. Angelini, G. et al. in Histocompatibility Testing (eds Albert, E. D., Baur, M. P. & Mayr, W. R.) 582-584 (Springer, New York, 1984).

 14. Hui, K. M. et al. in Histocompatibility Testing (eds Albert, E. D., Baur, M. P. & Mayr,
- Hu, K. M. et al. in Histocompatibility Testing (eds Albert, E. D., Daur, M. P. & Mayr, W. R.) 590-594 (Springer, New York, 1984).
 Tieber, V. L. et al. J. biol Chem. 261, 2738-2742 (1986).
 Kourilsky, P. Biochimie 65, 85-93 (1983).
 Grosse-Wilde, H., Doxiadis, I. & Brandt, H. in Histocompatibility Testing (eds Albert, E. D.,

- Baur, M. P. & Mayr, W. R.) 249-264 (Springer, New York, 1984).

 18. Denaro, M. et al. EMBO J. 3, 2029-2032 (1984).

- Mengle-Gaw, L. et al. J. exp. Med. 160, 1184-1194 (1984).
 Widera, G. & Flaveli, R. A. EMBO J. 3, 1221-1225 (1984).

- Cairns, J. S. et al. Nature 317, 166-168 (1985).
 Cairns, J. S. et al. Nature 317, 166-168 (1985).
 Angellini, G. et al. Proc. natn. Acad. Sci. U.S.A. (in the press).
 Maxam, A. M. & Gilbert, W. Proc. natn. Acad. Sci. U.S.A. 74, 560-564 (1977).
 Sanger, F., Nicklen, S. & Coulson, A. R. Proc. natn. Acad. Sci. U.S.A. 74, 5463-5467 (1977).
- Gorski, J. et al. J. exp. Med. 162, 105-116 (1985).
 Gregersen, P. K. et al. Proc. natn. Acad. Sci. U.S.A. 83, 2642-2646 (1986).

Hepatitis B virus DNA integration in a sequence homologous to v-erb-A and steroid receptor genes in a hepatocellular carcinoma

Anne Dejean*, Lydie Bougueleret†, Karl-Heinz Grzeschik‡ & Pierre Tiollais*

* Unité de Recombinaison et Expression Génétique (INSERM U.163, CNRS UA.271) and † Unité d'Informatique Scientifique, Institut Pasteur, 28 rue du Docteur Roux, 75724 Paris Cedex 15, France

‡ Institut für Humangenetik der Westfalischen Wilhems-Universität, 4400 Munster, FRG

Hepatitis B virus (HBV) is clearly involved in the aetiology of human hepatocellular carcinoma (HCC)1 and the finding of HBV DNA integration into human liver DNA in almost all HCCs studied²⁻⁷ suggested that these integrated viral sequences may be involved in liver oncogenesis. Several HBV integrations in different HCCs^{8,9} and HCC-derived cell lines¹⁰⁻¹⁴ have been analysed after molecular cloning without revealing any obvious role for HBV. From a comparison of a HBV integration site present in a particular HCC8 with the corresponding unoccupied site in the nontumorous tissue of the same liver, we now report that HBV integration places the viral sequence next to a liver cell sequence which bears a striking resemblance to both an oncogene (v-erb-A) and the supposed DNA-binding domain of the human glucocorticoid receptor and human oestrogen receptor genes. We suggest that this gene, usually silent or transcribed at a very low level in normal hepatocytes, becomes inappropriately expressed as a consequence of HBV integration, thus contributing to the cell transformation.

We have previously reported the molecular cloning of the single integrated viral sequence present in the liver tumorous nodule of patient D and we have determined the sequences of the cellular-viral junctions8. The viral insertion was a continuous subgenomic fragment 1.4 kilobases (kb) long (Fig. 1a) containing the cohesive-end region, gene C and the beginning of gene pre-S1. We therefore used the 1.1-kb and 5.8-kb HindIII cellular fragments and the 1.8-kb EcoRI host-viral fragment (respectively referred to as LT (left tumour), RT (right tumour) and MT (medium tumour); Fig. 1a) to isolate the unoccupied site from a λ phage library of DNA extracted from the non-tumorous liver of patient D. This part of the liver did not seem to contain any integrated HBV sequences. Seven overlapping clones, hybridizing to one and/or the other of the three probes, were isolated and represented 32 kb of cellular DNA at the unoccupied site (Fig. 1b). Southern blots of restriction digests of the seven clones using total human DNA as a probe showed that the host sequence at the viral insertion site corresponds mainly to unique sequence DNA (Fig. 1a, b, solid bars). Comparison between the restriction maps of the unoccupied site (Fig. 1b) and the integrated site (Fig. 1a) did not reveal any major genomic rearrangements in the cellular DNA. Integration took place within a small EcoRI fragment of 400 base pairs (bp) which we subcloned and refer to as MNT (medium non-tumour)

To investigate whether HBV became integrated in the vicinity of a cellular gene in the human genome, we determined the nucleotide sequence¹⁵ of the normal allele. This sequence

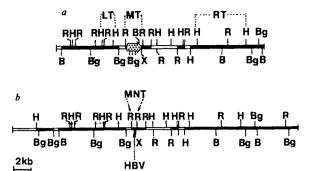


Fig. 1 a. Restriction map of the occupied site. This has previously been isolated from a library of cellular DNA extracted from the tumorous part of the liver of patient D8. The stippled region represents the 1.4-kb integrated HBV sequence. The arrowhead denotes the same orientation as the viral (+)strand30. Solid bars denote unique sequences and open bars regions containing repetitive cellular sequences. Restriction sites are: R, EcoRI; B, BamHI; Bg, Bg/II; H, HindIII; X, XhoI. The cloned 1.1-kb HindIII, 1.8-kb EcoRI and 5.8-kb HindIII cellular fragments are referred to as LT, MT and RT. b, Restriction map of the unoccupied site. The cloning experiment in which partial MboI digests of cellular DNA were cloned into λ L47.1 was as described previously¹¹. A library, made with cellular DNA from the non-tumorous part of the liver of patient D, was screened with LT, MT and RT as probes. Seven positive overlapping clones were analysed, representing 32 kb of cellular DNA. The cloned 400-bp EcoRI cellular fragment is referred to as MNT. The site of HBV integration within MNT is indicated by an arrow.

revealed the presence of an open reading frame (ORF) of 519 nucleotides which was interrupted in the middle by the viral insertion (Fig. 2). Since methionine codons were present only at the 3' end of the ORF, this region can only correspond to a single exon from a split gene. Two acceptor-like (A-L1, A-L2) and two donor-like (D-L1, D-L2) consensus sequences of splice junctions¹⁶ could be localized, respectively, at the 5' end and the 3' end of the ORF (Fig. 2). A computer-assisted analysis 17 showed that the region between A-L2 and D-L1 had a strong probability of being an exon. A search for related sequences in the NBRF protein data bank¹⁸ identified a remarkable homology (22 identities out of 49) between the translation product of the exon-like region of the ORF (amino-acid residues 69-117) and the amino-terminal region of the v-erb-A oncogene product (residues 8-58)19 (Fig. 3). Moreover, a significant homology has recently been reported between the v-erb-A protein and either the human glucocorticoid receptor (hGR)²⁰ or the human oestrogen receptor (ER)21. The alignment of the amino-acid sequence of hGR and ER with the exon-like protein product showed, in both cases, 19 identities out of 49 (Fig. 3). As already observed for v-erb-A, hGR²⁰ and ER²¹, the identity became greater beyond amino acid 96 of the ORF, which corresponds to a cysteine-rich region. In particular, the four cysteines conserved between v-erb-A, hGR and ER are present at the same position in the ORF. Although the homology continues for v-erb-A, hGR and ER-all derived from cDNA clones-no significant homology was found beyond residue 117 for the ORF. However, since the D-L1 sequence (next to residue 117) is strictly identical to the consensus sequence of a donor site, it could thus correspond to an exon/intron boundary.

The integration of HBV sequences interrupted the cellular open reading frame and generated a microdeletion of 7-12 bp (boxed in Fig. 4). This minor rearrangement provides evidence that the situation we are studying in patient D is probably very near the initial integration event. In addition to the microdeletion, the viral integration—interrupting the cellular ORF—generated a new viral-host hybrid sequence such that the first 29 codons of the viral pre-S1 gene became fused and in phase with the last 28 codons of the cellular exon (Fig. 4). Remarkably,

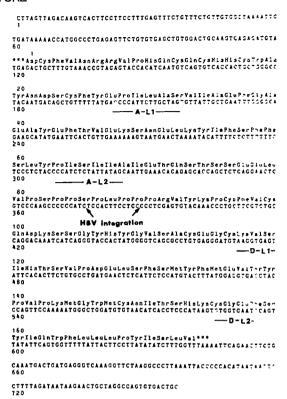


Fig. 2 Nucleotide sequence of the unoccupied site. Nucleotides are numbered at the left side. The deduced amino-acid sequence of the 519-bp open reading frame is shown above the nucleotide sequence. The amino-acid sequence is numbered from the first codon of the ORF. A large number of splice junction sequences have been reported¹⁶. The compilation of the data supports the consensus (C)₁N_TAG/G for acceptors and the consensus AG/GTAGT for donors. The two acceptor-like (A-L1 and A-L2) and donor-like (D-L1 and D-L2) sequences are underlined. The site of HBV integration in the middle of ORF is indicated by an arrow. The cloned 3.4-kb HindIII fragment, encompassing the unintegrated site in the normal allele, was sonicated, treated with the Klenow fragment of DNA polymerase plus deoxyribonucleotides (2 h, 15 °C) and fractionated by agarose gel electrophoresis. Fragments of 400-700 bp were excised and electroeluted. DNA was ethanol-precipitated, ligated to dephosphorylated Smalcleaved M13 mp8 replication form DNA and transfected into Escherichia coli strain TG-1 by the high-efficiency technique of Hanahan³¹. Recombinant clones were detected by plaque hybridization using the MNT (Fig. 1b) subclone DNA as a probe. Singlestranded templates were prepared from plaques exhibiting positive hybridization signals and were sequenced by the dideoxy chain termination procedure15 using buffer gradient gels3

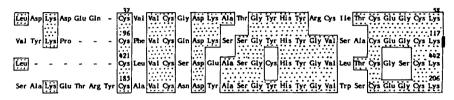
the viral genome became integrated a few nucleotides upstream from the most conserved Cys-rich portion of the ORF (Fig. 3), maintaining the integrity of this region.

Using a panel of 17 mouse-human and Chinese hamster-human somatic cell hybrid DNAs^{22,23}, we localized the ORF to chromosome 3 (data not shown), while the c-erb-A oncogene²⁴, hGR²⁵ and ER²⁶ have been mapped, respectively, to human chromosomes 17, 5 and 6. In preliminary experiments, we hybridized the MNT probe, encompassing the exon-like region of ORF, to a Northern blot of polyadenylated RNAs extracted from five human livers, but found no detectable transcripts. A large number of human fetal and adult tissues will have to be tested similarly to reveal any active transcription of this region.

The conserved Cys-rich region which extends over 60 aminoacid residues in v-erb-A protein, hGR and ER is thought to include the DNA-binding domain of the molecule^{20,21}. We can thus speculate that the corresponding homologous region of ORF, truncated by the exon-intron boundary, is part of a cellular gene that shares a common functional domain with hGR, ER

Fig. 3 Amino-acid sequence alignment of the v-erb-A oncogene protein19, the translation product of the exon-like region of ORF, the human glucocorticoid receptor (hGR)²⁰ and the oestrogen receptor (ER)²¹. The limits of the exon-like region of ORF, defined by A-L2 and D-L1 boundaries, are indicated by rectangles. To predict the location of exon-like regions, we used the discriminating program PREDICTOR¹⁷ Two subsets of the GenBank data library, containing either only exon or only intron sequences, were taken as reference pool. The program PROBE3-EXPLOR3 (ref. 18), allowing the search for ambiguous nucleic or peptidic patterns, was used to screen both the NBRF (proteins) and the GenBank (DNA) data banks. These programs were run on a MV8000 32-bit minicomputer. Amino-acid residues 69-117 from the ORF were aligned with amino-acid residues 8-58 from p75gag-erb-A, residues 397-442 from

V- <i>61b-A</i>	:		Lys Hi																			
ORF	:		Glu Th				1	• • • • •				_	1	ı	Pro	Ser					• • •	
hGR	•		Met Ar																			
ER	:	Asp	Asn Ar	Ārg	Gln	Gly	Gly	Arg	Ċlu/	\rg[A.	la Ser	Thr	Asn	Авр	Lys	Gly	Ser	Met	Ala	Met	Glu
																			нвν	√ in	tegra	tion



hGR and residues 115-206 from ER. Identical residues are boxed and gaps are indicated by dashes. The HBV integration site, upstream from the cysteine-rich region, is indicated.

and v-erb-A gene products and which could exert a transcriptional regulatory function on specific genes.

Although the way in which HBV participates in the formation of a liver cancer is unknown, the experiments reported here could promote our understanding of one possible mechanism of HBV carcinogenesis. In patient D the viral integration, interrupting the exon-like region (Fig. 2), created a chimaeric viralhost open reading frame (Fig. 4). The HBV insertion took place a few nucleotides upstream from the beginning of the putative DNA-binding domain. Since a viral promoter has been defined by in vitro transcription approximately 30 nucleotides upstream from the initiator codon of the pre-S1 gene²⁷, we suggest that, in the tumorous part of the liver, a readthrough transcription occurred from the viral promoter. Although protein or RNA from the tumour is no longer available to test this hypothesis, it is most probable that inappropriate activation of the putative gene as a consequence of HBV integration resulted in expression of a truncated protein at greater levels than that of the native protein. This protein could participate directly in the subsequent cell transformation.

Several arguments suggest that hormonal factors are involved in human hepatocarcinogenesis. The incidence of HCC is threeto sixfold greater in males¹, and the use of oral contraceptives in females is associated with the development of hepatic adenoma²⁸. Moreover, the ability of oestrogenic hormones to function as promoters of neoplastic development in rat liver has been clearly demonstrated²⁹. The finding that HBV sequences have become integrated into a putative cellular gene sharing homology with the steroid receptor genes is therefore intriguing and suggests that, in some cases, hormonal and HBV carcinogenesis may be directly related.

Received 5 February; accepted 16 April 1986.

- 1. Beasley, R. P. & Hwang, L. Y. in Viral Hepatitis and Liver Disease (eds Vyas, G. N., Dienstag, J. L. & Hoofnagle, J. H.) 209-214 (Grune & Stratton, New York, 1984 2. Charkraborty, P. R., Ruiz-Opazo, N., Shouval, D. & Shafritz, D. A. Nature 286, 531-533
- 3. Bréchot, C., Pourcel, C., Louise, A., Rain, B. & Tiollais, P. Nature 286, 533-535 (1980).

- Berchot, C., Gray, P., Valenzuela, P., Rall, L. B. & Rutter, W. J. Nature 286, 535-535 (1980).
 Bréchot, C. et al. Proc. natn. Acad. Sci. U.S.A. 78, 3906-3910 (1981).
 Shafritz, D. A., Shouval, D., Sherman, H. I., Hadziyannis, S. J. & Kew, M. C. New Engl. J. Med. 305, 1067-1073 (1981).
- 7. Chen, D. S., Hoyer, B. H., Nelson, J., Purcell, R. H. & Gerin, J. L. Hepatology 2, 42S-45S (1982).
- Dejean, A., Sonigo, P., Wain-Hobson, S. & Tiollais, P. Proc. natn. Acad. Sci. U.S.A. 81, 5350-5354 (1984).
- Rogler, C. E. et al. Science 230, 319-322 (1985).
- Koshy, R. et al. Cell 24, 215-223 (1983).
 Dejean, A., Bréchot, C., Tiollais, P. & Wain-Hobson, S. Proc. natn. Acad. Sci. U.S.A. 80, 2505-2509 (1983). 12. Shaul, Y. et al. J. Virol. 51, 776-787 (1984).
- 13. Mizusawa, H. et al. Proc. natn. Acad. Sci. U.S.A. 82, 208-212 (1985).



Fig. 4 DNA sequences at the HBV integration site. The sequences of the left and right host-viral DNA junctions at the occupied site (upper sequence) are compared with the human DNA sequence at the unoccupied site (lower sequence). The bold-face letters indicate the viral sequence. Nucleotides of the ORF and the HBV genome³³ are numbered. Homologous nucleotides between the two sequences are indicated by sloping lines. The 7-bp CACTTCC present in the normal allele and deleted after the viral integration in the occupied site is boxed. Because HBV DNA and cellular DNA shared a 2-bp and 3-bp sequence homology at a point coincident, respectively, with the left and right host-viral junctions (dashed lines), the deleted fragment could be up to 12 bp long. The DR2 copy of the 11-bp viral direct repeat specifically involved in HBV integration⁸ is indicated. The putative chimaeric protein, generated by the HBV inversion, between the first 29 amino acids of the viral pre-S1 gene product and the last 28 amino acids of the cellular exon protein product is partially represented at the fusion

We thank Drs Christian Bréchot, Pierre Sonigo, Simon Wain-Hobson and Jean Weissenbach for advice and discussion and Louise-Marie Da for typing the manuscript. This work was supported by NIH grant CA97300-02, the Economic European Community and the Faculté de Médecine Lariboisière Saint-Louis (University of Paris VII).

- Yaginuma, K., Kobayashi, M., Yoshida, E. & Koike, K. Proc. natn. Acad. Sci. U.S.A. 82, 4458-4462 (1985).
- 4438-4402 (1963).

 15. Sanger, F., Nicklen, S. & Coulson, A. R. Proc. natn. Acad. Sci. U.S.A. 74, 5463-5467 (1977).

 16. Mount, S. M. Nucleic Acads Res. 10, 459-472 (1982).

 17. Claverie, J. M. & Bougueleret, L. Nucleic Acids Res. 14 (in the press).

 18. Claverie, J. M. & Sauvaget, I. Cabios 1, 95-104 (1985).

- Debuire, B. et al. Science 224, 1456-1459 (1984)
- Weinberger, C., Hollenberg, S. M., Rosenfeld, M. G. & Evans, R. M. Nature 318, 670-672
- Green, S. et al. Nature 320, 134-139 (1986).
 Johannsmann, R., Hellkuhl, B. & Grzeschik, K. H. Hum. Genet. 56, 361-363 (1981).
 Huerre, C. et al. Ann. Genet. 27, 5-10 (1984).
 Spurr, N. K. et al. EMBO J. 3, 159-163 (1984).

- Hollenberg, S. M. et al. Nature 318, 635-641 (1985).
 Walter, P. et al. Proc. natn. Acad. Sci. U.S.A. 82, 7889-7893 (1985).
 Rall, L. B., Standring, D. N., Laub, O. & Rutter, W. J. Molec. cell. Biol. 3, 1766-1773 (1983).
 Edmonson, M. A., Henderson, B. & Benton, B. New Engl. J. Med. 294, 470 (1976).

- Wanless, I. R. & Medline, A. Lab. Invest 46, 313-320 (1982).
 Tiollais, P., Pourcel, C. & Dejean, A. Nature 317, 489-495 (1985).
 Hanahan, D. J. molec. Biol. 166, 557-580 (1983).
 Biggin, M. D., Gibson, T. J. & Hong, G. F. Proc. natn. Acad. Sci. U.S.A. 80, 3963-3965 (1983).
- 33. Galibert, F., Mandart, E., Fitoussi, F., Tiollais, P. & Charnay, P. Nature 281, 646-650 (1979).

Analysis of deletions in DNA from patients with Becker and Duchenne muscular dystrophy

Louis M. Kunkel and co-authors*

Division of Genetics, The Children's Hospital, Boston, Massachusetts 02115, USA

Duchenne muscular dystrophy (DMD) is an X-linked recessive genetic disorder for which the biochemical defect is as yet unknown. Recently, two cloned segments of human X-chromosome DNA have been described which detect structural alterations within or near the genetic locus responsible for the disorder^{1,2}. Both of these cloned segments were described as tightly linked to the locus and were capable of detecting deletions in the DNA of boys affected with DMD. In an attempt to determine more precisely the occurrence of these deletions within a large population of DMD patients and the accuracy of one of the segments, DXS164 (pERT87), in determining the inheritance of the DMD X chromosome, the subclones 1, 8 and 15 were made available to many investigators throughout the world. Here we describe the combined results of more than 20 research laboratories with respect to the occurrence of deletions at the DXS164 locus in DNA samples isolated from patients with DMD and Becker muscular dystrophy (BMD). The results indicate that the DXS164 locus apparently recombines with DMD 5% of the time, but is probably located between independent sites of mutation which yield DMD. The breakpoints of some deletions are delineated within the DXS164 locus, and it is evident that the deletions at the DMD locus are frequent and extremely large.

The previously described deletions of the DXS164 region and the XJ-1.1 junction clone^{1,2} were assumed to be large, for neither set of cloned segments exhibits any common sequence overlap and yet both cloned segments are absent from most of the same deletion DNA samples². To increase the possibility that a particular deletion would exhibit a break within cloned DNA, the DXS164 region was expanded further by chromosome walking³ in human genomic libraries constructed in the phage vector EMBL-3 (ref. 4). Following five bidirectional walks, a 137kilobase (kb) contiguous stretch of DNA was obtained from the DXS164 region. All DNA segments obtained from the 137 kb of DNA were subcloned in plasmid vectors and segments of unique sequence were identified for the entire length. The two previously described subclones (pERT87-1 and -8; ref. 1) and a new unique-sequence segment (pERT87-15) which also detects restriction fragment length polymorphisms (RFLPs; ref. 5) were sent to other investigators interested in DMD.

The three DXS164 subclones, which are spaced over a 50-kb

section, were tested for deletion by hybridization against the DNA isolated from males exhibiting the DMD and BMD phenotype. The results of this analysis for 1,346 males are presented in Table 1. As the results were obtained in many different laboratories, they are presented separately for each laboratory. Of all DMD and BMD males tested, 6.5% show deletions at the DXS164 locus, a slightly lower percentage than that found previously1. A difference was observed in the incidence of deletions between DMD males with a clear family history of the disease (8.3%) and those with no family history (5.8%). Such a difference might be a reflection of the incidence of deletion mutation in maternal and paternal meiosis. Any true sporadic case of DMD where the mother is not a carrier of the disease represents a mutation which must occur only in female meiosis with no paternal contribution. Familial cases would be assumed to have a contribution of both male and female meiotic deletion events. Thus, if the frequency of deletion mutations at the DMD locus were nearly equal in males and females, one might assume that a higher incidence of deletions, as presented in Table 1, would be observed in familial cases. Prediction of affected individuals in families segregating a deletion which is assumed to be the primary genetic cause of the disease (of more than 150 normal boys, no deletions were observed) should be highly accurate.

As indicated in Table 1, two boys with BMD were found to have a deletion of the DXS164 region. Linkage analysis has shown that the locus for BMD is localized near, or is a potential allele of, DMD⁶⁻⁹. The finding of deletions in the DNAs of BMD males which overlap with deletions found in DMD males suggests that if they are two separate loci they are indeed close to one another. Alternatively, if BMD and DMD are caused by different alleles at the same locus, then the milder BMD phenotype might be expected to be the result of a low-level expression of the DMD/BMD gene product. If this were the case, the BMD deletions might not involve DNA sequences that are absolutely necessary for the expression of the DMD/BMD gene product.

The three DNA probes from the DXS164 region that were distributed to other investigators each recognize the informative RFLP alleles given in Table 2. The separate RFLP alleles of pERT87-1 and -8 exhibit a degree of disequilibrium and are only informative in ~60% of women tested, despite there being many different enzyme-defined loci. The three separate loci of pERT87-15 defined by different enzymes, although in some degree of disequilibrium with each other, are closer to equilibrium with the pERT87-1 and -8 loci. When the three enzyme-defined loci of the pERT87-15 probe were used in combination with the BstXI locus of pERT87-8 and the XmnI locus of pERT87-1, 25 of 28 (89%) unrelated women at risk for DMD or BMD were observed to be informative for linkage between one or more of the RFLP-detecting loci and the disease locus.

^{*} J. F. Hejtmancik & C.Th. Caskey, Institute of Molecular Genetics, Baylor College of Medicine, Houston, Texas 77030, USA; A. Speer, Central Institute of Molecular Biology, Academy of Science DDR, 1115 Berlin, DDR; A. P. Monaco, W. Middlesworth, C. A. Colletti, C. Bertelson & U. Müller (Division of Genetics), M. Bresnan (Department of Neurology), F. Shapiro (Department of Orthopedics), U. Tantravahi, J. Speer & S. A. Latt (Division of Genetics, DMD Diagnostic Laboratory), The Children's Hospital, Boston, Massachusetts 02115, USA; R. Bartlett, M. A. Pericak-Vance & A. D. Roses, Division of Neurology, Duke University Medical Center, Durham, North Carolina 27710, USA; M. W. Thompson, P. N. Ray & R. G. Worton, Department of Genetics, Hospital for Sick Children, Toronto, Ontario, Canada M5G 1X8; K. H. Fischbeck, Neurology Department, Hospital of the University of Pennsylvania, Philadelphia, Pennsylvania 19104, USA; P. Gallano, M. Coulon, C. Duros, J. Boue & C. Junien, INSERM 473, Chateau de Longchamp, 75016 Paris, France; J. Chelly, G. Hamard, M. Jeanpierre, M. Lambert & J.-C. Kaplan, Institut de Pathologie Moléculaire, INSERM 129, Chu Cochin, 75014 Paris, France; A. Emery, Medical School, Teviot Place, Edinburgh EH18 9GA, UK; H. Dorkins, S. McGlade & K. E. Davies, Nuffield Department of Clinical Medicine, John Radcliffe Hospital, Oxford OX3 9DU, UK; C. Boehm, Department of Pediatrics, Johns Hopkins University, Baltimore, Maryland 21205, USA; B. Arveiler & C. Lemaire, Laboratoire de Génétique Moléculaire des Eucaryotes, CNRS and INSERM U184, Faculté de Médicine, Strasbourg, France; G. J. Morgan & M. J. Denton, Department of Pathology, Prince of Wales Hospital, Sydney, New South Wales 2031, Australia, J. Amos, Eunice Kennedy Shriver Center, Waltham, Massachusetts 02254, USA; M. Bobrow, F. Benham, E. Boswinkel, C. Cole, V. Dubowitz, K. Hart, S. Hodgson, L. Johnson & A. Walker, Paediatric Research Unit, United Medical and Dental Schools of Guy's and St Thomas's Hospitals, Hammersmith Hospital, London SE1 9RT, UK; L. Ro

Table 1 Structural alterations detected at the DXS164 locus in DMD males

	C	linical descriptio	n		Deletions	
Contributing laboratory	DMD-F	DMD-S	BMD	DMD-F	DMD-S	BMD
R. Bartlett, Durham*	11	9,	2	3	1	0
M. Bobrow, London	75	50	24	7	2	1
T. Caskey, Houston	22	18	0	5	3	0
K. Davies, Oxford†	42	68	0	0	2	0
A. de la Chapelle, Helsinki	10	20	2	0	1	1
M. Denton, Sydney*	12	15	0	6	0	0
R. Doherty, Rochester	32	61	8	4	4	0
A. Emery, Edinburgh†	0	30	0	0	0	0
M. Ferguson-Smith, Glasgow	37	44	17	3	3	0
K. Fischbeck, Philadelphia*	25	27	4	1	1	0
U. Francke, New Haven	. 11	1	1	1	0	0
C. Greenberg, Manitoba	3	0	1	1	0	0
P. Harper, Cardiff	50	43	35	4	1	0
V. Ionasescu, Iowa City	16	21	5	2 .	1	0
C. Junien, Paris	51	2	0	1	1	0
C. Boehm, Baltimore	12	5	0	1	0	0
J. C. Kaplan, Paris	52	29	7	3	2	0
L. Kunkel, Boston*	14	29	0	1	3	0
JL. Mandel, Strasbourg	12	13	0	0	0	0
P. Pearson, Leiden	43	24	8	5	3	0
A. Read, Manchester†	22	32	0	2	2	0
G. Romeo, Genova	7	6	10	1	1	0
A. Speer, E. Berlin†	51	0	18	1	0	0
U. Tantravahi, Boston	8	1	0	2	0	0
R. Worton, Toronto*	32	3	3	0	1	0
Total	650	551	145	54	32	2
Percentage				8.3%	5.8%	1.4%
Overall total			1,346		88 (6.5%	

The DNAs isolated from 1,346 DMD and BMD males from separate kindreds were cleaved with various restriction enzymes. Diagnosis of DMD and/or BMD was established by characteristic history, physical examination, increased CPK levels and, in many cases, a positive muscle biopsy¹⁹⁻²¹. Following separation of digested DNA by electrophoresis, the DNA samples were hybridized²² with one or more of the DXS164 subclones pERT87-1, pERT87-8 and pERT87-15. Not all samples were hybridized with all the subclones, but most were hybridized with pERT87-8. The investigator's laboratory in which the DNA isolations and, in most cases, the hybridizations were accomplished are indicated. The patients were divided into three categories: DMD-F, DMD males from a family in which there was more than one affected individual or, in a few cases, where the mother had an elevated CPK, but no clear family history of DMD; DMD-S, DMD males where there was no family history of the disease and the mother had a normal CPK value; BMD, males who exhibited the less severe X-linked myopathy. The number of boys studied within each of these three categories is shown for each laboratory. Deletions were defined as complete absence of hybridization for a DXS164 subclone and the number of individuals with absent fragments is given in each category. Those DMD males who exhibited deletions were representative of the clinical spectrum for DMD and included males who were mentally retarded as well as those not mentally retarded. Many DMD boys who were diagnosed as mentally retarded did not exhibit a deletion of DXS164 subclones. Those BMD males who exhibited deletion of DXS164 subclones were both on the more severe side of the BMD clinical spectrum, but both were wheelchair-bound later than a typical DMD patient: one was from a familial case of BMD and the other was a sporadic occurrence of BMD. Both are functioning well in their mid-twenties and one male is still able to drive a car.

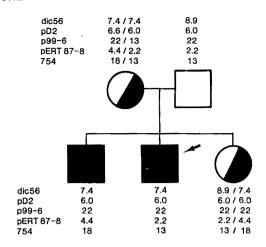
* Most of these DNA samples were obtained from the individual listed and were sent to L.M.K. in Boston, where they were tested for deletion. † Most of these DNA samples were sent to K.E.D. at Oxford, where they were tested for deletion. K.E.D. received other DNA samples from Dr Schwarts (Denmark) and Drs Ch. Coutelle, Spiegler, Herrmann and Szibor (FRG).

Segregation analysis of these RFLP-detecting loci in multiple families at risk for BMD and DMD has shown that recombinants are possible between DXS164 and the disease locus; one such recombinant is shown in Fig. 1. The family consists of two affected sons and a daughter whose level of creatine phosphokinase (CPK) and muscular hypertrophy indicate a carrier status. The boy indicated by an arrow in the figure has clearly received from his mother a 2.2-kb hybridizing BstXI fragment for pERT87-8, whereas his affected brother and carrier sister have each received a 4.4-kb fragment. Thus, the X chromosome of the boy carrying the 2.2-kb fragment must be the result of a recombination event between DXS164 locus and DMD.

To determine more accurately the meiotic exchange points in this family and to minimize the possibility of sample error, the same family was also tested for segregation with other Xp cloned loci. The PstI RFLP detected by the cloned probe 754 (DXS84; ref. 10) also exhibited recombination in the same individual, whereas the other loci, DXS41 (99-6) and DXS43 (D2)^{11,12}, appear to be non-recombinant. This is an unexpected result based on previous notions of gene order for these loci on the

X chromosome $^{10-15}$. Physical mapping of these marker loci using panels of hybrid cells 16,17 containing translocation chromosomes from two independent X; autosome translocations found in females with DMD localize DXS164 (ref. 14), DXS41 and DXS43 (refs 11, 12) on the pter side and DXS84 (refs 13, 17) on the centromere side of the translocation breakpoints. If the translocation exchange points in these two patients are in the DMD gene^{17,18}, the order of these loci would be as presented in Fig. 1 ('old order'). The recombination data of Fig. 1 are inconsistent with this order in this particular family. There must be a recombination event between DMD and DXS84(754), one between DMD and DXS164(pERT87-8), and another between DXS164(pERT87-8) and DXS41(99-6) for this latter marker to appear non-recombinant. The presumed order would require three meiotic exchanges within a region of previously closely linked markers^{9,15}. An alternative, and perhaps more likely explanation is that the DMD mutational site in this family maps between DXS41 and DXS164 and a single recombination (indicated at the bottom of Fig. 1) between DXS164 and the DMD mutation site would explain the results.

Fig. 1 Segregation of five Xp cloned loci in a DMD family. O, Females; □, males; ■, DMD-affected individual; ②, DMD carrier. DNA was isolated11 from five members of a DMD kindred. Diagnosis of DMD was established as described in Table 1 legend, and the mother was judged to be a carrier of the disease as she exhibited an increased concentration of CPK^{19,20} and had given birth to two affected individuals. The mother, though, had no knowledge of any other case of DMD in her family. The daughter was judged to be a carrier as she had extremely elevated CPK (relative to other female carriers) and exhibited hypertrophy of the leg muscles, although no weakness. The DNA samples were cleaved with the various restriction enzymes appropriate for each of the cloned DNA probes. Gel electrophoresis, transfer and hybridization were as described previously11. The different loci were tested by hybridization with the following cloned DNA fragments (given from the most distal): DXS143, dic56; DXS43, pD2; DXS41, p99-6; DXS164, pERT87-8; and DXS84, 754 (the most proximal). The various cloned segments had been physically mapped previously 10-14. The numbers above and below each symbol indicate the size of hybridizing restriction fragments (alleles). Segregation of the locus DXS143 (ref. 23) is included to show that the samples from the non-recombinant boy and the father were not inverted. Two possible orders for the loci are indicated at the bottom of the figure; the first places the DMD locus at the point where the translocation breaks occur in two females with DMD; the second order (new order) represents an interpretation of the results obtained in the family study.



OLD ORDER: pter: pD2: p99-6: pERT 87-8: DMD: 754: cen
Recombination
points: X X X

? NEW ORDER: pter: pD2: p99-6: DMD: pERT 87-8: 754: cen
Recombination
points:
X

In the cases where DXS164 has been observed to recombine with DMD (eight known instances) and where DXS84 was also informative (five instances), both markers were recombinant. These results are consistent with the fact that the mutations giving rise to DMD in some families lie distal to DXS84, two translocation breaks in Xp21 (refs 16, 17) and the DXS164 locus. Thus, DXS164 may lie between these two translocation breaks and additional sites of mutation, all of which yield the phenotype of DMD and/or BMD. Alternative explanations for the linkage results could include a different X-linked locus with a phenotype very similar to DMD or new mutations which would appear as recombinants. Potentially consistent with the latter possibility is the observation that only one of the eight DXS164 recombinants observed occurs in the third generation or thereafter in a multi-generation DMD family.

For whatever reason, the exclusive use of DXS164 cloned probes as linked markers would lead to some mistakes when predicting the inheritance of the DMD X chromosome. This result has major implications for the prediction of the DMD genotype. Although the exact error rate is difficult to calculate (because only recombinants for other closely linked markers were tested for the segregation of DXS164 clones), best estimates can be made from the observation that approximately one-half of DXS84 recombinants (estimated at 10% recombination; ref. 9) are also DXS164 recombinants. This leads to the assumption that DXS164 will be in error in predicting the DMD X chromosome 5% of the time. It is strongly advised that the DXS164 locus be used in combination with other Xp21 flanking markers to construct an Xp21 haplotype. Given that the DXS164 locus seems to be localized between mutations found in different families which yield the DMD phenotype, DXS164 should not be considered as a flanking marker to DMD with other Xp21 loci. In a diagnostic situation, it would be unknown in which direction the particular mutation actually occurred relative to DXS164. Combined multi-locus information should improve the accuracy of genotype prediction in DMD families, assuming, of course, that the observed prediction errors for the DXS164 locus are caused by recombinants and not by new mutations or a different, as yet uncharacterized, locus.

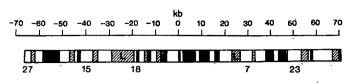
The deletions observed in the DNAs of boys with DMD (and also BMD) provide the means to start to define important

segments of Xp21 which might be involved in the normal functioning of the DMD locus. Therefore, 53 of the 88 DNA samples which constituted deletions for the three DXS164 subclones distributed were tested for the absence or presence of additional subclones from the entire 137 kb of DNA from the DXS164 locus. A representative hybridization analysis is shown in Fig. 2 for five DXS164 subclones hybridized to nine different deletion DNA samples. The subclones are located within the DXS164 locus on either side of pERT87-1 and -8, and the five subclones combined can detect size differences between PstI-hybridizing fragments over 45 kb of the DXS164 locus. Among the nine deletion DNA samples, five showed no DXS164-hybridizing PstI fragment. The remaining four DNA samples exhibited some fragments but not others; these samples thus have breakpoints within the DXS164 locus, and one (Fig. 2, lane 3) of the breakpoints is preliminarily determined as an altered PstI hybridizing fragment. By using additional subclones from the DXS164 locus, each breakpoint can be mapped more precisely to a specific subregion. Once localized to a specific region, the appropriate restriction enzyme can be chosen to best demonstrate the actual breakpoint (within 100-1,000 base pairs (bp)).

Table 2 RFLP-detecting subclones of DX3164

	Insert size		Allele (k		Allele frequency		
Subclone	(kb)	Enzyme	p	q	p	q	
pERT87-1	1.3	BstNI	3.1	2.5/0.6	0.63	0.37	
-		XmnI	8.7	7.5	0.66	0.34	
pERT87-8	1.3	BstXI	4.4	2.2	0.6	0.4	
-		Taq I	2.7/1.1	3.8	0.71	0.29	
pERT87-15	1.5	BamHI	7.1/2.3	9.4	0.62	0.38	
-		TaqI	3.1	3.3	0.67	0.33	
		XmnI	1.6/1.2	2.8	0.68	0.32	

The three DXS164 subclones are listed together with the sizes of their cloned human DNA inserts. The enzyme site variation detected by each probe is represented by the sizes of the hybridizing fragments and the respective frequencies of the common allele (p) and the rare allele (q). The allele frequencies were calculated in each case from the results obtained with over 75 X chromosomes.



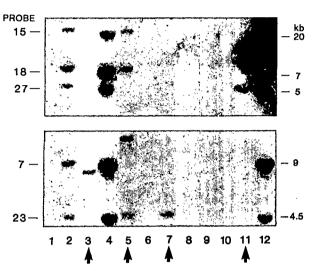


Fig. 2 Demonstration of four deletion breakpoints within the DXS164 locus. The DXS164 locus was expanded by chromosome 'walking' described prevously1. A schematic drawing of 137 kb of contiguous human DNA is presented at the top. Solid bars represent regions of repeated DNA sequences; open boxes represent regions of unique sequence. Cross-hatched boxes represent moderately repeated sequences, and two copies of LINE are indicated by the letter L. The numbers beneath the schematic diagram give the designations for five of the unique-sequence subclones used to determine the extent of deletions in DNA samples from nine DMD males. After digestion with PstI, each DNA sample was tested for the presence or absence of various human PstI fragments by hybridization²² with the various subclones. In the two different autoradiographs presented, the hybridizing PstI fragment for each subclone is indicated to the left of the figure; these are evident in lanes 2, 4 and 12, where the DNA samples isolated from individuals who do not bear deletions of DXS164 subclones are presented. The sizes of the respective PstI hybridizing fragments for normal individuals are given to the right of the figure. The DXS164 subclones pERT87-18, -15 and -27 were radiolabelled separately¹¹ and hybridized simultaneously to a nitrocellulose filter containing the 12 immobilized PstIcleaved DNA samples. The DXS164 subclones pERT87-7 and -23 were also radiolabelled separately and hybridized together to a duplicate nitrocellulose membrane with the same immobilized PstI-cleaved DNA samples. The different hybridization intensities of the PstI fragments were due to differences in specific activity and hybridization characteristics of the individual probes. Lines 4 and 12 contained 5 µg of PstI-cleaved DNA, whereas the others each contained $\sim 1~\mu g$. Lanes 1, 6 and 8-10 show no hybridization for any of the five DXS164 subclones. Lanes 3, 5, 7 and 11 (arrowed) exhibit at least one DXS164-hybridizing PstI fragment. The deletion DNA sample in lane 3 exhibits an absence of the subclones (left-hand side), pERT87-27, -15 and -18 and has a single altered PstI fragment for one of the subclones on the right-hand side (either pERT87-7 or -23). The altered fragment is presumably detected by the 23 subclone, and the hybridization results indicate that the deletion breakpoint occurs near pERT87-23 and the deletion extends in a leftward direction. The DNA sample in lane 7 exhibits similar hybridization results to the sample in lane 3, but the pERT87-23 hybridizing PstI fragment is normal in size. This DNA sample is presumed to have a different deletion breakpoint between pERT87-7 and pERT87-23 compared with that in lane 3 and the deletion also extends to the left. The DNA sample in lane 5 exhibits a normal-sized PstI hybridizing fragment for pERT87-23, a rare allele of a PstI RFLP detected by pERT87-7 (~10% of both normal and DMD males exhibit this larger PstI fragment) and normal-sized hybridizing PstI fragments for pERT87-18 and -15. The pERT87-27 subclone exhibited no hybridization. This DMD male has not been previously shown to have a deletion of pERT87-8 or -1 and has a deletion which starts between pERT87-15 and pERT87-27 and extends also to the left. The DNA sample in lane 11 carries a deletion which breaks near that presented in lane 5, but the deletion extends in the opposite direction. pERT87-27 hybridizes to a normal-sized PstI fragment whereas the remaining subclones are absent.

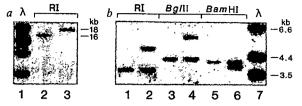


Fig. 3 Demonstration of deletion breakpoints for two independent deletions. Restriction enzyme cleavage, radiolabelling and hybridization were as described in Fig. 2 legend and ref. 1. In a, a deletion sample previously shown to carry pERT87-1 and a normal-sized hybridizing PstI fragment, showed no hybridization for pERT87-8 or other subclones to the left of this one. Subclone pERT87-14, between pERT87-1 and -8, was used to detect by hybridization an altered EcoRI fragment in the deletion DNA sample (lane 2; compare with a normal-sized EcoRI fragment in lane 3). The normal EcoRI fragment stretches across pERT87-8 and, based on other restriction enzyme sites in the region, the breakpoint of this deletion has been determined to fall between the right side of pERT87-8 and a PstI site 1.5 kb farther to the right. b, Demonstration of a deletion breakpoint detected with the pERT87-1 subclone. The deletion sample originally shown to be a deletion for pERT87-15 and -8 exhibits a break just to the left of pERT87-1. Lanes 1, 3 and 5, EcoRI, Bg/III and BamHI digests, respectively, of a normal male; lanes 2, 4 and 6, EcoRI, BglII and BamHI digests, respectively, of DNA isolated from a female heterozygous for the deletion. Both EcoRI and Bg/II reveal a larger altered fragment than BamHI. The deletion breakpoint lies ~500-1,000 bp to the left of pERT87-1.

Figure 3 shows two such determinations for two independent deletions. In one case (Fig. 3a, lane 2), an altered hybridizing EcoRI fragment is detected with the pERT87-14 subclone (located between pERT87-8 and pERT87-1). Comparison of the size of the altered EcoRI fragment with that seen in normal individuals (Fig. 3a, lane 3) and the knowledge that pERT87-8 is absent indicate that this deletion breakpoint maps between the pERT87-8 segment and an unaltered PstI site 1.5 kb towards pERT87-14. In the other example, different-sized hybridizing fragments for EcoRI (5.0 kb), BglII (5.8 kb) and BamHI (3.9 kb) were observed in the DNA sample isolated from a female heterozygous for a deleted X chromosome. A sample isolated from an unaffected male (Fig. 3b, lanes 1, 3, 5) exhibited the normal hybridizing fragments for the three enzymes.

Most deletions were found to be larger than 137 kb, for no subclone from within the entire cloned region was found to be. present. Among the 57 deletions tested, 24 showed the presence of some subclones but not others (the data are summarized in Fig. 4); these were deletions which had breakpoints within previously cloned DNA of the DXS164 locus. Fourteen deletions break on the left side of the cloned DNA and extend in the rightward direction off the DXS164 map towards the centromere (the direction of the DXS164 map relative to the centromere was established by analysing some deletion samples with the XJ-1.1 cloned segment; see Fig. 4 legend). Nine deletions break on the right of the map and extend in a leftward direction away from the centromere. Although some deletions are presented as similar, most have been shown to have independent breakpoints within the DXS164 locus (see Fig. 4 legend) and are schematically presented together when the breakpoints are near each other. It is apparent from Fig. 4 that there is a common region which is absent from almost all deletions except the six shown in the lower part of the figure. This region of common deletion overlap may be slightly biased due to the fact that the first probe made available to other investigators was pERT87-8, which resides near the overlap region. Further studies on additional DMD boys using all the DXS164 subclones should confirm whether this common region of overlap contains DNA sequences important for the expression of the DMD phenotype, or whether it represents an ascertainment bias.

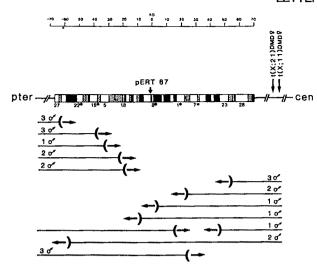


Fig. 4 A schematic representation of deletion breakpoints in the DXS164 locus. Fifty-seven DNA samples (53 samples shown to be deletions of one of the distributed subclones and 4 additional DNA samples shown to be deletions of either XJ-1.1 (ref. 2) or other DXS164 subclones) were tested for the absence or presence of various DXS164 subclones as presented in Figs 2, 3. Twenty-four of the 57 DNA samples showed the presence of at least one DXS164-hybridizing PstI fragment, whereas the remaining 33 DNA samples exhibited no DXS164-hybridizing PstI fragmentthe entire 137 kb was missing. By using a combination of subclones including those exemplified in Fig. 2, the approximate positions of the 24 different breaks were determined and are indicated by a bracket with an arrow indicating the direction of the missing DNA. Certain breakpoints which were similar are combined, and the number of males combined is indicated at the side of the figure. Nine deletion breakpoints were determined to the extent where an aberrant hybridizing restriction fragment was identified; these are localized within a few kilobases within the DXS164 locus. Nine deletions were determined to be different from the first nine, as revealed by the pattern of their hybridization with DXS164 subclones, but an altered restriction fragment has yet to be identified and these are thus only localized to within 1-5 kb. Six deletion breakpoints (the most recently acquired) were only mapped to 10-30-kb regions of the DXS164 locus and have not been definitely shown to differ from the other 18. Some of the deletions presented have also been tested for hybridization with the previously described clone XJ-1.1 (ref. 2): of those tested that break within DXS164 and extend to the right, all show no hybridization with XJ-1.1. For those tested that break in DXS164 and extend to the left, XJ-1.1 is present. The hybridization results with XJ-1.1 allow localization of the DXS164 subclones relative to the centromere as well as the (X; 21) translocation breakpoint, as indicated in the figure. Four of the six deletion DNA samples depicted at the bottom of the figure were not determined to be deletions by the original subclones pERT87-1, -8 or -15; two were found to be deletions for the XJ-1.1 cloned segment and were subsequently mapped with additional DXS164 clones, and the remaining two deletions were detected only with the leftmost DXS164 subclone, pERT87-27.

Screening of boys with additional pERT87 subclones and with the XJ-1.1 clone detected four deletions which would not have been detected with the originally distributed clones. These deletions were found among 269 boys who had been shown previously not to carry deletions of the pERT87-1, -8 or -15 subclones. These four deletions are not included in the data presented in Table 1 but are shown in Fig. 4; it is assumed that the true proportion of DMD and BMD boys who have deletions of portions of their X chromosomes would be greater than that presented in Table 1, where only three probes were used. Analysis of DMD or BMD DNA samples with the most distal pERT87-27 subclone, the three central subclones pERT87-1, -8 and -15, and the XJ-1.1 subclone should detect most of the deletions that are currently detectable.

The breakpoints of six deletions are different from most others; these are shown at the bottom of Fig. 4. One deletion is completely encompassed within cloned DNA and removes only 45 kb of DNA. Three deletions break within this 45-kb region and extend off the map towards the centromere; two of these were originally detected by the more centromeric cloned segment XJ-1.1 and subsequently mapped within the DXS164 locus. Two other deletions (detected with subclones of DXS164 other than pERT87-1, -8 and -15) break at the extreme left end of the cloned DNA and extend off the map for an undetermined distance. The central location of DXS164 subclones 1, 8 and 15 to DMD and/or BMD mutational sites, inferred from family studies and translocation breakpoint mapping, is substantiated by these additional deletion DNA samples. The profile of deletion breaks indicates that there must be a large segment of DNA which, when disrupted, can yield the phenotype of DMD and/or BMD. The fact that large deletions yield a DMD phenotype similar to that of other DMD boys who have not been demonstrated to bear deletions, indicates that the product of the locus can be either completely absent or aberrant and still yield a similar clinical picture.

The pattern of deletions implies that the gene(s) responsible for DMD must lie on a very large segment of X-chromosomal DNA. This is substantiated by the fact that recombinants are observed between cloned segments in the region and some disease mutation sites. For the future of diagnosis, the deletions represent a ready means of obtaining additional cloned segments from the other side of those deletions that break within DNA that has already been cloned. These junctional fragments from deletion patients are presently being cloned and the development of new RFLP-detecting probes to mark the entire region in which mutation can yield DMD and BMD is imminent. The deletion breakpoints also demarcate the regions of the DXS164 locus that might contain information important for the expression of the gene responsible for DMD and/or BMD. Analysis of these breakpoints at the level of the nucleotide sequence may also elucidate the mechanism underlying the deletions.

We thank all the families and patients involved in this study. We also acknowledge the many funding agencies who provided support for this work, especially the Muscular Dystrophy Association of America, the Muscular Dystrophy Group of Great Britain and Northern Ireland, the Muscular Dystrophy Association of Canada, and members of the European Alliance of Muscular Dystrophy Associations. We also thank the clinical geneticists, paediatricians and neurologists who brought to our attention the many Duchenne and Becker muscular dystrophy patients.

Received 26 March: accepted 1 May 1986.

```
1. Monaco, A. P. et al. Nature 316, 842-845 (1985).
```

Ray, P. N. et al. Nature 318, 672-675 (1985). Bender, W. et al. Science 221, 23-29 (1983).

Frischauf, A. M. et al. J. molec. Biol. 170, 827-842 (1983). Botstein, D. et al. Am. J. hum. Genet. 32, 314-331 (1980).

Brown, C. S. et al. Hum. Genet. 71, 62-74 (1985). Fadda, S. et al. Hum. Genet. 71, 33-36 (1985).

Wilcox, D. E. et al. Hum. Genet. 70, 365-378 (1985). de la Chapelle, A. (ed.) Human Gene Mapping 8 (Karger, Basel, 1985) Hofker, M. H. et al. Hum. Genet. 70, 148-156 (1985).

Aldridge, J. et al. Am. J. hum. Genet. 36, 546-564 (1984).
 de Martinville, B. et al. Am. J. hum. Genet. 37, 235-249 (1985)

^{13.} Francke, U. et al. Am. J. hum. Genet. 37, 250-267 (1985)

Kunkel, L. M. et al. Proc. natn. Acad. Sci. U.S.A. 82, 4778-4782 (1985)

Drayna, D. et al. Science 230, 753-758 (1985).
 Mohandas, T. et al. Proc. natn. Acad. Sci. U.S.A. 77, 6759-6763 (1980)

Worton, R. et al. Science 224, 1447-1449 (1984).
 Jacobs, P. A. et al. Am. J. hum. Genet. 33, 531-538 (1981).

Pearce, J. M. S. et al. J. Neurol. Neurosurg. Psychiat. 27, 181-185 (1964)
 Emery, A. E. H. & Holloway, S. Hum. Hered. 27, 118-126 (1977).
 Appel, S. H. & Roses, A. D. in The Metabolic Basis of Inherited Disease (ed Stanbery, J. B.) 1470-1495 (McGraw-Hill, New York, 1983).

Southern, E. M. J. molec. Biol. 98, 503-517 (1975). Middlesworth, W. et al. Nucleic Acids Res. 13, 5723 (1985).

^{24.} Singer, M. F. Int. Rev. Cytol. 76, 67-112 (1982).

Carcinogen-specific mutation and amplification of Ha-ras during mouse skin carcinogenesis

Miguel Quintanilla, Ken Brown, Martin Ramsden* & Allan Balmain

Beatson Institute for Cancer Research, Switchback Road, Bearsden, Glasgow G61 1BD, UK

Cellular proto-oncogenes can be activated by both point mutations and chromosomal translocations, suggesting that there may be a direct link between exposure to agents which damage DNA and genetic change leading to malignancy (see refs 1, 2 for reviews). Several groups have therefore analysed mutations found in cellular oncogenes of tumours induced by particular physical or chemical carcinogens³⁻⁹. Here, we have analysed the molecular changes at different stages of carcinogenesis in mouse skin tumours induced by initiating and promoting agents. Over 90% of tumours, including premalignant papillomas, initiated with dimethylbenzanthracene (DMBA) have a specific A -> T transversion at the second nucleotide of codon 61 of the Harvey-ras (Ha-ras) gene. The frequency of this mutation was dependent on the initiating agent used, but not on the promoter, suggesting that the mutation occurs at the time of initiation. The mutation was heterozygous in most papillomas tested, but was homozygous or amplified in some carcinomas. The development of further chromosomal changes at the c-Ha-ras gene locus is therefore a common feature of tumour progression.

One of the consequences of ras gene mutation is that the resultant altered proteins (p21) exhibit aberrant mobilities on SDS gels^{10,11}. Alterations at codon 12 give rise to more slowly migrating forms of p21, while mutations at the other frequently affected locus around codon 61 usually produce rapidly migrating forms. Figure 1B (lane 5) shows the normal Kirsten-ras (Ki-ras) p21 immunoprecipitated from NIH 3T3 cells by monoclonal antibody Y13-259 (ref. 12). Transformants induced by transfection with DNA from a papilloma (Fig. 1B, lane 1) or a carcinoma (lane 3) synthesize in addition a p21 product encoded by the transforming Ha-ras gene, as shown using the Harveyspecific monoclonal antibody YA6-172, which immunoprecipitates only the faster migrating species (Fig. 1A, lane 1). Although the parental NIH 3T3 cells produce only small amounts of Harvey p21, a band can be detected after immunoprecipitation with YA6-172, which migrates at the front edge of the Ki-ras p21 band (Fig. 1A, lane 3). Comparison of lanes 1 and 3 of Fig. 1A indicates that the transforming Ha-ras encoded by the tumour DNAs has a substantially higher mobility on SDS gels and probably results from a mutation in the region of the gene surrounding codon 61. In an analysis of representative foci induced by seven tumours, six were shown to synthesize rapidly migrating forms of Ha-ras p21; four of these are shown in Fig. 1C, together with a slowly migrating p21 (lane 5) in a transformant induced by DNA from a Sencar carcinoma. We conclude from this analysis that most skin tumours initiated with DMBA probably have mutations around codon 61 of the mouse Ha-ras gene, but a minority exhibit mutations at or around codon 12.

Restriction fragment length polymorphisms (RFLPs) have been used to demonstrate directly the presence of mutated *ras* genes in samples of DNA from human or animal tumours^{7,13,14}. To attempt this experimental approach, we first obtained a genomic clone of the normal mouse cellular Ha-*ras* gene and sequenced coding exons 1 and 2 which contained, respectively, the putative mutable sites at codons 12 and 61 (M.R., K.B., F.

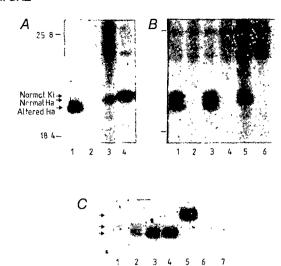


Fig. 1 Immunoprecipitation of ras p21 from NIH 3T3 transformants. A, Lanes 1, 2: NIH 3T3 transformant obtained by transfection with DNA from a primary carcinoma. Lanes 3, 4: NIH 3T3 cells. Lysates were immunoprecipitated with antibody YA6-172 (lanes 1, 3), normal rat serum (lane 2) or antibody Y13-259 (lane 4). B, NIH 3T3 transformants obtained by transfection with DNA from a papilloma (lanes 1, 2) or a carcinoma (lanes 3, 4). Lanes 5, 6: normal NIH 3T3 cells. Lysates in lanes 1, 3 and 5 were immunoprecipitated with Y13-259 and those in lanes 2, 4 and 6 with normal rat serum. C, NIH 3T3 transformants obtained by transfection with DNA from individual papillomas (lanes 1-3) or carcinomas (lanes 4, 5), all immunoprecipitated with YA6-172. Lanes 6 and 7: lysates from NIH 3T3 cells immunoprecipitated with YA6-172 or normal rat serum respectively.

Methods. Isolation of DNA by lysis of frozen tumours in 5 M guanidinium thiocyanate and centrifugation through CsCl has been described previously^{3,9}. NIH 3T3 transformants obtained by calcium phosphate-mediated transfection of DNA from primary tumours were grown to subconfluence in Special Liquid Medium (Flow) containing 10% fetal bovine serum. Cultures were labelled by incubation for 18 h in methionine-free medium containing 5% dialysed fetal bovine serum in the presence of 35S-methionine (NEN; specific activity 1,000 Ci mmol⁻¹, 200 μCi per ml of medium). Cells were lysed essentially as described by Furth et al.12 and aliquots $(3-5 \times 10^7)$ acid-precipitable c.p.m.) of the lysate incubated with monoclonal antibody YA6-172 or Y13-259, or normal rat serum. Antigen-antibody complexes were precipitated with protein A-Sepharose coated with rabbit anti-rat IgG (Sera Labs). Precipitates were washed six times in lysis buffer and run on 12.5% polyacrylamide gels as described by Laemmli²⁵. Gels were treated for fluorography with Enlightening (NEN), dried and exposed to Kodak film at -70 °C using intensifying screens.

Fee, R. Krumlauf and A.B., manuscript in preparation). The sequence around codon 61, which appeared to be the most frequently mutated locus in DMBA-initiated tumours, is shown in Fig. 2B. Clearly, an $A \rightarrow T$ transversion at this position could give rise to a new restriction site for the enzyme XbaI. Digestion with XbaI of DNA samples from the NIH 3T3 transformants shown in Fig. 1 revealed the presence of novel hybridizing fragments in all but one of the foci tested (Fig. 2A, lane a). This particular focus is that which exhibited the slowly migrating p21 (Fig. 1C), presumably because of a codon 12 mutation, and would therefore not be expected to show any change in the sequence of codon 61. Most foci had novel fragments of \sim 4 and 8 kilobases (kb) but some had aberrant bands due to the loss of one or more of the flanking XbaI sites during integration of the transfected DNA (Fig. 2A, lanes f-h).

The XbaI polymorphism enabled us to verify that the codon 61 mutation was present in the primary mouse skin tumours, and was not an artefact of the transfection procedure. Table 1 shows that 90% of DMBA-initiated tumours from three mouse strains had the same mutation. Figure 3A, lanes a and e, shows

^{*} Present address: Glaxo Research Laboratories, Ulverston, Cumbria LA129DR, UK

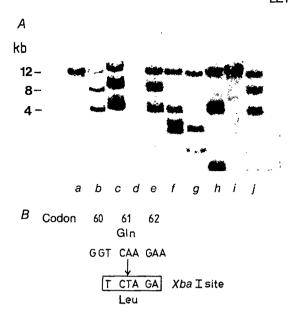


Fig. 2 XbaI polymorphism in NIH 3T3 transformants. A, DNAs derived from NIH 3T3 transformants obtained by transfection with papilloma (lanes d-h, j) or carcinoma (lanes a-c) DNAs were digested with XbaI and hybridized on Southern blots with an Ha-ras-specific probe. Lane a contains DNA from a transformant with the slowly migrating p21 protein shown in Fig. 1C. Lane i contains DNA from a spontaneous NIH 3T3 transformant and has the same hybridization pattern as normal DNA. B, Induction of an XbaI polymorphism by a specific mutation at codon 61. Digestion of normal mouse DNA with XbaI gives rise to a 12-kb fragment containing the mouse c-Ha-ras gene. Mutation of the middle base of c codon 61 from A to A would give rise to a new A site, generating tumour-specific fragments of A and A kb.

Methods. Aliquots (10 μg) of DNA from different transformants were digested with a 5-10-fold excess of XbaI (BioRad) under the conditions recommended by the suppliers. DNAs were run on 1% agarose gels, and transferred to nitrocellulose filters (Sartorius) according to Law et al. 26. Purified insert from the plasmid BS9 (ref. 27) was nick-translated and blots were hybridized at 42 °C in 50% formamide buffer as described previously 3. Blots were normally washed to a final stringency of 0.5×SSC at 65 °C, then exposed to Kodak X-OMAT film for 1-3 days at -70 °C with intensifying screens.

the typical pattern observed in 90% of the papillomas. Both the normal 12-kb band and those derived from the mutated allele are evident, and in almost all cases the band corresponding to the normal fragment is the most intense. Since histological analysis shows that papillomas consist predominantly of epithelial cells with a relatively small proportion of contaminating stroma cells, we conclude that the mutation is probably heterozygous in these premalignant tumours. A small proportion (\sim 10%) of the papillomas tested showed no evidence of the XbaI polymorphism (see, for example, Fig. 3A, lane d).

Figure 3A also shows the results of an analysis of a series of carcinomas initiated with DMBA. All the carcinomas from NIH mice exhibited the XbaI polymorphism, but in some cases, the relative intensity of the bands diagnostic of the mutated allele was considerably stronger than in the papillomas (Fig. 3A, lanes b, f-h, k). Figure 3B shows the pattern obtained after rehybridization of the same blot with a single-copy probe for the mouse interleukin-3 (IL-3) gene¹⁵. Comparison of the relative band intensities demonstrates that the mutated allele of the c-Ha-ras gene has become amplified in the carcinomas shown in lanes f-h. Those shown in lanes b and b, which contain more DNA and therefore do not provide clear evidence of amplification, nevertheless exhibit a change in the relative amounts of 'normal' 12-kb and 'mutated' 4- and 8-kb fragments. This result suggests that homozygosity may have developed in these cases, although

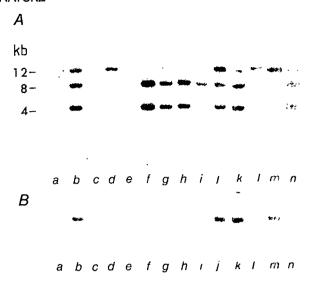


Fig. 3 Demonstration of the XbaI polymorphism in primary tumours. A, Lanes a, d and e: DNAs obtained from DMBA initiated primary papillomas. Lanes b, c and f-k contain NIH carcinoma DNAs. The pattern obtained with normal DNA is shown in lane l. Lanes m and n contain respectively DNA from spontaneously transformed NIH 3T3 cells and an NIH 3T3 transformant obtained by transfection with DNA from a papilloma with the codon 61 polymorphism. DNAs were digested with XbaI, run on agarose gels and hybridized with an Ha-ras-specific probe as described in Fig. 2 legend. B, Autoradiograph showing the ~ 1 -kb band obtained by rehybridization of the blot shown in A with a complementary DNA probe for the IL-3 gene¹⁵ (provided by A Dunn).

loss of the normal allele is difficult to prove because of the presence of some normal cells in the tumours. Yet another pattern is seen in the carcinomas in lanes c, i and j, which have similar band ratios to the papillomas.

The high frequency of the XbaI polymorphism in DMBAinitiated tumours allowed us to determine whether this mutation is carcinogen-specific, or is detected in tumours induced by different carcinogenic initiators or promoters. Chryserobin is a strong tumour promoter and a derivative of anthralin16. Compounds of this type are structurally unrelated to tetradecanoyl phorbol 13-acetate (TPA), do not bind to the phorbol ester receptor¹⁷ and presumably have a different site of action within the target cell. The results shown in Table 1 suggest that the nature of the promoter used does not influence the frequency of the specific XbaI polymorphism seen in DMBA-initiated tumours. However, of a total of 12 tumours from NIH mice initiated with N-methyl-N'-nitro-N-nitrosoguanidine (MNNG), comprising six papillomas and six carcinomas, none showed the restriction fragments diagnostic of the mutation. The carcinogen MNNG is a direct-acting methylating agent and might therefore not be expected to induce the same types of mutation as DMBA¹⁸. Since the mice were initiated by a single treatment with the carcinogen, the presence of the polymorphism in tumours initiated with one type of initiator, but not with another, suggests that the Ha-ras gene mutations occur at or very close to the time of initiation.

Zarbl et al.⁷ recently showed that specific $G \rightarrow A$ transitions occur consistently at the second nucleotide of codon 12 of the rat c-Ha-ras gene in rat mammary carcinomas induced by a single treatment with nitrosomethylurea (NMU). As this particular mutation is exactly that predicted on the basis of the known mechanism of action of NMU¹⁸, Zarbl et al. concluded that NMU interacts directly with codon 12 of the ras gene. Our observation that Ha-ras mutations in DMBA-initiated tumours occur predominantly at adenosine residues is compatible with previous results on the metabolism and binding of DMBA to

Table 1	in tumours			
Strain	Tumour	Initiator	Promoter	No. positive
				no. tested
Sencar	Papilloma	DMBA	TPA	12/14
	· .	DMBA	Chryserobin	5/5
NMRI	Papilloma	DMBA	TPA	2/2
NIH	Papilloma	DMBA	TPA	3/3
Sencar	Carcinoma	DMBA	TPA	0/2*
NMRI	Carcinoma	DMBA	TPA	3/3
	(transplanted)		•	
NIH	Carcinoma	DMBA	TPA	8/8
NIH	Papilloma	MNNG	TPA	0/6
NIH	Carcinoma	MNNG	TPA	0/6

Mice were initiated with 25 µg DMBA or 600 µg MNNG, dissolved in 200 µl acetone., Promotion was carried out twice weekly by treatment with an acetone solution of TPA (12.5 μg) or chryserobin (50 μg)¹⁶

One tumour has an Ha-ras mutation, presumably at codon 12 (see Fig. 1C, lane 5).

DNA in mouse skin. Dipple and co-workers have shown that benzo(a)pyrene, which is about 30-fold weaker as an initiating agent than DMBA, exhibits a corresponding decrease in the amount of binding to deoxyadenosine, but not deoxyguanosine, residues^{19,20}. The relative carcinogenic potency of these two aromatic hydrocarbons may be related to their abilities to bind to, and therefore induce mutations at; deoxyadenosine. The mutations in DMBA-induced tumours are not exclusively A > T transversions, however, as a small proportion of tumours are activated at codon 12, presumably by changes at one of two G residues.

If Ha-ras gene mutation is critically involved in initiation of mouse skin carcinogenesis, the introduction of a mutated gene into epidermal cells in vivo should be able to substitute for treatment with the initiating chemical. We have shown recently that the viral Ha-ras gene of Harvey sarcoma virus can act as an initiator of two-stage skin carcinogenesis21. These results support the conclusion that Ha-ras gene mutation occurs during initiation, but this event in itself is insufficient for tumorigenesis because even epidermal cells initiated with the viral Ha-ras gene required promoter treatment before papillomas developed

These studies suggest that mutation and amplification of ras genes may occur at different stages of carcinogenesis. It is possible that the additional changes involving the mutated allele may take place at the time of carcinoma development, or may be present in a sub-set of papillomas with a high probability of malignant conversion²². Indeed, one of 22 papillomas in the present studies showed amplification of the mutated allele (data not shown). We do not know whether these changes are accompanied by loss of the normal allele of the Ha-ras gene; loss of the normal allele has been seen in a carcinogen-induced thymic lymphoma²³ and in human tumour cell lines¹³, and loss of one Ha-ras allele has been reported in a series of bladder carcinomas²⁴. Chromosomal changes of this kind may represent late events in tumour development in some, but by no means all, mouse skin carcinomas.

M.Q. is the recipient of an EMBO long-term Fellowship and K.B. is supported by a Training Fellowship from the MRC. We thank I. B. Kerr for histological diagnosis of tumours, Francis Fee and Sheena Young for technical assistance, and J. Paul for critical reading of the manuscript. Some of the tumours used in this study were supplied by G. T. Bowden, T. Slaga and J. Di Giovanni. The Beatson Institute is funded by the Cancer Research Campaign.

Received 26 Feburary; accepted 7 May 1986.

- 1. Klein, G. & Klein, E. Carcinogenesis 5/429-435 (1984).
- Rein, G. & Alein, E. Carting and S. 422-435 (1984).
 Balmain, A. Br. J. Cancer 51, 1-7 (1985).
 Balmain, A. & Pragnell, I. B. Nature 303, 72-74 (1983).

- 4. Sukumar, S., Notario, V., Martin-Zanca, D. & Barbacid, M. Nature 306, 658-661 (1983).
 5. Guerrero, I., Calzada, P., Mayer, A. & Pellicer, A. Proc. natn. Acad. Sci. U.S.A. 81, 202-205 (1984)
- Eva, A. & Aaronson, S. Science 220, 955-956 (1983). Zarbl, H., Sukumar, S., Arthur, A. V., Martin-Zanca, D. & Barbacid, M. Nature 315, 382-386
- Guerrero, I., Villasante, A., Corces, V. & Pellicer, A. Science 225, 1159-1162 (1984).
 Balmain, A., Ramsden, M., Bowden, G. T. & Smith, J. Nature 307, 658-660 (1984).
 Seeburg, P. H., Colby, W. W., Capon, D. J., Goeddel, D. V. & Levinson, A. D. Nature 312, 71-75 (1984).
- Yuasa, Y. et al. Nature 303, 775-779 (1983).
 Furth, M. E., Davis, L. J., Fleudelys, B. & Scolnick, E. M. J. Virol. 43, 294-304 (1982).
- 13. Santos, E. et al. Science 223, 661-664 (1984).
- Fujita, J. et al. Nature 307, 464-466 (1984).
 Fung, M. C. et al. Nature 307, 233-237 (1984).
- DiGiovanni, J. & Boutwell, R. K. Carcinogenesis 4, 281-284 (1983).
 Delclos, K. B., Nagle, D. S. & Blumberg, P. M. Cell 19, 1025-1032 (1980).
 Margison, G. P. & O'Connor, P. J. Chemical Carcinogens and DNA Vol. 1 (ed. Grover, P.) (CRC Press, Florida, 1978).
- Sawicki, J. T., Moschel, R. C. & Dipple, A. Cancer Res. 40, 1580-1582 (1983).
 Dipple, A., Sawicki, J. T., Moschel, R. C. & Bigger, C. A. H. in Extrahepatic Drug Metabolism and Chemical Carcinogenesis (eds Rystrom, J., Montelius, J. & Bengtsson, M.) 439-448 (Elsevier, Amsterdam, 1983).
- Brown, K. et al. Cell (in the pr
- 22. Hennings, H., Shores, R., Mitchell, P., Spangler, E. F. & Yuspa, S. H. Carcinogenesis 6, 1607-1610 (1985).
- Guerrero, I., Villasante, A., Corces, V. & Pellicer, A. Proc. natn. Acad. Sci. U.S.A. 82, 7810-7814 (1985).
- Fearon, E. R., Feinberg, A. P., Hamilton, S. H. & Vogelstein, B. Nature 318, 377-380 (1985). Laemmli, U. K. Nature 227, 680-682 (1970).
- Law, D. J., Frossard, P. M. & Rucknagel, D. L. Gene 28, 153-158 (1984).
 Ellis, R. W. et al. J. Virol. 36, 408-420 (1980).

Site-directed mutagenesis of the regulatory light-chain Ca²⁺/Mg²⁺ binding site and its role in hybrid myosins

Fernando C. Reinach*, Kivoshi Nagai† & John Kendrick-Jones†

* Ludwig Institute for Cancer Research and † MRC Laboratory of Molecular Biology, MRC Centre, Hills Road, Cambridge CB2 2QH, UK

The regulatory light chains, small polypeptides located on the myosin head, regulate the interaction of myosin with actin in response to either Ca2+ or phosphorylation. The demonstration that the regulatory light chains on scallop myosin can be replaced by light chains from other myosins has allowed us to compare the functional capabilities of different light chains1, but has not enabled us to probe the role of features, such as the Ca2+/Mg2+ binding site, that are common to all of them. Here, we describe the use of site-directed mutagenesis to study the function of that site. We synthesized the chicken skeletal myosin light chain in Escherichia coli and constructed mutants with substitutions within the Ca²⁺/Mg²⁺ binding site. When the aspartate residues at the first and sixth Ca2+ coordination positions are replaced by uncharged alanines, the light chains have a reduced Ca2+ binding capacity but still bind to scallop myosin with high affinity. Unlike the wild-type skeletal light chain which inhibits myosin interaction with actin, the mutants activate it. Thus, an intact Ca²⁺/Mg²⁺ binding site in the N-terminal region of the light chain is essential for regulating the interaction of myosin with actin.

The myosin regulatory light chains belong to a family of calcium-binding proteins which includes calmodulin and troponin C²⁻⁴. These are composed of four EF hands or domains, each consisting of an α -helix E, a divalent cation binding loop and an α -helix F (refs 5-7). In the myosin regulatory light chains, deletions and non-conservative substitutions at critical positions have destroyed the Ca²⁺/Mg²⁺ binding ability of three of the loops, so that only the N-terminal domain has retained the ability to bind divalent ions⁸⁻¹¹.

The regulatory light chains are non-covalently bound to the heavy chains in the neck region of myosin heads 12-15. They can be subdivided into three functional classes: (1) in molluscan muscles, they inhibit myosin interaction with actin in the absence of Ca²⁺ and Ca²⁺ relieves this inhibition¹; (2) in vertebrate smooth muscle and non-muscle cells, Ca²⁺ binding to calmodulin activates a kinase which phosphorylates the regulatory light chains and thus 'switches on' myosin interaction with actin^{16,17}; (3) in vertebrate striated muscles, they do not appear to have a primary role in actomyosin regulation^{18,19}.

When the regulatory light chains are removed from scallop myosin by EDTA, myosin interaction with actin as measured by the actin-activated myosin MgATPase is 'desensitized' to Ca²⁺ and Ca²⁺ sensitivity can be restored when the scallop light chains rebind^{20,21} (Table 1). Regulatory light chains from a wide

Table 1 Effect of the light-chain mutants on Ca²⁺ regulation in desensitized scallop myofibril-regulatory light chain hybrids

Desensitized scallop myofibrils	Actomyosin -Ca ²⁺ (µmol H ⁺ m	+Ca ²⁺
Control	0.163	0.152
+scallop LC	0.050	0.263
+rabbit LC	0.050	0.081
+chicken LC	0.058	0.102
+ E. coli LC	0.050	0.069
+ mutant 442 LC	0.262	0.233
+mutant 452 LC	0.229	0.200
+ mutant 463 LC	0.251	0.231

The desensitized scallop myofibril-regulatory light chain hybrids were prepared as described in Fig. 2B legend. Their actin-activated Mg AT-Pase activities were measured at 25 °C in a final concentration of 36 mM KCl, 3 mM MgCl₂, 2 mM MgATP and either 0.1 mM EGTA (-Ca²⁺) or 0.1 mM EGTA and 0.15 mM Ca²⁺ (+Ca²⁺) by the pH-stat assay procedure as described previously¹. Samples (1 mg) of each of the hybrids were solubilized in 0.6 M KCl, 1 mM MgATP, pre-mixed with 0.5 mg skeletal muscle F-actin (actin filaments) in a final volume of 200 µl, and then diluted to 5 ml to give the final assay conditions shown above. The mutant light chains remain bound to the desensitized scallop myosin under these assay conditions. These ATPase assays were repeated with three other desensitized scallop myofibril preparations and with the light chain/mutant hybrids prepared under the various conditions described in Fig. 2B legend. We observed that under all the conditions tested the native and wild-type vertebrate light chains always inhibited the actin-activated myosin ATPase whereas the mutant light chains always activated the ATPase. LC, light chain.

variety of myosins will also bind to desensitized scallop myosin to form hybrid myosins and their function can be assayed¹. The three classes of light chains regulate the actin-activated ATPase of hybrid scallop myofibrils as follows: those from molluscan muscles regulate in a calcium-dependent fashion, whereas those from vertebrate smooth muscle and non-muscle cells regulate in a phosphorylation-dependent manner¹⁷ and those from vertebrate striated muscles inhibit the ATPase activity²². There is no evidence that the divalent cation binding site in any of these three classes of regulatory light chains is involved in Ca²⁺ regulation^{11,23}, and thus the precise role of this site is not known. We have prepared chicken skeletal regulatory light-chain mutants with genetically engineered substitutions in the Ca²⁺/Mg²⁺ binding loop, determined the Ca²⁺ binding capacity of these mutants and assayed their regulatory function using desensitized scallop myofibrils.

A plasmid plcIIFXMLC was constructed which directed the synthesis of a fusion protein consisting of the N-terminal 31 amino-acid residues of λ cII protein, the blood coagulation factor X_a recognition site and the complete chicken myosin light-chain (MLC) polypeptide (Fig. 1). Because the amino-acid sequence near the factor X_a cleavage site, Arg-Ala-Pro-Lys, resembles the thrombin cleavage site in fibrinogen²⁴, we digested the fusion protein CIIFXMLC with bovine thrombin. This enzyme cleaved the fusion protein at a single site to yield a

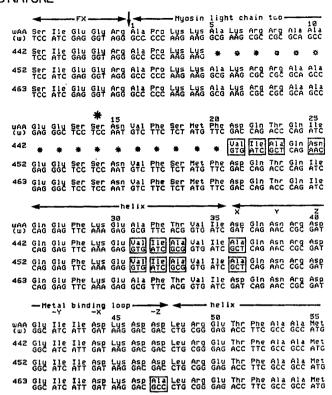
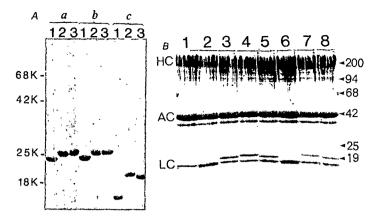


Fig. 1 Sequence of the factor X recognition site (FX) and the first 55 amino acids of the myosin regulatory light-chain clone present in pLcIIFXMLC Arrow, thrombin cleavage site. The nucleotide and amino-acid sequences of the wild-type light chain (wAA), mutants 442, 452 and 463 are indicated. Where the nucleotide and amino-acid sequences of the three mutant light chains are different from the wild type the residues are boxed. The deletion present in clone 442 is marked with asterisks. The residues involved in the α -helix-Ca/Mg binding loop- α -helix, which are believed to form a EF-hand structure, are indicated. The six residues believed to be involved in the Ca/Mg coordination are also indicated (X, Y, Z, -Y, -X, -Z). The phosphorylation site is indicated with a large asterisk.

Methods. Construction of the expression plasmid. The EcoRI insert of clone Agt11/L10 containing the whole coding region of chicken myosin light chain 2 (see Fig. 5 of ref. 25 for sequence) was treated with the Klenow fragment of DNA polymerase in the presence of dNTP to obtain flush ends and cloned into the SmaI site of M13mp19. A clone (M13MLC) containing the insert with the 5' end of the messenger RNA facing the universal priming site, was selected. A Sau96I fragment of M13MLC from position 33 to 253 was isolated, treated with Klenow DNA polymerase in the presence of dNTP to obtain flush ends, and cloned in the StuI site of M13mp11 (ref. 27). A clone (M13mp11FXMLC1) where the Ala codon of the insert was in-frame with the FX recognition sequence and facing the universal priming site of M13, was selected. The Ncol (position 194)-HindIII (polylinker) fragment from M13MLC was then cloned into the NcoI-HindIII-cleaved M13mp11FXMLC1 to obtain M13mp11FXMLC2. This clone contains the whole MLC coding and 3' noncoding region linked in-frame to the FX recognition site. The BamHI fragment from M13mp11 FXMLC2 containing FX sequences and MLC sequences up to position 364 was cloned into the BamHI site of pLcII (ref. 28) and a clone (pLcIIFXMLC1) with the FX recognition sequence in-frame with the first 31 amino acids of cII was selected by restriction enzyme analysis. Finally, the NcoI (194)-HindIII (polylinker) fragment of M13MLC was cloned into NcoI-HindIII-cleaved pLcIIFXMLC1 to obtain pLcIIFXMLC2. This clone contains the pL promoter of λ followed by nutL, nutR, tR₁ and the first 31 amino acids of cII. The sequence at the junction of FX and MLC is shown. The EcoRI-HindIII fragment of pLcIIFXMLC2 was subcloned into M13mp19 to obtain M13mp404. Single-stranded templates of M13mp404 were used to sequence the final construct with the help of synthetic oligonucleotides spaced along the insert. Construction of mutants. Single-stranded DNA from clone M13mp404 and oligonucleotides synthesized using the phosphotnester method (5'GGTGATCGCTCAGAACC to change Asp 36 to Ala and 5'TAAGGACGCCCTGCGGG also to change Asp 47 to Ala) were hybridized and extended with Klenow DNA polymerase and transfected into BMH-71-18-mutL (ref. 29). Mutant clones were identified by hybridization with the mutagenic oligonucleotide²⁷, plaque-purified and the whole *EcoRI-HindIII* insert was sequenced before recloning into pLmp10 (ref. 28). Restriction enzymes were from New England Biolabs, Klenow DNA polymerase from Boehringer Mannheim and T4 DNA ligase was purified from strain NM989 (ref. 30). M13 constructs were grown in TG-1 (ref. 29) and pLcII constructs in QY13 (ref. 31).

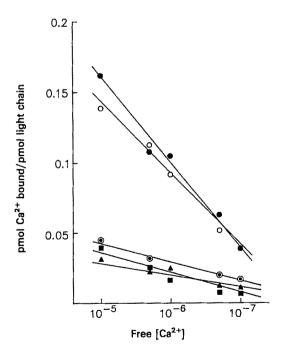
Fig. 2 A, Purification of light-chain mutants; B, SDS-PAGE (10-20% acrylamide gradient gel) of desensitized scallop myofibril/regulatory light chain hybrids. A, SDS (15%)-PAGE of: (1) mutant 442; (2) mutant 452; and (3) mutant 463 at the different stages in the purification procedure: a, cell/pellet fractions after 4 washes with Triton X-100 solution; b, mutant light-chain fusion proteins cIIFX-MLC after purification on DEAE-cellulose; c, mutant light chains after removal of the bacterial leader sequence by thrombin cleavage and DEAE-cellulose chromatography. The gels were calibrated using the following M_r standards: 68,000 (68K), bovine serum albumin; 42K, actin; 25K, rabbit skeletal muscle myosin A_1 (LC₁) light chain; 18K, rabbit myosin regulatory (LC₂) light chain. B, The hybrids were as follows: 1, control, desensitized scallop myofibrils alone; 2, +scallop light chains; 3, +rabbit skeletal muscle myosin light chains; 4, +chicken breast muscle myosin light chains; 5, +E. coli-synthesized light chains (wild type); 6, +light-chain mutant 442; 7, +mutant 452; and 8, +mutant 463. The following M_r standards were used: 200K, myosin heavy chain; 94K, phosphorylase; 68K, bovine serum albumin; 42K, actin; 25K, rabbit myosin A_1 (LC₁) light chain; 19K, chicken myosin LC₂ light chain. HC, myosin heavy chain; AC, actin; LC, light chains. The myofibril samples have been overloaded so that the light chains, which are present only as ~4% of the total



protein, can be clearly distinguished. In scallop myosin the two types of light chains (structural and regulatory) have the same mobility, and desensitization leads to the removal of only the regulatory light chains from the myosin²¹

to the removal of only the regulatory light chains from the myosin²¹.

Methods. A, QY13 cells containing pLcIIFXMLC or the mutated constructs were grown at 30 °C in 2×TY medium (containing 25 µg ampicillin per ml). At $A_{600\,\mathrm{nm}} = 0.8$ the cultures were quickly warmed to 42 °C and maintained at this temperature for 15 min, then grown at 37 °C for 3.5 h. The cell pellets were prepared as described 31, washed four times with 0.5% Triton X-100, 1 mM EDTA (shown in a) 32, dissolved in 6 M urea, 50 mM Tris-HCl, pH 7.5, 0.5 mM MgCl₂, 0.5 mM dithiothreitol (DTT), dialysed against the same solution for 3 h and then applied to a 11×4 cm DEAE-cellulose column (Whatman DE-52) equilibrated in the same solution. The fusion proteins were eluted with a linear gradient (500+500 ml) from 0 to 80 mM NaCl in the 6 M urea solution, and the peak fractions concentrated in an Amicon ultrafiltration cell with a PM-10 membrane (b). The proteins (5 mg ml⁻¹) were dialysed against two changes of 100 mM NaCl, 40 mM Tris-HCl, pH 8.0, 0.5 mM DTT and then digested at 20 °C for 2.5 h with thrombin (enzyme/protein (w/w) ratio 1:250). The digests were diluted with an equal volume of 4 M urea, 25 mM Tris-HCl, pH 7.5, 0.5 mM MgCl₂, 0.5 mM DTT (to reduce the NaCl concentration to 50 mM), loaded onto a 8×4 cm DEAE-cellulose column equilibrated in 2 M urea, 25 mM Tris-HCl, pH 7.5, 0.5 mM MgCl₂, 0.5 mM DTT and the light chains eluted with a linear gradient (400+400 ml) from 50 to 150 mM NaCl in the 2 M urea solution. The light chains were concentrated by ultrafiltration with an Amicon PM-10 membrane (c) and their protein concentrations measured assuming an E¹⁰⁰₁₀₀₀ = 5.5 (recovery > 80% of the initial fusion protein). Final yield was 20 mg purified light chain per 1 of bacterial culture. B, Scallop myofibrils were prepared and desensitized at 27 °C as described previously²¹. The hybrids were prepared by incubating desensitized scallop myofibrils (~2 mg ml⁻¹) in 50 mM NaCl, 4 mM MgCl₂, 5 mM phosphate buffer, pH 7.0, 0.2 mM DTT with the light chains and mutants at a 1.5:1 light chain/myosin heavy chai



polypeptide which co-migrated with the chicken skeletal myosin light chain on SDS gels. N-terminal sequence analysis of the cleaved protein gave the sequence Ala-Pro-Lys-Lys-Ala-Lys-Arg, which is identical to the N terminus of the light chain 10,25 except for the absence of the trimethyl blocking group on the N-terminal alanine residue²⁶. This light chain synthesized in E. coli bound to desensitized scallop myofibrils and inhibited the

Chicken breast muscle myosin light chain; , E. coli-synthesized light chain (wild type); ②, mutant 463; 🏔, mutant 452; 🌉, mutant 442.

Methods. Ca²⁺ binding was measured using a procedure adapted from that of Kawasaki et al.27 using a 96-well Microtiter hybrid dot manifold assembly (BRL, No. 1050 MM) and a nitrocellulose membrane filter (Schleicher & Schuel PH79, 0.1 μ m). Aliquots (2-5 μ l) containing 4-10 μ g of light chains/mutants were applied to the walls of the wells of the manifold and mixed with 250 µl of solution with the appropriate free Ca²⁺ concentration (10⁻⁵-10⁻⁷ M Ca²⁺ in 50 mM NaCl, 0.1 mM MgCl₂, 10 mM imidazole buffer, pH 7.0). These solutions were prepared using an apparent binding constant for Ca/EGTA at 25 °C and pH 7.0 of $3 \times 10^6 \,\mathrm{M}^{-1}$ (ref. 33) and with a final concentration of 5-20 μM ⁴⁵Ca/EGTA (specific activity 200-900 c.p.m. pmol⁻¹). The samples were mixed, incubated at 20 °C for 5 min and rapidly filtered on a vacuum pump. A fresh 250-µl aliquot of the appropriate Ca2+ solution was added and incubated at 20 °C for a further 5 min, and then filtered under vacuum. The nitrocellulose filter membrane was dried, wrapped in Saran wrap and autoradiographed at $-70\,^{\circ}\text{C}$ for 2 h. The regions of the nitrocellulose membrane containing the light chains/mutants could be identified from the autoradiograph and by the indentation caused by pressure and were excised with a one-hole punch, 'dissolved' in Aquasol-2 (NEN Research Products) and counted. Control wells with no added protein, but washed with the appropriate Ca/E01A-containing solutions, were used to correct for background. This procedure was checked by measuring the Ca²⁺ binding of the wild type and mutant light chains by the Hummel-Dryer technique³⁰ at 10^{-5} M free Ca²⁺ Ca²⁺ binding measurements were also carried out in the absence of Mg²⁺ and the binding curves obtained were very similar (~5-10% increase in Ca²⁺ binding) to those shown here in the presence of $100 \, \mu M \, Mg^{2+} \, Mg^{2+}$ was wells with no added protein, but washed with the appropriate 45Ca/EGTAincluded to eliminate background low-affinity nonspecific divalent cation

Fig. 3 Ca²⁺-binding ability of the regulatory light chain and mutants. O,

ATPase activity in an identical manner to the native regulatory light chain of chicken skeletal muscle.

binding. Binding measurements were repeated at least three times under each set of conditions.

In the divalent cation binding domains of the calcium-binding proteins, the acidic residues at the coordination positions X and -Z are conserved and are believed to bind to Ca^{2+} (refs 3, 4; Fig. 1). To inhibit Ca^{2+} binding in the light chain, we have separately replaced Asp 36 and Asp 47 with Ala at the X and

-Z coordination positions by oligonucleotide-directed mutagenesis. We sequenced a representative clone (463) of the Asp 47 → Ala mutant and showed that it contains no other substitutions. All the 36 clones sequenced in the experiment to produce the Asp 36 -> Ala mutant had three additional amino-acid substitutions in the E helix preceding the binding loop (Fig. 1). During the screening for Asp 36 -> Ala mutants, we found a clone (442) which contained in addition a deletion of 16 amino acids spanning the phosphorvlation site and four further amino-acid substitutions in the N-terminal region (Fig. 1). These mutants were produced in E. coli, purified and cleaved with thrombin. As expected, the protein produced from clone 442 was smaller (relative molecular mass $(M_r) \approx 17,000$) than the other mutants $(M_r \approx 19,000)$ (Fig. 2A).

We measured the relative Ca2+ binding abilities of the wildtype and mutant light chains at 10^{-7} to 10^{-5} M free Ca²⁺ and found that the Ca2+ binding capacities of the mutants were lower than that of the wild-type and native light chains (Fig. 3). All the mutants bound to desensitized scallop myfibrils with an affinity comparable with that of the wild type made in E. coli and native chicken myosin regulatory light chains (Fig. 2B). Table 1 shows that when scallop myofibrils were reconstituted with chicken skeletal myosin light chains or those of the wild type made in E. coli, the ATPase activity was inhibited both in the presence and absence of Ca²⁺, whereas the mutant light chains activated the ATPase to a level comparable with that observed with the scallop light chains in the presence of Ca²⁺. This shows that the mutant light chains have lost the ability to inhibit the interactions of myosin with actin and instead lock the actin-activated myosin ATPase in the 'on' state. Thus, they appear to bind to the myosin heavy chains in the correct positions needed to prevent the decrease in ATPase activity observed with the unregulated myosin heads (see Table 1 for control).

Furthermore, our results show that the first domain in the regulatory light chain really is the site with high affinity for divalent cations. The existence of light chains that differ in their physiological activities, a suitable myosin assay system and the generation of functional mutants in E. coli should allow us further to dissect the structural features responsible for myosin regulation.

We thank Drs Max Perutz, Hugh Huxley, Alexander MacLeod, Clive Bagshaw, Jane Mitchell, Sandra Citi, Lesley Clayton and Richard Turner for critically reading the manuscript; Ross Jakes for performing the N-terminal sequence analysis; Dr Peter Esnouf for the gift of factor X and thrombin; and Dr Hans C. Thøgersen for purified thrombin and for pointing out the similarity of the thrombin cleavage site in CIIFXMLC and fibrinogen. K.N. was supported by NIH grant RO1 HL 31461-02, F.C.R. was partially supported by CNPg grant 20.0694, Brazil.

Received 20 February; accepted 8 May 1986.

- 1. Kendrick-Jones, J., Szentkiralyi, E. M. & Szent-Gyorgyi, A. G. J. molec. Biol. 104, 747-775
- 2. Baba, M. L., Goodman, M., Berger-Cohn, J., DeMaille, J. G. & Matsuda, G. Molec. biol. Baba, M. L., Goodman, M., Berger-Conn, J., Derviante, J. G. & Maissua, Evol. 1, 442-455 (1984).
 Kretsinger, R. H. CRC Crit. Rev. Biochem. 8, 119-174 (1980).
 Kretsinger, R. H. & Nockolds, C. E. J. biol. Chem. 248, 3313-3326 (1973).
 Babu, Y. S. et al. Nature 315, 37-40 (1985).

- Herzberg, O. & James, M. N. G. Nature 313, 653-659 (1985).
- Sundaralingam, M. et al. Science 227, 945-948 (1985).
 Collins, J. H. Nature 259, 699-700 (1976).
- Collins, J. H. Nature 239, 039-100 (1970).
 Kendrick-Jones, J. & Jakes, R. in Boehringer International Sympsium on Myocardial Failure (eds Rieker, G., Weber, A. & Goodwing, J.) 28-40 (Springer, Berlin, 1976).
 Matsuda, G., Suzuyama, Y., Maita, T. & Umegane, T. FEBS Lett. 84, 53-56 (1977).
 Bagshaw, C. R. & Kendrick-Jones, J. J. molec. Biol. 130, 317-336 (1979).

- Bagshaw, C. R. Bochemistry 16, 59-67 (1977).
 Craig, R. et al. J. molec. Biol. 140, 35-55 (1980).
 Vibert, P. & Craig, R. J. molec. Biol. 157, 299-319 (1982).
 Flicker, P. F., Wallimann, T. & Vibert, P. J. molec. Biol. 169, 723-741 (1983).
 Adelstein, R. S. & Eisenberg, E. A. Rev. Biochem. 49, 921-956 (1980).

- Kendrick-Jones, J. et al. J. molec. Biol. 165, 139-162 (1983).
 Leavis, P. C. & Gergely, J. CRC Crit. Rev. Biochem. 16, 235-305 (1984).
 Persechini, A., Stull, J. T. & Cooke, R. J. biol. Chem. 260, 7951-7954 (1985).
- 20. Szent-Gyorgyi, A. G., Szentkiralyi, E. M. & Kendrick-Jones, J. J. molec. Biol. 74, 179-203
- 21. Chantler, P. D. & Szent-Gyorgyi, A G. J. molec. Biol. 138, 473-492 (1980).

- 22. Kendrick-Jones, J. et al. in Basic Biology of Muscles: A Comparative Account (eds Twaton, B. M., Levine, R. J. C. & Dewey, M. M.) 255-272 (Raven, New York, 1932)

 23. Bagshaw, C. R. & Kendrick-Jones, J. J. molec. Biol. 140, 411-433 (1980)

 24. Blombäck, M., Blombäck, B., Mammen, E. F. & Pradsad, A. S. Nature 218, 314-318 (1983)

- 25. Reinach, F. C. & Fischman, D. A. J. molec. Biol. 181, 411-422 (1985) 26. Hendry, G. D. et al. FEBS Lett. 144, 11-15 (1982).

- Kawasaki, H., Kasai, H. & Okuyama, T. Analyt. Biochem 148, 297-302 (1935)
 Nagai, K. & Thogersen, H. C. Nature 309, 810-812 (1984).
 Carter, P., Bedouelle, H. & Winter, G. Nucleic Acids Res. 13, 4431-444) (1935)
- 30. Murray, N., Bruce, S. A. & Murray, K. J. molec. Biol. 132, 493-505 (1979)
 31. Nagai, K., Perutz, M. F. & Poyart, C. Proc. natn. Acad. Sci. U.S A. 82, 7252-7255 (19.5)
- Marston, F. A. O. et al. Biotechnology 2, 800-804 (1984)
- 33. Marston, S. B. Prog. Biophys. molec. Biol. 41, 1-41 (1983).

Enzymatic activity of the conserved core of a group I self-splicing intron

Jack W. Szostak

Department of Molecular Biology, Massachusetts General Hospital, Boston, Massachusetts 02114, USA

Splicing of the Tetrahymena ribosomal intron was first studied by Cech et al.1,2, who subsequently demonstrated that the intron RNA catalyses its own excision from a primary transcript to yield mature ribosomal RNA^{3-5} . This intron shares several short conserved sequences and a common secondary structure with several other introns 6-9, some of which have also been shown to self-splice 10,11. Here I show that the conserved core of the Tetrahymena intron can act in trans to catalyse the sequence-specific cleavage and addition of guanosine to a separate RNA substrate.

Cech et al. proposed that self-splicing occurs by a series of trans-esterification reactions in which the total number of phosphodiester bonds is conserved^{4,12,13}. Each step involved the concerted breakage and formation of a specific phosphodiester bond, catalysed by a single phosphoester transferase activity contained within the intron RNA itself. In the first step, the 3' hydroxyl of a guanosine 12,14 attacks the phosphodiester bond between the 5' exon and the intron. That bond is broken and a new one is formed between the guanosine and the 5' end of the intron, thus conserving the total number of phosphodiester bonds. The second step is another exchange reaction; in this case the phosphodiester bond between the 3' end of the intron and the 3' exon is broken and a new one is formed between the 5' and 3' exons. In the third step, the intron circularizes itself in yet another trans-esterification reaction.

Examination of potential secondary structures shows that all three of these reactions may take place in a very similar structural context (Fig. 1). In each case, the reaction is between one strand of a short region of double-stranded RNA and a guanosine residue which can be either free G or the 3' nucleotide of a chain. Steps one and three are completely analogous, while step two is the reverse reaction. The similarity of the substrates for the three reactions strengthens the view that the entire splicing process is catalysed by a single enzyme activity. If the substrate was defined by local sequence and structure, and not by the overall folding of the intron, it seemed likely that the enzyme might also be capable of catalysing the reaction on an exogenously supplied template. Figure 2 shows the structure of the conserved core of the Tetrahymena rRNA intron, drawn according to Davies et al.6. This segment of the intron contains the conserved P, Q, R and S sequences of Davies et al., but not the flanking secondary structures. The secondary structure of the core is supported by a considerable degree of phylogenetic comparison^{6,9}, and some structural analysis^{15,16}.

The hypothesis that this conserved core contains the enzymatic activity was tested by constructing a series of plasmids (Fig. 3) that could be transcribed in vitro by T7 RNA polymerase to yield RNA molecules that could be tested for self-splicing or trans-esterification activity. The first experiment involved the insertion, downstream of a T7 RNA polymerase promoter, of

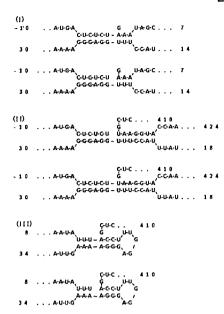


Fig. 1 Substrates for the RNA enzyme. The first transesterification reaction (I) is between a free G residue and an A residue that is part of a stem-loop structure. The double-stranded stem is formed between the exon-intron junction sequence, and the internal guide sequence^{6,9}. Release of the G-intron allows a more extensive pairing between the internal guide sequence and the 3' intron-exon sequence (II). The intron ends in G, which is placed in the same position as the incoming G in reaction I. Catalysis of the reverse reaction then results in loss of the intron and joining of the 5' and 3' exons. Circularization of the intron (III) takes place in a similar sequence and secondary structure context. The first nucleotide of the intron is +1 in the sequence coordinate system.

a DNA restriction fragment spanning the entire intron. As expected, RNA transcribed in vitro from this DNA and gelpurified was able to perform all three steps of the self-splicing process when incubated in buffer containing Mg2 guanosine. A series of RNAs truncated at different 3' positions was generated by cleavage of the DNA template with restriction endonucleases, followed by T7 RNA polymerase runoff transcription. The enzyme ScaI cuts just inside the 3' end of the intron, and templates cleaved with this enzyme yield RNA molecules lacking the 3' intron-exon junction. Remarkably, these transcripts still splice, apparently finding new acceptor splice sites within the intron sequence. The enzyme NheI cuts the DNA 20 nucleotides 3' of the conserved core, while BglII cuts within the core region. Transcription of NheI-cut DNA yielded enzymatically active RNA, as incubation of the gelpurified RNA with guanosine in splicing buffer resulted in the appearance of smaller RNA products. The RNA resulting from transcription of Bg/II-cut DNA was inert. All subsequent experiments were therefore done with transcripts of NheI-cut DNA.

The extent of 5' sequences required for enzymatic activity was determined by constructing internal deletions. Since the RNAs synthesized from these templates lack all of the sequences at which splicing normally takes place, an exogenous substrate was added to assay for trans-esterification activity. The three plasmids used to generate the shortened catalytic RNAs are shown in Fig. 3; pLG8 and pLG9 delete intron sequences to within 84 and 51 nucleotides of the conserved core (the first nucleotide of the P3 segment, GACCGUCA, in Fig. 2), while in pSZ243, all intron sequences farther than 9 nucleotides from the core are deleted. These catalytic RNAs were tested on a substrate prepared by T7 RNA polymerase transcription of pSZ241 cut with DraI. This generates a 119-nucleotide RNA containing the sequences that are the substrate for the first trans-esterification reaction (Fig. 1). The substrate RNA begins

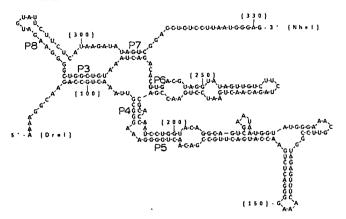


Fig. 2 Secondary structure of the conserved core of the RNA enzyme. All of the group I introns are characterized by conserved sequence elements and a conserved secondary structure. The conserved pairing regions P3, P4, P5, P6, P7 and P8 are labelled in accordance with the model of Davies et al.⁶. The nucleotide coordinates are numbered from the beginning of the intron. The segment of the Tetrahymena rRNA intron illustrated here corresponds to the T7 transcript of plasmid pSZ243 digested with NheI. Thus, reaction (I) (Fig. 1) involves the action of this catalytic core on sequences 100 nucleotides upstream, and reaction (II) involves substrate sequences both upstream and downstream from the conserved core.

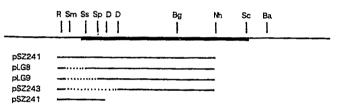


Fig. 3 Plasmids and transcripts used in the present study. The location of the intron relative to certain restriction sites is indicated by the heavy-lined segment. Plasmid pSZ241 contains the entire intron flanked by exon sequences. It was constructed by inserting the HinfI fragment of pTre1 (obtained from E. H. Blackburn) into the SmaI site of the T7 transcription vector pST53 (obtained from S. Tabor). Enzymatically active RNAs were generated by transcription of BamHI, ScaI or NheI digests of this DNA with T7 RNA polymerase. Plasmid pLG8 was generated by partial digestion of pSZ241 with SspI, complete digestion with SmaI, followed by blunt-end ligation. Plasmid pLG9 was generated by digestion of pSZ241 with SmaI and SphI, treatment with T4 polymerase to generate blunt ends, followed by blunt-end ligation. pSZ243 was constructed by blunt-end ligation of the gel-purified DraI fragment of pSZ241 into SmaI-cut pSZ241, followed by NheI digestion and recircularization. Substrate RNA was made by T7 transcription of DraI-cut pSZ241 DNA. All transcripts were purified by acrylamide-urea gel electrophoresis.

with 25 nucleotides of vector sequences, followed by 32 nucleotides of the 5' exon and the first 62 nucleotides of the intron. Activity was assayed by mixing catalytic RNA with substrate RNA in the presence of labelled GTP. The activity of the full-length intron RNA and of the three deletion derivatives was assayed (Fig. 4). All of the catalytic RNAs were able to cleave the substrate RNA at the exon-intron junction. The major labelled product is formed by the addition of GTP to the 5' end of the intron sequence. No incorporation of labelled G is observed in the absence of RNA enzyme. Since the pSZ243-NheI transcript contains only the conserved core sequence flanked by 10-20 nucleotides at each end, the conserved core does in fact contain the enzyme activity responsible for the trans-esterification reactions.

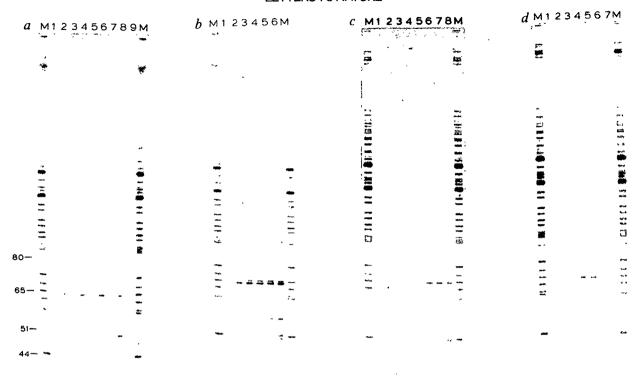


Fig. 4 Products of RNA-catalysed trans-esterification. a, Activity of deletion derivatives. Lane 1 contains substrate (transcript of DraI-cut pSZ241) but no enzyme (catalytic RNA). Lanes 2, 4, 6 and 8 contain enzyme and substrate; lanes 3, 5, 7 and 9 contain enzyme but no substrate. Lanes 2 and 3 show the addition of G and cleavage of substrate by the T7 transcript of NheI-cut pSZ241. Lanes 4 and 5 contain transcript of NheI-cut pLG8, lanes 5 and 6 contain the pLG9-NheI transcript, and lanes 7 and 8 contain the pSZ243-NheI transcript. The major product runs just below the 65-nucleotide marker, and corresponds to the GTP-intron sequence addition product. All reactions were done in the presence of 10 mM NH₄Cl, 20 mM MgCl₂, 30 mM Tris-HCl pH 7.4 and 0.2 mM aurin tricarboxylic acid. Incubations were for 30 mm at 58 °C. Catalytic RNAs were assayed at a concentration of ~50 nM, substrate RNAs were present at 0.5 μM, and α-labelled GTP at 2 5 μM. Size markers (Lanes M) are the 'A'-lane of a dideoxy-terminated sequence analysis reaction using a primer corresponding to the first 17 nucleotides of the substrate transcript, and DNA of pSZ241 as template. Sizes are 31, 32, 33, 44, 45, 48, 51, 58, 59, 60, 62, 65, 66, 68, 72 and 80 nucleotides for the region of interest. b, Time course of reaction. Aliquots were removed at 0, 15, 30, 45, 60 and 90 min (lanes 1-6) from a reaction of the enzymatically active pSZ243-NheI transcript, with α-labelled GTP and the pSZ241-DraI transcript as substrates. Reaction conditions were as for a. c, Optimal Mg²⁺ concentration. Reactions were as in b for 30 min, except that the Mg²⁺ concentration was varied. Reactions in lanes 1-8 contained 0, 2, 5, 10, 20, 30, 50 and 100 mM Mg²⁺, respectively. d, Temperature optimum. Reactions were as in b for 15 min, except that the temperature was varied. Lanes 1-7 show reactions incubated at 42, 46, 50, 54, 58, 62 and 66 °C, respectively.

The initial experiments used reaction conditions similar to those of Bass and Cech¹⁴. Characterization of the core enzyme, however, revealed some changes in optimum reaction conditions. The optimal Mg2+ concentration had increased from the 5 mM reported for the intact intron, to 20-40 mM (Fig. 4). This may reflect the difference between the intramolecular reaction of the intact intron and the intermolecular reaction, which requires a close interaction between separate substrate and enzyme molecules. This is supported by the effect of the volume excluder polyethylene glycol, which had a strong rate-enhancing effect at low Mg²⁺ concentration, but very little effect at a higher Mg²⁺ concentration. The temperature optimum of the reaction was a remarkably high 58 °C (Fig. 4), which was particularly surprising in view of the relatively short double-stranded region in the substrate stem loop and the short base-paired regions characteristic of the core enzyme itself. It is likely that the structure of the enzyme is stabilized by numerous tertiary interactions, and that the enzyme in turn stabilizes the structure of

The major products of the *trans*-esterification reaction clearly correspond to those expected by sequence-specific cleavage and GTP addition at the exon-intron boundary. Several minor products are visible, and may reflect a decreased sequence specificity of the small enzyme RNA. The identity of the major product

of the reaction was confirmed by examining the products of cleavage of 5'-end labelled RNA and uniformly labelled RNA (data not shown). The 3' fragment is not seen when 5' labelled RNA and cold G are used. With uniformly labelled RNA, the mobility of the 3' fragment is approximately 1 nucleotide faster if GTP rather than G is used as co-substrate, as expected from the extra negative charge contributed by the triphosphate moiety. The expected 57-nucleotide 5' fragment is seen with both 5' and uniformly labelled substrate RNA, but in submolar yield relative to the 3' fragment, probably because of splicing onto other substrate or enzyme sequences. In addition, other fragments are seen when labelled substrate RNA is used, possibly due to an inherent hydrolytic activity of the enzyme.

The observation that the self-splicing intron can be dissociated into an enzymatically active core and distinct substrate sequences should facilitate the genetic and biochemical analysis of both enzyme and substrate. Experiments with modified substrates should define the aspects of the substrate that are recognized by the enzyme. It should be a straightforward matter to define the minimal sequences required for enzymatic activity. Mutations in the enzyme which have specific effects on the binding of the RNA substrate or the guanosine co-substrate, or on the rate or nature of the reaction, should be informative with respect to the mechanism of catalysis. In addition, the constraints

that such information will place on enzyme structure and enzyme-substrate interactions will facilitate the development of models of the tertiary structure of the enzyme.

It is widely thought that RNA catalysis played an important part early in the evolution of life, before the evolution of protein synthesis. Sharp has suggested that early RNA replicases worked by splicing together short oligonucleotides in a template-directed manner¹⁷. An RNA polymerase-like activity of the Tetrahymena intron has recently been reported¹⁸. Mutations that lead to a loss in sequence specificity might result in a more general polymerase activity. It may therefore be possible to design an RNA replicase made of RNA by introducing a relatively small number of changes into the Tetrahymena intron core.

I thank Stan Tabor and Charles Richardson for gifts of T7 RNA polymerase, Laura Glew and Anne Gerber for technical assistance, and Andrew Murray for comments on the manuscript. This work was supported by a grant from Hoechst AG.

Received 25 February; accepted 15 April 1986.

- Zaug, A. J. & Cech, T. R. Cell 19, 331-338 (1980).
 Grabowski, P. J., Zaug, A. J. & Cech, T. R. Cell 23, 467-476 (1981).
 Kruger, K. et al. Cell 31, 147-157 (1982).
 Zaug, A. J., Grabowski, P. J. & Cech, T. R. Nature 301, 578-583 (1983).
 Zaug, A. J., Kent, J. R. & Cech, T. R. Science 224, 574-578 (1984).
- Davies, R. W., Waring, R. B., Ray, J. A., Brown, T. A. & Scazzochio, C. Nature 300, 719-724
- Michel, F. & Dujon, B. EMBO J. 2, 33-38 (1983). Cech, T. R. et al. Proc. natn. Acad. Sci. U.S.A. 80, 3903-3907 (1983).
- Waring, R. B., Scazzochio, C., Brown, T. A. & Davies, R. W. J. molec. Biol. 167, 595-605
- Garriga, G. & Lambowitz, A. M. Cell 38, 631-641 (1984).
 Horst, G.v.d. & Tabak, H. F. Cell 40, 759-766 (1985).
- Cech, T. R., Zaug, A. R. & Grabowski, P. J. Cell 27, 487-496 (1981).
 Cech, T. R. Cell 34, 713-716 (1983).
- 14. Bass, B. & Cech, T. R. Nature 308, 820-826 (1984).
- Inoue, T. & Cech, T. R. Proc. natn. Acad. Sci. U.S.A. 82, 648-652 (1985).
 Tanner, N. K. & Cech, T. R. Nucleic Acids Res. 13, 7759-7779 (1985).
- 17. Sharp, P. A. Cell 42, 397-400 (1985)
- 18. Zaug, A. J. & Cech, T. R. Science 231, 470-475 (1986).

Mechanism of recognition of the 5' splice site in self-splicing group I introns

Gian Garriga*, Alan M. Lambowitz*, Tan Inoue† & Thomas R. Cech‡

University of Colorado, Boulder, Colorado 80309, USA

* Edward A. Doisy Department of Biochemistry, St Louis University School of Medicine, St Louis, Missouri 63104, USA † Salk Institute, La Jolla, California 92037, USA ‡ Department of Chemistry and Biochemistry,

Group I introns include many mitochondrial ribosomal RNA and messenger RNA introns and the nuclear rRNA introns of Tetrahymena and Physarum 1-6. The splicing of precursor RNAs containing these introns is a two-step reaction. Cleavage at the 5' splice site precedes cleavage at the 3' splice site, the latter cleavage being coupled with exon ligation⁷⁻⁹. Following the first cleavage, the 5' exon must somehow be held in place for ligation. We have now tested the reactivity of two self-splicing group I RNAs, the Tetrahymena pre-rRNA and the intron 1 portion of the Neurospora mitochondrial cytochrome b (cob) pre-mRNA, in the intermolecular exon ligation reaction (splicing in trans) described by Inoue et al. 10. The different sequence specificity of the reactions supports the idea that the nucleotides immediately upstream from the 5' splice site are base-paired to an internal, 5' exon-binding site, in agreement with RNA structure models proposed by Davies and co-workers^{2,3} and others^{4,5,11}. The internal binding site is proposed to be involved in the formation of a structure that specifies the 5' splice site and, following the first step of splicing, to hold the 5' exon in place for exon ligation.

When the dinucleotide CpU or pCpU is incubated with the Tetrahymena pre-rRNA, the RNA is cleaved exactly at its 3'

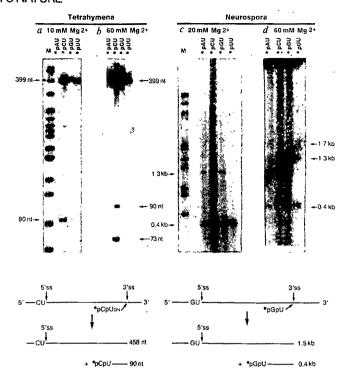


Fig. 1 Intermolecular exon ligation. Tetrahymena pre-rRNA was incubated with ³²P-pApU, ³²P-pCpU, ³²P-pGpU or ³²P-pUpU in Tetrahymena reaction conditions (10 mM Mg²⁺)(a) or Neurospora reaction conditions (60 mM Mg2+) (b). Neurospora cob pre-mRNA was similarly incubated in Neurospora reaction conditions (20 mM Mg²⁺) (c) or 60 mM Mg²⁺ (d). Tetrahymena and Neurospora reaction conditions are defined below. The diagrams at the bottom show trans-splicing reactions for Tetrahymena and Neurospora RNAs (not drawn to scale).

Methods. Tetrahymena pre-rRNA was prepared by transcription of pT7TT1A3, a phage T7 promoter version of the SP6 promotercontaining plasmid pSPTT1A3 (ref. 20). Neurospora cob intron 1 RNA was prepared by transcription of pSP64-H2a, using SP6 RNA polymerase at 40 °C in the absence of spermidine 12. Dinucleotides ApU, CpU, GpU and UpU (Pharmacia, P-L Biochemicals) were end-labelled using polynucleotide kinase and [\gamma^{32}P]ATP^{10}. Each labelled dinucleotide ran as a single band on a 20% polyacrylamide gel; the dinucleotides were not significantly cross-contaminated by this criterion. Splicing reactions were carried out by incubating 1.17 pmol of the Neurospora transcript or 0.03 pmol of the Tetrahymena transcript with 32P-pCpU, 32P-pApU, 32P-pGpU ³²P-pUpU (12 nmol for Neurospora, 0.2 nmol for Tetrahymena) for 1 h in 5 µl of reaction media. The experiment in a was carried out under Tetrahymena reaction conditions: the reaction media contained 200 mM NH₄Cl, 10 mM MgCl₂, 50 mM EPPS (N-2-hydroxyethylpiperazine-N'-2'-propanesulphonic acid)-HClpH 7.5, and the splicing reactions were carried out at 30 °C. These conditions differ somewhat from those used previously 10. The experiments in b, c and d were carried out under Neurospora reaction conditions: the reaction media contained 50 mM NH₄Cl, 20 or 60 mM MgCl₂, and 50 mM EPPS-HCl pH 7.5, and the splicing reactions were carried out at 37 °C. The reactions were terminated by addition of EDTA (100 mM), and RNAs were precipitated with ethanol three times before analysis. Tetrahymena RNAs (a and b) were analysed on an 8% polyacrylamide (20:1, acrylamide: bisacrylamide) gel containing 7 M urea, 90 mM Tris-borate, 2.5 mM EDTA. Neurospora RNAs (c and d) were glyoxalated and analysed on a 1.6% agarose gel²¹; ethidium bromide staining confirmed that equal amounts of RNA had been loaded on each lane. The gels were dried and analysed by autoradiography.

splice site and the dinucleotide is covalently ligated to the 3' exon¹⁰. This reaction can be explained as an intermolecular version of exon ligation, because it occurs with oligonucleotides whose sequence resembles that of the 5' exon (CUCUCU), and their site of attachment is identical to that of exon ligation. Except for the terminal uridine residue, the sequence preceding

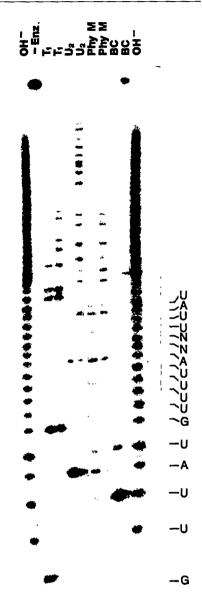




Fig. 2 RNA sequencing of the 32 P-pGpU-labelled 0.4-kb RNA. The 0.4-kb Neurospora RNA (conditions of Fig. 1d, 3 h incubation) was purified by gel electrophoresis. The RNA was then sequenced by partial hydrolysis with ribonucleases and alkali $(OH^-)^{22-24}$. Ribonuclease T_1 is specific for G residues, ribonuclease U_2 for A residues, ribonuclease Phy M for A and U residues, and Bacillus cereus (BC) ribonuclease for C and U residues. '-Enz.' shows RNA incubated under the conditions used for RNase T_1 , but in the absence of enzyme. 3'ss, 3' splice site; the boxed GU represents RNA sequencing reactions were analysed on a gel containing 22% polyacrylamide (20:1, acrylamide: bisacrylamide), 7 M urea, 90 mM Tris-borate, 2.5 mM EDTA.

the 5' splice site is not conserved among group I introns. For example, among other group I introns that have been found to be self-splicing in vitro, the first intron of the Neurospora cob gene is preceded by CUGGGU (ref. 12) the yeast rRNA intron by AGGGAU (ref. 13) and intron 5a of the yeast cytochrome oxidase subunit 1 gene by AUGAUU (refs 14, 15). If each of

these sequences defines a 5' splice site because it pairs with a sequence within the intron, the intermolecular exon ligation reaction should show a preference for oligonucleotides of different sequence. On the other hand, if the reaction of the Tetrahymena pre-rRNA with CpU reflects its interaction with one of the sequence elements that is conserved among group I introns, or some unanticipated higher nucleophilicity of CpU compared with the other dinucleotides, then CpU might be the most reactive dinucleotide towards all the precursor RNAs.

Truncated versions of the Tetrahymena pre-rRNA and Neurospora cob pre-mRNA were synthesized in vitro using either SP6 or T7 RNA polymerase. The transcripts were incubated with ³²P-labelled dinucleotides (³²P-pNpU_{OH}) under either Tetrahymena or Neurospora conditions (see Fig. 1 legend) in reaction media containing different concentrations of MgCl-Figure 1a and b shows incubation of the Tetrahymena RNA with the four labelled dinucleotides under optimal splicing conditions for that intron (Tetrahymena conditions, 10 mM MgCl₂) or under Neurospora conditions in a reaction medium containing 60 mM MgCl₂. In both cases, incubation with ¹²PpCpU resulted in labelling of a 90-nucleotide RNA band that is the product of intermolecular ligation of pCpU to the 3' exon. (Size was measured as 92 nucleotides relative to DNA markers, the size of 90 nucleotides is based on sequence of the DNA I The identity of this band was confirmed by partial digestion of the 90-nucleotide (90-nt) band with RNase T1 (data not shown) A number of other bands were also labelled, particularly under the high-Mg²⁺ conditions. The 399-nt band labelled by pCpU and pUpU was shown previously to result from reopening of the circular intervening sequence (IVS)16. The band slightly larger than the IVS labelled by pGpU and the 73-nt band labelled by pCpU under high-Mg²⁺ conditions were not observed previously with other in vitro transcripts incubated under somewhat different conditions¹⁰; their identities are unknown. Under both sets of conditions, the trans-splicing reaction showed a strong preference for pCpU. We observed no trans-splicing with pApU or pUpU, and incubation with pGpU resulted only in very inefficient labelling of a band of ~90 nt (<5% of the reaction with pCpU; Fig. 1a).

Trans-splicing of the Neurospora RNA showed the different specificity predicted for the interaction between the dinucleotide and the putative 5' exon-binding site. Figure 1c and d shows incubations of the Neurospora RNA with the four labelled dinucleotides in solutions containing 20 mM MgCl, and 60 mM MgCl₂, respectively. In both reaction media, incubation with pGpU gave a prominent labelled RNA of the size expected for the 3' exon (0.4 kilobases (kb); Fig. 1c,d). The identification of this RNA as the trans-splicing product is confirmed below. We observed no trans-splicing with pCpU, which is the most reactive dinucleotide for the Tetrahymena RNA. However, incubation with pApU and pUpU gave about 10% and 20%, respectively, of the extent of reaction with pGpU. The relative reactivities of the four dinucleotides in the putative trans-splicing reaction were roughly the same in reaction media containing 10, 20, 30 and 60 mM Mg²⁺. Considered together, the results show that the Neurospora trans-splicing reaction has the specificity predicted for base pairing with the 5' exon-binding site, but that the specificity appears to be somewhat less stringent than that for the Tetrahymena RNA. The trans-splicing reaction for Neurospora RNA also seems to be less efficient than that for the Tetrahymena RNA and requires higher concentrations of precursor RNA and dinucleotide (see Fig. 1 legend) The inefficiency of the specific reaction with pGpU necessitated loading more RNA per lane, which may make competing reactions with pApU and pUpU appear more prominent. We note, however, that pCpU shows no trans-splicing reaction whatsoever, indicating that this dinucleotide must be somehow incompatible with the exon-binding site.

To confirm that intermolecular exon ligation had in fact occurred for the Neurospora RNA, the 0.4-kb RNA labelled by



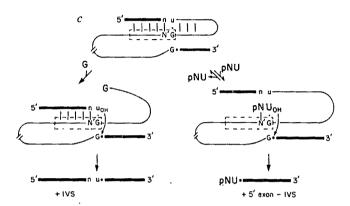


Fig. 3 Internal binding site model accounts for the sequence specificity of the exon ligation reaction. Structures of N. crassa cob pre-mRNA¹² (a) and T. thermophila pre-rRNA^{3,5} (b) are shown. Lower case letters, exons; capital letters, introns; •, 3' splice site. Boxed nucleotides indicate the portion of the internal guide sequence proposed to pair with the 5' exon^{2,3}. The pairing of the 3' exon with an adjacent portion of the internal guide sequence, which is not supported by mutation analysis²⁵, has been omitted from the diagrams. The interaction that holds the 3' splice site in place is therefore left unspecified. c, Generalized model for the role of the internal binding site. Left, normal exon ligation; right, intermolecular ligation of dinucleotides. The dinucleotide competes with the 5' exon of the intact precursor RNA for binding to the internal guide sequence. When the dinucleotide binds, its free 3'-hydroxyl group is directed towards the phosphorus atom of the phosphate at the 3' splice site in such a way as to facilitate nucleophilic attack. The result is covalent attachment of the dinucleotide to the 3' exon, an intermolecular version of exon ligation.

³²P-pGpU was purified and its sequence determined as shown in Fig. 2. The sequence confirmed that ³²P-pGpU had become covalently attached to the 3' exon by a phosphodiester linkage. The sequence of the 3' exon was the same as determined by Helmer-Citterich et al.¹⁷ and Burke et al.¹⁸.

Incubation of the Neurospora RNA with all four dinucleotides resulted in labelling of two larger bands of 1.7 and 1.3 kb, in addition to the 0.4-kb band. These larger bands are more prominently labelled under the high-Mg2+ conditions (Fig. 1c,d). Their sizes are those expected for the excised intron (1.3 kb) and intron plus 3' exon (1.7 kb). Because Neurospora cob intron 1 was not observed to undergo cyclization under any conditions tested previously¹², labelling of an intron-sized RNA by circle reopening16 was not anticipated. One possibility, therefore, is that labelling of the 1.3- and 1.7-kb bands reflects inefficient selfsplicing initiated by the dinucleotide substituting for the normal guanosine cofactor. The Tetrahymena RNA has been reported to show inefficient splicing with nucleoside triphosphates other than GTP9. Again, these competing reactions may appear more prominent here because of the inefficiency of the trans-splicing reaction with the Neurospora intron.

In the previous study of trans-splicing with the Tetrahymena intron, the two trinucleotides tested, UCU and UUU, had the

relative reactivities predicted for base-pairing with the putative 5' exon-binding site 10. In analogous experiments, the trinucleotides GGU, AGU and GAU were tested with the Neurospora RNA, and in each case the extent of reaction was greater than with the dinucleotide GU (data not shown). The increased reactivity of GGU might be explained on the basis of increased base-pairing interactions with the active site, while the reactivity of the other two trinucleotides might be explained as a combination of base-pairing and increased base-stacking interactions. Any such interpretation was clouded, however, by the unexpected finding that in 10 mM MgCl₂ the Tetrahymena RNA reacted efficiently with GGU and GAU, and to a smaller extent with AGU, to give RNAs of the size expected for trans-splicing to the 3' exon (91 nt). Partial RNA sequence analysis with RNase T₁ confirmed that GGU was accurately spliced to the 3' exon (data not shown). Thus, although Watson-Crick base-pairing with the 5' exon-binding site may be an important determinant of the trans-splicing reaction, additional interactions must also contribute to determining the extent of reaction with trinucleotides. Base stacking or non-Watson-Crick hydrogen-bonding might allow certain trinucleotides to interact with the normal binding site. Alternatively, the trinucleotide might interact with other, at present unidentified, binding sites within the intron.

Although the findings for trinucleotides were unexpected, our results show that Neurospora cob intron 1 RNA, like the Tetrahymena RNA, undergoes a specific trans-splicing reaction with dinucleotides. If the ligation of dinucleotides to the 3' splice site is an intermolecular version of exon ligation, then each precursor RNA should show the greatest reactivity with the dinucleotide whose sequence is homologous to that of the 3' end of its 5' exon. This prediction is satisfied by the relative reactivity of the Neurospora pre-mRNA with pGpU compared with other dinucleotides and of the Tetrahymena pre-rRNA with pCpU compared with other dinucleotides.

The relative reactivities of the different dinucleotides is most easily explained if each intron contains an exon-binding site that is complementary to the last two nucleotides of its own 5' exon. This requirement is fully met by the internal guide sequence model of Davies et al.². The internal guide has a different sequence in each intron, but a portion of the sequence is always complementary to the 6 or so nucleotides in the 5' exon immediately preceding the intron. The only conserved nucleotide is a G in the internal guide which pairs with the conserved U at the 5' splice site. Similar structural models incorporating the 5' exon-internal guide sequence pairing have been proposed by Michel et al.^{4,5} and Bos et al.¹¹.

Figure 3 shows the proposed mechanism by which the internal guide sequence promotes the intermolecular exon ligation reactions. The 5' exon is bound to the internal guide, but in the absence of cleavage by guanosine the exon does not have a free 3' hydroxyl group, so it cannot attack the 3' splice site. When the dinucleotide transiently displaces the 5' exon, its free 3' hydroxyl group attacks the 3' splice site.

In the normal exon ligation reaction, the 5' exon-binding site is proposed to serve two functions. It is responsible for choice of the 5' splice site, that is, the site at which free guanosine or GTP attacks. Thus, the guanosine-binding site¹⁹ must be in a fixed position relative to the 5' exon-binding site, perhaps by way of a direct interaction⁹. In addition, the binding site orients the 5' exon in proximity to the 3' splice site, helping to lower the activation energy for the exon ligation reaction. It therefore helps to determine the accuracy of reactions at both the 5' and 3' splice sites.

Recently, site-specific mutagenesis studies have confirmed that the sequence GGAGGG at nucleotides 22-27 of the *Tetrahymena* intron is the 5' exon-binding site^{26,27}.

We thank S. Walstrum and O. Uhlenbeck (University of Colorado) for their gift of trinucleotides. This work was supported by NIH grant GM26836 to A.M.L. and by NIH grant GM28039 and American Cancer Society grant NP374B to T.R.C.

Received 17 March; accepted 15 April 1986.

- Burke, J. & RajBhandary, U. L. Cell 31, 509-520 (1982).
- 2. Davies, R. W., Waring, R. B., Ray, J. A., Brown, T. A. & Scazzocchio, C. Nature 300, 719-724 (1982).
- 3. Waring, R. B., Scazzocchio, C., Brown, T. A. & Davies, R. W. J. molec. Biol. 167, 595-605

- Michel, F., Jacquier, A. & Dujon, B. Biochimie 64, 867-881 (1982).
 Michel, F. & Dujon, B. EMBO J. 2, 33-38 (1983).
 Cech, T. R. et al. Proc. natn. Acad. Sci. U.S.A. 80, 3903-3907 (1983).
 Zaug, A. J., Grabowski, P. J. & Cech, T. R. Nature 301, 578-583 (1983).
- Cech, T. R. Cell 44, 207-210 (1986).
 Inoue, T., Sullivan, F. X. & Cech, T. R. J. molec. biol. 189, 143-165 (1986).
 Inoue, T., Sullivan, F. X. & Cech, T. R. Cell 43, 431-437 (1985).
- 11. Bos, J. L. et al. Cell 20, 207-214 (1980).
- 12. Garriga, G. & Lambowitz, A. M. Cell 39, 631-641 (1984).
- 13. Tabak, H. F., Van der Horst, G., Osinga, K. A. & Arnberg, A. C. Cell 39, 623-629 (1984).
 14. Hensgens, L. A. M., Bonen, L., de Haan, M., Van der Horst, G. & Grivell, L. A. Cell 32, 379-389 (1983).
- 15. Van der Horst, G. & Tabak, H. F. Cell 40, 759-766 (1985).

- Sullivan, F. X. & Cech, T. R. Cell 42, 639-648 (1985).
 Helmer-Citterich, M., Morelli, G. & Macino, G. EMBO J. 2, 1235-1242 (1983).
 Burke, J. M., Breitenberger, C., Heckman, J. E., Dujon, B. & RajBhandary, U. L. J. biol. Chem. 259, 504-511 (1984).

 19. Bass, B. L. & Cech, T. R. Nature 308, 820-826 (1984).

 20. Price, J. V. & Cech, T. R. Science 228, 719-722 (1985).

 21. McMaster, G. K. & Carmichael, G. G. Proc. natn. Acad. Sci. U.S.A. 74, 4835-4838 (1977).

- Donis-Keller, H. Nucleic Acids Res. 7, 179-192 (1979).
 Lockard, R. E. et al. Nucleic Acids Res. 5, 37-56 (1978).
- 24. Donis-Keller, H. Nucleic Acids Res. 8, 3133-3142 (1980)
- 25. Been, M. D. & Cech, T. R. Nucleic Acids Res. 13, 8389-8408 (1985).
- 26. Waring, R. B., Towner, P., Minter, S. J. & Davies, R. W. Nature 321, 133-139 (1986).
- 27. Been, M. D. & Cech, T. R. (submitted).

Intermolecular binding of xanthan gum and carob gum

P. Cairns, M. J. Miles and V. J. Morris

AFRC Institute of Food Research, Norwich Laboratory, Colney Lane, Norwich NR47UA, UK

Gels are a representative state for polysaccharides in both natural and retificial systems. The nature of the inter-chain associations within the junction zones is important and models for such interactions between like polysaccharides are based on X-ray diffraction studies of oriented gels. Here we describe the extension of such studies to a binary gel (xanthan-carob) in order to characterize for the first time intermolecular binding between different polysaccharides. Xanthan-carob binding has been proposed to explain gelation of the mixtures and as a model for host-pathogen recognition and adhesion of Xanthomonas bacteria within plant vascular systems. Our data suggest that the established model 1-7 is incorrect and point to an alternative association mechanism.

Xanthan has a repeat unit^{8,9} based on a cellulose backbone with alternate glucose residues O-3-substituted with a trisaccharide side chain. Carob has a mannan backbone that is incompletely O-6-substituted with galactose² and a mannose/galactose ratio of 3.55 (ref. 10). Xanthan-carob binding is postulated to involve a mixed cooperative interaction in which the xanthan helix is retained (Fig. 1). We tested this model by X-ray fibre diffraction studies of oriented xanthan-carob gels, since this is

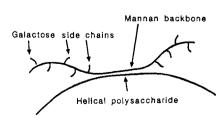


Fig. 1 Schematic diagram of the proposed binding of the xanthan helix to the bare mannan backbone of the galactomannan carob. Analogous models have been proposed¹⁻⁴ to explain the interaction between galactomannans and certain algal polysaccharides.

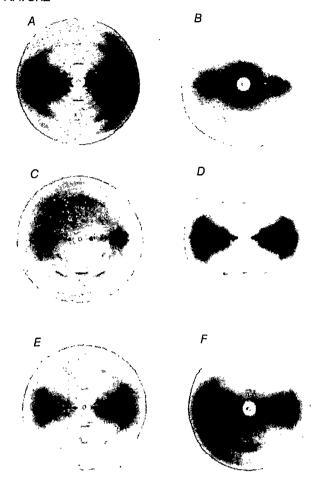


Fig. 2 X-ray fibre diffraction patterns recorded for polysaccharides and polysaccharide mixtures. Gels were cut into strips and stretched to induce alignment. Non-gelling mixtures were cast onto glass or PTFE substrates, dried to films, cut into strips and aligned by stretching. The X-ray wavelength was 0.154 nm; the camera was flushed with helium to reduce scattering. Pictures were calibrated with calcite. A, Xanthan, stretched 300%; B, carob, stretched 300%; C, carob, stretched 300% and stored at room temperature for 3 yr; D, mixed gel: 25% xanthan/75% carob, stretched 300%; E, mixed gel: 50% xanthan/50% carob, stretched 300%; F, non-gelling mixture: 50% xanthan/50% carob, prepared at room temperature, stretched 100%.

the only method available to examine polysaccharide ordered structures at atomic resolution and has provided reliable models for structures in the hydrated state¹¹.

Under conditions appropriate for studying fibres prepared from mixed gels, pure xanthan and carob gave the fibre patterns shown in Fig. 2A, B. Storage of carob fibres enhanced crystallinity (Fig. 2C). Diffraction data obtained for fibres prepared from xanthan-carob mixed gels are shown in Fig. 2D, E and these new X-ray patterns provide evidence for xanthan-carob binding.

Optical rotation measurements are sensitive to the helix-coil transition¹² and were used to monitor helix formation in xanthan samples. Thorough mixing of carob with xanthan in the helical conformation at room temperature did not lead to gelation. X-ray diffraction data on fibres prepared from such mixtures (Fig. 2F) showed reflections characteristic of pure xanthan (Fig. 2A) with no evidence of carob crystallization or carob-xanthan co-crystallization. Gelation only occurred when these mixtures were heated (95 °C) above the xanthan helix-coil transition temperature (T_c) and then re-cooled to room temperature. Oriented gels yielded fibre patterns of the type shown in Fig. 2D, E. T_c is particularly sensitive to the presence of divalent cations

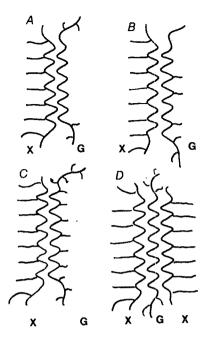


Fig. 3 Schematic representation of possible xanthan (X)-galactomannan (G) binding. Possible binding between a xanthan backbone and: A, bare mannan regions of the galactomannan backbone; B, randomly substituted galactomannan; C, galactomannan containing galactose on alternate mannose residues. D, Simplest xanthan-galactomannan sandwich structure.

in the medium¹³. When carob was mixed with xanthan in the presence of sufficient calcium chloride such that $T_c > 100$ °C, and the samples were heated (95 °C) and re-cooled to room temperature, they did not gel; this suggests that denaturation of the xanthan helix is necessary if intermolecular association and gelation is to occur. Glucose and mannose differ only in the orientation of the hydroxyl substituent at C-2, suggesting the possibility of binding between the sterically compatible cellulose backbone of xanthan and the mannan backbone of carob.

Optical rotation studies¹⁴ on xanthan-galactomannan mixtures coupled with enzymatic studies¹⁵ on xanthan-carob mixtures suggest that only small segments of both backbones could be involved in binding, with the remaining xanthan reforming the helical conformation. Alignment of mixed junction zones will also lead to alignment of xanthan helices. Thus, reflections characteristic of aligned xanthan should be neglected in Fig. 2D, E in order to characterize the mixed junction zone. The first meridional reflection for the mixed junction zones corresponds to an interplanar spacing of 0.52 nm, characteristic of cellulose¹⁶ or mannan¹⁷, supporting binding between the backbones but ruling out simple binding schemes of the type shown in Fig. 3A-C. To achieve the correct interplanar spacing appropriate to the first meridional reflection, it would be necessary to stagger the positions of the xanthan side chains (Fig. 3D) although the stoichiometry of such sandwich structures is undefined. The mixed junction zone patterns are equivalent to carob patterns for which only 0kl reflections are allowed. The simplest answer would be to permit growth of a sandwich structure in the b and c directions but to restrict growth in the a direction. However, streaking of layer line reflections characteristic of such laminar structures was not observed. The alternative is to envisage a structure periodic in the b and c directions but aperiodic in the a direction.

The data presented here constitute the first example of a conformational modification of one polysaccharide by a noncovalent interaction with another polysaccharide. The structural similarity of the xanthan and carob backbones accounts for the

specificity of the interaction and also explains why X-ray diffraction studies 10,18,19 have failed to reveal proposed 1-7 intermolecular binding between galactomannans and the structurally incompatible algal polysaccharides k-carrageenan and furcellaran. The data support suggested co-crystallization of cellulose with galactomannans²⁰ or xyloglucans²¹⁻²³ in complex plant cell walls. Binding of extracellular xanthan to plant cell wall components is only likely if helix formation is incomplete. This cannot, however, exclude possible host-pathogen interactions because such extracellular assembly is normally biochemically controlled.

Received 17 March; accepted 9 May 1986.

- 1. Morris, E. R., Rees, D. A., Young, G., Walkinshaw, M. D. & Darke, A. J. molec. Biol. 110, 1-16 (1977).

 2. Dea, I. C. M. & Morrison, A. Adv. Carbohyd. Chem. Biochem. 31, 241-312 (1975).

 3. Dea, I. C. M. Am. chem. Soc. Symp. Ser. 150, 439-454 (1981).

 4. Dea, I. C. M., McKinnon, A. A. & Rees, D. A. J. molec. Biol. 68, 153-172 (1972).

- McCleary, B. V. Carbohyd. Res. 71, 205-230 (1979).
 Tako, M., Asato, A. & Nakamura, S. Agric. biol. Chem. 48, 2995-3000 (1984).

- Tako, M., Asato, A. & Nakamura, S. Agric biol. Chem. 48, 2995-3000 (1984).
 Tako, M. & Nakamura, S. Carbohyd. Res. 138, 207-213 (1985).
 Jansson, P. E., Kenne, L. & Linberg, B. Carbohyd. Res. 45, 275-282 (1975).
 Melton, L. D., Mindt, L., Rees, D. A. & Sanderson, G. R. Carbohyd. Res. 46, 245-257 (1976).
 Miles, M. J., Morris, V. J. & Carroll, V. Macromolecules 17, 2443-2445 (1984).
 Rees, D. A., Morris, E. R., Thom, D. & Madden, J. R. in The Polysaccharides Vol. 1 (ed. Aspinall, G. O.) 195-290 (Academic, London, 1982).
 Norton, I. T., Goodall, D. M., Frangou, S. A., Morris, E. R. & Rees, D. A. J. molec. Biol. 125, 221, 204 (1984).
- 175, 371-394 (1984).
- 13. Lambert, F., Milas, M. & Rinaudo, M. Int. J. biol. Macromolec. 7, 49-52 (1985).
- Dea, I. C. M. et al. Carbohyd. Res. 57, 249-272 (1977).
 McCleary, B. V., Amado, R., Waibel, R. & Neukom, H. Carbohyd. Res. 92, 269-285 (1981).
- Васкwell, J., Gardner, K. H., Kolpak, F. J., Minke, R. & Claffey, W. B. Am. chem. Soc. Symp. Ser. 141, 315-334 (1980).
- 17. Frei, E. & Preston, R. D. Proc. R. Soc. B169, 127-145 (1968).
- Cairns, P., Miles, M. J. & Morris, V. J. Int. J. biol. Macromolec. 8, 124-127 (1986).
 Cairns, P., Miles, M. J., Morris, V. J. & Brownsey, G. J. Carbohyd. Res. (in the press).
- 20. Marchessault, R. H., Buléon, A., Deslandes, Y. & Goto, T. J. Colloid Interface Sci. 71, 375-382 (1979).
- Bauer, W. D., Talmadge, K. W., Keegstra, K. & Albersheim, P. Pl. Physiol. 54, 174-187 (1973).
 Aspinall, G. O., Molloy, J. A. & Graig, J. W. T. Can. J. Biochem. 47, 1063-1070 (1969).
 Taylor, I. E. P. & Atkins, E. D. T. FEBS Lett. 181, 300-302 (1985).

Erratum

Molecular distinction between fetal and adult forms of muscle acetylcholine receptor

M. Mishina, T. Takai, K. Imoto, M. Noda, T. Takahashi, S. Numa, C. Methfessel & B. Sakmann

Nature 321, 406-411 (1986)

THE first sentence in the summary to this article should read: "Distinct classes of acetylcholine receptor channels are injected with combinations of the bovine α -, β -, γ - and δ - or the α -, β -, δ - and ε -subunit-specific messenger RNAs.'

Corrigendum

Near-ultraviolet and visible spectrophotometry of comet Halley from Vega 2

G. Moreels, M. Gogoshev, V. A. Krasnopolsky, J. Clairemidi, M. Vincent, J. P. Parisot, J. L. Bertaux, J. E. Blamont, M. C. Festou, Ts. Gogosheva, S. Sargoichev, K. Palasov, V. I. Moroz, A. A. Krysko & V. Vanysek

Nature 321, 271-273 (1986)

In this letter in Nature's comet Halley supplement, an incorrect address was given for one of the authors. V. Vanysek's correct address is: Charles University, 15000 Prague, Czechoslovakia.

Imaging cells with acoustic microscopy

from M. Issouckis

The interaction between the mechanical waves of scanning acoustic microscopy (SAM) and the mechanical features of living cells makes a novel contribution to the characterization of biological materials.

High resolution scanning acoustic microscopy, or SAM, provides an opportunity to investigate the microstructure of materials on, and under, the material surface. In biology, acoustic imaging of living cells, mucous coats and cuticle structures has been very successful. The imaging of these biological objects has been described by M. Hoppe and J. Bereiter-Hahn¹. This paper uses their work with living cells as a springboard for discussing high resolution SAM and SAM image interpretation in the life sciences.

The heart of the high resolution SAM (Fig.1) is its lens assembly. A focused ultrasound wave (of frequencies between 1 and 2 GHz), generated by means of a pizoelectric transducer, is used to probe the sample. This same transducer receives the reflected wave, which is subsequently processed. By scanning in a roster fashion, an image is formed that represents the interaction between the acoustic material and the elastic properties of the sample material.

Some requirements of SAM imaging impose limitations on the types of samples that can be studied. As in high resolution light microscopy, high resolution SAM requires lenses with short focal length. Consequently, the depth of focus is small. In addition, attenuation (absorption) of acoustic waves by the intermedium limits the distance between lens and specimen.

These features restrict the application of acoustic microscopy to very small objects; that is, those that are very flat and in a plane parallel to the scanning plane of the acoustic lens. Flat structures such as insect wings and scales, and cells attached to glass or any other planar surface, fulfil these conditions.

Although observations of cell or organelle damage by ultrasound have been reported for lower frequencies (20 kHz, 5 MHz)^{2,3} damage to living cells does not occur with gigahertz frequencies. Experiments have shown that after more than one hour's exposure to 1 GHz ultrasound, sensitive epidermal cells still exhibit normal locomotive behaviour. These findings are consistent with theoretical expectations, which predict a decrease in cell damage as frequencey increases because the amplitude of particle displacement induced by a longitudinal wave is limited by the wavelength.

Interpretation

Some properties of SAM can also confound image interpretation. Images of biological samples, in particular, often

show interference lines due to the substructure supporting the sample. In materials science applications, the smooth surface of a specimen represents the structure that is to be investigated. In the case of biological objects, however, the samples are located on a planar surface to which they adhere.

This situation complicates the interpretation of acoustic images by producing

on the incompressible interior cytoplasm8,9.

The mechanical properties and surface profiles of living cells result from the interaction of elements of the cytoskeleton with each other, with the cell membrane, and with the supporting substratum. Microtubules and stress fibres stiffen the cytoplasm and, together with adhesion to a substratum, cause deviations of cell shape from a sphere. This model allows an



Fig.1 An Ernst Leitz scanning acoustic microscope (ELSAM) in its commercial configuration.

interference between the waves reflected at different interfaces. These interfaces include the surface of the substratum, the medium-facing surface of the cells and, depending on the distance of a cell to the substratum, the substratum-facing cell surface.

Comparable relations are found in reflection-contrast microscopy⁴⁻⁷. Light reflected from separate interfaces causes a pattern of interference lines. The pattern indicates the surface curvature of cell at the medium-facing surface and at the surface opposed to the substrate. In this case, optical path differences that determine the course of the interference lines depend on refractive indexes and the thickness of the layers between interfaces.

Similarly, with the scanning acoustic microscope, layer thickness and acoustic impedance (which corresponds to the refractive index in optics) govern the interference pattern. But whereas light absorption is negligible in most living cells, attenuation can contribute considerably to image formation in SAM.

The internal structures of cells can also alter image generation by reflection and scattering. In general, an animal cell can be considered as a hydraulic system enclosed by a semipermeable membrane to which a contractile fibrillar system (containing actin and probably myosin) is linked. This system exerts some pressure

understanding of acoustic images of living

Mechanical disturbances by the scanning movement of the SAM lens and flow of the interconnecting medium, which are caused by sound emission in the cavity of the lens, loosen the contact of cells to a substratum. In those cells that withstand this stress, density in stress fibre arrangement is enhanced considerably.

Internal reflections

In the images of Xenopus heart cells (Fig. 2), stress fibres are clearly shown as arcs near the periphery of the cell. The dark circles concentric with the nucleus. The difference in contrast between the sample mounted on plastic (top panel) and the sample mounted on glass (bottom panel) is apparent.

The peripheral region of the plasticmounted cell is relatively flat; its thickness is approximately $\lambda/2$ at the outer dark interference ring, increasing to about $\lambda/4$ in the outer bright region. For these estimations a phase shift of $\lambda/2$ at the interface to the medium with higher acoustic

impedance is considered.

The small distances between central interferences indicate an increased slope; that is, the thickness of the sample increases in the region. The contrast of an interference line may vary considerably throughout its course, so that a dark line may



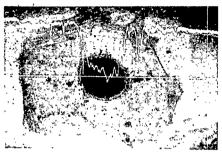


Fig.2 SAM images of endothelial cells from Xenopus laevis tadpole hearts (XTH-2 cells) using ×625 magnification and a frequencey of 1.6 GHz. The image width is 200 µm. Top panel: a sample mounted on plastic gives an interference image with stress fibres and cell topography clearly visible. The contrast of the cell fringes is related to stiffness conferred by intracellular structures. Bottom panel: a sample mounted on glass gives a more poorly defined attenuation image.

become very faint at some points (Fig. 2). However, this is not caused by a local thickness change, but by locally diminished reflectivity.

The structural basis for this reduced reflectivity is a weakened stiffness, visualized by the low contrast that is due to a diminished elastic modulus of the cortical cytoplasm. At this "weak region" the membrane can bulge out, and a thickening appears. The dark interference fringe close to the cell margin increases in contrast, indicating higher reflectivity.

The complexities posed by interference and contrast changes make SAM image interpretation a challenging task, but the information that can be gleaned from this complexity makes scanning acoustic microscopy a valuable technique for exploring the substructure of the smallest unit of life.

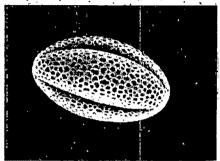
Matthew Issouckis is at E. Leitz Instruments Ltd, 48 Park Street, Luton LUI 2HP, UK.

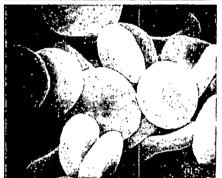
- 1. Hoppe, M. & Bereiter-Hahn, J. IEEE Trans. Sonics Ultra-
- sonics Vol. SU-32 (2). 289 (1985). Cachon, J. & Chachon, M. Biol. Cell. 40, 23–32 (1981). Cachon, J., Cachon, M. & Bruneton, J.N. Biol. Cell 40, 69–72 (1981).
- 4. Bereiter-Hahn, J., Fox, C H. & Thorell, B. J. cell. Biol. 82, 767-779 (1979).
- Beck, K. & Bereiter-Hahn, J. Microchim. Acta. 84, 153 178 (1981).
- Gingell, D. J. cell. Sci. 49, 237–247 (1981).
 Gingell, D. & Todd, I. J. biophys. biochem. Cytol. 26, 507 - 526 (1979).
- 8. Bereiter-Hahn, J., Strohmeier, R., Kunzenbacher, I.,
- Beck, K. & Voth, M. J. cell. Sci. 52, 289 311 (1981). 9. Strohmeier, R. & Bereiter-Hahn, J. Expl cell. Res. 154,

Setting the stage for microscopy

A collection of instruments and accessories for microscopy and image analysis closes with immunology product selections.

JEOL is offering a scanning electron microscope at a price that is more typical of advanced optical models (Reader Service No. 100). The T100, a compact and relatively simple instrument, is aimed at

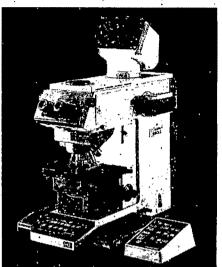




Micrographs from Jeol's new 'scopes. Rape pollen, top panel; control blood, bottom panel.

laboratories engaged in medical or botanical research and sold for £15,000 (UK). Image contrast and brightness controls are available along with a fast scan facility for TV viewing. The T100 features a single magnification adjustment that spans ×15 to ×100,000 with electronic readout. Equipped with several information channels, Jeol's microscope can be fitted with attachments for elemental analyses such as characteristic X-rays and cathodoluminescence.

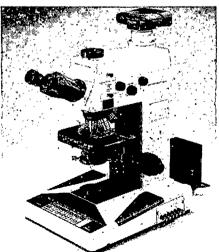
photomicrographic microscope system for research goes under the name of the New Vanox S/T from Olympus (Reader Service No. 101). Olympus says it has provided the Vanox with a flexibility that allows a wide variety of uses. The instrument has LB series objectives for super widefield observation; the eyepiece field number reaches 26.5. A motorized revolving nosepiece will alternate between six objectives at the touch of a button, whilst Köhler illumination shifts the lighting for the range of magnifications between ultra-low and high magnifying objectives. Four photographic eyepieces | The Microphot design for photomicrography.



Olympus makes flexibility its forte.

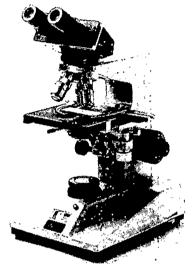
supply magnifications between 2.5× and $5\times$. Olympus designed its £18,000 (UK) machine with a rotatable stage for proper specimen alignment, and a light intensity control system based on ND filter conversion maintains constant colour temperatures regardless of light intensity.

The Microphot-FX, Nikon's new photomicrography system, combines the optical performance of the CF Plan Apocromat and Achromat series with versatile photomicrography (Reader Service No. 102). Nikon says the new instrument has 1 per cent spot or 30 per cent average exposure measurement switching, direct light measurement, direct image projection, and movable measurement area. The Microphot is also available with the



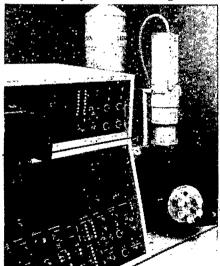
photographic attachment as an option, when photomicrography is a secondary purpose. Nikon also make several optical accessories as options, including phase contrast, diascopic fluorescence and interferometry equipment.

Straight from West Germany, an expanded range of Zeiss microscopes is being distributed by Gallenkamp in the United Kingdom (Reader Service No. 103). The company now includes "budget priced" stereo and compound microscopes, as well as more sophisticated instruments from the manufacturer. Microscopes for student work and routine research applications have been added to



Zeiss technology in the UK via Gallenkamp. the list. Gallenkamp claims its new selection is ideal for biological and materials examination.

Joining Philips' display at Micro '86 will be the company's latest scanning electron



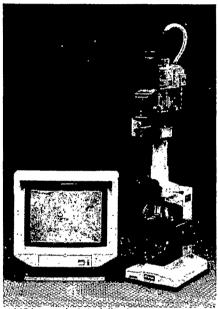
Part of Philips' Micro '86 display.

microscope, the 525M (Reader Service No. 104). The SEM 525M, part of a field of multi-purpose microscopes, offers a large specimen chamber and motorized stage with six-inch movement. Philips will | The flow cytometer for stationary cells.

also have on exhibit the CM10, a microprocessor-controlled transmission electron microscope. The system operates through a small VDU with a divided screen and soft-key controls. An energydispersive analyser set-up called EDAX PV 9900 will also make an appearance at the conference.

A sharper image

For full colour image analysis, Analytical Measuring Systems has a semi-automatic

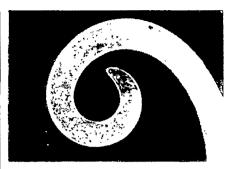


AMS has analysis in full colour.

system with software that runs on IBM PCs or compatibles (Reader Service No. 105). The VIDS III Colour uses a threegun video camera to obtain micro- or macroscopic sample images, and according to AMS, is particularly well-suited to applications in histology, cytochemistry and mineralogy. The VIDS III software can measure features within the images that are designated using a graphics tablet.

A fluorescence analysis workstation from Meridian Instruments can perform quantitative analyses of anchoragedependent cells without disturbing sterile conditions (Reader Service No. 106). Meridian's ACAS 470 system employs computer control and x-y stage positioning to direct a focused laser beam. Whilst





A spiral nematode posed for this photomicrograph, which won the Nikon Small World competition in 1985. (Reader Service No. 107). Nikon's annual contest is international and open to anyone interested in photography through microscopes. Both subject matter and microscopy technique are unrestricted. Past winners have come from disciplines as diverse as marine science and dentistry. This year's deadline was 27 June, but it is not too early to be eveing up the 1987 competition. Twenty contestants will receive awards, with the first place photographer winning a \$3,000 vacation or the equivalent in Nikon equipment. Last year's winner, who captured the image above, was J.D. Eisenback from Blacksburg, Virginia.

preserving cell attachment to extracellular matrix, the beam carries out optimal fluorescence excitation, cell sorting by laser ablation or physical separation on film, cell surgery and photobleaching of discrete areas. The workstation can also perform automated repetitive analysis on single cells or fields of cells.

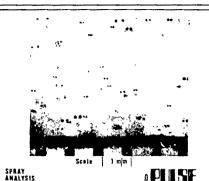
Quantel is exhibiting a high-speed digital image processing device at Micro '86 that it says can improve the contrast and



Making images CRYSTAL clear.

sharpness of images to analytical quality in real-time (Reader Service No. 108) Quantel calls its system CRYSTAL and claims the instrument can increase through-put as well as statistical validity CRYSTÂL also includes a second framestore for a reference image that can be compared to the sample input image in real-time. Quantel says CRYSTAL's features are beneficial in the inspection and analysis of non-conducting specimens. The £15,500 (UK) system is effective with ion beam, scanning optical and scanning microscopes as well as electron microscopes.

Polyscan is a fully automatic image analyser with flexible software control (Reader Service No. 109). Reichert-Jung



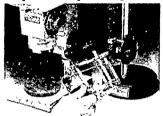
'PULSE' instrumentation equipment will produce time separated images of sprays and aerosols as

time separated images of sprays and aerosols as illustrated in this photograph

If you are concerned with the atomization of FUELS - SOLVENTS - PAINTS CHEMICALS this picture is important to you VELOCITY - SIZING DISTRIBUTION can be assessed from such pictures which will help you improve the efficiency of your spraying equipment and conserve expensive materials

Reader Service No.14

SINCED INSTRUMENTS Xenopus oocytes injection?



SINGER MKI MICROMANIPULATOR

We also offer a Microsyringe Kit. Write to:

Singer Instrument Co. Ltd. Treborough Lodge Roadwater, Watchet Somerset TA23 0QL England. Tel. (0984) 40226 Telex: 337492 Comcab G

Reader Service No.50

Activity Monitor

Track that rat, insect, fish, limb Tracking unit accepts input from video camera or recorder, and outputs the location of a high contrast object in the TV image. Interfaces for BBC, Apple, IBM-PC.

> HVS IMAGE ANALYSING LTD. 22 Cromwell Road, Kingston, KT2 6RE, England. Tel: 01-546 9090

> > Reader Service No.16



Medwire Div. stocks a wide variety

TEFLON COATED*

Platinum alloys, stainless steel, silver, multistrand and single strand available for prompt shipment. Write for descriptive brochure and price lists.



Medwire Div. Affiliate of Sigmund Cohn Corp 123 So. Columbus Ave. Mt. Vernon, N.Y. 10553 914-664-5300 'Reg. TM of E I. Dupont Reader Service No.49

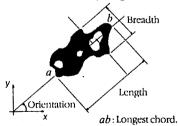


Processing by Polyscan can be customized.

developed the system with an extensive image processing library that enables customized programs to be constructed using a program editor. Polyscan accepts inputs from microscopes, video tape recorders, photometers and photographs and uses synchronous network architecture for real-time processing. For complex images, the system also allows semi-automatic measurement via a cursor-controlled digitizer.

Digithurst Ltd makes non-contact measurement and image analysis packages that perform data processing with standard microcomputers such as the IBM PC (Reader Service No. 110). The company's range can accommodate most types of microscopes, with camera mounts for optical microscopy. Digithurst's Micro-Scale software directs the detection of cell boundaries and outlines, growth rate determinations and measurements including area, length, counting, orientation to field and minimum and maximum diameters. A MicroStat statistics package provides derivation of statistical results and graphical presentation.

Joyce-Loebl introduced an image analysis system earlier this year called µMagiscan that will be displayed at Micro '86 (Reader Service No. 111). The package is based on a modified IBM PC, with software composed of test, analysis and statistics routines. The µMagiscan analysis



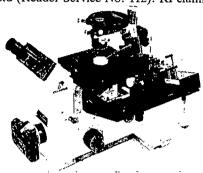
Joyce-Loebl's analyser takes on new

menu is capable of establishing working conditions, pre-processing to optimize the image state and detecting, selecting and measuring designated objects. Joyce-Loebl combined several hardware features to create µMagiscan, including a colour graphics adaptor board, a 10 MB Winchester disk and a Microsoft Mouse. The total µMagiscan package sells for less than £15,000 (UK) and consists of the computer, graphics boards, colour moni-

tor, camera, mouse, software and an Epson printer.

Microtools

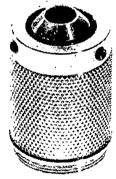
Inverted microscopes such as the Olympus IMT-2, the Nikon Diaphot and the Zeiss IM35 are the targets for a micromanipulator from Research Instruments Ltd (Reader Service No. 112). RI claims



micromanipulator that specializes in inversion.

that the TDU500 is the first leveroperated micromanipulator to use flexural hinges in its fine movement. According to the company, these hinges can provide sub-micrometre positioning accuracy. The instrument has a single lever for x-y-z fine movement, and levels for coarse x, yand z motion. Toolholders for one or two microtools are available on different TDU500 models.

Landmarks aren't easy to find under magnification, so EBETC Corp sells a \$63 (US) slide marker that puts an inked ring on slide locales that need to be identified (Reader Service No. 113). The ring is

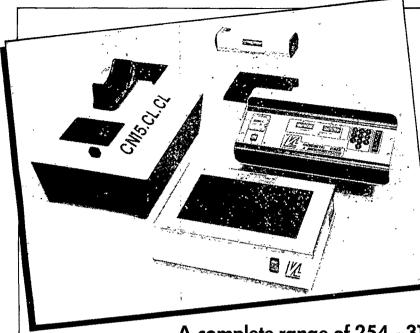


EBTEC marks the spot on microscope slides.

repeatable and concentric with the optical axis; marking will not break or damage slides. EBTEC's device fits any standard optical microscope with RMS objective thread, and the mark can be removed with solvent. EBTEC calls the marker "indispensible" for cytology, pathology, industry electron microscopy and applications.

Immunology addendum

Using plate electrodes to generate a uniform field, an electrophoretic blotting apparatus from Idea Scientific will execute Western blots in 30 minutes (Reader Service No. 114). Idea's GENIE has titanium



any **U.V.** problems?

l upon

254 - 312 - 365 nm lamps Portable lamps U.V. darkrooms Fluorescent tables U.V. radiometers Eprom erasers

A complete range of 254 - 312 - 365 nm U.V. Generators for your FLUORESCENT ANALYSIS (DNA - RNA - TLC...)

LOOKING FOR EXPORT AGENTS

BP 66 - Torcy - Z.I. Sud - 77202 Marne-la-Vallèe Cedex 1 France - Tél. : (1) 60.06.07.71 + - Télex VILBER 691 062 F

Reader Service No.23

Cutting or Polishing Specialized Materials?

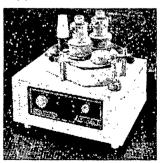


8

Applications

Semiconductors Electro-optics Lasers Fibre optics Soft and brittle materials Ceramics Teeth, bones **Rocks** Minerals

If minimum cutting loss, high surface finish, low material damage, flatness and parallelism are important, then Malvern's wide range of precision cutting, dicing, polishing and lapping machines provide the answer. A comprehensive range of accessories and technical support are available.



Malvern Instruments Ltd., Spring Lane South, Malvern, Worcestershire, WR14 1AQ, Telephone: (06845) 68415. Telex: 339679

SCIENCE AND TECHNOLOGY

Whatever the subject...refer to MACMILLAN DICTIONARIES

DESIGNED FOR STUDENTS

The paperback Macmillan Dictionary Series combines new and established works of teaching and reference with an attractive series format.

- * authoritative definitions and explanations of all current terminology written by experts
- * lucidly written entries with thorough cross referencing
- * regular new editions keep the student up to date with the latest research, practice and technology
- * a clear layout for easy reference
- * prices range from just £7.95 to £9.95

NEW IN 1986 ...

MACMILLAN DICTIONARY OF BIOTECHNOLOGY

320pp 0 333 40875 € March 1986

MACMILLAN DICTIONARY OF THE HISTORY OF SCIENCE Edited by W. F. BYNUM, E. J. BROWNE and ROY PORTER March 1986 528pp 0 333 34901 6 68.95

MACMILLAN DICTIONARY OF PERSONAL COMPUTING

AND COMMUNICATIONS DENNIS LONGLEY and MICHAEL SHAIN 0 333 42170 1 August 1986 320pp

MACMILLAN DICTIONARY OF PHYSICS

MARY P. LORD August 1986

320pp

MACMILLAN DICTIONARY OF IMMUNOLOGY FRED ROSEN, LISA STEINER and EMIL UNANUE

256рр

Macmillan Press, Houndmills, Basingstoke, Hants RG21 2XS, UK Not available in USA.



MONOCLONAL ANTIBODIES FOR BLOOD GROUPING

*Anti A, Anti B, Anti AB.

*Anti D (Rho)

Anti M. Anti N Anti Lewis a, Anti Lewis b

*ask for one hundred liter batches

MEDIA AND SERA FOR TISSUE CULTURE

DNA PROBES for Viral Diagnostic EBV, HTLV-III-LAV

EUROBIO

20, boulevard Saint-Germain - 75005 PARIS Tél.: (1) 43.25.20.33. - Telex: 201 236 F



Reader Service No.43

– NEW EDITION –—

INFORMATION SOURCES IN BIOTECHNOLOGY, 2nd Edition **Anita Crafts-Lighty**

"This book is a model. As such it should be in the hands of every librarian and information officer..." Process Biochemistry

"...very useful. No comparable work is available." Choice

First Edition—Choice Outstanding Academic book 1984-5

Revised and updated throughout, this new edition provides even more practical, incisive evaluations of both the traditional and more elusive sources of information in biotechnology. It will bring you right up to date by systematically and critically reviewing the many different sources available in:

 Trade and research literature
 Market surveys
 Company directories
 Conference Reports • Secondary sources—abstracts, title lists, indexes, bibliographies

PLUS—Greatly expanded sections on • Conference proceedings • Reading lists of introductory books • New information on • international organizations • Books out of print • How to set up and run information services • What is available for those seeking state-of-the-art coverage

A full index of publishers and addresses is included.

320pp \$100.00 0-943818-18-4 August 1986 £50.00 0-333-39290-6

CONTENTS

- 1. What is Biotechnology? The Science and the Business
- 2. Information Sources in Biotechnology—Outline of Types

 3. Monographs, Book Series and
- Textbooks
- 4. Conferences and Their Proceedings
- 5. Trade Periodicals and Newsletters 6. Research and Review Periodicals
- 7. Abstracting and Secondary Sources
- 8. Computer Databases/Databanks
- 9. Patents and Patenting
- Market Surveys
 Directories of Companies,
 Products and Research
- 12. Organizations
- 13. Providing Library and Information Services in Biotechnology

Publishers' Addresses Appendices and Tables Index

Order now on FREE APPROVAL by

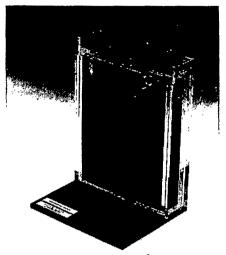
mail or phone. We accept all major credit cards.

We accept all major credit cards.

US/Canada—Mail to:
Stockton Press, 15 East 26th Street, New
York, N.Y. 10010. To order by phone, call
toll-free 800-221-2123. In N.Y., call 212-4811334. NYS residents add sales tax. Shipping
and handling costs added to billed orders.
Prepay and save s/h charges. Place a
Standing Order and receive a 5% discount
on this and all future editions

Standing Order and receive a 5% discou on this and all future editions. UK/Rest of World—Mall to: Elaine Coles, Globe Book Services, Ltd., FREEPOST, Brunel Road, Houndmills, Basingstoke, Hants RG21 2BR, England Basingstoke, Hants KGZ1 2BK, Englar Telephone: Basingstoke (0256) 26222 Charges for Postage and Packing: UK: £2.00 per order, Libraries free. Continental Europe: £2.00 per book. Rest of World: £3.50 per book. FREEPOST applies UK only. Globe Book Services, a division of Macmillan Publishers Ltd

plates coated with a thin layer of platinum which can blot gels up to 17 cm long. The GENIE also features an insertable loading tray that the company says will help achieve bubble-free loading. Idea's



The uniform field theory comes to electrophoresis.

machine requires less than one litre of buffer. Another version is available for gels up to 32 cm long.

Becton-Dickinson has recently released a new monoclonal antibody for B cell studies (Reader Service No. 115). The antibody, called Anti-Leu-16, reacts with an antigen found on human B cells in peripheral blood, tonsil and lymph node tis-



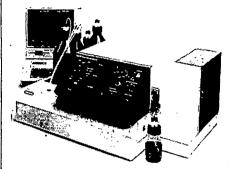
Becton-Dickinson's tool for trailing B cells.

sue. The antigen appears on approximately 10 per cent of peripheral blood lymphocytes, according to B-D. The company also says Anti-Leu-16 will not react with T cells or granulocytes and exhibits marginal reaction with monocytes. Available in purified form or as a fluorescein or phycoerythrin conjugate, the antibody can be used for B cell enumeration in peripheral blood, B cell isolation and studies of B cell neoplasms and activation.

Erratum: streptavidin pricing

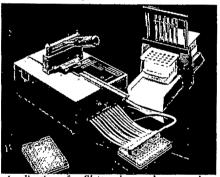
A review published in the 29 May issue of *Nature* (Vol. 321, p. 543) gave an incorrect price for Porton Products Ltd's streptavidin. In the United Kingdom, the chemical costs £5 per 0.5 mg, not 100 mg as previously stated. Porton Products sells streptavidin in 100 mg quantities for £1,000.

The latest version of Bio-Rad's MAPS (Monoclonal Antibody Purification System) kit has been designed specifically



MAPS dedicated to particular purifications.

for the purification of mouse IgG from ascites fluid (Reader Service No. 116). The kit, called Affi-Gel Protein A MAPS II, consists of protein A with MAPS buffers optimized for binding, elution and regeneration. Bio-Rad says the binding buffer increases the protein A-agarose capacity for IgG from less than 1 mg per ml to 6 to 8 mg per ml of gel. The elution buffer, the company claims, gives quantitative elution of bound IgG, and the regeneration buffer provides for up to 12 cycles. The entire kit contains the materials necessary to purify 500 mg of murine antibody.

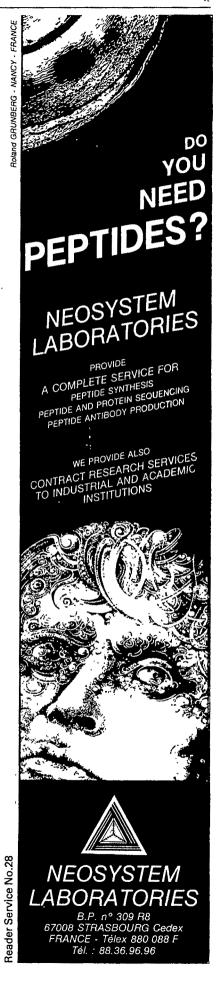


Applications for Skatron's new harvester keep growing.

Skatron is promoting a new cell harvester as an aid in receptor binding studies (Reader Service No. 117). The company describes a procedure that is intended to reduce the time and costs involved in filtration and reduce the levels of nonspecific binding. With Skatron's instrument, twelve incubation samples can be simultaneously filtered under reduced pressure. Another component, the Filterpunch, transfers the filter disks six at a time to scintillation vials. Skatron's cell harvester can also be employed in studies of HTLV-III/LAV infections.

These notes are compiled by Karen Wright from information provided by the manufacturers. To obtain further details about these products, use the reader service card bound inside the journal.

Prices quoted are sometimes nominal and apply only within the country indicated.



Will industry support higher education?

from Richard Pearson

Since 1980, government support for UK universities has dropped by over 11 per cent in real terms. Can new initiatives from industry soften the blow?

In the United Kingdom, higher education is now halfway through a decade of declining expenditure. Caught by the twin pressures of an attack on public expenditure and the reducing size of the population of 18-year-olds over the period to 1996, the University Grants Committee (UGC) and National Advisory Board (NAB) are trying to organize and manage a cash-constrained and reducing system. Overlaying these problems is the increasing pressure for higher education to become more directly relevant to the needs of the economy and increase the share of expenditure going to the 'vocational' disciplines, and engineering and technology in particular. Yet not only has this switch to higher cost courses got to be made within a shrinking budget but the physical infrastructure has also to be brought up to date with increasingly expensive technology which itself can often become obsolete within a few years.

Last year the Organization for Economic Cooperation and Development (OECD) reported on the problem of an "ageing infrastructure" and obsolete equipment in many OECD countries1. For twenty years, funding allocated for research has not matched the needs of the research community, and since the 1970s the cost of equipment has grown at a rate of 4 per cent above the inflation rate. In the United States it was estimated in 1982 that at least \$1,000 million was needed to bring university research equipment up to date. Many universities there now look to industry for help, and the tax regime makes donations tax deductable for companies. Although the majority of research and development funds for universities still come from government in one form or another, private industry has increased its spending on academic research and development by some 80 per cent since 1980 while government support has risen by only 34 per cent. It was estimated that US industry provided \$400 million to university research and development in 1984. Corporate motivation is clear: such investment aids graduate recruitment and gives access to teaching and research staff and facilities - all tax deductable. Several new university-based research centres have been established in recent years, such as that at Stanford, where 20 companies each paid \$750,000 towards new buildings, and then \$100,000 annually for three years to support education, research and administration. New centres have also opened in Texas and North Carolina. Other ventures involve consortia of small companies, while others have matching state support.

In the United Kingdom the government sees this model as one way in which higher education can ease its funding problems. In 1985 it made available an additional £43 million under the 'Engineering and Technology programme' to provide an extra 5,000 undergraduate places in information technology and related subjects in the universities and polytechnics. A condition of part of that funding was that the recipient institutions should raise significant industrial support. In the event, assistance valued at over £24 million was forthcoming in the form of equipment donations, project work, student sponsorship, research and teaching by industrial staff. Industrial support is also given to many other courses and institutions, although it is impossible to assess the total contribution in the United Kingdom with any accuracy. In addition to this direct support for higher education, there is a growing programme of collaborative activities under national and international research programmes such as Alvey and Esprit, and those more directed at training, such as CASE awards and the Teaching Company Scheme administered by the UK Science and Engineering Research

The majority of such links are negotiated at a personal level between individual academics and research or training staff in industry. As such, links have in the past developed on a very ad hoc basis. Now a number of major UK companies are seeking to develop corporate policies towards their support for higher education and are appointing 'campus coordinators' to draw together the company's activities with individual institutions in a more coherent way. They are still, however, a comparative rarity. While most collaboration is still on a one-off basis, with 'donations' often taking the form of payments in kind, there are some notable new jointly funded centres, such as the Leicester Biocentre which is funded by a consortium of companies to carry out fundamental research in biotechnology, and the recently announced Information Technology Institute organized by Cranfield Institute of Technology and supported by £4 million from over 20 high-tech companies. It is to be a commercial research and training centre running both short courses and degree programmes. The most common form of industrial collaboration remains, however, the provision of project work for students.

There is a growing interest in collaboration in both higher education and industry, and a recent survey of information technology departments showed that 86 per cent wanted to increase the level of collaboration, the remainder being satisfied with their current activities. Ironically, a 'lack of academic staff and time' was acting as a constraint to increasing the level of collaboration in two out of three departments, yet such collaboration is seen as an essential way of boosting resources. There were also concerns by one in three departments that there was a lack of industrial interest or that the interest was too short term and piecemeal2. Another problem was that out of date equipment reduced the attractiveness to industry, while many institutions still have over-bureaucratic procedures and uncertain guidelines by which academics can take on paid consultancy and outside work. In some institutions payments are supposed to be negotiated through the department with the individual receiving little direct cash reward, while in others staff are free to sell their time for personal gain. If industrial support is to grow and be seen as an integral part of an academic's timetable and reward structure, in part compensating for a low academic salary, then the institutions will need to be clearer and more positive towards the development and management of such links. And indeed some academics will have to start sharing their additional income with their full-time employers. It will take time for the links to develop as fully and as far as they have in the United States. The ultimate question for the United Kingdom is whether the industrial support will build on government funding or be seen as another reason for further reducing central expenditure on higher education and increasing the reliance or market forces.

Richard Pearson is at the Institute of Manpower Studies, Mantell Building, University of Sussex, Brighton BNI 9RF, UK.

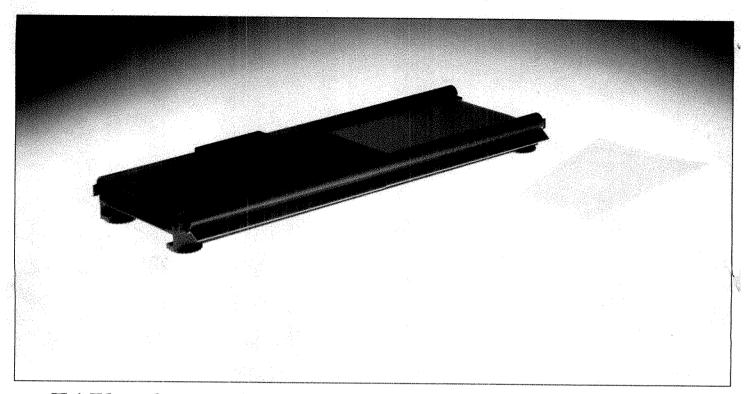
- Science and Technology Policy Outlook (OECD, Paris, 1985).
- Connor, H. & Pearson, R. Information Technology Manpower into the 1990s (Institute of Manpower Studies, Brighton, 1986).

1021011C INTERNATIONAL WEEKLY JOURNAL OF SCIENCE

Volume 322 No.6075 10-16 July 1986 £1.90



NMR IMAGINO OF A SINGLE CELL



Why buy the fastest gel casting system if you're short on time?

LKB's UltroMould is the fastest way to cast an electrofocusing gel. But if you want more productive results in even less time, you'll stop casting gels altogether.

There's a new alternative. A dried gel with an immobilized pH gradient. The Immobiline DryPlate." You'll get very high resolution and sample load. Put an end to drift, conductivity gaps and batch variations. The Immobiline DryPlate offers you today's most advanced electrofocusing opportunities. With runs that give you more information, a technique with outstanding flexibility and a system that provides unrivalled value for money. Time and again.

Our new brochure tells you why. It also contains the unique User Electrofocusing Guide – an invaluable aid to improving your results. Naturally if you've got the time, we'll be happy to show you UltroMould casting gels faster than you ever thought possible. But if you're truly short on time, just get a copy of "Immobiline DryPlate" – for modern electrofocusing.

Immobiline is a registered trademark of LKB-Produkter AB.

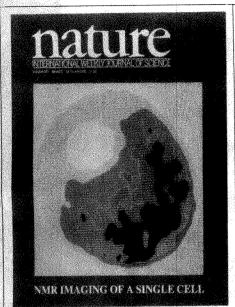


 $LKB-Produkter\ AB,\ Box\ 305,\ S-16126\ Bromma,\ Sweden.\ Tel.\ 08-9800\ 40,\ telex\ 10492$

Antwerp (03)218 93 35 · Athens-Middle East +30(1)894 73 96 · Beijing 89 06 21 · Copenhagen (01)29 50 44 · Hong Kong (852)5-55 55 5 · London (01)657 88 22 Lucerne (041)57 44 57 · Madras (044)45 28 74 · Moscow (095)255-6984 · Munich (089)85 830 · Paris (01)64 46 36 36 · Rome (06)39 90 33 · Stockholm (08)98 00 40 Tokyo (03)293-5141 · Turku (021)678 111 · Vienna +43(222)92 16 07 · Washington (301)963 3200 · Zoetermeer (079)31 92 01 Over 60 qualified representatives throughout the world.

nature

NATURE VOL. 322 10 JULY 1986



A nuclear magnetic resonance (NMR) image of a single Xenopus laevis ovum. The new technique of NMR imaging microscopy, described on page 190 and discussed in News and Views, can be performed on intact living systems with no sectioning, fixing or staining. The cell nucleus is clearly visible (light blue) and the cytoplasm displays heterogeneity. NMR provides information on the state of the water in cytoplasm and nucleus and chemical-shift imaging then gives an indication of the chemical composition of the cytoplasm.

OPINION	
Europe in trouble over aviation	97
Broadcasting by numbers	
NEWS	
Space vehicles	98
Indian science	
Scientific American	99
Others have problems too	
AIDS	100
OECD report	
Launch vehicles	101
Nature conservation	
National Science Foundation	102
Eucalyptus clean-up	
Vane back to basics	
Animal welfare	103
Eiffel in orbit	
US nutritional research	104
Young Hungarian academics protest	
Information technology	105
Chinese science	
CORRESPONDENCE-	
RGO to Manchester?/Prehistoric	
protection/Screwworm fly/	
Environment and nuclear power	106
Fig. 1 Add - 第4年 - Last 1	
NEWS AND VIEWS	
Looking for gravitational errors	109

Immunology T-cell receptor: gam	ma
gene product surfaces Miranda Robertson	110
Particles and the Universe	
Neil Turok	111
Archaeology: Towards a scientific	
approach Patricia Phillips	112
Clandestine sex in trypanosomes	
Keith Vickerman	113
European collaboration on dynan	nic
atmospheric fronts K A Browning, B J Hoskins,	
PR Jonas & A J Thorpe	114
Nuclear magnetic resonance: Firs	t
sight of a single cell	
John Mallard	115
Anoxic oceans and short-term carbon isotope trends	
Wayne D Goodfellow	115
Surface water acidification	-
Hans M Seip	117
-SCIENTIFIC CORRESPOND	ENCE-
Human gene cloning: the storm	
before the lull?	-
J Schmidtke, M Krawczak & D N Cooper	119
Immunotoxins to combat AIDS	
A Surolia & M P Ramprasad	119
Earthquake prediction and	
electric signals P Varotsos, K Alexopoulos,	A.
K Nomicos & M Lazaridou	120
The stability of zoological	
nomenclature	
R M Feldman	120
BOOK REVIEWS	
A Life in Science	
by Sir Nevill Mott RV Jones	121
Image Analysis: Principles	***
& Practice	
PW Hawkes	122
The Unfinished Universe by L B Young	
P W Atkins	
Continuum Theories in Solid	
Earth Physics	
R Teisseyre, ed.	122
Peter J Smith Natural Selection in the Wild	123
by J A Endler	
JSJones	124
COMMENTARY	
The mystery of declining tooth de	ecay
M Diesendorf	125
REVIEW ARTICLE	
Pathogenesis of lentivirus infection	ons
A T Haase	130

AKIICITO	
Pb isotope evidence in the	
South Atlantic for	
migrating ridge-hotspot interactions	
B B Hanan, R H Kingsley	
& J-G Schilling	137
The second secon	
Identification of a putative	
second T-cell receptor	
M B Brenner, J McLean.	
D P Dialynas, J L Strominger.	
J A Smith, F L Owen.	
J G Seidman, S Ip, F Rosen	
& M S Krangel	145
LETTERS TO NATURE	- 6
Infrared polarimetry of the nucleus of	
Centaurus A: the nearest blazar?	
J Bailey, W B Sparks,	
JH Hough & DJ Axon	150
JIIIOGH W. D. G. CHAVE	
The soft γ-ray burst GB790107	
JG Laros, E E Fenimore, MM Fikani.	1
R W Klebesadel, C Barat,	
G Chambon, K Hurley, M Niel.	
G Vedrenne, S R Kane, V G Kurt.	1
G A Mersov & V M Zenchenko	152
OAMEIOU TII Zememonii	
Evidence for an asymptotic lower	
limit to the surface dipole magnetic	1
field strengths of neutron stars	
E P J van den Heuvel.	
J A van Paradijs & R E Taam	153
JAvanrandon societa	
Inhibition of convective collapse of	
solar magnetic flux tubes by	
radiative diffusion	
P Venkatakrishnan	156
Lake acidification and the land-use	3
hypothesis: a mid-post-glacial analogue	
V J Jones, A C Stevenson	
& R W Battarbee	157
Non and have produced by the Secretary	
Non-axisymmetric behaviour of	
Olduvai and Jaramillo polarity	
transitions recorded in north-central	
Pacific deep-sea sediments	* # #
E Herrero-Bervera & F Theyer	159
Late Palaeozoic to early Mesozoic	
evolution of Pangaea	
R A Livermore, A G Smith	
&FJVine	162
X I J VIIIC	2.02.42
Mantle heterogeneity beneath the	
Nazca plate: San Felix and	
Nazca plate: San Felix and Juan Fernandez islands	
Nazca plate: San Felix and Juan Fernandez islands D C Gerlach, S R Hart.	165
Nazca plate: San Felix and Juan Fernandez islands	165
Nazca plate: San Felix and Juan Fernandez islands D C Gerlach, S R Hart.	165
Nazca plate: San Felix and Juan Fernandez islands D C Gerlach, S R Hart.	

Nature® (ISSN 0028-0836) is published weekly on Thursday, except the last week in December, by Macmillan Journals Ltd and includes the Annual Index (mailed in February). Annual subscription for USA and Canada US \$240. USA and Canadian orders to: Nature, Subscription Dept. PO Box 1501, Neptune, NJ 07753, USA. Other orders to Nature, Brunel Road, Basingstoke, Hants R621 2XS, UK. Second class postage paid at New York, NY 10012 and additional mailing offices. Authorization to photocopy material for internal or personal use, or internal or personal use, of internal or use, of internal or personal use, of internal or use, of int

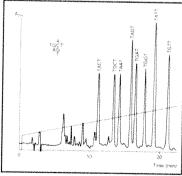


No other medium combines such high selectivity with such versatility. MinoRPC is unparalleled. It is optimised to give you fast, high resolution results.

To ensure high reproducibility, we have developed a special synthesis. You can always rely on MinoRPC to be the same every time we make it; every time you use it. And for that extra efficiency and reproducibility, you can work at elevated temperatures, carefully controlled by the Pharmacia high performance Column Heater.

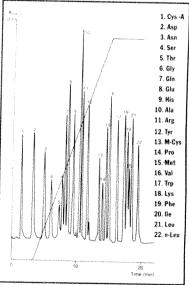
MinoRPC reflects the high standard you've come to expect from Pharmacia. Our contribution to high performance liquid chromatography has already brought success to thousands of chromatographers.

Share the success. Contact your local Pharmacia representative for more information on columns prepacked with MinoRPC.



SEPARATION OF OLIGONUCLEOTIDE: "WOBBLE SEQUENCES."

MinoRPC IS PART OF THE FPLC * SYSTEM, TODAY'S MOST VERSATILE AND BIOCOM-PATIBLE CHROMATOGRAPHY PROGRAM FOR THE FAST SEPARATION OF BIOMOLECULES



ANALYSIS OF PTH-DERIVATIZED AMINO ACIDS



That important research article you've been looking for located instantly!



If you store your copies of Nature for future reference, then the annual index of subject and author is an essential part of your collection. These comprehensive annual indexes are available for all issues of Nature from 1971 to 1985.

Prices and address for orders are set out below.

Annual Subscription Pr	ices	
UK & Irish Republic		£104
USA & Canada		US\$240
Australia, NZ &		C) C) C) C)
S. Africa	Airspeed	£150
3. Atrica	Airmail	£190
Continental Europe	Airspeed	£125
India		£120
IIIdia	Airspeed Airmail	£190
1		Y90000
Japan Rest of World	Airspeed	£120
Rest of World	Surface	
	Airmail	£180
Orders (with remittance	e) to:	
USA & Canada	UK & Rest of	f World
Nature	Nature	
Subscription Dept	Circulation I	Dept
PO Box 1501	Brunel Road	
Neptune	Basingstoke	
NJ 07753	Hants RG21	2XS LIK
USA	Tel: 0256 29	
(The addresses of Natu		
facing the first editorial		ces are snow
Sec.		
Japanese subscription e		4.4
Japan Publications Trac		ta
2-1 Sarugaku-cho 1-cho		
Chiyoda-ku, Tokyo, Ja	pan :	
Tel: (03) 292 3755		
Personal subscription ra	ates: These are a	vailable in
some countries to subsc	ribers paving by	personal
cheque or credit card. I	Details from:	•
USA & Canada	UK & Europ	e
Nature	Felicity Park	ter
65 Bleecker Street	Nature	
New York	4 Little Esse	x Street
NY 10012, USA		2R3LF, UK
Tel: (212) 477-9600	Tel: 01-836 (6633
Back issues: UK, £2.50	LISA & Canada	11886.00
(surface), US\$9.00 (air		
(surface), £4.00 (air)	J. INCOLOR PORTO	. 20.00
PACE 1 1 1 1 1 1 1 1 1 1 1 1 1 1 1 1 1 1 1		
Binders		
Single binders: UK, £5		
Rest of World, £7,75. S		
& Canada \$32.00; Rest	of World, £22.0	0
Annual Indone (1071)	005)	

Annual indexes (1971-1985)

Nature First Issue Facsimile

Nature in microform

UK, £5.00 each: Rest of World, \$10.00

UK, £2.00; Rest of World (surface), \$3.00; (air) \$4.00

Write to University Microfilms International, 300

North Zeeb Road, Ann Arbor, MI 48106, USA

Bacterial scavenging of Mn and Fe in a mid- to far-field hydrothermal particle plume	diagramma
J P Cowen, G J Massoth & E T Baker	169
Genetic selection for reproductive photoresponsiveness in deer mice C Desjardins, F H Bronson & J L Blank	172
Hybrid formation between African trypanosomes during cyclical transmission	
L Jenni, S Marti, J Schweizer, B Betschart, R W F Le Page, J M Wells, A Tait, P Paindavoine, E Pays & M Steinert	173
Analysis of human T-lymphotropic virus sequences in multiple	
sclerosis tissue S L Hauser, C Aubert, J S Burks, C Kerr, O Lyon-Caen,	
G de The & M Brahic and Lack of evidence for involvement of	176
known human retroviruses in multiple sclerosis A Karpas, U Kämpf, Å Sidèn, M Koch & S Poser Reply: H Koprowski, E C De Freitas, M E Harper, M Sandberg-Wollheim,	177
W A Sheremata, M Robert-Guroff, C W Saxinger, Flossie Wong-Staal & R C Gallo	178
A functional T3 molecule associated with a novel heterodimer on the surface of immature human thymocytes I Bank, R A DePinho, M B Brenner J Cassimeris, F W Alt & L Chess	179
Thy-1 functions as a signal transduction molecule in T lymphocytes and transfected B lymphocytes R A Kroczek, K C Gunter,	
R N Germain & E M Shevach Human T-cell γ genes contain N segments and have marked junctional variability T Quertermous, W Strauss, C Murre, D P Dialynas,	181
J L Strominger & J G Seidman	184
Newly replicated DNA is associated with DNA topoisomerase II in cultured rat prostatic adenocarcinoma cells W G Nelson, L F Liu	
& D S Coffey Nuclear magnetic resonance	187

imaging of a single cell

& M Hintermann

J B Aguayo, S J Blackband,

J Schoeniger, M A Mattingly

Cephalosporin antibiotics can be modified to inhibit human leukocyte elastase
J B Doherty. B M Ashe.
L W Argenbright, P L Barker.
R J Bonney. G O Chandler.
M E Dahlgren, C P Dorn Jr.
P E Finke. R A Firestone.
D Fletcher, W K Hagmann.
R Mumford. L O'Grady.
A L Maycock, J M Pisano.
S K Shah. K R Thompson
& M Zimmerman

192

-NATURE CLASSIFIED

Professional appointments — Research posts — Studentships — Fellowships — Conferences — Courses — Seminars — Symposia:

Back Pages

Next week in Nature:

- Solar oscillations
- Lightning photography
- Earth's core formation
- Memory in zirconia
- Tropical Atlantic "El Niño"
- Amazon dynamics
- Cyclic GMP in Paramecium
- Mitochondrial membrane permeability
- T-cell-mediated cytotoxicity
- Novel role for tRNA

-GUIDE TO AUTHORS

Authors should be aware of the diversity of Nature's renderships and should strive to be as widely understood as possible.

Review articles should be accessible to the while readenship.

Most are commissioned, but unsoluted reviews are welcome
(in which case prior consultation with the office is desirable).

Scientific articles are research reports whose conclusions are of general interest or which represent substantial advenges of understanding. The fext should not exceed 3.000 words and six displayed from (figures plus tables). The article should include an italic heading of about 50 words.

Letters to Nature are ordinarily 1.000 words long with no more than four displayed items. The first paragraph (not exceeding 150 words) should say what the letter is about, why the study it reports was undertaken and what the conclusions are

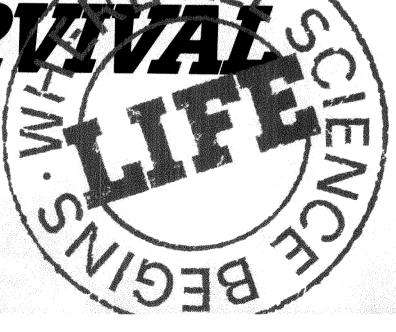
Matters arising are brief comments tup to 5000 words (on articles) and letters recently published in Nature. The originator of a Matters Arising contribution should initially send by mainscript to the author of the original paper and both parases should, wherever possible, agree on what is no be submitted.

Manuscripts may be submitted either to London or Washington, Manuscripts should be typed (double specing) or one side of the paper only. Four copies are required, each accompanied by copies of lettered artwork. No title should exceed Wichardeter in length. Reference lists, figure legends, etc., should be asparate sheets, all of which should be manuscred. Addressing tions, symbols, units, etc. should be identified on one edge of the manuscript at their lists appearance.

References should appear sequentially indicated by superscripts, in the test and should be abbreviated according to the World List of Scientific Periodiculs, fourth edition (Butterworth 1963-65). The first and last page numbers of each refrequenshould be etted. Reference to books should clearly indicates the publisher and the date and place of publication. Unpublished articles should not be formally referred to unless accepted or submitted for publication, but may be mentioned in the text.

Each piece of artwork should be clearly marked with the author's name and the figure number. Original artwork should be unlettered, Suggestions for cover illustrations are welcome. Original artwork tand one copy of the manufectiff will be returned when manuscripts cannot be published.

NEVER COMPROMISE BETWEEN HIGH RESOLUTION SURVE



nature

NATURE VOL. 322 to JULY 1986

Europe in trouble over aviation

Europe's failure to make a common market of itself is typified by the continuing muddle over civil air transport policy. The time has come to change that.

Fig. European Community is miscalled the "common market". So much is clear from the evidence that repeatedly comes to light of how its tolerance of restraints on free trade are crippling for the economy of Europe (see, for example, *Nature* 322, 2; 1986). But most of the time, the scale of this self-inflicted damage is hard to assess. Even the brashest of economists would be at a loss to tell what price Europe pays for its decision to forgo the benefits of a sensible division of labour among competing companies in fields such as electronics or general manufacturing. But in air transport the disbenefits are conspicuous.

Most European governments maintain civil airlines ostensibly as a means of enabling private persons to move from one place to another, but then come to regard them as extensions of the national persona, along with their national anthems and national flags. Europeans pay for these conceits in two ways: by extra taxes which allow governments to subsidize national airlines, and then by the higher fares which also partly compensate for inefficiency. It is especially scandalous that the European Commission should for so long have tolerated a state of affairs that cramps what should be one of the essential elements of the Europe it seeks, people's freedom to move about. It is similarly outrageous that the benefits of a now-traditional technology should be so widely withheld from 300 million people.

Now, luckily, some governments are becoming restive, with the Commission showing signs of waking up to its responsibilities. Motives are, inevitably mixed. The British government, which has been pressing for reform for the best part of three years, is eager that its own nationalized airline, which has been forced by the deprivations of recent years to become efficient and which is about to be sold as a going concern, should be able to compete more freely for the untapped market in European air travel. It would also be a legislative convenience if the government, when "privatizing" British Airways, were able to dispense with the usual monopolies by saying that competition is free. (There are at least two other privately held British airlines that could compete more effectively if allowed.) The Netherlands government is in a similar condition, eager that aviation should become a business rather than a branch of government.

The crucial step that may eventually unlock the jam is that the European Court has ruled that the Treaty of Rome, which created the "common market" in the first place, applies to aviation as to other kinds of business. At last, the Commission seems to have woken up. There is now talk that it will be writing to European airlines, possibly this week, with a warning that they must stop price-rigging and their other restrictive practices. The snag is that the Commission's only sanction is to take offending companies to the courts, not a speedy remedy. That is why hopes still centre on the prospect of a deal between the governments.

But what? The difficulty is that even the most fervent advocates of liberalized European air traffic seem to shrink from outright deregulation. Even the visionaries suppose that air traffic within the ten member states of the Community will continue to be regulated by a series of bilateral agreements between governments, so that aircraft bound from, say. Rome to London calling at Paris will not be free to pick up extra passengers on the second leg of their flight unless that right has been separately negotiated. Instead, the hopefuls model their ambitions on the present agreements between the British government and those of The Netherlands and Belgium, which allow all airlines to fly between designated point at the frequencies they choose, and with whatever fares they fix, provided that both governments choose not to object. These arrangements are better than nothing, but fall short of what they might be. What Europe needs, in this connection as in others, is true competition. In particular, it should be understood that subsidizing airlines is as illegal as subsidizing, say, motor manufacturers (for, otherwise, wasteful carriers will be perpetuated), that airlines of any European nationality may fly between any pair of cities already connected by scheduled services and that there should be no restraint on the ownership, within Europe, of privately held airline companies. That is what the airline business will have to come to in the end. The European Commission should face up to that now, not later. Until it does, the benefits of a simple technology will remain in escrow.

Broadcasting by numbers

Another British government has failed again to find a way of living without the BBC.

If we have enemies like that, what need have we of friends? That must be the reaction of the British Broadcasting Corporation (BBC) to last week's report of the committee under Professor Alan Peacock set up just over a year ago to find politically more palatable ways of supporting British public broadcasting, which is at present done by requiring those who use television receivers to buy an annual licence to make the practice legitimate. The Peacock committee came into being to spare the present government and its successors (of all parties) the periodic problem of deciding how much the licence fee should be, which is politically as popular as deciding by what degree politicians' salaries should be increased. The present government's suspicion (conviction?) a year ago was that advertising was the answer.

Expectations have not been realized. Peacock says that there is not enough advertising to sustain both public service broadcasting and the commercial stations. That is why the BBC is temporarily relieved. But then the committee goes off in a quite unexpected and technological direction, saying that the problem of financing the BBC independently of government decisions about a licence fee will be solved in the distant future, when it becomes possible to ensure that people pay each time they watch a television programme put out by the public broadcasting network. To the Peacock committee, it seems a minor matter that the technology for bringing this about, easily designed on the back of an envelope, is still far beyone most manufacturers' ken. It is nevertheless odd that a committee apparently willing to accept its marching orders, to devise alternative financing. should have sought refuge in technological futurology from the awkward truth that free-market remedies in present circumstances would kill standards. It would have been better to say outright that the BBC, for all its many faults, is probably worth keeping the way it is.

Space vehicles

British HOTOL closes in on French Hermes

BRITAIN'S horizontal take-off and landing space plane, HOTOL, could be in space by 1998, according to the director of the British National Space Centre (BNSC). Roy Gibson. A bid to make it a European project will be made at the next (October) council meeting of the European Space Agency (ESA). HOTOL, which was little more than a gleam in a British Aerospace designer's eye a couple of years ago, thus seems to be racing ahead. With its launch date brought forward, what once seemed almost science fiction is now in direct conflict with the more conventional French project Hermes, in which a mini-shuttle could be launched on top of a cryogenic Ariane-5 rocket around 1995.

But will HOTOL work? According to British Aerospace, the design incorporates a "breakthrough" in air-breathing engine technology which makes it possible to move ahead with off-the-shelf technology rather than the completely new engineering needed for the US National Aeronautics and Space Administration's "National Aerospace plane" (NASP) programme. The NASP programme is aimed at pushing ahead with research in high temperature materials and computational hypersonic fluid dynamics to enable, early next century, the creation of a whole class of vehicles from long-range airliners to spacecraft capable of airbreathing propulsion at speeds of Mach 5-12. By comparison with HOTOL, NASP is "technology driven" according to the British Aerospace Launch Vehicles Project Manager, Bob Parkinson. "HOTOL is a conceptual, not a technological breakthrough", Parkinson claims.

According to Parkinson, "we saw a way of doing the propulsion system that noone else has spotted.... We took the engine concept to Rolls-Royce" and HOTOL began to roll. That was a couple of years ago. But the "breakthrough" is still classified. Commentators have suggested the engine might precool inlet air with its liquid hydrogen fuel, to increase the density of the air and allow the production of a more compact engine. A Rolls-Royce spokesman said that the same engine, once the vehicle reached Mach 5, would be switched to liquid oxygen oxidant to complete the push into

Professor J.E. Ffowcs Williams, of the Department of Engineering at the University of Cambridge, many of whose staff work on Rolls-Royce contracts, said that though he knew little about the project he believed it would benefit from publicity at

this stage. Arthur C. Clarke, the science fiction writer, said from Colombo last week that he invented the idea of the airbreathing engine for space vehicles "40 years ago". But Clarke could not speculate on the British Aerospace design because "I don't know anything about engines and aerodynamics".

Meanwhile, Gibson and others backing the British space effort have the task of raising money from abroad for what is estimated as a \$4,500-million project to produce two flying HOTOL vehicles by 1998, without the freedom to expose the HOTOL "breakthrough". Nevertheless, says Gibson, BNSC has made "progress" in getting HOTOL declassified, as the classification was much more commerical than military. "We've been able to lift the veil enough to make a tour round Europe", seeking participants.

According to Gibson there remain a few technological "hoops", but all should be clear a year or so from now. The British plane is to present ESA members in October with a proposal for a four-year, \$400-million HOTOL feasibility study; but this will clash, politically at least, with the simultaneous effort being made by the French to win participants in a cheaper. \$48-million study of their Hermes space shuttle. Hermes is ahead on the political timetable, as ESA passed an "enabling resolution" approving the study in June (only the money is yet to be found); and it is also ahead on the engineering timetable (as the French space agency CNES has been working on Hermes far longer than the British on HOTOL). But Germany has been hesitating to give full support to Hermes, and according to a Bonn research ministry spokesman, HOTOL has already won the heart of his minister. Heinz Reisenhuber.

France has said it will go it alone with Hermes if it cannot raise European support. Britain, however, is sounding equally bullish about HOTOL. According to Gibson, whose first British space plan will go to ministers this week, participation of the French in the HOTOL programme would not be essential.

There is no French technology that can ot be found or developed elsewhere, ac ording to Gibson, and even French money may not be essential. It is not inconceivable, therefore, that HOTOL will go ahead like Concorde, the Anglo-French supersonic airliner, as a bi-national project, though this time the nations involved may be Britain and West Germany.

Robert Walgate

Indian science

Making the numbers count

Bangalore

TITE gulf between the industrialized nations of both East and West and developing countries such as India is dramatically illustrated in the latest batch of statistics from the Indian Department of Science and Technology. In one year, India's spending on research and development amounts to just US\$1.52 per head of population, compared to \$361.22 in Switzerland, the country at the top of the league. The United States spends \$303.9. Sweden \$242.26 and Japan US\$231.1. With India at the lower end of the scale are the Philippines (\$1.65) and Pakistan (\$0.49).

The pattern is similar when research spending is seen as a percentage of gross national product (see table) or when the

Expenditure on research and development as percentage of gross national product (1982)

Sweden	4.9
Hungary	3.3
Czechoslovakia	3.8
United States	2.5
Japan	2.4
West Germany	2.4
India	0.85
Greece	0.2
Pakistan	0.2
Philippines	0.2

science enterprise is assessed in terms of the number of scientists and technologists per head of population. Compared with nearly 140 per thousand of population in the United States, for instance. India boasts a mere 2.63 per thousand. Yet in a country as big as India this means there were 2.47 million scientist and technologists in 1985, up from 1.95 million ion 1980.

It is this two-million-plus science workforce that Prime Minister Mr Rajiv Gandhi sees as the key to India's welfare in the twenty-first century. His new science policy identifies three levels of projects: "missions", where scientists will need to put proven technology to work to solve specific problems: "thrust areas"; and "blue-sky" basic research. The emphasis in each area, is to be on the possible benefits for the "common man", most particularly India's rural population.

Five of the "missions" have already been selected — improving drinking water, campaigning against illiteracy, telecommunications, a vaccination programme for children and in agriculture a major effort to improve oil seeds. The "thrust areas" so far proposed are computer technology and biotechnology — frontier disciplines requiring major investment but with the potential to give immediate results.

Radhakrishna Rao

Scientific American

Unwanted fly in merger ointment

THE fate of 141-year-old Scientific American, which claims to be the oldest periodical in the United States, hung in the balance earlier this week, after an agreement by the board of Scientific American Inc. to merge with a West German publisher had been confused by a rival bid from Mr Robert Maxwell, the British publisher and owner of Pergamon Press. Mr Maxwell was bidding through the vehicle of the public company, BPPC, in which he holds a controlling interest. It will be for the shareholders in Scientific American Inc., which is not quoted on the stock exchanges, to decide whether to accept the board's proposal or that from Maxwell.

The board's proposal, agreed at a meeting in New York on 30 June, is that the West German company Verlagsgruppe Georg von Holtzbrinck of Stuttgart should be allowed to offer the shareholders of the US company \$258 for each of their shares, amounting to a total of \$52.6 million for the company as a whole.

Holtzbrinck's business centres on the publication of the newspaper Handels-blatt, a financial daily, but the company has been since 1981 a partner in the publication of the German edition of Scientific American (under the title Spektrum) and has recently been expanding into the US publishing industry by the acquisition of book-publishing companies.

Under the proposed arrangement, which includes the sale of the book publisher W.H. Freeman Inc., Scientific American would continue to operate as an independent enterprise, with Mr Gerard Piel continuing as chairman of the management board and his son, Mr Jonathan Piel, as editor and publisher. The younger Piel said last week that Holtzbrinck was enthusiastic about his plans for increasing the coverage of news in the magazine.

The present uncertainty is an ironic outcome of a process extending over the past three months, since the impending sale of Scientific American Inc. was first announced, and during which the New York investment (merchant) banker Salomon Brothers was commissioned by the board to conduct a "regulated auction" of the company. This is a process by means of which potential bidders can be screened so as to exclude unwanted owners. Sealed bids were received on 16 June from seven different organizations, including one from Maxwell of \$34 million.

Even the idea that Scientific American might be put on the block would have seemed strange a short while ago; during the 1960s, the monthly magazine was among the most successful of internationally circulating publications, both commercially and in reputation. In spite of its antiquity, Scientific American's success is

entirely a post-Second-World-War phenomenon deriving from the acquisition of the title by Gerard Piel and Denis Flanagan, the editor until four years ago.

The need to sell the company has largely arisen because of the discontent of some shareholders. The proportion of shares controlled by Gerard Piel is believed to be about one-sixth, not enough to prevent a sale. The largest shareholder, with 32 per cent, is Mr Arthur Seckler, well known for charitable works.

The company's announcement last week of the agreement with Holtzbrinck said that the board had confirmed this arrangement in spite of the receipt of a letter "from the bidder who had originally offered the lowest price... purporting to raise that offer to \$61 million".

Although the company says that it has legal grounds for not recommending Maxwell's bid to its shareholders, there is no obvious reason why the shareholders collectively should not let strictly financial considerations determine their decisions. The next step is, apparently, that Holtzbrinck will make a formal offer to buy the shares. A spokesman in Maxwell's office said this week that it would be for the board of *Scientific American* to consider the BPPC offer in the "light of its fiduciary

responsibilities to shareholders".

The uncertainty has nevertheless caused consternation among authors of W.H. Freeman, who appear to be alarmed at the transfer of ownership to Maxwell. Dr Harvey Lodish of the Massachusetts Institute of Technology says that he will not revise the first edition of his successfully published book if the threatened deal goes ahead. Dr Peter Atkins of the University of Oxford, whose successful textbook Physical Chemistry is published in the United States by W.H. Freeman, says that neither the shareholders nor the purchaser should be in doubt that the sale may be that of a "shell" if Freeman authors choose to defect.

Professor Martin Rees (Institute of Astronomy, University of Cambridge), who is writing a book for Freeman but who has not yet signed a contract, says that he is more offended by statements in a circular letter to BPPC shareholders three months ago explaining the basis which the titles of 361 titles of scientific journals were transferred from Pergamon Press to BPPC in exchange for £240 million. The circular says that, because scientists are more concerned with quality than price. prices of journals can (and have been) increased "well above the rate of inflation". In 1985, the prospectus says, the 361 journals will make a profit "before sales commission" of £23.7 million on a turnover of only £49 million. John Maddox

Others have problems too

POPULAR science magazines have suffered serious falls in advertising revenue recently from which even the relatively serious *Scientific American* has not been excepted. According to the US Publishers' Information Bureau, *Scientific American*'s advertising revenues have fallen by 27 per cent in the past year. The slump in the home computer market is one reason; although corporate advertising partly made up the shortfall, it too fell in the last year. Sales, at around 600,000 copies, are down from a peak of 720,000 in the late 1970s, mainly because of competition from the more popular magazines.

Mr Gerard Piel, chairman of Scientific American Inc., denies, however, that reduced revenues were the immediate cause of the sale; rather, he blames the "extremely turbulent corporate market" of recent years and the "staggering" frequency of mergers which threatened Scientific American with the possibility of a takeover by an unfriendly bidder who would not uphold the magazine's standards.

Falling advertising revenues are. however, blamed for the demise two weeks ago of *Science 86*, the popular publication of the American Association for the Advancement of Science. Time Inc. bought the magazine's assets for \$6 million and turned the subscriber list over to its own popular magazine Discover, which can use the Science 86 logo for 2 years. Discover has, however, been drifting away in recent months from science towards being a general consumer/ current affairs magazine. Science 86's advertising revenues dropped by 50 per cent in two years. Editorial staff are being "terminated".

Why has there been such a precipitous decline in advertising in popular science magazines? Different people have different answers, but the decline of the home computer market — and competition from specialized home computer magazines — is frequently mentioned. Some advertising agencies believe that readers of such magazines are not sufficiently consumerminded, and that similarly affluent readers can be reached to greater effect in consumer magazines, which are also read by more people per copy. Others point to proliferation of popular science magazines in the early 1980s. But many agree that one more magazine will have to go before equilibrium is reached. The most vulnerable, by common consent, is Science Digest. Its advertising revenues fell by 50 per cent in the past year, and even the wealthy Hearst Corporation is unlikely to continue supporting a loser for ever. Tim Beardsley

AIDS

New centres for clinical trials

Washington

As the number of cases of acquired immune deficiency syndrome (AIDS) continues to snowball, finding an effective therapy becomes increasingly urgent. The US National Institute of Allergy and Infectious Diseases (NIAID) announced last week that it was committing \$100 million over the next five years to speed the search for a therapy.

Fourteen AIDS treatment evaluation units will be set up around the United States to test drugs that have shown some promise, either by blocking replication of the virus that causes AIDS, or by strengthening immune system function. Therapies likely to be tested in the first year of trials include the anti-viral compounds azidothymidine, foscarnet, HPA-23, ribavirin, interferon-alpha and possibly dideoxycitidine. In announcing the new units, Anthony Fauci, director of NIAID, said a successful treatment would probably combine an anti-viral drug with an immune modulator. But combination therapies will be tested only after each single agent is tested.

A Data Safety Monitoring Board will evaluate the progress at each centre recommending new directions on initial results. To streamline exchange of information among the 14 units, NIAID plans to award a contract this September for a trial coordinating centre.

While Fauci estimates that some 2,000 patients will be included in trials by the end of the first year of the programme, the centres are not intended for treatment of the nearly 22,000 people with AIDS in the United States. Plans for placebo-controlled clinical trials has renewed the debate over the ethical justification of such an approach. Robert Levine, chairman of the Yale University School of Medicine Institutional Review Board, has suggested that using historical controls may be an "ethically less problematic" research design than placebo controls.

But Walter Dowdle, AIDS coordinator

Centres named

The fourteen institutions receiving NIAID funds are: Harvard University; John Hopkins University; Memorial Sloan-Kettering Cancer Center; New York University; Stanford University; University of California, Los Angeles; University of California, San Diego; University of California, San Francisco; University of Miami; University of Pittsburgh; University of Rochester; University of Southern California; University of Texas M.D. Anderson Hospital and Tumor Institute; and University of Washington.

for the Department of Health and Human Services Public Health Service (PHS), says that controlled trials are the "most compassionate way to go". Dowdle argues that, in the long run, only placebo-controlled trials will show which therapies are truly effective. Dowdle is also sceptical about providing experimental drugs to patients not involved in clinical trials. As no agent has been shown to be safe and effective against the AIDS virus, providing unproven drugs to patients could accelerate the course of their disease.

Critics of the government's response to the AIDS problem say that the present

administration has not gone far enough in dealing with the problem. In an occasionally heated congressional hearing last week chaired by Representative Ted Weiss (Democrat, New York), Martin Hirsch of Harvard University testified that it is "a national tragedy that so few patients" are in controlled clinical trials for AIDS therapies. Dowdle and Fauci defended NIAID's plans, but when questioned, Fauci admitted that additional money would allow NIAID to support another five centres whose applications had received favourable reviews. Weiss was quick to insist that PHS should request the money in its 1987 budget. After the hearing, Dowdle said PHS was considering asking for more cash, but no decision had yet been made. Joseph Palca

OECD report

Sweden number one for research

Sweden "has more to teach than to learn" about research and technology policy, according to a team of distinguished examiners for the Organisation of Economic Cooperation and Development (OECD) whose report on Sweden has just been released*. Swedish industry spends more on research and development per unit of turnover than even Japanese industry, according to the report. Over the past 15 years, Swedish business has raised its receipts from patents sold abroad eightfold—while its payments for foreign technology licences has risen only fourfold.

Despite this success, the examiners complain, Sweden pays university professors only 50 per cent more than it pays university janitors. University posts remain unfilled and there is a danger that the education system will not continue to provide the technically trained manpower that Sweden's established high-technology industry needs. Between 1970 and 1984, the numbers of doctoral graduates in physics, chemistry and mathematics in Sweden fell 50-75 per cent. OECD lays the blame on a system of loans, repayable after graduation, to cover higher education fees. Loans discourage students from entering research careers. A further degree means further debts, and a doctorate does not lead to higher salaries, or at least not sufficiently high to pay off the extra debt.

Yet Sweden depends on science. Its pharmaceutical and biomedical industry spends 17–18 per cent of its turnover on research and development. Including government spending, Swedish spending per head of population on biomedical research is higher than that of the United States, the OECD examiners claim.

Swedish communications engineering, environmental research, energy-saving equipment, paper-making technologies and robotics are equally advanced. The

use of robots in Swedish industry had reached 29.9 per 10,000 workers by 1981—the highest in the world, ahead of Japan (13.9 in the same year) and the United States (4.0).

The examiners congratulate Sweden on its enlightened workforce, and the "generally pro-science and technology attitude" in the country. This might be attributed, they suggest, to a strong programme by the national council for planning and coordination of research (FRN) in the schools, teaching children about energy problems, cancer, food and the like, an effort the examiners describe as "unprecedented in OECD countries with the possible exception of Japan".

The level of expenditure aimed at industrial development is now so high, however, that Sweden is in a class of its own, with no other country to learn from. Sweden is itself now an experiment, which other countries will watch with interest, to see the effects of this strategy.

A constant theme throughout this report from OECD, however, is that Sweden must beware of taking its renowned egalitarianism too far, at least in research. Swedish success in biomedicine, for example, is traced to the Nobel prize winner Theodor Svedborg and his successors at Uppsala; and the chemical industry to Nobel himself and precision instrumentation to Hasselblad. "We recommend that allocation of funds be made to individuals of excellence, with far-reaching plans, not to fields... and that high quality results be recognized by easy and substantial funding." **Robert Walgate**

*OECD Reviews of National Science and Technology Policies: Sweden (OECD Paris. 1986). The review panel consisted of: Guy Ourisson, director. Institut de Chimie des Substances Naturelles, Gif sur Yvette, France: Walter Zegveld, director, Policy Studies and Information Group, TNO, Delft, The Netherlands; Derek Denton, director, Howard Florey Institute, of Medicine. University of Melbourne, Australia: and Yrjo Toivola, managing director, Vaisala Oy, Helsinki, Finland.

Launch vehicles

France and US explain failures

AFTER third-stage ignition failures which destroyed two of the last three launches, the European space rocket Ariane looks set to go back to the makers for six months. The independent commission of inquiry which reported in Paris last week attributed Ariane's latest problems, and uncertain ignitions and failures early in the programme, to the small size of the "pyrotechnic" that lights the engine.

This view appears to counter speculation in the Los Angeles Times earlier this week that senior French sources believed Ariane had been sabotaged, but Jacqueline Schenkel of the Arianespace Washington office would say this week only that sabotage "had been practically ruled out". Certain questions are in fact "still being investigated" she said.

Ariane's third-stage, liquid hydrogenoxygen engine is ignited by a four-second pyrotechnic burning in the combustion chamber. But sometimes the fuel has failed to ignite; at others it has back-fired and gone out or faltered but continued. Ignition has proved to be sensitive to too many factors. The tolerances of the process have to be broadened, the commissioin says, and the easy solution is a bigger pyrotechnic.

This will take approximately six months, but in the face of similar launch difficulties in the United States with the shuttle and conventional rockets, Arianespace is still enjoying a burgeoning order book. Orders for 36 satellites to be placed in orbit at a net cost of some £1,000 million are still in hand, the company says.

Meanwhile, in Washington, explanations for US rocket failures abounded last week. At the Pentagon, the Air Force explained why its Titan 34D booster exploded seconds after lift-off. Over at the National Aeronautics and Space Administration (NASA), an investigation revealed faulty wiring as the cause of the failure of a Delta rocket on 3 May. Neither investigation showed fundamental flaws in rocket design, and launches could resume as soon as new prelaunch procedures can be implemented.

The Titan's problems started when rubber insulation apparently pulled away from the steel wall of the solid rocket motor (SRM) shortly after lift-off. This allowed combustion products to reach the booster wall, weakening it to the extent that it could no longer withstand the pressures inside the booster. Approximately 9 seconds after SRM ignition, the rocket exploded, causing \$70 million damage to the launch pad and adjacent facilities.

The Titan 34D SRMs are similar in design to those used on the space shuttle, but have a different manufacturer — United Technologies rather than Morton Thio-

kol. The commission investigating last January's shuttle disaster concluded that a failute of the O-ring seals caused the Challenger accident. But General Nathan Lindsay, who headed the Air Force investigation, said the O-ring seals joining the solid rocket segments "did not contribute to the [Titan 34D] mishap".

Lindsay does not believe that the accident represents a flaw in the SRM design. He pointed out that 940 booster segments have launched successfully without a problem. The Air Force plans to upgrade its inspection procedures of the solid rocket motor segments, but otherwise is

making no major alterations in the Titan 34D as a result of the accident. Lindsay expects that Titan 34D flights will resume within a year.

The problems of the Delta rocket were primarily electrical, according to NASA's investigation. A short in the main engine control circuits caused both the main and altitude engines to shut down. Without controlling thrust from the engines, the Delta broke apart in the atmosphere and was destroyed by ground controllers. Vibration at lift-off apparently caused the erosion of some insulation in a wiring harness, leading to the short circuit. NASA's investigation board recommended redesign of parts of a wiring harness, as well as increased attention to detail in construc-Robert Walgate & Joseph Palca tion.

Nature conservation

Too many of the wrong trees?

In a country as stripped bare of woodland as Britain, it might seem certain that the planting of new forests would be universally welcomed. But last week, all the nation's major voluntary conservation bodies



joined hands in a report protesting against the rapid growth of Britain's forests.

The report comes from Wildlife Link, which represents 24 conservation organizations with a total membership of 1.4 million. It is not more trees that they find objectionable but that present government policy, grants and tax relief favour a type of forest practice which they believe is damaging to the environment. The pace of planting has certainly increased: nearly 5.5 million acres of new forest a year, double that of fifty years ago. And, says the report, much of that is in massive monocultures, usually of Sitka spruce, that are transforming open land habitats and destroying the flora and fauna of moorland, heath, bog and sand dune. Two and a half million acres have gone since 1919. Vast areas of Scotland are now "tree farms" which destroy wildlife and are utterly different from any native forest that might once have grown there.

The critique by the conservation organizations comes a week after the publication by the Nature Conservancy Council of Nature conservation and afforestation in Britain, which details the increasing conflict between forestry interests and conservation needs. Each of the arguments for further massive plantations - that there is still plenty of open land left; that, as much of what is now open land was once forest, afforestation is a return to a more natural environment; and that forests support more wildlife than open ground - is examined and found wanting. Nor does the report find economic arguments compelling. Although Britain imports 90 per cent of its timber so that the need for increased domestic production would seem vital, forestry gives a low return on capital invested and takes up funds that might be better spent elsewhere.

The conservation bodies would like to see more sensitive planting, particularly using native tree species, in a manner that would help to increase the diversity of wildlife and avoid damage to unique open habitats. Various possible new planning control methods are suggested, but the first task remains to notify all Sites of Special Scientific Interest (SSSI) and to ensure that they are adequately protected. One possibility might be a stronger regulatory role for the Forestry Commission which processes applications for forestry grants. But the commission would first have to strike a better balance between timber production and protection of the environment in its own activities.

In the longer run, new and more attractive forestry schemes may appear. There is pressure within the European Community to reduce excess food production by converting relatively fertile farmland to forests. These lowland forests could be of native hardwoods and support rich wildlife communities; quite different from the massive forests being grown on the northwestern moorlands.

Alun Anderson

National Science Foundation

Grant applications go paperless

Washington

EXPRES, the National Science Foundation (NSF)'s plan to make grant application all electronic, will take off at the end of this month. NSF hopes the project will streamline its review process and serve as a prototype for the exchange of scientific information between different computer environments. But success depends largely on factors outside NSF's control.

Formally titled Experimental Research in Electronic Submission, EXPRES

Eucalyptus clean-up

New Delhi

India's northern state of Haryana appears to have found one solution for a major problem of developing countries — how to dispose of sewage cheaply. A five-year project at the Central Soil and Salinity Research Institute (CSSRI) at Karnal has revealed that untreated sewage is just the thing to encourage eucalyptus forests to grow on wasteland.

When the CSSRI scientists began their project back in 1981, they simply pumped sewage into trenches on wasteland and planted eucalyptus trees on ridges between them. Now the wastelands have turned into eucalyptus forests, previously used sewage ponds have disappeared and there a fewer mosquitoes.

"Land disposal of sewage is the cheapest and most cost-effective method of disposing of urban waste waters as it utilizes the entire biosystem - soil and vegetation as a living filter", says Dr Ranbir Chabbra, a senior soil scientist at CSSRI. Untreated sewage contains large quantities of plant nutrients but the presence of pathogens, heavy metals, pesticides and above all its odour makes it unsuitable for growing agricultural crops and vegetables. But these considerations do not affect its use for growing trees which are used as timber and fuel but not as food, says Chabbra. As the trees act as biopumps, they prevent water-logging and thus groundwater pollution.

There are two reasons why the eucalyptus system is particularly attractive to the Haryana towns. First, CSSRI has shown that one hectare of eucalyptus irrigated by sewage water can earn the municipalities a gross return of Rs 9,700 (£600) in the first year and Rs 28,000 (£1,800) in the second year. The sludge accumulating in the furrows, which can be sold as manure, is a bonus. Second, the technology raises the prospects of developing plantations into green belts and scenic parks. No wonder the project has the approval of the state forest department as well as the pollution control board. K.S. Jayaraman would shift proposal development, submission and review from reams of paper to the realm of computer workstations, so that a proposal could be distributed from its origin to NSF, and from NSF to reviewers, entirely by electronic transmission. Because the grant-seeking community is both technologically and geographically diverse, NSF thinks the scheme makes the perfect guinea pig for research on information exchange. The foundation receives ten copies each of 37,000 proposals from about 2,400 organizations in an average year.

The inspiration for EXPRES came from the NSF office that processes grant proposals, and gained impetus when Erich Bloch, a former vice-president at IBM, became NSF director in 1984. The foundation expects to announce two award recipients in September, and has earmarked \$2 million for EXPRES in fiscal year 1987.

Although the duration of the awards is three years, funding for the remaining two is not "set in concrete". Competition for the awards may be keen nonetheless: an interest meeting last month drew more than 30 people, and nearly 200 organizations have requested project solicitations.

Part of the reason that EXPRES has sparked this response has to do with its applicability beyond the paper-shuffling procedure at NSF; as project manager Alvin Thaler claims, "the grant process is just a handle to grab hold of the whole problem of communicating scientific information". Ultimately, however, the project's implementation depends upon concurrent developments in computer standardization to lay the groundwork for open information exchange. EXPRES pilot installations will intially use NSFNET, a network that links the foundation's supercomputers and is itself still in its formative years. Although NSFNET currently conforms to DARPA protocol (a system developed by the Department of Defense), it will eventually adopt the universal Open Systems Interconnection (OSI) standards of the International Standards Organization. But OSI standards are also in their infancy, putting another question mark in the EXPRES timetable.

The birth of EXPRES, therefore, needs to be closely attended by the groups responsible for computer standards, such as the National Bureau of Standards and the American National Standards Institute.

The project may also have an ally in the Virginia-based Corporation for Open Systems (COS), an organization conceived just last year to accelerate implementation of OSI by coordinating industry efforts towards standardization. With 55 members, including IBM, AT&T and Digital Equipment Corporation, COS could

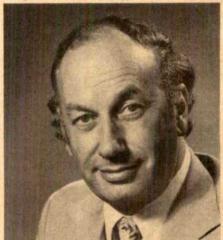
hasten the industry-wide compliance that NSF needs to make EXPRES operable. The view from COS is clear: programme manager Vance Mall says that if all concerned parties pool their efforts, EXPRES could be up and running by 1990.

Karen Wright

Vane back to basics

WITH the financial backing of Glaxo, the British pharmaceutical company, Sir John Vane is going back to his pharmacological roots, a year after leaving the Wellcome Foundation, of which he was research director.

Vane will direct the new William Harvey Research Institute at St Bartholomew's Hospital Medical College, situated close to



St Bartholomew's Hospital, where William Harvey established that blood circulates, but even closer to Smithfield, London's central meat market. Funds will be available for about a dozen scientists plus support staff for at least five years to carry out research on cardiovascular disease, with particular emphasis on atherosclerosis and eicosanoids, the area of research for which Sir John shared the 1982 Nobel prize for Physiology or Medicine.

The first of Vane's priorities is to stock the institute with Watenabe rabbits or other animal models of human atherosclerosis. With these and with the aid of cell culture and his own cascade bioassay system, Vane intends to improve the understanding of the pharmacology of cardiovascular disease. Against the trend, he has no plan to use the techniques of molecular genetics in the institute's research.

In return for financing the new institute, Glaxo has first rights on any discovery of commercial interest to it. Sir John is the second top Wellcome researcher to be snapped up by Glaxo; earlier this year, Dr Pedro Cuatrecasas left his position as head of research at Burroughs Wellcome, the US subsidiary of Wellcome plc, to set up a US research operation for Glaxo Ltd.

Peter Newmark

Animal welfare

Laboratory animals unprotected

Tokyo

DEBATE over the welfare of laboratory animals in Japan has been sparked by reports from a French scientist that monkeys at Kyoto University's Inuyama Primate Research Institute have been shamefully maltreated. Bernadette Brésard, who carried out research at the institute last year, has revealed to French magazines that monkeys were routinely restrained in "monkey chairs" for months on end. Behind this one incident lies a much deeper problem: the lack of clear, enforceable regulations on the treatment of laboratory animals in Japan.

Brésard came to Japan last year with an

Eiffel in orbit

FRENCH engineers, clearly inspired by the recent refurbishment and laser-lighting of the French-built Statue of Liberty in New York, are now planning to put an Eiffel Tower in space.

The object of a competition, announced last month by the Eiffel Tower Company (Société Nouvelle d'Exploitation de la Tour Eiffel), is to design a structure for the space age "as audacious and imaginative as that of Gustave Eiffel for the age of steam". Designs must be for a durable structure visible to the naked eye and symbolizing



"universal communication, the great dream of our times". Otherwise, the structure is to be useless: it must have "no commercial or military function", but "peaceful" and "scientific" uses can be considered. The three best projects will be selected by a jury of scientist, space engineers and artists this October, for prizes of up to \$20,000. There will also be a junior category for under-15s. Actual construction of the winners' projects, however, is not guaranteed.... Further information may be obtained from: La Tour Eiffel de l'Espace, Champ de Mars, 75007 Paris, France.

orang utan, Dou-dou, and a chimpanzee, Chloé, which were exchanged for Japanese macaques from Inuyama. The Inuyama centre, funded by the Ministry of Education, Science and Culture (MESC), was set up as the nations's key primate research centre. But after being recruited by MESC to continue her research on cognitive ethology Brésard soon found herself embroiled in an arguement.

The monkeys were confined day and night for several months in makeshift chairs with a stock-like clamper device around their necks so that electrical recordings could easily be taken from their brains. The monkeys' necks became ulcerated and their testicles degenerated because of the prolonged immobilization.

Horrified by the monkeys' condition, Brésard requested their immediate release, but she was told by members of the psychology department to which she belonged that they had "no right to ask the researchers to release their monkeys as long as they considered it essential for their experiments". Instead, Brésard was nominated to join an informal working group on animal welfare set up by associate professor Toshio Asano of the psychology department who also chaired the institute's ad hoc animal welfare committee. But, frustrated by the working group's prolonged deliberations, Brésard turned to the French magazines, Geo and La vie des bêtes.

No sooner did the articles appear than the Japanese embassies in France and Switzerland were inundated with complaints and the Foreign Ministry asked MESC to investigate. But the Inuyama researchers pointed out that they had been acting within Japanese law and government guidelines.

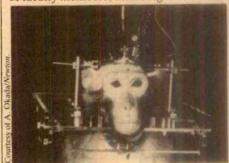
Whereas Western nations have been tightening up guidelines and introducing new laws, Japan still has regulations that are full of loopholes and leave interpretation largely to the "common sense" of the researcher. For example, in Article 5 of the guidelines issued by the Prime Minister's office in 1980, researchers are told to "minimize the pain and suffering of laboratory animals by, for example, giving anesthetics", "provided this does not interfere with the purpose of the experiment".

The regulations have no teeth. There is no system of licensing or government inspection to check that researchers follow the guidelines, no process of review of research proposals, and no requirement to report the number or type of animals used or the experiments carried out. Hence the fine of up to 30,000 yen (£120) for cruel treatment has little chance of being levied.

There are no vociferous anti-vivisectionist groups in Japan campaigning for

animal rights, as there are in the West. The Japan Animal Welfare Society is a moderate group that seeks to reduce experimentation on animals and to alleviate their suffering.

Recognizing that Japan lags behind in animal welfare, the Inuyama ad hoc committee headed by Asano drew up guidelines for the care and use of laboratory primates based on the US National Institutes of Health 1985 guide. Published in April shortly after Brésard left, the Inuyama guide is backed up by an institutional monitoring committee composed of faculty members, including at least one



who is involved in animal experiments; one who is not; and a veterinarian.

With implementation of the guide, conditions for the restrained monkeys have been considerably improved at Inuvama, says Asano. Chairing beyond 24 hours is no longer permitted without consent from the monkey committee, and no requests for chairing beyond 24 hours. have so far been made. When the monkeys are not being used for experiments. attempts are made to bring them together in social groups. Minimum cage sizes are defined and, although cages at Inuvama do not all come up to standard, Asano says they will soon get the 300 cages they require, despite a price of about 150,000 yen (£600) per cage.

The Inuyama guide is now attracting attention. At the annual convention of the Primate Society of Japan in Nagoya in mid-June, members were urged to draw up their own guidelines following that of Inuyama. But the Inuyama guide avoids discussion of an issue that has dominated debate in the West; pain in laboratory animals.

A symposium on this topic was held in Tokyo at the end of May by the Laboratory Animal Society of Japan, but the participants tied themselves up in semantic knots and no significant progress was made.

Although changes have now been made at Inuyama, other institutes are under no obligation to adopt new guidelines. Nor is there any way of checking up what conditions are like in private industry, where there is no requirement to report experiments. Changes in legislation are not at present being considered by the government, but there may be changes in attitude if concerned groups continue to grow in strength.

David Swinbanks

US nutritional research

Your grant is what you eat

Washington

NUTRITIONISTS find themselves divided on the activities of United Sciences of America (USA) Inc. Founded just six months ago, USA intends to put some \$1.2 million a year into nutritional research; the trouble is that the company's profits come from "network marketing" of "revolutionary dietary supplements". Despite USA's distinguished scientific board, many experts are sceptical about the value of dietary supplements for the general population and object to USA's advertising.

USA was founded last year by Robert M. Adler, a telecommunications entrepreneur. Its promotional videos make much of the claimed scientific merit of USA's preparations; a slickly produced 1985 video features views of huge computer rooms where research data is stored, and brief shots of the covers of Nature and the New England Journal of Medicine. The scientific advisory board includes two Nobel prizewinners and other well-known medical researchers. Critics allege, however, that not enough is known about some of the ingredients to recommend dietary supplements.

In addition to a retainer (at least for some members), members of the scientific advisory board get first shot at USA's research awards. Two weeks ago, at a meeting at its Dallas headquarters, USA approved its first twelve awards totalling \$600,000, of which several went to board members. But the meeting also spawned disagreement among the advisory board on the company's use of members' names for endorsements. One member, Dr Alexander Leaf of Harvard Medical College, threatened to resign unless his name was removed from endorsements.

According to Dr Jeffrey Fisher, USA vice-president for product development, the company will eventually offer a nutritional plan, a weight management plan and an aerobic fitness plan. The catchword is "optimal health". So far only the nutritional plan is on the market: it consists of a preparation of vitamins, trace elements and amino acids billed as rich in anti-oxidants; a "fibre energy bar" that includes a complex mixture of carbohydrates and a proprietary blend of cotton seed and surimi protein; a calorie control formula, again with special proteins; and a marine lipid concentrate containing omega-3 fatty acids, antioxidants and garlic extract.

Many of the ingredients are the subject of legitimate research. But many nutritionists question the strength of the evidence on which USA's products are based. Some, such as Dr Robert Good of the University of Southern Florida, chairman of the scientific advisory board, be-

lieve that indirect evidence is sufficient to recommend that the public take, for example, fish oils. But others, such as Henry Kamin of Duke University, who recently chaired a controversial National Research Council dietary study, believe that to offer fish oil supplements to the general public is "grossly premature".

Kamin — and many others — believes that epidemiological evidence (such as the low rate of heart disease among eskimos who eat a lot of fish) should not be used as a basis to "stuff people with fish oils" until possible hazards of long-term use are evaluated. Even if they could benefit some individuals, nobody has any idea of what would be a good dosage of omega fatty acids, according to Kamin. One of USA's recent research awards was to Leaf to investigate the effects of different levels of fish-oil supplements on blood chemistry.

Kamin also argues that there is no need for special protein blends with good amino-acid balance when the typical US citizen daily eats more than three times the amount necessary. He questions the relevance of the scientific advisory board's expertise; although a celebrity cast, few if any members are primarily nutritionists, a point admitted by Fisher.

Other features of the USA products are also contentious. Victor Herbert of Mount Sinai School of Medicine says there is "no evidence" that taking supplementary doses of vitamins E and C above national recommended daily allowances has any protective effect against cancer, a conclusion reached by the National Academy of Sciences in 1982.

USA's advertising is careful not to make any claims about specific health benefits, which would in the eyes of the Food and Drug Administration make the product a drug needing trials for safety and efficacy. But the 1985 video, which dwells darkly on environmental pollution and blames it for high heart disease and cancer rates, manages to suggest directly that USA's products might counter these hazards.

Leaf, chairman of the department of preventative medicine and clinical epidemiology at Harvard Medical College and a member of the scientific advisory board, is quoted in USA promotional materials as saying that "the four formulas of USA Inc. together constitute a nutritional plan that is the finest and most complete I have ever seen". But Leaf denies making such a statement and says he thought he had been "a little naive" in his dealings with USA Inc., having been told only that he would serve as a consultant. Leaf said he was threatening to resign from the advisory board unless his name was removed from product endorsements and that other members had made similar protests. The American Heart Association's logo is also apparently used in the video without permission.

USA's sales method is a source of concern to some. Described by Fisher as "as innovative as the programs", it involves individuals becoming "associates" of the company and then recruiting more associates — similar to "pyramid selling". The Food and Drug Administration points out that it is difficult to police claims made for products sold in private. But Dr Robert Morin of the University of California at Los Angeles, another member of the advisory board, contends that the instructional materials provided by USA Inc. make "network selling" preferable to simple counter sales.

Good says the dietary programme has been established "within conventional scientific wisdom" to provide "undernutrition without malnutrition". Good admitted that he had not seen USA's promotional video. But he is a believer in the benefits of anti-oxidants, which may inhibit some ageing processes. Good says he has been able to forestall death of genetically short-lived animals in all species so far studied, and believes there are sufficient data to promulgate cautiously dietary supplements to the public. And Good believes that a weight-reduction plan must include protein supplements.

Fisher admits that early videos were "too hypish" and says later versions were toned down. And he admits that there is debate about some nutrients in USA products but says science is coming around to USA's point of view.

Tim Beardsley

Young Hungarian

SZEGED University's Department of Natural Sciences has called on the Hungarian government to cut military spending and uneconomic large-scale projects and to devote the money saved to improving higher education and the standard of living of young graduates. Although such issues have been raised before in Hungary's underground press, this is the first time that they have been explicitly stated in an official context, at least since the discussions that led up to the 1956 uprising.

The Szeged group, which consists of young academic and graduating students, submitted its proposals to the Congress of the Hungarian young communist movement in May. Officially they were ignored and, according to some unconfirmed reports, copies of the university newspaper, Szegedi Egyetem, which carried the proposals, have been impounded.

Even apart from the proposal that military spending should be "rationalized", the Szeged document is bound to be controversial. One proposal is that the univer-

Information technology

Where next for Alvey?

Britain's Alvey programme, aimed at strengthening the information technology industries through collaborative research with the universities, appears to be at a critical stage. Last week's Alvey conference made clear that the programme, now halfway through its five-year life, has produced enough successes to excite government, universities and industry. But nobody is sure how to keep the momentum going to ensure long-term industrial success.

The 600 delegates at the conference at the University of Sussex were clearly optimistic about the future. The Alvey programme is a unique attempt to break down the barriers between the universities and industry in key areas of information technology: very-large-scale integrated circuits, software engineering; intelligent knowledge-based systems; and man/ machine interfaces. To ensure industrial involvement, even the smaller basic research projects carried out at universities must have an industrial "uncle" - someone from industry who will alert colleagues when an idea begins to look worth industrial development.

Three hundred and three projects are now under way at a cost of almost £200 million to the government plus a somewhat smaller amount from industry. One hundred and eight companies are participating alongside 53 universities and polytechnics (Imperial College, Edinburgh and Cambridge form the first league), a

academics protest

sities be given real, not merely symbolic, control over their budgets and the right to choose their own officials, rather than have them appointed by the state.

A further suggestion is that student grants should be pegged to keep pace with inflation and that less weight should go to means testing of family income. This would favour better-off families and is liable to be opposed by Party hard-liners.

Another proposal raises the whole question of the relationship between workers and intellectuals in a socialist state. In Hungary, entitlements to annual leave, pension rights and priority for housing are all related to length of service at a particular enterprise. Young graduates entering the system thus find themselves disadvantaged because they are five years behind in acquiring benefits compared with a worker who entered employment direct from school. The Szeged group is now asking for the years of study to be counted in the employment record — a seemingly modest proposal but one with clear political overtones. Vera Rich level of cooperation that Minister of State for Information Technology Geoffrey Pattie described as "probably unprecedented in peacetime". But as John Alvey, who originally proposed the programme, put it, "we have won some victories, but haven't won the war". The test will be the international marketplace. If saleable products cannot be produced, then Britain's industrial position will fall back still further.

Much discussion centred on what must be done to prevent this happening. Those actively involved in research tended to concentrate on the details: is there not, for example, an easier way to cope with drawing up cooperative agreements? Big delavs have been caused. And would it not be wiser to have a central research institute instead of distributing work throughout the participating laboratories? Advantages of the former are that it quickly creates a critical mass of expertise and avoids duplication. But it can too easily become an ivory tower. The really big questions, spelled out by Pattie, were of government support and the balance between national and international programmes. Although everyone would like funding to continue, the pre-competitive research of Alvey must be commercially exploited and the postgraduates who have been trained persuaded to move on to industry.

For the balance between international and national funding, critical decisions must be made soon. The huge industrial high-technology programmes, ESPRIT and RACE (for information and communication technology), lie within the European "research and development framework programme", designed to shape policy for the next five years. The outline of the programme is now before the European Community's science ministers. Where will the post-Alvey programme fit? According to Pattie, international programmes cannot substitute for national ones, for the latter are necessary to give strength in collaborative projects.

A formal "After Alvey" committee, chaired by Sir Austin Bide, has already been set up and will report in the autumn. Submit your evidence to Sir Austin, said Pattie: "no decision has been predetermined" and "real decisions" will be made. But as one iconoclast at the meeting put it, "can any number of collaborative programmes be a substitute for the rationalization of Europe's information technology industries?" Without markets and companies of the size found in United States and Japan, can Europe's excellent research ever be successfully exploited?

Alun Anderson

Chinese science

Legal protection for scientists

CHINA is to have a new law to protect societies from "outside interference". Addressing the third national congress of the Chinese Association for Science and Technology (CAST) last month, Song Jian, minister in charge of the State Science and Technology Commission, noted that the proposed law would give "official status to scholarly societies and define their role". It would regulate their relationship with the Communist Party, the government and state-owned collective and individual enterprises. Song said, as well as guaranteeing that their work could proceed "along normal lines".

China has 138 learned societies and organizations with 1.8 million members, who, in their turn, according to Song, are "in touch with a further five million scientists and technicians". The need for legal protection for scientific and learned research has been much discussed in the Chinese media during the past two months, in connection with the thirtieth anniversary of the launching of the "double hundred" policy ("Let a hundred flowers bloom, let a hundred schools of thought contend") which in recent years has been restored to official favour. The Constitution of the Peoples' Republic of China (Article 47) stipulates that "citizens have freedom to engage in scientific research, literary and artistic creation and other cultural activities", but this did not save scientists and scholars during the cultural revolution. Promulgating a specific law to cover learned activities, however, is felt to be sufficient, in the words of the People's Daily, to "ensure the implementation of the 'double hundred' without any intervention by or hindrance from either 'leftist' or 'rightist' tendencies".

The new law, and the "double hundred" policy itself will not give the scholars total independence. Social scientists, economists and philosophers will be allowed, within their learned environments, to investigate and consider non-Marxist theories. If they are asked to provide recommendations for practical implementation in production or society, however, they must base their proposals on sound Marxist principles. The natural scientists come off somewhat better, since, according to the Peoples' Daily and other leading commentators, the natural sciences can only flourish properly when kept clear of misleading ideological and philosophical labels. Frequent reference has been made recently to the Qingdao genetics forum of August 1956, which broke the monopoly of Lysenkoism in China as the exemplar of the proper "contention" of scientific ideas. Vera Rich

Why not move RGO to Manchester?

SIR—Alun Anderson's News article (Nature 321, 799; 1986) on the move of the Royal Greenwich Observatory (RGO) neglected to report that the Science and Engineering Council (SERC) also considered the possibility of moving it to Manchester. In fact, Manchester presented a powerful case, so why will RGO not move here?

SERC found the merits of Cambridge and Manchester to be finely balanced but simply considered the Cambridge case "to be even stronger". A world-beating centre of excellence is clearly what it was seeking, but that should not automatically favour Cambridge. The recent review by the University Grants Committee (UGC) rated Manchester's Physics and Astronomy Department, including Jodrell Bank, as outstanding, and here RGO would have formed the nucleus of a centre every bit as excellent as that we can expect in Cambridge. Did a beleaguered regional university just lose to the charisma of the old establishment?

An important inconsistency in the council's reasoning is that while claiming to be planning for the 1990s, it has allowed itself to be unduly influenced by the short-term consideration of minimizing disruption. Moreover, it does not give any reasons why the disruption caused by a move to Manchester should exceed that of a move to Cambridge. Could this be prejudice by the staff of RGO itself?

Alun Anderson's worries about costs are very relevant, but here Manchester had a strong advantage which was ignored. Construction of a new building to house RGO in Cambridge was apparently considered no more expensive than minor internal alterations to the suitable vacant premises in Manchester.

The council blithely asserts that both Manchester and Cambridge "have excellent communications" - sweeping Manchester's overwhelming superiority in this regard under the rug. The RGO staff will have to make regular trips to the new observatory in the Canary Islands; Manchester's international airport offers frequent direct flights and is just 20 minutes' drive from the university, whereas Cambridge to Gatwick airport is a long and awkward journey. It will be many years before Stansted will offer a service as good as already exists from Manchester. In addition, Manchester's rail and motorway connections to the rest of the country are far superior, which, together with its more central geographical location, would make RGO here much more readily accessible to astronomers around the country.

But the most disappointing aspect in my view is the missed opportunity for some positive action to redress the north/south

economic imbalance. The number of new jobs at stake is rather small, but the relocation of an influential and sophisticated scientific research organization to the north-west would be a morale-boosting statement of confidence in northern science and industry. Its demands for local specialized high technology, computer software and so on would be of much greater industrial benefit here than in the already thriving area around Cambridge.

We may never know what clinched the decision in favour of the old university and the south. But we should be told because it caused extra expense and could be to the lasting detriment of British astronomy outside Cambridge.

JERRY SELLWOOD

Department of Astronomy, The University, Manchester M13 9PL, UK

Prehistoric protection

SIR—The letter by Fernández and others' on radon in the Altamira cave shows how lax the standards of radiation safety were in Europe before 10,000 BC. Assuming that they worked a 40-hour week, I estimate that the palaeolithic painters received an annual radiation dose of 130 mSv from radon daughters. This would not be permitted under the Euratom legislation to which the European Community is now subject²: the dose limit for workers is 50 mSv in a year and indeed all exposures must be kept as low as reasonably achievable.

M.C. O'RIORDAN National Radiological Protection Board,

Chilton, Didcot, Oxfordshire OX11 0RQ, UK

Fernández, P.L. et al. Nature 321, 586 - 588 (1986).
 Official Journal of the European Communities, No L246/1, 17 September 1980.

Speaking up

Sir—David Swinbanks (*Nature* **321**, 374; 1986) seems to doubt the relevance of the speech I made when accepting the Japan Prize.

An example of scientists not speaking up in time was the destruction by a Christian mob, around AD 415, of the famous library in Alexandria. That event set back civilization 1,000 years.

If third-century scientists had been able to enlighten the public, and if the government and the clergy had spoken out loudly and clearly at every opportunity, that set back would not have occurred. If we do not speak up now, our civilization may be destroyed for more than 1,000 years.

While in Japan, I learned that the United States is expected to provide a great deal of money for research for the Australia

Strategic Defense Initiative (SDI) by West Germany (25 per cent), Great Britain (18 per cent) and Japan (13 per cent). The preliminary budget is \$60,000 million simply for research; development is not mentioned. You cannot blame the British Prime Minister for not refusing a subsidy to the British economy of 18 per cent of \$60,000 million.

President Dwight Eisenhower warned against the military-industrial complex, which has a momentum of its own. It has now extended far beyond the United States.

I also said in Japan that President Reagan has a better chance of achieving a nuclear freeze and a reduction of the nuclear arms race than any previous president. He should be told what scientists feel.

W.J. KOLFF

Division of Artificial Organs, Department of Surgery, University of Utah, Dumke Building, Salt Lake City, Utah 84112, USA

Screwworm fly

SIR—In the past twenty years, despite one or two minor setbacks, the New World screwworm fly, Cochliomya hominivorax, has been eliminated from the southern United States and all but the most southern areas of Mexico. It is difficult to accept that this is due, as suggested by J.L. Readshaw (Nature 320, 407; 1986), solely to climatic conditions adverse to the survival of the fly during this period. It is surely more than a coincidence that this occurred concurrently with the major sterile insect release method eradication campaign in the region.

This campaign, by the US Department of Agriculture, has apparently eliminated this major agricultural pest, which caused losses of many million dollars to cattle ranchers in the southern United States and Mexico.

A related species, Chrysomya bezziana, widespread in South-East Asia and Papua New Guinea, is one of the most serious exotic animal disease threats to Australia. The United States has been most generous in sharing sterile insect release technology. This has enabled Australia to develop methods which it is hoped will be effective in eradicating any incursion of Chrysomya bezziana into this country. Whatever the beneficial effects of climate to the North American programme, the tropical climate in northern Australia has convinced us that rapid application of the US technology would be our major defence response.

R.W. GEE

Australian Agricultural Health and Quarantine Service, Department of Primary Industry, Barton, ACT 2600, Australia

Anti-darwinism in Japan

SIR-L.B. Halstead's article1 on the socalled Imanishi phenomenon, the popularity of the writings of Kinji Imanishi, emeritus professor of Kyoto University, among intelligent laymen in Japan, attempts to relate the phenomenon to the character of Japanese society and its scientific community. Imanishi points out that the competition and selection in Darwin's view of nature derive from the cultural and religious ethos of Western paternalistic society, whereas the Japanese view is maternal, one that sees the inherently harmonious nature of the living world.

After holding a visiting professorship at the department of geology and mineralogy of Kyoto University, Halstead explained the Imanishi phenomenon by pointing out that the present world, Japan in particular, is demonstrably a world of competition, struggle and disharmony. In such a world or society, Halstead writes, "Imanishi's theory can satisfy the dreams and aspirations of people in a desperate rat-race, serving as a dream-scape sentimentality. Unhappily it has no place in scientific understanding of the real world."

Halstead's observation is rational, axiomatic and persuasive. Yet it creates a certain disharmony in the minds of "average laymen" in Japan. It reminds us of Niels Bohr, who extended his complementarity principle in quantum mechanics to the realm of human concerns beyond natural science. He states that the rational scientific approach is only one way of dealing with the world around us. A given approach seems fragile and senseless when applied within the framework (cultural tradition) of another, but is forceful and convincing within its own frame².

One of the central concepts of Imanishi's evolution theory, the principle of life-style partitioning which later evolved into the idea of the harmonious nature of the living world, arose out of his early research on aquatic insect larvae, mayflies in particular, in freshwater streams. On the basis of recent researches in freshwater, marine and terrestrial habitats in experimental ecology which demonstrated that interspecific competition takes place in 90 per cent of all cases studied, Halstead claims that the statistical foundation of Imanishi's theory no longer stands. He adds: "this seems to have little effect on either the standing or on the public reception of Imanishi's ideas so long as he states he is not an ecologist, since then ecologists cease to discuss his theories. When Imanishi further states he is not a scientist, fellow scientists no longer feel there is any need to discuss his ideas." Thus Halstead concludes his article with the statement that vigorous debate and scientific confrontation are not part of the cultural tradition in Japan"... originality and innovation flourish in secret enclaves — Kyoto University saloon and coffee houses - beyond the experience of the ordinary Japanese, condemned, as they are, to the rigid authoritarian feudal society that masquerades as one of the advanced nations of the world."

My understanding is different. When Imanishi states he is not an ecologist, he is warning with A.N. Whitehead³ that the narrowness in the selection of evidence in science is the chief danger to the construction of a holistic world view. When Imanishi states he is not a scientist, he is proposing that the ultimate concern and responsibility of a scientist should be to free contemporary intelligent laymen from their cultural fragmentation by making them more conscious of the way in which art, morality, religion and science have become specialized, censorial, constrictive to the unbroken wholeness of our cultural experience.

As Halstead points out, the fundamental divide in man's view of the evolution of life has been the degree of emphasis placed either on observed variations among individuals or on the features held in common. Then the harmonious nature of the living world exemplified by the phenomenon of altruism and habitat segregation becomes susceptible to an explanation in terms of natural selection. It would then be a responsibility of a careful scientist to try to replace words such as competition and selection by more objective terms or words that do not change the essential scientific tenets of darwinism but greatly change their aesthetic, moral and religious connotations. Without a critical usage of the words, the notion of the survival of the fittest, for example, would become a tautology of the selection of the selected or the survival of survivors1.

It is encouraging that the progress of molecular genetics over recent years has developed new concepts such as evolution by gene multiplication' and concerted or coincidented evolution which are not inconsistent with Imanishi's ideal of the evolution of the harmonized holospecia in which all the individuals of a species evolve simultaneously when the time becomes ripe.

Needless to say, we are only beginning to understand the origin and the evolution of life. At present, we do not even know whether the evolution was gradual or sudden. As a rule, darwinian selection is more important over long periods of time and Motoo Kimura's picture of molecular evolution by random statistical fluctuation without selection (neutral theory)⁷ is more important over short periods. In reality the evolution must have been a complicated process with incidents of rapid change (punctuated equilibrium - development in bursts of evolution)' separated by long periods of slow adaptation.

Finally, one of the persistent concerns of intelligent laymen in Japan since the time of the Meiji Restoration (1868) has been why science in the modern and current sense emerged in a restricted area of the world (Western Europe) and in a restricted period of time (early Middle Ages). It is commonly held that the synthesis of the Judeo-Christian conception of open-ended time and the Benedictine Order's motto "laborare est orare" lent progress and activism to the course of the history of Western civilization. We agree with Halstead that one of the secret enclaves of Kvoto University besides coffee houses, the Institute of the Humanities, where Imanishi's basic ideas and concepts took shape, was modelled after a medieval monastery in feudal Europe, though not of genuine Benedictine style.

Noboru Hokkyo

Bioenergy Division, Energy Research Laboratory, 1168 Moriyamacho, Hitachi, Japan 316

- 1. Halstead, L.B. Nature 317, 587 589 (1985)
- 2. Weisskopf, V.F. Physics Today December 1985, 36-41 3. Hall, D.L. in Buddhism and American Thinkers (eds. Inada, K.K. & Jacobson, N.P.), 14-15 (State University of New York Press, Albany, 1984).
- Eigen, M. Naturwiss, 58, 465-523 (1971)
- Ohno, S. Japan J. Hum. Genet. 26, 97 103 (1982). Ohta, T. Genet. Res. Camb. 41, 47 53 (1983)
- Kimura, M. Nature 217, 624-626 (1968)
- Gould, S.T. & Eldredge, N. Paleobiology 3, 115-119

Aussie disclaimer

SIR-With reference to the News and Views article by Tony Thulborn entitled "Taxonomic Tangles from Australia" (Nature 321, 13; 1986), I wish to state that The Australian Journal of Herpetology and its Supplementary Series have no connection whatsoever with any of the Australian Journals of Scientific Research

AJSR is a series of 10 journals published by the Commonwealth Scientific and Industrial Research Organization in collaboration with the Australian Academy of Science. The biological science journals in this series are The Australian Journal of Botany and its Supplementary Series, The Australian Journal of Zoology and its Supplementary Series. The Australian Journal of Agricultural Research, The Australian Journal of Biological Sciences. The Australian Journal of Marine and Freshwater Research, The Australian Journal of Plant Physiology and Australian Wildlife Research.

R.W. CROMPTON (Chairman, Board of the Australian Journals of Scientific Research) Australian Academy of Sciences, GPO Box 783, Canberra, ACT 2601, Australia

Roman Khesin-Lur'e

SIR-Vera Rich, in her comments on the Lenin prizes for science in the Soviet Union (Nature 321, 6; 1986), was very sceptical about the merit of this award given to Dr R. Khesin-Lur'e, merely because the award citation dated his publications in biochemical genetics from 1960 when "Lysenkoism was then in full swing". Rich also stated that "it would be interesting to know where Khesin Lur'e published his work at that time, and what part, if any, he played in the overthrow of Lysenkoism". Unfortunately, my old friend R.B. Khesin-Lur'e is unable to answer these questions. The prize was given to him posthumously. Because he was indeed a very prominent scientist, I hope that my brief reply may serve as a short obituary.

Roman Beniaminovich Khesin-Lur'e was born in 1922 and graduated from Moscow University as a geneticist in 1945. His PhD study was carried out under the supervision of the prominent Soviet geneticist A.S. Serebrovsky. In 1948, immediately after Lysenko's "coup", Khesin-Lur'e was dismissed from Moscow University. In 1949-53 he worked as an ordinary technician at the Institute of Biological and Medical Chemistry in Moscow, and in 1954-59 as a lecturer in biochemistry at the Medical Institute in Kaunas. In 1959, he started research work as senior scientist in biochemical genetics at the biological division of the Institute of Atomic Energy in Moscow, where Academician Igor Kurchatov gave protection to many Soviet geneticists who were not able to find work in the academy system or in colleges of higher education. From 1978, Khesin-Lur'e (who is better known in Soviet literature simply as Khesin) worked at the Institute of Molecular Genetics of the Academy of Sciences of the USSR and was, in fact, a founder of this institute.

It is enough to look through Chemical Abstracts for 1959-65 to find out that R.B. Khesin was able to publish many of his works during the period of Lysenko's domination. They were published usually in journals, such as Biochimija, Medizinskaya Khimija, Zhurnal Vsesoyznogo Khim. Obshestva and in different volumes, such as Aktual'nye Voprosy Sovremennoi Biokhimii, starting from Vol. 1 in 1959 and covered many subjects relevant to biosynthesis of proteins and nucleic acids. In 1960, Khesin published his well known (in the Soviet Union) book Biokhimija Tsytoplasmy (Biochemistry of Cytoplasm), which was published by the publishing house of the Academy of Sciences of the USSR. Khesin-Lur'e did play a very important role in "the overthrow of Lysenko" and did so primarily by his honest and intensive research in an extremely difficult situation. He died from

cancer in 1985, very soon after he was i nominated for the Lenin prize.

Lenin prizes in science are not international and the evaluation of scientific merit for them is, of course, a matter for Soviet scientists to decide. The very fact that Vera Rich has apparently never heard the name Khesin-Lur'e before is certainly not sufficient reason to doubt his contribution to science and his integrity as a scientist.

ZHORES A. MEDVEDEV Division of Genetics. National Institute for Medical Research, Mill Hill. London NW7 IAA, UK

Environmentalism

SIR-David Pearce rightly criticizes the nuclear industry in his review of Tony Hall's book, Nuclear Policy: The History of Nuclear Power in Britain, for having neither the traditions nor the capabilities to handle "environmentalism" when it emerged as a popular and political force. The industry was not alone in failing to appreciate the threat of this movement. It has taken some time for the true motivations of some "environmentalists" to emerge. Many of them seem to be seeking some sort of non-industrial Arcadia irrelevant to the needs of today's world, dominated by the problems of developing countries attempting to achieve some improvement in their living standards in the face of relentless pressures from population growth.

For example, Edward Goldsmith in an editorial in the Ecologist asks "How are we to power our expanding industrial society?". He considers the prospects for oil, coal and renewable sources of energy and concludes "The answer is that there is no alternative (to nuclear power)... no nuclear power — no industrial society... the nuclear power station has become the symbol of the industrial way of life... The industrial way of life is squalid, mediocre and unfulfilling. Progress is an illusion.'

The consequences of such views are well illuminated by J. Gordon Edwards' who points to the enormous amount of damage done by so-called environmentalists using as an example the DDT story. where concern about trace quantities of this material has had untold harmful consequences on malaria eradication programmes.

The world's problems may be soluble through the continuing application of science and technology that has already led to dramatic improvements in infant survival, public health and life expectancy, to a transformation of India from a continent threatened by starvation to a net food exporter, and to the harnessing of nuclear energy to enable the world to survive the depletion of its fossil fuel reserves and avoid the risks of climatic

change from their consumption. They will not be solved by the pursuit of rural Utopias inconsistent with today's population and its aspirations.

The Chernobyl accident should result in a major re-examination of the safety of nuclear plants throughout the world. We must ensure that the lessons of the accident are learned and applied, as happened, at least in the West, after Three Mile Island. But the predictable calls for a run-down of the world's nuclear programmes as a result of Chernobyl is as sensible as a call for the world to do without agricultural chemicals as a result of Bhopal.

P.A.H. SAUNDERS

Environmental and Medical Sciences Division. Harwell Laboratory, Didcot. Oxon OX11 9PS, UK

- Pearce, D. Nature 320, 403 (1986).
- Fearce, D. Nature 320, 403 (1986).
 Goldsmith, E. Ecologist 6, 310 (1976).
 Gordon Edwards, J. Nature 320, 391 (1986).

Sir—The leading article "What future for nuclear power?" (*Nature* **321**, 367; 1986) contained criticisms of Western environmental movements and impugned the motives of their membership.

Surely imprecation via an examination of motives as a substitute for argument is slightly insulting to the readers of Nature or any other journal bent on the promotion of serious discussion.

Apart from the fact that criticism based on an examination of motives is irrefutable in practical terms, it also substitutes mud-slinging for discussion. It is tempting to suggest that the aspiration of the mudslinger is that some of the mud may stick. But mud-slinging merely obscures issues and never contributes to serious debate.

The Western environmentalist movement has raised serious doubts, based on cogent arguments, about the efficacy and safety of nuclear power. It is these arguments that should be addressed; the reasons why the participants raised them, apart from concern with efficacy and safety, are of little significance.

Focusing on this matter, at the expense of arguing your case, results either from the arrogant assumption that environmentalists are of little consequence because of their populist origins and so their views on nuclear power must also be of little consequence, or a tacit recognition that the environmentalist argument presents problems for those who support the nuclear power programme. If the latter, why not admit it, and if the former, shame on you!

BARRIE PEARSON

13 Knoll Cottage Residential Park, Winfrith, Dorchester, Dorset DT2 8LD, UK

Looking for gravitational errors

The idea that there may be forces between macroscopic objects other than those caused by gravity is no longer an outrage. But precisely what is meant remains unclear.

THERE is always a special attraction in the discovery in the published literature of a surprising truth that other people have overlooked. This is no doubt one of the extra reasons why close attention was paid to the announcement earlier this year, by Fischbach et al. that the Eotvos experiments, first published in the 1920s and widely regarded since then as a proof that the gravitational force between massive objects is independent of their chemical constitution, concealed evidence that there is a force other than gravity between ordinary material objects (see Nature 319, 173; 1986). The proposal is not nearly as heterodox as it may at first have seemed. Most obviously, there have repeatedly been suggestions that the constant in Newton's law of gravitation (called G) is smaller when measured in laboratoryscale experiments than the value required to account for geophysical phenomena.

The article by Fischbach et al. originally appeared in Phys. Rev. Lett. (56, 3; 1986). The essence of its conclusions was that the published errors in the Eotvos measurements of the gravitational attraction between different kinds of substances (carried out with a torsion balance) could be accounted for if there is a force with a characteristic range of about 200 m whose strength depends on the baryon number (only roughly proportional to the mass) of the interacting materials. Now the same journal has published three papers which take the argument a little further, but which have the virtue of suggesting how the matter might be settled.

It is not really surprising that effects such as that described by Fischbach et al., if real, should have been overlooked for half a century. In spite of the exquisite accuracy with which it is possible to describe gravitational systems such as planets in orbit about a central mass such as the Sun, these successes cannot exclude the possibility that short-range forces between material objects may exist. Moreover, in systems such as these, where only relative masses matter to a first approximation, uncertainties may be arbitarily accommodated in either G or in the planetary and solar masses. This is one reason why it is notoriously a minor scandal that G is, even now, known a little less accurately than one part in 10⁵.

For the sake of clarity, it is worth recalling the form in which the Fischbach result is put. Most simply, G can be set equal to G_0 , the value of the gravitational constant ensuring that the centres of gravity of the two objects do not change with the oscillation). The oscillation itself was intended to provide a signal of known frequency

at infinity, multiplied by a factor differing from one by the addition of a relatively small distance-dependent exponential term of the form $\exp^{-(rl)}$. The distance lthen represents the scale over which departures from strict compliance with Newton's inverse-square law may be expected. The supposed constant by which the exponential factor is multiplied is a measure of the strength of the non-newtonian effect. The characteristic length was estimated at 200 m, with a possible error of 50 m in either direction. The constant of proportionality is most distinctive for being negative, meaning that apparently gravitational forces are smaller at smaller distances, or that the extra force is repulsive; its magnitude is such as to affect gravitational attraction by a few tenths of a per cent at zero distance.

It is also, of course, possible that some of the uncertainty in the value of G arises because of attempts to reconcile irreconcilable measurements of gravitational forces on the very large scale and the very small. If, indeed, there is an extra force of interaction perceptible over distances of a few hundred metres only, laboratory measurements of gravitation, going back to Cavendish, will differ systematically from those inferred from astronomical observations. Certainly one of the consequences of the reinterpretation of the Eotvos experiments by Fischbach et al. is that future attempts to narrow the errors in measurements of gravitational force will diligently segregate short-range from long-range measurements.

Two of the clutch of three articles now published by Physical Review Letters are, like Fischbach et al., of an archival character. Both David A. Neufeld of Harvard University (56, 2344; 1986) and S. Nussinor of Tel Aviv University (56, 2350; 1986) go back to the records of an experiment by L.B. Kreuzer first published in 1968 (Phys. Rev. 169, 1007; 1968). The objective was to carry out a kind of dynamical equivalent of Cavendish's direct measurement of the gravitational force between two static objects. For this purpose, Kreuzer used as gravitating masses containers with equal volumes of liquid within which were embedded oscillating masses of density equal to that of the surrounding fluid (which is a neat way of ensuring that the centres of gravity of the two objects do not change with the oscillation). The oscillation itself was intended

that, with luck and clever design, might be picked out easily from among the inevitable noise. Kreuzer's objective was to distinguish between the "passive" and "active" or dynamic gravitational fields caused by moving masses; his conclusion was that they could differ by, at most, one part in 20.000.

Both Neufeld and Nussinov now point out that the same measurements can be interpreted in terms relevant to the new Fischbach force. For, by good luck, the fluid in the Kreuzer experiment was a mixture of halogen-containing hydrocarbons different in chemical constitution from the solid rods of Teflon suspended in them. The difference is enough to account for a significant difference, for each unit mass. in baryon number, which is a measure of the content of protons and neutrons in a material (whereas the mass of the same material is the same quantity modified by what the nuclear physicists call the packing fraction, or the nuclear binding energy, of the elementary constituents of the materials).

Both Neufeld and Nussinov now argue that the Kreuzer measurements probably provide a more sensitive test of the implications drawn from the Fischbach analysis than an attempt to repeat the Eotvos experiments as such. Indeed, on various interpretations of the Kreuzer measurements, the intermediate-range field of force suggested by the re-analysis is already a little beyond the bounds of likelihood. Neufeld suggests that if the Eotvos measurements are to be repeated. it would be most profitable to do so at the foot of a tall cliff, where the effects of natural gravitational asymmetry would be most apparent.

P. Thieberger from the Brookhaven National Laboratory (56, 2347; 1986) is even more lyrical on the subject: repeating the Eotvos measurements at the bottom and the top of a tall cliff could be the most sensitive measurements yet bearing on the existence (or otherwise) of the intermediate force. (The University of Bath, sited on the top of such a cliff, is well placed, among others.) Given this enthusiasm it is certain that there will now be a host of proposals for the re-measurement of gravity by classical devices. The driving force may be the prize of pinning down the intermediate force. It must be hoped that one by-product will be the even more important definition of an accurate value John Maddox

Immunology

T-cell receptor: gamma gene product surfaces

from Miranda Robertson

THERE are various phenomena in cellular immunology that might demand a second antigen receptor on the surface of T lymphocytes; and as a T-cell specific receptor gene not encoding any part of the known antigen receptor, the gamma gene might have been expected to account for one of them. In fact, however, as has been remarked at intervals in these pages^{1,2}, it has been extraordinarily difficult to find out what the gamma gene is for; and until now, no protein product had been isolated to provide clues. On pages 145 and 179 of this issue34 two groups report the detection of the gamma gene product in a receptor complex on the surface of human T lymphocytes; and a third paper shortly to appear elsewhere' describes what is almost certainly the same putative receptor but without the evidence that it contains the gamma chain. The data in these reports suggest that the gamma gene is expressed on a small subset of circulating T cells; but there is no obvious way of fitting the gamma chain into any of the immunological phenomena still awaiting a biochemical basis. Before explaining how the receptor came to be detected and why it is difficult to reconcile with any of the roles envisaged for it, I shall briefly recapitulate what is known of the genes encoding the antigen receptor of T cells.

Of three functionally defined subsets of T cells, two — the helper and cytotoxic cells - are now known to express a receptor that is a heterodimer comprising one alpha and one beta chain, each encoded by a gene that is assembled by somatic rearrangement from a large and diverse pool of separate gene segments. This device for generating combinatorial diversity is familiar from immunoglobulin genes and seems to be the hallmark of those surface structures of lymphocytes that are responsible for specific antigen recognition. It is by that criterion alone that the gamma gene has been presumed to participate in the specific recognition of antigen.

The gamma gene was discovered fortuitously in the course of an attempt to isolate the alpha-chain gene (for which it was mistaken), and seems to be essentially similar in structure and organization to the alpha and beta genes, though with significantly more limited variability. There is no firm evidence that its expression is associated with any particular functional subset of T cells; and indeed in most mature T cells it is abortively rearranged—that is, the assembled gene segments

give rise to a transcript that cannot be translated into protein. This and the fact that it seems to be transcribed at relatively high levels early in thymic ontogeny have led several people to focus on the possibility that the gamma gene product has a specific role early in the ontogeny of T lymphocytes when it is believed that T cells 'learn' their unique pattern of dual recognition. The crucial feature of the Tcell receptor is that it is designed, or selected, or both, so as to recognize antigen only when it is associated on the surface of a cell with a molecule encoded by the major histocompatibility complex (MHC). This means T cells must be capable of activation by binding 'self' MHC when it is associated with antigen, but not when it is on its own. If the gamma chain plays a part in the development of this so-called MHC restriction then it is pivotal to the understanding of cellular immunity.

At this point it is only fair to say that the interesting findings described in the three papers I have mentioned earlier give no particular indication of any such role. The findings themselves are as follows.

The assumption from which all three groups started was that any antigen receptor on a T cell would probably be coexpressed with T3. T3, a multi-chain complex expressed on all T cells, is believed to be responsible for transducing the activation signal when the receptor heterodimer binds antigen. It is closely but noncovalently associated with the alpha-beta heterodimer and any mutation that prevents the appearance of the receptor heterodimer also prevents the appearance of T3 (ref.6). Nonetheless, there are lymphocytes that express T3 in the absence of the alpha and beta chains: they seem to account for about 3-8 per cent of peripheral blood lymphocytes (PBL)3.5. The presumption is that in these cells T3 may be co-expressed with some other receptor, for which indeed some evidence has already been reported'.

The biochemical definition of the receptor complex has however become possible only with the availability of large numbers of these relatively rare cells. As they report in this issue, Brenner et al.' succeeded in growing two T3+ alpha-beta cell lines from the PBL of immunodeficient patients (in normal individuals they are rapidly overgrown by alpha-beta cells); also in this issue, Bank et al. report the cloning of a cell with this phenotype after having selected for T4 T8- cells

(believed to be immature thymocytes); and Weiss et al.5 found a T3+ alpha-betaleukaemia. Much the most detailed biochemical analysis is that of Brenner et al... who report that their cell lines (which are 50 per cent T4-T8- and 50 per cent T4 T8⁺) express T3 in association with two chains: one of relative molecular mass 55,000 (55K) that binds antibodies raised against synthetic peptides representing gamma gene sequences; and a 40K peptide which they designate the delta chain. Bank et al. have a heterodimer in which a 60K protein is associated with a 44K chain that is recognized by the anti-gamma antibodies; and Weiss et al.5 find only a single 55-60K chain which they have not yet tested for reactivity with anti-gamma antibodies.

Clearly there are some discrepancies in the data from the three sources; but they are probably trivial. The difference in the size of the gamma chain identified by Brenner et al. and that of Bank et al. may for example be due to differences in glycosylation. On the other hand, the failure of Weiss et al. to find a second chain for their putative receptor is not surprising: it is not always easy to detect both chains of the established alpha-beta heterodimer; and besides, Brenner et al. and Banks et al. find that the gamma chain is not disulphide-linked to the second putative receptor chain. This distinguishes the new receptor complex from any other antigen receptor and may encourage speculation about the formation of alternative complexes between gamma and, say, beta chains; which brings us to the question of what the receptor is for. Only Bank et al. have functional data: they find that anti-T3 antibodies can induce both cytotoxicity and interleukin-2 secretion in their cloned cells, which thus seem to have the expected attributes of a normal T cell.

There are two cell types still in search of a receptor: natural killer (NK) cells, which may be related to T cells; and suppressor T cells. Do these data fit either of them? NK cells, like the cloned cells of Bank et al., have a T8-T4 phenotype and they are of course cytotoxic; but there is good evidence that they do not transcribe gamma genes.

Suppressor cells belong to an elusive regulatory subset of T cells that do not express the alpha-beta heterodimer that is common to the better-established helper and cytotoxic subsets. Might a gamma-delta complex be the suppressor receptor? Because of the rather ill-defined nature of this subset it is hard to rule this possibility out; but suppressor cells might be expected to constitute more than 3-8 per cent of PBL, and there is no obvious reason why, if cytotoxic and helper cells can use the same pool of receptor genes, suppressor cells should need a different one.

Finally, what of the postulated role of the gamma chain in T-cell ontogeny? It

cannot be excluded. But it is very difficult to imagine how an immature thymocyte expressing a given gamma-delta heterodimer could be selected for the properties of a subsequent alpha-beta heterodimer: so gamma would have to be co-expressed for at least some of the time with alpha or beta or both (and indeed a scheme of this sort is envisaged in one of the theories on the early role of gamma9); however there is no evidence that this occurs and Brenner et al. and Bank et al. know there are no functional alpha or beta transcriots in their cells while Weiss et al. find beta transcripts but there is no evidence that they are functional. It remains possible nonetheless that the alpha and beta genes are functionally rearranged later and a two- (or one-and-a-half10) receptor system might operate at some stage in ontogeny.

Co-expression of gamma and the alphabeta heterodimer as the basis for dual recognition of antigen and MHC in mature T cells¹⁰ can probably be excluded

because dual specificity for MHC and antigen can be conferred by transfection with the alpha and beta genes alone".

One would have thought there was already quite enough cellular immunology to satisfy any demand for a phenomenon to fit a molecule; but it begins to look as though to understand the gamma gene it may be necessary to invent still more of

- 1. Gefter, M. & Marrack, P. Nature News and Views 321, 116
- (1986). Robertson, M. *Nature News and Views* **317**, 768 (1985).
- Brenner, M. et al. Nature 322, 145 (1986). Bank, I. et al. Nature 322, 179 (1986).
- Weiss, A., Newton, M. & Crommie, D. Proc. natn. Acad. Sci. U.S.A. (in the press).
- Weiss, A. & Stobo, J. J. exp. Med. 160, 1284 (1984). Bushkin, Y., Kunkel, H.G., Pernis, B. & Wang, C.-Y. in Cell Biology of the Major Histocompatibility Complex
- (eds Pernis, B. & Vogel, E.) 173 (Academic, New York,
- Ritz, 1. et al. Science 328, 1540 (1985).
- Raulet, D.H., Garman, R.D., Saito, H. & Tonegawa, S. Nature 314, 103 (1985). 10. Pernis, B. & Axel, R. Cell 41, 13 (1985).
- 11. Dembic, Z. et al. Nature 320, 232 (1986).

Miranda Robertson is Biology Editor of Nature.

Particle physics

Particles and the Universe

from Neil Turok

COSMOLOGY is now the main arena in which fundamental theories of particle physics can be tested — an exciting stream of data on the large-scale structure of the Universe is just beginning to appear. It is also interesting that particle physics experiments designed to detect the 'dark' matter in the Universe directly should become operational in the next few years. Developments in these areas were discussed at a recent meeting*.

The most recent observations support earlier indications that the Universe has a lot of structure on quite large scales. This is very important for theories of particle physics. In most theories the matter has not moved about much on these scales since the Big Bang and so the observations provide a fairly direct 'window' on what the very early Universe was like.

Five years ago, the Bootes void, a region about 60 Megaparsecs (Mpc) across apparently devoid of bright galaxies was discovered. On the average, such a region would contain a thousand galaxies. More recently it was found that clusters of galaxies are themselves significantly clustered on a similar scale. Now two further observations support the existence of largescale structure.

The first, discussed by Joseph Silk in a recent News and Views article (Nature **320**, 12; 1986), is the result of measuring redshifts of galaxies in a thin slice of the Universe out to 150 Mpc. The measurement reveals a 'foamy' distribution of

Second ESO/CERN symposium: Cosmology, Astronomy and Fundamental Physics, Munich 17–21 March 1986.

galaxies, most of them lying on sheets surrounding large, almost empty holes of radii up to 50 Mpc. A problem with these data is that no correction has been made for peculiar velocities — the redshifts are simply interpreted as being the result of Hubble flow. Peculiar velocities produced by local gravitational infall can produce such sheets as artefacts. But even if this is the explanation, the data seem to indicate large coherent velocities in the distribution of galaxies over large scales.

The second observation confirms this point of view. Richard Bond and Sidney van den Bergh described in a recent News and Views article (Nature 320, 489; 1986) a large region of radius about 50 Mpc around our Galaxy that appears to be moving coherently with a velocity of about 1,000 km s⁻¹ relative to the microwave background. This is a significant fraction (about a fifth) of the Hubble flow on that scale.

These observations are bad news for the most popular current theory of the origin of fluctuations in the Universe. This is based on the notion of 'quantum fluctuations' produced by a field in the process of causing an inflationary stage in the very early Universe. One of the early successes of the inflation model was that it predicted a reasonable spectrum, the Z'eldovich spectrum, for the fluctuations. However, inflationary models require an artificial adjustment of parameters to very small values to give the perturbations a reasonable amplitude. There was consensus at the meeting that although inflation re-

mains a very good idea, no aesthetic model in which it is realized has vet been

Quantum fluctuations have several attractive aspects for cosmologists. They are linear, adiabatic and have a gaussian probability distribution. So it is comparatively easy to calculate their effects. Inflation clearly predicts that the cosmology density parameter Ω is very close to unity. In conjunction with arguments from nucleosynthesis, this requires the Universe to be dominated by non-baryonic

The first models to be looked at in detail were universes dominated by hot dark matter such as massive neutrinos, which free stream out of dense regions and erase perturbations on the scale of galaxies. As a result galaxies form much too late. Hot dark matter models appear to predict fluctuations in the cosmic microwave background marginally larger than the observational upper bounds (G. Efstathiou, Cambridge). But some criticism was made of the statistics used in obtaining the bounds (F. Melchiorri, Rome); there is agreement that the bounds usually quoted are too low by a factor of at least two.

The next models were universes dominated by cold dark matter, for example, axions, photinos or quark 'nuggets'. These models have the opposite problem (J. Primack, Santa Cruz). Although galaxies formed early enough, there is very little structure on large scales - in particular the correlations between clusters of galaxies are hard to understand. One way out is to invoke biassing — the idea that visible matter (stars) formed only at the peaks of the underlying matter distribution. Galaxies formed above some threshold, clusters formed at a higher threshold and so on. With a gaussian distribution, this increases the correlations of clusters, although not on scales as large as 50 Mpc. Voids are another possibility. Here, the large-scale structure appears as a statistical artefact of our seeing only a small fraction of the matter in the Universe. The underlying distribution of matter is very smooth, and coherent velocities on the scales which have now been observed were less than 160 km s . With a large degree of confidence, these models now seem to be ruled out.

The main alternative theory of the ongin of structure involves cosmic strings. relativistic defect lines which are predicted to form in the early Universe by many Grand Unified Theories and superstring theories. Loops of cosmic string chopped off a network seem to have just the right properties to seed the formation of galaxies and clusters of galaxies (see Hogan, C. Nature News and Views 320, 572; 1986). Interestingly, cosmic strings are able to produce the required small- and largescale structure in either hot or cold dark matter universes. In the former, small loops of string survive the free streaming and go on to seed galaxies, whereas in the latter, larger loops provide the large-scale structure. Cosmic string theories produce a correlation of clusters of galaxies remarkably similar to what is observed. Detailed calculations of the large-scale coherent velocities produced by cosmic strings have yet to be made. With hot matter these will almost certainly be large enough, and even with cold matter the fluctuations on large scales caused by large loops are much larger than with quantum fluctuations.

There remains the crucial question of the dark matter. Evidence from galactic rotation curves and from the dynamics of galaxy clusters suggests that dark matter does exist, but this is quite consistent with the simplest explanation: an $\Omega = 0.1$ Universe dominated by large planets (Jupiters) (M. Rees, Cambridge). But recent results from the infrared survey IRAS give a measurement of Ω on very large scales of around unity (M. Rowan-Robinson, Queen Mary College, London). If confirmed these results will reinforce ideas of the fundamental simplicity of our Universe, and the question of what the nonbaryonic matter is will become more

Particle physics has already come up with a plethora of candidate particles for the non-baryonic matter, none very well motivated. The massive neutrino received a lot of interest after Lyubimov et al. (Phys. Lett. 94B, 266; 1980) reported a mass for the electron neutrino in the cosmologically interesting range, around 30 eV, some time ago. However, a recent

experiment using more sophisticated apparatus disagrees with this value, setting an upper bound of 18 eV on the electron neutrino mass (K. Winter, CERN). The possibility remains that the Universe is dominated by the (very likely heavier) muon or tao neutrinos.

Some very interesting new ideas for detecting cold dark matter particles have been proposed recently (P. Smith, Rutherford Appleton Laboratory). The axion is probably the best candidate, being very light (about 10^{-s} eV) and very weakly coupled to other matter. Axion decay into two photons can be stimulated by a tuned oscillating field in a resonant cavity, and several experiments to detect axions by this method are under way.

Small pure crystals or lumps of superconducting metal can be used to look for more massive (about 10-1,000 GeV) weakly interacting particles like photinos or sneutrinos. Such a particle colliding with 1 mm³ of silicon at 50 mK would cause a recoil in the nucleus it collided with sufficient to heat the crystal by 5 mK. With existing technology, this can be detected with an accuracy of 1 per cent. A detector containing 1kg of such crystals would be expected to see from 1 to 1,000 events per day if these particles dominated the Universe. The experiments will probably take 2-3 years to set up and will open up a new area of particle physics; at the very least they will provide invaluable information on what the dark matter is not.

Neil Turok is in the Department of Theoretical Physics, Imperial College of Science and Technology, London SW7 2BZ, UK.

Archaeology

Towards a scientific approach

from Patricia Phillips

ARCHAEOLOGY, the study of our past, developed in a humanistic framework, although basic methods such as observation of stratigraphy were borrowed from contemporary sciences. Recently, more sophisticated techniques have been developed and refined to provide a basis for many types of archaeological investigation. But in the United Kingdom more money is needed to keep pace with current excavations and fieldwork and to apply the new techniques to the many artefacts and ecofacts generated by government-funded programmes over the past two decades. This is the message of a new report¹ archaeology must be science-based in fact, not just in name

Many archaeological finds, from whole sites to individual buildings, early industrial structures and assemblages of artefacts and ecofacts, fail to be exploited to their full scientific potential. Much more use should be made, both of established scientific techniques and of newly developed methods, to maximize the information from each archaeological find.

Readers of Nature will be familiar with some of the more recent applications of science to archaeology, such as refined radiocarbon measurement techniques permitting very small samples to be accurately dated. At the accelerator laboratory in Oxford, individual charred wheat grains from Danebury hill fort, England and from Mycenaean Greece have been successfully dated2. The European treering chronology, based mainly on German and Irish oaks, can be traced back more than 7,000 years', and small sequences of tree rings have been used to 'recalibrate' radiocarbon dates from the Neolithic period onwards4. Another dating technique, thermoluminescence, originally used on ceramics and ancient hearths, is being applied to burnt flint, and to windblown sediments: these applications offer new opportunities for dating on Palaeolithic sites, and are particularly useful beyond the present precision of radiocarbon (~ 40,000 years before present). One of the first examples was the dating of two burnt flints from the site of Terra Amata, Nice, to 230,000 years before present⁵.

Aerial photography on various scales is being intensively used by archaeologists. Satellite photographs are generally on too large a scale to be useful, but LANDSAT images have been used to trace broad aggradational features (ancient levee systems) in Mesopotamia⁶. Below-ground features showing up on oblique aerial photographs can now be mapped more precisely by using relatively simple computer programs, for instance, multi-point \ projective transformation7. Geophysical instruments have been refined and developed, and include soil-sounding radar, which has been tested at Sutton Hoo, and side-scan sonar, used in underwater archaeology8. Detailed air photographs or geophysical plots have increasingly been used as the basis for archaeological interpretation, since they are less costly than excavation. Although this is a valid exercise, especially for examining large landscapes, such interpretations need to be checked by excavation.

Where excavation does occur, automatic recording of information on microcomputers is becoming more widespread, and topographical survey before and during excavations has been revolutionized by the electronic distance meter. In 1984 this instrument was used to survey a Lincolnshire long barrow and adjacent excavation trench in only four hours.

Studies of past environments, in terms of soils, sediments, pollen grains and molluscs, are a standard feature of site investigations of all time periods. Increasingly sophisticated and precise techniques have been developed (for example, soil thin-sectioning and diatom analysis).

All the structures which archaeologists excavate, from scarcely visible shadows of postholes and pits to walls of brick or stone, can be characterized or finger-printed scientifically, although frequently the lack of funds prevents this from taking place. Some techniques, such as thin-sectioning or physical chemical analysis, are well established, but need to be expanded to all relevant raw materials in buildings and other structures.

New methods are also needed to study the composition of common artefact types, such as flint tools or some types of pottery, where extensive work using atomic absorption spectroscopy or neutron-activation analysis has only been partially successful in separating out source materials. Early metal artefacts are also difficult to characterize satisfactorily. However, their composition is becoming

better understood, both as larger series are investigated and with the application of lead isotope analysis. This relatively new method can identify the sources of ancient coins and metal artefacts. More recently, inductively coupled plasma spectroscopy has been used to characterize stone, pottery, metal and glass.

During the 1970s and 1980s the scanning electron microscope and its auxiliary tool, the electron microprobe, were increasingly used to investigate the structure and composition of archaeological artefacts and ecofacts, from crucibles and coin moulds to fragments of wood scabbard and sheepskin scabbard lining10. The scanning electron microscope is also useful as an addition to standard microscopy in microwear analyses. These studies of the polishes, striations and residues which indicate how a tool was used, and on what material, have expanded widely in western Europe since the mid 1970s. Although the high magnification of the analyses (at least 280 ×) restrict the numbers of artefacts that can be studied, the method is objective, and has allowed significant progress in the study of stone and bone tools. For instance, the method demonstrated that flint flakes found found beside a Neolithic trackway in the Somerset Levels, United Kingdom, were used to cut reeds and whittle wood".

New methods are being developed to age skeletons12 and to determine past diets. Blood grouping on ancient bone, to identify relationships between ancient mummified or buried bodies, a widely exploited technique, particularly in Hungary, has been applied to few individuals from British tombs. However, the publicity surrounding 'Lindow Man', whose 2,500-year-old body was found in a Cheshire peat bog, enabled a wide range of tests to be applied (from standard X rays and scanning electron micrographs to Xero radiographs, nuclear magnetic resonance, computer tomographic scans and surgery using a fibre optic endoscope) 13 . \square

- 1, Review of Science-Based Archaeology, 1985 (SERC, 1986).
- Gillespie, R., Gowlett, J.A.J., Hall, E.T., Hedges, R.E.M. & Perry, C. Archaeometry 27, 237 (1985).
 Pearson, G.W., Pilcher, J.R., Baillie, M.G.L., Corbett, D.M. & Qua, F. Radiocarbon, Calibration Issue (in the
- 4. Pearson, G.W. & Stuiver, M. Radiocarbon Calibration Issue (in the press).

 5. Wintle, A. & Aitken, M. Archaeometry 19, 111 (1977).
- Adams. R. McC. Heartland of Cities (University of Chicago Press. 1981).
- Haigh, J.G.B. Proc. 22nd Symp. Archaeom. (ed. Aspinall, A. & Warren, S.E.) (1983).
- Joyce, C. New Scient. 108, 36 (1985).
 Northover, J.P. & Gale, N.H. Proc. 22nd Symp. Archive. acom. (eds Aspinall, A. & Warren, S.E.), 284 (1983).
 10. Tite, M.S. et al. and Cronyn, J. et al. in The Archaeologist
- and the Laboratory. Council Brit. Archaeol. Rep. No. 58 (ed. Phillips, P.) 50: 24 (1985).
- 11. Morris, G. Somerset Levels Papers 10 (eds Coles, J.M. &
- Orme, B.J.) 96 (1984). 12. Samson, C. Thesis, Univ. Sheffield (1984). 13. Connolly, R.C. Anthrop. Today 1, 15 (1985).

Patricia Phillips is a Reader in the Department of Archaeology and Prehistory, University of Sheffield, Sheffield S102TN, UK.

Parasitology

Clandestine sex in trypanosomes

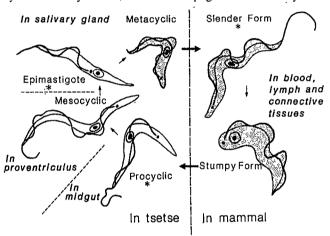
from Keith Vickerman

ALTHOUGH few biologists would question that eukaryotic organisms once needed sex to reach levels of cell complexity denied to prokaryotes, there is room for doubt over whether many unicellular eukaryotes have had cause to retain it. Indeed there is a complacent conviction among those who study them that a haploid genome and short doubling time enable the asexually reproducing protist to look natural selection in the face — and survive without the gene-shuffling benefits of meiosis and syngamy. So the demonstration of hybrid formation in sleepingsickness trypanosomes after transmission by the tsetse fly vector, described on page

A further source of genetic variation in trypanosomes may lie in the kinetoplast (mitochondrial DNA) close to the base of the flagellum (see figure). This unique structure contains about 100 20-kilobase (kb) maxicircles (corresponding to the mitochondrial genome in other eukaryotes) interlocked with several thousand 1-kb minicircles whose sequences alter during vegetative growth, providing another possible system of genome reassortment. The function of the minicircles (other than maintaining the network) is a complete mystery. Maxicircle deletions or disruption of the network are associated with loss of ability of the single mitochondrion.

> which is repressed in the mammalian host, to become activated in the vector.

> Trypanosomes ingested by the bloodfeeding tsetse fly embark on a long and complicated cycle of development multiplication, first in the vector's gut and later in its salivary glands (see figure)4. Hitherto the trypanosome cycle has revealed no obvious gamete or zygote stages. Yet Jenni and colleagues' find that



Developmental cycle of Trypanosoma brucei. Shaded areas, stages expressing variable antigen genes; asterisks, multiplicative stages.

173 of this issue, exposes a surprising and hitherto clandestine activity on the part of these important parasites, and one which calls for reassessment of several aspects of

One reason for doubting the existence of sexuality in trypanosomes was that these organisms have their own ways of generating genotypic diversity, regardless of sex, and these have received much attention in recent years. The tsetse fly-transmitted parasites have met the principal challenge to their survival in the blood of an antibody-producing host by evolving an elaborate genetic mechanism for repeatedly changing the antigenic nature of their protective glycoprotein coat2. Only one of 1,000-2,000 variable antigen genes is expressed at a time and expression can occur only at a chromosomal telomere. The switching process usually involves DNA rearrangements in order to get the new gene into the telomere expression site. These rearrangements provide a system of recombination and reassortment of variable antigen genes during asexual multi-

the mixture of two parental trypanosome stocks followed by tsetse transmission can result in stocks of non-parental phenotype which are heterozygous for parentalhomozygous isoenzyme and variable antigen gene restriction fragment markers. These findings come some years after the observation by Tait5 that the frequency of enzyme electrophoretic variants in a natural population of Trypanosoma brucei conforms to the Hardy-Weinberg equilibrium, suggesting that mating and meiosis occur, and that allele segregation takes place in an orthodox mendelian fashion. Bloodstream T. brucei appear to be diploid6, so if this gene-exchange system is a conventional one meiosis and 'gamete' formation must take place in the vector.

But where in the fly does this clandestine sex occur? The most likely place would be in the salivary glands where the attached epimastigote forms are crowded together under conditions of extreme intimacy; the epimastigote might perhaps furnish gametes, the non-dividing mammal-infective metacyclics derived from them might be zygotes.

The question of trypanosome ploidy will become more confusing with a further publication from groups in Basel and Brussels reporting that Feulgen spectrophotometry gives a metacyclic nuclear DNA content which is half that of the bloodstream form7. The obvious interpretation is that haploid metacyclics give rise to diploid blood infections after mating in the mammalian host. This seems unlikely. Finding a mate would be more difficult in the mammal than in the fly. Furthermore, metacylic-derived clones from heterozygous stocks fail to give rise to homozygous recombinants in blood infections, as they should if metacyclics are haploid, but remain heterozygous*. One possible interpretation of the data presented in this issue, however, is that the hybrids are tetraploid. In order to settle this point their DNA content should now be compared with that of parental stocks.

Clearly, much more work is needed to characterize the new genetic system and the first step should be examination of the progeny from reciprocal back crosses and the generation of an F₂ by mixing different hybrid clones to establish that classical meiosis and recombination occur. So far meiosis appears to be confined to eukaryotes which have conventional mitosis, while trypanosome nuclear division with its non-condensing chromosomes and peculiar spindle apparatus is highly unconventional.

The technique of pulsed-field gradient electrophoresis used for separating small chromosomes has revealed an extraordinarily large number of chromosomes in T. brucei: in addition to several 2,000-kb chromosomes there are about six of intermediate size (200-700 kb) and about 100 minichromosomes (50-100 kb)9. This multitude of chromosomes appears to provide an abundance of telomeres for expression of variable antigen genes. How the countless daughter chromosomes segregate at mitosis is difficult to imagine as electron microscopy shows that the intranuclear mitotic spindle contains only a few microtubules and less than 10 of the structures identified as kinetochores10. Not surprisingly, the intermediate and minichromosomes show considerable variation in size and number between trypanosome stocks and even size variation during successive generations of a

Jenni, L. et al. Nature 322, 173 (1986). Steinert, M. & Pays, E. Br. med. Bull. 41, 149 (1985).

clone. Using existing hybrid progeny it should be possible to examine the inheritance of chromosome variation and of kinetoplast DNA; in the maxicircles of the latter, restriction enzyme polymorphisms have already been identified. so markers are available11

The demonstration of sexuality in Trypanosoma brucei is of importance in the interpretation of epidemiological data. In epidemics of acute sleeping sickness several zymodemes (parasite populations distinguished by their isoenzyme profile) are found in the human population and it now seems possible that such epidemics might arises as a result of genetic exchange between existing zymodemes¹². It will be interesting to see if T. brucei throughout Africa is divided into

reproductively isolated populations. Experimentalists will want to know whether there are restrictions to hybridization; for example, the occurrence of mating types common in other eukaryotes; whether trypanosome sexuality is associated only with late-stage fly infections (most of our knowledge of development in the vector comes from early-stage infections); and whether differences in nuclear DNA content are simply a matter of ploidy or whether gene amplification and chromosome diminution also play a part. Undoubtedly, further surprises are in store

Keith Vickerman is Regius Professor of Zoology at the University of Glasgow, Glasgow G12 8QQ, UK.

Meteorology

European collaboration on dynamic atmospheric fronts

from K.A. Browning, B.J. Hoskins, P.R. Jonas and A.J. Thorpe

METEOROLOGY is a science that depends on the collaborative links between those involved in developing basic theories and in data collection, analysis and forecasting. The European Mesoscale Frontal Dynamics Project, an intensive programme for observing and modelling active cold fronts passing over north-west Europe, should improve both our understanding of frontal structure and the predictions of the associated mesoscale rainfall distributions. The observational phase of the project is planned for the autumn of 1987, and until then theoretical and modelling work will attempt to define precisely the type and scope of the data to be collected. The project will include university groups, national meteorological offices and research organizations in the United Kingdom, France and the Federal Republic of Germany.

An atmospheric front marks a transition zone between air of markedly different properties, such as temperature or moisture content (see Fig. 1). It is remarkable that air flow should generate such sharp zones, with horizontal scales in the atmosphere of only a few tens of kilometres, rather than maintaining a weaker, broader thermal contrast between equator and pole. In the terms of this definition, frontogenesis — the formation of fronts — is a fundamental fluid dynamical problem. Because rain and snowfall are concentrated at fronts, the problem is of considerable meteorological importance. It is now believed that one of the major challenges in weather forecasting is to predict the variations of precipitation on space and timescales of the order of a hundred kilometres and a few hours that I

are typically associated with fronts in midlatitudes. Such mesoscale variations are intermediate between the 1,000-km scale of depressions and the 10-km and smaller scales of individual convective clouds. Although predictions of the large-scale patterns of depressions and anticyclones are

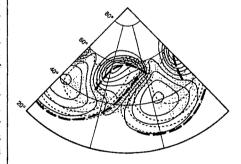


Fig. 1 Model simulation of an atmospheric frontal system¹³. Solid lines, surface pressure contours every 8 mb; dashed lines, low-level temperature contours every 8 K. Areas of strong ascent and descent, respectively, are shown heavily and lightly stippled. Heavy dashed lines, maximum in the low-level vorticity, corresponding to the position of fronts.

now rather accurate even for four days ahead, it is difficult to predict accurately the smaller storms and bands of rain embedded within depressions.

The influential 50-year-old Norwegian model^{1,2} of fronts is now thought to be misleading in several respects: for example, it imagines a depression as forming at a pre-existing frontal discontinuity whereas the modern view is that fronts form after a major depression or cyclone starts to grow. In other words, frontogenesis is now generally thought to follow

Stuart, K. Molec. biochem. Parasitol. 9, 93 (1983).
 Vickerman, K. Br. med. Bull. 41, 105 (1985).

Tait, A. Nature 287, 536 (1980).
 Gibson, W.C., Osinga, K.A., Michels, P.R.M. & Borst, P. Molec, biochem. Parasitol. 16, 231 (1985).

^{7.} Zampetti-Bosseler, F. et al. Proc. natn. Acad. Sci. U.S.A.

Zampetti-bosseier, F. et al. Proc. nan. Acad. 3ct. 0.334.
(in the press).
 Tait. A. et al. Parasitology 90, 89 (1985).
 Van der Ploeg, L.H.T. et al. Cell 37, 77 (1984).
 Vickerman, K. & Preston, T.M. J. Cell Sci. 6, 365 (1970).
 Gibson, W.C., Borst, P. & Fase-Fowler, F. Molechiochem. Parasitol. 15, 21 (1985).
 Gibson, W.C. & Wellde, B.T. Trans. R. Soc. urop. Med. Uro. 26 (21) (1985).

Hyg. 79, 671 (1985).

cyclogenesis rather than vice versa. But the model still holds in some situations for example, when mature fronts approach the north-east Atlantic, a wave cyclone of scale 200 km can develop on a cold front, producing an intensification of rainfall over north-west Europe. The reasons for the generation of these waves will be investigated by the new project.

There have been several significant advances since the Norwegian model was formulated. First, the westerly flow in mid-latitudes was shown to be unstable, leading to the periodic growth of the familiar depressions or cyclones. This predicts 'quasi-geostrophic' theory' rather accurately the horizontal scale and rate of growth of these systems. Although it suggests that in certain regions of the cyclone the conditions are favourable for the formation of fronts, it predicts that it would take an infinite time to produce the observed near-discontinuity. The formation of a front in a short time interval (of the order of one day) was shown to be caused by a non-linear feedback mechanism at the front', neglected in the quasigeostrophic model. This feedback can be described approximately as follows. As air rises just ahead of the front, its rotation about a vertical axis increases essentially to conserve the fluid dynamical analogue of angular momentum. This increase in rotation forces more low-level convergence and hence more ascent. An assumption of this 'semi-geostrophic' model is that the flow remains in a balanced state; that is, the role of high-frequency motions remains merely one of adjustment of the mass and the wind field to each other.

Where, then, are the essential missing links in present-day understanding of the processes responsible for the formation and structure of fronts? The major factor omitted in the semi-geostrophic model is the role of moisture and the consequent clouds and precipitation. Ideas in the past 5 years concerning the basic structure and dynamics of fronts have led to some insight into the production and organization of frontal rainfall. The main questions still to be answered by the new project concern interactions between the proces-

Erratum

In the article by Frank Westheimer (Nature 319, 534; 1986) references 8 and 9 should have read: 8. Milstein, S. & Cohen, L.A. J. Am. chem. Soc. 94, 9158 (1972); 9. Modrich, P. & Zabel, D. J. biol. Chem. 251, 5866 (1976). Professor Westheimer's permanent address is: Department of Chemistry, Harvard University, Cambridge, Massachusetts 02138, USA.

Corrigendum

In the article 'The class number problem' by Ian Stewart (29 May p. 474) the example of Fermat's theorem that "every prime of the form 6n+1 can be written as x^2+3y^2 for integers x and y" should have read: 31 is such a prime, and 31 $= 2^2 + 3.3^2$.

ses responsible for rainfall and those ultimately determining the development of the front.

Other aspects that will be investigated include the assumption that frontal regions are one of the most active parts of the atmosphere with respect to the exchange of air (and pollutants) between the stratosphere and the troposphere. The tropopause, the base of the stable stratosphere, is typically at a height of about 10 km above the surface, but it becomes highly distorted locally in frontal zones. Such are the vertical circulations at fronts that the tropopause has been observed to descend to within 3 km of the Earth's surface as a narrow 'intrusion'. Within the intrusion relatively dry and stable stratospheric air is brought far down from its normal location, to be mixed into the tropospheric air. The relative position of the intrusion with the surface front is thought to help to determine the degree of development or suppression of the convection that produces localized areas of heavy frontal rainfall. It is possible to track the position of the intrusion by monitoring tracers such as ozone or water vapour, using satellite or aircraft-borne detectors.

An essential hypothesis of semi-geostrophic theory, that of balanced flow, has recently been questioned - see the News and Views article by K. Emanuel', who reported suggestions that frontogenesis is halted if the flow becomes unbalanced, that is, if the operation of the non-linear feedback mechanism leading to the sharp front is prevented by the smaller-scale motion at the front. But recent highresolution observations and modelling work do not seem to support this idea".

A special field programme is needed because the theoretical models cannot be tested using only the data collected by routine weather-observing networks. These observations of temperature, humidity and winds in the upper air have a horizontal resolution of about 300 km, whereas fronts may be characterized by a scale of only 50-100 km. The weather radar networks currently being developed over much of western Europe can provide rainfall data and an indication of the presence of dynamical features over a wide range of scales from hundreds of kilometres down to less than 10 km, but these observations are not sufficient to define the dynamical and thermodynamical structure. Satellite cloud imagery also provides some information on cloud structure down to small scales but it gives limited quantitative information on atmospheric structure (see Fig. 2).

The planned experiment will focus on the western parts of the English Channel. southern England and northwestern France, where fronts approaching from the west (the dominant direction of movement) will be relatively unaffected by lift- l



Fig. 2 Satellite photograph (NOAA-9 visible imagery) of the cloud patterns associated with an atmospheric frontal system broadly res embling that modelled in Fig. 1 (courtesy of The University of Dundee)

ing over hills. It is intended that the conventional upper-air observations over the area of the experiment will be enhanced for short periods centred on the passage of fronts.

Extra observing systems will be used to obtain data over the range of scales required. These systems include specially instrumented aircraft such as a Dormer 128 (ref. 10) operated by German scientists to measure winds and turbulence, and a Hercules aircraft, operated by the UK Meteorological Office, with the capability of ejecting dropsondes that can make frequent measurement profiles of temperature, humidity and wind. Various kinds of ground-based Doppler radar, operated by French scientists", will provide detailed three-dimensional wind fields within areas of rainfall as well as continuous wind profiles within the clear air. Powerful computing facilities will support the running of mesoscale forecast models both in the United Kingdom and France These models are still in their intancy and it is expected that the data sets obtained in the new project will enable their basic hypotheses and predictions to be tested and improved.

- Bjerknes, J. Geophys. Publikus over 1, 143-393.
- Bjerknes, I & Solberg H. Gosphis, Par. Los. 11 1
- Charney J.G. J. Met. 4, 135 (1947) Eady, E. I. Tellio 1, 33 (1949)
- 5. Hoskins, B.J. & Bretherton, F.P.J. a.m., Sci. 29, 1
- Browning, K.A. Mer. Mag. 114, 293(11983)
- 7. Emanuel, K.A. Name News and Views M5, 974 (858) 8. Shapiro, M.A. Mon weath Rev. 112, 1634 (1984) 9. Cullen, M.J.P. & Purser, R.J. J. attern. No. 41, 1577
- Vorsmann, P. Proc. 13th Congr. Int. Council Actor. .. Sci. 1226(1984)
 Foot J.S. *NERC News J.* 3, 2 (1986)
 Gilet, M., Sauvageot, H. & Testud, J. *Fig.* 2200, Co. 1
- Radar Meteorol 15 (1984)
- 13. Hoskins, B.J. Quart. J.R. Met. Sci. 169, (15-3)

K.A. Browning and PR Jonas are at the Meteorological Office, London Road, Brack-nell RG12 2SZ, UK, B.J. Hoskins and A.J. Thorpe are in the Department of Meteorologs. University of Reading, PO Box 239, Reading RG6 2AU, ÚK.

Nuclear magnetic resonance

First sight of a single cell

from John Mallard

A PAPER on page 190 of this issue describes the first nuclear magnetic resonance (NMR) images of a single cell. This offers the exciting possibility of fineresolution NMR imaging of cells and collections of cells. The magnetic-field strengths which are used in clinical imaging range from 0.02 to 1 tesla, with about 0.1-0.5 tesla being the norm, but by going to 9.4 tesla and limiting the volume to be studied to a couple of hundred micrometres in thickness, the authors achieve spatial resolutions in the image of the order of 10 to 30 micrometres.

There was much excitement in 1980 when the first clinically useful images of the thorax and abdomen of a patient with multiple cancer deposits were obtained using the technique of NMR imaging^{2,3}. This was the realization of a goal first mooted in the early 1970s (refs 4,5) and bursued in several laboratories since then. By 1984 more than 200 machines were being used in hospitals", with 15 companies manufacturing them.

Nevertheless, I believe that the full potential of this powerful new imaging technique has still to be realized. What is being imaged is the hydrogen protons of water (and fat) in the body, and the parameters which contribute to the formation of contrast in the image are the proton density (or water concentration); the two magnetic resonance relaxation times t_i and t_i ; and the proton movement. The time t_1 is dependent on the interplay of the water molecules and their macromolecular environment, while t_2 is related to the interplay of the water molecules among themselves, and by carefully choosing the sequence, timing and duration of magnetic-field gradients and radio-frequency pulses one can tailor the image to emphasize one or other of these parameters to emphasize one or other aspect of water use in that tissue being imaged.

Because some of the images show vivid anatomical detail of soft tissue, such as the brain, they are immediately compared by radiologists with the images obtained by the X-ray methods, particularly X-ray tomography or X-ray scanning. Naturally, much effort is now being expended in finding which regions of the body and which disease or which abnormality this new imaging technique is better or worse at than these other existing procedures.

Although this exploratory stage is necessary, it is important not to lose sight of the fact that the signals forming the image are from a quite different source than those from X-rays. The X-ray images are formed by differential absorption of

X-rays by the electron clouds of the larger, heavier atoms in the body, whereas these new signals come largely from the nuclei of the hydrogen atoms of the water in the body. The movement of the protons in and out of the imaging volume also influence the signals, and there is now much effort to harness this to show blood flow in major vessels and even to measure the amount of flow, and deviations from it, in these vessels.

No doubt we will now see a rapid exploration of the new NMR instrument described in this issue and a comparison of what it can do with the other micro-

scopic techniques. At first sight this will include the study of material which is alive, and perhaps the really new distinctive feature may be the imaging of the dynamic processes of tissue fluid flow and diffusion. Might not the knowledge gained from the NMR microscope lead us back into attempting to obtain safely a much finer spatial resolution in clinicial images than can be achieved now? Might it also help us to understand the really new contribution of NMR to medicine?

- Aguayo, J.B. et al. Nature 322, 190 (1986).
- Mallard, J.R., Hutchison, J.M.S. et al. Int. Symp. Med. Radionuclide Imaging 117 (IAEA, Vicnna, 1980).
 Smith, F.W. et al. Lancet i, 78 (1981).
- Damadian, R. et al. Ann. N.Y. Acad. Sci. 222, 1048 (1973). Lauterbur, P.C. Nature 242, 190 (1973).
- 6. Mallard, J.R. Proc. R. Soc. B226. 391 (1986).

John Mallard is Professor of Medical Physics at the University of Aberdeen, Aberdeen AB9

Earth sciences

Anoxic oceans and short-term carbon isotope trends

from Wayne D. Goodfellow

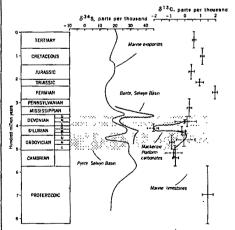
THE relationship between catastrophic geological events, mass mortality of species and sudden shifts in carbon isotope levels was demonstrated for the first time at the Cretaceous-Tertiary mass-extinction boundary, where negative δ¹³C values (see figure legend) were found to be associated with an iridium anomaly¹. Similar relationships between platinoid anomalies and short-term carbon fluctuations have been shown at the Permian-Triassic², Frasnian-Famennian³, Precambrian-Cambrian and, most recently, Proterozoic-Palaeozoic' boundaries. At other stratigraphic boundaries, a shift in carbon isotope values has been observed with no associated metal anomalies6. Many of these changes have been attributed to reductions of the biomass, although other factors may be important.

Changes in carbon isotope values in marine carbonates are influenced by many factors, such the level of mixing of the oceans, fractional preservation of organic matter and biological productivity. Changes in carbon fluxes with time are also important although they are unlikely to explain the relatively short-term and sudden decreases recorded at some System boundaries.

Because living organisms preferentially accumulate carbon-12, an increase of biomass is reflected by a corresponding proportional decrease in the carbon-12 in dissolved carbonate. The converse is also true — a decrease in biological productivity is recorded by an increase in the carbon-12/carbon-13 ratio. Although

there is general agreement that perturbations in productivity can generate changes in carbon isotope ratios in carbonates. the cause(s) of these shifts at a particula. horizon is often unclear.

The recent data of Magaritz et al.5 were obtained from a section from the Siberian Platform spanning the Proterozoic-



Short-term 848 trends in pyrite and barite from the Selwyn Basin and global evaporites in and corresponding curves for δ¹³C charges in carbonates from the Mackenzie Platform and global carbonate11. Small dots, ventilated water column; large dots, water column stratified with anoxic waters.

$$\delta^{13}C = \begin{bmatrix} \frac{^{13}C/^{12}C \text{ sample}}{^{13}C/^{12}C \text{ standard}} - 1 \end{bmatrix} \times 1,000 \text{ parts per thousand}$$

$$\delta^{34}S = \begin{bmatrix} \frac{^{14}S/^{32}S \text{ sample}}{^{34}S/^{32}S \text{ standard}} - 1 \end{bmatrix} \times 1,000 \text{ parts per thousand}$$

Palaeozoic boundary. The $\delta^{\iota 3}C$ values increase 15 m below the Vendian-Tommotian boundary and decrease at the boundary. The authors interpret these changes as a reflection of an initial bloom in biomass followed by a decrease in productivity on the basis of two lines of evidence. First, the association of highly negative δ¹³C values with the Vendian-Tommotian boundary indicates, by analogy with negative isotope shifts observed at other system boundaries, a decrease in productivity; and second, a major phosphogenic episode near the end of the Precambrian is evidence for increased productivity, which perhaps explains the trend to more positive $\delta^{13}C$ values during most of the Vendian.

One of the problems with this approach is that the Precambrian-Cambrian boundary has not yet been defined and the Vendian-Tommotian is just one of several being considered by the boundary committee of the Commission on Stratigraphy. The question of synchroneity with the proposed Precambrian-Cambrian contact (China C marker) of Hsü et al. cannot, therefore, be answered. Without supporting evidence for global catastrophism, such as coincidental anomalies in the platinoid elements, it is impossible to determine whether these isotope shifts reflect local or global processes.

Although the sedimentation rate is poorly constrained, the time span represented by anomalous δ¹³C values is probably large. Magaritz et al. are therefore dealing with relatively long-lived isotope changes that span tens of metres of section compared with the short-term effects that have been measured at mass-extinction boundaries' 4. Any short-term perturbations which exist cannot be resolved because of the large sample spacing.

The problem with the use of phosphate deposits as indicators of a biomass bloom is that most of these deposits are poorly constrained in time, making correlations with boundary events difficult. Furthermore, the lack of a clear relationship between trends of short-term changes in carbon isotopes and phosphogenic episodes indicates that phosphate deposits do not reflect, at least on a global scale, periods of increased productivity. But major phosphate deposits do occur at the onset of episodes of vertical mixing after periods of oceanic stability7, which suggests that other factors, such as the ventilation of anoxic oceans, influenced the isotope composition of dissolved carbonate.

During the history of the Earth, the oceans were not always as well mixed or ventilated as they are today. Major periods during which the oceans were stratified with an upper oxygenated and lower anoxic water column have been identified for the Mesozoic^b and Palaeozoic9. Carbonates precipitated from the lower anoxic water column are enriched

from Nature 34, 249; 15 July 1886 100 years ago Captain Ericsson's Pyrheliometer

in ¹²C because of the oxidation of organic matter by sulphate-reducing bacteria, as shown by the simplified reaction:

$$2CH,O + SO_4^{3-} \rightarrow H,S + 2HCO_5^{3-}$$

Because the amount of carbonate generated by this process is directly proportional to the fraction of sulphate reduced to sulphide, and as this fraction controls the δ^uS value (see figure legend) in the product sulphide, & S values in pyrite provide a measure of the amount of organic carbon oxidized in anoxic basins. As shown in the figure for the Palaeozoic Selwyn Basin of northwestern Canada, δ⁴S values increase during periods of ocean stratification until they approach or exceed those for coeval sulphate precipitated from the upper ventilated water column^{9,10}. Carbonates precipitated from the anoxic water column have δ¹³C values as low as -10 parts per thousand.

On the adjacent Mackenzie Platform, carbonates deposited from the upper water column during the Ordovician and Silurian display δ¹¹C values more positive than those for average carbonates" (see figure). The ventilation of the oceans, by contrast, should result in a shift to more negative δ^{13} C values caused by the mixing of isotopically light carbon from the anoxic water column with surface waters. This relationship is illustrated for the Mackenzie Platform by a deflection to more negative values in carbonates of the late Silurian (see figure).

The similarity of short-term carbon isotope trends in carbonates from the Mackenzie and Siberian platforms, both in the magnitude of the isotope shifts and in the polarity, indicates that biomass is not the only factor that influenced isotope ratios across the Vendian Tommotian boundary. This is particularly true to: stratigraphic horizons where synchroneity of events cannot be determined and where there is no supporting evidence for global catastrophism. More isotope and geochemical studies of carefully controlled sections sampled in detail across event boundaries are needed -- only then will the processes controlling the tractionation of carbon isotopes be fully understood

- 1. Hsu, K.J. et al. Science 216, 249 (1982)
- Dao-Yi, X. et al. Native 314 154 (1985) Playford, P.E., McLaten, D.J. Orth. C.J. Green, J.S. & Goodfellow, W.D. Science 226 437 Co 84
- Hsü, K.J. et al. Nature 316 809 (1985)
- Magaritz, M., Holser, W. L. & Kirschook, J.L. N. 320, 258 (1986). Shackleton, N.J., Imbrie, J. & Hall M. & I.
- Lett. 65, 233 (1983).
- Sheldon, R.P. A. Rev. Larth Ser 9 Series Scholle, P. A. & Arthur M. A. Bu'll Ass. Proc. 16. 64, 67 (1980).
- Goodfellow, W.D. & Jonasson, J.R. Go., vg. 12 553
- Claypool, C.E., Holset, W. L. Soxi J. R. & Z. k. L. C.
- Geol. 28, 199 (1980) Veizer, J., Holser, W.L. & Wilms, C.S. G. acci-cosmochim, Acta 44, 579 (1980)

Wayne D. Goodfellow is at the Geological Survey of Canada, 601 Booth Stree: Ottawa Ontario KIA OE8, Canada.

Palaeoecology

Surface water acidification

from Hans M. Seip

Few topics have been the subject of so much recent debate as acid precipitation. Are there other causes for the surface water acidification and the dramatic loss of fish populations observed particularly in Scandinavia, but also in other parts of Europe and in North America? Palaeoecological studies, such as the one described on page 157 of this issue', support deposition of compounds of anthropogenic origin as the primary cause.

It is now generally accepted that the recent increase in acidity (H+ concentration) of precipitation is caused by anthropogenic emissions of sulphur and nitrogen oxides. Recent surface-water acidification is also well documented. Although there is a reasonably good correlation in space and time between acid precipitation and water acidification, it is difficult to prove a causal relationship.

The main alternative hypothesis was originally forwarded by Rosenqvist2, who believes that soil acidification caused by changes in land use is the most important cause of the recent water acidification. Although this view is not generally accepted, it has some support3 and there is a consensus on which processes to consider; the differences arise in their relative importance.

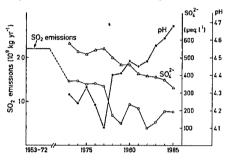
Because most of the precipitation will come into close contact with the terrestrial part of most catchments, acid soil is a prerequisite for acid water. Changes in the chemical properties of the soil, as well as changes in the hydrology5, affect the water chemistry. Several studies demonstrate soil acidification in Scandinavia and in Central Europe, which at least partly seems to be caused by acid deposition. Except for agricultural areas, estimation of H⁺ fluxes to the soils supports the importance of acid deposition in acidification.

Water acidification depends not only on soil properties, but also critically on the concentration of 'mobile' anions, particularly sulphate, nitrate and chloride, that move easily through the terrestrial part of the system. Because a charge balance must exist in any solution, increased anion concentration will lead to increased cation concentration, including increases in H+ and aluminium in runoff from acid soils. In most areas, the most important mobile anion seems to be sulphate; nitrate is mainly taken up by the vegetation but may affect water acidity, particularly during snow melt.

It is difficult to quantify the relative importance of acid deposition and other causes of water acidification. Simulation models indicate that increased sulphur | the diatom record. Despite some uncer-

deposition may cause a considerable decrease in the pH of surface water while deposition may cause similar increases^{6,7}. These theoretical calculations are supported by observations around Sudbury (see figure), where the emissions have been dramatically reduced since 1972 and surface water quality is improving. Conversely, a historical approach used in three Norwegian studies did not reveal a relationship between land-use changes and loss of fish populations8.

Jones et al. combine a detailed palaeoecological study of vegetation changes from the last glaciation until the present day around a lake in Galloway, Scotland,



The decreasing emissions at Sudbury, Ontario, have resulted in decreasing sulphate concentrations and acidity in the Clearwater lake 14.

with estimates of historical pH values using the diatoms in the lake sediments. Despite the rather dramatic changes in vegetation from a forest to an acid peatland, the pH of the lake remained surprisingly stable between 5.4 and 6.0 until the recent acidification started in about 1850. Although this study considers vegetation changes in particular detail, other palaeoecological results support the conclusion that acid deposition is a necessary condition for the recent acidification 9-12. For example, the pH of a lake in the Adirondack Mountains, United States, was about 5.7 during the period 1800-1950 despite major logging operations in the catchment. From about 1950 the inferred pH dropped to about 4.7 (ref. 12).

How reliable are these results? One complication is that the distribution of diatoms depends not only on pH, but also on other factors, such as the concentrations of humic substances and major ions in the water. The dependence on the content of humic substances has been used to infer changes from moderately acid humic water to more acid clear water in two Norwegian lakes, presumably because of acid deposition¹³. Seasonal variations in water acidity are often important and it is not clear how acid episodes are reflected in tainties in interpretation, palaeoecological methods may be the best way to determine the importance of acid deposition.

Can we draw the general conclusion that water acidification does not occur in an area without acid deposition? The diatom studies usually give inferred pH values of more than 5 in pre-industrial times for lakes that are now acidified. This agrees with the observation that fresh water in 'clean' areas seldom has a pH less than 5.0. There are simply not enough anions to balance the charge of high concentrations of H+ and aluminium ions. There are exceptions — highly coloured water may contain enough organic anions to make it more acid. But the recent acidification is not caused by increased concentration of organic compounds.

Sea-spray deposition with high concentrations of Cl and Na+ may also cause acidification if sodium is retained and H+ ions are released from the soil. But in a stable terrestrial system there will be no long-term accumulation of Na* and therefore only episodic acidification from sea-spray; in an aggrading system sodium may accumulate for longer periods.

Afforestation causes important changes in hydrology and soils, and several studies in the United Kingdom show more acid and aluminium-rich waters in afforested compared with non-forested areas in exposed regions. It is not clear whether a similar acidification would occur in areas with natural precipitation. The forest 'filters' the air and thus increases the deposition of both anthropogenic and natural compounds. Increased sulphate concentration in runoff may therefore be the main cause of acidification here.

In conclusion, there is at present little solid evidence for recent water acidification in areas not exposed to acid deposition. If occurring, it is likely to be found in areas with high sea-salt influence and recent vegetation changes such as afforestation, but the primary cause is evidently anthropogenic emissions of sulphur compounds.

- 1. Jones, V.J., Stevenson, A.C. & Battarbee, R.W. Nature
- 322, 157 (1986). Rosenqvist, I.Th. Sci. Total Environ. 10, 39 (1978).
- Krug, E.C. & Frink, C.R. Science 221, 520 (1983). Rosenqvist, I.Th. & Seip, H.M. Kjemi 46, 13 (1986). Whitehead, P.G., Neal, C. & Neale R. J. Hydrol. (in the press).
- 6. Reuss, J.O. & Johnson, D.W. J. environ. Qual. 14, 26
- 7. Rustad, S., Christophersen, N., Seip, H.M. & Dillon, P.J. Can, J. Fish. Aquat. Sci. 43, 625 (1986).
- 8. Drabløs, D. Sevaldrud, I. & Timberlid, J.A. in Ecological Impact of Acid Precipitation (eds Drabløs, D. & Tollan, A.) 367 (SNSF, Oslo, 1980).
- Battarbee, R.W., Flower, R.J., Stevenson, A.C. & Rippey, B. Nature 314, 350 (1985).
- Battarbee, R. W. Phil. Trans. R. Soc. B305, 451 (1984).
- 11. Renberg. I. & Hellberg. T. Ambio 11, 30 (1982)
- 12. Charles, D.F. Verh. Internat. Verein. Limnol. 22, 559
- 13. Davis, R.B., Anderson, D.S. & Berge, F. Nature 316, 436
- 14. Dillion, P.J., Reid, R.A. & Girard, R. Water Air Soil Pollut. (in the press).

Hans M. Seip is at the Centre for Industrial Research, Blindern, 0314 Oslo 3, Norway.

SCIENTIFIC CORRESPONDENCE

Human gene cloning: the storm before the lull?

SIR-Hardly a week goes by without an article in Nature describing the cloning of a human DNA sequence. Yet it is barely nine years since the first cloning of a human gene sequence, chorionic somatomammotropin, was reported in Nature¹. Since then, some five hundred different human gene sequences plus many anonymous DNA segments, have been reported in a total of nearly 2,500 independent published articles2 (as evidenced in Gene Communications, a quarterly updated newsletter obtainable from the authors on request). Such an exponential increase in knowledge accumulation is by no means unique. Examples of this phenomenon have included the literature explosions associated with cyclic AMP after the introduction of the second messenger hypothesis in 1958² and the discovery and analysis of hereditary amino acidopathies after the advent of chromatographic methods'.

We calculate that were the present growth in the number of reports of cloned genes to be maintained, their number would overtake the total number of biological publications in 1992 and that of all scientific publications by 1994 (Fig. 1), still leaving the majority of the human genome untouched. However, this year the first signs of a plateau are becoming evident. It is interesting to speculate upon the various factors which might affect publication rates over the next few years.

A slow-down factor could be the finite size of the human genome (3×10^9) base pairs) — although the number of gene sequences which it contains, perhaps in excess of 100,000, is sufficiently large to ensure that there is a long way to go before any law of diminishing returns begins to operate. But given its limited and already stretched resources, the scientific community will sooner or later have to decide whether it can afford the not inconsiderable redundancy so characteristic of research efforts in this area.

This redundancy of effort is apparent from the number of independent reports of the cloning of certain human DNA sequences. For example, the cloning of adenosine deaminase and of T-cell receptor α and β chain cDNAs have each been achieved eight times. There are 17 separate reports of a cloned c-mvc genomic sequence and 33 independent reports of the cloning of the β -globin gene, although, in fairness, some of these are mutant alleles. While a certain degree of competition is to be expected and indeed welcomed in science, redundancy on this scale clearly calls for some more effective means of coordinating research efforts at the international level. It is, however, to be expected that no such let-up is likely in the hunt for those gene sequences deemed worthy of commercial exploitation. Presumably, strong competition will still characterize the drive to clone genes coding for proteins of economic and/or medical importance. Furthermore, an ever increasing number of laboratories are involving themselves directly or indirectly with cloning and mapping the human genome. The synthesis of molecular biology and human genetics seems able to attract an increasing number of adherents. How long the cloning fashion will be able to lure young researchers remains an open question, but for most laboratories, cloning is not an end in itself, but a means to an end, for example, functional analysis, spawning further booms in clone analysis.

One further factor which will affect publication rates is the future editorial policy of the eighty or so journals that at present publish these reports. Although to some extent offset by the likely future increase in journal numbers, the number of published cloning reports should tend to decline as a result of a probably tightening-up of standards and criteria for article acceptability. It is anticipated that authors will be expected to report on a larger number of sequences, a more complete sequence or to have undertaken in-depth structural or functional studies. Cloning data may in the forseeable future have to be relegated to an information repository in the form of an electronic data base, a development which will be accelerated by

novel, more effective cloning, genome walking and sequencing strategies. It remains to be seen whether the level of acceptance of such novel means of data storage and transfer is sufficient for any appreciable effect to become apparent in the near future. Perhaps the rate of human gene cloning

may even decline because people are simply getting bored with it. But it is also true that man's feeling of self-importance will probably not be satisfied until the last bit of his genome has been sequenced and filed somewhere.

> JÖRG SCHMIDTKF MICHAEL KRAWCZAK

Institut für Humangenetik. Gosslerstasse 12d, D-3400 Göttingen, FRG

DAVID N. COOPER

Department of Neurochemistry, Institute of Neurology, University of London. Queen Square, London WC1N 2NS, UK

1. Shine, J. et al. Nature 270, 494 (1977)

- Jost, U.-P. & Rickenberg, H.V. A. Rev. B. Am. 40, 271
- 3. Scriver, C.R. Br. med., Bull. 25, 35 (1969) 4. Palca, J. Nature 321, 371 (1986)

Immunotoxins to combat AIDS

SIR—Of the three therapeutic approaches to acquired immune deficiency syndrome (AIDS) suggested by Klatzmann and Montagnier¹, Singer and Shearer have highlighted the possibility of attenuation of the CD4⁺ cells, which are the host for the virus associated with AIDS (HTLV-III/LAV), by infusing monoclonal anti-CD4 or anti-class II HLA reagents.

A more reasonable approach, we suggest, would be to use immunotoxins' conjugates of a specific antibody and a plant or bacterial toxin — directed specifically to the CD4 cells. The toxic moiety is a ribosome inactivating protein (RIP), either a single A chain or both an A chain and a B chain (which is a monovalent lectin). Immunotoxins containing A-chain RIPs have a definite advantage over the two-chain RIPs as they can be made absolutely target specific'. There is now good evidence that only one molecule of the enzymatic, toxic A chain entering the cytoplasm of a cell is sufficient to bring about the cell's destruction by totally inactivating its protein-synthesizing machinery⁵. Immunotoxins offer the advantage of providing both specificity of targeting through the antibody moiety and extremely effective inhibition of messenger RNA translation (which is increased by orders of magnitude by the product of the tat-III gene of HTLV-III/LAV in infected cells') by virtue of the toxophore moiety.

By subverting the stratagem used by the virus for its replication, the administration

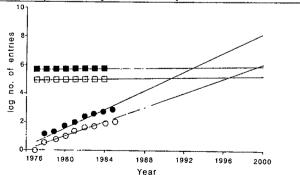


Fig.1 Exponential growth of publications per annum on cloned human DNA sequences: all reports (filled circles) and first reports on protein coding sequences (open circles). For comparison the number of publications covered by Biological Abstracts (open squares) and Science Citation Index (filled squares) are given.

of immunotoxins would greatly diminish the number of virus particles released, over a period of time, into the circulation following the destruction of CD4⁺ cells. As a consequence of this reduced number of viral particles thus released, they could probably be neutralized effectively by the antibodies already present in the patient's blood. On the other hand, infusion of anti-CD4 antibody alone (which by itself cannot attenuate the viral population) would release far greater numbers of viral particles. As a result, the neutralizing capacity of the circulating antibodies may be considerably reduced. The injection of antiviral antibodies to neutralize the virus would then be required. Because of the antigenic drift8 noted with this virus, extraneous infusion of anti-HTLV-III/LAV antibodies may not be particularly helpful in neutralizing the large pool of HTLV-III/LAV released by treatment with anti-CD4 antibodies.

Thus the administration of immunotoxins in miniscule amounts (as RIPs act in a catalytic manner) might forestall the spread of AIDS virus. Moreover, as only a small proportion of CD4+ cells are infected by the virus and as fresh peripheral blood lymphocytes of AIDS patients do not show the presence of viral DNA, there will probably be no necessity for immuneenhancing therapy with immunotoxins.

Avadhesha Surolia M.P. RAMPRASAD

Indian Institute of Science, Molecular Biophysics Unit, UGC Centre of Advanced Study, Bangalore 560 012, India

- Klatzmann, D. & Montagnier, L. Nature 319, 10 (1986).
- Singer, A. & Shearer, G.M. Nature 320, 113 (1986).
- Uhr I W. I. Immun. 133, 6 (1984).
- Barbieri, L. & Stirpe, F. Cancer Surv. 1, 489 (1982).
 Thorpe, P. E. et al. J. biol. Chem. 116, 447 (1981).
 Eiklid, K. et al. Expl Cell Res. 126, 321 (1980).

- Rosen, C.A. et al. Nature 319, 555 (1986). Laurence, J. Scient. Am. 253, 84 (1985).

Earthquake prediction and electric signals

SIR-In a comment in News and Views' P.W. Burton discussed our publications in Tectonophysics² on the prediction of the epicentre and the magnitude of earthquakes within a time window of 7 to 115 hours, based on the monitoring of the simultaneous changes of the electric field of the Earth observed at a number of sites. Burton expressed doubts about the claimed connections between earthquakes and the precursor signals, especially during periods of high seismicity. Of course, there is a high probability of an earthquake occurring somewhere within, the time window, but we have isolated a large number of events in both time and seismic region.

A recent case, with an exceedingly small probability of having been predicted by chance, illustrates our point. On 17

December 1985, we presented a prediction to the session of the Greek Special Committee on Earthquake Prediction, which was recently established by the Greek Ministry of Public Works and consists of geologists, seismologists and physicists. The electric signals allowed two solutions, one for an event of magnitude 4.8 in the sea to the south of Kalamata (southern continental Greece) and the other for a 5.2 mag event on the coast of Asia Minor near the island of Samos. Forty hours later a 5.2 mag event occurred within 150 km of the site expected from the second solution. As no earthquake with M > 4.7 had occurred within the 75,000-km² area 36.7-40.0 °N and 25.0-27.5°E for at least the previous 14 months. the time-probability is smaller than 10⁻². Obviously the probability of simultaneously predicting the time, epicentre and magnitude is appreciably smaller.

Another recent case is the following: On 29 March 1986 a 6.1 mag event occurred at 38.3°N-25.3°E. Four days earlier the government had been officially informed of an impending 6.1 mag earthquake. The error in the prediction of the epicentre was less than 50 km.

P. VAROTSOS K. Alexopoulos K. Nomicos M. Lazaridou

Knossou 36, Ano Glyfada, 165 61 Athens, Greece

- Burton, P.W. Nature 315, 370-371 (1985).
- Varotsos, P. & Alexopoulos, K. *Tectonophysics* **110**, 73, 99 (1984).

The stability of zoological nomenclature

Sir-As one of those cast by Erzinclioglu and Unwin (Nature 320, 687; 1986) as "having a legalistic turn of mind", I would like to protest the spirit, as well as the content, of their letter which was intended to detail the inadequacies of the International Code of Zoological Nomenclature and to protest the "tyranny of the Commission".

First, the writers do not seem to understand the meaning of stability in the sense of the code. Stability has never been taken to mean that a name shall remain unchanged and unchangeable: the preamble of the Code states that, "All its [Code] provisions and recommendations are subservient to these ends [promoting stability and universality in the scientific names of animals] and none restricts the freedom of taxonomic thought or action." Further, the plenary powers of the Commission, defined in Article 79, outline the responsibility of the body to maintain stability and specifically refer to the suppression of a senior homonym as a potential option in assuring stability.

With regard to a few specific points raised by Erzinclioglu and Unwin, the

Code has, for several editions, made a clear distinction between the endings of names and the name of the taxon. Thus, changing the ending of a species name to agree with that of the genus in no way constitutes a change of names.

A similar observation, of course, applies to the authors' argument regarding elevation of subfamily groups to the family level. The reasoning behind the rules governing change of rank within the family-group seems altogether clear and I cannot imagine such a change could cause confusion

In their lengthy summary of the change of species names for the medically important African fly Auchmeromyia luteola, or perhaps I should say A. senegalensis, the writers do not seem to be offended by the change in generic placement, which presumably occurred before their entry into the world of nomenclature, but only by the discovery of an obscure senior homonym and subsequent name replacement. Their irritation is misplaced and might better have been directed at the author(s) of Catalogue of the Diptera, who chose to offer a replacement name rather than to maintain the well-known name and refer the matter to the Commission. This option has existed for years and is the rational way to resolve this kind of problem and assure stability.

Erzinclioglu and Unwin seem particularly confused regarding the relationship between the rules of nomenclature and the classification of organisms. Adherence to the principles of cladism or, for that matter, "traditional" systematics have no bearing whatsoever on the value of the Code.

Finally, those of us who "mindlessly" adhere to the Code resent the notion that anarchy is the only sane alternative to felt weaknesses in the rules. There is, and always has been, the alternative of petition for change in the document. In my opinion the present Code constitutes an improvement, in some areas, over the previous edition. There remain very real problems regarding application of the rules to collective groups and ichnotaxa — problems that will probably never be resolved to everyone's satisfaction — but there is a mechanism within the rules to allow change to be proposed.

I find it ludicrous to consider the Commission as a group of hooded tyrants whose purpose it is to impose their arbitrary will upon the scientific community, from which, of course, they were elected. It may come as some consolation to Erzinclioglu and Unwin to note that by the act of expressing their interest in nomenclature, they have qualified themselves for nomination to election to the Commission.

RODNEY M. FELDMANN

Department of Geology, Kent State University. Kent, Ohio 44242, USA

The path to solid success

R.V. Jones

A Life in Science. By Sir Nevill Mott. Taylor & Francis: 1986. Pp. 198. £15, \$30.

Nevill Mott's concise autobiography shows how fortunate he was in his parents. They had both been research students at Cambridge under J.J. Thomson, and throughout their lives he could share with them his professional experiences in a happy manner rarely granted to a physicist. They could thus take informed pleasure in his first success in research, the prediction in 1929 — on the basis of the new quantum mechanics — of the way in which α-particles would be scattered by helium nuclei.

They could also enjoy pen-pictures of life in Copenhagen with Niels Bohr, in Göttingen in the earliest days of quantum mechanics, and back in Cambridge with Rutherford and Dirac. Writing of his Cambridge and Copenhagen periods, Mott twice uses the phrase "sink or swim" to describe the then prevailing atmosphere in which research students were expected to fend for themselves. This will ring true to those of us who entered physics before 1939.

His time as a student ended in 1929 with appointment to a lectureship with W.L. Bragg in Manchester. He held this for only a year, before an invitation from A.M. Tyndall took him to Bristol as professor of theoretical physics at the age of 28. Protected from administration by Tyndall, one of the wisest of laboratory heads, Mott pursued his developing interests in solid state physics; and over the next dozen years he became senior author of three notable books, "Mott and Massey" Theory of Atomic Collisions, "Mott and Jones" Theory and Properties of Metals and Alloys and "Mott and Gurney" Electronic Processes in Ionic Crystals. He was only 31 when elected to the Royal Society — "Nowhere near a record", he tells us, for "Paul Dirac was elected when he was 28".

The Second World War brought Mott into contact with the Army, first at Anti-Aircraft Command, then at the Army Operational Research Group at Petersham and finally at Fort Halstead as Superintendent of Mathematical Research in Armaments. Those who knew him before 1939 were struck by the way the war brought him out of his shell. As for many of us, he was now working with soldiers and grappling with practical problems of the utmost importance. I remember his contribution to the construction of reflecting screens of chicken wire for radar aerials: if a particular mesh would let 10 per cent of the energy leak backwards, then halving the pitch of the mesh would roughly halve the leakage: but if instead of using extra wire in the closer mesh, the same amount were woven into a second screen placed behind the first, then each screen would only let through 10 per cent of the radiation incident upon it, and so the double screen would let through only one per cent. But while Robert Watson-Watt could well have appreciated the elegance of this idea, I cannot imagine him being so happy with Mott's giving the credit, as he does, to Edward Appleton for the use of pulse methods in radar.

The experience at AA Command gave Mott "a deep respect for the professional soldier". At the same time the war led him to realize the importance of industry to Britain, and the benefits that could ensue

taken not by him but by the body of fellows. Tizard had experienced the same thing at Magdalen in Oxford where, as the Dictionary of National Biography records, he found it difficult "to pilot controversial issues through a very varied and independent-minded body of fellows". "Looking back", Mott writes, "on both my election and my resignation, it seems like one of Snow's novels; we used to say that Snow 'didn't know the half of it".

When he resigned from Caius in 1966 Mott still had another five years in the Cavendish chair, where he devoted much effort to teaching, both in the university and in schools. He chaired the physics committee of the Nuffield Scheme, where the main idea was "learning by doing". But, he writes,

I would have hated to do it this way. To me the laws of physics are to be approached through mathematics, and their validity and beauty become clear when expressed in mathematical form. My hero was Clerk Maxwell rather than Faraday....

He also had reservations, although he did his best for the scheme, over the Treve-



Nobel quintet— (left to right) Philip W. Anderson, W.H. Brattain, Nevill Mott, John Bardeen and J.H. Van Vleck. Anderson, Mott and Van Vleck were joint Laureates in 1977, and Brattain and Bardeen (with William Shockley) in 1956. Bardeen was again a winner in 1972, with Leon Cooper and J. Robert Schrieffer.

if university science were more closely linked to it. This was one factor that led him to return to Bristol rather than accept a chair he was offered in Cambridge.

The post-war years in Bristol scintillated with success. Mott succeeded Tyndall as head in 1948, and was surrounded by a galaxy of talent that included C.F. Powell, C.R. Burch, P.H. Fowler, F.C. Frank and J.W. Mitchell. But when, in an act of self-sacrifice, W.L. Bragg left the Cavendish chair in 1953 to restore the fortunes of the Royal Institution, Mott accepted appointment as his successor—just too late for his mother to be told of this "overwhelming honour".

In 1959 Mott also became Master of Caius College, Cambridge: surprisingly, it had become fairly common in Cambridge for an individual to be head of a college, as well as of a large laboratory. Mott found the two jobs very different. In the laboratory, after listening to opinions, he took the key decisions himself: in college he was expected to abide by decisions

lyan scholarships initiated by Kurt Hahn: "It was dangerously near 'character rather than intellect' which was of course anathema to me". He was happiest with his chairmanship of the Royal Society's education committee, writing a report in 1979 on the needs of talented children. The report concluded "that mixed ability teaching could be successful only with exceptionally able teachers"; instead "our working party believed that as far as possible talented children should advance at their own pace, and with this in view favoured 'setting' in science and mathematics from 13 years onwards".

Relinquishing the mastership of Caius gave Mott more time for research, and his interest was aroused by the properties of non-crystalline semi-conductors. His contributions to the theory, which have continued after his retirement from the Cavendish in 1971 to the present day, were recognized by the award of a Nobel Prize in 1977. So while advances in theoretical physics are nearly always made by

young men, Mott's best-rewarded work has been done, most remarkably, in retirement — an exemplary encouragement to us all.

As for his method of creative reasoning. some clue may be gained from Smoluchowski's retrospective comment on the early days of solid state physics: "Mott... and his colleagues horrified us by their 'simple' visualizable and seemingly uncomplicated models and mathematics". So, with his models such as "swollen atoms", Mott is in a tradition expressed by H.G.J. Moseley in 1914: "the French point of view is essentially different from the English. Where we try to find models and analogies, they are quite content with laws". By his practice, then, Mott has a foot in one camp, and by his professed predilection for laws, also a foot in the other. Bestriding both, his is one of the most sustained lives of success in physics, recognized by numerous medals and 27 honorary doctorates.

A Life in Science is written with great economy, throwing laconic sidelights on many issues into which Mott's pursuit of science has drawn him. "Kindness with firmness" is a pervading trait, the former being exemplified in his remark that "The greatest pleasure in life is putting others on the way to success", the latter in stopping the project for a linear accelerator in Cambridge in one of his first acts as Cavendish professor.

In the deepening attention that many in science are giving to religion, Mott's own personal statements on the matter will be appreciated. In 1929 he wrote to his fiancée, "If you wanted to become a Roman Catholic, I should want to die. The trouble is that I can't think about the institution because it fills me with absolute physical disgust...". While this pristine view has been much mellowed by age and by an appreciation of the services performed by many devoted Catholics, "something of my antagonism remains". But Mott feels no such antagonism for the Anglican Church: indeed in retirement he has been baptized and confirmed as a member, and he devotes a whole chapter of the book to religion. He regularly attends church

finding it helpful to worship God in company with other people. If some things that are repeated in the Creed do not correspond with what I believe, such as 'born of the Virgin Mary', I accept what is said because to me the Christian religion is the sum of the beliefs of Christians throughout the ages, not only those of our present generation.

Each man's religion is a matter for himself, and we can only be grateful to one who has spent a long life so eminently in science for exposing so frankly his personal conviction.

R.V. Jones. 8 Queen's Terrace, Aberdeen ABI IXL, UK, is Emeritus Professor of Natural Philosophy in the University of Aberdeen.

Getting the picture to tell the story

P.W. Hawkes

Image Analysis: Principles & Practice. Joyce-Loebl:1986. Pp.250. Pbk £35, \$50. *

THERE are four grand themes of digital image processing: acquisition and coding; enhancement; restoration; and analysis, including pattern recognition. This last activity differs from the others in that the result is not a better image or one that is transformed in some way, but information about its contents. The information often comes in the form of a histogram or tables of data. In a karyogram, for example, the properties of the various chromosomes present might be listed; in quality control in a manufacturing process, certain dimensions might be monitored and the process interrupted if these exceeded preset limits; in aerial cartography, areas of forest and field, river and lake, factories and dwellings might be recognized, measured and their relative separations characterized in some way.

There have been many books on image analysis but none quite like this one — in

* Available from Rosalyn Kell, Joyce-Loebl, Marquisway, Team Valley, Gateshead, Tyne & Wear NE11 OQW, UK, or Bill Burnip, Joyce-Loebl, c/o Nikon Inc., 623 Stewart Avenue, Garden City, New York 11530, USA.

simple language, and with ample illustration, it enables the reader to use a commercial image analyser to the best advantage. The coverage is broad but is not correspondingly shallow, though the mathematical foundations of the various operations are rarely described. The text covers acquisition and digitization, but it will be used principally for its chapters on image processing, detection and measurement techniques. These introduce the reader to the ways of locating specific structures, of amending images by erosion or dilation (sic), of identifying and coding boundaries, and of characterizing shape, among many related topics. Subsequent chapters deal with colour images, computing (almost too brief to be useful) and a number of case studies. Each chapter ends with a bold-face summary; these read \r more like collections of great thoughts than scientific abstracts: "classification is a useful technique, but can become complex if many different kinds of measurements are used" gives an idea of their profundity.

Excusably, the anonymous authors had the Joyce-Loebl analyser in mind, but the book is not unduly partisan and gives an exceedingly clear and easily assimilated account of a great deal of disparate material. There is no better book for anyone involved with these machines who would be daunted by a more mathematical account.

P.W. Hawkes is Maître de Recherche at the Laboratoire d'Optique Electronique du CNRS, BP 4347, F-31055, Toulose Cedex, France.

Disordered thoughts

P.W. Atkins

The Unfinished Universe. By Louise B. Young. Simon & Schuster: 1986. Pp.239. \$17.95.

THE argument of this book is that a great creative process is taking place within the Universe, with us as witnesses and participants, and that matter has an innate tendency to achieve greater complexity. Form is emerging like a butterfly from a chrysalis, and the process that began when quarks coalesced into protons is now moving towards its culmination. The argument depends on a specific rejection of the view that the Universe is running down into a state of disorder.

The case in favour of this formative tendency is passionately argued, and it is plain from the style of the exposition that Mrs Young is deeply in love with the world and with her vision of science, and longs to share her wonder and awe. Such books should be approached with a special cast of mind, for it is important not to allow the style to obscure the content. This is espe-

cially true of one wrapped in a jacket bearing messages from three highly respected scientists, one of whom claims that the book releases us from the stifling imprisonment of the Second Law of thermodynamics, another that Mrs Young's view that a creative process is taking place "is an idea... of great importance" and a third who finds it a strangely beautiful guide.

I feel outnumbered, for I find it none of these things. Passion there certainly is, and I can see why some might find the prose "lovely". I will disregard the little slips that don't matter very much (such as ascribing seven electrons to chlorine and the heat of the Earth to thermonuclear reactions in its core). I will also largely ignore (but it set my antennae waving) the author's rejection of the concept of force and its replacement by some kind of vague, non-quantified, tendency of particles to congregate into more complex form (p.41). I will concentrate instead on the central idea, that the Second Law cannot fully account for the phenomena of the world, and particularly for the phenomenon of life. Mrs Young admits (p.120) that the trend postulated by the Second Law is the opposite of the one she proposes, and therefore her thesis depends on her ability to demonstrate the Law's invalidity and incompleteness.

I can see why Mrs Young thinks it inadequate: it is because she appears not to have understood it. Chapter 6 is a travesty of thermodynamics. In the first place, a waterfall (p.119) is an excellent example of a process on which, as expressed, the Law is silent. Secondly, when the Law is first presented (p.119) it is stated in terms of the tendency of the entropy of a system to increase, without it being emphasized that the system must be isolated. A partial recovery is made three pages later when Mrs Young reminds us that physicists have "explained" (her quotation marks) the apparent spontaneous local emergence of order by insisting that the Second Law refers to a totally closed (by which she should mean isolated) system. However, she rejects this "explanation" by remarking (p.123) that it is not possible to ascribe numerical values to "the different levels of complexity" of a system, which I take to be the denial of the view that the entropy change in a system can be expressed quantitatively. That of course is silly: huge tables of thermodynamic data exist and other data can result from well-defined experiments. One of the main objects of statistical thermodynamics is to do this very calcu-

Slippery language erects false tests. In what should be a technical account of entropy and its calculation, the author asks (p.124) "how can we place a value on the creation of the first living thing?" as a paraphrase of "what is the change of entropy of the system?". Moreover, in a book on the application of thermodynamics to life, surely one should expect to find a discussion of the behaviour of open systems, dissipative structures and entropy production in states far from equilibrium?

Far from being a release from the stifling imprisonment of the Second Law, the book is an essay based on misunderstanding. Far from being a strangely beautiful guide it is a snare for those with a passion to know but not the ability to judge. Far from being important enough to be published and await its time (p.227), the central thesis is nonsense. I am sorry to be so harsh, for I can sympathize with the author's passion.

P.W. Atkins is University Lecturer in Physical Chemistry at the University of Oxford, and a Fellow of Lincoln College, Oxford, UK.

New in paperback

- Time Frames: The Rethinking of Darwinian Evolution and the Theory of Punctuated Equilibria by Niles Eldredge. Publisher is Touchstone (Simon & Schuster), price is \$8.95. For review see Nature 316, 683 (1985).
- Imagery in Scientific Thought by Arthur I. Miller. Publisher is MIT Press, price is \$8.95. £8.95. For review see Nature 314, 689 (1985).

Down to physicists

Peter J. Smith

Continuum Theories in Solid Earth Physics. Edited by R. Teisseyre. *Elsevier:1986. Pp.566. Dfl. 290, \$107.50.*

THE American geologist M. King Hubbert was wont to startle his audiences with the proposition that as science advances it becomes not more complex but simpler. This is, of course, one of those intellectual teases that is both true and false but more false than true. What King Hubbert had in mind was the plethora of apparently disparate observations and unrelated hypotheses which, once plate tectonics had been discovered, could be summarized as a paradigm in half a page. He had a nice philosophical point, but one that ignores the fact that working Earth scientists are not primarily philosophers. Students and researchers, forced to look behind the simplifying mega-patterns of the Earth, are all too aware not only of the increasing complexity but also of the growing burden of knowledge represented by ever more detailed observations, hypotheses and interpretations.

There is, moreover, a quite different sense in which King Hubbert's dictum is suspect. His exemplifier, plate tectonics, is essentially a theory of what happens rather than of how or why. It has been clear for some time now that the latter questions can only be addressed in terms of the solid-state physics of the Earth's interior, a development that raises complexity to bewildering heights for those versed only in conventional geological methods. Continuum Theories in Solid Earth Physics, which originated in Poland, proves the point with a vengeance. About 80 per cent mathematical and requiring a good working knowledge of tensor analysis applied to continuous media, the book demonstrates just how "non-geological" the fundamental problems of Earth behaviour really are.

The topics on the agenda here are the theory of Somigliana dislocations and its application to earthquake mechanics and aseismic creep; fracture theory and its relevance to seismology; the mechanics of continuous media with special reference to seismology; the behaviour of porous media; the theory of thermal stress in the Earth's interior; thermal convection; the nature of electromechanical and magnetomechanical coupling; and magnetohydrodynamic processes in the Earth's core as the source of the geomagnetic field. In each case, although the emphasis is on mathematical development, due attention is paid to the need to relate theory to the results of observation and experiment (not always a feature of books of this kind) and for the most part there is sufficient |

description to enable the non-mathematically inclined to get at least the gist of what is going on. It is interesting, too, to note that the Poles are far more familiar with what goes on in the West (and Japan) than are Western scientists with developments in Poland. As a result, there is little evidence here of a "Polish view" of Farth physics and thus, in contrast to many treatises emanating from the Soviet Union, no false impression of the subject having originated and developed quite separately in the East.

Whilst this commendable internationalism gives point to the publication of the book in Poland, it is less easy to see the merit in making a somewhat coals-to-Newcastle translation into English. The very lack of parochialism has the ironic consequence that there is little, if anything, here to be learned by Western Earth scientists. Nor, even if there were no comparable texts already in the West. would the volume be a suitable text for the uninitiated. As D.L. Turcotte and G Schubert so ably showed in Geodynamics: Applications of Continuum Physics to Geological Problems (Wiley, 1982), it is perfectly possible to teach Earth physics without tensors and get through to a wider audience into the bargain.

Peter J. Smith is Reader in Earth Sciences at the Open University, Walton Hall, Milton Keynes MK76AA, UK.





Tema 5 – Proceedings of the 5th International Symposium on Trace Elements in Man and Animals

edited by C.F.Mills if Bromner and J.K.Chesters

Accounts of recent studies of the biological role of the essential trace elements of the biochemical and pathological effects of defects, or excess, and of the significance of such problems in human and animal is different presented. This volume includes reports both of the scientific discussions that followed presentation of marity of these papers and of workshop so is root that considered problems associated with the detection of trace elemint related disorders.

Tema 5 will be of great interest to research workers on trace elements ar well as lecturers inutritionalist , pathologists and veterinarian .

244 × 187mm hardback 978r p ISBN 0-85198-533 X UK £43-00 Americas US \$81 '0 Rest of World £4730

Obtainable from major bookse, σ_{γ} or direct from

C.A.B. International, Farnham (150) of Farnham Royal, Slough St. 2,33N is K. Tell Farnham Common (02814) 267.

How important is natural selection?

J.S. Jones

Natural Selection in the Wild. By John A. Endler. Princeton University Press:1986. Pp.336. Hbk \$40, £26.65; pbk \$13.95, £9.30.

THE most influential evolutionary book of the past ten years is, without doubt, Motoo Kimura's Neutral Theory of Molecular Evolution, and of the decade before that R.C. Lewontin's The Genetic Basis of Evolutionary Change. Lewontin pointed out the difficulties of explaining molecular polymorphism using traditional models of natural selection acting at single loci, while Kimura argued cogently that the most important force in controlling the evolutionary fate of most newly arising mutations is not selection but random genetic drift. This relegation of natural selection to the role of evolution's policeman, who acts mainly to remove alleles deviating from an acceptable norm and ignores the vast majority of genes in populations, is now central to large parts of theoretical population genetics, to molecular evolution and to the reconstruction of phylogenies. John Endler's impressive book attempts to restore natural selection to its traditional place as the driving force of evolution. It may become an evolutionary classic of the next decade.

As Endler points out, the term "natural selection" has meant very different things to different people. After wandering briefly in the philosophical fog which is thicker in evolutionary biology than in any science apart from psychology, he produces a definition of selection close to the Darwinian one - variation, inheritance and genetic differences in the chances of reproduction — or even to that of Oscar Wilde, that "nothing succeeds like excess". Natural selection does not necessarily lead to evolution, and it includes many biological processes apart from differential mortality. Indeed, a survey of experiments on selection in nature suggests that inherited differences in survival are less important than are those associated with mating ability, fertility or fecundity.

There have been numerous attempts to measure selection in the wild. Many of these have failed because of poor experimental design, and Endler suggests a number of ways in which selection might acceptably be demonstrated in natural populations. He discusses ten kinds of information that can identify selection, from simple correlations of gene frequency with environment, to comparisons of the same genes in related species, and

to demographic studies and experimental perturbation of populations in nature. The road to detecting selection has many pitfalls. Endler finds 25 reasons why we might fail to detect it when it does exist but, comfortingly, only 21 ways in which selection might be identified when in fact it is not operating. His extensive analysis of work on natural selection in the wild suggests that strong selection on morphological characters and polymorphic alleles -selection of the intensity used by animal and plant breeders — is commonplace in nature, and that the general assumption that differences in fitness of more than about 10 per cent are rare is simply incorrect. It is nevertheless rather depressing to learn that there is as yet no case in which natural selection acting over an organism's whole lifetime has been measured. It is also true that if size and shape are controlled by many genes of individually small effect, then strong selection on morphological characters may still allow genetic drift to determine the evolutionary fate of most mutations at such loci. This distinction between natural selection on the phenotype and the genotype may yet bridge the gap between those who emphasize the importance of random change in evolution and those who hold the views so eloquently put forward in this

Endler himself is sanguine that "as our knowledge...increases, perhaps natural selection will become easily detectable at the biochemical and even the molecular level". Although ecological genetics has a

long way to go before this hope will be fulfilled, it is nevertheless true that a hypothesis that selection acts on a particular system is, like the search for the North West Passage, intrinsically productive even if it is wrong. All too often great pyramids of theory have been balanced on a mere assumption that selection is unimportant: the neutral theory has been much more of a stimulus to theoretical than to experimental studies of evolution. Theory frequently asks us to measure the unmeasurable, and experiments on the genetics of populations in nature are often designed in such a way as to produce results which cannot be interpreted. What is needed is a joint approach to the problem of the importance of selection in evolution: to use one of the quotations from Dr Johnson which preface each chapter, \ there is nothing

more pleasant, or more instructive, than to compare experience with expectation, or to register from time to time the difference between idea and reality. It is by this kind of observation that we grow daily less liable to be disappointed.

Natural Selection in the Wild is a unique blend of ideas about evolution set against the reality of studying it in nature. All evolutionists should read the book: it will disappoint none of them, whatever their preconceptions about the importance of natural selection.

J.S. Jones is a Lecturer in the Department of Genetics and Biometry, University College London, 4 Stephenson Way, London NWI 2HE, UK.

THE INVAGINATE GASTRULA AND THE PLANULA

A giddy little Gastrula, gyrating round and round, Was thought to show the way we got our enteron profound: A little whirlpool in its wake maintained a tasty store, A pocket sank to lodge it all, and left a blastopore.

As a larval epigram this description earns a prize, But as sketching adult ancestry can only win surprise, And when you note all early orders fixed upon the rocks, You feel a slight embarrassment, the first of many shocks.

The foremost inconsistency is the simple, solid fact That the Hydrozoan larva, the mouthless *Planula*, is packed With a jumbled mass of gastric cells that drop in, slow or fast, And show no slightest cavity till the larval stage has passed.

The larva then becomes attached, and shortly stands erect, Nourished by the yolky stores the inner cells eject: Their shrinkage leaves a growing space, the early enteron, Round which a layer of cells remains, and lines the outer one.

Some tentacles are sprouted then, say 2, then 4 and 8, And not till all is ready does the mouth break through quite late. If mouth and gut arose at first from one invagination, What roundabout procedure's here! What needless complication!

Invagination surely is a thing of later date—Procedure speeded up to suit the embryonic state:
The cells as loose irregulars build up the lower grades,
And yield but slowly, step by step, to organised brigades.

Reason in rhyme — this poem is an attack by Walter Garstang on Haeckel and his followers, who, in support of their "biogenetic law", invented an ancestor for all metazoans (the Gastrea theory) and claimed to be able to trace the evolution of the gut from a dimple in the surface of the primordial metazoan. It is reproduced from a new paperback reprint of Garstang's Larval Forms and Other Zoological Verses, published by University of Chicago Press. Price is \$5.95, £4.95.

The mystery of declining tooth decay

from Mark Diesendorf

Large temporal reductions in tooth decay, which cannot be attributed to fluoridation, have been observed in both unfluoridated and fluoridated areas of at least eight developed countries over the past thirty years. It is now time for a scientific re-examination of the alleged enormous benefits of fluoridation.

FLUORIDATION consists of raising the concentration of the fluoride ion F⁻ in water supplies to about 1 part per million (p.p.m.) with the aim of reducing dental caries (tooth decay) in children. In fluoridated areas, there are now many longitudinal (temporal) studies which record large reductions in the incidence of caries¹. The results of these and of fixed time surveys have led to the 'fluoridation hypothesis', namely that the principal cause of these reductions is fluoridation.

Until the early 1980s, there had been comparatively few longitudinal studies of caries in unfluoridated communities. Only a small minority of the studies in fluoridated areas had regularly examined control populations, and there seemed to be little motivation to study other unfluoridated communities. But during the period 1979-81, especially in western Europe where there is little fluoridation, a number of dental examinations were made and compared with surveys carried out a decade or so before. It soon became clear that large reductions in caries had been

occurring in unfluoridated areas (see below). The magnitudes of these reductions are generally comparable with those observed in fluoridated areas over similar periods of time.

In this article, these reductions are reviewed and attention is also drawn to a second category of caries reduction which cannot be explained by fluoridation. This category is observed in children described by proponents of fluoridation as having been 'optimally exposed', that is, children who have received water fluoridated at about 1 p.p.m. from birth. The observation is that caries is declining with time in 'optimally exposed' children of a given age. In some cases, the magnitudes of these reductions are much greater in percentage terms than the earlier reductions in the same area which had been attributed to fluoridation.

The problem of explaining the two categories of reduction goes well beyond the field of dentistry: contributions from nutritionists, immunologists, bacteriologists, epidemiologists and mathematical

statisticians, amongst others, may be required.

Caries in unfluoridated areas

Table 1 lists over 20 studies which report substantial temporal reductions in caries in children's permanent teeth in unfluoridated areas of the developed world. In many of these cases, the magnitudes of these reductions are comparable with those observed in fluoridated areas and attributed to fluoridation.

Several of these studies give clues as to factors which are unlikely to be the main causes of the reductions. A comparison of the 1954 and 1977 dental health surveys in Brisbane^{2,3} indicates to a reduction of about 50% in caries, as measured by the number of decayed, missing and filled permanent teeth (DMFT) per child and averaged over the age groups, in the 23year period. The 1977 survey distinguished between children who took fluoride tablets regularly, irregularly or not at all. Although there were differences in caries incidences between the three categories (which could reflect factors unrelated to fluoride levels), even the "no tablet" group had on average 40% less caries experience than that recorded in 1954. So fluoride tablets were not the principal cause of the reductions observed in Brisbane.

The first Sydney study⁴ showed that children with "naturally sound" teeth increased from 3.8% in 1961 to 20.2% in 1967 and 28% in 1972. The paper, which was titled enthusiastically "The Dental Health Revolution", was originally used widely to promote fluoridation in Australia. The authors stated that: "Almost certainly, the availability of fluoride both in tablet form and delivered through town water supplies has been the predominant factor.... These very large reductions represent a modern triumph of preventive health care"4. Yet the major proportion of the reported improvement had already occurred before Sydney was fluoridated in 1968. Moreover, no evidence was presented that fluoride tablets were widely used in the 1960s. Fluoride toothpaste was only introduced into Australia in 1967³. Although the index "naturally sound" teeth is unsuitable for more detailed

Table 1 Studies reporting large reductions in dental caries in unfluoridated areas

Location	on .	Years surveyed	References
Australia	Brisbane	1954, '77	2, 3
	Sydney	1961, '63, '67	4
Denmark	Various towns	1972, '79	53
Holland	The Hague	1969, '72, '75, '78	38
	Various towns	1965, '80	11
New Zealand	Auckland (parts)	1966, '74, '81	12
Norway	Various towns	1970, '80	54
Sweden	Various towns	1973, '78, '81	39
	North Sweden	1967, '77	55
United Kingdom	Bristol	1970, '79	56
	Bristol	1973, '79	56
	Devon	1971, '81	37
	Gloucestershire	Annually from 1964	37*
	Isle of Wight	1971, '80	57
	North-West England	1969, '80	58
•	Scotland	1970, '80	59
	Shropshire	1970, '80	10
	Somerset	1975-79 annually	60
	Somerset	1963-79	61
United States	Dedham, Mass.	1958, '74	40
	Norwood, Mass.	1958, '72, '78	40
	Massachusetts: sample of schools	1951, '81	41
	Ohio	1972, '78	62

^{*} Unpublished communication from J. Tee (1980), Area Dental Officer, Gloucestershire, to R. J. Anderson et al.³⁷

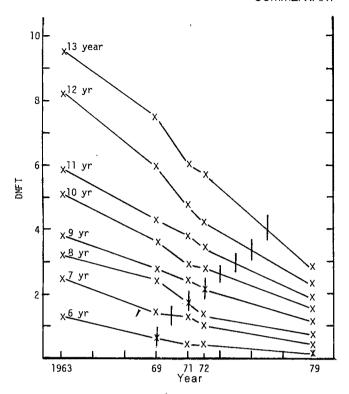


Fig. 1 Decline in caries, as measured by DMFT, in Tamworth, Australia, for children in age groups 6 years to 13 years. Data compiled from refs 14, 15. The vertical line cutting graph for each age group denotes year at which maximum possible benefit from fluoridation was reached.

Tamworth was fluoridated in 1963.

studies which distinguish decayed, missing and filled teeth, the populations examined were very large (over 9,000 children at each examination) and the results clear-cut.

A second Sydney study⁵ used the DMFT index, but was irrelevant for establishing any link with fluoridation, since it reported only on examinations in 1963 and 1982, but not around 1968 when Sydney was fluoridated. As in several other fluoridation studies, the key data were either not collected or not reported⁶. Although the two Sydney papers have an author in common (James S. Lawson, a senior officer of the New South Wales Health Commission), the second paper does not even cite the first. This suggests that, once it became clear that the first Sydney study contained evidence unfavourable to fluoridation, it was a source of embarrassment to some fluoridation proponents who are apparently trying to denigrate it.

However, independent confirmation of the large reductions in caries before fluoridation reported in the first Sydney study⁴ is readily obtained by comparing the results of two surveys^{7,8} separated by 20 years by Barnard. These surveys showed that the mean DIMF index ('1' denotes a permanent tooth which cannot be restored) for school children aged 13 and 14 declined from 11.0 in 1954-55 to 6.0 in 1972. The four years from 1968, when fluoridation commenced in Sydney, to

1972, would not have contributed significantly to the decline in caries prevalence in this age group⁹.

The authors of one of the British studies cited in Table 1 point out that sales of fluoride toothpaste in the United Kingdom were less than 5% of total sales in 1970, but rose to more than 95% of sales in 1977. They quote unpublished annual data from unfluoridated parts of Gloucestershire, collected from 1964 onwards, which show substantial improvements in children's teeth before the use of fluoride toothpaste became significant.

Many of the studies in the Netherlands, reviewed by Kalsbeek¹¹, were carried out to evaluate the effectiveness of the school

dental health programme. Temporal reductions in DMFT of about 50% occurred between 1970 and 1980, whether or not the children had taken part in the dental health education program. Kalsbeek also reviewed the use of fluoride tablets and toothpaste and concluded from the data that "factors other than the effects of different fluoride programmes must play a role."

The study in the partly fluoridated city of Auckland, New Zealand¹², examined the influence of social class (which reflects environmental and lifestyle factors, such as diet) as well as fluoridation on dental health as measured by the levels of dental treatment received by children. The paper showed that treatment levels have continued to decline in both fluoridated and unfluoridated parts of the city and that these reductions are related strongly to social class, there being less caries in the "above average social rank" group than in other children. Thus the main ethical argument for fluoridation, that it should assist the disadvantaged, is not borne out by this study.

Fluoridation's benefits

On 15 December 1980, the Dental Health Education and Research Foundation, one of the main fluoridation promoting bodies in New South Wales (NSW), issued a press release entitled, "Fluoridation dramatically cuts tooth decay in Tamworth" 13. This document, which highlighted results of a study conducted by the Department of Preventive Dentistry, Sydney University, and the Health Commission of NSW, stated in part:

Tamworth's water supply was fluoridated in 1963, and the last survey in the area was conducted in August 1979. It shows decay reductions ranging from 71% in 15-year-olds to 95% in 6-year-olds... All those surveyed were continuous residents using town water.

The "95%" reduction actually corresponded to a reduction in DMFT from 1.3 in 1963 to 0.1 in 1979¹⁴, which is 92%. The press release implied incorrectly that all this reduction was due to fluoridation. However, it has been claimed ever since

Table 2 Extent of fluoridation in Australia, 1977 and 1983

State or territory	. Capital city	Year city fluoridated*	% Of state fluoridated†	% Of state fluoridated† in 1983
ACT	Canberra	1964	100	100
Tasmania	Hobart	1964	74	77
NSW .	Sydney	1968	81	81
WA	Perth	1968	83	83
SA	Adelaide	1971	71	70
Victoria	Melbourne	1977	0.7 then 73	71
Queensland	Brisbane	Not fluoridated	10	5

^{*} Each capital city has the majority of the population of its state or territory.

[†] That is, the percentage of population of state/territory which drinks fluoridated water. Data from Annual Reports of Director-General of Health, for example ref. 17.

the commencement of fluoridation that the maximum possible benefits from fluoridation are obtained in children who have drunk fluoridated water from birth. Sixyear-olds would have done this by 1969, when, according to the published data15, they had a DMFT index of 0.6. The further reduction in caries in optimally exposed 6-year-olds, observed in years following 1969, cannot be due to fluoridation.

Thus, one can say that at best fluoridation could have approximately halved the DMFT rate in 6-year-olds between 1963 and 1969. (Since there was no control population, one could also say that at worst fluoridation might have had no effect in that period.) But from 1969 to 1979, caries in 6-year-olds was reduced a further 83%, by some other factor(s) than fluoridation.

Figure 1 shows that the unknown factors caused in children of each age from 6 years to 9 years similar large reductions in caries. Unfortunately, there are no published data for Tamworth beyond 1979 or in the years between 1972 and 1979, and so it cannot be confirmed whether the large reductions observed^{14,15} from 1972 to 1979 in children aged 10 to 15 were also due to these unknown factors.

A similar reduction beyond the maximum possible for fluoridation is observed for children of each age from 6 to 9 in the published data from Canberra¹⁶. which cover the period from 1964, the stated year of fluoridation, to 1974. In particular, DMFT rates declined by 50% in 6-year-olds from 1970 to 1974 and by 54% in 7-year-olds from 1971 to 1974. These reductions in optimally exposed children cannot be due to fluoridation. Published post-1974 data are needed to check on further reductions in optimally exposed children aged over 9 years.

From 1977 onwards, data have been systematically collected from the school dental services in each Australian state and territory^{9,17}. Table 2 shows the degree of fluoridation in each of these states/territories in 1977 and 1983 and also the dates of fluoridation of the capital cities of these regions. Each of these cities dominates the population of the state or territory in which it lies. The evidence presented in Fig. 2 and Table 2 suggests that states and territories which had been extensively fluoridated for at least 9 years before 1977 (Tasmania, Western Australia and New South Wales) had qualitatively similar large reductions in caries from 1977 to 1983 as a state which was only extensively fluoridated in 1977 (Victoria) and a state which had a small and declining fraction of fluoridation (Queensland). Although the results of the school dental health survey are recorded by age and state, the data have only been published^{9,17,18} so far for ages 6-13 averaged in each state, or for each age for the whole of Australia. There is evidence that the use of fluoride tooth-

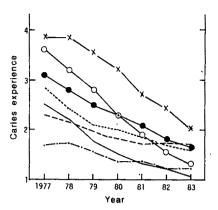


Fig. 2 Decline in the average number of (permanent) teeth per child with caries experience in each Australian state and the Australian Capital Territory as observed in school dental services17. 'Caries experience' can be one or more decayed, missing or filled teeth, and consists of an average for children aged 6-13 years. See Table 2 for information on the extent of fluoridation in each state/territory in 1977 and 1983 and the year when the main population centre of each state/territory was fluoridated. ×, Victoria; ○, Tasmania; ●, Queensland; - - ---, SA; ---, NSW; ---, WA; ·-·-·, ACT.

paste in Australia reached a high plateau around 1978, so these observed reductions in caries can be due neither to fluoride toothpaste9 nor to fluoridated water.

It is to be hoped that similar data on caries reductions in "optimally exposed" children will be sought in other fluoridated countries. In a region of Gloucestershire, United Kingdom where the main water supply was naturally fluoridated with 0.9 p.p.m. fluoride until 1972, reductions in caries of 51% were observed in 12-yearold children between 1964 and 197919. Factors other than fluoridated water must have caused these reductions. After 1972, the main water supply was drawn from a bore with less than 0.2 p.p.m. fluoride, so a recent survey of caries there would be of great interest.

Benefits overestimated?

In some fluoridated areas (for example Tamworth, Australia), temporal reductions in caries have been wrongly credited to fluoridation. The magnitude of these reductions is similar in both fluoridated and unfluoridated areas, and is also generally comparable with that traditionally attributed to fluoridation. Can it be concluded that communities which prefer not to fluoridate, either because of concern about potential health hazards²⁰⁻²⁵ or for ethical reasons (for example compulsory medication; medication with an uncontrolled dose), do not necessarily face higher levels of tooth decay than fluoridated communities? In other words, is it reasonable to ask whether it could be generally true that a major part of the benefits currently attributed to fluoridation is really due to other causes?

Such a hypothesis would seem to be possible in principle because it is well known that fluoridation is neither 'necessary' nor 'sufficient' (the words between inverted commas being used in the formal logic sense) for sound teeth; that is, some children can have sound teeth without fluoridation, and some children can have very decayed teeth even though they consume fluoridated water25.

To confirm or refute the hypothesis, it is necessary (but not 'sufficient') to examine the absolute values of caries prevalence in fluoridated and unfluoridated areas. If it is true that the absolute values of caries prevalence in some unfluoridated areas are comparable with those in some unfluoridated areas of the same country, then the hypothesis is supported (but not proven), and there would be a strong case for the scientific reexamination of the epidemiological studies which appear to demonstrate large benefits from fluoridation.

The earliest set of studies comparing caries in fluoridated and unfluoridated areas were time-independent surveys of caries prevalence in areas with 'high' natural levels of fluoride in water supplies, conducted by H. T. Dean and others in the United States²⁶. The surveys purported to show that there is an "inverse relationship" between caries and fluoride concentration. From the viewpoint of modern epidemiology, these early studies were rather primitive. They could be criticized for the virtual absence of quantitative, statistical methods, their nonrandom method of selecting data and the high sensitivity of the results to the way in which the study populations were grouped²⁵.

Results running counter to the alleged inverse relationship have been reported time-independent surveys naturally fluoridated locations in India², Sweden²⁸, Japan²⁹, the United States³⁰ and New Zealand^{31,63}. The Japanese survey²⁹ found a minimum in caries prevalence in communities with water F-concentrations in the range 0.3-0.4 p.p.m.; above and below this range, caries prevalence

increased rapidly.

These surveys²⁷⁻³¹ also selected their study regions nonrandomly. But recently Ziegelbecker32 attempted to make a selection close to a random sample by considering 'all' available published data on caries prevalence in naturally fluoridated areas. His large data set, which includes Dean's as a sub-set, comprises 48,000 children aged 12-14 years drawn from 136 community water supplies in seven countries. He found essentially no correlation between caries and log of fluoride concentration. The surveys²⁷⁻³² are generally omitted from lists1 of studies on the role of fluoridation in caries prevention.

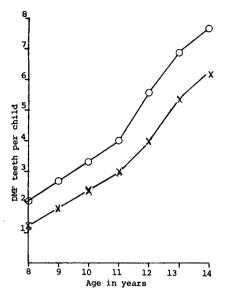


Fig. 3 The variation with age of decayed, missing and filled permanent teeth (DMFT) in fluoridated test towns (×) and unfluoridated control towns (O) in Britain, graphed from data published by the UK Department of Health³³. Note that the rate of increase of DMFT is essentially the same in both groups. Children in the fluoridated areas have an average only one less cavity than children of the same age in the unfluoridated areas.

Further evidence can be drawn from Fig. 2. In 1983, the absolute value of caries prevalence in the Australian state of Queensland (which is only 5% fluoridated) was approximately equal to that in the states of Western Australia (83% fluoridated) and South Australia (70% fluoridated).

The classical British fluoridation trials at Watford and Gwalchmai were longitudinal controlled studies. In this regard they were better designed than the majority of other studies which have been conducted around the world. However, as in the case of almost all other surveys, the examinations were not 'blind'. The review of the British trials by the UK Department. of Health after 11 years of fluoridation showed that children in fluoridated towns had approximately one less DMFT (that is, essentially one less cavity) than children of the same age in unfluoridated towns (see Fig. 3). The rate of increase in caries with age was the same in both populations³³

Thus there are a number of counter-examples to the widely-held belief that "All studies show that communities where water contains about 1 p.p.m. fluoride have about 50% lower caries prevalence than communities where water has much less than 1 p.p.m. fluoride".

At this point the empirical data presented here may be summarized as follows. In the developed world:

- (1) there have been large temporal reductions in caries in unfluoridated areas of at least eight countries;
- (2) there have been large temporal reductions in several fluoridated areas which cannot be attributed to fluoridation;
- (3) the absolute values of caries prevalence in several fluoridated areas are comparable with those in several unfluoridated regions of the same country.

Hence there is a case for scientific reexamination of the experimental design and statistical analysis of those studies which appear to prove or "demonstrate" that fluoridation causes large reductions in caries. Indeed the few re-examinations which have already been done confirm that there are grounds for concern.

The original justification for fluoridation in the United States, Britain, Canada, Australia, New Zealand and several other English-speaking countries was based almost entirely on the North American studies, which were of two kinds. The limitations of the first set, the time-independent surveys conducted in naturally fluoridated areas of the United States²⁶, have been referred to above.

The second set of North American studies consists of five longitudinal studies-carried out at Newburgh, Grand Rapids, Evanston and Brantford (two studies)-which commenced in the mid-1940s. Only three of them had controls for the full period of the study. These studies were criticized rigorously in a detailed monograph by Sutton³⁴, on the grounds of inadequate experimental design (for example, no 'blind' examinations and inadequate baseline measurement), poor or negligible statistical analysis and, in particular, failure to take account of large variations in caries prevalence observed in the control towns. The second edition of Sutton's monograph contains reprints of replies by authors of three of the North American studies and another author, together with Sutton's comments on these replies. It is difficult to avoid the conclusion that Sutton's critique still stands. Indeed, this was even the view of the profluoridation Tasmanian Royal Commission³⁵. Yet, in major, recent reviews of fluoridation, such as that by the British Royal College of Physicians³⁶ these North American studies are still referred to as providing the foundations for fluoridation, and Sutton's work³⁴ is not cited.

An examination has just been completed of the experimental design of all of the eight published fluoridation studies conducted in Australia. One (Tasmania) is a time-independent survey. Four (Townsville, Perth, Kalgoorlie and the second Sydney study) are longitudinal studies with only two examinations of the test group and either no control or only a single examination of a comparison group. The remaining three studies (Tamworth, Canberra and the first Sydney study) have several examinations of the test group, but no comparison group at all. Thus there has not been a single controlled longitudinal study in Australia. (M.D., to be published). Moreover, it has been shown above that three of the Australian studies (the first Sydney⁴, Tamworth^{14,15} and Canberra16) inadvertently provide evidence V that some other factor(s) than fluoridation is/are playing an important role in the decline of caries prevalence.

Hence the hypothesis that fluoridation has very large benefits requires reexamination by epidemiologists, mathematical statisticians and others outside of the dental profession. The danger of failing to perform scientific research on the mechanisms underlying the large reductions in caries discussed in this paper is that the strong emphasis on fluoridation and fluorides may be distracting attention away from the real major factors. These factors could actually be driving a cyclical variation of caries with time³⁷. It is possible that the condition of children's teeth could return to the poor state observed in the 1950s, even in the presence of a wide battery of F-treatments.

Causes of caries reductions

Many of the authors who reported the reductions in unfluoridated areas acknowledged that the explanation has not yet been determined scientifically^{11,37-41}. It is after all much easier to perform a study which measures temporal changes in the prevalence of a multifactorial disease than to identify the causes of such changes.

Nevertheless, the authors of some of these studies have speculated that important causes of the reductions which they observe might be topical fluorides^{38,53} (such as in toothpastes, rinses and gels), fluoride tablets^{4,38}, school dental health programmes⁹, a lower *frequency* of sugar intake³⁹, the widespread use of antibiotics which may be suppressing *Streptococcus mutans* bacteria in the mouth⁴¹, the increase in total fluoride intake from the environment^{9,42}, or a cyclical variation in time resulting from as yet unknown causes³⁷.

The present overview has revealed that several of the studies contain evidence against some of these proposed factors. We have seen that the Brisbane study³ and

the Dutch review¹¹ suggest that fluoride tablets may not be important; the Sydney study⁴, one of the British studies¹⁰ and the Dutch review¹¹ each provides evidence against fluoride toothpaste; and the Dutch review11 found no benefit in their school dental health education programmes.

Although there is evidence that fluoride toothpaste cannot be an important mechanism of caries reduction in some of the studies reported here, it must be stated that, unlike the case of fluoridation, there are also a few well-designed randomised controlled trials which demonstrate substantial reductions in caries from fluoride toothpaste⁴³. Hence, the hypothesis can be made that topical fluorides sometimes improve children's teeth, although they are not necessary. So topical fluorides may comprise one of several factors contributing to the solution of the scientific problem of explaining the reduction in tooth decay.

Leverett⁴² has speculated that the caries reductions in his smaller set of unfluoridated locations may be due to "an increase in fluoride in the food chain, especially from the use of fluoridated water in food processing, increased use of infant formulas with measurable fluoride content, and even unintentional ingestion of fluoride dentifrices." This hypothesis cannot explain the reductions in prefluoridation Sydney⁴, or those in unfluoridated parts of Gloucestershire which started in the late 1960s¹⁰. The ingestion of fluoride toothpastes (and gels) by young children is well documented and could account for an intake of about 0.5 mg F per day in the very young⁴⁴. But the food processing pathway is unlikely to be significant in western Europe where there is hardly any fluoridation, and infant formulas which are made up with unfloridated water will give only small contributions. Thus it appears that Leverett's hypothesis may at best be relevant to a minority of the studies listed in Table 1.

Here, the working hypothesis is presented that fluoridation and other systemic uses of fluoride, such as fluoride tablets, have at best a minor effect in reducing caries: that the main causes of the observed reductions in caries are changes in dietary patterns, possible changes in the immune status of populations and, under some circumstances, the use of topical fluorides. Indeed, a promising explanation is that the apparent benefit from fluorides is derived from their topical action. Then, since fluoridated water has a fluoride ion concentration 10⁻³ times that of fluoride toothpaste, its action in reducing caries is likely to be much weaker.

It is known that immunity plays a role in the development of caries, as it does with other diseases. Research is currently in progress to try to develop a vaccine against caries⁴⁵⁻⁴⁷. None of the data presented in the present paper provides evidence against immunity as a factor.

Dentists often argue against changes in dietary patterns as a major factor, on the grounds that sugar consumption has remained approximately constant in most developed countries over the past few decades. However, this is a simplistic argument. First, crude industry figures on total sales of sugar in developed countries contain no information on the distribution of sugar consumption with age and time of day. The form of sugar ingested-for example in canned food, soft drinks or processed cereals-may also be important. Second, tooth decay is increasing together with increases in sugar and other fermentable carbohydrates in the diet in several developing countries^{48,49}. This was also the case with Australian aborigines, even when their water supplies consisted of bores containing fluoride at close to the "optimal" concentration for the local climate^{50,51} Third, there is more to diet than sugar. For instance, there is some evidence, even conceded occasionally by pro-fluoride bodies⁵², that certain foods which do not contain fluorides (for example wholegrain cereals, nuts and dairy products) may protect against tooth decay. So the whole question of the relationship between total diet and tooth decay needs much greater input from nutritionists and dietitians.

Perhaps the real mystery of declining tooth decay is why so much effort has gone into poor quality research on fluoridation, instead of on the more fundamental questions of diet and immunity.

The main body of this research was performed while the author was a principal research scientist in the CSIRO Division of Mathematics and Statistics, Canberra.

Mark Diesendorf is at the Human Sciences Program, Australian National University. GPO Box 4, Canberra ACT 2601, Australia,

- 1. Murray, J. J. & Rugg-Gunn, A. J. Fluorides in Caries Prevention 2nd Edn (Wright, Bristol, 1982).

 2. Kruger, B. J. Aust. J. Dent. 59, 162-166 (1955).
- McEniery, T. M. & Davies, G. N. Community Dent. oral Epidem. 7, 42-50 (1979).
- 4. Lawson, J. S., Brown, J. H. & Oliver, T. I. Med. J. Aust. 1, 124-125 (1978).
- Burton, V. J., Rob, M. I., Craig, G. C. & Lawson, J. S. Med. J. Aust. 140, 405-407 (1984).
 Sutton, P. R. N. Med. J. Aust. 141, 394-395 (1984).
- Barnard, P. D. NHMRC Spec. Rep. Ser. 8, 30-43 (National Health & Medical Research Council, Canberra, 1956).
- 8. Barnard, P. D., Clements, F. W. Int. dent. J. 26, 320-326 (1976).
- Carr, L. M. Aust. dent. J. 28, 269-276 (1983).
- 10. Anderson, R. J., Bradnock, G. & James, P. M. C. Br. dent. J. 150, 278-281 (1981).
- 11. Kalsbeek, H. J. dent. Res. 61 (Special Issue), 1321-1326 (1982).
- 12. Colquhoun, J. Community Dent. Oral Epidemiol. 13, 37-41 (1985). 13. Dental Health Education & Research Foundation, News
- Release, Sydney, 15 December 1980.
- Barnard, P. D. Dent. Outlook 6(4), 46-47 (1980).
 Martin, N. D. & Barnard, P. D. Dent. Outlook no. 23, 6-7 (May, 1970); no. 33, 2-3 (May, 1972); no. 41, 6-7 (December, 1973).
- 16. Carr, L. M. Aust. dent. J. 21, 440-444, (1976).
- 17. Australia, Director-General of Health, Annual Report 1983-84, Table 69 (1984); Annual Report 1981-82, Table 66 (1982). Australian Government Publishing Service, Can-
- 18. Carr, L. M. Aust. dent. J. 27, 169-175 (1982).
- Anderson, R. J. Br. dent. J. 150, 354-355 (1981).
 Rose, D. & Marier, J. R. Environmental Fluoride, 1977 (National Research Council of Canada, Ottawa, 1977).
- 21. Waldbott, G. L., Burgstahler, A. W. & McKinney, H. L. Fluoridation: the Great Dilemma (Coronado, Lawrence, Kansas, 1978).

- 22. Tsutsui, T., Ide, K. & Maizumi, H. Mutat. Res. 140, 43-48 (1984).
- Tsutsui, T., Suzuki, N., Ohmori, M. & Maizumi, H., Mutat. Res. 139, 193-198 (1984). Tsutsui, T., Suzuki, N. & Ohmori, M. Cancer Res. 44, 938-941 (1984).
- Diesendorf, M. Commun. Hith Stud. 4, 224-230 (1980).
 McClure, F. J. (ed.) Fluoride Drinking Waters (US Department of Health, Education & Welfare, Public Health Service, Bethesda, Maryland, 1964). 27. Amrit, T. & Joshi, J. L. Conference Int. Soc. Fluoride Res.,
- New Delhi, November, Abstr. 15 (1983). 28. Forsman, B., Commun. dent. Oral Epidem. 2, 132-148
- (1974).
- 29. Imai, Y., Jan. J. Dent. Health 22, 144-196 (1972).
- 30. Zimmermann, E. R., Leone, N. C. & Arnold, F. A. J. Am. med. Ass. 50, 272-277 (1955).
- 31. Hewat, R. E. T. New Zealand dent. J. 45, 157-167 (1949).
- 32. Ziegelbecker, R. Fluoride 14, 123-128 (1981).
- Dept of Health, Report No. 122, HMSO, London (1969).
- utton, P. R. N. Fluoridation: Errors and Omissions in Experimental Trials 2nd edn (Melbourne University Press, Melbourne, 1960).
- Report of the Royal Commission into Fluoridation of Public Water Supplies (Government Printer, Hobart, Tasmania, 1968).
- 36. Royal College of Physicians, Fluoride, Teeth and Health (Pitman Medical, London, 1976). 37. Anderson, R. J., Bradnock, G., Beal, J. F. & James, P. M.
- C. J. dent. Res. 61 (Special Issue), 1311-1316 (1982). 38. Truin, G. J., Plasschaert, A. J. M., Konig, K. G. & Vogels,
- A. L. M. Commun. Dent. oral Epidem. 9, 55-60 (1981). 39. Koch, G. J. dent. Res. 61 (Special Issue), 1340-1345 (1982).
- 40. Glass, R. L. Caries Res. 15, 445-450 (1981).
- DePaola, P. F., Soparkar, P. M., Tavares, M., Allukian Jr, M. & Peterson, H., J. dent. Res. 61 (Special Issue). 1356-1360 (1982).

- 42. Leverett, D. H. Science 217, 26-30 (1982)
- 43. James, P. M. C., Anderson, R. J., Beai, J. F. & Bradnock. G. Commun. Dent. oral Epidem. 5, 67-72 (1977).
- 44. Ekstrand, J. & Ehrnebo, M. Canes Res. 14, 95-102 (1980). Ekstrand, J. & Koch, G, J. Dent Res. 59, 106 (1980)
- 45. Lehner, T., Russell, M. W. & Caldwell, J. Lancet i, 995 997 (1980).
- 46. McGhee, J. R. & Michalek, S. M., Am. Rev Microbiol. 35,
- 595-638 (1981).

 47. Smith, G. E., Trends pharmac, Sci. (in the press)
- 48. Newbrun, E. Science 217, 418-423 (1982) 49. Sheiham, A. Int. J. Epidemiol. 13, 142-147 (1984)
- 50. Barrett, M. J. & Williamson, J. J. in Aust den J 17, 37 50 (1972),
- 51. Brown, T. in Better Health for Abongines (eds Hetzel, B et al.) 97-101 (University of Queensland Press, Brisbane
- 52. Australian Nutrition Foundation, Dent. Outlook 11(2), 47-51 (1985).
- Fejerskov, O., Antoft, P. & Gadegaard, E., J dent. Res 61 (Special Issue), 1305-1310 (1982).
- von der Fehr, F. R. J. dent. Res. 61 (Special Issue), 1331-1335 (1982).55. Mansson, B., Holm, A. K. Ollinen, I. 55. Mansson, B., Holm, A. K., Ollinen, I. & Grahnen, H. Swed
- dent. J. 3, 193-203 (1979).
 56. Andlaw, R. J., Burchell, C. K. & Tucker, G. J. Caries Res.
- 16, 257-264 (1982). 57. Mainwaring, P. J. & Naylor, N. M. J. dent Res. 60, 1140
- (1981). 58 Mitropoulos, C. M. & Worthington, H. V. J dent Res 60,
- 1154 (1981). 59. Downer, M. C. J. dent. Res. 61, 1336-1339 (1982)
- Palmer, J. D. Br. dent. J. 149, 48-50 (1980).
 Anderson, R. J. Br dent. J. 150, 218-221 (1981).
- 62. Zacherl, W. A. & Long, D. M. J. dent. Res 58, 227 (1979) 63. Hewat, R. E. T. & Eastcott, D. F., Dental Caries in New Zealand, pp. 75-76, 79 (Medical Research Council of New Zealand, 1955).

Pathogenesis of lentivirus infections

Ashley T. Haase

Department of Microbiology, University of Minnesota, 420 Delaware St, SE, Minneapolis, Minnesota 55455, USA

Following infection of animals or humans, lentiviruses play a prolonged game of hide and seek with the host's immune system which results in a slowly developing multi-system disease. Emerging knowledge of the disease processes is of some relevance to acquired immune deficiency syndrome (AIDS), which is caused by a virus possessing many of the characteristics of a lentivirus.

LENTIVIRUSES, a subfamily of retroviruses (Table 1), derive their name from the slow time course of the infections they cause in humans and animals¹⁻¹⁰. The persistence and spread of these viruses, despite host defences, and the origins and slow evolution of the diseases they cause, pose fascinating problems in pathogenesis which have assumed a new significance with the addition of the agent of acquired immune deficiency syndrome (AIDS) to the subfamily. This review summarizes the increasingly coherent picture of the pathogenesis of lentivirus infections, and discusses the relevance of these concepts to the behaviour and control of the AIDS virus.

Visna-maedi and central issues

Lentiviruses cause chronic diseases affecting the lungs, joints, nervous, haematopoietic and immune systems of humans and animals (Table 1). The prototypic lentiviruses, visna and maedi, derived their Icelandic names from the prominent symptoms (wasting and shortness of breath) of the neurological and pulmonary diseases they cause in sheep. In fact, it is the same virus² that is responsible for both maedi, the more prevalent pulmonary disease, and visna, a paralytic condition showing some resemblance to multiple sclerosis 11-15. These two diseases reached epidemic proportions in Iceland in the 1940s about a decade after the virus was inadvertently introduced into Iceland by sheep imported from Germany. An Icelandic physician, Bjorn Sigurdsson, investigated the outbreaks of visna and maedi, showed that a filterable agent caused them12, and discovered the long incubation period and protracted course of disease that distinguish slow infections¹⁶. Sigurdsson introduced the term slow infection¹⁷ to capture the novel timescale of disease and the experimental design needed to demonstrate transmissibility, thus setting the stage for the discovery of slow diseases in man¹⁸.

In natural and experimental infections of sheep (Fig. 1a), the aetiological agent of visna-maedi replicates at the site of entry (the lung in natural infections) and subsequently spreads via the bloodstream or by other routes, such as the cerebrospinal fluid (CSF). The infected animal mounts a defensive response which has both nonspecific components, such as phagocytic cells, and specific humoral and cellular-immune elements 19,20. These defence mechanisms are effective against extracellular virus but are generally unable to eradicate the infectious agent altogether. Virus persists in many organ systems and continues to circulate in blood and tissue fluids. In the lungs and central nervous system (CNS), tissue is destroyed in areas where inflammatory cells have collected, and eventually this burden of pathological change becomes apparent as shortness of breath or partial paralysis and weight loss. In natural infections, animals generally become symptomatic in the second year of infection and die after a protracted and progressive illness.

This brief description of the major events of infection in visna-maedi is intended to bring out three salient problems in understanding the pathogenesis of slow infections: (1) How does

virus persist and spread in the face of a vigorous and sustained immune response by the host? (2) What causes destruction of tissue? (3) Why do these pathological events evolve so slowly?

Virus gene expression and persistence

The best current explanation for the persistence of lentiviruses is the immunologically silent nature of the infection. Most infected cells harbour the virus in a latent state in which viral antigens are not produced in sufficient quantities for detection and destruction of the infected cell by immune-surveillance mechanisms²¹. To show the magnitude of these damping effects, evidence for and molecular measures of the restricted virus gene expression in vivo have been set against a background of the growth of virus under permissive conditions in tissue culture in Figs 1 and 2 and Table 2. In tissue culture, visna virus reproduces rapidly to high titre and destroys the host cell^{22,23}. In this lytic and productive cycle, genetic information is transferred from the RNA genome of the infecting virus to a DNA intermediate

Table 1 Retrovirus subfamilies					
Subfamily	Disease	Natural hosts			
Oncoviruses	Cancer	Man, animals, birds and reptiles			
Spuma viruses	Inapparent infections	Man, animals			
Lentiviruses	Slow infections	Man, animals			
Visna-maedi virus	Pneumonia, meningoencephalitis	Sheep, goats			
Progressive pneu- monia virus (PPV)	Pneumonia	Sheep, goats			
Caprine arthritis encephalitis virus (CAEV)	Arthritis, pneumonia, meningoencephalitis	Goats, sheep			
Zwoegerziekte	Pneumonia, meningoencephalitis	Sheep			
Equine infectious anaemia virus (EIAV)	Fever, anaemia	Horses			
AIDS virus (HIV)	Immune deficiency, encephalopathy, myelopathy	Man			

The retrovirus subfamilies shown are currently accepted taxonomic divisions¹²¹. The EIAV and AIDS virus are provisionally included in the lentivirus subfamily because they, too, cause slow infections and have other properties in common with visna-maedi¹²²⁻¹³¹: cell fusion and other cytopathic effects in tissue culture; virion morphology; polypeptide composition; large envelope glycoproteins; shared antigenic determinants in the major structural protein (gag); similar size and structure of their genomes; nucleotide and amino-acid sequence homologies largely confined to conserved regions of gag-pol.

in the cell^{24,25} which serves as a template for the synthesis of thousands of copies of genomic and messenger RNAs (Table 2a). The latter are translated into millions of copies of structural virion proteins²⁶ and infectious progeny (50–100 per cell) subsequently assemble at the cell surface. The infected cells degenerate, either individually or after fusion²⁷, within 3 days.

By contrast, replication of virus in animals is highly focal and unproductive, even in relatively homogeneous populations of cells which serve as substrates for permissive growth in tissue culture: the number of copies of viral RNA in choroid plexus of infected animals is about two orders of magnitude less than in infected choroid plexus cells in culture (Table 2). Synthesis of viral RNA, antigens and virus is confined to one in a hundred to thousands of cells (Table 2b)²⁸. This focal and restricted growth cycle has been revealed by methods for quantitative analysis of virus replication at the single-cell level (in situ hybridization)²⁹ and, more recently, by methods that combine macroscopic screening of tissue with single-cell resolution (Fig. 2)30. The fundamental question of why virus growth should be so different in cells in culture from that in tissues is unanswered, but viral RNA synthesis has been defined as the major point in the virus growth cycle at which virus gene expression is blocked28.

Visna thus has two kinds of life cycle, somewhat analogous to bacteriophage λ in *Escherichia coli*: a productive and lytic life cycle in vitro and a latent life cycle in sheep, figuratively referred to as lysogeny on a grand scale³. This is probably overstated, as visna virus is not integrated into the host cell genome, àt least in tissue culture³¹, but it does epitomize the notion of the clandestine state of the virus as the mechanism by which it eludes the host's defences.

Trojan horse mechanism

A similar mechanism can be invoked to explain the continued spread of virus in the bloodstream, cerebrospinal fluid and other fluids that contain immune cells and neutralizing antibody. In this mechanism, a mobile cell, predominantly if not exclusively a monocyte^{32,33} in the case of visna virus, conceals the virus genome and conveys it without detection to other sites. Evidence for this Trojan horse mechanism again comes from in situ hybridization analyses of CSF, where infected cells are concentrated³². (The frequency of leukocytes carrying visna virus in the bloodsteam—about 1 in 10⁶ cells—is too low to be detected directly.) The CSF data³² provide evidence of (1) restricted levels of viral RNA accumulation in monocytes; (2) circulation of the latently infected monocytes in tissue fluids containing neutralizing antibody; and (3) transfer of infectious virus between monocytes and choroid plexus cells under conditions of close contact between the cells. These data satisfy the major predictions of the Trojan horse hypothesis.

Inapparent infections and latency

The theme of restricted virus gene expression is the dominant motif of lentivirus infections. In animals, infections are frequently not apparent, with no obvious pathological sequelae for periods that approximate the normal lifespan of the host. In the United States, for example, lentivirus infection of sheep is widespread and probably largely asymptomatic³⁴. There are flocks of sheep in Germany in which antibodies to virus are present in 50 per cent of the serum samples³⁵ and in which clinical symptoms of maedi have never been observed. Importation of silently infected sheep like these from Germany was presumably responsible for the outbreaks of maedi and visna in Iceland⁴.

The AIDS virus also establishes persistent and non-cytopathic infections in normal human lymphocytes³⁶. In the persistently infected cultures, virus production may be absent or limited (but can be induced), in keeping with the definition of latency³⁷. By extrapolation, similar virus-host cell interactions provide a mechanism for the AIDS virus to escape neutralization and

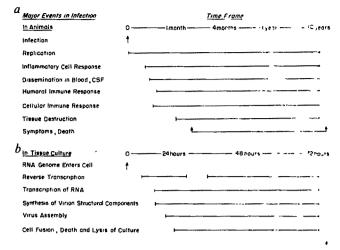


Fig. 1 Time course of animal lentivirus infection. The major events and strikingly different timescale of infection in animals (a) and tissue culture (b) can be seen.

other defences, but also a basis for the comforting observation that inapparent infection and a carrier state are common in infected patients³⁸.

Population spread

Animal lentivirus infections are transmitted between animals, probably by virus inside monocytes and macrophages in secretions (little if any cell-free virus is detectable). The aetiological agents of visna and maedi enter adult sheep by the respiratory route and lambs by a gastrointestinal route in colostrum^{2,4}. The appearance of disease in epidemical form requires special conditions such as those in Iceland, where sheep from many parts of the island are housed together for several days each year². This practice may have been as important in the rapid spread of the disease as the greater susceptibility of the Icelandic than German sheep to lentivirus infection.

AIDS is transmitted similarly. Virus is introduced into the bloodstream through sexual contact, intravenous drug administration with contaminated needles or administration of blood and blood products³⁶. It is not known whether the virus is transferred inside cells, but this is obviously of great importance in predicting the efficacy of conventional vaccine strategies to interdict further spread of AIDS. As in visna, perinatal transmission is also important, although it is not known whether this occurs in utero or postnatally.

There is no evidence of germline transmission of animal lentiviruses from mother to offspring, and endogenous lentiviruses are exceptional³⁹, in contrast to the situation with

Table 2 Comparison of the growth of visna virus in animals and in tissue culture

Type of infection	Cells positive for viral RNA (%)	Average no. of copies of viral RNA per infected cell	Cells with viral antigen (%)
a, Tissue culture (choroid plexus cells 3 days after infection)		5,000	90
b, Sheep (choroid plexus, alveolar macrophage monocytes, glial cells to 3 weeks after infec	; 3 days	50-150	0.001

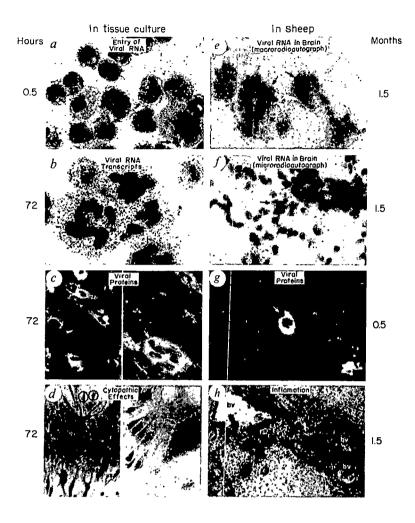


Fig. 2 Life cycles of an animal lentivirus in tissue culture and sheep. a, b, Autoradiographs of visna virus RNA detected by in situ hybridization. The number of copies of viral RNA in individual cells is proportional to the number of grains over the cell and the length of exposure2 At 0.5 h after infection (at a multiplicity of infection of 3 plaque-forming units per cell) about 30 copies of viral RNA enter the cell, often apparently inside a vacuole (arrows, a). By 72 h the cells contain about 5,000 copies of viral RNA²⁶, often in giant cells. Visna virus RNA can be localized anatomically in infected animals to regions surrounding the ventricles (arrows, e) using combined macroscopic-microscopic screening³⁰. In this method whole brain sections are hybridized to a virus-specific probe labelled with 125 I. The γ emission of 125 I produces a latent image of viral RNA on X-ray film placed against the tissue section after hybridization. The single-cell location of viral genes is determined from a microscopic autoradiograph produced by coating the section with nuclear track emulsion. The Auger electrons emitted by ¹²⁵I produce latent images with good resolution at the cellular level. The average copy number in the cells in the brain is about two orders of magnitude less than that in infected tissue culture (for example, number of grains over the cell in tissue culture 72 h after infection requires an exposure of a few hours; for a probe of the same specific activity, about 3 weeks would be needed to produce the number of grains in the cells in brain)30. In tissue culture there are ~106 copies of major viral protein (gag) easily detected in most cells by immunofluorescence with monospecific antibodies (c; the arrow indicates a giant cell with the visna gag polypeptide in the cytoplasm)4,127 Only rare cells with viral antigens can be detected in the infected animal (g). The infection in tissue culture leads directly to cell death with lysis of the culture in 72-96 h (d). Arrows indicate giant cells in various states of degeneration; individual dying cells are circled. In animals, tissue damage accumulates over months to years (h) and is indirectly caused by inflammatory cells (the dark-staining lymphocytes, plasma cells, monocytes, macrophages that surround the blood vessles (bv) and collect in foci in the tissue of this section of brain from a paralysed sheep¹⁻⁷.

oncogenic retroviruses. The exogenous nature of lentiviruses may reflect their infrequent opportunities to interact with the host genome. Only a few cells are infected in the animal, replication is restricted²⁸ and integration may be rare³¹. The failure of the viral genome to form covalent linkages with the host chromosome probably has a structural basis, as the topological precursor for retrovirus integration is likely to be circular DNA⁴⁰, and in cells infected with visna virus circular molecules are rare (the predominant structure is a nicked or gapped linear duplex)⁴¹. That is not to say that integration of lentivirus genomes cannot occur—integrated as well as unintegrated forms of AIDS virus⁴², equine infectious anaemia virus (EIAV)⁴³ and caprine arthritis and encephalitis virus (CAEV)⁴⁴ have been described.

Variant and common determinants

Antigenic variation is an additional or alternative mechanism for the persistence and spread of the lentiviruses. In this instance, the emergence of mutant viruses with an altered envelope glycoprotein, the antigen to which neutralizing antibody is directed⁴⁵, is the postulated mechanism by which virus temporarily escapes immunological inactivation. Gudnadottir's proposal that 'antigenic drift' might account for the survival of visna virus for such a long time in infected animals² was subsequently supported and fully developed by Narayan and his collaborators. They showed that antigenically distinct viruses could be isolated from sheep persistently infected with visna virus⁴⁶, and that these variants arise by point mutations in the *env* gene, which encodes the virion envelope glycoprotein^{45,47}. In visna,

however, variants do not replace the infecting serotype by antibody selection and, in most long-term infections, the inoculum virus strain persists and spreads without the emergence of antigenic variants^{48,49}. For these reasons it seems unlikely that antigenic variation is a necessary or important means of dissemination of visna virus.

For EIAV, the case for antigenic variation as an important mechanism of virus dissemination is more persuasive. There are cycles of virus replication in which cell-free virus is isolated from serum or plasma, and each new isolate from a cycle is refractory to neutralization by antibody that neutralized previous isolates^{50,51}. This immunologically dictated succession fulfils the expectations of the antigenic variation model for persistence and spread of viruses, and, as in visna virus infections, occurs primarily through point mutations in the env gene⁵². But this is not the sole basis for persistence and spread. By the end of the first year, cyclic replication of EIAV is superseded by an inapparent carrier state in which continued dissemination of virus within the host, or to new hosts, is again accomplished by latently infected macrophages⁹. Because this conversion to a Trojan horse mechanism of spread may be a consequence of production of antibody to all strains of EIAV, identification of these common antigenic determinants for neutralization would clearly be important in designing broadly effective vaccines.

It would be premature to predict the role of antigenic variation in AIDS infections, but isolates of the AIDS virus from different individuals differ genotypically⁵³, and this genomic diversity is greatest in the region of the *env* gene⁵⁴. If these genetic changes

are mirrored phenotypically, it will pose serious problems for vaccine development and provide an additional mechanism for the AIDS virus to persist and spread in individuals and populations.

Immunopathogenesis

Pathological changes in lentivirus infections are for the most part indirectly mediated by the immune and inflammatory response of the host. In visna, the coordinate reduction of inflammation and tissue lesions⁵⁵ with immunosuppression suggests that it is the inflammatory cell response (Fig. 2) that causes tissue damage. In the brain, this process is demyelinating¹¹⁻¹⁵ because at least one of the infected cell targets is the oligodendrocyte⁵⁶, the cell in the nervous system which provides the myelin sheath (identified unambiguously by a new method that combines immunocytochemistry, cell-specific antibodies and in situ hybridization⁵⁷; Fig. 3). The rare infected cell containing viral antigen probably provokes and sustains this inflammatory response⁵⁶, which then causes tissue damage by mechanisms that are not understood in any detail but could involve interleukin-mediated amplification of the response with indiscriminate damage to uninfected cells ('innocent bystanders') in the area. Lesions in the lungs and joints of infected animals in maedi virus and CAEV infections are also the result of the exuberant inflammatory response. In the lung, infiltration of lymphocytes and monocytes into the alveolar wall interferes with gas exchange; in the joints^{58,59}, the inflammatory cell infiltrate leads to the destruction of the cartilage perhaps by activating chondrocytes to elaborate matrix degrading factors⁶⁰, much as in rheumatoid arthritis.

Both lymphoproliferative changes (enlargement, necrosis) and immune complexes participate in the immunopathology of equine infectious anaemia^{9,61}. The characteristic anaemia is the result of phagocytosis and haemolysis of erythrocytes that first become coated with a viral haemagglutinin and then with antivirus antibody and complement. Circulating immune complexes of EIAV and antibody also elicit fever and cause glomerulone-phritis when they are deposited in the kidney. The, as yet unexplained, glomulerosclerosis and thrombocytopenic purpura of AIDS may similarly be immune complex diseases^{62,63}.

Immunopathology, however, cannot account for all the manifestations of lentivirus infections. There is an inflammatory component in the progressive encephalopathy that occurs frequently in children and adults with AIDS⁶⁴⁻⁶⁶, but in AIDS encephalopathy and myelopathy⁶⁷, inflammation is overshadowed by vacuolation and degenerative changes that are more like those in a paralytic disease of mice caused by some types of murine leukaemia viruses⁶⁸.

Immunodeficiency and cachexia

The agent of AIDS differs most profoundly from the lentiviruses of animals in its effects on the immune system. Immunodeficiency is the hallmark of AIDS^{10,69}, whereas in animal lentivirus infections the immune response is relatively normal or selectively impaired. (In natural US infections, particularly with CAEV, animals ordinarily produce little if any neutralizing antibody⁷⁰.) Until recently, the reasons for this distinction seemed relatively straightforward: the AIDS virus homes to a receptor on the surface of helper T cells^{71,72} and was thought to cause AIDS by destruction and depletion, or dysfunction, of this central element of the immune system. The animal lentiviruses infect monocytes in such small numbers that the impact on immune function is minor³².

It is becoming increasingly evident that this view is oversimplistic, inasmuch as infection of T4 lymphocytes (about 1 positive cell in 20,000-100,000 by in situ hybridization⁷³) is as infrequent in AIDS as it is in visna. To account for the large effects on the absolute number of T4 cells and immune function in AIDS, more complex mechanisms need to be invoked, including some that recall the theme of immunopathology in lentivirus

Immunocytochemistry with anti-oligodendrocyte antibody in situ hybridization Radioautography

Fig. 3 Determination of virus host cell tropism by the simultaneous detection assay⁵⁷. Brain sections from a paralysed sheep infected with visna virus were reacted with anti-oligodendrocyte antibody, and the reaction was visualized by immunocytochemical methods. After in situ hybridization with a visna virus-specific probe, the developed autoradiograph was examined to locate cells (oligodendrocytes) which stained with the antibody and also had an increased number of silver grains such as that shown in the figure. This method identifies the oligodendrocyte unambiguously as one of the types of cells infected by visna virus⁵⁶.

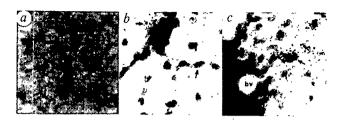
infections. For example, viral envelope glycoprotein shed from productive cells could make large numbers of uninfected cells targets for an autoimmune response directed to viral antigen bound to the T4 receptor. Alternatively, the network of interactions in the immune system should in time lead to an antiidiotypic response to antibody to the viral glycoprotein. This anti-idiotypic antibody might also be directed against the T4 antigen and viral receptor. This hypothetical reconstruction of the immune response provides a rationale for understanding the production of anti-lymphocyte antibodies in AIDS⁷⁴, and a basis for a paradoxical and potentially hazardous approach to treatment by immunosuppression⁷⁵. The latter could also theoretically relieve a block in the expansion, differentiation or function of T4 cells mediated by another subset of lymphocytes infected with the AIDS virus. Just as plausible, however, are direct mechanisms leading to immunodeficiency, for example, continued recruitment of uninfected T4 lymphocytes into the infectious process, destruction of precursors or the release of immunosuppressive virion components analogous to the p15E protein of feline sarcoma virus 76,77.

One of the unexplained symptoms of infection, the cachexia or wasting ('slim disease' is the name given to one form of AIDS in Uganda⁷⁸), might be partly attributable to interactions of lentiviruses with macrophages. In addition to inanition from concurrent enteropathic infections (possibly including AIDS virus) and diarrhoea which contribute to these manifestations of the infection, lentiviruses might, as the result of infection of monocytes, cause release of cachexin, a factor that inhibits adipocyte gene expression and the production of lipogenic enzymes⁷⁹.

Form and tempo of pathology

Visna virus gene expression is markedly curtailed in most infected cells in tissues²⁸, but there are a few cells in which levels of viral RNA approach those in productively infected tissue culture⁵⁶. These gradations in gene expression (Fig. 4) are tightly correlated with detection of viral antigens, the intensity of the inflammatory response, and tissue damage, as would be expected if gene expression determines the form and tempo of pathology. At one end of a spectrum of virus gene expression are a silent majority of infected cells with minimal levels of viral RNA and antigens, enabling the virus to persist and spread. Towards the other end of the spectrum is the occasional cell with higher levels of viral RNA and the antigens responsible for the continuing inflammatory cell response and inadvertent destruction of tissue at a rate commensurate with the scanty production of the inciting antigens. At the extreme end of the spectrum is the lytic

Fig. 4 Quantitative in situ hybridization used to demonstrate correspondence between virus gene expression and inflammatory response. Brain sections from a paralysed sheep infected with visna virus were hybridized with a virus-specific probe. In the developed and stained microautoradiographs there is a gradient in gene expression that correlates with the intensity of inflammation. a, A region with no inflammation and background levels of hybridization; b, as the number of copies of viral RNA increases, larger numbers of grains appear over cells (arrows) adjacent to small collections of dark-staining mononuclear cells; c, the largest numbers of inflammatory cells around blood vessels (bv) and tissue are adjacent to infected cells (arrow) with grain counts equivalent to hundreds to thousands of copies of viral RNA typical of productive infections in tissue culture. Viral antigens are occasionally demonstrable in cells with the highest concentrations of viral RNA56



infection in tissue culture, where destruction of cells is a rapid and direct result of virus growth under permissive conditions of replication. These cytopathic effects are more likely to be due to the abundance of virion components (probably the envelope glycoprotein) capable of fusing and killing the cell from within and outside²⁷ than to the high concentrations of extrachromosomal DNA which have been advanced as one explanation for these cytotoxic effects of retroviruses⁸⁰; experimental conditions can be contrived in visna-infected tissue culture (blocking superinfection with antibody)⁸¹ where fusion and cell death occur at DNA concentrations equivalent to those in tissues²⁸ at which cytopathic effects are never observed.

Regulatory mechanisms and control

The major thrust of this review on lentivirus pathogenesis is that the major issues of persistence, spread and the rate and mechanisms of cell death translate into more objective questions about the factors that control lentivirus replication. Indeed, the central fact and unresolved mystery in visna is why the replication of virus is restricted in the same relatively homogeneous and non-dividing population of cells that supports abundant replication after explantation²¹ or in non-dividing cells in cultures derived from the same tissues81. Many factors have been investigated that might potentially account for restriction; they fall into two general categories (extracellular and intracellular), and pertain to tissue culture systems or living hosts. The latter is an important distinction, because there are many examples of regulatory mechanisms that operate in tissue culture but bear little relationship to reality. For instance, one can establish persistent infections in tissue culture with visna virus in which the cells contain high concentrations of viral antigens, whereas the concentrations are low in infected sheep (A.T.H., unpublished). Moreover, antigenic variants of visna virus appear in a logical succession based on antibody selection in vitro⁸², but not in infected animals^{48,49}; and gene dosage effects in tissue culture⁸¹ apparently do not operate in vivo⁸³. The discussion below therefore concentrates on regulatory mechanisms which meet the test of relevance at the organismal level and which might be exploited in the control of lentivirus infections.

Sanctuaries and vaccines

In natural and experimental visna, dissemination of virus by extracellular routes largely ceases with the appearance of neutralizing antibody¹⁹, acting perhaps in concert with viral inhibitory factors in serum and CSF^{84,85}. Neither humoral nor cellular immunity, however, plays a significant part in maintaining latency, since immunosuppression does not relieve the restriction in virus gene expression^{55,86}.

The experience with animal lentivirus vaccines is unfortunately too limited to give much direction to vaccine development. Veterinary practices of identifying infected sheep by serological testing and removing them from flocks have been successful in controlling lentivirus infections of animals^{1,7,87}. No vaccine for

visna or maedi is available because of intractable difficulties in developing an inactivated virus or envelope component vaccine that will induce neutralizing antibody. Vaccinated sheep do produce complement-fixing antibody but are not protected. Moreover, natural infections are transmitted to lambs by cells in the colostrum of mothers carrying neutralizing antibody. This mechanism of transmission and the possibility of cell-cell spread⁸⁸ would circumvent conventional strategies for disease control. Lentiviruses also take refuge from immune defences in the central nervous system. Thus, vaccines alone cannot be expected to be wholly effective in preventing lentivirus infection, but may favourably alter the outcome by reducing at the outset of infection the number of cells with the potential to contribute to pathological changes.

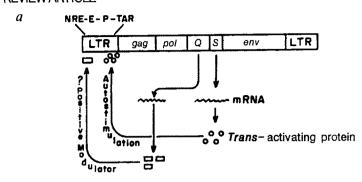
In AIDS, neutralizing antibody^{89,90} titres are low⁹⁰, virus in semen⁹¹ and saliva⁹² is partly cell-associated⁹³, and the brain is infected as a potential sanctuary for virus in a significant segment of the infected population^{64,94-96}. These considerations, and potential difficulties in vaccine development, underscore the importance of the practical measures and behavioural advice currently recommended to limit the spread of AIDS³⁶.

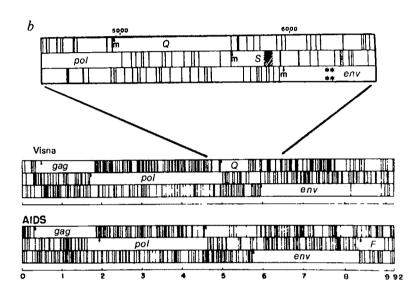
Intracellular mechanisms and antisense vaccine

Because viral gene expression directly or indirectly mediates cell damage, measures that limit gene expression should moderate or present the pathological consequences of infection. DNA synthesis is a logical point in the virus life cycle at which to intervene with drugs that inhibit reverse transcription or, like interferon, act intracellularly. The experience with the effects of inhibitors of viral DNA synthesis ^{97,98} and interferons ^{99,100} is limited to *in vitro* experiments which suggest that some benefit might be achieved ¹⁰⁰. In AIDS, inhibitors of reverse transcription have already undergone clinical trials, with demonstrable but temporary inhibition of virus replication and little alteration in clinical status ¹⁰¹. Sustained treatment with newer and less toxic drugs may induce long-term remissions ¹⁰².

Transcription and translation of the lentivirus genome are also potential targets for therapy. The major controlling elements for lentivirus gene expression are located at the 5' end (long terminal repeat, LTR) and centre of the genome (Fig. 5a, b). The lentiviral LTR, in common with other retroviruses, has promoter and enhancer domains and two additional domains, designated NRE and TAR in Fig. 5, which have negative or positive effects respectively on gene expression $^{103-105}$. The transactivating region (TAR) is responsive to a gene product encoded in a short open reading frame S (Fig. 5b) 103 . The transactivating gene product (TAT) of this open reading frame acts post-transcriptionally 106 to stimulate gene expression by 500-1,000-fold and is required for replication 107,108 . Modest stimulation by transactivation has also been described recently for visna virus 109 , which is comparable to that of the AIDS virus when the entire LTR of visna virus is used in the assay (K. Staskus, C. Rosen, W. Haseltine and A.T.H., unpublished). If transactivation has also been described as a sample of transactivation and A.T.H., unpublished).

Fig. 5 Speculations on control of lentivirus gene expression. a, Schematic illustration of a prototypic lentivirus genome and a speculative representation of control of gene expression. Transcription of the major genes of the virus is controlled by promoter (P) and enhancer (E) regions in the LTR. A trans-activating protein (O) encoded by the short open reading frame S binds to a region (TAR) to stimulate gene expression. The gene product of open reading frame Q also binds to the LTR to up-regulate transcription. The overall organization of the genomes of visna virus and the AIDS virus is shown in b with the controlling region in the centre of the genome with Q and S. (Modified from refs 103-110.) m, Initiator Met codon; F, an additional open reading frame in HIV (human immunodeficiency virus); asterisks in env indicate the hydrophobic signal sequence.





activation in visna is also effected post-transcriptionally, it could not account for the restricted gene expression in infected sheep which is primarily a result of diminished accumulation of viral RNA²⁸, but it could account for the discrepancy between the relatively high concentration of virus RNA in some cells and the lack of infectivity⁸³.

The reduction in transcription in infected animals was most recently speculated to be due to repressor activity of a putative DNA-binding protein, the basic and hydrophilic gene product of conserved open reading frames (Q) in visna¹¹⁰ and the AIDS virus¹¹¹⁻¹¹⁴. But there is now evidence that the Q gene product is a second positive regulatory factor, because deletion of Q slows the growth of the AIDS virus and delays the development of cytopathic effects¹¹⁵. Highly productive and rapidly progressive lytic infections may require co-expression of both factors, as might occur, for example, during activation of macrophages (CAEV) or lymphocytes^{116,117}.

One possible approach to the control of lentiviruses that anticipates the importance of the regulatory proteins encoded by the Q and S genes, and exploits antisense in mRNA¹¹⁸⁻¹²⁰, is the development of defective virus vectors which would stabilize the dormant state of infection. In one such project in progress in the visna model (K. Staskus, E. Retzel and A.T.H., unpublished), the trans-activating gene in infectious viral DNA is replaced by its antisense counterpart. Defective virus, produced by co-transfecting cells with the viral antisense DNA and with S gene DNA in an inducible expression vector, will have an identical host range to wild-type virus. It will therefore serve as a vector to introduce the antisense gene into cells already harbouring standard virus. In the co-infected cells, trans-activation should at first drive production of additional defective virus to

disseminate the antisense vector. Thereafter, the antisense vector should halt *trans*-activation and return the infected cells to a latent state. Of course, before there could be any assurance that the pathological consequences of infection may be prevented, this approach must overcome some theoretical and practical difficulties—particularly superinfection barriers in cells producing AIDS virus and the need to establish co-infection in a large pool of cells with a non-replicating virus.

Conclusions

The lentiviruses are responsible for slow infections of animals and man. Investigations of animal lentivirus infections have previously been directed to the inherently interesting issues of pathogenesis raised by this novel class of infections, parallels to such chronic diseases of man as multiple sclerosis and rheumatoid arthritis, and, to a much lesser extent, practical means of diagnosing, treating and preventing disease. With the knowledge that the causative agent of AIDS is a distant relative of the animal lentiviruses, these objectives have assumed a new and compelling urgency. Restricted gene expression is the general underlying mechanism in the persistence and spread of lentiviruses and the slow evolution of the diseases they produce. This restriction maintains the lentivirus genome in the cell in a covert state, and justifies the optimistic prediction that the commonest form of infection in AIDS, inapparent infection, will prevail for much, if not all, of the natural lifespan of the host. On a more pessimistic note, there is no guarantee that chronic infections will not ultimately progress to some form of illness; or that conventional approaches to prevention and treatment will be successful. These approaches may be frustrated by the ability of all lentiviruses to survive in intracellular and organ

(brain) sanctuaries or to elude host defences through antigenic variation. The prospects of developing vaccines to neutralizing determinants common to all strains of virus, designing vectors to maintain silent infections, and the general progress in lentivirus and AIDS research, are grounds for the hope that these problems will be resolved.

I thank my colleagues for their contributions to some of the research described in this review and for their helpful comments: Samuel Baron, Michael Bishop, Hubert Blum, Michel Brahic, Susan Carpenter, Phil Cheevers, Martin Dworkin, Anthony

Fauci, Adam Geballe, Jeffrey Harris, Colin Jordan, Jay Levy, Hal Minnigan, Opendra Narayan, Neal Nathanson, Michael Osterholm, Richard Peluso, Gudmundur Petursson, Richard Price, Ernest Retzel, Frank Rhame, Jane Scott, Katherine Staskus, Linda Stowring, Howard Temin, Betty Traynor, Lloyd Turtinen, Harold Varmus, Peter Ventura, Peter Vogt, Simon Wain-Hobson and Stephen Wietgrefe. I also thank NIH, National Multiple Sclerosis Society, American Cancer Society and Veterans Administration for support, and Jan Torma and Colleen O'Neill for preparation of the manuscript.

- 1. Thormar, H. & Paisson, P. A. Perspect. Virol. 5, 291-308 (1967).
- Gudnadottir, M. Prog. med. Virol. 18, 336-349 (1974).
 Haase, A. T. Curr. Topics Microbiol. Immun. 72, 101-156 (1975).
- De Boer, G. F., Terpstra, C. & Houwers, D. J. Bull. Off. int. Epiz. 89, 487-506 (1978).
 Brahic, M. & Haase, A. T. Comparative Diagnosts of Viral Diseases Vol. 4, Ch. 15 (Academic, New York, 1981).

- Narayan, O. & Cork, L. C. Rev. infect. Dis. 7, 89-98 (1985).
 Nathanson, N. et al. Rev. infect. Dis. 7, 75-82 (1985).
 Coggins, L. Comparative Diagnosis of Viral Diseases Vol. 4, Ch. 16 (Academic, New York,
- Cheevers, W. P. & McGuire, T. C. Rev. infect. Dis. 7, 83-88 (1985).

- Wong-Staal, F. & Gallo, R. C. Nature 317, 395-403 (1985).
 Sigurdsson, B., Palsso, P. A. & Grimson, H. J. Neuropath. exp. Neurol. 16, 389-403 (1982).
 Sigurdsson, B. & Palsson, P. A. Br. J. exp. Path. 39, 519-528 (1958).
 Sigurdsson, B., Palsson, P. A. & Van Bogaert, L. Acta neuropath. 1, 343-362 (1962).
- Georgsson, G., Palsson, P. A., Panitch, H., Nathanson, N. & Petursson, G. Acta neuropath. 37, 127-135 (1977).

- 37, 127-135 (1977).

 15. Georgsson, G. et al. Acta neuropath. 57, 171-178 (1982).

 16. Sigurdsson, B. Br. vet. J. 110, 255-270 (1954a).

 17. Sigurdsson, B. Br. vet. J. 110, 341-354 (1954b).

 18. Gajdusek, D. C. Science 197, 943-960 (1977).

 19. Petursson, G., Nathanson, N., Georgsson, G., Panitch, H. & Palsso, P. A. Lab. Invest. 35, 402-412 (1976).
- 20. Griffin, D. E., Narayan, O. & Adams, R. J. J. infect. Dis. 138, 340-350 (1978).
- Haase, A. T., Stowring, L., Narayan, O., Griffin, D. & Price, D. Science 195, 175-177 (1977).
 Sigurdsson, B., Thormar, H. & Palsson, P. Arch. ges. Virusforsch. 10, 368-371 (1960).

- Thormar, H. Virology 19, 273-278 (1963).
 Haase, A. T. & Varmus, H. E. Nature new Biol. 245, 237-239 (1973).
- Haase, A. T. & Varmus, H. E. Nature new Biol. 245, 237-239 (1973).
 Haase, A. T., Traynor, B. L., Ventura, P. E. & Alling, D. W. Virology 70, 65-79 (1976).
 Brahic, M., Filippi, P., Vigne, R. & Haase, A. T. J. Virol. 24, 74-81 (1977).
 Harter, D. H. & Chopping, P. W. Virology 31, 279-288 (1967).
 Brahic, M., Stowring, L., Ventura, P. & Haase, A. T. Nature 292, 240-242 (1981).
 Haase, A., Brahic, M., Stowring, L. & Blum, H. Meth. Virol. 3, 189-226 (1984).
 Haase, A. T. et al. Virology 140, 201-206 (1985).
 Harris, J. D. et al. Proc. natn. Acad. Sci. U.S.A. 81, 7212-7215 (1984).
 Palvace, B. Haase, A. Stowring, L. & Burnete, M. & Mantyra, P. Virology 147, 231-324.

- 32. Peluso, R., Haase, A., Stowring, L., Edwards, M. & Ventura, P. Virology 147, 231-236 (1985).

- Narayan, O. et al. J. gen. Virol. 59, 245-256 (1982).
 Cutlip, R. C., Jackson, T. A. & Laird, G. A. Am. J. vet. Res. 38, 2091-2093 (1977).
 de Boer, G. F. & Houwers, D. J. in Aspects of Slow and Persistent Infections (ed. Tyrrell, D. A. J.) 198-221 (Elsevier, Amsterdam, 1979).
 Hoxie, J. A., Haggarty, B. S., Rackowski, J. L., Pillsbury, N. & Levy, J. A. Science 229, 1981-1981 (1982).
- 1400-1402 (1985). 37. Folks, T. et al. Science 231, 600-602 (1986).
- 38. Curran, J. W. et al. Science 229, 1352-1357 (1985). 39. Barban, V. et al. J. Virol. 52, 680-682 (1984).
- Panganiban, A. & Temin, H. Cell 36, 673-679 (1984).
 Harris, J. D. et al. Virology 113, 573-583 (1981).
 Shaw, G. M. et al. Science 226, 1165-1171 (1984).

- Rice, N. R., Simek, S., Ryder, O. A. & Coggins, L. J. Virol. 26, 577-583 (1978).
 Yaniv, A., Dahlberg, J. E., Tronick, S. R., Chiu, I.-M. & Aaronson, S. A. Virology 145, 340-345 (1985).
 Scott, J. V., Stowring, L., Haase, A. T., Narayan, O. & Vigne, R. Cell. 18, 321-327
- (1979).
- 46. Narayan, O., Griffin, D. E. & Chase, J. Science 197, 376-378 (1977)
- Clements, J. E., Pederson, F. S., Narayan, O. & Haseltine, W. A. Proc. natn. Acad. Sci. U.S.A. 77, 4454-4458 (1980).
 Lutley, R. et al. J. gen. Virol. 64, 1433-1440 (1983).
- 49. Thormar, H., Barshatzky, M. R., Arnesen, K. & Kozlowski, P. B. J. gen. Virol. 64, 1427-1432 Inormar, H., Barshatzky, M. R., Arnesen, R. & Kozlowski, F. B. J. gen. Virol. 94, 1427-1432 (1983).
 Kono, Y., Kobayashi & Fukunaga, Y. Arch. ges. Virusforsch. 41, 1-10 (1973).
 Salinovich, O. et al. J. Virol. 57, 71-80 (1986).
 Montelaro, R. C., Parckh, B., Orrego, A. & Issel, C. J. J. biol. Chem. 259, 10539-10544 (1984).
 Wong-Staal, F. et al. Science 229, 759-762 (1985).
 Hahn, B. H. et al. Proc. natn. Acad. Sci. U.S.A. 82, 4813-4817 (1985).

- 55. Nathanson, N., Panitch, H., Palsson, P. A., Petursson, G. & Gorgsson, G. Lab. Invest. 35,
- 444-451 (1976). Stowring, L. et al. Virology 141, 311-318 (1985).
 Brahic, M., Hasse, A. T. & Cash, E. Proc. natn. Acad. Sci. U.S.A. 81, 5445-5448 (1984).

- Branic, M., Riasse, A. I. & Lish, E. Froc. nath. Acad. Sci. U.S.A. 81, 3443-3446 (1984).
 Crawford, T. B., Adams, D. S., Cheevers, W. P. & Cork, L. C. Science 207, 997-999 (1980).
 Klevjer-Anderson, P., Adams, D. S., Anderson, L. W., Banks, K. L. & McGuire, T. C. J. gen. Virol. 65, 1519-1525 (1984).
 Jasin, H. E. & Dingle, J. T. J. clin. Invest. 68, 571-581 (1981).
 McGuire, T. C. & Henson, J. B. in Progress in Medical Virology (ed. Hotchin, J.) 229-247
- (Karger, New York, 1974).

 62. Rao, T. K. et al. New Engl. J. Med. 310, 669-673 (1984).

 63. Cooper, D. A. et al. Lancet 1, 537-540 (1985).

 64. Shaw, G. M. et al. Science 227, 177-182 (1985).

- Epstein, L. G. et al. Ann. Neurol. 17, 488-496 (1985).
 Price, R. W., Navia, B. A. & Cho, E.-S. Neurol. Clin. 4, 285-301 (1986).

- 67. Petito, C. K. et al. New Engl. J. Med. 312, 874-879 (1985).
- Fello, C. R. et al. New Engl. J. Med. 311, 1286–1291 (1984).
 Scligmann, M. et al. New Engl. J. Med. 311, 1286–1291 (1984).
- Narayan, O., Sheffer, D., Griffin, D. E., Clements, J. & Hess, J. J. Virol. 49, 349-355 (1984).
- Dalgleish, A. G. et al. Nature 312, 763-767 (1984).
 Klatzman, D. et al. Nature 312, 767-768 (1984).
- Harper,, M. E., Marselle, L. M., Gallo, R. C. & Wong-Staal, F. Proc. natn. Acad. Sci. U.S.A. 83, 772-776 (1986).
- Williams, R. C. Jr, Masur, H. & Spira, T. J. J. clin. Immun. 4, 118-123 (1984). Klatzmann, D. & Montagnier, L. Nature 319, 10-11 (1986).
- Pahwa, S., Pahwa, R., Saxinger, C., Gallo, R. C. & Good, R. A. Proc. natn. Acad. Sci. U.S.A. 82, 8198-8202 (1985).
- 77. Mathes, L. E., Olsen, R. G., Hebebrand, L. C., Hoover, E. A. & Schaller, J. P. Nature 274, 687-689 (1978). 78. Serwadda, D. et al. Lancet ii, 849-852 (1985).
- 79. Torti, F. M., Dieckmann, B., Beutler, B., Cerami, A. & Ringold, G. M. Science 229, 867-869
- 80. Temin, H. M., Keshet, E. & Weller, S. K. Cold Spring Harb. Symp. quant. Biol. 44, 773-778 (1980).
- 81. Hanse, A. T. et al. Virology 119, 399-410 (1982).
- 82. Narayan, P., Clements, J. E., Griffin, D. E. & Wolinsky, J. S. Infect. Immunity 32, 1045-1050

- (1981).

 3. Geballe, A. P., Ventura, P., Stowring, L. & Haase, A..T. Virology 141, 148-154 (1985).

 4. Thormar, H. & Sigurdardottir, B. Acta path. microbiol. 55, 180-186 (1962).

 5. Thormar, H., Wisniewski, H. M. & Lin, F. H. Nature 279, 245-256 (1979).

 6. Narayan, O., Griffin, D. E. & Silverstein, A. M. J. Infect. Dis. 135, 800-806 (1977).

 7. Houwers, D. J. & Schaake, J. Ir Vet. Microbiol. 5, 445-451 (1984).

 8. Filippi, P., Vigne, R., Querat, G., Jouanny, C. & Sauze, N. J. Virol. 42, 1057-1066 (1982).

 89. Robert-Guroff, M., Brown, M. & Gallo, R. C. Nature 316, 72-74 (1985).

 90. Weiss, R. A. et al. Nature 316, 69-72 (1985).

 91. Zagury, C. et al. Science 226, 449-451 (1984).

 92. Groopman, J. E. et al. Science 226, 447-449 (1984).

 93. Levy, J. A. et al. Ann. intern. Med. 103, 694-699 (1985).

 94. Levy, J. A., Hollander, H., Shimabukuro, J., Mills, J. & Kaminsky, K. Lancet il. 586-588

- Levy, J. A., Hollander, H., Shimabukuro, J., Mills, J. & Kaminsky, K. Lancet ii, 586-588 (1985).
- 95. Ho, D. D. et al. New Engl. J. Med: 313, 1493-1497 (1985).
- Resnick, L. et al. New Engl. J. Med. 313, 1493-1549 (1985).
 Hasse, A. T. & Levinson, W. Biochem. biophys. Res. Comm.
 Sundquist, B. & Larner, E. J. Virol. 30, 847-851 (1977). nun. 51, 875-880 (1973).
- Carroll, D. et al. J. infect. Dis. 138, 614-617 (1978).
- 100. Narayan, P., Sheffer, D., Clements, J. E. & Tennekoon, G. J. exp. Med. 162, 1954-1969

- Broder, S. et al. Lancet II, 627-630 (1985).
 Mitsuya, H. et al. Proc. natn. Acad. Sci. U.S.A. 82, 7096-7100 (1985).
 Sodroski, J. G. et al. Science 227, 171-173 (1985).
 Rosen, C. A., Sodroski, J. G. & Haseltine, W. A. Cell 41, 813-823 (1985).
 Arya, S. K., Guo, C., Josephs, S. F. & Wong-Staal, F. Science 229, 69-73 (1985).
 Rosen, C. A. et al. Nature 319, 555-559 (1986).
- Dayton, A. I., Sodroski, J. G., Rosen, C. A., Goh, W. C. & Haseltine, W. A. Cell 44, 941-947 (1986).
- 108. Fisher, A. G. et al. Nature 320, 367-371 (1986). 109. Hess, J. L., Clements, J. E. & Narayan, O. Science 229, 482-485 (1985). 110. Sonigo, P. et al. Cell 42, 369-382 (1985).
- 111. Sanchez-Pescador, R. et al. Science 227, 484-492 (1984). 112. Ratner, L. et al. Nature 313, 277-284 (1985).

- 113. Muesing, M. A. et al. Nature 313, 450-458 (1985). 114. Wain-Hobson, S., Sonigo, P., Danos, O., Cole, S. & Alizon, M. Cell 40, 9-17 (1985). 115. Sodroski, J. et al. Science 231, 1549-1553 (1986).
- 116. Narayan, O., Kennedy-Stoskopf, S., Sheffer, D., Griffin, D. E. & Clements, J. E. Infect. Immunity 41, 67-73 (1983). 117. Zagury, D. et al. Science 231, 850-853 (1986).
- Ital. Izant, J. G. & Weintraub, H. Science 229, 345-352 (1985).
 Coleman, J., Hirashima, A., Inokuchi, Y., Green, P. J. & Inouye, M. Nature 315, 601-603 (1985).
- 120. Pestka, S., Daugherty, B. L., Jung, V., Hotta, K. & Pestka, R. K. Proc. natn. Acad. Sci.
- Pestka, S., Daugherty, B. L., Jung, V., Hotta, K. & Pestka, R. K. Proc. natn. Acad. Sci. U.S.A. 81, 7525-7528 (1984).
 Weiss, R., Teich, N., Varmus, H. & Coffin, J. (eds) RNA Tumor Viruses 2nd edn (Cold Spring Harbor Laboratory, New York, 1982).
 Haase, A. T. Microbiol. Pathogenesis 1, 1-4 (1986).
 Gonda, M. A. et al. Science 227, 173-177 (1985).
 Roberson, S. M., McGuire, T. C., Klevjer-Anderson, P., Gorham, J. R. & Cheevers, W. P. J. Virol. 44, 755-758 (1982).
 Gogolewski, R. P., Adams, D. S., McGuire, T. C., Banks, K. L. & Cheevers, W. P. J. gen. Virol. 66, 1233-1240 (1985).
 Chiu, L.-M. et al. Nature 317, 366-368 (1985).

- Virol. 66, 1233-1240 (1985).
 Chiu, I.-M. et al. Nature 317, 366-368 (1985).
 Stowring, L., Haase, A. T. & Charman, H. P. J. Virol. 29, 523-528 (1979).
 Weiland, F., Matheka, H. D., Coggins, L. & Hartner, D. Archs Virol. 55, 335-340 (1977).
 Stephens, R. M., Casey, J. W. & Rice, N. R. Science 231, 589-594 (1986).
 Montagnier, L. et al. Virology 144, 283-289 (1985).
 Barin, F. et al. Science 228, 1091-1096 (1985).

Pb isotope evidence in the South Atlantic for migrating ridge—hotspot interactions

B. B. Hanan, R. H. Kingsley & J-G. Schilling*

Graduate School of Oceanography, University of Rhode Island, Kingston, Rhode Island 02881, USA

Variations of Pb isotopes in basalts erupted along the Mid-Atlantic Ridge suggest that heterogeneities in the upper mantle beneath the South Atlantic are highly structured and dominated by distinct east-west channels connecting the off-ridge plumes with the westward-migrating ridge. These preferential flows are superimposed on a broad radical dispersion of the St Helena and Tristan plumes into the asthenosphere before the ridge overrode these plumes.

WE have recently discovered the presence of short-wavelength geochemical and bathymetric anomalies along the Mid-Atlantic Ridge (MAR) axis just opposite the off-ridge Tristan da Cunha, St Helena and Circe hotspots^{1,2}. We proposed that these anomalies are the result of preferential flow along sublithospheric channels which have developed between the mantle upwelling zones (hotspots) and the westward-migrating MAR since it overrode these hotspots ~80 Myr ago. The ridge in this case acts as a sink and the plume a source of mantle materials. The model was initially developed by Morgan³ for the Galapagos and the Reunion hotspots, purely on the basis of tracks left by anomalous constructional volcanism on the sea floor. The model has received support from the observation that the length of these geochemical anomalies and the magnitude of the associated residual elevation anomalies along migrating mid-ocean ridges both generally decrease as the square root of distance between these migrating ridge segments and related hotspots⁴.

In the South Atlantic, we have also noted that the large geochemical dispersion observed within these spike-like geochemical anomalies may be the result of irregular mixing along these lateral flow channels, between the plume-derived material and the large-ion lithophile element (LILE)-depleted asthenosphere. Furthermore, as the South Atlantic hotspots and the LILE-depleted asthenosphere have distinct signatures in Sr, Nd and Pb isotopic space^{5,6}, a test of the connecting flow channel model and proposed mixing can easily be made by measuring the isotopic composition of basalts derived from these regions. Distinct mixing trajectories are predicted in such isotopic space¹. This is also possible with Pb isotopic ratios alone. In this case, the mixing along the connecting channels between each of these hotspots and the LILE-depleted asthenosphere source should form distinct binary mixing arrays on two-dimensional Pb isotopic ratio diagrams, as the Tristan-Gough-Discovery hotspot(s) have Pb isotopic signatures distinct from that of St Helena and the source of typically LILE-depleted mid-ocean-ridge basalts (MORB)^{5,6} (Fig. 2b). However, no prediction can be made for the Circe mixing trend since this off-ridge hotspot has not yet been sampled. Its influence on the MAR was initially suspected on the basis of geophysical and morphological criteria only1. Note also that according to these predictions, referred to here as model 1, all binary mixing trends should converge towards the compositional range of the LILE-depleted endmember source for the area (Fig. 2b).

We report on 62 Pb isotope analyses of the same basalts previously analysed for major elements and trace element abundance ratios, such as La/Sm and Nb/Zr, which were instrumental in revealing the spike-like anomalies along the MAR in the South Atlantic (Fig. 1). The Pb isotope analyses were performed on carefully selected fresh glass chips if available; otherwise, pillow interiors were used. All of the samples were carefully hand-picked, cleaned and briefly leached with hydrochloric acid

to remove possible surface contaminants. Our results are listed in Table 1, along with some details of the analytical method. We will refer to the isotopic ratios ²⁰⁶Pb/²⁰⁴Pb, ²⁰⁷Pb/²⁰⁴Pb and ²⁰⁸Pb/²⁰⁴Pb as 6/4, 7/4 and 8/4, respectively.

Pb isotope test

For comparison with our model 1 predictions, Fig. 2a shows our actual Pb isotope results plotted on an 8/4 versus 6/4 diagram. As a first-order independent discriminant, we have divided the MAR basalts from 2°S to 47°S into four geographical populations on the basis of the La/Sm variation previously reported¹ (see Fig. 1b). These populations are: 2-12° S, including the Circe spike-like anomaly; the 12-22° S segment, including the St Helena spike-like anomaly; 22-30.75°S, an apparently 'normal' ridge segment with (chondrite-normalized) $(La/Sm)_N < 0.75$, showing a slight increase southward; and 30.75-47°S, a segment which includes the Tristan-Gough-Discovery spike-like anomaly. The exact boundaries between these four geographical populations were chosen where the (La/Sm)_N appears to reach a minimum (Fig. 1b). Using these populations, Fig. 2a shows that the St Helena-MAR population (12-22°S) follows a linear array pointing towards the field occupied by the off-ridge St Helena hotspot, and the 30.75-47° S population shows a broad cluster slightly elongated towards the field occupied by the off-ridge Tristan-Gough-Discovery hotspots. However, the 2-12°S MAR population does not form a single linear array; instead at least two linear arrays seem required by the data. The subpopulation from the 7-12° S segment comprising the Circe spike anomaly branches out from that of the St Helena array towards higher 8/4 ratios, presumably pointing towards values representing the Circe off-ridge hotspot rather than the nearby Ascension island. The Pb isotope data reinforce our previous inference^{1,4} that the influential hotspot in this region is located east rather than west of the MAR and may be beneath Circe Seamount¹. The origin of Ascension Island remains uncertain. Rather than being a hotspot itself, its formation may be related to tectonic adjustment in the region, involving MAR rift jumps and migration caused by the Circe hotspot, as well as perhaps the presence of the Ascension fracture zone In contrast, the subpopulation from 2-7°S (just north of the Circe anomaly) is among the least radiogenic Pb found in ocean-floor basalts, and is indistinguishable from that of the St Helena binary mixing array in the 8/4 versus 6/4 diagram, but, in fact, would show a higher slope on a 7/4 versus 6/4 plot (using data from Table 1). The same grouping and mixing array patterns just described in terms of 8/4 versus 6/4 would also be evident in the 8/4 versus 7/6 diagram, which includes the variation of all four isotopes of lead. On the other hand, there is more scatter and the mixing arrays are not as readily separated in the 7/4 versus 6/4 diagram, because the Tristan and apparently the Circe mantle plume sources lie closer to the

Table 1 Lead isotope ratios* in dredged basalts from the Mid-Atlantic Ridge, 2-47° S									
Sample†	Lat. (°S)	Long. (°W)	Depth (m)	²⁰⁶ Pb/ ²⁰⁴ Pb	(±)‡	²⁰⁷ Pb/ ²⁰⁴ Pb	(±)‡	²⁰⁸ Pb/ ²⁰⁴ Pb	(±)‡
EN061 2D-1g	2.24	12.40	3,885	17.829	(13)	15.456	(12)	37.319	(37)
EN061 3D-1	3.43	12.22	3,045	17.804	(23)	15.443	(20)	37.278	(48)
EN061 4D-1g	4.27	12.20	2,300	17.681	(13)	15.422	(11)	37.119	(27)
EN061 5D-1g	5.18	11.52	3,300	17.762	(13)	15.440	(11)	37.239	(27)
EN061 5D-3A	5.18	11.52	3,300	17.640	`(9)	15.417	(8)	37.077	(20)
EN061 6D-1g	6.31	11.32	3,218	17.899	(6)	15.462	(6)	37.368	(15)
EN061 7D-1g	7.51	13.46	4,025	18.888	(20)	15.582	(18)	38.517	(45)
EN061 8D-1g	8.01	13.40	3,390	18.925	(32)	15.560	(27)	38.525	(68)
EN061 8D-1	8.01	13.40	3,390	18.972	(11)	15.602	(9)	38.641	(23)
EN061 8D-2A	8.01	13.40	3,390	18.426	(10)	15.520	(9)	37.975	(22)
EN061 9D-1	8.61	13.27	2,205	19.079	(18)	15.595	(16)	38.922	(44)
EN061 10D-1	9.11	13.32	2,663	18.983	(18)	15.597	(15)	38.715	(38)
EN061 10D-2	9.11	13.32	2,663	18.880	(7)	15.575	(7)	38.548	(16)
EN061 10D-3	9.11	13.32	2,663	18.864	(11)	15.599	(9)	38.526	(23)
EN061 11D-1A	9.62	13.23	1,680	19.286	(11)	15.625	(9)	39.097	(24)
EN061 12D-1	9.93	13.12	2,205	19.151	(15)	15.583	(12)	38.875	(30)
EN061 13D-1	10.55	13.01	3,288	18.403	(12)	15.531	(10)	38.095	(40)
EN061 14D-1g	11.05	13.04	3,438	18.245	(13)	15.505	(11)	37.832	(29)
EN061 15D-1	12.03	14.41	3,253	18.605	(14)	15.552	(13)	38.109	(42)
EN061 16D-1g	12.68	14.66	3,575	18.642	(7)	15.535	(6)	38.183	(18)
RC16 6D-1	13.47	14.75	2,752	18.231	(6)	15.489	(5)	37.858	(13)
KOIO OD I	13.77	14.75	2,732	18.225	(12)	15.476	(10)	37.814	(26)
RC16 7D-1g	14.08	14.46	3,534	18.207	(12)	15.492	(11)	37.730	(25)
EN061 17D-1g	14.66	13.49	2,862	18.625	(21)	15.558	(18)	38.176	(43)
EN061 18D-1g	15.46	13.26	2,860	18.881	(4)	15.546	(4)	38.403	(12)
EN061 18D-1g	15.46	13.26	2,860	18.870	(7)	15.537	(6)	38.372	(16)
EN061 18D-1 EN061 18D-2A	15.46	13.26	2,860	18.364	(17)	15.482	(14)	37.892	
EN061 19D-1g	16.82	14.32	3,837	18.549	(14)	15.546	(12)	37.892 37.995	(35)
EN061 20D-1g	17.33	14.18	3,465	18.518	(10)	15.521	(9)	37.971	(29) (22)
EN061 22D-1g	18.38	12.84	3,675	18.727	(7)	15.546	(6)	38.091	
EN061 22D-1g EN061 23D-1g	18.98	12.30	3,537	18.786		15.563	(24)		(15)
E14001 2313-1g	10.90	12.30	3,337	18.803	(28)	15.587		38.291	(58)
EN063 2D-5g	21.50	11.82	3 460	18.316	(20)		(14)	38.371	(22)
	23.49	13.39	3,460	18.328	(13)	15.511	(12)	37.836	(28)
EN063 7D-5g	23.49 24.52		3,630		(4)	15.500	(3)	37.840	(9)
EN063 9D-5	24.32 24.95	13.36	4,010	18.295	(16)	15.511	(13)	37.965	(33)
EN063 10D-5g		13.19	3,105	18.337	(11)	15.504	(10)	37.941	(23)
EN063 12D-5g	26.00	13.90	2,670	18.307	(17)	15.504	(14)	37.925	(40)
EN063 14D-5g	26.99	13.52	3,610	18.336	(18)	15.520	(11)	37.888	(41)
EN063 14D-5	26.99	13.52	3,610	18.304	(11)	15.504	(11)	.37.924	(28)
EN063 17D-5g	28.54	12.54	3,240	18.164	(15)	15.524	(13)	37.941	(33)
EN063 22D-5g	30.50	13.77	3,125	18.254	(14)	15.499	(11)	38.013	(24)
EN063 24D-5g	30.98	13.46	3,530	18.347	(9)	15.511	(8)	37.983	(36)
EN063 23D-5g	31.51	13.41	3,400	18.322	(17)	15.517	(14)	37.983	(35)
AII107-7 25-1	31.83	13.58	2,349	18.272	(13)	15.507	(12)	38.013	(27)
	24.02	45.50	2 2 42	18.265	(6)	15.496	(6)	37.986	(14)
AII107-7 25-1B	31.83	13.58	2,349	18.290	(8)	15.531	(7)	38.096	(18)
AII107-7 25-2	31.83	13.58	2,349	18.324	(10)	15.548	(9)	38.124	(22)
AII107-7 20-3	33.71	14.25	1,759	18.134	(3)	15.517	(3)	37.948	(9)
AII107-7 18-28	34.55	15.15	2,694	18.122	(3)	15.493	(3)	38.091	(8)
AII107-7 17-71g	35.28	15.73	3,386	18.315	(3)	15.540	(3)	38.268	(10)
AII107-7 15-3g	36.56	17.59	2,459	18.245	(10)	15.539	(9)	38.235	(22)
AII107-7 14-43g	37.19	17.52	2,399	18.258	(7)	15.544	(6)	38.307	(14)
AII107-7 14-77	37.19	17.52	2,399	18.318	(13)	15.544	(10)	38.435	(27)
AII107-7 13-1	37.83	17.14	2,199	18.120	(17)	15.486	(16)	37.961	(33)
AII107-7 10-1g	38.88	16.24	2,169	18.172	(17)	15.535	(14)	38.215	(35)
AII107-7 9-38	39.70	16.05	2,473	18.151	(18)	15.488	(17)	38.108	(34)
AII107-7 7-10g	40.44	16.75	2,612	18.164	(9)	15.500	(8)	37.977	(26)
AII107-7 7-3	40.44	16.75	2,612	18.177	(13)	15.503	(12)	38.001	(30)
AII107-7 6-20g	41.25	16.60	2,394	18.100	(7)	15.539	(6)	38.076	(20)
AII107-7 4-4g	42.91	16.37	2,802	18.064	(23)	15.538	(21)	38.082	(54)
AII107-7 2-38	46.21	13.64	2.699	18,070	(10)	15.530	(10)	38.127	(22)
AII107-7 2-53	46.21	13.64	2,699	18.084	(10)	15.549	(6)	38.176	(20)

^{*} The Pb isotopic ratios were normalized on the basis of replicate measurements of NBS SRM981, using Todt et al's values (ref. 47). Duplicate analyses are on different pieces from the same sample. The discrimination factor averaged 0.97 ± 0.06 (2 standard errors) % per mass unit. The isotopic ratios were measured at URI on a VG Micromass 30B single collector, double focusing, thermal ionization mass spectrometer. A standard ion exchange procedure was used to separate Pb prior to mass spectrometry (ref. 49).

† g in sample identification stands for glass, otherwise pillow interiors.

‡ Errors in parentheses are 2 standard errors of the last significant figures, taking into account within-run precision and the uncertainty in the discrimination correction. Ph blanks are <0.15 ng on sample sizes up to 0.5 ng and are perligible.

discrimination correction. Pb blanks are <0.15 ng on sample sizes up to 0.5 g and are negligible.

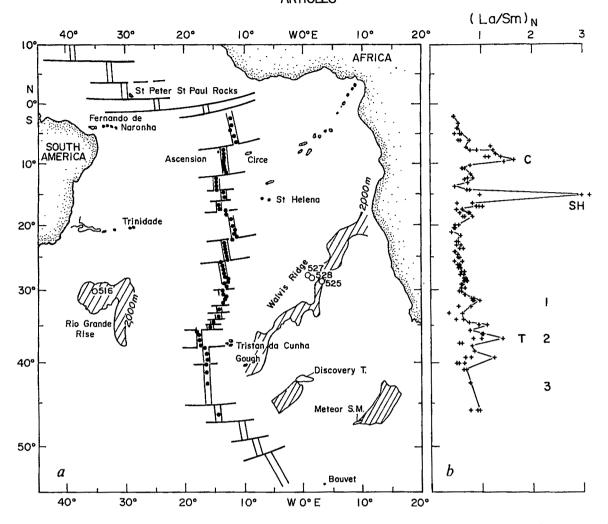


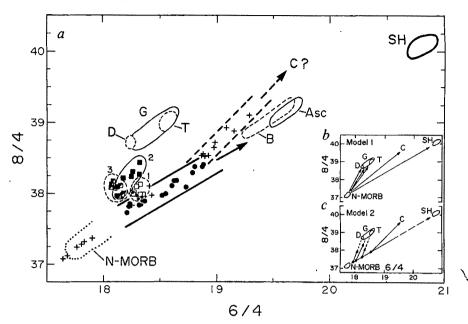
Fig. 1 a, Tectonic map of the South Atlantic showing the location of dredged basalts along the MAR, DSDP holes 525A, 528, 527 and 516F (open circles), off-ridge hotspots (islands) and their tracks (hatched areas of seamount chains). b, Corresponding latitudinal variation of chondrite-normalized La/Sm in dredged basalts from the MAR-axis. Note spike-like anomalies opposite Circe (C), St Helena (SH) and in the vicinity of the Tristan-Gough-Discovery hotspots (T). Note that there may be at least three distinct small spikes (1, 2, 3) in the latter broader anomaly. These geochemically anomalous ridge segments are also accompanied by anomalous elevation of the ridge axis (see ref. 4); they may reflect lateral sub-crustal plume flow feeding the spreading ridge axis from the corresponding off-ridge hotspots. The analytical uncertainty in the (La/Sm_N) is less than the size of the symbols.

LILE-depleted asthenosphere-St Helena binary mixing array in terms of 7/4. Overall, the mixing systematics described above are self-consistent among the different projections in Pb isotope ratio space. The three distinct arrays are also statistically recognizable in a 6/4-7/4-8/4 three-dimensional space using the method of principal component analysis. This statistical test will be discussed elsewhere (D. A. Fontignie, J.G.S. and B.B.H., in preparation).

Thus, overall, our first-order test of the hotspot sourcemigrating ridge sink and flow connection is essentially positive in the broad sense that the data indeed reveal distinct binary mixing arrays pointing towards respective fields representing the South Atlantic off-ridge hotspots. However, there are also some important differences. Notably, the three binary mixing arrays do not readily converge towards the field occupied by the LILE-depleted asthenosphere source and thus do not form the fan-tail arrangement of binary arrays initially expected (see model 1 in Fig. 2b). Instead, both the Circe binary array comprising the 7-12° S spike population and the 30.75-47° S MAR spike population tend to intersect that of the St Helena-MAR spike population at different levels of 6/4, as if the end-member LILE-depleted asthenospheric source in these regions were already isotopically polluted with a component rich in 6/4, perhaps composed of the St Helena type of material. The details

are more evident when the 30.75-47° S population is subdivided into three segments (30.75-34° S, 34°-39° S, 39°-47° S). This is done on the basis that the migrating MAR could have overridden three different hotspots in the region, Tristan, Gough and Discovery, thus producing three distinct lateral channels; also from the fact that basalts from these three hotspots indeed have distinct 6/4 (Fig. 2a); and finally that three small (La/Sm)_N spikes are also observed along the 30.75-47° S MAR segment (spikes 1, 2, 3 in Fig. 1b). Figure 2a shows that the 30.75-34° S subpopulation forms an array pointing towards the field for Tristan Island, which is geographically located closest to this segment. The southern subpopulation (39-47°S) is subparallel to the former and points towards the field of the off-ridge Discovery Tablemount, which is also closest to this segment. And finally, the MAR segment closest to Gough Island forms another subparallel array intermediate in position between the former two arrays, although overlapping significantly with the other two arrays in terms of 6/4. This is expected as the field occupied by Gough Island basalts reflects a relatively large range in 6/4 which overlaps that of Discovery Tablemount and Tristan Island (Fig. 2). The fact that the north-south zoning along the MAR in terms of 8/4 versus 6/4 space is essentially the same as for the three off-ridge hotspots, indeed, supports the possible presence of a strongly laminated east-west mantle flow pattern,

Fig. 2 8/4 versus 6/4 Pb isotope covariation diagram showing the South Atlantic MAR basalts in relation to: the field occupied by South Atlantic island basalts from off-ridge hotspots, including Discovery (D), Gough (G), Tristan (T), Bouvet (B), Ascension (Asc) and St Helena (SH) (taken from ref. 28); and the field occupied by normal MAR basalts from the North Atlantic (N-MORB) (taken from refs 16, 28, 30, 48). The island fields include analytical uncertainties. Symbols for basalts from the South Atlantic MAR segment subpopulations, based on the distribution of spike-like La/Sm anomalies shown in Fig. 1b, are: 2-12°S, including C-spike (crosses, heavy dashed-line array); 12-22° S, including SH-spike (filled circles, heavy-line array); 22-30.75° S (small dots); 30.75-34°S, including T-1 spike (open squares, thin dashed-line envelope); 34-39°S, including T-2 spike (filled squares, thin full-line envelope); and 39-47°S, including T-3 spike (half-filled squares, thin dashed-line envelope). The analytical uncertainties are less than the size of the symbols. Note: how basalts from the La/Sm spike-bearing MARsegment subpopulations tend to form distinct linear arrays pointing towards the field occupied by the geographically related off-ridge hotspots; two dis-



tinct linear arrays are required by the 2-12° S population. Geographically these correspond to segment 2-7° S (crosses overlapping with N-MORB field), which points towards St Helena or Ascension (but this is not the case on a 7/4 versus 6/4 plot; see also Fig. 5): and the 7-12° S segment (heavy dashed-line array), which points neither towards St Helena nor Ascension Island, but rather towards a field presumably occupied by the large Circe Seamount shown in Fig. 1 (8°15′ S, 9°20′ W)—presumably the influential off-ridge hotspot at this latitude. Three crosses present between these two arrays (samples EN61 8D-2, 13D-1 and 14D-1g), located on the two lower flanks of the C-spike of Fig. 1b, do not readily fit either of these two arrays (see also Fig. 5). b, Idealized binary mixing model 1 initially expected to account for the spike-like geochemical anomalies shown in Fig. 1b. Basalts from each spike would form a vector representing binary mixing between a pure, LILE-depleted, asthenosphere end-member source and plume material of Pb isotope composition characteristic of the off-ridge hotspot sources present at the corresponding latitude of these MAR spikes. c, Idealized binary mixing model 2, reflecting a possible interpretation of the Pb isotope distribution actually observed and shown in a. Distinct binary-mixing vectors are preserved between the off-ridge plumes and a LILE-depleted end-member which is no longer constant in accomposition, but is polluted (enriched) to various extents with a St Helena-plume-type end-member material whose contribution increases southward along the MAR. Presumably, the broad background pollution of the LILE-depleted source would have taken place before the migrating MAR sink passed over this hotspot. Black dots at the intersection of the binary mixing vectors D, G and T with the SH-LILE-depleted asthenosphere binary would give the Pb isotope composition of the polluted LILE-depleted asthenosphere at the latitudes of the C, SH and T(-1, -2, -3) geochemical anomalies shown in Fig. 1.

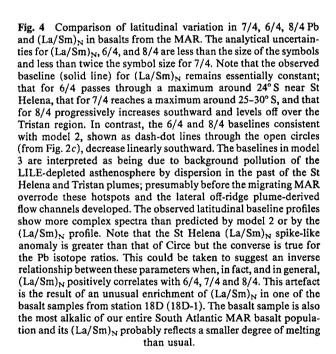
or distinct channels along which binary mixing is predominant, but the LILE-depleted asthenosphere source end-member entering the binary mixture is apparently itself already polluted with a 6/4-rich component (such as St Helena-type material). The influence of this 6/4-rich pollutant apparently decreases southward in some systematic way. An idealized sketch of such an updated mixing model is illustrated in Fig. 2c, where it is referred to as model 2. In this idealization, the pollutant of the LILE-depleted asthenosphere would be of the St Helena type only.

In terms of Pb isotope space, it appears that the MAR basalt variation within the Circe-related spike (2-12°S) and the Tristan-Gough-Discovery-related spike (30.75-47° S) may represent mixtures of at least three pure end-member isotopic components, whereas the St Helena-related spike (12-22°S) is dominantly a mix of only two pure end-member components. Physically, however, the Pb isotope data do not contradict the possibility that along each of the proposed lateral channels and beneath the MAR, the mixing would have taken place between only two types of material, as initially proposed; that is, the surrounding asthenosphere polluted to various extents (depending on the region) and the mantle plume material derived from each of the South Atlantic off-ridge hotspots. An important question which pertains to constraining or deciphering the overall dynamics of the mantle beneath the South Atlantic, is to establish more closely the nature of the background pollutant and map its possible geographical distribution. Is it random? Or does it bear some kind of a relationship with the location of St Helena or some other hotspot? Or, for instance, how does it relate to the so-called DUPAL¹⁰ anomaly? If random, the pollution could, for example, be the result of minor addition of metasomatic fluids, whereas if it bears some relation to the location of St Helena it could be related to the dispersion of this mantle plume into the surrounding athenosphere by convection¹¹⁻¹⁵. Insight may also be gained into the mantle flow pattern with depth by comparing our MAR profile with the semi-hemispherical DUPAL anomaly revealed from isotope systematics of ocean island volcanism¹⁰, as it is generally thought that MORBs are sampling a rather shallow upper mantle, whereas ocean island volcanism seems to tap deeper sources.

Asthenosphere pollution

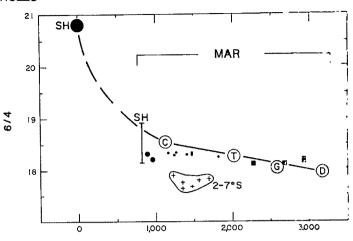
First, we will briefly pursue the consequences of our updated idealized model 2 in Fig. 2c. The intersections of the four binary mixing arrays formed by the MAR anomalies associated with Circe, Tristan, Gough and Discovery with the St Helena-LILEdepleted asthenosphere binary, would provide essentially the mean Pb isotopic value of the polluted asthenosphere endmember present beneath the MAR near the intersection with each of the four proposed connecting channels. Remarkably, Fig. 3 shows that these mean values are inversely related to radial distance from the St Helena hotspot, which would suggest that the extent of pollution of the asthenosphere is related to the St Helena plume location and may be a reflection of its broad dispersion into the upper mantle by convection. Thus, although a significant portion of the plume has been deflected along the connecting lateral channel since the migrating MAR overrode this hotspot, the remaining fraction may at the same time and to a lesser extent have been distributed radially into the upper mantle. The radial dispersion could also have taken place earlier, when the ascending plume was totally intraplate

Fig. 3 Plot of 6/4 Pb isotopic composition of the hypothetical model 2, LILE-depleted, St Helena-polluted, asthenosphere present beneath the MAR axis at the latitude of the C, SH and T-1, T-2 and T-3 spike-like anomalies shown in Fig. 1 (intersections of the migrating MAR axis with the lateral flow channels from offridge plumes located east of the ridge), as a function of radial distance from St Helena hotspot to these intersections. The uncertainties are of the order of the size of the surrounding circles. See Fig. 2c for method used in determining these hypothetical endmember Pb isotopic compositions (dots). The apparent negative correlation suggests that the extent of pollution of the LILEdepleted asthenosphere about the St Helena hotspot, by dispersion, may have been radial in the past (before the migrating MAR axis overrode the St Helena hotspot). Also superimposed is the Pb isotopic variation of basalts with normal ridge segments (that is (La/Sm)_N<0.63 in Fig. 1b). N-MORBs from segments 12.5-14.5°S (large dots); 20.5-30.75°S (small dots), 34.6-40.4°S (squares) tend to follow the negative correlation, but segment 2-7°S is clearly not related by radial dispersion-pollution model 2, suggesting additional complications.

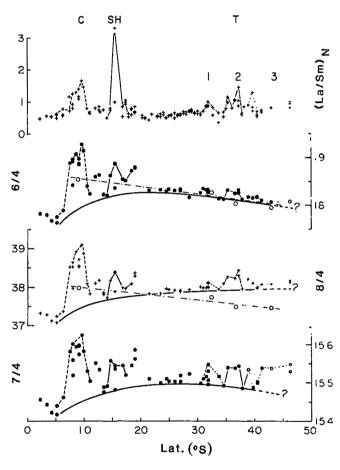


and spread on encountering the rigid lithosphere above. Alternatively, the radial dispersion or pollution could reflect a redistribution due to secondary cellular convection in the upper mantle in the region¹¹⁻¹⁵.

We can further test the radial distribution pattern of the pollutant suggested by our model 2 interpretation in two ways. First, we superimpose in Fig. 3 the Pb isotope variations actually observed along the ridge segments located in between those that contain the $(La/Sm)_N$ spike-like anomalies; that is: the segments from 2-7° S, 12.5-14.5° S, 20.5-30.75° S and 34-35° S. On the basis of the $(La/Sm)_N$ variations, these segments would appear to be essentially 'normal' and unaffected by plumes (that is $(La/Sm)_N < 0.63$ and normal ridge elevation). The Pb isotopic vairation along these segments with respect to radial distance from St Helena should follow the same pattern as predicted by our new model 2 interpretation. Figure 3 shows that the match



Radial distance to St Helena (km)



is generally poor, particularly for the 2-7°S and 12.5-13.5°S segments, suggesting additional complications or some inconsistencies in interpretation. The second test is made by comparing, on one hand, the (La/Sm)N and Pb isotopic profiles along the MAR and, on the other, the 6/4 and 8/4 Pb isotopic baselines observed with those suggested by contamination model 2 (Fig. 4). Between the Circe, St Helena and Tristan-Gough-Discovery spike-like anomalies, the (La/Sm), ratio returns to a baseline value that would be considered as typical of normal ridge segments in the North Atlantic or Pacific. In contrast, the baselines for the three Pb isotope ratios do not stay constant. The baseline for 6/4 goes through a maximum around 24°S, and that of 7/4 perhaps around 25-30 °S, whereas the baseline for 8/4 keeps increasing southward and tends to level off over the Tristan Platform transect. In contrast to these observations, the model 2 interpretation indicates that the 6/4 and 8/4

baselines should decrease linearly southward. The latitudinal Pb isotope ratio profiles thus show more complex spectra than predicted by model 2 or by the (La/Sm)_N profile, with spikes at the latitude of the hotspots as for the (La/Sm)_N (resulting from the channelling of the plumes), superimposed on a broader background variation related to dispersion into and pollution of the asthenosphere, perhaps by two rather than a single hotspot. We will refer to the two-background-pollutant model as model 3. Two major background pollutants of the asthenosphere are apparent from the following reasoning. First, the component rich in 6/4 reaches a maximum near 24°S close to St Helena Island, which suggests that its source may indeed be St Helena. On the other hand, the background pollutant component rich in 7/4 and 8/4, which seems to reach a maximum further south in the vicinity of the Tristan-Gough-Discovery hotspots, may be related to this group of hotspots, since these hotspots are also characterized by high 7/4 and 8/4 but relatively low 6/4 (Fig. 2). Such an 8/4- and 7/4-rich pollutant of the asthenosphere has also been observed in the Indian Ocean and has been attributed to pollution by a hotspot with Kerguelen-type Pb (refs 16-20).

The details of the two-component pollution of the asthenosphere source in the South Atlantic (model 3) is best revealed by studying the relative Pb isotopic variation (6/4, 7/4, 8/4) in a triangular diagram, using first only basalts with (La/Sm)_N< 0.63. These MAR basalts lie outside the three noted (La/Sm)_N spikes and usually would be considered as derived from the so-called LILE-depleted asthenosphere. The location of the transition zone where the St Helena type of pollutant fades out and the Tristan type becomes more dominant, is readily detectable in such a triangular diagram²¹ (Fig. 5a). From 2° S to 24° S the mixing line is essentially binary between the LILE-depleted source and the St Helena type of pollutant, the latter increasing fairly systematically southward to reach a maximum at 24° S. where the St Helena-type pollutant is felt most (see sequence along this trend). South of 24°S, the trend becomes ternary, with the influence of the Tristan-type pollutant becoming progressively more important and the St Helena type decreasing southward, while the 207Pb-rich component characterizing the N-MORB's source stays constant. Further south the trend systematically reverses, as the pollutants from both Tristan and St Helena decrease southward and the contribution from the N-MORB's source increases slightly. Note that the 24-47° S population overlaps the field found for the so-called normal MORBs from the three Mid-Indian-Ocean Ridges 16-20. Finally, we note that had the Tristan-type pollutant south of 24° S along the MAR not been present, the trend would have shown a reversal of the sequence along the same St Helena-asthenosphere mixing trend. The systematics observed with respect to the St Helena and Tristan hotspot locations is thus remarkably clear on such a triangular diagram (Fig. 5).

In comparison, MAR basalts located within the anomalous spikes depart from this sequence and form mixing-vector-like trends, which again tend to be directed towards the fields occupied by their respective plume end-members (Fig. 5b). The exact proportions of the two types of plume pollutants in the asthenosphere beneath the MAR sampling profile, or the mixing proportion within the spikes, cannot be more quantitatively described, as this would require knowing the Pb concentration in such plumes which are unknown and which need not be the same. There is also no guarantee that the Pb isotopic composition of the sources of the island basalts are representative of the pure end-member plumes. In fact, the vector-like trend formed by Tristan-Gough Islands and Discovery Tablemount themselves (Fig. 5b) suggests both a progressive southward increase in the LILE-depleted asthenospheric component (relatively rich in ²⁰⁷Pb) and a progressive decrease in the ²⁰⁶Pb-rich St Helenatype pollutant with increasing distance from St Helena Island. Thus, the extent of pollution of the asthenosphere by the St Helena-derived pollutant appears to be spatially widespread

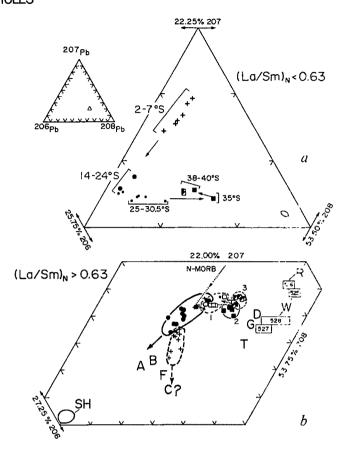
beneath the South Atlantic. It may have partly diluted neighbouring plumes as well, and the pollution may have taken place for quite some time. In fact, the spatial southward decrease in 6/4 pollution is also observable in the past, across the Walvis Ridge, from basalts recovered from the north-south DSDP drill hole sequence 527, 528, 525 (ref. 22) (Figs 2a and 5b). According to the fixed hotspot reference frame²³, these basalts were also erupted beneath the Tristan hotspot and slightly northward.

Finally, there is also a suggestion of a temporal increase of the St Helena pollutant with time from the vector-like sequence exhibited in Fig. 5b by lavas from the Rio Grande Rise, Walvis Ridge, Discovery Tablemount, Gough and Tristan da Cunha. For example, basalts from the Rio Grande Rise (produced at the Tristan Hotspot, 86 Myr ago; ref. 24), followed by Walvis Ridge basalts (69-71 Myr; ref. 25), are progressively less polluted in 6/4 relative to modern basalts from Tristan Island $(<10^5 \text{ yr}; \text{ ref. 26})$. In this time versus extent of 6/4 pollution sequence, the Discovery basalt (25 Myr old; ref. 27) comes third, and Gough, fourth (2-6 Myr; ref. 26), although in this case the radial distance from these two hotspots to St Helena is greater than from Tristan. A more detailed scrutiny of temporal and spatial relationships is not warranted here, as some of these basalts need first to be age-corrected for radiogenic Pb buildup since erupted (once parent/daughter concentrations become available).

Mantle dynamics beneath the South Atlantic

The concept of pollution of the LILE-depleted asthenosphere by the random disperson of blobs by convection as they ascend through the asthenosphere, was first suggested by Allègre and co-workers^{15,17-19}. Their arguments are based on a rather coarse sampling of the mid-ocean ridge system in the Atlantic, East Pacific and Indian Oceans at ~100-500 km intervals. Their comparative study shows that the pollutant in the Indian Ocean appears generally to be rich in 8/4 (Kerguelen or Tristan type) relative to the North Atlantic or East Pacific where such a pollutant has not been observed, but instead a pollutant rich in 6/4, similar to St Helena type, may be present and responsible for the elongation of the MORB field in the 7/4 versus 6/4 diagram²⁸⁻³². These observations have led Allègre and coworkers to suggest the blob cluster model, or provinciality of blob types^{15,17-19}. In contrast, our more detailed sampling (30-100 km intervals) of the North Atlantic³³ the Galangoos³⁴⁻³⁶ 100 km intervals) of the North Atlantic³³, the Galapagos and now the South Atlantic^{1,2}, has led us to pursue the more deterministic, fixed plume source-migrating ridge model^{1,3,37}. The Pb isotope evidence presented for the South Atlantic lends some support to both models and helps merge the two models towards describing a more realistic picture of upper-mantle dynamics. Our results show that heterogeneities in the upper mantle beneath the South Atlantic are not randomly distributed. but highly structured and dominated by east-west laminations, with streaks of identifiable isotopic signature corresponding to that of the hotspots located approximately at these latitudes east of the MAR. Thus, the probable existence of lateral sublithospheric channels, or tongues, connecting these off-ridge plumes and the westward migrating MAR at shallow depth in the upper mantle is substantiated by our Pb isotope test. An important fraction of the present plume flow around these hotspots is apparently strongly skewed along these distinct channels, which may have developed since the migrating MAR ridge sink has overridden the plumes. Mixing of plume-derived material with the asthenosphere along these channels appears irregular and apparently not purely binary as initially thought on the basis of trace element abundance ratios only, with the possible exception of the MAR-St Helena channel. The depleted asthenosphere beneath the South Atlantic appears to have also been broadly polluted by at least two distinct components, one of the St Helena type, the other of the Tristan type. The degree of pollution is apparently directly related to distance to these hotspots. The St Helena-related pollutant seems to be more

Fig. 5 Triangular plot of relative abundances of Pb 206, 207 and 208 in MAR basalts from the South Atlantic. a, With (La/Sm)_N< 0.63 (only N-MORB). Note that N-MORBs from the 2-24° S ridge segment suggest an array which reflects dominantly binary mixing between the LILE-depleted asthenosphere and the St Helena-type plume source (rich in 206Pb), with St Helena's contribution to the mix increasing southward (a pollution model of the asthenosphere dominated by St Helena). In contrast, N-MORBs from segment 25-35° S reflect ternary mixing between the LILE-depleted asthenosphere, St Helena and Tristan (rich in ²⁰⁸Pb) plume-type sources of pollutants, with Tristan's contribution to the mix increasing southward to the detriment of St Helena's, whereas the LILEdepleted source's contribution stays essentially constant. Southward, past Tristan, N-MORBs from segment 38-40°S are still reflecting ternary mixing, but with both St Helena and Tristan's types of pollutants of the LILE-depleted asthenosphere now decreasing southward. The analytical uncertainties are given by the error polygon in the lower right corner of the plot. b, With (La/Sm)_N>0.63 (basalts from the C, SH, and T-1, T-2, T-3 spike highs shown in Fig. 1b). Also plotted are averages of basalts from relevant South Atlantic off-ridge hotspots, and range for basalts from DSDP holes 525A, 527 and 528 on the Walvis Ridge (W) and 516F on the Rio-Grande Rise (R) (data uncorrected for age); and for reference, the N-MORB trend of Fig. 5a (dotted line). Note how the SH spike points towards the St Helena island field, the T-1, 2, 3 spikes towards Tristan-Gough-Discovery off-ridge hotspot fields, and the C-spike towards values corresponding neither to Fernando De Noronha (F), Bouvet (B), nor Ascension (A), but presumably Circe seamount (C). Note also that the three odd basalts discussed in Fig. 2 are part of the ternary mixing for N-MORBS discussed in a, and that the off-ridge Tristan (T), Gough (G) and Discovery (D) hotspots are progressively less enriched in the St Helena, ²⁰⁶Pb-rich, pollutant, moving radially southward from St Helena Island. See text for discussion of DSDP holes. Symbols used are the same as defined in Fig. 2.



widespread and to have polluted the plumes ascending, apparently at a rate increasing with time, towards the south within the past 80 Myr.

These observations are not unexpected within the framework of the migrating ridge sink-plume source model, which includes three critical stages of plume dispersion into the asthenosphere: (1) intraplate, when dispersion was at a maximum: (2) ridge-centred, when dispersion was at a minimum; and (3) off-ridge-channel-connected, when dispersion is intermediate^{1,4}. According to plate reconstruction models^{23,38,39}, the time-spans for these three stages for St Helena are respectively 75-90, 0-15 and 110 Myr, whereas for Tristan these are 60, 20-40 and 60-80 Myr. Thus, for comparable plume size or flux, the radial dispersion of the St Helena plume is expected to be more widespread than for the Tristan plume.

Within the frameworks of both the blob cluster model¹⁵ and the DUPAL anomaly10, one could conclude that the MAR region between 24 and 35°S marks the transitional boundary between the 8/4 Pb-rich, Kerguelen-Tristan blob cluster which dominates the Indian Ocean, and the 6/4 Pb-rich St Helena blob cluster which dominates the Atlantic, north of this boundary. However, in detail the pattern of pollution and dispersion is more complicated, apparently of smaller scale and tied to local hotspots. Sampling of the mid-ocean ridge system in the vicinity of the Bouvet triple junction suggests that the influence of the Bouvet plume, whose Pb isotope signature is intermediate between the Tristan-Kerguelen and the St Helena type (Figs 2a and 5b), can be detected and seems to extend irregularly over ~300-1,700 km along the three plate boundaries branching from the triple junction⁴⁰⁻⁴². Further north, we have seen that the extent of asthenosphere pollution, and the geochemical nature of the pollutants along the mid-ocean ridge system, are closely tied to the types of plume present in their vicinity. This tends to rule out a background pollution of the asthenosphere beneath the region by random addition of LILE-rich metasomatic fluids migrating from deeper zones of the Earth's mantle. Instead, the background pollution observed is more likely to reflect the dispersion at shallow depths of the South Atlantic plumes. However, the mechanism of dispersion of these plumes (or vertical chains of blobs) remains uncertain. It could be the result of a complex mantle convection pattern in the asthenosphere (see refs 11-15). Or, the dispersion could simply be the result of a radial flow of the plumes discharging into the asthenosphere, particularly when they were totally intraplate and had not yet sensed the effect of the spreading ridge axis (the sink). Or for that matter, both mechanisms may well have been operative⁴³. Our isotopic data does not allow such distinction.

Finally, we consider the observation that the Pb isotopic ratios seem to be more sensitive than the La/Sm or Nb/Zr ratios at detecting the broad background plume-related pollutant along the so-called normal ridge segments, as illustrated by the discrepancies in the baselines shown in Fig. 4. A proper understanding of such discrepancy, which at first may appear paradoxical, is important as it pertains to constraining not only the trace element and isotopic ratios, but also the elemental concentrations in the various plumes relative to that of the LILE-depleted asthenosphere, particularly of the elements in the denominator of these trace element or isotope ratios. In turn, this should help in constraining, or even mapping, the relative mass distribution of the different pollutants affecting the asthenosphere, and help understanding the mechanisms of dispersion heterogeneities and mantle dynamics in general. Two factors may contribute to the different sensitivities in detecting asthenosphere pollutants. One stems from mixing, the other from partial melting. First, it should be recalled that in mixing two reservoirs with distinct trace element or isotope ratios, the ratio in the

mixture is usually not linearly related to the mass-fraction entering the mix, unless the concentration ratio 'n' between the plume source (pollutant) and the asthenosphere source, of the chemical species in the denominator of such trace element or isotope ratios is unity^{44,45}. The parameter 'n' controls the curvature of the hyperbolic mixing curves. The greater is 'n', the more readily can a small fraction of the pollutant entering the mixture be detected. Since Pb isotopic ratios are more sensitive in revealing the plume pollutants in the South Atlantic than the (La/Sm)_N ratio (or the Nb/Zr analogue¹), it suggests that 'n' for Pb is greater than for Sm or Zr. In other words, Pb appears to be more incompatible than Sm or Zr. This is apparently also the case around Iceland²⁹, where 'n' for basalts derived from the Iceland plume relative to those derived from the LILE-depleted source south of 60° N is ~4 for Pb but only 1.5 for Sm (ref. 46). Although the ratio 'n' measured in the basalts is not necessarily identical to the ratio in the sources of these basalts, as it is affected by operative degrees of partial melting beneath Iceland and south of 60° N, the relative variation of 'n' among various trace elements is helpful.

Another mechanism suggested by G. Waggoner (personal communication) may be invoked if the plume-derived dispersed heterogeneities (pollutant) affecting the LILE-depleted source beneath the MAR have suffered some melt extraction in the recent past, but before the final partial melting stage taking place directly beneath the MAR axis. If this were the case, incompatible elements which partition preferentially into such melts would also be preferentially removed, thus generating residual plume material (plumes being dispersed towards the ridge) with lower ratios of highly incompatible to moderately incompatible elements (such as La/Sm or Nb/Zr). These residual plumes would thus have intermediate trace element ratios between that of the original plume and the LILE-depleted asthenosphere. In contrast, these dispersed residual plumes would still have a Pb isotope composition similar to that of the original plume even after a 100-200 Myr residence time in the asthenosphere, because of the long half-lives of the radioactive parents U and Th. The more different the trace element or

isotope ratio of the plume-derived pollutant is from that of the LILE-depleted asthenosphere, the more readily can it be detected in the mixture sampled along the MAR, even if the ratio 'n' discussed earlier is unity. The plausibility of this mechanism for the South Atlantic will depend on knowing better the dynamics and thermal structure of the upper mantle, to determine over what depth range the dispersion of these plumes and partial melting may take place. The question also requires a detailed analysis of relative rates, including the ridge migration and horizontal velocities of the plume domains being dispersed both along the proposed channels and radially.

Although the origin of mantle heterogeneities and mechanism of dispersion in the upper mantle remains an open question, we believe that some of the major discrepancies remaining between the different models discussed here may be more a reflection of the different scales of sampling existing along the mid-ocean ridges, rather than being of real substance. The evidence for upper mantle flow lamination in the South Atlantic would probably not have been detected had a sampling at intervals of 100-500 km been used, as currently available in the Indian Ocean¹⁶⁻²⁰. Morgan³ initially developed the model of plume source-migrating ridge sink and connecting channel on the basis of the track of constructional volcanism on the sea floor between the Reunion hotspot and the eastward-migrating Central Indian mid-ocean ridge. It would be of great interest to find out if a denser sampling of the region might reveal, in addition to the general background Kerguelen-Tristan pollutant already observed 16-20, some well-defined, spike-like geochemical anomalies along this ridge opposite the Reunion hotspot, as well as opposite other hotspots in the Indian Ocean, as our model predicts and sparse existing data already suggest^{18,19}

The sampling and initial stage of this study was done in collaboration with G. Thompson and S. Humphris (WHOI). Samples from Cruise EN63 were provided by H. Sigurdsson (URI). We also benefited from fruitful discussions with G. Waggoner and M. Cole. Assistance from S. Benson, B. McCully and the staff at RINSC are appreciated. This work was supported by the NSF.

Received 24 February; accepted 29 May 1986.

- 1. Schilling, J-G., Thompson, G., Kingsley, R. & Humphris, S. Nature 313, 187-191 (1985). Humphris, S. E., Thompson, G., Schilling, J-G. & Kingsley, R. H. Geochim. cosmochim. Acta 49, 1445-1464 (1985).
- Morgan, W. J. J. geophys. Res. 83, 5355-5360 (1978). Schilling, J-G. Nature 314, 62-67 (1985).
- Gast, P. W., Tilton, G. R. & Hedge, C. Science 145, 1181-1185 (1964).
 Zindler, A., Jagoutz, E. & Goldstein, S. Nature 298, 519-523 (1982).

- Brozena, J. M. J. geophys. Res. 91, 497-510 (1986).

 Van Andel, T. H. & Heath, G. R. Mar. Geophys. Res. 1, 5-36 (1970).

 Van Andel, T. H., Rea, D. K., Von Herzen, R. P. & Hoskins, M. Bull. geol. Soc. Am. 84, 1527-1546 (1973).
- 10. Hart, S. R. Nature 309, 753-757 (1984).
- Richter, F. M. & Ribe, N. M. Earth planet. Sci. Lett. 43, 212 (1979).
 Richter, F. M., Daly, S. F. & Nataf, H-C. Earth planet. Sci. Lett. 60, 178-194 (1982).

- Olsen, P., Yuen, D. A. & Balsiger, D. J. geophys. Res. 89, 425-436 (1984).
 Hoffman, N. R. A., McKenzie, D. P. Geophys. J. astr. Soc. 82, 163-206 (1985).
 Allègre, C. J., Hamelin, B. & Dupre, B. Earth planet. Sci. Lett. 71, 71-84 (1984).
 Cohen, R. S., Evensen, N. M., Hamilton, P. J. & O'Nions, R. K. Nature 283, 149-153 (1980).
- Dupré, B. & Allègre, C. J. Nature 142-146 (1983).
 Hamelin, B. & Allègre, C. J. Nature 315, 196-199 (1985).
- 19. Hamelin, B., Dupré, B. & Allègre, C. J. Earth planet. Sci. Lett. 76, 288-298 (1986).
- 20. Price, R. C., Kennedy, A. K., Sneeringer, M. R. & Frey, F. A. Earth planet. Sci. Lett. (in
- Cannon, R. S. Jr., Pierce, A. P., Antweiler, J. C. & Buck, K. L. Econ. Geol. 56, 1-38 (1961).
 Richardson, S. H., Erlank, A. J., Duncan, R. A. & Reid, D. L. Earth planet. Sci. Lett. 59, 327-342 (1982).
- 23. Morgan, W. J. Tectonophysics 94, 123-139 (1983).

- 24. Mussett, A. E. & Barker, P. F. Init. Rep. DSDP Leg. 72, 467-470 (1983).
- Moore, T. C. et al. Bull. geol. Soc. Am. 94, 907-925 (1983).
 Baker, P. E., Gass, I. G., Harris, P. G. & Le Maitre, R. W. Phil. Trans. R. Soc. A256, 439-578
- Kempe, P. R. C. & Schilling, J-G. Contr. Miner. Petrol. 44, 101-115 (1974).
 Sun, S. S. Phil. Trans. R. Soc. A297, 409-445 (1980).
 Sun, S. S., Tatsumoto, M. & Schilling, J-G. Science 190, 143-147 (1975).

- 30. Dupré, B. & Allègre, C. J. Nature 286, 17-22 (1980).
- Dupré, B., Lambret, B., Rousseau, D. & Allègre, C. J. Nature 294, 552-554 (1981).
 Hamelin, B., Dupré, B. & Allègre, C. J. Earth planet. Sci. Lett. 67, 340-350 (1984).

- Antietti, B., Dupre, B. & Allegre, C. J. Earin pianet. Sci. Lett. 61, 340-350 (1984).
 White, W. M. & Schilling, J.G. Geochim. cosmochim. Acta 42, 1501-1516 (1982).
 Schilling, J.-G., Kingsley, R. H. & Devine, J. D. J. geophys. Res. 87, 5593-5610 (1982).
 Verma, S. P. & Schilling, J.-G. J. geophys. Res. 87, 10838-10856 (1982).
 Verma, S. P., Schilling, J.-G. & Waggoner, D. G. Nature 306, 654-657 (1983).
 Stein, S. H., Melosh, J. & Minster, J. B. Earth planet. Sci. Lett. 36, 51-62 (1977).
 Morgan, W. J. in The Sea Vol. 7 (ed. Emiliani, C.) 443-487 (Wiley, New York, 1981).

- Duncan, R. A. Tectonophysics 74, 29-42 (1981).
 Dickey, J. S. Jr., Frey, F. A., Hart, S. R. & Watson, E. B. Geochim. cosmochim. Acta 41, 1105-1118 (1977)
- 41. Le Roex, A. P. et al. J. Petrol. 24, 267-318 (1983).
- Le Roex, A. P. et al. Contr. Miner. Petrol. 90, 367-380 (1985).
 Olson, P. & Singer, H. J. Fluid. Mech. 158, 509-529 (1985).
- Vollmer, R. Geochim. cosmochim. Acta. 40, 283-295 (1976)
- 45. Langmuir, C. H., Vocke, R. D., Hanson, G. N. & Hart, S. R. Earth planet. Sci. Lett. 37, 380-392 (1978).
- 46. Schilling, J-G. Nature 242, 564-571 (1973).
- 47. Todt, W., Cliff, R. A., Hanser, A. & Hofmann, A. W. Terra Cognita 4, 209 (1984).
- 48. Tatsumoto, M. Earth planet. Sci. Lett. 38, 63-87 (1978).
- 49. Tilton, G. R. Earth planet. Sci. Lett. 19, 321-329 (1973).

Identification of a putative second T-cell receptor

Michael B. Brenner**, Joanne McLean*, Deno P. Dialynas*, Jack L. Strominger**, John A. Smith^{§††}, Frances L. Owen^{||}, J. G. Seidman^{||}, Stephen Ip[#], Fred Rosen^{||} & Michael S. Krangel***

* Division of Tumor Virology, Dana-Farber Cancer Institute; † Departments of Rheumatology and Immunology, Brigham and Women's Hospital, Department of Genetics; ** Department of Pediatrics, Children's Hospital, Harvard Medical School, Boston, Massachusetts 02115, USA

Department of Schools, Department of Fediatrics, Cambridge, Massachusetts 02138, USA Departments of Molecular Biology and †Pathology, Harvard Medical School, Boston, Massachusetts 02115, USA

Cancer Research Center, Tufts Medical School, Boston, Massachusetts 02111, USA

"T cell Sciences, Inc., Cambridge, Massachusetts 02139, USA

Framework monoclonal antibodies have identified a population of human lymphocytes that express the T3 glycoprotein but not the T-cell receptor (TCR) α - and β -subunits. Chemical crosslinking experiments reveal that these lymphocytes express novel T3-associated polypeptides, one of which appears to be the product of the Ty gene. The other polypeptide may represent a fourth TCR subunit, designated To.

UNDERSTANDING T-cell recognition of antigen and the restriction of this process by major histocompatibility complex (MHC)encoded antigens has been an important goal in immunology. A major step forward occurred with the immunochemical identification of clone-specific disulphide-linked heterodimers on T cells, composed of subunits termed TCR α and β (relative molecular mass (M_r) 50,000 (50K) and 40K, respectively)¹⁻³. Genes that rearrange during thymic ontogeny and encode the TCR $\beta^{4,5}$ and α^{6-8} subunits were isolated either by subtractive hybridization or by probing with oligonucleotides.

A unique feature of the human TCR $\alpha\beta$ was the observed co-modulation², co-immunoprecipitation^{9,10} and required coexpression¹¹ of the TCR $\alpha\beta$ molecules with the T3 glycoprotein, which suggested that these two structures were related. Subsequently, the direct physical association of the two protein complexes was demonstrated by chemically crosslinking the TCR $\alpha\beta$ molecules to the T3 glycoprotein and identifying the components of the crosslinked complex as the TCR β -subunit and the T3 glycoprotein 28K subunit¹². A T3 counterpart is similarly associated with murine TCR $\alpha\beta^{13,14}$.

A third gene that rearranges in T cells, designated $T\gamma$, has been identified in mouse¹⁵⁻¹⁷ and man^{18,19}. Ty gene rearrangements occur in lymphocytes with suppressor-cytotoxic as well as helper phenotypes and may produce a large number of $T\gamma$ chains 18-23. However, the function of the $T\gamma$ gene is unknown. Furthermore, neither the protein encoded by the Ty gene nor its possible association with other structures (as occurs with TCR $\alpha\beta$ and T3 glycoproteins) has been defined.

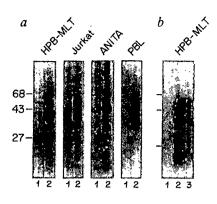
It appears increasingly likely that the TCR $\alpha\beta$ molecule alone determines both antigen recognition and MHC restriction on at least some T cells^{24,25}. However, it is unclear whether this receptor accounts for the process of T-cell selection during thymic ontogeny or for all antigen-specific recognition by mature T cells. For example, suppressor T lymphocytes remain an enigma; in some cases they delete or fail to rearrange TCR β genes^{26,27}. Thus, it is of great importance to determine whether a second T-cell receptor exists, to define its structure (particularly with regard to the possible use of the $T\gamma$ gene product) and ultimately to understand its function(s).

Here, framework monoclonal antibodies that react with shared determinants on human TCR $\alpha\beta$ molecules were used to identify peripheral blood lymphocytes (PBL) that were T3⁺ but did not react wth these monoclonal antibodies. We reasoned that such lymphocytes might express non- α , non- β T3-associated structures and that such molecules might represent a second T-cell receptor complex. This strategy resulted in the identification of a T3-associated molecular complex on the surface of human lymphocytes that do not express detectable TCR a and β transcripts or polypeptides. We suggest that this complex is a putative second T-cell receptor.

Monoclonal antibodies

A murine framework antiserum that recognizes most human TCR $\alpha\beta$ molecules has been reported previously²⁸. Subsequently, a murine monoclonal antibody, called β Framework 1 (β F1), that is reactive with shared determinants on the human TCR β -chain was obtained (M.B.B. et al., in preparation). The βF1 antibody reacts with most T3⁺ human PBL and is capable of immunoprecipitating the TCR $\alpha\beta$ heterodimer from all human T-cell lines examined that have $\alpha\beta$ T-cell receptors and express the T3 glycoprotein. Immunoprecipitations from a panel of T-cell lines using β F1 demonstrate this reactivity as well as the heterogeneity of the TCR α - and β -subunits from different receptors (Fig. 1a). Like the framework antiserum²⁸, this monoclonal antibody does not stain the surface of living T cells, but will react specifically with both membrane and cytoplasmic T-cell receptors after partial solubilization of the lymphocyte plasma membrane with 70% ethanol. Double staining of human PBL with fluorescein-conjugated anti-T3 monoclonal antibody and biotinyl- β F1 monoclonal antibody, followed by phycoerythrin-conjugated avidin reveals that β F1 recognizes 95-97% of peripheral blood T3⁺ lymphocytes. However, it clearly defines a small population of T lymphocytes that is $\beta F1^-$, yet $T3^+$ (Fig. 1c).

A second framework monoclonal antibody, WT31, initially thought to recognize the T3 antigen²⁹, has recently been shown to react with a common epitope of human TCR $\alpha\beta^{36}$. While double staining with anti-T3 monoclonal antibody (OKT3) and WT31 revealed that each antibody blocks binding of the other, one-colour fluorescence indicated that WT31 typically recognizes 1-3% fewer cells in peripheral blood than does anti-T3 (data not shown). WT31 efficiently binds to the surface of T cells (for example, in fluorescence-activated cell sorter (FACS) analyses) and is capable of immunoprecipitating the TCR $\alpha\beta$ molecules, albeit inefficiently, from radiolabelled detergent lysates³⁰ (see also Fig. 1b, lane 3). Thus, β F1 and WT31 appear to recognize all but a small fraction of human peripheral blood T3⁺ cells, and define a subpopulation that is T3⁺ but unreactive



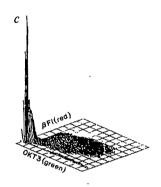


Fig. 1 Reactivity of framework monoclonal antibodies recognizing TCR $\alpha\beta$. a, Immunoprecipitates from 125 I-labelled lymphocyte lysates were analysed by SDS-PAGE. The radioiodinated T-cell leukaemia lines HPB-MLT and Jurkat, the human T-lymphotropic virus type 1-transformed cell line ANITA and resting PBL were solubilized in 1% Triton X-100 and immunoprecipitated with a control antibody, normal mouse serum (NMS) (lane 1 for each cell line) or framework antibody to TCR $\alpha\beta$, antibody β F1 (lane 2 for each cell line). b, ¹²⁵I-labelled lymphocytes were solubilized in 0.1% Triton X-100 and immunoprecipitated with NMS (lane 1), anti-T3 antibody, UCHT-1 (ref. 40) (lane 2) or framework antibody to TCR $\alpha\beta$, WT31 (lane 3). The efficiency of immunoprecipitation with WT31 was improved at the lower concentration of Triton X-100 used here. c, Two-colour FACS analysis of normal adult PBL using anti-TCR $\alpha\beta$ and anti-T3 monoclonal antibodies. PBL were stained first with FITC-conjugated anti-T3 antibody (OKT3) and then with biotinyl-anti-TCR $\alpha\beta$ antibody (βF1) followed by phycoerythrin-conjugated avidin (PE-avidin, Becton Dickinson). Red and green fluorescence were measured in comparison with nonspecific control FITC- and biotin-conjugated monoclonal antibodies (data not shown). Cells unreactive with either antibody are non-T cells (lower left corner); cells that are doubly positive, reacting with both OKT3 and β F1, make up the large population of lymphocytes in the centre of the grid; cells that are \$\beta F1^{-}\$ but OKT3⁺ comprise the narrow group of lymphocytes (4% of the T3+ cells) observed along the x-axis.

Methods. Viable lymphocytes were isolated by Ficoll-Hypaque density gradient centrifugation for both SDS-PAGE and FACS analyses. For SDS-PAGE, lymphocytes were radioiodinated by the lactoperoxidase technique, solubilized in 1% Triton X-100 and immunoprecipitated using 1 µg of specific antibody (\$\beta F1\$ or UCHT-1) or 1 µl of NMS. Monoclonal antibody 187-1 (3 µg) was used as a second antibody for β F1 and UCHT-1 (ref. 47). The immunoprecipitates were then analysed by SDS (10.5%)-PAGE under reducing conditions. The ¹²⁵I-labelled molecules were visualized by autoradiography as described previously28. Two-colour cytofluorographic analysis was performed by first staining PBL with FITC-OKT3 for 45 min at 4 °C. After washing, the lymphocytes were fixed in 1% paraformaldehyde for 15 min at 23 °C and then incubated in 70% ethanol in phosphate-buffered saline (PBS) for 5 min at -20 °C. After further washing, the cells were stained with biotinyl-\$\beta\$F1 followed by PE-avidin. Analysis was performed on an Ortho cytofluorograph.

Table 1 Phenotypes of cell lines derived from PBL of immunodeficiency patients

			% Positive for:					
Cell line	Source	Description	WT31	T3	T4	T8		
1	IDP1	Allo	50	100	11	50		
2	IDP1	WT31 ⁺ sort	100	100	70	28		
3	IDP1	WT31 ⁻ sort	0	100	0	62		
4	IDP2	Fresh PBL	61	63	38	16		
5	IDP2	PHA	100	96	18	80		
6	IDP2	Allo	2	100	0	43		
7	IDP2	PHA	. 12	93	1	18		

The description of each cell line indicates either the conditions for activation of the lymphocytes, or their source. Alloantigen (allo)-activated cultures were stimulated with irradiated allogeneic PBL at weekly intervals. Mitogen (phytohaemagglutin, PHA)-activated lines were stimulated with a 1:1,000 dilution of PHA (Difco) at culture initiation. WT31⁺ and WT31⁻ sorted cell lines 2 and 3 (sort) were obtained from IDP1 cell line 1 by cell sorting analysis. All cell lines were propagated in vitro in media composed of RPMI 1640, 10% human serum and conditioned media containing 2-5 units of IL-2 as described previously³⁴. Viable lymphocytes were isolated by Ficoll-Hypaque density gradient centrifugation and stained with 0.5 µg of WT31, OKT3, OKT4 or OKT8 (Ortho, Raritan, New Jersey) for 30 min at 4 °C. After washing, the cell pellets were stained again with fluorescein isothiocyanate (FITC)-conjugated goat anti-mouse F(ab')2 fragments. FACS analyses were performed on an Ortho cytofluorograph or a Coulter Epics as described previously³⁷. Specifically stained positive cells were determined relative to a negative control profile for each cell line (stained with nonspecific control monoclonal P3X63Ag8). Cells having fluorescence intensity channel numbers greater than the intercept of the negative control profile with the baseline were counted as positive, and the per cent positive was calculated relative to the total number of cells counted.

with both of these framework monoclonal antibodies against the TCR $\alpha\beta$ molecules. Evidence that the T3⁺ lymphocytes that are unreactive with β F1 are also unreactive with WT31 is presented below. We have used WT31 primarily for FACS analyses and β F1 primarily for immunoprecipitation studies.

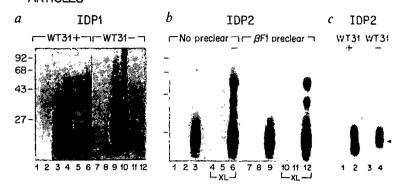
Isolation of WT31⁻T3⁺ lymphocytes

Efforts at growing the WT31⁻T3⁺ population from normal adult PBL proved difficult, as the WT31⁺T3⁺ lymphocytes usually overgrew the WT31⁻T3⁺ cells after mitogenic stimulation. However, growth of the WT31⁻T3⁺ population from the PBL of immunodeficiency patients was successful. Immunodeficiency patient 1 (IDP1) suffered from the bare lymphocyte syndrome, and lacked class II MHC antigen expression on lymphoid cells^{31,32}, while immunodeficiency patient 2 (IDP2) suffered from an ectodermal dysplasia syndrome³³ and displayed poor *in vitro* T-cell proliferative responses to mitogens.

After activation of PBL from IDP1 with alloantigen and propagation in conditioned media containing interleukin-2 (IL-2)³⁴, the resultant cell line was observed to be ~50% WT31⁺T3⁺ and 50% WT31⁻T3⁺ (Table 1, cell line 1). Subsequent sorting of this cell line yielded homogeneous populations of WT31⁺T3⁺ cells and WT31⁻T3⁺ cells (Table 1, cell lines 2 and 3, respectively).

Cell lines were also obtained from IDP2; 63% of the PBL from IDP2 were T3⁺ and 1-3% fewer cells (61%) were WT31⁺, which is typical of normal PBL (Table 1, cell line 4). Activation of these IDP2 PBL with either phytohaemagglutinin (PHA) or alloantigen and propagation in vitro with conditioned media resulted in several cell lines, including a homogeneous WT31⁺T3⁺ cell line (Table 1, cell line 5), a homogeneous WT31⁻T3⁺ cell line (cell line 6) and, on a third occasion, a cell line that was 88% WT31⁻T3⁺ (with 12% contaminating WT31⁺T3⁺ cells) (cell line 7). Note that the WT31⁻T3⁺ popula-

Fig. 2 SDS-PAGE of cell surface T3 and T3-associated (crosslinked) molecules from IDP1 and IDP2 cell lines. a, IDP1 cell lines 2 (WT31⁺) and 3 (WT31⁻) were ¹²⁵Ilabelled as described in Fig. 1 legend. Radioiodinated, intact lymphocytes were then either crosslinked by incubation in PBS (pH 8) containing 50 µg ml⁻¹ DSP (evennumbered lanes) or mock-incubated (odd-numbered lanes). The cells were then solubilized in 1% Triton X-100 and immunoprecipitated as described previously¹². Lanes 1, 2, 7 and 8 were immunoprecipitated with NMS. Lanes 3, 4, 9 and 10 were anti-T3 immunoprecipitates using UCHT-1. Lanes 5, 6, 11 and 12 were anti-TCR $\alpha\beta$ immunoprecipitates using β F1. Note that T3-associated molecules (40-55K) on the anti-T3 immunoprecipitations were detected at higher levels in the crosslinked samples than in the non-crosslinked samples. b, IDP2 cell line 7



(88% WT31⁻T3⁺) was ¹²⁵I-labelled and either treated with DSP [crosslinked samples (XL) lanes 4-6 and 10-12] or mock-incubated (non-crosslinked samples, lanes 1-3 and 7-9). Immunoprecipitations were performed using NMS (lanes 1, 4, 7 and 10), anti-T3 antibody UC117-1 (lanes 3, 6, 9 and 12) and anti-TCR $\alpha\beta$ antibody β F1 (lanes 2, 5, 8 and 11) either without (left-hand side) or with (right-hand side) preclearing of TCR $\alpha\beta$ molecules using β F1. Note that a small fraction of radiolabelled TCR $\alpha\beta$ was detected in lanes 2 and 5 (without preclear) but not with the β F1 preclear (lanes 8 and 11). c, IDP2 cell lines 5 (WT31⁺T3⁺) and 7 (88% WT31⁻T3⁺) were ¹²⁵I-labelled, solubilized in 1% Triton X-100 and immunoprecipitated using NMS (lanes 1 and 3) or anti-T3 antibody UCHT-1 (lanes 2 and 4). The T3 heavy subunit (27K) appeared similar in these two cell lines, while the T3 light subunits (19-25K) did not (compare lanes 2 and 4 below the arrowhead). Methods. ¹²⁵I-labelling, solubilization in 1% Triton X-100, immunoprecipitation and visualization after SDS (10.5%)-PAGE by autoradiography were performed as described previously¹²⁸. Chemical crosslinking of intact radiolabelled lymphocytes using DSP (50 μ g ml⁻¹) in PBS (ρ H 8) was for 30 min at 23 °C, as described previously¹²⁸. After immunoprecipitation, all samples were examined by SDS-PAGE under reducing conditions using 5% 2-mercaptoethanol, which cleaved both the disulphide bonds between protein subunits and the DSP chemical crosslink.

tion contained both T4⁻T8⁺ and T4⁻T8⁻ cells (cell lines 3, 6 and 7). Further phenotypic analyses revealed that this population was T11⁺ but negative for natural killer cell markers such as Leu 7, Leu 11 and OKM1 and for the immature thymocyte marker T6 (data not shown).

WT31⁻ T3⁺ cells are negative for TCR $\alpha\beta$

Having identified WT31⁺T3⁺ and WT31⁻T3⁺ populations, we sought to determine whether these lymphocytes expressed TCR $\alpha\beta$ molecules that could be immunoprecipitated by β F1. While β F1 immunochemically defined a heterodimeric structure on the surface of 125 I-labelled WT31+T3+ IDP1 lymphocytes (Fig. 2a, lane 5), it failed to recognize a similar protein on the WT31-T3+ population from the same individual (Fig. 2a, lane 11). Similar analysis of IDP2 cell lines revealed a trace of TCR $\alpha\beta$ on the 88% WT31⁻T3⁺ cell line 7 (Fig. 2b, lane 2) consistent with the 12% contamination with WT31+T3+ cells. Thus, the WT31-T3+ cells, identified by the lack of cell surface reactivity with antibody WT31 on FACS analysis, were also βF1, as determined by lack of TCR $\alpha\beta$ on immunoprecipitation. Note that all WT31+T3+ and WT31-T3+ cell lines expressed similar amounts of T3 as determined by FACS analysis (data not shown) and by immunoprecipitation with anti-T3 antibody (Fig. 2a, lanes 3 and 9, and c, lanes 2 and 4). However, the T3 molecule on WT31⁻βF1⁻T3⁺ lymphocytes was not identical to that on WT31+BF1+T3+ cells, as revealed SDS-polyacrylamide gel electrophoresis (SDS-PAGE). One- (Fig. 2c) and two-dimensional (data not shown) gel analysis indicated that the difference in T3 was restricted to the light T3 subunits, which reproducibly exhibited different SDS-PAGE mobilities (Fig. 2c, arrowhead).

To determine whether the WT31 $^{-}\beta$ F1 $^{-}$ T3 $^{+}$ population lacked TCR $\alpha\beta$ molecules, or alternatively expressed TCR $\alpha\beta$ molecules that failed to react with the monoclonal antibodies used, we analysed the cells for messenger RNAs encoding the TCR α and β proteins. 32 P-labelled complementary DNA clones encoding TCR α , TCR β and T γ were used to probe Northern blots containing whole-cell RNA from WT31 $^{-}\beta$ F1 $^{-}$ T3 $^{+}$ and WT31 $^{+}\beta$ F1 $^{+}$ T3 $^{+}$ IDP2 cell lines and from HPB-MLT, which is known to contain mRNAs for TCR α , TCR β and T γ . No TCR α or β mRNA transcripts were detected in the RNA from the WT31 $^{-}\beta$ F1 $^{-}$ T3 $^{+}$ IDP2 cell line 6 (Fig. 3 α , α -probe, lane 1; or β -probe, lane 1), whereas expression of both was clearly detectable in RNA from HPB-MLT (Fig. 3 α ; α -probe, lane 2; and β -probe, lane 2). Notably, T γ mRNA was present in the

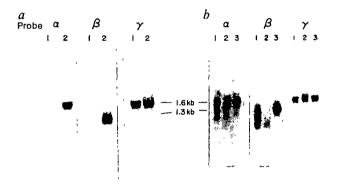


Fig. 3 Northern blot analysis of RNAs isolated from 1DP2 cell lines using TCR α , TCR β and T γ cDNA probes. a, Total RNA (15 µg) isolated from IDP2 cell line 6 (WT31⁻) (lane 1 for each probe) and from T-cell leukaemic line HBP-MLT (lane 2 for each probe) was fractionated on a 1.5% agarose gel containing 2.2 M formaldehyde, transferred to nitrocellulose and hybridized with TCR α , TCR β and T γ probes. b, Total RNAs (2 µg) isolated from IDP2 cell line 5 (WT31⁺T3⁺) (lane 1 for each probe), IDP2 cell line 7 (88% WT31⁻T3⁺) (lane 2 for each probe) and HPB-MLT (lane 3 for each probe) were analysed as in a.

Methods. RNA preparation, electrophoresis, transfer to nitrocellulose and hybridization with 32 P-labelled, nick-translated probes $(1-3\times10^8~\text{c.p.m.}~\mu\text{g}^{-1})$ were done as described previously 41 . The α -chain probes were the human cDNA clones pGA5 (ref. 8) in α and L17 α (ref. 42) in β ; the β -chain probes were human cDNA clones 12A1 (ref. 43) in α and L17 α (ref. 43) in β . The β -chain probe was an β -coal ragment derived from human cDNA clone T γ -1 (ref. 36). Radioactive bands were visualized by autoradiography using intensifying screens. In the experiment shown in β , all probes were labelled to almost identical specific activity, and identical exposure times were used.

WT31⁻T3⁺ cells at a level comparable to that in HPB-MLT (Fig. 3a, γ -probe, lanes 1 and 2). Thus, the WT31 β F1 T3⁺ lymphocytes lacked TCR α and β mRNA. Subsequent experiments on cell lines that were mostly WT31⁻T3⁻ corroborated this result. For example, Northern blot analysis of IDP2 cell line 7 (88% WT31⁻T3⁺) in comparison with IDP2 cell line 5 (WT31⁺T3⁺), as well as with HPB-MLT cells, revealed only a trace of TCR α or β mRNA in the 88% WT31⁻T3⁺ cells (con-

sistent with the 12% contamination with WT31⁺T3⁺ cells) (Fig. 3b, lane 2 for each probe). Further, most of the β transcripts that could be detected were 1.0 and not 1.3 kilobases (kb) long and were probably nonfunctional³⁵. In contrast, the IDP2 cell line 5 (WT31⁺T3⁺) expressed levels of both RNA species which were comparable to those in HPB-MLT (Fig. 3b, lane 1 for each probe). However, like the WT31⁻T3⁺ line shown in Fig. 3a, both the WT31⁻T3⁺ and the WT31⁺T3⁺ lines showed levels of T γ RNA comparable to that in HPB-MLT (Fig. 3b, γ -probe).

Thus, the WT31⁻T3⁺ cells lacked α and β T-cell receptor mRNA (by Northern analysis) and α and β T-cell receptor proteins (by immunoprecipitation and FACS analysis). The presence of T γ mRNA in WT31⁻T3⁺ cells, while consistent with T γ protein expression, could not be taken as strong evidence for this, as many human cell lines that express T γ mRNA of normal size may express full-length transcripts that are out of frame because of defective joining of the V (variable) and J (joining) regions³⁶.

Non- α , non- β T3-associated molecules

We used chemical crosslinking to determine whether proteins analogous to the TCR $\alpha\beta$ molecules existed on the WT31-BF1-T3+ cells. This technique has demonstrated the physical association of the TCR $\alpha\beta$ molecules with the T3 glycoprotein¹². The bifunctional, cleavable reagent dithiobissuccinimidyl propionate (DSP), was used to crosslink 125Ilabelled surface proteins of viable T lymphocytes. After crosslinking, the lymphocytes were solubilized in non-ionic detergent and immunoprecipitated with anti-T3 antibody. As expected, in the WT31⁺ β F1⁺T3⁺ lymphocytes the TCR α - and β -chains were found to be crosslinked to T3. For example, TCR $\alpha\beta$ molecules and T3 were found in anti-T3 or βF1 immunoprecipitates from crosslinked IDP1 cell line 2 (WT31+T3+) (Fig. 2a, lanes 4 and 6). However, despite the lack of reactivity with β F1 and the lack of TCR α or β mRNA, IDP1 cell line 3 (WT31⁻T3⁺) and IDP2 cell line 7 (88% WT31-T3+), both also expressed two protein subunits (55K and 40K) that specifically crosslinked to T3 (Fig. 2a, lane 10 and b, lane 6). Note that the mobilities of these T3-associated molecules were clearly different from those of the TCR α - and β -chains from WT31⁺T3⁺ cell lines (compare Fig. 2a, lanes 4 and 10, or b, lanes 5 and 6).

As IDP2 cell line 7 (88% WT31 $^-$ T3 $^+$) contained 12% WT31 $^+$ T3 $^+$ cells (accounting for the weak β F1 immunoprecipitates noted; Fig. 2b, lane 2), the lysate from these cells was precleared of TCR $\alpha\beta$ protein using β F1. After preclearing, no residual β F1-reactive material could be detected (Fig. 2b, lanes 8 and 11). When this β F1-precleared lysate from crosslinked cells was immunoprecipitated with anti-T3, 55K and 40K subunits were still detected (Fig. 3b, lane 12).

Because these WT31 $^-\beta$ F1 $^-$ T3 $^+$ cell lines do not apparently express TCR α and β mRNAs, the molecules found specifically crosslinked to T3 on their cell surfaces cannot represent proteins encoded by the known TCR α or β genes. We therefore considered the possibility that one of these polypeptides represents the product of the rearranging T γ gene.

Isolation of T3-associated 55K subunit

cDNA clones representing the rearranging human $T\gamma$ gene would encode a polypeptide with a predicted M_r of 40,000 (ref. 36). However, unlike the murine $T\gamma$ gene, which does not reveal any N-linked glycosylation sites¹⁵, the human $T\gamma$ gene has five potential sites for N-linked glycosylation, four of which are located in the constant region³⁶. As a $T\gamma$ protein has not been isolated previously, it is unknown how many of these potential sites are used. However, a fully glycosylated human $T\gamma$ protein may have a M_r of ~55,000. The heavy chain of the non- α , non- β T3-associated subunits identified on the WT31 $^-\beta$ F1 $^-$ T3 $^+$ IDP1 and IDP2 cell lines described in the present report had a relative mobility of 55K on SDS-PAGE (Fig. 2a, b). To determine whether this T3-associated heavy chain was serologically cross-

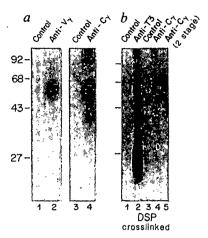


Fig. 4 Immunoprecipitations from IDP2 cell line 7 by anti-V. and anti-C₇ antisera. a, Triton X-100-solubilized, ¹²⁵I-labelled IDP2 cell line 7 (88% WT3 T3 +) was denatured (see below) and then immunoprecipitated with NMS (lane 1) or normal rabbit serum (lane 3) and with anti-V, antiserum (lane 2) or anti-C, antiserum (lane 4). Note that a specific band was observed at M_r 55,000 in both the anti-V, and anti-C, immunoprecipitations. The additional band at Mr 90,000 was not reproducibly observed in the anti-C₂ immunoprecipitations (see b). b, DSP-crosslinked native lysates (1% Triton-100) from ¹²⁵I-labelled IDP2 cell line 7 were immunoprecipitated with NMS (lane 1) or with anti-T3 antibody UCHT-1 (lane 2). Alternatively, the lysate was denatured (as described below) and immunoprecipitated with either normal rabbit serum (lane 3) or anti-C, antiserum (lane 4). An additional aliquot of lysate was subjected to a two-stage immunoprecipitation: polypeptides were immunoprecipitated with UCHT-1, and were eluted from the immunoadsorbent under denaturing and reducing conditions, in order to break the DSP crosslink. Immunoprecipitation from this eluate was then performed using anti-C, antiserum (lane 5)

Methods. 125 I-labelling, solubilization and immunoprecipitation were performed as described for Fig. 1. Native lysates (1% Triton-100) were denatured by adding SDS (final concentration 1%) and dithiothreitol (final concentration 2 mM) followed by heating the mixture for 5 min at 68 °C. After cooling, iodoacetamide was added (20 mM final concentration) and samples were diluted by adding 4 vol. of 1.5% Triton X-100 in Tris-buffered saline (pH 8). The initial immunoprecipitate in the experiment depicted in lane 5 of b was denatured and subsequently partially renatured in a similar manner²⁸. Samples were immunoprecipitated with 10 μl of anti-C. or anti-V, antiserum, 1 µg of UCHT-1 or 1 µl of NMS or normal rabbit serm and analysed by SDS (10.5%)-PAGE under reducing conditions (5% 2-mercaptoethanol). Peptides corresponding to deduced V, or C, amino-acid sequences (residue numbers noted in the text) were synthesized on a Beckman 990 or an Applied Biosystems 430A peptide synthesizer using the method of Merrifield44. Peptide purity was assessed by HPLC and peptide sequences were confirmed by amino-acid analysis. Peptides were coupled to keyhole limpet haemocyanin (KLH) at a ratio of 50 peptides per KLH molecule⁴⁵. Mice and rabbits were immunized with the V_{γ} or C_{γ} peptides, respectively. Animals were injected at 3-week intervals and the antisera screened for binding reactivity on peptide-KLH and peptide-bovine serum albumin conjugates to ascertain the presence of peptide-specific antibodies.

reactive with or identical to the $T\gamma$ protein, antisera were raised against synthetic peptides representing, respectively, a stretch of 17 amino acids (residues 5-21) from the variable region (anti- V_{γ} antiserum) and a stretch of 20 amino acids (residues 117-136) from the constant region (anti- C_{γ} antiserum) of the $T\gamma$ amino-acid sequence deduced from a human cDNA clone³⁶. Both the anti- C_{γ} antiserum and the anti- V_{γ} antiserum immunoprecipitated a molecule with a $M_{\rm r}$ of 55,000 from the denatured lysate of ¹²⁵I-labelled WT31 $^{-}\beta$ F1 $^{-}$ T3 $^{+}$ cells (Fig. 4a, lanes 2 and 4). Such molecules could not be immunoprecipitated from lysates of ¹²⁵I-labelled HPB-MLT cells, which express only nonfunctional $T\gamma$ mRNA³⁶ (data not shown).

To demonstrate that the 55K molecule immunoprecipitated by the anti- C_{γ} and anti- V_{γ} antisera was, in fact, the heavy subunit that crosslinked to T3, an additional experiment was performed (Fig. 4b). A sample of DSP-crosslinked lysate from the WT31⁻βF1⁻T3⁺ cells was first immunoprecipitated with anti-T3, again demonstrating the association of 55K and 40K subunits with T3 (Fig. 4b, lane 2). In parallel, another aliquot of the crosslinked lysate was immunoprecipitated with an anti-T3 monoclonal antibody, and the immunoprecipitated T3-crosslinked polypeptides were eluted from the immunoadsorbent, under denaturing and reducing conditions in order to break the DSP crosslink. This eluate was then re-precipitated with anti-C, antiserum; the 55K subunit that crosslinked to T3 was re-precipitated by the antiserum (Fig. 4b, lane 5), indicating that the 55K subunits defined by these two approaches were identical.

Conclusions

Framework monoclonal antibodies (β F1 and WT31) against the TCR $\alpha\beta$ molecules were used to identify and isolate a WT31⁻\beta F1⁻T3⁺ lymphocyte population from the PBL of two immunodeficiency patients. By the criteria of both immunoprecipitation analysis with framework monoclonal antibody and Northern blot analysis using TCR α - and β -specific cDNA probes, polyclonal human T-cell lines of this phenotype were shown to express neither TCR $\alpha\beta$ mRNA transcripts nor polypeptides. Nevertheless, chemical crosslinking studies using the cleavable DSP reagent revealed the existence of a protein complex associated with the T3 glycoprotein on the surface of these cells. The heavier of the two subunits that crosslinked to T3 (55K) was also immunoprecipitated by two different antisera, one generated against a 17-amino-acid synthetic peptide corresponding to a part of the variable region and another generated against a 20-amino-acid synthetic peptide corresponding to a part of the constant region of the deduced amino-acid sequence of a rearranged $T\gamma$ gene^{19,36}. Thus, it seems that the 55K protein is the T γ protein encoded by the rearranging T γ gene¹⁵ (or, less likely, a protein highly cross-reactive with it). Final proof of this, however, must await protein sequence determination and comparison with the deduced amino-acid sequences of rearranged Ty cDNA clones. The 40K polypeptide appears to be a novel fourth T3-associated protein that we term $T\delta$ (Fig. 2a, b). The T γ and T δ polypeptides may form a T3-associated heterodimeric structure $(T\gamma\delta-T3)$ on these cells that is analogous to the previously described T-cell receptor complex (TCR $\alpha\beta$ -T3). Alternatively, since the cell lines examined are polyclonal, the 55K and 40K polypeptides may occur as monomeric T3-associated subunits on individual T-cell clones.

The complex described here has several important characteristics that might be expected for a second T-cell receptor, that is, it is physically associated with T3 and one of the T3-associated chains is recognized by several anti-Ty antisera. We do not know at present whether the Ty and To components are distinct gene products, whether they are covalently linked via an interchain disulphide bond, whether they display clonal heterogeneity on T cells, or if ligands that react specifically with this protein complex are capable of triggering cell proliferation or factor production as occurs with the TCR $\alpha\beta$. However, in another study, human thymus-derived clones of the same phentoype as the IDP1 and IDP2 cell lines described here (β F1⁻T3⁺) were stimulated to proliferate and to secrete IL-2 in response to anti-T3 antibodies (see page 179 of this issue⁴⁶). Thus, pending the outcome of peptide mapping and additional functional experiments, the T3-associated complex demonstrated here represents a likely candidate for a second T-cell receptor.

The function of the WT31^{- β}F1⁻T3⁺ cells is unknown. Ty mRNA expression is highest early in murine thymic ontogeny and declines thereafter, suggesting that the Ty polypeptide may be functionally important only early in thymic ontogeny^{37,38}. Since the putative second T-cell receptor complex reported here has been identified in immunodeficiency patients, it may be expressed on cells arrested at an early stage of thymic ontogeny in these patients. For example, about 50% of the WT31 $^-\beta$ F1 $^-$ T3 $^+$ cells were T4 $^-$ T8 $^-$ T3 $^+$, which is similar in phenotype to an identified subpopulation of human thymocytes (ref. 39 and J. Allison and L. Lanier, personal communication). However, it is clear that the $\beta F1^{-}T3^{+}$ phenotype occurs on a subpopulation of normal human PBL (Fig. 1c). These PBL may similarly express the non- α , non- β T3-associated complex described here. If so, this putative second T-cell receptor may occur on mature cells of a lineage which is separate, although related, to that of TCR αβ-expressing T cells. Additional characterization of these novel T3-associated molecules and the cells that express them may further our understanding of T-cell ontogeny as well as mature T-cell function.

We thank Drs W. Tax, I. Trowbridge and P. Beverley for providing monoclonal antibodies, Drs S. Burakoff, T. Springer and J. Fraser for critical comments on the manuscript, and B. Hoffman for assistance with two-colour cytofluorographic analysis. This work was supported by grant ACS-NY-IM-425, NIH grant 5-RO1-AI15669, grant 2P050AI21163 and by grants from the Leukemia Research Foundation and from Hoechst Aktiengesellschaft.

Note added in proof: The 55K and 40K T3-associated polypeptides on IDP2 cell lines are not disulphide-linked.

```
Received 20 May; accepted 30 May 1986.
```

- Allison, J. P., McIntyre, B. W. & Bloch, D. J. Immun. 129, 2293-2300 (1982).
 Meuer, S. C. et al. J. exp. Med. 157, 705-719 (1983).
 Haskins, K. et al. J. exp. Med. 157, 1149-1169 (1983).
 Yanagi, Y. et al. Nature 308, 145-149 (1984).

- Hedrick, S. M., Nielsen, E. A., Kavaler, J., Cohen, D. I. & Davis, M. M. Nature 308, 153-158 (1984).
- Chien, Y. et al. Nature 312, 31-35 (1984).
 Saito, H. et al. Nature 312, 36-40 (1984).

- 8. Sim, G. K. et al. Nature 312, 771-775 (1984).
 9. Reinherz, I. L. et al. Proc. natn. Acad. Sci. U.S.A. 80, 4104-4108 (1983).
 10. Oettgen, H. C., Kappler, J., Tax, W. J. M. & Terhorst, C. J. blol. Chem. 259, 12039-12048
- 11. Weiss, A. & Stobo, J. D. J. exp. Med. 160, 1284-1299 (1984).
- Brenner, M. B., Trowbridge, I. S. & Strominger, J. L. Cell 40, 183-190 (1985).
 Allison, J. P. & Lanier, L. L. Nature 314, 107-109 (1985).
- 14. Samelson, L. E. & Schwartz, R. H. Immun. Rev. 81, 131-144 (1984). 15. Saito, H. et al. Nature 309, 757-762 (1984).
- Kranz, D. M. et al. Nature 313, 752-755 (1985).
 Hayday, A. C. et al. Cell 40, 259-269 (1985).
- Lefranc, M.-P. & Rabbits, T. H. Nature 316, 464-466 (1985).
 Murre, C. et al. Nature 316, 549-552 (1985).
- 20. Quertermous, T. et al. Science 231, 252-255 (1986).
- 21. LeFranc, M.-P., Forster, A., Baer, R., Stinson, M. A. & Rabbitts, T. H. Cell 45, 237-246
- Iwamoto, A. et al. J. exp. Med. 163, 1203-1212 (1986).
 Zauderer, M., Iwamoto, A. & Mak, T. W. J. exp. Med. 163, 1314-1318 (1986).
 Yague, J. et al. Cell 42, 81-87 (1985).

- 25. Dembic, Z. et al. Nature 320, 232-238 (1986).
- Hedrick, S. M. et al. Proc. natn. Acad. Sci. U.S.A. 82, 531-535 (1985).
 Blanckmeister, C. A., Yamamoto, K., Davis, M. M. & Hammerling, G. J. J. exp. Med. 162,
- 28. Brenner, M. B., Trowbridge, I. S., McLean, J. & Strominger, J. L. J. exp. Med 160, 541 551 (1984).
 29. Tax, W. J. M., Willems, H. W., Reekers, P. P. M., Capel, P. J. A. & Koene, R. A. P. Nature
- Spits, H. et al. J. Immun. 135, 1922-1928 (1985).
 Griscelli, C. et al. in Primary Immunodeficiencies (eds Seligmann, M. & Hitzig, H.) 499-504
- (North-Holland, Amsterdam, 1980).

 32. Hadam, M. R., Dopfer, R., Han-Harmut, P. & Niethammer, D. in Progress in Immunodeficiency Research and Therapy Vol. 1 (eds Griscellu, C. & Vossen, J.) 41-50 (Elsevier, Amsterdam, 1984).
- Levin, L. S. et al. J. Pediat. 90, 55-61 (1977).
 Brenner, M. B. et al. J. Immun. 135, 384-390 (1985).
- 35. Yasunobu, Y. et al. Nature 312, 521-524 (1984).
 36. Dialynas, D. P. et al. Proc. natn. Acad. Sci. U.S.A. 83, 2619-2623 (1986).
- 37. Raulet, D. H., Garman, R. D., Saito, H. & Tonegawa, S. Nature 314, 103-107 1985)
- Snodgrass, H. R., Dembic, Z., Steinmetz, M. & von Boehmer, H. Nature 315, 232-233 (1985)
 De la Hera, A., Toribio, M. L., Marquez, C. & Martinez-A. C. Proc. natn. Acad. Sci. U.S.A. 82, 6268-6271 (1985).
- 40. Beverley, P. C. & Callard, R. E. Eur. J. Immun. 11, 329-334 (1981).
- Krangel, M. S. EMBO J. 4, 1205-1210 (1985).
 Leiden, J. M., Fraser, J. D. & Strominger, J. L. Immunogenetics (in the press)
- Leiden, J. M. & Strominger, J. L. Proc. natn. Acad. Sci. U.S.A. (in the press).
 Merrifield, R. B. J. Am. chem. Soc. 85, 2149-2154 (1963).
- 45. Liu, F.-T., Zinnecker, M., Hamaoka, T. & Katz, D. H. Biochemistry 18, 690-697 (1979). 46. Bank, I. et al. Nature 322, 179-181 (1986).
- 47. Yelton, D. E., Desaymard, C. & Scharff, M. D. Hybridoma 1, 5-11 (1981).

Infrared polarimetry of the nucleus of Centaurus A: the nearest blazar?

J. Bailey*, W. B. Sparks†, J. H. Hough‡ & D. J. Axon§

- * Anglo-Australian Observatory, PO Box 296, Epping, NSW 2121, Australia
- † Astronomy Centre, University of Sussex, Falmer, Brighton BN1 9QH, UK
- ‡ Physics Department, Hatfield Polytechnic, College Lane, Hatfield AL10 9AB, UK
- § Nuffield Radio Astronomy Observatory, University of Manchester, Jodrell Bank, Macclesfield, Cheshire, SK11 9DR, UK

As one of the nearest examples of an active galaxy, NGC5128 (Centaurus A) has been studied in detail over a wide range of wavelengths1. The nucleus of the galaxy is seen clearly in the X-ray, radio and infrared, but is obscured in the optical by the prominent warped dust lane. We have made polarization observations of the infrared nucleus at wavelengths from 1.2 to 3.8 µm. We find that after correction for the polarization caused by the dust lane, and for dilution by starlight, the nucleus has a large intrinsic polarization of $\approx 9\%$ at position angle 147°. This position angle is perpendicular to the direction of the X-ray and radio jet. We interpret the polarized emission from the nucleus as synchrotron radiation from a region whose magnetic field is parallel to the jet direction. The properties of the Cen A nucleus are essentially identical to those of the much more luminous blazars 17. This suggest that blazar-type activity extends over a very wide range in luminosity, and low-luminosity blazars may be common in elliptical galaxies.

Polarimetry and photometry of NGC5128 in the J(1.20 µm), H(1.64 µm) and K (2.19 µm) bands were obtained on 26 June 1985. Polarimetry in the L' band (3.8 µm) was obtained on 2 and 3 July 1985. All observations were made using the 3.9-m Anglo-Australian telescope and the Hatfield polarimeter². The position angles were calibrated using an internal calibration polarizer and standard stars for J, H and K, and an observation of the W33A infrared source³ for L'. The J, H and K observations were each obtained through apertures of nominal size 8, 4.5 and 2.25 arc s, centred on the peak 2.2-µm signal. Some vignetting was introduced by the wire grid polarizer, so the response was not flat over the full aperture. The seeing disk size was ~1 arc s (full width at half maximum) and the photometry was calibrated using standards observed through the same set of three apertures. The photometry and polarimetry results are given in Table 1.

Optical polarimetry of several points in the dust lane has been published by Elvius and Hall⁴. These observations show typical polarization position angles of $\sim 115^{\circ}$ near the nucleus. This polarization can be understood as being caused by absorption

Table 1 Polarimetry and photometry of NGC5128						
Aperture (arc s)	Band	Magnitude	P de (%) θ (deg			
2.25	J	12.60	4.94 ± 0.42	123.9 ± 2.3		
	Н	10.96	4.63 ± 0.20	136.4 ± 1.3		
	K	9.60	6.63 ± 0.14	144.8 ± 0.3		
4.5	J	11.48	4.43 ± 0.14	119.3 ± 1.2		
	Н	9.95	2.80 ± 0.08	128.6 ± 0.8		
	K	8.98	4.22 ± 0.10	144.4 ± 1.4		
	L'		6.1 ± 0.9	146 ± 6		
8.0	J	10.67	2.99 ± 0.14	118.4 ± 0.8		
	Н	9.24	1.94 ± 0.06	124.9 ± 0.8		
	K	8.32	2.39 ± 0.11	139.6 ± 1.5		

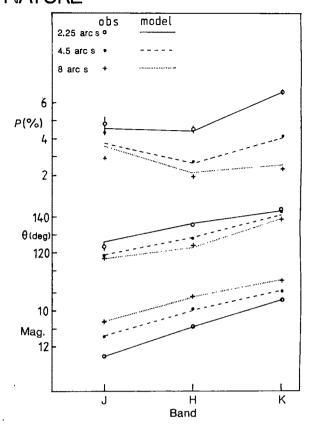


Fig. 1 Observations (points) of the polarization, position angle and magnitude of NGC5128 (Cen A) compared with the predictions (lines) of a model composed of a power-law polarized nucleus stellar component and dust lane polarization, as described in the text. Aperture sizes: $2.25 (\bigcirc, ---)$; $4.5 (\bigcirc, ---)$ and $8 (+, \cdots)$

by dust grains aligned by a magnetic field in the plane of the dust lane; thus, it can be expected to display the same wavelength dependence observed for interstellar polarization in our own Galaxy⁵, and decrease into the infrared. The polarizations we observe in the J band in the largest aperture show approximately the same position angle as this dust lane component, but as we go to smaller apertures and longer wavelengths we find increasing polarizations, and a tendency for the position angle to swing to larger values. This effect can be readily understood if the very red point-source nucleus⁶ has its own intrinsic polarization with a position angle different from that caused by the dust lane. Smaller apertures and longer wavelengths give increasing contributions of the nucleus relative to the stellar component of the galaxy, and thus a total polarization and position angle closer to that of the nucleus.

Using the multi-aperture observations we can derive the flux and polarization of the annuli between 2.25 and 8 arcs, and between 4.5 and 8 arcs. Although there are differences between the two annuli, the K-band polarizations are very small (~0.5%, compared with the 6.63% measured in the smallest aperture), confirming that the polarization is predominantly due to the nucleus itself. The light contained within the smallest aperture will be that from the polarized nucleus itself, and the contribution from starlight. We can reasonably assume that the starlight within the smallest aperture has the same colours and polarization as those observed for the annuli. We can set reasonable limits on the relative contributions to the flux, by requiring that the nuclear flux at J must be greater than zero, but must not be so large that the surface brightness of the stellar component would decrease inwards.

Using the above procedure, we find a range of values of the polarization of the nucleus. The K polarization must be in the range 8.8-11.1%, the H polarization in the range 7.2-15.4%, and the J polarization must be >7.1%. The smallest values correspond to the largest flux contributions from the nucleus. Thus, this analysis suggests a polarization which is either relatively flat with wavelength or increases to the blue.

We have obtained a good fit to the data with a model consisting of the following components (see Fig. 1 and Table 2): (1) A power-law nucleus with a wavelength-independent polarization of 9% at position angle 147°, spectral index 5.3, and J-band flux of 3.0 mJy. (2) A stellar component with spatial flux distribution adjusted to fit the J photometry, and colours equal to those observed for the 4.5-8 arcs annulus. (3) A polarization due to the dust lane, applied to both of the above components, following a Serkowski law with $P_{\text{max}} = 7\%$, $\lambda_{\text{max}} = 0.55 \,\mu\text{m}$ and position angle = 115° .

The fit is generally good. The discrepancies in the J-band polarization are probably due to the patchy nature of the dust lane⁷, causing its polarization to change over the spatial scale of the observations. Slight discrepancies in the fit to the flux indicate that a power law is not an accurate representation of the spectrum. A reddened power law may fit the data better, but the degree of reddening appropriate for the nucleus is uncertain. The L' polarization is a little lower than predicted by the model, perhaps indicating some additional source of dilution (such as thermal radiation from the dust lane as seen at 10 µm

There is evidence that the nucleus of Cen A has a much higher extinction than the A_v of 5-6 mag (ref. 9) due to the dust lane. The silicate optical depth implies $A_V = 22 \text{ mag}$ (ref. 10), and the hydrogen column density derived from X-ray absorption implies $A_v = 45 \text{ mag}$ (ref. 11). However, the wavelength dependence which we observe for the polarization of the nucleus does not rise to the blue steeply enough for the polarization to be due to dichroic absorption in this thick dust shell. A small contribution to the polarization arising from the dust shell, in addition to a flatter intrinsic polarization from the nucleus, cannot be

The position angle of the X-ray jet is $53 \pm 1^{\circ}$ (ref. 11), and that of the radio jet is $55 \pm 7^{\circ}$ (ref. 12). The polarization position angle we observe for the nucleus is almost exactly perpendicular to these jet position angles and suggests that the polarized infrared radiation is associated with the inner jet. Antonucci¹³ has noted other cases of radio galaxies with polarization perpendicular to the radio structure.

Models proposed for the nucleus of Cen A14-16 explain its infrared flux as synchrotron radiation, with inverse Compton scattering of the infrared photons giving rise to X-ray emission. Our observation of high polarization for the infrared nucleus provides strong support for such synchrotron models. The observed position angle then indicates that the magnetic field must be aligned predominantly along the jet direction. The only other plausible origin for the infrared nucleus is thermal reradiation by dust grains, which could produce a high polarization if the emitting grains has a high degree of alignment. However, Grasdalen and Joyce¹⁰ have considered this thermal

Received 24 January; accepted 10 April 1986.

- 1. Ebneter, K. & Balick, B. Publs astr. Soc. Pacif. 95, 675-690 (1983)

- Ebneter, K. & Balick, B. Publs astr. Soc. Pactf. 95, 675-690 (1983).
 Bailey, J. & Hough, J. H. Publs astr. Soc. Pactf. 94, 618-623 (1982).
 Capps, R. W., Gillett, F. C. & Knacke, R. F. Astrophys. J. 226, 863-868 (1978).
 Elvius, A. & Hall, J. S., Bull. Lowell Obs. VI, 123-134 (1964).
 Serkowski, K. in Methods of Experimental Physics Vol. 12A (ed. N. Carleton) 361-414 (Academic, New York, 1974).
 Becklin, E. E. et al. Astrophys. J. 170, L15-L19 (1971).
 Giles, A. B. Mon. Not. R. astr. Soc. 218, 615-627 (1986).
 Telesco, C. M. Astrophys. J. 226, L125-L128 (1978).
 Harding, P., Jones, T. J. & Rodgers, A. W. Astrophys. J. 251, 530-532 (1981).
 Grasdalen, G. L. & Jovee, R. R. Astrophys. J. 208, 317-322 (1976).

- Grasdalen, G. L. & Joyce, R. R. Astrophys. J. 208, 317-322 (1976).
 Feigelson, E. D. et al. Astrophys. J. 251, 31-51 (1981).
- Burns, J. O., Feigelson, E. D. & Screier, E. J. Astrophys. J 273, 128-153 (1983).
 Antonucci, R. J. Astrophys. J. 278, 499-520 (1984).

Table 2 Components of flux within a 2.25 arcs aperture

Band	Flux of nucleus (mJy)	Flux of Galaxy (mJy)	Total flux (mJy)	Magnitude	P (%)	θ (deg)
J	3.0	12.0	15.0	12.60	4.57	125.4
H	15.7	25.6	41.3	10.99	4.49	136.6
K	74.5	32.2	106.7	9.46	6.66	144.0

re-radiation model and find that it cannot account for the observed infrared flux.

The class of blazars¹⁷ includes the BL Lac objects and the highly polarized quasars. Such objects are considered to be normally found in the nuclei of giant elliptical galaxies, possess compact radio sources with flat or inverted spectra and highly polarized, smooth optical/infrared continua, and are subject to violent variability. The observation of a highly polarized infrared continuum shows that all of these properties are shared by the nucleus of Cen A, with the possible exception of violent variability. There is no evidence for variability of the infrared nucleus of Cen A, although this may be due to insufficient observations. The existence of variability of the Cen A nucleus at X-ray wavelengths is well established11. Studies of BL Lac objects show that the most violently variable objects are those of highest luminosity, with low-luminosity objects tending to show less variability and polarization with preferred position angles¹⁷. Similar effects can be seen in individual objects, such as BL Lac, which shows well-defined position angles when it is faint18 Thus, the absence of violent variability in Cen A, which is substantially less luminous than a typical blazar, need not preclude it being closely related to such objects. BL Lac objects typically show polarization which is either flat with wavelength of decreases to the red^{19,20}, consistent with what we see in Cen A.

The luminosity of the Cen A nucleus in the 1-2-\mu m region is

uncertain due to the unknown extinction, but is probably <10⁴² erg s⁻¹. The luminosities of BL Lac objects²¹ in the same spectral region range from 10⁴⁴ to 10⁴⁷ erg s⁻¹. However, the existence of blazar activity at such low luminosities is not surprising. Individual blazars (for example, 3C279²²) can vary by as much as a factor of 500. This range presumably reflects changes in the accretion rate onto a massive black hole. It is also thought that relativistic beaming may result in enhancements in apparent luminosity of up to a factor of 100 in the most luminous objects²³. Thus, a blazar which is currently at a low accretion rate, and is not beamed towards us, could have a luminosity lower by a factor of ≥50,000 than that of the most luminous examples. Cen A may well be such an object. Other probable examples of low-luminosity blazar activity are IC5063, which has an infrared nucleus 24 which we have recently found to be highly polarized, and NGC1052²⁵. Such objects may be relatively common, but in galaxies at distances much greater than that of Cen A they would become very difficult to find, because the stellar flux from the galaxy would dominate over the polarized non-thermal emission from the nucleus.

- Perola, G. C. & Tarenghi, M. Astr. Astrophys. 25, 461-465 (1973).
 Grindlay, J. E. Astrophys. J. 199, 49-53 (1975).

- Grindiay, J. E. Astrophys. J. 199, 49-53 (1975).
 Angel, J. R. P. & Stockman, H. S. A. Rev. Astr. Astrophys. 18, 321-361 (1980).
 Brindle, C. et al. Mon. Not. R. astr. Soc. 214, 619-638 (1985).
 Bailey, J., Hough, J. H. & Axon, D. J. Mon. Not. R. astr. Soc. 203, 339-344 (1983).
 Brindle, C., Hough, J. H., Bailey, J. A. Axon, D. J. & Hyland, A. R. Mon. Not. R. astr. Soc. 203, 339-344 (1983). Soc. (submitted).
- 21. Impey, C. D., Brand, P. W. J. L., Wolstencroft, R. D. & Williams, P. M. Mon. Not. R. astr. Soc. 200, 19-40 (1982).
 Eachus, L. J. & Liller, W. Astrophys. J. 200, L61-L62 (1975).
 Blandford, R. D. & Rees, M. J. Proc. Pittsburgh Conf. BL Lac Objects (ed. Woife, A. M.)

- 328-341 (University of Pittsburgh Press, 1978). Axon, D. J., Bailey, J. & Hough, J. H. Nature 299, 234-236 (1982)
- 25. Rieke, G. H., Lebofsky, M. J. & Kemp, J. C. Astrophys. J. 252, L53-L56 (1982)

Tucker, W., Kellogg, E., Gurskey, H., Giacconi, R. & Tanabaum, H. Astrophys. J. 180, 715-724 (1973).

The soft γ -ray burst GB790107

J. G. Laros*, E. E. Fenimore*, M. M. Fikani*, R. W. Klebesadel*, C. Barat†, G. Chambon†, K. Hurley†, M. Niel†, G. Vedrenne†, S. R. Kane‡, V. G. Kurt§, G. A. Mersov§ & V. M. Zenchenko§

- * Los Alamos National Laboratory, Los Alamos, New Mexico 87545, USA
- † Centre d'Etude Spatiale des Rayonements, 31029 Toulouse, France ‡ Space Sciences Laboratory, University of California, Berkeley, California 94720, USA
- § Space Research Institute, 117810 Moscow GSP-7, USSR

Nearly all of the known y-ray bursts (GRBs), when observed over the energy range ~30 keV to 1 MeV, have intensity spectra that can be described in terms of several-hundred-keV exponential functions. The Venera 11 and Venera 12 KONUS data indicate that, in addition to these 'normal' GRBs, there might exist a separate class of short, soft events^{1,2}. There can be little doubt that bursts with spectra that seem anomalously soft (e-folding energy ≤30 keV) do exist, and that the most convincing known examples—GB790305b (the famous 5 March burst, including its follow-on events), GB790324 (and its follows-ons) and GB790930—generally have atypically short durations of ~0.1-0.25 s. (Three of the 11 GB790305b follow-on events were longer³.) However, because most GRB instruments were designed primarily for observations above ~100 keV, events with very soft spectra have not been well enough studied to be classified unambiguously. Here we present the results of fortuitous detections of GB790107 (determined in ref. 2 to have a soft spectrum) with instrumentation better suited for the study of such bursts. Above 20 keV the spectrum is indeed much softer than any other cosmic event observed through the apertures of these experiments, and does not appear to belong to the general GRB spectral distribution. However, in the 5-15-keV range the spectrum is very flat. Statistical arguments indicate that soft-spectrum events might belong to a disk population, but this is not a strong conclusion.

By virtue of their ~20-keV thresholds, the KONUS experiments have been, until now, the only sources of data on bursts (apart from the 5 March event) with spectra that might be anomalously soft. These observations, although valuable, have significant limitations imposed by the KONUS 20-keV thresholds and 4-s accumulation times for spectral measurements. Clearly, information at lower energies and with better time resolution is required for the study of events having typical energies of ≤30 keV and durations of ~0.2 s. However, experiments with appreciably lower energy thresholds must be collimated to avoid excessive background rates caused by the diffuse X-ray background. Thus, we were fortunate to have simultaneously observed GB790107 down to 5 keV with 0.5-s spectral time resolution with a collimated instrument on the International Cometary Explorer (ICE) spacecraft⁴, and down to 13 keV with 0.25-s resolution with a collimated instrument on Prognoz 7 (P7)⁵. Unfortunately, however, GB790107 was not observable by most GRB instrumentation, due to low instrumental sensitivities below 30 keV. Thus, the detection in the near future of additional similar events could perhaps best be accomplished by examining the 5-100-keV ICE real-time data record, which spans ~6 yr at high duty cycle, with good spatial coverage and 0.5-s time resolution. (As mentioned below, we have already searched the equivalent of a 70-day, 100%-duty-cycle block of these data.)

Because of the brevity of GB790107 and the fact that its spectrum was too soft to trigger the high time-resolution memories of most GRB experiments, a well-resolved time history (energy-integrated) was obtained only by the KONUS experiment (Fig. 1 inset). The outburst had a duration of ~ 0.2 s and

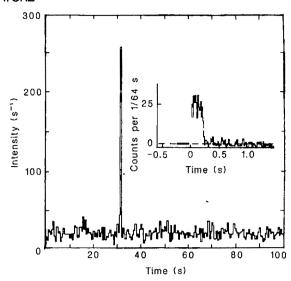


Fig. 1 Time histories of GB790107. The inset is the KONUS energy-integrated time history, and the main plot is the ICE 25-40-keV response. This was one of the most intense cosmic events ever seen in ICE data in this band, but its flux above ~100 keV was unobservable at current instrumental sensitivities.

a rather flat-topped profile. The ICE response in the 25-40-keV band (Fig. 1) is one of the most intense ever recorded by that instrument from a cosmic source. The P7 and ICE data records do not resolve the main spike, but the continuous ICE time coverage with 0.5-s resolution allows one to search for slow structure, such as '5 March-like' pulsations. As can be seen from Fig. 1, there are no indications of any such structure, although appropriately scaled-down GB790305b pulsations would not be observable.

Figure 2 shows the GB790107 spectral data. Because of the uncertainty in the source location, the absolute normalizations of the spectra measured by the collimated instruments on P7 and ICE are uncertain by about ±25%. The normalizations used in the figure assume the highest source exposures that are consistent with the time-of-arrival error box. Also, a spacecraft strut that is sometimes in the ICE field of view could give rise to an additional 25% systematic error below 15 keV for this event. Our conclusions are not affected by either the normalization or the 'strut-absorption' uncertainties. Above ~30 keV the spectrum is extremely steep for a GRB, corresponding to a temperature of ~10 keV if fit by a Planck function or ~30 keV if fit by optically thin thermal bremsstrahlung. (The GB790305b and GB790324 follow-on events had similar temperatures².) However, our data show that the steepness does not extend to lower energies; the 5-7-keV upper limit is comparable to the measured intensity at 30 keV. The high-energy 'tail' which seems to be present in the KONUS spectrum was not detected by the other experiments, even though their sensitivities were adequate. Even without the tail, simple models can reproduce the data only if some means of explaining the lack of low-energy photons is provided. It may be noteworthy that the thermal cyclotron model, with its lack of emission below the first harmonic, can provide a 'natural' low-energy cutoff if the magnetic field in the emission region is $\sim 10^{12}$ G.

The time history and spectral information give some insight concerning whether GB790107 belongs to, or is closely related to, any other known class of high-energy transient. First, we note that the only other cosmic events having a comparable 25-40-keV intensity in ICE records (GB781104b, GB790305b, GB820801 and GB840304) were among the most powerful GRBs ever observed at energies >100 keV. At these 'typical' GRB energies, GB790107 is at least ~2 orders of magnitude weaker than the aforementioned strongest bursts. None of the ~100 other known ICE events had an intensity in the 25-40-keV band

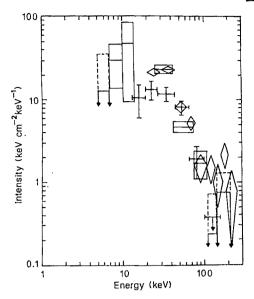


Fig. 2 GB790107 spectra. The plot is non-standard for γ-ray bursts in that it is an intensity spectrum rather than a number spectrum. This representation generates a clearer picture of the very steep GB790107 spectrum. Rectangles, ICE; crosses, P7; diamonds, KONUS data. The upper limits are shown at 10 (solid lines) and, for ICE, 2\sigma (dashed lines) confidence levels. The integration times for the spectra are 0.5 s for ICE and P7, and 4 s for KONUS. The burst duration was 0.2 s.

greater than one-quarter that of GB790107. It is therefore difficult, but not impossible, to believe that GB790107 is a member of the 'classical' GRB population. Furthermore, its short duration and high (>10 keV) temperature set it well apart from X-ray bursters, and its brevity and lack of a prominent gradual X-ray component differentiate it from solar flares. The only events both spectrally and temporally similar to GB790107 are the follow-on events associated with GB790305b and GB790324. (GB790107 does resemble spectrally the impulsive components of some solar flares, and a weak, gradual component could have gone undetected. This might be a clue to the emission mechanism.)

The GB790107 localization information is derived from wavefront arrival times at Venera 11, P7 and ICE, and from the responses of the collimated ICE and P7 instruments. The error box (more properly, the 'error arc') is defined by the intersection of the following areas: (1) the P7/KONUS arrival-time annulus of radius 33.475 \pm 0.012° centred at $(\alpha, \delta)_{1950} = 15 \text{ h} 43 \text{ min } 53.6 \text{ s}$, -18° 04′ 53"); (2) an 8° full-width band, centred on the ecliptic plane, inferred from the relative ICE response; and (3) a region ~15° by 20°, centred near $(\alpha, \delta) = (18 \text{ h } 20 \text{ min, } -25°)$, determined from the P7 response. The intersection of these regions is a curved strip, 8° by 0.024°, whose midpoint is at $(\alpha, \delta)_{1950}$ = (18 h 05 min 36.8 s, $-23^{\circ}26'22''$) or $(l_2, b_2) = (7.36, -1.71)$. A search through catalogues of flare stars, pulsars and high-energy emitters (~25,000 objects) revealed two in the box. These were the pulsar PSR1804-27 (ref. 6) and V2 57, an early-type star with emission lines⁷. In this region of the sky there are several catalogued objects per square degree, so chance coincidences are not unlikely. Also, due to its own location uncertainty, the pulsar may not be in the GRB error box.

Perhaps the most significant question about the error box concerns what its proximity to the galactic centre (GC) tells us about the spatial distribution of this type of event. The following additional facts are relevant: (1) The localized events that are spectrally and temporally most similar to GB790107 (that is, GB790305b and GB790324) are located at $(l_2, b_2) = (275, -33)$ and (47, 4). (2) GB790930, the most certain (in our judgment) other identification of a short event with a soft spectrum, did not produce a response in ICE, and was therefore at least 30°

from the GC (but not necessarily out of the plane). (3) If the flat top of the GB790107 time history is caused by the Eddington limit, then the distance to the source is ~1 kpc, and the low longitude is due to chance. (4) The ICE experiment, whose field of view always includes most of the GC region, has not observed a single additional cosmic event with a comparably soft spectrum. (Our searches have included lists of suspected events^{1,2,8,9} based on their short durations or published spectra, as well as an arbitrary 70-day-equivalent data block. The other ~10 short events observed by ICE had hard spectra.) These facts all imply that there is not much concentration in galactic longitude, although the three known locations are at low latitudes. A disk distribution may thus be indicated but this is not a strong conclusion.

There remain many basic questions concerning the spatial, temporal (both frequency of occurrence and time history) and spectral distributions of soft bursts. Until we obtain some of the answers (or the basic GRB mechanism becomes well understood) we cannot state definitively that GB790107 and other soft events constitute a true 'class', as opposed to being merely 'extreme' examples of GRBs.

The Los Alamos authors thank R. Robinson, whose efficient and well-organized data reduction methods have enabled us to use the ICE and Pioneer Venus Orbiter databases to an extent not previously possible. We also thank R. Epstein for carefully reading the manuscript and providing helpful comments. This work was supported by the US Department of Energy and NASA under contract NAS5-22307, and by CNES contract 82-212. Note added in proof: We have recently discovered multiple (perhaps >50) recurrences of GB790107 in 1983. This confirms its similarity to the March 1979 repeating sources, and strengthens the interpretation that these objects are members of a distinct 'class'.

Received 24 February; accepted 19 March 1986.

- Mazets, E. P. et al. Astrophys. Space Sci. 80, 3-143 (1981). Mazets, E. P., Golenetskii, S. V., Guryan, Yu. A. & Ilyinski, V. N. Astrophys Space Sci. 84, 173-189 (1982).
 Golenetskii, S. V., Ilyinski, V. N. & Mazets, E. P. Nature 307, 41-42 (1984)
 Anderson, K. A. et al. IEEE Trans. Geosci. Electron. GE-16, 157-159 (1978)
 Barat, C. et al. Space Sci. Instrum. 5, 229-235 (1981).

- Manchester, R. N. & Taylor, J. H. Astr. J. 86, 1953-1973 (1981).
- Wackerling, L. R. Mem. R. astr. Soc. 73, 153-319 (1970). Norris, J. P. et al. Nature 308, 434-435 (1984).
- Barat, C. et al. Astrophys. J. 285, L791-L800 (1984).

Evidence for an asymptotic lower limit to the surface dipole magnetic field strengths of neutron stars

E. P. J. van den Heuvel & J. A. van Paradijs

Astronomical Institute 'Anton Pannekoek', University of Amsterdam, Roetersstraat 15, 1018 WB Amsterdam, The Netherlands

R. E. Taam

Department of Physics and Astronomy, Northwestern University, Evanston, Illinois 60201, USA

The discovery of a second millisecond binary radio pulsar¹, PSR1855+09 (period P=5 ms), with a relatively wide circular orbit and low mass function indicates that the incidence of such systems (see also refs 2, 3) among the galactic radio pulsar population is $\sim 4 \times 10^{-3}$. The generally accepted model for the origin of these systems is that they have descended from low-mass X-ray binaries in which a weakly magnetized neutron star³ was spun-up by the accretion of matter from an evolved low-mass (≤1.2 M_{\odot}) companion star, which has now ended its life as a helium white dwarf³⁻⁸. We show here that, based on the incidence of the progenitor low-mass X-ray binaries (LMXBs), the observed incidence of millisecond binary radio pulsars can be explained only if, at their present low field strength of $\sim 10^9$ G, the decay timescale of neutron-star surface magnetic dipole moments is $\geq 10^9$ yr. This possibility has been advanced by Kulkarni⁹, who estimates, based on the optical detection of the counterpart of the weak-field binary radio pulsar PSR0655+64, that this pulsar is old ($>5 \times 10^8$ yr) and hence that the magnetic field decay timescale becomes very large ($>10^9$ yr) for field strengths $\leq 10^{10}$ G. Our findings provide independent support for this possibility.

The progenitor LMXBs, in which the companion stars are evolved, are strong sources, of X-ray luminosity $L_{\rm X} \simeq (0.2-1)\times 10^{38}\,{\rm erg\,s^{-1}}$, such as the strong galactic bulge sources, Sco X-1 and Cyg X-2 (ref. 10). There are at most 30-50 such sources in the Galaxy¹¹, of which about a dozen are located in the galactic bulge. The typical X-ray lifetime of these systems, based on their accretion rates (\dot{M}) of $\sim (0.2-1)\times 10^{-8}\,M_{\odot}\,{\rm yr}^{-1}$ and companion mass $\sim 1\,M_{\odot}$, is $\sim 2\times 10^8\,{\rm yr}\,{\rm (ref.\,12)}$. This implies a formation rate of these luminous LMXBs of at most $(1.5-2.5)\times 10^{-7}\,{\rm yr}^{-1}$. Assuming all such systems to leave millisecond binary radio pulsars, the number of millisecond binary radio pulsars formed during the $\sim 1.5\times 10^{10}\,{\rm yr}$ lifetime of the Galaxy is $\sim 3\times 10^3$ (in a steady state, their formation rate will be the same as that of the luminous LMXBs).

As pointed out by Taam and van den Heuvel¹³, the presently available data on magnetic field strengths of neutron stars in binaries are consistent with the hypothesis that neutron stars are born with surface dipole field strengths $B_s = 10^{12} - 10^{13}$ G, which decay exponentially on a timescale of $\sim 5 \times 10^6$ yr for $\sim 7-10$ e-foldings, that is, down to at least 10^9-10^{10} G. In order to become a millisecond pulsar, that is, to reach $P_{\text{rot}} \leq 5 \text{ ms by}$ spin-up, B_s should have decayed to $<3 \times 10^9$ G before the end of the accretion spin-up phase, as otherwise, even at $\dot{M} = \dot{M}_{\rm Edd}$ (the accretion rate corresponding to the Eddington limit), such a short period cannot be reached (see refs 8, 13, references therein, and equation (1), below). If the surface dipole fields of such pulsars were to keep decaying beyond this value on a timescale of $\sim 5 \times 10^6$ yr, the field strengths of these millisecond pulsars would drop below 5×10^7 G within $\sim 2 \times 10^7$ yr after the end of the accretion spin-up phase, rendering them virtually unobservable as pulsars (no known radio pulsar has a field strength of $<4.5\times10^8$ G). With the formation rate in the Galaxy derived above, this maximum lifetime of $\sim 2 \times 10^7$ yr as a millisecond pulsar would imply that, at any time, at most only three to five millisecond binary radio pulsars would be observable in the entire Galaxy. The total number of active radio pulsars in the Galaxy is estimated to be $(1-5) \times 10^5$ (ref. 14), leading to an expected incidence of millisecond binary pulsars among radio pulsars of at most 6×10^{-6} to 6×10^{-5} .

In contrast with the above estimate, among the ~ 500 known radio pulsars, there are already two millisecond binary pulsars (1953+29 and 1855+09). The distances of these two systems as inferred from their dispersion measures (~ 3 and 0.3 kpc, respectively) are in the same range as those of most of the known radio pulsars. The incidence of binary millisecond pulsars in the general pulsar population is therefore likely to be of the same order as their incidence among the known sample of pulsars, which is $\sim 4 \times 10^{-3}$. This is $\sim 10^2 - 10^3$ times higher than expected under the assumption that at $B_s < 3 \times 10^9$ G the fields continue to decay on a timescale of $\sim 5 \times 10^6$ yr.

Apparently, the latter assumption cannot be correct. The only solution to this problem seems to be that, once the surface dipole field strength has decreased to $\leq 3 \times 10^9$ G, the decay timescale of the field has increased by a factor of 10^2-10^3 over that at $B_s = 10^{12}-10^{13}$ G. Therefore, at $B_s < 3 \times 10^9$ G the field decay timescale must thus be at least $\geq 10^9$ yr, and possibly $\geq 10^{10}$ yr. As the fields of the binary radio pulsars PSR1913+16 and PSR0655+64 are already close to this boundary $(2.2 \times 10^{10}$ and 1.3×10^{10} G, respectively; see ref. 13), they may be expected to

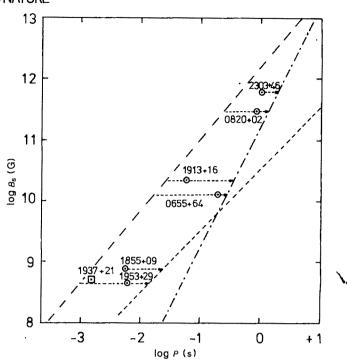


Fig. 1 B_s versus P diagram, showing the positions of the six binary pulsars with known \dot{P} values, together with the 'spin-up line', P_{\min} ($\dot{M}_{\rm Edd}$, B_s), given by equation(1) (———), the deathline³ (—·—·) and the P_f line (the final period reached after a Hubble time, if spin-down proceeds at constant B_s (---). The figure shows that spun-up pulsars with $B_s < 6.10^9$ G need longer than a Hubble time to reach the deathline (assuming evolution at constant B_s).

decay much more slowly than the fields of young, strong-field pulsars. These pulsars may therefore be considerably older than their formal ages, calculated with a field-decay timescale of $\sim 5 \times 10^6$ yr, would indicate. This gives independent support for the high age ($\ge 10^9$ yr) of PSR0655+64 as inferred from the faintness of the optical counterpart of its companion.

With an incidence of at least $\sim 4 \times 10^{-3}$ among the $(1-5) \times 10^{5}$ radio pulsars in the Galaxy, the total number of active binary millisecond pulsars is expected to be between at least ~ 400 and 2,000. Among these, the fraction in globular clusters is expected to be an order of magnitude less than one would infer on the basis of the incidence of LMXBs in such clusters. This is because in a globular cluster a neutron star in a binary may many times capture a fresh companion by means of an exchange collision¹⁵⁻¹⁷, thus lengthening its X-ray lifetime by an order of magnitude. Based on the number of strong sources in globular clusters (~ 10), this yields a formation rate of millisecond pulsars of $5 \times 10^{-9} \, \mathrm{yr}^{-1}$ in the globular cluster population, which, with a lifetime of $10^9 - 10^{10} \, \mathrm{yr}$ yields $\sim 5 - 50 \, \mathrm{active}$ binary millisecond pulsars. A pulsar survey of globular clusters would therefore be valuable.

Upper limits to the ages of the six binary radio pulsars with known period derivative (\dot{P}) can be obtained by assuming that they have all been spun up during the accretion phase to the shortest possible spin period P_{\min} (\dot{M}, B_s) , and have subsequently spun down as radio pulsars to their present pulse periods, at a constant value of B_s . P_{\min} is given by 8,13,18

$$P_{\min} = (1.9 \text{ ms}) B_9^{6/7} (M/1.4 M_{\odot})^{-5/7} (\dot{M}/\dot{M}_{\rm Edd})^{-3/7} R_6^{18/7}$$
 (1

where B_9 is the neutron-star magnetic field in units of 10^9 G, M is the mass of the neutron star, \dot{M} the accretion rate and R_6 the neutron-star radius (in units of 10^6 cm). With $\dot{M}=\dot{M}_{\rm Edd}$, $M=1.4~M_{\odot}$ and $R_6=1$, the values of $P_{\rm min}$ in Table 1 are obtained. The spin-down time from this period to the presently observed

Table 1 Observed and calculated parameters for the six binary pulsars with known \dot{P} -values²⁶, for the case of evolution at constant magnetic field

Binary pulsar	, P (s)	$B_{\rm s}$ (10°G)	P_{\min} (ms)	Max age (10 ⁹ yr)	P _f (s)	$P_{\text{t.o.}}$ (s)	$\frac{\Delta t_{\text{i.o.}}}{(10^9 \text{ yr})}$
PSR0655+64	0.196	12.6	16.7	3.9	0.38	0.30	5.3
PSR0820+02	0.865	300	252	0.124	9.1	1.36	0.2
PSR1855+09	0.0054	0.8	1.57	0.68	0.025	0.07	
PSR1913+16	0.059	22	24.8	0.097	0.67	0.36	4.2
PSR1953+29	0.0061	0.45	1.0	2.9	0.014	0.05	
PSR2303+46	1.066	660	500	0.033	Very long	1.8	0.08

Calculations assume $M = 1.4 M_{\odot}$, $I_{45} = R_6 = 1$.

spin period, at constant B_s, is then obtained by integrating the spin-down equation²:

$$(P\dot{P}) = R_6^6 I_{45}^{-1} B_s^2 / (1.024 \times 10^{39}) \text{ s}$$
 (2)

where I_{45} is the moment of inertia of the neutron star in units of 10⁴⁵ g cm². The resulting ages, listed in Table 1, are upper limits to the ages of these pulsars, because if B_s at the end of the spin-up phase was larger than at present, their true ages will be smaller.

Table 1 shows that PSR2303+46, PSR0820+02 and PSR1913+16 cannot be older than $\sim 0.33 \times 10^8$, 1.2×10^8 and 1.0×10^8 yr, respectively. On the other hand, PSR1855+09. PSR0655+64 and PSR1953+29 might be as old as 0.7×10^9 , 4×10^9 and 3×10^9 yr.

Table 1 also lists the final spin period, P_t , attained by each pulsar, one Hubble time (~1.5×10¹⁰ yr) after its birth at P = P_{\min} , if the surface dipole field remains constant. These periods are derived from the integration of equation (2), which yields

$$P(t)^2 = P_0^2 + 1.95 \times 10^{-21} R_6^6 I_{45}^{-1} B_9^2 t$$
 (3)

Also shown in Table 1, as well as in Fig. 1, are the turn-off periods, Pt.o of these pulsars, corresponding to the 'deathline' (see ref. 3), for evolution at constant B_s , and the lifetimes, $\Delta t_{t.o.}$, until reaching the deathline.

Table 1 and Fig. 1 show that the four binary pulsars with the largest B_s values will reach the deathline within one Hubble time. If their fields were to decay, their final periods would be shorter and they might remain observable for a Hubble time. (Note, however, that PSR1913+16 will coalesce with its companion due to gravitational radiation losses within $\sim 3 \times 10^8$ yr, long before it reaches the deathline 19.) On the other hand, PSR1855+09 and PSR1953+29 do not reach the deathline within a Hubble time. (The same holds for the 1.55-s single pulsar PSR1937 + 21, which has $B_c = 5 \times 10^8$ G, and is also expected to have had a history of spin-up in a binary system, although of an entirely different type (see refs 13, 20, 21, and references therein).) These three pulsars may therefore 'live forever'. These conclusions are in agreement with and provide added support for the findings of Kulkarni⁹.

As to the interpretation of the 'asymptotic' field strength: according to the work of Ruderman and co-workers²² the crustal currents that support the huge exterior magnetic field (~10¹²-10¹³ G) of a newborn neutron star decay on a timescale of ~10⁷ yr by ohmic dissipation. In contrast, any residual magnetic field arising from core currents will have a much longer lifepossibly longer than a Hubble time-due to proton superconductivity in the core (see also refs 23, 24). In this interpretation, the resulting asymptotic field strength is not expected to be the same for all neutron stars, as the strength of the core currents, frozen in at the time of collapse, will depend on the individual history of the parent star (for example, its rotation and magnetic field).

An alternative, purely phenomenological interpretation, consistent with the observations listed in Table 1, is that magnetic fields of non-accreting neutron stars do not decay at all (a

possibility suggested by Kundt²⁵), but that accretion gradually weakens the field. Indeed, in the long-lived (≥108 yr) LMXBs which produced the binary millisecond pulsars PSR1953+29 and PSR1855+09, the neutron stars are expected to have accreted >0.1 M_{\odot} , and possibly as much as 1.0 M_{\odot} (refs 7, 13). The same holds for the millisecond pulsar PSR1937+21 (refs 8, 18). On the other hand, PSR2303+46, PSR1913+16 and PSR0655+46, which have much stronger fields than the three millisecond pulsars, are expected to have accreted $\leq 0.01 M_{\odot}$, as they have descended from massive X-ray binaries in which the accretion phase lasted $<10^6$ yr (refs 7, 8, 13). The same holds for PSR0820+02, where, again, the accretion phase lasted less than a few million years^{7,8,13}.

We cannot offer an explanation for a possible relationship between field decay and amount of matter accreted. It seems conceivable, however, that both the crustal and interior structure of a newborn neutron star that formed in the liquid state at $T > 10^{10} \,\mathrm{K}$ and subsequently cooled and underwent crustal freezing²², is quite different from that of a neutron star that subsequently underwent considerable accretion at relatively low temperatures ($T < 10^8$ K).

It is not now possible to decide which of the two alternative interpretations of the asymptotic field behaviour is the correct one, although the first-mentioned one appears most plausible to us.

After submission of this paper we received a preprint by Bhattacharya and Srinivasan²⁷, who independently, and from a somewhat different viewpoint, also reached the conclusion that the decay timescale of the magnetic fields of binary millisecond pulsars must be $\sim 10^9$ yr.

We thank S. Kulkarni for a preprint and stimulating correspondence, which provided an important trigger for the work reported here.

Received 26 February; accepted 9 April 1986.

- 1. Segelstein, D. J., Taylor, J. H., Rawley, I. A. & Stinebring, D. R. IAU Circ. No. 4162 (1986).
- Boriakoff, V., Buccheri, R. & Fauci, F. Nature 304, 417-419 (1983). Rawley, L. A., Taylor, J. H. & Davis, M. M. Nature 319, 383-384 (1986).
- Savonije, G. J. Nature 304, 422-423 (1983). Paczynski, B. Nature 304, 421-422 (1983).
- Joss, P. C. & Rappaport, S. A. *Nature* 304, 419-421 (1983). Van den Heuvel, E. P. J. & Taam, R. E. *Nature* 309, 235-237 (1984). Van den Heuvel, E. P. J. *J. Astrophys. Astr.* 5, 209-233 (1984).

- Van den Heuvel, E. F. J. J. Astrophys. Astr. 5, 209-235 (1984).
 Kulkarni, S. R. Astrophys. J. (in the press).
 Webbink, R. F., Rappaport, S. A. & Savonije, G. J. Astrophys. J. 270, 678-693 (1983).
 Bradt, H. L. V. & McClintock, J. E. A. Rev. Astr. Astrophys. 21, 13-66 (1983).
 Sutantyo, W. & Van den Heuvel, E. P. J. in The Evolution of Galactic X-ray Binaries (eds. Truemper, J., Lewin, W. H. G. & Binkmann, W.) 183-187 (Reidel, Dordrecht, 1986).
 Taam, R. E. & Van den Heuvel, E. P. J. Astrophys. J. 305 (in the press) (1986).
 Lyna A. G. Manchetter P. N. & Taulor, I. H. Man. Not. R. astr. Soc. 213 (613-639) (1985).
- Lyne, A. G., Manchester, R. N. & Taylor, J. H. Mon. Not. R. astr. Soc. 213, 613-639 (1985).
 Hut, P. & Verbunt, F. in Cataclysmic Variables and Low-Mass X-ray Binaries (eds Lamb,

- Hut, F. & Vertonnt, F. in Cataciysmic Variables and Low-Naiss A-ray Binaries (eds Lamb, D. Q. & Patterson, J. 103-106 (Reidel, Dordrecht, 1983).
 Krolik, J. H., Meiksin, A. & Joss, P. C. Astrophys. J. 282, 466-480 (1984).
 Hut, P. & Paczynski, B. Astrophys. J. 284, 675-684 (1984).
 Alpar, M. A., Cheng, A. F., Ruderman, M. A. & Shaham, J. Nature 300, 728-730 (1982).
 Weisberg, J. M. & Taylor, J. H. Phys. Rev. Lett. 52, 1348-1350 (1984).
 Jeffrey, L. C. Nature 319, 384-386 (1986).

- 21. Van den Heuvel, E. P. J. & Bonsema, P. F. J. Astr. Astrophys. 139, L16-L17 (1985)
- Flowers, E. & Ruderman, M. A. Astrophys. J. 215, 302-310 (1977).
 Harvey, J., Ruderman, M. A. & Shaham, J. Phys. Rev. D (in the press).
 Muslimov, A. G. & Tsygan, A. I. Sov. Astr. Lett. 11, 80-83 (1985).
- Kundt, W. Astr. Astropys. 98, 207-210 (1981).
- 26. Dewey, R. J., Maguire, C. M., Rawley, L. A., Stokes, G. H. & Taylor, J. H. Nature (in the
- 27. Bhattacharya, D. & Srinivasan, G. Curr. Sci. 55, 327-330 (1986).

Inhibition of convective collapse of solar magnetic flux tubes by radiative diffusion

P. Venkatakrishnan

Indian Institute of Astrophysics, Bangalore 560034, India

Interaction of convection with a magnetic field leads to an intermittent distribution of magnetic flux¹. Such a process operating on the solar surface can lead to 'equipartition' fields of 700 G (ref. 2). These fields are further prone to a convective instability and eventually collapse to kilogauss intensity3-5. I show here that radiative diffusion can inhibit this collapse to a varying degree, depending on the field strength and the thickness of the flux elements. As a consequence, one would expect the field strength of the photospheric magnetic flux elements to depend on their sizes. It is shown that at one end of such a distribution there would be kilogauss tubes with small dispersion in field strength and large dispersion in size. At the other extreme of the spectrum would be thin tubes of fairly constant size but with a wide range in field strength, from kilogauss intensities to the equipartition values of 700 G. High-resolution observations from space-borne telescopes should reveal the existence of the latter variety of tubes.

An approximate but effective method of examining the stability of magnetic equilibria resembling solar flux tubes is to use the slender-flux-tube equations ⁶. The linearized equations for slender, radiating, optically thin flux tubes have been considered by Webb and Roberts ⁷ in the context of radiative damping of tube waves. One can use the same equations for optically thick tubes by re-defining the radiative relaxation time τ_R of ref. 7 as $\tau_R = 4\chi/r_0^2$ where χ is the radiative diffusivity and r_0 is the cross-sectional radius of the tube ⁸. For mathematical simplicity and to focus attention on the physics of the problem, we assume isothermal stratification in the tube. The imposition of boundary conditions of vanishing velocity perturbation at the two ends of the tube on equation (12) of ref. 7 (after correcting a misprint in that equation by replacing Λ^2 with Λ_0) leads to the following dispersion relation:

$$\tilde{\sigma}^3 + a_2 \tilde{\sigma}^2 + a_1 \tilde{\sigma} + a_0 = 0 \tag{1}$$

where $a_0 = \varepsilon b_0/\delta$, $a_1 = -\{(1-\gamma)(1+\beta_0)/2 - \gamma b_0\}/\delta$, $a_2 = \varepsilon (1+\beta_0/2)/\delta$, $\delta = (1+\gamma\beta_0/2)$, $b_0 = 1/16 + \pi^2 n^2 \Lambda_0^2/d^2$, $\varepsilon = \tau_D/\tau_R$, $\tilde{\sigma} = \sigma \tau_D$ and $\tau_D = (\Lambda_0/g)^{1/2}$. Here, σ is the complex frequency of the perturbation, assumed to grow in time as $e^{\sigma t}$, β_0 is the ratio of gas pressure to magnetic pressure in the tube, n is the harmonic of the perturbation, d is the length of the tube, Λ_0 is the isothermal scale height of the atmosphere and g is the acceleration due to gravity. To simulate a superadiabatic temperature gradient (necessary for convective collapse) one must assume $\gamma < 1$. Although this is strictly unphysical, it may be used for purely illustrative purposes. Note that choosing a non-isothermal stratification leads to a quartic equation in $\tilde{\sigma}$ (ref. 8). (An algebraic error in an earlier analysis for isothermal stratification 9 resulted in a quartic rather than a cubic equation.)

Inspection of the discriminant of equation (1) shows that increase of ε (the ratio of the dynamical to the radiative timescale) leads to a decrease of the growth rate for a tube which is convectively unstable at $\varepsilon = 0$. This decrease continues until $\tilde{\sigma}$ acquires an imaginary part, when the discriminant vanishes. It can also be seen, by examining the terms of leading power in ε (for $\varepsilon > 1$) in the expression for the real part of $\tilde{\sigma}$, that the growth rate tends asymptotically to a constant value.

What are the implications of the above results for solar flux tubes? A straightforward inference is the inhibition by radiation of convective collapse of the tubes. Increase of ε implies decrease of r_0 for a given diffusivity χ . Thus, thinner tubes will

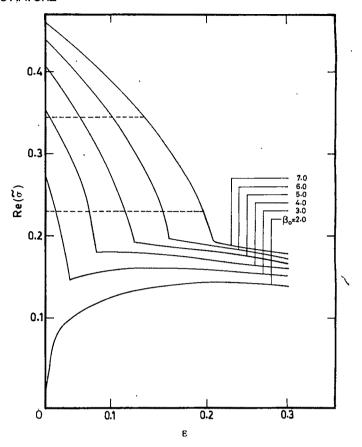


Fig. 1 Plot of Re $(\tilde{\sigma})$ against ε for different values of β_0 . Dashed lines at Re $(\tilde{\sigma})$ = 0.345 and 0.230 correspond to flux-tube lifetimes of 10 and 15 min, respectively.

collapse to a lesser extent than thicker ones. We shall now examine this phenomenon in a more quantitative manner, without forgetting the simplifications inherent in the assumption of isothermal stratification. We choose Λ_0 corresponding to 10^4 K (representing the region of largest convective instability due to hydrogen ionization), $\gamma=0.7$ (to yield a very high superadiabaticity of ~ 0.4) and d=1,200 km, assuring a stable tube at $\beta_0 \simeq 2.0$ for $\varepsilon=0$. With this choice of parameters, Fig. 1 shows the real part of $\tilde{\sigma}$ as a function of ε for different values of β_0 . We assign a value $\beta_0=7.0$ for the equipartition field of 700 G, so that $\beta_0=2.0$ corresponds to kilogauss intensity. Notice the curious cusps in the curves, which correspond to the transition from purely growing modes to overstable modes.

In the Sun, the flux tubes are presumably jostled around, with frequent rearrangement of the field lines into different concentrations 10,11 . Thus, a given tube probably exists as a separate identity for a finite lifetime, dictated externally by its environment. Tubes with growth times larger than such externally dictated lifetimes can therefore be considered as 'stable'. In Fig. 1, two horizontal lines (dashed) are drawn at $Re(\tilde{\sigma}) = 0.345$ and 0.230. These correspond to stable tubes with lifetimes of 10 and 15 min, respectively.

The 10-min timescale is representative of the normal granulation which rearranges the field lines 10, whereas the 15-min timescale represents the facular granules 12. From the intersection of these horizontal lines with the curves for different values of β_0 (Fig. 1), one can construct a plot of ε versus β_0 , showing the demarcation of stable and unstable regimes in $\varepsilon - \beta_0$ space. By choosing $\chi = 10^{10}$ cm² s⁻¹ (consistent with the solar value at 10^4 K)¹³ and assuming magnetic flux conservation as well as depth-independent β_0 for the tube, one can write the photospheric radius of the tube as $r_{\rm ph} = (p_{\rm ion}/p_{\rm ph})^{1/4} \cdot (4\tau_{\rm D}/\varepsilon)^{1/2}$ km, where $p_{\rm ion}/p_{\rm ph}$ is the ratio of the pressure at 10^4 K to photo-

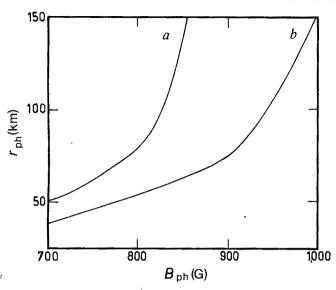


Fig. 2 Predicted photospheric cross-sectional radius of magnetic flux tubes as a function of their field strength, for stable tubes of lifetime 10 (a) and 15 (b) min.

spheric pressure and the dynamical timescale τ_D is expressed in seconds. Similarly, the surface magnetic field can be written as $B_{\rm ph} = 700\sqrt{8/(1+\beta_0)}$ G, remembering our assignment of $\beta_0 = 7.0$ to a 700-G tube. Figure 2 shows the resulting plot of $r_{\rm ph}$ versus $B_{\rm ph}$ for the two values of lifetime.

We conclude that stable tubes on the Sun would show a typical distribution of field strength versus size (Fig. 2). At one end of the spectrum, there would be intense kilogauss tubes with small dispersion in strength but large dispersion in size. At the other extreme of the distribution, there would be a group of thin tubes of fairly constant size but with a continuous distribution of field strengths ranging from kilogauss levels down to equipartition values of 700 G. The tubes observed until now from ground-based telescopes¹⁴ have perhaps belonged only to the stronger variety; observations from the new space-based telescopes should reveal the existence of the tubes at the thin end of the spectrum. A further prediction which can be made from Fig. 2 is that longer-lived tubes of a given size are magnetically more intense.

We emphasize the simple isothermal nature of the model which led to the above predictions: for a more precise prediction of the size distribution, the flux-tube model must be improved. A stability analysis¹⁵ of such an improved model has shown a similar influence of the radiative diffusion on the convective collapse, although the instability was not examined in the ε - β_0 plane as we have done here. Finally, it must be remembered that mechanisms other than convective interaction might create strong tubes below the photosphere, which could emerge above the surface by buoyancy. In this case, the curves in Fig. 2 should be taken as the stable limit of the weakest field for a given size, or conversely the limit of the largest tube of a given strength. Thus, curves like these can be used to distinguish between tubes concentrated by convection and those formed otherwise.

I thank Dr B. Roberts for comments.

Received 8 January; accepted 16 April 1986.

- Proctor, M. R. E. & Weiss, N. O. Rep. Prog. Phys. 45, 1317-1379 (1982).
 Parker, E. N. Cosmical Magnetic Fields, 268 (Clarendon, Oxford, 1979).
- Webb, A. R. & Roberts, B. Sol. Phys. 59, 249-274 (1978). Spruit, H. C. & Zweibel, E. G. Sol. Phys. 62, 15-22 (1979).
- Unno, W. & Ando, H. Geophys. astrophys. Fluid Dyn. 12, 107-115 (1979). Roberts, B. & Webb, A. R. Sol. Phys. 56, 5-35 (1978).
- Webb, A. R. & Roberts, B. Sol. Phys. 68, 87-102 (1980). Venkatakrishnan, P. J. Astrophys. Astr. 6, 21-34 (1985).
- Venkatakishnan, P. in Proc. MPA/ LPARL Workshop theor. Probl. high-resol. sol. Phys. (ed Schmidt, H. U.) 200-203 (Max-Plank-Institute für Physik und Astrophysik, Garching,
- 10. Schmidt, H. U., Simon, G. W. & Weiss, N. O. Astr. Astrophys. 148, 191-206 (1985).

- 11. Nordlund, A. in Proc. MPA/LPARL Workshop theor. Probl. high-resol, sol. Phys. (ed. Schmidt, H. U.) 101-123 (Max-Plank-Institute für Physik und Astrophysik, Garching, 1985).
- 12. Muller, R. Sol. Phys. 52, 249-262 (1977).
- Spruit, H. C. thesis, Univ. Utrecht (1977).
 Spruit, H. C. & Zwaan, C. Sol. Phys. 70, 207-228 (1981).
 Hasan., S. S. Mon. Not. R. astr. Soc. 219, 357-372 (1986).

Lake acidification and the land-use hypothesis: a mid-post-glacial analogue

Vivienne J. Jones, Anthony C. Stevenson & Richard W. Battarbee

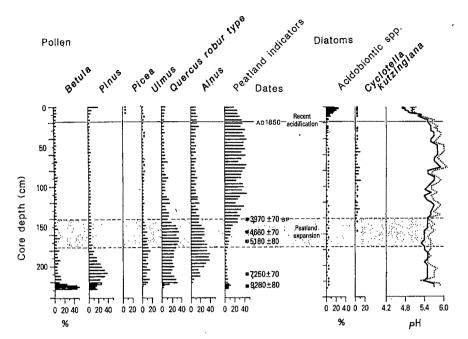
Palaeoecology Research Unit, Department of Geography, University College London, 26 Bedford Way, London WC1H 0AP, UK

It has been suggested that the recent acidification of lakes owes more to catchment soil acidification than to acid deposition. This can be tested by assessing the effect of catchment soil changes on lake acidity during earlier periods of post-glacial time, when acid deposition can be assumed to have been minimal. In the United Kingdom the mid-post-glacial formation of blanket mires in the catchments of lakes senstive to acidification provides a suitable analogue. Here we use the results of a pollen and diatom study of a sediment core from a recently acidified lake in Galloway, south-west Scotland³, to show that the lake was acid (pH 5.5-6.0) before peat formation and that no acidification occurred while peat was developing in the catchment. Acidification to pH values <5 occurs only after AD 1850, during the period of increasing acid emissions from fossil fuel combustion. We conclude that soil acidification is not the likely cause of the very low pH values found in many acidified lakes today.

Many lakes in Europe and North America have been acidified in recent decades³⁻⁸; however, arguments persist over the possible causes of acidification. Rosenquist¹, supported by Krug and Frink², has argued that the increase in the quantity of raw humus in lake catchments as a result of land-use change is of primary importance, and Pennington⁹ has attempted to illustrate this process by reference to the post-glacial development of acid lakes in the English Lake District. On the other hand, Seip¹⁰ has explained how sulphate anions from acid precipitation can carry H+ from soils with low acid-neutralizing capacity into surface waters, and Battarbee et al. 11 have used palaeolimnological techniques to show that an increase in acid deposition is the only plausible hypothesis to explain the acidification of Galloway lakes with non-afforested catchments, partly by showing that a land-use change as postulated by Rosenquist has not occurred in this region.

Although there is theoretical support and empirical evidence for both mechanisms of surface water acidification, we would like to know which is more important in the recent acidification of lakes in areas where both processes have been occurring2. Palaeoecological techniques can be used to separate these factors by considering the influence of catchment changes on a lake at a time when sulphur emissions from industrial sources can be assumed to have been minimal. Such time controls are superior to spatial controls because they allow us to study lakes in areas of high acid deposition, which have already been shown to be recently acidified. Moreover, many important variables such as lake morphometry and the ratio of catchment to lake area can be held constant. Suitable pre-industrial sites and time periods can be identified by pollen analysis and 14C dating.

In the United Kingdom the mid-post-glacial expansion of blanket mire vegetation in upland areas provides the ideal test situation. The replacement of forest vegetation by Calluna heathland and the leaching and paludification of mineral soils to create acid peatland environments has been well established



LETTERS TO NATURE

Fig. 1 Composite pollen and diatom diagram for a core from the Round Loch of Glenhead. including ²¹⁰Pb and ¹⁴C dates and pH reconstruction based on Index B (refs 5, 19) and multiple regression of pH preference groups11 Peatland indicators are Calluna vulgaris, Sphagnum, Cyperaceae, Succisa and Potentilla; acidobiontic spp. are Tabellaria quadriseptata, T. binalis and Navicula hofleri. Solid line, Index B (Galloway); dotted line, multiple regression.

by palaeoecologists 12,13. Blanket mires of this kind dominate the catchments of lakes in Galloway which have been strongly acidified since 18503. For one of these sites, Round Loch of Glenhead, we have carried out pollen analysis and ¹⁴C dating of a complete post-glacial sediment core to identify and date the development of blanket mire in the area, and we have used diatom analysis to reconstruct the pH history of the loch before, during and after the catchment change.

Pollen data from Round Loch (Fig. 1) show a complete early post-glacial forest succession from Betula-Pinus (9,280± 80 yr BP at 223-227 cm, Fig. 1) to Pinus-Ulmus-Quercus, and then to Quercus-Ulmus-Alnus woodland (7,250 ± 70 yr BP at 208-213 cm, Fig. 1). The woodland was subsequently replaced by an acid peatland dominated by Calluna, Cyperaceae and Sphagnum between 6,000 and 4,000 vr BP. Following this, few changes occurred until the recent afforestation in the region in the past 30 yr, indicated by the increased Pinus and Picea values in the uppermost sediment (Fig. 1). A detailed pollen stratigraphic examination of the catchment peatland (V.J.J., unpublished data) confirms that the pollen changes in the lake core reflect changes in the local region, and ¹⁴C dates for the inception of peat formation in the catchment indicate that acid organic soils were gradually replacing mineral soils and covering exposed bedrock from 9,000 yr BP onwards.

In spite of the early development of acid soils, the diatom record (Fig. 1) shows that neither this nor the later expansion of blanket peats caused an acidification of the lake. On the contrary, at the time of blanket mire expansion there was an increase in Cyclotella kutzingiana, a planktonic species that is rarely found in any abundance below $pH \sim 5.5$, and an increase in Fragilaria virescens, a species with circum-neutral pH preference. These changes indicate a small but significant increase in mean water pH, reflected in the pH reconstruction (Fig. 1), and suggest that leaching of sub-soil mineral horizons by more acidic soil water was responsible for an increase in alkalinity of the lake water. In general, the data show that Round Loch had a pH between ~5.5 and 6.0 throughout the post-glacial period, until the recent post-1850 acidification, when pH fell by almost one unit to the present value of \sim 4.7.

Previous studies of long-term lake acidification in the United Kingdom¹⁴⁻¹⁸ appear to be in conflict with these findings, as they all show an acidification trend during the early millennia of the post-glacial period. However, in none of these cases was

the early post-glacial diatom flora as acid as at the Round Loch. probably because none was situated on granitic bedrock, and in all cases the post-glacial acidification trends did not result in a diatom flora characteristic of acid lakes (that is, with negative alkalinity). These data are therefore consistent in showing that nowhere did soil acidification and blanket mire formation during the post-glacial period result in the lowering of lake water pH below $\sim 5.0-5.5$.

Soil acidification does not necessarily lead to surface-water acidification, especially where surface waters have low alkalinity and where acids generated in organic horizons can be neutralized by cation exchange and weathering in mineral horizons. Results from the studies cited above 14-18 show that acidification of lakes from alkaline to slightly acid conditions has occurred during the early post-glacial period, probably as a result of catchment soil changes. The Round Loch data, however, indicate that soil acidification is not a sufficiently effective mechanism to explain the very high levels of acidity found in contemporary acidified lakes. The hypothesis can be rejected in Galloway and must be open to serious question in other regions.

This work was carried out while V.J.J. was supported by a. NERC research studentship. We thank D. Harkness (East Kilbride) for ¹⁴C dates, and R. S. Clymo, S. J. Phethean, R. J. Flower, S. T. Patrick, N. J. Anderson and P. Raven for help with fieldwork. John Theaker and his NCC staff kindly transported our equipment to the site.

Received 10 February; accepted 18 April 1986.

- Rosenquist, I. T. Scl. tot. Environ. 10, 39-49 (1978).
- Krug, E. C. & Frink, C. R. Science 221, 520-525 (1983). Flower, R. J. & Battarbee, R. W. Nature 305, 130-133 (1983).
- Berge, F. Norg. tek-naturvitensk. Forsk. 11, 1-18 (1975).
 Renberg, I. & Hellberg, T. Ambio 11, 30-33 (1982).
 Davis, R. B., Norton, S. A., Hess, C. T. & Brakke, D. F. Hydrobiologia 103, 113-123 (1983).
 Tolonen, K. & Jaakkola, T. Ann. Bot. Fenn. 20, 47-78 (1983).
- Charles, D. F. Verh. int. Verein. theor. angew. Limnol. 22, 559-566 (1984). Pennington, W. Rep. Freshwat. biol. Ass. 52, 28-46 (1984).
- Seip, H. M. in Ecological Impact of Acid Precipitation (eds Drablos, D. & Tollan, A.) 358-366 (Norwegian Institute for Water Research, Oslo, 1980).
- Battarbee, R. W., Flower, R. J., Stevenson, A. C. & Rippey, B. Nature 314, 350-352 (1985).
 Moore, P. D. Nature 256, 267-269 (1975).
- Pennington, W. Phil. Trans. R. Soc. B248, 205-244 (1964).
 Round, F. E. New Phytol. 56, 98-126 (1957).
- 15. Haworth, E. Y. J. Ecol. 57, 429-441 (1969).
- 16. Crabtree, K. Mitt. int. Verein. theor. agnew. Limnol. 17, 165-171 (1969).
- 17. Pennington, W., Haworth, E. Y., Bonny, A. P. & Lishman, J. P. Phil. Trans. R. Soc. B264, 191-294 (1972).
- 18. Evans, G. H. New Phytol. 69, 821-874 (1970).
- 19. Flower, R. J. Hydrobiologia (in the press).

Non-axisymmetric behaviour of Olduvai and Jaramillo polarity transitions recorded in north-central Pacific deep-sea sediments

Emilio Herrero-Bervera* & Fritz Theyer†

* Hawaii Institute of Geophysics, University of Hawaii, 2525 Correa Road, Honolulu, Hawaii 96822, USA † Department of Geological Sciences, University of Southern California, University Park, Los Angeles, California 90089, USA

The causes of the reversals of the Earth's magnetic field can be investigated by studying the palaeomagnetic record preserved in rocks. A proper documentation of reversal phenomena should yield valuable information about the generation of the field. Deep-sea sediments provide a globally and temporally distributed set of polarity transition records. Our studies²⁻⁴ of the Olduvai (1.88-1.72 Myr)¹ and Jaramillo (0.94-0.88 Myr)¹ subchrons using deepsea sediments showed that the time-averaged behaviour of the geomagnetic field during these reversals proved to be reliably recorded, independent of the latitude and longitude of the sample site. Here we test some phenomenological transition models and present directional data, virtual geomagnetic poles (VGPs) and related directions in rotated declination, inclination (D', I') space⁵, using two records of the Olduvai reverse-normal-reverse (R-N-R) and two records of the Jaramillo R-N-R polarity transitions. These data are better explained by the flooding rather than the standing field model, but they also indicate a degree of asymmetry of the transitional field.

The palaeomagnetic data presented here are associated with a pair of sequential reversals (R-N and N-R) from a fully azimuthally-oriented piston core^{2,6,7} (K78030; 18°55.9' N, 160°70.8' W) taken near the Hawaiian island of Kauai. The other two records are from two other fully azimuthally-oriented piston cores^{2,6,7}: K76113 from low latitude (2°40.1' N, 178°45.1' W) and K7501 from a mid-latitude site (37°22.4' N, 179°36.1' W), which encompass the Olduvai reversals (R-N, K76113 and N-R, K7501).

The transitions studied were sampled using a 'high-resolution' technique²⁻⁴. The measurements derived from each sample represent a signal averaged from as little as 200 to as much as 1,000 years of post-depositional remanent magnetization (PDRM) history (considering the sediment accumulation rates of the cores studied). Thus, with a typical 3-mm offset between boxes, field fluctuations of periods between 200 and 600 years should, at least theoretically, be within the reach of our high-resolution technique. The four records discussed here are characterized by high palaeomagnetic stability of the samples within and outside the transition zones²⁻⁴.

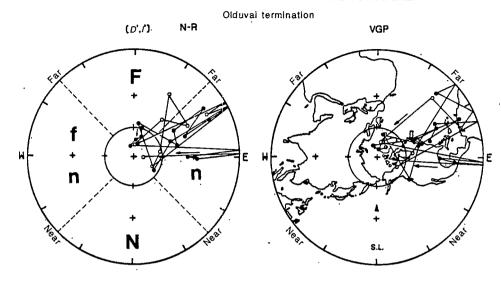
Figures 1 and 2 show the highly detailed VGP paths associated with the two sets of transitions. The VGPs are plotted with respect to their site longitude⁵ and are those which represent intermediate directions, as well as some outside the transition zones. The pattern of change in field directions is clear for the two transitional sets (Olduvai and Jaramillo subchrons) and is sufficient to apply Hoffman's8 test (to distinguish between the flooding model and the existence of a stationary (non-reversing) portion of the field during axial dipole decay and regeneration, using palaeomagnetic data corresponding to back-to-back (R-N and N-R) polarity transitions). During the onset of the Olduvai subchron R-N transition (core K76113), the VGPs representing the field remain southerly while migrating to nearly equatorial latitudes. The ancient field apparently underwent a rapid set of 'flips' during the transition, like those observed in several other detailed records^{9,10}. From the southerly latitudes, the VGPs migrate up to the Northern Hemisphere to the expected normal field direction. The path is clearly near-sided and is longitudinally confined. In the N-R reversal (core K7501) at the termination of the Olduvai subchron, a different sequence is observed. The termination path is more complicated than the onset path and is characterized by more intermediate VGPs (fewer in the Southern Hemisphere with respect to the VGPs in the Northern Hemisphere) and bigger loops in its traverse from northern latitudes to southern latitudes. These loops may show rapid fluctuations of the transitional field. The path can be classified as a far-sided path even though some of the VGPs he in the near-sided section of the plot (±90° from the site longitude). This path also exhibits a longitudinal confinement, as does the onset transitional path. Thus, both reversals are characterized by transitional VGP paths which lie along meridional bands on either side of the 90° meridian, but the paths are not completely antipodal.

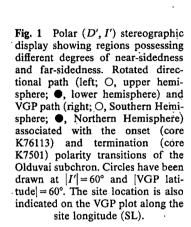
Analysis of the two Jaramillo transitional paths recorded by core K78030 (Fig. 2) shows that the two paths are dissimilar even though they represent records of a back-to-back transition zone from the same site. For instance, the R-N records display intermediate VGPs lingering at low southerly latitudes in the vicinity of the 90° meridian, with a sudden transit to the Northern Hemisphere where big loops occur before the final move to the expected normal direction. The path could be classified as near-sided because most of the intermediate VGPs reside within ±90° of the site longitude. The N-R Jaramillo transition path is more complicated than the R-N Jaramillo path. The VGPs in the Northern Hemisphere linger briefly before their transit to southern latitudes where they seem to migrate, forming loops in the Southern Hemisphere before their final move to the expected reversed field direction. This path is hard to classify as near-sided or far-sided because the VGPs lie on both sides of the meridian 90° from the site longitude. Thus, the transitional field of these two reversals was different. A characteristic of both the Olduvai sets and the Jaramillo sets is that the paths are not antipodal. A comparison of all four paths—between sites and within sites—shows that they are characterized by individual features peculiar to each transition; and overall, the data indicate that the reversal process is asymmetric, such that each reversal sense is associated with a different field configur-

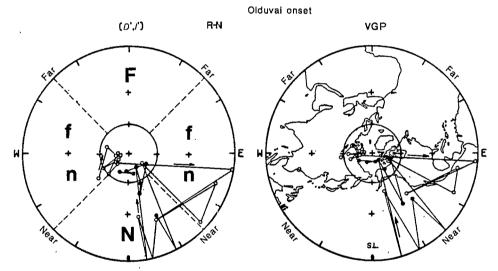
Figure 1 shows the VGP data, as well as the transition data rotated using Hoffman's method⁵. The polar (D', I') stereographic plot clearly shows that at the onset of the Olduvai subchron (K76113) the field displays an initial near-sided vector movement in quadrant 'n' (the first 10 rotated directions which are apparently closer to the reversed polarity and which represent the initiation of the reversal—still not part of the transitional field); then, a swing to the other quadrant 'n'; and finally a movement to normal polarity in the 'N' region of the diagram. These last two steps are part of the strictly transitional field behaviour. Thus, from this record alone, it can be concluded that the field geometry during the onset of the Olduvai reversal is consistent, but not uniquely so, with a hypothesized transi-

Table 1 Results of rotated intermediate directions and VGPs of Olduvai and Jaramillo polarity transitions

Transition	Sense of transition	VGP	(D',I')
Jaramillo			
Termination	N-R	ſ	f
K78030			
Onset	R-N	n-f	N
K78030			
Olduvai			
Termination	N-R	f	f
K7501			
Onset	R-N	n-N	n-N
K76113			







tional palaeofield geometry which is significantly zonal (rotated directions in the 'N' region of the (D', I') diagram), as well as a non-axisymmetric palaeofield geometry (rotated transitional directions in the 'n' region). Figure 1 also shows the transitional characteristics of the termination of the Olduvai subchron (core K7501). The record displaying the rotated (D', I') directions shows that the path lies on the far-side region of the polar diagrams. Initially, the reversal is controlled by a consistent axisymmetry, and during the middle and final stage of the reversal the field was apparently dominated by non-axisymmetric terms; most of the rotated directions are located in the 'f' region.

The two transitional records (Olduvai reversals) present entirely dissimilar characteristics. For instance, the rotated directions of the R-N reversal record are near-sided, whereas the rotated directions of the N-R record are far-sided. The two records do not present antipodal directions; instead, at different stages of the reversals some of the directions are consistent with a dominating axisymmetry and others with non-axisymmetric terms.

The rotated directions and VGP paths for the two back-to-back reversal records of the Jaramillo subchron (core K78030, from \sim 300 km from Kauai) are shown in Fig. 2. The (D', I') rotated directions of the R-N reversal record of the Jaramillo subchron display almost a total dominance of a consistent axisymmetry.

Such rotated directions are located in the 'N' region of the polar diagram. This reversal record shows that at the initial stage of the transition some of the directions are located on the far side of the polar diagram, and at some stage two directions are in the 'n' quadrant. Nevertheless, the path could be classified as near-sided. Figure 2 also shows the N-R reversal path of the Jaramillo subchron. This is a unique path with respect to the other three paths presented here: it is more complex than the R-N Jaramillo path and displays rotated directions on both the near and far side of the polar diagram. One group of rotated directions is in close proximity to the $D' = 90^{\circ}$ great circle (that is, the plane containing the horizontal east-west line and the axial dipole field direction). Other groups of directions are along the $D' = 180^{\circ}$ great circle (the plane containing the north-south line and the axial dipole field direction). In general, this transitional record is characterized by stages of the reversal that are in the 'N', 'n' and 'f' regions of the polar projection plot, although the path lingers mostly in the far-sided region of the diagram.

Each of the records presents individual characteristics, perhaps indicating that the harmonic content of each is different, even in the case of the two records of the Jaramillo subchron taken from the same core³. From a study of two older (Pliocene) Kauai back-to-back reversal records, Bogue and Coe concluded that those two paths are distinctly near-sided¹⁰⁻¹². Our nearby

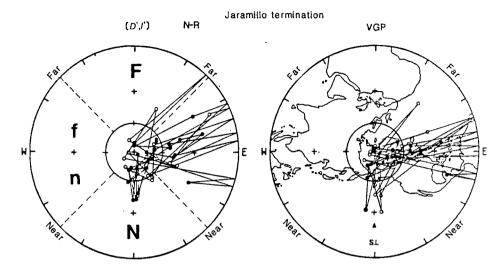
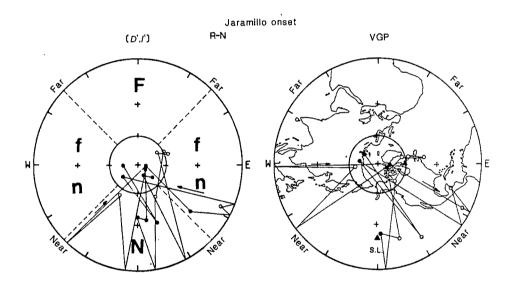


Fig. 2 Polar (D', I') stereographic display showing regions possessing different degrees of near-sidedness and far-sidedness. Rotated directional path (left) and VGP path (right) associated with the onset and termination polarity transitions of the Jaramillo subchron (core K78030). Circles have been drawn at $|I'| = 60^{\circ}$ and |VGP| latitude |VGP| at the site location is also indicated on the VGP plot along the site longitude (SL). Symbols as in Fig. 1.



core (K78030) that recorded the Jaramillo back-to-back reversals indicate that the R-N record is near-sided, whereas the N-R record is classified as a far-sided path using Hoffman's terminology. However, certain common characteristics must be taken into consideration. One is the site dependence of the transitions: the two R-N reversal records are near-sided and the two N-R reversal records are far-sided, or at least most of the rotated directions are on the far side of the diagram (for example, Olduvai termination). All four transition records show intermediate rotated directions residing in regions 'n' and 'f' that are only marginally near- and far-sided respectively (see Table 1). All four records are unambiguously associated with significantly non-axisymmetric transitional fields. Another common feature of these paths is that all tend to reside on the American continent. As shown in Figs 1 and 2, the VGP paths are clustered about the 90° meridian. This area is also where the VGP paths from Crete are located¹³.

Which of the current models for transitional field behaviour explains the characteristics of the Olduvai and Jaramillo records discussed here, the standing field model¹⁴⁻¹⁶ or the flooding model^{17,18}? The former predicts identical transitional field behaviour for repeated reversals as observed from a single site, and requires the postulated standing field to persist for several million years, whereas the latter treats the Earth's fluid core as a distributed source of magnetic field in which polarity transi-

tions begin with a localized reversal of field sign in a small region of the core, an effect that consequently spreads or floods through the rest of the source region. If the reversal starts at either of the poles or at the equatorial zone of the core, basically axial quadrupolar, or axial octupolar fields, respectively, will predominate during the intermediate stages of the reversal process. For the purely axisymmetric, and consequently the simplest cases, the flooding will begin at a pole (a predominantly quadrupolar transitional field) or along the equatorial band of the fluid core (an octupolar field at the midpoint of the reversal). Depending on the sense of the reversal and the hemisphere of the observer, the VGP path will be near-sided (same longitude as the site) or far-sided (180° away from the site). This is the basis of Hoffman and Fuller's method¹⁹ for determining the origin point of flooding, which involves the comparison of palaeomagnetic records of both R-N and N-R reversals.

The standing field model cannot successfully explain the diverging behaviour of the paths because it predicts identical transitional field behaviour for repeated reversals when viewed from a single site. Moreover, Bogue and Coe¹¹ have shown that the palaeointensity records of the Kauai transitions are not consistent with the standing field model. The same conclusion was reached by a palaeointensity study of the Steens Mountain polarity transition²⁰.

The generalized flooding model can successfully explain these data. For the two successive reversals (Jaramillo subchron), the model predicts (so long as a reversal is initiated at the same zone in the core each time) transitional VGP paths that differ in longitude by 180°. In general, for core K78030 the two records are not antipodal (R-N near-sided and N-R far-sided), and the same conclusion can be drawn from the Olduvai subchron paths, even though the two records are from two different localities. The salient directional features shared by all of these records are the overall longitudinal confinement of most intermediate VGPs and respective rotated directions well to the east of the sites; and the typical location of the intermediate VGPs over the Americas, the southeastern Pacific and the western Atlantic. None shows smooth pole-to-pole paths; all define major loops (including east-west swings, for example, in the Olduvai onset record, Fig. 2) before settling into the expected opposite polar positions. The important issue here is that the VGP paths are not antipodal. The rotated directions of all these data prove that the reversal process is asymmetric, such that each transition sense is associated with a different field configuration. Indications that the flooding process is itself asymmetric have been recently reported from the studies of the Kauai and Steens Mountain transitions 11,20

Financial support for this study was provided by the Hawaii Institute of Geophysics (HIG), the Office of Naval Research

grant N00014-75-0209, a cooperative research agreement between NOS/NOAA and HIG, and NSF grant EAR84-00058. The HIG Core Analysis Laboratory was supported by NSF grant OCE82-01962. Editorial assistance was provided by Diane Henderson and is gratefully acknowledged. This is HIG contribution no. 1763.

Received 1 July 1985: accented 23 April 1986.

- Berggren, W. A. et al. Quat. Res. 13, 277-302 (1980).
 Herrero-Bervera, E., thesis, Univ. Hawaii, Honolulu (1984).
- 3. Theyer, F., Herrero-Bervera, E., Hsu, V. & Hammond, S. R. J. geophys. Res. 90, 1963-1982
- Herrero-Bervera, E., Theyer, F. & Helsley, C. E. J. geophys. Res. (submitted).
- Hoffman, K. A. J. geophys. Res. 89, 6285-6292 (1984).
 Seyb, S. M., Hammond, S. R. & Gilliard, T. Deep Sea Res. 24, 943-950 (1977).
- Hammond, S. R., Seyb, S. M. & Theyer, F. Earth planet. Sci. Lett. 44, 167-175 (1979).
 Hoffman, K. A. Phys. Earth planet. Inter. 24, 229-235 (1981).
 Watkins, N. D. Geophys. J.R. astr. Soc. 17, 121-149 (1969).
 Bogue, S. W. & Coe, R. S. Nature 295, 399-401 (1982).

- Bogue, S. W. & Coe, R. S. J. geophys. Res. 89, 10341-10354 (1984).
 Hoffman, K. A. Phil. Trans. R. Soc. A306, 147-159 (1982).

- Valet, J.P., Laj, C. & Langereis, C. G. Nature 304, 330-332 (1983).
 Hillhouse, J. & Cox, A. Earth planet. Sci. Lett. 29, 51-64 (1976).
 Mankinen, E. A., Donnelly-Nolan, J. M., Grommé, C. S. & Hearn, B. C. Jr Prof. Pap. U.S.
- geol. Surv. 1141, 67-82 (1981). 16. Liddicoat, J. C. Phil. Trans. R. Soc. A 306, 121-128 (1982).
- Hoffman, K. A. Science 196, 1329-1332 (1977).
 Hoffman, K. A. Earth planet Sci. Lett. 44, 7-17 (1979).
- 19. Hoffman, K. A. & Fuller, M. Nature 273, 715-718 (1978).
- 20. Prévot, M., Mankinen, E. A., Coe, R. S. & Grommé, S. C. J. geophys. Res. 90, 417-448 (1985).

Late Palaeozoic to early Mesozoic evolution of Pangaea

R. A. Livermore*, A. G. Smith* & F. J. Vine†

* Department of Earth Sciences, University of Cambridge, Downing Street, Cambridge CB2 3EQ, UK

† School of Environmental Sciences, University of East Anglia, Norwich NR4 7TJ, UK

Several possible configurations of the Pangaea supercontinent have been suggested for the interval from late Carboniferous to early Triassic. Here we re-examine the palaeomagnetic basis for these models, emphasizing the trends of the paths of apparent polar wander for the individual components of the supercontinent rather than simply averaging poles of presumed similar age. Two of the alternatives, Pangaea B and C, may result from averaging poles of dissimilar age along common polar wander paths, giving rise to spurious tectonic displacements. The most likely model appears to be the formation, in late Devonian time, of a modified Pangaea (A2) followed by evolution to the traditional configuration (A) during the Triassic.

Hallam¹ reviewed geological information concerning the possible configuration of the Pangaea supercontinent in Permo-Carboniferous time and concluded that the evidence favours an unchanged configuration from the late Carboniferous to the Jurassic. However, the palaeomagnetic data disagree with such a model. In particular, late Palaeozoic poles from Gondwanaland are distinct from those obtained for the northern continents when plotted on the 'traditional' Pangaea reconstruction. Solutions to this problem range from an anticlockwise rotation of Laurasia relative to Pangaea of ~20° about a pole in the western Sahara²⁻⁵, to a rather larger rotation of $\sim 35^{\circ}$ about a different pole⁶⁻¹¹, to a drastic model in which northwestern South American is juxtaposed with southern Europe¹². These solutions have been designated Pangaea-A2, Pangaea-B and Pangaea-C respectively^{1,10}. Figure 1 shows the alternative reconstructions for the Permian, plotted on the same scale and in palaeomagnetic

Most of the contrasts between the competing models are due to differences in palaeolongitude of the component fragments: thus, palaeomagnetic data from a restricted interval of geological time cannot easily distinguish between these alternatives. However, a careful examination of the apparent polar wander paths of the component continental blocks for a longer period of time may allow some of the models to be discounted. This is the approach we have followed in our re-evaluation of the palaeomagnetic data.

Carefully selected palaeomagnetic poles from the interval 180-320 Myr (ref. 13) have been returned to their palaeogeographical positions in the alternative reconstructions. The data have then been sampled in 20-Myr non-overlapping windows and Fisher statistics calculated for the various continental fragments in an attempt to examine the implications of the various models.

The poles were selected from recent lists of data thought to represent the ancient geomagnetic field direction, such as those given by Embleton¹⁴ for Australia and East Antarctica, by Van der Voo15 for North America, and by Brock16 for Africa and Madagascar. In addition, more recent results (to 1983) have been incorporated. Results for which the time of magnetization could not be estimated to within 25 Myr were excluded. All the poles used conform to the minimum reliability criteria of McElhinny¹⁷ and are based on studies in which AF (alternating-field) and/or thermal cleaning techniques were employed. Results from within or east of the Urals have not been included because of the likelihood of relative motions between Europe and Siberia during at least part of the period of interest. Stratigraphic ages have been referred to the timescale of Harland et al. 18 and K-Ar dates have been standardized to the decay constants given by Steiger and Jaeger¹⁹. The assigned ages, together with the absence of Russian data and the inclusion of some more recent studies, constitute the chief differences between this dataset and that used by Morel and Irving¹⁰.

Any time window for data grouping must be narrow enough to preserve the main features of apparent polar wander (APW) paths, yet broad enough to allow sufficient poles to be included to define precise means. A width of 20 Myr was chosen as the minimum presently permitted by the number and quality of available data. Having returned the poles to the various reconstructions, Fisher statistics were calculated in Africa-fixed coordinates for each continent within each window, assuming a geocentric axial dipole field. The means and their associated A₆₃ standard error circles are given in Table 1 for the four

Fig. 1 Alternative models of the Pangaea supercontinent, orientated using early Permian (270 Myr) palaeomagnetic data. Orthographic projection. a, Pangaea-A, constructed using published sources²⁶⁻³¹: this is comparable to the classic reconstructions of Wegener³² and Bullard et al.³³. b, Pangaea-A2 reconstruction, obtained by applying an additional rotation of 20° about a pole in the north-west Sahara to Laurentia-Baltica, after ref. 2. c, Pangaea-B reconstruction, obtained using the rotations of Irving¹¹ for Laurentia, Baltica and Gondwana. d, Pangaea-C of Smith et al.¹², showing a large Tethyan offset of Gondwana and the northern continents of several thousand kilometres.

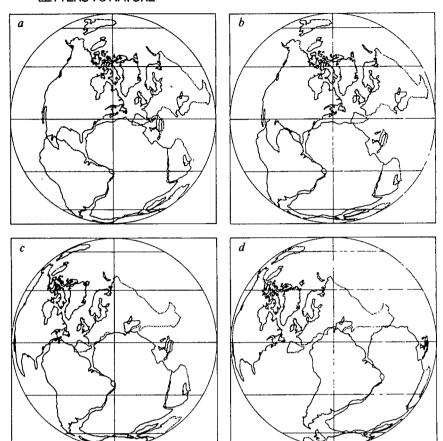


Table 1 Mean poles of continental fragments with respect to the different Pangaea reconstructions, with Africa fixed in present-day coordinates

				Mear	n pole					
	Pang	aea-A	Panga	nea-A2	Pang	aea-B	Pang	aea-C		
Age (Myr)	Lat. (deg)	Long. (deg)	Lat. (deg)	Long. (deg)	Lat. (deg)	Long. (deg)	Lat. (deg)	Long. (deg)	A_{63} (deg)	<i>N</i> *
Europe										
210	61.5	239.0	44.2	253.3						1
230	54.9	227.3	39.0	243.4						1
250	50.8	216.2	36.8	233.7	47.9	248.6	38.2	263.0	1.9	5
270	37.3	226.6	22.0	238.2	33.9	240.1	32.2	245.6	1.8	19
290	34.3	224.5	19.3	235.9	33.0	236.1	33.7	241.9	3.0	8
310	33.9	220.0	19.8	231.9	35.5	232.6	37.4	241.3	4.8	7
North Americ										
190	66.8	242.4	49.1	256.7					2.9	6
210	70.0	233.0	53.0	252.4					4.7	4
230	62.2	215.9	47.7	238.4					6.2	4
250	55.9	222.1	40.7	239.9	45.6	254.4	31.3	266.4	2.9	8
270	46.3	218.0	32.1	233.6	42.5	241.4	35.3	255.4	1.5	11
290	36.6	225.7	21.4	237.3	31.9	236.7	29.8	243.8	2.8	3
310	37.1	221.1	22.7	233.6	34.9	234.2	33.5	244.3	2.9	3
Africa										
190	70.1	246.6							3.9	7
210	67.2	246.1							6.4	5
230	67.3	250.9							4.3	6
250	60.6	261.0								2
270	31.7	241.8							5.3	3
290	29.0	240.0								1
310	16.1	242.5		•						1
South Americ	a									
190	50.8	242.2								2
210	68.2	228.2								1
230	58.4	247.3							3.4	5
250	50.1	252.4							4.2	5
270	46.5	243.2					•			2
290	23.2	237.9								2
310	23.3	230.5							4.4	4

^{*} N is the number of poles averaged to obtain the mean pole for an interval.

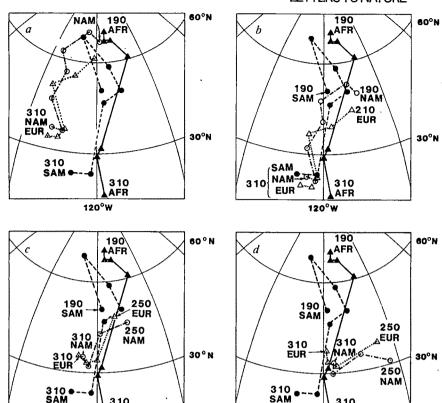
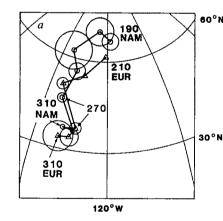


Fig. 2 Positions of mean palaeopoles and standard error (A_{63}) circles relative to an Africa-fixed Pangaea-A reconstruction, showing the general agreement of trends. However, detailed examination reveals differences in timing; for example, the 270-Myr means for Europe and North America disagree, as do those for South America and Africa. Lambert Equal Area projection. a, North America (\bigcirc) and Europe (\triangle) . b, South America (\bigcirc) and Africa (\triangle) .

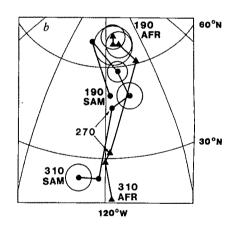
Fig. 3 a, APW paths of the northern (North American, European) and southern (African, South American) continents plotted relative to Pangaea-A in Africa-fixed coordinates. Symbols as for Fig. 2. Equal area projection. b, As for a but plotted relative to Pangaea-A2. The discrepancy between northern and southern continents before 210 Myr is now reduced, although the timing of motion along the common path varies between continents. c, As for a, but plotted relative to Pangaea-B for the interval 250-310 Myr. d, As for c, but plotted relative to Pangaea-C.

120°W



ĀFR

120°W



models. Note that no results are given for times younger than 250 Myr for either B or C, as these models were only intended for Permo-Carboniferous time.

Figure 2 illustrates the poles calculated with respect to Pangaea-A. Figure 2a shows that the trends of the APW paths for Europe and North America, especially for pre-Triassic time for which more reliable data are available, are very similar. Apart from the oldest two intervals, however, the A_{63} circles do not overlap and there is a clear offset in age along the common path. On the other hand, there is good agreement between the 290-, 270- and 250-Myr poles from North America and the 270-, 250- and 230-Myr poles for Europe, respectively. This suggests a possible error in intercontinental correlation of up to 20 Myr, or widespread remagnetization of the North America formations after a similar period of time. Similarly, although less obviously, the paths for South America and Africa (Fig. 2b) follow broadly similar northward routes, but with quite large divergences for individual windows, for example, 260-280 Myr.

Part of these differences may be attributable to dating errors for individual results, coupled with rapid polar wander. The discrepancies do appear to be systematic, however, and one suspects that a more fundamental problem exists concerning the accuracy of the stratigraphic correlations on which most of the assigned ages are based. In addition, many poles derive from studies of non-fossiliferous red sediments, for which the mechanism of remanence acquisition remains to be clearly demonstrated.

The observed differences cast considerable doubt on the Pangaea-B and -C reconstructions, because both of these models were constructed by moving Laurasia and Gondwanaland until their Permian and late Carboniferous poles coincided. If there are systematic errors in the correlation of these poles, then these reconstructions may be viewed as artefacts of the dating errors. An example of this may be seen in the Pangaea-B model, which requires a small ocean separating Europe and North America to satisfy an observed difference between their mean palaeopoles¹⁰. If, as suspected, this difference arises from dating errors along a common polar wander path, then no such separation (for which geological evidence is absent) is required.

One conclusion that can be drawn from the foregoing is that comparison of APW path segments is to be preferred to the simple averaging of supposedly contemporaneous poles. Figure 3 shows the polar wander paths for the four main continents (North America, Europe, Africa and South America) plotted with respect to Pangaea-A, A2, B and C in Africa-fixed coordinates. Figure 3a, b clearly illustrates the discrepancy between the paths for the northern and southern continents in the Pangaea-A reconstruction for times before 210 Myr, and the improvement for this time interval obtained if one assumes Pangaea-A2.

In Fig. 3c, d the paths are superimposed for reconstructions B and C, respectively, but only for the period 310-250 Myr, because it is only for this earlier period that these reconstructions have been suggested. With the exception of Pangaea-B for a period of time centred on 270 Myr, there is little similarity between the polar wander paths for the northern and southern continents in either reconstruction. We stop short of suggesting an evolution A2 to B to A2 to A, which would imply implausibly high rates of plate motion, and on the basis of the comparison of APW paths consider it unlikely that Pangaea ever existed in the form of configuration B or C.

It now seems clear from palaeomagnetic, biogeographical and stratigraphic evidence that the configuration of Pangaea immediately before its disruption was similar to that portrayed in Fig. 1a. For earlier times, uncertainty remains. There is doubt about the precise timing of the final collision between Gondwanaland and Euramerica which brought Pangaea into being. Depending on the interpretation of Devonian palaeopoles from Gondwana, this collision may have occurred either during the early Carboniferous or as early as late Devonian²⁰. The exact configuration at these times is not known with certainty, but published reconstructions favour Pangaea-A221,22

Several workers^{3,5} have noted the close agreement between the fossil faunas and tectonic structures of southern North America (such as the Oachita and Marathon belts) and those of northern South America (such as the Venezuelan Andes), and have suggested that better alignment of similar provinces can be achieved when the tighter A2 fit is adopted. If an A2 to A transition is accepted, the geological problem is that of locating the structures along which the transition took place, and determining their nature and displacement. A suitable zone of transcurrent motion is most plausibly located along part of the present-day continental margins of eastern North America and north-west Africa. To accommodate such motion in a simple fashion, the Euler pole for A2 would need to be modified, as it does not agree in detail with such a transition zone. This subject will be dealt with elsewhere.

The notable Permo-Triassic volcanism of the Alpine region sensu lato, interpreted as representing the break-up of the region, was followed by the subsidence of huge late Triassic and early Jurassic carbonate platforms, whose creation pre-dates the Pangaea^{23,24}. The Alpine cycle began in Triassic or possibly Permian time, but the Atlantic Ocean did not begin to open until the middle Jurassic. The observed tectonic pattern might well reflect mid- to late-Triassic plate margins formed by the A2 to A transition.

In view of this discussion of polar wander paths, and the geological arguments advanced by Hallam¹, both Pangaea-B and Pangaea-C seem less likely candidates, possibly resulting from uncertainties in the dating of components of remanence and/or intercontinental stratigraphical correlation. The most probable evolution appears to be formation of a supercontinent resembling Pangaea-A2 during the late Devonian21, followed by Permo-Triassic readjustments involving dextral shear, and the reorganization of fragments in the Gulf of Mexico and Mediterranean regions. This was accompanied by rapid motion of all the major continents with respect to the poles. Siberia and the Asian components of Pangaea (Kazakhstan, China, and so forth) were probably sutured to Europe during Permo-Triassic time¹⁷. By the late Triassic, Pangaea-A was in existence, and, although probably undergoing extension in early Jurassic time, remained intact as a supercontinent until break-up in the middle Jurassic²⁵.

This work was funded by a NERC studentship and grant number GR3/4405. This is Cambridge Earth Sciences contribution 761.

Received 13 January; accepted 9 April 1986.

- 1. Hallam, A. Nature 301, 499-502 (1983).
- Van der Voo, R. & French, R. B. Earth Sci. Rev. 10, 99-119 (1974).
 Van der Voo, R. et al. Geology 4, 177-180 (1976).
 Scotese, C. R., Bambach, R. K., Barton, C., Vander Voo, R. & Ziegler, A. M. J. Geol. 87,
- 217-277 (1979).
- 5. Walper, J. L. in The origin of the Gulf of Mexico and the Early Opening of the Central North Atlantic Ocean (ed. Pilger, R. H.) 87-98 (Louisiana State University, Baton Rouge, 1980) 6. Vine, F. J. Palaeontol. Ass. spec. Pap. 12, 61-77 (1973).
- Irving, E. Nature 270, 304-309 (1977)
- Westphal, M. Nature 267, 136-137 (1977).
- Kanasewich, E. R., Havskov, J. & Evans, M. E. Can. J. Earth Sci. 15, 919-955 (1978)
 Morel, P. & Irving, E. J. geophys. Res. 86, 1858-1872 (1981).
 Irving, E. Geophys. Surv. 5, 299-333 (1983).

- Smith, A. G., Hurley, A. M. & Briden, J. C. Phanerozoic Palaeocontinental Maps (Cambridge University Press, 1981).
- Livermore, R. A. thesis, Univ. East Anglia, Norwich (1985).
 Embleton, B. J. J. in Palaeoreconstruction of the Continents (eds McElhinny, M. W. & Valencio, D. A.) 77-92 (American Geophysical Union, Washington, 1981)

 15. Van der Voo, R. in Palaeoreconstruction of the Continents (eds McElhinny, M. W. & Valencio.
- D. A.) 159-176 (American Geophysical Union, Washington, 1981)
- 16. Brock, A. in Palaeoreconstruction of the Continents (eds McElhinny, M. W & Valencio, D A.) 65-76 (American Geophysical Union, Washington, 1981).

- A.) 65-76 (American Geophysical Union, Washington, 1981).
 McElhinny, M. W. Palaeomagnetism and Plate Tectonics (Cambridge University Press., 1973).
 Harland, W. B. et al. A Geologic Timescale (Cambridge University Press, 1982).
 Steiger, R. H. & Jaeger, E. Earth planet. Sci. Lett. 36, 359-362 (1977).
 Kent, D. V., Dia, O. & Sougy, J. M. A. in Plate Reconstruction from Palaeozoic Palaeomagnet-
- ism (eds Van der Voo, R., Scotese, C. R. & Bonhommet, N.) 99-115 (American Geophysical Union, Washington, 1984).
- 21. Livermore, R. A., Smith, A. G. & Briden, J. C. Phil Trans. R. Soc. B309, 29-56 (1985) 22. Scotese, C. R. in Plate Reconstruction from Palaeozoic Palaeomagnetism (eds Van der Voo.
- R., Scotese, C.R. & Bonhommet, N.) 1-10 (American Geophysical Union, Washington, 1984).
- Pamic, J. J. Ann. Soc. geol. Nord. CIII, 133-141 (1983).
- Pamič, J. J. Tectonophysics 109, 273-307 (1984).
 Sheridan, R. E. et al. geol. Soc. Am. Bull. 93, 876-886 (1982).
- - Le Fort, J.-P. Mar. Geol. 37, 355-369 (1980)
- 27. Klitgord, K. D. & Schouten, H. Eos 63, 307 (1982).
- Rabinowitz, P. D. & LaBrecque, J. J. geophys. Res. 84, 5973-6002 (1979).
- Norton, I. O. & Sclater, J. G. J. geophys. Res. 84, 6803-6830 (1979)
 Segoulin, J. & Patriat, P. Bull. Soc. géol. Fr. 23, 603-607 (1981)
- Smith, A. G. & Hallam, A. Nature 225, 139-144 (1970).
 Wegener, A. The Origin of the Continents and Oceans (Methuen, London, 1924). 33. Bullard, E. C., Everett, J. E. & Smith, A. G. Phil. Trans. R. Soc. A258, 41-51 (1965).

Mantle heterogeneity beneath the Nazca plate: San Felix and Juan Fernandez islands

D. C. Gerlach*‡, S. R. Hart*, V. W. J. Morales† & C. Palacios†

* Department of Earth, Atmospheric and Planetary Sciences, Massachusetts Institute of Technology, Cambridge,

Massachusetts 02139, USA

† Departmento de Geosciencias, Universidad del Norte, Casilla 1280, Antofagasta, Chile

The islands of San Felix, San Ambrosio and the Juan Fernandez group comprise one of the few subaerial occurrences of intraplate oceanic volcanism between the Mid-Atlantic Ridge and the East Pacific Rise south of 20°S, and are therefore valuable in the assessment of large-scale geochemical heterogeneities in the Earth's mantle 1-3. We present here the results of a preliminary Sr, Nd and Pb iosotpic study of basic lavas from these islands. All samples show a moderate Dupal³ signature (anomalous Sr. Nd and Pb isotopic compositions). Basalts from the Juan Fernandez group lie close to the mantle plane4, whereas basalts from San Felix display unusual isotopic characteristics which plot well below the Nd-Sr oceanic array. Based on this data, we propose the delineation of a new mantle array, linear in Nd-Sr-Pb isotopic space, with Tubuaii and Walvis Ridge as end members. The mixing relationships exhibited by this array suggest that both end members are geographically contiguous, and probably reside in delaminated sub-continental lithosphere.

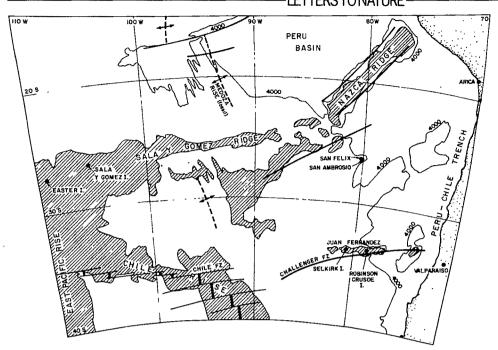


Fig. 1 Generalized tectonic map of the South-East Pacific, showing the location of San Felix, San Ambrosio Juan Fernandez islands (modified from ref. 42). Shaded areas represent depths less than 3,500 m; 4,000 m contours are also shown. Dashed lines represent extinct spreading ridges. San Felix and San Ambrosio are not related to present or older spreading systems or fracture zones, nor is there any convincing older hot-spot trace extending to the east from these islands. The Juan Fernandez islands lie along an eastwest-trending bathymetric ridge, probably associated with the Challenger fracture zone; this ridge may represent a hot-spot trace, as some bathymetric expression can be traced up to 500 km eastwards. Robinson Crusoe island lies on ~38-Myr-old crust; San Felix and San Ambrosio lie on ~42-Myr-old crust.

The Juan Fernandez islands are located on a N80° E-trending aseismic ridge, the Juan Fernandez Ridge, whereas San Felix and San Ambrosio do not appear to be associated with any significant tectonic or topographic feature (Fig. 1). San Felix and San Ambrosio (26°25′ S, 79°59′ W) are small (<3-4 km²), and located 20 km apart; although no historic eruptions have been reported, fresh-looking pahoehoe lava flows and fumarole activity on San Felix were observed by Willis and Washington⁵. These islands are mainly platforms bounded by steep cliffs, and consist largely of interbedded lavas and deeply weathered pyroclastics intruded by dikes⁵.

166

The Juan Fernandez islands include one large island, Robinson Crusoe (~50 km², at 33°37′ S, 78°50′ W), a much smaller nearby islet, Santa Clara, and A. Selkirk Island, 200 km to the west. Robinson Crusoe island is heavily eroded, with no historic record of volcanic activity, although evidence of submarine volcanism immediately west of Robinson Crusoe has been reported^{6,7}. An extensive volcanic sequence of >2,200 m thickness is exposed on Robinson Crusoe island⁸. The lowest unit (Punta Larga, >800 m thick) consists of extensive basalt flows with rare interbedded pyroclastics. The middle unit (Puerto

Ingles, \sim 1,200 m) consists of olivine-phyric to picritic basalts interbedded with a relatively greater proportion (\sim 30%) of pyroclastics. Basalt samples from this unit have been dated by K-Ar at 3.1-3.5 Myr (ref. 9). The youngest unit (Bahia del Padre, \sim 250 m thick) is made up mainly of pyroclastics, with minor olivine basalt flows.

Samples collected from San Felix in 1923 by Willis⁵ include weathered tuff, trachyte and basanite. Of these, we chose for analysis one fresh basanite and one sample of basanite glass, occurring as small inclusions in a palagonitized basanite tuff (Table 1); a fresh tephritic basalt⁵ from San Ambrosio was also analysed. Basalts from Robinson Crusoe are transitional to alkalic, and vary in freshness and olivine phenocryst content.

The basanites from San Felix and San Ambrosio are similar in major- and trace-element composition (D. Gerlach and S. R. Hart, unpublished data) to basanites from alkalic suites of Atlantic oceanic islands such as Fernando de Noronha, St Helena and Tristan da Cunha (refs 10, 11; D. Gerlach and J. Stormer, unpublished data). The basalts of Robinson Crusoe are similar in their major- and trace-element compositions to transitional and alkalic basalts from several Hawaiian vol-

Sample no.*	Lithology†	SiO ₂	K ₂ O	RЬ	Sr	Ba	⁸⁷ Sr/ ⁸⁶ Sr	¹⁴³ Nd/ ¹⁴⁴ Nd	²⁰⁶ Pb/ ²⁰⁴ Pb	207 Pb/ 204 Pb	²⁰⁸ Pb/ ²⁰⁴ Pb
1 (30MT0182)	AOB	46.71	0.75	15.3	452	182	0.703714 ± 41	0.512847 ± 16		_	_ •
2 (5MT0283)	TAB	48.27	1.04	20.3	554	244	0.703654 ± 23		19.042	15.596	38.872
3 (11MT0182)	AB	47.00	0.75	7.6	430	229	0.703512 ± 27	0.512882 ± 19	19.094	15.595	38.899
4 (28MT0182A)	AOB	45.82	1.11	26.0	629	279	0.703779 ± 25	0.512818 ± 19	19.214	15.627	39.099
5 (59MT82B3)	TAB	47.75	0.74	18.6	483	180	0.703634 ± 30		19.129	15.609	38.999
6 (14MT0182)	TAB	48.13	0.50	2.7	461	243	0.703581 ± 25	0.512835 ± 18	19.045	15.597	38.886
7 (10MT0283)	AOB	46.01	0.90	18.6	497	239	0.703762 ± 42	0.512831 ± 37	19.130	15.595	38.958
8 (52MT0282)	В	48.24	0.72		_		0.703629 ± 25	0.512840 ± 40		_	- .
9 (55MT0282)	В	47.61	1.48				0.703625 ± 26	0.512855 ± 18		_	_
10 (99653)	Bs	45.56	3.27	71.4	1447	891	0.704120 ± 27	0.512585 ± 19	18.960	15.569	38.871
11 (99656)	Bs	43.48	3.06	66.3	1359	815	0.704122 ± 18	0.512552 ± 16	19.312	15.602	39.329
12 (99657)	Te	45.88	2.32	51.8	1218	689	0.703983 ± 27	0.512732 ± 17	18.913	15.569	38.844

Chemical and isotopic techniques are as described elsewhere ³⁸⁻⁴⁰. SiO₂ (samples 1-10) by XRF, K₂O, Rb, Sr and Ba by isotope dilution; SiO₂ analyses of samples 11 and 12 are from ref. 5. Abundances are reported on an anhydrous basis. Sr and Nd isotope ratios are reported relative to 0.708000 for E+A standard, and 0.512640 for BCR-1; 2 σ precision refers to least significant figures. Pb isotope data corrected for fractionation, ratio by ratio, using results for NBS SRM 981; absolute values adopted for this standard (16.9373, 15.4925, 36.7054) are from ref. 41. Reproducibility of Pb ratios is better than 0.03% per AMU; in-run precision is a factor of 5 better. Samples 1, 3-7 also analysed for ⁸⁷Sr/⁸⁶Sr after HCl leaching, with identical results to above values.

^{*} Samples 1-7 are from Puerto Ingles unit, 8 and 9 from Punta Larga unit, Robinson Crusoe island (Juan Fernandez group), arranged in order of increasing age. Samples 10 and 11 are from San Felix Island; 12 is from San Ambrosio Island.

[†] A, alkali; B, basalt; O, olivine; T, transitional; Bs, basanite; Te, tephrite.

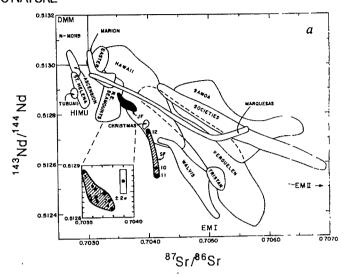
canos¹²⁻¹⁵. Alteration by weathering may have affected alkalielement abundances in some samples notably numbers 3 and 6, which are characterized by abnormally high K/Rb ratios (Table 1).

Samples from Robinson Crusoe display relatively narrow ranges in ⁸⁷Sr/⁸⁶Sr (0.70351-0.70378), ¹⁴³Nd/¹⁴⁴Nd (0.51282-0.51288) and ²⁰⁶Pb/²⁰⁴Pb (19.04-19.21) (Table 1), and lie close to the mantle plane of Zindler et al.4. The two samples from San Felix are characterized by relatively higher 87Sr/86Sr and lower ¹⁴³Nd/¹⁴⁴Nd, whereas the San Ambrosio sample is intermediate between San Felix and Robinson Crusoe (Table 1, Fig. 2a). With regard to their Pb isotopic compositions, samples from San Felix, San Ambrosio and Robinson Crusoe show a moderate Dupal signature³, with relatively high ²⁰⁷Pb/²⁰⁴Pb and ²⁰⁸Pb/²⁰⁴Pb ratios for a given ²⁰⁶Pb/²⁰⁴Pb ratio (Fig. 3). The San Felix samples plot well below the Nd-Sr mantle array, whereas basalts from Robinson Crusoe plot approximately within the mantle array, although on the low side (Fig. 2a). Other volcanic samples which plot below the Nd-Sr mantle array include basalts from St Helena¹⁶, the New England Seamounts¹⁷, Tubuaii¹⁸ and various volcanics from continental settings such as the Leucite Hills19, the Permian Oslo Rift20 and the Scottish Tertiary basalts^{21,22}.

Contamination of mantle-derived magmas at relatively shallow levels by old, granulitic crustal materials^{21,22} tends to produce similar deviations to the low side of the Nd-Sr oceanic array, but this is not a likely explanation for islands in an oceanic setting such as San Felix. Sources for oceanic islands with radiogenic Pb signatures such as San Felix and St Helena cannot have been produced by recycling of upper continental crust into the mantle, as this would displace the data along or to the right of the Nd-Sr mantle array²³ (Fig. 2a). An alternative hypothesis, similar to those of Vollmer et al.¹⁹ for the Leucite Hills volcanics and of Menzies and Wass²⁴ for the Kiama xenoliths, suggests that sources of volcanics plotting below the Sr-Nd mantle array were created during an ancient mantle enrichment event in which depleted upper mantle was metasomatized or modified by lightrare-earth-element-enriched, Rb-poor agents. In the case of islands with radiogenic Pb signatures, this metasomatizing agent would also need to have high U/Pb ratios.

The number of 'components' proposed for oceanic mantle basalt sources has steadily increased over the past few years; at least four now seem to be needed^{25,26}, and as many as five have been proposed^{2,27}. Although there is some agreement as to the isotopic signatures of these components, their identification with reservoirs of specified genesis is still controversial. The depleted upper mantle (DMM²⁶) is generally acknowledged to be the source region for mid-ocean-ridge basalts (MORB). The St Helena-type component (HIMU²⁶) is variously identified with ancient subducted oceanic crust^{4,27,28}, metasomatized mantle²⁵ or lower mantle which has lost Pb to the core²⁹⁻³¹. The other two necessary components have enriched isotopic signatures ($\varepsilon_{\rm Nd}$ < bulk earth): one, represented by the Walvis Ridge³² is called EM I²⁶; the other¹⁶, represented by Samoa and the Society islands, is called EM II²⁶ (see Fig. 2). These enriched mantle sources have been variously ascribed to mantle metasomatism^{31,33}, subduction of sediments or continental crust^{16,23}, subduction of altered oceanic crust^{27,28} or delamination of subcontinental lithosphere³⁴. Other reservoirs, with characteristics intermediate to the above four may exist as well (such as primitive undepleted mantle^{35,36}).

As discussed above, the San Felix data extend unusually far below the Nd-Sr array (Fig. 2a) and might be interpreted as evidence for a new mantle component, or as evidence that EM I is an end-member to San Felix, rather than to Walvis Ridge. However, the Sr-Pb plot (Fig. 2b) clearly shows that San Felix does not have ²⁰⁶Pb/²⁰⁴Pb ratios suitable for EM I. Rather, it is likely that San Felix is itself a mixture of EM I- and HIMU-type sources. Hart et al.³⁷ have shown that the lowest-Nd samples from Tubuaii, St Helena, New England seamounts, Comores,



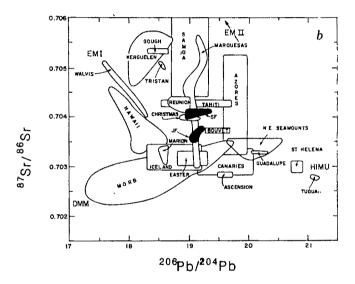


Fig. 2 Nd-Sr (a) and Sr-Pb (b) isotope plots showing San Felix, San Ambrosio and Robinson Crusoe basalt data in comparison with fields for other oceanic island basalts (see refs 2-4). Sample numbers as in Table 1. JF, Juan Fernandez field (individual samples shown in expanded inset in a); SF, San Felix/San Ambrosio data; MORB, mid-ocean-ridge basalts. Locations of four possible endmember mantle components (DMM, HIMU, EM I, EM II) are from ref. 26; see text for discussion. In a, note the linear arrangement of the lowest extensions of the fields for Tubuaii, St Helena, New England seamounts, San Felix and Walvis Ridge. These low-Nd samples also lie on a line in b.

San Felix and Walvis Ridge define a single linear vector in Sr-Nd-Pb space, originating on the mantle plane⁴ near Tubuaii and extending downwards to Walvis. This group of islands shows intra-island isotopic arrays which do not lie along this HIMU-EM I vector, but which extend upward from it toward the mantle plane (though not toward any common end-member on the plane). The implication is that each of these island suites contains a pure (though variable) mixture of HIMU and EM I, and that this mixing preceded the mixing with other components which generated the observed intra-island arrays. In this context, the Juan Fernandez basalts, which lie close to the mantle plane, represent the second mixing end-member of the San Felix-San Ambrosio array. Although this does not settle the question of how the various mantle components came into being, it does suggest that EM I and HIMU are contiguous and related in an evolutionary or kinematic sense, relative to the EM II and DMM components. One scenario would place the EMI and HIMU

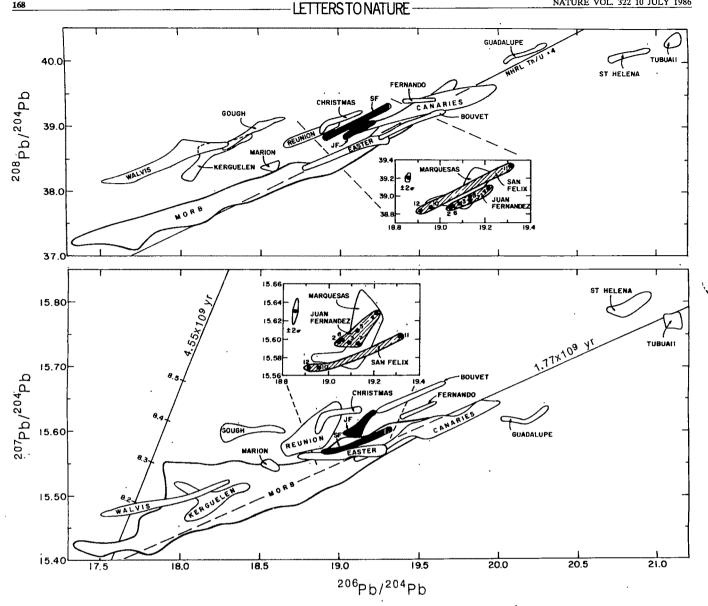


Fig. 3 Pb-Pb-Pb isotope plot showing San Felix, San Ambrosio and Robinson Crusoe data in comparison with fields for other oceanic islands (refs 2-4). JF, Juan Fernandez; SF, San Felix/San Ambrosio; individual data points are shown in expanded insets, with sample numbers as in Table 1; 20 precision estimates are also shown. The Northern Hemisphere reference line (NHRL) of Hart³ is shown for reference, as is a 4.55×10^9 yr geochron (with single-stage μ values indicated at tick-marks). Note that the San Felix/Juan Fernandez data overlap with the data for the Marquesas Islands¹⁸, both in this plot (inset) and in Fig. 2b; however, no overlap exists in Fig. 2a. As in Fig. 2, the low-Nd island samples are also linearly aligned in Pb-Pb-Pb space, (the New England seamount data is not shown on this plot, to avoid graphic confusion). This Tubuaii-Walvis array in fact defines a remarkable 'cross-array' on a 208 Pb/204 Pb - 206 Pb/204 Pb plot, which also includes the fields of a number of 'normal'-Sr-Nd islands.

components in the subcontinental lithosphere; delamination of this lithosphere, followed by mixing with other mantle components, could provide the mixing chronology outlined above³⁷.

We thank H. Banks (Smithsonian Institution) for providing the San Felix samples and K. Burrhus, M. Lezie, A. Gray and P. Guise for excellent technical support. This research was supported by NSF grant EAR 83-08809 (S.R.H.) and by NERC (D.C.G.).

Received 23 December 1985; accepted 1 April 1986.

- 1. Dupré, B. & Allègre, C. J. Nature 303, 142-146 (1983).
- White, W. M. Geology 13, 115-118 (1985).
 Hart, S. R. Nature 309, 753-757 (1984).

- A. Zindler, A., Jagoutz, E. & Goldstein, S. Nature 298, 519-523 (1982).
 Willis, B. & Washington, H. S. Bull. geol. Soc. Am. 35, 365-384 (1924).
 Richards, A. F. Catalogue of Active Volcanos Vol. 14, 41-44 (International Volcanological Association, Rome, Italy, 1962).

- Association, Rome, 11814, 1902.

 7. Fitzroy, R. Ř. geogr. Soc. Lond. J. 6, 311-343 (1836).

 8. Morales, V. W. J. thesis, Univ. del Norte, Chile (1985).

 9. Booker, J., Bullard, E. C. & Grasty, R. L. Geophys. J. R. Astr. Soc. 12, 469-471 (1967).

 10. Baker, I. Bull. geol. Soc. Am. 80, 1283-1310 (1969).

- 11. Baker, P. E., Gass, I. G., Harris, P. G. & Le Maitre, R. W. Phil. Trans. R. Soc. A256, 439-578
- (1969). 12. MacDonald, G. A. & Katsura, T. J. Petrol. 5, 82-133 (1964).
- Feigenson, M. D., Hofmann, A. W. & Spera, F. J. Contr. Miner. Petrol. 84, 390-405 (1983).
 Chen, C.-Y. & Frey, F. A. Nature 302, 785-789 (1983).
 MacDonald, G. A., Abbott, A. T. & Peterson, F. L. Volcanos in the Sea: the Geology of
- Hawaii (University of Hawaii Press, Honolulu, 1983).

 16. White, W. M. & Hofmann, A. W. Nature 296, 821-825 (1982).

 17. Taras, B. D. & Hart, S. R. Chem. Geol. (in the press).

 18. Vidal, Ph., Chauvel, C. & Brousse, R. Nature 307, 536-538 (1984).

- Vollmer, R., Ogden, P., Schilling, J.-G., Kingsley, R. H. & Waggoner, D. G. Contr. Miner. Petrol. 87, 359-368 (1984).
- Jacobsen, S. B. & Wasserburg, G. J. U.S. geol. Surv. Open File Rep. 78-701, 194-196 (1978).
 O'Nions, R. K., Carter, S. R., Evensen, N. M. & Hamilton, P. J. A. Rev. Earth planet. Sci.
- O'Niolis, R. N., Carter, S. R., Evenisch, N. M. & Hamilton, P. J. A. Rett Earth planet. Sci. 7, 11-38 (1979).
 Thirlwall, M. F. & Jones, N. W. in Continental Basalts and Mantle Xenoliths (eds Hawkesworth, C. J. & Norry, M. J.) (Shiva, Nantwich, 1983).
 Cohen, R. S. & O'Nions, R. K. Earth planet. Sci. Lett. 61, 73-84 (1982).
 Menzies, M. A. & Wass, S. Y. Earth planet Sci. Lett. 65, 287-302 (1983).
 Tatsumoto, M., Unruh, D., Stille, P. & Fujimake, H. Proc. 27th int. geol. Congress 11,

- 485-501 (1984).
- 26. Zindler, A. & Hart, S. A. Rev. Earth planet. Sci. 14, 493-571 (1986).
- Allègre, C. J. & Turcotte, D. L. Geophys. Res. Lett. 12, 207-210 (1985).
 Hofmann, A. W. & White, W. M. Earth planet. Sci. Lett. 57, 421-436 (1982).
- Vidal, Ph. & Dosso, L. Geophys. Res. Lett. 5, 169-172 (1978).
 Allegre, C. J., Brevart, O., Dupré, B. & Minster, J. Phil. Trans. R. Soc. A297, 447-477 (1980).

- 31. Vollmer, R. Nature 270, 144-147 (1977).
- Richardson, S. H., Erlank, A. J., Duncan, A. R. & Reid, D. L. Earth planet. Sci. Lett. 59, 327-342 (1982).
- Menzies, M. & Murthy, V. R. Am. J. Sci. 280A, 622-638 (1980)
- McKenzie, D. & O'Nions, R. K. Nature 301, 229-231 (1983) DePaolo, D. J. & Wasserburg, G. J. Geophys. Res. Lett. 3, 743-746 (1976).
- Schilling, J. G. Nature 242, 565-569 (1973).
- 37. Hart, S., Gerlach, D. C. & White, W. M. Geochim. cosmochim. Acta (in the press).
- 38. Hart, S. R. & Brooks, C. Contr. Miner. Petrol. 61, 109-128 (1977).
 39. Richard, P., Shimizu, N. & Allègre, C. J. Earth planet. Sci. Lett. 31, 269-278 (1976).
- Mannes, G., Minster, J.-F. & Allègre, C. J. Earth planet. Sci. Lett. 39, 14-24 (1978). Todt, W., Cliff, R. A., Hanser, A. & Hofmann, A. W. Terra Cognita 4, 209 (1984).
- Plate Tectonic Map of the Circum-Pacific Region (American Association of Petroleum Geologists, Tulsa, 1981).

Bacterial scavenging of Mn and Fe in a mid- to far-field hydrothermal particle plume

James P. Cowen*, Gary J. Massoth & Edward T. Baker

Pacific Marine Environmental Laboratory, National Oceanographic and Atmospheric Administration, Seattle, Washington 98115-0070, USA

* Present address: Hawaii Institute of Geophysics, University of Hawaii, 1000 Pope Road, Honolulu, Hawaii 96822, USA

The horizontally advected plumes which originate from buoyant hydrothermal fluid discharges and subsequently mix with entrained ambient sea water have been detected hundreds of kilometres from their vent sources by distinctive chemical hydrothermal tracers such as ³He, Mn and Fe (refs 1-6). Non-conservative plume tracers, such as Mn and Fe, undergo dynamic oxidation-precipitation reactions as the plume is advected away from the vent sources^{1,4,7,8}. Although some of these transformations may be mediated by microbial activity^{9,10}, hydrothermal plumes have largely escaped microbiological examination beyond tens of metres from their vent origins^{11,12}. Microbe-metal interactions in a hydrothermal plume were specifically addressed during our recent expedition (Vent-Plume '85) to the southern Juan de Fuca Ridge (SJFR). The early results, reported here, provide strong evidence of major microbiological influence over Mn scavenging and particulate-Mn distributions.

Microbiological studies of deep-sea hydrothermal vents have been concerned primarily with defining the metabolic processes involved and measuring the magnitude of chemosynthetic productivity (for a review see ref. 13); only a few studies have addressed microbe-metal interactions 11,14. Nearly all of these studies have been confined to the immediate vicinity of the vents. Recently, however, far-field hydrothermal influence has been suggested in bacterial capsule-metal (Mn and Fe) interactions within 50 km of the East Pacific Rise (EPR) at 20° N (ref. 9). Even more recently, elevated microbial biomass has been reported in hydrothermal plumes 100 m above the SJFR vent field10

Fig. 1 Total suspended matter (TSM) isopleths (in µg l⁻¹) for CTD 6 horizontal tow; the horizontal axis represents the perpendicular distance from the valley axis. The sawtooth pattern (dashed) shows the tow-path. The inset shows the relative orientation of CTDs 5 and 6 and the axis of the SJFR (the circle indicates the approximate location of the 4.5-km vertical profile shown in Fig. 3A, B). The arrow marks the plume lateral boundary, and corresponds to similar arrows in Fig. 3C, D. TSM values were derived by the normalized conversion of relative light-scattering values.

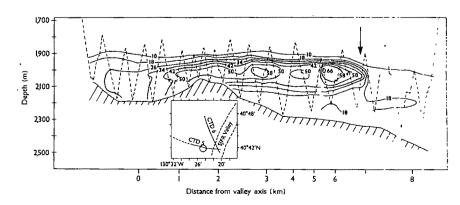
In the present study, the extensive plume (see Fig. 1) emanating from the SJFR axial valley, an area of documented hydrothermal activity¹⁵⁻¹⁸, was tracked in real time with a sensitive electronics package⁶; a rosette of 30-litre Niskin sample bottles was used to sample the plume selectively. Sea water was collected within the plume vertical maximum at distances of 0.9-8.2 km west of the SJFR axial valley, as well as from a vertical cast taken 4.5 km west of the valley (Fig. 1). Samples were analysed for numbers of metal-depositing and total bacteria (Fig. 2A, B; refs 9, 19) and total particulate Fe and Mn (ref. 20); individual particles were also analysed by transmission electron microscopy-energy dispersive X-ray spectrometry (TEM-EDS⁹). The TEM-EDS analyses show that most of the total suspended particulate Fe is present as amorphous hydrous Fe-oxide precipitates (Fig. 2C, D, 3); thus, estimates of relative background Fe-precipitate abundance were made from TEM sections.

Measurements of total suspended matter (TSM) concentrations indicate the depth of the well-defined plume maximum (2,050-2,150 m) at 4.5 km from the nearest hydrothermal source (Figs 1, 3A). Temperature (not shown), dissolved Mn, and particulate Fe anomalies verified the hydrothermal origin of the plume (Fig. 3A). Maxima in the numbers of total bacteria (Fig. 3A) and in two independent biochemical indicators of biomass (ATP and lipopolysaccharides; C. Winn and J.P.C., unpublished data) clearly coincide with the plume depths. The vertical profile of bacterial capsule numbers is less consistent than, but similar to, the corresponding particulate Mn profile: both show generally elevated values at plume depths, increasing towards the bottom (Fig. 3B). Capsules are distinguished by the tremendous surface areas of the extracellular polymer matrices and by the heavy-metal deposits associated with them (Figs 2A, 3A; refs 9, 21).

A horizontal profile through the off-axis plume maximum showed consistently high particle and Fe-precipitate concentrations up to 6.9 km away from the axial valley, beyond which they decline rather sharply (Fig. 3C). Capsule numbers remain high out to a distance of 7.5 km, with a possible gradual decline moving off-axis. Capsule numbers in the first 7.5 km correspond to the maximum values of the vertical profile taken at 4.5 km from the axis (Fig. 3B).

X-ray microanalysis of individual particles revealed large deposits of Mn and Fe associated with the bacterial capsules (Fig. 4A). No other type of plume particle examined so far shows TEM-EDS-detectable (>1,000 p.p.m.) Mn (Fig. 4A). Microanalysis of the common Fe precipitates showed that large concentrations of Mn are not incorporated during the spontaneous chemical precipitation of iron. Furthermore, capsule Mn deposits increase with distance from vents, whereas Fe deposits decrease (Fig. 4A). Such trends are consistent with the total particulate Fe and Mn data (Fig. 3C). These results, together with the high concentration of capsules in the plume. indicate that the bacterial capsules effectively scavenge hydrothermal Mn and thereby influence the partitioning of Mn in the plume.

Radiotracer experiments (Fig. 4B) and elevated microbial



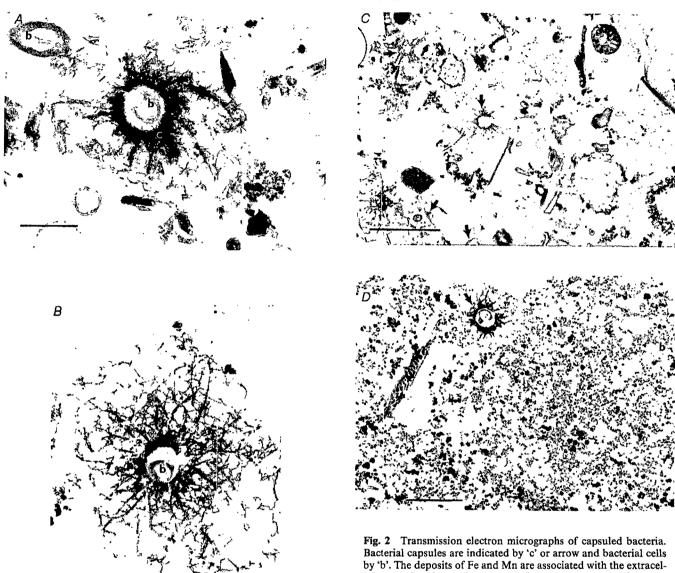


Fig. 2 Transmission electron micrographs of capsuled bacteria. Bacterial capsules are indicated by 'c' or arrow and bacterial cells by 'b'. The deposits of Fe and Mn are associated with the extracellular matrix of organic polymers (capsule or glycocalx). A, B: Scale bars, 1 μm. Lower-magnification micrographs (C, scale bar, 4 μm; D, scale bar, 2 μm) reveal the low (C) or high (D) relative abundance of amorphous Fe precipitate. Bacterial capsules are present in both C and D.

biomass at plume depths suggest that microbial metabolic activity enhances Mn scavenging. Ehrlich¹⁴ has found that some vent microbial mat bacteria exhibit Mn²⁺ oxidizing activity which is associated with cell envelopes and is peculiar to bacteria from vent environments. We do not know whether such activity extends to the capsules discussed here. Alternatively, the observed metal deposition may be non-enzymatic or proceed from some form of metabolic involvement to a predominantly inorganic process.

On the other hand, capsules probably do not have a major role in Fe scavenging or particulate Fe distributions within the plume extending from the axial valley to at least 7 km off-axis. The dominant presence of the amorphous hydrous Fe-oxide precipitates overwhelms the capsule Fe contributions in this portion of the plume. The absence of significant metabolically enhanced ⁵⁹Fe uptake (Fig. 4B) reflects this. Unfortunately, the radiotracer experiments cannot be extended to elucidate the specific mechanism of Fe deposition onto the bacterial capsules. Nevertheless, we postulate that the structural and chemical nature of the capsules themselves may be responsible for the

deposition^{9,22}. The additional involvement of continuously synthesized or recycled enzymes, chelators or other Fe-binding factors may be unnecessary. The occurrence in sediments of a high percentage of empty capsules with elevated Fe and Mn deposits relative to suspended capsules adds indirect evidence in support of passive or surface-enhanced metal deposition⁹.

The origin of bacteria, and especially capsuled bacteria, in hydrothermal plumes is not clear. Greatly elevated biomass has been found in the emitted vent fluids at the Galapagos vent¹². However, Lupton et al.²³, using hydrographic data to characterize the origin of the hydrothermal plume which resides ~200 m above an active hydrothermal field on the Endeavor segment of the JFR^{24,25}, estimated that the plume layer was composed of at least 70% entrained water which had been transported from deeper in the water column. Capsuled bacteria appear to be enriched in near-bottom waters and surface sediments⁹. Furthermore, Fe- and Mn-encapsuled bacteria are common in microbial mats surrounding hydrothermal vents¹¹. It is conceivable, therefore, that the high numbers of capsuled bacteria found in the mid- to far-field plume of the SJFR originated, in part, from

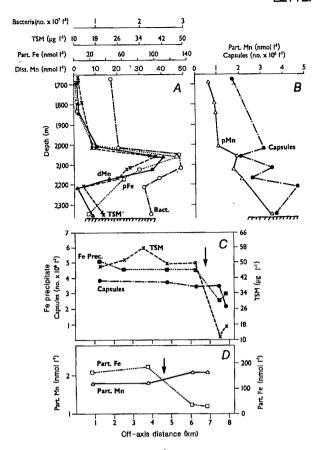


Fig. 3 A, B, Data from a vertical profile taken 4.5 km west of active hydrothermal vent fields, SJFR (40° 42.4' N, 130° 26.1' W), including: A, bacteria numbers, total suspended matter, particulate Fe and dissolved Mn; and B, capsule numbers and particulate Mn. C, Data from the plume maximum along tow-path CTD 6 include capsule numbers, Fe-precipitate relative abundance and particle concentration (TSM). Particulate Fe and Mn from tow-path CTD 5 are given in D. Arrows in C and D indicate the off-axis distance at which the respective tows intersect the plume lateral boundary, as indicated by the arrow in Fig. 1 in the case of CTD 6. Open and closed circles, bacteria and capsule numbers, respectively; open and closed triangles, particulate and dissolved Mn; open and closed squares, total particulate Fe and amorphous Fe precipitate; crosses, TSM concentrations. Bacterial numbers were obtained by filtering 60-100-ml subsamples through black Nucleopore filters (0.2 µm, 13 mm) and using epifluorescent (DAPI) direct counting methods; standard errors for 20 counting fields were 3-6%. Ratios of capsuled bacteria to total bacteria were determined by TEM. Bacteria numbers (DAPI) and capsule/bacteria ratios were determined from the same sample collection bottle for each data point. Capsule numbers were calculated by multiplying bacteria numbers by the ratio of capsules to total bacteria9; TSM concentrations were derived from light-scattering values (attenuation); and relative Fe precipitate abundance was estimated from TEM samples.

the entrainment of near-bottom waters in the vicinity of the - vents. Subsequently, deposition of Mn onto the entrained capsules could proceed within the dissolved-metal-rich plume waters. The latter model would also help to explain the overall vertical profiles for capsules, but not for uncapsuled bacteria. The origin of the latter could be the original emitted vent waters¹² or in situ activity.

Our data provide strong evidence of major microbiological contributions to the scavenging of Mn and particulate Mn distributions throughout off-axis hydrothermal particle plumes. The microbes provide exceptionally large and chemically suitable surface areas (the capsule) for metal deposition. There is also

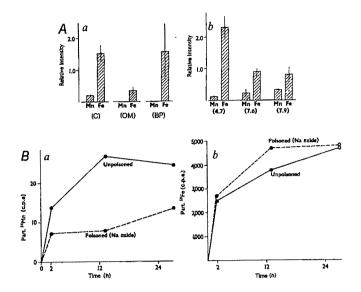


Fig. 4 A, Analysis of individual particles from hydrothermal plume maxima by micro-elemental analysis (TEM-EDS spectrometry); samples used were left completely unstained and analysed with a LINK EDS interfaced with a JOEL 100C STEM. a, Average relative Mn and Fe peak intensities for capsules (C), other minerals (OM) and background Fe precipitate (BP); b, capsule metal deposits at three distances (4.7, 7.6 and 7.9 km) west of the SJFR axial valley; error bars show ±1 s.e. B, Large-volume (6.5 litre) 54Mn and 59Fe uptake experiments using water from the hydrothermal particle plume maximum at 4 km west of the SJFR. Experiments were run in the dark at 2-4 °C; large (2-1) volumes were used for each subsample, providing highly representative samples of filtered particles. a, Particulate 54Mn (in counts per s) versus time; b, particulate 59Fe versus time. Note difference in vertical scales.

evidence that microbes may have a significant direct metabolic role in Mn, but not Fe, scavenging.

We thank Kamuron Gurol for help with sample collection; Lynda Wilkinson, Marie Cantino, Mary Carney and Carla Stehr for technical assistance; the National Marine Fisheries and Dale Johnson and John Baross of the University of Washington for use of their analytical facilities: and William Lavelle and Richard Feely of PMEL, NOAA for helpful reviews. This research was supported by Pacific Environmental Laboratory of NOAA and the National Research Council, National Academy of Sciences.

Received 17 January; accepted 18 April 1986.

1. Weiss, R. F. Earth planet. Sci. Lett. 37, 257-262 (1977).

Welss, R. P. Laun planet. Sci. Lett. 51, 297-202 (1977).
Bolger, G. W., Betzer, P. R. & Gordeev, V. V. Deep Sea Res. 25, 721-733 (1978).
Klinkhammer, G. P. Chem. Geol 29, 211-226 (1980).
Lupton, J. E. et al. Earth planet. Sci. Lett. 50, 1149-1161 (1980).

Lupton, J. E. & Craig, H. Science 214, 13-18 (1981). Baker, E. T., Lavelle, J. W. & Massoth, G. J. Nature 316, 342-344 (1985).

Edmond, J. N. et al. Nature 297, 187-191 (1982). Trefry, J. H. et al. Geophys. Res. Lett. 12, 506-509 (1985)

Cowen, J. P. & Bruland, K. W. Deep Sea Res. 32, 253-272 (1985).
 Winn, C. D., Karl, D. M. & Massoth, G. J. Nature 320, 744-746 (1986).

 Jannasch, H. W. & Wirsen, C. O. Appl envir. Microbiol. 41, 428-538 (1981).
 Karl, D. M., Wirsen, C. O. & Jannasch, H. W. Science 207, 1345-1347 (1980).
 Jannasch, H. W. & Nelson, D. C. in Current Perspectives in Microbial Ecology (eds Klerg, M. J. & Reddy, C. A.) (American Society for Microbiology, Washington, 1984).

Ehrlich, H. L. Envir. biogeochem. Ecol. Bull. 35, 357-366 (1983).

Delaney, J. R., Johnson, M. P. & Karsten, J. L. J. geophys. Res. 86, 11747-11750 (1981).

Normark, W. R. et al. Geology 11, 158-163 (1983).

Normark, W. R. et al. Eos 66, 116 (1985).
 Normark, W. R. et al. Eos 66, 116 (1985).
 Crane, K. et al. J. geophys. Res. 90, 727-744 (1985).
 Porter, K. G. & Feig, Y. S. Limnol. Oceanogr. 25, 943-948 (1980).
 Feely, R. A., Massoth, G. J. & Landing, W. M. Mar. Chem. 10, 431-453 (1981).
 Cowen, J. P. & Silver, M. W. Science 224, 1340-1342 (1984).
 Karsten, J. L. et al. Eos 65, 1111 (1984).

23. Hammond, S. E. et al. Eos 65, 1111 (1984) Lupton, J. E. et al. Nature 316, 621-623 (1985).

25. Ghiorse, W. C. & Hirsch, P. Arch. Mikrobiol. 123, 213-226 (1979).

Genetic selection for reproductive photoresponsiveness in deer mice

Claude Desjardins, F. H. Bronson & James L. Blank

Institute of Reproductive Biology, Department of Zoology, University of Texas, Austin, Texas 78712, USA

Seasonal breeding is common in mammals, particularly in habitats outside the tropics. Climate and availability of food are the ultimate factors that usually dictate the optimal time of year for a mammal to breed; however, day length (photoperiod) often serves as the proximal cue to signal the onset or cessation of seasonal reproduction¹. Some individuals in some populations of deer mice are reproductively responsive to photoperiod, while other individuals in the same population are not. As shown here, selection can dramatically alter the frequency of photoresponsiveness in a laboratory population in only two generations. To our knowledge this is the first demonstration of selection for reproductive photoresponsiveness in any mammal. By implication, some wild populations of deer mice must use multiple, genetic-based reproductive strategies, and the degree to which each such strategy is exhibited must be subject to rapid change in response to both seasonally and momentarily changing climatic and dietary conditions.

In the northern United States and southern Canada, members of the rodent genus *Peromyscus* usually exhibit a well-defined breeding season. Reproduction is largely limited to the spring and summer when food is plentiful, the climate benign and photoperiod long^{2,3}. Several northern populations of *Peromyscus* have been tested in the laboratory for reproductive responsiveness to photoperiod. Using similar techniques it has been found that reproduction is inhibited by short (winter) day lengths in most but not all of the individuals in these populations^{4–8}. This variation could be attributable to experiential factors encountered either prenatally or postnatally^{9–11}, or it could have a genetic basis. We explored this question by determining the degree to which reproductive photoresponsiveness could be manipulated by artificial selection.

Our test animals were derived from the third generation of a breeding colony of deer mice (*Peromyscus maniculatus nebrascensis*) originally collected near Rapid City, South Dakota (44° N, 103°W). The heterogeneity of this colony's response to photoperiod has been established previously: all individuals mature and breed on long day lengths (light:dark cycle of 16 h:8 h) but only some individuals reach sexual maturity and breed on short day lengths (light:dark = 8:16)⁴.

To begin our selection experiment, 40 pairs were mated on long day lengths, then the females were exposed to short day lengths early in pregnancy. The offspring of these females were defined as the parental generation, and they were weaned at 21-23 days old, maintained one per cage, and the sexes segregated in different animal rooms. The animals were maintained on short day lengths until 8 weeks of age, when their reproductive maturity was assessed. Females were laparotomized, their uteri were recorded as either infantile or partially or fully developed, and their ovaries were examined for corpora lutea as evidence of pubertal ovulation. Testes of males were measured externally using calipers. In each case only completely infantile or fully mature individuals were retained as breeding stock for the next generation.

After 10 weeks on long day lengths to allow sexual maturation of the animals that had been 'suppressed' by short day lengths, two genetic lines were initiated. A reproductively photoresponsive line was begun by mating animals that had remained infantile when reared on short day lengths, and a non-photoresponsive line was begun by mating animals that had matured despite being raised on short photoperiods. Using similar procedures

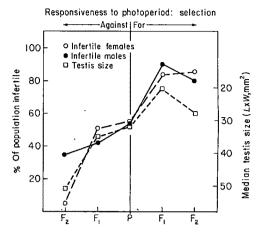


Fig. 1 Change in the frequency of reproductive photoresponsiveness in a laboratory population of deer mice after two generations of selection for and against this trait. The parental generation (P) consisted of 194 individuals of both sexes; 71 of these animals were discarded when they showed intermediate levels of reproductive development at 8 weeks old. Our non-photoresponsive line was begun with 24 pairs, which produced 68 offspring, of which 16 pairs were selected to produce the 43 individuals in the F₂ generation. Our photoresponsive line also was begun with 24 pairs, which produced 83 offspring, of which 16 pairs were selected to produce the 47 individuals in the F₂ generation. L, Length; W, weight.

the resulting two F_1 generations were again directionally selected to produce two F_2 generations.

Figure 1 shows that exposure to a short photoperiod inhibited the reproductive development of about half of the parental generation, while remaining animals were unresponsive to this cue. After two generations of selection only 5% of the females in the non-photoresponsive line had infantile ovaries and uteri when examined at 8 weeks old, as opposed to 86% in the responsive line $(P < 0.001, \chi^2)$. Comparable figures for males with infantile testes were 35% and 80% for the nonresponsive and responsive lines, respectively $(P < 0.01, \chi^2)$. Median testis size at 8 weeks of age also was changed markedly by selection (P < 0.001, median test).

The divergence seen in Fig. 1 confirms a genetic basis for at least some of the variation in reproductive photoresponsiveness that has been observed in deer mice. Indeed, the rapidity with which our two experimental lines diverged suggests that this trait has a high heritability. Two facts argue against the possibility that selection for rate of reproductive development itself was a factor in our experiment 12. First, our assessments of reproductive maturity were made at 8 weeks of age, which is well after the normal onset of fertility in this species. Second, during our selection experiment we always eliminated all animals showing an intermediate level of reproductive development.

Northern populations of deer mice are routinely and predictably exposed to severe winters in their natural habitats. In theory, a rigid use of photoperiod to limit breeding to the spring and summer months would seem to offer a great advantage in this region. Strict reliance on photoperiod would avoid wasted reproductive effort during the normally harsh winters; also, it would allow a long period of metabolic preparation for a short and intense breeding season. Further, it would enforce the many behavioural and physiological adjustments necessary for survival during harsh winters (for example, food hoarding, moulting, metabolic change¹³⁻¹⁵). Nevertheless, occasional winter breeding has been recorded at surprisingly high latitudes in deer mice¹⁶⁻¹⁸; this seems to occur either during climatically benign winters, or when some individuals are able to locate energetically favourable microenvironments characterized by an abundant food supply. Obviously, such breeding is done by animals that are unresponsive to short photoperiods.

Against this background then, our results suggest that selection for and against reproductive photoresponsiveness must be an exceptionally dynamic process in Peromyscus. Many northern populations of this genus must be composed of two or more phenotypes that vary genetically in their reproductive responsiveness to photoperiod. Animals that are not responsive to short day lengths could breed in the summer, but they would probably suffer high mortality during a typically harsh winter. On the other hand, should such individuals encounter a mild winter, or should they find a suitable microclimate during a harsh winter, they could reproduce and thereby add their genes to the population at a time when its size is at its lowest point. Thus, one can visualize a continual balancing of these selective forces, with the result being a highly labile trait whose frequency in a population could shift markedly over short periods of time.

The potential for dynamically changing, multiple reproductive strategies within Peromyscus populations has been suggested previously¹⁹. The present demonstration of successful selection for reproductive photoresponsiveness—the first in any mammal-reinforces this possibility. Indeed, the use of multiple reproductive strategies within a population is probably not limited to mid-latitudinal populations of Peromyscus, and may not even be limited to photoperiodic regulation^{8,20,21}. Most species of small rodents have short life expectancies, and most environments are relatively unpredictable for animals whose lifespans are measured in weeks or months. Reproductive success under such conditions must require great flexibility in reproductive strategies. The prevailing concept that the reproductive traits of a population have been exclusively tailored to the average, long-term physical and dietary characteristics of its habitat probably is not applicable to many populations of small mammals.

We thank Donald W. Caroll and Janet Darrow for their assistance with this research, and Janet Young for preparing the illustrations. This research was supported in part by grant AG00958 from the National Institute of Aging, grant HD-13470 from the National Institute of Child Health and Human Development, and NSF grant PCM 8208389.

Received 3 March; accepted 14 April 1986.

- 1. Sadleir, R. M. F. S. The Ecology of Reproduction in Wild and Domestic Mammels (Methuco, London, 1969).
- Millar, J. S. Spec. Publ. Carnegie Mus. nat. Hist. 10, 253-266 (1984)
 Bronson, F. H. Biol. Reprod. 32, 1-26 (1985).

Desjardins, C. & Lopez, M. J. in Testicular Development, Structure and Function (eds Steinberger, A. & Steinberger, E.) 381-388 (Raven, New York, 1980)

- Steinberger, A. & Steinberger, E. J. 361-386 (Raven, New 1018, 1980)

 5. Johnston, P. G. & Zucker, I. Biol. Reprod. 44, 983-989 (1980).

 6. Desjardins, C. Biol. Reprod. 24, 23A (1981).

 7. Lynch, G. R., Heath, H. W. & Johnston, C. M. Biol. Reprod. 25, 475-480 (1981).

 8. Desjardins, C. & Lopez, M. J. Endocrinology 112, 1398-1406 (1983).

 9. Hoffman, K. Biol. Reprod. 30 Suppl. 1, 55 (1984).

- 10. Horton, T. H. Can. J. Zool. 62, 1741-1746 (1984). 11. Stetson, M. H., Elliott, J. A. & Goldman, B. D. Biol. Reprod. (in the press)

Drickamer, L. C. Behav. neur. Biol. 31, 82-90 (1981).
 Vogt, F. D. & Lynch, G. R. Am. Zool. 18, 109 (1978)

- Zucker, I. in Biological Rhythms and Their Control Mechanisms (eds Suda M., Hayaisha, O. & Nakagawa, H.) 369-381 (Elsevier, New York, 1979).
- 15. Blank, J. L. & Desjardins, C. in Survival in the Cold (ed Heller, C) (Fisever, New York, in the press). Scheffer, T. H. J. Mammal. 5, 258-260 (1924)
- 17. Linduska, J. P. J. Wildl. Mgmt 6, 353-363 (1942). 18. Brown, H. L. Ecology 26, 308-309 (1945).

- Fairbairn, D. J. Can. J. Zool. 55, 862-871 (1977).
 Blank, J. & Desjardins, C. Am. J. Physiol. 248, R181-R189 (1985).
- 21. Murton, R. K., Westwood, N. J. & Thearle, R. J. P. J. Reprod. Fert. Suppl. 19, 563-577 (1973)

Hybrid formation between African trypanosomes during cyclical transmission

L. Jenni*, S. Marti*, J. Schweizer*, B. Betschart*, R. W. F. Le Paget, J. M. Wellst, A. Taitt, P. Paindavoine§, E. Pays§ & M. Steinert§

* Swiss Tropical Institute, Socinstrasse 57, CH-4051 Basel, Switzerland

† Department of Pathology, University of Cambridge, Cambridge CB2 1QP, UK

‡ Department of Genetics, University of Edinburgh, West Mains Road, Edinburgh EH9 3JN, UK

§ Department of Molecular Biology, Free University of Brussels, 1640 Rhode-St-Genese, Belgium

Trypanosomes of the species Trypanosoma brucei reproduce primarily by binary fission, but the frequency of enzyme electrophoretic variants in natural populations of T. brucei has provided indirect evidence for the existence of a sexual cycle¹⁻³. These studies, coupled with studies of restriction fragment length polymorphisms of genes encoding glycolytic enzymes⁴, have also provided evidence for T. brucei being diploid. Here we report direct evidence of gene exchange between two different clones of trypanosomes after mixed infection and full cyclical development in the tsetse fly vector.

Two cloned trypanosome populations (247-L and 386AA) were fed, either separately or as an equal mixture, through a membrane to different groups of tsetse flies (see Fig. 1). Flies showing the presence of metacyclic-stage trypanosomes (indicating completion of full cyclical development) were allowed to feed on mice and the resulting bloodstream infections (386AAA, 723C and 247LA) passaged to produce trypanosome lysates. In addition, a single clone (723CA) was isolated⁵ and then re-transmitted through a tsetse fly to yield the trypanosome populations 723CAB and 723CAE (Fig. 1). From an independent mixed transmission of the two parental clones, two further

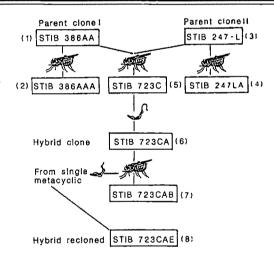


Fig. 1 Pedigree of mixed-infection experiment. Clone STIB 247-L is a derivative of the primary isolate STIB 247, obtained from Coke's hartebeest in the Serengeti National Park, Tanzania, in (ref. 8). Clone STIB 386AA is derived from TH 114/78 E (020), isolated in 1978 from a patient on the Ivory Coast9. Glossina morsitans centralis (ILRAD colony) were fed through a membrane on bloodstream trypanosomes from each clone mixed in equal proportions (total of 6×10⁷ trypanosomes per ml). Two further groups of G.m. centralis were fed at the same time on each of the two clones separately (6×10^7) trypanosomes 1). The flies were maintained at 28 °C in 75% relative humidity; they were membrane-fed three times a week on rehydrated pig blood¹⁰. All clones were established using the hanging-drop method of Van Meirvenne et al.⁵.

clones (723VI-L and 723VI-M) were derived directly from the metacyclic stage.

The two cloned stocks used in mixed tsetse fly transmission were screened for electrophoretic variation using starch gel electrophoresis or isoelectric focusing (IEF) and were found to differ in five enzymes—phosphoglucomutase (PGM), isocitrate dehydrogenase (ICD), alkaline phosphatase (AP), malic enzyme A (MEA) and malic enzyme B (MEB) (Fig. 2). Four of the enzymes show single bands of activity which differ in electrophoretic mobility between the two clones, while in the fifth enzyme (MEB), one clone shows a three-banded pattern and the other a single-banded pattern of identical mobility to the fastest band of the first clone.

The parental clones (numbered 1 and 3 in Fig. 1), the clones derived from separate cyclical transmission of these clones (2) and 4) and the clones derived from mixed transmission (6, 8 and 723VI-L) were screened by starch gel electrophoresis or IEF for the enzymes AP, ICD, PGM, MEA and MEB; Fig. 2 shows the results. The enzyme phenotypes of the parental clones remained unchanged after transmission through the tsetse fly. whereas the enzyme phenotypes of the stocks derived from the mixed transmission were found to differ from those of either parental clone and appeared to be heterozygous for the variant alleles for which the parental clones were homozygous (AP, ICD, PGM and MEA). These results are not due to the presence of mixtures of the parental clones in the tsetse-transmitted progeny, as populations 6, 7 and 8 are clones or directly derived from clones. Thus, mixing of the two parental stocks, followed by transmission through the tsetse fly, results in populations with non-parental phenotypes which are hybrid or heterozygous for parental homozygous markers. Identical results were obtained on analysis of clone 723VI-L, which is derived from a metacyclic form of an independent mixed transmission. These results clearly demonstrate that new, non-parental phenotypes (and therefore genotypes) can be generated by transmission of mixed trypanosome clones through tsetse flies. In addition, the transmission of either parental clone individually or the cloned hybrid progeny (clone 6) results in no alteration of the enzyme markers, implying that individual cloned stocks are stable in terms of phenotype and genotype after tsetse fly transmission.

Probes detecting restriction fragment length polymorphisms (RFLPs) in the genomic DNAs of the parental trypanosome clones were prepared as described in Fig. 3 legend. Southern hybridization of these probes with digests of DNA prepared from hypanosome clones 1, 2, 3, 4, 7, 9 and 10 revealed simple patterns of inheritance. Two probes, pDB9 (Fig. 3a,d) and pBG11 (not shown), revealed that the parental clones are homozygous and differ at the sites detected; the hybrid clones are heterozygous. Probe pBE2 (Fig. 3c) detected a family of fragments generated by EcoRI. The hybrid clones inherited all but one of these parental fragments. The results in Fig. 3c are compatible with most of the sites detected in the parental clones being homozygous, and those in the hybrid clones being heterozygous. Examples of markers that are heterozygous in one parent and homozygous in the other have been found using single-copy probes. Among these probes, pBE9 (Fig. 3b,e) detected an instance of the hybrids behaving as homozygotes and not inheriting all the fragments detected in the parents. This result, together with the non-inheritance of the arrowed band in Fig. 3c, demonstrates that the hybrids differ from both parents. The hybrid genotypes have also been detected in trypanosomes isolated from the field, suggesting that they occur naturally.

The DNAs of parental and hybrid trypanosome populations were analysed with DNA probes for variant surface antigen genes (see Fig. 4). The probes are specific for the genes encoding the AnTat 1.1 and 1.8 antigens which have been characterized previously in *T. brucei* stock EATRO 1125 (ref. 6). Both probes, in conjunction with a variety of restriction enzymes (not all shown here), provide restriction patterns that differ between the two parental clones; this result is in keeping with the considerable restriction polymorphism of antigen-specific sequences observed in *T. brucei*. As shown in Fig. 4, the mixed cyclical transmissions gave rise to 'hybrids' with different patterns of reassortment. The pattern revealed in the hybrids by the AnTat 1.1 probe (Fig. 4a) included all the fragments from both parents. The AnTat 1.8 probe (Fig. 4b) revealed a pattern combining all

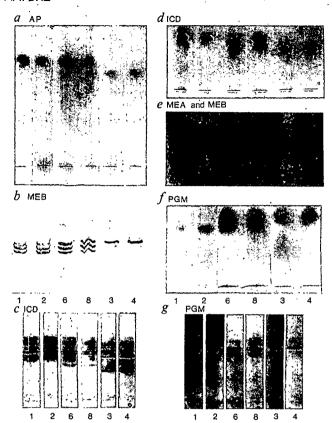


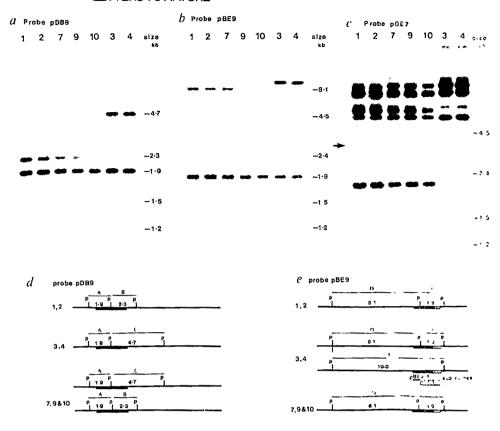
Fig. 2 Starch gel electrophoresis (a, d, e, f) and isoelectric focusing (b, c, g) of extracts of purified trypanosome clones 1-4, 6 and 8. After completion of electrophoresis or focusing, the gels were stained for alkaline phosphatase (AP, a), phosphoglucomutase (PGM, f and g), malic enzyme A (MEA and MEB, e), isocitrate dehydrogenase (ICD, c and d) and malic enzyme B (MEB, b). The methods and buffer systems used for these separations have been described previously 3,11,12 . The derivation and relationships of the trypanosome populations are shown in Fig. 1.

the fragments from parent 1 with only some fragments characteristic of parent 2. Clearly, some AnTat 1.8 gene family members (indicated by arrows in Fig. 4) were not transmitted to the progeny. The reassorted patterns were conserved through successive clonings and retransmission.

The results presented here directly demonstrate, for the first time, that genetic exchange occurs in T. brucei. Clearly, by mixing two trypanosome clones and transmitting the mixture through tsetse flies, trypanosome populations of non-parental phenotype and genotype are produced. With all the markers used, except for the gene probes AnTat 1.8 and pBE9, the progeny derived from mixed transmission of the two trypanosome clones were hybrid or heterozygous for parental markers. The restriction patterns of all these markers would fit a mendelian model of meiosis of the parental strains followed by fusion of a haploid stage, but other interpretations could be proposed to explain the results. The demonstration of genetic exchange in T. brucei potentially opens up a new field of trypanosome researchgenetic analysis—which should allow the genome to be manipulated. However, considerable further analysis is required to define the basic properties of this new genetic system and to determine whether meiosis occurs; such analysis is currently being undertaken.

This work was supported by grants from the Swiss NSF (to L.J.), the trypanosomiasis component of the UNDP/World Bank/WHO Special Programme for Research and Training in Tropical Diseases (L.J., M.S.), the Wellcome Trust (A.T.) the Overseas Development Administration of the UK (R.W.F.LeP.), the MRC, UK (J.M.W.), the Commission of the European

Fig. 3 Detection of RFLPs in parental and hybrid trypanosomes. a-c, The results of Southern hybridizations with probes detecting RFLPs in enzyme digests of parental (1-4) and hybrid (7, 9, 10) DNAs. In d and c, homozygous chromosome fragments are represented by a single line; heterozygous chromosome fragments are shown as double lines. Fragments detected by the probes in Southern blots of PstIdigested trypanosome DNAs are lettered A-F. Heavy bars indicate the cloned fragments used as probes. DNA preparations are numbered as in Figs 1, 2 and 4. a Is interpreted in d as indicating the presence of homozygous marker fragments in the parental clones, and heterozygous markers in the hybrids; pDB9 detects two fragments in the parental stocks 1-4. Fragment A is detected in trypanosome clones 1-4, fragment B in clones 1 and 2 and C in 3 and 4. The hybrids (7, 9 and 10) are all heterozygous for fragments B and C. In b the homozygous marker fragments in clones 7, 9 and 10 appear to have segregated from homozygous × heterozygous parental combinations (e). Probe pBE9 detects two fragments, D and E, in 1, 2, 7, 9 and 10 and an additional fragment, F, in the heterozygous parental stocks 3 and 4. Fragment F is detected because of



polymorphism at the Pst1 site in the cloned sequence. Pst1 subclones (pBE9-1 and pBE9-2) both hybridize to fragment F. The inheritance of a number of fragments detected with probe pBE2 (c). One fragment (arrowed in 1 and 2) is not inherited by hybrid clones 7, 9 and 10. Methods. Bloodstream-form trypanosomes were transformed to procyclic trypanosomes in Dulbecco's modified Eagle's medium (DMI M) containing 10% fetal bovine serum at 28 °C over irradiated fibroblast feeder layers (2,000 rad; Flow 2002 cells). Procyclic organisms were grown to late log phase in SDM 79 medium¹³, and DNA prepared using standard procedures^{14,15}. Genomic clones were prepared from a reference strain of T. brucei (8/18)¹³. Genomic DNA was digested with EcoRI and 2.5-5.1-kilobase fragments purified by electroclution from an agarose gel¹⁵. These fragments were ligated with EcoRI-digested pJSC73 (ref. 16) and used to transform Escherichia coli HB101 Colonies containing plasmids with inserts were detected by the colour selection method 16 and plasmids prepared by a rapid isolation procedure. After electrophoresis in 0.8% agarose, the plasmids were transferred to nitrocellulose filters and hybridized with nick-translated total genomic DNA from the reference strain $(1-2\times10^8 \text{ c.p.m.})$ per μg DNA)^{18,19}. Filters were washed three times for 30 min each in $2\times SSC$ plus 0.1°. SDS at 65 °C, and exposed to Fuji X-ray film at -70 °C for up to 5 days, with an intensifying screen. Recombinant plasmids yielding the weakest signals in our conditions identified single- or low-copy number sequences. Southern hybridization 8 of these probes to trypanosome DNAs from parental and hybrid clones digested with different restriction enzymes was used to detect RFLPs; filters were washed under conditions of high stringency (0.1 × SSC, 0.1% SDS at 65 °C) and autoradiographed.

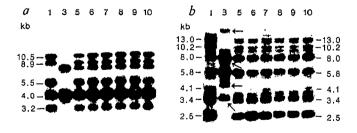


Fig. 4 Detection of restriction fragments specific for the genes encoding the antigens AnTat 1.1 (a) and AnTat 1.8 (b) in parental and hybrid trypanosomes. The different DNA preparations (1, 3, 5-8) are numbered according to the pedigree shown in Fig. 1. Tracks 9 and 10 contain DNAs from hybrid clones (723VI-L and 723VI-M) obtained in an independent mixed transmission experiment. The antigen-specific fragments of the hybrids (tracks 5-10) appear to be a combination of those of the two parental clones (tracks 1 and 3), except for the arrowed fragments in lane 3, which are not transmitted to the progeny.

Methods. The AnTat 1.8 and 1.1 probes were prepared as described previously6, then nick-translated and hybridized to Southern blots of genomic PstI digests, obtained as described in Fig. 3 legend.

Communities (M.S.), the ILRAD/Belgian Research Centers Agreement for Collaborative Research (M.S.) and the ILRAD/Swiss Research Centers Agreement for Collaborative Research (L.J.). We thank Dr R. Brun, D. Richner and C. Kunz for technical assistance with in vitro cultivation and Dr D. G. Godfrey for supplying the trypanosome stock 8/18.

Received 2 December 1985; accepted 15 April 1986.

- 1. Tait, A. Parasitology 86, 29-57 (1983).
- Gibson, W. C., Marshall, T. F. de C., Fidel, L. & Godfrey, D. G. Adv. Para at 18, 175 (1980).
- Tait, A. Nature 287, 536-538 (1980).
 Gibson, W. C., Osinga, K. A., Michels, P. A. M. & Borst, P. Melec. Birchim Forcus 16, 231-242 (1985).
- Van Meirenne, N., Janssens, P. G. & Magnus, E. Annis Soc heige Wed trep 55, 1 20 1975 Pays, E. et al. Nucleic Acids Res. 8, 5965-5981 (1980).
- Paindavoine, P. et al. Parasitology 92, 31-50 (1986).
- Geigy, R. & Kauffmann, M. Acta trop. 30, 12-48 (1973)
 Felgner, P. et al. Tropenmed. Parasit. 32, 134-140 (1981)
 Bauer, B. & Wetzel, H. W. Bull. ent. Res. 65, 563-565 (1976)

- Betschart, B., Wyler, R. & Jenni, L. Acta trop. 40, 25-28 (1933)
 Tait, A., Babiker, E. A. & Le Ray, D. Parasitology 89, 311-326 (1984)
 Brun, R. & Schónenberger, M. Acta trop. 36, 289-292 (1979)
 Williams, R. O., Young, J. R. & Majiwa, P. A. O. Nature 299, 417-420 (1993)
- McDonnell, M. W., Simon, M. N. & Studier, F. W. J. molec. B. et. 110, 112 (1977)
 Cordingley, J. S., Taylor, D. W., Dunne, D. W. & Butterworth, A. F. Gene 26, 25-3 (1983)
- 17. Holmes, D. S. & Quigley, M. Analyt. Biochem. 114, 193 (1981) 18. Southern, E. M. J. molec. Biol. 98, 503-513 (1975).
- 19. Maniatis, T., Jeffrey, A. & Kleid, D. C. Proc. natn. Acad. Sci. U. S. A. 72, 11. 5. 1134 (1971)

Analysis of human T-lymphotropic virus sequences in multiple sclerosis tissue

S. L. Hauser*†, C. Aubert*, J. S. Burks‡, C. Kerr§, O. Lyon-Caen||, G. de The¶ & M. Brahic*

- * Institut Pasteur, 75724 Paris Cedex 15, France
- † Department of Neurology, Massachusetts General Hospital, Boston, Massachusetts 02114, USA
- ‡ Rocky mountain MS Center, University of Colorado Medical School and the Denver VAMC, Denver, Colorado 80262, USA
- § Department of Neuropathology, Children's Hospital Medical Center, Boston, Massachusetts 02114, USA
- || Hôpital de la Salpêtrière, 75651 Paris Cedex 13, France
- ¶ Faculté Médecine Alexis Carrel, 69372 Lyon Cedex 8, France

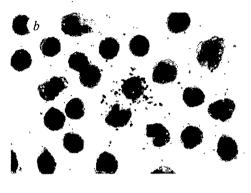
Several observations suggest that retroviral infection is involved in the pathogenesis of the human demvelinating disease multiple sclerosis (MS). First, lymphadenopathy-associated virus/human T-lymphotropic virus type III (LAV/HTLV-III), the agent of acquired immune deficiency syndrome (AIDS), has been shown to be neurotropic in man1. Second, the genetic organization of the lentivirus visna, which causes a chronic demyelinating disease of sheep, closely resembles that of LAV/HTLV-III². Recently, Koprowski and colleagues reported that MS is associated both with raised levels of circulating antibodies to HTLV-I and with the presence of HTLV-I-specific RNA within cell lines derived from the cerebrospinal fluid (CSF)3. Here we report that no HTLV-I-like or LAV/HTLV-III-like sequences can be detected, by in situ hybridization, in central nervous system (CNS) tissues from MS patients, and that no specific HTLV-I-like signal in peripheral blood mononuclear cells or in CSF cell lines is characteristic of MS. Furthermore, enzyme-linked immunosorbent assay (ELISA) analysis of circulating and CSF antibodies for HTLV-I reactivity fails to distinguish between MS and control groups.

Tissue blocks of active white matter lesions from 12 MS patients were selected for the presence of inflammation, macrophage infiltration and active demyelination; in some cases variable gliosis was also present (Fig. 1a). In situ hybridization was performed on serial sections, using a probe complementary to the long terminal repeat, pX, gag, pol and env regions of the HTLV-I genome, a probe complementary to the entire LAV/HTLV-III genome, and a control pBR322 probe. No specific RNA sequence was detected in any section following autoradiographic exposure times of 1 and 2 weeks.

Circulating mononuclear cells from 18 MS patients and 18 control individuals were separated by density gradient centrifugation, mounted on acetylated slides by cytocentrifugation and fixed. Table 1 shows the results of in situ hybridization with the HTLV-I and pBR322 probes. Cells were defined as positive when the number of grains counted was greater than five times background (Fig. 1b). It is noteworthy that both the HTLV-1 and pBR322 probes labelled a small number of cells $(10^{-4}-10^{-5}$ cells counted) in approximately half of both the MS and control samples. The morphology of cells labelled by both probes was heterogeneous and included small cells with scant cytoplasm, presumably lymphocytes, and, prominently, some larger cells with cloven or bi-lobed nuclei (Fig. 1c). Eosinophils, which were occasionally present in some samples, were also labelled by each of the probes; nonspecific labelling of this cell type during in situ hybridization has been noted previously4; no differences were present between the MS and control populations (Table 1).

CSF lines were derived from three individuals with active MS by stimulation with phytohaemagglutinin-P and by expansion with medium supplemented with interleukin-2 (Biotest). No positively labelled cells were detected in any of the three lines following in situ hybridization with the HTLV-I probe (10⁵ cells counted per sample) (Table 1). Analysis of peripheral blood





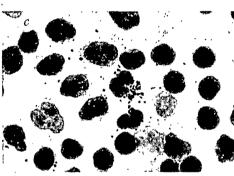


Fig. 1 a, Perivascular and parenchymal inflammation is present at the edge of an active MS plaque (haematoxylin-eosin). b, In situ hybridization of peripheral monuclear cells with the HLTV-I DNA probe. The figure shows a typical small round cell which was labelled by the HTLV-I probe. c, A peripheral blood mononuclear cell with a cloven nucleus is labelled by the HTLV-I probe. Methods. a, For this study, fresh frozen necropsy (n = 11) or biopsy (n=1) brain material was derived from patients with clinically definitive and pathologically confirmed MS. The MS material used is part of a larger collection which has been described previously⁶. Serial sections from each frozen tissue block were mounted on pretreated slides^{4,7}, fixed with ethanol acetic acid (3:1 vol/vol), and hybridized in situ as described elsewhere, including pretreatments with acid, heat and proteinase $K^{4,7}$. DNA probes for HTLV-I, LAV/HTLV-III and pBR322 sequences were labelled by nick translation with 35S to a final specific activity of 2×105 d.p.m. per ng. After washing, slides were dipped in Kodak NTB-2 emulsion, exposed for 11 days, developed and counterstained with a Giemsa stain. b, Cells were prepared by density gradient centrifugation, mounted on microscope slides with a cytocentrifuge and fixed in 0.5% formaldehyde, 0.5% glutaraldehyde, 0.1 M phosphate buffer pH 6.0, 1.6% glucose, 0.002% CaCl₂, 1.0% dimethyl sulphoxide⁸. In situ hybridization was performed as described above for brain

mononuclear cells from each of these patients had shown that several positive cells were detected with both the HTLV-I and pBR322 probes at the time that the CSF lines were established.

Serum antibody reactivity against HTLV-I was measured by ELISA, and no differences were found between a larger group of MS and control patients (Fig. 2). Serum from one MS patient was strongly reactive with HTLV-I, a finding confirmed by

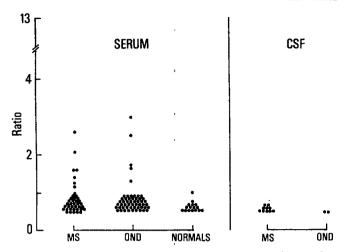


Fig. 2 Distribution of antibodies to HTLV-I in MS patients and controls. Coded serum and CSF samples were tested by the Biotech HTLV-I ELISA test using as antigen semipurified disrupted HTLV-I virions produced by the HUT-102 cell line9. The level of positivity was estimated by the ratio of absorbance between the test serum and the average of duplicate negative sera. OND, other neurologi-

immunoblot analysis. Sera from two other MS patients were weakly reactive by ELISA but negative by immunoblot. Serum from one control, a patient with amyotrophic lateral sclerosis, was weakly reactive against HTLV-I both by ELISA and immunoblot. CSF samples from 10 MS patients were uniformly unreactive to HTLV-I by ELISA (Fig. 2). CSF and brain material was available from one MS patient whose serum was reactive to HTLV-I by ELISA, and in this patient no CSF antibodies or viral RNA in brain tissue was found.

These results fail to confirm a recent report implicating infection with an HTLV-I-like virus in MS³. It is unlikely that this discrepancy is due to a difference in patient selection, as the MS population chosen for our study consisted of patients with both the relapsing-remitting and the chronic progressive forms of the disease and included patients from both Europe and the United States. The present study also represents the first analysis of HTLV sequences in MS brain material and the negative results obtained contrast with the finding that LAV/HTLV-III-specific sequences can be detected by in situ hybridization in the brains of some AIDS patients¹, a finding confirmed in our laboratory Vazeux and M.B., in preparation). The absence of circulating antibodies to HTLV-I in this population is also in striking contrast to the consistent findings of one of us (G.deT.) in patients with tropical spastic paraparesis⁵.

These results do not rule out the possibility that a small percentage of MS patients might be found to have an associated HTLV-I infection. In the present study, the one patient (of 42

Table 1 In situ hybridization of mononuclear cells in multiple sclerosis

		Specific r with H	
Source	Diagnosis	Present	Absent
Peripheral blood	Multiple sclerosis $(n=18)$	2	16
·	Control individuals $(n=18)\dagger$	3 .	15
Cerebrospinal fluid	Multiple sclerosis $(n=3)$	0	3

^{*} Specific hybridization with the HTLV-I probe was defined as those samples in which cells were labelled only with HTLV-I or in which the frequency of cells labelled with this probe was greater than that present with the control pBR322 probe.

tested) showing a strong serological response to HTLV-I was of French origin and not distinguishable on clinical grounds from the other MS patients studied. It also remains possible that an as yet undefined retrovirus is present in MS. In this regard, the extensive antigenic and sequence diversity which exists between different retroviruses makes it likely that other methods will be required to identify the presence of such agents in human disease states.

We thank Dr Masakazu Hatanaka for the generous gift of HTLV-I cloned DNA, Dr S. Wain-Hobson for the gift of LAV/HTLV-III cloned DNA, Drs Byron Waksman and Elisabeth Tournier for helpful discussions and B. MacMillan for technical assistance. This work was supported by the National Multiple Sclerosis Society, the Moseley Foundation of Harvard University, the Philippe Foundation, the Centre National de la Recherche Scientifique, the Foundation pour la Recherche Médicale and the Association pour la Recherche sur la Sclérose en Plaques. The MS tissue bank is supported by grants from the Veterans Administration and the National MS Society.

Received 27 March; accepted 21 April 1986.

- 1. Shaw, G. M. et al. Science 227, 177-182 (1985).
- Sonigo, P. et al. Cell 42, 369-382 (1985).
 Koprowski, H. et al. Nature 318, 154-160 (1985).
- 4. Haase, A. T., Brahie, M., Stowring, L. & Blum, H. in Methods of Virology (eds Maramorsch, H. & Koprowski, H.) 189-226 (Academic, San Diego, 1984).
- Gessain, A. et al. Lancet II, 407-410 (1985).
- 6. Hauser, S. L. et al. Ann. Neurol. (in the press).
- Brahic, M. & Haase, A. T. Proc. natn. Acad. Sci. U.S.A. 75, 6125-6129 (19°8)
- 8. Brahic, M., Haase, A. T. & Cash, E. Proc. natn. Acad. Sci. U.S.A. 81, 5445-5448 (1984)
- 9. Saxinger, C. & Gallo, R. C. Lab. invest. 49, 371-377 (1983).

KOPROWSKI ET AL. REPLY ON PAGE 178.

Lack of evidence for involvement of known human retroviruses in multiple sclerosis

Abraham Karpas*, Ursula Kämpf*, Åke Sidèn†, Michael Koch‡ & Sigrid Poser§

- * Department of Haematological Medicine, Cambridge University
- Clinical School, Hills Road, Cambridge CB2 2QL, UK † Department of Neurology, Karolinska Institute,
- Huddinge University Hospital, S-141186 Huddinge, Sweden
- ‡ VåC, Karlsborg S-54601, Sweden
- § Department of Neurology, Georg-August University, Göttingen, FRG

The recent report by Koprowski et al.1 that human T-cell lymphotropic retroviruses (HTLVs) may be involved in the development of multiple sclerosis (MS) has aroused much interest². The report was based largely on immunological evidence, using enzymelinked immunosorbent assays (ELISAs) with viral antigens or disrupted virions. We have accordingly sought confirmation by screening sera and cerebrospinal fluid (CSF) samples from MS patients against cell lines infected respectively with adult T-cell leukaemia (ATL) virus (ATLV/HTLV-I) of Japanese cells (MT-1 and MT-2 lines), our own isolate from British black patients with ATL, the MoT cell line which produce HTLV-II, and our own T-cell line containing a local isolate of acquired immune deficiency syndrome (AIDS) virus (C-LAV/HTLV-III). We have failed to find antibodies against these retroviruses in the sera or CSF. Furthermore, neither virus could be isolated from the peripheral white blood cells of two MS patients.

We have used the cell-based immunoperoxidase (IP) method, which we developed and found to be a highly sensitive test³ for antibodies to the AIDS virus and to ATLV/HTLV-I. In both tests, virus-infected cells which produce large quantities of the viral antigen were used. Each sample was tested in duplicate and also included a control (non-infected cells). The results of the IP reaction could be clearly distinguished by the naked eye

[†] Includes 11 individuals with a variety of non-MS neurological diseases and 7 normal controls.

and verified by examination under conventional low-power microscopy. This allows for the elimination of false readings associated with radioactivity of ELISA counters.

Table 1 lists the origin and clinical state of the sera and CSF and shows that we failed to detect antibodies to the oncoviruses (ATLV/HTLV-I, HTLV-II) or to the lentiviruses (LAV/HTLV-III) in any of the 46 sera and 15 CSF from MS patients.

In our preliminary studies we also tried to isolate a retrovirus from the peripheral white blood cells (WBC) of two patients with MS. The WBC were separated on Ficoll before being divided into two parts. One part was co-cultivated with fresh

Table 1 Results of retrovirus tests

		ATLV/ HTLV-I	HTLV-II	LAV/ HTLV-III
UK:	Paired, MS sera	0/15	0/15	0/15
OIL.	MS CSF	0/15	0/15	0/15
	Paired, OND sera	0/20	0/20	0/20
	OND CSF	0/20	0/20	0/20
Sweden: MS sera		0/21	0/21	0/21
Germ	any: MS sera	0/10	0/10	0/10
Japanese ATL sera		5/5	5/5	0/5
	h black ATL sera	3/3	3/3	0/3
Britis	h homosexuals' sera	0/61	0/10	61/61

MS, multiple sclerosis; CSF, cerebrospinal fluid; OND, other neurological diseases, including suspected but not confirmed MS; ATL, adult

human cord WBC and the other part was cultured with the Karpas T cells³. If ATLV/HTLV-I or HTLV-II were involved in MS, one might expect the cord WBC to become infected and express the viral antigen. In contrast, if an AIDS-like lentivirus was involved, one would have expected cell lysis of both the cord T cells and our T-cell line, or at least development of an antigen that reacted with sera containing antibodies to LAV/HTLV-III or ATLV/HTLV-I.

The two cultures of cord cells, and the two cultures of our T-cell line, which were co-cultivated with the WBC from the MS patients, were tested for the expression of ATLV/HTLV-I and LAV/HTLV-III after 2 and 4 weeks in culture, using the IP method. Neither the cord WBC nor our T-cell line expressed any antigens that reacted with human sera containing antibodies to ATLV or to LAV. Since sera of patients with ATLV contained antibodies which cross-reacted with HTLV-II, one would expect these sera to react with HTLV-II-infected cells if a related virus is involved in MS.

In summary, we failed to detect any antibodies against ATLV/HTLV-I and HTLV-II or LAV/HTLV-III in the sera and CSF samples from MS patients, nor could either of these viruses be isolated from the WBC. The claim to the presence of antibodies which react with the known human retroviruses is based on ELISA tests. We now know that some of the ELISA systems may give a high rate of false-positive results. The report that 37% of Israeli Falashas were ATLV/HTLV-I-positive has turned out to be wrong, probably due to the ELISA method⁴. Similarly, it has been repeatedly reported that some of the ELISA test kits used for AIDS screening give a high rate of false-positives^{5,6}. The results of such ELISA methods might cause premature claims to the involvement of HTLV in MS.

The possible viral aetiology of MS remains enigmatic; should a retrovirus eventually prove to be a pathogenic factor, it is likely to be distinct from the known human retroviruses.

We thank Professor P. Lachmann for providing some of the serum/CSF samples.

Received 4 March; accepted 21 April 1986.

- 1. Koprowski, H. et al. Nature 318, 154-160 (1985).
- Newmark, P. Nature 318, 101 (1985).
- Karpas, A., Gilsson, W., Bevan, P. C. & Oates, J. K. Lancet ii, 695-697 (1985).
 Karpas, A., Masyan, S. & Raz, R. Nature 319, 794-795 (1986).
 Prentice, R. L., Collins, R. J. & Wilson, R. J. Lancet ii, 274-275 (1985).
- Hernandez, J. M., Argelagues, E. & Canivell, M. Lancet I, 1389 (1985).

KOPROWSKI ET AL. REPLY: We are pleased that other investigators^{1,2} have undertaken the difficult task of searching for the involvement of retroviruses in multiple sclerosis. However, it is difficult for us to compare the results of our study³ with the data presented by Hauser et al. and Karpas et al. The first study used a commercially prepared kit for HTLV-I antibody while the second used visual detection of HTLV-I antibody by immunoperoxidase on infected cells. The drawback of both these assays is that the concentration of the HTLV group-specific (gag) antigen p24 in the kit is unknown and is considerably lower in cells than that used for our antibody determinations by ELISA. Despite this, the results of Hauser et al.1 with MS sera and normal controls are almost identical to the results shown in our Fig. 23. The discrepancy between our results and theirs with other neurological disease (OND) patients may be explained if we knew which OND patients were tested by Hauser et al.1. While Karpas et al.2 may find their immunoperoxidase test sensitive enough to detect antibodies in extremely high-titred AIDS⁴ and in eight leukaemia sera, we expect that this assay would not detect low-titred (HTLV-I cross-reactive) antibody found in MS patients. Because of the fluctuation of the HTLV p24 antibody levels, it does not make sense to search with low-sensitivity assays for antibodies in a single sample of either serum or cerebrospinal fluid of MS patients. 'False-positives' in our ELISA were excluded by specific competitive inhibition assays³.

The inability of Hauser et al.1 to detect retroviral sequences by in situ hybridization may be due to several factors: (1) use of complementary DNA probes rather than the much more sensitive riboprobes^{5,6}; (2) the stringency conditions under which the test was run (not mentioned by Hauser et al.1 but crucial in our assay); (3) restriction of sensitivity of the test by nonspecific hybridization with pBR322 plasmid alone. Hauser et al. provide neither positive controls showing the limitation of the sensitivity of the test nor controls confirming the presence of hybridizable RNA in the lymphocytes.

In the light of the considerable time and effort invested in the isolation of the human retroviruses I, II and III, it is not surprising that Karpas et al.2 failed to isolate the 'MS virus' from two randomly chosen MS samples in 4 weeks. We also emphasize points repeatedly made in our report that detectable antibodies are: present in low titre; cross-reactive, that is, not reactive specifically against the test HTLV; and, most importantly, present only sporadically in cerebrospinal fluid and sera during the course of disease. Karpas et al.² made a point that if HTLV is involved in MS, it is "distinct from the known human retroviruses". We agree and that was precisely our conclusion.

> HILARY KOPROWSKI* ELAINE C. DEFREITAS* MARY E. HARPERT MAGNHILD SANDBERG-WOLLHEIM‡ WILLIAM A. SHEREMATA§ MARJORIE ROBERT-GUROFFT CARL W. SAXINGERT FLOSSIE WONG-STAALT ROBERT C. GALLOT

* The Wistar Institute, 36th and Spruce Streets, Philadelphia, Pennsylvania 19104, USA † Laboratory of Tumor Cell Biology, National Cancer Institute, National Institutes of Health, Bethesda, Maryland 20892, USA ‡ Department of Neurology, University Hospital, University of Lund, S-22185 Lund, Sweden § Department of Neurology, University of Miami School of Medicine, Miami, Florida 33101, USA 1. Hauser, S. L. et al. Nature 322, 176-177 (1986).

- Karpas, A. et al. Nature 322, 177-178 (1986).
- 3. Koprowski, H. et al. Nature 318, 661 (1985). Karpas, A. et al. Lancet ii, 695 (1985).
- Cox, K. M. et al. Devl Biol. 101, 485 (1984).

6. Harper, M. E. et al. Proc. natn. Acad. Sci. U.S.A. 83, 771 (1986).

A functional T3 molecule associated with a novel heterodimer on the surface of immature human thymocytes

Ilan Bank*, Ronald A. DePinho†, Michael B. Brenner‡, Judy Cassimeris*, Frederick W. Alt† & Leonard Chess*

Departments of * Medicine and † Biochemistry, College of Physicians and Surgeons, Columbia University, New York, New York 10032, USA

‡ Division of Tumor Virology, Dana-Farber Cancer Institute, Harvard Medical School, Boston, Massachusetts 02115, USA

The known T-cell receptors (TCRs) involved in the recognition of antigen and major histocompatibility complex (MHC) molecules are glycoproteins comprised of polymorphic disulphide-linked α and β -chains 1-5. The genes encoding these chains are homologous to immunoglobulin genes and consist of V (variable), J(joining) and C (constant) regions that rearrange during development⁶⁻¹³ TCRs are expressed relatively late in thymocyte development and only in association with an invariant molecular complex of proteins termed T3 (refs 3, 14). Immature thymocytes do not express the TCR-T3 complex but do express messenger RNA encoding a third rearranging T-cell receptor-like gene, termed T γ (refs 13, 15–20). Here we report a clone of normal immature T4T8 human thymocytes, designated CII, which does not express mature mRNA for $T\alpha$ or $T\beta$ genes, but does express high levels of $T\gamma$ mRNA. This clone also expresses high levels of surface T3, and antibodies to T3 induce immunologically relevant functions in CII cells. Immunoprecipitation of CII surface-labelled proteins with anti-T3 co-precipitates a T3 molecular complex together with two additional and novel peptides of relative molecular mass (M,) 44,000 (44K) and 62,000 (62K).

To isolate immature T4⁻T8⁻ cells, human thymocytes were treated with anti-T4 and anti-T8 antibodies, and T4⁺ and T8⁺ cells were removed by rosetting with anti-mouse immunoglobulin-coupled red cells^{15,20-22}. The original thymocyte population contains cells expressing the T11, T3, T6, T4 and T8 antigens (Fig. 1a). In contrast, the non-rosetting population lacks T4- and T8-bearing cells but expresses the T11 and T6 surface antigens (Fig. 1b)^{20,23}. The T4⁻T8⁻ cells constituted 3.5% of the total thymocyte population and the number of these cells expressing T3 varied between 0 and 5%. To generate continuous cell lines, T4T8 cells were cultured with interleukin-2 (IL-2) and feeder cells. Over a short culture period (4 days), T4⁻T8⁻ cells lost expression of T6 and 80-90% of the cells expressed high levels of T3 (Fig. 1c). Cloning of these cells yielded several T3⁺T4⁻T8⁻ cell lines, one of which, CII, was studied in further detail. CII remains an IL-2- and feeder celldependent cell line which continues to be T3⁺, T4⁻ and T8⁻ (Fig. 1d). We confirmed the T4⁻T8⁻ phenotype of CII by Northern blot analysis. Neither the 3.0-kilobase (kb) T4 mRNA nor the 2.4-kb T8 mRNA was expressed in CII (refs 24, 25 and data not shown).

We next assessed whether the T3 molecule on CII cells was functional. Mature T cells can be activated by anti-T3 antibody in the presence of the phorbol ester 12-o-tetradecanoyl phorbol acetate (TPA) to secrete IL-2^{26,27}. When CII cells were stimulated with TPA in the presence of anti-T3 antibody (OKT3), significant amounts of IL-2 were produced (Fig. 2a). In contrast, TPA alone or anti-T11 (OKT11A) and TPA resulted in only minimal IL-2 release. In addition, CII, like mature T cells, could be activated to proliferate by OKT3 in the presence of monocytes²⁸. A monocyte-enriched (E⁻) population was irradiated and added to CII cells in the presence or absence of anti-T3 or control anti-T11 antibody. Anti-T3 but not anti-T11 induced a significant proliferative response which required the presence of E⁻ cells (Fig. 2b). Neither CII cells nor irradiated E⁻ cells

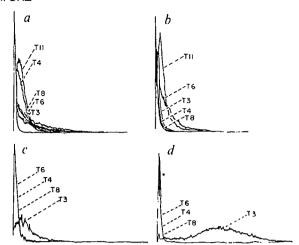


Fig. 1 Cytofluorographic analyses of fresh thymocytes (a), freshly selected T4 T8 thymocytes (b), cultured T4 T8 cells (c) and the clone CII (d) Methods. Thymus tissue was obtained from children 2-11 years old undergoing cardiac surgery, and single-cell suspensions were prepared. To obtain T4-T8- cells and the reciprocal T4+T8+ cells, unfractionated thymocytes were treated for 30 min at room temperature with a combination of OKT4 (1/1,000 of ascites) and OKT8 (1/2,000 of ascites), and rosetted with ox red blood cells coupled to rabbit anti-mouse IgG at a final haematocrit of 2.5% ^{34,35}. Rosetting (T4⁺ and T8⁺) cells were separated from non-rosetting (T4T8-) cells by Ficoll-Hypaque density centrifugation. The rosetting red cells were lysed with Tris-buffered ammonium chloride to obtain a pure $T4^+T8^+$ population²². $T4^-T8^-$ cells were cultured at 1×10^6 cells ml⁻¹ in the presence of 0.5×10^6 cells ml⁻¹ of irradiated (7,000 rad) B-lymphoblastoid cells, in a final volume of 2 ml in 12-well tissue culture plates (Costar). Recombinant IL-2 (100 U ml⁻¹; Hoffman-La Roche), and 1% phytohaemagglutinin (Gibco) were added. The final medium for all cultures was Iscove's modified Dulbecco's medium (Gibco) supplemented with 1% penicillin-streptomycin (Gibco) and 10% fetal calf serum (Hyclone), and cultures were grown in a humidified atmosphere with 5% CO, at 37 °C After 4 weeks of bulk culture, cells were cloned at limiting dilutions in 96-well round-bottom plates with lymphoblastoid feeders and expanded under conditions similar to those used in the initial bulk culture. For cytofluorographic analysis, 105 cells were incubated at room temperature with a 1/2,000 dilution of the appropriate antibodies (OKT11, OKT6, OKT4, OKT8 or OKT3) for 30 min. The cells were then washed and incubated for an additional 30 min at 4 °C with fluorescein-conjugated goat anti-mouse immunoglobulin (G/M FITC) (Cappel Laboratories) and washed. The cells were analysed on a Model 30-H Cytofluorograf (Ortho Instruments). The results shown represent analysis of 104 cells for each population as indicated

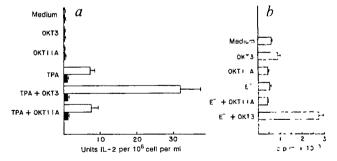


Fig. 2 Activation of CII cells by anti-T3 antibodies to secrete 1L-2 and proliferate. a, CII cells (open bars) or B-lymphoblastoid cells (closed bars) were washed and placed in 96-well microtitre plates in fresh medium at a concentration of 0.5 × 10⁶ cells ml⁻¹ in a final volume of 200 μl. TPA (Sigma) was added to the cultures at 5 ng ml⁻¹. OKT3 or OKT11A was added at a final concentration of 1/500 of ascites fluid. After 24 h, the supernatants were collected and added to the murine IL-2-dependent CTLL cell line²⁷. After overnight incubation at 37 °C in a humidified atmosphere with 5°s CO₂, the proliferation of CTLL was assessed by ³H-thymidine incorporation over an additional 6 h. A standard reference curve was obtained for each experiment, and the IL-2 units calculated as described previously³⁶. The results shown are expressed as units of IL-2 produced per 10⁶ cells ml ¹, and represent the mean±1 s.d. of triplicate wells. b, CII cells were washed and placed at 1×10⁶ cells in a volume of 200 μl in 96-well flat-bottom plates. E⁻ cells, obtained from normal donor peripheral blood mononuclear cells, were irradiated (2,000 rad) and added at 0.5×10⁶ cells ml⁻¹ (ref. 37) OKT3 and OKT11A were added at 1/500 dilution of ascites fluid. Plates were cultured as described previously. Proliferation was assessed after 48 h of culture by ³H-thymidine incorporation³⁷. The results shown represent the mean±1 s.d. of triplicate wells.

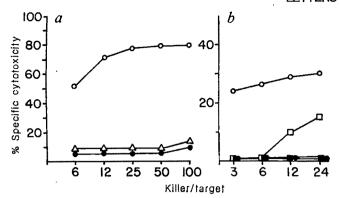


Fig. 3 Induction of cytotoxicity by OKT3 in CII cells. a, CII cells were added alone (\bullet), with OKT3 (O) or with OKT11A (\triangle) to 51 Cr-labelled U937 cells, and specific cytotoxicity was calculated (y-axis) at the indicated killer/target ratios. b, CII cells were added alone (solid symbols) or in the presence of OKT3 (open symbols) to 51 Cr-labelled U937 cells (circles) or 51 Cr-labelled K562 cells (squares). Methods. K562 and U937 cells were grown in culture medium containing

Methods. K.562 and U937 cells were grown in culture medium containing 10% fetal calf serum under culture conditions described in Fig. 1' legend. For each experiment, 10⁶ viable cells were removed from the cultures and treated with ⁵¹Cr-sodium chromate (Dupont), washed and placed (5,000 cells per well) in U-shaped 96-well plates (Costar). CII cells were added at the indicated killer/target ratios in a final volume of 200 μl. OKT3 and OKT11A (1/500 final dilution of ascites fluid) were added at the beginning of the assay. After 4 h of incubation of 37 °C in a humidified atmosphere containing 5% CO₂, 100 μl of the spun supernatants were removed and ⁵¹Cr content measured ³⁷. Specific cytotoxicity was calculated from the formula: specific cytotoxity = (experimental ⁵¹Cr release – spontaneous ⁵¹Cr release)/(total ⁵¹Cr release – spontaneous ⁵¹Cr release). Total ⁵¹Cr release was assessed by Triton lysis of the ⁵¹Cr-labelled cells.

alone proliferated. Since anti-T3 is also known to induce cytotoxicity in normal T cells, we studied its effect on the induction of killing by CII cells²⁹. We found that the addition of OKT3 to CII induced killing of ⁵¹Cr-labelled U937 macrophage targets (Fig. 3a). Untreated CII cells or CII cells treated with anti-T11 were not cytotoxic. In other experiments we found that anti-T3 induced CII cells to kill the natural killer cell target K562 (Fig. 3b). Taken together, these experiments demonstrate that antibody perturbation of the T3 molecule on CII results in the induction of immunological functions analogous to those observed in mature T lymphocytes.

Because the functional T3 molecule is physically associated with the T-cell receptor on mature T cells, it was of interest to determine whether the CII cells expressed mature $T\alpha$ and $T\beta$ mRNA, and to determine whether CII expressed Ty mRNA, known to be present in T4⁻T8⁻ murine thymocytes. Total RNA from CII cells as well as from thymocyte subpopulations (T4⁻T8⁻ and T4⁺T8⁺), mature T cells, B-lymphoblastoid cells and HeLa cells was assayed by Northern blotting procedures for hybridization to 32 P-labelled T α -, $T\beta$ - and T γ -specific complementary DNA probes (Fig. 4). HeLa cells and the lymphoblastoid cells did not express mature $T\alpha$, $T\beta$ or $T\gamma$ mRNA. In contrast, peripheral T cells, expressed the mature 1.7-kb $T\alpha$ mRNA and a mature 1.3-kb T β mRNA, but did not express T γ mRNA¹³. Freshly isolated T4⁻T8⁻ cells expressed Tγ mRNA as well as both the 1.3-kb mature T β mRNA and the 1.0-kb D-J(diversity-joining regions) β transcript. In addition, these cells expressed an immature 1.4-kb $T\alpha$ transcript but not the mature 1.7-kb $T\alpha$ mRNA¹³. The T4⁺T8⁺ thymocyte population, thought to contain cells at a more advanced stage of development, did not express Ty mRNA, but did express both the mature 1.3-kb $T\beta$ mRNA and to a lesser degree the 1.0-kb $T\beta$ transcript. We did not detect the 1.7-kb $T\alpha$ mRNA in the $T4^{+}T8^{+}$ population, but observed only the immature 1.4-kb $T\alpha$ transcript.

The CII cell line expressed high levels of $T\gamma$ mRNA but did not express the mature 1.3-kb $T\beta$ mRNA or the mature 1.7-kb $T\alpha$ transcript. However, CII cells did express the immature 1.0-kb $T\beta$ transcript and a faint band between 1.0 and 1.4 kb

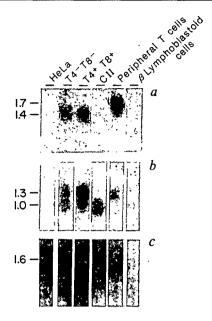


Fig. 4 Stage-specific expression of T-cell receptor (TCR) genes: a, α ; b, β ; c, γ . Approximately 6 μg of total RNA from each of the cell populations indicated was fractionated by formaldehyde/agarose gel electrophoresis, transferred to nitrocellulose or Nytran and assayed for hybridization to 32 P-labelled human $T\alpha$, $T\beta$ and $T\gamma$ cDNA probes (kindly provided by T.W. Mak and described elsewhere 6,38,39). Hybridization conditions were performed as described previously 40 .

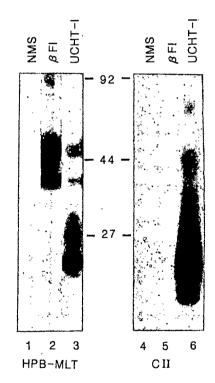


Fig. 5 SDS-PAGE analysis of T3 and T3-associated molecules from CII and HPB-MLT. ¹²⁵I-labelled detergent lysates from T-leukaemia cell line HPB-MLT and thymic clone CII were examined by SDS-PAGE. Immunoprecipitations were performed with nonspecific control antibody (normal mouse serum (NMS) in lanes 1 and 4, framework monoclonal antibody to the β -chain of the T-cell receptor (β FI) in lanes 2 and 5, and anti-T3 antibody (UCHT-1) in lanes 3 and 6 (ref. 29)).

anti-T3 antibody (UCHT-1) in lanes 3 and 6 (ref. 29)). Methods. 125 I-labelling was performed using the lactoperoxidase technique. Following radiolabelling, 10^7 lymphocytes were solubilized in Tris-buffered saline (pH 8) containing 1% Triton X-100. Lysates were immunoprecipitated using 1% I NMS, 1% pf I monoclonal antibody or 1% UCHT-1 monoclonal antibody. Immunoprecipitated proteins were resolved by SDS-PAGE (10.5% acrylamide) and radiolabelled species were visualized by autoradiography as described previously 14 .

which may correspond in part to the immature 1.4-kb $T\alpha$ transcript. Taken together, these data suggest a developmental progression of human $T\alpha$, $T\beta$ and $T\gamma$ gene expression similar to that observed in murine thymocytes, with γ genes expressed earliest, followed by β and then α gene expression^{13;15-17}. In this light, CII cells represent an early stage of thymocyte development in which γ genes are expressed in the absence of mature α and β gene expression.

The above data demonstrate that T3 surface expression in CII occurs in the absence of the expression of mature $T\alpha$ or $T\beta$ genes. Therefore, it was important to determine whether the T3 molecule on CII cells was physically associated with other surface proteins. For this, we immunoprecipitated 125 I-labelled surface proteins with anti-T3 as well as with antibodies to framework determinants of the β -chain Immunoprecipitated proteins were analysed by SDS-polyacrylamide gel electrophoresis (PAGE) under reducing conditions (Fig. 5). Immunoprecipitation of CII by anti-T3 revealed a T3 molecular complex (18-28K) that co-precipitated with two additional bands which migrated at 44K and 62K (Fig. 5, lane 6). In contrast, no bands were seen when CII was immunoprecipitated with β F1 (Fig. 5, lane 5). Immunoprecipitations of the control mature HPB-MLT cell line with anti-T3 revealed, as described previously, a T3 molecular complex co-precipitating with bands migrating at 40K and 49K (Fig. 5, lane 3)14. In addition, immunoprecipitation of HPB-MLT with BF1 revealed the 49K and 40K bands, representing the T α and T β chains¹⁴.

Our data demonstrate that the functional T3 molecule on the CII cells, although not associated with the $\alpha\beta$ heterodimer, is associated with a novel heterodimer of 44K and 62K. This structure is not seen on HPB-MLT cells (Fig. 5, lanes 2, 3) and has not been identified previously on human thymocytes or mature T cells. The finding of high levels of Ty mRNA expression in CII raises the possibility that one of the subunits of the 44/62K structure on CII could be encoded by the Ty gene. However, definitive designation of one of the subunits as a γ peptide must await amino-acid sequence analysis and comparison with deduced T γ protein sequence from CII T γ cDNA.

Surface expression of T3 is thought to mark a mature stage of T-cell development, and recent studies have suggested that surface T3 expression may depend on T α and T β expression^{26,31}. Our studies show definitively, however, that T3 can be expressed on immature thymocytes lacking $T\alpha$ and $T\beta$. Nevertheless, the concept that expression of surface receptor molecules may be essential for T3 surface expression may be correct, as CII cells do express a T3-linked 44/62K structure. Our studies, showing that antibodies to the T3 molecule associated with this heterodimer induce proliferation, IL-2 release and cytotoxicity, strengthen this idea by suggesting that the T3-44/62K complex on CII is functional. It has been speculated that precursor thymocytes may bear self-MHC receptors involved in the selection of the mature T-cell receptor repertoire intrathymically^{13,15,32,33}. If the CII cells described here do express self-MHC receptors, a candidate structure for this receptor is the T3-44/62K complex.

It is noteworthy that the 44/62K structure is not coimmunoprecipitated by anti-T3 antibodies from mature T cells¹⁴. This finding does not preclude its presence in a non-T3-linked form. Conceivably, mature T cells express a non-T3-linked 44/62K receptor, which might bind self-MHC molecules and participate in recognition of the antigen-MHC complex along with the T3-linked T-cell receptor. This hypothesis would permit independent interactions of the non-T3-linked 44/62K receptor with self-MHC. Such interaction would not necessarily induce autoreactivity because the T3 molecule may be essential for signal transduction26

We thank Dr T. W. Mak for $T\alpha$, $T\beta$ and $T\gamma$ cDNA probes and Dr F. Beverley for UCHT-1 monoclonal. Supported by NIH grants AI 14969 and AI 20698 to L.C.

Note added in proof: We have now immunoprecipitated solubil-

ized and 125 I-labelled proteins from C2 using anti-T3 and the anti-v-chain sera described by Brenner et al. 30. Immunoprecipitated proteins were analysed by SDS-PAGE under reducing conditions. The anti-y sera identifies the T3-associated 44K protein in CII.

Received 2 June; accepted 12 June 1986.

- 1. Allison, J. P., McIntyre, B. W. & Block, D. J. Immun. 129, 2293-2300 (1982).
- Haskins, K. et al. J. exp. Med. 157, 1149-1169 (1983).
 Meuer, S. C. et al. J. exp. Med. 157, 705-719 (1983).
- 4. Kappler, J. et al. Cell 35, 295-302 (1983).
- Meuer, S. C., Acuto, O., Hercend, T., Schlossman, S. F. & Reinherz, E. L. A Rev. Immun 2, 23-50 (1984).
- Yanagi, Y. et al. Nature 308, 145-149 (1984).
 Hedrick, S. M., Cohen, D. I., Nielsen, E. A. & Davis, M. M. Nature 308, 149-153 (1984). 8. Saito, H. et al. Nature 309, 757-762 (1984).

 9. Hedrick, S. M., Nielsen, E. A., Kavaler, J., Cohen, D. I. & Davis, M. M. Nature 308,
- 153-158 (1984).
- Fabbi, M., Acuto, O., Smart, J. E. & Reinherz, E. L. Nature 312, 269-271 (1984).
 Hannum, C. E., Kappler, J. W., Trowbridge, I. S., Marrack, P. & Freed, J. H. Nature 312, 65-67 (1984).
- 12. Sim, G. K. et al. Nature 312, 771-775 (1984).
- Kronenberg, M., Sim, G., Hood, L. E. & Shastri, N. A. Rev. Immun. 4, 529 591 (1986)
 Brenner, M. B., Trowbridge, I. S. & Strominger, J. C. Cell 40, 183-190 (1985)
- Raulet, D. H., Garman, R. D., Saito, H. & Tonegawa, S. Nature 314, 103-107 (1985).
 Samelson, L. E. et al. Nature 315, 765-768 (1985).
- 17. Trowbridge, I. S., Lesley, J., Trotter, J. & Hyman, R. Nature 315, 666-669 (1985).
 18. Chien, Y. et al. Nature 312, 31-35 (1984).
- 19. Saito, H. et al. Nature 312, 36-40 (1984)
- Reinherz, E. L. & Schlossman, S. F. Cell 19, 821-827 (1980).
 Mathieson, B. J. & Fowlkes, B. J. Immun. Rev. 82, 141-173 (1984).
 Thomas, Y. et al. J. Immun. 128, 1386-1390 (1982).
 Howard, F. P. et al. J. Immun. 126, 2117-2122 (1981).

- Howard, F. F. et al. J. Immun. 124, 293-104 (1985).
 Maddon, P. J. et al. Cell 42, 93-104 (1985).
 Littman, D. R., Thomas, Y., Maddon, P. J., Chess, L. & Axel, R. Cell 40, 23'-246 (1985).
 Weiss, A. et al. A. Reu. Immun. 4, 593-619 (1986).
 Hara, T. & Fu, S. M. J. exp. Med. 161, 641-656 (1986).
 Van Wauwe, J. P. & Goosens, J. G. J. Immun. 124, 2708-2713 (1980).
 Mentzer, S. J., Barbosa, J. A. & Burakoff, S. J. J. Immun. 135, 34-38 (1985)

- 30. Brenner, M. B. et al. Nature 322, 145-149 (1986).

- Ohashi, P. S. et al. Nature 316, 606-609 (1985).
 Zinkernagel, R. M. et al. J. exp. Med. 147, 882-896 (1978).
 Pernis, B. & Axel, R. Cell 41, 13-16 (1985).
 Kung, P. C., Goldstein, G., Reinherz, E. L. & Schlossman, S. F. Science 206, 34 '-349 (1979). 35. Reinherz, E. L., Kung, P. C., Goldstein, G. & Schlossman, S. F. J. Immun. 123, 2894-2895
- (1979).
- Gillis, S. & Smith, K. A. Nature 268, 154-156 (1977).
 Bank, I. & Chess, L. J. exp. Med. 162, 1294-1303 (1985).
 Yanagio, Y., Chan, A., Chin, B., Minden, M. & Mak, T. W. Proc. natn. Acad. Sci. U.S.A 82, 3430-3434 (1985).
- 39. Yoshikai, Y. et al. (submitted).
- Zimmerman, K. A. et al. Nature 319, 780-783 (1986).
 Gillis, S., Ferm, M. M., Ou, W. & Smith, K. A. J. Immun. 120, 2027-2032 (1978).
 Friedman, S. M., Hunter, S. B., Thomas, Y. & Chess, L. J. Immun. 125, 2202 2207 (1980).

Thy-1 functions as a signal transduction molecule in T lymphocytes and transfected B lymphocytes

Richard A. Kroczek, Kurt C. Gunter, Ronald N. Germain & Ethan M. Shevach

Laboratory of Immunology, National Institute of Allergy and Infectious Diseases, National Institutes of Health, Building 10, Room 11N311, Bethesda, Maryland 20892, USA

Thy-1, a glycoprotein of relative molecular mass 25,000 (25K), is a major constituent of the cell surface of mouse thymocytes, peripheral T cells and neurones1. In man, Thy-1 is present on neurones and on a small percentage of thymocytes, but is absent from peripheral T cells2. The amino-acid3,4 and complementary DNA⁵⁻⁷ sequences of Thy-1 indicate that it has a structure similar to an isolated V (variable region) domain of immunoglobulin⁴. Although the function of Thy-1 is unknown, the ability of different anti-Thy-1 monoclonal antibodies to activate murine T cells8, induce functional changes in neuronal cells in vitro 10 suggests that Thy-1 is involved in transmembrane signalling. We now show that crosslinking of murine Thy-1 triggers a rapid rise in the cytoplasmic free calcium concentration ([Ca2+]i), not only in murine T cells and Thy-1.2-transfected human T cells, but also in murine Blymphoma cells transfected with the murine thy-1.2 gene. These results indicate that the generation and transduction of the signal leading to the rise in [Ca2+]; is independent of the T-cell receptor and other T-cell-specific molecules. The preservation of the [Ca2+]1modulating function of Thy-1 in various lymphoid cells of two species further suggests that the necessary signal either originates in the Thy-1 molecule itself or is generated in concert with a highly conserved molecules(s) associated with Thy-1.

To define the cell surface and the intracellular requirements for signal transduction via Thy-1, several previously characterized cell lines which do not naturally express Thy-1, including the human T-cell tumour Jurkat E6.1 (ref. 11) and the murine B-lymphoma lines NBL.DUB¹², M12.4.1 (ref. 13) and WEHI 231 (ref. 14), were transfected with a murine genomic thy-1.2 clone. In Fig. 1, the fluorescence observed after staining of the murine T-cell hybridoma P.4.4 (a) with the anti-Thy-1 monoclonal antibody 3H11 is compared with that seen after staining of the thy-1.2-transfected clones Jurkat J14C9 (b), NBL.23C5 (c), M12.46E5 (d) and WEHI.40C2 (e). Because volume measurements demonstrated a very similar cell size in the populations examined, the amount of Thy-1.2 expressed by the cells could be estimated from the degree of fluorescence observed. Compared with P.4.4 (100%), the highest levels of Thy-1 were found on NBL.23C5 (88.3%); lower amounts were seen on M12.46E5 (40.9%), J14C9 (31%) and WEHI.40C2 (8.9%). Although the thy-1.2-transfected cell clones were reactive with a large panel of anti-Thy-1 monoclonal antibodies, they failed to bind antibody G7, which is mitogenic for resting murine T cells8. The parental lines Jurkat E6.1, NBL.DUB, M12.4.1 and WEHI 231 showed no reactivity with any of the anti-Thy-1 antibodies tested (results not shown).

As a rapid rise in $[Ca^{2+}]_i$ is an early event in a large number of cell activation models¹⁵, including the activation of T cells¹⁶⁻²⁰, we measured $[Ca^{2+}]_i$ after crosslinking of Thy-1 on the surface of the transfected cell lines as well as on murine thymocytes, peripheral T lymphocytes and the T-cell hybridoma P.4.4. For these measurements we used the fluorescent indicator Quin-2, which is trapped intracellularly, binds Ca²⁺ with a 1:1 stoichiometry, and shows increased fluorescence on binding Ca²⁺ (ref. 21). The cells to be tested were first loaded with Quin-2, incubated with rat antibodies 3H11 and 3A7, which recognize independent epitopes on Thy-1 (ref. 22), and washed. The preincubation with the two monoclonal antibodies did not change the resting [Ca²⁺]_i (results not shown). The cells were then reacted with MAR 18.5, a mouse antibody to rat κ -chains which does not bind to human or murine T or B cells²³. Preincubation with two anti-Thy-1 monoclonal antibodies gave better quantitative results with thymocytes, normal T cells and the T-cell hybridoma P.4.4, whereas identical tracings were obtained when only one anti-Thy-1 monoclonal antibody was used for preincubation of Jurkat J14C9 and the B-cell lines NBL.23C5 and M12.46E5 (results not shown). The tracings of Quin-2 fluorescence observed after crosslinking of Thy-1 on the various cell populations are shown in Fig. 2. After the addition of MAR 18.5, a rapid rise in [Ca²⁺]_i was seen in murine thymocytes (Fig. 2a), normal T cells (b) and the T-cell hybridoma P.4.4 (c). A similar result was observed in the transfected human cell line Jurkat J14C9 (Fig. 2d). As J14C9 expresses the T3 complex, which is known to trigger a rise in [Ca²⁺]_i (ref. 18), we compared the effect of crosslinking Thy-1 with the effect of antibody OKT3 (ref. 24) in the Quin-2 assay; the response to OKT3 (Fig. 2e) was more rapid and resulted in a greater rise in [Ca2+], which then reversed more quickly.

When the Thy-1 molecule on the transfected B-cell lines was subjected to the same crosslinking procedure using monoclonal antibodies 3H11/3A7 and MAR 18.5, both NBL.23C5 (Fig. 2f) and M12.46E5 (Fig. 2g) demonstrated a rapid rise in $[Ca^{2+}]_i$. In contrast, WEHI.40C2 (Fig. 2h) failed to respond in analogous experiments. As a positive control, the addition of a purified anti-IgM antibody preparation, which is known to increase $[Ca^{2+}]_i$ by crosslinking surface immunoglobulin²⁵, gave a positive signal in all three transfected B-cell lines (Fig. 2k-m). In general, anti-IgM antibodies produced a higher initial rise in $[Ca^{2+}]_i$, but crosslinking of both surface immunoglobulin and

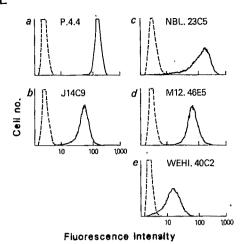
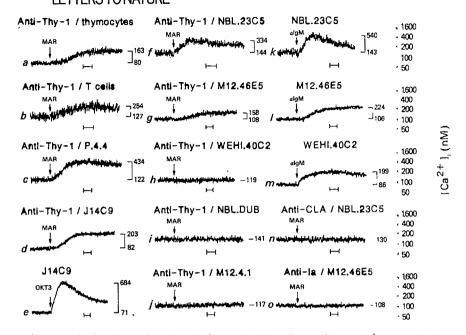


Fig. 1 Flow microfluorimetric analysis of Thy-1 expression on the T-cell hybridoma P.4.4 (a) and on the thy-1.2-transfected cell lines J14C9 (b), NBL.23C5 (c), M12.46E5 (d) and WEHI.40C2 (e). Cells (1×10^6) were preincubated with excess anti-Thy-1 antibody 3H11 (ref. 33) (-) for 30 min at 4 °C, then washed three times with Hanks' balanced salt solution containing 0.1% NaN3 and 3% fetal calf serum. The cells were then stained with excess fluorescein isothiocyanate (FITC)-conjugated antibody MAR 18.5, which is specific for rat κ light chains²³, and 3×10^4 viable cells (as determined by propidium iodide exclusion) were analysed on a fluorescence-activated cell sorter (FACS II: Becton Dickinson). The broken line indicates background fluorescence with FITC-MAR 18.5 alone. Control staining of the parental (Thy-1-negative) cell lines Jurkat E6.1, NBL.DUB, M12.4.1 and WEHI 231 yielded results identical to the FITC-MAR 18.5 background of the respective transfectants (results not shown). Measurements of cell volume were performed on a cell analyser (Becton Dickinson). Calculations indicated a cell-surface ratio for P.4.4/J14C9/NBL.23C5/-M12.46E5/WEHI.40C2 of 1:1.41:0.93:0.96:0.85. The T-cell hybridoma P.4.4 was produced as described previously³⁴; thy-1.2transfected cell lines were produced as described in detail elsewhere²⁷. Briefly, an 8.2-kilobase (kb) EcoRI fragment containing the complete thy-1.2 gene was cloned into the EcoRI site of the pSV2gpt vector³⁵. Spheroplasts were produced from Escherichia coli HB101 and fused to Jurkat E6.1 and to the murine B-cell lines. Expression of the Ecogpt gene in transfected cells enabled selection and long-term maintenance of cells in the presence of mycophenolic acid, hypoxanthine and xanthine. Colonies which grew out of selection were cloned at limiting dilution and analysed for Thy-1.2 expression by flow microfluorimetry.

Thy-1 produced a similar sustained elevation of [Ca²⁺]_i. The reason for the differential behaviour of WEHI.40C2 remains to be determined, but it is possible that the relatively low expression of Thy-1 on the surface of this cell line (see Fig. 1) prevented an effective crosslinking of the bound anti-Thy-1 monoclonal antibodies by MAR 18.5.

Several control experiments were performed in order to rule out nonspecific effects of the crosslinking procedure on [Ca²⁺]_i. First, when the parental (Thy-1-negative) lines of the responsive transfected T- and B-cell lines were preincubated with antibody 3H11 or 3A7, washed, and then reacted with MAR 18.5, no increase in [Ca²⁺], was seen in NBL DUB (Fig. 2i), M12.4.1 (Fig. 2j) or Jurkat E6.1 (result not shown). Second, a number of monoclonal antibodies to other cell-surface antigens present on the cell lines were subjected to crosslinking with MAR 18.5 in the Quin-2 assay; no elevation of [Ca²⁺]_i was seen in either NBL.23C5 preincubated with a monoclonal antibody to the common leukocyte antigen (CLA; Fig. 2n) or M12.46E5 preincubated with an anti-Ia monoclonal antibody (Fig. 20). Negative results were also observed when NBL.23C5 was pretreated with a monoclonal antibody recognizing H-2, and when M12.46E5 was pretreated with antibodies to H-2, CLA or B220. Furthermore, negative results were obtained with P.4.4 after preincubaFig. 2 Tracings of Quin-2 fluorescence representing [Ca²⁺]_i in Thy-1-bearing and thy-1.2-transfected cells. The scale for the ordinate has been standardized by appropriate optical reduction of the tracings; the scale bar in each record represents 1 min. a IgM, anti-IgM antibody.

Methods. In a modification of the method described by Tsien et al.²¹, the cells to be assayed (5×10⁶ ml⁻¹) were loaded in culture medium with a final concentration of 15 µM Quin 2-AM for 20 min. After loading, the cells were washed twice with Dulbecco's phosphate-buffered saline, resuspended in the same buffer to a concentration of 5×10⁶ ml⁻¹ and used immediately after equilibration at 37 °C for 5 min. Where indicated, Quin-2loaded cells (1×10^7) were preincubated with monoclonal antibody (250 µl of 1:10 ascites of 250 µl of purified antibody; 1 mg ml⁻¹) for 15 min at 37 °C and washed twice more. Fluorescence intensity was measured with a Perkin Elmer fluorescence spectrophotometer LS-5 (excitation 339 nm, emission 492 nm). The cuvette chamber was kept at 37 °C, and the cell suspension continuously stirred. After



a baseline had been established, antibody MAR 18.5 (1:100 ascites) or OKT3 (1:100 ascites) or anti-IgM antibodies (10 µg ml⁻¹) were added Maximum fluorescence (F_{max}) was determined by lysing the Quin-2-loaded cells with 0.1% Triton X-100. Minimum fluorescence (F_{min}) was obtained after addition of EGTA (4 mM) and sufficient Tris buffer to raise the pH to 8.3. Approximate values for cytoplasmic free Ca calculated using the formula: $[Ca^{2^{+}}]_{ix} = 115 \text{ nM} (F_x - F_{min})/(F_{max} - F_x)$ (ref. 21). The following antibodies were used for preincubation: 3H11 (Thy-1)³³, 3A7 (Thy-1)³³, M1.4/42.3.9.8 (H-2 common determinant)³⁶, M1/9.3.4.HL.2 (CLA)³⁶, FD441.8 (LFA-1)³⁷, M5/114 (Ia common determinant)38 and RA3-3A1 (B220)39. The affinity-purified anti-IgM antibodies (given by Dr Junichiro Mizuguchi) were prepared as described previously40.

tion with antibodies to H-2, CLA and lymphocyte function antigen (LFA-1) (results not shown). Thus, numerous lymphocyte surface antigens failed to act like Thy-1 in inducing a rise in [Ca²⁺]_i, demonstrating the specificity of the latter effect.

The ability of Thy-1 to act as a signal transducing molecule was first noted when it was recognized that anti-Thy-1 antibodies present in rabbit antisera to mouse brain were responsible for the T-cell mitogenic effects of such antisera²⁶. More recently, we and several other groups have confirmed and extended these studies by demonstrating that certain monoclonal anti-Thy-1 antibodies can activate resting murine T cells, as well as T-cell hybridomas and cytotoxic T-cell clones^{8,9}. Furthermore, we have shown recently that after crosslinking, a large number of unselected, non-mitogenic anti-Thy-1 antibodies (including 3H11 and 3A7) are capable of inducing a vigorous proliferative response in murine T cells and interleukin-2 (IL-2) production in thy-1.2transfected human Jurkat clones in the presence of phorbol esters; IL-2 production could be observed in murine T-cell hybridomas even in the absence of a co-stimulator^{22,27}. Our previous results, together with the present data, demonstrate that in every case in which crosslinking of Thy-1 elicited a rise in [Ca²⁺]_i, this was followed by functional responses in the T-cell populations studied.

The ability of crosslinked Thy-1 to trigger a rise in [Ca²⁺]_i in thy-1-transfected B cells clearly indicates that the signal delivered is independent of the T-cell antigen receptor and other T-cell-specific molecules. The preservation of the signalling function of Thy-1 in several lymphoid cell types of two species could be explained by a model in which Thy-1 associates, not only in murine B and T cells but also in human T cells and presumably in rodent and human neuronal cells, with a highly conserved molecule responsible for the rise in $[Ca^{2+}]_i$. Alternatively, the triggering signal leading to a rise in $[Ca^{2+}]_i$ may be generated by the Thy-1 molecule itself. Recent results indicate that Thy-1 is anchored directly to a cell membrane lipid, probably phosphatidylinositol^{28,29}. Whether this peculiar mode of membrane integration is related to the function of Thy-1 is at present unknown, but it is interesting to note that breakdown products of membrane phosphoinositides are involved in receptor-mediated signalling events, including changes in [Ca²⁺]; (reviewed in ref. 30).

The formulation of a hypothesis concerning the role of Thy-1 in the ontogeny and function of T cells is complicated by the differences in tissue distribution between species. The results of the present study are compatible with the view that Thy-1 has a critical role as an inducer of an alternative pathway of T-cell activation, in a manner similar to that proposed for the T11 antigen on human thymocytes and T cells^{31,32}. Thus, Thy-1 may represent a phylogenetically primitive pathway of cellular triggering which may have evolved prior to the antigen-specific receptor and which may function primarily in triggering thymocyte growth and differentiation. Whether this model is correct, and whether Thy-1 plays a similar part in transduction of intercellular differentiation signals in other Thy-1-bearing cell types, remains to be determined.

We thank David Scott for the NBL.DUB cell line, Art Weiss for the Jurkat subline E6.1, Linette Edison for the flow microfluorimetry studies, and Shirley Starnes for secretarial assistance. R.A.K. was supported by a grant from the Deutsche Forschungsgemeinschaft.

Received 13 January; accepted 9 April 1986.

- Reif, A. E. & Allen, J. M. Nature 209, 521-523 (1966).
- Foon, K. A. et al. J. Immunogenet. 11, 233-243 (1984). Campbell, D. G., Gagnon, J., Reid, K. B. M. & Williams, A. F. Biochem. J. 195, 15-30 (1981)
- Williams, A. F. & Gagnon, J. Science 216, 696-703 (1982). Seki, T. et al. Science 227, 649-651 (1985).
- Seki, T., Moriuchi, T., Chang, H.-C., Denome, R. & Silver, J. Nature 313, 485 487 (1985).
 Seki, T. et al. Proc. natn. Acad. Sci. U.S.A. 82, 6657-6661 (1985).
- Gunter, K. C., Malek, T. R. & Shevach, E. M. J. exp. Med. 159, 716-730 (1984). MacDonald, H. R., Bron, C., Rousseaux, M., Horvath, C. & Cerottini, J.-C. Eur. J. Immun. 15, 495-501 (1985).
- 10. Leifer, D., Lipton, S. A., Barnstable, C. J. & Masland, R. H. Science 224, 503-306 (1984)
- Weiss, A., Wiskocil, R. L. & Stobo, J. D. J. Immun. 133, 123-128 (1984).
 Ling, M., Linvat, D., Pillai, P. S. & Scott, D. W. J. Immun. 134, 1449-1454 (1985).
- 13. Glimcher, L. H. et al. Nature 298, 283-284 (1982).

- 14. Boyd, A. W. & Schrader, J. W. J. Immun, 126, 2466-2469 (1981).
- 15. Rubin, R. P., Weiss, G. B. & Putney, J. W. (eds) Calcium in Biological Systems (Plenum, New York, 1985).
- 16. Tsien, R. Y., Pozzan, T. & Rink, T. J. Nature 295, 68-71 (1982).
- Nisbet-Brown, E., Cheung, R. K., Lee, J. W. W. & Gelfand, E. W. Nature 316, 545-547 (1985).
 Weiss, A., Imboden, J., Shoback, D. & Stobo, J. Proc. natn. Acad. Sci. U.S.A. 81, 4169-4173
- 19. Imboden, J. B., Weiss, A. & Stobo, J. D. J. Immun, 134, 663-665 (1985).
- Weiss, M. J., Daley, J. F., Hodgdon, J. C. & Reinherz, E. L. Proc. natn. Acad. Sci. U.S.A. 81, 6836-6840 (1984).
- Tsien, R. Y., Pozzan, T. & Rink, T. J. J. Cell Biol. 94, 325-334 (1982).
- 22. Kroczek, R. A., Gunter, K. C., Seligmann, B. & Shevach, E. M. J. Immun, 136, 4379-4384
- 23. Lanier, L. L., Gutman, G. A., Lewis, D. E., Griswold, S. T. & Warner, N. L. Hybridoma 1, 125-131 (1982).
- Kung, P. C., Goldstein, G., Reinherz, E. L. & Schlossman, S. F. Science 206, 347-349 (1979).
 Pozzan, T., Arslan, P., Tsien, R. Y. & Rink, T. J. J. Cell Biol. 94, 335-340 (1982).
 Maino, V. C., Norcross, M. A., Perkins, M. S. & Smith, R. T. J. Immun. 126, 1829-1836 (1981).

- 27. Gunter, K. C., Kroczek, R. A., Shevach, E. M. & Germain, R. N. J. exp. Med. 163, 285-300
- 28. Low, M. G. & Kincade, P. W. Nature 318, 62-64 (1985).
 29. Tse, A. G. D., Barclay, A. N., Watts, A. & Williams, A. F. Science 230, 1003-1008 (1985).
- Berridge, M. J. Biochem. J. 220, 345-360 (1984).
 Fox, D. A. et al. J. Immun. 134, 330-335 (1985).

- Meuer, S. C. et al. Cell 36, 897-906 (1984).
 Lögdberg, L., Gunter, K. C. & Shevach, E. M. J. immun. Meth. 79, 239-249 (1985).
 Glimcher, L. H. & Shevach, E. M. J. exp. Med. 156, 640-645 (1982).
- Mulligan, R. C. & Berg, P. Proc. natn. Acad. Sci. U.S.A. 78, 2072-2076 (1981).
 Springer, T. A. in Monoclonal Antibodies (eds Kennett, R. H., McKearn, T. J. & Bechtol,
- K. B.) 185-217 (Plenum, New York, 1980). 37. Sarmiento, M. et al. Immun. Rev. 68, 135-169 (1982).
- Bhattacharya, A., Dorf, M. E. & Springer, T. A. J. Immun. 127, 2488-2495 (1981).
 Coffman, R. L. & Weissman, I. L. Nature 289, 681-683 (1981).
- Sieckmann, D. G., Asofsky, R., Mosier, D. E., Zitron, I. M. & Paul, W. E. J. exp. Med. 147, 814-829 (1978).

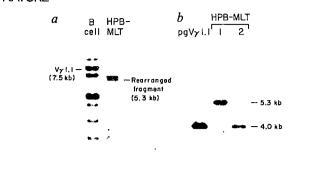
Human T-cell γ genes contain Nsegments and have marked junctional variability

Thomas Ouertermous*, William Strauss†, Cornelis Murret, Deno P. Dialynast, Jack L. Strominger & J. G. Seidman †

* Cardiac Unit, Department of Medicine, Massachusetts General Hospital, Fruit Street, Boston, Massachusetts 02114, USA † Department of Genetics, Harvard Medical School, 25 Shattuck Street, Boston, Massachusetts 02115, USA ‡ Department of Biochemistry and Molecular Biology, Harvard University, 7 Divinity Street, Cambridge, Massachusetts 02138, USA

The γ -chain genes are encoded by immunoglobulin-like gene segments in germline DNA which rearrange during the somatic development of T cells to form an active gene¹⁻⁷. The protein produced by these genes has not been identified and the diversity of the proteins that the genes can express has not been determined. We expect that the diversity of expressed y-chains is produced by the same three mechanisms that produce diversity of other immunoglobulin-like genes: (1) germline variable (V) and joining (J) region repertoires; (2) somatic mutation; and (3) junctional diversity^{8,9}. To define the contribution of each of these mechanisms to the generation of γ -chain diversity, several γ -chain complementary clones and rearranged γ -chain genes have been characterized. Most of these clones seem to encode a defective y-chain, the variable- and constant-region portions being joined such that they would not be translated in the same reading frame. Here we report that the germline J-region diversity of the human T-cell \gamma-chain is very limited and that somatic mutation does not contribute to the diversity of the γ -chains encoded by the cloned segments. However, the junctional diversity of these γ -chain genes is extensive. We suggest that N sequences (template-independent sequences) have been inserted enzymatically into all of the y-chain genes characterized.

The repertoire of germline V and J_{γ} segments encoded in the human genome is small. Recent studies have demonstrated that the human genome contains 12 variable-region segments,



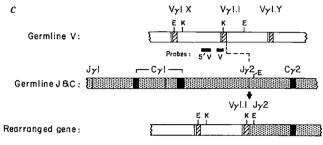
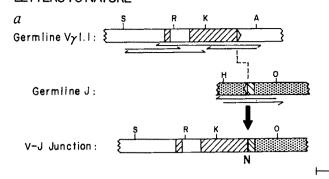
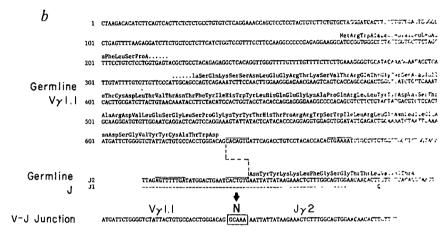


Fig. 1 Southern blots of germline and HPB-MLT $V_{\nu}1$ variable regions (a) and cloned $V_{\gamma}1.1$ (pgV $\gamma1.1$) and size-selected HPB-MLT genomic DNA (b). a, B-cell (Epstein-Barr virus-transformed B-cell line, LAZ 509) and HPB-MLT T-cell line DNA was digested with EcoRI, size fractionated on a 0.9% agarose gel, transferred to nitrocellulose and hybridized to a ^{32}P nick-translated variableregion probe from pTy-1 (ref. 12). The rearranged fragment was identified by its hybridization to both V and J probes. Samples were run on the same gel, fragment sizes were determined by co-migration with γ DNA digested with HindIII. b, Plasmid pgV γ 1.1 contains a 7.5-kb EcoRI fragment which hybridizes to the V probe, and was cloned into SP6 from an EMBL 3A human placental library using standard techniques¹². HPB-MLT DNA was digested with EcoRI and size fractionated on a preparative 0.8% agarose gel¹²; the fraction which contained the rearranged fragment was identified by hybridization to a genomic J probe. pgVy1.1 DNA was digested with KpnI and electrophoresed on the same 0.9% agarose gel with the EcoRI-digested size-selected HPB-MLT DNA (lane 1) and the size-selected DNA digested with KpnI (lane 2). DNA was transferred to a nitrocellulose filter and hybridized to 32 P-labelled 5' V probe (c). c, Variable- and constantregion exon arrangement was determined by nucleotide sequence analysis and hybridization to the cDNA pTγ-1. Variable-region exons are shown by hatching, constant exons are solid, the constant locus of the choromosome is stippled. Probes 5' V and V were isolated by cleavage of pgV γ 1.1 (ref. 12). Abbreviations: E, EcoRI, K, Kpn I. Scale bar, 1 kb.

making up four separate families (refs 6, 7 and W.S., T.Q. and J.G.S., unpublished results). At least six of the V segments can recombine with J segments encoded in the γ -chain constantregion locus (Fig. 1c and ref. 6). Two J segments were identified by restriction fragment analysis in the γ -chain locus. To determine the difference between the amino-acid sequences encoded by the two J segments and to define their contributions to the rearranged genes, we have determined their nucleotide sequences¹⁰. The J regions and 1,000 base pairs (bp) of flanking sequence were determined. The 49-bp J segments encode identical peptides (they differ by only 1 bp; Fig. 2b; ref. 7). Homology between the two loci extends outside the coding region with >95% homology over the 500 bp from the J segment in either direction. The finding of extensive homology between the human $J_{\gamma}1$ and $J_{\gamma}2$ indicates that the human constant-region locus has duplicated recently, since the divergence of mouse and human, and that the J_{γ} segment does not contribute to y-chain diversity.

Fig. 2 Restriction map and DNA sequence of germline $V_{\gamma}1.1$, $J_{\gamma}2$ (also $J_{\gamma}1$), and the rearranged V-J junction and N segment. a, Variable (図) and joining segments (図) are indicated in germline and rearranged configuration. The germline variable region and constant region (図) are joined by somatic recombination. Open arrowheads represent recombination signals; the restriction fragments used for nucleotide sequence analysis are indicated by horizontal arrows. Abbreviations: S, SacI; R, Rsal; K, KpnI; A, Sau3A; H, HindIII; O, Dral; N, N segment. b, Complete sequence of $V_{x}1.1, J_{x}1, J_{x}2$ and V-J junction as determined from sequence analysis of pgV γ 1.1, pJ γ 1, pJ γ 2 and cDNA pTy-1, respectively. Splice signals are indicated by dotted lines over appropriate nucleotides; recognition sequences for recombination are overlined. Nucleotides not encoded in germline V or J segments are boxed and labelled N. Scale bar in a, 100 bp.





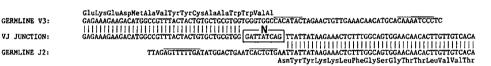


Fig. 3 Comparison of germline V, 3 and $J_{\gamma}2$ sequence with the V-J junction of cDNA pT γ -15. Heptamer and nonamer recombination sequences are overlined. Nucleotides not derived from germline sequence are boxed and labelled N. Vertical lines indicate identity of compared sequences.

The contribution of somatic mutation and junctional variation to the diversity of expressed γ -chains can be determined by comparing the nucleotide sequences of the germline V and Jsegments with the nucleotide sequence of the y-chain messenger RNA in particular T cells. We have previously obtained a full-length cDNA clone, pTy-1, which corresponds to y-chain mRNA from the T cell HPB-MLT (ref. 11). Southern blot analysis of germline (B-cell) DNA using the variable-region probe obtained from this cDNA clone indicated that the human genome contains a family of eight hybridizing variable-region gene segments (Fig. 1a), all except two of which have been deleted from the HPB-MLT genome (Fig. 1a, HPB-MLT). Most of the germline variable-region segments were cloned by screening an EMBL3A human placental library using the pTy-1 Vregion probe (data not shown and ref. 12). To determine which of these variable-region fragments was joined to the J segment to form the rearranged gene expressed in HPB-MLT, we compared the restriction enzyme map 5' of the rearranged γ -chain gene with the restriction enzyme map 5' of the germline variableregion genes (Fig. 1a and our unpublished results). Only one germline variable-region gene segment (designated $V_{\gamma}1.1$) yielded a 4.0-kilobase (kb) KpnI digestion fragment that hybridized to a 5' V probe and co-migrated with a fragment produced by KpnI digestion of purified rearranged fragment (Fig. 1b). Thus, $V_{\gamma}1.1$ is the germline variable-region fragment that underwent recombination with $J_{\gamma}2$ to produce the rearranged gene expressed in HPB-MLT (Fig. 1c).

Any differences between the nucleotide sequence of $V_{\gamma}1.1$ and the variable region utilized in HPB-MLT either occurred

by somatic mutation or are caused by polymorphic differences between the two individuals from whom the genes were obtained. To determine the extent of the differences between the two genes, we have determined the nucleotide sequence of $V_{2}1.1$ (Fig. 2a). We found that this germline variable-region gene is like other immunoglobulin and T-cell β -chain V segments and is encoded in two exons, a hydrophobic leader segment and a variable region. The conserved heptamer and nonamer sequences, thought to play an important part in somatic recombination and found 3' of all immunoglobulin-like V-region segments, are observed 3' of the $V_{\gamma}1.1$ variable region. The $V_{\gamma}1.1$ sequence was compared with the nucleotide sequence of the variable region expressed in HPB-MLT (Fig. 2b). Because there are no differences between the two variable-region genes, we conclude that somatic mutation has not occurred within this variable region since it underwent recombination to form the rearranged gene found in HPB-MLT. The sequence of a genomic rearranged γ gene utilizing this V region has been published recently and differs at a single nucleotide⁷. This difference could be a result of sequencing error, polymorphism or somatic mutation. If the difference is a product of somatic mutation, it is not important in generating y-chain diversity, since it is a silent mutation and does not affect the γ -chain amino-acid sequence.

The availability of germline V and J sequences as well as the nucleotide sequence of the cDNA expressed from the rearranged gene allows us to examine the mechanisms that produce diversity at the V-J junction. Comparison of the germline $V_{\gamma}1.1$ and $J_{\gamma}2$ sequences with the HPB-MLT cDNA sequence (Fig. 2h) indicates that 5 bp have been inserted between V and J during

Fig. 4 Junctional variability of rearranged γ genes. pT γ -1, pT γ -10, pT γ -15 are cDNAs, pT γ R4 is a rearranged genomic clone. λ S γ 12 and λ K γ 20 are rearranged genomic clones described in ref. 7. The nongermline nucleotides (labelled N segment) of pT γ -1, λ S γ 12 and pT γ -15 were determined by direct comparison with germline sequence (Figs

REARRANGED GENE	VARIABLE REGION	N SEGNENT	JOINING REGION
pTγ-1 (HPB-MLT)	GGG GTC TAT TAC TGT GCC ACC TGG GAC AG	CGGACG AAT	TATTATAAGAAACTCTTT
λSγ12	GGG GTC TAT TAC TGT GCC ACC TGG		TATTATAAGAAACTCTTT
pTγ-15 (HSB-2)	GCC GTT TAC TAC TGT GCT GCG TGG		TATTATAAGAAACTCTTT
		PREDICTED N SEGMENT	
pTyR4 (JURKAT)	GTG GTG TAC CCA TGT GCC TGT CAG ATC CT		TAAGAAACTCTTT
pTy-10 (HSB-2)	GCT ACC TAC TAC TGT GCC TTG TGG GAG GT		FATTATAAGAAACTCTTT
\lambda Ky20	GCT ACC TAC TAC TGT GCC TTG		FATTATAAGAAACTCTTT

2, 3 and ref. 11). The variable regions have been aligned at the second conserved cysteine codon and $V_{\gamma}1.1$ used as a guide to predict the 3' end of the variable regions in pT γ R4 and pT γ -10. A predicted N segment was thus derived for pT γ R4 where germline sequence was not available. pT γ -10 and $\lambda K \gamma 20$ use the same V and J region but the sequences differ at the V-J junction, indicating that at least one of them has an N segment. Since the germline sequence of this variable region is not known, pT γ -10 has been arbitrarily chosen to represent a complete V region and the 3' end predicted by comparison with $V_{\gamma}1.1$. This conservative analysis results in a 5-bp N segment in $\lambda K \gamma 20$. It is possible that pT γ -10 contains up to 9 bp of N sequence. The entire germline J sequence is encoded in pT γ -1; J-segment bases missing in the other clones are indicated by blank spaces.

somatic recombination. New sequences of this type have been identified in rearranged immunoglobulin and T-cell receptor β -chain genes and result either from additional germline diversity (D) segments or sequences inserted enzymatically in a template-independent fashion $(N \text{ segments})^{8,9}$.

We have investigated whether there are additional base pairs between the V and J segments of other rearranged γ -chain genes by cloning a partial y-chain cDNA (pTy-15) from the T-cell line HSB-2, which would encode another defective ychain (Fig. 3). This cDNA contains a γ -chain V region which we have designated V_{x3} and which is a member of a different variable-region gene family (data not shown). The 3' end of the V₂3 gene was cloned on a 9.5-kb EcoRI fragment isolated from a subgenomic library produced from size-selected Jurkat DNA. Nucleotide sequence analysis of the germline V_r3 variable region and the HSB-2 cDNA (pTγ-15) identified no differences between the germline gene and the expressed cDNA in the coding portion. This sequence identity suggests that the rearranged y-chain genes found in mature T cells have not been subjected to extensive somatic mutation. However, during the recombination that joined this V to J, 9 bp have been inserted between the V and J segments.

To determine whether additional sequences are inserted between the V and J sequences of other rearranged γ -chain genes, we have isolated a rearranged genomic γ -chain gene (pT γ R4) and another cDNA (pT γ -10). The germline V-region segments that were involved in the formation of these rearranged γ -chain genes have not been sequenced. However, we can predict the location of the 3' end of the germline variable region by aligning the codons encoding the conserved cysteine residues (Fig. 4). Thus, using $V_{\gamma}1.1$ as a guide, this analysis predicts the presence of a 13-bp additional sequence in one rearranged gene and a 1-bp addition in the other (Fig. 4).

The additional bases inserted between the V and J segments are probably added enzymatically during site-specific recombination and represent N segments. Evidence for a D segment between V and J segments in the immunoglobulin heavy-chain genes and the T-cell antigen receptor β -chain genes has been obtained by the identification of recombined D-J segments in plasmacytomas or T cells¹³⁻¹⁵. The human γ -chain J segments rearrange to produce six different variable regions⁶. In more than 50 T-cell lines and tumours (corresponding to more than 100 rearranged chromosomes) no other rearrangements that might represent D-J recombination have been detected (ref. 6 and J. Greenberg, T.Q., J.G.S. and J. Kersey, unpublished results). Although the exact origin of N segments is not known, a model for their generation has been proposed which involves terminal transferase^{16,17}. In other immunoglobulin-like gene rearrangements, N segments have been described only in association with D segments^{8,9}. Rearranged immunoglobulin lightchain genes seem to use neither D nor N segments. The human y-chain gene provides the best evidence for an immunoglobulinlike gene that does not have a D segment but contains N segments.

Rearranged murine γ -chain genes have also been identified which contain two or three additional base pairs between the V and J segments^{2,3,18}. Although it has been proposed that these additional base pairs may represent a D or N segment, there is no evidence for a separate D segment. Although both the murine and human rearranged γ -chains have additional nucleotides separating the V and J segments, the rearranged human genes have considerably longer N segments than the murine genes (Fig. 4). The 9- and 13-bp N segments found in rearranged human γ -chain genes are as long as the total sequence found separating many T-cell receptor β -chain and immunoglobulin V and J regions^{8,9}.

The human γ gene can further produce junctional diversity by altering the site of recombination in V- and J-region segments. Eight bases at the 3' end of the germline $V_{\gamma}3$ segment are absent in the rearranged gene (Fig. 3), and up to eight bases are lost from the 5' germline J sequence during recombination (Fig. 4). Flexibility in the site of recombination is thought to be an important source of variable-region diversity among other immunoglobulin-like genes and apparently occurs in the formation of rearranged γ -chain genes.

An important feature of all four rearranged y-chain genes described here is that they are rearranged in a way that will not produce an active gene. However, Lefranc et al. have recently described two y-chain genes that have rearranged so that they encode productive γ -chain transcripts⁷. Comparison with the germline variable-region sequences presented here suggests that both of these genes have N segments inserted between V and J segments (Fig. 4). The apparently high rate (four of six) of ineffective γ -chain gene rearrangement may represent the high price paid to achieve such flexibility of V-J joining. Presumably, the defective γ -chain genes rearranged in many mature T cells are not functional and these T cells do not have a requirement for functional γ -chain expression. One possibility is that junctional variability represents a by-product of a mechanism of recombinational inactivation of the y-chain gene; that is, the y-chain genes might rearrange during development of the T cell to produce a functional y-chain and subsequently undergo a second rearrangement as a feature of terminal T-cell differentiation. We have noted previously the infrequent use of $C_v 1$ in T cells, and we suggest that functional rearrangements of $J_{\nu}1$ occur in early T cells and may be lost during somatic development.

The human γ -chain derives little combinatorial diversity from two virtually identical J segments, although the possibility of further diversity resulting from rearrangement to other J-C loci has not been excluded. There seems to be little somatic mutation in the genes that have been sequenced. However, significant variability is introduced at the V-J junction by N segments and variation in the V and J recombination site. These mechan-

187

isms appear to be more active in the human γ -chain locus than in the murine locus. Although the mechanisms by which Nsegments are inserted into the V-J junction are unclear, this region in immunoglobulin proteins plays a significant part in determining antigen-binding specificity¹⁹. Thus, we believe that the junctional variability of the y-chains will have an important role in determining their function in the immune response.

T.O. is the recipient of NIH training grant T32-HL-07208, D.P.D. is supported by a fellowship from the Damon Runyon-Walter Winchell Cancer Fund, J.L.S. is the recipient of NIH grant AN-30241, and J.G.S. is supported by a grant from the Mallinkrodt Foundation and NIH grants AI-19938 and AI-18436.

Received 17 February; accepted 10 April 1986.

- Saito, H. et al. Nature 309, 757-762 (1984)
- Hayday, A. C. et al. Cell 40, 259-269 (1985).
- Kranz, D. M. et al. Nature 313, 752-755 (1985). Murre, C. et al. Nature 316, 549-552 (1985).
- Lefranc, M. P. & Rabbitts, T. H. Nature 316, 464-466 (1985). Quertermous, T. et al. Science 231, 252-255 (1986).
- Lefranc, M. P., Forster, A. & Rabbitts, T. H. Nature 319, 420-422 (1986).
- 8. Tonegawa, S. Nature 302, 575-581 (1983).
- Kronenberg, M., Siu, G., Hood, L. E. & Shastri, N. A. Rev. Immun. (in the press).
- Maxam, A. M. & Gilbert, W. Meth. Enzym. 65, 499-560 (1980).
 Dialynas, D. P. et al. Proc. natn. Acad. Sci. U.S.A. 83, 2619-2623 (1986).
- Dialynas, D. P. et al. Proc. natn. Acad. Sci. U.S.A. 83, 2619-2623 (1986).
 Maniatis, T., Fritsch, E. F. & Sambrook, J. Malecular Cloning: A Laboratory Manual (Cold Spring Harbor Laboratory, New York, 1982).
 Sakano, H., Kurosawa, Y., Weigert, M. & Tonegawa, S. Nature 290, 562-565 (1981).
 Kavaler, J., Davis, M. M. & Chien, Y. Nature 310, 421-423 (1984).
 Siu, G. et al. Nature 311, 344-350 (1984).

- Su, G. et al. Nature 31, 344-350 (1984).
 Alt, F. & Baltimore, D. Proc. natn. Acad. Sci. U.S.A. 79, 4118-4122 (1982).
 Desidero, S. et al. Nature 311, 752-755 (1984).
- 18. Heilig, J. S. et al. Nature 317, 68-70 (1985).
- 19. Early, P. & Hood, L. Cell 24, 1-3 (1981).

Newly replicated DNA is associated with DNA topoisomerase II in cultured rat prostatic adenocarcinoma cells

William G. Nelson*, Leroy F. Liu† & Donald S. Coffey*

* Departments of Pharmacology, Urology and Oncology and of † Biological Chemistry, Johns Hopkins University School of Medicine, 600 North Wolfe Street, Baltimore, Maryland 21205, USA

DNA topoisomerases have been proposed to function in a variety of genetic processes in both prokaryotes and eukaryotes1-3. Here, we have assessed the role of DNA topoisomerase II in mammalian DNA replication by determining the proximity of newly synthesized DNA to covalent enzyme-DNA complexes generated by treating cultured rat prostatic adenocarcinoma cells with teniposide. Teniposide (VM-26), an epipodophyllotoxin, is known to interact with mammalian DNA topoisomerase II so as to trap the enzyme in a covalent complex with DNA⁴⁻⁹. We have found that the teniposide-induced trapping of such complexes requires MgCl₂, is stimulated by ATP and is inhibited by novobiocin. The formation of covalent complexes seems to be reversible on removal of teniposide. Furthermore, analysis of the covalent complexes formed between ³H-thymidine pulse-labelled DNA and topoisomerase II following teniposide treatment reveals a direct association of the enzyme with nascent DNA fragments. Our results suggest that DNA topoisomerase II may interact with newly replicated daughter DNA molecules near DNA replication forks in mammalian cells.

We assayed for the appearance of teniposide-induced covalent complexes between topoisomerase II and newly replicated DNA in cultured Dunning R3327-G rat prostatic adenocarcinoma cells. For this we used a potassium-sodium dodecyl sulphate (K-SDS) precipitation procedure specific for protein-linked DNA^{9,10}. Monolayer cultures of growing cells were pulse-

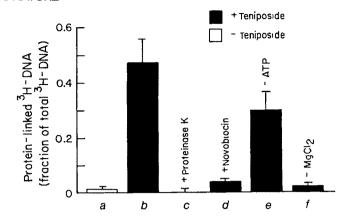


Fig. 1 Covalent linkage of pulse-labelled DNA to protein following temposide treatment requires an activity characteristic of mammalian topoisomerase II. The fraction of pulse-labelled ³H-DNA linked to protein (protein-linked ³H-DNA/total ³H-DNA) was determined for. a, control, lysates from cells incubated in buffer I without teniposide, b, teniposide, lysates from cells incubated with 20 µM teniposide; c, lysates from teniposide-treated cells that had been digested with 200 µg ml 1 proteinase K for 30 min at 50 °C; d, lysates from cells incubated with teniposide in buffer 1 supplemented with 2 mM novobiocin; e, lysates from cells incubated with teniposide in buffer I without ATP; f, lysates from cells incubated with teniposide in buffer I without MgCl₂. Protein-linked ³H-DNA fractions are expressed as means ± s.e.m.

Methods. Monolayer cultures of growing Dunning R3327-G rat prostatic adenocarcinoma cells were pulse-labelled for 90 s at 37 °C by exposure to ³H-thymidine (54 Ci mmol⁻¹) in complete medium (RPMI 1640 supplemented with 10% fetal calf serum, 25 nM dexamethasone, 100 U ml penicillin, 100 U mi streptomycin). Immediately after pulse labelling, the cells were permeabilized in situ by gently washing first for 5 min, and then again for 10 min at 4 °C with buffer E (0.5% Nonidet P-40, 10° glycerol, 10 mM NaCl, 5 mM MgCl2, 1 mM EGTA, 1 mM phenylmethylsulphonyl fluoride in 10 mM sodium phosphate, pH 6.5). In preparation for teniposide treatment, the cells were rinsed twice for 5 min at 4 °C with buffer I (100 mM NaCl, 5 mM MgCl₂, 1mM EGTA, 0.1 mM dithiothreitol, 0.5 mM ATP in 10 mM sodium phosphate, pH 6.5), buffer I without MgCl2, buffer I without ATP, or buffer I supplemented with 2 mM novobiocin. The rinsed, permeabilized cells were then incubated for 30 min at 37 °C in the same buffer with 0.2% DMSO (a) or with 20 µM teniposide and 0.2% DMSO (b f) before being lysed in lysis buffer (2% SDS and 10 mM EDTA in 10 mM Tris, pH 8.0). The lysates were subjected to the K-SDS assay^{9,10}. Briefly, for the non-denaturing K-SDS assay, 500 µl of 120 mM KCl were added to an equal volume of SDS lysate. The mixture was heated to 65 °C for 10 min, cooled at 4°C for 5 min and then centrifuged at 1,500g for 5 min at 4°C. The K-SDS-protein precipitate was recovered and washed by resuspending the precipitate in 1 ml of wash buffer (100 μg ml⁻¹ calf thymus DNA, 20 μg bovine serum albumin, 100 mM KCl, I mM EDTA in 10 mM Fris pH 8.0) and heating at 65 °C for 10 min. The wash mixture was then cooled at 4°C for 5 min and centrifuged at 1,500g for 5 min at 4°C. After five washes, the amount of protein-linked ³H-DNA was determined by dissolving the final precipitate in 1 ml of water before counting in 10 ml of Aquasol-2 (NEN). The total amount of ³H-DNA was determined by assessing the amount of trichloroacetic acid-insoluble ³H-DNA in the lysates.

labelled for 90 s with ³H-thymidine; in order to limit the ³Hthymidine pulse duration to 90 s, the cells were placed on ice and permeabilized immediatedly after labelling. The permeabilized cell monolayers were then treated in situ with teniposide in the absence of exogenous deoxynucleoside triphosphates before being lysed in SDS. When SDS lysates from these cell monolayers were subjected to the K-SDS assay, 3H-DNA was recovered along with the K-SDS precipitate (Fig. 1b). Digestion of the lysates with proteinase K reduced the amount of K-SDSprecipitable ³H-DNA by >99% (Fig. 1c), confirming the specificity of the K-SDS assay for protein-linked DNA. Markedly less topoisomerase II-linked ³H-DNA was detected when the topoisomerase II inhibitor novobiocin was included during teniposide treatment (Fig. 1d), while omission of teniposide (Fig. 1a), ATP (Fig. 1e) or MgCl₂ (Fig. 1f) from the incubation mixture resulted in a reduced amount of enzyme-linked ³H-DNA, as expected for a topoisomerase II reaction⁴ 6,8,10.

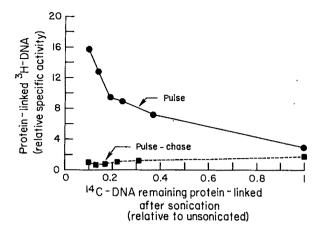


Fig. 2 Enrichment of newly replicated DNA with teniposide-induced covalent DNA-protein complexes. Cultured Dunning R3327-G rat prostatic adenocarcinoma cells that had been labelled for 72 h with 0.05 μCi ml⁻¹ ¹⁴C-thymidine (60 mCi mmol⁻¹) were incubated with 20 μCi ml⁻¹ ³H-thymidine (54 μCi mmol⁻¹) in complete medium for 90 s at 37 °C (pulse, •) or exposed to 20 μCi ml⁻¹ ³H-thymidine for 90 s and then incubated in 40 μM unlabelled thymidine in complete medium for 45 min at 37 °C (pulse-chase). Both pulse and pulse-chase labelled cells were permeabilized, treated with teniposide and lysed in lysis buffer as described for Fig. 1. Then, in order to progressively reduce the size of DNA remaining protein-linked, the lysates were sonicated for 0, 5, 10, 15, 20 and 30 s with a Branson Model W140 Sonifier at setting 2 before being subjected to the K-SDS assay as for Fig. 1. The specific activity of ³H-DNA in total DNA [(protein-linked ³H-DNA c.p.m./protein-linked ¹⁴C-DNA c.p.m.)/(total ³H-DNA c.p.m./total ¹⁴C-DNA c.p.m.)] was determined. This relative specific activity was plotted as a function of ¹⁴C-DNA remaining protein-linked after sonication (normalized to the unsonicated protein-linked ¹⁴C-DNA value).

Furthermore, protein-linked ³H-DNA complexes could be reversed by >60% after incubating the teniposide-treated monolayers in the absence of teniposide for 4 h at 37 °C. The time dependence of reversal (data not shown) was similar to that observed using purified topoisomerase II⁵.

³H-thymidine pulse and pulse-chase labelling experiments revealed that newly replicated DNA was specifically enriched within the teniposide-induced topoisomerase II-DNA complexes. Briefly, monolayer cultures that had been labelled previously for 72 h with ¹⁴C-thymidine were incubated with ³Hthymidine for 90 s (pulse) or exposed to ³H-thymidine for 90 s and then incubated with a 100-fold excess of unlabelled thymidine for 45 min (pulse-chase). Immediately following pulse or pulse-chase labelling, the cell monolayers were permeabilized, treated with teniposide, and then lysed in SDS. At this point, the SDS lysates were sonicated for various lengths of time in order to progressively reduce the average fragment size of DNA remaining covalently bound to topoisomerase II. The topoisomerase II-linked DNA fragments in the sheared lysates were then recovered usng the K-SDS precipitation procedure. The results of these experiments (see Fig. 2) indicated that as the amount of K-SDS-precipitable 14C-DNA was reduced by sonication, protein-linked DNA from pulse-labelled cells became progressively enriched in ³H-DNA (that is, the specific activity of protein -linked ³H-DNA relative to the specific activity of total ³H-DNA became >1). In contrast, protein-linked DNA from pulse-chase labelled cells was not enriched in ³H-DNA following sonication. In the absence of teniposide treatment, neither pulse-labelled nor pulse-chase labelled cells displayed any enrichment of ³H-DNA among protein-linked DNA, whether sonicated or not.

We believe that the association of pulse-labelled DNA with topoisomerase II-DNA covalent complexes may reflect a functional interaction of topoisomerase II with newly replicated DNA. However, another possible explanation for the observed

enrichment of newly replicated DNA with teniposide-induced topoisomerase II-DNA covalent complexes is that DNA at the replication fork might be more readily accessible for spurious binding to abundant nuclear proteins like topoisomerase II than is bulk nuclear DNA. We therefore treated pulse-labelled permeabilized cells with camptothecin, a plant alkaloid reported to trap covalent mammalian DNA topoisomerase I-DNA complexes¹¹, and found that camptothecin generated covalent protein-DNA complexes but failed to reveal any enrichment of ³H-DNA among protein-linked DNA after sonication.

Furthermore, the enrichment for pulse-labelled ³H-DNA with topoisomerase II-linked DNA was not limited to our permeabilized cell system. We found that for short ³H-thymidine labelling times, intact cells exposed to teniposide also contained protein-linked DNA enriched in ³H-DNA following sonication (Table 1). Cell monolayers that had been labelled previously with ¹⁴C-thymidine were incubated with ³H-thymidine for 5, 10, 20 and 30 min. In order to trap topoisomerase II-DNA complexes in the intact cells, teniposide was added to the ³H-thymidine incubation medium for the final 5 min of ³H-thymidine labelling. When the cells were lysed in SDS and sonicated, topoisomerase II-linked DNA enriched in ³H-DNA was recovered along with the K-SDS precipitate (see Table 1). The enrichment for ³H-DNA was greater for shorter ³H-thymidine labelling times.

Table 1 Teniposide treatment of intact cells reveals an enrichment of newly replicated DNA with covalent protein-DNA complexes

³ H-thymidine labelling time (min)	Protein-linked ³ H-DNA (relative specific activity)
5	19.1 ± 0.3
10	11.3 ± 0.3
20	7.7 ± 0.7
30	6.4 ± 0.1

Cultured Dunning R3326-G rat prostatic adenocarcinoma cells that had been labelled for 72 h with 0.05 Ci ml $^{-1}$ $^{14}\text{C-thymidine}$ (60 mCi mmol $^{-1}$) were incubated with 20 Ci ml $^{-1}$ $^{3}\text{H-thymidine}$ (54 Ci mmol $^{-1}$) in complete medium for 5, 10, 20 or 30 min at 37 °C. To trap topoisomerase II-DNA covalent complexes, teniposide was added to the $^{3}\text{H-thymidine-containing medium}$ to a final concentration of 20 μM (0.2% dimethyl sulphoxide, DMSO) for the final 5 min of $^{3}\text{H-thymidine labelling}$. Following $^{3}\text{H-thymidine labelling}$ and teniposide exposure, the cell monolayers were lysed directly in SDS lysis buffer and the SDS lysates were sonicated for 30 s with a Branson Model W160 Sonifier before being subjected to the K-SDS assay described in Fig. 1 legend. The specific activity of $^{3}\text{H-DNA}$ in total DNA was determined as for Fig. 2 and is expressed as the mean \pm s.d. The $^{3}\text{H-thymidine labelling}$ time dependence of this relative specific activity is given.

Topoisomerase II forms covalent complexes with DNA in the presence of teniposide such that each subunit (mammalian topoisomerase II is a homo-dimer) can be found in covalent linkage through a tyrosine to a 5'-phosphate on the cleaved substrate DNA^{5,10}. We sought to determine whether teniposideinduced covalent protein-DNA complexes were formed exclusively with unreplicated parental DNA near the replicating fork or whether nascent daughter DNA strands could be isolated with the complexes. In order to detect teniposide-induced complexes between topoisomerase II and nascent daughter DNA strands, 3H-thymidine pulse and pulse-chase labelled cells were permeabilized, treated with teniposide and lysed in SDS (as in Fig. 2). The SDS lysates were sonicated and then analysed by using the K-SDS assay under both denaturing (single-stranded DNA; lysates heated to 100 °C for 10 min) and non-denaturing (double-stranded DNA) conditions. We predicted that if covalent complexes were trapped near DNA replication forks, but only on unreplicated parental DNA, we should not detect denatured DNA enriched in ³H-DNA in sonicated lysates from pulse-labelled cells. We found instead that when lysates from

Fig. 3 Nascent DNA strands can be isolated in covalent linkage with topoisomerase II following teniposide treatment. Following sucrose gradient centrifugation, the fractions of the total protein-linked 3H-DNA (72-h label, a) and newly synthesized DNA (90-s label, b) recovered from each gradient were plotted as a function of fraction number (from the top). Arrows in a denote the position of the 2S (28 base pair, bp) and 13S (2,657 bp) markers determined by analysing aliquots from each fraction for ³²P c.p.m. Methods. Dunning R3327-G rat prostatic adenocarcinoma cells growing in culture were labelled with $20 \,\mu\text{Ci ml}^{-1}$ $^3\text{H-thymidine}$ (54 $\mu\text{Ci mmol}^{-1}$) for 90 s or with 1 $\mu\text{Ci ml}^{-1}$ $^3\text{H-thymidine}$ for 72 h in complete medium at 37 °C. Permeabilized monolayers treated with 20 μM teniposide (as for Fig. 1) were lysed in 1 ml of alkaline lysis buffer (0.2 M NaOH, 0.2 M NaCl, 10 mM EDTA). The alkaline lysates were carefully applied to 30-ml 5-20% sucrose gradients on top of 5-ml 50% sucrose cushions in alkaline buffer (0.1 M NaOH, 0.9 M NaCl, 10 mM EDTA) and centrifuged in an SW27 (Beckman) rotor for 15 h at 4 °C at 25,000 r.p.m. For DNA size markers plasmid pLY-1, a 2,679-bp pBR322 derivative, was digested with *EcoRI* and *ClaI*, and then end-labelled by fill-in with $[\alpha^{-3^2}P]$ dATP in the presence of unlabelled dGTP, dCTP and TTP using the Klenow fragment of DNA polymerase I (ref. 19), ²P-labelled 28- and 2,657-bp DNA fragments. s°_{20,w} Values for the fragments under alkaline sedimentation conditions were estimated to be 2S (for the 28-bp fragment) and 13S (for the 2,679-bp fragment), respectively²⁰. The labelled fragments were applied as internal markers in the gradient containing the alkaline lysate from the 72-h-labelled cells. After centrifugation 1.5-ml fractions were collected from the top of each centrifuge

tube by displacement with 70% sucrose. Fractions were neutralized by the addition of 0.1 ml 1.5 M HCl in 0.4 M Tris (pH 8.0). After the addition of 0.25 ml of 2×SDS lysis buffer and 0.25 ml of 240 mM KCl, 0.5-ml aliquots

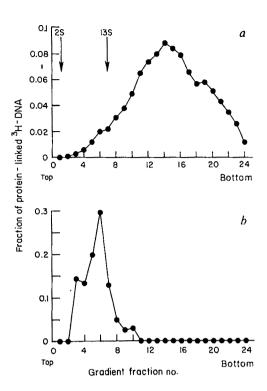
from each fraction were subjected to the K-SDS assay for protein-linked

DNA as described for Fig. 1 (with two washes).

teniposide-treated pulse-labelled cells were sonicated for 30 s (as in Fig. 2), the denaturing K-SDS assay revealed an enrichment of 3H-DNA among topoisomerase II-linked singlestranded DNA (13.7 \pm 1.3-fold) similar to that detected with the non-denaturing K-SDS assay for topoisomerase II-linked double-stranded DNA (13.4 ± 1.3-fold). Sonicated lysates from pulse-chase labelled cells failed to display any enrichment for ³H-DNA among topoisomerase II-linked DNA, regardless of whether the K-SDS assay was run under denaturing or nondenaturing conditions.

Further evidence that topoisomerase II might form covalent complexes directly with nascent DNA fragments in the presence of teniposide was provided by alkaline sucrose density gradient sedimentation studies. Pulse-labelled or uniformly labelled cells were permeabilized, treated with teniposide, dissolved in NaOH and then applied to alkaline sucrose gradients (see Fig. 3). After centrifugation, the gradient fractions were subjected to the K-SDS assay for protein-linked DNA. Similar to the findings of Chen et al.5, we found that most topoisomerase II-linked ³H-DNA from uniformly labelled cells treated with teniposide sedimented to a size of 25-35S (Fig. 3a). Topoisomerase IIlinked ³H-DNA from pulse-labelled cells treated with teniposide sedimented to a size (<12S) characteristic of nascent DNA chains (Fig. 3b).

Our results indicate that mammalian DNA topoisomerase II can be isolated in covalent linkage with newly replicated DNA molecules near the site of DNA synthesis, following teniposide treatment of permeabilized cultured rat prostatic adenocarcinoma cells. The close proximity of the teniposide-induced covalent complexes to the replicating fork suggests that DNA topoisomerase II may be actively involved in the replication of mammalian cell DNA. These findings are consistent with the identification of topoisomerase II as a component of the mammalian replitase12 malian replitase¹², a multi-enzyme complex responsible for DNA replication^{12,13}, and with the demonstration of topoisomerase II within the nuclear matrix¹⁴, the subcellular site for eukaryotic DNA synthesis15. An increase in topoisomerase II activity in rat liver following partial hepatectomy further supports a role for topoisomerase II in mammalian DNA replication¹⁶.



Previous studies on the role of DNA topoisomerase II in eukaryotic DNA replication have emphasized the importance of a topoisomerase II double-strand DNA passage activity in resolving the products of DNA synthesis prior to mitotic segregation¹⁷. However, our observation that mammalian DNA topoisomerase II covalent complexes may be located near the replicating fork suggests that the enzyme may also function during replication fork progression in mammalian cells. Cairns 18 recognized the need for an effective swivel in his description of the replication of covalently closed DNA molecules. We speculate that a mammalian DNA topoisomerase II, located near the replication fork in association with daughter DNA molecules, might be able to remove parental helical turns that have been passed through the fork to the daughter strands.

We thank Drs E. R. Barrack and G. L. Chen for helpful suggestions and comments, and R. Middleton for assistance in typing this manuscript. This work was supported by grants GM 27731 and AM 22000. W.G.N. is supported by the Medical Scientist Training Program Grant 5T32 GM 07309.

Received 17 January: accepted 15 April 1986

- Wang, J. C. A. Rev. Biochem, 54, 665-697 (1985).
- Liu, L. F. CRC crit. Rev. Biochem. 15, 1-24 (1983).
 Gellert, M. A. Rev. Biochem. 50, 879-910 (1981).
- Ross, W., Rowe, T., Glisson, B., Yalowich, J. & Liu, L. Cancer Res. 44, 5857-5860 (1984).
- Chen, G. L. et al. J. biol. Chem. 259, 13560-13566 (1984).

 Glisson, B. S., Smallwood, S. E. & Ross, W. E. Biochim. biophys. Acta 738, 74-79 (1984).

 Long, B. H., Musial, S. T. & Brattain, M. G. Cancer Res. 45, 3106-3112 (1985).

 Yang, L., Rowe, T. C. & Liu, L. F. Cancer Res. 45, 5872-5876 (1985).
- Rowe, T. C., Chen, G. L., Hsiang, Y.-H. & Liu, L. F. Cancer Res. (in the press)
- 10. Liu, L. F., Rowe, T. C., Yang, L., Tewey, K. M. & Chen, G. L. J. biol. Chem. 258, 15365-15370 (1983).

 11. Hsiang, Y.-H., Hertzberg, R., Hecht, S. & Liu, L. F. J. biol. Chem. 260, 14873–14878 (1985).

- Noguchi, H., Reddy, G. P. V. & Pardee, A. P. Cell 32, 443-451 (1983).
 Reddy, G. P. V. & Pardee, A. B. Proc. natn. Acad. Sci. U.S.A. 77, 3312-3316 (1980).
 Berrios, M., Osheroff, N. & Fisher, P. A. Proc. natn. Acad. Sci. U.S.A. 82, 4142-4146 (1985).

- Pardoll, D. M., Vogelstein, B. & Coffey, D. S. Cell 19, 527-536 (1980).
 Duguet, M., Lavenot, C., Harper, F., Mirambeau, G. & DeRecondo, A. M. Nucleic Acids Res. 11, 1059-1075 (1983).
 DiNardo, S., Voeikei, K. & Sternglanz, R. Proc. natn. Acad. Sci. U.S.A. 81, 2612-2620 (1984).
- 18. Cairns, J. Cold Spring Harb. Symp. quant. Biol. 28, 43-46 (1963).

 19. Maniatis, T., Fritsch, E. F. & Sambrook, J. Molecular Cloning, A Laboratory Manual (Cold Spring Harbor Laboratory, New York, 1982). 20. Studier, F. W. J. molec. Biol. 11, 373-390 (1965).

Nuclear magnetic resonance imaging of a single cell

James B. Aguayo*, Stephen J. Blackband, Joseph Schoenigert, Mark A. Mattingly‡ & Markus Hintermann‡

Massachusetts 01821, USA

Division of NMR Research, Department of Radiology, * Wilmer Ophthalmological Institute, and † Department of Biological Chemistry, Johns Hopkins University School of Medicine, Baltimore, Maryland 21205, USA Bruker Medical Instruments, Manning Park, Billerica,

Nuclear magnetic resonance (NMR) imaging^{1,2} is now an established tool in clinical imaging and competes favourably with conventional X-ray computerized tomography (CT) scanning³. The drive behind NMR imaging has primarily been in the area of whole-body imaging, which has been limited clinically to fields of up to 1.5 T (60 MHz). It is recognized that there may be substantial advantages in obtaining images with sub-millimetre spatial resolution^{4,5}. Also, there may be benefits to imaging at higher fields, since the signal increases as the square of the magnetic field. Using a modified 9.5 T 89-mm-bore high-resolution NMR spectrometer, we have now obtained the first NMR images of a single cell, demonstrating the advent of the NMR imaging microscope. The NMR microscope is expected to have considerable impact in the areas of biology, medicine and materials science, and may serve as a precursor to obtaining such resolutions on human subjects.

The spectrometer was equipped with a set of magnetic field gradient coils with corresponding control units and power supplies capable of producing gradients for spatial delineation in excess of 20 G cm⁻¹. In addition, a radiofrequency (r.f.) modulator, a linear amplifier, waveform memories for gradient and r.f. control, and image display facilities were interfaced with the spectrometer. Radiofrequency excitation and reception were performed using a 5-mm horizontal solenoid. The studies presented here used a spin-echo imaging technique^{7,8}. The delay between the excitation and the acquisition of the spin-echo (TE) and the time between excitation pulses (TR) are given for each image in the figure legends.

The cells used in these studies were ova obtained from Xenopus laevis (African clawed toad) by standard surgical extraction techniques⁹. The ova were mechanically stripped of ovarian tissue and maintained in Barth's solution, and ova in different stages of oogenesis were placed in a 1.1-mm (inside diameter) tube and imaged. Figure 1 shows that the nucleus is clearly resolved, with heterogeneity in the cell cytoplasm seen as two regions of differing intensity corresponding to the animal and vegetal poles of the ovum. The differences in image intensity result from proton density variations, differences in relaxation times, or a mixture of the two. The water in the cell cytoplasm is distinct from the free water surrounding the cell, as has been suggested by some investigators¹⁰. The water signal from the nucleus is distinct from that of the cytoplasm and is indistinguishable from that of the free water surrounding the cell, suggesting that nuclear water is less strongly bound than cytoplasmic water. The signal-to-noise ratio of these images indicates that a greater spatial resolution can be obtained in similar times. To date, a resolution of 10×13 μm with a 250-μm slice width has been achieved (Fig. 2), although greater resolutions are expected to be possible. The nucleus of the ovum in Fig. 2 is clearly resolved, and a greater signal is obtained from the animal pole of the ovum than from the vegetal pole. Such data are obtained in acceptable experimental times (see Figs 1-4) and can be directly related to morphological regions within the cell.

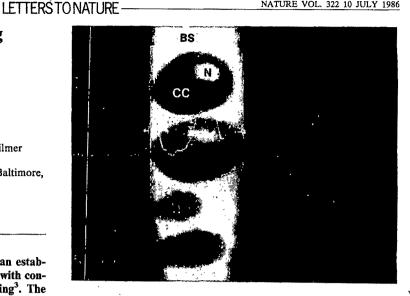


Fig. 1 NMR image of four ova from Xenopus laevis at different. stages of oogenesis. The image represents a slice 500 µm thick lengthwise through the tube containing the intact ova. The image matrix is 256×256, which corresponds to a spatial resolution of 16×27 μm. Zero-filling was not used in any of the following images as a means of improving resolution because we noted no significant improvement in image quality. A spin-echo pulse sequence was used with a TE of 16 ms and a TR of 1 s, resulting in an imaging time of 4 min and 16 s. The image shows the clear distinction between the cell nucleus (N) and the cell cytoplasm (CC). The profile across one of the cells demonstrates a signal-to-noise ratio for the nucleus of ~15:1. The cell was surrounded by Barth's solution (BS).

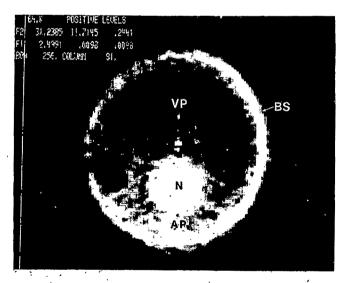


Fig. 2 NMR image representing a transverse slice across a glass tube containing a stage 4 X. laevis ovum; it has a spatial resolution of $10 \times 13 \,\mu\text{m}$ and a slice width of 250 μm . The spin-echo pulse sequence used a TE of 16 ms, a TR of 4 s, and produced a data array of 128 × 128. Four experiments were averaged and thus the total imaging time was 32 min and 8 s. Although the image is relatively grainy, the differences between the cell nucleus and different zones of the cytoplasm are easily discerned. VP, vegetal pole; AP, animal pole.

We have also been able to infer information about the chemical composition of the cell. A chemical shift artefact in the form of an adjacent, slightly overlapping image was noted in early cell experiments (Fig. 3). This artefact slowly disappeared as the cells remained in the imaging system for longer periods of time. Earlier data11 imply that this artefact is due to

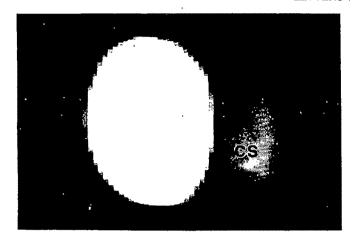
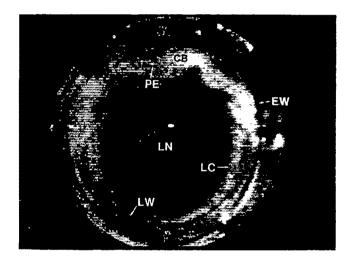


Fig. 3 (Left) NMR image showing a transverse section of a cell in a glass tube. The image acquisition parameters were the same as those of Fig. 1. The display constraints were adjusted so that low signal intensities can be easily observed. Under these display conditions the water signal from the cell appears as a solid white disk. To the right of this disk is a chemically shifted image (CS), which corresponds to the signal arising from the lipid content of the cell. The small dark area at the top of the chemical shift corresponds to the nucleus, indicating that there is little lipid within the nucleus.

Fig. 4 (Right) NMR micrograph of a mouse eye. The 256×256 data array has an in-plane resolution of 16×27 µm and a slice width of 250 µm. Only one data acquisition was used, with a TE of 16 ms and a TR of 2 s, resulting in an imaging time of 8 min and 32 s. The eye was placed in buffer solution within a 4.1-mm capillary tube. Considerable care was taken to ensure that there were no air bubbles around the eye, as these considerably distort the image. The image, from bottom to top, corresponds roughly to the eye, from side to side, although the presence of only one part of the ciliary body indicates that the imaging plane is tilted slightly from this equatorial plane. BS, buffer solution; LN, lens nucleus; LW, lens wall; LC, lens cortex; EW, eye wall; V, vitreous; CB, ciliary body. The dark patches in the surrounding buffer solution are due to extra-ocular material that remained after extraction.



the presence of lipid in the cytoplasm. Further studies should confirm the temporal dependence of this lipid. We speculate that the cell metabolizes these lipids during the experiment.

Figure 4 shows an image of a mouse eye to illustrate the clarity of images obtained at these high field strengths. The eye (~3.4 mm in diameter) was freshly extracted from a CD albino mouse. Structures within the eye are sharply resolved at a resolution of 16×27 µm, and the image definition is comparable to that of conventional NMR images. The resolution of this image is less than that of the ovum image in Fig. 2 because the object is larger; a larger matrix and hence a longer imaging time would have been required to obtain an image of the entire object. However, there is sufficient signal to obtain better resolutions on such samples, since both eye and cell images were obtained with an r.f. coil of the same diameter. The use of a zoom imaging technique should allow imaging of a small section of an object at high resolutions¹².

The slice widths within these images are considerably larger than the in-plane spatial resolution, primarily to reduce imaging times and improve the signal-to-noise ratio in the image. We

anticipate being able to use much smaller slice widths with these resolutions by efficient use and balance of imaging delays, r.f. coil design, imaging technique and higher fields. We note that in optical transmission microscopy the 'slice width' is determined by the physical width of the sample, which is often fixed, sectioned and stained. NMR imaging can be performed on intact living systems. No sectioning, fixing or staining was required to produce these NMR images and thus they are not subject to artefacts inherent in these procedures.

As expected, because the samples we studied were small, we observed no r.f. penetration problems. Also, no alterations in morphology were seen at this high field. Whether attenuation of r.f. energy at these frequencies will be a problem for larger samples and whether the high fields used are indeed harmful to living systems is unknown. Even if this should prove to be the case, we anticipate that a small-bore NMR microscope, as demonstrated here, will in itself prove to be a valuable tool in many spheres of science.

We thank J. D. Glickson, V. P. Chacko, H. M. Cheng, J. Windle and C. D. Paella for technical assistance.

- Mansfield, P. & Morris, P. G. Adv. magn. Res. Suppl. 2 (1982).
- 3. Kressel, H. Y. Magnetic Resonance Annual (Raven, New York, 1985).
 4. Lauterbur, P. C. IEEE Trans. nucl. Sci. NS-31, No. 4 (1984).
- Mansfield, P. & Grannell, P. Phys. Rev. B12, 3618 (1975).
 Abragam, A. The Principles of Nuclear Magnetism (Clarendon, Oxford, 1961).
- 7. Hutchinson, J. M. S. Proc. int. Symp. NMR Imaging (Bowman Gray School of Medicine.
- Winston-Salem, North Carolina, 1981).

 8. Kumar, A., Welti, D. & Ernst, R. R. J. magn. Res. 18, 69-83 (1975).

 9. Ziegler, D. H. & Morrill, G. A. Deul Biol. 60, 318 (1977).

 10. Mathur-De Vre, R. Prog. Biophys. molec. Biol. 35, 103 (1979).

- 11. Slack, J. M. W. From Egg to Embryo (Cambridge University Press, 1983)
 12. Luyten, P. R. & Hollander, J. A. Proc. Soc. magn. Res. Med., 1021 (19-23 August 1985)

Received 24 February; accepted 13 May 1986.

1. Lauterbur, P. C. Nature 242, 190-191 (1973).

Cephalosporin antibiotics can be modified to inhibit human leukocyte elastase

James B. Doherty, Bonnie M. Ashe,
Lawrence W. Argenbright, Peter L. Barker,
Robert J. Bonney, Gilbert O. Chandler,
Mary Ellen Dahlgren, Conrad P. Dorn Jr,
Paul E. Finke, Raymond A. Firestone, Daniel Fletcher,
William K. Hagmann, Richard Mumford,
Laura O'Grady, Alan L. Maycock, Judith M. Pisano,
Shrenik K. Shah, Kevan R. Thompson
& Morris Zimmerman

Merck Sharp and Dohme Research Laboratories, Rahway, New Jersey 07065, USA

Several laboratories, including our own, have reported the synthesis and activity of certain low relative molecular mass inhibitors of mammalian serine proteases1-4, especially human leukocyte elastase (HLE, EC 3.4.21.37), an enzyme whose degradative activity on lung elastin has been implicated as a major causative factor in the induction of pulmonary emphysema⁵, and which is present in the azurophil granules of human polymorphonuclear leukocytes (PMN). Normally, these granules fuse with phagosomes containing engulfed foreign material (such as bacteria), and HLE, in combination with other lysosomal enzymes, catabolizes the particles^{6,7}. Under certain pathological conditions, however, PMN become attached to host protein (elastin fibres, basement membrane, connective tissue, immune complexes)8,9, and in response to this adherence, the granules may fuse with the PMN outer membrane and release their contents, including HLE, directly onto the tissue10 Besides emphysema, HLE may also contribute to the pathogenesis of disease states such as adult respiratory distress syndrome¹¹. and its potential involvement in rheumatoid arthritis 12 makes HLE inhibitors of considerable interest. It is known that cephalosporin antibiotics (for example, cephalothin (compound I, Table 2)) are acylating inhibitors of bacterial serine proteases which help synthesize the cell wall by performing a transpeptidation reaction on a peptidyl substrate bearing a D-Ala-D-Ala terminus¹³. We now report that neutral cephalosporins (that is, compounds not bearing a free carboxyl at position C-4) can be modified to become potent time-dependent inhibitors of HLE.

Cephalosporins bearing substituents in the 7α position are potent inhibitors of HLE (Table 2; details of the chemical synthesis of these compounds will be reported elsewhere). The corresponding 7β isomers are either weaker inhibitors or inactive. The preference for α over β substituents is perhaps due to the fact that HLE cleaves L-L-amino acid peptide linkages whereas the target enzymes for β -lactam antibiotics cleave D-D-amino-acid peptide bonds, and thus 7α -substituted cephems

Table 1 Kinetic constants for inactivation of HLE by substituted cephalosporins

Compound	$K_{i}\left(\mathbf{M}\right)$	$k_2 (\mathrm{s}^{-1})$	$k_2/K_i (\mathrm{M}^{-1} \mathrm{s}^{-1})$
XIII	$1.2 \times 10^{-6} \\ 1.8 \times 10^{-7}$	0.023	19,000
XXII		0.029	161,000

Rates of reaction versus time were measured at constant substrate and enzyme concentration, but varying inhibitor concentration. Data were computer fitted to the non-linear regression progress curve absorbance $= V_s \, r + (V_0 - V_s) \, (1 - \mathrm{e}^{-kt})/k + C$ (where $V_0 = \text{initial velocity}, \, V_s = \text{final velocity}, \, k = \text{observed rate constant}, \, t = \text{time and } C = \text{constant}$ integration), which assumes first-order enzyme inactivation. K_i and k_2 were calculated from a reciprocal plot of k versus inhibitor concentration.

may be better mimics of mammalian substrates. Further, we have found that the enzyme prefers smaller substituents in the 7α position, possibly because HLE cleaves proteins preferentially at sites where the P-1 (ref. 14) position is occupied by a relatively small alkyl substituent¹⁵. In the case of the alkyl ether series (compounds XIII → XIV → XV → XVI, Table 2), a rapid decrease in activity with increasing length of the alkyl group is observed. Branched groups (XVII) are also less active. The unsubstituted analogue (X) is inactive, but the 7α -fluoro derivative (XXI) is highly active, indicating that the inductive nature of the substituent has a strong effect on the rate of acylation. That inductive effects are not of overwhelming importance, however, is amply demonstrated by the fact that the 7α -ethyl analogue (XI) is a very potent inhibitor of the enzyme, almost as active as the isosteric 7α -methoxy derivative (XIII). Finally, aromatic rings can be tolerated by the enzyme; the 7α -phenyl analogue (XXIII) is roughly equipotent as an inhibitor to XIII, and in the ether series both XVIII and XX (but curiously not XIX) gave good inhibition of the enzyme.

The effects of modification of other parts of the cephalosporin nucleus have also been examined. With respect to the oxidation state of the sulphur, we have found that sulphones are generally the most active members of a series, with the (S)-sulphoxides and sulphides usually being an order of magnitude less active, and the (R)-sulphoxides being characteristically the least active of the series (compare compounds XIII \rightarrow XXV \rightarrow XXIV \rightarrow XXVI and XIV \rightarrow XXVIII \rightarrow XXVIII \rightarrow XXVIII \rightarrow XXVIII \rightarrow XXVIII \rightarrow XXVIII \rightarrow XXIX; Table 2).

Modification of the functionality at position C-4 has been studied extensively (compounds XXXI-XLII; Table 2). As noted earlier, the free acids are generally poor inhibitors of HLE. In fact, carboxylates even more remote from the nucleus (for example, compound XXXIX) also result in a loss of inhibitory activity. Considering that HLE is an endopeptidase that cleaves peptide linkages between non-ionic amino acids, the enzyme preference for neutral molecules (at least those not bearing a charge in close proximity to the active site) is understandable. Decreasing the steric bulk of the ester (XIII-> XXXIII → XXXII → XXXI) leads to some increase in activity. Incorporation of a benzene ring into the ester moiety (XXXIV) leads to a >10-fold enhancement in activity over XIII. Here again, placing a carboxyl at the C-4 position of the benzyl group yields a compound which is ~10-fold less active (XXXV), although still possessing substantial activity. The N-benzyl amide analogue (XXXVII) is ~100 times less active than the benzyl ester, but conversion of this secondary amide to a tertiary amide (XXXVIII) almost completely restores the inhibitory capacity of the molecule, leading to the interesting hypothesis that the s-cis amide conformation is required to fit the benzyl group appropriately into the active site. Note also that even a simple hydrogen at the C-4 position (XLI) still gives an entity with some inhibitory capability.

Most of the potent inhibitors in Table 2 cause time-dependent inhibition of HLE. (In Table 2 the compounds are evaluated according to their ability to cause 50% reduction in enzyme activity after an incubation period arbitrarily chosen to be 2 min. Greater inhibition is observed at longer times.) Preliminary kinetic data are consistent with a mechanism involving reversible complex formation followed by acylation of an active-site residue to produce the inactivated species (scheme 1). This

Scheme 1
$$E+I \xrightarrow[k_{-1}]{k_1} E \cdot I \xrightarrow{k_2} E-I \rightarrow Further modification?$$

$$Acylated$$

$$enzyme$$

$$K_i = k_{-1}/k_1$$

scheme is similar to those describing the initial steps in the

Table 2 Activity of substituted cephalosporins against HLE

		(O) _n			
		Χ			
		Y			
		N	- A		
		OAC OAC			
		Ž			
Compound No.	X	Y	Z	n	IC _{so} (µg ml ⁻¹)
1	H	ThCH ₂ CONH*	CO₂H	0	>20
II .	H	ThCH ₂ CONH	$CO_2C(CH_3)_3$	0	>20
Ш	H	ThCH ₂ CONH	$CO_2C(CH_3)_3$	2	>20
IV	H	CH ₃ CONH	$CO_2C(CH_3)_3$	2	>20
V	CH ₃ CONH	Н	$CO_2C(CH_3)_3$	2	>20
VI	Н	CF ₃ CONH	$CO_2C(CH_3)_3$	2	>20
VII	CF ₃ CONH	н	$CO_2C(CH_3)_3$	2	2
VIII	H	HCONH	$CO_2C(CH_3)_3$	2	15
IX	HCONH	Ħ	$CO_2C(CH_3)_3$	2	2
X	Н	• Н	$CO_2C(CH_3)_3$	2	>20
XI	CH ₂ CH ₃	H	$CO_2C(CH_3)_3$	2	1
XII	H	OCH ₃	$CO_2C(CH_3)_3$	2	>20
XIII	OCH ₃	H	$CO_2C(CH_3)_3$	2	0.5
XIV	OCH ₂ CH ₃	Н	$CO_2C(CH_3)_3$	2	1.5
XV	O(CH ₂) ₂ CH ₃	Н	CO ₂ C(CH ₃) ₃	2	20
XVI	$O(CH_2)_3CH_3$	H	$CO_2C(CH_3)_3$	2	>20
XVII	OCH(CH ₃) ₂	H	$CO_2C(CH_3)_3$	2	>20
XVIII	OC ₆ H ₅	Н	CO ₂ C(CH ₃) ₃	2	0.8
XIX	OCH ₂ C ₆ H ₅	H	CO ₂ C(CH ₃) ₃	2	>51
XX	OCH ₂ CH ₂ C ₆ H ₅	H	CO ₂ C(CH ₃) ₃	2	2.5 0.03
XXI	F	Н	CO ₂ C(CH ₃) ₃	2	0.03
XXII	CI	Н	CO ₂ C(CH ₃) ₃	2	0.02
XXIII	C ₆ H ₅	H	CO ₂ C(CH ₃) ₃	ő	5
XXIV	OCH ₃	Н	CO ₂ C(CH ₃) ₃	1(S)	2
XXV	OCH ₃	H H	CO ₂ C(CH ₃) ₃	1(R)	>20
XXVI	OCH,		CO ₂ C(CH ₃) ₃	0	>20
XXVII	OCH ₂ CH ₃	H H	$CO_2C(CH_3)_3$ $CO_2C(CH_3)_3$	1(S)	17
XXVIII	OCH ₂ CH ₃	п Н	$CO_2(CH_3)_3$ $CO_2(CH_3)_3$	1 (R)	>20
XXIX XXX	OCH ₂ CH ₃ Cl	H	$CO_2(CH_3)_3$ $CO_2C(CH_3)_3$	0	0.5
XXXI	OCH ₃	H	CO ₂ C(CH ₃) ₃	2	0.08
XXXII	OCH ₃	H	CO ₂ CH ₃ CH ₃	2	0.07
XXXIII	OCH ₃	H	$CO_2CH_2CH_3$ $CO_2CH(CH_3)_2$	2	0.3
XXXIV	OCH,	H	CO ₂ CH ₂ Ph	2	0.03
XXXV	OCH ₁	H	CO ₂ CH ₂ PH(4-CO ₂ H)	2	0.2
XXXVI	OCH ₃	H	$CO_2CH_2H(4CO_2H)$ $CON(CH_3)_2$	2	0.6
XXXVII	OCH ₃	H	CONHCH ₂ Ph	2	2
XXXVIII	OCH ₃	H	CON(CH ₃)CH ₂ Ph	2	0.06
XXXIX	OCH ₃	H	CONHCH ₂ CO ₂ H	2	>20
XL	OCH,	H	CONHCH ₂ CO ₂ C(CH ₃) ₃	2	0.9
XLI	OCH,	H	H	2	2
XLII	OCH ₃	Ĥ	CO ₂ H	2	>20
ALCOHOLOGY CONTRACTOR			■ **		

HLE was isolated as described previously^{2,3}. Purified HLE was assayed spectrophotometrically at 25 °C by continuous monitoring of the release of p-nitroaniline from Boc-Ala-Ala-Pro-Ala-p-nitroaniline at 410 nm. Incubation mixtures contained inhibitor, 0.2 mM substrate (both added in dimethyl sulphoxide; DMSO), DMSO (10% final concentration) and enzyme (added last) in 0.05 M trimethylaminoethanesulphonic acid, pH 7.5. The reaction was followed for 10 min and the rate after 2 min (r) was determined from the slope of the progress curve at that time. Per cent inhibition was determined by $100 \times [1 - (r_{\text{inhibitor present}}/r_{\text{inhibitor absent}})]$. IC₅₀ (concentration of inhibitor giving 50% inhibition) was determined from a plot of % inhibition versus log inhibitor concentration. Except for compounds which gave less than 50% inhibition at 20 μ g ml⁻¹, all inhibitors were studied over a concentration range that produced 15-90% inhibition.

inactivation of β -lactamases by various β -lactams^{16,17}. Table 1 shows kinetic constants for inactivation by compounds XIII and XXII. Both compounds are potent inhibitors (K_i values micromolar or less which rapidly and irreversibly inactivate the enzyme). Preliminary data suggest that certain other β -lactams may function solely as competitive (reversible, non-time-dependent) inhibitors of HLE. Further mechanistic details are being examined. Experiments are also under way to elucidate the structural features of β -lactams which are responsible for rapid inactivation.

Table 3 shows the relative inhibition of several different serine proteases by a representative set of cephalosporins. Most of the compounds in this series are excellent inhibitors of porcine pancreatic elastase (PPE) as well as HLE, and to a lesser extent α -chymotrypsin. This series shows no significant activity against trypsin or human cathepsin G, although some activity is seen against human thrombin, and one compound (XVIII) shows trace activity against plasmin. Interestingly, compound XX shows unusual activity against chymotrypsin, implying that an appropriate chain length has been achieved to allow the phenyl

^{*} Th, 2-thienyl.

[†] The compound is insoluble at higher concentrations.

Table 3 Selectivity of modified cephalosporins against various serine proteases IC., (up ml-1)

2200 5 Secretary of incomes depiniosporms against various serine processes (Lgg ini							
Compound	HLE	PPE	ChT	Cat G	Trypsin	Plasmin	Thrombin
XIII	0.5	<0.1	7-8	>50	>50	≫20	6
XXIV	5 :	15	≫20	>50	»20	n.d.	n.d.
XXV	2	7	>20	≫20	≫20	»20	»20
XIV	1.5	0.5	10	≫20	≫20	≫20	≫20
XVIII	0.8	5	5	≫20	≫20	20	1 %
XX	2.5	0.5	< 0.5	≫20	≫20	»20	»20

Both elastases were assayed with 0.2 mM Boc-Ala-Pro-Ala-p-nitroanilide as described in Table 1 legend. Other proteases were assayed similarly using Ac-Ala-Ala-Pro-Phe-pNA (chymotrypsin), Cbz-Gly-Pro-Arg-pNA (trypsin and thrombin) and tosyl-Gly-Pro-Lys-pNA (plasmin) (all at 0.2 mM). Cathepsin G was assayed with 0.2 mM Boc-Tyr-p-nitrophenyl ester in 0.05 M PIPES buffer, pH 6.5, containing 10% DMSO at 25 °C by measuring the production of p-nitrophenol at 348 nm. IC₅₀ values were obtained as described for Table 1. HLE and cathepsin G (Cat G) were prepared as described previously^{2,3}. Porcine pancreatic elastase (PPE) was obtained from Sigma Biochemicals, bovine α -chymotrypsin (ChT) and bovine tryspin were obtained from Worthington, and human thrombin and human plasmin were obtained from Boehringer Mannheim. n.d., not determined

group to bind in the S₁ enzyme binding site.

One biological effect of elastase inhibitors is illustrated by the following observations. Microvascular haemorrhage can be part of an inflammatory response when PMN infiltrate inflamed tissue^{18,19}. Stetson and Good²⁰ postulated that this vascular damage may result from release of PMN proteases during phagocytosis. Argenbright et al.21 have shown that microvascular haemorrhage follows the intradermal injection of soluble human PMN granule contents into rabbits, and that this haemorrhage is dependent on HLE activity. Table 4 demonstrates that this

Table 4 Inhibition of microvascular haemorrhage by compound XIII

	Haemorrhage		In vitro activity	
	Blood vol./ skin site(µl)	% Inhibition	% Inhibition	
PMN extract +DMSO	86.5 + 12	,		
PMN extract +100 µg XIII PMN Extract	0.8 + 1.6	98	100	
+2.8 µg XIII PMN extract	22.1+10	75.	84	
+1.5 µg XIII	73.7 + 18	14	25	

Intradermal microvascular haemorrhage was produced in rabbit skin by the injection of components derived from human PMN granules. Haemorrhage was quantitated by measuring the 30-min accumulation of ⁵⁹Fe-autologous red blood cells in the injected skin sites. The data are expressed as the change in blood content as a result of PMN extract injection (for example, the $5.0 \pm 1.9 \mu l$ blood per site measured in vehicle injected sites has been subtracted from all other sites). Inhibition of haemorrhage was obtained by adding XIII directly to the PMN extract before injection. All sites received 0.4% DMSO. In vitro activity was determined by assaying a sample of PMN extract with and without addition of XIII against synthetic substrate according to previously published procedures15.

haemorrhage is inhibited by compound XIII, and further, that inhibition of haemorrhage correlates well with inhibition of HLE activity as measured in vitro.

Our study is the first reported demonstration that the appendages of a β -lactam nucleus, which has proved to be such an important source of bacterial enzyme inhibitors, can be modified to produce compounds that are potent inhibitors of human serine proteases. The implications of this work for further enzyme inhibitor design are clear, and we will shortly be reporting on the mechanism of this inhibition as well as our results with other B-lactam nuclei.

We thank Drs P. Davies, A. S. Rosenthal and T. Y. Shen for their support and encouragement in this work, Drs B. G.

Christensen, F. P. DiNinno, R. W. Ratcliffe, E. Walton and the staff of the Synthetic Chemical Research Department for aiding in the advancement of this research, Mr J. Smith for analytical support and Mrs Carol D. Babish for help in preparing this manuscript.

Received 14 March; accepted 18 April 1986

- Powers, J. C. Am. Rev. respir. Dis. 127, 854-858 (1983).
 Zimmerman, M. et al. J. biol. Chem. 255, 9848-9851 (1980).
- Ashe, B. M., Clark, R. L., Jones, H. & Zimmerman, M. J. biol. Chem. 256, 11603-11606
- Moorman, A. R. & Abeles, R. J. J. Am. chem. Soc. 104, 6785-6786 (1982).
- Mittman, C. (ed.) Pulmonary Emphysema and Proteolysis 1-537 (Academic, New York,

- Thorne, K. J. I., Oliver, R. C. & Barrett, A. J. Infect. Immun. 14, 555-563 (1976).
 Blondin, J. & Janoff, A. J. clin. Invest. 58, 971-979 (1976).
 Starkey, P. M. & Barrett, A. Biochem. J. 155, 265-271 (1976).
 Schmidt, W. & Havemann, K. Hoppe-Seylers Z. physiol. Chem. 355, 1077-1082 (1974).
 Henson, P. M. J. Immun. 167, 1547-1557 (1971).
 Sprung, C. L., Schultz, D. R. & Clerch, A. R. New Engl. J. Med. 304, 1301-1302 (1984).
- 11. Velvart, M. Rheumatol. Int. 1, 121-130 (1981).
 13. Ghuysen, J.-M. in The Bacterial D-D Carboxypeptides/transpeptidase Enzyme System, 115-143 (University of Tokyo Press, 1976).
- Schechter, I. & Berger, A. Biochem. biophys. Res. Commun. 27, 157-162 (1967).
 Zimmerman, M. Colloquium Ges. biolog. Chem. 30, 186-195 (1979).
- Brenner, D. G. & Knowles, J. R. Biochemistry 23, 5833-5839 (1984).
 Brenner, D. G. & Knowles, J. R. Biochemistry 23, 5839-5846 (1984).
- Stetson, C. A. Ir J. exp. Med. 94, 347-358 (1951).
 Thomas, L. in The Inflammatory Process 456-459 (Academic, New York, 1965).
- 20. Stetson, C. A. & Good, R. A. J. exp. Med. 93, 49-64 (1951).
- 21. Argenbright, L. W., Ashe, B. M., Zimmerman, M. & Bonney, R. J. Fedn Proc. 43, 405 (1984).

New product news in *Nature*

- New on the market. Four pages of information 7 August: on new and novel items for the laboratory.
- 14 August: Computers in the laboratory. The latest in information technology and computer services.
- American Chemical Society. This issue will 28 August: include coverage of new equipment presented
 - at the ACS meeting to be held in Anaheim from 7th to 10th September.
- New on the market. More items of general 4 September: interest.
- Nature's Eighth International Conference. The 11 September: conference 'Exploring the Human Genome' will be held in conjunction with an exhibition of relevant equipment. Both conference and exhibition are to be held in Boston, running from 15 to 17 September.

Manufacturers are requested to send press releases on new products for consideration in the above issues to Nature's London office or to:

Karen Wright,

Nature.

1134 National Press Building, Washington DC 20045, USA

102111E

Volume 322 No.6076 17-23 July 1986 £1.90

Author Index

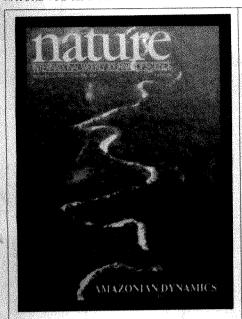
AMAZONIAN DYNAMICS

The collector that can't lose a drop, doesn't waste your time and won't cost a fortune.



nature

NATURE VOL. 322 17 JULY 1986



The Amazon basin rainforest in Madre de Díos. southeastern Perú. The meandering of the river crodes the old rainforest and creates point-bar deposits that promote primary succession. The river dynamics disturb all types of rainforest in the western Amazon as the forests are mostly growing on soils of floodplain origin. The resulting age heterogeneity contributes to the wide species diversity in the Upper Amazon. See page 254. The Author Index for volume 321 faces page 292.

OPINION

Court Africa note out of hand

DOUGH ATTICA gets out of mana	
Trouble on the farm	195
Shutting barn doors	196
NEWS	
European research	
German universities	197
Spain	
India	198
The deutschmarks that count	
US technology	199
AIDS	
Eureka	200
Patent law	
Space vehicles	201
West Germany	
Energy	202
US education	
Chernobyl	203
CORRESPONDENCE	and the second second
Risks of medical research/	
Monkeys/Computers	204
NEWS AND VIEWS	www.marananinide
	40*
Test ban made more respectable	205
RNA and hot-water springs	300
E.G. Nisbet	206

	name and the second
What makes nearby galactic clusters	
all move as one?	207
Joseph Silk New role for transfer RNA	207
	208
An unfolding story of protein	
translocation	1
James E Rothman	
& Roger D Kornberg	209
Are there two functional classes of	
glutamate receptors? Charles F Stevens	210
Ocean Drilling Program:	210
Palaeoclimatic linkage between	
high and low latitudes	
Leg 108 shipboard scientific party	211
Thyrotrophin-releasing hormone:	Ī
New applications in the clinic	212
Ewan C Griffiths	212
Biological chemistry: Long-range electron transfer	and the same of th
RJP Williams & D Concar	213
Obituary: Dame Honor Fell	
Ilse Lasnitzki	214
-SCIENTIFIC CORRESPONDENC	·c
	,C
Visual observation of lightning	
propagation D G Baker & A Baker-Blocker	215
Controversial glycosaminoglycan	213
conformations	
B Casu, J Choay, D R Ferro,	Version of the second
G Gatti, J-C Jacquinet.	
M Petitou, A Provasoli,	
M Raggazzi, P Sinay & G Torri	215
Ulcerative rhabdovirus in fish	
in South-East Asia G N Frerichs, S D Millar	
& R J Roberts	216
BOOK REVIEWS	
The Red and the Blue: Intelligence,	
Treason and the Universities	
by A Sinclair	
William Cooper	217
Verification: How Much is Enough? by A S Krass	
Dennis Fakley	218
Ecological Knowledge and	
Environmental Problem-Solving	- Contraction of the Contraction
by the Committee on the Applications	
of Ecological Theory to	Jahren John
Environmental Problems	210
Michael J Crawley	219
Mobilizing Against AIDS: The Unfinished Story of a Virus	
by E K Nichols	
Peter Newmark	220

-REVIEW AR	TICL	and the same
------------	------	--------------

Geochemical constraints on core formation in the Earth J H Jones & M J Drake

371

-ARTICLES

Binding of a specific ligand inhibits import of a purified precursor protein into mitochondria M Eilers & G Schatz

228

232

234

LETTERS TO NATURE

In	frared helioseismology: detection
of	the chromospheric mode
	Deming, D A Glenar, H U Käufl.
A	A Hill & F Espenak

Shape memory behaviour in partially stabilized ceramics M V Swain

Unusual conditions in the tropical Altantic Ocean in 1984 SGH Philander

236

Interannual variability in the tropical Atlantic P.J.Lamb, R.A. Peppler & S Hastenrath

238

240

245

251

Equatorial Atlantic Ocean temperature and current variations during 1983 and 1984 R H Weisberg & C Colin

Oceanic conditions in the tropical Atlantic during 1983 and 1984

P Hisard, C Henin, R Houghton. B Piton & P Rual 243

Annual change of sea surface slope along the Equator of the Atlantic Ocean in 1983 and 1984 E J Katz, P Hisard, J-M Verstraete

& SL Garzoli Atmospheric conditions in the Atlantic sector during 1983 and 1984

JD Horel, VE Kousky & MT Kagano 248 Influence of the Atlantic, Pacific and Indian Oceans on Sahel rainfall TN Palmer

River dynamics and the diversity of Amazon lowland forest

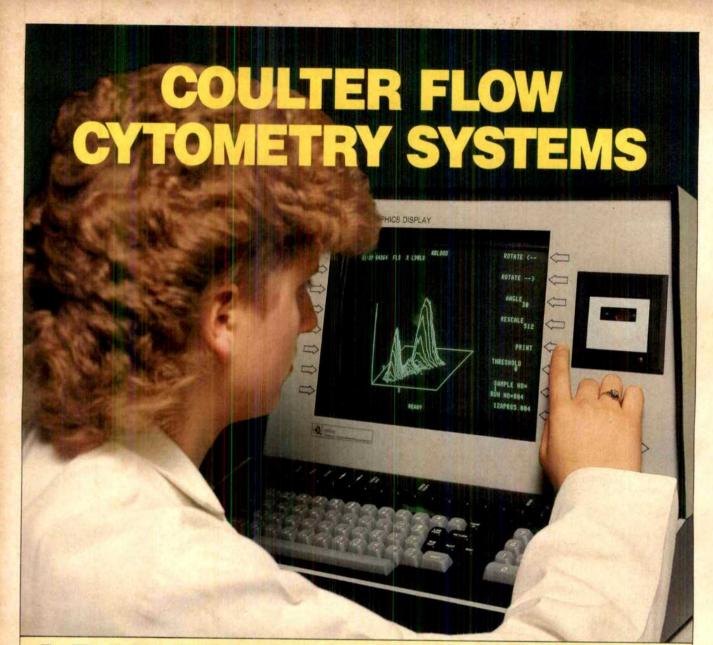
J Salo, R Kalliola, I Häkkinen. Y Mäkinen, P Niemelä, M Puhakka, & PD Coley

Contents continued overleaf

Nature® (ISSN 0028-0836) is published weekly on Thursday, except the last week in December, by Macmillan Journals Ltd and includes the Annual Index (mailed in February). Annual subscription for USA and Canada US \$240. USA and Canadian orders to: Nature, Subscription Dept, PO Box 1501, Neptune, NJ 07753, USA. Other orders to: Nature, Brunel Road, Basingstoke, Hants RG21. ZXS, UK. Second class postage paid at New York, NY 10012 and additional mailing offices. Authorization to photocopy material for internal or personal use, or internal or personal use, or internal or personal use, or internal or personal use of specific clients, is grainted by Nature to libraries and others registered with the Copyright Clearactional Reporting Service, provided the base fee of \$1.00 a copy plus \$0.10 a page is paid directly to CCC, 21 Congress Street, Salem, Massachusetts 01970, USA. Identification code for Nature: 0028-0836/86 \$1.00 + \$0.10. US Postmaster send address changes to: Nature, 65 Bleecker Street, New York, NY 10012. Published in Japan by Macmillan Shuppan K.K., Eikow Building, 1-10-9 Hongo, Bunkyo-ku, Tokyo, Japan. © 1986 Macmillan Journals Ltd.

Hopping Conduction in Solids by H Böttger and V V Bryksin

David R Rosseinsky



A RANGE TO SUIT YOUR NEEDS

The Coulter family of Flow Cytometry Systems are easy to use, accurate and versatile. Combining an unparalleled choice of system sophistication and technical quality, they are the natural choice for the clinical and research laboratory. More than 500 EPICS systems are in use worldwide in these and many other applications.

The Coulter family comprises:-

EPICS C Series: simple to operate automatic systems

(shown above)

EPICS 54 Series: low-cost, versatile instruments for

routine and research use

EPICS 74 Series: high performance instruments with single or dual laser system capability.

EPICS 75 Series:

the most sophisticated system available offering single or dual lasers with an additional dye laser for three colour analysis/sorting.

All are backed up by Coulter Electronics superlative reputation for quality, service and reliability.

For further information and advice on the Coulter Flow Cytometry System to best suit your needs, write to or 'phone Coulter Electronics Ltd, Northwell Drive, Luton, Beds. LU3 3RH. Tel: (0582) 582442, Telex: 825074.

Coulter Electronics Limited

Northwell Drive, Luton, Beds. LU33RH. Tel: (0582) 582442. Telex: 825074.

systems

CS® Artfully Advancing the **Science of Flow Cytometry**



289

290

Normal maturation involves

NATURE'S FIRST ISSUE FACSIMILE



REPRODUCED. ORDER YOUR OWN COPY AND DISCOVER HOW SCIENCE HAS ADVANCED SINCE 1869! PRICES AND ADDRESS FOR				
ORDERS ARE SI	**************************************	W.		
Annual Subscription Pr UK & Irish Republic	ices	£104		
USA & Canada		US\$240		
Australia, NZ &		21.50		
S. Africa	Airspeed	£150 £190		
Continental Europe	Airmail Airspeed	£125		
ndia	Airspeed	£120		
	Airmail	£190		
apan	Airspeed	Y90000		
Rest of World	Surface Airmail	£120 £180		
Orders (with remittance) ISA & Canada lature Libert (With the Control of the Control Libert (With the Control Libert (Wit	UK & Rest of Nature Circulation E Brunel Road Basingstoke Hants RG21: Tel: 0256 292: re's editorial offic page)	Pept 2XS, UK 42		
Japanese subscription e Japan Publications Tra 2-1 Sarugaku-cho 1-cho	ding Company Lt ome	d		
Chiyoda-ku, Tokyo, Ja	pan			
Tel: (03) 292 3755 Personal subscription r some countries to subscription or credit card. I	cribers paying by			
USA & Canada	UK & Europ			
Nature 65 Bleecker Street	Felicity Park Nature	er		
New York	4 Little Essex	Street		
NY 10012, USA Fel: (212) 477-9600	London WC Tel: 01-8366	2R 3LF, UK 633		
Back issues: UK, £2.50 (surface), US\$9.00 (air (surface), £4.00 (air)	; USA & Canada r); Rest of World,	. US\$6.00 £3.00		
Binders Single binders: UK, £5 Rest of World, £7.75.5 & Canada \$32.00; Res	Set of four: UK, £ t of World, £22.00	da \$11.50; 15.00; USA		
Annual indexes (1971-1 UK, £5.00 each; Rest of				
Nature First Issue Facs	imila			

UK, £2.00; Rest of World (surface), \$3.00; (air) \$4.00

Write to University Microfilms International, 300 North Zeeb Road, Ann Arbor, MI 48106, USA

Nature in microform

systematic changes in binocular	
visual connections in Xenopus laevis S Grant & M J Keating	258
Measurement of the intracellular free calcium concentration in salamander rods	
P A McNaughton, L Cervetto & B J Nunn	261
Mediation of thalamic sensory input by both NMDA receptors	and the second of the second
and non-NMDA receptors TE Salt	263
Frequency-dependent involvement of NMDA receptors in the hippocampus: a novel synaptic mechanism C E Herron, R A J Lester, E J Coan	2.6
& G L Collingridge The inducible cytotoxic	265
T-lymphocyte-associated gene transcript CTLA-1 sequence and gene localization to mouse chromosome 14 J-F Brunet, M Dosseto, F Denizot, M-G Mattei, W R Clark, T M Haqqi, P Ferrier, M Nabholz, A-M Schmitt-Verhulst, M-F Luciani & P Golstein	268
Voltage-gated Ca2+ entry into	yr ng yngo gy myddiddiodiodio
Paramecium linked to intraciliary increase in cyclic GMP J E Schultz, T Pohl	
& S Klumpp	271
Expression of peptide chain release factor 2 requires high-efficiency frameshift	promptypes and additional process of the second
WJCraigen & CTCaskey	273
A mouse locus at which transcription from both DNA strands produces mRNAs complementary at their 3' ends	
T Williams & M Fried	275
Overlapping transcription units in the dopa decarboxylase region of <i>Drosophila</i>	
C A Spencer, R D Gietz & R B Hodgetts	279
The RNA required in the first step of chlorophyll biosynthesis is a chloroplast glutamate tRNA A Schön, G Krupp, S Gough, S Berry-Lowe, C G Kannangara & D Söll	281
Quantitative analysis of	
structure-activity relationships in engineered proteins by linear free-energy relationships A R Fersht, R J Leatherbarrow & T N C Wells	284
Directional electron transfer in ruthenium-modified horse heart	A 1900
rumemum-moumed norse neart	

R Bechtold, C Kuehn.

C Lepre & SS Isied

-MATTERS ARISING

Diversity of haematopoietic stem cell growth from a uniform population of cells N M Blackett, E Necas & E Frindel Reply: N N Iscove, M C Magli & N Odartchenko

DNA fingerprint analysis in immigration test-cases W G Hill

Reply: A J Jeffreys, J F Y Brookfield & R Semeonoff

X;autosome translocations in females with Duchenne or Becker muscular dystrophy

V Dubowitz Reply: R G Worton

291

-NATURE CLASSIFIED

Professional appointments — Research posts — Studentships — Fellowships — Conferences — Courses — Seminars — Symposia:

Back Pages

Next week in Nature:

- Do miracles happen?
- Looking for extraterrestrials
- Early Universe structure
- Moon's terrestrial origin
- Climate and acid rain
- Mortar and pestle revisited
- Oral rabies vaccine for foxes
- Vanadium-base nitrogenase

-GUIDE TO AUTHORS

Authors should be aware of the diversity of Nature's readership and should strive to be as widely understood as possible.

Review articles should be accessible to the whole readership.

Most are commissioned, but unsolicited reviews are welcome
(in which case prior consultation with the office is desirable).

Scientific articles are research reports whose conclusions are of general interest or which represent substantial advances, of understanding. The text should not exceed 3,000 words and six displayed items (figures plus tables). The article should include an italic heading of about 50 words.

Letters to Nature are ordinarily 1,000 words long with no more than four displayed items. The first paragraph (not exceeding 150 words) should say what the letter is about, why the studyit reports was undertaken and what the conclusions are.

Matters arising are brief comments (up to 500 words) on articles and letters recently published in *Nature*. The originator of a Matters Arising contribution should initially send his manuscript to the author of the original paper and both parties should, wherever possible, agree on what is to be submitted.

Manuscripts may be submitted either to London or Washington). Manuscripts should be typed (double spacing) on one side of the paper only. Four copies are required, each accompanied by copies of lettered artwork. No title should exceed 80 characters in length. Reference lists, figure legends, etc., should be on seperate sheets, all of which should be numbered. Abbreviations, symbols, units, etc., should be identified on one copy of the manuscript at their first appearance.

References should appear sequentially indicated by superscripts, in the text and should be abbreviated according to the World List of Scientific Periodicals, fourth edition (Butterworth 1963-65). The first and last page numbers of each reference should be cited. Reference to books should clearly indicate the publisher and the date and place of publication. Unpublished articles should not be formally referred to unless accepted or submitted for publication, but may be mentioned in the text.

Each piece of artwork should be clearly marked with the author's name and the figure number. Original artwork should be unlettered. Suggestions for cover illustrations are welcome. Original artwork (and one copy of the manuscript) will see returned when manuscripts cannot be published.

286



THE 19th MIAMI WINTER SYMPOSIUM ADVANCES IN GENE TECHNOLOGY: THE MOLECULAR BIOLOGY OF DEVELOPMENT

February 9 - 13, 1987

Hyatt Regency Hotel / University of Miami / James L. Knight International Center • Miami, Florida U.S.A.

SCIENTIFIC PROGRAM

MONDAY, FEBRUARY 9 · CONTROL OF GENE EXPRESSION

This session is sponsored by the Dupont Company— Biotechnology Systems Division

Eric H. Davidson, California Institute of Technology, Pasadena Differential Genomic Expression in the Sea Urchin Embryo

Robert T. Tjian, University of California, Berkeley Transcriptional Regulation in Animal Cells

Peter Gruss, Universitaet Heidelberg, Heidelberg Control of Gene Expression in Stem Cells and Terminally Differentiated Cells

Allan C. Spradling, Carnegie Institution of Washington Regulation of Drosophila Chorion Gene Amplification

Heiner Westphal, National Institutes of Health, Bethesda
Oncogenesis and Insertion Mediated Mutagenesis in Transgenic
Mice

THE FEODOR LYNEN LECTURE
"The Molecular Basis of Differential Gene Expression"
DONALD D. BROWN

Carnegie Institution of Washington, Baltimore SPONSORED BY: GIBCO/BRL – Division of Life Technologies

TUESDAY, FEBRUARY 10 . EARLY DETERMINATION

Walter J. Gehring, University of Basel, Basel Homeotic Genes and the Genetic Circuits Controlling Development

Christiane Nuesslein-Volhard, Friedrich Miescher Laboratorium der Max Planck Gesellschaft, Tuebingen Maternal Genes Organizing the Anteroposterior Pattern of the

Drosophila Embryo
Frank H. Ruddle, Yale University, New Hover

Frank H. Ruddle, Yale University, New Haven

Homeo Box Gene Control and Expression in Mouse and Man

H. Robert Horvitz, Massachusetts Institute of Technology, Cambridge

Genes that Control Aspects of Nematode Development John C. Gerhart, University of California, Berkeley Axis Determination in the Amphibian Embryo

Hugh R. Woodland, University of Warwick, Coventry Early Events in Tissue Determination in Amphibian Embryos

DISTINGUISHED SERVICE AWARD
John C. Kendrew, St. John's College, Oxford and
Max F. Perutz, Medical Research Council, Cambridge, UK
Introduced by: James D. Watson, Cold Spring Harbor

SPONSORED BY: Elsevier Science Publishers, B.V.

The Miami Winter Symposia wishes to acknowledge and thank our major sponsors for their support:

Boehringer Mannheim

Elsevier Science Publishers

Biosearch, Inc.

GIBCO/BRL

Dupont Company

Schleicher & Schuell

REGISTRATION INFORMATION

ADVANCE REGISTRATION — Mail the registration form along with a check (made payable to: **Miami Winter Symposia**) to our mailing address: Miami Winter Symposia, P.O. Box 016129, Miami, Florida 33101, U.S.A. Our street address is: Medical Research Building, University of Miami School of Medicine, 1600 N.W. 10 Avenue, Miami, Florida 33136.

The registration fee provides for: admittance to all scientific and poster sessions; scientific and publisher exhibits; the book of Short Reports, which will be given out at registration, a final program booklet which will be mailed in advance of the meeting; and, attendance at the social functions. A late registration fee of \$25 will apply to all registrations received after December 31. Cancellation retunds will not be honored if the request is received after December 31, and there will be a \$25 fee for any registration cancellation. Refunds will be mailed after the Symposium.

SYMPOSIUM REGISTRATION will begin in the Hyatt Regency Hotel/ University of Miami/James L. Knight International Center, level three, at 5:00 p.m. on Sunday, February 8. The scientific sessions will be held in the James L. Knight Theater, level three. Exhibits will be on level three, all located within the Center.

FREE COMMUNICATIONS will be held as poster sessions on Monday, Tuesday, and Thursday, February 9, 10, and 12, from 9:00 a.m. until 10:30 a.m. See instructions for submitting a poster.

ORAL PRESENTATIONS OF SELECTED POSTERS — Additional oral presentations will be selected from submitted posters.

WEDNESDAY, FEBRUARY 11 · DIFFERENTIATION

Howard Green, Harvard Medical School, Boston Involucrin: The Gene and The Protein

Bernardo Nadal-Ginard, The Children's Hospital, Boston Generation of Complex Contractile Protein Phenotypes through Promoter Selection and Alternative RNA Splicing

Tom Curran, Roche Research Center, Nutley Control of C-FOS Induction in PC12 Cells

William R. Jeffery, University of Texas, Austin Muscle Cell Determination in Ascidian Embryos

THURSDAY, FEBRUARY 12

CELL SURFACE & TISSUE INTERACTIONS

James A. Weston, University of Oregon, Eugene Environmental Regulation of Neural Crest Cell Behavior

William H. Kinsey, University of Miami School of Medicine, Miami Role of Tyrosine Kinases in Embryonic Development

William J. Lennarz, M.D. Anderson Hospital, Houston Cell-Surface Proteins in Gastrulation and Skeleton Formation

Masatoshi Takeichi, Kyoto University, Kyoto Cadherin Adhesion Molecules Associated with Animal Morphogenesis

Urs S. Rutishauser, Case Western Reserve University, Cleveland Developmental Biology of a Neural Cell Adhesion Molecule

MORPHOGENESIS

Susan V. Bryant, University of California, Irvine Cellular Interactions in Vertebrate Limb Patterning

David R. Soll, University of Iowa, Iowa City

Gene Expression and the Opposing Programs of Differentiation
and Dedifferentiation in <u>Dictyostelium discoideum</u>

Hans R. Bode, University of California, Irvine Patterning In Hydra

FRIDAY, FEBRUARY 13 . GENE THERAPY

This session is sponsored by Biosearch, Inc.

Richard C. Mulligan, Whitehead Institute, Cambridge, MA Prospects for Gene Therapy

Theodore Friedmann, University of California, San Diego In Vitro and In Vivo Models for Gene Therapy

Mario R. Capecchi, University of Utah, Salt Lake City
High Frequency Targeting of Genes to Specific Sites in the Mammalian
Chromosome

Beatrice Mintz, Fox Chase Institute, Philadelphia Hematopoietic Stem Cell Development With and Without Foreign Genes

TRAVEL INFORMATION

EASTERN AIRLINES is the official airline of the Miami Winter Symposia. Call Eastern's Special Convention Desk for 50% discounted fares. Eastern will handle your travel arrangements regardless of whether or not they service your city. Make your reservations by calling Eastern's toll-free number, 800-468-7022 (in Florida, 800-282-0244). Be sure to refer to the Easy Access number, EZ2P9, when speaking with the Eastern agent. You can have your travel agent write your ticket, or have Eastern send it to you along with an invoice for payment. Or pay for the ticket by other convenient methods that Eastern can suggest. Eastern has made attending this meeting as simple as possible.

HOTEL INFORMATION

The Symposium and all other functions will take place at the Hyatt Regency Hotel / University of Miami / James L. Knight International Center, 400 S.E. 2 Avenue, Miami, Florida 33131-2197. Rooms have been reserved in the hotel for Symposium participants at rates that represent a considerable reduction below those normally prevailing. They are available only to Symposium registrants and accompanying members and only for the nights of February 7 – 13, inclusive. Please complete the hotel reservation form and mail it directly to the hotel.

THE 20th MIAMI WINTER SYMPOSIUM • FEBRUARY 8 – 12, 1988
Advances in Gene Technology: Protein Engineering
Hyatt Regency / University of Miami / James L. Knight International Center

If you desire information about this meeting, send your name and address to: Miami Winter Symposia, P.O. Box 016129, Miami, FL 33101, U.S.A., or call 1-800-MIAMI-87.

NATURE VOL. 322 17 JULY 1986

195

South Africa gets out of hand

The present sad condition of the Republic of South Africa is unlikely to last for very long. But the timescale of general impatience may be dangerously short.

WHAT can be done and what should be said about the growing crisis in South Africa? Nature has no competence in the matter, which lies outside the terms of reference implicitly defined by a readership of professional scientists. Of course, there are some aspects of the condition of South Africa on which science has a bearing. There can be no genetic basis for the inequitable and offensive system of apartheid, which is not to say that apparent differences in the attainment of different races may not be induced by the systematic social deprivation of one (or several) of them. It is also pertinent, as in the argument begun just under a year ago by the thoughtless Southampton organizers of September's World Archaeological Congress, that academics outside South Africa cannot ostracize fellow-intellectuals working at South African institutions without irreparably and permanently damaging the cause of international scholarship. But there are also some commonsense considerations that deserve more attention than they are being given.

Those outside South Africa wishing to encourage change should prudently begin with an assessment of the time over which their hopes are likely to be realized. The temptation is to miscalculate that the system of apartheid is so near collapse that only modest pressure from outside will send it tumbling. This is why the cry for general economic sanctions is now widespread, not merely from outside South Africa, but by many of the black leaders within the republic. But that underestimates the capacity for survival of the Nationalist South African government. One of the most distasteful features of the apartheid system is that many of the black workers on whom the economy depends belong titularly not where they work but to artificial living places many miles away, to which they are supposed to return when they are out of work. If sanctions were effective enough to hurt the economy of South Africa, the republic government would be acting within its own laws if it chose to send the unemployed off to their "homelands" to starve in obscurity. The process would be difficult but not impossible, and would buy more time. Is it possible that well-wishers outside South Africa have allowed their distaste of the present system to lead them to too sanguine a view of the weakness of a government whose determination is, in other connections, its hallmark?

But if not sanctions, what? That is the general dilemma. The simplest answer is "selective sanctions", by which is meant a variety of schemes ranging from the cancellation of permission for South African aircraft to land elsewhere to a collective decision not to buy South African exports of certain kinds, fruit for example. But if full sanctions would not produce the intended effect, can half-sanctions succeed? (A few symbolic actions might nevertheless be worthwhile.) The difficulty running through these tortuous considerations is the frustration of governments elsewhere that they have no obvious means except the passive device of sanctions legally to influence internal affairs in South Africa.

Luckily, that does not imply that nothing can be done. Although the international banking system has been quietly helping to bring about the "disinvestment" in South Africa for which well-wishers have been asking, would it not now make sense, as

a condition for the continued operation of South African companies as subsidiaries of companies registered elsewhere, that they should promptly follow employment practices of the kind that would be expected of them outside South Africa, treating people of different races on an equal footing and providing for the disadvantaged the kind of technical training that would allow them to function properly in their jobs? The cost could be high. but not necessarily greater than that of sanctions and certainly less than the cost of the international chaos that will supervene if South Africa falls apart. Indeed, it might even be worthwhile to encourage the South African subsidiaries of overseas corporations to break the apartheid laws, as Barclays Bank has just done by lending money to a black employee to buy a house in a district reserved for whites. When industrialized governments do not shrink from telling companies to instruct their overseas subsidiaries to which customers they may and may not sell high technology, why should they shrink from using this power constructively within South Africa?

Trouble on the farm

The problems now facing farmers will not go away overnight.

Most developed countries have long since been forced by economic reality to reduce the scale on which they maintain once-traditional industries such as shipbuilding and steel manufacture. In many places, farming will be the next in line. So much has been clear for several years, some would say decades. Much of the food that farmers in developed countries now grow with the crucial help of government subsidies could already be grown more cheaply elsewhere, in Australia, New Zealand, Argentina and Zimbabwe, for example. As time passes, the list of potential suppliers of temperate foodstuffs will be or could be increased by the addition of many now-developing countries, which would conform well with Adam Smith's principle that the economic use of resources requires a division of labour: in the modern world, some must grow food and others make computers.

That is what the textbooks say. The reality is very different. The subsidies industrialized governments pay their farmers, which have ensured over the years that the industrialized world is awash with food that impoverished nations cannot afford to buy, serve a multitude of functions, not all of them respectable, Occasionally, the old strategic argument still surfaces that a country less than self-sufficient in food production is vulnerable to starvation in time of war, but this can hardly carry weight when most governments fear that future wars will be over before most people know they have begun, and when government warehouses are in any case filled to the brim with food that nobody wants. The social argument, that the farming community is the repository of an invaluable tradition whose erosion would spell the loss of crucial elements in the constitution of advanced societies, contrasts oddly with the continual war between farmers and many of the societies in which they are embedded over environmental issues, for example. (Too often. farmers cut the figure of state-licensed vandals.) That farming is a social problem is, on the other hand, undeniable: the plight of farmers (and their banks) in the Middle West of the United States during the past two years is one vivid proof. The nub of the difficulty is that most industrialized governments, after decades of encouragement of increased farm production, now find themselves morally committed to a large group of people whose lives have been spent in farming, who have no wish to do anything else and who are not outstandingly fitted to do other things. Governments also recognize, of course, that farmers are also voters, often noisy.

This dilemma is nicely illustrated by the state of British farming. Last year was in many ways disastrous. The government's Annual Review of Agriculture 1986 (HMSO, Cmnd 9708), published at the beginning of the year, showed that as a consequence of the appalling weather, farm income fell in 1985 by 43 per cent compared with the previous year, which had been a good year. In a year when there were 240,000 farms in Britain (a steadily declining number), farmers and their spouses were left with a cash income of merely £1,154 million, just about half the total scale of subsidy for British farmers last year (£2,205 million) and even less than the proportion of the farming subsidy (£1,308 million) provided by the Common Agricultural Policy by means of which European farming is sustained at an uneconomically high level.

In 1985, in other words, it would have been cheaper for the British taxpayer merely to have provided farmers with the cash they are supposed to have earned from their farming operations and to have bought in their production from the huge stocks of food the Community has built up over the years. Yet farmers are plainly undismayed by this alarming calculation. Farmers spent more on new machinery and building than the cash that stayed in their pockets, while the price of farm land remained buoyant, as the real estate dealers say.

Can this state of affairs be allowed to continue? Common sense says no. Now even the British government seems to be having second thoughts. In the past few weeks, there have been repeated hints that the scale of traditional farming must decline. One common suggestion is that farmers must take to growing other things than the traditional crops, and that British farmers should in particular take to growing trees. The prospect is not cheerful. So long as the incentive is financial, the trees that farmers grow will be cheap and nasty (see Nature 322, 101; 1986) like those favoured by the Forestry Commission. Environmental conflicts are more likely to be sharpened than diminished in the process. But trees grow slowly, and will not provide the continuing employment that farmers have come to regard as their birthright, even though the taxation system could no doubt be modified in such a way as to put £1,000 million plus in their pockets every year. Why not instead bite the unpalatable bullet, and draw up a long-term strategy for the industry that will properly quantify the supposed non-economic benefits, set these off against the equally intangible but important disbenefits of enforced rural life, and declare that the time will have to come, some years from now, when farming will be run on economic lines?

Shutting barn doors

The consequences of the Chernobyl accident are about to become diplomatic, thanks to IAEA.

When the Soviet reactor at Chernobyl, north of Kiev, went out of control on 26 April, it quickly became apparent, in Sweden where the fallout was first detected and, then, elsewhere in Western Europe, that the formal arrangements for dealing with trans-frontier radioactive pollution are inadequate. At the outset, there was no obvious means by which the Soviet Union could be required to provide fuller information about the character and the scale of the release of radioactive material

from the Chernobyl reactor. (It is now clear that the Soviet officials in charge of the reactor were not themselves aware of what had gone wrong, and that they may even have concealed what they knew about the scale of the accident from Moscow.) Inevitably, the Soviet Union was subjected to a great deal of verbal drubbing from Western governments, many of them eager to complain that Soviet secretiveness, a long-standing nuisance, had become a danger to other people's lives. Yet, curiously, it has been overlooked that, for the past three years, the International Atomic Energy Agency (IAEA) at Vienna has been nursing a kind of international agreement on trans-frontier radioactive pollution. At a conference opening at Vienna later this month, the agency is hoping to turn its draft agreement into an agreement that will stick.

Before this laudable exercise is written off as an attempt to shut the stable (or barn) door after the horse has bolted, some consideration should be given to the complexity of the issues that will arise during the coming weeks. The starting-point for IAEA's conference is the set of recommendations produced in April 1984 on the management of nuclear accidents that might cause fallout beyond the boundaries of the states housing faulty reactors and other nuclear facilities. Sensibly, indeed inevitably, the experts concluded that there should be an element of planning in advance.

Each reactor operator should have a well-defined set of criteria for telling when an accident must be taken seriously, must tell the authorities in neighbouring states about these criteria and must then identify, also in advance, the nuclear installations that are potentially a source of international trouble. All that makes sense, as does the requirement that there should be identified communications links by which news of accidents may be signalled if and when they happen. What IAEA now seeks, in the chastened atmosphere after Chernobyl, is an agreement between its member states that these modest guidelines will be adopted. Whether it will succeed is another matter.

Here are some of the impediments to agreement at Vienna. In many places, the exact design of nuclear installations and even their intended function is still a secret, for either military or quasi-military reasons. The Soviet Union, which declares the nature of its operating reactors to IAEA as a matter of course, says little about its other facilities such as separation plants. France is similarly coy about the division between the civil and military aspects of its nuclear plants.

Other states such as India and Israel (both members of IAEA but non-signatories of the Non-Proliferation Treaty) think they have an interest in keeping their neighbours guessing about their nuclear programmes, believing that their own security will be enhanced if they can give the impression of being capable of making nuclear weapons. Such states will not readily fall in with the suggestion that they should disclose the nature of their nuclear installations.

But even elsewhere, where a state has nothing (or nothing much) to hide, there will be a profound reluctance to say in advance that this or that nuclear plant is in principle capable of going wrong, and of causing trouble to others. Indeed, it is easy to imagine how information of that kind could be used malevolently by those who believe that Chernobyl gives them a licence to halt the nuclear industry in its tracks.

So this month's meeting at Vienna is bound to be a tense affair. Even enlightened governments will be uneasy about the disclosures they will be asked to make. Yet their long-term interest is precisely the kind of undertstanding on the management of major nuclear accidents that IAEA's guidelines would set in place. If one consequence will be the abatement of senseless secrecy in the management of nuclear installations, that will be an uncovenanted benefit of what is, in any case, an essential measure. And the fear that too much openness will put too much ammunition in the hands of the anti-nuclear people is unreal; part of the trouble now is that too many authorities have been too secretive for too long.

European research

Framework programme poses political questions

It began to emerge clearly last week that the scale of the European Commission's new "framework programme" of cooperative research and development in Europe is so large that a phase of real interaction between international and national research policies in Europe is now beginning, with national programmes the likely "losers" as research becomes more international.

This internationalization of science seems to be becoming a particular possibility in Britain, where technology minister, Mr Geoffrey Pattie, said last week that he had "no trouble" with the content of the European Commission's 1987-91 "framework programme", the definitive version of which the Commission should place before member states in the next few weeks.

Pattie's support, though qualified when it comes to matters of scale, is significant because, in line with Britain's current presidency of the European council of ministers. Pattie will preside for the next six months over the research council. And Britain attaches "considerable importance" to concluding political negotiations over the content and financing of the programme by the end of this year, Pattie

Pattie is concerned, however, at the possible cost of the programme (earlier this year, the Commission was seeking a near tripling of present spending from the present 4,300 million European Currency Units'); he demands more critical preassessment and analysis of Commission projects and says a final decision on fund-

ing may go to cabinet level.

In fact, Pattie's concern reflects the wider issue: that the levels of research spending recommended by the Commission are at last reaching a politically noticeable level. From around 2 per cent of member states' net research and development budgets, the Commission has moved in its framework programme to nearer 4-6 per cent. In individual projects, the levels are even higher: in materials science, for example, where European national spending lags far behind that of the United States and Japan, initial Commission spending proposals in the framework programme reached a fifth of all European research. This seemed to be going well beyond the mere "catalysis" of European collaboration for which the European Commission has previously argued; and at these levels it has begun to be difficult even for enthusiasts of European collaboration - like Mr Pattie - to argue that European research programmes should l

not substitute for national research, but add to it. Increases in European programmes are in danger, in Britain at least, of causing reductions in corresponding national ones.

Thus, in money-conscious Britain, where many of the financial issues are clearest, Treasury sources stress that ministries benefiting from any substantial increase in Commission research funding by winning grants — will have to account for these receipts, and may have their national support commensurately reduced. This near-automatic system of "attribution" of Commission receipts could affect a number of national programmes, not least because British researchers appear to be particularly effective at winning Commission support: last year, Britain won 27 per cent of available Commission research funding, although the country pays only 20 per cent of the Commission's total budget. In research, Britain's receipts exceed "juste retour"

Paradoxically, however, this success of British scientists in winning funds from Brussels could in future be penalized by Treasury insistence on the attribution of receipts. Increases under the framework programme could thus conflict with the research of the Department of Energy, and particularly of the Department of Trade and Industry. The Commission's plan to boost its pilot-scale "stimulation programme" — which has successfully combined basic research groups in joint research throughout Europe - could result, under the Treasury attribution rules, in a commensurate decrease in the funds of the research councils, or the universities directly. Sir David Phillips, who is both chairman of the Advisory Board for the Research Councils (which distributes basic research funding in Britain) and a member of the CODEST scientific committee which advices the Commission on science policy, admits that "a key question" now is how far, and whether, national budgets should be cut to support European cooperation. This is why Pattie considers that finding the money for the framework programme may become an issue for the whole government.

The Treasury itself remains unconvinced by the Commission's arguments for an increase in research, and opposes Pattie's view that the framework should not substitute for national programmes. Pattie himself feels he unfortunately gets little help from the Commission — which however important the programmes proposed tends to argue by exhortation.

More detailed and precise arguments are necessary, Pattie says. The framework programme itself should therefore include an important element of assessment to ensure and detail the "effectiveness" and "relevance" of projects and to sharpen arguments for ministers.

Despite the drive for "effectiveness" of the framework programme, however, "flat out market considerations cannot be the order of the day". Pattie insists, because the research-oriented framework programme must take into account the needs of the smaller countries in Europe. These have felt neglected by the quite separate (non-Commission) Eureka technology programme, in which market forces are to the fore. But framework research should have a long-term relevance to European technological competitiveness. An increase in industrial participation, on a sliding scale, as Commission research projects developed, would sharpen Commission programmes Pattie suggested. It would help "to keep testing out the project on industry" and to "make people shape up". Robert Walgate

German universities

In the past fifteen years, federal and Länder (regional) governments have spent DM38,000 million to create an extra 300,000 places at West German universities. But the era of expansion is now near its end, according to the commission for university building.

In its sixteenth framework plan, published last week, the commission recommends that a further DM9,000 million be spent between now and 1990. High priority is given to the extension of natural science and engineering faculties, among them a new faculty of informatics in Karlsruhe, the next phase of the new Biozentrum in Würzburg and a new centre for interdisciplinary research in Frankfurt. The greater part of the money, however, will go for medical institutions and clinics.

The Federal Minister of Education, Dorothee Wilms, emphasized that the goal of 850,000 university places had not yet been reached, but would be brought close with the creation of another 20,000 places in the near future. Although there are now signs of a downward trend in the number of students entering university, there are still around 1.3 million students. far more than there are places. Students have grown accustomed to overcrowded lecture theatres without room even to sit on the floor and inadequate library and laboratory space. As the deputy commission head, Anke Brunn, pointed out, there is no sign of the feared "education catastrophe", the collapse of education due to excess student numbers.

Jürgen Neffe

Spain

More university reforms needed

Barcelona

THERE are said to be two national spectacles in Spain, bullfights and "oposiciones", the recruiting system for the civil service. It is a matter of discussion which one is the bloodier. Reforms in access to university and CSIC (Spanish Science Research Council) positions have modified the "oposiciones", but recent experience suggests that some of the most controversial elements of the system still exist.

Spanish professors and researchers in public institutions are considered as civil servants and therefore have permanent tenure, which tends to create lethargy in many Spanish institutions. That was certainly the opinion, before coming to power, of many members of the Socialist Party, now starting its second four-year term in Spanish central government. Recent regulations have led to invited professors and research staff recruited on short-term contracts. The reforms introduced in universities and in CSIC in the past four years have, however, maintained the traditional civil service system and the selection by "oposiciones"

The spectacle itself is much less colourful than it used to be. The "oposiciones", in the nineteenth-century tradition but modified in the 1930s during the Second Spanish Republic, used to be a series of public examinations, theoretical or practical, designed to choose the ablest candidate for the job. Now, a candidate has to pass only two examinations, one on his personal curriculum and the second on a subject related to his field of research. A committee formed for every position or groups of similar positions makes its decision by voting and without appeal. The committee can put any kind of questions to the candidate. In some cases, the experience may be traumatic for candidates, committees (which may sit for weeks before reaching a decision) and for departments.

The Law for University Reform has introduced two important modifications. One is that universities now have the right to appoint two of the five-member committee that selects the candidates; the other three members are chosen by a computer at random from the list of professors of the same field.

The second change is that university departments may propose a "profile" of the candidate. The experience of the past two years shows that the result has normally been to slant appointments to specific people already working in the same department. The actual result is an increase in in-breeding in university departments and many people are worried about the long-term consequences. Hundreds of new positions are being advertised as a

consequence of the Law of University Reform; for example, the Autonomous University of Barcelona has had nearly 300 new positions in 1986 alone. But the rules may be modified in the near future in the light of experience.

In CSIC, the system shows some important differences. On the one hand, positions are advertised once a year and relate to specific institutes and specific subjects; on the other hand, since last year, all committee members are appointed by the president of CSIC and often include members of university departments as well as CSIC staff. In each of the past two years, about 200 positions have been advertised, after a long time without openings. Last year around 400 candidates applied for the positions. In some fields such as molecular biology, there were four candidates for each position,

which means that in many cases only one candidate applied, or none. This result has been interpreted as showing the need for a long-term policy for recruiting research personnel and for attracting scientists now working abroad. New statutes for CSIC are expected to be issued before the end of this year that will include a different structure for research staff.

The "oposiciones" was a system designed more than a hundred years ago to make Spanish public administration more accessible. It has been widely recognized that a new system would be needed before the end of the twentieth century to select the appropriate people for research or universities. But the rules of Spanish administration are difficult to change, and the recent regulations have tried to adapt an obsolete system to modern Spanish society.

It is generally felt in universities and CSIC that further steps are needed in any case to achieve a flexible and efficient recruiting system for Spanish higher education and research. **Pedro Puigdoménech**

India

Space programme uncertainty

New Delh

INDIA is still not sure when or how to get its multipurpose Insat I-C satellite launched into geostationary orbit to provide continuity in its space-based meteorological, television and telecommunications services.

Under a contract with the US National Aeronautics and Space Administration (NASA), the satellite, along with an Indian payload specialist, was to have been carried by the space shuttle this month. The indefinite postponement of shuttle flights after the Challenger explosion, and uncertainty about the availability of the alternative Delta rockets, has upset the schedule of the Indian Department of Space (DOS).

According to DOS secretary Professor U.R. Rao, negotiations are now going on with the European Space Agency for Insat 1-C to be accommodated in one of the Ariane launches before the end of 1987. With Ariane solidly booked for the next two years, and with its own schedule upset by the failure of the Ariane-IV launch in March, it is likely that Insat 1-C may not leave the ground before 1988. India's only functioning satellite, Insat 1-B, has been taking the full work load since August 1983 after its companion, Insat 1-A, was disabled by on-board power failure. The US Ford Aerospace Corporation, which built the three satellites for India. has been asked to deliver a fourth, Insat 1-D, by 1988.

Continuity of the satellite service is important, for India now relies significantly on Insat 1-B for weather forecast, television broadcast and telephone links be-

tween remote places. The satellite provides 4,000 two-way telephone circuits and has helped to network India's 173 television and 91 radio stations, as well as beaming television programmes directly to 2,000 community receivers in villages and relaying educational programmes to 1,953 schools and 62 colleges.

Insat 1-B is the only geostationary satellite over the Indian Ocean providing meteorological images to the world, and duplicate Insat weather data are supplied daily to the United States. Apart from ensuring continuity of services, India is anxious to get Insat 1-C launched as soon as possible to avoid possible political complications arising out of delay in occupying the allotted slot in the geostationary orbit. India will continue to rely on foreign launchers, as it is unlikely to be able itself to put satellites into geosynchronous orbit before the year 2000.

Insat 1-C is not the only project beset by delay. The test flight of the Augmented Satellite Launch Vehicle (ASLV), designed to lift a 150-kg payload, was scheduled for last year but has yet to take place. The launch of an Indian-built remote-sensing satellite from the Soviet Union, scheduled for September this year, has been postponed. India's only operational rocket, SLV-3, has not flown for the past two years.

According to DOS, the destruction of major facilities at its east coast Sriharikota launch complex is one reason for the slowdown of space activities. The complex was damaged in a cyclone two years ago and plans are afoot to shift it to a safer location.

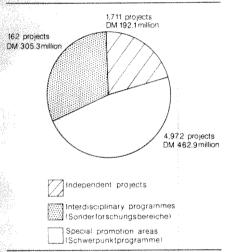
K.S. Jayaraman

The deutschmarks that count

Hamburg

THE annual meeting of the Deutsche Forschungsgemeinschaft (DFG), the West German Science Foundation, was held in Bonn last week. DFG's new president, Hubert Markl, pointed out that all DFG's activities were met with a budget of less than DM 1,000 million, just two per cent of the nation's research and development expenditure and, more significantly, only 60 per cent of the amount spent to subsidize the public theatres.

In 1985, DFG spent DM 982.6 million for the support of research and researchers, with 74 per cent going on personnel costs. Most of the money came from the federal government (DM 578.6 million) and the Länder (DM 397.4 million); expenditure was divided as below.



Markl rejected criticisms by the Wissenschraftsrat, the senior science advisory board, which had earlier said that doctoral education in West Germany is both too long and ineffective. Some 4,000 doctoral students are supported by DFG. Doctoral research is carried out in well controlled projects of quality, Markl said. He singled out for praise the contribution made by female scientists.

Chancellor Helmut Kohl made a speech in which he said that "quality and performance have reached a higher level", partly due to a retreat from the politicization of science. Despite increasing debate on the dangers of nuclear power and of science in general following the Chernobyl disaster, Kohl demands that politics should be kept out of science.

Hans-Werner Franke, the president of the Länder Ministers of Culture, Education and Church Affairs (Kultusministerkonfernz), demanded that the existing university system should be consolidated even with a decreasing student population. That may create a chance to switch some resources to research and to much-needed Jürgen Neffe reforms.

US technology

Making rivals work together

FROM the outset, the US Microelectronics and Computer Technology Corporation (MCC) was risky business. The plan to bring together arch-competitors in the semiconductor and computer industries in a cooperative research institute had no precedent, and even the Justice Department considered challenging the consortium's formation. After operations began in 1983, MCC president Admiral Bobby Inman struggled for over a year to bring first-rate talent to the facilities in Austin, Texas. Then a long silence ensued.

That silence has only recently been broken. MCC is now drawing cautious sketches of the technology it has transferred to its "shareholders" (the 21 companies that invest in and preside over MCC), Despite the slump in the computer industry, the consortium's membership has now more than doubled, and includes such giants as Honeywell, 3M and Control Data. MCC's budget has reached \$65 million a year and its staff is near capacity with 440 employees.

Seven programmes are under way, focusing on semiconductor packaging, software technology, computer-aided design and advanced computer architecture. Each company pays \$500,000 for a share in MCC, and then foots a portion of the bill for each programme in which it participates.

The shareholders also contribute staff - approximately 35 per cent of MCC's employees are "on loan" from shareholder companies. One representative from each company joins the board of directors and one the technical advisory board. Among developments that have already reached shareholders are a model for building expert systems, an editor to aid graphic design of semiconductor circuitry and an improved process for tapeautomated bonding which packs silicon chips tightly together on circuit boards and enables denser interconnections to be

The new technology is important, but what excites industry is whether the research structure of MCC can provide a new model. Inman says he and his managerial crew have vowed to minimize bureaucracy — "an everyday battle" — and to nurture the type of environment that encourages creativity. The three-level management hierarchy permits autonomy and quick decision-making within research ranks.

And MCC scientists are freed from the vagaries of market forces. The ability to provide stable funding and support is just part of the "psychic income" that keeps MCC laboratories alive, says vice-president and chief scientist John Pinkston.

MCC has invested heavily in its staff: \$20,000 to \$70,000 each for private computer workstations that in typical laboratories would be shared by up to four people. Although the aim is pre-competitive, collaborative research, the opportunities for collaboration are not unlimited. Because all programme information is considered proprietary unless declared otherwise, informal exchange between different programmes is discouraged.

Similarly, MCC scientists must bear in mind the expectations of their shareholders. Although they acknowledge that its goals are long-term, the shareholder companies are anxious to see MCC pay off. But shareholders have so far been reluctant to provide the brightest of their own staff for MCC.

Inman cites technology transfer as the most pressing problem confronting MCC. "We are delivering technology at a level of complexity that not too many of these companies are used to dealing with," he claims.

To enhance communication, quarterly updates and semi-annual research reviews bring shareholder and MCC scientists together regularly. Project teams throw "coming out parties" for newly-assembled technology packages, attended by all participating shareholders. Seminars and technical meetings take place frequently throughout the year. 3M and DEC have even moved their research and development headquarters to Austin.

Will MCC survive? Several industry consortia that have sprung up in MCC's wake pose no challenge, but the multi-billion-dollar budgets of the research and development teams at IBM and AT&T Bell Laboratories dwarf MCC's allotment. And the extent to which companies will capitalize upon MCC's legacy remains uncertain. Unequal gains could force out some shareholders and cause rancour

among those that remain.

Finally, the diversity of interests represented at MCC may curtail its expansion into key programmes that would help fill the gap created by such a shake-out. One example is Inman's drive for a manufacturing technology programme, which "raised a lot of welts" at a technical meeting last spring, according to one person who attended. The proposed programme is both too specific to draw broad support among shareholders, and too close to applied science to prevent competitive

But the adventurous spirit that created MCC may sustain it through the transitions ahead. With its unique position in industry research, the consortium has a rare opportunity to test alternatives.

Karen Wright

AIDS

US wins round in patent row

Washington

A US CLAIMS Court last week dismissed a suit brought by the Institut Pasteur in Paris against the United States — representing its National Cancer Institute (NCI) — over the development of a blood test for antibodies to the virus causing acquired immune deficiency syndrome (AIDS). Lawyers for the French research institute expressed confidence that the claims court decision would be reversed on appeal. But the legal issues raised by the Pasteur lawsuit may have a chilling effect on all international exchange of research materials.

Pasteur's case is based on a form signed by Mikulas Popovic, a colleague of Robert Gallo at NCI, when he accepted samples of a virus being studied at Pasteur by Luc Montagnier.

On 15 September 1983, Montagnier presented data at a Cold Spring Harbor symposium attended by Gallo and Popovic about a virus he called LAV. At the time, both Gallo and Montagnier were looking at a retrovirus as a possible causative agent for AIDS. On 23 September, one week after the Cold Spring Harbor meeting, Popovic signed a receipt accepting two isolates of LAV (Mkt-1B and JBB LAV) as well as anti-interferon sheep serum. The receipt stipulated that these materials would be used only for biological, immunological and nucleic acid studies, and would not be used for "industrial purposes without the prior written consent of the Director of the Pasteur Institute". NCI and Gallo have maintained that they adhered to those conditions. But Pasteur's lawsuit claims that Gallo and his associates used the LAV isolates in research that has since led to development of a commercial diagnostic test kit.

The claims court refused to decide the issue of whether the LAV isolates were used improperly. Instead, Judge James Merow based his ruling on whether or not the document Popovic signed constituted a contract with the United States. NCI argued that neither Popovic nor Gallo had authority to commit the United States to a binding contract. The court decided that even if the receipt did constitute a contract, the French institute had not followed appropriate procedures for settling contract disputes - in this case first submitting a claim to the Department of Health and Human Services — and dismissed the case.

James Swire, a lawyer for the Institut Pasteur, described the ruling as "roadblock, nothing more". Swire says it is a "sad day for international scientific research" when NCI disavows agreements of its principal investigators.

Reaction from the Department of

Health and Human Services was low key. A spokesman said the department was "pleased" by the court's ruling, and expressed hope that it would "provide impetus to resolving this matter". The claims court decision has no direct effect on a separate proceedings being conducted by the US Patent Office on a disputed patent claim for the AIDS antibody blood test (see *Nature* 320, 96; 1986). The Patent Office has awarded a patent to Gallo for his version of the blood test, but that patent could revert to Montagnier and the Institut Pasteur pending the outcome of the proceedings.

The claims court decision raises important questions about the legal standing of documents signed by researchers when exchanging research materials. J. Edward Rall, deputy director of the National Institutes of Health (NIH) for intramural re-

search, says collaborative agreements are usually entered into on a person-to-person basis. But Rall says most researchers at NIH are aware that there are certain documents they cannot sign.

In 1981, NIH associate director Philip Chen drafted a sample response for NIH scientists to use when requested to sign agreements accompanying cell lines. Researchers must reply that they cannot sign agreements containing waivers or indemnification agreements. They can, however, promise not to share the cell lines without permission from the supplying laboratory.

Scientists have not had to worry about the legal aspects of cooperation before. Both Chen and Rall say litigation is making some grow wary. Rall worries that if things grow worse lawyers may "subvert straightforward scientific collaboration" with legal arguments that will not be appreciated. "It may be that no one will sign anything any more", says Chen.

Joseph Palca

Eureka

Soviets feel left out of Europe

THE Eureka conference in London last month revealed a stance contrary to the Helsinki Accords, according to the official Soviet media. The "obvious tendencies" among participants to limit participation in scientific and technological cooperation to West European countries is seen, at best, as an impediment to the close contacts between countries irrespective of political orientation that were the goal of the Final Act, and at the worst as a means of diverting the supposedly peaceful Eureka programmes for military ends.

Much play has been made of an alleged French distinction between Eureka and the US Strategic Defense Initiative (SDI): SDI is a programme which has a civilian application, while Eureka is a civilian programme capable of a military application.

According to the official Soviet newsagency TASS, Western "political and industrial circles" have recently shown increased interest in the "military aspects of Eureka", while Aleksandr Bovin, a Moscow commentator, stressed that such "giants" as Siemens, Philips and Thomson want to take part simultaneously in both Eureka and SDI. There have been indications in the world press, Bovin said, that Bulgaria, Hungary, Czechoslovakia, Yugoslavia and East Germany are interested in working "within the Eureka framework", but the Western countries do not wish to admit countries that do not share their "ideas about the supreme values'

The Soviet stance may be due partly to pique. In their own opinion, as an eminent Soviet arms control expert, General Nikolai Chervov, stressed at the Royal have been replaced ledgement that, in economic crisis, the cafford to participate.

Institute of International Affairs last week, the Soviets have made a major concession to the West by softening their demands on SDI: instead of requiring that any arms control treaty outlaw all SDI-related research, they will now accept the compromise that such research be confined to the laboratory stage. Apart from some ironic questions about what, in the context of SDI, constitutes a laboratory, there has been virtually no Western response to this concession.

As for the alleged wish of the West to exclude the socialist countries from Eureka, the problem is a far wider one than a single programme. The whole idea of Eureka, as Bovin rightly noted, is to deal with leading edge technologies — lasers, computers, robots and biotechnology — precisely the fields affected by the Co-Com embargo on technology transfer. Furthermore, even if Eureka does include some programmes that would not come under Co-Com, the Socialist countries cited by Bovin have been remarkably quiet about their wish to participate.

The exception in the socialist bloc is East Germany whose leader, Erich Honecker, has publicly expressed some interest in participation, possibly within the framework of the existing intra-German trade arrangements, and, to a lesser extent, Yugoslavia (which technically ranks as a non-aligned country), where an initial interest now seems to have been replaced by a tacit acknowledgement that, in its state of endemic economic crisis, the country simply cannot afford to participate. Vera Rich

Patent law

Boost for Canadian drug research

Washington

AFTER a long and painful gestation, the Canadian government has finally given birth to proposals for changes in patent law. The amendments, actively sought by the pharmaceutical industry, will restore to patent holders exclusive rights to sales of patented drugs. In exchange, the government will require pharmaceutical companies to double their current research commitments in Canada.

Since 1969, Canada has had a unique law that allows generic drug manufacturers to obtain licences to produce patented drugs at any time. Once approved for sale by the health protection branch of the Department of Health and Welfare, generic manufacturers are in most cases obliged only to pay a 4 per cent royalty to the patent holder. Major, multi-national drug companies argue that this "compulsory licence" system discourages domestic investment and cuts sharply into profits. But for consumers, the benefits are obvious. A government report last year estimated that Canadians are saving \$220 million a year in drug costs under this arrangement.

Knowing that changing the compulsory licence system will provide political hay for the opposition, the government has several times delayed introduction of the amendments. But as the government has a 70-seat majority, the bill should pass into law unscathed. The government hopes to deflect some consumer criticism by establishing a new Drug Prices Review Board that can remove the protection from compulsory licences for companies whose prices rise too high.

Under the new laws, which will be presented to parliament in the fall but will apply from 27 June this year, companies will not be subject to compulsory licences for ten years. An additional ten years' protection from compulsory licences is offered to companies that manufacture a new drug in Canada. In exchange for such protection, the government has set targets for research expenditure by drug companies. Companies must increase research and development outlay to 8 per cent of sales by 1990, and 10 per cent by 1995. Research expenditure is now running at 5 per cent. Failure to comply with these targets could mean loss of protection from compulsory licences.

Other changes will bring Canada's patent laws in line with practices in most industrialized countries. Following the European model, patent applications will be open to public inspection 18 months after submission. Canada also plans to move away from the US system of awarding patents on a "first to invent" basis in favour of the European "first to file" ap-

proach. The government will also change patent terms from 17 to 20 years, and ratify the patent cooperation treaty.

While pharmaceutical industry trade groups have not yet formally endorsed the proposals, at least one pharmaceutical company is enthusiastic about them. Merck & Co. is moving immediately to complete plans for a Cdn\$20 million addition to its research complex in Montreal and expects to begin construction next year. By 1990, Merck estimates it will spend an additional \$100 million on research and development as well as creating 50 new scientific posts in Canada.

While victories are being won in Canada, the pharmaceutical industry has not been so fortunate in its dealings with the United States. For years, US drug companies have been seeking a change in the law to allow them to manufacture and export drugs that are not approved for sale in the United States.

Earlier this year an industry-approved bill reached the floor of the Senate, and the House was poised to consider similar legislation. But at the last moment, opponents added amendments so unpalatable to the industry that it withdrew its support for the legislation. The amendments would have placed tighter controls on export of infant formulas, and required additional notification procedures for exports of certain drugs.

Joseph Palea

Space vehicles

A short flight for Japan's shuttle

Tokyo

This is not the year for space flight. First it was the US Challenger, then Europe's Ariane, now Japan's shuttle has crashed to Earth seconds into its maiden flight. The craft's loss, however, is not a major setback — the shuttle was only a two-metre plastic model.

Last month, scientists from Japan's Institute of Space and Astronautical Sciences (ISAS), the space institute that earlier this year sent two probes to Halley's comet, test-flew a model of an orbital



re-entry vehicle. The white twin-finned shuttle was released at 1,000 m from a helicopter flying at 200 km per h 5 km off the Akita coast of Japan.

Equipped with a three-axis accelerometer, an angular velocity meter, a geomagnetic attitude sensor, an air-pressure sensor and a microprocessor, the model was supposed to be controlled from the ground and to relay information on altitude, attitude and velocity. But no sooner

was the shuttle set free than it looped the loop, turned into dive and 35 seconds later plunged headlong into the sea

A second test a few days later with a back-up model was more successful. After release, the shuttle remained airborne and glided steadily for 4.2 km while descending from 800 to 500 m. But it then veered left, failed to respond to correction signals from the ground, and 48 seconds later dived into the sea.

The ISAS team nevertheless considers the experiments a partial success. The telemeter system performed flawlessly and relayed data to Earth which show that the on-board roll stabilizer and yaw damper struggled valiantly to keep the shuttle on a steady course. But with no more models and a limited annual budget of only 100 million yen (£400,000), no further tests are planned this year.

The ISAS Working Group on Winged Vehicles, set up in 1982, is headed by Professor Makoto Nagatomo and has been carrying out computer simulation studies, wind tunnel tests and the present ballistics tests on Japan's shuttle of the future. Once a working model is made, the group hopes to attach a bigger version to a single-stage S-520 sounding rocket — but that would require an increase of two orders of magnitude in its budget, and funds are not yet forthcoming from the Ministry of Education, Science and Culture.

Beyond that, Nagatomo has outlined plans to develop a Highly Manoeuvrable Experimental Space (HIMES) Vehicle by incorporating a cryogenic engine into the shuttle. The HIMES vehicle could then be used as a self-contained re-usable sounding rocket or even as an orbital re-entry vehicle. But ISAS has no ambitions to build a manned shuttle — that is the preserve of the National Aerospace Laboratory and the National Space Development Agency.

David Swinbanks

West Germany

Terror against technology

Hamburg

KARL HEINZ Beckurts, a renowned physicist and one of the most important research managers in West Germany, was killed by terrorists of the Rote Armee Fraktion (RAF), in Munich on his way to work on 7 July. He and his driver, Eckhard Groppler, were victims of a 10-kg bomb, which was ignited electronically as they passed it in their car on their way from Beckurts' home in the Munich commuter village Strasslack to his Siemens office, where he worked as head of the department of research and technics, employing 36,000 workers.

Beckurts, who was born on 16 May 1930 in Rheydt, studied physics in Göttingen, first at the university and then at the Max-Planck-Institut for physics, where he finished his doctorate in 1956. Two years later he became head of the department for neutron physics and reactor technics at the Kernforschungszentrum in Karlsruhe. He moved to the Kernforschungszentrum in Jülich in 1970, and during his ten-year stay was responsible for its reorganization, introducing institutes for biotechnology and contact surface research. He then went to Siemens and became head of the research department.

Apart from his work there and his participation in the Grossforschungseinrichtungen, he taught in Karlsruhe and as an honorary professor in Bonn and Heidelberg. He is said to have been responsible for Siemens' leap into high-technology research.

Beckurts was also a keen supporter of the nuclear programme and it may be this that made him a target for the terrorists. He had fought for his conviction that, even after the Chernobyl disaster, a stable energy supply for West Germany must include nuclear power in the foreseeable future. Beckurts was also head of the Arbeitsgruppe Kernenergie of the Bund Deutscher Industrieller.

It is evident that in planning the killing the terrorisis took into account his support for puclear power as well as the new political situation in West Germany. There is now not only argument over quitting the nuclear programme, but also clashes between demonstrators and police in Brokdorf and Wackersdorf which prove the potential for violence on both sides and the readiness of a few to carry out criminal actions. RAF apparently seeks support from those who have already decided to abandon legal forms of action. A letter found near the site of the bombing "accused" Beckurts of having supported, apart from the nuclear programme, the US Strategic Defense Initiative (SDI) and the European research programme Eureka, described as programmes to further the "strategic reorganization of research and production". It is no surprise that a man like Beckurts was involved in consultation on Eureka and SDI, He had, however, committed himself to SDI, and, in spite of Siemens' participation, was not at all enthusiastic about Eureka.

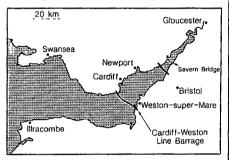
The assassination was apparently planned long in advance. Beckurts' name had been found on a list discovered in an apartment used by terrorists after the killing of Ernst Zimmermann, head of the

Motor- und Turbinen-Union, last year. Friedrich Zimmermann, Minister of the Interior, told the press that the Siemens manager had been warned. Safety measures will not, however, be tightened up. According to Zimmermann, there is no absolute protection against a remote-controlled bomb: not a very promising outlook for other endangered scientists. But laws regulating the right to demonstrate and the police law may well be tightened up. Political commentators say that this might have been a tactical aim of RAF, because more severe clashes could give them wider support or even new members from whom to recruit. Jürgen Neffe

Energy

Power from the Severn waters

THE world's largest tidal power-generation project came a step closer to realization last week with the decision of the UK Secretary of State for Energy to back a £5.5 million advanced feasibility programme. The decision was triggered by a new report showing that a 16-km barrage



across the Severn Estuary could be used to generate 14.4 TWh of electricity a year, six per cent of the nation's demand.

The idea of tapping the awesome energy of the Severn's tides — their 30 ft range puts them among the world's highest - has been around for a long time. In 1981, a committee under the chairmanship of Sir Hermann Bondi reported that a barrage was technically feasible. That provided enough encouragement for a more detailed study to be carried out by the Severn Tidal Power Group, a group of six major construction companies, with backing from the government. The report published last week says that the barrage, containing 192 turbine generators, could be built by the year 2000: six years of preconstruction development and seven years of construction, providing 44,000 jobs, would be needed. A further programme will now look in more detail at costs, performance and regional and environmental issues, as well as investigating a smaller tidal barrage scheme for the estuary of the River Mersey.

Two major issues have dominated discussion of the barrage scheme: the cost of the electricity it will generate in comparison with conventional power stations and

the effect it will have on the environment, particularly on the huge area of water behind the barrage.

Serious environmental problems are not foreseen by the report. Water will still flow into the Severn Estuary and it is believed that there would be little change in the salinity of the water or in the rate at which pollutants would move out to sea. But the tidal range behind the barrier would fall by half: although it would still be well within the range found elsewhere in Britain, there is no doubt there would be changes, which are not yet predictable, in the estuary's ecology. Ships using the Severn would be largely unaffected as locks will be provided in the barrage.

Calculating the costs of generated electricity has been more difficult as it depends on making projections into the next century. Electricity would be generated as the tide ebbed and rushed through the line of turbines. Pumping will add more energy: around high tide, when the level of the water either side of the barrier is the same, water can be pumped over the barrier. Later, when the tide has fallen, the extra water can be allowed to run out to give a net energy gain. The gain can be further increased if cheap rate electricity can be used for pumping and the generated electricity returned to the grid at peak rate times. One problem, of course, is that the time when electricity is generated is determined not by demand but by the tides. That, says the Severn Tidal Power Group, is not necessarily a problem: coal-fired stations can be kept on spinning reserve and brought up to full power as the tidal generators slow down.

Taking into account the need for this back-up, the tidally generated electricity seems likely to be marginally more expensive that nuclear-generated electricity but cheaper than coal-generated electricity. As it is unlikely that a large number of new nuclear power stations will be built this century, there should be room for tide power.

Alun Anderson

US education

Liberal colleges ask for more

EMPHASIZING their "significant and increasingly important contribution to America's scientific manpower pool", a group of fifty leading US liberal arts colleges say they will need to spend an additional \$1,000 million in the next decade to continue providing undergraduate training for future scientists. That conclusion appears in a preliminary draft report writ-

Earned doctorates in empirical and life sciences

Institution	Percentage
Cal Tech	37.5
Harvey Mudd*	37.2
MIT	18.6
Reed*	12.8
UC San Diego	10.8
Swarthmore*	8.2
Haverford*	7.5
Carnegie Mellon	6.4
Wabash*	6.4
Chicago	6.2

Percentage of graduates earning doctoral degrees comparing 50 liberal arts colleges with 20 top rated universities, Starred institutions are among 50 liberal arts colleges.

ten by Sam Carrier and David Davis-Van Atta of Oberlin College, presented last month at a conference on the future of science at liberal arts colleges.

The report is the second in a series assessing the role of small colleges as a training ground for scientists. The 1985 report showed that liberal arts colleges were relatively immune to a nationwide decline in the numbers of new students expressing an interest in majoring in a science discipline. Nearly 30 per cent of entering freshmen at the 50 liberal arts colleges included in the report said they were planning to major in science, compared with a national average of only 5 per cent. Women continue to represent a rising percentage of baccalaureate degrees in the sciences. More than 40 per cent of all undergraduate degrees for women in the 50 colleges were in the sciences.

The report attributes a large part of this strong showing to the close link between teaching and faculty research on the small campuses. Measures of academic distinction show graduates of the liberal arts colleges fare well when compared with graduates from larger universities. Carrier says the importance of liberal arts colleges is the quality of the students they produce as much as the quantity.

A problem for the smaller colleges is a stratification of faculty. At present their science faculties are overwhelmingly male (89 per cent), nearly all white (96 per cent), mostly in tenured positions (69 per cent) and relatively old (average age 44 years). The age distribution is skewed, with relatively few faculty younger than 30 or older than 55.

The 1986 report identifies the investments needed to maintain a strong position. Assuming a 1.1 per cent growth in faculty positions will be needed in the next decade, paying for these positions will cost an estimated \$369 million. To continue to attract a strong faculty, \$532 million will be needed to support faculty research, and an additional \$150 million for new laboratories and classrooms.

Appropriate ways of increasing investment in undergraduate science education have been a hot topic at the National

Science Foundation (NSF) recently. A National Science Board task committee chaired by Homer Neal (see Nature 320, 479; 1986) called on NSF to increase its support for undergraduate education to \$100 million annually. But NSF must still decide how to implement the Neal report recommendations, and must then win approval for new expenditures from the White House Office of Management and Budget and the Congress.

Carrier believes that the liberal arts colleges would fare well in competition for new NSF grants, but he expects a mix of federal, corporate and foundation support will be necessary to achieve financial goals. A third report to be produced by next summer will assess the issue of where the money should come from.

Joseph Palca

Chernobyl

Inquest continues on nuclear power

al improvements into the design of its nuclear power stations, according to Viktor Sidorenko, deputy chairman of the USSR State Committee for the Supervision of Safe Working Practices in the Nuclear Power Industry. But the type of improvement will be determined only after a detailed study has been made of the causes of the Chernobyl disaster.

In a statement released through the TASS news agency last week, Sidorenko said that his committee had been repeatedly asked, during the past few weeks, whether every reactor should have a dome-type containment building, which would prevent the emission of radioactive material into the external environment. Before Chernobyl, the Soviet stance had been that such containment buildings were unnecessary, and were merely a way for capitalist constructors to increase their profits. Sidorenko, however, took a slightly different line: that containment buildings are simply an alternative approach to safety, and that the Soviet system of modular "strong boxes", as used at Chernobyl, is a valid equivalent. It would be difficult to say at this stage, Sidorenko stated, whether a containment building would have reduced the scale of the Chernobyl emission.

Whether the two approaches are truly equivalent is a moot point. As a recent open letter to the International Atomic Energy Agency (IAEA) from an unofficial team of Polish scientists stressed, Soviet reactors have only two levels of containment, not as in the West, three. The more cautious purchasers of Soviet VVER reactors — Finns, Hungarians and Poles - have therefore insisted on a Western-style containment building being incorporated into the design.

Certainly the "modular strong-box"

THE Soviet Union is to introduce structur- 1.; approach failed to work for the RBMK reactor at Chernobyl, although, as Boris Semenov, deputy chairman of the USSR State Committee for Nuclear Energy, said in an interview with the Moscow Literaturnaya Gazeta in June, the design was intended to be sufficient to stop the leakage of radioactive material from the worst possible accident that could be foreseen: an instantaneous transverse rupture of the pressure header of the main circulation pumps.

One of the tasks of the government commission set up immediately after the accident is to determine and report on its cause or causes. Its other, and even more pressing duty, is to "eliminate the consequences" of the disaster. Since this is proving an extremely complex task, the report, which since the end of May has been promised "shortly", is not yet complete. (The arduous nature of the twofold task has, so far, worn out at least four, and possibly five, commission chairmen, all deputy premiers of the USSR.) Even without the official findings, and in spite of reports of faulty construction at Chernobyl, which appeared in the Ukrainian press before the accident, at least one Soviet official is quite sure that neither the design nor the construction of the Chernobyl plant was to blame.

Two days after Sidorenko's statement to TASS, Aleksei Makhukhin, First Deputy Minister of Power and Electrification, told the other official Soviet news agency, Novosti, that the accident seems to have been due to "a coincidence of several highly improbable and hence unforeseeable failures". Nevertheless, he admitted, although neither design nor construction was at fault, additional measures would be introduced to ensure greater safety of nuclear power engineer-Vera Rich

-CORRESPONDENCE-

A threat to medical progress

SIR—There have in recent years been several examples of a trend that has serious scientific and public importance, and in particular is liable to inhibit the development of medicine.

Any medical or surgical intervention carries, as is accepted, some degree of risk. Before devices or drugs are cleared for public use, they are subjected to close scrutiny and extended trials, and are released only if the risks are found to be acceptably small in relation to the much more substantial benefits. For example, it is accepted that the use of an intra-uterine device involves some slight increase in the risk of pelvic infection, but substantially less than the risks resulting from pregnancy, and it is equally accepted that all drugs carry some risk of undesired sideeffects.

However careful and extensive the trials may be, the release of a device or drug to the public provides data on a very much larger scale; this relationship is inevitable and unavoidable. In due course, further risks may come to light, usually those which are so small that they could not have been statistically significant in the original trials.

What is then liable to happen is that the manufacturer is subjected to lawsuits by people who have nothing to lose, and in particular clients of lawyers in those countries that permit contingency fees. These cases are tried and assessed by judges and juries who are not in general scientifically trained or knowledgeable, and who are unlikely to understand statistics or statistical causality. It is then probable that one or more of these cases will succeed, and it can afterwards be said that "it has been established by a court" that the substance or device is harmful.

The manufacturer is then on the horns of a dilemma. If it does not fight the lawsuits then it loses immediately. If it does fight them it may be put to enormous costs even if it wins, and by resisting the claims it is almost certain to attract hostile publicity, in particular media attention in which it is assumed and reiterated, without evidence, that what has been supplied is unquestionably harmful. The problem is so serious that once anything is even alleged against a supplier of a drug or a medical device, there may be little option than for the supplier to go into liquidation.

If this trend continues, it may well become commercially impossible for companies to develop anything new in medicine, and this would have serious public implications.

Of course some drug companies and other large firms have not been blameless, just as others have displayed a commendably responsible attitude. The problem is lawsuits and media emotionalism is almost entirely undiscriminating between those that have behaved well and those that have behaved badly. False sympathies are aroused by the media representing the problem as the little man or woman up against the commercial giant, but it needs to be remembered that it is the large company, rather than the retailer or physician, that is sued because it is only against a large corporation that large damages can be won, amounting in some recent cases to as much as £1 million.

Every sympathy and help is indeed due to someone damaged, in any circumstances, by medical intervention, but indiscriminate treasure-hunt suits do not fulfil this function and they confer a disbenefit on everybody who might need medical help in the future. The courts in this country have generally taken a responsible stand (and been castigated for it) by suppressing reports relating to a case sub judice; and when the report is eventually released, it may prove to be not evidence but only hearsay and unsupported assertion. Further legislative adjustment does however seem to be necessary, above all to strengthen discrimination in the assessment of alleged blame.

P.B. FELLGETT

University of Reading, Department of Cybernetics, 3 Earley Gate, Whiteknights, Reading RG6 2AL, UK

Monkeyed about

Sir-Tim Beardsley's News item "Monkey business: Bolivia asks for animals back" (Nature 319, 610; 1986) mentions squirrel monkeys and owl monkeys from Bolivia. The scientific names for both species are misspelled. For squirrel monkeys the correct spelling would have been Saimiri sciureus boliviensis, not "Saimiri scioureous boliviensis". Further, the appropriate nomenclature for Bolivian squirrel monkeys would have been Saimiri boliviensis boliviensis\.

For owl monkeys, the correct spelling would have been Aotus trivirgatus, not "Actus trivirgatusson". Further, the correct nomenclature would have been Aotus azarae. According to Hershkovitz², virtually all the owl monkeys in Bolivia should belong to one of two subspecies of Aotus azarae. Aotus exhibits substantial between-population chromosomal variation, and it is clear that it should not be regarded as a monotypic species (as has often been the case in the biomedical research community).

There is a clear need for primates and other animals used in biomedical and bethat the combination of contingency-fee | havioural research to be accurately identi- | Strand, London WC2R 2LS, UK

fied. For imported primates, specific sites of origin should be included in import documents and animal records. Too often scientists do not correctly identify their animal subjects, even in reports published in the best journals. Appropriate identification of primates should be a minimum requirement for their use and importation.

I urge all scientists who use primates to make a special effort to identify the animals they use, including geographic origin, and correctly to report this information in all published materials. For bibliographic assistance, scientists should make use of the services of the Primate Information Center at University of Washington.

J. ERWIN

American Journal of Primatology, PO Box 65481, Washington, DC 20035-5481, USA

Hershkovitz, P. Am. J. Primatol. 6, 257–312 (1984).
 Hershkovitz, P. Am. J. Primatol. 4, 209–243 (1983).

Tim Beardsley replies: The names were copied faithfully from the US Fish and Wildlife Service's import documents; there is no universally recognized taxonomy of squirrel and owl monkeys.

Soviet computers

SIR-Vera Rich reports skilfully on the planned changes in the administration of Soviet higher education (Nature 321, 716; 1986). Quite apart from the fact that one shudders a little whenever the Central Committee (or even someone like Sir Keith Joseph) announces that "we have plans for you", the situation in Soviet science is actually pretty grim for those who have to put up with it (even when they have all the privileges that come with the high status of an "Academician").

For example, at a recent meeting of the Academy of Sciences in Moscow, a very eminent scientist complained in public that not only was he short of computing power, which put him two or three years behind his American opposite number, but he gained a distinct impression that there were influential people around in Soviet science who did not think computers were essential. As a result he had to resort to "unusual ways" of acquiring his computer facilities (one imagines, either by smuggling them out of Western countries, or using the telephone to communicate with a computer in the United States).

The fact is that Soviet science is run by an establishment that makes our own University Grants Committee and Science and Engineering Research Council look like a collective of enterprising young men.

S.CHOMET

Department of Physics, King's College London (KOC), University of London,

Test ban made more respectable

A new study suggests that even the smallest nuclear explosions cannot be successfully hidden in holes beneath the ground, which makes a test-ban treaty a better proposition.

WHETHER or not there is eventually a comprehensive ban on nuclear tests, it will never be possible for politicians and others to claim that the academic community has failed to give the matter the attention it deserves. So much should be clear from the long account which occupies the first 71 pages of the current issue of Reviews of Geophysics, published by the American Geophysical Union, of the argument by which J.F. Evernden and two colleagues have been able to show that even attempts to hide underground explosions of nuclear weapons by conducting them in underground cavities cannot be successful (24, 143; 1986).

The question whether nuclear explosions might be concealed from the prying seismometers of invigilators first became a public issue in the 1950s, in the years preceding the abortive negotiations of a fully comprehensive test ban. In the event, the three governments in negotiation of the question, the Soviet Union, the United Kingdom and the United States, settled instead for a ban on all but underground tests, partly at least because of the belief that sizeable underground explosions might be effectively concealed by "decoupling" them from the surrounding medium. People were set to work ingeniously devising paper schemes for building spherical cavities in salt mines by solution mining and other methods. There was talk of muffling the seismic noise generated by explosions by factors of 50 or even 100. In the more recently aborted negotiation of a comprehensive test ban, in 1979, the three negotiating powers seem to have agreed to set aside the difficulty of concealment by decoupling, but the question has more recently been given a new lease of life and would no doubt be a stumblingblock again if serious negotiations on a comprehensive test ban were under way.

Not surprisingly, the question has an intrinsic as well as forensic interest. What really happens to the seismic signal of an underground explosion carried out in a cavity of some kind? Evernden is at the US Geological Survey at Menlo Park in California; the fellow authors of his latest contributions to the literature of the test ban are C.B. Archambeau (University of Colorado) and E. Cranswick (US Geological Survey), both at Boulder, Colorado.

The conclusion is heartening. According to Evernden *et al.*, it should now be possible to detect underground explosions in, say, the Soviet Union yielding explo-

sive energy equivalent to 1 kilotonne of conventional explosive even when these are fully decoupled from the surrounding rock. This, the authors say, could be accomplished by means of 15 monitoring stations outside the Soviet Union and by a network of 25 automatic seismic stations within the territory of the Soviet Union if they were so disposed as to make the most efficient use of the data gathered. The conclusion is heartening because, in the most recently aborted set of negotiations on the subject, the two major powers had agreed that each would provide house room for exactly 10 such stations.

How has this cheering result been obtained? Those who read the article by Evernden et al., as Evernden's earlier work on the same subject, will be struck by the way the argument is founded uncontentiously on empirical data. The starting point, for example, is a widely accepted formula (due to J.A. Sharpe and first published in 1942) describing the displacement field caused by an explosion in a supposedly homogeneous elastic material as a function of distance and of the frequency of the signal.

The physics of the process is well understood but none the less interesting for that reason. There is no doubt that an explosion in a cavity can in principle muffle the seismic signals from an underground explosion, partly because of the energy absorbed by the compression of the surrounding medium (air) and partly because of the sheer size of the cavity, which may imply that the pressure of the expanding explosive wave may be less, by the time that reaches the walls of the cavity, than that required to stimulate shock-wave propagation into the rock. And the result of that is that the wave from a decoupled explosion expands outwards, when it reaches the surrounding rock, even less efficiently than will the wave from a welltamped explosion.

It is good to be reminded by the article of Evernden et al. that the US authorities have in their time been obliging in their willingness to allow these predictions to be verified experimentally. Indeed, the authors make good use of the experiment conducted beneath the Nevada desert in the 1960s, when one nuclear explosion was used to make a cavity and another, smaller and later, was used to test the then current understanding of decoupling.

The essence of the argument now published turns on the dependence of dis-

placement at a distance from an explosion of any kind, decoupled or not, on the frequency at which the seismic signals are measured. Simply, the amplitude of the seismic signals is roughly a constant up to a certain value and then appears inversely proportional to the square of the frequency. Moreover, this "corner frequency" is itself a function of the magnitude of the explosion.

The practical consideration is that while the reduction of the seismic amplitude caused by decoupling in the low-frequency range may be very large, amounting to a factor of as much as 100, the disparity in the high-frequency range may be much less, a factor of 10 or so. What Evernden and his associates now propose is that the detection of decoupled explosions will be most efficient in the highfrequency region. Although the magnitude of the seismic displacements is itself reduced by the inverse-square variation of displacement with frequency, modern instruments could cope with that. But the reduced signal strength at higher frequencies explains why it is necessary to increase the number within the Soviet Union from the 10 talked of in 1979 to 25 now.

This latest contribution to the literature of the detection of decoupled explosions will surely not be the last on the subject. Indeed, Evernden and his colleagues raise hares fit for half a dozen investigations. There is, it seems, a possibility that decoupled explosions may be distinguished from well-tamped explosions, raising the possibility that attempted violations of a comprehensive test ban might be detectable. The limits of the sensitivity of detection arise, it turns out, from the confusion caused by wind-driven micro-seismic activity; the network of 25 internal stations is so chosen as to make use of the efficient propagation of high-frequency signals through the shelf structures of mainland Asia. Perhaps the most serious drawback in a system for detecting explosions as sensitively as that now proposed is that quite modest explosions of conventional chemicals would be detectable, raising the awkward possibility that the proposals for on-site inspection of suspicious places, one of the unprecedented provisions of the most recent draft treaty, would too often raise demands for inspection when none was called for. But that is not a serious obstacle to an agreement between governments prepared to take modest John Maddox

Origin of life

RNA and hot-water springs

from E.G. Nisbet

THE discovery that RNA molecules can extrude introns which can then act as enzymes (refs 1,2; see the recent News and Views article' by Frank Westheimer) makes the notion that life began from RNA very attractive. The most likely site for the inorganic construction of an RNA chain, which would have occurred in the Archaean, is in a hydrothermal system. Only in such a setting would the necessary basic components (CH4, NH3 and phosphates^{1,5}) be freely available. Suitable pH (fluctuating around 8) and temperatures around 40°C are characteristic of hydrothermal systems on land. Furthermore, altered lavas in the zeolite metamorphic facies, which are rich in zeolites, clays and heavy metal sulphides, would provide catalytic surfaces, pores and molecular sieves6 in which RNA molecules could be assembled and contained. If the RNA could then replicate in such a setting with the aid of ribozymes and without proteins, the chance of creating life becomes not impossible but merely wildly unlikely.

Models of self-replication

A self-replicating von Neumann machine needs a list of instructions (DNA and RNA in life); a set of organs (proteins) to help in the replication of the list; and a container which protects a local degree of order so that the components can find each other. In some models the container is dispensed with by the assumption that the oceans were a 'soup' of organic molecules. This is most improbable, as the Archaean oceans were probably rapidly processed through lavas in submarine hydrothermal systems at temperatures of several hundred degrees.

In the modern Earth, a volume of sea water equivalent to the entire oceanic volume passes through the mid-ocean ridge hydrothermal systems in about 10⁷ years⁸, whereas in the early Archaean this circulation time was probably 10° years or less ".". Unless the production rate of organic molecules in the ocean and atmosphere was high, the soup was probably clear and with chemistry not greatly different from today. Furthermore, NH, and CH, would not be present in any significant amounts as they would have had very short lifetimes in the atmosphere". It therefore seems unlikely that life began in the open ocean.

In other models12, the nucleic acid 'list' is dispensed with and proteins are called on to replicate themselves, but in this case it is difficult to see how the mechanism of replication could have the necessary specificity. The subsequent evolution of

nucleic acids would have to be from information in polyamino acids, which is not according to the central dogma. In an alternative model13, the list is based on clay minerals which can replicate themselves and do not need a protective container; but it is not clear how a daughter could detach itself from the parent and assume an independent existence.

In contrast to these interesting but complex models, the discovery that RNA can splice out a length of itself, which can then act as an enzyme¹⁻³, suggests a much simpler path to life. RNA is not only a list, but can also help⁷ to replicate the list. What is needed to complete the model is the third component, a suitable container or environment in which an RNA molecule could be assembled and could detach daughter ribozymes, yet still retain access to them.

A shallow-level hydrothermal system is the most likely setting in which all the necessary components could have been assembled to create a polynucleotide. First, only in hydrothermal systems could significant partial pressures of CH, and NH, exist in the Archaean Earth.

Second, hydrothermal systems carry large quantities of phosphorus, which has been dissolved out of basalt glass'. Typical mid-ocean ridge basalts contain 0.1-0.2 per cent P₂O₅, virtually all of which is lost to solution on the passage of hydrothermal fluids5. In the earliest Archaean the flux released by this route would have been much greater than today, and would have dominated the global supply of phosphorus, especially in the absence of a large sedimentary inventory on the continents.

The third reason for favouring a hydrothermal setting is the availability of inorganic catalysts. Altered basalts and pillow breccia consist of a porous fabric which includes a complex microcrystalline aggregate of zeolites, clay minerals and heavy metal sulphides, as well as albite, carbonates and relict primary phases. Enormous volumes of water flow through such altered rocks, with varying pH, chemical content and temperature, depending on the activity of the driving volcanic heat source and the local geology. Zeolite minerals can act as molecular sieves6, allowing the passage of small molecules while retaining large molecules. They also have remarkable and highly specific catalytic properties similar to enzymes¹⁴; the catalytic effects of clay minerals¹⁵⁻¹⁷ are well known. The abundant pores and cavities in altered basalt would provide an extraordinary assortment of inorganic containers lined with

zeolite molecular sieves, ranging in size from the zeolite cage⁶ (about 11 Å) to cavities several centimetres long.

If a molecule of RNA capable of selfreplication formed in this setting it would be in a fabric of altered rock, probably in a pore surrounded by a molecular sieve of zeolite. The pH of some Icelandic hydrothermal systems fluctuates in the range 7.5-8 (in contrast to submarine systems which are acid); such systems also have large regions at temperatures around 40°C; and the concentrations of Mg²⁺ and Cl ions in the hydrothermal systems would favour replication of RNA.

The RNA world

In a recent News and Views article18. Walter Gilbert postulated that the first stage of evolution was in an RNA world. In this model world, life consisted of selfreplicating RNA molecules and used recombination and mutation to explore new functions and adapt to new niches. Eventually a wide range of enzymic activities would develop by using RNA co-factors. Later, RNA would begin to bind and synthesize proteins which would eventually take over the enzymic role. A hydrothermal system would be ideal for providing the amino-acid components in this process¹⁹. In such a world, replicating systems in pores in altered rock close to the water-rock interface could pass from pore to pore in the altered lava, by chance as hydrothermal systems varied. They would eventually colonize their habitat to the extent of available resources. Any molecule which could replicate more faithfully by isolating itself from the random catalytic effects of zeolites and clays (once so useful, by now a source of error) would be strongly favoured by natural selection 10. A system which learned to surround itself with a bag of lipids would be more successful at reproduction and would be pre-adapted to life in the open ocean.

- Zaug, A.J. & Cech, T.R. Science 23, 470 (1986).
- Guerrier-Takada, C. & Altman, S. Science 223, 285 (1984). Westheimer, F.H. Nature News and Views 319, 534
- Arnorsson, S. & Svavarsson, H. Geochim. cosmochim. Acta 46, 1513 (1982). Staudige!, H. & Hart, S.R. Geochim. cosmochim. Acta 47,
- 337 (1983). Newsam, J.M. Science 231, 1093 (1986).
- von Neumann, J. Theory of self-replicating machines (University of Illinois Press, Urbana, 1966).

- versity of Hillions Press, Ordana, 1900).

 8. van Andel, Tj. H. Nature 305, 178 (1983).

 9. Bickle, M.J. Earth planet. Sci. Lett. 40, 301 (1978).

 10. Nisbet, E.G. J. molec. Evol. 21, 289 (1985).

 11. Abelson, P.H. Proc. natn. Acad. Sci. U.S.A. 55, 1365 (1965).
 12. Fox. S.W. & Dose, K. Molecular Evolution and the Origin
- of Life (Dekker, New York, 1977). Cairns-Smith, A.G. Genetic Takeover (Cambridge Uni-
- versity Press, 1982). Wright, P.A. et al. Nature 318, 611 (1985).
- Bernal, J.D. The Origin of Life (Weidenfeld and Nicholson, London, 1967).
- Odom, D.G. et al. J. molec. Evol. 12, 365 (1979). Gilbert, W. Nature News and Views 319, 618 (1986).
- Cortiss, J.B. et al. Oceanologica Acta Spec. Pub. 59 (1980).

E.G. Nisbet is in the Department of Geological Sciences, University of Saskatchewan, Saskatoon, S7N OWO, Canada.

Cosmology

What makes nearby galactic clusters all move as one?

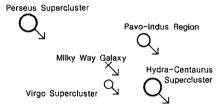
from Joseph Silk

No matter how hard cosmologists try, they have been unable to come up with a simple scenario that simultaneously explains both galaxy formation and the large-scale frothy structure of the galaxy distribution. One class of models, characterized by cold dark matter in the form of weakly interacting elementary particles, does well at explaining small-scale structures, but stumbles at the hurdle of the clustering of galaxy clusters. Another class, characterized by hot dark matter in the form of massive neutrinos or dark baryons such as burnt-out stars or black holes, shows promise of matching the large-scale structure, but at the cost of failing to form galaxies early enough in the Universe. The one point of consensus is the existence of pervasive dark matter, although the lack of any evidence as to its nature has opened the floodgates of speculation. More exotic avenues are being explored, the most promising of which involves cosmic strings, relics from the very early Universe which can act as seeds for the growth of structure on both small and large scales (see Hogan, C. Nature News and Views 320, 572; 1986).

It is premature to tell whether strings will be the cosmic panacea. But no sooner have cosmologists recovered from the momentous discovery of the bubble-like structure of the galaxy distribution on scales of tens of megaparsecs (Mpc) (see my News and Views article, Nature 320, 12; 1986), a remarkable new result is being announced. That our Local Group of galaxies is whizzing through space at a speed of about 600 km s⁻¹ towards a direction not far from the southern constellation of Centaurus is well known. This motion shows up as an unambiguous dipole anistropy in the cosmic microwave background (CMB) radiation, seen as a slight heating of the radiation in the direction in which we are moving and as a slight cooling in the reverse direction. Recently it has been reported that our Local Group is not a lone wanderer in intergalactic space, but that galaxies throughout a vast region of about 100 Mpc in extent are companions in its headlong rush. Evidence for this alarmingly coherent large-scale flow has been independently found by two groups.

David Burstein (Arizona State University) and co-workers from six other institutions spanning the globe from Pasadena to Herstmonceux (R. Davies, A. Dressler, S. Faber, D. Lynden-Bell, R. Terlevich & G. Wegner) have presented data on some 400 elliptical galaxies evenly distributed

on the sky. The measured parameters (central velocity dispersions, effective radii and total magnitudes) defined a sufficiently good correlation that enable distances to be inferred once distance-independent parameters (such as velocity dispersion and total magnitude) have been measured. This survey, the results of which were presented at a recent meeting in Hawaii and reported in the News and Views article by Richard Bond and Sidney van der Bergh (Nature 320, 489; 1986), shows that there is a bulk motion of about 700 km s⁻¹ of essentially all galaxies within $60 h^{-1}$ Mpc of the Local Group (h = 1 if the Hubble constant is 100 km s⁻¹ Mpc⁻¹, or $h = \frac{1}{2}$ if the Hubble constant is half of this value). The direction of this motion is towards galactic longitude $l = 299^{\circ}$ and latitude $\vec{b} = +1^{\circ}$ and within 20° from the apex of the dipole motion which yields the Local Group motion relative to the CMB.



350,000,000 LIGHT YEARS

A traveller at rest with respect to the microwave background radiation looking down on the superclusters would see them moving with about the same velocity in about the same direction. The arrows represent, to scale, the velocities the traveller would see.

(Graphic by David Burstein.)

Another group, working at Imperial College London (Collins, C., Joseph, R. & Robertson, N. Nature 320, 506; 1986) obtained infrared photometry for an allsky sample of the class of galaxies termed Sc at a mean distance of 50 h^{-1} Mpc. Again, by adopting the known correlations between their derived distancedependent parameter (infrared luminosity) and distance-independent parameters (infrared colour or central velocity dispersion) either absolute distances or Hubble velocities can be inferred once the correlations are calibrated. Comparison of Hubble velocity with the observed recession velocity for about 45 galaxies led Collins and colleagues to infer a bulk streaming velocity of 970 (± 300) km s⁻¹ in a direction towards $l = 305^{\circ}$, $b = 47^{\circ}$ that, within their large quoted uncertainty, is consistent with Burstein et al.'s result.

To many astronomers, this is a case of déjà vu. The large-scale motion amounts to a confirmation of the Rubin-Ford effect, a motion of the Local Group relative to a shell of Sc galaxies at $\sim 50 h^{-1}$ Mpc that, following its initial discovery in 1976 by Vera Rubin and Kent Ford, has generally been disbelieved until now. After all. the inferred direction of motion was nearly orthogonal to the apex of the Local Group motion relative to the CMB. This neglect may have been unjustified. Indeed, the first indication of a large-scale bulk motion came with the confirmation by several groups that the Local Group is falling towards the Virgo cluster at ~ 250 km s⁻¹ and in a direction some 45° away from the apex of its CMB motion. This means that, in the reference frame of the CMB, the entire Virgo Supercluster, including the Local Group at a distance of some $10 h^{-1}$ Mpc from Virgo, is moving at ~ 400 km s⁻¹ in the direction of Hydra-Centaurus

The new data on ellipticals tell us that clusters in Hydra - Centaurus in the south. and in Perseus and Pisces in the north. separated by a distance of $\sim 60 h^{-1} \text{Mpc}$. are all sharing a common motion with Virgo, whose amplitude may be as large as 700 km s⁻¹. We are all moving towards a region behind the Hydra-Centaurus clusters. According to Burstein et al., there is an additional component of random motion of $\sim 300 \text{ km s}^{-1}$ for individual clusters superimposed on the bulk flow. Finally, of course, the CMB must represent the ultimate local rest frame. It is reassuring that A. Yahil, D. Walker and M. Rowan-Robinson have confirmed in a study of IRAS galaxies that at a depth of $\sim 200 h^{-1}$ Mpc, the galaxies are indeed at rest with respect to the CMB (Astrophys. J. Lett. 301, L1; 1986). (Similar results were reported last summer at the Princeton dark matter symposium (in the press) by A. Meiksen and M. Davis.)

Reconciling these new data with existing models of large-scale structure will be a difficult task as no model predicts such large velocities. If the interpretation of the data holds up then something must be pulling us; exactly what is not clear. Indeed, it has been argued by N. Vittorio, R. Juszkiewicz and M. Davis (Nature in the press) that confirmation of the large-scale bulk motion will invalidate all hot or cold dark matter models that rely on inflationgenerated random phase perturbations of a Friedmann cosmology. Less attractive models may work: these include low-density Friedmann cosmologies containing either hot or cold dark matter, together with primordial seeds that have triggered early galaxy formation. The seeds might be cosmic strings, as proposed by T. Kibble, A. Vilenkin and Ya B. Zel'dovich (see Hogan, C. Nature News and Views **320**, 572; 1986), or rare objects that have injected sufficient energy via supernova

explosions to explosively amplify the perturbed mass scale up to galactic dimensions, as discussed by J. Ostriker & L. Cowie (Astrophys. J. Lett. 243, 127; 1981) and S. Ikeuchi (Publ. astr. Soc. Japan 33, 211; 1981).

The one source of solace is that the large-scale bulk motion does seem to be a likely consequence of the existence of the Hubble bubbles. These apparent voids, on scales up to $50\ h^{-1}$ Mpc, could have been generated by the large-scale flows which would evidently be present in a hot dark matter-dominated universe. Of course, these flows must have maintained considerable coherence to preserve the well-defined bubble surfaces on which the galaxies are found. If this were the case, the bubble interiors should be genuinely devoid of matter.

There is an alternative, needless to say,

offered by advocates of cold dark matter namely that the voids are illusory, simply reflecting the large-scale inhomogeneity of the luminous matter, concentrated into great clusters and into ridges of galaxies, from the relatively smooth dark matter distribution. Such a situation could arise if only the highest peaks in the primordial fluctuation spectrum managed to form galaxies. But however this biasing arose, one consequence is inevitable: the large-scale flows must turn out to be an artefact of observational error. Astronomers are now rushing to verify the reality of the large-scale flows: their confirmation promises to mark a turning point in cosmology.

Joseph Silk is in the Astronomy Department at the University of California, Berkeley, California 94720, USA.

Biochemistry

New role for transfer RNA

from Robert Haselkorn

BIOCHEMISTRY is conservative, and as a rule the same biochemical step is carried out in pretty much the same way throughout the kingdoms, microbes and man alike. It is unusual, therefore, that this rule is broken by a basic step in the biosynthesis of haem and chlorophyll. These molecules are both modified forms of a conjugated ring molecule called a tetra pyrrole nucleus, made by the condensation of several molecules of the amino acid *δ*-amino-levulinic acid. But it turns out that δ-amino-levulinic acid is made in very different ways in the cells of animals and plants. As Schön et al. report in this issue (Nature 322, 281; 1986), a glutamyl transfer RNA molecule participates in this pathway in chloroplasts.

Labelled acetate and glycine were shown 40 years ago (Shemin, D. & Rittenberg, D. J. biol. Chem. 166, 621; 1946) to be the exclusive precursors of the carbon atoms of haem in mammals and, later, in photosynthetic bacteria. Subsequent work showed that acetate entered the tricarboxylić acid cycle and the key step in the synthesis of hacm is the condensation of the cycle intermediate succinyl CoA, with glycine, to make δ -amino-levulinic acid. This is then transported from the mitochondria to the cytoplasm where subsequent steps in porphyrin biosynthesis occur. When the radioactive tracer experiments were eventually repeated using plant extracts (Beale, S.I., Gough, S.P.& Granick, S. Proc. natn. Acad. Sci. U.S.A. 72, 2719; 1975), it was found that the carbon atoms of δ-amino-levulinic acid were not derived from acetate and glycine but from α -ketoglutarate via glutamate.

During the past decade it was shown

that glutamate is reduced to glutamic semialdehyde and the latter transaminated to produce δ-amino-levulinic acid in chloroplast extracts. Various mechanisms were proposed for the glutamate reduction, some involving phosphorylated intermediates. Participation of RNA in the conversion of glutamate to δ -amino-levulinic acid was first indicated by work at the Carlsberg Laboratory in Copenhagen and at the University of Iowa (Huang, D.-D. et al. Science 225, 1482; 1984). Evidence that the RNA is a glutamyl-tRNA was obtained independently by W.-Y. Wang in Iowa, S.I. Beale at Brown University and the group of D. Söll at Yale University. In this issue, Söll's group reports that the intermediate in barley chloroplasts is one of three isoaccepting glutamyl-tRNAs. This tRNA, which has the unusual modified base 5methylaminomethyl-2-thiouridine in the first anticodon position, is the only one that functions as a substrate for the reduction to glutamic-semialdehyde. Whether this glutamyl-tRNA also functions in protein synthesis is not yet known. The tRNA is encoded in chloroplast DNA.

The two alternative paths to δ-amino-levulinic acid arose, I believe, separately in the heterotrophic and photosynthetic bacteria on the one hand and in cyanobacteria on the other. Heterotrophic bacteria are the evolutionary precursors of mammalian mitochondria while cyanobacteria are the ancestors of chloroplasts. Succinyl CoA and glycine are available raw materials in heterotrophic bacteria, but succinyl CoA is in short supply in most cyanobacteria, which lack the complete tricarboxylic acid cycle. Reduction of an

organic acid to an aldehyde proceeds nicely via an ester intermediate; what better source of glutamate ester than glutamyl-tRNA, already on hand for protein synthesis? To avoid competition for the same intermediate, the glutamyl-tRNA used to make δ-amino-levulinic acid should be modified to prevent its use in protein synthesis, but whether that is actually the case remains to be determined, as noted above.

The failure to observe incorporation of glycine into porphyrins in plants and most green algae suggests that the chloroplast pathway provides δ-amino-levulinic acid for all biosynthesis in plants. What is wrong with plant mitochondria? Where did they come from? Plant mitochondrial DNA is much larger than its mammalian counterpart, replete with direct and inverted repeats that recombine frequently to generate an array of circular molecules. Some plant mitochondrial DNA sequences are homologous to chloroplast DNA; at least one such sequence originated in the chloroplast because it encodes a major chloroplast enzyme. Other plant mitochondrial DNA sequences have nuclear homologues, suggesting a history of rather promiscuous exchange of genetic material between organelles in the evolution of plants. With δ -amino-levulinic acid supplied by chloroplasts, selection for the mitochondrial pathway in plants would be relaxed and the relevant genes could have been lost in the shuffle.

An exception to the general proposal that plants lack the glycine-succinyl CoA condensation pathway is known. The alga Euglena, evolutionarily bizarre in other respects, has been shown to contain both pathways (Weinstein, J. & Belae, S.I. J. biol. Chem. 258, 6799; 1983). However, so far the green algae Chorella and Chlamydomonas, as well as cyanobacteria, are believed to contain only the plant pathway to δ -amino-levulinic acid. A number of the outstanding questions raised by Schön et al. could be approached conveniently by the isolation and characterization of mutants, for which Chlamydomonas and Anacystis appear to be the organisms of choice. Useful in this connection could be a compound called gabaculine (5-amino-1,3-cyclohexadienyl acid) that probably inhibits the transaminase that converts glutamic semialdehyde to δ -amino-levulinic (Gardner, G. & Gorton, H.L. Plant Physiol. 77, 540; 1985). A collection of mutants resistant to gabaculine ought to include a few that affect the tRNA and the tRNA ligase as well as the transaminase. Examination of the δ -amino-levulinic acid pathway in fungi would also be rewarding from an evolutionary viewpoint.

Robert Haselkorn is in the Department of Molecular Genetics and Cell Biology, University of Chicago, Chicago, Illinois 60637, USA.

Cell biology

An unfolding story of protein translocation

from James E. Rothman and Roger D. Kornberg

THE general rule of co-translational protein secretion and membrane insertion is faced with a growing number of exceptions. Many cases are now known in which translation can be completed before membrane translocation. The difficult enough issue of how a nascent polypeptide traverses a membrane and folds up on the other side has, therefore, given way to the more general and seemingly impossible problem of how a fully folded, soluble protein can pass the permeability barrier of a lipid bilayer. Fundamental insight into this problem comes from the ingenious experiment of Eilers and Schatz, described on page 228 of this issue1, which implies that proteins unfold as they are imported into mitochondria. The existence of enzymes that unfold proteins has been indicated in other contexts; such activities may have broad significance.

Newly made proteins potentially can cross several translocational-competent membranes in the cell. For proteins targeted for import into mitochondria and the endoplasmic reticulum, the specificity is usually determined by the nature of the amino-acid sequence at the extreme amino terminus. Mitochondrial precursors have a leader peptide or signal sequence that is usually charged and hydrophilic. Proteins targeted to the endoplasmic reticulum, on the other hand, have a signal peptide that is mostly hydrophobic in character.

To test whether a protein unfolds as it crosses the mitochondrial membrane, Eilers and Schatz produced a fusion protein consisting of a mitochondrial signal peptide linked to the amino terminus of a well-characterized enzyme that is not normally translocated across any membrane, dihydrofolate reductase. They could then ask whether the translocation of dihydrofolate reductase into mitochondria (measured in a now standard type of cell-free system) is affected by a small molecule (the inhibitor, methotrexate) that binds tightly to the active site of the enzyme. If dihydrofolate reductase crosses the membrane in its folded form, then the binding of methotrexate should be without effect on transport (the methotrexate would simply be transported as well). But if the enzyme must be unfolded in order to cross, then methotrexate should profoundly inhibit uptake, by stabilizing the folded structure of enzyme.

The results of Eilers and Schatz show that import of dihydrofolate reductase (but not other mitochondrial precursors)

is virtually abolished by methotrexate. Moreover, the K_i for inhibition of import is the same as the binding constant of methotrexate to the active site of dihydrofolate reductase. Direct evidence that methotrexate binding stabilizes the compact, folded form of the enzyme comes from proteolytic digestion studies. Only the amino-terminal signal peptide and not the remainder of the fusion protein is accessible to digestion, whereas both parts of the molecule are degraded in the absence of ligand binding.

The bipartite nature of the dihvdrofolate reductase fusion protein, with an exposed amino-terminal signal peptide and compact core, fits nicely with the finding by Schleyer and Neupert2 that transport into mitochondria is at least a two-step process. First the amino-terminal signal and some additional sequence traverses the membrane; then the rest of the chain follows. Schleyer and Neupert trapped protein precursors between steps, in the act of translocation, by using low temperatures, both in vitro and in vivo. In the two cases examined (the beta subunit of F, ATPase and cytochrome c_i), the polypeptide chain is caught with its amino terminus penetrating the matrix space (shown by cleavage of its signal peptide) but with much of its mass still on the outside of the mitochondrion where it is susceptible to external proteolytic attack. Only the first step of import requires energy, derived from the mitochondrial membrane potential, because the remainder of the process occurs when the temperature is raised in the presence of energy poisons. The energy that drives protein unfolding must be introduced in the first step, even though complete unfolding may only occur later.

A similar multi-stage process involving protein unfolding may operate during protein translocation across endoplasmic reticulum and across bacterial plasma membranes. It was recognized several years ago3.4 that protein transport across bacterial membranes can occur posttranslationally, as in mitochondria. Only recently, however (as discussed in the recent News and Views article⁵ by Schatz), has it become apparent that translocation across the endoplasmic reticulum membrane can also occur post-translationally, although in at least some cases the completed chain must still be attached to the ribosome6. This suggests that all forms of translocation may have common mechanistic features⁵, possibly including an unfolding step.

Previously, all the evidence had suggested that transport across endoplasmic reticulum membranes was unique in being coupled to protein synthesis, implying that already folded chains are unable to cross. It now appears that when a precursor is unable to cross the endoplasmic reticulum post-translationally it is the fault of the precursor and not of the translocation machinery. Such a precursor simply does not put its best foot forward. apparently folding in such a way as to obscure its signal sequence. As would be expected, post-translational import of proteins by the endoplasmic reticulum requires energy, although in the form of a nucleoside triphosphate, rather than a membrane potential. One wonders whether energy is also used here for an initial step in which the signal sequence traverses the membrane.

Is the machinery that drives protein unfolding limited to membranes? If such a machine were free in the cytoplasm and operated under the same principles, it could unfold selected sets of proteins with selectivity being based on the appropriate 'signal' on the protein (analogous to the endoplasmic reticulum and mitochondrial signal sequences). For example, if a proteolytic activity were built into an unfolding machine, then selected proteins would be degraded as they were unfolded in the cytoplasm. Proteolysis would be ATP-dependent because of the need for energy in unfolding, and it would be limited to substrate proteins unfolded within the machine. Indeed, the ATP-dependent protease from Escherichia coli that is responsible for the degradation of partially denatured proteins seems to couple unfolding to proteolysis in such a fashion.

This remarkable enzyme, described by Goldberg and colleagues ', degrades a polypeptide chain into small, acid-soluble peptides, starting from one end and finishing off the chain it is degrading before it starts another. This processive degradation requires sustained ATP hydrolysis which, Goldberg and co-workers suggest. rapid translocation of the enzyme along its polypeptide substrate Were such an enzyme mounted in a membrane (deprived of its protease activity), it would translocate a polypeptide substrate past itself and across the membrane. The ATP-dependent protease from E. coli thus seems to represent the first known protein translocator.

The power of unfolding enzymes could also be harnessed for constructive purposes. Such enzymes could even catalyse the fundamental process of protein folding. Although this process is generally viewed as spontaneous, because isolated polypeptides can re-fold efficiently, artificial manoeuvres such as the gradual removal of a denaturing agent are often required. Wrongly folded structures

otherwise form and persist. Misfolded proteins in a cell might be recognized by virtue of the chain they expose and then be actively unfolded to allow the folding process to repeat itself rapidly until a compact structure of minimum energy is achieved. Such catalysis of folding by unfolding enzymes would set a minimum stability for a correctly folded structure.

The situation would be analogous to the action of helix-destabilizing proteins such as E. coli recA^{10,11}, and single-strand binding proteins¹² in catalysing the reassociation of DNA single strands. These proteins presumably bind to the sugarphosphate backbone of DNA and destroy wrongly paired duplexes of limited size that would otherwise persist for some time, allowing the strands to reassociate repeatedly until a stable structure, paired in the correct register along its entire length, is achieved. Proteins that act in a similar fashion to facilitate protein folding might recognize and bind to the backbone of a polypeptide chain. Such proteins would act in concert with other factors, such as an enzyme discovered long ago, which facilitates thiol-disulphide interchange during protein folding until the correct (most stable) arrangement of disulphide bonds is achieved¹³⁻¹⁵.

The exciting possibility emerges that cells have a set of unfolding enzymes. When they span membranes such as those of the mitochondrion or rough endoplasmic reticulum and have the appropriate signal-recognition machinery to provide the specificity for initial entry of the protein substrate, they catalyse translocation and unfolding. When a protease activity is built into the unfolding enzyme, selected proteins can be degraded as they are unfolded. One can even imagine an unfolding enzyme lacking proteolytic activity that still recognizes incorrectly folded proteins. Such an enzyme would correct the errors by allowing misfolded polypeptide chains a chance to try again. Is it possible that the rapid acquisition of a three-dimensional structure, one of the few processes in cells that seems to occur without the aid of enzymes, may in fact receive help? This unfolding story is far from wrapped up.

- Eilers, M. & Schatz, G. Nature 322, 228 (1986)
- Schleyer, M. & Neupert, W. Cell, 43, 339 (1985).
 Date, T., Zwizinski, C., Ludmerer, S. & Wickner, W. Proc. natn. Acad. Sci. U.S.A. 77, 827 (1980).

Randall, L. Cell, 33, 231 (1983).

- 5. Schatz, G. Nature News and Views 321, 108 (1986). 6. Perara, E., Rothman, R. & Lingappa, V. Science 232, 348
- Goldberg, A. & Waxman, L. J. biol. Chem. 260, 12029
- (1985). 8. Waxman, T. & Goldberg, A. J. Cell Biochem. (in the
- press). 10. McEntee, K., Weinstock, G.M. & Lehman, I.R. Proc.
- natn. Acad. Sci. U.S.A. 76, 2615 (1979).

 11. Bryant, F.R. & Lehman, I.R. Proc. natn. Acad. Sci. U.S.A. 82, 297 (1985).
- 12. Christiansen, C. & Baldwin, R.L. J. molec. Biol. 115, 441
- Goldberger, R.F., Epstein, C.J., & Anfinsen, C.B. J. biol. Chem. 238, 628 (1963).
- Venetianer, P. & Straub, F.B. Biochim. biophys. Acta 67, 166 (1963). Lambert, N. & Freedman, R.B. Biochem. J. 228, 635

James E. Rothman is in the Department of Biochemistry and Roger D. Kornberg is in the Department of Cell Biology at Stanford University School of Medicine, Stanford, California 94305,

Neurotransmission

Are there two functional classes of glutamate receptors?

from Charles F. Stevens

A RECENT article in Nature1 and two that appear on page 263 and 265 of this issue2.3, help to clear up some mysteries about excitatory synaptic transmission in the brain. Neurones that respond to the excitatory neurotransmitter glutamate generally possess at least two distinct classes of receptors, classified by the artificial agonists that excite them, into NMDA (for N-methy-D-aspartate) and non-NMDA types. Under normal recording conditions the NMDA type has rarely seemed to operate. The two articles in this issue show that the NMDA receptor is, indeed, used and define some conditions that determine its use, whereas the earlier article shows why two distinct classes of neuronal glutamate receptors may be useful.

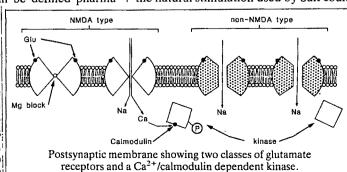
Acidic amino acids, especially glutamate, are to the brain what acetylcholine is to the neuromuscular junction. That is, where acetylcholine is used for excitatory synaptic transmission between nerve and muscle, glutamate is used at brain excitatory synapses. It is likely to be that more than half the neurones found in the brain use glutamate as their neurotransmitter.

At least three distinct classes of glutamate receptors can be defined pharma-

cologically. One class responds to NMDA, whereas the other classes respond to kainate and quisqualate. evidence Some suggests that the kainate and quisqualate receptors may be separate, but these two receptor types! are often classed together and often only two main classes of receptors - NMDA and non-NMDA — are distinguished. Amino-phosphonovalerate (APV) is a specific blocker for the NMDA receptor class but general glutamate receptor blockers that work on all classes are also available. Many neurones have high densities of binding sites for NMDA and are strongly excited when NMDA is applied directly to their surface. Although this excitation is effectively blocked by small doses of APV, this antagonist generally has little effect on excitatory transmission produced by stimulating presynaptic axons. Such excitation, however, is well blocked by broad-spectrum glutamate receptor antagonists. Therefore excitatory synaptic transmission must be normally mediated by the non-NMDA receptor class but what, then, is the function of NMDA class of receptors?

Salt² has investigated the contribution of NMDA receptors to synaptic transmission on the thalamus and has found, as is the case of other synapses, that the blocker APV has no effect on the baseline discharge of thalamic neurones and does not alter the response of the thalamic neurones to electrical stimulation of the excitatory pathways that project there. NMDA receptors would thus seem not to be involved in synaptic transmission in the thalamus. However, when natural stimuli are used, for example puffs of air instead of electric shocks, APV almost completely blocks the response of these same thalamic neurones. In other words, NMDA receptors appear to be used when the stimulation is natural but not when afferent pathways are stimulated synchronously with electric shocks.

A clue to how this paradoxical result could arise is provided by the observation of Herron et al.3. Although the conditions of their experiments differ from those of Salt, they find, using only electrical stimulation, that the intensity and pattern of stimulation can favour the participation of NMDA receptors in the response of a neurone. Their findings can be explained in several different ways, one of which is that NMDA receptors respond preferentially to low concentrations of glutamate and non-NMDA receptors respond to higher concentrations. By the same explanation, the natural stimulation used by Salt could



perhaps give rise to lower agonist concentrations than would synchronous stimulation, thereby favouring the use of NMDA receptors in one case and non-NMDA receptors in the other. Although further experiments will be needed to sort out the precise mechanisms involved, NMDA receptors are clearly there to be used.

But why are two classes of receptors required? One important difference between the two receptor classes is that the efficacy of synaptic transmission using NMDA receptors (but not the non-NMDA type) depends strongly on the voltage of the postsynaptic cell: if the membrane potential of a neurone is quite negative, NMDA applied directly has no effect whereas NMDA is quite effective in causing excitation (depolarization) if the neurone is already excited (depolarized). This property is, as far as we know, unique to NMDA receptors and arises through an interesting mechanism^{4.5}. NMDA always causes channels to open, but at negative voltages the channels are immediately blocked by physiological concentrations of magnesium ions whereas at more positive voltages the magnesium ions are driven out of the pore and the NMDA channel can excite the neurone by permitting sodium ions to flow in.

The paper by McDermott et al. demonstrates another important distinction between NMDA receptor channels and their non-NMDA counterparts: activation of NMDA receptors permits not only sodium but also calcium ions to flow into the cell and to produce significant increases in

the local calcium concentration.

One important consequence of this calcium flux in at least some neurones has been suggested following an observation first made by Saitoh and Schwartz⁶ and recently confirmed and extended by Miller and Kennedy⁷. A kinase regulated by calcium, known to be present in the postsynaptic membrane, appears clustered at many excitatory synapses, so that glutamate action on NMDA-type receptors would produce a calcium influx and consequently activate this kinase. The recent studies reveal that, when sufficiently stimulated by calcium, this kinase phosphorylates itself, and the phosphorylated enzyme then remains active even when calcium concentrations return to resting low levels. Activation of NMDA-type channels then can activate a kinase and switch the metabolic state of the postsynaptic region. Precisely which proteins the kinase phosphorylates, what function they have and whether this effect is a basis for learning and memory as is widely suspected, are questions whose answers should not be long in coming.

- MacDermott, A.B. et al. Nature 321, 519 (1986).
- Salt, T.E. Nature 322, 263 (1986).
- Herron, C.E. et al. Nature 322, 265 (1986).
 Nowak, L. et al. Nature 307, 462 (1984).
- Mayers, M.L., Westbrook, E.L. & Guthrie, P.B. Nature 309, 261 (1984).
- Saitoh, T & Schwartz, J.H. J. Cell Biol. 100, 835 (1985).

7. Miller, S.G. & Kennedy, M.B. Cell 44, 861 (1986).

Charles F. Stevens is in the Department of Molecular Neurobiology, Yale University Medical School, New Haven, Conneticut 06510,

Ocean Drilling Program

Palaeoclimatic linkage between high and low latitudes

from the Leg 108 shipboard scientific party*

One of the major questions in palaeoceanography concerns the linkage between the polar components of the climate system (ice sheets, sea ice and polar oceans) and the low-latitude ocean-atmosphere components (surface ocean, upwelling regions, wind circulation and land climate). Potential linkages between high and low latitudes have been proposed for timescales ranging from the early Cenozoic12 to the late Pleistocene^{3,4}. The central question is whether the two portions of the system are independent or interdependent, and if interdependent, to what degree and through which linkages?

The answer to these questions is important for the current debate on the relative contributions of ice-volume variations and ocean-temperature changes to the δ¹⁸O record, particularly in low-latitude planktonic foraminifers. It is also important in understanding long-term aridityhumidity cycles on the African continent, which seem to be driven by orbital insolation variations5, but which may also depend on evaporation from equatorial surface waters. In addition, the transfer of carbon from the surface to the deep ocean in productive upwelling regions may provide global climatic feedback via atmospheric CO, levels.

Between 21 February and 17 April, Leg 108 of the Ocean Drilling Program (ODP) cored more than 3,800 m of sediment at 12 sites in the eastern equatorial Atlantic (Fig. 1). At the coarse resolution achieved with our shipboard analyses, the initial results suggest a broad-scale late Neogene linkage between the polar and equatorial responses, but further shore-based analyses at the resolution of orbital periods (20,000-100,000 yr) will be necessary to determine the kind of link.

Results from three sites (657, 658 and)

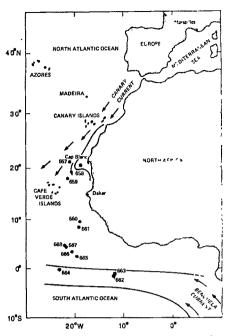


Fig. 1 Sites cored by Leg 108. Arrows, major current systems; dotted areas, regions of strong Plio-Pleistocene upwelling and divergence

659) in and outside the upwelling system driven by Northern Hemisphere trade winds along the north-west African margin suggest a substantial intensification of coastal upwelling since 3 million years (Myr) ago. A progressive intensification during the past 3-2.5 Myr also emerges from analyses of sediment at three sites along the south equatorial divergence (662, 663 and 664). In both locations, these conclusions are based on increases in the content of opaline silica (diatoms) and organic carbon in layers increasingly rich in terrigenous silt and clay from the late Pliocene to the Pleistocene. These indicators become more abundant in successively deeper Plio-Pleistocene CaCO, minima, probably at orbital rhythms (Fig. 2). Our conclusions are further supported by changes in the frequency of cool-indicator nannotossils. planktonic foraminifers and diatoms. In addition to local divergence and upwelling driven by northern and southern trade winds, some of the response in each region may also represent increased equatorwards advection of cool water by stronger eastern boundary currents in each hemisphere (Fig. 1).

The level of resolution of the shipboard

^{*} Co-chief scientists: W. Ruddiman (Lamont-Doherty Geological Observatory), M. Sarnthein (Geologisch Palaontologisches Institut, Universitat Kiel), ODP Staff Scientist, I Baldauf (Texas A & M Univ.), Also, J Backman (Univ. Stockholm), J. Bloemendal (Univ. Rhode Island), W Curry (Woods Hole Oceanographic Inst.), P. Farrimond (Univ. Bristol), J.-C. Faugeres (Univ. Bordeaux I) 1 Janeecs Bristol, J.-C. Faugeres (Univ. Bordeaux 1) I Janeces (Lamont-Doherty Geological Observatory), Y. Katsur (Univ. Tsukuba), H. Manivit (Univ. Paris VI), J. Mazzullo (Texas A & M Univ.), J. Mienert (Univ. Kiel), E. Pokras (Lamont Doherty Geological Observatory), M. Raymo (Lamont Doherty Geological Observatory), P. Schultheiss (Inst. Oceanographic Sci.), R. Stein (Univ. Giessen) 1 Lauxe (Scripps Inst.) J.-P. Valet (CNRS), P.P. Weaver (Inst. Oceanographic Sci.), H. Yasuda (Kochi Univ.).

analytical signals (approximately 50,000 yr) does not allow us to distinguish between whether these trends developed slowly over the past 3 Myr or whether they developed with abrupt step-like changes in amplitude. Regardless, a clear firstorder correlation exists between this equatorial trend and that seen in polar climates. Northern Hemisphere ice sheets first attained sufficient size to initiate ice rafting in the subpolar North Atlantic at 2.5 Myr (refs 7,8). Moderate-scale variations in ice-sheet size during the past 2.47 Myr then culminated in the large-amplitude 100,000-yr cycles during the past 650,000 yr (refs 9,10). The changes in equatorial upwelling/divergence show about the same late Pliocene onset and Plio-Pleistocene intensification (Fig. 2).

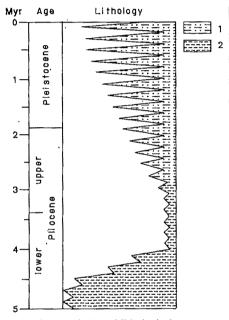


Fig. 2 Schematic log of lithological sequences obtained in and near north-west African margin upwelling area (sites 657, 658 and 659) and equatorial divergence area (sites 662, 663 and 664). CaCO, cycles increase in amplitude progressively from 3-2.5 Myr until the present, with non-carbonate lithology consisting mainly of silty clay with opaline (diatom) silica and minor amounts of organic carbon. I, Silty clay with diatoms; 2, red clay.

In addition to the north polar and equatorial changes, there is also evidence of northwards expansion of the Antarctic Circumpolar Current and the Antarctic polar front at and after 2.7-2.6 Myr (ref. 11). The fact that all three regions experienced nearly simultaneous changes complicates direct cause-and-effect interpretations. Similar first-order synchroneity of responses in polar regions and equatorial oceans has also been noted for the late Miocene 12-14

The exact polar-equatorial linkage thus remains unknown. Eventually, the question will best be answered by orbital-scale analysis of the long Leg 108 sequences using the numerical approaches pioneered by Project SPECMAP10. At this level of

analysis, the more exact criteria for defining climatic interdependence (analysis of orbital rhythms, phasing and coherence) will narrow the range of explanations.

There are already some suggestions of linkages from orbital-scale studies of conventional piston cores. Late Pleistocene surface-ocean coolings along the north-west African margin appear to vary with the size of Northern Hemisphere ice sheets4.15. In contrast, the equatorial surface waters have a predominant 23,000-vr signal in the late Pleistocene; not only is the dominance of this rhythm different from the distribution of orbital power in the ice sheets, but the equatorial seasurface temperature response leads ice volume by several thousand years¹⁶. Because the geographical equator lies south of the thermal equator in a region of Southern Hemisphere influence, the equatorial surface ocean may be forced from high southern latitudes on orbital timescales. Thus, the two primary upwelling/divergence regions in the tropical/ subtropical eastern Atlantic may be driven from opposite polar regions.

Fine-scale analyses will be aided by new correlation techniques introduced on Leg 108. Previous Deep Sea Drilling Project (DSDP) and ODP palaeoceanographic legs, despite coring two offset holes with the hydraulic piston cores at some sites, have had difficulty obtaining continuous sections; disturbed cores and incomplete recovery of some sections create gaps in the sediment sequence and thus in the climatic record. Only DSDP Leg 94 succeeded in verifying continuity of section in detail (tens of centimetres) at sea by tracking CaCO, layering in core photographs and then spot-coring any gaps.

ODP Leg 108 introduced a more sophisticated strategy that should be applicable to future palaeoceanographic legs in regions of large lithological variability. We measured two signals (P-wave velocity and magnetic susceptibility) at intervals of 3 cm or less on unsplit cores, which allowed correlation of the records at the offset holes to within a few centimetres. As a result, laboratory analyses of the various upwelling/divergence or tradewind signals are provided with a 'road map' showing precisely which sections to analyse from the offset holes to obtain a complete record of each site. In addition, P-wave and magnetic susceptibility signals contain orbital-scale rhythms and may prove as useful as some of the more conventional palaeoclimatic indicators.

We found evidence of one major Neogene change in palaeo-deep-water circulation: preservation of CaCO, was poor before 4.6-3.8 Myr, with red clay below 4,000 and dissolved calcareous sedimens above (Fig. 2). After that time, preservation markedly improved, with CaCO, preserved to well below 4,000 and less dissolution of the shallower calcareous sections. This change appears to represent the culmination of a cyclical long-term late Neogene trend towards improving CaCO, preservation that began in the late Miocene. An accompanying increase in sedimentation rates was more narrowly bracketed at several sites between 4.6 and 3.8 Myr. This change in the CaCO, compensation depth is the major equatorial Atlantic deep-water shift of the Plio-Pleistocene.

- 1. Shackleton, N.J. & Kennett, J.P. Init. Rep. DSDP Leg 29.
- 743 (1980).
 Matthews. R.K. & Poore, R.Z. Geology 8, 501 (1980). Cline, R.C. & Hays, J.D. Mem. geol. Soc. Am. 145, 464
- Sarnthein, M. et al. in Geology of the Northwest Africa Continental Margin (eds von Rad, U. et al.) 545 (Springer, Berlin, 1982).
- Kutzbach, J.E. Science 214, 59 (1981).
- Flohn, H. J. Met. Soc., Japan 60, 268 (1982)
- Backman, J. Stockh. Contr. Geol. 32, 115 (1979). Shackleton, N.J. et al. Nature 307, 620 (1984).1
- Shackleton, N.J. & Opdyke, N.D. Quat. Res. 3, 39 (1973).
 Imbrie, J. et al. in Milankovitch and Climate II, 269 (1984).
- 11. Cicsielski, P.F. & Weaver, F.M. Init. Rep. DSDP Leg 71, 461 (1983).
- Kennett, J.P. N.Z. Jl Geol. Geophys. 10, 1051 (1977).
- Thunell, R.C. Mar. Micropal. 6, 71 (1981). Denton, G.H. & Armstrong, R.L. Am. J. Sci. 267, 1121
- 15. Thiede, J. Meteor Rep. C28, 1 (1977).
- McIntyre, A., Ruddiman, W. & Karlin, K. Transact. Am. geophys. Un. 66, 931 (1985).

Thyrotrophin-releasing hormone

New applications in the clinic

from Ewan C. Griffiths

As a result of research reported at a recent meeting*, it seems likely that thyrotrophin-releasing hormone (TRH) and its analogues are about to attract interest as novel therapeutic agents in various neurological disorders. TRH, the tripeptide L-pyroglutamyl-L-histidyl-L-prolineamide (Burgess, R. et al. Nature 226, 321; 1970), acts as a hypothalamic hormone in stimulating the release of thyrotrophin (and other hormones) from the anterior pit-

*Therapeutic uses of TRH, Santa Barbara, California, 6-8

uitary. More than 70 per cent of the total brain content of TRH however, is found outside the hypothalamus and several initial studies suggested that it might be useful clinically as an antidepressant. But none of the analogues produced proved useful, so interest in the hormone declined.

One particular line of research that has re-awakened interest in TRH now is the demonstration that TRH can reverse induced states of shock and spinal injury (J.W. Holaday, Washington DC; A.I. Faden, San Francisco; S. Amir, Rehovot). In endotoxic, anaphylactic, lipoxygenase-induced and leukotriene-induced shock, TRH has proved a remarkable agent in increasing survival and reversing depressed cardiovascular and respiratory function. In spinal cord trauma, this neuropeptide was particularly effective, though not in dog and gerbil models of brain ischaemia. In a rat model of cerebral ischaemia (Latham et al. Regul. Peptides 13, 80; 1985), two TRH analogues given intraventricularly have been dramatically effective: RX 77368 (pGlu-His-[3,3'-dimethyl] ProNH₃) and CG3509 (orotyl-His-ProNH₃).

One area of clinical relevance for TRH is in motor neurone disease or amyotrophic lateral sclerosis. There are improvements in muscle tone and function after intravenous TRH treatment in some, but not all, patients with motor neurone disease and other types of spasticity (W.K. Engel, Los Angeles; B. Brooks, Madison). Other preliminary findings on the improvement of muscular functions in motor neurone disease used intrathecal administration (T. Munsat, Boston). These three studies suffer from short duration of action of TRH which has a half-life of 4 min or less. To overcome this, R. Guiloff (Westminister Hospital, London) has undertaken a clinical trial in patients with RX 77368, an analogue that binds well to TRH receptors and, compared with other analogues, is extremely stable and potent (my own observations). The patients treated with RX 77368 had significant improvements in speech, respiratory function, tongue movements and swallowing and decreased spasticity. There was also a marked increase in force of muscle contraction and in motoneurone activity.

How does TRH and its analogues work in motor neurone disease? Some clues have come from the work of Valerie Askansas (Los Angeles) who finds that motoneurones grown in culture in the presence of TRH show increases in choline acetyltransferase activity and neurite outgrowth, so perhaps the hormone is a neurotrophic agent. Further evidence for a neurotrophic effect has come to light through the reported reversal by TRH of neuronal damage caused by the substance P antagonist spantide (Freedman, J. et al. Expl Brain Res. 62, 175; 1986), and the stimulation of myelin lipid synthesis in chick neural cultures (Kanamoto, Y. et al. Brain Res. 371, 201; 1986). In patients with motor neurone disease, there is a loss of TRH and TRH receptors in the spinal cord (laminae II and ÎX). TRH is known to excite a-motoneurone activity and may act at several central and peripheral neuronal sites to cause the improvements observed in motor neurone disease.

Further potential applications arise from the variety of central nervous system actions attributed to TRH. In an animal model of Alzheimer's disease (neuronal damage induced by AF 64A, a nitrogen I mustard derivative of choline), another TRH analogue MK771 (L-pyro-2-aminoadipyl-His-thiazolidine-4-carboxamide) was reported by A. Horita to reverse the decrease in choline acetyltransferase activity. Because Alzheimer's disease is believed to involve a cholinergic deficit, perhaps TRH and its analogues could be used to reverse this deficiency. In view of the antiopioid actions of TRH (except in prolactin release and analgesia), it might be useful in treating narcolepsy and, through its analeptic effects, in the reversal of anaesthesia. Similarly, there is no really satisfactory therapy for either stroke or spinal injury and although there may be a time-limit on the effectiveness of the hormone, this is another possible use.

Such a list of previously untreatable

conditions has not gone unnoticed by the pharmaceutical companies, and besides motor neurone disease, clinical trials are being planned or are already under way with TRH and its analogues in spinal injury. Perhaps there is greater scope for the more stable analogues with enhanced duration of action, and choice of the best one from a long list of analogues now available can be assisted by both biological studies and theoretical prediction of conformation (Ward, D.J. et al. Regul Peptides 13, 73; 1985). After being thought of only as an ineffective antidepressant and a means of testing anterior pituitary function, TRH is making a comeback.

Ewan C. Griffiths is Lecturer in Physiology at the University of Manchester Medical School. Manchester M13 9PT, UK

Biological chemistry

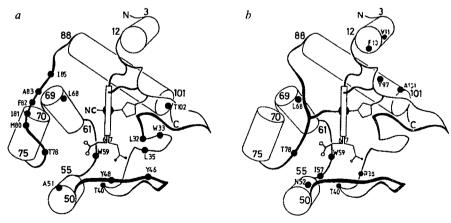
Long-range electron transfer

from R.J.P. Williams and D. Concar

THE basis of many biological processes, including many fundamental steps of energy transduction in membranes, depends on long-range (10-20 Å) electron transfer. The postulation of these electron hops, based on observations of complex biological pathways, was necessary as soon as it was realized some twenty years ago that the metal centres of electrontransfer proteins are embedded in folds some 5-10 Å from the surfaces of the proteins. That such processes were possible was then demonstrated by theoretical and solid-state studies. But the recent results of S. Isied and colleagues, reported elsewhere in this issue (Bechtold, R. et al. *Nature* **322**, 286; 1986), apparently throw

much of our subsequent knowledge of these processes into question.

The concept of long-range electron-hop reactions originally met with scepticism from inorganic chemists, who analysed reactions in small well-defined complexes in solution. Recently, several groups of biochemists and inorganic chemists (or bio-inorganic chemists) decided therefore that a thorough attack on the problem was necessary to show the constraints on through-protein electron hopping in solution systems. The protein cytochrome c is the major experimental object. Different approaches to the problem include protein to protein electron transfer; free small molecule (ferrocyanide) to protein



a, The fold of cytochrome c. Black spots, residues known to be affected by redox state changes. The larger effects are towards the bottom and left corner. The major change Met 80 - ALa 85 on substitution at the iron (in b) by CN*. Other residues known to be affected are shown as black spots. Grosser effects are towards the bottom left-hand corner. These diagrams are of cytochrome c from tuna. The site labelled W33 in a is equivalent to His 33 in horse cytochrome c, the species studied by Isied and co-workers. His 33 is the bound site of electron-transfer ruthennum reagents and is in a conformationally stable region. Lys 13 and 72 are on the front protrucing edge of the protein by the haem where reagents such as $[Fe(CN)_0]^1$ bind

transfer; and bound (crosslinked) small molecules (usually ruthenium complexes) to protein electron transfer. The last method, in avoiding the need to determine independently the binding constants and sites of the reagents, is particularly attractive, and it is this method that Isied and collaborators have used to produce their disturbing results.

Before discussing the results of Isied's group in detail, we will briefly describe the ribbon structure of cytochrome c (see figure). X-ray diffraction studies of crystals of the protein and nuclear magnetic resonance studies of the protein in solution leave no doubt that the ribbon structure undergoes only a small change from the Fe(11) to the Fe(111) state. Nuclear magnetic resonance additionally provides a dynamic map of fluctuations and their energetics in the protein and has also been used to analyse the structural change and energetics associated with substitution at the iron (see figure). This is a first-order groove-opening reaction dependent on the breaking of the Fe(111)-methionine 80 bond and some small protein rearrangement involving a concerted movement of the section of the protein mainly under the haem. As a result of these studies, the following position was firmly established before the report of Isied's group.

- (1) Electron transfer is a reversible phenomenon, which is axiomatic for self-exchange. Provided differences in redox potential are taken into account for forward and back reactions, there is no doubt about reversibility of electron transfer to or from free anions (ferrocyanide), bound cations (ruthenium derivatives) or other proteins (cytochromes b). There were no known gated bimolecular reactions involving cytochrome c.
- (2) A small activation energy is associated with electron transfer for all three types of reaction with some small protein rearrangement (see figure), but electron transfer could not involve a step as energetic as the Fe-Met bond break or ring flips that is, electron transfer has an activation energy of 10-20 kJ and not of the order of 50-100 kJ.
- (3) There is an understandable distance dependence for electron-hop transfer with a rather higher transmission coefficient than expected from theory. This helps to allow long-range (10–15 Å) electron transfer at rates as fast as is commonly found in protein-to-protein electron hopping. Protein-small molecule (free or bound) electron transfer is usually somewhat slower and complicated by solvent relaxation energies, that is, the same type of relaxation, but larger, as that of the small conformation change in the metal protein on redox change, where the protein is the effective solvent.
- (4) Electron transfer at these low redox potentials has little dependence on the chemical (amino acid) between the

Dame Honor Fell FRS (1900–1986)

DAME Honor Fell FRS, who died on 22 April, was the pioneer of the technique of organ culture by which small organs or organ rudiments can be successfully grown in vitro. In such cultures the various tissue components and their spatial relationship and function are preserved so that the explanted organ closely resembles the parent tissue in vivo. In her hands the method proved particularly suitable for the study of developmental processes in fetal organ rudiments but has since been adopted and is still used for the cultivation of adult tissues.

Using this method she made a major contribution in the elucidation of the processes involved in skeletal development. She showed that both avian and murine limb bone rudiments have a remarkable capacity for self-differentiation and will grow and differentiate in the same manner in vitro as the organs in situ. She further showed that both growth and differentiation could be modified by extrinsic factors, such as vitamins and hormones.

An important example of this modification is the influence of vitamin A on the differentiation of cartilage and ectoderm. She showed that vitamin A added to the culture medium of avian ectoderm modified the direction of epithelial differentiation. The vitamin suppresses normal keratinization and induces mucus-secreting ciliated epithelium instead associated with an increase of sulphur uptake by the metaplastic cells. In embryonic cartilage the vitamin causes a severe breakdown of the matrix with a loss of metachromasia.

This finding formed an important link with her more recent investigations into

the mechanisms involved in joint damage in arthritis. To simulate the rheumatoid pannus she grew pig articular cartilage in association with synovium and showed that the synovium, either in direct contact with the cartilage or in medium conditioned by synovial cells, has, like vitamin A, a deleterious effect on the cartilage ground substance, leading to a loss of proteoglycans and collagen, and of metachromasia.

Together with her colleagues at the Strangeways Research Laboratory, Cambridge, United Kingdom, she traced this effect to a factor secreted by the synovial cells, now identified as the polypeptide catabolin/IL1. Her finding constituted a major advance in the understanding of joint destruction in arthritis and forms the basis of much vigorously pursued international research in this field.

Honor Fell obtained her PhD in Zoology at Edinburgh University in 1923 and the same year joined Dr T.S.P. Strangeways at what was then the Cambridge Research Hospital. After his death in 1926 she became Director of the Laboratory now renamed Strangeways Research Laboratory in 1928, a post she held until 1970.

Under her directorship the small laboratory grew to a major institute of worldwide reputation. In the post-war years the laboratory became a focal point for visiting biologists from abroad whom she trained in *in vitro* methods and who came to rely on her advice, guidance and encouragement, which were unstintingly given. She was one of the most outstanding biologists of this century and her death means the end of an era in biomedical science.

Ilse Lasnitzki

centres, whereas at high potential aromatic groups can act as hopping stations.

The experiments of Isied and collaborators throw all of these conclusions into question. Their results seem to show that the electron-transfer rate, properly corrected for redox potential, can be dependent on the *direction* of electron transfer, that is, it is irreversible. This means that different micro-states are involved for the reaction Ru(II) to Fe(III) and Fe(II) to Ru(III) in cytochrome c. Unless there is a gross experimental error in the characterization of species (for example, in structure) this means that this electron transfer can be gated.

The authors offer explanations as to how this could come about and they refer to the conformational states of cytochrome c we have described above. It has to be admitted that some states, such as those involved in the flipping of certain aromatic rings and groove openings, do involve activation energies of up to 100 kJ per mole, but it is hard to see how these motions could have anything to do with the electron-transfer steps in only one

direction, especially as they are not involved in the other reactions described above. This is not to say that in some proteins, such as cytochrome P-450, electrontransfer reactions are not gated — in the case of P-450 they are gated by substrate binding. But in the very simple case under discussion we have a puzzle on our hands, in that one set of observations is completely out of line with all the others. Clearly the puzzle can be resolved only with a large series of measurements.

Given the importance of the observations of Isied and colleagues it is essential that at least one other group of inorganic chemists makes the same study independently. Until that is done we face the data with bewildered amazement, frankly hoping that they will go away. If they do not, we must re-examine a considerable part of our thinking about protein energy states and not just about electron transfer.

R.J.P. Williams and D. Concar are in the Department of Inorganic Chemistry at the University of Oxford, South Parks Road, Oxford OX1 3QR, UK.

SCIENTIFIC CORRESPONDENCE

Visual observation of lightning propagation

Sir-Reliable scientific observers' have reported discerning direction of movement and propagation in long-duration horizontal lightning flashes. With measured velocities between $5.6 \times 10^{\circ}$ and 1.1× 10⁴ m s⁻¹ for horizontal flashes⁴, lightning approaches the upper threshold for detection of movement by the human eye.

During a nocturnal thunderstorm over Ann Arbor on 9 June 1985, we were able to observe and photograph cloud-to-air lightning that appeared to propagate so slowly that we were able visually to observe apparent movement. The photograph of one of these lightning flashes reproduced here neither supports nor contradicts the visual observation of propagation, since it represents a time exposure. Because this photograph shows only a large, widely branched lightning flash, we were prompted to review both the physics of the flash and the limitations of the human visual system to better understand what we perceived.

Even a long-duration lightning flash (≥ 0.4 s) is too brief to allow interpretation of the observation, since the duration of a perceptual experience is around 0.4 s for the dark-adapted visual system5, even following the briefest stimuli. The time frame is also too fast to allow the eve to track the flash; so what we must have observed was the temporal ordering of the flash.

A lightning flash usually consists of successive discharges (strokes) along the same channel, and channel sections have been observed to propagate with a mean

pause time of 0.06 s, with about four pause { times per horizontal channel. The fovea of the eve is able to determine temporal order perfectly with a pause of 0.3s between the onset of two targets. Thus the time frame of propagation of long-duration horizontal lightning flashes is more than adequate for the visual processing system to resolve temporal ordering. If the mean duration of such a flash is 0.43 s (ref. 4), the flicker rate of the flash would be around 17 Hz, well below the critical fusion frequency, but too fast for the individual strokes to be counted accurately'.

The initial visual stimulus of the lightning flash shown below was probably a single channel extending downwards from the base of the clouds. The image of the initial and subsequent channels would be renewed in the observer's visual system with each stroke of the flash, enhancing the perception of movement and propagation for the observer.

DENNIS G. BAKER

Department of Atmospheric and Oceanic Science,

University of Michigan,

Ann Arbor, Michigan 48109, USA Anita Baker-Blocker

Advance Science Consultants, Ann Arbor, Michigan 48107, USA

- D'Abbadie, A. Nature 35, 342 (1887).
 Krider, E.P. Weather 29, 24-27 (1984).
- Brook, M. & Vonnegut, B. J. geophys. Res. 65, 1302-1303 (1965).
- Brantly, R.D., Tiller, J.A. & Uman, M.A. J. geophys. Res.
- Haber, R.N. & Standing, L.G. Can. J. Psychol. 24, 216-229
- McKee, S.P & Taylor, D.G. J. opt. Soc. Am. A(1) 620-627
- Ganz, L. Handbook of Sensory Perception Vol. 5 (Academic, New York, 1975)

Controversial glycosaminoglycan conformations

Sir-The issue of the ring conformation of the α-L-idopyranuronate residue in dermatan sulphate, heparan sulphate and heparin — three important biological classes of glycosaminoglycans — was recently debated by Rees et al.1. At least for dermatan sulphate, the authors explained how a postulated conformational equilibrium of the iduronate residue between a prevalent 'C₄ and a minor 'C₁ chair form was compatible with experimental observations, including extreme susceptibility of dermatan sulphate to periodate oxidat-

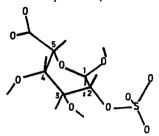
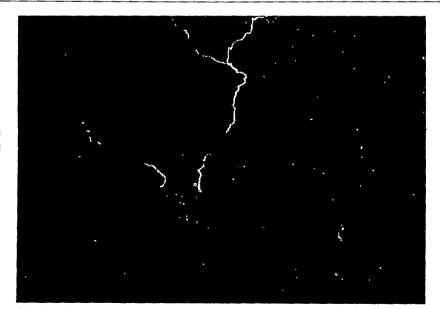


Fig. 1. The ²S₀ skew-boat conformation for the 2-O-sulpho α-L-iduronate residue.

ion. It was stated that "also possible are various distorted chairs and skew boats but these are not discussed here since their consideration would constitute a second order of analysis". This last statement prompts us to air our own views on this controversy

In a recent work², a detailed forcefield study of the conformational characteristics of methyl 4-O-methyl-2-Osulpho-α-L-idopyranosiduronate demonstrated that the ring may indeed adopt three nearly isoenergetic conformations ¹C₄, ⁴C₁ and the skew boat ²S₀. The vicinal coupling constants ${}^3J_{\rm ini}$ observed for heparin and various heparin oligosaccharides containing (I₂₅), the 2-sulphate iduronate residue⁴, were subsequently interpreted' in terms of conformeric coupling constants computed by using the Karplus-like equation proposed by Altona and colleagues' and the molecular geometry obtained from force-field calculations2. For heparin and synthetic oligosaccharide sequences contained in heparin, the I_{2s} residue shows considerable populations of only two conformations, ¹C₄ and ²S₀, the percentage of the skew boat ²S_a found (40 to 64%) being a function of the sequence. A similar analysis has been achieved for the non-sulphated α-Iiduronate residue in dermatan sulphate (D.R.F., A.P. and M.R., unpublished data). The vicinal coupling constants of the iduronate ring observed in dermatan sulphate were computed by means of Altona's relationship' relating the 'J_{int} to the dihedral angles H-C-C-H, which were obtained from force-field calculations on methyl α -L-idopyranosiduronate. iduronate residue in dermatan sulphate



Cloud-to-air discharge emanating from cloud base of about 2 km at 4:30 a.m. EDT on 9 June 1985 at Ann Arbor, Michigan, USA, photographed with a Chinon camera with a 58mm lens at f/1.8, with the shutter held open until after the flash ended, using Kodachrome ASA 25 35-mm slide film.

was shown to be in equilibrium between ${}^{1}C_{4}$ (58%) and ${}^{2}S_{0}$ (42%).

We have also analysed data for various naturals or synthetic (J.-C.J., T. Chiba and P.S., unpublished data) glycosides of non-sulphated L-iduronate. A considerable population of the two chair conformers ${}^{1}C_{4}$ and ${}^{4}C_{1}$ has been found, in this particular case where the α -L-iduronate residue is unsubstituted at position 4. The main difference between the two sets of coupling constants corresponding to the presence of either ${}^{2}S_{0}$ or ${}^{4}C_{1}$ lies in the value of $J_{3,4}$ which in the former case remains small, even when $J_{3,4}$ is quite large.

Finally, 4-unsubstituted glycosides of 2-O-sulpho- α -L-idopyranuronate exist mainly (> 90%) in the $^{1}C_{4}$ conformation as also evidenced by the observation of longrange coupling constants ($J_{1,3}$ and $J_{2,4}$ from 0.5 to 1 Hz) in synthetic as well as disaccharides and oligosaccharides (B. Perly and M.P., unpublished data) derived from heparin.

The participation in the conformer equilibrium of α -L-iduronate residue located *inside* a glycosaminoglycan chain of the well-defined 2 2 S_n skew boat, which results in a quasi-equatorial orientation of its hydroxyl groups, is an equally plausible explanation for the observed susceptibility to periodate oxidation of unsulphated L-iduronate residue in glycosaminoglycans.

Moreover, the unique conformational flexibility of α -L-iduronate residues may explain some important binding and related biological properties of dermatan sulphate, heparan sulphate and heparin.

B. Casu*, J. Choay†, D.R. Ferro‡,
G. Gatti§, J.-C. Jacquinet||,
M. Petitou†, A. Provasoli‡,
M. Ragazzi‡, P. Sinay|| & G. Torri*

* Istituto di Chimica e Biochimica
"G. Ronzoni",
via G. Colombo 81,
20133 Milano, Italy
† Institut Choay,
46 Avenue Théophile Gautier,
75782 Paris Cedex 16, France
‡ Istituto di Chimica delle
Macromolecole del CNR,

via E. Bassini 15/A,
20133 Milano, Italy

§ Bruker Spectrospin, Via Pascoli 70/3,
20133 Milano, Italy

[Laboratoire de Biochimie Structurale,
U.A. 499, U.F.R. de Sciences
Fondamentales et Appliquées,

rue de Chartres, B.P. 6759, 45067 Orléans Cedex 2, France

- Rees, D.A., Morris, E.R., Stoddart, J.F. & Stevens, E.S. Nature 317, 480 (1985).
- Ragazzi, M., Ferro, D.R. & Provasoli, A. J. Comput. Chem. 7, 105–112 (1986).
- Gatti, G., Casu, B., Homer, G.K. & Perlin A.S. Macro-molecules 12, 1001–1007 (1979).
- Torri, G. et al. Biochem. biophys. Res. Commun. 128, 134–140 (1985).
- Ferro, D.R. et al. J. Am. Chem. Soc. (in the press).
 Haasnoot, C.A.G., De Leeuw, F.A.A.M. & Altona. C. Tetrahedron 36, 2783-2792 (1980).

- Gatti, G., Casu, B., Torri, G. & Vercellotti, J.R. Carbohydr, Res. 68, C3-C7 (1979).
- Sanderson, P.N., Huckerby, T.N. & Nieduszynski, I.A. Glyconconjugate J. 2, 109-120 (1985).
 Jacquinet, J.C., Petitou, M., Choay, J. & Sinaÿ, P. XIIII.
- Intern. Carbohydr. Symp., Utrecht. 68 (1984).
 Huckersby, T.N., Sanderson, P.N. & Nieduzynski, I.A. Carbohydr. Res. 138, 199-206 (1985).

Ulcerative rhabdovirus in fish in South-East Asia

SIR-Annual outbreaks of a severe ulcerative disease with high mortalities of wild and pond cultured freshwater fish have been reported throughout South-East Asia since 1980'. The condition is characterized by the appearance of large, deep ulcers on the body and/or head with varying degrees of destruction of the underlying tissues. Many species are considered to be susceptible but the striped snakehead (Ophicephalus striatus), one of the economically most important species, has perhaps suffered the most severe losses. Pollution of the natural waterways and fish ponds with insecticides and herbicides, particularly paraquat, is believed by some workers to be the major cause of disease whereas others consider the nature, distribution and pattern of spread of the outbreaks to be more consistent with an infective condition.

Between October 1985 and February 1986, wild and pond cultured fish showing varying degrees of skin ulceration were obtained from widely dispersed locations in Thailand and Burma and subjected to virological examination. Portions of liver, kidney and spleen were removed from affected fish, homogenized in Hanks' balanced salt solution, clarified by low-speed centrifugation and the supernatants

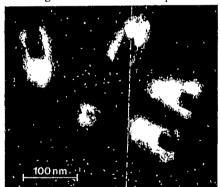


Fig. 1 Rhabdovirus particles from second passage on snakehead cells.

decontaminated by filtration through 450-nm membrane filters. Monolayer cultures of a cell line derived from snakehead fry were prepared using Leibovitz L-15 medium supplemented with 10% fetal calf serum as growth medium and 1 ml aliquots of filtered supernatant added to 25cm cultures. After allowing absorption for 1h at room temperature the cultures were overlaid with 7 ml maintenance medium (L-15 + 2% serum) and incubated at 28°C. Cytopathic effects developed between 3 and 14 days post-inoculation. Cells

became granular, rounded up, detached from the monolayer and lysed. This progressed at varying rates over some days until virtual total destruction of the monolayer had occurred leaving only fine, granular debris in the culture medium. Aliquots of media were inoculated onto fresh snakehead cell cultures to confirm transmissibility of the effect.

Electron microscope examination of phosphotungstic acid stained pellets obtained following ultracentrifugation of cell culture fluids from passaged samples revealed bullet-shaped virus particles (Fig. 1). The overall dimensions of these typical rhabdoviruses were $120 \pm 10 \,\mathrm{nm} \times$ 80 ± 5 nm. Morphologically indistinguishable particles were recovered in cell culture from diseased snakeheads from the Bangkok region of central Thailand, Chiang Mai in northern Thailand, Udornthani in northern Thailand and snakehead and freshwater eel (Fluta alba) from the Rangoon area of Burma. The size of the particles corresponds closely with that of other recognized fish-pathogenic rhabdoviruses2-5, but further studies are required to determine the relationship of the ulcerative disease isolates to these pathogens.

Although a virus infection has always been recognized as the possible primary cause of disease and virus-like particles of varying morphology have been observed in the tissues of diseased fish, this is the first report of the isolation of a single virus type from more than one species of diseased fish in widely separated geographical areas. However, many diseases of fish cause clinical signs only in adverse environmental conditions and this ulcerative condition seems such a disease. The fact that outbreaks occur in Thailand only during the cooler months of the year suggests that a falling water temperature may be a prime stress factor in this region but other environmental conditions may be precipitating factors elsewhere. Overall we consider the balance of evidence to implicate the rhabdovirus as the likely primary causal agent of the disease.

This work was supported by the UK Overseas Development Administration and FAO. We thank Dr Wattana Wattanavijarn, Chulalongkorn University, Bangkok for facilities and assistance.

G.N.FRERICHS S.D. MILLAR R.J. ROBERTS

Institute of Aquaculture, University of Stirling, Stirling FK9 4LA, UK

- FAO Technical Co-operation Project Rebort 4508 (Department of Fisheries, Ministry of Agriculture and Cooperatives, Bangkok, 1985).
- De Kinkelin, P., Galinard, B. & Bootsma, R. Nature 241, 465-467 (1973).
- Cohen, J. and Lenoir, G. Ann. Rech. vet. 5, 443–450 (1974).
 Hill, B.J., Underwood, B.O., Smale, C.J. & Brown, F. J.
- gen. Virol. 27, 369-378 (1975).
 5. Ahne, W. Archs Virol. 48, 181-185 (1975).
- Wattanavijarn, W. et al. Thai. J. vet. Med. 13, 51-58 (1983);
 14, 31-39 (1984). (In Thai).

Two Cambridge cultures

William Cooper

The Red and the Blue: Intelligence, Treason and the Universities. By Andrew Sinclair. Weidenfeld & Nicolson: 1986. Pp.179. £12.95. To be published in the United States by Little, Brown.

I THOUGHT I couldn't bear to read another book about Burgess, Maclean et al. — or even a book in which they appeared as characters. I'm allergic to spies. SNEAKS ALL, I call them; regarding the CIA, KGB and MI5 as having more in common with each other than they have with the rest of us. As for the sneaks themselves, some of them are so eaten up with the vanity of sneakery that they can't resist sneaking for both sides at once! Vain and trivial people. Were the CIA, KGB and MI5 disbanded tomorrow, the difference in our world ten years hence would be insignificant.

Burgess, Maclean, Philby and Blunt appear throughout as characters in Andrew Sinclair's The Red and the Blue, to which he gives the more explanatory subtitle, "Intelligence, Treason and the Universities". I found I could read the book with admiration and approval. The universities in question are chiefly Cambridge and the period covered begins with the First World War and ends in the present day; the central feature of that period in Cambridge being the glorious era of physical discovery in the Cavendish Laboratory, discovery in atomic and nuclear physics which had a revolutionary impact on world history. The glory was at its peak in the years around 1932 — just when Burgess, Maclean, Philby and Blunt embarked on their private pettifogging tricks that have so hypnotized the British popular press. Mr Sinclair, however, judges his perspective on the whole Cambridge scene with a combination of independence, accuracy and understanding. (He took a double first in History at Trinity College, Cambridge.) His interpretation owes much to the concept of "The Two Cultures", first publicized by C.P. Snow in 1959 — which is when Mr Sinclair graduated, so he only arrived on the scene in person ten years after the half-way mark in his story.

From the end of the First World War to the beginning of the second, the scientific culture is epitomized, obviously, by the Cavendish Laboratory — Rutherford, Chadwick, Blackett, Cockcroft, Rutherford's remarkable Russian protégé, Kapitsa, and others. Kapitsa founded a very influential open club, where scientists could publicly exchange information about their discoveries. The literary culture is epitomized by a secret society called The Apostles, "a self-electing élite of

those who considered themselves the brightest and best in contemporary literature and philosophy", its members drawn from the privileged classes, male and mostly from Eton, no scientists — Keynes, G.E. Moore, Wittgenstein, E.M. Forster, Bertrand Russell and others. They were given to passionate mutual admiration; devotion to the growth of private virtues (in natural reaction against the collective madness of the earlier war); personal liberation in pursuit of beauty, love and truth — and furthermore, pursuit of beautiful young men, known to them in its platonic form as The Higher Sodomy... oh dear! It is a truth universally unacknowledged that extremely clever people can be ineffably silly: high intelligence is not automatically bonded with commonsense. The Apostles had their Bloomsbury offshoot, known as the Bloomsberries: Lytton Strachey, Leonard and Virginia Woolf, Clive Bell and Vanessa Bell and Duncan Grant, and others. Mr Sinclair takes his stand thus:

In terms of fundamental discoveries that would change our understanding of the structure of the world, the interchanges at the Kapitsa Club made the conversazione of the Society of the Apostles seem small beer. Science and technology derived from it would transform human societies, while the military application of atomic research would disturb international relations. Any political or social changes brought about by members of the Apostles could only be trivial. Yet the Apostles had the gift of the pen and the power of the word. They backed into publicity. Their clandestine doings became famous. Along with associates in Bloomsbury, rarely in the field of human endeavour has so much been written about so few who achieved so little. As for the Kapitsa Club, rarely in the field of human discovery has so little been written about so few who achieved so much.

In rebelling against the conventions of the past generation and looking inward with admiration upon themselves, the Society of the Apostles became vulnerable to invasion by Communism during the thirties, when the liberal-minded classes, if not some of the privileged classes, were very properly reacting against Nazism and Fascism. Burgess, Maclean, Philby and Blunt were Apostles converted to active Communism - a secret élite within a secret élite... Mr Sinclair traces their careers, through rightly being overt Soviet supporters when Russia was a major ally of the British during the war, to "moles" working their way, unvetted by virtue of |

Apostolic cachet, incredibly into British Intelligence when the West reverted to anti-Communism and the Cold War. Mr Sinclair estimates the military damage they did as trivial, exceeded by the damage done by Fuchs and Pontecorvo, "whose actions only accelerated inevitable discoveries by months or the odd year." More serious was the damage they did to the course of research in those sciences that were of interest to the politicians and the military in prosecuting the Cold War and the armaments race.

Mr Sinclair takes the point that until the tide turned with the advent of war, research was "open", its findings publicly available without restriction: the absence of restriction was, and still is, regarded by scientists as essential to the speediest and most effective advance of their research There was nothing secret about the discussions of the Kapitsa Club, and when Kapitsa was forcibly recalled to Russia in 1934 he took with him the common assumption that co-operation between his institute and the Cavendish would continue. That assumption was steadily eroded as the politicians and the military on both sides laid hands on nuclear physics; and it was in effect destroyed altogether in 1945 at the bombing of Hiroshima and Nagasakı: as Oliphant put it, "This has killed a beautiful subject". Mr Sinclair adds. "Fuchs's conviction on charges of espionage, followed by the defections of Burgess and Maclean, further soured the possibility of scientific collaboration. Espionage as usual had poisoned reciprocity. Treason was the enemy of reason." Well said! The story is a tragic one; the nature of science permanently marred by its use for unthinkable slaughter; human endeavour brought low by human weakness.

To end on a lighter note, let me earn my fee as a critic by finding fault. Occasional looseness in writing, for example "by months or the odd year". Occasional lapses of judgement, for example equating the damage of Fuchs and Pontecorvo - Fuchs actually was a nuclear physicist. whereas Pontecorvo's speciality was cosmic rays. Occasional failures in proofreading, for example "Sir Wallace Aken" was Sir Wallace Akers. For my taste too many names per inch of text — the index is a veritable list of All Those People You Would Like To Have Known But Never Had The Chance To Meet. And I began to feel that Mr Sinclair was tiring, his thinking becoming more dispersed, towards the end — when both cultures were themselves becoming more fragmented, more dispersed. Such fault-finding I simply dismiss in the face of the book's major achievement.

William Cooper, Savile Club, 69 Brook St. London WI, is the pseudonym of the novelest Harry Hoff. Methuen recently republished his book The Struggles of Albert Woods

Observing arms control

Dennis Fakley

Verification: How Much is Enough? By Allan S. Krass. *Taylor & Francis: 1986.* Pp.271. £25, \$45.

CURRENT arms control treaties, such as the 1963 Partial Test Ban, 1967 Outer Space, 1972 Sea-Bed, 1972 Anti-Ballistic Missile, 1975 Biological Weapons and 1978 Environmental Modification agreements, contain little or no provision for cooperation between the signatories on measures to verify that the obligations in the treaties are being observed. This lack of verification provisions can be attributed either to the effectiveness of so-called national technical means of verification or to the relative unimportance of the treaties from a security viewpoint. Other treaties, which have been negotiated (but not ratified) or have been discussed - Threshold Test Ban, Peaceful Nuclear Explosions, Strategic Arms Limitations II, Comprehensive Test Ban, Chemical Weapons — are considered to be much more security-sensitive, and thus to require special measures to verify compliance. Western dissatisfaction with negotiated or proposed verification arrangements for these treaties accounts, in part, for the failure to complete them.

Any analyst of arms control verification is faced with a surfeit of American sources and a dearth of Soviet ones. In consequence, it is difficult to maintain a balance between American and Soviet views, upon which a verification regime has to depend. Professor Krass quotes extensively from American sources on both American and Soviet positions — without recognizing that the latter may be inaccurately reflected — and finds ample support for his conclusions.

In the Introduction, verification is taken to be the action of demonstrating compliance with treaty obligations. However, an arms control treaty usually requires the parties concerned to refrain from some specified activities rather than to undertake them; hence, verification has to be concerned with demonstrating an absence of non-compliance. As Professor Krass observes, a negative cannot be proved, but he could have pointed to the possibility of developing measures to provide sufficient assurance that treaty obligations were not being flouted.

The first main chapter, "Technology", is an account of the monitoring capabilities of satellite photography, ground-and satellite-based radars, seismology, nuclear explosion detectors, electronic signals interceptors and safeguards systems of the type operated by the Inter-

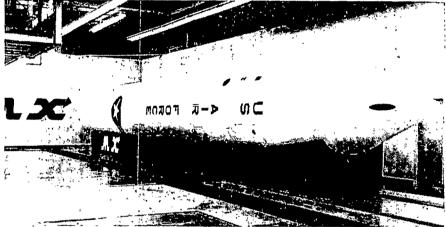
national Atomic Energy Agency (IAEA). While reference is made to some of the problems of achieving the theoretically available performances from these systems, such difficulties are largely discounted in the conclusion that a substantial number of arms control bans or limits could be verified with a high degree of reliability. This would not be universally endorsed.

In the next chapter, "Politics", Professor Krass outlines two major differences between the American and Soviet political approaches to arms control verification. He contrasts the American requirement, as a negotiating precondition, for assurance on the verifiability of an arms control measure, with the Soviet requirement for a definition of the measure to be negotiated before the question of

confident that any American attempt to circumvent a treaty would inevitably become public knowledge — and sooner rather than later.

American bureaucracy certainly complicates the process of arms control negotiation, and the separation of executive and legislative functions means that Presidential proposals are not necessarily enacted. This would not, however, appear to warrant Professor Krass's suggestion that verification provisions should be made less technically precise to avoid the risk of misunderstanding in Congress. On the contrary, precision is essential if the scope for genuine differences in interpretation is to be minimized.

It is undoubtedly true that the assessment of whether a verification regime is adequate depends on the prevailing politi-



Full-scale mockup of the MX intercontinental ballistic missile developed by the US Air Force

verification is discussed. He also compares their respective positions on on-site inspection, suggesting that they may be held for not entirely honourable reasons. He is, perhaps, over-optimistic about these differences becoming smaller.

Professor Krass appears to underestimate the importance of the fact that the closed nature of Soviet society militates against American confidence in treaty compliance. The American authorities recognize that, if the Soviet Union decided that it would be worthwhile violating an arms control obligation, it would not be constrained by public opinion. While not necessarily believing that the Soviet Union would deliberately enter into an agreement with the intention of disregarding its obligations, the possibility that it might do so leads the Americans to presume that treaty violations would occur unless they were made too unattractive by the verification provisions of the treaty. It is no argument to claim that the American intelligence services have been successful, in the post-war era, in penetrating the screen of Soviet military security. The successes are known but the failures may not be apparent until it is too late. On the other hand, the Soviet Union, no matter what it says, can be reasonably !

cal climate. This leads Professor Krass to conclude that unreasonable demands should not be made of the verification arrangements lest they become unacceptable with a change of political opinion. His conclusion is consistent with the underlying theme of the book, i.e. that arms control measures are needed so urgently that even risky compromises are justified if they lead to a negotiated agreement. He does not offer the option of postponing arms control agreements until robust verification measures become available.

It is highly questionable whether any real and stable arms control agreement can be reached as long as there is the present lack of trust between East and West, and Professor Krass rightly questions whether verification arrangements would build or undermine international confidence. He appears to believe that it needs a certain leap of faith to generate a modicum of trust between the superpowers to serve as a nucleus on which confidence could grow. Otherwise, verification arrangements are likely to reinforce existing prejudices. This is consistent with the view that it is futile to seek to resolve political differences between East and West by purely technical means; at best, they can only contribute to a process which has been politically initiated.

In the third and final main chapter. "Technology and Politics", Professor Krass attempts to correlate the technical and political issues he has raised. He examines the legitimacy of various verification technologies and sees the possibility of friction arising from the lack of an adequate international legal and institutional framework to regulate them. He also discusses how to deal with real and mistaken assessments of treaty non-compliance, and recommends that charges should be pursued vigorously only in cases where the suspected violation could have military significance; the political implications of breaches should largely be disregarded to avoid a threat to the continuation of the treaty. This would demand a tolerance which many might consider unrealistic. It would have been interesting to have had a deeper analysis of the different attitudes of the United States and the Soviet Union towards treaty compliance, and a recognition that "one man's compliance could be another's violation".

On-site inspection has for long been a bone of contention in arms control negotiation. Professor Krass argues that inspection rights have in some cases been sought for other than technical reasons, and that the effectiveness of on-site inspections in many arms control contexts has not been established. He predicts that there are insurmountable obstacles to any agreement on mandatory rights of inspection at other than pre-determined locations and that any inspection rights will be granted only when there is a reasonable degree of trust between parties to the treaty. Irrespective of the technical case for on-site inspection, politically it has become one of the measures by which the intentions of the Soviet Union will be judged.

Professor Krass deals only briefly with multilateral arms control but he would welcome an internationalization of verification. Here he fails to recognize that a sovereign state cannot possibly risk delegating to an international body responsibilities for activities that might impinge on its fundamental security interests. The safeguards regime operated by the IAEA does not provide a precedent.

If readers expect to find quantitative answers to the question posed in the title of this book, they will be largely disappointed. Professor Krass does, however, provide much relevant information in an easily digestible form and, so long as the reader recognizes the viewpoint from which he writes, the book will serve as a useful introduction to some of the issues of arms control verification.

Dennis Fakley, 14 Coval Gardens, London SW147DG, was formerly Assistant Chief Scientific Adviser (Nuclear) at the Ministry of Defence, and was Deputy Leader of the British Delegation during the 1977 – 1980 Comprehensive Test Ban negotiations. The opinions expressed in this review are his own.

Committee ecology

Michael J. Crawley

Ecological Knowledge and Environmental Problem-Solving: Concepts and Case Studies. Committee on the Applications of Ecological Theory to Environmental Problems, chairman Gordon H. Orians. National Academy Press, Washington DC: 1986. Pp. 388. Pbk \$24.50. Distributed in Britain by Wiley £28.60.

This is a curious book. Its origins lie in the recognition, by the Board on Basic Biology of the United States National Research Council's Commission on Life Sciences, that it should be concerned with the basic biology of ecosystems. The first aspect of ecology to receive the Board's attention was the current status of ecological concepts, and their applicability to specific environmental problems. Following a workshop in 1979, a committee was established under the chairmanship of Gordon Orians. This book represents the fruits of its labours.

There are two parts to the report. The first attempts to encapsulate "ecological knowledge" as it relates to environmental problem-solving. The second consists of 13 case-studies, selected to illustrate the use of ecological information in dealing with a wide variety of environmental problems. The intended audience is "those who prepare, receive, and use environmental evaluations and management plans; legislators and regulators concerned with environmental issues; and teachers and students in the natural and environmental sciences". Given this audience, the section "Kinds of Ecological Knowledge and Their Application" in the first part of the book has to be judged as unsatisfactory; it varies between being unacceptably shallow and downright misleading. A great many of the statements, though undoubtedly true (and probably both worthy and important), are so brief as to be unintelligible. Take this, for example: "many ecological interactions are characterized by strong non-linear effects brought about by slight changes in key factors". One would need a thorough grounding in theoretical ecology to get the real message.

A number of specious fallacies also get recycled in this part of the book. For example, on p. 28, we read that "the greatest number of individuals of a species that the environment can support is called the carrying capacity (K)". This is wrong; K is the equilibrium population size in models such as the logistic. In discrete-time versions of the logistic, overshoots of K are possible and perfectly reasonable, representing population sizes temporarily in excess of equilibrium. Again, on the same page, we find this gem: "Many pest

species, such as weeds, are poor competitors". Tell that to any gardener! Weeds are *exceptionally* competitive; rather, the point here is that many of them are short-lived, and also are rather unlikely to recruit from seed under shady conditions.

The second half of the book is much better, and the case-histories are carefully chosen and extremely interesting. They include well-known examples such as the biological control of California red scale, the Garki project on malaria control in West Africa, management of the North Pacific halibut fishery and the environmental effects of DDT. More recent studies include research on nuclear radiation, eutrophication, forest felling policy and wildlife managment. It would have been good to see more of them. allowing the inclusion of topics such as acid rain. desertification, release of genetically engineered organisms, the regulation of human population growth and so forth.

At the end of each case-study is a kind of headmaster's report by the editors. These "Committee Comments" are one of the highlights of the book, and have a delightfully superior tone about them -"relevant ecological theories, for the most part, proved inspirational or didactic, rather than directly applicable", or "it is interesting that the scoping of this project (and in fact, most of applied ecology) is somewhat myopic"! Another unintended bonus lies in a liberal sprinkling of parenthetical one-liners of the utmost inscrutability. For instance: "(if plants can be regarded as predators on photons)"; "(all predators must eat regularly)"; the guts of herbivores are "(technically outside their bodies, inasmuch as no cell membrane has to be crossed)"; or "(all CO2 molecules can be treated as identical)"!

The recommendations that emerge, however, are laudable. In carrying out environmental projects, managers are urged to: (1) involve scientists from the beginning; (2) treat projects as experiments; (3) publish information; (4) set proper boundaries on projects: (5) use natural history information; (6) be aware of interactions; (7) be alert for possible cumulative effects; (8) plan for heterogeneity in space and time; and (9) prepare for uncertainty and think probabilistically. This scheme would have made an excellent plan for the first section of the book, where the ecological principles underlying each of the recommendations could have been explained in context. As things are, however, the first half of the report is as weak as the second half is strong, and the book stands as a monument to the pitfalls of committee authorship.

Michael J. Crawley is a Lecturer in Ecology at Imperial College, Silwood Park, Ascot, Berkshire SL5 7TY, UK.

AIDS without emotion

Peter Newmark

Mobilizing Against AIDS: The Unfinished Story of a Virus. By Eve K. Nichols. Institute of Medicine/National Academy of Sciences/Harvard University Press: 1986. Pp.198. Hbk \$15; pbk \$7.95. To be published in Britain on 18 August, hbk £12.75, pbk £6.75.

IT HAS become commonplace to describe as astounding the rate at which research on the AIDS virus has proceeded since the first isolation of the virus at the Pasteur Institute just over three years ago. The pace continues, so that the writer of any book on the subject faces an impossible task in trying to be fully up to date.

Although, in theory, handicapped in this regard by basing her book on a conference held in 1985, Eve Nichols has been able to add new information as recent as this April. Nonetheless, she has missed out on key new discoveries including that of a new gene in the virus and of what seems to be a second AIDS virus in some Africans. This just goes to prove the point about the rate of research, which is matched only by the rate of publication of books on AIDS. But Eve Nichols seems to have performed as good a job as anyone in writing a sensible account for an educated public.

The meeting to which the book owes its origins was the annual conference of the Institute of Medicine in the United States. There were about a dozen speakers, including both Luc Montagnier of the Pasteur — the only non-American — and Robert Gallo of the National Institutes of Health. Each of the eight chapters in the book is based on a few of the talks, and the scientific, medical and public health aspects of AIDS are all dealt with in a straightforward and unemotional way.

Care is taken to tread a middle course between the pessimists and the optimists on issues such as the rate of spread of AIDS in heterosexual populations and the prospects of effective vaccines or therapy. Adequate attention is drawn to such

• AIDS: Papers from Science, 1982 – 1985 is a collection of 108 research papers and reports, edited by Ruth Kulstad, that have appeared in Science. Arranged chronologically, the papers show the progress in AIDS research and indicate the directions in which it might go. An introduction by Dr Myron Essex, chairman of the Department of Cancer Biology at the Harvard University School of Public Health, provides an overview of AIDS research. Available from the American Association for the Advancement and Science, Marketing Dept. A, 1333 H St NW, Washington DC 20005, priced Hbk \$32.95, pbk \$19.95 plus \$1.50 p+p.

thorny questions as whether AIDS should be made a notifiable disease, so that contacts could be traced, when guarantees of confidentiality seem to have a way of being less than cast iron and when there is growing discrimination against even healthy carriers of the virus by employers and insurance companies.

The book comes complete with a glossary and a list of organizations (only American) to contact for help and information. Also included, as appendices, are the Public Health Service recommendations on preventing transmission in the workplace, care of infected children and reducing the risk of transmission. There is additional advice on how to prevent transmission, but none on how to put into practice one of the recommendations:

"Everyone should know the infection status of his or her sexual partners; those who are not infected should avoid intercourse with those who are infected".

Were this not a book aimed at the public, and particularly the public of the United States, it would be more fair to criticize the lack of recognition of some of the European contributions to the understanding of AIDS. In the same vein, it is a pity that less than two pages are devoted to the exceedingly serious problems of AIDS in Africa. But then, does the American public at large care about African AIDS? And for that matter, how many African countries would welcome a book such as this which dealt with their own AIDS problem for their own people? Peter Newmark is Deputy Editor of Nature.

Nimble electrons

David R. Rosseinsky

Hopping Conduction in Solids. By Harald Böttger and Valerij V. Bryksin. Akademie-Verlag, Berlin/Royal Society of Chemistry: 1986. Pp.398. DM 140, £44.

"LOVELY 'OPS", murmurs the drill sergeant quaffing a pint of beer in the television advertisement, while watching a platoon of recruits hop past him. So it is with electrons, which in certain solids move, and conduct, by hops from site to site. The other kind of electron motion, within the extended bands allowed by multi-centre wave functions pervading condensed matter, has curiously enough never acquired a complementary term like "swanning" or "floating" or even "shining": it is simply band conduction. Metals have it anyway, but crystalline semiconductors have bands only of high energy separated by a gap from the states populated by the bulk of electrons, which requires an energy input to mobilize the electrons. Most of the vast structure of solid state physics encompasses band systems, and the recent interest in hopping arose largely from the fact that amorphous semiconductors have irregular structures generating sites which are envisaged to lie within the gap. As these are more or less discrete from the bands, and each other. so are the motions of visiting electrons, hence the designation "hops". Nevill Mott's 1977 Nobel prize was in part awarded for his studies of amorphous semiconductors, and those who in the 1970s based their learning on Austin and Mott, and Mott and Davis, will be avid readers of the text at hand.

Professor Böttger in Magdeburg and Dr Bryksin in Leningrad have themselves contributed substantially to the subject and here provide a comprehensive account of the theory of the hopping mech-

anism. After elaboration of Hamiltonians for the hopping system, the small polaron model is described, in which the charge in question, together with the self-entrapping reciprocal effect on its ambience, represent the moving entity. The theoretical framework is then applied to observations on disordered systems. Ionic and atomic hopping are addressed next, and the final chapter is an up-dating of the material to mid-1985, inserted in proof as an addendum to the 1983 manuscript. This is perhaps not an entirely conformtable addition but it represents an excellent way of circumventing publication delays, fulfilling the aim of the series, of which this book is a member, to provide quick dissemination of information. Other authors and publishers could profitably follow suit. Part of the commendable immediacy has apparently been achieved by direct authorship without the intervention of a translator. Nearly a third of the references are those added in proof, which is indicative of the recent growth of interest in the mechanism.

If the book is somewhat austere in aspect it is quite readable withal. Few, however, who are not involved in the minutiae of conduction or electron transfer within solids will approach it lightly, but, besides physicists, solid state chemists will increasingly find the need for recourse to one or other aspect of the exposition. Siteto-site electron transfer occurs in (chemical) mixed-valent solids where the sites are regular and rigorously defined, but such promising, even ideal, routes towards verifications of the theories have not yet entered the province of the monograph. Biological electron transfer between donor and acceptor sites is of the same kind as that considered here, and so the ramifications of this quite complex motion will extend across the sciences perhaps by discrete hops.

David R. Rosseinsky is a Reader in the Department of Chemistry, University of Exeter, Exeter EX4 4QD, UK.

Geochemical constraints on core formation in the Earth

John H. Jones & Michael J. Drake

Lunar and Planetary Laboratory, University of Arizona, Tucson, Arizona 85721, USA

New experimental data on the partitioning of siderophile and chalcophile elements among metallic and silicate phases may be used to constrain hypotheses of core formation in the Earth. Three current hypotheses can explain gross features of mantle geochemistry, but none predicts siderophile and chalcophile element abundances to within a factor of two of observed values. Either our understanding of metal-silicate interactions and/or our understanding of the early Earth requires revision.

CORE formation has been described as perhaps the single most important thermal event in the history of the Earth¹. This description is certainly true if the core formed by segregation of metal in an initially homogeneous body the size of the present Earth, as the heat liberated in such an event would raise the temperature of the Earth by ~2,000 °C (ref. 2). However, less extreme models in which core formation is concomitant with accretion appear to be more probable³. Regardless of whether core formation resulted in catastrophic changes in the Earth. better knowledge of the core-forming event would certainly elucidate important aspects of the histories of the Earth and Moon⁴.

Geochemists have traditionally divided the chemical elements into four classes: (1) lithophile—those elements which prefer to be combined with oxygen and which typically reside in rocky material; (2) siderophile—elements which prefer to be in the metallic state; (3) chalcophile—elements preferring to be associated with sulphur; and (4) atmophile—elements so volatile that they are typically concentrated in a planet's atmosphere. Obviously, membership in one of these classes is not invariant, but is modulated by the ambient conditions. For example, as the temperature increases, elements which normally exist as solids or liquids will vaporize and become gases, and, in fact, the classes of lithophile, siderophile and chalcophile are typically subdivided into groups of elements of similar volatility.

In principle, the record of core formation is contained in the siderophile and chalcophile element contents of rocks derived from the Earth's mantle. Certainly these elements are much more depleted in the upper mantle than lithophile elements of similar volatility, implying that they record a depletion event unseen by the lithophile elements—presumably core formation. In practice, these elemental abundances have been attributed to either gross disequilibrium between the core and upper mantle, or mixing of siderophile- and chalcophile-element-rich material into the upper mantle after core formation, or both^{5,6}. In this view, little information about core formation may be obtained from mantle siderophile and chalcophile elements because their abundances were established either after core formation ceased or as the results of processes which never approached equilibrium. The evidence cited for disequilibrium between mantle and core during core formation is simply that the concentrations of siderophile and chalcophile elements in mantle-derived rocks are orders of magnitude higher than would be expected if these rocks had ever equilibrated with metal⁶. Furthermore, many of the siderophile elements in the Earth's mantle exist in chondritic proportions (that is, with elemental abundance ratios characteristic of primitive meteorites (chondrites) which have not undergone chemical processing). Thus, successful models of core formation and for siderophile and chalcophile element abundances in the Earth's upper mantle must be able to explain both high abundances and the apparently unfractionated ratios of some (but not all) element pairs.

Models of core formation are further complicated by our lack of knowledge of the chemical composition of the core. All models of the Earth's core require the presence of a 'light element' to reduce the overall density³. If the light element is sulphur, silicon or carbon, then these elements were probably dissolved into the metal (which eventually formed the core) at low pressure as the Earth grew by accretion, and may be relevant to understanding the core-forming process. If the light element is oxygen or a mixture of oxygen and lithophile elements which have followed oxygen into the core, then the light element must have been incorporated at high pressure⁴ and may not have played a role in establishing the siderophile and chalcophile element abundances of the upper mantle.

The behaviours of siderophile trace elements in complex, natural metal-silicate systems are poorly known. This lack of knowledge has led us to determine partition coefficients (Ds; for definition, see below) between solid metal, sulphur-bearing metallic liquid and silicate liquid for a suite of siderophile and/or chalcophile elements under controlled laboratory condi- $(T = 1,250-1,270 \,^{\circ}\text{C};$ $P \leq 1$ bar). These partition coefficients, together with estimates of the mantle abundances of the same elements, may be used to evaluate three physically plausible but very different hypotheses of core formation. These hypotheses are: (1) inefficient core formation, involving equilibrium between solid and liquid metals and silicates, with a small fraction of solid and liquid metal remaining trapped in the mantle, subsequently to be oxidized7; (2) equilibrium between an Fe-S-O metallic liquid and the mantle⁸; and (3) heterogeneous accretion involving a late 'veneer' of oxidized chondritic material which did not segregate into the core^{6,9}. In each of these hypotheses, metal is added to the surface of the growing Earth, and initial interaction between metal and silicate will occur at relatively low pressures. Hence, our partition coefficients, which are obtained at low pressure, may be applicable. Later, we shall return to this point and further discuss the importance of pressure on partitioning equilibria.

A fourth hypothesis, that siderophile and chalcophile element abundances in the Earth's upper mantle were established by partitioning between metal and silicate at very high pressures, perhaps at the core-mantle boundary, will not be explored for three reasons. First, metal-silicate partition coefficients have not been determined at megabar pressures, precluding quantitative evaluation. Second, evidence discussed below suggests that siderophile and chalcophile element concentrations in the mantle were established no later than 3.5 Gyr ago. Thus, material must have been efficiently cycled from the core-mantle boundary to the upper mantle and have been well mixed in <1 Gyr. Such effective mixing appears problematical. Third, it seems unlikely that equilibration of siderophile elements between the core and lower mantle would have preserved chondritic ratios of elements such as Ni and Co, which differ greatly in their siderophile tendencies.

	Table 1 Experimental conditions and results							
Element	T (°C)	$-\log f_{O_2}^*$	D _(SM/LM) (range)	D _(LS/LM) (range)	%S _{LM} ‡	N§		
w	1,250-1,270	12.3-12.5	20 (15-30)	~1 (0.12-1.9)	19-24	3		
Re	1,250-1,260	13.0-13.5	51 (51->60)	$5 \times 10^{-4} (5 \times 10^{-3} - 5 \times 10^{-5})$	23-24	2		
Ir	1,270	12.5-13.2	46 (41–52)	$5 \times 10^{-5} (5 \times 10^{-4} - 5 \times 10^{-6})$	22-23	2		
Mo	1,260	_	2.45	` <u> </u>	25	0		
Ni	1,270	12.5	1.24	$2 \times 10^{-4} (4 \times 10^{-4} - 1 \times 10^{-4})$	23	1		
Co	1,260	12.6-12.7	2.3 (2.2-2.5)	0.0075 (0.0060.010)	24-25	ä		
Au	1,270	12.2-13.0	1.0 (0.97-1.1)	$10^{-4} (3 \times 10^{-4} - 5 \times 10^{-5})$	20-22	2		
P	1,250	12.6	0.28	0.24	18	1		
Ga	1,270	12.5	3.5 (2.6-4.3)	0.8 (0.6-1)	19-22	2		
Ag	1,250	12.7-13.0	~0.01	0.01 (0.01-0.014)	23-27	2		
Pb	1,270	12.2	BDL¶	0.15	20	1		

- * Calculated from the Fe content of the solid metal and the FeO content of the silicate glass using the iron-wüstite data of ref. 41.
- ‡ Weight per cent sulphur in liquid metal phase.
- § Number of individual experiments which contained silicate melt.
- All experiments contain Ni but only one sample (the most oxidized sample to receive a high-neutron-flux irradiation) contained measurable Ni in the silicate glass. The range for $D_{(LS/LM)}$ is that for two analyses of the same glass.
 - ¶ Below detection limit.

The first three hypotheses will be explored in more detail. First, however, we will discuss constraints obtained from experimental and natural samples which must be satisfied by any successful model of core formation in the Earth.

Constraints

Partition coefficients. Our experimental partitioning techniques have been described elsewhere 10 and will not be repeated in detail here. In general, samples containing Fe-Ni metal, natural pyrite (FeS₂), synthetic basaltic glass and a tracer element are placed in an alumina crucible and sealed in an evacuated silica tube with a separate Fe-metal-silica assemblage designed to maintain the oxygen fugacity of the system (f_{O_2} , equivalent to the partial pressure of oxygen) near the quartz-fayalite-iron (QFI) buffer (thus ensuring that iron metal is a stable phase). Quenched samples of coexisting solid metal (SM), liquid metal (LM) and liquid silicate (LS) are analysed by electron microprobe. If the tracer concentration in the silicate glass is too low for microprobe analysis, aliquots of glass are separated from metal and analysed by instrumental neutron activation. Table 1 gives experimental conditions and results for W, Re, Ir, Mo, Ni, Co, Au, P, Ga, Ag and Pb—a suite of elements which covers a wide range of nebular condensation temperatures (volatilities) and geochemical behaviour. In this suite W, Re and Ir are the most refractory and Ag and Pb are the most volatile.

Siderophile abundances in the bulk Earth. The presumed extraction of most of the siderophile and chalcophile elements to the core makes calculation of the bulk-Earth concentrations of these elements difficult or impossible. However, on the basis of lithophile elements, which do not readily combine with Fe or S, we infer that the bulk Earth is approximately chondritic in composition. We do not mean to imply by this that the Earth is compositionally identical to the group CI chondrites, but that refractory siderophile elements should be present in chondritic relative proportions and that more volatile elements may be depleted to varying degrees. Figure 1 shows the concentrations of siderophile and chalcophile elements in several types of chondritic meteorites. Refractory siderophile elements are usually present in higher concentrations than in group CI, while more volatile elements are typically depleted. Again, although the concentrations of siderophile and chalcophile elements in the bulk Earth are unknown, it is reasonable to require that models of bulk-Earth abundances of these elements be consistent with siderophile and chalcophile element concentration patterns in chondrites.

Siderophile abundances in the upper mantle. During the past decade, a large quantity of high-quality data on mantle samples (such as lherzolites) and basalts has become available. Morgan

et al.⁶ and Jagoutz et al.¹¹ have presented convincing evidence that their lherzolite samples (or at least their most 'fertile' lherzolite samples) have not undergone large amounts of partial melting, and hence are most likely to record primitive mantle abundances, at least for the compatible elements. Thus, when possible, we have used the mantle abundance estimates of refs 6 and 11. For the incompatible elements P, Mo and W, abundances are inferred from the trace-element systematics of basalts (see below). These estimates are listed in Table 2.

Mineral-melt partitioning in basalts. The partitioning of Ni and Co and between minerals and silicate melts is moderately well known from laboratory experiments, but these elements are the exception rather than the rule. For most of the elements in our suite, solid silicate (SS)/liquid silicate (LS) partition coefficients for element i (${}^{i}D_{SS/LS}$) must be evaluated from element correlations in natural basalts. For example, a comparison of data for basalts and ultramafic xenoliths on Re versus Ir and Au versus Ir diagrams from ref. 12 implies that ${}^{Au}D_{SS/LS}$ and ${}^{Re}D_{SS/LS}$ are of order unity, but that ${}^{Ir}D_{SS/LS}$ is ~ 50 . (Note in Table 1 that during core formation, trivially small fractions of Au, Re or Ir enter the silicate phase, making the exact value of these particular silicate partition coefficients of little consequence. Also, although the host phase of Ir during silicate partial melting is unknown, the large differences in partitioning behaviour between Au and Ir strongly imply that the host is an oxide or silicate.)

Drake¹³ has used element *i* versus La diagrams to make geochemical distinctions between terrestrial, lunar and eucritic basalts. Many siderophile and chalcophile elements, when plot-

Table 2 Siderophile and chalcophile element abundances in the upper mantle

Element	Concentration/CI*	Ref.	
w	0.11	15	
Re	0.0075	6	
Ir	0.0075	6	
Mo	0.064	15	
Ni	0.19	11	
Co	0.21	11	
Au	0.02	6	
P	0.058	14	
Ga	0.3	11	
Ag	0.087	6	
Рb	0.09†	42	

- * Concentrations normalized to CI chondrite ref. 43.
- † Mean of total Pb and unleachable Pb.

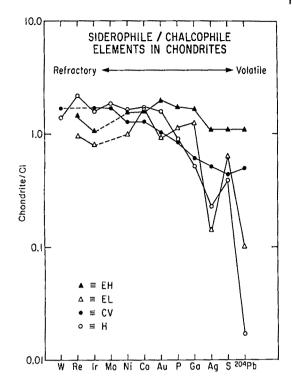


Fig. 1 Siderophile and chalcophile element abundances for four different types of chondritic meteorites (A, EH; △, EL; ●, CV; O. H), normalized to the concentrations of these elements in CI chondrites. Elements on the left are more refractory and elements on the right are more volatile. Relative to CI chondrites, refractory siderophile and chalcophile elements are typically enriched in other chrondrite types and volatile siderophile and chalcophile elements are typically depleted. Chondritic materials provide estimates of the siderophile and chalcophile element abundances that may be expected in the bulk Earth (see text). Data are from the following sources: E, chondrites, refs 45 (Re, Ir, Ni, Au, Ag), 43, 46 (Co, Ga), 43, 47 (P), 43, 48 (S), 43, 49 (204 Pb); CV, chondrites, refs 50 (Ir, Co, Ni, Au, Ga), 43, 51 (Re, Ag), 43, 52 (W), 53 (Mo), 43, 47 (P), 43, 54 (S), 43, 55 (204 Pb); H chondrites, refs 43, 56 (W, Re, Ir, Mo, Ni, Co, Au, P, Ga, S) 43, 57 (Ag), 43, 58 (204 Pb). When only one reference is given, both the chondrite group analysis and the CI normalization analysis are reported in that reference. When two references are given, the first is the source of the CI normalization.

ted on such a diagram, form linear trends which yield information on the depletion of element i in the mantle (relative to chondritic abundances) and permit the partition coefficient of i between basalt and mantle residuum to be estimated. For example, Ga concentrations in basalts increase by a factor of two, while La concentrations increase by two orders of magnitude in natural terrestrial samples¹³. If we assume that this basalt trend is formed by differing degrees of equilibrium partial melting of similar mantle sources and that $^{\text{La}}D_{\text{SS/LS}} \leq 10^{-2}$, then $^{\text{Ga}}D_{\text{SS/LS}} \simeq 0.4$. Correlations of Pb with La show almost exactly the same variation as the Ga-La diagram, implying that Pb Dss/Ls is also ~ 0.4 . The good (approximately 1:1) correlation of P, W and Mo with La or another lithophile incompatible element in basalts^{14,15} implies that these elements are all very incompatible in silicate systems. Diagrams of phosphorous, W and Mo versus incompatibile elements are also the best means of ascertaining the mantle abundances of these elements 14,15. Analyses of Ag in terrestrial basalts are very scarce; however, based on the available data16,17, Ag appears to be weakly incompatible like Ga and Pb. Consequently, we have adopted a value of $^{Ag}D_{SS/LS} =$ 0.4, although it could be larger. For example, the MORB (midocean-ridge basalt) data of ref. 17 are consistent with values of $^{\mathrm{Ag}}D_{\mathrm{SS/LS}}$ between 0.1 and 0.5, for 5% equilibrium partial melting.

Summary. Table 3 lists our adopted partition coefficients. As we shall see below, the uncertainty associated with these partition coefficients, while often large, is of the same order as the uncertainties regarding the physical conditions under which core formation occurred. In this sense at least, we feel that zeroth-order modelling, using the data of Tables 2 and 3, is justified. We will now examine hypotheses for core formation in the light of these data.

Hypotheses

Inefficient core formation. The segregation of the core from the mantle is envisaged as an equilibration between four phases, namely, solid silicate, liquid silicate, solid metal and liquid metal, followed by incomplete separation of metal from silicate. Equilibrium between these four phases is described by three sets of partition coefficients (D) for each element at specified temperature, pressure and oxygen fugacity: D(solid metal/sulphur-bearing metallic liquid), D(liquid silicate/sulphur-bearing

Element	$D_{(LS/LM})$	$D_{(SM/LM)}$	$D_{\rm (SS/LS)}$
W	1	36	0.01
Re	5×10^{-4}	83	1
Ir	5×10^{-5}	83	50
Mo	8×10 ⁻⁴ *	2.45	0.01
Ni	2×10^{-4}	1.33	10 ⁺
Co	7×10^{-3}	2.3	3Ϋ
Au	1×10^{-4}	1.3	1
P	0.24	1.7	0.02
Ga	0.8	6.0	0.4
Ag	0.01	0.01	0.4
Pb	0.15	0	0.4

* Calculated from our data and that of ref. 25.

metallic liquid) and D(solid silicate/liquid silicate) where ${}^{i}D_{(\alpha/\beta)}$ is defined to be the weight concentration of element i in phase α divided by the weight concentration of element i in phase β .

The partitioning behaviour of the elements in the experimental suite can be generalized in the case of this hypothesis. Mantle concentrations of Au, Ir, Mo, Ni and Re are determined almost solely by the amount of trapped metal phases. Silver is concentrated nearly exclusively in the trapped metallic liquid; P, W, Ga, Co and Pb are intermediate in their siderophilic tendencies. Nickel, Co and Ir and compatible $(D_{SS/LS} > 1)$ in solid silicates (or oxides); W, P and Mo behave as very incompatible elements $(D_{SS/LS} \ll 1)$; and other elements are intermediate in their silicate-system compatibility.

Physical conditions of core formation. The fractions of metal and silicate in the Earth are taken to be 0.3 and 0.7, respectively, the relative masses of the present core and mantle. The proportions of solid metal and liquid metal are determined by assuming that the principal light element in the core is sulphur. Our experiments (see below) were conducted so that our metallic liquids contained ~25 wt% S. Thus, if the present core contains 8-12 wt % S (ref. 18), use of our experimental data in model calculations requires that the metal assemblage which segregated to form the core was 30-50% molten at the time of metal-silicate equilibration.

The degree of partial melting of silicate materials during core formation is virtually unknown. If the Earth's accretion and core formation occurred rapidly, it seems inconceivable that high degrees of partial melting could have been avoided'; however, the mantle samples themselves give no evidence for extensive melting early in the Earth's history. Spinel lherzolites throughout the world are very similar in composition and

[†] Ni and Co $D_{\rm (SS/LS)}$ values estimated from ref. 44; all others estimated from natural basalt systematics (see text).

texture¹⁹. If lherzolites are undepleted in elements that are strongly concentrated in basalts, these lherzolites are described as 'fertile' (that is, able to produce basalt). Large chemical differences are not observed between the fertile spinel lherzolites and the fertile garnet lherzolites¹⁹. Small differences between garnet and spinel lherzolites may exist²⁰, but the overall chemical similarity between these rock-types implies a mantle which is chemically homogeneous down to at least the depth of the sources of garnet lherzolites (~150 km; ref. 21). If large degrees of partial melting (>20%) occurred in the early Earth, even minor density differences between solid and melt would be expected to lead to phase separation and the formation of a magma ocean²². Subsequent crystallization of this hypothetical magma ocean would be unlikely to result in a chemically homogeneous upper mantle. Rather, it would be expected that the formerly molten portion of the mantle would resemble large mafic intrusions with pronounced vertical zoning, as observed in the Stillwater and Skaergaard intrusions and inferred for the Moon^{23,24}. Even if such zoning was largely homogenized by subsequent mantle convection, it is surprising that apparently no remnants remain within the continental lithospheres. The uniform chemical composition of mantle lherzolites (the samples from which our mantle siderophile and chalcophile element abundances are mainly derived), coupled with plausible physical theories of core formation which predict continuous core formation as the Earth grows from the mass of Mars to its present mass³, lead us to opt for low degrees (≤20%) of silicate partial melting.

The ambient oxygen fugacity during core formation was most likely below the iron-wüstite (IW) oxygen buffer (see later discussion), but is otherwise imprecisely constrained. Thus we allow for isothermal variation in oxygen fugacity in our coreformation model. In practice, this means that we allow $D_{\rm LS/LM}$ to change with oxygen fugacity in an ideal manner, as defined by Rammensee²⁵. The $^{1}D_{\rm LS/LM}$ values in Table 3 are appropriate for a log $f_{\rm O_2}$ of -12.75 at 1,250-1,270 °C (approximately one log unit below the QFI oxygen buffer).

Model calculations. The inefficient core formation hypothesis may be tested mathematically using the formalism outlined below:

(1) After equilibration among the four relevant phases, most of the solid and liquid metal drains away and does not communicate further with the overlying mantle. This process is subject to the constraint of mass balance, so that

$${}^{t}C_{\text{Earth}} = {}^{t}C_{\text{SM}}X_{\text{SM}} + {}^{t}C_{\text{LM}}X_{\text{LM}} + {}^{t}C_{\text{SS}}X_{\text{SS}} + {}^{t}C_{\text{LS}}X_{\text{LS}}$$
 (1)

where Xs are mass fractions, ${}^{i}Cs$ are mass concentrations of element i and SM, LM, SS and LS refer to solid metal, liquid metal, solid silicate and liquid silicate, respectively. Reiterating the constraints outlined above,

$$X_{\rm SS} + X_{\rm LS} = 0.7 \tag{2}$$

$$p = X_{LS}/(X_{SS} + X_{LS}) \le 0.2$$
 (3)

$$X_{\rm SM} + X_{\rm LM} = 0.3 \tag{4}$$

$$0.3 \le X_{LM} / (X_{LM} + X_{SM}) \le 0.5$$
 (5)

where p is the fraction of the silicate portion of the system which is molten. In terms of partition coefficients (D) and degree of partial melting, equation (1) becomes

$${}^{i}C_{Earth} = {}^{i}C_{LM}[{}^{i}D_{SM/LM}(0.3 - X_{LM}) + X_{LM} + 0.7{}^{i}D_{SS/LM}(1 - p) + 0.7{}^{i}D_{LS/LM}p]$$
(6)

As partition coefficients have been measured, ${}^{l}C_{Earth}/{}^{l}C_{LM}$ may be calculated for assumed values of p and X_{LM} . The sensitivity of this calculation to the assumptions of equations (2)–(5) should, in general, be acceptably small. For example, the permissible variation in the total masses of the various reservoirs (solid metal, liquid metal, and so forth) is probably about a factor of

two, and the effects of factor-of-two uncertainties translate into two-fold changes in calculated concentrations.

(2) A small amount of trapped solid metal (X'_{SM}) and trapped liquid metal (X'_{LM}) remains behind in the upper mantle. The concentration of element i in the mantle is then given by

$${}^{i}C_{\text{mantle}} = {}^{i}C_{\text{LM}}X'_{\text{LM}} + {}^{i}C_{\text{SM}}X'_{\text{SM}} + {}^{i}C_{\text{SS}}(1-p) + {}^{i}C_{\text{LS}}p$$
 (7)

if X'_{SM} and X'_{LM} are small (~0.01).

Rearranging as in equation (6), we obtain

$${}^{i}C_{\text{mantle}} = {}^{i}C_{\text{LM}} \left(X'_{\text{LM}} + {}^{i}D_{\text{SM/LM}} X'_{\text{SM}} + {}^{i}D_{\text{SS/LM}} (1 - p) + {}^{i}D_{\text{LS/LM}} p \right)$$
(8)

(3) As ${}^{i}C_{\text{mantle}}$ is known from mantle nodules and basalts, ${}^{i}C_{\text{LM}}$ may be calculated for assumed values of p, X'_{LM} and X'_{SM} . If ${}^{i}C_{\text{LM}}$ is known then ${}^{i}C_{\text{Earth}}$ can also be calculated from equation (6). The credibility of the chosen values for the model parameters may be evaluated by comparing the calculated ${}^{i}C_{\text{Earth}}$ to the concentration of element i in CI chondrites (${}^{i}C_{\text{CI}}$). Values of ${}^{i}C_{\text{Earth}}$ for refractory elements which deviate by an order of magnitude from 2-3 × ${}^{i}C_{\text{CI}}$ are defined as unacceptable, and new values for the model's parameters are chosen.

There are five important adjustable parameters: $X_{\rm LM}$, p, $f_{\rm O_2}$, $X'_{\rm LM}$ and $X'_{\rm SM}$. However, it must be emphasized that it is unknown in detail if the measured partition coefficient values are exactly appropriate. We note that low-pressure (1 bar) partition coefficients may be relevant, in that new metal accreting to the Earth is deposited at the surface, and metal-silicate equilibrium is likely to be achieved at relatively shallow depths before the metal largely segregates into the centre of the growing planet. Nevertheless, we should probably be content if any set of model parameters can be found which, assuming an Earth with chondritic relative proportions of refractory elements (2-3 × CI), will predict mantle abundances of siderophile and chalcophile elements to within a factor of two. Better fits, while mathematically pleasing, may have no physical significance.

Results. Jones and Drake⁷ have evaluated inefficient core formation as a means of reconciling the high abundances of siderophile and chalcophile elements in mantle materials with a reducing (that is, low- f_{O_2}) core-forming event. Early results were encouraging, but increasing the number of constraints on the model (that is, increasing the number of elements to be modelled) has led to progressively poorer model results. Figure 2 shows a 'best fit' calculation of bulk-Earth concentrations for our suite of siderophile and chalcophile elements. The refractory elements W to Mo have concentrations of $\sim 2 \times CI$ in the bulk Earth, a reasonable value. The more volatile elements show various degrees of depletion. Au and P concentrations appear low compared with those of more volatile elements.

Calculated Co and Ni abundances are such that the Co/Ni ratio in the Earth is within 10% of chondritic (a requirement of our model), but this agreement is somewhat contrived as Co and Ni are not concentrated in the same phase. Nickel is contained mainly in the metallic phases, whereas Co is retained by the silicates. Maintaining a chondritic Ni/Co ratio in the bulk Earth by our model requires trapping large amounts of metallic liquid (~2.5 wt %) in the mantle. Although this amount of trapped liquid is not inconsistent with theoretical estimates²⁶, the retention of this S-bearing liquid leads to unreasonably high S concentrations (~6,000 p.p.m.) in the mantle, in contrast to the observed concentration of <300 p.p.m. S (ref. 19).

Furthermore, because we allow for isothermal variation in oxygen fugacity (and, therefore, in ${}^{i}D_{LS/LM}$ as well), our best-fit oxygen fugacity is $\sim 1-1.3$ log units more oxidizing than the oxygen fugacity necessary for the present mantle FeO concentrations to have been established by equilibration with metal at 1 bar. This disagreement is not necessarily a problem, as an oxygen buffer such as QFI will become slightly more oxidizing with pressure (by ~ 1 log unit per 50 kbar), but more work is needed to define the relative effects of pressure and oxygen fugacity on siderophile and chalcophile element partitioning.

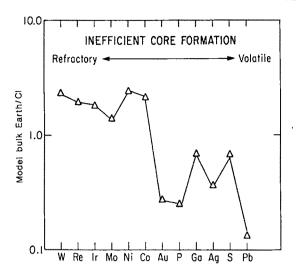


Fig. 2 Calculated bulk-Earth abundances of a suite of 12 siderophile and/or chalcophile elements. Elements are listed in the same order as in Fig. 1. The model of calculation is that of inefficient core formation (see text). The physical conditions of core formation and the amount of trapped metal phases are varied until the calculated refractory siderophile element abundances are 2-3×CI for the bulk Earth and the Ni/Co ratio of the bulk Earth is within 15% of chondritic. Clearly, geologically reasonable conditions can be chosen so that these two constraints are satisfied. A consequence of the calculation is that volatile elements are found to be depleted in the bulk Earth. A drawback of this type of model is that calculated S abundances for the upper mantle are >20 times higher than is actually observed. Best-fit model parameters: trapped metallic liquid (25 wt% S), 2.5%; trapped metal, 0.04%; degree of silicate partial melting, 10%; $\log f_{\rm O_2} = -12.35$; S concentration in core, 10%

Thus, even though it is possible to calculate bulk-Earth concentrations of many siderophile and chalcophile elements which are not unreasonable, the consequences of inefficient core formation are not totally attractive. If this model is to be viable, there must be substantial changes in the values of partition coefficients due to an uninvestigated intensive variable (such as pressure). Such variations are certainly not out of the question, especially as the Fe-FeS eutectic composition is known to be pressure-sensitive²⁷.

Equilibrium between an Fe-S-O metallic liquid and mantle silicates. This model has been proposed by Brett⁸, and accounts successfully for the upper-mantle abundances of a subset of siderophile and chalcophile elements. The model postulates equilibrium between metal and silicate phases and does not resort to trapping small fractions of metal in the mantle. The main difference between this model and previous equilibrium core-formation models is that no solid metal is present. It recognizes that liquid metal/silicate partition coefficients may be lower than solid metal/silicate partition coefficients (Table 3). The redox conditions postulated by Brett⁸ are rather oxidizing, in accordance with the absence of solid metal. This model is mathematically testable using partition coefficients and mass balance constraints in a similar manner to that outlined above. Generalizations concerning element partitioning are also as above.

Although at first sight this hypothesis seems successful, there are significant difficulties which appear to invalidate it. For example, the refractory element Mo was calculated by Brett⁸ to be present in the Earth's mantle at $59 \times \text{CI}$ abundance. Although this value is much closer than typical fits obtainable with solid metal/silicate partition coefficients, we consider this to be an unacceptably high value. In addition, although unknown to Brett⁸ at the time, the value of 3.65×10^{-3} which he used for the Ni liquid silicate/liquid metal partition coefficient is very large

(compare with our value of 2×10^{-4} in Table 3) and, in turn, implies an oxygen fugacity too high to be consistent with the low FeO content of the Earth's upper mantle. For example, at 1,250 °C, we predict that the oxygen fugacity required for Brett's Ni partition coefficient is ~ 1 log unit more oxidizing than the Fe-FeO (IW) oxygen buffer. Under these conditions, the activity of Fe in an Fe-S-O metallic liquid will be much less than the activity of FeO in any coexisting silicates. The very low iron content of the upper mantle (<10 wt %) implies that any metallic liquid postulated to have been in equilibrium with the upper mantle (under oxidizing conditions) had an even lower iron activity than the present mantle.

The possibility that core formation in the upper mantle occurred by separation of a metallic liquid with a very low iron activity deserves further exploration. In the Fe-Si system at 1,600 °C, for example, the iron activity at the midpoint of the binary system is ~0.05 (ref. 28). In the Fe-S system at 1,600 °C the iron activity at the midpoint of the system is ~ 0.13 (ref. 29). Non-ideal interactions between iron and non-metals can drastically reduce the activity of iron, even at fairly high iron concentrations in the liquid. Conversely, decreasing the temperature may minimize the non-ideal effects of non-metals. For example, at the eutectics of the Fe-S and Fe-Si systems, where the mole fraction of iron is definitely less than unity, iron metal is stable and the activity of iron in the liquid must also be unity. The complex interaction of intensive variables (pressure, temperature, non-metal concentrations, oxygen fugacity) make quantitative prediction of liquid activities difficult.

Although we cannot rule out highly oxidizing conditions during core formation on physical-chemical grounds, we note that fractionations of the noble refractory siderophile elements are much more probable in this model than in other models of core formation. Because noble siderophile elements appear to be present in chondritic relative abundances in the Earth's mantle, this is an important consideration. In the inefficient core formation model, mantle abundances of the noble refractory siderophile elements are 'buffered' towards chondritic ratios by trapped metal, contrary to the assertion of Morgan³⁰. In 'late-stage veneer' models , of course, no noble siderophile element fractionations are possible because the material is simply added to the upper mantle without chemical processing.

Figure 3 shows the results of recalculating bulk-Earth abundances for Brett's model by extrapolating our internally consistent set of partition coefficients to higher $f_{\rm O_2}$. In this model $X_{\rm LM}=0.3$, the degree of silicate partial melting is 20%, and $f_{\rm O}$ is allowed to vary between IW and QFM (quartz-fayalite-magnetite, an oxidizing buffer at which iron metal is unstable). Our inefficient core formation model results from Fig. 2 are shown for comparison. The refractory siderophiles (W, Re, Ir, Mo), rather than being enriched relative to CI, are severely depleted. We conclude that Brett's equilibrium core formation model is no more viable than our own, although this conclusion is subject to the same caveat as before—that high-pressure partitioning data are virtually non-existent.

Heterogeneous accretion/'chondritic veneer'. The most recent advocates of this type of model are Morgan et al.6 and Wänke9, who have suggested that material accreted to the Earth became progressively more oxidized as accretion proceeded. Early accretion and core formation was dominated by highly reduced materials, and metal effectively segregated siderophile and chalcophile elements to the centre of the growing planet. By the end of accretion, an influx of more oxidized materials had caused core formation to cease because metal was no longer stable. In this model, moderately siderophile elements such as Ni and Co stopped segregating to the core when the Earth's accretion was 80-90% complete; the noble siderophile elements such as Ir and Au ended their segregation into the core when accretion was ~99% complete. This model predicts that moderately siderophile elements should be present in the mantle in chondritic ratios, at abundances of 0.1-0.2 × CI, and that the noble

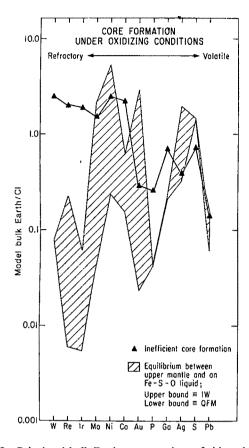


Fig. 3 Calculated bulk-Earth concentrations of siderophile and chalcophile elements assuming equilibrium between an Fe-S-O liquid and a mantle which is 20% partially molten (T=1,250 °C). The shaded region shows the calculated concentrations for a range of oxygen fugacities, ranging from IW (upper bound) to QFM (lower bound). Bulk-Earth abundaces calculated by the inefficient core formation model are shown for comparison (Δ). The assumption that the core formed in relatively oxidizing conditions, without any trapping of metals by the mantle, leads to the conclusion that the Earth is depleted in refractory siderophile elements, contrary to the expectations based on Fig. 1.

siderophile elements should be present in chondritic ratios at $\sim 0.01 \times CI$ abundances.

This class of hypothesis has gained favour in the past decade, in spite of the requirement that extensive physical mixing of material into the upper mantle must occur after core formation. Impact processes alone seem incapable of such fine-scale mixing (witness the heterogeneity of meteorite-derived siderophile elements in lunar samples), but sustained sub-solidus mantle convection may be adequate, particularly if mantle convection is layered. The mixing process must be capable of homogenizing Fe, Co and Ni at the scale of basalt generation by 3,500 Myr BP and be capable of homogenizing Ir at the hand-sample scale by today^{7,31}.

In this regard, it is possible that samples of the upper mantle which have been stored in continental lithospheres for considerable times (without the benefit of sub-solidus convective mixing over geological time) place even tighter constraints on the rate of mixing required to homogenize mantle siderophile elements. Jagoutz et al.³² have presented evidence that 2,700 Myr-old eclogites have been stored in the lower continental lithosphere for long periods of time (100-2,000 Myr) without participating in mantle mixing processes. More dramatically, Boyd et al.²¹ have argued that eclogitic and garnet peridotitic material, transported to the surface by kimberlite eruption, was emplaced in the lower continental lithosphere as long ago as 3,000-3,500 Myr. Thus, it is quite possible that the isolation of con-

Table 4 Test of the multi-component accretion model

Element	Concentration before second episode of core formation (C/CI)	Concentration after removal of metal* (C/CI)
Ni	0.2	0.2
Co	0.2	0.2
P	0.2	0.2
Mo	0.2	0.064
Ga	0.2	0.2
W	0.2	0.2

^{*} Just enough metal is removed to lower the Mo concentration from 0.2 to 0.064×CI (see text).

tinental shield lithospheres from mantle convection and the homogenization of Ir that we observe today in continental lithospheric materials were both complete by 3,500 Myr ago. We question whether mantle convection was capable of such rapid, fine-scale mixing.

Another way of making the same observation is to note that Ir contents of Iherzolites from beneath old cratons (such as Southern Africa), from beneath younger continental margins (such as the southwestern United States) and from mantle overlying oceanic hot-spots (Hawaii) are essentially identical¹⁹. The lithospheres beneath southern Africa and the southwestern United States were not obviously isolated from mantle convection at the same time, and the lithosphere beneath Hawaii has presumably never been isolated to the same degree as continental lithospheres. Iridium homogenization was apparently complete by the time of the formation of the earliest continental lithospheres.

Regardless of absolute rates of mantle mixing, the moderately siderophile elements are a sensitive test of the heterogeneous accretion hypothesis. Table 4 shows our model results using the partition coefficients of Table 3. For simplicity we have quantized accretion and core formation (before the accretion of the last 1%—the hypothesized 'late-stage veneer') into two parts: the first 80% of material accreted is highly reduced, the last 20% is more oxidized. This approach permits us to model core formation as two discrete events: the first, which removed all siderophile and chalcophile elements from the early-accreted 80% of the Earth, and a second event which removed only noble siderophile elements (such as Ir and Au) from the late-accreted 20%. A justification of this simple approach is that, because of the large difference in the metal/silicate partition coefficients between Co and Ni, continuous core formation during the last 20% of accretion would be unlikely to preserve the approximately chondritic Co/Ni ratio of the upper mantle (Table 2). Thus, at the beginning of the second model core-forming event, most (if not all) siderophile and chalcophile elements were present at $\sim 0.2 \times CI$ abundances in the upper mantle, as defined by present Ni and Co abundances. At this time we allow just enough separation of metal to lower the Mo concentration from 0.2×CI to its present value of 0.064×CI (Table 2), and we observe the effect of this separation on the other siderophile elements. As can be seen from Table 4, no moderately siderophile element other than Mo is affected, even though W and P are clearly depleted relative to Co and Ni in the present mantle (Table 2).

The heterogeneous accretion hypothesis results in additional predictions which are inconsistent with observed elemental abundances in the Earth's upper mantle. First, the amount of metal which was extracted from the last 20% of accreting material must have been trivial, and the high $f_{\rm O_2}$ requires that that metal must have been Ni-rich (because of the decreased stability of Fe-rich metal). If we assume that as much as 10% of the total Ni was removed during the last core-forming event (consistent with the approximately chondritic Co/Ni ratio of the upper mantle), then only 0.02% metal was removed. It would

seem that a substantially molten upper mantle would be required to separate this minute amount of metal, and, as we have already discussed, there is no evidence for a pervasive terrestrial magma ocean. Second, if the last 20% of accreted material was sufficiently oxidized to effectively halt core formation, it is expected that this material would have been enriched in volatile elements and oxidized species. If the last dregs of core formation removed only a few hundredths of a per cent of metal, it is not possible for substantial amounts of S to have been taken to the core (S is cosmically more abundant than Ni). All chondritic materials contain 2-6 wt% S. If the material which made up the last 20% of the Earth's accretion even approached chondritic composition, we would expect that the crust and upper mantle would contain 4,000-12,000 p.p.m. S: not appreciably different from the prediction of the inefficient core formation hypothesis, and in contradiction to observed S abundances of <300 p.p.m. in the Earth's upper mantle¹⁹.

In this context we note that Morgan³³ has refined his abundance estimates of incompatible noble siderophile elements (for example, Au and Re) in spinel lherzolites, and finds that the noble element ratios are remarkably chondritic. Obviously, this observation strengthens the arguments for a 1% chondritic 'latestage veneer'. Furthermore, Morgan shows that the S/Se ratio of spinel lherzolites is chondritic and advocates that the S and Se abundances of the upper mantle were established by the same 'late-stage veneer' process. The implication of Morgan's work appears to be that, before the last 1% of accretion, the mantle was sulphur-free. In principle, this may remove some of the difficulties with S which were discussed above, although it is still unclear whether such low S abundances during the last 20% of the Earth's inhomogeneous accretion are compatible with the more oxidizing conditions postulated for this stage of accretion9.

We note that the consistency of the siderophile element abundances inferred from basalts, spinel lherzolites and garnet lherzolites implies that the siderophile elements of the upper mantle are likely to be homogeneously distributed to a depth of at least 500 km—a scale consistent with models of upper mantle convection³⁴. If 1% of the mass of the upper mantle were added by a uniform flux of planetesimals and if this same population were responsible for the production of a 2.5-km megaregolith on the Moon²⁴, we would expect that the lunar megaregolith would contain ~200% of chondritic material—a physically impossible value which is about two orders of magnitude higher than the ~1.5 wt% of meteoritic material measured in lunar soils²⁴. The Moon would have to be well-mixed to a depth of 400 km in order to be consistent with the terrestrial 'late-stage veneer', yet estimates of mantle abundances of noble siderophile elements¹³ show no evidence of such mixing. Of course, it is possible that the Moon formed after the Earth accreted its final 1% of mass, although available isotopic evidence points to comparable ages for both objects35.

Although we find some elements of the heterogeneous accretion/'chondritic veneer' hypothesis attractive, this hypothesis contains as many quantitative difficulties as the inefficient core formation and metallic liquid/silicate equilibrium core formation hypotheses. It is not clear to us which, if any model of core formation should be preferred.

Conclusions

The preceding discussion emphasizes that none of the current hypotheses of core formation in the Earth survives quantitative scrutiny. For any of the hypotheses to be correct, our present knowledge of the relevant relative partition coefficients must be accurate to perhaps no better than a factor of two. We emphasize that the volume of $(P-T-f_{O_2})$ space which has been investigated in our partitioning studies (as well as those of others) is small and should be extended.

This failure of all hypotheses to quantitatively model core formation and siderophile and chalcophile element abundances in the upper mantle is disappointing, in that a detailed picture of the history of the early Earth is important to our understanding of many consequential issues, such as the origin of the Moon and the subsequent geological evolution of the Earth. What, if any, statements about core formation may be made with such confidence that they will go unchallenged?

Lack of equilibration between core and upper mantle. All viable models for the explanation of the high abundances of siderophile and chalcophile elements in the mantle implicitly assume that the core and upper mantle have not communicated over geological time. An immediate consequence of this assumption is that either convection in the mantle is layered and the upper and lower mantles communicate only with great difficulty, or the mantle which we sample today was incorporated into the subcontinental lithosphere extremely early. In fact, these two possibilities are not mutually exclusive; in any case the upper mantle and core have not equilibrated since the last addition of siderophile elements to the upper mantle.

Antiquity of siderophile and chalcophile elements in the upper mantle. However the abundances of siderophile and chalcophile elements were established, they are unlikely to have changed over geological time. Evidence from basalts indicates that the Co, Fe and Ni contents of the upper mantle have not changed since 3,500 Myr (ref. 31) and that 'future leads' cannot be explained in terms of continuous core formation³⁶. Siderophile and chalcophile element concentrations in the upper mantle were established early in the history of the Earth and are not the result of secondary processes.

The redox state of the early Earth. All models of core formation seem to require that the mantle has become more oxidized over geological time. If the FeO content of the upper mantle is the result of equilibration with metal, then the consistent FeO content of 8-10 wt% in fertile mantle nodules appears to limit the oxidation state of the early Earth to oxygen fugacities less than ~1.5-2.0 log units below the QFI buffer. (For a discussion of the assumptions involved in this calculation see ref. 37.) This estimate should be accurate and is tantalizingly close to the oxygen fugacity of the metal-olivine-pyroxene reaction of ref. 38. If the FeO content of the mantle was not established by reaction with metal but, rather, by later admixture of FeO-rich material, then the calculated oxygen fugacity is an upper limit to that obtaining during core formation. If the FeO content of the mantle was due primarily to reaction with a metallic liquid, rich in non-metals⁸, the oxygen fugacity was probably still within two log units of IW. In all these cases the mantle was once very reduced and its oxygen fugacity must have changed over geological time to its present oxidized state (that is, from near IW (or lower) to QFM; ref. 39). If the oxygen fugacity calculated at the beginning of this section is accurate, no reactions other than the Fe metal-olivine-pyroxene reaction³⁸ need be postulated; if the calculation is only an upper limit, it may be necessary to consider seriously the hypothesis that the Earth is predominantly made of enstatite-chondrite-like material.

Also, we note that the moderately low non-metal concentrations (8-12%) inferred for the core (compared with the high concentrations (~30%) of S and O in the metallic liquid of Brett⁸) appear to require that models of core formation which postulate large amounts of Fe-S-O-rich liquids cannot apply throughout the core formation process. If non-metal-rich metallic liquids contributed significantly to core formation, then additional metal, containing little or no S or O, is required to account for the observed non-metal concentrations in the present core. The easiest means of achieving such a dichotomy is probably through inhomogeneous accretion, in which earlier core-forming events were S-O-poor and later events were S-O-rich. Thus, even models which postulate oxidizing conditions for core formation may require that the oxygen fugacity changed during planetary accretion and core formation, becoming more oxidizing with time.

Future directions. We emphasize again that only a very small

volume of (P, T, f_{O_2}) -space relevant to core formation has been investigated. Two obvious areas for new experimental explorations are those of high pressure and higher oxygen fugacity. For example, from our work on iron meteorites⁴⁰, we have gained example, from our work on iron meteorites⁴⁰, we have gained some insight into the possible role of pressure. Many siderophile trace element-non-metal interactions in metallic liquids appear to be explicable in terms of a simple non-metal-avoidance model. Siderophile trace element-sulphur interactions are often ~10 times stronger than Fe-S interactions, which are known to be pressure-sensitive. (Specifically, the composition of the eutectic point in the Fe-FeS binary system becomes more Fe-rich as

pressure increases²⁷.) Extrapolating from the Fe-S system, it is possible that siderophile element-non-metal interactions will be strong functions of pressure. Quantitatively successful models of core formation may require accurate and detailed assessments of the (P, T) state of the early Earth.

This work was supported by NASA grant NAG 9-39. We thank H. Doane and the Reactor Facility of the University of Arizona for assistance; D. Hill and W. V. Boynton for help with neutron activation analyses; D. Stevenson and F. Richter for discussions; and R. Brett, D. J. Malvin, J. W. Morgan and H. E. Newsom for helpful reviews.

- Brett, R. Rev. Geophys. Space Phys. 14, 375-383 (1976).
 Urey, H. C. The Planets (Yale University Press, New Haven, 1952).
 Stevenson, D. J. Science 214, 611-619 (1981).

Ringwood, A. E. Origin of the Earth and Moon (Springer, Berlin, 1979). Ringwood, A. E. Geochim. cosmochim. Acta 35, 223-230 (1971).

- Morgan, J. W., Wandless, G. A., Petrie, R. K. & Irving, A. J. Proc. Lunar planet. Sci. Conf. 11, 213-233 (1980).
- 7. Jones, J. H. & Drake, M. J. Eos 62, 1073-1074 (1981); Proc. Lunar planet. Sci. Conf. 13, 369-370 (1982); 15, 413-414 (1984); 16, 412-413 (1985). Brett, R. Geochim. cosmochim. Acta 48, 1183-1188 (1984).

- Wänke, H. Phil Trans. R. Soc. A303, 287-302 (1981).
 Jones, J. H. & Drake, M. J. Geochim. cosmochim. Acta 47, 1199-1209 (1983).
- Jagoutz, E. et al. Proc. Lunar planet. Sci. Conf. 10, 2031-2050 (1979).
 Chou, C.-L., Shaw, D. M. & Crocket, J. H. J. geophys. Res. 88, A507-A518 (1983).
- 13. Drake, M. J. Geochim. cosmochim. Acta 47, 1759-1767 (1983).

- Newsom, H. E. & Drake, M. J. Geochim. cosmochim. Acta 47, 93-100 (1983).
 Newsom, H. E. & Palme, H. Earth planet. Sci. Lett. 69, 354-364 (1984).
 Laul, J. C., Keays, R. R., Ganapathy, R., Anders, E. & Morgan, J. W. Geochim. cosmochim. Acta 36, 329-345 (1972).
- Hertogen, J., Janssens, M.-J. & Palme, H. Geochim. cosmochim. Acta 44, 2125-2143 (1980).
 Brown, J. M., Ahrens, T. J. & Shampine, D. L. J. geophys. Res. 89, 6041-6048 (1984).
- 19. Basaltic Volcanism Study Project Basaltic Volcanism on the Terrestrial Planets (Pergamon
- Oxford, 1981).
- 20. Palme, H. & Nickel, K. G. Geochim. cosmochim. Acta 49, 2123-2132 (1985). 21. Boyd, F. R., Gurney, J. J. & Richardson, S. H. Nature 315, 387-389 (1985)

- Walker, D., Stolper, E. M. & Hays, J. F. J. geophys. Res. 83, 6005-6013 (1978).
 Hofmeister, A. M. J. geophys. Res. 88, 4963-4983 (1983).
 Taylor, S. R. Lunar Science: A Post-Apollo View (Pergamon, Oxford, 1975).
- 25. Rammensee, W. thesis. Univ. Mainz (1978). 26. Stevenson, D. J. in Workshop on the Early Earth: The Interval from Accretion to the Older
- Archean (eds Burke, K. & Ashwal, L. D.) 76-78 (LPI tech. Rep. 85-01, Lunar and Planetary Institute, Houston, 1985).
 Usselman, T. M. Am. J. Sci. 275, 278-290 (1975).
- 28. Hultgren, R., Pramod, D. D., Hawkins, D. T., Gleiser, M. & Kelley, K. K. Selected Values of the Thermodynamic Properties of Binary Alloys, 871-883 (American Society of Metals, Metals Park, 1973).
- Sharma, R. C. & Chang, Y. A. Metall. Trans. 10B, 103-108 (1979).
 Morgan, J. W. Nature 317, 703-705 (1985).
 Delano, J. W. & Stone, K. Proc. Lunar planet. Sci. Conf. 16, 181-182 (1985).

- Jagoutz, E., Dawson, J. B., Hoernes, S., Spettel, B. & Wänke, H. in Workshop on the Early Earlh: The Interval from Accretion to the Older Archaen (eds Burke, K. & Ashwal. L. D.) 40-41 (LPI tech. Rep. 85-01, Lunar and Planetary Institute, Houston, 1985).
- Morgan, J. W. J. geophys. Res. (in the press).
- Richter, F. M. Earth planet. Sci. Lett. 73, 350-360 (1985).
 Swindle, T. D., Caffee, M. W., Hohenberg, C. M. & Taylor, S. R. in Origin of the Moon (Lunar and Planetary Institute, Houston, in the press).
 Newsom, H. E., White, W. M. & Jochum, K. P. Proc. Lunar planet. Sci. Conf. 16, 616-617
- 37. Newsom, H. E. J. geophys. Res. 90, C613-C617 (1985).
- Larimer, J. W. Geochim. cosmochim. Acta 32, 1189-1209 (1968).
- 39. Arculus, R. J. A. Rev. Earth planet. Sci. 13, (1985).
 40. Malvin, D. J., Jones, J. H. & Drake, M. J. Geochim. cosmochim. Acta (in the press).
- Meyers, J. & Eugster, H. P. Contr. Miner. Petrol. 82, 75-90 (1983).
 Zartman, R. & Tera, F. Earth planet. Sci. Lett. 20, 54-66 (1973).
- Anders, E. & Ebihara, M. Geochim. cosmochim. Acta 46, 2363-2380 (1982). Irving, A. J. Geochim. cosmochim. Acta 42, 743-770 (1978).
- Hertogen, J., Janssens, M.-J., Takahashi, H., Morgan, J. W. & Anders, E. Geochim. cos-mochim. Acta 47, 2241-2255 (1983).
- Sears, D. W., Kallemeyn, G. W. & Wasson, J. T. Geochim. cosmochim. Acta 46, 597-608 (1982).
- Von Michaelis, H., Willis, J. P., Erlank, A. J. & Ahrens, L. H. Earth planet. Sci. Lett. 5. 383-386 (1969).
- Moore, C. B. in Handbook of Elemental Abundances in Meteorites (ed. Mason, B.) 137-142

- Moore, C. B. in Fundation of Elemental Aduntances in Meteorites (ed. Mason, B.) 157-142 (Gordon and Breach, New York, 1971).
 Manhes, G. & Allègre, C. J. Meteoritics 13, 543-548 (1978).
 Kallemeyn, G. W. & Wasson, J. T. Geochim. cosmochim. Acta. 45, 1217-1230 (1981).
 Anders, E., Higuchi, H., Ganapathy, R. & Morgan, J. W. Geochim. cosmochim. Acta 40, 1111, 1120 (1922). 1131-1139 (1976).
- 52. Morgan, J. W. et al. Nature 224, 789-791 (1969).

- Palme, H. & Rammensee, W. Earth planet. Sci. Lett. 55, 356-362 (1981).

 Mason, B. Space Sci. Rev. 1, 621-646 (1963).

 Tatsumoto, M., Unruh, D. M. & Desborough, G. A. Geochim. cosmochim. Acta 40, 617-634
- 56. Mason, B. Handbook, of Elemental Abundances in Meteorites, 55, (Gordon and Breach, New York, 1971).
 57. Laul, J. C., Ganapathy, R., Anders, E. & Morgan, J. W. Geochim. cosmochim. Acta 37,
- 329-357 (1973)
- 58. Tatsumoto, M., Knight, R. J. & Allègre, C. J. Science 180, 1279-1283 (1973).

ARTICLES

Binding of a specific ligand inhibits import of a purified precursor protein into mitochondria

Martin Eilers & Gottfried Schatz

Biocenter, University of Basel, CH-4056 Basel, Switzerland

Methotrexate, a folate antagonist, blocks import into mitochondria of mouse dihydrofolate reductase fused to a mitochondrial presequence. Methotrexate does not mask the presequence, but stabilizes the dihydrofolate reductase moiety. It does not inhibit import of the authentic precursor from which the presequence is derived. This suggests that dihydrofolate reductase must at least partly unfold in order to be transported across mitochondrial membranes.

TRANSLOCATION of proteins across biological membranes is a key step in the intracellular sorting and secretion of proteins. Although much is known about protein movement across various membrane systems¹, it is unclear how hydrophilic, charged proteins translocate through the hydrophobic core of a phos-

pholipid bilayer. In particular, it remains unanswered whether a protein must unfold during the transport process² or whether it can translocate in a folded state³, perhaps through transient non-bilayer domains in the target membrane⁴. We have approached this question by fusing the presequence of an im-

Fig. 1 Expression and purification of mouse DHFR carrying a mitochondrial presequence. The fusion gene encoding the first 22 residues of the yeast cytochrome oxidase subunit IV presequence linked to mouse DHFR5 was excised from the yeast-E. coli shuttle vector pLGS-D5pCoxIV-DHFR6 with BamHI and treated with Bal31 to remove flanking sequences. The ends were filled-in with the large (Klenow) fragment of E. coli DNA polymerase and the shortened fusion gene was cut with HindIII at its 3' end. A fragment of the expected size was isolated?00 and cloned into a 'TAC'-expression vector²¹ (pKK 223-3; Pharmacia) using a filled-in EcoRI site at one end and a HindIII site at the other. E. coli HB101 (ref. 22) transformants resistant to antifolates (500 μg trimethoprim ml⁻¹ or 5-10 μg 1,3-diamino-7-benzylpyrrolo-[3,2/f]quinazoline ml⁻¹) were screened by colony immunoblotting²³ using a polyclonal antiserum against mouse DHFR. Plasmid pKK-pCoxIV-DHFR (a) was isolated from a transformant giving a strong signal with the anti-mouse DHFR antibody. P_{TAC}, TAC-promoter; rrnB, ribosomal transcription terminator; Amp^r, \(\beta\)-lactamase gene. The insert shows the first 29 amino acids of the fusion protein, consisting of 22 amino acids of the subunit IV presequence (1-22), 6 amino acids introduced by the cloning procedure (I-IV) and the first methionine of mouse DHFR. E. coli transformed with plasmid pKK-pCoxIV-DHFR were grown to the late logarithmic phase on LB medium²⁴, induced for 2 h at 37 °C with 1 mM isopropyl- β -thiogalactoside, and harvested. In these induced cells, the fusion protein represented ~1% of the total cellular protein. All subsequent steps were performed at 0-5 °C. The cells were osmotically shocked to release most of the periplasmic contents25, then suspended in 250 mM KCl, 20 mM KP, pH 8.0, 1 mM EDTA, 1 mM EGTA and 0.1 mM phenylmethylsulphonyl fluoride (PMSF). The shocked cells were gently lysed by adding lysozyme to 0.4 mg ml⁻¹ and, after 30 min, octyl-polyoxyethylene (given by Dr J. Rosenbusch, Biocenter) to 1%. The lysate was diluted 10-fold with 20 mM KP_i pH 7.0, 1 mM EDTA, 0.1 mM PMSF, mixed with 0.1 vol. of 2% protamine sulphate, stirred for 15 min, and centrifuged at 6,000g for 10 min. The supernatant was chromatographed on a CM-cellulose column in the presence of 0.5% octyl-polyoxyethylene, 0.1 mM PMSF, using a linear KCl gradient (25-500 mM). Fractions exhibiting DHFR activity²⁶ were pooled, dialysed overnight against 20 mM KP, pH 5.8, and subjected to affinity chromatography on methotrexate-Sepharose⁸, using 4.5 mM dihydrofolate in 1 M KCl, 20 mM KP, pH 8.0, as eluent. b, A silver-stained²⁷ SDS/12% polyacrylamide gel. Lanes 1 and 5, authentic mouse DHFR; 2-4, purified fusion protein (36, 108 and 360 ng, respectively). Protein was assayed as described elsewhere⁵.

ported mitochondrial protein to mouse dihydrofolate reductase (DHFR)⁵, and studying the translocation of the fusion protein into isolated yeast mitochondria.

The fusion protein

Hurt et al.^{5,6} have fused the first 22 residues of the presequence of yeast cytochrome oxidase subunit IV (an imported mitochondrial protein) to the N-terminus of mouse DHFR (a cytosolic protein), and shown that the resulting fusion protein is imported and proteolytically processed by isolated yeast mitochondria or by mitochondria in living yeast cells. DHFR lacking an attached presequence is not imported. In all properties studied, import of the fusion protein into mitochondria resembled import of authentic mitochondrial precursor proteins.

When we expressed the fusion protein in *Escherichia coli* (Fig. 1a), the bacterial cells became resistant to high levels of the folate antagonists trimethoprim and 1,3-diamino-7-benzyl-pyrrolo-[3,2/f]-quinazoline, indicative of elevated intracellular levels of DHFR. When the cells were rapidly lysed in NaOH and analysed by immune blotting with antiserum against mouse DHFR, only undegraded fusion protein was detected (not shown); thus, this protein is enzymatically active *in vivo*.

The fusion protein was purified from the *E. coli* transformants by cation-exchange chromatography in the presence of a nonionic detergent, followed by affinity chromatography on Sepharose derivatized with the folate antagonist methotrexate⁸. The purified fusion protein was nearly homogeneous as judged by SDS-polyacrylamide gel electrophoresis (Fig. 1b); by this procedure, 1 litre of an *E. coli* culture harvested in late logarithmic phase yielded 180 µg of purified fusion protein.

The fusion protein appeared to aggregate within the *E. coli* cells and required detergent for efficient extraction (not shown). Once extracted, however, it remained soluble even on removal of the detergent. The purified soluble fusion protein exhibited

DHFR activity; its specific activity (13 U mg⁻¹) was lower than that of authentic mouse DHFR (31 U mg⁻¹) but the fusion protein might have retained traces of methotrexate that had leaked off the affinity column. The $K_{\rm m}$ values for NADPH were 0.58 μ M for the fusion protein and 0.54 μ M for authentic DHFR. For technical reasons, $K_{\rm m}$ values for dihydrofolate could not be measured precisely, but they, too, were similar (0.13-0.31 μ M).

We conclude that the attachment of a presequence to the amino-terminus of DHFR does not significantly alter the protein's enzymatic properties, and therefore probably does not greatly alter the protein's conformation: the presequence and attached 'mature' sequence probably represent separate domains. The experiments reported below support this view.

Blockade of fusion protein import

The purified fusion protein was imported by energized yeast mitochondria (Fig. 2a). When 35 ng of purified fusion protein was incubated with 120 µg of de-energized yeast mitochondria, 7 ng (20%) was found in association with the mitochondria (Fig. 2a, lane 2) but was not imported: it remained accessible to externally added proteinase K (lane 3). On incubation with energized mitochondria, however, 42% (15 ng protein) of the fusion protein molecules were imported: they were cleaved to a smaller species (Fig. 2a, lane 4) which was inaccessible to externally added protease (lane 5). When the mitochondrial membranes were disrupted with detergent, the imported molecules, too, became accessible to added protease; under these conditions, they were cleaved to a proteolytic fragment (Fig. 2a, lane 6) distinctly smaller than that generated on import into mitochondria (compare lanes 5 and 6). Methotrexate (55 nM) inhibited mitochondrial import of the fusion protein by 89%; binding to the mitochondrial surface was decreased by only 17% (Fig. 2b; all lanes correspond to those of Fig. 2a

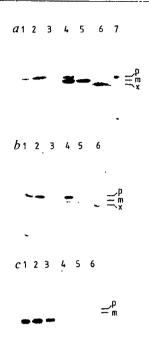


Fig. 2 Methotrexate blocks import of the fusion protein into isolated mitchondria. a, Lanes 1 and 7, 3.5 ng fusion protein (10% of the amount added to mitochondria); 2 and 3, fusion protein incubated with de-energized mitochondria (1 µg valinomycin ml was present); 4-6, fusion protein incubated with energized mitochondria. The samples shown in lanes 3 and 5 had been treated with proteinase K after import; that in lane 6 had been treated with proteinase K in the presence of 1% Triton X-100. p and m, uncleaved and cleaved fusion protein, respectively; x, proteaseresistant degradation product of DHFR. Relative molecular masses (M_rs) were 25,000 (25K), 22K and 21K for p, m and x, respectively. b, Same as a, except that all incubations contained 55 nM methotrexate, and lane 7 was omitted. c, Import of the fusion protein into energized mitochondria in the presence of the following concentrations (nM) of methotrexate: lane 1, 0.83; 2, 2.75; 3, 8.3; 4, 27.5; 5, 83; 6, 275. Import conditions as in a, lane 5. Methods. E. coli transformed with pKK-pCoxIV-DHFR were pulse-labelled for 30 min at 37 °C with 2 mCi of carrier-free 35 SO₄ (>1,000 Ci mmol⁻¹) in synthetic minimal medium supplemented with 1 mM isopropyl- β -D-thiogalactoside and all amino acids except cysteine and methionine²⁸. The fusion protein was then isolated as described in Fig. 1 legend except that affinity chromatography was omitted. Fractions eluted from CM-cellulose were analysed for fusion proteins by SDS-polyacrylamide gel electrophoresis and fluorography. Appropriate fractions were pooled and dialysed overnight against 100 mM KCl, 20 mM HEPES-KOH pH 7.4, 1 mM EDTA, 1 mM dithiothreiol, 0.1 mM PMSF. Aliquots of the purified fusion protein (35 ng; 1.5×10° c.p.m. per mg protein) were incubated with isolated yeast mitochondria (120 µg protein) for 30 min at 30 °C and the mitochondria were analysed for imported fusion protein²⁹. Internalization was ascertained by treating the re-isolated mitochondria with 50 µg proteinase K (250 µg ml⁻¹) for 30 min at 0 °C before electrophoretic analysis. The amount of added fusion protein was quantitative by calibrated immune blotting6, using authentic mouse DHFR as a standard.

except that methotrexate was added to all incubations). Methotrexate inhibited import of the fusion protein at roughly the same concentration at which it inhibited the enzymatic activity of pure mouse DHFR (Fig. 2c), the $K_{\rm m}$ values for inhibition of import and of enzymatic activity being 4.1 and 3.8 nM, respectively (data not shown). The result suggests that methotrexate blocks mitochondrial import of the fusion protein by binding to the catalytic syte? on DHFR.

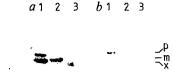


Fig. 3 A hydrophobic folate antagonist also blocks import of the fusion protein into yeast mitochondria. All incubations were carried out as described in Fig. 2 legend. a, Lanes 1, 2 and 3 show, respectively, fusion protein incubated with energized mitochondria and left untreated, treated with proteinase K or treated with proteinase K in the presence of 1% Triton X-100. b, Same as a, except that all incubations contained 1 μ M 1,3-diamino-7-benzylpyrrolo-[3,2/f]-quinazoline.

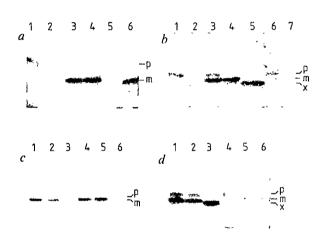


Fig. 4 Methotrexate only inhibits mitochondrial import of fusion proteins containing DHFR. All proteins tested for import were synthesized by coupled transcription/translation14 in the presence of 35S-methionine. Import into isolated yeast mitochondria was assayed as described in Fig. 2 legend. a, Authentic precursor to yeast cytochrome oxidase subunit IV. Lane 1, de-energized mitochondria; 2, de-energized mitochondria, plus protease; 3-5, energized mitochondria left untreated, treated with protease, or treated with protease and 1% Triton X-100, respectively; 6, energized mitochondria in the presence of 250 nM methotrexate, followed by protease treatment. For p, m and x, see Fig. 2. p, 17K; m, 14K. b, Fusion protein containing the first 22 residues of the subunit IV presequence attached to mouse DHFR. Lanes 1-5, analogous to those of a; 6, energized mitochondria plus 50 nM methotrexate; 7, energized mitochondria, protease treatment, plus 50 nM methotrexate. p, 25K; m, 22K; x, 21K. c, Authentic precursor to the yeast mitochondrial isozyme alcohol dehydrogenase III. Lanes 1-3, no methotrexate; 4-6, plus 15 nM methotrexate; 1 and 4, energized mitochondria; 2 and 5, energized mitochondria, protease-treated; 3 and 6, energized mitochondria, protease-treated, plus Triton X-100. p, 40K; m, 37K. d, Fusion protein containing the first 27 residues of the alcohol dehydrogenase III precursor attached to mouse DHFR. Lanes correspond to those of c. p, 25K; m, 22K; x, 21K.

Import of the purified fusion protein into mitochondria is also blocked by 1,3-diamino-7-benzylpyrrolo-[3,2/f]-quinazoline, a membrane-permeant antifolate (ref. 10 and R.L. Then, personal communication) (Fig. 3). The inhibition of import of the fusion protein is, therefore, not simply a consequence of the inability of methotrexate to cross biological membranes.

To demonstrate that methotrexate is not a general inhibitor of mitochondrial protein import, we tested its effect on

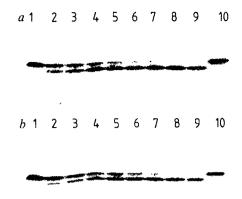


Fig. 5 Methotrexate does not inhibit the action of mitochondrial processing protease on the presequence attached to DHFR. a, Lane 1, no incubation with protease; lanes 2-9, incubation with protease for 1.5, 2.5, 5, 7.5, 10, 15, 20 and 30 min, respectively; lane 10, incubation for 30 min in the presence of 1 mM 1,10-phenanthroline, a relatively specific inhibitor of the matrix protease. b, Same as a, except that all incubations contained, in addition, 70 nM methotrexate.

Methods. The fusion protein containing the first 22 residues of the subunit IV presequence attached to mouse DHFR was synthesized in vitro in the presence of ³⁵S-methionine (see Fig. 4 legend) and incubated with the partially purified ¹⁵ processing protease. Samples were precipitated with 5% trichloroacetic acid and analysed by SDS/12% polyacrylamide gel electrophoresis and fluorography.

mitochondrial import of four different proteins: (1) the authentic precursor to cytochrome oxidase subunit IV¹¹; (2) the authentic precursor to yeast alcohol dehydrogenase III (a mitochondrial isozyme¹²); (3) mouse DHFR linked to the first 22 residues of the cytochrome oxidase subunit IV presequence⁵ (that is, the fusion protein described above); and (4) mouse DHFR linked to the first 27 residues of the alcohol dehydrogenase III precursor¹³. Each of the four proteins was synthesized in vitro by coupled transcription-translation in the presence of 35Smethionine and tested for cleavage and import by isolated yeast mitochondria. Methotrexate blocked import of only the two fusion proteins (Fig. 4b, d); it did not measurably affect import of the two authentic precursors whose presequences had been used to construct the fusion proteins (Fig. 4a, c). Thus, methotrexate blocked mitochondrial import of only those proteins containing a DHFR moiety.

Methotrexate binding

Binding of methotrexate to the fusion proteins could trigger an interaction between the DHFR domain and the attached presequence, rendering that presequence inaccessible to the mitochondrial import machinery. Two observations make this possibility unlikely. First, methotrexate did not significantly affect binding of the fusion proteins to de-energized mitochondria (Figs 2, 4); as DHFR lacking a presequence does not bind to mitochondria14, binding of the fusion proteins shows that the presequence is accessible. Second, methotrexate did not significantly inhibit removal of the attached presequence by the processing protease partially purified15 from the yeast mitochondrial matrix (Fig. 5). Methotrexate did, however, partially protect the DHFR moiety against degradation by low concentrations of thermolysin (Fig. 6). Incubation of the purified fusion protein with thermolysin in the presence of methotrexate caused accumulation of a degradation intermediate whose size corresponded to that of DHFR lacking a presequence (Fig. 6, lanes 5-11). Methotrexate also protected authentic DHFR against thermolysin; in that case, however, no smaller intermediate was detected (not shown). Thus, it is likely that the cleaved-off

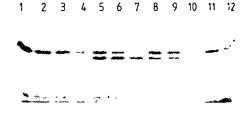


Fig. 6 Methotrexate protects DHFR against degradation by thermolysin. ³⁵S-labelled purified fusion protein (7.5 ng; see Fig. 1 legend) was incubated for 30 min at 43 °C in 0.1 M HEPES-KOH pH 7.4, 2 mM CaCl₂ in the absence of protease (lane 1) or with 5.6 ng (lanes 2, 5, 8, 11), 11.2 ng (lanes 3, 6, 9, 12) or 28 ng (lanes 4, 7, 10) of thermolysin, either in the absence of methotrexate (lanes 1-4), or in the presence of 16.5 μM (lanes 5-7), 660 nM (lanes 8-10) or 66 nM (lanes 11, 12) methotrexate. The final volume in each case was 50 μl. Samples were then mixed with 5 μl of 0.2 M EGTA and analysed by SDS/12% polyacrylamide gel electrophoresis and fluorography.

fragment which is not protected from thermolysin by methotrexate is indeed the presequence. Control experiments (not shown) established that methotrexate at a concentration as high as $7 \mu M$ did not affect the action of thermolysin on yeast hexokinase or chicken ovalbumin.

Implications for protein translocation

How does methotrexate block import of the DHFR-containing fusion proteins into mitochondria? We can exclude the possibility that it blocks mitochondrial protein import per se or causes masking of the presequence. Amost certainly, it also does not induce a major structural change in the DHFR moiety: extensive X-ray crystallographic studies on the interaction between chicken DHFR and antifolates have revealed only a minor displacement of Tyr 30 and Glu 31 (refs 9, 16). These data should also apply to mouse DHFR as the amino-acid sequences of the two enzymes show 77% homology 17,18. Such extensive sequence homology predicates close resemblance of the three-dimensional structures?

It could be argued that methotrexate by itself might not be able to pass membranes and thereby might block translocation of any protein to which it is bound. This possibility is rendered highly unlikely by the finding that 1,3-diamino-7-benzylpyrrolo-[3,2/f]-quinazoline also blocks import of the purified fusion protein; this folate antagonist is uncharged and highly hydrophobic and has been shown to pass freely through cell membranes of yeast¹⁰ and E. coli (R.L. Then, personal communication).

The combined evidence strongly suggests that folate antagonists block the translocation of DHFR through mitochondrial membranes by preventing unfolding of the protein. This view is in accord with the crystallographic evidence on the interaction between antifolates and DHFR and the protection data described here. By binding tightly to DHFR, antifolates impede unfolding of the enzyme. In line with this interpretation is the recent observation of a translocation intermediate during the import of the precursors of the F_1 -ATPase β -subunit and cytochrome c_1 into Neurospora mitochondria¹⁹. This intermediate accumulated at low temperature and appeared to span both mitochondrial membranes, as it remained accessible to an externally added protease even though the presequence had already been cleaved off by the matrix-located processing protease. To allow such an orientation, at least the amino-terminal portion of the imported proteins must have been partially unfolded. Neither of these observations, however, give any indication as to how extensive the unfolding must be to allow movement of the protein across a membrane. The purified, translocationcompetent fusion protein described here should be a valuable tool for investigating this question.

This study was supported by grants 3.394-0.83 and 3.660-0.84 from the Swiss NSF. We thank Dr J. Kraut (University of California, San Diego) for sending us the unpublished crystallographic coordinates of chicken DHFR; Drs R. L. Then and D.

Stüber (Hoffman-La Roche Co., Basel) for gifts of antifolates and mouse DHFR, respectively; Dr E. Mehler (Biocenter, Basel) for valuable advice; W. Oppliger for technical assistance; and M. Probst and L. Schwörer for typing the manuscript.

Received 1 April; accepted 22 May 1986.

- 1. Wickner, W. T. & Lodish, H. F. Science 230, 40u-407 (1985).
- Blobel, G. & Dobberstein, B. J. Cell Biol. 67, 835-851 (1975).
 Randall, L. L. & Hardy, S. J. S. in Modern Cell Biology Vol. 3, 1-20 (Liss, New York, 1984).
- Cullis, P. R. & De Kruijff, B. Biochim. biophys. Acta 559, 399-420 (1979).
 Hurt, E. C., Pesold-Hurt, B. & Schatz, G. FEBS Lett. 178, 306-310 (1984)
- 6. Hurt, E. C., Pesold-Hurt, B., Suda, K., Oppliger, W. & Schatz, G. EMBO J. 4, 2061-2068
- Chang, A. C. Y. et al. Nature 275, 617-624 (1978).
- Kaufman, B. T. & Pierce, J. V. Biochem, biophys. Res. Commun 44, 608-613 (1971). Volz, K. W. et al. J. biol. Chem. 257, 2528-2536 (1982).
- 10. Castaldo, R. A., Gump, D. W. & McCormack, J. J. Antimicrob. Ag. Chemother, 15, 81-86

- Maarse, A. C. et al. EMBO J. 3, 2831-2837 (1984).
 Young, E. T. & Pilgrim, D. B. Molec. cell. Biol. 5, 3024-3034 (1985).
 Van Loon, A. P. G. M., Brändli, A. & Schatz, G. Cell 44, 801-812 (1986).
 Hurt, E. C., Pesold-Hurt, B. & Schatz, G. EMBO J. 3, 3149-3156 (1984).

- 15. Böhni, P. C., Daum, G. & Schatz, G. J. biol. Chem. 258, 4937-4943 (1983).
- 16. Matthews, D. A. et al. J. biol. Chem. 260, 381-391 (1985).
- 17. Kumar, A. A., Blankenship, D. T., Kaufman, B. T. & Freisheim, J. H. Biochemistry 19, .
- Stone, D. & Phillips, A. W. FEBS Lett. 74, 85-87 (1977).
 Schleyer, M. & Neupert, W. Cell 43, 339-350 (1985).
- 20. Dretzen, G., Bellard, M., Sassone-Corsi, P. & Chambon, P. Analyt. Biochem. 112, 295-298
- Amann, E., Brosius, J. & Ptashne, M. Gene 25, 167-178 (1983).
 Bolivar, F. & Backman, K. Meth. Enzym. 68, 245-268 (1979).
- Stanley, K. K. Nucleic Acids Res. 11, 4077-4092 (1983)
- 24. Maniatis, T., Fritsch, E. F. & Sambrook, J. Molecular Cloning: A Laboratory Manual (Cold Maniaus, I., Fritsch, E. F. & Samorook, J. Molecular Cloning: A Laboratory Manual (Cold Spring Harbor Laboratory, New York, 1982).
 Neu, H. C. & Heppel, L. A. J. biol. Chem. 240, 3685-3692 (1965).
 Gupta, S. V. et al. Biochemistry 16, 3073-3079 (1977).
 Wray, W., Boulikss, T., Wray, V. P. & Hancock, R. Analyt. Biochem. 118, 197-203 (1981).
 Van Loon, A. P. G. M., Maarse, A. C., Riezman, H. & Grivell, L. A. Gene 26, 261-272 (1983).

- 29. Gasser, S. M., Daum, G. & Schatz, G. J. biol. Chem. 257, 13034-13041 (1982).

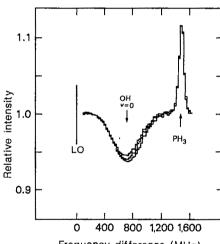
LETTERS TO NATURE

Infrared helioseismology: detection of the chromospheric mode

Drake Deming*, David A. Glenar†, Hans Ulrich Käufl*, Andrew A. Hill† & Fred Espenak*

* Planetary Systems Branch, NASA/Goddard Space Flight Center, Greenbelt, Maryland 20771, USA † Department of Physics, Colgate University, Hamilton, New York 13346, USA

Observations of velocity waves from the 5-min p-mode oscillations in the solar sub-photospheric cavity have permitted a number of important inferences about physical conditions and differential rotation in the solar interior¹. Models also predict the existence of an overlying acoustic cavity, defined by reflections between the temperature minimum and the sharp rise from chromospheric to coronal temperatures²⁻⁵. Observations of chromospheric emission features^{6,7}, the cores of strong absorption lines⁸⁻¹¹ and the farinfrared continuum¹² have established that chromospheric oscillatory power is shifted to higher frequencies than is the case for the sub-photospheric cavity. However, it remains to be established that this oscillatory power is sufficiently localized to indicate the presence of resonant modes at frequencies close to the predicted eigenfrequencies. We have obtained time-series observations of an infrared (11-µm) solar OH absorption line profile, on two consecutive days, using a laser heterodyne spectrometer to view a 2-arc-s portion of the quiet Sun at disk centre. A power spectrum of the line-centre velocity shows the well-known photospheric p-mode oscillations very prominently, but also shows a second feature near 4.3 mHz. A power spectrum of the line intensity shows only the 4.3-mHz feature, which we identify as the fundamental (n = 1)p-mode resonance of the solar chromosphere. The frequency of the mode is observed to be in substantial agreement with the eigenfrequency of current chromospheric models. A time series of two beam difference measurements shows that the mode is present only for horizontal wavelengths >19 Mm. The period of a chromospheric p-mode resonance is directly related to the sound travel time across the chromosphere, which depends on the chromospheric temperature and geometric height. Thus, detection of this resonance will provide an important new constraint on chromospheric models.



Frequency difference (MHz)

Fig. 1 Sample line profiles obtained on 16 June 1985 in three consecutive integrations, showing changes in the solar line profile and stability in the PH₃ gas-cell line. LO, local oscillator (13C16O₂ P(12), 903.74974 cm⁻¹); OH, R22(27.5)f rotational transition of OH, PH₃, phosphine absorption feature.

We measured the Doppler shift and line intensity of a 903.769cm⁻¹ (11.065-µm) OH absorption feature with a 2-arc-s field of view (full width at half-maximum, FWHM) centred on the solar disk, and not following the solar rotation. We used the Goddard laser heterodyne spectrometer at the McMath telescope of the National Solar Observatory, in June 1985. The design and operation of the instrument are discussed in ref. 13. The R22(27.5)f rotation transition of OH was measured using a peak-power stabilized laser local oscillator operating on the I-band, P(12) transition of $^{13}C^{16}O_2$ at $903.7497\,\mathrm{cm}^{-1}$. The observations were made in the optically null-balanced mode described in ref. 14. In this mode, the instrument uses a 27-Hz mirror-chopper to alternately place the Sun and a local hightemperature black body on the detector. Line profiles are measured in the optical difference spectrum. To monitor the laser stability, an absorption cell containing phosphine (PH₃) at 0.5 torr was placed in the black-body (BB) beam. A PH₃

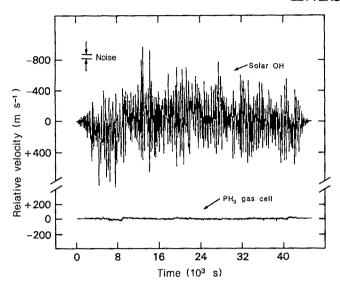


Fig. 2 Time series of line-centre velocity for the solar OH feature and PH₃ gas-cell line. The velocity scales are of opposite sense because the lines occur in opposite side bands. Both time series were apodized using a 10% cosine bell. The 1σ statistical noise level for a single solar measurement is 26 m s^{-1} and is indicated in the upper left. The corresponding 1σ level for the PH₃ line is 5 m s^{-1} .

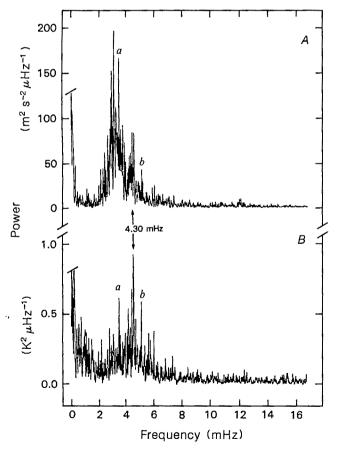


Fig. 3 Power spectra of line velocity (A) and line intensity (B), calculated from the concatenated data of 15 and 16 June, and smoothed to $20 \,\mu$ Hz resolution. The line velocity was measured in metres per second and the line depth was measured in kelvins. The peaks near zero frequency in both spectra are due to instrumental effects, and are not of solar origin. The arrows indicate the solar chromospheric mode at 4.30 mHz, and the features labelled 'a' and 'b' are discussed in the text.

absorption feature is thus recorded simultaneously with the solar OH feature in each 30-s integration. In Fig. 1, three consecutive integrations show the solar OH feature near the centre, and the PH₃ feature near 1,450 MHz. The PH₃ line appears inverted because each result is obtained as a difference spectrum (Sun-BB). A gaussian profile is fitted to each line to determine the line centre position, and line intensity (depth) relative to the continuum. It is evident from Fig. 1 that the solar line shows large fluctuations in both line centre frequency and line intensity. These fluctuations are not seen in the PH₃ gas-cell line, indicating that potential instabilities in the local oscillator frequency are negligible.

Our Sun-centre time series spanned a total of 2 days (15-16 June), with a total of 18.7 h of data. Figure 2 shows apodized velocity time series for 16 June. The results of the PH2 profile fitting are displayed below the solar results to show the overall instrument stability. The solar time series shows r.m.s. (rootmean-square) velocity fluctuations of ~300 m s⁻¹, greatly in excess of the $26 \,\mathrm{m \, s^{-1}}$ (1 σ) error associated with a single measurement. The only instrumental effect which is noticeable in Fig. 2 is represented by a slow drift in both time series, which is corrected near 8,600 s. This is caused by changes in the spectral baseline due to changes in the detector response. The leastsquares algorithms which compute the line shape parameters cannot fully compensate for these baseline drifts, because the bandpass of the heterodyne spectrometer is so narrow. However this instrumental effect has no impact for the present purpose, because it propagates into the power spectra only at the lowest frequencies.

Velocity and line intensity power spectra from both days of observations were calculated using the method of Deeming¹: the velocity spectrum is shown in Fig. 3A. The spectrum of the concatenated data has been smoothed to a resolution of 20 µHz (FWHM) to suppress the side-lobes produced by the night-time data gap. We checked the extent of side-lobe contamination by calculating power spectra of continuous sine waves with the same data sampling. The velocity spectrum shows the dominant 3-mHz band from the subphotospheric cavity. Individual modes in this band cannot be distinguished because of the lack of spatial wavenumber resolution. The second most prominent feature is the relatively narrow band of power near 4.3 mHz, which we identify as a chromospheric resonance. The integrated power in the range 3.86-4.47 mHz produces an r.m.s velocity amplitude of 50 m s⁻¹. This is too large to be attributed to instrumental drifts or solar image motion at this frequency. The reality of the 4.3-mHz feature is confirmed in Fig. 3B, which shows the power spectrum of the line depth. In this figure the photospheric p-modes are essentially absent; only the 4.3-mHz feature is evident. The central peak in this spectrum occurs at 4.30 ± 0.01 mHz, in very close agreement with the locus of frequencies predicted by Ando and Osaki³ for radial order n = 1. Two other peaks, labelled 'a' and 'b', are also prominent in both spectra at identical frequencies. They occur at 3.39 mHz (a) and 4.96 mHz (b). Although they do not correspond to overtones of higher radial order (n>1), we speculate that they may represent resonances due to different components in an inhomogeneous chromosphere.

Several factors lend confidence to our identification of the n=1 chromospheric resonance. (1) Our infrared observations sample the upper photosphere, where the chromospheric mode becomes increasingly prominent relative to the photospheric mode¹⁶. (2) The mode is observed at a frequency in close agreement with the predicted eigenfrequency. (3) The mode is clearly present in power spectra of the line intensity as well as the line velocity. It is distinguished from the photospheric pmodes by being relatively more prominent in the line intensity spectrum. This is expected, as the temperature perturbation associated with the chromospheric mode will be less affected by radiative damping¹⁷. (4) Compared with many previous chromospheric observations, our data are of relatively long

duration, making our result more representative of average conditions in the upper solar atmosphere. (5) The lack of solar activity at the time of our observations provided optimum conditions for the existence of a resonance.

In addition to the power spectra of Fig. 3, we have also examined power spectra from a 1-day sequence of dispersionline shapes, obtained on 18 June 1985 by chopping our 2-arc-s field of view between two locations on the solar disk separated by 26 arc s (see ref. 13). These data allow us to derive the velocity and line intensity difference between these two locations, and power spectra of these quantities show no evidence of the chromospheric mode. This implies that the mode is being coherently subtracted in these data; therefore, its horizontal wavelength must exceed the 19-Mm chopping distance. A long horizontal wavelength for this mode is also consistent with the low-spatial-resolution data of Lindsey and Kaminski¹², provided that we identify the chromospheric mode as producing the 3-6-mHz oscillatory power which they observed in the intensity

Received 10 February; accepted 23 April 1986.

- Christensen-Dalsgaard, J., Gough, D. & Toomre, J. Science 229, 923-931 (1985). Bahng, J. & Schwarzschild, M. Astrophys. J. 137, 901-913 (1963). Ando, H. & Osaki, Y. Publs astr. Soc. Japan 29, 221-233 (1977).

- Ulrich, R. K. & Rhodes, E. J. Jr Astrophys. J. 218, 521-529 (1977). Christensen-Dalsgaard, J. & Frandsen, S. Soi. Phys. 82, 165-204 (1983).
- Orrall, F. Q. Astrophys. J. 143, 917-927 (1966).
- Athay, R. G. & White, O. R. Astrophys. J. Suppl Ser. 39, 333-346 (1979). Cram, L. E. Astr. Astrophys. 70, 345-354 (1978).
- Kneer, F., Newkirk, G. Jr & von Uexkull, M. Astr. Astrophys. 113, 129-134 (1982)

of the far-infrared solar continuum. This situation was anticipated by Christensen-Dalsgaard and Frandsen⁵, who commented that "modes whose horizontal wavelength is much longer than the scale of the inhomogeneities feel only the mean structure of the atmosphere, . . . therefore our results may apply

We thank J. Goldstein for assistance in the observations, J. Faris for preparation of CO₂ mixtures, the staff of the National Solar Observatory for their support of our experiment, and our colleagues Drs T. Kostiuk and M. J. Mumma for their efforts in the development of the laser heterodyne technique at Goddard. D.A.G. was supported by NASA/Goddard Space Flight Center as a NASA/ASEE summer faculty fellow, and by NASA/Goddard Space Flight Center grant NAG 5-478. The present investigation was supported by RTOP 188-41-55 to Dr Mumma. A.A.H. received support from Colgate University's Division of Natural Sciences; D.D., D.A.G. and H.U.K. were guest investigators at the National Solar Observatory.

- Dame, F., Gouttebroze, P. & Malherbe, J. M. Astr. Astrophys. 130, 331-340 (1984).
 von Uexkull, M., Kneer, F., Mattig, W., Nesis, A. & Schmidt, W. Astr. Astrophys. 146, 192-194 (1985).
- Lindsey, C. & Kaminski, C. Astrophys. J. 282, L103-L106 (1984).
- 13. Glenar, D., Deming, D., Espenak, F., Kostiuk, T. & Mumma, M. J. Appl. Opt. 25, 58-62
- 14. Deming, D., Hillman, J. J., Kostiuk, T., Mumma, M. J. & Zipoy, D. M. Sol. Phys. 94, 57-74 (1984).
- 15. Deeming, T. J. Astrophys. Space Sci. 36, 137-158 (1975).
- 16. Leibacher, J., Gouttebroze, P. & Stein, R. F. Astrophys. J. 258, 393-403 (1982).
- 17. Noyes, R. W. & Leighton, R. B. Astrophys. J. 138, 631-647 (1963).

Shape memory behaviour in partially stabilized zirconia ceramics

M. V. Swain

CSIRO Division of Materials Science, Locked Bag 33, Normanby Road, Clayton, Victoria 3168, Australia

Shape memory behaviour has been observed in a variety of metallic alloys. It is usually associated with specific materials which on being deformed to various degrees of inelastic strain, return to their original shape on heating. The essential requirement is that they undergo reversible martensitic (diffusionless) phase transformations on heating and cooling. The past decade has seen considerable scientific and technological interest in ceramics containing zirconia (ZrO₂), a material that exhibits such martensitic transformations. This interest has arisen because of the high strengths and toughness that can be achieved in such materials by a stress-induced volume-expanding phase transformation about the crack tip1. Observations are reported here of shape memory behaviour in a zirconia alloy partially stabilized with magnesia, at temperatures a few hundred degrees higher than reported for metallic alloys. The reversible deformation strains are relatively small, 0.5%, and are limited by the brittleness of the ceramic material. In the MgO-PSZ material the phase exhibiting the martensitic behaviour is the minor phase and occurs as precipitates in a stable

In the course of thermal cyclic testing of magnesia-partiallystabilized-zirconia (MgO-PSZ) material (J. E. Excel, M. Marmach and M. V. S., unpublished results) a behaviour very similar to the so-called shape memory effects of certain metallic alloys was observed. Shape memory behaviour was first observed about 40 years ago in various metallic alloys, and has since found technological applications². The metallic alloys based on compositions containing NiTi or CuAlNi have attracted much interest. The copper-containing alloy has created interest recently through an attempt to increase the temperature at which the deformation remains reversible³.

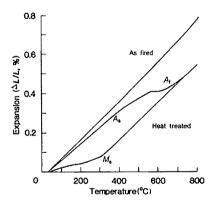


Fig. 1 Thermal expansion curves for the as-fired and heat-treated MgO-PSZ.

The essential requirement for shape memory alloys is that they undergo reversible martensitic phase transformations on heating and cooling, and this usually also means that the twin boundaries of the lower-symmetry (lower-temperature) phase must be sufficiently mobile or glissile to enable reorientation on the application of stress. The twin boundaries within the lowtemperature phase must then consist of partially or fully coherent interfaces, to enable reversal on heating. Deformation of the alloy under load usually takes place below the martensitic start temperature, M_s , with non-linear strain being accommodated by the reorientation of the twin laths within the microstructure. It is also possible to achieve such non-linear strain above M_s but below a specific temperature, M_d , by a stress-induced transformation. On heating materials that have been deformed in either manner to above the $A_{\rm f}$ temperature, where the lowertemperature crystal structure completely reverts back to the high-temperature phase, the bodies return to their original prestrained states. The reversal of the deformation begins at the temperature at which the reverse martensitic phase change starts, A_s , and is complete at A_f . Shape memory behaviour has usually been described for metals where the entire alloy is single phase, although some data exist for NiTi alloys containing minor volume fractions of intermetallic precipitates².

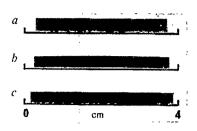


Fig. 2 Optical micrographs of the as-fired (a) and heat-treated (b) material after thermal cycling to 800 °C under a flexural stress of 200 MPa. c, Thermal cycling of a deformed bar to 800 °C in the absence of stress leads to the near complete reversal of the deflection.

PSZ ceramics are a new class of strong and tough materials that may be fabricated to use a martensitic transformation to increase their toughness1. The tetragonal phase of zirconia undergoes a martensitic transformation to monoclinic zirconia, accompanied by a 4-6% volume dilation and 9% shear strain. The temperature at which this transformation takes place is dependent on the solute content, precipitate size and matrix constraint, if any, imposed on the tetragonal material. To optimize the toughness of these materials, the content and size of the tetragonal grains or precipitates is adjusted so that M_s is just below the temperature of interest. The application of tensile stresses, for example about a crack tip, can trigger the volumeexpanding transformation, leading to crack-tip shielding and a higher fracture toughness. With this mechanism a 10-fold increase in K_{1c} is achievable in optimum alloy compositions⁴. In addition to the increased toughness, recent studies have shown that the application of stress may lead to ductile behaviour due to the tetragonal to monoclinic induced transformation, and deformation strains of 0.25% have been reported5-

The present observations were noted during thermal cycling tests on MgO-PSZ alloys in four-point flexure. These materials, containing 9.4 mol % MgO, consisted of coarse grains (~50 μm) of a cubic zirconia matrix with ~35 vol. % tetragonal zirconia precipitates in the as-fired state. Some of these bars were heattreated (at 1,100 °C for 9 h) to partially destabilize the tetragonal precipitates on cooling; that is, M_s was above room temperature. Example of the thermal expansion curves of the as-fired and heat-treated materials are shown in Fig. 1. The M_f temperature of the aged material was below room temperature and the monoclinic content of the polished surface as determined from the 111 X-ray diffraction peaks⁸ was 15%. Details of the heat treatment of MgO-PSZ materials are discussed elsewhere⁹ The thermal expansion hysteresis of PSZ alloys is much larger, particularly in the temperature axis, than most metallic alloys, and has been attributed to the constrained nature of the transforming precipitates¹⁰.

Thermal cycling tests consisted of loading rectangular bars, $3 \times 4 \times 40$ mm, in a four-point flexure, dead-weight loading jig, such that the tensile stress at the outer fibre was 200 MPa. No difference in behaviour was detected between specimens that had a ground or polished surface. The inner and outer spans of the flexure jig were 15 mm and 30 mm. The bars were slowly heated at $100 \,^{\circ}\text{C}$ h⁻¹ to $800 \,^{\circ}\text{C}$ and held for 2 h before cooling at $100 \,^{\circ}\text{C}$ h⁻¹. The as-fired material on such a thermal cycle behaved as anticipated for an elastic non-creeping body, whereas the heat-treated material was quite bent after such a cycle. A comparison of the two bars after such a thermal cycle under load is shown in Fig. 2a, b. On re-heating the bent bar to $800 \,^{\circ}\text{C}$ at the same heating and cooling rates in the absence of stress, it returned almost completely to its original shape, as seen in Fig. 2c.

The permanent strain in the outer fibre of the bent bar after thermal cycling under load was calculated from the radius of

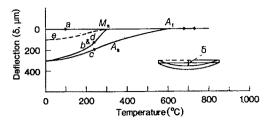


Fig. 3 A plot of the non-elastic deflection of the heat-treated material on heating and cooling under stress (corrected for thermal expansion of as-fired material). a, Heating under load (200 MPa); b, cooling under load (200 MPa); c, re-heating under load (200 MPa); d, cooling under load (200 MPa); e, cooling without load.

curvature, ρ , using the simple relationship

$$\varepsilon = t/2\rho \tag{1}$$

where t is the beam thickness. This analysis assumed that the neutral axis remains in the middle of the deformed bar. Recent studies of stress-induced transformation during flexure have shown that the neutral axis is displaced⁶, and the above estimate for the strain is slightly conservative. From equation (1) the retained deformation strain at room temperature was found to be 0.42%, which is much larger than the deformation strains (typically 0.2%) reported in peak-toughness MgO-PSZ and CeO₂-PSZ alloys loaded in tension or flexure⁵⁻⁷. The retained inelastic strain after re-heating to 800 °C and cooling to room temperature in the absence of external stress was 0.14%. The influence of applied stress on the extent of deformation strain and retained strain after re-heating in the absence of stress is being investigated and will be reported elsewhere.

To determine when the deformation was taking place, a linear variable displacement transducer (LVDT) was used to monitor the movement of the loading arm during heating and cooling. On heating and cooling the loading rams expanded and contracted substantially more than the specimen deformation. However, by subtracting the thermal expansion and contraction of the as-fired material from that of the heat-treated material it was possible to deduce the temperature at which deformation began. An additional experiment of re-heating the bent specimen under load was also performed to evaluate if, and at what temperature, the deformation reversed. The corrected deflection of the bar with temperature during heating and cooling on the first and second thermal cycles is shown in Fig. 3. Also shown are the $M_{\rm s}$, $A_{\rm s}$ and $A_{\rm f}$ temperatures determined from the thermal expansion curve in Fig. 1.

The results in Fig. 3 show that the bar begins to deform on cooling at temperatures $\leq M_s$. On re-heating under load the bar begins to return to its original shape at temperatures below A_s and the process seems to be complete by A_t . On cooling, the deformation is identical to the initial cycle at temperatures below M_s . These observations are very similar to the observations in metallic shape memory alloys. The main differences are that the temperatures at which the deformation and reversal occur are hundreds of degrees higher in the MgO-PSZ and the extent of deformation strain is much less. There appears to be a small remnant of irreversible deformation associated with reheating above A_f in the absence of stress. This behaviour is also observed in metallic alloys, which exhibit a large hysteresis between M_s and A_f (ref. 2).

Crystallographic analysis of the orientation relationships of transformed monoclinic zirconia precipitate in a cubic matrix is an area of active research. Recent detailed transmission electron microscopy (TEM) of the twinned monoclinic precipitates in MgO-PSZ has shown that 12 different crystallographic variants exist¹¹. It has also been observed that the twin orientations in the monoclinic structure could differ from precipitate to precipitate and were dictated by the local stress state.

Microcracks, observed at the interface between matrix and precipitate, accommodated lattice strains which arose, particularly at specific twin domain/interphase boundaries. More recently, Hannink et al. 12 used a technique of in situ TEM straining of almost identical MgO-PSZ alloys using electron-beam heating and subsequently annealing transformed precipitates in the same manner. They also observed that the orientation of the monoclinic twin variants of individual precipitates is dependent on the superimposed local stress state. On annealing, the precipitates revert back to their original tetragonal shape, regardless of the pre-existing twin variants. In these TEM experiments, there was no attempt to monitor the temperature of the foil and therefore determine the M_s and A_s of individual precipitate. However, some residual strain did remain after annealing, particularly at sites where microcracking was observed when the precipitate was in the twinned monoclinic form. The presence of such residual strain sites may well contribute to the destabilization of some of the associated metastable tetragonal precipitates in a preferred manner on cooling. This would lead to some residual strain after re-annealing in the absence of a biasing or superimposed stress on the body, and may account for the slight residual deflection of the beam.

The present experiments strongly support the contention that shape memory behaviour, due to a martensitic reaction, occurs in PSZ ceramics. The application of a biasing stress as the body cooled through the M_s temperature leads to a deflection of the specimen which could be almost completely removed on annealing above the $A_{\rm f}$ temperature. Although the present experiments have been carried out with MgO-PSZ alloys, it is anticipated that similar behaviour would be observed in other zirconiatoughened ceramics with the appropriate phase assemblage. [Since submitting this manuscript, shape memory behaviour has also been observed in a fine-grained yttria (Y₂O₃)-PSZ ceramic (M. Matsui and T. Soma, personal communication.] At this stage it is uncertain what contribution the volume dilation associated with the transformation makes to the deformation strain developed in cooling through M_s under load. In addition, the ability of the stiff non-transformable cubic matrix phase to absorb the large deformations during cooling and heating through M_s and A_s under load is not understood. The limited strains associated with the inelastic deflection and subsequent recovery on annealing with the investigated MgO-PSZ alloy are so small that it is too early to speculate about technological applications of such shape memory behaviour. However, the much higher temperatures at which this behaviour is being observed in PSZ materials, and the ability to vary the M_s and $A_{\rm f}$ temperatures to >1,200 °C by the addition of hafnium oxide, may provide technological opportunities unavailable for metallic shape memory alloys. The upper temperature application limit for zirconia ceramics, like metallic alloys, will be controlled by the temperature at which the internal elastic strains responsible for the shape memory effect are relaxed by thermally activated processes.

The provision of specimens by J. Excel and M. Marmach is appreciated, as are discussions with and access to unpublished work of R. H. J. Hannink, L. R. F. Rose, N. Kennon, D. Dunne and M. J. Bannister. I thank H. G. Scott and Professor A. P. Miodownik for constructive comments.

Received 28 November 1985; accepted 2 May 1986.

- Garvie, R. C., Pascoe, R. T. & Hannink, R. H. J. Nature 258, 703-705 (1975).

 Metals Forum 4, 125-190 (1981).

 Duerig, T. W., Albrecht, J. & Gessinger, G. H. J. Metals 32, 14-20 (1982).

 Swain, M. V. & Rose, L. R. F. Advances in Fracture Research, ICF6 Vol. 1 (eds Valluri, S. R. et al.) 473-494 (Pergamon, Oxford).

 5. Swain, M. V. Acta metall. 33, 2035 (1985).

- Marshall, D. B. J. Am. ceram. Soc. 69, 173-180 (1986).
 Tsukuma, K. & Shimada, M. J. mater. Sci. 20, 1178-1184 (1985).
 Garvie, R. C. & Nicholson, P. Bull Am. ceram. Soc. 55, 303-305 (1972).
- Hannink, R. H. J. & Swain, M. V. J. Aust. ceram. Soc. 18, 53-62 (1982).
 Hannink, R. H. J., Johnson, K. A., Pascoe, R. T. & Garvie, R. C. Adu. Ceram. 3, 116-136
- 11. Muddle, B. & Hannink, R. H. J. J. Am. ceram. Soc. (in the press).
- 12. Hannink, R. H. J., Potter, R. J. & Marshall, D. B., J. Am. ceram. Soc. (in the press).

Unusual conditions in the tropical Atlantic Ocean in 1984

S. G. H. Philander

Geophysical Fluid Dynamics Laboratory/NOAA, Princeton University, Princeton, New Jersey 08542, USA

During the first half of 1984, oceanic and atmospheric conditions in the tropical Atlantic were, in many respects, similar to conditions in the Pacific Ocean during El Niño: the upper ocean was unusually warm in the eastern part of the basin, rainfall was heavy over the normally arid regions to the south of the Equator, and coastal upwelling was inhibited in regions (southwestern Africa) where this is a seasonal phenomenon. The change in sea-surface temperatures, which resulted when unusual eastward currents to the south of the Equator transported warm surface waters towards Africa, contributed to the change in atmospheric conditions. The altered atmospheric conditions, in turn, contributed to the change in the oceanic circulation and the change in the sea-surface temperature.

Figure 1 contrasts the sea-surface temperatures (SSTs) in the tropical Atlantic in June 1983 and June 1984. The higher SSTs in 1984 were associated with exceptionally heavy rainfall over northeastern Brazil and the coastal zone of southwestern Africa but were also associated with a persistence of the drought in the Sahel, the region to the south of the Sahara desert. This happened because the Intertropical Convergence Zone¹ (ITCZ), the narrow east-west band of rising air, cloudiness, and heavy rainfall onto which the south-east and north-east trades converge, was displaced unusually far southward during 1984. Such a displacement of the ITCZ is also a feature of El Niño in the Pacific Ocean. However, the other important feature of El Niño, eastward movement of the atmospheric convective zone that is normally over the western equatorial Pacific, had no counterpart in the Atlantic during 1984. In the Pacific the eastward movement of the region of heavy rainfall and low sea-level pressure, towards the arid eastern equatorial Pacific where sea-level pressure is normally high, results in negatively correlated variations in the eastern and western sides of the ocean basin. During the warm event in the Atlantic, by contrast, the increase in rainfall and decrease in sea-level pressure was fairly uniform in the east-west direction.

The dominant change in the Atlantic was not a zonal one—the low-pressure convective zone over the Amazon Basin was not dislodged from the continent-but was a meridional one associated with the equatorward movement of the ITCZ. The ITCZ is the principal region of rainfall over the tropical Atlantic Ocean and the adjacent land. Seasonally it moves between the Equator and 15 °N, approximately, so that northeastern Brazil has a rainy season in March and April when the ITCZ is furthest south, whereas the Sahel (10 °N to 15 °N in west Africa) has a rainy season centred on August when the ITCZ is furthest north. Because of this dependence on the ITCZ for rainfall, latitudinal precipitation gradients are enormous: annual mean rainfall along the west African coast is 1,939 mm at Bissau (12 °N), 542 mm at Dakar (15 °N) and 123 mm at Nouakchott (18 °N). These statistics make it clear that slight variations in the position of the ITCZ, which has a very small north-south extent, have a major effect on rainfall variations in west Africa. The unusual southerly position of the ITCZ in 1984 contributed significantly to the persistence into 1984 of the drought in the Sahel, and to the heavy rainfall and floods in northeastern Brazil and the coastal zone of equatorial and southwestern Africa, including Angola.

Atmospheric convective zones over the ocean are usually over the warmest surface waters. The ITCZ, for example, is in the neighbourhood of the Equator when SSTs in that region are at

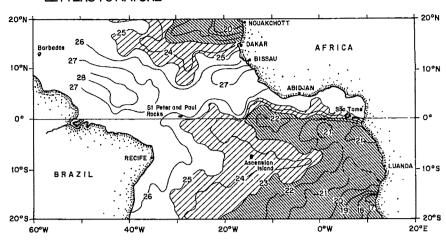
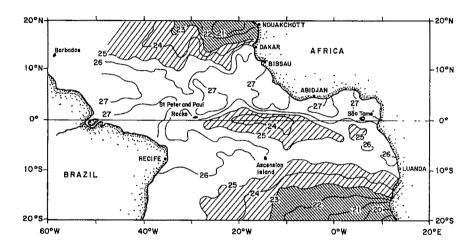


Fig. 1 Sea-surface temperatures (°C) in the tropical Atlantic Ocean in June 1983 (top) and June 1984 (bottom).



a maximum (March and April) and it moves northward when SSTs at, and to the south of the Equator in the central and eastern Atlantic start to fall. Interannually, southward displacement of the ITCZ is correlated with, and in models is effected by, an increase in SST to the south of the Equator and a simultaneous decrease in SST farther north^{2,3}. SST variations in the tropical Atlantic, therefore, influence rainfall variations over Africa and Brazil. There are, however, other factors that influence the position of the ITCZ and the rainfall. Palmer³ finds that, in a general circulation model of the atmosphere, SST variations in the tropical Pacific Ocean have a significant effect on the position of the ITCZ over the Atlantic Ocean. This result suggests that the atmospheric convergence onto the region of unusually high SST in the eastern tropical Pacific in 1983 was the cause of the intense trade winds over the Atlantic in 1983. Palmer's calculations indicate that the high SST in the Atlantic during 1984 should have weakened the trade winds over the Pacific. Such a weakening was not observed—the trade winds over the Pacific were stronger than usual in 1984—possibly because SST in the tropical Pacific during 1984 were much lower than normal. There are factors, other than SST, that influence the atmospheric circulation in the tropics. For example, it has been suggested that an expansion of the Northern Hemisphere circumpolar vortex and an equatorward displacement of the subtropical high-pressure belt affect the tropical circulation and the rainfall of the Sahel⁴⁻⁷. The degree to which SST variations in the tropical Atlantic affect rainfall in the Sahel appears to be modest⁸ but there are indications that these SST variations have a more pronounced effect on rainfall over northeastern Brazil and southwestern Africa.

SST variations over large parts of the ocean are determined primarily by changes in the local flux of heat across the ocean surface. In the tropical oceans, however, SST variations are

strongly influenced by changes in the large-scale oceanic circulation, in response to changes in the surface winds. On seasonal and interannual timescales the strength of the wind determines the intensity of the oceanic circulation and the magnitude of the associated thermal gradients in the ocean. These gradients are reflected in SST patterns. For example, SST is uniformly high in March and April when the winds are relaxed and drive a weak circulation. The seasonal strengthening of the winds in May intensifies the oceanic circulation and increases the horizontal thermal gradients both in the surface and subsurface. The strong westward surface flow to the south of 3°N now transports warm surface waters from the Gulf of Guinea in the east to the western side of the ocean basin so that SST is much lower in the southeastern equatorial Atlantic than in the west. The unusually weak surface winds in 1984 maintained relatively small thermal gradients in the tropical Atlantic Ocean, primarily because isotherms in the Gulf of Guinea were exceptionally deep during the early months of 1984 (refs 9-11). An unusual eastward current between the Equator and 5 °S carried warm water into the Gulf of Guinea. Some of this water flowed southward along the African coast and suppressed coastal upwelling as far south as Angola and Namibia¹². Simulations of oceanic conditions in the tropical Atlantic during 1984 with a realistic general circulation model are in progress and should provide a coherent picture of how the circulation changed during the warm event.

From an oceanographic point of view, the unusual conditions in the tropical Atlantic Ocean during 1984 were caused by changes in the surface winds. From a meteorological point of view, the unusual winds were in part attributable to changes in the SST. This circular argument suggests that interactions between the ocean and atmosphere were of central importance. These interactions are crucial both seasonally and interannually.

(The large seasonal variations in SST near the Equator both influence the movements of the ITCZ and are influenced by the movements of the ITCZ which determine changes in the surface winds.) Interannual variations in the Atlantic Ocean can be viewed as perturbations to the seasonal cycle. In 1984, the seasonal migrations of the ITCZ took it further south than normal and it remained in a southerly position longer than normal. An unusual southward displacement of the ITCZ is also a feature of El Niño events in the Pacific Ocean. An additional feature of El Niño, but apparently not a feature of interannual variability in the Atlantic, is an eastward displacement of atmospheric convective zones at the western extreme of the ocean basin. Most studies 13-15 of interactions between the ocean and atmosphere in the tropics concern this zonal movement of convective zones. Studies of the air-sea interactions and the other factors that control the latitudinal movements of the ITCZ will shed light not only on phenomena such as droughts in western Africa and northeastern Brazil, but also on El Niño.

Finally, how often do warm events such as that of 1984 occur? The previous warm event with a comparable amplitude to the south of the Equator occurred in 1963 when the arid regions of southwestern Africa experienced severe floods, and a suppression of the coastal upwelling. However, the few available long time-series records show that there is considerable variability from year to year8. This variability is associated with the timing of the major feature of the seasonal cycle, the northward movement of the ITCZ. This movement starts abruptly so that the associated intensification of the south-east trades is sudden. In some (cold, dry) years, this happens as early as February, in some (warm, wet) years as late as June. Over the next decade, special oceanographic and meteorological measurements will be made in the tropical Atlantic to document this variability. This will be part of the international TOGA program, to study interannual variability of the tropical oceans and global atmosphere, over a 10-year period that started in 1985.

Received 17 January: accepted 18 April 1986.

- Horel, J. D., Kousky, V. E. & Kagano, M. T. Nature 322, 248-251 (1986).
 Moura, A. D. & Shukla, J. J. atmos. Sci. 38, 2653-2675 (1981).
- 3. Palmer, T. N. Nature 322, 251-253 (1986).
- Winstanley, D. Nature 243, 464-465 (1973)
- Winstanley, D. Nature 245, 190-194 (1973).
- Angell, J. K. & Korshover, J. Mon. Weath. Rev. 102, 669-678 (1974). Lamb, P. J. Tellus 30, 240-251 (1978).

- Lamb, P. J. Tellus 30, 240-251 (1978).
 Lamb, P. J., Peppler, R. A. & Hastenrath, S. Nature 322, 238-243 (1986).
 Hisard, P., Henin, C., Houghton, R., Piton, B., & Rual, P. Nature 322, 243-245 (1986).
 Katz, E. J., Hisard, P., Verstraete, J.-M. & Garzoli, S. L. Nature 322, 245-247 (1986).
 Weisberg, R. & Colin, C. Nature 322, 240-243 (1986).
 Shannon, L. V., Boyd, A. J., Brundrit, G. B. & Taunton-Clark, J. J. mar. Res. (in the press).
 Philander, S. G. H., Yamagata, T. & Pacanowski, R. C. J. atmos. Sci. 41, 604-613 (1984).
 Cane, M. A. & Zebiak, S. E. Science 228, 1085 (1985).

- 15. Anderson, D. L. T. & McCreary, J. P. J. atmos. Sci. 42, 615-629 (1985).

Interannual variability in the tropical Atlantic

Peter J. Lamb*, Randy A. Peppler* & Stefan Hastenrath†

* Climate and Meteorology Section, Illinois State Water Survey, Champaign, Illinois 61820, USA

† Department of Meteorology, University of Wisconsin, Madison, Wisconsin 53706, USA

The anomalous meteorological and oceanic conditions in the tropical Atlantic basin during 1983-84 can be seen as an extreme example of a common historical pattern. Here we present time series of rainfall in subsaharan West Africa (SWA) and north-east Brazil (NEB), which show that departures in 1983-84 were severe, but not unprecedented. The associated sea surface temperature (SST) anomaly patterns included one that had previously been shown to accompany earlier years of extreme rainfall in SWA and NEB, and others that contained key elements of that pattern. The pattern concerned was recently shown to be a major mode of tropical Atlantic SST variation.

Figure 1 documents the interannual variation of rainfall in two contrasting parts of the tropical Atlantic basin, SWA (11-18° N) and NEB (3-8° S). Their rainy seasons, which occur at different times of the year (July-September core in SWA and March-April core in NEB), are associated with the two extremes of the annual cycle of the latitudinal position of the Intertropical Convergence Zone (ITCZ)¹. Each time series shown contains the yearly averages of normalized departures for a fixed set of stations (20 in SWA, 30 in NEB). The value for the year j is given by

$$\dot{X}_{j} = \frac{1}{N_{i}} \sum_{i=1}^{N_{j}} \frac{r_{ij} - \bar{r}_{i}}{\sigma_{i}}$$

where r_{ij} is that year's rainfall total at station i, \bar{r}_i and σ_i are respectively the mean and standard deviation of station i's yearly totals for the base period used (1941-82 for SWA, 1913-56 for NEB), and N_i is the number of stations with complete records in year j. The statistical advantages of this rainfall index formulation were originally summarized by Kraus², and its viability has

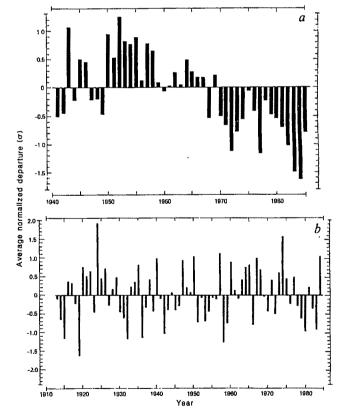
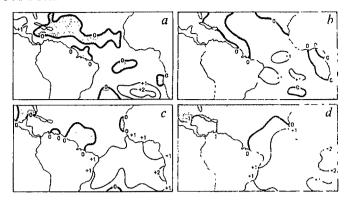


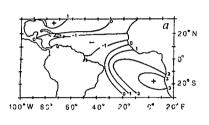
Fig. 1 Time series of yearly averages of normalized rainfall departures (in units of σ) for a, subsaharan West Africa (April-October) for 1941-85, and b, north-east Brazil (March-April) for 1913-84.

been confirmed by Katz and Glantz³. Further details on its use in this context appear in refs 4-6, where earlier versions of the time series were previously published for 1941-82 (SWA) and 1912-73 (NEB).

It is clear from Fig. 1 that 1983-84 was a period of anomalous rainfall in both SWA and NEB. Those two years were SWA's driest during 1941-84, and constituted the most recent extension

Fig. 2 Sea surface temperature (SST) anomaly maps (°C) for January 1983 (a), August 1983 (b), March 1984 (c) and August 1984 (d), from ref. 13. The March 1983 map would have been a better indicator of conditions during the NEB rainy season than that for January 1983, but was not available.





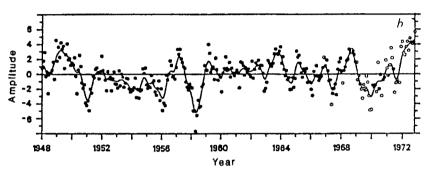


Fig. 3 Principal component 2 extracted from monthly normalized SST departures for 1948-72 (from ref. 12). a, Loadings multiplied by 10; b, amplitudes, with curve showing the result of applying a 13-point low-pass filter.

of a drought that has persisted, with very little respite, since 1968 (Fig. 1a). The widespread severity of the 1983-84 SWA drought conditions is fully documented in refs 7 and 8. Rainfall in that zone was also extremely deficient in 1972, 1977 and 1982, and moderately deficient during several other years since 1968, including 1985. Three moderately severe SWA drought years also occurred in the 1940s. The period spanning 1950-58, in contrast, was one of abundant rainfall in SWA, with strong positive departures in most of these years; weaker positive departures characterized 1959-67. SWA has thus experienced a pronounced decline of rainfall since the early 1950s.

In contrast to SWA, the anomalous 1983-84 rainfall in NEB consisted of both an extremely dry (1983) and an extremely wet (1984) year (Fig. 1b); each was among the 6-8 driest/wettest since 1913, and both ranked second in that regard for 1959-84. The stronger anomalies for this region are scattered throughout the record, which exhibits pronounced year-to-year variation. NEB rainfall shows little evidence of long-term trend, unlike that for SWA (Fig. 1). Hastenrath and Kaczmarczyk⁹ found that the variance of NEB rainfall includes a stronger high-frequency component (for example, periods of 2.5 and 5 yr) than does that of the Senegal river discharge, which reflects SWA rainfall. Much of the Senegal variance is centred on 30 yr, as is implied by the SWA time series in Fig. 1a, while NEB has a substantial portion of its interannual variance concentrated around 14 years. Preliminary reports (not shown) suggest that NEB rainfall was as abundant in 1985 as in 1984.

Figure 1 of ref. 10 documents the large-scale tropical Atlantic SST fields of June 1983 (a month lying between very deficient NEB and SWA rainy seasons; see Fig. 1 and discussion above) and June 1984 (lying between most abundant NEB and very deficient SWA rainy seasons). When converted to anomaly form, the 1984 pattern (see Fig. 2c, d) in particular is extremely similar to the one which has previously been shown to accompany earlier SWA drought and NEB flood years. That pattern, which was first identified by Lamb¹¹ (for SWA drought) and Hastenrath and Heller⁶ (for NEB flood), contains warmer than average surface water to the south of 10° N and east of 30° W, a feature that extends to at least 20° S, and colder than average surface

water to its immediate north and west. This pattern has been confirmed by the recent work of Lough¹², who showed it is a major mode of variation of tropical Atlantic SST (Fig. 3). The results of Lamb¹¹ and Lough¹² (including Fig. 3) collectively suggest that the above pattern has characterized many deficient SWA rainy seasons (for example, those in 1913, 1921, 1949, 1968, 1972 and, to a lesser extent, 1971), and did not occur during two periods (1927-34, 1950-56) when SWA was droughtfree (see Fig. 1). Furthermore, the magnitude of the pattern's correlation with SWA rainfall, as obtained using Lough's¹² principal component amplitudes shown in Fig. 2, is in the range 0.51-0.66 (26-44% of rainfall variance explained), depending on the timescale of the analysis. Hastenrath and Heller⁶ found that the same anomaly pattern characterized an SST composite for 10 extremely wet NEB years, and that the opposite pattern emerged from a treatment of 10 extremely dry NEB years.

Although the above SST anomaly pattern was not fully present during the very deficient 1983 SWA rainy season (Fig. 2b), the strong positive departures centred on the Equator probably displaced the zone of maximum SST southwards of its long-term average position. Lamb11 found the latter displacement to be an important consequence of the above SST anomaly pattern, and one that coincided with SWA drought. Note also that the positive SST departures in August 1983 were stronger between 5° N and 20° S than between 5 and 20° N. The SST anomaly field just before the deficient 1983 NEB rainy season (Fig. 2a) was also different in part from the NEB drought SST pattern described above. However, Fig. 2a does display the relatively large pool of abnormally cold water to the south of the Equator and the predominance of positive SST departures between 0 and 10° N. The 0-10° S SST anomaly pattern changed considerably from January to August of 1983 (Fig. 2a, b), in contrast to 1984 (Fig. 2c, d).

This research was partially supported by NOAA grants NA86AA-D-MC007 and NA86AA-D-AC065 and NSF grant ATM 84-13575. P.J.L. is also affiliated with the Department of Atmospheric Sciences, University of Illinois. We thank Phyllis Stone, Rebecca Runge and Linda Riggin for technical assistance.

Received 10 April: accepted 9 June 1986.

- Hastenrath, S. Mon. Weath. Rev. 112, 1097-1107 (1984).
 Kraus, E. B. Mon. Weath. Rev. 105, 1009-1018 (1977).
 Katz, R. W. & Glantz, M. H. Mon. Weath. Rev. 114, 764-771 (1986).
- Lamb, P. J. Nature 299, 46-48 (1982).
- Lamb, P. J. J. Clim. 3, 419-422 (1983).

- Lamb, P. J. J. Clim. 3, 419-422 (1985).
 Hastenrath, S. & Heller, L. Q. Jl R. met. Soc. 103, 77-92 (1977).
 Lamb, P. J. Z. Gletscherk. Glazialgeol. 21, 131-139 (1985).
 Nicholson, S. E. J. Clim. appl. Met. 24, 1388-1391 (1985).
 Hastenrath, S. & Kaczmarczyk, E. B. Tellus. 33, 453-462 (1981).
- 10. Philander, S. G. H. Nature 322, 236-238 (1986). 11. Lamb, P. J. Tellus 30, 240-251 (1978); Mon. Weath, Rev. 106, 482-491 (1978); Clim. Monit.
- 11, 46-49 (1982). 12. Lough, J. M. Mon. Weath. Rev. 114, 561-570 (1986).
- 13. Climate Diagnostics Bulletin (Climate Analysis Center, Washington, February 1983, August 1983, March 1984, August 1984).

Equatorial Atlantic Ocean temperature and current variations during 1983 and 1984

Robert H. Weisberg* & Christian Colin†

* Department of Marine, Earth, and Atmospheric Sciences, North Carolina State University, Raleigh, North Carolina 27695-8208, USA † ORSTOM, 24 Rue Bayard, 75008 Paris, France

The equatorial regions of the Earth's oceans are climatically sensitive ones because of the zonal sea-surface temperature contrasts observed there1. Equatorial sea-surface temperature normally varies on an annual cycle with the prevailing trade winds but deviations from this cycle may have significant global implications as occurred for example during the 1982-83 Pacific Ocean El Niño/Southern Oscillation event². Understanding the annual and interannual variability of the tropical oceans has therefore been the goal of several measurement programmes. In the Atlantic Ocean, the Seasonal Response of the Equatorial Atlantic (SEQUAL) Experiment and the Programme Francais Ocean et Climat dans l'Atlantique Equatorial (FOCAL) have provided a basin-wide and synoptic data set over two annual cycles. We present here results from surface moored current meters which were one of several fixed and shipborne measurement systems employed by SEOUAL and FOCAL. We will describe the evolution of the upper ocean thermal and zonal velocity component variations in relation to forcing by the trade winds, show differences observed along the Equator at 28° W and 4° W, and compare the oceans responses at these locations during 1983 and 1984. The synoptic data realizations of these years differed from climatology and these differences are related to the rapidly varying nature and intensity of the wind stress in a given year. Changes in wind stress from year to year result in interannual variability as a modulated annual cycle and 1984, a year of weak winds relative to 1983, offers a case in point. The zonal sea-surface temperature gradient vanished along the Equator in 1984 during the season when it normally would have been a maximum.

The data were collected using vector averaging current meters suspended beneath taut moored surface buoys at depths of 10, 50, 75, 100, 150, and 200 m on the Equator at 28° W and at depths of 10, 35, 60, 85, and 110 m, on the Equator at 4° W. Sampling intervals for velocity and temperature were 15 min and these data have been low pass filtered to exclude fluctuations occurring at timescales shorter than 10 days to focus on the

Essentially, it is the zonal integral of easterly wind stress near the Equator that causes the annual cycle in the upper equatorial ocean velocity and temperature fields. Currents are generated which redistribute mass and together with equatorial long waves emanating from the boundaries these provide the mechanisms by which the ocean tends to adjust to the large-scale wind stress variations^{3,4}. Time series of surface wind velocity were collected during SEQUAL and FOCAL at St Peter and Paul Rocks (1° N, 29° W) and from buoys moored along the Equator at 24° W, 15° W and 4° W. The former are the most complete and they are representative of the temporal variations over the western twothirds of the equatorial Atlantic⁵⁻⁷. Katz et al.⁸ show the details of the wind stress variability during 1983-84 and the following large-scale features are noted for qualitative discussion. During 1983 the easterly component of surface wind stress intensified rapidly beginning in mid-April and remained strongly developed through mid-December. It then relaxed rapidly and remained weak through mid-May before intensifying rapidly again. Immediately before the seasonal intensifications during both years were short lived (around one week) relaxation events where the already weak easterlies got even weaker or reversed to become westerlies.

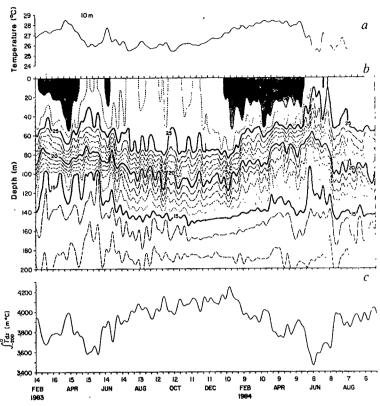
The effects of these variations in easterly wind stress on the upper ocean thermal and eastward velocity component fields are apparent in the SEQUAL and FOCAL data. Figure 1 shows the temperature variability over the upper 200 m on the Equator at 28° W along with the temperature at 10 m which is approximately equal to sea-surface temperature (SST) and the verticallyintegrated temperature which is proportional to heat content. Beginning in mid-April 1983, and coincident with the onset of increasing easterlies, a rapid shoaling of the isotherms and an attendant reduction in heat content is observed. This proceeds for around 1 month after which the isotherms deepen and the heat content increases to a relatively steady state lasting from August to December. Beginning in mid-December 1983 and coincident with the relaxation in easterly wind stress is a further deepening of the isotherms and an increase in heat content (peaking around mid-January) followed by shoaling through April. The thermocline has now completed one cycle in response to the winds and a repetition of this begins again during mid-May 1984 when the easterly wind stress intensifies again. The responses of the thermocline on the Equator at 28° W to the annual large-scale variations in easterly wind stress may, therefore, be summarized as sequences of shoaling and deepening (or conversely) leading to adjusted states. Accompanying these transitions are changes in the vertically-integrated temperature or heat content.

SST behaves differently to the thermocline depth. Note that while SST decreases to a minimum as the thermocline shoals beginning in mid-April 1983, it then remains low even after the thermocline has deepened to its adjusted state. In so doing, minimum SST on the Equator at 28°W coincides with a deepened thermocline and increased local heat content. The opposite occurs following the mid-December easterly wind stress relaxation resulting in maximum SST on the Equator at 28°W after the thermocline has shoaled and the local heat content has decreased.

Corresponding plots for the eastward velocity component, its vertical integral, and surface value are shown in Fig. 2. The flow is primarily eastward over the entire 200 m domain with only intermittent westward flow at the surface associated with the south equatorial current (SEC). The core of the equatorial undercurrent (EUC) is observed between 50 and 100 m and its position moves downward with the thermocline as the latter adjusts to increased easterly wind stress around June and July of both 1983 and 1984. While the vertical position of the EUC core migrates annually with the thermocline a clear annual variation in EUC speed or transport is not readily apparent.

Similar plots for the temperature and eastward velocity component observed on the Equator at 4°W are shown in Figs 3 and 4 respectively. The thermocline at 4°W also undergoes a sequence of shoaling followed by deepening beginning in Mid-April 1983 and again in mid-May 1984, and a sequence of deepening followed by shoaling beginning in mid-December 1983. Several important differences between the responses at both longitudes are evident, however. First, the shoaling/deepening and deepening/shoaling sequences at 4° W are of longer duration and larger magnitude than those at 28° W.

Fig. 1 Thermal structure observed over the upper 200 m on the Equator at 28° W from February 1983 to October 1984. a, The temperature at 10-m depth; b, isotherm depths as a function of time; c, vertically integrated temperature proportional to heat content. The data have all been low pass filtered to remove fluctuations with timescales <10 days. Temperatures >27°C are stippled to highlight the warmest surface temperatures relative to the thermocline depth.



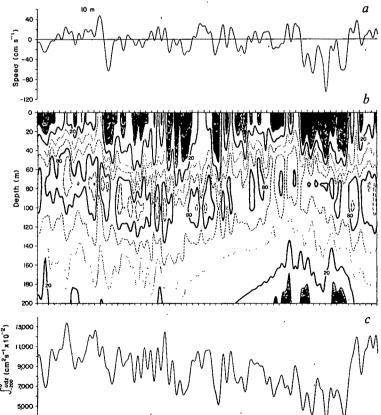
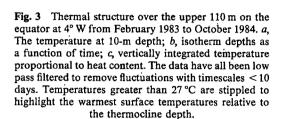
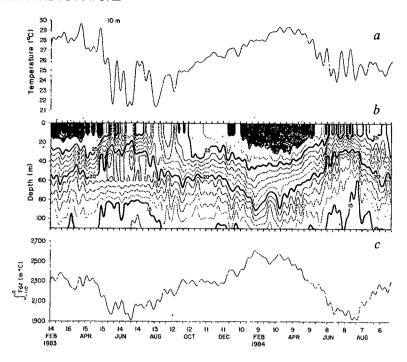


Fig. 2 Eastward component of velocity (u) observed over the upper 200 m on the Equator at 28° W from February 1983 to October 1984. a, u at 10 m depth; b, u isotach depths as a function of time; c, the vertical integral of u. The data have all been low-pass filtered to remove fluctuations with timescales <10 days. Regions of westward flow are stippled.

This is true for both the vertical position of a given isotherm within the thermocline as well as for SST. Not only does the Gulf of Guinea have the coldest SST along the Equator in the Atlantic Ocean during summer, it also has the warmest SST during winter. Owing to the increased duration of the response sequences the annual variations show a more sinusoidal appear-

ance at 4° W than at 28° W (where the thermocline attained an adjusted equilibrium to increased easterly wind stress for several months in 1983). Because it takes longer for the thermocline at 4° W to adjust to increased easterlies than at 28° W, SST is more nearly in phase with the thermocline at 4° W although SST still remains low even after the thermocline begins to deepen there.





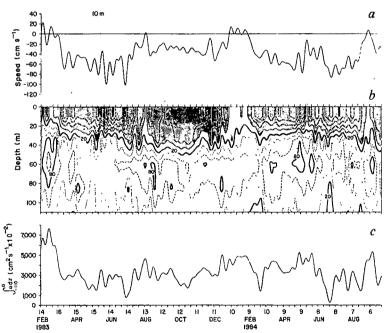


Fig. 4 Eastward component of velocity observed over the upper 110 m on the Equator at 4° W from February 1983 to October 1984. a, u at 10-m depth; b, u isotach depths as a function of time; c, the vertical integral of u. The data have all been low-pass filtered to remove fluctuations with timescales <10 days. Regions of westward flow are stippled.

Second, we observe an additional shoaling period at 4°W between October and December 1983 which is not evident at 28°W. Third, the deepening response at 4°W beginning in mid-December 1983 is much more pronounced than that at 28°W resulting in a well-defined peak in vertically integrated temperature at 4°W during February and March 1984. The corresponding change in dynamic height between the surface and 110 m due to the increased temperature is ~8 dynamic cm in agreement with the FOCAL hydrographic section data obtained at that time⁸.

In the zonal velocity component, the principal difference between 4° W and 28° W is a much more persistent and stronger westward SEC on the surface at 4° W. Below the surface and down to the observational limit of 110 m the flow is eastward and the position of the EUC core deepens with the thermocline as at 28° W.

Before SEQUAL and FOCAL our view of the annual cycle was based on climatologically-averaged monthly fields derived

from decades of ship reports⁹⁻¹¹. Linear and non-linear numerical models¹²⁻¹⁴, driven by climatological wind fields, have been successful in emulating the vertically integrated climatological thermal field. The new basin-wide synoptic data show significant differences between the annual cycle of a given year and the climatological mean annual cycle. Rather than a slowly varying response nearly in phase with the easterly wind stress component the thermocline undergoes sequences of deepening and shoaling varying in both duration and magnitude along the Equator. These differences are related¹⁵ to the rapidly varying nature of the wind stress observed in any given year versus the slowly varying nature of the climatology; a property inherent in averaging data from many years with varying phase. Historical shipboard observed wind data when displayed by individual years 16 rather than averaged show that rapid transitions are, indeed, the normal occurrence. Variations in the wind stress development from year to year will, therefore, give rise to interannual variability as a modulated annual cycle and this is evident in comparing the 1984 and 1983 responses; years of relatively weak and strong surface easterlies respectively^{8,17}. At 28° W, the shoaling portion of the annual cycle shows the 20°C isotherm some 20 m higher in May and June 1984 than in 1983. At 4° W. the deepening portion of the cycle shows the 20 °C isotherm some 30 m deeper in February and March 1984 than in 1983. The zonal distribution of upper ocean heat content was therefore different during these years with more heat in the eastern side of the basin during 1984.

SST along the Equator was also quite different. In 1984, from June to August, SST was roughly 1 °C colder at 28° W (25 °C versus 26 °C) and 3 °C warmer at 4° W (24.5 °C versus 21.5 °C) than over the same period in 1983. Consequently, during the cold season of 1984, the zonal SST gradient along the Equator had essentially vanished when it normally should have been a maximum. During the warm season (February and March) SST was warmer by roughly 1 °C at both 28 °W and 4° W in 1984 than in 1983. These SST differences seem to be linked with the differences reported in the position of the Intertropical Convergence Zone¹⁷ during these years.

While vertically integrated temperature and SST both differed from 1983 to 1984 it is reiterated that these two quantities are not related in a simple manner. At 28° W minimum SST coincides with a deepened thermocline. At 4°W minimum SST occurs while the thermocline is deepening. In either case, vertically integrated upper ocean temperature or heat content alone is not adequate to account for air-sea heat exchange since this process depends on SST.

Variations in the velocity field appear to be more complicated than those in the temperature field and the relative importance of horizontal and vertical advection in the heat balance has not yet been assessed. Note that at 28° W during March-June 1983 the transport per unit width on the Equator was nearly double the amount observed during those months in 1984.

We have presented a subset of the SEQUAL and FOCAL moored current meter data showing the evolution of the annual cycle in upper ocean zonal currents and temperature along the Equator. Differences found between climatological data inference and synoptic data realization are related to the rapidly varying nature of the easterly surface wind stress component observed in any given year versus the slowly varying climatology. In 1984, a year of relatively weak winds compared with 1983, the eastern portion of the basin showed increased values of vertically integrated temperature and SST during the winter/spring and summer seasons respectively. These changes in the zonal distribution of temperature along the Equator in the Atlantic Ocean have similarities with the El Niño occurrences in the Pacific Ocean.

This work was supported by the Oceanography Section, NSF under grant number OCE-8211848 and by ORSTOM, Paris. We thank T. Y. Tang and T. Weingartner for helpful discussions.

Received 21 January; accepted 16 April 1986.

- Bjerknes, J. Tellus 18, 820-828 (1966).
 Rasmusson, E. M. & Wallace, J. M. Science 222, 1195-1202 (1983).
- 3. Moore, D. W. & Philander, S. G. H. in The Sea Vol. 6 (eds Goldber, E. et al.) 319-361 (Wiley-Interscience, New York 1977).
 4. Cane, M. & Sarachik, E. S. J. mar. Res. 35, 395-432 (1977).
 5. Garzoli, S. & Katz, E. J. Geophys. Res. Lett. 11, 715-718 (1984).

- 5. Katz, E. J. Geophys. Res. Lett. 11, 726-728 (1984).
 7. Payne, R. E. Geophys. Res. Lett. 11, 719-721 (1984).
 8. Katz, E. J., Hisard, P., Verstraete, J. M. & Garzoli, S. L. Nature 322, 245-247 (1986).
 9. Hastenrath, S. & Lamb, P. J. Climatic Atlas of the Tropical Atlantic and Eastern Pacific
- Ocean (University of Wisconsin Press, 1977).

 10. Hellerman, S. Deep-Sea Res. Suppl. II 26, 63-75 (1979).

 11. Merle, J. Tran. Doc. ORSTOM 82 (1978).
- 12. Busalacchi, A. J. & Picaut, J. J. phys. Oceanogr. 13, 1564-1588 (1983).
- Busslacchi, A. J. & Ficaut, J. J. pnys. Oceanogr. 13, 1504-1588 (1985).
 Philander, S. G. H. & Pacanowski, R. C. Geophys. Res. Lett. 11, 802-804 (1984).
 du Penhoat, Y. & Treguier, A. M. Geophys. Res. Lett. 11, 799-801 (1984).
 Weisberg, R. H. & Tang, T. Y. J. geophys. Res. 90, 7117-7128 (1985).
 Servain, J., Picaut, J. & Merle, J. J. Phys. Oceanogr. 12, 457-463 (1982).

- 17. Horel, J. D., Kousky, V. E. & Kagano, M. T. Nature 322, 248-251 (1986).

Oceanic conditions in the tropical Atlantic during 1983 and 1984

P. Hisard*, C. Henin*, R. Houghton†, B. Piton‡ & P. Rual#

- * ORSTOM/LPDA, Universite Pierre et Marie Curie, 4 Place Jussieu, 75005 Paris, France
- † Lamont-Doherty Geological Observatory of Columbia University, Palisades, New York, 10964, USA
- ‡ ORSTOM/COB, BP 337, Brest, France

During 1983 and 1984 oceanographers from France and the USA conducted an extensive field programme in the tropical Atlantic Ocean. The principal goal was to document the annual cycle, but unexpectedly a difference was observed between the two years. We describe here the observed variations in the thermal field and in the zonal currents along several meridians. In early 1984, the upper ocean especially on the eastern side of the ocean basin was substantially warmer than during the corresponding period a year earlier. Most of this change in the heat content was the result of a deeper thermocline. During this time an unusual eastward surface current appeared to the south of the Equator undoubtedly contributing to large zonal heat fluxes. The decrease in the surface winds¹ between 1983 and 1984 is presumably responsible for these changes. Inspection of the few available long records reveals that in the Atlantic warm events such as that of 1984 are rare and that the previous event with comparable amplitude occurred in 1963.

Oceanic conditions in the tropical Atlantic have a pronounced annual cycle which is almost in phase with the annual changes in the surface winds. When the winds near the Equator are relaxed, in March and April, horizontal thermal gradients are at a minimum and the surface currents are weak and westward. These currents feed the Brazilian coastal current which flows northwestward into the Gulf of Mexico. The intensification of the south-east trade winds from May onwards results in a dramatic change in the oceanic circulation. The westward surface flow, to the south of 3° N approximately, accelerates while an intense eastward surface current appears between 3° N and 9° N approximately². The Brazilian coastal current now veers offshore near 5° N to maintain the eastward flow3. The associated changes in the thermal field include a deepening of the isotherms in the western equatorial Atlantic, especially in the neighbourhood of 3° N, and an elevation of isotherms of the Gulf of Guinea and near 9° N in the western side of the ocean basin⁴. These changes in the thermal structure affect the sea-surface temperatures which decrease at, and to the south of, the Equator in the central and eastern Atlantic once the south-east trade winds start to strengthen.

The field work conducted in 1983 and 1984 was part of the Seasonal Response of the Equatorial Atlantic (SEQUAL) and Français Ocean et Climat dans l'Atlantique (FOCAL)

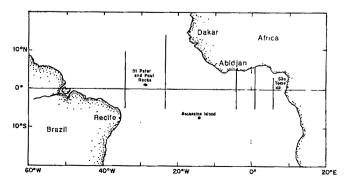


Fig. 1. Equatorial Atlantic Ocean with the meridional sections used in this study.

programmes, and it provided extensive observations of the thermal structure in the equatorial Atlantic during that period. Preliminary results from the first year (1983) measurements are given elsewhere⁵. Data for this study were derived from several sources. These include meridional hydrographic sections along 34° W, 23° W, 4° W, 1° E and 6° E (Fig. 1) that were made four times each year by the research vessels *Capricorne* and *Nizery*. On these sections, temperature and salinity were measured by means of a CTD (conductivity temperature/depth), currents were measured by means of a profiler⁶ at the station locations shown in Fig. 2. Additional data were derived from aircraft and ship-of-opportunity expendable bathythermographs.

We shall confine our discussion to the temperature structure along 23° W, 4° W and 6° E measured in January-February and in July-August of 1983 and 1984. The depth of the 20 °C isotherm along these sections is shown in Fig. 2. The 20 °C isotherm lies within the thermocline and is thus representative of the thermal structure in the upper 100 m of the water column. The most striking difference between the sections made in the two years is the increase in the average temperature of the upper ocean. between February 1983 and February 1984. This warming was most pronounced in the Gulf of Guinea where the thermocline in some places was 30 m deeper than normal in February 1984 throughout the entire section. The equatorial temperature profiles shown in Fig. 3 illustrate this change. In 1983, the thermocline depth was approximately equal to the climatological mean value, whereas in 1984 it was approximately three standard deviations below the mean. This condition was so anomalous that in January and February 1984 the thermocline which usually slopes downward to the west was practically horizontal⁸. Time series measurement along the Equator indicate that the unusual warming started as early as November 1983 and persisted into May 1984. The warm water that accumulated in the Gulf of Guinea was unusually saline which indicates that its origin was the western side of the ocean basin.

Sections along 23°W show that the meridional gradient of shallow isotherms (not shown in Fig. 2) increased significantly to the south of the Equator between February 1983 and February 1984. This implies an eastward geostrophic current between the Equator and 5°S in February 1984. Normally the surface flow in this region is westward. Direct measurements with current profilers averaged over 0-20 m depth confirm this unusual eastward current which penetrated into the Gulf of Guinea (Fig. 4). The current is absent from sections made in April 1984 but appears again in July 1984. Presumably this current played an important role in transporting warm saline surface waters into the Gulf of Guinea thus increasing the average temperature of the upper ocean in that region. There is evidence that the eastward north equatorial countercurrent, to the north of 3° N. also contributed to the unusual accumulation of warm surface waters in the eastern equatorial Atlantic. Some of this warm water flowed southward along the African coast and may be a factor in inhibited coastal upwelling as far south as Angola and Namibia¹⁰.

The change in the surface winds^{1,8} between 1983 and 1984 was presumably responsible for the change in the oceanic circulation between those two years. The westward winds maintain the zonal density gradients in the ocean so that the unusually weak winds in early 1984 resulted in the reduction of the zonal slope of the thermocline during January and February and the associated eastward transfer of warm surface waters. That this transfer occurred primarily in the eastward current to the south of the Equator, and in the eastward north equatorial countercurrent to the north of 3° N approximately, suggests that there were significant changes in the curl of the wind during 1984. The curl is large in the neighbourhood of the Intertropical Convergence Zone (ITCZ) which is usually over the north equatorial countercurrent to the north of 3° N. It is intriguing that from satellite cloud images in early 1984 a second ITCZ was observed to the south of the Equator where the unusual eastward current

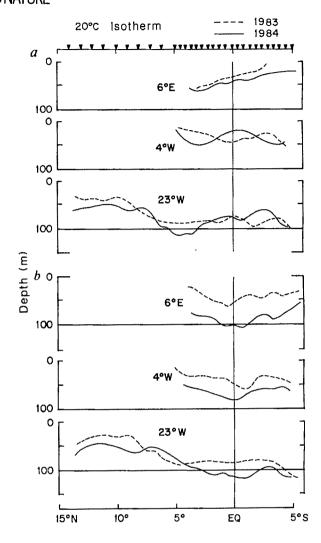


Fig. 2 Meridional sections of the depth of the 20 °C isotherm along 6° E, 4° W, and 23° W longitude during July-August (a) and January-February (b) for 1983 (dashed line) and 1984 (solid line).

CTD station locations indicated at top.

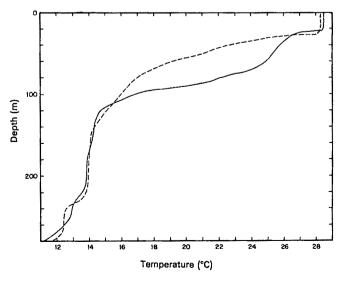


Fig. 3 Profiles of the temperature on the Equator at 4°W in February 1983 (dashed line) and 1984 (solid line).

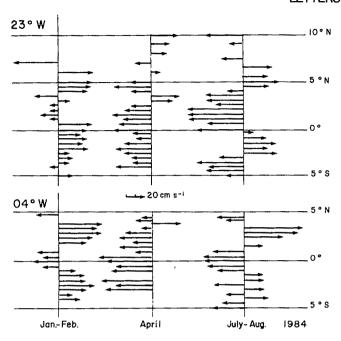


Fig. 4 The zonal component of the 0-20 m surface currents (arrows to the right are eastward) as measured along 23°W and 4° W in January-February, April and July-August 1984.

appeared (J. Citeau and B. Guillot, personal communication). The relations between this current, the ITCZ, and the curl of the wind are now being studied. Another topic under investigation is the relation between the north-westward flowing Brazilian coastal current and the eastward currents. This coastal current, as mentioned earlier, absorbs water from the westward currents and, in turn, maintains the eastward flow to the north fo 3° N approximately. It is not yet known whether the unusual eastward current to the south of the Equator in early 1984 was fed by the Brazilian coastal current.

There are many similarities between oceanographic conditions in the tropical Atlantic in 1984 and 1963 when a comparable warm event occurred. Not only were sea-surface temperatures exceptionally high in 1963, but there were also reports of unusual eastward surface currents to the south of the Equator, and of the intrusion of warm saline water into the coastal regions of Angola and Namibia where local coastal upwelling was inhibited¹¹⁻¹⁴. Occurrences such as these are very similar to but much less frequent than El Niño events in the Pacific Ocean. In the Atlantic, interannual variability on shorter timescales has a relatively small amplitude but is, nonetheless, of considerable interest because the physical processes involved in the major events are likely to be the same as those involved with smaller amplitudes.

This work was supported in part by ORSTOM and by the NSF (grant OCE 81-17554). We thank S. G. H. Philander for assistance. This is Lamont-Doherty Geological Observatory contribution no. 3967.

Received 17 January; accepted 18 April 1984.

- 1. Horel, J. D., Kousky, V. E. & Kagano, M. T. Nature 322, 248-251 (1986).
- Katz, E. J. & Garzoli, S. L. J. mar. Res. 40, 307-327 (1982).
- Bruce, J. G. & Kerling, J. L. Geophys. Res. Lett. 11, 779-782 (1984). Merle, J. & Arnault, S. J. mar. Res. 43, 267-288 (1985).
- Weisberg, R. W. (ed.) Geophys. Res. Lett. 11, 713-803 (1984). Duing, W. & Johnson, D. Deep Sea Res. 19, 259-276 (1972).

- 7. Houghton, R. W. J. phys. Oceanogr. 13, 2079-2081 (1983).

 8. Katz, E. J., Hisard, P., Verstraete, J. M. & Garzoli, S. L. Nature 322, 245-247 (1986).

 9. Weisberg, R. & Colin, C. Nature 322, 240-243 (1986).
- Shannon, L. V., Boyd, A. J., Brundrit, G. B. & Taunton-Clark, J. J. mar. Res. (in the press).
 Mazeika, P. A. J. geophys. Res. 73, 5819-5828 (1968).
 Reid, J. L. Nature 203, 182 (1964).
- Hisard, P. Oceanol. Acta 3, 69-78 (1980).
- 14. Voituriez, B. Oceanogr. Tropic. 18, 185-199 (1983).

Annual change of sea surface slope along the Equator of the Atlantic Ocean in 1983 and 1984

Eli Joel Katz*, Philippe Hisard†, Jean-Marc Verstraete‡ & Silvia L. Garzoli*

- * Lamont-Doherty Geological Observatory of Columbia University. Palisades, New York 10964, USA
- † Université P.-M. Curie, 4 Place Jussieu, 75230 Paris, France ‡ O.R.S.T.O.M., 195 Rue Saint Jacques, 75005 Paris, France

For two years beginning in October 1982, oceanographic observations were made in the equatorial Atlantic to investigate the relationship between sea level, wind stress, sea surface slope (zonal pressure gradient, thermocline depth) and equatorial currents. Here we describe the sea surface slope derived from three complementary methods: hydrographic stations, pressure gauges and inverted echo sounders. The latter two have the advantage of yielding continuous time series, but depend on the hydrographic stations for an absolute reference. Together, the three provide a detailed description of the temporal variation of the sea surface slope which is then compared to a wind-stress time series. The dominant signal, in both sea slope and wind stress, is the annual cycle, although amplitude and phase vary interannually. The annual increase in sea surface slope along the Equator in the western and central basins lags the onset of the south-east trade wind. During the boreal winter of 1983-84 a strong rise in sea level occurred against the African coast, accompanied by a levelling of the sea surface to the west. At the same time, an almost complete relaxation of eastward wind stress on the Equator was observed near the centre of the basin.

The sea surface along much of the Equator in the Atlantic and Pacific oceans slopes upward to the west. This slope reflects a shallowing of the thermocline toward the east and results in a zonal pressure gradient in the uppermost 100 m which is essential to the existence of the Equatorial Undercurrent¹. The

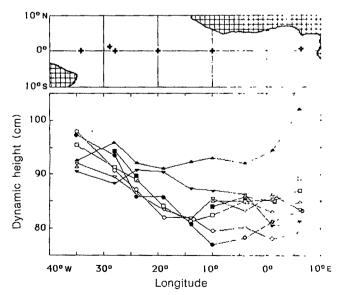


Fig. 1 Quarter-annual dynamic height of the sea surface, relative to 500 m. □ (■), October-November 1982 (1983); △ (▲), January-February 1983 (1984); ∇ (**V**), April-May 1983 (1984);) (**•**), July-August 1983 (1984). Individual points are either mendional averages of casts within 0.5° of the Equator or zonal averages of casts within a 5° band along the Equator. Locations of inverted echo sounders, a wind recorder and pressure gauges discussed in the text are indicated in the chart above. The shaded areas are the bounding continents.

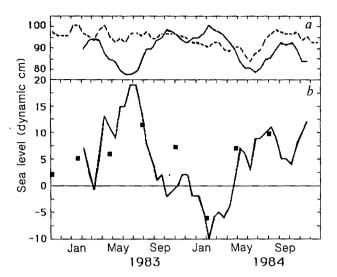


Fig. 2 Sea level difference (b) between St Peter and St Paul Rocks (29° W) and São Tomé island (7° E) . The individual traces are shown in a (dashed line, 29° W ; solid line, 7° E). The dynamic level at each site is determined by comparison with hydrocast dynamic height, 0 relative to 500 m. The differences in dynamic height from nearby hydrographic stations (near the Equator at 28° W and 6° E) are shown as points, although the casts were not simultaneous.

latter is a major zonal current in the tropics which, in 1979, transported an annual average of 20×10^6 m³ s⁻¹ of near-surface water from west to east in the Atlantic^{2,3}. A change in the mean level of the sea surface is a direct indication of a change in heat storage in the upper few hundred metres of that region, and a zonally differential change in mean level varies the acceleration force imposed on the fluid by the zonal pressure gradient.

The pressure gradient has a seasonal signal: weak in the boreal spring followed by a stronger gradient in the summer and autumn⁴⁻⁶. Six quasi-synoptic observations, obtained during three different years, found gradients at the surface ranging from 0.7 to 7.3×10^{-5} dyn g⁻¹ (ref. 4). (The values are reported as accelerations obtained by dividing the pressure gradient by a density of $\sim 1 \, \mathrm{g \ cm^{-3}}$). Furthermore, the seasonal cycle is roughly in phase with the zonal wind field, both as reported by the ships during the discrete hydrographic observations and as compiled from the historical record⁴. Incomplete observations during 1979 of wind, sea surface height in the west and transport of the equatorial currents were compared to a simplified windforced model with encouraging results⁷.

Hydrographic data were obtained during eight cruises of both the Capricorne and Nizery between October 1982 and August 1984. Figure 1 shows the result of this work as the dynamic height at the surface, relative to 500 m. Gradients derived from the data west of the Gulf of Guinea are shown in a later figure. The slope of the sea surface in the Gulf is generally weak and without a preferred direction, except in January-February 1984, when there was a rapid rise in height approaching the African coast.

Pressure gauge data (Fig. 2) were obtained at 7° E and 29° W. The sensors were placed at depths of <10 m (in order to be equivalent to tide gauges), adjacent to the only two equatorial islands in the Atlantic; namely, São Tomé (0°15' N, 6°40' E) and St Peter and St Paul Rocks (0°55' N, 29°21' W). Half-monthly averages were compared with the average of several hydrocasts, each made seven times at each site during the record in order to get a consistent dynamic level between the two sites. The standard deviation of the difference between hydrographic and pressure gauge data, after adjustment for the mean, was ± 3 cm. The difference between the two gauges is plotted in Fig. 2b.

As shown in Fig. 1, the difference in dynamic height between 7° E and 29° W combines both the westward upward slope and the Gulf of Guinea slope. Thus the negative (westward downward) slope shown in Fig. 2 from December 1983 to mid-April 1984 is not a basin-wide reversal in surface tilt, but probably a neutral slope over much of the basin and a large height increase against the African coast. It confirms the suggestion from the hydrographic data that this condition did not occur in the previous 12-month period. The second clear contrast between the two years is the size of the positive difference in the summer, which was only half as large in 1984. This is not seen in the hydrographic data because of the discrete sampling.

Of the six inverted echo sounders deployed along the Equator during 1983-84, results from the four at 34° W, 28° W, 20° W and 10° W are discussed here. (A record at 1° W showed no substantial difference from that at 10° W and a short record at 38.5° W is omitted.) An inverted echo sounder is similar to a tide gauge in that it provides a measure of the vertically integrated temperature of the entire water column. To convert this to dynamic height, the hydrocasts are used to determine mean values, and historical data⁷ are used to relate a change in the observed travel time to a change in dynamic height. The standard deviation of the difference between the sounder-derived dynamic height and the hydrographic data is ±2 dynamic cm.

The four resulting time series were low-pass filtered to remove tides and inertia-gravity waves. A linear regression analysis was then performed zonally on the data once every 10 days: the result is shown in Fig. 3, along with an indication of the goodness of fit. Also shown is the pressure gradient estimated from the hydrocast data (Fig. 1) for the same region. The 17-month time series derived from the four sounders shows the development of the zonal pressure gradient in the boreal spring of 1983, its gradual relaxation over a 9-month period and its subsequent redevelopment in 1984. This redevelopment occurred very rapidly during the first 20 days of June; the 1984 maximum exceeded that of 1983 by ~20%.

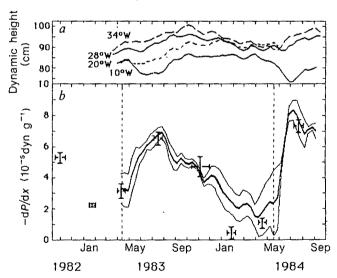


Fig. 3 Dynamic height (a) and zonal pressure gradient (b) between 34° W and 10° W along the equator. The solid line in b is the gradient computed at 10-day intervals from four inverted echo sounder records (shown in a). The bounding curves are determined from the standard error of the slope of the linear regression and, while not a true measure of statistical significance, they are a measure of linearity. The points (with error bars) are from the hydrocast data (Fig. 1) for the same region. The horizontal bar shows the time interval during which the casts were made; the vertical bar indicates the standard error of the slope (from a linear regression of (typically) six averages as plotted in Fig. 1). The dashed lines indicate the time of onset, each year, of the south-east trade wind (see Fig. 4).

In general, the hydrocast data (points in Fig. 3) yielded the same gradients, but with one important discrepancy. In the latter half of January 1984, the hydrographic data show no significant gradient. From Fig. 1 we note that this section (solid triangles. apex up) recorded an unusual sea surface slope, and a higher surface at every site (except for the westernmost location) than at any other time in the two years. Also, the 1984 surface is typically 10 cm higher than at the comparable time in 1983, increasing to nearly 20 cm near the eastern boundary. This anomaly is indirectly confirmed by the pressure gauge data (Fig. 2), which further suggests that this situation, although most pronounced near the time of the survey, was sustained during the months of January-March.

In contrast, the sounders did not indicate a minimum in pressure gradient during these months. Neither the sounder at 10° W, nor the one at 1° W not included in Fig. 3, indicated a high surface height. Indeed, the comparison between sounders and hydrocasts at these two sites showed discrepancies of 6 and 8 cm, several standard deviations more than the general result from the comparison. We cannot yet explain the different results from the two observational methods.

The objective of obtaining a time series of the zonal pressure gradient is to compare it with the synoptic wind field. The annual cycle of the trade winds along the Equator and west of the Gulf of Guinea results from the meridional migration of the Intertropical Convergence Zone (ITCZ), which is located near the Equator at the beginning of the year and reaches to beyond 10° N six months later. Horel et al.8 remark on a rapid relaxaton of the near-surface wind field between November 1983 and January 1984, during which time the ITCZ shifted southward and then remained south of the Equator until May. Unlike the oceanographic data, which have only a meager and patchy historical base, the meteorological data are sufficiently complete for Horel et al.8 to conclude that conditions over the Atlantic in 1983-84 constituted an extreme event.

Our interest here is in the surface wind field directly over the Equator, in the band from the Gulf of Guinea to the South American coast. To characterize that wind field a wind recorder was placed on St Peter and St Paul Rocks: Fig. 4 shows the zonal wind stress computed from this record. From the historical data we know that this location is typical of the central and western reaches of the equatorial Atlantic, with stress increasing from east to west⁹. The record in Fig. 4 shows sudden increases in westward wind stress in the boreal spring of each year. A similar picture was obtained at the same site in 1979¹⁰ and in 1985 (S.L.G. and E.J.K., unpublished data), but the date of onset varies each year over a range of \sim 2 months.

The low wind stress observed from mid-January to May 1984 reflects the southerly location of the ITCZ in early 1984. The negative (eastward) stress in May is unusual. In an objective analysis of ship-reported winds (1964-84), Jacques Servain (personal communication) computed a monthly average eastward wind stress in the area of St Peter and St Paul Rocks only for May and June 1968. In 1983 and 1984, the onset of high wind stress leading to the seasonal trade wind occurred on 5 April and 19 May, respectively. These dates are indicated by dashed lines in Fig. 3, and they show the near simultaneity of the westward wind onset and the build-up of the zonal pressure gradient. A lag-correlation calculation between the data of Figs 3 and 4 indicates that the ocean surface height lagged the wind (at this one site) by 10-15 days. We note that the lower wind stress in mid-1984, relative to 1983, is associated with a larger maximum zonal pressure gradient in 1984.

The quarter-annual hydrographic surveys provide the densest set of classical observations yet obtained in the equatorial Atlantic, and the inverted echo sounder array is unique. The data confirm our previous understanding that the basin comprises two different regions of response, roughly delineated by the Gulf of Guinea. To the west of the gulf the hydrographic sampling proved adequate to define the annual variation of the

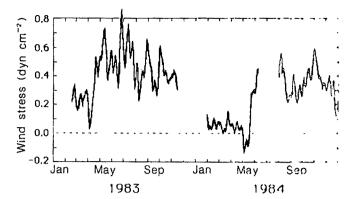


Fig. 4 Low-pass-filtered westward wind stress at St Peter and St Paul Rocks (29° W), 1983-84. The filter admits >95° of the variance for frequencies less than 0.1 cycle per day

zonal pressure gradient, relative to the results from the continuously sampling sounders. The range of values, 0-8 x 10⁻⁵ dyn g⁻¹, is comparable to earlier estimates. The previous low value, obtained in the spring of 1963, was also associated with a particularly strong relaxation of the trade winds⁴. Both methods of observation show a slow and nearly monotonic decrease in zonal pressure gradient from August 1983 until May 1984, followed by a sharper and larger increase in gradient in the spring of 1984, relative to 1983. The hydrocast data show an anomalously high surface (deep thermocline) in January-February 1984 not evident in the sounder data: this difference needs further investigation.

The pressure gauge data (Fig. 2) compare the western central region with the eastern boundary of the Gulf of Guinea and also show an annual signal superimposed on an interannual difference in level. Around July of each year, a peak is seen in the sea surface height difference between west and east, and a minimum is found to occur around February. In 1984 the minimum is strongly negative (that is, the thermocline is deeper in the east), in agreement with the hydrocast data.

The zonal wind stress from 29° W (Fig. 4) has a boxcar-like time dependence: low in the boreal spring when the ITCZ is at or near the Equator and high when the south-east trade winds prevail. There is however an interannual difference, with the amplitude of the zonal stress in 1984 consistently lower than that in 1983 by ~0.15 dyn cm⁻² throughout the entire year. The lower stress during 1984, however, resulted in a larger zonal pressure gradient west of the Gulf of Guinea which, unless opposed by other differences, would be expected to alter the equatorial circulation. The timing of the onset of the south-east trade winds is closely correlated with the build-up of the zonal pressure gradient. Our data imply a response time for the ocean of 10-15 days.

We acknowledge the financial support of the NSF (grants OCE 81-17000 and OCE 82-09892) and O.R.S.T.O.M. C. Henin and B. Piton collaborated with P.H. in obtaining the hydrographic data; G. Philander made helpful comments on an early draft. Lamont-Doherty Geological Observatory contribution no. 3966.

Received 15 January; accepted 27 March 1986.

- 1. Fofonoff, N. P. & Montgomery, R. B. Tellus 7, 518-521 (1955)
- Katz, E. J. et al. Oceanol. Acta 4, 445-450 (1981).
- Burkov, V. A., Zubin, A. B., Titov, V. B. & Kharlamov, A. I. Societ Met. H. Srol. 9, 81 . .
- Katz, E. J. et al. J. mar. Res. 35, 293-307 (1977).
- Merle, J. Atlas Hydrologique Saisonnier de l'Océan Atlantique Intertre, cui (Fra. 24x & Documents de l'O.R.S.T.O.M. No. 82) (Paris, 1978).
- Lass, H. U. et al. Oceanol. Acta 6, 3-11 (1983).
 Katz, E. J. & Garzoli, S. J. mar. Res. 40, 307-327 (1982)
- 8. Horel, J. D., Kousky, V. E. & Kagano, M. T. Nature 322, 248-251 (1985)
 9. Hastenrath, S. & Lamb, P. J. Climate Atlas of the Tropical Atlantic and Lastern Polytic
- Oceans (University of Wisconsin Press, Madison, 1977).

 10. Garzoli, S. L., Katz, E. J., Panitz, H. J. & Speth, P. Oceanol. Acta 5, 281 20. (1982)

Atmospheric conditions in the Atlantic sector during 1983 and 1984

John D. Horel*, Vernon E. Kousky† & Mary T. Kagano‡

* Climate Research Group, Scripps Institution of Oceanography, La Jolla, California 92093, USA † Climate Analysis Center, National Meteorological Center, NWS/NOAA, Washington DC 20233, USA

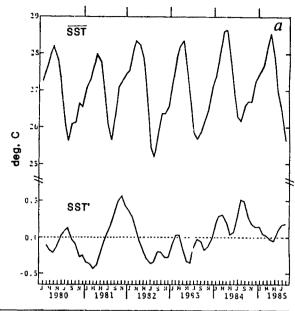
‡ Instituto de Pesquisas Espaciais, 12.200 Sao Jose dos Campos, SP. Brazil

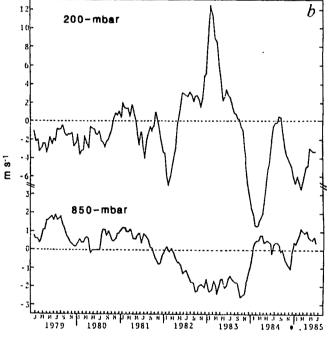
The dramatic global climate variability during the period from 1982 to 1984 has presented a unique opportunity to diagnose and interpret the role of air/sea interactions over the tropical oceans. Recent reviews have summarized the observational and numerical evidence for air/sea interactions over the equatorial Pacific Ocean associated with the El Niño/Southern Oscillation (ENSO) phenomenon¹⁻³. Here we present details of the atmospheric conditions in the Atlantic sector between 1983 and 1984. During the latter half of 1983, the atmospheric circulation over the equatorial Atlantic underwent a dramatic reversal: surface trade winds were substantially reduced; surface pressures decreased; and cloudiness and rainfall increased over the ocean and adjacent regions of north-east Brazil. These regional changes over the equatorial Atlantic coincided with planetary-scale adjustments in the tropical atmosphere. While the atmospheric circulation over the tropical Pacific was experiencing an extraordinary departure from normal during 1983, as evidenced by a reversal in direction of the surface winds, the circulation over the Atlantic was in a building-up phase with stronger than usual surface winds. As the atmospheric circulation over the Pacific returned to normal during the latter half of 1983, the trade winds over the Atlantic relaxed.

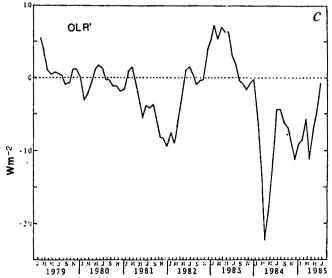
To place the atmospheric conditions over the Atlantic sector during 1983-84 in context, it is helpful to review the salient features of the global tropical circulation during this period. More detailed accounts of the month-to-month variability of the global circulation are given in the seasonal reviews⁴⁻¹⁰ and monthly Climate Diagnostics Bulletins. Over the equatorial Pacific, the largest climatic anomaly of the atmosphere-ocean system during the past 100 years was observed during the latter half of 1982 and early part of 1983 (refs 1-3). The conditions during this period represented an extreme 'warm' phase of the ENSO phenomenon, where 'warm' refers to the unprecedented increase in sea surface temperature in the equatorial Pacific. Some of the significant atmospheric circulation features observed during this period are: weakening of the Pacific trade winds and strengthening of the Atlantic trade winds: reduction of surface pressures over the eastern equatorial Pacific and increased pressures over Indonesia and the equatorial Atlantic; torrential rainfall over the central and eastern equatorial Pacific and drought over Indonesia and north-east Brazil.

While the 1982-83 ENSO warm phase in the equatorial Pacific has been well documented, its collapse during mid-1983 and

Fig. 1 Indices of: a, monthly averaged sea surface temperature (top) and departures (bottom) of the monthly averages from the climatological means 18; b, 200-mbar zonal wind anomalies (top) and 850-mbar zonal wind anomalies (bottom); c, monthly anomalies of outgoing long-wave radiation. The indices are based on observations within the region 5° N to 5° S and from 35° W to 10° W. The anomalies of 850- and 200-mbar wind (outgoing long wave radiation) are computed with respect to the 1978-83 (1974-83) base period. To smooth month-to-month irregularities in the data, a 3-month running mean filter has been applied to the indices. The 1980-85 mean anomaly has been removed from the sea surface temperature anomaly index, to compensate for trends in the long-term sea surface temperature record.







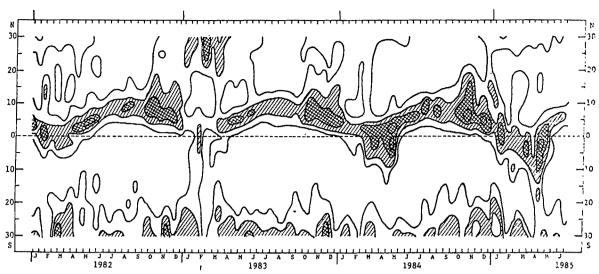


Fig. 2 Time versus latitude plot of outgoing long-wave radiation (OLR) averaged over the latitude band 20-35° W. OLR values > 240 W m⁻² are indicated by a lack of hatching; hatching denotes OLR values between 220 and 240 W m⁻²; cross-hatching indicates values less than 220 W m⁻²; the contour interval is 20 W m⁻².

subsequent reversal into a 'cold' ENSO phase have received less attention. In many respects, the tropical circulation during 1984 was as unusual as that during the preceding year: decreased ocean temperatures in the central equatorial Pacific and increased temperatures in the equatorial Atlantic; strengthening of the Pacific trade winds and weakening of the Atlantic trade winds; higher pressures over the eastern equatorial Pacific and decreased pressures over Indonesia and the equatorial Atlantic; dry conditions over the central equatorial Pacific and above normal rainfall over Indonesia and north-east Brazil.

Briefly, the anomalous atmospheric conditions during 1983 (1984) over the equatorial Pacific can be explained largely in terms of the atmospheric response to the unusually warm (cold) ocean surface^{1-3,11-13}. Similar processes undoubtedly had a role over the equatorial Atlantic during 1984. Because of the sensitivity of the tropical atmosphere to relatively small changes in equatorial sea surface temperature, sea surface temperature is often regarded more as an atmospheric variable than an oceanic one. In the following, we will contrast the changes in sea surface temperature in the equatorial Atlantic to those in the overlying atmosphere during 1983–84. In addition, we will compare the relative magnitudes and durations of the anomalous conditions in the Atlantic sector during this period to those over the Pacific associated with ENSO.

Figure 1 contrasts a number of indices of the sea surface temperature and selected atmospheric fields. The month-to-month changes in sea surface temperature averaged over the central equatorial Atlantic from 5° N to 5° S and 35° W to 10° W are shown in Fig. 1a for the period 1980–85. During every year, sea surface temperature exhibits a pronounced annual cycle with the highest (lowest) temperatures during February-April (August-October)^{14,15}. Note that the warmest ocean surface (>28.5°C) was evident during February-May 1984. In contrast, averages of sea surface temperature for the central equatorial Pacific exhibit less of an annual cycle and more variability from year to year^{16,17}.

The departures from climatology¹⁸ of central equatorial Atlantic sea surface temperature are also shown in Fig. 1a. Large positive anomalies were observed in late 1981; however, these occurred primarily during the cool phase of the annual cycle. Sea surface temperature was near or slightly below normal from mid-1982 until late 1983. After the beginning of 1984, the sea surface became anomalously warm in the equatorial Atlantic, with peak anomalies occurring during August-September. The anomalies decreased thereafter but remained positive until June 1985. The magnitude (<1 °C) of the sea surface temperature

increase in the equatorial Atlantic during 1984 is modest compared with that in the Pacific during 1983 (2-3 °C).

To first order, the fluctuations in the atmospheric circulation over the equatorial Atlantic can be viewed as perturbations of the mean zonally oriented circulation cell characterized by rising motion over the Amazon Basin, surface inflow from the Atlantic trade winds (directed from east to west), and outflow aloft (directed from west to east). Superimposed on this mean zonal circulation are large seasonal meridional migrations of the Intertropical Convergence Zone (ITCZ), an east-west oriented band of extensive cloudiness and rainfall. Indices of 850-mbar zonal wind (indicative of the surface trade-wind field) and 200-mbar zonal wind (representative of the flow in the upper troposphere) for the region used for the sea surface temperature index are shown in Fig. 1b. Positive (negative) values of the 850-mbar wind index indicate weaker (stronger) than normal surface trade winds over the equatorial Atlantic. The most striking features of the near-surface wind field are the gradual buildup of the trade winds during mid-1982 and their rapid relaxation between November 1983 and January 1984. The effects of these changes in surface wind stress on the ocean circulation are discussed in refs 19-24.

The out-of-phase relationship between near-surface and upper tropospheric winds is evident in Fig. 1b. In contrast to the near-surface winds, year-to-year fluctuations in the upper tropospheric winds are strongly modulated by the annual cycle such that the largest anomalies are observed from January to April of 1983 and 1984.

Figure 1c shows the month-to-month changes in outgoing long-wave radiation averaged over the region used for the other indices. Outgoing long-wave radiation provides an indication of cloudiness and deep tropical cumulus convection: positive (negative) anomalies of outgoing long-wave radiation indicate warmer (colder) cloud-top temperatures and less (more) cloudiness and rainfall than usual. Rainfall and cloudiness were inhibited during February-May 1983 while they increased substantially during February-May 1984.

As mentioned above, variations in cloudiness and rainfall over the equatorial Atlantic are strongly modulated by the seasonal meridional migrations of the ITCZ. The ITCZ normally extends furthest south and straddles the Equator in the western and central Atlantic from February to April. Figure 2 shows the meridional migrations of the ITCZ during the period from 1982 to 1985 in terms of a time-latitude plot of outgoing long-wave radiation averaged over the longitude band 20° W to 35° W. Note that the ITCZ was noticeably weak and slightly further north

during February-April 1983, compared with the other years. During March-May of 1984 and 1985, the ITCZ was vigorous and expanded southward.

The variations in cloudiness and rainfall evident in Figs 1c and 2 for the equatorial Atlantic extend westward into the region of north-east Brazil. Figure 3 contrasts the distribution of anomalous rainfall during 1983 and 1984 during the normally rainy seasons of March-May. The anomalies of rainfall at each station have been normalized by the climatological mean rainfall for that season so that the figures are not biased towards the Amazon regions, which receive more rainfall than the drought-prone areas of north-east Brazil. During 1983, most stations in north-east Brazil measured less than half of their normal rainfall amounts for that season, whereas the opposite was true during 1984.

Half-monthly values of sea-level pressure were substantially lower over the entire South Atlantic during 1984 in comparison with corresponding periods during 1982-83 (not shown). The reduction in surface pressure is consistent with the decreased strength of the trade winds. Sea-level pressure in the eastern tropical Atlantic returned to pre-1984 levels by September-November 1984. However, in the western tropical Atlantic, sea-level pressure remained lower than that during 1982-83 until June 1985.

The temporal and spatial evolution of the variations in ocean surface temperature and atmospheric circulation can be summarized as follows. Beginning in early 1984, sea surface temperature began to rise sharply across the entire equatorial strip, particularly to the south of the Equator. The warmest temperatures were observed along the Equator from March to May 1984, the season during which the equatorial Atlantic is normally warmest. Anomalies of roughly 1 °C in sea surface temperature persisted through the remainder of 1984 to the south of the Equator, while temperatures were normal or slightly below normal to the north of 5 °N. Although temperatures in the eastern equatorial ocean returned to near normal by early 1985, abovenormal temperatures remained in the western Atlantic until June 1985.

The atmospheric circulation over the tropical Atlantic during early 1983 was in a highly perturbed state, with higher pressures than normal, stronger surface trade winds, a weakened and northward-displaced ITCZ, and drought over north-east Brazil. As the surface temperatures in the equatorial Atlantic were close to normal during this period, it is unlikely that this anomalous atmospheric circulation was forced from below. Concurrent with the anomalous circulation over the Atlantic, an extreme warm phase of ENSO was observed over the equatorial Pacific. As the low-frequency fluctuations of the tropical atmosphere are highly coupled over long distances, it is plausible that the anomalous conditions over the Atlantic were a remote readjustment of the tropical circulation to the unusually intense convection and rising motion over the eastern equatorial Pacific. Possible links between the warm phase of ENSO in the Pacific and weakening of the Atlantic ITCZ and drought in north-east Brazil have been discussed elsewhere²⁵.

During the period from November 1983 to January 1984, the surface trade-wind and surface pressure fields weakened. The reduction in surface wind stress led to alterations in the circulation and thermal fields of the equatorial Atlantic. As sea surface temperatures rose during early 1984, the Atlantic ITCZ shifted southwards and remained near and to the south of the Equator in the vicinity of the warmest sea surface temperature (>27 °C) until May. The anomalous pattern of near-normal sea surface temperatures to the south of the Equator and below-normal temperatures to the north of the Equator has been linked before to abundant rainfall in north-east Brazil and drought over the sub-Sahel regions of Africa^{26,27}.

Although surface pressures and surface trade winds increased perceptibly over the eastern Atlantic and north of the Equator towards the end of 1984, the ITCZ again migrated south of the

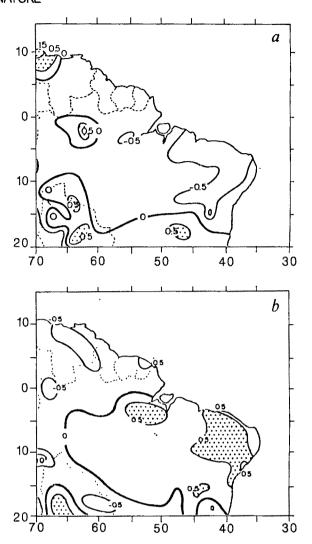


Fig. 3 Normalized precipitation deviations over north-east Brazil during a, March-May 1983 and b, March-May 1984. Values are calculated by determining the precipitation deviations from the mean and then dividing by the mean. The contour interval (in non-dimensional units) is 0.5; stippling indicates regions where seasonal rainfall totals were >0.5 of the seasonal mean.

Equator during February-May 1985 in the western Atlantic. This led to another season with above-normal rainfall in northeast Brazil. Sea surface temperatures gradually returned to near normal by the end of May 1985 in the equatorial Atlantic, and rainfall in sub-Sahel regions of Africa during the 1985 rainy season was much more plentiful than that during the previous two years.

The atmospheric circulation observed during the warm 1984 Atlantic event has many similarities to the warm 1983 ENSO event over the Pacific. The weakened trade winds, southward displacement of the ITCZ and enhanced equatorial convection are also features common to warm events in both the Atlantic and Pacific regions. However, several features are distinctly different. A major component of the warm Pacific event is the east-west shift of convection from the maritime continent towards the dateline and 'see-saw' of surface pressure, with lower pressures in the southeastern Pacific and higher pressures over the maritime continent¹⁻³. In contrast, the observed changes in cloudiness over the Atlantic were oriented primarily meridionally; convective activity over the Amazon basin exhibited little east-west movement during 1984 and pressures were reduced nearly uniformly across the southern Atlantic. Furthermore, the magnitude of the circulation changes in the Atlantic sector are

considerably weaker (roughly one half to one third) than those during the 1983 Pacific warm event and even slightly weaker than those during other such Pacific warm events, for example, those of 1972 and 1957.

The development of an unusually warm equatorial Atlantic, relaxed trade winds, and southward-displaced ITCZ are consistent with current theories on air/sea interaction over equatorial oceans. However, the conditions over the Atlantic during 1983-84 constitute an extreme event, much like the extreme nature of the 1982-83 warm event in the Pacific.

We thank Kathy Stevenson and John Knopman for assistance. Partial support for J.D.H. was provided by the Climate Dynamics Program under NSF grant ATM 84-04548. These results were presented at the CCCO Tropical Atlantic Panel Meeting held in Rio de Janiero, Brazil 9-13 September 1985. The Climate Diagnostics Bulletin is prepared by staff of the Climate Analysis Center, National Weather Service, Washington

Received 30 January: accepted 10 April 1986.

- 1. Philander, S. G. H. Nature 302, 295-301 (1983).
- Gill, A. E. & Rasmusson, E. M. Nature 306, 226-234 (1983)
- Rasmusson, E. M. & Wallace, J. M. Science 222, 1195-1202 (1983).
 Quiroz, R. S. Mon. Weath. Rev. 111, 1685-1706 (1983).

- Chen, W. Y. Mon. Weath. Rev. 111, 2371-2384 (1983).
 Ropelewski, C. F. Mon. Weath. Rev. 112, 591-609 (1984)
- Bergman, K. H. Mon. Weath. Rev. 112, 1441-1456 (1984). Ouiroz, R. S. Mon. Weath. Rev. 112, 1894-1912 (1984).
- Wagner, A. J. Mon. Weath. Rev. 113, 149-169 (1985). 10. Ropelewski, C. F. Mon. Weath. Rev. 113, 664-679 (1985).
- 11. Keshavamurty, R. N. J. atmos. Sci. 39, 1241-1259 (1982).
- Blackmon, M. L., Geisler, J. E. & Pitcher, E. J. J. atmos. Sci. 40, 1410-1425 (1983).
 Shukla, J. & Wallace, J. M. J. atmos. Sci. 40, 1613-1630 (1983).
- 14. Weare, B. C. Q. Jl R. met. Soc. 103, 467-478 (1977).
- Merle, J., Fieux, M. & Hisgard, P. Deep Sea Res. 26 (Suppl. 11), 77-102 (1979).
- Weare, B. C., Navato, A. R. & Newell, R. E. J. Phys. Oceanogr. 6, 671-678 (1976).
 Horel, J. D. Mon. Weath. Rev. 110, 1863-1878 (1982).
- Reynolds, R. W. NOAA Tech. Rep. 31 (1982).
 Philander, S. G. H. Nature 322, 236-238 (1986).
- Lamb, P. J., Peppler, R. A. & Hastenrath, S. Nature 322, 238-243 (1986).
 Palmer, J. N. Nature 322, 251-253 (1986).

- Hisard, P., Henin, C., Houghton, R., Piton, B. & Rual, R. Nature 322, 243-245 (1986).
 Katz, E. J., Hisard, P., Verstraete, J. M. & Garzoli, G. L. Nature 322, 245-247 (1986).
 Weisberg, R. W. & Colin, C. Nature 322, 240-243 (1986).
- Kousky, V. E., Kagano, M. T. & Cavalcanti, I. F. A. Tellus 36A, 490-504 (1984).
 Hastenrath, S. & Heller, L. Q. Jl met. Soc. 103, 77-92 (1977).
- 27. Lamb, P. J. Mon. Weath. Rev. 106, 482-491 (1978).

Influence of the Atlantic, Pacific and Indian Oceans on Sahel rainfall

T. N. Palmer

Meterological Office, Bracknell, Berkshire RG12 2SZ, UK

Folland et al. have reported that persistently dry and wet periods of several years in the Sahel have been accompanied by global-scale patterns of sea-surface temperature (SST) anomaly. They also demonstrated that the response of a general circulation model (GCM) of the atmosphere to an observed composite SST difference field between a number of such dry and wet periods showed substantial reduction in Sahel rainfall compared with values from a simulation with climatological SSTs. I examine here the same model's response to the individual components of the composite SST difference field in the Atlantic, Pacific and Indian Oceans. It is found that over the western Sahel, the Atlantic and Pacific fields have a comparable effect in reducing rainfall whereas the Indian Ocean field produces a slight enhancement. Results suggest that, over the eastern Sahel, the Indian Ocean has the dominant role in reducing rainfall.

Figure 1 shows the worldwide SST difference field between the five driest and five wettest years in the Sahel after 1949 and is discussed in more detail in ref. 1. Note that whilst this field

does represent differences between extreme years, values in the South Atlantic are not as large as anomalies (>2 K) observed during the exceptional warm event of 1984 (ref. 2). Similarly, values over the east Pacific are not as large as observed anomalies following the 1982/83 El Niño event³.

Results were obtained from several 180-day fixed July integrations of the Meteorological Office 11-layer GCM4 using the full difference field in Fig. 1, and its components in the three principal oceans. The integrations are identified as follows. The control integration has fixed climatological average July SSTs, and the anomaly integration (TOT) has the full field in Fig. 1 added to these values. Integrations ATL, PAC and IND have only those SSTs in Fig. 1 from the Atlantic, Pacific and Indian Oceans respectively, added to climatological values (see ref.) for a description of rainfall and low level moisture flux in the control integration).

Figure 2 shows 180-day mean-rainfall difference fields between the four anomaly integrations and the control. As discussed in ref. 1, in TOT (Fig. 2a) there is a coherent and substantial reduction in rainfall across the Atlantic and the Sahel, by up to 50% of the model's climatological mean. For integration ATL (Fig. 2b), the pattern of rainfall reduction over the Atlantic and the Western Sahel is similar to, but ~30% weaker than, that for integration TOT. Over the eastern Sahel, the reduction in rainfall is much less substantial in ATL.

For integration PAC, surprisingly at first sight, there is a similar pattern of rainfall reduction to that in TOT and ATL. Over the Atlantic, values are smaller than in ATL, and the rainfall enhancement to the south is absent. However, inland, over the Sahel, rainfall reduction seems to be larger than that in ATL

Results from IND are different. Inland, over the western and central Sahel, an enhancement in rainfall of over 1 mm per day is apparent. Further east, over Sudan and northern Ethiopia, there is a decrease in rainfall by up to 50% of climatological values. Finally, over the western Indian Ocean itself, values are strongly enhanced. (Although not shown, rainfall over the eastern Indian Ocean is also increased.)

An assessment of whether these rainfall anomalies are significant was made by calculating a t-variant from the six pairs of non-overlapping 30-day mean values of the control and anomaly integrations. If the conditions of the t-test were satisfied, then anomalies with |t| > 2 would be accepted at about the 7% significance level, using a two-sided test. t-Values with magnitude >2 shown stippled in Fig. 2. The reduction in rainfall across the Atlantic and into the extreme western Sahel is extremely-reproducible for experiment TOT whilst values of t are smaller in this region for ATL and, except for a small neighbourhood of the West African coast, t < 2 in PAC. In experiment IND, the increase in rainfall over the Indian Ocean is significant, as is the principal area of decrease over Sudan. In TOT, and more so in ATL, the increase in rainfall over north-east Brazil appears to be highly reproducible (although the northern summer is not the main rainy season in this area).

The addition of the SST anomaly in ATL reduces the meridional gradient of Atlantic SST just south of the intertropical convergence zone (ITCZ). As a result, the Atlantic Hadley cell south of the ITCZ is weakened and, as Fig. 3 shows, the low-level south-east Trade Winds are weakened. The flux of moisture into the ITCZ is reduced, producing less latent heating there, consistent with the weaker Hadley cell.

Whilst the main change in precipitation occurs over the Atlantic, Fig. 3a shows that reduction in low-level flow into the ITCZ also reduces the south-west monsoon flow into the western

As mentioned above, the composite positive SST anomaly in Fig. 1 is considerably weaker, particularly in the Gulf of Guinea, than SST anomalies observed during the exceptional warming of 1984. Hence, it is very likely that a more marked weakening of the south-west monsoon flow into the western Sahel would

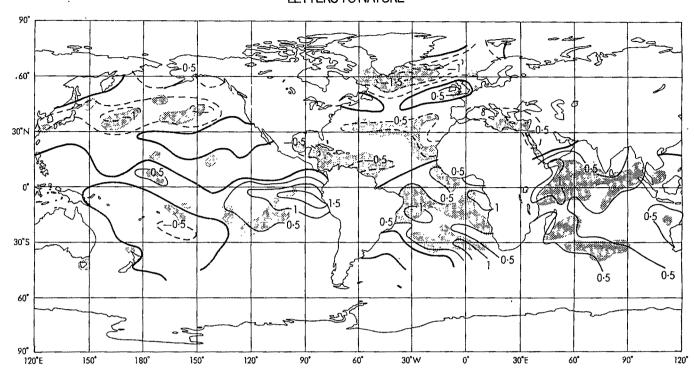


Fig. 1 SST for July to September. Average of 1972, 1973, 1982, 1983, 1984 (dry years) relative to average of 1950, 1952, 1953, 1954, 1958 (wet years). Contour interval, 0.5 °C. Shaded areas are different from zero at the 90% level of significance according to a *t*-test.

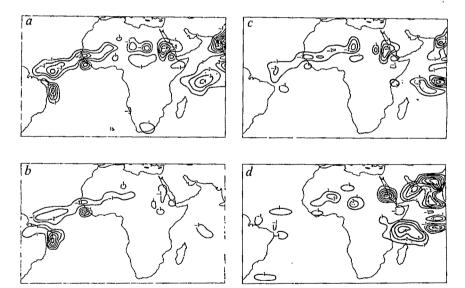
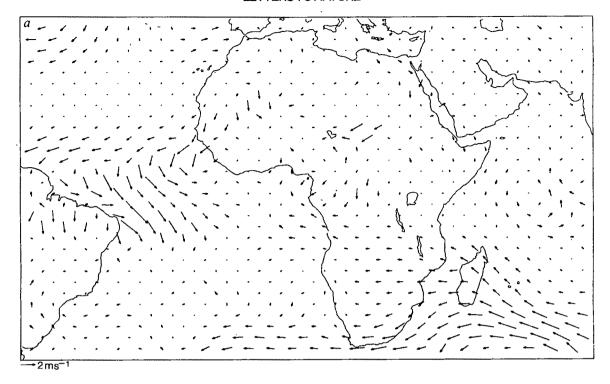


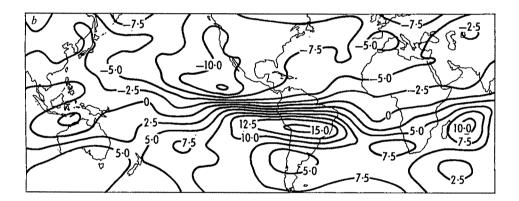
Fig. 2 Rainfall anomaly (relative to control integration) for experiment with: a, Full SST anomaly in Fig. 1 (TOT); b, Atlantic portion of Fig. 1 only (ATL); c, Pacific portion of Fig. 1 only (PAC); d, Indian Ocean portion of Fig. 1 only (IND). Contour interval, 1 mm per day. Stippling indicates areas where the magnitude of the t-variate exceeds 2.

have resulted if the 1984 SST anomalies had been used in place of those in Fig. 1. We hope to test this speculation in a future integration

Whilst the SST anomaly field in Fig. 1 has negative values over 1 K in the north Pacific, the principal influence of SST anomalies in PAC on rainfall is over the tropical Pacific. With water at 28 °C or warmer extending across most of the tropical Pacific north of the Equator in the climatological normal, the anomaly near the dateline in Fig. 1 produces a substantial increase up to 10 mm per day over the central and west Pacific, whilst anomalies west of Central America (which weaken the meridional SST gradient there) are associated with a reduction of the maximum of rainfall west of Mexico by up to 10 mm per day. Previous GCM studies with El Niño SST anomalies 5 have

shown that enhanced latent heat release in the central equatorial Pacific excites an atmospheric Kelvin wave which can propagate across the Atlantic and Africa without complete dissipation. As a result the equatorial upper troposphere is warmed, geopotential height is raised and anomalous equatorial westerlies are produced, in agreement with results from thermally forced linear equatorial β -plane models⁶. Figure 3b shows the 250-mbar streamfunction anomaly from PAC. The north-to-south gradient indicates that the anomalous non-divergent wind in the tropics at 250 mbar indeed has a westerly component, strongest over the east Pacific, but extending over the Atlantic and Africa. The wind anomalies have a baroclinic vertical structure near the ITCZ over the Pacific, Atlantic and Sahel, with an easterly component at low levels.





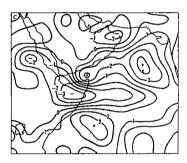


Fig. 3 a, 950-mbar wind anomaly for experiment ATL; b, 250-mbar streamfunction anomaly (×10⁶ m² s⁻¹) for PAC; c, 250-mbar divergence anomaly $(\times 10^{-6} \,\mathrm{s}^{-1})$ for IND.

This again reduces the south-west monsoon flow into the western Sahel, and thereby the supply of moisture for precipitation. The fact that there is no significant increase in rainfall over the Atlantic south of the ITCZ in PAC is consistent with the divergent circulation anomalies being mainly east/west oriented ('Walker cell') rather than north/south ('Hadley cell') as in ATL.

Results from IND are more easily understood. In Fig. 2d, there was substantial enhancement of rainfall over the Indian Ocean; Figure 3c shows anomalous divergence at 250 mbar associated with this enhancement. The correspondence between divergence and rainfall arises from the local thermodynamic balance in the tropics7 between adiabatic cooling by vertical motion and latent heat release. The main area of descent required by mass continuity appears to be located over Ethiopia and Somalia, consistent with the rainfall decrease there. The anomalous low-level wind in this region (not shown) flows from land to ocean, similar to Fig. 3a for ATL.

The tropical Atlantic therefore has a role in modulating rainfall over the Sahel, and was probably paramount during the exceptional 1984 season. On the other hand, effects from either the Pacific or Indian Ocean cannot be ignored. Hence, a com-

plete understanding of variability of rainfall in the Sahel involves consideration of the entire tropical circulation. As such, these model results are in agreement with the observational correlations between worldwide SST and Sahel rainfall, discussed by Folland et al.1.

However, results from the t-test also show that over most of the Sahel, rainfall anomalies were quite variable. On the other hand, a stronger and more significant response to SST anomalies in this area might be expected if coupling between rainfall, ground reflectivity and soil moisture capacity4 were built into the model.

C. K. Folland and D. E. Parker supplied the SST data shown in Fig. 1. I also thank them for many useful discussions.

Received 4 November 1985; accepted 2 April 1986.

- 1. Folland, C. K., Palmer, T. N. & Parker, D. E. Nature 320, 602-607 (1986).
- Philander, S. G. H. Nature. 322, 236-238 (1986).

- Critiander, S. O. H. Nature 322, 250-238 (1988).
 Gill, A. E. & Rasmusson, E. M. Nature 306, 229-234 (1983).
 Cunnington, W. M. & Rowntree, P. R. Q. II R. met. Soc. (in the press).
 Palmer, T. N. in Coupled Ocean Atmosphere Models (Elsevier, Amsterdam, 1985).
 Gill, A. E. Q. II R. met. Soc. 444-462 (1980).
 Webster, P. J. J. astmos. Sci. 38, 554-571 (1981).

River dynamics and the diversity of Amazon lowland forest

Jukka Salo*, Risto Kalliola*, Ilmari Häkkinen*, Yrjö Mäkinen*, Pekka Niemelä*, Maarit Puhakka* & Phyllis D. Coley†

* Department of Biology, University of Turku, SF-20500 Turku, Finland † Department of Biology, University of Utah, Salt Lake City, Utah 84112, USA

We suggest here that large-scale natural forest disturbance and primary succession in the lowland rainforests of the Peruvian Amazon is caused by lateral erosion and channel changes of meandering rivers. Our results indicate that in the upper Amazon region, primary succession on newly deposited riverine soils is a major mode of forest regeneration. Landsat imagery analyses show that 26.6% of the modern lowland forest has characteristics of recent erosional and depositional activity; 12.0% of the Peruvian lowland forest is in successional stages along rivers. This successional development is used to classify the western Amazon rainforests according to their geomorphological erosion-deposition pattern. We also propose that by causing high site turnover, disturbance and variation in forest structure, the river dynamics may be a major factor creating and maintaining the high betweenhabitat (β -type) species diversity characterizing the upper Amazon¹

The degree of forest disturbance caused by river-channel erosion was studied in $>0.5\times10^6\,\mathrm{km^2}$ of the Peruvian Amazon by using analyses of Landsat MSS (multi-spectral scanner) images (visual analysis). The disturbance is caused by the lateral erosion and channel changes of the meandering and braided white-water rivers (rich in fine suspended inorganic solids; see refs 2–7) of the western periphery of the Amazon region^{8–12}. Patterns of primary succession on newly deposited riverine soils were examined in more detail along the Rio Madre de Dios and Rio de los Amigos in the Madre de Dios region of southeastern Peru in 1982. The work was continued at the Cocha Cashu biological station at Manú National Park in 1983–86.

Twenty-two Landsat images of the Peruvian headwater region were surveyed for indications of former riverine erosion (Fig. 1, Table 1). In the analyses, we defined three erosional-depositional formations: (1) present floodplain formation, (2) previous floodplain formation, unquestionable floodplain origin; and (3) forests on denuded soils, which includes all the forests beyond the present or previous floodplains (these are probably also of former floodplain/lacustrine origin^{13,14}, derived from the depositional processes described here).

(1) Forests on the present floodplains are the areas most recently subjected to lateral erosion and channel migration. They were detected on the images by delimiting the areas covered by the present meander plains, which were defined as the areas containing the present meanders and the most recent channel cutoffs and oxbow lakes. This area, which has recently undergone several cycles of complete lateral erosion, may be further divided into two distinct types: sequential successional forest and mosaic forest (Fig. 2). Active deposition occurs on the inside of the meander bends, by point bar accretion, and with time meander migration has produced a series of meander scrolls; these form a sequence of ridges running parallel to the river course, on which a sequential primary forest succession takes place. The sequential succession proceeds undisturbed until the migrating river channel cuts the meander from a different angle.

According to the repetitive nature of river dynamics, the migration of the river channel course creates a mosaic of successional forests within the present meander plain. The mosaic forest is composed of patches of differentially aged sequential

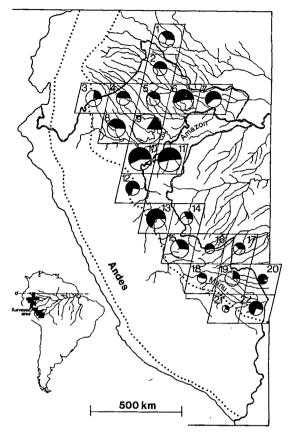


Fig. 1 The distribution and areas of riverine disturbance in the Peruvian Amazon basin. Each of the 22 squares represents one Landsat image (182.5×182.5 km). The sizes of the circles give the area (km²) of total floodplain (see text and Table 1 for details), representing the disturbed area covered by sequential floodplain generations. The black sectors represent the area of the forests on the present floodplains (sequential successional and mosaic forests). The white sectors show the area of the forests on the previous floodplains, indicating transitional forest. Inset, orientation map.

successional forests and patches of forests originating from a succession on the sites of former oxbow lakes. The annual floods further modify the mosaic pattern. The total area covered by the present floodplains is 12.0% of the area analysed.

(2) The area covered by former floodplain formations was defined by identifying the areas of flat surface topography without the convex-concave morphology¹⁵ (indicating surface erosion; for details see refs 16-19) characteristic of the upper Amazon forests on the oldest alluvium of diverse nature. The surface processes acting on Amazon abandoned floodplains change from depositional to erosional with increasing age²⁰. The area characterized by lack of the convex-concave topography is also scattered with isolated oxbow lakes, thus confirming the fluvial/floodplain origin of this formation. We believe that the successional status of forests growing on the soils of previous floodplains is transitional, as the mode of forest regeneration takes place increasingly through secondary succession, promoted by light gaps.

Previous floodplain formations cover 14.6% of the area analysed. The geomorphology of the old floodplains remains highly heterogeneous and is composed of a mosaic of abandoned river channels, oxbow lakes and sedimentary beds of different ages. This heterogeneity gives rise to densely packed plant communities of different ages and origin. In contrast to forests under the influence of present floodplains, older areas of floodplain are scattered throughout the analysed area, indicating major channel changes in the recent history of the western Amazon river system.

(3) The area beyond the present and previous floodplain

Table 1 Peruvian Amazon basin areas subjected to riverine disturbance

No. in Fig. 1	Landsat scene		Analysed area*	Forests on present floodplains (sequential and mosaic forest)		Forests on previous floodplains (transitional forest)		Total floodplain		
	Path	Row	Date	(km ²)	Area (km²)	(%)	Area (km²)	(%)	Area (km²)	% Of total
1	007	60	2 October 1972	29,900	2,050	6.9	3,650	12.2	5,700	19.1
2	007	61	2 October 1972	27,000	2,050	7.6	2,150	8.0	4,200	15.6
3	009	62	29 September 1973	15,700	1,350	8.6	4,650	29.6	6,000	38.2
4	008	62	24 July 1977	21,400	1,900	8.9	2,000	9.3	3,900	18.2
5	007	62	8 December 1973	24,400	1,900	7.8	2,700	11.1	4,600	18.9
6	006	62	7 December 1973	33,300	5,150	15.5	4,050	12.1	9,200	27.6
7	005	62	3 February 1973	26,300	4,000	15.2	2,300	8.7	6,300	23.9
8	800	63	10 September 1973	29,700	3,250	10.9	4.050	13.7	7,300	24.6
9	007	63	2 October 1972	24,000	2,950	12.3	15,950	66.5	18,900	78.8
10	007	64	8 December 1973	25,600	7,050	27.5	4,950	19.4	12,000	46.9
11	006	64	7 December 1973	30,300	9,800	32.3	8,000	26.4	17,800	58.7
12	007	65	2 October 1972	13,600	2,800	20.6	1,200	8.8	4,000	29.4
13	006	66	24 August 1981	20,600	6,600	32.0	3,200	15.5	9,800	47.6
14	005	66	11 July 1979	26,600	950	3.6	1,850	6.9	2,800	10.5
15	005	67	27 April 1976	16,600	2,150	12.9	4,450	26.8	6,600	39.7
16	004	67	5 September 1975	32,200	950	2.9	750	2.4	1,700	5.3
17	003	67	28 October 1975	26,000	1,050	4.0	1,650	6.3	2,700	10.3
18	004	68	7 July 1976	17,100	700	4.1	800	4.7	1,500	8.8
19	003	68	22 August 1976	25,400	1,250	4.9	4,350	17.1	5,600	22.0
20	002	68	29 July 1975	26,300	1,600	6.1	100	0.4	1,700	6.5
21	003	69	3 December 1975	4,000	300	7.5	900	22.5	1,200	30.0
22	002	69	29 July 1975	19,800	2,300	11.6	1,400	7.1	3,700	18.7
otal				515,800	62,100	12.0	75,100	14.6	137,200	26.6

Forests on the present floodplains are undergoing primary and early succession on newly deposited riverine soils. The present floodplain formation is composed of the sequential successional and mosaic forests. Forests on the previous floodplains represent the area covered by a series of older floodplain formations (transitional forest). The analyses are based on visual analysis of 1:10⁶ Landsat images MSS 7, except scenes 007.63 and 007-65, which are MSS 6.

formations has the convex-concave surface erosion pattern. The origin and geomorphology of these areas is unknown, but the erosion pattern is found on both floodplain and lacustrine (Belterra clay type) deposits. As the processes operating on the floodplains change towards erosional, the topography becomes similar to that of the areas of convex-concave relief^{15,20} (see Fig. 2).

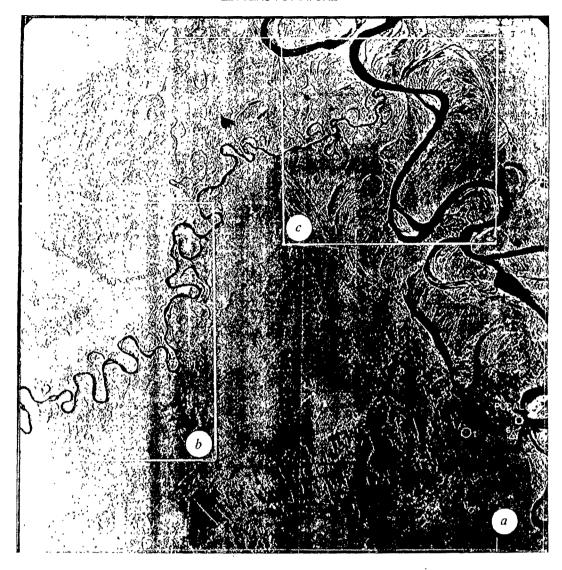
In the western Amazon, the structure of the denuded topmost sedimentary layer has been only locally surveyed $^{8-12,21-24}$. However, there is good reason to believe that after the glacial periods of the Quaternary, the Andean tills, re-worked by rivers, formed a belt of highly heterogenous sedimentary beds in front of the foothills of the Eastern Cordillera 24 . In Peru and Bolivia, the uppermost sedimentary bed, called the Iñapari Formation, overlies the Tertiary red beds $^{25-28}$, especially at sites of high river erosion banks ('cerros'). Recent radiocarbon dates of four samples collected from three 35-m eroding channel banks along the Rio Acre, Bolivia, show that these sediments were deposited between $5,575\pm105$ and $10,085\pm150$ yr BP (ref. 28). These data indicate the youth of the Iñapari Formation, although the stratigraphy of the samples may merely reflect a local sedimentation pattern within the Rio Acre region.

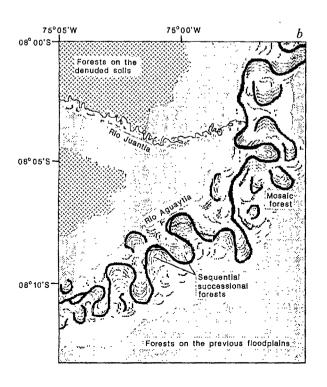
To evaluate the rate of forest regeneration within the areas of sequential successional and mosaic forests, an analysis of a 70-km section of the Rio Manú from the Cocha Cashu station (11°53′ S, 71°24′ W; 350 m above sea level) to Boca Manú (12°15′ S, 70°55′ W, 320 m a.s.l.) was carried out. We compared 1962-63 aerial photographs with a 1976 Landsat image (276296-135752-7). The mean lateral erosion rate of the meander bends during the 13-yr period was 12 m yr⁻¹. During this period, the total area of newly created depositional land subject to primary succession was 12.0 km², representing 3.7% of the present flood-plain formation area (325 km²).

The typical pattern of riparian primary succession (sequential successional forest) is summarized in Fig. 3, where characteristics of the successional meander forest which is common along most of the western Amazon lowland rivers²⁹ are emphasized. Extreme zonation of vegetation occurs during the early phases of succession (up to the Ficus-Cedrela zone³⁰). This zonation is initially created by the instability of the youngest point bar deposits ('beaches') on the inner curve of the meander (see Fig. 3 for details). Tessaria integrifolia (Asteraceae) is the first pioneer tree to appear, because its seedlings can tolerate the arid and unshaded conditions of this environment. Invasion by other successional trees is possible only after modification of the microclimate by Tessaria. At this stage, competition between species may further influence the zonation pattern.

The traditional view of the Amazon rainforests has emphasized stability, with the dominant mode of forest regeneration occurring in light gaps created by fallen trees. Estimated tree-fall frequencies from several lowland tropical forests indicate that 3-5% of the forest is in the first 5 years of regeneration in light gaps³¹⁻³³. Our results show that the lateral erosion and channel changes of rivers repeatedly disturb all types of forest in the western Amazon lowlands, and thus create a mosaic of forests with higher age heterogeneity than could have resulted from regeneration in light gaps alone. Also, the nature of forest regeneration is fundamentally different in these two processes. The erosional disturbance is much more severe than disturbances caused by tree-falls. Regeneration on newly exposed fluvial deposits ('beaches') must start with the earliest phases of primary succession. Regeneration in tree-falls is due to growth of established saplings or of a well-developed seed bank. Finally, areas of riparian succession occur in long, continuous and dynamic strips along recent and abandoned river channels. This spatial

^{*} In the analysis, Andean rifts and areas shaded by clouds or other turbulence are excluded. The total area of each image is 33,300 km²





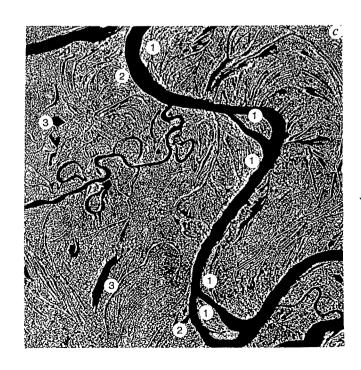


Fig. 2 (Left) a, Side-looking airborne radar (SLAR) image of the floodplain mosaic formed by the white-water river Ucayali at Pucallpa, Perú (8°15' S, 74°40' W). b, Simplified map of the forest disturbance site in a. The sequential successional forest is created on both sides of the meandering rivers Aguaytía and Juantía. As the meandering proceeds, the sequential successional forest is cut from different angles and a mosaic forest structure is created. During the annual flood cycle, sedimentation modifies the sequential meander scroll topography towards the flat topography of the former floodplain area. The previous floodplains are generally at a topographically higher level than the present floodplains. The denuded forest areas (upper left corner) representing the surface erosion relief pattern (convex-concave morphology) are being laterally eroded by the Rio Juantía. The transitional forest (lower right corner) is developing towards the denuded pattern. c, Detailed map of forest ground development. 1, Sites of intense primary succession at meander points leading to sequential successional forest. 2, Mosaic and transitional forest subject to lateral erosion at the outer curve of the meanders. 3, Isolated oxbow lakes. Based on ONERN SLAR image SC-18 3.A.

distribution differs markedly from the scattered distribution of light gaps.

We also propose that forest disturbance due to modern and past river dynamics is partially responsible for the high biological diversity in the upper Amazon basin^{34–36}, for several reasons. First, many distinct habitats are generated by erosional and depositional activity of rivers. As the forest succession and river bank erosion proceed, a mosaic of forests of different ages and on different soils is created (Fig. 2). A good example of this is the species richness of the Tambopata and Manú reserves in southeastern Peru^{30,36}, both of which are located at sites which have been, and still are, modified by relatively small meandering rivers (Rio Tambopata and Rio Manú, respectively) causing closely packed, small-scale habitat mosaics. Second, the habitats are highly stable in species composition and are relatively shortlived, so there is insufficient time for competitive exclusion³ Finally, the floodplains may differ profoundly in water and soil chemistry, mode of alluvial sedimentation, and case-historical bio-geographical events.

The river dynamics may also represent a mechanism leading to a pattern of equal allopatric speciation, as has been proposed to operate in the context of the Pleistocene refuges³⁸. The Pleistocene refuge theory states that the basis for the prevailing high species richness of the Amazon lowlands was laid down during the arid phases of the Pleistocene³⁹. During this time, the continuous forest was repeatedly fragmented into savannah-bordered isolates. Owing to the dynamic nature of the topmost sedimentary layer in the western Amazon, both floodplains separated by old denuded-soil forests and the denuded-soil

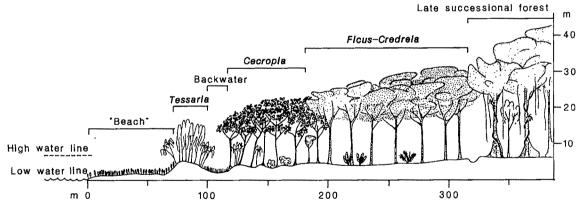


Fig. 3 Riparian succession in the sequential successional forest next to the Rio Manú at the Cocha Cashu biological station (11°53' S, 71°24' W). The scheme is a simplified transect of the Cocha Cashu meander loop from the point (left) towards the neck. The 'beach' is created by the deposition of river sediment on the point bar of the meander bank. The dominating species (~99%) is Tessaria integrifolia (Asteraceae). The persistence of Tessaria seedlings depends on the stability of the 'beach', successful colonization reaching maturity is expected to take place only once in a 4-yr period. Other primary successional species include: Baccharis salicifolia (Asteraceae), Cassia reticulata (Leguminosae), Cyperus spp. (Cyperaceae), Ipomoea spp. (Convolvulaceae), Ochroma lagopus (Bombacaceae) and Panicum spp. (Poaceae). The Tessaria-Gynerium zone is situated on the youngest point bar, the topography of which is accentuated by the deposition of sandy river sediment during the annual flooding of the river, predominantly during December-April. In the middle part of the zone, stands of reproductive Tessaria of equal age predominate. Both sides of the zone are dominated by Gynerium sagittatum (Poaceae). Gradually, Tessaria is replaced by Gynerium. The zone harbours seedlings of Cecropia cf. tessmannii (Moraceae), Cedrela odorata (Meliaceae) and Ficus insipida (Moraceae). The 10-30-m-wide backwater depression marks the previous position of the river channel, before accretion of the youngest point bar. During the high-water period the depression is often used as a secondary channel, or chute, as a result of turbulence in the flood waters. The backwater depressions run parallel to the river and their number in meander loops varies according to the local turbulence patterns. In the middle of the backwater depression runs a belt of Hymenachne donacifolia (Poaceae). The edges of backwater depressions are invaded by young Cecropia trees. As the backwater belt becomes subject to lesser annual flooding, the Cecropia forms a closed canopy over the belt. Before this, the stagnant water prevents the invasion of other trees or Gynerium. The Cecropia zone is located on the older meander scrolls with intermediate former backwater depressions. The dominating soil type is still fluvial sand. The forest is dominated by Cecropia tessmannii, forming an open canopy at 14-18 m. The gaps in the canopy promote patches of declining Gynerium. The gaps are filled by Caseara sp. (Flacourtiaceae), Cedrela odorata, Erythrina spp. (Leguminosae), Ficus insipida, Guarea sp. (Meliaceae) and Sapium sp. (Euphorbiaceae). The understorey includes members of the families Euphorbiaceae, Melastomataceae, Piperaceae and Acanthaceae. The topography in the Ficus-Cedrela zone is more gentle than in the previous stages due to the sedimentation of alluvial silt which is deposited annually during the flooding period, forming a layer above the riverine sands of the meander scrolls and chutes. The zonation characterizing the vegetation in the previous phases is diminishing. The closed forest canopy is formed mainly by fruiting Ficus insipida and Cedrela odorata. The understorey is dominated by thick growth of Heliconia spp. (Musaceae). The Ficus-Cedrela forest is characterized as the first zone containing palms. The topography of the late successional forest (mosaic forest) is generally flat, with minor depressions and gentle hills. The forest structure is further diversified by autogenic succession promoted by light gaps.

forests themselves may act as isolates within which biological differentiation can occur. There is a growing body of evidence that the number of species confined only to floodplain or denuded-soil forests is exceptionally high in the Amazon⁴ If the rivers repeatedly form new major floodplains and abandon old ones, subsequent secondary contact of formerly separated river systems, floodplains and denuded-soil forests may lead to species dynamics similar to the refuge pattern.

The ecological consequences of river dynamics and riparian primary succession also have profound implications for the conservation policies of the Amazon. As a major part of the forest has gone through riparian succession, the first phases of succession may be essential in determining the structure of the later successional forest. Conservation programmes based solely on the Pleistocene refuge theory may not preserve the present dynamic mechanism underlying the maintenance of high species diversity.

We thank F. S. Chapin, D. Davidson, I. Hanski, E. Haukioja, S. Hinneri, D. Janzen, O. Järvinen, K. J. Laine, O. V. Lindqvist, S. Neuvonen, D. Pearson, M. Räsänen, J. Tuomi, K. Viherkoski, P. Voss and T. Vuorisalo for constructive comments. J. Terborgh, L. Emmons and other workers at the Cocha Cashu biological station, Peru, provided invaluable help during the field work. T. Laurikainen and M. Mustonen drew the figures. ONERN, Lima, provided the SLAR and aerial photos of the monitored sites. The research was sponsored by the Academy of Finland under agreement 29/103 and by the Turku University Foundation.

Received 26 November 1985: accented 23 April 1986

- 1. Gentry, A. H. Pl. Syst. Evolut. 137, 95-105 (1981).
- Sioli, H. Forsch. Fortschr. 26, 274-280 (1950).
 Sioli, H. Geol. Rdsh 45, 608-633 (1957).

- Sioli, H. Amazoniana 1, 74-83 (1965).
 Fittkau, E. J. Münster. Forsch. Geol. Paläeont. 20/21, 35-50 (1971).
- 6. Meade, R. H., Dunne, T., Richey, J. E., de M. Santos, U. & Salati, E. Science 228, 488-490 (1985)
- 7. Junk, W. J. & Furch, K. in Amazonia (eds Prance, G. & Lovejoy, T. E., 3-17 (Pergamon, Oxford, 1985). Liu, K.-b. & Colinvaux, P. A. Nature 318, 556-557 (1985).

- 9. Servant, M. & Villarroel, R. Cr. hebd. Séanc. Acad. Sci., Paris 288, 665-668 (1979).
 10. Servant, M., Fontes, J.-C., Argollo, J. & Saliège, J.-F. Cr. hebd. Séanc. Acad. Sci., Paris 292, 1209-1212 (1981).
- Servant, M., Fontes, J.-C., Rieu, M. & Saliège, J.-F. C.r. hebd. Séanc. Acad. Sci., Paris 292, 1295-1297 (1981).
- Soubies, F. Cah ORSTOM, sér. Géal. XI, 133-148 (1980).
 Putzer, H. in The Amazon, Limnology and Landscape Ecology of a Mighty Tropical River and its Basin (ed. Sioli, H.) 15-46 (Junk, Dordrecht, 1984).
- 14. Irion, G. in The Amazon (ed. Sioli, H.) 201-214 (Junk, Dordrecht, 1984).
- Eden, M. J., McGregor, D. F. M. & Morelo, J. A. Z. Geomorph. 26, 343-363 (1982).
 Sombroek, W. G. Amazon Soils (Centre for Agricultural Publications and Documentation, Wageningen, 1966).

- Tricart, J. Annis Géogr. 84, 1-54 (1977).
 Mousinho de Meis, M. R. Revta bras. Geogr. 30, 3-20 (1968).
 Colinvaux, P. A., Miller, M. C., Liu, K.-b., Steinitz-Kannan, M. & Frost, I. Nature 313, 2007 (1998).
- 42-45 (1984).

 20. Klammer, G. in The Amazon (ed Sioli, H.) 47-83 (Junk, Dordrecht, 1984).

 21. Rüegg, W. & Rosenzweig, A. Soc. Geol. Perú Vol. Jubilar 113, 1-24 (1949).

 22. Gibbs, R. J. Bull. geol. Soc. Am. 78, 1203-1232 (1967).

 23. Irion, G. in Neotropische Ökosysteme (ed Müller, P.) 163-167 (Junk, The Hague, 1976).

- 24. Putzer, H. Mitt. Geol. Inst. TU Hannover 8, 87-96 (1968).
 25. ONERN Inventario, Evaluación e Integración de los Recursos Naturales de la Zona de los
- Ríos Inambari y Madre de Dios (Lima, 1972). 26. ONERN Inventario, Evaluación e Integración de los Recursos Naturales de la Zona Iberia-Iñapari (Lima, 1977).

- Iñapari (Lima, 1977).
 Paula Couto, C. de Iheringia 5, 3-17 (1978).
 Campbell, K. E. & Frailey, D. Quat. Res. 21, 369-375 (1984).
 Ule, E. Bot. Jb. 40, 114-172, 398-443 (1908).
 Terborgh, J. Five New World Primates (Princeton University Press, 1983).
 Hartshorn, G. S. Biotropica Suppl. 12, 23-30 (1980).
 Uhl, C. & Murphy, P. G. Trop. Ecol. 22, 219-237 (1982).
 Dourojeanni, M. J. R. & Ponce, C. F. in Los Parques Nacionales del Perú (eds Dourojeanni, M. J. R. & Ponce, C. F.) 176-201 (Infaco, Madrid, 1978).
 Hiccarracion, E. Ferweten Paul (INIV. EAO). PERI 181 (2002, 7, 1983).
- 34. Encarnacion, F. Proyecto PNUD/FAO/PER/81/002 7, 1983. 35. Lao, R. Rev. Forest. Perú 3, 1-61 (1969).
- 36. Brown, K. S. News Lepid. Soc. 1984, 45-47 (1984). 37. Connel, J. H. Science 204, 1344-1345 (1978).
- 38. Haffer, J. Science 165, 131-137 (1969)
- Prance, G. T. in Amazonia (eds Prance, G. T. & Lovejoy, T. E.) 146-165 (Pergamon, Oxford, 1985).
- Kinzey, W. G. & Gentry, A. H. in Primate Ecology: Problem-Oriented Field Studies (ed. Sussman, R. W.) 89-100 (Wiley, New York, 1979).
- 41. Remsen, J. V. & Parker, T. A. Biotropica 15, 223-231 (1983).
 42. Erwin, T. & Adis, J. in Biological Diversification in Tropics (ed Prance, G. T.) 358-371
- (Columbia University Press, New York, 1982).
 43. Pires, J. M. in *The Amazon* (ed. Sioli, H.) 581-602 (Junk, Dordrecht, 1984).

Normal maturation involves systematic changes in binocular visual connections in Xenopus laevis

S. Grant* & M. J. Keating†

National Institute for Medical Research, Mill Hill, London NW7 1AA, UK

Systematic changes in neuronal connections have been observed during the development of many vertebrate neuronal systems. These changes have usually involved a refinement from an initial exuberance of connections¹⁻⁴ or a response to some experimental perturbation⁵⁻⁸. Here we report on a system of neuronal connections, which, during a protracted developmental period, undergo ordered changes in response to normally occurring changes in functional requirements. In the frog Xenopus laevis, interocular alignment changes markedly during late larval and post-metamorphic life, producing a progressive enlargement of the binocular portion of the visual field^{9,10}. An intertectal system links the two mid-brain optic tecta and is concerned with the neural representation of binocular visual space. In the adult animal, connections in this system link corresponding points (points receiving information from one locus of binocular visual space) on the two tecta. Changes in eye position with development, however, change the set of corresponding points. Therefore, if the intertectal connections link corresponding tectal points throughout development, they must undergo an ordered change with time. We present electrophysiological evidence that the intertectal connections do, indeed, undergo such changes in response to changes in eye alignment, and that the changes are major.

In the late larval Xenopus the two eyes face laterally and there is no fronto-superior binocular visual field. As metamorphic climax approaches, changes in skull shape produce frontal and dorsal migration of the two eyes. This movement persists into post-metamorphic and adult life. Optical methods were used to determine the relative alignment of the two optic axes and the extent of the two monocular visual fields^{9,10}. These measurements indicated that the interocular angle changes from 160° at stage 60 (ref. 11), the onset of metamorphic climax, to 50° in adult life. The monocular visual field remains relatively constant between 195° and 200° throughout this period. The binocular visual field (the area of overlap of the two monocular visual fields) thus increases from ~35° at stage 60 to 45° at stage 62, 100° at stage 66 (the completion of metamorphic climax) and ~150° in adult life. This growth of the binocular visual field with age is plotted, on right eye-centred coordinates, in Fig. 1.

In the adult each optic tectum receives two projections of binocular visual space, one through each eye. The contralateral visuotectal projection is the product of the direct retinal fibre input from an eye to its contralateral optic tectum. The system of intertectal connections conveys visual information from the contralateral to the ipsilateral tectum and thus underlies the ipsilateral visuotectal projection 12-18. Figure 2 shows the four visuotectal projections in a normal adult. The adult ipsilateral visuotectal projection displays several characteristics: it arises from the full extent of the binocular visual field, it is topographically ordered, and is in register with the contralateral visuotectal projection to that optic tectum. Figure 2 legend outlines the analysis by which the pattern of functional intertectal connections may be determined from the visuotectal projections.

To determine whether the pattern of intertectal connections changes during normal development, visuotectal projections were mapped electrophysiologically in 52 animals from stage

^{*} Present address: Department of Anatomy, Medical College of Pennsylvania, 3200 Henry Avenue, Philadelphia, Pennsylvania 19129, USA

[†] To whom correspondence should be addressed.

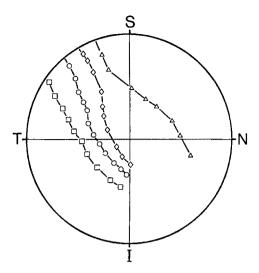


Fig. 1 Developmental changes in the extent of the binocular visual field in Xenopus. For these measurements, animals were placed at the centre of an Aimark projection perimeter (radius 33 cm) with the optic axis of the right eye aligned with the fixation point of the perimeter. The larger circle represents the visual field of the right eye, subtending some 200° of solid angle about the origin of this polar coordinate representation of visual space. The animal is thus positioned such that the right eye is looking out from the surface of the page. N, T, S and I are the nasal, temporal, superior and inferior poles of the visual field of the right eye. Reversible ophthalmoscopic methods used to determine the boundaries of the two monocular visual fields were those described by Grobstein and Comer⁹. The symbols represent the optically-determined naso-superior boundary of the visual field of the left eye at different developmental stages. The results are presented as mean observations from animals at stage 62 (\triangle , n=2), stage 66 (\diamondsuit , n=3), 3 months after metamorphosis (O, n=3) and adulthood $(\Box, n=4)$. Neither the range nor standard error bars are shown as they were of the same order of size as the symbols. The binocular visual field at any developmental stage is the overlap of the two monocular visual fields and is that area between the symbols and the naso-superior periphery of the visual field of the right eye.

Table 1 Degree of registration of ipsilateral and contralateral visuotectal projections to one tectum at different developmental ages

Age	Nasotemporal disparity (deg.)	Superoinferior disparity (deg.)
Stage $60-64 \ (n=107)$	1.5 ± 12.6	3.2 ± 10.0
Stage 66 $(n = 129)$	1.3 ± 10.0	0.3 ± 9.7
$3MAM \qquad (n=121)$	3.2 ± 10.8	0.2 ± 9.4
12MAM (n = 165)	0.8 ± 12.8	0.5 ± 7.4
Adult $(n=137)$	0.3 ± 9.9	0.4 ± 7.9

Values are mean ± s.d. MAM, months after metamorphosis. n, Number of electrode penetrations.

60 to adulthood. Detailed maps permitting such analysis were obtained in animals at stage 60 (2), stage 62 (4), stage 64 (5), stage 66 (10), and post-metamorphically at 2 weeks (8), 6 weeks (2), 3 months (10), 1 yr (7) and adulthood (4). Figure 3 shows representative results from animals at stages 62 and 66 and 3 months after metamorphosis. We found that, at all developmental ages studied, the ipsilateral visuotectal projection arose only from the binocular portion of the visual field and effectively occupied the entire binocular visual space then existing. This projection thus increased in size with age as the binocular visual field enlarged. There was a corresponding increase in the proportion of the tectal surface occupied by the ipsilateral visuotectal projection.

Table 1 provides data on the degree of registration between the ipsilateral and contralateral visuotectal projections to one

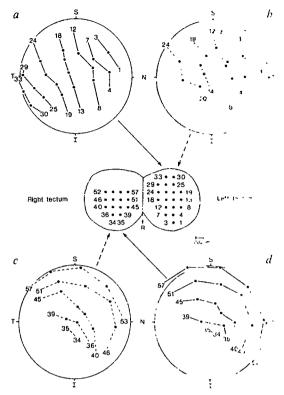


Fig. 2 The contralateral and ipsilateral visuotectal projections in a normal adult Xenopus. This animal, anaesthetized with MS 222 (ethyl m-aminobenzoate; Sigma) and subjected to partial craniotomy, was placed in an Aimark projection perimeter with its right eye centred (see Fig. 1 legend). The diagrams of the optic tecta show their outlines, transposed from a photograph of the dorsal surface, upon which a 100-µm grid was superimposed. Rostral is indicated by the direction of the midline arrow labelled R. Numbers and intermediate dots on the tectal diagram represent the sites of vertical microelectrode penetrations. Large circles denote perimetric chart representations of the visual field, with the optic axis of the right eye centred on the fixation point of the perimeter as in Fig. 1. The animal was not moved within the coordinate frame during the recording session, thus the four chart representations plot identical areas of visual space. For each microelectrode position the centre of the region in visual space, stimulation of which produced evoked unitary potentials at that electrode site, when viewed by either the right or the left eye, is indicated by the corresponding number of intermediate dots on the relevant chart representation. a, The contralateral visuotectal projection through the right eye; b, the ipsilateral visuotectal projection through the left eye; c, ipsilateral visuotectal projection through the right eye; d, contralateral visuotectal projection through the left eye. The indirect nature of the ipsilateral visuotectal pathway is denoted by the discontinuous lines within and from the visual field representations. N, T, S and I are the nasal, temporal, superior and inferior aspects of the visual field of the tested eye. Note that the two visual projections to each tectum are in register, for example, equivalent visual field positions 35 in c and d project through both right and left eyes to microelectrode position 35 in the right tectum. The pattern of intertectal connections may be derived from the visuotectal projections as follows: right tectal position 35 is receiving visual input from visual field position 35 through the contralateral left eye. This visual field position is identical to field position 21 which projects through the left eye to left tectal position 21. The presence of an ipsilateral visuotectal response at the left tectal position 21 indicates that visual information, conveyed from the left eye directly to right tectal position 35, has been relayed through the intertectal system to left tectal position 21. When this type of analysis is extended to other parts of the visuotectal projections through the left eye, it yields the overall pattern of intertectal connections relaying information from the right to the left tectum. Similar analysis of the visuotectal projections through the right eye to both tecta reveals the pattern of intertectal connections from the left to the right tectum. The latter are, in fact, the reciprocal of those from the right to the left tectum.

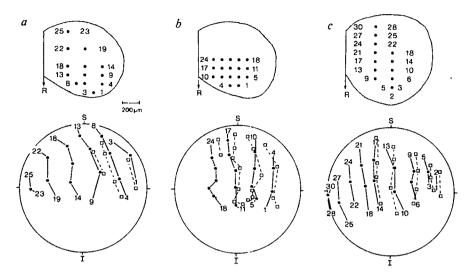


Fig. 3 Contralateral and ipsilateral visuotectal projections to the left tectum in representative animals at: a, stage 62; b, stage 66; and c, 3 months after metamorphosis. Conventions are essentially similar to those of Fig. 2, except that the two visuotectal projections are superimposed. The contralateral projections are represented by closed circles linked by continuous lines, the ipsilateral projections by open squares linked by dotted lines. Projections to the right optic tectum were also mapped but are not shown

tectum at various developmental ages. The nasotemporal and superoinferior disparities between the two visual field positions to one tectal locus were measured and the results grouped by developmental age. Apparently, there were no systematic disparities at any developmental age, indicating that throughout development the ipsilateral visuotectal projection through one eye was in register with the contralateral visuotectal projection through the other eye.

The patterns of intertectal connections at various stages of development from stage 60 to adulthood were determined from the visuotectal projections by the method outlined in Fig. 2 legend. To compare the connections at different developmental stages, it is necessary to know the nature of tectal growth during this period. We have recently reported¹⁰ the results of a detailed study on histogenetic and hypertrophic growth of both the retina and the tectum from stage 60 to adulthood. Summarizing the tectal results briefly, there was no significant tectal histogenesis during this period. From stage 60 until 3 months after metamorphosis there was little change in the linear dimensions of the tectum although these did increase thereafter. Tectal cell density counts indicated that this increase in tectal size was uniformly hypertrophic; this information was used to construct the diagram in Fig. 4, which shows the different points on the left optic tectum to which a given site near the rostral pole of the right optic tectum projects, via the intertectal system, at different developmental stages. When the ipsilateral visuotectal projection first appears at stage 60, the rostral pole of the right tectum is linked to a rostral region in the left tectum. As development proceeds through metamorphosis and juvenile life into adulthood, this same area of the right tectum is linked progressively to more caudal left tectal areas. Similar results are obtained if we consider other points on the right tectum participating in the intertectal system. With time, progressively more caudal right tectal areas are incorporated into the system, these project initially to rostral left tectal areas and are then displaced more caudally on the left tectum as new input arrives from the right tectum. The intertectal system itself is not a direct link but involves a synaptic relay in the nucleus isthmi¹⁴⁻¹⁸. Our present data do not allow us to determine which component(s) of the tecto-isthmo-tectal pathway is involved in this normal developmental plasticity. Other studies 17,19,20, however, suggest that it is the crossed isthmo-tectal projection that is the plastic component.

We conclude that the normal maturation of the intertectal system in *Xenopus laevis* is a highly plastic process. In response to the changing functional requirements presented by changing interocular alignment, the intertectal system undergoes a continuous and systematic change in its functional connections.

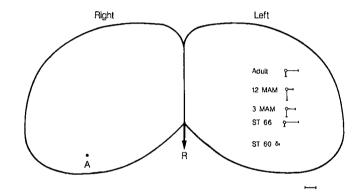


Fig. 4 Illustration of the changing intertectal connections during normal development in Xenopus. This diagram was constructed from patterns of intertectal connections derived, as explained in Fig. 2 legend, from animals of different developmental ages. For simplicity, the changing links of only one right tectal position (A) are shown. The diagram shows the positions on the left tectum which, at different stages of development, receive intertectal connections from the given position (A) near the rostral pole of the right tectum (MAM, months after metamorphosis; Ad, adult). As animals of different ages are involved in this analysis, allowance had to be made for tectal growth during this period (see text). The tectal diagrams represent tecta in adult animals. In plotting the results from younger animals on these tecta, the necessary corrections for tectal growth have been made. The open circles on the left tectum indicate the mean position for animals of that age (stage 60, n=2; stage 66, n=10; 3MAM, n=10; 12MAM, n=7; adult, n=4). The bars indicate the standard deviation in the rostro-caudal and medio-lateral tectal axes, except in the case of the two stage-60 animals, where they indicate the range. The rostro-caudal tectal positions of all age groups shown are statistically different from each other. Intertectal connections from the rostral region of the right tectum project, with age, to progressively more caudal positions on the left tectum. The converse is also true. As the normal intertectal projection is reciprocally symmetrical, this diagram also shows that, with age, intertectal connections from the left tectum to the rostral region of the right tectum arise from progressively more caudal tectal positions. Calibration bar, 200 μm.

The fact that the normal development of this system entails such continuous synaptic adjustments may explain why it is capable of responding with major readjustments to experimental perturbation of interocular alignment, as, for example, by early eye rotation 17,19,21-23. In both normal development and following eye rotation, the intertectal connections alter so as to link the new set of corresponding tectal points. Visual deprivation disrupts the normal development of the intertectal system 20,24,25

and prevents the readjustment of intertectal connections following eve rotation²⁴.

In the cat the first few months of postnatal life see a maturation of eye alignment²⁶⁻³¹ involving maturational changes in cortical and callosal systems associated with binocular vision3,31-33. These systems are also able to adjust following experimental alteration of eye alignment^{7,8,34-36}. It has been suggested that critical periods of experience-dependent development in both binocular visual³⁷⁻⁴⁰ and binaural auditory⁴¹ systems reflect a requirement for neuronal systems to adjust to growth-related changes in interocular or interaural geometry. In Xenopus the developmental changes in interocular geometry are particularly marked; the intertectal system in this species provides a clear demonstration that a neuronal system subserving binocular integration does, in fact, undergo extensive functional rewiring during normal maturation.

Received 11 November 1985; accepted 21 April 1986.

- 1. Redfern, P. A. J. Physiol, Lond. 209, 701-709 (1970).
- Crepel, F., Mariani, J. & Delhaye-Bouchaud, N. J. Neurobiol. 7, 567-578 (1976). Innocenti, G. M., Fiore, L. & Caminiti, R. Neurosci. Lett. 4, 237-242 (1977).
- LeVay, S., Wiesel, T. N. & Hubel, D. J. comp. Neurol. 191, 1-51 (1980).
 Raisman, G. Brain Res. 14, 25-48 (1969).
- 6. Hubel, D., Wiesel, T. N. & LeVay, S. Phil. Trans. R. Soc. B278, 377-409 (1977).
- 7. Lund, R. D., Mitchell, D. E. & Henry, G. H. Brain Res. 144, 169-172 (1978).
- Berman, N. E. & Payne, B. R. Brain Res. 274, 201-212 (1983).
 Grobstein, P. & Comer, C. Nature 269, 54-56 (1977).
- 10. Grant, S. & Keating, M. J. J. Embryol. exp. Morph. 92, 43-69 (1986).

- 11. Nieuwkoop, P. D. & Faber, J. A Normal Table of Xenopus laevis (D. ad.n.) 2nd edn
- (North-Holland, Amsterdam, 1967). 12. Gaze, R. M. & Jacobson, M. Q. Ji exp. Physiol. 47, 273-280 (1962).
- Keating, M. J. & Gaze, R. M. Q. Jl exp. Physiol. 55, 284-292 (1970)
 Glasser, S. & Ingle, D. Brain Res. 159, 214-218 (1978)
- Grobstein, P., Comer, C., Hollyday, M. & Archer, S. M. Brain Res 156, 117 123 (1978).
 Gruberg, E. R. & Udin, S. B. J. comp. Neurol. 179, 487-500 (1978).
- 17. Udin, S. B. & Keating, M. J. J. comp. Neurol. 203, 575-594 (1981)
- Grobstein, P. & Comer, C. J. comp. Neurol. 217, 54-74 (1983)
 Udin, S. B. Nature 301, 336-338 (1983).
- 20. Keating, M. J. & Kennard, C. Neuroscience (in the press).

 21. Gaze, R. M., Keating, M. J., Szekely, G. & Beazley, L. Proc. R. Soc. B175, 107, 147 (1973).
- Keating, M. J. Proc. R. Soc. B189, 603-610 (1975).
 Keating, M. J. Proc. R. Soc. B189, 603-610 (1975).
 Keating, M. J. Beazley, L., Feldman, J. D. & Gaze, R. M. Proc. R. Soc. B191, 445-466 (1975).
 Grant, S. & Keating, M. J. J. Physiol., Lond. 320, 19P-20P (1981).
- 26. Sherman, S. M. Brain Res. 37, 187-203 (1972).
- Olsen, C. R. & Freeman, R. D. Nature 271, 446-447 (1978)
 Elberger, A. J. Expl Brain Res. 36, 71-85 (1979).

- von Grünau, M. W. Expl Brain Res. 37, 41-47 (1979).
 Pettigrew, J. D. J. Physiol., Lond. 237, 49-74 (1974).
- 31. LeVay, S., Stryker, M. P. & Schatz, C. J. J. comp. Neurol. 179, 223-244 (1973) 32. Innocenti, G. M. Science 212, 824-827 (1981).
- Hubel, D. & Wiesel, T. N. J. Neurophysiol. 28, 1041-1059 (1965)
 Schlaer, R. Science 173, 638-641 (1971).
- Innocenti, G. M. & Frost, D. O. Nature 280, 231-234 (1979)
 Dürsteler, M. R. & von der Heydt, R. J. Physiol, Lond. 345, 87 105 (1983)
- 37. Keating, M. J. Br. med. Bull. 30, 145-151 (1974).

- Keating, M. J. Br. med. Bull. 30, 142-131 (1974).
 Blakemore, C. in Handbook of Sensory Physiology Vol. 8 (eds Hedl, F., Lebowitz, M. & Teuber, H. L.) 377-436 (Springer, New York, 1978).
 Pettigrew, J. D. in Neuronal Plasticity (ed. Cotman, C. W.) 311-330 (Raven No. York, 1978).
 Mitchell, D. E. in Development of Perception Vol. 2 (eds Aslin, J. N., Alberts, S. R. & Peterson, M. R. 3-43 (Academic, New York, 1981).
 Merzenich, M. M., Jenkins, W. M. & Middlebrooks, J. C. in Dynamical Aspect. of Neurotical Function (eds Edelman, G. M., Gall, W. E. & Cowan, W. M.) 397-424 (Wiley, New York, 1984). York, 1984).

Measurement of the intracellular free calcium concentration in salamander rods

P. A. McNaughton, L. Cervetto* & B. J. Nunn

Physiological Laboratory, University of Cambridge, Downing St, Cambridge CB2 3EG, UK

Measurement of the free calcium concentration within a photoreceptor outer segment has been considered an important aim since the proposal by Hagins and Yoshikami^{1,2} that the primary event in phototransduction is a release of Ca2+ inside the cell. More recent evidence3-6 has cast doubt on the calcium hypothesis, and the observations of Yau and Nakatani⁷ and Matthews et al.⁶ suggest that the internal Ca2+ concentration ([Ca2+],) may decrease after a flash of light. In the present study we have measured [Ca2+], directly by using a new method for incorporating the Ca-sensitive photoprotein aequorin into an isolated rod. We report that the light response is accompanied by a decrease in [Ca²⁺]_i, caused by the closure of light-sensitive channels which are the main route for Ca2+ entry into the outer segment. Of the Ca2+ entering through light-sensitive channels, about 95% is sequestered by a rapid and reversible buffering mechanism. Calcium is removed from the cell by an electrogenic pump³ in which 3 Na⁺ ions are exchanged for each Ca²⁺; the pump is highly active and the free Ca2+ in the cell declines with a time constant of ~0.5 s after a flash of light.

A rod mechanically isolated from the retina of the tiger salamander, Ambystoma tigrinum, was drawn, inner segment first, into a suction pipette, leaving the outer segment projecting into a solution which could be rapidly changed⁴. A whole-cell recording pipette was sealed against the outer segment membrane, and the membrane was broken by suction or by a pulse of current^{6,8,9}. Aequorin was then ejected from a fine plastic pipe inserted as close as possible (~100 µm) to the mouth of the whole-cell pipette, and was allowed to diffuse into the rod outer segment (ROS). The whole-cell pipette was gently withdrawn after ~10 min; the membrane usually reseals, leaving the aequorin-loaded rod in the suction pipette. Rods were loaded

with up to 4×10^4 counts using our method, corresponding to $\sim 4 \times 10^6$ aequorin molecules in the cell.

In normal Ringer's, the calcium concentration in the ROS is below the limit of resolution of the present method, and no significant change in [Ca²⁺]; could be detected during the response to a flash of light. From the cell in which the best loading was obtained, an upper limit of 0.6 µM (at the 95% confidence level) could be set for the free calcium concentration both in the dark and at the plateau of the light response.

The calcium concentration can be increased to detectable levels by using the phosphodiesterase inhibitor IBMX (3isobutyl-1-methylxanthine) which increases the intracellular level of cyclic GMP and consequently opens light-sensitive channels^{5,10,11}. Figure 1 shows that when IBMX was applied to the outer segment the light-sensitive current increased, and a burst of light was recorded from the aequorin-loaded cell. If the exposure to IBMX was prolonged the light-sensitive current oscillated, and each current maximum was accompanied by a burst of aequorin light emission. These results are difficult to reconcile with the idea that intracellular Ca2+ acts directly to close light-sensitive channels, since the light-sensitive current and free [Ca²⁺], increase at the same time. A more likely explanation is that light-sensitive channels are permeable to Ca2 (for which there is other evidence^{3,4,12}) and that [Ca^{2*}], rises because of the increase in light-sensitive current in the presence of IBMX. The oscillatory response to IBMX application was not seen in unloaded rods, and must be connected with absorption of the aequorin light by the photosensitive mechanism of the rod itself.

The effects of a flash of light on [Ca²⁺]_i were investigated in the experiment shown in Fig. 2. As in Fig. 1, [Ca2+], was first increased to measurable levels by applying IBMX, and a bright flash was then delivered at the peak of the increase in current (Fig. 2, trace 1). The flash caused a delayed decline in [Ca²⁺], and the free calcium level after the flash at no time exceeded that observed in the absence of a flash. A small, slowly declining inward current is visible at the plateau of the light response (marked with a triangle in trace 1 of Fig. 2a). This current has been attributed to the operation of a light-insensitive electrogenic Na/Ca exchange which reduces the Ca²⁺ level within the cell after a flash of light^{3,7,10}. Figure 2c supports this interpretation as the time course of the decrease in [Ca²⁺], correlates with the integral of this 'pumping current'.

^{*} Permanent address: Istituțo di Neurofisiologia del CNR, via San Zeno 51, 56100 Pisa, Italy.

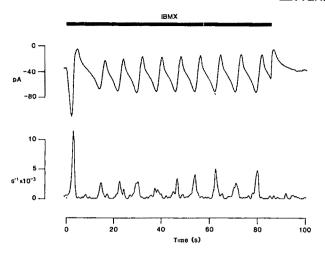


Fig. 1 Effect of exposure of the outer segment of an isolated rod loaded with aequorin to the phosphodiesterase inhibitor IBMX (0.5 mM). The upper panel shows the light-sensitive current recorded with a suction pipette. The lower panel shows the aequorin light output, expressed as rate of disintegration. The rate of disintegration was calculated as the ratio of the recorded count rate to the total counts in the cell, which were 5×10^3 ; the latter value was obtained by lysing the cell in 1 mM CaCl₂ at the end of the experiment and summing back the counts expended during the experiment. The period of oscillation was 8.3 s, and the peak aequorin light output occurred 0.63 s after the peak current. Methods. The traces were low-pass-filtered at 20 Hz; the aequorin light signal was in addition filtered digitally by convolving with a gaussian function of standard deviation 275 ms. This filtering operation does not cause a temporal shift. Composition of the normal Ringer's was (in mM): NaCl 110, KCl 2.5, MgCl₂ 1.6, CaCl₂ 1, glucose, 3, HEPES 10, neutralized to pH 7.6 with TMAOH (tetramethylammonium hydroxide). Composition of the solution filling the whole-cell pipette was (in mM): K-aspartate 110, EGTA 0.02, MgCl₂ 3, Na₂ATP 1, Na₂GTP 1, PIPES 10, neutralized to pH 7.2 with KOH. Aliquots of aequorin (0.1 µl at 20 mg ml⁻¹) were dialysed against the filling solution before use. The aequorin light was collected with a ×100 lens mounted on a Zeiss IM35 inverted microscope, and was focused onto the cathode of a photomultiplier tube (EMI 9789B) mounted in place of the binocular head. Single photons were counted by a Brookdeal quantum photometer. An aperture mounted at an intermediate image plane limited light collection to an area slightly greater than that of the outer segment.

Aequorin light came principally from the outer segment, as little

light was recorded with the aperture positioned over the inner segment¹³. The aperture was removed before lysis of the cell at

the end of the experiment.

The influx of Ca²⁺ into the cell can be measured directly by exposing the ROS to a solution in which all permeant ions have been replaced by Ca²⁺. Figure 3 shows an experiment of this kind. The influx of Ca²⁺ on exposure to isotonic Ca²⁺ was followed by a rise in the emission of light from the aequorin and a subsequent closure of light-sensitive channels. In contrast to the experiment of Fig. 2 (in the presence of a normal concentration of Na), there was little decline in the light emission after the closure of the channels; the observed slow decline in Fig. 3c is attributable largely to consumption of aequorin by the large increase in [Ca2+]i. On restoration of a normal concentration of Na, there was a rapid decline in [Ca2+], and a large light-insensitive pumping current. The rate of decline of free [Ca²⁺]; on restoration of Na was ~30 μM s⁻¹, compared with a rate of $< 0.6 \,\mu\text{M s}^{-1}$ in the absence of Na (see Fig. 3 legend). This experiment shows that the maximal activity of the Na/Ca exchange is at least 50 times greater than that of other Ca pumps in the outer segment membrane.

In the experiment shown in Fig. 3, the total charge flowing during the application of isotonic Ca^{2+} was 46 pC and the total charge transferred by the pump was 20.6 pC, consistent with a $3 \text{ Na}^+/1 \text{ Ca}^{2+}$ stoichiometry for the pump³. In this experiment

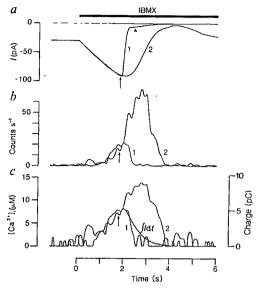


Fig. 2 Effect of a flash of light on [Ca²⁺]_i. a, Light-sensitive current obtained with a light flash (4.0×10⁴ Rh*) delivered at the arrow (trace 1), or in the dark (trace 2). The triangle marks the pumping current at the plateau of the light response. b, The aequorin light output. c, [Ca²⁺]; calculated from the rate of disintegration of aequorin by using a calibration curve supplied by Dr J. Blinks. Over the range $0.1 \,\mu\text{m} < [\text{Ca}^{2+}] < 30 \,\mu\text{m}$ and with free $[Mg^{2+}] = 1$ mM, the curve was well fitted by the function $[Ca^{2+}] =$ A(rate of disintegration)^y, where $A = 4.67 \times 10^{-5} \text{M}$ and y = 0.417. The integral of the pumping current (smooth trace, right-hand ordinate) is also shown in c. Traces are the mean of five presentations. The gaussian filter for the aequorum trace had a standard deviation of 65 ms. Total counts in the cell were 5.3×10^3 , and we assumed for the purpose of calculating [Ca2+]; that 26% of the aequorin was in the outer segment since this was the maximum fraction of the total counts which could be exhausted by a rapid elevation of [Ca2+]i.

the suction pipette collected 52% of the outer segment current, as judged by the ratio of bright flash responses recorded by the whole-cell pipette to those recorded by the suction pipette at the start of the experiment. From this collection ratio, and taking an outer segment volume of 2 pl, of which half is assumed to be occupied by the disks, we calculate that the total $[Ca^{2+}]_i$ increased by 458 μ M in the cytoplasmic space of the outer segment; the observed rise in $[Ca^{2+}]_i$ was less than this value by a factor of ~20, showing that about 95% of the Ca^{2+} entering the outer segment is bound and is not free to interact with aequorin. The binding mechanism must be rapid and reversible, as there was a good temporal correlation between the change in $[Ca^{2+}]_i$, as measured from the aequorin light output, and the integrals of both the Ca^{2+} influx and the pumping current.

Figure 4 shows the results of an experiment in which a large increase in light-sensitive current resulted from exposure to low external Ca^{2+} (ref. 4) in the absence of IBMX. In this experiment the increase in current did not cause an increase in [Ca]_i, but on return to Ringer's containing 1 mM Ca there was a large influx of calcium through light-sensitive channels and an increase in aequorin light emission. The subsequent decline in $[Ca^{2+}]_i$ correlates well with the time course of charge transfer by the pump (see Fig. 4c). The rate of decline was slower than in the experiments of Figs 2 and 3, perhaps because of the build-up of Na_i during the preceding large current flow. From the total charge transferred by the pump we calculate that 24% of the current flowing on return to normal Ringer's was carried by Ca^{2+} .

The results described here can be used to estimate the normal free $[Ca^{2+}]_i$ when the rod is bathed in Ringer's. In the presence of a bright light $[Ca^{2+}]_i$ is likely to be low, in view of our finding that the main route of entry is via the light-sensitive channel.

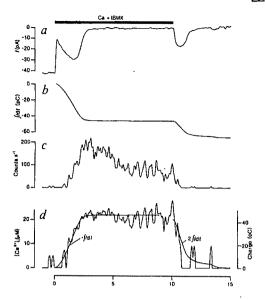


Fig. 3 a, Membrane current recorded during exposure to an isotonic CaCl₂ solution containing (in mM): CaCl₂ 77.6, HEPES 10 (pH 7.6), IBMX 0.5. The junction current has been subtracted⁴. The elevation in Ca²⁺ caused an initial rapid suppression of current, due to an external action⁴, followed by a rise due to the inhibition of phosphodiesterase by the IBMX. The subsequent decrease is due to closure of light-sensitive channels by the aequorin light emission; the light-sensitive current remained completely suppressed until after the end of the trace shown in a. b, Integral of the membrane current in a, beginning from the time of admission of isotonic Ca²⁺. Note that the integral of the current carried by Ca^{2+} is approximately double that of the pumping current. c, The aequorin light output. d, Calculated change in $[Ca^{2+}]_i$ (noisy trace, left-hand ordinate) based on the assumptions outlined in Fig. 2 legend. Based on these assumptions, no decline in $[Ca^{2+}]_i$ is observed during exposure to isotonic Ca^{2+} , and the rate of decline on restoration of Na is 30 µM s⁻¹. If instead we make the extreme assumption that all the aequorin is in the outer segment, then the rate of decline of $[Ca^{2+}]_i$ is $0.6\,\mu\text{M}\,\text{s}^{-1}$ during the exposure to isotonic Ca²⁺. Total counts in the cell were 4.6×10³. The smooth traces (right-hand ordinate) in d compare the time courses of the integrals of the light-sensitive and pumping currents with the time course of the change in [Ca²⁺],.

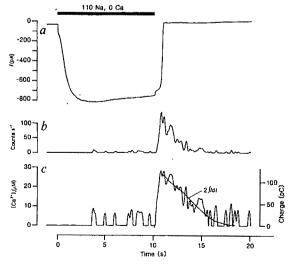


Fig. 4 Membrane current (a), aequorin light output (b) and $[Ca^{2+}]_i$ (c) during exposure to Ringer's containing 0 Ca and 2 mM BAPTA¹⁴. The smooth trace (right-hand ordinate) in c is the integral of the pumping current observed after all light-sensitive channels had been closed by the strong aequorin light emission. The absence of bumps at the beginning of the traces in b and c, which was not seen in other records, is not significant. Total counts in the cell, 1.86×10^3 . For other details, see Fig. 2 legend.

After a bright flash of light the pumping current at the plateau of the response declines with a time constant of ~ 0.5 s, and carries a total charge of ~0.5 pC, as measured with a suction pipette^{7,10}. If we assume a current collection efficiency of 50% and if the pump operates as a $3Na^{+}/1Ca^{2+}$ exchange, this charge transfer corresponds to a change in total [Ca²⁺]; of 10 µM when distributed over an effective outer segment volume of 1 pl. If 95% of this Ca²⁺ is bound, the free [Ca²⁺]_i in the dark will be 0.5 µM, which is slightly below our present detection limit of 0.6 µM. As we find that the time course of decline of free [Ca²⁺ correlates well with the time course of the integral of the pumping current, we expect that the effect of a bright flash will be to reduce [Ca²⁺], from its dark level of ~0.5 μM to a much lower level with a time constant of ~ 0.5 s.

This work was supported by the MRC and by an EMBO fellowship (to L.C.). B.J.N. is a Lister Institute Research Fellow. We thank Drs J. R. Blinks and P. H. Cobbold for supplies of aequorin and for advice, and Professor A. L. Hodgkin, Dr T. D. Lamb and Mr L. Lagnado for helpful discussions.

Received 12 December; accepted 17 April 1986.

- 1. Hagins, W. A. A. Rev. Biophys. Bioengng 1, 131-158 (1972).
- Hagins, W. A. & Yoshikami, S. Expl Eye Res. 18, 299-305 (1974). Yau, K.-W. & Nakatani, K. Nature 311, 661-663 (1984).
- Hodgkin, A. L., McNaughton, P. A. & Nunn, B. J. J. Physiol., Lond. 358, 447-468 (1985). Fesenko, E. E., Kolesnikov, S. S. & Lyubarsky, A. L. Nature 313, 310-313 (1985). Matthews, H. R., Torre, V. & Lamb, T. D. Nature 313, 582-585 (1985). Yau, K.-W. & Nakatani, K. Nature 313, 579-582 (1985).

- 8. Hamill, O. P., Marty, A., Neher, E., Sakmann, B. & Sigworth, F. J. Eur. J. Physiol. 391, 85-100 (1981)
- Cobbs, W. H. & Pugh, E. N. Nature 313, 585-587 (1985).
- Cervetto, L. & McNaughton, P. A. J. Physiol., Lond. 370, 91-109 (1986).
 Capovilla, M., Caretta, A., Cavaggioni, A., Cervetto, L. & Sorbi, R. T. Prog. Retinal Res.
- 2, 233-247 (1983).
- 12. Capovilla, M., Caretta, A., Cervetto, L. & Torre, V. J. Physiol., Lond. 343, 295-310 (1983).
- Cervetto, L., McNaughton, P. A. & Nunn, B. J. J. Physiol., Lond. 371, 36P (1986).
 Tsien, R. Y. Biochemistry 19, 2396-2404 (1980).

Mediation of thalamic sensory input by both NMDA receptors and non-NMDA receptors

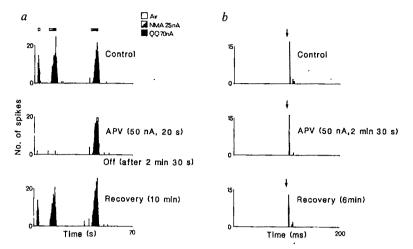
T. E. Salt

Department of Physiology, University College, Cardiff, PO Box 78, Cardiff CF1 1XL, UK

Excitatory amino acids such as L-glutamate and L-aspartate are well established as neurotransmitter candidates in the mammalian central nervous system¹, and three types of receptor for these substances have been proposed, characterized by the agonists N-methyl-D-aspartate (NMDA), kainate and quisqualate¹. All these receptors have been suggested to have synaptic roles in excitatory transmission in the brain¹⁻⁷. Here I demonstrate that NMDA receptors play a crucial role in the observed response of ventrobasal thalamus (VB) neurones to natural stimulation of somatosensory afferents, but do not appear to be responsible for the short-latency excitation seen on electrical stimulation of the afferents, which is apparently mediated by excitatory amino-acid receptors of the non-NMDA type. This result indicates an involvement of both NMDA and non-NMDA receptors in the responses of VB neurones to stimulation of somatosensory afferents, depending on the mode of stimulation of the pathway.

Recordings, using extracellular iontophoretic electrodes, were made from single neurones in the ventrobasal thalamus of rats anaesthetized with urethane (1.2 g per kg intraperitoneal). Responses of VB neurones to physiological stimulation of hair or vibrissa follicle afferents (using an air jet) and iontophoretic application of N-methylaspartate (NMA) and either kainate (14 neurones) or quisqualate (14 neurones), were challenged

Fig. 1 Peristimulus time histograms of action potentials recorded from a single VB neurone with one barrel of a five-barrelled iontophoretic electrode. Action potentials were discriminated on the basis of amplitude and waveform. The vertical axis of each histogram is the number of action potential spikes counted into epochs of either 250 ms (a) or 1 ms (b). Each drug barrel of the electrode contained one of the following: N-methylaspartate (NMA, 0.2 M, pH 8.0), quisqualate (QQ, 25 mM in 75 mM NaCl, pH 8.0), kainate (KA, 0.1 M, pH 8.0), APV (50 mM in 150 mM NaCl, pH 8.0), kynurenate (KYN, 50 mM, pH 8.0), acetylcholine (ACh, 0.5 M, pH 3.5), carbamylcholine (CCh, 0.2 M, pH 4.0) or 1 M NaCl. Automatic current balancing was used in this experiment, but qualitatively identical results were found in experiments where balancing was not performed. In three experiments a sevenbarrelled electrode was used. a, Top record shows the control responses (averaged over two trials) of a neurone to an air jet, directed so as to deflect the hairs within its receptive field, and to iontophoretic application of NMA



and QQ. The three stimuli were applied at the time and for the durations indicated by the bars above the record. The middle record shows the responses of the same neurone to the same three stimuli, but during the concurrent ejection of APV. APV antagonized the responses to the air jet stimulus and NMA, but had little effect on the response to QQ. The bottom record shows the same sequence, but 10 min after termination of the APV ejection when responses to the air jet and NMA had recovered to their control levels. b, Response of the same neurone as in a to electrical stimulation (0.1-ms pulse, 10 V, 0.5-Hz repetition rate) of the afferent pathway delivered via needle electrodes within the peripheral receptive field. In all experiments the stimulus intensity was adjusted to the minimum necessary to evoke a short-latency response. The time of stimulation is indicated by an arrow above each histogram. The records are averaged over 20 trials. The middle record shows the response of the neurone to the stimulus during the ejection of APV. The antagonist had little effect on the electrically evoked response, even though the APV ejection was for a longer duration than that necessary to antagonize responses to the air jet and NMA.

with concurrent application (0-50 nA) of the selective NMDA antagonist D-2-amino-5-phosphonovalerate $(APV)^1$. This antagonist was found to antagonize the responses to NMA but not responses to kainate or quisqualate, and had little effect on the spontaneous activity of VB neurones. It was also possible to antagonize the responses of the VB neurones to the physiological stimulus by 42-100% (mean = 80%), using the same APV ejection currents, in 26 of the 28 neurones studied in this way (Fig. 1a). The response of 11 of these neurones to single-pulse electrical stimulation of the afferent pathway was then studied. The

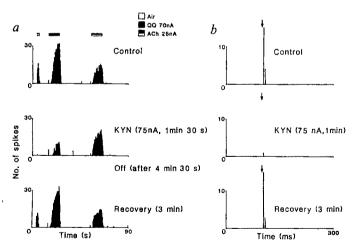


Fig. 2 a, Similar records to those in Fig. 1, but from another neurone which responded to the air jet stimulus and to iontophoretic ejection of QQ and ACh applied as indicated by the bars above the records. Below the control record is shown the same sequence during the ejection of kynurenate (KYN). A complete antagonism of the air jet response was evident, and the responses to QQ were also greatly reduced. No reduction in the response to ACh was seen. The bottom record shows recovery from the effects of kynurenate 3 min after the end of the antagonist ejection. b, Responses of the same neurone to single-pulse electrical stimulation in its peripheral receptive field at the time indicated by the arrows (15 trials). Middle record shows the response of the neurone during the ejection of kynurenate. The antagonist greatly reduced the response to the stimulus.

short-latency (4-10 ms) response evoked by such a stimulus was challenged with the same iontophoretic current of APV that had previously been found to be effective against NMA and the physiologically evoked response, and in all of these cases the antagonist was found to be ineffective against the electrically evoked response (Fig. 1b). In contrast, the broad-spectrum excitatory amino-acid antagonist kynurenate^{4,8} (10-150 nA), which antagonized the responses of VB neurones to quisqualate in addition to the responses to NMA and the physiological stimulus, blocked the responses to electrical stimulation by 54-100% (mean = 86%) in 11 neurones (Fig. 2). Responses to the cholinergic agonists acetylcholine and carbamylcholine remained largely unaffected by kynurenate, although in some cases a small excitatory effect of the antagonist became evident.

These results suggest that an excitatory amino acid functions as the transmitter mediating the responses of VB neurones to stimulation of second-order sensory afferents. This mechanism is consistent with those suggested previously^{9,10}, and with data on the retino-geniculate projection^{11,12}. In addition, it seems likely that the excitation observed in response to stimulation of the afferent pathway is composed of at least two separate components. The first of these components, which can be selectively evoked at short latency by single-pulse electrical stimulation in the peripheral receptive field, is apparently mediated by excitatory amino-acid receptors of the non-NMDA type, as it is antagonized by kynurenate but not by APV. It is unlikely that this response is resistant to APV because the response has a high safety factor, as threshold stimulus intensities were used and the response could be antagonized by kynurenate, which might be expected to be ineffective if the response had a high safety factor. The finding that the response of VB neurones to physiological stimulation of the sensory afferents is greatly reduced by the selective NMDA antagonist APV implies an additional response component, which is mediated by NMDA receptors and which is recruited during physiological stimulation. It is tempting to speculate that it is the pattern of afferent activity which governs the recruitment of the APV-sensitive response, as the response of the VB neurones to the air jet is a train of action potentials (typically of frequency ~20 Hz) lasting for the duration of the stimulus (0.5-2 s), while the response to the single-pulse electrical stimulus is one or two action potentials. To test this possibility further, electrical stimulation was performed in 20-Hz trains on 10 neurones in which APV was found to antagonize the physiologically evoked response. For nine of these neurones, APV was found to antagonize the response to the stimulus train. In particular, the later components of the response appeared more susceptible to APV (Fig. 3). Note that the APV-sensitive component of this response does not appear to be larger than the APV-insensitive component; this suggests that the APV-insensitive component becomes less effective during the stimulus train, possibly because of activation of inhibitory processes in the thalamus¹³. Clearly, experiments using intracellular recording would provide further information on this matter.

It is conceivable that, under physiological conditions, the NMDA receptor component potentiates an already present, but possibly sub-threshold, excitatory input mediated by non-NMDA excitatory amino-acid receptors (presumably of the kainate or quisqualate type). This hypothesis is attractive in view of recent work which shows that responses of neurones to NMDA are subject to voltage-dependent blockade by Mg2+ ions in the physiological concentration range for Mg²⁺ (refs 6, 14, 15), and it is noteworthy that a postsynaptic potential involving a short-latency non-NMDA component and an NMDA component of longer latency have been found in the spinal cord of Xenopus¹⁶. The recruitment of NMDA receptors could be a purely synaptic phenomenon similar to the APV-sensitive longterm potentiation observed in the hippocampus⁷, and might involve one type of excitatory amino acid being released onto both NMDA and non-NMDA receptors. Alternatively, the two types of response could be mediated by two afferent pathways to the thalamus which terminate on the same neurone. Evidence for such multiple pathways already exists 17,18

The NMDA receptor-mediated response of VB neurones to physiological stimulation of afferents provides a possible site of action for the dissociative anaesthetic ketamine, which has been shown to possess NMDA antagonist properties^{6,19}. This contrasts with previous findings in the dorsal horns of the spinal cord²⁰ and medulla³, where NMDA antagonists were found to be ineffective in blocking responses to air jet deflection of hairs and vibrissae. As there are no major procedural differences between the present experiments and those performed on the medullary dorsal horn³, it seems likely that the observed difference reflects a regional difference between the dorsal horn and thalamus. Thus, it is possible that the thalamus is a major site for the anaesthetic action of ketamine.

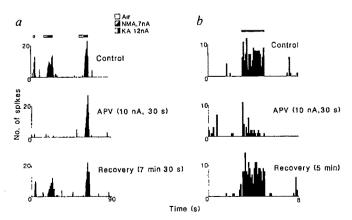


Fig. 3 a, Similar records to those in Fig. 1 (500 ms epochs), but from a neurone responding to air jet stimulation and iontophoretically applied NMA and kainate (KA). APV selectively and reversibly antagonized the responses to the air jet and NMA. b, Records from the same neurone as in a, showing the responses to a train of electrical stimuli (20 Hz, 0.1-ms pulse, 2 s duration, 100 ms epochs, 5 trials). The time of stimulation is indicated by the vertical lines above the top record. The middle record shows the response of the neurone during the ejection of APV, and the bottom record shows the recovery after termination of the APV ejection.

I thank Ms V. Crimmins for technical assistance. This work was supported by the MRC (UK).

Received 14 January: accepted 16 April 1986.

- Watkins, J. C. & Evans, R. H. A. Rev. Pharmac. Tox. 21, 165-204 (1981)
 Davies, J. & Watkins, J. C. Brain Res. 327, 113-120 (1985).
 Hill, R. G. & Salt, T. E. J. Physiol, Lond. 327, 65-78 (1982).
- Herrling, P. L. Neuroscience 14, 417-426 (1985).
- Crunelli, V., Forda, S. & Kelly, J. S. J. Physiol., Lond. 341, 627-640 (1983).

- Crunell, V., Forda, S. & Keily, J. S. J. Physiol., Lond. 341, 621-640 (183).

 Thomson, A. M., West, D. C. & Lodge, D. Nature 313, 479-481 (1985).

 Collingridge, G. L., Kehl, S. J. & McLennan, H. J. Physiol., Lond. 334, 33-46 (1983).

 Perkins, M. N. & Stone, T. W. Brain Res. 274, 184-187 (1982).

 Haldeman, S., Huffman, R. D., Marshall, K. C. & McLennan, H. Brain Res. 39, 419 425 (1972).

 10. Ben-Ari, Y. & Kelly, J. S. J. Physiol, Lond. 251, 25P-27P (1975).

 11. Crunelli, V., Leresche, N. & Pirchio, M. J. Physiol, Lond. 365, 40P (1985).

 12. Kemp, J. A. & Sillito, A. M. J. Physiol, Lond. 323, 377-391 (1982).

 13. Andersen, P., Eccles, J. C. & Sears, T. J. Physiol, Lond. 174, 370-399 (1964).

 Name J. Breschier, J. R. & Sallito, A. Marker, P. Hecher, A. & Perchier, A. Name

- 14. Nowak, L., Bregestovski, P., Ascher, P., Herbert, A. & Prochiantz, A. Nature 307, 462-465
- 15. Mayer, M. L. & Westbrook, G. L. J. Physiol., Lond. 361, 65-90 (1985)
 - Dale, N. & Roberts, A. J. Physiol., Lond. 363, 35-59 (1985)
- Hongo, T. & Koike, H. in The Somatosensory System (ed. Kornhuber, H. H.) 218 226 (Georg Thieme, Stuttgart, 1975).
- 18. Albe-Fessard, D., Berkley, K. J., Kruger, L., Ralston, H. J. III & Willis, W D. Brain Res Ren. 9, 217-296 (1985).
- Anis, N. A., Berry, S. C., Burton, N. R. & Lodge, D. Br. J. Pharmac. 79, 565-575 (1983)
 Anis, N. A., Heradley, P. M., Lodge, D. & West, D. C. J. Physiol., Lond 328, 199 (1982)

Frequency-dependent involvement of NMDA receptors in the hippocampus: a novel synaptic mechanism

Caroline E. Herron, Robin A. J. Lester, Elizabeth J. Coan & Graham L. Collingridge

Department of Pharmacology, University of Bristol, Medical School, University Walk, Bristol BS8 1TD, UK

Acidic amino acids, such as L-glutamate, are believed to be excitatory neurotransmitters in the mammalian brain 1,2 and exert effects on several different receptors named after the selective agonists kainate, quisqualate and N-methyl-D-aspartate (NMDA)1. The first two receptors, collectively termed non-NMDA receptors, have been implicated in the mediation of synaptic transmission in many excitatory pathways in the central nervous system (CNS), whereas NMDA receptors, with few exceptions, do not appear to be involved2; this is typified in the hippocampus where there is a high density of NMDA receptors3 yet selective NMDA receptor antagonists, such as D-2-amino-5-phosphonovalerate (APV), do not affect synaptic potentials⁴⁻¹¹. NMDA receptors have, however, been shown to be involved in long-term potentiation (LTP) in the hippocampus⁶⁻¹¹, a form of synaptic plasticity¹² which may be involved in learning and memory¹¹. NMDA receptors have also been found to contribute to epileptiform activity in this region 13,14. We now describe how NMDA receptors can participate during high-frequency synaptic transmission in the hippocampus, their involvement during low-frequency transmission being greatly suppressed by Mg2+. A frequency-dependent alleviation of this blockade provides a novel synaptic mechanism whereby a single neurotransmitter can transmit very different information depending on the temporal nature of the input. This mechanism could account for the involvement of NMDA receptors in the initiation of LTP and their contribution, in part, to epileptic activity.

Experiments were performed on transverse hippocampal slices prepared from adult female rats as described previously¹⁵. The standard perfusion medium comprised (in mM): NaCl 124, NaHCO₃ 26, NaH₂PO₄ 1.2, KCl 3 or 5, MgSO₄ 1 or 2, CaCl₂ 2, D-glucose 10. Extracellular and intracellular recordings were obtained from the CA1 cell body region using electrodes containing NaCl (1-4 M) and CH₃COOK (3 M), respectively. The Schaffer collateral-commissural pathway was stimulated with single shocks delivered at 10-30-s intervals to elicit 'low-

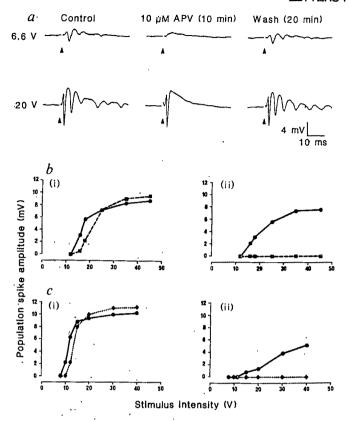


Fig. 1 Effects of NMDA antagonists on field potentials recorded extracellularly from the CA1 cell body region in response to low-frequency stimulation of the Schaffer collateral-commissural pathway. a, Effect of 10 μM APV on responses at two stimulus intensities (6.6 V and 20 V). b, Amplitude of the primary (i) and secondary (ii) population spikes as a function of stimulus intensity in control medium (continuous line) and in the presence of 20 μM APV (broken line) in another hippocampal slice. c, Data presented in the same manner as b for a different slice, showing the effects of 100 μM Mg²⁺.

frequency' synaptic responses and for periods of 200 ms at 10-ms intervals to evoke 'high-frequency' responses. The selective NMDA antagonist APV was administered via the perfusion medium (flow rate $1-2 \text{ ml min}^{-1}$). In the absence of APV, high-frequency stimulation often produced LTP of the excitatory postsynaptic potential (e.p.s.p), therefore periods of high-frequency stimulation were delivered first in the presence and subsequently following washout of APV. The data were tested for significance (P < 0.05) using paired Student's t-tests.

Field potentials were recorded from the CA1 cell body region in response to low-frequency stimulation of the Schaffer collateral-commissural pathway with no $\mathrm{Mg^{2+}}$ in the bathing medium ¹⁶. At low stimulus intensities the synaptic response was greatly suppressed (Fig. 1a) or abolished by 10 or 20 μ M APV. In contrast, at higher stimulus intensities, the secondary population spikes were abolished while the primary population spike was little affected by APV (Fig. 1a, b), presumably because non-NMDA excitatory amino-acid receptors could sustain this component of the response⁶. These effects were fully reversible and seen in all 10 hippocampal slices examined. An identical pattern of antagonism was also observed with $\mathrm{Mg^{2+}}$ (100 μ M) in all four slices tested (Fig. 1c).

These results demonstrate for the first time that NMDA receptors mediate a synaptic response in hippocampal neurones that has as low a threshold as that of non-NMDA receptors, provided Mg²⁺ is absent from the extracellular medium; this could be accounted for by the neurotransmitter having a high affinity for NMDA receptors, which would only be seen functionally when the Mg²⁺ block of NMDA channels was removed. The con-

centrations of Mg^{2+} (dose-dependent over the range $20-500~\mu M$) that affect this component are the same as those that directly block postsynaptic responses to $NMDA^1$ and are much lower than those expected to affect significantly transmitter release¹⁷ or membrane stabilization¹⁸; they are also much lower than the generally accepted levels of Mg^{2+} in extracellular fluid. It is likely, therefore, that a major action of Mg^{2+} in the hippocampus is to exert a powerful controlling influence on synaptic transmission by a direct interaction with the NMDA receptor system.

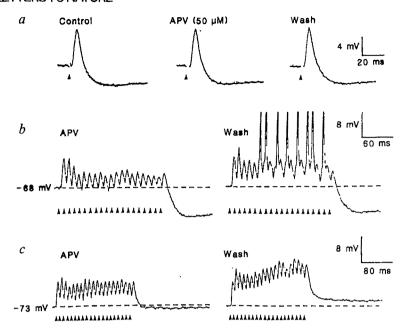
A second series of experiments was performed to determine the extent of the involvement of the NMDA receptor system in synaptic transmission in the hippocampus in the presence of physiological concentrations of Mg²⁺ (1-2 mM). Passive membrane properties, determined for 27 CA1 neurones (resting membrane potential -69±1 mV; input resistance, calculated near the resting membrane potential, $27 \pm 1 \text{ M}\Omega$), were not altered significantly by APV (20 or 50 µM). Stimulation of the Schaffer collateral-commissural pathway at low frequencies evoked a fast e.p.s.p. which was unaffected by APV (Fig. 2a). Measurements (mean ± s.e.m.) of peak amplitude and duration at 50% of peak amplitude in control solutions $(8.3 \pm 0.6 \text{ mV}; 9.6 \pm 0.8 \text{ ms})$ and in the presence of APV $(8.4\pm0.6 \text{ mV}; 9.3\pm0.6 \text{ ms})$ were not significantly different (n=32). The inhibitory postsynaptic potential (i.p.s.p.) which followed the fast e.p.s.p. was generally unaffected by APV (Fig. 2a).

In contrast to the lack of effect on low-frequency synaptic responses, APV had a marked effect on the synaptic response generated by high-frequency stimulation. During highfrequency stimulation, fast e.p.s.ps were associated with a slow depolarizing potential. APV (20 or 50 µM) had no effect on fast e.p.s.ps evoked during high-frequency stimulation (Fig. 2c); it did, however, reduce the size of the associated slow depolarization, measured from the pre-stimulus membrane potential to the base of the fast e.p.s.ps, in 17 of 22 neurones examined (Fig. 2b, c). The mean (\pm s.e.m.) amplitude of the depolarization. measured at 140-150 ms into the high-frequency train, for these 17 cells in the presence and after washout of APV, was $5.3 \pm$ 0.9 mV and $8.3 \pm 1.0 \text{ mV}$, respectively. The size of the NMDA receptor-mediated potential calculated individually for each cell varied between 0.9 and 5.1 mV (mean \pm s.e.m., $3.0 \pm 0.2 \text{ mV}$). This NMDA receptor-mediated e.p.s.p. became apparent in some cells as early as the second fast e.p.s.p. in the high-frequency train (Fig. 2b, c).

The lack of effect of APV on low-frequency synaptic transmission in the Schaffer collateral-commissural pathway is in agreement with previous reports using extracellular recording⁵⁻⁹. but contrasts with a recent intracellular study which reported that APV depressed the fast e.p.s.p. 19. The latter effect can be attributed to the use of high concentrations of the racemic mixture of APV, which has previously been shown to depress synaptic transmission in this pathway by an action unrelated to NMDA-receptor antagonism⁷. As low-frequency synaptic responses in this pathway can be reduced by broad-spectrum excitatory amino-acid antagonists, such as y-D-glutamylglycine⁶, it is believed that receptors of the kainate or quisqualate (that is, non-NMDA) type are responsible for fast e.p.s.ps. The present study has shown that an NMDA receptor-mediated e.p.s.p. can be recorded in this pathway during high-frequency stimulation, but the slow nature of this synaptic response as well as its activation characteristics clearly distinguished it from the fast e.p.s.ps. The observation that the NMDA receptormediated synaptic potential could often be detected as early as the second fast e.p.s.p. during high-frequency stimulation (see Fig. 2b, c) demonstrates that as few as two appropriately timed synaptic inputs may activate the NMDA receptor system in the hippocampus.

The finding that in the absence of Mg²⁺, low-frequency stimulation activates a low-threshold NMDA receptor-mediated synaptic response, implies that NMDA receptors are normally acted on by the neurotransmitter released by low-frequency

Fig. 2 Effect of 50 µM APV on synaptic responses recorded intracellularly in CA1 neurones in response to stimulation of the Schaffer collateral-commissural pathway. a, Averages of five successive records of synaptic potentials evoked at 30-s intervals before (control), during and after washout of APV. b, Single records of responses of the same cell to high-frequency stimulation (20 shocks at 10-ms intervals) in the presence and following washout of APV. The e.p.s.p.s shown in a (centre and right-hand records) were obtained immediately before the two respective periods of high-frequency stimulation. c, Single records of responses to high-frequency stimulation in another cell. The times of stimulation are indicated by arrowheads and stimulus artefacts have been blanked out for clarity. Stimulus intensity and membrane potentials were constant throughout. Action potentials in b are truncated.



stimulation. It is not necessary, therefore, to postulate that high-frequency stimulation is required either to release an additional agonist for NMDA receptors or to increase neurotransmitter release sufficient to activate the NMDA receptors due to their localization or activation characteristics. A simpler hypothesis^{20,21} which agrees fully with the present observations is that a single neurotransmitter acts simultaneously on both non-NMDA and NMDA receptors but that the latter are prevented from participating appreciably in low-frequency synaptic transmission by Mg²⁺. During high-frequency stimulation this Mg²⁺ blockade of the NMDA receptor system may be temporarily alleviated, allowing Ca²⁺ and Na⁺ to enter via the NMDA channels^{6,22-25}, and lead to the induction of LTP²⁶. This inward movement of cations through the NMDA channels could account for the slow e.p.s.p. recorded in the present study. It is likely that depolarization of the synaptic membrane, caused in part by temporal summation of fast e.p.s.ps, could be the mechanism by which the blockade is reduced. In this respect, it has been shown using cultured neurones that Mg2+ directly blocks NMDA-gated channels and that this block is reduced by membrane depolarization²⁷. In addition, it has been reported recently that pairing single afferent synaptic inputs with postsynaptic depolarization can activate the NMDA receptor system and elicit LTP28

It has been shown that NMDA receptors are involved in epilepsy²⁹. In the presence of convulsant drugs, an NMDA receptor-mediated potential has been recorded extracellularly in the hippocampus during brief periods of high-frequency stimulation⁸, and a small NMDA receptor-mediated component of the fast e.p.s.p. recorded extracellularly²¹ or intracellularly^{13,14} has been detected during low-frequency stimulation. The latter effect has been explained on the basis of removal of the Mg²⁺ block of NMDA channels, the necessary depolarization being provided by the fast e.p.s.ps prolonged by the action of the convulsant drug¹⁴. Such a mechanism could operate at the centre of an epileptic focus where synaptic inhibition may be impaired. The present results suggest a second way in which the NMDA receptor system may contribute to epileptic activity—by amplifying the synaptic output in response to a high-frequency input in the presence of fully functional synaptic inhibition (that is, absence of convulsant drugs). The synchronized, high-frequency discharge of neurones in epileptic tissue would provide ideal conditions for the activation of the NMDA receptor system such that this system could contribute to the propagation of epileptic activity through normal brain tissue.

It is now widely believed that NMDA receptors are important for synaptic plasticity in the hippocampus, but their function elsewhere in the brain is generally less clear. Although it is probable that NMDA receptors will be found to be involved in plastic processes in other regions of the CNS (for example, the cerebral cortex), their involvement in the discharge pattern of spinal interneurones¹, transmission of afferent sensory input³⁰ and generation of locomotor patterns³¹ is also indicated. As ions are a potent NMDA antagonist in all regions of the brain so far examined, it is likely that a synaptic mechanism similar to that proposed here for hippocampal neuronal transmission will apply throughout the CNS.

Since submission of this manuscript, it has been reported³² that postsynaptic hyperpolarization during conditioning reversibly prevents the initiation of LTP. These authors proposed that this was caused by the hyperpolarization preventing activation of voltage-gated calcium channels. On the basis of our present findings, we suggest a refinement of this hypothesis: that hyperpolarization prevented LTP by opposing the depolarization necessary to alleviate the Mg²⁺ block of NMDA channels.

This work was supported by the MRC and the Royal Society.

We thank Dr J. C. Watkins for gifts of APV.

Received 6 January; accepted 28 April 1986.

- Watkins, J. C. & Evans, R. H. A. Rev. Pharmac. Tox. 21, 165-204 (1981).
 Watkins, J. C. Trends pharmac. Sci. 5, 373-376 (1984).
 Olverman, H. J., Jones, A. W. & Watkins, J. C. Nature 307, 460-462 (1984).
 Crunelli, V., Forda, S., Collingridge, G. L. & Kelly, J. S. Nature 300, 450-452 (1982).
 Koerner, J. F. & Cotman, C. W. Brain Res. 251, 105-115 (1982).
 Collingridge, G. L., Kehl, S. J. & McLennan, H. J. Physiol., Lond. 334, 33-46 (1983).
 Collingridge, G. L., Kehl, S. J. & McLennan, H. J. Physiol., Lond. 338, 27P (1983).
 Wigström, H. & Gustafsson, B. Neurosci. Lett. 44, 327-332 (1984).
 Harris, E. W., Ganong, A. H. & Cotman, C. W. Brain Res. 323, 132-137 (1984).
 Slater, N. T., Stelzer, A. & Galvan, M. Neurosci. Lett. 60, 25-31 (1985).
 Morris R. G. M. Anderson, E. Lynch, G. S. & Baudey, M. Nature, 319, 774-776 (1985).

- Morris, R. G. M., Anderson, E., Lynch, G. S. & Baudry, M. Nature 319, 774-776 (1986).
 Bliss, T. V. P. & Lømo, T. J. Physiol., Lond. 232, 331-358 (1973).
- Hynes, M. A. & Dingledine, R. Soc. Neurosci. Abstr. 10, 229 (1984).
 Herron, C. E., Williamson, R. & Collingridge, G. L. Neurosci. Lett. 61, 255-260 (1985).
 Collingridge, G. L., Kehl, S. J. & McLennan, H. J. Physiol., Lond. 334, 19-31 (1983).
- Coan, E. J. & Collingridge, G. L. Neurosci. Lett. 53, 21-26 (1985). Katz, B. & Miledi, R. J. Physiol., Lond. 168, 389-422 (1963).
- Hille, B., Woodhull, A. M. & Shapiro, B. I. Phil. Trans. R. Soc. B270, 301-318 (1975)
 Hablitz, J. J. & Langmoen, I. A. J. Neurosci. 6, 102-106 (1986).

- Collingridge, G. L. Trends pharmac. Sci. 6, 407-411 (1985).
 Wigström, H., Gustafsson, B. & Huang, Y.-Y. Acta physiol. scand. 124, 474-478 (1985).
 Dingledine, R. J. Physiol., Lond. 343, 385-405 (1983).
 Heinemann, U., Hamon, B. & Konnerth, A. Neurosci. Lett. 47, 295-300 (1984).

- Ascher, P. & Nowak, L. J. Physiol., Lond. (in the press).
 MacDermott, A. B., Mayer, M. L., Westbrook, G. L., Smith, S. J. & Barker, J. L. Nature
- 321, 519-522 (1986).
- 26. Lynch, G., Larson, J., Kelso, S., Barrionuevo, G. & Schottler, F. Nature 305, 719-721 (1983).

- 27. Nowak, L., Bregestovski, P., Ascher, P., Herbet, A. & Prochiantz, A. Nature 307, 462-465
- 28. Wigström, H., Gustafsson, B., Huang, Y.-Y. & Abrahams, W. C. Acta physiol. scand. 126, 317-319 (1986).
- Soli-317 (1980).
 Croucher, M. J., Collins, J. F. & Meldrum, B. S. Science 216, 889-901 (1982).
 Salt, T. E. Nature 322, 263-265 (1986).
- 31. Dale, N. & Roberts, A. J. Physiol, Lond. 348, 527-543 (1984).
- 32. Malinow, R. & Miller, J. P. Nature 320, 529-520 (1986).

The inducible cytotoxic T-lymphocyte-associated gene transcript CTLA-1 sequence and gene localization to mouse chromosome 14

Jean-François Brunet, Magali Dosseto, François Denizot, Marie-Geneviève Mattei*, William R. Clark‡, Tariq M. Haqqi, Pierre Ferrier, Markus Nabholzt, Anne-Marie Schmitt-Verhulst, Marie-Françoise Luciani & Pierre Golstein

Centre d'Immunologie INSERM-CNRS de Marseille-Luminy, Case 906, 13288 Marseille Cédex 9, France INSERM U.242, CHU Timone, 13385 Marseille Cedex 5, France. † Swiss Institute for Experimental Cancer Research, Epalinges CH-1066, Switzerland.

Classical phenomenological approaches to the study of the mechanism of T-cell-mediated cytotoxicity 1-3 have now given way to a search for molecules involved in this function; this is attempted either by subcellular and biochemical fractionation of material from cytotoxic cells^{4,5}, or through the characterization of molecules recognized by cytotoxicity-inhibiting monoclonal antibodies (see ref. 6 for a review). Molecules having a role in cytotoxicity may also be identified by detecting the corresponding messenger RNA transcripts. Such an approach may include, as a first step, the search for transcripts as specific as possible to cytotoxic T cells; only secondarily can their actual relevance to cytotoxicity be investigated. We report here the preparation and systematic screening of a differential complementary DNA bank, in which we detected three distinct messenger RNA transcripts (CTLA-1, CTLA-2 and CTLA-3) present in various cytotoxic T cells but not (or less so) in a range of non-cytotoxic lymphoid cells. We describe the co-inducibility of these transcripts and of cytoxicity in thymocytes and hybridoma cells, the sequence of CTLA-1 cDNA, its protein homology with serine esterases and the localization of the corresponding gene to mouse chromo-

A library was derived from cDNA obtained by subtractive hybridization⁷⁻¹¹ between cDNA from the B10.BR anti-H-2K^b cytotoxic T-cell clone KB5C20 (ref. 12; hereafter designated T_c) and mRNA from the B-lymphoma M12.4.1 (ref. 13; hereafter designated B). The 8,300 recombinant cDNA clones obtained were subjected to three successive rounds of screening with radioactive cDNA probes prepared from a range of cytotoxic and non-cytotoxic cells. In the first round of screening, 230 of the 8,300 cDNA clones gave a signal with a T_c probe but not with a B probe. These 230 T_c B clones were subjected to a second round of screening using radioactive cDNA probes from T_c, B, T_h (T-helper cells, that is, the T-lymphoma EL4), thymocytes or brain. The results are summarized in Table 1. The 230 clones fell into a number of specificity patterns, with only 73 of them remaining 'T_c-specific'.

These 73 clones were hybridized with cDNA probes made from (1) RDM4, another non-cytotoxic T-cell lymphoma, detecting no clones, (2) EL4 cells, now activated with phorbol myristate acetate, which detected five 'activation-associated'

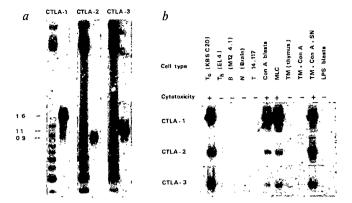


Fig. 1 Size and specificity patterns of CTLA-1, CTLA-2 and CTLA-3 RNA transcripts. Northern blots of RNA from the T_c clone KB5C20 (a) and from 11 cytotoxic and non-cytotoxic cell types (b) were probed with the inserts of plasmid M41D12, M41G12 or M11E6, representive of CTLA-1, CTLA-2 and CTLA-3, respectively. Cell types were as in Table 1, plus: T14.117, a hybridoma between a T-helper cell clone and the BW5147 thymoma²⁴; MLC cells, A/J spleen cells stimulated for 5 days in vitro with C57BL/6 irradiated spleen cells; TM+Con A, C57BL/6 thymocytes incubated for 24 h in the presence of 5 µg ml⁻¹ of Con A; TM+Con A+SN, TM+Con A further incubated for 5 days in the presence of IL-2-containing supernatant from PMA-stimulated EL4 C116 cells. At the time of RNA extraction, the cells were tested for cytotoxicity and classified as cytotoxic (+) or noncytotoxic (-) according to the criteria given in Table 1. In a, an end-labelled 123-bp ladder (BRL) was used as a size marker. In b, a control actin probe gave a distinct band in all lanes (not shown). Methods. Total RNA (10 µg per lane) was run for 3-6 h at 2.5 V on a 1.1% formaldehyde-agarose gel, in MOPS buffer, then transferred to nitrocellulose filters. Inserts, obtained either from CsCl-purified plasmids or from minipreparations of plasmids, digested with PstI and separated on 2% LMP (low melting point) agarose (BRL) gels, were labelled by random priming²⁵ and used as probes on Northern blots. Blots were prehybridized in 5×SSC, 50% formamide, 5 × Denhardt's, 5 mM EDTA, 0.1% SDS, 50 mM phosphate buffer pH7 and 7% dextran sulphate, at 42 °C for 4-12 h. Hybridization was in the same buffer, to which the probe was added at 10⁶ d.p.m. ml⁻¹, for 12 h at 42 °C. Washes were for 10 min in 2×SSC, 0.1% SDS and for 30 min in 0.2×SSC, 0.1% SDS at 65 °C.

clones, (3) lipopolysaccharide (LPS)-stimulated blasts, detecting two clones, and (4) a mixture of 2-day-old and 3-day-old cytotoxic concanavalin A (Con A) blasts, which failed to detect nine cDNA clones that previously were found to be positive with a T_c probe. The latter clones might, therefore, be associated with long-term in vitro growth of T cells rather than with cytotoxicity. Also, 8 of the 73 T_c⁺ clones proved to be negative with a subtracted (T_c-B) cDNA probe, which was taken as an indication of non-T_c-specificity. Altogether, after this third round of screening, only 50 T_c-specific cDNA clones were retained for further study.

In order to identify clones corresponding to the same genes, inserts (of 200 to 1,400 base pairs, bp) from individual clones were purified and hybridized to all of the 50 clones. This approach identified five groups of cDNA clones. Of these, on the basis of transcript size as determined by Northern blotting (Fig. 1a), three groups were clearly distinct. These were designated CTLA-1, CTLA-2 and CTLA-3, and included at least 3, 3 and 39 cDNA clones, respectively. Transcripts were detected as single bands of 1.6 kilobases (kb) for CTLA-1, 0.9 kb for CTLA-2 and 1.1 kb for CTLA-3 (Fig. 1a). CTLA-1, CTLA-2 and CTLA-3 transcripts were present in all the cytotoxic cell populations tested (T-cell clones, mixed leukocyte culture cells, Con A blasts and thymocytes activated with Con A plus interleukin-2 (IL-2)-containing EL4 supernatant). The CTLA-1 transcript was not detected in brain cells or in a range of non-

Table 1	Pattern of specificity of selected clones from a subtracted (T _c -B) cDNA
	library

		Probe			No. of cDNA
T _e	T_h	TM	В	N	clones
•	_		-	_	40
+	_	_	_	-	73
+	+	_	_	_	23
+	_	+	_	_	41
+	+	+	_		24
+	+	+	+	_	4
+	+	+	_	+	4
+	+	+	+	+	13

Two hundred and thirty $T_c^+B^-$ clones were transferred to filters and probed by hybridization with radioactive cDNA derived from, respectively, T_c (cytotoxic T-cell clone KB5C20), T_h (EL4 thymoma), TM (C57BL/6 thymocytes), B (M12.4.1 B-lymphoma cells) and N (C57BL/6 brain cells). + Indcates that a given collection hybridized detectably with the cDNA probe used, – that it did not. A few cDNA clones were lost during transfers and are not included. Forty clones did not give any positive signal and were considered false positives from the initial screening. Reciprocally, 17 clones gave a signal with the B probe and were considered false negatives from the initial screening. Only the 73 T_c -specific clones were subjected to further screening, although some of the rejected clones may be of interest in their own right.

Methods. Unselected total RNA was extracted by the LiCl method²⁰ from clone KB5C20 and the B lymphoma M12.4.1. Poly(A)+ RNA was selected by two passages over oligo(dT)-cellulose. KB5C20 single-stranded (SS) cDNA was synthesized from 5 µg of poly(A)* RNA in 100 mM Tris-HCl pH 8.3, 100 mM KCl, 10 mM MgCl₂, 10 mM dithiothreitol, 1 mM each of dA, dT and dG, 0.1 mM dC, 50 μ Cl ³²P-dCTP, oligo(dT₁₀) at 2 U ml⁻¹ and 6 U of reverse transcriptase (super RT, Stehelin) for 1 h at 42 °C. Single-stranded cDNA (1.3 μ g) was hybridized to M12.4.1 poly(A) * RNA (2 μ g μ l * 1) in 10 μ l of 0.4 M phosphate buffer pH 7.5, 1 mM EDTA, 0.1% SDS, overlaid with paraffin oil, for 20 h at 68 °C. After dilution in preheated 0.12 M phosphate buffer, the reaction was fractionated on a 1-ml hydroxyapatite column at 65 °C. The single-stranded fraction was precipitated in 50 mM EDTA pH 8, 0.1% cetylpyridinium bromide as described else-, except that an additional ethanol precipitation step was performed. The subtractive hybridization was repeated once, followed by an homologous hybridization with KB5C20 poly (A)+ RNA. The double-stranded fraction was precipitated as before, resuspended in H2O and the RNA hydrolysed in 0.1 N NaOH. Thirty nanograms of single-stranded cDNA was recovered at this stage, that is, 6.4% of initial cDNA (notwithstanding nonspecific losses). Second-strand synthesis and elongation, S₁-nuclease digestion and dC tailing were performed as described elsewhere²². Fourteen nanograms of tailed cDNA were annealed to dGMP-tailed Pst1-cut pBR322 plasmid (NEN) and used to transform Escherichia coli strain C600 according to the procedure of Hanahan²³. A total of 8,300 tetracyclineresistant, β -lactamase-negative (selected using Ampscreen, BRL) bacterial colonies containing recombinant plasmids were individually picked and grown into microtitre plate wells, replicated onto nitrocellulose filters and hybridized to 32 P-labelled cDNA synthesized as described above (however, with 50 μ M each of cold dG and dT, and 100 μ Ci each of 32 P-dT and 32 P-dG) from poly(A)⁺ RNA extracted from the following cells: Te (KB5C20) and B (M12.4.1) for a first round of differential screening, and the same plus T_h (thymoma EL4 C116), TM (C57BL/6 thymus) and N (C57BL/6 adult brain) for a second round on the $T_c^+B^$ clones selected in the first round. The results of this second round are presented above. Hybridizations were in 50% (v/v) formamide, 5×SSC, 5×Denhardt's, single-stranded DNA, for 48 h at 42 °C; washes were twice for 30 min each in 2×SSC, 0.1% SDS and twice for 30 min each in 0.2×SSC, 0.1% SDS at 65 °C. All the cells mentioned in this paper were tested, at the time of nucleic acid extraction, for their cytotoxic activity (or lack of it) in a conventional 4-h 51Cr-release test in the presence of the lectin Con A on both EL4 and RDM4 target cells. Cells were considered cytotoxic if they gave more than 20% specific Cr-release at a 20:1 effector to target cell ratio. In the absence of Con A, Tc specifically lysed EL4 but not RDM4 target cells, and induced PC60 cells lysed YAC target cells. To avoid contamination with feeder cell material, before extraction of RNA, Tc were grown for three passages without allogeneic feeder cells in the presence of EL4 C116 supernatant.

cytotoxic lymphoid cells (B-lymphoma cells, LPS blast cells, EL4 cells, normal thymocytes, Con-A-pulsed thymocytes, and hybridoma cells between a helper cell clone and BW5147 thymoma cells), even on overexposed films (Fig. 1b). The CTLA-2 transcript was detected in none of the non-cytotoxic cells at the exposure shown in Fig. 1b; with a longer exposure, faint bands appeared for all cells but the EL4 and B-lymphoma cells. The CTLA-3 transcript was detected in thymocytes and LPS blasts at the exposure shown in Fig. 1b, albeit less markedly than in the cytotoxic cells. These deviations from a strict T_c specificity had not been detected with the less sensitive methods used in the initial rounds of screening.

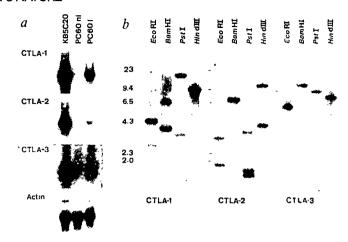
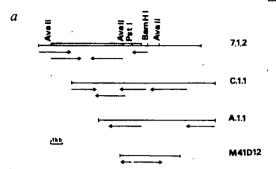


Fig. 2 Inducible transcription and Southern patterns of CTLA genes. a, Northern blots of RNA from KB5C20 (positive control) and non-induced (ni) or induced (i) PC60 hybridoma cells were probed with plasmid inserts representative of CTLA-1, CTLA-2 and CTLA-3, respectively, and with a control actin probe (given by M. Buckingham via C. Goridis); induction of PC60 cells also led to the appearance of cytotoxicity (not shown). Exposure times were different for each probe. b, Southern blots of DNA from mouse liver cells, cut with the indicated restriction enzymes, were probed with the same plasmid inserts; the numbers on the left are HindIII-derived size markers (in kb). Identical patterns were obtained with BALB/c liver, B10.BR liver or KB5C20 DNA (not shown)

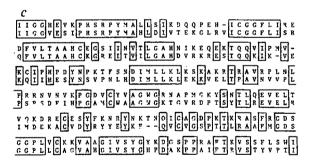
Methods. Northern blots were performed and probed as described in Fig. 1 legend. PC60 hybridoma cells were induced by adding IL-1- and IL-2-containing supernatant to PC60 cells as described previously²⁶ (we used the PC60-21-14-4 subclone of PC60). For Southern blots, DNA was prepared and purified by centrifugation to equilibrium in CsCl essentially as described elsewhere27, except that a higher concentration of Tris and EDTA was used in homogenizing buffer. Genomic DNA (10 µg) was digested to completion with EcoRI, BamHI, PstI or HindIII according to the conditions specified by the manufacturer (Boehringer Mannheim), electrophoresed for 16 h in 0.8% agarose gel in TAE (tris-acctate-EDTA) buffer and transferred to Gene Screen Plus (Du Pont). Blots were prehybridized for 6 h at 65 °C in 6 × SSC, 5 × Denhardt's. 1% SDS, 10 mM EDTA and 150 µg ml⁻¹ denatured salmon sperm DNA. Probes were labelled²⁵ to high specific activity (1.6 × 10⁹ c.p.m. μg⁻¹). Hybridization medium was as above plus 10% dextran sulphate and denatured probe (8×106 c.p.m. ml-1). Blots were hybridized overnight, then washed down to $0.2 \times SSC$ at 65 °C for 100 min, dried and exposed to film overnight.

Expression of the CTLA transcripts was induced under conditions (addition of IL-2) which led to the differentiation of non-cytotoxic thymocytes into cytotoxic cells (Fig. 1b); this, however, might reflect the differential growth on stimulation of a small subpopulation of precursor cells already making these transcripts. We therefore used PC60 hybridoma cells¹⁴ which are constitutive for growth but inducible for cytotoxicity; all three CTLA transcripts, which in non-induced PC60 cells were not or only barely detectable, appeared in PC60 cells when cytotoxicity was induced (Fig. 2a). Thus, in both thymocytes and hybridoma cells there was a correlation between induction of cytotoxicity and induction of the three CTLA transcripts.

We then wondered whether CTLA-1, which gave the clearest association (Fig. 1b) and induction (Fig. 2a) results, was homologous or identical to a previously sequenced molecule. The cDNA sequence that we obtained (Fig. 3) was not significantly homologous to any of the sequences in the Los Alamos Gene Bank. However, the translated protein sequence showed significant homology, but not identity, with known serine esterases (Fig. 3).



goet lys life leu leu leu leu leu AACACTCTTGACGCTGGGACCTAGGCGGCCTTCCGGGGAAG ATG AAG ATC CTC CTG CTA CTG CTG thr less ser less its ser arg thr lys sits gly glu ite ite gly gly his glu val lys 28
ACC TTG TCT CTG GCC TCC AGG ACA AAG GCA GGG GAG ATC ATC GGG GGA CAT GAA GTC AAG 195 pro his ser arg pro tyr dest als leu leu ser ile lys asp glo glo pro glu als ile TGT GGG GGC TTC CTT ATT CGA GAG GAC TTT GTG CTG ACT GCT CAC TGT GAA GGA AGT ile ale ann val the feu gly ala his ann lle lyn glu gln glu lyn the gln gin ATA ATA AAT GTC ACT TTG GGG GCC CAC AAC ATC AAA GAA CAG GAG AAG ACC CAG CAA wal life oro met wal lys ywa life oro his pro and tyr san oro lys the one ser and GTC ATC CCT ATG GTA AAA TGC ATT CCC CAC CCA GAC TAT AAT CCT AAG ACA TTC TCC AAT map lie met leu leu lys leu lys ser lys ala lys arg thr arg ala val arg pro leu 127 GAC ATC ATG CTG CTA AAG CTG AAG AGT AAG GCC AAG AGG ACT AGA GCT CTG AGG CCC CTC 492 san leu pro arg arg ann val ann val tya pro gly sap val cyn tyr val ain gly trp. AAC CTG CCC AGG CGC AAT GTC AAT GTG AAG CCA GGA GAT GTG TGC TAT GTG GCT GGT TGG GGA AGG ATG GCC CCA ATG GGC AAA TAC TCA AAC ACG CTA CAA GAG GTT GAG CTG ACA GTAB12 gin lys asp arg gin cys gin ser lyr phe lys asn arg lyr asn lys thr asn gin CAG AAG GAT COG GAG TOT GAG TCC TAC TTT AAA AAT COT TAC AAC AAA ACC AAT CAG teu val cys lys val als als gly ite val ser tyr gly tyr ivs asp gly ser pro CTT GTG TGT AAA AAA GTG GCT GCA GGC ATA GTT TCC TAT GGA TAT AAG GAT GGT TCA CCT pro arg als phe thr lys wal ser ser phe leu ser trp ale lys lys thr met lys ser246 CCA CGT GCT TTC ACC AAA GTC TCG AGT TTC TTA TCC TGG ATA AAG AAA ACA ATG AAA AGC849 AGC TAA CTACAGAAGCAACATCGGATCCTGCTCTGATTACCCATCGTCCTAGAGCTGAGTCCAGGATT918 GCTCTAGGACAGGTGGCAGGATCTGAATAAAGGACTGCAAAGACTGGCTTCATATCCATTCACAAGGA 986 CCAGCTCTGTCCTTGGCAGGCCAATGGAACACCTCTTCTGCCACCATGCTGTGACAACCCAACTGACATC 1054 TTCCTATGGAAATTTGCCCTCTCCACAAAAGAAGTAGAATGTTTGCATTGGAGCTGGGCATGCTCTGCTC 1126 CCCTCAGTGCCCCGAGAATGTTATCTAATGCTAGTCATCATTAATAGCTCCCTACAGAACTTTCATACA 1195 GTTGCACCCAAGTTGCTGATGTGTTCTCTAGAATAGAGCAAGAAATAGTAAAACAGAATTCCTTTTGCCT1264 CTCTGTACTATTTTCCCCCAAATACCAAGATTTGTATGTTTTATAAAGCTAATTTCCTTATCAAATGA 1332 CATCTTTAATTTTTACATTAATGGCTTATTTTCAAGGTACAACCTGATTTTTTTATGGACAAAAATG 1400



Southern patterns of liver DNA tested with probes from the three CTLA families showed a small number of bands (Fig. 2b), indicating that the corresponding genes are present as either one copy or a small number of copies per haploid genome. The respective patterns were the same for KB5C20 DNA (not shown), thus providing no detectable evidence for CTLA gene rearrangements in T cells. The chromosomal localization of the CTLA-1 gene was determined by in situ hybridization. Only one major binding site was found, in the D segment of mouse chromosome 14 (Fig. 4), interestingly in a region to which the T-cell receptor (TCR) α -chain gene has been mapped¹⁵. Experiments in progress, taking advantage of the cross-hybridization of CTLA-1 mouse probes to human DNA (not shown), suggest that CTLA-1 and TCR α genes might be co-localized on human chromosomes also.

Thus, we have detected three 'CTLA' genes whose transcription is induced preferentially or exclusively in cytotoxic T lymphocytes. A first question raised by these results is the nature of the CTLA protein products. That CTLA-1 is a cytotoxic T-cell-associated serine esterase is reminiscent of the detection

Fig. 3 The sequence of CTLA-1 cDNA and its protein translation. a, Sequencing strategy. The open reading frame of 741 nucleotides is indicated by a box on clone 7.1.2. b, cDNA sequence and the predicted amino-acid sequence. The open reading frame starts from the first ATG downstream of the stop codon at position 79. The 3'-untranslated region ends with the consensus polyadenylation signal AATAAA. There is a potential N-linked glycosylation site at Asn 70. The conceptual amino-acid sequence shows clustered homologies with trypsin-related serine-esterases, in particular around the serine-esterase active-site residues His, Asp and Ser (here at positions 64, 108 and 203, respectively). c, Alignment of the rat group-specific serine esterase sequence²⁸ with that of CTLA-1 from Ile 21 to Ile 240. The overall homology is 46%; identical stretches of sequence are boxed. Given the highly hydrophobic leader sequence in the NH2-terminal region, the potential site of cleavage of an activation peptide at Arg 15 or perhaps rather Lys 17, and the sequence homology with the initial residues of serine esterases, the putative active CTLA-1 protein would start at Ala 18 and therefore be 230 amino acids long.

Methods. KB5C20-derived single-stranded cDNA was synthesized as described in Table 1 (except that 4 mM Na-PP_i was included in the reaction), made double-stranded using RNase H (BRL), Pol I (Boehringer) and E. coli lipase (BRL) as described by Gubler and Hoffman²⁹ (except that the incubation was for 1 h at 12 °C and 1 h at 16 °C), tailed by TdT (NEN; 20 U μg⁻¹ in 50 μl of 200 mM KCaCo pH7.2, 1 mM CoCl₂, 500 μg ml⁻¹ bovine serum albumin, 5 μM dCTP for 40 min at 15 °C), and size-fractionated on 1.5% agarose. Slices corresponding to 1.2-1.6 kb were electroeluted and double-stranded cDNA annealed to the PstI site of dG-tailed PUC9 (NEN); transformation was as described in Table 1. The library was screened with the 450-bp PstI fragment of M41D12 which detected 10 clones, of which the 3 longest were analysed. Sequences were obtained by the dideoxy chain-termination method³⁰ for the two PstI fragments of M41D12 subcloned in M13, and by chemical cleavage³¹ following the strategy shown in α

in cytotoxic T cells of such enzymes at the protein level¹⁶. A comparison of partial sequences showed that CTLA-1 and the C11 clone described by Lobe *et al.*¹⁷ were almost identical; differences in the Northern patterns are being investigated. A second, key question—whether the CTLA products are actually involved in the mechanism of cytolysis—could be investigated by using anti-sense mRNA technology^{18,19}; the probable serine esterase activity of CTLA-1 suggests that it might have a profactor-activating role. Irrespective of the answers to these questions, it will be interesting to study the regulation of expression of the CTLA-1 gene in particular, which maps near the TCR α gene and is induced on differentiation into cytotoxic T-cells.

We thank C. Goridis, B. Jordan, B. Malissen and M. Pierres for advice and for reading of the manuscript, M. Pierres for the gift of T14.117 hybridoma cells. J. Sire and R. Sodoyer for advice and help in DNA sequencing, and M. Masson (Pasteur Institute) for computer searches in gene and protein sequence banks. We thank Dr Bleackley (Edmonton) for a crucial suggestion and for a comparison of a partial sequence. W. R. C. was supported by an Eleanor Roosevelt Fellowship and T.M.H. by the Founda-

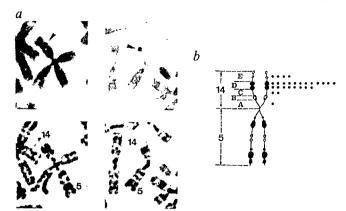


Fig. 4 Localization of the CTLA-1 gene to mouse chromosome 14 by in situ hybridization with the CTLA-1 probe C.1.1. a, Two partial WMP mouse metaphases, showing the specific site of hybridization to chromosome 14. Top, arrowheads indicate silver grains on Giemsa-stained chromosomes, after autoradiography. Bottom, chromosomes with silver grains were subsequently identified by R-banding. b, Diagram of WMP mouse Rb(5; 14) chromosome, indicating the distribution of labelled sites. In the 85 metaphases examined, there were 152 silver grains associated with chromosomes and 27 of these (17.7%) were localized on chromosome 14. The distribution of grains on this chromosome was not random: 74% of them mapped to the D band, with a maximum in the distal D3 part of this band (for banding nomenclature, see ref. 32).

Methods. In situ hybridizations with probe C.1.1 were done using metaphase spreads from a male WMP mouse in which all the autosomes (except 19) are in the form of metacentric robertsonian translocations (given by J. L. Guénet, Pasteur Institute, Paris). Con A-stimulated lymphocytes were cultured at 37 °C for 72 h, with 5-bromodeoxyuridine added for the final 7 h of culture (30 µg per ml of medium) to ensure a chromosomal R-banding of good quality. Total C.1.1. plasmid DNA was tritium-labelled by nick-translation to a specific activity of 10⁸ c.p.m. μ g⁻¹. The radiolabelled probe was hybridized to metaphase spreads at a final concentration of 2 μg per ml of hybridization solution, as described previously³³. After coating with nuclear track emulsion (Kodak NTB 2), the slides were exposed for 8 days at 4 °C, then developed. To avoid any slipping of silver grains during the banding procedure, chromosome spreads were first stained with buffered Giemsa solution and metaphases photographed. Then chromosome banding was realized by the fluorochrome-photolysis-Giemsa (FPG) method described by Camargo and Cervenka³⁴, and metaphases photographed again before analysis.

tion pour la Recherche Médicale. Other support was through institutional grants from INSERM and CNRS and through a specific grant from the Association pour la Recherche contre le Cancer.

Received 7 April; accepted 25 April 1986.

- Henney, C. S. Contemp. Topics Immunobiol. 7, 245-272 (1977).
 Golstein, P. & Smith, E. T. Contemp. Topics Immunobiol. 7, 273-300 (1977).
 Martz, E. Contemp. Topics Immunobiol. 7, 301-361 (1977).
- 4. Henkart, P. A., Millard, P. J., Reynolds, C. W. & Henkart, M. P. J. exp. Med. 160, 75-93
- (1984).

 Podack, E. R. & Konigsberg, P. J. J. exp. Med. 160, 695-710 (1984).

 Golstein, P. et al. Immun. Rev. 68, 5-42 (1982).

 Timberlake, W. E. Devl Biol. 78, 497-510 (1980).

 Yanagi, Y. et al. Nature 308, 145-149 (1984).

- Hedrick, S. M., Cohen, D. I., Nielsen, E. A. & Davis, M. Nature 308, 149-153 (1984).
 Saito, H. et al. Nature 309, 757-762 (1984).
- 11. Sims, J. E., Tunnacliffe, A., Smith, W. J. & Rabbitts, T. H. Nature 312, 541-545 (1984). 12. Albert, F., Buferne, M., Boyer, C. & Schmitt-Verhulst, A.-M. Immunogenetics 16, 533-549
- Hamano, T., Kim, K. J., Leiserson, W. M. & Asofsky, R. J. Immun. 129, 1403-1406 (1982).
 Conzelmann, A., Corthésy, P., Gianfriglia, M., Silva, A. & Nabholz, M. Nature 298, 170-172
- 15. Kranz, D. M. et al. Science 227, 941-945 (1985)
- Pasternack, M. S. & Eisen, H. N. Nature 314, 743-745 (1985).
 Lobe, C. G., Havele, C. & Bleackly, R. C. Proc. natn. Acad. Sci. U.S.A. 83, 1448-1452 (1986).
- 18. Izant, J. G. & Weintraub, H. Cell 36, 1007-1015 (1984).
- Rubinstein, J. L. R., Nicolas, J.-F. & Jacob, F. C.r. hebd. Acad. Séanc. Acad. Sci., Paris 299, 271-274 (1984).

- 20. Auffray, C. & Rougeon, R. Eur. J. Biochem. 107, 303-314 (1980)
- Geck, P. & Nasz, I. Analys. Biochem. 135, 264-268 (1983).
 Maniatis, T., Fritsch, E. F. & Sambrook, J. in Molecular Cloning A Laboratory Manual Maniaus, I., Fritsch, E. P. & Sambrook, J. III Molect (Cold Spring Harbor Laboratory, New York, 1982).
 Hanahan, D. J. molec Biol. 166, 557-580 (1983).
 Pont, S. et al. Eur. J. Immun. 15, 1222-1228 (1985).

- Feinberg, A. & Vogelstein, B. Analyt. Biochem. 137, 266-267 (1984)
 Erard, F. et al. J. exp. Med. 160, 584-599 (1984).
- 27. Kaiser, K. & Murray, N. E. in DNA Cloning Vol. 1 (ed. Glover, D. M.) (IRL Fress, Oxford,
- 28. Woodbury, G., Katunuma, N., Kobayashi, K., Titani, K. & Neurath, H. Buchemeur. 17. 811-819 (1978).
- 29. Gubler, U. & Hoffman, B. J. Gene 25, 263-269 (1983).
- Sanger, F., Nicklen, S. & Coulson, A. R. Proc. natn. Acad. Sci. U.S.A. 74, 5463-5467 (1977). Chuvpilov, S. A. & Kravchenko, V. V. FEBS Lett. 179, 34-36 (1984). Nesbitt, M. N. & Francke, U. Chromosoma 41, 145-158 (1973).

- 33. Mattéi, M. G. et al. Hum. Genet. 69, 268-271 (1985).
- 34. Camargo, M. & Cervenka, J. Am. J. hum. Genet. 34, 757-780 (1982).

Voltage-gated Ca²⁺ entry into Paramecium linked to intraciliary increase in cyclic GMP

Joachim E. Schultz, Thomas Pohl & Susanne Klumpp

Pharmazeutisches Institut der Universität Tübingen, Morgenstelle 8, 7400 Tübingen, FRG

Inward Ca2+ currents exist in many excitable tissues and are linked to regulation of several cellular processes such as cyclic GMP formation 1-4. In *Paramecium*, a graded Ca²⁺/K⁺ action potential regulates swimming behaviour⁵⁻⁷. Voltage-gated Ca²⁺ channels localized in the excitable ciliary membrane^{8,9} conduct a depolarizing influx of Ca²⁺ and translate changes in membrane potential into a transient Ca²⁺ signal which triggers ciliary reversal, that is, backward swimming^{5,6}. A guanylate cyclase that is activated specifically by Ca²⁺ has already been characterized in the ciliary membrane¹⁰. By using behavioural mutants of *Paramecium* with reduced^{6,11,12} or exaggerated^{13,14} Ca²⁺ currents, we now demonstrate in an intact animal a direct link between the voltage-gated inward Ca2+ current and an elevation of cyclic GMP levels. Although the increased cyclic GMP level does not directly influence swimming behaviour, the combination of electrophysiology, biochemistry and genetics possible with Paramecium offers an opportunity of identifying the role of cyclic GMP levels in cell behaviour.

In several Paramecium strains, increasing the external K' concentration from 5 to 25 mM enhances ciliary Ca²⁺ permeability and causes a reversal of ciliary beating and consequently of the swimming direction⁵⁻⁷, a response similar to the avoidance displayed by Paramecium in adverse situations. This reversal lasts for 5-10 s and is mediated by the influx of Ca2+ into the cilia. In Paramecium tetraurelia wild-type 51s, the concentration of cyclic GMP increases from 3.8 to 5.5 pmol per mg protein 3-5 s after the addition of K^+ (Fig. 1a). The increase is moderate because the influx of Ca²⁺ leads to an inactivation of the Ca²⁺ channel within 5 ms^{5,15}. Consequently, the Ca²⁺-dependent guanylate cyclase is only briefly stimulated. Therefore, Ba2+ was used to increase the excitability of the Ca2+ channels by decreasing their rate of inactivation, thereby producing a more sustained (if somewhat slower) Ca²⁺ entry^{11,15,16}. Addition of 3 mM Ba²⁺ to wild-type Paramecium evoked a rapid, large and transient increase in cyclic GMP (Fig. 1b). The level of cyclic GMP attained a maximum 5-10s after stimulation and returned towards resting levels after 30 s. In the presence of Ba²⁺ the backward swimming response continued for ~60 s, indicating that the level of cyclic GMP does not directly control backward swimming. The effect of Ba²⁺ was specific, as 3 mM of Mg², Ca²⁺ or Sr²⁺ did not elicit the avoidance reaction or an increase in cyclic GMP. Moreover, the temperature dependence of the Ba²⁺-stimulated increase in cylcic GMP indicates that it is not the ion current itself but a subsequent step that is responsible for the effect. At 0 °C Ba²⁺ does not evoke an increase in cyclic

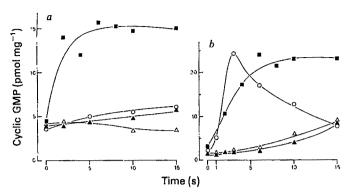


Fig. 1 Time-dependent increase in cyclic GMP concentrations in Paramecium tetraurelia wild-type 51 s (O), mutant pawn A (d4-94. △), double mutant pawn A/pawn B (▲) and mutant dancer (d4-614,) after a sudden increase in the concentration of K from 5 to 25 mM (a) or after addition of 3 mM Ba^{2+} (b). Methods. Early stationary cells grown in a bacterized hay infusion or in axenic complex medium²⁶ were collected by centrifugation at 250g, washed and equilibrated for 2 h at 40,000 cells ml (90,000 cells = 1 mg protein) in buffer containing $50 \,\mu\text{M}$ Ca²⁴ 5 mM K⁺, 10 mM MOPS pH 7.2. For stimulation, 250 µl of 40 mM K⁺ (a) or 6 mM BaCl₂ (b) in equilibration buffer were added to 250 µl of cells. Viability and behaviour were checked microscopically before and during the experiments. Incubations were stopped by adding perchloric acid (final concentration 1 M). Cyclic GMP was determined by radioimmunoassay using rabbit antibodies against cyclic GMP and 125I-iodinated 2-O'-succinyl-cyclic GMP-L-tyrosinylmethylester (for details see ref. 27). Cross-reactivity of the antibody with cyclic AMP was <5%. No cyclic GMP was found when samples were digested with phosphodiesterase isolated from pig brain before the assay. We did not detect cyclic GMP in the incubation medium nor did we observe differences in behaviour or cyclic GMP levels between cells grown in bacterized medium and those grown axenically.

GMP, although influx of Ca²⁺ does occur¹⁷; we attribute this effect to the lower activity of guanylate cyclase at this temperature.

Because both Ba2+ and Ca2+ compete for the inactivation site on the channel, the electrophysiological and behavioural effects of Ba2+ stimulation depend on the ratio of these cations in the medium^{16,18}. We established dose-response curves for Ba²⁺ in the presence of various Ca²⁺ concentrations. The ED₅₀ (50% effective dose) values for Ba²⁺-stimulated cyclic GMP levels in the presence of 3, 50 and 1,000 μ M Ca²⁺ were 0.1, 2 and 10 mM, respectively (Fig. 2), reflecting the competition between Ca² and Ba²⁺. Ba²⁺ elicited a concentration of cyclic GMP of only 15 pmol mg⁻¹ at 3 μ M Ca²⁺, compared with 28 pmol mg⁻¹ at an external Ca²⁺ concentration greater than 50 μ M (Fig. 2). Thus, low external Ca²⁺, leading to reduced Ca²⁺ influx^{16,19}, is correlated with considerably reduced production of intracellular cyclic GMP. Obviously, release of Ca²⁺ from intraciliary storage sites, if it occurred, was not involved in stimulating cyclic GMP production. Ba2+ itself does not stimulate guanylate cyclase activity in vitro²⁰ or antagonize Ca²⁺-mediated activation (Fig. 3). Importantly, the ED₅₀ of 9 μM Ca²⁺ for guanylate cyclase activation was not affected by the presence of 1 mM Ba²⁺ (Fig. 3). Thus we conclude that during an action potential Ca²⁺ enters the cilia with Ba²⁺ and directly stimulates ciliary guanylate cyclase.

Further evidence for a link between the inward Ca²⁺ current and intraciliary cyclic GMP production can be obtained by studying mutants possessing defects in ion conductances^{5-7,11,12}. 'Pawn' mutants lack voltage-gated Ca²⁺ channels^{11,12,16} and therefore cannot swim backwards. In agreement with electrophysiological and behavioural observations^{6,11,12}, we found that addition of 3 mM Ba²⁺ to pawn A or pawn A/pawn B cells did not stimulate cyclic GMP biosynthesis as in wild-type cells (Fig. 1b). 'Atalanta' mutants lack the axonemal response to Ca²⁺

despite having normal Ca2+ channels, so they are unable to reverse the direction of the ciliary beat and cannot swim backwards^{12,21}. Addition of 3 mM Ba²⁺ to atalanta cells produced an increase in the cyclic GMP concentration, from 4.6 pmol to 18.0 pmol mg⁻¹ after 10 s; as expected, this is comparable to the response of wild-type cells and reflects the fact that atalanta mutants have an intact inward Ca2+ current. Dancer mutants possess Ca²⁺ channels which inactivate more slowly and incompletely, resulting in enhanced inward Ca²⁺ currents^{13,14}. 'Dancer' cells display much longer periods of backward swimming when depolarized by K⁺ than wild-type Paramecium¹³. Thus, K⁺ stimulation should have a profound effect on the cyclic GMP content of dancer cells if the inward Ca2+ current is linked to intraciliary guanylate cyclase activation. Indeed, K+ evoked a fourfold increase in the concentration of cyclic GMP in dancer cells (Fig. 1a). In Ba²⁺-stimulated dancer cells, levels of cyclic GMP remained higher than those in comparably stimulated wild-type Paramecium (Fig. 1b). These observations are compatible with the defect in Ca^{2+} -channel inactivation in the dancer

The differences in cylic GMP production in vivo between wild-type and mutant Paramecium could be caused by different activities of guanylate cyclase. Therefore, enzyme activities were measured in cilia from all Paramecium strains used. The mean guanylate cyclase activity in wild-type and mutant preparations was 175 pmol per min per mg. We also investigated a possible involvement of phosphodiesterase in the regulation of cyclic GMP concentration. Using partially purified cyclic GMP phosphodiesterase from Paramecium, we found no effect of Ca²⁺ or Ba²⁺. Thus, inward flow of Ca²⁺ apparently stimulates intraciliary cyclic GMP production directly. Previously, we have shown by immunocytochemistry that cyclic GMP is predominantly localized in the cilia of Paramecium²²; this corroborates the link between voltage-gated Ca²⁺ influx and Ca²⁺-regulated guanylate cyclase.

Sophisticated control loops involving Ca²⁺ and cyclic nucleotides probably operate in most cells^{23,24}. In particular, hormonally stimulated production of cyclic GMP in metazoan tissues—for example, in brain¹, smooth muscle² and neuroblastoma cells³—has been demonstrated to depend on the presence of Ca²⁺. However, guanylate cyclases regulated by physiologically meaningful Ca²⁺ concentrations have not been found.

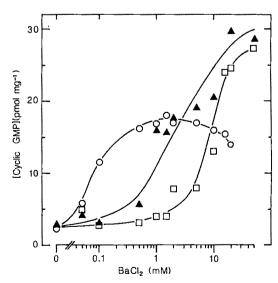


Fig. 2 Dose-response curves for Ba²⁺-stimulated cyclic GMP production in *Paramecium tetraurelia* wild-type 51 s in the presence of 3 (\bigcirc , n=5), 50 (\triangle , n=13) and 1,000 (\square , n=3) μ M Ca²⁺ in the equilibration and incubation buffer. Additions of Ba²⁺ were made to yield the indicated concentrations without affecting the concentration of other buffer constituents. Measurements were made 10 s after Ba²⁺ addition. For methods see Fig. 1 legend.

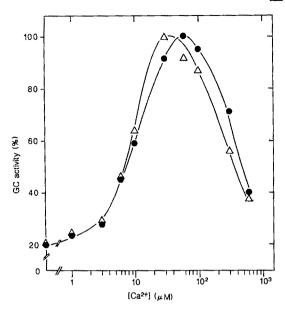


Fig. 3 Dose-response curve for Ca²⁺-stimulated guanylate cyclase (GC) in ciliary membranes from Paramecium. Membranes were washed with 60 µM EGTA followed by two washing steps with buffer to remove the chelator. All reagents were purified by treatment with Chelex. The remaining Ca2+ concentration was <1 µM. Activity was determined for various concentrations of Ca^{2+} in the absence (\bullet) or presence (\triangle) of 1 mM Ba²⁺. 100% activity corresponds to 1,560 pmol cyclic GMP per mg per min.

Here, we have demonstrated for the first time an unequivocal link between an inward Ca²⁺ current and enhanced cyclic GMP production.

In Paramecium the voltage-gated Ca2+ channels in the ciliary membrane serve as a mediator of all excitatory (that is, depolarizing) stimuli. In response to depolarizing receptor potentials, an action potential starts with a Ca²⁺ influx. Internally, Ca²⁺ has at least four effects: the inactivation of the Ca²⁻ channels within 5 ms, the activation of a Ca2+-dependent K+ efflux after 100 ms (ref. 25), the reversal of the direction of the ciliary power stroke, and the production of the second messenger cyclic GMP. That the electrophysiology, genetics and biochemistry of Paramecium can be studied in combination holds great promise for elucidating the molecular events of basic cellular processes controlled by cyclic GMP. At present, there are insufficient data to assign a common function for cyclic GMP in all cells but the functional relationship between cyclic GMP and Ca²⁺ in many tissues (for example in rod outer segments, which are phylogenetically a rudimentary cilium⁴) suggests that similarities in the regulation of cyclic GMP in different cellular systems will be found.

We thank Dr C. Kung (University of Wisconsin, Madison) for the Paramecium mutants. This work was supported by the Deutsche Forschungsgemeinschaft (SFB 323).

Received 19 February; accepted 21 April 1986.

- 1. Ferrendelli, J. A., Rubin, E. H. & Kinscherf, D. A. J. Neurochem, 26, 741-748 (1976).
- Takayanagi, I., Hisayama, T. & Kotsugai, T. Jap. J. Pharmac. 31, 831-834 (1981). El-Fakahany, E. & Richelson, E. Proc. natn. Acad. Sci. U.S.A. 77, 6897-6901 (1980).

- El-Fakahany, E. & Richelson, E. Froc. natn. Acad. Sci. U.S.A. 77, 6897-6901 (1980).

 Cohen, A. I. Curr. Topics Membranes Transp. 15, 215-229 (1981).

 Eckert, R. & Brehm, P. A. Rev. Biophys. Bioengng 8, 353-383 (1979).

 Kung, C. & Saimi, Y. A. Rev. Physiol. 44, 519-534 (1982).

 Naitoh, Y. in Electrical Conduction and Behaviour in 'Simple' Invertebrates (ed. Shelton, A. B.) 1-48 (Clarendon, Oxford, 1982). 8. Ogura, A. & Takahashi, K. Nature 264, 170-172 (1976). 9. Dunlap, K. J. Physiol, Lond. 271, 119-133 (1977).

- Klumpp, S. & Schultz, J. E. Eur. J. Biochem. 124, 317-324 (1982).
 Oertel, D., Schein, S. J. & Kung, C. Nature 268, 120-124 (1977).
 Kung, C., Chang, S. Y., Satow, Y., van Houten, J. & Hansma, H. Science 188, 898-904 (1975).
 Hinrichsen, R. D. & Saimi, Y. J. Physiol., Lond. 351, 397-410 (1984).
 Hinrichsen, R. D., Saimi, Y. & Kung, C. Genetics 108, 545-558 (1984).
 Brehm, P., Eckert, R. & Tillotson, D. J. Physiol., Lond. 306, 193-203 (1980).

- 16. Ling, K.-Y. & Kung, C. J. exp. Biol. 84, 73-87 (1980).
- 17. Browning, J. L., Nelson, D. L. & Hansma, H. Nature 259, 491-494 (1976) 18. Naitoh, Y. & Eckert, R. Z. vergl. Physiol. 8, 453-472 (1968).
- Satow, Y. & Kung, C. J. exp. Biol. 78, 149-161 (1979).
 Klumpp, S., Kleefeld, G. & Schultz, J. E. J. biol. Chem. 258, 12455-12459 (1983)
- Hinrichsen, R. D. & Kung, C. Genet. Res. 43, 11-20 (1904).
- Klumpp, S., Steiner, A. L. & Schultz, J. E. Eur. J. Cell Biol. 32, 164-170 (15-33)
 Rapp, P. E. & Berridge, M. J. J. theor. Biol. 66, 497-525 (1977)
- 24. Berridge, M. J. Adv. Cyclic Nucleotide Prot. Phosphor. 17, 329-315 (1984) 25. Satow, Y. & Kung, C. J. exp. Biol. 88, 293-303 (1980).
- Van Wagtendonk, W. J. in Paramecium: A Current Survey (ed van Wagtendonk, W. J. 339-378 (Elsevier, Amsterdam, 1974).
- 27. Delaage, M. A., Roux, D. & Cailla, H. L. Molecular Biology and Pharmacology of Cycle Nucleotides (eds Falco, G. & Paoletti, R.) 155-170 (Elsevier, Amsterdam, 19"8)

Expression of peptide chain release factor 2 requires high-efficiency frameshift

William J. Craigen & C. Thomas Caskey

Institute for Molecular Genetics, Department of Biochemistry, and Howard Hughes Medical Institute, Baylor College of Medicine. Houston, Texas 77030, USA

Peptide chain release factors are soluble proteins that participate in the stop codon-dependent termination of polypeptide biosynthesis. In Escherichia coli, two release factors are necessary for peptide chain termination: release factor 1 (RF1) specifies UAGand UAA-dependent termination whereas release factor 2 (RF2) specifies UGA- and UAA-dependent termination1. Release factors are found in low concentrations relative to other translation factors², suggesting that their expression is tightly regulated and, accordingly, making the study of their structure-function relationship difficult. RF1 and RF2 exhibit significant sequence homology, probably reflecting their similar functions and perhaps a common evolutionary origin³. DNA and peptide sequencing have suggested the existence of a unique mechanism for the autogenous regulation of RF2 in which an in-frame UGA stop codon requires an obligatory +1 frameshift within the coding region of the RF2 gene. In this report we present in vitro experimental results consistent with the autogenous regulation of RF2. Additionally, we used RF2-lacZ gene fusions to demonstrate that autogenous regulation occurs, at least in part, by premature termination at the in-frame stop codon. since deletion of this stop codon leads to overproduction of the RF2-LacZ fusion protein. Frameshifting at this premature termination codon occurs at the remarkably high rate of 50%.

DNA sequencing demonstrated that the RF2 gene contains a UGA (opal) stop codon in-frame with the initiator methionine codon at codon position 26. Peptide sequencing of the amino terminus of RF2 confirmed that a +1 frameshift must occur at this position for the complete translation of intact RF23. Since RF2 uniquely recognizes opal stop codons⁴, RF2 may autoregulate when present in excess by prematurely terminating its own synthesis at codon 26.

To test this hypothesis we have used an in vitro coupled transcription/translation system to determine whether excess RF2 protein can suppress the translation of plasmid-encoded RF2. This system has been used to demonstrate autogenous translational regulation for a number of ribosomal protein operons⁵. Figure 1 shows the result of adding varying amounts of purified RF2 to the reaction mixture. Using the plasmidencoded β -lactamase as an internal standard it can be seen that RF2 production is reduced by increasing concentrations of added RF2. The addition of purified RF1 has no measurable effect (results are summarized in Fig. 2), and conversely the addition of RF2 has no measurable effect on RF1 synthesis (data not shown). We conclude that, at least in vitro, RF2 18 regulated at the translational level by its own gene product.

To determine whether this in-frame stop codon is the actual regulatory mechanism, and to measure the rate of frameshifting

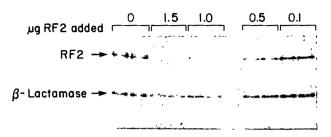


Fig. 1 In vitro autogenous regulation of RF2. A coupled transcription/translation system (Amersham) is used to demonstrate autogenous regulation of RF2. To a 30-µl reaction mixture containing ³⁵S-methionine, the indicated amount of purified RF2 protein ¹⁵ was added and the reaction started by the addition of 1 µg pRF2-1. The reaction was incubated at 37 °C for 30 min, followed by a 15-min chase with cold methionine, and the reaction products were displayed on a 12% SDS-polyacrylamide gel. The overall efficiency of the reaction is somewhat inhibited by the addition of RF2. Each reaction was performed in duplicate, and the complete experiment performed three times.

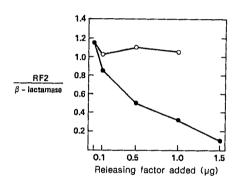


Fig. 2 A summary of the *in vitro* translation data for RF1 (O) and RF2 (\bullet). Band intensity was measured with a Helena Laboratories Auto-scanner densitometer and the intensity plotted as a ratio of RF2 to β -lactamase. The effect of purified RF1 protein was assessed as described in Fig. 1 legend for RF2, and plotted similarly. A representative experiment is depicted in the graph.

at this stop codon, RF2-lacZ gene fusions were constructed both with and without codon 26. It was assumed that these fusion proteins would be inactive for release factor activities and thus would not contribute to their own regulation. The construction of the gene fusions is shown diagrammatically in Fig. 3. Briefly, DNA restriction fragments containing 300-400 base pairs (bp) of 5' flanking sequence and either the first 12 codons (pEAB-1) or 67 codons (pEAB-2) of RF2 were inserted into a restriction site polylinker in the 5' coding region of the lacZ gene encoded on plasmid p9AB1. The lacZ promoter was subsequently removed by Bal31 digestion, and production of a fusion protein was confirmed by immunoprecipitation of 35S-methioninelabelled protein using anti-RF2 antibodies (Fig. 4). Only the pEAB-2 fusion protein is immunoprecipitable with anti-RF2 antibodies; presumably the pEAB-1 product lacks a sufficient RF2 sequence to be recognized by the anti-RF2 antibodies.

Bacteria harbouring these gene fusions were assayed for β -galactosidase activity, and the results are shown in Table 1. Several conclusions can be drawn from these results: first, since a high-level activity is seen with the gene fusion lacking codon 26, we conclude that the stop codon may be the only means by which RF2 expression is regulated, although we cannot exclude the possibility of an as yet undescribed 5' sequence, or sequences between codon 12 and 25, being involved in RF2 regulation.

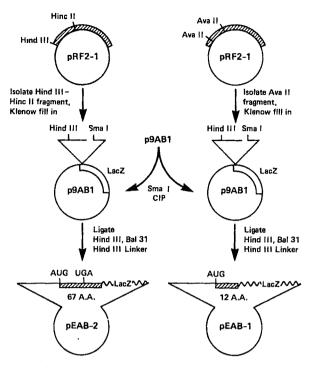


Fig. 3 The strategy for constructing RF2-lacZ fusion genes. The plasmid pRF2-1 contains the entire RF2 gene with 400 bp of 5' flanking DNA. Two DNA fragments containing the RF2 promoter. the initiating AUG, and either 12 codons or 67 codons of the coding region were isolated by restriction enzyme digestion and low melting agarose gel electrophoresis. Both fragments were made blunt-ended with the Klenow fragment of E. coli pol I, and ligated into SmaI-cut and dephosphorylated p9AB1. This plasmid contains the entire coding region of lacZ with a polylinker inserted in the amino-terminal end, and confers ampicillin resistance (provided by Bob Weiss, University of Utah). After ligation, the hybrid plasmid was redigested at a 5' flanking HindIII site, the adjacent lac promoter removed by Bal31 digestion, and a HindIII linker inserted to assess the size of the deletion. Plasmids containing an equivalent amount of 5' flanking DNA from the RF2 gene were selected for further study. The final plasmids are indicated at the bottom; pEAB-1 lacks the frameshift region, while pEAB-2 contains it.

This high level of activity also indicates that the RF2 gene contains a strong promoter, as underscored by the threefold greater activity of pEAB-1 over the parent plasmid activity. Second, by comparing the β -galactosidase activity of each RF2-LacZ fusion, a rate of frameshifting across the opal stop codon can be determined. Since pEAB-2 exhibits 50% of the β -galactosidase activity of pEAB-1, in the presence of normal levels of endogenous RF2 the ribosome can be assumed to frameshift at this rate. Thus, without a compensatory suppression of translation by excess RF2, the region around the in-frame stop codon permits a remarkably high level of frameshifting.

	Table 1	High-efficiency frameshifting
Plasmid	>	β-Galactosidase activity
pEAB-1		1.3×10^{4}
pEAB-2		6.4×10^{3}
p9AB1		4.5×10^{3}

 β -Galactosidase activity of RF2-LacZ fusion proteins. The assay was performed, and the units of activity calculated, according to Miller¹⁷. Bacteria were grown in minimal A medium supplemented with amino acids. The host strain is Su1675, a $recA^-$ derivative of CSH36 (Δ (lacpro), Laci⁻), provided by Bob Weiss. Plasmid copy number was determined by the method of Uhlin and Nordström¹⁸, and found to be essentially identical for all three plasmids.

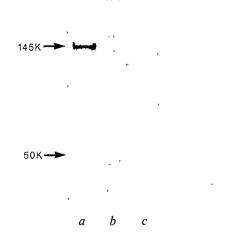


Fig. 4 Immunoprecipitation of RF2-LacZ fusion proteins. Exponentially growing E. coli, grown in minimal A medium¹⁷, was labelled with ³⁵S-methionine for 1 h and cell lysates made and immunoprecipitated with anti-RF2 antibodies, as described in Caskey et al. 16, except that the proteins were electrophoresed through an 8% polyacrylamide gel. a, Immunoprecipitated proteins from cells containing pEAB-2; b, from cells containing pEAB-1; c, from cells containing the parent lacZ plasmid p9AB-1. The band seen in a at a relative molecular mass of 145K (145,000) represents the RF2-LacZ fusion protein. The plasmid pEAB-1 fails to make an immunoprecipitable fusion protein, probably due to insufficient RF2 sequences being present, while the LacZ protein encoded on p9AB-1 fails to react with anti-RF2 antibodies. The bands seen at the 50 K position correspond to the endogenous RF2 protein.

Several factors influence the rate of frameshifting. Codon context has been shown to be important in determining the capacity of a particular codon to frameshift, with certain codons and their cognate transfer RNAs being inherently more 'shifty', and particular surrounding sequences having marked effects on the rate of frameshifting⁶. In certain circumstances the identity of the base found 3' to a shifty codon seems to play an important part in determining the rate of frameshifting at that codon, perhaps by allowing codon/anticodon mismatch and ribosome slippage⁷. Codon context has also been shown to effect the efficiency of nonsense suppression⁸, missense suppression⁹ and in vitro misreading of UGU codons¹⁰. Since previous examples of frameshifting were uniformly low-frequency events, factors involved in the recognition of stop codons by RF2 may be still another factor contributing to this high-efficiency frameshifting.

Natural frameshifting is involved in the expression of several prokaryotic and eukaryotic genes. Translation of the major coat protein of phage T7 (ref. 11), the gag-pol fusion protein of Rous sarcoma virus¹², and the analogous overlapping open reading frames of the yeast Ty912 transposable element¹³ involve an obligate frameshift event, although the exact position of the frameshift in these genes is unknown. In some of the above examples frameshifting may provide a mechanism for maintaining a fixed ratio of two separate proteins. For RF2 it seems that the frameshift is solely a means of regulating RF2 translation.

Elaborating the mechanism of frameshifting requires, as a first step, identifying the neighbouring sequences required for high-level frameshifting. Since RF2 exhibits a very high rate of frameshifting relative to artificial frameshift mutations¹⁴, RF2 may provide a unique model system for refining the rules of frameshifting, and for studying the mechanism of stop codon

W.J.C. was supported by the Baylor College of Medicine Medical Scientist Training Program GM07330. This research was supported by NIH grant GM34438 and the Howard Hughes Medical Institute.

Received 24 March: accepted 13 May 1986.

- 1. Caskey, C. T. Trends biochem. Sci. 5, 234-237 (1980).
- 2. Klein, H. A. & Capecchi, M. R. J. biol. Chem. 256, 1055-1061 (1971) 3. Craigen, W. J., Cook, R. G., Tate, W. P. & Caskey, C. T. Proc. natn. Acad. Soc. U.S.A. 82, 3616-3620 (1985).
- Scolnick, E., Tompkins, R., Caskey, T. & Nirenberg, M. Proc. gatn. Acad. Sci. U. S.A. 61, 768-774 (1968).
- 5. Nomura, M., Jinks-Robertson, S. & Miura, A. in Interaction of Translational and Transcrip tional Controls in the Regulation of Gene Expression (eds Grunberg-Manage, M. & Safer
- B.) 91-104 (Elsevier, Amsterdam, 1982). 6. Weiss, R. Proc. natn. Acad. Sci. U.S.A. 81, 5797-5801 (1984).
- Weiss, R. & Gallant, J. Genetics (in the press).
 Bossi, L. J. molec. Biol. 164, 73-87 (1983).
 Murgola, E. J., Pagel, F. T. & Hijazi, K. A. J. molec. Biol. 175, 19-27 (1984).
- Carrier, M. J. & Buckingham, R. H. J. molec. Biol. 175, 29-38 (1984)
 Dunn, J. J. & Studier, F. W. J. molec. Biol. 166, 477-535 (1983)

- Junn, J. J. & Studier, F. W. J. molec. Bibl. 100, 417-335 (1963)
 Jacks, T. & Varmus, H. E. Science 230, 1237-1242 (1985).
 Clare, J. & Farabaugh, P. Proc. natn. Acad. Sci. U.S.A. 82, 2829-2833 (1985).
 Atkins, J. F., Elseviers, D. & Gorini, L. Proc. natn. Acad. Sci. U.S.A. 69, 1192-1196 (1972).
 Caskey, C. T., Scolnick, E., Tomkins, R., Milman, G. & Goldstein, J. Met.). Enzim. 20. 367-375 (1971).
- 16. Caskey, C. T., Forrester, W. C., Tate, W. P. & Ward, C. J. Bact. 158, 365-365 (1984)
- 17. Miller, J. H. Experiments in Molecular Genetics, 355 (Cold Spring Harbor Laboratory, New York 1972)
- 18. Uhlin, B. E. & Nordström, K. Plasmid 1, 1-8 (1977).

A mouse locus at which transcription from both DNA strands produces mRNAs complementary at their 3' ends

Trevor Williams & Mike Fried

Department of Tumour Virus Genetics, Imperial Cancer Research Fund, Lincoln's Inn Fields, London WC2A 3PX, UK

The organization and large size of the mammalian cell genome allows spatial separation of different transcription units. In those cases where more than one species of messenger are synthesized from the same cellular DNA sequence, they have been found to be generated from transcription proceeding in the same direction. These mRNAs always share regions of homology and can differ from one another as a result of differential processing (splicing and/or polyadenylation) or alternative initiation 1-14. In contrast, complementary mRNAs transcribed from opposite strands of the same cellular DNA sequence have not previously been observed. Here we have identified a region of mouse DNA at which processed mRNAs from two adjacent convergent transcription units overlap by 133 base pairs (bp) at their 3'-untranslated ends. One of the transcription units appears to encode a second mRNA which does not contain this overlapping region. This represents the first description of the natural occurrence of processed mammalian cell mRNAs transcribed from opposite strands of the same DNA sequence. The implications of these complementary regions in normal gene regulation are discussed in the context of the finding that the artificial introduction into cells of DNA constructs synthesizing anti-sense RNAs complementary to regions of mRNA transcribed from a chromosomal gene, can inhibit the gene's activity, presumably by the formation of double-stranded RNA¹⁵⁻¹⁹.

We have used the 'expression selection' technique to isolate cellular DNA sequences with enhancer-like properties (expression sequences) by virtue of their ability to reactivate a test gene lacking its own 5' regulatory sequences^{20,21}. A 19kilobase (kb) EcoRI fragment of mouse cellular DNA containing the normal chromosomal location of the previously identified cellular expression sequence²⁰ has been cloned and characterized and found to encode a number of transcription units (T.W. and M.F., in preparation). The 746-bp PvuII/EcoRI subfragment (Fig. 1a) found at the right-hand end of the 19-kb clone is present as a single-copy sequence when used to probe Southern blots of mouse genomic DNA (Fig. 1b). In contrast, when this fragment is used to probe Northern blots of mouse poly(A)⁺ RNA, it hybridizes to two transcripts, of 1.2 and 3.0 kb (Fig. 1c). The presence of overlapping regions of the two

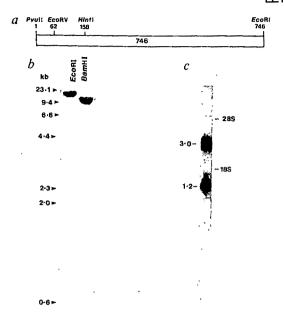


Fig. 1 Southern and Northern analysis of the 746-bp PvuII-EcoRI mouse cellular DNA fragment. a, Restriction map of the 746-bp PvuII-EcoRI fragment. This fragment was derived from one end of a 19-kb EcoRI clone (T.W. and M.F., in preparation) which contains a copy of a previously isolated mouse expression sequence²⁰, and which is subcloned into EcoRI/SmaI-cleaved pEMBL 8(+)³⁶. The PvuII, EcoRV, HinfI and EcoRI sites are indicated. b, Detection of a single copy of the 746-bp sequence in the mouse genome. A Southern blot of mouse genomic DNA digested with either EcoRI or BamHI was hybridized to the 746-bp probe. The numbers on the left show the sizes of the DNA markers (in kb). c, Northern blotting analysis of BALB/c TS-A-3T3 poly (A)⁺ RNA hybridized to the 746-bp fragment identifies two distinct mRNA species of 3.0 and 1.2 kb. On the right are shown the positions of the 28S and 18S ribosomal RNA markers.

Methods. For Southern blotting, 16 μg of BALB/c 3T3 DNA was digested with either EcoRI or BamHI, fractionated by electrophoresis on a 0.8% agarose gel, and transferred to nitrocellulose as described previously³⁷. For Northern blotting, total cellular RNA was prepared from BALB/c TS-A-3T3 cells²⁵ by the guanidinium/CsCl method³⁸ and poly(A) selected on oligo(dT)-cellulose; 5 μg of poly(A)⁺ RNA was fractionated on a 1% agarose/formaldehyde gel and transferred to nitrocellulose after partial alkaline hydrolysis³⁸. Hybridization conditions were identical for Northern and Southern blotting and both types of blot were washed to a stringency of 0.5× SSC at 68 °C essentially as described previously³⁷.

mRNAs was initially suggested by the finding that when uniformly labelled single-stranded probes specific for either strand of the 746-bp fragment were annealed to poly(A)+ RNA, both strands produced S₁-nuclease-resistant products, and the sum of these products was greater than 746 nucleotides. To more accurately localize the transcripts and determine the extent of their overlap, 3'S₁-nuclease mapping was performed using either a 746-nucleotide probe 3'-labelled at the EcoRI site or a 684nucleotide probe 3'-labelled at the EcoRV site at position 62 (Fig. 2a, probes A and B respectively). The probes were annealed to mouse RNA, and the S₁-nuclease-resistant products fractionated on polyacrylamide gels. Probe A, homologous to the top (A) strand, protects a 500-bp fragment (Fig. 2b, lane 3), locating a splice donor or polyadenylation site around nucleotide 242. Probe B, homologous to the bottom (B) strand, mainly protects a 310-bp fragment (Fig. 2c, lane 3), locating a splice donor or polyadenylation site around residue 372, but on the opposite strand. This indicates that the transcripts are derived from opposite strands and overlap by ~130 nucleotides.

To analyse the overlapping region in detail, complementary DNA clones corresponding to both transcripts were isolated

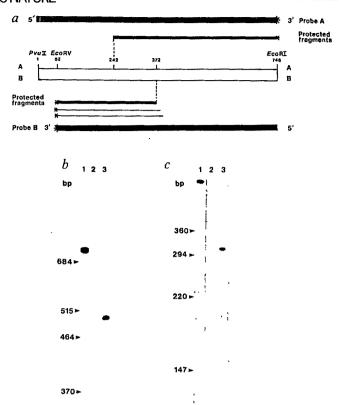
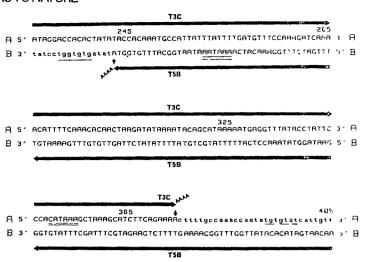


Fig. 2 Identification by 3' S₁ mapping of a region of mouse DNA where convergent transcription units overlap. a, Diagrammatic representation of the probes used for 3' S₁ mapping and the overlapping protected fragments. The open box represents the 746-bp fragment, with the A strand at the top and the B strand at the bottom. Nucleotide (nt) numbers above the DNA fragment are given from the PvuII site. The 746-nt probe A is illustrated by the solid box at the top, and is 3'-end-labelled at the EcoRI site (indicated by *). The 684-nt probe B, 3'-end-labelled at the EcoRV site, is similarly shown at the bottom. The major fragments protected in b and c are represented by the thick lines between the probes and the genomic sequence; the minor bands in c are represented similarly by thin lines. b, 3' S_1 mapping using the 746-nt probe A homologous to the A strand (see a). Lane 1, untreated probe; lane 2, probe plus 40 µg yeast RNA; lane 3, probe plus 40 µg BALB/c TS-A-3T3 total RNA. Marker DNA sizes are given on the left (in bp). c, 3' S₁ mapping using the 684-nt probe B homologous to the B strand (see a). Lane 1, untreated probe; lane 2, probe plus 40 μg yeast RNA; lane 3, probe plus 40 μg BALB/c TS-A-3T3 total RNA. Marker DNA sizes are given on the left (in bp).

Methods. The 746-bp fragment subcloned in pEMBL 8(+) was cleaved with either EcoRI (for probe A) or EcoRV (for probe B). Probe A was 3'-end-labelled at the EcoRI site using Klenow polymerase and ³²P-dATP and re-cut at the BamHI site present in the pEMBL 8(+) polylinker sequence. Probe B was 3'-end-labelled at the EcoRV site using T₄ DNA polymerase and ³²P-TTP and re-cut with EcoRI. Probes A and B were then prepared by electroelution after fractionation on 1% agarose gels. Procedures for RNA/DNA hybridization and S₁-nuclease digestion were essentially as described elsewhere³⁹. S₁-protected products were analysed by electrophoresis on 4% (b) or 6% (c) polyacrylamide gels containing 50% urea.

from a mouse cell cDNA library and sequenced. Figure 3 shows the relationship of the cDNAs T3C and T5B to the sequence of the 746-bp genomic fragment. The 3' 374 nucleotides of T3C (up to the start of the poly(A) tract) are homologous to the genomic sequence of the A strand from nucleotide 1 to 374. In addition, the 3' 505 nucleotides of T5B (up to the start of the poly(A) tract) are homologous to the genomic sequence of the B strand from position 746 to 242 (nucleotide numbers corre-

Fig. 3 A comparison of the genomic sequence of the 746-bp fragment with the cDNA sequences of T3C and T5B in the region of the overlap. The extent and orientation of the cDNAs are shown by the thick, solid arrowed lines above or below the sequence. Upper-case letters indicate sequences present in the processed poly(A)+ RNA; lower-case letters denote sequences 3' of the poly(A) addition sites. The vertical arrows indicate the last nucleotide of the genomic sequence which is homologous to the sequence of either T3C (A strand) or T5B (B strand). Beyond these positions the presence of poly(A) tracts in the cDNAs distinguishes them from the genomic sequence. The postulated poly(A) addition signals for both transcripts are indicated by double underlining. The postulated poly(A) addition signal for transcripts homologous to the B strand is the canonical AAUAAA⁴⁰, while that for transcripts homologous to the A strand, which may display microheterogeneity in the nucleotide used for poly(A) addition, is the much rarer CAUAAA⁴¹. The TG nucleotide blocks seen downstream of many poly(A) addition sites are underlined⁴²⁻⁴⁵. In contrast, the consensus sequence CAYUG, postulated to be important in the 3' processing of primary transcripts⁴⁶, is not seen in the vicinity of the poly(A) addition site for either transcript.



Methods. A cDNA library was constructed from BALB/c TS-A-3T3 poly(A)⁺ RNA as described elsewhere⁴⁷, with the following modifications: after second-strand synthesis the cDNA was repaired with T₄ DNA polymerase and ligated into λgt10 (ref. 48) after the addition of EcoRI linkers. cDNAs T3C and T5B were isolated on the basis of their homology to the 746-bp genomic fragment, and their EcoRI cDNA inserts were subcloned into pAT153. The sequence of the 746-bp fragment and the cDNA clones T3C and T5B in the region of the overlap was obtained for both strands by the dideoxy method⁴⁹ after appropriate restriction fragments had been subcloned into either M13mp18 or M13mp19 (ref. 50).

spond to the A strand sequence in Fig. 2). Thus, the two cDNAs analysed here are derived from mRNAs transcribed from opposite strands of the 746-bp genomic fragment (T3C from the B-strand template and T5B from the A-strand template) and overlap by 133 nucleotides at their 3' ends (Fig. 3), which is in agreement with the 3' S₁ mapping data presented in Fig. 2. The minor bands observed using probe B (Fig. 2c, lane 3) may be due to microheterogeneity in the choice of site for poly(A) addition²²⁻²⁴, in which case the exact extent of the overlap for processed mRNA would depend on which nucleotide was used for poly(A) addition for mRNAs homologous to the A strand (corresponding to cDNA T3C).

To determine which of the $poly(A)^+$ RNA species in Fig. 1c corresponded to which cDNA clone, a truncated fragment of T3C (deleted 3' to the HinfI site; see Fig. 4e) lacking the 3' overlapping sequences was used as a probe for Northern blotting and found to hybridize only to the 1.2-kb mRNA species (Fig. 4, compare a and b). When the cDNA clone RMC4, which is homologous to T5B but is truncated at its 3' end and contains only 18 bp of the overlapping sequences (Fig. 4c,e), was used as a probe for Northern blotting, it hybridized to 3.0-kb mRNA, but not to the 1.2-kb mRNA (Fig. 4c). Probe RMC4 also hybridized to a 2.4-kb mRNA (Fig. 4c,e), which was not visible if the 746-bp genomic clone was used as a probe (Fig. 4b). However, when used to probe Southern blots of mouse genomic DNA, clone RMC4 was found to represent single-copy sequence in the genome (data not shown); this suggests that, in addition to the transcripts homologous to the B strand which have been polyadenylated in the 746-bp fragment, typified by T5B (see Figs 3, 4e), there is an alternative shorter transcript terminating before the overlapping region of the 746-bp genomic sequence is reached (Fig. 4e). Further experiments will be necessary to determine whether the 2.4-kb poly(A)⁺ species is derived from this transcription unit by alternative 3' exon usage or alternative polyadenylation. We are presently cloning the mouse genomic DNA adjacent to the 746-bp fragment in order to further analyse the relationship of the 2.4-kb mRNA to the 3.0-kb mRNA.

The presence of the 1.2-kb and 3.0-kb mRNAs was assessed by Northern blotting in several normal and transformed clonal cell lines (Fig. 4d). No differences were detected in the ratios of the steady-state levels of the two mRNAs between normal BALB/c 3T3 cells and their transformed derivative BALB/c

TS-A-3T3 cells²⁵. However, the ratios of the steady-state levels of the two mRNAs in F9 (ref. 26) and MH15 (ref. 27) teratocarcinoma cells differed from those found in differentiated mouse cells (Fig. 4d). In the undifferentiated cells, the 3.0-kb mRNA appears to be down-regulated with respect to the 1.2-kb mRNA.

The function of the 1.2-, 2.4- and 3.0-kb mRNAs remains to be determined. However, in this context, the 5' end of the gene encoding the 1.2-kb mRNA maps in close proximity to the expression sequence²⁰ and displays a number of properties which are normally associated with housekeeping genes (T.W. and M.F., in preparation). The structures of the 3.0-kb and 2.4-kb mRNAs are presently being characterized.

The overlapping transcripts described here raise several interesting questions concerning the organization of genetic information and the control of gene expression. The mammalian genome characteristically contains individual genes separated by large regions of untranscribed DNA. In the present report we have identified a mouse genetic locus at which two processed poly(A)+ RNA species transcribed from opposite strands overlap by 133 nucleotides at their 3' ends. This finding implies a complex sequence organization in this region as the poly(A) addition signal for one transcript is contained in the exon sequence of the other, and vice versa. In addition, for those vertebrate genes in which it has been studied, transcription does not terminate at the poly(A) addition site but continues for some distance downstream. Therefore, the sequences that may be involved in the transcriptional termination or processing of one transcript are also probably encoded in the sequence giving rise to the transcript from the other strand, and vice versa. Therefore, it may be significant that the overlap is in the 3'-untranslated region of both mRNAs. Such overlapping transcripts have been identified previously in mammalian viruses, for example, the early and late mRNAs of polyoma virus overlap by 50 nucleotides and those of simian virus 40 by 87/88 nucleotides, although there is temporal control of the expression of these opposite strands2

In prokaryotes the formation of double-stranded RNA by the hybridization of complementary transcripts is important in the regulation of gene expression and replication. Such a mechanism has been shown to be responsible for the inhibition of translation of the *ompF* (ref. 29) and IS10 transposase³⁰ genes, and the control of replication of the plasmid ColE1 by inhibiting RNA

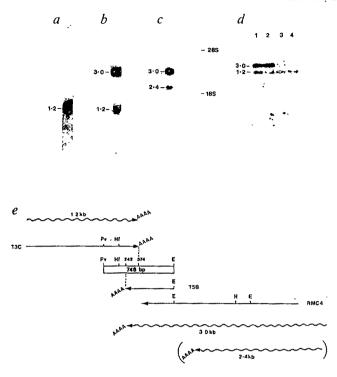


Fig. 4 Analysis of mRNAs homologous to the overlapping region. a, Northern blot analysis of BALB/c TS-A-3T3 poly(A)⁺ RNA to determine which mRNA is homologous to cDNA clone T3C (see e). A fragment of T3C lacking sequences 3' of the Hinf1 site (nucleotide 158 on the genomic sequence shown in e) and so missing the overlapping sequence, was used as a probe. b, Northern blot analysis of BALB/c TS-A-3T3 poly(A)+ RNA hybridized to the 746-bp fragment. c, Northern analysis of BALB/c TS-A-3T3 poly(A)+ RNA hybridized to cDNA RMC4 (see e) identifies mRNAs of 3.0 kb and 2.4 kb. cDNA RMC4 was isolated from a cDNA library derived from mouse mammary tumour virus-transformed mouse cells (given by R. Moore) on the basis of its homology to the 746-bp genomic fragment. RMC4 is truncated at its 3' end 115 bp before the poly(A) addition site and so lacks all but 18 bp of the overlapping sequences that would hybridize to the 1.2-kb mRNA. d, Northern blot analysis of mouse poly(A) RNA from differentiated cell lines (lane 1, BALB/c TS-A-3T3; lane 2, BALB/c 3T3) and undifferentiated teratocarcinoma cell lines (lane 3, MH15; lane 4, F9) hybridized to the 746-bp fragment. e, Organization of cDNA clones and transcripts in the vicinity of the 746-bp fragment. The 746-bp cellular DNA sequence is indicated by an open box. The straight lines represent the cDNA clones, with the arrows showing the direction of transcription and AAAA indicating the presence of a poly(A) tail. The dotted lines between the 746-bp fragment and T3C or T5B indicate the extent of the cDNAs with respect to the sequence of the genomic A strand; the last nucleotide of each cDNA is given above the 746-bp fragment (see Fig. 3). Wavy lines indicate the positions of the mRNAs, with their direction of transcription shown by arrows, and the poly(A) tails indicated by AAAA. The wavy line in parentheses represents the 2.4-kb mRNA which is related to the cDNA clone RMC4 but which terminates before the EcoRI site is reached (see c). The positions of relevant restriction enzyme sites are indicated: E, EcoRI; Pv, PvuII; H, HindIII; and Hf, HinfI. RNA preparation and Northern blotting procedures were identical to those described in Fig. 1 legend.

priming³¹⁻³³. In eukaryotes the introduction of anti-sense RNA, or vectors expressing anti-sense RNA, into cells has been used as a tool for the inhibition of gene product expression^{15,16}. In a cytoplasmic location, anti-sense RNAs which are complementary to the 5' sequence of a mRNA have been found to be more inhibitory than anti-sense RNAs complementary to the 3' sequence. This effect appears to be mediated by the ability of anti-sense RNAs to inhibit the translation of the specific mRNA

to which they are complementary 17,18. However, when anti-sense transcripts are expressed in a nuclear location, inhibition probably occurs via the formation of double-stranded RNA, which prevents the transport of sense transcripts from the nucleus; in this case, sequences complementary to the 3' portion of the sense transcript are as potent as those complementary to the 5' sequences 19. In addition, in Saccharomyces cerevisiae the CYC1 gene and an adjacent gene are convergently transcribed from opposite strands, but transcription termination signals located between the two genes normally ensure that transcripts from one gene do not read-through into the other gene and vice versa. The deletion of these termination signals generates overlapping convergent transcription from opposite strands and has a marked deleterious effect on the mRNA levels yielded from both transcription units34

Therefore, the two overlapping transcripts described here may display some novel mechanism of control of mammalian gene expression. First, if the overlapping transcripts were expressed at the same time, it might be expected that RNA polymerase complexes travelling in opposite directions along a DNA duplex might encounter a considerable degree of steric hindrance, especially as transcription probably continues past the poly(A) addition site³⁵. Second, although the abundance of the mRNAs is fairly low (<0.01% for each of the two mRNA species), the local concentration of the two opposite-strand transcripts in the vicinity of the 3'-ends of the transcription units might favour RNA duplex formation with concomitant inhibition of RNA processing and/or transport from the nucleus. Thus the two strands might be only rarely transcribed and their mRNAs very stable, or there might be some temporal or spatial control of expression such that their transcription occurs at different times in the cell cycle or from different alleles. Alternatively, coincident convergent transcription might be involved in controlling the expression of one or both of these transcripts. For example, it may be that when transcription of the 1.2-kb mRNA species is required, the shorter, non-overlapping 2.4-kb mRNA is generated from the opposite strand. Finally, an effect on the translation of either the 1.2-kb or the 3.0-kb mRNA by the overlap cannot be excluded. Further studies on the transcription of this mouse genomic locus may answer some of these questions.

We thank Drs P. Goodfellow, N. Jones, I. Kerr, P. Nurse and M. Parker for helpful discussions, and Mrs G. Briody and Mrs C. Middlemiss for typing the manuscript.

Received 28 February; accepted 15 April 1986.

- 1. Alt, F. W. et al. Cell 20, 293-301 (1980).
- Early, P. et al. Cell 20, 313-319 (1980).
 Rosenfeld, M. G. et al. Nature 304, 129-135 (1983).
- 4. Medford, R. M., Nguyen, H. T., Destree, A. T., Summers, E. & Nadal-Ginard, B. Cell 38,
- 5. Kornblihtt, A. R., Umezawa, K., Vibe-Pedersen, K. & Baralle, E. EMBO J. 4, 1755-1759

- (1985).
 6. de Ferra, F. et al. Cell 43, 721-727 (1985).
 7. Leonard, W. J. et al. Science 230, 633-639 (1985).
 8. Setzer, D. R., McGrogan, M., Hunberg, J. H. & Schimke, R. T. Cell 22, 361-370 (1980).
 9. Tosi, M., Young, R. A., Hagenbuchle, O. & Schibler, U. Nucleic Acids Res. 9, 2313-2323 (1981).
- 10. Setzer, D. R., McGrogan, M. & Schimke, T. J. biol. Chem. 257, 5143-5147 (1982).
- Setzer, D. R., McGrogan, M. & Schinke, I. J. biol. Chem. 237, 5143-5147 (1982).
 Parnes, J. R. & Robinson, R. R. Nature 302, 449-452 (1983).
 Sakakibara, M., Mukai, T., Yatsuki, H. & Hori, K. Nucleic Acids Res. 13, 5055-5069 (1985).
 Milner, R. J. et al. Cell 42, 931-939 (1985).
 Schibler, U., Hagenbuchle, O., Wellauer, P. K. & Pittet, A. C. Cell 33, 501-508 (1983).
 Izant, J. G. & Weintraub, H. Cell 36, 1007-1015 (1984).
 Izant, J. G. & Weintraub, H. Science 229, 345-352 (1985).
 Tant, D. A. Pecantr. Acid. Sci. MS. 42, 2444 (1985).

- Herland, D. A. Poc. natn. Acad. Sci. U.S.A. 82, 144-148 (1985).
 Harland, R. & Weintraub, H. J. Cell Biol. 101, 1094-1099 (1985).
- Kim, S. K. & Wold, B. Cell 42, 129-138 (1985).
- 20. Fried, M. et al. Proc. natn. Acad. Sci. U.S.A. 80, 2117-2121 (1983).
- 21. Ford, M., Davies, B., Griffiths, M., Wilson, J. & Fried, M. Proc. natn. Acad. Sci. U.S.A. 82, 3370-3374 (1985).
- Sasavage, N. L., Smith, M., Gillam, S., Woychik, R. O. & Rottman, F. M. Proc. natn. Acad. Sci. U.S.A. 79, 223-227 (1982).
- 23. Wiedemann, L. M. & Perry, R. P. Molec. cell. Biol. 4, 2518-2528 (1984)
- Simonsen, C. C. & Levinson, A. D. Molec. cell. Biol. 3, 2250-2258 (1983).
 Ruley, H. E., Lania, L., Chaudry, F. & Fried, M. Nucleic Acids Res. 10, 4515-4524 (1982).
- Bernstine, E. G., Hooper, M. L., Grandchamp, S. & Ephrussi, B. Proc. natn. Acad. Sci. U.S.A. 70, 3899-3903 (1973).
- 27. Solter, D. & Knowles, B. Proc. natn. Acad. Sci. U.S.A. 75, 5565-5569 (1978).

- 28. Tooze, J. (ed.) DNA Tumour Viruses 2nd edn (Cold Spring Harbor Laboratory, New York,
- Mizuno, T., Chou, M.-Y. & Inouye, M. Proc. natn. Acad. Sci. U.S.A. 81, 1966-1970 (1984).
 Simons, R. W. & Kleckner, N. Cell 34, 683-691 (1983).
- 31. Tomizawa, T.-I., Itoh, T., Selzer, G. & Som, T. Proc. natn. Acad. Sci. U.S.A. 78, 1421-1425
- 32. Cesareni, M., Muesing, M. A. & Polisky, B. Proc. natn. Acad. Sci. U.S.A. 79, 6313-6317 (1982).
- Tomizawa, J.-I. & Itoh, T. Cell 31, 575-583 (1982)
- 34. Zaret, K. S. & Sherman, F. Cell 28, 563-573 (1982)
- Birnstiel, M. L., Busslinger, M. & Strub, K. Cell 41, 349-359 (1985).
 Dente, L., Cesareni, G. & Cortese, R. Nucleic Acids Res. 11, 1645-1655 (1983).
- Hayday, A., Ruley, H. E. & Fried, M. J. Virol. 44, 67-77 (1982).
- Maniatis, T., Fritsch, E. F. & Sambrook, J. in Molecular Cloning: a Laboratory Manual (Cold Spring Harbor Laboratory, New York, 1982).

 39. Favaloro, J., Triesman, R. & Kamen, R. Meth. Enzym. 65, 718-749 (1980).

 40. Proudfoot, N. J. & Brownlee, G. G. Nature 263, 211-214 (1976).

- Wickens, M. & Stephenson, P. Science 226, 1045-1051 (1984).
 Taya, T. et al. EMBO J. 1, 953-958 (1982).
- 43. Woychik, R. P., Lyons, R. H., Post, L. & Rottman, F. M. Proc. natn. Acad. Sci. U.S.A. 81, 3944-3948 (1984).
- Gil, A. & Proudfoot, N. J. Nature 312, 473-474 (1984).
 McLauchlan, J., Gaffney, D., Whitton, J. L. & Clements, J. B. Nucleic Acids Res. 13, 1347-1368 (1985).
- 46. Berget, S. M. Nature 309, 179-182 (1984). 47. Gubler, U. & Hoffman, B. J. Gene 25, 263-269 (1983).
- Huynh, T. V., Young, R. A. & Davis, R. W. in DNA Cloning: a Practical Approach Vol. 1 (ed. Glover, D. M.) 49-78 (IRL, Oxford, 1985).
- Sanger, F., Nicklen, S. & Coulson, A. R. Proc. natn. Acad. Sci. U.S.A. 74, 5463-5467 (1977).
 Yanisch-Perron, C., Vicira, J. & Messing, J. Gene 33, 103-119 (1985).

Overlapping transcription units in the dopa decarboxylase region of *Drosophila*

Charlotte A. Spencer, R. Daniel Gietz & Ross B. Hodgetts

Department of Genetics, University of Alberta, Edmonton, Alberta, Canada T6G 2E9

The many examples of overlap in the genes of various viruses and bacteria illustrate that the parsimonious utilization of the coding capacity of DNA is relatively common amongst prokaryotes (for review, see ref. 1). The recent discovery of a pupal cuticle gene within an intron of the completely unrelated Gart locus in Drosophila² shows that overlapping transcription units also exist in higher organisms. However, the prevalence of such phenomena is unknown. We report here a quite different situation of overlap between the 3' termini of a pair of convergent transcription units in another region of the Drosophila genome. This 88-base-pair (bp) genomic region encodes the 3' terminus of the messenger RNA for the enzyme dopa decarboxylase (Ddc) and, in opposite orientation, the 3' terminus of the adjacent gene whose function is unknown. An analysis of the temporal and spatial distribution of the two transcripts within the organism shows that high levels of both transcripts are never concordant. However, within the testes, where the 3' transcript is maximally expressed, low levels of Ddc transcript were detected. This result raises the possibility that a hybrid molecule involving the two transcripts forms in vivo or that transcription interference occurs, with concomitant regulatory implications.

Previous work has shown that the dopa decarboxylase region of Drosophila, as defined by the deficiency DF(2L)TW130 (ref. 3), contains a cluster of 18 genes, 14 of which appear to function in cuticle development and catecholamine metabolism⁴. Four genes, including Ddc, have been mapped within a 12-kilobase (kb) region and primary transcripts from these genes account for ~10.5 kb of the genomic DNA⁵. This tight clustering of genes has complicated our previous analysis of Ddc transcripts⁶, because the DNA probes we used in that study were found to encompass both Ddc and its 3'-adjacent transcription unit7. Strand-specific RNA probes revealed that the 3'-adjacent transcript originated on the opposite strand from that of the Ddc transcript and a hybridization of Northern blots to a series of nested single-stranded probes showed that the 3' termini of the Ddc gene and the adjacent gene apparently lie on opposite sides of the HpaI site shown in Fig. 1. However, subsequent analysis of the DNA sequence in this region showed that putative polyadenylation signals for the two genes are present on opposite sides of the HpaI site (see Fig. 1). This result suggested the possibility of a slight amount of overlap between the two transcripts in the vicinity of the HpaI site. We have now obtained complementary DNA clones for both Ddc and the 3'-flanking gene, and a comparison of their DNA sequences with the genomic DNA sequence confirms that an 88-bp overlap between the two 3' termini exists.

A cDNA library in λgt10 was made using poly(A)⁺ RNA from newly eclosed adults as described elsewhere8. Two clones each of Ddc and the 3'-flanking gene were chosen for further analysis. The inserts, which ranged in size from 1.1 to 2.0 kb, were re-cloned into M13mp19 and the ends of each fragment were sequenced (Fig. 2). Clones ACP, ACQ and ACR represented intact 3' termini, as revealed by tracts of oligo(dT) (or oligo(dA), depending on their orientation within the cloning vector) not found in the genomic sequence. The polyadenylation site of the 3'-adjacent gene was assigned unambiguously from the two cDNA clones of different length (ACQ and ACR); it is indicated by an asterisk beneath the genomic sequence in Fig. 2. A canonical polyadenylation signal sequence, 5'AATAAA3', lies 16 bases upstream of the terminal C residue (boxed in Fig. 2). The polyadenylation site for the Ddc gene (indicated by an asterisk above the genomic sequence in Fig. 2) could not be assigned unambiguously from the cDNA sequence because of

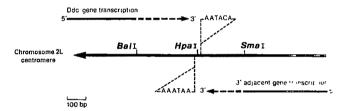
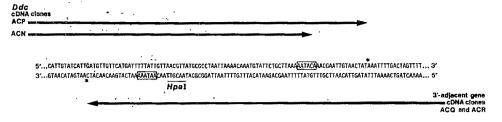


Fig. 1 Mapping the 3' termini of Ddc and the adjacent gene. The figure summarizes the results of our earlier work in which strandspecific RNA probes were used in a Northern analysis of poly(A) RNA from the mature larval and young adult stages of Drosophila7. Single-stranded Ddc-specific probes indicated that transcription of this gene terminated in the Ball-Hpal interval, while probes specific for the flanking gene indicated that its transcripts terminated in the HpaI-SmaI interval. Possible polyadenylation signals, chosen on the basis of their similarity to the eukaryotic consensus sequence 5'AATAAA3' (see ref. 9), were obtained from genomic DNA sequence analysis. Their precise locations with respect to the HpaI site are shown in Fig. 2.

the uncertainty caused by a run of adenine residues in the genomic sequence. However, we believe the site chosen at the T residue in Fig. 2 is the most likely one, based on its similarity the eukaryotic polyadenylation addition sequence 5'...Py\(^1\)A...3' (ref. 9); a hexameric sequence (5'ATTACA3') which could control poly(A)+ addition at this residue lies 16 bases upstream of it. Although this sequence appears to be an inefficient signal for transcription termination¹⁰, the other possible hexamers 5'AACAA3' and 5'AATTAA3' lie 38 and 43 bases upstream, farther than any reported in the most recent review9.

The extent of overlap that we have found between the 3' termini of the poly(A)⁺ mRNAs may reflect an even greater overlap between the unprocessed, non-adenylated transcripts, assuming that transcription termination occurs in Drosophila 1 kb or farther downstream of the $poly(A)^+$ signal sequence, as is known to occur in other systems. The overlap also raises the intriguing possibility that a sense/anti-sense hybrid might exist in vivo, with regulatory implications for the expression of one

Fig. 2 Genomic DNA sequence in the region of overlap between the *Ddc* transcription unit and the 3'-flanking gene. The sequence of both strands of the genomic DNA was determined by the dideoxynucleotide method of Sanger¹⁵ and constitutes part of a 5-kb sequence including the entire *Ddc* gene⁸. Poly(A) signal sequences are boxed. Methods. Sequences of the cDNA



molecules near their 3' termini were obtained from single- or double-stranded templates in which the cDNA constructs were cloned into M13mp19. The cDNA libraries were prepared from poly(A)⁺ adult RNA as described elsewhere⁸. Ddc-specific clones were identified using a nick-translated HpaI genomic fragment which extends 3.6 kb upstream of the HpaI site shown in Fig. 1. Although this fragment actually includes the 3'-terminal 26 nucleotides of the flanking gene, the extent of homology between the probe and the 3' gene is insufficient to generate a stable hybrid under the conditions used. Clones of the 3'-flanking transcription unit were identified using the strand-specific probe 10 (ref. 7), which is homologous to the HpaI-SmaI interval shown in Fig. 1.

or both mRNAs. We therefore undertook analyses of the temporal and spatial distribution of Ddc transcripts and of the 3'-adjacent transcripts during the life cycle of Drosophila. Our earlier work indicates that the developmental expression of the two genes is quite different. Maximum levels of dopa decarboxylase occur in 18-h embryos, at each larval moult, at pupariation and at adult eclosion11. The 3'-adjacent transcript, however, is abundant only in adult stages and in 1-4-h embryos⁷. These data make it unlikely that the region of overlap between the two transcripts has biological significance during embryonic or larval life. However, both transcripts are present in adult flies (Fig. 3). Between 0 and 4 days, the level of mature Ddc transcript (the 2.0-kb species^{6,12}) decreases, although substantial amounts of the 3.0-kb Ddc species are still present (Fig. 3a). High levels of the 3'-adjacent transcript are present in both newly eclosed and 4-day-old adults and an obvious sexual dimorphism in both the amount and size distribution of this transcript is apparent (Fig. 3b).

To further define the distribution of the two transcripts within adults, we prepared RNAs from several dissected fractions of newly eclosed adults and quantitated the two transcripts by dot hybridization (Fig. 4). Control experiments (not shown) indi-

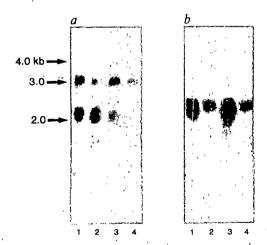


Fig. 3 Northern analysis of transcript levels in male and female adults. Duplicate samples of poly(A)⁺ RNA (5 μ g) were subjected to Northern analysis as described previously⁷. The autoradiogram in a shows the hybridization response to the *Ddc*-specific RNA probe 5 prepared by in vitro transcription of a 1.5-kb genomic fragment including \sim 600 bp from the 3' end of *Ddc*⁷. b, The response to probe 4 (ref. 7), transcribed from the opposite strand of the same genomic fragment and therefore complementary to transcripts of the 3'-adjacent gene. Lanes 1, newly eclosed male; 2, newly eclosed female; 3, 4-day-old adult male; 4, 4-day-old adult female.

cated no detectable hybridization to either of the strand-specific probes in purified ribosomal or $poly(A)^-$ cytoplasmic RNA from young adults. The pattern of Ddc expression in whole heads, thoraces and abdomens of both males and females (Fig. 4a) is consistent with a distribution of the enzyme in epidermal¹³ and neural tissue¹⁴. The higher concentration of Ddc transcripts in male abdomens (Fig. 4a, dot 7) than in female abdomens (a, dot 3) probably results from the contribution of testicular Ddc transcripts (a, dot 8) to the male abdominal sample. Longer exposures indicated a very low but detectable level of Ddc transcript in dissected ovaries (Fig. 4a, dot 4).

The pattern observed for the 3'-adjacent transcripts appears almost complementary to that of the *Ddc* transcripts (Fig. 4b): low, but detectable levels of the former transcript occur in both male and female heads and thoraces, and in female abdomens and ovaries. Clearly, though, the 3'-adjacent gene transcripts accumulate primarily in the testes (Fig. 4b, dot 8). A Northern analysis of total RNA samples from the dissected tissue samples confirmed that the male-specific size distribution of the 3'-adjacent gene transcripts (Fig. 3b) is also seen in the testes. Similarly, the female-specific size distribution (Fig. 3b) is identical to that contributed by ovaries and 2-h embryos (data not shown).

The data presented here, and our previous work⁷, indicate that high levels of the two overlapping transcripts are found only within young adults. However, the maximal steady-state levels of the two transcripts occur in different tissues. *Ddc* transcripts are confined primarily to the epidermis of males and females whereas transcripts of the 3'-adjacent gene accumulate primarily in the testes. The presence of low levels of *Ddc* transcript in the testes makes this the most likely place for formation

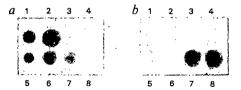


Fig. 4 Tissue distribution of transcripts of *Ddc* and the 3'-adjacent gene. RNA dot-blots were hybridized with: a, RNA probe 12, which is homologous to only RNA molecules transcribed from the 3'-flanking gene⁷; and b, RNA probe 5, which is homologous to only *Ddc* transcripts⁷. Total RNA was extracted as described previously from newly eclosed animals that had been dissected in D-20 medium¹⁷. Twelve animal equivalents were spotted in each case. RNAs in dots 1-4 were obtained from female samples, those in dots 5-8 from males. Dots 1, 5, heads; dots 2, 6, thoraces; dots 3, 7, abdomens; dots 4, 8, isolated gonads. The lengths of the two probes and their respective specific activities were similar, thus the intensities of the dots in a and b represent the relative steady-state levels of the two transcripts.

of a sense/anti-sense hybrid molecule containing both transcripts. However, confirmation of this possibility must await further detailed functional analysis of the 3'-adjacent transcription unit and in situ studies of the cell-specific distribution of both species of transcript. While this is only the second known example of overlapping genes in Drosophila, such arrangements in eukaryotes may be more common than previously supposed.

We thank Drs Larry Marsh and Ted Wright for sharing unpublished results. A studentship (C.A.S.) and a fellowship (R.D.G.) from the Alberta Heritage Fund for Medical Research are gratefully acknowledged. This research was supported by grant A6377 from NSERC (Canada).

Received 28 March: accepted 28 April 1986.

- 1. Normark, S. et al. A. Rev. Genet. 17, 499-525 (1983).
- 2. Henikoff, S., Keene, M. A., Fechtel, K. & Fristrom, J. W. Cell 44, 33-42 (1986).
- Wright, T. R. F., Hodgetts, R. B. & Sherald, A. F. Genetics 84, 267-285 (1976).
 Pentz, E. S. & Wright, T. R. F. Genetics 112, 843-859 (1986).
 Eveleth, D. D. & Marsh, J. L. Genetics 114 (in the press).

- Gietz, R. D. & Hodgetts, R. B. Devl Biol. 107, 142-155 (1985).
 Spencer, C. A., Gietz, R. D. & Hodgetts, R. B. Devl Biol. 114, 260-264 (1986).
 Eveleth, D. D. et al. EMBO J. (submitted).
 Birnstiel, M. L., Busslinger, M. & Strub, K. Cell 41, 349-359 (1985).

- Wickens, M. & Stephenson, P. Science 226, 1045-1051 (1984).
 Kraminsky, G. P. et al. Proc. natn. Acad. Sci. U.S.A. 77, 4175-4179 (1980).
- 12. Beall, C. J. & Hirsh, J. Molec. cell. Biol. 4, 1669-1674 (1984).
- Scholnick, S. B., Morgan, B. A. & Hirsch, J. Cell 34, 37-45 (1983).
 Livingstone, M. S. & Tempel, B. L. Nature 303, 67-70 (1983).
- Sanger, F., Nicklen, S. & Coulson, A. R. Proc. natn. Acad. Sci. U.S.A. 74, 5463-5467 (1977).
 Chen, E. Y. & Seeburg, P. H. DNA 4, 165-170 (1985).
- 17. Echalier, G. & Ohanessian, A. C.r. hebd. Séanc. Acad. Sci., Paris D268, 1771-1773 (1969).

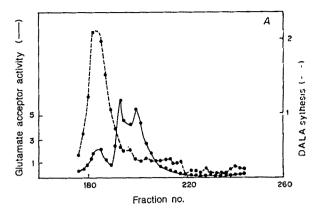
The RNA required in the first step of chlorophyll biosynthesis is a chloroplast glutamate tRNA

Astrid Schön*, Guido Krupp, Simon Gought, Sandra Berry-Lowet, C. Gamini Kannangarat & Dieter Söll‡

Department of Molecular Biophysics and Biochemistry, Yale University, PO Box 6666, New Haven, Connecticut 06511, USA † Department of Physiology, Carlsberg Laboratory, Gamle Carlsberg Vej 10, 2500 Copenhagen Valby, Denmark

A molecule of chlorophyll is synthesized from eight molecules of δ -aminolevulinate (DALA), the universal precursor of porphyrins. The light-regulated conversion of glutamate to δ -aminolevulinate in the stroma of greening plastids involves the reduction of glutamate to glutamate-1-semialdehyde and its subsequent transamination¹⁻⁵. The components performing this conversion have been isolated from barley^{1,2} and Chlamydomonas⁵ and separated into three fractions by serial affinity chromatography on Blue Sepharose and haem-1,5 or chlorophyllin-Sepharose². The complete reaction can be performed in vitro in a reconstituted assay by combining all three fractions. An RNA is the essential component of the chlorophyllin-Sepharose-bound fraction^{2,3}. By nucleotide sequence analysis, we have now identified this RNA as a chloroplast glutamate acceptor RNA. Glutamate attached by an aminoacyl bond to the 3'-terminal adenosine of this RNA is a substrate for the enzyme(s) which perform the subsequent reactions. This reaction represents a novel role for transfer RNA: participation in the metabolic conversion of its cognate amino acid into another metabolite of low relative molecular mass which subsequently is not used in peptide bond synthesis.

The ultraviolet spectrum of the haem- or chlorophyllin-Sepharose-bound fraction showed the characteristics typical of



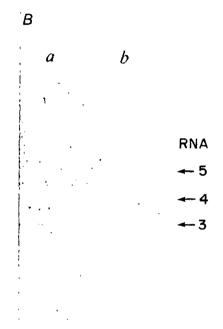


Fig. 1 Purification of RNADALA, A, HPLC fractionation. RNA was recovered from the chlorophyllin-Sepharose-bound fraction by phenol extraction, precipitated with ethanol and injected into 250×9-mm column packed with trioctylmethylammonium chloride-coated 5µ Hypersil ODS (refs 2, 37). Separation was achieved with a 4-h linear gradient from 0.5-2.3 M ammonium acetate (pH 5.1). Fractions 181-187 were pooled and the RNA was precipitated with ethanol. Glutamate acceptor activity and δ-aminolevulinate synthesis were determined as described elsewhere². B, Gel purification. For further purification, aliquots of the pooled HPLC fraction (5 µg dry RNA) were dissolved in 8 M urea containing 0.03% of tracking dyes and loaded into 10-mmwide slots of 15% polyacrylamide sequencing gels $(20 \times 40 \times$ 0.2 cm); electrophoresis was at 1,500 V until Sigma brilliant blue had reached the bottom of the gel8. Gels were stained with toluidine blue 0 and RNA was recovered as described previously³⁸. Lane a, RNA species present after HPLC fractionation; lane b, separation of partially purified RNAs (recovered from incompletely resolved RNA bands 3-5 in a less extensive electrophoresis). RNAs 1-3 were tested for their ability to function in δ -aminolevulinate biosynthesis (see Table 1).

nucleic acids. From these data and the fact that ribonuclease treatment of this fraction destroyed its ability to support δ aminolevulinate formation in the reconstitution assay, it was concluded that RNA is the active principle in the haem- or chlorophyllin-Sepharose-bound material^{2,3}. Phenol extraction of this material and HPLC fractionation led to the separation of three fractions of glutamate acceptor activity (Fig. 1A). Only the first species was able to support δ -aminolevulinate formation in the reconstitution assay (Fig. 1A). From this HPLC fraction

^{*} Present address: Institut für Biochemie, Universität Würzburg, D-8700 Würzburg, FRG.

[‡] To whom correspondence should be addressed.

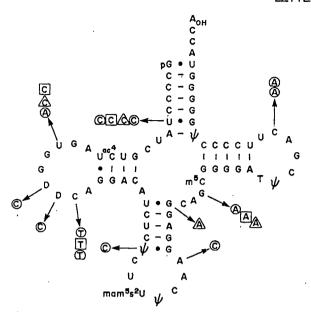


Fig. 2 Nucleotide sequence of RNADALA. The sequence was determined by base-specific enzymatic and chemical cleavage of the 5'- and 3'-end-labelled RNA6-9. Modified nucleotides were identified by the method of Stanley and Vassilenko⁶. Ambiguities due to the tight secondary structure and the lability of mam⁵s²U were resolved by mobility shift analysis11 of fragments generated either by complete digestion with RNase T₁ or by partial cleavage with aniline⁹. Arrows indicate differences in primary structure from chloroplast tRNA^{Glu} genes of the following species: Nicotiana tabacum¹⁹, squashed circle; Vicia faba²⁰ and Pisum sativum²¹, squares; spinach²², triangle; Euglena gracilis²³, round circle. The sequence is identical to a wheat (Triticum aestivum) tRNAGlu gene.

a homogeneous active RNA species, referred to as RNADALA, was purified by polyacrylamide gel electrophoresis (Fig. 1B, Table 1). Analysis of the nucleotide sequence of this RNA was complicated by the fact that it contained a chemically labile base and possessed an extremely stable secondary structure. Chemical and enzymatic sequence analysis of the 3'- and 5'-endlabelled RNA⁶⁻⁹, as well as fingerprinting of post-labelled RNA¹⁰, established the structure of a tRNA (Fig. 2). The labile base in the first position of the anticodon was identified as 5-methylaminomethyl-2-thiouridine (mam⁵s²U). This was established by co-migration of the [5'-³²P]-nucleoside monophosphate¹¹ with the authentic marker nucleotide prepared from Escherichia coli tRNA Glu₂ (refs 12, 13) in several thin layer chromatographic systems¹⁴⁻¹⁷ as well as by its sensitivity to cyanogen bromide12 and its behaviour in a mobility shift analysis 11. The nucleotide mam 5s 2U has previously been found exclusively in the tRNAs of prokaryotic organisms 18. Its occurrence in chloroplast tRNA supports the endosymbiont theory of the prokaryotic origin of organelles¹⁹. The anticodon sequence UUC (unmodified) suggests a glutamate tRNA, in agreement with its

amino-acid acceptor properties (Fig. 1).

Comparison with known tRNA^{Glu} gene sequences (no other chloroplast tRNA^{Glu} species have been sequenced to date) showed high homology to tRNAGiu genes from chloroplasts of higher plants²⁰⁻²⁵: the known wheat (Triticum aestivum) gene has a sequence identical to the barley RNADALA. The sequence from tobacco (Nicotiana tabacum) differs in only three bases, the sequences from broad bean (Vicia faba), pea (Pisum sativum) and spinach (Spinacea oleracea) differ in four positions, whereas the sequence from Euglena gracilis shows nine differences (Fig. 2). One distinctive feature of tRNA^{Glu} of chloroplast origin, the A53:A61 pair^{22,23} (the last base pair in the $T\psi C$ -stem), is also present in this tRNA. The RNA^{DALA} requires an intact 3'-terminal CCA end for its

ability to support δ -aminolevulinate formation. This was demon-

strated by inactivating the glutamate acceptor and δ aminolevulinate-synthesizing activity of the RNA by partial exonucleolytic digestion with snake venom phosphodiesterase and subsequent restoration by repair of the 3'-terminal CCA end with tRNA nucleotidyl transferase²⁶ (Table 1). The linkage between glutamate and RNA was identified as an authentic aminoacyl bond after labelling the 3'-end of the purified RNA with $[\alpha^{-32}P]$ ATP by use of nucleotidyl transferase and charging with 14C-glutamate using the Blue Sepharose-bound enzyme fraction. The terminal ¹⁴C-glutamyl-³²P-adenosine 5'-phosphate was recovered after cleavage with nuclease P₁ and identified by thin layer chromatography¹⁴, using as a marker ¹⁴C-glutamyladenosine 5'-phosphate derived from pure aminoacylated E. coli tRNAGlu2 (data not snown). These findings indicate that, as in aminoacyl-tRNA, the α -carboxyl group of glutamate is probably aminoacylated. However, we cannot rule out the possibility that amino-acid activation involves the y-carboxyl group.

The presence of an enzyme-associated RNA in the chloroplast led to questions of whether, in barley, RNADALA is encoded in the chloroplast DNA and whether the location of the gene is the same in widely different plant species. Although it is generally believed that organellar RNAs are encoded in the organellar DNA, RNA transport into the mitochondrion has also been described²⁷. Hybridization experiments were performed using genomic and chloroplast DNAs from various plant species, including unicellular algae. To allow comparisons with the available HindIII bank of the barley chloroplast genome²⁸, and because the sequence of RNA^{DALA} shows a unique HinfI restriction site in the T-loop region, HindIII and HinfI treatments were chosen for Southern hybridizations. To avoid artefacts

Table 1 Characterization of the RNA required for δ -aminolevulinate biosynthesis

- Josynthesi	s	
	Glutamate to δ-aminolevulina conversion (c.p.m. above background	ite
•	per 10 µg RNA)	(%)
Expt 1	per to he ktivity	(70)
No RNA (background)	(19,000)	0
HPLC fraction (Fig. 1a)	200,900	100
Expt 2		
Gel purified RNA (Fig. 1b)		,
Band 3	15,900	8
Band 4	243,500	121
Band 5	12,500	6
Expt 3		
Snake venom phosphodiesterase inactivated RNA	3,950	2
RNA repaired with tRNA nucleotidyltransferase	150,700	,75

δ-Aminolevulinate synthesis was assayed in a mixture containing 0.5 mM ATP, 1 mM NADPH, 25 mM MgCl₂, 1 mM dithiothreitol (DTT), 0.3 M glycerol, 0.1 M Tricine-NaOH (pH 7.9), 0.25 mg Blue Sepharose-bound protein, 0.4 mg unbound protein and 2.5 µCi ¹⁴C-glutamate (275 ci mmol⁻¹; 330,000 c.p.m. pmol⁻¹) in a total volume of 0.5 ml. 10-50 µg RNA was used per assay. The conversion of glutamate to δ-aminolevulinate was determined as described elsewhere². For exonuclease inactivation of RNA, 100 µg of HPLC-purified RNA was incubated for 20 min at room temperature with $2\,\mu g$ snake venom phosphodiesterase in 50 mM Tris-HCl (pH 8), 10 mM MgCl₂. The material was then phenol extracted and ethanol precipitated. Reactivation was performed with 50 µg of this RNA in 0.4 ml, containing 25 µM ATP, 25 μM CTP, 10 mM MgCl₂, 8 mM DTT, 40 mM Tris-HCl (pH 8) and 62.5 µg (0.6 U) of tRNA nucleotidyl transferase. After incubation for 45 min at 37 °C, the RNA was phenol extracted, ethanol precipitated and assayed for reconstitution activity as described above, 3'-End labelling of the gel-purified active RNA species was performed with 5 µg RNA by scaling down these protocols and substituting [5'-32P]ATP (3,000 Ci mmol⁻¹, 36 pmol) for ATP.

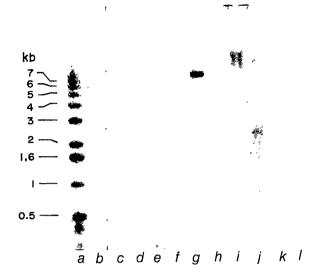


Fig. 3 Hybridization of RNA^{DALA} to genomic and chloroplast DNA. Restricted DNA $(1-2 \mu g)$ was separated on a 0.7% agarose gel and blotted onto nitrocellulose paper³⁹. Hybridization was performed in $6 \times SSC$, $3 \times Denhardt's$ solution and 0.1% sodium pyrophosphate for 1 h at 42 °C. Nonspecifically bound probe was removed by washing the filter with $2 \times SSC$ at 42 °C. The lanes contained: a, DNA size markers; b, barley genomic DNA; c, d, barley chloroplast DNA; e, f, tobacco genomic DNA; g, h, tobacco chloroplast DNA; i, j, Chlamydomonas reinardii genomic DNA; k, l, Chlamydomonas reinhardii chloroplast DNA. All samples were digested with HindIII, and d, f, h, j and l were also digested with Hinf1.

created by the secondary structure of the RNA, fragments generated by complete digestion with RNase T₁ or by controlled aniline cleavage⁹ (size range 15-30 nucleotides) were used for hybridization. All chloroplast DNAs showed one prominent signal of 7-10 kilobases (kb) in length and two bands of low intensity, whereas the nuclear DNA preparations gave no specific hybridization signal (Fig. 3). HinfI cleaved the prominently hybridizing HindIII fragments into DNA of lower relative molecular mass. Although the nuclear genomes obviously contain DNA sequences related to RNA^{DALA}, the presence of a strongly hybridizing DNA fragment in all chloroplast DNAs make it unlikely that this RNA is encoded in the nucleus.

A few examples exist for the involvement of tRNA in reactions other than protein biosynthesis, among them the synthesis of aminoacyl-phosphatidyl-glycerol²⁹, the N-terminal addition of amino acids to proteins³⁰ and the formation of pentapeptide bridges in bacterial cell walls³¹. More recently, tRNA has been reported to be an essential component of the ubiquitin- and ATP-dependent proteolytic system of mammalian cells³². The transamination of glutamyl-tRNA^{GIn} to yield glutaminyl-tRNA^{GIn} in Bacillus megatherium is an example of enzymatic conversion of an amino acid already linked to a tRNA³³. However, in contrast to the case reported here, glutamine formed in this reaction is then donated into peptide linkage during the

process of protein biosynthesis. For the normal requirements of intermediary metabolism in *Bacillus*, glutamine is formed by glutamine synthase^{33,34}.

Two of the three glutamate isoacceptors in barley chloroplasts are unable to substitute for the specific RNA required in δ -aminolevulinate synthesis, although they are efficiently charged by aminoacyl-tRNA synthetases present in the enzyme preparation². This raises the question of whether the RNA $^{\text{DA}}$ is tRNA species specialized just for δ -aminolevulinate formation and not used for protein biosynthesis in the chloroplast. Although the anticodon in RNA $^{\text{DALA}}$ is more highly modified than in other known tRNA $^{\text{Glu}}$ species, the answer to this question must await the results of in vitro protein synthesis experiments comparing all three pure tRNA $^{\text{Glu}}$ species. A case of such tRNA specialization is seen in Staphylococcus, where some tRNA species participate in cell wall biosynthesis but not in protein synthesis 31 .

The fact that chlorophyll biosynthesis is a light-induced process involving the concerted expression of a number of nuclear and chloroplast genes raises several questions concerning the regulation of gene expression. Of particular interest regarding the occurrence of three chloroplast glutamate isoacceptors is the question of whether they are encoded by a single gene, thus differing only in their base modifications, or whether they are derived from differentially regulated individual genes.

The formation of δ -aminolevulinate from glutamate is specific for plant chloroplasts and blue-green algae (for example, cyanobacteria³⁵). An outline of the enzymatic reaction scheme in plants based on our current knowledge is shown in Fig. 4. There are at least three distinct reactions performed by a complex set of enzymes and an RNA moiety. ATP-dependent ligation of glutamate to the RNA DALA by an aminoacyl bond is the reaction initiating this metabolic pathway. It remains to be determined whether this reaction is carried out by the normal chloroplast glutamyl-tRNA synthetase active in the glutamylation of all three chloroplast tRNA species (Fig. 1a) or whether a special enzyme is used. The glutamyl-RNA ligase present in the Blue Sepharose-bound fraction has recently been purified (P. Bruyant, unpublished). The subsequent reduction of the glutamate, activated by attachment to the RNA, is an interesting new type of reaction in which RNA is the 'cofactor' for a dehydrogenase. The fact that only one of the three tRNA Glu isoacceptors is recognized by the dehydrogenase raises interesting questions about the importance for proper recognition of primary structure and of the nucleoside modification pattern of the tRNAs. Depending on the position of the activated carboxyl group in glutamate, an additional enzyme, a hydrolase (indicated by the short arrow in Fig. 4) may be required to cleave glutamate-1-semialdehyde from the RNA^{DALA}. In the final step, free glutamate-1-semialdehyde is then the substrate for a specific aminotransferase. The RNADALA has been sequenced and identified by Southern hybridization analysis as a chloroplast tRNA^{Glu}. The fact that the RNA hybridized to chloroplast DNA of many different plant species and that a required RNA was also demonstrated for Chlamydomonas3 and Chlorella36 suggests that the RNA-dependent formation of δ -aminolevulinate for chlorophyll synthesis occurs in all plants.

Fig. 4 Scheme of the first steps of chlorophyll synthesis. For details see text.

Glutemote

Giu-RNA^{DALA}

Giutamate -1semialdehyde DALA

A.S. was supported by a fellowship of the Deutscher Akademischer Autauschdienst; G.K. was a Postdoctoral Fellow of the Deutsche Foreschungsgemeinschaft; S.B-L. is a Postdoctoral Fellow of the US NSF. We thank Drs H. Cudny and M. Deutscher for their gift of purified tRNA nucleotidyl transferase. Some of the DNA samples from chloroplasts and nuclei were provided by Drs A. Cheung and J. Palmer. We thank Professor Diter von Wettstein for initiating the cooperative work. This work was supported by a NIH grant.

Received 14 February; accepted 15 April 1986.

- Wang, W.-Y., Gough, S. P. & Kannangara, C. G. Carlsberg Res. Commun. 46, 243-257 (1981). Kannangara, C. G., Gough, S. P., Oliver, R. P. & Rasmussen, S. K. Carlsberg Res. Commun 49, 417-437 (1984).
- Huang, D.-D. Wang, W.-Y., Gough, S. P. & Kannangara, C. G. Science 225, 1482-1484 (1984).
- 4. Kannangara, C. G., Gough, S. P. & von Wettstein, D. in Development in Plant Biology Vol. 2 (eds Akoyonoglou, G. & Akoyonoglou, J. H.) 147-160 (Elsevier, Amsterdam, 1978).
- Wang, W.-Y., Huang, D.-D., Stachon, D., Gough, S. P. & Kannangara, C. G. Pl. Physiol. 74, 569-575 (1984).
- 6. Stanley, J. & Vassilenko, S. Nature 274, 87-89 (1978).
- Donis-Keller, H., Maxam, A. M. & Gilbert, W. Nucleic Acids Res. 4, 2527-2537 (1977).
 Krupp, G. & Gross, H. J. in The Modified Nucleosides in Transfer RNA II: A Laboratory Manual of Genetic Analysis, Identification and Sequence Determination (eds Agris, P. F. & Kopper, R. A.) 11-58 (Liss, New York, 1983).
- Peattie, D. A. Proc. natn. Acad. Sci. U.S.A. 76, 1760-1764 (1979).
 Domdey, H., Jank, P., Sänger, H. L. & Gross, H. J. Nucleic Acids Res. 5, 1221-1236 (1978).
- 11. Silberklang, M., Gillum, A. M. & RajBhandary, U. L. Meth. Enzym. 59, 58-109 (1979).

- 12. Ohashi, Z., Harada, F. & Nishimura, S. FEBS Lett. 20, 239-241 (1972)
- Munninger, K. O. & Chang, S. H. Biochem. biophys. Res. Commun. 46, 1837-1842 (1972).
 Nishimura, S. in tRNA: Structure, Properties and Recognition (eds Schimmel, P. R., Söll,
- D. & Abelson, J. N.) 551-552 (Cold Spring Harbor Laboratory, New York, 1979). Saneyoshi, M. & Nishimura, S. Biochim, biophys. Acta 204, 389-399 (1979).
- 16. Gupta, R., Randerath, E. & Randerath, K. Nucleic Acids Res. 3, 2915-2921 (1976).
- 17. Raba, M. et al. Eur. J. Biochem. 97, 305-318 (1979)
- Kava, M. et al. Lat. J. Botcheth. 91, 303-318 (1977).
 Sprinzl, M., Moll, J., Meissner, F. & Hartmann, T. Nucleic Acids Res. 13, r1-r49 (1985).
 Fox, G. E. et al. Science 209, 457-463 (1980).
 Quigley, F. & Weil, J. H. Curr. Genet. 9, 495-503 (1985).

- 21. Ohme, M., Kamogashira, T., Shinozaki, K. & Sugiura, M. Nucleic Acids Res. 13, 1045-1056
- Kuntz, M., Weill, J. H. & Steinmetz, A. Nucleic Acids Res. 12, 5037-5047 (1984).
 Rasmussen, O. F., Stummann, B. M. & Henningsen, K. W. Nucleic Acids Res. 12, 9143-9153
- Holschuh, K., Bottomley, W. & Whitfield, P. R. Pl. molec. Biol. 3, 313-317 (1984)
- 25. Hollingsworth, M. J. & Hallick, R. B. J. biol. Chem. 257, 12795-12799 (1982).
- Silberklang, M., Gillum, A. M. & Rajbhandary, U. L. Nucleic Acids Res. 4, 4091-4108 (1978).

 Martin, R. P., Schneller, J. M. Stahl, A. J. C. & Dirheimer, G. Nucleic Acids Res. 4, 3497-3511
- 28. Poulsen, C. Carlsberg Res. Commun. 48, 57-80 (1983).
- Nesbitt, J. A. & Lennartz, W. J. J. biol. Chem. 243, 3088-3095 (1968).
 Leibowitz, M. J. & Soffer, R. L. Biochem. biophys. Res. Commun. 36, 47-53 (1969).
- Bumsted, R. M., Dahl, J. M., Söll, D. & Strominger, J. L. J. biol. Chem. 249, 4787-4796 (1974).
- 32. Ciechanover, A., Wolin, S., Steitz, J. A. & Lodish, H. F. Proc. natn. Acad. Sci. U.S.A. 82, 1341-1345 (1985).
- Wilcox, M. & Nirenberg, M., Proc. natn. Acad. Sci. U.S.A. 61, 229-236 (1968).
- Whender, D. J. & Hoch, J. A. Microbiol. Rev. 44, 57-82 (1980). McKie, J., Lucas, C. & Smith, A. Phytochemistry 20, 1547-1549 (1981). Weinstein, J. D. & Beale, S. I. Archs Biochem. Biophys. 239, 87-93 (1985).
- Bischoff, R. E., Graeser, E. & McLaughlin, L. J. Chromat. 257, 305-315 (1983)
- 38. Beier, H., Barciszewska, M., Krupp, G., Mitnacht, R. & Gross, H. J. EMBO J. 3, 351-356 (1984).
- 39. Maniatis, T., Fritsch, E. F. & Sambrook, J. Molecular Cloning, a Laboratory Manual (Cold Spring Harbor Laboratories, New York, 1982).

Quantitative analysis of structure—activity relationships in engineered proteins by linear free-energy relationships

Alan R. Fersht, Robin J. Leatherbarrow & Tim N. C. Wells

Department of Chemistry, Imperial College of Science and Technology, London SW7 2AY, UK

Protein engineering is being used increasingly to study the fine details of the structure and activity of enzymes. How can small effects of mutation on activity be reliably quantified and systematized, and artefacts be recognized? A traditional means of doing this in organic chemistry is the use of linear free-energy relationships that link changes in rate constant for a reaction to changes in its equilibrium constant as the structure of the reagents is altered-Brønsted or Hammett plots1. We now find that the same type of plot may be applied to enzymatic reactions for variation of the structure of an enzyme with mutation. The activities of many mutant tyrosyl-transfer RNA synthetases fit structureactivity relationships which relate the rate constant for the formation of enzyme-bound tyrosyl adenylate (E.Tyr-AMP) to its equilibrium constant with enzyme-bound tyrosine and ATP (E.Tyr.ATP). This reaction results in an increase in binding energy between certain side chains of the enzyme and the side chain of tyrosine and the ribose ring of ATP. Plots of rate against equilibrium constant for a series of enzymes mutated in the relevant positions indicate that 71% of the binding energy change occurs on formation of the transition state for the chemical reaction and 90% occurs on formation of the E.Tyr-AMP.PP, complex. Other mutations show a different behaviour which is diagnostic of residues that specifically bind the transition state. Linear free-energy plots show trends and allow exceptions to be readily noted. That the activities of a large number of mutants conform to linear freeenergy equations is the best evidence yet that mutation of an enzyme can probe general properties and trends in the relationship between structure and activity.

Mutants of the tyrosyl-tRNA synthetase, which catalyses the formation of tyrosyl adenylate [equation (1)], have been gener-

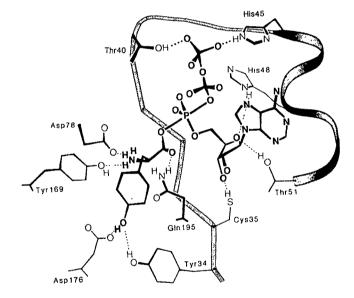


Fig. 1 Side chains of the tyrosyl-tRNA synthetase from Bacillus stearothermophilus which form hydrogen bonds with the transition state of ATP and tyrosine during the formation of tyrosyl adenylate (from ref. 5).

ated by site-directed mutagenesis and studied by kinetics²⁻⁴.

$$E+Tyr+ATP \Leftrightarrow E.Tyr-AMP+PP_i$$
 (1)

These mutants have been altered in side chains that make hydrogen bonds with the substrates (Fig. 1). Model building followed by mutagenesis has revealed that there is a major catalytic factor caused by just two side chains that contribute binding energy to the γ -phosphate of ATP only when it is in the transition state (Thr 40 and His 45)⁵. Further, the binding energies of groups far removed from the site of reaction are also used to increase the chemical rate constants for the reaction (Tyr 34, Cys 35, His 48, Thr 51 and Tyr 169)⁶. Subsequent studies have measured the complete free-energy profiles for activation of tyrosine by the mutant enzymes^{7,8}. The comparison of these

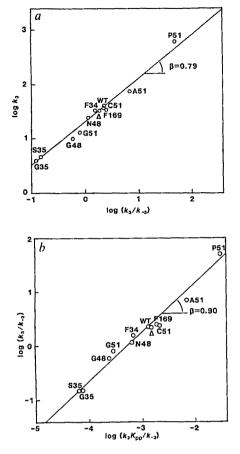


Fig. 2 a, Plot of $\log k_3$ against $\log (k_3/k_{-3})$ for equation (5) for mutation of Tyr 34, Cys 35, His 48, Thr 51 and Tyr 169. The mutations are indicated by the one-letter code apart from Δ , which represents the truncated enzyme lacking the tRNA-binding domain 10. Data are from refs 6 and 7 and T.N.C.W. (unpublished). The plot is equivalent to a plot of $G_{[E,Tyr-ATP]} - G_{E,Tyr-ATP}$ against $G_{E,Tyr-AMP,PPi} - G_{E,Tyr-ATP}$, where G is Gibbs free energy and [E,Tyr-ATP] is the transition state. b, Plot of $\log (k_3/k_{-3})$ against $\log (k_3 K_{pp}/k_{-3})$. This is equivalent to a plot of $G_{E,Tyr-AMP,PPi} - G_{E,Tyr-ATP}$ against $G_{E,Tyr-AMP} - G_{E,Tyr-ATP}$. Note that individual variations in rate and equilibrium constants are seen as deviations from the regression line.

with the profile for wild-type enzyme gives the apparent binding energy of the relevant side chain with the substrates, transition states and intermediates throughout the reaction. These data have been analysed in each individual case to show how the changes in binding energy affect the rate and equilibrium constants for the interconversion of free and enzyme-bound species. Several of the side chains that bind the side chain of tyrosine and the ribose ring of ATP appear to stabilize the enzyme-bound tyrosyl adenylate complex (E.Tyr-AMP) more than the transition state for its formation and more still than the initial enzyme-substrate ternary complex (E.Tyr.ATP)^{7,8}. By this type of analysis, we are building up a picture of how each side chain contributes to catalysis.

The question most frequently asked about this approach is: How do we know that alteration of a side chain by mutagenesis does not cause additional structural changes in the enzyme which lead to artefactual results? X-ray crystallography of mutants can provide important evidence but may miss a series of small changes or the existence of conformational changes in solution. Further, although crystallography and spectroscopy can solve the structures of the stable states of the enzyme and its substrates, they do not give direct information on the structure

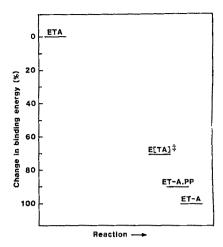


Fig. 3 Summary of the average binding-energy changes calculated for residues Tyr 34, Cys 35, His 48, Thr 51 and Tyr 169 on going from the E.Tyr.ATP complex (ETA) to the transition state (E[TA][‡]) to the first intermediate, E.Tyr-AMP.PP, (ET-A.PP), to the final intermediate, E.Tyr-AMP (ET-A).

which is important for the determination of rate, the transition state. The only way this can be probed experimentally at present is by kinetics. A possible way of both probing the structure of the transition state and detecting artefacts is the use of linear free-energy plots. In these, plots of rate constant against equilibrium constant are made for a reaction in which the structures of the reagents are systematically varied. The plots can give information on how much the transition state resembles starting materials or products. The plots assume that there is the relationship between the equilibrium constant K of a reaction and the rate constant k for the formation of products of the general form:

$$k = AK^{\beta} \tag{2}$$

where A and β are constants. The plot of $\log k$ against $\log K$ when equation (2) holds is a straight line of slope β [equation (3)].

$$\log k = \text{constant} + \beta \log K \tag{3}$$

Since $\log k$ is proportional to the free energy of activation of the reaction, ΔG^{\dagger} , and $\log K$ is proportional to the free-energy change for the equilibrium, ΔG_{e} , equation (3) is equivalent to:

$$\Delta G^{\dagger} = \text{constant} + \beta \Delta G_{\bullet} \tag{4}$$

A qualitative interpretation of equations (2) to (4) is that, all things being equal, a value of β which is close to zero means that the transition state resembles starting materials, and a value of β close to 1 means that the transition state resembles products. Linear free-energy relationships in simple organic reactions generally measure the inductive effects of groups on rate and equilibrium constants. In enzymatic reactions, however, changes in structure remote from the seat of reaction result in changes of binding energy (ref. 9 and A.R.F., unpublished). Can linear free-energy relationships be applied to the changes in rate and equilibrium constants which occur when enzyme structure is varied as in a site-directed mutagenesis experiment? If so, the values of β will, in general, measure the fractions of total changes in binding energy.

We have measured all the necessary rate and equilibrium constants defined in equation (5) to construct plots for different stages of the reaction.

$$E \stackrel{K_{i}}{\rightleftharpoons} E.Tyr \stackrel{K'_{a}}{\rightleftharpoons} E.Tyr.ATP \stackrel{k_{3}}{\rightleftharpoons} E.Tyr-AMP.PP_{i} \stackrel{K_{pp}}{\rightleftharpoons} E.Tyr-AMP$$
(5)

As Fig. 2 shows, a plot of $\log k_3$ against $\log(k_3/k_{-3})$ for mutants in the side chains which bind the side chain of tyrosine and

the ribose ring of ATP fits an excellent straight line of slope $\beta = 0.79$. This means that 79% of the binding-energy change on E.Tyr.ATP going to E.Tyr-AMP.PP_i is realized in the transition state for the reaction. Also plotted in Fig. 2 is $log(k_3/k_{-3})$ against $\log(k_3 K_{\rm pp}/k_{-3})$. This is in reality a plot of the change in binding energy on going from E.Tyr.ATP to E.Tyr-AMP.PP; against the change in going from E. Tyr. ATP to E. Tyr-AMP+PP_i. The slope of 0.9 shows that 90% of the change in binding energy on forming E.Tyr-AMP occurs at the stage of formation of E.Tyr-AMP.PP_i. Figure 3 summarizes the changes in binding energy. There is a gain in binding energy on going from the ternary complex E.Tyr.ATP to the enzyme-bound tyrosyl adenylate complex, E.Tyr-AMP; 71% of this binding energy is realized in the transition state and 90% in the other intermediate. E.Tyr-AMP.PPi.

The above type of behaviour applies when the residues concerned show a uniformly progressive change in binding energy as the reaction proceeds. A different pattern is expected when the mutation involves residues that bind the transition state of the substrates well but bind the unreacted substrates and products only poorly. Such behaviour should lead to values for β which are much greater than 1. For example, in the extreme case, where a residue binds only at the stage of the transition state, mutation of that residue will not affect the equilibrium constant of the reaction but will affect the rate; that is, β should tend to infinity. This is found quite dramatically with residues Thr 40 and His 45 (Fig. 4), which have already been implicated

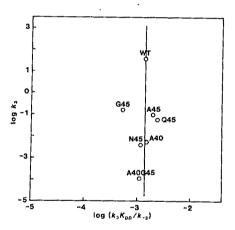


Fig. 4 Plot of $\log k_3$ against $\log (k_3 K_{pp}/k_{-3})$ for the mutation of residues Thr 40 and His 45 which are involved in transition-state binding only⁵. This is equivalent to a plot of $G_{\text{[E.Tyr-ATP]}}$ $G_{\text{E.Tyr.ATP}}$ against $G_{\text{E.Tyr.AMP}} - G_{\text{E.Tyr.ATP}}$. Data are from ref. 5 and R.J.L. (unpublished).

in such a mode of catalysis⁵. The very high value of β found indicates that they are highly specific for the transition state.

It is quite remarkable that plots in Fig. 2 are so similar to those found for linear free-energy relationships in simple organic reactions. Indeed, the fit to such plots is as good as many examples from physical organic chemistry. Why are the linear free-energy relationships followed so well considering the likelihood of disturbing the structure of the protein? The answer is probably because we have restricted our mutations to the most conservative changes, which have made only small perturbations in the structure.

The demonstration that certain structural changes of the tyrosyl-tRNA synthetase cause changes in rate which may be described satisfactorily by linear free-energy equations is important for the following reasons. First, the equations combine the data from many experiments and so bring order to them. Second, they quantify aspects of the transition state structure; in particular, they show how much the interactions in the transition state resemble those in the enzyme-substrate and the enzymeintermediate complexes. Finally, the equations show trends; any mutant that deviates from the trend is immediately apparent.

The last point is particularly important. The results of any one individual mutation can be challenged on the grounds that the mutation might cause a significant change in the protein structure. However, when a whole series of mutational experiments can be fitted to a linear free-energy equation, there is overwhelming evidence that each mutant shows part of a general phenomenon of the relationship between structure and activity. This type of analysis can be applied to any enzymatic reaction where both rate and equilibrium constants may be measured.

Received 6 May; accepted 5 June 1986.

- Jencks, W. P. Chem. Rev. 85, 511-517 (1985).
 Winter, G., Fersht, A. R., Wilkinson, A. J., Zoller, M. & Smith, M. Nature 299, 756-758 (1982).
- Fersht, A. R. et al. Angew. Chem. int. Edn Engl. 23, 467-473 (1984).
- Fersht, A. R. et al. Nature 314, 235-238 (1985).
 Leatherbarrow, R. J., Winter, G. & Fersht, A. R. Proc. natn. Acad. Sci. U.S.A. 82, 7840-7844
- Wells, T. N. C. & Fersht, A. R. Nature 316, 656-657 (1985).
 Wells, T. N. C. & Fersht, A. R. Biochemistry 25, 1881-1886 (1986).

- Ho, C. K. & Fersht, A. R. Biochemistry 25, 1891-1897 (1986).
 Fersht, A. R. Enzyme Structure and Mechanism 2nd edn, Ch. 12 (Freeman, San Francisco, 1985
- 10. Waye, M. M. Y., Winter, G., Wilkinson, A. J. & Fersht, A. R. EMBO J. 2, 1827-1829 (1983).

Directional electron transfer in ruthenium-modified horse heart cytochrome c

Rolf Bechtold, Christa Kuehn, Chris Lepre & Stephan S. Isied*

Department of Chemistry, Rutgers, State University of New Jersey, New Brunswick, New Jersey 08903, USA

Cytochrome c can be modified by [(NH₃)₅Ru^{II/III}-] specifically at the imidazole moiety of histidine 33, and we have recently discussed the thermodynamics and kinetics of electron transfer within this modified protein¹⁻⁵. X-ray crystal structures of the oxidized and reduced forms of tuna cytochrome c^6 indicate that the separation between the haem group of cytochrome c and the ruthenium label is 12-16 Å. Internal electron transfer from the [(NH3)5Ru11-] centre to the Fe(III) haem centre occurs with a rate constant $k \approx 53 \text{ s}^-$ (25 °C) ($\Delta H^{\ddagger} = 3.5 \text{ kcal mol}^{-1}$, $\Delta S^{\ddagger} = -39 \text{ EU}$), as measured by pulse radiolysis. The measured unimolecular rate constant¹, $k \simeq$ 53 s⁻¹, is on the same timescale as a number of conformational changes that occur within the cytochrome c molecule⁷⁻⁹. These results raise the question of whether electron transfer or protein conformational change is the rate limiting step in this process. We describe here an experiment that probes this intramolecular electron transfer step further. It involves reversing the direction of electron transfer by changing the redox potential of the ruthenium label. Electron transfer in the new ruthenium-cytochrome c derivative described here is from haem(II) to the Ru(III) label, whereas in $(NH_3)_5$ Ru-cytochrome c the electron transfer is from Ru(II) to haem(III). Intramolecular electron transfer from haem(II) to Ru(III) in the new ruthenium-cytochrome c described here proceeds much slower (>105 times) than the electron transfer from Ru(II) to haem(III) in the (NH₃)₅Ru-cytochrome c. We therefore conclude that electron transfer in cytochrome c is directional, with the protein envelope presumably involved in this directionality.

^{*} To whom correspondence should be addressed.

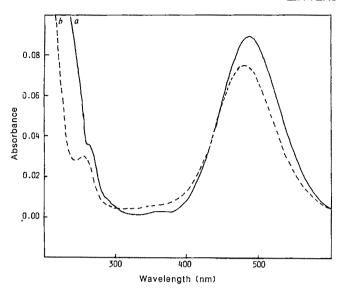


Fig. 1 a, Ultraviolet-visible spectrum of the Ruⁿ(NH₃)₄(isn)-peptide fragment containing His 33. b, Ultraviolet-visible spectrum of the model complex, trans-[Ru(NH₃)₄(isn)-N-acetylhist-aminet²⁺.

The new ruthenium-modified cytochrome c has trans-[Ru(NH₃)₄(N \bigcirc C \bigcirc)]- covalently bound to His 33

and was synthesized using techniques described earlier³. Ruthenium analysis by direct coupled plasma atomic absorption spectroscopy showed the presence of 1 mol of ruthenium per mol of iron. The ultraviolet-visible spectra of the oxidized derivative indicated no difference from that of native cytochrome c(III). Comparison between the tryptic digests of the native cytochrome c and the $[Ru(NH_3)_4(isn)-cyt\,c]$ (isn = isonicotinamide) by HPLC showed the presence of a new fragment in the ruthenium-modified product. The amino-acid composition of this fraction (Asp, 1.04; Thr, 0.97; Gly, 2.01; Leu, 1.62; His, 0.94; Pro, not detected) corresponds to amino acids 28-35 of cytochrome c. (The new cleavage site for trypsin may have resulted from the hydrophobicity of the isonicotinamide ligand in combination with the positive charge of the ruthenium centre.)

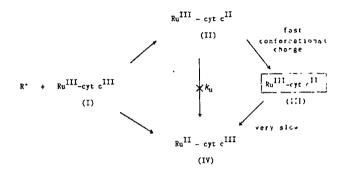
The ultraviolet-visible spectrum of this peptide fragment after reduction with ascorbic acid (Fig. 1a) closely resembles that of the model compound trans-[Ru^{II}(NH₃)₄(isn)(N-acetylhist-amine] (Fig. 1b). Figure 2a shows a differential pulse polarogram (DPP) of [Ru(NH₃)₄isn-cyt c]. Two waves are observed, one corresponding to the haem iron (II/III) of cytochrome c (0.26 V versus normal hydrogen electrode (NHE)) and the other corresponding to [Ru^{II/III}(NH₃)₄isn-] (0.44 V versus NHE). Figure 2b shows the DPP of [(Ru(NH₃)₅-cyt c] for comparison¹.

A spectrophotometric titration of the fully reduced ruthenium-modified cytochrome c, $[Ru^{II}(NH_3)_4 isn-cyt c^{II}]$, with the trans- $[Ru(NH_3)_4 (isn)_2]^{3+}$ oxidant $(E^\circ = 0.70 \text{ V};$ estimated from ref. 10), was carried out to determine the stoichiometry of the oxidation. Colour changes in the trans- $[Ru(NH_3)_4 (isn)_2]^{3+}$ species during titration enable the oxidation of the haem and the ruthenium sites to be observed sequentially. Two mol of trans- $[Ru(NH_3)_4 (isn)_2]^{3+}$ oxidant were required per mol of the cytochrome c derivative.

The kinetics of intermolecular oxidation of the haem site in $[Ru^{II}(NH_3)_4]$ isn-cyt c^{II} with $[Fe(CN)_6]^{3-}$ or $trans-[Ru(NH_3)_4-(isn)_2]^{3+}$ is similar to the oxidation of native cytochrome c(II) by inorganic oxidizing agents¹¹. This indicates similar environments of the haem site in the native and the modified protein.

As Fig. 2 shows, the two ruthenium-cytochrome c derivatives, $[Ru(NH_3)_4 isn-cyt\ c]$ and $[Ru(NH_3)_5 - cyt\ c]$, possess Ru(II/III) potentials approximately equidistant in the positive and negative directions, respectively, from the potential of Fe(II/III) haem $(\Delta E^\circ = 0.18 \text{ V} \text{ and } 0.11 \text{ V})$. Thus, on the basis of driving force¹², the rate of intramolecular electron transfer from cytochrome c(II) to $[Ru^{II}(NH_3)_4 isn-]$ should be equal to or slightly greater than the rate of intramolecular electron transfer measured from $[Ru^{II}(NH_3)_5]$ to cytochrome c(III) $(k \approx 53 \text{ s}^{-1})$.

Reduction of a solution of [Ru^{III}(NH₃)₄isn-cyt c^{III}] in 0.1 M phosphate buffer pH 7 (scheme 1) with the radicals derived from



Ru = Ru(NH₃)₄(isn)-

Scheme 1

either isopropanol or formate (R') using pulse radiolysis techniques is shown in Fig. 3.

The haem site is reduced at the expected rate¹, but no intramolecular electron transfer is observed from the Fe(11) haem to the $[Ru^{III}(NH_3)_4 isn-]$ site on the timescale of the experiment (2 s). This result is completely unexpected when compared with the $[Ru(NH_3)_5$ -cyt c] derivative. In both the $[Ru(NH_3)_4 isn-$ cyt c] and the $[Ru(NH_3)_5$ -cyt c] derivatives, the ruthenium is bound to the identical His 33 site and the difference in driving

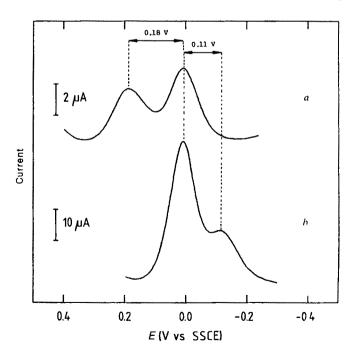


Fig. 2 Differential pulse polarograms of $[Ru(NH_3)_4(isn)-cyt\ c]$ (a) and $[Ru(NH_3)_5-cyt\ c]$ (b); volts versus standard saturated calomel electrode (SSCE); 2-mm gold disk electrode; scan rate = 2 mV s^{-1} ; pulse amplitude, 25 mV; approximately 0.25 μ mol $[Ru^{III}-cyt\ c^{III}]$ in 0.1 M NaClO₄, 0.01 M bipyridine, 0.08 M phosphate buffer, pH 7.

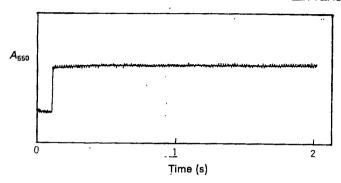


Fig. 3 Absorption change at 550 nm for the reduction of [Ru^{III}(NH₃)₄(isn)-cyt c^{III}] with isopropanol radical. The small absorbance increase at long times in the pulse radiolysis experiment is due to the reduction of the haem site in Ru(III)-cyt c(III) by secondary radicals. A similar increase in absorbance is observed at long times with the native cytochrome c(III).

force between each ruthenium complex and the haem iron is of a similar magnitude.

Scheme 1 shows the proposed sequence of events after reduction of [Ru^{III}(NH₃)₄isn-cyt c^{III}] using pulse radiolysis or chemical techniques. Following reduction, species II and IV are rapidly formed. ku is the expected rate constant for intramolecular electron transfer between species II (the kinetically stable product) and species IV (the thermodynamically stable product). However, no such reaction is observed and

Table 1 · Chemical and pulse radiolysis reduction of $[Ru^{II}(NH_3)_4isn-cyt c^{III}]$

Reductant*	% Haem reduced	%[Ru ^{III} (NH ₃) ₄ (isn)-His 33] reduced
$[Ru(NH_3)_6]^{2+}$	80 ± 10	20 ± 10
CO_2^-	40 ± 5	60±5 ·
(CH₃)₂ĊOH	60 ± 5	. 40±5

Data were obtained by monitoring the increase in absorbance at wavelength $\lambda = 550 \,\mathrm{nm}$ for the reduction of the haem site and the increase in absorbance at $\lambda = 504$ nm for the reduction of the Ru(III) site. * One mol of $[Ru(NH_3)_6]^{2+}$ was used per mol $[Ru^m(NH_3)_4$ isn-cyt c^m . CO₂ and (CH₃)₂COH were formed by pulse radiolysis from formate and 2-propanol, respectively.

instead species II undergoes a rapid (conformational) change to species III. Species III is long-lived (several hours), but can be converted to species IV by the use of a mediator, $[Ru(NH_3)_5 pyridine]^{3+}$ (redox potential, $E^\circ = 0.3$ V versus NHE, in between the reduction potentials of cytochrome c and the $[Ru^{II}(NH_3)_4 isn]$ sites). This mediator oxidizes the haem c(II), resulting in the formation of [Ru(NH₃)₅pyridine]²⁺ which in turn reduces the [Ru^{III}(NH₃)₄isn] site on cytochrome c by intermolecular reactions, as observed from spectral changes on the haem and the ruthenium sites. If species III is generated and kept without this mediator, it decays by a bimolecular pathway on a timescale of several hours ($k \approx 10 \pm 8 \text{ M}^{-1} \text{ s}^{-1}$; studied over a concentration range of 5-50 μM). The chemical reduction of $[Ru^{III}(NH_3)_4$ isn-cyt c^{III}] with 1 mol of $[Ru(NH_3)_6]^{2+}$ resulted in the formation of the kinetic intermediates II and III (scheme 1 and Table 1), as observed in the pulse radiolysis experiment.

The combined results of these ruthenium modification experiments constitute strong evidence for directional electron transfer in horse heart cytochrome c, where the intramolecular electron transfer pathway for the reduction of the haem site is more facile than that for the oxidation of the haem by the Ru(III) complex. This type of behaviour probably results from a conformational change in the protein, such that when cytochrome c(III) is reduced to cytochrome c(II), the reduced haem possesses a high kinetic barrier for intramolecular oxidation from a long distance (12-16 Å). It is noteworthy that intermolecular oxidation of cytochrome c(II) by redox reagents such as cobalt phenanthrolines and ferrocene is very rapid, presumably because there is no restriction on the approach of the oxidant to a favourable haem site for reduction, an option not available in this long-range intramolecular oxidation reaction in Ru(NH₃)₄isn-cyt c.

Earlier work on cytochrome c by Tabushi et al. 13,14 using stopped-flow circular dichroism techniques showed the presence of intermediates formed during the reduction of cytochrome c(III), but not during re-oxidation. These results led the authors to suggest that the reduction pathway is different from the oxidation pathway¹³. Furthermore, theoretical and experimental evidence showed conformational differences between the oxidized and reduced forms of cytochrome c in solution 15-18

This directionality of electron transfer in cytochrome c may have great significance in the biological function of cytochrome c, as it may mean that cytochrome c and perhaps other electron transfer proteins undergo electron transfer accompanied by conformational changes. These conformational changes can modify the barrier for electron transfer in different directions. Our observations also call for a differentiation between the formalisms used to describe electron transfer in small molecules and those needed for electron transfer proteins. For example, the meaning of the term 'self exchange' for an electron transfer protein should be redefined, since a multi-step process is involved in the electron exchange of these proteins.

We thank Dr Harold Schwarz (Brookhaven National Laboratories) for his help in the pulse radiolysis experiments, and acknowledge the support of NIH grant GM 26324 and NSF grant 840552. S.S.I. is the recipient of NIH Career Development Award (AM 00732) (1980-85) and a Camille and Henry Dreyfus Teacher Scholar Award (1981-85).

Received 24 March; accepted 18 April 1986.

^{1.} Isied, S. S., Kuehn, C. & Worosila, G. J. Am. chem. Soc. 106, 1722-1726 (1984).

Sied, S. S., Worosila, G. & Atherton, S. J. J. Am. chem. Soc. 104, 7659-7661 (1984).
 Steed, S. S., Worosila, G. & Atherton, S. J. J. Am. chem. Soc. 104, 7659-7661 (1982).
 Yocum, K. et al. Proc. natn. Acad. Sci. U.S.A. 91, 7052-7055 (1982).
 Nocera, D. G., Winkler, J. R., Yocum, K. M., Bordignon, E. & Gray, H. B. J. Am. chem. Soc. 106, 5145-5150 (1984). Yocum, K., Winkler, J. R., Nocera, D. G., Bordignon, E. & Gray, H. B. Chemica Scr. 21,

^{29-33 (1983)}

Takano, T. & Dickerson, R. E. J. molec. Biol. 153, 95-115 (1981).
 Creutz, C. & Sutin, N. Proc. natn. Acad. Sci. U.S.A. 70, 1701-1703 (1973).

^{8.} Creutz, C. & Sutin, N. J. biol. Chem. 249, 6788-6795 (1974).

Moore, G. et al. Discuss. Faraday Soc. 74, 311-379 (1982).
 Zwickel, A. M. & Creutz, C. Inorg. Chem. 10, 2395-2399 (1971).
 Wherland, S. & Gray, H. B. in Biological Aspects of Inorganic Chemistry (eds Addison, A. W., Cullen, W. R., Dolphin, D. & James, B. R.) 289-368 (Wiley, New York, 1977).
 Isied, S. S. & Taube, H. Inorg. Chem. 15, 3070-3075 (1976).
 Tabushi, I., Yamamura, K. & Nishiya, T. J. Am. chem. Soc. 101, 2785-2787 (1979).
 Tabushi, I., Yamamura, K. & Nishiya, T. Tetrahedron Lett. 49, 4921-4924 (1978).
 Bosshard, H. R. & Zürrer, M. J. biol. Chem. 255, 6694-6699 (1980).

Rackovsky, S. & Goldstein, D. A. Proc. natn. Acad. Sci. U.S.A. 81, 5901-5905 (1984).
 Williams, G., Clayden, N. J., Moore, G. R. & Williams, R. J. P. J. molec. Biol. 183, 447-460

^{18.} Margoliash, E. & Schejter, A. Adv. Protein Chem. 21, 113-286 (1966).

Diversity of haematopoietic stem cell growth from a uniform population of cells

THE stochastic model for haematopoietic stem cell differentiation 1 with the addition of a maturation pathway and a 'resting' G_0 phase provides unifying explanations for three characteristics of the growth of colonies developing in the spleens of irradiated mice that have been injected with haematopoietic cells (Fig. 1).

First, it predicts that a homogeneous cell population can produce a high proportion of visible colonies that disappear between the 7th and 12th day of colony growth, with a nearly equal number of cells appearing during this interval; however, this requires the proviso that the self-renewal probability of colonyforming cells does not increase from the normal steady-state value until a few days after the irradiation and injection of haematopoietic cells. Second, the tiny transient erythroid colonies (devoid of colony-forming cells) observed in erythropoietically stimulated irradiated mice² can be predicted if there is a reduction in the threshold size for visibility, due to the increased contrast of more mature erythroid cells. Thus, these colonies may be produced by the same homogeneous population of multipotential cells producing the late-disappearing and lateappearing colonies, but such colonies are those which run out of stem cells early, 60% predicted theoretically³, and so are not usually seen. Third, the late appearance of colonies (with higher colonyforming content) observed after injection of bone marrow cells from donor mice that have been treated with the anticancer agent 5-fluorouracil⁴ can be predicted by a 15% reduction in the number of maturing cell generations.

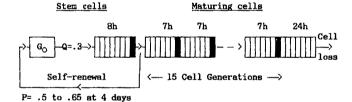
Physical cell separation shows unambiguously that spleen colony-forming cells are heterogeneous, but does not argue forcibly for the existence of a separate subpopulation of committed spleen colony-forming cells comparable in number to the multipotential population. We therefore suggest that the experimental results of Magli et al.5 fail to provide satisfactory evidence for the widely accepted claim "that the spleen colony method measures pluripotential stem cells only where macroscopic colonies are scored 11 days or later". Moreover, up to 80% of 10-day colonies contain colony-forming cells⁶. Thus, there is no compelling reason for scoring colonies later than 10 days, with the attendant increase in such technical problems as fewer countable colonies, linearity of colony counts with number of cells injected due to their larger size, possible migration from other sites, appearance of endogenous colonies and more frequent difficulty with animal survival. Moreover, these date do not necessarily require a reassessment of work carried out over the past 20 years using this important assay for haematopoietic stem cells.

This highly oversimplistic model with quite uncontroversial assump lions, demonstrates that results previously explained by postulating separate stem cell populations or selective drug sensitivity can be explained elegantly by a homogeneous population responding in different ways. Unless the minimum number of assumptions required . explain particular experimental data is found, it is unlikely that we will acquire a better understanding of the nature and regulation of haematopoietic stem cells. Our unifying model reverses the tendency to postulate a new cell population each time a new type of experimental result is observed. Elsewhere it is shown that these conclusions support the specific mechanism for the regulation of the number of haematopoietic stem cells proposed previously⁷, that they provide a straightforward explanation for the 'puzzle' concerning stem cell regeneration from cells with impaired self-renewal capacity⁸ and that the equation³ for calculating sel!-renewal has been misapplied.

N.M.B. is temporarily employed by the 'Association pour la Recherche sur le Cancer' and E.N. is holder of an INSFRM Fellowship.

N. M. BLACKETT E. NECAS E. FRINDEI

Laboratoire de Cinétique Céllulaire (U250), Institut Gustave Roussy, Villejuif, France



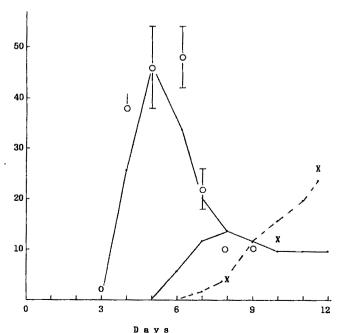


Fig. 1 Model with parameters predicting 40% loss of 7-day colonies and the number of colonies visible during growth. a, normal bone marrow (.); b, a reduction in the number of cell generations from 15 to 13 compared with experimental results, \times ref. 4; c, a threefold reduction in the diameter threshold for colony visibility compared experimental results. O ref. 2.

- Till, J. E., McCulloch, E. A. & Simonovico, L. Proc. vatn. Acad. Sci. U.S.A. 51, 29-36 (1964)
- Gregory, C. J., McCulloch, E. A. & Till, J. I. I. et Ph. stol. 86, 1-8 (1975).
 Vogel, H., Niewisch, H. & Mattoli G. J. ver. Physiol. 72,
- 221-228 (1968).

 4. Hodgson, G. S. & Bradley, T. R. Nature 251, 381-382
- (1979).

 5 Maoli M. C. Iscove, N. N. & Ovartshori, N. N. 1978
- Magli, M. C., Iscove, N. N. & Ocartcherko N. Nature 295, 527-529 (1982).
 Dumenil, D., Sainteny, F. & Frind, J. F. Ceuk, ma Rev. 6,
- Dumenil, D., Sainteny, F. & Frind, F. Estin mat Rev. 6, 753-760 (1982).
 Blackett, N. M. & Botnick, L. J. Blood Cells 7, 417-423.
- (1981).
- 8. Schofield, R. & Lajtha, L. G. Blood Cells 9, 45" 173 (1983)

ISCOVE ET AL. REPLY—Blackett, Necas and Frindel show that our observations of transient and late-appearing splcen colonies can be simulated by assuming an initially homogeneous colony-forming cell population and making an ad hoc adjustment of self-renewal probability. They conclude that our data do not prove that only the later colonies arise from pluripotential cells capable of extensive proliferation, and therefore claim that "there is no compelling reason for scoring colonies later than 10 days ...".

The essential point of our report was that early colonies are transient, and that the later-appearing multilineage colonies which contain primitive precursors are not derived from the early colonies. Therefore, the character of later colonies could no longer be invoked as proof of the primitiveness of the cells originating the early colonies. Faced with transient early colonies that had no primitive cells and contained practically only terminally differentiating erythroid cells, and now lacking any evidence for derivation from pluripotential precursors, we proposed the straightforward interpretation: that early and late colonies arise from different kinds of cell, and that the early transient colonies might in fact arise from committed precursors possessing limited proliferative potential.

There is an important additional consequence of the unrelatedness of early and late colonies which concerns the question of probability of 'self renewal'. The concept that this probability could increase during the development of spleen colonies was originally invoked to explain their increasing relative content of primitive precursors with time. An increase in self renewal probability during the course of spleen colony growth is the central assumption in the simulation performed by Blackett et al. However, our result removed both the need for this postulate and the evidence supporting it.

The important issue now is whether both early and late spleen colonies arise from an initially homogeneous precursor cell population. There is now abundant evidence that they do not: (1) Eight-day spleen colony-forming units (CFU-S[8]) are killed by 5-fluorouracil, while CFU-S[12] are relatively spared². (2) In sublethally irradiated mice, CFU-S[7] initiate DNA synthesis whereas CFU-S[11] do not³. (3) CFU-S[7] are twice as sensitive as CFU-S[11] to photoinactivation by the membrane-binding agent merocyanine 540 (ref. 4). (4) CFU-S[7] are resistant to inactivation by anti-Qa-m2 antibody plus complement, while most CFU-S[12] are inactivated⁵. (5) CFU-S sorted on the basis of binding of pokeweed mitogen segregate into a population high in proliferative capacity and ability to generate primitive precursors, and a second population having lower proliferative capacity and relatively enriched in CFU-S[7] (ref. 6). Sorting on the basis of H33342 staining⁷ and anti-H-2K binding similarly segregates cells forming early and late spleen colonies.

These experiments show conclusively that early and late spleen colonies are derived from different and separable types of precursor cells, and directly refute the model proposed by Blackett et al. Until contrary evidence appears, the available negative evidence provides more than adequate reason to question the notion

that spleen colonies scored at early times arise from pluripotential precursors with extensive proliferative potential.

N. N. ISCOVE European Molecular Biology Laboratory, Postbox 10 22 09.

D-6900 Heidelberg 1, FRG M. C. MAGLI

Ontario Cancer Institute, 500 Sherbourne Street, Toronto, Canada M4X 1K9

N. Odartchenko

Swiss Cancer Institute, CH-1066 Epalinges sur Lausanne, Switzerland

- 1. Magli, M. C., Iscove, N. N. & Odartchenko, N. Nature
- 295, 527-529 (1982). 2. Hodgson, G. S. & Bradley, T. R. Nature 281, 381-382
- 3. Chertkov, J. L. & Drize, N. J. Cell Tissue Kinet. 17, 247-252
- 4. Meagher, R. C. et al. J. cell. Physiol. 116, 118-124 (1983). 5. Harris, R. A. et al. Nature 307, 638-641 (1984)
- 6. Johnson, G. R. & Nicola, N. A. J. cell. Physiol. 118, 45-52
- (1984).

 7. Baines, P. & Visser, J. W. M. Expl Hemat. 11, 701-708 (1983).
- 8. Visser, J. W. M. et al. J. exp. Med. 59, 1576-1590 (1984).

DNA fingerprint analysis in immigration test-cases

RECENTLY, Jeffreys et al.1 used 'fingerprints' of mini-satellites to check maternity in an immigration case. I do not dispute their conclusion that the boy (X) seeking immigration was the son of the putative mother (M), and not the son of an unrelated woman or of a sister of M, but their statistical analysis includes some deficiencies.

A complete analysis of the pedigree, which involved X, M and three undisputed offspring (B, S1 and S2) of M, requires construction of a series of likelihoods taking account of the distribution of DNA bands in each individual, for example information about homozygosity of particular mini-satellites is provided by whether or not all the sibs shared any particular band. It is useful first, however, to reanalyse the summary data given by Jeffreys et al.1 in which, having assumed that X had the same father as B, S1 and S2, they deduced that 25 fragments, all of which were present in M, must have been inherited from X's mother. Following Jeffreys et al., I assume that shared bands represent identical alleles at a hypervariable locus, and that the frequency (x) is the same for all bands. For the model where M is the aunt of X, I have computed the probability that M has the band and X has inherited his from a sister of M (Table 1). The relevant likelihood ratio is $L_{\rm a}/L_{\rm m} = 0.63^{25} \doteq 10^{-5}$. Jeffreys et al. computed, instead, the probability that M and a sister (assumed, but not stated, not to be an identical twin) share a band, which is not relevant because the band has to be

transmitted to X. Their value of 0.62 is so close to 0.63, however, that overall probabilities are little different.

The basic data on the 95 bands observed and the computation of likelihood in terms of the p_{ijk} , the prior probabilities of occurrence of the bands in different family members, are given in Table 2. Computation of pijk for each model is straightforward, but tedious.

For models unrelated (u) and mother (m) all possible genotypes of mother and father have to be considered. For example, if both are heterozygotes for a band, the prior frequency of the mating is $4q^2(1$ $q)^2$, i=1 since M has the band, and the conditional probabilities that k=0, 1, 2and 3 are 1/64, 9/64, 27/64 and 27/64, respectively; the conditional probability that j = 0 is 1/2 - q/2 under model u and 1/4 under model m. Summation over combinations of genotypes gives the p_{ijk} .

For model a, where M is the aunt, a two-stage process can be used. First, all possible matings among the parents of M and her sister and for these the conditional probabilities of each genotype of M and of the band inherited by X from his mother (that is, M's sister) have to be enumerated. For example, if both the grandparents are heterozygotes, the joint probability that M is a heterozygote and X does not inherit the band from his mother is 1/4. From these data, prior probabilities of each of the possible inheritance patterns can be computed as a function of q. Second, these alternatives have to be taken with each possible genotype of the father, and the conditional probabilities that X has the band and the number of sibs with the band computed. For example, if r_3 denotes the prior probability that M is a heterozygote and X does not inherit the band from his mother, the prior probability of the corresponding mating of M to a heterozygote is $2q(1-q)r_3$, i=1 (M is a heterozygote), j=0 with probability 1/2, and k=0 with probability 1/64. Subsequent summation yields the p_{iik} .

The likelihoods can be obtained for any value of q, but as there is no prior knowledge of band frequency in the Ghanaian population, q has to be estimated for each model by maximizing the likelihood. The important likelihood ratio is $L_a/L_m =$ 0.000035 (Table 3) which, though six times higher than the probability ratio calculated by Jeffreys et al., is still very small. If the likelihood computations are repeated with q = 0.14, the value previously used¹, the corresponding ratio is much reduced (1.3×10^{-7}) ; and 0.14 was at the upper end of frequencies observed in British caucasians². Also, because frequencies of bands differ2, these likelihood calculations overestimate L_a/L_m if M is indeed the mother.

There are many assumptions in these analyses, but there seems no justification in avoiding a formal method whatever the

Table 1 Probability that M carries the band and X has a maternally derived band for each model in the reduced analysis

Model	Probability	Likelihood ratio
M unrelated to X (u)	qx	$L_{\rm u}/L_{\rm m} = 0.26^{25} = 2.4 \times 10^{-15}$
M aunt of X (a)	q(1+x)/2	$L_{\rm u}/L_{\rm a}=0.413^{25}=2.5\times10^{-10}$
M mother of X (m)	\boldsymbol{q}	$L_{\rm a}/L_{\rm m} = 0.63^{25} = 9.6 \times 10^{-6}$

x, Band frequency, assumed to be the same for each band (x = 0.26); q, allele frequency $(x=2q-q^2).$

Table 2 The number of bands (n_{ijk}) present in the sample with i = (0)1 if the band is (absent) present in M, j = (0)1 if the band is (absent) present in X, k = 0, 1, 2, 3 is the number of sibs with the band, and computation of likelihood

	Band absent in $X(j=0)$			Band present in $X(j=1)$			(j = 1)		
No. of sibs	0	1	2	3	0	1	2	3	
Band absent in M $(i=0)$	-	10	4	0	0	7	9	2	
Band present in M $(i=1)$	2	5	8	4	3	13	13	15	

 p_{ijk} Probability corresponding to n_{ijk} . The log likelihood is computed conditional on the occurrence of the band in at least one individual, with summation excluding the 000 class: $\ln L = \sum_{i} \sum_{k} \sum_{k} n_{ijk} [\ln p_{ijk} - \ln p_{000}].$

Table 3 Maximum likelihood estimates of allele frequency (q_{max}) for each model, together with corresponding log likelihoods (ln L) and likelihood ratios in the full analysis, assuming B, S1, S2 and X all have the same father

Model	q_{max}	$\ln L$	Likelihood ratios
u	0.32	-256.78	$L_{\rm u}/L_{\rm m} = 2.1 \times 10^{-9}$
a	0.26	-247.05	$L_{\rm u}/L_{\rm a} = 5.9 \times 10^{-5}$
m	0.18	-236.78	$L_{\rm a}/L_{\rm m} = 3.5 \times 10^{-5}$

model. As more information about the frequencies and inheritance of the minisatellites becomes available, the models can be refined and the obvious power of the DNA-fingerprint technique utilized. Nevertheless, I do not believe that comparisons such as these give positive identification as suggested¹, only evidence that alternatives are highly unlikely.

I thank John Brookfield for providing the basic data, Susan Brotherstone for computational assistance, and members of Leicester University's Genetics Department for financial assistance.

WILLIAM G. HILL

Institute of Animal Genetics University of Edinburgh, West Mains Road Edinburgh EH9 3JN, UK

JEFFREYS ET AL. REPLY—We thank Professor Hill for his rigorous statistical analysis of the DNA fingerprint data of this immigration test-case. We are pleased that the new analysis gives ranges of values

for the likelihood ratios which are broadly similar to ours. We reiterate that even the new analysis includes a number of assumptions. The maximum likelihood values of q are based on only one family, and will be inaccurate. It is assumed that there is no variation in q between bands. and it is assumed that bands with the same mobility are always allelic and that bands with different mobilities never are.

We admit that we have not provided positive identification of the mother of X in a mathematical sense, since no probability calculation could do this. However, we believe that the probability of error in this case is so low that it would be legally appropriate to treat the test as providing positive identification.

> A. J. JEFFREYS J. F. Y. BROOKFIELD R. SEMEONOFF

Department of Genetics, University of Leicester, Leicester LE1 7RH, UK

X; autosome translocations in females with Duchenne or Becker muscular dystrophy

RAY et al.1 recently documented their efforts at isolating the gene for Duchenne muscular dystrophy by studying DNA cloned from the breakpoint of an X;21 translocation associated with Duchenne muscular dystrophy. However, the female patient² from whom this X-chromosomal material was derived³, clearly had Becker muscular dystrophy and not Duchenne dystrophy, as she was 20 years old and still ambulant. It thus seemed timely to critically review all the reported cases of muscular dystrophy in females associated with an X; autosome translocation (Table 1) in order to try and designate them as Duchenne or Becker type.

Duchenne muscular dystrophy is an Xlinked condition with onset in early childhood and a rapidly progressive course, so that the vast majority of affected boys lose the ability to walk by the age of 12 years⁴; Becker muscular dystrophy has an identical pattern of muscle involvement but follows a more benign course, and affected males will remain ambulant beyond 16 years of age and usually into adult life⁵. Inevitably there will also be occasional cases who may fall in the grey zone between the two and be a little milder than the usual Duchenne but not quite as mild as the usual Becker type and lose ability to walk between 13 and 16 years.

Careful attention has been paid to the diagnosis of male cases of either Duchenne or Becker dystrophy in the application of restriction fragment length polymorphism (RFLP) studies and detection of deletions. It would seem logical to pay the same attention to the initial diagnosis in the X:autosome translocation females from which the DNA sequences are cloned, rather than loosely referring to them all as Duchenne muscular dystrophy, as seems to have been the current practice.

Of the twelve cases documented to date, four⁶⁻⁹ conform closely to Duchenne dystrophy and a further four¹⁰ 13 also seem to have a Duchenne severity but are still too young to be certain. One additional case¹⁴ is probably a Duchenne but was only published in abstract form with no mention of the age, which had to be surmised from the date of birth and timing of the abstract (approximately 14 years); she was said to be "unable to walk without assistance", which is also difficult to interpret. One case² conforms to Becker type and another¹⁵ also seems likely to be, but is too young (13 years) to be certain about ambulation beyond 16 years. The remaining case16 (published only in abstract form) has insufficient clinical data to draw any conclusions. Two of these cases are somewhat atypical, one10 having an associated dysmorphic syndrome and the other9 an associated Turner's syndrome.

Recent studies¹⁷⁻²⁰ have shown that the gene locus for Becker muscular dystrophy is very close to that for Duchenne and it seems likely that the two conditions are allelic. Studies with some of the probes (for example pERT 87.8)21 have shown deletions in approximately 9% (5'57) of cases of Duchenne muscular dystrophy but none with cases of Becker muscular dystrophy.

In the report of Ray et al.1, only one Duchenne dystrophy patient out of 50 studied showed a deletion for their XJ-1 clone, and this was also the only case which showed a deletion for pERT 87. In

Jeffreys, A. J., Brookfield, J. F. Y. & Semeonoff, R. Nature 317, 818-819 (1985).
 Jeffreys, A. J., Wilson, V. & Thein, S. L. Nature 316, 76-79 (1985).

Table 1 X; autosome translocations in girls with muscular dystrophy

	•		-	-				
Reference	Autosomal breakpoint	Age at reporting	Age of onset	Loss of ambulation	Still walking	IQ	Conclusions	
Canki et al. (1979)10	3q13	4 уг	10 mth	-	+	R	? DMD*	
Lindenbaum et al. (1979) ⁶	1p34	8 yr	<2 yr	+(8 yr)		N	DMD†	
Greenstein et al. (1980) ¹⁶	11q13	16 yr	?	?	?	?	? DMD or BMD	
Jacobs et al. (1981) ⁷	5q35	9 yr	4 yr		+	N	DMD	
Zatz et al. (1981)8	6q21	11 yr	5 yr	+(10 yr)		N	DMD .	
Emanuel et al. (1983) ¹¹	9p22	9 yr	<2 yr	` - `	+	R	? DMD	
Nielsen et al. (1983)15	11q23	13 yr	<2 yr	_	+	N	? BMD	
Perez Vidal et al. (1983) ¹²	6q16	4 <u>1</u> yr	<3 yr	-	+	?	? DMD	
MacLeod et al. (1983)14	2q36	?14 yr	<2 yr	+	••••	R	? DMD	
Verellen-Dumoulin et al. (1984) ²	21p12	20 yr	2 yr	_	+	N	BMD	
Bjerglund-Nielsen (1984)9	9p21	23 yr‡	<2 yr	+(12 yr)	_	R	DMD§	
Saito et al. (1985) ¹³	4q26	3 yr	2 yr		+	?	? DMD	

- N, normal; R, retarded; DMD, Duchenne muscular dystrophy; BMD, Becker muscular dystrophy.
- * Associated dysmorphic syndrome.
- † Personally examined.
- # Died.
- § Associated Turner's syndrome.

addition, all five patients of Monaco et al.21 with deletions for pERT 87 were found to have deletions for XJ-1.

Although all the reported cases of X; autosome translocation with muscular dystrophy have apparently had the breakpoint in the same region of the short arm of the X chromosome (Xp21), there may be variations from case to case in the exact location of the breakpoint²². It may thus be of interest and importance when cloning sequences from these X-chromosome breakpoint regions, and applying them in the detection of RFLPs close to the Duchenne/Becker dystrophy genes, and looking for deletions in individual male cases, to know whether the original source came from a Duchenne or a Becker type case, and in addition to have adequate documentation of the dystrophic nature of the underlying muscle disorder.

Note added in proof: A further case, conforming to Duchenne severity, with an X:5 translocation, has recently been documented by Nevin et al.23.

VICTOR DUBOWITZ

Department of Paediatrics & Neonatal Medicine and Jerry Lewis Muscle Research Centre, Royal Postgraduate Medical School, Hammersmith Hospital, Du Cane Road, London W12 0HS, UK

- 1. Ray, P. N. et al. Nature 318, 672-675 (1985).
- 2. Verellen-Dumoulin, C. et al. Hum. Genet. 67, 115-119 Worton, R. G. et al. Science 224, 1447-1449 (1984).
- Dubowitz, V. Muscle Disorders in Childhood (Saunders, London, 1978).
- 5. Emery, A. E. H. & Skinner, R. Clin. Genet. 10, 189-201
- 6. Lindenbaum, R. H. et al. J. med. Genet. 16, 389-392 (1979). 7. Jacobs, P. A. et al. Am. J. hum. Genet. 33, 513-518 (1981).
- Zatz, M. et al. J. med. Genet. 18, 442-447 (1981).
 Bjerglund Nielsen, L. & Nielsen, I. M. Ann. Génét. 27, 173-177 (1984).
- 10. Canki, N., Dutrillaux, B. & Tivadar, I. Ann. Génét. 22. 35-39 (1979). 11. Emanuel, B. S., Zackai, E. H. & Tucker, S. H. J. med. Genet.
- 20, 461-463 (1983).

- 12. Perez Vidal, M. T. et al. Rev. Neurol. (Barcelona) XI. 51, 155-158 (1983).
- 13. Saito, F. et al. Hum. Genet. 71, 370-371 (1985).
- MacLeod, P. M., Holden, J. & Masotti, R. Am. J. hum. Genet. 35, 104A (1983).
- 15. Nielsen, L. B. et al. Clin. Genet. 23, 242 (1983).
- 16. Greenstein, R. M. et al. Cytogenet. Cell Genet. 27, 268
- 17 Kingston, H. M. et al. J. med. Genet. 20, 255-258 (1983). 18. Kingston, H. M. et al. Hum. Genet. 67, 6-17 (1984).
- Brown, C. S. et al. Hum. Genet. 71, 62-74 (1985).
 Dorkins, H. et al. Hum. Genet. 71, 103-107 (1985).
- 21. Monaco, A. P. et al. Nature 316, 842-845 (1985).
- Boyd, Y. & Buckle, V. J. Clin. Genet. 29, 108-115 (1986).
 Nevin, N. G. et al. J. med. Genet. 23, 171-173 (1986).

WORTON REPLIES—Dubowitz raises a very valid concern about the phenotypes of girls with myopathic disease secondary to an X; autosome translocation. Certainly the X;21 translocation patient whose junction has been cloned has a mild form of muscular dystrophy more like the Becker form of the disease and should perhaps be reclassified as such.

However, there are two very important points to be made about the translocation patients in general. First, all have translocation exchange points in band Xp21 despite the fact that some have a severe (Duchenne) phenotype and others appear to have the milder (Becker) phenotype. This fits with the linkage data that map the gene for both Becker and Duchenne muscular dystrophy to this region of the X chromosome. As Dubowitz points out the two diseases may in fact be due to allelic mutations at the same locus. Thus, although it is important to have the phenotype of patients accurately described, the Duchenne and Becker variants of muscular dystrophy may simply represent different manifestations of the same disease.

The second important point, and one not discussed by Dubowitz, is that the expression of muscle disease in these girls who are heterozygous for the mutation (translocation) is a function of the nonrandom inactivation of the normal X chromosome carrying the wild-type allele. In many of the girls examined, the preference for normal X inactivation is not complete; up to 10% of the lymphocytes examined displayed a late replicating (inactive) translocation X and an early replicating (active) normal X. If this pattern holds in muscle, a proportion of the nuclei in a multi-nucleated myotube may be capable of producing the normal gene product. Since the 50% level of gene product expected of a non-translocation carrier female is sufficient to prevent the disease, a level of 5% or 10% may well be sufficient to modify the severity of the disease. In translocation patients a mutation at the 'Duchenne gene', therefore, may result in a Becker phenotype. This complicates the picture and suggests that neither term is really appropriate to the translocation females. Only through detailed genetic studies of the Becker/Duchenne muscular dystrophy locus will the true relationship between the two diseases be understood.

R. G. WORTON

The Hospital for Sick Children, 555 University Avenue, Toronto, Ontario, Canada M5G 1X8

Matters Arising

Matters Arising is meant as a vehicle for comment and discussion about papers that appear in Nature. The originator of a Matters Arising contribution should initially send his manuscript to the author of the original paper and both parties should, wherever possible, agree on what is to be submitted. Neither contribution nor reply (if one is necessary) should be longer than 500 words and the briefest of replies, to the effect that a point is taken, should be considered.

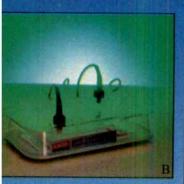
10210116C INTERNATIONAL WEEKLY JOURNAL OF SCIENCE

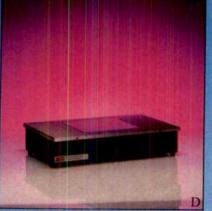
Volume 322 No.6077 24-30 July 1986 £1.90

TERRESTRIAL ORIGIN OF THE MOON

A better way to get uniform band sp Wedge-shap







No longer need you resort to multiple loading with its increased time and greater required sample volumes. Whether for nucleotide separations in agarose gels or sequencing in acrylamide gels, the technique of wedge-shaped field strength gradients lets you get linearly spaced bands for maximum resolution and ease of reading. Two new instrument systems from LKB render the technique rapid, reliable

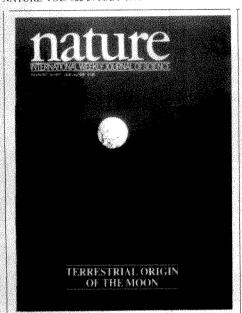
and above all, reproducible.

In the Maxiphor" horizontal electrophoresis unit (A), it is the simplest thing in the world to pour wedge-shaped agarose bridge gels directly on the central platform when adjustable legs beneath the cathode dam are extended. Gels can be run rapidly at high power even without external buffer circulation, the half-litre reservoir providing enough internal cooling capacity even at 500 volts. Want to use the Maxiphor for constant thickness bridge or submarine gels? Just as easily done. And you can run up to 40 samples every time.

For greatest economy and speed in fragment separations, the sibling Miniphor™ unit (B) with its integral cooling jacket lets you run submarine gels at very high power. Companion to both units is the LKB constant power supply (C) that permits regulation to 1 volt or 1 milliamp with 1 minute precision for automated runs. And completing the system is the MacroVue" transilluminator (D) whose optical design permits you to detect as little as 1 ng DNA in a single band. This instrument makes publication grade photography easy.

nature

NATURE VOL. 322 24 JULY 1986



Reviewing the chemistry of the Moon. Ringwood (p.323) suggests that the close relationship between the lunar and terrestrial mantles means that the Moon was once part of the Earth. Giant impacts could have thrown parts of the Earth's mantle into orbit, to subsequently accrete afresh to form the Moon. Photo: Kim Taylor/Bruce Coleman Ltd.

OPINION	************
Half-way report on Chernobyl	293
Packing for the summit?	
Research directions	294
NEWS	
Soviet inquiry	295
US and Pakistan	
AIDS	296
Japan	
More dead penguins	
Engineered organisms	297
Space antiques	
hedge against inflation	
Chinese science	
OECD indicators	298
Getting tough on doctorates	
Berlin arrest riddle	
UK universities	299
SDI	300
UK star wars consortium launched	
US space Now it's save French science!	
CORRESPONDENCE	
Embryo research/etc.	302
NEWS AND VIEWS	uququunun marani v
Gentle warning on fractal fashions	301
Rabies control: Vaccination of wildl	
reservoirs	***
Roy M. Anderson	304

Roy M. Anderson

Carl Scheele (1742-1786) and the discovery of oxygen		Studies on Plant Demography: A Festshrift for John L Harper	
	305	J White ed.	
Lunar cycles in lake plankton	-	and	
Geoffrey Fryer	306	The Population Structure of	
Signs of language in the brain		Vegetation. Handbook of	
John C Marshall	307	Vegetation Science, Vol. 3	
New semiconducting polymers		I White ed.	
RH Friend	308	Peter D Moore	320
Meteorites: Window on the early	300		
		COMMENTARY	
Solar System	309	What to believe about miracles	
Derek Sears	309	RJBerry	321
Geometry: Exotic structures		NJ Delly	44 B
on four-space	210	REVIEW ARTICLE	and the second second second
Ian Stewart	310		
Galactic haloes need computers		Terrestrial origin of the Moon	323
George Efshathiou	311	A E Ringwood	
Nitrogen fixation:		ARTICLES	
A role for vanadium at last			
R Cammack	312	Primordial density fluctuations and	
-SCIENTIFIC CORRESPONDENC	c	the structure of galactic haloes	
SCIENTIFIC CONNEST ONDENC	L	PJQuinn, JKSalmon & WH Zurek	329
Observation of 110m Ag in		793 × 3	
Chernobyl fallout		The cytoplasmic carboxy terminus of	
G D Jones, P D Forsyth		M13 procoat is required for the	
& PG Appleby	313	membrane insertion of its	
Characteristics of Chernobyl		central domain	
radioactivity in Tennessee		A Kuhn, W Wickner & G Kreil	335
E A Bondietti & J N Brantley	313		
Human lipocortin similar		LETTERS TO NATURE	
to ras gene products		Detection of planetary systems and	
TZMunn & GIMues	314	the search for evidence of life	
	J.T.	BF Burke	340
Evolutionary 'classics' may		DIDUIK	en canada
self-destruct	315	A space telescope for infrared	
A Rossiter	313	spectroscopy of Earth-like planets	
Recent discoveries of		JRP Angel, AYS Cheng	
a supermass in the Universe	217	& N.I Woolf	341
H Arp	316	the second secon	
Espresso coffee emporia		An explanation of the east - west	
take note		asymmetry of Io's sodium	
A Parsons	316	cloud	
BOOK REVIEWS		NThomas	343
DOONKEVIEWS			on a set orderpoint
Scientists and Journalists: Reporting		A class of narrow-band-gap	
Science as News		semiconducting polymers	
S M Friedman, S Dunwoody and		S A Jenekhe	345
C L Rogers eds			
David Dickson	317	Extraordinary effects of mortar-and-	
Coastal and Estuarine Sediment		pestle grinding on microstructure	
Dynamics		of sintered alumina gel	
by KR Dyer		W A Yarbrough & R Roy	347
JR L Allen	318	AND	
Spinors and Space-time, Vol. 2:		Crustal structure of the northern	13
Spinor and Twistor Methods in		Alpha Ridge beneath the	
		Arctic Ocean	
Space-Time Geometry		D A Forsyth, I Asudeh.	200
by R Penrose and W Rindler		A G Green & H R Jackson	349
Abhay Ashtekar		The second secon	
Climatic Change and World Affairs		Melting of a model chondritic	
(Revised Edition)		mantle to 20 GPa	
		more come, a real	18 M W -
by C Tickell Nicholas A Rupke	319	E Ohtani, T Kato & H Sawamoto	352

Nature* (ISSN 0028-0836) is published weekly on Thursday, except the last week in December, by Macmillan Journals Ltd and includes the Annual Index (mailed in February). Annual subscription for USA and Canada US \$240. USA and Canadian orders to: Nature, Subscription Dept. PO Box 1501, Neptune, NJ 07753, USA. Other orders to: Nature, Brunel Road, Basingstoke, Hans RO21, 2XS, UK. Second class postage paid at New York, NY 10012 and additional mailing offices. Authorization to photocopy material for internal or personal use, or operation as of specific clients, is granted by Nature to libraries and others registered with the Copyright Clearance Center (CCC) Transactional Reporting Service, provided the base fee of \$1.00 a copy plus \$0.110 a page is paid directly to CCC, 21 Congress Street, Salem, Massachusetts 01970, USA, Identification code for Nature: 0028-0836/86 \$1.00 + \$0.10. US Postmaster send address changes to: Nature, 85 Bleecker Street, New York, NY 10012. Published in Japan by Macmillan Shuppan K.K., Eikow Building, 1-10-9 Hongo, Bunkyo-ku, Tokyo, Japan © 1986 Macmillan Journals Ltd.

TGF-BETA

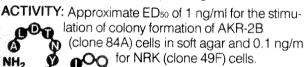
TRANSFORMING GROWTH FACTOR TYPE BETA

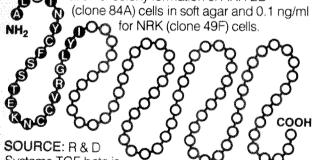
TGF-beta is an extremely stable. multi-functional growth factor, active in picomolar quantities. The effect of the molecule is largely governed by the cell line under investigation.

Some of the more notable reported effects are:1

- Reversibly confers the transformed phenotype
- Provides synergistism with EGF and/or TGF-alpha
- Inhibits growth of certain carcinoma cell lines
- Inhibits terminal differentiation of pre-adipocytes
- Promotes in vivo wound healing
- · Mimics the effects of ras oncogene transfection
- Induces c-sis expression

PURITY: greater than 96 percent homogeneous by silver-stained gels, amino acid analysis and N-terminus sequencing





Systems TGF-beta is prepared from fresh porcine platelets. Based on its molecular weight, amino acid analysis and N-terminus sequencing (22 a.a.), it is indistinguishable from TGF beta prepared from human sources.

TO ORDER: Call 1 (800) 328-2400 or to request information or technical bulletins (In Minnesota call 612-379-2956).

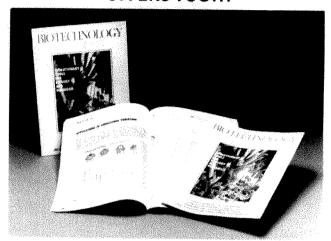
1For a more complete description and list of references, request R & D Systems Technical



R & D Systems, Inc. 614 McKinley Place N.E. Minneapolis, MN 55413

BIO/TECHNOLOGY

The International Monthly for Industrial Biologists OFFERS YOU...



MORE NEWS, FEATURES. **EVALUATIONS and ORIGINAL RESEARCH BY TOP EXPERTS** THAN ANY OTHER SINGLE **BIOTECHNOLOGY PUBLICATION...**

SUBSCRIBE NOW!

ORDER FORM

- ☐ YES please send me a subscription to Bio/Technology
- □ Lenclose payment of:

In US: ☐ 1 year US\$78 ☐ 2 years US\$129 (SAVE US\$27!)

In UK: □1 year £70 □ 2 years £119 (SAVE £211)

In Australia: ☐ 1 year A\$130 ☐ 2 years A\$221 (SAVE A\$39!) Elsewhere: ☐ 1 year US\$112 ☐ 2 years U\$\$190 (SAVE U\$\$34!)

in Japan write to: Macmillan Shuppan k.k., Eikow Building, 10-9 Hongo 1-Chome, Bunkyo-ku, Tokyo 113, Japan

- ☐ I enclose my cheque made payable to BIO/TECHNOLOGY
- ☐ Please charge my credit card account
- ☐ American Express ☐ Mastercard ☐ Visa

Account No Expiry date Signature Name. Address

In US Send to: Bio/Technology Customer Relations, PO Box 316, Martinsville, N.J. 08836, U.S.A.

Elsewhere send to: Circulation Manager, Macmillan Journals, Brunel Road, Basingstoke, Hampshire, RG21 2XS U.K.

- Copies outside US despatched by Airspeed
- * Ali orders require pre-payment

7818



NATURE BINDERS

Your copies of Nature are invaluable for future reference so why not give them the treatment they deserve and file them neatly in our special Nature binders?

Ordering address and prices for one or a set of four are listed below.

Annual Subscription Pr	ices	
UK & Irish Republic		£104
USA & Canada		US\$240
Australia, NZ &		
S. Africa	Airspeed	£150
	Airmail	£190
Continental Europe	Airspeed	£125
India	Airspeed	£120
*******	Airmail	£190
Japan	Airspeed	Y90000
Rest of World	Surface	£120
ASSOCIATE TO STATE	Airmail	£180
Orders (with remittance	e) to:	
USA & Canada	UK & Rest of	World
Nature	Nature	
Subscription Dept	Circulation D	ept
PO Box 1501	Brunel Road	Can Co.
Neptune	Basingstoke	
NJ 07753	Hants RG21	2XS, UK
USA	Tel: 0256 292	
(The addresses of Natu	re's editorial offic	es are shown
facing the first editorial		
Japanese subscription e	nguiries to:	
Japan Publications Tra		d
2-1 Sarugaku-cho 1-cho		
Chiyoda-ku, Tokyo, Ja		
T 1 (00) 200 2755	•	

Tel: (03) 292 3755

Personal subscription rates: These are available in some countries to subscribers paying by personal cheque or credit card. Details from:

Back issues: UK, £2.50; USA & Canada, US\$6.00 (surface), US\$9.00 (air); Rest of World, £3.00 (surface), £4.00 (air)

Binders

Single binders: UK, £5.25; USA & Canada \$11.50; Rest of World, £7.75. Set of four: UK, £15.00; USA & Canada \$32.00; Rest of World, £22.00

Annual indexes (1971-1985) UK, £5.00 each; Rest of World, \$10.00

Nature First Issue Facsimile UK, £2.00; Rest of World (surface), \$3.00; (air) \$4.00

Nature in microform Write to University Microfilms International, 300 North Zeeb Road, Ann Arbor, MI 48106, USA

Mel	ting	of ga	rnet	per	ido	tite	to	13 G	Pa
and	the	early	hist	ory	of t	he	upp	er	
man	tle								

CM Scarfe & E Takahashi

Evidence from the Parana of south Brazil for a continental contribution to Dupal basalts C J Hawkesworth, M S M Mantovani, PN Taylor & Z Palacz

Acidity of Scottish rainfall influenced by climatic change T D Davies, P M Kelly,

P Brimblecombe, G Farmer & R J Barthelmie

Simultaneous outflow of fresh water and inflow of sea water in a coastal spring

C Drogue & P Bidaux
Sign language aphasia during

left-hemisphere Amytal injection A Damasio, U Bellugi, H Damasio, H Poizner & J Van Gilder

Electrokinetic shape changes of cochlear outer hair cells

B Kachar, W E Brownell, R Altschuler & J Fex

Ionic basis of membrane potential in outer hair cells of guinea pig cochlea J F Ashmore & R W Meech 368

Lithium-induced respecification of pattern in Xenopus laevis embryos K R Kao, Y Masui & R P Elinson

Oral vaccination of the fox against rabies using a live recombinant vaccinia virus

J Blancou, M P Kieny, R Lathe, J P Lecocq, P P Pastoret, J P Soulebot & P Desmettre 373

Preferential expression of a defined T-cell receptor β-chain gene in hapten-specific cytotoxic T-cell clones

U Hochgeschwender, H U Weltzien, K Eichmann, R B Wallace & JT Epplen

Alternative splicing of murine
Tcell receptor β-chain transcripts
M A Behlke & D Y Loh
379

Synergism between immunoglobulin enhancers and promoters J V Garcia, Lê thi Bich-Thuy,

J Stafford & C Queen

Expression of human adenosine deaminase in murine haematopoietic progenitor cells following

retroviral transfer
J W Belmont, J Henkel-Tigges,
S M W Chang, K Wager-Smith,
R E Kellems, J E Dick,
M C Magli, R A Phillips,
A Bernstein & C T Caskey

The alternative nitrogenase of Azotobacter chroococcum is a vanadium enzyme

R L Robson, R R Eady, T H Richardson, R W Miller, M Hawkins & J R Postgate

388

Botulinum C2 toxin ADP-ribosylates actin

K Aktories, M Bärmann, I Ohishi, S Tsuyama, K H Jakobs & E Habermann

AMOOF!! AND

MISCELLANY

100 years ago

354

356

359

361

363

365

371

376

383

311

390

-NATURE CLASSIFIED

Professional appointments — Research posts — Studentships — Fellowships — Conferences — Courses — Seminars — Symposia:

Back Pages

Next week in Nature:

- The dark night sky
- Terrestrial orbital motion
- Magnetic reversal periodicity
- Dating Le Moustier
- Swordfish ancestor
- Molecular basis of memory
- Cystic fibrosis mechanism
- Cytopathic effect of AIDS virus

GUIDE TO AUTHORS

Authors should be aware of the diversity of Nature's readership and should strive to be as widely understood as possible.

Review articles should be accessible to the whole readership.

Most are commissioned, but unsolicited reviews are welcome
(in which case prior consultation with the office is desirable).

Scientific articles are research reports whose conclusions are of general interest or which represent substantial advances of understanding. The text should not exceed 3,000 words and six displayed items (figures plus tables). The article should include an italic heading of about 50 words.

Letters to Nature are ordinarily 1,000 words long with no more than four displayed items. The first paragraph (not exceeding 150 words) should say what the letter is about, why the study it reports was undertaken and what the conclusions are.

Matters arising are brief comments (up to 500 words) on articles and letters recently published in Nature. The originator of a Matters Arising contribution should initially send his manuscript to the author of the original paper and both parties should, wherever possible, agree on what is to be submitted.

Manuscripts may be submitted either to London or Washington). Manuscripts should be typed (double specing) on one side of the paper only. Four copies are required, each accompanied by copies of lettered artwork. No title should exceed 80 characters in length. Reference lists, figure legends, etc. should be on seperate sheets, all of which should be numbered. Abbreviations, symbols, units, etc. should be identified on one copy of the manuscript at their first appearance.

References should appear sequentially indicated by superscripts, in the text and should be abbreviated according to the World List of Scientific Periodicals, fourth edition (Butterworth 1963-65). The first and last page numbers of each reference should be cited. Reference to books should clearly indicate the publisher and the date and place of publication. Unpublished articles should not be formally referred to unless accepted or submitted for publication, but may be mentioned in the text.

Each piece of artwork should be clearly marked with the author's name and the figure number. Original artwork should be unlettered. Suggestions for cover illustrations are welcome. Original artwork (and one copy of the manuscript) will be returned when manuscripts cannot be published.

WINORPC UNPARALLED SELECTIVITY



NATURE VOL. 322 24 JULY 1986

Half-way report on Chernobyl

The Soviet Union has published this week only the least interesting parts of its report on the Chernobyl disaster. More needs to be said.

Human error is always a convenient explanation for catastrophe. It has the advantage, for the managers of great enterprises, that a few heads can be made to roll with some publicity without interfering too directly with the underlying programme. This is the spirit in which the surviving managers of the Soviet Union's still ambitious nuclear programme will no doubt be relieved by the publication earlier this week of an abridged version of the report on the Chernobyl disaster drawn up by the official investigating committee (see page 295). None of this implies that the explanation is incorrect. There is no reason to disbelieve the Soviet statement that the managers of the plant at Chernobyl behaved foolishly and "irresponsibly", or that they deserve to lose their jobs. Indeed, most Soviet statements about Chernobyl have been shown to have been accurate.

Nevertheless, the public interest in the Chernobyl disaster stems from the general concern that the world at large should have such a good understanding of how the accident happened that it is possible to make rational decisions about the future use of nuclear power as a source of electricity. Some, no doubt, seek further information so as to berate the hapless managers of nuclear industries elsewhere. Others seek the same information in the hope that it will demonstrate that nuclear power stations can be safely operated. The curiosity of both groups is legitimate, and must be satisfied. So must be that of the people most directly affected, the population of the region stretching for 400 square kilometres around the plant. The need now is for such a full disclosure of the circumstances leading to the accident that people will be able to judge for themselves whether the Chernobyl managers were as feckless as they are now said to be.

On present evidence, there is a long way to go before the circumstances are plain. It is said that those responsible at Chernobyl had been engaged in "experiments" not authorized by the licensing authorities when the accident happened, but there is no way of telling whether this was idle technological curiosity (unlikely on the eve of the May holiday) or, instead, a desperate attempt by unorthodox means to bring a wayward reactor under control. Similarly, there is not yet a sufficient explanation of the course of the accident itself. Monitoring stations elsewhere now clearly suggest that there was a second release of radioactive material from the reactor on the second day, presumably as a consequence of a further increase of the internal temperature. but the explanation remains for the time being hidden. Yet until this information is available, people outside the Soviet Union will remain on tenterhooks. There is again no reason to fear that the Soviet Union will not keep its promise to tell all. But this once secretive government now experimenting with openness clearly still has a lot to learn.

The Soviet managers of the nuclear industry need also to learn a little more caution about reactors of the type that went wrong at Chernobyl. One of the defects of this type of reactor is that the system becomes more reactive when water is lost from the cooling system, either because it leaks away or because it turns into steam. The consequence is an uncomfortable degree of instability which can also be a source of danger when something else goes wrong. But Soviet reactors of this type also lack the large pressure-tight containment vessels that would be required

of them in the United States and most other places. It must now be a matter of grave concern whether the other reactors of this type, of which are more than twenty still in operation in the Soviet Union, can be safely allowed to continue.

In one respect, the Soviet government has responded constructively to the delivery of the report by setting up a new ministry with responsibility for the design and construction of new reactors. Obviously the intention is that the Soviet nuclear industry should in future be run on lines more appropriate for a military organization (which, in the circumstances, may be the best solution, although one conflicting with Mr Gorbachev's belief that there are too many ministries as there are). But the Soviet authorities should also pay some attention to the possible lity that there may be other, better, solutions. Notoriously, Soviet industry is perennially crippled by the bureaucratic environment in which it must function. Part (but only part) of the trouble is that managers are responsible both to the government agency or ministry which has built their plant and to the Communist Party, working through its local and regional committees. This is a recipe for the division and even dilution of responsibility. At Chernobyl, it seems to have a been a recipe for disaster as well. Nobody would expect that a single nuclear accident would persuade the Soviet Union to forsake the path Lenin mapped out, but there is good reason why the Soviet Union should now be asking whether its present arrangements for the management of industry are the only means by which the dictatorship of the proletariat can be exercised.

The plight of those exposed to fallout near Chernobyl but not acutely injured remains to be determined. Strictly speaking, it is a matter for the Soviet government, in its dealings with its own people, to decide. This week's statement says that those affected by the enormous disruption caused by the accident will be compensated, though it is not clear what that means. But there is a great need that there should be close medical surveillance of those affected for several decades to come. It is not merely that there is a great deal to learn about the effects of low-level radiation exposure, or that there are ethical considerations which require that those now at greater risk from cancer than most others should be given as timely a warning as possible, but that this is a chance for the Soviet Union to make good its previously poor record for compassion.

Packing for the summit?

There may be a Soviet-US summit this year if only a package of agreements can be found.

OPTIMISM earlier this year that 1986 would be the year in which the first arms control agreement this decade would be signed seems to be strengthening again, against the odds, and in spite of the succession of disagreements between the two major powers that have studded the past few months. And while the latest developments amount to nothing more substantial than straws in the wind, they do suggest that the two sides will eventually talk to each other, at a summit meeting later in the year. That is something for which many people will be grateful. But the likely

content of any agreement that may emerge is still a matter for conjecture. What is going on?

The straws in the wind are several. The Soviet Foreign Minister in London last week referred to the summit meeting as if it had already been arranged, apparently anticipating events. At the Stockholm meeting within the framework of the Helsinki agreements on European security, the Soviet Union has dropped its previous demands that air movements should be notified as part of the package of "confidence-building measures" on which the negotiators have been working since the beginning of 1985; now there is a chance of something to be signed at Vienna in November. Less formally, the Pugwash organization seems to have had a constructive meeting in Moscow earlier in the month. leaving many of the participants with the impression that the Soviet side is both eager for a test ban and willing to be flexible about the terms in which it might be drawn. Then President Reagan has made an encouraging speech, saying that there is much that might be done with the most recent set of proposals to the bilateral negotiations at Geneva, suggesting that an agreement may in due course emerge. Why all this sweetness and light?

The simple explanation is that both the Soviet and the US leaders wish there to be a summit, but that the Soviet side is determined that it will not allow itself this time to return emptyhanded, as in many ways it did from last year's meeting at Geneva. And the practical question is whether there is a deal of some kind that would satisfy Mr Gorbachev without sticking in Mr Reagan's throat (or the throats of his colleagues in the US administration). In many ways, guessing what the package will contain is like a children's nursery game, except that it seems clear that there can be no substantial agreement on the main issues at Geneva — reductions of strategic weapons, regulation of intermediate-range missiles and the Strategic Defense Initiative (SDI). So what else? Agreement to ratify unratified treaties, such as the threshold test-ban treaty whose provisions require the exchange of seismic data relevant to the monitoring of tests, would be a sensible step forward — one that should have been taken several years ago. But the Soviet Union, with its unilateral moratorium on testing still in force after nine months. seems anxious to secure substantial improvement in this field. That is apparently why so much attention is being paid to the several variations on the test-ban theme suggested at an informal meeting in Washington earlier in the year — comprehensive test bans whose start is delayed, or which may be interrupted occasionally. It should not hurt either side to put together a package of proposals along these lines. The obvious snag is that such a package would, by definition, not touch the centre of the problem of arms control, the regulation of major strategic weapons already deployed.

That is why the two participants in the summit should be most of all concerned to reach a new understanding on the principles by which future arms negotiations will be conducted. Too much has changed in the past few years for most people's comfort. President Reagan, who came to office nearly six years ago with a long string of cogent complaints against the then existing agreements (SALT II in particular), but who found himself forced by events and pressure from his electorate to take arms control more seriously, has now further muddied the waters by suggesting that SDI seriously offers a way round the present strategic doctrines based on mutual deterrence by the threat of a catastrophic nuclear exchange. But the plain truth is that SDI will never be as effective as its enthusiasts claim, and will probably yield nothing more than a space-borne early warning system whose existence will not substantially change the present strategic balance (if that is what it is). So the summit will be a wasted opportunity if it does not yield an understanding of the ways in which SDI has changed (or, rather, left unchanged) the rules of arms control. For pride's sake, President Reagan would need such an understanding to be limited in time, but that should be no problem.

Research directions

The British government plans to evaluate its research. But there are pitfalls.

Not much has yet been heard from Mr Kenneth Baker, the successor in the British government to Sir Keith Joseph at the Department of Education and Science, about his plans for the administration of research. Perhaps inevitably, most of his time seems to have been spent on the urgent problems of how to restore contentment and achievement to the schools, whose bruising dispute with the government over pay, working conditions and career prospects has left deep scars. Yet Mr Baker cannot overlook the problems thrown up in the past few years by the government's insistence that the costs of reorganizing (or cutting) the research councils should be met from within a static budget. Already, the political calendar has reached the point at which final estimates for the next financial year are being drawn up. Moreover, unless Mr Baker is careful (and quick), he may find that this important part of his parish has been taken away from him.

That is one implication of the decision, announced at the end of last month, that there will be a unit within the Cabinet Office for the assessment of science, technology and the relationship between them. The plan is that there should be a small group of people, run by a senior (but not too senior) civil servant, with the task of throwing light on the relationship between research spending and such benefits as may ensue. The hope is that the government will then be better placed to decide which expenditures on research will yield the greater benefits. Although the unit will be chiefly concerned with what government departments at present spend on research on their own account, and may thus be a means by which some external appraisal of the civil value of defence research is at last attained, it is inevitable that the boundaries will be fuzzy, and that the new unit's opinions will overlap with those of other organizations, the Advisory Board for the Research Councils in particular. Given its place within the bureaucracy, the new unit could powerfully influence the pattern of all publicly sponsored research.

So will the unit come to sensible conclusions? Even the passage of time may not be enough to tell, for the new unit (which still lacks a head) will almost certainly operate behind closed doors. And because its existence springs from the British government's well-known impatience with the notion that there is no way of telling in advance what investments in research are likely to be profitable, there can be no assurance that the unit will recognize as impediments to its work the two serious objections to over-closely directed research: the circumstance that successful innovation requires that companies should be both technically well-equipped and well-placed in the market and the temptation (from which civil servants are not immune) to be swept up by fashion. Mr Baker's own first claim on public attention, his advocacy of information technology as a means not merely of making Britain prosperous but of curing unemployment at the same time, was plainly timely in the early years of this government, but has not produced the expected benefits for the simple reason that Britain lacks sufficient technical skill to make full use of the opportunities that abound in information technology. It is especially shocking that the University Grants Committee, in its recent set of circulars to British universities, should have had to explain that the annual intake of students to engineering schools cannot be increased more quickly for lack of suitable school-leavers.

That is but one illustration of the truth that there is more to the problem of winning benefit from research than the backing of good ideas with sufficient funds. The most obvious pitfall for the new Cabinet Office unit is that it will be blind to pitfalls such as these. The danger is especially great because the unit's work will not necessarily be public. Even at this late stage, there may be a case for changing that.

Soviet inquiry

Chernobyl accident is blamed on human error

THE Chernobyl disaster was due to human factors or, in the words of the official dispatch, "a whole series of crude violations of the regulations for the operation of reactor installations". Such was the decision of a special session of the Politburo last weekend, after considering the report of the governmental commission that has been working at Chernobyl since the accident on 26 April. The full text of the report is expected to be published in mid-August.

According to the Politburo statement, during the night of 25/26 April, unauthorized investigations into the operating conditions of the turbogenerators were carried out on the Number 4 set, while it was out of service for a planned overhaul. Just what form these "experiments" took is unclear. The dispatch merely stated that the management and specialists of the power station had neither prepared themselves for the experiments nor coordinated them with the appropriate authorities, although they were legally bound to do so. Furthermore, there was no proper supervision of the experiments, nor were proper safety measures enforced while they were in progress. Several high officials have been dismissed for allowing this situation of "irresponsibility, negligence and lack of discipline" to develop.

By putting the blame squarely on the Chernobyl crew, the report would seem to exonerate the Soviet nuclear power programme and, in particular, the design of the RBMK reactor. But the unauthorized, unsupervised "experiments" could possibly have a more ominous explanation. In mid-May, some three weeks after the accident, there were some veiled references in the Soviet media to "experiments" at Chernobyl, followed by unattributed and unofficial reports that a malfunction on the Number 4 reactor had developed on the afternoon of 25 April, and that an emergency crew was still struggling to close it down when the explosion occurred. In this case, the "experiments" would refer to unauthorized or incorrect shutdown procedures, possibly undertaken as a last resort. In all events, the Politburo statement still fails to explain how an experiment with the turbogenerator could cause an explosion in the reactor.

Although the report was, presumably, completed only shortly before the Politburo meeting, the Soviet Procurator's Office has already instituted criminal proceedings against "the persons guilty of the accident at Chernobyl". In view of Mr Gorbachev's current drive for "open-

ness", the trial is likely to be accorded maximum publicity. The Politburo statement outlines the charges against the accused: 28 people dead, damage to the health of a large number of people, including 203 cases of radiation sickness so far, the cost of large-scale prophylactic work (including medical checks on several hundred thousand people), 1,000 km² of agricultural land taken out of production, the closure of various enterprises, the cost of evacuation and the rehousing of the evacuees, the loss of power production. The direct losses due to the accident are estimated at 2,000 thousand million roubles.

For the moment, the Politburo seems more concerned to ensure that such negligence will not occur again. Four senior officials have been dismissed: Evgenii Kulov, chairman of the state committee for safety in the nuclear power industry, G.A. Shasharin, a deputy minister of power and electrification, Aleksandr Meshkov, a first deputy minister of medium engineering, and Ivan Emelyanov, a deputy director of a research and development institute. In addition, all have been subjected to "rigorous Party penalties", as has also Bryukhanov, the former director of the Chernobyl power station who was dismissed in May

The Minister for Power and Electrification, Anatolii Mayorets, was allowed to retain his post, but suffered a Party reprimand, and the public humiliation of being told that the Politburo had taken into account that he had only recently been appointed to the job, and that, "if he did not draw the appropriate conclusions", he would suffer a more severe penalty.

A new All-Union Ministry of Nuclear Energy has been established, in order to "raise the level of management and responsibility" in the nuclear power industry, and plans are under way for the retraining and requalification of nuclear power personnel. The use of simulators in training programmes is to be expanded, presumably to familiarize personnel with emergency procedures.

Furthermore, although the RBMK reactor design appears to have been officially exonerated, the Politburo has issued an urgent "demand" to all ministries and departments that they should draw up and implement additional measures to ensure the safety of existing reactors — and an appeal to scientists of the world to cooperate in developing a new generation of fission and, in the longer term, fusion reactors.

Vera Rich

US and Pakistan

Agreement on technology

Washington

THE United States and Pakistan have signed an agreement to establish a framework for trade in high technology goods. The agreement will make it easier for Pakistan to obtain mainframe computers and modern telecommunications equipment but will also provide specific assurance that Pakistan will neither divert the goods to other countries, nor use them in ways not approved by the United States.

Pakistan Foreign Minister Yaqub Khan and US Secretary of State George Shultz signed the agreement at the White House last week during the visit of Prime Minister Mohammad Khan Junejo. Last year the United States signed a similar memorandum of understanding with India during Mr Rajiv Gandhi's trip to Washington. The Indian agreement has far greater economic significance than that being worked out with Pakistan. Trade with India amounts to approximately \$1,600 million per year, according to Commerce Department figures, and something like \$75 million of that is in high technology equipment, including computers.

By contrast, trade with Pakistan amounts to only \$350-400 million per year, with most of that consisting of aircraft, soya bean oil and heavy industrial equipment. According to a Commerce Department official, Pakistan is just beginning to automate its government, and with no domestic computer industry it will have to import everything it needs.

But the real significance of the Pakistan agreement may be political. Ken Flamm, a research associate at the Brookings Institution in Washington, says that the trade agreement will smoothe the Pakistani feathers, ruffled by the lack of an arrangement such as that already offered to India. At the same time it will give the United States some control over the way in which the high technology equipment is

The United States is primarily worried that Pakistan might use computers obtained under the agreement to further a nuclear weapons programme. While the United States does not believe that Pakistan now possesses nuclear weapons, if takes the view that Pakistan could produce such weapons in a fairly short space of time. Prime Minister June to took some pains during his visit to emphasize the peaceful nature of Pakistan's nuclear programme. A joint statement issued by the two governments affirmed the Prime Minister's support of "US efforts to promote arms control and the non-proliferation of nuclear weapons". Joseph Palca **AIDS**

Confused ethics of blood testing

Will the publication this month of the results of compulsory blood tests for the acquired immune deficiency syndrome (AIDS) virus in potential military recruits in the United States has provided valuable, and to some extent disturbing, information on the spread of the virus, monitoring attempts in Britain are foundering on ethical and bureacratic rocks,

According to Sir Richard Doll, who has been asked by the British Medical Research Council to try to overcome the problems, all concerned are agreed that it would be unethical to take blood specifically for AIDS testing without informing those being tested of the purpose and result of the test. But the contentious question is whether the testing of blood samples taken for completely different purposes should be allowed.

Those who argue against such tests do so on the grounds that it would be unethical not to pass on the result of positive tests to the individuals concerned and yet unethical also to inform them because of the lack of prior consent. Those for whom the need to monitor the spread of the virus is paramount advocate that tests are carried out in an anonymous way so that it would be literally impossible to identify the individual that provided the blood sample. The justification for brushing the ethical problem under the carpet is that without information on the spread of the virus, it will be hard to persuade those at risk, including politicians, of the need for preventive measures.

As sexual transmission is the only way by which the virus can spread in the general population, it is necessary only to monitor blood samples from sexually active groups. One obvious source of such samples for anonymous testing would be antenatal clinics, but the Royal College of Obstetricians and Gynaecologists has objected to the idea. Another source being investigated is sexually-transmitted disease clinics, which have the advantage of including both sexes.

At present, the compulsory tests on potential blood donors provide the only source of information on the spread of the AIDS virus in the British population at large. Among 140,000 potential new donors tested between February and May this year, 7 individuals (or 0.05 per thousand) had a positive test. From October 1985, when the testing began, until May 1986, the rate was 0.02 per thousand but it is impossible to determine the rate per donor, according to Dr Harold Gunson, who collates the figures, because a substantial but unknown number of donors have given blood on more than one occasion during that period.

Prevalence among new donors is the

best figure to monitor for a trend but none is yet discernible, says Gunson, who is in the process of determining the sex and age distribution of the donor pool so that prevalences can also be worked out on that basis. The overall prevalence among UK blood donors is about 20-fold less than it was in August 1985 in the United States, the latest period for which figures are available.

The UK Ministry of Defence is opposed to the compulsory testing of potential military recruits. But in the United States that source has provided valuable figures on the prevalence of the virus in a sexually active heterosexual population.

Figures published in the 4 July Morbidity and Mortality Weekly Report show that the overall prevalence from October

1985 to March 1986 was 1.4 per thousand Figures varied widely by region and age group, ranging from 0.2 to 10.1 per thousand. The latter figure was for those of 26 or more in the central states on the Atlantic seaboard. At last month's huge AIDS conference in Paris, a figure of 20 per thousand was given for 18-25 year old recruits from Manhattan. Just over 300,000 potential recruits have been tested overall, with 459 positive results. The prevalence rate in males was three times that of females.

Seropositive applicants are excluded from military service, illustrating the growing discrimination that discourages people from agreeing to be tested and physicians from the prospect of having to inform anyone who has not specifically agreed to be tested of a positive result. Exclusion from life insurance and the possibility of losing one's job are added discouragements. **Peter Newmark**

Japan

Islanders put environment first

JAPAN'S Liberal Democratic Party (LDP) won a landslide victory throughout Japan in the double election on 6 July, except in Miyakejima, a tiny Pacific Island south of Tokyo, where the party suffered a crushing setback. Local and worldwide opposition from environmentalists to government plans to build a US military airfield on the island probably helped to sway

Miyakejima is an idyllic volcanic isle blessed with coral reefs, luxuriant tropical vegetation and two rare endemic species of bird, the Izu Island thrush (Turdus celaenops) and Ijima's willow warbler (Phylloscops ijimae). But if military planners have their way, the island will become an "aircraft carrier" for US Navy warplanes to practice night landing.

The local islanders, however, have put up dogged resistance to the government's plan. All attempts by the Defense Agency to hold public hearings on the issue have failed and two island assemblymen have been threatened with recall for failing to voice their opposition to the airfield. In the general election the Japan Socialist Party won easily over LDP with a vote double that of the previous election. International support for the islanders cause has grown rapidly and they can now count British royalty amongst their allies.

In late May, the Wild Bird Society of Japan reported that the Duke of Edinburgh, president of the World Wildlife Fund, had written to Prime Minister Yasuhiro Nakasone and the US Department of Defense appealing for the plan to be called off to protect wildlife in the island. Following this the International Council for Bird Preservation passed a resolution in June opposing the airfield's construction.

The Environment Agency carried out a survey in the area of the planned construction after a volcanic eruption in 1983 and concluded that "artificial objects would destroy the area if put up in defiance with harmony of the scenery". But the agency has yet to clarify its official position.

Numerous LDP delegations have visited the island to try and woo the islanders with promises of investment. But to no avail. As one islander put it: "important people from the LDP say they will make the island a 'mountain of treasure' but the island is already a mountain of treasures"

David Swinbanks

More dead penguins

THE mysterious mortality of rockhopper and gentoo penguins observed in the Falkland Islands (see Nature 322, 4; 1986) has now spread to Argentina. But the Argentine National Atomic Energy Commission (CNEA) has ruled out the possibility, suggested at a press conference at the Soviet Embassy in Buenos Aires, that radioactivity is involved. According to the Soviets. the four British ships sunk during the 1982 Falklands conflict had been carrying nuclear weapons, the casings of which had leaked, contaminating the waters. The CNEA scientists, however, are preserving a proper academic detachment on the issue. Asked to comment on the deaths of some 300 penguins near Piero Deseado, they stated categorically that, even if some radioactive material had escaped into the sea, the concentration would have been far too low to be dangerous. Vera Rich

Engineered organisms

Confusion over European rules

THE announcement this week of a new and supposedly safe vaccine against rabies (see pages 304 and 373) may bring to a head a simmering conflict in Europe over whether to permit the release of genetically engineered organisms.

The new vaccine is a version of the vaccinia virus, which is related to smallpox but much less dangerous, engineered to express a protein from the coat of the rabies virus, and thus create immunity in any creature inoculated with the vaccine. Target populations are foxes in Europe and raccoons on the east coast of the United States. Both, in principle, could be fed the vaccine in infected bait.

Developed by the French genetic engineering company Transgène in Strasbourg, the vaccine will be commercialized by Mérieux of Lyons, where chief scientist Philippe Desmettre said last week that there are no immediate plans for field trials. French regulations require approval of such trials by the ministries of health and agriculture, but Mérieux has not so far applied for permission. The company has supplied vaccine for tests by the Wistar Institute in Philadelphia, but use of the vaccine in the wild is likely to take place in Europe first, said Desmettre

In Europe, there is no general agreement on how to regulate field trials. Denmark has jumped the gun and already imposed controls; in West Germany and

in the European Parliament, the Green Party is pressing for action to prevent the release of genetically engineered organisms, but in Britain, France, the Netherlands and elsewhere there seems little concern. In the midst of this confusion, the European Commission is attempting to create a little order rather than see yet another European market divided by multifarious regulations. But the Commission itself is a house divided, with those representing scientific, industrial and agricultural interests in conflict with the environment directorate.

Nevertheless, Commission officials said last week that a paper on the problem is now circulating and is likely to be presented to the European Council of Ministers towards the end of this month. This, however, would merely alert ministers that there is an issue to be discussed and it is not even clear at what council the issue would be thrashed out. The European Parliament, whose irritant value — if not real power — is steadily increasing in the European pantheon, will debate a hardhitting report on the same issues by Dutch socialist Phili Viehoff, later this year. Not only will Viehoff present her report, but six other committees covering biotechnology and the environment will also table positions, leading to what could be an acrimonious debate.

The Commission itself is aiming to sub-

mit joint safety proposals to Council by April next year — Denmark's "banning" of the release of engineered organisms, hailed as a success by Europe's greens, is not a major obstacle, for trials are not truly "banned" although they must be referred to the government for approval.

In the next few weeks, a major report should appear by the Organisation for Economic Cooperation and Development (OECD) in Paris on "safety considerations in the use of recombinant DNA". It is said by those who have seen it to be a "very reassuring report", arguing that risks are small. Britain is expected to base its own guidelines on the OECD recommendations.

Robert Walgate

Chinese science

Back to your work units

CHINA is to introduce new rules on foreign study. Although the number of people sent abroad to study at government expense is to remain at its present level, the mix will be different. There will be more emphasis on those applied disciplines necessary for China's modernization programme, and less opportunity for students to go abroad immediately after completing their first degrees. On the other hand, the number of people with masters' degrees who go abroad to work for a doctorate will be increased. Students who go abroad at their own expense (mainly the children of top officials, plus the lucky few who have wealthy relatives abroad) will be given greater "guidance" to ensure that their chosen studies also conform with the state plan.

The changes are meant to ensure a sufficient supply of trained personnel to satisfy the demands of "work units" throughout the country. "Poaching" of graduates from their assigned jobs is now a problem in China. Understaffed enterprises frequently offer substantial and fringe benefits to well-trained recruits; they even advertise in newsletters which flourish in spite of official disapproval. The new rules should frustrate the "poachers". From this year onward, most of the quotas for government-sponsored students will be assigned to enterprises and work units in need of trained staff; the latter will then select who is to go abroad.

Foreign study, it is stressed, is not meant to be simply a means of self-betterment. Those who obtain a doctoral degree abroad will not now be permitted to stay on just to acquire a still higher qualification. Instead, they will have to return to an appropriate job in China for several years, before being sent abroad again. This, it is explained, will better help them coordinate their studies with China's needs.

Space antiques hedge against inflation

Washington

"MUSEUM piece" is an apt term for a satellite the US Air Force plans to launch next October. Although it is now called the Polar Beacon Experiment and Auroral Research (Polar BEAR) satellite, for eight years it hung in the Smithsonian Institution's National Air and Space Museum in Washington as a Transit 5A, an example of an early navigational satellite.

The satellite's transformation came at the hands of the Johns Hopkins University Applied Physics Laboratory (APL) in Laurel, Maryland. APL, the contractor for Polar BEAR, realized that the satellite shared many components with the Transit 5A and Oscar satellites it had built in the 1960s and early 1970s for the Air Force. In 1975, the Smithsonian was looking for an example of an early navigational satellite to hang in its new museum. APL offered an Oscar 17, with flight-tested components, that was made to look like the earlier Transit 5A. To get its Oscar satellite back, APL offered the Air and Space Museum an untested back-up Transit 5A satellite that had been on display at APL. By using the older parts, a saving of about \$2 million was

achieved on the \$15 million bill for the satellite. Much of the saving came from the solar panels. All but one of the thousands of solar cells on the panels worked perfectly when APL tested them.

A Scout launch vehicle will carry the Polar BEAR satellite into a circular polar orbit from Vandenberg Air Force Base in California. The Air Force will use the satellite for experiments to improve communications over the poles. In addition, an Auroral Imaging Remote Sensor will study the aurora borealis.

This is not the first time that the Air and Space Museum has transferred an exhibition piece to active duty. The University of Iowa borrowed part of the attitude control system on the museum's Applications Technology Satellite for its Plasma Diagnostic Package that flew aboard Spacelab 2 on the shuttle last summer. A foot restraint system, once used on Skylab and donated by the National Aeronautics and Space Administration (NASA) to the museum was used by shuttle astronauts. NASA also borrowed Skylab's shower, but only for developmental studies for the manned Joseph Palca Space Station.

OECD indicators

Science statistics prove slippery

RESULTS for 1983 and data for a few countries for 1984–85 suggest a "definite slowing down" of research and development spending in the industrialized countries, according to the latest "science and technology indicators" report* by the Organisation for Economic Cooperation and Development (OECD).

Some doubts remain about the figures. The rate at which data are accumulated, checked and reported by governments means that most data in the OECD tables end in 1983 and the latest trends are hard to spot. Between 1979 and 1983, research and development expenditure in the OECD states (most of the non-Communist industrial world from the United States to Japan) had been rising rapidly.

Other points made by the OECD study are that up to 1983:

Research and development became

Getting tough on doctorates

How to make do with little might be thought of as the theme of the new corporate plan from Britain's Economic and Social Research Council. Taking inflation into account, the £23.6 million budget is lower than it has been for a decade and ways have to be found to be more selective.

The major move is to take £2 million from the budget for postgraduate awards and shift it to research over the next five years. The shift is largely dictated by complaints over the appalling performance of doctoral students supported by the council. Only 20 per cent of students submit theses within four years and around half never write up their research at all.

The council is now to take a tough stand. Institutions where fewer than 10 per cent of students submit theses within four years will be banned from taking on new students for two years. By 1989, 60 per cent of students must submit theses before new funds will be awarded. No action is planned against individual students: supervisors are to be held responsible. One hundred studentships will go over the next two years.

More money is to go into research but the council is to tighten the reins. Expenditure is to be concentrated on "research initiatives" where the council determines what will be done rather than on research grants where researchers choose for themselves. While this gives some assurance of the quality of research, it does, as the plan points out, lessen the chances of throwing up "original ideas with high future value". Economic and social charge in contemporary Britain is the current key research area.

Alun Anderson

more concentrated in the largest countries.

- Japanese research and development grew faster than that in any other country.
- The United States remained the largest research performer, with the countries of the European Economic Community (EEC) second.
- Japan spent "substantially less" than the EEC countries in total.
- Research and development kept pace with or exceeded economic growth in most countries. Exceptions are Switzerland, Australia and the United Kingdom during 1981–83.
- Most OECD government funding went to defence and space programmes.
- Basic research received about 15 per cent of total OECD research and development funds in 1981.
- Industry increased its role in relation to government as a research and development spender, exept in Switzerland.

The value of OECD's figures on higher education research is questionable, however, according to a British research team which has just reported to the British Advisory Board to the Research Councils (ABRC). The report will not be published until the autumn, but its authors have indicated that OECD data are limited by their reliance on national government interpretations of the "Frascati agreement" of the 1960s, which was supposed to codify the reporting and comparison of national research statistics but has since lost its real effectiveness due to changes in institutional structures. Governments may also stretch the meanings of terms to suit their political convenience.

Some of the more glaring problems thrown up by the British work, which relates only to higher education, are in the varying definition of universities, and the attributions of government laboratory spending. Japan, apparently, attributes half of the total budgets (including salaries) of its 1,000 or so colleges, few of which are at full university level, to "research"; and the United States lumps the research of its big defence laboratories such as Lawrence Livermore and Los Alamos in with that of the universities. In the DM 20,000 million German university accounts DM 5,000 million is distributed in part as research, but turns out on analysis to be income from hospital beds, through certain medical universities' private health schemes.

The most anomalous of the six countries analysed by the British group is Japan, but European countries as a whole also suffer in a major way by excluding all international research facilities (such as the Organisation for European Nuclear Research, CERN) from their higher educa-

tion statistics. (The United States, by contrast, includes its big science facilities such as Fermilab in its university figures.)

Altogether, the feeling in British science policy circles is that such anomalies allow the all-powerful Treasury to decry OECD figures which show declining research spending in Britain. That is why an independent, in-depth study was commissioned. It is believed to leave no escape from the conclusion that British research in the higher education sector has indeed been undergoing a relative decline — which is what, of course, everyone knew but could not prove.

Robert Walgate

Academician's Berlin arrest riddle

A PUZZLING diplomatic incident involving East and West Germany was resolved on Monday, when the West German authorities decided it would not be in the public interest to prefer charges against Professor Herbert Meissner, deputy general secretary of the East German Academy of Sciences.

Meissner had been on what the East Germans described as a routine business trip to West Berlin, travelling on a diplomatic passport, when he was arrested for shop-lifting. He was subsequently taken to Munich where he was questioned by BND, the West German intelligence service. He then, in some unexplained way, appeared in Bonn, at the East German permanent mission. The head of the mission, Herr Lothar Glienke, then lodged a strong protest at the West German Chancellor's office.

According to Glienke, the charges against Meissner were totally fabricated, his journey to Munich was "abduction", and his interview with BND had included the use of pressure and blackmail to try to make him betray his country. Glienke had therefore demanded an immediate guarantee from the chancellor's office that Meissner would be able to return to East Germany immediately, and that his diplomatic passport and personal papers would be returned.

The West Germans, however, maintain that the shoplifting charge was genuine, and that instead of answering the questions of the West German police, Meissner had demanded to be taken to BND in Munich, saying that he wanted to defect. A spokesman for the West German government, Herr Friedhelm Ost, stated, moreover, that Meissner combined his duties for the academy with work for the East German Ministry of State Security.

Either explanation of Meissner's movements last week leaves a number of questions unanswered. The West German decision to drop charges will, however, presumably bury these questions in diplomatic obscurity. Vera Rich

UK universities

Research gradings stir emotions

British university departments that received poor marks in the recent University Grants Committee (UGC)'s assessment of research may have a chance to be re-rated if they can do better. Sir Peter Swinnerton-Dyer, chairman of UGC, spoke of the need for machinery to pick up those that improve "dramatically" in giving evidence to the House of Lords Select Committee on Science and Technology last week. But no general reassessment is expected for 4–5 years and 15 per cent of the money available to the universities is now to be distributed according to the quality of research.

The assessment has provoked considerable outrage. Departmental groups have been rated as below average, average, above average or "starred" — of outstanding merit by international standards. But angry academics writing to *The Times* describe the assessment as "wholly lacking in intellectual credibility" and its methodology as "questionable", "extremely crude" and "seriously defective".

Many researchers even protest that they have been given no indication of how the ratings were arrived at. But the method was actually straightforward: "individual judgement helped by some factual records", as a member of UGC put it. Last year, a letter was sent to all universities requesting short (500-600 word) profiles of their departmental "cost centres" together with a list of five recent publications demonstrating the quality of research in each cost centre. Cost centres are larger units than departments: mathematics and chemistry have their own cost centres, but the biological sciences are divided into biochemistry and "other biological sciences", and the physical sciences into physics and "other physical sciences".

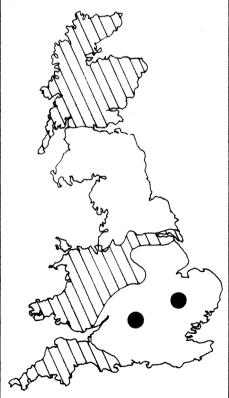
UGC's committees (for physics, biology, and so on), each with some 12-15 members then divided up into smaller subcommittees and parcelled out the replies. Further evidence was added: the number of grants and research studentships gained from the research councils over the past three years, the level of support from the large medical charities, the numbers of Royal Society fellowships held, "new blood" posts gained over the past three years and money gained from industry. Opinions were sought and meetings convened with the research councils which gave their private rather than corporate views.

At the end of this first stage, cost centres were scored on a scale of 1 to 5; where there were many departments in one cost centre (zoology, genetics and biology are all "other biological sciences"), some subcommittees scored individual departments. Final adjustments were made at

meetings of whole committees where personal knowledge of outstanding researchers, or those that had slipped from their prime, counted for much. It was then decided not to mention specifically the below-average departments, nor to say how below average they were, but to issue just three ratings and the "stars".

Given the way the assessment was done, huge surprises cannot be expected; en masse the results confirm popular prejudice (see map). In the celtic north and west and parts of the Midlands, below-average cost centres are in the majority, often by a very considerable margin. London (with a few exceptions), the south and north of England and Edinburgh and Glasgow are in the black. Towering above all are Oxford and Cambridge, the latter with a staggering 32 starred departments and none below average.

But it is not all so simple. Even universities with poor overall ratings may contain departments of excellence — Dundee with stars for biochemistry and applied mathematics for example. Do these indicate a few individuals' outstanding efforts? And there are whole universities which go against trends. Warwick had seven stars



In the hatched areas universities have less than one above average cost centre for each one below average; at the two black dots (Oxford and Cambridge) there are nineteen or more above average for each below average; in other areas the ratio varies from one to ten above average (University of Warwick) to below average.

and no below-average departments: does this suggest others might learn from its management?

Critics, on the other hand, would say that nothing useful can be gained from the assessment. The chief objection is that it was grossly unfair to look at cost centres rather than individual departments. Several different departments often had to share a single report and pool the five examples of their recent work, so that some researchers went virtually unrepresented. The problem is most severe for small arts departments where, as one historian put it, research on Ancient Greece, might be judged from a work on modern Europe.

Sir Peter Swinnerton-Dyer agrees that the assessment results have not been "perfect" here. Small departments may also have been penalized because there seems to have been little effort to look at productivity per staff member rather than a few examples of excellence. Science Citation Index, with weighting for quality of the journal cited, might have provided a database.

Another criticism is that the style of a university has not been taken into account. Salford, for example, scores rather poorly but has been held up by British Prime Minister Mrs Margaret Thatcher as a model university for its success in creating jobs. A cut in funding because it fails to reach certain research norms may be regarded as an implicit judgement of its aims. Other university departments simply feel they have been wholly misjudged — and can provide evidence that they should be rated differently. But no general appeal mechanism is planned.

Perhaps the most telling criticisms of the assessment are of the effect it may have. What made the assessment necessary is that funds need to be concentrated on research that will prove outstanding. A monolithic judgement may not do this but simply fulfil its own prophecies. Departments that have, in the past, been poorly funded by the research councils are likely to have gained poor ratings and will now find life even more difficult as they lose UGC funds. The judgement of UGC may make it harder for them to find funds from other sources too.

But, if it is original ideas that should be funded, it can be argued that the more independent sources of funds there are the better. How will poorly rated departments, among them those that contain a few excellent people, now get back on their feet? Sir Peter advised that universities should continue to fund the good and pick out for help those that can improve. He saw little to be gained by putting money into bad departments. Harsh advice perhaps, but the chairman of UGC knows, perhaps better than anyone, how little money there is to spare for university research. Alun Anderson

SDI

UK scientists should take care

British scientists thinking of participating in Strategic Defense Initiative (SDI) research might do well to consider their legal position carefully. An incident in the United States in which basic research results were suddenly classified and what has recently become known about British Ministry of Defence (MoD) guidelines suggest that scientists may find it hard to protect their rights of free publication.

The terms of British involvement in SDI are enshrined in a memorandum of understanding between the British and United States governments. A research contract is placed by the SDI Organization (SDIO) in Washington, an office separate from the Pentagon, in one of five classified, military Project Areas, or in the \$100 million Innovative Science and Technology (IST) programme for basic science.

Exactly what regulations cover the latter programme are unclear. The SDI Participation Office in the MoD promises scientists the right to publish work that is also receiving SDI funding, with the provision that a copy of the paper of presentation is delivered to it and SDIO in Washington before publication.

Fundamental research will thus be free, as has often been claimed by the university liaison officer of the Ministry of Defence SDI office, George Gallagher Daggitt. But will this always be true? In response to a letter from Paul Labbett (8 April 1986), research contracts officer at Imperial College, London, Daggitt wrote: "It is however conceivable that exceptions to this rule could arise if there is the likelihood of disclosing operational capabilities and performance characteristics of developing military systems. In this case the contract for the work will clearly stipulate that responsibility for the release of information lies with the sponsoring office" (that is, SDIO in Washington).

The case of a US high-energy physicist, Dr Andrew Sessler, shows that successful SDI research can easily be classified. His team's work on the free electron laser was guaranteed open for publication until he showed how gigawatt power outputs were possible in March 1985. SDIO immediately classified the entire experiment and the results. The work, largely paid for by the Department of Energy, was part of the civil fusion reactor programme. But as Sessler took a small grant from SDIO it became the sponsor. The work was classified top secret (Sessler and his staff were threatened with expulsion and jail if they released details) for 13 months until April this year, when the results alone were de-classified. The experimental details are still classified.

SDIO is free to classify what it sees fit. The memorandum can offer no guarantees that fundamental science will be open for publication. MoD Guidelines say a review procedure is available "so that appropriate representations can be made". But SDIO in Washington has the final say. A significant number of British scientists have applied for funding under IST: there are 36 individual proposals, and 2 consortia.

The memorandum embodies the principle that there will be no guaranteed work although the figure of \$1,500 million was floated early on. Days before the memorandum of understanding was signed, the British draft contained a schedule of work in three categories: commercial work from research into manufacture worth \$1,000 million, government contracts for research worth \$250 million and university research up to \$250 million. How much will British companies and individual researchers actually gain in SD1? From \$50 to \$100 million in total, estimates MoD.

MoD can identify five commercial contracts worth a total of \$1 million. Another 12 contracts are in negotiation, each worth around \$2 million. The first round of IST proposals might bring another \$10 million. Government-to-government business could rise from the present \$15 million to \$50 million.

The government agreed a special research contract for the work in which it is the principal or subcontractor. The Letter of Offer and Acceptance negoti-

ated to cover the first two contracts, "written according to patent law" according to the SDI Office in the MoD, acts as a standard contract for SDI research and is said to safeguard the rights of ownership of technology. The letter is secret and applies only to government work. Yet it is said to embody the best definition of intellectual property right, and to safeguard technology produced in SDI for the researcher concerned.

Why should it be secret? And why cannot other researchers use the definition of intellectual property right? MoD says it is for private individuals and companies to get the best deal they can for themselves even though the memorandum of understanding was intended to act as an umbrella agreement for all participants. The Americans insisted on this arrangement.

Government work can only be research, not manufacture, and must stay within the terms of the 1972 Anti-Ballistic Missile (ABM) Treaty according to the memorandum of understanding.

A joint MoD/Foreign Office Arms Control Unit has a veto on government research proposals that threaten to stray beyond other treaty obligations. If a British company were to design, prototype, test or build a component of SDI, however, it is unclear in the memorandum whether or not such proposals could be vetoed.

The right to own technology originating in a research contract funded either by SDIO (as basic science), or in a subcontract with a US company (on project work), is not defined in the memorandum. This is thought to have contributed to the

UK star wars consortium launched

A CONSORTIUM of eleven UK defence contractors has bid jointly for the first Strategic Defense Initiative (SDI) contract worth \$9.9 million, the European Architecture Study, let to the Ministry of Defence by the Strategic Defense Initiative Organization (SDIO) in Washington, DC.

Ian Sutherland, a director of Marconi, said that this "team" will share out research work if it secures the entire study and would work together as "UK Ltd" on the SDI contracts that follow on. These could be worth tens of millions of dollars.

The group includes defence contractors GEC-Marconi, British Aerospace, Barr & Stroud and Shorts, electronics companies Thorn EMI, Racal and Ferranti, the Royal Ordnance Factory, and computer software houses CAP Scientific, Scicon and Software Sciences.

The architecture study will consider how an SDI system could operate in Europe. Four subcontracts will be awarded, probably in September, in computer systems, weapons, battle management and command, control and communication. Few contracts have yet been awarded to British companies. Sutherland said Marconi has sold "£4 million worth of hardware", including exotic electronic components such as thyratrons (which switch very high currents quickly) and silicon-on-sapphire semiconductors (which are relatively unaffected by radiation). In addition, Marconi Projects has two research subcontracts worth under \$250,000.

Up to 12 other proposals are in the pipeline, including those for electromagnetic guns, battle management, lethality and target hardening, very high speed integrated circuits, high-energy lasers, advanced sensors and particle beams.

SDIO in Washington has also requested access to the Ministry of Defence's results from the Teal Ruby experiment which considered strategic defence from short-range and mid-range missile attack. But the Australian government, which collaborated in the experiment, is set against SDI participation and Australian permission is necessary before results can be released.

Paul Walton

low take-up of work by companies. Background research, that is existing company data on intellectual property rights defined by patent or copyright, can be protected. But foreground research, that produced during a funded contract, is not protected by the memorandum.

As things stand, a US prime contractor would be legally entitled (under US law) to patent foreground research, denying use to the originator for 17 years. This patent defines the owner as the body which pays, not the individual or organization which completes the research.

A further problem for British researchers is that the memorandum does not waive those items of US law, in particular the Export Administration Act, that make



At least we've proved the existence of Black Holes ...

it difficult for items of technology or technical data in the form of proposals or descriptions to be passed freely between Britain and the United States.

Technology transfer law still applies to SDI work. "Both Governments will make every effort to process within 30 days requests for export licences for technical data packages or other controlled information for direct bidding", according to the memorandum. In practice, clearance can take several months, by which time an SDI contract will have been let. Visits to secure sites, to closed conferences, or to discuss classified information with a partner in the United States requires prior clearance, and full vetting, of any person by the US authorities. It is likely that positive vetting will be carried out by US embassy staff in the United Kingdom. Most British citizens will be required to sign the Official Secrets Act.

The memorandum is "secret in perpituity", or top secret. A full debate on British participation has been requested by Labour MP Tam Dalyell but denied on the basis that the United Kingdom has negotiated a good deal which the United States does not wish other allies to know of in detail. All the UK opposition parties, Labour, Liberal and Social Democrats, have pledged that they will do away with the memorandum and pull out of SDI.

Paul Walton

US space

Shuttle faces more delay

Washington

THE US National Aeronautics and Space Administration (NASA) announced last week that shuttle flights will not now resume before 1988, despite earlier estimates that the shuttle might fly again as soon as next summer. Although disappointing, the delay, say NASA officials, is necessary to complete a review of the design and testing of the solid rocket motors (SRMs) responsible for last January's shuttle accident.

In a report requested by President Reagan, NASA spelled out its plans for implementing the recommendation of the Rogers Commission on the accident (see Nature 321, 637; 1986). NASA hopes to redesign the SRMs so that existing hardware can be used, but there are alternatives using completely new hardware in case that plan is frustrated. At NASA's request, the National Research Council (NRC) has established an independent oversight group, chaired by H. Guyford Stever, to superintend the redesign.

Other hardware modifications recommended by the Rogers Commission included improvements in the tyre, brake and nose-wheel steering systems. NASA says that some of those improvements were under way at the time of the accident, and that the other modifications are in hand. Until the improvements are judged a success, the shuttle will continue to land at Edwards Air Force Base in California, where there is a longer landing strip. Ultimately NASA hopes to land shuttles at the Kennedy Space Center in Florida where they are launched. NASA also plans a thorough review of all critical safety items on the shuttle, and a second NRC oversight panel is being formed to watch over that process as well. Not surprisingly, safety issues are uppermost in the minds of most NASA officials. Waivers allowing marginal parts to be used in launches will be few and far between, says one NASA official.

NASA has also begun two separate reviews of its much criticized management practices. One will look at the shuttle programme, the other at NASA as a whole. Many at NASA involved in the shuttle have either left the agency or been transferred since the accident. The latest casualty is Lawrence Mulloy, director of the SRM programme at the beginning of the year, who resigned last week after having been transferred from that programme.

NASA has yet to make a final decision about crew escape systems, but preliminary conclusions suggest that no approach will provide a safe escape route under all conditions. But further attention is to be paid to procedures for aborting launches, including one scheme for transatlantic escape.

The Rogers Commission pointed out that total reliance on the shuttle for launches had put heavy pressure on NASA to increase its launch rate: NASA hopes that the pressure will be partly reduced by the new policies it has adopted on the choice of cargo for the shuttle bay, but it is also now backing the claims of other agencies that there should be a mixed fleet of launch vehicles, including expendable rockets. Responding to a request from Congress, NASA has asked NRC to form a third panel that will evaluate launch rates and the balance between manned and unmanned launch systems. Edward David, president of Exxon Research and Engineering Company, will chair this committee

Joseph Palca

Now it's save French science!

FRENCH scientists appear to be getting more and more like their British colleagues — absolutely desperate. But in one way the French are going further. Discovering that appeals to their own government over recent cuts have failed (no doubt in part because, as it is said, the new science minister is uninterested in politics), they have gone to the lengths of producing an international petition: "Save CNRS" (the principal French research council).

"We the undersigned members of the international scientific community", the petition reads, "wish to express our grave concern regarding the policy followed by the French government. The policy has already resulted in: budget cuts (more than FF 4,000 million — £400 million); 25 per cent reductions in new posts for 1986; a

decision to cut the number of scientists employed by government in 1987; the smallest ratio of research spending to gross national product in the West; and the suppression of the CNRS Comité National." The Comité is a decision-making body whose loss brings to a standstill the whole administrative machinery of the CNRS—including the setting up of new posts and grants.

The petition calls for the French government to reinstate the Comité National, and reverse the new downward trend in jobs and cash for French science. What it fails to do, however, is to give an address to which to send the completed petition. But interested readers could always try the French Prime Minister, Jacques Chirac, at the Matignon... Robert Walgate

European research priorities

SIR-The Advisory Subgroup on Human Reproduction of the European Medical Research Council (EMRC)* has published recommendations for research related to in vitro fertilization and embryo transfer and has sought to identify priority areas in human reproduction research deemed particularly suitable for investigation by European scientists2

The subgroup has noted the decrease of financial support for human reproduction research, particularly in the development of new and safe methods for fertility regulation, from both the public and private sectors'. This contrasts strikingly with the recommendations for increased support for reproduction research by all sectors called for by 146 governments at the International Population conference in Mexico City in 1984, where particular emphasis was placed on the special needs of developing countries4.

The subgroup believes that the scientific community has a particular contribution to make to research on new methods for fertility regulation for three reasons: its well-established record in this field, its long-standing tradition of providing medical and scientific assistance to developing countries and the close collaboration between its medical research councils and the European pharmaceutical industry.

In order to facilitate this collaboration, the subgroup held a consultation with representatives of interested European pharmaceutical companies in October 1985. At a meeting of the subgroup alone in April 1986, the following recommendations, which represent the views of the subgroup and do not necessarily reflect the views of the industry participants in the earlier consultation, were drawn up.

- (1) Steps should be taken, separately and jointly, by both industry and the medical research councils to increase the priority given to research on new methods of fertility regulation and on related fundamental research.
- (2) The requirements for clinical trials of new contraceptive drugs and for the approval of such drugs for public use vary from country to country and are deemed unnecessarily complex in certain instances. The subgroup recommends that these requirements be modernized and standardized.
- (3) A marked increase in the number and magnitude of liability lawsuits has caused some companies to withdraw from the fertility regulation field, and is one of the primary reasons for decreased work in this field. The subgroup recommends that European MRCs and industry representatives should work together to forestall this problem which threatens progress in this
- (4) In view of the challenges confronting

science to develop new methods of fertility regulation, the subgroup recommends consideration of the establishment of a European funding mechanism for reproduction research, sponsored and funded by industry and the MRCs and dedicated to the support of European research and research training adapted to the jointly derived requirements of both the private and public sectors.

E. Nieschlag (Chairman of the EMRC Advisory Subgroup)

MPG Clinical Research Unit for Reproductive Medicine, Steinfurter Str. 107 4400 Münster, FRG

*The advisory subgroup includes: E. Nieschlag (chairman), Max Planck Clinical Research Unit for Reproductive Medi-cine, University of Münster; B.M. Baccetti, Institute of Zoology, University of Siena; L. Cedard, Maternite Cochin, Paris; P. Corfman, Special Programme of Research, Development and Research Training in Human Reproduction, World Health Organization, Geneva (observer); F. Haseltine, National Institute of Child Health and Human Development. Bethesda (observer); E.D.B. Johansson, Pharmacia AB, Uppsala; D.W. Lincoln, MRC Reproductive Biology Unit, Edinburgh: C. Robyn, Hôpital Universitaire Saint Pierre, Brussels; R. Vihko, Department of Clinical Chemistry, University of Oulu; G.H. Zeilmaker, Department of Endocrinology, Growth and Reproduction, Erasmus University, Rotterdam

- Lancet. II., 1187 (1983)
- Lancet, I, 1228 (1984). Atkinson, L.E., Lincoln R., Forrest J.D. Family Planning
- perspectives, 17, 196 (1985).
 Report of the International Conference on Population. United Nations Publication E/CONF. 76/19, New York

Henderson Island

SIR-In 1983 there was international concern when a strip-miner from West Virginia proposed to establish a settlement on Henderson Island in the Pitcairn group of the central South Pacific, as it was thought to be one of the few raised atolls still comparatively unaffected by human activity1. As much of the case for preserving the island depends upon its undisturbed state. we are now concerned to observe a statement in an influential journal that: "The recent discovery of several Polynesian occupational sites on Henderson' shows that the island had, in fact, been inhabited in prehistoric times. On the basis of vertebrate remains from one of these sites we can now show that this period of human occupancy was accompanied by extinction and a consequent decrease in the species diversity of the island... The biota of Henderson Island can thus no longer be regarded as being in an unaltered state."3

As this statement is liable to be quoted in support of further proposals for development of Henderson Island, it deserves some scrutiny.

The past Polynesian presence, which was already noted in our recent contribution on the birds of the island, had so little impact that it is difficult to detect. Its only observed effects appear to have been the

introduction of the Polynesian rat Rattus exulans, and perhaps some plants, and the possible extermination of some widespread but unobtrusive seabirds, whose survival may have been overlooked, and pigeons of the genus Ducula, attributed to two species because the wings were comparatively small whereas the jaw and legs were rather large.

The alternative possibility that instead of two additional species of pigeon occurring on one very small island alongside the small one which still survives, the pigeon bones may have belonged to a single large species showing the reduction in the wings common in insular birds, and also found in the flightless Henderson rail Porzana atra, which will be the next species at risk if the island is developed, is not discussed

The list of petrels of the genus Pterodroma reported to survive in the group3 does not agree with our experience⁴, and it is rather surprising that all the bones should be identified as P. alba when it is doubtful whether this is distinguishable osteologically from one of the other species which is now commoner, P. arminjoniana.

It is to be hoped that this contribution will not be allowed to count against the case for preserving the island, which is apparently still at risk.

W.R.P. BOURNE

Department of Zoology, The University. Aberdeen, UK

A.C.F. DAVID

Oak End, West Monkton, Taunton, Somerset, UK

- Fosberg, F.R., Sachet, M.-H. & Stoddart, D.R., Atoll Res. Bull. 272, 1–47, (1983).
- Binoto, Y.S. J. Soc. Ocean. 39, 57-67 (1983). Steadman, D.W. & Olson, S.L. Proc. nam. Acad. Sci. U.S.A. 82, 6191-6195 (1985).
- 4. Bourne, W.R.P. & David, A.C.F. Notornis 30, 233-252

More bright ideas

SIR-We read with interest of Greg Ojakangas's award-winning proposal to use a ROOPH (Readily Operative Overhead Protection by Hippos) in the event of nuclear attack (*Nature* 321, 373; 1986).

We wish to suggest the use of BOOBS (Blockade of Overhead Objects by Baby Seals) based on the same principle.

Canada could supply the animals (having an abundance of baby seals, especially in recent years) in return for protection. Use of an indigenous species has strategic and financial advantages, and, unlike hippos, baby seals are already cold-adapted for deployment at high altitudes or in winter (nuclear or otherwise).

> MARK RAGAN KATHY SCHWARTZENTRUBER

1141 Oxford Street, Halifax, Nova Scotia, Canada B3H 3Z1

Gentle warning on fractal fashions

The novel idea that fractal structures can support high-energy lattice vibrations may not be the philosophers' stone that some have suggested.

FRACTAL structures are understandably one of the captivating fashions of our times. Even without the proselytizing of B.b. Mandelbrot (as in The Fractal Geometry of Nature (Freeman, New York; 1983)), the subject would by now have been dragged into prominence by the host of practical applications to which it lends itself. The simplest problems are those of the aggregation of particles onto a growing aggregate, where there is now a host of demonstrations that the density of such a structure is a decreasing function of its size, most graphically described by means of a "dimension" smaller than that of the space in which it grows. But it is plain that biological applications must also abound. For are not large polymer molecules put together by the aggregation of monomers onto a growing backbone candidate fractal structures?

This line of enquiry has already been productive. Some polymer structures do indeed turn out to be fractal structures, while the suspicion has grown up that the properties of some important biological molecules are in many ways a consequence of their supposed inherent fractal character. But fashions that are too pervasive can also be misleading, and require occasional correction. That is the chief interest in an elegant paper by J.A. Krumhansl (Phys. Rev. Lett 56, 2696; 1986) of Cornell University which, in the gentlest manner, warns people against the tendency to look for fractal explanations everywhere.

Krumhansl's topic is also interesting and potentially important. His startingpoint is a series of speculations about the interaction in molecules such as those of haemoglobin of the central iron atoms with the surrounding ring of porphyrin rings and the protein structures to which they are in turn attached. Changing the spin states of the central iron atoms requires a substantial amount of energy, greater than that corresponding to the mostly low-energy vibrations of the usual protein chain. So how can a larger amount of energy be exchanged with a protein environment? Fashionably, there seems recently to have been a tendency to invoke fractal phenomena of a new kind, those pertaining to the vibration of fractal structures of various kinds.

The mere idea that it might be possible to calculate the vibration frequencies of a fractal structure is naturally surprising. To be sure, it should in principle be possible

to deal with any specific fractal structure provided there is enough computer power to hand. One common model is that in which the particles in an aggregate are replaced by masses (all of the same size) which are then supposedly connected to their neighbours with springs with identical elastic properties. Since most simulations of fractal structures begin life on an underlying lattice with well-defined properties, solving the vibrational problem is essentially a calculation of the vibrations of a lattice in which there are patches missing. And even though each different arrangement of patches should in principle give rise to a distinctive set of vibration frequencies, the fact that the geometrical properties of aggregates can be described in gross terms (by their fractal geometry) means that it is reasonable to look for general properties of the vibrational spectrum of a fractal lattice.

It is nevertheless remarkable that so much has been accomplished in just over a decade. The frequency spectrum of a reasonably well-behaved solid (with three space dimension) is a function proportional to the square of the frequency. So much has been known since Debye and others took up the question of the specific heat of solids early in this century. At low frequencies, fractal structures have the same kind of vibrational spectrum; longer waves do not recognize that there are patches of the lattice missing.

The surprise (but a little thought will show that it is not really that surprising) is that the vibrational spectrum of a fractal structure includes a large proportion of high-frequency vibrations. Crudely, there must be within a fractal structure patches filled with particles which are nearly isolated from the rest of the structure, and which then perforce vibrate internally at lower frequencies because they are denied the opportunity for taking part in the large-scale long-wavelength vibrations involving the operation of the lattice as a whole.

This conclusion obviously neatly fills the bill required by the haemoglobin problems. If fractal structures not merely admit but require an unexpectedly large proportion of vibrations at high frequency (or, more strictly, short wavelength), there will be opportunities for the exchange of relatively large amounts of energy between, say, haem iron atoms and the surrounding haemoglobin molecule. But there is one snag: the peculiarly

fractal vibrations are also localized (to the patches of the lattice which are themselves almost geometrically isolated), so that the rate of energy exchange will not be great. Is it possible to circumvent that difficulty?

Krumhansl's paper is not so much a protest as a demurring. He does not question the possibility that fractal structures may sustain short wavelength vibrations (which, being cousins of more familiar photons, have inevitably been called fractons), but he does insist that the statement cannot be turned around in such a way that every solid with an anomalous vibration spectrum can be inferred to be a fractal structure of some kind.

The issue is of some importance because of the way in which estimates of the vibrational spectra of real solids (most simply made by measuring the specific heat as a function of temperature) have been used to make structural inferences. This has become especially fashionable in the study of amorphous solids, often said to be fractal over short distances. For starters, Krumhansl offers the example of the monatomic indubitably three-dimensional solid selenium, whose vibrational spectrum is as anomalous as it could be.

Krumhansl's explanation is both simpler and more persuasive. The anomalous vibrational frequency-spectra are often merely consequences of anisotropy of the forces between the atoms in a vibrating structure. Where proteins are concerned, for example, the forces are not central but are directed along the chemical bonds by which atoms are joined. And, in other circumstances, bond-bending forces become dominant.

The effect of Krumhansi's gentle broadside will not be to discourage interest in fractal structures. Quite possibly, the effect may be the reverse of that (no bad thing in itself). But this is an interesting case, which seems to happen more and more often, of how an explanation in search of a phenomenon may lay claim to far more territory than it can handle.

For the time being, and perhaps for a long time to come, progress in the field of fractals hangs crucially on numerical simulation. The results are convincing but not suggestive. They tend to confirm conjectures but not to suggest them. One day, it may all be different. Let us hope so.

John Maddox

Rabies control

Vaccination of wildlife reservoirs

from Roy M. Anderson

CERTAIN major infectious diseases of man and his livestock persist endemically in so-called reservoir populations of wild mammals. In Europe, two important examples are those of rabies and bovine tuberculosis. Such infections are usually difficult to control and past efforts have often centred on the widescale slaughter or culling of the reservoir host species in the absence of more effective measures. But in this issue (Blancou, J. et al. Nature 322, 373; 1986) the production of a recombinant vaccinia virus is described that may be an important step towards the control of rabies by vaccination.

Rabies, an acute viral infection of the central nervous system, has throughout human history been one of the most feared of all diseases because of the distressing clinical symptoms it induces and their invariably fatal outcome. The current epidemic in Europe (see figure) is characterized by a high incidence in the red fox (Vulpes vulpes), which accounts for more than 70 per cent of all reported cases, and populations of this species are believed to constitute the principal reservoir of infection. Tuberculosis in cattle (Mycobacterium bovis) is of less cause for concern to man but the infection can result in serious economic losses to the beef and dairy industries and it can present a threat to public health in the absence of milk pasteurization. In many regions of Western Europe populations of the badger (Meles meles) form an important wildlife reservoir of tuberculosis.

In both examples difficulties have been encountered in the design and implementation of effective control measures. A significant factor is the widespread public concern at the slaughter of wildlife for the control of diseases that are of limited significance to human health and welfare. Human deaths resulting from rabies in Europe, for example, have been of the order of 1-4 per annum over the past two decades. In contrast, crude estimates suggest that a minimum of 11/4 million foxes are killed annually by rabies control programmes in Europe (Zimen, E. The Red Fox, Junk, The Hague, 1980). Economic as well as conservation issues are also of relevance. A recent report commissioned by the British government suggests that the cost of badger culling to reduce the incidence of bovine tuberculosis in cattle herds far outweighs the economic benefit of control (Badgers and bovine turberculosis, HMSO, 1985).

The major problem, however, concerns the limited success achieved by wildlife culling. The extensive slaughter of foxes in countries such as France and West Germany has slowed the rate but not stopped the spread of rabies across mainland Europe. Similarly, efforts to remove social groups of badgers infected with bovine tuberculosis in areas of England and Wales have reduced the incidence of cattle-herd infection but they have not eliminated the problem. These experiences have stimulated a search for alternative or supplementary methods of

control and, in the cases of rabies, much attention has been focused on the development of safe vaccines for use in wildlife populations.

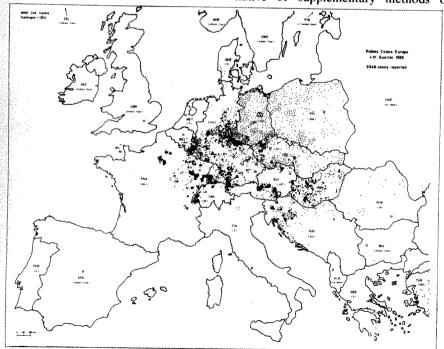
It is in this context that the work of Blancou et al. is important. Vaccines based on inactivated or attenuated rabies virus have been available for some time but their use to immunize wildlife has been restricted by poor efficacy and fears over their safety. Wildlife is vaccinated by consumption of inoculated baits (chicken heads or sausages) but this oral route of immunization for inactivated vaccines fails to induce strong protection. Oral administration of attenuated vaccines is better and appears to create effective immunity but the instability of the attenuated strains and the possibility of reversion to full virulence have prevented their use in natural habitats. Blancou and coworkers report the successful development and testing in foxes of a recombinant vaccinia virus harbouring the gene encoding the rabies surface antigen. Oral and intradermal inoculation give good protection against challenge with the wild rabies virus. The safety, efficacy and ease of administration of this new vaccine should soon lead to large-scale field trials in wild populations of foxes.

The development of a safe and effective vaccine, although essential, is only a first step in the control of infection within a population. The creation of sufficient herd immunity to block transmission is dependent on various economic and other factors, the biology and demography of the target host species and the epidemiology of the virus. A central question in the implementation of mass vaccination is what proportion of the target population must be immunized to halt disease spread. A related issue is the relationship of this critical proportion with factors such as fox density and spatial distribution.

A body of epidemiological theory is available today to help answer these questions. Simple mathematical models of the transmission of rabies in fox populations suggest that the critical proportion of animals, p, that must be effectively immunized to eradicate the infection is approximately given by

 $p > 1 - K_T/K$

Here, K_T is the critical density of foxes necessary for the endemic persistence of rabies and K is the carrying capacity of the habitat or the magnitude of fox abundance in the absence of rabies (Anderson, R.M. et al. Nature 289, 765; 1981). Epidemiological observations on rabies persistence in different habitats that support varying densities of foxes suggest that the value of K_T is approximately 0.3-0.5 foxes km⁻². The value of K is determined by the mixture of habitat types in an area and within Europe it typically lies in the range of 0.1 to 4 foxes km⁻² (Harris, S. & Rayner, J.M.V. J. anim. Ecol. 55, 575; 1986). In



some urban and suburban areas fox density may be much higher $(7-10 \text{ foxes km}^{-2})$. The equation shows clearly that the required degree of vaccine-induced herd immunity is greater in dense fox populations than in sparse ones; for K=2 foxes km⁻² the required degree of herd immunity is predicted to be approximately $80 \text{ per cent } (K_T = 0.4 \text{ km}^{-2})$. In urban areas with dense populations for example, $(K=7 \text{ km}^{-2})$ the required level of protection is predicted to be roughly 95 per cent. These figures are depressingly high and question the practical feasibility of mass vaccination as a means of control.

A further problem is created by the demography of the reservoir host species. The fox has a high fecundity (an average birth rate of 4–5 cubs per litter each year) and a short life expectancy (between 1.5–2.5 years from birth). These observations imply that a high proportion of fox populations are young animals in their first or second year of life. As such the maintainance of high levels of herd immunity would require repeated (preferably annual) cohort immunization with the aim of exposing young foxes to inoculated baits at as young an age as is practically possible.

The development of a safe wildlife vaccine as described by Blancou et al. is

clearly an important step towards the control of rabies. In practice it will undoubtedly be of value to block transmission in areas of low fox density (given that the vaccine can be produced and delivered cheaply). But in areas of high fox density, such as many urban areas in Europe (where the risk of transmission to man and his domestic animals is greatest), mass vaccination will probably have to be supplemented by culling to reduce the target level of immunization (the degree of herd immunity) required to prevent rabies persistence.

The new vaccine's greatest value may well be in the immunization of domestic animals and pets as opposed to wildlife reservoir species. In Latin America, Asia and Africa, for example, rabies in dogs presents the major threat to man (most of the estimated 15,000 annual human deaths caused by rabies occur in these regions). In densely populated urban areas, with large free-roaming dog and cat populations, baits inoculated with a safe recombinant vaccine is potentially a very attractive method of reducing the risk of

Roy M. Anderson is Professor of Parasite Ecology in the Department of Pure and Applied Biology at Imperial College, University of London, London SW7 2BB, UK.



gases, only one of which (occupying about a quarter of the volume) attracts phlogiston. This latter gas he termed Feuerluft (fire air) and eventually isolated it by heating concentrated nitric acid with charcoal, absorbing in milk of lime the red fumes of nitrogen dioxide generated. The oxygen remaining was formed by the thermal decomposition of the acid.

Scheele came close to anticipating Lavoisier by considering the possibility that during combustion fire air combines with the burning body, but he eventually concluded that the gas unites with phlogiston forming heat — which, like most of his contemporaries, he regarded as a material. This hypothesis enabled Scheele to explain why, in a few cases, a calx could be restored to a metal by heat alone, whereas normally the presence of a substance rich in phlogiston (for example, charcoal) was necessary.

Although misled by his belief in phlogiston, Scheele's record of achievement during his short life is remarkable. He discovered radiant heat, noting the similarity of its properties to those of light. His investigation of fluorite, pyrolusite and molybdenite led, respectively, to the discoveries of hydrofluoric acid, chlorine and molybdenum. He discovered glycerol and isolated a dozen previously unknown organic acids. A minor mystery surrounds his discovery of the toxic hydrocyanic acid, resulting from his investigation of the pigment Prussian blue, for he described its taste and smell.

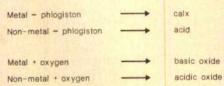
From the age of fifteen Scheele worked in various pharmacies in Sweden until, in the summer of 1775, he acquired his own pharmacy from the widow of Herman Pohl in the small town of Köping. Though subsequently offered academic posts he refused to leave his practice. A few days before his death in 1786 he married Pohl's widow and made her his heiress.

History of chemistry

Carl Scheele (1742–1786) and the discovery of oxygen

from E. L. Scott

THE birthday of oxygen is generally taken to be 1 August 1774, the day on which Joseph Priestley used a twelve-inch lens to focus the Sun's rays on the red calx of mercury (HgO), thereby liberating a gas in which "a candle burned...with a remarkably vigorous flame" (Priestley, J. in Experiments and Observations on Different Kinds of Air Vol. ii, 34; Johnson, London, 1775). But at least two years before that the Swedish chemist Carl Wilhelm Scheele, who died two hundred years ago, had already isolated oxygen. Moreover, Scheele's discovery was a confirmation of his belief in the existence of the gas, whereas Priestley's discovery was



A comparison of the phlogiston and oxygen theories of combustion. Lavoisier, like his predecessors, did not distinguish between an acidic oxide and the acid which it forms on combining with water.

totally unexpected.

transmission to man.

Scheele's experiments and conjectures are described in his only book, Chemische Abhandlung von der Luft und dem Feuer (Uppsala and Leipzig, 1777), translated into English in 1780 (Scheele, C.W. Chemical Observations and Experiments on Air and Fire (trans. Forster, J.R.) Johnson, London, 1780). Within a few years the French chemist Lavoisier named the gas oxygène, believing it to be present in all acids, and had demonstrated its role in combustion. Previously, for more than a century, burning and the calcination of metals had been explained in terms of phlogiston - a 'principle' present in all metals and inflammable non-metals. On the application of sufficient heat, the phlogiston was thought to be attracted by the surrounding air, leaving a calx in the case of a metal and an acid when the substance burned was a non-metal.

Scheele, in several experiments carried out in closed vessels observed the diminution in volume of the air and the failure of the residual air to support combustion, processes now recognizable as oxidation. He concluded that air consists of two

E.L. Scott is a retired schoolmaster and historian at Spring Hill, Careby, Stamford, Lincolnshire PE9 4EA, UK.

Ecology

Lunar cycles in lake plankton

from Geoffrey Fryer

Rнутные behaviour is an almost universal attribute of animals, the most familiar example being that of activity by day and resting by night, or vice versa. A cycle related to the movements of heavenly bodies is also shown by many intertidal animals, the lunar cycle being associated with that of the tides. These rhythms are sometimes intrinsic (or endogenous): they continue, at least for a time, when the cycle is broken experimentally. More puzzling are rhythms associated with the lunar cycle shown by certain freshwater animals, of which only a few cases are known. Some African insects with aquatic larvae emerge only at certain phases of the Moon. Maciej Gliwicz (Ecology 67, 883; 1986) now demonstrates a lunar cycle in planktonic crustaceans, a cycle that is not intrinsic but is imposed on the organisms by a predator. The study reveals a fascinating set of ecological relationships; it remains to be seen whether as yet undiscovered adaptations are involved.

In the Cahora Bassa Reservoir, Zambezi Valley, Mozambique, four cladocerans (a ctenopod and three anomopods; see figure) and two copepods (a calanoid and a cyclopoid) show changes in numerical abundance that are clearly synchronized with the lunar cycle. Such a pattern could only be revealed by frequent sampling. Monthly sampling might greatly over- or underestimate numbers, depending on the starting date, and might fail to detect the very considerable fluctuations in population size.

How can this cycle be explained? Birth rates are such that the fluctuations cannot be attributed to changes in the fecundity of these rapidly reproducing organisms. Maximum death rates, however, occur around full Moon and changes in death

DIAPHANOSOMA

BOSMINA

CERIODAPHNIA

DAPHNIA

O.5

AUG SEP OCT NOV DEC JAN FEB MAR APR MAY JUN

Changes in population size of cladocerans in relation to the lunar cycle in Cahora Bassa Reservoir. Vertical broken lines, full Moon.

rates are clearly responsible for the fluctuations. The culprit is *Limnothrissa miodon*, a sardine-like clupeid fish native to Lake Tanganyika. Introduced to Lake Kariba, it has moved downstream and colonized Cahora Bassa. It feeds avidly on planktonic crustaceans, and calculations show that its depredations can account for even the most drastic declines observed in its planktonic prey.

There are changes in abundance of Limnothrissa adults, evidently short-lived in Cahora Bassa; annual changes in zooplankton abundance are related to these. but lunar fluctuations are not. Lunar fluctuations are caused by changes in feeding efficiency of the predator at different phases of the Moon. Limnothrissa feeds intensively throughout the night at full Moon, following the vertically migrating plankton to the surface: on moonless nights it is too dark for efficient hunting, so the predator disperses over a wide range of depths. Diaphanosoma and Ceriodaphnia begin to decline a few days before full Moon, as one might expect. In Bosmina and Daphnia, however, maximum death rates tend to occur after full Moon. Why should this be?

Gliwicz finds that stomachs of Limnothrissa are always fuller soon after full Moon than just before it, despite the similar light intensities and the fact that plankton is always more abundant before than after full Moon. Feeding intensity depends on the time of moonrise: before full Moon there is moonlight as soon as the sun sets and the plankton does not rise very near the surface; after full Moon there is complete darkness for between one and three hours, during which time the plankton ascends to the surface. When the full moon rises, its appearance is particularly

sudden in Cahora Bassa, which lies in a gorge. Plankton that has previously risen to near the surface is thus suddenly exposed to predation by Limnothrissa and is heavily cropped. Daphnia and Bosmina are apparently particularly vulnerable to this trap. This is the first time that such lunar cycles have been demonstrated, but Gliwicz thinks he can detect others in published data on planktonic Cladocera in temperate lakes cycles probably overlooked at the time as inherent sampling variations.

Since the classical work of Hrbáček (Verh. int. Ver.

Limnol. 13, 394; 1961) and of Brooks and Dodson (Science 150, 28; 1965) which shows how the introduction of a predator can alter the species composition of a plankton community, predation has been shown to have profound selective effects on the size, transparency and even on the gross morphology of planktonic anomopod cladocerans. The avoidance of predators has also long been considered to be a possible explanation of the phenomenon of vertical migration, and seems in some cases certainly to be involved. But dramatic fluctuations in abundance related to the lunar cycle suggest that planktonic crustaceans have not been able to evolve a complete response to increased predation at the time of full Moon. Avoidance of the surface waters on moonlit nights certainly reduces the effects of predation, but the trap set by the timing of sunset and moonrise is more difficult to detect and avoid.

Are such problems real or do they exist only in the human mind? Planktonic animals certainly suffer enormous mortality when caught in the Moon trap — yet they survive, and in sufficient numbers to build up their populations again within a lunar month. Fecundity may be the adaptive mechanism here: it might be advantageous to purchase grazing rights in rich pastures at the high price of periodic heavy payments.

The patterns of emergence of two African insects may be relevant to this hypothesis. In Lake Victoria the mayfly Povilla adusta emerges with a sharp peak of abundance on the second to fourth nights after full Moon (Hartland-Rowe, R. Revue zool. Bot. afr. 63, 185; 1958); in Lake Bangweulu the midge Chironomus brevibucca does so on the third to fifth nights (Fryer, G. Bull. ent. Res. 50, 1; 1959). Such synchronized emergence has the obvious advantage of facilitating the finding of mates. Swarming and spawning of marine organisms, essentially polychaetes, with similar lunar rhythms takes place at similar Moon ages. P. Korringa (Mem. geol. Soc. Am. 67, 917; 1957) has shown how marine animals might use moonlight to time and to synchronize their maturation, and this explanation fits the observed emergence times of P. adusta and C. brevibucca. In both species emergence takes place very near the phase of the Moon when the insects are most vulnerable to predation, and both are eaten extensively. Again, however, these species may find it advantageous to pay this price to achieve synchronized emergence at a convenient phase of the Moon. In the case of C. brevibucca, the numbers emerging are so immense that even heavy predation is trivial.

Geoffrey Fryer is at the Windemere Laboratory of The Freshwater Biological Association, Ambleside, Cumbria LA22 OLP, UK.

Cognitive neurophysiology

Signs of language in the brain

from John C. Marshall

THOSE of us with intact hearing are often inclined to dismiss the manual communication of deaf people, discussed in a study reported on page 363 of this issue', as a mishmash of pantomime and iconic signals, eked out by finger spelling. In many teaching institutions committed to strict 'oralism', signing was (and in some instances still is) firmly suppressed, with disastrous consequences for the deaf child's educational attainment2; even in academic discussion, sign language was frequently

regarded as, at best, a primitive pidgin, and not a 'real' language.

Yet in Europe, true sign languages, with all the formal complexity and expressive power of spoken language, are known to exist in (at least) Austria, Denmark, Finland, France, Germany, Norway, Portugal, Rumania, Sweden, Switzerland, the Soviet Union, the United Kingdom and Yugoslavia. These different, often mutually unintelligible languages, which have little or no superficial similarity with the local spoken languages, have been passed down through the generations from deaf parents to their deaf (and often hearing) children.

American Sign Language (ASL) branched off from

French Sign Language some two hundred years ago, and the current intense interest in the linguistic structure of ASL derives in large measure from the pioneering work recently undertaken by Ursula Bellugi and Edward Klima' at the Salk Institute in California. Once the formal structure of manual signing had been elucidated - how hand configuration,

position and movement through space (including change in hand configuration) combine to express vocabulary and syntax - it was clear that ASL is indeed a fullyfledged language that can serve every day conversation, intellectual argumentation, wit and poetry4. But now there arises an interesting issue about the neuronal substrate for sign.

The basic complementary organization of the duplex human brain is between speech processing (committed to the left

Movement trajectories of grammatical processes (courtesy of U. Bellugi).

cerebral hemisphere) and visuo-spatial together with visuo-manipulative processing (committed in the main to the right hemisphere). A central question in the psychobiology of language is thus whether the underlying specialization of the left hemisphere is restricted to auditory-vocal language (that is, speech), or rather includes a more 'abstract' representation of linguistic form (grammar), irrespective of the mode in which it is expressed

Natural sign languages provide a privileged insight into this question. Such a system simultaneously qualifies as a language and as an extremely complex and precise set of gestures, executed in space and perceived visually. Nonetheless, studies of disorders in the expression and comprehension of sign consequent upon unilateral brain damage show that, just as with aphasia for spoken language, it is left hemisphere damage that provokes these sign language aphasias67; by contrast, in deaf patients with extensive right hemi-

sphere damage, signing is little disturbed. although many non-language visuo-spatial tasks (including drawing) may show severe impairment 8.9. It would seem, then, that it is language per se (not solely speech perception and production) that is lateralized to the left cerebral hemisphere. Grammatical structure is processed by the left hemisphere even when the overt physical realization of that structure involves a visuo-spatial medium.

The case now reported by Damasio, Bellugi, Damasio, Poizner and Van Gilder demonstrates in even stronger fashion that the above conclusion is warranted. Their patient, a young woman with normal hearing, spoke English but was also proficient in ASL as a second language; she earns her living as an inter-

> preter and counsellor for deaf people whose native language is ASL. Unfortunately, she suffered increasingly from frequent partial complex seizures that could not be controlled pharmacologically. gical intervention - resection of the temporal lobe was therefore considered. But which temporal lobe (left or right) should be ablated? Bilateral temporal lobectomy results in a gross amnestic syndrome that precludes any kind of normal life; removal of the language-dominant temporal lobe could result in aphasic impairment that would destroy the patient's livelihood.

The application advanced in vivo brain imaging techniques showed anatomic and metabolic

asymmetries consistent with normal left hemisphere processing of speech in the patient. More direct evidence for the control of language skills was then obtained by barbiturate injection. The brief inactivation of frontal and central areas of one hemisphere (which include languagecommitted cortex) can be achieved by injection of sodium amytal into the ipsilateral carotid artery. When this was performed, a reversible lesion (pharmacologically induced) of the left hemisphere produced in the patient a temporary aphasia for English and ASL; left cerebral dominance for both language systems was thereby indicated, and the severity and the duration of the sign language impairment was even greater than in spoken English. Subsequent neurosurgical intervention - partial resection of the right temporal lobe - was found, three and twelve months post-operatively, to have produced no neuropsychological impairment of either English or sign language.

Damasio, A., Bellugi, U., Damasio, H., Poizner, H. & Van Gilder, J. Nature 322, 363 (1986).
 Conrad, R. The Deaf School Child: Language and Cog-

nitive Function (Harper and Row, London, 1979).

3. Klima, E.S. & Bellugi, U. The Signs of Language (Harvard

University Press, Cambridge, 1979).

4. Klima, E.S. & Bellugi, U. Sign Language Studies 8, 204,

Bellugi, U., Poizner, H. & Zurif, E. in Neural Models of Language Processes (eds Arbib, M.A., Caplan, D. & Marshall, J.C.) 217 (Academic, New York, 1982).
 Kimura, D. Sign Language Studies 33, 291 (1981).
 Poizner, H., Bellugi, U. & Iragui, V. Am. J. Physiol. 246, 1988. (1984)

R868, (1984). Kimura, D., Davidson, W. & McCormick, C. W. Brain and

Kimura, D., Davidson, W. & McCormick, C. W. Brain and Language 17, 359 (1982).
 Poizner, H., Kaplan, E., Bellugi, U. & Padden, C. Brain and Cognition 3, 281 (1984).
 Marshall, J. C. Cognition 17, 209 (1984).

The patient continued to manipulate the spatial syntax of ASL with the same fluency she had shown pre-operatively. Dr A. Damasio reports (personal communication) that the patient has been seizure-free since the operation and has successfully returned to her demanding work as a sign-language interpreter.

These results, then, provide further testimony for the modular organization of the human brain; different domain-specific cognitive representations are computed by the two halves of the adult brain, irrespective of the physical form whereby

those representations are made manifest. It is, however, possible that by virtue of their combined linguistic and visuospatial nature, the facile acquisition of signs requires both hemispheres to be fully intact. Damasio, Bellugi and their colleagues now intend to investigate how easily their patient can learn new signs, including the quite distinct space structures of Chinese Sign Language.

John C. Marshall is in the Neuropsychology Unit, Neuroscience Group, Radcliffe Infirmary, Oxford OX2 6HE, UK.

Solid-state physics

New semiconducting polymers

from R.H. Friend

THE discovery in 1977¹ that the addition of small amounts of strong oxidizing or reducing chemicals to polyacetylene (doping) produces levels of conductivity typical of metals contradicted long-held views that electrons in organic semiconductors necessarily have low mobilities. Progress since then has been impeded by the limited availability of polymers with desirable properties and also by difficulties in processing them. This constraint has been loosened by S.A. Jenekhe, who on page 345 of this issue² reports the smallest energy gap yet obtained in an organic polymer, which brings closer the

use of this class of compounds as semiconductors and transparent conductors.

The feature common to the organic semiconductor class of polymers is the presence of pon each atom on the chain, giving a conjugated structure which can be represented (slightly misleadingly) by alternation of 'double' and 'single' bonds. Overlap of adjacent p, orbitals gives welldelocalized π electron wavefunctions and high electronic mobilities. These polymers do not conform to the models that work for inorganic semiconductors.

Whereas it is can be said that threedimensionally bonded inorganic semiconductors are semiconductors by accident (that is, there happens to be an energy gap between the highest occupied and lowest unoccupied levels), the same is not true for 'one-dimensional' polymeric semiconductors, where it is energetically favourable to set up the interatomic spacings along the chain so that there is an energy gap between the highest π and the lowest π^* levels.

The semiconductor gap in the *trans*-isomer of polyacetylene is caused by alternation of bond lengths along the chain;

this dimerization introduces an energy gap between the occupied π 'bonding' states (which have high electron density in the short, double bonds) and the unoccupied π^* states (with electron density in the long, single bonds). The strength of the bond alternation, and hence the size of the energy gap, is determined by the trade-off between the cost in elastic strain energy associated with the distortion and the reduction in π electron energy that it achieves. The observed gap is approximately $1.5 \, \mathrm{eV}$.

The particular novelty in trans-polyacetylene is that the sense of bond alter-

Bond-alternation defect (shown as the neutral defect) separating the degenerate A and B phases of trans-polyacetylene (above); and a positively charged bipolaron defect on a poly(phenylene) chain, showing the quinonoid character within the defect (B phase) and benzenoid character (A phase) elsewhere on the chain (below).

nation is not determined, so that there are two, degenerate phases, labelled A and B in the figure. In consequence the chain can support stable defects in the bond alternation sequence, separating the A and B phases as shown in the figure. These topological defects, which have an associated 'non-bonding' p, level, are calculated to move along the chains as low-mass particles and possess most of the qualities of solitary waves (solitons). Furthermore, the result of adding charge to the chain, through chemical doping or following photoexcitation, is always to create these defects, which can be positively charged

(p_z level empty, spin 0), neutral (one electron on p_z level, spin $\frac{1}{2}$) or negatively charged (p_z level doubly occupied, spin 0). This is in contrast to the doping of traditional, inorganic semiconductors in which added charges are present as holes in the valence band or electrons in the conduction band.

For most of the other conjugated polymers that have been synthesized, the sense of bond alternation along the chain is determined, and the A and B phases are non-degenerate. For the polyphenylene chain illustrated in the figure, the benzenoid (A) phase is lower in energy than the quinonoid (B) phase. The usual consequence of this is that there is now an additional contribution to the semiconductor gap (π levels are of benzenoid character, π^* levels quinonoid), and indeed this is true in many cases, including polyphenylene (3 eV) and polythiophene (2 eV). Soliton defects are no longer stable, although in pairs they can form 'polaron' defects with a short length of B phase on the chain. Although the polaron defect is not stable on a neutral chain, it does provide the cheapest way of accommodating charges added to the chain, either as a singly charged polaron or as a doubly charged bipolaron (see figure).

Hence the discovery of conjugated polymers with band gaps smaller than that of polyacetylene was unexpected. To obtain these small band gaps it is necessary to design the polymer so that the energy difference between the A and B phases is as

small as possible, and this is apparently achieved in polyisothionaphthene' which has a gap of slightly more than 1 eV. An alternative strategy is to design a polymer which is forced to have alternating sequences of the A and B phases along the chain so that there is little difference in the benzenoid/quinonoid character in the π and π^* states. Jenekhe has achieved this for a class of thiophene-derived polymers that reduce the gap to as low as $0.75 \, \mathrm{eV}$.

Narrow-gap conjugated polymers will extend the scope both for applications and for fundamental investigations. Much as for

inorganic semi-conductors, narrow-gap materials should show high electronic mobilities. In the context of the polymers, the soliton and polaron defect states will be delocalized and have low effective masses. This is desirable for many semi-conductor applications and, in addition, these materials can be transparent in the visible part of the spectrum and are thus of use as transparent conductors.

Beside the tuning of electronic properties that is now achieved with new synthetic routes, processibility via a soluble phase, either a 'precursor' polymer or a conjugated polymer with soluble side

groups', is now routine. Well-crystallized and highly oriented films of several precursor-route polymers can obtained by stretch orientation during transformation; these films have allowed the first experimental investigations of the anisotropy of electron motion along or between chains78. Although electron motion along chains is easy, it is important to recognize that the degree of contact between the π electron wavefunctions on adjacent chains is quite strong, and that interchain electron motion is not difficult. Experiments using oriented polyacetylenes demonstrate that the quantum yield for photogeneration of charged pairs is higher when the band-gap illumination is polarized perpendicular, rather than parallel, to the

chains, so that the photons absorbed transfer electrons between chains. The scope for development of the highly dichroic properties of these materials is vast.

- Chiang, C.K. et al. Phys. Rev. Lett. 39, 1098 (1977)
- Jenekhe, S.A. *Nature* **322**, 345 (1986). Su, W.P., Schrieffer, J.R. & Heeger, A.J. *Phys. Rev.* B**22**,
- Campbell, D.K., Bishop, A.R. & Rice, M.J. in Hanbook of Conducting Polymers (ed Skotheim, T.J.) (Dekker, New
- Wudl, F., Kobayashi, M., Colaneri, N., Boysel, M. & Hee-
- ger, A.J. Molec. Cryst. Liq. Cryst. 118, 199 (1985). Calvert. P. Nature News and Views 304, 487 (1986).
- Kahlert, H. & Leising, G. Synth. Metals (in the press). Townsend, P.D. & Friend, R.H. in Synth. Metals (in the

R.H. Friend is in the Cavendish Laboratory University of Cambridge, Cambridge CB3 OHE. UK.

Meteorites

Window on the early Solar System

from Derek Sears

It is an oft-repeated truism that meteorites are a window on the early Solar System. They are, however, complex: the astronomer B. Pagel once remarked, after taking a cursory glance through the window, that "the oracle is . . . wrapped in obscurity of truly Delphic proportions". Fortunately, Pagel was unduly pessimistic, because the window sometimes clears to present a unique and fascinating picture of places and processes as they were 4,600 million years ago, as shown in a recent paper by David Wark2.

One of the most important developments in the study of meteorites over the past few decades is the realization that some meteorites retain a better record of the nebular phase of their history than others; these primitive or type 3 chondrites contain many individual components with particular significance for deciphering the earliest history of solid matter in the Solar System. Some of the better-studied components are the silicate aggregates called chondrules3; the finegrained, almost smoke-like, matrix4; certain kinds of metal grains; and the graphite-magnetite aggregates6. But the objects which have attracted the most attention are calcium-aluminium-rich inclusions (CAIs), one of which is the subject of Wark's paper.

Wark describes a CAI discovered in the Allende meteorite shortly after it fell in 1969. The inclusion (CAI 3643) consists of a core, mantle and crust. The crust appears to have been formed by rapid episodic condensation and aggregation in a compositionally unchanging gas. The core consists predominantly of hibonite, a mineral which is one of the first to condense in a gas of solar composition, whereas the mantle and crust consist predominantly of melilite, which is thought to form by re-

action between the hibonite and the gas. The core has the texture of a material which formed by deposition from a vapour. There are many metal nuggets in the centre of the core which consist of highly refractory trace elements, whereas those in the outer parts of the core contain elements of less refractory nature - it is as if they mopped up the elements missing from the nuggets at the core's centre. Other refractory trace elements, the rareearth elements, show a steady decrease in abundance with increasing volatility, as if the formation of the CAI occurred over the same temperature interval as the elements were condensing.

All these details are consistent with an episodic condensation and accretion of the core, with the mantle and crust being made by later episodes of condensation onto the earlier-formed solids. The processes occurred at high temperatures and involve solids which are refractory to various degrees. Once formed, the entire assemblage suffered several alteration processes at much lower temperatures. with evidence for metamorphism, metasomatism and the introduction of a vapour rich in halogens, alkali metals and iron.

Many who have worked on this CAI have suggested that the inclusions, or some material in them, were not formed in our Solar System, but were transported here from interstellar space during or just before the formation of the Solar System. This idea is rooted in the unusual isotope ratios frequently encountered in the inclusions. It was long believed that the isotopes in our Solar System became thoroughly mixed during its formation. CAIs also contained several short-lived radioactive isotopes at the time they were formed. Some of the nuclides have very short half-lives (for example *Al, 0.72

million years), which has suggested that the event which ejected the isotopes into the interstellar medium (say, a supernova explosion) was that which triggered the formation of the Solar System. Thus, the condensation sequences would have occurred in the expanding and cooling shells of ejected supernova materials

An alternative view is that interstellar material, with essentially normal chondritic composition, entered the primordial solar nebula at cosmic velocities and became heated in a manner analogous to meteorites entering the atmosphere ". The evaporation sequence as the material is heated would be the reverse of the condensation sequence, so that CAIs can be regarded as distillation residues rather than high-temperature condensates

Wark points out that the properties of CAI 3643 are not consistent with ideas that involve exposure to various chemical environments. Although the zones in the inclusion, and the radial gradients in mineralogy and refractory-element chemistry, imply different temperature regimes for the aggregation processes, they must have occurred quickly for the differences to have persisted, and they must have occurred in a gas which did not change very much in its composition. Instead, Wark suggests that the CAI formed in a single place and over a fairly restricted time interval; he favours the formation of the CAI by episodic condensation and aggregation during localized transient heating events in the asteroid belt.

Wark's paper will not lay to rest the idea that CAIs are extra-Solar System in origin. It is always possible, although unlikely, that the various extra-Solar System atmospheres that have been postulated were compositionally very similar and movement from one to another was very rapid. It is also possible that not all CAIs were created in the same way. But Wark provides a clear indication that, in at least this instance, the condensation and accretion sequence was followed episodically and in a very restricted regime of time and environment. In this sense, our window on the early Solar System has cleared a little, and provided us with a view that can be obtained in no other way.

- Pagel, B. Observatory 99, 162 (1979)
- Paget, B. Observatory 99, 102 (14777).

 Wark, D. A. Earth planet, Sci. Lett. 77, 129 (1986).

 King, E. A. (ed.) Chondrules and Their Origins (Lanus and Planetary Institute, Houston, 1984).
- Huss, G.R., Keil, K. & Taylor, G.J. Geochim, cosmis-chim, Acta 45, 33 (1981).
- Rambaldi, E.R., Scars, D.W. & Wasson, J.T. Nature 287.
- Scott, E.R.D., Taylor, G.J., Rubin, A.E., Okada, A. & Keil, K. Nature 291, 544 (1981).
- Grossman, L. A. Rev. Earth planet Sci. 8, 559 (1980). Cameron, A.G.W. & Truran J. W. Icarus 36, 447 (1977).
- Lattimer, J.M., Schramm, D.N. & Grossman, L. Astro-phys. J. 219, 230 (1978).
- Wood, J.A. Earth planer. Sci. Lett. 70, 11 (1981).
- 11. Wood, J.A. Earth planet. Sci. Lett. 56, 32 (1981)

Derek Sears is in the Department of Chemistry at the University of Arkansas College of Arts and Sciences, Fayetteville, Arkansas 72701, USA.

Geometry

Exotic structures on four-space

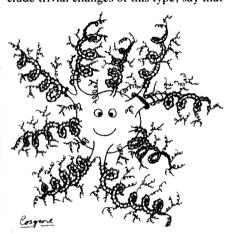
from Ian Stewart

ONE of the biggest surprises in topology was the discovery in 1982 that fourdimensional euclidean space does not have a unique structure as a differentiable manifold. The existence of an 'exotic' structure on four-space was proved by Michael Freedman, by combining his techniques for analysing four-manifolds (J. diff. Geom. 17, 357; 1982) with a new and startling result due to Simon Donaldson (J. diff. Geom. 18, 279; 1983). A question that immediately arose was how to classify all such structures: in particular, how many are there? Robert Gompf (J. diff. Geom. 18, 317; 1983) found four distinct differentiable structures - the standard one plus three exotics. A fifth universal' structure (containing all the others) was found by Freedman and Larry Taylor. And now Gompf has shown (J. diff. Geom. 21, 283; 1985) that there exists an uncountable infinity of exotic structures on four-space.

A differentiable manifold is a multidimensional analogue of a smooth twodimensional surface. The idea is of central importance in mathematics and has applications throughout the physical sciences. For example, the motion of the Moon, the Earth and the Sun under their mutual gravitational influence corresponds to the motion of a point on an 18dimensional 'phase space' having three dimensions of position and three of momentum for each body. The original idea goes back to Bernhard Riemann in 1854; in its modern form it is due to Hermann Weyl in the 1930s. An ndimensional manifold is a collection of overlapping 'patches', each looking like a piece of *n*-dimensional euclidean space. Each patch inherits a coordinate system, which means than on each overlap there are two distinct coordinate systems - one from each patch. These do not necessarily agree; but if each is related to the other by a differentiable transformation, then the system of patches is said to define a differentiable structure on the manifold.

For example consider an ordinary twodimensional sphere. This can be considered as two overlapping patches, each forming rather more than a hemisphere. For example, in geographical terms, let one patch be everything south of the Tropic of Cancer, and let the other be everything north of the Tropic of Capricorn. The overlap is an equatorial band between the two tropics. Each patch is a distorted circular disk, and it is not hard to find coordinate systems on the disks that provide smooth overlaps. An *n*-dimensional hypersphere can be defined by an analogous construction, using two balls in *n*-dimensional space.

It is easy to see that a given manifold can have many different differentiable structures, that is, systems of smoothly overlapping patches. But the obvious examples are related in an essentially trivial way. Start with a manifold M and a differentiable structure S. Take any continuous one-to-one correspondence of M with itself and apply it to all of the patches describing S, to get a new set of patches S'. Then, in general, S' is different from S, but the patches of S' fit together to give the same manifold as those of S. To exclude trivial changes of this type, say that



Artist's impression of an exotic four-space. The structure resembles ordinary four-space at the centre, but becomes more and more complicated as it approaches infinity, putting out branched tentacles in all directions. This conjectural picture compresses four dimensions into two, and is correct, if at all, only in spirit. An explicit description of the true geometry is not yet known.

under these circumstances S and S' are 'equivalent'. Then a more interesting question arises: can there be several inequivalent differentiable structures on the same manifold?

Early results suggested not: for example, it was proved in the 1950s that if the manifold is three-dimensional then there is a unique differentiable structure up to equivalence. However, matters took an unexpected turn in 1963 when John Milnor proved that the seven-dimensional hypersphere has at least two inequivalent differentiable structures: the 'standard' one and another exotic one. A detailed study of these exotic spheres revealed that there are exactly 28 inequivalent differentiable structures on the 7-sphere.

Even so, it was not expected that this kind of trouble would show up in ordinary euclidean *n*-space. Indeed it was known

that for $n \neq 4$ there is a unique differentiable structure. The conjecture that uniqueness holds for all euclidean spaces lay at the heart of smoothing theory, a method for studying non-differentiable manifolds by providing them with a differentiable structure. So it was quite a shock when Freedman and Donaldson showed that four-dimensional space behaves in a completely different and rather horrifying way. There exist 'exotic R's', that is, differentiable structures on four-space that are not equivalent to the standard one (see figure).

The problem is to tame these unruly structures by imposing some comprehensible order on them. Which brings us back to the question: how many exotic R's are there? Mathematicians distinguish many different 'sizes' of infinity. The cardinal of a set is the size of infinity that corresponds to it. The smallest cardinal, called aleph-zero, or countable infinity, is that corresponding to the set $\{1,2,3,\ldots\}$ of positive integers. A set is countably infinite if it can be put into one-to-one correspondence with the positive integers. Many sets — pairs of integers, the rational numbers, the algebraic numbers — are countably infinite. But the set of real numbers cannot be put in one-to-one correspondence with the positive integers, and is said to be uncountably infinite. There is a consistent arithmetic of infinite cardinals; it has its own bizarre logic, and there are many pitfalls. For example, it is possible for one set to contain another (and thus be 'bigger') even though both sets have the same cardinal.

Gompf first found a family R, of exotic R^4s , where s and t are positive integers, with the property that R, embeds in R, if and only if $s \le u$ and $t \le v$. In particular R_{ij} is equivalent to R_{us} only when s = u and t= v. This provides a countably infinite set of inequivalent exotic R4s. Clifford Taubes has now developed a generalization of Donaldson's results, inspired by an observation of Freedman that such a generalization would imply the existence of an uncountable infinity of exotic R's. This idea can be applied to Gompf's construction, and it yields an even more extensive family of exotic R's. It is probable - but not yet certain - that these results give the correct cardinal for the set of all exotic R's. That does not mean that Gompf's examples exhaust all possibilities, because 'larger' sets can have the same cardinal. Indeed Taubes's set is smaller than Gompf's, yet the cardinal is the same in both cases.

The set of all exotic R's also carries a natural algebraic operation, the 'end-sum'. There are a number of analogous operations in topology. The simplest combines two knots to yield their 'sum' by tying both in the same piece of string. Similarly the connected sum of two manifolds can be obtained by cutting a small

disk out of each and gluing a tube between the holes that result. (Milnor showed that such a construction applied to his 28 exotic 7-spheres turns them into a very nice algebraic object: a group.) The end-sum of two exotic R's is obtained by 'gluing them together at infinity'. To find an abstract description of the structure of the set of all exotic R's under the end-sum operation is a problem of central importance. It would not only classify them all, but also explain how they relate to each other.

The importance of these ideas for mathematics is manifest. We know that four-dimensional space differs in a dramatic and rich way from all other dimensions. It is obviously of fundamental interest to explore exactly how and why this occurs.

The relevance to applied science is not

so clear: the 'standard' structure on fourspace is after all the one suggested by physical observation. But the influence of mathematics and applications on each other, while profound, is seldom immediate and hardly ever direct. For example the existence of exotic R's is established by combining some recent ideas in quantum physics — gauge field theories — with some extremely abstract techniques of modern topology. The same combination is appearing in basic questions about unifying the forces of nature. A fundamental mathematical truth is important because, once proved true, it stays true. Exotic R's are abroad in the world, and the world is changed - forever.

Ian Stewart is at the Mathematics Institute, University of Warwick, Coventry CV47AL, ÚK.

Computational cosmology

Galactic haloes need computers

from George Efstathiou

OBSERVATIONS of rotation in spiral galaxies suggest the presence of dark material in haloes surrounding the luminous component. Little is known about the nature of this dark matter — it could be black holes, ultra-small 'stars' or even elementary particles such as massive neutrinos, photinos or gravitinos. However, the way that the rotation speed varies with distance from the centre of a spiral suggests that the mass in the halo increases linearly with radius. This behaviour is important for at least two reasons. The first concerns the origin of the observed spatial distribution and whether it arises naturally from small perturbations which grow by the action of gravity. The second concerns the total extent of the dark haloes, and whether there is enough dark matter so that the Universe will eventually collapse back to a singularity. The first of these questions is addressed by P.J. Quinn, J.K. Salmon and W.H. Zurek elsewhere in this issue (Nature 322, 329; 1986) and both questions were among those discussed at a recent meeting*.

Quinn et al. use computer simulations which model the gravitational interactions between a large number of mass points to study the formation of structure in an expanding universe under various assumptions concerning the initial conditions. If the mass points are initially distributed at random (white noise), then the haloes that form in the simulations are more centrally concentrated than indicated by the observations. But the authors also show that density fluctuations with significant contributions from long-wavelength perturbations (more like 'pink noise'), develop

haloes with a linear mass distribution resembling that around spirals.

Interestingly, the pink-noise irregularities arise naturally if the dark matter is in the form of weakly interacting massive particles such as gravitinos. The evolution of structure in such models has been investigated using computer simulations by C.S. Frenk et al. (Nature 317, 595; 1985) who showed that the model broadly accounts for the distribution of mass in haloes

and their abundance in space.

But what relation do these studies have to the models of galactic distribution and clustering that follow from cosmic string theories? There are very significant differences: the underlying assumption of the gravitating mass-point studies is that statistics of the initial fluctuations are gaussian, whereas strings introduce considerable skewness — which may lead to clustering and superclustering; furthermore numerical models of the strings developed so far exclude gravitational forces. The two types of study clearly need to be combined in a single model, but the computer code to do the job has not yet been written — largely because of the power and time that are necessary to handle simultaneously gravitating mass points, strings and internal string forces.

Why do we need computer simulations at all in such problems? The answer lies in the non-linear nature of gravitation. In general, it is not possible to study the evolution of a gravitating system of mass points by analytic methods unless one adopts highly restrictive assumptions such as spherical symmetry. Furthermore, in the cosmological context described above, halos do not evolve as isolated systems. Rather they form through a complicated

series of mergers between smaller subunits. It seems unlikely that we will readily develop an analytic theory capable of reliably modelling such events. Yet can we believe computer simulations which typically contain less than 50,000 mass points. some six orders of magnitude less than the number of stars in one galaxy? Does the artificial 'graininess' or the presence of boundaries in computer simulations adversely affect the results? The answer is ves in some cases and no in others, and it is up to the numerical experimenter to convince his readers of the reliability of key conclusions by applying appropriate tests. Sadly, this has not always been done in the past and many researchers, in other fields as well as in cosmology, remain sceptical of the computer simulations.

There are also other issues. In the present mass-point studies, essentially any 'clump' that forms is considered to be a galactic halo. The familiar flattening of galaxies into disks does not occur because it requires dissipating forces, such as radiative cooling from high-density gas. Consideration of these effects requires a hybrid program that can handle both gas dynamics and gravitational mass-point interaction. Since a full model must also take into account feedback effects where star formation can raise intergalactic gas temperatures from microwave background levels to 10,000 K, the ultimate computer model of galaxy formation is bound to be highly complex.

Much larger simulations could be achieved by using improved algorithms, a new generation of supercomputers, or both, as discussed at the meeting. Most present-day computers are simple uniprocessor machines: the current generation of supercomputers such as the Cray-XMP or Cyber-205 achieve a high performance by applying the same instruction simultaneously to many pieces of data which belong to a 'vector'. The US National Science Foundation has set up several centres for large-scale scientific computing where the computers will be coarse-grained parallel machines such as the ETA-10. This enormous computer consists of &

100 years ago **Animal Intelligence**

A REMARKABLE instance of animal intelligence has lately come under my notice. In a neighbour's bungalow in this district two of our common house-swallows (Hirundo javanica) built their nest on top of a lamp that hangs in the dining-room. As the lamp is either raised or depressed by chains fixed to a central counterweight, these chains pass over pulleys fixed to a metal disk above, on which the nest was placed. The swallows built over each pulley a little dome, allowing sufficient space, both for wheel and chain to pass in the hollow so constructed. without danger to the nest, which was not only fully constructed, but the young birds were reared without further danger

From Nature 34, 265; 22 July 1886

^{*}Use of computers in stellar dynamics, 2-4 June 1986, Institute for Advanced Study, Princeton, New Jersey, USA.

Cyber-205 machines with a massive shared memory. At the other end of the spectrum, fine-grained parallel machines such as the Connection Machine use many simple processors which communicate with each other via a complicated network of interconnections.

The optimal algorithm for solving the gravitational n-body problem clearly depends on the architecture of the machine. Existing programs such as Aarseth's famous n-body code can easily be adapted for vector machines and will be used extensively at the supercomputer centres. Algorithms for very fine-grained computers (which use many simple processors) are likely to be quite different. Several ingenious possibilities were described at the meeting (Joshua Barnes, Institute for Advanced Study, Princeton).

Very few cosmologists and astrophysicists have thought seriously about building their own special-purpose supercomputer, yet it is feasible to acquire the

necessary skills (Gerald Sussman, MIT). Sussman also argued that it is now possible to build one-off machines to study the stellar dynamical evolution of, say, an entire globular star cluster containing one million stars.

But even the globular cluster problem is not entirely stellar dynamical. At some point during evolution, the finite sizes of stars may become important, as may mass-loss and other astrophysical effects. In the case of cosmological simulations, our lack of knowledge of gas dynamics and star formation impose severe limitations on our understanding. Supercomputers will undoubtedly make a major impact in cosmology and astrophysics, but in many cases they will solve only idealized problems. Theorists will still have plenty to do in applying the results to real stellar systems.

George Efstathiou is at the Institute of Astronomy, University of Cambridge, Road, Cambridge CB3 0HA, UK. Madingley

Nitrogen fixation

A role for vanadium at last

from R. Cammack

FIFTY years after Bortels reported that vanadium could substitute for molybdenum as a trace element essential for nitrogen fixation in the soil bacterium Azotobacter vinelandii, Robson et al., on page 388 of this issue², report conclusive evidence for an alternative vanadiumcontaining nitrogenase from A. chroococcum, a result made possible by recent developments in the genetics of nitrogenfixing bacteria. Robson et al. produced a mutant strain in which the structural genes for the normal molybdenum-containing nitrogenase are deleted and demonstrate that the alternative nitrogenase uniquely requires vanadium for its synthesis, and in stoichiometric amounts.

The complex, nitrogen-fixing enzyme nitrogenase has two types of protein component, both containing iron-sulphur clusters. One of these components, the iron-molybdenum protein, also contains a cluster of unknown structure, the iron-molybdenum cofactor (Fe-Mo-Co): there is compelling evidence that this is the site at which dinitrogen is reduced to ammonia. The function of the other component is to 'pump' electrons, using energy from ATP, into the iron-molybdenum protein. The vanadium-containing nitrogenase appears to have a very similar arrangement, a structure containing vanadium presumably substituting for the Fe-Mo-Co, although the proteins involved are the products of different genes.

Chemically, the substitution of vanadium for molybdenum makes good sense. The two elements are capable of | its presence was not detected. A recent |

similar oxidation-reduction reactions at low redox potentials. Model compounds for the nitrogenase reaction that can catalyse the reduction of dinitrogen to ammonia have been synthesized, most containing molybdenum, although complexes of vanadium are also effective3.

Ironically, although nitrogenase was partially purified from vanadium-grown A. vinelandii about 15 years ago and several of its catalytic properties, such as decreased sensitivity to cobalt inhibition, correctly described, the significance of vanadium in this system was not recognized. This was partly because of the extreme difficulty of obtaining growth media that were sufficiently molybdenum-free, which meant that all nitrogenase preparations contained a certain amount of molybdenum. It must have seemed unreasonable at the time to assume that there existed a second nitrogenase system with almost identical protein structure to the molybdenum nitrogenase system, which rapidly decomposes during purification and has very little activity in the conventional acetylene-reduction assay. Instead it was concluded that vanadium had a 'sparing' effect, stabilizing the molybdenum nitrogenase when molybdenum was in short supply. The idea that all nitrogenases contain molybdenum became firmly established and molybdenum was routinely added to all growth media for nitrogen-fixing organisms. Because the synthesis of the vanadium nitrogenase is repressed even by traces of molybdenum, survey of the literature showed that Bortels' 1930 paper describing a requirement for molybdenum in nitrogen fixation has been cited 55 times, while his 1936 paper describing the alternative use of vanadium was cited 4 times.

The more recent discoveries stem from the work of Bishop⁵ who, in the face of much initial scepticism, demonstrated the presence of a second nitrogenase system in A. vinelandii grown in molybdenumdeficient conditions. He obtained a nif mutant which could not express the conventional molybdenum nitrogenase, but which could still grow by fixing nitrogen in the absence of molybdenum. He showed that these 'pseudo-revertants' were tungstate resistant and expressed a different nitrogenase whose activity (as measured by hydrogen production) was less sensitive to inhibition by acetylene, carbon monoxide or tungstate. It appears that it was the vanadium present as a contaminant in tungstate that allowed Robson et al.2 to discover the vanadium enzyme.

Azotobacter synthesizes the molybdenum nitrogenase in preference to the vanadium nitrogenase when molybdenum is available presumably because the molybdenum enzyme is more stable, and possibly catalyses less of the wasteful side-reaction in which hydrogen is produced. Although molybdenum is difficult to remove from laboratory media, it may become a limiting factor in some soils, and hence the capacity to make the alternative nitrogenase confers a selective advantage. A question of great interest is whether other nitrogen-fixing organisms, and in particular the economically important rhizobia, are capable of making the vanadium nitrogenase.

Macara⁶ has described vanadium as "an element in search of a [biochemical] role". It is known that vanadium in extremely small amounts is a nutritional requirement for many types of organism, possibly including higher animals'. The sea-squirt Ascidia nigra contains high concentrations of V(III) ions in specialized blood cells. Vanadium is also accumulated by the toadstool Amanita muscaria8 and a vanadium-containing bromoperoxidase has recently been isolated from a seaweed, Ascophyllum nodosum9. With the establishment of vanadium in nitrogenase, its role is beginning to emerge.

- 1. Bortels, H. Zentbl. Bakt. ParasitKde Abt. II 95, 193 (1936)
- Robson, R.L. et al. Nature 322, 388 (1986). Nikonova, L.A., Isaeva, S.A., Pershikova, N.I. & Shilov,
- A.E. J. molec. Catal. 1, 367 (1975). Bortels H. Arch, Mikrobiol. 1, 333 (1930).

- Bishop, P. Trends biochem, Sci. 11, 225 (1986). Macara, I.G. Trends biochem. Sci. 5, 92 (1980).
- Nechay, B.R. Fedn Proc. 45, 123 (1986)
- Gillard, R.D. & Lancashire, R.J. Phytochemistry 23, 179
- De Boer, E., Van Kooyk, Y., Tromp, M.G.M., Plat, H. & Wever, R. Biochim. biophys. Acta 869, 48 (1986).

R. Cammack is a Reader in the Department of Biochemistry, King's College London, Campden Hill Road, London W87AH, UK.

SCIENTIFIC CORRESPONDENCE

Observation of ^{110m}Ag in Chernobyl fallout

Sir—The initial radiometric flurry of interest in fission products with relatively short half lives following the Chernobyl reactor accident has been replaced with concern about the entry of fission products with longer half-lives into the food chain.

The movement and slaughter of lambs in Wales, Cumbria and Scotland has recently been prohibited due to the identification of lamb meat containing abnormally high levels of 134 Cs (T_{12} =2 yr) and 137 Cs (T_{12} =30 yr).

The radiometric laboratory of the Department of Physics at the University of Liverpool, which houses several low-level γ-ray counting systems, has been employed to carry out measurments on various dairy and meat products originating from North Wales. The low-level counting systems consist of high-efficiency, hyperpure germanium detectors with Compton suppression shields enclosed in lead castles to reduce background radiation. All systems are efficiency calibrated so that radionuclide concentrations can be determined.

A recent study of beef and lamb products in this laboratory revealed the presence of the radionuclide 110m Ag ($T_{1/2}$ =250 days) in both beef and lamb liver but not in other meats from the same animals. This radionuclide is readily identified by the presence of a γ -ray line of 658 keV alongside the characteristic 662 keV line of 137 Cs, although several other γ -rays including those at 447, 620, 707, 764, 885 and 937

keV provide an unambiguous identification of 100s Ag.

A relevant portion of the γ-ray spectrum shown in Fig. 1 indicates the excellence of the detection system with its low background contribution and the clear resolution of the 658 and 662 keV lines.

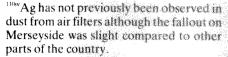
Although the levels of Hum Ag are small in both the beef and lamb liver, this radio-nuclide has not been observed in any other samples measured in this laboratory including air filters, rainwater and milk measured on 5–9 May 1986, nor in other meats and from ecological studies since.

In the beef liver we observed 23 ± 1 Bq kg⁻¹ of ^{110m} Ag, 19 ± 1 Bq kg⁻¹ of ¹³⁴Cs and 21 ± 1 Bq kg⁻¹ of ¹³⁷Cs. In lamb liver we observed 74 ± 1 Bq kg⁻¹ of ^{110m}Ag, 30 ± 1 Bq kg⁻¹ of ¹³⁴Cs and 48 ± 1 Bq kg⁻¹ of ¹³⁷Cs.

The radionuclide ^{110m}Ag is unlikely to arise as a fission product of ²³⁵U. A=110 is near the minimum of the saddle point in the asymmetric mass distribution arising from the fission of ²³⁵U by thermal neutrons. Also, a neutron-rich mass chain of A=110 produced in fission would terminate after successive β -decays at the stable nucleus ¹¹⁰ Pd before ^{110m}Ag could be reached.

A more plausible explanation is that the ^{110m}Ag is generated via the ¹¹⁰ Cd (n,p) ¹¹⁰Ag reaction. Cadmium has been widely used in nuclear reactors as a neutron absorber for control purposes, however, following the Chernobyl reactor accident, cadmium may well have been used to try to control self-sustaining fission after the core meltdown.

As liver acts as a filter for large particles in the blood it is perhaps surprising that

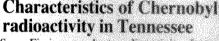


Further study of the lungs, liver and kidneys of animals reared in the areas of heavy fallout may provide yet more information concerning the Chernobyl accident.

G. D. Jones

P. D. FORSYTH P. G. APPLEBY

Oliver Lodge Laboratory, University of Liverpool, Liverpool L69 3BX, UK



Sir-Fission product radioactivity from the Chernobyl reactor accident was first detected in air samples at Oak Ridge. Tennesee on 10 May 1986. The aerodynamic sizes of the aerosol-associated fission products were evaluated in four measurements made during the period 7 May to 13 June, using Sierra high-volume cascade impactors and low-background intrinsic germanium coaxial and well detectors. Additional air and precipitation samples were also obtained over this period. The Chernobyl activity was mostly sub-micrometre in size, and the particle size increased significantly over the measurement period. Only a small fraction of the aerosol "I was soluble in CHC1,. Both 134,137 Cs and 183 Ru were less soluble than natural radioactivity, indicating some association with aerosols produced by the accident.

Two distinct phases in airborne radioactivity were evident in our measurements. The first phase lasted from 10 to 17 May and was characterized by a "Cs/" Ru activity ratio of ~1.5, resembling the airborne fission products and deposition. reported in Finland on the 28-29 April The second phase began on 18 May, when precipitation from a convective storm yielded much higher "Ru and "Ba activities, relative to "Cs, than previously found in air or precipitation. This resulted in 137 Cs/ 102 Ru ratios of <0.8, similar to that calculated from British data³. Subsequent air and precipitation samples showed that this lower 137Cs/103Ru ratio persisted until 13 June. Table 1 summarizes these

The change in ¹⁰Cs/¹⁰⁰Ru ratio on 18 May is interpreted as reflecting separate releases from the reactor which were meteorologically and/or temporally isolated. Two separate maxima in radioactivity were reported in Sweden, one on 28 April and one in the first week of May. The highest measured air concentration of ¹⁰⁰Ru, 3.7 mBq m⁻³, occurred in the 20–23 May sample By 3 June, ¹⁰¹Ru had declined to 0.1 mBq m⁻³. We have also measured the amount of aerosol ¹³¹I and its chemical

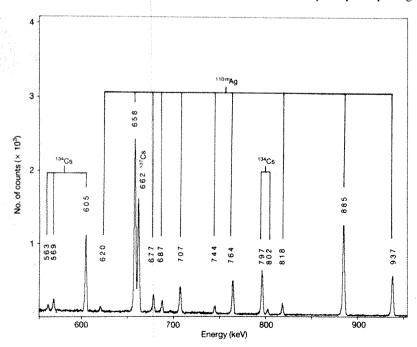


Fig. 1 A partial γ-ray spectrum arising from a sample of liver from a Welsh lamb. The count time was 57,700s. The lines are labelled by their energies in keV and by the originating radionuclides ^{110m}Ag, ¹³⁴Cs and ¹³⁷Cs.

Table 1 137Cs: fission product ratios (calculated as of 16 May 1986) measured in air (aerosol fraction) or precipitation

Fission product										
	¹⁴⁰ Ba*									
	28									
	ND									
	ND									
	ND									
	2.54									
	2.04									
	ND									
	ND									
	ND									
	1.78									
	3.9									
1.7	6.8									
֡	Cs 106Ru 17 ND 10 ND 14 ND 13 ND 10 4.60 15 2.69 18 ND 19 ND 17 ND 1									

^{* 140} Ba or derived from 140 La, assuming secular equilibrium.

Table 2 Activity median aerodynamic diameters (µm) or Chernobyl fission products and cosmogenic ⁷Be measured at Oak Ridge

	The state of the s						
Date	131	¹³⁷ Cs	¹³⁴ Cs	103Ru	106Ru	140Ba	⁷ Ba
7-16 May	0.37	0.40	0.40	0.37	ND	ND	0.38
20-23 May	0.32	0.48	0.43	0.44	0.44	0.45	0.39
30 May-3 June	ND	0.67	0.66	0.60	ND	ND	0.48
6-13 June	ND	0.72	0.71	0.62	ND	ND	0.36

ND, not detected or measured with >25% uncertainty.

composition. One of the cascade impactors operated from 7 to 16 May had a charcoal-impregnated final filter instead of the normal glass-fibre filter. Based on the 134I distributions on both charcoalequipped and normal impactors, we have estimated that ≤40% of the airborne ¹³¹I was aeorsol-associated. The actual fraction may have been smaller, as the efficiency of the filter for trapping gaseous 131I at high flow rate is not known. Both the Finnish and Swedish reports indicated that $\sim 15\%$ of the 13 I measured on 28 May was gaseous. If that fraction is applied to the Finnish data', the resulting ratio (1.0) agrees well with our aerosol "Cs/" I ratio from the 7-16 May measurement (0.89; see Table 1). Despite these qualifications, it is apparent that very little gas-to-aerosol transformation of [31] occurred during its transit to the United States.

Aerosol "I speciation was examined using methods previously applied to weapons fallout. The <0.41-µm aerosol ¹³I fraction, in both the 7-13 and 20-23 May measurements, consisted of $\sim 20\% I$. or I (or other CHC1, soluble species). No IO, was detected, in contrast to what was found for weapons-derived (ref. 4). The 0.41- to 0.73-µm fractions from these measurements showed similar CHC1,-soluble fractions.

Table 2 lists the mean aerodynamic sizes of aerosol-associated fission products reaching Tennessee. The fission product sizes increased considerably during the measurement period. By contrast, cosmogenic Be, which is initially associated with very small aerosols, is continually being added to the aerosol population. In the first two impactor measurements, ≤2% of the fission products were found to be larger than 2.1 µm, strongly suggesting the absence of any significant mechanical suspension of reactor material into the free troposphere. The behaviour and sizes of the fission products are consistent with the long-range transport of isotopes released by volatilization, which condensed on or with ambient or accident-produced aerosols. We did not find "Zr or rare-earth fission

products in our samples.

About 27% of the 144,147Cs and 46% of the Ru was not rapidly dissolved in cold 2M HC1. This behaviour is very different from what is observed for natural 'Be, Pb or 212Pb, which become associated with natural aerosols by surface condensation and are quite soluble. This poor solubility may indicate that some of the aerosol-associated fission products were

incorporated into reactor-derived materials which condensed in the hot plume leaving the reactor core. Autoradiographic evidence of such aerosols has been reported3.

This work was sponsored by the Office of Health and Environmental Research, US Department of Energy, under contract DE-ACO5-840R21400 with Martin Marietta Energy Systems, Inc.

> ERNEST A. BONDIETTI J.N. BRANTLEY

Environmental Sciences Division, Oak Ridge National Laboratory Oak Ridge, Tennessee 37831, USA

- Savolainen, I. Finnish Cent. Radiat. nucl. Safety Rep. No. STUK-B-VALO 44 (1986).
- Fry, F.A., Clarke, R.H. & O'Riordan, M.C. Nature 321.
- Devell, L. et al. Nature 321, 192–193 (1986).
 Perkins, R.W. Hith. Phys. 9, 1113-1122 (1963)

Human lipocortin similar to ras gene products

SIR—Wallner et al. recently reported the sequence of a human lipocortin complementary DNA clone. We divided the predicted amino acid sequence of lipocortin into several fragments and, using the similarity matrix comparison program FASTP², the fragments were searched against each other in order to locate any regions of internal homology. Analysis of the computer alignments of the fragments, combined with visual alignment using the nucleic acid sequence as a guide, revealed that, except for the first 43 amino acids, the protein sequence is composed of four repeats (Fig.1). Statistical evaluations of all pairwise alignments of the repeats indicate a strong homology between most of them (Table 1). Com-

Table 1 Similarly scores (z) of the alignments of the lipocortin repeats

Α	В	z(s.d.)
I + II	III + IV	24.4
I	11	11.8
I	Ш	8.5
I	IV	11.4
П	Ш	9.3
П	IV	19.4
III	IV.	3.7

The FASTP program first identifies regions of sequence similarity, and then scores the aligned identical and differing residues in those regions by means of an amino acid replaceability matrix. The statistical significance of the alignment score between the repeat listed under A and the repeat under B is expressed as the similarity score (z), which is the number of standard deviations (s.d.) that the alignment score differs from the mean of the alignment scores obtained when A was compared to 100 random shuffles of sequence B. I + II and III + IV are amino acids 44-199 and 200-346, respectively. Scores between z = 3 and z = 6 are considered possibly significant, between 6 and 10 probably significant, and greater than 10 significant2,

[†] Based on four stages from two cascade impactors.

[‡] Aerosol ratio calculated from total 131 I, assuming 15% aerosol1.

ND, not detected or measured with >25% uncertainty.

- 44 PSSDVAALHKA-IMVKGVDEATIIDILTKRNNAQRQQIKAAYLQETGKPLDETLKKALTGHLEEVVLALLKTP 115
- 11 116 AQFDADELRAA-MKGLGTDEDTLIEILASKTNKEIRDINRVYREELKRDLAKDITSDTSGDFRNALISLAKGDRSEDFGVNEDL 198
- III 199 ADSDARALYEAGERRKGTDVNVFNTILITTRSYPQLRRVFQKYTKYSKHDMNKVLDLELKGDIEKCLTAIVKCATSKP 275
- 276 AFF-AEKLBQA-MKGVGTRHKALIRIMVSRSEIDMNDIKAFYQKMYGISLCQAILDETKGDYEKILVALCGGN 346 (COGH)

Fig. 1 Alignment of the four repeats in lipocortin. The complete predicted amino acid sequence is shown except for the amino-terminal 43 residues. Two asterisks indicate positions where three or four identifal matches, occur, and single asterisks where one or two pairs of residues are the same.

		* *	*		** *	*	.*	**	****		**		*	*	*	. *				**	
Lipocortin	78	QQIKA	AYLQETG	KPLDETI	KKALT	GHLE	EVVL	ALLK	TPAQ	PDAI	DELRAA	MKGL	GTI	EDT	LIE	ILA	SRTN	KEIRI	INR	LVYR	157
c-K-ras2a	22	QLIQN	if vde ye	PTIEDSY	RKOVV	IDGE:	TCLLI	DILD	TAGQI	EEYS	SAMRDQ	YM	RT(GEGI	LC-	VFA	INNT	KSFEI)1HH	i-Yr	97
Lipocortin	158			* . SDTSGDE																	236
c-K-ras2a				EDVPMVI	- 1																

Fig. 2 Alignment of the predicted amino acid sequences of human lipocortin and the human protooncogene e-K ras2a12. Identities are indicated by asterisks and favoured amino-acid substitutions by dots. Favoured amino-acid substitutions¹³ are defined by pairs of residues belonging to one of the following groups: S,T,A,G and P;N,D,E and Q;R,K, and H;M,I,L and V;F,Y and W.

parison of the nucleotide sequences of the four repeats, aligned as in Fig. 1, revealed 41% homology on average, with repeat II being 50% homologous to repeat IV. This suggests that the four repeats evolved from a common sequence by means of gene duplication events. To what extent these structural units are congruent with the functionally active fragments' lipocortin remains to be determined.

After original submission of this correspondence, Kretsinger and Creutz' described three regions in lipocortin which are homologous to a 17 amino acid consensus sequence" from nine peptide fragments of the four related proteins P36, pll, calelectrin and endonexin. The homologous areas of lipocortin that were identified by these authors are amino acids 56 to 72 in repeat I and the corresponding areas of repeats II and IV (Fig. 1).

To find additional homologies to other proteins, we searched the predicted amino acid sequence of lipocortin against 3,061 sequences in the Protein Sequence Database of the Protein Identification Resource (PIR)16. The FASTP program revealed a strong homology between lipocortin and the mammalian ras protooncogene products, which are thought to interact with phospholipase C in a Gprotein like fashion. The similarity score (z = 8.1 standard deviations) of the alignment between lipocortin and c-K-ras2a (Fig.2) is higher than the scores found by comparing ras to any of the known Gprotein sequences.

TERRY Z. MUNN GABRIELE I. MUES

Department of Psychiatry, University of Texas Health Science Center at Dallas. Dallas, Texas 75235, USA

- 1. Wallner, B.P. et al. Nature 320, 77 (1986).
- 2. Lipman, D.J. & Pearson, W.R. Science 27, 1435 (1985).

- Blackwell, G.J. et al. Nature 287, 147 (1980)
- Hirata, F. J. biol. Chem. 256, 7730 (1981) Cloix, J.F. et al. Br. J. Pharmac. 79, 313 (1983)
- DiRosa, M. et al. Prostaglandins 28, 441 (1984). Errasfa, N. et al. Biochem. biophys. Res. Commun. 847. 247 (1985).
- Kretsinger, R.H. & Creutz, C.E. Nature 320, 573 (1986).
- Geisow, M.J. et al. Nature 320, 636 (1986).
- Barker, W.C. et al. Report of the National Biomedical Research Foundation (Georgetown University, Washington DC 1984)
- Fleischman, L.F. et al. Science 231, 407 (1986)
- McGrath, J.P. et al. Nature 304, 501 (1983). Dayhoff, M.P. et al. in Atlas of Protein Sequence and
- Structure Vol.5, Suppl. 3 (ed. Dayhoff, M.O.) 345-352 (National Biomedical Research Foundation, Washington

Evolutionary 'classics' may self-destruct

SIR-While respectively amused and bemused to see myself described as young, at 30, and as an entomologist, never having studied entomology, I feel compelled to comment on the further plethora of misinformation contained in Sibatani's recent letter', which attempted to defend the theory of evolution of Japanese scientist Imanishi against criticisms by Beverly Halstead2. At the outset let me make it clear that, contrary to Sibatani's implication in his final paragraph, my views on Imanishi's theory of evolution have not changed as a result of working with Kazumi Tanida nor do I retract any of the advice I gave to Beverly Halstead during his stay in Japan.

As the author and I have never met, the complete misrepresentation of my standpoint and persona are, perhaps, understandable. Unfortunately, the conclusions and arguments forwarded seem similarly based on a complete unacquaintance with the subject. Confusion regarding the concepts in question is evident, as typified by the paralogistic statement "... preferences may well partially overlap and are thus unlikely to explain the almost total segregation...observed...", and is also ap-

parent in the superficial dismissal of Halstead's supporting references. An informed reading of refs 3-5 will reveal them to demonstrate that groups of aquatic insects aggregate due to certain environmental and physical factors, and not due to any inherent species "protoidentity", as Imanishi would contend.

Reference 4 shows how selection of a physical variable by mayfly nymphs can "contribute significantly to the occurrence of highest densities on certain substrates and explain density shifts noted by other investigators in the field", thus adequately explaining Imanishi's wholly anecdotal field observations.

As only 0.3% of ref. 6 is concerned with "temporal segregation", it can hardly be said to "deal" with that topic, and in fact shows field and laboratory evidence of the importance of physical factors in the distribution of two sympatric trichopteran larvae. The extremely strictured rebuff, that physical preferences are accepted but may well overlap, seems to have been formulated in splendid detachment from harsh ecological reality. Rivers are not clinal continua and habitat quality can vary both temporally and spatially. Although various individual factors can affect life history parameters and maximize individual fitness". life history and distribution patterns usually represent a compromise between an interacting complex of biotic and environmental factors.

Competition itself is an interaction's. and so the attempted tautological evasion of the significance of the contents of ref. 7 fails, but does emphasize the need for a standardized definition of competition and its occurrence16

As for the quoted confirmatory evidence in the net-spinning Hydropsychidae", I feel that samples taken on only three occasions, two of which were 7 years apart, do not form an adequate logistic base for such conclusions, and the apparent loss of one species from the site during the sample period may actually provide evidence for competitive displacement or exclusion. Furthermore, in this family, the documented sequential downstream species-replacement, sometimes overlapping, sometimes disjunct, is well known12, detailed studies having revealed it to be mainly related to variations in the physical factor gradients down the length of a watercourse 12-15, while at the microhabitat level, species coexisting differed in their biotic and physical factor preferences, results agreeing with theoretical arguments based on resource partitioning16 and depressibility17.18. The regular spacing in some sites indicates territoriality, itself a form of intraspecific competition19. Larvae may fight for net sites and also possess an ultrasonic stridulatory mechanism which is used agonistically to repel intruders and to defend the site³⁶. In this family therefore, the evidence for

inter- and intra-specific competition is overwhelming and the distribution patterns are easily explained in terms of orthodox neo-darwinian theory. However, although a growing body of research has shown competition to play a critical role in determining habitat selection, survivorship and, ultimately, Darwinian fitness in some stream insects21, in other species, for example, mayfly larvae, little interspecific interaction was evident under certain conditions 12.23. There exist an immense variety of possible interspecific interactions, and dangers are inherent in overemphasizing any single aspect, and in overgeneralizing from observations taken either over a limited period. in a limited situation, or on a restricted range of species.

Scientific evidence should be based upon sound scientific data, and in this respect Imanishi's theory is found to be seriously wanting. Viewed from the ethereal realm of the philosopher, biological phenomena often differ in quite fundamental aspects than when viewed from the quantitative world of the scientist. Thus, Imanishi may have suffered the singular misfortune of basing his evolutionary theory upon non-quantitative observations made in a situation where little or no interaction occurred during the observation period. Such vague and essentially untestable theories are always difficult to disprove, but quantitative evidence usually eventually supercedes bad philosophy. As Wordsworth so eloquently phrased it, "Our meddling intellect misshapes the beauteous form of things", yet accuracy is the goal we seek. In this respect, the proposed translations of Imanishi's 'classics' may prove productive since, in addition to being "unrefined and crude"1, subjective analysis, coupled with the quantitative evidence from a growing body of research may reveal them to contain the ingredients of their own implausibility.

ANDREW ROSSITER

Laboratory of Animal Ecology,

Kyoto University,

Sakyo-ku,

Kyoto 606, Japan

- 1. Sibatani, A. Nature 320, 492 (1986).
- Halstead, L.B. Nature 317, 587 (1985). Barber, E.W. & Kevern, N.R. Hydrobiologia 43, 53-75
- 4. Wright, L.L. & Mattice, J.S. Aquatic Insects 3, 13-24 (1981).
- Hawkins, C.P. & Sedell, J.R. Ecology 62, 387-397 (1981).
- Cummins, K.W. Ecol. Monogr. 34, 271 295 (1964). Schoener, T.W. Am. Nat. 122, 240 285 (1983).
- Sweeney, B.W. in Ecology of Aquatic Insects (eds Resh, V.H. & Rosenberg, D.M.) (Praeger, New York, 1984).
- Krebs, C.J. Ecology: The Experimental Analysis of Distribution and Abundance (Harper & Row, New York, 1978).
 Ferson, S. et al. Am. Nat 127, 571 576 (1986).
 Tanida, K. Physiol. Ecol. Jap. 21, 115 130 (1984).
 Edington, J.M. & Hildrew, A.G. Caseless Caddis Larvae of the British Lieu (EPA P. De. No. 120).
- of the British Isles (FBA Pub. No. 43, 1981).

 13. Edington, J.M. & Hildrew, A.G. Verh. int. Verein, theor. agnew. Limnol. 18, 1549–1558 (1979).
- 14. Boon, P.J. Hydrobiologia 57, 167-174 (1978).
- 15. Hildrew, A.G. & Edington, J.M. J. Anim. Ecol. 48, 557
- 576 (1979).
 May, R.M. & MacArthur, R.H. Proc. natn. Acad. Sci. U.S.A. 69, 1109 1113 (1972).

Royama, T. J. Anim. Ecol. 42, 693-726 (1974)

- 18. Hassell, M.P. & May, R.M. J. Anim. Ecol. 42, 693-726
- Odum, E.P. Fundamentals of Ecology (Saunders, Philadelphia, 1971).
- Jansson, A. & Vuoristo, T. Behaviour 71, 168~186 (1979).
 Hart, D.D. in Stream Ecology: Application and Testing of General Ecological Theory (eds Barnes, J.R. & Minshall, G.W.) (Plenum, New York, 1983).
- Peckarsky, B.L. & Dodson S.I. Ecology 61, 1275 1282
- 23. Corkum, L.D. & Clifford, H.F. in Advances in Ephemeropteran Biology (eds Flannagan, J.F. & Marshall, K.E. (Plenum, New York, 1980).

Recent discoveries of a supermass in the Universe

Sir-A pair of quasars with very similar redshifts was recently interpreted as a pair of images produced by a gravitational lens of enormous mass'. However, I and the other astronomers who originally discovered the quasars23 pointed out that this pair belonged to a tight association of five quasars on the sky. The spatial grouping alone was equivalent to a 20 sigma density enhancement. The similarities in redshift of these quasars — four were at redshifts z=0.9, 1.0, 1.0 and 1.1 — had in addition only a chance of $\approx 10^{-4}$ of being accidental. Later it was shown4 that all the densest concentrations of quasars known in the sky had this concentration of redshifts around $z \approx 1$.

For gravitational lens advocates to now fasten on certain aspects of only two obiects in these physical groups which fit their interpretation — and totally ignore the other information which does not fitis tantamount to distorting the scientific data.

The enormity of the derived mass also makes it clear that there is no result which is sufficiently absurd to force rejection of the original assumption. A scientific theory must be capable of being disproved which apparently this is not.

A fascinating sequel quickly emerges when it is shown that the two supposed images of the same object are not identical in the reds. The simple conclusion which follows is that these two quasars, which have almost identical spectra, are really two separate objects. But then what happens to the arguments for the original gravitational lens? (called Q0957+561; see refs 6-8).

The argument that it had to be a gravitational lens rested on the claim that there was no other explanation for how the spectra could be so similar. (Actually one was considerably redder than the other.) What is the evidence now for gravitational

In general we should not disguise the fact that gravitational lens theories are really just another variation of 'hidden mass' or 'dark matter' hypotheses. Just as undetected (or undetectable) matter is supposed to close the Universe, so unmeasured mass in clusters of galaxies is supposed to explain large redshift dispersions

and unseen and implausibly distributed mass is supposed to explain flat rotation curves in spiral galaxies. Until scientific detection and measures of these hypothesized entities is made they should be recognized as really just statements that some part of our current physical laws are contradicted by the observations.

HALTON ARP

Max-Planck-Institut für Astrophysik. Karl-Schwarzschild-Str. 1, D-8046 Garching b. München, FRG

- Turner, E.L. et al. Nature 321, 142 (1986).
 Hazard, C., Arp, H. & Morton, D.C. Nature 282, 271 (1979)
- Arp. H. & Hazard, C. Astrophys. J. 240, 726 (1980).
- Arp, H., 307~352 (Universite de Liege, Institut d'Astrophysique, 1983); Quasars Redshifts and Controversies. (Interstellar Media, Berkely, California, 1986).
- Shaver, P. & Christiani, S., Nature in press. Walsh, D., Carswell, R.F. & Weymann, R.J. Nature 279, 381 (1979).
- Weymann, R.J., et al. Astrophys. J. 233, L43 (1979).
- Young, P., Gunn, J.E., Kristian, J., Oke, J.B. & Westphal, J.A. Astrophys. J. 241, 507 520 (1980).

Espresso coffee emporia take note

SIR—Apfel and Davy's report (Nature 321, 658; 1986) of the superheating of water by microwave ovens is totally consistent with empirical evidence obtained while using our laboratory microwave oven for preparing hot drinks (a practice sure to get us into hot water with our safety officer). I had placed a cup of tap water in the microwave and set it to boil but at first was prevented from making the drink by an experiment that required attention. On the third occasion of activating the oven, I responded to the timer bell by rushing to the oven, removing the cup and stirring my hot chocolate powder into the water which promptly erupted into a foaming cascade.

An interpretation of this dramatic event was that the water had become superheated and that the chocolate powder simply provided nucleation sites for the water to boil. In the light of Apfel and Davy's quantitative study of the superheating of water in microwave ovens it would seem that the explanation was correct. As well as offering supportive evidence and perhaps a cautionary tale, we think that a practical application of this phenomenon with coffee might be the production of energy-efficient espressos!

ANTHONY PARSONS

Department of Biology, University of York, York YOI 5DD, UK

Scientific Correspondence

Scientific Correspondence is intended to provide a forum in which readers may raise points of a rather technical character which are not provoked by articles or letters previously published.

Tensions in science

David Dickson

Scientists and Journalists: Reporting Science as News.
Edited by Sharon M. Friedman, Sharon Dunwoody and Carol L. Rogers.

Free Press/Collier Macmillan: 1986. Pp.333. \$24.95, £25.

SHORTLY after taking over as the new administrator of the US National Aeronautics and Space Administration at the end of May, Dr James C. Fletcher delivered a stinging attack on the way that the US news media had covered the Challenger accident and its aftermath. Speaking to an audience of aerospace executives, he claimed that the media had acquired a "deep and unwarranted suspicion of NASA", reflected in its highly critical investigations of the agency's management, and that the resulting coverage could do "irreparable damage" both to the space programme and to the nation.

As several journalists were quick to point out, there was a certain irony in Fletcher's remarks. For NASA has always depended, perhaps more than any other US government agency, on heavy media coverage of its activities to generate the public enthusiasm needed to justify a continued investment of funds. Furthermore, studies of the agency's relations with the media in the 1960s suggest that a "myth of invincibility" had been deliberately developed, sustained by a lack of critical reporting, and became a factor in creating the conditions leading to the Apollo fire in 1969 in which three astro-nauts died.

Fletcher's remarks, however, highlight the ambiguity that surrounds public perceptions of science and technology in modern culture. Both are viewed as sources of trust and authority, but at the same time both are seen as containing threats that undermine the assumptions on which this trust is based. The ambiguity is reflected in two very different aspects of science journalism, and the tension between them emerges from a close reading of Scientists and Journalists, a collection of essays by working journalists, media sociologists and practising scientists.

The core of the book is a series of presentations delivered to a symposium organized by the American Association for the Advancement of Science. To these have been added further contributions which, while not exhaustive in their coverage (other views are referred to in a valuable annotated bibliography), nevertheless highlight many of the complexities of what is often considered a one-dimensional debate. Furthermore, although Scientists and Journalists is written primarily for an American readership, the perspectives on display are equally applicable to the practice of science journalism

in other countries, Britain in particular.

Several articles in the volume provide detailed accounts of the way that the different actors concerned with the communication of information about science see their professional responsibilities. An articulate statement of the journalist's role is provided by Christine Russell, a science writer on the Washington Post, while that of the public relations officer is described by Carol Rogers, who is responsible for such activities at the AAAS.

Other articles give insights either into the social factors that influence how science journalists operate as a community, or into the challenges to prevailing approaches to writing about science. In the first category Sharon Dunwoody, who teaches journalism at the University of Wisconsin, describes the existence of a "science writing inner club", made up primarily of experienced journalists from the main news media in the United States, and the way this "club" can influence what is treated as news by other science journalists. In the second category, Jon Franklin, a Pulitzer prize winner who writes for the Baltimore Evening Sun, tells how he has developed a highly-personal, narrative style of science writing. A closely annotated version of one of his essays, describing a surgeon's unsuccessful attempt to remove a brain tumour, provides useful hints for conveying scientific information in a readable and absorbing manner.

Taken together, these somewhat heterogenous contributions give a valuable overview of many of the issues that are likely to confront either journalists or scientists as each side struggles to make sense of the other.

At the same time, several of the authors address, sometimes only in passing, the question "where do we go from here?" And it is on this point that the tensions and disagreements arising from the ambiguities described at the beginning of this review begin to appear. For example, implicit in many of the contributions, as indeed in much of the current debate about the "public understanding of science" on both sides of the Atlantic, is that better science journalism will result from closer collaboration between scientists and journalists. Thus Dunwoody suggests the need to develop a "shared culture" of reporters and scientists which, she considers, has already developed from virtual non-existence to "a kind of fragile, neophyte state". Rae Goodell, however, a teacher of science writing at the Massachusetts Institute of Technology, uses an analysis of the recent controversy over the safety of recombinant DNA experiments to argue that an excessively close relationship can enable scientists to manipulate the media to their own advantage

Elsewhere, divergent views about the social function of science journalism reveal themselves as reflections of broader differences over desirable forms of social decision-making. Thus Jon D. Miller suggests that the main target for news about science, particularly those aspects relevant to policy issues, should be those at or near the top of the political tree. Under normal circumstances, he says, "I don't think any useful purpose would be served by directing policyrelevant information to the nonattentive segment of the public" (those he defines as lacking either a high degree of interest in science policy, or a "functional understanding of the process of terminology of science"). In contrast, David W. Crisp, a reporter for a local newspaper in Texas



NASA has depended on the media to generate public enthusiasm for its activities.

ASA

who won an award for his coverage of the federal government's proposal to build a nuclear waste dump near his town, describes how under certain conditions the science journalist can be thrust into the role of providing crucial information to those who might otherwise be deprived of it — or who distrust other sources.

Sadly, but perhaps wisely, the editors have not attempted to pull together the wide variety of points of view represented in the book. If they had done, they would have found considerable evidence to support the argument that a closer relationship between working scientists and journalists would undoubtedly be more comfortable for science. But whether it would necessarily be equally beneficial to the non-scientific community is less clear. As William Bennett, editor of the *Harvard Medical School Health Letter*, points out, the journalist's role of "informed sceptic" is vital to the health of a science-

based democracy. And this role is never a straightforward one; in science, even more than in politics or the arts, the definition of "informed" is often open to dispute.

Nevertheless scientists who are quick to attack critical reporting of their work, or that of their colleagues, should consider a thoughtful comment from David Crisp: "Good scientists and good journalists," says Crisp, "have a great deal in common: an ingrained skepticism toward established dogma, conventional wisdom and the tyranny of commonsense; an eye for accuracy and detail; the ability to deal impartially with facts that don't fit the theory; and contempt for the pernicious theory that all passionately held ideas are of equal value".

David Dickson, Le Billehou, 91190 Gif-sur-Yvette, France, is the European correspondent for Science, and the author of the New Politics of Science (Pantheon, 1984).

Dynamic insights

J.R.L. Allen

Coastal and Estuarine Sediment Dynamics. By Keith R. Dyer. Wiley:1986. Pp.342. £36, \$63.35.

SEDIMENT transport dynamics is of great importance in several disciplines, each of which, in its traditional garb, approaches the subject from a special standpoint and with particular perceived needs. This is why it is so hard to write about it well. Sedimentologists and geomorphologists are best able to discuss the outcomes of sediment transport, namely what, in the form of sedimentary textures, structures and larger scale formations, has to be explained. From fluid dynamicists and rheologists come the necessary theoretical and experimental insights into the roles of fluid motion and particle mechanics in sediment transport. Engineers, with their emphasis on an empirical, pragmatic approach, are best equipped to provide from contemporary environments and from the laboratory many of the additional links necessary for the appreciation of sediment transport and its real effects in quantitative terms.

Writing about sediment dynamics as expressed in shallow-marine environments, Dr Dyer rightly attempts to blend these three traditional approaches — sadly, still a rare venture. The result is a lucidly written book which, if with limitations here and there on the descriptive and theoretical sides, and a singular lack of photographic illustrations, is up to date and largely a success.

The book begins with a brief survey of the subject and a sketch of sediment production and the geological context of

modern shallow-marine sedimentation. Next come discussions of sediment particles as such and the fluid flow; more emphasis could usefully have been placed on the diversity and significance for transport of particle shapes, and on mass transport currents in waves. Chapter 3 covers sediment entrainment, one-way transport in suspension and as bedload, and bedforms (inadequately characterized). The following brief chapter examines sediment movement under waves, but the resulting bedforms are again ill-characterized and the origin of wave ripples is not explored. The further treatment of sediment suspension includes useful accounts of stratification by suspended particles and the suspension profile under waves.

In Chapter 7 Dyer compares sediment transport-rate formulae and sketches the important but under-researched topic of transport beneath waves and waves combined with currents. Not surprisingly, given the author's background, the treatment of cohesive sediments is excellent, except for the surprising omission of the by no means negligible mass-movement processes. Estuarine and coastal sedimentation are well summarized, as are beach processes, but the important role of storms in causing unusual sediment transport in these environments is ignored. An extensive bibliography (c. 1,000 items) and a short index conclude the book. Readers should beware equations 3.6 and 11.17, incorrectly set, and a mis-spelling of Bernoulli. Regrettably, SI units are eschewed.

This book has its faults. But it broadens our appreciation of sediment dynamics in shallow-marine environments, and deserves to be read and used.

J.R.L. Allen is a Professor in the Department of Geology, University of Reading, Whiteknights, Reading RG6 2AB, UK.

Framework for twistors

Abhay Ashtekar

Spinors and Space-Time. Vol. 2 Spinor and Twistor Methods in Space-Time Geometry. By R. Penrose and W. Rindler. Cambridge University Press: 1986. Pp.501. £45, \$89.50.

Twistors were invented by Roger Penrose about 20 years ago. Since then he and his research group have worked on the subject steadily and have built it into a thriving branch of mathematical physics. The goal of the twistor programme is very ambitious - first to recast and then further develop all of known physics within a framework in which space-time itself is a derived, secondary object. Considering that relatively few individuals have been involved in the programme, the results to date are most impressive from a mathematical standpoint. Indeed, even if it should turn out that the ideas cannot be taken any further because of some intrinsic limitation, the fact that so much of the basic mathematical structure underlying relativistic physics can be constructed without a direct reference to space and time is, in itself, sufficient to make this endeavour fascinating. It is therefore regrettable that most mathematical physicists know virtually nothing about twistor theory. In part, this is because very little of the recent literature on the subject is accessible to non-specialists. The second volume of Spinors and Space-Time is intended to remedy this problem, and it does so very satisfactorily.

The authors first introduce the basic ideas of twistor theory, including some of the recent developments, and then go on to discuss a number of constructions of use in general relativity which are simplified and, in some cases, inspired by this theory. Since the relevant results and equations from Vol. 1 are recalled at the beginning of the book, readers familiar with 2-component spinors can go directly to Vol. 2.

The introduction to twistor theory is fairly detailed. Readers are first exposed to the non-local relation between the geometry of twistor space and of Minkowski space-time; they are then shown that the momentum angular-momentum structure of particles and fields can be coded in a natural way in the twistor picture; and, finally, they are presented with the description of the zero rest mass fields in terms of contour integrals and cohomology on the twistor space. It is remarkable that, although the relation between the twistor space and space-time is non-local, solutions to physically interesting local differential equations in spacetime can be represented in a natural way in twistor space. This interplay between cohomology on complex manifolds and solutions to differential equations on real manifolds is extremely interesting, because it brings together two otherwise unrelated branches of mathematics in an unexpected way. The outstanding application of these ideas to general relativity is the definition of quasi-local quantities which attempts to capture the notion of total energy-momentum and angular momentum associated with the region of space-time enclosed by a topological 2sphere. The current status of this definition and its consequences is described in detail. In addition, several mathematical results on null congruences, on algebraic classification of curvature tensors and on asymptotic structure of space-time at null infinity, which are simplified and illuminated by the use of twistor methods and the spin coefficient techniques, are presented in varying degrees of detail and completeness.

This is primarily a work in mathematics rather than physics. The emphasis is on illustration of the power and elegance of certain techniques rather than on provision of a comprehensive treatment of topics that are of direct application in general relativity. Consequently, the discussion is not uniform; points dealing with twistoral ideas and spin coefficient methods are treated thoroughly, while those requiring ideas from elsewhere are often mentioned only briefly.

Overall, there is a considerable difference between this volume and its companion. Volume 1 (reviewed in Nature 313, 607; 1985) appeared as a finished, definitive work that could be used in courses as well as by individual researchers. Volume 2, on the other hand, has a mixed flavour. Parts of it, such as the treatment of quasi-local mass, report the current state of the art. These parts have the style of lecture notes rather than that of a monograph. Furthermore, none of the chapters has an introductory section to map out the material that follows. Consequently, it is sometimes difficult to see where one is headed, and only those readers who are already familiar with more conventional treatment of topics such as gravitational radiation theory, and energy-momentum and angular momentum in general relativity, will be able to appreciate the simplifications and insights provided by twistor methods. Volume 2, therefore, is primarily for researchers who want to understand the spirit of twistor theory and for teachers of courses on general relativity who want to broaden their knowledge of the field.

Abhay Ashtekar, a Professor of Physics at Syracuse University, New York, is currently at the Institute of Theoretical Physics, University of California, Santa Barbara, California 93106, USA.

Strategy for future weather

Nicholas A. Rupke

Climatic Change and World Affairs, Revised Edition. By Crispin Tickell. Center for International Affairs, Harvard University/University Press of America: 1986. Pp.76. \$17.50; pbk \$7.25. Distributed in Britain by Eurospan, 3 Henrietta Street, London WC2E 8LU. Hbk £16.55; pbk £7.30.

ERRATIC blocks and boulders, strewn across much of northern Europe and North America, reminded our ancestors of the waters of the biblical deluge. By around 1840, the Swiss naturalist Louis Agassiz concluded that these erratics had been put in place by gigantic ice sheets, and were evidence of a former Ice Age.



Heavy cloud in the southern hemisphere, as seen from Apollo 17. The photo extends from the Mediterranean to the Antarctic.

Thus began the scientific study of glacial climatic change in the geological past — change which, during the most recent, Quaternary Period of Earth history, has included half a dozen ice ages alternating with warmer interglacial stages. Simultaneously, however, our awareness of the vast extent of geological time has grown and, as a result, the historic reality of climatic upheaval has receded into the dim distance of "millions of years" before (or after) us.

Crispin Tickell's "brilliant short book" (to quote from Lord Zuckerman's introduction to the British edition) warns us, however, against a false sense of security and an après nous le déluge complacency. Our seemingly stable climate is in fact a vulnerable and changeable product of a

great many astronomical and terrestrial factors. Moreover, man himself has become a potentially destabilizing factor as a consequence of large-scale environmental mismanagement, such as the pollution of the air with carbon dioxide, aerosols and other industrial wastes which change the heat balance of our atmosphere.

Much has already been written about the threat to world climate - some authors demonstrating the scientific complexity and uncertainties of the issue, others giving free rein to doomsday predictions of imminent catastrophe in the form of a new and prolonged Arctic winter or, conversely, of the precipitous melting or surging of polar icecaps and a consequent rise in sea level. In this revised edition of a book first published in 1977 Tickell again succeeds in walking the tightrope between these two approaches: he presents an intelligible account of world climate in all its scientific complexity, but does so without letting the reader

lose a sense of the reality and potential immediacy of a calamitous deterioration. After all, only a relatively small change of a few degrees Celsius in mean global temperature would suffice to trigger an irreversible feedback process of glacial expanse or retreat at the poles.

The author (who is Permanent Secretary of the Overseas Development Administration in London) has examined the subject with the eyes of both science and international affairs. In a "call for action" he forcefully argues for the need to get some form of international agreement on how to cope with future climatic crises. More specifically, Tickell proposes that administrative responsibility be given to the World Cli-

mate Program (adopted in 1979 by the World Meteorological Organization) as the custodian of a series of climatic agreements. These should cover all major experiments and actions (industrial and military) which affect the climate. Furthermore, an international code of good climatic behaviour should be adopted and enforced by means of various economic measures.

Beginners and specialists alike will find Climatic Change and World Affairs lucid and stimulating, particularly if they are interested in science policy and international cooperation in the study of weather and climate.

Nicholas A. Rupke is a geologist and an historian of science at Wolfson College, Oxford OX2 6UD, UK.

Vegetative roots differ

Peter D. Moore

Studies on Plant Demography: A Festschrift for John L. Harper. Edited by James White. Academic: 1985. Pp.416. Hbk £45, \$59.50; pbk £22, \$29.50.

The Population Structure of Vegetation. Handbook of Vegetation Science, Vol.3. Edited by James White. Dr W. Junk: 1985. Pp.669. Dfl. 310, \$97.50, £85.95.

THROUGHOUT the history of plant ecology there have been profound disagreements over the most realistic, or at least the most intellectually profitable, way of studying vegetation. Is vegetation simply a "fortuitous juxtaposition of plant individuals", as maintained by Gleason? Or is it an orderly assemblage of recurrent plant associations, as conceived by certain schools of phytosociology? Plant population biology is essentially the product of an individualistic way of thinking: it is concerned with the interactions between adjacent members of a population, their growth, reproduction and mortality. But the overview of vegetation which the phytosociologist seeks to present must still recognize populations of plants, perhaps co-evolved, as the elemental structures from which higher levels of organization

Two approaches to the subject are thus possible: we can begin with vegetation and work down towards the individual, or we can begin with the individual in its population and gradually extend towards the more complex interactions of the community. In the books under review we find the two schools of thought effectively and separately illustrated, which is a credit to James White who edited both volumes.

John Harper, to whom the first book is dedicated in celebration of his sixtieth birthday, is rightly regarded as the founding father of plant population biology, and his perspective on the subject is essentially Darwinian and analytical; a view of architecture that begins with the

R.K. Peet has edited Plant Community Ecology: Papers in Honour of Robert H. Whittaker, which contains papers written by Whittaker's past colleagues and students after his death in 1980. Rather than review Whittaker's own contributions. Peet chose to illustrate current applications of approaches Whittaker developed and to show recent advances which have grown from his pioneering work. The papers are arranged in four sections, representing areas of plant community ecology which were strongly influenced by Whittaker: Methods of community analysis. Analysis of gradients, Community dynamics and Species Diversity. Published by Dr W. Junk as Vol. 7 of the "Advances in Vegetation Science". Pp.332. Dfl. 200, \$68, £55.50.

bricks. This collection of papers by his past students amply demonstrates the value of such an approach. Take John Ogden's work on forests, for example. In this type of habitat the long life-history of the individual gives an impression of stability, but population studies reveal a constant turnover, a mosaic of recovery stages from past disturbances — what Henry Horn has described as a "preemptive crazy quilt" of vegetation.

Mobility, of course, is a special problem for plants, but one that must be overcome if the patchwork of opportunities in the environment is to be fully exploited. Noble illustrates the effectiveness of birds in transporting seeds even when the birds in question cannot fly, as in the case of the gut carriage of *Nitraria* by emus in Australia.

Turkington, on the other hand, expands on the value of vegetative growth by stolons in clover. Clones can spread extensively in this way (some ecologists even talk of such plants "foraging"), but though the propagation of vegetative clones provides a form of mobility it can lead to a general lack of genetic diversity. In Turkington's view, the input of new genotypes by somatic mutation and occasional germination of new individuals is adequate to provide this required genetic variability.

Studies such as these on clover can lead to confusion about what really constitutes an individual plant. One approach is to consider a plant as a collection of relatively independent units. This idea of modular growth, where each module is the product of a single meristem, is particularly attractive and is exemplified here by Michelle Jones's report of her work on silver birch. In the case of trees, the branching systems differ in their "modular dynamics" because they are influenced by neighbours and respond by the formation of varying crown geometries. The implications of such studies for forestry are further developed by Miguel Franco.

The total collection of papers provides a wide range of examples from current studies in plant population biology. Most of these have originated from Harper's work and ideas, and are now taking root and ramifying.

In The Population Structure of Vegetation, James White is at pains to encourage the recognition of the complementarity of the demographic and sociological approaches. But it is vegetation that is quite recognizably the starting point of most of the papers included here, rather than population studies on individual species. Perhaps the key to the difference in thinking lies in the paper by T.A. Rabotnov on the dynamics of plant coenotic populations. But what, we may be forgiven for asking, is a coenotic population? It is defined as the sum of the individuals of a species within a plant community (the phytocoenosis), and is a concept arrived at by Rabotnov himself (the founding father of the Soviet plant coenotic population biology to whom this book is dedicated) as a result of the mental dissection of vegetation into its interacting components.

One of the consequences of this way of looking at population biology is the need to examine the demography of many different species at the same time; the detailed analysis of one species is of little value in isolation. Inevitably this leads to less-rigorous, less-numerical conclusions than typify the Harper school, but it also encourages the tendency to classify plants according to their interactive "strategies" as a means of simplifying community description. Some interesting proposals have resulted. The threefold classification of plants into "violents", "patients" and "explerents" by Ramenskii, for example, foreshadows the work of Grime, who also summarizes his current views in this volume. But such simple classification systems are not universally adopted by the contributors. Indeed, Grubb provides a detailed argument against the use of such models, demanding a much more critical attitude to the use of such terms as "stress", "tolerance", "dominance", "disturbance" and "competition", and calling for more attention to be given to the factors which permit coexistence among plants.

One prominent aspect of this book are the contributions of Soviet scientists, and Markov's paper on the use of permanent quadrats in the Soviet Union opens up for Westerners a useful window on Eastern ecology. Most of the Soviet papers are concerned with coenotic population research in steppic environments, but more occidental studies are also included, from chalk grasslands in the Netherlands to the cedar groves of the south-eastern United States. There are even some contributions that wander slightly from the "coenotic" theme, such as the demographic study of Plantago major and P. lanceolata by van der Aart. But even here the main emphasis is upon the variation in demography according to the plant's habitat - paths, hay fields, dunes, roadsides, pastures and so on — so the community remains the centre of interest.

Perhaps the most remarkable feature to emerge from these two books is the great difference in the starting point and the approach found in each and yet their tendency to generate lines of convergence. These lines will undoubtedly culminate in fruitful fusions, possibly under the diplomatic eye of James White, the sole common factor. Meanwhile, the balanced botanist must obviously have access to both.

Peter D. Moore is Reader in Ecology in the Department of Biology, King's College London (KQC), 68 Half Moon Lane, London SE24 9JF, UK.

What to believe about miracles

from R.J. Berry

Differences of interpretation within the Church of England have stimulated a re-examination of the "miracles" as recounted in the Bible.

Two years ago I was one of 14 signatories of a letter to the Times about miracles All of us were professors of science in British universities; six were Fellows of the Royal Society. We asserted: "It is not logically valid to use science as an argument against miracles. To believe that miracles cannot happen is as much an act of faith as to believe that they can happen. We gladly accept the virgin birth, the Gospel miracles, and the resurrection of Christ as historical events. . . Miracles are unprecedented events. Whatever the current fashions in philosophy or the revelations of opinion polls may suggest, it is important to affirm that science (based as it is upon the observation of precedents) can have nothing to say on the subject. Its "laws" are only generalizations of our experience...

A leading article in Nature accepting our statement on the nature of scientific laws, dissented from our conclusion about miracles, terming them "inexplicable and irreproducible phenomena (which) do not occur - a definition by exclusion of the concept. . . the publication of Berry et al. provides a licence not merely for religious belief (which, on other grounds is unexceptionable) but for mischievous reports of all things paranormal, from ghosts to flying saucers".

Subsequent correspondents disagreed. For example, Clarke objected that "your concern not to license 'mischievous reports of all things paranormal' is no doubt motivated in the interest of scientific truth, but your strategy of defining away what you find unpalatable is the antithesis of scientific"; MacKay4 emphasized that "for the Christian believer, baseless credulity is a sin - a disservice to the God of truth. His belief in the resurrection does not stem from softness in his standards of evidence, but rather from the coherence with which (as he sees it) that particular unprecedented event fits into and makes sense of a great mass of data. . . . There is clearly no inconsistency in believing (with astonishment) in a unique event so well attested, while remaining unconvinced by spectacular stories of 'paranormal' occurrences that lack any comparable support".

The credibility of belief in miracles has resurfaced in a report of the Church of England bishops⁵. The *Times* commented: "Did the two key miracles at the centre of the Christian faith, the Virgin Birth and the Resurrection, really happen?... The

that belief in miracles, at least where they are central to the faith, is thoroughly intellectually respectable. . . "6.

It would be easy to decry the criteria or standards of proof accepted by the bishops, but their integrity is presumably not in doubt. It is more profitable to enquire whether miracles are really credible, and, if so, what are the circumstances where they might be expected.

Natural law

"In an earlier age, miracles would have been one of the strongest weapons in the armoury of apologetic. A man who did such things must at the very least have the power of God with him. Jesus himself is represented as using this argument when he said, 'If it is by the finger of God that I cast out demons then the kingdom of God has come upon you' (Luke 11:20). For us today, by one of those twists that make up intellectual history, miracles are rather an embarrassment. We are so impressed by the regularity of the world that any story which is full of strange happenings acquires an air of fairytale and invention"7. The historical twist referred to by Polkinghorne was an inevitable consequence of the separation of observation (or test) from interpretation, which is the essential feature of what we call science. Before the sixteenth century "how" and "why" questions were answered in much the same way: acorns fell to the ground so that new oaks might grow; rain came so crops might flourish and people feed; and so on. The realization that the same event could be interpreted in more than one way led to an emphasis on mechanism, and therefore on the uniformity and predictability of natural events, with a consequent restricting of divine activity to the ever-decreasing gaps in knowledge. God became unnecessary, except as a rationalization for the unexplainable⁸.

By the seventeenth century scientists were using the "laws of nature" in the modern sense, and the physical and (increasingly) the biological worlds were regarded as self-regulating causal nexi. God was merely the "First Cause", and could intervene in the world only by breaking or suspending the "natural laws". Locke and Hume used the determinism of newtonian physics to argue that natural laws were inviolable, and therefore that miracles could not happen9. Their conclusion seemed to be vindicated exercise has established one thing clearly: I in the nineteenth century when the dar-

winian revolution purged from biological systems the simple notion of purpose and created pattern. And as Cupitt says, "religion was more badly shaken when the universe went historical in the nineteenth century than it had been when it went mechanical in the seventeenth century" The futility of believing in a god unable to do anything exposed the problem that spurred the English bishops to re-affirm that miracles could happen"

Miracles and mechanisms

Defenders of miracles have tended to descend into an unconvincing mysticism or an assault on determinism. A few decades ago, it was fashionable to claim that physical indeterminancy gave God enough freedom to control events. Biological indeterminancy is a live debate now, particularly in sociobiology. For example, Lewontin (unlikely to argue that miracles are common or important) strongly attacked the reality of biological laws beyond "very special rules of comportment or particular physical entities . . . If we are to find biological laws that can be the models for social laws, they will surely be at the level of laws of population. laws of evolution, laws of organization, But is is precisely such laws that are absent in biology, although many attempts have been made to erect them"

However, the case for miracles does not depend on indeterminancy, since the intellectual orthodoxy stemming from Hume's underlying thesis is not as strong as it is usually made out to be. C.S. Lewis pointed this out succinctly: "We must agree with Hume that if there is absolutely 'uniform experience' against miracles, if in other words they have never happened. why then they never have. Unfortunately we know the experience against them to be uniform only if we know that all the reports of them are false. And we know the reports to be false only if we know already that miracles have never occurred. In fact, we are arguing in a circle"

Exposing the fallacy of Hume's attack on miracles also reveals that it is based on an unjustified assumption, that events have only a single cause and can be fully explained if that cause is known. This is logically wrong. For example, an oil painting can be "explained" in terms either of the distribution of pigments or the intention and design of the artist; both explanations refer to the same physical object but they complement rather than conflict. In the same way, a miracle may be the work of (say) a divine up-holder of the physical world rather than a false observation or unknown cause. Such an interpretation does not depend on any irruption into a causal network, since the determinism of the machine is only one of the levels of the phenomenon (sensu Polanyi15).

'Complementary" explanations causation are excluded only by making the reductionist assumption that a single identifiable cause is the sole effect operating in a particular situation. This assumption is common, but unnecessary and restrictive. Medawar has dissected this clearly: "That there is indeed a limit upon science is made very likely by the existence of questions that science cannot answer and that no conceivable advances of science would empower it to answer. These are the questions that children ask — the 'ultimate questions' of Karl Popper. I have in mind such questions as: How did everything begin? What are we all here for? What is the point of living? Doctrinaire positivism — now something of a period piece — dismissed all such questions as nonquestions or pseudoquestions such as only simpletons ask and only charlatans of one kind or another profess to be able to answer. This peremptory dismissal leaves one empty and dissatisfied because the questions make sense to those who ask them, and the answers to those who try to give them; but whatever else may be in dispute, it would be universally agreed that it is not to science that we should look for answers. There is then a prima facie case for the existence of a limit to scientific understanding.

As far as miracles are concerned, this means that they are impossible to prove or disproye on normal scientific criteria; we accept the possibility of their occurrence by faith, and equally deny them by faith. Even if we know or deduce the mechanism behind a miracle, this does not necessarily remove the miraculous element. For example, the Bible tells us that the Israelites crossed the Red Sea dry-shod because "the Lord drove the sea back by a strong east wind all night and made the sea dry land" (Exodus 14:21); the significance of the miracle lies in its timing and place rather than its actual occurrence.

Implications

The act of faith that denies the possibility of miracles is a straightforward reductionist judgement. Miracles by themselves are always susceptible to an explanation other than the miraculous (even if they have physical manifestations, such as "spontaneous" healing or the Empty Tomb), so the value of the reductionist assumption can be best tested by its implications. These were spelt out with depressing clarity in the nihilism of Jacques Monod[®], and comprehensively answered by W.H.

dualism of Sherrington, Eccles and Popper which is kin to the complementarity espoused above19.

There are implications of embracing a reductionist determinism which impinge on two recent controversies: creationism and the definition of human life. Creationism is largely an insistence that God made the world in a particular way, without using "normal" evolutionary mechanisms. Part of this claim stems from a restricted interpretation of the Bible, but it has the effect of prescribing that God acted in an interventionist fashion. Notwithstanding, it is entirely consistent with both evolutionary biology and Bible texts to maintain that God worked "complementarily" with genetic processes so that the world is both a causal outcome of mutation, selection, and so on, but also a divine creation. The creationist position is at odds with both scientific and theistic understanding^{20,21}. Individual human life has a physiological and genetic continuity with that of other humans (and indeed, other animals); the value of individual life lies not in genetic uniqueness (cancers and hydatidiform moles are also genetically unique) but in being (in Christian language) "made in the image of God". This imago is not a physical entity, and it is a category mistake to confuse it with genetic coding or mental function. Notwithstanding, defenders of the inviolability of the early embryo make this precise mistake. The imago is a non-biological attribute, and there is no logical (or scriptural²²) reason for assuming that it is present from conception. If this simple point was realized, the ethical debate over developments in human reproduction could proceed more sensibly.

The conventional view of miracles is that they depend on supernatural intervention in, or suspension of, the natural order. Some theologians have been overimpressed with scientific determinism. and have attempted a demythologized (miracle-free) religion. This endeavour is now unfashionable, but it is worse than that; Nebelick called it "a speculativedevice imposed on unsuspecting persons. . . based on false presuppositions about both science and the scientific world view"23. This is no help to scientists, and an interventionalist God will always be an embarrassment to us.

I believe that the interpretation that miracles are a necessary but unpredictable consequence of a God who holds the world in being is more plausible and more scriptural than deist interventionism. This does not mean that apparent miracles should be approached with any less objectivity than we would employ for any scientific observation; our standards of evidence should be just as rigorous. Those who deny the possibility of miracles are exercising their own brand of faith; this is Thorpe who expounded a version of the | based on a questionable assumption, and |

one which creates problems with its implications. Miracles in the New Testament are described as unusual events which are wonders due to God's power, intended as signs. Confining oneself wholly to this category (leaving aside the question of whether other sorts of miracles occur), this makes at least some miracles expectable and non-capricious, and independent of any knowledge of their mechanism.

In his exposition of the "Two Cultures". C.P. Snow described the scorn of the one for the other as intellectual Ludditism²⁴. Miracles are examples of events which may easily be denied by an illegitimate reductionist Ludditism; scientific reality will be hindered in the process. A doctrinaire disbelief in miracles is not "more scientific" than a willingness to accept that they may occur. Some years ago Sir George Porter wrote: "Most of our anxieties, problems and unhappiness today stem from a lack of purpose which was rare a century ago and which can fairly be blamed on the consequences of scientific inquiry. . . There is one great purpose for man and for us today, and that is to try to discover man's purpose by every means in our power. That is the ultimate relevance of science"25. He was not writing specifically about miracles, but his argument applies. Miracles are not inherently impossible or unbelievable, and acceptance of their existence does not necessarily involve credulity, but does involve recognizing that science has limits.

Professor R.J. Berry is at the Department of Zoology, University College London, Gower Street, London WC1E 6BT, UK.

- The Times (London) (13 July 1984).
- Nature 310, 171 (1984). Clarke, P.G.H. Nature 311, 502 (1984).
- MacKay, D.M. Nature 311, 502 (1984)
- The Nature of Christian Belief (Church House, London,
- The Times (London) (6 June 1986).
- Polkinghorne, J. The Way the World Is (SPCK. London, 10831
- Coulson, C.A. Science and Christian Belief (Oxford University Press, 1955).
 Brown, C. Miracles and the Critical Mind (Eerdmans,
- Grand Rapids, 1984). Cupitt, D. The Sea of Faith (BBC, London, 1984).
- 11. Harris, M.J. Easter in Durham (Paternoster, Exeter, 12. Berry, R.J. Free to be Different (ed. Stott, J.R.W.) Ch.5
- Berry, R.J. Pree to be Different (ed. Stott, J.R.W.) Ch.S (Marshall, Morgan & Scott, Basingstoke, 1984).
 Lewontin, R.C. Population and Biology (ed. Keyfitz, N.) Ch.1 (Ordina, Liege, 1985).
 Lewis, C.S. Miracles (Bles, London, 1974).
- 15. Polanyi, M. Knowing and Being (Routledge & Kegan-Paul, London, 1969).
- 16. Medawar, P. The Limits of Science (Harper & Row, New
- 17. Monod, J. Chance and Necessity (Collins, London, 1971). 18. Thorpe, W.H. Purpose in a World of Chance (Oxford University Press, 1978).
- 19. MacKay, D.M. Freedom of Action in a Mechanistic Universe (Cambridge University Press. 1979); Human Science and Human Dignity (Hodder & Stoughton, London, 1979)
- 20. Midgley, M. Evolution as a Religion (Methuen, London,
- 21. Berry, R.J. Epworth Rev. 13, 74-85 (1986).
- Rogerson, J.W. Abortion and the Sanctity of Human Life, (ed. Channer, J.H.) Ch.4 (Paternoster, Exeter, 1985).
- Nebelick, H.R. Scot. J. Theol. 37, 239 (1984).
- Snow, C.P. The Two Cultures (Cambridge University Press, 1975)
- 25. Porter, G. The Times (London) (21 June 1975).

Terrestrial origin of the Moon

A. E. Ringwood

Research School of Earth Sciences, Australian National University, Canberra, ACT 2601, Australia

Abundance patterns of siderophile elements in the Earth's mantle have been determined by complex processes connected with internal segregation of a metallic core amounting to 32% of the Earth's mass. Although the lunar core may be only 2% of the lunar mass and formed in very different conditions to the Earth's core, the lunar siderophile pattern is closely related to that of the Earth's mantle, implying that the material in the Moon derived mainly from the Earth's mantle after core formation. New models for the accretion of the Earth which require impacts by large planetesimals in the presence of a corotating primitive terrestrial atmosphere provide a mechanism for transferring material from the Earth's mantle into geocentric orbit as a ring of proto-lunar planetesimals, from which the Moon later accreted.

More than a century ago, Darwin¹ studied the tidal evolution of the Earth-Moon system and concluded that the Moon had been torn out of the Earth's mantle by a tidally induced fission process. Subsequently, it was realized that this would explain the anomalously low density of the Moon compared with the bulk Earth. Darwin's hypothesis enjoyed several decades of popularity before lapsing into obscurity after Jeffreys² had demonstrated that the proposed fission mechanism was physically unsound. Thereafter, it was generally considered that the low density of the Moon could be explained by an extension of the same processes responsible for causing marked differences between the intrinsic densities of the terrestrial planets (see refs 3, 4). Essentially, the Moon was regarded as having formed by processes analogous to those experienced by independent planets.

Jeffreys3, Urey4 and many others explained the intrinsic density variations between the terrestrial planets by assuming that they are composed of varying proportions of silicate (initial density, $\rho_0 = 3.3 \text{ g cm}^{-3}$) and nickel-iron ($\rho_0 = 7.9 \text{ g cm}^{-3}$) phases, each being essentially of constant composition. According to this model, Mercury and Mars contain ~65% and 20% of metal phase respectively whilst Earth and Venus possess intermediate metal contents. The model implies that the Moon contains <5% of metal phase. Urey^{5,6} proposed that physical processes occurring in the solar nebula before accretion of the planets had caused variable degrees of fractionation of iron particles from silicate particles in different regions of the nebula. Subsequent accretion of planets in particular regions reflected these pre-existing metal/silicate inhomogeneities. The major role attributed to metal/silicate fractionation in the solar nebula was supported by measurements which seemed to show that the abundance of iron in the Sun was lower by a factor of 5 than is found in Earth, Mars and chondritic meteorites. Urey's interpretation became widely accepted and has been reflected in subsequent cosmogonic models^{7,8}

Since 1959, I have argued that the mechanisms invoked by the above hypotheses to explain the metal/silicate fractionations were physically implausible and therefore attempted to develop a cosmogonic model aimed at minimizing the role of this process⁹⁻¹¹. The model proposed that the relative abundances of iron and the common lithophile elements (Mg, Si, Ca, Al) were the same in Mars, Earth and Venus, and were similar to those in the Sun and in chondritic meteorites. Differences in density between Mars, Venus and Earth were caused by differing oxidation states, a variable which was readily explained on cosmochemical grounds.

This interpretation received substantial support in 1969 when a more accurate determination of the relative abundance of iron in the Sun showed that it was similar to that in chondrites 12. Moreover, new space probe measurements have since provided precise values of the densities of Venus and Mars and of the martian moment of inertia. It was readily demonstrated that the gross physical (and chemical) properties of Venus, Earth and Mars were explicable in terms of models based on chondritic abundances of major elements, differing in mean oxidation state, with Mars being significantly more oxidized than Earth and Venus 11. The only planet displaying the effects of major metal/silicate fractionation is Mercury. Several authors have suggested that its high density, implying a high iron content, may be caused by specialized conditions of accretion, owing to its position nearest to the Sun 8,10.

These considerations have an important bearing on the origin of the Moon. During the period 1950-70, most scientists treated the Moon as representing an extreme case of the general process of iron/silicate fractionation which was believed to have occurred between Sun and planets, and between the planets themselves. In this sense, it was regarded as an 'independent planet', which, owing to special circumstances, had accreted in orbit around the Earth or had been captured into Earth orbit.

However, we now recognize that the Moon must have accreted in a region of the Solar System between Earth, Mars and Venus, and probably close to the Earth. Currently, there is no evidence requiring iron/silicate fractionation between these planets and the Sun. From this perspective, the high depletion of metallic iron in the Moon must be recognized as a truly remarkable phenomenon. This led me in 1960 to revive Darwin's hypothesis that the material now in the Moon was derived from the Earth's mantle by a fission process, albeit employing a different mechanism¹³ from that proposed by Darwin. Analogous fission-related hypotheses were also developed during the 1960s by Wise¹⁴, Cameron¹⁵ and O'Keefe¹⁶. Subsequently, I abandoned the fission mechanism and developed another model in which the Moon was formed from material evaporated from the Earth's mantle in a high-temperature regime caused by rapid accretion of the Earth^{10,11,17-19}.

If the Moon were indeed derived from the Earth's mantle, one might hope to find supporting evidence in a comparison of the chemical compositions of both bodies. Unfortunately, there are divergent views among geochemists regarding the major element composition of the Moon. Some believe that the Moon's composition is similar to that of the Earth's upper mantle 11,20,21, whereas others 22,23 believe that refractory elements are markedly

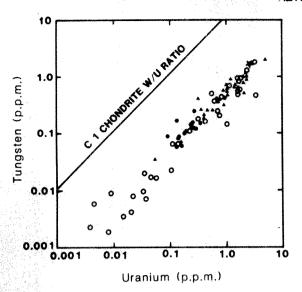


Fig. 1 Tungsten (siderophile) and uranium (lithophile) concentrations in terrestrial and lunar rocks. ○, Earth's mantle; ★, upper crust; ♠, lunar mare; ♠, lunar highlands. The W/U ratios in both bodies are remarkably similar despite the fact that core formation within the Earth caused tungsten to be relatively depleted in the upper mantle by a factor of ~25 compared with the primordial C1 W/U ratio (solid line). The lunar samples include both mare and highland rocks, showing that the lunar W/U ratio is of global significance. (After refs 33, 49, 52.)

enriched in the Moon. But is there any other source of compositional evidence which points unambiguously towards a terrestrial origin? I believe that the answer is provided by the siderophile geochemistry of Earth and Moon.

Siderophile geochemistry

The abundance patterns of siderophile elements in the Earth's mantle display some remarkable characteristics. For example, Ni, Co, Cu, Fe, Ga, W, Mo, P, As, Sn, Ag and Ge are present at levels ranging between 1 and 16% of their primordial abundances^{24–28}. Little relationship exists between the partition coefficients for these siderophile elements between silicate and metallic iron phases, and their relative abundances in the mantle. The platinoids, Au, Re, S, Se and Te, are present in the mantle at $\sim 0.3\%$ of their primordial abundances^{25,27–29}. Most of the above siderophiles are considerably overabundant in the mantle compared with expectations based on experimentally determined partitions between silicate and metallic iron phases.

Chromium and vanadium, which display distinct siderophile tendencies above 1,500 °C (refs 30, 31), are significantly depleted in the mantle by factors of 2 and 1.5, respectively²⁵. These depletions almost certainly reflect their partial entry into the core³². Manganese also displays a fourfold depletion which may be caused either by entry into the core^{20,32,33} and/or by loss due to volatility²⁴.

The above patterns have evidently been caused by a combination of several complex processes, as yet incompletely understood, which occurred during the segregation of a metallic core, amounting to 32% of the Earth's mass. Partitions of siderphiles would have been affected by the very high pressure (P) and temperature (T) regime under which this process operated, and by the presence in the core of $\sim 10\%$ of light elements, probably consisting mainly of oxygen³⁴. It is also widely believed that the terrestrial siderophile pattern was substantially influenced at an advanced stage of accretion by the physical mixing into the mantle of an oxidized, solar nebular condensate in conditions which did not permit equilibration with metal phase $^{20,27-29}$.

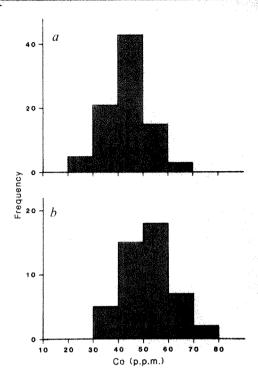


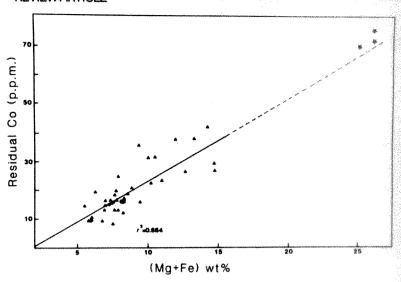
Fig. 2 Comparison of Co abundances in terrestrial oceanic tholeiites (a, mean Co = 43 p.p.m.) and in lunar low-Ti mare basalts (b, mean Co = 51 p.p.m.) (from ref. 53).

The particular combination of processes which generated the siderophile signature of the Earth's mantle probably did not operate to the same extent in all planets and differentiated planetesimals. Accordingly, it is expected to be unique to the Earth, or to an Earth-like planet. This expectation can be tested by comparing the terrestrial siderophile signature with the siderophile signature of the parent body of shergottites35-38 which is widely identified as Mars^{39,40}. As with the Earth, most siderophiles (such as, Co, Ni, P, W, Ge, Mo, Au and Ir) are substantially overabundant compared with expectations based on equilibrium partitions between silicate and metallic iron phases. There are, however, very significant differences between the martian and the terrestrial signatures. In shergottites, W and P are present at levels about 5-10 times higher than the Earth, while Cu, Ni, As, T1 and In are depleted by factors of 5-20. Moreover, Mn and Cr are present in primordial C1 abundances, whereas these elements are depleted in the Earth. In addition, the oxygen isotope composition of shergottites is significantly different from that of the Earth 41,42. Dreibus and Wänke 36 have pointed out that the differences between the martian and terrestrial siderophile signatures could be explained by differences in the mode of accretion of both planets, combined with the presence of a large quantity of sulphur in the martian core.

The siderophile signature displayed by the silicate phase of the eucrite parent body (EPB) differs in turn from those of the Earth and Mars. In this case, the siderophile abundances reflect a close approach to chemical equilibrium between silicate and iron phases during segregation of the core in the EPB. In consequence, many siderophiles (for example, Ni, Co, Cu, Ga, Mo and Ir) are relatively depleted by factors varying between 3 and 50 in the EPB silicate phase compared with the Earth's mantle⁴³⁻⁴⁵. On the other hand, Mn, V and Cr are present in primordial abundances, in contrast to their depletion in the Earth's mantle^{32,43}.

The above discussion highlights the unique nature of the siderophile signatures in the mantles of planets and planetesimals which have differentiated to produce substantial metallic cores. The siderophile signature of the Moon, in which

Fig. 3 Cobalt in primitive lunar volcanic glasses (★) and Apollo 16 highland breccias (▲, corrected for meteoritic contamination) plotted against (Mg+Fe). Note that the solid line representing the best fit to the highland breccia data projects directly into the field of primitive volcanic glasses, showing that the lunar Co/(Mg+Fe) ratio is of global significance. (After ref. 53.)



a metallic core probably amounts to <2% of its mass, is therefore likely to be of considerable interest.

Lunar siderophile signature

The importance of lunar siderophile geochemistry to the problem of the Moon's origin was emphasized by O'Keefe⁴ O'Keefe and Urey47. A comparative study of siderophile abundances in terrestrial and low-Ti lunar basalts, carried out by Ringwood and Kesson", concluded that the average abundances of a particular group, including Fe, Co, Ni, W, P, S and Se, were similar within a factor of ~2. Pointing to the unique factors responsible for the siderophile signature of the terrestrial mantle and its derived basalts, they concluded that "the similarity in siderophile elements between the Moon and Earth's mantle therefore implies that the Moon was derived from the Earth's mantle after the Earth's core had segregated". They also recognized that another group of siderophiles (Ga, Cu, Ge, As, Ag, Au, Sb, Re) was genuinely depleted in the Moon compared with Earth and ascribed this to loss as volatile species. Delano and Ringwood⁴⁴ made a parallel study of the siderophile chemistry of lunar highland breccias, after applying corrections for meteoritic contamination. They found that the indigenous siderophile signature in the lunar highlands closely resembled that of the low-Ti mare basalts and terrestrial basalts, thereby reinforcing the previous conclusion.

Wänke and co-workers in Mainz independently arrived at very similar conclusions^{48,49}, based on detailed studies of the geochemical behaviour of W and P in terrestrial rocks and in lunar highland rocks and basalts (Fig. 1). Wänke et al. 50,51 extended these conclusions by demonstrating the occurrence of a substantial component in the Apollo 16 highlands breccias. possessing very similar Ni/Mg and Co/Mg ratios to the Earth's mantle. Wänke and Dreibus 20,32,33 also drew attention to the genetic significance of similar Cr, V and Mn abundances in the Moon and in the Earth's mantle. As noted earlier, these elements are significantly depleted in the mantle, primarily because of their partial entry into the Earth's core. Wänke et al.50 also recognized that another group of highly siderophilic elements was depleted in the Moon compared with the Earth's mantle. They attributed this depletion not to volatility (as proposed by Ringwood and Kesson²⁴) but to selective extraction by segregation of a small metallic core within the Moon.

Tungsten and cobalt provide good examples of moderately siderophilic elements whose geochemical behaviour in the Earth are well understood. In oxidized form, W is an incompatible element and behaves similarly to U during magmatic fractionation. Hence the W/U ratio in terrestrial rocks remains approximately constant over a wide concentration range (Fig. 1)^{33,49,52}.

Tungsten and uranium are both refractory elements and were accreted by the Earth in chondritic relative abundances 23,49. Because of its siderophile nature, W was depleted in Earth's mantle by a factor of 25 owing to its entry into the Earth's massive core. The W/U ratios of lunar mare and highland rocks are almost identical to those of terrestrial rocks (Fig. 1). In view of the similar U abundances in the Earth's mantle and Moon¹¹, the W abundances in both bodies must display a corresponding similarity.

Unlike W, Co is a compatible element which is not strongly fractionated (relative to Mg and Fe) during magmatic differentiation. Abundances of Co in terrestrial tholeittes and lunar low-Ti mare basalts are shown in Fig. 2 and are very similar^{24,53}. Figure 3 demonstrates a good correlation between Co and (Mg+Fe) in lunar highland breccias. Moreover, the highland Co/(Mg+Fe) ratio is identical to that displayed by the least fractionated lunar mare basaltic magmas as represented by volcanic glasses, confirming that the lunar Co/(Mg+Fe) ratio is also a global characteristic. Experimental investigation⁵³ of the distribution of Co between a primitive lunar volcanic glass, liquidus olivine and metal phase confirmed that the Co content of the lunar mantle was very similar to that of Earth's mantle.

The conclusion by both Canberra and Mainz groups that the similarity in abundances of a particular group of siderophile elements in the Earth's mantle and Moon unequivocally implies that the material in the Moon has been derived from the Earth's mantle created considerably controversy. Most lunar scientists were reluctant to accept the proposition that the vexed question of the Moon's origin could be settled by such a 'simple' argument. Nevertheless, the controversy had beneficial results because it stimulated the acquisition of additional analytical data on the abundances of siderophile elements in lunar and terrestrial rocks, and on partition coefficients of siderophiles between metal and silicate phases. The demonstration⁵² that molybdenum was depleted in the Moon by a factor of ~30 was particularly significant, since the depletion of this highly siderophilic element could not be ascribed to volatility, and pointed towards extraction by a small metallic lunar core⁵

The new data have been combined with earlier results in Fig. 4 as a plot of abundance ratios of siderophile elements in the Earth's¹¹ mantle and Moon verus their metal/silicate partition coefficients. Analogous but less comprehensive diagrams have been constructed by Wänke and Dreibus³³ and by Newsom⁵². It is seen that the abundances of elements less siderophilic than nickel (Mn, V, Cr, Fe, W, Co, P, S, Se) are similar (within a factor of 2) in both bodies. Elements more siderophilic than nickel (Cu, Mo, Re, Au) are depleted to degrees which correspond well with their metal/silicate partition coefficients. Nickel

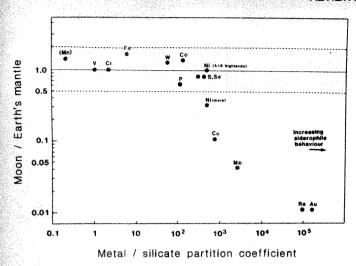


Fig. 4 Abundance ratios of siderophile elements in the Moon and Earth's mantle versus their metal/silicate partition coefficients. Partition coefficients used for compatible elements, Mn, V, Cr, Fe, Co and Ni, are based on measured distributions between olivine and Fe-metal phases^{30,31,53,79}. Partition coefficients for generally incompatible elements W, P, S, Mo, Re and Au, are for basaltic melts and Fe-metal phases^{40,80-83}. Positions of Se and Cu were estimated by interpolation from the free energies of formation of their oxides. Abundance data for siderophile elements in the Moon and Earth's mantle are from the following sources: Mn, refs 24, 25; V, Cr, refs 24, 25, 79; Fe, refs 24, 25; W, refs 24, 25, 49, 52; P, refs 24, 25, 33, 44; Co, refs 24, 25, 53; S, Se, ref. 24; Ni, refs 50, 53; Cu, refs 24, 25; Mo, refs 27, 52; Re, Au, refs 24, 29, 84, 85. Brackets around Mn indicate the possibility that its depletion in the Moon and Earth might be related to volatility rather than siderophile behaviour²⁴.

presents an interesting case and has been studied extensively; it is depleted by a factor of ~ 3 in the source regions of the most primitive lunar basalts^{33,53-55} but is present in terrestrial abundances (relative to Mg) in breccias at the A16 lunar highlands site^{50,53}.

Wänke and colleagues^{33,50,52} have shown that the depletions (below terrestrial levels) of highly siderophilic elements shown in Fig. 4 can readily be explained by separation of a small metallic core amounting to <1% of the lunar mass. This would not markedly affect the abundances of moderately siderophilic elements but would have strongly depleted the highly siderophilic elements. The presence of a small (<2% by mass) lunar core is strongly suggested by the lunar moment of inertia coefficient⁵⁶ ($I/MR^2 = 0.391 \pm 0.002$) and by the observation of a phase shift in the forced precession of the lunar figure⁵⁷.

The composition of the lunar core is constrained by the nickel and cobalt abundances of lunar mantle silicates. The nickel content of the lunar mantle can be determined using a procedure identical to that used to determine its abundance in the Earth's mantle, that is by measuring the nickel content in the olivine crystallizing on the liquidus of the most primitive, unfractionated basaltic magmas derived from the lunar interior. Ringwood and Seifert⁵³ used this technique to demonstrate that the olivine of the lunar mantle contains ~900 p.p.m. Ni. Moreover, they showed that any metal in equilibrium with lunar olivine would contain at least 40% nickel. It is reasonable to expect that lunar mantle silicates would have equilibrated with metal phase during segregation of the lunar core. Thus the lunar core is required to contain at least 40% Ni in sharp contrast to the Earth's core, which contains ~5% Ni (ref. 53). An analogous technique has been applied⁵³ to a totally independent data-set to demonstrate that the cobalt content of the lunar core is also higher than that of the Earth's core. The gross dissimilarities in chemical compositions between the lunar and terrestrial cores have important implications for hypotheses of lunar origin.

Implications for lunar origin

Previously, it was shown that the lunar and terrestrial siderophile signatures differ fundamentally from those of the shergottite parent body (Mars) and the EPB. The reasons why the terrestrial siderophile signature is likely to be unique to the Earth or an Earth-like planet have also been documented. Figure 4 provides a striking illustration of the close relationship between the abundances of siderophiles in the Earth's mantle and the Moon. The moderately siderophile elements in the Moon are clearly 'Earth-like'. Although the highly siderophilic elements are greatly depleted in the Moon compared with Earth, this can be readily explained by segregation of a small amount (<1%) of a Ni-rich metal phase (~40% Ni) from parent material of terrestrial composition to form a lunar core. I conclude that the close relationship between the lunar and terrestrial siderophile signatures depicted in Fig. 4 provides definitive evidence for the terrestrial origin of the Moon, as argued previously by the Canberra and Mainz groups. This is further supported by the identity in oxygen isotope compositions between Earth and Moon and their dissimilarity with those of shergottites and differentiated meteorites41,42

Could these abundance patterns be explained in terms of an origin of the Moon as an "independent planet" 23 ? Newsom 52 has attempted to show that the lunar abundances of W, P, Ni and Co could be explained by this hypothesis. His model requires the separation within the Moon of an iron-rich metallic core amounting to $\sim 5\%$ of the lunar mass. The model can be rejected on the following grounds.

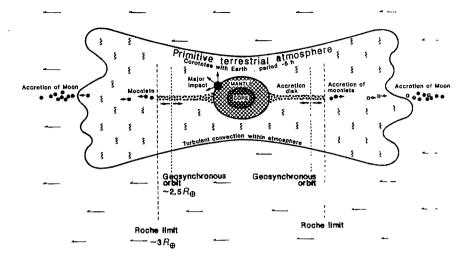
- (1) Current geophysical and petrological models of the Moon agree that its FeO content lies between 8 and 17% (refs 21, 50). If the lower limit is accepted, an iron core amounting to 5% of the lunar mass would lead⁵⁸ to a mean lunar density exceeding 3.40 g cm⁻³ in contradiction to its observed density of 3.34 g cm⁻³. The discrepancy is increased if the more widely accepted estimate of 13-16% FeO in the lunar mantle is used. (2) Experimental data cited previously show that the lunar core is Ni-rich; this causes a decrease in the effective metal/silicate partition coefficients for W (ref. 49), p (ref. 59) and Co (ref. 53) as compared with pure iron. Newsom's model therefore requires a metal core constituting substantially more than 5% of the lunar mass.
- (3) The size of the lunar core is constrained to be <2% of the lunar mass by the seismic observations of Nakamura *et al.*⁶⁰ who state that "the radius of a low-velocity (molten) core cannot be greater than about 350 km because normal transmission of P waves to that depth is observed".
- (4) The model fails to explain the similar abundances of Mn, Cr, V, S and Se in the Moon and the terrestrial mantle (Fig. 4) and their variable depletions as compared with primordial abundances.

More generally, the 'independent planet' hypothesis of lunar origin encounters a series of additional difficulties, which cumulatively are quite lethal.

- (i) The siderophile signature of the terrestrial mantle was established by a series of complex processes occurring during the segregation of a large (32% $M_{\rm E}$) metallic core within the Earth. If the Moon had formed as an independent planet, it would be quite incredible if its very different conditions of accretion, followed by segregation of a relatively small ($\sim 2\% M_{\rm m}$) core possessing a composition grossly different to the Earth's core, and formed in a totally different P, T environment, had, nevertheless, produced a siderophile signature similar to the Earth's mantle.
- (ii) The dilemma of providing a plausible mechanism for explaining the depletion of iron in the Moon, as compared with Earth, Venus and Mars, is not resolved.
- (iii) Previous attempts to solve this problem have relied on

- Solar nebula (mainly H2)

Fig. 5 Model showing the formation of the Moon via the ejection of material from the Earth's mantle by impacts from late-accreting planetesimals in the presence of a corotating primitive terrestrial atmosphere.



highly speculative physical mechanisms to fractionate metal from silicate in the nebula, before accretion of the Moon⁶¹. However, in these models, the composition of the metal phases accreted by Earth and Moon would be similar, that is Fe-rich and Ni, Co-poor. This is contrary to the evidence cited previously that the lunar core is actually Ni, Co-rich and quite different in composition to the Earth's core.

(iv) Some workers⁶² have attempted to interpret the Moon as having formed from an earlier generation of planetesimals which accreted in the solar nebula and then melted and differentiated analogously to the eucrite parent body. These were subsequently fragmented and their metal cores somehow removed, leaving the Moon to accrete from the differentiated silicate mantles. The major differences already noted between the siderophile signatures of the Moon and the silicate phase of the EPB are unexplained by this model. Moreover, the mechanisms proposed for removing the metal cores are highly implausible^{63,64}.

Making of the Moon

The geochemical evidence reviewed previously can apparently only be satisfied if the Moon was formed from material derived from the Earth's mantle after the core had segregated. Provision of the energy and angular momentum required to remove >1% of the Earth's mass and place it into orbit represents a rather formidable challenge. For two decades, I have argued that the energy was provided by the Earth's own gravitational energy of accretion and that the requisite angular momentum was transferred from the rapidly rotating Earth to protolunar material by a corotating primitive terrestrial atmosphere.

According to these models 10,11,17-19, accretion of the Earth

occurred before dissipation of the primordial gases of the solar nebula. Accretion was accompanied by the formation of a primitive terrestrial atmosphere comprised mainly of hydrogen gravitationally captured from the solar nebula⁶⁵⁻⁶⁷. The primitive atmosphere was coupled to the Earth's rotation through turbulent viscosity and hydromagnetic torques and was thereby spun out into a corotating disk (period ~5 h). During the later stages of accretion of the Earth, high temperatures were produced by a combination of rapid accretion and thermal insulation by the primitive atmosphere. In these conditions, material from the mantle was evaporated into the primitive atmosphere and spun out into the disk. As the primitive atmosphere cooled and was dissipated, the silicate components were precipitated to form a ring of Earth-orbiting planetesimals. Further fractionation due to volatility occurred during the precipitation process, since the more volatile components would be precipitated at relatively low temperatures, forming micrometre-sized smoke particles. These remained coupled to the escaping gases and hence were removed from the system. The Moon accreted from the ring of devolatilized Earth-orbiting planetesimals.

The principal problem with this scenario was the short timescale (~106 yr) over which the Earth must have formed if the gravitational potential energy of impacting planetesimals was to have generated the sustained high temperatures necessary to evaporate part of the upper mantle during the late stages of accretion. An attractive alternative is provided by the models of Hartmann and Davis⁶⁸, and of Cameron and Ward⁶⁹. These authors invoke one or a few impacts by giant, late-accreting planetesimals to evaporate material from the Earth's mantle and place it into orbit. The planetesimals are believed to have sizes ranging between a substantial fraction of the lunar mass and the size of Mars⁷⁰. The physical processes envisaged⁷¹ are quite closely related to those of my earlier models. Rather than achieve high mantle-evaporation temperatures via the 'steady-state' liberation of gravitational potential energy from a continuum of relatively small impacts over a short accretion timescale (1 Myr), giant impact models achieve these conditions in one or a few transient ultrahigh energy events, and permit a much longer accretion timescale for the Earth (such as 10^7-10^8 yr).

Although the giant impact model is currently attracting considerable interest, it is not free from potential problems. It is expected to lead to complete melting of the entire Earth^{70,72}, this should have caused efficient differentation of the mantle accompanied by formation of a massive 4,500-Myr terrestrial crust, contrary to observation¹¹. Complete melting of the Earth and subsequent crystallization of the mantle should also have been accompanied by near-quantitative degassing of volatiles such as CO₂, N₂, Cl and inert gases. This implication is not readily reconciled with available geochemical evidence^{4,5,73}.

Accordingly, I now prefer a model intermediate between my earlier rapid-accretion models and the current giant impact models (Fig. 5). A key role in lunar genesis continues to be played by the primitive terrestrial atmosphere which corotates with the Earth, extending as a disk perhaps out to 5 Earth radii $(R_{\oplus})^{65,74,75}$. The atmosphere would extend the effective radius of capture of incoming planetesimals. This factor might have contributed to a relatively short rotation period for the Earth.

During most of the Earth's accretion, small planetesimals would be captured by the atmosphere and would spiral down to the equatorial plane, forming an accretion disk. Large planetesimals would impact the Earth directly; their ejecta would be captured by the atmosphere and transferred to the accretion disk. Within the disk, planetesimals orbiting inside the geosynchronous limit would experience gas drag and spiral

inwards to the Earth. Beyond the geosynchronous radius, the atmosphere, coupled to the Earth by hydromagnetic torques, would be rotating faster than the keplerian velocities of the planetesimals, which consequently would be driven outwards. However, as the mass of the Earth continued to grow by accretion, the geosynchronous orbit expanded so that most of this material was eventually accreted by the Earth.

It is possible to form the Moon only at a late stage of accretion when the Earth had developed nearly to its present size and core formation was complete (or nearly complete). At this stage, impacts of many large (100 < R < 1,000 km) but not necessarily giant (R > 1,000 km) planetesimals at velocities exceeding 12 km s⁻¹ would vapourize ~5 times their own mass of target material and would shock-melt 100 times their own mass⁷⁶. The shockmelted material would probably form a spray of devolatilized droplets. Rapid expansion of the impact cloud would cause acceleration to high velocities^{70,71}. As the cloud expanded and cooled, selective condensation of the less volatile components would have produced more liquid droplets which subsequently solidified. Highly volatile elements condensed only at relatively low temperatures, forming smoke particles.

The corotating primitive atmosphere is believed to have had an essential role in transferring angular momentum from the solid Earth to impact-evaporated gases and liquid spray, so that a substantial proportion of the ejected material was placed in circular, equatorial orbits. The devolatilized droplets.(1-10 mm) and coarser condensates accreted to produce an assemblage of devolatilized planetesimals. Most planetesimals probably

accreted in orbits smaller than the geosynchrous limit ($\sim 2.5~R_{\oplus}$ for a rotation period of 5 h). They would have lost energy through dissipation in the corotating atmosphere and hence spiralled back to Earth. However, a significant proportion of planetesimals would have been formed beyond the geosynchronous limit. They would have been accelerated by gas-drag. causing them to spiral outwards, beyond Roche's Limit $(\sim 3 R_{\oplus})$. Here they would have accreted into moonlets, which continued to spiral outwards (through gas drag) to the boundary region between the corotating primitive terrestrial atmosphere and the solar nebula. Accretion of moonlets to form the Moon occurred in this region, possibly at a distance of \sim 5 R_{\oplus} (Fig. 5).

It remains to consider the significance of the higher FeO content of the Moon compared with the Earth's mantle^{54,75}. Actually, the Mn (ref. 24), Co (ref. 53) and W (ref. 33) abundances in the Moon may also be slightly but significantly higher than in the Earth's mantle (Fig. 4). It has been suggested 33,77 that the excess FeO was derived from planetesimals involved in the major impacts. This explanation might apply also to the excesses of Mn, Co and W. The planetesimals accreting at a late stage on the Earth may well have been oxidized, containing no free metal phase⁷⁸. The excess Fe, Mn, Co and W might be explained if the impact ejecta included ~20% of the projectile, Under the high temperatures pertaining, a limited degree of autoreduction is likely to have occurred, yielding ~1% of Nirich metal phase which ultimately segregated to form the lunar core.

```
1. Darwin, G. H. Phil. Trans. R. Soc. 170, 447-530 (1879).
```

- Jeffreys, H. Mon. Not. R. astr. Soc. 91, 169-173 (1930).
- 3. Jeffreys, H. Mon. Not. R. astr. Soc. Geophys. Suppl. 4, 62-71 (1937). 4. Urey, H. C. The Planets (Yale University Press, New Haven, 1952).
- 5. Urey, H. C. in Physics and Chemistry of the Earth, Vol. 2 (eds Ahrens, L., Press, F., Rankama, K. & Runcorn, S.) 46-76 (Pergamon, London, 1957).

- Urey, H. C. Yb. Phys. Soc. Lond. 14-29 (1957).
 Anders, E. A. Rev. Astr. Astrophys. 9, 1-34 (1971).
 Grossman, L. Geochim. cosmochim. Acta 36, 597-619 (1972).
- 9. Ringwood, A. E. Geochim. cosmochim. Acta 15, 257-283 (1959). 10. Ringwood, A. E. Geochim. cosmochim. Acta 30, 41-104 (1966).
- 11. Ringwood, A. E. Origin of the Earth and Moon (Springer, New York, 1979).
 12. Garz, T. et al. Nature 223, 1254-1256 (1969).
- Garz, I. et al. Nature 223, 1234-1236 (1969).
 Ringwood, A. E. Geochim. cosmochim. Acta 20, 241-259 (1960).
 Wise, D. U. J. geophys. Res. 68, 1547-1554 (1963).
 Cameron, A. G. W. Icarus 2, 249-257 (1963).
 O'Keefe, J. A. J. geophys. Res. 74, 2758-2767 (1969).
 Ringwood, A. E. Earth planet. Sci. Lett. 8, 131-140 (1970).

- Ringwood, A. E. Phys. Earth planet. Inter. 6, 366-376 (1972).
 Ringwood, A. E. Composition and Petrology of the Earth's Mantle (McGraw-Hill, New York, 1975)
- 20. Wänke, H. & Dreibus, G. in Tidal Friction and the Earth's Rotation Vol. 2 (eds Brosche, Waine, T. & Dreitois, G. In Tidan Friction and the Earth School Not. 2 (eds Biose P. & Sundermann, J.) 332-344 (Springer, Berlin, 1982).
 Warren, P. H. & Wasson, J. T. Proc. 10th Lunar planet. Sci. Conf. 2, 2051-2083 (1979).
 Taylor, S. & Jakes, P. Proc. 5th Lunar Sci. Conf. 2, 1287-1305 (1974).
 Ganapathy, R. & Anders, E. Proc. 5th Lunar Sci. Conf. 2, 1181-1206 (1974).
 Ringwood, A. E. & Kesson, S. E. The Moon 16, 425-464 (1977).

- Sun, S. Geochim. cosmochim. Acta 46, 179-192 (1982).
 Jagoutz, E. et al. Proc. 10th Lunar planet Sci. Conf. 2, 2031-2050 (1979).
- Newsom, H. & Palme, H. Earth planet. Sci. Lett. 69, 354-264 (1984).
 Morgan, J. W., Wandless, G., Petrie, R. & Irving, A. Tectononophysics 75, 47-67 (1981).
- Chou, C., Shaw, D. & Crocket, J. J. geophys. Res. Suppl. 88, A507-A518 (1983).
 Brey, G. & Wänke, H. Lunar planet. Sci. 14, 71-72 (1983).
- Rammensee, W., Palme, H. & Wänke, H. Lunar planet. Sci. 14, 628-629 (1983).
 Dreibus, G. & Wänke, H. Lunar planet. Sci. 10, 315-317 (1979).
- 33. Wänke, H. & Dreibus, G. in Origin of the Moon (Lunar and Planetary Institute, Houston, in the press).
- 34. Ringwood, A. E. Proc. R. Soc. 395, 1-46 (1984)
- 35. Dreibus, G. et al. Lunar planet. Sci. 13, 186-187 (1982).
- Dreibus, G. & Walke, H. Proc. 27th int. Gool. Congr. 11, 1-20 (1984).
 Laul, J. C. et al. Geochim. cosmochim. Acta (in the press).
- 38. Stolper, E. Earth planet. Sci. Lett. 42, 239-242 (1979).
- Wood, C. & Ashwal, L. Proc. 12th Lunar planet. Sci. Conf. 2, 1359-1375 (1981).
 Pepin, R. O. Nature 317, 473-474 (1985).

- Clayton, R. N. & Mayeda, T. Proc. 6th Lunar Sci. Conf. 2, 1761-1769 (1975).
 Clayton, R. N. & Mayeda, T. Earth planet. Sci. Lett. 62, 1-6 (1983).
- Dreibus, G. & Wänke, H. Z. Naturforsch, 35a, 204-216 (1980).
 Delano, J. W. & Ringwood, A. E. The Moon and Planets 18, 345-425 (1978).

- Newsom, H. J. geophys. Res. Suppl. 90, C613-C617 (1985).
 O'Keefe, J. A. Naturwissenschaften 59, 45-52 (1972).

- O'Keefe, J. A. & Urey, H. C. Phil. Trans. R. Soc. 285, 569-575 (1977).
 Dreibus, G., Spettel, B. & Wänke, H. Proc. 7th Lunar Sci. Conf. 3, 3383-3396 (1976).
 Rammensee, W. & Wänke, H. Proc. 8th Lunar Sci. Conf. 1, 399-409 (1977).
 Wänke, H., Dreibus, G. & Palme, H. Proc. 9th Lunar planet. Sci. Conf. 1, 83-110 (1978).
- Wänke, H., Dreibus, G. & Palme, H. Proc. 10th Lunar planet. Sci. Conf. 1, 611-626 (1979). Newsom, H. in Origin of the Moon (Lunar and Planetary Institute, Houston, in the press),
- 53. Ringwood, A. E. & Seifert, S. in Origin of the Moon (Lunar and Planetary Institute, Houston,
- in the press).

 Delano, J. W. in Origin of the Moon (Lunar and Planetary Institute, Houston, in the press).
- Wolf, R. & Anders, E. Geochim. cosmochim. Acta 44, 2111-2124 (1980).
 Blackshear, W. & Gapcynski, J. P. J. geophys. Res. 82, 1699-1701 1(977)
- 57. Yoder, C. F. Abstr. Conf. on the Origin of the Moon, 6 (Kona, Hawaii, 1984).
 58. Toksoz, M., Dainty, A., Solomon, S. & Anderson, K. Rev. Geophys. Space Phys. 12, 539-567
- 59. Newsom, H. & Drake, M. Geochim, cosmochim, Acta 47, 93-100 (1983).
- Nakamura, Y. et al. Proc. 7th Lunar Sci. Conf. 3, 313-3121 (1976).
 Ruskol, Y. L. in Soviet-American Conf. on the Cosmochemistry of the Moon and Planets (eds Pomeroy, J. H. & Hubbard, N. J.) 812-822 (NASA, Washington DC, 1977).

- Smith, J. V. Lun. Sci. 5, 718-720 (1974).
 Mizuno, H. & Boss, A. Icarus 63, 109-133 (1985).
 Harris, A. & Kaua, W. Icarus 24, 516-524 (1975).
 Hayashi, C. in Fundamental Problems in the Theory of Stellar Evolution (eds Lamb, D. & Schramm, D.) 113-128 (International Astronomical Un ion, 1981).
- 66. Hayashi, C., Nakazowa, K. & Nakagawa, Y. in Protostars and Planets Vol. 2 (University of Arizona Press, 1986).
- 67. Sekiya, M., Hayashi, C. & Nakazawa, K. Prog. theor. Phys. 66, 1301-1316 (1981). 68. Hartmann, W. K. & Davis, D. Icarus 24, 504-515 (1975). 69. Cameron, A. G. L. & Ward, W. R. Lun. Sci. 7, 120-122 (1976).

- 70. Cameron, A. G. L. Icarus 62, 319-327 (1985).
- Stevenson, D. J. Abstr. Conf. on the Origin of the Moon, 60 (Kona, Hawaii, 1984).
 Stevenson, D. J. Abstr. Conf. on the Origin of the Moon, 60 (Kona, Hawaii, 1984).
 Benz, W., Slattery, W. & Cameron, A. G. W. Lunar planet. Sci. 17, 40-41 (1986).
 Rubey, W. W. Geol. Soc. Am. Spec. Pap. 62, 631-650 (1955).
 Walker, J. C. Precambr. Res. 17, 147-171 (1982).

- 75. Ringwood, A. E. in Origin of the Moon (Lunar arnd Planetary Science Institute, Houston, in the press).

- Boslough, M. & Ahrens. T, J. Lunar planet. Sci. 14, 63-64 (1983).
 Delano, J. D. & Stone, K. K. Lunar planet. Sci. 16, 181-182 (1985).
 Turekian, K. & Clark, S. P. Earth planet. Sci. Lett. 6, 346-348 (1969).
 Seifert, S. & Ringwood, A. E. Lunar planet. Sci. 17, 789-790 (1986).
- Newsom, H. & Drake, M. Geodim. cosmochim. Acta 46, 2483-2489 (1982).
 Haughton, D., Roeder, P. & Skinner, B. Econ. Geol. 69, 451-467 (1975).
 Rammensee, W. thesis, Mainz Univ. (1978).

- 83. Kimuar, K., Lewis, R. & Anders, E. Geochim. cosmochim. Acta 38, 683-701 (1974)
- 84. Hertogen, J., Janssens, M. & Palme, H. Gochim. cosmichim. Acta 44, 2125-2143 (1980).
- 85. Wolf, R., Woodrow, A. & Anders, E. Proc. 10th Lunar planet. Sci. Conf. 2, 2107-2129

Primordial density fluctuations and the structure of galactic haloes

P. J. Quinn*†‡, J. K. Salmon†‡ & W. H. Zurek‡

N-body models used to study the formation of structure in $\Omega=1$ universes reveal that the mass profiles of the collapsed structures—galactic haloes—are intimately related to the power spectrum of initial, gaussian, density perturbations. In particular, flat rotation curves observed in disk galaxies are obtained only when the exponent of the power law $P(k) \sim k^{\circ}$ is, on the megaparsec scale, less than -1, but not as small as -3. These results have important implications for various cosmological models.

THE structures observed in the Universe on the galactic and larger scales are believed to have been seeded by primordial density perturbations¹. These perturbations were presumably imprinted much earlier by a process such as inflation²⁻⁴. Later, they were modified in the course of the radiation-dominated era (redshift $z > 2.5 \times 10^4 \Omega h^2$). Both this initial imprinting, and the more recent modifications depend sensitively on the composition of matter in the Universe and on the physics at very high energies. Therefore, an understanding of the formation of structure from initial, seed perturbations is essential for cosmology as well as for particle physics.

We now explore, by means of computer modelling, the formation of collapsed and virialized structures in Einstein-deSitter $(\Omega=1)$ universes. We focus on a class of model universes characterized by gaussian, scale-free density perturbations. Their power spectra:

$$P(k) = Ak^n \tag{1}$$

are completely specified by the normalization constant A and the exponent n. k is the wavenumber. The white noise case corresponds to n=0. Scale-free perturbations in an $\Omega=1$ universe result in hierarchical clustering⁵⁻¹⁰, which is both reasonably easy to analyse and often a good approximation of more complicated and more realistic models. We shall also simulate the formation of haloes in CDM (cold dark matter) universes¹¹⁻¹³. Indeed, we shall normalize our scale-free power spectra so that on a 'galactic scale' they have similar power to the CDM case. The influence of Ω on the structure of galactic haloes will be treated elsewhere (W.H.Z., P.J.Q. and J.K.S., manuscript in preparation).

Observations of rotational velocities in disk galaxies indicate that the bulk of the mass of these objects is invisible 'dark matter'. Moreover, this dark matter is distributed so that the rotational velocities of stars, H II regions and neutral hydrogen 14-18 are approximately independent of radius out to distances near to and even well beyond the optical radius of the galaxy. This implies a density (ρ) of dark material that, at large radii, falls off like;

$$\rho(r) \sim r^{-2} \tag{2}$$

or alternatively, the mass profile:

$$M(r) \sim r \tag{3}$$

We will demonstrate that mass profiles of this kind can be obtained when the initial density perturbations have at least as much energy on the large scale as they have on the small scale,

n < -1. This conclusion has been anticipated analytically by the 'secondary infall' models proposed by Gunn and Gott¹⁹. In particular, using the secondary infall paradigm, Hosimann and Shaham²⁰ have conjectured that the average density profile should be related to the power-law exponent n by

$$\rho(r) \sim r^{-\gamma} \tag{4}$$

where

$$\gamma = \frac{3(3+n)}{(4+n)} \tag{5}$$

for n>-1, and should relax to $p\sim r^{-2}$ for -1>n>-3. Our results are in approximate agreement with these conclusions for n>-2, even though the process of formation of collapsed objects does not seem to conform with the secondary infall picture.

Computer simulations

A gaussian field of initial density perturbations can be reproduced by writing:

$$\Delta \rho(\vec{r}) = \rho(\vec{r}) - \langle \rho \rangle$$

$$= \sum_{\vec{k}} |\delta_{\vec{k}}| e^{-i\phi_{\vec{k}}} e^{-i\vec{k}\cdot\vec{r}}$$
(6)

Here $|\delta_{\vec{k}}|$ are the absolute values of the complex amplitudes of all the modes and $\phi_{\vec{k}}$ are their phases. One can realize power spectrum $P(\vec{k})$ by choosing:

$$\delta_{\vec{k}} = \sqrt{2P(\vec{k})} R_{\vec{k}}^{\delta} \tag{7a}$$

$$\phi_{\mathcal{E}} = 2\pi R_{\mathcal{E}}^{\phi} \tag{7b}$$

where $\{R_{\vec{k}}^{\delta}, R_{\vec{k}}^{\phi}\}$ are a pair of random numbers with distributions which are, respectively, gaussian in the interval $(0, \infty)$, and uniform in the interval (0, 1].

We have found it extremely useful to implement different power spectra by using the same set of random number pairs. This allows us to model 'the same' fragment of the universe with different power laws and therefore to bring out systematic changes which would otherwise be overwhelmed by the random nature of the initial perturbations.

The density distribution can be faithfully represented in the form given by equation (6) only when, on the scales of interest, the amplitude $\sigma = \sqrt{\langle (\Delta \rho)^2 \rangle}$ is much smaller than the average density;

$$\sigma \ll \langle \rho \rangle$$
 (8)

This follows not just from the trivial requirement that ρ be positive; beyond the linear regime mode-mode interactions induce correlations between modes which in turn invalidates

^{*} Space Telescope Science Institute, 3700 San Martin Drive, Baltimore, Maryland 21218, USA.
† Theoretical Astrophysics, California Institute of Technology, Pasadena, California 91125, USA
‡ Theoretical Astrophysics, Los Alamos National Laboratory, Los Alamos, New Mexico 87545,

the assumption of gaussian density perturbations and makes the use of equation (6) impossible (see ref. 1).

We guarantee the validity of equation (6) by adjusting the normalization constant A in equation (1) so that mass fluctuations on the scale-of-interest (Λ) are small:

$$\left[\frac{\delta M}{M}\right]_{\Lambda} = 0.06\tag{9}$$

We impose the same condition on $\delta M/M$ for the CDM models. It will be useful but will entail no loss of generality, to refer to this chosen scale A by analogy with the CDM case—for which A can be estimated by comparison with present-day galaxy correlation functions 12,13,21—as the 'megaparsec scale'. In other words, we anticipate that 'galactic haloes' will form from Λ-sized fragments of the initial distribution after a time interval corresponding to the Hubble time. With this convention in mind we can now state that our models are initiated with the Hubble constant $H_o = 100 \text{ km s}^{-1} \text{ M pc}^{-1}$ at $z_{\text{int}} = 24$ and are evolved for ~10,000-14,000 Myr beyond the conventional present which for this set of initial conditions occurs at an unrealistically short time of 6,700 Myr after the big bang. It is essential to keep in mind that for the power law models the above convention is nothing but a convention as the scale-free nature of $P(\vec{k})$ implies. Our results—density profiles of haloes—are independent of the value of H_0 . The Hubble constant influences only the total values of the masses of haloes, but not their shapes.

The initial conditions are imprinted on a system of 64^3 particles, each of them with a conventional mass of $m = 1.02 \times 10^9 M_{\odot}$, $\Omega = 1$. They represent a $(10 \text{Mpc})^3$ section of the model universe. The initial conditions are imposed using the Zel'dovich 'growing mode' method^{1,20,22} which deforms the cubic lattice of particles in the desired manner. The evolution of the system to z = 0 is then simulated by a Fourier (cloud-in-cell) code with a 64^3 mesh.

The Fourier methods are inaccurate on scales smaller than a few mesh spacings. Therefore, we use it only to set up initial conditions for the N-body simulations. These are provided by the output of the Fourier code at z=5.25 and/or z=10.1. (We do not want to generate initial conditions this late in the history of the universe, as by then the inequality (8) is no longer valid and equation (6) cannot be trusted.) The use of the Fourier code allows us to employ sufficiently many particles at very early times to imprint initial conditions without the danger of introducing errors via shot noise or aliasing (ref. 21 and work in preparation). Moreover, using this technique we can obtain the first 'blurred' but, nevertheless, informative pictures of the model at z=0.

Two kinds of N-body runs are used. Low-resolution simulations use particles with a mass $M_L = 27 \,\mathrm{m}$. A sphere with a diameter of 10 Mpc cut out from the Fourier cube provides the initial conditions. Each of the low resolution particles has the location and the velocity of the centre of mass of a $3 \times 3 \times 3$ fragment of the original Fourier lattice. However, particle masses are now close to $3 \times 10^{10} \,\mathrm{M}_\odot$ which means that a typical galactic halo will contain no more than ~100 particles. Therefore, to investigate smaller scale structures we have employed a different mapping of the Fourier particles onto the N-body initial conditions.

High-resolution runs use a one-to-one mapping in a chosen sphere of 2 Mpc radius, and a very low-resolution mapping (64 Fourier particles to one N-body particle) towards the outskirts of the model. Masses in the transition region between 2 and 3 Mpc take on intermediate values. The resulting multi-resolution system is evolved using the N-body code for a time comparable to the corresponding low-resolution run (see Fig. 1).

Typically 5,000-7,000 particles are evolved and a run is completed within 2-4 hrs of Cray-1 CPU time. Usually more than one high-resolution sphere-of-interest is chosen for each low-resolution model. Therefore, the same fragment of the universe is modelled using three distinct resolutions. All of the N-body runs use a smoothing length of 10 kpc. Note that on the scales

on which all three resolutions are expected to be accurate, all of them yield comparable results. Low-resolution runs are then used to extract information about the large-scale structure, mergers, and so on. The results of these runs will be discussed elsewhere. Here we shall concentrate on the small-scale information contained in the high-resolution runs. Specifically, we shall consider the density profiles of haloes, that is objects with masses between $10^{11} M_{\odot}$ and $10^{12} M_{\odot}$.

Halo density profiles

Figure 2 contains a graphic summary of the key results discussed in this section. Two conclusions are immediately apparent: (1) the high-resolution portions of the particle plots in Fig. 2 contain related structures (the 'same' halo can be usually identified in the figures corresponding to the neighbouring values of n). (2) The realizations with more power on small scales (larger n) have larger numbers of more compact haloes. In particular, while the model with n=-2.75 exhibits only two reasonably well developed haloes, there are about 10 such structures of various sizes for n=1. Moreover, models with a lot of power on the large scale exhibit more pronounced 'caustics' and 'filaments'. The CDM model is the closest in appearance to the n=-1 and n=-2 cases. This is not unexpected: the effective exponent of the cold dark matter power spectrum is close to -1.5 on the megaparsec scale.

Most of the haloes in the high resolution region contain only high-resolution particles. However, some of them are contaminated by heavy particles that have entered from the low-resolution part of the model. The results given below are inferred from haloes that contain ≤10% of these heavies by mass. (In fact, only 10% of the analysed halos had more than 1 or 2 heavies).

For the densities given by equation (4), the mass profile (the mass within radius r) is given by the relation:

$$M(r) \sim r^{3-\gamma} \tag{10}$$

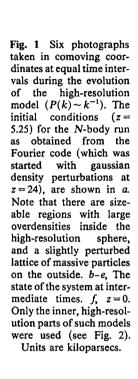
The corresponding rotational velocity inferred for such M(r) is;

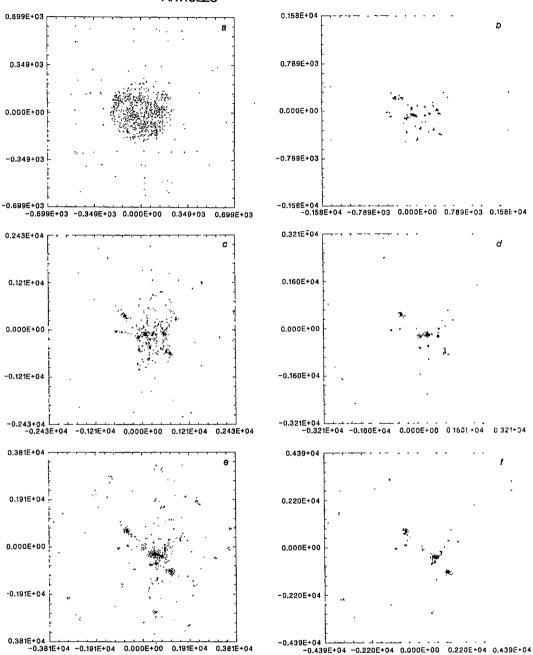
$$v(r) \sim r^{(2-\gamma)/2} \tag{11}$$

The circular rotational velocities of haloes obtained in the computer experiment are for a subset of the haloes shown in Fig. 2. We also indicate there the velocity profile predicted by equation (5).

Models with n=1 and n=0 produce centrally condensed haloes with the mass falling off faster than in the flat rotation case. The typical slope of the density profile is well approximated by the value of γ inferred from equation (5) although a systematic discrepancy can also be noted: densities tend to fall off faster than equation (5) would have it. In particular, rotation curves are not quite flat for n=-1 but clearly flatten for CDM as well as for the n=-2 case. In all cases when n>-1 rotation curves flatten at radii between 10 and 20 kpc. (The resolution of our N-body code is 10 kpc and does not allow us to comment on the structure on the innermost parts of the halo.) It is interesting that virtually all haloes formed in a simulation with a given power law have very similar rotation curves.

The situation is different when n = -2.75. Now the rotational velocities are still rising at r = 50 kpc and some of them do not flatten even in the 100 kpc range. This seems to imply that the structure of these haloes is inconsistent with the conclusions of Hoffman and Shaham, who conjecture that flat rotation curves will form even for n = -3. It is unlikely that such haloes with rising rotation velocities are a temporary, unstable phenomenon: We have checked the slope of the density profile at z = -0.5, at a time equal to 14,000 Myr. It is still rising and equation (5) still provides as good an estimate as a flat rotation profile. More relevant in understanding this discrepancy is probably the systematic increase of the size of the soft core with n decreasing to -3. This trend is visible already for n = -2. Indeed, rotation profiles between 100 and 200 kpc, not shown in Fig. 2, are quite





flat for n = -2.75. Therefore, the relevant part of Fig. 2 may be showing just the soft core parts of the haloes for this case. Moreover, the treatment given in ref. 20 breaks down for n < -3. Hence, it is not too surprising that its predictions for n = -2.75 are inaccurate. Indeed, one should be surprised that the arguments of Hoffman and Shaham give as good an estimate of the resulting density profiles as they do, as the assumptions on which they are based are only approximately valid.

The mass profile of the cold dark matter haloes is reasonably close to the flat rotation curve variety out to 100-150 kpc. Beyond that distance rotation profiles begin to fall off. The rotation parameters (λ) of the collapsed objects are typically in the 0.05-0.1 range ($\lambda = |E|^{1/2}J/GM^{5/2}$, where E is the total energy of the halo, J its angular momentum, M its mass, and G is the gravitational constant.) This is consistent with our earlier findings^{24,25} as well as with a number of other cold dark matter simulations²⁶.

We have concluded that the mass profiles of collapsed, virialized objects in the $\Omega=1$ universe initiated with an effective power law spectrum on the galactic scale are determined over the range of interest by the value of n. Equations (4) and (5)

give a fair estimate of the corresponding density profiles. Although a power spectrum translates unambiguously into a rotation curve, one should keep in mind that the reverse argument is not so straightforward: The fact that a flat rotation curve is observed, often allows, within the errors, a range of halo density profiles. Moreover, baryonic material in the dissipative process of settling in the centre of the core will inevitably steepen the final rotation curve²⁷.

Comparisons with theory

Gunn and Gott have developed the secondary infall scenario based on the assumption that the formation of collapsed objects in an overdense region begins from the density peak which in due course accretes surrounding shells of material ¹⁹ Each of these shells is thought to be much less massive than the already collapsed and virialized core. Assuming spherical symmetry, one can show that material from each consecutive shell will be eventually deposited at a radius:

$$r = \frac{r_{\rm m}(\beta - 1)}{2} \tag{12}$$

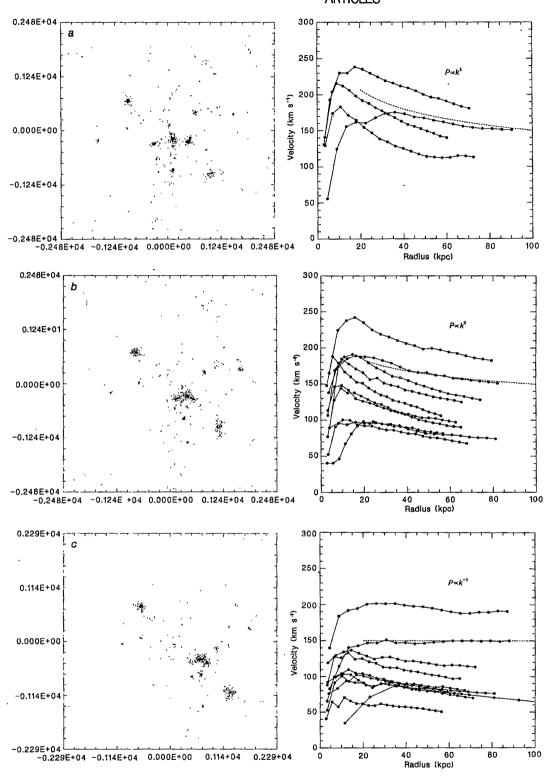


Fig. 2 The formation of haloes in an EinsteindeSitter $(\Omega = 1)$ universe different power spectra. Particle plots show only the inner, highresolution regions. The exponent of the power law is indicated in the plots of the rotation velocities. The rotation profile predicted by $\rho(r) \sim r^{-3(3+n)/(4+n)}$ is indicated by dashed line. A scaled down average rotation profile of Sc spirals, ref. 15, is plotted along with the CDM haloes.

around the centre, where $r_{\rm m}$ is the radius of maximum expansion, and β characterizes the density of the already virialized core:

$$\rho(r) \sim r^{-\beta} \tag{13}$$

With a few additional assumptions, this can be used to calculate the density profile. The maximum radius of expansion for a spherically symmetric density perturbation with the initial relative overdensity δ_i is given by:

$$r_{\rm m} = r_{\rm i} \frac{1 + \delta_{\rm i}(r_{\rm i})}{\delta_{\rm i}(r_{\rm i}) - (\Omega_{\rm i}^{-1} - 1)}$$
 (14)

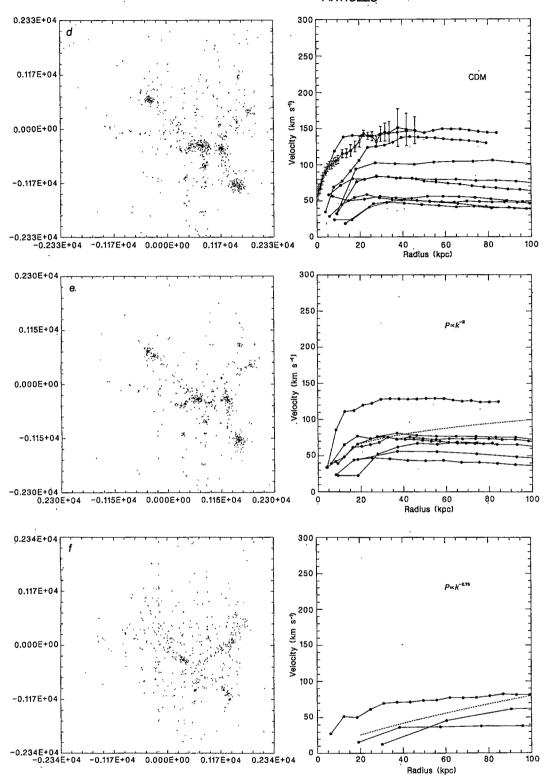
Here δ_i characterizes the initial overdensity inside the sphere of radius r_i :

$$M(r < r_i) = \left(\frac{4\pi}{3}\right) r_i^3 \langle \rho \rangle (1 + \delta_i(r_i)) \tag{15}$$

In the case considered here $\Omega_i = 1$. Therefore, the final density of the halo is:

$$\rho(r) \sim \delta_{\rm i}(r_{\rm i}(r))^3 \tag{16}$$

Hoffman and Shaham²⁰, following Peebles¹², argue that in a universe with a scale-free spectrum of initial density perturba-



tions, given by equation (1), the relative overdensity around a local maximum can be estimated by:

$$\delta_{i} \sim \left(\frac{r_{i}}{r_{\lambda}}\right)^{-(3+n)} \tag{17}$$

Here r_{λ} is the characteristic smoothing distance ^{12,20,28}, related to the distance between the peaks. Consequently, the final density of the collapsed halo is given by:

$$\rho(r) \sim (r_i(r))^{-3(3+n)} \tag{18}$$

To express the right-hand side of this relation in terms of the distance from the halo centre we use equation (14) together with equation (17) to obtain:

$$=\frac{r_{\rm m}(\beta-1)}{2}$$

$$\sim \frac{(\beta - 1)}{2} \left(\frac{r_{\rm i}}{r_{\rm i}}\right)^{4+n} \tag{19}$$

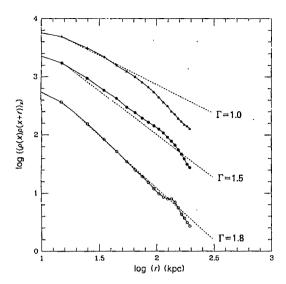


Fig. 3 Density autocorrelation functions, equation (21), for the particles in the high-resolution portions of some of the power law models. The prediction of the hierarchical clustering scenariopower law with the exponent given by equation (22)—is indicated by the dashed line. Results for: \triangle , n = -2; \bigcirc , n = -1; \bigcirc , n = 0respectively. Note that each curve has been offset vertically by an arbitrary amount for clarity.

Therefore.

$$\rho(r) \sim \left(\frac{r}{r_{\lambda}}\right)^{-3(3+n)/(4+n)} \tag{20}$$

Our derivation of equation (20) paraphrases a more detailed discussion in ref. 20.

Hoffman and Shaham, following Fillmore and Goldreich²⁹, conjecture that the mass profiles with $M \sim r^{1+\epsilon}$, $\epsilon > 0$, are unstable. Therefore, they conclude that haloes with $\gamma < 2$ will relax into flat rotation curve haloes. This additional conjecture has not been so far confirmed by our computer models. The key difference between the situation analysed by Fillmore and Goldreich and our computer simulations may be due to the absence of angular momentum in the spherically symmetric, self-similar calculations reported in the ref. 29. Large angular momenta may stabilize haloes with rising rotation curves.

The analysis leading to equation (20) hinges on assumptions which are at best only approximately valid: (1) The initial overdensity profile, equation (17), is a reasonable estimate of the actual density profile only for a limited range of initial radii. When $r < r_{\lambda}$, near the peak, $\delta_i(r_i)$ is flatter than equation (17) would suggest. Moreover, for larger r, fluctuations of overdensity soon begin to exceed the systematic behaviour given by equation (17)^{20,28}. Therefore, the derivation is based on an assumption which is approximately accurate only for a rather limited range of radii. (2) A detailed discussion by Bardeen et al.28 shows that the criterion implicitely used by Hoffman and Shaham to define density maxima is biased towards unusually broad peaks. (3) The density profile around correctly chosen density maxima falls off more steeply than equation (17) would have it. This difference may account for the discrepancy between the rotation curves predicted on the basis of equation (20) and the steeper rotation profiles obtained in our simulations. (4) The paradigm of the secondary infall onto a peak does not appear to be valid in the course of collapse leading to the formation of the haloes considered here. In particular, merging of smaller, already collapsed objects (see Fig. 1) appears to be a better description of the formation process. This is at odds with the picture of shells deposited spherically symmetrically onto a pre-existing core. In

spite of all these problems equations (4) and (5) give a reasonably accurate prediction of the density profiles of the collapsed objects. Discrepancies, which we have already pointed out in the previous section, are worth further study.

Scale-free spectra lead to a self-similar clustering hierarchy⁵⁻¹⁰ Peebles has pointed out that the density autocorrelation function in an evolved region of such a hierarchical universe should have a power law form⁶:

$$\langle \rho(x)\rho(x+r)\rangle_x = r^{-\Gamma}$$
 (21)

with an 'hierarchical' exponent Γ given by:

$$\Gamma = \frac{3(3+n)}{(5+n)} \tag{22}$$

This Γ differs from the γ in the density formula, equation (5). We have verified (see Fig. 3) that this estimate for Γ is indeed correct in the high-resolution portions of our models. Note, perhaps not unexpectedly, that when the density autocorrelation is calculated only for the particles inside the haloes—that is, for x chosen from within the perimeter of the halo, but for an arbitrary r in the notation of equation (21)—it is considerably steeper, with the effective power law exponent close to the one given by equation (5).

Conclusions

Our numerical experiments provide clear evidence of a direct connection between the form of the power spectrum responsible for the gaussian density perturbations and the rotation curves of the resulting haloes. In particular, $P(k) \sim k^n$ with $n \sim -1 \rightarrow -2$ leads to flat rotation curves in present day galactic haloes. Power law spectra with n > -1 give haloes with rotation curves steeper than observed. This puts severe constraints on the shape of the power spectrum in the range corresponding to 1 Mpc. Furthermore, baryon condensation in the central parts of the halo can be expected to further steepen the rotation profile²⁷. This indicates that density perturbations with the preponderance of the power on small scales are untenable as models for galaxy formation. On the other hand, baryon condensation can probably flatten rising rotation curves inside broad soft cores, making n = -1 or n = -2 attractive. The cold dark matter power spectrum falls into the category of spectra producing haloes compatible with observations. Further studies to determine the environment dependence of other halo properties (such as the radii of their soft cores, angular momenta, and eccentricities) are underway.

We thank Stirling Colgate, Richard Epstein, Mike Fall, Yehuda Hoffman, Craig Hogan, Robert Hotchkiss, Nick Kaiser, Jeremy Ostriker and Martin Rees for stimulating discussion and help. Completion of this project would have been impossible without the large amounts of computer time provided by Los Alamos National Laboratory, Caltech and the Space Telescope Science Institute. We thank Kate Quinn for helping to prepare the manuscript.

Received 14 February; accepted 23 May 1986.

- Peebles, P. J. E. The Large Scale Structure of the Universe (Princeton University Press, 1980). Guth, A. Phys. Rev. D23, 347-356 (1981).
- Linde, A. D. Phys. Lett. 108B, 389-393 (1982).
- Albrecht, A. & Steinhardt, P. J. Phys. Rev. Lett. 48, 1220-1223 (1982).

- Albrecht, A. & Steinhardt, P. J. Phys. Rev. Lett. 48, 1220-1223 (1982).
 Press, W. H. & Schechter, P. Astrophys. J. 187, 425-438 (1974).
 Peebles, P. J. E. Astrophys. J. 189, L51-L53 (1974).
 Gott, J. R. & Recs, M. J. Astr. Astrophys. 45, 365-376 (1975).
 Gott, J. R. & Turner, E. L. Atrophys. J. 216, 357-371 (1977).
 White, S. D. M. & Rees, M. J. Mon. Not. R. astr. Soc. 183, 341-358 (1978).
 Faber, S. M. in Astrophysical Cosmology (eds Bruck, H. A., Coyne, G. & Longair, M.) 191-217 (Pontifica Academia Scientiarium, 1982).
 Peebler, B. F. E. Atrophys. J. 421, 11, 15 (1982).
- Peebles, P. J. E. Astrophys. J. 263, L1-L5 (1982).
 Peebles, P. J. E. Astrophys. J. 277, 470-477 (1984).

- Humenthal, G. R., Faber, S. M., Primack, J. R. & Rees, M. J. Nature 311, 517-525 (1984).
 Rubin, V. C., Ford, W. K. & Thonnard, N. Astrophys. J. 238, 471-487 (1980).
 Rubin, V. C., Burstein, D., Ford, W. K. & Thonnard, N. Astrophys. J. 289, 81-104 (1985).
 Bosma, A. thesis, Univ. of Gronigen (1978).
 Carignan, C. & Freeman, K. C. Astrophys. J. 294, 494-501 (1980).
 van Albada, T. S., Bahcall, J. N., Begeman, K. & Sancisi, R. Preprint (Princeton Univ., 1985).

- Gunn, J. E. & Gott, J. R. Astrophys. J. 176, 1-19 (1972).
 Hoffmann, Y. & Shaham, J. Astrophys. J. 297, 16-22 (1985).
 Efstathiou, G., Davis, M., Frenk, C. S. & White, S. D. M. Astrophys. J. Suppl. 57, 241-260
- 22. Zeldovich, Ya. B. Astr. Astrophys. 5, 84-89 (1970).
- 23. Davis, M., Efstathiou, G., Frenk, C. S. & White, S. D. M. Astrophys. J. 292, 371-394 (1985).
- Quinn, P. J., Salmon, J. K. & Zurek, W. H. IAU Symp. 117 (in the press).
 Zurek, W. H., Quinn, P. J. & Salmon, J. K. IAU Symp. 117 (in the press).
- Frenk, C. S., White, S. D. M., Efstathiou, G. & Davis, M. Nature 317, 595-597 (1985).
- Blumenthal, G. R., Faber, S. M., Flores, R. & Primack, J. R. Astrophys. J. 301, 27-34 (1986).
 Bardeen, J. M., Bond, J. R., Kaiser, N. & Szalay, A. S. Astrophys. J. 304, 15-61 (1986).
- 29. Fillmore, J. A. & Goldreich, P. Astrophys. J. 281, 1-8 (1984).

The cytoplasmic carboxy terminus of M13 procoat is required for the membrane insertion of its central domain

Andreas Kuhn, William Wickner & Günther Kreil

Molecular Biology Institute and Department of Biological Chemistry, University of California, Los Angeles, California 90024, USA

The M13 coat protein spans the Escherichia coli plasma membrane with its amino-terminus facing the periplasm. It is made as a precursor—the procoat—with a typical leader peptide. Mutations which destroy the basic character of the carboxy-terminal domain of procoat, a domain which is oriented towards the cytoplasm, block membrane assembly, while insertion of three lysyl residues near the carboxy terminus partially restores assembly. Thus the information specifying membrane insertion of M13 procoat protein is found in its mature region as well as the leader and is not simply decoded in an amino to carboxy direction.

MANY secreted and membrane proteins are made with basic, amphiphilic leader (signal) peptides of 15 to 30 residues at their amino-terminus¹⁻³. Leader peptides are removed by an endoprotease, the leader peptidase⁴, after the pre-protein has crossed the membrane. Although leader peptides are essential for the processes of secretion and membrane assembly⁵, their precise roles have been the subject of speculation (reviewed in ref. 6) and are not yet established. Careful compilation and analysis^{2,3} have shown that certain features, such as the distribution of charged and apolar residues, are common among leader peptides. In contrast, there is no apparent sequence conservation among the mature regions of secreted proteins or extracytoplasmic domains of transmembrane proteins. This has led to the concept that the information specifying protein translocation into, or across, a membrane lies solely in leader peptides⁷.

Mutations in bacterial proteins which impair their export to the plasma membrane, periplasm or outer membrane can define domains which are relevant to this process. Almost all available mutations which affect the translocation of the λ receptor or the maltose-binding protein are in the leader region⁸. Furthermore, deletion of the carboxy-terminal regions of β -lactamase⁹ or maltose-binding protein¹⁰ has no effect on their export. These studies supported the concept that the leader peptide is sufficient to specify translocation.

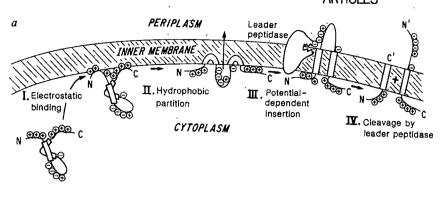
However, other studies have implicated the mature region of pre-proteins in membrane transit processes. In bacteria, protein translocation is a late or post-translational event¹¹⁻¹³, suggesting that the carboxy-terminus may have a necessary role. Indeed, fusion proteins comprised of the leader peptide of a secreted protein and the carboxy-terminal region of a cytoplasmic protein cannot cross the plasma membrane 14,15. Furthermore, Silhavy and colleagues 16 have shown that over half of the 'mature' region of the λ receptor must be present in a fusion protein to permit export. The relative roles of the leader and mature domains of a pre-protein during its export across the plasma membrane of Escherichia coli have thus remained undefined.

Membrane assembly of procoat

We have studied the biosynthesis of M13 coat protein, a small protein (relative molecular mass (M_r) 5,280) which spans the inner membrane of M13-infected cells¹⁷. It is made as a precursor, termed procoat $(M_r, 7,628)$, with a 23-residue leader peptide (Fig. 1). Our working model of procoat membrane assembly is shown in Fig. 1a. Procoat has two hydrophobic domains (drawn as rectangles in Fig. 1), one in the leader and one which spans the membrane in mature coat protein. Its membrane insertion is not coupled to either secA or secY function 18 or to polypeptide synthesis¹⁹, but does require the transmembrane electrochemical potential²⁰. Transmembrane procoat is cleaved by leader peptidase to yield coat protein and the leader peptide, which is rapidly degraded. The biosynthesis of this protein has been studied extensively, both in vivo and in crude and reconstituted in vitro reactions^{21,22}. However, only a few mutants of this protein have been described.

In a recent study, we cloned the procoat gene and used in vitro mutagenesis with hydroxylamine to create mutations²³. More than 40 mutants were identified, of which 3 were in the leader sequence near the leader peptidase cleavage site²⁴. These three mutations affected the cleavage of procoat by leader peptidase, yet did not prevent procoat insertion across the membrane. In fact, despite careful screening, no mutations were identified which blocked membrane insertion. Examination of the 111 transitions which hydroxylamine could potentially cause in this gene of 219 base pairs (bp) revealed that only 68 would lead to amino-acid substitutions, and most of these would be quite conservative. Current mutagens only yield a very limited variety of mutants. Thus the failure to create export-defective mutations in the mature domain of secretory and membrane proteins, with currently available mutagens cannot be taken as evidence that such mutations cannot occur.

In the present study, we have circumvented this problem by directly altering the carboxy-terminus of procoat with recom-



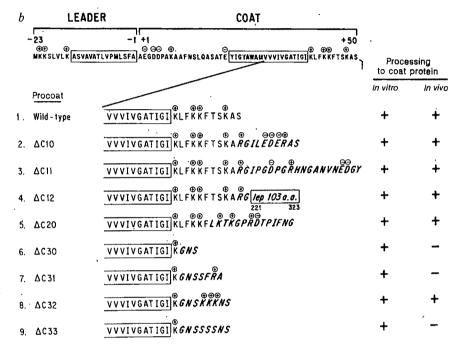


Fig. 1 a, A working model for the membrane insertion of M13 procoat. b, Construction of procoat mutants.

Methods. The procoat gene was cloned into the pING-1 vector²³ and excised by digestion with Sall and EcoRI. It was purified by electrophoresis in 0.7% agarose and then partially cleaved with AluI. This restriction endonuclease can cleave the procoat gene after the second base of the codon of the COOHterminal serine and after the codon for lysine +40. The partially digested procoat gene was inserted into the pING plasmid which had previously been digested with SalI and SmaI. This yielded plasmids Δ C10 and Δ C30, respectively. As a second step, the plasmid $\Delta C10$ was cut with EcoRI and ligated with the EcoRI fragment of leader peptidase. This contains the codons for the COOH-terminal region of leader peptidase, starting at isoleucine 221 and extending 52 bp beyond the stop codon. The resulting plasmids $\Delta C11$ and $\Delta C12$ contained this fragment in the opposite and same orientations as the leader peptidase gene, respectively. In ΔC12, the reading frame of the leader peptidase gene is retained, yielding a fusion protein. The same EcoRI fragment was also inserted into the plasmid $\Delta C30$. This yielded only one phenotype, represented by plasmid ΔC31. Finally, the two complementary oligonucleod(AATTCGAAGAAGAAG) d(AATTCTTCTTCTG) were synthesized and ligated into plasmid AC30 which had been digested with EcoRI. Depending on the orientation, this resulted in the insertion of three lysine (Δ C32) or three serine (Δ C33) residues. During screening for the clones Δ C11 and Δ C12, a new phenotype was observed which corresponded neither to the parent plasmid Δ C10 nor to Δ C12. This plasmid, termed $\Delta C20$, was shown by sequencing to have a deletion which alters the amino-acid sequence of procoat after residue

+45.

binant DNA techniques, including oligonucleotide-directed mutagenesis. We find that the basic character of the carboxy terminus of procoat is as essential for its membrane assembly as the leader peptide.

Carboxy-terminal mutations

The sequence of wild-type M13 procoat, and of mutations which we have created near the carboxy-terminus, are listed in Fig. 1b. The mutants are designated 'AC' to indicate the deletion of procoat near the carboxy terminus. The first digit after the C indicates which restriction site was used for the construction, while the second simply lists the various derivatives made at that site. All the AC constructions migrated at their expected M_r on SDS-polyacrylamide gel electrophoresis. Each was readily cleaved to its mature size in cell-free detergent extracts, as expected for the known substrate specificity of leader peptidase (ref. 25 and Figs 2, 4). We have shown previously that such cleavage is at the amino terminus, and is due to leader peptidase²⁴. In addition, the in vitro conversion of procoat to coat was shown to be inhibited by purified leader peptide (data not shown). Since these mutant procoat proteins are substrates for leader peptidase, their processing in vivo is an accurate indicator of whether they have assembled across the plasma

Procoat mutants Δ C10, Δ C11 and Δ C12 retained all but the carboxy-terminal serine of procoat, while adding 10, 20 or 105 polar amino-acid residues. Each of these mutant procoats rapidly chased to its respective mature form, though some of the precursor was lost to cytoplasmic degradation (Fig. 3, lanes

1, 2; 7, 8; 9, 10; odd-numbered lanes are pulse-labelled; evennumbered lanes are chased for 60 s). Since it has been suggested that the assembly properties of procoat are a function of its small size, we characterized the largest of these mutants, Δ C12, in detail. To create this mutant, a restriction fragment encoding the carboxy-terminal 103 polar amino-acid residues of leader peptidase was joined (in-frame) to the 3' end of the procoat gene. Its membrane assembly and orientation are indicated diagrammatically in Fig. 4a. In vitro, Δ C12 is synthesized as a precursor (Fig. 4b, lane 1) which can be cleaved to its mature M, by leader peptidase (Fig. 4b, lane 2). In vivo, even a brief pulse-label reveals largely mature $\Delta C12$ (Fig. 3, lane 9, and Fig. 4c) and only a small amount of precursor. This presumably simply reflects membrane assembly during the additional time needed to synthesize the 103 extra carboxy-terminal residues. Correct assembly was confirmed by protease mapping (Fig. 4c). Cells. synthesizing $\Delta C12$ were pulse-labelled with methionine, then chilled and treated with Tris, sucrose and EDTA to permeabilize the outer membrane. These cells, or cells lysed with detergent, were digested with proteinase K for the indicated times. Aliquots were immunoprecipitated with antiserum to coat protein or to leader peptidase and analysed by SDS-polyacrylamide gel electrophoresis (PAGE) and fluorography. Although a small fraction of the cells lysed during the experiment, the precursor form of $\Delta C12$ was largely inaccessible to protease, though it was completely degraded when the cells were lysed with detergent. The mature form of Δ C12 was cleaved to a form of sightly lower M_r by proteinase K added to intact spheroplasts. This lower M_r form retained the carboxy-terminal

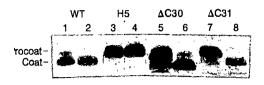


Fig. 2 Sensitivity of wild-type and mutant procoats to digestion by leader peptidase in detergent mixed micelles. E. coli HJM114bearing plasmids with either the wild-type or various mutant procoat genes (as noted) were grown at 37°C in minimal medium 9 (ref. 32) containing 0.5% fructose and a supplement of the mixed amino acids, less methionine. At an absorbance at 600 nm of 0.05, arabinose was added to 0.5% and growth continued for 2 h. Each culture (1 ml) was then labelled for 30 s with 50 µCi 35S-methionine (1,000 Ci mmol⁻¹). Cultures were added to 0.25 ml of 30% sucrose, 0.6 mg ml^{-1} lysozyme, 0.03 M EDTA, 3% (v/v) Triton X-100, and 100 µg ml⁻¹ DNase I. Each sample was frozen in a dry ice/ethanol bath, then thawed and incubated for 30 min at 0 °C. Aliquots (0.2 ml) were either held on ice (lanes 1, 3, 5, 7) or incubated at 37 °C (lanes 2, 4, 6, 8) for 1 h, then analysed for procoat and coat by immunoprecipitation, SDS-PAGE and fluorography. Procoat H5 is a mutant in the leader peptidase target site of procoat²⁴.

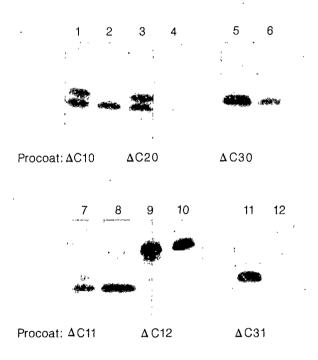


Fig. 3 Phenotypes of ΔC mutant procoats. Recombinant plasmids were transformed into wild-type E. coli HJM114. Cultures were grown overnight at 37 °C in M9 minimal medium containing ampicillin and glucose. Fresh overnight cultures were diluted 1:100 into M9 minimal medium containing 0.5% arabinose and grown at 37 °C to a density of 3×10^8 cells per ml. Aliquots were pulselabelled for 30 s with $10~\mu Ci$ of $^{35} S$ -methionine, then chased for either 5 s (odd-numbered lanes) or 60 s (even-numbered lanes) in the presence of unlabelled methionine. Samples were precipitated with trichloroacetic acid and analysed by immunoprecipitation, SDS-PAGE and fluorography.

leader peptidase immunological determinants, but was no longer immunoprecipitable by antiserum to coat protein (Fig. 4c). Δ C12 therefore has the expected orientation across the plasma membrane, with its amino terminus facing the periplasm and its carboxy terminus exposed to the cytoplasm. Mutants Δ C10 to Δ C12 demonstrate that simply elongating the carboxy terminus of procoat does not interfere with membrane assembly.

Procoat Δ C20 has lost the original carboxy-terminal 5 residues of procoat, including lysine +48, and in their place has sub-

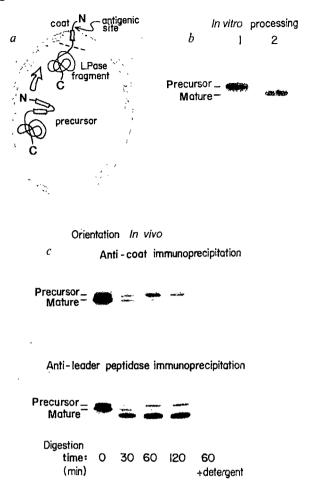


Fig. 4 Procoat Δ C12 is translocated across the membrane and processed. a, Schematic representation of the cellular localization of procoat Δ C12 and coat Δ C12. b, Plasmid-directed synthesis of procoat Δ C12 in vitro and its cleavage to a mature form by purified leader peptidase. c, Protease-accessibility of procoat and coat Δ C12.

Methods. Purified plasmid DNA encoding procoat ΔC12 was added to cellular extracts (S-30) of E. coli HJM114 in the presence of 0.4% arabinose, 0.5% Triton X-100 and purified ara C protein (200 μg ml⁻¹; a gift from Dr G. Wilcox, Ingene Inc.). Incubation was at 37 °C for 1 h under the conditions described by Zalkin et al.³³ either in the absence (lane 1) or in the presence (lane 2) of 50 μg ml⁻¹ purified leader peptidase⁴. For c, exponentially growing cells were pulse-labelled with ³⁵S-methionine for 1 min and osmotically shocked by mixing with an equal volume of ice-cold 60 mM Tris-HCl, pH 8.0, 40% sucrose, 20 mM EDTA. These cells were incubated with proteinase K (1 mg ml⁻¹) for the indicated times without (lanes 1-4) or with (lane 5) 2.5% Triton X-100. The samples were then immunoprecipitated with antibodies to coat (upper panel) or to leader peptidase (lower panel) and analysed by SDS-PAGE and fluorography.

stituted 14 polar, basic residues. It also assembles across the plasma membrane and is processed to coat protein (Fig. 3, lane 3), though this assembly reaction is inefficient. Δ C20 procoat was inaccessible to added proteinase K in spheroplasts, while the mature Δ C20 was degraded (Fig. 5a), confirming that processing reflected membrane assembly. Both the precursor and mature forms of Δ C20 were rapidly degraded in vivo (Fig. 3, lane 4). The precursor form is far more stable in a htp, lon strain (Fig. 6b), which lacks the cytoplasmic, ATP-dependent lon protease²⁶, indicating that procoat Δ C20 is normally degraded by the cytoplasmic lon protease in wild-type cells. The mature form of Δ C20 is still degraded, presumably by a different proteinase.

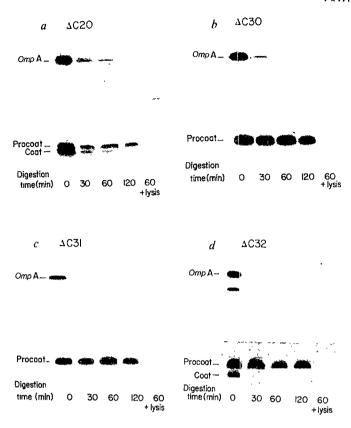


Fig. 5 Protease-accessibility to test for insertion of procoat into the membrane. Exponentially growing cultures of LC 137 which bore plasmids coding for procoat Δ C20 (a), Δ C30 (b), Δ C31 (c), or Δ C32 (d) were pulse-labelled with ³⁵S-methionine for 1 min, chased with an excess of L-methionine for 1 min, and osmotically shocked by thorough mixing with an equal volume of ice-cold 60 mM Tris-HCl pH 8.0, 40% sucrose, and 20 mM EDTA. Proteinase K (Boehringer) was added to a final concentration of 1 mg ml⁻¹ and incubated at 0 °C for the indicated times. For some samples, the cells were lysed by addition of 2.5% Triton X-100. Proteinase K was inactivated by addition of phenylmethanesulphonyl fluoride (Sigma) and 20% trichloroacetic acid. The acid precipitates were collected by centrifugation, twice resuspended in ice-cold acetone, sedimented and resuspended in 50 µl of 10 mM Tris-HCl (pH 8), 2% SDS and incubated for 5 min at 95 °C. Each sample was then diluted with 1 ml of 2% Triton X-100, 0.1 mM EDTA, 0.15 M NaCl, 10 mM Tris-HCl pH 8.0 (buffer A) and mixed with 15 µl of a 10% suspension of formalin-fixed, SDS-washed Staphylococcus aureus¹¹ for 30 min. The S. aureus cells were removed by centrifugation. Antiserum to M13 coat protein and the outer membrane protein (Omp A) was added to the supernatant and incubated overnight. After addition of 15 µl of a 10% suspension of S. aureus cells, the samples were incubated for 1 h and centrifuged. The cells were sequentially suspended in buffer A and buffer A minus detergent and collected by centrifugation. They were then mixed with electrophoresis sample buffer, boiled and applied to 19% polyacrylamide gels in SDS containing 6 M urea. After electrophoresis, the gels were fixed, incubated in salicylate, dried and fluorographed11.

Altering the carboxy terminus

In the mutant Δ C30, the carboxy-terminal 10 residues of procoat were replaced by the sequence Gly-Asn-Ser. This yields a precursor which contains 66 rather than 73 residues and which lacks 3 of the 4 lysyl residues present in the cytoplasmic 'tail' of the wild-type protein. Surprisingly, this change at the carboxy terminus of procoat completely prevents its processing (Fig. 3, lanes 5, 6). Since procoat Δ C30 is an excellent substrate for leader peptidase *in vitro*, the absence of *in vivo* processing indicates that it failed to insert across the plasma membrane.

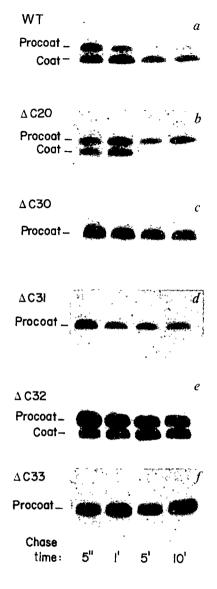


Fig. 6 In vivo processing of procoat mutants. Exponentially growing cultures of E. coli LC 137 (htp⁻, lon⁻) with plasmids coding for wild-type (a) or mutant (b-f) procoat were pulse-labelled with ³⁵S-methionine for 30 s and chased with an excess of L-methionine for the indicated times. Samples were analysed by immunoprecipitation, SDS-PAGE and fluorography.

The mutant precursor is slowly degraded in wild-type cells but not in the htp, lon mutant (Fig. 6c). This provides a second criterion that procoat Δ C30 remains in the cytoplasm. Procoat Δ C30 was also found to be inaccessible to protease in intact spheroplasts (Fig. 5b), confirming that it does not insert across the plasma membrane. These results cannot be explained by any combination of leader, stop-transfer and start-transfer sequences⁷; they are readily explained if procoat Δ C30 fails to form a spontaneous insertion domain⁶.

A derivative of Δ C30 was obtained by inserting the EcoRI fragment of the leader peptidase gene into the EcoRI site of the Δ C30 gene. In either orientation, the fragment has only a short open reading frame, yielding procoat mutants of either 70 or 72 residues. Twelve such clones were investigated by pulse-chase experiments of the type described in Fig. 6, but the observed assembly phenotype was in each case the same as for Δ C30. One such plasmid, Δ C31, was sequenced and shown to encode a procoat mutant of 70 residues. The extra seven residues added after lysine +40 of the wild-type sequence are all hydrophilic and include one arginine. Although this precursor is nearly as

large as wild-type procoat and has two positive charges in its carboxy-terminal region, it still cannot translocate across the plasma membrane. It has the following properties: (1) it can be cleaved by leader peptidase in detergent extracts (Fig. 2, lanes 7, 8), but is not processed in vivo (Fig. 3, lane 11); (2) it is rapidly degraded in wild-type cells (Fig. 3, lane 12) but not in cells which lack the cytoplasmic lon protease (Fig. 6b); and (3) it is inaccessible to added protease in spheroplasts (Fig. 5c). Apparently, restoration of neither size nor overall polarity was sufficient to allow translocation of this mutant procoat.

We therefore devised a test of whether the basic charge at the carboxy terminus of procoat was essential for potein translocation. Two complementary oligonucleotides were synthesized which contained EcoRI linkers at their termini and, depending on the orientation, specified three codons for lysine or for serine. The two oligonucleotides were annealed and cloned into the EcoRI site of Δ C30. The resulting procoat mutants showed different behaviour in pulse/chase experiments. Procoat $\Delta C32$, which has three lysines introduced near its carboxy terminus by the oligonucleotides, can insert into the plasma membrane (Figs 5d, 6e), though at a somewhat lower efficiency than wild-type procoat. In contrast, insertion of the oligonucleotide in the other direction, which created procoat Δ C33 with three added seryl residues, did not restore membrane assembly (Fig. 6f). These results indicate that it is the basic charge in the short carboxyterminal domain of procoat which is essential for its insertion across the membrane.

Conclusions

We have shown that the precise sequence of the carboxy terminus of procoat is not required for membrane assembly, yet its basic character is essential. The signal hypothesis, as originally proposed²⁷ and as modified⁷, postulates a vectorial decoding of linear information contained in 'signal' and 'stoptransfer' sequences of a membrane protein in the amino to carboxy direction. Our results demonstrate that the entire procoat protein has a role in the membrane assembly process. The carboxy terminus of procoat does not resemble a signal or stop-transfer sequence. It is highly polar, while apolar amino acids dominate signal or stop-transfer sequences. Since the carboxy terminus of procoat faces the cytoplasm, our results rule out a linear amino-to-carboxy decoding of this protein's assembly information. We suggest that the entire protein folds in a fashion competent for membrane insertion, as suggested by the membrane trigger hypothesis²⁸. Such a folded structure has recently been termed a spontaneous insertion domain⁶.

Received 13 January; accepted 28 April 1986.

- 1. Milstein, C., Brownlee, G. G., Harrison, T. M. & Mathews, M. B. Nature new Biol. 239, 117-120 (1972).
- vonHeijne, G. Eur. J. Biochem. 133, 17-21 (1983)
- Perlman, D. & Haivorson, H. O. J. molec. Biol. 167, 391-409 (1983).
 Wolfe, P. B., Silver, P. & Wickner, W. J. biol. Chem. 257, 7898-7902 (1982).

- Carlson, M. & Botstein, D. Cell 28, 145-154 (1982).
 Wickner, W. T. & Lodish, H. F. Science 230, 400-407 (1985).
 Blobel, G. Proc. natn. Acad. Sci. U.S.A. 77, 1496-1500 (1980).
 Michaelis, S. & Beckwith, J. A. Rev. Microbiol. 36, 435-465 (1982).

- Koshland, D., Sauer, R. T. & Botstein, D. Cell 30, 903-914 (1982).
 Ito, K. & Beckwith, J. Cell 25, 143-150 (1981).
 Ito, K., Date, T. & Wickner, W. J. biol. Chem. 255, 2123-2130 (1980).
 Koshland, D. & Botstein, D. Cell 20, 749-760 (1980).
- Randall, L. L. Cell 33, 231-240 (1983).
 Moreno, F. et al. Nature 286, 356-359 (1980).

- Kadonaga, J. T. et al. J. biol. Chem. 259, 2149-2154 (1984).
 Hall, M. H., Schwartz, M. & Silhavy, T. J. J. molec. Biol. 156, 93-112 (1982).
 Wickner, W. Proc. natn. Acad. Sci. U.S.A. 73, 1159-1163 (1976).

The carboxy terminus and leader peptide of procoat are not the only regions which are essential for its membrane assembly. We have also found that the introduction of an arginine at position +30 (the centre of the membrane-spanning domain) in place of the normal valine residue blocks membrane assembly (A.K., G.K. and W.W., manuscript in preparation). Thus the hydrophobic domain +20 to +40 is not only a 'membrane anchor', but is also required to initiate the membrane insertion process.

Our current working model of coat protein biogenesis is presented in Fig. 1a. Procoat may need its basic carboxy terminus in order to bind electrostatically to the membrane acidic lipid head groups. Both apolar domains, that in the leader and the apolar membrane anchor of the mature protein, may participate in partition into the apolar fatty acyl core of the membrane. Insertion of the central, polar domain across the membrane would then be driven by the membrane electrochemical potential, followed by cleavage to yield the mature coat protein. This speculative model may provide a framework for designing future studies.

Other proteins, with different assembly characteristics, may also require information encoded throughout their sequence for insertion across the bacterial plasma membrane. Procoat protein is representative of a class of proteins which do not require the sec-encoded functions for their export 18,29. We have also examined the biosynthesis of leader peptidase, an inner membrane protein which requires at least secA and secY function for its membrane assembly¹⁸. Leader peptidase spans the plasma membrane, with its amino terminus facing the cytoplasm and its carboxy terminus exposed to the periplasm³⁰. A polar, central domain which is carboxy-terminal to the membrane-spanning region is essential for the membrane assembly of leader peptidase (R. Dalbey and W.W., manuscript in preparation). Mutations have also been described in the mature regions of λ receptor¹⁶ and pre-maltose binding protein³¹ which affect their export. These results suggest that, in general, various domains of bacterial proteins in addition to the leader sequence may participate in the process of membrane assembly.

We thank Dr Satoshi Miura for performing the experiment shown in Fig. 6b, Dr Pierre Prentki for help with DNA sequencing and Marilyn Rice and Douglas Geisser for technical assistance. This work was supported by a grant from the NIH and a contract from Ingene, Inc. A.K. is a fellow of the Schweizerischen Stiftung fuer medizinisch-biologische Stipendien and the European Molecular Biology Organization. G.K. is a Visiting Professor of the UCLA Molecular Biology Institute.

- Wolfe, P. B., Rice, M. & Wickner, W. J. biol. Chem. 260, 1836-1841 (1985).
 Date, T. & Wickner, W. T. J. Virol. 37, 1087-1089 (1981).
 Date, T., Goodman, J. M. & Wickner, W. Proc. natn. Acad. Sci. U.S.A. 77, 4669-4773 (1980).
- 21. Date, T., Zwizinski, C., Ludmerer, S. & Wickner, W. Proc. natn. Acad. Sci. U.S.A. 77,
- 827-831 (1980).
- Wickner, W. Trends biochem. Sci. 8, 90-92 (1983).
 Kuhn, A. & Wickner, W. J. biol. Chem. 260, 15907-15913 (1985).
 Kuhn, A. & Wickner, W. J. biol. Chem. 260, 15914-15918 (1985).
- 25. Dierstein, R. & Wickner, W. EMBO J. (in the press).
- Goff, S. & Goldberg, A. L. Cell 41, 587-595 (1985).
 Blobel, G. & Dobberstein, B. J. Cell Biol. 67, 852-862 (1975).
- Wickner, W. A. Rev. Biochem. 48, 23-45 (1979).
 Oliver, D. B. & Beckwith, J. Cell 25, 765-772 (1981).
- Wolfe, P. B., Wickner, W. & Goodman, J. J. biol. Chem. 258, 12073-12080 (1983).
 Bankaitis, V. A., Rasmussen, B. A. & Bassford, P. J. Jr Cell 37, 243-252 (1984).
- 32. Miller, J. Experiments in Molecular Genetics (Cold Spring Harbor Laboratory, New York,
- 33. Zalkin, H., Yanofsky, C. & Squires, C. L. J. biol. Chem. 249, 465-475 (1974)

Detection of planetary systems and the search for evidence of life

Bernard F. Burke

Department of Physics, Massachusetts Institute of Technology, Cambridge, Massachusetts 02139, USA

The Solar System is our only example of a planetary system, and the Earth is the only known instance of a planet harbouring life. The formation of planetary systems may occur commonly among stars like the Sun, but whether life arises frequently, rarely, or is a unique event is more problematical. Astrometric techniques capable of detecting major planets (similar to Jupiter, Saturn and Uranus) orbiting nearby stars are currently active ¹⁻⁴, but detection of an Earth-like planet is beyond current techniques. Direct imaging of planetary systems (refs 5, 6; B. M. Oliver, unpublished data) is even more challenging, and current opinion seems to have dismissed the possibility of imaging a planet as small as the Earth. The problem is not an impossible one, however: by combining radioastronomy and optical methods, images of Earth-like planets orbiting nearby stars should be obtainable, and their atmospheres could be studied spectroscopically for evidence of life.

Consider the problem of optically detecting an Earth-like planet in orbit about the nearby G5 star τ Ceti, ~3 pc distant. Except for a numerical factor near unity, the signal-to-noise considerations are the same for both interferometric and filledaperture systems. For a planet of diameter d, albedo η (assuming isotropic scattering), in a circular orbit of radius a at maximum elongation, the ratio of planetary to stellar photon flux (S_p/S_s) is $(\eta/16)$ $(d/a)^2$. The flux from an Earth-like planet with a=1 AU is indeed feeble: $(S_p/S_s) = 1.8 \times 10^{-10}$. More explicitly, the total photon flux of τ Ceti is 8.5×10^9 photons m⁻² s⁻¹, and the scattered planetary flux would be 1.5 photons m⁻² s⁻¹. Thus one must have a stable system that permits long integrations, and the flood of photons from the parent star must be reduced. The general system requirements, for a star at distance D whose flux would be S_0 if it were at distance D_0 , can be specified in terms of the effective collecting area A, the relative gain $G(\theta)$ for the star offset by an angle θ (G=1 at peak response) and signal-to-noise ratio r after integration time t: $A/G = r^2$ $(S_s/S_p)^2 (D/D_0)^2/(tS_0)$. For t = 10 h, $r = 10 \sigma$ (where σ is the standard deviation), and using the parameters for τ Ceti $(S_p/S_s =$ 1.8×10⁻¹⁰, $D = D_0$ and $S_0 = 8.5 \times 10^9$ photons m⁻² s⁻¹), detection of an Earth-like planet requires $(A/G) \approx 10^7$ m². As any system would surely have a finite bandwidth, this must be a lower limit. Collecting area and side-lobe suppression are therefore key considerations.

Radio aperture-synthesis techniques have achieved remarkable success, starting from the earliest Cambridge work^{7,8}, and culminating in the Very Large Array (VLA)9. A study of the relationship between the optical and radio cases 10 indicates that, with the signal-to-noise ratio treated in the shot-noise limit, as noted above, the radio concepts carry over to the optical domain. The ability to perform lengthy integrations (K. I. Kellerman et al., personal communication) recently achieved a theoretical signal-to-noise ratio of 5σ after averaging for 76 h with the VLA) gives interferometry a definite advantage if coherent averaging is possible. It is natural, therefore, to consider extending the method to shorter wavelengths, and the optical case will be considered here, leaving infrared possibilities as a separate exercise. Optical interferometry on the ground is limited by 'seeing' fluctuations, and a space-based system would be free of such troubles. The possibilities for space-borne inteferometry have received attention in the past year or so^{11,12}. The dispersedfringe technique^{13,14} provides a solution of the 'white fringe' problem, and at the same time guarantees that every fringe-

visibility measurement retains information on the spectral distribution. For the present problem, the nearby star can provide a phase reference if the equipment is properly designed, thus providing coherent averaging. We therefore consider an interferometric system in space, having a total collecting area of 10-100 m² (the latter is admittedly ambitious). One can immediately see that the gain, G, must be between -50 and -60 dB. With a more realistic 10% bandwidth, the required gain must therefore be in the range -60 to -70 dB. This immediately rules out any interferometric system having uniformly illuminated apertures, because the side-lobe level would be much too high. The aperture illumination must therefore be tapered (apodized, in optical terminology). A simple example (not necessarily optimum) can be given by assuming a Hanning function taper, that is, one with amplitude proportional to $(1+\cos(\pi r/r_0))/2$. The effective area is halved and the half-power primary beam width is increased, but the side-lobe level is decreased markedly.

If a planet like the Earth were orbiting τ Ceti, its maximum elongation would be 0.28 arcs. For this case, we assume an optical array of Hanning-tapered primary apertures, 1.5 m in diameter. With a desired signal-to-noise ratio of 10σ , a bandwidth that admits 10% of the photons, and an integration time of 10 h, it follows that a mean side-lobe level of $-70 \, dB$ and a collecting area of 10 m² would be needed. This would be achieved by a 10-element array, using only photons of wavelength $\lambda > 5.000$ Å. This assumes, of course, that 'noise side-lobes' generated by optical imperfections are not important. Hence, one must be concerned with the optical quality of the system, and Ruze's theory15 for imperfect antennas applies. If the r.m.s. tolerance of the mirrors is $\lambda/60$ over distances ≥ 1 cm, a demanding but not impossible specification, the 'noise' sidelobes due to irregularities induced in the wavefront will be well below -70 dB, a conclusion consistent with the recent work of Mauron¹⁶. Detection of planets orbiting τ Ceti and other close stars, notably the dozen or so Sun-like stars within 6 pc, should therefore be possible.

We next examine spectrometric possibilities. The Earth's oxygen was almost certainly generated by life, probably by bluegreen algae¹⁷, and a high oxygen abundance in the atmosphere of another planet would be a strong indication that life existed there. Owen¹⁸ proposed looking for the oxygen A-band absorption at 7,600 Å, but he did not discuss how it could be done. He thought that Hartley ozone bands beyond 3,000 Å would be hard to distinguish from the Metropoulos-Beutler bands (3,400-2,600 Å) of sulphur dioxide. With the spectroscopic resolution afforded by the dispersed-fringe correlator, however, this is not the case, provided the signal-to-noise ratio is sufficient. The ozone absorption, being at short wavelength, is easier to detect than the oxygen A-band because the side-lobe level is low. It appears that an integration time of $\sim 100 \,\mathrm{h}$ would give $10 \,\sigma$ detection, and SO₂, if present, could also be seen. Detection of the oxygen A-band is more delicate: the required resolution of 80 Å restricts the available photons, while, for fixed aperture size, the long wavelength dictates a raised side-lobe level. Nevertheless, it appears that an integration time of 100 h would give 10σ detection if the star could be kept within 1 marcs of the second null in the diffraction pattern.

Objections can be raised on several points, but there are ready replies. Scattered light, especially from zodiacal particles, might well be present. The signal level is so extended and weak that no problems arise for a zodiacal belt comparable to that of our Solar System. In reply to the objection that high photon efficiency has been assumed, note that present CCD (charge-couple device) detectors already have high photon efficiency. Read-out noise would be no problem because the background starlight effectively floods the field. Even if no further advances are made in the design of photon detectors, the required increase in integration time will be no more than a factor of two. Starlight scattered within the telescopes must be minimized, but careful optical design, as in a coronagraph, should avoid the problem.

The prospects are sufficiently encouraging to justify more intensive examination of interferometric systems in space. The present example has concentrated on the detection of Earth-like planets with familiar life forms, but in general one might expect that a planet teeming with life is likely to exhibit dramatic departures from chemical equilibrium in its atmosphere 19,20. Encouraging results from a successful instrument of the scale described in this note might well encourage more ambitious systems that might examine the ~50 F, G and K stars within 10 pc (J. C. Tarter, unpublished data). In the present discussion, the detection and study of Earth-like planets has been the principal aim; clearly, major planets could be detected easily and quickly by a similar interferometric system, and manifold opportunities would be opened in many other fields of astrophysical research.

I thank T. M. Donohue, F. D. Drake, A. K. Dupree, R. Giacconi, J. M. Moran (who provided apodization calculations), B. M. Oliver, M. Shao, R. D. Reasenberg and J. C. Tarter for helpful comments. B.F.B. was supported in part by a Smithsonian Regents Fellowships.

Received 10 September 1985; accepted 17 April 1986.

- 1. Black, D. C. Bull Am. astr. Soc. 16, 767-769 (1984).
- Shao, M. et al. Bull. Am. astr. Soc. 16, 750-757 (1984).
- York, D. G. et al. Bull. Am. astr. Soc. 16, 775 (1984). Reasenberg, R. D. Bull. Am. astr. Soc. 16, 758-766 (1984).
- Ken Knight, R. G. Icarus 36, 422-423 (1978).
- Bracewell, R. N. & MacPhie, R. H. Icarus 38, 136-147 (1979). Ryle, M. & Hewish, A. Mon. Not. R. astr. Soc. 120, 220-230 (1960).
- Ryle, M. Nature 239, 435-438 (1972).
- Napier, P. J., Thompson, A. R. & Ekers, R. D. Proc. IEEE 71, 1295-1320 (1983).
- Burke, B. F. Eur. Space Ag. spec. Publ. 226, 177-183 (1985).
 Reasenberg, R. D. (ed.) Bull Am. astr. Soc. 16, 747-837 (1984).
- 12. Eur. Space Ag. spec. Publ. 226 (1985).
 13. Labeyrie, A. in Optical and Infrared Telescopes for the 1990s (ed. Hewitt, A.) 786-788 (Kitt Peak National Observatory, Tucson, 1980).

 14. Stachnik, R. & Labeyrie, A. Sky Telesc. 67, 205-209 (1984).

 15. Ruze, J. Proc. IEEE 54, 633-640 (1966).

- Mauron, N. thesis, Univ. Marseilles (1984).
 Cloud, P. Am. Scient. 62, 54-66 (1974).
- 18. Owen, T. in Strategies for Search for Life in the Universe (ed. Papagiannis, M. D.) 177-185 (Reidel, Dordrecht, 1980).
- Margulis, L. & Lovelock, J. E. Icarus 21, 471-480 (1974).
 Papagiannis, M. IAU Trans., 323-329 (1982).

A space telescope for infrared spectroscopy of Earth-like planets

J. R. P. Angel, A. Y. S. Cheng & N. J. Woolf

Steward Observatory, University of Arizona, Tucson, Arizona 85721, USA

Owen has reviewed the potential for detecting life on Earth-like planets of nearby stars, from atmospheric spectra. The presence of oxygen, as revealed, for example, by the 7,600-A absorption band, would be of particular significance. But even the direct detection of a Jupiter-like planet around the nearest star is a formidable task, perhaps just possible with the Hubble Space Telescope^{2,3} or with a Michelson interferometer operating at 40µm wavelength4. Earth-like planets, being fainter and closer in, are still more difficult. Here we show that a space telescope of 16 m diameter, apodized in a new way, could image and measure oxygen in the thermal infrared spectra of earthlike planets up to 4 pc away. Several interesting candidate stars lie within this distance.

Observation of our own Solar System from a distance of 4 pc would reveal the Earth at an angular distance of 0.25 arc s from the Sun, and nearly 10¹⁰ times fainter in visible light. Burke⁵ argues that a multi-element interferometer in space could be capable of optical detection and spectroscopy. As we discuss below, this would require mirrors of extraordinary precision. Figure 1 shows the advantage of observing in the infrared. The Earth's thermal flux (measured in photons) is about 20 times

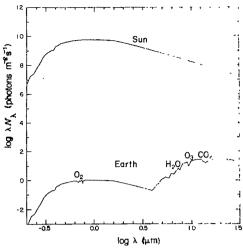


Fig. 1 Fluxes of the Sun and Earth as seen from 4 pc. Detection of spectral features in the photon noise limit depends on the photon flux N_{λ} in a given bandwidth, hence the quantity plotted is $\log(\lambda N_{\lambda})$. The Sun's smoothed flux is from ref. 12. The Earth's optical flux assumes a constant albedo of 0.4 and isotropic emission with the O2 band strengths from ref. 1. The infrared features are an average from ref. 6, normalized to be consistent with re-radiation of 60% of absorbed sunlight.

its optical reflected flux, while the solar flux at 10 µm is 35 times weaker than at 0.7 µm. As photon noise is a limiting factor, these are very significant advantages. Fortunately, the presence of oxygen results in a strong absorption feature (due to ozone) just below 10 µm, near the peak of the thermal spectrum. Figure 1 shows the main O₂ and O₃ features in the Earth's spectrum. An unambiguous detection of ozone needs a spectrum with a resolution of 1 µm and a signal-to-noise ratio of ~20.

A telescope for optical or infrared imaging should form a diffraction pattern with very low side-lobes at the radius of the planet. The side-lobe intensities depend on the size and geometry of the telescope pupil, the wavelength λ , controlled variations in transmission or reflectivity (apodization) and phase errors across the pupil. In general, a mirror will have phase errors on different spatial scales l. At an angle θ from a star, the scattering will be determined predominantly by errors of wavelength $l \approx$ λ/θ . If the surface errors on this scale are random, with an r.m.s. amplitude equal to $\delta(l)$, then the maximum realizable gain G, the intensity at the diffraction pattern centre compared with that at θ , is given approximately by

$$G(\theta) \simeq \frac{D^2 \theta^2}{8\pi \delta(l)^2} \tag{1}$$

where D is the telescope diameter. The exact value of G depends on the statistical character of the surface irregularities^{7,8}. The form of the residual scattered light will be a speckle pattern. Note that $G(\theta)$ depends only on the radiation wavelength through $\delta(l)$.

Consider first the problem of visible light imaging. The planet's image will be separated from that of the star by at least several times the radius of the first Airy minimum, depending on telescope aperture, and apodizing solutions have been developed in this domain capable of realizing extremely lowside-lobes. However, the tolerance on phase errors is very severe. Simply to overcome the photon noise of scattered starlight requires a gain of $\ge 10^7$ (ref. 5). Probably the most perfect mirror made to date is that of the 2.4-m-diameter Space Telescope, for which δ on the scale of 40 cm appropriate for visible light is ~5 nm (ref. 9). Thus, $G(0.25 \text{ arc s}) \approx 1.5 \times 10^4$, nearly 1,000 times smaller than required.

The only way to increase G is to decrease δ and/or increase D. For example, the goal of $G = 10^7$ could be achieved in an 8-m mirror if δ were 0.6 nm on a scale of 40 cm. The trouble is

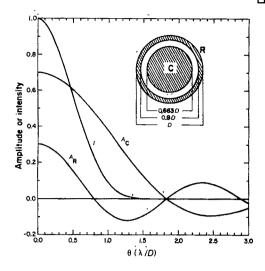
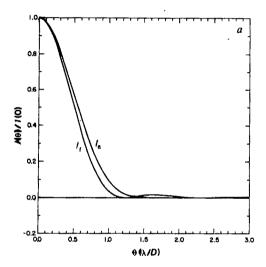


Fig. 2 Radial profiles of diffraction by a circular aperture apodized as shown, with a clear centre aperture C and outer annulus R. Curves $A_{\rm C}$ and $A_{\rm R}$ are the amplitudes from C and R, and I is the resulting intensity.



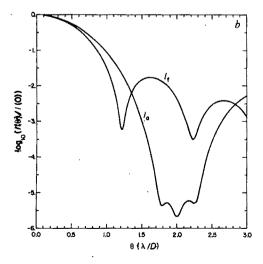


Fig. 3 Intensity of the diffraction patterns of the apodized aperture in Fig. 2 (I_a) and of a filled circular aperture (I_f) with the same outer diameter, plotted on different scales: a, linear; b, logarithmic. The intensities include broadening by bandwidth $\Delta \lambda / \lambda = 0.1$.

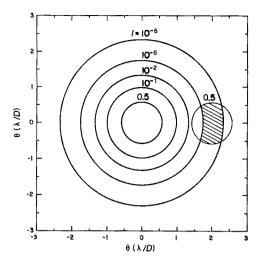


Fig. 4 Contour map of the intensity of the star's diffraction pattern, again with broadening by $\Delta\lambda/\lambda = 0.1$. The I = 0.5 contour of a planet's image is shown centred on the dark band, with the hatched area showing where the planet would be detected.

that even if the surface were finished to this accuracy, the remaining starlight is not a uniform background, but forms a speckle pattern. The speckles will look like a cluster of barely resolved stars of 21st magnitude, in which is hidden a 28th magnitude planet. Calibration of the 'star' field is almost impossible, as it is sensitive to path-length changes of only a few angstroms. These will probably arise as the telescope is rotated to move the planet's relative position or repointed to calibrate on another star. Burke⁵ argues that optical interferometry can control phase errors, but this will be a very difficult problem.

For these reasons we turn to the possibility of imaging the thermal emission, with greatly reduced requirements for gain and hence surface accuracy. The technical problems are still formidable, but if overcome will lead to a more secure observation. The telescope mirror must be large, at least 10 m in one dimension, to overcome the fundamental limits of diffraction at 10 µm wavlength. The mirror must be cooled to ≤80 K, to reduce the telescope thermal background to a level below that of the zodiacal background and scattered stellar radiation. Such cooling may well be possible by largely passive thermal control in an appropriate orbit. For example, since the cryogen was exhausted, the IRAS (Infrared Astronomy Satellite) mirror has settled to a passive equilibrium temperature near 100 K (ref. 10).

The Airy diffraction pattern of the star formed by a simple round aperture of 10 m has a first minimum at 0.25 arc s radius, at 10 µm wavelength. However, the dark ring is not a deep or broad enough null to allow an effective search for a planet. After consideration of various single-mirror and array configurations, we find the best search beam can be made by a circular aperture apodized in a new way. A very dark and broad first minimum would be produced if the wave amplitude at the first dark ring were made to have an inflection with zero gradient. This can be approximated accurately by masking a circular pupil with an obscuring annulus, as shown in Fig. 2. The second dark ring of the outer transmitting annulus is arranged to coincide with the first dark ring of the inner disk. By correct choice of the mask radii (0.663 and 0.9 of the full radius), the amplitude slopes can be made nearly equal and opposite, yielding a very dark ring at radius $\theta = 1.83 \lambda/D$. For the planet at 0.25 arc s to appear centred in this ring at 10 µm wavelength, the full mirror diameter must be 16 m.

Fine-tuning of the relative areas of the disk and ring components can yield a moderately high gain over a wide band, or very high gain over a narrower band. To determine which is better, consider the background of zodiacal emission. It would clearly be optimum to have the residual stellar flux weaker than

this background. The most recent estimate from IRAS of the zodiacal flux at the ecliptic pole is a grey body at 275 K with optical depth $\tau = 7.1 \times 10^{-8}$ (G. Rieke, personal communication). If the planetary system under observation is similar to the Solar System, and is viewed perpendicular to its orbital plane, its own zodiacal emission will be twice as bright, vielding a total background τ of 2.13×10^{-7} . The spatial resolution element d Ω of the apodized telescope is $(\lambda/D)^2$, and in this element, for $\lambda = 10 \,\mu\text{m}$ and $D = 16 \,\text{m}$, we obtain a photon flux λN_{λ} of 850 photons m⁻² s⁻¹. This is 5×10^{-6} of the 10- μ m stellar flux of Fig. 1. Thus the gain should be significantly better than 10⁵, to avoid stellar emission contributing to the background shot noise.

Figure 3 shows a version of the apodization which gives a gain of 3×10^5 , averaged over a dark annular ring in the image plane 1.73 $\lambda/D < \theta < 2.32 \lambda/D$. The amplitude passes through zero at three closely spaced radii. The profiles have been broadened by a bandwidth $\Delta \lambda / \lambda = 0.1$. The central maximum is only a little broader than for the unapodized case, while high throughput is maintained 63% that of the unapodized full aperture.

The signal-to-noise ratio of such a telescope can be computed with reference to Fig. 4, which shows the 50% contour of a planet's image seen against the star's diffraction pattern. Radiation from the planet would be measured with the shaded region of solid angle $d\Omega = 2.2 \times 10^{-13}$ sr, which contains 25% of its total flux. Assuming a combined telescope and detector efficiency of 50%, the signal from the Earth at 4 pc would be 30 electrons s⁻¹. Zodiacal emission would give a signal of 3,000 electrons s⁻¹, while the scattered light from the star in the same region would give a signal of 900 electrons s⁻¹. The shot noise fluctuations of the combined background would thus be ± 62 electrons s⁻¹, and the signal-to-noise ratio about unity in 4 s of integration. An integration of 30 min would be needed to achieve the desired signal-to-noise ratio of 20. We would use two-dimensional imaging detector with a tunable filter. The initial search would be made at one or a few wavelengths at the 0.25 arcs radius, and at larger radii with smaller or more conventional apodizing masks. Once a planet is located and an ephemeris calculated, its spectrum would be accumulated over a few hours by repeated scanning through the full wavelength interval.

Given an apodization solution that can, in theory, give very acceptable performance, we return to a discussion of mirror surface accuracy. For the 16-m mirror, phase errors on a scale of l=8 m will be the most important, and from equation (1) for $G = 10^6$ these should be <4 nm for the theoretical apodization gain of 3×10^5 not to be compromized. The mirror needs comparable accuracy to that of the Space Telescope on large scales, but could be less perfect on smaller scales. A 16-m mirror to these specifications could be assembled in space from lightweight rigid segments prefabricated on the ground. These should be made from glass that has zero expansion coefficient at the ~80 K operating temperature, such as high silica borosilicate with a conveniently low fusion temperature of ~1,200 °C (ref. 11). The placement of the segments to form the large surface would have to be accurate to 4 nm. Such accuracy could be achieved by a servo loop to adjust the segment heights to correct errors in the star's diffraction pattern measured in ultraviolet light. This pattern is the same at different wavelengths, except that the effect of phase errors is magnified as the square of the wavelength ratio. Small phase errors in the 10-µm pattern will give error signals magnified by 1,000 at 3,000 Å and 10,000 at 1,000 Å, provided that spatial variation in ultraviolet and infrared reflectivity are controlled to the 0.1% level. The effect of 4 nm surface errors will be to introduce speckle structure in the dark ring at ~10 times the planet brightness. In the initial search this structure must be calibrated out by rotation of the telescope.

The search for earthlike planets and oxygen could conceivably be carried out with a less expensive, one-dimensional telescope configuration, but with inferior results. Consider, for example, a 4 m by 12 m rectangular mirror launched in the space shuttle

and apodized in a manner similar to that described, to give a response with two very dark fringes 0.25 arc s on either side of the central bright fringe. The planet could, in principle, be detected by rotation to compare the brightness of the two fringes, in the manner proposed by Bracewell and MacPhie⁴. However, it appears that the full dark ring formed by a round telescope will give a much better chance to reject spurious signals from phase errors, as well as more pixels. Furthermore, the inferior resolution solid angle of the smaller collecting area would result in a signal-to-noise ratio limited by zodical background which is four times worse. Each spectral point would thus take 16 times longer (8 h) and be less secure.

It is interesting that consideration of a single observational goal has led to a very specific solution: a round 16-m-diameter telescope, cooled to <80 K and with a figure essentially diffraction-limited in visible light. Its size is similar to that proposed for the large deployable reflector (LDR) project, but it is cooled and of higher surface quality. It would bring great power to many of the most fundamental problems of astrophysics, in addition to the search for life. We believe it merits further study as part of NASA's long-range plans.

A corollary of this work is that life on Earth could have been detected during the past 10° years from thousands of planets beyond the wave of man-made radio emission, by an infrared telescope of 100-200 m diameter.

We acknowledge valuable discussions of this work with Bob Brown, Bernie Burke and Frank Low. Research in Innovative Optics for Space has been supported at Steward Observatory by NASA grant NAGW-121.

Received 11 November 1985; accepted 11 March 1986.

- 1. Owen, T. Strategies for the Search for Life in the Universe (ed. Papagiannis, M. D. 177-185
- (Reidel, Dordrecht, 1980). 2. Davies, D. W. Icarus 42, 145-148 (1980).
- Breckindge, J. B., Kuper, T. G. & Shack, R. V. Opt. Enging 23, 816-820 (1984)
 Brackewell, R. N. & MacPhie, R. H. Icarus 38, 136-147 (1979).
 Burke, B. F. Detection of Life in Other Planetary Systems, Nature (in press).

- Rose, H. et al. The Handbook of Albedo and Thermal Earthshine (Environmental Research Institute of Michigan, Ann Arbor, Rep. No. 190201-I-T, 1973).
- Ruze, J. Proc. IEEE 54, 633-640 (1966).
 Elson, J. M., Bennett, H. E. & Bennett, J. M. Applied Optics and Optical Engineering Vol. 7 (eds Shannon, R. R. & Wyant, J. C.) pp. 191-244 (Academic Press, New York, 1979).

 9. Bahcall, J. N. & Spitzer, L. Scient. Am. 247, 40-51 (1982).

 10. Mason, P. V. & Mount, K. JPL Memo (10 Feburary 1984).
- 11. Angel, J. R. P. Proc. South-west Conference on Optics (eds McDowell, R. S. & Gerada, J. B.)
- Proceedings of the SPIE, 542, 32 (1986). 12. Allen, C. W. Astrophysical Quantitites (Clowes, London, 1973).

An explanation of the east-west asymmetry of Io's sodium cloud

Nicolas Thomas

Rock Cottage, Kinnerley, Oswestry SY10 8DF, UK

Since the discovery of a cloud of neutral sodium atoms accompanying the jovian satellite, Io, in its orbit1, asymmetries of part of the cloud (region B)2 have often been noted3-6. Brightness variations with orbital longitude^{3,4} and asymmetries found by comparing images taken at orbital longitudes differing by 180° (ref. 5) have been explained as effects of solar radiation pressure7. Given that the vast majority of neutrals precede Io in its orbit, and that sputtering of Io is the principal source mechanism, Matson et al.8 postulated a hemispherical source centred 60° towards the sub-Jupiter point from the centre of the leading hemisphere to explain the general cloud shape. However, soft collisions with plasma ions may be important and call for a reassessment⁹. I show here that, given reasonable assumptions, the east-west brightness asymmetry can be explained by temporal changes in the number of emitting atoms in the cloud caused by atmospheric shielding of the surface. Three types of SO₂ atmosphere have been proposed for Io. Matson and Nash¹⁰ used the phenomenon of sub-surface cold-trapping to produce a model in which sputtering of the entire surface is possible. Following measurements of sputtering yields¹¹, it has been shown^{12,13} that surface sputtering alone cannot balance observed loss rates from the plasma torus and hence cannot maintain the observed stability.

The second type of model¹²⁻¹⁴ is an atmosphere in which the sputtering ions cannot strike the surface but do sputter material from the atmosphere. In atmospheric sputtering, the bound gas serves as a target, and recoil collisions occur, leading to escape. Kumar himself¹⁴ recognizes the problems with this type of model. First, neutral sodium has to be present in large quantities in the atmosphere, where it is liable to rapid charge exchange. To reproduce the size of the cloud, a surface electron concentration 5 times higher than observed 15,16 was found to be necessary in this model. Second, sputtering of the polar caps would not be possible, and rapid atmospheric mixing 13 due to pressure gradients would lead to bright cap formation, contrary to observation 17.

The third type of model^{18,19} is based on the equilibrium vapour pressure (EVP) of SO₂ controlling the atmospheric pressure. As Io's surface temperature varies from <87 K on the night side to > 130 K at the sub-solar point, and the EVP of SO₂ increases by seven orders of magnitude over this range 10,20 , the atmosphere is characterized by high pressures and atmospheric sputtering on the day side and low pressures and surface sputtering on the night side and at the poles. Thus at eastern elongation, 90° beyond superior conjunction, the co-rotating plasma strikes the night side and removes sodium and SO₂ from the surface, whereas at western elongation the plasma cannot strike the surface (except at the poles), and hence SO₂ in larger quantities is removed from the atmosphere. This idea implies an asymmetrical sodium source which should be reflected in changing numbers of atoms in the cloud and consequent brightness variations. Some authors, citing ref. 6, have suggested that the cloud is strikingly symmetrical between eastern and western elongations^{9,21}, and that therefore an anisotropic source is not appropriate. However, the work of Murcray and Goody⁶ is not conclusive. They state that "there may be a slight trend toward lower intensities in the exposures on the western side of Jupiter" (see also refs 3 and 4) and that they "are unable to judge from the data themselves whether or not we are seeing a real temporal change in the cloud". Thus an asymmetrical sodium source is not ruled out.

A simple model may be used to determine whether the idea is consistent with observations. The total ejection rate is taken as

$$\Gamma = kA \tag{1}$$

where k is the ejection rate per unit area. A is the cross-sectional area of Io exposed to the sputtering, as defined by

$$A = \frac{\pi r^2 - E}{2} (1 + \cos(\phi + \Phi)) + E \tag{2}$$

where

$$E = 4 \int_{-\infty}^{r \sin(\pi/2 - \theta)} (r^2 - y^2)^{1/2} dy$$
 (3)

in which θ is the latitude above which no protection is afforded to the surface at any time, ϕ is the angular departure of Io from eastern elongation (Sun-centred coordinates) and r is the radius of Io. Φ (see Fig. 1) is an angle accounting for the process described by Cummings et al.²² which invokes neutral mized near Io's surface as a source of sputtering ions. Interaction with the co-rotating electrical field would concentrate sputtering towards Io's inner face, thus explaining the relatively large number of sodium atoms inside Io's orbit. Inclusion of this term may be consistent with Io's longitudinal albedo asymmetry²³, showing the darkest hemisphere to be centred \sim 45° nearer the

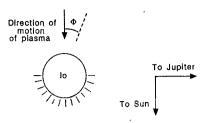


Fig. 1 At eastern elongation ($\phi = 0^{\circ}$), the higher-density day-side atmosphere (shaded) is sheltered from the incident plasma and affords no protection to the surface. The Φ term in the calculation accounts for the process described by Cummings et al.²².

sub-Jupiter point than the trailing hemisphere. Darker colour both on this hemisphere and at the poles is associated with radiation damage²⁴⁻²⁶ and lack of surface SO_2 due to surface sputtering²⁷⁻²⁹. In general accordance with these observations, Φ is taken to be $\pi/6$.

The equation for the total loss rate is taken as

$$\Xi = \frac{n(1 - e^{(-t/L)})}{t} \tag{4}$$

where L is the mean lifetime of sodium atoms in the cloud before ionization, n is the total number of atoms in the cloud and t is the time step. Thus the change in the total number of sodium atoms is

$$\frac{\mathrm{d}n}{\mathrm{d}t} = \Gamma - \Xi \tag{5}$$

Shemansky³⁰ calculated a value for L of 1 h; however, it has been suggested that this is only approached in the immediate vicinity of Io⁹. Arguments in favour of longer neutral sodium lifetimes are supported by high-resolution profiles of the sodium D_2 -line showing high-velocity wings dependent on Io's orbital phase. Implied velocities are as high as 18 km s^{-1} with respect to Io, blueshifted at eastern elongation and redshifted at western elongation³¹. A sputtered sodium atom would take just over 6 h to reach the leading edge of the cloud at this speed. Brown et al.⁹ consider that the average sodium lifetime in region B is between 5 and 10 h. They also point out that the velocity distribution and cloud structure can be explained by elastic collisions. The wings on the D_2 -line profiles are strongest when Io is on Jupiter's magnetic equator³¹. As the peak ion density in the torus is on or near the magnetic equator³², the higher density should lead to more collisions and hence more sodium atoms at high velocity.

Figure 2, calculated by step-by-step integration of equation (5) (for $t \ll L$) with a shooting method, shows a brightness reduction consistent with 20-25% brightness asymmetries^{3,4}. Furthermore, the latitude above which surface sputtering can occur on the day side is consistent with that predicted by Pearl et al.'s¹⁸ EVP atmospheric model.

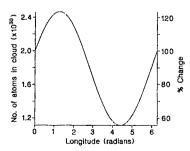


Fig. 2 Brightness variation as a function of orbital phase for Io's sodium cloud, assuming an anisotropic source caused by atmospheric shielding of the surface. Longitude is measured from eastern elongation. Day-side surface exposed to co-rotating plasma at latitudes greater than 75°; average sodium atom lifetime, 6.0 h.

Figure 3a shows the brightness reduction as a function of lifetime, maintaining the exposure latitude at 75°, and Fig. 3b shows the result of keeping the lifetime constant while varying the exposure latitude. Increasing the lifetime requires an increase in the exposure latitude to achieve the same brightness change. Thus sodium lifetimes and exposure latitudes are tightly constrained but are consistent with the EVP atmospheric models, surface brightness and SO₂ distributions and sodium velocity distributions. For example, Φ values $> \pi/4$ are inconsistent with observation. For $\Phi = \pi/6$, the lifetime is constrained to lie between 3 h ($\theta = 60^{\circ}$) and 8 h ($\theta = 90^{\circ}$). The lower limit is inconsistent with the velocity distribution. Near-direct sputtering of

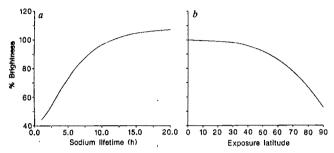


Fig. 3 Brightness changes at western elongation as a function of a, sodium atom lifetime (exposure latitude = 75°) and b, exposure latitude (mean sodium lifetime = 5 h). Brightness at eastern elongation = 100%.

the trailing hemisphere ($\Phi = 10^{\circ}$) gives a looser bracket for the lifetime of $10 \pm 4 \text{ h}$.

Further temporal variations may result from volcanic activity, in which the driving volatile may protect the surface near the vent, leading to a short-timescale reduction in brightness of the cloud.

To estimate whether surface sputtering can produce sufficient quantities of sodium atoms to populate the cloud and, ultimately, the torus, knowledge of the sputtering yields is required; however, a rough value can be obtained by using the yields estimated for SO₂ (ref. 11). Taking the O⁺ ion impact yield of 50 as a lower limit for the lower-mass Na atom and estimating that ~3% of the sputtered material would escape from Io, then 1.5 Na atoms per impact would escape from a pure sodium surface. Using 2×10^{9} m⁻³ for the ion concentration in the , the number of sodium atoms produced would be 1.7×10^{14} m⁻² s⁻¹. Multiplying by the cross-sectional area of Io gives a total of $\sim 1.8 \times 10^{27}$ Na atoms s⁻¹ produced from one hemisphere if the surface were 100% sodium. Kumar¹⁴ states that the required rate to populate the cloud is 8.3×10^{25} atoms s^{-1} . This allows us to put a limit of $\sim 4.7\%$ on the percentage surface coverage of sodium. However, Kumar's required population rate is relatively low, a value of $\sim 10^{27}$ Na atoms s⁻¹ having been quoted elsewhere⁹. Unless the sputter yield is substantially higher (by more than a factor of 4), surface sputtering would be capable of supplying this quantity only if a high proportion of the surface were composed of sodium and its compounds, although the higher value makes the alternative case for atmospheric sputtering of sodium even more difficult.

I thank Michael Woolfson and Beryl Leatham-Thomas for their assistance with this work.

Received 17 February: accented 29 April 1986.

- 1. Brown, R. A. in Exploration of the Planetary System (eds Woszczyk, A. & Iwaniszewska, C.) 527-531 (Reidel, Hingham, 1974).
- 2. Brown, R. A., Goody, R. M., Murcray, F. J. & Chaffee, F. H. Astrophys. J. 200, L49-L53
- Bergstralh, J. T., Matson, D. L. & Johnson, T. V. Astrophys. J. 195, L131-L135 (1975).
 Bergstralh, J. T., Young, J. W., Matson, D. L. & Johnson, T. V. Astrophys. J. 211, L51-L55
- 5. Goldberg, B. A., Garneau, G. W. & LaVoie, S. K. Science 226, 512-516 (1984).
- Murcray, F. J. & Goody, R. M. Astrophys. J. 226, 327-335 (1978).
 Smyth, W. H. Astrophys. J. 234, 1148-1153 (1979).
- 8. Matson, D. L., Goldberg, G. A., Johnson, T. V. & Carlson, R. W. Science 199, 531-533 (1978).

- 9. Brown, R. A., Pilcher, C. B. & Strobel, D. F. in Physics of the Jovian Magnetosphere (ed.
- Dessler, A. J.) 197-225 (Cambridge University Press, 1983).

 10. Matson, D. L. & Nash, D. B. J. geophys. Res. 88, 4771-4783 (1983).
- Johnson, R. E., Garret, J. W., Boring, J. W., Barton, L. A. & Brown, W. L. J. geophys. Res. 89, B711-B715 (1984).
- 12. Kumar, S. J. geophys. Res. 89, 7399-7406 (1984).
- Cheng, A. F. J. geophys. Res. 89, 3939-3944 (1984).
 Kumar, S. Icarus 61, 101-123 (1985).
- 15. Kliore, A. J. et al. Icarus 24, 407-410 (1975).
- 16. Kliore, A. J. IAU Collog. 57 (1980).
- Kildle, K. J. 1975 College, St. (1995).
 Minton, R. B. Commun. lunar planet. Lab. 10, 35-39 (1973).
 Pearl, J. et al. Nature 280, 755-758 (1979).
- Fanale, F. P., Banerdt, W. B., Elson, L. S., Johnson, T. V. & Zurek, R. W. in The Satellites of Jupiter (ed. Morrison, D.) 756-781 (University of Arizona Press, Tucson, 1982).
 Honig, R. E. & Hook, H. O. RCA Rev. 21, 360-368 (1960).
- Kumar, S. & Hunten, D. in The Satellites of Jupiter (ed. Morrison, D.) 782-806 (University of Arizona Press, Tucson, 1982).
- Cummings, W. D., Dessler, A. J. & Hill, T. W. J. geophys. Res. 85, 2108-2114 (1980).
 Nash, D. B. & Johnson, T. V. Icarus 38, 69-74 (1979).

- Moore, M. H. Icarus 59, 114-128 (1984).
 Radford, H. E. & Rice, F. O. J. chem. Phys. 33, 774-776 (1960).
 Young, A. T. Icarus 58, 197-226 (1984).
- Young, A. T. Icarus 58, 197-226 (1984).
 Soderblom, L. A. et al. Geophys. Res. Lett. 7, 963-966 (1980).
 Howell, R. R., Cruikshank, D. P. & Fanale, F. P. Icarus 57, 83-92 (1984).
- 30. Shemansky, D. E. Astrophys. J. 236, 1043-1054 (1980).
- Trafton, L. & Macy, W. Astrophys. J. 215, 971-976 (1977).
 Bagenal, F. & Sullivan, J. D. J. geophys. Res. 86, 8447-8466 (1981).

A class of narrow-band-gap semiconducting polymers

Samson A. Jenekhe

Honeywell Inc., Physical Sciences Center, Bloomington, Minnesota 55420, USA

Scientific interest in electrically conducting polymers and conjugated polymers in general has been widespread among workers in polymer science, chemistry, condensed matter physics, materials science and related fields since the discovery of doped conductive polyacetylene^{1,2}. Many doped conducting organic polymers with conductivity spanning the range from insulator to near-metallic (~10⁻¹⁵-10³ ohm⁻¹ cm⁻¹) are now known¹⁻¹³. Of prime importance and fundamental interest in the continuing experimental and theoretical search for new conducting, and perhaps superconducting, polymers is the achievement of small or vanishing values for the semiconductor band gap (E_g) , which governs the intrinsic electronic, optical and magnetic properties of materials. Existence of a finite $E_{\rm g}$ in conjugated polymers is thought to originate principally from bond-length alternation, which is related to the Peierls instability theorem for one-dimensional metals 14-17. Here I describe a novel class of conjugated polymers, containing alternating aromatic and quinonoid segments, whose members exhibit intrinsic band gaps as low as 0.75 eV, the smallest known value of $E_{\rm p}$ for an organic polymer.

Among conjugated polyenes, polyenynes, and related polymers, polyacetylene (PA), (-CH=CH-)_m, has the smallest band gap, with a value of 1.5 eV (ref. 3). Among the aromatic and hetero-aromatic conjugated polymers, polythiophene (PT) (Fig. 1a with X = S) has the smallest band gap, with a value of -2.1-2.2 eV (refs 8, 13). In the search for narrower-band-gap polymers, the strategy of substitution on existing main-chain polymers or formation of co-polymers has not generally been successful. An important exception is the annelated 3,4-benzo derivative of polythiophene, polyisothianaphthene (PITN), which has an E_g value of only 1.13 eV. Wudl et al. have attributed the difference in E_g values between PT and PITN to contribution of quinonoid resonance structure (Fig. 1b) in the case of PITN and a lack of such contribution in PT13. I have argued elsewhere that a large part of the ~ 1 eV difference in $E_{\rm e}$ values of PT and PITN is attributable to co-planarity of polymer repeating units in PITN and its lack in PT¹⁸. However, introduction of quinonoid character into the main chain of an aromatic conjugated polymer can be expected to reduce the band gap.

Fig. 1 a, Aromatic ground-state structure of hetero-aromatic polymers (for example, X = S, polythiophene; X = N - H, polypyrrole). b, Quinonoid ground-state structure of hetero-aromatic polymers of a. c, Ground-state structure of novel tunable, narrow-band-gap, conjugated polymers containing alternating aromatic and quinonoid segments, some of which exhibit the smallest E_g values known for organic polymers.

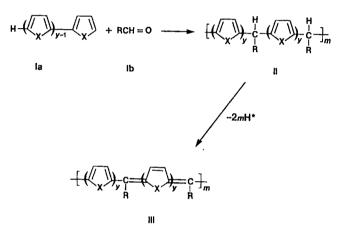


Fig. 2 Two-step synthesis of polymers with alternating aromatic and quinonoid segments, with quinonoid character Q = 1/2 (x = y in Fig. 1c).

In fact, we have already observed a similar effect in polycarbazoles 10 . Also, Bredas 19 has recently shown theoretically, using valence effective hamiltonian (VEH) calculations, that as quinonoid structure is introduced into polythiophene geometry (Fig. 1a, b) $E_{\rm g}$ decreases linearly with increasing quinonoid character 19 .

Figure 1c shows a class of hetero-aromatic conjugated polymers designed to incorporate aromatic and quinonoid segments in the main chain, which we hoped would exhibit small $E_{\rm g}$ values. This class of polymers displays several interesting general features:

(1) The quinonoid character is given in terms of integer molecular parameters (x, y) which could be subject to synthetic manipulation. Neglecting possible end-group effects, the fraction of the chain with quinonoid character is Q = y/(x+y). Thus, Q = 0, 1/2, 2/3, 3/4, 4/5, ... when y/x = 0, 1, 2, 3, 4, ... and Q = 1/3, 1/4, 1/5, 1/6, ... when y/x = 1/2, 1/3, 1/4, 1/5, The limiting cases of Q = 0 (y = 0 or $x \to \infty$) and Q = 1 (x = 0 or $y \to \infty$) correspond respectively to polymers with chain structures a and b (Fig. 1). The hypothetical polymer b, relative to a and polymers of intermediate compositions, has a lower but nonetheless finite E_g^{19} . The parameter Q could in principle be related to bond-length alternation Δr ($= d_1 - d_2$) by some function $f(\Delta r)$, where d_1 and d_2 are the C—C and C=C bond lengths respectively. The value of Q when $\Delta r = 0$ and of Δr when E_g is minimum would be of interest in understanding the origin of E_g in conjugated polymers.

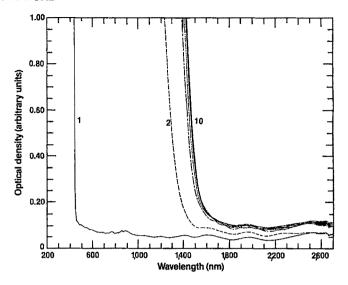


Fig. 3 Optical absorption spectra of thin films of polymer precursor PTTB (1), and conjugated derivatives (2-10), which are the polymers in Fig. 1c.

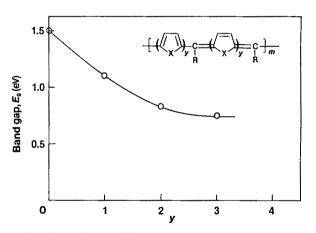


Fig. 4 The band gap $E_g(y)$ of the polymers in Fig. 1c with X = S, R = Ph and x = y. The E_g value at y = 0 is that of trans-PA.

- (2) The ground-state structure of this class of polymers is two-fold degenerate in the sense of *trans*-PA, when Q=1/2 or $x=y=1,2,3,4,\ldots$ In fact, when x=y=0 (Q=0) and R=H we obtain polyacetylene; however, the uniqueness of polyacetylene is preserved by its Q=0 value. Soliton excitations have been postulated for *trans*-PA on the basis of its degenerate ground-state structure²⁰. Thus, soliton excitations may be anticipated in the degenerate or symmetric (Q=1/2) polymers of Fig. 1c. However, it is unclear to what extent a finite Q will influence such excitations relative to *trans*-PA.
- (3) If the hetero-atom (X) is neglected, the polymer backbone is essentially an alternating co-polymer of *trans-cisoid* and *cistransoid* forms of polyacetylene.
- (4) Doping in aromatic (for example, poly-p-phenylene) and hetero-aromatic (Fig. 1a) polymers leads to polarons and bipolarons as the charged species, presumably by increasing the quinonoid character (Q) of the chain^{21,22}. As the present class of polymers already has Q > 0, it is uncertain how much more, if any, quinonoid character can result from doping.
- (5) As macromolecules, these polymers have an unusual 'expandable' constitutional repeating unit (CRU), consisting of alternating aromatic and quinonoid segments. Conceivably, a material with a very high molecular weight (say 10^7) could result from a small chain length (say m=1), simply by increasing x and y. If such materials could be synthesized this suggests that the electronic and optical properties would be more sensitive to x and y than to the polymer chain length m. These

features and questions warrant a detailed theoretical investigation.

Polymers of the type shown in Fig. 1c, with x = y = 1, 2 or 3 (Q=1/2) have been experimentally realized for various X and R by a two-step synthetic technique, shown in Fig. 2. First, non-conjugated precursor polymers containing alternating sp³ carbon atom (-CRH-) and hetero-aromatic conjugated units D were synthesized by condensation polymerization of the appropriate monomer, dimer or trimer (Ia) with aldehydes (Ib), where D is 2,5-thiophenediyl, $5,5'-\alpha$ -bithiophenediyl or $5,5'',\alpha$ terthiophenediyl. Second, the precursors (II) were converted to the conjugated polymers with alternating aromatic and quinonoid segments (III) by oxidative elimination of the bridge hydrogens. This two-step synthesis could also be used to achieve the asymmetric polymers of Fig. 1c; that is, those with $Q \neq 1/2$. Note that the basic linear structure of the conjugated polymers (III) is the same as that of the precursors (II); the structure of the precursors (II) was readily established by infrared spectra. The precursor polymers have been characterized by infrared and electronic spectra, elemental analysis, studies of molecular weight, and thermal analysis. Evidence of the elimination of the bridge hydrogens is provided principally by infrared and electronic spectra; insolubility of polymers III compared to polymers II provides additional proof of elimination. Details of the syntheses of the conjugated polymers and their precursors are described elsewhere (refs 18, 23 and S.A.J. in preparation). The smallest band gaps were obtained with X = S. Also, E_{α} values were less sensitive to the side-group R.

Figure 3 shows the optical absorption spectra for thin films (\sim 0.1-0.2 µm) of a polymer with R = phenyl, X = S and x = y = 3. Curve 1 is the optical absorption spectrum of the polymer precursor, poly- $(5,5',\alpha$ -terthiophenediyl benzylidene) (PTTB). Curve 2 is that of a conjugated derivative (Fig. 1c) which has an $E_{\rm g}$ of 0.83 eV (1,500 nm) and corresponds to the product of elimination after 7.1 min of reaction. On exhaustive elimination (curves 2-10) the band gap narrows to a constant value of 0.75 eV (1,650 nm). Similar results of band-gap narrowing to a constant value during elimination have been obtained for x =y = 1 and 2: y = 1, $E_g = 1.1$ eV; y = 2, $E_g = 0.83$ eV.

Figure 4 shows the band gap as a function of y for X = S and x = y. The point shown at y = 0 is that for trans-PA; this is because the general polymer repeating unit shown in Fig. 3 contains 8y + 2 carbon atoms in the main chain, which naturally reduces to polyacetylene in the limit y = 0. The asymptotic value of $E_g(y)$ is ~ 0.7 eV, which is already closely approached at y=3.

As expected, the proposed polymers do exhibit narrow band gaps. Although the quinonoid character Q qualitatively explains why $E_{\rm g}$ is smaller in this class of polymers, relative to PT, it does not explain why the band gap decreases with y at a constant Q, as observed. If there is a linear relationship between $E_{\rm g}$ and Q, it will be approximately $E_g = 2.2 - 2.05Q$, using the band gap of PT (2.2 eV, Q = 0) and the $E_{\rm e}$ value of 0.15 eV calculated for Q = 1 by Bredas¹⁹. The expected E_g value of 1.18 eV at Q = 1/2is close to the 1.1 eV found for y = 1, but the other values of the band gap at Q=1/2 cannot be explained by this linear equation at all. This is due to the degeneracy of the case Q = 1/2. Both the generally small band gaps in this class of polymers and the decrease of E_g with y can be explained in terms of the more primitive concept, the bond-length alternation Δr . The decrease of E_{α} with y is consistent with the decrease in Δr with expansion of the polymer repeating unit. From the theoretical calculations of Grant and Batra¹⁶ for trans-PA and those of Bredas¹⁹ for PT, a linear relationship of the form $E_g = E_g^0 + b\Delta r$ appears to hold. We have obtained the same value of b = 11.50 eV/Å from the two different calculations 16,19 ; however, $E_g^0 = 0$ for trans-PA¹⁶ and $E_g^0 = 0.705 \text{ eV}$ for PT¹⁹. This linear equation and the observed band gaps give estimated bond alternations of 0.034, 0.011 and 0.004 Å for y = 1, 2 and 3, respectively, compared to 0.13 Å for PT. It will be interesting to compare these estimated bond alternation values with those

computed or measured directly. Even from these estimates it is clear that nearly uniform bond lengths are attained at y = 3 and yet the band gap is as high as 0.75 eV due primarily to E_a^0 Existence of a finite E_g^0 further distinguishes aromatic and hetero-aromatic conjugated polymers from polyenes¹⁹, and raises the question of its origin, as only the amount above E_{\bullet}^{0} can be attributed to bond alternation. Narrower band gaps would imply negative bond alternation ($\Delta r < 0$), in which carbon-carbon double bonds are longer than single bonds. In principle, as the calculations of Bredas suggest¹⁹, the proposed hetero-aromatic polymers (Fig. 1c) with $Q \to 1$ could exhibit band gaps smaller than E_g^0 , but such members of this class of polymers have yet to be synthesized.

Obviously, other hetero-aromatic or aromatic polymers with structures similar to Fig. 1c, and hence similar properties, can be expected when the hetero-aromatic units, $(C_4H_2X)_{y,x}$, are replaced by phenyl (Ph), p-phenylene oligomers, or other groups capable of both aromatic and quinonoid bonding structures. After we had already synthesized the polymers described here we became aware of the theoretical work of others, predicting a narrow band gap for a structurally related hypothetical (not yet synthesized) polymer. Boudreaux et al.²⁴ have calculated a band gap of 1.17 eV and predicted the existence soliton excitations in poly-p-phenylenemethine, $(-Ph-CH=Ph=CH-)_m$

This work has been partly supported by the US Office of Naval Research. The technical assistance of Marcia Hansen is appreciated.

Received 31 March; accepted 4 June 1986.

- 1. Shirakawa, H., Louis, E. J., MacDiarmid, A. G., Chiang, C. K. & Heeger, A. J JCS chem.
- Commun., 578 (1977).
 2. Chiang, C. K. et al. Phys. Rev. Lett. 39, 1098-1101 (1977).
- Chien, J. C. W. Polyacetylene: Chemistry, Physics and Materials Science (Academic, Orlando,
- 1987. Ivory, D. M. et al. J. chem. Phys. 71, 1506-1507 (1979). Clarke, T. C. et al. J. Polym. Sci. Polym. Phys. 20, 117-130 (1982).

- Diaz, A. F., Kanazawa, K. K. & Gardini, G. P. JCS chem. Commun, 635 (1979).

 Kanazawa, K. K. et al. Synth. Metals 1, 329-336 (1980).

 Tourillon, G. & Garnier, F. J. electroanal. Chem. 135, 173-178 (1982), 161, 407-414 (1984). Wellinghoff, S. T., Kedrowski, T., Jenekhe, S. A. & Ishida, H. J. Phys. (ollog. 44, 677-681
- Jenekhe, S. A., Wellinghoff, S. T. & Deng, Z. Synth. Metals 10, 281-292 (1985)
 Jenekhe, S. A., Wellinghoff, S. T. & Reed, J. F. Mol. Cryst. Liq. Cryst. 105, 175-189 (1984).
 Greene, R. L. & Street, G. B. Science 226, 651-656 (1984).
 Wudl, F., Kobayashi, M., Colaneri, N., Boysel, M. & Heeger, A. J. Mol. Cryst. Liq. Cryst.

- 118, 199-204 (1985).
 Peierls, R. E. Quantum Theory of Solids, 108 (Oxford University Press, London, 1955).
 Ovchinnkov, A. A., Ukrainskii, I. I. & Krentsel, G. V. Soviet Phys. Usp. 15, 575-591 (1973).
 Grant, P. M. & Batra, I. P. Solid State Commun. 29, 225-229 (1979)
 Simon, J. & Andre, J.-J. Molecular Semiconductors, 166-173 (Springer, New York, 1984).

- Sandi, S. A. Macromolecules (submitted).
 Bredas, J. L. Mol. Cryst. Liq. Cryst. 118, 49-56 (1985).
 Su, W. P., Schrieffer, J. R. & Heeger, A. J. Phys. Rev. B 22, 2099-2111 (1980). Phys. Rev. Lett. 42, 1698-1701 (1979). 21. Bredas, J. L., Themans, B., Andre, J. M., Chance, R. R. & Silbey, R Synth. Metals 9,
- 265-274 (1984).
- 22. Bredas, J. L., Chance, R. R. & Silbey, R. Phys. Rev. B26, 5843-5854 (1982). 23. Jenekhe, S. A. Macromolecules (submitted).
- Boudreaux, D. S. et al. Phys. Rev. B31, 652-655 (1985).

Extraordinary effects of mortar-andpestle grinding on microstructure of sintered alumina gel

W. A. Yarbrough & Rustum Roy

Materials Research Laboratory, The Pennsylvania State University. University Park, Pennsylvania, USA

The use of the mortar and pestle in the laboratory dates back to the earliest attempts to understand and use the materials around us. Even now, it is difficult to imagine an alternative to crushing and grinding for the preparation of many samples. Traditionally, mortar-and-pestle mixing or grinding has been held to be a relatively mild and controlled process, although it was recognized that the grinding of materials harder than the material of the mortar and pestle would result in some contamination. Thus, good practice forbade grinding of, for example, mullite and alumina in agate mortars. That this technique is not so innocuous was demonstrated by Dachille and Roy1 with respect to the stresses generated. They showed that phases usually obtained only at 10-20 kbar can be obtained metastably by simple grinding in a laboratory mortar. There are numerous examples of solid-state phase transformations being produced by prolonged or intense comminution², two of the best-documented cases of stress/shear-induced transformation being the conversion of calcite to aragonite¹, and of quartz to amorphous silica^{3,4}, both by prolonged grinding in a laboratory mortar and pestle. Here we show that the very small amounts of material generated by the wear of mortar and pestle surfaces by even mild grinding can also have substantial effects on the microstructure and transformation kinetics of certain ceramic systems so treated.

Materials prepared by the sol-gel method are typically obtained as non-crystalline or poorly crystallized metastable solids which may then be calcined for densification and/or transformation to a more stable crystalline phase. In the preparation of dense non-crystalline solids (glasses), uncontrolled crystallization or devitrification is undesirable, as this usually leads to a loss of mechanical integrity and other desired properties, such as transparency. In other materials, where a given stable crystalline phase may be the desired product, the kinetics of transformation and the microstructure of the material obtained can be controlled by 'seeding' with the desired phase or with chemically dissimilar materials having, or readily transforming to, the desired structure.

Seeding with crystals of the expected or desired phase has long been used as an aid in the study of phase equilibria, and the importance of even minor amounts of a second phase, isostructural with a stable phase of the composition under study, has already been noted^{5,6}. In particular, we have reported the remarkably enhanced transformation kinetics obtained by seeding sol-gel-derived materials⁷⁻¹⁰. This may well turn out to be a route to a new class of crystalline solids: nanocomposites (dior multiphasic solid aggregates), where the size range of the monophasic regions is ~1-100 nm. One of the striking properties of a structurally diphasic xerogel (for example, boehmite sol mixed with an α -alumina sol) is the solid-state epitaxy which occurs on heating, with considerably accelerated kinetics. Thus, Fig. 1 (taken from ref. 9) compares the differential thermal analysis (DTA) of a monophasic boehmite sol with that of a diphasic sol of boehmite and various amounts of α -alumina. Seeding with amounts as small as 0.08 wt % results in a marked lowering of the transformation temperature. Moreover, there is a marked change in the microstructure of the alumina formed.

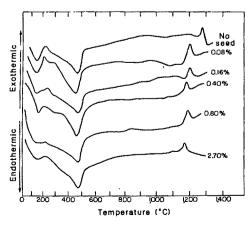
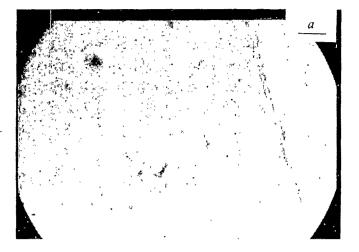


Fig. 1 DTA results showing the effect of seeding with various amounts of α -alumina on the transformation temperature of boehmite gel.



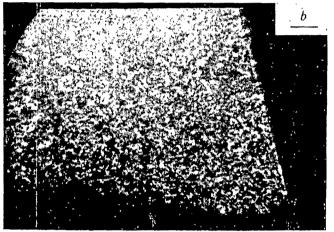


Fig. 2 Boehmite gel fragment prepared from water 'ground' in Diamonite mortar and pestle as seen after calcination at 1,200 °C for 2 h: a, Bright-field transmitted light; b, crossed polars. Scale bars, 10 µm.

In the unseeded material, monocrystalline cells $\sim 10~\mu m$ across are formed, whereas in the seeded material, the grain size is $<1~\mu m$ (ref. 10).

The mortar and pestle experiment was conducted using a Fisher Scientific Co. 'Diamonite' (corundum) mortar and pestle. After thoroughly cleaning the mortar and pestle, 200 ml of deionized water was added to the mortar. The water was slowly 'ground' in the mortar using only light to moderate pressure for 5 min. This water, slightly turbid with suspended detritus from the wear of the mortar and pestle surfaces, was then used to prepare a boehmite (aluminium oxide monohydrate) sol using 13.90 g of a commercially available microcrystalline boehmite. (Dispereal, Remet Chemical Co.) The boehmite was peptized using 15.0 ml of 1.00 M HNO₃; the sol was then dried at 90-95 °C to produce a boehmite xerogel. A second batch of xerogel was prepared in precisely the same manner using the same lots of material (water, acid and boehmite), the only modification being the use of a mortar and pestle of agate instead of Diamonite. Fragments of these xerogels were lightly crushed in an agate mortar and pestle. Calcination was performed in air using a Lindberg model 51524 furnace equipped with a model 59256-E1 controller (Lindberg Co.). This furnace uses exposed MoSi₂ elements and had been modified by installing a type S thermocouple positioned just above the sample for accurate temperature measurement. The maximum calcination temperature was 1,200 °C for a period of 2 h, which is sufficient to convert all of the material to α -alumina. The powders were dispersed in immersion oil and examined with a polarizing microscope.



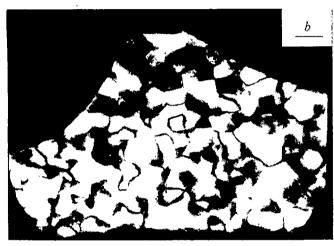


Fig. 3 Boehmite gel fragment prepared from water 'ground' in agate mortar and pestle as seen after calcination at 1,200 °C for 2 h: a, Bright-field transmitted light; b, crossed polars. Scale bars,

Alpha aluminium oxide (α -alumina) is anisotropic and uniaxial negative. Assuming that a sufficient crystallite size is attained on transformation, its birefringence makes observation in a polarizing microscope relatively easy. Figures 2 and 3 show transmitted-light photomicrographs (Figs 2a and 3a in brightfield transmitted light; Figs 2b and 3b using crossed polars) of the calcined powders. Transformation occurs by the nucleation and growth of the α phase in a matrix of very finely divided and poorly crystallized transitional aluminas (δ and θ). The microstructure exhibited in Fig. 2 is identical to that obtained in a xerogel seeded with α -alumina or with materials having the corundum crystal structure; that seen in Fig. 3 is identical to that seen with unseeded or non-isostructurally seeded gels.

Scientists almost universally use milling or grinding in a mortar and pestle as a means of preparing powdered materials, in industry as well as in the laboratory. It is so routine that in many cases no report is made of the materials and methods used¹¹. Enhanced transformation kinetics and nucleation frequency in milled materials have been variously attributed to particle size effects¹² and possibly lattice strain¹³. Dynys and Halloran¹³, in fact, considered and rejected the possibility that detritus from milling was responsible for these effects. In their experiment, α -alumina milling debris was collected, dried and dry-mixed (at 1 wt%) with powders obtained from the calcination of ammonium alum. Pressed pellets were prepared and fired in air. No effect could be seen either by transmission electron microscopy or by comparison of the transformation kinetics of doped and undoped material. Assuming that the nature of the interface between seed and bulk phase, and the uniformity of seed distribution, are of controlling importance, it is not surprising to find that the efficacy of seeding depends on how the seed phase is produced and introduced to the bulk material. Effects due to the method of seed introduction have been observed previously¹⁴. This demonstration of the power of trace contaminants introduced by grinding has led us to question our common laboratory and commercial practice

This work was supported by a grant from the Air Force Office of Scientific Research, AFOSR grant no. 83-0212.

Received 17 March; accepted 24 April 1986.

- 1. Dachille, F. & Roy, R. Nature 186, 34-71 (1960).
 2. Lin, I. J., Nadiv, S. & Grodzian, D. J. M. Miner. Sci. Enging 7, 313-136 (1975).
- 3, Ray, R. C. Proc, R. Soc. A102, 640-642 (1923).
- 4. Dale, A. J. Trans. Br. ceram. Soc. 23, 211-216 (1923).
- 5. Ervin, G. & Osborn, E. F. J. Geol. 59, 331-384 (1951) 6. Roy, D. M. Am. Miner. 39, 140-143 (1954).

- 6. Roy, D. M. Am. Miner. 39, 140-143 (1934).
 7. Suwa, Y., Roy, R. & Komarneni, S. J. Am. ceram. Soc. (in the press)
 8. Roy, R., Suwa, Y. & Komarneni, S. in Ultrastructure Processing of Costact, (i.a. ce. 23)
 Composites (eds Hench, L. L. & Ulrich, D. R.) (Wiley, New York, 1973)
 9. Suwa, Y., Komarneni, S. & Roy, R. J. Mater. Sci. Lett. 5, 21-24 (1976)
 10. Yarbrough, W. A. & Roy, R. J. Mater. Res. (submitted)

- Guglielmi, M. & Principi, G. J. Non-Cryst. Solids 48, 161-175 (1982)
 Gregory, A. G. & Veasey, T. J. J. Mater. Sci. 7, 324-332 (1973)
- Dynys, F. W. & Halloran, J. W. J. Am. ceram. Soc. 65, 442-448 (1952)
- 14. Bykhovskii, A. I. Solid State Transformations (eds Sirota, N. N., Gorshii, F. K. & Vani. V. M.) (Institute of Solid State Physics and Semiconductors, Academy of Sciences of the Byelorussian SSR, Minsk; Transl. by Consultants Bureau, New York, 1965)

Crustal structure of the northern Alpha Ridge beneath the Arctic Ocean

D. A. Forsyth*, I. Asudeh*, A. G. Green* & H. R. Jackson†

* Lithosphere and Canadian Shield Division, Geological Survey of Canada, 1 Observatory Crescent, Ottawa, Ontario, Canada K1A 0V3 † Atlantic Geoscience Centre, Geological Survey of Canada, Bedford Institute of Oceanography, PO Box 1006, Dartmouth, Nova Scotta, Canada B2Y 4A2

Beneath the Arctic Ocean, the Alpha Ridge complex is the principal tectonic feature between the Canada Basin and the Lomonsov Ridge. Here we report on analysis of seismic refraction data along the Alpha Ridge and within the basin area 175 km to the north (Fig. 1), which, together with geological and aeromagnetic constraints, indicates that the Alpha Ridge is characterized by regions of continental-like thickness but has probably resulted from an oceanic mode of development. The ridge flank thins towards the North Pole but may extend as far north as 88° N, and is therefore >500 km wide in the region near 110° W. Consequently, south of the pole along 110° W, typical oceanic crust beneath the eastern Makarov Basin may be present only locally, if at all. Similarities between the velocity structures of the Alpha Ridge and the Iceland area suggest that the Icelandic structure may be a currently active analogue for the Alpha Ridge.

The 1983 CESAR (Canadian Expedition to Study the Alpha Ridge) crustal refraction survey consisted of a 200-l.m 'strike' line with 7-8-km station spacing along the CESAR South Ridge (C.S.R. in Fig. 1) of the Alpha complex, a parallel 120-km-long 'basin' line north of 87° N, in what we considered to be the Makarov Basin, and a 175-km 'dip' line connecting the other two lines. In addition, an 80-km 'camp' line with an effective spacing of 1-2 km was recorded along the CESAR North Ridge (C.N.R. in Fig. 1). All lines were effectively reversed, the strike line was also recorded to each end from a central shotpoint. The camp and basin lines were shot along the line and recorded at the ends. Multi-element arrays1 on the ice surface recorded

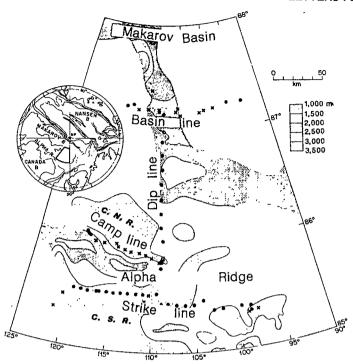


Fig. 1 Location of the CESAR refraction profiles. ●, Recorder location; ×, shot location.

A a a b a construction of the construction of

Fig. 2 CESAR strike line. A, comparison of section shot from west end (b) with first-arrival and PmP reflection synthetic section (a). The data (b) are shown with true amplitudes, after application of a bandpass filter (2.5-10.0 Hz). B, Velocity model derived from analysis of reversed strike line data. Velocities (km s⁻¹) are followed by gradients (s⁻¹), in parentheses. Note the central region of relatively lower average velocity.

energy from 100-500-kg shots detonated at depths of 100 m (end shots) to 200 m (line shots). We report here the crustal models determined from the strike and basin line data sets. Interpretations of the dip and camp line data are consistent with these models (I.A., A.G.G. and D.A.F., in preparation).

As in most marine surveys, reverberations in the water and sediment layers are common in the CESAR data, and secondary energy arriving later but with apparent P-wave velocity similar to that of the first arrivals can be traced up to several seconds after the first arrivals (Fig. 2A). A thorough study of the nature of these multiples using synthetic seismogram modelling techniques produced water depth estimates in good agreement with known values, and determined that sediment cover was generally <1 km over the ridge area. Sediment thicknesses varying from zero to 1 km were observed independently from air-gun reflection data gathered at the main camp on the ice as it drifted from the central region of the strike line to C.N.R.² (Fig. 1).

The first-arrival waveform of the strike line data remains remarkably similar and continuous for distances up to ~ 100 km. Within this range, the first-arrival waveforms recorded from the central and eastern shotpoints are similar to the data section in Fig. 2A. There is little evidence of reflected arrivals from midor upper-crustal boundaries; the data suggest considerable lateral homogeneity in the upper crust. At distances > 100 km the first-arrival waveform uniformity is gradually lost to the effects of deeper lateral velocity variations and reflected arrivals from the crust-mantle boundary. The maximum reflected energy is concentrated in the distance range 150–180 km. The wideangle reflected energy and the cross-over to first-arrival velocities of ~ 8.1 km s⁻¹ in the distance range 180–200 km require a relatively thick crustal section.

In Fig. 2A, the synthetic section generated³ from the western shotpoint through our proposed crustal model is compared to the observed data. The strike line model results from synthetic seismogram modelling of the sections from each end of the line and the data recorded from the centre shotpoint. Overlapping and reversed ray paths demonstrate that the model is relatively

well constrained to a depth of \sim 24 km. The exact shape of the anomalous triangular zone of lower average velocity, the velocity structure of the lower crust and the depth of the crust-mantle transition are more weakly constrained. In Fig. 2B the dashed and dotted lines represent velocity or velocity gradient changes (heavy dashes indicate regions constrained by ray-trace modelling). The crust-mantle transition is shown as a solid line to represent the velocity step required to produce the wide-angle reflections in Fig. 2A.

Figure 2B includes the time delays required by variations in water depth and by our best estimates of sediment cover thickness. Beneath the sediments, the upper crust is characterized by a laterally uniform velocity of 5.1 km s⁻¹ and a gradient of $\sim 0.23 \text{ s}^{-1}$. At 9 km depth the velocity gradient diminishes to 0.05 s⁻¹ and 0.10 s⁻¹, in the eastern and western regions respectively, to satisfy times and amplitudes of first-arrival energy at distances <90 km. These gradients lead to mid-crustal velocities of 7.3 km s⁻¹ in the eastern part of the model, and upper-mantletype velocities of near 8.0 km s⁻¹ at similar depths in the west. The anomalous central region beneath the topographic high (Fig. 1), with a near-constant velocity of 6.8 km s⁻¹, is required to match times and amplitudes of first arrivals beyond 100 km. The depth of the crust-mantle transition cannot be determined confidently from first-arrival data because reversed upper mantle arrivals beyond a distance of 190 km were not well defined. However, given the control on mid- to upper-crustal velocity structure and the position and amplitude of first arrivals and wide-angle reflections (Fig. 2A), our modelling indicates a crustmantle transition at 38-40 km depth beneath the central and eastern regions and mantle-type velocities at 24 km depth beneath the western region. Tests using a range of plausible crustal and upper mantle velocities suggest a possible range of crustal thicknesses of 36-44 km for the eastern and central regions.

Reduced to a water depth of 2.5 km, reversed basin line sections to distances up to 60 km show a continuity of waveform remarkably similar to the strike line data (compare Figs 2A and

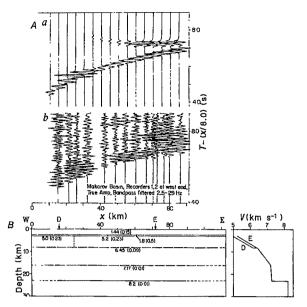


Fig. 3 CESAR basin line. A, comparison of section recorded at west end (b) with first-arrival and PmP reflection synthetic section (a). The data (b) are shown with true amplitudes, after application of a bandpass filter (2.5-29 Hz). B, Velocity model derived from analysis of reversed data obtained at each end of the line.

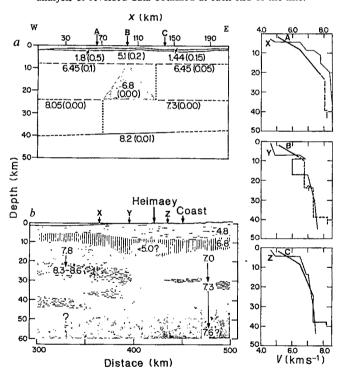


Fig. 4 Comparison of strike line velocity model (a) with model of Iceland-Reykjanes Ridge⁸ (b). Velocity-depth profiles A and X, B and Y and C and Z are compared at right.

3A). Beneath the sediments both data sets require a velocity of $5.1-5.2 \text{ km s}^{-1}$ and a gradient of $\sim 0.23 \text{ s}^{-1}$. Thus, the uppermost 15 km of the basin model (Fig. 3B) appear laterally homogeneous and closely resembles the western region of the strike line.

Features observed on the basin line but not observed on the strike line include indications of reflected energy closely following the first arrivals at ~ 30 km distance, and a large amplitude secondary event starting at ~ 60 km. The nearer source reflections result from the larger velocity difference in the western part of the basin (Fig. 3B). Note that the upper-crustal velocity gradient is uniform across the basin. We interpret the high-

amplitude secondary events starting at 60 km as reflections from the crust-mantle transition, similar to those observed on the strike line beyond 120 km. Again, the depth to the crust-mantle transition is poorly constrained, with our best estimate of 23 km being the mean of a range from 21 to 25 km.

Taylor et al⁴ point out that the short-wavelength magnetic anomalies in the area of Fig. 1 closely follow the bedrock topography of the Alpha Ridge, and they propose that ridge material extends farther south beneath the sediments of the Canada Basin than is indicated by the bathymetry. Similarly, the basin line, with a crustal thickness of ~23 km and a velocity structure similar to the Alpha Ridge, suggests that the ridge complex extends to ~200 km north of the strike line. These results support the suggestion⁵ that the Alpha Ridge complex extends almost to the edge of the Lomonosov Ridge, and is therefore >500 km wide in this region.

The upper-crustal velocity of 5.1 km s⁻¹ immediately underlying a thin sediment cover, the apparent lateral homogeneity along the strike of the ridge, the high-intensity magnetic anomalies⁴ and the vesicular, highly altered volcanic samples dredged from an Alpha Ridge scarp⁶ favour the identification of the upper crustal medium as oceanic layer 2. The greater lateral variation at mid- and lower-crustal depths seems to reflect a more complex tectonic evolution.

The continental-type thickness indicates that the Alpha Ridge, like the Ontong-Java and Manihiki plateaus of the Pacific plate⁷, is an oceanic plateau of problematic origin. Jackson² has outlined the similarity of the Alpha Ridge morphology and shallow structure to that seen on the Manihiki plateau. Certainly, the available geological and geophysical evidence suggests that both the Alpha and Manihiki features are characterized by an overthickened oceanic-type crust. A closer tectonic analogue to the Alpha structure may be Iceland today. Figure 4 shows a comparison of the velocity structure along the strike of the Alpha Ridge with the structure along the strike of the Mid-Atlantic system from the Reykjanes Ridge to Iceland. The lateral change from a structure characteristic of oceanic crust beneath the flank of the Reykjanes Ridge to a structure with 'anomalous mantle' beneath Iceland itself resembles the structure along the Alpha Ridge. Note that the crustal structures that have been derived from seismic refraction data may be compared only to depths of ~40 km; Icelandic structure below 40 km is not based on direct refraction data. Comparisons of velocity structures for particular sections of the respective models show:

(1) Thick oceanic sections beneath both the Alpha Ridge and Iceland, with typical layer 2 and layer 3 velocities and a similar velocity-depth profile for the thickened 'anomalous crust' beneath the active area of Iceland and the region beneath the eastern end of the Alpha Ridge profile (Z and C in Fig. 4). The greatest difference between the crustal responses is the interpreted wide-angle reflection coda that indicate significant energy return from a crust-mantle transition near 40 km depth beneath the Alpha Ridge. The absence of similar energy return from beneath Iceland is probably related to the present plume and spreading activity. Comparable activity would have ceased in the Alpha Ridge area during late Mesozoic times².

(2) A central zone (Y and B in Fig. 4), characterized in the Icelandic case by low-velocity regions representing possible magma chambers, and in the Alpha Ridge case by a region of lower velocity gradient. Neither Icelandic nor Alpha Ridge data sets can further resolve the zone of required time delay. In the Icelandic case the lower-velocity regions have been explained as zones of high melt concentration. In the older Alpha Ridge structure, the zone of lower velocity gradient may represent an ancient melt zone which has cooled to yield a higher velocity than in the much younger, still active zone beneath Iceland.

(3) A more normal oceanic velocity-depth profile for the flank of the Reykjanes Ridge and western part of the Alpha Ridge (X and A in Fig. 4), with upper-mantle velocities appearing in the 20-23 km depth range.

Note that, in general, comparable velocities are reached at ~3 km shallower depths on the Icelandic sections than on the Alpha Ridge sections. Although technique resolution may be debated, the results are consistent with the present elevation difference between Iceland (+1.5 km) and the Alpha Ridge (-1.5 km). It is suggested that most of the differences between the velocity-depth profiles may be accounted for by normal thermal decay and subsidence.

We greatly appreciate the valuable discussions and constructive critiques offered by Drs P. Morel-à-l'Huissier, I. Reid, J. R. Weber and M. J. Berry. This is Geological Survey of Canada contribution no. 11086, CESAR contribution no. 7.

Received 10 January; accepted 21 April 1986.

- .1. Mair, J. A. & Lyons, J. A. Can. J. Earth Sci. 18, 724-741 (1981). 2. Jackson, H. R. Geol. Surv. Pap. Can. 84-22 19-23 (1985).
- Spence, G. D., Whittail, K. P. & Clowes, R. M. Bull. seism. Soc. Am. 74, 1209-1223 (1984).
 Taylor, P. T., Kovacs, L. C., Vogt, P. R. & Johnson, G. L. J. geophys. Res. 86, 6323-6333 (1981).
 Weber, J. R. & Sweeney, J. F. J. geophys. Res. 90, 663-677 (1985).
- Van Wagoner, N. A. & Robinson, P. T. Geol, Surv. Pap. Can. 84-22, 47-57 (1985).
- Carlson, R. L., Christensen, N. I. & Moore, R. P. Earth planet. Sci. Lett. 51, 171-180 (1980).
- 8. Gebrande, H., Miller, H. & Einarsson, P. J. Geophys. 47, 239-249 (1980).

Melting of a model chondritic mantle to 20 GPa

Eiji Ohtani*, Takumi Kato† & Hiroshi Sawamoto†

- * Department of Earth Sciences, Ehime University, Matsuyama 790,
- † Department of Earth Sciences, Nagoya University, Nagoya 464, Japan

Calculations of the thermal evolution of the Earth during accretion suggest that the outer layer may once have been molten, perhaps to a depth of 1,000 km or more^{1,2}. If such global melting did occur, fractionation processes could have produced a chemical stratification in the mantle. Recent technical developments in experimental petrology have made it possible to achieve temperatures in excess of 2,000 °C at a pressure of 20 GPa^{3,4}, thereby permitting studies of multi-component systems under conditions that prevail in the Earth's mantle. We have conducted melting experiments using a composition in the five-component system CaO-FeO-MgO-Al₂O₃-SiO₂ (CFMAS) corresponding to a model chondritic mantle, and find that the liquidus phase changes from olivine to majorite at a pressure between 12 and 15 GPa. The liquid coexisting with majorite at 20 GPa has a peridotitic composition. In addition, because the CaO/Al2O3 ratio of the liquidus majorite at 20 GPa is lower than that of the sub-solidus majorite, partial melting and majorite fractionation at the base of the upper mantle could produce a peridotitic liquid with a CaO/Al₂O₃ ratio greater than that of the chondritic starting material, consistent with current views on mantle geochemistry.

Cosmochemical studies (see, for example, refs 5, 6) suggest that the composition of the bulk Earth is close to chondritic in terms of the major lithophile and refractory elements, such as Mg, Si, Al and Ca. The bulk mantle may contain these elements in ratios close to chondritic. Assuming that the core is composed of iron with ~16 wt % light elements, a mass balance calculation⁷ gives a value of ~0.1 for the Fe/(Fe+Mg) (atomic) ratio of the mantle.

We therefore chose as our starting material a model chondritic mantle composition of 50.18 wt% SiO₂, 3.62% Al₂O₃, 7.16% FeO, 36.18% MgO and 2.86% CaO, in which the ratios of Mg, Si. Al and Ca are chondritic⁸, while the iron content is Fe/(Fe+ Mg) = 0.1. The samples were prepared by mixing the reagents and heating the mixture at 1,150 °C in an atmosphere with controlled oxygen partial pressure. The starting material after

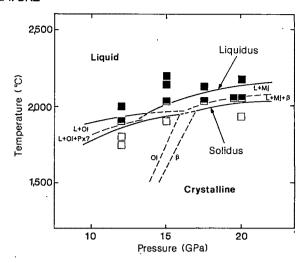


Fig. 1 Melting relations of a model chondritic mantle to 20 GPa. □, Sub-solidus; ≡, crystal+liquid; ≡, super-liquidus; L, liquid; Ol, olivine; Px, clinopyroxene; β , modified spinel; Mj, majorite.

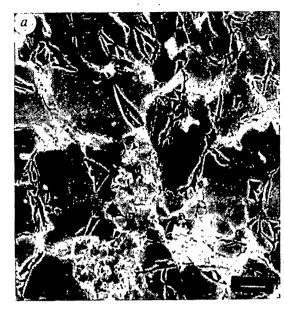
heating comprised olivine, pyroxenes and a small amount of anorthite.

The apparatus used was an MA8-type high-pressure apparatus³, driven by the guide block/uniaxial press system of Nagoya University, and with a heating assembly similar to that described in ref. 4. The heating element used for the present experiments is a composite of tungsten carbide and diamond. The graphite sample capsule was placed between sheet heaters in the pressure medium, which is made of sintered magnesia containing 8 mol % CoO. A tungsten-rhenium (W25% Re-W3% Re) thermocouple, 0.2 mm in diameter, was placed in contact with the sample capsule, without making electrical contact with the heater. The furnace components and pressure medium were heated to ~1,000 °C for 1 h to remove water. The charge was dried again in an oven at 170 °C for a few hours immediately before the experiments.

The pressure was calibrated using the resistance changes associated with phase changes in Bi, Pb, ZnS and GaAs. A temperature correction was applied to the pressure values calibrated at room temperature, based on the phase boundary curves determined at pressures below 15 GPa by in situ X-ray diffraction experiments⁹. The resulting uncertainty in the pressure values was ± 0.6 GPa at 15 GPa and ± 2 GPa at 20 GPa.

The pressure was applied first, after which the temperature was increased to the desired value and held constant for ~2 min. The charge was quenched by turning off the electrical power to the furnace. The run products recovered after quenching were examined by X-ray powder diffraction, optical and scanning electron microscopy and electron probe microanalyser (EPMA) analysis. The melt is identified under the scanning electron microscope by the presence of fibrous or dendritic texture, which has been established as diagnostic of quenching from liquid at very high pressure^{3,4}.

The conditions and the results of the high-pressure runs are summarized in Fig. 1 as a phase diagram. The run made at 12 GPa and 1,900 °C indicated that olivine is the liquidus phase; thus, the partial melt formed at this pressure is richer in SiO₂ than the starting material with chondritic mantle composition. This result is consistent with melting experiments on the natural peridotite KLB1 (ref. 10). The sub-solidus mineralogy at this pressure is olivine, clinopyroxene and garnet. Figure 2a shows the back-scattered electron image of the charge adjacent to the thermocouple junction, quenched at 20 GPa and 2,050 °C. In this portion of the charge the liquid coexists with two phases; majorite and modified spinel. Figure 2b shows the highertemperature portion of the same charge, in which the quenched



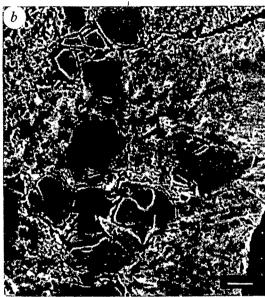


Fig. 2 Back-scattered electron images of the partially molten textures of the model chondritic mantle composition quenched at 20 GPa. In a, the quenched liquid (bright parts) is located in interstices between majorite (light grey crystals) and modified spinel (dark grey crystals). In b, the quenched liquid, now an aggregate of fine dendritic quench crystals, is coexisting with majorite (large grey crystals). Scale bars, 10 μm.

liquid coexists with granular majorite crystals as a liquidus phase. The temperature difference between the two portions of the charge should have been <100 °C, on the basis of a measurement of the temperature distribution in a similar furnace system¹¹. The sub-solidus mineralogy at 20 GPa is a mixture of majorite and modified spinel. Majorite was also observed as the liquidus phase at pressures of 15 and 17.5 GPa. The present experiments clearly demonstrate a change of the liquidus phase from olivine to majorite at a pressure between 12 and 15 GPa for the model chondritic mantle composition.

The compositions of minerals coexisting with a liquid, and of those observed under sub-solidus conditions (~1,930 °C), at 20 GPa were determined by EPMA and are given in Table 1. Note that the CaO/Al₂O₃ ratio of majorite above the solidus is lower than that observed under sub-solidus conditions; CaO and FeO contents of majorite decrease by partial melting. The partition coefficient K_D of Mg and Fe between majorite and

Table 1 Chemical compositions (wt %) of minerals and partial melt in the model chondritic mantle at 20 GPa

	Ga I	MS I	Ga II	MS II	Ga III	Liq III
SiO ₂	56.29	42.89	54.83	42.37	54.24	47.7 ± 2.5
Al ₂ Õ3	4.50	0.29	8.16	1.51	9.70	2.7 ± 1.5
FeO	2.48	4.17	1.88	2.75	1.48	5.1 ± 1.0
MgO	32.60	53.63	34.08	54.22	34.29	40.4 ± 2.5
CaO	3.98	0.09	1.97	0.05	1.14	3.3 ± 1.5
Total	99.85	101.07	100.92	100.90	100.85	99.2
Atomic rat	ios					
Al/Si	0.094	0.008	0.177	0.042	0.211	
Ca/Al	0.802	0.250	0.218	0.023	0.107	
Fe/Mg	0.043	0.044	0.031	0.028	0.024	

Ga I and MS I, majorite and modified spinel under sub-solidus conditions; Ga II and MS II, majorite and modified spinel coexisting with a liquid (Fig. 2a); Ga III and Liq III, majorite and coexisting liquid.

modified spinel is near unity at 20 GPa and >1,930 °C.

The composition of the liquid adjacent to majorite crystals in Fig. 2b was measured by EPMA with a diffused beam, ~15 µm in diameter. As the liquid could not be quenched to a glass (quench crystals of modified spinel, majorite and clinopyroxene were formed during quenching), the liquid composition (Table 1) was obtained by averaging measurements obtained over an area of >50 × 50 µm. The liquid is highly magnesian and peridotitic in composition. The FeO contents of the liquid and coexisting minerals shown in Table 1 are lower than would be expected from the starting composition; this is because some of the FeO was reduced to metal during heating at high pressure and temperature. (Small dispersed grains of metallic iron were observed in the charge.) The determination of the liquid composition has a large uncertainty, because of the heterogeneity of the aggregates of quench crystals formed from a liquid during quenching. Nevertheless, our result supports the generation of peridotitic magma by majorite fractionation at the base of a chondritic upper mantle. The low value of CaO/Al₂O₃ in the liquidus majorite implies that the partial melt has higher than chondritic CaO/Al₂O₃.

The partially molten zone may have extended to the deep upper mantle, or even to the lower mantle in the final stage of the accretion of the Earth^{1,2}. If the zone extended to the base of the upper mantle, the majorite fractionation and upward transportation of the peridotitic liquid could have produced a largely molten, peridotitic upper mantle 12-14, and a majoriteenriched transition zone. The upper mantle formed by the process would have a higher than chondritic CaO/Al₂O₃ ratio, as shown in the present experiment. Thus, the suggestion of Pulme and Nickel¹⁵ that the upper mantle has a high CaO/Al₂O₃ ratio, compared with the chondritic value, is consistent with an upper mantle chemistry derived from majorite fractionation by partial melting in the deep upper mantle.

This work was supported by grants 59740186 and 60121007 from the Ministry of Education, Science and Culture, Japan.

Received 26 March; accepted 21 April 1986.

- Kaula, W. H. J. geophys. Res. 84, 999-1008 (1979).
- Hayashi, C., Nakazawa, K. & Mizuno, H. Earth planet. Sci. Lett. 43, 22-28 (1979). Ohtani, E. & Kumazawa, M. Phys. Earth planet. Inter. 27, 32-38 (1981).
- Kato, T. & Kumazawa, M. Phys. Earth planet. Inter. 41, 1-5 (1985). Ganapathy, R. & Anders, E. Geochim. cosmochim. Acta Suppl. 5, 1181-1209 (1974).
- Anderson, D. L. J. geophys. Res. 88, B41-B52 (1983). Liu, L. G. Geochem. J. 16, 287-310 (1982).
- Anders, E. & Ebihara, M. Geochim. cosmochim. Acta 46, 2363-2380 (1982) Akimoto, S., Yagi, T. & Inoue, K. in High-Pressure Research: Applications in Geophysics
- Akimoto, S., Yagi, T. & Inoue, K. in High-Pressure Research: Applications in Ge (eds Manghnani, M. H. & Akimoto, S.) 595-602 (Academic, New York, 1977).
 Takahashi, E. & Scarfe, C. M. Nature 315, 566-568 (1985).
 Irifune, T. & Hibberson, W. O. High Temp. high Press. 17, 575-579 (1985).
 Herzberg, C. T. & O'Hara, P. J. Geophys. Res. Lett. 12, 541-544 (1985).
 Walker, D. & Herzberg, C. T. Eos 66, 403-404 (1985).
 Ohtani, E. Phys. Earth planet. Inter. 38, 70-80 (1985).

- 15. Pulme, H. & Nickel, K. G. Geochim. cosmochim. Acta 49, 2123-2132 (1985).

Melting of garnet peridotite to 13 GPa and the early history of the upper mantle

Christopher M. Scarfe* & Eiichi Takahashi

Institute for Study of the Earth's Interior, Okayama University, Misasa, Tottori-Ken 682-02, Japan

By analogy with the evolution of the Moon, it has been suggested that the Earth may have had a 'magma ocean' or liquid outer layer before 3,800 Myr ago. 1. Its presence would have had profound implications for the primary stratification of the mantle into upper mantle, transition zone and lower mantle^{2,3}. An essential constraint on this hypothesis is a knowledge of the high-pressure melting characteristics of mantle material, generally assumed to be peridotite in the upper mantle. We recently described the first melting experiments on mantle peridotite to 14 GPa. Using spinel lherzolite KLB-1 from Kilbourne Hole, New Mexico, we showed that partial melts close to the solidus at 5-7 GPa are komatiitic in composition and that the solidus and liquidus converge at high pressures. Here we report further melting experiments on garnet lherzolite PHN1611 from Thaba Putsoa, Lesotho. We confirm the convergence of the solidus and liquidus and we show a negative dT/dP slope for the liquidus above 7 GPa. These observations are briefly discussed in terms of their importance to the petrological evolution of the upper mantle and the presence of a magma ocean in the early Archaean.

PHN1611 is a sheared garnet peridotite⁵. The bulk composition is given in Table 1 along with analyses of the constituent mineral phases. The composition (Mg/Mg+Fe=0.87; CaO/Al₂O₃=1.19) is close to pyrolite⁶ and is thought to represent undepleted or fertile mantle lherzolite⁷. The melting relationships of PHN 1611 at pressures ≤ 3.5 GPa have been previously reported, both for the anhydrous rock⁸⁻¹⁰ and in the presence of H₂O (ref. 9) and CO₂ (ref. 11).

Experimental methods and calibration procedures are similar to those in our previous report and are fully described elsewhere¹². The major technological innovation was the use of the 5,000-ton uniaxial, split-sphere, 6-8-type, multi-anvil apparatus developed by Ito^{13,14}. The apparatus incorporates a large sample volume and is capable of pressures of at least 30 GPa and temperatures >2,000 °C. Our experiments are the first melting studies on natural rock material using the split-sphere apparatus.

Figure 1 shows that at 1 atmosphere the temperature interval between the liquidus and solidus of PHN1611 is 500 °C: the solidus is at 1,125 °C, the liquidus at ~1,625 °C. With increasing pressure, however, at 5 GPa the solidus is at 1,700 °C and the liquidus at 1,975 °C. At still higher pressures the solidus increases more gradually, to 1,825 °C at 13 GPa. In contrast, at pressures >7 GPa the liquidus temperature no longer increases, but decreases to 1,900 °C at 13 GPa. The negative slope of the liquidus allows the liquidus and solidus to converge, until at 13 GPa the melting interval is <100 °C. In our previous study of KLB-1, results above 10 GPa suggested convergence of the solidus and liquidus, but the results were not definitive enough to confirm convergence⁴.

New determinations of the melting curve of diopside extend the results of Boyd and England¹⁵ from 5 to 13 GPa. Figure 2 shows the melting curve of diopside, along with the melting curves for forsterite¹⁶ and pyrope¹⁷. The diopside melting curve flattens at pressures between 7 and 13 GPa and varies little from 2,000 °C. This behaviour contrasts with that of the melting curve for forsterite, which approximates a straight line with a slope of dT/dP = 41 °C GPa⁻¹ (ref. 16). However, the curvature of the diopside curve is similar to the strong curvature shown by

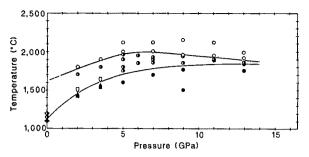


Fig. 1 Phase diagram showing the melting of garnet peridotite PHN1611 to 13 GPa. Experiments close to the liquidus were typically 1 min in duration; however, experiments close to the solidus and in the sub-solidus ranged from 10 to 150 min. Uncertainties in pressure and temperature are discussed in detail elsewhere 12. Because of possible hydration problems, all sample and pressure assemblies were heated with a propane torch before final assembly and were stored in an oven at 120 °C. O, Super-liquidus; O, crystals+liquid; sub-solidus. Open and filled arrowheads show solidus brackets from refs 8-10.

the melting curve for pyrope, which is attributed to a possible change in Al^{3+} in the melt from 4- to 6-coordination with oxygen¹⁷. Preliminary results by Ohtani and Irifune¹⁸ for diopside to 10 GPa also suggest a flattening of the melting curve at pressures >8 GPa. At 7-13 GPa, diopside melt does not quench to a glass but exhibits prismatic quench crystals. Note, on the other hand, that at \leq 5 GPa diopside melt can be quenched to a glass⁵. This could imply a change of melt structure above and below 7 GPa.

It is possible that the negative slope of the peridotite liquidus above 7 GPa is due to the solution of CO₂ or CO in the melt as a result of reduction of iron oxides in the charge by graphite from the graphite capsule. Carbon dioxide reduces melting temperatures at lower pressures 11,19; however, both the solidus and liquidus should be affected. Microprobe analyses of carbon in two charges (CMS 62, 13 GPa, 1,920 °C; CMS 52, 11 GPa, 1,900 °C) by T. Furuta (Ocean Research Institute, University of Tokyo) show concentrations of <0.5 wt % using Al metal as a conductive coating. At this stage, however, these analyses must be considered preliminary because no special precautions were used to exclude carbon during polishing of the charges and because the analyses involved the development of special techniques.

The compositions of melts and coexisting crystals have been reported for spinel lherzolite KLB-1 in our previous paper⁴. The results for PHN1611 are very similar and we report here only analyses of the composition of near-solidus olivine, clinopyroxene and garnet as a function of pressure (Table 1). The major point is that above ~ 5 GPa at temperatures ≥ 1.750 °C the near-solidus assemblage is olivine + clinopyroxene + garnet. Orthopyroxene was not identified and must be excluded at high pressures by solution of the enstatite component in both clinopyroxene and garnet (Fig. 3). When compared with the composition of the starting material, with increasing pressure the Si and Mg/Mg+Fe contents of the garnet increase and the Al content decreases. At the same time, the clinopyroxene becomes depleted in Al and Ca and enriched in Fe. These trends may be compared with previous work on the sub-solidus phase relationships of PHN 1611 (ref. 20), and on pyroxene-garnet solid solution relationships in Mg- and Fe-rich systems²¹ and in the system CaO-MgO-Al₂O₃-SiO₂ (CMAS; ref. 22). Note, however, that any differences may be accounted for by the much higher temperatures of the present experiments compared with temperatures of ≤1.500 °C in previous work. Recently, natural garnets from the upper mantle with pyroxene in solid solution have been described by Moore and Gurney23. These garnets, found as inclusions in diamond in kimberlite, have similar compositions to garnets in the experiments.

^{*} Permanent address: Department of Geology and Institute of Earth and Planetary Physics, University of Alberta, Edmonton, Canada T6G 2E3.

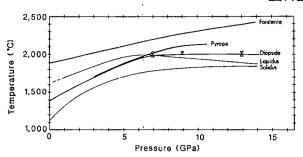


Fig. 2 Melting curves for forsterite, diopside and pyrope, superimposed on the phase diagram for PHN1611. Brackets at high pressures for diopside are from the present study.

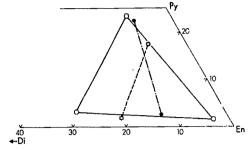


Fig. 3 Garnet-pyroxene chemical relationships projected on to the plane pyrope-enstatite-diopside in CMAS. O, PHN1611 starting material; ●, charge CMS41 (5 GPa, 1,750 °C); 菜, charge CMS64 (13 GPa, 1,850 °C).

The present results for garnet lherzolite PHN1611 confirm our previous work on spinel lherzolite and show the convergence of the solidus and liquidus of mantle peridotite at pressures >7 GPa. This result had been anticipated by Herzberg²⁴. Below, we discuss three implications of the results.

First, the question arises as to whether complete convergence takes place between the liquidus and solidus at some pressure above 13 GPa, or whether the curves approach each other but do not actually join (see refs 24-28). In a multi-component system with solid solutions, complete convergence may not occur but a close approach is possible. Therefore, it is anticipated that at a pressure close to 15 GPa the slope of the liquidus will again become positive and a cusp or inflection will be generated where olivine is replaced by garnet-pyroxene solid solution (majorite)^{12,24}. At this cusp, for small temperature excursions across the solidus, melts would be close to the bulk composition of upper mantle peridotite.

Second, because of the negative $\mathrm{d}T/\mathrm{d}P$ slope of the liquidus, melts in equilibrium with olivine in the pressure interval 7-13 GPa may be denser than olivine, in order to satisfy the Clapeyron relationship. However, note that the Clapeyron relationship is strictly applicable only to systems where the liquid and solid compositions are identical; in a natural multi-

component system where liquids and coexisting crystals have different compositions, additional terms are required^{24,29,30}. Olivine flotation was not confirmed in our experiments, but we believe this may be due to the very short run durations near the liquidus and to the presence of temperature gradients in our charges¹². The possibility that melts at high degrees of partial melting are more dense than olivine has profound implications for melt-crystal dynamics at depth in the Earth. The most obvious conclusion is that melts, once formed at depths >200 km, may not be able to rise to shallower levels, but will remain concealed at depth. The density cross-over between liquid and crystals results from the greater compressibility of silicate melts at high pressure compared with their coexisting crystalline solids^{29,31}. Several petrogenetic possibilities related to this observation have been discussed elsewhere ^{12,24-27,29,31,32}.

Third, it has been suggested that the Earth may have possessed a liquid or partially molten 'magma ocean' during the early stages of its evolution 2,3,26,32 . A similar concept has been discussed in relation to the evolution of the Moon¹. Our present results suggest that because of the close approach of the solidus and liquidus at pressures of ~ 15 GPa, the Earth could have had a subterranean molten layer of broadly lherzolitic composition. Whether the eutectic-like melting behaviour implies that the

	PHN1611 Pyr		PHN1611 starting material				CMS41: 5 GPa, 1,750 °C			CMS64: 13 GPa, 1,850 °C		
		Pyrolite	Gt	Срх	Орх	Ol	Gt	Срх	Ol	Gt	Срх	Ol
SiO ₂	44.54	45.20	42.68	54.79	56.26	40.42	42.85	55.78	40.78	46.92	56.03	40.81
TiO ₂	0.25	0.71	0.80	0.30	0.23	0.03	0.24	0.05	0.01	0.51	0.07	0.04
$Al_2\tilde{O}_3$	2.80	3.54	21.15	2.41	1.34	. 0.10	21.05	2.58	0.14	15.74	1.57	0.12
FeO(total)	10.24	8.47	8.63	5.14	7.04	11.44	5.78	5.40	8.26	7.29	6.07	11.46
MnO	0.13	0.14	0.26	0.13	0.13	0.14	0.17	0.10	0.12	0.19	0.09	0.10
MgO	37.94	37.48	20.66	20.32	32.66	48.06	23.97	28.25	49.64	23.88	23.91	46.95
CaO	3.32	3.08	4.30	13.03	1.59	0.13	3.96	6.20	0.28	3.72	9.73	0.22
Na ₂ O	0.34	0.57	0.07	1.50	0.34	ND	0.10	0.51	0.05	0.13	0.91	0.06
K₂Õ	0.14	0.13										
P ₂ O ₅	ND	0.06										
Cr ₂ O ₃	0.29	0.43	1.46	0.49	0.21	0.05	1.46	0.37	0.17	1.18	0.27	0.11
NiO	ND	0.20										
Total	99.99	100.01	100.01	98.11	99.80	100.37	99.58	99.24	99.45	99.56	98.65	99.87
Mg/Mg+Fe 0.5(Al+Cr)		0.887	0.810	0.875	0.892	0.882	0.881	0.903	0.915	0.854	0.876	0.878
[0.5(Al+Cr)+Fe+Mg+Ca]			0.234	0.032	0.016		0.225	0.026		0.176	0.020	
Ca/[0.5(Al+Cr)+Fe+Mg+Ca]			0.083	0.278	0.030		0.073	0.121		0.072	0.200	

According to recent studies (F. R. Boyd, personal communication), PHN1611 may have been affected by metasomatism immediately before eruption; however, the magnitude of any compositional changes is unclear. Analyses of experimental charges were performed at Misasa with a JEOL JXA-5A microprobe. Conditions for wavelength-dispersive analysis were a 15-kV accelerating voltage, a beam current of 20 nA and counting times of 40-70 s. Data reduction using ZAF corrections. ND, Not determined.

upper mantle itself is a partial melt sweated out of the whole mantle^{26,27,33}, and whether on cooling and crystallization the layer would fractionate olivine by flotation and garnet solidsolution by settling^{2,3,26,27}, thus inducing some mineralogical stratification of the upper mantle, are questions that go beyond the scope of this paper. However, the melting phase relationships of garnet peridotite presented here provide a starting point for modelling the early Earth and the evolution of its upper mantle.

This study was supported by grants 58460042 and 59540525 from the Ministry of Education, Science and Culture of Japan. C.M.S. acknowledges the support and hospitality of ISEI and travel funds from Canadian NSERC grant IC-0214 and the University of Alberta Central Research Fund, Samples of PHN1611 were supplied by Drs F. R. Boyd and P. H. Nixon. We thank Dr E. Ito for advice and use of his apparatus. Comments by Drs D. L. Anderson, F. R. Boyd, C. T. Herzberg, E. Ito, Y. Matsui and D. Walker helped to improve the manuscript.

Received 3 December 1985; accepted 16 April 1986.

- 1. Warren, P. H. A. Rev. Earth planet. Sci. 13, 201-240 (1985).
- Anderson, D. L. J. geophys. Res. 84, 6297-6298 (1979). Anderson, D. L. Science 223, 347-355 (1984).
- Takahashi, E. & Scarfe, C. M. Nature 315, 566-568 (1985).
- Nixon, P. H. & Boyd, F. R. in Lesotho Kimberlites (ed. Nixon, P. H.) (Lesotho National Development Corporation, 1973).

- 6. Ringwood, A. E. in Advances in Earth Sciences (ed. Hurley, P. M.) (Massachusetts Institute of Technology, Cambridge, 1966). Shimizu, N. Earth planet. Sci. Lett. 25, 26-32 (1975).
- Kushiro, I. in Lesotho Kimberlites (ed. Nixon, P. H.) (Lesotho National Development Corporation, 1973).
- Mysen, B. O. & Kushiro, I. Am. Miner. 62, 843-865 (1977).
- Harrison, W. J. Yb. Carnegie Instn. Wash. 78, 562-568 (1979).
 Wendlandt, R. F. & Mysen, B. O. Am. Miner. 65, 37-44 (1980).
- Takahashi, E. J. geophys. Res. (in the press).
 Ito, E. & Yamada, H. Advances in Earth and Planetary Sciences Vol. 12 (Reidel, Dordrecht, 1982). 14. Ito, E., Takahashi, E. & Matsui, Y. Earth planet. Sci. Lett. 67, 238-248 (1984).
- Boyd, F. R. & England, J. L. J. geophys. Res. 68, 311-323 (1963).
 Ohtani, E. & Kumazawa, M. Phys. Earth planet. Inter. 27, 32-38 (1981).
- 17. Ohtani, E., Irifune, T. & Fujino, K. Nature 294, 62-64 (1981)
- Ohtani, E. & Irifune, T. Seism. Soc. Jap. Abstr. C51, 243 (1985).
 Eggler, D. H. Am. J. Sci. 278, 305-343 (1978).
- Akaogi, M. & Akimoto, S. Phys. Earth planet. Inter. 19, 31-51 (1979).
 Akaogi, M. & Akimoto, S. Phys. Earth planet. Inter. 15, 90-106 (1977). 22. Yamada, H. & Takahashi, E. in Kimberlites II: The Mantle and Crust-Mantle Relationships
- (ed. Komprobst, J.) (Elsevier, Amsterdam, 1984). 23. Moore, R. O. & Gurney, J. J. Nature 318, 553-555 (1985)
- 24. Herzberg, C. T. Phys. Earth planet. Inter. 32, 193-202 (1983).
- Ohtani, E. Earth planet. Sci. Lett. 67, 261-272 (1984).
 Ohtani, E. Phys. Earth planet. Inter. 38, 70-80 (1985).
- Herzberg, C. T. & O'Hara, M. J. Geophys. Res. Lett. 12, 541-544 (1985).
- Walker, D. Contr. Miner. Petrol. 92, 303-307 (1986).
- Nigden, S. M., Ahrens, T. J. & Stolper, E. M. Science 226, 1071-1074 (1984).
 Walker, D. & Agee, C. Eos 67, 405 (1986).
 Stolper, E. M., Walker, D., Hager, B. H. & Hays, J. F. J. geophys. Res. 86, 6261-6271 (1981).

- Nisbet, E. G. & Walker, D. Earth planet. Sci. Lett. 60, 103-113 (1982).
 Takahashi, E., Matsui, Y. & Ito, E. Proc. 10th Symp. Antarctic Meteorites, 59-60 (National Institute of Polar Research, Tokyo, 1985).

Evidence from the Parana of south Brazil for a continental contribution to Dupal basalts

C. J. Hawkesworth*, M. S. M. Mantovani†, P. N. Tavlor[‡] & Z. Palacz*

- * Department of Earth Sciences, The Open University, Milton Keynes, MK7 6AA, UK
- † Departamento de Geofisica, Instituto Astronomico e Geofisico. Universidade de Sao Paulo, Caixa Postal 30627, 01051 Sao Paulo SP,
- ‡ Department of Earth Sciences, University of Oxford, Parks Road, Oxford OX1 3PR, UK

It has been suggested^{1,2} that the oceanic upper mantle preserves a large scale isotope anomaly, Dupal², which may be thousands of millions of years old. New Nd-, Pb- and Sr-isotope data on the continental volcanic rocks of the Parana, south Brazil, reveal 'enriched' isotopic ratios, with $^{87}\mathrm{Sr}/^{86}\mathrm{Sr} = 0.705-0.716$ and $\varepsilon_{\mathrm{Nd}} =$ -2.5 to -8, similar to those from other continental flood basalt provinces. Their ²⁰⁷Pb/²⁰⁴Pb ratios are higher than those of midocean-ridge basalts (MORB) at comparable ²⁰⁶Pb/²⁰⁴Pb, and even though the basalts appear to have been derived from lithospheric sources within the sub-continental mantle, they preserve isotope and trace element ratios similar to those in oceanic basalts with the Dupal signature in the South Atlantic. The implied link between these continental flood basalts and Dupal oceanic volcanics raises the possibility that in some areas the Dupal anomaly marks a comparatively shallow-level feature in the Earth's mantle.

The Parana is one of the largest known continental flood basalt provinces (106 km²). Most age determinations cluster around 130-120 Myr (ref. 3), so that the Parana appears to be contemporaneous with the Etendeka volcanics in Namibia and the opening of the South Atlantic⁵. The Parana rocks range from tholeiitic basalts to rhyodacites and rhyolites. The more evolved rocks tend to occur at higher stratigraphical levels, and in a large regional study by Bellieni et al.⁶ they comprised ~16% of the rocks analysed.

Geochemically the Parana volcanics consist of two apparently discrete groups characterized by different minor and trace ele-

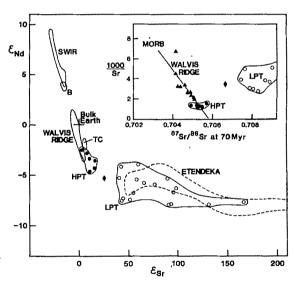


Fig. 1 Plot of $\varepsilon_{\rm Sr}$ versus $\varepsilon_{\rm Nd}$, comparing Parana data with those from: SWIR, south-west Indian Ridge; B, Bouvet; TC, Tristan da Cunha, the Walvis Ridge, and the low-Ti Etendeka rocks from Namibia 12,22,26,27. ●, HPT; ○, LPT; ◆, a transitional basalt. Inset, 1,000/Sr versus ⁸⁷Sr/⁸⁶Sr for the Walvis Ridge (A) and Parana rocks (after ref. 22).

ment abundances and 87Sr/86 ratios6-9. The HPT (high phosphorus and titanium) rocks have high P2O5, TiO2, Sr and LREE (light rare-earth element) contents but, at least in the samples analysed here, restricted major element contents (SiO₂= 49.3-53.9%, MgO = 5.0-4.3%) and initial 87Sr/86Sr (0.7048-0.7058). LTP (low phosphorus and titanium) rocks exhibit a full range from basalt to rhyolite, but have low P₂O₅ and TiO₂ (<0.3 and 2.0%, respectively), and high and variable initial 87Sr/86Sr (0.7076-0.7160). Mantovani et al.8 explained the striking increase in 87Sr/86Sr with differentiation in the LPT rocks in terms of crustal assimilation during high-level fractional crystallization (AFC). However, they and others⁶⁻⁹ have argued that the HPT and LPT series were derived from sources with different minor and trace element features, and probably different 87 Sr/ 86 Sr, of ≈ 0.705 and ≈ 0.707 respectively.

Regional studies of the Parana have demonstrated that, as in

Table 1 Parana volcanics											
	SiO*	TiO ₂ *	Rb*	Sr*	Sm*	Nd*	⁸⁷ Sr/ ⁸⁶ Sr†	¹⁴³ Nd/ ¹⁴⁴ Nd†	²⁰⁶ Pb/ ²⁰⁴ Pb†	²⁰⁷ Pb/ ²⁰⁴ †	208 Pb/ 204 Pb†
GB 28ab	49.6	3.87	34	736	11	58	0.70540	0.512437 ± 8	17.558	15.506	38.090
GB 33ab	49.4	3.76	22	740	10	50	0.70499	0.512451 ± 24	17.087	15.445	37.240
GB 23ab	49.5	3.62	54	816	11	53	0.70565	0.512415 ± 14	17.159	15.482	37.659
GB 45ac	49.5	3.85	14	755	11	53	0.70540	0.512351 ± 16	16.629	15.501	38.132
GB 13af	50.9	3.53	22	663	10.5	49.0	0.70581	0.512368 ± 14	17.062	15.447	37.388
GB 41ac	50.8	3.44	43	304	11.6	58.4	0.70705	0.512328 ± 20	17.727	15.529	38.315
GB 57da	48.7	1.43	10	254	4.61	19.9	0.70755	0.512330 ± 14	18.495	15.628	38.621
GB 43ab	48.9	1.86	59	329	5.8	25	0.70856	0.512221 ± 16	18.096	15.593	38.639
GB 20a	49.5	0.80	15	188	2.58	10.6	0.70924	0.512413 ± 26	18.299	15.602	38.566
GB 40bb	49.7	0.90	9	199	3.05	12.9	0.70779	0.512389 ± 24	18.523	15.631	38.655
GB 45ab	50.6	1.75	16	375	6.2	29	0.70846	0.512207 ± 24	17.942	15.583	38.356
GB 50ac	50.9	1.69	41	259	5.8	20	0.70918	0.512281 ± 20	18.358	15.622	38.642
GB 18ac	51.1	0.99	22	228	3.85	16.6	0.70951	0.512302 ± 20	18.068	15.624	38.323
GB 39aa	51.2	1.77	21	271	5.8	22	0.70907	0.512339 ± 8	18.820	15.664	38.797
GB 44ad	51.5	1.72	41	305	5.0	26	0.70824	0.512194 ± 18	17.201	15.497	37.442
GB 2ah	53.1	0.87	35	237	4.73	22.2	0.71187	$0.5\dot{1}2193 \pm 20$	18.269	15.617	38.541
GB 6ac	54.2	1.22	50	225	6.61	28.7	0.71196	0.512184 ± 18	18.521	15.633	38.855
GB 36aa	54.5	1.75	72	255	6.10	28.1	0.71220	0.512319 ± 34	18.420	15.651	38.370
GB 53ab	55.0	1.43	73	138	7.2	35	0.71588	0.512177 ± 14		_	
GB 54a	57.6	1.48	54	168	7.82	37.2	0.71769	0.512199 ± 20	19.024	15.705	38.957
H 295	53.2	1.42	38	178	4.6	20	0.71239	0.512258 ± 18	18.687	15.658	38.800
H 205	54.1	1.44	43	196	5.7	22	0.71100	0.512308 ± 16	18.624	15.660	38.926
T 4	53.3	1.29	37	303	5.1	24	0.71213	0.512266 ± 16	18.764	15.682	39.919
T 23	69.5	0.97	139	148	8.5	38	0.72009	0.512202 ± 10	19.114	15.727	38.987

* Data from ref. 8 except for Sm and Nd results with three significant figures, which are by isotope dilution.

† Measured ratios. Analytical errors = 0.007% for ${}^{87}Sr/{}^{86}Sr$ and 0.11% for Pb. ${}^{87}Sr/{}^{86}Sr$ in NBS987 = 0.71018 ± 4 and ${}^{143}Nd/{}^{144}Nd$ in BCR-1 = 0.51262 ± 2 . Pb isotope ratios corrected for -0.1%/AMU mass fractionation, assessed from repeated analysis of NBS 981.

the Karoo¹⁰⁻¹¹, the northern rocks are predominantly high-Ti, whereas those in the south are low-Ti (ref. 10). Our samples, for which fuller descriptions are given elsewhere⁸, are from close to the probable boundary between high- and low-Ti provinces⁹. Most are from a detailed section at 28 °S, in which high-Ti rocks are confined to a 200-m segment (30%) near the base.

All samples have higher $^{87}\text{Sr}/^{86}\text{Sr}$ and lower $^{143}\text{Nd}/^{144}\text{Nd}$ ratios than the bulk Earth (Table 1). HPT rocks show restricted ε_{Sr} (from 4 to 16) and ε_{Nd} (from -2.5 to -4.6), and plot on an extension of the so-called mantle array (Fig. 1). The LPT rocks have slightly lower ε_{Nd} (from -3.7 to -7.9), but higher and more variable ε_{Sr} , plotting in a flat-lying field on the ε_{Nd} - ε_{Sr} diagram similar to that for contemporaneous lavas in Namibia which are also low-Ti (refs 11-13).

Pb isotope data for the Parana define arrays sub-parallel to MORB, but displaced to higher $^{207}\text{Pb}/^{204}\text{Pb}$ and $^{208}\text{Pb}/^{204}\text{Pb}$ (Fig. 2). The slope of the array in the $^{207}\text{Pb}/^{204}\text{Pb}-^{206}\text{Pb}/^{204}\text{Pb}$ diagram corresponds to an apparent age of $\sim 2,000$ Myr, and the array yields a single-stage model μ value of 8.11. The Pb isotopes straddle the first-stage geochron for 120 Myr (the best estimate of eruption age), with the HPT rocks generally having less radiogenic Pb ($^{206}\text{Pb}/^{204}\text{Pb}$ from 17.06 to 17.73) than the LPT (Fig. 2).

Crustal contamination is a possibility during continental magmatism^{14,15}. For the Parana, the present consensus is that the HPT exhibit no clear signs of significant contamination⁶⁻⁹. They evolved in an environment characterized by high Ti, Ta and Sr abundances, and with trace element ratios similar to OIB (ocean island basalts), presumably in the sub-continental mantle. In contrast, the striking changes in isotope ratios with SiO₂ in the LPT are due to open-system differentiation within the crust, and determination of the isotope ratios of uncontaminated LPT remains problematical. Published models emphasize that primitive HPT and LPT magmas had different isotope and trace element ratios, perhaps with $\varepsilon_{\rm Sr} = 30$ -40 (and by implication from Pb-Sr correlations, $^{206}{\rm Pb}/^{204}{\rm Pb} = 18$) in uncontaminated LPT

On the ²⁰⁷Pb/²⁰⁴Pb-²⁰⁶Pb/²⁰⁴Pb diagram the HPT and LPT

data lie on sub-parallel, slightly en echelon, trends (Fig. 2). The LPT field is dominated by progressive contamination, with more radiogenic Pb in the higher SiO₂ rocks. The HPT rocks, which show no evidence of crustal contamination, plot approximately on the extension of the LPT trend at less radiogenic compositions, and define an apparent isochron age of 1,800 ± 400 Myr (MSWD=0.7), with a model μ value of 8.1. This age is very similar to a Pb-Pb age of $2,180 \pm 180 \,\mathrm{Myr}$ (model $\mu = 8.06$) recently reported by Mantovani et al.16 for nine composite samples of basement rocks from beneath the Parana, and the simplest interpretation is that the major crust-forming event in this area took place ~2,200 Myr ago, and that in the following 200-300 Myr mantle material stabilized within the continental lithosphere. Such material probably included mantle depleted after crust extraction, and variably enriched by trapped melts and fluids. It was later remobilized in the Parana event, and from the initial isotope ratios of the HPT rocks, it had average U/Pb=0.08, Sm/Nd=0.27 and Rb/Sr=0.049. Comparison with measured trace element ratios in the HPT indicates that in this model Sm/Nd was on average reduced by 18%, and Rb/Sr increased by 8%, during melting and subsequent fractionation.

Coupled crust-mantle domains have been invoked elsewhere ^{13,17,18}, but the question is whether material from the continental lithosphere subsequently contributes to the composition of the oceanic basalts ^{19,20}.

Hart's recent survey of isotopic data from both oceanic and rift-related continental basalts indicated that, while many scatter around a Pb/Pb array that includes most MORB, there are areas where the basalts are consistently displaced to relatively high $^{207}\text{Pb}/^{204}\text{Pb}$ and $^{208}\text{Pb}/^{204}\text{Pb}^2$ (ref. 2). Termed the Dupal anomaly, one such area is in the South Atlantic (Fig. 3), where rocks with $\Delta7/4>10$ and $\Delta8/4>100$ tend also to have high $^{87}\text{Sr}/^{86}\text{Sr}$, ($\Delta\text{Sr}>45$). The relation between Pb and Sr isotopes is complex, and although the relatively high- $^{207}\text{Pb}/^{204}\text{Pb}$ rocks tend to have higher $^{87}\text{Sr}/^{86}\text{Sr}$, there is no simple correlation between $^{87}\text{Sr}/^{86}\text{Sr}$ and $^{206}\text{Pb}/^{204}\text{Pb}$ along the Pb/Pb arrays.

Variations in 207 Pb/ 204 Pb and 208 Pb/ 204 Pb require long-lived variations in U/Pb and Th/Pb (>10⁹ yr), but they may be

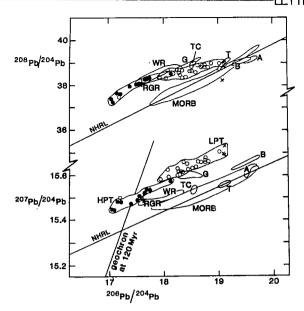


Fig. 2 Pb-isotope diagrams. Parana symbols as in Fig. 1. NHRL, the Northern Hemisphere Reference Line from ref. 3. RGR, Rio Grande Rise; WR, Walvis Ridge; TC, Tristan de Cunha; G, Gough; T, Trinidad; A, Ascension, B, Bouvet^{22,28}

interpreted as evidence either for old, anomalous regions in the sub-lithospheric mantle, or for the introduction of anomalous Pb from lithospheric reservoirs. Hart² preferred the former because recent injection of crustal material would tend to generate Pb/Pb arrays at a high angle to the MORB trend, rather than sub-parallel to it. Weaver et al.21 demonstrated that in the South Atlantic, basalts from the area of the Dupal anomaly are characterized by higher La/Nb, Th/Ta, Th/U, Ba/La and Ba/Nb than basalts from outside the anomaly. Such high ratios are relatively unusual in OIB and were attributed by Weaver et al. to the introduction of a few per cent of pelagic sediment. In contrast, Richardson et al.22 suggested that a similar component in the Walvis Ridge basalts was derived from enriched (metasomatized) material comparable to that proposed for the continental lithosphere.

A feature of the Dupal anomaly in the South Atlantic is that it appears to be restricted to an area between those of continental volcanism associated with continental break-up, Parana and Etendeka (Fig. 3). Moreover, both the HPT and the more primitive LTP rocks have the relatively high ⁸⁷Sr/⁸⁶Sr and ²⁰⁷Pb/²⁰⁴Pb ratios which define the Dupal anomaly in oceanic areas. LTP rocks, however, have minor and trace element features markedly different from OIB (for example, low Ti), which precludes any simple relation between the LPT rocks and oceanic magmatism (see also Fig. 1 inset). By contrast, the HPT rocks have many similarities with OIB.

For all three isotope systems, and for 1/Sr-87Sr/86Sr, it is remarkable that the HPT Parana rocks plot at the end of the Walvis Ridge trend (Figs 1 and 2). In addition, the HPT lie at the high-Ba/Nb end of a striking positive correlation between Ba/Nb and $\Delta 7/4$ for South Atlantic basalts in the Dupal area²³. Thus, HPT rocks were either derived from source regions similar to the enriched component invoked for the Walvis Ridge, or they at least contain more of that component. This component has distinctive low ²⁰⁶Pb/²⁰⁴Pb, similar to that inferred for portions of the sub-continental mantle from studies of lamproites and mantle xenoliths 24,25

The Dupal signature has been identified in ocean islands such as Gough and Tristan da Cunha, on the Walvis Ridge², and in the HPT rocks of the Parana. It has been suggested that it was derived from either enriched lithosphere²², or recycled sediments²¹, but since both probably reflect subduction processes they may prove difficult to distinguish.

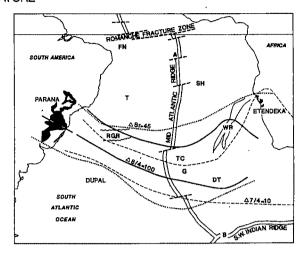


Fig. 3 Sketch map of Dupal anomaly isotope contours in the South Atlantic, after ref. 2. $\Delta 7/4$ and $\Delta 8/4$ are measures of the deviation of individual Pb isotope analyses from the NHRL, (Fig. 2). $\Delta 7/4 = [^{207}\text{Pb}/^{204}\text{Pb}_s - ^{207}\text{Pb}/^{204}\text{Pb}_{\text{NHRL}}]100; \Delta 8/4 \text{ is calculated similarly, but } \Delta \text{Sr} = [^{87}\text{Sr}/^{86}\text{Sr}_s - 0.7]10^4.$

The presence of Dupal features in both oceanic and continental flood basalts, and their apparent restriction in the South Atlantic to areas between the Etendeka and the Parana, implies a close link between continental and oceanic magmatism. One interpretation is that the Dupal geochemistry is due to a deepseated upwelling³ that both initiated continental break-up and was responsible for the Dupal signature. However, that requires that the trace element and isotope characteristics of the Karoo and Parana basalts are from deep-seated sources, rather than from within the continental lithosphere as presently believed^{4,10,11}, and it would conflict with suggestions that the mantle sources of both Karoo and Parana basalts are locally of similar age to the overlying crust 12,12,16. An alternative interpretation is that, at least in the South Atlantic, the Dupal is a relatively shallow-level phenomenon which evolved in the continental lithosphere. In this model, the Dupal signature occurs between the areas of continental volcanism because in those areas lithospheric mantle had been significantly heated and remobilized before continental break-up. Remobilization of such material detaches it from the lithospheric plates and hence enables it to contribute to oceanic volcanism as the continents move apart and the ocean basin develops.

We thank Peter van Calsteren, Andrew Gledhill and Roy Goodwin for help with the isotope analyses, and Peter van Calsteren and Nick Rogers for comments on the manuscript. Borming Jahn and Jon Patchett provided thoughtful reviews. Travel grants for M.M. were provided by FAPESP, the British Council and CNPq, and for this work the laboratories at the Open University and Oxford were supported by NERC.

Received 18 November 1985; accepted 22 April 1986.

- Dupre, B. & Allégre, C. J. Nature 303, 142-146 (1983).
- Hart, S. R. Nature 309, 753-757 (1984).
- Cordani, U. G., Sartori, P. L. & Kawashita, K. Anls Acad. brasil. Cienc. 52, 811-818 (1980).
- Erlank, A. J. et al. Geol. Soc. S. Afr. spec. Publ. 13, 195-245 (1984). Rabinowitz, P. D. & La Breque, J. J. geophys. Res. 84, 5973-6002 (1982).
- Bellieni, G. et al. J. Petrol. 25, 579-618 (1984).
- Atalla, L. T. et al. IAVCEI-IAGC Reykjavik 52, 62 (1982).
- Mantovani, M. S. M. et al. J. Petrol. 26, 187-209 (1985). Bellieni, G. et al. Neues Jahrbuch. Miner. Abh. 150, 273-306 (1984).
- Cox, K. G. in Continental Basalts and Mantle Xenoliths (eds Hawkesworth, C. J. & Norry, M. J.) 139-157 (Shiva, Orpington 1983).

- Duncan, A. R., Erlank, A. J., March, J. S. & Cox, K. G. Geol. Soc. S. Afr. spec. Publ. (1984).
 Hawkesworth, C. J. et al. Geol. Soc. S. Afr. spec. Publ. 13, 341-354 (1984).
 Hawkesworth, C. J. et al. in Continental Basalts and Mantle Xeonoliths (eds Hawkesworth,
- C. J. & Norry, M. J.) 111-138 (Shiva, Orpington, 1983).
 14. Patchett, P. J. Nature 283, 559-561 (1980).
- Huppert, H. E. & Sparks, R. S. J. Earth planet. Sci. Lett. 74, 371-386 (1985).
 Mantovani, M. S. M., Hawkesworth, C. J., Taylor, P. N. & Palacz, Z. Abstr. Vol. IAVCEI. N.Z. 181 (1986).
- 17. Leeman, W. P. Lunar planet Sci. XIII, 431-432 (1982).

- 18. Cohen, R. S., O'Nions, R. K. & Dawson, J. B. Earth planet. Sci. Lett. 68, 209-220 (1984).
- Hofmann, A. W. & White, W. M. Earth planet. Sci. Lett. 57, 421-436 (1982).
 McKenzie, D. P. & O'Nions, R. K. Nature 301, 229-231 (1983).
 Weaver, B. L., Wood, D. A., Tarney, J. & Joron, J. L. J. geol. Soc. Lond. (in the press)
- Richardson, S. H., Erlank, A. J., Duncan, A. R. & Reid, D. L. Earth planet Sci. Lett. 59, 317-342 (1982).
- Hawkesworth, C. J., van Calsteren, P., Rogers, N. W. & Menzies, M. A. in Mantle Metasomatism (eds Menzies, M. A. & Hawkesworth, C. J.) (Academic, in the press).
- Kramers, J. D. Earth planet. Sci. Lett. 42, 58-70 (1979).
 Le Roex, A. P. et al. J. Petrol. 24, 267-318 (1984).
- 25. Erlank, A. J. et al. in Mantle Metasomatism (eds Menzies, M. A. & Hawkesworth, C. J.) (Academic, in the press).

 26. Le Roex, A. P. et al. J. Petrol. 24, 267-318 (1984).
- 27. O'Nions, R. K., Hamilton, P. J. & Evensen, N. M. Earth planet. Sci. Lett. 34, 13-22 (1977). 28. Sun, S. S. Phil. Trans. R. Soc. A297, 409-445 (1980).

Acidity of Scottish rainfall influenced by climatic change

T. D. Davies*, P. M. Kelly†, P. Brimblecombe*, G. Farmer† & R. J. Barthelmie†

* School of Environmental Sciences, and † Climatic Research Unit, School of Environmental Sciences, University of East Anglia, Norwich NR47TJ, UK

Although there are clear links between acidic deposition and synoptic meteorology¹, the effects of climatic change have been largely neglected. It is demonstrated here that long-term variations in the atmospheric circulation and associated changes in trajectory characteristics on timescales of years and longer can affect deposition levels within the United Kingdom, masking the effects of changing emissions. This study provides empirical support for the suggestion that climatic change may need to be considered in the assessment of emission control strategies2.

The potential importance of climatic change in influencing precipitation acidity has been acknowledged3-6 but not assessed, although significant changes in climate and the atmospheric circulation have occurred in the European area over the past 100 yr (refs 7-9). As the frequency and character of air trajectories between regions varies, the relative importance of different source regions for deposition in a particular area will alter. Moreover, other physical and chemical processes in the atmosphere which influence deposition may also be affected. The spatial pattern of deposition over Europe as a whole could alter and climatic change may explain the apparent disagreement between recent trends in European pollutant emissions and precipitation composition 10,11.

Here, we consider the link between recent fluctuations in precipitation acidity (H+ concentration) at Eskdalemuir in Scotland (Fig. 1) and variations in the frequency of various atmospheric circulation types over the United Kingdom extracted from the Lamb Catalogue of Daily Weather Types¹². This catalogue provides a succinct characterization of the synoptic circulation and extends back to 1861 enabling the study of long-term trends. On an annual basis, three Lamb Weather Types (LWTs) account for much of the variance in the circulation over the United Kingdom: Westerly (W); Anticyclonic (A); and Cyclonic (C)8. A-types produce little rainfall although they may be of ultimate importance for acidic deposition¹. C- and W-types together produce ~50% of the precipitation in the UK; no other type accounts for more than ~10%.

We have undertaken trajectory analyses for the C- and Wtypes to determine their significance for acidic deposition at Eskdalemuir. The synoptic situation characterized by the Ctype¹² is such that, when there is frontal precipitation over Scotland, back-trajectories often originate over England or adjacent continental Europe (work in preparation). This is likely to lead to relatively acidic precipitation over Scotland 13,14. W-types. on the other hand, are more commonly associated with maritime trajectories and less-polluted rainfall in Scotland¹³. Variation in



Fig. 1 Location of precipitation-collecting station used in this study: E, Eskdalemuir. The shaded areas represent major pollution sources, H+ concentration data available for this station include: a, bulk-monthly, 1958-78 (Meteorological Office); b, daily, 1973-77 (Warren Spring Laboratory), c, daily, November 1977 to September 1982 (EMEP), same collector as b. Further details are available elsewhere 14,20

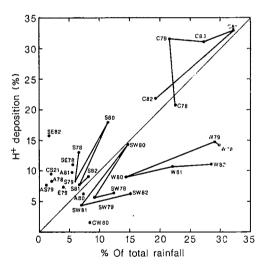


Fig. 2 Relationship between Lamb Weather Type, percentage of total H+ deposition and precipitation amount at Eskdalemuir (annual values derived from EMEP daily data). Only LWTs contributing >7.5% of annual H⁺ deposition and >7.5% of annual precipitation have been included. For clarity, the points for the major LWT contributors have been joined. The acid content of annual precipitation is dominated by C-type and W-type events. C-type events account for about 30% of the total H⁺deposition and around 25% of the total rainfall; the respective values for W-type events are ~12% and 25%. Although other LWTs make significant contributions to the concentration or dilution of precipitation acidity in certain years (S-type and SE-type events in particular), the acid content of annual precipitation is dominated by C- and W-type associated rainfall. C-type events make the major contribution of all LWTs to concentrating H+ levels (a large average departure in the +y direction from the equality line combined with a substantial contribution to the total rainfall) whereas W-type rainfall makes the major contribution to diluting H+ levels (greatest departure in the -y direction from the equality line along with a large contribution to the annual rainfall). C, Cyclonic; CS, cyclonic-southerly; CW, cyclonic-westerly; W, westerly; A, anticyclonic; S, southerly; SE, southeasterly; SW, southwesterly; E, easterly.

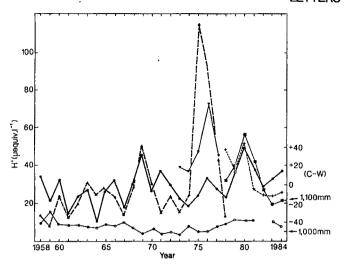


Fig. 3 Annual values of the C-W index, rainfall total for Eskdalemuir and volume-weighted H⁺ concentration data for Eskdalemuir (for sources, see Fig. 1). The average H⁺ concentration for seven collectors distributed through Scotland is also shown (data provided by J. N. Cape). The reliability of the monthly bulk collector data should be viewed with extreme caution²⁰. Unfortunately, they represent the only long-term records of precipitation acidity for the UK. Bottom curve, annual rainfall (mm); ▲ and dashed line, Eskdalemuir monthly H⁺; ▼ and light solid line, Eskdalemuir daily H⁺; ■ EMEP daily H⁺; ● and heavy solid line, C-W; + and dotted line, Scotland regional H⁺.

wind speed between these types may also affect precipitation acidity¹³, as may other characteristics of the weather types. On the basis of our analysis of trajectories associated with the two LWTs, we conclude that these indicators of the general state of the local circulation can be used as a surrogate for case-related trajectory analysis; an expedient which allows us to explore the historical dimension of acidic deposition.

Analysis of the daily EMEP precipitation composition data¹⁴ for Eskdalemuir for the period January 1978 to October 1982 shows the prevalence of C-types in acidic episodes¹. These episodes, periods of high deposition on the day-to-day timescale, were first ranked according to order of magnitude. Then, the LWTs associated with the largest episodes each year (in total accounting for one-third of the total H⁺ deposition in that year) were identified. The resulting frequency of C-types (~10 events per year) was four to five times that of the nearest contenders, the S-type (Southerly) and the W-type.

In determining the significance of the individual weather types for total H⁺ deposition, precipitation amount is also important. Figure 2 illustrates the relationship between H⁺ deposition, precipitation amount and LWT. C-type events account for between 20 and 25% of total H⁺ deposition; W-types for 10-15%. C-type rainfall is high and relatively acid; W-type rainfall is similar in amount but lower in acidity. A simple index of the influence of atmospheric circulation variation on H⁺ deposition can, therefore, be devised by subtracting the number of W-type days from the number of C-type days (the C-W index). This should be related to volume-weighted H⁺ concentration in precipitation. More complex indices which included other LWTs and weighting to account for relative importance were devised but did not differ substantially in terms of information content from the C-W index.

Figure 3 shows the annual C-W index for the period 1958-84 during which rainfall H⁺ concentration observations for Eskdalemuir are available. Despite problems with the reliability of the earlier acidity data, the overall relationship between these variables is clear, confirming that shifts in the atmospheric circulation do play a part in the determination of deposition

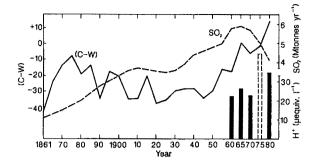


Fig. 4 Five-year means for: the C-W index (1861-64, 1865-69, and so on); SO_2 emissions estimated from published data²² (the data must be considered notional before 1950); and 5-yr volume-weighted H⁺ concentrations at Eskdalemuir using the Meteorological Office bulk monthly data and the EMEP daily data. In the latter case, the pentade 1975-79 is represented differently to highlight: the anomalous nature of the 1975-76 period; and the use of two different data sources during this interval.

levels in the Eskdalemuir region.

The relationship breaks down in certain years: for example, 1971 and, most notably, 1975 and 1976. The period of greatest acidity during the latter years, June 1975 to July 1976, was coincident with a severe drought over England and Wales¹⁵⁻¹⁷. Frontal depressions were steered further north over the UK than usual and, although there was a drought in the South, Scotland received between 70 and 110% of its 'normal' rainfall. Synoptic patterns which are recognized to produce acidic episodes frequently affected Scotland. Ozone concentrations were also high over the UK during this period¹⁸ and this may have influenced sulphate production¹⁹ and led to greater rainfall acidity, further complicating the situation.

The C-type count for the 1975-76 period was low and, in this case, the simple C-W index was not a good measure of the atmospheric factors affecting production, transport and deposition. A more sophisticated index may be needed. Nevertheless, the correlation between the annual C-W index and the H⁺ concentration data for the period 1958-84 is statistically significant. A correlation analysis yields a coefficient of 0.38, significant at the 5% level (the coefficient is 0.59 if the years of 1975 and 1976 are excluded). The relationship between these variables cannot be stationary in time because of changes in other important factors such as varying emissions. A more appropriate measure of association may, therefore, be a sign test on the year-to-year fluctuations. In this case, the test statistic is significant at the 0.1% level (data were included for all years during the period 1958-84).

Figure 4 shows the long-term history of the C-W index. Allowing for the anomaly in the mid-1970s, the 5-yr volume-weighted H⁺ concentrations at Eskdalemuir show a closer match with this record than with that of UK emissions of SO₂. (Sulphate has been the anion best correlated with precipitation acidity in Scotland²⁰.) Besides the strong relationship on the year-to-year timescale, there may also be a link on longer timescales. Unfortunately, the H⁺ record is too short to test this point statistically

This association between climatic change and precipitation acidity in the UK shows that the climate dimension must be taken into account in any consideration of the acid rain issue. Our index could be criticised on the grounds of oversimplicity and further work is needed to determine whether other indicators are more appropriate. Nevertheless, this analysis demonstrates that, as climate changes, deposition levels can vary even in the absence of alterations in emissions. As well as compounding the problem of assessing emission control strategies², this complicates the determination of the effects of past emissions. Climatic change may produce biological damage in its own right

or in conjunction with pollutants²¹, and it may also exert an indirect influence via its contribution to acidic deposition variability.

This work is funded by the UK Department of Environment and the Commission of the European Community. We thank Dr J. N. Cape (Institute of Terrestrial Ecology), Mr A. Martin (Central Electricity Generating Board), Dr J. G. Irwin (Warren Spring Laboratory) and Dr A F. Tuck (Meteorological Office) for helpful advice and for permission to use their data. We also thank Dr F. B. Smith (Meteorological Office) and Dr B. E. A. Fisher (CEGB) for their valuable comments. The Norwegian Institute for Air Research was particularly helpful with the provision of data as were the Central Electricity Research Laboratories.

Received 15 January; accepted 2 May 1986.

- 1 Smith F. R. & Hunt R. D. Atmos Ennir 12, 461-477 (1978).
- 2. Streets, D. G., Lesht, B. M., Shannon, J. D. & Veselka, T. D. Envir. Sci. Technol. 19, 887-893 (1985).
- Munn, R. E. & Rodhe, H. Tellus 23, 1-13 (1971).
- Fisher, B. E. A. in Sulphur in the Environment (ed. Nriagu, J. O.) 243-295 (Wiley, New York, 1978).
- Ottar, B. Almos. Envir. 12, 445-454 (1978).
 Rodhe, H. & Granat, L. Almos. Envir. 18, 2627-2640 (1984).
- Kouler, H. & Ginald, L. Minos. Linux, 184, 6027-2040 (1994).
 Lamb, H. H. Climate: Present, Past and Future Vol. 2 (Methuen, London, 1977).
 Jones, P. D. & Kelly, P. M. J. Climat. 2, 147-157 (1982).
- Hess, P. & Brezowsky, H. Ber. Deut. Hett. 15, No. 113 (1969).
- Cape, J. N. et al. Atmos. Envir. 18, 1921-1932 (1984).
 Clarke, P. A., Fisher, B. E. A. & Scriven, R. A. Atmos. Envir. (in the press).
- Lamb, H. H. Geophysical Memoir No. 116 (HMSO, London, 1972).
 Fowler, D. & Cape, J. N. Atmos. Envir. 18, 1859-1866 (1984).
- Schaug, J., Dovland, H. & Skjelmoen, J. E. ECE Co-operative Programme for Monitoring and Evaluation of the Long-range Transmission of Air Pollutants in Europe, Data Reports. October 1977-September 1982 (Chemical Co-ordinating Centre, Norwegian Institute for
- Air Research, Oslo, various years).

 15. Murray, R. Met. Mag. 106, 129-145 (1977)
- Ratcliffe, R. A. S. Met. Mag. 106, 145-154 (1977).
 Doornkamp, J. C., Gregory, K. J. & Burn, A. S. (eds) Atlas of Drought in Britain 1975-76 (Institute of British Geographers, London, 1980).

 18. Simpson, D. Report LR 536 (AP)M (Warren Spring Laboratory, Stevenage, 1985).

 19. Martin, A. & Barber, F. R. Atmos. Envir. 19, 1091-1102 (1985).

 20. UK Review Group on Acid Rain, Acid Deposition in the UK (Warren Spring Laboratory,

- Stevenage, 1983).
 21. Binns, W. O. & Redfern, D. B. Forrestry Commission Research and Development Pap. 131
- (Forestry Commission, Edinburgh, 1983). 22. Irwin, J. G. *Envir. Hith* 93, 212-220 (1985).

Simultaneous outflow of fresh water and inflow of sea water in a coastal spring

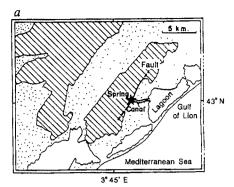
Claude Drogue & Pascal Bidaux

Laboratoire d'Hydrogéologie, Université des Sciences et Techniques, Place E. Bataillon, 34060 Montpellier Cedex, France

The ability of sea water to flow into coastal or submarine cavities is surprising, in view of the fact that sea level is, for water, a level of minimum gravitational potential where it can perform no work. To achieve a lower potential requires energy, the provision of which is an example of a completely original aspect of the interaction between subterranean hydrodynamics and marine hydraulics. We have studied a spectacular example of the simultaneous outflow of fresh water and inflow of salt water at a karstic spring running into a salt-water lagoon on the French Mediterranean coast, and we suggest here a hypothesis to account for the surprising doublelayered, two-directional flow observed.

The flow of sea water into cavities is known to occur in, among other places, the Bahamas, Florida and Greece, where limestone which is in contact with the sea displays considerable karst development and is very permeable. There appear to be various causes-proved or supposed-for the inflow of sea water¹⁻⁵; the examples described in the literature are continuous or periodic but consist of either inflow of sea water or outflow of fresh water. The two types of flow never occur simultaneously.

The work described here reveals the possibility of a more complex coastal phenomenon in which two flows-outflow and



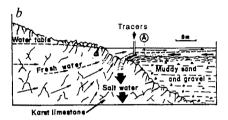


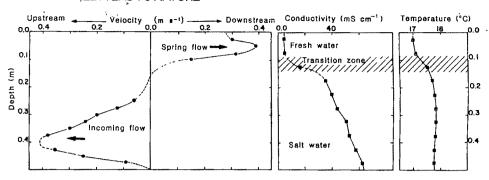
Fig. 1 a, Map showing the location of the Source de la Roubine. The carbonate massif has an area of 55 km² and consists of Mesozoic limestone and dolomite. It is only part of the aquifer feeding the spring; other massifs located further north also contribute to the supply. The deposits of Quaternary and Cenozoic clay, loam and sand in the plain are several hundred metres thick and cover Mesozoic limestone which extends beneath the sea. The level of the Mediterranean has undergone a number of fluctuations since the end of the Neogene, and during some periods was lower than it is today¹⁰⁻¹³. These regressions caused deep penetration by rainfall infiltrating into the carbonate massifs which had emerged, accompanied by intense internal corrosion and the formation of cavities by dissolution (karst topography). Thus, the aquiferous structure which formed in the depths of the carbonate mass is mainly below sea level today, and the Source de la Roubine is a spring of very recent formation. Movement of water starts in the form of a rising current in the deep palaeokarst. b, Cross-section of the spring showing the double flow (vertical exaggeration 5:1). Tracers were injected into the stream of salt water through a pipe, as shown in the drawing. Measurements of velocity, conductivity and temperature were made along the vertical marked 'A'.

inflow—are concomitant and superposed. The study was carried out at a spring on the Mediterranean coast (Source de la Roubine, Fig. 1a), which is at the edge of an extremely karstic carbonate massif and quaternary clay-marl deposits several hundred metres thick in the coastal plain. The spring and flow run along a 2.5-km channel into a lagoon (sea water). The discharge can attain a value of 6 m³ s⁻¹, and is 0.1-0.2 m³ s⁻¹ at normal low-water functioning of the spring, that is, when the spring is flowing. Inflow of salt water occurs only during such times of low discharge⁶.

In the absence of rain, rises of several tens of centimetres are observed in the water level near the spring and last from a few hours to 4-5 days. While the water level changes in this way, a current of salt water runs along the bottom of the channel below the fresh water and in the opposite direction, enters one or two of the springs and disappears into the aquifer. At the same time, water continues to run out of the other springs and flows towards the lagoon on top of the salt water (Fig. 1b).

The interface between the two flows can be clearly seen in vertical profiles of electrical conductivity and temperature. (Fig. 2). The conductivity of the water from the spring is 4.2-4.3 mS cm⁻¹ (at 25 °C), whereas that of the lagoon water varies from 48 to 56 mS cm⁻¹ according to the season. Although for reasons of convenience the spring water is referred to as 'fresh', the mean electrical conductivity of spring water in limestone soil far from the coast is 0.6 mS cm⁻¹ with a Cl⁻ ion content of

Fig. 2 Observations of velocity, conductivity and temperature, showing the superposition of the two streams. Maximum velocities of the two currents running in opposite directions are almost the same. The discharge of the fresh-water stream is 0.18 m³ s⁻¹; that of the salt-water stream beneath is 0.20 m³ s⁻¹. The superposition of fresh water is also shown by the observations of conductivity and temperature. The lagoon water is warmer than the spring water.



 $15-35 \text{ mg l}^{-1}$ (the water in the lagoon has a Cl⁻ content of $18,000 \text{ mg l}^{-1}$).

The temperature of the spring is relatively stable, at 17.3 ± 0.5 °C. In contrast, the lagoon water is subject to wide temperature variations: from 5-10 °C in winter to 25-28 °C in summer. The monitoring of inflow with time revealed some remarkable features. The beginning of the double-flow phenomenon has a sudden effect on conductivity values: this is proof of the poor miscibility of fresh and salt water. The temperature, however, varies progressively even before the appearance of salt water. This is caused by the fact that the advance of the salt water in the bottom of the channel pushes the fresh spring water already affected by the outside temperature back towards the spring.

With regard to the hydraulic mechanism, it would appear that the variations in the water level at the spring are caused by variations in the level of the lagoon on the west bank. The measurements (Fig. 3) show that they are not caused by tide;

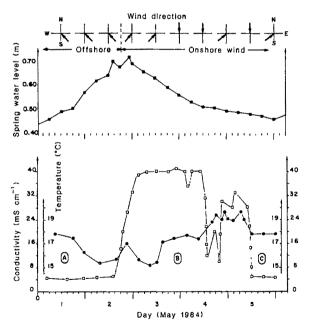


Fig. 3 Example of the time-evolution of conductivity (□) and temperature (●) in the spring into which the salt water flows, compared with water levels in the spring (■) and with wind direction (arrows). A, No inflow of salt water, but start of return flow is indicated by a fall in temperature. This is fresh water in the channel affected by the outside temperature. B, Inflow has started suddenly and is revealed by stable conductivity; however, temperatures are irregular. This is the effect of the thermal heterogeneity of the water in the lagoon. The lowest temperature of the water flowing in is 14.9 °C; the highest is 19.8 °C (the temperature of the spring water is 17.8 °C). C, Inflow ceases suddenly. The spring flows normally once more. Inflow occurs when there is a rise in water level of 0.35 m caused by easterly winds.

however, it was observed that the variations are associated with certain wind directions. The spring is on the west bank; easterly winds cause the water level to rise on this side and fall on the east bank. The rapid rise in level on the western side thus sets up a hydraulic gradient in the salt water, directed towards the spring. Progress of salt water towards the spring is encouraged by the low hydraulic gradient of the fresh water in the channel ($\sim 0.01\%$) and by the near-zero slope of the bottom of the channel.

The superposition of the two flows and the low apparent miscilibity of the two streams are caused by the differences in density (spring water: 0.9994 kg dm⁻³ at 25 °C; sea water (in the lagoon): 1.0258 kg dm⁻³).

Finally, it might be thought that the salt water which runs into the aquifer reappears in spring flow after dilution and could be the cause of the salinity of the spring. Tracers were injected into the saline inflow in order to test this hypothesis, and no trace of the dye was observed in fresh water to the spring during an observation period which lasted several months. It would thus appear that the two flows are probably separate in the aquifer itself.

It is likely that part of the salt water mixes with water from the aquifer, but the origin of most of the salinity of the spring water is undoubtedly contamination of deep ground water by the penetration of sea water into the karst⁷⁻⁹ (salt-water encroachment; Fig. 4). When lagoon water has flowed in, it probably runs by gravity to the interface of the salt-water encroachment. It may then be taken by groundwater flow to springs under the lagoon or under the sea.

In conclusion, we note that geological structures which could

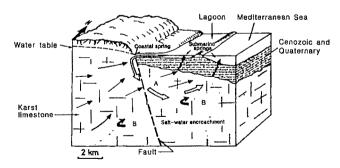


Fig. 4 Diagrammatic representation of the karstic aquifer and the organization of flows. Fine arrows, fresh water; bold and shaded arrows, salt water. The flow of salt water that runs into the spring must descend by gravity through the aquifer (A) to the deep salt-water encroachment (B). This flow is then carried to submarine springs. There is thus double contamination of underground water by sea water: from below in the aquifer and from above. Note that the large-scale flow of water into the spring carries large quantities of organic matter into the underground zone; this could form the basis for a totally unknown biotope. (For reasons of simplicity, the arrows in A do not show any dispersion that may take place in the aquifer.)

enable this phenomenon to occur are very common on the limestone coasts around the Mediterranean. Equivalent structures also exist on ocean coasts: we have observed such features in Miocene limestone in south-east Java (Gunung Sowu) and in southern Portugal (Algarve).

Received 27 January: accepted 28 April 1986.

- Stringfield, V. T. & Legrand, H. E. J. Hydrol. 14, 139-157 (1974).
 Stringfield, V. T. & Legrand, H. E. J. Hydrol. 9, 387-404 (1969).
 Maurin, V. & Zoelt, J. Int. Ass. Sci. Hydrol. Bull. 74, 423-438 (1967).
 Fuller, M. L. Geol. Soc. Am. Bull. 18, 221-232 (1906).
- Geze, B. La Géographie 69, 193-208 (1938).
 Derozier, Ph. thesis, Univ. Montpellier (1984)
- Kohout, F. A. J. geophys. Res. 65, 2133-2141 (1960).
 Henri, H. R. Int. Ass. Sci. Hydrol. Bull. 52, 478-487 (1960).
- 9. Cooper, H. H., Kohout, F. A., Henri, H. R. & Glover, R. E. U.S. Geol. Surv. Wat. Supply Pap. No. 1613-C (1964). 10. Hsu, K. J. et al. Init. Rep. DSDP 42, 1053-1078 (1978)

- Steckler, M. S. & Watts, A. B. Nature 287, 425-429 (1980).
 Aloisi, J. C., Monaco, A. & Thommeret, J. Rev. Géogr. phys. Geol. dynam. 2, 13-22 (1975).
- 13. Monaco, A. & Thommeret, J. C.r. hebd. Séanc. Sci., Paris. D274, 2280-2283 (1972).

Sign language aphasia during left-hemisphere Amytal injection

Antonio Damasio*, Ursula Bellugi†‡, Hanna Damasio*, Howard Poizner† & John Van Gilder*

- * Department of Neurobiology, University of Iowa College of Medicine, Iowa City, Iowa 52242, USA
- † Laboratory for Language and Cognitive Studies, Salk Institute for Biological Studies, 10010 North Torrey Pines Road, La Jolla, California 92037, USA

Although it has been established that the left cerebral hemisphere subserves spoken language, the nature of brain organization for sign language remains relatively unexplored. The issue is especially important because sign language displays the complex linguistic structure of spoken languages, but conveys it through manipulation of visuo-spatial relations1, thereby exhibiting properties for which the hemispheres of hearing individuals show opposing specializations. We had the unique opportunity to study a hearing signer proficient in American sign language (ASL), during the left intracarotid injection of a barbiturate (the Wada test), and before and after a right temporal lobectomy. The subject was a strong righthander. Neuropsychological and anatomical asymmetries suggested left cerebral dominance for auditory-based language. Emission tomography revealed lateralized activity of left Broca's and Wernicke's regions for spoken language. The Wada test, during which all left language areas were rendered inoperative, caused a marked aphasia in both English and ASL. After partial ablation of the right temporal lobe, the abilities to sign and understand signing were unchanged. These data add further support to the notion that anatomical structures of the left cerebral hemisphere subserve language in a visuo-spatial as well as an auditory mode.

Recent research has shown that ASL has developed as a fully autonomous language. It has complex organizational properties shared by the spoken languages of the world, but it also has grammatical devices not derived from spoken language; thus, ASL is a separate language, not a manual rendering of English. At all structural levels, the surface forms of a signed language are deeply influenced by the modality in which it develops. This is displayed most distinctively in the pervasive use of spatial contrasts and spatial manipulations to express syntactic function. At the syntactic level, for example, nouns are associated with arbitrary points in signing space, pronoun signs are directed toward those points for anaphoric reference, and verb signs move between them in specifying grammatical relations². Thus a grammatical function served in many spoken languages by case marking or by linear ordering of words is fulfilled in ASL by essentially spatial mechanisms. Since sign languages utilize visuo-spatial channels, several investigators have assumed that structures in the right cerebral hemisphere are likely to have a major role in the reception and production of these languages. Indeed, the issue is quite controversial and many studies do suggest a special role for the right hemisphere in mediating signs³.

Our study was performed in a 27-yr-old hearing woman, a native English speaker who learned ASL at an age of 18 yr. She is a college graduate with a MS degree in rehabilitation of the deaf, and works at a community agency as interpreter and counsellor for deaf people. She uses ASL daily in her work and is a skilled signer. She had her first seizure, of the partial complex type, at age 13 yr, but had never had generalized tonic-clonic seizures. The seizures did not hamper her intellectual or emotional development, but in recent years the episodes had become more frequent and refractory to drug therapy. Because they were interfering with her professional activity she sought surgical treatment. She is a right-hander (in Geschwind's version of Oldfield's laterality index, she scored +90), and so are both her parents. Comprehensive neuropsychological evaluation failed to reveal any abnormality of language, visuo-spatial or other higher cognitive abilities. Her full-scale intelligence quotient (Wechsler Adult Intelligence Scale-Revised) was 105, with no discrepancy between the verbal and performance scales. Her dichotic listening performance for words showed a right-ear advantage. Computer tomographic scan and cerebral angiography revealed brain asymmetries suggestive of left language dominance (left>right occipital width on computer tomography; left sylvian angle = 105°; right sylvian angle = 130°, in angiography). Recording from depth electrodes showed a right anterior temporal focus. There was no mirror focus.

Single photon emission tomography (SPET) using xenon-133 as radiotracer revealed a normal resting pattern⁴. A second SPET procedure was performed during a language activation task, a verbal rhyme detection paradigm modified from Knopman⁵. The subject compared words presented through earphones with a memorized target word and was asked to respond with left foot flexion to those words that rhymed with the memorized target. SPET revealed increased signal in the left Broca and Wernicke regions (see Fig. 1), indicating that processing of English was lateralized to the left.

Injection of a barbiturate (sodium amobarbital; Amytal) was made into the left carotid system (due to a persistent right trigeminal artery, no injection was possible in the right side). The procedure was videotaped and both English and ASL examiners were in attendance. The patient developed a right hemiplegia and aphasia in both English and ASL. During the recovery period, correct English responses appeared at 4 min, preceding those in ASL by $1\frac{1}{2}$ min, a substantial time interval in this procedure. The patient's signing was markedly impaired, including sign paraphasias, perseverations, neologisms and grammatical errors. Interestingly, since she was hearing and could sign and speak at the same time, we could compare her responses in two languages simultaneously. This revealed a frequent mismatch between word and sign, with English mostly correct but ASL often incorrect in both meaning and form (see Fig. 2).

The extent of the surgical resection was documented by postoperative advanced magnetic resonance imaging (see Fig. 3). It encompassed the right hippocampus, parahippocampal gyrus, amygdala and both polar and anterolateral right temporal neocortex. The primary and secondary auditory association cortices contained in the middle and posterior first temporal gyrus were spared, as was area 37.

Neuropsychological re-evaluation at 3 and 12 months comprised all the tests administered pre-operatively, to assess attention, perception, language, memory and reasoning. The scores were virtually unchanged, including those of the Boston Diagnostic Aphasia Examination⁶, dichotic listening, recognition and recall of previously learned visual stimuli, geographical orienta-

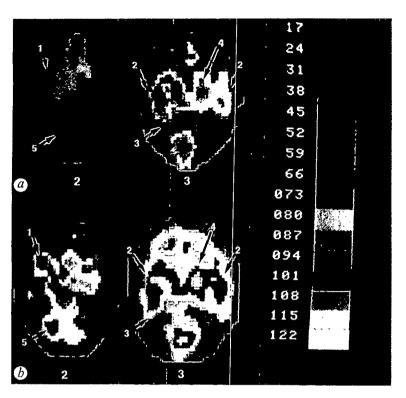
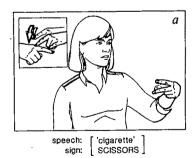


Fig. 1 Cuts 2 and 3 of a six-slice Tomomatic SPET study at rest (a) and during a verbal rhyme detection task (b). During activation there is an increase of radiosignal in Broca's region, that is, in the left frontal fields 44 and 45 indicated by arrow 1, and a bilateral increase of signal in auditory cortices indicated by arrow 2. In the left hemisphere the signal increase extends into Wernicke's area, that is, the posterior sector of area 22 (arrow 3). During activation there is also an increase in the right basal ganglia (arrow 4) and left cerebellar hemisphere (arrow 5), related to the motor activity of the left foot required to signal appropriate rhyme detection.

tion, immediate visual memory (Benton's visual retention test), and copy and 15-min recall of a visual pattern (Rey-Osterrieth figure). The learning of new visuo-spatial and visual object memories was not assessed. There were no detectable neurological abnormalities. Most importantly, however, analysis of videotaped spontaneous signing and structured signing interviews confirmed the patient's own impression that her ability to sign and understand signing had not been compromised at all. Intensive analysis of her videotaped signing showed, for example, that her noun to pronoun ratio was in the normal range, her use of ASL morphological structures was unchanged, and there were no errors in her use of the spatially organized syntax of ASL before or after the right temporal lobectomy.

The impairment of ASL during the Wada test is associated with pharmacologically induced dysfunction in the territory of

the left middle and anterior cerebral arteries⁷. The structures clearly affected during the test included the left Broca and Wernicke areas, the left dorsolateral parietal lobe (especially the inferior parietal lobule), the middle and lower rolandic cortices, the left basal ganglia and possibly territories of both the lateral temporal lobe and the anterolateral frontal lobe⁸. The cerebral territories supplied by the left posterior cerebral artery (namely, the mesial and part of the lateral occipital lobe, and the mesial occipito-temporal and occipito-parietal regions) were probably unaffected. This indicates that a fully operational right hemisphere and partially operational, interconnected, left visual cortices could not prevent the impairment in sign language. Thus ASL may be especially dependent on the normal function of left hemisphere cortices, as is the case with auditory-based languages.



b a second secon

speech: ['orange' sign: [Neologism] ORANGE/SCISSORS blend



Speech: ['cat'].
Sign: [Neologism].
different ORANGE/SCISSORS blend

Fig. 2 Three errors produced by the patient during left Wada injection. In identifying an object presented, the patient produced an English word and an ASL sign simultaneously, and the two differed. In a, the patient correctly said 'cigarette' but simultaneously signed 'scissors' to a presented cigarette. In b, the patient correctly said 'orange' to a presented orange, but signed a form that was like a blend of two signs in ASL—the handshape of 'orange' and the place and movement of 'scissors'. In c, the patient correctly said 'cat' to a picture of a cat, but signed another blend, this time with the handshape of 'scissors', the place of articulation of 'orange' and the movement of 'scissors'. The combinations of parameters from different signs produced nonsense forms that were well-formed in ASL but were meaningless. It is of interest that during recovery from the left Wada injection, the patient frequently responded in speech and sign simultaneously-a unique possibility for languages in different modalities—with a mismatch between the two languages and the sign more often in error. Inserts in the upper left-hand corner of the

illustrations indicate the correct ASL signs.

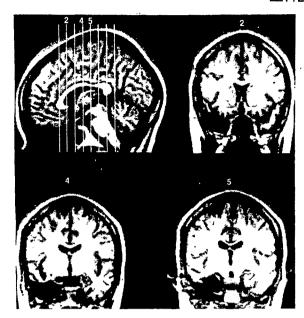


Fig. 3 Magnetic resonance images obtained after surgery with an inversion recovery technique; magnetic field, 0.5 T. Resolution was 2 mm in the plane of cut. The top left-hand image is a midsagital cut showing the mesial aspect of one hemisphere. The vertical lines represent the level and incidence of the coronal cuts. Cuts 2, 4 and 5 are reproduced depicting the area of right temporal lobe ablation. Hippocampus, parahippocampal gyrus, fourth, third and second temporal gyri are missing. The first (superior) temporal gyrus is intact.

A major point of interest concerns the rate of recovery of the languages. During the final period of dysfunction, after the use of English had returned and the paralysis subsided, the patient still made errors in ASL. Considering that the recovery from barbiturate action must have taken place gradually and have occurred last in the outer border of the middle cerebral artery territory, that is, in a C-shaped watershed region containing visual and somatosensory cortices that we believe are especially crucial for ASL processing, it is possible that the ASL delay reflected the continued dysfunction of those cortices at a time when the core territories of the middle cerebral artery (which contain the classic speech cortices) had already returned to normal. An alternative explanation for this lag would need to invoke the fact that ASL was a second language and propose that its neural representation might thus be more vulnerable, a rather unsatisfactory hypothesis. In fact, one might have expected a second language, and especially a visuo-spatial language, to have been primarily represented in the non-English dominant hemisphere, in which case the left Wada test would not have interfered with ASL operations at all.

The lack of post-operative signing defects suggests that right anterior temporal structures medially and laterally do not have a significant role in signing or in comprehension of previously learned signs. It is possible that these areas are pertinent to the learning of ASL but certainly not to the production of ASL once learned, that is, the right hippocampal/parahippocampal complex and the polar and anterolateral temporal cortices were involved in neither the generation nor the detection of the complex visuo-spatial and motor patterns of ASL that had been learned pre-operatively. It might be argued that this patient's seizure would have so disorganized the structure of the right hemisphere that any ability normally dependent on it would have been transferred to the healthy left hemisphere. This possibility is unlikely considering: (1) the mild and circumscribed neuropathological changes encountered in the block of ablated tissue; (2) the lack of a mirror focus in the opposite hemisphere; (3) the lack of any pre-operative symptom or sign suggestive of right hemisphere dysfunction; (4) the late onset of the seizures; and (5) the fact that they never interfered with the acquisition of skills or the development of a normal personality.

Our findings provide the rare opportunity of relating the processing of ASL to a circumscribed set of brain structures in the left hemisphere, in a subject who has unequivocal left-sided functional dominance for English, and who has anatomical brain asymmetries also favouring the left hemisphere. Furthermore, the findings suggest that the right hippocampal system is not involved in active processing of ASL. Our results should be seen in the perspective of other converging evidence on the respective roles of left and right hemisphere in ASL⁹⁻¹¹. Studies of unilateral lesions in deaf signers show that lesions to the left hemisphere cause sign aphasia, affecting different structural levels of the language, while lesions to the right hemisphere produce marked spatial deficits but leave expressive language intact12. Thus, the underlying specialization of the left hemisphere for language does not seem to rest on speech or sound. nor on the form of the signal, but rather on the linguistic function

We thank Dr Paul Eslinger for performing the neuropsychological assessment, Drs Karim Rezai and Val Dunn for their collaboration in the SPET and magnetic resonance imaging studies, Mr Ozzie Diaz-Duque and Ms Charissa Lansing for their assistance with sign language procedures during the Wada test and David Corina, Maureen O'Grady, Lucinda O'Grady and Diane Lillo-Martin for their help with the sign language analysis. This research was supported in part by NINCDS grant PO NS 19632-02 (to A.D. and H.D.), NSF grant BNS 83-09680 and NIH grants HD13249, NS15175, NS19096 (to U.B. and H.P.).

Received 15 October 1985; accepted 10 April 1986.

- Klima, E. S. & Bellugi, U. The Signs of Language (Harvard University Press, 1979)
 Bellugi, U. Signed and Spoken Language: Biological Constraints on Language: Form, 115-140 (Verlag Chemie, Weinheim, 1980).
- 3. Poizner, H. & Battison, R. in Recent Perspectives on American Sign Language (eds Lane, H. & Grosjean, F.) 79-101 (Erlbaum Associates, Hilsdale, 1980)
- 4. Rezai, K. et al. Neurology 34(3), 204 (1984).
- 5. Knopman, D. S., Rubens, A. B., Klassen, A. C. & Meyer, M. W. Arch. Neurol. 39, 487-493 (1982).
- 6. Goodglass, H. & Kaplan, E. The Assessment of Aphasia and Related Disorders (Les & Goodgiass, H. & Kapian, E. The Assessment of Aphasia and Related Distracts
 Febiger, Philadelphia, 1983).
 Wada, J. & Rasmussen, T. J. Neurosurg. 17, 266-282 (1960).
 Damasio, H. Arch. Neurol. 40, 138-142 (1983).
 Hoeman, W., Criswell, E., Wada, A. & Ross, D. Neurology 32, 1020-1023 (1982)
 Bellugi, U., Poizner, H. & Klima, E. A. Hum. Neurobiol. 2, 155-170 (1983)

- 11. Poizner, H., Kaplan, E., Bellugi, U. & Padden, C. Brain Cognition 3, 281 306 (1984)
 12. Bellugi, U., Poizner, H. & Klima, E. S. What the Hands Reveal About the Brain (Braford
- Books, Cambridge, Massachusetts, in the press).

Electrokinetic shape changes of cochlear outer hair cells

Bechara Kachar*, William E. Brownell†, Richard Altschuler‡ & Jörgen Fex‡

Laboratories of * Neurobiology and ‡ Neuro-Otolaryngology, NINCDS, National Institutes of Health, Bethesda, Maryland 20892, USA

Departments of Neuroscience and Surgery (ENT), Box J-244, University of Florida, Gainesville, Florida 32610, USA

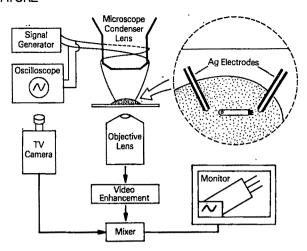
Rapid mechanical changes have been associated with electrical activity in a variety of non-muscle excitable cells¹⁻⁵. Recently, mechanical changes have been reported in cochlear hair cells⁶⁻⁶ Here we describe electrically evoked mechanical changes in isolated cochlear outer hair cells (OHCs) with characteristics which suggest that direct electrokinetic phenomena are implicated in the response. OHCs make up one of two mechanosensitive hair cell populations in the mammalian cochlea; their role may be to modulate the micromechanical properties of the hearing organ through mechanical feedback mechanisms⁶⁻¹⁰. In the experiments described here, we applied sinusoidally modulated electrical potentials across isolated OHCs; this produced oscillatory elongation and shortening of the cells and oscillatory displacements of intracellular organelles. The movements were a function of the direction and strength of the electrical field, were inversely related to the ionic concentration of the medium, and occurred in the presence of metabolic uncouplers. The cylindrical shape of the OHCs and the presence of a system of membranes within the cytoplasm—laminated cisternae¹¹—may provide the anatomical substrate for electrokinetic phenomena such as electrosmosis^{12,13}.

Isolated OHCs were prepared from the organ of Corti of guinea pig by non-enzymatic mechanical dissociation^{7,8}. A 100-µl volume of culture medium containing isolated cells was placed on a microscope slide and viewed with video-enhanced microscopy (Fig. 1). Isolated OHCs attach to the microscope slide at either the synaptic or the stereociliar end. Sinusoidal potential gradients at 2-30 Hz and <1 mA (0.8-1.5 V peak-topeak) were passed across OHCs by means of a pair of silver-wire electrodes placed 200-300 µm apart (Fig. 1). About 100 isolated OHCs from 34 cochleae were analysed from experiments recorded on videotape.

Oscillatory movement of the cell's free end, corresponding to elongation and shortening of the cell in response to the electrical stimulation, was visualized in over 80% of the OHCs. Oscillatory movement of intracellular organelles located around the cell axis was observed in ~15% of the OHCs. Maximal responses of up to 0.3-0.4 µm amplitude about a resting position (Figs 2, 3) were obtained when the cells were longitudinally aligned with the direction of the electrical field. We could not distinguish oscillatory movements from brownian movement for amplitudes smaller than 50 nm. Most OHCs showed elongation with positive potential gradients and shortening with negative potential gradients, when the ground electrode was placed near the end of the cell that was attached to the substrate (Figs $2\dot{a}-d$, 3a,b,d). Less than 20% of the OHCs showed the opposite response polarity. Organelle movement, when detectable in cells that also responded with length changes, was in-phase with the movement of the free end of the cell (Fig. 3d,e). Organelle movement was also observed in some cases when both the stereociliar and synaptic ends were attached to the slide. Oscillatory movements of organelles or changes in cell length were not observed in red blood cells, Deiters' or Hensen's cells which co-isolate with the OHCs.

These electrically evoked responses persisted for several hours after dissociation. The responses were unchanged when the cells were incubated for 1 h in medium containing dinitrophenol (2 mM) or iodoacetic acid (2 mM), both of which are inhibitors of ATP production and commonly used to test for energy requirements^{14,15}. The responses were enhanced by lowering the ionic concentration by 20–25% (this was achieved by isotonic dilution of the medium with a sucrose solution). Some cells showed little or no movement in the standard medium but exhibited robust movement after ionic dilution; this effect was reversed by replacing the diluted medium with the original medium (Fig. 3 d).

The symmetry of the sinusoidal displacements, their apparent independence of ATP involvement, and the enhanced responses after ionic dilution are difficult to reconcile with conventional contractile mechanisms. However, electrophoresis ^{13,16} and electro-osmosis ^{12,13} might provide the motive force underlying both the length changes and the oscillatory organelle movements. Such electrokinetic phenomena are a function of applied voltage and are enhanced in medium of low ionic concentration ^{12,17}. Electro-osmosis is a field-induced movement of fluid adjacent to a charged surface as a consequence of the electrophoretic migration of counterions ^{12,13,17-19}. When electro-osmosis occurs in a tube with closed ends, a pressure difference develops between the tube ends ¹⁹. If the tube wall is elastic it can deform (elongate or shorten), or if it is rigid the flow of liquid along



Schematic diagram of the video-enhanced light microscopy³¹ system used in the present experiments. An inverted Zeiss Axiomat was operated in the differential interference contrast mode and equipped with a ×100, 1.3-NA Planapo objective, a 0.63-NA condenser fully illuminated with a 100-W mercury lamp and a Newvicon Dage-68 (MTI) video camera for contrast enhancement. The magnification of the image on the TV monitor was ×20,000. Experiments were carried out in droplets of medium (Leibovitz L-15 with 1% bovine serum albumin and 10 mM HEPES). A droplet containing cells was placed on a microscope slide which had been pretreated with polylysine. Isolated OHCs in most cases adhere to the slide surface at either the basal (synaptic) of apical (stereociliar) region. Stimulation was achieved with a pair of Teflon-insulated no. 30 silver-wire electrodes placed 200-300 µm apart and mounted on the microscope condenser lens. The electrode pair was lowered into the droplet and oriented in relation to individual OHCs by rotating the microscope stage. The voltage waveform was displayed on an oscilloscope screen and the video image mixed with that of the video-enhanced image of the OHC. The response of the cells to electrical stimulation were analysed by frame-by-frame playback of videotape-recorded experiments. Time resolution was limited to 17 ms, corresponding to the duration of a single non-interlaced video frame. Photographs and measurements were taken from a TV monitor.

the wall is counterbalanced by a flow in the opposite direction at the centre of the tube¹⁸.

OHCs display structural features that are favourable for electrokinetic effects. OHCs are elongated cylinders, 4-9 µm wide and 15-70 µm long, and they contain parallel membranes that form the laminated cisternae along the lateral plasma membrane¹¹ (Fig. 2f). The function of the cisternae is unknown. The closely apposed membranes may be an optimal substrate for an electro-osmotic effect¹². Cytoplasmic fluid movement in relation to the plasma and cisternal membranes would produce pressure variations and changes in cell shape.

Evidence that bulk fluid oscillatory movement is induced by potential gradients is provided by the fact that all organelles in the axial region of the cytoplasm move in concert and to an equal extent, not with different amplitudes as expected for an inhomogeneous population of organelles with different electrophoretic mobilities. In addition, free cytoplasmic organelles from disrupted cells fail to respond to the same electrical gradients.

It is unknown why different OHCs show different polarity of the displacement responses. Structural and metabolic differences between OHCs isolated from different turns or different rows in the cochlear spiral^{20,21} may alter the balance of forces resulting from the electro-osmotic fluid drag and the electrophoresis of soluble metabolites¹⁶ as well as of components of the membrane¹³ and of the cytoskeleton.

The requirement of video enhancement to visualize the shape changes and the intracellular organelle movements limited our

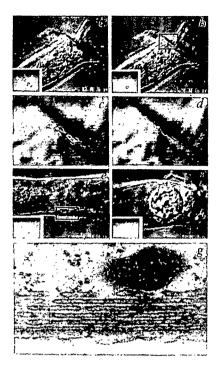


Fig. 2 Mechanical responses of OHCs to transcellular stimulation. a, Video-enhanced image of the stereociliar end of an OHC at the positive phase of a sinusoidal stimulus (oscilloscope screen shown at lower left); the active electrode lies outside the field of view to the right, the ground electrode is positioned near the synaptic end of the cell to the left of the field of view. The time is indicated at the lower right. b, Image of the same cell as in a during the negative phase of the stimulus. c, d, Higher magnification of the images enclosed by the rectangle at the stereociliar end of OHC shown in a and b respectively; the lower arrow in c indicates a reference point in the screen with fixed coordinates, the upper arrow indicates the edge of the cell image. The OHC was longer during the positive phase (a and c) of the stimulus and shorter during the negative phase (b and d). e, f, Images of the middle (e) and synaptic end (f) of another cell; cytoplasmic organelles are clearly visualized. g, Thin-section electron micrograph from a region of OHC equivalent to that outlined by the rectangle in e, showing the laminated cisternal system adjacent and parallel to the plasma membrane. This system is found between the cuticular plate and the nucleus. There are 6-8 cisternae in guinea pig OHCs; the outermost layer is parallel to and 30-35 nm from the lateral plasma membrane and each layer is parallel to its neighbours and separated from the next layer by 15-20 nm¹¹. Magnifications: a, b, e, f, $\times 1,500$; c, d, $\times 7,500$; g, $\times 40,000$.

ability to resolve cycle-by-cycle changes beyond 30 Hz. However, we were able to see vibration and blurring of the image of OHCs in response to electrical stimulation above 100 Hz. In addition, Ashmore and Brownell²², reproducing our experimental conditions but using a linear position detector, recorded changes in cell length in response to stimulations in excess of 8 kHz.

OHCs in situ have no attachments at the lateral surfaces except for synaptic contacts at the base of the cell and an apical band of tight junctions with Deiters' cells in the reticular lamina. This tight junction constrains current flow in vivo; its absence in vitro would lead to current shunting around the cell. Therefore, the actual potential gradients driving the motile process in our experiments may approach the physiological values²³ (7 V m⁻¹) measured near OHCs in vivo. Furthermore, smaller physiological potential gradients would produce smaller displacements which would be more compatible with observed magnitudes of vibrations of the cochlear partition—of the order of angstroms at the threshold of hearing. The free lateral surfaces of OHCs permit free expression of length changes which in turn

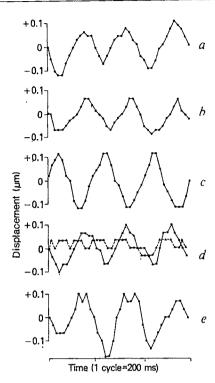


Fig. 3 Displacement evoked by 5-Hz sinusoidal transcellular stimulation, a-d. Plots of movement of the free end of OHCs: e is a plot of organelle movement. a, Apical end movement (same cell as in Fig. 2a-d), b. Basal end movement (same cell as in Fig. 2f). c, Example of free end movement of opposite polarity to that shown in a and b. d, Circles represent free end movements at reduced ionic concentration; triangles represent movements of the same cell under the same stimulus conditions, but using the original medium. We assume that a decrease in extracellular ionic strength leads to a decrease in the intracellular ionic strength; in support of this assumption are the findings of low resting potentials and input impedances of OHCs in vitro^{7,32}, consistent with a highly permeable plasma membrane. e, Organelle movement in the same cell as d under conditions of reduced ionic concentration; the response sinusoid is less regular because of concurrent brownian motion of the organelles.

affects the micromechanics of the cochlear partition^{7,24}. A change in the OHC length will change the separation between the reticular lamina and the basilar membrane and affect cochlear transduction^{7-10,25-27}. There is evidence that the efferent olivocochlear synapses on OHCs may modify the microm-echanics of the latter^{27,28,33}. In addition, electrical potentials (cochlear microphonics)²⁹ that vary at acoustic frequencies are generated by mechano-electrical transduction associated with the OHCs³⁰, which increases the significance of an electrokinetic basis for OHC length changes by permitting shape changes in the audio-frequency ranges.

We thank Remy Pujol for the electron micrograph shown in Fig. 2g. This research was supported in part by research grants BNS-12174 from NSF(USA), NS-19050 from NINCDS and a research stipend from INSERM (France) to W.E.B.

Received 6 February; accepted 22 April 1986.

- Iwasa, K., Tasaki, I. & Gibbons, R. C. Science 210, 338-339 (1980).
- Tasaki, I. & Birne, P. M. Brain Res. 301, 265-272 (1984). Tasaki, I. & Nakaye, T. Science 223, 411-413 (1984).

- Brown, K. T. & Murakami, M. Nature 201, 626 (1964).
 Hill, B. C., Schubert, E. D., Nokes, M. A. & Michelson, R. P. Science 196, 426-428 (1977).
- Crawford, A. C. & Fettiplace, R. J. Physiol., Lond. 364, 359-379 (1985).
 Brownell, W. E., Bader, C. R., Bertrand, D. & Ribaupierre, Y. Science 227, 194-196 (1985).
- Zenner, H. P., Zimmermann, U. & Schmitt, U. Hearing Res. 18, 127-133 (1985).
- Davis, H. Hearing Res. 9, 79-90 (1983).
 Dallos, P. in Contemporary Sensory Neurobiology (eds Correia, M. J. & Perachio, A. A.) 207-230 (Liss, New York, 1985).
- 11. Saito, K. Cell Tissue Res. 229, 467-481 (1983).

- 12. McLaughlin, S. & Mathias, R. T. J. gen. Physiol. 85, 699-728 (1985).
- 13. Poo, M. A. Rev. Biophys. Bioengng 10, 245-276 (1981).
- Chance, B., Williams, G. R. & Hollunger, G. J. biol. Chem. 278, 439-444 (1961).
 Epstein, M. L., Sheridan, J. D. & Johnson, R. G. Expl Cell Res. 104, 25-30 (1977).
- Horwitz, B. Neuroscience 12, 887-905 (1984).
 Balasubramanian, A. & McLaughlin, S. Biochim. biophys. Acta 685, 1-5 (1982).
- Morrison, F. A. & Osterele, J. F. J. chem. Phys. 43, 2111-2115 (1965).
 Nee, T. W. J. Chromatography 105, 231-248 (1975).

- Lim, D. J. J. acoust. Soc. Am. 67, 1686-1695 (1980).
 Bohne, B. A. & Carr, C. D. J. acoust. Soc. Am. 77, 153-158 (1985).
 Ashmore, J. & Brownell, W. E. J. Physiol., Lond. (Abstr.) (in the press).
- 23. Brownell, W. E., Manis, P. B., Zidanic, M. & Spirou, G. A. J. Acoust. Soc. Am. 74, 792-800
- 24. Brownell, W. E. & Kachar, B. in Peripheral Auditory Mechanisms (eds Allen, J. B. et al.) (Springer, New York, 1986).
 25. Strelioff, D., Flock, A. & Minser, K. E. Hearing Res. 18, 169-175 (1985).
 26. Weiss, T. F. Hearing Res. 7, 353-360 (1982).
 27. Brown, N. C. & Nutall, A. J. Physiol., Lond. 354, 625-646 (1984).

- Mountain, D. C. Science 210, 71-72 (1980).
 Wever, E. G. Physiol. Rev. 46, 102-127 (1966)
- Dallos, P. A. Rev. Psychol. 32, 153-190 (1981).
 Inoue, S. J. Cell Biol. 89, 346-356 (1981).
- 32. Flock, A. & Strelioff, D. Hearing Res. 15, 11-18 (1984).
- 33. Siegel, J. H. & Kim, D. O. Hearing Res. 6, 171-182 (1982).

Ionic basis of membrane potential in outer hair cells of guinea pig cochlea

J. F. Ashmore & R. W. Meech

Department of Physiology, The Medical School, University of Bristol, University Walk, Bristol BS8 1TD, UK

Mammalian hearing involves features not found in other species, for example, the separation of sound frequencies depends on an active control of the cochlear mechanics1,2. The force-generating component in the cochlea is likely to be the outer hair cell (OHC), one of the two types of sensory cell through which current is gated by mechano-electrical transducer channels sited on the apical surface3. Outer hair cells isolated in vitro have been shown to be motile^{4,5} and capable of generating forces at acoustic frequencies⁶. The OHC membrane is not, however, electrically tuned, as found in lower vertebrates⁷⁻⁹. Here we describe how the OHC resting potential is determined by a Ca²⁺-activated K⁺ conductance^{10,11} at the base of the cell. Two channel types with unitary sizes of 240 and 45 pS underlie this Ca2+-activated K+ conductance and we suggest that their activity is determined by a Ca2+ influx through the apical transducer channel, as demonstrated in other hair cells 12. This coupled system simultaneously explains the large OHC resting potentials observed in vivo 13,14 and indicates how the current gated by the transducer may be maximized to generate the forces required in cochlear micromechanics.

Outer hair cells were isolated from the guinea pig cochlea and maintained in vitro at room temperature with no obvious change in their morphology for about 4 h (Fig. 1A; see also Fig. 1 legend). Their input conductance and resting potential, measured using whole-cell recording techniques¹⁵, were found to depend on the contents of the recording pipette. When the pipette contained 140 mM K⁺, the input conductance ranged from 25 to 40 nS (Fig. 1B, a). Typical resting potentials were -15 to -40 mV and only exceptionally were more negative. Comparable results were obtained with conventional high-resistance micropipettes (J.F.A., unpublished). Cells equilibrated with pipettes containing 140 mM Na⁺ had a lower input conductance $(2.9\pm0.9 \text{ nS } (\pm \text{s.d.}), n=6; \text{ Fig. } 1B, b)$. A low input conductance (4.8 nS) was also obtained with pipettes containing 100 mM CsCl. There was no significant difference in input conductance when the external Cl was replaced by gluconate. We conclude that under our experimental conditions the hair cell membrane is relatively impermeable to Cl⁻ and is more permeable to K+ than to Na+ by a factor of at least 5. Furthermore, hair cells in vivo have input conductances of $\geq 20 \text{ nS}^{16}$; thus, the values reported here suggest that the isolation procedure introduces little change in membrane leakage.

In some experiments with 140 mM Na⁺ in the recording pipette, depolarizing current pulses elicited what appeared to be a slowly developing active response (Fig. 1B, b). Such responses were not seen when the pipette contained 140 mM K⁺ (Fig. 1B, a) unless it also contained the Ca²⁺ buffer BAPTA¹⁷ (Fig. 1B,c). With 10 mM BAPTA in the recording pipette. intracellular levels of calcium would be expected to fall below 10⁻⁸ M. Thus the observed decrease in input conductance is consistent with a membrane K⁺ conductance gated by internal Ca²⁺ (ref. 18). Cells loaded with BAPTA and 140 mM K⁺ from the pipette had a final mean resting potential of -60 mV (n = 7)after equilibration (2-3 min), even though the initial resting potential was close to -10 mV. We attribute the increase in resting potential to a rise in internal K+ and the contribution of a small (<3 nS at -60 mV) residual K⁺ conductance.

When BAPTA-containing cells were studied under voltage clamp, step changes in membrane potential produced a large capacitive transient followed by a steady inward current (with hyperpolarizing pulses) or a slowly developing outward current (with depolarizing pulses; Fig. 2A). Both inward and outward currents were reduced or blocked by externally applied Cd²⁻¹ which blocks Ca2+ currents in many different tissues19 (Fig. 2B, c).

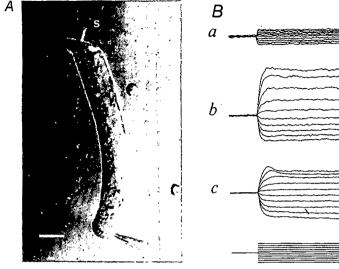
The residual ionic currents in saline containing 1 mM Cd2+ appeared to be largely time-independent; they were smaller in the outward direction than in the inward direction (Fig. 2B. C) but this anomalous rectification was not characterized further. In Fig. 2D, currents recorded in Cd²⁺ have been subtracted from those recorded in normal saline to show the Cd2+-sensitive fraction. The Cd2+-sensitive current makes only a minor contribution to the total membrane conductance (1-4 nS at -60 mV): it appears even at membrane potentials more negative than -100 mV, that is, beyond the normal operating range for Ca²⁺ channels, and is unlikely to be the remains of the Ca²⁺-activated K⁺ conductance because it appears even in cells containing 50 mM BAPTA. We propose, instead, that it crosses the membrane via the transducer pathway which, in other vertebrate hair cells, is known to be closed by Ca2+-channel blockers12

A prominent component of the Cd²⁺-sensitive current is apparent during membrane depolarization as a slowly developing outward current; this appears even in cells containing 50 mM BAPTA and its tail-current, seen when the membrane is repolarized, reverses at $\sim -50 \text{ mV}$ (not shown) and so it too may be associated with the transducer channel. However, H⁺ conductances appear in this voltage range in some cells and they are also blocked by Cd²⁺ (refs 20, 21). A rapidly developing Cd²⁺sensitive Ca2+-activated K+ current has been reported in isolated hair cells from the sacculus of the bullfrog⁷ but its time-course and voltage-dependence do not correspond to the Cd²⁺-sensitive currents reported here.

Single-channel recordings revealed several distinct channel populations which underlie some of the conductances observed in whole cells. In the cell-attached mode²² at least two populations were evident: an uncharacterized voltage-dependent channel with a unit conductance of ~30 pS, and a range of larger conductance channels (40-65 pS) subsequently identified as two populations of Ca²⁺-activated K⁺ channel. Unitary K⁺ currents recorded from such cell-attached membrane patches reversed direction at potentials between -20 and -30 mV, which is consistent with decreased levels of internal K+ in isolated cells.

Current records from single Ca2+-activated K+ channels were obtained with inside-out patches of membrane²³ taken from the basolateral region of the outer hair cells. One type of channel had a unit conductance of 233 ± 33 pS (n = 10) when bathed bilaterally in 140 mM KCl (Fig. 3A). This type of channel resembles the large-conductance Ca^{2+} -activated K^+ channel described in a variety of other systems²⁴⁻³¹ because its probability of opening increased with elevated Ca2+ at the internal membrane surface (Fig. 3C).

In addition to the large-conductance channel, a second class



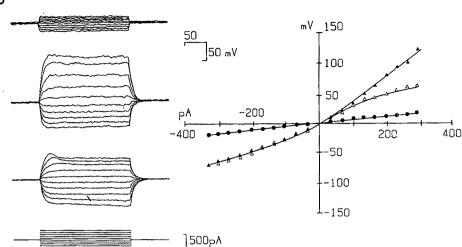
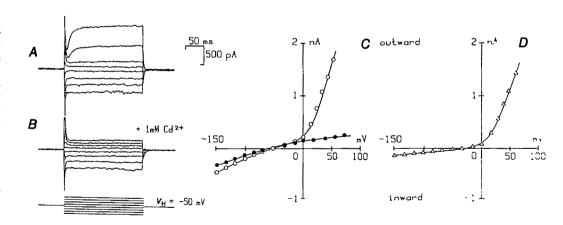


Fig. 1 Membrane permeability of isolated outer hair cells. A, An isolated outer hair cell of the guinea pig cochlea. The cell length indicates that the cell originates from the low-frequency end of the cochlea. The mechano-electrical transducer and stereocilia (s) on the apical surface face endolymph when in situ. Patch recordings were made on the basal surface as shown. Scale bar, 10 µm. B, Effect of different internal ions on membrane conductance of outer hair cells. The figure shows the changes in voltage observed during step changes in current, obtained in the whole-cell recording mode¹⁵ when the membrane potential had reached a steady level, that is, after 1-3 min (separate experiments with fluorescent dyes suggest that this corresponds to the time required for the cell contents to reach a steady state). The pipette contained: a, KCl, 140 mM, MgCl₂, 2 mM, 6.5×10^{-8} M Ca²⁺ (using 500 μ M EGTA/Ca²⁺ buffer), HEPES 5 mM; pH 7.6. Cell resting potential -29 mV. b, Same as in a except that NaCl replaced KCl. Cell resting potential +17 mV. In some cells depolarizing current pulses elicited a small, slowly developing active response on the rising phase of the trace. c, Same as in a except that 10 mM BAPTA (BDH) replaced the EGTA/Ca² buffer in the pipette. Cell resting potential -63 mV. C, Steady-state current/voltage curves obtained from the data in B. O, Data from a; A, data from b; \triangle , data from c. Zero on the voltage axis corresponds to the resting potential. Data were corrected for series resistance of the pipette (20-45 M Ω) in each cell.

Methods. Guinea pigs (300-500 g) were killed by rapid cervical dislocation, and their cochlear coils dissected out into L-15 medium (Gibco) using a fine needle. The apical two turns only were used; they yielded outer hair cells which were 55-80 µm long and had an electrical capacitance in whole-cell clamp of 24-32 pF. Each coil was removed into a 140-µl aliquot of medium containing 0.3 mg ml⁻¹ trypsin (Sigma type III S) for 30 min. The cells were mechanically dissociated and the volume increased to 300 µl in the microscope chamber. The major ions in L-15 medium are Na⁺ (145 mM), K⁺ (5.4 mM), Mg²⁺ (1.8 mM), Ca²⁺ (1.26 mM), Cl⁻ (147 mM) and phosphate buffer. Cells were observed under 40 × WI DIC optics. Patch recordings were made from the basal part of the cell using an EPC-5 amplifier (List Electronic). Pipettes were pulled on a two-stage puller, (BB-CH, Mecanex) and used without further treatment. Seal resistances >2 GΩ were obtained before whole-cell recording. Experiments were performed at room temperature (19-21 °C).

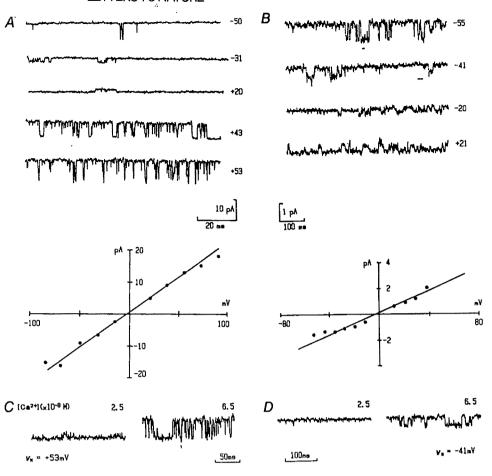
Fig. 2 Cd2+-sensitive K+ conductance in outer hair cells recorded under voltage clamp. The pipette was filled as for Fig. (10 mM BAPTA included). No cancellation of the capacitive transients was made; time constant 1.7 ms. Holding potential $(V_H) = -50 \text{ mV}.$ Step increment, 34 mV. A, 5 min after whole-cell recording conditions had been established. B, After addition of 1 mM Cd2+ to the bath. C, Currentvoltage curves showing:



O, steady currents during depolarizing or hyperpolarizing pulses in normal saline (data from A); •, steady currents in 1 mM Cd²⁺ (data from B). D, Cd²⁺-sensitive currents obtained by subtraction of Cd²⁺-resistant currents from currents observed in normal saline. The pipette series resistance (38 M Ω) measured in the bath was used to compensate C and D. Maximum slope conductance in A was 32 nS.

of Ca^{2+} -activated K^+ channel was found (Fig. 3B,D) which had a smaller single unit conductance, 44 ± 17 pS (n=6), when bathed bilaterally in 140 mM KCl. Ca²⁺-activated K⁺ channels with comparable conductances (25-92 pS in 140 mM K⁺) have been described in other vertebrate tissues^{27,32}. Like the largeconductance channel, this channel 'turned on' at Ca²⁺ levels between 2.5×10^{-8} and 6.5×10^{-8} M (with EGTA buffer, pH 7.6) but its kinetics were less complex. We have investigated the possibility that it was a fragment of some other channel. We found that membrane patches generally had either large- or small-conductance channels and at no time did we observe large-conductance channels decomposing into smaller ones. The selectivity of the two Ca²⁺-gated channels for K⁺ over Na⁺ was about the same; the reversal potential shifted by 35-55 mV per 10-fold reduction of K⁺ at the inside surface. In these experiments we found that Na+ at the internal surface of the membrane produced a 'flickery' block of both types of K^+ channel at positive membrane potentials^{31,33,34}.

Fig. 3 Ca²⁺-activated K⁺ currents in outer hair cells. Single channels recorded from inside-out patches. A, Large-conductance Ca²⁺-activated K+ channels observed at different patch potentials, as indicated; inward current downwards. The channel open probability increased with depolarization of the intracellular surface of the isolated patch (~30 mV for an e-fold change). The pipette contained (in mM): 140 KCl, 1.25 CaCl₂, 2 MgCl₂, 5 HEPES pH 7.4; the cytoplasmic face was bathed in 140 mM KCl, 6.5×10^{-8} M Ca²⁺ (500 μM EGTA/Ca²⁺ buffer), 2 mM MgCl₂, 5 mM HEPES pH 7.6. In bilateral 140 mM KCl, the unit slope conductance was 220 pS, measured from well-resolved openings. The K/Na permeability of this channel, determined by altering K+ at the cytoplasmic surface, was ~7:1. Recording bandwidth (via 4pole Bessel filter) 1.6 kHz. B, Small-conductance Ca²⁺-activated K⁺ channel observed under the same conditions as in A. Unit slope conductance 45 pS. Recording bandwidth 880 Hz. Large-conductance (C) and small-conductance (D) channel types are activated by levels of Ca2+ at their intracellular surface that are greater than 2.5×10^{-8} M. Values shown alongside each record show the prevailing Ca2+ concentration (in µM) at the cytoplasmic sur-



face; this was changed using a continuous flow system³⁸. The holding potential $V_{\rm H}$ (+53 mV for large-conductance channel; -41 mV for small-conductance channel) was the same for both Ca²⁺ solutions. In 2.5×10⁻⁸ M Ca²⁺ the channels were generally inactive at voltages between -70 and +70 mV. EGTA buffers were used throughout.

In summary, we have been able to convert isolated outer hair cells with a high input conductance and low resting potential into cells with a resting potential near normal; we have done this by introducing the Ca2+ buffer BAPTA into the cell interior and by raising the level of internal K⁺. We have also identified two populations of channels which underlie this resting Ca²⁺activated K⁺ conductance. In vivo the transducing surface of an outer hair cell faces a K⁺-rich endolymph at a potential of +80 mV; the basolateral surface faces a perilymph with the composition of normal extracellular fluid, and the cell resting potential is close to -80 mV^{13,14,35,36}. Isolated outer hair cells will tend to lose their internal K⁺ because the large K⁺ reservoir which drives K⁺ across the apical surface in vivo is absent when the isolated cells are placed in normal (5.5 mM) $\rm K^+$ saline. Low levels of internal $\rm K^+$ and a gain of $\rm Na^+$ would account for the low resting potentials of isolated cells, the reversal potential of K⁺-selective channels in the cell-attached mode and their 'flickery' block at positive membrane potentials.

Our demonstration, in isolated cells, of a Cd2+-sensitive conductance at potentials more negative than -100 mV leads us to suppose that outer hair cells have a transduction channel much like that described by Ohmori for chick vestibular hair cells¹². Such channels have a high permeability for Ca²⁺ and are blocked by Ca2+-channel blocking agents. Perhaps damage to the cochlea due to noise (which often involves outer hair cells) arises from a reduced Ca2+ influx through the disrupted transduction pathway. The reduced activity of the Ca2+-activated channels that we have described would account for the previously reported decrease in K⁺ permeability in noise-damaged cells³⁷

At no time during whole-cell recording did we observe an oscillatory ringing of the membrane potential like that found in auditory hair cells of lower vertebrates⁷⁻⁹. The voltage-dependent channels we have observed were activated at voltages outside the normal range for mammalian cells^{13,14}, therefore we conclude that transduction in outer hair cells and lower vertebrate hair cells operates along different principles.

Isolated outer hair cells exhibit motile responses when current is injected into them⁴⁻⁶. This movement may be seen even in Cd²⁺-containing solution and it appears to depend on transmembrane current rather than on the polarity of the axially flowing component. The function of the Ca²⁺-activated K⁺ conductance may be to clamp the cell close to its K⁺ equilibrium potential and maximize the inward driving force for cations across the transduction channel at the apical surface. In this scheme the large outward current generated across the basolateral surface would directly couple the sensory stimulus to the cell's mechanical response.

This work was supported by the MRC, R.W.M. is a Wellcome Trust Senior Lecturer in Physiology.

Received 12 December 1985; accepted 18 April 1986.

- Brown, M. C. & Nuttall, A. L. J. Physiol., Lond. 354, 625-646 (1984).
- Davis, H. Hearing Res. 9, 79-90 (1983).
 Pickles, J. O. Prog. Neurobiol. 24, 1-42 (1985).
- Ashmore, J. F. J. Physiol., Lond. 364, 4P (1985).
 Brownell, W. E., Bader, C. R., Bertrand, D. & de Ribaupierre, Y. Science 227, 194-196 (1985).
- Ashmore, J. F. & Brownell, W. E. J. Physiol., Lond. (in the press). Lewis, R. S. & Hudspeth, A. J. Nature 304, 538-541 (1983).
- Ashmore, J. F. & Pitchford, S. J. Physiol, Lond. 364, 39P (1985).

- Crawford, A. C. & Fettiplace, R. J. Physiol., Lond. 312, 377-412 (1981).
 Meech, R. W. Comp. Biochem. Physiol. 42A, 493-499 (1972).
- 11. Meech, R. W. & Standen, N. B. J. Physiol., Lond. 249, 211-239 (1975).
- 12. Ohmori, H. J. Physiol, Lond. 359, 189-218 (1985).
- 13. Cody, A. R. & Russell, I. J. Nature 315, 662-665 (1985)
- 14. Dallos, P., Santos-Sacchi, J. & Flock, A. Science 218, S82-584 (1982).

 15. Hamill, O. P., Marty, A., Neher, E., Sakmann, B. & Sigworth, F. J. Pflügers. Arch. ges Physiol. 391, 85-100 (1981).
- Russell, I. J. Nobel Symp. 63, (in the press). Tsien, R. Y. Biochemistry 19, 2396-2404 (1980)
- Meech, R. W. A. Rev. Biophys. Bioengng 7, 1-18 (1978).
 Hagiwara, S. & Byerly, L. A. Rev. Neurosci. 4, 69-125 (1981). 19. падумага, 5. & Byerty, L. A. Kev. Neurosci. 4, 69-123 (1981).
 20. Byerly, L., Meech, R. & Moody, W. Jr. J. Physiol., Lond. 351, 199-216 (1984).
 21. Thomas, R. C. & Meech, R. W. Nature 299, 826-828 (1982).
 22. Sigworth, F. J. & Neher, E. Nature 287, 447-449 (1980).
 23. Horn, R. & Patlak, J. Proc. natn. Acad. Sci. U.S.A. 77, 6930-6934 (1980).

- Barrett, J. N., Magleby, K. L. & Pallotta, B. S. J. Physiol., Lond. 331, 211-230 (1982). Cook, D. L., Ikeuchi, M. & Fujimoto, W. Y. Nature 311, 269-271 (1984). Findlay, I. J. Physiol., Lond. 350, 179-195 (1984).

- Inoue, R., Kitamura, K. & Kuriyama, H. Pflügers Arch. ges. Physiol. 405, 173-179 (1985).
- Marty, A. Nature 291, 497-500 (1981).
- Maruyama, Y., Petersen, O. H., Flanagan, P. & Pearson, G. T. Nature 305, 228-232 (1983). Wong, B. S., Lecar, H. & Adler, M. Biophys. J. 39, 313-317 (1982). Yellen, G. J. gen. Physiol. 84, 157-186 (1984).

- Grygorczyk, R., Schwarz, W. & Passow, H. Biophys. J. 45, 693-698 (1984).
- Marty, A. Pflügers Arch. ges. Physiol. 396, 179-181 (1983). Singer, J. J. & Walsh, J. V. Jr Biophys. J. 45, 68-70 (1984)
- Bosher, S. K. & Warren, R. L. Nature 273, 377-378 (1978).
- Bosher, S. K. Acta oto-lar. 90, 219-229 (1980). Konishi, T. & Salt, A. N. Expl Brain Res. 40, 457-463 (1980).
- Yeilen, G. Nature 296, 357-359 (1982).

Lithium-induced respecification of pattern in Xenopus laevis embryos

Kenneth R. Kao, Yoshio Masui & Richard P. Elinson

Department of Zoology, University of Toronto, Toronto, Ontario, Canada M5S 1A1

Much interest in vertebrate embryology is now focused on early pattern formation in the frog, Xenopus laevis. In this species, the body plan is specified by a stable positional system set up by a cytoplasmic rotation in the zygote that occurs before first cleavage1-4. Perturbation of this initial cellular event by a variety of means causes permanent distortions of the positional system4 Until now it has not been possible to alter the positional system after it has been specified. However, we report here that lithium, when applied after specification of the body plan, can respecify the positional system of the Xenopus embryo such that dorsal, axial structures develop from cells that otherwise contribute to ventral structures. Lithium is usually considered to have negative effects on early embryo development⁸⁻¹⁰, but our results show that lithium can act in a positive manner to produce structures which represent the uppermost values of the positional system. This discovery introduces a convenient means to study cellular and molecular mechanisms of early vertebrate pattern expression.

When dejellied 32-cell Xenopus laevis embryos are exposed to Li+ (such as 20% Steinberg's solution with 0.3 M LiCl for 6 min) they develop exaggerated head or dorso-anterior structures. They form multiple eyes or large bands of retinal pigment, and in some batches of eggs, the embryos develop a long proboscis. These embryos resemble morphologically those produced by exposure to deuterium oxide (D2O) before axis specification, and are considered to have enhanced dorsal structures4. Backström9 reported similar results which he considered to be Li*-induced 'ventralization'. However, the parallels between the morphologies produced by Li⁺ and those produced by D2O suggest that Li⁺ is causing enhancement of dorsoanterior development.

To confirm that Li+ causes dorso-anterior development, we applied Li⁺ to cleavage stage embryos which had been irradiated with ultraviolet (UV) light before first cleavage^{6,7}. UV-irradiated embryos lack all dorsal structures including the central nervous system, notochord and somites, and they remain as a radially symmetric ventral mass. However, dorsal structures can be

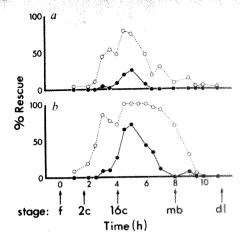


Fig. 1 Rescue of dorso-anterior development by LiCl in radially symmetric, ventral embryos produced by UV-irradiation. The horizontal axis represents the time in hours following fertilization with corresponding stages of development, f, fertilization; 2c, two cells; 16c, sixteen cells; mb, mid-blastula; dl, dorsal lip. The vertical axes represent the percentage of embryos showing axis development in response to 0.2 M Li⁺(a) and 0.3 M Li⁺(b) (35-87 embryos per treatment group). O, Percentage of embryos showing dorsal development, ranging from those showing somites and tail fin (IAD) grade 4) to those showing dorso-anterior radial development as in Fig. 2a and 2b. , Percentage of embryos showing exclusive dorsoanterior development. Note the peak in sensitivity to Li* at 5 to 6 hours of development (32 to 64 cells). As judged from the area under each curve, the higher concentration of Li⁺ was able to effect more rescue than the lower concentration.

Methods. Xenopus laevis eggs were fertilized and dejellied as described previously12. The vegetal poles were irradiated with UV light fort 2 min at a distance of $2\frac{1}{2}$ cm through a quartz slide within 30 min after fertilization. For these experiments, we used a pulse treatment of a high Li+ concentration for short duration in order to resolve the period of Li+ sensitivity. Irradiated embryos were incubated for 5 min at various times after fertilization in solutions of either 0.2 M or 0.3 M LiCl dissolved in 20% Steinberg's solution. Irradiated embryos not treated with LiCl developed into radially symmetric, ventral embryos. A few (usually <1%) develop a small tail fin but with no dorso-anterior development. After the LiCl treatment, embryos were thoroughly washed several times with 20% Steinberg's solution immediately and intermittently for several hours thereafter. All experiments and raising of embryos were done at 20 °C. Embryos were scored for development when untreated controls were at stage 4013

rescued when these ventralized embryos are exposed to Li during early cleavage. Two different patterns of rescue emerge from such treatment: dorso-posterior and dorso-anterior rescue. The dorso-posterior embryo is identical to the grade-4 axisdeficient embryo classified by Scharf and Gerhart's index of axis deficiency (IAD)7. The grade-4 embryo has somites and a tailfin but completely lacks a head. The other type of rescued embryo develops only dorso-anterior structures. Some develop a head with a cement gland and small amount of retinal pigment (Fig. 2a), while others have radial dorso-anterior development with a wide band of retinal pigment and a cement gland encircling the head (Fig. 2b). The frequency of embryos displaying exclusive dorso-anterior rescue and those showing rescue of any dorsal structures depends on dosage of Li* and the time of treatment (Fig. 1). The most sensitive period for rescuing UV-irradiated embryos with Li⁺ is between the 32- and 64-cell stages. Thus, the presence of dorsal structures in embryos otherwise lacking them suggests that Li⁺ is activating, some time during early cleavage, those components that are responsible for dorsal differentiation.

The radial arrangement of dorso-anterior structures produced by Li⁺ treatment suggests that Li⁺ is acting evenly around the embryo. We microinjected Li+ into specific cells of UV-irradi-

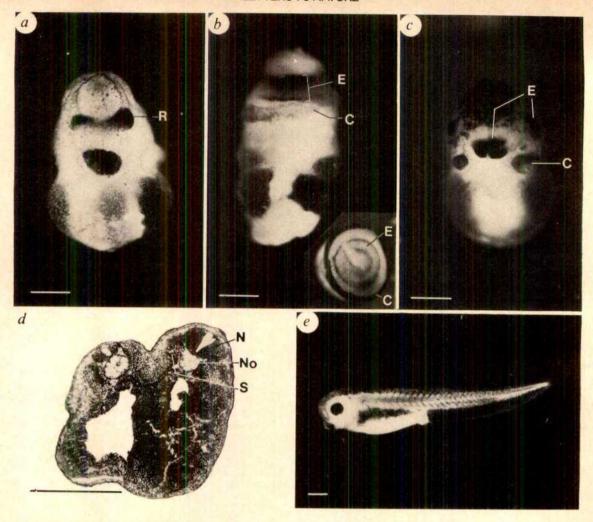


Fig. 2 a, X. laevis embryo exposed to UV light prior to first cleavage and then treated with 0.3 M LiCl for 5 min at the 32-cell stage. Note the presence of retinal pigment (R) which would not develop without LiCl exposure. b, An embryo with dorso-anterior radial symmetry. This embryo, like that in a, was UV-irradiated. Exposure to 0.3 M LiCl for 5 min 4.5 h following fertilization (16-32 cells) restored dorso-anterior development, causing rescue of eye (E) and cement gland (C) in a radial manner (inset: top view of radial, anterior embryo). c, A 'Janus twin' embryo exhibiting duplication of dorso-anterior structures. This embryo was injected with 4 nl of 0.3 M Li⁻¹ into a ventral, vegetal cell at the 32-cell stage. The eyes (E) and cement gland (C) of the head on the right side are labelled. d, A section just posterior to the head of an embryo displaying duplication of the head with one posterior axis. This embryo was microinjected similarly to the embryo in c. Embryos were fixed, sectioned in paraplast and stained as described previously¹². The duplicate axis is unlabelled. No, notochord; N, neural tube; S, somites. See Fig. 4 for experimental details. e, A control, untreated embryo at stage 40. Scale bars, 0.5 mm.

ated embryos to try to restore dorso-anterior development to one side of the embryo and thereby rescue normal development. Embryos at the 32-cell stage were used because they could be easily injected without significant leakage, and were most sensitive to rescue by Li+. Microinjection of Li+ into a cell in the vegetal-most tier caused significant rescue of normal development in a dose-dependent manner (Fig. 3). We used the IAD to quantify axis development, because the embryos developed morphologies identical to those defined by the IAD scale. For example, in Fig. 3, vegetal cell injections of 0.3 M Li+ reduced the average IAD to 2 in embryos which would otherwise develop into grade 4.9 or 5 embryos. Out of 81 embryos, 30% were scored as grade 0 (normal), 13% as grade 1 (slightly microcephalic), 16% as grade 2 (cyclopic), 17% as grade 3 (microcephalic), 16% as grade 4 (acephalic), and 8% as grade 5 (radial ventral). We could not assign an IAD score to embryos injected with solutions of Li⁺ greater than 0.3 M. These concentrations approach lethal levels and in the surviving embryos, there is an over-enhancement of dorso-anterior structures so that the embryos tend towards radial dorso-anteriorization. Injection of Li+ into an animal cell gave a lower frequency of rescue than with vegetal cell injections. It remains to be determined whether

the injected vegetal cell is altered by Li⁺ or whether it acts as a local source of Li⁺.

The restoration of bilateral symmetry in UV-irradiated embryos by Li+ microinjection prompted us to determine whether dorsal structures are duplicated in normal embryos when they are microinjected with Li+. We microinjected into vegetal lower-tier cells as this injection gave the best rescue of UV-irradiated embryos. From 112 embryos microinjected with Li⁺ into a ventral, vegetal cell, we obtained 97 embryos that had duplication of dorso-anterior structures (Fig. 4). Most of these embryos developed into 'Janus' twins (Fig. 2c) that lack posterior development but consist of two heads which have normally formed eyes and cement glands. A small number (~5%) developed into twins which have a single posterior axis but with twinned heads, central nervous systems, notochords and somites (Fig. 2d). Injection into a dorsal cell failed to duplicate dorsal structures. Out of 97 embryos injected into a dorsal, vegetal cell, 89 survived to form a single body axis. Most (~80%) developed normally, but the remainder developed enhanced dorso-anterior structures, similar in external appearance to the 'imbalanced' embryos produced by Cooke5

To see whether dorsal rescue is specific for Li+, we microinjec-

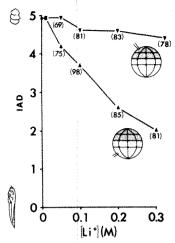


Fig. 3 Rescue of normal development by Li⁺ microinjection into radially symmetric ventral, embryos, Embryos were fertilized and irradiated with UV light as described in Fig. 1, and then microinjected with 3-5 nl of LiCl dissolved in distilled H2O or 200% Steinberg's solution at varying concentrations (horizontal axis) into either a top mostanimal tier cell (♥) or lowest vegetal tier cell (▲). The embryos for each experimental group were scored for axis development (vertical axis) using the index of axis deficiency (IAD)[†]. An IAD score of 0 indicates normal development whereas a score of 5 indicates complete lack of dorsal structures with only radial ventral development. The average IAD is plotted here for each group of injected embryos. Note that the average IAD is reduced in both animal and vegetal cell injections, but more significantly in the latter. Microinjection of >0.3 M Li⁺ increased the frequency of dead embryos and the formation of exclusively dorsoanterior embryos that are not scorable with the IAD. The numbers in brackets refer to numbers of embryos injected with LiCl at the indicated concentration. (For 0.01 M LiCl, 78 embryos were microinjected in the animal cell and 86 embryos were injected into the vegetal cell. At 0 M, 269 control embryos were scored.)

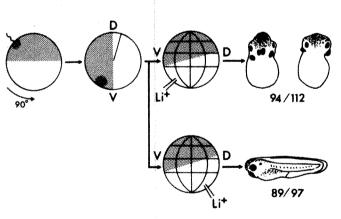


Fig. 4 Summary of twinning experiments. Fertilized eggs were placed in a 5% solution of Ficoll (Pharmacia) in 20% Steinberg's solution and rotated within 30 min after fertilization with the sperm entry point (SEP) towards gravity. The rotation ensures the position of the dorsal side of the embryo (D) as 180° opposite the SEP (ventral side, V) in the meridian passing through the SEP and the animal-vegetal axis. Eggs were kept in this orientation for 20 to 30 min and the dorsal (upper) side was marked with Nile blue sulphate14. After the rotation period, eggs were allowed to orient normally in 20% Steinberg's solution with the vegetal pole downwards. At the 32-cell stage, embryos were microinjected either in a ventral, vegetal-most cell or a dorsal, vegetal-most cell with 3-5 nl of 0.3 M LiCl dissolved in 200% Steinberg's solution. At stage 40, the embryos were scored for development either as having a single body axis or with duplicated dorso-anterior development. The twins resulting from ventral cell injection are usually Janus twins with two diametrically opposed anterior ends, although some show closely approximated heads as in Fig. 2c.

ted 4 nl of 0.4 M solutions of NaCl, KCl, CsCl, RbCl or NH₄Cl, 50 mM solutions of CaCl2 or MgCl2, or a 10 mM solution of ZnCl₃ (higher concentrations of the latter three salts usually killed the embryos). All solutions were made up in 200% Steinberg's solution which, when injected alone into UV-irradiated embryos, did not cause rescue. Among the cations tested, only Li⁺ was able to cause significant rescue of dorsal structures.

Based on cell transplant experiments Gimlich and Gerhart¹¹ showed that a vegetal, dorsal cell at the 32-cell stage carried sufficient information to promote complete dorsal development. This information is translated by inductive cell interactions during cleavage to form dorsal elements. Our experiments show that Li⁺ is able to cause expression of dorsalizing information in cells that otherwise lack or do not express this information. Thus, the potential for cells to undergo dorsal development exists radially around the embryo even after axis specification. and such development will occur when stimulated by Li* at the appropriate time.

The ability to produce radial dorsal embryos with L should facilitate investigations on the molecular and cellular differences between dorsal and ventral pattern formation in X. laevis.

We thank JoAnn Render for initial discussions. This work was supported by a grant to R.P.E. from NSERC, Canada.

Received 12 March; accepted 25 April 1986.

- Elinson, R. P. Symp. Soc. dev. Biol. 38, 217-234 (1980).
- Gerhart, J. C., Ubbels, G., Black, S., Hara, K. & Kirschner, M. Nature 292, 511-516 (1981). Vincent, J.-P., Oster, G. F. & Gerhart, J. C. Devl Biol. 113, 484-500 (1986).
- Scharf, S. R., Vincent, J-P. & Gerhart, J. C. UCLA Symp. molec. cell. Biol. 19, 51-73 (1984).
- Cooke, J. Nature 319, 60-63 (1986).
- Grant, P. & Wacaster, J. F. Devl Biol. 28, 454-471 (1972).
- Scharf. S. R. & Gerhart, J. C. Devl Biol. 99, 75-87 (1983)
- Lehmann, F. Einführung in die physiologische Embryologie (Birkhauser, Basel, 1945). Backström, S. Archiv. Zool. 6, 527-536 (1954).

- Masui, Y. Experientia 17, 1-6 (1961).
 Gimlich, R. & Gerhart, J. C. Deul Biol. 104, 117-130 (1984).
 Kao, K. R. & Elinson, R. P. Deul Biol. 107, 239-251 (1985).
 Nieuwkoop, P. D. & Faber, J. Normal Table of Xenopus laevis (Daudin) (Elsevier, Amsterdam, 1967).
- 14. Kirschner, M. W. & Hara, K. Mikroskopie 36, 12-15 (1980)

Oral vaccination of the fox against rabies using a live recombinant vaccinia virus

J. Blancou*, M. P. Kieny†, R. Lathe†, J. P. Lecocq†, P. P. Pastoret‡, J. P. Soulebot§ & P. Desmettre§

- * Ministère de l'Agriculture, Centre National d'Etudes sur la Rage et la Pathologie des Animaux Sauvages, BP 9, 54220 Malzeville, France
- † Transgène SA, 11 rue de Molsheim, 67000 Strasbourg, France ‡ Faculté de Médecine Vétérinaire, Université de Liège,
- 45 rue des Vétérinaires, 1070 Bruxelles, Belgique
- § Rhône-Mérieux, Laboratoire IFFA, 254 rue Marcel Mérieux, 69342 Lyon, France

Rabies, a viral disease affecting all warm-blooded animals, is prevalent in most parts of the world1, where it propagates amongst wild animals, particularly the fox and dog. The public health and economic consequences of infection in man and livestock are well known. Attempts to control the disease by vaccinating wild carnivores with inactivated or attenuated rabies virus remain controversial, and we have instead evaluated here the potential of a recombinant vaccinia virus to protect foxes against the disease. We have found that the administration of vaccinia virus (VV) or a recombinant harbouring the rabies surface antigen gene (VVTGgRAB) is innocuous to foxes. The recombinant virus can elicit the production of titres of rabies-neutralizing antibodies equal or superior to those obtained with conventional vaccine, and 108 plaque-forming units (PFU) of VVTGgRAB administered subcutaneously, intradermally or orally confers complete protection to severe challenge infection with street rabies virus.

Table 1 Rabies-neutralizing antibodies and resistance to challenge

Vaccine and route	Dose (PFU)	Animals	Rabies neutralizing antibody titre*	Mean titre	Resistance to challenge†	Fraction surviving
No vaccine		#	0	NA		0/6
Conventional vaccine subcutaneous‡		440	1.21	1.49	+	2/2
		441	1.77		+	•
VVTGgRAB, intradermal§	10 ⁸	446	3.03	2.82	+	2/2
		449	2.61		+	-,
VVTGgRAB, subcutaneous§	108	439	3.03	NA	+	2/2
		442	0		+	-, -
VVTGgRAB, oral scarified	108	437	1.91	2.4	+	4/4
	4.00	438	2.33		+	., .
		447	2.61		+	
		452	2.75		+	
VVTGgRAB, oral	104	408	1.35	NA	+	1/4
, , , , , , , , , , , , , , , , , , ,		427	0		-	-, .
		428	0			
		429	Õ		***	
	10^{6}	416	0.8	0.4	+	2/4
		425	0.8	• • • • • • • • • • • • • • • • • • • •	<u>.</u>	- , ·
		426	0			
		430	0			
	10^{8}	414	2.33	2.57	+	4/4
		431	2.61		+	•, •
		433	2.61		+	
		451	2,75		+	
VVTGgRAB in bait	108	411	1.07	1.8		4/5
		412	1.63	***	+ .	٠, ٥
		420	2.61		+	
		423	2.19		+	
		424	1.49		+¶	

Rabies neutralizing antibody titres were determined in accordance with recommendations laid down by the World Health Organisation²⁷. Titres are expressed as the log₁₀ of the final neutralizing dilution (FND). For conversion to international units (IU) IU = 59/[antilog (3.5 - log FND)]. Foxes were monitored for 50 days following challenge and the presence of rabies virus in the brain of the animals succumbing to challenge was verified by immunoflorescence (not shown). Challenge virus GS6 (street virus comprising salivary glands from rabid foxes dispersed in phosphate-buffered saline (PBS) (20% w/v) as described previously²⁸) was injected in a volume of 1 ml containing 5,700 mouse LD₅₀ units (intracerebral), ~17,000 fox LD₅₀ units (intramuscular). Vaccinia Copenhagen strain and VVgRAB were grown on tissue culture cells as described elsewhere²⁹. Supernatants were recovered, the cell pellets homogenized, recentrifuged and pooled with the supernatant. Virus was purified by sedimentation through a sucrose cushion (36% w/v) for 2 h, 14,000 r.p.m., Beckman SW28 rotor. Pellets were suspended into PBS, sonicated briefly and banded by centrifugation on a sucrose gradient (20-40% w/v; 12,000 r.p.m., 45 min, SW28) before diluting (PBS) to the required concentration. Virus was titred on BHK21 cells. NA, not applicable.

* Only the 28-day titre is given.

- †+, Resisted challenge, -, succumbed to rabies. All animals not resisting died between 15 and 25 days after challenge.
- ‡ 'Rabisin ND' vaccine, lot 5532; neutralizing antibody titres obtained with live attenuated virus are similar (not shown).
- § Virus was inoculated intradermally as described (see text); subcutaneous injections were performed in a volume of 1 ml.
- Virus was administered by direct application into the mouth by syringe (vol. 1 ml).
- ¶ Two animals were observed to have ingested only a part of the vaccine.
- # Four animals were vaccinated with vaccinia virus Copenhagen strain, two animals received no treatment.

Transmission of rabies occurs predominantly through biting. Large quantities of virus are shed in the saliva and the aggressive behaviour of the rabid animal facilitates transmission. Infection by this route is invariably fatal and an immune population is therefore never established. Prophylactic measures have aimed at eliminating or reducing the population of the principal reservoir through poisoning or gassing², though a decrease in the carrier population density rarely reduces the rate of advance of the disease front³. In Europe, culling of foxes has reduced the number of rabies outbreaks but has not contained the disease. Vaccination, perhaps supported by culling in low-density fox populations, seems more likely to be effective than mere destruction of foxes⁴. An immune population is better able to limit the spread of the disease than one which is sparse but susceptible^{4,5}.

Oral administration could facilitate the vaccination of large numbers of wild foxes and this was first attempted in North America and Europe^{6,7}. Live attenuated rabies virus introduced into chicken heads, sausages or dog biscuits and distributed in the wild has been successfully used to vaccinate wild foxes⁸, and field trials are in progress in Switzerland, West Germany⁹ and Canada (C. D. MacInnes, personal communication).

However, the virus is often unstable and attenuated viruses retain pathogenicity for rodents and can revert to virulence¹⁰. Furthermore, inactivated rabies virus is ineffective when administered orally¹¹. A novel vaccination strategy, in which a recombinant vaccinia virus bearing a foreign antigen coding sequence is used as the immunizing agent¹²⁻¹⁴, seemed to hold some promise for the vaccination of foxes against rabies.

The causative agent of rabies is a rhabdovirus, and the glycoprotein (G) which traverses the envelope surrounding the virus, is the sole viral protein capable of inducing and reacting with virus-neutralizing antibodies or of conferring protection against rabies^{15,16}. The relative innocuity of vaccinia virus, which has been used extensively to control and eradicate smallpox in man¹⁷, has stimulated its development as a cloning and expression vector, and derivatives expressing surface antigens from influenza, hepatitis B and herpes simplex have been used to confer protection against these diseases¹⁴. We recently developed a recombinant VV (VVTGgRAB) expressing the rabies G coding sequence¹⁸ and found that mice scarified with the live recombinant virus VVTGgRAB resisted severe challenge with street rabies virus¹⁸⁻²⁰. VV itself is an enveloped virus and

the recombinant VVTGgRAB presenting rabies G protein elicited protection against rabies even after chemical inactivation¹⁹. We therefore extended our investigations to wild foxes.

Vaccinia virus (Copenhagen strain) was first tested for innocuity to foxes. European foxes (Vulpes vulpes) of both sexes captured in the wild and raised in captivity as described previously²¹ were inoculated with live vaccinia virus. Two animals (nos 445, 448) received VV by injection (vol. 0.1 ml) into the depilated skin of the back and two further animals (446, 449) received the recombinant VVTGgRAB by the same route. 102, 104, 106 or 108 PFU of virus were injected at triplicate sites and cutaneous reactions monitored for 15 days.

Mild localized inflammation was observed at the sites of injection with 106 or 108 PFU of virus, and in one animal (445) at 102 and 104 PFU. In all cases inflammation regressed spontaneously within 8 days. Cutaneous reaction was significantly greater with the wild-type strain of VV than with the recombinant VVTGgRAB strain (not shown). No lesions appeared elsewhere than at the site of injection and there was no evidence here of contact transmission of vaccinia virus between animals. In test animals receiving live recombinant vaccinia virus by direct application into the mouth (Table 1) no impairment of digestive or alimentary function was observed.

We subsequently examined the ability of the recombinant virus to elicit the production of antibodies directed against rabies virus. Animals inoculated intradermally, subcutaneously or orally with VVTGgRAB were bled on days 0, 8, 14 and 28; serum was separated and titred for the presence of rabiesneutralizing antibodies. High titres of neutralizing antibodies were present in sera from all but one animal treated with 108 PFU of VVTGgRAB (Table 1). Further, scarification of oral mucous membranes before oral administration (to facilitate penetration of the virus) did not yield improved titres of neutralizing antibodies. All animals presented only low levels of antibody capable of neutralizing VV (not shown), in agreement with other reports²².

Direct protection testing was then performed. Twenty-eight days after vaccination, animals were challenged by injection of 5,700 mouse LD₅₀ (50% lethal dose) units of rabies virus. All 12 animals recieving 108 PFU of VVTGgRAB either orally or parenterally resisted challenge (Table 1). One animal (442) exhibiting undetectable levels of rabies-neutralizing antibodies also resisted challenge, attesting to the relevance of cell-mediated immunity in defence against rabies 16,23. Control animals receiving no vaccine succumbed to the disease after 15-25 days. Two animals injected subcutaneously with a commercial inactivated (adjuvanted) vaccine similarly resisted challenge, although virus-neutralizing antibodies were present at a reduced level (Table 1). Oral administration of conventional (inactivated) vaccine has previously been shown to be ineffective11.

Animals receiving less than 108 PFU of VVTGgRAB showed a clear dose-dependent response, with one out of four and two out of four animals surviving challenge after oral administration of 10⁴ and 10⁶ PFU of VVTGgRAB, respectively (Table 1).

Oral administration is the only route appropriate to the vaccination of wild animals. Accordingly, the vaccine must be presented in a form suitable for ingestion. We thus prepared 'Plastipak capsules (a gift from Dr Wandeler) containing 108 PFU of VVTGgRAB, inserted them into chicken heads (one capsule per head into the beak) and distributed them to test animals (one per fox). These animals similarly produced high titres of rabies-neutralizing antibodies and resisted severe challenge with rabies virus (Table 1).

Transmissibility is a major factor determining the impact of a live vaccine on a wild population. We therefore sought to establish whether animals vaccinated with VVTGgRAB might transmit the virus by contact with untreated control animals. Four test animals (two male, two female) were acclimatized (4 days) to sharing a pen (2 m²) with an animal of the opposite sex. One animal from each pair received 108 PFU of live

VVTGgRAB by direct application into the mouth (vol. 1 ml). Serum samples were collected from both vaccinated and control animals at 14 and 28 days, and intramuscular challenge with live rabies virus (see Table 1 legend) was performed at 28 days.

All vaccinated animals presented high titres of rabiesneutralizing antibodies (mean 2.72 at 28 days, units as in Table 1) and resisted challenge. In three out of four control animals no rabies-neutralizing antibodies were detectable and these animals succumbed to challenge (not shown). Surprisingly, the fourth control animal (523, female) presented significant levels of rabies-neutralizing antibodies (1.35 and 0.97 at 14 and 28 days, respectively) and resisted severe challenge infection.

Subsequent investigations into possible mechanisms of transmission revealed that both the relevant vaccinated male (517) and control female 523 consistently displayed aggressive behaviour, and reciprocal biting was observed within a few minutes of oral vaccination. Contamination of bite wounds with VVTGgRAB may, in this instance, have been sufficient to effect immunization. Such a mode of transmission requires a combination of rather exceptional circumstances, and we surmise that contact transmisson of VVTGgRAB in the field is likely to be

We have shown that vaccinia virus and its recombinant VVTGgRAB bearing the rabies surface antigen are innocuous to healthy foxes; indeed, the thymidine kinase-negative recombinant may be more innocuous than wild-type strains of vaccinia virus²⁴. Our recombinant virus can confer complete protection to severe challenge infection with rabies virus. Similar experiments are in progress with other animal vectors of rabies, notably the skunk and racoon25. Importantly, presentation to foxes of the live recombinant, encapsulated and introduced into chicken heads, also yields animals resisting severe challenge infection. Procedures for the production, stabilization and distribution of vaccinia virus are fully established26. Due to its efficacy, innocuity and stability, the recombinant virus may be a candidate for the large-scale vaccination of wild foxes and, possibly, other feral or domestic animals.

We thank H. Koprowski and T. Wiktor for helpful discussion and for communicating unpublished data, R. Thomas for his practical suggestions concerning this study, D. Schmitt, K. Dott, J. Bailly, M. Sleve and E. Cain for technical assistance and N. Monfrini and L. Schneider for help in preparing the manuscript. We dedicate this manuscript to the late Dr T. Wiktor.

Received 10 March; accepted 18 April 1986.

- Steck, F. Symp. zool. Soc. Lond. 50, 57-75 (1982).
- Debbie, J. G. in Report on Rabies, 22-27 (Veterinary Learning Systems, Princeton, 1983).
- Toma, B. & Andral, L. Adv. Virus Res. 21, 1-36 (1977). Anderson, R. M., Jackson, H. C., May, R. M. & Smith, A. D. M. Nature 289, 765-771 (1981).
- Andral, L. & Blancou, J. Rev. Sci. Tech. Off. int. Epiz. 1, 927-959 (1982).
 Baer, G. M., Abelseth, M. K. & Debbie, J. G. Am. J. Epidemiol. 93, 487-490 (1974)
- Mayr, A., Kraft, H., Haeger, O. & Haake, H. Zentbl. VetMed. 19, 615-625 (1972). Blancou, J. Rec. Méd. Vét. 155, 733-741 (1979).
- Schneider, L. G., Cox, J. H. & Muller, W. W. Rev. Ecol. (Terre Vie) 46, 265-266 (1985).
- 10. Pépin, M. et al. Annls Inst. Pasteur Virol. 136E, 65-73 (1985).
- 11. Blancou, J., Andral, L., Aubert, M. F. A. & Artois, M. Bull. Acad. vés. Fr. 55, 351-359 (1982).
- 12. Panicali, D., Davis, S. W., Weinberg, R. L. & Paoletti, E. Proc. natn. Acad. Sci. U.S.A. 16. 5364-5368 (1983).
- Smith, G. L., Mackett, M. & Moss, B. Nature 302, 490-495 (1985).
 Smith, G. L., Mackett, M. & Moss, B. Biotechnol. genet. Engng Rev. 2, 383-407 (1984).
- Wunner, W. H., Dietzschold, B., Curtis, P. & Wiktor, T. J. J. gen. Virol. 64, 1649-1656 (1983).
- 16. Kieny, M. P., Desmettre, P., Soulebot, J. P. & Lathe, R. Prog. ver. Microbiol. Immun. 3 (in
- the press).
- 17. Rehhehani, A. M. Microbiol, Rev. 47, 455-509 (1983) 18. Kieny, M. P. et al. Nature 312, 163-166 (1984).
- Wiktot, T. J. et al. Proc. natn. Acad. Sci. U.S.A. 81, 7194-7198 (1984).
- 20. Lathe, R. et al. in Vaccines 85 (eds Lerner, R., Chanock, R. & Brown, F.) 157-162 (Cold
- Spring Harbor Laboratory, New York, 1985).

 21. Dubreuil, M., Andral, L., Aubert, M. F. A. & Blancou, J. Ann. Rech. Vet. 18, 9-21 (1979).
- Appleyard, G. & Andrews, C. J. gen. Virol. 23, 197-200 (1974). Wiktor, T. J. Dev. biol. Standard. 40, 225-264 (1978).
- Buller, R. M., Smith, G. L., Moss, B., Cremer, K. & Notkins, A. L. in Vaccines 85 (eds Lerner, R., Chanock, R. & Brown, F.) 163-167 (Cold Spring Harbor Laboratory, New York, 1985).
- 25. Wiktor, T. J. Inst. Pasteur Symp. Vaccines and Vaccination (in the press).
- World Health Organisation Tech. Rep. Ser. 323 (WHO, Geneva, 1966).
 Kaplan, M. M. & Koprowski, H. La Rage: Techniques de Laboratoire 3rd edn (World Health Organisation, Geneva, 1974).
- 28. Blancou, J., Aubert, M. F. A., Andral, L. & Artois, M. Rev. Med. vet. 136, 1001-1015 (1979).
- 29. Drillien, R., Tripier, F., Koehren, F. & Kirn, A. Virology 79, 369-380 (1977)

Preferential expression of a defined T-cell receptor β-chain gene in hapten-specific cytotoxic T-cell clones

Ute Hochgeschwender*†, Hans Ulrich Weltzien†, Klaus Eichmann†, R. Bruce Wallace* & Jörg T. Epplen*

* Junior Research Unit and † Department of Cellular Immunology, Max-Planck-Institut für Immunbiologie, D-7800 Freiburg, FRG

A multitude of different antigens can be recognized by T cells through specific receptors. Both the α - and β -chains of the T-cell receptor contribute to the antigen recognition portion1. The repertoire of β -chain variable region (V_{β}) gene segments is limited to some 20 elements²⁻⁴ which seem to be used randomly in different T cells^{2,5,6}. Diversity at the β-chain level can be created in several ways^{2,3,7-12}; a multiplicity of germline gene segments; combinatorial diversity by rearranging different V, diversity (D), joining (J) and constant (C) region elements; junctional diversity by joining gene segments at different sites; N-region diversity, that is, insertion of random nucleotides at junctional sites; and somatic mutation¹³. However, the major sources and the extent of diversity of the T-cell receptor are unclear. To address this issue, 42 H-2Kb-restricted, 2,4,6-trinitrophenyl (TNP)-specific cytotoxic T-cell (Tc) clones from C57BL/6 mice were characterized with respect to expression of different β-chain gene segments in messenger RNA using specific oligonucleotide probes. We report here that nearly half of the T_c clones use identical elements for productive β-chain gene rearrangement. Thus, there is a restriction in the use of β-chain gene segments in this panel of T_c clones which favours a particular $V_{eta}\!-\!D_{eta}\!-\!J_{eta}\!-\!C_{eta}$ combination with a defined D_{α} element.

A collection of 42 class I (H-2K^b) restricted cytotoxic T-cell clones possessing specificity for the hapten TNP has been established ¹⁴. In order to isolate and characterize the expressed T-cell receptor β -chain gene of a randomly chosen T-cell clone, a complementary DNA library was constructed in the bacteriophage vector λ gt11 from total cellular RNA of T_c clone 112-2. The nucleotide sequence of a β -chain cDNA clone (pBJ2.1) was determined as $V_{\beta}3$ - $D_{\beta}112$ -2- $J_{\beta}2$ -6- $C_{\beta}2$ (nomenclature according to ref. 2; $V_{\beta}3$ is termed $V_{\beta}2B4$ in ref. 7 and $V_{\beta}13$ in ref. 3), whereby $D_{\beta}112$ -2 is a segment of seven nucleotides partly different from the known germline sequences of $D_{\beta}1$ -1 or $D_{\beta}2$ -1 (Fig. 1a).

Synthetic oligonucleotides were prepared which were specific for the V, D and J segments of T_c clone 112-2 (Fig. 1a) in order to determine the frequencies with which the $V_{\beta}3$, $D_{\beta}112-2$ and J_{β} 2-6 gene segments are used in the panel of T_{c} clones. Furthermore, oligonucleotides specific for the $C_{\beta}1$, $C_{\beta}2$ and C_{α} gene elements were used for sequential Northern blot or direct gel hybridizations. An example is shown in Fig. 1b in which hybridizations of an RNA gel with the set of oligonucleotide probes reveal the individual elements expressed in β-chain mRNAs of the different T_c clones. We found that 19 out of 42 (45%) T_c clones use the same V_{β} 3 gene segment as T_c clone 112-2 (see Fig. 2). Moreover, whenever the V_B 3 gene segment is expressed, it is always rearranged to D_{β} 112-2, J_{β} 2-6 and C_{β} 2 as in T_c clone 112-2 (see Figs 1b, 2). Therefore, 45% of the H-2Kb/TNP-specific T_c clones must use identically composed β-chain genes for the T-cell receptors. In half of the remaining T_c clones, different V_{β} and D_{β} elements are joined to the $J_{\beta}2-6-C_{\beta}2$ gene segments, while 30% of all T_c clones use additional V_{β} , D_{β} and J_{β} elements in connection with either $C_{\beta}1$ or $C_{\beta}2$.

To obtain additional evidence that the D elements used in individual T_c clones are identical—in particular with regard to the V-D and D-J junctions—probes were designed with one

or two base mismatches at the borders of the $D_{\beta}112\text{-}2$ element (see Fig. 3). EcoRI-digested DNA of cDNA clone pBJ2.1 was probed with the perfectly matched $D_{\beta}112\text{-}2$, the D_{I} (one mismatch at the D-J junction), the D_{II} (two mismatches at the D-J junction) and the D_{III} (one mismatch at the V-D junction) probes under various conditions (Fig. 3). Only the perfectly matched $D_{\beta}112\text{-}2$ probe was able to form stable hybrids under the standard conditions employed. Corresponding results were observed in RNA hybridization experiments (data not shown). Therefore, the finding that 45% of T_{c} clones give positive signals with the $D_{\beta}112\text{-}2$ probe indicates that very similar or identical D elements are being expressed.

The $V_{\beta}3$, $D_{\beta}112-2$ and $J_{\beta}2-6$ oligonucleotide probes were also employed in the DNA hybridization analysis of the panel of H-2K^b/TNP-specific T_c clones using different restriction enzymes. As an example, Fig. 4 shows the gel hybridization pattern obtained with EcoRI-digested DNA from three Tc clones and B6 liver (Fig. 4). Using the $V_{\beta}3$ probe, two germline gene segments were detected in B6 liver DNA, while the band of high relative molecular mass (M_r) corresponds to the $V_{\beta}3$ band of the B10.A mouse (refs 2, 12 and our unpublished results). Sequence analysis of the coding region of the B6 germline $V_{\rm g}3$ element revealed identity with the known segment from B10.A mice. Southern blot and DNA gel hybridizations of all V_B 3positive T_c clones revealed identical productive V_B3 rearrangements (data not shown), suggesting that only the element of the high- M_r band is used. With the $V_B 3$ and $J_B 2$ -6 probes, in addition to germline elements, rearranged gene segments were detected in T_c clones. Hybridization of the D_{β} 112-2 oligonucleotide to the DNAs produced a signal exclusively in a T_c clone in the same position as the productively rearranged $V_{\beta}3$ and $J_{\beta}2$ -6 elements (Fig. 4). The hybridization specificity and design of the D_{β} 112-2 probe (Fig. 1a) ensures that a positive signal can be obtained only when D_{β} 112-2 is rearranged to the V_{β} 3 and J_{β} 2-6 gene segments. All the T_c clones that scored positive for the complete preferentially expressed V_{β} gene showed the single D_{β} 112-2 band of Fig. 4 (data not shown). In additional Southern blot hybridization, the rearrangements of the $C_{\beta}1$ and $C_{\beta}2$ loci were investigated in T_c clones which did not hybridize with V_a 3. D_{β} 112-2 or J_{β} 2-6 probes. Nick-translated and oligonucleotide probes specific for the $J_{\beta}1$ and $J_{\beta}2$ clusters revealed heterogeneous rearrangements in $J_{\beta}1$ for the $C_{\beta}1$ -positive T_{c} clones and in $J_{\beta}2$ for the $C_{\beta}2$ -positive T_{c} clones (data not shown). With regard to the productive rearrangements, this heterogeneity stands in contrast to the uniformity observed in the group of T_c clones that express the defined V_{β} gene.

Although there have been no similar studies of T-cell receptor β-chain diversity in an antigen-specific restricted immune response, data are available on Southern hybridization experiments of cytochrome c-specific T-helper (Th) hybridomas15 and bulk T-cell lines specific for hen egg white lysozyme5. Both reports present evidence that similar or identical β-chain gene rearrangements have occurred in the DNA of their isolated Th cells from the same immune response. It is assumed, therefore, that these T_h cells express identical V_{β} genes. Our investigation shows clearly that in a collection of T_c clones specific for the same antigen (H-2Kb/TNP), a defined complete T-cell receptor β-chain gene is preferentially expressed. The reasons for this are unknown, but the situation is reminiscent of observations of humoral immune responses; in the mouse the antibody response to certain model antigens¹⁶⁻¹⁹ is characterized by the dominant expression of one or a few related immunoglobulin heavy-chain V-region genes by antibody-secreting lymphocytes. In contrast to the similarities to V-gene expression in B- and T-cell receptors in defined immune responses, the choice of the D segment appears to be restricted only in the β -chain of T_o clones. D-region identity is not found in specific humoral immune response. In immunoglobulins, the V regions of heavy chains are often almost identical, whereas the D segments are extremely variable 16-18, although antigen recognition is

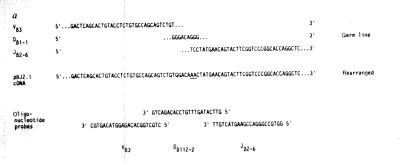
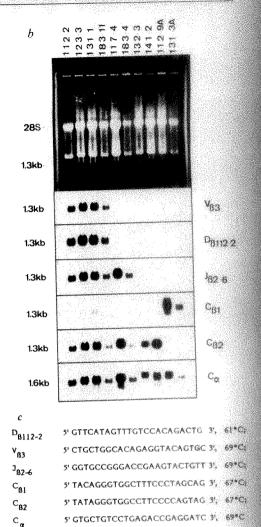


Fig. 1 a, Sequences of the V_{β} , D_{β} and J_{β} gene segments in germline configuration and after rearrangement in the TNP-specific T_c clone 112-2, illustrating junctional and N-region diversity. cDNA clone pBJ2.1 is compared with published germline gene segments $V_{\beta}3$ (ref. 7), $D_{\beta}1$ -1 (ref. 11) and $J_{\beta}2$ -6 (ref. 7). At least two nucleotides (underlined) at the D-J joining of pBJ2.1 are encoded by neither the germline D_{β} nor the J_{β} segment. The oligonucleotide probes $V_{\beta}3$, $D_{\beta}112$ -2 and $J_{\beta}2$ -6 are complementary to the mRNA and depicted below the cDNA sequence. b, Gel hybridization analysis of RNA from 10 different T_c clones specific for H-2Kb/TNP using six different $J_{\beta}2$ -P-labelled oligonucleotide probes specific for different T-cell receptor gene segments. kb, kilobases.

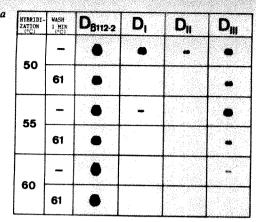
Methods. a, A cDNA library was constructed from total cellular RNA of Tc clone 112-2 in the bacteriophage vector Agt11. Screening was carried out according to ref. 22, using a nick-translated probe (AK1)²³ which hybridizes with the constant region of the T-cell receptor β-chain gene. Positive clones were isolated and plaque purified. A hybridizing cDNA clone from the 112-2 library was subcloned into pUC12 (pBJ2.1) and into M13mp9. Sequence analysis of pBJ2.1 was carried out according to Sanger et al.24. The sequence of the 740-base-pair (bp) insert of pBJ2.1 consists of the 3' end of a V_{β} (~100 bp), a D_{β} and a J_{β} element as well as a complete C_{β} (including some 50 bp of 3' untranslated sequence). b, RNA from cultured cells was extracted in the presence of guanidinium thiocyanate²⁵ and pelleted by centrifugation through a 5.7 M caesium chloride cushion. RNA (10 µg) was denatured in the presence of formaldehyde and agarose gel electrophoresis was performed26. The ethidium bromide-stained gel was photographed under ultraviolet light (top) and dried27 or blotted onto GeneScreen (NEN). Oligonucleotides were synthesized on an automated DNA synthesizer and radiolabelled using $[\gamma^{-32}P]ATP$ and T4 polynucleotide kinase²⁸. All hybridizations and washing steps were carried out according to ref. 18. c, The same gel has been hybridized consecutively with various probes (in the order given) at 60 °C and was washed for 1 min at the indicated temperatures. The washed gel was exposed to Kodak XAR-5 films using Quanta III (Dupont-Cronex) intensifying screens for approximately 40 h. After each exposure, probes were removed by washing the gel in 5 mM EDTA at 60 °C. Washing efficiency was monitored by control exposures.



	Designation
8-chain gene segments	of T _C clones
Ĩ	

PERHINE	HIBBER	HIMBE		11.2-2
	Millilli	HIHHH	allanin	112~3
V _{B3}	D ₆₁₁₂₋₂	Jan. 6	Cap	117-3
***************************************	200000000000000000000000000000000000000	*********	202000000	122-1
			Hillish II	122-6
				123-1
	Million .			123-3
				131-1
lumming	bonnel			133-2
45%	45%			
Sources	Browned			162-1
				163-2 177-1
				182-5
	11/19/11/11	69%		183-2
		07.0		183-6
				183-9
			humani	183-11
			81%	187-2
	MILLION IN			112-6A
ļ	1			117-1
				117-4
1	1			131-2
				132-4
1				137-L
	1	3163.33		183-3
				183-3.1
1	1			183-4
	1	M. C. Carlotte		183-7
1	1		331050	132-3
1		1		141-2
1	1			161-1 163-4
		1		183-1
	Ì		etataketa	112-9A
	1	1	11111	113-4A
1	1	1	1	117-2A
i	1		CBI	121-1
1			11111	131-3A
1			19%	142-2A
1	1	1	11111	143-2A
1	1		1111	147-1

Fig. 2 T-cell receptor β-chain genes of H-2Kb/TNP-specific To clones. The 42 T_c clones are listed according to their β-chain gene structure as determined by Northern blot or RNA gel hybridizations with specific oligonucleotide probes (see Fig. 1b legend for a description of the probes). The panel of T_c clones was derived from seven individual mice. Briefly, 5-6-week-old female C57BL/6 mice were immunized with TNP^{29,30}. Cultures from spicens of immunized mice were established 10 days later with immune spleen cells and irradiated B6 spleen cells coupled with TNP as stimulator cells in medium containing interleukin-2. From 32 independent cell lines, 42 T_c clones were derived from cultures containing on average 0.5 cells per culture. According to Poisson statistics, at least 77% of the 42 clones should have been derived from a single cell while up to 10 may have been derived from 2 or more cells 4 T_c clones were grown in the presence of stimulator cells and interleukin-2 by weekly restimulation. Cells were collected for extraction of RNA and DNA 4 days after restimulation. At the time of RNA and DNA extraction, Tc clones investigated have been in continuous culture for 5-8 months. In some cases the cells had been frozen, then thawed and regrown for RNA and DNA extraction (indicated by 'A'). T_c clones were tested for cytotoxic function and H-2Kb/TNP specificity at monthly intervals in a 51Cr-release assay. Clones were numbered according to the series of immunization, the individual mouse, the individual cell line derived from the spleen of a certain mouse and the cultures obtained after cloning: for example, T_c clone 112-2 is from series 1, mouse 1, line 2, clone 2.



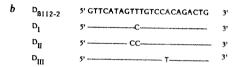


Fig. 3 a, Hybridization specificity of the oligonucleotide probe $D_{\rm B}$ 112-2 and three derivatives with base mismatches at the V-Dand D-J junctions. pBJ2.1 (3 μg) was digested with EcoRI, divided into six identical aliquots and subsequently subjected to electrophoresis in a 0.75% agarose gel³¹. After denaturation, neutralization and drying of the gel²⁷, the six individual lanes were cut. b, Gels strips were consecutively hybridized with the D_B 112-2 probe and its derivatives. After hybridization at the indicated temperatures, each gel strip was washed in 6×SSC at room temperature. Half of the gel strips were then washed for 1 min at 61 °C as indicated. Steps were exposed for 15 h without intensifying screen. After each hybridization the probe was removed and gel strips re-exposed to exclude any remaining signal.

maintained. This indicates that the D regions of heavy chains are involved in idiotypy^{20,21}. There is no obviously analogous role for the D region in the T-cell receptor β-chain.

The finding that 45% of the H-2Kb/TNP-specific T_c clones express very similar or identical D_{β} elements is unexpected in view of the fact that the $D_{\beta}112-2$ element is not identical to known germline D_{β} elements. If the germline D_{β} 1-1 element is assumed to be used, at least two bases (AA) at the borders of the D_{β} - J_{β} junction are not germline encoded (see Fig. 1a) and consequently are generated by a random process². If one assumes that the β -chain D region is important for antigen

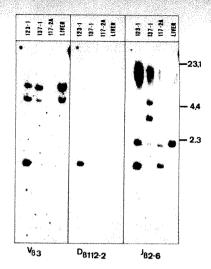


Fig. 4 Analysis of DNA from T_c clones specific for H-2K^b/TNP and from liver of the B6 mouse.

Methods. Cellular DNA was extracted modified according to ref. 31. DNA (10 µg) prepared from T_c clones was digested to completion with the restriction enzyme *EcoRI*. DNAs were electrophoresed in 0.75% agarose gels³¹. After denaturation and neutralization the gel was dried²⁷ and hybridized consecutively with the oligonucleotide probes J_{β} 2-6, D_{β} 112-2 and V_{β} 3. (See Fig. 1b legend for a description of the probes.) The gel was exposed for 4 days with intensifying screens. M_r markers are indicated in

binding and that the dinucleotide AA of the AAC codon for asparagine is critical for TNP recognition, then its presence in nearly half of the T_c clones would be due to selection by the antigen. On the other hand, the D_{β} 112-2 element might be encoded by a hitherto undescribed D_{β} segment in which the preferential combination of this D element with $V_B 3$ and $J_B 2-6$ could also be explained by selective forces. We have found evidence (from additional oligonucleotides covering the V_{β} 3- D_{B} 112-2 junction) for independence of the V_{B} 3 and D_{B} 112-2 elements; it remains to be seen how the D_{β} 112-2 element is in fact generated.

We thank Hannelore Thoma and Ulrike Pflugfelder for tissue culture work, Gary McMaster for Agt11 DNA, Lore Lay for art work, and Rosemary Schneider for secretarial assistance. R.B.W. was recipient of a research award from the Alexander von Humboldt-Stiftung. This work was partially supported by the Deutsche Forschungsgemeinschaft. R.B.W. was on sabbatical leave from Beckman Research Institute of the City of Hope, Duarte, California 91010, USA.

Received 16 January; accepted 24 April 1986.

- 1. Yagüe, J. et al. Cell 42, 81-87 (1985)
- Barth, R. K. et al. Nature 316, 517-523 (1985).
- Behlke, M. A. et al. Science 229, 566-570 (1985). 4. Davis, M. M. A. Rev. Immun. 3, 537-560 (1985)
- Goverman, J. et al. Cell 40, 859-867 (1985).
- 6. Rupp, F., Acha-Orbea, H., Hengartner, H., Zinkernagel, R. & Joho, R. Nature 315, 425-427 (1985).
- 7. Chien, Y., Gascoigne, N. R. J., Lee, N., Kavaler, J. & Davis, M. M. Nature 309, 322-327
- 8. Malissen, M. et al. Cell 37, 1101-1110 (1984)
- Gascoigne, N. R. J., Chien, Y. H., Becker, D. M., Kavaler, J. & Davis, M. M. Nature 310, 387-391 (1984).
- Kavaler, J., Davis, M. M. & Chien, Y.-H. Nature 310, 421-423 (1984).
 Siu, G. et al. Nature 311, 344-350 (1984).
 Patten, P. et al. Nature 312, 40-46 (1984).
- Augustin, A. A. & Sim, G. K. Cell 39, 5-12 (1984).
- 14. Weltzien, H. U., Kempkes, B., Jankovic, D. L. & Eichmann, K. Eur. J. Immun. 16, 631-639
- 15. Hedrick, S. M. et al. Proc. natn. Acad. Sci. U.S.A. 82, 531-535 (1985).

- 16. Schilling, J., Clevinger, B., Davie, J. W. & Hood, L. Nature 183, 35-40 (1980).
- Schming, J., Clevinger, B., Davie, J. W. & Hood, L. Nature 193, 35-40 (1950).
 Gearhart, P. J., Johnson, N. D., Douglas, R. & Hood, L. Nature 291, 29-34 (1981).
 Kaartinen, M., Griffiths, G. M., Markham, A. F. & Milstein, C. Nature 304, 320-324 (1983).
 Manser, T., Huang, S.-Y. & Gefter, M. L. Science 226, 1283-1288 (1984).
 Gridley, T., Margolies, M. N. & Gefter, M. J. Immun. 134, 1236-1244 (1985).

- Radbruch, A. et al. Nature 315, 506-508 (1985).
 Benton, W. D. & Davis, R. W. Science 196, 180-182 (1977).
- 23. Rinaldy, A., Wallace, R. B., Simon, M. M., Becker, A. & Epplen, J. T. Immunogenetics 21. 403-406 (1985).
- Sanger, F., Coulson, A. R., Barell, B. G., Smith, A. J. H. & Roe, B. J. molec. Biol. 143, 161-178 (1980).
- Chirgwin, J. M., Przybyla, A. E., MacDonald, R. J. & Rutter, W. J. Biochemistry 18, 5294-5299 (1979).

- Thomas, P. S. Proc. natn. Acad. Sci. U.S.A. 77, 5201-5205 (1980).
 Tsao, S. G. S., Brunk, C. F. & Pearlman, R. E. Analyt. Biochem. 131, 365-372 (1983).
 Miyada, C. G., Reyes, A. A., Studencki, A. B. & Wallace, R. B. Proc. natn. Acad. Sci. U.S.A. 82, 2890-2894 (1985)
- Shearer, G. M. Eur. J. Immun. 4, 527-533 (1974).

- Snearet, G. M. Lut. J. Dinnaud. 3, 227-223 (1974).
 Fujiwara, H. & Shearer, G. A. J. Immun. 126, 1047-1051 (1981).
 Maniatis, T., Fritsch, E. F. & Sambrook, J. Molecular Cloning: A Laboratory Manual (Cold Spring Harbor Laboratory, New York, 1982).

Alternative splicing of murine T-cell receptor β -chain transcripts

Mark A. Behlke & Dennis Y. Loh

Howard Hughes Medical Institute, Departments of Medicine, Microbiology, and Immunology, Washington University School of Medicine, St Louis, Missouri, 63110, USA

Variable processing of heteronuclear RNA into multiple, defined species of messenger RNA is a well-established phenomenon in a number of systems, including myelin basic protein1,2, calcitonin3, troponin T4 and immunoglobulins5-7. Within a single B cell, immunoglobulin heavy-chain peptides often exist as two related but distinct species, a membrane-bound form and a secreted form, both of which originate from the same germline constant(C)-region gene via alternative RNA processing pathways5. Furthermore, at certain stages of B-cell development, a single variable(V)-region element can be concurrently expressed in immunoglobulins of both the IgM and IgD isotypes, presumably resulting from the alternative splicing of one variable-region exon to different constantregion genes^{6,7}. We report here the existence of an alternative RNA splicing pathway available to murine T-cell receptor (TCR) β -chain transcripts. Sequence analysis of β -chain complementary DNA clones reveals a C_0 1 species containing a 72-base pair (bp) insertion between the joining (J_{eta}) and C_{eta} elements. This sequence is inserted via an alternative splicing pathway available to $C_{\beta}1$ transcripts. The optional exon is located between the $J_{\beta}1$ cluster and the first exon of C_{β} 1. Interestingly, this element can be spliced to $C_B 2$ in the New Zealand White mouse, in which the $C_B 1$ gene is deleted^{8,9}. Use of the alternative splicing pathway varies between 1% and 18% of total C_{β} clones, depending on the source of isolation.

We previously reported the nucleotide sequences of a series of murine TCR β -chain variable-region genes identified from 15 V_{β} - C_{β} -containing cDNA clones 10. All 15 of these clones contain a somatically rearranged V_{β} - D_{β} - J_{β} element and a C_{β} element, of which 13 clones have the V_{β} - D_{β} - J_{β} element spliced in the expected manner to the C_{β} element. The remaining two clones were both found to contain an identical 72-bp insertion between their J_{β} and C_{β} elements. The insertion of this 72-bp sequence maintains the open translational reading frame seen in conventionally spliced J_{β} - C_{β} -containing cDNAs and results in the addition of 24 extra codons precisely at the J_{β} - C_{β} splice junction 11.12. As such, the 72-bp insertion appears to define the existence of a new exon which is available for alternative splicing of β -chain transcripts. We call this new exon C_{β} 0.

Of the two clones initially found to include this novel sequence, clone B/C-61 contains $V_{\beta}10-D_{\beta}1.1-J_{\beta}1.6-C_{\beta}0-C_{\beta}1$ and clone B/C-77 contains $V_{\beta}8.2-D_{\beta}1.1-J_{\beta}1.6-C_{\beta}0-C_{\beta}1$. (V_{β} nomenclature follows that of Barth *et al.*¹³, as described in Behlke et al.14). Subsequently, a third cDNA clone (B/C-04) which also contained the C_80 exon was obtained. This clone contains $J_{\beta} 1.3 - C_{\beta} 0 - C_{\beta} 1$ and is truncated within the J_{β} element. The nucleotide sequences of these three cDNA clones are presented in Fig. 1a. These clones all originated from a BALB/c thymus cDNA library; two out of four V_{β} -containing clones examined from this library10 contained the alternatively spliced C_{β} 0 exon. To determine whether alternatively spliced C_{β} 0- C_{β} containing clones could be detected in lymphoid tissue other than thymus, the two oligonucleotide probes described in Fig. 1c were used to screen an unamplified B6 spleen cDNA library. Four C_{β} 0-containing clones were identified from a total of 301 that were C_{β} positive. Three of these four clones contain V_{β} elements; their DNA sequences are presented in Fig. 1b. Clone B6-26s contains $V_{\beta}12-D_{\beta}1.1-J_{\beta}1.1-C_{\beta}1$, clone B6-34 contains $V_{\beta}6-D_{\beta}1.1-J_{\beta}1.1-C_{\beta}1$, and clone B6-73 contains $V_{\beta}1-D_{\beta}1.1-$

Table 1 Relative expression of the C_80 exon in cDNA libraries

cDNA library	$C_{\beta}0$	$C_{oldsymbol{eta}}$	Frequency of $C_{\beta}0$	Frequency of $C_{\beta}1$	Total no. of clones screened
C57BL/6 spleen	4	301	1.3%	27%	350,000
C57BL/6 thymus	14	267	5%	32%	60,000
NZW thymus	26	146	18%	*	40,000

cDNA libraries were constructed and screened as described in the legends to Figs 1 and 3. Libraries were also screened with nick-translated probes specific for $C_{\beta}1$ and $C_{\beta}2$; these probes contain only 3' untranslated (UT) sequence and were subcloned from C_{β} 1- and C_{β} 2-containing cDNA clones. It is not clear whether the frequency of C_{β} 0-containing clones in unamplified cDNA libraries reflects the actual frequency of these species in vivo. While we have no way of directly addressing this question for C_8 0-containing transcripts, we can make such a comparison for a different subset of β -chain transcripts. The C57BL/6 spleen cDNA library has been screened for V_{β} usage (complete data to be presented elsewhere); out of 154 C_{β} -positive clones examined, 102 hybridize to probes specific for the 16 known murine V_{β} subfamilies 14, including 19 clones which hybridize to $V_{\beta}8.2$. Thus, 19% (19/102) of known V_{β} -containing clones and 12% (19/154) of total C_{β} -containing clones contain V_{β} 8-subfamily genes in our B6 spleen cDNA library. The anti-TCR monoclonal antibodies F23.1 and KJ16-133 recognize 19% and 13%, respectively, of peripheral T cells in B6 mice^{30,31}. These reagents are believed to identify a subset of β -chain peptides expressing elements of the three-member $V_{\beta}8$ subfamily ^{14,32}. Thus, expression of at least one subset of β -chain clones in our cDNA library approximates the known level of expression of this same subset in vivo. We presume the same will be true for C_{β} 0-containing clones.

* Does not apply.

 $J_{\beta}1.4-C_{\beta}1$. Clone B6-27 (not shown) contains $C_{\beta}0$ spliced as expected to $C_{\beta}1$, but does not contain an identifiable J_{β} or V_{β} element 5' to $C_{\beta}0$. The seven $C_{\beta}0$ -containing clones described above use five different V_{β} elements and four different J_{β} elements, thus the alternative splicing pathway does not prefer any particular J_{β} or V_{β} sequence.

All seven C_{β} 0-containing clones obtained thus far also contain C_{β} 1, implying that the C_{β} 0 exon should be located between the $J_{\beta}1$ cluster and $C_{\beta}1$ in the genome. A BALB/c genomic library was screened with a C_{β} probe, and a phage was isolated which contained both the $J_{\beta}1$ cluster and $C_{\beta}1$. As expected, C_{B} 0-specific probes hybridize to this genomic clone. A restriction map of the $J_{\beta}1-C_{\beta}1$ region of this phage is presented in Fig. 2a, and the nucleotide sequence of the C_B0 -hybridizing region is presented in Fig. 2b. The nucleotide sequence of the C_80 exon and its flanking introns closely match the consensus donor and acceptor splice sites established by Breathnach and Chambon¹⁵ (Fig. 2c), and the splice sites predicted by such an analysis are in complete agreement with the actual nucleotide sequences of the spliced C_{β} 0-containing cDNAs in Fig. 1. We conclude that the inclusion of the $C_{\beta}0$ exon in transcripts represents a naturally occurring alternative splicing pathway and is not an aberrant event or cloning artefact.

Thus far, $C_{\beta}0$ -containing clones have only been identified in cDNA libraries constructed from heterogeneous populations of T cells, such as from thymus or spleen, and not in libraries constructed from cloned T cells. From such data we cannot determine whether the 1.3% incidence of $C_{\beta}0$ expression seen in C57BL/6 spleen reflects a low level of alternatively spliced message in all $C_{\beta}1$ -expressing cells or if a particular subset of $C_{\beta}1$ -expressing cells selectively express $C_{\beta}0$ at higher levels. Two cDNA libraries we examined from cloned T cells both proved to have their V_{β} elements productively rearranged to $J_{\beta}2$ - $C_{\beta}2$ (ref. 10), and no $C_{\beta}0$ - or $C_{\beta}1$ -containing clones were obtained. Molecular analysis of several $C_{\beta}1$ -expressing T-cell clones have been reported $^{13,16-18}$, but no $C_{\beta}0$ -containing cDNAs were described in these reports. A thorough examination of

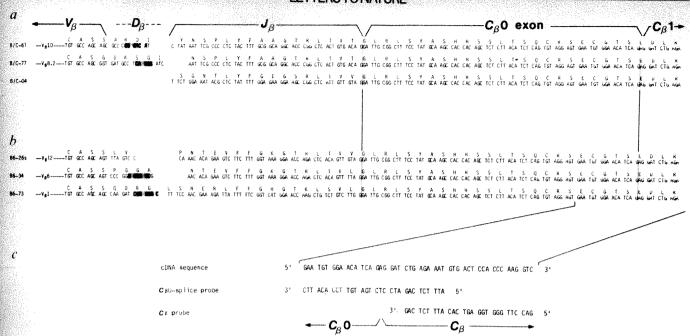


Fig. 1 Nucleotide and amino-acid (one-letter code) sequence of alternatively spliced TCR β -chain cDNAs. a, Isolates from BALB/c thymus. Clones containing a 72-bp insertion between the J_{β} and C_{β} elements are presented. Nucleotide and predicted amino-acid sequences begin at the 3' conserved cysteine codon of the V_{β} element and extend into the 5' end of C_{β} . Additional V_{β} or C_{β} sequence is not included as these sequences are well established $^{10-14,19}$; V_{β} gene segments are identified according to the nomenclature of Barth et al. a described in Behlke et al. Sequences contributed from the germline D_{β} 1.1 element are shaded while J_{β} gene segments are aligned separately. The J_{β} and C_{β} splice junctions are demarcated, and the 72-bp insertion has been labelled C_{β} 0. b, Isolates of three V_{β} -containing alternatively spliced cDNAs from C57BL/6 spleen. c, Design of C_{β} and C_{β} 0-specific synthetic oligonucleotide probes. The nucleotide sequences of alternatively spliced cDNA clones at the C_{β} 0- C_{β} splice junction are given, under which are aligned the sequences of two synthetic oligonucleotides which are complementary to the original cDNA sequence. The C_{β} 0-splice probe spans the C_{β} 0- C_{β} splice junction and is specific for clones in which the C_{β} 0 exon has been spliced to C_{β} . The C_{β} probe is complementary only to actual C_{β} coding sequence and hybridizes to all C_{β} -containing clones which extend sufficiently 5' to contain this sequence.

Methods. a, A BALB/c thymus cDNA library was screened with a TCR C_β-specific probe¹⁰. Random clones were subcloned into pUC12 and their nucleotide sequences were determined by the method of Maxam and Gilbert²⁵. b, A C57BL/6 spleen concanavalin A blast cDNA library (previously described¹⁰) was screened with a C_β0-specific oligonucleotide probe, as described below. C_β0-containing cDNAs were subcloned into pUC12 and their nucleotide sequences were determined by the method of Maxam and Gilbert²⁵. ³²P-labelled oligonucleotide probes were hybridized at 68 °C in 0.9 M NaCl, 0.18 M Tris pH 7.4, 0.012 M EDTA, 2× Denhardt's solution, and 20 μg ml⁻¹ salmon sperm DNA; washing was performed at 55 °C in 0.75 M NaCl, 0.075 M sodium citrate (5× SSC)²⁶.

several C_{β} 1-expressing T-cell clones for C_{β} 0 expression will be required to resolve this point.

The absence of $C_{\beta}0$ -like alternative splicing products in $C_{\beta}2$ containing transcripts can be explained in several ways. First, it may be that a $C_{\beta}0$ analogue $(C_{\beta}0')$ exists between the $J_{\beta}2$ cluster and C_{β} 2 but that this element has diverged far enough from the C_{β} 0 sequence described here so that our synthetic oligonucleotide probes do not cross-hybridize with it. Our first three $C_{\beta}0$ - $C_{\beta}1$ -containing clones were identified from an analysis of randomly isolated C_{β} -positive thymus cDNA clones (Fig. 1a). All subsequent C_{β} 0-containing clones were identified by hybridization to an oligonucleotide probe, which would select against the isolation of $C_{\beta}0'-C_{\beta}2$ -containing clones if this probe did not cross-hybridize to the putative $C_{\beta}0'$ sequence. A small number of C_{β} 2-containing clones have been examined for this possibility, and no $C_{\beta}0'-C_{\beta}2$ clones were found. While this may suggest that variable RNA splicing occurs exclusively in $C_{\beta}1$ transcripts, it is also possible that an insufficient number of $C_{B}2$ clones has been examined. However, we note that both nicktranslated and oligonucleotide probes specific for C_B0 do not hybridize to murine C_{β} 2-containing genomic clones (data not shown), and that no sequence with an open reading frame and >50% homology to C_8 0 can be found within 900 bp 5' of the first exon of C_{β} 2 (ref. 19).

It has been reported that the New Zealand White (NZW) mouse contains a germline deletion which includes both $C_{\beta}1$ and the $J_{\beta}2$ cluster⁸, suggesting that a $J_{\beta}1-C_{\beta}2$ -containing species should account for all NZW β -chain transcripts. The

deletion of $C_{\beta}1$ in the NZW mouse is thought to have resulted from a homologous recombination event between the first exon of $C_{\beta}1$ and the first exon of $C_{\beta}2$ (ref. 9). The sequence 5' to the single C_{β} coding region should therefore be of $C_{\beta}1$ origin, implying that the $C_{\beta}0$ exon will be present in NZW. To look for the existence of a $C_{\beta}0$ - $C_{\beta}2$ -containing species and examine $C_{\beta}0$ expression in the altered chromosomal context of the NZW mouse, an unamplified NZW thymus cDNA library was screened with the C_{β} and $C_{\beta}0$ -splice oligonucleotide probes. Of 146 C_{β} -positive clones identified, 26 hybridized to the $C_{\beta}0$ -splice probe. Thus, 18% (26/146) of the C_{β} -containing clones in the NZW thymus library use the $C_{\beta}0$ alternative splicing pathway. This frequency is significantly higher than the 1.3% level seen earlier in the C57BL/6 spleen cDNA library.

Two of these $26 C_{\beta}0$ -containing clones were randomly chosen for further analysis. The DNA sequences of these two clones were determined and are presented in Fig. 3. Clone NZW 8 is truncated within V_{β} coding sequence but was found to contain $V_{\beta}12-D_{\beta}1.1-J_{\beta}1.1-C_{\beta}0-C_{\beta}2$; clone NZW 22s is full-length and contains $V_{\beta}5.2-D_{\beta}1.1-J_{\beta}1.4-C_{\beta}0-C_{\beta}2$. While the $V_{\beta}12$ sequence seen in clone NZW 8 is identical to a V_{β} sequence reported previously 10, the V_{β} sequence in clone NZW 22s has not been reported; we note, however, that this sequence is 88% homologous at the nucleotide level to the published $V_{\beta}5.1$ sequence 3 and is therefore presumed to represent the second member of a three-member V_{β} gene subfamily, whose existence was inferred from Southern blot analysis using the $V_{\beta}5.1$ sequence as a probe 13 , 14.

Fig. 2 Genomic localization of the C_β0 exon. a, Restriction map locating C_β0 between J_β1 and C_β1. B, BamHI; R, EcoRI; K, Kpni; kb, kilobase. b, Nucleotide sequence of the C_β0 exon and flanking introns. Nucleotide sequence is given beginning at the EcoRI site, as shown c, Analysis of splice donor and acceptor sites. The nucleotide sequence of the C_β0 exon and its flanking introns is compared with the consensus donor and acceptor splice-site sequences reported by Breathnach and Chambon¹⁵. Py, pyrimidine; Pu, purine.
Methods. A BALB/c genomic library (EcoRI partial digest in Charon 4A, as described earlier²⁷) was screened with a C_β probe. Restriction maps of C_β-positive isolates were determined, and a clone was identified that was consistent with the map of the C_β1 locus reported earlier by Gascoigne et al. Exon elements were located by hybridization. For b, the 2.2 kb EcoRI fragment containing C_β0 and C_β1 was subcloned into pUC12 and the nucleotide sequence of the indicated region was determined by the method of Maxam and Gilbert²⁵.

GATTGC---CATCAGGTA

CAG

Expression of the $C_{\beta}0$ exon has been seen to vary from 1.3% of C_{β} -containing cDNA clones in a C57BL/6 spleen library to 18% of C_{β} -containing clones in an NZW thymus library. Direct comparison of the relative levels of $C_{\beta}0$ expression between these two libraries is difficult to interpret, however, because of uncertainty over the effects of the NZW $C_{\beta}1$ deletion on $C_{\beta}0$ expression. To better contrast the frequency of $C_{\beta}0$ expression between thymus and spleen, we constructed a C57BL/6 thymus cDNA library and screened a portion of the unamplified library with the C_{β} and $C_{\beta}0$ -splice oligonucleotide probes. Fourteen $C_{\beta}0$ -containing clones were identified from a total of 267 C_{β} -positives (Table 1). Thus 5% (14/267) of the C_{β} -containing clones in the C57BL/6 thymus library use the alternative splicing pathway.

Consensus splice sequence

Actual genomic sequence

C_B0-containing cDNA clones represent a species of mRNA that is expressed at levels ranging from 5% to 1.3% of total C_B-containing clones in our C57BL/6 thymus and spleen libraries, respectively. A lower level of $C_{\beta}0$ expression in spleen than in thymus could be specifically regulated, or it could simply parallel a lower level of overall $C_B 1$ usage in spleen. To address this possibility, the C57BL/6 thymus and spleen cDNA libraries were re-screened with probes specific for the 3'-untranslated sequence of $C_{\beta}1$ and $C_{\beta}2$; it was determined that $C_{\beta}1$ was present at levels of 32% and 27% of total C_{β} -positive clones in the thymus and spleen libraries, respectively (Table 1). The $C_{\beta}0$ element was present in 16% of thymic $C_{\beta}1$ clones and 5% of splenic $C_{\beta}1$ clones. No $C_{\beta}2$ clones were found to contain a C_{β} 0-hydrizing element. As the relative level of C_{β} 1 usage does not change significantly between thymus and spleen, the decrease in $C_{\beta}0$ usage may result from some kind of specific

down-regulation of this pathway independent of $C_{\beta}1$ usage in general.

Interestingly, this is not the first report of an alternative RNA splicing pathway in a T-cell-specific transcript. The murine Lyt 2 gene has been shown to produce two species of mRNA via alternative splicing²⁰. The relative proportions of the two mRNA species were seen to differ between thymus and spleen; in parallel with our observations of alternative splicing in TCR β -chain, expression of the minor species of Lyt 2 mRNA was seen to be higher in thymus than in spleen.

Insertion of the $C_{\beta}0$ exon between a J_{β} element and the C_{β} element maintains the expected J_{β} - C_{β} translational reading frame, and the new exon itself encodes a 24-codon open reading frame. Thus, there is no obvious reason to suspect that $C_{\beta}0$ -containing β -chain transcripts should not be translated in parallel with other C_{β} -containing transcripts. While we have no data directly demonstrating the existence of a $C_{\beta}0$ -containing protein species, it seems reasonable to propose that such a species should actually exist, leading to the prediction that, in some circumstances, surface TCR could be a mixed population composed of both $C_{\beta}0$ -containing and $C_{\beta}0$ -excluding β -chain peptides.

Some predictions can be made from the primary sequence of the new exon regarding the potential effects its insertion may have on β -chain protein structure. The translated amino-acid sequences from Fig. 1 were analysed using the algorithm of Chou and Fasman²¹. The C_{β} 0 sequence was found to occupy a region of low β -sheet and α -helix potentials with moderate reverse-turn probability, leading to a composite prediction of a random-turn secondary structure throughout this region. Inter-

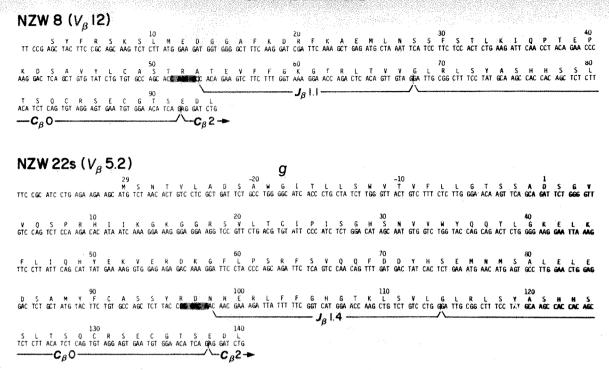


Fig. 3 Nucleotide and amino-acid sequences of the V-D-J regions from two C_{β} 0-containing isolates from an NZW thymus cDNA library. Sequences contributed from germline D_{β} 1.1 are shaded, while I_{β} , C_{β} 0 and C_{β} 2 gene segments are underlined. Nucleotides between D_{β} and J_{β} segments are proposed N-region insertions. The cDNA library was constructed from oligo(dT)-cellulose-selected NZW thymus RNA²⁶ in the λ gt10 cloning vector as described by Huynh et al.²⁸, with modifications²⁹. Library screening was done with ³²P-labelled oligonucleotide probes as described for Fig. 1c; C_{β} 0-positive clones were subcloned into pUC12 and their DNA sequences determined by the method of Maxam and Gilbert²⁵.

estingly, these parameters are very similar to those generated for the hinge region of human $\gamma 1$ immunoglobulins (data not shown). In addition, the $C_{\beta}0$ sequence contains two nearly adjacent cysteine residues in a region predicted to be hydrophilic by the algorithm of Hopp and Woods²². If these residues do not bond to each other, they may be available to form inter- or intra-chain disulphide bonds not usually present in the β -chain peptide. It is interesting to speculate that the presence of this sequence promotes the association of β -chain with a peptide other than α -chain (for example, γ -chain).

While it is not clear whether the $C_{\beta}0$ exon actually has any functional significance in vivo, it may be relevant to note that $C_{\beta}0$ is expressed at a fourfold higher level in thymus than in spleen. Decreased peripheral expression might simply reflect that few C_B 0-expressing T cells escape the thymus to become splenic T cells. Alternatively, it might reflect specific downregulation of the C_{β} 0 splicing pathway as cells leave the thymus. In regard to developmental regulation, we note that most $C_{\beta}0$ containing cDNAs isolated from thymus are also V_{β} -containing,

Received 3 March; accepted 18 April 1986.

- Takahashi, N., Roach, A., Teplow, D., Prusiner, S. & Hood, L. Cell 42, 139-148 (1985).
 deFerra, F. et al. Cell 43, 721-727 (1985).
 Amara, S., Jonas, V., Rosenfeld, M., Ong, E. & Evans, R. Nature 298, 240-244 (1982).
 Breitbart, R. et al. Cell 41, 67-82 (1985).

- Early, P. et al. Cell 20, 313-319 (1980).
 Moore, K. et al. Proc. natn. Acad. Sci. U.S.A. 78, 1800-1804 (1981).
- Blattner, F. & Tucker, P. Nature 307, 417-422 (1984).
 Kotzin, B., Barr, V., Palmer, E. Science 229, 167-171 (1985).
 Noonan, D. et al. J. exp. Med. 163, 644-653 (1986).

- Noonan, D. et al. J. exp. New. 103, 044-053 (1986).
 Behlke, M. et al. Science 229, 566-570 (1985).
 Chien, Y., Gascoigne, N., Kavaler, J., Lee, N. & Davis, M. Nature 309, 322-326 (1984).
- 12. Gascoigne, N., Chien, Y., Becker, D., Kavaler, J. & Davis, M. Nature 310, 387-391
- 13. Barth, R. K. et al. Nature 316, 517-523 (1985). 14. Behlke, M., Chou, H., Huppi, K. & Loh, D. Proc. natn. Acad. Sci. U.S.A. 83, 767-771
- Breathnach, R. & Chambon, P. A. Rev. Biochem. 50, 349-383 (1981).
- 16. Rupp, F., Acha-Orbea, H., Hengartner, H., Zinkernagel, R. & Joho, R. Nature 315, 425-427 (1985).

suggesting that the more immature thymic 'D-J' type transcripts²³ may express the C_B0 exon at lower levels than mature V-D-J transcripts. The thymus cDNA libraries examined here were constructed from tissue obtained from 6-week-old animals; it would be interesting to see whether the frequency of $C_{\beta}0$ expression varies with the developmental stage of the thymus. Further, we do not know whether the $C_{\beta}0$ splicing pathway is unique to the murine system or if it is also available to human TCR β -chain transcripts. In this regard, we note that no sequence with recognizable homology to $C_{\beta}0$ is present in the published human $C_{\beta}1$ sequence²⁴, although only a small portion of the intron between the $J_{B}1$ cluster and $C_{B}1$ has been reported.

We thank Mr Joseph Leykam for assistance with protein analysis and Madline Pearlman for manuscript preparation. This research was supported by funds from the Howard Hughes Medical Institute (D.Y.L.) and NIH Research Service Award GM 07200, Medical Scientist, from the National Institute of General Medical Sciences (M.A.B.).

- Morinaga, T., Fortedar, A., Singh, B., Wegmann, T. & Tamaoki, T. Proc. natn. Acad. Sci. U.S.A. 82, 8163-8167 (1985).
 Goverman, J. et al. Cell 40, 859-867 (1985).

- Goverman, J. et al. Cell 40, 859-867 (1985).
 Malissen, M. Cell 37, 1101-1110 (1984).
 Zamoyska, R., Vollmer, A., Sizer, K., Liaw, C. & Parnes, J. Cell 43, 153-163 (1985).
 Chou, P. & Fasman, G. A. Rev. Biochem. 47, 251-276 (1978).
 Hopp, T. & Woods, K. Proc. natn. Acad. Sci. U.S.A. 78, 3824-3828 (1981).
 Siu, G. et al. Nature 311, 344-350 (1984).

- Toyonaga, B., Yoshikai, Y., Vadasz, V., Chin, B. & Mak, T. Proc. natn. Acad. Sci. U.S.A. 82, 8624-8628 (1986).
 Maxam, A. & Gilbert, W. Proc. natn. Acad. Sci. U.S.A. 74, 560-564 (1977).
 Maniatis, T., Fritsch, E. & Sambrook, J. in Molecular Cloning, A Laboratory Manual (Cold Spring Harbor Laboratory, New York, 1982).
 Loh, D., Bothwell, A., White-Scharf, M., Imanishi-Kari, T. & Baltimore, D. Cell 33, 85-93
- (1983).
- 28. Huynh, T., Young, R. & Davis, R. in DNA Cloning: A Practical Approach (ed. Glover, D.)
- 49-78 (IRL, Oxford, 1984). 29. Gubler, V. & Hoffman, B. Gene 25, 263-269 (1983). 30. Roehm, N. et al. J. Immun. 135, 2176-2182 (1985).
- 31. Staertz, U., Rammensee, H., Benedetto, J. & Bevan, M. J. Immun. 134, 3994-4000 (1985). 32. Sim, G. & Augustin, A. Cell 42, 89-92 (1985).

Synergism between immunoglobulin enhancers and promoters

J. Victor Garcia, Lê thi Bich-Thuy, Jeannine Stafford & Cary Queen

Laboratory of Biochemistry, National Cancer Institute, National Institutes of Health, Bethesda, Maryland 20892, USA

Enhancers are DNA sequences that stimulate transcription from eukaryotic promoters1-3. This stimulatory effect can be exerted over large distances and from a position either 5' or 3' of a promoter. Enhancers have been found in the genomes of many viruses, and in some cellular genes such as those encoding immunoglobulin heavy chain^{4,5} and κ light chain^{6,8}. An important feature of both viral and cellular enhancers is the ability of each enhancer to stimulate transcription from many promoters other than the one with which it is found associated1,2. However, the question of whether cellular enhancers stimulate their 'own' promoter more efficiently than other promoters has apparently not been investigated. We show here that the k light-chain enhancer stimulates a k promoter about 20-fold more than it stimulates either the simian virus 40 (SV40) early promoter or a metallothionein (MT) promoter, two promoters that are very sensitive to other enhancers. Similarly, the heavy-chain enhancer stimulates a heavy-chain promoter much more than it stimulates the SV40 and MT promoters. This synergism between immunoglobulin enhancers and promoters might be due to the action of a protein that binds specifically to each of the regulatory elements.

To measure the effects of different enhancers, we used the chloramphenicol acetyltransferase (CAT) assay9, which has been widely employed for that purpose (see, for example, refs 10, 11). Four sets of plasmids were constructed. Plasmids used to determine the effect of enhancers on the SV40 early promoter were derived from pA10cat2 (ref. 10) which here is called pAcat (Fig. 1a). To determine the effect of enhancers on a κ gene promoter from the mouse myeloma MOPC 41 (ref. 12) we constructed the plasmid pKcat (Fig. 1b); in this plasmid, a fragment extending from an EcoRI site about 1,100 base pairs (bp) before the κ transcription start site to 25 bp beyond the start site was connected to the cat gene via a BglII adapter. Similarly, a fragment of the mouse 17.2.25 heavy-chain gene 13,14 extending from ~2,000 bp before the promoter start site to 44 bp beyond the start site, was connected to the cat gene to form the plasmid pHcat. These plasmids also include the origin of replication of SV40 (ori), without the SV40 enhancer, in order to make them more analogous to pAcat (Fig. 1). Finally, the effect of enhancers on the mouse metallothionein-I (MT-I) promoter was determined using the plasmid pMcat. This plasmid is similar to pKcat and pHcat, except that the immunoglobulin gene segments are replaced by a fragment extending from an EcoRI site ~1,900 bp before the transcription start site of the MT gene to a BglII site located 64 bp after the start site 15. On all plasmids, the initiating ATG of the cat gene is the first ATG codon after the expected transcription start site.

Three DNA fragments containing known enhancers from murine viruses or genes were inserted into each of the plasmids pAcat, pKcat, pHcat and pMcat at the sites indicated in Fig. 1. The polyomavirus and κ light-chain gene enhancers were, respectively, contained on the 238-bp and 473-bp fragments used previously 16, and the heavy-chain enhancer was contained on a 682-bp XbaI-EcoRI fragment 4.5. The enhancers were inserted in the same orientation with respect to the direction of cat transcription that they have relative to the polyoma Tantigen, κ and heavy-chain genes. Plasmids containing the polyoma virus, κ and heavy-chain enhancers are designated with the suffixes P, K and H, respectively. All transfection experiments were performed on S194 cells (ATCC TIB 19), a mouse

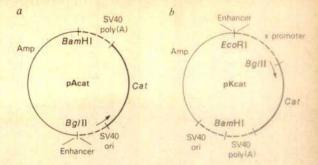


Fig. 1 Schematic diagrams of plasmids (not to scale). Arrows indicate the approximate initiation sites and direction of transcription from the SV40 early and κ promoters. Enhancers were inserted by means of Bg/II linkers into pAcat and by EcoRI linkers into pKcat. a, pAcat is the plasmid pAl0cat2 of ref. 10, and does not contain the SV40 enhancer. b, The part of pKcat from the EcoRI site counterclockwise to the BamHI site was taken from pLT1 (ref. 6), and the part from the Bg/II site to the BamHI site is the HindIII-BamHI fragment of pSV2cat9. The plasmids pHcat and pMcat are similar to pKcat, with the κ gene segment replaced by heavy-chain and MT gene segments, respectively. Plasmids were constructed by standard methods; details available on request.

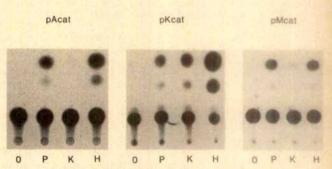


Fig. 2 CAT assays of extracts from transfected cells. The cells were transfected with the indicated plasmids containing the enhancers noted beneath the lanes: 0 (no enhancer), P (polyoma), K (κ) and H (heavy chain).

Methods. For each plasmid, one plate containing ~10⁷ S194 cells was transfected as described elsewhere⁸, except that the transfection was done in 1 ml with 5 μg DNA. After 24 h, an additional 15 ml of medium was added to each plate, and CdCl₂ to 6 μM was added to the cells transfected with the pMcat plasmids. Cells were harvested after another 24 h and CAT assays performed as described elsewhere⁹, using half of the extract from each plate and a 1-h incubation.

immunoglobulin (α, κ) myeloma line that we have found to have high transfection efficiency (unpublished data).

The plasmid pAcat and derivatives were transfected in parallel into S194 cells. After 48 h, the cells were lysed and tested for CAT activity9; Fig 2 shows the results of a typical experiment. The geometric means of the determinations of per cent 14Cchloramphenicol conversion for three separate experiments, using two sets of independently isolated plasmids, are shown in Table 1; all numbers have been normalized to the values for pAcatP rather than for pAcat, because the values for the latter are much smaller and may therefore be less reliable. Insertion of the k enhancer into pAcat led to only a 4.2-fold increase (0.008 to 0.034) in transcription of cat, as measured by CAT synthesis, while the polyoma and heavy-chain enhancers respectively produced increases of 125- and 236-fold. These results are consistent with the finding that the k enhancer is only 5% as effective as the heavy-chain enhancer in stimulating a β-globin promoter7. Two additional plasmids, identical to pAcatK and pAcatH except with the orientations of the enhancer fragments reversed, were transfected at the same time as the other plasmids,

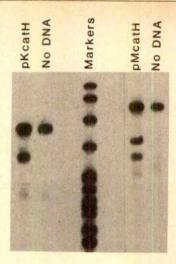


Fig. 3 S₁-nuclease assay of RNAs from transfected cells. S194 cells were transfected with the indicated plasmids, containing the polyoma early region, or were mock-transfected without DNA. After 48 h, total RNA was extracted from the cells and assayed as described elsewhere. The topmost band in each lane ran at the position of intact probe. The markers were an *Hpa*II digest of pBR322; sizes (in nucleotides) were: 622, 527, 404, 309, 242, 238, 217, 201, 190, 180, 160 and 147.

and yielded mean normalized CAT values of 0.038 and 0.70, respectively. Thus, reversing the orientation had no significant effect on the κ enhancer while it reduced the effect of the heavy-chain enhancer by a factor of \sim 3.

Corresponding data were obtained for the plasmid pKcat, in which the κ promoter is linked to the cat gene (Fig. 2, Table 1). In contrast to the pAcat results, the κ enhancer stimulated transcription of the cat gene on pKcat more than did the polyoma enhancer, and the heavy-chain enhancer stimulated cat transcription by much more. In fact, the κ enhancer and the heavy-chain enhancer increased CAT synthesis by 88-fold (0.017 to 1.49) and 829-fold, respectively. Hence, the κ enhancer apparently stimulated transcription from the κ promoter about 20 times more efficiently than from the SV40 promoter, and the heavy-chain enhancer stimulated κ transcription about four times more than SV40 transcription. These results cannot be caused by the κ promoter being generally more sensitive to enhancers than the SV40 promoter, because the polyoma enhancer stimulated the κ promoter less than it did the SV40 promoter.

However, to verify that the phenomenon was not caused by a pecularity of the SV40 promoter, we used pMcat, a plasmid very similar to pKcat in which a metallothionein promoter replaces the κ promoter. 24 h after transfection of pMcat and its derivatives into S194 cells, cadmium was added to the medium to induce the MT promoter. The results (Fig. 2, Table 1) were analogous to those for the pAcat plasmids. In fact, the κ en-

Table 1 Effect of enhancers on different promoters

Enhancer	Plasmid					
	pAcat	pKcat	pMcat	pHcat		
None	0.008	0.017	0.041	< 0.01		
Polyoma	1.00	1.00	1.00	1.00		
K	0.034	1.49	0.19	0.58		
Heavy chain	1.89	14.1	0.92	15.3		

Each value is the geometric mean of determinations of per cent chloramphenical conversion after three independent transfections, and is normalized to the values for the polyoma enhancer. hancer stimulated transcription from the MT promoter only 4.6-fold, again about 20-fold less than from the κ promoter. Similarly, the heavy-chain enhancer increased transcription from the MT promoter much less than from the κ promoter. When cadmium was omitted from the medium, the amount of CAT synthesis from all the pMcat plasmids was decreased about fivefold, so that the amount of stimulation by the various enhancers remained approximately the same.

Finally, data were obtained from the pHcat plasmids, which have the heavy-chain promoter linked to cat (Table 1). The plasmid pHcat itself, which has no enhancer, expressed CAT at a very low level, precluding its accurate quantification. Moreover, whereas the heavy-chain enhancer stimulated the SV40 and MT promoters about as well as did the polyoma enhancer (Table 1), the heavy-chain enhancer stimulated the heavy-chain promoter 15.3 times more than did the polyoma enhancer. This result and the low level of heavy-chain promoter activity without any enhancer imply an especially effective interaction between the heavy-chain promoter and enhancer. Relative to the polyoma enhancer, the k enhancer stimulated the heavychain promoter more (0.58) than it stimulated the SV40 or MT promoters (0.034 and 0.19) but less than it stimulated the κ promoter (1.49). Taking all the data together, the strongest synergism exists between the k enhancer and promoter and between the heavy-chain enhancer and promoter, but there is also synergism between any pair of immunoglobulin gene elements.

Our results were not affected by fluctuations in transfection efficiency of the plasmids into the S194 myeloma cells. Indeed, each set of plasmids was independently transfected in parallel three times. The multiplicative standard deviations¹⁷ of the values for each plasmid were less than 1.6, except for pKcatH (1.82). In other experiments, the pKcat and pMcat plasmids were mixed with the plasmid pCH110, which contains a gene for β -galactosidase¹⁸, before transfection. Extracts of the transfected cells were assayed for both CAT and β -galactosidase activity. The β-galactosidase values for the four pKcat plasmids had a multiplicative standard deviation of only 1.02, and for the pMcat plasmids only 1.06. Hence, the transfection efficiencies for the plasmids within each experiment were very similar. Moreover, after normalization to the results for pKcatP and pMcatP, the CAT values for the plasmids carrying the k and heavy-chain enhancers showed no significant differences from the values in Table 1.

Many studies have shown that enhancers do not alter the start point of transcription from the promoters that they stimulate (see, for example, refs 1, 4, 19). In particular, we have shown that in lymphoid cells, transcription initiates from the same place in the κ promoter when it is stimulated by either the κ or polyoma enhancers 16. To further verify the location of the transcription start sites in the experiments presented here, we extracted RNA from S194 cells 48 h after they had been transfected with pKcatH or pMcatH. The RNAs were analysed using an S₁-nuclease assay, with double-stranded probes labelled at the EcoRI site in the cat gene 9, and respectively extending to the MaeIII site 5' of the κ promoter 20 or to the SacI site 5' of the MT promoter 15. In initial S₁ experiments, no signals were detected clearly from pKcatH or pMcatH, probably because of instability of the cat RNA.

To increase the signal, we inserted the polyoma early region into pKcatH and pMcatH. This region has been shown to increase the amount of RNA transcribed from transfected plasmids by allowing them to replicate in mouse cells, thus increasing the amount of DNA template 6,8,21 . The S_1 analysis of RNA from cells transfected with the modified pKcatH plasmid (Fig. 3) revealed a strong band of a length corresponding to transcripts from the usual κ start site 6 . The RNA from cells transfected with the modified pMcatH plasmid yielded two bands (in addition to residual intact probe): the length of the stronger, upper band corresponds to transcripts from the usual MT start site 15 ;

the lower band presumably represents transcripts initiating ~40 bp farther downstream. Both bands were also present when the MT promoter was stimulated by the polyoma enhancer in pMcatP, but were much weaker when there was no enhancer present on the plasmid (not shown). The shorter transcript from the MT promoter has not been observed previously¹⁵, but the probe used in that study would probably not have detected it.

An attractive explanation for the observed synergism between immunoglobulin enhancers and promoters is that one or more proteins specifically bind to all of these regulatory regions. The existence of such proteins might be reflected in sequence homologies between the regulatory regions. Such homologies

Received 16 April; accepted 20 May 1986.

- 1. Banerji, J., Rusconi, S. & Schaffner, W. Cell 27, 299-308 (1981).

- Moreau, P. et al. Nucleic Acids Res. 9, 6047-6068 (1981).
 Fromm, M. & Berg, P. J. molec. appl. Genet. 1, 457-481 (1982).
 Banerji, J., Olson, L. & Schaffner, W. Cell 33, 729-740 (1983).
 Gillies, S. D., Morrison, S. L., Oi, V. T. & Tonegawa, S. Cell 33, 717-728 (1983).
- Queen, C. & Baltimore, D. Cell 33, 741-748 (1983). Picard, D. & Shaffner, W. Nature 307, 80-83 (1984).
- Queen, C. & Stafford, J. Molec. cell. Biol. 4, 1042-1049 (1984)
- Gorman, C., Moffat, L. & Howard, B. Molec. cell. Biol. 2, 1044-1051 (1982).
 Laimins, L. A., Gruss, P., Pozzatti, R. & Khoury, G. J. Virol. 49, 183-189 (1984).
- Herbomel, P., Bourachot, B. & Yaniv, M. Cell 39, 653-666 (1984).
 Seidman, J. G. & Leder, P. Nature 276, 790-795 (1978).

have indeed been observed²². Recently, direct evidence of a protein that binds both immunoglobulin promoters and enhancers has been obtained²³. The results presented here may help to explain the negative findings of searches for cellular enhancers that use a heterologous promoter as the assay24. Many enhancers in cellular genes may, like the k enhancer, efficiently stimulate only their own or related promoters.

We thank L. Laimins, F. Lee and D. Hamer for providing pAcat, pCH110 and the MT promoter, respectively. We thank C. Mock and B. Miller for photographic and sectarial assistance. and M. Singer for reviewing the manuscript. L.T.B.-T. was partially supported by INSERM, France.

- 13. Loh, D. Y., Bothwell, A. L. M., White-Scarf, M. E., Imanishi-Kari, T. & Baltimore, D. Cell
- Grossched, R. & Baltimore, D. Cell 41, 885-897 (1985).
 Hamer, D. H. & Walling, M. J. molec. appl. Genet. 1, 273-288 (1982).
 Foster, J., Stafford, J. & Queen, C. Nature 315, 423-425 (1985).
- 17. Snedecor, G. W. & Cochran, W. G. Statistical Methods 6th edn., 330 (lowe State University
- 18. Hall, C., Jacob, E., Ringold, G. & Lee, F. J. molec. appl. Genes. 2, 101-109 (1983)
- 19. Levinson, B., Khoury, G., Vande Woude, G. & Gruss, P. Nature 295, 368-572 (1982).
- 20. Seidman, J. G., Max. E. E. & Leder, P. Nature 280, 370-375 (1979).
- 21. Deans, R., Denis, K. A., Taylor, A. & Wall, R. Proc. natn. Acad. Sci. U.S.A. 81, 1292-1286
- 22. Falkner, F. G. & Zachau, H. G. Nature 310, 71-74 (1984).
- Singh, H., Sen, R., Baltimore, D. & Sharp, P. A. Nature 319, 154-158 (1986).
 Weber, F., de Villiers, J. & Schaffner, W. Cell 36, 983-992 (1984).

Expression of human adenosine deaminase in murine haematopoietic progenitor cells following retroviral transfer

John W. Belmont*, Jenny Henkel-Tigges*, Stephen M. W. Chang*, Karen Wager-Smith*, Rodney E. Kellems†, John E. Dick‡, M. Cristina Magli‡, Robert A. Phillips‡, Alan Bernstein‡ & C. Thomas Caskey*

* Institute for Molecular Genetics and Howard Hughes Medical Institute and † Department of Biochemistry, Baylor College of Medicine, Houston, Texas 77030, USA ‡ Ontario Cancer Institute and Mt Sinai Hospital Research Institute. Department of Medical Genetics and Biophysics,

University of Toronto, Toronto, Ontario, Canada M4X 1K9

Adenosine deaminase (ADA) deficiency, an autosomal recessive inborn error of metabolism, leads to severe combined immune deficiency in man1. This enzyme, although constitutively expressed in most tissues, is expressed at high level in immature T cells, and study of the pathophysiology of the disorder indicates that increased deoxyadenosine or altered methylation capacity have toxic effects on T-cell maturation1. Although bone marrow transplantation can correct the immune deficiency^{2,3}, this therapy is associated with graft-versus-host disease and incomplete immune restoration, and so our laboratory and others have sought to develop a method of gene replacement as a possible treatment for the disease4. Moreover, characterization of the complementary DNA of the human ADA gene and some of its mutants^{5,6} makes it possible to design gene transfer strategies. We have now subcloned a human adenosine deaminase cDNA into the retrovirus shuttle vector pZIP-SV(B), and in this way have isolated a cell line, 4.2T, which produces high titres of replication-defective retrovirus which have been used to transfer the gene for human ADA to mouse bone marrow cells. Transfer and expression of the neomycin-resistance gene (neo) and the ADA gene in murine bone marrow colony-forming units (CFU) was demonstrated by in vitro colony formation in the presence of the antibiotic G418 or 9xylofuranosyladenine plus deoxycoformycin, respectively. Isoenzyme analysis also showed human ADA expression in the cultured mouse bone marrow.

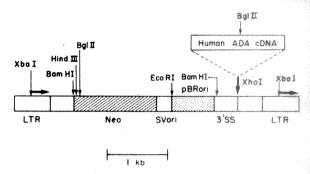
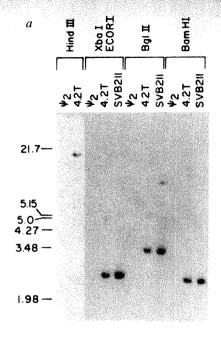


Fig. 1 Construction of the 4.2T cell line. The SV(B) plasmid vector was cleaved with XhoI, filled in with Klenow and treated with calf intestinal phosphatase (CIP). The pADA2115 plasmid containing a full-length human ADA cDNA was cleaved with EcoRI and DdeI, thus removing the 3' poly(A) addition site, filled in with Klenow and blunt-end ligated to the SV(B) vector. The SVBADA211 plasmid was isolated by banding in CsCl, and 10 µg purified DNA was used to transform PA-12 (ref. 9) cells by CaPO_a precipitation. Supernatant from these cells, containing the transiently expressed SVBADA211 virus with an amphotropic envelope, was collected at 48 h and used to infect ψ_2 cells. These cells were placed in Dulbecco's modified Eagle's medium (DMEM) with 10% FCS containing G418 (300 µg mf⁻¹). Ninetysix G418-resistant clones were selected and placed in 11AAU (1.1 mM adenosine, 50 mM alanosine, 1.0 mM uridine) plus 50 nM deoxycoformycin (dCf). Two cell lines, 4.1T and 4.2T, were able to grow in this selective medium, and 4.2T had both higher expression of human ADA and higher titre virus production. LTR, long terminal repeat. SVori, SV40 origin of replication; pBRori, origin of replication from pBR322; 3'SS, 3' splice site; kb, kilobases.

The development of a biological gene transfer system based on highly infectious retroviruses opens the way to efficiently introducing genes into rare cell populations⁷⁻¹⁰, and several studies have recently demonstrated that the neo gene can be transferred into murine haematopoietic progenitors and stem cells using retroviral vectors¹¹⁻¹⁵. However, ADA gene transfer is hampered by the need to fulfil several requirements: (1) the production of a high-titre ADA vector without concomitant production of replication-competent virus, (2) expression of the transferred ADA gene in the target cells (that is, in marrow stem cells and their differentiated progeny), and (3) adequate expression at the tissue level in the test animal (ADA in thymus



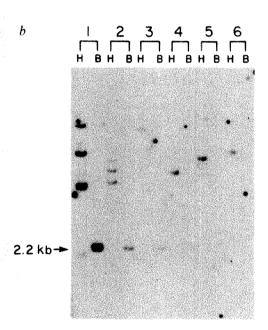


Fig. 2 a, Southern analysis of 4.2T. b, Southern analysis of 4.2T-infected cells. H, digestion with *HindIII*; B, digestion with *Bam* I. Lanes 1-6 represent individual clonal cell lines.

Methods. a, Genomic DNA was prepared from cultured ψ_2 and 4.2T cells by standard techniques. 10 µg of genomic DNA or 40 pg of plasmid was digested overnight with the indicated restriction enzymes, separated on 0.8% agarose, Tris-acetate-EDTA buffered gel at 40 V for 16 h. The gels were blotted onto nylon membrane, prehybridized overnight and probed with nick-translated neo insert at 42 °C with 50% formamide. The filters were washed in 0.1 × SSC at 60 °C and then autoradiographed overnight. b, NIH 3T3 cells were infected with supernatants from 4.2T. After 48 h the cells were placed in DMEM with 300 µg ml⁻¹ G418. The surviving cells were clonally selected and grown in DMEM plus G418. Genomic DNA was extracted, digested with either HindIII (H) or BamHI (B). Filter hybridization with ³²P-neo was as described in A. Cell lines with apparent multiple inserts (lanes 1, 2) are being recloned to establish homogeneity.

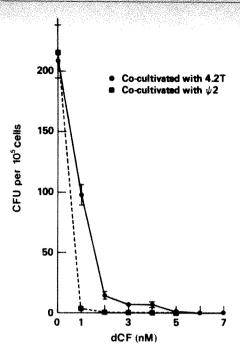


Fig. 3 Selection of CFU for ADA expression. Co-cultivation of 4.2T and mouse marrow cells was identical with that described in Table 1. After 24 h co-cultivation, the non-adherent cells were collected and plated in IMDM with 1% methylcellulose cultures with 5 μ M XylA and varying concentrations of dCF. CFU were counted at 7 days. Data represent averages of duplicate culture from two separate experiments $\pm\,s.e.m.$

and spleen). The present experiments investigated these problems in committed bone marrow progenitor cells. The vector pZIP-SV(B)10 (Fig. 1) was chosen because it allows the neo gene to be used as a dominant selectable marker for expression. The cell line 4.2T was formed by infection of the ψ_2 packaging line by defective amphotropic SVBADA211 virus. This line was clonally isolated after sequential selection in G418¹⁶ and then 11AAU (1.1 mM adenosine, 50 mM alanosine, 1.0 mM uridine) plus 50 nM deoxycoformycin (dCF)¹⁷. These selections require expression of neomycin phosphotransferase and increased ADA expression. The amount of dCF added makes the selection very stringent and thus rapidly identifies cells showing maximal expression of the transferred ADA gene. Of 96 G418-resistant isolates screened in this way, the 4.2T line had the highest expression of human ADA. The titre on NIH 3T3 mouse fibroblasts is $\sim 2 \times 10^4$ CFU per ml (G418 resistance). Southern analysis of 4.2T (Fig. 2a) indicated that the cell line has a single proviral insert. In addition, the 4.2T provirus was identical with plasmid pSVBADA211 using several internal restriction cuts, indicating that the selection procedure did not engender a gross rearrangement of the provirus. Southern analysis of cell lines infected with virus produced by 4.2T showed intact internal provirus structure (Fig. 2b). This also strongly suggests that the basic transcriptional unit of the provirus was not altered during selection. A more subtle alteration—for example, point mutations-cannot be ruled out, however.

The 4.2T cell line was then used to test the transfer and expression of the *neo* and ADA genes in murine haematopoietic cells. Mouse bone marrow was co-cultivated with 4.2T cells for 24 h according to the protocol of Dick *et al.*¹³. Non-adherent cells were replated in liquid media for 48 h with or without preselection in G418. These cells were then replated in semisolid media in the absence or presence of G418 to determine the proportion of resistant CFU. Table 1 indicates that approximately 10% of CFU acquire G418 resistance when co-cultivated with 4.2T. Co-cultivation with ψ_2 gives no G418-resistant colonies, indicating the specificity of the effect. Metabolic selec-

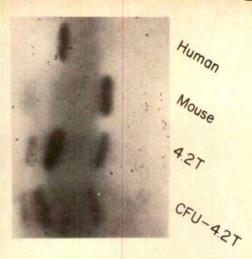


Fig. 4 Isoenzyme analysis of ADA in G418-selected infected bone marrow cells. Lane 1, HeLa cell (human) extract; lane 2, ψ2 cell (mouse) extract; lane 3, 4.2T; lane 4, CFU co-cultivated with 4.2T cells. The infection of mouse bone marrow cells was identical with that described in Table 1 except that the 4.2T cells were irradiated (1,500R, Gamma-cell 100, 137Cs source) before co-cultivation. Cells from CFU cultures were collected by repeated washing to remove the methylcellulose. Cell extracts were made by freezing and thawing in 20 mM Tris-HCl, pH 7.5. Supernatants were cleared by 15 min spin in a microcentrifuge. Cell extracts were loaded on a prefocused 1-mm-thick pH 4-5 polyacrylamide isoelectric focusing gel. Focusing was stopped after 3-4 h and the gel was soaked in 50 mM Tris-HCl pH 8.0 for 20 min. The gel was then stained for ADA enzyme activity using an agar overlay by standard methods17.

tion of CFU for increased expression of ADA was also performed using 9-xylofuranosyl adenine (XylA) plus dCF18 in a similar protocol (Fig. 3). XylA plus dCF was used for ADA selection because it gives a sharper inflection on survival curves than 11AAU for both fibroblasts and CFU. These data show a preferential survival of CFU co-cultivated with 4.2T compared with those co-cultivated with ψ_2 . At medium concentrations of dCF (2-4 nM), the per cent resistant CFU was comparable to the results obtained with G418 selection. To confirm the expression of human ADA in these cultured marrow cells, the cells were pooled from G418-selected cultures, and freeze-thaw extracts were prepared and run on an isoelectric focusing gel (Fig. 4). A band corresponding to the human ADA was detected only in CFU arising from 4.2T-infected marrow. Carryover of human enzyme activity from 4.2T virus-producer cells is highly unlikely since the monolayer was irradiated and there were two rounds of removal of adherent cells before replating in semisolid media. However, we cannot rule out a contribution to the observed expression by more mature non-colony-forming marrow cells.

These preliminary studies show that by exploiting the selectability of the ADA gene, cell lines producing high-titre retrovirus can be rapidly selected. The endogenous ADA gene can be amplified using 11AAU plus dCF¹⁷, and it may therefore be possible to increase virus production by amplification of the ADA-containing provirus. We have also shown that this particular SV(B)-human ADA construction is expressed well in murine haematopoietic cells after infection in vitro. There are several reports indicating problems with expression in retroviral constructs containing two genes^{19,20}. Furthermore, expression of a particular retroviral construct in mature marrow cells and committed progenitors does not guarantee that the same retroviral vector will function well after infection of more primitive stem cells. Indeed, preliminary data indicate significant loss of expression of neo in the differentiated progeny of infected CFU (ref. 21 and J.E.D. et al., manuscript in preparation). It is generally considered that constructs that use separate promoters

Table 1 Selection of CFU for neo expression

Preselection	Selection	ψ_2	4.2T
_	_	240 ± 26	218 ± 20
_	G418	0	24±5
G418	-	0	19±5
G418	G418	0	7±2

 ψ_2 or 4.2T cells (1×10⁶) were plated in 100-mm tissue culture dishes (Corning) in Iscove's modified Dulbecco's medium (IMDM, Gibco) with 25% fetal calf serum (FCS). The next day 4×106 bone marrow cells from the tibias and femurs of C3H/HeJ or C57B16/J (Jackson Laboratories) were placed in each dish in IMDM supplemented with bovine serum albumin (BSA), soybean lipid, Fe-saturated transferrin (Boehringer Mannheim), penicillin-streptomycin (Gibco), 10% FCS, 10% WEHI3B-conditioned medium, α-thioglycerol and 2 μg ml-1 Polybrene (Sigma). Twenty-four hours later, non-adherent cells were washed off and plated in fresh 100-mm Petri dishes (Falcon) with or without selective drugs (preselection). After 48 h recovery, the non-adherent cells were again collected, counted and 1×105 cells were plated in 1 ml IMDM with 1% methylcellulose (Fluka). These cultures had either no drug selection, or 1 mg ml⁻¹ G418. CFU (>200 cells) were counted 7-10 days after initiation of the semisolid cultures. Data are expressed as averages of three separate experiments ±s.e.m.

for each cDNA (two transcriptional units) give better expression in target cells. The SV(B) construction used here has only one transcriptional unit. We presume that expression in the target cell is dependent on the particular features of each construction and that it is premature to predict how a construction will behave at the stages of virus production and target cell expression. Other constructs using both double-promoter and unspliced designs are under investigation in our laboratory.

Somatic gene transfer techniques may allow a number of difficult biological problems to be addressed. Several reports indicate its usefulness in investigating cell lineage relationships in the haematopoietic system 13,14, and similar hierarchy studies may be undertaken with other tissues if infection is carried out at multiple developmental stages. Retrovirus gene transfer may also be useful for the study of oncogenesis22,23, while transfer of poorly understood genes into haematopoietic cells (for example, T1a or T11 antigen) may help to clarify their functional role. Finally, this technique may allow safe and effective treatment of ADA deficiency and various other inborn errors of metabolism by somatic gene therapy.

Received 2 May; accepted 5 June 1986.

1. Kredich, N. & Herschfield, M. The Metabolic Basis of Inherited Disease, 1157-1183 (McGraw-Hill, New York, 1983).

2. Parkman, R., Gelfand, E. W., Rosen, F. S., Sanderson, A. & Hirshhorn, R. New Engl. J.

Med. 292, 714-719 (1975).

- Med. 292, 714-719 (1973).

 Polmar, S. H. et al. New Engl. J. Med. 295, 1337-1343 (1976).

 Anderson, W. F. Science 226, 401-409 (1984).

 Adrian, G. S., Wiginton, D. A. & Hutton, J. J. Molec. cell. Biol. 4, 1712-1717 (1984).

 Bonthron, D. T., Macham, A. F., Ginsburg, D. & Orkin, S. H. J. clin. Invest. 76, 894-897
- 7. Bernstein, A., Berger, S., Huszar, D. & Dick, J. Genetic Engineering, Principles and Methods Vol. 7, 235-261 (Plenum, New York, 1985). Mann, R., Mulligan, R. C. & Baltimore, D. Cell 33, 153-159 (1983)

- Miller, A. D., Low, M.-F. & Verma, I. M. Molec. cell. Biol. 5, 431–437 (1985).
 Cepko, C. L., Roberts, B. E. & Mulligan, R. C. Cell 37, 1053–1062 (1984).
 Joyner, A., Keller, G., Phillips, R. A. & Bernstein, A. Nature 305, 556–558 (1983).
 Williams, D. A., Lemischka, I. T., Nathan, D. G. & Mulligan, R. C. Nature 310, 476–480 (1984)
- Dick, J. E., Magli, M. C., Huszar, D., Phillips, R. A. & Bernstein, A. Cell 42, 71-79 (1985).
 Keller, G., Paige, C., Gilboa, E. & Wagner, E. Nature 318, 149-154 (1985).
 Eglitis, M. A., Kantoff, P., Gilboa, E. & Anderson, W. F. Science 230, 1395-1398 (1985).
- 16. Colbère-Garapin, F., Horodniceanu, F., Kourilsky, P. & Garapin, A. C. J. molec. Biol. 150, 1-14 (1981).
- Yeung, C.-Y. et al. J. biol. Chem. 258, 8338-8345 (1983).
 Yeung, C.-Y., Riser, M., Kellems, R. E. & Siciliano, M. J. Molec. cell. Biol. 3, 2191-2202 (1983).
- Emerman, M. & Temin, H. M. Cell 39, 459-467 (1984).
 Joyner, A. L. & Bernstein, A. Molec. cell. Biol. 3, 2191-2202 (1983).
- 21. Williams, D. A., Orkin, S. H. & Mulligan, R. C. Proc. nam. Acad. Sci. U.S.A. 83, 2566-2570 (1986)
- 22. Wolf, L. & Ruscetti, S. Science 228, 1549-1552 (1985).
- 23. Berger, S. A., Sanderson, N., Bernstein, A. & Hawkins, W. D. Proc. natn. Acad. Sci. U.S.A. 82, 6913-6917 (1985).

The alternative nitrogenase of Azotobacter chroococcum is a vanadium enzyme

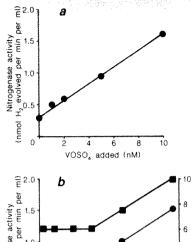
Robert L. Robson, Robert R. Eady, Toby H. Richardson, Richard W. Miller*, Marie Hawkins & John R. Postgate

AFRC Unit of Nitrogen Fixation, University of Sussex, Brighton BN1 9RQ, UK * Chemistry and Biology Research Institute, Agriculture Canada, Ottawa, Canada K1A 0C6

The requirement for molybdenum in biological dinitrogen fixation, first reported by Bortels1, is due to its involvement at or near the site of reduction of N₂ in conventional nitrogenase. To date, all nitrogenases which have been purified to homogeneity consist of an iron protein (component 2) and a molybdoprotein (component 1)2. Azotobacter vinelandii, an obligately aerobic diazotrophic bacterium, has two systems for nitrogen fixation: a conventional nitrogenase involving molybdenum and an alternative system which functions under conditions of Mo deficiency and does not require the structural genes for conventional nitrogenase3-6. The properties of the nitrogenase in extracts of comparable deletion strains of A. vinelandii are consistent with a two-component system^{6,7} in which the component 1-containing fraction has no detectable Mo (ref. 6). Recently, an alternative nitrogen fixation system has been demonstrated in Azotobacter chroococcum strain MCD1155, in which the structural genes for conventional nitrogenase are deleted8. We demonstrate here that nitrogen fixation by this strain depends on vanadium and we show that its purified nitrogenase is a binary system in which the conventional molybdoprotein is replaced by a vanadoprotein.

A. chroococcum NCIMB 8003 contains conventional nitrogenase when grown diazotrophically in a medium containing molybdate⁹. The genes which encode the polypeptides for this nitrogenase (nifH for the Fe-protein, Ac2; nifD and nifK for the α and β subunits of the MoFe-protein, Ac1) have been cloned as a contiguous cluster from this organism¹⁰. Strains in which this gene cluster was deleted, constructed by a genereplacement technique, were incapable of N₂ fixation when molybdate was provided, but developed feeble acetylene reduction activity indicative of nitrogenase in Mo-deficient medium8. A derivative, MCD1155, defective in uptake hydrogenase activity and resistant to up to 5 mM sodium tungstate (an inhibitor of molybdate uptake or assimilation in azotobacter^{11,12}), grew in N₂, and exhibited ¹⁵N incorporation from ¹⁵N₂, acetylene reduction and nitrogenase-dependent H₂ evolution. Growth and nitrogenase activity in MCD1155 apparently required relatively high (2.5 mM) concentrations of sodium tungstate8.

The most probable reason for so high a tungstate requirement is that our tungstate was contaminated with traces of an element (or elements) required for diazotrophy in this strain, We therefore tested cultures which grew poorly, in the N-deficient, Modeficient medium of Fig. 1, for stimulation of growth by Na₂SeO₃ $(29 \mu M)$, MnCl₂ $(15.2 \mu M)$, CuSO₄ $(0.6 \mu M)$, NiCl₂ $(0.2 \mu M)$, CoCl₂ (5 µM), FeSO₄ (50 µM), ZnSO₄ (7 µM), CaCl₂ (100 µM), Na_2MoO_4 (10 nM or 100 μ M), Na_3BO_3 (81 μ M) or $NaReO_4$ (10 μM). None stimulated growth. However, VOSO₄ at low concentrations restored growth; Fig. 1a shows that nitrogenase activity as measured by H2 evolution was proportional to added VOSO4 between 1 and 10 nM. From these data we deduced a specific activity for H₂ evolution in air of 120 pmol per min per pg atoms V. Mo, V-starved organisms responded rapidly and in a biphasic pattern to V (Fig. 1b); a rapid two fold activation of hydrogen-evolving activity seen after 30 min was followed by a slower progressive increase in activity over 10 h. Growth was evident after 6 h. We conclude that vanadium is required for diazotrophic growth of this strain.



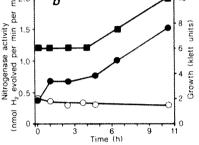


Fig. 1 Influence of vanadium on diazotrophic growth and nitrogenase activity in A. chroococcum MCD1155. a, Organisms were inoculated to 5×10^6 cells ml $^{-1}$. VOSO $_4$ was added and nitrogenase activities were measured in cultures by following H $_2$ evolution. Maximum activities obtained after 48 h at 30 °C are plotted. b, Organisms were inoculated to 5×10^7 ml $^{-1}$. At time zero, VOSO $_4$ was added to 10 nM. Nitrogenase activity was determined at intervals by following H $_2$ evolution over 15 min. Growth was determined using a Klett-Summerson photoelectric colorimeter and is shown for the V-supplemented culture only (\blacksquare). No growth was observed without added V. \blacksquare , Nitrogenase activity with V added; \bigcirc , without V added.

Methods. A. chroococcum MCD1155 was routinely grown in air at 30 °C in (g per l of distilled H_2O): sucrose 20; $K_2HPO_4 \cdot 3H_2O$, 0.64; KH_2PO_4 , 0.16; Na_2SO_4 , 0.142; $MgCl_2 \cdot 6H_2O$, 0.203; $CaCl_2 \cdot 2H_2O$, 0.074; $FeC_6H_5O_7$, 0.0335; Na_2WO_4 , 0.734. To test for the influence of V on growth and nitrogenase activity, organisms were grown without added tungstate until residual level was

The apparent requirements for high levels of tungstate could have been due to: (1) competitive exclusion of traces of molybdenum, (2) use of W in place of V via an inefficient uptake system or (3) contamination of our tungstate source with traces of V. We eliminate possibility (1) because, in shaken flasks with the Mo-free medium, diazotrophic growth of MCD1155 depended on tungstate concentration up to 2.5 mM, but addition of normal levels of molybdate (100 µM) to cultures containing 2.5 mM tungstate did not inhibit growth. Our studies do not conclusively eliminate explanation (2), but we favour explanation (3) because we have detected trace contamination (22 p.p.m. V) of our tungstate source and, in the presence of 2.5 mM tungstate, added vanadium did not stimulate growth.

Nitrogenase activity in extracts of MCD1155 prepared as in Fig. 2 had properties and requirements similar to those of conventional nitrogenases. Activity measurable as H₂ evolution, acetylene reduction or ammonia production was ATP- and reductant-dependent (data not shown). The activity was highly sensitive to irreversible inactivation by O₂, unlike the enzyme in crude extracts of the parent strain grown in molybdenum-sufficient conditions.

MCD1155 nitrogenase was purified essentially as described in Fig. 2 legend. Two readily separable yellow-brown coloured protein components were purified to homogeneity by a combination of ion-exchange and gel-filtration chromatography (Fig. 2). Both proteins were essential for activity. We refer to these

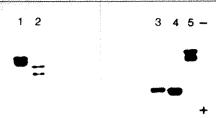


Fig. 2 Polyacrylamide gel electrophoresis of nitrogenase components of A. chroococcum MCD1155. Lanes 1 and 5, Acl 2.9 μg and 2.9 μg, respectively; lane 2, Acl* 2 μg; lane 3, Ac2* 11.0 μg; lane 4, Ac2 2.7 μg.

Methods. Organisms were grown in 400 l of the medium described in Fig. 1 legend with 40 µM VOSO4 added. Cells were collected at mid-exponential growth, resuspended in 50 mM HEPES buffer pH 8.0 and disrupted by French pressure cell treatment. Nitrogenase was purified under strictly anoxic conditions and separated into two components using a combination of DEAE-Sephacel chromatography in 50 mM Tris-HCl buffer pH 8.0 and gel filtration in 50 mM Tris-HCl buffer pH 8.0, 50 mM MgCl₂ essentially as described for nitrogenase from Klebsiella pneumoniae²⁶. Both proteins were then subjected to a linear NaCl gradient (0.25-0.4 M NaCl; total volume 300 ml) on DEAE-Sephacel equilibrated with 50 mM Tris-HCl pH 8.0 to remove contaminating proteins. Purified components were subjected to treatment with 1% SDS and 1% β -mercaptoethanol, electrophoresed as described previously²⁷ and stained wth Coomassie brilliant blue. Nitrogenase components (Ac1* and Ac2*) are compared with samples of conventional nitrogenase (Ac1 and Ac2) purified from A. chroococcum grown in Mo-sufficient conditions9.

components as Ac1* for the large protein and Ac2* for the small protein, where the asterisk distinguishes these proteins from the nitrogenase from Mo-sufficient cultures of the parent strain. Some physico chemical properties of the proteins are given in Table 1. Neither component contained significant amounts of Mo. V was present in stoichiometric amounts in Ac1* but not Ac2*. In the final purification step the highest levels of vanadium eluting from the column corresponded with the peak of activity for Ac1* (Fig. 3). Ac2* resembles a typical nitrogenase Feprotein. Ac1* resembles MoFe-proteins in subunit structure, although one of the two subunits is apparently smaller than that of Ac1 (Fig. 2). The presence of V in Ac1* is unlikely to be adventitious because it is present in stoichiometric amounts in purified protein of high specific activity (Table 1). This finding correlates with our observation that V is required for diazotrophy in MCD1155. Furthermore, our estimate of the specific activity for the vanadium stimulation of nitrogenase in whole cells (120 pmol H₂ evolved per min per pg atoms V) agrees closely with the activity per vanadium in the purified protein (160 pmol H₂ evolved per min per pg atoms V). Compared with H⁺ and N₂ as substrates, C₂H₂ is a poor substrate for the V nitrogenase (Table 1).

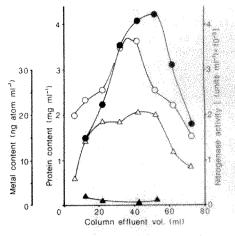


Fig. 3 Correlation of vanadium content of Ac1* with nitrogenase activity. The figure shows the elution profile of the larger component of nitrogenase (Ac1*, M_r 210,000) from DEAE-Sephacel under the conditions described in Fig. 2 legend. Nitrogenase activity (♠), Mo (♠) and V (△) and protein (○) contents of fractions across the peak are compared. Vanadium was estimated by atomic absorption spectroscopy on wet-ashed samples, while molybdenum was estimated colorimetrically²⁸. Quench corrections were made by the inclusion of internal standards for both metals. Nitrogenase activity was determined by complementation of fractions with Ac2* and assayed as ATP-dependent H₂ evolution as described elsewhere²⁶ (units of activity are nmol H₂ per min).

Reports that V can substitute for Mo for diazotrophy in azotobacters can be traced to Bortels¹³. Nicholas et al. 14 showed that nanomolar levels of V stimulated growth of A. chroococcum NCIMB 8003 in a Mo-deficient medium, which agrees with our findings for MCD1155. Becking15 showed that V replaced Mo in most strains of A. vinelandii and A. chroococcum tested. Biochemical studies on the vanadium effect led McKenna et al.16 and Burns et al.17 to prepare a crude V-nitrogenase from A. vinelandii and A. chroococcum which they proposed was the conventional nitrogenase in which Mo had been replaced by V. Some of the properties of their V-nitrogenase (for example, low electron allocation to acetylene) resemble ours. However, their preparations contained significant levels of residual Mo and their findings were attributed to a sparing effect of V on the amounts of Mo required for activity of conventional nitrogenase molvbdoprotein¹⁸. Our present findings confirm the reality of a V-nitrogenase but assign it to genetic determinants distinct from those of the Mo-nitrogenase which probably specify the alternative nitrogenase proposed by Bishop and his colleagues3-3, who suggested4 an involvement of V.

We propose in future to refer to conventional nitrogenase as Mo-nitrogenase and the alternative genetically distinct

Table 1 Comparison of physicochemical properties of components of Mo- and V-nitrogenase components of A. chroococcum

Marketine in the second of the		Metal content Subunit (g atoms mol ⁻¹)		Specific activities (nmol product per min per mg protein)			
	M_{r}	M_r	Мо	V	H ₂	NH_3	C_2H_4
Acl*	210,000	55,000 50,000	< 0.107	1.6	1,374	350	516
Acl	227,000	60,000	1.9	ND	2,138	1,521	1,924
Ac2*	60,000	31,500	0.012	0.04	1,107	507	999
Ac2	64,000	30,000	0.2	ND	1,993	1,361	1,830

For V-nitrogenase components (Ac1* and Ac2*), native and subunit relative molecular masses (M_r s) were determined by thin-layer gel filtration in Sephadex G-200 Superfine and SDS-electrophoresis as described elsewhere²⁶. Metal contents and activities were determined as described for Fig. 3. M_r and metal content of Ac1 and Ac2 are from ref. 9. Nitrogenase activity was measured as described in ref. 26, Ac1* (102 μ g) was complemented with Ac2* (1 mg); Ac2* (72 μ g) was complemented with Ac1 (0.14 mg). Ac1 (58 μ g) was complemented with Ac2 (0.32 mg); Ac2 (86.4 μ g) was complemented with Ac1 (0.29 mg). ND, not determined.

nitrogenase as V-nitrogenase, and the component proteins of the V-nitrogenase of Azotobacter chroococcum as Ac1* and Ac2* using the generally accepted nomenclature of Eady et al. 19. A. chroococcum contains two unlinked nifH genes encoding different Fe-proteins. The second copy $(nifH^*)$ that we have recently cloned and sequenced is likely to encode Ac2* (ref. 20). We have also shown that a nifK-like sequence, which might encode one of the Acl* subunits identified here, is present in the genome of MCD1155 (ref. 8).

Vanadium stimulates N2 fixation in Xanthobacter (Mycobacterium) flavus21 and Clostridium butyricum29. In Nostoc muscorum tungstate- or chromate-resistant mutants became dependent on these ions, respectively, but not molybdate, for N₂ fixation²², a situation which may parallel the apparent dependence of MCD1155 on tungstate. Thus, if azotobacters are not unique in this respect, vanadium may be a key element in the nitrogen cycle especially since it is more abundant in soils and fresh water than is molybdenum²³. Furthermore, it suggests that chemical systems based on vanadium which catalytically reduce N₂ (refs 24, 25) may have more biological significance than has hitherto been recognized.

We thank Simon Harrison for bulk growth of MCD1155, and Beryl Scutt and Brenda Hall for typing the manuscript.

Received 4 March: accepted 13 May 1986

- Bortels, H. Arch. Mikrobiol. 1, 333-342 (1930).
- Burgess, B. K. in Advances in Nitrogen Fixation Research (eds Veeger, C. & Newton, W. E.) 103-114 (Nijhoff/Junk, Pudoc, 1984).

- 3. Bishop, P. E., Jartneski, D. M. L. & Hetherington, D. R. Proc. natn. Acad. Sci. U.S.A. 77,
- 4. Bishop, P. E., Jarlenski, D. M. L. & Hetherington, D. R. J. Bact. 150, 1244-1251
- Bishop, P. E. & Eady, R. R. in Nitrogen Fixation Research Progress (eds Evans, H. J., Bottomley, P. J. & Newton, W. E.) 622 (Nijhoff, Dordrecht, 1985).
 Hales, B. J., Case, E. E. & Langosch, D. in Nitrogen Fixation Research Progress (eds Evans, H. J., Bottomley, P. J. & Newton, W. E.) 612 (Nijhoff, Dordrecht, 1985).
- Chisnell, J. R. & Bishop, P. E. in Nitrogen Fixation Research Progress (eds Evans, H. J., Bottomley, P. J. & Newton, W. E.) 623 (Nijhoff, Dordrecht, 1985).
 Robson, R. L. Archie. Microbiol. (in the press).
 Yates, M. G. & Planqué, K. Eur. J. Biochem. 60, 467-476 (1975).

- 10. Jones, R., Woodley, P. R. & Robson, R. L. Molec. gen. Genet. 197, 318-327 (1984).
- Takahashi, H. & Nason, A. Biochim. biophys. Acta 23, 433-435 (1957).
 Keeler, R. F. & Varner, J. E. Archs Biochem. Biophys. 70, 585-590 (1957).
 Bottels, H. Zentre. Bakteriol. Parasitenk. Abt. II 95, 193-218 (1936).

- 14. Nicholas, D. J. D., Fisher, D. J., Redmond, W. J. & Wright, M. A. J. gen. Microbiol. 22, 191-205 (1960).
- Becking, J. H. Pl. Soil 2, 171-201 (1962).
- 16. McKenna, C. E., Benemann, J. R. & Traylor, T. C. Biochem. biophys. Res. Commun. 41, 1501-1508 (1970).
- 17. Burns, R. C., Fuchsman, W. H. & Hardy, R. W. F. Biochem. biophys. Res. Commun. 42, 353-358 (1971).
- Beneman, J. R., McKenna, C. E., Lie, R. F., Traylor, T. G. & Kamen, M. D. Biochim. biophys. Acta 264, 25-38 (1972).
- 19. Eady, R. R., Smith, B. E., Cook, K. A. & Postgate, J. R. Biochem. J. 128, 655-675 (1972).
- Robson, R., Woodley, P. & Jones, R. EMBO J. 5, 1159-1163.
 Krylova, N. B. Doki. Mosk. Sef Kokhoz. Akad. 84, 293-299 (1963).
- Singh, N. H., Vaishampayan, A. & Singh, R. K. Biochem. biophys. Res. Commun. 81, 67-74 (1978).
- 23. Bowen, H. J. M. Trace Elements in Biochemistry (Academic, London, 1966). 24. Denisov, N. T., Efimov, O. N., Shuvalova, N. I., Shilova, A. K. & Shilov, A. E. Russ. J.
- phys. Chem. 44, 1693-1694 (1970). Nikinova, L. A., Ovchařenko, A. G., Eflmov, O. N., Avilov, V. A. & Shilov, A. E. Kin. i. Kat. 13, 1602–1603 (1972).

- Kat. 13, 1602-1603 (1972).

 6. Eady, R. R. Meth. Enzym. 69, 751-776 (1980).

 7. Laemmli, U. K. Nature 227, 680-685 (1970).

 8. Bulen, W. A. & Le Comte, J. R. Proc. natn. Acad. Sci. U.S.A. 51, 979-989 (1966).

 9. Jensen, H. L. & Spencer, D. Proc. Linn. Soc. N. S. Wales 72, 73-86.

Botulinum C2 toxin ADP-ribosylates actin

K. Aktories*, M. Bärmann†, I. Ohishi‡, S. Tsuyama‡, K. H. Jakobs§ & E. Habermann*

- * Rudolf-Buchheim-Institut für Pharmakologie der Universität Giessen, Frankfurter Strasse 107, D-6300 Giessen, FRG
- † Institut für Pharmakologie und Toxikologie der Universität Giessen, D-6300 Giessen, FRG
- ‡ College of Agriculture, University of Osaka Prefecture, Sakai, Osaka 591, Japan
- § Pharmakologisches Institut der Universität Heidelberg, D-6900 Heidelberg, FRG

ADP-ribosylation of regulatory proteins is an important pathological mechanism by which various bacterial toxins affect eukaryotic cell functions. While diphtheria toxin catalyses the ADPribosylation of elongation factor 2, which results in inhibition of protein synthesis, cholera toxin and pertussis toxin ADP-ribosylate N_s and N_i, respectively, the GTP-binding regulatory components of the adenylate cyclase system, thereby modulating the bidirectional hormonal regulation of the adenylate cyclase^{1,2}. Botulinum C2 toxin is another toxin which has been reported to possess ADP-ribosyltransferase activity3. This extremely toxic agent is produced by certain strains of Clostridium botulinum4 and induces hypotension5, an increase in intestinal secretion6, vascular permeability and haemorrhaging in the lungs. In contrast to botulinum neurotoxins, the botulinum C2 toxin apparently lacks any neurotoxic effects5. Here we report that botulinum C2 toxin ADPribosylates a protein of relative molecular mass 43,000 (43K) in intact cells and in cell-free preparations. We present evidence that the 43K protein substrate is actin, which is apparently mono-ADPribosylated by the toxin. Botulinum C2 toxin also ADP-ribosylated purified liver G-actin, whereas liver F-actin was only poorly ADPribosylated and skeletal muscle actin was not ADP-ribosylated in

either its G form or its F form. ADP-ribosylation of liver G-actin by botulinum C2 toxin resulted in a drastic reduction in viscosity of actin polymerized in vitro.

Botulinum C2 toxin is a binary toxin and consists of two components, C2-I and C2-II, with relative molecular masses $(M_r s)$ of ~50K and 100K, respectively⁴. Both components are actually completely separate proteins which interact to cause the toxic effects. The 50K component, which is non-toxic in intact tissue, apparently represents the ADP-ribosyltransferase³. The 100K component appears to be involved in the binding of the toxin to intact cells⁶ and probably enables the enzymatically active component C2-I to enter the cell. Therefore, we used the combination of C2-I and -II for studies in intact cells and the isolated C2-I component for studies in cell-free preparations. In platelet lysates, C2-I toxin ADP-ribosylated a 43K protein, predominantly located in the cytosolic fraction (Fig. 1a). ADPribosylation of a 43K protein was also found in lysates of S49 lymphoma cells, hamster adipocytes, chicken embryo fibroblasts and neuroblastoma x glioma hybrid cells (NG 108-15) and in brain homogenates (not shown). As botulinum C2-I toxin ADPribosylated a protein with a M, similar to those of the N, and N_i proteins, the substrates of cholera and pertussis toxin, respectively, we studied the ADP-ribosylated substrates of all three toxins by SDS-gel electrophoresis. As shown in Fig. 1b, the 43K substrate of botulinum C2 toxin was clearly separated from the cholera toxin and pertussis toxin ADP-ribosylated regulatory components, N_s and N_i, respectively, of the adenylate cyclase system. When intact S49 lymphoma cells were pretreated with botulinum C2 toxin (components I and II), the subsequent C2-I-induced ADP-ribosylation of the 43K substrate protein in cell-free preparations was largely decreased (Fig. 2a). These findings suggest that the substrate of botulinum C2 toxin is identical in intact cells and in cell-free preparations. C2-Iinduced ADP-ribosylation of the 43K protein in platelet cytosol was time- and concentration-dependent. In the presence of 5 µM NAD, maximal ADP-ribosylation was seen at $\sim 1 \mu g \text{ ml}^{-1}$ toxin after 2 hours of incubation. That the ADP-ribosylation of the 43K protein was a mono-ADP-ribosylation under the conditions

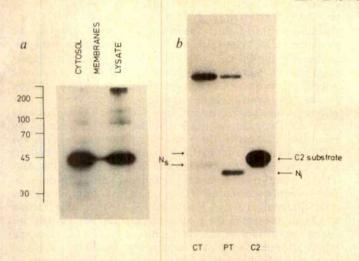


Fig. 1 Polyacrylamide gel analysis of radioactive products resulting from ADP-ribosylation catalysed by botulinum C2-I toxin, cholera toxin and pertussis toxin. a, ADP-ribosylation of a 43K protein in human platelet lysate, crude platelet membranes and platelet cytosol by botulinum C2-I toxin. b, ADP-ribosylation of the N_a and N_i proteins, and of the 43K C2 substrate in crude membranes of S49 lymphoma cells by cholera toxin (CT), pertussis toxin (PT) and botulinum C2-I toxin (C2), respectively.

Methods. a, Human platelets were isolated as described pre-viously11, then lysed by freezing and thawing in a hypotonic medium containing 10 mM triethanolamine-HCl (pH 7.4) and 5 mM EDTA. Platelet cytosol was obtained by centrifuging the lysate for 15 min at 30,000g. The pellet was washed twice with the hypotonic buffer then used as the crude platelet membrane fraction. ADP-ribosylation was carried out in a buffer containing 10 mM thymidine, 5 mM MgCl₂, 1 mM EDTA, 1 µg ml⁻¹ C2-I toxin, 0.5 μM [α-32P] NAD (~600,000 c.p.m.), 0.5 mM ATP and 50 mM triethanolamine-HCl (pH 7.4). Protein concentration was 50-200 µg per tube. After incubation of 37 °C for 1 h, the reaction was stopped by adding 1 ml of trichloroacetic acid (20% w/v). The resulting pellet was washed with ether and dissolved in 50 µl of electrophoresis buffer. SDS-gel electrophoresis was performed according to Laemmli12. Gels were stained with Coomassie blue, destained and subjected to autoradiography for 24-48 h. Thereafter, the protein bands containing the radioactive label were cut from destained gels, solubilized in the presence of 1 ml of 30% hydrogen peroxide and counted for 32P. ADP-ribosylation of the 43K protein in platelet lysate, crude membranes and cytosol was 24.7, 7.6 and 28.3 pmol ADP-ribose per mg protein per h, respectively. b, Crude S49 lymphoma cell membranes, prepared essentially as described elsewhere13, were incubated with 100 µg ml-1 cholera toxin, 40 µg ml⁻¹ pertussis toxin or 1 µg ml⁻¹ C2-I toxin for 45 min at 37 °C in medium containing 1 μM [α-32P]NAD (~1 µCi per tube), 10 mM thymidine, 10 mM arginine, 5 mM creatine phosphate, 0.1 mg ml⁻¹ creatine kinase, 5 mM MgCl₂, 1 mM EDTA, 0.5 mM ATP, 0.5 mM GTP and 50 mM triethanolamine-HCl (pH 7.4). Cholera toxin and pertussis toxin were preactivated by incubation in the presence of 20 mM dithiothreitol (DTT) for 10 min at 37 °C.

used is indicated by the following observations. First, whereas the total amount of the ADP-ribosylation increased with length of incubation, the M_r of the labelled substrate remained constant. Second, addition of snake venom phosphodiesterase hydrolysed the protein-bound radioactivity and resulted in the formation of 5'AMP (not shown).

The similarity between the relative molecular mass of the labelled protein and that of actin led us to study whether the platelet microfilament protein was ADP-ribosylated by botulinum C2-I toxin. After incubation with anti-actin antibodies but not with non-immune rabbit serum, protein A-agarose precipitated the toxin-labelled platelet cytosolic protein (Fig. 3a). In addition, immunoblotting with anti-actin antibodies clearly demonstrated that the antibodies recognized the labelled 43K protein (Fig. 3b). Both findings strongly indicated that actin

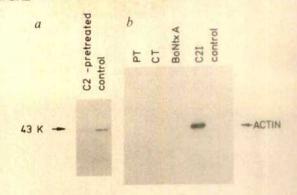


Fig. 2 a, Effect of pretreatment of intact S49 lymphoma cells with botulinum C2 toxin on the subsequent ADP-ribosylation of cell lysates. b, Effects of botulinum C2-I toxin, cholera toxin, pertussis toxin and botulinum neurotoxin A on the radiolabelling of liver Gractin

Methods. a, S49 lymphoma cells were treated for 24 h without (control) or with botulinum C2 toxin (5 μg l⁻¹ component I plus 10 μg l⁻¹ component II), then crude membranes were prepared and treated with botulinum C2-I toxin (1 μg ml⁻¹) in the presence of [α-3²P]NAD. SDS-gel electrophoresis and autoradiography were performed as described in Fig. 1 legend. b, Purified liver G-actin (100 μg ml⁻¹), prepared according to Jaberg¹⁴, was incubated without (control) or with 1 μg ml⁻¹ C2-I toxin (C21), 200 μg ml⁻¹ preactivated cholera toxin (CT), 30 μg ml⁻¹ preactivated pertussis toxin (PT) or 80 μg ml⁻¹ botulinum neurotoxin A (BoNtx A) in the presence of 0.5 μM [α-3²P]NAD (~500,000 c.p.m. per tube) as described in Fig. 1 legend.

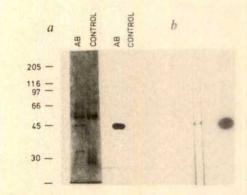


Fig. 3 Immunoprecipitation and immunoblotting of the platelet 43 K protein labelled by botulinum C2-I toxin. a, SDS-gel electrophoresis and autoradiography of the ADP-ribosylated C2-I toxin substrate immunoprecipitated by anti-actin antibodies (AB) but not by non-immune serum (Control). b, Immunoblot and autoradiography of the 43 K platelet cytosolic protein ADP-ribosylated by C2 toxin.

Methods. a, Platelet cytosol (~200 µg protein) was ADP-ribosylated as described in Fig. 1 legend, except that NAD and MgCl2 was at 1 µM and 0.5 mM, respectively and the total volume was 0.5 ml. Toxin-ADP-ribosylated platelet cytosol (200 µl), freed from unreacted [\alpha^{32}P]NAD by gel-filtration, was incubated in 1% Triton X-100, 1% deoxycholate, 0.1% SDS, 150 mM NaCl and 50 mM Tris-HCl (pH 7.2) with 100 µl of rabbit polyclonal antibodies (0.1 mg ml-1) for 12 h at 0 °C in a total volume of 400 µl. The antibodies were raised against heat- and SDS-denatured pig liver actin and affinity-purified over a column of rabbit skeletal muscle actin coupled to Sepharose 4B. Then, 20 µl of protein A-agarose (Sigma) was added for 1 h. The immuno-protein-A-agarose complex was separated by centrifugation, washed twice and analysed by SDS-gel electrophoresis. b, Anti-actin antibodies recognized the ADP-ribosylated toxin substrate. Immunoblotting was performed according to Towbin et al. 15 with peroxidase-coupled swine IgG to rabbit IgG (Dakopatts) as second antibody and 4-chloro-1naphthol as peroxidase substrate.

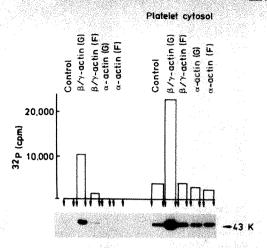


Fig. 4 Botulinum C2-I toxin-induced ADP-ribosylation of actin. For ADP-ribosylation purified liver G-actin (200 µg ml⁻¹) and F-actin (160 µg ml⁻¹) and rabbit muscle G-actin (200 µg ml⁻¹) and F-actin (110 µg ml⁻¹), prepared according to Pardee and Spudich¹⁶, were incubated without or with human platelet cytosol (170 µg ml⁻¹) in the presence of 1 µg ml⁻¹ botulinum C2-I toxin and 0.2 μM ³²P-NAD (~250,000 c.p.m. per tube) for 15 min at 37 °C. Reaction medium, SDS-gel electrophoresis, autoradiography and 32P measurements were as described in Fig. 1 legend.

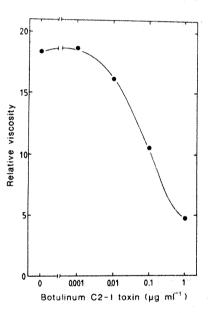


Fig. 5 Effect of C2 toxin-induced ADP-ribosylation on β/γ -actin polymerization, measured as relative viscosity.

Methods. Liver G-actin (30 µM) was incubated in the presence of 1 mM NAD, 10 mM thymidine, 0.5 mM MgCl₂, 0.5 µM ATP and 50 mM triethanolamine-HCl (pH 7.4) without or with botulinum C2-I toxin at the indicated concentrations for 1 h at 37 °C. Thereafter, the samples were placed on ice. Polymerization was initiated in 140 µl of the pretreated actin solution by adding 20 µl of a medium containing 16 mM MgCl₂, 1.6 mM ČaCl₂, 4.0 mM ATP, 0.8 mM DTT and 16 mM Tris-HCl, pH 7.5. Measurements were made after 10 min at 25 °C. Viscosity was determined using the falling-ball device described by Pollard and Cooper¹⁷. Relative viscosity is the quotient sample viscosity (η_s) divided by the buffer viscosity (η_a) .

was the protein ADP-ribosylated by botulinum C2 toxin. Furthermore, purified liver G-actin was a good substrate for botulinum C2-I toxin (Fig. 2b). In contrast, cholera toxin and pertussis toxin did not ADP-ribosylate the isolated microfilament protein. Botulinum neurotoxin A, which has no enterotoxic effects8, showed no ADP-ribosyltransferase activity with platelet lysates (not shown), brain homogenates (not shown), with purified liver G-actin. Interestingly, only the G-form of liver actin was a good substrate for the ADP-ribosylation by botulinum C2-I toxin. The F-form of liver actin was much less ADP-ribosylated, and purified α-actin from rabbit skeletal muscle was not ADP-ribosylated in its G- or F-form (Fig. 4)— Thus, it seems that botulinum C2 toxin-induced ADP-ribosylation is highly specific for β/γ -actin in its G-form. The slight ADP-ribosylation of liver F-actin may be due to a minor fraction of G-actin present in the F-actin preparation. Accordingly, we found that phalloidin, which specifically binds to F-actin and which stabilizes this form9, impaired or abolished the toxininduced ADP-ribosylation (data not shown). The addition of platelet cytosol to G-actin further increased the amount of ADP-ribosylation, suggesting that an additional factor present in the cytosolic fraction facilitated the ADP-ribosylation reaction. In contrast, the addition of platelet cytosol did not increase the ADP-ribosylation of liver F-actin or muscle α -actin.

In order to study whether the ADP-ribosylation of actin caused any change in the functional properties of the microfilament protein, we compared the viscosity of control and C2-I toxin-pretreated actin 10 min after induction of polymerization of actin with MgCl₂. When actin was pretreated with increasing concentrations of botulinum C2-I toxin, the relative viscosity of the polymerized actin solution was decreased in a concentration-dependent manner (Fig. 5). At 1 µg ml⁻¹ C2-I toxin, the relatve viscosity of ADP-ribosylated actin was reduced by about 72% compared with the control preparation, indicating that the polymerization of the modified actin was largely impaired.

Taken together, the data presented show that botulinum C2 toxin induces the ADP-ribosylation of β/γ -actin. This covalent modification subsequently alters at least one functional property of the microfilament protein, actin polymerization. It is suggested that the ADP-ribosylation of actin is the pathophysiological basis of the toxic effects of botulinum C2 toxin, for example, the increase in vascular permeability, gut secretion and haemorrhaging of the lungs. Recent findings that the C2 toxin induces rounding up and subsequent lysis of cultured cells, can also be interpreted in this sense 10. Botulinum C2 toxin, which clearly discriminates between non-muscle and skeletal muscle actin, appears to be an important tool for studying the physiological processes which involve non-muscle actin.

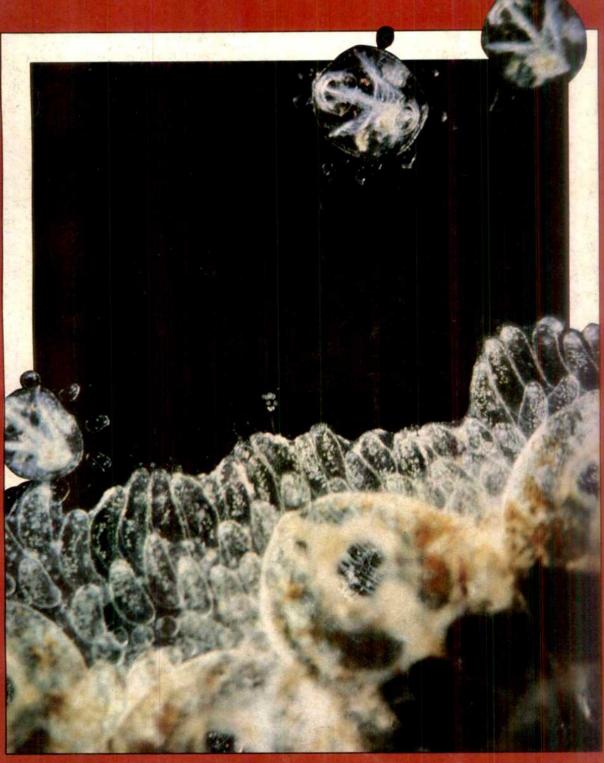
Received 21 January; accepted 7 May 1986.

- Foster, J. W. & Kinney, D. M. CRC crit. Rev. Microbiol. 11, 273-297 (1985).
- Gill, D. M. & Woolkalis, M. Ciba Fdn Symp. 112, 47-69 (1985). Simpson, L. L. J. Pharmac. exp. Theor. 230, 665-669 (1984).
- Ohishi, I., Iwasaki, M. & Sakaguchi, G. Infect. Immunity 30, 668-673 (1980). Simpson, L. L. J. Pharmac exp. Ther. 223, 695-701 (1982).
- Ohishi, I. Infect. Immunity 40, 691-695 (1983) Ohishi, I. Infect. Immunity 40, 336-339 (1983)
- Simpson, L. L. Pharmac. Rev. 33, 155-188 (1981)
- Wieland, T. Naturwissenschaften 64, 303-309 (1977).
- Wieland, I. Audurwissenschapter G., 303-303 (1971).
 Ohishi, I. Miyake, M., Ogura, H. & Nakamura, S. FEMS Microbiol. Lett. 23, 281-284 (1984).
 Jakobs, K. H., Saur, W. & Schultz, G. Naunyn Schmiedeberg's Arch. Pharmac. 302, 285-291
- 12. Laemmli, U. K. Nature 227, 680-685 (1970)
- 13. Jakobs, K. H., Gehring, U., Gaugler, B., Pfeuffer, T. & Schultz, G. Eur. J. Biochem. 130, 605-611 (1983).
- Jaberg, B. Z. Naturforsch. 38c, 829-833 (1983).
- Towbin, H., Staehelin, T. & Gordon, J. Proc. natn. Acad. Sci. U.S.A. 76, 4350-4354 (1979)
 Pardee, J. D. & Spudich, J. A. Meth. Enzym. 85, 164-181 (1982).
- 17. Pollard, T. D. & Cooper, J. A. Meth. Enzym. 85, 211-230 (1982).

nature

INTERNATIONAL WEEKLY JOURNAL OF SCIENCE

Volume 322 No.6078 31 July-6 August 1986 £1.90.



PLANKTONIC KIN RECOGNITION



Electrophoresis then and now

Then, in the early 70's, this was the latest thing in electrophoresis.

Now, it's the mid 80's, and there's a powerful new concept in high resolution electrophoresis.

PhastSystem

Run and stain SDS-PAGE gels in about 1 hour

PhastSystem combines precision equipment and new high-performance PhastGelTM media to give you:

- Fast results: from short separation times and quick protein staining. In total, SDS-PAGE and IEF each take about 1 hour. The resolution is superb.
- Quick staining: coomassie takes about 30 minutes, and silver staining about an hour.
- Reproducibility: you have automated, programmable control over running and staining conditions.

Try it for yourself!



nature

NATURE VOL. 322 31 JULY 1986

nature



Adults of Botryllus schlosseri. The planctonic larvae of this ascidian settle and metamorphose into sessile adults which fuse with one another to form colonies. On page 456 of this issue Grosberg and Quinn show how larvae from the same parent colony settle closer to their kin than to unrelated larvae.

OPINION	
Cafechism for nuclear power Teaching by numbers	393 394
NEWS	
British radioactivity	395
Paying for old lambs Genetic engineering UK research grants	396
Human genome	397
New career for Brenner Biotechnology	398
West German nuclear power Atomic power	399
Chernobyl French budget Terrorists strike again US – Japan trade	400
High-technology trade Science Digest dies	401
CORRESPONDENCE	
Gulf protest/RGO thumb up for Cambridge/Japanese education	402
NEWS AND VIEWS	
Catching atoms in beams of light Pattern formation: Descartes and the fruitfly	403

Geoffrey North

A bacterial haemoglobin MF Perutz Neural models: Networks	405
for fun and profit James A Anderson	406
Chloride ions and cystic fibrosis Maynard Case	407
Genetic management in zoos Andrew F Read- & Paul H Harvey	408
Archaeology: A new chronology for the French Mousterian period Paul Mellars Obituary: Adrian Edmund Gill (1937–1986) Peter D Killworth	410
-SCIENTIFIC CORRESPONDENC	
Example 2	412 412
BOOK REVIEWS	ndaga and constitu

Neurophilosophy: Toward a Unified Science of the Mind-Brain by P Smith Churchland 413 Philip Kitcher **Optical Interferometry** by P Hariharan 414 OS Heavens **Visual Cognition** ed. S Pinker Stuart Sutherland 415 Skeletal Muscle. Handbook of Microscopic Anatomy, Vol.2, Part 6 by H Schmalbruch 415 Malcolm Irving The Origins of War by A Ferrill William McNeil 416 The Encyclopaedia of Reptiles and **Amphibians** eds T Halliday & K Adler The Encyclopaedia of Insects

Kelvin on an old, celebrated hypothesis	
E Harrison	417
REVIEW ARTICLE	
The long and the short of	
long-term memory	
— a molecular framework	
P Goelet, V F Castellucci,	
S Schacher & E R Kandel	419

COMMENTARY

ed. CO'Toole

John Crothers

404

 ΔR	TI	1	FC
$\neg \cdot \cdot$	111	11	L b

Petrological and tectonic segmentation	
of the East Pacific Rise.	
5°30′ – 14°30′N	
CH Langmuir, JF Bender	
& R Batiza	422
property control of the control of t	

Global temperature variations between 1861 and 1984 P D Jones, T M L Wigley & P B Wright

-LETTERS TO NATURE

Observation of terrestrial orbital
motion using the cosmic-ray
Compton-Getting effect
DJ Cutler & DE Groom

Prospecting for planets in	
circumstellar dust:	
sifting the evidence from β Pictoris	
DJDiner & JF Appleby	43

Radio observations of PKS2314+03	
during occultation by comet Halley	
S K Alurkar, R V Bhonsle	
& A K Sharma	

Imaş	ging the outflow of ionospheric
ions	into the magnetosphere
YT	Chiu, R M Robinson,
\dot{G} R	Swenson, S Chakrabarti
& D	S Evans

Periodicity of the	Earth's magnetic
reversals	
R B Stothers	

Th	ermohaline intrusions created
iso	pycnically at oceanic fronts
are	inclined to isopycnals
JD	Woods, R Onken
& J	Fischer

Effects of surface heat flux during the	
1972 and 1982 El Niño episodes	
R K Reed	449

Uplift of the shores of the western
Mediterranean due to Messinian
desiccation and flexural isostasy
S E Norman & C G Chase
AND THE RESIDENCE OF THE PROPERTY OF THE PROPE

416

Thermoluminescence dating of	
Le Moustier (Dordogne, France)	
H Valladas, J M Geneste.	
J L Joron & J P Chadelle	45
A mutative encepter for the	

A putative ances	tor for the	****
swordfish-like ic	hthyosaur	
Eurhinosaurus		
C McGowan		454
	Contents continu	ed overleaf

Nature* (ISSN 0028-0836) is published weekly on Thursday, except the last week in December, by Macmillan Journals Ltd and includes the Annual Index (mailed in February). Annual subscription for USA and Canada US \$240. USA and Canadian orders to: Nature, Subscription Dept. PO Box 1501. Neptune, NJ 07753, USA. Other orders to Nature, Brunel Road, Basingstoke, Hants RG21 2XS, UK, Second class postage paid at New York, NY 10012 and additional mailing offices. Authorization to photocopy material for internal or personal use, or internal or operational use. Or internal or personal use, of internal or personal use, or internal or operational use. Or internal or operational use, or internal or operational use, or internal or operational use. Or internal or operational use, or internal or operational use, or internal or operational use. Or internal or operational use, or internal or operational use. Or internal or operational use, or internal or operational use. Or internal or operational use. Or internal or operational use, or internal or operational use. O

444

430

434

439

441

444

450

NEWANTI JODIES

ESEARCH

nur für in vitro-Gebrauch

Antibodies to

Kat. Nr. D 7324

0047 Ch. 8.

HTLV-III gp 120

Menge 2 ml

Lagerung 4°C

Made in Germany

Biochrom KG Leonorenstr. 2-6 · D-1000 Berlin 46

inity purified sheep antibodies the HTLV-III/LAV proteins.

Kat.-Nr.

gp 120 D 7324 gp 41 D 7323 p 24 D 7320

intibodies are generated against nthetic peptides representing itopes of the proteins. estern blot analysis is used to rify specificity and reactivity.

or additional information contact:

JOCHROM KG Leonorenstr. 2–6 D-1000 Berlin 46 Tel.: (030) 7718047

Telex: 185 821 bio d Reader Service No.19

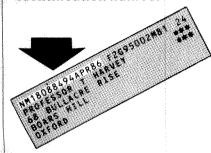
DEFINED CELL CULTURE MEDIA · DIAGNOSTICS · SYNTHETIC PEPTIDES



Biochrom KG

SUBSCRIPTION SERVICE

Your mailing label contains vour unique subscriber identification number



To ensure prompt service, please quote this number whenever you speak or write to us about your subscription

HELP US TO HELP YOU

Annual Subscription Pri	ces	
UK & Irish Republic		£104
USA & Canada		US\$240
Australia, NZ &		
S. Africa	Airspeed	£150
	Airmail	£190
Continental Europe	Airspeed	£125
India	Airspeed	£120
	Airmail	£190
Japan	Airspeed	Y90000
Rest of World	Surface	£120
	Airmail	£180
Orders (with remittance) to:	

UK & Rest of World USA & Canada Nature Nature Subscription Dept PO Box 1501 Circulation Dept Brunel Road Basingstoke Hants RG212XS, UK Tel: 025629242 Neptune NJ 07753

(The addresses of Nature's editorial offices are shown facing the first editorial page)

Japanese subscription enquiries to: Japan Publications Trading Company Ltd 2-1 Sarugaku-cho 1-chome Chiyoda-ku, Tokyo, Japan

Tel: (03) 292 3755 Personal subscription rates: These are available in some countries to subscribers paying by personal cheque or credit card. Details from:

USA & Canada UK & Europe Felicity Parker 65 Bleecker Street New York NY 10012, USA Nature 4 Little Essex Street London WC2R 3LF, UK Tel: (212) 477-9600

Back issues: UK, £2.50; USA & Canada, US\$6.00 (surface), US\$9.00 (air); Rest of World, £3.00 (surface), £4.00 (air)

Binders Single binders: UK, £5.25; USA & Canada \$11.50; Rest of World, £7.75. Set of four: UK, £15.00; USA & Canada \$32.00; Rest of World, £22.00

Annual indexes (1971-1985) UK, £5.00 each; Rest of World, \$10.00

Nature First Issue Facsimile

UK. £2.00; Rest of World (surface), \$3.00; (air) \$4.00

Nature in microform Write to University Microfilms International, 300 North Zeeb Road, Ann Arbor, MI 48106, USA

The genetic control and consequences of kin recognition by the larvae of a colonial marine invertebrate RK Grosberg & JF Quinn

Genetically restricted suppressor T-cell clones derived from lepromatous leprosy lesions R L Modlin, H Kato, V Mehra,

E E Nelson, F Xue-dong, T H Rea,

PK Pattengale & BR Bloom

Cloned suppressor T cells from a lepromatous leprosy patient suppress Mycobacterium leprae reactive helper T cells THM Ottenhoff.

D G Elferink, P R Klatser

& RRP de Vries

Retinal ganglion cells lose response to laminin with maturation J Cohen, J F Burne, J Winter

& P Bartlett

Chloride and potassium channels in cystic fibrosis airway epithelia MJ Welsh & CM Liedtke

Role of the HTLV-III/LAV envelope in syncytium formation and cytopathicity J Sodroski, W C Goh,

C Rosen, K Campbell & W A Haseltine A chromosomal rearrangement in a

P. falciparum histidine-rich protein gene is associated with the knobless phenotype LG Pologe & JV Ravetch

Long-range restriction site mapping of mammalian

genomic DNA WRABrown&APBird 477

Primary sequence of a dimeric bacterial haemoglobin from Vitreoscilla

S Wakabayashi, H Matsubara & D A Webster

MATTERS ARISING

Homology between IgE-binding factor and retrovirus genes K W Moore & C L Martens Reply: T Miyata, H Toh 484 & M Ono

NATURE CLASSIFIED

Professional appointments -Research posts - Studentships -Fellowships — Conferences – Courses — Seminars — Symposia:

Back Pages

Next week in Nature:

- Life as a cosmic phenomenon
- X-ray photoionized nebula
- Silicon under the microscope
- New cyclodextrins

456

459

462

465

467

470

474

481

- Novel gene regulation
- Trypanosomal clone
- Bacterial gene from plant
- Chloroplast DNA sequence
- Australopithecus boisei only 2.5 million years old

GUIDE TO AUTHORS

Authors should be aware of the diversity of Nature's readership and should strive to be as widely under stood as possible.

Review articles should be accessible to the whole regidership. Most are commissioned, but unsolicited reviews are welcome (in which case prior consultation with the office is desirable).

Scientific articles are research reports whose conclusions are of general interest or which represent substantial advances of understanding. The text should not exceed 3,000 words and six displayed items (figures plus tables). The article should include an italic heading of about 50 words.

Letters to Nature are ordinarily 1,000 words long with no more than four displayed items. The first paragraph (not exceeding 150 words) should say what the letter is about, why the study it reports was undertaken and what the conclusions are.

Matters arising are brief comments (up to 500 words) on articles and letters recently published in Nature, The originator of a Matters Arising contribution should initially send his manuscript to the author of the original paper and both parties should, wherever possible, agree on what is to be submitted.

Manuscripts may be submitted either to London of Washington. Manuscripts should be typed (double spacing) on one side of the paper only. Four copies are required, each accompanied by copies of lettered artwork. No title should exceed 80 characters in length. Reference lists, figure legends, etc. should be on separate sheets, all of which should be numbered. Abbreviations, symbols, units, etc. should be identified on one copy of the manuscript at their first

References should appear sequentially indicated by superscripts, in the text and should be abbreviated according to the World List of Scientific Periodicals, fourth edition (Butterworth 1963-65). The first and last page numbers of each reference should be cited. Reference to books should clearly indicate the publisher and the date and place of publication. Unpublished articles should not be formally referred to uniless accepted or submitted for publication, but may be mentioned in the text.

Each piece of artwork should be clearly marked with the author's name and the figure number. Original artwork should be unlettered. Suggestions for cover illustrations are welcome. Original artwork (and one copy of the manuscript) will be returned when manuscripts cannot be published.

Important: Manuscripts or proofs sent by air courses should be declared as "manuscripts" and "value \$5" for prevent the imposition of Customs duty and Value Added Tax in the United Kingdom.

Requests for permission to reproduce material from Nature should be accompanied by a self-addressed tand, in the case of the United Kingdom and United States, stamped) envelope

NEWS • FEATURES

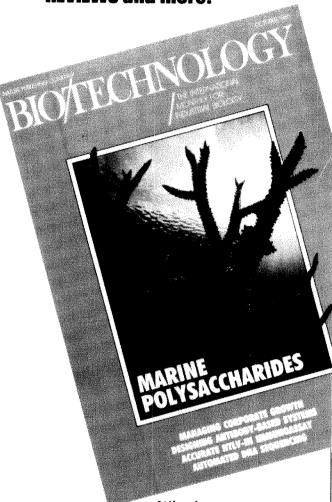
ORIGINAL RESEARCH

PRODUCT EVALUATIONS

INDUSTRIAL APPLICATIONS

JOB OPENINGS

BOOK and PRODUCT REVIEWS and more!



Whether you are involved in the engineering, scientific or commercial aspects of biotechnology, this is the one magazine you can't afford to be without.

For details of our special 2-year subscription offer and a FREE SAMPLE COPY phone Za Dale on (01) 836 6633 (UK) or Paige Beaver (212) 477 9600 (US) OR write to

Bio/Technology Macmillan Journals Ltd 4 Little Essex Street London WC2R 3LF UK

Bio/Technology 65 Bleeker Street New York NY 10012 **USA**

EDITORIAL OFFICES

London: 4 Little Essex Street, WC2R 3LF Telephone: (01) 836 6633 Telex: 262024

Washington: 1134 National Press Building, DC 20045 Telephone: (202)

Tokyo: Eikow Building, 10-9, Hongo 1-Chome, Bunkyo-ku, Tokyo 113

Telephone: (93) 816 3756/7 Telex: 2722634 MSKKJ

Editor: John Maddos

Deputy Editor: Peter Newmark

Editorial Staff: Jennifer Altman, Alun Anderson, Philip Campbell, Maxine Clarke, Philip Campbell, Maxine Clarke, Laura Garwin, Sarah Hargreaves, Tim Lincoln, Geoffrey North, Miranda Robertson, Charles Wenz, Nigel Williams and Karen Wright (Washington)

Washington Correspondents: Tim Beardsley and

Tokyo Correspondent: David Swinbanks European Correspondent (in London): Robert Walgate

Art & Design: Joel Chernin, Wai Sing Tang and Elizabeth Terrell

Administration: Mary Sheehan, Michelle Ashman, Juhette Bedborough, Angela Brown, Sara Dallas (Washington), Zoe James Geraldene Lambert, Maureen Palmer, Meg Taylor and Penclope Walker (Washington)

Publisher: Elizabeth Hughes Managing Director: Ray Barker Promotion Manager: Felicity Parker International Advertisement Manager:

European Display Advertisement Manager:

Sales Executives: Julia Tindall, Louise Smith Group Classified Advertisement Manager:

Nature New York Office 65 Bleecker Street, New York, NY 10012 Telephone: (212) 477-9600 Telex: 668497 UW

President: Gary M. Rekstad

American Advertising Manager: Henry Dale Classified Advertising Manager: Marianne Ettisch

Circulation Director: Paul E. Siman Canadian Display & Classified: Peter Drake. 17 Pine Crescent, Toronto, Ontario M4E 1L1—(416) 690-2423

Display Advertising Representatives

New York: Nature Office

Chicago: Didier & Broderick, Inc.—(312) 498-4520 San Francisco: Jobson/Jordan/Harrison/Schulz. Inc--(415) 392-6794

Los Angeles & Pasadena: Jobson/Jordan/ Harrison/Schulz, Inc.—(818) 796-9200

New England: Denis J. O'Malley-(212) 477-9623 Mid-Atlantic: Denis J. O'Malley-(212) 477-9623

Southeast: Nature New York Office

Spring, Texas: Jobson/Jordan/Harrison/Schulz, Inc.-(713) 376-2368

Australia: Gus Bartel, Gus Bartel & Associates—(075) 466 577

France: Françoise Teisseyre, Mediatess—(1) 46 22 51 54

West Germany and Austria: Franz Schrecklinger. TMW Top Media Werbegesellschaft GmbH, Frankfurt—(69) 72 60 46

Switzerland: Verena Loewenthal-Hugi, 8103 Unterengstringen — (01) 750 55 11

Israel: Daniel Zimet, Zimet Advertising & Publishing—(03) 221083 Italy: Luigi Rancatí, Rancati Advertising—(02) 7531 445

Japan: Mashy Yoshikawa, Orient Echo Inc. --

Netherlands and Belgium: Adele Struvck.

Astra, Netherlands—(03404) 23265 Scandinavia: Andrew Karnig, Andrew Karnig & Associates, Sweden—(08) 4400 05



Nature® ISSN 0028-0836 Registered as a newspaper at the British Post Office © 1986 Macmillan Journals Ltd Vol. 322 No. 6078 31 July 1986

nature

SAMERIAGE 32 VILLAY 1986

19

Catechism for nuclear power

Governments should urgently give attention to the consequences of Chernobyl on public opinion of nuclear power — and should correct some of the damage they have done.

High is a question from an examination paper in the final examination for students following the course in Logic for the Modern World, offered by the University of the Sticks, on which people may wish to brood.

 \mathbf{Q} . Even small doses of radiation exposure are potentially harmful to people, and should be avoided.

Nuclear power stations, and the nuclear industry in general, are sources of artificial radiation to which people may be exposed.

"Therefore nuclear power stations should not be built.

"Either explain in no more than 250 words which of the three statements in this syllogism is invalid or outline in no more than 50,000 words an alternative energy policy for your country of nationality, drawing attention to such social consequences as you can foresee."

Like most examination questions, this example begs a host of other questions, mostly unexamined. But the example is not nearly as hypothetical as it may seem. Especially in the aftermath of the Chernobyl accident, but not exclusively on that account, the imputed logic is increasingly coming to dominate the policies of governments across the world. And while there remains what may be called a hard core of people who believe that nuclear power remains an economic necessity, the syllogism cannot as easily as they would wish be demolished in the prescribed 250 words.

Radiation

Those familiar with exercises like these will nevertheless quickly know the truth, that the insidious errors are in the premise. Once that has been swallowed, the conclusion tends to follow as night follows day. Nuclear power stations and the nuclear industry in general are, indeed, sources of radiation to which people, either workers in the nuclear industry or the general population. may be exposed. The British population, and British farmers in particular, have recently been given a dramatic proof of that by the decision of the agriculture ministry to ban the sale of fat lambs on the flimsy grounds that some were found to contain just over 10 per cent of the amount of Chernobyl caesium that would have been permitted by the emergency reference levels promulgated earlier this year by the British National Radiological Protection Board (see Nature 321, 798; 1986). Earlier, the whole European Community had been reminded that power stations are potentially powerful sources of radiation by the decision, at Brussels, that imports of foodstuffs from Eastern Europe would be prohibited while the content of radioactivity exceeded 600 Bu per kg. 6 per cent of the same reference level. The effect of these and other decisions has been to dramatize the truth that nuclear power stations are potential sources of radioactivity, which may be geographically widespread. The lesson will now be firmly embedded in the public consciousness, as it should be. So, given the premise, the conclusion follows that nuclear power stations are an abomination and should not be built.

As it happens, the bulk of the premise is also correct. "Even small doses of radiation exposure" are indeed potentially harmful to people. The days have long since gone when it was permissible for politicians and others to canvass the idea that there is a

"threshold" dose below which no damage of any kind is done to living organisms. While much remains to be learned about the biological consequences of small doses of radiation, the best assumption is that the probability of a particular kind of damage is proportional to the radiation dose, however small. To be sure, it is possible that in the causation of some kinds of cancer by radiation (or even other agents), where two separate damaging interactions between radiation and tissues may be required to trigger the neoplastic process, the risk of damage may be proportional to the square of the dose. But, in the present state of ignorance, nobody would go to the stake for that hypothesis. which would in any case only partially restore the respectability of the notion that there are thresholds below which no damage of this particular kind — carcinogenesis — is done. And where genetic damage is in question, there seems (at least for the time being) no sensible alternative to the proposition that the risk of damage is proportional to the dose.

Risk

The circumstance that different kinds of radiation exposure are potentially damaging in different ways does not undermine the validity of the first part of the premise in the examination question, although this circumstance enormously complicates both the estimation of risk and the general understanding of why radiation is hazardous. It is now a familiar circumstance that different sources of radiation, natural or artificial, must be dealt with differently in the estimation of biological effects. Naturally occurring radon (on account of its decay products) and airborne radioactivity are potentially causes of lung cancer to the extent that they are trapped in the airways of the lungs. Naturally occurring potassium-40 and artifical caesium (as in British post-Chernobyl lambs) once ingested, expose the internal organs of the body almost equally to potentially damaging doses of radis ation. Both plutonium-239 and strontium-90 concentrate in bones and are a threat to bone marrow, but, becquerel for becquerel, plutonium-239 is more damaging than strontium because alpha particles deposit their energy along shorter paths of ionization. And so on. There is far too little public understanding of the sophistication now applied by the radiological protection people as a matter of routine to the unravelling of the once-daunting complexity. Yet none of this qualifies the general principle that the potential hazard of a radiation dose (of a particular kind) is probably proportional to its amount.

The catch in the premise is the hanging qualifier in the premise, the seemingly innocent phrase "and should be avoided". This, of course, is not so much the starting point for a syllogism but the conclusion of some other. Moreover, whether premise or conclusion, it cannot be taken by reasonable people as an absolute injunction against radiation exposure. If it were such, the whole pattern of civilized life would already, during the half-century in which understanding of the hazards of radiation have accumulated, have been transformed. People would no longer live, or be allowed to live, at high altitudes or even high latitudes, on account of the extra doses of cosmic radiation to which they are there exposed. Old granite shield areas, where radon in the atmosphere accounts for up to a third of natural exposure.

would be evacuated. Jet aircraft would be disallowed. And so on

The truth, of course, is that the principle that radiation exposure is best avoided is not now, and never can be, absolute. Merely to rationalize present patterns of life, people have to acknowledge that the heavily loaded part of the premise must be extended somehow, perhaps to read "should be avoided whenever possible" or, more tangibly, "should be weighed in a costbenefit calculation and then, when the costs exceed the benefits, avoided". The snag for the simplifiers is that any such qualification undermines the logic of the syllogism. Only if the interdiction of radiation exposure is absolute does the conclusion follow that nuclear power stations must never be built. In all other circumstances, the most that can be said is that the benefits of nuclear power must be weighed against the costs, one of which is the potential damage done by radiation exposure, both as a matter of routine (to workers at reprocessing plants) and after accidents (as at Chernobyl).

All this is familiar stuff. For thirty years, those who build (or would build) nuclear power stations have been saying just this. It may be true that, for much of that period, the professionals have been less than frank about the potential scale of the hazards, but nobody has sought to conceal the need for a rational trade-off between risks and benefits. What Chernobyl might rationally have accomplished is a demonstration that, within a well-run nuclear programme, the avoidance of major reactor accidents deserves even more attention than it has received since the close attention given to the problem by the monumental Rasmussen study just over a decade ago. It is also possible to argue that it is worth paying something extra to avoid self-imposed risks, such as those unavoidably attending a nuclear industry, on the principle that there is a difference between unavoidable sources of risk (cosmic rays, for example) and those that are self-imposed. Yet even that seductive argument leaks. By what tests is it virtuous to claim (as the British Labour Party now does) that nuclear power should be replaced by coal when one of the few certainties in the trade-off is that many more miners will be killed per gigawatt-hour in the coalmining industry than members of the public by exposure to the radiation accompanying the routing operation of a nuclear industry?

If Chernobyl and its consequences were to lead to a more public re-examination of these questions in the countries where nuclear power is potentially an economic benefit, nobody would complain. The trouble is that the accident has come at a time when the populations most likely to need nuclear power in the decades ahead have been dissuaded from regarding the issues calmly by siren voices seeming to proclaim that there is such a thing as a free lunch — electricity without the risk to those who consume it. The sad truth is that governments are often unwittingly the abetters of these seductive propagandists, as when European governments band together to settle on a limit for the contamination of imported foodstuffs that provocatively plays over-safe. They seem not to have appreciated that, by taking such a line, they have gone a long way to accepting the loaded premise of the false syllogism which will be used against them when they plan to build a nuclear reactor. Is it too late to ask that they should mend their ways?

Teaching by numbers

A British committee has produced an enlightening report on future trends in education.

What is the difference between a teacher and a teaching machine? This question, widely asked in the sense pejorative of teachers a decade or more ago, has usually been answered by the claim (usually on behalf of teachers) that even the best teaching machines are merely mechanical, incapable of firing the imagination and the aspirations of students. For the most part, the teachers' case has been vindicated by the appalling quality of

what has previously been passed off under the label of educational technology. Some teaching machines have been literally machines whose mastery required not merely skills available to, say, high-school students, but those of ambidextrous conjurors as well. Others have looked like books but have been seen, on casual inspection, to be ways of drilling students in lessons which it is possible, but inappropriate, to learn by rote, leaving the real work to be done by real teachers. It is no wonder, that after a brief fashion for educational technology in the 1960s, the exercise should have been discredited. But equally, now that professional people are agog with the idea that "expert" systems should be used as aids to judgement in fields as different as medicine and engineering, it is natural that the old claims of educational technology should be dusted off and re-examined.

One result, in Britain, is a sensible slim document by a government committee called the Information Technology Advisory Panel, set up when Mr Kenneth Baker, now Secretary of State for Education and Science, was the British government's cheer leader for the information revolution. One irony is that most of the panel's recommendations urge that the government should spend money on investigation and research on the application of information technology; Mr Baker, in his new role, would have to foot the bill. Another is that the panel was subsumed last April in another government committee, the Advisory Committee on Applied Research and Development, whose most recent public report some weeks ago consisted of an extended wringing of hands over the parlous condition of the British software industry, from which many of the defunct panel's members spring. Yet, curiously, the panel's report (Learning to live with IT, HMSO £4.00) is just the judicious blend of enthusiasm for change and caution about the means by which it may be accomplished that endears a committee to its discriminating followers.

On the leading question, not directly answered by the panel, the difference between a teacher and a machine is that the teacher alone can serve as an intelligent critic of an individual student's learning. Machines, of course, can automatically assess a student's performance by criteria written in their programs, providing reinforcement exercises whenever these seem necessary. But even as machines are now, or are likely to be tomorrow, there is only a poor prospect that they will be able to handle the unexpected difficulties that arise in most people's learning, among which the recurring question "Why bother?" is the most frequent. In one of its rosier passages, the panel does venture the guess that the simulation of the teacher's skills by sufficiently expert systems is not impossible, but for the most part it recognizes that the immediate need is for experiment and investigation to define the bounds of what may be possible.

The belief that the time has come for another wave of interest in new educational technology is even stronger than the panel says. First, and most notoriously, this is a time when few technically advanced societies are able to recruit enough skilled teachers for what are considered essential tasks, teaching mathematics or science more widely, for example. Shortages are especially acute in the field with which the panel is chiefly concerned, information technology. Second, because of the rapidly changing ethos of the high school, students are no longer content to sit and watch teachers make marks with chalk on the walls of the rooms they inhabit but appear (to teachers) to be subversively bent on deciding for themselves what they wish to learn, which is often a recipe for learning (too late, as things are) from their mistakes. Third, there is much more to learn, in circumstances in which the educationalists have not so far been able to devise a curriculum for the modern teenager. Fourth, this is a time when the old advocacy of the cause of continuing education has become an economic necessity; one package of youthful skills no longer lasts a lifetime. How, in these circumstances, can anybody resist this modest committee's appeal for a modest subvention of a programme to find out what computers have to offer students? Not, surely, Mr Kenneth Baker?

British radioactivity

Sellafield remains at the centre of the storm

LIVING with radiation in Britain has come to require the intellectual stamina for digesting a plethora of technical and often conflicting documents. This is the experience of the past few weeks, which have seen the publication of the first report from the newly appointed Committee on Medical Aspects of Radiation in the Environment (COMARE); the government's response to a critical report on waste management from the House of Commons Select Committee on the Environment; and a further slew of documents from the National Radiological Protection Board (NRPB).

COMARE, which owes its existence to a recommendation of the report two years

Paying for old lambs

Confusion persists in Britain about arrangements for compensating farmers for the consequences of the ban on the sales of lamb after the accident at the Soviet nuclear power station at Chernobyl. Farmers affected, in North Wales and Cumbria, have been told that the British agriculture ministry will pay compensation to farmers able to show they have suffered loss by having to keep lambs off the market for so long that they no longer qualify for the premium prices paid for lean animals.

But suggestions that the British government will pass the bill, which might amount to £10 million, onto the Soviet government, are premature. That, a spokesman at the agriculture ministry said last week, would be a matter for the Foreign and Commonwealth Office.

Restrictions of the sale of lambs through agricultural markets are being progressively removed, and now apply only to the Lake District region of Cumbria. They were introduced at the beginning of last month because the caesium-134 content of lambs from the affected regions exceeded 1,000 Bq per kg, a limit adopted by the ministry as an "action level" after an ad hoc meeting of a European Community advisory committee. The Emergency Reference Level recommended by the National Radiological Protection Board (NRPB) earlier this year is ten times as much, or 10,000 Bq per kg.

As yet, it seems, no British farmer has made a formal application for compensation. There appears to be no plan to compensate farmers for reduced prices from the sales of lamb from farms outside the two affected areas.

ago by Sir Douglas Black about the occurrence of excess leukaemia deaths around the Sellafield reprocessing plant, ironically begins its life by correcting in its *First Report* (HMSO, £4.40) the Black report's calculations.

The unexpectedly high incidence of leukaemia in the neighbourhood of the reprocessing plant, first publicized by a television company, is now accepted as a valid observation which was, in fact, the stimulus for Sir Douglas Black's inquiry. The conclusion of that report was that leukaemia incidence in the neighbourhood of the plant, especially among people born in the 1950s, was indeed greatly in excess of the expected average incidence but not necessarily inconsistent with random fluctuations within the small population concerned.

The committee is however exercised by the discovery that the Black inquiry, which was provided with an official history of radioactive discharges from the Sellafield plant, including that from the fire in the core of a plutonium-producing reactor in 1957, was not told of an incident in which fission products from spent uranium fuel elements had been released to the environment in 1954 and 1955.

The circumstances are odd, and have come to light because of representations by Dr Derek Jakeman, now a reactor physicist at the Winfrith Heath Research Establishment of the UK Atomic Energy Authority (UKAEA), but an employee at the Sellafield (then called Windscale) establishment in the 1950s. Jakeman was one of two employees who called attention to the unsuspected release of radioactivity from the two plutonium reactors on the basis of measurements of soil from his garden near the plant.

Jakeman said this week that irradiated uranium metal fuel elements occasionally incorrectly discharged from the plutonium reactors in 1954 and 1955 would lodge inaccessibly behind a concrete shield and would be allowed to oxidize in the ambient air. He estimated at the time that several kilograms of uranium and associated fission products would have been discharged in oxide form to the local environment. His revised estimate is that a total of 30 kg of uranium and its associated fission products would have been released over a period of perhaps two years; a formal report on Jakeman's reconstruction of this leakage will be published by the Winfrith establishment in the next few days.

What concerns COMARE is that infor-

mation about this release was not provided to the Black inquiry, and that a search of UKAEA archives since carried out did not uncover a reference to the incident. The committee says that the "way in which these data came to light is unsatisfactory and undermines our confidence in the adequacy and the completeness of the available data". The committee nevertheless accepts that the increased radiation doses to young people living nearby in the 1950s are at once less than the natural background and insufficient to account for the leukaemia incidence.

The recalculation of the exposure of the Sellafield population to artificial radioactivity has been carried out by NRPB (NRPB-R171-Addendum) in the light of the further information about the uncontrolled oxidation of fuel elements in 1954-55, information about other recorded discharges report to the Black inquiry and new assumptions about the rate of absorption of plutonium and americium in the gut which have recently been recommended by the International Commission on Radiological Protection (ICRP). The effect is to increase the expected incidence of leukaemia as a consequence of discharges from the Sellafield plant by roughly two-thirds, giving an expected number of cases of 0.16 among the study population of 1,255, which is statistically much less than the 4 cases on which controversy continues to centre. NRPB's recalculation also distinguishes between the effects on bone marrow of radiation with high and low linear-energy transfer (LET) in tissues; its report says that although the biological effects of high-LET radiation may have been underestimated, supposing that the degree of underestimation would suffice to explain the four known cases of leukaemia would require that the incidence of leukaemia on account of natural radiation would be much greater than is observed away from nuclear plants.

Sellafield is also the chief focus of the British government's reply to the House of Commons select committee's report, which argued on 12 March that the new reprocessing plant being built at Sellafield to handle oxide fuel from pressurized water reactors should be abandoned. The government now says (Radioactive Waste, Cmnd 9852, £3.40) that the financial consequences of abandonment would involve the waste of £600 million already spent on the plant.

More significantly, the government's response also holds robustly to the view that extracting fissile material from spent uranium fuel is a necessary preparation for the next century "when nuclear power will have an essential contribution to make". In other respects, as in its willingness to specify limits for the discharge of gaseous radioactivity to the atmosphere, the government is conciliatory.

Genetic engineering

Hepatitis vaccine wins approval

Washington

THE US Food and Drug Administration last week approved for the first time the sale of a human vaccine made by recombinant DNA techniques. The vaccine, for hepatitis B, is to be manufactured by Merck, Sharp and Dohme of West Point, Pennsylvania, under the name Recombivax HB, and was developed in collaboration with Chiron Corporation of Emeryville, California.

Recombivax has a potential world market of hundreds of millions of doses for, unlike existing hepatitis-B vaccines, production is not limited by the need for plasma from infected patients. But at \$100 for the course of three injections, the vaccine costs about the same as conventional plasma-derived vaccines and is far too expensive for mass immunization programmes in countries where the disease is most common.

In East Asia and tropical Africa, more than 10 per cent of the population are chronic carriers, and active hepatitis and related cirrhosis are major causes of mortality. Worldwide there are about 300,000 liver cancer deaths per year, most of them thought to result from hepatitis-B infection. In the United States there are 200,000 new cases of hepatitis each year. Those most at risk are offspring of infected mothers, health-care workers, intravenous drug users and male homosexuals.

Although a plasma-derived vaccine, also sold by Merck, has been available in the United States since 1981 only 3 - 30per cent of high risk groups have been vaccinated, partly because of fears that the vaccine might transmit acquired immune deficiency syndrome (AIDS). Although Merck says these fears are groundless the company hopes that the recombinant vaccine, which is produced in yeast cells, will prove more acceptable to members of high-risk groups.

Recombivax is made intracellularly in yeast cells that express the hepatitis-B surface antigen. Since early successes were reported in Nature (298, 347; 1982), a more complex expression system has been developed, and improvements in expression and scale-up work done by Merck. Patents governing the process are held by the University of California, by Chiron and by the University of Washington. But there is a continuing dispute over some patent rights to the viral genome with Pierre Tiollais' group at Institut Pasteur in Paris, which was the first to obtain a complete viral sequence. The US Patent Office is likely to declare an "interference procedure" to consider the French claims. In the short term, the factor that will limit use of the recombinant product is price. Dr Joseph Melnick of Baylor Col-

lege of Medicine estimates that the price of a treatment would have to come down to around \$1 to be widely used in mass immunization campaigns in the poorest countries, but is optimistic that the potentially unlimited supply of new vaccine will lead to its widespread use.

Dr William McAleer of Merck is also optimistic, believing that the recombinant vaccine made in yeast will in the long term become cheaper than the existing plasmaderived product. McAleer argues that constructing a suitable high-yielding clone has been the most expensive part of development; extraction and purification procedures are inherently cheaper for yeast-derived than for plasma-derived vaccines, because inactivation steps and innocuity testing are less elaborate.

The hepatitis-B antigen particles in

Recombivax are not identical to those from infected humans because they do not include polypeptides coded by the "pre-S' regions of the viral coat gene. In addition, lipid membrane in the particles is from yeast rather than human cells. Nevertheless, about 95 per cent of volunteers immunized in trials developed a strong antibody response and are presumed to be protected. But Chiron has already produced an experimental vaccine that does include pre-S polypeptides, and it is hoped that it will provoke immunity in those who do not respond to the Recombivax HB.

Recombivax is Chiron's first therapeutic product to gain marketing approval and the company expects it to earn at least \$100 million a year. The only competitor is sold in Singapore by Smith Kline-RIT, a subsidiary of SmithKline Beckman based in Belgium. But Institut Pasteur in Paris and Genentech in the United States are likely to enter the market and then prices may fall. **Tim Beardsley**

UK research grants

Research board pleads for more

EACH year seems to deepen the despair of Britain's Advisory Board for the Research Councils (ABRC). In its annual claim for research funds, now under consideration by the Secretary of State for Education and Science, it finds need to reiterate, in bold type, that scientific research is relevant to "national needs". A series of increases in science spending over the next three years is called for.

The argument the report seems repeatedly to try to drive into the minister's mind is that the new technologies, principally



biotechnology and information technology, that the government hopes will revitalize the economy, are science-based and crucially dependent on advances in basic research. Demands on the science base, particularly from industry, are thus increasing while the volume of scientific research performed is falling because funds are not available. Evidence of the failure to keep up with other countries in investment can be seen in the brain drain

an describer de la companya de la c

of scientists from the United Kingdom and in a study from the Science Policy Research Unit that shows the per capita expenditure on science in to be the lowest in the industrialized world.

The report protests that everything that can be done to make better use of available money has been done. Dozens of research units have been closed, and more than 3,000 jobs lost to try to give better value for money.

But very little scope remains. If, as the report speculates, it is the government's intention to have a much smaller science base in Britain, there is not even enough money for an orderly transition.

By 1990, the volume of research supported will be some 10 per cent less than at the beginning of the 1980s, despite the value of the science budget having been maintained. The trouble is that the costs of scientific equipment and materials rise much more rapidly than does inflation and this needs to be reflected in the budget.

To end the erosion of research the board asks for an increase over present figures (some £614 million in 1986-87) of £35 million in 1987-88, £50 million in 1988-89 and £60 million in 1989-90. In addition, the Science and Engineering Research Council needs an immediate £9 million to compensate for recent rises in the cost of its subscriptions to international laboratories.

The signs are that the government will be hard to persuade. A white paper (policy document) released last week rejected recommendations from a select committee that the science budget be increased annually by at least three per cent above inflation. **Alun Anderson**

Human genome

No consensus on sequence

Washington

"Can it be done? Yes. Will it be done? Yes." With those words, Donald Fredrickson, president of the Howard Hughes Medical Institute, introduced a conference sponsored by his institute on the sequencing of the human genome. But as Fredrickson quickly acknowledged, the questions of how it should be done, when, by whom and who should pay are still up in the air.

What emerged from the conference was a consensus that a physical map of the genome, consisting of an ordered set of cosmids, should be constructed as soon as possible. There is also considerable support for a restriction fragment length polymorphism (RFLP) map.

But few are as enthusiastic when it comes to contemplating the task of sequencing the estimated 3,500 million base pairs in the human genome. "I'm in favor of it", says Cold Spring Harbor director James Watson, "and everyone else at Cold Spring Harbor is against it." The reason is money. Watson thinks there is wide support for starting initial mapping, but many feel that a commitment to determining the sequence will draw resources from other activities.

John Tooze, executive secretary of the European Molecular Biology Organization (EMBO), agrees it would be a disaster if current projects had to compete for funds with the sequencing project. Tooze believes European governments would be hard-pressed to find additional funds, making competition inevitable.

Leroy Hood of California Institute of Technology says it would be a "serious mistake" to jump into a full-scale sequencing project now, as automation will speed sequencing by one or more orders of magnitude in the next few years. Ironically, one of the factors that sparked interest in the sequencing project was the imminent commercial appearance of the automated DNA sequencer that Hood helped to develop (see *Nature* 321, 674; 1986).

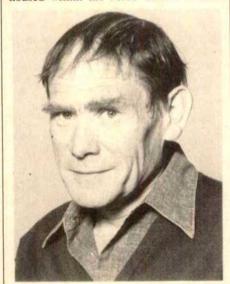
A sequence for the entire human genome, while itself a goal, is only a tool for a better understanding of human genetics, points out Eric Lander of the Whitehead Institute in Cambridge, Massachusetts. Just knowing the sequence tells you almost nothing, argues Lander; it will be useful only when coupled with a better understanding of the structure and function of proteins. Toward that end, Tooze says the European Molecular Biology Laboratory will be putting more of its resources into biocomputing and crystallography.

There has been no dearth of meetings to discuss the sequencing project this year,

and there are more to come. In February, the Howard Hughes Medical Institute conducted a preliminary meeting on the topic in Florida. In March, the Department of Energy hosted a meeting in Santa Fe, New Mexico, and in June the topic was the focus of a Cold Spring Harbor symposium (see *Nature 322*, 11; 1986). Next month, the National Academy of Sciences will air its views at a meeting in Woods Hole, Massachusetts, and in October the National Institutes of Health will discuss what their role in the project ought to be.

New career for Sydney Brenner

DR Sydney Brenner, director of the Medical Research Council (MRC) Laboratory of Molecular Biology in Cambridge, is soon to have a chance to give up administration and pursue his own personal research. This week, MRC announced that it has set up a new Molecular Genetics Unit which Brenner will head from 1 October this year until his retirement. The unit will be a small one, of 4 or 5 researchers, housed within the MRC Centre in Hills



Sydney Brenner

Road, Cambridge. Four hundred thousand pounds will be provided to establish the unit and a budget of £200,000 a year awarded thereafter. Research at the unit will concentrate on areas in which Brenner has already won international renown: methods of gene mapping; the characterization of genes affecting the development of the nervous system in Caenorhabditis elegans; and aspects of gene evolution. Dr Aaron Klug, who won the Nobel prize for Chemistry in 1982, will succeed Dr Brenner as director of the Laboratory of Molecular Biology.

Alun Anderson

Enthusiasm for starting the sequencing project continues to run high at the Department of Energy. The department has already started constructing a physical map of the human genome, as well as supporting research on database management and automated data entry. But its cost estimates for the sequencing project have dropped considerably during the past year — down by an order of magnitude from the \$3,000 million that was thought necessary at the March meeting.

In spite of uncertainty about how best to proceed with the project, Sydney Brenner, director of the Medical Research Council Laboratory of Molecular Biology in Cambridge, United Kingdom says that everyone interested in medical research ought to be interested in the sequence of the human genome. Those that are not, says Brenner, "have to be considered a subject for appropriate treatment".

Joseph Palca

David Swinbanks in Tokyo adds: It would take US \$600 million and 30 years to sequence the entire human genome by a "sequencing factory" according to Akiyoshi Wada, professor of biophysics at Tokyo University. While that may seem a lot, he estimates that if it was done by 100 experts it would take \$1,100 million — and 250 years.

Since 1981, Wada's group has been trying to develop an automated DNA sequencing system in collaboration with industry under the support of the Science and Technology Agency. A robot that performs DNA fragment separation according to the Maxam-Gilbert or Sanger M13 protocol (see Nature 307, 193; 1984) has been developed with Seiko Instruments and Electronics Co. And Toyo Soda Manufacturing Co. has designed a specific DNA extractor with high base resolution, while Fuji Photo Film Co. has created a system for mass production of films for gel electrophoresis.

Now Seiko and Hitachi Software Engineering Co. are competing in development of machines to read the gels and type out the sequence. By combining these operations, Wada estimates that it should be possible to sequence one million base pairs per day.

Once a working system is developed, Wada thinks that sequencing should be extended to all parts of the genome, not just those of immediate interest. He compares the operation with geographic mapping, which is carried out irrespective of the "profitability" of the area to be mapped.

If a sequencing factory can be built, Wada emphasizes that it would not be "Japan Incorporated" against the rest of the world. He wants an international centre that would be open to scientists of all nationalities and intended for the benefit of all mankind.

Biotechnology

Regulations please nobody

Washington

CONTROVERSY continues in the United States over the federal government's proposals to regulate biotechnology. At a recent congressional hearing, representatives of the American Society for Microbiology, the Environmental Law Institute and the Ecological Society of America all criticized the administration's plan to exempt from high-level review environmental releases of intergeneric organisms whose introduced genetic material is "well-characterized and contains only non-coding regulatory regions".

The administration's latest proposals on biotechnology regulation were published after much delay on 26 June. They recognize that non-living products of genetic engineering technology should be regulated in the same way as conventionally made products, but require that environmental releases of engineered organisms containing DNA from different genera or from a known pathogen should receive high-level review. The exemption for transferred non-coding regulatory sequences applies whether or not the donor organism is a known pathogen.

The proposals were examined last week at a joint hearing by three subcommittees of the House of Respresentatives' Science and Technology Committee. Monica Riley, chairman of the American Society for Microbiology, said that "strain construction that places a strong, effective regulatory sequence in a position of control over any particular gene can increase the expression of that gene many fold", thus affecting a microorganism's capacity to compete. Riley also pointed out that regulatory sequences carry specific determinants that turn genes on or off; changing the signals to which a gene responds could constitute a substantial change in the biology of the recombinant organism.

Some congressional staff speculate that this criticism from respected professional bodies might persuade the administration, which is anxious not to overburden the emerging biotechnology industry, to remove the exemption. Industry organizations publicly support the administration's proposals, but some privately concede that the non-coding exemption could undermine public support and they would rather have it removed.

Meanwhile, the administration's plan has come under attack from a more predictable quarter. Jeremy Rifkin of the Foundation on Economic Trends has sued the government for omitting to conduct an environmental impact statement and failing to keep an adequate record of its development.

Tim Beardsley

West German nuclear power

The fast breeder is stumbling

Hamburg

REIMUT Jochimsen, Social Democratic Economy Minister of Nordrhein-Westfalen, has put aside political questions and called for a halt to the fast-breeder programme on scientific grounds. Fulfilling his earlier promise to keep scientific and political issues separate, he has published an expert opinion (roughly 100 pages long) written by co-workers in his ministry, where grave doubts are raised about the safety of the 300 MW prototype reactor. The problems are enough, Jochimsen emphasizes, to make the fast breeder the most expensive misinvestment ever in industrial history.

The report clearly shows that politicians have been careless in trusting the calculations of engineers from the reactor building and operating companies, in particular those of the Schnellbrüter-kraftwerksgesellschaft (SBK), on which many of the 17 permits already granted were based. Under certain very adverse conditions, a runaway reaction could take place. In contradiction to earlier claims, there are serious doubts about the breeder's safety.

In 1984, experts of the companies involved said in court that a disastrous failure of the ventilation system was impossible. This expert opinion proved wrong when after less than two years of routine test running (without nuclear fuel cells) two of the ventilation devices failed. The experts also excluded absolutely the possibility that oil could enter the radioactive primary system of the reactor. But that happened. Never, they said, could water and sodium, the reactors' primary coolant, meet. But that too has happened.

Parts of the reactor, which must never fail, are called "holy" by the technicians. But some of them have been found to be not safe under any conditions. A grating to hold the fuel cells, for example, can rust. Jochimsen said that for such parts a "repeatable control" is necessary, which is impossible in the planned prototype. Rust has also (as long ago as 1980) been found in the reactor tank, and technicians have found weaknesses in weld seams. The method of estimating the probability of a runaway accident was not scientific, the report says. All the Gesellschaft für Reaktorsicherheit (the company responsible for reactor safety) did was to ask selected experts if they though such an accident likely. Another analysis, carried out at the Kernforschungszentrum Karlsruhe, was found to be incorrect due to a faulty computer program.

Opponents of the Jochimsen report, such as the leader of the Nordrhein-Westfalen Christian Democrats, Kurt Biedenkopf, say that its arguments are

false. The truth, they say, is that Jochimsen is executing the Social Democratic Party's decision to stop the nuclear programme. A representative of the Ministry of Research and Technology said that Jochimsen's political intentions are evident because the minister published his paper only 11 days after the Nordrhein–Westfalen members of the Social Democrats had decided to stop the breeder. This accusation is hard to believe, however, for the report cannot have been produced so quickly.

Critics have not attacked the technical arguments presented, Jochimsen points out, but only produced political arguments. The head of SBK, August Wilhelm Eitz, argues that all necessary modifications will be made. But that still leaves one key objection from Jochimsen: in the foreseeable future, there is no acceptable place and method for disposing of the nuclear waste from the reactor.

The Social Democrats now want to go further. In Nordrhein-Westfalen, permission will not be given for new sites for nuclear plants. The party is working on a bill to be introduced into the Bundestag in the autumn. According to representatives, it demands that no nuclear plants at all should be permitted to run in West Germany, even those already built. Preferential treatment for nuclear energy should be ended. In addition, the Social Democrats will introduce clear standards of radiation analysis and protection to avoid the confusion experienced after the Chernobyl disaster. The law, which could come into force if the Social Democrats win next year's federal elections. would also automatically terminate the DM7,000 million breeder. The Nordrhein-Westfalen government cannot enforce a decision on its own because the federal government can make it grant permission for the fast breeder reactor.

Heinz Riesenhuber (CDU), Minister of Research and Technology, has already mentioned that option in an interview, but he knows that it is unlikely to be successful. On the other hand, if he abandoned the project he could save more than DM200 million. The problem is very delicate and the legal situation unclear. If the project is stopped without definite technical reasons, the power supplier will get back the DM1,400 million it paid. Belgium and the Netherlands will also want their DM1,600 million returned. If, however, Jochimsen's paper is telling the truth, the reimbursement need not exceed the present value of the plant, which would not be very high, given a plant too dangerous to run. A meeting planned for September should make things clear.

Jürgen Neffe

Atomic power

No nuclear doubts for Japan

Tokvo

By 2030, Japan will have more than 120 nuclear power reactors supplying over half the country's electricity needs. Fastbreeder reactors will be on line, and fuel evele facilities will provide a large proportion of the nuclear industry's enriched uranium requirements, reprocess most of its spent fuel and store all its waste. Such is the "vision" of Japan's nuclear industry outlined in a report recently submitted to the Ministry of International Trade and Industry by the nuclear subcommittee of the Advisory Committee of Energy. But where will all these nuclear plants be located and will the Japanese public willingly accept them?

Japan has 32 reactors generating nearly 25 million kilowatts, putting Japan behind the United States, the Soviet Union and France in total nuclear capacity. Twenty-six per cent of Japan's electricity is nuclear generated.

According to the report, nuclear power capacity will more than double to 62 million kilowatts by the end of this century and, assuming a growth in Gross National Product of 2.5 per cent, rise to 137 million kilowatts by 2030 to provide 58 per cent of Japan's needs. This will require the construction of 116 new reactors at the rate of 2 or 3 a year. Ten new reactors are under construction and seven more are planned.

Two areas in Fukui and Fukushima prefectures contain most of the nation's nuclear plants. Their presence has brought economic benefits but there is resistance to further expansion. The town of Ohi in Fukui Prefecture, for example, has earned more than Y11,000 (£47 million) in fixed property revenue funds, grants from the central and local government and redemption taxes during the past 15 years. But plans to double the number of reactors in the town to four have led to mass demonstrations; in 1984 1,400 riot police had to be mobilized to contain thousands of demonstrators protesting outside public hearings in the town.

The subcommittee's report makes several recommendations to promote public understanding of nuclear power so that expansion can proceed "smoothly". Safety should be strictly maintained in the plants to ensure the public's understanding of the "safety" of nuclear power. Nuclear power technology should be explained in simple, easy-to-understand terms, and the central and local government should positively promote nuclear power in school education.

Japan certainly has an enviable safety record, with far fewer shutdowns due to accidents than for example, the United States. But accidents do occur, such as the leak of low-level radioactive waste at the

Tsuruga power plant in 1981 and the exposure of an official of the International Atomic Energy Agency to traces of plutonium earlier this year.

A key element in future plans is the construction of a huge fuel cycle facility for uranium enrichment, fuel reprocessing and low-level waste storage in Aomori Prefecture at a cost of one million million yen (£4,300 million). But this facility, for which approval was granted by the prefectural government in 1985, has yet to gain the unanimous approval of the local fishing cooperative and the start of construction has been delayed.

Fishing cooperatives wield considerable political power in Japan as do other blocks of rural voters who traditionally support the ruling party. Promises of Y177,000 million yen (£750 million) in contracts for local companies and 1,400 jobs have won approval for the project from other sections of the local community.

If the Aomori complex is completed on schedule in the 1990s, it will provide 30 per cent of Japan's enriched uranium requirements by the year 2000, and will be capable of reprocessing most of the spent

fuel that is now sent to French and British facilities. According to the report, a second fuel reprocessing plant will be built in Japan in 2010 to meet increased demand.

Low-level radioactive waste will be stored at Aomori in a plant with an eventual capacity of 3 million 200-fitre drums. It will be capable of dealing with all Japan's low-level waste produced by 2030 and beyond.

Greatest growth over the next 45 years is seen in establishing the fuel cycle. Expenditure is expected to amount to Y70,000 million million yen (£300,000 million) by 2030. The only note of restraint in this bullish assessment of the future of Japan's nuclear industry is in regard to fast-breeder reactors, commercial operations of which are predicted to start in 2020, ten years later than expected.

But a big question mark hangs over the locations of the proposed new plants. The report calls for the establishment of 20 new sites without clearly stating where they will be. Development of new siting technology is advocated so that nuclear plants can be placed underground, on the sea, and close to population centres. Clearly Chernobyl has not shaken the confidence of Japan's nuclear power planners.

David Swinbanks

Chernobyl

Experimental speculations

THE Soviet Politburo, apparently responding to a torrent of questions about the mysterious "unauthorized experiment" said to have been under way when the Chernobyl reactor accident occurred on 26 April, said last week that the power station crew was attempting to operate the reactor at a low power, below that for which it was designed.

From the beginning, Soviet statements have said that the Chernobyl reactor was operating at 7 per cent of full power at the time of the accident. Many reactor engineers in the West now consider that the most likely explanation of the Soviet statement is that those concerned were trying out some scheme for operating the reactor's housekeeping functions from the station turbine proper, and not from the stand-by diesel sets provided to guard against disconnection from the Soviet electricity grid.

While operating at full power, reactors are naturally able to deal with this "hotel" load from their own production of electricity, but the removal of fission product heat from a shutdown reactor requires an external source of power. Measurements of fallout from Chernobyl suggest that the reactor had been shut down for some hours before the first release of radioactivity began, which would suggest that the decay heat of the fission products

would by then amount to some 4 per cent of the total power, less than the 7 per cent quoted by Soviet sources.

Dr David Hicks, director of the UK Atomic Energy Authority's water reactor programme (chiefly concerned with the safety of pressurized water reactors) said earlier this week that such an operation, well outside the power range for which the Soviet RBMK reactors are designed, could well have made the Soviet reactor prone to the instabilities for which it is known, especially because a core which had been in use for 1.5 years would have accumulated such a load of fission products that the production of even a few per cent of full power by fission would have required that the control rods should be to a large extent withdrawn.

The occurrence of steam voids within the cooling system would, in these conditions, have created power excursions which it might have been difficult to control by means of the control rods, which move in narrow water channels where their free fall is impeded. Hicks emphasized, however, that his theory of what may have happened is only one of many.

Much of what is known of the Soviet reactors derives from three consultations in the mid-1970s when British and Soviet designers exchanged information about the RBMK and its British analogue.

French budget

Bleak prospect for researchers

THE French government research budget for 1987 is now more or less complete. No figures have been released, nor are they likely to be before September, but the indications are that the spending power of French scientists will at best be pegged at around the levels of 1985. There may also be redundancies, as the Prime Minister, Jacques Chirac, has ordered a 1.5 per cent across-the-board cut in government employment. There is hope, however, that the job losses will be partly compensated by a growth in the recruitment of young scientists, under a government scheme to counter youth unemployment.

The worsening prospects for French scientists, coming after the boom years of the early 1980s, were heralded by an 8 per cent cut in the science budget made in April, just a month after the new government came to power. The change shows

Terrorists strike again

Hamburg

THE terror against technology in West Germany continues. Following the killing of Siemens research manager Karl Heinz **Beckurts by terrorists of the Rote Armee** Fraktion (RAF), a bomb exploded at the Fraunhofer Institute for Laser Research in Aachen at 5 a.m. on Thursday last week. The total damage has not vet been estimated, but some sensitive machines seem to have been affected. In a letter found near the site, a "Fighting force Sheban Atlouf" admitted its responsibility for the attack. The institute, which is part of the Technical University of Aachen, is carrying out research only on the introduction and use of laser techniques for industrial and medical purposes, according to the head of the institute, Professor Herziger.

RAF struck again last Friday at 5 a.m. This time their chosen target was more in line with their announced aim of hitting military and nuclear research institutes. The bomb exploded outside the head-quarters of Dornier GmbH, owned by Daimler Benz, in Immenstaad. Only a wall and about 250 windows were damaged.

Police think that this may be the beginning of a series of bombings against what RAF calls the "Militärisch Industrieller Komplex". Last year, when some bombs exploded near institutes for biotechnology and gene research, the new aim of the terrorists became clear. In the underground newspaper Sabot, anonymous sources have announced that "harmless" people in various institutes will face assassination. Protection for such a wide range of imperilled people and institutes cannot be given. Scientists have a hard challenge to face.

Jürgen Neffe

how depressingly shallow-rooted was the science policy-making system instituted by the previous administration during its five years in power. Research, it seems, never became a proper political and administrative fiefdom, and now the parts of the old estate, the ministry of research and technology, have been scattered among the ministries from which they were first confiscated in 1981.

The result, according to one senior French scientist, is that there can no longer be a science policy in France. Rather, research will get the scraps of the budget that are left after the real political carnivores — the ministers responsible for police and defence, among others, in this government — have torn at it. Only then will the minister of research and higher education, the well-meaning physicist Alain Devaquet, have a chance to form a policy. The importance for research and technology of having a politically powerful champion (in the previous French government it was Jean-Pierre Chevènement, who led the largest single wing of the socialist party) has never been clearer. Without power, the budget determines the policy; with it, the reverse is possible.

The Conseil Supérieur de la Recherche et de la Technologie (CSRT), the independent group of high-level scientific advisers to Devaquet, is already well aware of the sea-change facing French science, but seems powerless to act. Having seen the outline budget for 1987, the Conseil has been forbidden by Devaquet to speak of it. The minister will present his budget, which given inflation and the April cuts would need a 6 per cent increase in current francs to retain the spending power of 1985, probably in September. Only then will CSRT, of which Devaquet is ex-officio chairman, be free to publish its "advice"

Nevertheless, François Kourilsky, the Marseilles immunologist and scientific president of CSRT, has dared to warn that any suppression of scientific jobs would have "long-term effects incommensurate with the economies achieved", and to demand that the government "finish and publish a research and technology policy" This may come with Devaquet's awaited presentation, but the feeling is now clear in France that science has returned to the doldrums of the 1970s. Then, ministers in the Délégation Générale à la Recherche Scientifique et Technique (DGRST) who were responsible for "coordinating" the research budget in the prime minister's office were renowned for their fine forward-looking speeches in the Assemblée Nationale - but for their almost total lack of power to influence real Robert Walgate events.

US-Japan trade

No easy end to chip war

Washington

An agreement is expected early this week in the long and increasingly bitter negotiations between Japan and the United States on semiconductor trade. The United States is seeking greater access to Japanese markets for US semiconductor manufacturers, and an end to "dumping" of Japanese semiconductors on international markets. As both legal and self-imposed deadlines loom, negotiations have entered what a spokesman for the US semiconductor industry termed "a period of trench warfare".

For more than a year, the US semiconductor industry has been pursuing a trade complaint against Japan over access to Japanese semiconductor markets. US chips now account for only 10 per cent of sales in Japan according to US industry figures, as opposed to 83 per cent of sales in the United States and 55 per cent of sales in Europe. In late May, US Trade Representative Clayton Yeutter worked out a framework for concluding the trade case, known as the 301 case after the section of the Trade Act of 1974 that covers unfair trade practices. Included in the framework is the resolution of two other complaints that Japanese companies are selling erasable programmable read-only memory chips (EPROMs) and 256 kilobyte dynamic random access memory chips (256K DRAMs) below their production costs. A preliminary judgement made last year by the Department of Commerce found Japanese companies guilty of dumping in violation of international trade agreements. But in early July, both sides reached a tentative agreement to drop the dumping cases so that negotiations in a comprehensive agreement could continue. Since June, US and Japanese negotiators have been trying to forge an agreement under Yeutter's framework, but so far without success. Without a final decision to stop the dumping cases this week, permanent dumping duties will be imposed on all imported Japanese EPROMs and 256K DRAMs.

Opening Japanese markets to US goods is not straightforward. Despite the power of the Japanese Ministry of International Trade and Industry, it cannot force Japanese companies to buy US chips. The Japanese government has offered to open a special office to assist foreign companies in making semiconductor sales.

Japanese semiconductor producers are large, vertically integrated companies that can subsidize losses in their semiconductor division to purchase market share, an option not open to generally smaller US firms. No agreement will

change this situation.

A document leaked to the Financial Times of London gave details of a working draft of the agreement. The United States would agree to drop its dumping cases. and Japan would try to increase US market share in semiconductors to 20 per cent. To prevent future dumping disagreements, the United States would request

WITH a self-imposed deadline of Saturday, 26 July for concluding the negotiations, Japanese representatives were no doubt surprised when the US team announced on Friday that negotiations had to stop at 1 p.m. The reason? The Trade Representative's office had scheduled its annual picnic for that day, and not even Washington's current heat wave was going to stop plans for a softball game during the picnic.

immediate consultations between the two governments. These consultations would be limited to 14 days, in contrast to the year it now takes to resolve dumping issues. If dumping is suspected, the Japanese government will encourage its industry to provide documentation for the legitimacy of its sales figures.

Even if an agreement is reached, chip prices in Japan will probably stay comparatively low, and US importers are likely to find "loopholes" - purchasing semifinished goods containing chips or buying chips at Tokyo discount stores. Nevertheless, Japanese companies do appear to be worried by the agreement. They find it blatantly unfair and one-sided, placing Japan at a disadvantage to South Korea, Taiwan and especially to US companies that will have access to Japanese production costs under anti-dumping agreements. Japanese industry sees this agreement as being largely beyond their control, having arisen out of the politically close relationship between President Reagan and Prime Minister Nakasone.

As talks moved into the eleventh hour, both sides seemed intransigent. Three US manufacturers complained formally to the Department of Commerce that Japanese companies were trying to cut last minute deals at bargain prices with US customers before signing an agreement. By 30 July a decision has to be made on the EPROM dumping case, and the next day President Reagan must announce what action he will take in the 301 trade case. As *Nature* goes to press, it is impossible to say what the likely outcome would be.

The US industry is frustrated by the current negotiations. It believes it has an open and shut case against the Japanese both for dumping and for closing their markets. Hopes for agreement may have given way to a desire for retaliation against Japan for its trade practices. But a comprehensive agreement is still the ultimate goal. At stake could be nothing short of the future of the US semiconductor industry. Joseph Palca & David Swinbanks

High-technology trade

Anger over supercomputer veto

OFFICIALS at the British Embassy in Washington hope that they can soon resolve "without major compromise" the difficulties of British academics in obtaining US-manufactured supercomputers. Intensive discussions have been taking place over an issue that last week sparked a debate in the House of Commons.

The trouble began when the University of London Computer Centre found that its purchase of a Cray I supercomputer had been blocked by US government regulations. A condition of sale of the supercomputer is that scientists from Eastern Bloc countries and China must not gain access to the machine. But the centre's director, Richard Field, says that although the scientific standards of work carried out on the machine will be monitored, it is not possible to police all the computer's users to ensure there are no scientists from proscribed countries among them.

What has really enraged British opposition politicians is that the computer the centre wants is second-hand and already in Britain; all that has been requested is its transfer from the Atomic Energy Authority's Harwell laboratory. That the United States can control the movement of a computer inside Britain is described by Liberal Member of Parliament Mr Paddy Ashdown, who initiated the House of Commons debate, as a "flagrant breach of British sovereignty". And it became clear during the debate that while this may be the first time US controls have hit academics, British high-technology companies have had difficulties with US government regulations for some time. Indeed, Ashdown claims that one British company was effectively driven out of business by US sanctions.

The US regulations come on top of the COCOM agreement that regulates the export of strategically sensitive goods from members of the North Atlantic Treaty Organisation and Japan. British companies that wish to export manufactured goods containing any US component (as do most electronic products) now find themselves having to apply for a licence from both the UK Department of Industry and the US Department of Commerce.

Ashdown's exhortations to take on the United States did not go down well with the government. The official response, from Minister of Information Technology Mr Geoffrey Pattie, was that "if we could compel the United States to withdraw . . . the problem could be eliminated easily, but we cannot . . . and US reaction to a direct and comprehensive challenge . . . cannot be predicted". Rather than accept the opposition view of British Prime Mini-

ster Margaret Thatcher's "craven subservience to President Reagan". Pattie dwelt on the overall advantages to Britain of commercial and scientific links with the United States — plus the new efforts to reduce that dependence by strengthening links with Europe in large-scale development programmes. Problems with the United States have to be dealt with by a "case-by-case" approach, he says.

This view is scarcely welcome to British Embassy officials in Washington who have to do the case-by-case negotiations and hope for a more general understanding. An agreement is needed soon if research at the University of London is not to be severely disrupted. The computer should be delivered next month according to the contract, on which a prepayment has already been made. If the computer is not in place by the end of the year, the contract will be void and the computer centre will have to do what it can to seek redress. Any decision will also have a bearing on a contract for delivery of a Cray to the Science and Engineering Research council's Rutherford Appleton Laboratory next year. Alun Anderson

Science Digest dies

Washington

Science Digest last week became the latest casualty of the turmoil hitting popular science magazines. Hearst Magazines, its publisher, announced that the September issue of Science Digest will be the last. The subscription list and licensing rights to the name have been bought by Time Inc., publisher of Discover, for an undisclosed sum.

The announcement came as a shock to editorial staff, who have been given a week to clear out their desks. Hearst had been trying unsuccessfully to sell the magazine for several months before finally deciding to cease publication, mainly because of a drastic fall in advertising revenues (see Nature 322, 99; 1986). Hearst expects to retain and reassign about a third of the 26 Science Digest staff.

Time Inc. also recently bought for \$6 million the logo and subscription list of Science 86, the popular science magazine published until last month by the American Association for the Advancement of Science; its readers will be offered Discover instead. Science Digest subscribers will be offered a choice of various Time publications. A spokesman for Time Inc. said that Hearst had already made the decision to cease publication of Science Digest before Time agreed to buy the subscription list: the Science Digest logo is not likely to be used.

-CORRESPONDENCE-

GAP protest over South Africa

Sir—We wish to bring to the attention of the scientific community the circumstances that led to the cancellation of the Third International Workshop of the Group for Aquatic Primary Productivity (GAP) scheduled for 29 April—4 May in Durban, South Africa.

GAP was established in 1980 under the aegis of the International Society for Limnology and the International Association for Ecology to provide a forum for oceanographers and limnologists studying theoretical and methodological aspects of primary production in marine and fresh waters. Successful GAP Workshops were held in Konstanz, West Germany, in 1982 and Haifa, Israel, in 1984.

When the International Committee of GAP accepted the invitation of our South African colleagues to hold the third workshop in that country, we were aware of potential problems. It was clear that some scientists, as individuals, would choose not to attend an event in a country whose governmental racial policies are morally repugnant to most, if not all, of us. This viewpoint is understandable and such a decision is the prerogative of each individual.

We did not expect, however, to be faced with a situation in which a significant number of our colleagues who had expressed their intention to attend the workshop were expressly forbidden to do so by their superiors or administrations. In at least one case, a young scientist was threatened with jeopardizing his future career if he participated in any capacity at the GAP meeting. As a result of such pressures, the number of prospective participants in the workshop became so limited that we were reluctantly forced to cancel the meeting.

GAP is a scientific organization affiliated to the International Council of Scientific Unions (ICSU). For many years, ICSU has striven to guarantee the freedom of bona fide scientific exchange. The Principles of Universality as formulated by the ICSU Standing Committee on the Free Circulation of Scientists are basic to all ICSU objectives and have been reaffirmed by the latest ICSU General Conference in Ottawa in October 1984. Actions that deny scientists' freedom to travel to legitimate scientific activities are a flagrant and dangerous violation of these principles.

Science is an international endeavour, unfortunately tainted by political realities. It behoves the scientific community to be vigilant in maintaining its rights of free exchange and circulation. The forced cancellation of the GAP Workshop has no impact on the South African government's racial policies and only serves to increase the isolation of our colleagues

who are largely counted among the liberalizing forces there. We can only caution the scientific community that, alas, this will not be the last encroachment upon the Principles of Universality and advise vigorous and early protest in future instances.

Tom Berman (Chairman, GAP International Committee)

Israel Oceanographic &Limnological Research Ltd, The Yigal Allon Kinneret Limnological Laboratory, POB 345, Tiberias, Israel

RGO move OK

SIR—The decision of the Science and Engineering Research Council (SERC) to move the Royal Greenwich Observatory (RGO) to the University of Cambridge is a historic decision, whose consequences are not fully realized by Nature. Your leading article (Nature 322, 1: 1986) belittles the SERC choice as being based on the unwillingness of RGO staff to travel north of the Trent. This point-scoring ignores the facts that ex-RGO staff hold positions at the Royal Observatory, Edinburgh (ROE) — there has been a good history of staff interchange between RGO and ROE — and that large numbers of the RGO staff spend a large proportion of their time working and living overseas on La Palma and elsewhere. Jerry Sellwood's pro-Manchester letter (322, 106; 1986) comments on the decision by raising issues irrelevant to astronomy, such as national policies of regional development and an alleged prejudice by everybody against Manchester.

In deciding to move RGO to Cambridge, SERC is consolidating one of the world's great centres for astronomy, bringing radio, theoretical and optical astronomy together with the instrument science and engineering on which the progress of astronomy depends. It is true that many RGO staff (including ourselves) and many British astronomers opposed the move, and that the University of Sussex's astronomy programme could be damaged, an issue that SERC should address in the future. But we believe that of the choices SERC set itself the decision to move to Cambridge is best for British astronomy as a whole.

We hope that the Secretary of State for Education and Science, taking proper account of the financial arguments, will stick with the clear scientific decision of SERC. Further vacillation would prolong the problems for RGO and British astronomy; surely astronomers in the United Kingdom now need to put this matter be-

hind them and move confidently into the twenty first century, getting on with the tasks at hand.

BOB ARGYLE, CHARLES JENKINS, DEREK JONES, ROBERT LAING, TOM MARSH, BILL MARTIN, PAUL MURDIN, MAX PETTINI, HANS SCHILD, KEITH TAYLOR, ROBERTO TERLEVICH, KEITH TRITTON, JASPER WALL Royal Greenwich Observatory,

Herstmonceux Castle, Hailsham, East Sussex BN271RP

Japanese education

SIR-I would like to add to Alun Anderson's News item (Nature 321, 6; 1986) on Japanese education from the viewpoint of an undergraduate student. The University Council recently decided to increase the opportunity for applicants to take the university entrance examination with the aim of increasing the flexibility of the universities. But I wonder if it will not produce another worse result; to standardize the quality of students and to rank more clearly all of the universities. The educational industry will also gain power, worsening the situation we call "the examination war ordeal". Even now, many applicants choose their universities only for their name value, and after entering have no clear object of study. To solve these problems, the universities must be given more independence and autonomous rights.

The PhD glut ("overdoctors" or unemployed PhD holders) is another difficult problem. If one wants to get a post in a university, one must put up with years as an overdoctor because of the low staff turnover. Otherwise one must move to private enterprise. For this reason, I think, Japanese basic research cannot develop fully.

SHINJI HIRANO

Faculty of Science, Kyoto University, Kitashirakawa, Sakyo-ku, Kyoto 606, Japan

Alun Anderson replies: I agree with Mr Hirano. All state universities have traditionally held their examinations on the same day, effectively preventing anyone from applying to more than one state university in any one year, a situation that commits candidates to the uncertain task of selecting a university with a pass mark thought likely to match the candidate's likely examination mark. Universities are now to be divided into groups with examinations on different days. But this may not solve the problem of universities forming a hierarchy according to their pass marks. Kyoto University law school, for example, fears that in future all its candidates will take both Tokyo and Kyoto University law school examinations and all those accepted for Tokyo will go there. That could have the immediate effect of converting Kyoto into a "secondrank" institution.

Catching atoms in beams of light

The past few weeks' excitement about the trapping of atoms in laser beams is well justified; the applications of the technique could be exciting.

THE notion that it might be possible to trap an atom in a single beam of light is, of course, nonsensical. Atoms capable of interacting with light of specified frequency will sense what is called radiation pressure, and be propelled along in the direction of the beam. This is how newly formed stars clear a nearly empty space in their immediate vicinity and, for that matter, how the outer regions of all stars are prevented from gravitational collapse upon themselves. It is only natural that people should not hitherto have sought to trap single atoms in a single laser beam.

That diffidence will now have to be dispensed with. A group from AT&T Bell Laboratories, in a continuation of work by A. Ashkin going back to the early 1970s, has indeed been able to trap a large collection of sodium atoms in a single laser beam. The group now reports (*Phys. Rev. Lett.* 57, 317; 1986) that it has been possible to gather as many as 500 atoms into a volume no more than 10 micro-metres in dimension, which corresponds to the respectable density of 10¹¹ atoms per cm³.

But how can such a feat be accomplished? Steven Chu, J.E. Bjorkholm, A. Ashkin and A. Cable have been able to start from a great deal of expertise accumulated over the years at their own establishment as well as from the many successes in recent years with different kinds of traps for atoms, usually built around combinations of electrostatic and magnetic forces. Devices of that kind, mostly elaborations of the Penning trap, have been widely used in recent years for the spectroscopy of isolated, or nearly-isolated, atoms.

The essential requirement for success appears, however, to have been the suspension of conventional belief. In a companion paper (ibid. 57, 310; 1986), J.E. Pritchard et al. rehearse the case for believing that optical trapping is impossible — before showing that not to be the case. The principle is simple enough. In a coherent beam of light, the flux of momentum is represented by the Poynting vector, which is proportional to the vector product of the electric and magnetic field intensities (and thus directed in the direction of an ordinary light beam). By an extension of the nineteenth-century Earnshaw's theorem in electrostatics, it then turns out to be the case that the Poynting vector must be divergenceless across any closed surface that does not contain a source or sink for radiation, just as the divergence of the electrostatic force must be divergenceless over a surface containing no electrostatic charges.

In the optical case, what this seems to imply is that the force on irradiated atoms, which must be in the same direction as the Poynting vector, will also be divergenceless and thus could not be formed in such a way as to be directed inwards everywhere on some closed surface. Ironically, say Pritchard et al., Ashkin is one of those to have argued that Earnshaw's theorem is a bar to laser trapping for atoms, thereby "discrediting these proposals and discouraging any others". One way round the difficulty would be to use light intensities varying with time, a technique that works with radio-frequencies; a temporarily inward array of forces can, for example, be switched off when a sufficient number of atoms have been corralled into some other kind of trap. Doing this at the frequency of optical radiation would be a different matter.

The essence of what Ashkin's group has now done is to use a strongly focused laser beam whose intensity profile is far from uniform but, rather, gaussian, with the peak intensity along the centre. Moreover, the laser generating the beam is tuned to a frequency some way below the natural resonance frequency of the sodium line, with the result that the force on sodium atoms can be controlled at an arbitrarily low level. In these circumstances, the only forces on sodium atoms that matter are those between the electric field of the laser beam and the electric dipole moments which they induce in atoms exposed to them. The forces depend on the detuning of the laser beam, but not as critically as the scattering.

The result is that sodium atoms can be made to move towards the most intense part of a non-uniform laser beam. To be sure, the magnitude of this effect is greater as the frequency of the laser approaches the resonance frequency (which is the condition when scattering could be a nuisance), which implies that a trade-off must be struck between the closeness of the approach to resonance and the steepness of the gaussian profile. That, says Ashkin's group, accounts for trapping on the axis of the laser beam. Trapping in the axial direction depends on the rapidity with which the beam is focused in space.

The actual success reported by Ashkin's group hangs crucially, as is acknowledged, on the way in which it has been possible to

start with sodium atoms "cooled", again by the use of laser beams, to an effective temperature of a quarter of a millikelyin. The idea there, implemented in the past few years, is that it is possible to rob an atom of its translation velocity in the direction of a beam of light whose trequency is well-defined by means of the transfer of momentum that occurs on scattering. The trick is to arrange the difference of the laser and the resonance absorption frequency of the atom so that the Doppler shift works in the direction of cooling, but does not as easily allow the transfer of momentum to atoms which are already nearly at rest. But if this works in one dimension, why not arrange that three lasers at right angles should bring a whole package of atoms to near-rest? This arrangement, called "optical molasses" for obvious reasons, was demonstrated only last year. In the new experiments, a package of atoms trapped in such molasses is used as the sources of material to be trapped by the single convergent laser beam, suitably detuned.

For the time being, everybody seems too breathless to wish to speculate where the new development will lead. It is nevertheless remarkable that the lifetime of a package of some hundreds of sodium atoms in such a trap can be as much as several seconds - virtually aeons by the frequency of the resonance absorption line. The lifetime of the trap is limited, for practical purposes, by the residual scattering of light by the atoms in the trap, from which they gain energy and an increased capacity to escape. One little refinement is that, according to Ashkin's group, it is possible to move the package of trapped atoms bodily from place to place, which is why AT&T Bell Laboratories, public relations people have coined the term "optical tweezers".

So what happens next? The insatiable curiosity of spectroscopists is only the most obvious suitor of the new device. The substantial density of atoms that seems to have been achieved suggests that it should be possible almost directly to simulate astrophysical processes in, for example, molecular clouds, especially if there is a chance of using the tweezers effect to mix together different materials. But, inevitably, there will soon also be better traps. Pritchard *et al.* have thoughtfully given no fewer than three recipes that will no doubt be quickly followed.

John Maddox

Pattern formation

Descartes and the fruitfly

from Geoffrey North

In recent years remarkable advances have been made in elucidating the developmental biology of the fruitfly Drosophila melanogaster, but despite the cloning and intensive analysis of many of the genes controlling morphogenesis, we still do not understand the processes of pattern formation in mechanistic detail. The evidence of a recent meeting*, however, suggests that this goal may at last be in sight. Perhaps the most telling signs of this are the links that are emerging between a complex and rapidly expanding set of data on the genetic control of embryonic segmentation on the one hand, and a theoretical model that can simulate many of the observations on the other.

The meeting also provided what seems likely to be the first identification of bona fide developmental morphogens, which define the anterior-posterior axis of *Drosophila* embryos. A gene implicated in the establishment of dorsal-ventral polarity has turned out to encode a serine protease, which as I shall explain may help to suggest a precise mechanism of pattern formation along this axis. And intriguing evidence was presented that these orthogonal axes might function like a Cartesian coordinate system, their points of intersection specifying different pattern elements at particular positions of the embryo.

Anterior-posterior axis

The polarity of the anterior-posterior axis of an insect is manifested both in the sequence of segments along its body and in the pattern within an individual segment. Various experiments suggest that this originates in localized morphogentic centres laid down in the egg from the onset of development. For example, the egg of the leaf-hopper Euscelis contains at its posterior end a ball of symbiotic bacteria, which can be experimentally moved within the egg. Such manipulations induce the development of posterior structures at inappropriate positions along the body axis, presumably because of cytoplasmic determinants carried with the ball of bacteria. Perhaps more dramatically, the ultraviolet irradiation of one or other pole of eggs of the midge Chironomus leads to the development of either double-headed or double-abdomen 'monsters', in which the untreated pole has apparently undergone a mirror-image duplication. On the basis of these and other experiments Sander' postulated that two gradients. one from either end, set up the anteriorposterior pattern of developing insects.

It has not, however, been clear how these striking results could be taken much further, so to bring the powerful techniques of classical and molecular genetics to bear on the problem Christianne Nüsslein-Volhard and collaborators (Max-Planck Institute, Tübingen) have attempted to reproduce the observations with Drosophila, which with a relatively small egg is less amenable to physical manipulation. They have succeeded, in a series of experiments involving various combinations of allowing cytoplasm to escape from the embryo through holes punctured at specific positions through the egg-case and transplantation of cytoplasm from one region to another'. For example, loss of cytoplasm from the anterior end causes loss of head structures and the development at the anterior pole of structures such as the telson normally only found at the posterior pole. If, in addition, posterior cytoplasm is transplanted to the anterior end the result is an embryo consisting of two abdomens arranged in mirror-image symmetry.

The phenotypes produced in these experiments can be reproduced by certain 'maternal-effect' mutations, in which the inability of the mother fly to make a wildtype gene product leads to the mutant embryonic phenotype. Thus bicoid mutants lack head structures (Nüsslein-Volhard) and oskar mutants lack an abdomen (R. Lehmann, Max-Planck Institute, Tübingen). Cytoplasm from the appropriate end of a wild-type embryo can rescue these mutants if injected into a specific region along their body axis, and in the case of bicoid mutants injection at the wrong site causes ectopic head development. The bicoid-oskar double mutants are particularly revealing: they lack both head and abdomen, and consist of juxtaposed posterior terminal structures which seem to be a kind of 'groundstate' made in the absence of information to the contrary. If such mutants are injected with wild-type cytoplasm from the anterior or posterior pole it is possible to correct one or other mutation, generating single mutant phenotypes in either normal or inverted orientation, depending on the end into which the cytoplasm is injected.

These results lead to a picture of mutually antagonistic determinants localized at either end of the egg with long-range effects on the nature and polarity of structures formed during development: whether they really generate formal 'gradients' is not yet clear. The bicoid

gene, which is located within the Antennapedia complex of homoeotic and segmentation genes, has been cloned, and Nüsslein-Volhard's in situ hybridization experiments show that it encodes a transcript localized at the anterior pole of the egg, presumably transported there from the transcriptionally active nurse cells to which the egg is connected.

The bicoid gene, therefore, has all the features of a gene encoding a developmental morphogen. The situation for oskar appears somewhat more complicated, for together with a small set of other maternal-effect genes, it seems to generate a signal at the posterior end that is transported anteriorly, where it has its effects on zygotic gene expression. In a model put forward by Hans Meinhardt (Max Planck Institute, Tübingen), a single gradient of maternal information is interpreted by the sequential activation along the anterior-posterior embryonic axis of the zygotic 'gap' genes, mutations of which cause the loss of large contiguous groups of segments. The results with bicoid and oskar are more consistent with Sander's proposal that there are morphogenetic centres at both poles of the embryo, but the 'gap' phenotype of oskar mutants supports the suggestion that the gap genes are the next stage in the developmental hierarchy after maternally expressed genes.

In Meinhardt's model, the gap genes (which he prefers to call cardinal genes) play a central part in initiating both the periodic pattern of segmentation and, via the homoeotic genes they are postulated to regulate, the sequential pattern of segment specification. Interest in this model has been fuelled by recent results that bear out several of its non-trivial predictions. For example, although different gap mutations delete large, overlapping regions of the embryo, Meinhardt predicted that they would be expressed in non-overlapping regions about half the length of the affected region — and in the case of Krüppel and hunchback this has turned out to be just the case (H. Jäckle, Friedrich Miescher Institute, Tübingen). Also confirmed has been the prediction that the loss of a given gap gene would cause the expression of the neighbouring gene to spread into its domain (Jäckle). In the model the gross non-autonomy of gap genes results from the central importance of the borders between the domains of gap gene expression in organizing the expression of the next set of genes in the postulated hierarchy, the pair-rule genes (the first to have a periodic pattern of expression): the loss of one gap gene eliminates two borders and hence a region of the embryo twice as long as that in which it is expressed.

Data on the expression of the segmentation genes of *Drosophila* are being obtained at a tremendous rate, and some

^{*5}th EMBO workshop on the molecular and developmental biology of *Drosophila*, Kolymbari, Crete, 21–29 June 1986.

of these have been discussed recently in News and Views. The main focus at present is to obtain clues as to how the genes interact by studying the effects of mutations in one gene on the expression of another. With so many genes apparently involved, however, the interpretation of such experiments is unlikely to be simple, and it was notable at the meeting that most of the experimentalists averred that they found Meinhardt's model a helpful framework in which to try to interpret their results. The film Meinhardt showed at the meeting of computer simulations based on his model demonstrated that it can closely simulate the evolving patterns of segmentation gene expression in wild-type and normal embryos that are observed experimentally.

Dorsal-ventral axis

A further set of maternal-effect mutations affects pattern-formation along the dorsal-ventral axis of the Drosophila embryo. Recessive mutations in at least 10 genes cause dorsalization of the embryo, and a series of experiments7.8 reviewed recently in News and Views9 has led to a model for the establishment of dorsalventral positional information by a morphogenetic product generated by these genes. One of this set, snake, has been cloned and sequenced, and encodes a protein with all the features of a serine protease (R. Delotto, University of Geneva). This is an exciting result, for serine proteases are made as inactive precursors activated by specific proteolytic cleavage, and in blood clotting and complement fixation chains of specific serine proteases are arranged in a cascade to amplify an initial signal in such a way as can readily be envisaged to be applied to the more glamorous problem of pattern formation. Both blood clotting and complement fixation generate products tightly localized in space close to the initial signal: the intriguing prospect is that such a signal, probably at the ventral pole, initiates a cascade of reactions which converts it into a set of coordinates along the dorsal-ventral axis. If this is true, other dorsalization genes should turn out to encode serine proteases.

Although the issue has been controversial, it is now generally accepted that during development the anterior-posterior axis of the Drosophila embryo is divided into polyclonal units called compartments, defined by the expression of sets of 'specifier' genes that determine their pathways of development. Whether the dorsal-ventral axis is divided into compartments analogous to those along the anterior-posterior axis is unclear. That this may be the case is suggested by recent work on another gene of the Antennapedia complex that has recently been cloned, zerknullt (zen)[™]. Mutations of this gene affect the differentiation of

A bacterial haemoglobin

from M.F. Perutz

HAEMOGLOBIN was believed to be a protein that evolved in eukaryotes, but a report elsewhere in this issue (Wakabayashi, S., Matsubara, H. & Webster, D.A. Nature 322, 481; 1986) describes a bacterial haem protein from Vitreoscilla that combines with molecular oxygen and has an amino-acid sequence with features characteristic of the globins.

There are only two amino-acid residues that are common to all the globins: a histidine that forms a covalent link with the haem iron; and a phenylalanine in position 1 of the loop made by helices C and D which wedges the haem into its pocket. All other residues are replaceable, but in 33 specific positions replacements are restricted to non-polar residues (Perutz, M.F., Kendrew, J.C. & Watson, H.C. J.molec. Biol. 13, 669; 1965).

The haem protein of Vitreoscilla does contain non-polar residues at almost all these positions, and it shows marked homology with the haemoglobin of the leguminous nodules of lupins, whose globin is encoded by a gene in the plant, rather than the symbiotic bacterium Rhizobium where the haemoglobin is concentrated. Most haemoglobins contain a histidine in a position distal to the haem, but the α -chain of the oppossum is an exception and contains a glutamine in-

stead. The alignment of the Vitreoscilla sequence by Wakabayashi et al. suggests that it also has a distal glutamine whose amino group could form a hydrogen bond with the bound oxygen, just as the distal histidine does in myoglobin (Phillips, S.E.V. & Schoenborn, B. Nature 292, 81; 1981). Homology between Vitreoscilla and other globins extends to helices B, C, E, F, G and H; helix **D** is missing as it is in the α -chains of mammalian haemoglobins, and homology ends at the A-B corner. The first 11 residues show no homology with the A helix, but this helix is unimportant because it is not in contact with the haem.

What is the function of this haemoglobin? The haemoglobin content of Vitreoscilla increases almost 50-fold when the oxygen concentration of the growth medium falls below 10 per cent of atmospheric. Apparently, species of this genus live in oxygen-poor environments; possession of the haemoglobin helps them to absorb oxygen for their aerobic metabolism. Is this an example of divergent or convergent evolution or of gene transfer from eukaryotes? Who can guess? We were not there when it happened.

M.F. Perutz is at the Laboratory of Molecular Biology, Hills Road, Cambridge CB2 2Q11.

dorsally derived embryonic tissues. Analysis of the cloned gene shows that it contains a homoeo box and is expressed in dorsal tissues of developing embryos. The evolution of the pattern of zen expression along the dorsal-ventral axis during development is reminiscent of genes such as Ultrabithorax that are expressed in a compartment-specific manner along the anterior-posterior axis, suggesting that zen may be involved in the specification of a dorsal-ventral compartment.

A Cartesian coordinate frame?

Meinhardt has suggested that the points on the surface on an insect embryo where dorsal-ventral and anterior-posterior compartment boundaries intersect might specify the positions of the imaginal disks that later in development generate the adult cuticle structures. Intriguing evidence that this could be true was reported by W. Gelbert (Harvard). Mutations of the decapentaplegic gene of Drosophila cause the loss of pattern elements derived from the centres of imaginal disks. Gelbert explained that clonal analysis shows that a normal decapentaplegic gene is required only in cells that abut the anterior-posterior compartment boundary of a disk for normal development.

Furthermore, using the cloned gene it has been found that decapentaplegic is expressed in a dorsal region of the embryo, later splitting into two stripes running along the anterior-posterior axis on either side of the embryo just where the two lines of imaginal disks later develop. So it could be that these stripes define dorsal-ventral compartment boundaries, and the spatial cue for disk formation is where they cross anterior-posterior compartment boundaries. I am sure that the founder of analytical geometry, René Descartes, would be pleased by this elegant application of his system of spatial coordinates to biological pattern formation.

- . North, G. Nature News and Views 311, 214 (1984) Sander, K. Adv. Insect Physiol. 12, 125 (1976)
- Frohnhofer, H.G., Lehmann, R. & Nusslein-Volhard (

- J. Embryol. exp. Morph. (in the press) Lehmann, R. & Nússlein-Volhard, C. Ceh (in the press) Meinhardt, H. J. Cell Sci. Suppl. 4, 35" (1986) Coulter, D. & Wieschaus, F. Nature News and Views 321, 272 (1996)
- Anderson, K.V., Jurgens, G. & Nusslein-Volhard, C. Cell
- 42, 779 (1985). 8. Anderson, K.V., Bokln, L. & Nusslein-Volhard C Cell
- Woodland, H. & Jones, E. Nature News and Views 319, 261
- 10. Doyle, H.J., Harding, K. Hoey, T. & Levine, M. Nature (in the press).

Geoffrey North is Deputy Biology Editor of

Neural models

Networks for fun and profit

from James A. Anderson

Knowing how the brain works is intrinsically interesting and could be practically useful. There have been many attempts to make artificial systems compute the way we seem to. Recently, there has been a renaissance of interest in what have been variously called neural models, brain models, neural networks and connectionist models. Two recent papers^{1,2} provide examples of how some important practical problems turn out to be well suited to computations based on neural networks, and applications using these networks may appear in the near future.

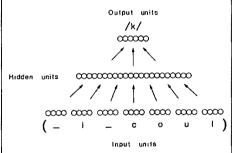
Connectionist systems were originally proposed as models for brain organization and for psychological functions such as association, concept formation and word recognition. But there has been a change in the past year — an adequate brain model must be able to compute something. It seems that even at their current state of development, the things that connectionist models compute effectively are now of interest to many scientists and engineers with practical problems.

There are several variants of connectionist models, but all have similar structure. They assume that there are a very large number of simple processing elements arranged in parallel arrays. Processing elements can either be simple Boolean devices with two allowable states (for example, on or off) or they can have continuously graded activity. Elements in the same group can be coupled together or can be joined to elements in other groups by connections with modifiable strengths. This interconnected system is largely based on the architecture of the mammalian cerebral cortex, with varying degrees of oversimplification: the properties of the elements are inspired by the properties of neurones and those of their modifiable connections by synapses.

There are two distinct aspects to the functioning of a connectionist system. First, the strengths of the interconnections must be specified. One way this can be done is by having the network learn a set of training activity patterns so it forms the appropriate connection strengths based on a learning rule. Most learning rules are variants of an idea proposed by Donald Hebb in 1949, that a connection strength is changed based on the simultaneous occurrence of activity on both sides of the connection. Another way is by simply knowing what the strengths should be to compute what it is you want to know. This is possible for some well-defined problems, and has the great advantage that a slow and sometimes unreliable learning process can be bypassed.

Second, when the connections are formed, the network must be provoked to perform the desired computation. An input pattern of activity is provided to start the system, then the initial pattern, through the interconnections, modifies itself and affects the activity of other connected elements to form a new pattern. This process may repeat for a number of steps until the network stabilizes, or it may run continuously. If the system works properly, the new patterns contain the results of the computation.

One example of a new application of networks is NETtalk, a program which converts text into spoken English (reads) developed by Terrance Sejnowski and Charles Rosenberg^t. Reading printed text



Schematic drawing of the network architecture for NETtalk. Input units are shown on the bottom of the pyramid, with 7 groups of 29 units in each group. A 29-unit group corresponds to a single letter, giving rise to a 7-letter window into the text. Each hidden unit in the intermediate layer receives inputs from all the input layers in the bottom layer, and in turn sends its output to all 26 units in the output layer. An example of an input string of letters is shown below the input groups, and the correct output phoneme for the middle letter is shown above the output layer. For 80 hidden units, which were used for the corpus of continuous informal speech, there was a total of 309 units and 18.629 weights in the network. (Figure and caption from ref.1.)

is typical of the rule-based systems used by humans. There are important rules and regularities in English spelling, but there are also many exceptions to the rules. Sejnowski and Rosenberg used samples of English text with the conversion of that text into phonetic symbols. As they then knew the input strings of characters and output strings of phonemes for many examples, they could modify connection strengths using an effective learning algorithm called back propagation, developed by David Rumelhart, Geoffrey Hinton and Ron Williams3, and independently by David Parker and by Yann Le Cun3.

This algorithm is able to learn effectively when there are several layers of modifiable connections between input and output. It is an error-correction technique that sends corrections 'backwards' from the output (where we can measure the error) to earlier layers with the appropriate strengths. NETtalk looks at seven input characters at once to generate an output phoneme, as pronunciation of a particular letter is strongly dependent on context. There are three layers of processing elements: an input layer, an output layer and a layer of 'hidden units' between input and output. After about a dozen hours of computer time on a VAX superminicomputer, the program was 'speaking' correctly more than 90 per cent of the words encountered in the input text. When a speech synthesizer was connected to the output, it generated quite understandable speech with occasional, usually minor, mispronunciations.

This simulation is much more than a curiosity. Sejnowski modelled the name of the simulation, NETtalk, after a commercial product of the Digital Equipment Corporation called DECtalk, a complex system developed over several years which speaks the words and characters appearing on a computer terminal. Sejnowski and Rosenberg, starting from zero, took less than three months to develop a functioning system that can do some of the same things.

A second example is the recent work of John Hopfield and David Tank². Hopfield had written two influential papers^{6,7} that pointed out some similarities between neural network computations and some problems in solid-state physics, for example, spin glasses, with a similar mathematical structure. He showed that the essence of the dynamics of a network computation in many cases is that the network is trying to put the state of the system in a minimum of what can be interpreted as an energy function in a physical system. This means that many of the powerful analytical tools available in physics can be carried over bodily to neural networks and might help towards understanding brain function.

The new paper by Hopfield and Tank² shows how a neural network can be applied to a practical problem that seems remote from brain function. They discuss the use of network model to estimate the answer to the 'travelling salesman' problem, the best-known example of a set of problems called np-complete by computer scientists. Like many good problems it is simple: a travelling salesman is given a number of cities to visit on his route. What sequence of cities gives the shortest total travel distance? To be certain the shortest route has been found, it is necessary to compute the distance for all possible routes. As the number of cities increases, the number of combinations to check

grows exponentially, and it rapidly becomes impractical to find the best solution. This problem is related to many optimization problems such as minimizing costs and maximizing efficiency.

Hopfield and Tank² show that a suitably designed neural network can compute a good estimate of the best solution. When checked, it is not the best solution but it is quite close to the best and can be computed quickly. Their technique is to arrange the system so that only allowable solutions to the problem can occur. For example, if the city is visited eighth on the circuit, then no other city can also be visited eighth. When one city is chosen for that position on the trip, it inhibits all the other candidates for the eighth position. No city can be visited twice, so if a city is chosen for one position on the route, it inhibits its potential appearances in other positions on the route. Hopfield and Tank constructed the connection strengths and the energy function so that as the state of the network evolves, the states corresponding to routes with small total distance grow at the expense of other routes. If the initial state of the system is random, the final state of the system corresponds to a route with a small total distance and is an allowable route. If the computation is repeated a few times with different initial states, the best solution is close to the actual solution of the problem. For many practical applications, this is good enough to be satisfactory.

But special algorithms for this problem are able to get better and faster estimates. and DECtalk works. So why bother with NETtalk and its potential descendents? One reason is that these two quite different problems are solved with techniques that are basically that same: interconnected sets of simple elements coupled with modifiable connections. Special-purpose hardware built to make one compute quickly will make the other compute quickly as well. Also, the algorithms for a network computation are highly parallel, that is, all the elements are computing their outputs simultaneously. Network computations are therefore well suited for parallel computers. For example, optical hardware, with its high speed, low precision, parallelism and high interconnectivity, is an excellent match for the requirements of network computations. Several groups are now building specialpurpose parallel hardware specifically for networks.

Once the hardware becomes available. it can be used for a wide range of problems, from optimization to learning rules for natural language, with only minor changes. Connectionist models may not give the best or fastest answer to any particular problem but will come up with a pretty good answer quickly. It is this potential flexibility and speed that makes practical applications so attractive. The brain may show similar computational flexibility and power for similar reasons.

James A. Anderson is in the Department of Psychology. Center for Neural Science and Center for Cognitive Science at Brown University, Providence, Rhode Island 02912, USA

Physiology

Chloride ions and cystic fibrosis

from Maynard Case

Cystic fibrosis, a lethal inheritable disease, seems to involve defective transport of chloride ions across epithelia. Such a defect could be caused by an alteration in the number, characteristics or regulation of Cl- channels in the plasma membrane of epithelial cells. Three recent articles1-3, one of which appears on page 467 of this issue', suggest it is the regulation of Cl-channel activity that is at fault.

The conventional electrophysiological studies on sweat gland ducts' and airway epithelia⁵ (which are both affected in cystic fibrosis) point conclusively towards the involvement of decreased Cl- transport in the pathophysiology of this disease. The nature of this transport defect has now been studied independently by Welsh and Liedtke^{1,2} and by Frizzell et al.³ using patch-clamp techniques.

The two groups have studied primary cultures of tracheal epithelial cells from normal subjects and cystic fibrosis patients and have recorded both from intact cells and excised, inside-out membrane patches. They both describe the presence of Cl -- selective channels on the apical membrane of these epithelial cells but under similar experimental conditions, Welsh and Liedtke observe only one type of channel whereas Frizzell et al. detect two channels. Also, the channel described by Welsh and Liedtke seems to be insensitive to Ca2+ but those described by Frizzell et al. are both Ca²⁺-sensitive.

Despite these apparent and important differences in the characteristics of the channels, which might perhaps reflect differences in tissue culture technique, the major findings of the two studies are similar. First, during recording from intact cells, Cl--channel activity can be elicited by adrenaline or cyclic AMP in normal but not cystic fibrosis cells; and second, in excised patches, the biophysical properties and kinetic behaviour of the channels are identical in both cell types. This suggests that the problem in cystic fibrosis relates not to the presence or absence of the Cl⁻ conductance but to the regulation of this conductance by a cyclic AMPdependent process.

Although both studies describe differ-

ences between normal and diseased cells only about half the intact normal cells respond to stimulation by opening Cl -channels whereas all excised patches from normal and diseased cells show activity. This may indicate active inhibition of the Cl channel so that excising the patch or stimulating the cell removes some sort of brake. If so, perhaps the brake-release mechanism is at fault in cystic fibrosis. Alternatively, there could be two populations of epithelial cells in normal subjects, but only one in cystic fibrosis patients.

These articles refocus our attention on the pathway generating cyclic AMP, but as adrenaline causes the normal accumulation of cyclic AMP in cultured airway cells from cystic fibrosis patients, presumably the defect lies downstream from cyclic AMP generation itself. If a cyclic AMP-dependent pathway is involved in the disease, this may help to explain the effects of the disease on the pancreas another prime target.

Secretion in the pancreas occurs across both acinar and ductal epithelia. Whereas the former is controlled by Ca'-mobilizing agonists (cholecystokinin and acetylcholine), secretion across the ducts is controlled by secretin, which seems to act exclusively via cyclic AMP. Hence these studies on airway epithelia support the hypothesis that pancreatic ductal secretion is faulty in the disease. However, as cystic fibrosis is thought to be associated with defective Cl secretion, it has always been a problem to explain why an epithelium lining the pancreatic ducts that secretes HCO₁, rather than Cl . should be affected (although this HCO, secretion is Cl-dependent). If the fault lies in the regulation of the anion channel rather than the channel itself, as this recent work suggests, this objection is overcome.

Maynard Case is in the Department of Physiology, University of Manchester, Manchester M13 9PT, UK.

^{1.} Sejnowski, T.J. & Rosenberg, C.R. The Johns Hopkins University Electrical Engineering and Computer Science Technical Report JHU/EECS-86/01 (Baltimore, Maryland,

Hopfield, J.J. & Tank, D.W. Biol. Cybernet. 5, 141 (1985). 3. Rumelhart, D.E., Hinton, G.E. & Williams, R.J. in Paral-lel, Distributed Processing: Explorations in the Microstructure of Cognition (eds Rumelhart, D.E. & McClelland, J.L.) (MIT, Cambridge, in the press).

Parker, D. MIT Tech. Rep. TR-47 (1085).

Yann Le Cun in Disordered Systems and Biological Organtiation (eds Bienenstock, E., Fogelman Soulie, F. & Weisbuch, G.) (Springer, Berlin, in the press).

Hopfield, J.J. Proc. natn. Acad. Sci. U.S.A. 79, 2554 (1982). Hopfield, J.J. Proc. natn. Acad. Sci. U.S.A. 81, 3088 (1984).

^{1.} Welsh, M.J. & Liedtke, C.M. Vature 322, 467 (1986)

Welsh, M.J. Science 232, 1648 (1986)
 Frizzell, R.A., Rechkemmer, G. & Shoemaker, R.I. Science 233, 558 (1986). Quinton, P.M. Nature 301, 421 (1983).

^{5.} Knowles M.R. Science 221, 1067 (1983).

Population biology

Genetic management in zoos

from Andrew F. Read and Paul H. Harvey

Animal populations in zoos tend to be small and, therefore, particularly susceptible to the loss of genetic variability. Such losses can have harmful effects on the fitness of individuals as well as reducing the evolutionary potential of populations1. Interest in the genetic management of zoo populations has recently taken on a fresh urgency² because of the increasing realization that captive breeding programmes are essential to prevent many species from becoming extinct. A new 13-chapter report, written by about 40 zoo managers, geneticists and population biologists3, introduces rather than solves many relevant problems, but should provide an important framework for future research.

The increasing size of the human population is causing large-scale degradation of tropical and temperate ecosystems that support most of the world's wildlife. If the human population achieves zero population growth in about 100 years, as some demographic studies forecast^{4,5}, and then begins to decline, it would take several centuries before viable populations of many animal species could be restored in the wild. Given such dismal prospects for the world's fauna, zoos must be prepared to act as stewards or as 'arks', to use the metaphor of Soulé et al.3. These authors point out that technical improvements may eventually provide other ways of maintaining populations (for example, by regenerating organisms from preserved zygotes). But in the meantime, they argue. about 2,000 species of terrestrial vertebrates, including 160 primates, 100 large carnivores, 100 artiodactyls, 800 birds and several hundred amphibians and reptiles, may have to be captively bred to save them from extinction.

The preservation of genetic diversity is becoming a primary goal of many captive breeding programmes. Juvenile mortality in captive species has been linked to the loss of genetic diversity after inbreeding. Similarly, the low level of heterozygosity in South African cheetahs Acinonyx jubatus jubatus may underlie the great difficulty these animals have breeding in captivity, their high degree of juvenile mortality and their extraordinary sensitivity to pathological viruses. Loss of genetic diversity could also limit the potential of a population to adapt to new environments when reintroduced to the wild.

If maintenance of genetic variation is to be a central aim of management, how should we measure it? Electrophoretically detected protein variation has been used to estimate the overall extent of genetic variation within populations. For example,

such tests identified the low level of heterozygosity in cheetahs⁸. Allozyme surveys can be used to distinguish outbred populations from genetically homogeneous inbred populations, but heterozygosity at a few protein-coding loci is not necessarily a good estimate of the overall genomic heterozygosity of an individual. For example, the average number of loci examined in routine electrophoretic surveys is about 20. As Hedrick and coauthors point out3, if the expectation of heterozygosity is the same at all loci; if the loci segregate independently; and if the 20 loci are examined from a pool of 1,000, the correlation, between heterozygosity for those loci and overall heterozygosity is only 0.14.

Furthermore, heterozygosity may be an

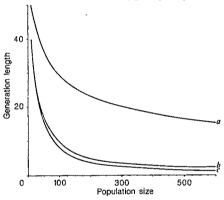


Fig. 1 Combinations of target population sizes and generation lengths required for a species to retain 90 per cent of the genetic variation of the source population for 200 years, given an exponential growth rate of 1.0 and founder population sizes of 10 (a), 20 (b) and the target number of individuals $(c)^3$. Species with long generation times can be maintained with fewer animals, and the size needed can be decreased dramatically by increasing the number of founders used to initiate the captive population.

insufficient measure of genetic variation. Allendorf argues that useful allelic diversity is largely caused by rare alleles that are likely to be lost early in a captive breeding programme, with only a minimal effect on heterozygosity3. Although heterozygosity is a good measure of the ability of a population to respond to selection in the short term (the first few captive generations), the number of alleles may be a more important indicator of the potential long-term response under continued selection. Thus, both high heterozygosity and high allelic diversity are desirable in species under consideration for reintroduction programmes. The problem, then, is to determine the number and distribution of alleles. Electrophoretic

techniques provide somewhat conservative estimates, whereas DNA sequencing is more accurate but more costly.

How many individuals of each endangered species should be kept in zoos? This depends on the amount of genetic variation to be maintained in the captive population over a specified amount of time. Soulé and co-authors set themselves the theoretical problem of keeping a captive population which, after 200 years, retains about 90 per cent of the genetic variation found in the original wild population3. This, they think, is the intuitive threshold between a tolerable loss of heterozygosity and potentially damaging homozygosity that provides enough time for the biotechnology to develop that will be necessary to maintain and regenerate species from preserved eggs, zygotes or tissues. Their model assumes random breeding in groups, equal sex ratios, non-overlapping generations and Poisson-distributed family sizes. The target captive population size depends on generation time, population growth rate and the number of interbreeding founders. The combinations of population sizes and generation lengths required for species with an exponential growth rate of 1.0 are shown in Fig. 1. Given that a major aim is to use resources as efficiently as possible, zoo managers are faced with the prospect of minimizing the number of individuals of each species held, while at the same time attempting to retain genetic variability within the captive population.

For a fixed number of founders, species with longer generation times require smaller target captive population sizes, because under the assumptions of the model there is loss of alleles only during reproduction. But the required target population sizes can be very sensitive to the number of individuals taken from the wild. For the values shown in Fig. 1, a large decrease in the target population size can be achieved by increasing the number of founders, at least up to 25 animals. (Fewer founders are needed in species with high population growth rates but, even with the highest rates of growth, the founder population should still be above six, otherwise more than 10 per cent of the genetic variability will be lost in the first generation.) Ideally then, captive propagation plans should aim to start with more than 20 founders (although the actual number depends on the rate of growth and generation time of the species in captivity), increase to the eventual population size in few generations (so that the effects of genetic drift are minimized and to ensure survival of the species in captivity) and then, if possible, artificially delay reproduction. Soulé and co-authors consider that breeding programmes should aim to maintain an effective population size of 200-300 individuals for more species.



Fig. 2 Przewalski's horse

The number of founders and reproductive rates of several endangered species currently in captive breeding programmes falls well short of those guidelines. The population of Przewalski's horse (Equus caballus przewalskii; Fig. 2), for example, has a growth rate of 0.1 and is derived from only 13 founders. According to Soulé's model there is no target population size which will allow the retention of more than 90 per cent of the original genetic variability.

Should populations be divided? Subdivision helps to protect populations from total extinction by epidemics or local disasters, and for this reason alone it is desirable to have more than one captive group of any endangered species. Foose and co-authors also point out that, if at least one breeding individual per generation is transferred between groups and there is no differential mortality according to genotype, the entire captive population is nearly equivalent to a single interbreeding unit

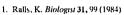
Which animals should be chosen for captive breeding programmes? This is by no means a trivial question. The choice of individuals for reintroduction to the wild must take into account the extent to which they are likely to be adapted to local conditions. For example, the Tatra Mountain ibex Capra ibex ibex became extinct in Czechoslovakia but was successfully reintroduced from Austria. Subsequently, C. i. aegagus from Turkey and C. i. nubiana from Sinai were added to the Czech herd. The resulting hybrids rutted in the early autumn, rather than in the winter as the local ibex did, and their young were born in February, the coldest month of the year. As a result the whole Czech population became extinct10.

Major problems facing captive breeding programmes include relaxation of natural selection and inadvertent selection for domestication. For example, selection for ease of handling may result in loss of predator escape behaviour. Frankham and co-authors conclude that selection in captivity can be minimized by adopting breeding plans designed to maximize genetic diversity'. As well as maximizing the number of founders, rapidly expanding and then subdividing the population, they suggest equalizing the genetic contribution of each of the founders to subsequent generations by manipulating family sizes. The only active selection they advocate is to cull animals with specific deleterious traits and outliers in morphological or fitness measures.

Any other forms of artificial selection must be justified. Selection for captive breeding success is clearly appropriate for rare species not yet capable of selfsustaining reproduction in captivity. In some cases it may be desirable to select against certain genotypes. Captive populations of Przewalski's horse, for example, have had genetic inputs from 12 wildcaught Przewalski's horses and one Mongolian domestic mare. The historical distribution of the breeding lines has resulted in two-thirds of the current population having genetic inputs from this mare. An interim breeding plan aimed at purifying the captive population by allowing matings only between animals lacking genetic input from the mare has begun. This selection will, of course, turther reduce the genetic diversity of the species. In the case of the Speke's gazelle Gazella spekei, selection for inbreeding tolerance was applied. This was inevitable because the captive population was facing serious inbreeding problems, had very few founders and no opportunity for input from the wild.

Hedrik and co-authors add a note of caution'. Successful reintroduction, they say, is more likely when genetic variation in a captive population is maintained in the form found in natural populations. The maintenance of the breeding and social structure found in the wild may be more important for a species than a programme designed only to retain maximum genetic diversity.

Several simulation models have been developed to assess the interacting effects of such competing management goals. These models assign a genotype to each founder and then, using pedigree data and demographic characteristics of popula-tions, subject the 'colony' to various management plans. One such computer experiment, reported by Dyke and coauthors', uses data from a real colony of captive rhesus monkeys to test the idea that removing some individuals from a single age group (usually early in life) and removing all older breeders with low reproductive rates would increase the



FOOSE, T. in Genetics and Conservation: a Reference for Managing Wild Animal and Plant Populations (eds Schonewald-Cox, C.M., Chambers, S.M., MacBryde, B. & Thomas, W.L.) 374 (Cummings, Menlo Park, Californ-tics)

- 3. Ralls, K. & Ballou J. (eds) Zoo Biol. 5 (1986).
- United Nations Pop. Bull. 14 (1982)
 World Bank World Development Reports (World Bank. Washington DC, 1984)

 6. Ralls, K. & Ballou, J. in Genetics and Conservation, a
- Reference for Managing Wild Animal and Plant Popula-uons (eds) Schonewald-Cox, C.M., Chambers, S.M., MacBryde, B. & Thomas, W.L.) 164 (Cummings, Menlo Park, California, 1983).
- 7. O'Brien, S.J. *et al. Science* 227, 1428 (1985). 8. O'Brien, S.J. Wildt, D.E., Goldman, D., Merril, C.R. & Bush, M. Science 221, 459 (1983)
- Crow, J.F. & Kimura, M. An Introduction to Population Genetics Theory (Harper & Row, New York, 1970),
 Greig, J.C. S. Afr. J. Wildl. Res. 9, 57 (1979).
- 11. Ryder, O.A. & Wedermeyer, E. A. Biol. Conservation 22,
- 259 (1982).
- 12. Templeton, A.R. & Read, B. in Genetics & Conservation: a Reference for Managing Wild Animal and Plant Popula-tions (eds Schonewald-Cox, C.M., Chambers, S.M., MacBryde, B. & Thomas, W.I.) 241 (Cummings, Menlo Park, California, 1983).



GIANT tube worms (Lamellibrachia sp.) have been found in Japan's deep-sea back yard, 1 km from the east coast of the Izu Peninsula, at a depth of 1,160 m. The worms, 60-70 cm in length, occur alongside giant clam (Calyptogena soyoae) colonies, the largest of which spans 200 by 80 m. Methane levels reach 10,000 at per litre a few centimetres above this 'vent' community which is aligned along a major fault associated with subduction of the Philippine plate beneath Japan. Photograph taken in May/June 1986 during a survey by the Japan Marine Science and Technology Center and the Ocean Research Institute, University of Tokyo. David Swinbanks

productivity above that obtained when individuals were removed at random. Productivity increases with minimal effects on the genetic variability of the population. The implementation of increased population growth rates need not, therefore, add significantly to the problems of genetic management.

Ultimately, the biological problems so carefully brought together in this volume may be dwarfed by financial and political

constraints. At present, zoos can sustain around 925 species of terrestrial vertebrates with captive population sizes of more than 250, far short of the 2,000 species that may need to be accommodated. This time around, the ark may be very crowded.

Andrew Read and Paul Harvey are in the Department of Zoology, University of Oxford, South Parks Road, Oxford OXI 3PS, UK.

Archaeology

A new chronology for the French Mousterian period

from Paul Mellars

THE classic sequence of 'Mousterian' industries recorded within the cave and rock shelters of southwestern France represents an important record of Neanderthal man, but the dating has been controversial. Dating of the Le Moustier site by thermoluminescence techniques, reported on page 452 of this issue', provides one of the first well-documented points of reference for the chronology of the sequence and therefore will require reanalysis of climatic and human changes during this period.

The time range of the Mousterian (broadly from 40,000 to 115,000 years before present (BP) — coinciding with the earlier part of the last glaciation) puts it effectively beyond the range of dating by means of conventional radiocarbon techniques, and even the refinements of the new accelerator mass spectrometer techniques of "C measurement are unlikely to extend for more than 10–20,000 years into the most recent part of the period².

All attempts to construct a detailed in-

ternal chronology for the Mousterian have had to rely either on complex and controversial correlations between the geological and palaeo-environmental sequences recorded in individual sites^{1,5}, or on equally contro-versial correlations between the character of the archaeological material recovered from the sites⁶. But thermoluminescence dating of burnt flint artefacts promises to put the dating of Mousterian sites on to a secure scientific footing.

No dating method is perfect and thermoluminescence dating of burnt flints depends on a rather complex series of calculations — and in some cases assumptions — involving not only the measurement of the thermoluminescence activity of the samples but also the environmental history of the sites and levels dated.

Fortunately there are several internal cross checks on the dates obtained for the Le Moustier sequence. The results of the thermoluminescence dating can be compared directly with the stratigraphic

sequence samples, and the dates obtained for the uppermost part of the sequence (containing an early Upper Palaeolithic industry) can be compared with the known age of these levels as documented by radiocarbon dating. In the latter case, thermoluminescence results turn out to be slightly older than would have been expected from radiocarbon evidence. but only marginally so, when allowance is made for the relatively large standard deviations attached to the thermoluminescence measurements. The consistency and internal coherence of the dates obtained for the different levels pro-vides strong corroborative evidence for the absolute chronology proposed for the Le Moustier sequence as a whole.

The present chronological structure of the French Mousterian hinges almost entirely on the correlation between the geological and archaeological successions in two key sites — Le Moustier on the one hand, and Combe Grenal (a major rockshelter site in the Dordogne valley) on the other. Previous interpretations of the geological evidence have assumed that the sequences in both sites span broadly the same range of time, and provide essentially parallel records of occupation throughout at least the greater part of the Mousterian sequence (that is, the 'Wurm I' and Wurm II' climatic phases of the current literature)³⁻⁵. Since the archaeological material recovered from the two sites is strikingly different, this interpretation carries with it the important implication that distinct industrial variants of the Mousterian were manufactured synchronously in southwestern France throughout most if not all the Mousterian period^{3,5}.

The new thermoluminescence dating of the Le Moustier sequence' argues against this intrepretation in several ways. In the first place, the earlier geological studies of Laville had postulated a substantial depositional hiatus within the uppermost part of the Le Moustier sequence (between the final Mousterian and earliest Upper Palaeolithic levels)⁴⁵ which is now seen to be untenable. More significantly, the new thermoluminescence dates show that the entire sequence of dated levels at Le Moustier (layers G to K) spans a period of only about 15,000 years, which is in sharp conflict with the earlier suggestion that these levels span a period of at least 30-35.000 years^{5.8}. Clearly, the present geological interpretations of the Le Moustier sequence will need to be substantially revised.

The long sequence of Mousterian levels recorded in the site of Combe Grenal^{9,10}, on the other hand, demonstrably spans a very much longer period. The basal levels of the sequence can be reliably attributed on both geological and archaeological grounds to the final part of the penultimate ('Riss') glaciation, while the overlying levels reveal a detailed pattern of climatic fluctuations which parallels almost exactly that recorded for the earliest stages of the last glaciation in recent studies of deep-sea cores (that is, stages 5 and 4 of the ocean-core sequence; see Fig. 1) 8.9.11-13. The geological evidence is reinforced by the archaeological record, which shows that classic 'Mousterian of Acheulian Tradition' industries - of the kind which occupy the greater part of the archaeological sequence at Le Moustier — occur only in the uppermost

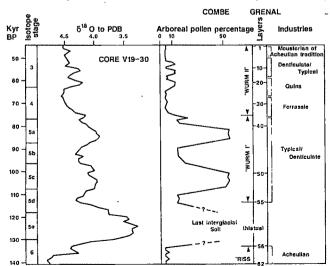


Fig. 1 Suggested correlation between the climatic sequence at Combe Grenal and the sequence of oxygen isotope stages recorded in deep-sea core V1930 (from refs 8, 9, 13 and N. J. Shackleton, personal communication). For details of archaeological sequences, see Fig.2.

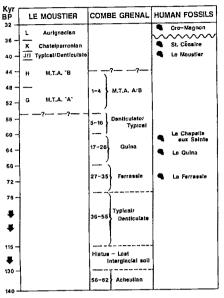


Fig. 2 Correlation between the archaeological sequences at Le Moustier and Combe Grenal implied by the new thermoluminescence dates for Le Moustier. The inferred chronological distribution of the principal Neanderthal remains from south-west France is shown in the right hand column (from refs 5, 10, 14, 15, 17). The sequence of Ferrassie and Quina Mousterian horizons at Combe Grenal is interrupted by a single level of 'Denticulate' Mousterian in layer 20, and three levels of either 'Typical' or 'attenuated Ferrassie' industries in layers 28-30; see ref. 17). M.T.A.; Mousterian of Acheulian Tradition.

occupation levels at Combe Grenal (see Fig. 2). The geological, archaeological and thermoluminescence evidence now converge in suggesting that the two sequences at Le Moustier and Combe Grenal represent essentially successive episodes in the total sequence of Mousterian occupation in south-west France, and together provide a largely complete record of human occupation in the area over a period of at least 70–80,000 years (Fig. 2).

This new chronology has radical implications for almost all aspects of our current understanding of the Mousterian period. In the first place it is now clear that any attempt to force the total pattern of climatic fluctuation during the earlier part of the last glaciation into a simple, two-fold scheme (that is, the 'Wurm I' and 'Wurm II' episodes referred to above) must be seen as a serious oversimplification of a much longer and more complex climatic succession. This in turn has direct implications for the interpretation of the archaeological record. Now that the archaeological sequences at Le Moustier and Combe Grenal can be seen to be successive rather than parallel, there can no longer be any objection to the hypothesis of a basic chronological sequence within three of the major industrial variants of the Mousterian within south-west France (that is, Ferrassie, followed by Quina, followed by Mousterian of Acheulian

Adrian Edmund Gill (1937–1986)

ADRIAN GILL, who died in hospital on 19 April after a sudden illness, will be remembered for his insight, and the almost uncanny ability he possessed to ask apparently very simple questions about ocean and atmosphere.

During the 1970s Gill - who took his doctorate under G.K. Batchelor at the University of Cambridge - began work on a seminal textbook (Atmosphere-Ocean Dynamics, published in 1982). The wide reading of both current and historical research that this involved led to the publication of many of the elegantly simple papers for which he will be remembered. His subjects included stability theory, thermal convection, internal and edge waves, and interactions between atmosphere and ocean. The lucidity of his book encapsulated his thinking for the current generation of students and researchers, and rapidly became a best-seller.

Simplicity was the key to the man and his thinking: Gill was a superb mathematician, yet one whose ability was seldom demonstrated, as this would confuse the message that he was anxious to get across not only to his theoretical colleagues but also to seagoing observationalists world-

wide. He was perpetually enthusiastic about discovering more of the physical world in which he lived. Those in Cambridge during his time there will recall the stub of pencil which lived in his jacket and which would always be in evidence at tea-time when some fluid dynamical problem would be hotly debated by those around him; or the essay on anomalous tidal flows in Greece that resulted from a family holiday in that country.

Gill travelled widely in the cause of science, and served on innumerable international working groups and committees. His concern with the world climate led to his becoming a founder member of the Committee for Climate Change and the Ocean, and to the conviction in the last years of his life that a model which coupled the global atmospheric circulation to the tropical ocean was the minimum necessary to understand short-term climatic variations such as El Niño. At the time of his death he was serving as the chairman of the Tropical Ocean-Global Atmosphere programme, one of the main components of the World Climate Research Programme, and had just been elected to the Roval Society. Peter D. Killworth

Combe Grenal had already suggested (see Fig. 2)^{3.5.6}. The same archaeological sequence is repeated in at least twelve other sites in the same region⁶.

Probably the most significant implications of the new dating however, are for the relative and absolute chronology of the various Neanderthal remains recovered from sites in south-west France. The famous Neanderthal skeleton from Le Moustier itself is known to have come from the uppermost part of the Mousterian sequence14 and therefore dated at about 40-45,000 years BP. By contrast, most of the other well-preserved Neanderthal finds are associated with archaeological material which is quite different from that recorded anywhere within the Le Moustier sequence but which compares closely with that recorded in the sequence of Ferrassie and Quina Mousterian levels at Combe Grenal 14.15. It would now appear that all of these finds including the famous 'classic' Neanderthal skeletons from La Ferrassie, La Quina and La Chapelle aux Saints - most probably date from the period of extremely harsh, glacial conditions represented by stage 4 of the ocean core sequence. If so, these finds must be dated at about 60-75,000 years BP. This is at least 15,000 years earlier than the Le Moustier skeleton, and probably 30,000 years earlier than the oldest finds of Homo sapiens sapiens forms from Cro Magnon and elsewhere (see Fig. 2).

followed by Mousterian of Acheulian | Exactly what implications this dating Tradition) — as the sequence recorded at | may have for current views on the re-

lationships between the various Neanderthal finds and their ultimate relationships with the Cro Magnon forms remains to be seen. It is already clear, however, that our whole perception of the chronology of human developments during the earlier part of the last glaciation is beginning to change and it may well be that further application of absolute dating techniques will reveal further surprises.

- Valladas, H., Geneste, J.M., Joron, J.L. & Cludelle, J.P. Nature 322, 452 (1986).
- Nature 322, 452 (1986).

 Hedges, R.E.M. & Gowlett, J.A.J. Sci. Acr. 254, 109 (1986).
- 3. Laville, H. World Archaeot 4, 321 (1973)
- Laville, H. Climatologie et Chronologie da Pale Juliagarea Périgord. Etude Sédimentologique de Depuis et Creates et sons Abris (Etudes Quaternaires, Université d. Provence Marseilles, 1975).
- Laville, H., Rigaud, J-P. & Sackett, J.R. Rock, Methers of the Perigord: Geological Strangraphy and Ares week rocks Succession (Academic, New York, 1980)
- 6. Mellars, P.A. Proc. Prehistoric Soc. 35, 134 (19-9)
- Aitken, M.J. Thermoluminescence Dairing (Neaderin New York, 1985).
- 8. Laville, H., et al. Bulletin de l'Institut de Geo! vei, du Bassin de l'Aquitaine (Bordeaux) 34, 219 (1983)
- Bordes, F., Laville, H. & Paquereau M.M. Aches de la Sociéte Luméenne de Bordeaux 103B 4-19 (1996).
 Bordes, F. A Tale of Two Caves (Harper & Row New York).
- York, 1972). 11. Shackleton, N.J. & Opdyke, N.D. Quat. Rev. 3, 33 (1873)
- Shackleton, N.J. Phil. Trans. R. Soc. B280, 160 (1977).
 Shackleton, N.J., Hall, M.A., Line, J. & Chang. Nature 306, 319 (1983).
- 14. Bordes, F. L'Anthropologie 63, 154 (1959)
- Vandermeersch, B. Annales de Palcontologie (Vertebrev) 51, 69 (1965).
- Stringer, C.B., Hublin, J.J. & Vandermeer and Pain The Origins of Modern Humans: a World Survey of the Food Evidence (eds Smith, F.H. & Spencer, F.) SI (Fox. New York, 1984).
- Bordes, F. Bullenn de la Sociéte Prehistorique I ra-aise 52, 426 (1955).

Paul Mellars is in the Department of Archaeology, Downing Street, Cambridge, CB2 3DZ, UK.

Speciation and our own species

SIR-It is dangerous to build a methodological artefact into dogma. Students of the modern biota are constrained to study those phenomena which are amenable to their methods. Allopatric speciation and other processes of phyletic branching can be studied using modern organisms. Speciation without branching (phyletic speciation) perhaps cannot, so it is sometimes denied1

There is some positive evidence that the transformation of Homo erectus into Homo sapiens was both more or less gradual² and occurred in different parts of the world¹⁵. The latter conclusion has been, and remains, especially common to students of East Asian and Australasian fossils. This evidence cannot simply be ignored with impunity. The phenomenon has been proposed for some other mammals also (refs 6-8 and M. Freudenthal, personal communication).

As discussed in more detail elsewhere 4.9. geographically extended phyletic speciation is a single process, not a matter of independent origin in different places in the manner of some polyploid species. The frequency of occurrence of such phyletic speciation remains controversial, but the mechanism itself consists entirely of a combination of generally accepted processes. These are, first, temporal continuity of regionally adaptive features; second, persisting gene flow from region to region; third, a single potential origin for each generally adaptive feature; and fourth, the spread of generally adaptive features by dispersal and natural selection within pre-existing regional populations elsewhere. The possibility of more than one place of partial or even complete origin is plausible for polygenic characters but it is unnecessary because of development or genetic interactions. 'Hitchhiking' and the like can partly homogenize neutral alleles and other DNA geographically. There is no more reproductive isolation at any one time than within normal species today. The above process is called speciation because it creates an entity which is adaptively (and in other respects) as distinct from its ancestor as are the species we see around us from their close contemporaneous relatives. Such differences are how paleontologists recognize allochronic species. If a later population could travel in time back to an earlier one, it might find itself reproductively isolated, but since this is both untestable and without causal effect, it is irrelevant to the pheromone. There is no implication as to how rapidly phyletic speciation may occur.

But one should not ignore the molecular evidence either, which points to differences of frequencies of variants among populations and even some qualitative

differences. These are used to construct distance matrices and phylogenetic trees, not all of which agree" even apart from the usual and (at this scale) unjustified11-13 assumption of equality of rates of change. However, in the absence of locally temporal calibration (with associated error of estimate), we really have no idea when the branchings occurred. Perhaps they really are different for different genetic elements; under selection, genomes need not disperse even approximately together. They may have occurred before the origin of H. sapiens14, in part during it, afterwards, or all three.

The suggestion 1,15 of a bottleneck in population size will be more convincing if enough genetic elements unrelated both functionally and chromosomally can be found to provide positive evidence. A bottleneck is now merely a plausible alternative; processes like meiotic drive and individual selection can mimic its results in particular cases, and different genetic elements now suggest different scenarios.

LEIGH M. VAN VALEN

Biology Department (Whitman), University of Chicago, 915 East 57th Street, Chicago, Illinois 60637, USA

- 1. Jones, J.S. & Rouhani, S. Nature 319, 449-450 (1986).
- Wolpoff, M.H. Paleobiology 10, 389 -406 (1985).
 Wu, R. & Dong, X. in Palaeounthropology and Palaeolithic Archaeology in the People's Republic of China (eds. Wu R. & Olsen, J.W.) 79-89 (Academic, Orlando, 1985).
 4. Wolpoff, M.H., Wu, X.Z. & Thorne, A.G. in *The Ori-*
- gins of Modern Humans (eds Smith, F.H. & Spencer, F.) 411-483 (Liss New York 1984).
- Smith, F.H. Z. Morph. Anthro. 75, 197 222 (1985).
- Martin, R.A. Science 167, 1504-1506 (1970). Martin, R.A. Evol. Monogr. 2, 1-36 (1979).
- Heintz, É.Bull. Soc. géol. Fr. 16 (7), 411-417 (1974).
 Van Valen, L.M. Perspect. biol. Med. 9, 377-383 (1966).
- Wainscoat, J.S. et al. Nature 319, 491-493 (1986).
 Gillespie, J. H. Proc. natn. Acad. Sci. U.S.A. 81, 8009-
- 8013 (1984). 12. Van Valen, L.M. J. molec. Evol. 3, 89–101 (1974).
- Johnson, M.J., Wallace, D.C., Ferris, S.D., Rattazzi, M.C. & Cavalli-Sforza, L.L. J. molec. Evol. 19, 255–271
- 14. Cann. R.L. Brown, W.M. & Wilson, A.C. Genetics 106. 479-499. (1984).
- Brown, W.M. Proc. nam. Acad. Sci. U.S.A. 77, 3605–3609 (1980).

The origins of chloroplasts in eukaryotes

SIR—While I agree with most of A.E. Walsby's News and Views comment on the significance of the discovery by Burger-Wiersma et al.2 of a filamentous prochlorophyte, I must take issue with his statement that the pairing or stacking of thylakoids (chlorophyll-bearing membranes) ". . . may be a quasi-mechanical consequence of the presence of chlorophyll b and the absence of phycobilisome structures . . . " and "may not therefore be of any phylogenetic significance". This neglects a fundamental difference in the organization of photosynthesis between cyanobacteria (and eukaryotic red algae) on one hand and prochlorophytes and green eukaryotes on the other.

In cyanobacteria the thylakoid membranes are laterally homogenous; both photosystem II (which seems to be specifically associated with the phycobilisomes) and photosystem I are distributed across the whole membrane. In green eukaryotes there is a segregation of function; photosystem II is largely or entirely concentrated in appressed membrane regions, while photosystem I is predominantly located in single membranes. Freezefracture electron microscopy shows that Prochloron thylakoids are laterally heterogeneous, with a very similar pattern of intramembrane protein particles to that seen in green algae and higher plants34. There is no a priori reason why either the presence of chlorophyll b or the absence of phycobilisomes would lead to this segregation and membrane specialization; the phylogenetic significance lies in the fact that Prochloron both has the same chlorophylls as higher plants and organizes its photosynthesis in the same way. It is conceivable that chlorophyll b could have arisen more than once, but hard to imagine that each time it would have been accompanied by the same major restructuring of the photosystem organization in the membrane.

Prochloron resembles the green chloroplast in another feature, the dispersed arrangement of its DNA5; cyanobacteria almost always have their DNA in a central nucleoid⁶. Burger-Wiersma et al.² report that their organism has a central nucleoid like that of cvanobacteria and unlike other prochlorophytes. They do not mention whether or not the thylakoids are stacked, and their published micrographs do not establish this clearly. Further electron microscopy to settle this point and freezefracture studies to establish whether or not the membranes are laterally heterogeneous are the next steps towards understanding the position occupied by Prochloron in the evolution of photosynthesis.

GUY COX

Electron Microscope Unit, University of Sydney, NSW 2006, Australia

- Walsby, A.E. Nature 320, 212 (1986).
- Burger-Wiersma, T. et al. Nature 320, 262 (1986). Giddings, T.H. Withers, N. & Staehelin, L.A. Proc. natu.
- Acad. Sci. U.S.A. 77, 352 (1980). Cox, G.C. & Dwarte, D.M. New Phytol. 88, 427 (1981).
- Coleman, A.W. & Lewin, R.A. *Phycologia* 22, 209 (1983).
 Coleman, A.W. *J. Phycol.* 21, 371 (1985).

Scientific Correspondence

Scientific Correspondence is intended to provide a forum in which readers may raise points of a scientific character. They need not arise out of anything published in Nature, but those that do should not be highly technical comments on Articles or Letters (where the Matters Arising section remains appropriate). П

Model of reduction

Philip Kitcher

Neurophilosophy: Toward a Unified Science of the Mind-Brain. By Patricia Smith Churchland. MIT Press: 1986. Pp.546. \$27.50, £27.50.

THE scholarly reading population divides naturally into two types. There are absorbers, people who like to be informed and who delight in the lucid presentation of unfamiliar ideas, facts and theories. Arguers, by contrast, like to fill the margins of their best-loved books with questions and comments (usually prefaced by "Yes but ...") and they prize ingenious defences of controversial theses. Patricia Churchland's new book should appeal to readers of both types.

Neurophilosophy offers an illuminating survey of contemporary neuroscience, and a review of recent developments in the philosophy of science and the philosophy of mind, which lead Churchland to a distinctive philosophical position and to a series of suggestions about how scientists and philosophers together might develop large explanatory theories of brain functioning. A leading theme of the entire book is that, in Quine's famous phrase, "there is no first philosophy". Philosophical reflection about the nature and function of minds must be informed and may be transformed - by the findings of the sciences. Conversely, philosophical synthesis of the ideas of various disciplines can prove profitable to the working scientist, to the neuroscientist as well as the psychologist, by removing conceptual blinkers and opening up new vistas for research. Churchland's philosophical naturalism may be anathema to those whose livelihood depends on keeping

"Churchland writes with the authority of an insider; one who has spent nearly a decade not only in polite conversation with neuroscientists but also with her hands in the brain."

philosophy pure, but it harmonizes beautifully with the efforts of other contemporary philosophers who have begun (or continued) a dialogue with one or another of the sciences. Moreover, *Neurophilosophy* provides an admirable illustration of how fruitful the exchange may be.

The first 235 pages present the main achievements of neuroscience past and present. Churchland writes with the authority of an insider, one who has spent nearly a decade not only in polite conversation with neuroscientists but also with her hands in the brain. She also understands clearly the predicament of the out-

sider, the curious absorber who can't tell the hypothalamus from the hippocampus. The result is a brilliant piece of exposition that should be read by anyone who is interested in what we currently know of the brain and its workings but who does not have the time to invest in a degree course in neuroscience. In my own experience, attempts to explain to non-professionals the intricacies of neuroanatomy and neurophysiology typically pile detail upon detail, technical term upon technical term, until the bewildered reader is lost in the mossy fibres. Churchland's account proves entertaining instead of soporific. partly because of her lively style, partly through the telling use of illustrations, but chiefly because of her organization of the material. What might have been a catalogue of cell types, neurotransmitters and brain areas becomes an exciting travel guide, in which we are informed both about the history of the discoveries concerned and about the nature (and limitations) of methods for acquiring information about the brain.

In the second part of her book, Churchland turns her attention to the philosophy of science and the philosophy of mind. She begins with an overview of twentiethcentury philosophy of science, in which she outlines the principal themes of logical empiricism and chronicles its death (or transfiguration?) under the impact of the ideas of Kuhn and Feyerabend. Her discussion sets the stage for a more intensive examination of the concept of "intertheoretic reduction". Churchland provides a model of reduction according to which theories are viewed as sets of sentences and reduction consists in the deduction of analogues of the statements of one theory (the reduced theory) from the principles of the other (the reducing theory).

The concept of reduction is important to Churchland because she sees the issue of the reducibility of psychology to neuroscience as the question in the philosophy of mind. Furthermore, to anticipate a little, finding an appropriate answer to this question and integrating it with our current neuroscientific knowledge might produce, as Churchland contends in the final chapter of her book, both improvements within neuroscience and a transformation of philosophy. The fundamental issue is approached carefully. After a penetrating discussion of varieties of mind-brain dualism - which will, I hope, diminish the fascination that some neuroscientists find in these hopeless doctrines — Churchland focuses on what she sees as the most sophisticated antireductionist position, the thesis that psychological states are functional states (that is, states that occupy a particular functional role in the life of an organism) which have extremely heterogeneous neurological realizations. Her critique of this position is integral to her development of her own views about psycho-physical reduction.

The kernel of Churchland's intricate and wide-ranging argument runs as follows. We should not expect neat reductions that provide simple and uniform identifications of the entities and properties discussed by the reduced theory using language from the reducing theory, and that derive "corrected versions" of the principles of the reduced theory which introduce only minor corrections. For such neat reductions are not to be found among the philosopher's paradigm cases from physics, let alone in the example, which Churchland takes to be more pertinent, of genetics. Moreover, even if the distinctions drawn by psychology should cut

"How can we make sense of mental activities without employing the ideas of folk psychology and assuming that thought involves the manipulation of symbols?"

across the divisions of neuroscience, this does not signify that psychology will persist as an autonomous science remaining irreducible to neuroscience. Rather, we ought to expect psychology and neuroscience to coevolve, so that their categories come to mesh with one another. Although this may demand the sacrifice of some everyday psychological notions, Churchland contends that folk psychology roughly that body of lore that we bring to the understanding and prediction of the behaviour of others — is in trouble anyway, and, in this connection, she cites the recent work of Stephen Stich and Daniel Dennett. If I interpret her correctly, the argument is clinched by appeal to the unity of science. Functionalists who flaunt the irreducibility of psychology are to be hoist with their own petard. Unity of scince demands that the barriers to reduction must be removed, and psychology (or neuroscience) must amend itself to suit.

I am not convinced by this line of reasoning. One source of my resistance lies in the fact that, while she is happy to advocate conceptual reform for psychologists, and though she explicitly considers the possibility that science might lead us to modify our philosophical concepts, that possibility is not taken seriously in the present context. Perhaps Churchland is right in thinking that something like the

question of reducibility of psychology to neuroscience is the fundamental problem in the philosophy of mind. Yet the analogy I draw from the case of genetics is that the philosophical concept of reduction is inadequate to the representation of the relations among many theories (or fields) of science*. To borrow Churchland's own terminology, I think that the concept of reduction may belong to folk metascience.

A second concern about her argument derives from a different way of appealing to the unity of science. One of the leading themes of functionalism is the view that there are generalizations about psychological processes — couched in terms of representation and computation — which apply to systems that are built out of very different materials. Assuming that such generalizations cannot be integrated into neuroscience, the functionalist may reasonably protest against their sacrifice on the altar of the unity of science on the grounds that they already contribute to a unified science by linking together the study of different forms of intelligence both artificial and natural. Churchland's apparently clinching argument thus seems to presuppose a particular view of how an ideally unified science must be organized, a view on which neuroscience stands as the neighbouring discipline to psychology. Functionalists who believe in unified science should adopt a different picture of its structure, and they may accuse Churchland of extracting more from a methodological principle than it can fairly

These reservations do not detract from the achievement of the second part of Neurophilosophy. Whether or not one agrees with her, Churchland has performed a great service for philosophers, psychologists and neuroscientists through her elaboration of the major positions and her clear presentation of arguments. Equally, the long and fascinating chapter that makes up the third and final part of the book, should serve as the starting point for serious interdisciplinary discussions.

We learned in Churchland's review of neuroscience that the various branches of the field are urgently in need of theory. Attention to the philosophy of mind offered the moral that philosophical conceptions, including those that strike us as untutored common sense, may have to be "reconfigured". But what are the prospects for theories in neuroscience? And how can we make sense of mental activities without employing the ideas of folk psychology and assuming that thought involves the manipulation of symbols? Churchland's final chapter outlines some

answers to these questions. She gives a lucid account of some recent research: the tensor network theory of Pellionisz and Llinas (and a related proposal by Paul Churchland), the parallel models of computation developed by Rumelhart and McClelland, and a hypothesis of Crick's about the neurobiology of attention. In each case, there appears to be an exciting symbiosis between naturalistic philosophy and theoretical neuroscience, with the liberation from conceptual chains leading to new prospects for developing theory.

Tensor network theory receives the most extended treatment. The core of the Pellionisz-Llinas proposal is that synaptic connections in the cerebellum can be viewed as an array for performing matrix multiplication. So, to simplify enormously, sensorimotor coordination might be achieved by means of the registering of information on a sensory map in the brain, the "computation" in the cerebellum of an appropriate vector in a motor map, and, as the result of the stimulation of the right region of the motor map, the activation of the proper muscles. The proposal is especially stimulating because the 'computation" does not involve manipulation of symbols. Algebra gives way to geometry. Churchland offers a succinct summary:

What is needed is a way to conceive of what nonsentential representing might be, and the tensor network theory provides that much, even if, in the end, it turns out not to be right [p.452].

Functionalists will be quick to protest that managing without symbol manipulation in the case of sensorimotor coordination is one thing, doing the same in the case of language learning quite another. Neuroscience can cope with the more mundane operations of the brain, but the higher cognitive functions require a more abstract treatment. Taken as a cautionary note, this is perfectly correct, but the point should not be overinterpreted. The work Churchland describes is extremely tantalizing, for neuroscience, for psychology and for philosophy. We do well to recognize exactly how far we have gone, but not to make unwarranted judgments about how far we may go.

Churchland is plainly optimistic, and her optimism may ultimately prove unjustified. But, whatever the outcome of the trends in theoretical neuroscience that she favours, the value of her book is independent of its more speculative claims and its more controversial arguments. While reading it, I was reminded of the comments of numerous friends, who mourn the good old days --- days when there were far fewer academic books, when books were read by several generations of graduate students, when the brief bright ideas emerged on journal pages but not in the more enduring medium of hard covers. Such people should be happy with Churchland, for she has given them a book of the old-fashioned sort, one that deserves to be read and pondered by philosophers, psychologists and neuroscientists for a good long time.

Philip Kitcher is Director of the Minnesota Center for the Philosophy of Science, 315 Ford Hall, 224 Church Street SE, Minneapolis, Minnesota 55455, USA. His most recent book is Vaulting Ambition: Sociobiology and the Quest for Human Nature (MIT Press, 1985).

Revival in optics

O.S. Heavens

Optical Interferometry. By P. Hariharan. *Academic: 1986. Pp.303.* \$58, £49.50.

OPTICS — until recently perhaps regarded as satisfactorily completed and with little more to be expected — has experienced a resurgence of interest since the arrival of the laser, a tool of almost infinite sharpness compared with the light sources previously available. The laser has not only made many traditional optical techniques more convenient, but has made possible methods such as holography which were hitherto practically impossible.

An account of optical interferometry can thus be expected to contain some new excitements to complement the more traditional material. In this sense, Hariharan's book is no disappointment: holography, holographic interferometry and speckle inteferometry — all post-laser subjects — are well covered in a mainly

readable fashion. There are some grumbles. The pedagogue tires of explaining to students why the term "phase of a photon" is completely meaningless, but here it is again. There is, too, an uneven quality to the book in that rather basic algebra is spelled out at length while a knowledge of Jones matrices is assumed. Some carelessness in checking the matching of symbols in text and figures has introduced glitches in reading, and many of the line diagrams could have been made clearer by the use of shading.

One instinctively draws a comparison between this book and the classic work of Steel, Interferometry, of which a new edition appeared in 1983 and which is now available in paperback (Cambridge, £12.95, \$24.95). They have much in common, since Steel's updating of the earlier (1967) book was thorough. The better diagrams of Steel's version and freedom from some of the blemishes referred to above, will probably mean that its sales will not suffer.

O.S. Heavens is Profeassor of Physics, University of York, York YO1 5DD, UK.

^{*}For a study of the example of genetics that seeks to develop more sophisticated metascientific concepts, see my article "1953 and All That. A Tale of Two Sciences" (*Philosophical Review* 93, 335-373; 1984)

How does the brain do it?

Stuart Sutherland

Visual Cognition. Edited by Steven Pinker. MIT Press: 1986. Pp.270. Pbk \$17.50, £17.50.

Many years ago, I put forward the following problem. A cross and a circle, horizontally aligned, are flashed onto the retina; regardless of the shapes' absolute positions, the subject has to determine which is on the left. As visual tasks go, it could hardly be simpler: the problem is that we have no idea how the brain does it. A scan from left to right (or vice versa) seems improbable. If, on the other hand, the coordinates of each shape are carried forward, how is this done and how is the comparison between the coordinates made in neural terms?

In the most original and important article in *Visual Cognition*, Shimon Ullman points to a series of similar problems. He asks what mechanism could trace out a closed curve to decide that it is closed and to determine which points lie inside and which outside it. The problem is a more precise version of the figure-ground effect, so beloved by the Gestaltists. Although the question can be stated more rigorously than in their day, we are no nearer a solution, at least in terms of brain mechanisms, for there is no difficulty in writing computer programs to carry out this task.

At the other extreme of vision are complicated problems which still defy computers, but which are solved by the brain by means that remain obscure. Perhaps the most difficult is that of visual recognition. Steven Pinker gives a judicious review of the subject, noting the many difficulties that beset current theories. We have of course moved on: nowadays Gestalt theorizing looks hopelessly vague, and the idea that recognition could be achieved by templates or by feature matching, which was being put forward in all seriousness only 20 years ago, now looks extremely naive. Some of the more recent ideas will probably survive, for example that, for the purposes of recognition, the brain builds an abstract and hierarchical structural description of an object. However, the exact nature of such descriptions, the methods by which they are derived from the retinal image, and how or indeed whether the same description is formed of an object regardless of viewpoint remain entirely open questions.

Half of the papers collected by Pinker are devoted to visual imagery and the ways in which people manipulate it, a subject on which there has recently been much research. There are a limited num-

ber of transformations that can be applied to the image of an object — it can, for example, be made to change size, to rotate or to change position. In all such changes, the imaged object passes through all intermediate points. One cannot suddenly replace an image of an upright letter with that of the same letter tilted through 90°. Steven Kosslyn has constructed an ingenious computer model which incorporates the processes required to manipulate imagery in the way people do. He describes his model and the results of submitting it to a series of tests, in which he uses consistent differences in people's ability to perform the different operations to demonstrate that they really are used by

Such questions as whether the tail of a horse ends above or below its kilees can only be answered by using imagery. But if for the purpose of recognition we construct structural descriptions, it is puzzling that the answer cannot be read off directly from them. Perhaps this relationship is only implicit in the description, making it necessary to generate an image from the structural description and derive the answer from that.

The present volume, originally a special issue of the journal *Cognition*, is useful in so far as it delineates the state of the art in a few branches of vision. It makes it clear that we have advanced mainly by discovering and making precise an increasing number of problems, and that theorizing is more rigorous than ever before. But although the secret of how the brain subserves vision has for some time appeared to be just around the corner, it still remains elusive. How, for instance, does my brain calculate that my typewriter lies to the left of my gin bottle?

Stuart Sutherland is Director of the Centre for Research on Perception and Cognition, University of Sussex, Brighton BNI 9QG, UK.

Morphological eye

Malcolm Irving

Skeletal Muscle. Handbook of Microscopic Anatomy, Vol.2, Part 6. By Henning Schmalbruch. Springer-Verlag: 1985. Pp. 440. DM 580.

THE PREVIOUS edition of this handbook was published in 1956, a time of revolution in muscle research. The idea that contraction involved the relative sliding of two sets of filaments was new, and the first clear electron micrographs of the side-by-side array of interdigitating filaments were still to be published. In the 30 years since then electron microscopes seem to have been focused on every structural feature in muscle, so that we now have a fairly complete picture of its ultrastructure, at

least down to a resolution of about 10nm. Parallel progress with other techniques has in many cases helped to reveal the functional significance of the structural specializations.

This new edition is therefore long overdue and, in attempting to review progress since the last one. Schmalbruch was confronted with an embarrassment of riches. He has reduced his subject to manageable proportions by concentrating on one approach to the study of muscle, which he describes as "muscle seen through the eves of a morphologist". This allows him to treat a wide range of biologically interesting phenomena from a unified viewpoint. The morphological aspects of neuromuscular transmission, contractile proteins and the mechanism of force generation, internal membranes and the regulation of contraction, metabolism and fibre types, development and regeneration are all dealt with in some depth. A wide range of other features, for example connective tissue, vascularization and the organization of motor units, are described more briefly. The emphasis is on mammalian muscle (including a section on non-skeletal striated types, but excluding cardiac muscle), though results from studies on other animals are discussed where they serve as useful experimental models. Pathological states are mentioned in passing but not treated systematically.

Schmalbruch has painstakingly organized and cross-referenced his material. which is also beautifully illustrated by over 200 micrographs and backed up by about 2,000 references. He does not hesitate to pepper the text with quantitative detail where it is available (thus we learn that a 10cm cell from a human biceps contains 3.000 nuclei), or to resort to descriptions of "amorphous densities" or "ill-defined periodic structures" where it is not. Technical issues, such as possible problems in the use of a particular fixative, are discussed where they might affect the interpretation of the literature. The rather empirical "morphologist's eye" approach adopted for most of the book often leaves the reader to draw his or her own conclusions from the data; sometimes, though, as in the section on myogenesis. Schmalbruch allows himself to discuss alternative hypotheses, giving freer rein to the morphologist's brain.

This book is more than an atlas of muscle structure, but less than a complete account of the structural basis of muscle function, and it will probably be of more use to the research worker than to the undergraduate. It should remain a useful reference volume for a long period—it not quite until the publication of the next edition, which at the present rate should appear sometime after the year 2010.

Malcolm Irving is in the Department of Bupphysics, King's College London (KQC), 26 29 Drury Lane, London WC2B 5RL, UK.

Neolithic battles

William H. McNeill

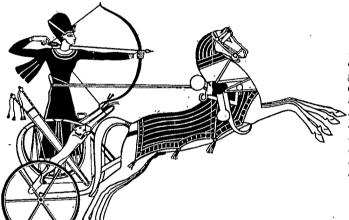
The Origins of War: From the Stone Age to Alexander the Great. By Arther Ferrill. Thames & Hudson: 1985. Pp.240. Hbk £12.50, \$19.95; pbk £5.95, \$10.95.

ARTHER Ferrill is a professor of ancient history at the University of Washington, Seattle, and in this book he advances two general propositions that are likely to surprise most readers, as they did me.

First, he describes a Neolithic "burst of organized warfare" in the Near East which, he argues, was "as important for the area as Alexander's conquest of Persia in the fourth century BC or the march of Islam in the seventh century AD" (pp. 27–28). New weaponry was part of this change: the bow, the sling, the dagger and the mace all start to appear in the archaeo-

the phalanx, which supplanted that form of warfare among the Greeks in the seventh century, were rudimentary indeed. Only in the second half of the fourth century BC, when Greek and Macedonian captains had learned the art of war from prolonged service as allies and mercenaries of the Persians, did Philip and Alexander successfully unite Greek-style heavy infantry with Persian combined arms - skirmishers, light and heavy cavalry, siege trains, a supply system and, not least, generalship capable of using all arms efficiently in mutual support. With that development. Ferrill claims, the art of war reached a plateau where it remained until after 1815. He supports the claim by refighting the battle of Waterloo with Alexander and his army in Napoleon's place, and concludes that the ancients might well have won, assuming some prior acclimatization to the noise of gunfire (pp.220-222).

Obviously, Ferrill's claim of Persian



Ramesses II in his war chariot at the Battle of Kadesh in 1285 BC: his lighter chariots and strategy gave him a tactical advantage against the Hittites. Ramesses' strategy and tactics showed a degree of military sophistication that was not seen in many later historical periods.

logical record between 12000 and 8000 BC. Regular military formations (column and line) made the use of such weapons more effective, and elaborate fortifications had to be built to protect against organized attack—all before settled agriculture had become widespread. Indeed, Ferrill suggests that fixed residence, dictated by the need for protective walls, may have led to the development of fixed agriculture (p.29), without, however, pressing the point as to which came first.

Ferrill's second proposition is that classical Greek warfare was backward and technically deficient compared with the military techniques and command system of the Persian empire. That empire, heir to Bronze Age empires and to the even more impressive Assyrian techniques of waging war, added a navy to combinedarms warfare on land, and could in addition support both branches with an adequate logistical system. By comparison, the Greek style of hurly-burly duelling between aristocratic horsemen (who Ferrill says, dismounted to fight in the eighth century: hence Homer's chariot tactics!) and the unsupported charge of

superiority in the fifth and fourth centuries requires him to explain away Greek victories on the plain of Marathon and at Plataea. His schematized accounts of the battles leave aside all the innumerable contested issues as to what actually happened. If Persian combined arms were so superior, why did they not prevail on these occasions? Ferrill's brief battle narratives simply do not show "that the Persians were defeated by their own mistakes", although he declares that this view "must surely be correct" (p.122).

Throughout, the author uses the style of an essayist, and simply asserts what must often be guesswork. He reaches for novelty of interpretation, and perhaps overreaches himself. But as long as one understands what treacherous ground he traverses, and how controversial most of his assertions are, the book makes good reading; and I, for one, was persuaded that the Neolithic "military revolution" in the Near East was as real and important as Ferrill says it was.

William H. McNeill is a Professor in the Department of History, University of Chicago, 5801 S. Ellis Avenue, Chicago, Illinois 60637, USA.

Good and the bad

John Crothers

The Encyclopaedia of Reptiles and Amphibians. Edited by Tim Halliday and Kraig Adler. The Encyclopaedia of Insects. Edited by Christopher O'Toole. George Allen & Unwin/Facts on File:1986. Both: Pp.152.£15, \$22.50.

THESE are the fifth and sixth volumes in the deservedly successful Unwin Animal Library. Previous titles have dealt with mammals (two volumes), birds and underwater life. The features uniting all these works are a systematic format, authoritative, concise text, and superb illustrations; all are beautifully produced and are a pleasure to read.

The Encyclopaedia of Reptiles and Amphibians must be the best book on herpetology currently available to the general reader - and there can be few professional zoologists working in related fields who will not welcome it onto their shelves. The extraordinary collection of colour photographs is augmented with quite excellent paintings. But, unlike many beautiful books, the text would stand on its own. It is arranged ordinally, with a small box at the beginning of each section describing the main features of the order (or sub-order) concerned — the number of species, their distribution, habitats, size, colour, reproduction and longevity. There are also separate sections on parthenogenesis, shedding of lizard tails and so on.

I was initially surprised to find no mention—in the systematic part—of the influence of temperature on sex determination in crocodilians, but the topic is discussed earlier in the general introduction to reptiles. Unlike *The Encyclopaedia of Mammals*, this volume does not include an appendix listing species, genera and families, and giving both the scientific and colloquial names. But that is just about my only criticism.

By comparison, the volume on insects is disappointing. The title is misleading, as the work seeks to cover most of the terrestrial arthropods, and for some reason it has been decided that all these invertebrates only justify 143 pages of text (the same as amphibians and reptiles), against 895 for the mammals. The 9,000 species of reptiles and amphibians have an entire book to themselves but the 11,500 species of millipedes, centipedes and their allies are covered in just four pages of this one. Even the 300,000 known species of Coleoptera (beetles) are given only twelve. The result, inevitably, is a very much more superficial account.

John Crothers is Warden of The Leonard Wills Field Centre, Nettlecombe Court, Williton, Taunton, Somerset TA44HT, UK.

Kelvin on an old, celebrated hypothesis

from Edward Harrison

Lord Kelvin in 1901 tested an "old and celebrated hypothesis" that if we could see far enough into space the whole sky would be occupied with stellar disks all of perhaps the same brightness as the Sun. Kelvin was the first to solve quantitatively and correctly the riddle of a dark night sky, a riddle that had been previously solved qualitatively by Edgar Allan Poe, and is now known as Olbers' paradox.

IN a paper¹ published in 1901, Lord Kelvin discussed various astronomical topics, such as the size and mass of the Galaxy, the velocities of stars, and the dark night-sky riddle. Kelvin's treatment of the riddle of darkness at night is of considerable scientific and historical interest; for the first time in the context of a static universe he solved the riddle quantitatively and correctly. This paper was reproduced in 1904 as the revised Lecture XVI in the Baltimore Lectures2. The omission of this paper from Kelvin's Mathematical and Physical Papers3 and from the complete bibliography of his works in Silvanus Thompson's Life of William Thomson4 may account for its neglect in numerous subsequent discussions of the so-called Olbers' paradox⁵⁻⁷.

The riddle of a dark starlit sky can be traced back to Thomas Digges in 1576 and Johannes Kepler in 1610⁸. The modern expression 'Olbers' paradox' gained popularity in ignorance of these contributions, and of those made by Otto von Guericke⁹ in 1672, Edmund Halley¹⁰ in 1721, Jean-Philippe Loys de Chéseaux¹¹ in 1744, and many others, all of which preceded the work by Wilhelm Olbers in 1823¹².

The riddle is easily stated in the form proposed by Olbers. Plausibly, space is unbounded and stars are scattered throughout space; a line of sight extended in any direction ultimately intercepts the surface of a star. Every point of the sky must blaze with starlight with no dark gaps between the stars. If most stars are like the Sun, the sky at every point must be as bright as the Sun's disk. The sky subtends a solid angle 180,000 times that of the Sun, so the starlit sky should be 180,000 times brighter than the Sun. But the sky at night is dark—hence the riddle.

Kelvin's analysis

The following parallels the analysis given by Kelvin. We assume for computational convenience that all stars are Sun-like, of radius a, and uniformly distributed. Let n be their number per unit volume. Then the number in a shell of radius q and thickness dq is $4\pi nq^2dq$. This number multiplied by $a^2/4q^2$ represents the fraction of the whole sky covered by stars viewed by an observer at the centre. To include geometric overlap of stellar disks, neglected by Kelvin, we

multiply by $\exp(-q/\lambda)$, where $\lambda = (\pi na^2)^{-1}$ is the mean free path of a light ray. Hence the fraction of the sky covered by stars in the shell is $\exp(-q/\lambda) dq/\lambda$. By integrating from q = 0 to q = r we obtain

$$\alpha = 1 - e^{-r/\lambda} \tag{1}$$

where α denotes the fraction of the sky covered by stellar disks out to radius r. In a distribution of stars of infinite extent the entire sky is covered $(\alpha = 1)$ and the average distance seen from any position is the background limit λ . We arrive at Kelvin's result (his equation (10)) when the radius r of the distribution of stars is small compared with the background limit, so that

$$\alpha \simeq \frac{r}{\lambda} = \frac{3N}{4} \left(\frac{a}{r}\right)^2 \tag{2}$$

where $N = 4\pi r^3/3$ is the total number of stars. This treatment by Kelvin elucidates that previously given by Halley, Chéseaux and Olbers.

Let each star have luminosity L. The contribution to the radiation density u at the centre from the stars in a shell is $(nL/c)e^{-q/\lambda}dq$, where c is the speed of light. By integrating as before we find

$$u = u^*(1 - e^{-r/\lambda})$$
 (3)

where $u^* = L/\pi a^2 c$ is the radiation density at the surface of a star¹³. Hence $u = u^*$ in any distribution of stars extending much beyond the background limit.

From equations (1) and (3) we obtain

$$\alpha = u/u^* \tag{4}$$

thus demonstrating the truth of Kelvin's remark that " α is the ratio of the apparent brightness of our star-lit sky to the brightness of our Sun's disc." In many recent discussions of the riddle this significant relation has received scant recognition.

Solutions

With his model of the Galaxy, consisting of a sphere of radius 10^3 pc (1 pc = 3.26 light-yr) containing 10^9 Sun-like stars, Kelvin found $\alpha = 4 \times 10^{-13}$, and said, "This exceedingly small ratio will help us to test an old and celebrated hypothesis that if we could see far enough into space the whole sky would be seen occupied with discs of stars all of perhaps the same

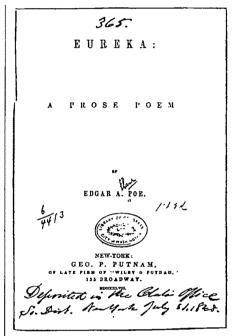


Fig. 1 The title page of Edgar Allan Poe's Eureka, published in June 1848, dedicated to Alexander von Humboldt, and based on a two-hour lecture, "The cosmogony of the universe". delivered at the Society Library, New York, in February 1848 while the Rev. Dr John Pringle Nichol, regius professor of astronomy at the University of Glasgow, was also lecturing in New York.

brightness as our own Sun."

We require, said Kelvin, a "great sphere" of stars, of radius λ ($\approx 10^{14}$ pc), to cover the sky with stellar disks. But starlight travelling from the outlying stars of such a great sphere takes 3×10^{14} yr to reach us. Using the theory that stars derive their energy by gravitational contraction, he said, we know that 108 yr is an upper limit for a stellar luminous lifetime. "Hence, if all the stars through our vast sphere commenced shining at the same time...at no one instant would light be reaching the Earth from more than an excessively small proportion of all the stars." In this remarkable argument Kelvin showed that the transit time of light from the background limit greatly exceeds the luminous lifetime of stars. If all stars began to shine at the same instant, we see light only from stars in the foreground, not from those in the distant background.

Relativity theory had yet to stress the

universality of $E = mc^2$, which provides a true maximum luminous lifetime $M_{\odot}c^2/L_{\odot}$ of $\sim 10^{13}$ yr for the Sun. This extreme value is still less than Kelvin's limit of 3×10^{14} yr and could not have altered his conclusion. It was not evident in Kelvin's day that the universe contains insufficient energy to create a bright starlit sky¹⁴. We now know that the conversion of all mass in the universe into thermal radiation would attain at most a temperature of 20 K, much less than the Sun's surface temperature of 6,000 K.

We may re-write equation (3) in the

$$u = u^*(1 - e^{-t/\tau}) \tag{5}$$

where t = r/c is the transit time of light from stars at distance r, and $\tau = \lambda/c$ is the transit time from the background limit. When α is small,

$$\alpha = u/u^* = t/\tau \tag{6}$$

thus confirming Kelvin's conclusion that the sky is dark because the transit time τ from the background limit greatly exceeds the maximum value of t equal to the stellar luminous lifetime. Equation (5) can be derived thermodynamically by considering the radiation density in a cavity containing luminous sources; t is then the timespan during which the sources emit radiation and τ the characteristic time required to fill the cavity with radiation in equilibrium with the sources14.

Edgar Allan Poe was perhaps the first to give a correct qualitative solution to the riddle of darkness. In 1845 he wrote¹⁵,

Look down into the abysmal distances!attempt to force the gaze down the multitudinous vistas of the stars, as we sweep slowly through them thus-and thus-and thus! Even the spiritual vision, is it not at all points arrested by the continuous golden walls of the universe?-the walls of the myriads of the shining bodies that mere number has appeared to blend into unity?

Three years later, in his masterpiece Eureka¹⁵, he formulated his most radical cosmological ideas. Concerning the riddle of darkness, he said,

Were the succession of stars endless, then the background of the sky would present us an uniform luminosity, like that displayed by the Galaxy-since there could be absolutely no point, in all that background, at which would not exist a star. The only mode, therefore, in which, under such a state of affairs, we could comprehend the voids which our telescopes find in innumerable directions, would be by supposing the distance of the invisible background so immense that no ray from it has yet been able to reach us at all.

A few lines he wrote, "I myself feel impelled to the fancy-without daring to call it more—that there does exist a limitless succession of Universes, more or less similar to that of which we have cognizance." By "Universes" he meant the

BALTIMORE LECTURES

MOLECULAR DYNAMICS AND

THE WAVE THEORY OF LIGHT

FOUNDED ON MR A. S. HATHAWAY'S STENOGRAPHIC REPORT OF TWENTY LECTURES DELIVERED IN JOHNS HOPKINS UNIVERSITY, DALTIMORE, IN OCTOBER 1884: FOLLOWED BY TWELVE APPENDICES ON ALLIED SUBJECTS

LORD KELVIN, O.M., G.C.V.O., P.C., F.R.S., &c.

PROPERTY OF THE ROLL, MODERN OF FOLKBOOK, PROPESSOR OF TATERNA COLLEGE, CAMBRIDGE, PROPESSOR OF TATERNA PHILOSOPHY OF THE UNIVERSITY OF

LONDON: C. J. CLAY AND SONS. CAMBRIDGE UNIVERSITY PRESS WAREHOUSE, AVE MARIA LANE. Stanob: 30. WRILINGTON STREET.

HALTIMORE:

PUBLICATION AGENCY OF THE JOHNS HOPKINS UNIVERSITY. 1904

Fig. 2 Title page of the Baltimore Lectures, published in 1904. Kelvin's solution of the riddle of darkness is given in Lecture XVI, pages 260-278. The solution does not appear in the original lecture notes of 1884, and was first published in 1901 in the Philsophical Magazine in a paper entitled "On ether and gravitational matter through infinite space".

Galaxy and other galaxies. The finite speed of light and the age of the starlit universe had come together in Poe's fertile mind, shedding new light on an old hypothesis.

Comments

Despite the widespread interest in Olbers' paradox in recent years, little attention has been paid to the pertinent comments in the nineteenth century by William Herschel, Olbers, Nichol, Poe, Thomas Dick, Friedrich Struve, Alexander von Humboldt, John Herschel, Richard Proctor, Hugo von Seeliger, Ellard Gore, Lord Kelvin and others^{6,9}

John Pringle Nichol, who introduced the word 'evolution' into astronomy and was regius professor of astronomy at Glasgow University from 1836 to 1859, greatly inspired both Kelvin and Poe. Kelvin acknowledged his debt when recalling his student days17,18. Much of Poe's knowledge of contemporary developments in astronomy came from Nichol's influential Views of the Architecture of the Heavens 19,20, to which he made reference in Eureka. Nichol's astronomy lectures stressed the importance of the transit time of light.

Kelvin pointed out that the supposition of uniform density is arbitrary, and "we ought in the greater sphere to assume the density much smaller than in the smaller sphere." Allowing for the reduced density of stars in the universe because of the wide separation between galaxies, the background limit of Poe's golden walls recedes to 10²³ light-yr. With a typical steller luminous lifetime of 1010 yr we see that the fractional coverage $\alpha = 10^{-13}$ departs little from Kelvin's value.

According to Kelvin the sky at night is dark because the radius of the starlit visible universe, equal to the time stars have been luminous multiplied by the speed of light, is small compared with the background limit, where the background limit is the distance to which stars must extend in order to cover the entire sky. Starlight emitted beyond the visible universe has yet to reach us. Kelvin thus solved the riddle in its original cosmological framework: a static universe of uniformly scattered, Sun-like stars. All variants of this primitive standard model seeking to solve the riddle by appeal to absorption, hierarchy, expansion or fatigued light merely achieve a state of greater darkness in a universe already dark.

Bondi⁵ resurrected the riddle within the context of the steady-state theory. Continually created stars shine unceasingly, according to this theory, and expansion maintains starlight at a constant level. Expansion is necessary (but not sufficient) for darkness, and Kelvin's solution fails in the steady-state model because of its non-conservation of energy.

More than once Kelvin said, "paradoxes have no place in science"21. He took the rationalist view that paradoxes lie in ourselves and not the external world. It is historically ironic that he was the first to solve quantitatively with utmost lucidity a riddle that later, when his work lay forgotten, became known as Olbers' paradox.

Edward Harrison is at the Department of Physics and Astronomy, University of Massachusetts, Amherst, Massachusetts 01003, USA.

- 1. Thomson, W. Phil. Mag. Ser. 6, 2, 161-177 (1901).
- Thomson, W. Phil. Mag. Ser. 6, 2, 161-177 (1901).
 Thomson, W. Baltimore Lectures on Molecular Dynamics and the Wave Theory of Light (Cambridge University Press, Clay & Sons, London, 1904).
 Thomson, W. Mathematical and Physical Papers (Cambridge University Press, 1882-1911).
- 4. Thompson, S. P. The Life of William Tomson, Baron Kelvin of Largs (Macmillan, Londo , 1910).
- Bondi, H. Cosmology (Cambridge University Press, 1952). Jaki, S. L. The Paradox of Olbers' Paradox (Herder, New York, 1969).
- 7. Harrison, E. R. Cosmology: The Science of the Universe (Cambridge University Press, New York, 1981).

 8. Harrison, E. R. Science 226, 941-945 (1984).
- Harrison, E. R. Darknesss at Night: The History of a Riddle
- (Harvard University Press, in the press).
 10. Halley, E. Phil. Trans. R. Soc. 31, 22-24; 24-26 (1720-21), 11. Loys de Chéseaux, J. P. Traité de la Comète, 223-229 (M. M. Boușequet, Lausanne, 1744).
- Olbers, H. W. in Astronomisches Jahrbuch für das Jahr 1826 (ed. Bode, J. E.) 110-121 (C. F. E. Späthen, Berlin, 1823);
- Edin. New Philos. J. 1, 141-150 (1826). 13. Harrison, E. R. Physics Today 27, 69-74 (1974).
- Harrison, E. R. Nature 204, 271-272 (1964).
 Poe, E. A. in The Science Fiction of Edgar Allan Poe (ed.
- Beaver, H.) 171-174 (Penguin, Harmondsworth, 1976). 16. Poe, E. A. Eureka: A Prose Poem (Putnam, New York, 1848); reproduced in The Science Fiction of Edgar Allan Poe (cd. Beaver, H.) 205-309 (Penguin, Harmondsworth,
- 17. Thomson, W. Nature 68, 623-624 (1903).
- Thompson, S. P. The Life of William Thomson, Baron Kelvin of Largs, Ch. 1 (Macmillan, London, 1910).
- onner, F. W. in All These to Teach (eds Bryan, R. A. et al. (University of Florida Press, Gainsville, 1965).
- Nichol, J. P. Views of the Architecture of the Heavens (Dayton & Newton, New York, 1842). 21. Thompson, S. P. The Life of William Thomson,

of Largs, 1125 (Macmillan, London, 1910).

The long and the short of long-term memory—a molecular framework

Philip Goelet, Vincent F. Castellucci, Samuel Schacher & Eric R. Kandel

Howard Hughes Medical Institute, Center for Neurobiology and Behavior, Columbia University College of Physicians and Surgeons, and New York State Psychiatric Institute, New York, New York 10032, USA

A single learning event initiates several memory processes with different time courses of retention. While short term memory involves covalent modification of pre-existing proteins, the finding that long-term memory requires the expression, during learning, of additional genes, makes it possible to analyse in molecular terms the induction and retention of long-term memory.

ANIMALS acquire new information about the world through mechanisms of learning, and retain that information through mechanisms of memory. Clinical and experimental observations indicate that memory is not a unitary process but is thought to have at least two forms, each of which subserves a family of time courses: a short-term form that can last seconds, minutes and hours, and a long-term form lasting days, weeks or years¹⁻⁵. To understand the mechanisms of the major forms of memory, it will be necessary to describe, in cellular and molecular terms, the inductive mechanisms used in the acquisition of information for each form of memory and the various molecular time-keeping steps involved in retaining the resulting memories.

Studies in certain invertebrates (Aplysia, Hermissenda and Drosophila) have shown that the acquisition and retention of information for short-term memory lasting minutes to hours does not require the synthesis of new proteins. Rather, it depends on second messenger-mediated covalent modifications of previously synthesized proteins that modulate the properties of nerve cells and their synaptic connections⁶⁻¹³. Acquisition involves the activation, by neurotransmitters, of receptor-linked enzymes responsible for the synthesis of intracellular messages. These second messengers activate protein kinases that phosphorylate substrate proteins required for the plastic neuronal modifications (Fig. 1, pathway 1). Retention of these plastic changes depends on the duration of the covalent modification of the substrate proteins and the maintained activity of the enzymes responsible for second-messenger synthesis.

Covalent modifications of the sort used in short-term memory have been proposed to become self-reinforcing for certain instances of long-term memory¹⁴⁻¹⁸. However, a variety of studies now indicate that during the acquisition of information whose memory lasts more than 1 day, specific nerve cells need to express genes that are not needed for short-term memory^{5,19-21}. These studies lead us to outline a specific molecular framework for the various time courses of long-term memory. We think it likely that the same modulatory neurotransmitters that act on the cell surface to induce cytoplasmic messengers during learning are not only important for short-term memory, but also lead, through either the same or additional second-messenger systems. to the activation of at least three other overlapping memory processes, each with its own time course of retention (Fig. 1, pathways 2, 3 and 4): (i) A self-reinforcing covalent modification of proteins, encoding for memory lasting many hours. (ii) A transient activation of effector genes for memory lasting more than 1 day, where the time course of memory retention is simply determined by the half-lives of the induced messenger RNAs and proteins. (iii) The induction of a gene sequence for memory lasting weeks or months, in which early regulatory genes lead to maintained alterations in the expression of late, effector genes. Here, the molecular time-keeping step for memory retention is in the maintenance of an altered mRNA transcription or processing state, much as it is in cellular differentiation.

Time window

Whereas short-term memory does not require the synthesis of new proteins⁶, behavioural studies of learning in vertebrates suggest that memory lasting days or weeks can be disrupted by the inhibition of protein synthesis^{5,19,22,23}. Particularly important for the arguments we develop below is the finding that long-term memory is most sensitive to disruption during and immediately after training. Vertebrates experience no deficit in long-term memory if exposure to the protein synthesis inhibitor is delayed by as little as 1 h after training ^{5,19,23}.

This time window for protein synthesis has been found in both lower vertebrates and mammals, and for learning processes that range in complexity from non-associative forms, such as sensitization, to associative forms, such as classical and instrumental conditioning. Although comparable data are lacking in humans, there is the interesting and analogous clinical observation that long-term memory for an experience is particularly susceptible to disruption by convulsions or trauma during and briefly after the experience. Because these findings were based on alterations in behaviour, the studies failed to answer the question of whether this sensitivity to disruption by protein synthesis inhibitors is a systems property of motivation, motor performance or some other complex brain system, or whether it actually reflects a fundamental property of long-term information storage in specific nerve cells of the circuit responsible for the modified behaviour.

This question has now been answered in invertebrates where the neuronal circuitry underlying behaviour and learning is better understood. Studies on long-term sensitization of the gill-withdrawal reflex in Aplysia demonstrate that the elementary synaptic connection between sensory and motor neurones, which is enhanced during short-term sensitization, is also enhanced during long-term sensitization²⁴. Examination of this connection in dissociated cell culture has shown that a single application of a facilitating transmitter enhances synaptic transmission for minutes, whereas four or more repeated applications lead to long-term facilitation lasting for over 24 h (ref. 20). In contrast to short-term facilitation at this synapse, the long-term facilitation associated with the memory of long-term sensitization is blocked by both translational and transcriptional inhibitors. As in vertebrates, transient blockage of protein synthesis in Aplysia during a 2-h training period is sufficient to block the retention of long-term facilitation assayed 1 day later (refs 20, 21, and V.F.C. et al., in preparation). Similarly, inhibition of both protein and mRNA synthesis after training has little effect on long-term memory assayed 1 day later.

These findings indicate that a critical and general feature of long-term memory characteristic of many forms of learning in vertebrates and perhaps also in human beings-a narrow time window during which new proteins must be synthesizedreflects a fundamental property in the storage of information by specific neurones and their connections. As a result, the findings lead to three specific molecular conclusions: (1) that the same extracellular signal (the same neurotransmitter) that initiates short-term memory also initiates long-term memory; (2) by contrast, there are genes and proteins necessary for the cellular mechanisms underlying long-term memory that are not required for the mechanisms of short-term memory; (3) whereas proteins and mRNAs critical for short-term memory are preexisting and turn over slowly, certain proteins and mRNAs necessary for long-term memory must be either induced or, if constitutively expressed, only transiently accessible to modification.

Constitutively expressed proteins

Several models of long-term memory have considered the participation of constitutively expressed proteins which are present in an inactive form prior to learning. Acquisition, during learning, involves the activation of these proteins, perhaps by means of covalent modification. Retention of the memory relies on self-reinforcing mechanisms which outlast the turnover times of both the modifications and the proteins themselves. In one such model, Crick¹⁴ proposed that acquisition of memory is achieved during learning by a system (perhaps a cytoplasmic second-messenger system) which shifts a dimer to an active state where both subunits are modified. This active state can then be retained despite turnover of a single subunit, by an enzyme which can modify one monomer only when the other is modified.

In a more detailed model, which has now received some experimental support, Lisman¹⁷ proposed that competing activities of an autophosphorylating kinase and an associated phosphatase make up a 'bistable switch'. Learning stimulates the phosphorylation of the kinase and thereby initiates its autophosphorylation. When the rate of autophosphorylation exceeds that of dephosporylation, phosphorylation of the kinase becomes independent of the stimulus provided by learning. Support for this aspect of the model derives from studies on the Ca²⁺/calmodulin protein kinase in which intramolecular autophosphorylation permits persistent activation of the kinase in the absence of Ca²⁺ (refs 16, 18). For Lisman's model to be independent of protein turnover either autophosphorylation must be intermolecular or subunit exchange must take place. Neither of these has yet been demonstrated.

Based on studies of long-term potentiation, Lynch and Baudry¹⁵ suggested a model involving the self-reinforcing disassembly of molecular assemblies. They found that during acquisition, Ca²⁺ influx produced by learning rapidly and irreversibly increased the number of glutamate receptors in the synaptic membrane by activating calpain, a protease that degrades fodrin, a structural protein in the postsynaptic cell. This degradation is proposed to be the means whereby changes in activity in the postsynaptic cell lead to the insertion of new glutamate receptors; these, in turn, enhance Ca²⁺ entry and provide the reinforcement necessary for the maintenance of the memory.

These three models, however, do not account for the requirement of protein and mRNA synthesis during learning for memory lasting one day or more. Conceivably, constitutively expressed proteins with self-reinforcing properties could share the pharmacological sensitivity of long-term memory if these proteins and their mRNAs were either rapidly turned over or only available to modification during a brief period of their biogenesis. We think, however, that in their present form these models readily account for memory processes lasting many hours. The extracellular signals and second-messenger systems responsible for short-term memory could therefore activate a

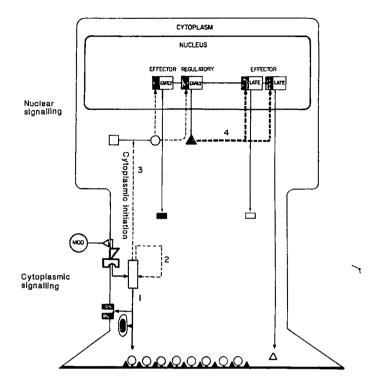


Fig. 1 Possible signalling systems used to activate memory systems with various time courses. For schematic reasons we have arbitrarily selected a presynaptic neurone at a synapse and consider how various acquisition processes could lead to the activation of retention processes with different time courses. These retention processes in turn initiate and maintain functional changes in ion channels, transmitter release mechanisms and structural changes at active zones. Similar changes in the properties and insertion of receptors are likely to occur in postsynaptic cells. In this model, a common extracellular signal, a transmitter released by modulatory neurones (MOD), acts on a presynaptic neurone to initiate separate memory processes with different durations. Short-term memory, which has a time course of minutes to hours (pathway 1), involves covalent modification of pre-existing proteins. Common components of cytoplasmic signalling [membrane receptor, transducing proteins, amplifier enzyme (adenylate cyclase, phospholipase C), cytoplasmic signal (cAMP, Ca²⁺, IT₃ triacylglycerol), protein kinase (A, B or C)] are used to modify target proteins (gated K⁺ channels, Ca²⁺ handling system, transmitter release mechanism). The duration of these modifications determines the retention of memory. For intermediate memory, this short-term memory system can be prolonged to last many hours by similar covalent modifications which are self-reinforcing (pathway 2), as in the case of autocatalytic phosphorylation of a protein kinase. Unlike these covalent modification mechanisms (pathways 1 and 2), the acquisition of long-term memory lasting more than 1 day (pathways 3 and 4) is dependent on the induction of new proteins (■, ▲). This induction is initiated by second messengers involved in short-term memory, which modify trans-acting regulators (open box linked to open circle) that activate both 'early effector' and 'early regulatory' genes. It is the induced synthesis of the proteins encoded by these genes, the early effector (11) and the early regulatory (A) proteins, that is blocked by the inhibition of protein synthesis during learning. Memory lasting for days is retained by the half-life of the effector proteins of early effector genes (pathway 3). Memory lasting weeks and months, longer than the half-life of effector proteins, is induced by the early regulatory genes whose protein products (which we call nuclear signals) trigger the maintained expression of late effector genes (pathway 4). Some of these additional acquisition steps (pathways 3 and 4) may require reinforcement by cytoplasmic signals to permit transition from shorter- to longer-term memory systems.

self-reinforcing mechanism to give a time course intermediate between short- and long-term memory (Fig. 1, pathway 2).

Induced proteins

We believe the sensitivity of long-term memory (lasting more than 1 day) to translational and transcriptional inhibitors during learning is best accounted for by inductive mechanisms, especially because the second messengers induced during learning (and responsible for the shorter forms of memory) are known to be potent gene activators in other systems^{25,26} (Fig. 1, pathways 3 and 4).

Particularly relevant for the discusson of learning are the peptide and biogenic amine hormones that activate receptors linked to enzymes involved in the synthesis of intracellular messengers. The detailed mechanisms by which these second messengers then regulate gene expression are unknown, but it is believed that they modify trans-acting regulators of transcription by either leading to their phosphorylation or binding to them directly, in a manner analogous to the binding of CAP protein by cyclic AMP in Escherichia coli^{27,28}. The modified transcription regulators could then act on enhancer DNA sequences of structural genes for long-term memory, much as do the DNA-binding proteins that mediate the transcriptional response to steroid hormones or heat shock^{29,30} (Fig. 1, pathway 3). With certain hormones, gene induction is relatively transient and parallels the period during which the hormone is present³¹. The duration of the physiological response is then carried by the stability of the mRNA and the half-life of the protein products. In the case of neurones, where the average half-life of protein is several days, the acquisition process for memory lasting days need, therefore, involve only transient activation of effector genes since the retention of memory could be accounted for by the turnover rate of the induced mRNA and protein products (Fig. 1, pathway 3). These considerations lead us to suggest that it will be important to look for alterations in gene expression, not only during the maintenance phase of memory but, more importantly, during the acquisition phase of memory, that is, during the learning process itself.

One objection to the possibility of genomic regulation of long-term memory that is sometimes raised relates to the question: how can a genomic change can lead to long-term alterations in some synapses of a neurone and not others? We suggest that synapse-specific alterations represent a special case of a larger issue frequently encountered in cell biology—the targeting of specific proteins to one rather than another site in the cell³²⁻³⁴. This problem is shared in many other contexts of cell biology. The transient modification at a given synapse produced by short-term memory could allow protein targeting to, recognition by, and stabilization at, that synapse.

Nuclear signals

Memories lasting many days to years clearly persist longer than the half-life of most proteins. In these cases, it is attractive to think of mechanisms for retention that are independent of protein and mRNA turnover, but which depend on persistent, rather transient changes in transcriptional state, changes that are maintained by cooperative or self-reinforcing mechanisms^{35,36} (Fig. 1, pathway 4). These mechanisms are used in cellular differentiation. Indeed, the often-drawn parallel between long-term memory and cellular differentiation³⁷⁻³⁹ has been strengthened recently by morphological studies of long-term sensitization of the gill-withdrawal reflex of *Aplysia*⁴⁰ and of long-term potentiation in the hippocampus⁴¹ which indicate that long-term memory is associated with growth of synaptic contacts.

Furthermore, the time window so characteristic of memory acquisition is also found in developmental processes in which 'early' genes act as regulators for the expression of 'late' effector genes. For example, the induction of growth and moulting in insects by ecdysone has been shown to alter the expression of

early genes whose induction regulates the expression of late genes. If ecdysone is given together with a protein synthesis inhibitor, the early genes are induced but the late ones are not; if the inhibitor is given several hours later, the late genes are induced normally⁴². A similar class of early genes has been studied more extensively in adenovirus where the nuclear oncogene E1A, an early gene, also regulates the expression of the late adenoviral genes⁴³. We suggest that protein synthesis inhibitors not only block the induction of effector proteins for memories lasting a few days, but also block the induction of nuclear signals used by early regulatory genes to activate long-lasting changes in the transcription or processing of the mRNA's of late effector genes. We believe, therefore, that much progress could be made by identifying possible nuclear signals used by early genes to communicate with late effector genes.

Particularly attractive candidates for nuclear signals in longterm memory acquisition are the products of 'competence' or 'immediate early genes' 44,45. These proteins are rapidly but transiently induced by hormones and growth factors whose prolonged presentation leads to cellular differentiation and growth. Although these early genes have yet to be shown to regulate the expression of specific effector genes in differentiation, the best-known members of this class, the proto-oncogenes c-fos and c-myc (which resemble the oncogene E1A), have several characteristics which may be relevant to nuclear signalling: (1), the genes respond to the specific cytoplasmic messengers shown to be involved in short-term memory, that is, cAMP, Ca²⁺ and diacyglycerol⁴⁶⁻⁴⁸. (2) The products of these genes are nuclear proteins⁴⁹ that are thought to affect transcription or mRNA processing⁵⁰. (3) The levels of the proteins and mRNA products, when induced, are only transiently increased because of their rapid turnover by degradative processes^{51,52}. (4) The oncogenic forms of these genes are capable of transforming cellular state⁴⁹.

We are not suggesting that c-fos and c-myc are the nuclear signals responsible for the establishment of memories lasting weeks; but we believe they represent prominent members of a large class of regulatory genes important for development (some of which may be induced during learning), whose protein products may have regulatory functions in the establishment of longer-lasting changes in cellular state. If induced nuclear regulatory proteins important for development prove also to be important for memory acquisition, it would have significance that would extend beyond the biology of learning. It would suggest the existence of common nuclear signalling systems, in the form of mRNA transcription and processing regulators, for long-lived cellular responses much as there are common cytoplasmic signalling systems for transient cellular responses.

Molecular reinforcement

We have proposed that the same extracellular signals that initiate short-term memory (Fig. 1, pathway 1) can initiate, through common intracellular messengers, additional acquisition steps for memory processes with more persistent retention mechanisms (Fig. 1, pathways 2-4). However, not every learning event gives rise to long-term memory. Often a single training trial produces only short-term memory. To produce long-term memory, repeated trials (repeated behavioural reinforcement) are required.

How is information for long-term memory distinguished from that for short-term memory? What are the molecular representations of the behavioural reinforcements necessary for initiating the various long-term memory processes (pathways 3 and 4 of Fig. 1)? To explain the specific activation of these additional acquisition steps, it will be necessary to determine whether the steps require quantitative changes in the levels or durations of the second messengers used in short-term memory, or whether qualitative changes are needed, such as the recruitment of other signalling systems, either cytoplasmic or nuclear. It will therefore be necessary not only to identify and characterize the effector

and regulatory genes whose transcription is activated during the acquisition of long-term memory, but also to delineate necessary molecular reinforcing events. However, the ability to pose some of the critical problems of long-term memory in molecular terms should allow an exploration of its various time courses in a variety of invertebrate and vertebrate learning systems, and thereby make it possible to explore long-term memory at its most fundamental level.

- 1. Ebbinghaus, H. Memory: A Contribution to Experimental Psychology (Dover, New York,
- James, W. The Principles of Psychology (Holt, New York, 1890).
 McDougall, W. Mind 10, 385-394 (1901).
- 4. Klatzky, R. L. Human Memory. Structures and Processes 2nd edn (Freeman, San Francisco,
- 5. Davis, H. P. & Squire, L. R. Psychol. Bull. 96, 518-559 (1984).
- Schwartz, J. H., Castellucci, V. F. & Kandel, E. R. J. Neurophysiol. 34, 939-963 (1971).
 Kandel, E. R. & Schwartz, J. H. Science 218, 433-443 (1982).

- Alkon, D. L. Science 226, 1037-1045 (1984).
 Farley, J. & Auerbach, S. Nature 319, 220-223 (1986).
 Livingstone, M. S. Proc. natn. Acad. Sci. U.S.A. 82, 5992-5996 (1985).
- 11. Quinn, W. G. in Biology of Learning (eds Marler, P. & Terrace, H.) 197-246 (Dahlem Konferenzen, Berlin, 1984).
- 12. Dudai, Y. Adv. Cyclic Nucleotide Protein Phosphoryl. Res. (in the press).
 13. L. TRE, J. H. Trends Neurosci. 8, 478-482 (1986).

- Crick, F. Nature 312, 101-102 (1984).
 Lynch, G. & Baudry, A. Science 224, 1057-1063 (1984).
- Saitoh, T. & Schwartz, J. H. J. Cell Biol. 100, 835-842 (1985).
 Lisman, J. E. Proc. natn. Acad. Sci. U.S.A. 82, 3055-3057 (1985).
- 18. Miller, S. G. & Kennedy, M. B. Cell (in the press).

 19. Agranoff, B. W. The Chemistry of Mood Motivation and Memory (Plenum, New York, 1972). 20. Montarolo, P. G., Castellucci, V. F., Goelet, P., Kandel, E. R. & Schacher, S. Soc. Neur Abstr. 11, 795 (1985)
- 21. Schacher, S., Montarolo, P. G., Castellucci, V. F., Kandel, E. R. & Goelet, P. Science (in
- 22. Flexner, J. B., Flexner, L. B. & Stellar, E. Science 141, 57-59 (1963).
- 23. Barondes, S. H. Short-Term Memory (eds Deutsch, D. & Deutsch, J. A.) 379-390 (Academic, New York, 1975).
- Frost, W. N., Castellucci, V. F., Hawkins, R. D. & Kandel, E. R. Proc. natn. Acad. Sci. U.S.A. 82, 8266-8269 (1985).
- Murdoch, G. H., Rosenfeld, M. G. & Evans, R. M. Science 218, 1315-1317 (1982).
- Waterman, M., Murdoch, G. M., Evans, R. M. & Rosenfeld, M. G. Science 229, 267-269

We thank Richard Axel and James H. Schwartz for their useful criticisms, Tom Abrams, Tom Curran, James Darnell, Thomas Jessell, James Morgan, Jeff Morgan and Charles Stevens for their comments on early drafts of this manuscript, Harriet Ayers and Andrew Krawetz for typing the manuscript, Louise Katz and Kathrin Hilten for help with the illustration, and the Helen Hay Whitney Foundation for their support (to P.G.).

- 27. de Crombrugghe, A., Bushby, B. & Bug, H. Biological Regulation and Development Vol. 3B (eds Goldberger, R. F. & Yamamoto, K. R.) 129-167 (Plenum, New York, 1984).
 28. Nagamine, Y. & Reich, E. Proc. natn. Acad. Sci. U.S.A. 82, 4606-4610 (1985).
- Yamamoto, K. R. A. Rev. Genet. 19, 209-252 (1985).
- 30. Ashburner, M. Heat Shock: From Bacteria to Man (eds Schlesinger, M. J., Ashburner, M. & Tissieres, A.) 1-9 (Cold Spring Harbor Laboratory, New York, 1982).
- Murdoch, G. H., Evans, R. M. & Rosenfeld, M. G. in Biochemical Actions of Hormones Vol. 12 (ed. Litwack, G.) 38-69 (Academic, 1985).
- Blobel, G. Proc anta. Acad. Sci. U.S.A. 77, 1496-1500 (1980).
 Sabatini, D. D., Kreibich, G., Morimoto, P. & Adesnik, M. J. Cell Biol. 92, 1-22 (1982).
- Schatten, S., D., Relection, G., Morindo, F. & Adesins, M. J. Cell Biol. 72, 1-22 (1982).
 Rothman, J. E., Scient. Am. 253 (3), 74-89 (1985).
 Razin, A. & Friedman, J. Prog. Nucleic Acid Res. molec. Biol. 25, 33 (1981).
 Groudine, M. & Weintraub, H. Cell 30, 131-139 (1982).
 Cajal, S. R. Histologie du Système Nerveux de l'Homme et des Vertèbres Vol. 2 (transl.
- Azoulay, L.) (Instituto Ramon y Cajal, Madrid, 1955). 38. Kandel, E. R. Harvey Lect. 73, 19-92 (1979).
- 39. Purves, D. & Lichtmann, J. W. Principles of Neural Development (Sinauer, Sunderland, Massachusetts, 1985). 40. Bailey, C. H. & Chen, M. Science 220, 91-93 (1983).
- Greenough, W. T. in Neurobiology of Learning and Memory (eds Lynch, G., McGaugh, J. L. & Weinberger, N. M.) 170-478 (Guilford, London, 1984).
- Richards, G. & Ashburner, M. Biological Regulation and Development Vol. 3B (eds Goldberger, R. F. & Yamamoto, K. R.) 213-253 (Plenum, New York, 1984).
- Nevins, J. R. CRC crit. Rev. Biochem. 12, 307-322 (1985).
 Cochran, B. H., Reffel, A. C. & Stiles, C. D. Cell 33, 939-947 (1983).
 Lau, L. F. & Nathans, D. EMBO J. 4(12), 3145-3151 (1985).
- Greenberg, M. E., Green, L. A. & Ziff, E. B. J. biol. Chem. 260, 14107-14110 (1985). Kruiger, W., Schubert, D. & Verma, I. M. Proc. natn. Acad. Sci. U.S.A. 82, 7330-7334 (1985).
- 48. Morgan, J. I. & Curran, T. Nature (in the press). 49. Weinberg, R. A. Science 230, 770-776 (1985).
- 50. Lewin, R. Science 233, 159 (1986). 51. Treisman, R. Cell 42, 889-902 (1985).
- 52. Blanchard, J.-M. et al. Nature 317, 443-445 (1985).

ARTICLES

Petrological and tectonic segmentation of the East Pacific Rise, 5°30′-14°30′ N

Charles H. Langmuir*, John F. Bender* & Rodey Batiza*

* Lamont-Doherty Geological Observatory, Palisades, New York 10964, USA † University of North Carolina at Charlotte, Charlotte, North Carolina 28223, USA * Washington University, St Louis, Missouri 63130, USA

Lavas from the fast-spreading East Pacific Rise are geochemically diverse even within a single tectonically defined spreading cell. Within such spreading cells, small offsets of the rise axis are often boundaries between petrologically distinct magmatic units which must be supplied independently from beneath the ocean crust. Volcanics erupted near the small offsets can have chemical characteristics similar to those previously found near transform faults.

IN April 1985, we carried out an extensive dredging program of the East Pacific Rise (EPR) between 5°30' N and 14°30' N. This region of the EPR is fast-spreading (9-11 cm yr⁻¹ full rate) and contains two major transform faults, the Siqueiros at 8°22' N and the Clipperton at 10°20' N (Fig. 1). There are several smaller offsets identified by Macdonald et al.1, which they named overlapping spreading centres (OSCs). Lonsdale^{2,3} identified similar features between 5°30' N and Siqueiros, which he called nontransform offsets. Our program was designed to examine the effects of transforms and smaller offsets on the chemistry of ocean ridge basalts, and through the chemistry to improve our understanding of magmatic processes along ocean ridges. Another aim of the study was to sample a substantial length of a fast-spreading ridge to test ideas about the relationship between spreading rate and the degree of observed mantle heterogeneity⁴⁻⁹.

Previous work on the chemistry of ocean ridge basalts erupted near transform faults suggested that proximity to transforms leads to several petrological effects, including cooler magmatic temperatures 10-12, eruption of a wider range of composition 12-15, higher-pressure fractionation 16,17 and slightly smaller extents of melting^{13,16}, which can lead to eruption of 'enriched' basalts when a veined mantle is present. These petrological effects, which collectively can be called a transform fault effect (TFE), make sense in terms of the cooling of lithosphere and asthenosphere that results from truncation of a spreading ridge by an offset 16,18. If these various effects are caused by lithospheric and asthenospheric cooling, the magnitude of the effect should correlate with the temperature (and hence, age) of the truncating lithosphere.

Earlier work also showed that there were abrupt changes in major and trace element chemistry across some transform faults

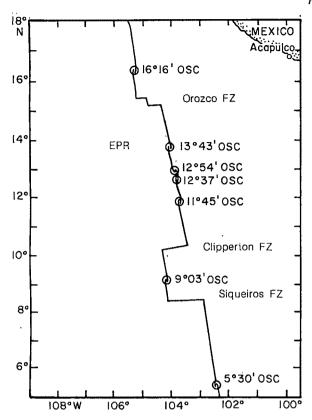


Fig. 1 Map showing general location of CHEPR expedition on the EPR, modified after ref. 1. The major transforms and overlapping spreading centres are indicated.

('transform discontinuities') at slow- and medium-spreading ridges 16,19,20. On this basis, it appeared that transforms might separate coherent geochemical units—lengths of ridge crest along which basalts are chemically related by crystal fractionation or different extents of melting 16. This idea, however, was based on sampling immediately adjacent to transforms, and needed to be tested by closely spaced sampling of a series of transform-bounded ridge segments.

The petrological variations associated with spreading centre offsets are just one aspect of a more general problem concerning the magmatic and tectonic segmentation of ocean ridges. Schouten and Klitgord²¹ introduced the useful concept of 'spreading cells' to describe transform-bounded ridge segments, and they showed that, in the Atlantic, spreading cells could be long-lived tectonic units. Francheteau and Ballard²² suggested that large portions of the EPR (~300 km) may be a single cell, although Ballard et al.²³ also noted the existence of secondary topographic highs separated by 'relay zones'. It has also been suggested 1.² that segmentation of the EPR needed to be considered in the context of both OSCs and transform faults, and thus could be <300 km.

The spreading cell idea has gradually evolved into a general magmatic model for ocean ridges. The centrepiece of this model is that there are magmatic injection centres regularly spaced along the ridge axis which correspond with long-wavelength bathymetric highs^{22,24,26}. Magma moves out from the central injection point along the ridge in a manner analogous to the observed rift eruptions on Iceland²⁵. Such an idea has received support from bathymetric studies²², from the location of hydrothermal fields^{22,26}, from interpretation of multi-channel seismic results²⁷, and from theoretical consideration of potential Rayleigh-Taylor instabilities during melt production beneath ocean ridges^{24,26,28}. In its simplest form, this central injection model predicts that the temperature of eruption of lavas should decrease regularly from a maximum at the bathymetric high at

the centre of a spreading cell to lower temperatures at the boundaries²⁹.

A contrasting, but not mutually exclusive idea, is that magma supply is not confined to the centres of long-wavelength cells, but that there are multiple injection centres distributed along the ridge, with edge effects at offsets which locally lead to cooler temperatures and possibly lower extents of melting (see refs 13-15; ref. 16, Fig. 12). The multiple injection model predicts less systematic long-wavelength variations in temperature and chemistry along axis except in the vicinity of large offsets, where the cold edge effect leads to lower-temperature lavas.

Thompson et al.29 recently presented preliminary petrological and photographic results from a short segment of the EPR between 10°20' and 11°45' N. They found at least five different basalt types, and suggested that they were separated into two discrete geographical units with edges at the Clipperton transform and the two OSCs identified by Macdonald et al.1. They also suggested that their data strongly supported the central injection model, and that each bathymetric high between OSCs or transforms was a single injection centre, away from which magmas became progressively more fractionated because of cooling during passage down axis. Inspection of their figures, however, reveals that the data show a narrow range in degree of fractionation $((Mg/Mg+Fe)=54\pm3(1\sigma))$ except for the dredge locations within 30 km of the Clipperton transform fault. In addition, there are at least two distinct magma types on each bathymetric high, which could be interpreted as evidence against the central injection model. Thus their data do not clearly discriminate between the central injection and multiple injection hypotheses.

Our dredging program was designed to recover samples on the appropriate scale to address the petrological significance of transform faults and smaller ridge offsets, and to discriminate between central injection and multiple injection models of ocean crust formation. The results and discussion which follow are the first-order results based on ~250 shipboard analyses of glass chips, supplemented by ~150 new major and trace element analyses on shore of hand-picked glass powders and 50 analyses of rare-earth elements (REE) by isotope dilution and neutron activation. A fuller evaluation based on data from chemical, mineralogical and isotopic studies will be given elsewhere.

Results

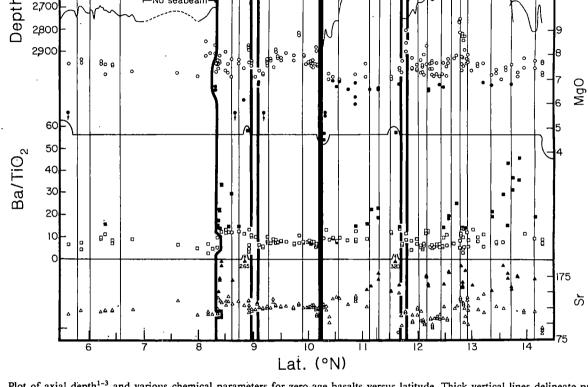
During the cruise, there were 122 successful dredges along 980 km of the EPR. Most of the dredge sites were located using a 12-kHz wide-beam echo sounder, conventional satellite navigation and large-scale versions of Sea Beam maps provided by Jeff Fox and Peter Lonsdale. All dredges were thoroughly described, and representative samples (~8 per dredge) were cut and had glass removed on board. Dredge tracks were usually made along axis and were usually kept to <1 km. One to four glasses per dredge were chemically analysed on board with a direct-current plasma emission spectrometer. The on-board analyses enabled us to determine where the significant changes in chemistry were occurring and to sample those areas more extensively.

Axial depth and linearity. A longitudinal profile of axial depth in our study area is shown in Fig. 2. The minimum depth was picked approximately every 2' of latitude from large-scale versions of the Sea Beam charts^{1,2}, and from our shipboard echo sounder data where there was no Sea Beam data between 7° N and the Siqueiros fracture zone. Macdonald et al.¹ pointed out many of the critical features of axial depth north of the Siqueiros transform. In particular, they noted the correspondence of OSCs with local maxima in axial depth. Although most of the depth profile in Fig. 2 is directly derived from the Macdonald et al.¹ maps, it differs from their profile in subtle but important ways. In particular, the Fig. 2 profile plots a single minimum depth except where two overlapping limbs of the EPR are completely unambiguous. The petrological data do not support the existence

၁Տ၀,

5°30'080

2,600



8°37' Deval

Siqueiros

No seabeam

Fig. 2 Plot of axial depth¹⁻³ and various chemical parameters for zero-age basalts versus latitude. Thick vertical lines delineate proposed spreading cell margins at the major OSCs and the two transform faults. Thinner vertical lines occur at small-offset OSCs and 'deviations from axial linearity' (devals) along the EPR, Filled symbols are for samples with MgO <7%, Ba/TiO₂ >14 and Sr >150 p.p.m., respectively. Ba/TiO₂ is a ratio similar to La/Sm. Normal, depleted ocean ridge basalts usually have Ba/TiO₂ ratios of 4-8. Enriched MORB with (La/Sm)_N>1 generally have Ba/TiO₂>23. Most chemical data were determined at sea by plasma emission spectrometry. Approximately 50 mg of glass chips were run for SiO₂, Al₂O₃, CaO, Na₂O, FeO, MgO, TiO₂, Sr and Ba. Because of approximate weights, sums were normalized to 99.5%. Precision based on 10 replicate analyses of a standard run on board as an unknown throughout the cruise was SiO₂, 0.5%; Al₂O₃, 2%; FeO, 1%; MgO, 1.5%; CaO, 2%; Na₂O, 1.5%; TiO₂, 2%; Sr, 2%; Ba, 10%. All data are 1σ in relative per cent (50.0±0.25 for SiO₂). Accuracy, based on samples rerun at Lamont, was worse than precision, and there were slight biases of as much as 3% relative for Na₂O and Sr. Some Ba values at sea were anomalously high, which we attribute to contamination with Mn-oxide rinds. Most high-Ba samples have been rerun at Lamont.

of an OSC at 11°15' N, and that OSC has been omitted.

The four large offsets in the region conveniently divide the EPR into five long-wavelength features, separated by the heavy vertical lines in Fig. 2. Across three of the four large offsets for which depths from both sides are shown there are distinct steps of >100 m in the axial depth. From Clipperton to the north end of the study area the axial depth increases substantially approaching the large offsets, giving a 'domed' shape to the long-wavelength features. South of Clipperton, 'domes' are not obvious, although depths do increase over short distances approaching the 9°03′ OSC and the northern side of the Siqueiros transform. Superimposed on all the long-wavelength features are shorter-wavelength (~25 km) undulations. Some of the deep points of these undulations correspond to the small-offset OSCs of Macdonald et al.1, but most do not. For example, just south of Clipperton there are several pronounced local depth anomalies even though there are no small-offset OSCs.

Another way of viewing the EPR is to note the changes in its strike. Lonsdale^{2,3}, for example, noted several kinks in the EPR between 4° and 6°S, Macdonald *et al.*¹ noted a 'regional sinuosity', and Ballard *et al.*²³ noted the existence of short

segments of slightly varying strike separated by what they called 'relay zones'. These changes in strike often occur where there are local depth maxima.

The petrological results presented below suggest that some of the short-wavelength variations in axial strike and depth are magmatically significant. Many of the short-wavelength undulations may be individual small volcanoes. Our initial inclination was to try and preserve a direct connection between the short-wavelength petrologic segmentation of the EPR and the 'spreading cell' concept. However, the short-wavelength structure of the EPR is likely to be temporally variable, and a fundamental feature of the 'spreading cell' idea21 is its connection with long-lived tectonic fabric of the ocean floor. Therefore, 'spreading cell' might be an appropriate term for each of the five long-wavelength bathymetric features in this area. Boundaries of spreading cells would be transforms or large-offset OSCs; these boundaries are relatively long-lived and usually have a significant change in axial depth across them. In addition, we suggest that the boundaries of the short-wavelength features within spreading cells be called 'devals' (or 'deviations from axial linearity'). The term 'deval' would include kinks, bends

(which are more gradual changes in strike than kinks) and small ridge offsets with or without overlap. (After the cruise, Batiza and Margolis³⁰ named one type of deval a 'SNOO', or small non-overlapping offset, and proposed a stochastic-spreading genetic model to account for such features.) We introduce the term 'deval' because the boundaries of the short-wavelength features can be petrologically important, yet their morphologic expression is diverse. There is not always an offset or overlap, hence terms which rely on these words are not general enough. Positions of some prominent devals are indicated in Fig. 2. Devals cannot always be identified with certainty on Sea Beam contour maps because of navigational inaccuracies, the nature of the contouring algorithm, and the subjective judgements involved in fitting separate Sea Beam swaths together by hand. Thus we give several examples of the importance of devals but do not present a comprehensive catalogue of their occurrence. Temperature, axial depth and width. One aim of the dredging program was to determine if there were systematic changes in the chemistry of basalts with changing depth of the EPR axis. Figure 2 shows the range of MgO contents of 200 glasses from our 100 zero-age dredge hauls. The magnesium content of glasses is directly proportional to liquidus temperature when olivine is close to the liquidus, hence the variations in MgO approximately reflect the relative variations in the quenching temperature of

Figure 2 shows that there is no overall correlation between the depth of the rise axis and the MgO content of the erupted lavas. The EPR between Clipperton and the 11°45′ OSC is, in general, a shallow segment, and yet it has the lowest mean MgO (that is, lowest temperature of erupted lava), while the adjacent ridge segment between the 9°03′ OSC and Clipperton, at approximately the same depth, has the highest mean MgO.

For each spreading cell defined by the major offsets, there is no overall correlation between MgO and distance from the centre of the segment. Some of the highest-MgO lavas occur near the centres of three of the five long-wavelength features, but so do lavas with average MgO contents. High-MgO lavas also occur at some of the margins of these features. Low-MgO, and even high-SiO₂ lavas occur immediately adjacent to the northern side of the Clipperton transform, the 9°03′ OSC and the 5°30′ OSC, but andesites also occur midway between Siqueiros and the 9°03′ OSC. Thus, in some cases, there may be a tendency for the centres of spreading cells to erupt hotter magmas, and the edges to erupt cooler magmas, but the data are noisy.

It is possible that on a shorter wavelength, samples from the centres of some of the secondary highs have higher MgO (for example, 9°50' N, 12°15' N and just south of Siqueiros). In most cases, however, our dredge spacing is not close enough to examine the detailed chemical variations for the secondary highs separated by devals.

In contrast to the complex and irregular relationship between MgO and depth, there may be a correlation between the mean regional MgO content and the mean regional width of the rise axis (Fig. 3). This correlation is not apparent over very short distances and for some unusual areas, such as just south of the 9°03′ OSC where the axis is exceptionally broad, but does apply when data are averaged over distances of ~50 km.

Macdonald et al. inferred from axial geomorphology that the cross-sectional shape of the rise axis reflected the robustness of the magmatic budget. The width in Fig. 3 is a crude measure of cross-sectional shape, and thus confirms much of Macdonald et al.'s discussion. In general, where the EPR is narrow and triangular, such as north of Clipperton, it reflects relative starvation of the magmatic budget. Erupted lavas tend to be cooler and to have low MgO, and show a pronounced edge effect. Where the EPR is broad, such as south of Clipperton, the magma supply is robust, the mean MgO content is higher and there is no perceptible edge effect either in terms of bathymetry or chemistry. The EPR also shows a substantial change in depth approaching Clipperton on the north, but is remarkably constant

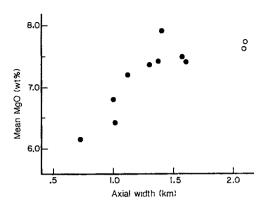


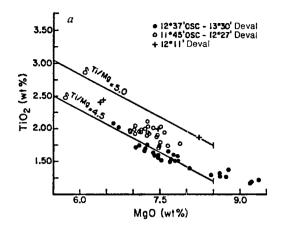
Fig. 3 Width of the EPR axis plotted against mean MgO content of the axis. Width was measured approximately every 2' of latitude as the distance between Sea Beam contours 40 m below the summit, using the maps from refs. 1-3. Standard deviations on the width estimated from this method are large, and the correlation should be regarded as qualitative.

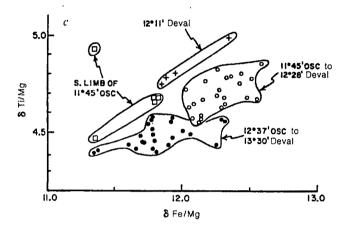
in depth on the south. Thus it may be the slope of the depth along axis rather than the absolute depth that correlates with magmatic temperatures. The bathymetry, shape of the rise axis and chemistry, therefore, do appear to be related, and reflect a balance between magma supply and edge effects. The balance can be highly variable even over short distances, such as across the Clipperton transform, and need not be related to position along a long-wavelength bathymetric feature.

As axial width seems to reflect the magmatic budget, one might expect a correlation between axial width and the presence of hydrothermal activity. It is also intriguing to speculate that the axial shape may reflect the width or depth of axial magma chambers.

Trace element geochemistry. Figure 2 also shows variations in Ba/TiO₂ ratios and Sr content of the basalt glasses. Both these parameters, but especially the Ba/TiO2 ratio, can be indices of enrichment of the mantle source. Ba/TiO2 is analogous to and correlates with the better known (La/Sm)_N ratio³¹. Normal ('N-type') MORB (mid-ocean-ridge basalt) glasses from both the Atlantic (~23 °N, 54 °N) and the Pacific (23° N and 44° N) have Ba/TiO₂ ratios between 2 and 12. Slightly more enriched, or transitional ('T-type') MORB, like those from the FAMOUS area along the Mid-Atlantic Ridge, have Ba/TiO2 ratios between 25 and 40. As Fig. 2 shows, several discrete lengths of ridge in our study area have Ba/TiO₂ ratios <12. Such N-type MORB occur from the 5°30' OSC to Siqueiros, from the 9°03' OSC north to Clipperton, and for the first 50 km north of Clipperton. From the 11°45' OSC to just south of the 12°37' OSC, 13 out of 15 dredges are N-type. Thus we recovered exclusively normal MORB from about two-thirds of the ridge length surveyed.

Surprisingly, one-third of the length of the EPR in this region contains at least some basalts more enriched than normal MORB. Such basalts occur from Sigueiros to the 9°03′ OSC, from a deval at 11°08' to the 11°45' OSC, around the 12°37' OSC, and around the 13°43′ OSC. In terms of regional distribution, the portions of the EPR which contain relatively enriched basalts are not systematically distributed with respect to the longwavelength bathymetric features discussed above. The most enriched basalts in the region occur just south of the large OSCs at 11°45' N and 9°03' N. Some basalts recovered near all of the OSCs in our study region (excluding 11°15') are more enriched than those recovered from the adjoining ridge segments. However, not every sample near OSCs is enriched. Devals also can be the location of relatively enriched basalts. In particular, basalts from the 8°37', 12°11' and 13°20' devals are more enriched than basalts from the axis immediately to the north and south (see Figs 2 and 5).





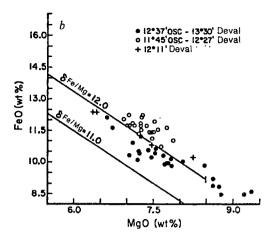


Fig. 4 Demonstration of major element variability along the EPR and the nature of the δ parameters. a, b, MgO/FeO and MgO/TiO₂ diagrams, all oxides in weight per cent. When the axes are rotated such that x' is parallel to the low-pressure fractionation path, then y', which is the δ value, reflects differences in the fractionation paths. Lines parallel to the x'-axis at different values of y' ($+\delta$) are shown for illustration. Samples with different δ values cannot be related to one another by low-pressure fractionation. c, Plot of δ Fe/Mg versus δ Ti/Mg showing distinct major element characteristics of different ridge segments. Samples from 12° to 12°28′ are completely distinct from those recovered between 12°37′ to 13°20′ N. Samples from near the deval at 12°11′ N plot separately, as do samples from south of the 11°45′ OSC.

The most notable feature of these data is the large number of occurrences of T-type MORB, and the significant number of dredges which recovered both T-type and N-type MORB. In the North Atlantic, T-type MORB are restricted to regions near hotspots, even where there are large offset transforms^{31,32}. Extensively sampled regions near the Kane fracture zone, for example, have yielded exclusively N-type MORB (ref. 32 and C.H.L. unpublished data). The fact that there are large regions with no enriched MORB, and discrete regions where enriched MORB are found, suggests that the mantle beneath this region of the EPR is not ubiquitously veined with enriched material.

Previously, it has been proposed that fast-spreading ridges are more homogeneous in their chemistry than slow-spreading ridges^{4,5,7}. The data in Fig. 2 demonstrate that basalt chemistry on a substantial portion of the EPR is not homogeneous, but instead is highly variable. Indeed, the mean Ba/TiO2 and the distribution of enriched material on the EPR between Siqueiros and 14° N is very similar to the ratio that can be inferred from rare-earth data from the South Atlantic, where there are multiple off-axis hotspots^{33,34}. These new data from the EPR are difficult to reconcile with correlations between spreading rate and the extent of geochemical variability which have been previously postulated. The data show that geochemical enrichment is not restricted to off-axis seamounts^{8,35}, but is quite common on axis as well. Thus, models which attempt to explain normal basalts on axis and both normal and enriched basalts off axis^{8,35,36} may need to be re-evaluated. Note, however, that the enriched basalts at zero age are preferentially located near offsets. Thus there may be lower extents of melting of a veined mantle beneath the offsets-suggesting that the offsets are at the margins of mantle melting anomalies. This explanation of the enrichment would be similar to that proposed for seamounts on older crust^{8,35}, but the spatial systematics leading to enriched basalts would occur

parallel rather than perpendicular to the rise axis. The remarkable consequence of this explanation is that even devals may be located at the margins of zones of mantle melting.

Chemical discontinuities across ridge offsets. The Sr and Ba/TiO₂ data in Fig. 2 show several abrupt, as well as some less abrupt, chemical changes across ridge offsets. There are prominent, abrupt chemical changes across the Siqueiros transform and the 11°45′ OSC. The 9°03′ OSC and 12°37′ OSC also bound distinct regions in Ba/TiO₂, but there is chemical 'noise' in the immediate vicinity of the boundary. A deval at 11°08′ divides discrete chemical regions as well. (Thompson et al.²⁹ suggested the 11°15′ OSC was a boundary, but we have two dredges, one at 11°10′ and the other at 11°20′, which have similar chemistry, suggesting that the actual boundary is south of 11°10′.)

The marked discontinuities in trace elements are also present in major elements-and the major elements reveal many more subtle discontinuities. Major elements are strongly affected by crystal fractionation, and usually suites of samples are required to define a regional trend, which can then be compared to another large region (see ref. 31). An example of such an approach is shown in Fig. 4a, b, where glasses from north of the 11°45' OSC to south of the 12°27' kink are compared with glasses from north of the 12°37' OSC to the 13°20' N bend. These illustrate a gross chemical distinction between these two regions, but it is useful to consider more detailed variations along axis which are not readily apparent from a presentation such as Fig. 4a, b. This can be done by rotating the axes so that the new reference frame has its x'-axis approximately parallel to the liquid line of descent after plagioclase has joined olivine on the liquidus, that is, for samples with ≤8.5% MgO. The values along the rotated y'-axis are given the δ notation because they reflect differences in the characteristic levels of Fe, Ti or Na of the various liquid lines of descent.

Figure 4c illustrates with major elements the discontinuities across the 11°45′ OSC and the 12°37′ OSC. The dredges from near the 12°11′ deval are distinct from the other data in the 11°45′ to 12°37′ ridge segment. Noting this distinction while at sea, we decided to halve our dredge spacing for this ridge segment to see if we could resolve smaller-scale segmentation. This segment was ideal for such a test, as there was an extended length of the EPR with no OSCs.

Figure 5 shows the results of this smaller-scale study. On the basis of the δ Ti/Mg parameter, this 50-km ridge segment appears to consist of three distinct chemical populations which are not related to one another by low-pressure fractionation processes. (One of the two sample groups from a single dredge appears to violate the regularity.) A small volcanic edifice with a relief of \sim 50 m and length of \sim 10 km (see Fig. 5) appears to consist of material with higher Ba/TiO₂ and δ Ti/Mg than the EPR immediately to the north and south. This small volcano is centred on the 12°11′ deval.

This small scale of petrological segmentation is not an isolated phenomenon. Figure 6 shows data for the ridge segment between Clipperton and the 9°17′ deval. This ridge segment is more homogenous in general than the segments which contain enriched basalts. There is a deval near 9°53′ N. Basalts from south of this feature are distinguishable from basalts north of it both in major and rare-earth elements. In both cases, each group is quite homogeneous, except right at the edges of the segments. Thus, in this region a deval separates two discrete petrological units.

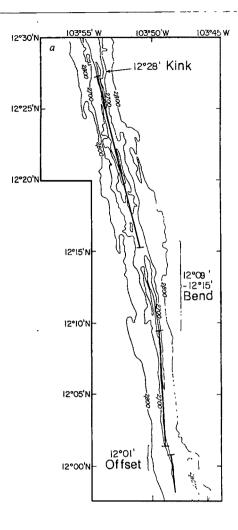
Occurrence of high-silica glasses. Glasses ranging in composition from basaltic andesite with 53% silica to dacite with almost 70% silica were recovered in three on-axis dredges and one off-axis dredge. Of these four dredges, three of them were near the major offsets—just north of the 9°03' OSC, just north of the 5°30' OSC and just north of Clipperton. Previously, high-SiO₂ glasses from the ocean flow have been recovered primarily from behind propagating rifts 14,37. Although other models which would lead to high-SiO₂ lavas are feasible, the occurrences on the northern limbs of these large-offset OSCs may imply that these limbs are propagating southwards. (On the basis of bottom photography, Thompson et al.29 also suggested that the east limb of the 11°45' OSC may also be propagating southward and Hekinian et al.40 suggested that the western limb of the 12°54' OSC may be propagating southward.) The fourth occurrence of high-SiO₂ glass is even more intriguing as it occurs 40 km north of the Siqueiros transform fault (Fig. 6d). It is not close to a major offset, but occurs just north of the deval at 8°37′ N (Fig. 6d). South of the deval are two dredges with normal basalts with no anomalous enrichment. At the deval there is slightly enriched basalt with higher light-rare-earth concentrations and Ba/TiO₂ ratio. The andesite occurrence is exactly analogous to the other occurrences of high-silica lavas (it is on the northern side of a right lateral offset), except that the offset is a deval rather than an OSC or transform.

Discussion

Recent studies have shown that there are several chemical effects which are often associated with transform faults; the results presented above suggest that chemical variations around some OSCs have many of these same characteristics. OSCs serve as the locus for the eruption of enriched basalts; more primitive, more differentiated and even silicic volcanics occur in their vicinity; and they serve as boundaries between chemically distinct ridge segments.

What is even more remarkable is that many of the chemical effects characteristic of transforms can also be present at very small bathymetric offsets (devals) which have only recently been able to be resolved as offsets with along-axis Sea Beam data^{1,2,23}.

The EPR thus seems to be magmatically segmented into petrological units which can have as boundaries, transforms, OSCs and devals. This segmentation is an order of magnitude



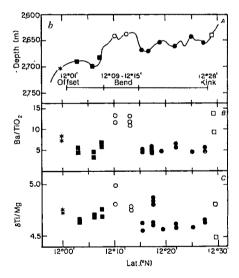


Fig. 5 Documentation of the fine scale of magmatic segmentation which can be present along the EPR. a, Sea Beam map¹ of the EPR from 12° to 12°30′ N. Locations of deviations from axial linearity (devals) are indicated. b, A, a depth profile of the axis and the dredge locations. B, Ba/TiO₂ ratios for basalt glasses from the dredges. C, δ Ti/Mg for the same glasses (see Fig. 4 for explanation of δ Ti/Mg). Note that with the exception of one sample group from the dredge at ~12°17′ N, the data separate into distinct, regionally coherent groups.

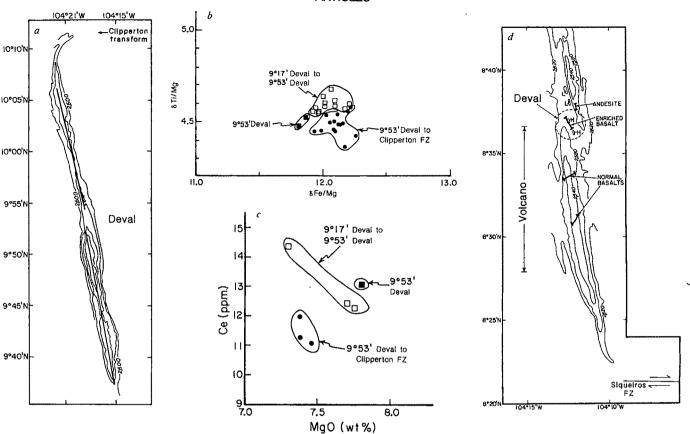


Fig. 6 a, Sea Beam map¹ of the EPR just south of the Clipperton transform fault. Note that the EPR seems to consist of a series of sausage-shaped volcanoes. b, Plot of δTi/Mg versus δFe/Mg, showing the distinct major element chemistry across the 9°53′ deval. c, Ce versus MgO, showing the distinction in rare-earth elements across the 9°53′ Deval. Ce was determined by isotope dilution. d, Sausage-shaped volcano north of the Siqueiros transform showing the systematic locations of andesite, normal basalt and enriched basalt.

smaller than long-lived spreading cells. For example, we find that the spreading cell of Francheteau and Ballard²², which includes the whole dome between 11°45′ N and the Orozco fracture zone, is made up of as many as 10 much smaller discrete magmatic segments. The two axial volcanoes of Lonsdale³ between the Gofar and Yaquina transforms may actually be 10 smaller-scale volcanic edifices. Each small segment of rise crest has its own bathymetric expression, and may have its own distinctive chemical signature.

Posible origins of devals. The origin of these features poses an interesting problem which is dependent on the interaction of magma supply with the stress regime at the rise axis, and which must relate in some way to OSCs. There is conceptual continuity across the range from large OSCs with substantial overlap and a deep overlap basin, to small OSCs with almost no decipherable basin, to devals with or without overlaps, and with no basin. This progression naturally suggests a familial relationship among these features and that a general concept may apply to all of them. The petrological data suggest that a starting point for such concepts should be that all the features are boundaries between regions with separate magma supply.

One possibility would be that the size and importance of the various offsets relates to the depth and scale of mantle upwelling. Transforms separate deep upwelling regions, and can remain distinct for up to 10^8 yr (ref. 21). At the other extreme, devals may reflect the last stage of melt segregation, at which small batches of magma ascend from beneath the crust to form axial magma chambers and associated volcanic cones. Individual devals may have a lifetime of $\leq 10^4$ - 10^5 yr. Large-offset OSCs would be intermediate features with intermediate lifetimes.

An important question is whether offsets propagate. Transforms in this region are quite stable and long-lived. The existence

of a volcanic edifice centred on a deval at 12°11' N leads us to speculate that new magmatic pulses may sometimes nucleate at a deval, and that (at least some) devals may not propagate but may be simply covered up by new volcanic construction. Thus, a deval may mark the edge of a constructional volcanic event, and may provide a nucleation site for the next volcanic pulse. Implications for OSCs. The discontinuities in chemistry documented above place constraints on models for the origin of OSCs. Both models^{1,2} suggest that OSCs separate regions of independent magma supply, and in this respect our data agree. Lonsdale's model², however, relies on the presence of a large magma chamber beneath OSCs, and in this respect is difficult to reconcile with the petrological data. Macdonald et al. suggested magma chambers were continuous beneath small-offset OSCs and that even for large-offset OSCs the magma chamber would become continuous once one OSC linked with another. They suggested that OSCs develop when a magma pulse interacts with this sinuosity of the ridge axis, and that the sinuosity results from previous OSCs. Thus, in their model OSCs are intimately connected with axial magma chambers. Our data suggest that OSCs, particularly those of large offset, may result from being at the margins of deep upwelling zones with fairly long wavelengths-the relationship with magma chambers is not at all clear. Between such large-offset OSCs there may be multiple devals which never were and never will become OSCs. Thus, large-offset OSCs and devals may reflect different stages, scales and depths of magma supply.

Note that there may be an asymmetry to the types of rocks recovered around the large-offset OSCs. All silicic rocks are on northern limbs. The most enriched rocks are on southern limbs, approximately on strike with the northern limbs. To the extent that silicic rocks reflect rift propagation, this suggests that the

northern limbs are propagating southwards. The southern limbs may be stagnating^{2,3}. The stagnating rift may be the locus of seamount formation because it is no longer an active spreading centre and hence eruptions pile up on the crust and form seamounts. Enriched basalt occasionally may occur because the OSCs are at the margins of the melting anomaly in the mantle where the extent of melting is less, and hence small-scale heterogeneities may be sampled. Sinton et al.37 have pointed out that absolute plate motions may be important for understanding some aspects of propagating rifts and Schouten et al.38 have attempted to relate off-axis seamount trends to absolute plate motions. Intriguingly, if all the northern limbs on this portion of the EPR are propagating southwards, then there may be a relationship with absolute plate motions, which have a northward component in this region.

Axial magma chambers. These petrological data seem to provide tight constants on the scale of mixing and homogenization of EPR lavas. The small, discrete chemical units along axis, some of which appear to require tapping of heterogeneous mantle, show that the processes of basalt genesis, including magma formation, segregation from the mantle, injection into the crust and eruption onto the ocean floor, do not homogenize EPR lavas. The only way that there could be a continuous axial magma chamber is if it has many separate regions of supply from below the crust and is not well mixed. Basaltic magma chambers in many geochemical models are envisaged as efficient mixing machines which buffer and homogenize magmas³⁹. This geochemical concept of a magma chamber is difficult to reconcile with our data. If, on the other hand, a physical magma chamber does exist, then the magma chamber must be variously fed. incompletely mixed, and hence substantially zoned and laterally heterogenous in its composition. However, if this were the case, why are most of the petrological data systematically distributed with respect to devals and OSCs? Therefore, while the data do not strictly require the physical absence of a magma chamber, they would be most consistent with magma chambers that are discontinuous, even with single spreading cells.

Conclusions

Systematic dredging of the EPR with an average spacing of 8 km has allowed a definition of the scale of magmatic diversity and segmentation along 700 km of a fast-spreading ridge. The data have definite implications for the two models of ocean crust formation discussed. Central supply of magma to the crust on the scale of spreading cells, even when such cells are defined by OSCs with finite offset, is difficult to reconcile with the data. Instead there seem to be multiple injection zones from the mantle into the crust. This does not mean that there are no petrological regularities with respect to spreading cells. Note that the most pronounced chemical offsets and most pronounced edge effects occur at the spreading cell boundaries, where there are also

discontinuities in axial depth. The long-wavelength anomalies must relate to the temperature structure and mass transfer processes within the underlying mantle. Apparently the mantle is variable on a much smaller scale than the long-wavelength anomalies, and this variability can be preserved through the crust formation process.

The data also have important implications for the effects of transform faults on the petrological evolution of the ocean crust. The south side of the Clipperton transform, where there is a cold edge, apparently has no petrological edge effect, unless it is on the adjoining, older plate. In contrast, there can be pronounced edge effects at devals, where there is no cold edge. Thus, in many cases there are edge effects, but not cold edge effects. This means that the previous emphasis on the cold edge as an explanation of the petrological manifestations associated with transform faults (and possibly propagating rifts) needs to be re-evaluated. Some aspects of the edge effects may be concerned with along-axis systematics of upwelling, melt segregation and distribution in the crust, and magmatic edges may exist even when there are not tectonic cold edges 13,16 (hence the occurrence of edge effects at devals). The cycle of magma supply to the ocean crust also seems to be able to overwhelm the tectonic cold edge, such as is occurring south of Clipperton. It is not clear from our zero-age data whether the cold edge has a time-averaged effect which only over the short term can be dominated by the magmatic budget.

Finally, the data show that enriched basalts are common at zero age on this portion of the EPR, although they do seem to occur preferentially at offsets. The general concept of fastspreading ridges being more homogeneous than slow-spreading ridges such as the Mid-Atlantic Ridge is no longer valid.

We thank the other members of the CHEPR team: Emily Klein, Pat Castillo, Jerry Ross, Terri Smith, Dan Miller, Tim O'Hearn, Mike Thatcher, Alex Biesada, Eliesir Duarte and Ron Comer for hard work and dedication. Captain Tom Desjardins and the crew of R/V New Horizon were also very helpful. Collaboration with Emily Klein has contributed substantially to this work. Jeff Fox and Peter Lonsdale gave us large-scale versions of Sea Beam maps which were essential for precision dredging. Geoff Thompson, Bill Bryan and Jim Natland provided preliminary data from cruises to the EPR. Conversations with or reviews by Bill Bryan, Dave Christie, Bob Detrick, Dan Fornari, Jeff Fox, Fred Frey, Dick Hey, Ellen Kappel, Jill Karsten, Kim Kastens, Peter Lonsdale, Ken Macdonald, John Mutter, Jim Natland, Mike Perfit, Paul Robinson, Jean-Guy Schilling, Hans Schouten, John Sinton, Geoff Thompson, and Dave Walker were very useful. This work was supported by NSF grant OCE84-11448 to C.H.L. at Lamont-Doherty Geological Observatory and OCE84-09660 to J.F.B. at the University of North Carolina at Charlotte. The Seed Money program at Lamont-Doherty provided part of the funds necessary to carry out the shipboard analyses.

```
Received 15 October 1985; accepted 3 June 1986.
```

- Macdonald, K., Sempere, J.-C. & Fox, P. J. J. geophys. Res. 89, 6049-6069 (1984).
- Lonsdale, P. J. geophys. Res. 88, 9393-9406 (1983). Lonsdale, P. J. Bull. geol. Soc. Am. 96, 313-327 (1985).

- Allègre, C. J., Hamelin, B. & Dupré, B. Earth planet. Sci. Lett. 71, 71-84 (1984). Cohen, R. & O'Nions, R. K. J. Petrol. 23, 299-324 (1982). Hamelin, B., Dupré, B. & Allègre, C. J. Earth planet. Sci. Lett. 67, 340-350 (1984).
- Batiza, R. Nature 309, 440-441 (1984). Zindler, A., Staudigel, H. & Batiza, R. Earth planet. Sci. Lett. 70, 175-195 (1984).
- Macdougall, J. D. & Lugmair, G. Nature 313, 209-211 (1985).
 Hekinian, R. & Thompson, G. Contr. Miner. Petrol. 57, 145-162 (1976).
- 11. Schilling, J. G. & Sigurdsson, H. Nature 282, 370-375 (1979).
- Christie, D. & Sinton, J. Earth planet. Sci. Lett. 56, 321-335 (1981).
 Bender, J., Langmuir, C. & Hanson, G. J. Petrol. 25, 213-254 (1984).
- Perfit, M. & Fornari, J. J. geophys. Res. 88, 10551-10572 (1983).
 Natland, J. Inil. Rep. DSDP 54, 833-850 (1980).
- Langmuir, C. & Bender, J. Earth planet. Sci. Lett. 69, 107-127 (1984).
 Sinton, J. & Christie, D. Eos 65, 1138 (1985).

- Fox, P. J. & Gallo, D. Tectonophysics 104, 205-247 (1984).
 Schilling, J.G., Kingsley, R. & Devine, J. J. geophys. Res. 87, 5593-5610 (1982).
 Machado, N., Ludden, J. & Brooks, C. Nature 295, 286-288 (1982).
- 21. Schouten, H. & Klitgord, K. Earth planet. Sci. Lett. 59, 255-266 (1982).

- Francheteau, J. & Ballard, R. Earth planet. Sci. Lett. 64, 93-116 (1983).
 Ballard, R., Hekinian, R. & Francheteau, J. Earth planet. Sci. Lett. 69, 176-186 (1984). 24. Whitehead, J., Dick, H. J. B. & Schouten, H. Nature 312, 146-148 (1984).

- Sigurdsson, H. & Sparks, S. R. J. Nature 274, 126-130 (1978).
 Crane, K. Earth planet. Sci. Lett. 72, 405-414 (1985).
 Mutter, J. et al. Geology 13, 629-632 (1985).
 Schouten, H., Klitgord, K. & Whitehead, J. Nature 317, 225-229 (1986).
- 29. Thompson, G., Bryan, B., Ballard, R., Hamuro, K. & Melson, W. Nature 318, 429-433
- Batiza, R. & Margolis, S. H. Nature 320, 439-441 (1986).
 Schilling, J.-G. et al. Am. J. Sci. 283, 510-586 (1983).

- Bryan, W., Thompson, G. & Ludden, J. J. geophys. Res. 86, 11815-11836 (1981)
 Schilling, J. G., Thompson, G., Kingsley, R. & Humphries, S. Nature 313, 187-191 (1985).
 Humphris, S., Thompson, G., Schilling, J-G. & Kingsley, R. Geochim. cosmochim. Acta 49, 1445-1464 (1985).
- 35. Batiza, R. & Vanko, D. J. geophys. Res. 89, 11235-11260 (1984).
- 36. Sleep, N. J. geophys. Res. 89, 10029-10041 (1984).
- 37. Sinton, J., Wilson, D., Christie, D., Hey, R. & Delaney, J. Earth planet. Sci. Lett. 62, 193-207 (1983).
- 38. Schouten, N., Whitehead, J. & Dick, H. Nature (in the press).
- O'Hara, M. J. Nature 266, 503-507 (1977).
 Hekinian, R., Augarde, J. M., Francheteau, J., Gente, P., Ryan, W. & Kappel, E. Mar. geophys. Res. 7, 359-377 (1985).

Global temperature variations between 1861 and 1984

P. D. Jones, T. M. L. Wigley & P. B. Wright*

Climatic Research Unit, School of Environmental Sciences, University of East Anglia, Norwich NR47TJ, UK

Recent homogenized near-surface temperature data over the land and oceans of both hemispheres during the past 130 years are combined to produce the first comprehensive estimates of global mean temperature. The results show little trend in the nineteenth century, marked warming to 1940, relatively steady conditions to the mid-1970s and a subsequent rapid warming. The warmest 3 years have all occurred in the 1980s.

GLOBAL mean surface air temperature is the most commonly used measure of the state of the climate system. When general issues of climatic change are addressed, global mean temperature change is often used as a yardstick; the age of the dinosaurs was warmer than today, the ice ages were colder, and so on. Paradoxically, in the present era of instrumental meteorology, with data coverage far better than at any earlier time, our knowledge of global mean temperature changes is still uncertain. Variations in global mean air temperature are of considerable importance, as they are a measure of the sensitivity of the climate system to external forcing factors such as changes in carbon dioxide concentration, solar output and the frequency of explosive volcanic eruptions. Quantifying the response of the climate to external forcing changes is a major goal of climatology and a prerequisite for predicting future climatic change. As a step towards this goal, we present here the first global synthesis of near-surface temperature measurements over the land and

Most earlier estimates of global and hemispheric mean temperature (see refs 1, 2) were based solely on data from land-based meteorological stations. Since >70% of the globe is ocean, one might suspect the global representativeness of such estimates, although on long timescales (≥decades) the thermal coupling between land and ocean should ensure that the land data largely mirror changes occurring over the oceans1. Recently, data from ships at sea collected for routine weather forecasting purposes, have been compiled by groups in the United Kingdom^{3,4} and the United States^{5,6}, and these data give us the potential to calculate improved estimates of global mean temperature. Apart from our own work⁷, the only previous attempt to analyse both land and marine data is that of Paltridge and Woodruff^{8,9}. These authors, however, failed to account for inhomogeneities in the marine data, which are substantial (see below and also refs 4 and 10). The quality and coverage of the land data they used was also less than adequate, but this is understandable because they were primarily interested in sea-surface temperature variations.

The land data we use are those from refs 11, 12. These have been carefully examined to detect and correct for non-climatic errors that may result from station shifts or instrument changes, changes in the methods used for calculating means, urban warming, and so on. Although problems still exist^{13,14}, the quality of these data is much better than that of material used in earlier studies. Area averages based on these data show medium to long timescale trends (≥10 yr) whose spatial consistency provides a strong pointer to the data's overall reliability^{1,11,12}. The marine data we employ are those in the COADS (Comprehensive Ocean Atmosphere Data Set) compilation⁶ which extends to 1979, and data from the Climate Analysis Center, NOAA,

for 1980-84. We use both sea surface temperatures (SST) and marine air temperatures (MAT).

Marine data problems

Both SST and MAT data contain 'inhomogeneities', variations resulting from non-climatic factors^{4.10,15}. For example, early SSTs were measured using water collected in uninsulated, canvas buckets, while more recent data come either from insulated bucket or cooling water intake measurements, with the latter considered to be 0.3-0.7 °C warmer than uninsulated bucket measurements¹⁰. For marine air temperatures, changes in the size and speed of ships, especially those increases associated with the sail to steam transition, are both thought to have influenced data homogeneity. In addition, many early air temperature observations were not taken in screened locations. Because of these non-climatic factors, both SST and MAT data must be corrected (or 'homogenized') to remove their effects.

Folland et al.4,16 and Folland and Kates17, using the UK Meteorological Office (UKMO) data bank3, attempted to overcome these problems by identifying specific sources of error, attempting to quantify these and using this information to make corrections to the raw gridded data. Such corrections have inherent uncertainties because of difficulties in their a priori quantification and a lack of knowledge of how most measurements were taken. Information on whether bucket or intake measurements were made has, in most cases, apparently been lost or never recorded. It has also been shown¹⁸ that supposedly homogeneous (that is bucket-only or intake-only) SST data series appear to have non-climatic changes that are similar to those found in mixed data series, suggesting that all historical data sets contain a mix of measurement types. Since 1945, however, it is generally assumed that available SST data contain a reasonably consistent mix of intake and bucket measurements18.

The Folland et al.⁴ corrected MAT and SST series have been compared with averages of land-based data by Jones et al.^{11,12}. Agreement is reasonable since the start of the twentieth century, although MAT values for the years 1942-45 appear to be too warm in both hemispheres. Before 1900, the marine and land series diverge markedly, with both marine series being about 0.3 °C warmer than the land data.

Correcting the COADS data

The COADS compilation contains some 63.25 million non-duplicated SST observations, of which 0.96 million have been 'trimmed' to remove extreme outliers⁵. While these are more data than in the UKMO SST set (which has about 46 million non-duplicated observations⁴), the effective area and density of coverage is very similar in both data sets. However, unlike the UKMO data set used by Folland *et al.*⁴, none of the data in COADS have been corrected for non-climatic effects. Our first task, therefore, was to homogenize the COADS data. We did

^{*} Present address: Max-Planck-Institut für Meteorologie, Bundesstrasse 55, 2000 Hamburg 13, FRG.

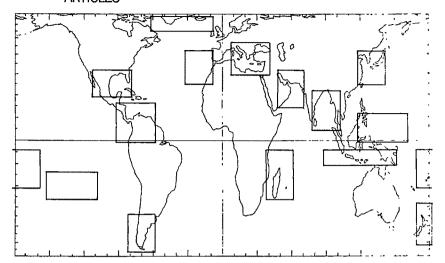


Fig. 1 Map showing the 15 regions where marine air temperatures and land-based temperatures were compared (Peters equal-area rectangular projection).

this by comparing marine and land data in areas where the two abut or overlap (coastal areas and around ocean islands).

The trimmed COADS data include monthly means and medians on a 2°×2° grid, together with the number of observations in a month and the mean observation date. We compressed the data onto a more manageable grid (5°×5° for MAT, 4°×10° for SST) after first eliminating values where the number and distribution of observations was likely to have produced unrepresentative monthly means, and expressed the values as anomalies from a 1950-79 reference period. As a test of data quality at this stage we calculated hemispheric mean values by appropriately weighting the gridded MAT and SST data (NH, Northern Hemisphere; SH, Southern Hemisphere). Year-to-year variations for these uncorrected data were found to be in excellent agreement with the UKMO corrected data (NHSST, r=0.86; NHMAT, r = 0.87; SHSST, r = 0.88; SHMAT, r = 0.75 over 1856-1979: correlation coefficients calculated using residuals from a 10-yr gaussian filter), but, as expected, the long-term (≥10 yr) fluctuations showed marked differences. Similar high frequency correlations between SST and MAT for the uncorrected COADS data (NH, r = 0.91; SH, r = 0.89) were higher than in the corrected UKMO data (NH, r = 0.81; SH, r = 0.80).

Because of the high SST-MAT correlation (see also ref. 19). SST data can be corrected by comparison with MAT data, once the latter have been corrected. For the MAT data, any attempt to assess, a priori, the magnitudes of errors arising from instrumental changes, changes in observation methods, and the effects of changes in ships' thermal inertia, speed and size (the latter determines the height at which observations were taken), must be fraught with uncertainty. Data reliability and long-term homogeneity can be far more convincingly demonstrated for the gridded land data than for the marine data because land station data homogeneities can be more easily identified, explained and corrected 11,12. We therefore use these data directly to correct the marine data. Fifteen regions (see Fig. 1) were chosen in which land and marine data are in close proximity. Area averages of annual mean MAT and land air temperature were calculated for each region using the uncorrected COADS data and the homogenized land data produced by Jones et $al.^{11,12}$. No attempt was made to consider night-time observations only, as used by Folland et al.4. In addition to the 15 pairs of area averages, annual mean coastal land time series were produced for both hemispheres and compared with the uncorrected hemispheric-mean MAT series.

The 17 land minus MAT time series were then examined for systematic differences between the land and marine data. For the period 1861-1979 (both marine and Southern Hemisphere land data are unrepresentative before 1861 because of poor data

coverage), five distinct periods could be discerned in all 15 regional land minus MAT time series and in the two hemispheric land minus MAT time series. The latter are shown in Fig. 2. The three main periods are: the period up to the 1880s when the MAT data appear to be too warm by 0.4-0.5 °C; the period from the 1900s to 1941 when the MAT data are too cold by 0.1-0.2 °C; and 1946-79 when there is no obvious bias. There is a strong upward trend in the land-minus-MAT difference between the mid 1880s and the late 1900s, and the war years, 1942-45, are marked by anomalously warm MAT values. The consistency between the hemispheres is clear from Fig. 2, and the land minus MAT data for the individual smaller regions, although showing greater inter-annual variability, all show the same features.

The nineteenth century land minus MAT data also show differences between the values before and after about 1873 (see Fig. 2). By examining land, MAT and SST data it can be shown that this difference is also likely to reflect a non-climatic

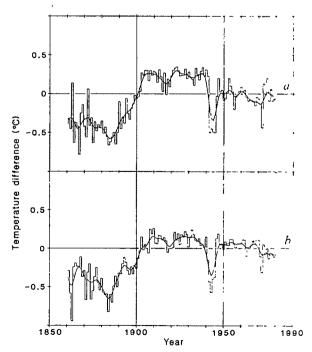


Fig. 2 Temperature differences: coastal land values minus uncorrected COADS marine air temperature values for the Northern (a) and Southern (b) Hemispheres. Smooth curves show 10-yr gaussian filtered values, padded at each end as described in ref. 11.

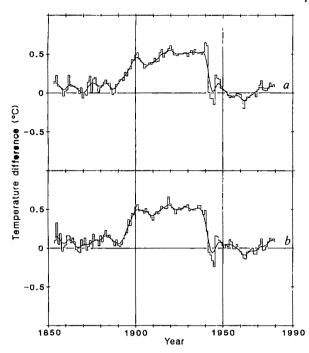


Fig. 3 Temperature differences: corrected marine air temperatures minus uncorrected sea surface temperatures for the Northern (a) and Southern (b) Hemispheres. Smooth curves show 10-yr gaussian filtered values.

inhomogeneity in either the MAT data or the land data, probably the former.

The means and standard deviations of the land minus MAT values are shown in Table 1. The consistency of these values strongly suggests that these land/MAT discrepancies are not climatic in origin. They may, therefore, be used to estimate annual correction factors for the MAT data in order to make these data compatible with the existing homogenized land data. Except for the 1942-45 period, when war conditions apparently prompted observers to measure temperature in unconventional locations⁴, the specific reasons for these non-climatic MAT fluctuations are not known. Although their reality cannot be questioned, there is clearly some uncertainty in the magnitude of the implied corrections.

The correction values we have used (added to the raw MAT data) are (°C): 1861-73, -0.40; 1874-89, -0.48; 1903-41, 0.17; 1942-45, -0.54; 1946-79, 0.0; with linear interpolation between

Table 1 Comparison between coastal land and MAT data

		1861-73	187489	1903-41	1942-45	1946-79
NH	$ar{X}$	-0.35	-0.50	0.23	-0.49	-0.02
	S	0.26	0.11	0.09	0.02	0.12
SH	$ar{X}$	-0.36	-0.53	0.10	-0.44	0.03
	S	0.23	0.14	0.09	0.09	0.10
NH (9 region	Χ̈́	-0.36	-0.42	0.17	-0.54	-0.03
average	$egin{array}{c} s(ar{X}) \ ar{X} \end{array}$	0.40	0.21	0.10	0.10	0.05
SH (6 region	Χ̈́	-0.61	-0.52	0.17	-0.44	0.05
average	$s(\bar{X})$	0.57	0.36	0.22	0.15	0.08
Correction		-0.40	-0.48	0.17	-0.54	0.00

 \bar{X} = mean land minus MAT value; s = corresponding standard deviation defined by $s^2 = (Y-1)^{-1}\Sigma(X_i = \bar{X})^2$ where X_j is the value in year j, and Y is the number of years; $s(\bar{X})$ = standard deviation of the means defined by $(s(\bar{X}))^2 = (n-1)^{-1}\Sigma(\bar{X}_i - \bar{X})^2$ where n is the number of regions (6 or 9), \bar{X}_i is the mean for region i and \bar{X} is the average value of \bar{X}_i . The last line shows the inferred correction which was added to the uncorrected annual MAT data.

1889 and 1903. Slightly different corrections were judged necessary for Southern Hemisphere data between 1941 and 1945: 1941, -0.14; 1942-45, -0.44. Most of the transition dates for these correction factors, which are based on a number of considerations, could be altered slightly with no appreciable effect on the resulting corrected MAT values. Although the 0.08 °C difference in the MAT corrections before and after 1873 may be inappropriate if it arises from a land data inhomogeneity, we judge this to be unlikely. It has the effect of slightly reducing the magnitude of the long-term MAT warming between the period before 1873 and today. The corrections generally reflect the mean land minus MAT values shown in Table 1, but the precise values used and the transition dates also take MAT-SST comparisons into account. Our corrections differ markedly from those applied by Folland et al.4 to their night-time MAT data. This is a clear indication of incompatibilities between the corrected UKMO MAT data and the homogenized land data (see also refs 11 and 12).

Having corrected the MAT data, we can now estimate the SST corrections required to ensure overall compatibility between the land, MAT and SST data by comparing the corrected MAT and raw SST values. Table 2 and Fig. 3 show the hemispheric mean differences between the corrected MAT data and the raw SST data. As with the MAT analysis, three distinct periods can

Table 2. Comparison between corrected MAT data and uncorrected SST data

		1861-89	1903-41	1942-45	1946-79
NH	$ar{X}$	0.08	0.49	-0.07	0.02
	·s	0.08	0.08	0.07	0.09
SH	$ar{X}$	0.07	0.50	-0.14	0.02
	s	0.04	0.05	0.08	0.08
Correction		0.08	0.49	-0.10	0.00

 \bar{X} = mean MAT minus SST value; s = corresponding standard deviation. The correction is the number added to the uncorrected annual SST data.

be discerned: pre-1890 when the SST data are slightly but consistently cooler than the MAT data; 1903-41 when SSTs are markedly cooler than MATs; and post-1945 when there is no consistent difference. Rather complex transitions exist between these three phases. The MAT-SST difference curves are essentially the same in both hemispheres. This is a strong indication that the differences reflect non-climatic effects, and it provides a valuable consistency check on the MAT corrections.

The implied SST corrections, are (°C): 1861-89, 0.08; 1903-41, 0.49; 1942-45, -0.10; 1946-79, 0.0; with linear interpolation between 1889 and 1903. For 1941 we applied a slightly different correction in the Southern Hemisphere, 0.19 °C. As for MAT, these corrections also differ somewhat from those used by Folland et al.⁴. In their analysis, SST values were adjusted to ensure compatibility with corrected MAT values, just as we have done. However, since their corrected MAT values must differ noticeably from those produced here, differences in the SST corrections will, in part, reflect these MAT differences.

In our analysis, the difference between the twentieth century SST correction factor before 1941 and after 1946 is 0.49 °C. This difference is in the range (0.3-0.7 °C) generally accepted for the difference between uninsulated bucket and intake SST measurements ^{18,20,21}. The precise reasons for the differences that we obtain between the nineteenth century and early twentieth century MAT and SST corrections are uncertain. For MAT, the change is likely to be related to the transition from sail to steam. Between 1880 and 1910, the percentage of steamship tonnage as a fraction of total shipping tonnage rose from ~25 to 75% (ref. 22). Noticeable increases in ship speed occurred over the period 1880-1900, and in ship size over the period 1890-1910

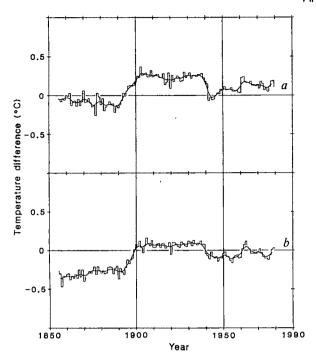


Fig. 4 Differences between the hemispheric-mean sea surface temperature values produced in the present work and those of Folland et al.⁴; Northern Hemisphere (a), Southern Hemisphere (b). Smooth curves show 10-yr gaussian filtered values. The implied warmth of the Folland et al. SH data relative to the NH (by ~ 0.2 °C), is due to their use of 1951-60 as a reference period. Conditions during this decade differed noticeably from the mean conditions during the reference period, 1950-79, used here (see

(ref. 22). These dates should be compared with the duration of the rising trends in land minus uncorrected-MAT data in both hemispheres shown in Fig. 2. Changes in MAT may be related to exposure changes attendant on the above, and to other changes in instrument exposure procedure which occurred over the same period. For SST, the main reasons for the change may be the standardization of the measuring technique and the introduction of more reliable instruments²³. It is also possible that, in the mid to late nineteenth century, many bucket temperatures were not taken in the shade²⁴. In addition, some of the earlier measurements may have been made with wooden rather than canvas buckets. The latter, being uninsulated and subject to evaporative cooling, produce lower temperature readings.

The overall differences between the hemispheric mean SST values produced here and those of Folland et al.4 are shown in Fig. 4. The results for an MAT comparison are similar. The discrepancies are large and comparable in magnitude to either set of corrections. The reasons for these differences stem mainly from the different correction factors applied to what are essentially similar raw data. Because there are several sources of data inhomogeneity, we have not attempted to correct for these individually. The result should be more complete than Folland et al.4 who attempted to make specific corrections for identified sources of inhomogeneity based on physical arguments. Our corrections synthesize the effects of several different factors. However, while they ensure compatibility between the marine and land data, the fact that the reasons for these corrections are uncertain must point towards some remaining uncertainty in our corrected marine data, especially in the nineteenth century.

Global mean temperatures ...

It is a relatively simple matter to produce estimates of annual global mean surface air temperature using the available (correc-

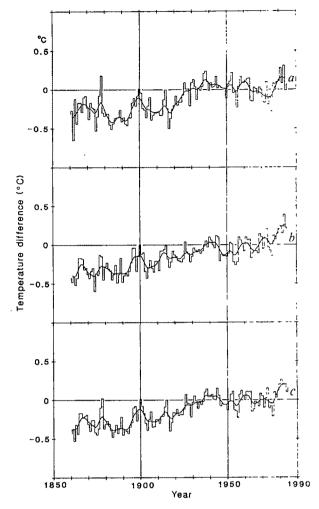


Fig. 5 Global (c) and hemispheric (Northern, a; Southern, b) annual mean temperature variations since 1861, based on seasurface temperature data to represent the marine domain and using weights corresponding approximately to the maximum coverage for the four domains (method two in the text). Smooth curves show 10-yr gaussian filtered values. 1980-84 values are based on SST data obtained from the Climate Analysis Center, U.S. National Oceanic and Atmospheric Administration (see ref. 29 for information about this data source). These data were adjusted to be compatible with the values in earlier years by comparing values in both hemispheres over the overlap period, 1970-79. The CAC data correlate highly with the COADS data (r=0.984 for the Northern Hemisphere mean and r=0.991 for the Southern Hemisphere mean).

ted) marine data and the most recent compilations of land data^{11,12}. There are three different ways in which global or hemispheric (land plus marine) averages can be calculated. The first method is to average only those grid point values (with appropriate cosine weighting) for which data exist. This is the way hemispheric means have been produced for the land data^{11,12}. The second and third methods assume that each of the four independent time series (NH and SH land and NH and SH marine, either SST or MAT) are, at all times, representative either of their maximum coverage or of the total areas of the four domains. The results obtained differ but little, and the use of either SST or MAT to represent the marine domains produces only minor differences. We therefore show only results using the second method based on SST data, obtained using

T global = 0.25NH land + 0.25NH SST + 0.2SH land + 0.3SH SST

(Fig. 5) where, after 1957, SH land includes Antarctic data from

Raper et al.25, updated. The insensitivity to the precise method of weighting arises because all time series are quite strongly

The reliability of the time series given in Fig. 5 as true hemispheric and global averages can be questioned because the spatial coverage, even at best, is less than 75% and because the coverage changes with time. Coverage is always much better in the Northern Hemisphere. Coverage before 1900 is generally less than one third of the globe, down to <20% in the 1860s. The question of representativeness of the land data has been considered in detail in refs 1, 11 and 12. Although marine coverage before 1900 is sparse, the spatial correlation length over the oceans is large and limited coverage should still give results representative of a much larger area. Nevertheless, there are large parts of the Southern Hemisphere that nearly always lack data, especially the southern oceans south of 45 °S and the whole of the southeastern Pacific (except near the South American coast). Before 1957, when most Antarctic data first became available, there are essentially no data at all for the globe south of 45 °S (refs 25, 26). Although this represents only ~15% of the area of the globe, temperature fluctuations at high latitudes are known to be larger than at lower latitudes and so can have a disproportionate effect on the global average^{12,27}. Any interpretation of Fig. 5 must bear in mind both these basic data deficiencies and the marine data uncertainties implied by

Received 10 February; accepted 28 May 1986.

- 1. Wigley, T. M. L., Angell, J. K. & Jones, P. D. in Detecting the Climatic Effects of Increasing Carbon Dioxide (eds MacCracken, M. C. & Luther, F. M.) 55-90 (U.S. Dept of Energy, 1985).
- 2. Hansen, J. et al. Science 213, 957-966 (1981).
- Shearman, R. J. Met. Mag. 112, 1-10 (1983).
 Folland, C. K., Parker, D. E. & Kates, F. E. Nature 310, 670-673 (1984).
- Woodruff, S. D. in Proc. 3rd Conf. on Climate Variations and Symp. on Contemporary Climate: 1850-2100, 14-15 (American Meteorological Society, Boston, 1985).
- Slutz, R. J. et al. Comprehensive Ocean-Atmosphere Data Set Release 1 (NOAA Environmental Research Laboratories, Boulder, 1985).
 Wigley, T. M. L., Jones, P. D. & Kelly, P. M. in The Greenhouse Effect, Climatic Change, and Ecosystems (eds Bolin, B., Döös, B. R., Jäger, J. & Warrick, R. A.) (SCOPE series,
- Wiley, in the press).

 8. Paltridge, G. W. & Woodruff, S. Mon. Weath. Rev. 109, 2427-2434 (1981).
- Paltridge, G. W. Mon. Weath. Rev. 112, 1093-1095 (1984).
- Barnett, T. P. in Detecting the Climatic Effects of Increasing Carbon Dioxide (eds Mac-Cracken, M. C. & Luther, F. M.) 91-107 (U.S. Dept of Energy, 1985).
- Jones, P. D. et al. J. Clim. appl. Met. 25, 161-179 (1986).
 Jones, P. D., Raper, S. C. B. & Wigley, T. M. L. J. Clim. appl. Met. 25 (in the press).
- Bradley, R. S., Kelly, P. M., Jones, P. D., Diaz, H. F. & Goodess, C. A Climatic Data Bank for the Northern Hemisphere Land Areas, 1851-1980, DoE Tech. Rep. No. TR017 (U.S. Dept of Energy, 1985).

Fig. 4. We note, however, that the latter do not affect the gross features of the global mean changes observed this century.

The global curve is extremely interesting when viewed in the light of recent ideas of the causes of climatic change^{1,2}. The data show a long timescale warming trend, with the three warmest years being 1980, 1981 and 1983, and five of nine warmest years in the entire 134-yr record occurring after 1978. With regard to the hypothesized warming due to increasing concentrations of carbon dioxide and other greenhouse gases, the overall change is in the right direction and of the correct magnitude 1,7,28. However, the relatively steady conditions maintained between the late 1930s and mid 1970s requires either the existence of some compensating forcing factor or, possibly, a lower sensitivity to greenhouse gas changes than is generally accepted.

We thank particularly C. K. Folland, D. E. Parker, P. M. Kelly, T. P. Barnett and D. J. Shea for useful comments. We thank D. E. Parker and C. K. Folland (UK Meteorological Office) for access to unpublished data used in Fig. 4 Scott Woodruff (Environmental Research Laboratories, US National Oceanic and Atmospheric Administration) for an early copy of the trimmed COADS data set, and the Climate Analysis Center, US National Oceanic and Atmospheric Administration, for the recent marine data used in Fig. 5. This work was funded by the Carbon Dioxide Research Division, US Department of Energy, grant no. DE-FGO2-86-ER60397.

- 14. Bradley, R. S. & Jones, P. D. in Detecting the Climatic Effects of Increasing Carbon Dioxide (eds MacCracken, M. C. & Luther, F. M.) 29-53 (U.S. Dept of Energy, 1985). Wright, P. B. Mon. Weath. Rev. 114 (in the press).

- Wight, F. B. Moll. Wealth. Reb. 114 (In the picss).
 Folland, C. K., Parker, D. E. & Newman, M. in Proc. 9th Annual Climate Diagnostics Workshop, 70-85 (U.S. Dept. of Commerce, NOAA, Washington DC, 1984).
 Folland, C. K. & Kates, F. E. in Milankovitch and Climate (eds Berger, A., Imbrie, J., Hays, J., Kukla, G. & Saltzman, B.) 721-727 (Reidel, Dordrecht, 1984).
- 18. Barnett, T. P. Mon. Weath. Rev. 112, 303-312 (1984).
- 19. Cavan. D. R. Mon. Weath. Rev. 108, 1293-1301 (1980).
- 20. Saur, J. F. T. J. appl. Met. 2, 417-425 (1963).
- James, R. W. & Fox, P. T. Comparative sea-surface temperature measurements, Marine Science Affairs Rep. No. 5, WMO Publ. No. 336 (Geneva, 1972).
- Kirkaldy, A. W. British Shipping, Its History, Organization and Importance (Kegan Paul, Trench, Trubner, London, 1919).
- Krümmel, O. Handbuch der Ozeanographie, Vol. 1 (Engelhorn, Stuttgart, 1907).
 Brooks, C. F. Mon. Weath. Rev. 54, 241-253 (1926).
- 25. Raper, S. C. B., Wigley, T. M. L., Mayes, P. R., Jones, P. D. & Salinger, M. J. Mon. Weath. Rev. 112, 1341-1353 (1984).
- Raper, S. C. B., Wigley, T. M. L., Jones, P. D., Kelly, P. M., Mayes, P. R. & Limbert, D. W. S. Nature 306, 458-459 (1984).
- 27. Kelly, P. M., Jones, P. D., Sear, C. B., Cherry, B. S. G. & Tavakol, R. K. Mon. Weath. Rev. 110. 71-83 (1982)
- 28. Wigley, T. M. L. & Schlesinger, M. E. Nature 315, 649-652 (1985). 29. Reynolds, R. W. & Gemmill, W. H. Trop. Ocean-Atmos. Newslett. No. 23, 4-5 (1984).

FTTERS TO NATURE

Observation of terrestrial orbital motion using the cosmic-ray Compton—Getting effect

D. J. Cutler* & D. E. Groom*

Department of Physics, University of Utah, Salt Lake City, Utah 84112, USA

* Present addresses: Instrumentation Laboratory, North 3939 Freya, Spokane Washington 99207, USA (D.J.C.); Supercollider Central Design Group, LBL 90-4040, Berkeley, California 94720, USA (D.E.G.)

Using underground observations, we have found a small diurnal amplitude modulation of the cosmic-ray muon intensity which agrees in amplitude and phase with a first-order relativistic effect due to the Earth's motion, as discussed by Compton and Getting more than fifty years ago. The parent particles are sufficiently rigid ($\sim 1.5 \, \mathrm{TeV}/c$) that solar and geomagnetic effects should be minor. The muon flux deep underground is relatively insensitive to near-surface meteorological effects, and temperature effects at production height would produce intensity variations nearly out of phase with the observed effect. Analysis of the arrival times of 5×10^8 muons during a period of 5.4 yr yields a fractional amplitude variation of $2.5^{+0.7}_{-0.6} \times 10^{-4}$, with a maximum near dawn, at $08:18\pm1.0$ h local mean solar time (LT). The expected amplitude is 3.40×10^{-4} , with the maximum at 06:00 LT.

Compton and Getting1 showed that a cosmic-ray detector with an energy threshold would observe an enhanced intensity when it moved along its direction of maximum sensitivity with respect to the rest frame of the cosmic-ray plasma. If the cosmicray energy distribution were a power law of the form $E^{-\gamma}$, then the fractional intensity enhancement above a fixed energy threshold should be

$$\frac{\Delta I(\theta)}{\langle I \rangle} = (2 + \gamma) \frac{v}{c} \cos \theta$$

where θ is the angle between the direction of detector sensitivity and its velocity vector. A term v/c arises because the detector sweeps out a column of the cosmic-ray plasma, another term 2v/c because the solid angle transformation increases the intensity in the direction of motion, and a term $(\gamma - 1)v/c$

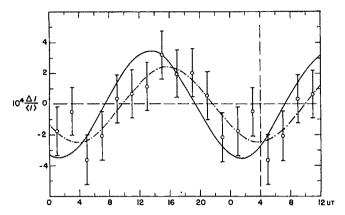


Fig. 1 Fractional muon intensity in 2-h intervals as a function of Universal Time. The dotted line is a two-parameter least-squares fit to the data; the solid curve is the *a priori* expectation due to the Earth's orbital motion. The error bars indicate a standard devation of $\sqrt{12/N_1}$, where a total of N_1 events were recorded.

because the Doppler shift of the energy spectrum changes the number of particles that exceed the detector's energy threshold. For a terrestrial detector at latitude λ sensitive to normally incident particles, and for $\gamma=2.75\pm0.03$ (ref. 2), the Earth's orbital velocity should lead to a diurnal amplitude modulation of $4.75\times10^{-4}\cos\lambda\cos^2{(i/2)}$, where i is the inclination of the Earth's axis. To first order in eccentricity there are no eccentricity effects. The effect should peak near dawn (06:00 LT), when the detector is sensitive in a direction most nearly parallel to that of the Earth's velocity.

The detector, located in a mine near Heber, Utah, was designed to measure the sidereal anisotropy of the cosmic-ray intensity, and is described in a report³ of the analysis of the first 3-yr data segment. Three layers of 100 plastic scintillators each were separated by concrete absorbers. The 25 × 154-cm counters were arranged in the north-south direction to optimize hourangle resolution. A detailed readout of triple-coincidence events permitted recognition of single muons at various angles. The muon threshold energy, as intensity-averaged over the topography, was 128 GeV. This energy corresponds to a median primary rigidity (momentum per unit charge) of 1,520 GeV/c (ref. 4), if 79% of the primaries are assumed to be protons. At this rigidity, the cyclotron radius of a particle at the Earth's orbit would be ~6 AU, and in interstellar space ($\mu \approx 2 \mu G$) about 170 AU, or 10⁻³ pc. Because of overburden details, the effective position of the detector was displaced 1.1° north of its actual position (to 41.7° N) and 9.3° east (to 110.8° W). As a consequence, 06:00 LT occurred at 13:24 Universal Time (UT), and at this latitude the expected fractional amplitude of the Compton-Getting effect should be 3.40×10^{-4} .

Data were recorded with an average muon trigger rate of 4.7 s⁻¹ between 4 January 1978 and 20 May 1983. The detector was operational 64% of the time; most of the down-time was the result of interrupted or ill-conditioned power. During this period 4.8×10⁸ muons were recorded in 60,500 half-hour summary records. After correcting for any dead channels⁵ and re-binning to correct for the hour-angle differences between different angular bins, the data were Fourier-analysed to search for spectral features near harmonics of (24 h)⁻¹. As a check, the data were also folded with sidereal and solar periods. Such 'folded light curves' agreed well with curves synthesized from the Fourier amplitudes. Figure 1 shows the results at the solar frequency. No evidence for solar harmonics higher than the first was found. Analysis of the sidereal frequency case will be published elsewhere.

Figure 1 also shows the *a priori* expectation discussed above (solid curve) and a two-parameter least-squares fit to the data (dash-dot curve). The least-squares fit has an amplitude of

 $2.47^{+0.72}_{-0.55} \times 10^{-4}$ and peaks at $15:42\pm1.0\,\mathrm{h}\,\mathrm{UT}$ (08:18 LT). The position-dependent amplitude is chosen from an off-centre Rayleigh distribution, as discussed in ref. 3. Quoted errors are such that the distance to the mean contains 34% of the area, in analogy to ±1 standard deviation (s.d.) errors for a normal distribution. The χ^2 for this fit is 3.8, which is unusually small for 9 degrees of freedom (d.f.). The probability of χ^2 being this small or less is $\sim8\%$. The data processing algorithms were tested for possible smoothing effects by processing Monte-Carlogenerated data with gaussian noise. As analysis of these data resulted in χ^2 s with expected values, we can only conclude that the low χ^2 observed with the real data is the result of a statistical fluctuation.

What other effects could confuse or mimic the Compton-Getting effect? Bending in solar magnetic fields should not be important at this rigidity, which was intentionally chosen to minimize such effects for the sidereal signal. The persistence of the sidereal signal reported in ref. 3 is evidence that this is the case. In addition, sidereal anisotropies have been reported at $500 \, \text{GeV/}c$ (refs 6, 7) and 1,000 $\, \text{GeV/}c$ (ref. 8), indicating that at even lower momenta the streaming direction in interstellar space is not lost in penetrating the Solar System. Even if directions were smeared by the solar fields, all that is required for observation of the diurnal Compton-Getting effect is that the cosmic-ray plasma moves with constant velocity in the Sun's rest frame.

According to detailed integrations by D. J. Cooke (personal communication), a normally incident 1,000-GeV/c proton at the Utah detector would have been deflected 1.2° to the east by the Earth's magnetic field. An analytical calculation with a simple dipole field model yields an effect which is slightly larger, but still negligible. However, this geomagnetic field might easily wash out the Compton-Getting effect at lower energies, where sensitivity to solar activity would also be expected.

Meteorological effects are more problematical. Most cosmicray muons come from meson decay in the upper atmosphere, at a mean height of ~200 mbar. Because the competition between interaction and decay is sensitive to air density, the muon intensity is greater when the stratosphere is warmer. More specifically, the fraction of pions with energy E_{π} which decay rather than interact at the mean production height is (1+ E_{π}/B_{π}), where the energy scale $B_{\pi} \approx 112 \text{ GeV}$ is proportional to temperature9. When kaons are included, the total temperature coefficient of $\Delta I/\langle I \rangle$ is $2.9 \times 10^{-3} \text{ K}^{-1}$. An effect as large as that expected from the Compton-Getting effect would thus occur if the diurnal temperature modulation of the upper atmosphere were as large as 0.1 °C; in fact, temperature effects larger than this are expected 10,11 . Similarly, a pressure coefficient of $-5.4 \times$ 10⁻⁵ mbar⁻¹ is expected, mostly because the increased muon range during a high-pressure period implies a higher energy threshold and therefore reduced intensity at the detector.

Meteorological effects have already received extensive attention ¹²⁻¹⁴, and we conclude that correlations between temperature and pressure in radiosonde data result in incorrect experimental coefficients¹⁵; that dominant pressure effects are not particularly correlated with the diurnal period and will thus tend to average out in a least-squares sense; and that radiosonde pre-flight setting errors of as much as ±1 K make detailed temperature corrections impossible. Our main evidence that temperature effects are small comes from the phase of the observed effect. A temperature-related maximum should occur several hours after solar noon, nearly out of phase with the observed effect. The amplitude reduction and slight phase lag which we observe is consistent with a temperature wave with amplitude 0.07 K and a maximum at 15:00 LT.

In principle, we might divide the data to simultaneously 'observe' two directions 90° apart, and by subtraction eliminate meteorological effects. In practice, most statistical significance is lost in the process. This approach has been used successfully at lower energies (where the counting rate is higher)¹⁶, but where

geomagnetic and solar effects are important.

The orbital motion Compton-Getting effect surely exists, and generations of cosmic-ray experiments have made corrections for it, and used evidence of some signal as evidence for freedom from solar modulation. At the same time, direct observation of the effect has been curiously rare. At 500 GeV/c, Davis and co-workers^{6,7} report consistency with the effect. Gombosi et al. 17 report it as below noise level in their air shower work at ~3× 10¹³ eV/c. The strongest evidence comes from a report by the Mt Norikura group 18, who report a 1.9-s.d. effect with the expected phase in their $\sim 10^{14} \text{ eV}/c$ air shower observations. The present results seem to represent the best confirmation to date of this classic effect.

This work was supported by NSF grant AST80-10727. The historical involvement of H. E. Bergeson, J. F. Davis, A. Larson, J. West and countless students is gratefully acknowledged.

Received 28 March; accepted 24 April 1986.

- Compton, A. H. & Getting, I. A. Phys. Rev. 47, 817-821 (1935).
- Ryan, M. J., Ormes, J. F. & Balasubrahmanyan, V. K. Phys. Rev. Lett. 28, 985-988 (1972).
 Cutler, D. J., Bergeson, H. E., Davis, J. F. & Groom, D. E. Astrophys. J. 1166-1178 (1981).
- T. K. J. geophys. Res. 79, 2281-2286 (1974); Proc. 2nd int. Cosmic-Ray Symp. Jap.
- Groom, D. E., Loh, E. C., Nelson, H. N. & Ritson, D. M. Phys. Rev. Lett. 50, 573-576 (1983).
- Davis, S. T., Elliot, H. & Thambyahpillai, T. Proc. 16th int. Cosmic-Ray Conf., Kyoto 4, 210-214 (1979).
- Davis, S. T., Elliot, H., Marsden, R. G., Thambyahpillai, T. & Dutt, J. C. Planet. Space Sci. 27, 733-738 (1979).
- Fenton, A. G. & Fenton, K. B. Proc. 14th int. Cosmic Ray Conf., Munich 4, 1482-1484 (1975).

 Barrett, P. H., Bollinger, L. M., Cocconi, G., Eisenberg, Y. & Greisen, K. Rev. mod. Phys. 24, 133-178 (1952).
- 10. Chapman, S. & Lindzen, R. S. Space Sci. Rev. 10, 3 (1969)
- 11. Finger, F. G. & McInturff, R. M. J. atmos. Sci. 25, 1116 (1968).
- 12. Dorman, L. I. Cosmic Ray Variations (State Publishing House, Moscow, 1957).
 13. Hashim, A., Speller, R. D. & Thambyahpillai, T. J. atmos. terr. Phys. 34, 1525-1535 (1972).
- Lyons, P. R. A., Fenton, A. G. & Fenton, K. B. Proc. 17th int. Cosmic Ray Conf., Paris 4, 300-303 (1981).
- 15. Cutler, D. J. & Groom, D. E. Proc. 17th int. Cosmic Ray Conf., Paris 4, 290-293 (1981).
- 16. Bercovitch, M. Proc. 17th int. Cosmic Ray Conf., Paris 10, 246-249 (1981).
- Gombos, T., Kota, J., Somogy, A. J. & Varga, A. Nature 255, 687-689 (1975).
 Nagashima, K. et al. Proc. 14th int. Cosmic Ray Conf., Munich 4, 1503-1508 (1975).

Prospecting for planets in circumstellar dust: sifting the evidence from β Pictoris

David J. Diner & John F. Appleby

Earth and Space Science Division, Jet Propulsion Laboratory, California Institute of Technology, 4800 Oak Grove Drive, MS 183-301, Pasadena, California 91109, USA

Spectroscopic evidence for an extended gaseous shell around the A5V star β Pictoris has been available for more than a decade¹⁻⁵. Recently, the presence of a vast circumstellar cloud of particles was deduced from Infrared Astronomy Satellite (IRAS) measurements of excess thermal flux⁶⁻⁸. This interpretation is supported by a near-infrared (0.89 µm) coronagraphic image of the region beyond 100 AU from β Pic, which shows scattered starlight in a configuration consistent with a disk viewed nearly edge-on9. Conceivably, the β Pic system may represent one phase of planetary evolution. From an analysis of visible photometry and their coronagraph data, Smith and Terrile9 suggested that planetary accretion has swept out an extensive (~30 AU) clearing at the centre of the disk. We report here a new analysis of the same data and the results of including the IRAS observations in the analysis. The consequent models do not produce a large inner clearing and suggest alternatively that significant particle number densities occur within several AU of the star. An illustrative case is used to evaluate the short-wavelength detectibility of circumstellar disks in less favourable orientations than that surrounding β Pic.

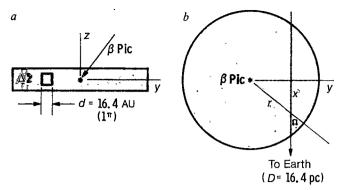


Fig. 1 Geometrical coordinates used in analysing the groundbased and IRAS observations of the disk orbiting β Pic. The disk is taken to be uniformly thick in the vertical direction and in an edge-on orientation as seen from Earth. a, Edge-on view; b, top

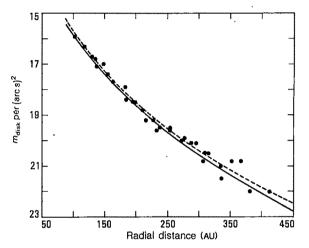


Fig. 2 Comparison of models for m_{disk} per $(\text{arc s})^2$ as a function of radial distance from β Pic (lines) with the observations of Smith and Terrile⁹ (filled circles). Dashed line, model derived from a fit to the coronagraph data only, assuming the modified gamma distribution for σ and g = 0.8. Solid line, model derived from a simultaneous fit to the coronagraph and IRAS measurements using g = 0.8 and $T_1 = 440$ K. Within the limits specified in the text, other choices for g and T_1 do not significantly affect the quality of the fit. The radial distribution parameters obtained for the models shown are $\eta = 0.15$, $\gamma = 0.50$ and $r_0 = 7.19$ AU for the 'coronagraph only' case and $\eta = 2.09$, $\gamma = 0.31$ and $r_0 = 0.03$ AU for the 'coronagraph + IRAS' case.

As a first step in modelling scattered light from the central star, it is appropriate to neglect attenuation of radiation traversing the disk and multiple-scattering effects. Thermal emission at 0.89 µm is justifiably ignored because the high radiating temperatures (for example, ~530 K at 200 AU) required to match the observed 0.89-µm brightness would make the disk brighter than the star at 2.2 µm, a wavelength at which no flux excess is observed8. In addition, because molecular scattering by the gaseous envelope of hydrogen inferred spectroscopically would require an H₂ abundance greatly exceeding the upper limit of $\sim 2M_{\oplus}$ (ref. 5; M_{\oplus} = mass of Earth), it is reasonable to interpret the observed features in the coronagraph data as starlight scattered by solid material. Integrating the scattering source function along the line of sight yields disk magnitude per (arcs)2 as a function of distance from the star:

$$m_{\rm disk}(y) \, \text{per (arc s)}^2$$

= $m_{\rm I} - 2.5 \log \frac{d^2}{4\pi} \int_{-\infty}^{\infty} \frac{\sigma[r(x, y)]}{x^2 + y^2} \, p[\Omega(x, y)] \, \mathrm{d}x$ (1)

Geometrical coordinates are shown in Fig. 1 and d = 16.4 AU

(1 arc s at the distance of β Pic from Earth), σ (AU⁻¹) is the radially varying scattering coefficient, p is the single-scattering phase function, assumed dependent only on the scattering angle Ω , and $m_{\rm I}$ is the I (0.89- μ m) magnitude of the star. We use $m_{\rm V}=3.85$ for the visual magnitude of β Pic¹⁰, and $m_{\rm V}-m_{\rm I}=0.23$ for an A5V star¹¹.

Smith and Terrile's analysis9 of the coronagraph data relied on several assumptions: an edge-on disk, a power-law distribution for the scattering coefficient (that is, $\sigma \propto r^{-\zeta}$) and isotropic scattering. In addition, because the absolute visual magnitude $M_{\rm V}$ of β Pic (2.78, based on a distance D of 16.4 pc) is 0.8 mag fainter than a typical A5 main-sequence star and 0.3 mag fainter than an A5 star on the zero-age main sequence (ZAMS)^{11,12}, they adopted a mean extinction of 0.5 mag relative to stars of the same type and luminosity class. This implies an optical depth of 0.46 in front of the star. Finally, because the power law is singular at the origin, they assumed $\sigma = 0$ for radial distances within an inner boundary whose location is governed by the adopted line-of-sight opacity in front of the star. From this analysis they concluded that the inner ~30 AU of the disk is relatively clear and that there is a fairly abrupt and substantial increase in disk opacity just outside the inner clear zone, beyond which σ decreases as the inverse cube of the radial distance. Under the assumption that the relative variation of σ is representative of changes in particle number density, a highly efficient mechanism must be invoked to explain the extensive clearing. As the inferred size of the clear region is of similar extent to our own Solar System, it is tempting to speculate that this paucity of material is the result of sweeping out by planetary accretion.

To test Smith and Terrile's model⁹ for uniqueness, we examined in detail several of their assumptions. First, we note that the inner clearing was artificially imposed a priori by the need to remove the singularity in the power law. To avoid this problem, we employed a continuous and bounded function for σ , namely, the modified gamma distribution¹³:

$$\sigma(r) = \sigma'(r/r_0)^{\eta} \exp\left[-(r/r_0)^{\gamma}\right] \tag{2}$$

The flexibility of this function allows for varying degrees of depletion at small r and rates of decay at large r. Second, instead of isotropic scattering, we used the Henyey-Greenstein phase function $p = (1 - g^2) (1 + g^2 - 2g \cos \Omega)^{-3/2}$ to represent more realistically the scattering by particulates¹⁴. In this expression, g is an asymmetry parameter equal to the average scattering angle cosine. Third, we examined all A5V stars in the Bright Star Catalogue¹⁰ with parallaxes >0.02 arcs (that is, within 50 pc, for which interstellar extinction is negligible). We find the cumulative mean and standard deviation of M_V for stars closer than 20, 30, 40 and 50 pc to be 3.45 ± 0.52 , 2.60 ± 0.81 , 2.53 ± 0.75 and 2.27 ± 0.73 , respectively, showing that the dispersion in M_V is comparable to or larger than the deviation of β Pic from the typical main-sequence and ZAMS values. Combined with the fact that the uncertainty of ± 2.9 pc in the distance to β Pic (D. Hoffleit, personal communication) corresponds to an additional 0.4 mag uncertainty in $M_{\rm V}$, we ascribe no statistical significance to the 0.5 mag extinction adopted by Smith and Terrile⁹. Noting furthermore that a correct assessment of the effect of disk opacity on $M_{\rm v}$ must include the scattering of light towards Earth in addition to attenuation of the direct stellar beam, we argue that the visible photometry does not provide a useful constraint on the optical properties of the disk. Instead, we included IRAS observations in our analysis.

The measured infrared magnitudes of β Pic are 2.66, 0.04, -2.75 and -3.41 at 12, 25, 60 and 100 μ m, respectively⁸. The magnitude scale is defined such that 0 mag at any wavelength corresponds to the flux from a black body at $T_{\rm ref}=10,000~{\rm K}$ radiating into a solid angle $S_{\rm ref}=1.57\times 10^{-16}$ ster. Using $T_*=8,500~{\rm K}$ as the effective temperature of an A5V star¹¹, we calculate the solid angle of β Pic from the K (2.2- μ m) magnitude⁸ of 3.47. The result implies $R_*/R_\odot=1.17$ (where R_* and R_\odot

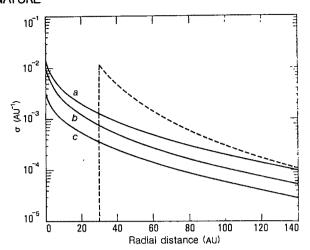


Fig. 3 Scattering coefficient σ at 0.89 μ m as a function of radial distance from β Pic, using the modified gamma distribution and fitting only the coronagraph data with several choices of g (a, 0.9; b, 0.8; c, 0.6). Smith and Terrile's model⁹, also derived using only their coronagraph data, is shown for comparison (dashed line) and predicts $\sigma = 1.17 \times 10^{-2} \, \mathrm{AU}^{-1}$ at 30 AU, no material inward of this distance, and an r^{-3} dependence beyond 30 AU. (These values are taken directly from ref. 9. We note, however, that use of Smith and Terrile's model assumptions and our equation (1) implies values of σ approximately a factor of five smaller.) Given the lack of direct near-infrared measurements within 100 AU, this figure demonstrates the sensitivity of the derived radial opacity distribution to the assumed functional form used to fit the data.

are, respectively, the radius of β Pic and that of the Sun). Because the IRAS fields of view are large relative to the disk dimensions implied by the coronagraph data, the measured infrared flux is equal to the sum of the stellar flux and the contribution from the entire disk. For an optically thin disk in which each element radiates isotropically, the orientation is immaterial and the simplest method of calculating the disk flux is to imagine a face-on rather than edge-on view. Letting B_{λ} denote the Planck function at wavelength λ , $T_{\rm d}$ the temperature of the disk at radius r, and Δz the vertical geometric thickness, and assuming for simplicity that the infrared absorption coefficient α is wavelength-independent at 12–100 μ m and follows the same radial distribution as the near-infrared scattering coefficient α (see equation (2)), we derive model infrared magnitudes

$$m_{\lambda} = -2.5 \log \left\{ \frac{\exp(c_2/\lambda T_{\text{ref}}) - 1}{D^2 S_{\text{ref}}} \left[\frac{\pi R_{*}^2}{\exp(c_2/\lambda T_{*}) - 1} + 2\pi r_0 \alpha' \Delta z \int_0^\infty \frac{(r/r_0)^{n+1} \exp[-(r/r_0)^{\gamma}] dr}{\exp[c_2/\lambda T_d(r)] - 1} \right] \right\}$$
(3)

where $c_2 = 1.43883$ cm K. Radiative equilibrium between the dust grains in the disk and the central star implies $T_d = T_1 r^{-1/2}$ (r in AU), where the temperature at 1 AU, T_1 , depends on the optical properties of the disk material.

The iterative method of nonlinear least-squares ¹⁵ was used to fit, first, the coronagraph data only and, second, the coronagraph and IRAS data simultaneously. At each iteration step, the 0.89- μ m solution was normalized to 19.5 mag (arc s)⁻² at 250 AU and the product $\alpha'\Delta z$ was determined by averaging the values required to match the 25- and 60- μ m observations. All integrals were evaluated numerically. Individual models were characterized by specifying values for the Henyey-Greenstein asymmetry parameter and the disk temperature at 1 AU. Due to the variety of mechanisms which promote removal of very small particles over long timescales, we assume grain sizes \geqslant visible wavelengths, in which case the limits ¹⁶ $0.6 \leqslant g \leqslant 0.9$ and the range ^{17,18} $200 \leqslant T_1 \leqslant 600$ K encompass a wide variety of particle

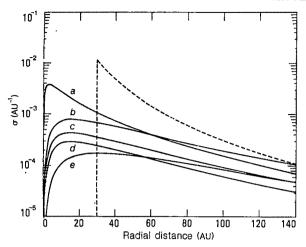


Fig. 4 Scattering coefficient σ at 0.89 μ m as a function of radial distance from β Pic, using the modified gamma distribution and fitting the coronagraph and IRAS data simultaneously for various choices of g and T_1 : a, $(g = 0.8, T_1 = 200 \text{ K})$; b, (0.9, 440); c (0.8, 440)440); d, (0.6, 440); e, (0.8, 600). The distribution at small radial distances is governed primarily by the IRAS results; note that a cooler disk requires larger opacity near the star to fit those data. Increased disk opacity is also required for higher values of g, to compensate for the decrease in amount of starlight scattered towards Earth. As an example of the magnitude of derived disk opacities, we use the case with g = 0.8 and $T_1 = 440$ K (model c) for illustration. We calculate a peak vertical (z-direction) infrared absorption optical depth of 1.5×10^{-3} , which occurs at 15 AU from the star in this model. The corresponding scattering opacity in the near-infrared depends on an assumed value for Δz : we compute in this case a peak vertical near-infrared scattering optical depth of 4.3×10^{-3} for each 10 AU of disk thickness. Note that in models a-e, significant disk opacity (50% of the peak value) is found within several AU of the star. Smith and Terrile's model⁹ is shown for comparison (dashed line).

sizes and complex refractive indices. The range for T_1 has been scaled from calculations performed for studies of the zodiacal cloud. Note that the value $T_1 = 440 \text{ K}$ is the equilibrium temperature for black-body grains.

The least-squares iteration was ended following negligible improvement in the sum of the squares of the residuals between the measurements and corresponding model magnitudes. Comparisons of our model 0.89-um magnitudes with the coronagraph data indicate excellent fits (see Fig. 2). When the IRAS data are excluded from the fitting procedure, the predicted infrared magnitudes, not surprisingly, do not match the IRAS data. For example, the model with g = 0.8 yields 12-, 25-, 60- and 100- μ m magnitudes of 0.80, -0.78, -2.28 and -2.89, respectively. Choosing $T_1 = 440 \text{ K}$ for illustration and including the IRAS data, these values become 2.55, -0.05, -2.66 and -3.66 mag. This is a satisfactory fit, especially in view of our simple assumptions. Thus, the introduction of further complexity into the modelling is not warranted until additional observations (such as spatially

resolved infrared data or coronagraphic images with greater radial coverage) become available. We note that the goodnessof-fit to the IRAS data is not particularly sensitive to g and that the warmer-disk models give better fits at 12-100 µm. The models which incorporate the IRAS data predict no flux excess at 2.2 µm and ~ 0.02 mag at 5 μ m.

The scattering coefficient at 0.89 µm derived by fitting the coronagraph data only is shown in Fig. 3 for several values of g. Figure 4 shows $\sigma(r)$ derived from simultaneous fits of the coronagraph and IRAS data for several combinations of g and T_1 . The Smith and Terrile model⁹ is reproduced in both figures. Note that for all of our models, significant opacity occurs well within the region which they inferred to be swept clear of material. Thus, these models indicate no sizeable inner clearing, particularly of the scale inferred by Smith and Terrile. It remains an open question whether planetary formation must be invoked to explain the distribution of disk material. Other mechanisms could account for a decrease in opacity close to the star, such as loss of particles due to radiative, electromagnetic or aerodynamic effects; or a change in particle properties such as a decrease in mean size.

One practical application of combined modelling of scattered and emitted radiation is in predicting the detectibility of randomly oriented circumstellar disks by coronagraphic imaging. The nearly edge-on orientation of the β Pic disk provides the most favourable condition for detection of scattered starlight. Taking m_{disk} per $(\text{arc s})^2 < 22$ as a reasonable ciriterion for detection (see Fig. 2) and using the case with g = 0.8 and $T_1 = 440$ K for illustration, we calculate that if the β Pic disk were in the less favourable face-on oreientation, it would be detectable by coronagraphic imaging at 100 AU from the star if its vertical geometric thickness (Δz) is greater than a few tenths of an AU and at 200 AU radial distance if $\Delta z \ge 4$ AU. IRAS has identified a number of stars with thermal infrared excesses, but with the exception of β Pic, attempts to obtain optical images of the material around those stars have, to our knowledge, not been successful.

In future, simultaneous acquisition of scattered-light and thermal infrared observations of stars with circumstellar shells or disks should be a promising method of determining the nature and distribution of orbiting material. Spatially resolved infrared observations, perhaps obtained interferometrically, combined with multi-spectral coronagraphic images with smaller occulting masks, would be very useful in characterizing circumstellar disk structure. The degrading effects of the terrestrial atmosphere probably dictate acquisition of such data from a spaceborne platform. Determination of the ubiquity of objects such as β Pic, evaluation of whether orientation of circumstellar disks is a critical factor governing their detectibility, and placement of such systems into the context of planetary evolution must await the collection and analysis of further infrared and coronagraphic observations.

We thank H. H. Aumann, J. Diner, M. S. Hanner, J. V. Martonchik, D. J. McCleese and J. A. Russell for helpful discussions and W. Wells for care in preparation of the manuscript. This work was carried out by the Jet Propulsion Laboratory, California Institute of Technology, under contract with NASA.

Received 13 January; accepted 7 April 1986.

^{1.} Sletteback, A. Astrophys. J. 197, 137-138 (1975)

^{2.} Sletteback, A. Astrophys. J. Suppl. Ser. 50, 55-84 (1982).

Sietteback, A. & Carpenter, K. G. Astrophys. J. Suppl. Ser. 53, 869-892 (1983).
 Kondo, Y. & Bruhweiler, F. C. Astrophys. J. 291, L1-L5 (1985).

^{5.} Hobbs, L. M., Vidal-Madjar, A., Ferlet, R., Albert, C E. & Gry, C. Astrophys. J. 293, L29-L33 (1985).

Aumann, H. H. Bull. Am. astr. Soc. 16, 483 (1984).
 Aumann, H. H. et al. Astrophys. J. 278, L23-L27 (1984)

Aumann, H. H. Publs astr. Soc. Pacif. 97, 885-891 (1985) 9. Smith, B. A. & Terrile, R. J. Science 226, 1421-1424 (1984).

^{10.} Hoffleit, D. & Jaschek, C. The Bright Star Catalogue (Yale University Observatory, New Haven, 1982).
Allen, C. W. Astrophysical Quantities (Athlone, London, 1981).

Crawford, D. L. Astr. J. 84, 1858-1865 (1979); 85, 621-622 (1980).

Deirmendiian, D. Electromagnetic Scattering on Spherical Polydispersions (Elsevier, New

^{14.} Irvine, W. M. Icarus 25, 175-204 (1975).

Bevington, P. R. Data Reduction and Error Analysis for the Physical Sciences (McGraw-Hill,

New York, 1969).

16. Hansen, J. E. & Travis, L. D. Space Sci. Rev. 16, 527-610 (1974).

17. Lamy, Ph. L. Astr. Astrophys. 35, 197-207 (1974).

18. Röser, S. & Staude, H. J. Astr. Astrophys. 67, 381-894 (1978).

Radio observations of PKS2314+03 during occultation by comet Halley

S. K. Alurkar, R. V. Bhonsle & A. K. Sharma

Physical Research Laboratory, Ahmedabad-380009, India

Strong interplanetary scintillations (IPS) were recorded at 103 MHz at Thaltej (23°02′ N, 72°36′ E) between 18 and 20 December 1985, when the quasar PKS2314+03 was occulted by the ion tail of comet Halley. The scintillation periodicities were near 1 s and their amplitudes decreased progressively as the source approached the end of the tail. The scintillating flux density on these days was 18.2, 11.4 and 4.7 Jy when the source was ~86° from the Sun. The r.m.s. density variations were 10, 6 and 3 electrons cm⁻³ on 18, 19 and 20 December respectively, and varied with distance r from cometary nucleus as $r^{-3.3}$. Assuming an ion velocity of 100 km s⁻¹, we show here that the observed periodicity of 1 s implies ion density inhomogeneities of the order of 100 km.

Comets develop ion or type I tails when they are 2-4 AU from the Sun¹. Plasma features such as kinks and knots seen in these tails are caused through interaction with the solar wind^{2,3}. Plasma density inhomogeneities in the solar wind scatter radio waves from a compact radio source and produce interplanetary scintillations that apparently broaden the radio source⁴. Attempts have been made to observe the angular broadening of radio sources as they were occulted by comet Arend-Roland⁵, and scintillations were observed during the occultation of radio source PKS2025-15 by comet Kohoutek⁶.

Regular observations of seven radio sources in the declination range +2° to +23° were made during December 1985 at Thaltej using a 10,000-m² correlation interferometer operating as a transit instrument at 103 MHz (ref. 7). Of these, six were scintillating sources. Sine and cosine outputs of the correlation receiver, together with a scintillometer⁸ output, were recorded

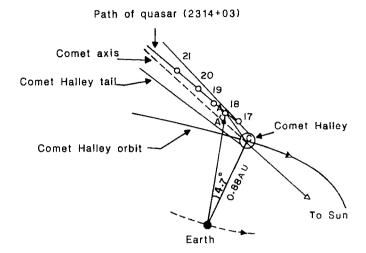


Fig. 1 Geometry, not to scale, of the occultation of PKS2314+03 (3C459) by comet Halley.

on a strip chart. These outputs, sampled 20 times per second, were recorded with time information on a digital magnetic tape. A real-time fast Fourier transform spectrum analyser (Model 512/S Rockland) can provide an average power spectrum of the scintillating source over a frequency range of 0.1-20 Hz.

Comet Halley was predicted to occult PKS2314+03 (or 3C459) during the period 17-21 December 1985. 3C459 is a scintillating source with \sim 70% of the total flux in the 0.45 arc s component⁹.

Figure 1 shows the geometry of the occultation for the period 17-21 December, for which the path of 3C459 as seen through the comet tail is indicated. The comet's position angle on 18 December was $\sim 66^{\circ}$, and the quasar on that day was 87.5° away from the Sun. Some relevant parameters of the occultation are summarized in Table 1. 3C459 has been observed since the

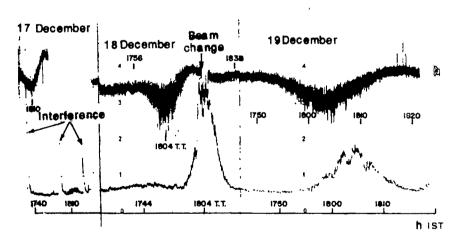
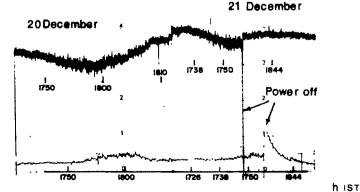


Fig. 2 103-MHz recordings of 3C459 during 17-21 December 1985. Top trace in each panel, sine receiver output; bottom trace, scintillometer output. Chart speed on 17 and 18 December was 5 and 10 cm h⁻¹, respectively, and 20 cm h⁻¹ thereafter. Note the strong scintillations on 18 and 19 December and weaker scintillations on 20 December.



beginning of December 1985, when it was $\sim 103^{\circ}$ from the Sun. Its average scintillating flux density was 3.5 Jy until 17 December, when the source was observed through the cometary tail at a distance of 0.08 AU from its nucleus.

On 18 December, however, as shown in Fig. 2, very intense scintillations were recorded when the distance from the comet nucleus to the point of intersection of the line of sight with the tail (AC in Fig. 1) was 0.12 AU. On 19 and 20 December the scintillations decreased progressively, when the corresponding distances were ~0.14 and 0.18 AU. Note that only sine and scintillometer outputs are shown in the recordings of Fig. 2, as the deflection due to 3C459 appears only on the sine response of the correlation receiver. On 21 December, when the source-comet distance was 0.2 AU, the scintillating flux density of 3C459 decreased to ~3.3 Jy.

Following the calibration procedure suggested by Duffett-Smith¹⁰ for estimating the mean source flux and the scintillating flux, IPS observations on 18-21 December, shown in Fig. 2, were analysed. The scintillometer outputs on these days correspond to r.m.s. scintillating flux densities of 18.2 ± 0.04 , 11.4 ± 0.04 , 4.7 ± 0.04 and 3.3 ± 0.04 Jy. Thus, the scintillation index, m (=r.m.s. scintillating flux/mean source flux) values become 0.42, 0.27, 0.11 and 0.08 respectively, for a mean source flux of 43 Jy.

Note that the average scintillating flux of 3C459 when it is $\sim 90^{\circ}$ away from the Sun is usually 3.5 Jy and reaches a maximum of ~ 12 Jy at 28-30°, when *m* begins to turn over at 103 MHz. Allowing for day-to-day maximum variations of 2-3 times 3.5 Jy, the measured scintillating flux values during the occultation by comet Halley are very significant.

The scintillation spectra (computed by the real-time spectrum analyser) obtained between 17 and 20 December are shown in Fig. 3. These were normalized with respect to the maximum value and are source spectra computed as the difference between 'on-source' and 'off-source' spectra, each averaged over 10 min. The spectra resemble typical IPS spectra¹¹, with a nearly flat low-frequency region below the spectral variations at \sim 0.2 Hz on 17 and 20 December, and at \sim 0.6 and 0.4 Hz on 18 and 19 December, respectively, when the scintillations were very strong. Auto-correlation analysis of the spectra gave average scintillation periodicities of 1.0 s.

The solar and ionospheric disturbances which might have caused these scintillations were studied using the data for the period 2-22 December 1985 (see ref. 12). Solar activity throughout this period was 'very low', while geomagnetic activity was 'quiet to unsettled', with no Sc-type magnetic storms. Furthermore, ionospheric beacon satellite data at very high frequency and ionograms at Ahmedabad did not indicate scintillation activity and spread-F respectively during this period.

An interplanetary transient or ionospheric scintillation causing the enhancement in scintillation of 3C459 was ruled out by studying IPS of 3C298, 3C318, 3C324, 3C368, 3C409 and 3C459, covering the declination range +2° to +23°, which were being regularly observed. Of these, 3C298 and 3C368 are within 8° declination of 3C459. Using many scintillating sources, Hewish et al. derived the shape and dynamics of large-scale interplanetary transients, which cover a typical solid angle of helio-

Table 1 Parameters of the occultation geometry Comet nucleus-Comet-Geocentric Solar Earthsource Date distance elongation (December along axis of comet of 2314+03 1985) (AU) (deg.) (AU) (deg.) 0.08 0.86 87.5 3.4 18 0.12 4.7 0.88 86.5 5.9 7.0 19 0.14 0.90 85.5 20 0.18 0.92 84.5 0.94 83.5 21 0.20

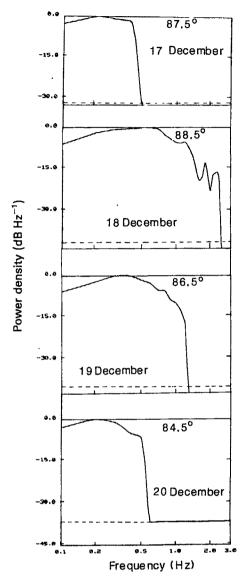


Fig. 3 Scintillation spectra of 3C459 on 17-20 December 1985. Dashed lines indicate noise level. Numbers in upper right-hand corners are solar elongations of 3C459.

longitude and latitude of $\pi/2$ sr. They also showed a strong correlation between enhancement in scintillation and total plasma density along the line of sight to a source. Except for 3C459, no other source showed enhanced scintillations during 18-20 December 1985, indicating that the enhancement was restricted to the direction of 3C459.

Thus, the strength of the observed scintillations in the direction of 3C459, and their progressive decrease from 18 to 21 December 1985 during the expected occultation of the source by comet Halley, strongly support our conclusion that the scintillations were caused by the scattering of the radio waves by density inhomogeneities in the ion tail of comet Halley.

The values of m on 18-21 December depend on the source-comet distance along the axis of the comet (A'C in Fig. 1), such that $m \propto r^{-3.3}$, where r in AU is the distance between the comet nucleus and A', the projection of A on the comet axis. For gaussian irregularities with weak scattering, and for a layer of thickness L containing density irregularities of scale size a, m is given by n4

$$m^2 = 2(\pi)^{1/2} r_a^2 \lambda^2 \langle \Delta N^2 \rangle aL$$

 λ is the wavelength of radiation passing through the scattering layer and r_e is the classical electron radius. In the case of comet

Halley, L is the thickness of its cylindrical ion tail, which is $\sim 10^5$ km (ref. 15).

The scintillation periodicities of 1 s imply scale sizes of density inhomogeneities in the cometary ion tail of 100 km (assuming their average velocity of 100 km s⁻¹ (ref. 16)), which compares well with scale sizes in the solar plasma estimated from IPS measurements17

Using the above formula, the average values of the r.m.s. density variations, $(\Delta N^2)^{1/2}$, in the ion tail are 10, 6 and 3 electrons cm⁻³ on 18, 19 and 20 December 1985, respectively. If the mean ion density in the tail of comet Halley is assumed to be 10^2 ions cm⁻³ (ref. 18) then $\Delta N = 10$ corresponds to 10% modulation of the mean density. This modulation is much higher than 4% for the solar wind at 0.1 AU.

Note that on 17 December 3C459 had just begun to be occulted by the comet Halley tail at a distance of ~0.08 AU from its nucleus. Average scintillations were observed on that day. This may be due to insufficient turbulence in that tail region. Also, ion density condensations in cometary tails cannot exist within 0.1 AU of the nucleus, due to the stabilizing effect of solar wind turbulence on the Kelvin-Helmholtz instabilities 16,19

The length of the plasma tail of comet Halley over which scintillations were observed up to 20 December was ~0.10 AU or 1.5×10^7 km, which is in good agreement with optical measurements15

We thank Professor S. P. Pandya for interest and the staff of Radio Astronomy and Ionospheric Groups for assistance. Discussions with Professors B. Buti and R. K. Varma were useful. We appreciate valuable suggestions by Dr P. J. Duffett-Smith of Cavendish Laboratory. Financial support for this work came from Departments of Space, Science & Technology, Government of India.

Received 30 January, accepted 25 April 1986.

- 1. Brandt, J. C. Introduction to Solar Wind (Freeman, San Francisco, 1970)
- Jockers, K. & Lust, R. Astr. Astrophys. 26, 113-121 (1973).

 Ip, W.-H. & Axford, W. I. Comets (ed. Wilkening, L. L.) 588-636 (University of Arizona) Press, 1982).
- 4. Hewish, A. & Symonds, M. D. Planet. Space Sci. 17, 313-320 (1969)
- 5. Whitfield, G. R. & Hogbom, J. Nature 180, 602 (1957).
 6. Ananthakrishnan, S., Bhandari, S. M. & Pramesh Rao, A. Astrophys. Space Sci. 37, 274-283.
- 7. Alurkar, S. K., et al. J. Inst. Electron. Telecommun. Engrs 28, 577-582 (1982)
- Nulkati, S., & F. dt. S. Miss. Letteron. Fetcommen. English 83, 717-76.
 B. Duffett-Smith, P. J., Mon. Not. R. astr. Soc. 177, 349-355 (1976).
 Readhead, A. C. S. & Hewish, A. Mem. R. astr. Soc. 78, 1-49 (1974).
 Duffett-Smith, P. J., thesis, Cambridge Univ. (1976).

- Scott, S. L. thesis, Univ. California, San Diego (1978).
 Preliminary Report and Forecast of Solar Geophysical Data (Joint NOAA-1 SAF Space Environment Services Center, 1985).

 13. Hewish, A., Tappin. S. J. & Gapper, G. R. Nature 314, 137-140 (1985).

 14. Little, L. T. Meth. Exptl Phys. 12c, 118-137 (1976).

 15. Jockers, K. Proc. ESO Workshop, Paris (1982).

 16. Ershkovich, A. I. Space Sci. Rev. 25, 3-34 (1980).

- 17. Readhead, A. C. S., Kemp, M. C. & Hewish, A. Mon. Not. R. astr. Soc. 185, 207 225 (1978)
 18. Schmidt, H. U. & Wegmann, R. Comets (ed. Wilkening, L. L.) 538-560 (The University of
- Arizona Press, Tucson, 1982).

 19. Buti, B. Astrophys. J. 252, L43-L47 (1982).

Imaging the outflow of ionospheric ions into the magnetosphere

Y. T. Chiu*, R. M. Robinson*, G. R. Swenson*, S. Chakrabarti† & D. S. Evans‡

* Space Sciences Laboratory, Lockheed Palo Alto Research Laboratories, Palo Alto, California 94304, USA

† Space Sciences Laboratory, University of California, Berkeley, California 94720, USA

‡ Space Environment Laboratory, National Oceanic and Atmospheric Administration, Boulder, Colorado 80303, USA

The discovery of ionospheric ion outflow into the magnetosphere has been considered a major advance in magnetospheric physics in the past decade. Satellite measurements in situ are, however, too localized to address the global scope of the phenomenon. It is therefore important to consider methods to image the global outflow of ionospheric ions into the magnetosphere. We consider below the concept and verification of imaging the global ionospheric outflow by using spectrophotometric observations of farultraviolet and extreme-ultraviolet solar lines resonantly scattered by ionospheric ions or exospheric neutrals in the auroral regions of the magnetosphere. We shall also present new satellite observations which verify the concept and show that this imaging capability is feasible with present technology.

Our concept of magnetospheric imagery proposed here originated with the interpretation of high-sensitivity, high-resolution observations of the solar 304-Å emission line intensity resonantly scattered by He⁺ in the plasmasphere. The observations were obtained by an extreme-ultraviolet telescope on the Apollo-Soyuz mission¹. The line intensities, measured while the instrument line of sight was spinning with the spacecraft, were shown to be in excellent agreement with line-of-sight He⁺ density distributions predicted by a kinetic equilibrium model of the plasmasphere2, when ionospheric densities measured simultaneously by the AE-C satellite at 300 km altitude were used as boundary conditions of the model. The success of this experiment and interpretation suggests that an image in line emissions resonantly scattered by magnetospheric ions of ionospheric origin or exospheric neutrals may similarly be converted into

an image of their density distribution in the magnetosphere. Furthermore, if spectrometric information is available, the flow speed and temperature of the ions or neutrals can be derived, so that an image of the ionospheric ion outflow into the magnetosphere in the high-latitude region can be made. (For reviews of various aspects of the ion outflow phenomenon, see refs 3-6.)

The generalization of concepts stemming from the earlier He II 304-Å work¹ requires a search for other emission lines, because the high-latitude ion outflows consist primarily of O and H⁺, as well as some He⁺ in the polar cap. We have determined that the solar O II 834-Å line can be used analogously to the He II 304-Å line to determine O+ distributions and outflow. The proton has no resonant scattering lines; however, outflowing hot H+ can charge-exchange with cold exospheric neutral atoms to produce hot outflowing H⁰ which can, in turn, resonantly scatter Doppler-shifted Ly- α from the Sun. Thus, the same principle can be applied to Doppler-shifted Ly- α observations to determine the hot H⁰ distribution. We show that our concept is workable, in principle, and is verifiable with current observations, although there is no imaging capability in currently available instruments. Details of data deconvolution will not be considered.

As both the He⁺ and O⁺ lines can be treated analogously, we discuss these two together. Figure 1 summarizes the results of observation and interpretation of the He⁺ line in the plasmasphere.

For the He⁺ and O⁺ lines in the auroral region, there are two important sources of illumination: (1) solar line emission, F_s , and (2) auroral line emission, $F_{\rm a}$, excited at ~100 km altitude by electron impact. The solar flux F_s is uniform but, as the auroral source is close to the region of resonant scattering, the geometric properties of F_a need to be included. The resonantly scattered O II 834-Å and He II 304-Å line intensities, I, seen above ~600 km altitude can be considered optically thin, especially as the auroral ionosphere is particularly tenuous. Thus, the intensity is given by

$$I = \int dL (F_s + F_a) \sigma_{rs} N_i(L)$$
 (1)

where σ_{rs} is the resonance scattering cross-section (=2.6× 10^{-13} cm² for the 834 Å line) and $N_i(L)$ is the ion density along the line of sight, L. This equation allows us to derive the

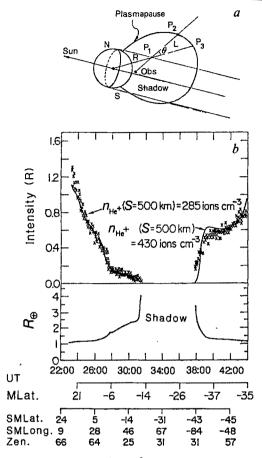
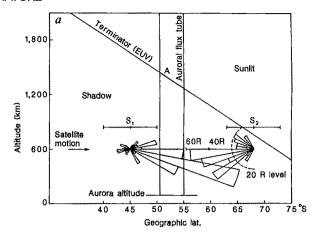


Fig. 1 Intensity of the He⁺ 304-Å line measured in a spin-scan of the Apollo-Soyuz photometer. The viewing geometry is shown in a. The satellite (OBS) measures the line intensity from the sunlit portion of the line of sight (L) between P₁ and P₂. The altitude (R₁) of the point P₁ which is the intercept of L with the terminator, is shown in b. The magnetic latitude of P₁ (MLAT), the satellite magnetic coordinates (SMLat., SMLong.) and the zenith angle of the line of sight (Zen.) are also shown. The agreement between the model (solid lines) and the data (crosses) demonstrates the capability of deriving the density distribution of He⁺ in the plasmasphere by imaging the 304-Å line intensity.

appropriate ion density distribution with the help of a theoretical profile superimposed on the viewing geometry shown in Fig. 1. The pecularities of the Earth's shadowing impose tomographic signatures (note the kinks in the line intensity profile) in much the same way as lead is used in X-ray tomography in the laboratory. A unique set of density model parameters can be determined.

We have been able to test this concept with the O II 834-Å line by using data from the University of California Berkeley extreme-ultraviolet spectrometer flown on board the P78-1 satellite. The P78-1 satellite was placed in a 600-km-altitude circular orbit, with an inclination of 97.7° and an orbital period of 96 min. The orbit is Sun-synchronous, precessing at 1° per day, with the spacecraft orbit lying essentially in the noon-midnight plane. The spectrometer is housed in the spinning wheel of the spacecraft, with the spin axis of the wheel perpendicular to the orbital plane. The spectrometer's line of sight is oriented 120° from the spin axis, and, as the wheel rotates at 11 r.p.m., the instrument line of sight sweeps out a cone, alternately viewing Earth and space, never looking closer than 30° to the Sun.

To test the magnetospheric O^+ imaging model, we have chosen a pass where a night-time aurora was observed by the instrument over the South Pole on 22 March 1979. The down-looking intensity profile of the O^+ 834-Å feature as a function of latitude indicates an auroral arc at ~45,000 s UT, centred between -50°



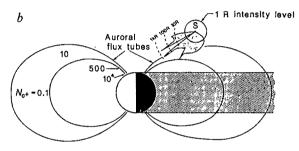


Fig. 2 a, Intensities of the O^+ 834-Å line as a function of the angle between the zenith and the line-of-sight direction of the extreme-ultraviolet (EUV) spectrometer aboard the satellite P78-1. Spin-angle intensity profiles accumulated during the intervals centred at S1 and S2 are shown. Wavelength-independent background has been subtracted. The location and extent of the auroral flux tube are determined by the measured zenith and nadir intensities. Note that the 834-Å source volumes are at altitudes as high as 2,000 km. b, Simulated O^+ 834-Å line intensity profile seen by a hypothetical satellite S at $4R_{\rm E}$ is shown on the nightside lobe of an auroral flux tube. The input O^+ density profile 9 as a function of distance along the field line is shown on the dayside lobe of the flux tube. Instrument sensitivity of 1 R is needed to image the distribution of O^+ on the entire auroral flux tube.

and -55° geographic latitude. Figure 2a shows spin-scan profiles of the O+ 834-A line accumulated for ~150 s, centred at two satellite locations S1 and S2 along the satellite path towards the South Pole, plotted as linear polar bar graphs according to the directions of the zenith-angle bins. The satellite was in the Earth's shadow at both points, viewing the auroral region forward from S1 and then backward from S2. From the forwardbackward anisotropy of the intensity pattern, it is clear that the instrument is viewing emissions from the auroral flux tube and that this is the predominant emission source at such high altitudes. The up-looking intensities of 1-20 R are of particular interest because they correspond to sources located at altitudes as high as 2,000 km. Using the model parameters of $N(O^+) \simeq$ 500 cm⁻³ at 2,000 km over a typical evening discrete-auroral-arc region of width ~200 km lit by solar and auroral 834-Å emissions, we found, for example, that the model predicts a luminosity of 6 R, in agreement with the up-looking intensities at S2, which include the sunlit and aurora-lit regions of the flux tube at 2,000 km. The extreme-ultraviolet background has been corrected for in the data and the 834-Å signal, though weak, stands out well above background.

The data clearly show that the auroral flux tube up to ~2,000 km can be imaged with an extreme-ultraviolet instrument at 834 Å. The intensity observed is in agreement with that expected from auroral flux tube models⁹. This verification allows

us to simulate what we may expect from the O⁺ line when viewed from a high-altitude platform. We have run a model of electric field and plasma distributions⁹ for a discrete arc with a total potential drop of 1 keV and O⁺ density of 500 cm⁻³ and H⁺ density of 70 cm⁻³ at 2,000 km, to simulate an average auroral flux tube. These densities are consistent with ISIS-2 observations¹⁰. The O⁺ densitites are shown at roughly appropriate locations on the sunlit auroral lobe in Fig. 2b. The solar flux is assumed to be 1.3 kR, and the auroral flux is ~1 kR (ref. 11) at ~100 km altitude. With such a model, one can simulate the expected intensity of the 834-Å resonance scattering line seen at any viewing geometry. Such a simulated intensity plot for the 834-Å line is shown on the nightside lobe of Fig. 2b, in which the intensity of a 360° spin-scan is shown as the mottled area centred around a hypothetical satellite, S, at $4 R_E$ (where R_E is the radius of the Earth). It is seen that instrument sensitivity to 1R is required to obtain a deconvolution of O⁺density distribution of the auroral flux tube to \sim 5 $R_{\rm E}$. The simulation is for the minimum outflow of an inverted V. Other sources of O+ outflow, such as conics and polar wind, add to the 834-Å intensity. Note that the simulation applies only to 834-Å emission of O+ accelerated upward by the inverted V. Such emissions have distinct Doppler shifts and broadenings. When the instrument is looking in the downward direction, the line core will be cluttered with 834-Å dayglow¹² (~0.5 kR) and nightglow¹³ (~1 R). These issues of background require high-resolution spectrometry, but we cannot address these issues here.

If our concept of magnetospheric imagery is valid, it would imply that solar Ly- α emissions should also be resonantly scattered by the hot H⁰ outflow created by charge-exchange interaction between the H⁺ outflow and neutral constituents of the exosphere. Such emissions are clearly distinguishable from the intense geocoronal background because such hot H⁰ will resonantly scatter solar Ly- α at Doppler-shifted wavelengths from the cold geocoronal line core. Note that the geocoronal Ly- α width corresponds to an exospheric temperature of ~1,000 K (~0.1 eV) for the cold H⁰; therefore, any H⁰ with higher energy is defined as hot for the present purposes. Our concept predicts the existence of a hot Ly- α emission source at the auroral magnetospheric flux tubes.

Evidence of such a hot emission source in the magnetosphere was obtained by the spectrophotometer flown on Spacelab 1. The instrument was equipped with an absorber specifically to eliminate the geocoronal Ly- α line core so as to study hot emission sources14 which are Doppler-shifted and/or broadened to the geocoronal line wings. An unexplained magnetospheric source of hot emissions with an intensity of ~200 R, after subtraction of interplanetary background, and ~20° wide in orbital angle was detected by the instrument¹⁴ at ~22:54 UT on day 341 of 1983. The viewing geometry projected onto the horizontal plane is illustrated in Fig. 3, showing the Spacelab 1 ground track at southern high latitudes. The hot emission source was observed in the zenith direction, perpendicular to the ground track and out of the plane of the figure. Within a few minutes of the event, the NOAA-7 satellite flew through the southern auroral region and the NOAA-8 satellite flew through the northern auroral region. Both detected auroral electrons in the vicinity of -65° to -70° geomagnetic latitudes, but virtually no protons above the instrument threshold were found. Assuming conjugacy, these two NOAA satellite observations approximately defined the low-altitude aurora as shown on Fig. 3. The hot emission source is clearly not from the direction of the low altitude aurora, whose intensity in Ly- α is usually \sim 6 kR and is emitted by the cold geocoronal H⁰. We conjecture that the hot emission of ~200 R originates from Dopper-shifted Lyα resonance scattering of solar emissions by the hot H⁰ which are produced by charge exchange between outflowing hot H+ and cold exospheric neutral atoms at several thousand kilometres up the auroral flux tube. If so, the source region is bounded below by the intercept of the equatorward edge of the auroral

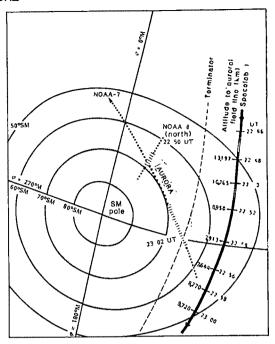


Fig. 3 Viewing geometry of Spacelab 1 observation 14 of an unaccounted-for Ly-α emission source in the magnetosphere. The source was observed between 22:50 and 22:57 UT, near the zenith direction.

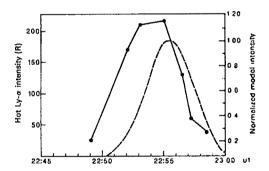


Fig. 4 Comparison of the observed hot Ly- α intensity profile (solid curve) with the expected model profile (dashed curve). The model curve is normalized to unity at 22:56 UT, when Spacelab 1 is at closest approach to the equatorward boundary of the auroral flux tube in the zenith direction. The model assumes that the unknown hot Ly- α source is the hot H^o produced by charge exchange between hot outflowing H⁺ and exospheric neutrals.

flux tube with the line of sight of the instrument. The altitudes of these equatorward intercepts are shown along the Spacelab 1 ground track on Fig. 3. Note that the closest approach of these equatorward intercepts to the instrument occurs near the observed hot emission source. This intercept is important in understanding why the source is highly localized.

To consider the source localization, we note that the intensity, I, of the hot emission can be written approximately in terms of the solar flux F_s ($\sim 250 \text{ kR}$)¹⁵, the resonance scattering cross-section σ_{rs} ($\sim 2.5 \times 10^{-13} \text{ cm}^2$) and the hot hydrogen density N_H

$$I \simeq F_{\rm s} \sigma_{\rm rs} \int_{z_{\rm r}}^{z_{\rm p}} \mathrm{d}z \, N_{\rm H}(z) \tag{2}$$

where z_e is the altitude of the equatorward intercept and z_p is the altitude of the poleward intercept of the line of sight with the auroral flux tube. Locally, the density of hot H^0 can be parameterized in terms of a scale height h along the field line

$$N_{\rm H} = N_o \exp -[(z - z_o)/h \sin \lambda] \tag{3}$$

where N_0 is the density at the reference altitude z_0 along the

field line at invariant latitude λ . For our case, z_p is much larger than z_e because the auroral field lines are approximately radial, yielding

$$I = F_s \sigma_{rs} h \sin \lambda N_o \exp -[(z_e - z_o)/h \sin \lambda]$$
 (4)

Thus, the intensity is expected to be an exponential function of the equatorward intercept z_e , and the width of the emission source is expected to be determined by the projected scale height $h \sin \lambda$.

Figure 5 shows the comparison between a modelling of the intensity according to equation (4) and the actual observations along the satellite ground track. The observed width is well fit with a scale height of ~1,000 km and, indeed, the intensity varies approximately with the equatorward intercept as an inverse exponential. The observed intensity is obtained by subtracting the fitted interplanetary hot emission background¹³ from the total hot emission to obtain the magnetospheric component of the hot emisson intensity. Even without assuming any longitudinal variations of the aurora, the two intensity curves shown in Fig. 4 are sufficiently similar in shape and location to support our conjecture and to explain the most significant feature that the magnetospheric hot emission source appears to be localized. Furthermore, using the peak intensity of ~200 R and the fitted

width of ~1,000 km, we can determine from equation (4) that the hot hydrogen source density is $\sim 30 \text{ cm}^{-3}$. This number density is quite reasonable, as the hot H⁰ includes all populations above ~ 0.1 eV.

We thank J. L. Bertaux for providing information on the Spacelab 1 observations.

Received 20 March; accepted 29 April 1986.

- 1. Chakrabarti, S., Paresce, F., Bowyer, S., Chiu, Y. T. & Aikin, A. Geophys. Res. Lett. 9, 151-154 (1982). Chiu, Y. T., Luhmann, J. G., Ching, B. K. & Boucher, D. J. Jr J. geophys. Res. 84, 909-916
- (1979).
- Shelley, E. G. Space Sci. Rev. 23, 465-497 (1979).
 Chiu, Y. T., Cornwall, J. M., Fennell, J. F., Gorney, D. J. & Mizera, P. F. Space Sci. Rev. 35, 221-257 (1983).
- Moore, T. E. Rev. Geophys. Space Phys. 22, 264 (1984).
- Johnson, R. G. Energetic Ion Composition in the Earth's Magnetosphere (Reidel, Dordrecht,
- Kumar, S., Chakrabarti, S., Paresce, F. & Bowyer, S. J. geophys. Res. 88, 9271-9279 (1983). Bowyer, S., Kimble, R., Paresce, F., Lampton, M. & Penegor, G. Appl. Opt. 20, 477 (1981).
- Chiu, Y. T. & Schulz, M. J. geophys. Res. 83, 629-642 (1978).
 Hoffman, J. H., Dodson, W. H., Lippincott, C. R. & Hammack, H. D. J. geophys. Res. 79,
- 4246-4251 (1974).
- 11. Paresce, F., Chakrabarti, S., Boyer, S. & Kimble, R. J. geophys. Res. 88, 4905-4910 (1983).
- 12. Chakrabarti, S., Paresce, F., Bowyer, S. & Kimble, R. J. geophys. Res. 88, 4898 (1983).
- Chakrabarti, S., Kimble, R. & Bowyer, S. J. geophys. Res. 89, 5660-5664 (1984).
 Bertaux, J. L., Goutail, F. & Kockarts, G. Science 225, 174-176 (1984).
- 15. Heroux, L. & Hinteregger, H. E. J. geophys. Res. 83, 5305-5308 (1978).

Periodicity of the Earth's magnetic reversals

Richard B. Stothers

National Aeronautics and Space Administration, Goddard Space Flight Center, Institute for Space Studies, 2880 Broadway, New York New York 10025, USA

Reversals of the Earth's magnetic field may occur with a certain regularity. Using observed percentages of normal and reversed polarity during different time intervals, Negi and Tiwari¹ detected several significant periodicities, notably one of 32-34 Myr. Raup² used the dates of individual reversals to propose a 30-Myr period in the frequency of reversals, although Mazaud et al.3 obtained a periodicity of only 15 Myr. Like Negi and Tiwari's other detected short periods, the 15-Myr period may be harmonically related to a basic 30-Myr period⁴. It has also been suggested that these are accidental periodicities arising in a short record^{5,6}, or are harmonics of the record length itself7. In fact, all of the cited studies have used different data, different record lengths and different methods of time-series analysis. Raup8 has consequently retracted his original claim. Here I present a much fuller analyis of the reversal record and show that a statistically significant period of ~30 Myr does formally exist, in spite of the cited differences.

For consistency with the most recent studies, most of the calculations reported here have used the dates given by Harland et al.9 for 296 magnetic reversals in the past 165 Myr. Raup² and Lutz⁷ displayed histograms of these dates in bins with widths of 5 and 8.27 Myr, respectively. Because 5 Myr is a harmonic of the suggested 30-Myr period, and 8.27 Myr is too long to reveal visually a 30-Myr period, an unbiased bin width of 4 Myr is used here to construct a new histogram, shown in Fig. 1. Inspection suggests that peaking of the magnetic reversal rate near both ends of the record will produce a very strong artificial periodicity of ~140 Myr, while the complete absence of magnetic reversals near the middle of the record (Cretaceous quiet interval) will create a strong first harmonic of ~70 Myr. Superimposed on the bowl-shaped histogram, however, there appears to be a possibly real oscillation of minor peaks with a period of ~30 Myr. Other published displays of the reversal frequency suggest a shorter wavelength of 15 or 20 Myr (refs 3, 10), but only the 30-Myr oscillation appears when the data are binned

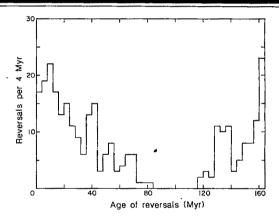


Fig. 1 Magnetic reversal frequencies shown in bins of width 4 Myr (data from ref. 9). Note the minor peaks spaced at ~30-Myr intervals.

in very short intervals, such as 1 Myr.

To proceed further, the dates of individual magnetic reversals may be analysed by using a technique in which the observed dates t_i $(i=1,2,\ldots,N)$ are fitted to a linear periodic function of the type $t = t_0 + nP$, where P is a trial period, t_0 is a trial value for the most recent epoch, and n is an integer. In the original formulation of the technique¹¹, I minimized $N\sigma^2$, the sum of the squares of the residuals for each trial epoch, to obtain a best fit for a selected trial period, and computed a 'residuals index' $(\sigma - \sigma_c)/P$, where $\sigma_c/P = [(N^2 - 1)/12N^2]^{1/2}$. Raup and Sepkoski¹², in independent work, searched for the arithmetic mean of the residuals that was closest to zero, and Lutz⁷ made a circular transformation to obtain phases of the observed data, the dispersion of which was then minimized by performing two trigonometric summations, as in Fourier analysis. Lutz's variation of the method allows a correction to be made for the unequal weighting of the dates which biases most, if not all, time-series analyses. However, as he showed that this effect is very small for the present data, I neglect it here and use the technique as originally formulated. Earlier versions, for both temporal¹³ and spatial¹⁴ problems, looked for either a leastsquares or maximum-likelihood solution for two unknowns and so did not compute the spectral information, or else assumed a known value for the most recent epoch.

The computed spectrum of the residuals index for the adopted dates of magnetic reversals (Fig. 2) displays many periodicities.

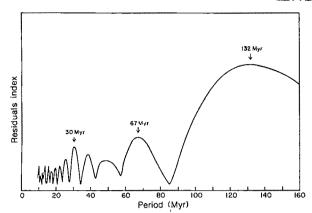


Fig. 2 Spectrum of residuals index for the complete time series of magnetic reversals, t = 0-165 Myr. The residuals index measures the goodness-of-fit of the observed times series to an assumed, perfectly periodic time series.

To determine their robustness, the record can be progressively truncated: successive cuts of 5 Myr are applied from the present time to as far back as 65 Myr ago (beginning of the Cenozoic Era). Table 1 lists the periods of all spectral peaks appearing at trial periods $P \ge 10$ Myr. A number of important features of this table should be noted. First, the longest period is always of the order of the length of the truncated record. (This period always has the highest spectral peak.) Second, the next-longest period is always nearly equal to one-half of the longest period. (This first-harmonic period has the next-highest spectral peak if the amount of truncation is <25 Myr.) Third, the dominant period occurring elsewhere in the computed spectra is 28-33 Myr. Its precise value oscillates down Table 1 in a discontinuous, saw-tooth fashion with a wavelength of ~30 Myr. The same wavelength of oscillation (with a slight phase shift) characterizes the neighbouring periods of 22-25 and 20-22 Myr, although the shorter periods of 18-19, 17-18 and 15-16 Myr vary down the table with a wavelength only half as large. Note that the percentage by which the period varies is smaller for the shorter periods, so that the variations of the four shortest periods, 13, 12, 11 and 10 Myr, are imperceptible. Thus, the more cycles a record contains, the less these cycles will be distorted by the record length.

The average values of the 12 periods that lie in the range 10-58 Myr are closely represented by the individual periods shown in the first row of Table 1, and are very close to what would be expected for an ideal time series consisting of six dates successively separated by 30.1 Myr. An explicit comparison of observed and expected periods is presented in Table 2, including a simple harmonic interpretation¹¹. The correlation coefficient between the 11 pairs of observed and expected periods (excluding the generating period of 30.1 Myr) is r = 0.997. The significance of this value has been tested by correlating the sequence of 11 observed periods with 5,000 simulated sequences, each consisting of 11 numbers drawn at random from the range 10-58 Myr and then ordered. Fewer than 0.1% of the simulated sequences showed $r \ge 0.997$. Since there is no a priori reason to expect precisely 11 periods to show up in the range 10-58 Myr. this represents a very conservative test of significance.

An independent test has been made by generating 5,000 artificial time series, each containing 296 dates selected randomly from the time interval 0-165 Myr and then ordered. The spectrum of the residuals index has been computed for each time series and compared with Fig. 2. Fewer than 0.1% of the synthetic spectra showed a residuals index at P=30 Myr that was higher than the observed peak. However, this test assumes 30 Myr as an a priori period and does not take into account the non-stationarities in the observed time series, as illustrated in Fig. 1.

Raup² performed a different significance test by randomizing the order of the observed time intervals. He found a low percentage (0.6%) of simulated cases in which the height of the observed spectral peak at $P = 30 \,\mathrm{Myr}$ was surpassed. Lutz detected the statistical significance of the observed peaks at shorter periods, but did not recognize their harmonic connection to the 30-Myr period. Instead, he associated these periods with the record length, an interpretation that was based on a limited truncation back to only 21 Myr BP. Additional evidence against Lutz's interpretation follows from an attempt to match the provisionally expected series of harmonics (1/2, 1/3, 1/4,...) of the longest period in each row of Table 1 to the rest of the observed periods along the same row. Discrepancies of up to 15% in the values of the observed periods occur, and not all of the observed periods can be successfully identified. The number of extraneous periods per row is three in one of the rows, two in six rows, and one in another six rows; only one row has no extraneous period at all.

Truncation of the record in the middle of the Cretaceous quiet interval provides a further test. Separate spectral analyses of the more recent time segment (t = 0-83 Myr, N = 196 dates) and the older time segment (t = 118-165 Myr, N = 100 dates) yield the following results for trial periods in the range 10-40 Myr. The more recent time segment contains five spectral peaks at periods of 32.7, 20.0, 15.9, 13.3 and 9.8 Myr; the older time segment contains three peaks at 29.9, 14.2 and 10.4 Myr. For comparison, two ideal time series consisting of three dates and two dates, respectively, with generating periods of 32.7 Myr and 29.9 Myr,

Table 1 Periods of the spectral peaks in time-series analyses of a progressively truncated record of magnetic reversals

t				Peri	ods (My	:)							
0-165	132	67	48	38	30*	25	22	19	17	16	13	12	11	10
5-165	128	65	48	37	29*	24	21	19	17	15	13	12	11	10
10-165	123	63	47	36	29*	24	20	18	17	15	13	12	11	10
15-165	117	60	46	33	28*	23	20		18	16	13	12	11	10
20-165	113	59	44	33*	28	22	20		17	15	13	12	11	10
25-165	109	57	42	32*	_	25	22	19	17	15	13	12	11	10
30-165	105	55	41	30*		24	21		18	16	13	12	11	10
35-165	102	52	40	29*		23	20		17	15	13	12	11	10
40-165	99	51	38	29*		23	20	19	17	15	13	12	11	10
45-165	96	49	34	28*	_	22	_		18	16	13	12	11	10
50-165	94	48	33*	28		22	-		18	15	13	12	11	10
55-165	93	47	32*			24		19	17	15	13	12	11	10
60-165	93	45	31*		—	23	_	19		16	13	12	11	10
65-165	96	43	30*			23	_	18	*****	15	13	12	11	10

^{*} Highest spectral peak for periods <58 Myr.

show high peaks only at 32.7, 21.8, 16.3, 13.1 and 10.9 Myr and only at 29.9, 14.9 and 10.0 Myr. The corresponding harmonic identifications are 1, 2/3, 1/2, 2/5 and 1/3, and 1, 1/2 and 1/3.

Several conclusions can be drawn from this comparison. One is that the 15-Myr period detected by Mazaud et al.3 in the more recent time segment is probably just a harmonic period, rather than the basic period. Although progressive truncation of this segment of the record back to 35 Myr BP leads, in some cases, to the highest spectral peak being at P = 13-15 Myr, comparison with the computed spectra of the corresponding ideal time series shows unambiguously that the generating period remains P =30 Myr (plus or minus the amount of period oscillation). Second, the presence of the 30-Myr period in the separate spectral analyses for t = 0-83 Myr and t = 118-165 Myr demonstrates that this periodicity is not being produced by the 35-Myr quiet interval. (Raup² came to the same conclusion.) Third, the abrupt shifts in the number of observed periods, going down Table 1, arise from the change in the number of cycles covered as the record is progressively truncated. For an ideal time series, the total number of integer multiples of harmonics that appear in

Table 2 Periods (Myr) of the peaks in spectral analyses of the magnetic-reversal and ideal time series

Observed series	Ideal series	Harmonic series	Harmonic series identification
48.2	48.0	45.2, 50.2	3/2, 5/3
38.0	40.5	40.1, 37.6	4/3, 5/4
30.1	30.1	30.1	1
25.2	24.0	24.1, 25.1	4/5, 5/6
_	22.0*	22.6, 21.5	3/4, 5/7
21.9	20.7	20.1, 21.5	2/3, 5/7
19.4	19.5	20.1, 18.8	2/3, 5/8
_	18.5*	18.1, 18.8	3/5, 5/8
17.2	17.3	17.2	4/7
15.5	15.1	15.1	1/2
13.4	13.1	12.9	3/7
12.0	12.0	12.0	2/5
10.9	11.0	11.3	3/8
10.0	10.0	10.0	1/3

^{*} Very low spectral peak.

the computed spectrum is by definition controlled by the value of the largest-occurring integer, which turns out to be equal to the number of cycles covered by the time series.

Three additional checks have been made of the above results. First, Fourier analysis has been applied to the histogram shown in Fig. 1. Spectral peaks were determined to occur with relative heights and absolute periods that agreed, within the resolution of the method, with the peaks found by linear analysis. To examine the effect of the obvious non-stationarities in Fig. 1, de-trending was performed by subtracting the strongest contributing Fourier components. Accordingly, the two longest cycles, corresponding to the 132-Myr and 67-Myr periods of Fig. 2, were successively removed. Fourier analysis of the residual data then showed the highest spectral peak occurring at 30.9 Myr, which was shifted only slightly from the original value of 30.4 Myr. A similar Fourier analysis of Raup's² and Lutz's⁷ histograms, as well as of a histogram with a 1-Myr bin width, yielded essentially identical results. This check shows that the method of analysis does not bias the results.

A second test concerned the possible influence of undetected magnetic reversals. If the unknown reversals are distributed randomly or proportionally among the known ones, their omission should not significantly affect the present results. To simulate their omission, the known magnetic reversals were systematically pruned from the record. Only the recent time segment t = 0-83 Myr was considered, and all fixed-polarity chrons of less than a certain length δt were excluded from the data set. As the missing chrons from the original record are probably shorter than 0.04 Myr (ref. 10), a very conservative test uses $\delta t \gg 0.04$ Myr. When $\delta t = 0.5$ Myr is used, the basic period of 30.1 Myr still emerges (N = 49 dates). Even with $\delta t =$ 1 Myr, the period remains 28.9 Myr (N = 19 dates).

A third check of the present results involved using two different sets of magnetic-reversal dates: those of Kent and Gradstein¹⁵ (t = 0-169 Myr, N = 283 dates) and of Lowrie and

Table 3 Summary of results for the basic period (P) and phase (t_0) of magnetic reversals

	Ref.	9 dates	Ref. 15	dates	Ref. 16	dates
Time range (Myr)	P (Myr)	t ₀ (Муг вр)	P	t_0	P	t ₀
(0-65)-170*	30.5	10	29.5	7	_	
0-170	30.1	10	29.9	7	_	
(0-35)-85*	28.0	14	29.0	10	28.0	14
0-85	32.7	9	28.8	7	32.1	9
115-170	29.9	10	26.9	-6	_	

^{*} Average of the truncation results.

Alvarez¹⁶ (t = 0-84 Myr, N = 174 dates). Analysis of these dates by the linear technique produced the results shown in Table 3. In view of the small number of cycles covered, the differences seem rather minor, the total spread among the periods being ±3 Myr. Using maximum-entropy analysis, Pal and Creer¹⁷ independently found the 32.1-Myr period in the data of ref. 16.

The above results suggest that a real periodicity exists in the record of magnetic reversals, supporting the claims of Negi and Tiwari¹ and of Raup². With fine tuning of the truncated-record results, the mean value of the basic period falls at 30.5 Myr (ref. 9 data) or 29.5 Myr (ref. 15 data). Shuter and Klatt's 18 136-Myr period is now seen to arise only from the record length. Like the basic period, the phase oscillates in a discontinuous: saw-tooth fashion with progressive truncation, and returns to its starting value every ~30 Myr. A best estimate of its mean value is $t_0 = 10 \pm 8$ Myr BP (ref. 9 data) or $t_0 = 7 \pm 8$ Myr BP (ref. 15 data). Note that t_0 represents the most recent epoch of the mean cycle and therefore is not necessarily equal to the most recent time of high magnetic-reversal frequency, unless the times are strictly periodic.

These results do not prove that there is a physical periodicity in the Earth's magnetic record, nor do they prove that any periodicity, real or accidental, is strictly regular. However, the already demonstrated^{4,19} coincidences in time between a high rate of magnetic reversals, heightened global tectonic activity, and impact cratering do at least suggest that periodic or episodic large-body impacts may trigger many of these disturbances.

I thank D. V. Kent, T. M. Lutz, P. L. McFadden, M. R. Rampino and D. M. Raup for helpful communications.

Received 9 December 1985; accepted 7 May 1986.

- 1. Negi, J. G. & Tiwari, R. K. Geophys. Res. Lett. 10, 713-716 (1983).
- Raup, D. M. Nature 314, 341-343 (1985).
- Mazaud, A., Laj, C., de Sèze, L. & Verosub, K. L. Nature 304, 328-330 (1983).
- Rampino, M. R. & Stothers, R. B. Science 226, 1427-1431 (1984).
- McFadden, P. L. Nature 311, 396 (1984).
- Mazaud, A., Laj, C., de Sèze, L. & Verosub, K. L. Nature 311, 396 (1984). Lutz, T. M. Nature 317, 404-407 (1985). Raup, D. M. Nature 317, 384-385 (1985).
- Harland, W. B. et al. A Geological Time Scale (Cambridge University Press, 1982).
- Lowrie, W. & Kent, D. V. Earth planet. Sci. Lett. 62, 305-313 (1983).
 Stothers, R. Astr. Astrophys. 77, 121-127 (1979).

- Raup, D. M. & Sepkoski, J. J. Proc. nain. Acad. Sci. U.S.A. 81, 801-805 (1984).
 Fraser, D. A. S. Statistics: An Introduction, 245 (Wiley, New York, 1958).
 Broadbent, S. R. Biometrika 42, 45-57 (1955); 43, 32-44 (1956).
 Kent, D. V. & Gradstein, F. M. in The Western Atlantic Region, Volume M of the Geology of North America (eds Tucholke, B. E. & Vogt, P. R.) (Geological Society of America, Boulder, in the press). Lowrie, W. & Alvarez, W. Geology 9, 392-397 (1981)
- Pal, P. C. & Creer, K. M. Nature 320, 148-150 (1986).
 Shuter, W. L. H. & Klatt, C. Astrophys. J. 301, 471-477 (1986).
- 19. Rampino, M. R. & Stothers, R. B. Nature 308, 709-712 (1984).

Thermohaline intrusions created isopycnically at oceanic fronts are inclined to isopycnals

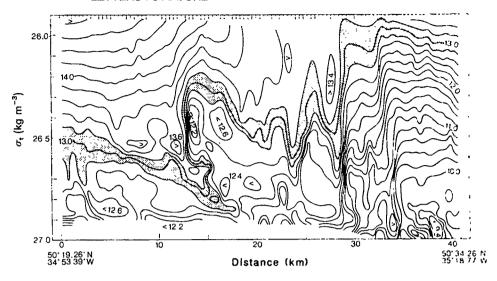
J. D. Woods*, R. Onken & J. Fischer

Institut für Meereskunde an der Universität Kiel, FRG

Thermohaline intrusions have often been observed extending several kilometres from ocean fronts1. They have a central role in models of mixing^{2,3}; however, their origin has been the subject of controversy. Laboratory studies led to the idea that intrusions might be formed by double diffusion⁴⁻⁶, in which case they would slope across isopycnals (surface of constant density). That signature has been identified in ocean fine-structure sections7. Observations of the three-dimensional structure of meandering fronts led to a different conjecture: that intrusions might be formed isopycnically by the ageostrophic circulation within unstable meanders on the frontal jet 1,8. In that conceptual model, double diffusion

^{*} Present address: NERC, Polaris House, North Star Ave, Swindon, Wiltshire SN2 1EU, UK.

Fig. 1 Density variation (σ_t) of isotherms in a vertical section across the North Atlantic polar front, surveyed with the Kiel Sea Rover apparatus in summer 1981. The horizontal resolution (400 m) is indicated by the tick marks on the upper axis; the vertical depth range lies between 30 and 80 m. The temperature range between the 12.8 °C and 13.2 °C isotherms is shaded.



does not initiate intrusions, but may extend and dissipate those created by frontal circulation. Here we present first the observed structure of such an intrusion and then the results of a dynamical model simulating the isopycnic generation mechanism at an unstable meandering front. We show that thermohaline intrusions formed isopycnically also slope across density surfaces, so there is no need to invoke double diffusion to explain such structures.

We have observed a thermohaline intrusion at a meander structure of the North Atlantic polar front. The section presented here (Fig. 1) was obtained by the Kiel Sea Rover towed CTD (conductivity/temperature/depth) system¹⁰. It represents a high-resolution snapshot of a thermohaline front in the seasonal pycnocline. The orientation of the section was almost perpendicular to the front which separates the warm and saline water in the anticyclonic meander-ridge, from the cold and fresh water in the cyclonic trough of the meander. Isopycnic analysis eliminated internal wave noise¹¹. The resulting product revealed strong thermohaline fine structure created by the three-dimensional frontal dynamics.

The 13 °C isotherm is folded in the vicinity of the major thermoclinicity signal. Relatively warm water is intruded into a region of cooler and fresher water, with the axis of the intrusion being clearly inclined to isopycnic surfaces. The horizontal extent of the fold was \sim 6 km and the vertical scale of the intrusion, estimated from the mean static stability profile, was \sim 10 m.

We modelled the development of a meandering front in two stages: (1) frontogenesis, which transforms the initial (largescale) baroclinicity and thermoclinicity into a jet with an associated T-S (temperature-salinity) front, and (2) instability of the jet. It is important that the initial condition for stage (2) is the output of stage (1), so that we can establish the sensitivity of intrusion structure to large-scale initial conditions. Our simulation of thermohaline intrusions was based on a primitive equation model with quasi-isopycnic coordinates¹². The first stage, describing frontogensis in two dimensions, was an extension of that described in ref. 9, with initial thermoclinicity described by horizontal isotherms. It gave the frontal structure shown in Fig. 2a. That was used as the initial conditions for the second stage¹³, a channel model based on the Bleck-Boudra quasi-isopycnic coordinate scheme¹², rigid side walls with free slip, and cyclic downstream boundary conditions. The grid has 10 isopycnic layers, each with a rectangular array of 32×64 grid points, spaced 2.5 km apart in the cross-stream direction and in the downstream direction. Meanders grow in response to an initial small perturbation in the stream function. In the present examples, the disturbance had downstream amplitude as shown by the streamlines at a depth of 25 m after 40 days of integration (Fig. 3a). The corresponding pattern of isotherms on an isopycnic surface (Fig. 3b) appears much more complicated, but is,

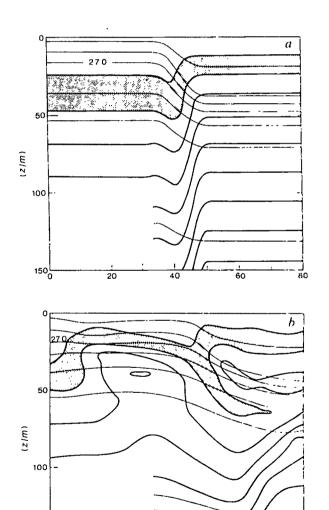


Fig. 2 Depth of isotherms (thick contours) and isopycnals (thin contours) in a vertical section of the upper 150 m in the model domain at positions indicated by the broken lines in Fig. 3 The temperature range between the 18 °C and 19 °C isotherms is shaded.

a, Initial conditions; b, day 40.

40

Distance (km)

60

20

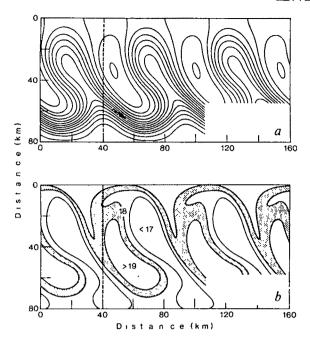


Fig. 3 a, Stream function at 25 m depth after 40 days of integration of the frontal meander model. The arrow indicates the flow direction. b, Temperature pattern on the isopycnic surface σ_t = 27.0 kg m⁻³ at day 40. The mean depth of this surface is ~25 m.

of course, consistent with the evolving streamlines. A vertical section through the meander (Fig. 2b) shows an intrusion of relatively warm, salty water into the cooler, fresher side of the front. Its axis is inclined to isopycnals. The 18-19 °C temperature range has a 20-km fold.

To understand the isopycnic mechanism of thermohaline intrusions at fronts, it is necessary to discriminate between kinematic and dynamic processes. The latter change the pressure gradient and accelerate the flow; the former do not. Kinematic frontogenesis is the result of a horizontal confluence acting on a passive scalar gradient, which becomes sharpened without changing the flow. The passive gradient of interest here is thermoclinicity, defined as the gradient of temperature on a surface of constant density. Dynamical frontogenesis is the result of a horizontal confluence acting on a dynamically active scalar gradient, which changes the flow as it becomes sharper. The active scalar gradient of interest here is baroclinicity, defined as the gradient of pressure along a surface of constant density. Both processes occur together where there is horizontal confluence of a body of water that is both thermoclinic and baroclinic; that is, one in which the isothermal surfaces are inclined to non-horizontal isopycnic surfaces—the necessary condition for the isopycnic mechanism of thermohaline intrusions. It depends on the kinematic folding of an isothermal surface by the total velocity field, comprising the externally imposed confluence plus the internal circulation arising from the dynamic response to that confluence.

Regional variation of air-sea interaction creates large-scale variations of temperature and salinity in the surface mixed layer. After subduction ¹⁴ into the interior these large-scale variations include both baroclinicity and thermoclinicity. Frontogenesis occurs where there is a confluence in the (mostly laminar-flow ¹⁵ and therefore isopycnic) circulation. The thermoclinicity is sharpened kinematically into a T-S front. The corresponding sharpening of the baroclinicity produces a jet, which is roughly in geostrophic balance with the density gradient. To simulate the cross-front shear that produces intrusions, we have to compute the ageostrophic component of flow associated with the acceleration of the jet. That is done by using the law of isopycnic potential vorticity (IPV) conservation, which states that IPV = $((\zeta + f)/h)$ (d/D) = constant, for a water column bounded by

a pair of isopycnals, where f is the planetary vorticity, and h is the spacing between a pair of isopycnals with mean density D and density difference d. According to this law, h varies with the absolute vorticity, $(\zeta + f)$. Relative vorticity of large-scale motion is negligible compared with f, so the initial IPV before frontogenesis is given by IPV = (f/h(0))/(d/D). As frontogenesis proceeds, changes in h are computed from the local Rossby number (Ro), $h(t)/h(0) = \zeta(t)/f = \text{Ro}(t)$. In practice, the jet scale is usually so small that changes in f can be neglected in comparison with changes in ζ . But as the jet accelerates, the cross-jet shear begins to develop significant relative vorticity (ζ) . The spacing between isopycnals adjusts accordingly, becoming greater on the cyclonic side, and smaller on the anticyclonic side. Continuity of mass is achieved by a cross-jet, ageostrophic flow¹⁶. The structure of this cross-jet circulation depends on the initial profile of the isopycnic gradient of IPV (IPVG)¹⁷. The spring subduction process tends to create a maximum of IPVG near the top of the seasonal thermocline¹⁸. In that case the cross-front ageostrophic circulation comprises a simple cell, with upwelling on the anticyclonic side and downwelling on the cyclonic side of the jet. The circulation tends to flatten isopycnals, limiting the final kinetic energy of the jet, preventing further narrowing and progressively decreasing its depth. The kinematic sharpening of frontal thermoclinicity, effected mainly by the external confluence, is modulated by divergence of the cross-jet ageostrophic circulation. It does not become as sharp as it would have done due to the confluence alone, but, nevertheless, ends up much narrower than the jet. The surface of thermoclinicity maximum, which may have been initially vertical, becomes tipped over, so that it slopes down from the cylonic side to the anticylonic, creating the well-documented slope of the temperature field at a front¹⁹. These characteristics (narrowness and slope of the thermoclinicity maximum relative to the baroclinicity maximum) are important for the structure of thermohaline intrusions which develop as the jet begins to meander unstably.

Frontogenesis, as described above, leads to a two-dimensional structure which can be used as initial conditions for modelling jet instability. The jet is normally unstable, with fastest-growing wavelength and growth rate dependent on the initial IPVG profile. As the meanders grow to large amplitude, they develop curvature vorticity which modulates the spacing between isopycnals, according to the law of IPV conservation described above. Ageostrophic flow from thinning regions to thickening regions advects isotherms isopycnically across the meandering jet core, with a complex vertical structure governed by the initial conditions (and ultimately by the profile of large-scale IPVG before frontogenesis). At any moment, the pattern formed by isotherms on each isopycnic surface depends on the initial thermoclinicity (before frontogenesis) and the time integral of the total flow, including both the geostrophic jet component and the ageostrophic vortex-stretching component.

Our model proves that the isopycnic motion in unstable fronts can produce thermohaline intrusions that slope across isopycnals, a property previously believed to be symptomatic of the double diffusion mechanism. It also emphasizes the three-dimensional character of the velocity field responsible for isopycnic intrusions: one must resist the temptation to seek two-dimensional explanations for intrusions observed in hydrographic sections. Finally, we emphasize that the structure shown in Figs 2 and 3 depended critically on our choice of initial conditions. Cross-isopycnal folding of isotherms is common, but the details vary. The strength of our model technique is that it permits us accurately to simulate the complicated development from explicit large-scale initial conditions to a meandering jet/front with high Rossby number.

Received 7 March; accepted 29 April 1986.

^{1.} Woods, J. D., Wiley, R. L. & Briscoe, M. G. Deep-Sea Res. 24, 253-275 (1977).

Joyce, T. J. phys. Oceanogr. 7, 626-629 (1977).
 Garrett, C. J. phys. Oceanogr. 12, 952-957 (1982).

- 4. Turner, J. S. J. geophys. Res. 83, 2887-2901 (1978).
 5. Turner, J. S. in Evolution of Physical Oceanography (ed. Warren, B. A. & Wunsch, C.) 236-262 (MIT, Cambridge, 1981).
- 6. Ruddick, B. R. & Turner, J. S. Deep-Sea Res. 903-913 (1979). 7. Gargett, A. E. J. geophys. Res. 83, 5123-5134 (1978).
- Gregg, M. G. & McKenzie, J. H. Nature 280, 310-311 (1979). Woods, J. D. Ocean Model. 32, 1-4 (1978).
- 10. Bauer, J., Fischer, J., Leach, H. & Woods, J. D. Ber. Inst. Meeresk. Univ. Kiel, FRG. No. 143 (1985).
- Leach, H., Minnett, P. J. & Woods, J. D. Deep-Sea Res. 32, 575-597 (1985).
 Bleck, R. & Boudra, D. B. J. phys. Oceanogr. 11, 755-770 (1981).
 Onken, R. thesis Univ. Kiel (1986).

- Woods, J. D. & Barkmann, W. Q. J. R. met. Soc. 112, 1-27 (1986).
 Woods, J. D. J. Fluid Mech. 32, 791-800 (1986).
- 16. Sawyer, J. S. Proc. R. Soc. A234, 364-362 (1956).
- Stammer, D. & Woods, J. D. Q. Jl R. met. Soc. (1986).
 Stammer, D. & Woods, J. D. Ber. Inst. Meeresk. Univ. Kiel, FRG (in the press).
- 19. MacVean, M. K. & Woods, J. D. Q. Jl R. met. Soc. 106, 293-311 (1980).

Effects of surface heat flux during the 1972 and 1982 El Niño episodes

R. K. Reed

Pacific Marine Environmental Laboratory, National Oceanic and Atmospheric Administration, Seattle, Washington 98115, USA

It has been suggested 1,2 that anomalous surface heat flux may be partly responsible for the initial warming that occurs in the eastern Pacific during El Niño events. Sea surface temperature, net surface heat flux, and winds in the equatorial Pacific are examined here for the 1972 and 1982 El Niño episodes. It is found that surface heat flux and sea surface temperature anomalies tend to have little or negative correlation; thus, surface flux is not of major importance in the formation of thermal anomalies in the central and eastern Pacific.

In northern summer of 1982 a large El Niño episode began. This event produced dramatic effects in the equatorial Pacific Ocean (disappearance of the equatorial undercurrent³, for example) and induced global changes in atmospheric conditions4. Initially, there was considerable discussion of the differences between this event and a 'canonical' episode. Further examination of some of these differences, however, revealed that they largely resulted from similar processes acting in the presence of different initial conditions⁵. It would be of interest to explore in some detail the morphology of the 1982 episode in comparison with a more typical event such as that of 1972. Special emphasis is placed on examining surface heat flux, in an effort to resolve its role in creating thermal anomalies.

The data used for this study were archived ship-of-opportunity weather reports. They were obtained from NOAA's National Climatic Data Center for the periods 1970-79 and January 1982-October 1983. The 1970-79 period was chosen primarily because this was the first data subset for which careful editing procedures had been used to eliminate duplicate reports and other erroneous data. The climatology during this decade was also found to agree closely with those based on longer periods⁶. Surface heat fluxes (insolation, net long-wave radiation, latent heat, sensible heat, and their sum—the net or total heat flux) were calculated from the individual weather reports using empirical formulas⁶, and the fluxes were averaged over 2° latitude by 10° longitude areas to obtain monthly values. Weather elements were also averaged to obtain monthly means.

Estimates of the standard errors of the mean values for each month were made from the calculated intra-month variances for the 2°×10° areas used below. Because the data are very heterogeneous, the estimates are biased high by natural spatial and temporal variability, but they do provide conservative guides. Keeping these caveats in mind, standard errors of the mean sea surface temperature and net heat flux, for an individual month, were calculated as 0.7 °C and 45 W m⁻²

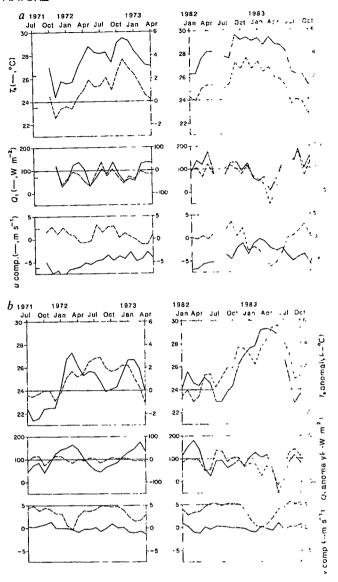


Fig. 1 a, Plots of mean monthly sea surface temperature (T_s , °C), sea surface temperature anomaly (individual monthly mean minus monthly mean for the period 1970-79), mean monthly net or total surface heat flux $(Q_t$, positive for flux into the ocean), net surface heat flux anomaly (individual monthly mean minus monthly mean for the period 1970-79), and the u (east)- and v (north)- components of wind velocity (in m s⁻¹) for the central equatorial Pacific (2° N-2° S, 140-160° W), July 1971-April 1973 and January 1982-October 1983. b, As a except for the eastern equatorial Pacific (2° N-6° S, 80-90° W).

Figure 1a presents information on the evolution of surface properties during both the 1972 and 1982 El Niño episodes for a region in the central Pacific (2° N-2° S, 140-160° W). When more than two of the original four 2°×10° areas had fewer than three observations, the data were omitted. Each monthly mean was typically based on > 10 observations. The east (u) and north (v) components of wind are shown rather than wind speed or anomalies.

During the 1972 episode, surface temperature (T_s) anomalies increased by 2.5 °C between February and May 1972. A further increase occurred during September-November, with a rapid decrease thereafter. (All of the positive temperature anomalies between April 1972 and February 1973 are greater than the standard error estimate above.) Both warming periods coincided with consistently negative surface heat flux (Q_i) anomalies, although some of the values are smaller than the error estimate.

The u-component of wind at this site decreased in magnitude through much of the period, but the winds did not become

The 1982 event evolved differently. There was a small increase in T_s anomaly between February and April 1982 and a large increase between July and September. Relatively constant values then occurred, followed by a fairly rapid decrease after March 1983. Q, anomalies were small before December 1982, but large negative values were present during January-April 1983. This period coincided with small u-component winds but large negative v-component winds, a very anomalous situation⁷.

An interesting difference between the events is that during 1982, formation of the anomalies in the central Pacific led similar changes at the eastern margin by one to two months (Fig. 1b): conversely, in 1972, warming in the central region seemed to generally lag that off South America. Although the magnitudes of the maximum anomalies during the two events in the central region were similar, the duration of anomalies >2 °C was considerably longer in 1982-83 than in 1972.

Figure 1b presents data for a region just off the South American coast (2° N-6° S, 80-90° W). This region has numerous ship-of-opportunity reports, and each 2° × 10° area generally had >20 observations. In 1972, the T_s anomaly appears to have largely formed during January to March, but a subsequent increase occurred from May to August. The second pronounced maximum in T_s , but not in T_s anomaly, in January-February 1973 gives the typical double-peak signature⁸. The Q_t anomalies during this episode were all very small, and the only unusual behaviour in winds is a sharp decrease in the southerlies during February-March 1972.

The first appreciable change in T_e anomaly in 1982 was an increase of 1.9 °C during April-May. (During this period of normal seasonal cooling there was only a small increase in T_{s} .) A second increase in T_s anomaly occurred between August and November 1982. A final warming event took place between February and May 1983, when the T_s anomaly reached +5.4 °C, and cooling started after June. Unlike the 1972 episode, Q anomalies were variable early in the event, but they were all negative from December 1982 to July 1983. The southerly winds were quite weak during January-May 1983, which was of longer duration, and later in the epsiode, than the comparable weakening during 1972.

Figure 1 shows that during both the 'canonical' event of 1972 and the 'summer' event of 1982, heat flux anomalies were small or negative during warming. Thus, surface heat fluxes do not seem to be a significant factor in forming thermal anomalies in the central and eastern ocean. Other studies^{6,9-11} provide support for this conclusion. What processes then produce the marked warming? The surface data set used here does not allow very definitive answers, but other studies (using subsurface thermal data, sea level data, and direct current measurements) have yielded essential agreement on the important mechanisms.

The initiation of warming near the Equator in the central and eastern ocean appears to be consistently induced by heat advection resulting from eastward-moving Kelvin waves^{12,13}. The effects will appear different depending on time of year⁵. If the event is initiated early in the year, as is typical, major warming will first appear off South America because thermal gradients are quite weak along the Equator in the central ocean in southern summer. If the event is triggered in mid-year, as in 1982, warming advances eastward across the ocean in the presence of strong east-west gradients in both the central and eastern ocean. During canonical events, final increases in temperature anomaly in the central ocean may result from a weakening or southward displacement of the South Equatorial Current¹². A southward displacement of this flow¹⁴ also appears to be a factor in the rapid rise in temperature anomaly (Fig. 1b) in early 1983, although the very weak winds then probably also resulted in reduced upwelling.

I thank G. Meyers and E. Sarachik for helpful discussions. The efforts of D. G. Kachel in retrieving the data and programming computations are appreciated. This study was suported by the Equatorial Pacific Ocean Climate Studies (EPOCS) program of NOAA. Contribution 774 from NOAA/Pacific Marine Environmental Laboratory.

Received 13 February; accepted 25 April 1986.

- 1. Weare, B. C. Science 221, 947-949 (1983)
- Leetma, A. J. phys. Oceanogr. 13, 467-473 (1983).
- Firing, E., Lukas, R., Sadler, J. & Wyrtki, K. Science 222, 1121-1122 (1983). Rasmusson, E. M. & Wallace, J. M. Science 222, 1195-1202 (1983).
- Harrison, D. E. & Schopf, P. S. Mon. Weath. Rev. 112, 923-933 (1984). Reed, R. K. J. geophys. Res. 88, 9627-9638 (1983).
 Wyrtki, K. & Meyers, G. The Tradewind Field Over the Pacific Ocean Part II. (Univ. Hawaii
- Wyrtki, K. & Meyers, G. The Tradewind Field Over the Pacific Ocean Part II. (URP. Rep. HIG-75-2, 1975).
 Busalacchi, A. & O'Brien, J. J. J. geophys. Res. 86, 10901-10907 (1981).
 Barnett, T. P. Mon. Weath. Rev. 112, 2388-2400 (1984).
 Gill, A. E. J. phys. Oceanogr. 13, 586-606 (1983).
 Gill, A. E. & Rasmusson, E. M. Nature 306, 229-234 (1983).
 Wyrtki, K. J. phys. Oceanogr. 7, 779-787 (1977).
 Lukas, R., Hayes, S. P. & Wyrtki, K. J. geophys. Res. 89, 10425-10430 (1984).
 Wyrtki, K. Goobar, Res. Lett. 21, 215 (1986).

- 14. Wyrtki, K. Geophys. Res. Lett. 12, 125-128 (1985).

Uplift of the shores of the western Mediterranean due to Messinian desiccation and flexural isostasy

Sonya E. Norman & Clement G. Chase

Department of Geosciences, University of Arizona, Tucson, Arizona 85721, USA

During the Messinian Stage (5.5 Myr, Miocene/Pliocene boundary) the 4.2×10^{23} m³ of water that now fills the Mediterranean evaporated. Evidence for this includes palaeogorges 1 km below the present Nile and Rhone valleys and evaporite deposits, sampled by cores and deep-sea drilling^{1,2}, that are thicker than 1 km over much of the Mediterranean³. Two-dimensional flexure models, presented here, indicate that the regionally compensated crustal unwarping from removal of the seawater load would lead to a Messinian geomorphology with an uplifted Mediterranean basin and shoreline bulges along its northwestern and southeastern coasts. These shoreline bulges would cause a reversal of downhill gradient direction in areas with low original seaward slopes. Such a profile would lead to a landward reversal of drainage in rivers with low discharge.

We used a cross-section north from Annaba, Algeria to Marseilles, France to determine present-day ocean depth, which we presume to have been comparable just before the last Messinian desiccation. Vertical deflection from removal of the seawater load along this profile was calculated from an equation derived by Hetenyi4 for distributed block loads and modified by Jordan⁵ for an elastic lithosphere. Figure 1 shows the flexure from 250 km inland in southern France to 300 km south of the coast. We assume a broken plate boundary along the African coast. (Flexure of the European coast is essentially the same for a broken plate as it would be for a plate unbroken at the African margin.) The calculation was first done with a twodimensional seawater load ('Water' in Fig. 1) and was repeated for several flexural rigidity values.

The removal of the load of only the present sea water gives us a flexural response representing the uplift caused by the last desiccation before the final infilling. Another calculation was made for removal of water and the 1.6-km-thick evaporites ('Salt' in Fig. 1). This unloading corresponds to the first Messinian dehydration of the Mediterranean, before its depth had been reduced by deposition of the thick evaporites. Finally, the flexure profiles were superimposed on the present-day topography.

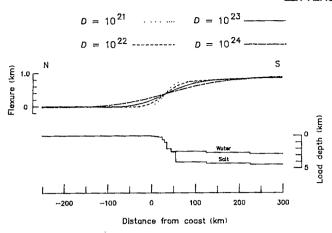


Fig. 1 Uplift of the Mediterranean Basin and 250 km inland on the French coast due to unloading of 2.6 km of water (density 1,000 kg m⁻³) for a range of values of flexural rigidity D (in N m). Load depth profiles are shown at the bottom. The flexure profiles are calculated for removal of present water load only. Topographic relief is not considered.

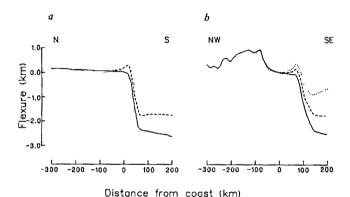


Fig. 2 Flexural effects combined with present topography, giving a regionally compensated palaeotopography profile from 200 km offshore to 300 km onshore, assuming $D = 10^{23}$ N m. Solid line, present profile; broken line, latest Messinian palaeotopography, calculated by removal of water load; dotted line, early Messinian palaeotopography, calculated by removing both water and salt loads (density 2,200 kg m⁻³). a, N7E through Rhone Valley, slight uphill gradient. b, N38W through Cape d'Agde, moderate uphill gradient.

Time-dependent viscous response of the upper mantle should not seriously affect our results. For the size of load and range of flexural rigidities considered here, and for reasonable mantle viscosities, the viscous relaxation time will be <10⁴ yr (ref. 6), while the time span of Messinian dehydration is probably $\sim 10^6$ yr, with episodes of partial refilling^{2,7,8}.

Figure 1 shows the calculated deflection patterns for the seawater load; the effect of superimposing topography on the calculated uplift from seawater and evaporite load is illustrated in Fig. 2. In calculating these palaeotopographic profiles, we work back from the present and show where the present-day topographic surface would have been deformed to by the flexural uplift. We have not estimated the pre-Messinian palaeotopography.

For all flexural rigidity values, the maximum uplift at the centre of the ocean basin is 0.85 km for removal of the seawater load, and 1.9 km for removal of the sea water and evaporites combined. Watts and Ryan9, employing a thermal subsidence model in this area, found the best value for the flexural rigidity D to be 10^{23} N m (this is used for all profiles in Fig. 2). Figure 2a through the Rhone valley (elevation gradient 0.5 m km⁻¹)

has an elevation at the shelf edge greater than that 50-300 km inland. The magnitude of the elevation difference and the location of the axis of lowest topography depends on the flexural rigidity. For $D = 10^{23}$ N m the shelf edge would have been raised 0.18 km above present sea level at the last desiccation (present seawater load removed) and 0.45 km at the first desiccation (seawater and evaporite load removed). The axis of lowest elevation would be 125 km inland from the present coastline for both models. The slight moat immediately off the shelf break is caused by the interaction of the sudden elevation drop with the increase in flexural uplift near the edge of the load. This moat is best developed for the initial uplift (dotted lines in Fig. 2).

Shoreline bulges with inland flexural depressions lead us to consider drainage reversals towards inland basins. There is, however, a problem with applying this to some of the major rivers of the Mediterranean, especially the Rhone. The presence of palaeogorges buried 1 km below present river valleys^{1,2,10} indicates that seaward flow probably persisted throughout the desiccation period. There is still the possibility that further upstream there was a drainage divide, or that during early stages of uplift there was a drainage reversal, but headward cutting (in this case, northward from the Mediterranean) eventually carved through the drainage divide, and cutting of the gorge at the coast was a later event.

The necessary condition for a reversal of drainage is that the change of gradient due to the uplift be faster than the downcutting rate of rivers. Even if large rivers, by virtue of their larger discharge and therefore increased excavating potential, managed to continue flowing in the same direction throughout the Messinian, this model predicts that smaller rivers, with their inherently weaker cutting potential would probably have reversed their drainage direction. Figure 2b demonstrates that a steeper original topographic gradient brings the on-land flexural basin closer to the palaeo-shore and makes it narrower. In addition to the formation of these shore-parallel moats, drainage patterns on the plateaus and in mountains were probably also altered by flexural warping.

This discussion is quantitatively applicable only to the northwestern Mediterranean, and the accuracy there is limited by the assumption of two-dimensionality. The same sort of model should apply to the southeastern Mediterranean, which also has thick evaporites³, although there the broken plate boundaries are more complex and the basin is narrower.

Topographic effects of flexural upwarping due to evaporation of the Mediterranean waters depend on the original topography and flexural rigidity. For southern France, southern Spain, northern Egypt and northern Libya, in areas with topography originally flat enough to have a shoreline bulge, major rivers probably excavated through the bulge as it formed, while lowdischarge rivers probably changed their course toward inland drainage basins. Uplift attending the first desiccation of the Mediterranean, before thick evaporite deposition, should have had about twice the amplitude of the uplift accompanying the last dehydration. Messinian palaeocurrent indicators, location of inland basins and better information on the depth, extent and character of palaeogorges on such rivers as the Rhone, as well as smaller rivers, would test these predictions.

Received 2 October 1985; accepted 1 May 1986.

^{1.} Hsu, K. J. in Messinian Events in the Mediterranean. Geodynamics Scientific Report No. (ed. Drooger, C. W.) 60-67 (North-Holland, Amsterdam, 1973).
 Hsu, K. J., Cita, M. B. & Ryan, W. B. F. Init. Rep. DSDP 13, 1203-1231 (1973).

Montadert, L., Letouzey, J. & Mauffret, A. Init. Rep. DSDP 42, 1037-1050 1978).

Hetenyi, M. Beams on Elastic Foundation (University of Michigan Press, Ann Arbor, 1946)

Jordan, T. E. Bull. Am. Ass. Petrol. Geol. 65, 12, 2506-2520 (1981)

Cathles, L. M. The Viscosity of the Earth's Mantle (Princeton University Press, 1975

Hsu, K. J. et al. Nature 267, 399-403 (1977). Cita, M. B. Am. Geophys. Un. Geodyn. Ser. 7, 113-140 (1982). Watts, A. B. & Ryan, W. B. Tectonophysics 36, 25-44 (1976). 10. Clauzon, G. Bull. Soc. géol. Fr. 24, 567-610 (1982).

Thermoluminescence dating of Le Moustier (Dordogne, France)

H. Valladas*, J. M. Geneste†, J. L. Joron‡ & J. P. Chadelle§

* Centre des Faibles Radioactivités, Laboratoire Mixte CNRS-CEA, Avenue de la Terrasse, 91190 Gif-sur-Yvette, France † UA 133 du CNRS; Direction des Antiquités Préhistoriques d'Aquitaine, 26-28 Place Gambetta, 33074 Bordeaux Cedex, France ‡ Groupe des Sciences de la Terre, Laboratoire Pierre Süe, CEN, Saclay, 91191 Gif-sur-Yvette, France § Direction des Antiquités Préhistoriques d'Aquitaine, 26-28 Place Gambetta, 33074 Bordeaux Cedex, France

The chronology of the Neanderthal cultures, commonly called Mousterian, which flourished between ~100,000 and 40,000 yr ago, has not been well established. The lower rock-shelter of Le Moustier provides one of the most important stratigraphic sequences, incorporating ten main Mousterian layers originally identified by Peyrony¹ and two early Upper Palaeolithic layers, the stratigraphy of which is mainly defined in terms of the regional climatic chronostratigraphy derived from the alpine glacial sequence¹⁻⁴. A correlation has recently been proposed between the chronostratigraphy of Dordogne and the past 125,000 yr of the wellestablished stratigraphy based on oceanic oxygen isotope ratios^{5,6}, but the lack of absolute datings of Mousterian settlements makes this correlation uncertain between 100,000 and 40,000 yr BP. We now report dates obtained by thermoluminescence measurements of 34 specimens of burnt flint recovered from the upper 3 m of the Mousterian deposits and from the superimposed Upper Palaeolithic layer. The dates, which range from 56,000 to 40,000 yr BP, allow us to correlate the cold sediment deposits of Le Moustier with cold intervals of the oxygen isotopic record of the Mediterranean Sea during isotopic stage 3.

Of the two major rock-shelters discovered at Le Moustier at the end of the last century, the upper or classic shelter was studied by Lartet and Christy (1863), whereupon Mortillet named the middle Palaeolithic industries Mousterian. The upper shelter was excavated at the beginning of the century^{1,7}. In the other shelter, which is located ~13.5 m below, several Mousterian traditions have been recognized^{1,2}, including typical Mousterian (layers B and J), Denticulate (layers F and I), and Acheulian tradition type A (layer G) and type B (layer H). The stratigraphic sequence, which is ~4 m thick, reveals two types of deposits: (1) the lower group of strata (layers A to F) is made up of waterlain sediments deposited by the floods of the Vézère River; (2) the upper group (layers G to L, Fig. 1a) consists of cryoclastic sediments in which the proportion of anthropological remains can be substantial (especially in layer H).

Each of the 12 main layers has been subdivided on the basis of sedimentation and pollen count data^{4,8}, and the whole sequence has been assigned to the early part of the last glacial period (ancient Würm in the chronostratigraphy of Dordogne^{5,6}). Layer K, overlying the most recent Mousterian layer, contains a mixture of Lower Perigordian (Chatelperronian) and Mousterian tool assemblages. The state of preservation of the Mousterian component in this assemblage suggests possible contamination from below. Layer K has been assigned to the beginning of the recent Würm²⁻⁶, ~35,000 yr ago.

Burnt flints have been widely used for thermoluminescence

Burnt flints have been widely used for thermoluminescence (TL) dating⁹⁻¹⁴; they are common near prehistoric hearths, where some will have been heated to a temperature high enough to erase the thermoluminescence acquired by the minerals during their geological history. Good agreement among the TL dates obtained¹⁵ with four quartz and three flint fragments for the upper Perigordian layer (Gravettian) of La Vigne Brun (Villerest,

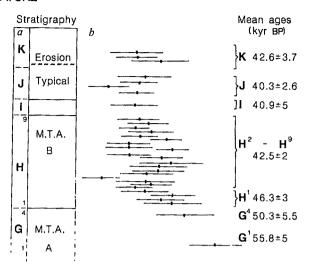


Fig. 1 a, The top Mousterian layers and the Upper Palaeolithic layers of the lower rock-shelter at Le Moustier^{1,4}. The thickness of this sequence is ~3 m. M.T.A., Mousterian of Acheulian tradition, type A (A) and type B (B). b, Horizontal bars representing the TL ages of the burnt flints from Le Moustier as a function of depth. The weighted ages calculated for the respective layers are listed at the right.

Loire, France) suggests that the TL of flint does not fade significantly.

The burnt flints were collected from a small area (30×40 cm) excavated in May 1982 in the north-east corner of the 'witness' sediments (level G to K). Approximately 80 flints of suitable size, showing signs of having been heated, were selected for TL examination. Of these, only 34 were sufficiently well burnt and had satisfactory TL characteristics. Three of these were from the middle part of layer K, 4 from layers J5 to J1, 1 from layer I3, 24 from layers H9 to H1 and 2 from layers G4 and G1. The bottom 1 m of Mousterian deposits (F to A) has not yet yielded burnt flints.

The methods used to treat the samples and to measure their palaeodose and annual dose rate have been described in detail elsewhere 15. The environmental γ dose rate was measured using 28 calcium sulphate dosimeters in copper capsules. These were inserted at the ends of 30-cm-deep horizontal auger holes, which were distributed at ~10-cm intervals from top to bottom, and left buried for 1 yr. As the archaeological layers are also ~10 cm thick, it was impossible to specify the exact location of each sample within a specific layer. The external dose rate received by the flints of a given layer was obtained by taking the average dose measured in the layer itself and in the two adjoining layers, and ranges from 0.33 to 0.54 mGy yr⁻¹ except in layer G. The uranium and thorium contents in the flints were measured by epithermal neutron activation inside a cadmium container^{16,17}, and the potassium content by neutron activation at the Institut Pierre Süe (CEN, Saclay). The internal dose rate usually represents ~50% of the total dose rate, which ranges from 0.67 to 0.90 mGy y⁻¹. The results are reported in Table 1.

The age of each flint and its statistical error are presented as a function of depth in Fig. 1b. The ages (weighted mean) derived for the respective layers range from $\sim 56,000$ to 40,000 yr BP (Table 2). Levels J and H, for which many burnt flints were available, have been dated with better precision (5-6%) than the other levels; for the latter, <3 samples were available and the precision of the results is only $\sim 10\%$.

The time span represented by the layers from which the dated flints were recovered (G to K) is estimated at $15,000 \pm 5,000$ yr. The paucity of data makes it impossible to determine whether there were any occupation gaps during the $\sim 10,000$ yr separating layers G1 from H1. On the other hand, virtually continuous

Table 1. Thermoluminescence results and radioactivity data for the flints from Le Moustier

		U*	Th*	, vr.	$D_{lpha}\dagger$	$D_{m{eta}}$ ‡	External dose§	Dose rate	D.I. d.	A
Layer	Sample	(p.p.m.)		K* — (p.p.m.)		(10 ⁻⁵ Gy	yr ⁻¹)		Palaeodose (10 ⁻² Gy)	Age (kyr BP)
K	3	0.823	0.473	334	22.2 ± 5.1	16.1 ± 0.9	44±6	83 ± 8	3.423 ± 218	41.3 ± 4.7
K	6	0.94	0.487	458	22.4 ± 2.7	18.8 ± 1.1	45±6	87 ± 6.7	$3,595 \pm 185$	41.5 ± 3.8
K	7	0.915	0.256	296	24.7 ± 3.9	16.5 ± 0.9	44.8 ± 6	86.5 ± 7	3.964 ± 322	45.8 ± 5.2
J5	24	0.687	0.352	300	19.2 ± 2	13.5 ± 0.8	42.7 ± 7	76 ± 7	$3,282 \pm 220$	43.2 ± 5
J2	52	0.801	0.455	394	23 ± 2.2	16.2 ± 0.9	40 ± 2	80±3	$3,334 \pm 252$	41.7 ± 3.5
J2	53	0.647	0.657	450	19.2 ± 4.2	15 ± 0.9	40.5 ± 2	75.2 ± 5	$2,715 \pm 210$	36.1 ± 3.7
J1	71	0.668	0.28	300	21.2 ± 3.8	13 ± 0.7	38.3 ± 3	72.8 ± 5	3.029 ± 161	41.6 ± 3.6
13	120	0.772	0.29	100	19.7 ± 2.7	12.9 ± 0.7	36.2 ± 5	69.3 ± 5.8	2.834 ± 194	40.9 ± 4.4
H9.	141	0.851	0.54	350	21.6 ± 2	16.8 ± 1	32 ± 3.5	71.4 ± 4	2.989 ± 223	41.9 ± 3.9
H9	142	0.719	0.62	430	17 ± 2.2	15.8 ± 0.9	32.6 ± 3.5	66 ± 4.2	$2,863 \pm 286$	43.4 ± 5.1
Н9.	150	0.907	0.42	360	23 ± 2.2	17.4 ± 1	33 ± 3.5	74 ± 4.2	3.040 ± 162	41.1 ± 3.2
H7D	200	0.844	0.31	340	21.9 ± 2.2	16 ± 0.9	30.8 ± 3	69.7 ± 3.8	$3,088 \pm 265$	44.3 ± 4.5
H7C	220	1.27	0.4	370	37.3 ± 4.3	22.7 ± 1.3	31.4 ± 3	92.5 ± 5.4	$3,907 \pm 227$	42.2 ± 3.5
H7B	242	0.715	0.63	500	19.5 ± 1.4	16.3 ± 0.9	30.4 ± 3	67.5 ± 3.5	$3,167 \pm 127$	46.9 ± 3
H4.	302	1.04	0.354	360	34.3 ± 4	19.1 ± 1.1	32.9 ± 3	86.9 ± 5.1	$3,471 \pm 256$	39.9 ± 3.8
H2E	360	0.93	0.3	300	29.5 ± 6	16.9 ± 1	35.1 ± 5	82.4 ± 8	3.298 ± 196	40 ± 4.4
H2E	362	1.11	0.4	421	26.5 ± 2.6	20.8 ± 1.2	35.4±5	83.5 ± 5.7	$3,301 \pm 245$	39.5 ± 4
H2E	363	0.462	0.944	630	16 ± 4.1	14.6 ± 0.8	35.5 ± 5	66.7 ± 6.5	$3,209 \pm 243$	48.1 ± 5.8
H2B	401	0.9	0.34	100	23 ± 2.6	14.9 ± 0.8	35.3 ± 5	74 ± 5.7	$2,979 \pm 183$	40.3 ± 4
H2B	402	0.89	0.35	333	26 ± 2.2	16.7 ± 1	34.6 ± 5	78.3 ± 5.5	$3,594 \pm 183$	45.9 ± 4
H2B	407	0.53	0.35	160	15.2 ± 1.5	10 ± 0.6	35 ± 5	60.8 ± 5.2	2.908 ± 270	47.8 ± 6
H2B	421	0.4	0.378	170	9.9 ± 0.9	8.3 ± 0.4	35.3 ± 5	53.9 ± 5.1	$2,458 \pm 191$	45.5 ± 5.6
H2B	423	1.07	0.454	440	29 ± 3.3	20.6 ± 1.2	34.6 ± 5	85.4 ± 6.1	$3,861 \pm 337$	45.2 ± 5.1
H2B	428	0.56	0.243	400	14.1 ± 2.6	12.1 ± 0.7	35.1 ± 5	62 ± 5.7	$2,693 \pm 173$	43.4 ± 4.9
H2A	443	1.32	0.45	440	40 ± 5.3	24.1 ± 1.4	34.3 ± 5	100 ± 7.4	$3,535 \pm 249$	35.3 ± 3.6
H2A	464	0.64	0.285	280	23.5 ± 3.8	12.4 ± 0.7	35 ± 5	71.6 ± 6.3	$3,058 \pm 305$	42.7 ± 5.7
H2A	480	1.25	0.525	380	29.9 ± 2.7	22.8 ± 1.3	35 ± 5	88.9 ± 5.8	3.884 ± 266	43.7 ± 4.2
H2A	482	1.01	0.462	400 -	30.8 ± 4.4	19.3 ± 1.1	35.1 ± 5	86.2 ± 6.7	3.551 ± 134	41.2 ± 3.6
H1	500	0.86	0.32	240	28 ± 2.5	15.4 ± 0.9	39 ± 5	83.1 ± 5.7	3.597 ± 277	43.2 ± 4.5
H1	501	1.05	0.39	390	30.6 ± 3	19.6 ± 1.1	39.3 ± 5	90.3 ± 5.9	$4,361 \pm 274$	48.3 ± 4.4
H1	502	1.12	0.44	340	32.5 ± 3	20.4 ± 1.2	38.7 ± 5	92.7 ± 5.9	$4,274 \pm 346$	46.1 ± 4.8
H1	503	0.844	0.336	220	21.3 ± 5	15.1 ± 0.9	39.1 ± 5	76.1 ± 7.1	$3,636 \pm 247$	47.7 ± 5.6
G4	570	0.594	0.76	400	16.9 ± 2	14.1 ± 0.8	47 ± 5	78.5 ± 5.5	3.952 ± 277	50.5 ± 5.5
Ġ1	571	1.3	0.3	270	33.9 ± 4.4	22 ± 1.3	84 ± 8	141 ± 9	$7,864 \pm 342$	55.8 ± 5

^{*} The values of U. Th and K each have an error of ±6%.

occupation is suggested by the many layers falling within the shorter time period separating layers H1 and K (6,000 \pm 3,000 yr). Note that, although the ages obtained for the highest Mousterian layer J (40,300 \pm 2,600 yr) and the overlying layer K (42,600 \pm 3,200 yr) are not in accord with the stratigraphy, the magnitude of the experimental errors makes the inversion more

Table 2 Weighted mean ages of levels in which flints were found

Layers	Mean ages (уг вр)
K	$42,600 \pm 3,200$
j	$40,300 \pm 2,600$
I	$40,900 \pm 5,000$
H _o to H ₂	$42,500 \pm 2,000$
H,	$46,300 \pm 3,000$
G_4	$50,300 \pm 5,500$
G_1	$55,800 \pm 5,000$

The errors (statistical plus systematic) at 68% confidence level have been assessed as in ref. 32. A systematic error of $\pm 7.5\%$ has been assumed for the external dose, to take into account possible past variations of the water content of the archaeological sediments (M. J. Aitken, personal communication).

apparent than real. Also, as noted earlier, layer K contained a mixture of Lower Perigordian (Chatelperronian) and Mousterian tools. Thus, it may have been Mousterian flints which were responsible for the date obtained for layer K.

These dates allow us to correlate the stratigraphy of Le Moustier4,5 with the isotopic record and chronology of deep-sea sediments. The ages obtained for levels G to K place their deposition during isotopic stage 3 (ref. 18). A detailed chronology of this stage has recently been proposed by correlating five ash layers contained in cores collected in the central Tyrrhenian Sea with terrestrial volcanic deposits dated by the ¹⁴C and/or the K-Ar method¹⁹. The temperature variations of the Tyrrhenian Sea are much larger than those of the open ocean; consequently, the Tyrrhenian Sea sediments provide an oxygen isotopic signal which is sensitive to both the water temperature and changes in the δ^{18} O content of the water²⁰⁻²². Nevertheless, the Tyrrhenian Sea, like the entire Mediterranean Sea, has yielded isotopic records showing features similar to those in the generally accepted oxygen isotope curve²³; indeed, the classical isotopic stages¹⁸ are easily recognized and within stage 3, a strong climatic variability with a succession of cold and warmer isotopic events has been described19.

. The Tyrrhenian record shows the same climatic trends as those deduced from the analysis of continental pollen in

[†] The β equivalent dose rate per unit of α flux was measured as in ref. 27 and the β equivalent annual dose of flints was calculated using specific fluxes deduced from ref. 28.

[‡] The β dose in flints was calculated using the specific values given in ref. 29. The γ internal dose is <0.01 mGy yr⁻¹.

[§] The external dose rate includes a cosmic contribution of $5-6\times10^{-5}$ Gy yr⁻¹. It has been calculated using the data given in refs 30 and 31; the estimated average thickness of overburden is 9-10 m.

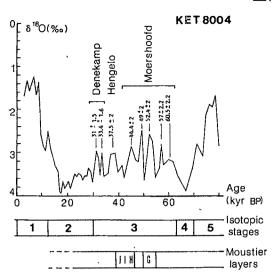


Fig. 2 The dated Mousterian layers are shown below the $\delta^{18}O(\%)$ variations measured in the core KET 8004 collected in the Tyrrhenian Sea. Estimates of the age of the oxygen isotopic events (light δ^{18} O peaks) have been calculated assuming a constant sedimentation rate between two well-dated ash layers¹⁹.

northern Europe, as well as in France and eastern Macedonia²⁴⁻²⁶; the well-dated oxygen isotope peaks (warm events) which occur between 60,000 and 30,000 yr BP (ref. 19) correlate with the continental interstadials dated by the 14C method²⁶. This record provides a fairly good comparison framework for the prehistoric stratigraphy, as it has been obtained in a climatic zone close to southern France.

The dated layers of Le Moustier are shown below the isotopic record of the Tyrrhenian Sea (Fig. 2). The cryoclastic sediments of layers G to K have yielded low pollen counts (<10%), which suggests that these layers were deposited during cold periods^{4,8}. The TL ages obtained for the above-mentioned layers suggest that their deposition occured during the cold periods which developed between 56,000 and 40,000 yr BP on the isotopic record.

We therefore conclude that TL dating of burnt flints should make it possible to obtain close correlation between the floating chronology of the Mousterian epoch based on stratigraphic evidence and the more absolute chronology derived from the isotopic record of sea cores.

The field research at Le Moustier has been supported by the L.S.B. Leakey foundation, Pasadena; California (grant for the Combe-Saunière Dating Project, 1981). We thank G. Valladas for his important contribution to this work and J. L. Reyss for radioactivity analyses. CFR contribution 760.

Received 5 March: accepted 30 April 1986.

- 1. Peyrony, D. Rev. Anthropol. 1-3; 48-76; 4, 6 (1930).
- Bordes, F. Livret Guide de l'excursion A4, Landes-Perigord, 38-87 (VIII Congrés INQUA, Paris, 1969).
- aville, H. & Rigaud, J. P. C: r. hebd. Séanc. acad. Sci., Paris D 276 3097-3100 (1973).
- Laville. H. in Etudes Quaternaires Mémoires (Marseille), 4 (1975).
- Laville, H. et al. Paleoclimat, 34, 219-241 (1983).

- Laville, H., Raynal, J. P. & Texier, P. J. in Bul. Soc. préh. franç. 81, 8-11 (1984). Bourlon, M. L'homme préhistorique 3, 7, 14 (1905). Paquereau. M. M. Quaternaria 18, 85-93 (1974-1975).
- Gosku, H. Y., Fremlin, J. H., Irwin, H. T. & Fryxell, R. Science 183, 651-654 (1974). Wintle, A. G. & Aitken, M. J. Archaeometry 19, 111-130 (1977).
 Valladas, H. PACT 2, 180-184 (1978).

- Huxtable, J. & Jacobi, R. M. Archaeometry 24, 164-169 (1982).
 Bowman, S. G. E. & Sieveking, G de G. PACT 9, 353-361 (1982).
 Aitken, M. J. Thermoluminescence Dating (Academic, New York, 1985).
 Valladas, H. thesis, Paris VI and Museum Nat. Hist. Nat. (1985).
- Chayla, B., Jaffrezic, H. & Joron, J. L. C. r. heòd. Séanc. Acad. Sci., Paris, 277, 273-275, (1973).
- Joron, J. L. thesis, Orsay (1974).
 Shackleton, N. J. & Opdyke, N. D. Quat. Res. 3, 39-55 (1973)
- 19. Paterne, M., Guichard, F., Labeyrie, J., Gillot, P. Y. & Duplessy, J. C. Mar. Geol. (in the
- 20. Emiliani, C. Quaternaria 2, 87 (1955).
- 21. Vergnaud-Grazzini, C. Science 190, 272-274 (1975).

- Thumell, R., Federman, A., Sparks, S. & Williams, D. Quat. Res. 12, 241-253 (1979).
 Ryan, W. B. F. in The Mediterranean Sea, (Stanley, D. J. ed.) 149-170 (Dorden, Hutchinson
- and Ross, 1972). Van Der Hammen, T., Wijmstra, T. A. & Zagwija, W. H. in The Late Cenozoic Glacial Ages (Turekian, K. K. ed) 391-424 (Yale University Press, Cambridge, 1971).
- Woillard, G. Quat. Res. 9, 1-21 (1978).
 Woillard, G. & Mook, W. G. Science 215, 159-161 (1982).
 Valladas, H. & Valladas, G. PACT 6, 171-178 (1982).
- Aiken, M. J. & Bowman, S. G. E. Archaeometry 17, 132-138 (1975).
 Bell, W. T. Archaeometry 21 243-245 (1979).
 Kvasnicka, J. Hlth Phys. 36, 521-524 (1979).
 Prescott, J. R. & Stephan, L. G. PACT 6, 17-25 (1982).

- 32. Aitken, M. J. Archaeometry 18, 233-238 (1976).

A putative ancestor for the swordfish-like ichthyosaur Eurhinosaurus

C. McGowan

Department of Vertebrate Palaeontology, Royal Ontario Museum, 100 Queen's Park, Toronto, Ontario, Canada M5S 2C6, and Department of Zoology, University of Toronto

Ichthyosaurs, extinct marine reptiles superficially similar to sharks and dolphins, flourished throughout most of the Mesozoic, but are best represented in the early Jurassic1-5. Hundreds of skeletons are known, principally from the Lower Liassic (Hettangian, Sinemurian and Lower Pleinsbachian) of south-west England and the Upper Liassic (Toarcian) of southern Germany⁶⁻⁹. Among the most specialized is Eurhinosaurus, unique for its long rostrum and shortened mandible, which confers a striking resemblance to the modern swordfish, Xiphias 1,5,10. Known only from the Upper Liassic of Germany, this monotypic genus, like most fossil species, appears suddenly, without antecedents 11-14. The recent discovery of a geologically older (Lower Liassic) ichthyosaur with a partially extended rostrum is therefore of considerable interest. As described here, this specimen, which is too large to be part of a growth series of Eurhinosaurus, appears to be ancestral, and could have given rise to Eurhinosaurus through changes in growth rates of the rostrum and mandible.

The incomplete skeleton of this new ichthyosaur was collected in Somerset in 1984 by D. Costin. It is described below as representing a new genus.

> Class Reptilia Order Ichthyosauria (Family designation awaits revision) Excalibosaurus gen. nov.

Etymology: Excalibur, the mythological sword of Arthurian legend; saurus, Greek (masculine) for lizard.

Diagnosis: Mandible shorter than skull, but exceeding 60% of skull length. Snout extends well beyond anterior tip of mandible, but length of snout (distance between tip of snout and anterior margin of orbit¹⁵) not greatly exceeding length of mandible.

Type species: Excalibosaurus costini gen. et sp. nov. (Fig. 1). Etymology: In honour of D. Costin, through whose diligence and generosity the material was collected and safely deposited in a museum.

Diagnosis: As for genus.

Holotype: Cc 881, a complete skull, with associated forefin, pectoral girdle, vertebrae and ribs, deposited in The City of Bristol Museum and Art Gallery, UK.

Locality and horizon: The foreshore near Lilstock, Somerset, UK (map ref. ST 196 463). Lower Liassic (Sinemurian), horizon provisionally given as the Bucklandi Zone (M. L. K. Curtis, personal communication).

Description: The elongated snout, which projects well beyond the tip of the mandible, distinguishes this from all other ichthyosaurs, except Eurhinosaurus huenei, where the disparity.

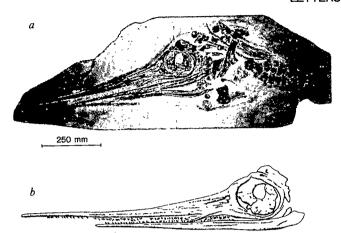
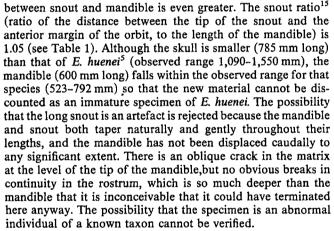


Fig. 1 Excalibosaurus costini gen. et sp. nov. Holotype (Cc881, City of Bristol Museum and Art Gallery). Lower Liassic (Sinemurian) of Lilstock, Somerset, a, Complete specimen; b, diagram of the skull. Scale bar, 250 mm.



Compared with most other Lower Liassic ichthyosaurs, the new species is relatively large, the skull length exceeding that of *Ichthyosaurus communis* and lying at the top end of the range for *I. tenuirostris*³. The new species is, however, smaller than most specimens referred to *Temnodontosaurus*². Its slender teeth extend along most of the free portion of the snout; *Eurhinosaurus huenei* similarly has a dentigerous 'sword'. Further preparation is needed, but the external naris appears bilobed, as in some

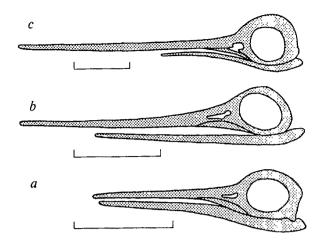


Fig. 2 Ichthyosaur skulls drawn to the same manidbular lengths (a, b), and to the same skull lengths (b, c). a, Ichthyosaurus tenuirostris (based on OUM J10305, Oxford University Museum, and IGS 51236, Institute of Geological Sciences, London) from Lower Liassic (Hettangian-Sinemurian), Street, Somerset. b, Excalibosaurus costini gen. et sp. nov., holotype, from Lower Liassic (Sinemurian), Lilstock, Somerset. The apparent difference in shape between a and b in the vicinity of the jaw joint is an artefact of preservation. c, Eurhinosaurus huenei (based on MNHP 1946-20, Museum National d'Histoire Naturelle, Paris, and FSF 4155, Forschungsinstitut Senckenberg, Frankfurt) from Upper Liassic (Toarcian), Holzmaden. The transition from a to c, via b, could have been effected through an elongation of the rostrum, followed by a reduction in the mandible. Scale bar, 250 mm.

specimens of E. huenet⁵. A similar naris occurs in I. tenuirostris, which has other features in common with the new taxon. This similarity could be used to support a relationship between the three taxa, but it is not a constant feature, and a somewhat similar naris occurs in Leptopterygius burgundiae⁵. The naris of the new species appears to be relatively large. The prenarial¹⁵ ratio (ratio of the distance between the tip of the snout and the anterior margin of the external naris, to the length of the mandible) is relatively higher (0.89) than in I. tenuirostris (0.60). The anterior end of the maxilla has been displaced, but the premaxillary ratio¹⁵ (ratio of the distance between the tip of the snout and the anterior tip of the maxilla, to the length of the mandible) is estimated to be 0.86. The orbital ratio¹⁵ (ratio of the diameter of the orbit to the length of the mandible) is 0.20. The forefin has three digits, with some indication of a fourth; there are

Table 1 Cranial and mandibular ratios for selected ichthyosaurs

		Cranial ratios				Mandibular ratios			
Species	Snout/ skull	Orbit/ skull	Premaxilla/ skull	Prenaris/ skull	Snout/ mandible	Orbit/ mandible	Premaxilla/ mandible	Prenaris/ mandible	
Excalibosaurus costini gen. et sp. nov.	0.80	0.16	0.66	0.68	1.05	0.20	0.86	0.89	
Ichthyosaurus tenuirostris (mean values)	0.75	0.23	0.54	0.62	0.72	0.21	0.52	0.60	
Modified specimen of I. tenuirostris*	0.83	0.16	0.67	0.74	1.09	0.21	0.88	0.97	
Eurhinosaurus huenei (mean values)	0.83	0.12	0.64	0.77	1.64	0.25	1.28	1.53	
Modified specimen of Excalibosaurus costini†	0.80	0.16	0.66	0.68	1.58	0.31	1.29	1.33	

Cranial ratios are measurements (such as the length of the snout) compared with the length of the skull, while in mandibular ratios they are compared with the length of the mandible.

^{*} I. tenuirostris modified by increasing the snout length such that the ratio skull length/mandibular length is the same as in E. costini.

[†] E. costini modified by reducing the length of the mandible such that the ratio mandible length/skull length is the same as in E. huenei.

usually four in I. tenuirostris and up to five in E. huenei. The forefin is about half the length of the mandible, as in I, tenuirostris, whereas in E. huenei it is relatively longer, often exceeding the length of the mandible. There are 12 elements in the longest digit (commencing with the epipodials¹⁶), which is within the observed range for I. tenuirostris, but there are usually more in E. huenei (up to 23). Fin structure, however, is often variable within species, especially in E. huenei⁵.

Aside from its longer snout, the skull of E. costini is similar to that of I. tenuirostris (compare Fig. 2b, a); this results in their having similar orbital ratios, but their other mandibular ratios, and their cranial ratios, are disparate (Table 1). However, if the snout of I. tenuirostris is increased in length until the ratio of skull length/mandibular length corresponds to that of E. costini, their cranial and mandibular ratios converge (Table 1). E. costini could therefore be derived from I. tenuirostris by an elongation of the snout.

E. costini is cranially similar to E. huenei, except in having a relatively longer mandible (Fig. 2b,c); this is reflected in the similarity of their cranial ratios, and the dissimilarity of their mandibular ratios (Table 1). However, if the mandible of E. costini is reduced to 400 mm, giving the same value for the ratio mandible length/skull length as in E. huenei (0.51), its mandibular ratios converge with those of E. huenei (Table 1). E. huenei could therefore be derived from E. costini by mandibular reduction.

If E. huenei evolved from a long-snouted ancestor like I. tenuirostris, through an intermediary like E. costini, what mechanism might have been involved? A change in growth rates of the rostrum and mandible during ontogeny seems plausible, and some insight is gained by studying ontogeny in Xiphias. Larval swordfish have mandibles extending to the tip of the skull¹⁷⁻¹⁹ whereas in adults the mandible is only about one-third of the skull length. These profound changes are effected by relatively small differences in growth rates between the mandible and rostrum (C. McG., in preparation). A small increase in the growth rate of the rostrum in an ichthyosaur like I. tenuirostris could therefore give rise to a descendant like E. costini with an elongated rostrum. This, in turn, could give rise to E. huenei by a reduction in the growth rate of the mandible. Such minor modifications would presumably require relatively small genetic changes, but the morphological, and consequent biological changes would be profound.

I thank M. A. Taylor for bringing the new material to my attention and also thank him, S. Swansborough and M. L. K. Curtis for their help in Bristol. I thank J. Mulock for his drawings; P. Purves for typing; R. Johnson and J. Thomason for reading the manuscript; C. E. McGowan for nomenclatural inspiration; and J. Campsie for classical advice. This research was supported by the Natural Sciences and Engineering Research Council of Canada, grant A 9550.

Received 6 January; accepted 1 May 1986.

- 1. Von Huene, F. Die Ichthyosaurier des Lias und ihre Zusammenhänge (Verlag von Gebrüder, Borntraeger, Berlin, 1922). McGowan, C. Life Sci. Contr. R. Ont. Mus. 93, 1-37 (1974a).
- McGowan, C. Life Sci. Contr. R. Ont. Mus. 100, 1-30 (1974b).
 McGowan, C. J. Paleont. 52, 1155-1162 (1978).
- McGowan, C. Palaeontographica 166, 93-135 (1979). Hauff, B. Palaeontographica 64, 1-42 (1921).
- Hauff, B. Das Holzmadenbuch (F. Rau, Öhringen, 1953).
- 8. Arkell, W. J. The Jurassic System in Great Britain (Oxford University Press, 1933).
- Palmer, C. P. Newsl. Stratigr. 2, 45-54 (1972).
 Jäger, G. Nova Acta Akad. Caesar. Leop. Carol. 25, 937-967 (1856).
- Jäger, G. Nova Acta Akad. Caesar. Leop. Carol. 25, 937-967 (1856).
 Darwin, C. On the Origin of Species (Murray, London, 1859).
 Eldredge, N. & Gould, S. J. in Models in Paleobiology (ed. Schopf, T. J.) 82-115 (Freeman, Cooper, San Francisco, 1972).
 Gould, S. J. Paleobiology 11, 2-12 (1985).
 Gingerich, P. D. Paleobiology 11, 27-41 (1985).
 McGowan, C. Can. J. Earth Sci. 13, 668-683 (1976).
 McGowan, C. Life Sci. occ. Pap. R. Ont. Mus. 20, 1-8 (1972).
 Arata, G. F. Bull. mar. Sci. Gulf Caribb. 4, 183-243 (1954).
 Yabe, H., Uevannei, S., Kikawa, S. & Watanabe, H. Reo. Nankat reg. Fish Res. Lab. 10.

- 18. Yabe, H., Ueyanagi, S., Kikawa, S. & Watanabe, H. Rep. Nankai reg. Fish Res. Lab. 10,
- 19. Markle, G. E. U.S. Dept. Commerce, NOAA tech. Rep. NMFS SSRF-675, 252-260 (1974).

The genetic control and consequences of kin recognition by the larvae of a colonial marine invertebrate

Richard K. Grosberg* & James F. Quinn†

* Department of Zoology and † Division of Environmental Studies, University of California, Davis, California 95616, USA

The evolution of altruism, cooperation and sociality should be favoured by mechanisms promoting interactions among relatives^{1,2}. In turn, the opportunity for such interactions should be enhanced where related individuals are spatially associated. The simplest explanation for association of kin invokes philopatric, or limited, dispersal3. Alternatively, kin recognition—which is known from a broad array of taxa^{4,5}—can produce similar associations. Neither the prevalence of kin recognition, nor aggregations of kin, are by themselves sufficient to demonstrate that kin recognition plays an important role in the production of nonrandom associations of relatives. To have such a role, kin recognition must promote or inhibit associations of kin beyond the effects of other processes, notably dispersal, that modify spatial patterns. Here we report the results of field experiments showing that sibling planktonic larvae of the sessile colonial ascidian Botryllus schlosseri settle in aggregations that are much stronger than expected from dispersal distance effects alone. Laboratory experiments indicate that larvae distinguish kin on the basis of shared alleles at a highly polymorphic histocompatibility locus known to regulate fusion between adult colonies. This kin recognition mechanism, along with limited dispersal of larvae, promotes co-settlement of histocompatible individuals. Consequently, the probability of fusion between adult colonies is far greater than that expected if larvae settled randomly.

Botryllus schlosseri colonies are founded after a sexually produced planktonic tadpole larva attaches to a firm substratum and metamorphoses. Repeated cycles of asexual multiplication produce a colony of morphologically and genetically identical zooids, connected by a blood vascular system. As in many colonial marine invertebrates, the larvae of several oviparous ascidians can metamorphose soon after release into the plankton⁶⁻¹⁰. In the case of B. schlosseri, our laboratory and field observations, as well as those of others¹¹, demonstrate that larvae can metamorphose—and many do—soon after escaping from their natal colony.

To determine the contribution of larval settlement behaviour to the spatial arrangement of sibling adult colonies, we examined the recruitment pattern of sibling colonies (<4 weeks old) that were founded by larvae, all derived from the same cross, and carrying a rare genetic marker. We identified the marker from an electrophoretic survey of 512 colonies living on the side of the Marine Biological Laboratory Supply Dock in the Eel Pond at Woods Hole, Massachusetts, USA. At the phosphoglucose isomerase locus (PGI), five electromorphs occurred, one of which (PGI-fast) was present in only two of the colonies surveyed. We cross-fertilized these two colonies, then assayed the F_1 colonies for *PGI-fast* homozygotes. One F_1 homozygote was selected as the source colony for marked larvae, and was positioned at the centre of a 1-m diameter circular asbestos-cement panel horizontally suspended 0.5 m below the dock. All zooids in a sexually mature B. schlosseri colony ovulate synchronously approximately weekly. Just before each ovulation, we returned the source colony to the laboratory, where we mated it with a sibling colony homozygous for the same marker allele, then repositioned the source colony on the panel. We left the panel in position for 4 weeks, then mapped and removed all B. schlosseri colonies that had recruited. Colonies were frozen at -80 °C, then analysed electrophoretically. We mapped the panel before any recruited colonies had reached sexual maturity; thus,

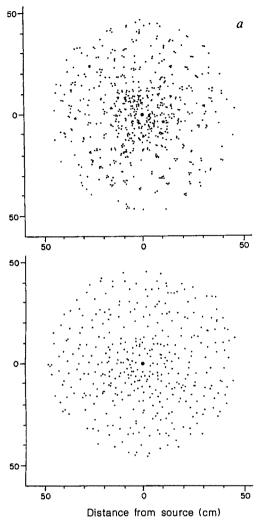


Fig. 1 Maps of the dispersion of Botryllus schlosseri (which settled on the undersurface of a 1-m circular asbestos-cement panel suspended below the Marine Biological Laboratory Supply Dock at Woods Hole, Massachusetts). Small dots depict the locations of colonies. The large dot marks the location of the source colony. a, Map of F₁ colonies (identified by the presence of the PGI-fast allele, see text) derived from source colony. b, Map of colonies not carrying the PGI-fast allele, thus, not derived from the source colony.

colonies homozygous for the *PGI* marker allele were assumed to be siblings originating from the source colony at the centre of the panel. Recruits not carrying the marker allele must have immigrated.

Figure 1a and b show respectively maps of marked and unmarked colonies. To test for spatial association among siblings, we computed the Clark and Evans¹² index of aggregation (R) based on nearest-neighbour distances between sibling colonies. R is the mean nearest-neighbour distance observed, divided by that expected if dispersion were random. Thus, randomly arranged individuals are expected to yield a value for R of 1.0. Values of R significantly <1 indicate aggregation, whereas values >1 indicate overdispersion. The sibling colonies were aggregated as tested by Clark and Evans' significance criteria (R = 0.769: P < 0.001). The unmarked immigrant colonies were significantly overdispersed (R = 1.227; P < 0.001). This overdispersion could result from larval behaviour, or could simply be an artefact of spacing due to colony growth¹³. In any case, the degree of aggregation of siblings differs even more from that of immigrants than it does from random (t-test; P < 0.001).

Figure 1a shows that sibling colonies are clustered around the source colony, perhaps because B. schlosseri larvae can settle

upon release into the plankton. To separate any aggregation caused by sibling recognition from that due to limited dispersal, we constructed a null model based on a bootstrap analysis 14 of the nearest-neighbour data. The locations of colonies were expressed in polar coordinates with the origin at the centre of the source colony: pseudosamples with the same distributions of distances and directions were chosen independently and randomly, with replacement, from the actual coordinates of sibling colonies. The randomized distance and direction coordinates are thus independent in the pseudosamples. This randomization procedure should preserve in the pseudosamples the overall aggregating effect of dispersal distance alone. However, smaller-scale aggregations due to interactions between immediate neighbours will be broken up by the randomization of the angular coordinates. For 500 randomizations, we calculated the value of R produced by the random model. In all cases, the values of R under the random model were substantially greater (mean = 0.897; s.d. = 0.023; range 0.824-0.964) than the observed R = 0.769. This analysis demonstrates that limited dispersal explains only about half the deviation of mean nearestneighbour distance from that expected if settlement were random.

The histocompatibility system known to control fusion and rejection between adult Botryllus colonies may provide a mechanism by which larvae recognize their siblings. Histocompatibility is controlled by a single mendelian locus such that two colonies sharing one or both alleles can fuse by their blood vascular systems. When colonies do not share an allele, rejection, accompanied by necrosis at the site of allogeneic contact, occurs 15-17. Fusion frequencies among pairs of Botryllus colonies collected in the field have been reported to range from 4 to 8% (refs 18, 19). In our studies on the Marine Biological Laboratory Supply Dock, of 500 pairs of colonies collected haphazardly along a 20-m transect, 22 pairs (4.2%) fused. According to the method of Curtis et al.²⁰, at equilibrium, approximately 100 equally frequent histocompatibility alleles would produce the fusion frequency observed in the Eel Pond population. Given such a high level of polymorphism at the histocompatibility locus, the likelihood that any two colonies will share a histocompatibility allele should depend primarily on their pedigree

Because the settled colonies in the field experiments were all full siblings, shared alleles at loci other than the histocompatibility locus could have been used for sibling recognition. Accordingly, we designed laboratory experiments to test whether larval settlement location is better predicted by the histocompatibility type or the relatedness of resident individuals. With a breeding programme using colonies of known histocompatibility genotypes (determined by fusion assays), in a factorial design, we varied independently the effects of pedigree relatedness and histocompatibility genotype of larvae and residents on distance between settled larvae and previously attached residents. Thus, there were four experimental treatments: (1) the residents and larvae were inbred, and shared one histocompatibility allele; (2) the residents and larvae were inbred, but did not share a histocompatibility allele; (3) the residents were fourth-generation outbred descendants of the parents of the larvae, with one shared histocompatibility allele; and (4) the same as (3), but residents and larvae did not share a histocompatibility allele. In outline, the breeding programme was as follows: for treatments (1) and (2), homozygous resident colonies of known histocompatibility genotype (AA) were derived from crosses between heterozygous sibling colonies (AB). Unfusible homozygous colonies (BB) were isolated from the same cross. In treatment (1), introduced larvae (AB) were derived from a cross between the AA and BB full-sibs. In treatment (2), introduced larvae (BB) were derived from a $BB \times BB$ cross from the same sibship used to generate the larvae in treatment (1). Therefore, the introduced larvae in treatments (1) and (2) bear the same pedigree relatedness to the residents, but differ in the presence

Table 1 Two-way analysis of variance on the distance between settled larvae and the nearest resident colony as a function of resident/larval relatedness and histocompatibility types

Source	Sum of squares	Degrees of freedom	F value (P)
Relatedness	57.2	1	1.35 (>0.25)
Histocompatibility type	3,708.5	1 .	87.46 (<0.001)
Replicate	39.8	2	0.47 (>0.63)
Relatedness/			
histocompatibility	174.1	1	4.10 (0.04)
Error	9,964.6	235	

Table 2 Summary of the mean distances between settled larvae and the nearest resident colony according to experimental treatment

Treatment	Mean (mm)	n
Siblings, no shared alleles	14.70	60
Siblings, one shared allele	7.80	60
Outbred, one shared allele	5.15	60
Outbred, no shared alleles	13.92	60

n, Number of observations for each treatment.

of an A histocompatibility allele. For treatments (3) and (4), either AA or BB larvae were introduced into Petri dishes with outbred residents carrying an A allele. These residents were derived after sequential outcrossing with different colonies taken from the field, none of which carried either an A or B allele. After each generation, a colony carrying the A allele was identified (with a fusion assay) and used for subsequent matings. After four generations of outcrossing, single zooids from a heterozygous colony carrying the A histocompatibility allele, and an unknown second allele (differing from B), were used as residents.

For each treatment, we established three replicates, each with 20 resident colonies. The resident colonies were founded by attaching single zooids from a colony of known genotype to random positions on the submerged undersurfaces of the tops of 150-mm plastic Petri dishes. Twenty-four hours later, the dishes were filled with seawater, sealed and kept in the dark. We then introduced 20 larvae through a port in the side of each dish according to the above treatments. One day later, we measured the distance from each settled larva to the nearest

The results of an analysis of variance show that the relatedness of residents and larvae has no discernible effect on nearestneighbour distances (Table 1). In contrast, where larvae and residents shared a histocompatibility allele, the larvae settled significantly closer to the residents (Table 1). Indeed, the mean nearest-neighbour distance between larvae and residents sharing a histocompatibility allele is roughly half that observed when no allele is shared (Table 2). Table 1 shows a marginally significant interaction between the two main effects that is difficult to interpret. However, the minor contribution that this interaction makes to the overall sum of squares suggests that the interaction is biologically unimportant in these experiments.

Our experiments do not eliminate the possibility that larval kin recognition and histocompatibility are closely linked, rather than identical, genetic traits. However, because larval kin recognition increases the likelihood of adjacent colonies being fusible—an otherwise improbable event given the polymorphism of the histocompatibility locus—there are functional grounds for expecting the two processes to be controlled by a single locus.

The promotion of co-settlement of histocompatible colonies, coupled with the restriction of fusion to closely related

genotypes, indicate that colony fusion may be beneficial, but only among kin. In colonial organisms such as Botryllus, fusion may benefit one, or both, members of a chimaera in several ways. First, colony fusion immediately increases colony size. Survivorship is known to be size-dependent in several colonial ascidians (refs 21, 22 and our unpublished observations), sponges^{23,24}, cnidarians²⁵⁻²⁸ and ectoprocts^{29,30}; hence, fusion may reduce the likelihood of total mortality^{29,30}. Second, if the onset of reproduction is size-dependent—as it appears to be in several cnidarians^{28,31} and ascidians^{6,21}—then fusion may lower the age at first reproduction of both members of the chimaera³² In colonial organisms where growth rate is size-dependent^{33,34}. fusion may also increase the probability of subsequent survival and reproduction. Indeed, fusion among juvenile colonial organisms is well known^{32,35}. Third, a chimaera may have different physiological attributes from either component colony, potentially increasing the range of environmental tolerance³² Finally, fused botryllid ascidians (like many other clonal taxa^{36,37}) freely exchange cells that can differentiate into gametes³⁸, and the rate of differentiation may vary genetically³⁸. Under these conditions, somatic cell parasitism, in which one member of a chimaera increases its reproductive output at the expense of the other, can occur³². However, because the polymorphism and genetics of the Botryllus histocompatibility system limit fusion almost entirely to closely related individuals, the parasitic losses, in evolutionary terms, would be considerably less than if the fused colonies were unrelated^{1,39}.

Another potential consequence of close association of kin is increased inbreeding. Laboratory studies suggest that selffertilization is deleterious in B. schlosseri⁴⁰ and, in some congeners, syngamy may not occur if sperm and egg carry the same histocompatibility allele^{41,42}. However, there is no evidence of inbreeding depression in the Eel Pond population of Botryllus schlosseri⁴³. Indeed, studies of other marine invertebrates in which closely related individuals are likely to cross-fertilize provide meagre evidence for inbreeding depression^{9,44}.

Botryllus schlosseri appears to be one of the first species where a functional—and perhaps evolutionary—link between kin recognition, historecognition and the enhancement of colony fusion has been experimentally demonstrated. The prevalence of limited dispersal⁹ and historecognition systems among sessile clonal marine invertebrates³² suggests that such a link may be found in other clonal organisms. Recent studies of congeneic mice show that haplotypic differences in the H-2 region affect mating behaviour⁴⁵; thus, histocompatibility markers could mediate kin recognition in other taxa. Whether the study of marine invertebrates will provide useful insights into the more complex dynamics of kin recognition in mobile, social vertebrates is unclear, but the analogies remain intriguing.

This research was funded by NSF grant OCE 84-07158 to R.K.G. The Committee on Research of the University of California at Davis provided additional support. We thank P. Sherman and M. Marthas for their useful comments.

Received 27 January; accepted 25 June 1986.

- Hamilton, W. D. J. theor. Biol. 7, 1-51 (1964).
 Holmes, W. G. & Sherman, P. W. Am. Zool. 22, 491-517 (1982).
 Shields, W. J. Philopatry, Inbreeding and the Evolution of Sex (State University of New York Press, Albany, 1982).
 Sherman, P. W. & Holmes, W. G. Fortschr. Zool. 31, 437-459 (1985).
 Keough, M. J. Evolution 38, 142-147 (1984).
- van Duyl, F. C., Bak, R. P. M. & Sybesma, J. Mar. Ecol. Prog. Ser. 6, 35-42 (1981). Olson, R. R. Ecology 66, 30-39 (1985).
- 8. Jackson, J. B. C. in Population Biology and Evolution of Clonal Organisms (eds Jackson, J. B. C., Buss, L. W. & Cook, R. E.) 297-356 (Yale University Press, New Haven, 1986). Jackson, J. B. C. J. mar. Res. (in the press).
 Kott, P. Proc. 2nd int. Coral Reef Symp. 1, 405-423 (1974).
 Grave, C. & Woodbridge, H. J. Morph. Physiol. 39, 207-247 (1924).
 Clark, P. J. & Evans, F. C. Ecology 35, 445-453 (1954).

- Simberloff, D. S. Ecology 60, 679-685 (1979).
 Efron, B. & Gong, G. Am. Statistn 37, 36-48 (1983).
- 15. Bancroft, F. W. Proc. Calif. Acad. Sci. 3, 138-186 (1903).
- 16. Oka, H. & Watanabe, H. Bull, biol, Stn Asamushi 10, 153-155 (1960), 17. Sabbadin, A. Atti. Accad. naz. Lincei Rc. 32, 1031-1035 (1962).

- 18. Mukai, H. & Watanabe, H. Proc. Japan Acad. 51, 44-47 (1975).
- 19. Karakashian, S. & Milkman, R. Biol. Bull. 133, 473 (1967).
- 20. Curtis, A. S. G., Kerr, J. & Knowlton, N. Transplantation 33, 116-123 (1982). 21. Bak, R. P. M., Sybesma, J. & van Duyl, F. C. Mar. Ecol. Prog. Ser. 6, 43-52 (1981).
- 22. Russ, G. R. Oecologia 53, 12-19 (1982).
- 23. Reiswig, H. R. Bull. mar. Sci. 23, 191-226 (1973).
- 24. Fry, W. G. in 4th Eur. mar. biol. Symp. (ed. Crisp, D. J.) 155-178 (Cambridge University
- Press, 1971).

 25. Highsmith, R. C., Riggs, A. C. & D'Antonio, C. A. Oecologia 46, 322-329 (1980).

 26. Wahle, C. M. Biol. Bull. 165, 778-790 (1983).

 27. Hughes, T. P. & Jackson, J. B. C. Ecol. Monogr. 55, 141-166 (1985).

- 28. Sebens, K. P. J. exp. mar. Biol. Ecol. 72, 263-285 (1983). 29. Buss, L. W. Proc. natn. Acad. Sci. U.S.A. 77, 5355-5359 (1980).
- Winston, J. E. & Jackson, J. B. C. J. exp. mar. Biol. Ecol. 76, 1-21 (1984).
 Fadlallah, Y. H. Coral Reefs 2, 129-150 (1983).
 Buss, L. W. Proc. natn. Acad. Sci. U.S.A. 79, 5337-5341 (1982).

- 33. Jones, W. E. Nature 178, 426-427 (1956).

- Notes, W. E. Nature 116, 426-427 (1936).
 Kaufmann, K. W. Oecologia 49, 293-299 (1981).
 Hidaka, M. Coral Reefs 4, 111-116 (1985).
 Buss, L. W. Proc. natn. Acad. Sci. U.S.A. 80, 1387-1391 (1983).
- 37. Nieuwkoop, P. D. & Sutasurya, L. A. Primordial Germ Cells in the Invertebrates (Cambridge University Press, 1981).
- Sabbadin, A. & Zaniolo, G. J. exp. Zool. 207, 289-304 (1979).
 Buss, L. W. & Green, D. R. Devl comp. Immun. 9, 191-201 (1985).
- 40. Sabbadin, A. Deel Biol 24, 379-391 (1971).
 41. Oka, H. in Profiles of Japanese Science and Scientists (ed. Yukawa, H.) 195-206 (Kodansha, Tokyo, 1970).
 42. Scofield, V. L., Schlumpberger, J. L., West, L. A. & Weismann, I. L. Nature 295, 499-502
- 43. Grosberg, R. K. Evolution (submitted).
- Strathmann, R. R., Strathmann, M. & Emson, R. H. Am. Nat. 123, 796-818 (1984).
- Yamazaki, K. E., Beauchamp, G. K., Bard, J., Thomas, L. & Boyse, E. A. Proc. natn. Acad. Sci. U.S.A. 79, 7828-7831 (1982).

Genetically restricted suppressor T-cell clones derived from lepromatous leprosy lesions

Robert L. Modlin*†, Hideyuki Kato‡, Vijay Mehra‡, Erica E. Nelson*†, Fan Xue-dong‡, Thomas H. Rea*, Paul K. Pattengale† & Barry R. Bloom‡

Section of * Dermatology and † Department of Pathology, University of Southern California School of Medicine, Los Angeles, California 90033, USA

‡ Department of Microbiology and Immunology, Albert Einstein College of Medicine, Bronx, New York 10461, USA

Leprosy is a spectral disease in which immune responses to Mycobacterium leprae correlate with the clinical, bacteriological and histopathological manifestations of disease^{1,2}, so study of its pathology provides insights into immunoregulatory mechanisms in man. At the tuberculoid pole, patients have few lesions in the skin which contain rare organisms and are able to mount strong cell-mediated immune responses to M. leprae antigens. In contrast, at the lepromatous pole, patients have disseminated skin lesions containing large numbers of acid-fast bacilli and are selectively unresponsive to antigens of M. leprae. M. leprae-induced suppressor cells derived from peripheral blood have been reported to be active in vitro³⁻⁶, yet their in vivo significance has remained unclear. Because the focal point of the immune response to M. leprae is the skin lesion consisting of lymphocytes and macrophages, we have recently developed methods for isolating lymphocytes from skin biopsies of leprosy patients. We report here that two T8 clones derived from lepromatous leprosy skin biopsies, in the presence of lepromin, suppress concanavalin A (Con-A) responses both of peripheral blood mononuclear cells and of T4 clones in an HLA-D (HLA, histocompatibility locus antigen)restricted manner. Moreover, these T8 clones suppressed responses of HLA-D-matched, but not HLA-D-mismatched antigen-responsive T4 clones to M. leprae antigens, indicating that T-cell suppression is major histocompatibility complex (MHC)-restricted at some level in man.

Initial immunohistological studies of skin lesions from patients across the spectrum revealed that cells bearing the T8

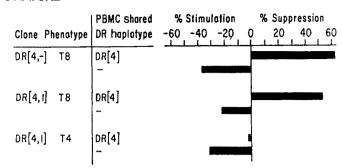


Fig. 1 HLA-D-restricted lepromin-induced suppression of Con A responses of normal peripheral blood mononuclear cells (PBMC) by T8 clones from lepromatous leprosy skin lesions.

Methods. Ellipsoid skin biopsy specimens obtained under local anaesthesia (1% lidocaine with adrenaline) from lepromatous leprosy patients, classified according to the criteria of Ridley and Jopling³⁰, were stripped of epidermis and subcutaneous fat and placed in a tissue sieve fitted with a 64-µm-mesh filter (Belleo Glass Inc.) on a Petri dish containing RPMI 1640 medium with 10% fetal calf serum¹². The tissue was cut into small pieces with a surgical scalpel and extruded through the mesh with a glass rod. The lymphocytes were isolated by Ficoll-Paque (Pharmacia) centrifugation, labelled with fluorescein isothiocyanate-conjugated monoclonal antibodies T4 and T8 (Coulter Immunology), and sorted using a FACS IV (Becton-Dickinson). Long-term culture lines were successfully established from T lymphocytes derived from skin lesions of lepromatous patients. T4 and T8 lymphocytes sorted by FACS to greater than 90% purity were seeded in 96-well flat-bottom Linbro microtitre plates (Flow Laboratories) at 1,000 cells per well. To each well were added 5×10⁵ lethally irradiated (5,000 rad) allogeneic feeder peripheral blood mononuclear cells, RPMI 1640 with penicillin/streptomycin, 10% human AB serum and 10% IL-2 (Electronucleonics). Cultures were incubated at 37 °C in 5% CO2. Every 3 or 4 days thereafter, the cultures were monitored with an inverted phase microscope, transferred to additional wells when necessary and fed with 50% fresh IL-2-containing medium. To avoid suppression from adherent suppressor cells found in blood of lepromatous patients, the lines were cultured with allogeneic or no feeder cells. Some lines were maintained for longer than 11 months using these techniques. Lines from two lepromatous patients It indicts the string tiese techniques. Lines from two epitomators patterns (J.G. and B.P.) were selected for subcloning. Clones were obtained by limiting dilution by seeding 0.3 cells per 20 μ l Terasaki well with 10% AB serum, 5-10% IL-2 and 10⁴ γ -irradiated allogeneic feeder PBMC for 1 week¹³. Positive wells were transferred to a 96-well plate and expanded as above, using 5×10^4 feeder cells, and then to 24-well plates using 5×10^5 feeder cells. When ready for study, T-lymphocyte clones were separated from non-viable cells over Ficoll-Paque and the phenotype was determined by FACS. Antibodies used included T4, T8, anti-HLA-DR (Becton-Dickinson) and anti-IL-2 receptor (Tac, kindly provided by Dr T. Waldmann, or from Becton-Dickinson). Measurement of antigen-induced suppressor activity of lesion derived T-lymphocyte clones was performed using the method of Mehra et al.³. 5×10^4 Cells of a particular T8 clone were admixed with 2×10^5 normal PBMC per microtitre well with and without Dharmendra lepromin (1:10). Con A (2.5 µg ml⁻¹) was added and ³H-thymidine incorporation of triplicate cultures measured at 3 days. Per cent suppression is calculated as 100— (c.p.m. Con A+lepromin/c.p.m. Con A)×100. For each clone, three HLA-DR-matched (A.K., M.R., H.K.) and three HLA-DRmismatched (B.L., G.P., M.S.) donors were used and the results were averaged. A non-reactive T4 clone derived from a lepromatous lesion was substituted for the T8 clones to control for the addition of cells. The c.p.m. above background obtained in the Con A controls averaged 27,471. The results obtained with the T8 clones admixed with the HLA-DR-matched cells differed significantly (P<0.001) when compared with either the T8 clones admixed with HLA-DR-mismatched cells or the T4 'filler' clone assayed with HLA-DR-matched cells, using the z-test approximation to the test for relative difference in Poisson data on actual c.p.m.

(Leu 2a) phenotype were present in excess in lepromatous granulomata as compared with tuberculoid⁷⁻¹⁰. Because the surface markers do not necessarily reflect lymphocyte function within lesions¹¹, simple procedures were developed to extract 10⁵-10⁶ lymphocytes from biopsies of leprosy skin lesions¹². The phenotypic distribution of these cells as determined by fluorescence-activated cell sorter (FACS) analysis was similar to that obtained using immunoperoxidase staining of the tissue sections (T4:T8=0.5:1) in lepromatous and T4:T8=2.0:1 from tuberculoid lesions). In lepromatous patients, the T4/T8 ratio of extracted cells was significantly different from that in blood, indicating that contamination from peripheral blood was negligible. Because we assumed that the lymphocytes in the lesions may be involved in specific immune reactivity and were likely

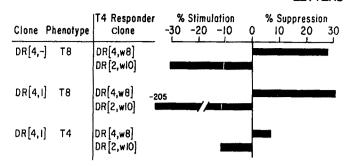


Fig. 2 HLA-D-restricted lepromin-induced suppression of Con A responses of T4 clones by T8 clones from lepromatous leprosy skin lesions.

Methods. Two antigen-reactive T4 clones were derived from skin and blood respectively of two tuberculoid leprosy patients, O.C. and I.B. A T4 line was obtained from peripheral blood by stimulating 1×10⁶ PBMC mI⁻¹ with Dharmendra lepromin (1:10) and 10% AB serum. On day 5, 10% IL-2 was added. On day 6 lymphoblasts were isolated on a Ficoll gradient, then recultured with lepromin, IL-2 and feeder cells. A T4 line was obtained from a tuberculoid skin lesion by extracting T4 cells as described in Fig. 1 legend, and culturing in the presence of lepromin and IL-2. The T4 line from skin was cloned by picking colonies at 4 days from a 35-mm Petri dish containing 1% methylcellulose in RPMI with lepromin (1:10), 10% AB serum, 10% IL-2, 10²-10⁴ lymphoblasts and 4×10^6 irradiated autologous feeder cells per ml. These two T4 lines had previously been found to respond to lepromin but not tetanus toxoid. The T4 line from blood was cloned by limiting dilution as described except that lepromin was included in the cultures at a 1:10 dilution. For testing, 10⁴ cells of an antigenreactive T4 clone were mixed with 105 irradiated autologous PBMC. Lepromin-induced suppression of the Con A response of these T4 clones was determined at 72 h in the presence or absence of 10⁴ cells of the T8 clones. A non-reactive T4 clone was substituted for the T8 clone to control for the addition of cells. The mean c.p.m. above background in three experiments for T4 clone O.C. was 19,059 c.p.m. and for the I.B. clone was 18,150 following Con A stimulation. The results obtained with the T8 clones when admixed with the HLA-DR-matched antigen-reactive T4 clone were significantly different (P < 0.001 by z-test) compared with either the T8 clones when assayed with the mismatched antigenreactive T4 clone or the control T4 'filler' clone admixed with the HLA-DR-matched antigen-reactive T4 clone.

to be activated in situ, cells from lesions were isolated, sorted for T4 and T8 cells and expanded in culture as long-term (up to 11 months) lines in the presence of irradiated feeder cells and interleukin-2 (IL-2) (ref. 12). The cells were cloned by limiting dilution (0.3 cells per well) as described by Lamb et al.13. T4 clones were grown in the presence of lepromin (a human-derived M. leprae preparation) and IL-2 plus autologous or HLA-D-matched feeder cells. T8 clones from lepromatous lesions were grown in the presence of γ -irradiated feeder cells and IL-2 but not antigen. Lepromin seemed to be inhibitory to the growth of T8 clones. The T-cell lines and clones studied expressed both HLA-DR monomorphic determinants and the Tac receptor for IL-2. The T8 clones grow rather slowly and have been difficult to expand in culture. Nevertheless, two clones were selected for study which were suppressive only on stimulation with antigen as described; they have been in culture for 12 and 6 months, respectively.

Because it has been previously observed that lepromatous patients have circulating antigen-specific suppressor T8 cells that inhibit mitogen-induced T-cell proliferation in vitro^{3,4}, lines containing predominantly T8 cells were initially screened for lepromin-induced suppression of the Con A responses of the peripheral blood mononuclear cells (PBMC) of normal donors¹². Lepromin-specific suppression of PBMC from random normal donors was observed in 13 of 32 T8 lines derived from

skin biopsies of 6 lepromatous leprosy patients and in none of 9 T8 lines derived from 6 tuberculoid lesions. The inconsistent suppression of T8 lines from the lesions prompted us to select for single-cell clones and consider possible HLA restriction of suppression.

The HLA types of the donors whose cells were studied are listed in Table 1. The ability of cloned T8 cells from two HLA-DR4 donors to suppress the Con A responses of a panel of six DR4-matched and -mismatched normal donors' PBMC was examined. As illustrated in Fig. 1, there was marked lepromin-induced suppression by the T8 clones of Con A responses of primary lymphocytes from donors sharing DR4 and not those mismatched for DR. There was no obvious correlation with HLA-A or -B-types in these combinations. A Tac⁺, IL-2-dependent T4 clone derived from lepromatous skin of one of the same DR4 donors was used in every experiment to control both for the effect of addition of cloned cells to the wells and for possible competition for IL-2 in the medium. In no case was suppression observed in this control.

Two lepromin-specific T4 clones were derived from blood and skin respectively of two strongly lepromin skin-test-positive patients of differing DR types with tuberculoid leprosy. The ability of the T8 clones to suppress the responses of these T4 clones to mitogen and specific antigen was tested. When DR4matched and DR-mismatched T4 clones and T8 clones were compared for lepromin-induced suppression of Con A responses at 72 hours, again there was striking suppression only of HLA-Dcompatible cultures (Fig. 2). Finally, since the relevance of the lepromin-induced suppression of mitogenic activity to the failure of lepromatous patients to respond to specific antigens remained to be established, we examined the effect of the T8 clones on proliferation of the T4 clones to specific antigen. Since the T4 clones proliferate in response to lepromin at 72 h and fail to show any alloreactivity to MHC-incompatible cells at that time, we were in a unique position to examine whether the T8 clones were capable of suppressing the proliferative response of T4 clones to specific antigen, and to ascertain whether such suppression was MHC-restricted. The results of three experiments (Fig. 3) revealed an HLA-D-restricted suppression by T8 clones of the responses of T4 clones to M. leprae antigens.

While some previous efforts to detect antigen-specific suppression by lymphocytes from lepromatous leprosy patients have not been successful^{14,15}, Ottenhof et al.¹⁶ have recently obtained data similar to those presented here indicating that T8 clones derived from blood of lepromatous patients are able to suppress specific responses of T4 clones from the same patients to lepromin. Nishimura and Sasazuki, who reported the suppression of streptococcal antigen responses of HLA-D-matched T cells by T8 cells from hyporesponsive donors¹⁷, have recently observed suppression of lepromin responses by T8 cells from lepromatous patients (Kikuchi, I., Uzawi, T. and Sasazuki, T.,

Table 1 HLA phenotypes of donor cells									
•	Donor	HLA-A	HLA-B	HLA-DR					
T8 clones									
	J.G.	24, 32	12, 18	4, —					
	B.P.	11, 29	7, 35	4, 1					
T4 clones		ŕ	.,	ŕ					
	I.B.	24, 31	61, 62	4, w8					
	O.C.	11, 24	38, —	2, w10					
Peripheral blood mononuclear cells		•	r	•					
	A.K.	2, 11	44, 60	4,					
	M.R.	28,	38, 60	4, —					
	H.K.	24,	61, —	4, w9					
	B.L.	26, 28	35, 51	w6, —					
	G.P.	1, 2	8, 60	2, —					
	M.S.	11, 23	45, 44	2, —					

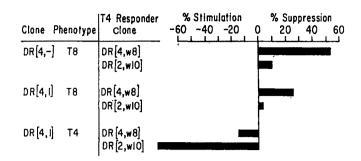


Fig. 3 HLA-D-restricted suppression of the antigen response of T4 clones by T8 clones. Antigen-reactive T4 cloned cells (104) were cultured with 105 irradiated autologous PBMC per 200-µl microwell in RPMI with 10% AB serum, with and without lepromin (1:10), and with and without 104 of each T8 clone. Thymidine incorporation was measured at 72 h. Per cent suppression was determined as 100 - (c.p.m. T4 clone + T8 clone/c.p.m. T4 clone) × 100. A non-reactive T4 clone was substituted for the T8 clone to control for the addition of cells. The mean c.p.m. above background for the lepromin-stimulated T4 clones was 33,662 c.p.m. for I.B. and 24,452 c.p.m. for O.C. respectively. The results obtained with the T8 clones when admixed with the HLA-DR-matched antigenreactive T4 clone were significantly different (P < 0.001 by z-test) compared with either the T8 clones assayed with the mismatched antigen-reactive T4 clone or the control T4 'filler' admixed with the antigen-reactive T4 clone.

in preparation). There are previous reports of T8 suppressor cell clones from human peripheral blood^{18,19}, but we believe that the present observations represent the first evidence that. at some level, human T-cell suppression may be HLA-Drestricted. More detailed analysis will be required to establish that the restriction is in fact localized to the HLA-D region and to learn whether DP, DQ or DR are involved. There is evidence from murine systems that effector suppression is mediated by Ia-positive T cells which are MHC class II-restricted²⁰⁻²²

The nature of the antigen recognized by the suppressor T8 clones remains to be established. We have previously reported that some T-suppressor cells appear to recognize the unique phenolic glycolipid of M. $leprae^{23}$. The recent successful expression of M. leprae antigens in Escherichia coli²⁴ should permit the delineation of protein antigens and epitopes recognized by T-suppressor and T-helper cells.

The existence of monocytes in lepromatous patients with the ability to suppress mitogen and antigen responses in vitro has been reported by a number of laboratories 3,5,6,25,26. The nonspecific nature of the monocyte suppression and the selective unresponsiveness of lepromatous patients to antigens of M. leprae suggest that more specific mechanisms must be involved as well. A number of lines of evidence suggest that T-suppressor cells may contribute to the failure of the immune system in lepromatous patients to kill and clear M. leprae from their lesions. Clearly, large numbers of M. leprae coexist in lesions with T8 cells which show antigen-induced suppressor activity in vitro. There is a marked diminution of T4 cells containing IL-2 in these same lesions, although many are positive for the IL-2 (Tac) receptor²⁷. We have found that the in vitro suppression of Con A responses by T8 cells from lepromatous patients is specific for the stage of the disease^{3,4}. Finally, T8 suppressor activity present in 10 lepromatous patients disappeared after successful immunotherapy by vaccination with live BCG together with killed M. leprae28

At least four possible mechanisms could be involved in the selective immunological unresponsiveness of lepromatous leprosy patients: (1) M. leprae or a secreted metabolic product could inhibit appropriate antigen presentation to T4 cells by macrophages, Langerhans or dendritic cells, resulting in development of T8 suppressor cells; (2) T8 suppressor cells could secrete a suppressor factor (TsF) that blocks responsiveness of specific T4 cells to M. leprae antigens; (3) T8 suppressor cells could lyse T4 cells in an antigen- and MHC-restricted manner; and (4) T8 cells could interact with and 'veto' antigenreactive T4 cells without killing them²⁹

We believe this to be the first report of isolation of genetically restricted T-suppressor cell clones from lesions of a human disease. Considerably more detailed study will be required to establish the precise nature of the genetic restrictions involved in unresponsiveness in man. Nevertheless, we hope that this approach will be useful in exploring the nature of genetic restrictions and receptor gene organization in suppressor T cells. and the role of these cells in regulating immunological unresponsiveness in man.

This work was supported by NIH grants AI 22187, AI 22553, AI 07118 and AI 02111; the UNDP/World Bank/World Health Organization Special Programme for Research and Training in Tropical Diseases (IMMLEP), National Hansen's Disease Center, Knights of St Lazarus of Jerusalem, Heiser Trust, Hartford Foundation, the US-Japan Leprosy Program, and the Irvington House Institute for Medical Research. P.K.P. is a Scholar of the Leukaemia Society. We thank Drs Jonathan Lamb, Geoffrey Gersuk and Roland Tcheng for help and advice on T-cell cloning, Ms Betty Donovan for secretarial assistance and Bryan Langholz for help with statistical analysis.

Received 16 December 1985; accepted 22 April 1986.

- Rea, T. H. & Levan, N. E. Archs Derm. 113, 345-352 (1977).
- Bloom, B. R. & Godal, T. Rev. Infect. Dis. 5, 765-779 (1983).
 Mehra, V., Mason, L. H., Fields, J. P. & Bloom, B. R. J. Immun. 123, 1813-1817 (1979).
 Bloom, B. R. & Mehra, V. Immun. Rev. 80, 6-28 (1984).
 Salgame, P. R., Birdi, T. J., Mahadevan, P. R. & Antia, N. H. Int. J. Lepr. 48, 172-177 (1980).
- Nath, I., Van Rood, J. J., Mehra, N. K. & Vaidya, M. C. Clin. exp. Immun. 42, 203-210 (1980). Van Voorhis, W. C. et al. New Engl. J. Med. 307, 1593-1597 (1982).
- 8. Modlin, R. L., Hofman, F. M., Taylor, C. R. & Rea, T. H. J. Am. Acad. Derm. 8, 181-189
- Modlin, R. L. et al. Clin. exp. Immun. 51, 430-438 (1983).
 Narayanan, R. B., Bhutani, L. K., Sharma, A. K. & Nath, I. Clin. exp. Immun. 51, 422-429 (1983).
- 11. Modlin, R. L. et al. Clin. exp. Immun. 60, 241-248 (1985).
- Modlin, R. L. et al. J. Immun. (in the press).
 Lamb, J. R. et al. J. Immun. 128, 233-238 (1982).
- 14. Stoner, G. L., Touw, J., Belehu, A. & Naafs, B. Lancet II, 543-547 (1978).

- 15. Nath, I., Van Rood, J. J., Mehra, N. K. & Vaidya, M. C. Clin. exp. Immun. 42, 203-210 (1980).
- Ottenhoff, R. H. M., Elferink, D. G., Klatser, P. R. & de Vries, R. R. P. Nature (in the press).
 Nishimura, Y. & Sasazuki, T. Nature 302, 67-69 (1983).
- 18. Bensussan, A., Acuto, O., Hussey, R. E., Milanese, C. & Reinherz, E. L. Nature 311, 565 567
- Rees, A. D. M. et al. in Human T Cell Clones, a New Approach to Immunoregulation (eds Feldmann, M., Lamb, J. R. & Woody, J. N.) (Humana, Clifton, New Jersey, 1985).
 Baxevanis, C. N. Ishii, N., Nagy, Z. A. & Klein, J. J. exp. Med. 156, 822-833 (1982)
 Dorf, M. E. & Benacerraf, B. Immun. Rev. 83, 23-40 (1985).
- Araneo, B. A. & Yowell, R. L. J. Immun. 135, 73-79 (1985).
 Mehra, V., Brennan, P. J., Rada, E., Convit, J. & Bloom, B. R. Nature 308, 194-196 (1984)

- Young, R. A. et al. Nature 316, 450-452 (1985).
 Salgame, P. R., Mahadevan, P. R. & Antia, N. H. Infect. Immunity 40, 1119-1126 (1983).
 Sathish, M., Bhutani, L. K., Sharma, A. K. & Nath, I. Infect. Immunity 42, 890-899 (1983).
 Modlin, R. L. et al. J. Immun. 132, 3085-3090 (1984).
- Mehra, V., Convit, J., Rubinstein, A. & Bloom, B. R. J. Immun. 129, 1946-1951 (1982).
 Miller, R. G. Immun. Today 7, 112-114 (1986).
 Ridley, D. S. & Jopling, W. H. Int. J. Lepr. 34, 255-273 (1966).

Cloned suppressor T cells from a lepromatous leprosy patient suppress *Mycobacterium leprae* reactive helper T cells

Tom H. M. Ottenhoff*, Diënne G. Elferink*, Paul R. Klatser† & René R. P. de Vries*

* Department of Immunohaematology and Bloodbank, University Hospital Leiden, 2333 AA Leiden, The Netherlands † Laboratory of Tropical Hygiene, Royal Tropical Institute, 1105 AZ Amsterdam, The Netherlands

Leprosy is a chronic infectious disease caused by Mycobacterium leprae. A characteristic feature of the disease is its remarkable spectrum of clinical symptoms correlating with the cellular immune responsiveness of the patient1. At one pole of this spectrum are tuberculoid patients displaying both acquired cell-mediated immunity and delayed type hypersensitivity against the bacillus²⁻⁴. At the other pole are lepromatous patients which show a specific T-cell unresponsiveneess against M. leprae⁵. In between those two poles variable degrees of tuberculoid and lepromatous features may be seen in borderline leprosy patients. Thus far, studies on the mechanism of the antigen specific unresponsiveness in lepromatous leprosy have been contradictory and difficult to interpret, probably because of the use of heterogeneous cell populations in those experiments⁶⁻¹⁰. We have now succeeded in cloning M. leprae stimulated T-helper (TH) as well as T-suppressor (TS) cells from a borderline lepromatous patient. The Ts-clones of this patient specifically suppress reponses of peripheral TH cells as well as TH clones induced by both M. leprae and other mycobacteria, but not unrelated antigen or mitogen. These Ts cells also completely suppress T_H cell responses against a M. leprae specific protein with a relative molecular mass of 36,000 (36K), suggesting the presence of a suppression inducing determinant on this 36K M. leprae protein.

In contrast to M. leprae-activated and interleukin-2 (IL-2)propagated T-cell lines and clones derived from tuberculoid leprosy patients, similar T-cell lines of (borderline) lepromatous leprosy patients consistently failed to show a proliferative response against M. leprae antigens presented by autologous or allogeneic histocompatibility locus antigens (HLA) class II matched antigen presenting cells (APC) (data not shown). This lack of proliferation by cultured T cells to M. leprae was also observed when the peripheral blood mononuclear cells (PBMNC) of such (borderline) lepromatous patients did proliferate to M. leprae. We selected one such a borderline lepromatous patient whose peripheral T cells did proliferate against M. leprae as well as to unrelated antigens like herpes simplex virus (HSV) and mitogen (phytohaemagglutinin; PHA) because this might enable us to study both helper and possibly suppressor T-cell responses against M. leprae. We then tested the M. leprae-non-responsive T-cell line on autologous antigen activated peripheral T_H cells, thereby circumventing allogeneic effects. As shown in Fig. 1, the M. leprae-non-responsive T-cell line suppressed specifically and strongly M. leprae but not HSV or PHA responses. Peripheral responding T cells were mainly positive for the CD4 antigen. The same result was obtained with five other M. leprae induced T cell lines of the same patient, all of which were antigen non responsive but IL-2 responsive.

Cloned T cells were derived from one such a line. None of these clones proliferated to *M. leprae* in the presence of APC, similar to the parental T-cell line (data not shown). All these clones suppressed *M. leprae* but not HSV-specific responses of peripheral T cells (Table 1). Peripheral T-cell responses against *M. tuberculosis*, *M. fortuitum* or PPD (purified protein derivative of *M. tuberculosis*) were also suppressed in variable degrees by

these T_S -clones. The cell surface marker phenotypes of the T_S -cell line and T_S clones are also shown in Table 1. All T_S -clones were CD3 positive, confirming the T-cell lineage nature of these cells. All T_S clones were also CD8 positive, whereas some showed a weak (1D8, 1D11) or clear (1E9) double staining for CD4. The simultaneous expression of CD4 and CD8 by peripheral T cells and T-cell clones has been reported recently 11,12 . The clones strongly expressed HLA-DR antigens whereas the expression of DQ and DP varied.

Recently the genes for the five major proteins of M. leprae have been cloned and expressed in Escherichia coli¹³. One of these five proteins is a M. leprae specific 36K protein¹³⁻¹⁵. This protein was recently shown to contain several different antigenic determinants capable of stimulating helper T cells. These determinants include both M. leprae specific and cross-reactive ones as defined by M. leprae specific and cross reactive T-helper clones from tuberculoid patients¹⁶. Peripheral T cells of the suppressor cell donor reacted with this 36K protein. This offered the possibility to determine whether these 36K reactive T_H cells could be suppressed by the autologous Ts cells. A negative result would indicate that the epitope(s) recognized by Ts cells resides neither on the 36K protein nor on the 36K reactive TH cells, thus enabling us to dissociate easily the induction of M. leprae reactive T_H and T_S. This is of course not only important for experimental purposes, but also for the prevention (vaccine) and maybe even therapy of leprosy. However, as shown in Fig. 2, the 36K response could be inhibited completely by the T_S cells. This result may indicate that the 36K protein in addition to helper epitopes also contains at least one suppressor epitope.

Table 1 T_S clones and line suppress the response of PBMNC to M. leprae and other mycobacteria but not unrelated antigen

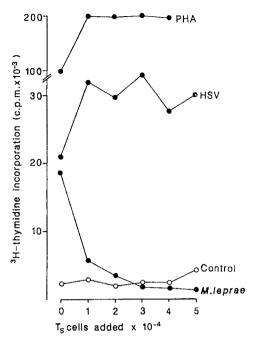
Ts clone	1D8	1D11	1E9	1D10	3D2	1G2	Ts line
[CD phenotype] % Suppression of response of PBMNC to:	[4,8]	[4,8]	[4(8)]	[8]	[8]	[8]	[4,8]
M. leprae	70	95	73	53	54	53	88
M. tuberculosis	24	55	70	44	39	ND	80
M. fortuitum	20	48	72	34	40	ND	91
PPD	2	44	56	50	50	ND	76
HSV	-250	12	8	-231	-56	5	-59

The results are expressed as the percentage suppression of peripheral T cell responses against the respective antigens after the addition of 3×10^4 T suppressor cells, as calculated with the formula (1-c.p.m. of peripheral T cells cultured in the presence of suppressor T cells/c.p.m. of peripheral T cells in the absence of suppressor T cells) $\times 100\%$. Peripheral T-cell responses in the absence of suppressor cells against M. leprae were: 21,920 c.p.m., against M. luberculosis: 26,570, against M. fortuitum: 15,605, against PPD:6,060 and against HSV:29,300. Responses in the absence of antigen were 970 c.p.m. All results are given as the mean c.p.m. of duplicate cultures. Standard deviations did not exceed 20%. The CD4,8 phentoypes of the T cell line and clones are shown. ND, not determined.

Methods. The cultures were set up as described in Fig. 1 legend. The antigens tested in addition were ultrasonicates of whole mycobacteria (20 µg ml⁻¹) and PPD (5.0 µg ml⁻¹). From the suppressor T-cell line, clones were prepared by cloning the cells (1D8, 1D10, 1D11:10 cells per well; 1E9, 3D2, 1G2; 0.5 cell per well) on the feeder cell mixture described in the legend of Fig. 1, supplemented with Leuko Agglutinin A (1 μg ml⁻¹) (Pharmacia) and expanding the cultures in the presence of exogeneous IL-2. This cycle was repeated several times. The cell surface marker phenotypes of the different T cells were determined by a standard indirect immunofluorescence technique as described in ref. 32. The monoclonal antibodies used were OKT3 (Ortho) for the CD3 marker, RIV-6 (anti-T4/leu 3; National Institute of Public Health, Bilthoven, Netherlands) for the CD4 marker, FK18 (anti-T8/leu2; gift of F. Koning) for the CD8 marker, B8.11.2 (anti HLA-DR; gift of B. Malissen), SPV-L3 (anti HLA-DQ; gift of H. Spits) and B7/21 (anti HLA-DP; gift of F. Bach) for respectively HLA-DR, DQ and DP antigens.

Fig. 1 Antigen specific suppression of *M. leprae* but not herpes simplex virus (HSV) or PHA induced proliferative peripheral T cell responses by a *M. leprae* induced and in IL-2 grown suppressor T cell line. The latter was added to 10⁵ PBMNC in concentrations of 0, 1, 2, 3, 4 or 5×10^4 cells per culture. The results are expressed as the mean c.p.m. of duplicate cultures (³H-thymidine incorporation). Standard deviations mostly did not exceed 20%. *M. leprae* antigens isolated from human lepromas and from armadillo infected tissue induced similar suppression.

Methods. PBMNC of a borderline lepromatous leprosy patient were isolated from heparinized venous blood by Ficoll-Isopaque density centrifugation (Pharmacy, University Hospital Leiden), washed three times in Hanks' balanced salt solution (Gibco) and resuspended in Iscove's modified Dulbecco's medium (IMDM; Gibco) supplemented with 100 µg ml⁻¹ streptomycin, 100 U ml⁻¹ penicillin (both Flow Laboratories) and 10% heat inactivated human AB serum. The diagnosis of this and other patients used for this study was based on regular clinical examination, lepromin skin test and skin biopsy histology by Dr D. L. Leiker, Department of Dermatology, University Hospital of Amsterdam, the Netherlands. A standard lymphocyte transformation test was set up with 105 PBMNC per culture, to which antigen was added. Antigens tested were Dharmendra lepromin, consisting of bacilli isolated from human lepromas (obtained from the Centre for Infectious Diseases, Center for Disease Control, Atlanta, USA; 1:80 dilution) and herpes simplex virus (obtained from the National Institute of Public Health, Bilthoven, The Netherlands; 1:64 dilution). From the start of the culture, either no or 1, 2, 3, 4 or 5×10^4 T cells of the nonresponsive T-cell line (see above) were added to the culture. The cultures were set up in flat-bottomed 96-well microtitre plates (Greiner), incubated at 37 °C in a fully humidified 5% CO2-air mixture for 5 days after which 1.0 µCi ³H-thymidine was added to each well; the cultures were collected 16 h later on glass-fibre filters using a semiautomatic sample harvester. 3H-TdR



incorporation was assessed by liquid scintillation counting. The T cell line was generated as described previously ^{16,30}. In brief, PBMNC were restimulated in vitro with an optimal concentration of Dharmendra lepromin (1:80) in 24-well tissue culture plates. T-cell blasts were then cultured for 10 days in the presence of 20% IL-2 containing medium (Lymfocult-T, Biotest). The cells were tested then for antigen-induced proliferation in the presence of autologous APC and antigen but failed to show a response. The cells were then restimulated with a feeder mixture consisting of irradiated autologous EBV-BC as autologous APC³¹ (10⁵ cells ml⁻¹), PBMNC from three or four random donors (10⁶ cells ml⁻¹) and Dharmendra lepromin (1:80). The cultures were further expanded in the presence of IL-2. The cells were then collected, tested again for non responsiveness against antigen and used for experiments. All cells were cultured in IMDM supplemented with 10% human AB serum.

This 36K epitope then would be the first M. leprae suppressor epitope on a M. leprae protein, because we consider it unlikely that the 36K protein would contain the M. leprae specific phenolic glycolipid, which has been reported to induce suppression of concanavalin-A stimulated PBMNC of lepromatous patients^{5,7}. The co-existence of both helper and suppressor epitopes on the 36K protein would closely resemble the situation for other immunogenic proteins like hen egg white lysozyme¹⁷, β-galactosidase¹⁸ and a 185K streptococcal protein¹⁹. For the first two protein antigens it has been shown that the putative suppressor epitope has to be situated on the same molecule or fragment as the helper epitope in order to induce suppression of the immune response^{20,21}. This may be true for the 36K protein as well. A second explanation however for the suppression of T_H cell responses against the 36K M. leprae protein would be that that T_S cells specifically recognize (an) idiotypic determinant(s) on the 36K responsive T_H cells. Whatever the mechanism of the observed suppression, it is clear the activation of antigen specific suppressor cells places constraints on the use of such proteins for prophylactic immunization. We hope that a suppressor epitope will turn out to be the right explanation, because then the rational design of a synthetic M. leprae vaccine would imply the selection of helper epitopes and/or the molecular dissociation of helper from suppressor epitopes²². If the mechanism would appear to be an anti-idiotypic one such a vaccine strategy would not easily result in the circumvention of M. leprae reactive suppression in susceptible individuals.

In order to obtain more insight in the specificity and mechanism of the supression mediated by these T_S clones, we isolated CD4-positive clones from the same patient that proliferated to *M. leprae* by cloning the cells relatively early (96 hours) after a single exposure to *M. leprae*. This procedure was followed because helper T-cell growth was reported to precede that of suppressor T cells in time²³. The thus isolated supposedly T_H clones responded to *M. leprae* specific or cross-reactive determinants, like was observed for tuberculoid patients and healthy contacts^{16,24} and were HLA-DR or -DP restricted in their response. As shown in Table 2, T_S clones could suppress both

 $M.\ leprae$ specific and cross-reactive T_H clones in a number of cases (1G2, 1D11). Other T_S clones appeared to suppress only some (1E9) or no (1D10) T_H clones, although suppressing the $M.\ leprae$ response of PBMNC. Apart from providing a (negative) control for the specific suppression on T_H clones, the latter observation may either indicate that in order to complete and/or amplify the suppressor circuit, cells other than the T_S clones have to be recruited. Alternatively, the T_S clones may be anti-idiotypic and would not suppress T_H clones (2F9, 2B2) which carry another idiotypic determinant than that seen by the T_S cell. However, probably the most important aspect of the data presented in Table 2 is the fact that the same T_S clones which suppressed T_H responses to cross-reactive mycobacterial anti-gens (T_S clones 1G2 and 1D11, see also Table 1) are also able

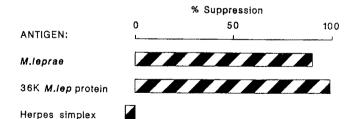


Fig. 2 Antigen-specific suppression of peripheral T-cell responses against a purified M. leprae 36K protein. The results are expressed as the percentage suppression after the addition of 3×10^4 T suppressor cells (see legend table 1). The response in the absence of T suppressor cells against the 36K protein was 12,020 c.p.m., against M. leprae 27,040 c.p.m., and against HSV 14,255. Responses with no antigen in the culture were 1,030 c.p.m. in the absence and 428 c.p.m. in the presence of the T suppressor cells. Standard deviations did not exceed 20%. The suppressor T-cell line was tested in this experiment. Similar results have now been obtained with T_S clones. The tested 36K protein was purified by affinity chromatography using monoclonal antibody F47-9-1 (refs 14, 15) coupled to cyanogen bromide-activated Sepharose 4B, followed by elution with 0.1 M diethylamine pH 11.5. The protein was tested in a concentration of 5.6 μ g ml⁻¹.

Table 2 T_S clones suppress the M. leprae response of some but not all M. lenrae reactive T., clones of the same nations

THE OLD INC.		ne patient	•			
	Proliferative T ₁₁ clone					
	2F9	2B2	2F6			
Proliferation to M. leprae: Proliferation to	+	+	+			
other mycobacteria:	-	±	+			
T _S clone added	Percer	ntage suppi	ression			
1G2	411	47	63			
1D11	55 .	52	62			
1E9	5	-1	30			
1D10	-51	-13	4			

Results are expressed as the percentage suppression (see table 1). M. leprae specific, (2F9), partly crossreactive (2B2) or completely crossreactive (2F6) T_H clones of the same patient were induced to proliferate by autologous irradiated APC and M. leprae antigen as described recently 16,26. Briefly, 10⁴ TLC cells were cocultured with 5×10⁴ APC (40 Gy irradiated) and Dharmendra lepromin (1:80) for 72 h, after which ³H-TdR was added as described in Fig. 1 legend. The mean c.p.m. of the T_H clones in the absence of suppressor T cells were 36,780 for 2F9, 8,252 for 2B2 and 8,694 for 2F6. At the start of the culture either no or 3×10^4 suppressor cells were added. Background proliferation in cultures containing T_H and T_S cells without antigen was always less than 440 c.p.m. The percentage of suppression was calculated as described in the legend of Fig. 1. Standard deviations did not exceed

to suppress a T_H clone directed against an M. leprae specific epitope. This might indicate that cross-reactive T_S clones as described in this paper although not M. leprae specific, could play an essential role in the M. leprae specific unresponsiveness observed in lepromatous leprosy. It is interesting that in several instances a marked depresson of M. tuberculosis and BCG responses has been noted in lepromatous leprosy patients 25,26. In the light of our findings this may be explained at least in part by M. leprae induced crossreactive Ts cells. We deliberately selected a borderline lepromatous leprosy patient, which was not unresponsive to M. leprae in order to be able to generate both T_H and T_S clones. Therefore we have to be cautious in generalizing this observation because it is generally assumed that lepromatous leprosy patients are nonresponsive to M. leprae but remain good responders towards other mycobacteria (reviewed in refs 1, 5). Interestingly, it has recently been suggested that such patients—in contrast to tuberculoid patients and healthy contacts—do not respond to cross reactive or common antigens on other mycobacteria, but rather to the species specific antigens except of course the M. leprae specific ones (refs 25, 27, 28; G. A. W. Rook, submitted for publication). The question then arises why the M. leprae induced crossreactive Ts cells could not also suppress TH responses against the species specific antigens of other mycobacteria than M. leprae. Extending the antigen bridging model (refs 20, 21) we propose that these T_S cells might only suppress T_H cells when both the suppressor epitope (that is, the crossreactive M. leprae suppressor epitope) and the helper epitope to which the M. leprae reactive T_H cells were induced originally (that is, either a M. leprae specific or a crossreactive helper epitope) are expressed by the same molecule. This prerequisite is not met in the case of T_H responses against the species specific helper epitopes of other mycobacteria than M. leprae: since these helper epitopes by definition are not situated on molecules shared with M. leprae, T_H responses against these non-M. leprae epitopes can evade suppression by cross-reactive T_S cells irrespective of the presence of a crossreactive suppressor epitope on that same molecule. Qualitative and quantitative differences in the sensitization towards those species specific helper epitopes in lepromatous leprosy patients might thus account for at least part of the heterogeneity observed in responsiveness against other mycobacteria in lepromatous leprosy.

Since the observed suppression of peripheral T_H-cell responses and T_H clones might be explained by cytotoxicity against either responding antigen specific TH cells or APC, we investigated whether peripheral cells activated by M. leprae or HSV, or autologous Epstein-Barr virus-B cells, pulsed or unpulsed with M. leprae, or M. leprae reactive TH clones could be lysed by suppressor cells. However, no specific lysis of these targets by the suppressor T-cell line and T_s clones was observed, whereas a control cytotoxic T-cell line specific for HLA-A2 strongly lysed all targets tested. Therefore these results excluded cytotoxicity as a possible mechanism of suppression.

Finally, we were interested to know whether these T_S clones were HLA-restricted or not and if so by which HLA molecules and epitopes. Modlin et al.29 have recently claimed that suppressor T cells from the skin lesions of lepromatous leprosy patients may be restricted by HLA-DR. Our own preliminary data obtained with both panel and family studies in which the To cells were mixed with allogeneic TH cells have indeed also shown evidence for some kind of restriction. However, this was not simply associated with HLA-class I, -DR or -DO alleles. Thus far, we have been unable to abolish the suppression with HLA-class I or HLA-DQ specific monoclonal antibodies, but HLA-DR antibodies could do so in certain TH-Ts cell combinations. Thus, although HLA-DR might be involved, the genetic restriction of T_S cells seems to be more complex than that of T_H cells.

The lines and clones described in this paper can be made available to interested colleagues.

We thank Professor J. J. van Rood for his support for this project; Dr. R. C. Good for M. leprae antigen; Professor D. L. Leiker for help and cooperation; the patients for donating blood; Earl Johanns and John Haanen for technical assistance; Fons UytdeHaag for HSV antigens; Madeleine de Wit for isolating the 36K protein; Arend Kolk for monoclonal antibodies; Jos Pool for assistance in the CML test and in preparing serum pools, Annemarie Termijtelen for helpful discussions and Ellen van der Willik for preparing of the manuscript. This study was supported in part by the Foundation for Medical Research (FUNGO grant 900-509-099), the Immunology of Leprosy (IMMLEP) component of the UNDP/WORLD Bank/WHO Special Programme for Research and Training in Tropical Diseases, the Netherlands Leprosy Relief Association (NSL). and the J. A. Cohen Institute for Radiopathology and Radiation Protection (IRS).

Received 21 January; accepted 21 April 1986.

- 1. Bloom, B. R. & Godal, T. Rev. infect. Dis. 5, 765-780 (1983).
- 2. Rees. R. J. W. Nature 211, 576 (1966).
- Patel, P. J. & Lefford, M. J. Infect. Immun. 19, 87-93 (1978).
- Lowe, C., Brett, S. J. & Rees, R. J. W. Clin. exp. Immun. 61, 336-342 (1985). Bloom, B. R. & Mehra, V. Immun. Rev. 80, 5-28 (1984).
- Mehra, V., Mason, L. H., Fields, J. P. & Bloom, B. R. J. Immun. 123, 1813-1817 (1979). Mehra, V., Brennan, P. J., Rada, E., Convit, J. & Bloom, B. R. Nature 308, 194-196 (1984).
- Nath, I., van Rood, J. J., Mehra, N. K. & Vaidya, M. C. Clin. exp. Immun. 42, 203-210 (1980). Sathish, M., Bhutani, L. K., Sharma, A. K. & Nath. I. Infect. Immun. 42, 890-899 (1983). Salgame, P. R., Mahadevan, P. R. & Antia, N. H. Infect. Immun. 40, 1119-1126 (1983).
- 11. Blue, M. L., Daley, J. F., Levine, H. & Schlossman, S. F. J. Immun. 134, 2281-2286 (1985).
- Farcet, J. P. et al. Eur. J. Immun. 15, 1067-1073 (1985). Young, R. A. et al. Nature 316, 450-452 (1985).
- Klatser, P. R., de Wit, M. Y. L. & Kolk, A. H. J. Clin. exp. Immun. 62, 468-473 (1985). Engers, H. D. et al. Infect. Immun. 48, 603-605 (1985). Ottenhoff, T. H. M. et al. Nature 319, 66-68 (1986).

- Ortennon, I. H. M. et al. Nature 319, 06-08 (1986).
 Wicker, L. S., Katz, M., Sercarz, E. & Miller, A. Eur. J. Immun. 14, 442-447 (1984).
 Goodman, J. W. & Sercarz, E. A. Rev. Immun. 1, 465-498 (1983).
 Lehner, T., Mehlert, A., Avery, J., Jones, T. & Caldwell, J. J. Immun. 135, 1437-1442 (1985).
 Oki, A. & Sercarz, E. J. exp. Med. 161, 897-911 (1985).

- Krzych, U., Fowler, A. V. & Sercarz, E. J. exp. Med. 162, 311-323 (1985).
 Mitchison, N. A. Nature 308, 112-113 (1984).
- Bensussan, A., Acuto, O., Hussey, R. E., Milanese, C. & Reinherz, E. L. Nature 311, 565-567
- 24. Mustafa, A. S. et al. Nature 319, 63-66 (1986).
- 25. Reitan, L. J., Closs, O. & Belehu, A. Int. J. Lepr. 50, 455-467 (1982).
- Godai, T., Myklestad, B., Samuei, D. R. & Myrvang, B. Clin. exp. Immun. 9, 825-831 (1971).
 Smelt, A. H. M., Rees, R. J. W. & Liew, F. Y. Clin. exp. Immun. 44, 507-511 (1981).
- 28. Stanford, J. L., Nye, P. M., Rook, G. A. W., Samuel, N. M. & Fairbank, A. A. Lepr. Rev. 52, 321-327 (1981).
- Modlin, R. L. et al. Nature (in the press).
 Ottenhoff, T. H. M., Elferink, B. G., Hermans, J. & de Vries, R. R. P. Human Immun. 13,
- 31. Elferink, B. G., Ottenhoff, T. H. M. & de Vries, R. R. P. Scand. J. Immun. 22, 585-589 (1985).
- 32. Haanen, J. B. A. G. et al. Scand. J. Immun. 23, 101-108 (1986).

Retinal ganglion cells lose response to laminin with maturation

J. Cohen*, J. F. Burne*, J. Winter† & P. Bartlett‡

* MRC Neuroimmunology Project, Department of Zoology, University College London, London WC1E 6BT, UK † Sandoz Institute for Medical Research, 5, Gower Place, London WC1E 6BN, UK

‡ Walter and Eliza Hall Institute of Medical Research, Royal Melbourne Hospital, Victoria 3050, Australia

The decisive role played by adhesive interactions between neuronal processes and the culture substrate in determining the form and extent of neurite outgrowth in vitro1,2 has greatly influenced ideas about the mechanisms of axonal growth and guidance in the vertebrate nervous system. These studies have also helped to identify adhesive molecules that might be involved in guiding axonal growth in vivo. One candidate molecule is laminin, a major glycoprotein of basal laminae3 which has been shown to induce a wide variety of embryonic neurones to extend neurites in culture4-8. Moreover, laminin is found in large amounts in injured nerves that can successfully regenerate but is absent from nerves where regeneration fails⁹⁻¹¹. However, it is unclear to what extent the mechanisms that regulate axonal regeneration also operate in the embryo when axon outgrowth is initiated. Here we have examined the substrate requirements for neurite outgrowth in vitro by chick embryo retinal ganglion cells, the only cells in the retina to send axons to the brain. We show that while retinal ganglion cells from embryonic day 6 (E6) chicks extend profuse neurites on laminin, those from E11 do not, although they retain the ability to extend neurites on astrocytes via a laminin-independent mechanism. This represents the first evidence that central nervous system neurones may undergo a change in their substrate requirements for neurite outgrowth as they mature.

In the chick retina most retinal ganglion cells (RGC) become post-mitotic between E3 and E7 (ref. 12), and during this period axon outgrowth is largely confined within the retina, optic stalk and tract. By E11 the production of RGC has virtually ceased and the majority of optic axons have entered their target tissue, the optic tectum¹³. To compare the behaviour of RGC in cultures of E6 and E11 retinal cells, we have used a monoclonal antibody against chicken Thy-1 glycoprotein¹⁴, an immunologically distinct homologue of mammalian Thy-1 (ref. 15). As previously shown for the immature rat retina^{16,17}, Thy-1 is restricted to RGC in cryostat sections of the embryonic chick retina (Fig. 1). Whereas optic nerve transection experiments in the rat suggest

Fig. 1 Localization of Thy-1 antigen in embryonic chick retina. Phase-contrast (a,c) and fluorescence (b,d) photomicrographs of E11 (a,b) and E20 (c,d) cryostat sections of retina. b, At stage E11, monoclonal anti-Thy-1 antibody binds only to cells in the retinal ganglion cell layer (RGC) and axons in the optic fibre layer (OFL) (d). At E20, immunofluorescence staining is more intense and extends also to the inner plexiform layer (IPL) but is absent from all other retinal layers. Both a and c show dorsal-central regions of retina adjacent to the optic nerve head. Scale bars, 50 μ m.

Methods. Whole eyes were fixed in paraformaldehydelysine-periodate 36 , cryoprotected with sucrose, infiltrated with OCT embedding compound, and frozen in liquid nitrogen. Cryostat sections $(6-10\,\mu\text{m})$ were cut in the horizontal plane, dried on polylysine-coated (PL) slides and incubated overnight at 4 °C with monoclonal anti-chick Thy-1 antibody (ascites fluid diluted 1:100) followed successively by incubation for 2 h at room temperature in biotinylated sheep anti-mouse immunoglobulin and streptavidin-fluorescein (Amersham; diluted 1:100). Sections were mounted in glycerol containing 1,4-diazobicyclo-(2,2,2)octane (DABCO) to inhibit fading of fluorescence 37 , and photographed on a Zeiss Universal microscope.

that some bipolar and amacrine neurones might also express Thy-1 in the mature retina¹⁸, most of these cells differentiate after E11 in the chick and are unlikely to account for a significant proportion of the Thy-1⁺ cells seen in our cultures.

Immunoreactive Thy-1 antigen was first detectable in situ at E5 as faint punctate deposits in the immature RGC layer (not shown). By E11 the antigen was also detectable in the optic fibre layer (OFL) (Fig. 1a, b), and at E20 it was found in regions containing RGC cell bodies, their axons and dendrites, but was absent from other retinal layers (Fig. 1c, d). In retinal suspensions at E6 and E11, 2-5% of these cells were Thy-1⁺ (not shown), including more than 90% of the larger (>10 μ m diameter) cell bodies.

When cells dissociated from E6 or E11 retina were plated on polylysine (PL) coated glass coverslips at a sufficiently low density ($\leq 50,000 \text{ cells cm}^{-2}$) to keep them separate, >80% of the Thy-1⁺ cells attached within 2 h. However, after 16 h < 10% had extended neurites and most had begun to degenerate. Similar results were obtained with a variety of substrates, including polyornithine, fibronectin, rat-tail collagen and fibroblast ghosts (not shown). However, when E6 cells were grown on laminin, most Thy-1+ cells (>75%; Fig. 3) extended long neurites (Fig. 2a, b); profuse, non-fasciculated outgrowth of Thy-1⁺ processes, which also stained with a monoclonal antineurofilament antibody RT97 (not shown), was evident within a few hours of plating, being maximal at 48-72 h, by which time some Thy-1+ RT97+ neurites extended distances in excess of 50 cell diameters (>600 μ m). By contrast, <10% of Thy-1 $^{+}$ cells in cultures of E11 retina extended neurites on laminin and this growth pattern was indistinguishable from that on polylysine (Figs 2c, d, 3). The same stage-dependent response was also seen on a substrate (ACM) consisting of polylysine binding material from culture medium conditioned by rat type-1 astrocytes¹⁹ (Fig. 3). Although we have not characterized the factor in ACM, previous studies with a variety of culture medium-derived neurite-promoting factors make it likely that the activity of ACM resides in a complex of laminin with heparan sulphate proteoglycan^{20,21}

A possible explanation for the failure of E11 Thy-1⁺ neurones to extend neurites *in vitro* is that as RGC mature, they become intrinsically unable to regenerate their axons. However, previous studies have demonstrated that rat RGC, which had extended axons to their retino-receptive targets in the brain, are able to regrow neurites when cultured on some substrates^{22,23}. Moreover, after optic nerve transection in adult rats, RGC have been shown to regrow axons into sciatic nerve grafts²⁴. These observations on mammalian RGC suggested that E11 chick RGC could extend neurites *in vitro* if given the appropriate









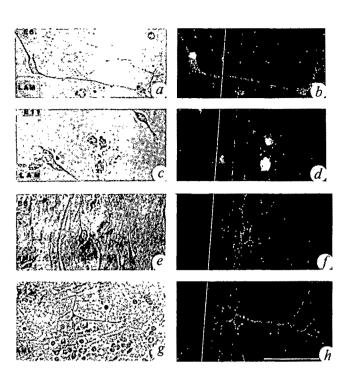


Fig. 2 Effect of maturation on neurite extension by Thy-1⁺ retinal neurones grown on laminin and astrocytes. The cells were photographed using phase-contrast (a, c, e, g) or fluorescein (b, d, f, h) optics. Note that while E6 Thy-1⁺ neurones extend neurites on laminin (LAM) (a, b) and type-1 astrocytes (AML) (e, f), E11 Thy-1⁺ neurones fail to extend neurites on LAM (c, d) but do so on AML (g, h). All Thy-1⁺ process-bearing cells also stained with a monoclonal antibody (RT97) against neurofilaments (not shown). On AML (e-h) Thy-1⁺ cells assumed a more complex morphology than on laminin (a-d). Scale bar, 50 μ m.

Methods. Retinas were separated from choroidal and scleral tissue, dissected free of pigment epithelium and incubated at 37 °C for 20 min in Ca²⁺, Mg²⁺-free Earle's balanced salts (BSS) plus 0.1% trypsin and bovine serum albumin (BSA, 3 mg ml⁻¹; Sigma). Tissue was removed and resuspended in BSS plus soybean trypsin inhibitor (SBT1, 0.52 mg ml⁻¹; Sigma), DNase (0.04 mg ml⁻¹; Sigma) and BSA and dissociated by repetitive trituration in a wide-bore Pasteur pipette to give a single-cell suspension. Homogeneous cultures of rat type-1 astrocytes (AML) were prepared from neonatal cerebral cortex tissue as described previously²⁸. (Rat, rather than chick astrocytes were used as a growth substrate as immature chick astrocytes do not express the astrocyte-specific marker GFAP³⁸ and could not, therefore, be reliably monitored for their purity in vitro. Preliminary experiments established that the neurite-outgrowth-promoting activity of rat type-I astrocytes was as effective with chick neurones as previously shown for rat neurones²⁵.) Laminin substrate was prepared by incubating PL-coated glass coverslips at room temperature for 2 h in a solution of laminin (10 µg ml⁻¹; BRL) in serum-free culture medium (see below), followed by two brief rinses in medium. Retinal cells (50,000) were plated onto pre-coated glass coverslips in Falcon multi-well plates and grown in Ham's F12 medium (Flow) supplemented with 0.5% fetal calf serum and the following (µg ml-100 BSA, 5 insulin, 100 transferrin, 6 progesterone, 16.1 putrescine and 5.6 selenium, as modified from Bottenstein and Sato³⁹. All cultures were incubated for 48 h at 37 °C in a humidified atmosphere of 5% CO₂, 95% air. Living cultures were labelled with monoclonal anti-Thy-1 antibody (ascites fluid diluted 1:100) for 30 min at room temperature, followed by biotinylated anti-mouse immunoglobulin and fluorescein-streptavidin as described in Fig. 1 legend, except that incubation times were shortened to 30 min. Coverslips were fixed in 95% ethanol/5% acetic acid, mounted in glycerol/DABCO and labelled cells photographed as described in Fig. 1 legend.

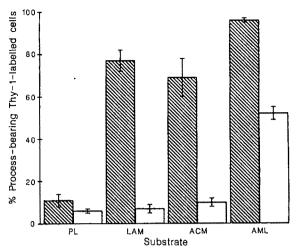


Fig. 3 Effect of laminin (LAM), ACM and AML on neurite outgrowth by E6 (SS) and E11 (□) Thy-1⁺ neurones. Most of E6 Thy-1+ neurones extended neurites on LAM, ACM and AML while only AML induced neurite outgrowth by E11 Thy-1+ neurones. Retinal cells (50,000) from E6 or E11 retinas were plated onto glass coverslips pre-coated with PL, LAM or AML as described in Fig. 2 legend. In experiments using ACM as substrate (PLbinding material from astrocyte-conditioned medium), PL-coated coverslips were incubated overnight in culture medium conditioned over confluent monolayers of rat astrocytes for at least 24 h. After 48 h of culture, coverslips were labelled with anti-Thy-1 antibody as described in Fig. 2 legend. After fixation the cultures were co-labelled with RT97 (ascites fluid, 1:200) for 30 min at room temperature followed by rhodamine-conjugated anti-mouse immunoglobulin 1:100; Cappell). Coverslips were then washed and mounted as described in Fig. 2 legend. The total number of Thy-1⁺ cells per coverslip (≥50 cells), and the number with Thy-1⁺/RT97⁺ processes longer than 3 cell diameters, were counted. The results shown are the mean (±s.e.m.) of at least four separate experiments. At E6 a significant difference (Student's t-test) was found between PL and LAM (P < 0.0006), PL and ACM (P < 0.04) and between PL and AML (P<0.0001). At E11 a significant difference was found between PL and AML (P < 0.0004) but no significant difference was found between PL and LAM (P > 0.7)or between PL and ACM (P>0.2).

substrate. We therefore cultured retinal cells on monolayers of purified rat brain astrocytes (AML) which consisted of >95% glial fibrillary acidic protein-positive (GFAP⁺) type-1 astrocytes with a flat fibroblast-like morphology¹⁹. Such cells are known^{25,26} to provide a highly adhesive substrate for the growth of neurites in vitro and possibly also in vivo^{27,28}. We found that on AML the majority of Thy-1⁺ neurones in cultures of both E6 and E11 retina extended long neurites (Figs 2e-h, 3). Moreover, the neurite-promoting effect of AML on Thy-1⁺ neurones seemed to depend on direct contact with the astrocytes and not on astrocyte-derived soluble factors, as the effect was abolished in co-cultures arranged to prevent contact²⁵.

An alternative explanation for our findings is that during maturation, RGC surface receptors for laminin are lost or modified. However, evidence against receptor down-regulation is provided by our experiments (not shown) with a monoclonal antibody, JG22, which is specific for a cell surface receptor complex that binds both laminin and fibronectin^{29,30}. When trypsinized suspensions of E6 and E11 retina were allowed to settle onto coverslips and labelled with JG22 antibody, over 80% of cells in the larger size range (>10 µm diameter), corresponding to the majority of Thy-1⁺ cells on duplicate coverslips, were JG22⁺ at both ages, and labelling was more intense at E11 than at E6. When cultured on a substrate permissive for neurite outgrowth, RGC cell bodies, neurites and growth cones were JG22⁺. Also, in immunostained tissue sections taken from the retinas of E6 and E11 chicks (not shown) RGC axons in the optic fibre layer and the optic nerve head were intensely JG22⁺

along their entire length. Therefore, these findings raise the possibility that the receptor complex on E11 RGC is modified so as to reduce its affinity for laminin. Alternatively, transduction mechanisms within the cells may be uncoupled from the binding event.

What is the nature of the molecules on the astrocyte surface which promote neurite outgrowth? Whereas brain astrocytes can produce laminin in vitro³¹, the failure of either pure laminin or ACM substrate to evoke a response from E11 RGC argues that the neurite-promoting activity of the astrocyte cell surface resides in either a modified form of laminin not represented in ACM, or in an entirely different molecule. Evidence against the first possibility was provided by further experiments (not shown) with JG22 antibody: whereas the antibody blocked most neurite outgrowth by E6 RGC on either laminin or ACM substrate, it failed to inhibit outgrowth by E6 or E11 RGC on AML. It may be that the neurite-promoting molecule on the astrocyte surface is one of the cell adhesion molecules previously shown to influence neurone-astrocyte interactions^{32,33}.

From days 6 to 11 of incubation in the chick embryo, maturation of the optic pathway is characterized by the transition from a predominantly retinal to a tectal phase of RGC axon outgrowth¹³. It is possible, therefore, that the change in substrate requirements for growth in vitro reflects a response by RGC in vivo to changes in the composition of the substrate that their growth cones encounter as they traverse the optic pathway. Such changes could be regulated by temporal or spatial mechanisms. Evidence for the former has come from an immunohistochemical survey with anti-laminin antibodies of the embryonic chick optic pathway throughout development. We have shown, using a sensitive immunohistochemical method, that in addition to its presence in basement membranes at the inner limiting membrane and pigment epithelium³⁴, laminin is also expressed by neuroepithelial cells throughout the optic pathway, within the retina, optic fissure, stalk and tectum during the earliest stages of maturation (between E3 and E7), becoming restricted to basement membrane locations only after E8 (ref. 35 and J.C., J.F.B. and J.W., unpublished observations). These findings suggest that laminin is a component of the physiological substrate for RGC axon extension during the earliest phase of outgrowth in vivo, and provide an explanation for our observations of the response of E6 RGC to growth on laminin in vitro. The mechanism whereby the maturation of RGC is accompanied by a loss of response to laminin remains to be elucidated. The fact that the timing of this change coincides with the arrival of the bulk of optic axons at the tectum raises the possibility that an alteration in the substrate requirements for axon extension may be one of the consequences of the transition from a target-independent to a target-dependent phase of RGC maturation. Future experiments should allow us to test whether optic tectum-derived factors can influence the substrate requirements in vitro for neurite outgrowth by RGC as a function of maturation.

We thank D. Gottlieb for supplying JG22 antibody, John Wood for RT97 antibody and Martin Raff and other members of the Neuroimmunology Group for helpful suggestions.

Received 18 March; accepted 21 May 1986.

- Bray, D. Nature 244, 93-96 (1973).
 Letourneau, P. C. Devl Biol. 44, 92-101 (1975)
- Timpl, R. H. et al. J. biol. Chem. 254, 9933-9937 (1979).
 Baron von Evercooren et al. J. Neurosci. Res. 8, 179-193 (1982).

- Manthorpe, M. et al. J. Cell Biol. 97, 1882-1890 (1983). Rogers, S. L. et al. Devl Biol. 98, 212-220 (1983). Smallheiser, N. R., Crain, S. M. & Reid, L. M. Devl Brain Res. 12, 136-140 (1984).
- Calof, A. L. & Reichardt, L. F. Devl Biol. 106, 194-210 (1984).
 Bignami, A., Chi, N. H. & Dahl, D. Expl Neurol. 85, 226-236 (1984).
 Hopkins, J. M., Ford-Holevinski, T. S., McCoy, J. P. & Agranoff, B. W. J. Neurosci. 5, 200-2004 (1984). 3030-3038 (1985).
- 11. Liesi, P. EMBO J. 4, 2505-2511 (1985).
- Kahn, A. J. Brain Res. 63, 285-290 (1973).

- Rager, G. H. Adv. Anat. Embryol. Cell Biol. 63, 1-92 (1980).
 Sinclair, C. M., Bartlett, P. F., Grieg, D. I. & Jeffrey, P. L. Brain Res. (in the press).
 Rostas, J. A. P., Shernan, A., Sinclair, C. M. & Jeffrey, P. L. Biochem. J. 213, 143-152 (1983).
 Beale, R. & Osborne, N. N. Neurochem. Int. 4, 587-595 (1982).
- 17. Barnstable, C. J. & Drager, H. C. Neuroscience 11, 847-855 (1984).

- Perry, V. H., Morris, R. J. & Raisman, G. J. Neurocytol. 13, 809-824 (1984)
 Raff, M. C. et al. J. Neurosci. 3, 1289-1300 (1983).
 Lander, A. D., Fujii, D. K. & Reichardt, L. F. Proc. natn. Acad. Sci. U.S.A. 82, 2183-2187
- 21. Davis, G. E., Manthorpe, M., Engvall, E. & Varon, S. J. Neurosci, 5, 2662-2671 (1985)
- Leifer, D., Lipton, S. A., Barnstable, C. J. & Masland, R. H. Science 224, 303-306 (1984).
 McCaffery, C. A., Raju, T. R. & Bennett, M. R. Devl Biol. 104, 441-448 (1984).
 So, K.-F. & Aquayo, A. J. Brain Res. 32, 349-354 (1985).
- Noble, M., Fok-Seang, J. & Cohen, J. J. Neurosci. 4, 1892-1903 (1984).
 Fallon, J. S. J. Cell Biol. 100, 198-207 (1985).

- Silver, J. & Sapiro, J. J. comp. Neurol. 202, 521-538 (1981).
 Kryanek, S. & Goldberg, S. Devl Biol. 84, 41-50 (1981).
- Greve, J. M. & Gottlieb, D. L. J. cell. Biochem. 18, 221-230 (1982).
 Horwitz, A. et al. J. Cell Biol. 101, 2134-2144 (1985).
 Liesi, P., Dahl, D. & Vaheri, A. J. Cell Biol. 96, 920-924 (1983).

- 32. Grummet, M., Hoffman, S. & Edelman, G. M. Proc. natn. Acad. Sci. U.S.A. 81, 267-271
- 33. Keilhauser, G., Faissner, A. & Schachner, M. Nature 316, 728-730 (1985)
- Adler, R., Jordan, J. & Hewitt, A. T. Devl Biol. 112, 100-114 (1985).
- Cohen, J. Neurosci. Lett. Suppl. 22, 36 (1985).
 McLean, I. W. & Nakane, P. K. J. Histochem. Cytochem. 22, 1077-1083 (1984).
- 37. Johnson, G. D. et al. J. immun. Meth. 55, 231-242 (1982). 38. Lemmon, V. Devl Brain Res. 23, 111-120 (1985).
- 39. Bottenstein, J. & Sato, G. H. Proc. natn. Acad. Sci. U.S.A. 76, 515-517 (1979)

Chloride and potassium channels in cystic fibrosis airway epithelia

Michael J. Welsh & Carole M. Liedtke

Laboratory of Epithelial Transport and Pulmonary Division, Department of Internal Medicine, University of Iowa College of Medicine, Iowa City, Iowa 52242, USA and the Cystic Fibrosis Center, Department of Pediatrics, Developmental Genetics and Anatomy, School of Medicine, Case Western Reserve University, Cleveland, Ohio 44106, USA

Cystic fibrosis, the most common lethal genetic disease in Caucasians, is characterized by a decreased permeability in sweat gland duct and airway epithelia. In sweat duct epithelium, a decreased Cl permeability accounts for the abnormally increased salt content of sweat1. In airway epithelia a decreased Cl permeability, and possibly increased sodium absorption, may account for the abnormal respiratory tract fluid^{2,3}. The Cl impermeability has been localized to the apical membrane of cystic fibrosis airway epithelial cells4. The finding that hormonally regulated Cl channels make the apical membrane CI permeable in normal airway epithelial cells suggested abnormal Cl channel function in cystic fibrosis. Here we report that excised, cell-free patches of membrane from cystic fibrosis epithelial cells contain Cl channels that have the same conductive properties as CI channels from normal cells. However, Cl channels from cystic fibrosis cells did not open when they were attached to the cell. These findings suggest defective regulation of Cl channels in cystic fibrosis epithelia; to begin to address this issue, we performed two studies. First, we found that isoprenaline, which stimulates Cl secretion, increases cellular levels of cyclic AMP in a similar manner in cystic fibrosis and non-cystic fibrosis epithelial cells. Second, we show that adrenergic agonists open calcium-activated potassium channels, indirectly suggesting that calcium-dependent stimulus-response coupling is intact in cystic fibrosis. These data suggest defective regulation of Cl channels at a site distal to cAMP accumulation.

Figure 1 shows a model of the cellular mechanism of Cl⁻secretion by airway epithelia⁶. Chloride enters the cell at the basolateral membrane coupled to Na⁺ on an electrically neutral co-transport process. Chloride then leaves the cell across a Cl⁻-conductive apical membrane; regulation of the Cl⁻ conductance determines, in part, the rate of transepithelial Cl⁻ secretion. Chloride channels produce the apical Cl conductance. Using the patch-clamp technique, we recently described a Cl channel from the apical membrane of normal human airway epithelial cells which had properties different from those of previously described Cl channels^{5,8}. The ion selectivity, response to inhibitors and activation by secretagogues indicate that this Cl

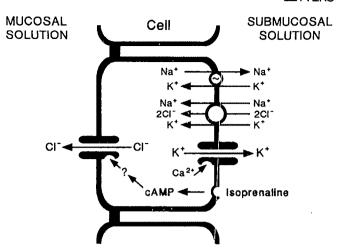


Fig. 1 Model of the cellular mechanism of Cl⁻ secretion. Chloride enters at the basolateral membrane via a NaKCl co-transport process that is inhibited by loop diuretics. The energy to drive intracellular Cl⁻ accumulation above electrochemical equilibrium comes from the movement of Na⁺ down its electrochemical gradient. A low intracellular Na⁺ concentration is maintained by the ouabain-inhibitable (Na⁺ + K⁺)ATPase. Potassium that enters the cell in exchange for Na⁺ and coupled to Cl⁻, exits from the cell across the basolateral membrane through Ca²⁺-regulated K⁺ channels. Chloride leaves the cell across the apical membrane through Cl⁻ channels.

channel is responsible for the apical Cl⁻ conductance in airway epithelia.

The decreased Cl⁻ permeability in cystic fibrosis (CF) apical membranes is therefore most probably due to abnormal Cl⁻ channel function. There are several possible ways to explain such a defect: it might result from an absence of Cl⁻ channels (such as faulty insertion into the cell membrane), from the presence of Cl⁻ channels with abnormal conductive or ion-selective properties, from inhibition of the Cl⁻ channels, or from faulty regulation of apical membrane Cl⁻ channels.

To address these possibilities, we examined single-channel currents in primary cultures of CF airway epithelial cells, to look for Cl⁻ channels with the same properties as those observed in non-CF cells. In excised cell-free patches of membrane from four preparations, we observed single-channel currents that were characteristic of Cl⁻ channels. Figure 2a shows tracings of the

current from an excised Cl⁻ channel, and Fig. 2b shows the single-channel current voltage (I-V) relation of that same channel. Figure 2b also shows that cation substitutions did not alter the I-V relation. In six patches the channel was exposed to cation gradients, either Na⁺ or K⁺, without a shift in reversal potential. In contrast, Fig. 2c shows that a Cl⁻ concentration gradient shifted the reversal potential, as expected for a channel that is selective for Cl⁻ over Na⁺. Calculation of the relative Cl⁻ to Na⁺ permeability, P(Cl/Na), from the Goldman-Hodgkin-Katz equation yielded a value of 6.5 ± 0.4 (mean \pm s.e.m., n=3). The I-V relation of a Cl⁻ channel from a non-CF cell is shown in Fig. 2b for comparison.

Several features indicate that in excised patches these channels are identical to non-CF Cl⁻ channels that are responsible for the apical Cl⁻ conductance and Cl⁻ secretion⁵. First, the conductance of the channel $(26\pm2 \text{ pS} \text{ measured at } 0 \text{ mV} \text{ with } 100 \text{ mV})$

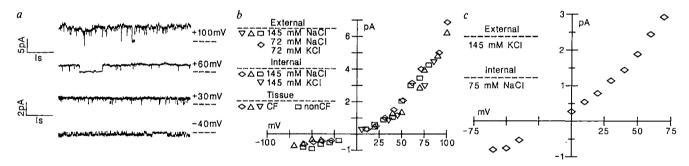


Fig. 2 Tracings and current-voltage relations of Cl⁻ channels. a, Single Cl⁻ channel currents recorded from an excised, inside-out patch at four holding voltages. Outward currents are shown as upward deflections. The current level when the channel is closed is given by the dashed line. The tracing shows substantial open-channel noise, a characteristic of the Cl⁻ channel. This channel was open most of the time and did not show marked voltage dependence of kinetics. The external (pipette) solution contained 72 mM NaCl, 72 mM KCl and 1 mM Ca²⁺ and the internal (bath) solution contained 145 mM NaCl and 5 mM EGTA (estimated Ca²⁺ concentration <1 nM). b, Current-voltage relation obtained from the channel shown in Fig. 2a (\diamondsuit); I-V relation with symmetrical 145 mM NaCl solutions (\triangle); and the relation when the external solution was 145 mM NaCl and internal solution was 145 mM KCl (∇). For comparison the I-V relation of a Cl⁻ channel obtained from non-CF cells is shown (\square)⁵. There is some variability in the absolute conductance of Cl⁻ channels from non-CF cells, however, Cl⁻ channels from CF cells did not show any appreciable difference from non-CF channels. c, I-V relation with 145 mM KCl externally and 75 mm NaCl, 150 mM sucrose and 2.5 mM EGTA internally. The observed reversal potential, approximately -13 mV, is close to the value expected for the Cl⁻ activity gradient (-15.4 mV). In contrast, the cation gradients across the channel would predict either positive or very large negative values for K⁺- or Na⁺-selective channels, respectively. We identified this channel in 19 of 198 successfully excised patches from CF cells, whereas under similar conditions it was observed in 2-10% of successfully excised patches from non-CF cells⁵. Methods. The technique used for constructing pipettes and seal formation 5,12 is similar to that described by Hamill et al.⁷. Either a Dagan Model 8900 or a List EPC 7 amplifier was used for voltage clamping and current amplifica

Model 8900 or a List EPC 7 amplifier was used for voltage clamping and current amplification. For some studies, currents were filtered (500-750 Hz) by an 8-pole Bessel filter, viewed on an oscilloscope and recorded on a strip-chart recorder. The 90% rise-time for a 2-cm deflection on the recorder was 3.5 mS. Results were analysed by hand. For other studies currents were filtered at 1 kHz and recorded (500 μ s sampling rate) and analysed with a laboratory computer system (Indec Systems). Pipette resistance was 2.5-10 M Ω and seal resistance was 3-30 G Ω . During seal formation and when recording in the cell-attached mode, bath solution contained (in mM): 140 NaCl, 1.2 CaCl₂, 1.2 MgCl₂ and 10 HEPES buffered with KOH (5 mM). All bath and pipette solutions contained 10 mM HEPES buffered to pH7.2, except the standard bath solution at pH7.4. Junction potentials that developed in the presence of asymmetrical salt solutions were directly measured with a 3 M KCl electrode and corrected for. Experiments were performed at room temperature (21-23 °C). Cells were studied 4 h to 3 days after plating. Voltages are reported in reference to the external surface of the membrane and outward (+) current refers to the flow of cations from internal to external surface of the patch, or anion flow in the opposite direction.

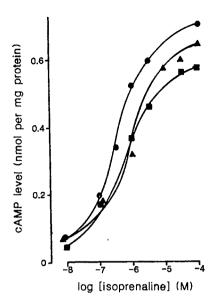


Fig. 3 Effect of isoprenaline on cellular levels of cAMP. Source of cells: ●, CF tracheal epithelium; ■, CF nasal epithelium; ▲, non-CF tracheal epithelium. To measure cellular concentrations of cAMP, the culture medium was replaced with Hank's balanced saline solution (HBSS) containing 10 mM HEPES pH 7.4 and (−)isoprenaline at varying concentrations. Isoprenaline was prepared and diluted in the same buffered salt solution. After incubation for 10 min at 37 °C, the medium was removed and cellular cAMP was released using dilute HCl (0.1 M). Cyclic AMP radioimmunoassay kits (Amersham) were used for measurement of cAMP levels. The cells were treated with 1 M NaOH to dissolve cellular protein which was measured according to the method of Lowry et al. 13, using bovine serum albumin as the standard. Cyclic AMP levels were calculated as nmol cAMP per mg protein.

symmetrical 145 mM Cl⁻, n=10) is the same as in normal humans. Second, the strong rectification of the I-V relation, even with symmetrical bathing solutions, is quite characteristic. Third, the selectivity for Cl⁻ over cations is similar. Fourth, there is an appreciable amount of open-channel noise (Fig. 2a) which we find characteristic of Cl⁻ channels from normal human cells. Fifth, the Cl⁻ channel blocker diphenylamine 2-carboxylate (1 mM) decreased single-channel current to 53% of control values (at +60 mV, n=1, data not shown), a response similar to that found in non-CF Cl⁻ channels. Sixth, the channel in CF and non-CF cells was not strongly voltage-gated, nor was it acutely regulated by internal Ca²⁺ concentration under these conditions; there was no apparent effect on excised channels of changing from 1 mM internal Ca²⁺ to less than 1 nM Ca²⁺ (5 mM EGTA and nominal Ca²⁺).

Although excised patches from CF cells had Cl channels with conductive and kinetic properties identical to those observed in Cl channels from non-CF cells, we never observed a Cl channel in the cell-attached recording mode, even though we looked for its activity following each successful seal and treated the cells with isoprenaline (5 μ M), adrenaline (1 μ M), 8-bromo-cAMP (100 µM) and/or forskolin (100 µM). In non-CF tracheal epithelial cells⁵ the Cl⁻ channel was observed in the cell-attached mode in 58% of 40 patches that contained Cl channels. In contrast, in CF cells the Cl channel was not observed cell-attached in the 19 patches that were shown to contain Cl⁻ channels after excision (P < 0.001 by χ^2 analysis). These findings suggest that Cl impermeability of the apical membrane in CF does not result from the complete absence of Cl channels or from the presence of Cl channels with abnormal conductive properties. Rather, they suggest that abnormal regulation of Cl channels produces the decreased Cl permeability8

To investigate regulation of ion transport in CF epithelial cells, two studies were performed. First, we measured intra-

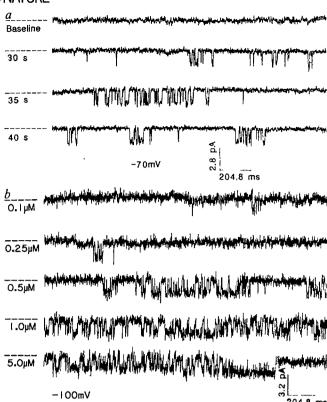


Fig. 4 Potassium channels in CF cells. a, Effect of adrenaline on K⁺-channel activity in a cell-attached patch. Sweeps were taken under baseline conditions and at the times indicated, following addition of adrenaline (1 μ M) to the bathing solution. The holding potential was -70 mV (membrane hyperpolarized). The pipette solution contained 72 mM KCl, 76 mM NaCl and 1 mM CaCl Downward deflections represent inward current. The dashed line indicates the current level when all channels are closed. b, Effect of internal Ca2+ on K+-channel activity in an excised, inside-out patch. Tracings were obtained from a single patch held at -100 mV The external (pipette) solution was 200 mM potassium glutamate and 5 mM MgCl₂; internal solution was 140 mM KCl. Internal Ca²⁺ concentrations indicated were achieved by buffering 5 mM EGTA with Ca²⁺ assuming a 1.5×10⁻⁷ M dissociation constant. Methods. Tracheas for cell culture were obtained from three patients at autopsy and nasal polyps were obtained from three patients at the time of polypectomy. Measurement of cAMP was made in cells from one trachea and nasal polyps from three patients, and electrophysiological measurements were made in cells from three tracheas and one culture of nasal polyps. The tissue was washed extensively with sterile HBSS containing (per ml) 100 U penicillin, 100 µg streptomycin, 50 µg tobramycin and 200 mg piperacillin, then incubated at 37 °C with antibiotics for 60 min. The wash and incubation cycles were carred out four times. The tissue was then incubated overnight with HBSS at 7 °C and the epithelium dissected free from the submucosal tissue the next morning. Epithelial cells were isolated according to the method of Liedtke and Tandler¹⁴ with the following modification. Dissected surface epithelium was incubated with collagenase (135 U ml⁻¹), 2 mM EGTA, 2 mM Mg²⁺ and DNase (2 mg ml⁻¹). Dispersed epithelial cells were recovered by centrifugation, washed in sterile HBSS to remove chelators and enzymes, and suspended in culture medium consisting of a 1:1 (v/v) mixture of Ham's F12 and Dulbecco's modified Eagle's medium containing antibiotics as indicated above. Total cell recovery ranged from 38×10^6 to 63×10^6 cells. Cell viability was 95-98% as assessed by fluorescent staining with acridine orange and ethidium bromide. An aliquot of the cell suspension was flown to M.J.W. for studies on single ion channels. The remaining cells were diluted in culture medium supplemented with 5 μM hydrocortisone, 5% fetal calf serum and (per ml) 1 μg insulin, 1 µg transferrin, 4 µg fibronectin and 1 µg epidermal growth factor. For cAMP assays, cells were plated onto collagen-coated plastic culture dishes at 500,000 cm⁻². For electrophysiological studies, cells were seeded at 5,000-20,000 cm⁻². Cultures were maintained at 37 °C in a humidified 5% CO₂ atmosphere

cellular levels of cAMP. Although the intracellular factors that directly regulate the Cl channel are unknown, circumstantial evidence suggests that cAMP is involved; many secretagogues. including β -adrenergic agonists, increase intracellular levels of cAMP and exogenous addition of cAMP stimulates Cl⁻ secretion^{9,10}. Figure 3 shows that the β -adrenergic agonist (-)isoprenaline caused a similar dose-dependent increase in cAMP levels in cultured CF and non-CF epithelial cells. The concentration of isoprenaline required to produce a halfmaximal increase in cAMP (EC₅₀) was $0.4\pm0.1~\mu\text{M}$ in non-CF tracheal epithelium (n = 3), $0.5 \pm 0.1 \mu M$ in CF nasal epithelium (n=3) and $0.4 \,\mu\text{M}$ in CF tracheal epithelium (n=1). The increase in cAMP was blocked by (\pm) propranolol, a β adrenergic antagonist, indicating that isoprenaline interacts with B-adrenergic receptors (data not shown). Both CF and non-CF cells showed a similar rank-order of potency for adrenergic agonists: isoprenaline > adrenaline > noradrenaline. Similar results have been obtained in the secretory coil of CF and non-CF sweat glands: isoprenaline produced identical increases in cellular levels of cAMP¹¹. Thus, if cAMP regulates the Cl⁻ channel, the defect in CF would probably lie somewhere distal to the production of cAMP.

470

Second, to further examine stimulus-response coupling in airway epithelia, we studied the K+ channels responsible for the basolateral K⁺ conductance¹². Stimulation of Cl⁻ secretion activates both apical Cl⁻ channels and basolateral K⁺ channels. Activation of K⁺ channels results from an increase in intracellular Ca2+ concentration. CF cells contained K+ channels with the same conductive and ion-selective properties as cells obtained from non-CF humans and dogs. Figure 4a shows that addition of adrenaline to the bathing solution activated a cellattached K⁺ channel. A similar response was observed on three occasions using isoprenaline and in cells from three of the four preparations studied. To show that the channel was regulated by the internal Ca²⁺ concentration, we used inside-out, cell-free patches as shown in Fig. 4b. Increasing the concentration of Ca²⁺ bathing the cytosolic surface of the patch increased the probability of finding the K⁺ channel open. The same response was observed in cells from all four patients. This apparently normal regulation of the Ca2+-activated K+ channel suggests that the metabolic steps between hormone binding and regulation of the K⁺ channel (that is, regulation of intracellular Ca²⁺ concentration) are intact in CF.

In conclusion, these results suggest that CF epithelial cells contain the same apical Cl- channel as non-CF cells. However, the channel does not open when attached to the cell. Thus, the data suggest that the apical membrane is Cl impermeable because of abnormal regulation of the Cl channel. However, the data also suggest that β -adrenergic agonists bind to their receptors, that cAMP accumulation is intact and that the K⁺ channel, which is involved in Ca-dependent stimulus-response coupling, is activated normally. Thus, we speculate that the Cl impermeability of CF epithelia results from a defect in the metabolism of some intracellular mediator, the presence of an intracellular inhibitor of the channel, or an abnormal regulatory site on the Cl channel itself.

We thank Phil Karp, Timothy R. Ruppert, Robin Wicks, Theresa Butwell and Vanessa Krumbholz for technical assistance. We especially thank the patients with cystic fibrosis and their families for allowing us to obtain the tissue required for these studies. This work was supported by grants from the NHLBI (HL-29851) and NIADDK (AM-27651), the Cystic Fibrosis Foundation (National organization and Rainbow Chapter) and the American Heart Association. M.J.W. is an Established Investigator of the American Heart Association.

Received 9 January; accepted 6 June 1986.

- Widdicombe, J. H., Welsh, M. J. & Finkbeiner, W. E. Proc. natn. Acad. Sci. U.S.A. 82, 6167-6171 (1985).
- Welsh, M. J. Science 232, 1648-1650 (1986).
- Welsh, M. J. in Physiology of Membrane Disorders (eds Andreoli, T. E., Hoffman, J. F., Fanestil, D. D. & Schultz, S. G.:) 751-766 (Plenum, New York, 1986).
- Hamill, O. P., Marty, A., Neher, E., Sakmann, B. & Sigworth, F. J. Pflügers Arch. ges. Physiol. 391, 85-100 (1981).
- Shoemaker, R. L., Rechkemmer, G. & Frizzell, R. A. Biophys. J. 49, 158a (1986).
 Smith, P. L., Welsh, M. J., Stoff, J. S. & Frizzell, R. A. J. Membrane Biol. 70, 217-226 (1972).

- Al-Bazzaz, F. J. Am. Rev. respir. Dis. 123, 295-298 (1981).
 Sato, K. & Sato, F. J. clin. Invest. 73, 1763-1771 (1984).
 Welsh, M. J. & McCann, J. D. Proc. natn. Acad. Sci. U.S.A. 82, 8823-8826 (1985).
- 13. Lowry, O. H., Rosebrough, N. H., Farr, A. L. & Randall, R. J. J. biol. Chem. 193, 265-275
- 14. Liedtke, C. M. & Tandler, B. Am. J. Physiol. 247, C441 (1983).

Role of the HTLV-III/LAV envelope in syncytium formation and cytopathicity

Joseph Sodroski, Wei Chun Goh, Craig Rosen, Kathryn Campbell & William A. Haseltine*

Department of Pathology, Dana-Farber Cancer Institute, Harvard Medical School and * Department of Cancer Biology. Harvard School of Public Health, Boston, Massachusetts 02115, USA

Acquired immune deficiency syndrome (AIDS) is characterized by marked depletion of the T4⁺ helper subset of T cells¹⁻³. The aetiological agent of the disease, the human T-lymphotropic virus type III (HTLV-III)/lymphadenopathy-associated virus (LAV), specifically kills T4⁺ cells in vitro⁴⁻¹⁰. Part of this specificity for the T4+ population residues in the relative efficiency with which HTLV-III infects these cells, as a result of a specific interaction between the T4 molecule and the virus envelope glycoprotein 11-13. In addition, the cytotoxic consequences of HTLV-III replication are dependent on cell type, as certain lymphoid and myeloid cells can be productively infected without notable cytopathic effect 14,15. Here we investigate the basis for the specific cytotoxicity of the virus, and report that high-level expression of the HTLV-III envelope gene induces syncytia and concomitant cell death in T4+ cell lines but not in a B-lymphocyte line. Syncytium formation depends on the interaction of envelope-expressing cells with neighbouring cells bearing surface T4 molecules. These results explain, at least in part, the specific cytopathic effect of HTLV-III infec-

The investigation of the envelope gene as a determinant of HTLV-III cytopathic effect was motivated by recognition that the exterior glycoprotein of several enveloped viruses is responsible for syncytium formation and contributes to the cytotoxic effects of infection¹⁶⁻²³. Moreover, previous findings ruled out a direct cytopathic role for the proteins unique to HTLV-III, including those encoded by the sor, 3' orf and tat-III (transactivator) genes. Viruses deleted for either or both of the sor and 3' orf genes replicate in and kill T4+ cells^{24,25}. Moreover, T4⁺ cell lines that express constitutively a functional tat_{III} gene product are viable²⁶

To determine whether the HTLV-III envelope gene was involved in the induction of syncytia and cell death, plasmids were constructed that produced high levels of the envelope glycoprotein. The construction of such plasmids was made possible by the finding that expression of the envelope gene directed by the HTLV-III long terminal repeat (LTR) is dependent on two other HTLV-III genes, tat-III and art²⁶⁻²⁹. Accordingly, these two functions were supplied in the initial experiments. The presence of the tat-III gene was guaranteed by using cells that express constitutively the tat-III gene product (Jurkat-tat-III and Raji-tat-III)30. The art function was supplied by using plasmids that were designed to express both the art and env proteins simultaneously (pIIIenv3-1 and pIIIenv3-2; ref. 29) (Fig. 1).

The T4⁺ Jurkat-tat-III cell line³⁰ was used as a recipient in these experiments. The gp160 and gp120 HTLV-III envelope

^{1.} Quinton, P. M. Nature 301, 421-422 (1983).

Knowles, M. R. et al. Science 221, 1067-1070 (1983).

^{3.} Yankaskas, J. R., Knowles, M. R., Gatzy, J. T. & Boucher, R. C. Lancet i, 954-956 (1985).

		Table 1	Syncytium formation	n following transfection of	cells		
Transfected DNA	Added antibody	Co-cultivated cells (%T4 ⁺)	Syncytia per 10 ⁷ cells	Transfected DNA	Added antibody	Co-cultivated cells (%T4 ⁺)	Syncytia per 10 cells
a, Jurkat-tat-III cells				b, Jurkat cells			
None	None	None	<1,000	ptat-I	None	None	23 ± 12
pIIIenv3-1	None	None	$38,000 \pm 10,000$	ptat-I	None	None	$2,005 \pm 120$
pIIIenv3-2	None	None	$29,000 \pm 8,000$	+pIenv3			•
pIIIenv3-D1	None	None	<1,000	ptat-I	None	None	$1,952 \pm 80$
pIIIenv3-FS1	None	None	<1,000	+pIenv3-FS2			
pIIIenv3-FS2	None	None	<1,000	ptat-I	None	None	30 ± 18
pIIIenv3-FS1 +pIIIenv3-FS2	None	None	$76,000 \pm 18,000$	+plenv3-FS1			
pIIIenv3-D1	None	None	58,000 + 13,000	c, Raji-tat-III cells			
+pIIIenv3-FS2			, ,	None	None	None	< 1.000
pIllenv3-D1	OKT8	None	$65,000 \pm 15,000$	pIIIenv3-1	None	None	<1,000
+pIIIenv3-FS2			, ,	pIIIenv3-D1	None	None	< 1,000
pIIIenv3-D1	OKT4	None	$51,000 \pm 12,000$	+pIIIenv3-FS2			,
+pIIIenv3-FS2			, ,	pIIIenv3-D1	None	Raji (0)	< 1.000
pIIIenv3-D1	OKT4A	None	$2,000 \pm 2,000$	+pIIIenv3-FS2		• • •	•
+pIIIenv3-FS2			, ,	pIIIenv3-D1	None	Raji-tat-III (0)	<1,000
pIIIenv3-D1	p982	None	53,000 + 16,000	+pIIIenv3-FS2		, ,	
+pIIIenv3-FS2	•		,	pIIIenv3-D1	None	HUT78 (30)	$11,000 \pm 4,000$
pIIIenv3-D1	12-8	None	$55,000 \pm 7,000$	+pIIIenv3-FS2			, , , , , ,
+pIIIenv3-FS2			,	pIIIenv3-D1	None	C8166-45 (>95)	$54,000 \pm 8,000$
pIIIenv3-D1	Wy	None	$30,000 \pm 13,000$	+ pIIIenv3-FS2		,	,
+pIIIenv3-FS2	-		,	pIIIenv3-D1	None	Jurkat (80)	$38,000 \pm 3,000$
pIIIenv3-D1	91-1	None	$35,000 \pm 8,000$	+pIIIenv3-FS2			
+pIIIenv3-FS2				pIIIenv3-D1	OKT4	Jurkat	$36,000 \pm 5,000$
pIIIenv3-D1	Pe	None	$44,000 \pm 14,000$	pIIIenv3-FS2			
+pIIIenv3-FS2				pIIIenv3-D1	OKT8	Jurkat	$41,000 \pm 7,000$
pIIIenv3-D1	Ba	None	$62,000 \pm 11,000$	+pIIIenv3-FS2			
+pIIIenv3-FS2				pIIIenv3-D1	OKT4A	Jurkat	<1,000
pIIIenv3-D1	K.C.	None	$57,000 \pm 9,000$	+pIIIenv3-FS2			
+pIIIenv3-FS2				pIIIenv3-D1	None	H9 (90)	$19,000 \pm 3,000$
pIIIenv3-D1	McD.	None	$50,000 \pm 13,000$	+pIIIenv3-FS2			
+pHIenv3-FS2				pIIIenv3-D1	OKT8	H9	$21,000 \pm 6,000$
				+pIIIenv3-FS2			
				pIIIenv3-D1	OKT4	H 9	$17,000 \pm 2,000$
				+pIIIenv3-FS2			
				pIIIenv3-D1	OKT4A	H9	<1,000
				+pIIIenv3-FS2			

For these experiments, ~10⁷ cells were transfected with 10 µg of each plasmid DNA using the DEAE-dextran technique³⁸. Immediately after transfection the cells were pelleted and incubated for 30 min at room temperature in 1 ml of medium containing a 1:200 dilution of monoclonal antibody OKT8, OKT4 or OKT4A (Ortho Pharmaceuticals). The cells were then suspended in 10 ml of fresh medium containing a 1:400 dilution of monoclonal antibody and incubated at 37 °C until the syncytia were counted. In subsequent experiments, the OKT4A antibody reduced syncytium formation by >90% at dilutions of 1:800. For patient antisera containing HTLV-III neutralizing activity (p982, 12-8, 91-1, Wy and Pe) as well as control patient sera (Ba, K.C. and McD.), transfected Jurkat-tat-III cells were grown in medium containing a 1:10 dilution of serum and syncytia counted as described below. Neutralizing activities of the p982, 12-8 and 91-1 sera were determined to be 1:64, 1:64 and 1:32, respectively, by David Ho and Martin Hirsch using methods described previously³⁴. Neutralizing activities of the Wy and Pe antisera were determined by Thomas Matthews and Dani Bolognesi to be 1:500 and 1:150, respectively, in their assay³⁶. Immediately after transfection of Raji-tat-III cells with the indicated plasmids, a threefold excess of untransfected cells of the type indicated was added to the culture. Values in parentheses represent the percentage of the added cells that were T4⁺, as estimated by indirect immunofluorescence¹¹. Syncytia for the Jurkat-tat-III and Raji-tat-III experiments were counted from the photographic prints to determine the number of syncytia. The values represent the mean of three independent experiments, with the range of values indicated. For the experiment using Jurkat cells, 10⁷ cells were aliquoted for counting at 72 h post-transfection. The values represent the mean (and range) of three independent experiments. The syncytia observed following transfection of the ptat-I and ptat-I+plenv3-FS1 DNAs contained

gene products³¹ were produced in these cells on transfection with either the pIIIenv3-1 or -2 plasmids (Fig. 2a, lanes 3, 4). The expression of these proteins was eliminated by either a frameshift mutation or a deletion in the region of the envelope gene that encodes the exterior glycoprotein (pIIIenv3-FS1 and -D1, Fig. 2a, lane 5; b, lane 4).

Marked syncytium formation was observed by 48 h after transfection of Jurkat-tat-III cultures with plasmids that express the envelope glycoprotein (Fig. 3b, c and Table 1a). In these experiments, at least 30-80-fold increases in syncytia were observed relative to control or mock-transfected cultures, representing 0.5-1% of transfected cells, a value consistent with the transient transfection frequency of human lymphoid cell lines (J.S. and

W.A.H., unpublished observations). Greater than 90% of the syncytia are unable to exclude vital dyes by 2 weeks after transfection, indicating the cytotoxic nature of the events accompanying syncytium formation (see, for example, Fig. 3h). The syncytium formation and cytopathic effect observed in experiments with the *env*-expression plasmids were indistinguishable from those seen following infection of Jurkat-tat-III-cells with HTLV-III (Fig. 3a).

Neither syncytium formation nor cell death was noted in cultures transfected with the plasmids containing mutations in *env* that prevent expression of the gp160 and gp120 proteins (Fig. 3d, Table 1a). However, both of these plasmids (pIIIenv3-FS1 and -D1) continued to express *art* gene function, as judged

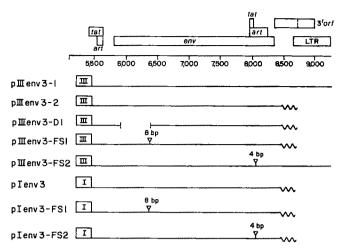


Fig. 1 Structure of the plasmids expressing art and env genes. The structure of the 3' half of the HTLV-III genome, based on the sequence of Ratner et al.32, is shown. The positions of the env gene, 3' orf gene and LTR are shown, together with the two coding exons of the tat-III and art genes in their respective reading frames. The position of a stop codon in the 3' orf gene of the parental proviral clone used in these studies, pHXBc2 (ref. 39), is denoted by a vertical broken line. In all the plasmids shown, LTR sequences from -167 to +80 for the HTLV-III LTR (boxes labelled III) or -353 to +326 of the HTLV-I LTR (boxes labelled I)⁴⁰ are located at nucleotide 5,496 of the sequence of Ratner et al. 32. The zig-zag lines represent signals for polyadenylation and splicing derived from the simian virus 40 early region⁴¹. The eight-nucleotide insertion (8 bp) in plasmids pIIIenv-3-FS1 and pIenv3-FS1 was introduced by digestion of either pIIIenv3-2 or pIenv3 with the restriction endonuclease Stul and insertion of 8-bp Xbal linkers before transfection of Escherichia coli. The construction of the other plasmids has been described previously²⁹. All plasmids were banded in CsCl before transfection.

by the ability of the plasmids to complement art-defective proviruses for gag or env gene expression²⁹.

Of special interest is the effect of another mutation present on plasmid pIIIenv3-FS2. The frameshift mutation of this plasmid interrupts the second coding exon of the art gene²⁹ and results in the replacement of the 104 carboxy-terminal envelope amino acids with 57 different amino acids³². The inability of the pIIIenv3-FS2 plasmid to synthesize env gene products can be complemented by co-transfection with plasmids expressing the art gene (pIIIenv3-D1 or -FS1) (Fig. 2a, lane 6; b, lanes 5-7). An altered env gene product capable of inducing syncytium formation and cell death was produced in this experiment (Table 1a, Fig. 3e, f), indicating that the 104 carboxy-terminal amino acids of the HTLV-III envelope are not required for these effects.

To determine whether expression of the HTLV-III envelope in the absence of tat-III or art functions is sufficient for syncytium formation and cytopathicity, plasmids containing the HTLV-I LTR 5' to the HTLV-III env gene were constructed (plenv3, plenv3-FS1 and plenv3-FS2; Fig. 1). One of these plasmids, plenv3-FS2, cannot encode a functional art product because of a frameshift mutation in the art gene coding sequences. plenv3-FS1 contains a frameshift mutation in the 5' portion of the env gene that encodes the exterior glycoprotein. These plasmids were transfected into Jurkat T-lymphocytes together with a plasmid (ptat-I) that expresses the trans-activator protein of HTLV-I33. The level of HTLV-III envelope expression and syncytium formation observed following transfection with plasmids plenv3 and plenv3-FS2 was lower than that observed using the trans-activated HTLV-III LTR as a promoter, but was at least 60-fold higher than that observed after transfection with plenv3-FS1 (Table 1b). The syncytia observed in this experiment were smaller (30-50 nuclei per syncytium) than those observed when the HTLV-III LTR was used as promoter (>200 nuclei per syncytium), but the viability of the syncytia was not appreciably different in the two experiments. We conclude that the HTLV-III tat-III and art genes are not required for either syncytium formation or cytopathicity consequent to env gene expression in T4⁺ lymphocytes.

To determine whether host cell factors might influence susceptibility to syncytium formation, a B-lymphocyte cell line that expresses constitutively the tat-III gene product, Raji-tat-III³⁰, was transfected with plasmids expressing the HTLV-III art and env genes. Raji-tat-III cells transfected with either pIIIenv3-1 or a combination of pIIIenv3-FS2 and pIIIenv3-D1 produced the gp160/120 envelope proteins at levels similar to those observed in Jurkat-tat-III cells (Fig. 2). Nonetheless, no syncytia or cytopathic effects were observed in the transfected Raji-tat-III cells (Table 1c).

To test whether the HTLV-III envelope glycoproteins synthesized in the Raji-tat-III cells were capable of inducing syncytia, the transfected Raji-tat-III cells were co-cultivated with various untransfected human lymphoid cell lines (Table 1c). Syncytia were observed within 72 h following addition of the human T-lymphocyte lines H9, Jurkat, C8166-45 and, to a lesser extent, HUT78 to the transfected Raji-tat-III cells. The syncytia formed in this experiment failed to exclude vital dyes within 7 days of their formation (data not shown). No syncytia were observed following addition of untransfected Raji or Raji-tat-III cells to the transfected cells. Thus, the transfected Raji-tat-III cells synthesized immunoprecipitable HTLV-III envelope proteins capable of inducing syncytia in a susceptible cell type.

Studies of animal retroviruses suggest that syncytium formation involves an interaction of virus-expressing cells with adjacent cells bearing receptors for the virus^{11,17-22}. The cells capable of forming syncytia following co-cultivation with Raji-tat-III

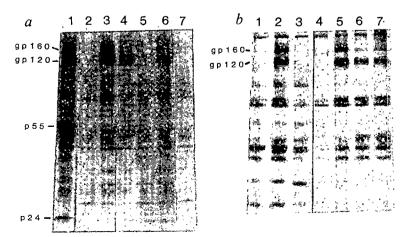


Fig. 2 Immunoprecipitation of transfected Jurkat-tat-III and Raji-tat-III cells. Jurkat-tat-III (a, lanes 1-7; b, lanes 4-7) or Raji-tat-III (b, lanes 1-3) cells were transfected by the DEAE-dextran procedure³⁷ using 10 µg of plasmid DNA; 48 h after transfection, cells were labelled with 35S-cysteine and cell lysates immunoprecipitated using an AIDS patient serum, RV119. The positions of the gp160 and gp120 env proteins and the p55 and p24 gag products are noted. Transfected plasmids were pHXBc2 (a, lane 1), pBR322 (a, lane 2), pIIIenv3-1 (a, lane 3), pIIIenv3-2 (lane 4), pIIIenv3-FS1 (lane 5), pIIIenv3-FS1 plus pIIIenv3-FS2 (lane 6), pIIIenv3-FS2 (a, lane 7 and b, lane 1), pIIIenv-D1 (b, lanes 3, 4), pIIIenv-D1 plus pIIIenv3-FS2 (b, lanes 2, 5-7). Transfected Jurkat-tat-III cells were incubated with monoclonal antibody OKT4 or OKT4A (b, lanes 6 and 7, respectively) as described in Table 1.

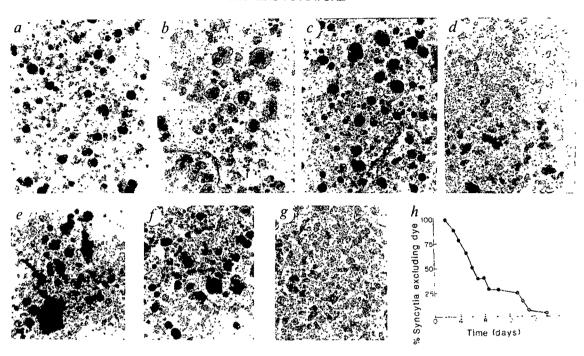


Fig. 3 Transfection of Jurkat-tat-III cells with plasmid DNAs. Approximately 10⁷ Jurkat-tat-III cells were transfected with 10 µg of plasmid DNA using the DEAE-dextran procedure³⁸, and the cells were photographed at various times after transfection (a-g, ×53). a, Jurkat-tat-III cells 5 days after transfection with plasmid pHXBc2, which generates replicating HTLV-III that kills the culture. b, c, Jurkat-tat-III cells 3 and 7 days, respectively, after transfection with plasmid pIIIenv3-1. The Jurkat-tat-III cells in d were transfected with plasmid pIIIenv3-FS1 7 days previously. e-g, Jurkat-tat-III cells 10 days after transfection with a combination of pIIIenv3-D1 and pIIIenv3-FS2, followed by treatment with OKT8, OKT4 and OKT4A, respectively. Treatment with monoclonal antibodies was as described in Table 1. h, Percentage of Jurkat-tat-III cells forming syncytia that exclude Trypan blue at various times after transfection with pIIIenv3-FS1 plus pIIIenv3-FS2. The transfected culture was fed every 3 days and aliquots removed for counting. Values were obtained by examining more than 200 random syncytia for uptake of Trypan blue. The curve shown is a typical experiment, with a maximum variation of 3 days in the time required for 50% dye exclusion in three separate experiments.

transfectants expressed the T4 molecule, which has been shown to be a component of the HTLV-III receptor¹¹⁻¹³. To examine the role of T-lymphocyte markers in syncytium induction by HTLV-III, Jurkat-tat-III cells were transfected simultaneously with two plasmids, pIIIenv3-D1 and pIIIenv3-FS2, the combination of which leads to high-level production of the env protein. The cells were then incubated with monoclonal antibodies directed against T8, T4 or T4A. Only the monoclonal antibody against T4A inhibited syncytium formation in the transfected Jurkat-tat-III cells (Fig. 3e-g, Table 1a). The absence of syncytia in the presence of the monoclonal antibody cannot be attributed to inhibition of env gene synthesis as levels of immunoprecipitable gp160/120 envelope proteins were similar regardless of the monoclonal antibody used for incubation (Fig. 2b, lanes 6, 7). The formation of syncytia following co-cultivation of envelopeexpressing Raji-tat-III cells with T4+ lymphocytes (Jurkat and H9) could also be inhibited by monoclonal antibodies against T4A but not by antibodies against T8 or T4 (Table 1c). Previous studies demonstrated that monoclonal antibodies against T4A but not against T4 or T8 could inhibit the interaction of the HTLV-III envelope with the T4 molecule¹³. These results suggest that the T4 epitope that interacts with the HTLV-III envelope is a necessary component in syncytium formation.

The ability of antisera from normal individuals and from HTLV-III-infected patients to inhibit syncytium formation by the HTLV-III envelope gene was assayed. The sera tested included some that previously were found to contain relatively high antibody titres that inactivate HTLV-III in virus neutralization tests³⁴⁻³⁶. All the patient sera tested contain antibodies to envelope glycoproteins as judged by radioimmune precipitation tests (not shown). None of the patient sera significantly inhibited syncytium formation by the HTLV-III envelope gene compared with control sera (Table 1).

The results presented here demonstrate that expression of the HTLV-III envelope results in marked syncytium formation and concomitant cell death indistinguishable from the effects of infection with HTLV-III itself. Syncytium formation does not occur in a cell line lacking the T4 molecule nor does it occur in the presence of antibodies known to interfere with the interaction between the HTLV-III envelope and T4. These results suggest that syncytium formation resulting from an interaction of the HTLV-III envelope with the T4 molecule is the basis for at least part of the specific cytotoxicity of HTLV-III for T4' cells. It is also likely that cell death will result from the expression of the HTLV-III envelope protein in an isolated cell that exhibits a high density of T4 surface antigen via an autofusion reaction that disrupts normal membrane function. The marked cytopathic effect of HTLV-III relative to most other retroviruses might be the consequence of several factors: the greater avidity of binding of the exterior glycoprotein for the receptor, efficient fusion activity of HTLV-III envelope domains, and high-level expression of virion components consequent to trans-activation.

Cells expressing the HTLV-III envelope glycoprotein, regardless of the level of expression of the T4 molecule, can serve to nucleate the formation of syncytia with uninfected cells that bear the T4 surface protein. This effect may contribute to the marked depletion of T4⁺lymphocytes observed in AIDS patients despite the small percentage of peripheral blood lymphocytes actively producing viral messages and protein at any given time³⁷.

The dependence of the cytopathic effect of HTLV-III on the interaction of the envelope glycoprotein with a T4 surface protein provides an explanation for the ability of the virus to infect but not kill cells that do not express high levels of the T4 molecule. Dalgleish et al. 11 observed that higher titres of anti-T4 antibodies are required to block infection by vesicular stomatitis

virus pseudotypes of HTLV-III than are necessary to inhibit syncytium formation, and suggested that more T4 molecules are required for syncytium formation than for infection by HTLV-

The antisera from HTLV-III-infected patients that we have tested exhibit at best slight inhibition of env gene-mediated syncytium formation or cytopathicity, even though they react with the envelope glycoprotein and are reported to inactivate virion infectivity³⁴⁻³⁶. Weiss *et al.*³⁵ also observed that most patient sera failed to inhibit syncytium formation. Inhibition of syncytium formation by antibodies is reported to be critical for the protective response to infection by other enveloped viruses²³. Failure to inhibit the fusion activity of the virus may account for the progression of HTLV-III-related diseases in the presence of antibodies reactive against the envelope glycoproteins, as cell-to-cell transmission of the virus may not be blocked in most patients.

Definition of both the binding and fusion domains of the HTLV-III envelope glycoprotein will be important for the development of strategies for protection against HTLV-III infection and consequent immune cell depletion.

We thank Drs George Shaw, Beatrice Hahn, Flossie Wong-Staal and Robert Gallo for the gift of the pHXBc2 provirus: Mary Fran McLane, Myron Essex, Dani Bolognesi, David Ho and Martin Hirsch for gifts of antisera; and Tanya Parks for manuscript preparation. W.A.H. is supported by a State of Massachusetts contract and by NIH grant CA21082. J.S. is a Special Fellow of the Leukaemia Society of America and is also the recipient of NIH grants CA40658 and CA42597. C.R. is the recipient of NIH postdoctoral fellowship CA07580 and NIH Contract FOD-0757. Both J.S. and C.R. are recipients of grants from the American Foundation for AIDS Research.

Received 14 April: accepted 4 June 1986.

- 1. Seligman, M. et al. New Engl. J. Med. 311, 1286-1292 (1984).
- Friedman-Kein, A. E. et al. Ann. intern. Med. 96, 693-700 (1982).
 Gottleib, M. S. et al. New Engl. J. Med. 305, 1425-1431 (1981).
 Gallo, R. C. et al. Science 224, 497-500 (1984).

- 5. Popovic, M., Sarngadharan, M. G., Read, E. & Gallo, R. C. Science 224, 497-500 (1984). 6. Sarngadharan, M. G., Popovic, M., Bruch, L., Shupbach, J. & Gallo, R. C. Science 224,
- 506-508 (1984). 7. Barre-Sinoussi, F. et al. Science 220, 868-871 (1983).
- Schupbach, J. et al. Science 224, 503-505 (1984).
- 9. Klatzmann, D. et al. Science 225, 59-63 (1984).
- 10. Vilmer, E. et al. Lancet i, 753-756 (1984).
- Dalgleish, A. et al. Nature 312, 763-767 (1984).
 Klatzmann, D. et al. Nature 312, 767-768 (1984).
- 13. McDougal, J. S. et al. Science 231, 382-385 (1986)
- 14. DeRossi, A. et al. Proc. natn. Acad. Sci. U.S.A. 83, 4297-4301 (1986).
- Gartner, S. et al. Science 233, 215-219 (1986).
 Poste, G. Int. Rev. Cytol. 13, 157-252 (1972).

- roste, C. Int. Rev. Cytot. 13, 151-252 (1972).
 Chatterjee, S. & Hunter, E. Virology 107, 100-108 (1970).
 Diglio, C. A. & Ferrer, J. F. Cancer Res. 36, 1056-1067 (1976).
 Klement, V., Rowe, W. P., Hartley, J. W. & Pugh, W. E. Proc. natn. Acad. Sci. U.S.A. 63, 753-758 (1969).
- 20. Nagy, K., Clapham, P., Cheingsong-Popov, R. & Weiss, R. A. Int. J. Cancer 32, 321-328 (1983).
- Redmond, S., Peters, G. & Dickson, C. Virology 133, 393-402 (1984).
 Pinter, A. et al. J. Virol. 57, 1048-1054 (1986).
 Richardson, C. D. & Choppin, P. W. Virology 131, 518-532 (1983).

- Sodroski, J. et al. Science 231, 1549-1553 (1986).
 Terwilliger, E., Sodroski, J., Rosen, C. & Haseltine, W. J. Virol. (in the press).
 Dayton, A., Sodroski, J., Rosen, C., Goh, W. C. & Haseltine, W. Cell 44, 941-947 (1986).
 Arya, S., Guo, C., Josephs, S. F. & Wong-Staal, F. Science 229, 69-74 (1985).
- 28. Sodroski, J., Patarca, R., Rosen, C., Wong-Staal, F. & Haseltine, W. A. Science 229, 74-77
- 29. Sodroski, J. et al. Nature 321, 412-417 (1986).
- Rosen, C. A., Sodroski, J. G., Campbell, K. & Haseltine, W. A. J. Virol. 57, 379-384 (1986).
 Allan, J. S. et al. Science 228, 1091-1093 (1985).
- Ratner, L. et al. Nature 313, 277-284 (1985).
 Sodroski, J., Rosen, C., Goh, W. C. & Haseltine, W. Science 228, 1430-1434 (1985).
 Ho, D., Rota, T. & Hirsch, M. New Engl. J. Med. 312, 649-650 (1985).
 Weiss, R. A. et al. Nature 316, 69-72 (1985).

- 36. Robert-Guroff, M. Brown, M. & Gallo, R. C. Nature 316, 72-74 (1985).
 37. Harper, M. E., Marselle, L. M., Gallo, R. C. & Wong-Staal, F. Proc. natn. Acad. Sci. U.S.A. 83, 772-776 (1986):
- 38. Queen, C. & Baltimore, D. Cell 33, 741-748 (1983).
- 39. Fisher, A. C., Collalti, E., Ratner, L., Gallo, R. C. & Wong-Staal, F. Nature 316, 262-265
- 40. Seiki, M., Hattori, S., Hirayama, Y. & Yoshida, M. Proc. natn. Acad. Sci. U.S.A. 80, 3618-3622
- 41. Mulligan, R. C., Howard, B. H. & Berg, P. Nature 277, 108-114 (1979).

A chromosomal rearrangement in a P. falciparum histidine-rich protein gene is associated with the knobless phenotype

Laura G. Pologe & Jeffrey V. Ravetch

DeWitt Wallace Research Laboratory, Memorial Sloan-Kettering Cancer Center, 1275 York Avenue, New York, New York 10021, USA

The significant morbidity and mortality associated with Plasmodium falciparum malaria results, in part, from the sequestration of parasitized erythrocytes in postcapillary venules, which may protect the parasite from splenic clearance^{1,2} and contribute to the pathogenesis of cerebral malaria³. This sequestration has been linked to the expression of parasite-induced knob structures on the surface of the infected erythrocyte which mediate the cytoadherence phenomenon^{4,5}. While knobs are necessary for cytoadherence, they are not sufficient, requiring both parasite- and host-encoded proteins⁶⁻¹⁰. Spontaneous mutants of P. falciparum have been isolated from in vitro cultures which lack the ability to express knobs and fail to cytoadhere11. A histidine-rich protein has been described which is associated with the knobby phenotype 12 and may be a constituent of the knob13. We now report the isolation of complementary DNA clones for a knob-associated histidine-rich protein (KAHRP) and demonstrate that in knobless mutants the gene for this protein has undergone a rearrangement, resulting in a deletion in the 3' coding sequence. Moreover, the chromosome to which the KAHRP gene maps is rearranged in these mutants, producing a telomeric location of the truncated gene. These observations explain the loss of expression of the messenger RNA and protein in such mutants and may explain the loss of the knob itself. The implications for the generation of spontaneous mutations in the parasite by this novel mechanism are discussed.

A cDNA library constructed to P. falciparum strain FcR-3 at the trophozoite stage was screened with a 1.8-kilobase (kb) EcoRI fragment derived from the histidine-rich protein gene of Plasmodium lophurae¹⁴ under reduced stringency (25% formamide, 10% dextran sulphate, 5×SSC, 7 mM Tris pH 7.6, 1 × Denhardt's buffer, 25 μg ml⁻¹ salmon sperm DNA at 40 °C; final wash = 0.1 × SSC, 0.1% SDS, 40 °C). cDNA clones which cross-hybridized with the avian gene were characterized further by restriction enzyme and Northern blot analysis to knobby (K⁺) and knobless (K⁻) RNA. Three overlapping cDNA clones (Fig. 1a) were characterized by DNA sequence analysis and shown to encode an open reading frame containing multiple polyhistidine sequences varying between 6 and 9 contiguous histidine residues (data not shown), a primary structure analogous to the P. lophurae gene¹⁴. These same clones were identified in the library using a cDNA probe to unique sequences in K⁺ mRNA constructed by subtractive hybridization¹⁵ between K⁺ and K⁻ clonal isolates. Northern blot analysis (Fig. 1b, c) demonstrated that stable mRNA transcripts of 4.2 kb accumulate in K+ but not K- isolates and are maximally expressed in trophozoites. Antibodies generated to the recombinant protein expressed in Escherichia coli recognize a protein (in FCR-3) of 80,000-90,000 relative molecular mass in K⁺ but not K⁻ isolates (Pologe and Ravetch, in preparation). This expression pattern is in agreement with the expression of a knob-associated histidine-rich protein described previously^{12,16}. Independent clonal derivatives of K⁺ parasites from a wide range of geographical isolates demonstrated expression of this RNA only in K+ isolates (see Fig. 1b). Thus, by virtue of its histidine-rich amino-acid sequence and expression in K+ and not K- isolates, these clones represent cDNA isolates for a KAHRP gene.

To investigate how the accumulation of stable transcripts for this gene has been lost in K isolates, DNA was isolated from K⁺ and K⁻ isolates, analysed with multiple restriction endonu-

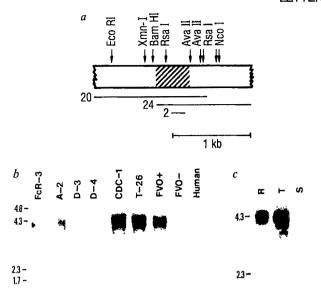


Fig. 1 a, Restriction map and cDNA clones for a knob-associated histidine-rich protein of P. falciparum. Cross-hatching, polyhistidine encoding sequences. Three overlapping cDNA clones are indicated with their numerical designation. b. Northern blot analysis of RNA isolated from multiple knobby (K+) and knobless (K-) isolates. Size markers are derived from P. falciparum and human rRNA sizes. FcR-3 is the non-clonal Gambian line established by Trager²⁵ and A-2 (K^+), D-3 (K^-) and D-4 (K^-) are clonal derivatives of that line²²; FVO⁺ is a K⁺ line cloned from a Vietnam isolate (ref. 26) and FVO⁻ a K⁻ clone derived from it²⁷; CDC-1 (ref. 28) is a Honduran isolate (K+) and T-26 is a Tanzanian isolate (K⁺). Two RNA species appear to be resolved for this KAHRP gene migrating at 4.1 and 4.2 kb. c, Stage specificity of KAHRP gene expression. R, rings; T, trophozoites; S, schizonts. The faint hybridization seen in the schizont lane may represent contamination of schizonts with trophozoites during synchronization. Methods. a, A cDNA library constructed in the PstI site of pUC-9 (ref. 29) was screened and the resulting clones characterized as described in the text. Overlapping clones were identified by restriction enzyme analysis and the fragment sizes verified by co-migration with genomic DNA. DNA sequence analysis was performed using the chemical degradation method of Maxam and Gilbert³ b, P. falciparum was grown in synchronous culture as described elsewhere 26 to obtain populations enriched for trophozoites (b) or rings and schizonts (c). 1 µg of total RNA was fractionated on agarose-formaldehyde gels, transferred to nitrocellulose and hybridized with nick-translated cDNA probes (specific activity 2×10^8 c.p.m. per μ g), under stringent conditions (50% formamide, 10% dextran sulphate, 5×SSC, 7 mM Tris pH 7.6, 1× Denhardt's, 25 μ g ml⁻¹ salmon sperm DNA; final wash = 0.1 × SSC, 0.1% SDS, 52 °C). These conditions were used for all stringent hybridization studies described. The 1.4-kb PstI insert of clone 20 was used in

cleases and probed with the cDNA clones illustrated in Fig. 1a. As shown in Fig. 2, the restriction fragments encoding this cDNA sequence are conserved in K⁺ parasites from two geographical isolates, as well as in clonal derivatives of these isolates. A single HindIII fragment of 10.5 kb is detected by these cDNA clones in K⁺ strains (lanes 1, 3), while two Xmn fragments of 8.1 and 3.4 kb are detected when clone 20 is used as a probe, as a result of an internal Xmn site in this cDNA clone (lanes 5, 6, 9). Similar studies on K⁺ isolates from Honduras (CDC-1) and Tanzania (T-26) reveal that the gene for this KAHRP is conserved (not shown). However, a DNA rearrangement has occurred in K⁻ isolates, resulting in more rapidly migrating species. The HindIII fragment is 6.1 kb in D-4 and 7.2 kb in FVO⁻ (Fig.

b and the 250-base-pair (bp) PstI insert of clone 2 for c.

2, lanes 2, 4). Similarly, the 5' Xmn fragment in FVO is unrearranged, while the 3' fragment, encoding the polyhistidine sequences, now migrates as a diffuse band of 2.3 ± 0.25 kb (Fig. 2. lane 10), K⁻ isolates D-3 and D-4 have lost the 5' Xmn site. resulting in a single rearranged Xmn fragment of 5.2 kb (Fig. 2, lanes 7, 8). This rearrangement has resulted in a deletion of DNA sequences corresponding to the 3' coding sequence of this gene. Restriction enzyme mapping of the strains shown in Fig. 2 with EcoRI, BamHI, XmnI, AvaII and HindIII, singly and in combination, using probes derived from both the 5' and 3' sequences of the KAHRP gene, demonstrated that the breakpoint of the deletion in different K- isolates varies by several hundred nucleotides. For clones D-3 and D-4, derived from FcR-3, the deletion breakpoint results in the loss of all histidineencoding sequences, while in FVO-, derived from a Vietnam isolate, the breakpoint retains polyhistidine sequences (see Fig. 3c). The rearranged DNA fragment observed in these K⁻ isolates migrates as a diffuse band (Fig. 2, lanes 2, 4, 7, 8, 10), implying that the DNA fragment that is generated varies in length in the different K-isolates. In addition, our restriction mapping studies suggest that a clustering of restriction enzyme cleavage sites has been introduced 3' of this gene in K⁻ isolates (data not shown).

The finding that a common restriction site had been introduced 3' of the rearranged gene in K isolates and the heterogeneity of the DNA fragment in these mutants suggested that the gene for the KAHRP in K isolates might have become relocated to the end of a chromosome. To test this hypothesis directly, DNA from FVO+ and FVO- parasites was subjected to Bal31 digestion for increasing lengths of time, then digested with the restriction enzyme HindIII. Southern blot analysis with the cDNA probe revealed that the 10.5-kb HindIII fragment is unaffected by Bal31 digestion in the K⁺ isolate (Fig. 3a), while the 7.2-kb HindIII fragment in the K isolate migrates as a 4.3-kb fragment after 30 min of Bal31 digestion (Fig. 3b). In other experiments, the 10.5-kb fragment remains undigested in this K⁺ isolate at 60 min while the DNA from the K⁻ isolate shows no detectable hybridization at 35 min (not shown). Similar analysis of A-2, D-3 and D-4 revealed increased susceptibility to Bal31 in the K⁻ isolates (data not shown). From the size of the truncated gene fragment in the K⁻ isolates, we can estimate that the rearrangement which has occurred in these mutants has relocated this gene within 2.5 kb of a telomere. Figure 3c summarizes findings regarding the structure of the KAHRP gene in K+ and K- isolates.

These observations suggested that there may be a chromosomal rearrangement in the K- isolates involving the KAHRP gene. P. falciparum chromosomes were separated by pulse-field gradient electrophoresis¹⁷ and hybridized with the cDNA clones isolated for the KAHRP (Fig. 4). The KAHRP gene maps to chromosome 2, which appears to be invariant in the K⁺ isolates used. However, the K⁻ isolates demonstrate a more rapidly migrating chromosome 2 which hybridizes with reduced intensity to the cDNA probe for this gene, due to the deletion within the KAHRP gene. As has been noted previously^{18,19}, P. falciparum isolates differ in their karyotype with respect to the size and number of chromosomes. For the clonal isolates FVO and FVO⁻, and also for the clonal isolates A-2 (K⁺), D-3 (K) and D-4 (K⁻), the only karyotypic difference observed is in chromosome 2. FcR-3, the non-clonal parent for A-2, D-3 and D-4, is perplexing in its karyotype when compared with its clonal isolates for chromosomes 1 and 4. The only chromosomal rearrangement, however, observed consistently for all K+ and K isolates, is seen for chromosome 2. Hybridization with the falciparum ribosomal RNA gene probe20 detected no difference in the clonal pairs (not shown), nor was there a difference when the gene for the glycophorin-binding protein GBP130 (ref. 21) was used. These results demonstrate that the DNA rearrangement found in K- isolates for the KAHRP gene is reflected at the chromosomal level, and may represent a large deletion from chromosome 2.

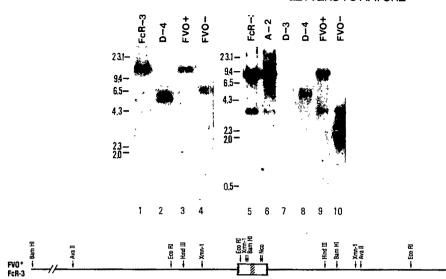
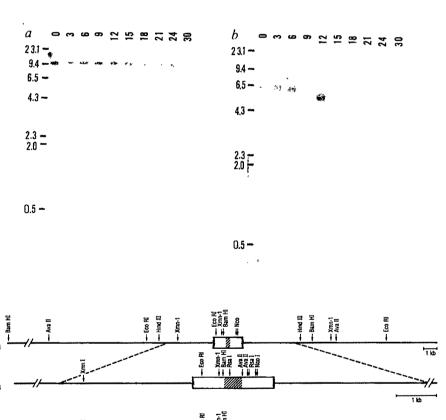


Fig. 2 Southern blot analysis³¹ of the KAHRP gene in DNA isolated from K+ and K- isolates. Lanes 1-4, HindIII digestions of DNA isolated from FcR-3 (lane 1), D-4 (lane 2), FVO+ (lane 3) and FVO- (lane 4) probed with a 5' PstI-Eco fragment of 250 bp derived from clone 20; lanes 5-10, XmnI digests of FcR-3 (lane 5), A-2 (lane 6), D-3 (lane 7), D-4 (lane 8), FVO+ (lane 9) and FVO (lane 10) probed with the Pstl insert of clone 20. Under the stringent conditions of hybridization and washing used, only one hybridizing fragment is detected for HindIII and two fragments for Xmn, as expected for K+ DNA. The genomic restriction map for this KAHRP gene is presented below the autoradiogram of the Southern blot. The cloned and sequenced region of the gene is indicated by the open box; hatching indicates the histidine-encoding sequences.

Fig. 3 a, b, Bal31 digestion of the KAHRP gene in K⁺ and K⁻ isolates. Numbers at the top of each lane refer to time in minutes. c, Summary of restriction maps of the KAHRP in K⁺ and K⁻ isolates. The breakpoints in FVO⁻, D-3 and D-4 are approximate, mapping to within the BamHI-AvaII fragment for FVO and the Xmn-EcoRI fragment for D-3 and D-4. The solid bar at the end of the maps for the K isolates indicates the end of a chromosome, as determined by the Bal31 experiments described above. Hatching indicates polyhistidine-encoding sequence.

Methods, a, b, FVO+ (a) and FVO- (b) DNA was obtained from these isolates as described elsewhere³², and digested with Bal31 according to the manufacturer's (NEB) specifications in a reaction containing 5 µg DNA, 1 U Bal31 in a total reaction volume of 175 µl. At the indicated time points, aliquots were brought to 20 mM EGTA, heated to 70 °C for 5 min and ethanol-precipitated. The DNA samples were digested with HindIII, fractionated on 1% agarose, Tris-acetate EDTA gels and transfer-red as described previously³¹. Hybridization under stringent conditions was performed using a 250-bp Pst-EcoRI fragment derived from clone 20 (see Fig. 1a). The rate of precession of the Bal31 was determined to be 80 bp min-1 based on digestion of λ DNA cut with HindIII under the conditions used for these experiments. The increased sensitivity of the gene in the K- isolate is seen. Analogous experiments performed with A-2 (K⁺), D-3 (K⁻) and D-4 (K-) revealed a similar pattern of increased Bal31 sensitivity (not shown) in the K- isolates. c, The restriction maps were generated using the enzymes indicated both singly and in combination. Sites within the cloned sequences were verified by DNA sequencing analysis.



These results demonstrate that the loss of expression of a KAHRP gene in knobless mutants is associated with a chromosomal rearrangement and deletion of part of the gene itself. The molecular mechanism which could account for the telomeric location for the truncated gene is under investigation. We do not know the extent of the deletion on chromosome 2, nor have we determined whether a reciprocal translocation involving telomeric exchange of DNA from chromosome 2 to some other

chromosome has occurred. The K⁻ phenotype occurs spontaneously in culture²², resulting in parasites which are otherwise wild type in their growth. If these mutants occur in vivo, they would presumably be selected against by splenic clearance, as has been shown²³. It is possible that K⁻ mutants accumulate in culture because of the absence of the negative selection exerted by the spleen in vivo. Thus, this chromosomal rearrangement may reflect a more general mechanism for mutation by the





Pulse-field gradient electrophoresis of P. falciparum chromosomes isolated from K+ and K- isolates. a, The ethidium bromide-stained gel pattern for various K⁺ and K⁻ isolates: b. an autoradiogram of the gel in a hybridized with a cDNA clone to the KAHRP gene.

Methods. Agarose blocks containing P. falciparum-infected erythrocytes were prepared as described previously^{17,18} using parasites grown in culture to parasitaemias of 10-20%. Chromosome separation was performed using the method of Schwartz and Cantor¹⁷ in 1% agarose, 0.5×TBE gels electrophoresed at 210 V for 22 h with a pulse frequency of 75 s in north-south and east-west directions. Following electrophoresis and staining in 1 µg ml⁻¹ of ethidium bromide, the gels were soaked in 0.25 M HCl for 1 h before transfer to nitrocellulose as described by Southern³¹. Hybridization under stringent conditions was performed using the nick-translated PstI fragment of clone 20. The strains are described in Fig. 1 legend. The numbering of the chromosomes is according to van der Ploeg et al.18, with chromosome 1 migrating at 700 kb and chromosome 6 at 2,000 kb.

parasite, resulting in the diverse karyotypes found in nature which could be of selective advantage in parasite survival. Although mechanistically this rearrangement may resemble the relocation of certain variable surface glycoprotein genes to telomeres in trypanosomes²⁴, the result of the K⁺ to K⁻ rearrangement is the loss of expression of a KAHRP gene. Analysis of these K⁺ to K⁻ mutations will provide an opportunity to determine the generality of chromosomal rearrangement in plasmodia and may yield insights into its mechanism.

This work was supported in part by grants to J.V.R. from the Rockefeller Foundation, the United Nations Development Programme-World Bank World Health Organization Special Programme for Research and Training in Tropical Diseases and US Army Contract DAMD17-85-C-5177. J.V.R. is a Pew Scholar and a recipient of an award from the Pew Scholars Program in the biomedical sciences, supported by the Pew Memorial Trust. L.G.P. is a fellow of the Schepp Foundation and supported in part by an Exxon Fellowship Training Grant in Molecular Biology. We thank Lex van der Ploeg for assistance with our PFG studies, Margaret Perkins, Lex van der Ploeg and Peter Model for critical reading of this manuscript, M. Samuels, H. Valsamis and A. Pavlovec for technical assistance, and Karen Yates and Mary Wentzler for secretarial assistance.

Received 28 January; accepted 23 April 1986.

- 1. Miller, L. H. Am. J. trop. Med. Hyg. 18, 860-865 (1969).

- Miller, L. H. Am. J. trop. Mea. Flyg. 18, 500-505 (1709).
 Barnwell, J. W., Howard, R. J. & Miller, L. H. Ciba Fdn Symp. 94, 117-136 (1983).
 Edington, G. M. Ann. trop. Med. Parasit. 48, 300-306 (1954).
 Trager, W., Rudzinska, M. A. & Bradbury, P. C. Bull. Wld Hith Org. 35, 883-885 (1966).
 Luse, S. A. & Miller, L. H. Am. J. trop. Med. Hyg. 20, 655-660 (1971).
 Udeinya, I. J., Schmidt, J. A., Aikawa, M., Miller, L. H. & Green, I. Science 213, 555-557 (1961).
- 7. Udeinya, I. J., Graves, P. M., Carter, R., Aikawa, M. & Miller, L. H. Expl Parasit. 56, 207-214 (1983).
- 8. Roberts, D. D. et al. Nature 318, 64-66 (1985).
- Leech, J. H., Barnwell, J. W., Miller, L. H. & Howard, R. J. J. exp. Med. 159, 1567-1575 (1984).
 Aley, S. B., Sherwood, J. A. & Howard, R. J. J. exp. Med. 160, 1585-1590 (1984).
 Schmidt, J. A. et al. J. clin. Invest. 70, 379-386 (1982).

- Kilejian, A. Proc. natn. Acad. Sci. U.S.A. 76, 4650-4653 (1979).
 Leech, J. H., Barnwell, J. W., Aikawa, M., Miller, L. H. & Howard, R. J. J. Cell Biol. 98, 1256-1264 (1984).
- 14. Ravetch, J. V., Feder, R., Pavlovec, A. & Blobel, G. Nature 312, 616-620 (1984).
- Hedrick, S. M., Cohen, D. I., Nielsen, E. A. & Davis, M. Mature 308, 149-153 (1984). Vernot-Hernandez, J.-P. & Heidrich, H.-G. Molec. Biochem. Parasit. 12, 337-350 (1984).

- 17. Schwartz, D. C. & Cantor, C. R. Cell 37, 67-75 (1984).
- 18. van der Ploeg, L. H. T. et al. Science 229, 658-660 (1985). 19. Kemp, D. J. et al. Nature 315, 347-350 (1985).
- Langsley, G., Hyde, J. E., Goman, M. & Scaife, J. G. Nucleic Acids Res. 11, 8"03-8717 (1983).
 Ravetch, J. V., Kochan, J. & Perkins, M. Science 227, 1593-1597 (1985).
- Trager, W. et al. Proc. natn. Acad. Sci U.S.A. 78, 6527-6530 (1981).
- Langreth, S. G. & Peterson, E. Infect. Immunity 47, 760-766 (1985)
 van der Ploeg, L. H. T., Schwartz, D. C., Cantor, C. R. & Borst, P. Cell 37, 77-84 (1984).
 Jensen, J. B. & Trager, W. Am. J. trop. Med. Hyg. 27, 743-746 (1978)
 Trager, W. & Jensen, J. B. Science 193, 673-675 (1976).

- Gritzmacher, C. A. & Reese, R. T. Science 226, 65-67 (1984).
 Bhasim, V. K. & Trager, W. Am. J. trop. Med. Hyg. 33, 534-537 (1984).
 Kochan, J., Perkins, M. & Ravetch, J. V. Cell 44, 689-696 (1986).
- Maxam, A. M. & Gilbert, W. Meth. Enzym. 65, 499-560 (1980).
 Southern, E. M. J. molec. Biol. 98, 503-517 (1975).
- 32. Goman, M. et al. Molec. Biochem. Parasit. 5, 391-400 (1982).

Long-range restriction site mapping of mammalian genomic DNA

William R. A. Brown & Adrian P. Bird

MRC Mammalian Genome Unit, King's Buildings, West Mains Road, Edinburgh EH9 3JT, UK

Molecular analysis of many problems in genetics would be facilitated by the ability to construct restriction site maps of long stretches of genomic DNA and to directly place genes on these maps. Pulsed-field gradient gel electrophoresis allows measurement of the size of DNA fragments up to at least 2,000 kilobase pairs (kb) long^{1,2} and we have used this technique here to map sites for one class of infrequently cutting restriction enzyme over a total of 1,500 kb of mouse genomic DNA. The sites for these enzymes tend to be clustered in the genome. These clusters may correspond to the short stretches of C+G-rich unmethylated DNA³ often associated with mammalian genes.

To construct long-range maps of genomic DNA, enzymes are needed which cut the DNA infrequently. Sites for enzymes which have a 6-base-pair (bp) recognition sequence composed entirely of inter-strand C·G base pairs and which include one or more CpG dinucleotides (C·G enzymes) are rare in the mammalian genome because the DNA is low in G+C and because the CpG dinucleotide occurs at only 20-25% of the frequency expected from base composition⁴. In addition, the CpG dinucleotide is often methylated at cytosine and this inhibits cleavage by many C · G enzymes (see Table 1). It occurred to us that cleavable sites for methylation-sensitive C·G enzymes should not be distributed randomly with respect to one another in mammalian DNA but should be concentrated in short stretches of genomic DNA called HTF islands³; this is predicted because HTF islands are 65% C+G, show no CpG suppression, and are unmethylated (see Table 1). As the rare inter-island sites are likely to be methylated and therefore resistant to cleavage, our calculations suggest that almost all cleavable sites for methylation-sensitive $C \cdot G$ enzymes will be in HTF islands. Two lines of evidence which support this prediction are shown in Fig. 1. When DNA of high relative molecular mass (M_r) is restricted with Nael, SacII or SmaI and analysed by pulsed-field gradient gel electrophoresis, the DNA in each digest is distributed from ~50 kb up to the limit of resolution, which in this experiment was at 650 kb; about 30% of the DNA in the sample was above this limit. The SacII recognition sequence (Table 1) includes two CpG dinucleotides while the recognition sequences for NaeI and SmaI contain only one, yet all three enzymes gave a similar distribution of fragments. This result suggests that these enzymes are cutting in regions of the genome which show no CpG suppression. The observation that the double and single digests all contained a similar distribution of fragments suggests that the sites for the different enzymes are close to one another.

The standard strategy for mapping of restriction sites in genomic DNA involves a series of single and double enzyme digests, gel electrophoresis, blotting and hybridization. In general, however, this technique does not work where the sites for different enzymes are clustered. An alternative mapping strategy is to regard a particular HTF island as a landmark and to use pulsed-field gel electrophoresis to measure the distance from sites in that known island to the flanking sites located tens or hundreds of kilobases away. We used this strategy to map about three HTF islands in the mouse genome. Two of these islands were isolated at random from genomic DNA³ and one was from the 5' end of the dihydrofolate reductase gene (dhfr)^{5,6}. Although our results were obtained using mouse DNA, this approach can be applied to the DNA of other mammals.

The first region of the genome studied was that which flanks island HTF 9. This island was isolated from mouse DNA³ and is known to be associated with transcripts that occur in several mouse tissues (P. Lavia, unpublished results). Island HTF 9 has two sites each for the enzymes NarI, SacII and SmaI and three sites for NaeI (Fig. 2a). We digested high- M_r DNA with each of the four enzymes. To check that the digest was complete at the sites within the island, we restricted an aliquot of each digest with EcoRI and, after conventional agarose gel electrophoresis, analysed the products with a probe which encompasses island HTF 9 (Fig. 2b). As no trace of the full-sized EcoRI fragment remained in any of the double digests, we concluded that each enzyme could cleave completely within island HTF 9. This check on digestion is necessary for the construction of an unambiguous map because Nael, Narl and Sacll show site-dependent heterogeneity in their reaction rates (see ref. 7 and below). We then fractionated DNA that had been digested with the infrequently cutting enzymes by pulsed-field gradient gel electrophoresis, and analysed the fractionated DNA by filter hybridization. The probes in this experiment flank island HTF 9, thus the size of any hybridizing restriction fragment localizes the restriction site with respect to the HTF island. The gels were run at a shorter pulse time than those shown in Fig. 1 to allow better resolution of the fragments of lower M_r . Analysis with the left-hand probe (Fig. 2c) revealed two hybridizing fragments in the Nael digest: a small weakly hybridizing fragment and a larger fragment close to the unfractionated DNA. The latter fragment was more accurately sized on a gel run at a longer pulse time, and measured ~375 kb (not shown). In addition, there was a NarI fragment of 140 kb, two SacII fragments (30 and 140 kb) and a weakly hybridizing SmaI fragment (140 kb). On the right-hand side of the island (Fig. 2d) we observed a NaeI fragment of ~105 kb and NarI, SacII and SmaI fragments each ~40 kb long. Together these results yield the restriction site map around island HTF9 shown in Fig. 2e. This map also indicates the estimated error in the restriction fragment sizes which we have measured from our data. A limitation of this sort of map is that it may be incomplete. Because we are making measurements about a single point, we are unable to map distal to sites which are cut to completion. A striking feature of the analysis shown in Fig. 2c is the presence of more than one hybridizing fragment in the NaeI and SacII digests, which means that although island HTF 9 is completely cleaved by these enzymes, it is flanked on one side by NaeI and SacII sites which are only partially cleaved. These sites are clustered with sites for other tested enzymes, thus they would be expected to represent uncharacterized HTF islands. A possible explanation is that the site-dependent kinetics of cleavage by NaeI and SacII⁷ is responsible for the partial cleavage. The possibility cannot be excluded, however, that incomplete cleavage is due to partial methylation at these sites. Whatever the cause, partial cleavage increases the amount of data from the experiments.

We have used the same strategy to construct long-range maps around island HTF 12 (Fig. 3) and the HTF island at the 5' end of dhfr (Fig. 4). Two technical points were important in the construction of the long-range maps (Figs 3e, 4e). First, island HTF 12 lacks any NarI sites and so we were unable to locate the ends of the 375-kb NarI fragment including island HTF 12.



Fig. 1 Pulsed-field gradient gel electrophoresis of high- M_r mouse DNA restricted with either NaeII, SacII or SmaI alone or in combination. The M_r markers are multimers of phage λ -cI857 DNA produced by annealing the cohesive ends in free soution (λ_n) .

Methods. For the preparation of high-M, DNA, BALB/c mouse thymocytes were encapsulated in agarose beads at a concentration of 5×10^7 per ml of beads¹¹. The beads, washed free of paraffin, were washed once in phosphatebuffered saline (PBS), once in Tris-EDTA buffer (TE: 10 mM Tris-HCl, 1 mM EDTA pH 7.5), then the nuclei were lysed with detergent by resuspending them at a concentration of 2×10^7 cells ml⁻¹ in 10 mM Tris, 0.05 M EDTA, 1% SDS pH 8.0 at room temperature, The suspension became like a jelly, presumably because of the release of DNA from cells at the periphery of individual beads, and so was thoroughly mixed by forcing it through the 2-mm orifice of a pipette. When the suspension of beads had become less viscous, the beads were washed twice in TE buffer and once in an EDTA/lauroyl sarcosine buffer (NDS: 0.5 M EDTA, 10 mM Tris-HCl, 1% lauroyl sarcosine pH 9.5) and finally resuspended in 2 vol. NDS. Proteinase K (Boehringer) was added to a final concentration of 500 µg ml suspension of beads was incubated at 55 °C for 48 h. This digest was then made to 50% (v/v) with glycerol and stored at -20 °C. For restriction enzyme digestion of DNA, beads were washed in TE buffer (pH 7.8) and residual proteinase K inactivated with 5 mM phenylmethylsulphonyl fluoride. The beads were restricted as follows: 120 µl of beads restricted with 15 U of NaeI in a total volume of 150 µl; 240 µl of beads restricted with 62 U SacII in a total volume of 300 µl; and 360 µl of beads restricted with 70 U SmaI in a total volume of 450 µl. These samples were incubated at the recommended temperature for 5 h, then washed in TE. The slurry of washed beads containing SacII-digested DNA was divided into two equally sized aliquots, one of which was digested with 14 U Nael. The slurry of beads containing Smal-digested DNA was subdivided into three equally sized aliquots, one of which was further restricted with 14 U NaeI and another with 50 U SacII. The second round of digests continued for 5 h and the beads were then washed and loaded onto the electrophoresis slots. An aliquot of washed beads (120 µl) was incubated for 10 h in restriction buffer at 37 °C as a control for nonspecific nuclease degradation. These beads were washed and loaded into the right-most well. The pulsed-field gradient gel electrophoresis chamber was based on the design of Carle and Olson² but was modified to take a 20×20 cm gel plate. Construction details may be obtained from W.R.A.B. The DNA sample to be fractionated was loaded into a well of dimensions $8 \times 2 \times 6.5$ mm. The total depth of the agarose gel was 7.5 mm. The agarose (Sigma type II; Medium EEO) concentration was 1.5% (w/v) and the electrophoresis buffer was 0.5 × TAE (TAE is 0.04 M Tris-acetate, 0.001 M EDTA). The run time in this experiment was 26 h, buffer temperature 8 °C, pulse time 30 s.

Second, we were unable to completely cleave the NarI site in the dhfr HTF island and so could not place the NarI sites which flank this gene. The consistent failure to cleave this particular NarI site may be the result of either-site-dependent heterogeneity in the reaction rate of this enzyme or partial methylation at this site. The former explanation is strongly supported by our finding that the same NarI site in a genomic clone of dhfr is not cleaved completely even in the presence of a 40-fold excess of enzyme (data not shown).

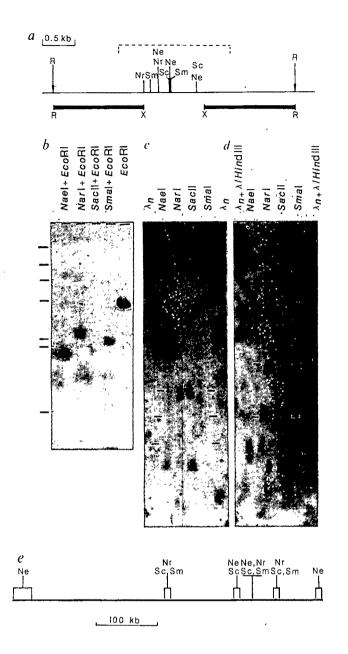


Fig. 2 Long-range mapping around island HTF9. a, Restriction site map of island HTF9. Ne, Nael; Nr, Narl; Sc, SacII; Sm, SmaI; X, XhoI; R, EcoRI. The probes used in the long-range mapping are indicated by the solid bars beneath the map. The broken line above the map indicates the extent of unmethylated DNA. b, Analysis of Nael, Narl, Sacli and Smal digestion at island HTF9. High-M, DNA that had either been restricted with Nael, Narl, Saell or Smal or incubated in restriction buffer without enzyme as described in Fig. 1 legend, was washed and restricted with EcoRI. Digests were fractionated by conventional 1% agarose gel electrophoresis and analysed using a 2.6-kb HindIII fragment including the whole island as a probe. The standards used in this gel were products of phage λ DNA restricted with HindIII. Some fragments are weaker than expected or undetectable on the blot because of their small size and also because low- M_r DNA fragments diffuse out of the beads during restriction and washing. The sizes of the restriction fragments seen in the digests were estimated as EcoRI 3.8 kb, NaeI+ EcoRI 1.8 kb, NarI+ EcoRI 2.5 kb, SacII+ EcoRI 1.8 kb and SmaI + EcoRI 2.2 kb. These values are consistent with each of the infrequently cutting enzymes cleaving at one or more of the respective sites in this island. c, Mapping to the left of island HTF 9. High-M, DNA restricted with Nael, Narl, Sacli or Smal was fractionated by pulsed-field gradient gel electrophoresis, transferred to GeneScreen Plus and analysed by hybridization using the left-hand Xhol-EcoRI fragment shown in a Conditions of electrophoresis: pulse time 22.5 s, run time 20 h, buffer temperature 18 °C; 300 V. d, Mapping to the right of island HTF 9. High-Mr DNA restricted and fractionated as described above was transferred to nitrocellulose and analysed by hybridization using the right-hand XhoI-EcoRI fragment shown in a. Conditions of electrophoresis: pulse time 8 4 s, run time 27 h, buffer temperature 8 °C, 300 V. The bars marked on the autoradiographs in c and d indicate the positions of the oligomers of phage λ cI1857 DNA run in the flanking tracks of these gels. The broken bars in d show the positions of the 23-kb fragment of a λ DNA/HindIII digest also run in the flanking tracks of this gel. The positions of these markers were determined by projecting the images of the ethidium bromide-stained gels onto the autoradiographs. e, Long-range map around island HTF 9. The map was constructed from the data shown in c and d and other similar experiments. In particular, there is a Nael site ~375 kb to the left of island HTF 9; this corresponds to a band towards the top of the NaeI track in the autoradiograph shown in a This band is beyond the markers on this particular gel and is not accurately sized at a short pulse time, therefore the size of this NaeI fragment was estimated from two other similar experiments in which the gel was run with a pulse time of 30 s. The error associated with fragment sizes is caused by the diffuseness of the hybridization signals. This uncertainty is indicated by the square brackets at the relevant restriction sites. The cluster of sites corresponding to HTF island 9 is underlined.

Methods. High-M, DNA was restricted with Nael, Narl, SacII or SmaI and analysed as described in Fig. 1 legend. The conditions of the pulsed-field gradient gel electrophoresis were chosen to optimize the resolution in the M_r range corresponding to the restriction site clusters. Filter transfer DNA from the pulsed-field gels was as follows: gels were incubated with gentle shaking in 0.25 M HCl for 40 min, rinsed in distilled water and incubated with gentle shaking in 0.5 M NaOH, 1.5 M NaCl for 60 min with one change. The gel was finally neutralized in 0.5 M Tris-HCl, 3 M NaCl pH 5.0 for 90 min with two changes. Transfer was done in $10\times$ SSC. Filters were hybridized to 20 ng of probe radiolabelled ¹³ to 2×10^9 c.p.m. μg^{-1} in a volume of 15 ml. GeneScreen Plus was hybridized according to conditions recommended by the manufacturer; nitrocellulose was hybridized in 5 × Denhardt's 5×SET, 0.1% SDS, 0.1% sodium pyrophosphate, 10% dextran sulphate at 65 °C. Filters were washed down to 0.2×SSC, 0.1% SDS, 0.1%

sodium pyrophosphate at 65 °C and autoradiographed for 2 weeks at -70 °C using an intensifying screen.

Table 1 Distribution of potential C-G endonuclease sites between bulk DNA and the HTF island fraction in mouse DNA

			m ⁵ C	No. of p sites per gen		Per cent sites	Sites per
Enzyme	Site	No. of CpGs	sensitivity*	Bulk DNA	Islands	in islands	island
Smal	CCCGGG	1	+	4.8	3.5	42	1.2
NaeI	GCCGGC	, 1	+	4.8	3.5	42	1.2
NarI	GGCGCC	1	+	4.8	3.5	42	1.2
SacII	CCGCGG	2	+	1.2	3.5	74	1.2

For the calculation of number of sites per haploid genome, we took the base composition of bulk DNA as 40% G+C, the CpG deficiency as 25% of the expected level, and the haploid genome size as 3×10^9 bp. HTF islands were assumed to comprise 1% of genomic DNA, to have a base composition of 65% G+C, and to show no deficiency of CpG.HTF islands of 500 to 2,000 bp have been found in mouse DNA, so for the purpose of calculation an average length of 1,000 bp has been assumed; this implies that there are 3×10^4 HTF islands per haploid genome and that they occur on average every 100 kb. The values for the number of sites in bulk DNA refer to the number of potential sites and do not take into account the effect of cytosine methylation which reduces the number of sites that can be cleaved by the enzyme.

* SmaI is a C·G enzyme which was known to be inhibited by methylation but nothing was known about the effects of methylation on the cleavage by other C·G enzymes. We tested NaeI, NarI and SacII by attempting to cleave the ribosomal DNA of Xenopus laevis either isolated in a molecular clone or in the sperm genome. Sequence data⁹ indicated that there are many sites for each of these enzymes within the untranscribed spacer of the ribosomal DNA and these could be cleaved in the molecular clone. The rDNA in sperm is 97% methylated at CpG (ref. 10) and was largely refractory to cleavage (not shown), thus we concluded that these enzymes are inhibited greatly by cytosine methylation.

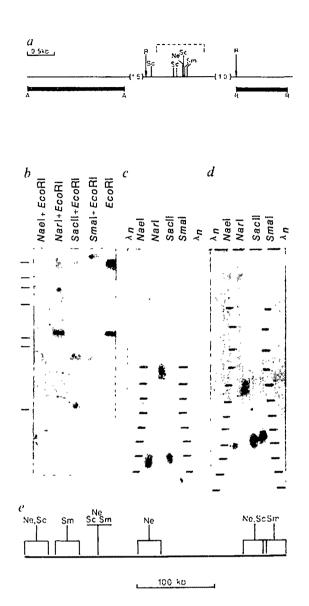


Fig. 3 Long-range mapping around island HTF 12. a, Restriction site map of island HTF 12. The probes used in the analysis shown in c and d are indicated by the bars beneath the map. The left-hand probe is an AccI fragment (abbreviated A). The right-hand probe is an EcoRI fragment. The broken lines indicate the extent of unmethylated genomic DNA. b, High-M, DNA either restricted with Nael, Narl, Sacll or Smal or incubated in restriction buffer without enzyme, was washed and EcoRI-restricted. Digests were analysed after conventional agarose gel electrophoresis using the central EcoRI fragment shown in a as a probe. Markers were the products of λ DNA restricted with HindIII. The sizes of the restriction fragments seen in the digests were estimated as (kb): EcoRI 2.45, Nael+ EcoRI 1.76, Narl+ EcoRI 2.53, SacII + EcoRI 1.7, Smal+ EcoRI 1.7. These values are consistent with Nael, SacII and Smal cleaving once within the island. c, Mapping to the left of island HTF 12. High-M_r DNA restricted with either Nael, Narl, Saell or Smal was fractionated by pulsed-field gradient gel electrophoresis and analysed by filter hybridization using the left-hand AccI fragment shown in a. Electrophoresis conditions: pulse time 30 s, run time 23 h, buffer temperature 15 °C, 300 V. d, Mapping to the right of island HTF 12. High-M_t DNA restricted and fractionated as above was analysed by filter hybridization to the right-hand EcoRI fragment. The electrophoresis conditions were as described for c. The bars on the autoradiographs show the positions of the oligomers of phage λ c1857 DNA run in the flanking tracks of these gels. e, Long-range map around island HTF 12. Construction details are given in Fig. 2 legend. The cluster of sites corresponding to island HTF 12 is underlined. Methods were as described in Fig. 2 legend except that all DNA samples were from within a single set of digestions and all filters were GeneScreen Plus

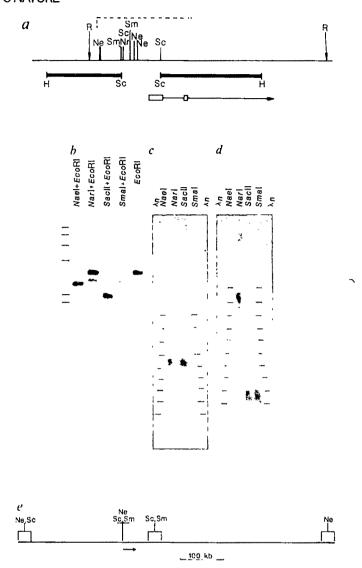


Fig. 4 Long-range mapping around the mouse dihydrofolate reductase gene (dhfr). a, Restriction site map of the HTF island at the 5' end of dhfr. The positions of the probes used in the analysis illustrated in b-d are indicated by the bars beneath the map. Also shown is the 5' end of the primary transcript. The first two exons are boxed. The broken lines above the map indicate the extent of unmethylated genomic DNA. H, HindIII. b, High-M. DNA either restricted with Nael, Narl, SaclI or Smal, or incubated in restriction buffer without enzyme, was washed and restricted with EcoRI. Digests were analysed after conventional agarose gel electrophoresis using the right-hand SacI-HindIII fragment shown in a as a probe. The products of phage λ DNA restricted with HindIII served as markers. The fragment sizes are as follows (kb): EcoRI 3.33, NaeI+ EcoRI 2.82, NarI+ EcoRI 3.33 and 2.93, SacII+ EcoRI 2.24, SmaI+ EcoRI 2.82. These values indicate that NaeI, SacII and SmaI all cleaved within this HTF island. The presence of an intact EcoRI fragment in the EcoRI + NarI double digest indicates that NarI did not cut completely in this island; this was also seen in a second experiment. c, Mapping to the left of dhfr. High-M, DNA restricted with either Nael, Narl, Sacll or Smal was fractionated by pulsed-field gradient gel electrophoresis and analysed by filter hybridization using the left-hand SacII-HindIII fragment described in a. Electrophoresis conditions: pulse time 30 s, run time 22 h, buffer temperature 16 °C, 320 V. d, Mapping to the right-hand side of dhf. High-M, DNA restricted and fractionated as above was analysed by filter hybridization using the right-hand SacII-HindIII fragment illustrated in a. Electrophoresis conditions: pulse time 30 s, run time 23 h, buffer temperature 15 °C, 300 V. The bars on the autoradiographs show the positions of the oligomers of phage λ c1857 DNA run in the flanking tracks of these gels. e, Long-range map around dhfr. The map was constructed on the basis of the data shown in c and d. The left-hand SmaI site was not mapped because a possible hybridizing fragment was obscured by a scratch on the autoradiograph shown in d. In a second experiment the Smal digest was only partially complete at the dhfr HTF island. The position of the 34-kb dhfr primary transcript is indicated by the arrow. The cluster of sites corresponding to the dhfr HTF island is underlined. DNA samples were all from within a single set of digests and all filters were GeneScreen Plus. For other details see Fig. 2 legend.

In the present study we have used pulsed-field gradient gel electrophoresis to map cleavable sites for the enzymes Nael, NarI, SacII and SmaI over ~1.5 million base pairs of the mouse genome. As predicted, the sites available for cleavage by these enzymes (in other words, non-methylated sites) occur in clusters which correspond to regions rich in non-methylated CpG. Additional recognition sites for the enzymes are present outside clusters but most of the potential sites in these regions are probably not cleaved because they are methylated. Making the assumption that sites of cleavage by more than one enzyme represent HTF islands, the average distance between islands in the mapped region is 109 kb (mean of seven values). The average distance between islands has been indirectly estimated as 100 kb (ref. 3), which agrees quite well with the present value. It is clear, though, that variation about the mean is considerable.

CpG-rich islands have now been found in association with many genes (reviewed in ref. 8), and it is likely that a high proportion of the 30,000 or so HTF islands are gene-associated. As many genes with HTF islands are already available as molecular clones, it will be possible to use the strategy of mapping from HTF islands to tackle a variety of longrange mapping problems. Moreover, the putative HTF islands identified by the map data may lead directly to new genes.

We thank Chris Tyler-Smith and Howard Cooke for comments on the manuscript, Patrizia Lavia and Donald Macleod for access to unpublished data, Jean Scott for a cosmid containing the 5' end of dhfr and Anne Deane for typing the manuscript.

Received 13 February; accepted 23 April 1986.

- Schwartz, D. C. & Cantor, C. R. Cell 37, 67-75 (1984).
 Carle, G. F. & Olson, M. V. Nucleic Acids Res. 12, 5647-5664 (1984).
- 3. Bird, A. P., Taggart, M., Frommer, M., Miller, O. J. & Macleod, D. Cell 40, 91-99 (1985).
- Swartz, M. N., Trautner, T. A. & Kornberg, A. J. biol. Chem. 237, 1961-1967 (1962).
 Tykocinski, M. L. & Max, E. C. Nucleic Acids Res. 12, 4385-4396 (1984).
- Crouse, G. F., Simonsen, C. C., McEwan, R. N. & Schimke, R. T. J. biol. Chem. 257, 7887-7897 (1982).
- 7. New England Biolabs Cat. (1985-86)
- 8. Bird, A. P. Nature 321, 209-213 (1986).
- Moss, T., Bosely, P. G. & Birnstiel, M. L. Nucleic Acids Res. 8, 467-485 (1980).
- 10. Macleod. D. & Bird, A. P. Nature 306, 200-203 (1983).
- 11. Cook, P. R. EMBO J. 3, 1837-1842 (1984).
- Southern, E. M. J. molec. Biol. 98, 503-517 (1975). 13. Feinberg, A. P. & Vogelstein, B. Analyt. Biochem. 132, 6-13 (1983).

Primary sequence of a dimeric bacterial haemoglobin from Vitreoscilla

S. Wakabayashi*, H. Matsubara* & D. A. Webster†

- * Department of Biology, Faculty of Science, Osaka University, Toyonaka, Osaka 569, Japan
- † Department of Biology, Illinois Institute of Technology, Chicago, Illinois 60616, USA

Vitreoscilla, a filamentous bacterium in the Beggiatoa family, synthesizes a soluble haemprotein which has two identical subunits of relative molecular mass 15,775 and two b haems per molecule¹. It is synthesized in relatively large quantities when the organism, a strict aerobe, is grown under hypoxic conditions². It forms a relatively stable oxygenated form which is spectrally similar to oxymyoglobin (oxyHb) and oxyhaemoglobin (oxyHb)3. The amino acid sequence of this protein has been determined and aligned to fit the helical regions of several animal and plant globins. This alignment is consistent with its being a structural homologue of the eucaryotic haemoglobins although it diverged from the others in the N-terminal region and may lack an A-helix. It showed the maximum sequence homology (24%) with lupin leghaemoblobin (Lb). Vitreoscilla Hb is the first bacterial haemoglobin to be sequenced. It may function to enable the organism to survive in oxygen-limited environments by acting as an oxygen storage-trap or to facilitate oxygen diffusion.

Partially purified preparations of this Vitreoscilla haemprotein, which was previously called soluble cytochrome o, contained NADH-cytochrome o reductase activity, exhibited slow turnover of the NADH, oxygen consumption, and it was presumed that this protein functioned as a soluble terminal oxidase³. An oxygenated form detectable in these preparations was subsequently observed to be the predominant species of the protein present in intact cells of the bacterium during aerobic respiration⁴. The latter result and more recent experiments have provided evidence against the function of this protein as an oxidase. A true membrane cytochrome o was identified by photolysis of CO-liganded intact cells at −100 °C and eventually purified, and a cytochrome d was also identified. The need for a soluble oxidase in the presence of these established membrane terminal oxidase became even less evident. When the CO-compound of the protein was photodissociated with a dve laser in the presence of oxygen, or when the oxygenated compound itself was photodissociated, recombination with oxygen occurred with no evidence of oxidation of the heme iron? is in contrast to results expected for a terminal oxidase and observed for cytochrome c oxidase but similar to what is observed for oxygen binding proteins like haemoglobin and myoglobin9. An infrared spectroscopic study of the stretch band for oxygen liganded to the heme iron showed that the absorption band was similar to those observed for oxymyoglobins and oxyhaemoglobins, evidence for a similar bent-end-on oxygenyltype bonding¹⁰. Finally, the results reported here show that the amino acid sequence has considerable homology with that of yellow lupin Lb II. Consequently, we have reconsidered the role of this protein as a terminal oxidase and now propose that it is a haemoglobin-like protein which will accordingly be called Vitreoscilla Hb hereafter.

A summary of the sequence analysis of Vitreosculla Hb is shown in Fig. 1. It consists of 146 amino-acid residues with a calculated relative molecular mass of 15,775 for the aposubunit, somewhat larger than the 13,000 estimated previously by SDS polyacrylamide gel electrophoresis¹. The sequence of the carboxymethylated protein was determined using trypsin and Staphylococcus V8 protease digestion, separation of peptides by HPLC on an ODS column, and manual and automated solidphase Edman degradations^{11,12}. The only technical difficulty that was encountered was in deducing the sequence near the C-terminus of the polypeptide chain.

Carboxypeptidase Y released alanine, leucine, valine, glutamate, and several other amino acids from the carboxymethylated protein, but no peptide with these amino acids as C-terminus was isolated. The C-terminal tryptic peptide, T-11, which could not be recovered from the HPLC column, was obtained by precipitating the digest with dilute acetic acid and although impure was successfully sequenced, but the C-terminal amino acid could not be determined because again carboxypeptidase Y digestion released many amino acids. Chymotryptic digestion of peptide T-11 gave three peptides, and their amino-acid compositions were in agreement with the sequence of T-11. Curboxypeptidase Y digestion of peptide C-3 released a small amount of glutamic acid. Since glutamic acid does not fit the cleavage site specificity of either trypsin or chymotrypsin we assigned peptide C-3 to be the C-terminal peptide of the cytochrome. Although Vitreoscilla Hb is the first bacterial haemoglobin to be sequenced, a soluble Rhizobium haemoglobin has been reported in free-living (cultured) cells of Rhizobium that is unrelated to Lb and has about the same molecular size as Vitreoscilla Hb13

The sequence of Vitreoscilla Hb is aligned for comparison with other haemobins in Table 1. It shows the greatest sequence homology with lupin Lb14. The final alignment shown was obtained from the initial computer alignment by positioning hydrophobic residues at the approximately thirty sites where internal hydrophobic residues are conserved in the normal globin structure¹⁵. This was accomplished with several

		Table 1	l Alignn	nent and s	equence	compari	son of Vitre	oscilla Hb with	several anim	nal and pla	int haemo	globins.			
Residue	. Helix			Haemog	lobin		***************************************	Residue	Helix			Haemog	lobin		
no. (R)	posn (H)	HΗbα	нньβ	SWMb	GHb	LLb	VHb	no. (R)	posn (H)	HΗbα	ннь <i>в</i>	SWMb	GHb.	LLb	VHb
1. 2 3 4 5 6 7 8 9 10 11 12 13 14 15 16 17	NA1 NA2 A1 A2 A3 A4 A5 A6 A7 A8 A9 A10 A11 A12 A13 A14 A15	V L S P A D K T N V K A A W G K V S	V H L T P E E K S A V T A L W G K V	V L S E G E W Q L V L H V W A K V D	GLSAAQRQVIAATWKDI	GALTES QAALVKS SWEEFN	M**DQQTINII)	84 85 86 87 88 89 90 91 92 93 94 95 96 97 98 99	EF2 EF3 EF4 EF5 EF6 EF7 EF8 F1 F2 F3 F4 F5	D DM PN ALS ALS DLH	D NLKGTFATLSELH:	K GHHEAELKPLAQSH	GDEGKMVAEMKAVGVRH:	VTGVVASDATLKNLGSVH:	NLPA*ILPAVKKI†AVK**
19 20 21 22 23 24 25 26	A16 AB1 B1 B2 B3	G A H A G	N V D	E A D V A	A G N D N G A	A N I P	K A* T V . P*	102 103 104 105 106 107 108	F9 F10 FG1 FG2	A H K L	C D K L	Á T K H	K G Y G D K H	V S K G	K H* C Q A G*
26 27 28 30 31 32 33 34 35 36 37 38 39 40 41 42 43 44 45 46 47 48 49 50 51 52 53 55 56 67 67 77 78 77 77 78 77 77 78 77 77 77 78 77 77	B4 B5 B6 B7 B8 B9 B10 B11 B12 B13 B14 B15 C1 C2 C3 C4 C5 C6 C7 CD1 CD2 CD3 CD4 CD5 CD5 CD6 CD7 D2 D3 D4 D5 D6 D7 E12 E13 E14 E15 E16 E17 E18 E17 E18 E18 E18 E18 E18 E18 E18 E18 E18 E18	GEYGAEALERMFLSFPTTKTYFPHF DLS HGSAQVKGHGKKVADALTNAVAHV	SEV G G E A L G R L L V V Y P W T Q R F F E S F G D L S T P D A V M G N P K V K A H G K K V L G A F S D G L A H L	*GHGQDILIRLFKSHPETLEKFDRFKHLKTEAEMKASEDLKKHGVTVLTALGAILKK	AGVGKDCLIKHLSAHPEMAAVFG FSG AS DPAVADLGAKVLAEIGVAVSHL	KHTHRFFILVLEIAPAAKOLFS FLKG TSEVPQNNPELQAHAGKVFKLVYEAAIQLE	· VLKEHGVTITTTFYKNLFAKHPEVR PLFDMGRQESLEQPKALAMTVLA***	109 110 111 112 113 114 115 116 117 118 119 120 121 123 124 125 126 127 128 129 130 131 132 133 134 135 136 137 138 139 140 141 142 143 144 145 146 147 148 149 150 151 152 153 154 155 156 157 158 159 160 161 162 163 164 165	FG4 G1 G2 G3 G4 G5 G10 G11 G13 G14 G15 G16 G17 G18 G19 G11 G13 G15 G16 G17 G18 G19 G11 H12 H11 H12 H11 H12 H11 H11 H12 H11 H12 H11 H12 H11 H12 H12	NV DPV NFKLLSHCLLVTLAAHLPAEFTPAVHASLDKFLASVSTVLTSKYR	"V D P E N F R L L G N V L V C V L A H H F G K E F T P P V Q A A Y Q K V V A G V A N A L A H K Y H	AIPIKYLEFISEAIIHVLHSRHPGNFGADAQGAMNKÄLEUFRKDIAAKYKELGYQG	HY-KGEYFEPLGASELSAMEHRIGGKMD~AAKDAWAAAYADTSGALISGLES:	VADAHFPVVKEAILKTIKEVVGAKWSEELNSAWTIAYDELAIVIKKEMDDAA .	·VAAAAHYPI.VGQELLGAIKEVLGDAATDDILDAWGKAYGVIADVFIQVEADLYAQAVE

R is an arbitrary residue number with the numbering beginning from the N-terminal of the globins with the longest N-terminal extension. H refers to the helix position in sperm whale myoglobin. The haemoglobins are: HHB α , human α -chain; HHb β , human β -chain; SWMb, sperm whale myoglobin; GHb, Glycera haemoglobin; LLb, lupin leghaemoglobin; VHb, Vitreoscilla haemoglobin. Sequence data for the first five proteins were taken directly from ref. 14, omitting three residues which were each inadvertently entered twice in the sequence for LLb presented there.

* Residues in Vitreoscilla Hb that match those in lupin Lb.
† Conserved, buried hydrophobic residues²³.

Fig. 1 Sequence analysis of Vitreoscilla Hb. T-, V- and C- refer to tryptic, Staphylococcus V8 protease and chymotryptic peptides, respectively. Arrows above the residues at N-terminal regions indicate the results of N-terminal sequence analysis of the apoprotein. Arrows (\rightarrow) , (\rightarrow) and (\leftarrow) show automated solid-phase (DITC method) Edman degradation, manual Edman degradation, and carboxypeptidase Y digestion, respectively. Dotted arrows indicate ambiguous identifications (---) or unrecovered residues by the solid-phase method (\rightarrow) .

25 T-2 ----Ash-Leu-Phe-Alc-Lys-His-Pro-Glu-Yol-Arg-Pro-Leu-Phe-Ash-Yet-Gly-Arg-Glg-Glu-Ser-Leu-Glu-Cir-Cit-Lys-Lu------65 70 75 3 3 Vol-Leu-Aig-Aig-Aig-Aig-Ain-Asn-fle-Gig-Asn-Leu-Pro-Aig-fle-Leu-Pro-Aig-7g1-Lys-Lys-Lys-Lie-2,5-4g,-4,5-4,-7,-7 ÷..... 133 105 -13 95 Alg-Alg-Alg-Mis-Tyr-Pro-He-Vol-Gly-Gln-Glu-Leu-Leu-Gly-Alg-He-Lys-Glu-Vol-Leu-Gly-No (A.S.). Tre-T-9 7-11 C-1 C-2

exceptions which are probably not important (Glu at G11 and Ser at E4). The final alignment has His at F8, the proximal ligand, and the invariant Phe at CD1. The usual residue at E7, His, the distal ligand, is replaced by Gln, which has been observed in the α -chain of opossum Hb and would also be capable of forming a hydrogen bond with the bound oxygen. There are 35 matches with the 153 residues of the lupin legHb. a 24% identity per length. The number of identical residues among these various globins is given in Table 2. Note that the number of identical residues between sperm whale Mb and

Table 2 Identical residues matrix: the number of matching amino acid residues among the sequences of the globins in Table 1

	HHbα	НΗЬβ	SWMb	GHb	LLb
$HHb\alpha$					
$HHb\beta$	60				
SWMb	38	33			
GHb	30	29	32		
LLb	23	23	26	23	
VHb	16	16	14	20	34

human Hb chains is approximately the same as that between Vitreoscilla Hb and Lb, which is indicative of significant homology. In addition to the identical matches there are 20 similar residue matches, such as Glu/Asp, Ser/Thr, Leu/Val/Ile, Phe/Tyr, and roughly another twenty 'neutral' matches. The N-terminal region of the Vitreoscilla Hb does diverge from the other globins listed in Table 1, and the A-helix appears to be incomplete or lacking.

It is premature to speculate whether Vitreoscilla Hb shares a common evolutionary ancestor with the plant and animal haemoglobins or is the product of convergent evolution. We found no notable sequence homology between Vitreoscilla Hb and various cytochromes by computer analysis. Some observed similarities in the primary sequences of various globins and b-type cytochromes led Runnegar to propose that all globins are monophyletic, the common ancestor being a b-type cytochrome¹⁶. The existence of bacterial haemoglobins implies that this common ancestor would have to be a bacterial b-type cytochrome.

The following observations relate to the function of Hb in Vitreoscilla. The cellular haem content is dependent on the dissolved oxygen in the growth medium and increases about 50-fold when the oxygen concentration falls below about 10% atmospheric²; most or all of this is due to an increase in the Vitreoscilla Hb17. Species in this genus tend to live in oxygenpoor environments such as stagnant ponds and decaying veget-

able matter18, they are unable to ferment sugars, and their metabolism appears limited to aerobic oxidation of amino acids¹⁹. An adaptation to hypoxic conditions by increasing the concentration of terminal oxidases in the cellular membrane is unlikely because enzymatically active membranes, which include chloroplast, inner mitochondrial, and bacterial cell membranes, already have a protein to lipid ratio of around 3:1. in contrast to a ratio of roughly 1:1 for most animal cell membranes²⁰. An increase in membrane terminal oxidase would likely result in destabilization of the membrane. On the other hand, the concentration of haemoglobin in erythrocyte cytoplasm is more than 80% that of the crystalline protein²¹. Thus, the concentration of Hb could increase to very high concentrations in Vitreoscilla cytoplasm, without adversely affecting its normal metabolism, where it could then function as an oxygen storagetrap to enable the organism to survive in oxygen poor environments. Alternatively, if it were localized near the bacterial plasma membrane it could function to facilitate oxygen diffusion to the membrane terminal oxidases²². Perhaps primitive haemoglobin first appeared to play a similar role during the evolution of aerobic respiration.

The authors are indebted to Drs Russell, F. Doolittle and Peter E. Wright for invaluable assistance with the sequence homologies. Most of this work was done while D.A.W. was on a sabbatical leave in Japan supported by US NSF grant INT-8212086. Partial support also came from the US PHS NIH grant GM27085.

Received 9 January; accepted 9 May 1986

- 1. Tyree, B. & Webster, D. A. J. biol Chem. 253, 6988-6991 (1978).
- Tyree, B. & Webster, D. A. J. tool Chem. 253, 0588-0591 (1978).
 Boerman, S. & Webster, D. A. J. Gen. appl. Microbiol. 28, 35-43 (1982)
 Webster, D. A. & Liu, C. Y. J. biol. Chem. 249, 4257-4260 (1974).
 Webster, D. A. & Orii, Y. J. biol. Chem. 252, 1834-1836 (1977).
- DeMaio, R. A., Webster, D. A. & Chance, B. J. biol. Chem. 258, 13768-13⁻¹ (1983) Webster, D. & Georgiou, C. Fedn Proc. 44, 1780 (1985).

 Orii, Y. & Webster, D. A. J. biol. Chem. 261, 3544-3547 (1986).

- Orii, Y. J. biol. Chem. 259, 7187-7190 (1984). McCray, J. A. Biochem. biophys. Res. Commun. 47, 187-193 (1972)
- Choc, M. G., Webster, D. A. & Caughey, W. S. J. biol. Chem. 257, 865-869 (1982)
 Wakabayashi, S., Matsubara, H., Kim, C. H. & King, T. E. J. biol. Chem. 257, 9315-9344
- 12. Minami, Y., Wakabayashi, S., Imoto, S., Ohta, Y. & Matsubara, H. J. Biochemistry (Tokus) 98, 649-655 (1985). Appleby, C. A. Biochim. biophys. Acta 172, 88-105 (1969).
- 14. Lesk, A. M. & Chothia, C. J. molec, Blol. 136, 225-270 (1980) 15. Perutz, M. F., Kendrew, J. C. & Watson, H. C. J. molec. Biol. 13, 669-678 (1965)
- Runnegar, B. J. Molec. Evol. 21, 33-41 (1984).
- 17. Lamba, P. & Webster, D. A. J. Bact. 142, 169-173 (1980).
- Pringsheim, E. G. J. gen. Microbiol. 5, 124-149 (1951).
- Mayfield, D. C. & Kester, A. S. J. Bact. 112, 1052-1056 (1972).
 Guidotti, G. An. Rev. Biochem. 41, 731-752 (1972).
- 21. Stryer, L. in Biochemistry, 847 (Freeman, San Francisco, 1975).
- Wittenberg, J. A., Bergensen, F. J., Appleby, C. A. & Turner, G. I. 1 birl Chem. 249, 4057-4066 (1974). 23. Pritsyn, O. B. J. molec. Biol. 88, 287-300 (1974).

Homology between IgE-binding factor and retrovirus genes

THE recent report by Toh et al.1 of sequence homology between segments of a cloned gene encoding rodent IgE-binding factor (IgE-BF)² and a gene encoding Syrian hamster intracisternal Aparticle (IAP)³ is an intriguing observation. However, we must express reservations about Toh et al.'s interpretations of the observed homology.

First, the authors claim that because the N-terminal third of the IgE-BF coding sequence shows no homology with their particular IAP gene, the IgE-BF gene must be "a hybrid gene which evolved...by integrating genes of viral origin". No evidence is presented by either Toh et al. or Martens et al.2 in support of the authors' assertions that the cloned IgE-BF gene is a hybrid gene or that it even contains a portion of a non-IAP gene at all. Neither report presents any genomic blot data to indicate whether homologous genes exist in the mouse or rat genomes. Here, the conclusions of Toh et al. are considerably weakened by the fact that their sequence comparison crosses species lines; they really have no justification for making any statement regarding the nature of IgE-BF sequences which do not show homology to their hamster IAP sequence. Thus, their assertion that the N-terminal third of the IgE-BF amino-acid sequence is unique to IgE-BF is speculative and not supported by their data.

The IgE-BF clone was derived by Martens et al. from a rat-mouse T-cell hybridoma. Toh et al. do not mention the possibility that the IgE-BF clone could represent a hybridoma-related recombination event, as opposed to an evolutionarily significant insertion of a retroviral-related sequence into "a cellular DNA region proximal (sic) to a primordial IgE-BF gene". Observations suggesting such an alternative explanation exist in the literature⁴⁻⁶. These data all demonstrate that in the mouse genome, IAP genes are mobile elements which can affect the expression of unrelated genes. Toh et al. overlooked the possibility that the structure of the cloned IgE-BF gene could have arisen by insertion (in the hybridoma) of an IAP sequence distal to the IgE-BF coding sequence, followed by transcription of this region and splicing of the "'IgE-BF', gag and pol" sequences. In view of this possibility, it is important to stress that the IgE-BF clone is a complementary DNA, rather than a genomic clone; Toh et al. make inferences of considerable import about the structure and evolution of a putative genomic gene from sequence comparisons involving only a cDNA clone.

Taken together, the arguments outlined above also cast doubt on the statement of

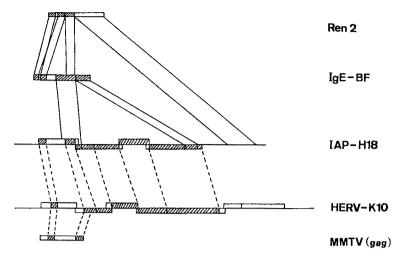


Fig. 1 Profiles of sequence homology of IgE-BF cDNA to mouse (Ren 2) and hamster (H-18) IAPs, human endogenous retrovirus (HERV-K10) and MMTV gag. Homologous regions are indicated by slanted lines. Regions where homologies exist at the DNA level and at the protein level are connected by vertical straight lines and dotted lines, respectively.

Toh et al. that a particular proteolytic cleavage of the precursor IgE-BF is more likely than another to generate the 11K (relative molecular mass 11,000) IgE-BF from the 60K species.

Thus, we believe that while the observations of Toh et al. are of interest, conclusions about their possible significance are speculative, and certainly premature in the absence of any experimental data examining the relationship of IgE-BF to IAP. A preliminary report of the homology of IgE-BF to mouse IAP genes appeared earlier, but was not cited by Toh et al.

KEVIN W. MOORE CHRISTINE L. MARTENS

Department of Immunology. DNAX Research Institute of Molecular and Cellular Biology, Palo Alto,

California 94304, USA

- 1. Toh, H., Ono, M. & Miyata, T. Nature 318, 388-389 (1985). Martens, C. L. et al. Proc. natn. Acad. Sci. U.S.A. 82, 2460-2464 (1985).
- Ono, M., Toh, H., Miyata, T. & Awaya, T. J. Virol. 55, 387-394 (1985).
- 4. Hawley, R. G., Shulman, M. J., Murialdo, H., Gibson, D. M. & Hozumi, N. Proc. natn. Acad. Sci. U.S.A. 79, 7425-
- 5. Kuff, E. L. et al. Proc. natn. Acad. Sci. U.S.A. 80. 1992-1996
- Kuff, E. L. et al. Nature 302, 547-548 (1985).
- 7. Martens, C. et al. in Immune Regulation (eds Feldmann, M. & Mitchison, N. A.) 121-130 (Humana, Clifton, New Jersey, 1985).

MIYATA ET AL. REPLY-We have shown previously1 that the IgE-BF cDNA from a rat-mouse T-cell hybridoma² exhibits a strong sequence homology to the Syrian hamster IAP3 at the nucleotide level in the 3' two-thirds of the protein-coding region, whereas the remaining 5' one-third shows obvious homology. This

homologous region of the IgE-BF cDNA, however, shows sequence homology to a mouse IAP (Ren 2)4 at the DNA level, but not to a distantly related human endogenous retrovirus, HERV-K10 (M.O. et al., in preparation) or to a mouse mammary tumour virus (MMTV)⁵ gag region, both of which share obvious homology with the hamster IAP at the protein level (Fig. 1). Moore et al.6 recently demonstrated sequence homology of the IgE-BF cDNA to mouse IAPs, represented by MIA14, over its entire regions. These results suggest that the nucleotide sequence corresponding to the 5' third of the IgE-BF coding region is unique to mouse IAPs or their close relatives. This unique region might have been derived very recently from a distantly related retrovirus or an endogenous retrovirus by a recombination mechanism, or from a primordial IgE-BF gene of cellular origin, as suggested previously1.

TAKASHI MIYATA HIROYUKI TOH

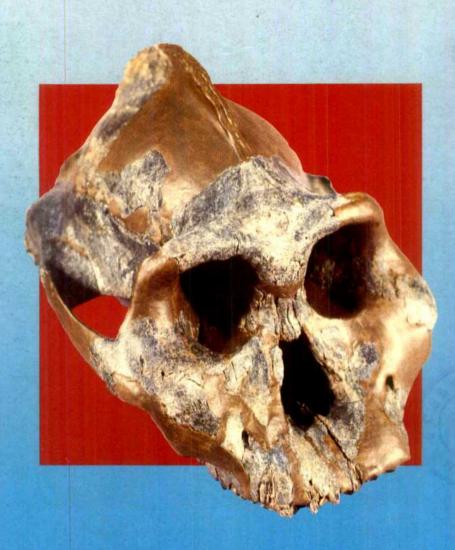
Department of Biology, Faculty of Science, Kyushu University, Fukuoka 812, Japan

MASAO ONO Department of Molecular Biology, School of Medicine, Kitasato University, Kanagawa 228, Japan

- 1. Toh, H., Ono, M. & Miyata, T. Nature 318, 388-389 (1985). Martens, C. L. et al. Proc. natn. Acad. Sci. U.S.A. 82, 2460-2464 (1985).
- Ono, M., Toh, H., Miyata, T. & Awaya, T. J. Virol. 55, 387-394 (1985).
- Burt, D. W., Reith, A. D. & Brammar, W. J. Nucleic Acids Res. 12, 8579-8593 (1984).
- Fasel, N. et al. Nucleic Acids Res. 11, 6943-6955 (1983).
 Moore, K. W. et al. J. Immun. 136, 4283-4290 (1986).

Volume 322 No.6079 7-13 August 1986 £1.90

Entered 29,1.87



EARLY HOMINID PHYLOGENY

IVIASSION The new force in bi

ZetaPrep® Technology. Engineered for mass ion exchange. Powered with a unique solid matrix. Thrusting you in to a new age of upstream purification. Boosting mass flow and volume flow with results that outdate every other known separation method. Giving you quantum savings in time and money.

Unique solid matrix!

Designed for highly efficient, ultrafast extraction of proteins, peptides and enzymes, the ZetaPrep solid matrix comes in a cartridge that's completely self-contained. With its unique, multi-directional radial flow, this patented rigid format offers optimal surface area for rapid bulk binding, plus the strength to withstand high flow rates.

All ZetaPrep housings and cartridges are completely sterilizable and compatible with standard equipment. Shown here is the ZetaPrep 100 for laboratory separations.

Economics you just can't ignore!

Capable of one-step puri-

fication and concentration with up to 80% purity or more, ZetaPrep will slash your production costs to a fraction of what they are today. Because ZetaPrep is so easy to operate, simple to automate and efficient in use, you'll cut expensive man hours to a minimum.

ZetaPrep's incredible flow lets you radically reduce total processing time. Gets you fast binding, wash and elution flow rates. And at least 10 times higher throughput. With no more packing problems. No more fines removal. Just all the benefits of a totally enclosed system—and yields that are truly astounding.

Amazing scale-up potential

LKB's comprehensive range of ZetaPrep cartridges and Multi-Cartridge Systems lets you select different sizes, extend in series or even couple in parallel for virtually unlimited flow rate and process capacity. With DEAE, QAE and SP functional groups, you can now exploit this amazing scale-up potential from lab, through pilot to fullscale industrial production. In biotechnology, pharmaceuticals or any other process that needs cost-effective purification of proteins and biopolymer products.



nature

NATURE VOL. 322 7 AUGUST 1986





EARLY HOMINID PHYLOGENY

The find of a new 'robust' hominid west of Lake Turkana. Kenya in sediments much older than previously associated with these forms throws into doubt the relationship with other species of Australopithecus, and more widely, the pattern of human phylogeny. From analysis of several features and comparison with a specimen from the Olduvai Gorge in Tanzania, the new find is considered to be A. boisei. See p.517. The implications of this find are discussed further on p.496...

OPINION	
Rigging the price of silicon chips	· 485
Selling the family silver	
Taxes make big waves	486
NEWS	
INCAAO	
US budget	487
Inventors' rewards	
Eurpean nuclear power	488
Made in Japan label on launchers	
Soviet/West German cooperation agre	
US-Japan trade	489
Technology journals	
European biotechnology	490
Transplant donor held up by red tape	
Plant research	491
US-Soviet exchange	
US space	492
US doctorates by sex	
New telescopes	493
More ocean dives	
Timber trade	
CORRESPONDENCE-	
Oppression in Chile/AGS	
indicated/Parapsychology	494
	., .
NEWS AND VIEWS-	
New ways with quasi-crystals	495
First X-ray-ionized nebula	.,,
A C Fabian	406

Human phylogeny revised again Eric Delson	496	LETTERS TO NATURE-	
Kinky variations of collagen John Galloway	497	Steep-spectrum radio lobes near the galactic centre	
Muscle contraction: through thick and thin	777	N E Kassim, T N LaRosa	522
Peter D Chantler	498	An interstellar line coincident	344
Fluid mechanics: G I Taylor and his influence		with the P(2,1) transition of hydronium (H ₁ O ⁻)	
Herbert E Huppert Catalysis: Designing porous solids	500	J M Hollis, E B Churchwell, E Herbst & F C De Lucia	524
John M Thomas Wonders of chloroplast DNA	500	Impact-induced atmospheres and	
John Gray MHC antigens and malignancy Hilliard Festenstein &	501	oceans on Earth and Venus T Matsui & Y Abe	526
Federico Garrido -SCIENTIFIC CORRESPONDENC	502 F-	The quasi-crystalline phase in the Mg-Al-Zn system	
The origin of Japanese HTLV-I	,	K Rajasekharan. D Akhtar. R Gopalan & K Muraleedharan	528
T Ishida & Y Hinuma Phosphoinositol more than skin deep	504	High-resolution transmission electron microscopy of silicon re-growth at	
PD Mier, FW Bauer & R Happle	504	controlled elevated temperatures R Sinclair & M A Parker	531
BOOK REVIEWS—		A new type of host compound	
In Search of the Big Bang by J Gribbin	505	consisting of α-zirconium phosphate and an aminated	
Joseph Silk Science Confronts the Paranormal by D Frazier, ed	505	cyclodextrin T Kijima & Y Matsui	533
CEM Hansel Physical Methods for Inorganic		Plume versus lithospheric sources for melts at Ua Pou, Marquesas	
Biochemistry by J Wright, W Hendrickson,		Islands R A Duncan, M T McCulloch,	
S Osaki and G James A J Thomson	506	H G Barsczus & D R Nelson	534
The Geology of China by Y Zunyi, C Yuqi and W Hongzhen	200	Geophysical evidence for the East Antarctic plate	
AMCŞengör	507	boundary in the Weddell Sea Y Kristoffersen & K Haugland	538
Community Ecology J Diamond and T Case, eds		Capacity of purified Lyt-2	
Colin Townsend The Sparrowhawk		T cells to mount primary proliferative and cytotoxic	
by I Newton John Andrews	508	responses to Ia	
COMMENTARY		tumour cells J Sprent & M Schaefer	541
The case for life as a cosmic phenomenon		Increased levels of myelin basic	
F Hoyle & N C Wickramasinghe	509	protein transcripts gene in virus-induced demyelination	
Detection of an X-ray-ionized nebula		K Kristensson, K V Holmes, C S Duchala, N K Zeller,	
around the black hole candidate binary LMC X-1		R A Lazzarini & M Dubois-Dalcq	544
M W Pakull & L P Angebault	511	Tumour necrosis factor α stimulates resorption and inhibits synthesis of	
2.5-Myr Australopithecus boisei from west of Lake Turkana, Kenya A Walker, R E Leakey, J M Harris		proteoglycan in cartilage J Saklatvala	547
& FH Brown	517	Contents continued over	·leaf

Nature® (ISSN 0028-0836) is published weekly on Thursday, except the last week in December, by Macmillan Journals Ltd and includes the Annual Index (mailed in February). Annual subscription for USA and Canada US \$240. USA and Canadaian orders to: Nature, Subscription Dept, PO Box 1501, Neptune, NJ 07753, USA. Other orders to Nature, Brunel Road, Basingstoke, Hants RG21 2XS, UK. Second class postage paid at New York, NY 10012 and additional mailing offices. Authorization to photocopy material for internal or personal use, or internal or personal use, or internal or personal use, or internal or personal use of specific clients, is granted by Nature to libraries and others registered with the Copyright Clearance Center (CCC) Transactional Reporting Service, provided the base fee of \$1.00 a copy plus \$0.10 a page is paid directly to CCC, 21 Congress Street, Salem, Massachusetts 01970, USA. Identification code for Nature: 0028-0836/86 \$1.00 + \$0.10. US Postmaster send address changes to: Nature, 65 Bleecker Street, New York, NY 10012. Published in Japan by Macmillan Shuppan K. K., Eikow Building, 1-10-9 Hongo, Bunkyo-ku, Tokyo, Japan. © 1986 Macmillan Journals Ltd.

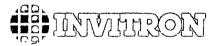
& FH Brown

A new era in cell culture has arrived. Invitron's Static Maintenance Reactor (U.S. Patent No. 4,537,860) is the result of a 15 year marriage of cell biology with bioengineering. This revolutionary cell culture bioreactor approaches—within a pharmaceutical environment—the condition under which cells exist in living tissue.

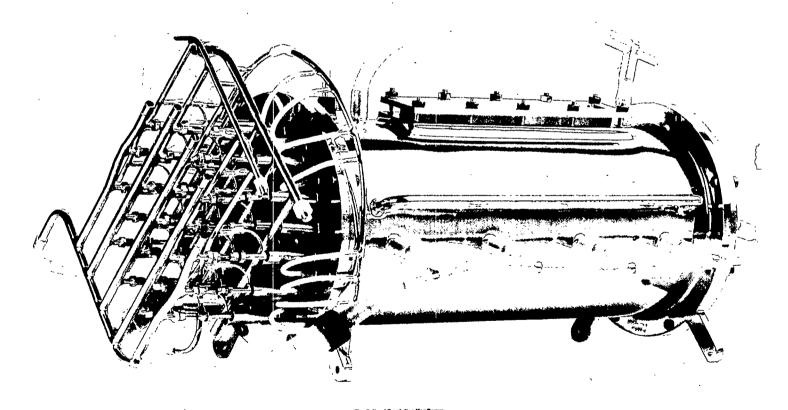
Just one of these reactors has the capacity to produce multi-gram quantities of product...everyday...for months at a time. Annualized, this means that each reactor has multi-kilogram capacity.

to the merketeletees

For further information contacts



W. File Manyland Arcs o Suffe and Transport (ICO CO) (ALCOHOLD)



Reader Service No.28

NATURE'S GUIDE TO HOW BRITAIN RUNS ITS SCIENCE

Nature's practical and useful wallchart has now been thoroughly updated. It provides a complete survey of the administration of British science. showing the functions, key personnel and finance of

- Government departments
- Public and independent bodies
- Research councils

Easily carried to meetings or hung as a wall poster for permanent reference, the new Nature wallchart is an ideal source of reference.

Prices: £4.75 (UK) US\$8.50 (USA/ Canada) £5.75 (All other countries) Airmail despatch

BUY YOURS NOW! From our offices in Basingstoke

Annual Subscription Pr	ices	
UK & Irish Republic		£104
USA & Canada		US\$240
Australia, NZ &	•	
S. Africa	Airspeed	£150
	Airmail	£190
Continental Europe -	Airspeed	£125
India	Airspeed	£120
	Airmail	£190
Japan	Airspeed	Y90000
Rest of World	Surface	£120
	Airmail	£180
Orders (with remittance	e) to:	
USA & Canada	UK & Rest of	World
Nature	Nature	., 0114
Subscription Dept	Circulation D	ent
PO Box 1501	Brunel Road	-1,-
Neptune	Basingstoke	
NJ 07753	Hants RG212	XS. UK
USA	Tel: 0256 2924	
(The addresses of Natur		
facing the first editorial		
Japanese subscription e	• •	
Japan Publications Trac		į
2-1 Sarugaku-cho 1-cho		
Chiyoda-ku, Tokyo, Ja		
Tel: (03) 292 3755	жи	
• •		
Personal subscription ra	ites: These are ava	ulable in
some countries to subsc	ribers paying by p	ersonal
cheque or credit card. F	letails from:	

cheque or credit card. Details from USA & Canada UK & E

UK & Europe Felicity Parker Nature 65 Bleecker Street New York NY 10012, USA Nature 4 Little Essex Street London WC2R 3LF, UK Tel: 01-836 6633 Tel: (212) 477-9600

Back issues: UK, £2.50; USA & Canada, US\$6.00 (surface), US\$9.00 (air); Rest of World, £3.00 (surface). £4.00 (air)

Binders Single binders: UK, £5.25; USA & Canada \$11.50; Rest of World, £7.75. Set of four; UK, £15.00; USA & Canada \$32.00; Rest of World, £22.00

Annual indexes (1971-1985)

UK, £5.00 each: Rest of World, \$10.00

Nature First Issue Facsimile

UK, £2.00; Rest of World (surface), \$3.00; (air) \$4.00

Nature in microform Write to University Microfilms International, 300 North Zeeb Road, Ann Arbor, M148106, USA

Post-translational insertion of a
fragment of the glucose transporter
into microsomes requires
phosphoanhydride bond cleavage
M Mueckler & H F Lodish

Role of ion flux in the control of c-fos expression

J I Morgan & T Curran

retinoblastoma mutation is independent of N-myc expression J Squire, A D Goddard, M Canton, A Becker, R A Phillips & B L Gallie

Tumour induction by the

Discrete cis-active genomic sequences dictate the pituitary cell type-specific expression of rat prolactin and growth hormone genes C Nelson, E B Crenshaw III,

R Franco, S A Lira, V R Albert, R M Evans & M G Rosenfeld

Transcriptional interference and termination between duplicated α-globin gene constructs suggests a novel mechanism for gene regulation N J Proudfoot

Cloning of a major surface-antigen gene of Trypanosoma cruzi and identification of a nonapeptide repeat DS Peterson, RA Wrightsman & J E Manning

Apparent eukaryotic origin of glutamine synthetase II from the bacterium Bradyrhizobium japonicum T A Carlson & B K Chelm

Ultrafast carotenoid to pheophorbide energy transfer in a biomimetic model for antenna function in photosynthesis M R Wasielewski, P A Liddell,

D Barrett, T A Moore & D Gust

Chloroplast gene organization deduced from complete sequence of liverwort Marchantia polymorpha chloroplast DNA K Ohyama, H Fukuzawa, T Kohchi, H Shirai, T Sano, S Sano, K Umesono, Y Shiki,

M Takeuchi, Z Chang, S Aota, H Inokuchi & H'Ozeki

-NEW ON THE MARKET

Tradition takes an unexpected turn

-NATURE CLASSIFIED

Professional appointments -Research posts — Studentships — Fellowships — Conferences — Courses — Seminars — Symposia:

Back Pages

Next week in Nature:

- Search for cosmic strings
- Solar activity in rocks

549

552

555

557

562

566

568

- Tropospheric hydroxyl radicals
- Amorphous alloys as fine particles
- Diamond formation
- Japan's first farmers
- Oncogenesis mechanisms
- Acoustic neuroma genetics
- Cryptic simplicity in DNA
- Lab computer networks

GUIDE TO AUTHORS

Authors should be aware of the diversity of Nature's readership and should strive to be as widely understood as possible.

Review articles should be accessible to the whole readership. Most are commissioned, but unsolicited reviews are welcome (in which case prior consultation with the office is desirable).

Scientific articles are research reports whose conclusions are of general interest or which represent substantial advances of understanding. The text should not exceed 3,000 words and six displayed items (hgures plus tables). The article should include an italic heading of about 50 words.

Letters to Nature are ordinarily 1,000 words long with no more than four displayed items. The first paragraph (not exceeding 150 words) should say what the letter is about, why the study it reports was undertaken and what the conclusions are.

Matters arising are brief comments (up to 500 words) on articles and letters recently published in Nature. The originator of a Matters Arising contribution should initially send his manuscript to the author of the original paper and both parties should, wherever possible, agree on what is to be submitted

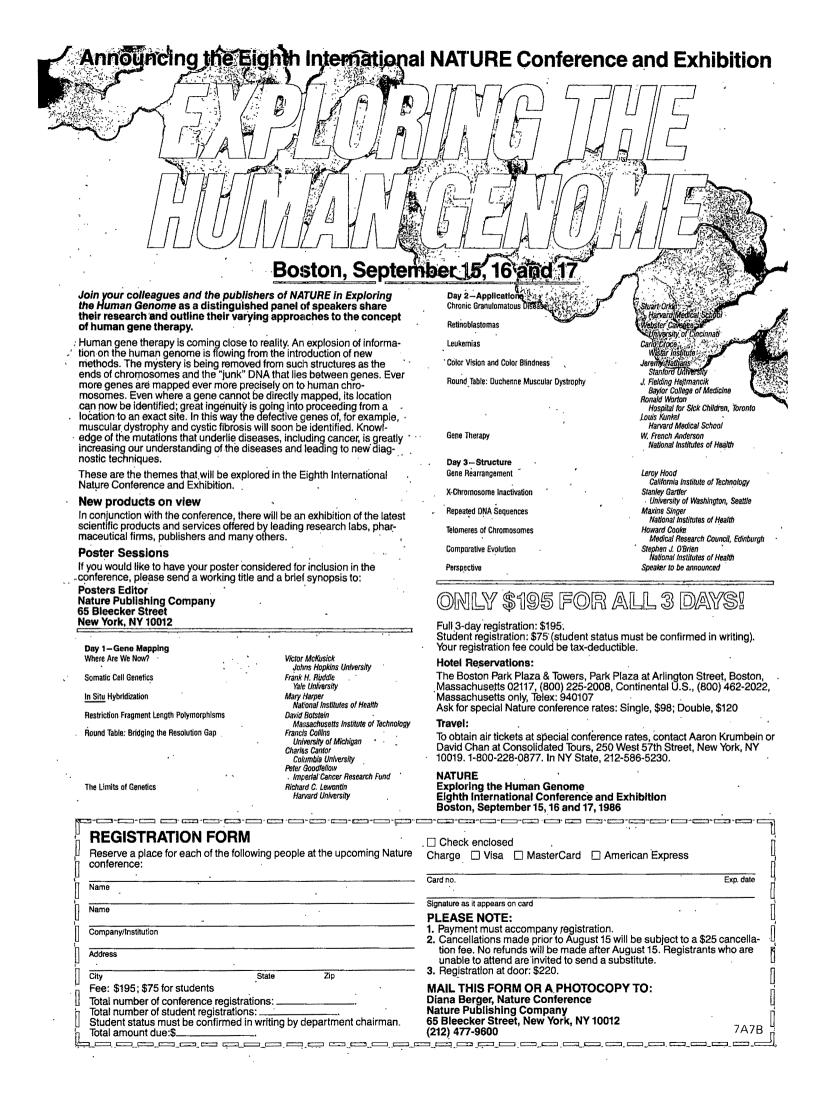
Manuscripts may be submitted either to London or Washington. Manuscripts should be typed (double spacing) on one side of the paper only. Four copies are required, each accompanied by copies of lettered artwork. No title should exceed 80 characters in length. Reference lists, figure legends, etc, should be on separate sheets, all of which should be numbered. Abbreviations, symbols, units, etc. should be identified on one copy of the manuscript at their first appearance.

References should appear sequentially indicated by superscripts, in the text and should be abbreviated according to the World List of Scientific Periodicals, fourth edition (Butterworth 1963-65). The first and last page numbers of each reference should be cited. Reference to books should clearly indicate the publisher and the date and place of publication. Unpublished articles should not be formally referred to unless accepted or submitted for publication, but may be mentioned in the text.

Each piece of artwork should be clearly marked with the author's name and the figure number. Original artwork should be unlettered. Suggestions for coverillustrations are welcome. Original artwork (and one copy of the manuscript) will be returned when manuscripts cannot be published.

Important: Manuscripts or proofs sent by air courier should be declared as "manuscripts" and "value \$5" to prevent the imposition of Customs duty and Value Added Tax in the United Kingdom.

Requests for permission to reproduce material from Nature should be accompanied by a self-addressed tand, in the case of the United Kingdom and United States, stamped) envelope.



NATURE VOL. 322 7 AUGUST 1986 . 485

Rigging the price of silicon chips

The agreement signed last week between Japan and the United States will not in the long run keep Silicon Valley healthy, and meanwhile will be a recipe for trouble.

ONLY a few days after one of the largest steel-makers in the United States, the conglomerate LTV, ran for the shelter of the US bankruptcy laws, trade officials in Washington were foolishly celebrating last week the agreement they have negotiated with their opposite numbers in Japan to regulate the sale of semiconductor memory chips between their manufacturers. The coincidence is striking and also chilling. LTV has been driven into queer street by the long decline in the demand for steel when the world is swimming with the capacity to produce . the stuff. During much of that time, the US government has done what it can to protect the domestic industry from overseas competition by a variety of restrictions on the free import of steel. Voluntary quotas have been negotiated with European steel-makers, while the policy of protection has been stiffened by the usual array of anti-dumping suits in the courts. The result is that the US steel industry has been kept alive, but only just.

Technically, the industry has limped along, maintaining existing plants without the funds to improve them to a point at which they might compete effectively with steel-makers in Japan and Korea. The companies involved have in the process been locked into a declining business when their long-term interests would have dictated diversification. What has happened to the US steel industry is yet another proof that, in a competitive world, protection is more often the kiss of death than a safeguard. How soon will this truth be demonstrated in the manufacture of silicon chips?

The new agreement is believed to cover something like 90 per cent of the semiconductor manufactures supplied by Japan to the United States. All the bread and butter in the trade will be regulated, but, almost by definition, the regulations will not apply to the most advanced components, those so novel that competition has not yet developed and whose lucky manufacturers can charge what prices they choose, not to mention the chips not yet invented. The agreement binds both signatories to ensure that chips are not sold for export at prices other than those defined as fair, which implies that manufacturers will have to recover in their prices not merely the marginal cost of production but also a contribution towards the capital costs of the plants in which chips are made.

Technically, the agreement is a recipe for endless bickering. Difficulties have arisen about the prices charged for chips because of the huge difference, in a capital-intensive business, between the marginal cost of production and that which fully amortizes the cost of the equipment with which chips are made. Who will now decide what production overheads are fair? But in practice, the effect of the agreement promises to be unambiguous: prices of chips of all kinds will be increased for everybody, often substantially.

For a time, no doubt, there will be rejoicing in Silicon Valley, the Californian hub of the US computer industry. Small companies whose backs have been against the wall for months on end will be able to walk tall again, sheltered from the formidable competition of Japanese manufacturers by increased prices. The new deal may not restore the full excitement of the 1970s, when for a time it seemed as if Californian entrepreneurs had stumbled on the modern equivalent of the philosophers'

stone, a way of turning silicon into gold. But there will be fewer lawyers preoccupied with the intricacies of Chapter XI, the provisions of the bankruptcy laws that allow a company to keep trading while protected from the most pressing claims of its creditors. Undoubtedly there will be a spell, of months and possibly years, during which the sales of the US chip-makers will increase, both in volume and in profitability.

Japanese manufacturers will be compelled to compete in other ways, two of which are easily foreseen. First, they will pay even more attention than is their present custom to the quality of what they manufacture and put on the market. Second, compelled by the agreement to charge more for what they sell at present and thus made even more profitable than they are now, they will invest even more enthusiastically in novel semiconductor devices. A few years from now. Silicon Valley will probably still be a high-cost producer, but may well have lost its present reputation for daring design behind the shield for foreign competition now being provided. That is what has happened to steel manufacture in the United States

Meanwhile, the economic cost of the new agreement will be felt throughout the world. To prevent manufacturers in Japan selling cheaply into the United States through the intermediary of third countries, price-fixing will apply to chips sold by both Japanese and US companies in, for example, Europe. One result will be that the prices of electronic equipment will be increased. Another will be that European chip-makers will enjoy the benefits being showered on Silicon Valley at a crucial time in their strategic history, when the case for making chips indigenously is stronger than it has ever been. Whether European companies will ever be able to match those in Japan in quality and cost is an open question, but now at least they will have an opportunity to do so. Is that what the United States intends?

That the new agreement will not serve its intended purpose, but others that cannot accurately be foreseen, is beyond dispute. Yet one malign side-effect is easily predicted. To the extent that the new agreement on chips establishes an inter-governmental cartel for the regulation of prices in international markets, it will be an awkward precedent that is bound to come to haunt the United States, hitherto an admirably staunch supporter of the doctrine that free trade is the only effective means of arriving at an economic division of labour in the world. Which other governments, in respect of other manufacturers, will now be tempted to follow suit? All they will have to dissuade them is the example of the Organization of Petroleum Exporting Countries (OPEC), now in collapse along with the price of crude oil.

Selling the family silver

Turning public into private enterprise is fashionable, but not best done by public servants.

LORD Stockton, previously Mr Harold Macmillan, last year startled the British government which he supports politically by reproving it for "selling the family silver" in order better to balance its accounts. The circumstances are now familiar, and by

no means exclusively British, even if the present British government is among the most zealous of those attempting to turn public into private enterprises. (M. Chirac's government in Paris seems anxious to follow suit, if President Mitterrand's reluctance is in the end overridden by the French Assembly.) Already a majority of the shares in the previously nationalized telecommunications network and the aerospace company have been sold to the public. The gas monopoly is to be sold later in the year, but there will be a long delay before the complicated water industry can be made private, and it remains to be seen whether the government can find a buyer for the motor-car manufacturer it owns who will be acceptable to its own supporters (who, with others, killed the attempt to sell part of it to US General Motors a few months ago).

Meanwhile (see, p.491), at the other end of the spectrum financially, the government has managed to work out a way of selling off its interest in the breeding of commercial crops through the Plant Breeding Institute at Cambridge (England). In principle, this is a sensible step to take. Like all the other research institutes operated by the Agricultural and Food Research Council (AFRC), the Plant Breeding Institute has had a rough and over-spartan time in the past few years. Budgets have been held stagnant or even cut, with the result that vacant posts have not been filled even when there is productive work for their potential occupants to do. But the institute differs from most others in that the benefits of the work it does are translated directly and tangibly into monetary terms. The new varieties developed at the institute are sold to farmers, in Britain and overseas, through bodies such as the National Seed Development Organization, which regularly makes a substantial profit on its operation that, under the present system, has been dutifully turned over to the British Treasury. Taken together and averaged over the years, the profits of the seed organizations are not very different from the costs of the research that has sustained them, which vividly illustrates the folly of having kept the institute on such short commons all these years. Now the breeding and marketing organizations are to be put up for sale as a package. There is a chance that the new entity will be able to make its way in the world relatively free from worry, and even more conscious of how its skills (widely acknowledged to be high) should be most effectively deployed.

That is the plus side of the account. The other is the decision that, in the process of privatization, the Plant Breeding Institute should be split in two. Plant breeding pure and simple (if there is such a thing these days) is part of the commercial package, but molecular biology will stay in the public sector. That, at least, is the intention, however little sense it makes when plant breeders the world over are bent on using genetic manipulation to give crop varieties characteristics they would not acquire naturally. If the institute is indeed sold off successfully (as seems likely), the new owners would promptly set out to recruit a team of molecular biologists to make up for the loss now being decreed. They would not have far to look.

None of this implies that research councils such as AFRC should withdraw from the molecular biology of plants. On the contrary, there is the strongest possible reason why the scale of effort in this field should be increased even in circumstances such as those in Britain, where farming is no longer strictly an economic activity (see Nature 322, 195; 1986). But the opportunity for spinning off a substantial team of people working in the field already should be regarded as a heaven-sent chance for creating another. This is a chance to sell the family silver and to get another set. Luckily, it is not too late for the government and AFRC to change their minds. Indeed, on the principle that the British government in its present mood is unlikely to increase the funds available for supporting basic research but, equally, is unlikely to have the gall to cut them even further, there is a strong case for scouring government departments for other parts of the public research enterprise that might be thrown to the commercial wolves.

Taxes make big waves

The effects of US tax reform will be felt far outside the United States.

BEFORE the summer is out, the US Congress will have put the finishing touches to the tax bill that is almost certain to be what the Reagan administration is remembered for. That, at least, is the plan, which is likely to be sustained by the way in which general enthusiasm for lower percentage rates of tax promises to. overcome taxpayers' attachment to the labyrinthine network of deductions from income they have long regarded as their birthright. While the marginal rates of tax are still to be determined, the mere idea that there may be just two, at 15 per cent and 27 per cent, will excite the envy of taxpayers elsewhere, many of whom are used to surrendering more than half of the extra they earn. Even if the rates at which optimistic congressmen are aiming cannot be achieved, or if it turns out that the extra taxes that business will have to pay are economically damaging and must be reduced, the simplicity of the new tax bill cannot fail to be seductive elsewhere.

There will be more immediate and specific consequences, one of which may benefit the economic partners of the United States. The details of the new bill are still being negotiated between the US Senate and the House of Representatives, and there is much to be worked out. The Senate version of the bill is generally considered friendlier to business, perhaps reflecting its Republican majority. By contrast, the House version generally provides greater savings to individual taxpayers. Arriving at a compromise that will be acceptable to at least a majority of legislators is proving to be at least as hard as analysts predicted it would be. But one feature likely to emerge intact is the proposed abolition of the tax shelter embodied in the device of the limited partnership; its effect will be to send venture capital scurrying to other places in the industrial world where investment in innovation is still encouraged by such means. The principle is that people may invest part of their income in some new venture, which may be a new company or even just a new project on which a company is engaged, pay no tax on that slice of income but pay capital gains tax on their profits if the venture should succeed. The device has been widely used in the past few years in, for example, the development of biotechnology. If, now, such opportunities are no longer available in the United States, individuals and corporations with income arising elsewhere will be tempted to look for them where they can. Already there are people in Europe calculating that the flow of venture capital across the Atlantic may be substantial.

The other side of that coin is that the dazzling attractions of the tax reform bill may, over a longer period of time, work in the other direction. Ever since the Second World War, the United States has been a magnet for technical people elsewhere. The canard that engineers in the United States are so busy at their profession that they have no time for teaching, with the result that the education of young engineers is in the hands of people from overseas, is at least a half-truth. Other governments are often alarmed enough to mount formal inquiries into what they call the brain drain, only to discover that their emigrating technical people proclaim that they are leaving for the United States only because working facilities are better there, or that they seek the chance of working alongside particular colleagues. But this is humbug, and should be recognized as such. Is there any reason to believe that technical people are immune from the prosperity that makes the United States attractive not merely to other professionals but to the army of unskilled people who seek the same haven? By that test, the rate at which technical people depart for the United States will only be accelerated when the tax bill passes. Are governments elsewhere reconciled to that alarming prospect? And will they choose to follow the only course by which they might convincingly respond, that of mimicking what is now happening in Washington?

US budget

Winners and losers worry about Gramm–Rudman

Washington

CLEAR signs emerged last week that the US Congress may be unwilling to support some of the increases in research funds proposed in President Reagan's budget for the next financial year, beginning in October. Faced with strong political pressure to reduce the federal budget deficit, the Appropriations Committee of the House of Representatives recommended providing the National Science Foundation (NSF) with \$136 million less than the \$1,686 million sought by the President, giving only a slight real increase over this year's level. A small cut of \$44 million from the President's request was also proposed for the National Aeronautics and Space Administration (NASA).

The still uncertain effect of last year's Gramm-Rudman deficit control act makes prediction of agencies' budgets difficult. But academic and scientific bodies did not hide their dismay last week that Congress had failed to support the 8 per cent increase sought by the President for NSF, the main federal source of support for non-military basic research. Jack Crowley of the Association of American Universities was disappointed that a key committee of Congress saw increased support for basic research as "an expendable priority". Others pointed out, however, that the committee had in the same legislation approved significant reductions for other agencies and that it had gone as far as it could to protect NSF.

The National Institutes of Health (NIH) are, however, another story. The House of Representatives excelled even its own customary generosity to NIH by voting to provide \$6,153 millon for the institutes, \$1,073 million more than the President's budget request and \$893 million more than the 1986 figure. The House specifically noted that it wanted to see 6,200 new extramural research grants next fiscal year, about 700 more than the administration wanted. While the Senate might temper the House's enthusiasm, there seems little doubt that Congress's strong support for NIH is unchanged from previous years.

During the House debate that preceded the vote, much was made of the growing death toll due to AIDS (acquired immune deficiency syndrome), and \$336 million was voted for efforts to combat the disease, \$133 million more than the President had requested.

Other appropriations bills on which the House has taken action include a bill providing funds for the Department of Energy. Here the House has also followed the pattern of previous years by voting to restore some of the large cuts proposed by the President in solar power and magnetic fusion research. But at the same time it cut \$536 million from the \$8,330 million budget request for the department's defence programmes, to take account of limits placed by Congress on growth of the Strategic Defense Initiative.

The House has, however, alarmed academic groups by allowing to pass in the same bill \$69.7 million for research and construction projects at eight named institutions that have not been through the usual process of authorization by Congress and have not been subject to peer review. Most scientific and academic bodies are opposed to Congress's growing tendency to provide funds for specific unreviewed construction projects from research budgets. But Congress seems in no mood to compromise. An amendment to delete funds for the unreviewed projects was defeated by 315 to 106. The Senate has yet to consider the matter, but recently defeated a move to delete funds in a Department of Defense emergency money bill for unreviewed projects at nine universities (see Nature 322, 4: 1986).

Most of the appropriations now at various stages of approval in the House have not reached the Senate. But the exact amounts specified by both houses could become largely irrelevant if, as some expect, a legislative formula is found to allow automatic cuts to be made to agencies' budgets to make them comply with the \$144,000 million budget deficit target specified by Gramm-Rudman.

Although the mechanism specified in Gramm-Rudman for making the automatic cuts was ruled unconstitional by the Supreme Court in July, efforts are under way to modify it. The court's objection was over the pivotal role played by the General Accounting Office in determining the size of the cuts; one proposal now under consideration would meet that difficulty by substituting the executive branch's Office of Management and Budget.

A preliminary estimate of the likely budget deficit next year will be made on 15 August and, if the target is exceeded by more than \$10,000 million, the necessary across-the-board cuts would then be calculated. If Congress has not by then completed appropriations for the next fiscal year, the 1986 levels will be used in the calculation, a prospect particularly alarming for agencies such as NSF that had been

in line for large increases. I ven it the automatic cuts are not made, however, there will be strong pressure on Congress to meet the targets in the Gramm-Rudman law.

Many congressional staff now consider it inevitable that the cuts will be triggered: slow economic growth has reduced expected revenues and a deficit of around \$220,000 million seems likely, it Congress sticks to the budget guidelines agreed earlier. The cuts would probably be much bigger than the 4.3 per cent made this year. But congressional elections in November could prove to be the wild eard Some observers think that Congress will yet devise some way of getting itself off the Gramm–Rudman hook before November.

Inventors' rewards

THIRTY-three British universities and colleges have gained permission to exploit financially inventions arising from research funded by the research councils. Until now the British Technology Group (BTG) has had right of first refusal for the commercial development of government-funded research, a process that its just released annual report shows is not without its dangers.

Last year, BTG, a state-owned management company formed to assist the commercialization of innovative ideas, had to spend more than a million pounds defending its patent rights. Most of the money went on fighting for the hovercraft — a great British invention back in 1959 now being put into use by the US Armed Forces. The trouble is they are not paying the royalties and "American lawyers are very expensive" as a BTG spokesperson put it. But BTG still managed an income of nearly £20 million from licensing and industrial projects.

Before being granted permission to try for similar profits on their own, the universities had to assure a scrutiny committee that they knew what they were about. The chief aim, in line with government policy. is to provide new incentives for individual researchers as well as their universities. That aim can be satisfied only by arrangements in which inventions with a potential for commercial exploitation can be spotted early; flexible routes for their exploitation, including setting up new companies and forming partnerships with industry, can be quickly set up; and inventors properly rewarded. That may mean the inventor will get all the proceeds if the invention has a low level of return, and the university gets a cut when bigger profits can be made.

Universities that have not yet received permission to exploit their inventions are likely to do so in the near future. Some, though, will continue to use existing arrangements with BTG. Alun Anderson

European nuclear power

Muddle over safety measures

A swingering attack on the European Economic Community (EEC)'s nuclear safety and public information record was delivered in Brussels last week by its commissioner for the environment, Stanley Clinton Davies. His remarks were apparently based on a new report from an expert committee — but those involved in the report's preparation claim it reaches wholly opposite conclusions.

The report, due to be published in a few months, was drawn up by those close to the nuclear industry and it supports its policies, according to Commission sources. It is regarded, however, only as advice and the European Commission is free to draw its own, even contradictory, conclusions.

Clinton Davies's interpretation was certainly affected by the uncoordinated response by European states to the Chernobyl nuclear disaster, which came late in the expert group's year-long deliberations. In that context, the commissioner felt it necessary to criticize the poor and late provision of public information in some countries (by implication, France), and the very disparate actions taken in response to contamination. "Everyone got under their own umbrella", said a Commission spokesman, and some umbrellas were big and others patchy.

The environment commissioner's objective in attacking national safety measures is thus clear: he believes there is a central coordinating role to be played by the European Commission in matters of setting nuclear safety levels and the rapid collection and dissemination of information across national boundaries in the ease of accidents. Thus Clinton Davies last week attacked, by implication, West Germany, Italy, the Netherlands, Belgium and others for failing to implement an EEC directive on "basic norms" for

Made in Japan label on launchers

Tokyo

Next week Japan takes its first big step towards independence from US rocket technology with the test launch of its new H-I rocket.

Throughout its 17-year history, the National Space Development Agency (NASDA) has depended on licensed US rocket technology to boost its satellites into orbit. Breaking with that tradition, the H-I has a domestically developed second-stage cryogenic engine, the LE-5. On its first test flight, a two-stage version will be flown; later flights will be of the full three-stage rocket. And, unlike its predecessors, the N-I and N-II, the rocket will also have a new Japanese-built inertial guidance system.

Scheduled to blast off on 13 August, the H-I will carry three inexpensive payloads into orbit; the Experimental Geodetic Payload (EGP), a hollow globe over two metres in diameter, covered in mirrors and laser reflectors, that will be used by the Maritime Safety Agency and the Geographical

Survey Institute for laser triangulation surveys; the Japan Amateur Satellite-1 (JAS-1) for ham radio enthusiasts; and a magnetic bearing flywheel to be tested in space before incorporation into future satellites. The total budget for the launch including the satellites is 16,000 million yen (about \$100 million).

From 1988 the rocket is planned to go into regular service placing communications, broadcast, meteorological and Earth resources satellites into geosynchronous orbit. But with a maximum payload capacity of only 550 kg, the H-I is still small by international standards, and by 1992 NASDA hopes to replace it with the H-II, a two-stage launcher, capable of boosting a 2,000 kg satellite into a geostationary orbit, that will be 100 per cent "made in Japan".

Although still not in the big space league, the H-II will allow Japan to compete in the international market for the launch of small to medium scale satellites in the 1990s.

David Swinbanks

emissions and radiation exposure, which had been due for ratification last April. Europe's principal nuclear states, Britain and France, are not in default on "basic norms", but according to a spokesman "most" of the 12 EEC nations have failed to implement another directive, on exposure to medical X rays.

Both radiation directives, agreed by the European Council of Ministers in 1984 (subject to ratification by national parliaments), are applications of the much older Euratom Treaty of 1957. This treaty is, in turn, one of the foundation stones of the European Communities and gives the European Commission wide powers to gather information and set standards of nuclear safety. The nuclear member states, in particular France, with nearly 70 per cent of its electricity demand met by nuclear power, are set firmly against such a role for the Commission. But in Brussels

it is felt that a clear, objective, international information system is urgently needed—otherwise the European public, including even the French, will lose confidence in nuclear power altogether. Last week Clinton Davies made a firm and specific proposal that such a system be set up, although he drew back from pressing for the wider powers that the Euratom Treaty would allow, but which for the moment seem politically inopportune.

As if to confirm the commissioner's views, the influential umbrella organization for European consumer associations. the Bureau Européen des Unions des Consommateurs (BEUC), which receives a small grant from the European Commission, also recommended such an international reporting system last week. In a 35-page report which collated official and published information on national responses to the Chernobyl disaster and its fallout, BEUC contrasted, among other things, the 3,700 becquerel per litre radiation level prescribed in France in milk with the 500 bq 1-1 upper limit in the Netherlands and Belgium, and the 20 bq 1-1 imposed during the Chernobyl affair in the German Länder of Hessen and

BEUC, with its large public backing through the consumer associations, also recommends in its report that the Commission adopt its full powers under the Euratom Treaty; that it set up a truly independent scientific committee to make recommendations on standards; that it prepare a European-wide contingency plan for any future accident, including one at a chemical plant; and that it develop a long-term post-Chernobyl research programme.

Robert Walgate

Soviet/West German cooperation agreed

Hamburg

WEST Germany and the Soviet Union have agreed on closer cooperation in science and technology. Foreign Minister Hans-Dietrich Genscher signed a framework treaty in Moscow two weeks ago which covers three sub-agreements on nuclear power, medical and agricultural research. Fifteen two-year programmes were agreed.

Then negotiations began in 1973, but soon came to a halt. Only when Chancellor Helmut Kohl met First Secretary Gorbachev in 1983 did both sides agree to continue the talks. A draft was ready in 1984 but in the new treaty the ministers add a note of their intention to work out a fourth,

additional sub-agreement on environmental protection.

The framework treaty is of particular importance in the light of Soviet efforts to make their nuclear power safe. The agreement includes clauses on exchange of information and scientists and the organization of meetings, exhibition and courses. Basic research may even be performed jointly in shared laboratories, but it is not yet clear what projects will be tackled. On the political side, the treaty is sure to help the progress of negotiations with East Germany on a similar treaty. Discussion began in 1973 but no agreement has been reached even after 27 meetings.

Jürgen Neffe

US-Japan trade

Truce agreed in chip war

Washington

Just minutes before midnight on 30 July, Japanese and US negotiators reached a comprehensive agreement on trade in semiconductors. Under the terms of the five-year agreement, the Japanese government will both help US semiconductor companies to increase their share of the Japanese market and stop Japanese companies from "dumping" chips on international markets. The US industry is well pleased with the agreement. But the industry knows that a key question remains; can it be enforced?

Reaching an agreement before midnight on 30 July was crucial. That was the statutory deadline for a Department of Commerce decision to impose permanent dumping duties on erasable programmable read-only memory (EPROMs). The Commerce Department had already made a preliminary judgement that Japanese manufacturers were dumping EPROMs — selling them at less than fair value considering their production costs — and chip importers have been posting bonds against possible imposition of duties. Under the agreement, both the dumping case against EPROMs, and a similar case against 256 kilobyte dynamic random access memory chips (256K DRAMS) with an 1 August deadline, will be suspended. In exchange, the Japanese government agrees to ensure its manufacturers sell products only at "fair market value". Also suspended is an unfair trading case being pursued by the office of the US Trade Representative, which could have resulted in sanctions against Japan.

To increase the US share of the Japanese semiconductor market, Japan will establish an organization to assist foreign manufacturers' sales efforts, and will also promote long-term relationships between US manufacturers and Japanese semiconductor users. While there is no specific target, the US market share in Japan is expected to increase to 20 per cent by the end of the five-year agreement. US sales at present account for 8–10 per cent of the Japanese market.

Another key element of the agreement, according to George Scalise of the Semiconductor Industry Association (SIA), is that US companies manufacturing in Japan will be given the same rights and privileges as Japanese companies, which is likely to increase the market share for the US industry.

In the week just before the signing of the agreement, Japanese manufacturers made a large number of sales to US customers. While the agreement on EPROM dumping became effective on 31 July, 256K DRAMS can be shipped to customers at any price agreed before 1 August until 15 September. After that, fair market pricing will prevail. But US industry spokesmen concede that a large number of chips can be delivered to US customers during that time. Sales of 256K DRAMs now account for 17 per cent of the total US semiconductor market.

To prevent future dumping, Japanese companies will provide data on pricing of EPROMs and 256K DRAMS to the Department of Commerce on a regular basis. The Japanese Ministry of International Trade and Industry will keep track of pricing data on other semiconductors, as well as products to be shipped to markets other than the United States. The United States

can request immediate 14-day consultations to resolve dumping questions and retains the right to initiate its own anti-dumping investigations that could result in the imposition of dumping duties. The issue of third-market sales, and the possibility that chips would be dumped in small countries for trans-shipment to major customers at cut-rate prices, proved especially divisive in the negotiations. Although Japanese companies never admitted to dumping during the negotiations. Michael Gadbaw of SIA says they nevertheless "promised never to do it again".

What gives US negotiators confidence that Japan will adhere to the terms of the agreement is the threat that the suspended dumping and unfair trade cases can be reinstituted. But many believe that it will take a lot of work to turn these commit ments into reality.

Joseph Palca

Technology journals

Time to learn Japanese

Washingtor

FEARFUL that US industry is not doing enough by itself to tap the voluminous output of Japanese scientific and technical literature, the US Senate is expected this week to agree to set aside \$1 million per year for efforts to make access easier. How the money will be spent has not yet been decided, but a possibility is that special representatives in Tokyo of the US Commerce Department will seek out the best from the Japanese literature and ensure that it is available in translation to US researchers.

Even supporters of the measure acknowledge, however, that the amount specified will do little to right the huge imbalance in the flow of technical information. The total number of US translators capable of handling difficult technical material in Japanese is small, perhaps only 200, with most of them working for one company. Japanese efforts to translate Western literature into Japanese, by contrast, are impressive: over 5,000 scientists and engineers are said to abstract routinely some 10,000 foreign and domestic journals, as well as other sources.

The Japanese Technical Literature Act directs the US Secretary of Commerce to redirect \$1 million from other Commerce Department activities to the monitoring and dissemination of Japanese technical developments. So far, the department has agreed to find only \$250,000. The act requires the department to consult businesses, professional societies and libraries in order to find out what is in most demand; it must, however, avoid offering material already sold by commercial companies.

A probable formula is that the Commerce Department's International Trade Administration will represent the Nation-

al Technical Information Service (NTIS also part of Commerce) in Tokyo, and will then offer the information culled to US industry and academic institutions for a nominal fee. NTIS already monitors some Japanese government publications, but spent only \$18,000 last year on translation. The future of NTIS is, however, uncertain; the federal government has proposed turning over the agency in whole or in part to the private sector, and NTIS staff fear they may never see the money The International Trade Administration. in contrast, already has ideas about what it would do with the promised \$250,000. produce another two of its in-depth reports on Japanese technology, four of which were produced recently for \$500,000 and were sell-outs.

By far the largest Japanese translating operation in the United States is the provate-sector Japanese Technical Information Service (JTIS) of Media, Pennsylvania, a subsidiary of University Microfilms. JTIS (which claims to employ most of the qualified Japanese translators in the United States) abstracts some 600 Japanese journals for its industry clients and offers full translations as requested. But at \$5,500 per year for a subscription to its abstract journal, sales have been restricted to major companies, with only 150 or so paid-up subscribers.

Justin Bloom, a former science adviser at the US Embassy in Tokyo, says that it JTIS's service fails to prosper it will show there is "no demonstrable US interest" in access to Japanese literature. But he is sceptical about the new act, describing it as "laudable in principle but meaning little in practice". Bloom says that in Tokyo, even with a staff of 22, he was hardly able to make an impact in monitoring Japanese technical literature.

European biotechnology

Parliament giving up alcohol

THE giant Italian food and agricultural company Ferruzzi is set to fight back after the European Parliament struck a blow against its plans to convert Europe's grain mountain into fuel alcohol. The plan, according to Ferruzzi, would create jobs, be environmentally benign, and give farmers a new deal. But, says a report adopted by parliament before the summer recess, the project would kill jobs in the oil industry and could produce far more pollution (in the form of biological oxygen demand) than all Europe's sewage. In Brazil, where a similar project has been under way since the 1970s, up to half a million jobs have been created, 80 per cent of them unskilled, says the report. There are no studies available, however, to indicate the possible impact in Europe, where educational and skill levels are higher and where technology is often cheaper than labour.

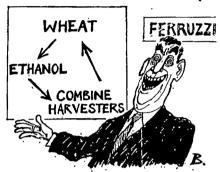
Ferruzzi, the company whose proposal led to the reports, was recently referred to the British Monopolies Commission for its thinly disguised attempt to take over British Sugar, the UK beet monopoly. But this has been only the latest event in the saga of the expansionist group, which already controls most of the sugar production in Italy and has a controlling stake in the leading French sugar manufacturer Beghin-Say. Control of British Sugar would give Ferruzzi one quarter of the sugar market of the whole European Economic Community (EEC). Through its alcohol project, the company has shown an almost equal interest in grain.

Ferruzzi's grain-to-alcohol plans would leave Scotch whisky producers standing. The group has proposed 12 conversion plants, costing upwards of \$560 million, and designed to take 15 million tonnes of cereals a year for conversion to alcohol.

The Ferruzzi plants would be built in France, where 94 per cent of Europe's grain surplus is grown (according to the European Parliament report). Naturally enough, the French farm minister François Guillaume, an ex-farming trade unionist, supports the Ferruzzi plan, and so do most of the French members of the European Parliament, but this was not enough last month to reject the parliamentary report, which itself rejected the production of bioethanol from raw materials "in present market conditions". The resistance to a large, precipitous bioethanol programme cut across all countries (other than France) and all parties; and although the parliament has little real power, its position will certainly give political weight to the European Commission (the EEC secretariat) which has also rejected the Ferruzzi proposal.

The principal reason for rejection is that the project is drastically uneconomic without vast EEC subsidies. Ferruzzi's plans would require grain at world market prices. The present EEC subsidy to grain farmers, guaranteeing the sale of their grain at inflated European prices, would therefore have to continue. Moreover, this would still not bring the alcohol down to saleable prices as a fuel additive, where it could displace either petrol itself or the

In other words, perpetual motion!



new lead-free anti-knock agents. At present prices of oil and of anti-knock agents, governments would also have to offer tax reductions on any alcohol-containing petrol sold, the Ferruzzi group says.

Such arguments would seem to rule the whole proposal out of hand—and certainly the canny Dutch ex-economics minister, Fran Adriessen, who is now European Commissioner for Agriculture, rejects it—if it were not for the renowned strength of certain European agricultural lobbies, particularly the French. Ferruzzi's president, Dr Paul Gardini, has promised that he will not let the issue rest. The possible carcinogenicity of some proposed

anti-knock agents is one new line to try.

Meanwhile, therefore, the vote at the European Parliament is just one further move in the game, which is continuing through a \$200,000 study on the social and economic impacts of a European gasohol programme. This independent report should be ready in draft by November, when it could in principle receive attention by the Commission during the British presidency of the European Council, the Commission's decision-making body. But Britain, committed to reforming the overproductive and costly Common Agricultural Policy is thought to see European gasohol as yet another "black hole" of European subsidy, and will not aid the Ferruzzi project even if the study recommends it.

The European Parliament did not reject the development of bioethanol plants on a 🔍 smaller scale, and at smaller rates of subsidy, than envisaged by Ferruzzi, however. Small plants could be of use to remote rural areas and parliament recommended Commission support for research and pilot projects along these lines. On the whole, however, the European Parliament, which has a higher representation of scientists than probably any national assembly in Europe, is of the opinion that the Ferruzzi plan would do damage to the more cautious and reasonable plans of the Commission to introduce biotechnology to European farms under its proposals for "stimulating agro-industrial development". These, involving pilot studies from post-research field trials of new crops to biotechnology-based processes, are not billed to remove the European food surpluses next year, but could, Commission officials hope, sow the seeds of a new European agriculture. A failed bioethanol programme could set such proposals back by years. Robert Walgate

Transplant donor held up by red tape

When Dr Robert Gale, the bone-marrow transplant specialist, flew to Moscow in May to treat the victims of the Chernobyl disaster, he took with him an essential piece of equipment for sorting cells, developed at Israel's Weizmann Institute. He also took an urgent request for help from an Israeli biologist, Michael Sherman, who himself needs a bone marrow transplant. Ironically, until he developed leukaemia last year, Sherman was employed at *Interyeda*, a commercial company established to develop innovations based on research conducted at the Weizmann Institute.

Michael Sherman is an emigrant from the Soviet Union, who settled in Israel some six years ago. The only possible related donor would be his sister, who still lives in Moscow. In February, as soon as she heard of her brother's illness, she immediately applied to OVIR, the Soviet passport department, for permission to go to Israel to donate the necessary marrow. There was no immediate reply, but after Gale's visit, the sister and her husband and children were called to the OVIR office. They were informed that a temporary visit to Israel on a Soviet passport was impossible due to "bureaucratic difficulties", and were advised to apply for permanent emigration to Israel. On 2 July, therefore, they filed the appropriate papers.

Shortly afterwards, Sherman says, "unpleasant things" began to happen. His sister was demoted to a lower-paid job, and, now "they are examining the possibility of firing her". It now appears, he says, that OVIR is treating the case as a routine request to emigrate, with all the delays that involves. And that, in Sherman's case, could well be too late.

Vera Rich

Success breeds privatization

THE British government is to go ahead with its plan to sell off its institutes for the development and marketing of new varieties of plants. The government has long seen the sale as politically desirable, given its philosophy that the role of the private sector should be expanded. But it was only last week that a merchant bank confirmed that the sale will also be financially profitable.

The two organizations to be sold, the National Seed Development Organization and the Plant Breeding Institute (PBI), might seem to form a natural couple. PBI, belonging to the Agricultural and Food Research Council (AFRC), runs large-scale programmes in plant breeding which have produced nearly all the new varieties sold by the National Seed Development Organization. This has been a profitable business, generating £4.65 million for the government last year. Given that support for plant breeding research at PBI cost just £2.5 million last year, the institutions are bound to seem an attractive buy.

In the short term, researchers in plant breeding may benefit from privatization. In recent years, they have suffered the same cuts in research council funds that have been felt elsewhere and one breeding programme, for Triticalae, the family that includes grasses and cereals, came close to being abandoned. Private industry should provide funds more closely related to profitability. But there must be some

The new owners want you to concentrate on improving coca-leaf yields...



doubts about the longer term. Before privatization, PBI's molecular genetics and cytogenetics sections will be split off and combined with other AFRC institutes to form a new Plant Sciences Institute. That, according to PBI's director Professor Peter Day, will threaten a much admired quality of the institute, its ability to "couple disparate activities" under one roof. Whether it makes sense to remove the plant breeding part of the institute from its more basic molecular genetics research section just when the impact of molecular genetics is beginning to be felt must be a matter of controversy.

Much will depend on the buyer. The favourite is the Agricultural Genetics Company, a private company partly own-

ed by the British Technology Group that was set up in 1984 and given first option to develop plant biotechnology discoveries made at AFRC institutes. Although the company is well placed to ensure that fruitful cooperation between the privatized institutes and the research laboratories of AFRC continues, it lacks size. It is still a small organization with fewer than 30 staff, based at Cambridge's Science Park. Big multinational agricultural companies are bound to recognize the appeal of the two institutes and to be able to offer far more money for them. The only reservation they are likely to have is that the Agricultural Genetics Company has already gained the right to commercialize

NEWS:

many of PBI's discoveries. Whether the government will accept the Agricultural Genetics Company's view that it is "the natural vehicle for maintaining the integrity and future development" of the institutes within the private sector should be decided within the next few months.

491

The future of the remaining "plant sciences" fragment of PBI is unclear. The new Plant Science Institute will be completed by the addition of the John Innes Institute, the Unit of Nitrogen Fixation at the University of Sussex and a small part of the Rothamsted Experimental Station. But no provision has been made to bring the various parts together at one site the "institute" will be more of an administrative convenience. Again, it is not clear if AFRC will itself profit from the sale of PBI or whether the proceeds will accrue directly to the Treasury. Alun Anderson

US-Soviet exchange

Relations thaw in the far north

Washington

An agreement between the University of Alaska at Anchorage and the Siberian Branch of the Soviet Academy of Medicine to study problems of human adaptation to circumpolar living was endorsed by a Soviet delegation visiting Washington last week. But last minute uncertainty about official Soviet participation pointed up the fragility of US—Soviet relations.

For five years, Ted Mala, associate professor of health sciences at the University of Alaska, has been trying to work out an agreement with Siberian scientists to study health issues relating to life in the far north. Mala wrote to Soviet leader Mikhail Gorbachev, who responded favourably to his suggestions for cooperation, and arranged meetings with officials of the Soviet health ministry as well as the medical workers' union. The US-Soviet Exchange Initiative Office, established after last winter's summit meeting between President Reagan and Mr Gorbachev to encourage people-to-people exchanges, supported Mala's efforts.

Last week an agreement between the University of Alaska and the Soviet Ministry of Health was due to be signed through the US-Soviet Exchange Initiative Office, and Mala was summoned from Alaska for the signing ceremony. But on arrival in Washington, the Soviet delegation declined to sign a formal agreement, saying the exchange could take place only under health agreements in effect since 1972. The delegation did sign what amounted to a memorandum of understanding saying that Mala could visit the Soviet Union to complete arrangements for the exchanges, but formal plans would have to be approved next by the US-USSR Joint Health Committee formed under the 1972 agreement — a committee that has not met for seven years.

Although health exchanges between the United States and Soviet Union have never stopped, there has been a slowing down in the past seven years. In 1972, the two countries signed two self-perpetuating agreements to cooperate in health sciences. The Joint Health Committee. consisting of senior health officials from both countries, met each year, but the United States cancelled the 1979 meeting following the Soviet invasion of Afghanistan. In recent years the climate has been changing, and a 1984 speech by President Reagan called specifically for the renewal of cooperation in the health sciences, a call given added impetus by last year's summit meeting.

A three-step plan has been worked out to improve relations. Surgeon General C. Everett Koop and Dr James Mason, director of the Centers for Disease Control, will visit the Soviet Union in October to discuss cooperation in the realm of public health. James Wyngaarden, director of the National Institutes of Health, will make a similar journey in November to discuss biomedical cooperation. Finally, the Joint Health Committee is to meet again next spring after nearly eight years.

As Mala's proposed exchange is strictly a private agreement between the University of Alaska and the Soviet Institute of Medicine, the US government has no control over what Mala plans to do. But the Soviet Union is placing things on a government-to-government basis. Harold Thompson, deputy director of the Office of International Health at the Department of Health and Human Services, says the US government is not happy with that arrangement, but does not feel that it should be allowed to interfere with exchanges.

Joseph Palca

US space

Continuing problems all round

Washington

THESE are trying times for US space scientists. The space shuttle is grounded until at least 1988, and when flights resume, competition for cargo space will be fierce. While there is discussion of launching scientific missions on expendable launch vehicles (ELV), for the time being nothing is decided. Planetary scientists are among the hardest hit. At the end of last month, they learned that new weight restrictions mean that neither the Comet Rendezvous Asteroid Flyby (CRAF) mission nor the Saturn orbiter (Cassini) can fly aboard the shuttle. This news follows a decision to abandon the shuttle/Centaur upper stage that would have been used to take Galileo to Jupiter (see Nature 321, 800; 1986). Bruce Murray, professor of planetary science at California Institute of Technology (Cal-



Moustafa T. Chahine—chief scientist at JPL. tech), puts it bluntly, "the US planetary program has collapsed":

For the Jet Propulsion Laboratory (JPL) in Pasadena, the delays will be especially difficult. JPL is run by Caltech for the National Aeronautics and Space Administration (NASA). Although JPL is engaged in a variety of projects from remote sensing to astrophysics to defence-related research, Solar System exploration has been its bread and butter. Fully 20 per cent of JPL's 1985 budget was spent on three planetary probes, Galileo, Voyager and the Venus radar mapper Magellan.

The uncertain future is beginning to take its toll on the staff of JPL, says Moustafa Chahine, its chief scientist. Chahine says morale is still high from Voyager's Uranus flyby last January, but senior scientists now face tough decisions. The median staff age at JPL is 42, and scientists are at a crucial juncture in their careers. "Would you commit yourself to 10 years of uncertainty?" asks Chahine rhetorically. Although nobody has yet left JPL, Chahine is certain that some will do so in the coming months.

That no major missions can be launched for at least three years does not necessarily have to be a drawback for planetary science, maintains Chahine. With a strong commitment from NASA, JPL would have no trouble assembling a team to plan new missions. Were planning to begin in 1988, a reasonable launch date would be the early 1990s, by which time either the shuttle or some other launch vehicle should be back in operation. Working on long-term projects is something JPL scientists are familiar with. What is needed, says Chahine, is a demonstration from NASA, in deed not just word, that planetary science will not be forgotten as NASA plans for the future.

JPL is not the only NASA centre to have taken a body blow from the delays in the space programme. Noel Hinners, director of the Goddard Space Flight Center in Greenbelt, Maryland, says Goddard also must cope with uncertainty. "Mentally, things are on hold", says Hinners. If the launch delays for Goddard projects such as the Gamma Ray Observatory or the Cosmic Background Explorer are of the order of one to two years, Hinners believes most key people will stay with the projects. But a delay of five years is a different story. Even keeping a launch team together for two or three years is tough, and Hinners reckons people will have to be laid off.

While the Hubble Space Telescope (HST) is in the same boat as the other major satellite launches, the delay seems to be less troubling to Garth Illingworth, deputy director of the Space Telescope Science Institute. He maintains that optical astronomers have never had a chance to become dependent on space-based observations, and can get by with existing ground facilities. "We are not really as subject to the feast or famine as the planetary people", he says.

James Welch, Space Telescope project director for NASA, agrees that principal investigators are unlikely to leave the project. But keeping the engineering team intact will not be easy, Directing routine maintenance while the satellite is in storage is not a stepping stone to career advancement. One challenging engineering problem has, however, recently cropped up for HST. NASA's heightened awareness of safety issues has prompted a re-evaluation of the natural frequency of satellite subsystems. If they coincide with the frequency of shock waves generated by the shuttle, there could be serious problems. Determining these frequencies is not easy, says Welch.

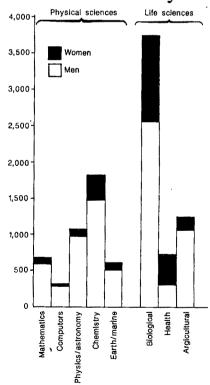
Although NASA and the Reagan administration have not yet enunciated a clear policy on alternative launch vehicles

to the shuttle, most members of the space science community see a new fleet of expendable launch vehicles as crucial. Tom Donahue, chairman of the National Academy of Sciences Space Science Board, told Congress last month that he supports the use of the Air Force's new Titan 34D7 to launch deep space missions. Donahue favours moving to the Titan 34D7 to launch Galileo, Magellan and Ulysses (the joint mission with the European Space Agency to study the Sun's polar region) even if it means postponing acquisition of an orbiter or slowing down work on the space station.

If there is any bright side to the current upheaval, Murray believes it may be the study of Mars. The Mars Observer, the first of a series of low-cost planetary probes, is scheduled for a 1990 launch, and could still make use of the shuttle. Murray says the Soviet Union is planning two major missions to Mars in the next five years, and there have been non-governmental discussions about a joint United States/Soviet Union mission. These factors may make Mars programmes attractive candidates for new funds.

Joseph Palca

US doctorates by sex



THE numbers of doctorates awarded to men and women in the United States in 1985, taken from a report from the National Science Foundation division of science resource studies. In total 4,531 doctorates were awarded in physical sciences (3,817 to men, 714 to women) compared with 5,748 in the life sciences (3,893 men, 1,855 women).

New telescopes

Shining mirrors at Apache Point

Washington

USING a new mirror technology and a new design, a consortium of five universities is planning to build a 3.5-metre telescope in New Mexico's Sacramento Mountains. With a recently awarded grant of \$3.74 million from the National Science Foundation (NSF), the Apache Point Observatory is scheduled to begin operation in 1988.

Apache Point's mirror is a smaller version of the type of mirror likely to be used for the National New Technology Telescope (NNTT). It is cast using borosilicate glass and spun as it is cast, allowing a closer first approximation of the desired parabolic shape. The new techniques result in lighter and less expensive mirrors, bringing the cost of observatories the size of Apache Point to a level manage-

More ocean dives

Tokvo

THE US submersible Alvin is scheduled to make its first visit to Japanese waters in 1987. Scientists from the United States and Japan have agreed plans for at least 85 dives to investigate the back- and fore-arc regions of the western Pacific.

Dives will be made in three areas; the Mariana Trough, a back-arc spreading centre, the Mariana fore-arc region which overlies the subducting Pacific Plate and the Sumisu back-arc rift northwest of the Ogasawara Islands.

Among the features to be investigated are a methane plume billowing up to 700 m above the floor of the Mariana Trough; diapiric seamounts bulging out of the seafloor of the Mariana fore-arc region; a chain of volcanoes that trends across the back-arc basin from the Northern Mariana Arc; and the Sumisu Rift which is thought to be a modern analogue of the setting for the Kuroko massive sulphide ore deposits on the Japanese mainland.

Funding for the project, which will run up a bill of a few million dollars, will be covered almost entirely by the US side.

Follow-up investigations of the survey area by the Japanese submersibles Shinkai 2000, and, when completed, Shinkai 6500, are expected to be made in the near future according to Hiroshi Hotta, director of the Deep-Sea Research Department of the Japan Marine Science and Technology Center (JAMSTEC), who will participate in the Alvin survey. In a recent review of policy, JAMSTEC decided to devote attention to the spreading ridges and rift basins in close proximity to Japan, such as the Okinawa Trough and Sumisu Rift. Also, in future, foreign scientists will be allowed to board Shinkai 2000. **David Swinbanks**

able by a small research consortium.

The five universities are not all equal partners in the project. The University of Chicago and the University of Washington will both contribute 31 per cent of the project costs, Princeton University and New Mexico State University 16 per cent and Washington State University the remaining 6 per cent. Bruce Margon of the University of Washington, chairman of the Astrophysical Research Consortium formed by the universities to build Apache Point, says viewing time will be allocated in accordance with contributions. Margon estimates the total cost of the project will be \$10 million.

Using private funds to build large observatories is a new trend. Several university groups have announced plans to build 7.5-metre telescopes, and the Keck Telescope, a 10-metre segmented mirror telescope that will be operated by California Institute of Technology and the University of California, is already under construction in Hawaii.

Several factors make Apache Point attractive. The observatory is the first designed for complete remote operation. Margon points out that this allows users to wait for appropriate conditions without having to make a pilgrimage to New Mexico. It will also be possible to divide a night's observation among astronomers at different institutions.

The performance of Apache Point may well exceed that of larger telescopes for certain problems. Keeping the structure housing the telescope to an absolute minimum will reduce atmospheric distortion caused by the heat from the observatory's own instruments. Sacramento Peak is also one of the darkest points in the United States, making it an attractive spot for observing extremely low light objects.

Perhaps most alluring to consortium members is that once built. Apache Point will be theirs to use as they please. Observing time is oversubscribed at the Kitt Peak National Observatory in Auzona and Cerro Tololo Inter-American Observatory in Chile. At Apache Point, says Margon, users will be able to tackle longer term and speculative projects

Joseph Palca

Timber trade

A little hope for tropical forests

AT long last the world has an international forum that could help avert the total destruction of tropical forests. All the major tropical timber producing and consuming nations agreed in Geneva last week to put into operation the International Tropical Timber Agreement. Among its clauses are those aimed at "sustainable utilization and conservation of tropical forests and their genetic resources, and at maintaining the ecological balance . . .".

The agreement has been twenty years in the making and has been held up for more than a year by a squabble over the location of its headquarters. Only after a fresh meeting broke up in disarray was agreement finally reached: the headquarters are to be established in Yokohama and its executive director is to be Mr Haji Freezailah, deputy director-general of forestry for Malaysia. This arrangement neatly ties together the world's biggest tropical timber producer, Malaysia, and the biggest consumer, Japan. But argument is continuing over the budget for the new organization and nobody yet knows how effective a body it will be.

The UN-sponsored agreement does not establish a cartel and has no powers to fix prices or to regulate exports. But it does provide a talking shop for 41 nations that between them account for 95 per cent of the world's trade in tropical timber and, uniquely for a trade agreement, it has among its principal goals the preservation of tropical forests so that they may be

managed as a renewable resource. Other aims, also intended to benefit timber producers in the developing world, are to promote research and development in tropical forest management and utilization and to encourage the processing of timber in producing countries to promote their industrialization and export earnings.

The Scandinavian countries have taken the lead in introducing into the agreement clauses aimed at protecting tropical forests. Voting rights have been equally distributed among producer and consumer countries and if a majority can be found there is every chance that these clauses can be translated into action. The chief obstacle is likely to be lack of money Several thousand million dollars need to be spent to halt tropical deforestation and the producer countries naturally feel that the bulk of the burden should be borne by the wealthy consumers. As a practical first step, the World Wildlife Fund is urging the appointment of an experienced forest ecologist to help run the agreement and prevent forest disasters; it also wants at least \$5 million to be set aside for conservation projects in the short term and says that prices for tropical timber should include the cost of reforestation, conservation and research on sustainable management. It is likely to be next spring, at the earliest, before the organization announces its initial budget and there is any indication of how successful it might be.

Alun Änderson

Academic oppression in Chile

Sir—On the afternoon of 1 July, we witnessed the siege and assault of the building of the School of Medicine of the University of Chile by a combined force of the military and the police. Military vehicles and troops first circled the quadrangle where the School of Medicine and its teaching hospital are located and then occupied both buildings. Among other actions, we saw a group of soldiers, armed with automatic weapons and with their faces painted black in combat camouflage, as they took twenty students as prisoners and made them lie face down on the floor of the hall of the School of Public Health.

Afterwards, another seventy students tried to take refuge in the classrooms of the department of physiology. The police broke in, took them out, and lined them up in the hall in order to arrest them. At that point, a professor implored the many faculty members gathered there to do something to prevent the students from being taken away. Her brave attitude created a vividly emotional atmosphere that allowed the dean of the faculty to persuade the police not to proceed to further arrests.

This episode was only one of the many assaults in the past weeks by combined military and police forces in several faculties of our university that have ended with violent arrests of students. These assaults typically include tear-gas bombing, the breaking into the university yards of heavily armed soldiers and vehicles and, in some cases, the destruction of installations and laboratory equipment. As a matter of fact, the action on 1 July was taken because the students were peacefully protesting against the arrest of 118 of their fellows, including the president and other members of the student council, which had occurred the day before inside the university main building. The student leaders were arrested invoking an article of the new Chilean constitution that allows special action to be taken against "terrorists that cause public alarm".

Student demonstrations have been aimed at ending the overt government intervention suffered by our universities since the 1973 military takeover; at the same time, the professors of the University of Chile have recently asked, through a referendum, for the resignation of the present principal of the university, a serving major general of the Army, and the election by the academic community of academic authorities.

On 2 July, Carmen Gloria Quintana, an 18-year-old student of the University of Santiago, and Rodrigo Rojas, a 20-yearold Chilean who had recently arrived from the United States where he was a resident, and who was collaborating as a computer programmer at the department of physiology of the University of Chile School of Medicine, were found with burns that extended over 60 per cent of their body surface. This event has been well documented by the world press.

On 10 July, the government arrested some prominent leaders of social institutions, who had concurred in the creation of an Assembly of Civilians, asking for the return of the country to a democratic regime. Among those arrested were Dr Juan Luis Gonzalez and Dr Francisco Rivas, president and secretary of the Chilean College of Physicians, and Professor Patricio Basso, president of the Association of Professors of the University of Chile.

We think that these events should stimulate reflection and action by the international academic community. In experimental sciences, insights of widespread relevance are obtained not from the observation of phenomena in their usual context but rather from taking them to extreme conditions. In Chile, the relationship betwen university, society and the political regime has been brought today to a grotesque extreme.

> Rosa Devés NORBEL GALANTI CARLOS VALENZUELA ENNIO A. VIVALDI

Facultad de Medicina, Universidad de Chile, Casilla 137-D Correo Central, Santiago, Chile

AGS vindicated

SIR-In recent months it has been widely reported that scientists at Advanced Genetic Sciences, Inc. (AGS) "knowingly falsified" data in an application to the US Environmental Protection Agency (EPA). EPA has now "concluded that there is no information to indicate that (AGS) knowingly falsified its application".

The original allegations of data falsification surfaced during a congressional subcommittee hearing, and were based upon an unsigned two-page handout and an 8 × 10 inch photograph. These documents were supposed to demonstrate inadequate experimental design and plant pathogenic effects of the recombinant Pseudomonads, and were purportedly the subject of an AGS cover-up. EPA now accepts this "evidence" was inaccurate.

Unfortunately our vindication from the charge of falsification will not automatically reverse the damage that has been done to the reputations of individual scientists at AGS. The uncritical reporting of these allegations has caused much damage; scientific fraud should not be taken so lightly.

An article in Nature (320, 472; 1986)

referred to the allegations as though they were established fact, perhaps because of a misunderstanding of the operating procedure of EPA's Office of Enforcement and Compliance Monitoring. The process of developing an "administrative complaint" is interactive and EPA's initial charges were apparently made more in the spirit of prosecutor than in the role of judge. In fact, the charges of data falsification were not supported by EPA's own data audit, the basis for the final retraction of those charges, which had already been completed when the initial complaint was

How and why did this situation lead to the publication of misleading, unjust and damaging reports? Somewhere between the deed and the reporting, the process of disseminating information went badly awry. It should be of concern to everyone when the news reaching the scientific community becomes subject to distortion by politics and sensationalism. It should be of concern to everyone that our case demonstrates the success of a frightening weapon the gratuitous accusation of fraud.

J. Bedbrook, P. Dunsmuir, J. LINDEMANN, T. SUSLOW, G. WARREN Advanced Genetic Sciences, Inc., 6701 San Pablo Avenue,

Oakland, California 94608, USA

• We are glad to clarify that the allegation of falsified data appeared only the EPA's formal complaint, not in its announcement that AGS would be fined \$20,000 (later reduced). But should not EPA be more careful about giving currency to allegations such as these, especially when it knows them to be unfounded? -Editor, Nature.

Parapsychology

SIR—Elitzur¹ criticizes Marks³ for having omitted "representative" works. I know of no work that could be acceptable as a case for parapsychology. As for the extraordinary instrumental sophistication proudly presented, my question is why such a complicated mess is necessary for the basically rather simple claims of psi such as telepathy, telekinesis and so on. If they existed, their demonstration should actually be simple.

There is an explanation for the complexity. The more complicated the experiment, the more likely it is that it will have errors that will be attributed to psi. At the same time, it becomes easier deliberately to introduce errors and more difficult and time-consuming for sceptics to find them. If anything, the mentioned counterhypothesis coincidence, artefact, selfdeception and fraud become more likely.

Amardeo Sarma

Kirchgasse 4, D-6101 Rossdorf 1, FRG

- Elitzur, A.C. *Nature* 321, 465 (1986).
 Marks, D.F. *Nature* 320, 119 124 (1986).

Hanover highlights all the latest developments

and industrial applications

in the field of biotechnology

From its very inception **BIOTECHNICA** Hanover has established itself as Europe's leading forum for research, development and practical applications in the field of biotechnology. The basis for the unprecedented success of BIOTECHNICA is two-fold. Firstly, the excellent program of symposia, workshops and lectures held by internationally renowned experts. And secondly, the user-oriented exhibition presented by leading manufacturers and research institutes.

The international congress – a meeting-place for experts

On three successive days, 16 internationally renowned experts will deliver papers on the application of biotechnology in the following fields:

Medicine/pharmacology

e.g. diagnostics and various approaches to therapy following cardiac infarction

Food production/ agriculture

including the optimization of agricultural produce and quality control in foodstuffs

Environmental protection

from biological methods of combating air pollution to the treatment of sewage

Seminars and workshops – a spotlight on research and its practical application

Research institutes, universities and leading manufacturers will utilize the comprehensive parallel program of talks, symposia and workshops in order to present their latest research findings, products and processes. Hanover illustrates how research findings can be transformed into marketable industrial processes and products.

In a series of special seminars organized by the European Community, BIOTECHNICA'86 will also present the most important results of the biotechnological research projects funded by the EC.

The 3rd US Seminar for Biotechnology, organized by the US Foreign Commercial Service, will also be held on all three days of BIOTECHNICA'86.

The exhibition – geared to industrial applications

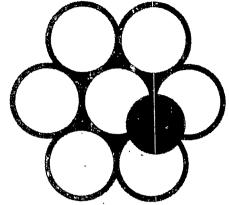
Over 200 research institutes and commercial firms will exhibit at BIOTECHNICA'86. The exhibition will highlight biotechnological processes and products, the latest developments in laboratory equipment and techniques, as well as new production technology. It's no surprise, therefore, that in 1985 some 3,500 professional visitors from 27 countries attended this comprehensive display.

At BIOTECHNICA Hanover'86 you can find out all you want to know about every major aspect of hiotechnology.

If you require more information please contact:
Deutsche Messe-und Ausstellungs-AG Abtlg. "Neue Projekte"
Messegelände, D-3000 Hannover 82
Tel.: (0) 511/89-2720

23rd-25th September 1986 2nd International Exhibition+Congress for Biotechnology





The British Journal of Cancer

The Scientific Journal of the Cancer Research Campaign

Editorial Board D.G. Harnden *Chairman*M.Moore *Editor*

G.E.D. Adams M.R. Alderson K.R. Harrap H. Harris

P. Alexander

J.S. Jenkins

K.D. Bagshawe

N.H. Kemp

M. Baum

B. Ketterer

R.J. Berry

L.J. Kinlen

G.D. Birnie

J.O.D. McGee

N.M. Bleehen

N.A. Mitchison

P. Brookes

A.M. Neville

T.A. Connors

J.G. Ratcliffe

D. Crowther

N.G. Testa

J. Denekamp

P.R. Twentyman M.A. Vessey

M.J. Embleton P. Gallimore

R.A. Weiss

J. Hardcastle

N.M. Wilkie

- * one of the leading cancer journals in the world publishing articles on all the relevant major scientific disciplines
- includes original papers and short communications submitted by scientists, researchers and oncologists throughout the world
- * regularly publishes proceedings of the meetings of the British Association for Cancer Research
- reports on other selected national and international conferences and symposia
- each issue contains authoritative book reviews
- provocative Correspondence, international Calendar of Events

Subscription Order Form

- To: Richard Gedye, the British Journal of Cancer, Farndon Road, Market Harborough Leigestershire LE16 9NR J.K.
- Please enter my subscription to the British Journal of Cancer for TWO YEARS commencing with the current year @ £250.00 thereby avoiding any price increase.
- Please enter my subscription to the British Journal of Cancer for ONE YEAR commencing with the current year @ £125.00
- C) I enclose a cheque made payable to Macmillan Journals for £*
- 1 I authorise you to charge my VISA*/ACCESS*/MASTERCARD* the amount

Credit card Account No

Signature Expiry date
All orders must be accompanied by cheque or credit card authorisation.

Subscription Information

ISSN 0007-0920

Frequency: Monthly - Two volumes per year

Language: English

Rates per year

UK & Éire: £125.00, USA/Canada: US\$275.00 (surface) US\$330.00 (airmail), Rest of World: £165.00 (surface) £200.00 (airmail)

Two Year Subscription

Save money and ensure an uninterrupted supply of the Journal – simply double the payment sent.

Please write in BLOCK CAPITALS

☐ Please send me a free sample copy of the British Journal of

MACMILLAN PRESS

New ways with quasi-crystals While theorists continue to brood about the properties of quasi-crystals, experimentalists have begun

to simulate them in the laboratory to tell how they behave.

WHETHER the unexpected fivefold geometrical symmetry of the manganesealuminium alloy MnAl, springs from an underlying quasi-crystalline structure, from twinning on a microscopic scale as Linus Pauling says (see *Nature* 317, 512: 1985) or from a quite different phenomenon not yet identified, the whole idea of fivefold symmetry has enlivened several groups of people. That the theorists should have jumped in the new pool feet first is not at all surprising, which is why it is a little shocking that there is still no straightforward way of writing down a formula that will specify which points in three-dimensional space are the permitted vertices of a quasi-crystalline lattice. (The best approach is still to suppose that a three-dimensional quasi-crystal is the projection of a six-dimensional lattice on a three-dimensional surface.) But now the experimentalists have joined the fray, with entertaining consequences.

That fivefold symmetry is unattainable in an infinite regular crystal lattice has been known since the allowable symmetries of crystal lattices were first enumerated in the nineteenth century. The quasi-crystal explanation of the MnAl., alloy, whose strange symmetry was first recognized by Schachtman, remains essentially that suggested more than eighteen months ago by D. Levine and P.J. Steinhardt (Phys. Rev. Lett. 53, 2477; 1984). A quasi-crystal is not a regular lattice in which all vertices can be reached from all others by displacements represented by integral multiples of some basic set of vectors. Instead, the argument goes, the directions of the lattice bonds drawn between nearest neighbours in the crystal lattice take only a finite number of values, but the distances between successive vertices along a line, far from being equal, as in a regular crystal, may take one of two (or more) values which are, of necessity, incommensurate - their ratio is an irrational number. In two dimensions, the prototype of a quasi-crystal is the Penrose tiling of the plane, a kind of party trick by which a plane surface can be filled by rhombi of two distinct shapes yielding local fivefold symmetry. In this case, the crucial irrational number is the old Greek golden mean, half the square root of 5 plus 1.

How do experimentalists weigh into such a field? Here is a neat example, based on the familiar observation in superconductivity that the magnetic flux within a sufficiently small superconducting loop will ideally be quantized in the sense of being an integral multiple of the elementary quantity hc/2e, where h is Planck's constant, c the velocity of light and e the charge of the electron. Only integral multiples of this magnetic flux are compatible with the condition that the superconducting loop carries no electric current. The origin of the condition is the requirement that the phase of the wave function describing electrons in the superconductor should be unambiguously defined.

Now a six-person group based mainly at the University of Pennsylvania but including Levine (op. cit.) has devised a clever experiment to show that magnetic fields can tell the difference between lattices that are regular and those that are merely quasi-crystalline (A. Behrooz, et al., Phys. Rev. Lett. 57, 368; 1986). What this group has done is to build a pair of twodimensional arrays of aluminium wires merely 50 nm in diameter, one of which is a quasi-crystal of holes in one dimension, the other almost a Penrose tiling. The group has then measured the superconducting properties of this array in the presence of magnetic fields of different strength with the objective of telling how quanta of flux are distributed among the differently shaped holes of the lattice.

Others have previously set out to tell what happens when regular (not quasiperiodic) superconducting meshes are immersed in a magnetic field. If the total amount of flux, supposed uniform, across the mesh is an integral number of flux quanta, no electric current need flow in any of the wires so as to ensure that the phases of the electron wave functions are well defined. One of the simplest ways of recognizing that state of grace is to measure the temperature at which the superconductive transition takes place. If the temperature is identical with that of the superconducting phase transition in the absence of a magnetic field, the inference is that the flux through each and every hole in the mesh is an integral multiple of the flux quantum. Otherwise the transition temperature will be reduced. Behrooz et al. refer to earlier results showing that when the total flux through a regular mesh is less than enough to provide one flux quantum through every hole, the transition temperature is most nearly normal when the field is enough to endow each hole in the mesh with a rational (as distinct from irrational) fraction of a single I flux quantum.

That is an obvious starting point for the experiments now described. The simplest trick is to make a mesh from 50 nm aluminium wires which are regularly spaced in one direction but whose spacing in the orthogonal direction is that of the Fabonacci sequence, whose spacings are related by the irrational golden mean. For practical purposes, there are holes of two different sizes whose areas are irrationally related to each other. The experimental result is striking, even startling. The temperature of the superconducting transition is most nearly normal when the average magnetic flux through each hole amounts to a number of flux quanta which is a power of the golden mean. The inference is that the most energetically favourable distribution of the magnetic flux is one on which as many holes as possible are threaded by integral numbers of flux units, which is what would be expected. It is nevertheless remarkable that it should in principle be possible to measure the irrational ratio of the dimensions of the mesh simply by measuring the transition temperature as a function of total flux through all the holes.

Similar results have been obtained with a network analogous to the Penrose tiling of the plane, but where the characteristic irrational ratio is the square root of 2 (Forgivably, the authors say that they were unable to make a true Penrose tiling with their microfabrication apparatus. which is nothing to be ashamed of: they managed 20,000 holes of two different shapes related by the square root of 21 Again the most favourable threading of the total flux through the different holes is that determined by the irrational number The principle is merely that the best configuration is that when the quantum condition is most often satisfied. What the practical applications will be is anybody's guess, but there could hardly be a more vivid proof of the quantization of magnetic flux.

As it happens, a calculation of a more general system of this kind, a randomly organized superconducting network, has been produced by two Argentinian physicists, J. Simonen and A. Lopez (Phys. Rev. Lett. 56, 2649; 1986). Again, the conclusion is that integral numbers of flux quanta are energetically favoured. Meanwhile, experimentalists are busily studying other quasi-periodic structures. Obviously there is a whole new world to explore. John Maddox

Astronomy

First X-ray-ionized nebula

from A.C. Fabian

The hottest objects in a galaxy, the binary X-ray sources, should produce the most highly ionized nebulae. Despite extensive calculations of the ionization state of gas around X-ray sources (McCray, R. et al. Astrophys. J. Lett. 311, L29; 1977), no such nebula had been found until M.W. Pakull and L.P. Angebault studied the Large Magellanic Cloud carefully, as they describe elsewhere in this issue (Nature 322, 511; 1986).

Spiral and irregular galaxies are dotted with nebulae excited by hot stars. The H II regions are ionized by the ultraviolet radiation from massive main-sequence stars and glow mainly through recombinationline radiation. The even hotter cores of evolved stars that have recently ejected their outer envelopes, the planetary nebulae, ionize substantial amounts of helium as well. Visible radiation from planetary nebulae give an estimate of the ultraviolet radiation field, and thus surface temperature, of hot stars. In principle, this is a relatively simple deduction if it is assumed that all the photons capable of ionizing gases such as hydrogen do so, and that the resulting photon luminosity in some recombination line can be estimated from the observations.

The major problem in the search for nebulae around X-ray sources is that they tend not to be in dense gas environments, so the luminosity of the nebulae is very low. Massive main-sequence stars, by contrast, are young and embedded in dense star-forming clouds. Moreover, planetary nebulae create their own dense surroundings in the ejected stellar envelope.

The X-ray ionized nebula discovered by Pakull and Angebault, LMC X-1, was the first X-ray source found in the Large Magellanic Cloud and is securely identified by them with an 07 III-V star. The star appears to be surrounded by a nebula of radius 5 pc that emits visible lines of hydrogen and ionized helium as well as of doubly ionized oxygen. The He II emission is simply explained by the recombination of He III ionized by extreme ultraviolet photons of energy greater than 54 eV. These photons imply a much harder spectrum than any normal star and are consistent with the X-ray source. The centring of the emission on the 07 star identifies it, or rather its binary companion, as the X-ray source.

The extreme ultraviolet spectrum of LMC X-1 is of particular interest because the source is a black-hole candidate. Pakull and Angebault estimate that the spectrum is flat below the X-ray observed photon energies of ~1 keV down through

the otherwise invisible extreme ultraviolet to the ultraviolet. This could be the thermal black-body emission from an accretion disk. The spatial extent of the surrounding He III zone is ~10 light years and so presumably indicates that the source has maintained that spectrum and luminosity for at least the past 10 years.

LMC X-1 is an unusual black-hole candidate as it seems to be stuck in a 'high-state' (White, N.E. & Marshall, F.E. Astrophys. J. 281, 349; 1984). The other black-hole candidates such as Cygnus X-1 switch between 'high'- and 'low'-states for about a month every year or so. (A high-state is characterized by a higher luminosity and steeper (softer) X-ray spectrum and a low state by the opposite.) An X-ray nebula around Cygnus X-1 should then appear as a set of rings around the source marking the past few high-

states. Unfortunately, the other blackhole candidates seem to be in low density regions and the He $\scriptstyle\rm II$ nebula more or less undetectable at present. Indeed, it is curious that LMC X-1 is in a high-density region. The formation of the compact object in a binary X-ray source is expected to impart a substantial velocity to the system by momentum conservation. LMC X-1 should then be a long way away from the region of its birth. Perhaps it just happens to be passing through a dense region.

Pakull and Angebault remark that the LMC X-1 He in region is similar to the narrow-line region of a Seyfert galaxy. We can expect more investigations of the narrow-line region of LMC X-1 to explore this similarity as well as more searches around other black-hole candidates and X-ray sources. Such investigations have already revealed a high-excitation emission-line region around another LMC binary, LHG83.

A.C. Fabian is at the Institute of Astronomy, University of Cambridge, Madingley Road, Cambridge CB3 0HA, UK.

Palaeoanthropology

Human phylogeny revised again

from Eric Delson

A newly recovered cranium of one of the early human species called robust australopithecines may well force palaeoanthropologists to reconsider the evolutionary relationships among all Australopithecus forms. On page 517 of this issue', Walker and colleagues describe two specimens (a partial lower jaw and a skull lacking most of the teeth and part of the skull roof) found in sediments on the west side of Lake Turkana, Kenya, dated about 2.5 million years (Myr) old. Many of those who have had the opportunity to study a replica of the skull feel that it is the most exciting fossil hominid found since 'Lucy' in 1974 (ref. 2).

The record of early humans (upright bipeds with small canines and apparently already partly expanded brains in comparison to body size) begins about 4-5 Myr ago in eastern Africa. The first wellpreserved remains are those from Laetoli about 3.7 Myr) and Hadar (3.3–3.0 Myr) generally termed A. afarensis. This species is often thought to be close to the base of the radiation of Plio-Pleistocene humans, but opinions differ widely on details. Later australopithecine species include the 'gracile' A. africanus of South Africa, 3.0-2.3 Myr in age; 'robust' A. robustus (and perhaps a distinct A. crassidens) from 1.9-1.6-Myr-old caves in South Africa; and the hyper-robust A. boisei from eastern Africa, well known between about 2 and 1.3 Myr ago. Based on his identification of isolated teeth and the revision of Omo chronology by Brown et al.³, Grine⁴ has argued that A. boisei may occur as early as 2.5 Myr ago in Lake Turkana basin. The earliest Homo fossils appear about 2 Myr ago in both eastern and southern Africa.

Although there is no consensus, most probably agree with the interpretation of Rak⁵ and of Kimbel and colleagues⁶ that A. afarensis is close to the common ancestor of two main lineages of early humans, one leading to Homo but unknown in the 2–3 Myr interval, the other passing through a 'gracile' stage to terminate in several robust species (of which the South African form is most like the common ancestor).

Others, especially Olson⁷, have suggested that A. afarensis is a mixture of two species, with most of the cranial and dental material being an early robust form based on shared features that are considered derived for the robust lineage, whereas Lucy and other less complete remains are like gracile forms and later Homo. Skelton et al. conclude that a third option is best: deriving both Homo and robust forms from A. africanus, with A. afarensis as an earlier ancestral stage.

The new robust fossils add to this already confusing picture. Walker *et al.*¹ make two main points in their analysis.

Age (Myr)

Possible evolutionary relationships among Plio-Pleistocene homínids. Solid lines, known ranges of taxa; dashed lines, probable range extensions and hypothesized relationships.

They argue first, that the new specimens can be included within the known species A. boisei; and second, that their antiquity now makes it impossible for South African A. robustus to have been ancestral to A.

In their Table 2, Walker et al. summarize the distribution among australopithecine taxa of 22 craniodental character states but their data do not, in my opinion, support allocation of KNM-WT 17000 to A. boisei. Of the 22 features, the new skull is apparently phylogenetically conservative in 11 and reasonably conservative in two more; in one (orbital height), it is similarly conservative in that only A. boisei is derived. In having the I² roots medial to the nasal margin, all postafarensis forms are linked indeterminately. Thus, 15 of 22 features are phylogenetically neutral. In four characters, WT 17000 is grouped squarely with the other robust forms by derived features, but then only three remain to place the skull within the robust group. Of these, the shape of the orbital margins links it to A. robustus, whereas foramen magnum shape is shared with A. boisei; in neither character, however, is the state known in A. afarensis nor can an ancestral condition be readily determined.

The absence of a maxillary fossula appears to be a second link to A. boisei, but only if Rak's interpretation of development of the fossula in the africanusrobustus lineage and loss by boisei is accepted. If the fossula and related anterior pillars are functionally linked to canine root size, the fossula could even be independently derived in the two South African species — I consider this character as yet of indeterminate polarity. Walker et al. add to these tabulated features the supposedly boisei-like nature of the infraorbital, nasal and zygomatic root regioins, but interpretations of those similarities differ among observers. We are thus left with only large overall size (and geography) as reasons for including WT 17000 within A. boisei and in the light of the quite distinctive mosaic of characters seen in WT 17000 (for example, prognathic lower face and lack of a bare area where the muscle crests join), I would have assigned it to A. boisei only hesitantly at best. Further analysis (including study of Olson's characters of the mastoid and nasal region) could well show WT 17000 to be a rare case in which a new hominid merits description as a new species.

On the question of phylogeny, Walker et al. have argued that the great age of the new material falsifies the hypothesis that A. robustus or a similar taxon was ancestral to A. boisei. But it is possible (although undemonstrated) that a form resembling A. robustus inhabited southern (or eastern) Africa between 3 and 2.5 Myr ago, giving rise to all of the post-2.5 Myr robust species including WT 17000. As the new skull (and Lucy before it) showed, predicting fossil morphology in barren time periods is a risky pursuit.

But it is morphology and not time that reveals which taxa (or samples) are most closely related, and in this case, it seems best to interpret the new West Turkana robust forms as representing a population near the divergence of the southern and eastern variants. Although retaining

many character states seen in A. afarensis (and perhaps A. africanus as well), the form represented by WT 17000 presents several features characterizing all robust forms but few specific to either boises or robustus. Its discovery leads paleoanthropologists to reassess the trends suggested by Rak for relating the gracile and robust species and the relationship of A. afarensis to all later species. The figure illustrates one such view.

- Walker, A., Leakey, R.E., Harris, J.M. & Brown F.H Nature, 322, 517 (1986).
- 2. Johanson, D.C. & Edey, M. Lucv (Simon & Schuster New
- 3. Brown, F.H., McDougall, I., Davis, T. & Maier, R. in Ancestors: The Hard Evidence (ed. Delson, F.) 82 (Liss New York, 1985).
- Grine, F.E. in Ancestors: The Hard Evidence ed Delson E.) 153 (Liss, New York, 1985)
- 5. Rak, Y. The Australopathecine Face (Academic, New York
- Kimbel, W.H., White, T.D. & Johanson, D.C. in Arcestors: The Hard Evidence (ed. Delson, F.) 120 (Ers. New) York, 1985).
- 7. Olson, T.R. in Ancestors: The Hard Evidence (cd. Delson
- E.) 102 (Liss, New York, 1985)

 8. Skelton, R.R., McHenry, H.M. & Drawhorn G.M. Curr Anthropol., 27, 21 (1986).

Eric Delson is Professor of Anthropology at the City University of New York and works in the Department of Vertebrate Palaeontology, the American Museum of Natural History, New York, New York 10024, USA.

Protein structure

Kinky variations of collagen

from John Galloway

DISCONTINUITIES compel our attention. They are a surprise, as much in the molecular biology of structural tissues as in everyday living. The principle of simplicity leads us to presume that a structure like the triple-helical collagen molecule, with its great uniformity of amino-acid sequence, will also be uniformly stiff and therefore straight or smoothly curving. Intuitively we do not expect it to kink abruptly. Perhaps that is why more than ten years have elapsed before a molecular model first aired in Nature in 1974 and elaborated two years later1.2 has now resurfaced3. In the intervening period the significance of the model has been considerably enhanced. Its interesting and novel feature - then only tentatively suggested1.2 but now formulated more concretely — namely that collagen molecules bend sharply at well-specified positions, now appears (or is thought to appear) in various tissues.

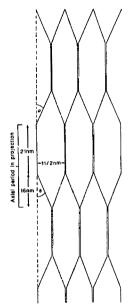
The collagen in question is that of the egg case of the dogfish Scyliorhinus caniculus. It differs from most known structural collagens in that it is secreted by epithelial cells rather than being produced by fibroblasts — a feature it shares, possibly significantly, with the better-known type IV collagen of basement membranes. It also differs from other, better-known, fibrillar collagens in forming a structure with an

axial period of 37 nm rather than the customary 67 nm. Under the electron microscope in transverse section it is seen to possess small crystalline regions in which a square lattice of side 11 nm is apparent. This is another unusual feature. as this sort of direct information has not been available for other collagens.

Briefly, the model (which is still schematic) is as suggested in the figure. The molecules (or groups of molecules) run parallel to the fibre axis along the edges of square prisms of side 11 nm and height 21 nm; they then bend more or less sharply through an angle of about 26° in a plane diagonally bisecting the prism: then run for another 16 nm; and then bend back and resume their course, again along the edges of square prisms but now displaced by exactly half the diagonal of the prism. that is, by $11/\sqrt{2}$ nm. This process continues for considerable distances. In this intriguing model, the simple relationship between successive prisms presumably results from segments of precisely the same length tilting alternatively 'right' and 'left'.

The lattice is, of course, extremely open. The side-to-side separation of the roughly close-packed collagen molecules in rat-tail tendon is about 1.5 nm. in marked contrast to the 11-nm separation seen in the egg-case collagen. Such an

open-work structure presumably provides an extended scaffolding or mesh which is then filled by the extra accessory proteins. It is difficult to avoid the conclusion that the large molecular tilt is the mechanism by which the open-work threedimensional mesh is rendered possible at all, and kept mechanically stable. It is worth remembering that regular, planehexagonal meshes of collagen molecules have been proposed as a feature of basement membranes4. This may turn out to be a particularly useful comparison if, as is now speculated', the egg-case colla-



Presumed arrangement of collagen molecules in planes diagonally bisecting the 11-nm square prisms, a molecular arrangement similar to the Z disks of striated muscle. $\theta = \tan^{-1}(11/16\sqrt{2}) \approx 26^{\circ}$.

gen is closely related to that of the basement membrane.

There remains the question of what features of amino-acid sequence cause the molecule to bend. Because little or nothing is known of the sequence of eggcase collagen, the question cannot be addressed directly, but it might be worth rehearsing some options borrowed from other, better-described collagens. Again because of the possible link, basement membrane collagen might offer a clue. Hoffmann et al. report' that the flexibility of the type IV molecule varies in a marked way along its length and claim this to be consistent with what is known of the amino-acid sequence of the molecule, namely that it contains several interruptions in the otherwise regular sequence of triplets, Gly-X-Y. This approach has led to a view of the molecule as a series of stiff, triple-helical segments connected by short lengths of flexible non-helix.

A similar mechanism certainly seems to operate in the best-described collagen kink — that found in the molecule C1q of the complement system. All three chains, A, B and C, of the triple-helical parts of

the molecule have been fully characterized. Close to the kink in A, threonine is inserted between two triplets; an alanine substitutes for a triplet glycine in C and an entire extra triplet is apparently inserted into B (ref.6).

On the face of it this interruptive mechanism would not be generally available to vertebrate fibrillar collagens where the amino-acid sequence within the triplehelical part of the molecule seems to be encoded exclusively by exons containing an integral multiple of 9m nucleotides (m = 5.6.11.12 and 18) so that each exon encodes an integral number of triplets (unless the interrupting part itself always consists of triplets). Invertebrate collagens are less constrained. Could bending be brought about by mechanisms not involving residues actually interrupting the triplet sequence? For example, some regions of the molecule might simply be less thermodynamically stable. Hoffman et al.5 suggest that because imino residues are usually thought to confer stability, their absence over short regions might reduce local stiffness.

It is perhaps worth considering another possible mechanism in this class. The most striking single feature of the sequence of 1,014 residues in the triple-helical part of the a_1 (I) chain is the presence of a solitary, idiosyncratically placed glycine. The sequence contains 1,014/3 = 338glycines, each in position 1 of the triplet, and one glycine, residue 311, in position 2. Such a small residue in place of a much bulkier one could well promote buckling, especially as the extra glycine is a feature of two out of the three chains (the $\alpha_2(I)$ chain does not have it).

At least two detailed models for the structure of rat-tail tendon invoke molecular kinking^{7,8} and both suggest possible kinking sites at the gap/overlap interfaces.

The 67-nm D-period, which includes one gap and one overlap region, is known to run through almost 234 residues and the whole triple helix runs through 4 gaps and 5 overlaps. Thus the overlap length is $1,014 - (4 \times 234) = 78 (D/3)$ residues. The position of the interfaces are given by 234n, where n = 0.1.2.3.4 and 234n + 78. When n = 1 the interface falls at residue 312, that is, within one residue of the additional glycine.

Without a lot more work this observation, although interesting, is obviously no more than that. If every molecule kinks at every interface, what mechanism is operating at the other seven potential kinking sites? Perhaps the molecule does not kink at every potential site. At least one other case of a double glycine within a triple helix, residue 73 of the B chain of Clq, is not associated with kinking9.

If kinking is an important and universal feature of collagens then the range of ways in which it is contrived are worth studying, as are the ways in which genes conserve such crucial structural features. Reid9 has pointed out that in the gene encoding the B chain of C1q the single intron is located inside the codon for the glycine (other examples are known) within the inserted triplet and speculates that it might play a part in conserving the kink as a functionally important feature.

- Knight, D.P. & Hunt, S. Nature 249, 379 (1974).
- Knight, D.P. & Hunt, S. *Tissue and Cell* 8, 183 (1976). Knight, D.P. & Hunt, S. *Tissue and Cell* 18, 201 (1986).
- Madri, J.A. et al. Ciba Fdn Symp. 108, 6 (1984). Hoffmann, H. et al. J. molec. Biol. 172, 325 (1984).
- Reid, K.B.M. Biochem. Soc. Trans. 11, 1 (1983). Woodhead-Galloway, J. Acta Cryst. B33, 1212 (1977).
- Fraser, R.D.B., MacRae, T.P. Miller, A. & Suzuki, E. J. molec. Biol. 167, 497 (1983).
- 9. Reid, K.B.M. Biochem. J. 231, 729 (1985).

John Galloway is at the Medical Research Council, 20 Park Crescent, London WIN 4AL, UK. The views expressed here are the personal views of the author.

Muscle contraction

Through thick and thin

from Peter D. Chantler

Two recent papers report observations that both confirm and extend our ideas about how muscle contraction is regulated. Knox et al. look at the role of tropomyosin in regulatory myosins, whereas Bennett and Bagshaw² investigate the non-specific divalent cation binding site of myosin, the major protein of the thick filament.

Regulation of muscle contraction can be divided broadly into two types: thin filament control and thick filament control. Thin filament control, typified by vertebrate skeletal muscle, is a function of actin, tropomyosin and troponin. During activation of muscle from the relaxed state, troponin senses the calcium signal,

causes tropomyosin to move in the groove of the actin helix and thereby removes the obstacle that prevented attachment of myosin heads (crossbridges) to actin this is the well-known steric blocking model (Fig. 1a-c). In thick filament control, exemplified by scallop myosin, regulation of actin-myosin interactions is controlled by conformational events on the myosin head subsequent to calcium binding at a specific site (Fig.2, site 2). Hence, there is no need for tropomyosin movement in this form of regulation: indeed, full regulatory behaviour is observed in the absence of tropomyosin.

A practical consequence of the steric blocking model, reported many years

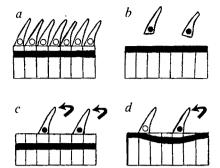


Fig. 1. The simplest explanation of rigor complex formation operative in thin filament regulation. Actin is represented as a set of 7 subunits; myosin heads can interact with only one subunit at once. Open circles, no bound ATP; closed circles, bound ATP; solid band, tropomyosin. Magnesium (>10 3 M) is present in all cases. a, Rigor. No ATP; myosin heads bind to actin as a tight complex, pushing tropomyosin out of the way. b, Relaxed situation. ATP $> 10^{-3}$ M, Ca²⁺ $< 10^{-7}$ M; myosin heads are prevented from binding to actin by tropomyosin assuming a blocking position. c, Active situation. ATP > 10^{-3} M, Ca^{2+} > 10⁻⁶ M; myosin heads attach to, then detach from, actin in a cyclic, force-generating manner; tropomyosin is displaced to a non-blocking position. d, Rigor complex formation Ratio of ATP to myosin heads < 1.0, Ca²⁺ < 10⁻⁷ M; rigor attachment of myosin heads, without bound ATP, pushes tropomyosin out of the way, thereby allowing heads possessing ATP to elicit force generation.

ago', was the ability of crossbridges to cycle in the absence of calcium and at low concentrations (less than 50 micromolar) of ATP. These observations were interpreted as follows: at low levels of ATP (no calcium, 1 millimolar magnesium) a finite population of nucleotide-free myosin heads exist. These form 'rigor' complexes with actin, in the process pushing tropomyosin away from its blocking position such that active myosin heads, possessing nucleotide, now have access to actin and can turn over (Fig. 1d). Similar results were not observed with scallop preparations³, a finding that has not been reported in full until now1

Because scallop adductor muscle is thought to be regulated solely by myosinlinked regulation, one would predict that there is no cycling of crossbridges in the absence of calcium at low levels of ATP, as such an effect seems to be a consequence of thin filament control. Nevertheless, several irksome observations have been made over the years: the X-ray diffraction patterns from contracting, rigor and relaxed molluscan muscle, interpreted as a movement of tropomyosin in the actin groove⁴; the presence of troponin subunits in some molluscan muscles⁵; and the apparent demonstration of a reversal of actomyosin relaxation at low ATP levels (by turbimetric assay) in both scallop and squid muscle⁶. Knox et al. principally address this latter point.

These authors examine the effect of low ATP concentrations on the relaxation of scallop myofibrils by ATPase, turbimetric and light-microscope techniques. Using ATPase, they observe no increase in activity at low ATP concentrations in the absence of calcium, which leads directly to the conclusion that no crossbridge cycling is allowed in regulated scallop myofibrils at reduced ATP levels, exactly as predicted for a myosin-linked system.

Curiously, the turbidity measurements of Knox et al. confirm earlier observations6 that reported an increase in optical density at reduced ATP concentrations, both in the presence and absence of calcium. These results appear to point to the exact opposite conclusion — that cycling is allowed at low ATP levels. This apparent contradiction was resolved by light microscopy: comparison with myofibrillar shortening indicates that turbidity cannot be equated with contraction, but instead appears to be associated with shrinking and swelling of the myofibrils'. Speculation that all forms of myosinlinked regulation will produce results similar to those obtained with scallop by Knox et al. should be tempered by the knowledge that tropomyosin can influence actin-activated ATPase rates in myosins controlled by light-chain phosphorylation.

Bennett and Bagshaw, on the other hand, examine the rate of release of divalent cations from myosin subfragments (proteolytic portions of the molecule), in particular, from the high-affinity, non-specific sites known to be localized on the regulatory light chains of all myosins (Fig. 2, site 1). Several years ago, Bagshaw and Reed' reported that the rate of dissociation of magnesium ions from this site on rabbit myosin subfragments was too slow to account for the rate of onset of contraction (complete within 100 milliseconds). They reached this conclusion by observing the decay of protein fluorescence consequent on chelation of the metal ion by EDTA in a stopped-flow apparatus. One criticism of this work is that measurement of the fluorescence signal was indirect and may have monitored a slower change on the protein that is subsequent to cation dissociation.

Bennett and Bagshaw⁶ have now repeated the measurements, this time monitoring events at the metal-binding site (Fig.2, site 1), and have extended them to include scallop myosin subfragments. They have taken advantage of a neat spectroscopic trick to overcome the problem that Mg2+ is spectroscopically transparent under the conditions required to monitor its binding to protein. The trick is that manganese ions (Mn2+) are not invisible by electron paramagnetic resonance and will give a tell-tale spectrum which becomes broadened when Mn2+ binds to the divalent cation site on the regulatory light chain, for which it competes effectively with Mg. Thus, by displacing bound Mg2, it was possible to monitor the decrease in signal of unbound Mn²⁺, thereby obtaining Mg²⁺ dissociation rate constants from both rabbit and scallop subfragments that are similar to the earlier measurements obtained by protein fluorescence (0.05-0.06 per second). Magnesium is therefore lost from these sites at a rate that is too slow for the ion to be replaced by activating concentrations of calcium (though one cannot exclude the possibility that some calcium is bound to the sites during a prolonged tetanus).

This result is no surprise to thick filament afficianados who have known for some time that these two high-affinity. non-specific sites exist in addition to the two calcium-specific sites (Fig. 2, site 2) located on scallop myosin, and it is this latter pair of sites that is responsible for the activation of contraction in scallop muscle. But for rabbit myosin there are no

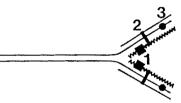


Fig. 2 Metal binding sites on myosin Site 1 is the Ca/Mg site, located on the regulatory light chain; site 2 is the calcium-specific control site, found on scallop myosin (its exact location is unknown but it requires ligands from both the regulatory light chain and the myosin heavy chain), site 3 is the active site on the myosin heavy chain where ATP binds (usually in association with a divalent cation).

alternative sites: if one excludes the highaffinity regulatory light-chain sites as calcium switches, as the work of Bagshaw and colleagues appears to have done, then one must conclude that no on/off divalent cation switch exists on the thick filament of rabbit skeletal muscle, a result in harmony with many earlier observations Although the activity of the ATPase site on rabbit myosin is undoubtedly influenced by the presence or absence of bound calcium and regulatory light chain. this influence is modulatory in nature, the true calcium switch being on the thin filament. The nature and location of the calcium-specific sites on scallop mysom is still unknown.

- Knox, M.K., Szent-Gvorgyi A.G. Treeblood, C.I. Weber, A. & Zigmond, S. J. Mioche Rev. Cell Meet. 7, 440 (1986).
- 2. Bennett, A.J. & Bagshaw, C.R. Buckern, J. 233, 473
- Bremel, R. D. & Weber, A. Naturenew Bact. 238,97 (1972). Vibert, P.J., Haselgrove, J.C., Lowy, J. & Poulse o. L.R. J. molec, Biol. 71, 757 (1972)
- 5. Lehman, W. Biochim, biophys. Acta 668, 339 (1981)
- 6. Toyo-oka, F. J. Biochem., Tokyo 85, 871 (1979) 7. Bagshaw, C.R. & Reed, G.H. ITBN Lett. 81, 386 (1977)

Peter D. Chantler is in the Department of Anatomy at the Medical College of Pennsylvania, 3200 Henry Avenue, Philadelphia, Pennsylvania 19129, USA.

Fluid mechanics

G.I. Taylor and his influence

from Herbert E. Huppert

SIR Geoffrey Ingram Taylor OM, FRS was one of the giants of physical science in this century. His work was at the centre of research on the mechanics of fluids and solids and their application to aeronautics, chemical engineering, meteorology, mechanical engineering, metal physics and oceanography. He had a distinctive style of research that brought penetrating insight into the fundamental nature of almost all the problems he considered. At the same time, he was generally able to



Sir Geoffrey Taylor investigating the motion of a fluid in a partially filled spinning cylinder. design simple but effective laboratory experiments that tested, and usually confirmed, his theoretical concepts. Taylor was born on 7 March 1886 and, at a recent meeting* to celebrate the centenary of his birth, it was asked whether the style of his work is still alive, and of value, to contemporary research workers.

Taylor liked to describe himself as an amateur scientist — by which he meant that he enjoyed working independently, with a minimum of help from others, and, of central importance, for pleasure. His scientific curiosity led him frequently to initiate new areas of research, only to lose interest in them after he had discovered the fundamental phenomena of one field, by which time the possibility of developing another novel field struck his imagination. After the tragic sinking of the Titanic in 1912, Taylor was invited to be the meteorologist on the old sailing ship Scotia, which had been requisitioned to investigate the motion of icebergs in the North Atlantic. While on board, he grasped the opportunity to design instruments attached to balloons and kites flown to heights of 2 km from the masthead of the ship. From these instruments, Taylor obtained the first reliable estimates of the transfer rates of momentum, heat and water vapour in the lower atmosphere. This work consolidated his interest in meteorology and turbulent diffusion and dispersion, to which he contributed so much in later years.

Taylor also originated important ideas in solid mechanics. A series of definitive experiments on various materials led him to develop a theory for 'dislocations' in metal crystals which predicted how cracks propagate and accounted for the observed strength of metal crystals. Motivated by conversations with Lord Rothschild, Taylor initiated the quantitative study of the swimming of microorganisms and, on the way, constructed a model of the tail of a spermatozoon from a metal-wire helix enclosed in a rubber sheath. The sheath rotated by the action of a wound-up rubber band anchored inside a head at one end of the helix. This model swam through glycerine at a rate that agreed with Taylor's theoretical prediction.

Because of the wide-ranging applicability of fluid and solid mechanics, and because of Taylor's ingenuity, his abilities were called on during the two world wars. In 1914 he helped to investigate the design and operation of military airplanes. While doing so he learnt to fly and make parachute jumps; operating as both experimenter and pilot he made the first pressure measurements over a wing in steady flight. During World War II he analysed and advised on a wide range of problems, including the rate of propagation of blast waves emanating from intense explosions.

Taylor produced more than 200 scientific papers spanning the years from 1909 to 1972. An example of his inventiveness occurs in his design of an anchor. Unhappy with the holding power and weight of the traditional anchor, Taylor created a totally new design, with a single hook shaped like a double-bladed, symmetrical plough-share. This was much lighter than traditional anchors yet had the same holding power. These 'CQR' anchors are now widely used in small vessels and are still the best available.

Is it still possible, and useful, to carry out current research in the style of G.I. Taylor? He used his intuition and just sufficient mathematics and experimentation to develop extraordinary insight into the general nature of the area being considered. As was clear from the recent meeting, this style, although not easy to \square imitate, is currently being used to good effect in several areas of fluid mechanics. The conference confirmed that current research in fluid mechanics, in contrast to some other subjects, permits important contributions to be made on a very broad range of problems. These include dynamical problems such as chaotic and turbulent behaviour in the atmosphere and oceans and in industrial contexts. Another important area concerns the formation of finger' patterns when fluid of one viscosity displaces fluid of another within a confined space — a subject also started by Taylor, who wanted to understand how oil could be recovered from porous rock by driving it up ahead of a heavier, less viscous water layer pumped into the base of the rock. Such questions continue to demand all the imagination and ingenuity of Taylor's successors and will be solved by individual scientists or small groups working on their own — and for pleasure.

Herbert E. Huppert is in the Department of Applied Mathematics and Theoretical Physics, University of Cambridge, Cambridge CB3 9EW, UK.

Catalysis

Designing porous solids

from John M. Thomas

A JET of hydrogen impinging in air on platinized, fibrous asbestos produces a spark. The famous nineteenth century German chemist, Döbereiner, capitalized on this phenomenon in the first commercial exploitation of heterogeneous catalysis. More than a million tinder boxes, containing compartments housing zinc and acid to generate the hydrogen, were made in the late 1820s and used as fire-lighting devices. The key to their operation is the degree of subdivision of the platinum engendered by the exceptionally large area of the fibrous support: no sparks are pro-

duced with platinum wires, rods or foils of low area. Chemists ever since have been seeking new large-area solids, especially those that function as synergistic catalysts with a supported metal — such as rhodium for the control of automobile emissions, or palladium for the production of many pharmaceuticals. But industrial catalysis is not the only driving force in this quest. Porous solids are also required as platforms for a range of immobilized enzymes, as improved columns in adsorption and ion-exchange chromatography, and for effecting gas separations such as meth-

^{*}Fluid Mechanics in the Spirit of G.I. Taylor, University of Cambridge, 24-28 March 1986.

clones derived from these tumours which either lack or have a relative deficiency of H–2K antigens tend to grow and metastasize more readily than similar cells transfected with and expressing an H–2K gene but that were originally H–2K deficient. Evidence was presented to suggest that surveillance by T lymphocytes is the most likely relevant anti-tumour host response in these experiments in that T cells recognize tumour-associated antigens only when associated with certain class I antigens (MHC restriction).

An apparently contradictory result is found (K. Kärre, Stockholm) in YAC -I tumour cells induced by Moloney virus where increased amounts of H-2 antigen expression is directly related to increased metastatic potential. But the host response in this case is apparently related to natural killer cell activity, which operates best in the absence of H-2 antigens on the target cells.

T-cell surveillence may be relevant however, as when large doses of these tumour cells are injected into preimmunized animals their growth is favoured by the absence of H-2 antigens. In individual primary AKR lymphomas the quantitative expression of H-2K and H-2D antigens correlates with the quantity of a murine leukaemia virus-encoded glycoprotein on the cell surface (P. Demant, Amsterdam). This could ensure the preferential elimination by cytotoxic T lymphocytes of cells with high levels of expression of viral antigens.

Although T-cell surveillance is clearly dependent on the presence of the relevant class I MHC molecule in most instances, there are exceptions in some AKR leukaemias (W. Schmidt, Essen) and in some human Burkitt lymphomas (E. Klein, Stockholm) which are resistant to T-cell cytoxicity even though the relevant restriction elements are apparently present. These findings stress the importance of the heterogeneity of the quality and quantity of the host's immune responses to tumours.

As the level of expression of H-2 antigens on syngeneic tumour cells is relevant for host-tumour interactions, it is important to elucidate the mechanisms of control. Three presentations were in agreement in proposing that DNA methylation is likely to be as important in regulating expression of both class I and II MHC antigens and also the Thy 1 antigen. C. David (Rochester) showed that Class II H-2 antigens are expressed after treating the BW 5147 thymoma line, with the demethylating agent 5-azacytidine; E.

Erratum

In the article by K.A. Browning et al. on atmospheric fronts (*Nature* 322, 114; 1986), Fig. 2 should have been rotated clockwise by 90 degrees to relate to the model simulation shown in Fig. 1.

Pareja (Granada) showed a similar result for class I antigens after treating an H-2-negative GR9 tumour cell clone with 5-azacytidine. He also showed differing methylation patterns that correspond to the different levels of expression of H-2 antigens on the various tumour cell clones

F. Grosveld (London) came closer to identifying a site of action by showing that the methylation of the 5' flanking region of the Thy 1 gene is responsible for the control of expression of this antigen. Possible transcriptional and post-transcriptional mechanisms mediated by transforming proteins of DNA tumour viruses that may also account for the regulation of class I antigen expression in SV40-transformed cells were indicated by P. Rigby (London). Ultimately these studies will open the way for the manipulation of host-tumour interactions through the regulation of syngeneic H-2 antigen expression.

Expression of aberrant H–2-like alloantigens by tumour cells was originally described about 10 years ago by the group of one of us (H.F.), soon followed by similar observations of others. There is new molecular evidence for the expression of an H–2D^d-like specificity on an H–2K AKR leukaemia (H.F.) and Schmidt described an aberrant H–2K¹-like molecule which is responsible for rejection of a tumour induced by the Rous sarcoma virus that does not express normal syngeneic Class I antigens.

H. Schreiber (Chicago), M. MacMillan (Los Angeles) and R. Goodenow (Berkeley) discussed the well-characterized novel class I MHC molecules identified on the ultraviolet radiation-induced fibrosarcoma 1591. What is of interest here is that the genes encoding two of these molecules have a high degree of homology with H-2L which is not normally expressed on cells of the H-2^k haplotype.

Thus chemicals or viruses may induce gene rearrangements that cause derepression of silent genes, leading to the appearance of aberrant H-2-like allogeneic molecules. The multiple Qa- and Tla-like genes that have a considerable degree of homology with H-2 genes could provide the genetic basis of aberrant MHC antigen expression. Such H-2-like molecules capable of eliciting an immune response may function as tumour-associated transplantation antigens, or be intrinsically suppressive in another genetic context. P. Demant (Amsterdam) and P. Stern (Liverpool) both showed class I-like products on embryonal carcinoma cells but disagreed on whether they were normal or aberrant products.

Expression of MHC antigens on human tumour cells was also considered. 'Extra' HLA class I-like specificities of the AW19 cross-reactive group on HTLV-I infected cells were described by D. Mann (NIH)

and were attributed to the high degree of cross-reactivity between virally induced tumour-associated antigens and these HLA specificities. P. Schrier and D. Ruiter (Leiden) and F. Ruiz-Cabello (Granada) both found a lower level of expression of class I HLA antigens in metastatic compared with primary melanomas but G. Parmiani (Milan) tound no difference between the level of class I MHC antigens in metastatic and primary melanomas.

Difficulties are encountered in interpreting the results of some of the other solid tissue human tumours studied. where extreme heterogeneity of MHC antigen expression in individual cells within the tumours is found. This is true for several solid tissue tumours, including breast carcinomas (J. Peña, Cordoba and M. Perez, Granada) and gastrointestinal neoplasia (M. Moore, Manchester). In a study of colorectal carcinomas Hammerling and Peña find a correlation between the loss of MHC class I antigen expression and the degree of cell dedifferentiation within the tumours. We believe that both these solid tumours and chemically induced tumours in mice arise from multiple clones having differing levels of expression of MHC antigens. Class II MHC antigen levels could thus be indicators for metastasizing melanomas (Ruiter: Parmiani).

C. Navarrete (London) reported difterential expression and function of MHC class II antigens (DR, DQ) on various acute leukaemic cells and cell lines. These findings may have important biological consequences in host-tumour interactions as was implied further by the data presented by A. van Leeuwen (Leiden) on the expression of TCA- (Tla-like) antigens on several human leukaemias.

Another question concerns the association of MHC antigens with particular tumours. M. Zijlstra (Amsterdam) demonstrated in mice that alleles of class II *I*–*A* control the type of lymphoma that develops (T,B or non T, non B) with MCF 1233 virus. T. Oliver (London) showed, significant positive association between HLA-DR5 antigen frequency and the development of seminomas in man.

It appears the genetic basis for the expression of aberrant MHC antigen specificities on tumour cells is probably the result of a series of gene-conversion events and DNA rearrangements involving pseudogenes and genes encoding differentiation antigens and by various initiating factors including toxic chemicals, radiation effects and viruses and influenced by host lymphokines.

Hilliard Festenstein is in the Department of Immunology, The London Hospital Medical College, London El 2AD, UK and Federica Garrido is in the Servicio de Analisis Clinicos Hospital Virgen de les Nieves, Granada 18012, Spain.

The origin of Japanese HTLV-Ī

SIR-Gallo and his colleagues' seem still to believe that African blacks came to Japan with the Portuguese in the sixteenth century, that HTLV-I (human T-lymphotropic virus type 1) adult T-cell leukaemia virus was transmitted from them to the Japanese people and then became highly endemic in Japan². But our studies^{4,5} strongly suggest that HTLV-I was already present in aboriginal Japanese in prehistoric times.

There are at least three ethnically distinguishable populations in Japan: the Ainu in the north the Ryukyuans in the south and the Wajin, or "Japanese", inhabiting the rest of the country. In our examination of the prevalance of HTLV-I in these ethnic populations46, we found that the incidence of virus carriers was highest in the Ainu and the Ryukyuans, not the Wajin, and that the seroprevalent frequencies in adults over 40 years old of these three ethnic groups were 45.2%, 33.9% and 1.1% respectively,4.

The Wajin, who constitute most of the present population of Japan, are considered to be descendents mainly of post-neolithic immigrants from the mainland in the Yayoi and the Kofun eras (300 BC to AD 600). The Ainu and Ryukyuans, who share several common physical and genetic traits, are considered to be relatively pure descendents of native Japanese populations. The Ainu in particular are regarded as descendents of the native population inhabiting mainly northern Japan from the pre-agricultural Jomon period, more than 2,300 years ago.

The highly endemic areas of the retrovirus in Japan have been demonstrated to be restricted to (1) the most northerly and southerly regions and (2) isolated areas in other regions^{5,7,8}. These native populations have been relatively unaffected by the Wajin, who are not HTLV-I carriers. In most other areas, however, the Wajin became predominant because of their higher technological skills, planting rice and making iron tools and arms, for example.

Gallo and his colleagues' state that "the Japanese word for monkey amakawa is... derived from the Portuguese word macaco, also meaning monkey, however, we do not call monkeys amakawa, but saru. Furthermore the Japanese word amakawa is derived from Macao, the Portuguese territory in China. It may be true that the Portuguese brought Africans and African monkeys to Japan, but there is no relation between the places where the Portuguese landed in Japan and the endemic area of HTLV-I9.10. Among the Ainu people living in Hokkaido (the most northerly island of Japan) there are no monkeys living outside zoos, HTLV-I is prevalent, but Roman Catholicism, which Gallo et al. say was imported from Portugal, is not. Thus, the hypothesis that Japanese HTLV-I derives from Africans brought by the Portuguese in the sixteenth century is inadequate. Alternatively, from our recent finding that HTLV-I is prevalent in northern Japan and the report of Gallo's group of the presence of HTLV-I carriers in the Arctic", we propose that, like simian HTLV-like virus, which is now found in Old World monkeys12 14, HTLV-I was originally prevalent in all humans, but that during human evolution it was lost from all but a few populations.

Finally, we think that it is premature to draw a conclusion on the origins of HTLV-I, because many populations have not yet been examined.

T. ISHIDA

Primate Research Institute, Kyoto University, Inuvama, Aichi 484, Japan

Y. HINUMA

Institute for Virus Research, Kyoto University, Sakyu-ku Kyoto 606,

- 1. Gallo, R.C. et al. Nature 320, 219 (1986).
- Gallo, R.C. et al. Nature 220, 217 (1980).
 Gallo, R.C. et al. Lancet li, 962–963 (1983).
 Wong-Staal, F. & Gallo, R.C. Nature 317, 395–403 (1985).
 Ishida, T. et al. J. Infect. 11, 153–157 (1985).
 Hinuma, Y. BioEssays 3, 205–209 (1985).
- Kohakura, M. et al. Jpn. J. Cancer Res. 77, 21–23 (1986) Hinuma, Y. et al. Int. J. Cancer 29, 631-635 (1982).
- 8. Maeda, Y. et al. Int. J. Cuncer 33, 717-720 (1984). 9. Hinuma, Y. et al. Luncet 3, 824-825 (1983).
- 10. Kurimura, T. et al. Jap. J. med. Sci. Biol 99, 25-28 (1986).
- 11. Robert-Guroff, M. et al. Int. J. Cancer 36, 651-655 (1985).
- Hayami, M. et al. Int. J. Cancer 33, 179-183 (1984).
- 13. Ishida, L. et al. Microbial. Immun 29, 839-846 (1985). 14. Ishida, I. et al. Microbiol. Immun 30, 315-321 (1986)

Phosphoinositol more than skin deep

SIR—Touqui et al. may have been too cautious in the discussion of their paper which showed that the phosphoinositol (PI) cycle is responsible for activation of phospholipase A, (PLA,) and initiation of the arachidonic acid cascade in platelets'. Our current studies of epithelial growth control provide data that are in line with their hypothesis, allowing us to interpret the findings of the Paris group in a broader context. It has long been recognized that a tissue responds to injury in two ways inflammation and regeneration - and that these are tightly coupled; indeed, in normal circumstances they are inseparable. From a teleological point of view this of course makes sense, but in mechanistic terms still awaits an explanation. We are now in a position to provide one, namely that both arms of the response are triggered by activation of the PI cycle.

As in certain other tissues, PLA, activity in human epidermis is calcium-dependent and appears to be inhibited by a lipocortin-like molecule': the epidermal inhibitor also seems to be modulated by phosphorylation3. Thus the findings of Touqui et al. may be extended to epidermis, a conclusion strengthened by the report that phorbol myristic acetate increases the synthesis of arachidonic acid metabolites by cultured keratinocytes. These metabolites include prostaglandins (responsible for vasodilation) and chemotactic agents, such as leukotriene B, which initiate invasion of the tissue by granulocytes.

The link with proliferation was originally suggested by observations that protein kinase C, following activation by diacylglycerol, phosphorylates (and hence activates) a membrane antiport which exchanges intracellular H+ for extracellular Na*. In several cell types the resulting increase in cytosolic pH causes entry of resting (G₀) cells into the mitotic cycle^[5,6]. Again, extrapolation to epithelia seems reasonable, since phorbol esters applied topically to skin cause a dramatic hyperproliferation.

Further evidence comes from our unpublished observation that inhibitors of the antiport and/or protein kinase C, such as amiloride, abolish the recruitment of G_n keratinocytes in human epidermis following experimental injury.

Thus the findings of Touqui et al. may well lead to a clearer understanding of the way in which a tissue responds to injury, one of the central problems in pathology. We would also note its relevance to psoriasis, a common skin disease with polygenic inheritance. The lesions of this disease are characterized by a continuous, chronic inflammation and secrete high levels of arachidonic acid metabolites7. The epidermis within the lesions is grossly hyperproliferative with a complete absence of G, cells' and PLA, activity increases in the entire epidermis of the patient which seems to result from an over-phosphorylation of the inhibitor3. It would seem that the PI cycle may be a rewarding field for research into the pathogenesis of this disease.

> P.D. MIER F.W. BAUER R. HAPPLE

Department of Dermatology, University of Nijmegen, 6524 M J Nijmegen. The Netherlands

- Touqui, L. et al. Nature 321, 177-180 (1986).
- Forster, S., Ilderton, E., Norris, J.F.B., Summerly, R. & Yardley, H.J. Br. J. Dermat. 112, 135-147 (1985).

- Halley, H.J. Bernat. 112, 133-14 (1983). Hichyshyn. A., Ilderton, E., Kingsbury, J.A. & Yardley, H.J. Br. J. Dermat. 111, 721-722 (1984) Galey, C.I., Ziboh, V.A., Marcelo, C.L. & Voorhees, J.J. J. im est. Dermat. 85, 319-323 (1985). Moolenaar, W.H., Tertoolen, L.G.J. & de Laat, S.W. Nature 312 371-374 (1984).
- Swann, K. & Whitaker, M. Nature 314, 274-277 (1985).
- Kragballe, K. and Voorhees, J.J. in *Psoriasis* (eds Roenigk, H.H. & Maibach, H.I.) 255-263 (Dekker, New York, 1985).
- 8. Bauer, F.W. in Textbook of Psoriusis (eds Mier, P.D. & van de Kerkhof, P.C.M.) 100-112 (Churchill Livingston, Lon-

Faith in the physicists

Joseph Silk

In Search of the Big Bang: Quantum Physics and Cosmology. By John Gribbin. Bantam/Heinemann: 1986. Pp. 413. Pbk \$9.95, Hbk £14.95.

SUSY GUTS is not a radical feminist, but a theory that is designed to unify the fundamental forces of nature. The reader will find this, along with many other esoteric facts, relieved by occasional gossipy anecdotes, in the latest book from prolific science writer John Gribbin.

In Search of the Big Bang completes a trilogy of major works on what Gribbin considers to be the most important scientific achievements of the twentieth century. Previous volumes were devoted to the nature of reality and quantum physics, and to the origin of life: here we move onto the ultimate issue of the creation of the Universe itself. The faint of heart may dispute the status of our cosmic origins as an equal partner to these other matters, but Gribbin unabashedly takes us on a grand tour of modern cosmology.

The difficulty is that cosmology is a science starved of data and not readily amenable to controlled experiments. We must take each glimpse of the Universe as it comes, no matter how confused or obscure it happens to be. Remote galaxies appear as they were acons ago, and thereby profoundly alter our normal sense of perspective if, for example, young galaxies were more luminous than the mature, nearby galaxies. It is as though we view the Universe through a distorting lens, and we have little sense of the nature of the distortion. And this applies to the galaxies, whose formation was only the most recent episode in the history of the Big Bang. Extrapolating backwards in time from the furiously receding galaxies we see today, we infer that the Universe was once a far more exotic, denser, hotter hostile place.

In many respects, the Big Bang is to modern cosmology what mythology was

to the ancients. To believe that we understand the very early Universe, the first microseconds of cosmic time, requires immense faith in the physicist's search for the ultimate union of the fundamental forces of nature, because direct evidence is completely lacking. Yet to the physicist, the vast energies attained in the immensely compressed primeval fireball that was once the Universe offer a unique testing ground for the latest theories of elementary particles. Exotic names, like photinos, strings or even superstrings, are reeled off as though they were the most natural state of matter, which perhaps they once were. Provided we accept theories of matter and gravity that are certainly correct at our present epoch and in our environment, then we are inevitably led by the Big Bang to a singular state near the origin of time.

Of course we are still awaiting the ultimate theory of everything, currently thought to be superstrings, which will explain the most important missing link in the puzzle, namely how it all began. Many physicists around the world are pursuing this ultimate goal that represents the union of gravity and quantum mechanics. However, we are not there yet, and opinions differ widely as to how far away we may be: according to Stephen Hawking, the end of physics is in sight, yet Sheldon Glashow argues that superstrings are only a mirage.

My only quibble with Gribbin's book is that he presents physicists and astronomers as gods whereas, in reality, they are no less fallible than other mortals. The Big Bang theory is an excellent description of the here and now, and of the not-so-longago and not-so-far-away. But one ought to take the extrapolations back to the begin-

ning of time with a healthy dose of scepticism. The Big Bang cosmology may yet be superseded, just as Newton's theory of gravitation was incorporated by Einstein into a new theory. Our more extreme extrapolations of space and time could prove to be equally false, or at least, incomplete.

In Search of the Big Bang is a remarkably readable guide, however, to the mysteries of cosmic creation. It is strong on personalities, from anecdotes about missed opportunities and Nobel prizes, to the story of the wealthy telescope builder and the mule skinner who paved the way to the realm of the nebulae. The first third of the book represents a historical development of cosmological data, and the second third provides a readable description of the classical Big Bang theory. The remainder is devoted to quantum physics and the very early Universe. Rife with speculation and liable to become largely irrelevant overnight, the last third of the book is the weakest section. But it is definitely worth reading, if only to find out how Kaluza, the founder of higher dimensional cosmology, learnt to swim.

Joseph Silk is a Professor in the Department of Astronomy, University of California. Berkeley California 94720, USA.

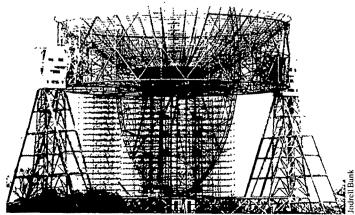
Fact or fiction?

C.E.M. Hansel

Science Confronts the Paranormal. Edited by Kendrick Frazier. *Prometheus: 1986 Pp.367. Pbk \$15.95, £12.95.*

SCIENCE Confronts the Paranormal contains a selection of articles published by the Committee for the Scientific Investigation of Claims of the Paranormal in its journal The Skeptical Inquirer. The book is divided into two sections. The first of them, "Assessing Claims of Paranormal Phenomena", is mainly concerned with parapsychology — including poltergeists. and the claims made by mediums and professional "psychics" - together with palmistry and iridology. The second section, "Evaluating Fringe Science", covers unidentified flying objects, fringe archaeology, creationism, the Turin shroud, astrology and the Loch Ness Monster.

The general approach is set out in the introduction and early chapters. Stephen Toulmin suggests that consideration of the manner in which new ideas have been opposed will "induce a certain modesty even about our skeptical doubts". Paul Kurtz also considers that the claims made by "paranormalists" should not be rejected out of hand. But over the history of scientific inquiry it is difficult to identify a new idea that has been rejected for long, provided that observations could be convided.



Jodrell Bank radio telescope nearing completion in April 1957. Taken from Bernard Lovell: A Biography by Dudley Seward, which includes a summary of Lovell's views on the nature and origins of the Universe, Now available in the USA (Salem House, \$21.95). For review, see Nature 312, 210;



The spoon-bending abilities of Uri Geller, a professional magician who claimed to be psychic, made headline news. Scientific tests of his powers have now become "little more than a collection of anecdotes"

firmed adequately or that a new hypothesis could be tested experimentally and confirmed by independent investigators.

Most of the claims examined in the first section are not new, but are dependent on ideas going back into prehistory that have failed to be accepted within science. They have not been totally rejected for scientists from many disciplines working within parapsychology have been attempting to provide repeatable experimental demonstrations of the various psychical phenomena for more than a century. When such a demonstration becomes available, it will then be necessary for the sceptics to see whether they can also confirm its findings. The main reason for examining such claims in advance of evidence supporting them is made clear by Kurtz: "... we are confi cerned not simply with paranormal beliefs in the laboratory but with their dramatization in the media".

Two types of investigation may be distinguished: first, experiments, in which the researcher decides on the experimental design and procedures to be adopted whilst the subject does as he is told; second, demonstrations, in which a person attempts to convince observers of his psychic powers. Here the investigator observes the subject while he performs under his own conditions, often reminiscent of those enjoyed by a conjuror in the music hall.

What has emerged from the experimental work is that attempts to confirm an original "positive" finding will either fail or "succeed" at a low level of significance, the result depending mainly on the experimenter. This has led to the conclusion within parapsychology that there is an "experimenter effect"; which is not dependent on the slap-happy nature of the investigation but on some new interaction between the experimenter and the hypothetical process being considered. Of particular interest here is the discussion of an experiment on "remote viewing" - or clairvoyance - reported in Nature (252, 602; 1974) by Targ and Puthoff of the Stanford Research Institute (SRI). The experiment was shown by Marks and Kamman (Nature 292, 177; 1981) to contain a schoolboy blunder that could account for the result. Marks himself reviews this and further experiments which claimed to indicate that the fault in the procedure made no difference to the result. His conclusion is that:

Well-controlled experiments never find the RV effect, while poorly controlled experiments nearly always do so. Data suppression, flawed methodology, and lack of replication lead to the conclusion that remote viewing is a cognitive illusion, an artefact of human error and wishful thinking.

An investigation of the second type is discussed by Martin Gardner in "How Not to Test a Psychic: The Great SRI Die Mystery". Uri Geller, a professional magician who claimed to be psychic, was tested during a visit to SRI where it was stated that he was able to name correctly the face uppermost on a concealed die on each of eight attempts and that he made no attempt on two occasions. After discussing means whereby any trained conjuror might have obtained similar results, and his attempts to find out more about the tests, Gardner writes:

What conclusion can we reach from all this? The most important is surely the following. What seemed to any reader of *Nature* to be a carefully controlled die test has now become little more than a collection of anecdotes.

The section on fringe science is concerned in the main with certain claims that are not inconsistent with contemporary scientific theory but that are not supported by evidence. A large amount of material is available here relating to matters that become headline news but are seldom reported fully and critically.

Science Confronts the Paranormal should be of considerable value to those puzzled by accounts of "paranormal" events appearing in the media, to teachers interested in the scientific method and to parents who are disturbed by what their children are taught. It could well be made compulsory reading for science correspondents and television producers.

C.E.M. Hansel is Emeritus Professor of Psychology at the University College of Swansea, Singleton Park, Swansea SA2 8PP, UK.

Wide sweep

A.J. Thomson

Physical Methods for Inorganic Biochemistry. By John Wright, Wayne Hendrickson. Shigemasa Osaki and Gordon James. *Plenum: 1986. Pp.384. \$71.40, £47.60.*

The task this book sets itself is ambitious. It attempts to cover the spectroscopic, diffraction and analytical methods used to probe the structural properties of the elements employed by living organisms. But, before beginning, the authors needed to decide whether to write a book about the methodology of the techniques, their principles and practice, or to describe the ways in which our understanding of biological systems has been advanced. This choice has not been made, and as a result most chapters fall short of meeting either goal.

The consequences of indecision are seen clearly in the chapter on the principles, practices and applications of nuclear magnetic resonance (NMR). Here the authors have slipped between three stools. Principles are stated briefly but inadequately, and it is doubtful that those readers who do not understand the basis of Fourier transform NMR, say, will be much clearer after reading this section. The description of practice extends to giving absurd detail for a circuit diagram of a low-pass noise filter — surely a topic for a technical manual — while applications are dealt with on an element-byelement basis; this makes a useful compendium, but hardly shows the powerful ways in which NMR has helped biologists.

To make things worse, the authors have tried to cover too many techniques, several of which are as yet of little established value in biological research. For example, nuclear quadrupole resonance (NQR) spectroscopy is an insensitive technique that has produced no information of biological significance. Electron spectroscopy (ESCA) is also out of place, whereas EXAFS (extended X-ray absorption edge fine structure) is not discussed even though it has had considerable impact. The sweeping scope has inevitably led to areas being tackled that are well outside the authors' competence — the statement that "there have been few temperaturedependent magnetic circular dichroism studies of transition-metal enzymes" is false and renders the chapter concerned out-of-date and inadequate.

Altogether, it is difficult to see the aim or the value of this book. Much of the material is available elsewhere, either in reviews or texts on the individual techniques written by more authoritiative authors.

A.J. Thomson is a Professor in the School of Chemical Sciences, University of East Anglia, Norwich NR4 7TJ, UK.

New frontier for stratigraphy

A.M.C. Şengör

The Geology of China. By Yang Zunyi, Cheng Yuqi and Wang Hongzhen. Oxford University Press: 1986. Pp.303. £55, \$79.

WITH 9.6 million km² China covers nearly one-fifteenth of the world's land area and is the third largest country in the world. The geology of this vast portion of our planet is now being studied by some 70,000 geological personnel in China. Their results are reported regularly in some 50 Chinese periodicals and monograph series, only a few of which contain English abstracts. The Geology of China, the second book of its kind since Li Siguang's (J.S. Lee's) 1939 classic bearing the same title, has been written by two stratigraphers and a metamorphic geologist to provide an up-to-date survey of the subject. It is based mainly on the immense amounts of both published and unpublished work done since the foundation of the People's Republic.

The book contains a total of 20 chapters, divided into four main parts. Part I ("Background") briefly reviews the development of geology in China and the physical features of the country. Part II ("Stratigraphy") is the backbone of the book, consistent with the dominant interest of the authors. Here, in the first chapter the stratigraphic terminology employed in the book is reviewed and a synopsis of the stratigraphic evolution of China is presented. The next three chapters deal with the Archaean and the Proterozoic eons and the Sinian system. Nine of the remaining ten chapters of Part II treat individual systems from the Cambrian to the Cretaceous, while the last describes, too briefly perhaps, the Cenozoic. In each chapter sedimentary rocks are discussed in terms of stable (platform), mobile (geosynclinal) and transitional sedimentation types — this was an unfortunate choice, which makes understanding of former sedimentary environments in terms of present-day settings difficult. Although boundary and correlation problems are considered for each system, palaeobiogeographic provinces are touched upon only in chapters on the Carboniferous and the Permian systems.

Part III ("Magmatic and Metamorphic Rocks of China") contains two chapters, one each for the two major rock groups. Here the treatment is mainly regional and chronological.

In the last part ("Geotectonic Development of China"), two chapters are devoted to the tectonic framework and geotectonic units, and the geotectonic

development of China respectively. Although much lip service is paid to plate tectonics, and the few palaeotectonic cross-sections are drawn in basic plate-tectonic terms, the underlying framework in both of these chapters is based on an unhappy marriage between a Soviet-style fixist philosophy and plate tectonic mobilism. The descriptions and arguments are made even more difficult for the reader to follow because of the authors peculiar employment of familiar terminology such as aulacogen and continental margin.

A serious limitation of the book is the almost complete lack of reference to foreign or cooperative research on Chinese geology. For example, Molnar and Taponnier's epoch-making studies on the neotectonics of China are not even mentioned. Further, there is no reference to the Franco-Chinese work on Tibet (absence of mention of the geophysical results is especially glaring), nor to the important magnetostratigraphic work by Liu Dongsheng and his co-workers on the loess deposits. Such omissions have in places led to some rather odd conclusions, such as the supposed late Mesozoic origin

and Cenozoic inactivity of the Altyn-Tagh fault.

The paucity of sketch-maps showing particular geological relationships and outcrops adds to the problem of comprehending both local and regional details, so the book is difficult to use to reinterpret the data in terms of models other than the authors'. Despite its deficiencies, however, The Geology of China is a must for those interested in the regional stratigraphy of this country. A subject and a stratigraphic index (both in Pinyin transliteration and in the original Chinese characters) increase the value of the book. as do the 19 black-and-white plates of fossils and photomicrographs of representative lithologies. However, readers would be well-advised to keep at hand either one of the post-1980 comprehensive editions of the Times Atlas or the Zhonghua Renmin Gongheguo Fen Sheng Dituji, for many of the places mentioned in the text are not on any of the maps in the book.

A.M.C. Şengör is Lecturer in Geology in the Faculty of Mines, Istanbul Technical University, 80394 Teşvikiye, Istanbul, Turkey.

A diverse life

Colin Townsend

Community Ecology. Edited by Jared Diamond and Ted J. Case. Harper & Row: 1986. Pp.665. \$37.50, £16.95.

Suppose, for the sake of argument, that the genetic code, instead of being determined solely by DNA, was co-determined by seven classes of macromolecule. Suppose, too, that in a given species the relative role of the macromolecules varied with age, season, weather conditions and time since the last glaciation, and also tended to differ between large and small species, ectotherms and endotherms, and herbivores and carnivores. If this were true, we would surely not have our present complete understanding of the code. And yet, as the editors of this volume point out, this is exactly the problem that ecologists face in trying to explain how the abundances of interacting species in a community are co-determined by competition. predation, herbivory, disease, parasitism, mutualism and disturbance. Later in the book we are told that studying ecology resembles what it would be like to conduct a chemistry experiment if the chemist were only a few angstroms long and lived for only a few microseconds!

Attempts to solve the daunting problems of variability and scale in community ecology demand a diversity of methodologies to obtain the data and a diversity of models to interpret them. The methods

include laboratory experiments, field observations, experiments in the field, "natural" experiments involving comparative observations at several contrasting outdoor sites, and reconstructions based on historical records in library and museum archives and in fossil assemblages. All figure prominently in this stimulating collection of 33 essays by 35 authors (34 from North America and one from England). The book is written with the professional researcher in mind, but undergraduates will find much of the material accessible.

Each of the five sections of the book opens with a scene-setting chapter. The first, by Jared Diamond, compares the merits of the different experimental approaches and is followed by an account of probably the most ambitious laboratory experiment on community assembly yet attempted — Michael Gilpin and his coworkers describe how the results from 28 species of fruit fly studied singly can be used to predict, with surprising accuracy, the outcome of pair-wise interactions or ten species combinations.

Section 2 is concerned with species introductions and extinctions. Competition between species for food or space is potentially a potent force in the structuring of communities, with species co-existing only if they exhibit some minimal differences in their resource requirements. If this potential is realized (and there is much debate about the point), competition must operate through a process of selective extinction. Michael Moulton and Stuart Pimm have come up with a novel

analysis of historical data to address this question. Records of success or failure of over 100 introductions of exotic bird species to Hawaii during the past 125 years permit calculations of how a species' risk of extinction depends on the number and morphological closeness of other species in the community—a role for competition is indicated in this case.

Section 3 discusses the problem of the appropriate choice of spatial and temporal scale in investigations of community ecology, and Section 4 contrasts equilibrium and non-equilibrium theories of community ecology. A recurring theme in these sections, and elsewhere in the book, is the importance of historical data. Paradoxically, although those who study modern communities regularly debate whether communities are at equilibrium, rarely have they consulted the fossil evidence. Margaret Davis emphasizes that on any time scale from a decade to 100,000 years climate does not fluctuate about a mean value, but exhibits long-term trends. Her data for forest trees, and those of Thomas Van Devender derived from plant and animal fossil remains in packrat middens in the Chihuahuan Desert, emphasize how communities have frequently become dismantled and reshuffled as species shift their geographical location differentially in response to changing climate.

The final sections deal with the variety of forces structuring communities and with the variety of kinds of community that exist. The message is that there is no single model to describe all communities - some are structured mainly by competition, some by predation, some by unpredictable disturbances and so on - but neither is every community unique. Thomas Schoener makes an initial assault on the problem of defining a minimum number of properties of organisms and environments that will enable us to say, for example, that for organisms of Type A, in environments of Type B, the dominant structuring force(s) will be of Type C (D, etc.). But there is still a long way to

Thirty years ago, a book about the multi-species level of ecological organization would probably have dealt almost exclusively with the flux of energy and nutrients between the environment and the community. More popular today is an approach to the understanding of multi-species assemblages based on knowledge of the dynamics of the constituent species populations. Indeed, the old distinction between population ecologist (a student of the abundance and distribution of individual species populations) and community ecologist seems to be fast breaking down.

Colin Townsend is a Lecturer in the School of Biological Sciences, University of East Anglia, Norwich NR47TJ, UK.

Bird cake

John Andrews

The Sparrowhawk. By Ian Newton. Poyser, Town Head House, Calton, Waterhouses, Staffordshire, UK/Buteo, PO Box 481, Vermillion, South Dakota 57069, USA:1986. Pp.396 + plates. £16, \$35.

IN THE battle being fought in many countries to protect rare or declining species. wildlife conservationists are often severely handicapped by lack of knowledge. What are the species' numbers and distribution? What are its requirements, and how can these be accommodated in a changing environment? Often the best we can do is to make an informed guess, always running the risk that error will harm the subject of our concern and weaken our modest influence still further. Against this background, Ian Newton's study of the sparrowhawk (Accipiter nisus) is valuable on two counts. First, it answers many of the questions relevant to the conservation of a bird much affected by human activities. Second, the research methodology and some of the conclusions may, with care, be applied to other accipiters and so advance research on them also.

Sparrowhawks breed in woods and forests across the Palearctic region from Ireland to Japan. In winter most of the boreal birds move south into the Middle East, India and south-east Asia. Close relatives occupy North America, Africa and southern Asia, the whole genus comprising about 50 species worldwide. Few escape the influence of mankind.

In Britain, progressive clearance reduced forest cover to 5 per cent of the land surface by the mid-nineteenth century, and accordingly restricted sparrowhawk distribution: then came the development of game preservation, and an era of intense persecution. Nonetheless, these evasive birds held on in small numbers, thinly but generally present over most of the country until, recently, organochlorine pesticides eliminated them from much of their range. Now, legal protection and, more importantly, changes in pheasant rearing methods have much reduced deliberate killing; afforestation has doubled the potential habitat and controls on organochlorines have permitted a rapid recovery in numbers over most of the country.

Newton, who is a senior ornithologist with the Natural Environmental Research Council, began his study of the species 14 years ago, selecting two areas of Scotland where he sought to trap and ring all individuals present and to find all their nests. From this basis he was able to explore the bird's ecology, making his own practical experiments to test hypotheses as the pro-

ject developed and drawing on other researchers' findings. The work was complicated (but made more rewarding) by the fact that male sparrowhawks are half the weight of the females, so that they differ greatly in habitat usage, range of prey taken and response to factors such as weather and inter-specific competition (not to mention being killed by their own fair sex!).

Many individual birds were studied throughout their lives, enabling Newton to provide here a detailed account of the species' hunting and prev selection, dispersal and migration, breeding mortality and population trends, and of the human impact on their well-being. Much of the material has already appeared in journals, but, like a cake, the book's ingredients gain from being mixed and cooked by a skilful hand. The text is supplemented by crisp monochrome photographs and line drawings, while copious figures present results graphically with the supporting data set out in appendices. There is a good bibliography and an extensive, helpful

Ian Newton has a well-deserved reputation for sound research and for presenting his results in a carefully reasoned and readable manner. *The Sparrowhawk* is well up to expectations; it will be enjoyed by amateur ornithologists and professionals alike.

John Andrews is Head of Conservation Planning at the Royal Society for the Protection of Birds, Sandy, Bedfordshire SG19 2DL, UK.



The sooty owl from Birds of Eucalypt Forests and Woodlands: Ecology, Conservation, Management. Published by Surrey Beatty & Sons Pty, 43-45 Rickard Road, Chipping Norton. NSW 2170, Australia (A\$47, US\$43), it is based on the proceedings of a conference organized by the Royal Australasian Ornithologists Union.

The case for life as a cosmic phenomenon

from F. Hoyle and N.C. Wickramasinghe

The arguments in support of life as a cosmic phenomenon are not readily accepted by a culture in which a geocentric theory of biology is seen as the norm.

A LEADING article in a recent issue of Nature explained that we had ourselves to blame for experiencing difficulties of an unusual kind in the publication of referencing of our work1. Our fault was that we had become caught up in the eccentric doctrine of panspermiology, a doctrine for which there was said to be little or no evidence. We have now been invited by the editor of Nature to explain why we differ from his judgement and why in our opinion there is indeed evidence in favour of our position. In our experience, people who become eccentric usually do so through a mental discontinuity, whereas we would claim to have progressed by a series of comparatively small steps over many years, with each step rather cautiously tested by either observation, experiment or calculation using generally accepted methods of deductive science.

Our ideas began in the middle 1950s with qualitative considerations on the nature of interstellar grains and with a straightforward generalization to interplanetary conditions of the well-known Urey-Miller prebiotic experiment². By the early 1960s we had added a refractory carbonaceous component to the ice-grain model of van de Hulst' and had begun to calculate the extinction of starlight to be expected from complex mixtures of ice and carbonaceous particles ". The correspondence between our results and the observed interstellar extinction of visible starlight was tolerable but not really good in view of the many adjustable parameters that were present in the calculations.

Eventually we discovered that appreciably better agreement could be obtained between observation and calculation provided the real part of the refractive index of interstellar grains was low, say 1.15, instead of being 1.3 as for ice or ~2.4 as for carbonaceous particles. A low refractive index turned out to be much better than the many-parameter adjustments we had formerly used. But what material could have a refractive index as low as 1.15? In seeking an answer to this question it was important that the grains be largely made up of cosmically abundant elements, because the amount of the observed extinction is so considerable that only abundant elements will suffice to give the necessary quantity of grains. Of materials based on common elements only solid hydrogen would have the required low refractive index it seemed. So for a while we investigated this possibility and

became enthusiastic about it ⁹. The trouble, however, turned out to be that solid hydrogen was too volatile and would evaporate away¹⁰. So it came about that we were left with an unsolved problem, and we had to put it aside for a decade until quite new ideas suggested themselves.

Organic polymers

From calculations made in 1968 of condensations occurring in large mass flows from astronomical objects we suggested that interstellar grains might contain a magnesium oxide-silicon oxide component and when a so-called silicate emission-band near 10 µm in the infrared was observationally discovered the following year we had a new topic to become en-thusiastic about¹² ¹⁶. Unfortunately as it seemed at the time, our former disappointing experience repeated itself. Following an initial approximate success in matching the laboratory absorption properties of mineral silicate particles to the infrared observations16, the situation did not improve as better laboratory measurements and better observations were made. Discrepancies that were unsatisfactory remained, as they do to this day. It was with mounting frustration that we began to look through mountains of chemical literature, searching for a substance made-up of common atoms with infrared properties similar around 10 µm to the astronomical observations. It was from this intensive literature search that the idea at last dawned on us that organic materials in the form of polymeric structures might make up a major fraction of the interstellar grains', and moreover that similar structures might be present in cometary dust15.

The step from inorganic to organic grains did not seem particularly revolutionary. Organic molecules in the gaseous interstellar medium had been discovered already by radioastronomers, although in nothing like the quantity of the grains, while as long ago as 1956 Platt had suggested the widespread presence of very tiny organic grains19. Still pursuing the infrared problem, we eventually found that among organic materials polysaccharides gave the best correspondence to the astronomical data20,21, and it was at exactly this point in our work that we began to experience hostility from the referees of journals and from the assessors of grant applications at what was then the Science Research Council. We realize now that because polysaccharides on the Earth are a biological product we had unwittingly made a contact that is deeply forbidden in our scientific culture, a contact between biology and astronomy. We did not see that we had sinned mortally and were deeply mystified since at first, we thought of polysaccharides as being produced abiologically. Nor did we realize that the cultural taboo that confronted us had already surfaced in 1870, only one year after the inception of this journal.

Only gradually did we come to understand the difficulties of producing very large quantities of organic material by abiological processes²⁵. The Fischer-Tropsch reaction, for example, which produces hydrocarbons from hydrogen and carbon monoxide depends on the use of carefully controlled catalytic surfaces. which would almost surely be quickly poisoned by corrosive sulphur compounds under cosmic conditions (it may be noted that the Fischer-Tropsch process could not be operated profitably to complete with natural oil at \$30 per barrel, even under the most expertly managed terrestrial conditions).

Biological solution

We are not sure of exactly what it was that caused biology to enter our perceptions. but we think it was noticing a series of drawings of a bacterium from which the internal water was progressively dried out. The cell wall remained in place as cavities developed in the interior, eventually yielding a particle of typically the size of an interstellar grain that was hollow. We realized at once that such a particle would behave with respect to visual light. to a close approximation like a particle of low refractive index, just the situation we had been seeking more than ten years earlier in the 1960s. We obtained an experimentally-defermined size distribution of bacteria from a standard manual and were quickly able to calculate how such a size distribution of hollow particles would behave with respect to the extinction of starlight. The result was a truly excellent fit to the astronomical data, the data we had attempted to fit without real success by our many-parameter models in the

On the strength of this result. Dr Shirwan Al-Mufti began to measure the infrared properties of a number of species of bacteria, finding to his and our surprise a remarkable constancy of absorption for

the wavelength range 3.3 to 3.5 µm, and a general constancy for the whole range from 3 to 4 µm (ref 24). If bacteria made up an appreciable fraction of the interstellar grains, as the observed extinction of visible starlight seemed to suggest, it was necessary therefore that the grains must possess the characteristic absorption pattern which Al-Mufti had measured in the laboratory. It happened not long after these experiments that the average absorption properties of grains along the whole path length from the galactic centre to the Earth was measured to a high degree of accuracy by Allen and D.T. Wickramasinghe³. The results, made at no less than 60 wavelengths between 3 and 4 um, agreed with the bacterial experiments to within an accuracy of typically about one small graticule division on a standard Perkin-Elmer pen chart, an accuracy that we, who had hoped for accuracy, found impressive²⁶.

We are aware that astronomers and chemists can be found who will claim that these results are not impressive, because equally good results could be obtained using plausible non-biological materials. Our answer is that equally good results have not been obtained using plausible non-biological materials. Such claims are advanced and listened to only because they are designed to be culturally acceptable, whereas our results, although based on careful observations, experiments and calculations are not culturally acceptable. In such a situation the critic is permitted to say anything at all without being weighed in the balance and found wanting.

Stellar replication

An attempt is often made to saddle us with the criticism that bacteria could not replicate in interstellar space. We have never said that they did. Our model is a cyclic one, with bacteria replicating as a byproduct of star formation in environments where replication can occur 27 29. Following star formation, a fraction of the bacteria produced are expelled into the interstellar medium. Some die, some survive — quite likely only a minority survive to become incorporated in further star formation processes, and so on around the cycle. Biological replication is an exponential process that can immensely outstrip all abiological processes. Granted sustained conditions for the growth of a bacterial culture, a single viable bacterium could grow to a mass of bacteria equal to the Earth in about nine days, a mass equal to the galaxy in about fifteen days, and a mass equal to the whole visible universe in about twenty days.

It is a necessary corollary that bacteria must be space-hardy, unless after arriving here on Earth mutations have destroyed properties which they possess intially was A viable strain of Streptococcus mitis was recovered after two years of exposure to

conditions on the surface of the Moon³¹. Bacteria can be taken down to near zero pressure and temperature without loss of viability, provided suitable care is exercised in the experimental conditions 12.33 Bacteria can survive after exposure to pressures as high as 10 tonnes cm⁻² (ref. 34) and after flash heating under dry conditions at temperatures up to 1,000 K (ref. 35). Viable bacteria have been recovered from the interior of an operating nuclear reactor. A fraction of bacteria remain viable even after extremely heavy flash doses of high energy radiation, upwards of a megarad, while it seems that bacteria can repair themselves continuously in a maintained environment of high radiation intensity, to the extent of repairing tens of thousands of breaks in their nucleic acid stucture 17.38. These are not properties one would have expected to evolve on the Earth, but they are all properties necessary for survival in space. Damage from ultraviolet light, which is often raised as a problem is actually no problem, because ultraviolet light is easily shielded against^{20,10}

An individual comet has only a small mass, but if one considers all the comets that are believed to exist in the presentday Oort cloud, and to have existed over the whole history of the Solar System, their combined mass could well be comparable to that of the outer planets Uranus and Neptune, about 1029 grams. If the ~10" stars of our Galaxy are typically endowed with similar quantities of cometary material, the total cometary mass for the whole Galaxy would be ~10⁴⁰ grams, very close to the mass of the interstellar grains.

We were led from this consideration to think of a swarm of comet-like bodies, present towards the outer regions of the Solar System in its early history, and being made warm in their interiors by radioactive heat, as the likely sites for early biological replication 42. As we put it on one occasion, such an individual cometary interior would be like a vast laboratory with a floor area of some thousand square kilometres and with a height comparable to that of the Empire State Building. If other dwarf stars are mostly like the Solar System, there could be more than 10²⁰ such laboratories in the Galaxy, which makes it only a matter of commonsense we believe to regard such bodies as a more favourable venue for the development of life than the initially sterile surface of a small planet like the Earth, which even today has a biosphere with a mass of not more than $10^{15} - 10^{19}$ grams.

Holding these views, it was easy for us to predict that an important fraction of the dust expelled from comet Halley would be organic in composition, that bacteria in the dust would become hollow as water within them dried out, thereby yielding particles with an average mass density less than I gm cm ', and that organic material at the surface of comet Hallev would be dark43. We have heard astronomers speaking of the surface material of comet Halley as being dark like tar, perhaps without realizing that tar is itself a biological product

It has often been suggested to us that our views might be tested by a suitable satellite experiment. Such an experiment would be expensive and difficult because of high impact speeds, as we saw in the recent Giotto encounter. Another suggestion often made is to send balloons or rockets into the high atmosphere with the aim of recovering viable bacteria from space. This has actually been done, repeatedly. On every occasion viable bacteria were obtained 44-48, and on every occasion the result was discounted because of the possibility, admittedly serious in some cases, of terrestrial contamination. When a result is culturally unacceptable it will always be discounted on some excuse or other. One cannot win that way.

The Earth is perpetually embedded in a halo of cometary material, of which some 1,000 tonnes enter the terrestrial atmosphere each year. Because of the low density of the upper atmosphere, incident small particles of the sizes of bacteria and viruses could land 'soft' without viability being destroyed by flash heating. After intervals ranging from months to years such particles eventually settle to ground level, where they would be added to the already-existing reservoir of bacteria and viruses. It is to the potential interaction of such incoming particles with plants and animals that one can best look for a direct verification of these ideas. For some years we have been much concerned with this interesting and informative mode of verification22.11. It is our opinion that a large body of facts exists to prove the correctness of the general picture outlined above. The topics themselves being in the medical field of epidemiology, would take us far away from the rest of the present article. Besides which, we are about to run out of the space the Editor has kindly allotted us, and so must refer the reader, if any should be interested, to a recent publication entitled: Viruses from Space . We have found it not a little odd to find our views taken more seriously, or at least received more politely, by the medical profession than they have been by astronomers and chemists, for whom we retain not a few rods in pickle.

- 1. Maddox, J. Nature 321, 723 (1986).
- 2. Hoyle, F. Frontiers of Astronomy, 100 103 (Heinemann, London, 1955).
- 3. van der Hulst, H.C. Rech. astr. Obs. Utrecht 11 (1946 and
- Hoyle, F, & Wickramasinghe, N.C. Mon. Not. R. astr. Soc. 124, 417 (1962).
- 5. Wickramasinghe, N.C. Mon. Not. R. astr. Soc. 126, 99

F. Hoyle and N.C. Wickramasinghe are at the Department of Applied Mathematics and Astronomy, PO Box 78, University College, Cardiff CF1 1XL, UK.

- Nandy, K. & Wickramasinghe, N.C. Pub. Roy. Obs. Edinburgh 5, No. 3 (1965).
- 7. Wickramasinghe, N.C. & Nandy, K. Nature 219, 1347
- 8. Hoyle, F., Wickramasinghe, N.C. & Reddish, V.C. Nature
- 218, 1124 (1968).
 Reddish, V.C. & Wickramasinghe, N.C. Mon. Not. R. astr. Soc. 143, 189 (1969).
- Greenberg, J.M. & de Jong, T. Nature 224, 251 (1969).
- 11. Hoyle, F. & Wickramasinghe, N.C. Nature 217, 415; 218,
- 12. Woolf, N.J. & Ney, E.P. Astrophys. J Lett. 155, L181
- Ney, E.P. & Allen, D.A. Astrophys. J. Lett. 155, L193 (1969).
- 14. Knacke, R.F., Guadstad, J.E., Gillett, F.C. & Stein, W.A. Astrophys. J. 155, L189 (1969).
- 15. Stein, W.A. & Gillett, F.C. Astrophys. J. Lett. 155, L197
- (1969).
 16. Hoyle, F. & Wickramasinghe, N.C. Nature 223, 459
- 17. Wickramasinghe, N.C. Nature 252, 462 (1974). Mon. Not. R. astr. Soc. 170, 11P (1975).

 18. Vanýsek, V. & Wickramasinghe, N.C. Astrophys. Sp. Sc.
- 33, L19 (1975).
- Platt, J.R. Astrophys. J. 123, 486 (1956).
 Hoyle, F. & Wickramasinghe, N.C. Nature 268, 610
- 21. Hoyle, F., Olaveson, A.H. & Wickramasinghe, N.C.

- Vature 271 229 (1978)
- 21. Nature 1, 327 (1870). 22. Hoyle, F. & Wickramasinghe, N.C. Living Comets (University College Cardiff Press. 1985).
- 23. Hoyle, F. & Wickramasinghe, N.C. Astrophys. Sp. Sc. 66,
- 77 (1979). 24. Hoyle, F., Wickramasinghe, N.C. Al-Mufti, S. & Ola-
- vesen, A.H. Astrophys. Space Sci. 81, 489 (1982). Allen, D.A. & Wickramasinghe, D.T. Nature 294, 239 (1981).
- 26. Hoyle, F., Wickramasinghe, N.C., Al-Mufti, S. & Ola-
- vesen, A.H. Astrophys. Space Sci. 83, 405 (1982).
 27. Hoyle, F. The Relation of Biology to Astronomy (Univer-
- sity College Cardiff Press, 1980).

 28. Hoyle, F. & Wickramasinghe, C. Space Travellers (University College Cardiff Press, 1981).
- Hoyle, F. & Wickramasinghe, N.C. in Comets and the Origins of Life (ed. Ponnamperums, C.D.) (Reidel, Dordrecht, 1981).
 Hoyle, F. & Wickramasinghe, N.C. Evolution from Space
- (Dent, London, 1981).
 31. Mitchell, F.J. & Ellis, W.L. Proc. Second Lunar Sci. Conf. 3, 2721 (1971).
- 32. Portner, D.M., Spiner, D.R., Hoffman, R.K. & Phillips, R. Science 259, 2047 (1961).
- 33. Hagan, C.A., Godfrey, J.F. & Green, R.H. Space Life Sci.
- 34. Al-Mufti, S. Hoyle, F. & Wickramasinghe, N.C. in Fundamental Studies and the Future of Science (ed. Wickrama-

- singhe, C.) (University College Caratif Press, 1984) 35. Hoyle, F., Wickramasinghe, N.C. & Al-Multi, S. Lordi
- Moon and Planets 35, 79 (1986)
 36. Fowler, E.B., Christenson, C.W., Jurwey T. F. & Scho fer, W.D. Nucleonics 18, 102 (1960)
- 37. McGrath, R.A. Williams, R.W. & Swartzendroner, D (Biophys. J. 6, 115 (1966).
- Nassim, A. & James, A.P. in Microbial Life et l'Airente Environnents (ed. Kushner, D.J. (Academic, New York)
- Weber, P. & Greenberg, J.M. Nature 316, 403 (1985)
- 40. Hoyle, F. & Wickramashinghe, C. Lifecloud (Dent. Lon don. 1977).
- Hoyle, F. & Wickramasinghe, C. Diseases from Space (Dent. London, 1979).
- Wallis, M.K. Nature 284, 431 (1980)
- 43. Hoyle, F. & Wickramasinghe, N.C. Cardiff Astrophysics and Relativity Preprint Series 121 (1986). Astrophys. Space Sci. (in the press).
- Imshentsky, A.A., Lysenko, S.V. & Luch S.P. Doolaal An. SSRR. 224, 223 (1975).
 Greene, W.W., Pederson, P.D., Lundgren, D.A. & Hag.
- Soffen, G.A. NASA Report N65 23980 (1965) Soffen, G.A. NASA Report N65 23980 (1965) Fulton, J.D. Appl. Microbial. 14, 237, 241 (1966)
- 48. Jayaweera, K. & Flanagan, P. Geophys Res Lett 9 94
- 49. Hoyle, F., Wickramasinghe, C. & Watkins, J. Viewes from Space (University College Cardiff Press 1986)

ARTICLES

Detection of an X-ray-ionized nebula around the black hole candidate binary LMC X-1

M. W. Pakull* & L. P. Angebault[†]

* Institut für Astronomie und Astrophysik, TU Berlin, Sekr, PN 8-1, Hardenbergstrasse 36, D-1000 Berlin 12, West Germany † European Southern Observatory, Karl-Schwarzschild-Strasse 2, D-8046 Garching, West Germany

Optical spectra of the black hole candidate X-ray binary LMC X-1 reveal that the system is surrounded by an extended, highly ionized He III region, N159F, which appears to be the long-sought-for example of an X-ray-photoionized nebula. The spatially resolved temperature and ionization structure allows us to measure the previously unobservable extreme ultraviolet (EUV) luminosity of an accreting compact object.

DESPITE a fairly accurate (±3 arc s) Einstein HRI (high-resolution imager) position for the bright (X-ray luminosity $L_X = 2 \times$ 10³⁸ erg s⁻¹) variable X-ray source LMC (Large Magellanic Cloud) X-1 (ref. 1), neither of the previously suggested optical counterparts²⁻⁴ can be excluded on positional ground alone (Fig. 1). The optical properties of the B5 I star R148 (V =12.2 mag) appear normal for its spectral type, including the slight radial velocity and photometric variations^{5,6} which are observed in most supergiants. More promising for an optical identification is the fainter (V = 14.5) O7 III-type star '32', which reveals the variable He II λ4,686 and λλ4,640-4,650 emission⁴⁻⁶ generally considered to be the hallmark of high-luminosity massive X-ray binary (MXRB) optical counterparts. Hutchings et al.6 have suggested that part of the 4,686-Å emission stems from the surrounding H II region N159F (refs 7, 8; see also Fig. 1); but these authors did not elaborate on this potentially important result.

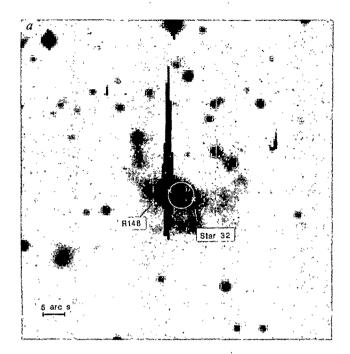
In order to study the reported radial velocity variations⁶ in star 32 which suggest that LMC X-1 might be a black hole (a conjecture which is supported by the interpretation of its extremely soft X-ray spectrum⁹), and to investigate possible X-ray heating effects on the H II region N159F, we have obtained long-slit spectra of this region. Our observations reveal a remarkable ionization structure, suggesting that we have observed the

first example of a spatially resolved X-ray-ionized nebula.

Observations

We carried out two-dimensional charge-coupled device (CCD) spectrophotometry 4 nights in December 1984, using the B&C spectrograph attached to the 3.6-m ESO telescope at La Silla, Chile. Here we are concerned mainly with the results of our observations on 21 December, which were obtained with a reciprocal dispersion of 114 Å mm⁻¹, resulting in a full width at half-maximum (FWHM) resolution of 5 Å in the wavelength range 3,600-5,200 Å. The relatively large width of the slit (2 arcs) made this configuration most suitable for the study of nebular emission from the surrounding H II region N159F. The slit orientations were chosen as shown in Fig. 1b: A, including both candidates R148 and star 32 and B, roughly perpendicular to the former orientation, including star 32. Two longerwavelength CCD spectra which also include the 5,000-6,700 Å region, at a lower resolution of 8 Å, were obtained in May 1985.

The images were flat-field- and extinction-corrected and calibrated in wavelength and flux from the observation of a He-Ar lamp and the spectrophotometric standard stars LLT1020, EG21 and L745-46A, respectively¹⁰, using the image processing facilities IHAP and MIDAS at ESO, Garching.



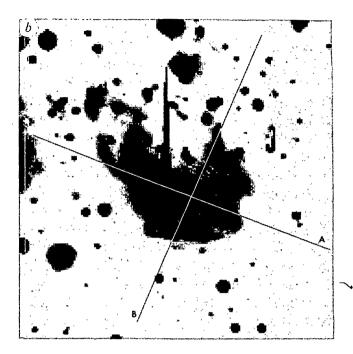


Fig. 1 Direct CCD images of N159F obtained with a Gunn r filter, emphasizing nebular $H\alpha$ emission. The HRI error circle (radius ~3 arc s) of LMC X-1 includes the 12.1-mag B5 I star R148 (strongly overexposed and elongated due to charge transfer effects from the read-out process of the CCD chip) and the presumed O7-III-type optical counterpart (star 32). The image of another fainter star (17 mag) can be seen close to R148. α and α were obtained from the same image with different high and low cuts, in order to emphasize the presence of stars (α) and nebular emission (α). The orientations of the slit in scans A and B are shown in α .

From the reduced images we measured the intensity of several nebular emission lines as a function of position along the slit. As suggested from inspection of Fig. 2, most emission lines are strongly enhanced in the vicinity of LMC X-1. H β , for instance, rises steeply from a background intensity of ~10 to a maximum value of 75 in units of 10^{-16} erg cm⁻² s⁻¹ arc s⁻² (Fig. 3). The extent of ~40 arc s (corresponding to 10 pc at the distance of the LMC) and total flux $F_{\beta} = 10^{-11}$ erg cm⁻² s⁻¹, corrected for interstellar extinction with optical reddening E(B-V) = 0.37

Table 1 De-reddened line strengths relative to H β (=100)							
Emission line	Position 1	Position 2					
[O II] 3,727 Å	285	391					
[Ne III] 3,868	42	8 .					
Ηδ 4,101	. 24	25					
Ηγ 4,340	48	48					
[O III] 4,363	7	1.0					
He I 4,471	2	4					
N 111/C 111 4,640-4,650	<1	<1					
He II 4,686	10	< 0.5					
[Ar IV] 4,711	2	<1 .					
Hβ 4,861	100	100					
[O 111] 4,959	` 171	49					
[O III] 5,007	538	157					
He I 5,876	10	10					
[O I] 6,300	8	4					
[O I] 6,364	. 2	2					
[N II] 6,548	8	10					
Ηα 6,563	. 286	286					
[N II] 6,584	29	34					
[S 11] 6,717*	32	34					
[S II] 6,731*	· 23	24					
$C(H\beta)$	0.582	0.302					

Probable errors in the relative intensity of strong lines $(I_{\lambda}/I_{\beta} \ge 8)$ are dominated by the relative uncertainty in our flux calibration (<10%). The accuracy of weaker intensities is limited by photon noise and reaches $\pm 40\%$ for the faintest detected emission.

(ref. 8), can be accounted for by a Strömgren-sphere model of uniform electron density ($N_{\rm e}=40~{\rm cm}^{-3}$), excited by the ultraviolet flux of an O7 star. Note that the B5 star R148 should not produce a substantial flux of H Lyman-continuum photons.

The [O III] emission is even more enhanced near LMC X-1. The [O III](λ 4,958+5,007)/H β line ratio, which is sensitive to the degree of excitation, peaks at 7.5±0.2, compared with a value of ~2.5 more than 20 arc s away (Fig. 4). The electron temperature derived from the λ 4,363/ λ (4,958+5,007) intensity ratio¹¹ around LMC X-1 is 13,500 K, which is ~5,000 K higher than in the more distant parts of the H II region.

Table 1 lists additional emission line intensities measured close to LMC X-1 and \sim 1.3 arc min away (positions 1 and 2, respectively; see Fig. 3a). Note the increasing ionization towards LMC X-1, as revealed by the [O II] $\lambda\lambda$ 3,726-3,729/H β and [Ne III] λ 3,868/H β line ratios at positions 1 and 2. To produce the high nebular excitation, the effective stellar temperature should exceed \sim 45,000 K (refs 12, 13); however, this is inconsistent with the $T_{\rm eff}$ = 35,000 K determined from the IUE (International Ultraviolet Explorer) study of star 32 (ref. 8).

The most convincing evidence for the presence of a source of high excitation is provided by our detection of extended He II λ 4,686 emission ('He III region', Figs 2, 5) with a diameter of 24 arc s, corresponding to 6 pc in the LMC. The formation by recombination of doubly ionized helium requires a substantial intensity of He⁺ Lyman-continuum photons ($h\nu > 54$ eV), which cannot be provided by even the hottest normal O-stars, as shown by the observation that this transition is never present in the spectra of normal H II regions but can be quite strong in planetary nebula (PN) with central star temperatures of $\sim 10^5$ K.

A PN-type nature of the He III region is, however, ruled out on the basis of the extreme population I environment in N159F and the large extent compared with the diameters of PN in the LMC, which do not exceed 4 arc s (ref. 14). Collisional ionization and excitation in a supernova remnant (SNR) shock can most probably also be excluded, as there is no indication of extended X-ray emission from LMC X-1¹⁵. Furthermore, our red spectra (see Table 1) do not show enhanced forbidden lines

^{*} Values obtained from observations with the 2.2 m telescope.

Table 2 Observed parameters for the X-ray-ionized nebula N159F around LMC X-1

	!
 X-ray spectrum	$L_{1-10 \text{ keV}} = 2 \times 10^{38} \text{ erg s}^{-1};$ thermal bremsstrahlung, $kT = 2 \text{ keV},$ $N_{12} = 9 \times 10^{21} \text{ cm}^{-2}$
Stellar spectrum	O7, $T_{\text{eff}}^1 = 37,000 \text{ K}$, $M_{\text{V}} = -5.0$, E(B-V) = 0.37
Ambient electron density	$N_e = 40 \text{ cm}^{-3}$, probably smaller near LMC X-1
Hβ luminosity	$L_{\rm H\beta} = 3.2 \times 10^{36} \rm erg s^{-1}$
He 11 λ4,686 luminosity	$L_{4,686} = 1.5 \times 10^{35} \text{ erg s}^{-1}$
H II region radius	$r_{\rm H}$ II = 5-6 pc
He III region radius	$r_{\rm He}$ III = 3 pc
O III electron temperature	$T_{\rm e} = 13,500$ K in the He III region
	9,000 K outside

due to low-ionization species such as O I, S II and N II often exhibited by SNRs¹⁶. Also, the λ 4,686 emission has the same (instrumental) width of 170 km s⁻¹ (FWHM) and radial velocity of 261 ± 10 km s⁻¹ (derived from our higher-resolution spectra) as the lower-excitation lines, suggesting that it is not produced in the high-velocity knots observed in many SNR¹⁷. Rejecting a PN or SNR nature, we are left with the hypothesis that LMC X-1 is responsible for the formation of the He-III region in N159F.

He II $\lambda 4,686$ photon counting

Before discussing our findings in the context of increasingly detailed models for X-ray-ionized nebula¹⁸⁻²², we take advantage of the 'photon counting' property of the He II $\lambda 4,686$ line in order to measure the hitherto unobservable EUV flux from LMC X-1.

Although our spectrophotometric mapping of N159F is not complete we can reasonably estimate a total flux $F_{4,686} = 1.2 \times 10^{-13} \,\mathrm{erg} \,\mathrm{cm}^{-2} \,\mathrm{s}^{-1}$ in the $\lambda 4,686$ line, assuming that our scans are representative of the spatial distribution of the emission. Correcting for interstellar absorption towards LMC X-1⁸ and taking 52 kpc for the distance to the LMC, we find (within a factor of 2) an emission-line luminosity $L_{4,686} = 1.5 \times 10^{35} \,\mathrm{erg} \,\mathrm{s}^{-1}$, this being proportional to the absorption rate of He⁺ Lyman-continuum photons, Q_4' , in the nebula:

$$Q_4' = \int_{54 \text{ eV}}^{\infty} L_{\epsilon} / \varepsilon (1 - \exp(-\tau_{\epsilon})) d\varepsilon$$

$$= \frac{L_{4,686}}{h\nu_{4,686}} \frac{\alpha_{\text{B}}(\text{He}^+, T)}{\alpha_{4,686}^{\text{eff}}(T)} = 2 \times 10^{47} \text{ s}^{-1}$$
(1)

where ε is the photon energy, $L_{\rm e}/\varepsilon$ is the photon number spectrum of LMC X-1 (emitted photons s⁻¹ keV⁻¹), $\alpha_{\rm B}$ (He⁺, T) the recombination coefficient summed over all levels above the ground state and $\alpha_{4,686}^{\rm eff}$ (T) the effective recombination coefficient for the emission of He II $\lambda 4,686$ photons (luminosity $L_{4,686}$), carrying an energy $h\nu_{4,686}$. Note that the ratio of these

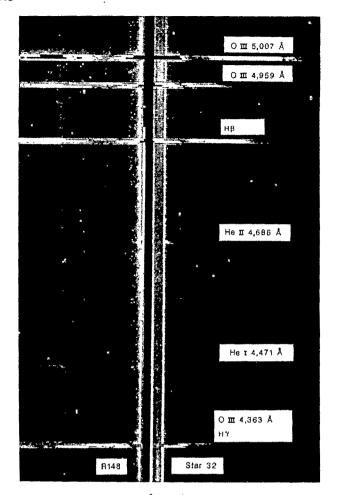
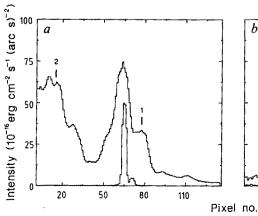


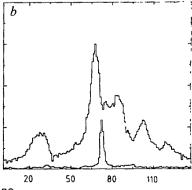
Fig. 2 A section of the 114 Å mm^{-1} two-dimensional spectrum (scan A) with the slit orientated in order to include R148 and star 32. The stellar continua appear as black (R148) and grey (star 32) vertical bands in this representation. The high and low cuts were chosen so as to emphasize faint nebular emission. Note in particular the extended distribution of He II $\lambda 4,686$ emission which peaks at the position of star 32. One pixel corresponds to 1.17 arc s × 2 Å.

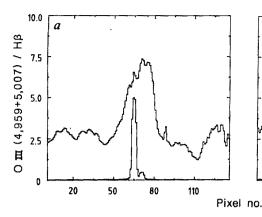
coefficients (\sim 5.2) depends only weakly on the electron temperature.

The optical depth due to He⁺, $\tau_{\varepsilon} = \int_{0}^{\infty} \sigma_{\varepsilon} N_{\text{He}^{+}} ds$ (where s is distance and σ_{ε} is the photoionization cross-section of He⁺, which decreases as ε^{-3} above the threshold of 54 eV) can be estimated by noting that He⁺ is the prevailing ionization stage outside the central parts of the He III region. This is shown by the fact that the (reddening-corrected) He/H recombination line ratio here, $I_{4,471}/I_{\beta} = 0.030 \pm 0.002$, implies a He⁺ abundance of

Fig. 3 Intensity of nebular $H\beta$ emission as a function of position along the slit (a, scan A; b, scan B). The nearby continuum flux has been normalized appropriately and subtracted to correct for the contribution of the stellar emission and H β absorption. The continua due to R148 and the 10 times fainter star 32 (scan A) and star 32 (scan B); which were scaled down by arbitrary factors, are shown in the lower curves to display their position with respect to the nebular emission along the slit. Note the strong enhancement of the emission nearthestars over a background level of 15 × 10⁻¹⁶ erg cm⁻² s⁻¹ (arc s)⁻². Marks 1 and 2 show positions where the nebular spectra summarized in Table 1 were extracted. 1 pixel = 1.17 arc s.







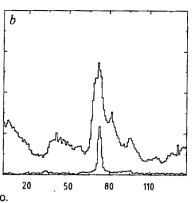
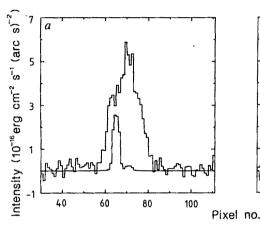


Fig. 4 The [O III] $(\lambda\lambda 4,959+5,007)/H\beta$ line ratio as a function of position along the slit (a, scan A; b, scan B). The lower curves are scans of the stellar and nebular continuum. The maximum value of 7.5 is reached near the position of star 32. 1pixel = 1.17 arc s.



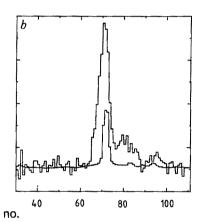


Fig. 5 The He II λ4,686 intensity as a function of position along the slit (a, scan A; b, scan B). Thd lower curves are scans of the stellar and nebular continuum. There is an unresolved component present due to stellar emission from star 32. The extended emission has a diameter of 24 arcs (He III region), corresponding to 6 pc at the distance of the LMC and is centred within 1 arcs on star 32.

 0.070 ± 0.005 , which is in fair agreement with the total average He abundance of 0.085 measured in LMC H II regions²³. A shell with a thickness of 3 pc and a He⁺ density of 3 cm⁻³ has an optical depth of ~40 at 54 eV. The nebula becomes optically thin, however, for He⁺ Lyman-continuum photons above $\varepsilon_u \approx 0.2-0.3$ keV. Accordingly, we can approximate Q_4' by

$$Q_4 = \int_{54 \, \text{eV}}^{\varepsilon_u} L_{\varepsilon} / \varepsilon \, d\varepsilon \tag{2}$$

provided that the intrinsic spectrum does not fall off too rapidly below $\varepsilon_{\rm u}$. At higher photon energies, K-edge photoionization of heavier elements, notably of oxygen at 0.53 keV, is the main opacity source, but these photons are less important for the He ionization balance.

The X-ray spectrum of LMC X-1, which has been observed between 0.6 and 20 keV with the HEAO-1 (High Energy Astrophysical Observatory) A2 MED and HED and Einstein SSS experiments⁹ and, coordinated with our optical investigation, with the Exosat observatory (S. Ilovaisky, personal communication), exhibits relatively strong low-energy absorption with an equivalent column density $N_{\rm H}$ of $(9\pm2)\times10^{21}$ equivalent H atoms cm⁻². Combining the column density with the optical reddening, E(B-V)=0.37 (ref. 8), we obtain the ratio $N_{\rm H}/E(B-V)=(2.4\pm0.6)\times10^{22}$ H atoms cm⁻² mag⁻¹, which is four times higher than the galactic value but agrees well with the LMC gas to dust ratio deduced from interstellar Lyman- α absorption profiles²⁴.

We note that the contribution from the H II Strömgren sphere $(r=5 \text{ pc}, N_e=40 \text{ cm}^{-3}; \text{ see Table 2})$ amounts to only 7% of the total equivalent column density, implying that most of the X-ray and optical absorption is due to an extended neutral envelope, visible in 21-cm surveys, with a total column density of 6×10^{21} H atoms cm⁻² (ref. 25).

Assuming that the kT=2 keV thermal bremsstrahlung model which represents a satisfactory fit to the Exosat ME (0.7-10 keV) observations of LMC X-1 ($L_{\varepsilon}=1.4\times10^{38}$ $g_{\rm ff}(\varepsilon)$ exp $(-\varepsilon/2$ keV) erg s⁻¹ keV⁻¹, where $g_{\rm ff}$ is the Gaunt factor²⁶; S. Ilovaisky, personal communication) can be extrapolated into the EUV,

and anticipating that photoelectric absorption between the X-ray source and the nebula is negligible (see below), we can integrate the differential photon rate L_e/ε to find (from equation (2)): $Q_4=3(4)\times 10^{47}$ photons s⁻¹ for $\varepsilon_{\rm u}=0.2$ (0.3) keV. The close agreement, within a factor of 2, with the value of Q_4 derived from He II $\lambda 4,686$ photon-counting arguments supports the validity of our approach, at least to a first approximation.

Because a power-law model with an energy spectral index $\alpha=1.7\pm0.1$ in the range 0.6-3 keV resulted in a substantially better fit to the Einstein SSS data⁹, we have also investigated how far this model might be valid at lower energies without violating our photon-counting constaint (equation (2)). If the power law extended down to 54 eV, we would expect a $\lambda4,686$ flux 50 times larger than actually observed. In order to produce the observed $\lambda4,686$ luminosity, the intrinsic X-ray spectrum from LMC X-1 should either be cut off below 0.2 keV or substantially flatten (α < 0) between 0.5 and 0.3 keV. The latter alternative qualitatively agrees with the 'cool disk' model²⁷ proposed to explain the spectra of accreting black holes in their high state.

Are the derived He⁺ Lyman-continuum flux from LMC X-1 and the ambient gas density consistent with the observed extent of the He III region? In the optically thin case the radius r_R of this region can be estimated by equating the rate of photoionization and recombination:

$$r_{\rm R} = \left(\frac{L_{\rm X}\gamma}{4\pi N_{\rm e}\alpha_{\rm B}({\rm He}^+, T)}\right)^{1/2} \tag{3}$$

where γ is the photoionization rate coefficient normalized to unit source intensity²¹:

$$\gamma = L_{\rm X}^{-1} \int_{\rm 54\,eV}^{\infty} L(\varepsilon) \sigma(\varepsilon) \frac{{\rm d}\varepsilon}{\varepsilon} \tag{4}$$

In the optically-thick limit, recombination occurs roughly at the Strömgren radius:

$$r_{\rm S} = \left(\frac{3Q_4}{4\pi N_{\rm He}^{++} N_{\rm c} \alpha_{\rm B}({\rm He}^+, T)}\right)^{1/3}$$
 (5)

Inserting the observed parameters from Table 2, we find $r_R \simeq r_S \simeq$ 2-3 pc, in good agreement with the radius of the observed He II $\lambda 4,686$ emission line region.

Here we have assumed that the He III region is observed in a static situation; that is, that the ionization front moving as $r(t) = r_{\rm eq}(1-\exp(-t/\tau_{\rm He II}))^{1/3}$ (where $\tau_{\rm He II} = (N_{\rm e} \alpha_{\rm B}({\rm H_e^+},T))^{-1}$ is the He⁺⁺ recombination timescale) has reached its equilibrium extent, $r_{\rm eq}$. $\tau_{\rm He II}$ (\approx 400 yr for $N_{\rm e}$ = 40 cm⁻³) therefore sets a lower limit to the time LMC X-1 has been X-ray active, and provides the timescale with which the structure of the He III region will react to variations of X-ray input from LMC X-1.

In order to estimate the fraction of doubly ionized He, we use the He II $\lambda 4,686/H\beta$ recombination line ratio, $I_{4,686}/I_{\beta}$, which reaches a maximum value of 0.095 ± 0.010 (corrected for stellar contribution and reddening) around star 32.

Using

$$\frac{\int N_{\text{He}^{++}} N_{\text{e}} \, ds}{\int N_{\text{H}^{+}} N_{\text{e}} \, ds} = \frac{I_{4,686}}{I_{\beta}} \frac{\alpha_{\beta}^{\text{eff}}(T)}{\alpha_{4,686}^{\text{eff}}(T)} \frac{h\nu_{\beta}}{h\nu_{4,686}}$$
(6)

and a He abundance of 0.085 (ref. 23), we find that, averaged over the line of sight towards LMC X-1, the ionization fraction amounts to $\overline{N_{\text{He}}}^{++}/\overline{N_{\text{He}}} = 0.10 \pm 0.01$. Even taking into account that the H II zone around star 32 is 2-3 times larger than the $\lambda 4,686$ emission line region, and allowing for a background contribution from N159F of 30% to the observed H β intensity, we find that He appears not to be fully ionized ($N_{\text{He}}^{++}/N_{\text{He}} \approx 0.4$) in the inner parts of the He III region, unless the density there is lower than in the ambient H II region. A decreasing density and the increase of temperature towards the X-ray source suggests an isobaric, rather than constant-density, cloud (see below).

Keeping in mind the uncertainty involved in the measurement of the de-reddened $\lambda 4,686$ flux, the fact that the extent of the He III zone reflects a time average of the X-ray luminosity, and that we did not take into account the diffuse radiation field from recombinations and transitions of heavy elements, we feel that our modified 'Zanstra temperature' argument provides a first clue to the otherwise unobservable EUV part of the emission from an accreting compact star.

So far we have not fully exploited the information provided by our spatially resolved spectroscopy concerning the ionization and temperature structure of the nebular region around LMC X-1. First, we note that the centre of gravity of the He II λ4,686 intensity profile in scan A (Fig. 5) coincides within 0.6 arc s with star 32. Here we have discarded the unresolved stellar component, which contributes ~10% to the observed flux. Scan B exhibits a more strongly peaked λ4,686 profile near star 32, with lower-intensity emission ~10 arc s to the north. Again, the centre of gravity of the extended emission deviates by <1 arc s from the star. We take this as convincing evidence that star 32 is the optical counterpart of LMC X-1.

A second point concerns the presence of a relatively strong nebular continuum in N159F. Here we find that the intensity in the continuum, I_{ν} (measured near $H\beta$), closely follows the variation of I_{β} along the slit (see Fig. 3), and has an I_{ν}/I_{β} ratio of $(5.0\pm0.6)\times10^{-14}\,\mathrm{Hz^{-1}}$, which is ~8 times higher than the value calculated from atomic processes (free-free, bound-free and two-photon emission²⁸) alone. This result implies an intimate mixture of gas and dust in N159F, which scatters stellar radiation from star 32 (and possibly R148) into our line of sight and also explains the extended ultraviolet continuum emission observed with the IUE around LMC X-1 (ref. 8).

Comparison with models

Drawing on early studies of the physical conditions prevailing in a gas cloud around a strong X-ray source^{18,19}, several investigators have extended the calculations by including important effects such as Auger emission, Compton heating and charge-transfer reactions. The most extensive calculations were per-

formed by Kallman and McCray²¹ and Kallman²², who explored the nebular response to several X-ray input spectra, assuming constant gas density and constant pressure clouds.

For a given X-ray spectrum the ionization and temperature structure depend only on the ratio of X-ray photon flux to particle density, $\zeta = L_{\rm X}/nR^2$ (ref. 18), where n is the particle density at a distance R from the source, provided that the cloud is optically thin. Radiative transfer effects become important for larger values of the column density scaling parameter $(L_{\rm X}n)^{1/2}$ (ref. 21), starting at low photon energies where the opacity is greatest. As shown above, N159F has an optical depth of 40 at the He⁺ ionization threshold, which then quickly drops to values $\ll 1$ for photons with $\varepsilon > 0.2-0.3$ keV.

Model 2 of ref. 21, which assumes a thermal-bremsstrahlungtype spectrum with kT = 10 keV, a luminosity $L_X = 10^3$ erg s⁻¹ and a constant ambient density of 10^3 cm^{-3} , has about the right column density scaling parameter to be compared with the observed X-ray heating and ionization effects around LMC X-1.

Helium is expected to be doubly ionized ($\mathrm{He^{2+}/He} > 0.9$) for $\zeta > 5$ (in cgs units). For increasing distance from the source, different ionization stages coexist, decreasing the relative abundance of $\mathrm{He^{++}}$ to <10% for $\zeta < 0.4$. The low efficiency of highenergy photons for the complete ionization of helium is clearly demonstrated by the model calculations of ref. 20 which assume input spectra with a low-energy cut-off at 1 keV. Here, $\mathrm{He^{++}}/\mathrm{He}$ drops below 0.1 for $\zeta < 100$, implying a He III region which is 16 times smaller than in model 2 of ref. 21. At the same total luminosity the soft ($kT = 2 \,\mathrm{keV}$) spectrum of LMC X-1 provides ~ 5 times more flux below 1 keV than the $kT = 10 \,\mathrm{keV}$ model; therefore, we consider an equivalent spectrum for LMC X-1, with $L_{\rm X} = 10^{39} \,\mathrm{erg \, s^{-1}}$ and $kT = 10 \,\mathrm{keV}$.

At an ambient density $N_{\rm e}=40~{\rm cm}^{-3}$ (Table 2), ionization parameters of 0.4 and 5 translate into distance of 2.6 and 0.7 pc from the X-ray source. The former radius closely agrees with the observed extent of the He II $\lambda 4,686$ emission and with the result of the previous estimate on the basis of simple recombination and Strömgren-sphere arguments.

Moving inward from $\zeta = 0.4$ to 5, the temperature increases from 1×10^4 to 1.8×10^4 K. Our O III observations qualitatively support this type of temperature structure, with T_e increasing by $\sim 5,000$ K from the outer to the inner parts of N159F (Table 2)

For a more quantitative comparison, one must take into account the distribution of O²⁺ ions within the nebula, which strongly deviates from that in model 2 due to the presence of the stellar ultraviolet continuum from star 32. Here the stellar radiation field keeps oxygen doubly ionized throughout the H II region (see Fig. 4), and therefore strongly weighs the observed [O III] line ratio towards lower temperatures.

The presence of the ultraviolet continuum from star 32 has another important effect on the ionization structure of N159F: it removes the H I and He I atoms, thus suppressing charge-transfer reactions. It has been argued²⁹ that this effect increases the column densities N_i^j of several multiply ionized trace elements by factors of 3 to 25, and moves the location of the shell in which a given ion is found outward by a factor of 1.4-6 in radius.

Using the scaling laws $N_i^{\rm i} \propto (L_{\rm X} n)^{1/2}$ (ref. 21) and taking into account the observed abundance in LMC H II regions²³, we can predict interstellar column densities of 5×10^{15} , 5×10^{14} and 8×10^{15} cm⁻² for the ions C IV, N V and O VI, respectively, which have resonance lines in the observable ultraviolet. These values are 1-2 orders of magnitude larger than those in the line of sight towards the galactic massive X-ray binaries HD153919 (ref. 30) and HD77581 (ref. 31) and should therefore be easily detectable in future high-resolution ultraviolet spectroscopy of LMC X-1.

As there is observational evidence for increasing temperature and decreasing density towards LMC X-1, isobaric X-ray nebular models might be more applicable for the situation prevailing in N159F. Here we note only that, according to ref. 22,

the assumption of constant pressure enhances the tendency to thermal instability in the cloud and increases the temperature and ionization gradients. The model spectra predict enhanced forbidden and semi-forbidden line intensities and relative suppression of optically allowed emission lines of highly charged ions, compared with the results obtained under the assumption of constant density.

Discussion

X-ray and ultraviolet studies of several massive X-ray binaries have revealed that these systems are imbedded in strong stellar winds (with typical mass loss rates of 10^{-7} - $10^{-6}~M_{\odot}~yr^{-1}$, where M_{\odot} is the mass of the Sun) emerging from the OB-type companions, which in turn will absorb most of the soft X-ray flux and cause variable P Cyg profiles of ultraviolet resonance lines formed in the wind^{32,33}. However, when the X-ray luminosity exceeds a critical value, the low-Z (atomic number) atoms which dominate the opacity of the wind will be nearly completely ionized. This situation probably prevails in the super-Eddington pulsar SMC X-1, where no indication for wind absorption has been found down to at least 0.5 keV (ref. 34). Following ref. 32 and assuming for simplicity a constant-velocity stellar wind, we find that the ionization parameter in the wind can be expressed

$$\zeta = 1.1 \times 10^{5} \left(\frac{L_{\rm X}}{2 \times 10^{38} \,\mathrm{erg \, s^{-1}}} \right) \left(\frac{a}{2 \times 10^{12} \,\mathrm{cm}} \right)^{-2} \times \left(\frac{v_{\rm w}}{1,500 \,\mathrm{km \, s^{-1}}} \right) \left(\frac{\dot{M}}{10^{-7} \,M_{\odot} \,\mathrm{yr^{-1}}} \right)^{-1} \left(\frac{r_{*}}{r_{\rm X}} \right)^{2}$$
(7)

where r_* and r_X are the distances from the O star and X-ray component, respectively, and \dot{M} denotes the mass loss rate. The units of L_X (2×10³⁸ erg s⁻¹; see Table 1), binary separation a (2×10¹² cm (ref. 6)) and stellar wind velocity v_w (1,500 km s⁻¹ (ref. 8)) have been chosen to match the observed parameters of LMC X-1. Using various mass-loss indices based on the profile of the C IV 1,548-1,550-Å ultraviolet resonance doublet³⁵, which has an absorption equivalent width of 2-4 Å (ref. 8), $10^{-7} M_{\odot}$ yr⁻¹ can probably be considered as an upper limit to the mass loss rate from star 32.

Such high ξ values are more than sufficient to completely ionize H and He (log $\xi > 1.4$), oxygen (log $\xi > 2$) and other low-Z atoms²¹ throughout the wind zone, with the possible exception of the X-ray shadow cast by the O star. Thus, the stellar wind in the LMC X-1 system is largely transparent to soft-X-ray and EUV photons, consistent with our observation that N159F is exposed to most of the EUV photons from an unabsorbed thermal bremsstrahlung or 'cool disk' spectrum.

We have shown that LMC X-1 is not just projected onto N159F but that the source is located within, and interacting with, the extreme population I environment. This has the important consequence that the interstellar medium around the X-ray binary is dense enough ($N_e = 40 \, \mathrm{cm}^{-3}$, Table 2) to reveal observable high excitation features. Keeping in mind that the extent and luminosity of the λ^4 ,686 emission scale with $(L_{\rm X}/n)^{1/2}$ and $L_{\rm X}$, respectively, we find that the surface brightness (intensity), $I_{4,686}$, in this approximation is directly proportional to the gas density; that is, $I_{4,686} \subset N_e$, independent of $L_{\rm X}$. Let us imagine an LMC-X-1-type source in a low-density environment, with $N=0.1 \, \mathrm{cm}^{-3}$ being typical for the general interstellar medium. The He III zone would then be 20 times more extended, emitting a $\lambda 4$,686 intensity of $4 \times 10^{-18} \, \mathrm{erg \, s^{-1} \, cm^{-2}}$ (arc s)⁻² (assuming negligible reddening), which comes close to the limit of detectability for today's instrumentation.

How can we explain the fact that, with the notable exception of LMC X-1, massive X-ray binaries are generally found far away from their birthplaces? According to evolutionary scenarios for MXRB (ref. 36, and references quoted therein)

the supernova explosion creating the compact component introduces an appreciable orbital eccentricity and systemic run-away velocity, $v^{\rm ra}$. When the OB star is sufficiently evolved (evolutionary timescale $\tau^{\rm eV}$) either to emit a strong stellar wind or fill its critical lobe, the system will enter the relatively short ($<10^5$ yr) X-ray phase.

For system parameters representing typical MXRB, $v^{\rm ra} = 40-100~{\rm km~s^{-1}}$ and $\tau^{\rm ev} = 3\times 10^6~{\rm yr}$, runaway distances of $d_{\rm ra} = 200~v_{70}^{\rm ra}~\tau_{6.5}^{\rm ev}$ pc (where $v_{70}^{\rm ra} = v'^a/70~{\rm km~s^{-1}}$ and $\tau_{6.5}^{\rm ev} = \tau^{\rm ev}/10^{6.5}~{\rm yr}$) from the site of formation are envisaged, displacing the X-ray binary far outside the average parent OB association and, thus far from the region of high interstellar density.

The fact that LMC X-1 is located within N159 (diameter 50 pc) argues for an exceedingly small $v^{\rm ra} (\le 20 \, {\rm km \ s^{-1}})$, which is consistent with the upper limit of $40 \, {\rm km \ s^{-1}}$ (ref. 6) to the systemic relative radial velocity with respect to the nebular emission. We cannot exclude with certainty, however, that LMC X-1 was born in one of the nearby OB associations (LH103, LH108) and is by chance now crossing N159F.

We note that the BH candidate system LMC X-3 should have had a different evolutionary history. In the framework of a recently proposed evolutionary scenario for the source³⁷, we find a runaway distance $d_{\rm ra} = 1.8 \, {\rm kpc} \, (v_{70}^{\rm ra} = 2, \, \tau_{6.5}^{\rm ev} = 3.8)$, which explains its location in the outskirts of the LMC more then 2° (corresponding to 2 kpc) away from the nearest region of recent star formation.

A possibily related high-excitation region has recently been discovered around the SNR 1E0102.2-7219 in the Small Magellanic Cloud, where a He II $\lambda 4,686$ -emitting halo surrounds the X-ray and optical remnant³⁸. The X-ray emission and its extrapolation towards lower energies, however, seems to be too weak to account for the ionization. Instead, a fossil H II region created by an ultraviolet flash during the supernova explosion or ultraviolet radiation from the SNR itself were proposed to be responsible for the excitation of the observed He III region.

Yet another candidate X-ray ionized nebula in the Magellanic Clouds was identified in the course of the present study, in the form of a shell-like structure in the light of [O III] centred on the ultra-soft LMC X-ray binary LHG83 (ref. 39). The question of whether the environment of the Magellanic Clouds is particularly favourable for the formation of observable X-ray-ionized nebulae (as seems to be the case for the formation of black holes⁴⁰), or whether some selection effect operates against their detection in the Galaxy, remains to be investigated. Further studies of galactic X-ray binaries at a sensitivity equal to or exceeding that of our observations will be necessary to search for galactic counterparts to N159F.

Conclusions

Our spectroscopic observations of LMC X-1 reveal that the black-hole-candidate binary is surrounded by a spatially resolved He III region, N159F, of ~6 pc in diameter. Within N159F the degree of ionization and the temperature strongly increase towards the X-ray source. We suggest that we are seeing the first example of an X-ray-ionized nebula, which is furthermore embedded in a more conventional H II region excited by the O7 star optical counterpart of LMC X-1 (star 32). Using simple photon-counting computations we have determined the previously unobservable EUV/soft-X-ray spectrum of an accreting compact object from the flux in the nebular He II $\lambda 4,686$ recombination line. Our results suggest that N159F is subjected to an essentially unabsorbed thermal bremsstrahlung (or related) X-ray spectrum, extending towards low energies to at least 0.054 keV. We show that, in contrast to the situation encountered in most galactic massive X-ray binaries, the X-ray luminosity of LMC X-1 is sufficiently high to nearly completely ionize the stellar wind from the early-type companion, which in turn becomes essentially transparent to EUV/soft X-ray photons. Evolutionary models have been shown to explain why strong X-ray binaries are generally located outside regions of enhanced interstellar gas density, implying that observable N159F-type X-ray-ionized nebula are quite rare phenomena.

X-ray photoionization is also thought to play a major role in the formation of emission lines in active galactic nuclei (see refs 41, 42 and referenced therein), and several models of X-rayionized nebulae have been tailored to account for the observed continua and emission lines in these objects. In this context the highly ionized nebula around LMC X-1 might be considered to be a scaled-down version of the narrow-emission-line region in Seyfert-2- and 1.5-type galaxies. Most importantly, the combination of high X-ray luminosity and moderately low ambient gas density realized for LMC X-1 allows a spatially resolved study

Received 10 February; accepted 30 May 1986.

- Cowley, A. P. et al. Astrophys. J. 286, 196-208 (1984).
 Jones, C. G., Chetin, T. & Liller, W. Astrophys. J. 190, L1-L3 (1974).
- Rapley, C. G. & Tuohy, I. R. Astrophys. J. 191, L113-L116 (1974). Pakull, M. W. IAU Circ. No. 3472 (1978).

- Pakull, M. W. JAU Circ. No. 3472 (1978).
 Pakull, M. W. Proc. IAU Symp. 108, 317 (1984).
 Hutchings, J. B., Crampton, C. & Cowley, A. P. Astrophys. J. 275, L43-L47 (1983).
 Dickel, H. R. Astrophys. J. 141, 1306-1317 (1965).
 Bianchi, L. & Pakuli, M. W. Astr. Astrophys. 146, 242-248 (1985).
 White, N. E. & Marshall, F. E. Astrophys. J. 281, 354-359 (1984).
 Stone, R. P. S. & Baldwin, J. A. Mon. Not. R. astr. Soc. 204, 347-353 (1982).
 Aller, L. N., Physics of Thermal Gaseous Nebulae (Astrophysics and Space Science Library, Vol. 11) (Paidel Doctreets, 1984) Vol. 11) (Reidel, Dordrecht, 1984).

- Yol. II) (Reddel, Dordrecht, 1984).
 Stasinska, G. Astr. Astrophys. 84, 320-328 (1980).
 Evans, I. N. & Dopita, M. A. Astrophys. J. Suppl. Ser. 58, 125-142 (1985).
 Jacoby, G. H. Astrophys. J. Suppl. Ser. 42, 1-18 (1980).
 Mauche, C. W. & Gorenstein, P. Astrophys. J. 302, 371-383 (1986).
 Dopita, M. A., Binette, L., D'Odorico, S. & Benvanuti, P. Astrophys. J. 276, 653-666 (1984).

- Danzier, I. J. Proc. IAU Symp. 101, 193-203 (1983).
 Tarter, C. B., Tucker, W. H. & Salpeter, E. E. Astrophys. J. 156, 943-951 (1969).
 Tarter, C. B. & Salpeter, E. E. Astrophys. J. 156, 943-951 (1969).
 Halpern, J. P. & Grindlay, J. E. Astrophys. J. 242, 1041-1055 (1980).
- 21. Kallman, T. R. & McCray, R. Astrophys. J. Suppl. Ser. 50, 263-317 (1982).

of the ionization, temperature and density structure, whereas active galactic nuclei appear largely unresolved in optical and ultraviolet observations.

We thank the European Southern Observatory for generous allotment of observing time and extensive use of reduction facilities in Garching; B. Reipurth for the CCD image, M. Mouchet for the 'red' spectra of LMC X-1 and the GSO staff for giving us the opportunity to observe at the 2.2 m telescope in the remote mode. L.P.A. acknowledges an ESO fellowship. Note added in proof: Our recent detection in extended [Ne V] A3426 emission around LMC X-1 with ionization potential (to produce the ion) of 97.1 eV provides further support to the X-ray-photoionization model of N159F.

- Kallman, T. R. Astrophys. J. 280, 269-281 (1984).
 Dufour, R. J. Proc. IAU Symp. 108, 353-360 (1984).

- Dufour, R. J. Froe IAC Symp. 108, 335-360 (1984).
 Koorneef, J. Astr. Astrophys. 107, 247-251 (1982).
 Mathewson, D. S. & Ford, V. L. Proc. IAU Symp. 108, 125-136 (1984).
 Karzas, W. & Latter, R. Astrophys. J. Suppl. Ser. 6, 167-212 (1961).
 Shakura, N. I. & Sunyaev, R. A. Astr. Astrophys. 24, 337-355 (1973).
 Osterbrock, D. E. Astrophysics of Gaseous Nebula (Freeman, San Francisco, 1974).
- McCray, R., Wright, C. & Hatchett, S. Astrophys. J. 211, L29-L33 (1977)
 Dupree, A. K. et al. Nature 275, 400-403 (1978).
- Dupree, A. K. et al. Astrophys. J. 238, 969-981 (1980).
 Hatchett, S. & McCray, R. Astrophys. J. 211, 552-561 (1977).
- 33. White, N. E. in Interacting Binaries (eds Eggleton, P. P. & Pringle, J. E.) 249-287 Reidel, Dordrecht, 1985).

- Marshall, F.E., White, N. E. & Becker, R. M. Astrophys. J. 266, 814-822 (1983).
 Garmany, C. D. & Conti, P. S. Astrophys. J. 293, 407-413 (1985).
 van den Heuvel, E. P. J. in Accretion driven X-ray sources (eds. Lewin, W. H. G. & van den Heuvel, E. P. J.) 303-341 (Cambridge University Press, 1983).
 van den Heuvel, E. P. J. & Habets, G. M. H. J. Nature 309, 598-600 (1984).

- Tuchy, I. R. & Dopita, M. A. Astrophys. J. 268, L11-L15 (1983).
 Pakull, M. W., Ilovaisky, S. A. & Chevalier, C. Space Sci. Rev. 40, 229-232 1985.
 Hutchings, J. B. Proc. IAU Symp. 108, 305-312 (1984).
 Osterbrock, D. E. Physica Scripta 17, 285-292 (1978).

- 42. Collin-Souffrin, S. Physica Scripta 17, 293-300 (1978).

2.5-Myr Australopithecus boisei from west of Lake Turkana, Kenya

A. Walker*, R. E. Leakey†, J. M. Harris‡ & F. H. Brown§

* Department of Cell Biology and Anatomy, Johns Hopkins University School of Medicine, 725 North Wolfe Street, Baltimore, Maryland 21205, USA

† National Museums of Kenya, PO Box 40658, Nairobi, Kenya ‡ Los Angeles County Museum of Natural History, 900 Exposition Boulevard, Los Angeles, California 90007, USA § Department of Geology and Geophysics, University of Utah, Salt Lake City, Utah 84112, USA

Specimens of Australopithecus boisei have been found in 2.5-Myr-old sediments west of Lake Turkana, Kenya. The primitive morphology of these early A. boisei suggests that robust and hyper-robust Australopithecus developed many of their common features in parallel and further that A. africanus is unlikely to have been ancestral to A. boisei.

THE 'hyper-robust' hominid Australopithecus boisei is wellknown from several East African Plio-Pleistocene deposits dated between 2.2 and 1.2 Myr (refs 1, 2). It has been thought of variously, as: the northern vicar of the equally well-known A. robustus3; the extremely specialized end-member of the robust clade4; an already developed species which immigrated from another, unknown area⁵; and as representing individuals at the large end of a single Australopithecus species that also encompasses A. robustus and A. africanus⁶.

There is a growing consensus that the east and south African samples are different enough to allow them to be placed in separate species¹⁻⁴. The type specimen of A. boisei is Olduval Hominid $5^{7.8}$.

These two robust species are placed in the genus Paranthropus by some authors9. Although recognizing that the two known samples overlap in time, some have advocated an ancestordescendant relationship with A. robustus giving rise to A. boisei. Perhaps the most compelling recent evidence for this last view

is Rak's exemplary study of the structure and function of the australopithecine face4. He has followed an evolutionary scheme in which the origins of the robust clade are in A. africanus, which is thereby removed from consideration as a human ancestor¹⁰. This scheme has not found universal acceptance^{11,12}.

Localities

Prospecting was carried out in 1985 in Pliocene sediments to the west of Lake Turkana, Kenya. It led to the recovery of two A. boisei specimens. A cranium and a partial mandible were discovered at two separate localities: sediments in the Lomekwi and Kangatukuseo drainages (see Fig. 1) at approximately 3°45′ N, 35°45′ E.

The general dip of strata is to the east in the Lomekwi drainage, but the strata at Lomekwi I from which the cranium was derived are deformed into a syncline by drag along a fault that truncates the section about 50 m east of the site. Several small faults cut the section west of the site, but it has been possible to link the

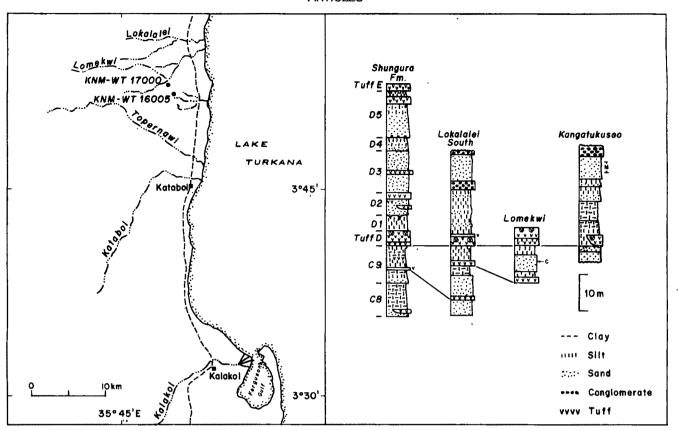


Fig. 1 Map and sections showing geographical and stratigraphic positions of KNM-WT 17000 and KNM-WT 16005. C, cranium; M, mandible.

short sections together by analysis of volcanic ash layers in the sequence. The total thickness of section immediately surrounding the site is less than 15 m, and the volcanic ash layer which caps the section is compositionally indistinguishable from Tuff D of the Shungura Formation. Earlier¹³, this tuff was referred to the informally designated Upper Burgi Tuff of the Koobi Fora Formation. With more numerous analyses it is now clear that the Upper Burgi Tuff also correlates with Tuff D, and an additional correlation datum is provided between the Shungura Formation and the Koobi Fora Formation. Tuff D has been

Table 1 Fossil mammals from the new australopithecine localities west
of Lake Turkana

Giraffa sp.
Aepyceros sp.
Connochaetes sp.
Parmularius cf. braini
Alcelaphini medium
Alcelaphini small
Menelikia sp.
Kobus sigmoidalis
Kobus sp. A
Kobus sp. B
Kobus sp. C
Kobus sp. D
Kobus sp. E
Kobus sp. F
Reduncini indet.
Reduncini large
Reduncini medium
Reduncini small
Tragelaphus nakuae
Tragelaphus sp.
. Bovini
Gazella aff. granti
Antidorcas recki
Antilopini

dated at 2.52 ± 0.05 Myr¹⁴. This age is an average computed from samples from the Shungura Formation in Ethiopia, and from the correlative unit at Kangatukuseo. The cranium derives from a level 3.8 m below Tuff D. Around 10 m below Tuff D there is a second ash layer. In the Lokalalei drainage, about 4 km northwest of the site, there are three ash layers exposed in sequence. The lowest correlates with a tuff in submember C9 of the Shungura Formation, and the upper two correlate with the two ash layers exposed at the site of the cranium. On this basis, the cranium is shown to lie within strata correlative with submember C9 of the Shungura Formation. Based on the K/Ar chronology of the Shungura Formation and scaling on the basis of constant sedimentation rates there, the cranium is estimated to be 2.55 Myr old. Using palaeomagnetic polarity boundaries as the basis of chronological placement, the age of the cranium would be ~2.45 Myr, as there is a slight discordance between the two chronologies¹⁵. Therefore, we believe that the age of the cranium can be confidently stated as 2.50 ± 0.07 Myr, including all errors. The sediments from which the cranium derives are overbank deposits of a large perennial river, probably the ancestral Omo.

The mandible from Kangatukuseo III derives from a level about 19 m above Tuff D. Tuff E is not exposed in Kangatukuseo, but it is exposed in the northern part of the Lomekwi drainage, and in the southern Lokalalei drainage. There, sediments correlative with Member D of the Shungura Formation are at least 26 m thick. On this basis, the mandible is assigned to the central part of Member D of the Shungura Formation, the best age estimate for which is 2.45 ± 0.05 Myr. The section is faulted east of the mandible site, and older sediments are exposed along the drainage east of that point. In fact, the entire section exposed in Kangatukuseo lies within an interval from ~25 m above Tuff D to 5 m below that tuff. The mandible was collected from a sandstone layer \sim 6 m thick, deposited by a large river system. Thin basalt pebble conglomerates intercalated in this part of the section show that the site lay near the boundary between sediments deposited by this large river, and alluvial fan deposits derived from the west.

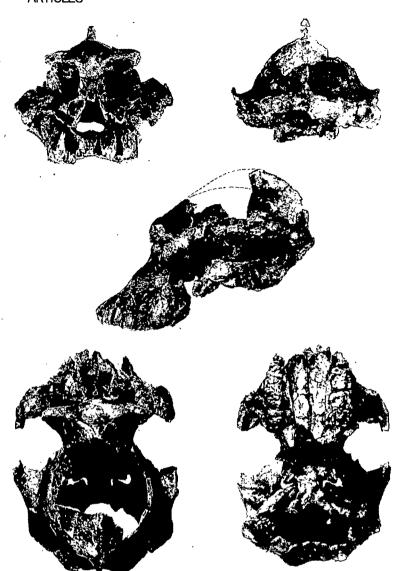


Fig. 2 Anterior, posterior, left lateral, superior and inferior views of cranium KNM-WT 17000.

Scale in cm.

The interval of section from which the australopithecine specimens were collected has also yielded over 200 fossils representing more than 40 other mammalian species (Table 1), including the skeleton of a ground-dwelling colobine and a relatively complete camel mandible. Bovids are the most common elements of the fauna at this level and most represent species that are otherwise known from the lower portion of the Omo Shungura succession. But whereas alcelaphines and impalas predominate at lower horizons west of Lake Turkana, reduncine bovids are the commonest fossils at the australopithecine sites reported here and are taxonomically different from those recovered slightly higher in the sequence. Elephas recki shungurensis is the common elephant at the localities considered here while Notochoerus scotti and Kolpochoerus limnetes are the common suids. Although all three taxa have lengthy Pliocene distributions, the West Turkana specimens closely match samples of these species from Omo Shungura Members C and D-thus supporting the estimate of age derived from the tuff analyses. The age estimate is corroborated by the apparent absence of the elephantids Loxodonta adaurora, Loxodonta exoptata and Elephas recki brumpti, and of the suids Nyanzachoerus kanamensis, Notochoerus euilus, Kolpochoerus afarensis and Potamochoerus sp., all of which occur in older horizons in the upper reaches of the Laga Lomekwi. Also missing from the australopithecine-bearing assemblage are the reduncine bovid

Menelikia lyrocera and equids of the genus Equus, both of which occur higher in the sequence.

Specimens

KNM-WT 17000 is an adult cranium with the following parts missing: all of the tooth crowns except a half molar and the right P³; some facial bone fragments which have spalled off the infilled maxillary sinus; most of the frontal processes and temporal plates of the zygomatics; the zygomatic arches themselves; a large part of the frontal and parietals superiorly (but a piece of the sagittal crest on the anterior part of the parietal is preserved); parts of both pterygoid regions inferiorly and the posterior part of the maxilla and palate on the right side; and the inferior part of the nuchal region of the occipital. There is no bilateral asymmetry and all bony contacts are sharp. There is no evidence of any plastic deformation and the brain case has retained its spheroidal shape (Fig. 2).

It is a massively-built cranium with a very large facial skeleton, palate and large cranial base, but with a small brain case. The palate and cranial base are roughly the same size as in Olduvai Hominid (O.H.) 5. The cranial base is about the same size as, but the palate is slightly larger than in, KNM-ER 406 (ref. 16). The cranial capacity is 410 ml (mean of five determinations by water displacement with a standard error of 4.32). This measurement is probably accurate since the orbital plates of the frontals,

occipital

Braincase relative to face

Nasoalveolar gutter present

Infraorbital foramen high

Maxillary fossula present

Greatest orbital height

Nasals wide above frontonasal suture

Inferior orbital margins soft laterally

Foramen magnum heart-shaped

Table 2 Compilation of features of Australopithecus species							
Feature	A. afarensis	A. africanus	A. robustus	A. boisei	KNM-WT 17000		
Position of I ² roots relative to	Lateral	Medial	Medial	Medial	Medial		
nasal aperture margins							
Divergence of temporal lines relative to lambda	Below	Above	Above	Above	Below		
Lateral concavity of nuchal plane	Present	Absent	Absent	Absent	Probably present		
Depth of mandibular fossa	Shallow	Deep	Deep	Deep	Shallow		
Temporal squama pneumatization	Extensive	Weak	Weak	Weak	Extensive		
Flat, shallow palate	Present	Absent	Absent	Absent	Present		
Subnasal prognathism	Pronounced	Intermediate	Reduced	Reduced	Pronounced		
Orientation of tympanic plate	Less vertical	Intermediate	Vertical	Vertical	Intermediate		
Flexion of cranial base	Weak	Moderate	Strong	Strong	Weak		
Relative sizes of posterior to anterior temporalis	Large	Intermediate	Small	Small	Large		
Position of postglenoid process	Completely	Variable	Merge	Merge	Completely		
relative to tympanic	anterior		superiorly	superiorly	anterior		
Tubular tympanic	Present	Intermediate	No	No	Intermediate		
Articular eminence	Weak	Intermediate	Strong	Strong	Weak		
Foramen magnum relative to tympanic tips	Anterior	Intermediate	Anterior	Anterior	Anterior		
Coronally placed petrous temporals	No	Variable	Yes	Yes	Yes		
Distance between M ¹ and temporomandibular joint	Long	Variable	Short	Short	Long		
P ³ outline	Asymmetric	Intermediate	Oval	Oval	Oval		
Relative size of C	Very large	Medium	Small	Small	Small		
Anterior projection of zygomatic	Absent	Intermediate	Strong	Very strong	Very strong		
Height of masseter origin	Lowest	Intermediate	High	High	High		
Canine jugum separate from margin of pyriform aperture	Yes	Variable	No	No	No		
Distinct subnasal and intranasal parts of clivus	Yes	Intermediate	No	No	No		
Relative size of post-canine teeth	Moderate	Large	Very large	Very large	Very large		
Robustness of zygomatic arches	Moderate	Strong	Very strong	Very strong	Very strong		
Common origin of zygomatic arch	M^1/P^4	P ⁴	P ⁴	P^3	\mathbf{P}^3		
C jugum	Prominent	Pronounced	Reduced	Lost	Lost		
Inclination of nuchal plane	Steep	Less steep	_	Variable	Less steep		
Compound temporonuchal crest	Present	Absent	Males only	Males only	Present		
Asterionic notch	Present	Absent	Absent	Absent	Probably present		
Medial inflection of mastoids	Strong	Reduced	Reduced	Reduced	Reduced		
Anterior facial pillars	Absent	Present	Present	Absent	Absent		
Length of nuchal plane relative to	Long	Intermediate	Long	Long	Long		

High

No

No

Yes

Yes

No

No

Middle

No

Yes

No

Low

Yes

Yes

No

Yes

Yes

No

Middle

the cribiform plate region of the ethmoid, one anterior clinoid and both posterior clinoid processes are preserved together with the rest of the cranial base. The missing cranial vault fragments can be reconstructed with fair certainty by following the internal contours all around them. This is the smallest published cranial capacity for any adult fossil hominid, although A.L. 162-28 from Hadar¹⁷ must have been smaller. Given the massive face and palate combined with a small brain case, it is not surprising that the sagittal crest is the largest ever in a hominid. Further, the sagittal crest joins completely to compound temporal-nuchal crests with no intervening bare area¹⁸. The foramen magnum position is far forward as in other robust Australopithecus specimens¹⁹.

The one complete tooth crown, right P³, is 11.5 mesiodistally by 16.2 buccolingually. This is bigger mesiodistally (md) than O.H. 5 (10.9) and smaller buccolingually (bl) (17.0)^{7,8}. These dimensions are completely outside the recorded range for A. robustus (9.2-10.7 md, 11.6-15.2 bl) and at the high end of the range for A. boisei (9.5-11.8 md, 13.8-17.0 bl)²⁰. Only the largest A. boisei mandibles found so far (for example, KNM-ER 729

and 3230²¹) would fit this cranium. It is unfortunate that the region of the occipital which would show the grooves for the occipital and marginal sinuses is missing, but the small sigmoid sinuses appear to have no contribution from transverse ones. Thus we feel that enlarged occipital and a marginal sinuses may have been present.

Low

Yes

Yes

No

Nο

No

Yes

Medial

Low

Yes

Yes

No

Nο

Yes

Yes

Middle

Most of the previously recorded differences between A. boisei and A. robustus have involved greater robustness in the former. In fact for those parts preserved in KNM-WT 17000, the definitions originally given by Tobias⁸ include only two characters that cannot be simply attributed to this robustness. One is that the supraorbital torus is 'twisted' along its length. Subsequent discoveries of A. boisei specimens show that O.H. 5 is extreme in its supraorbital torus development and that others are not so 'twisted'. The other character is that A. boisei palates are deeper anteriorly than those of A. robustus, in which they tend to be shallow all along the length. Recently, Rak⁴ has undertaken a study of the australopithecine face and has documented structural differences between the faces of all four species. Skelton et al.²² have just made a cladistic analysis of



Fig. 3 Occlusal view of mandible KNM-WT 16005. Scale in cm.

early hominids; Table 2 lists some of the characteristics given as typical of Australopithecus species by these authors (see ref. 22 and refs therein) as well as the condition found in KNM-WT 17000. For most features the new specimen resembles A. boisei.

There are some features of KNM-WT 17000 that differ from all other 'hyper-robust' specimens as well as from robust ones. The most obvious and important is the prognathic mid- and lower facial region. In superior view all other robust crania are so orthognathic that only a small part of the incisor region projects past the supraorbital tori. In KNM-WT 17000 the mid-face projects strongly past the tori and the anterior maxilla projects well forwards as a square muzzle. In summary, we regard this specimen as part of the A. boisei clade and view its differences from the younger sample as being either primitive, or part of normal intraspecific variation that has not been documented before, or both.

Mandible KNM-WT 16005 has the body preserved to the M₃ alveoli on the left and the M₂ alveoli on the right. The base is missing. The incisors and canines are, as judged from their roots, relatively very small and the post-canine teeth relatively very large. In its size, shape and proportions, KNM-WT 16005 is very similar to the Peninj mandible²³, except that the P₄ and M₁ of the latter are a little larger and the M₂ a little smaller than this specimen. KNM-WT 16005 is smaller than the mandible which KNM-WT 17000 possessed. Tooth measurements are given in Table 3, and the specimen is shown in Fig. 3.

Although future finds may show that KNM-WT 17000 is well within the range of variation of A. boisei, it is also possible that the differences will prove sufficient to warrant specific distinction. If the latter proves to be the case we suggest that some specimens from the same time period and from the same sedimentary basin (for example, Omo 1967-18 from the Shungura Formation) will be included in the same species. Omo 1967-18 is the type specimen of Paraustralopithecus aethiopicus Arambourg and Coppens²⁴. In our view, the appropriate name then would be Australopithecus aethiopicus.

Conclusions

The new specimens show that the A. boisei lineage was established at least 2.5 Myr ago and further that, in robustness and tooth size, at least some members of the early population were as large as any later ones. Although one authority suggested

that the robust australopithecines became smaller in skull and tooth size with time²⁵, most have pointed out that the available sample showed the opposite, that within A. boisei there has been an increase in size and robustness of the skull and jaws. This was apparently an artefact of sampling and is no longer correct.

Although recognizing that at least some populations of A. robustus and A. boisei overlapped in their time ranges, Rak⁴ hypothesized that the former was ancestral to A. boisei. This is no longer tenable. A. robustus shares with younger examples of A. boisei several features which are clearly derived from the condition seen in KNM-WT 17000. These include the cresting pattern—with the emphasis on the anterior and middle parts of the temporalis muscle—the orthognathism and the deep temporomandibular joint with strong eminence. At the same time KNM-WT 17000 is clearly a member of the A. boisei lineage, as demonstrated by the massive size, extremely large palate and teeth, the build of the infraorbital and nasal areas and the anterior position and low take-off of the zygomatic root.

Therefore, this new specimen shows that A. robustus is a related, smaller species that was either derived from ancestral forms earlier than 2.5 Myr and/or has evolved independently in southern Africa, perhaps from A. africanus. It has been suggested before that A. robustus was derived from A. africanus⁴, but by those who believed A. robustus then gave rise to A. boisei—an interpretation that is now unlikely.

The idea that A. africanus was the earliest species of a lineage in which A. robustus led to A. boisei is challenged by the new evidence. KNM-WT 17000 shows that all known A. africanus share features which are derived relative to it. Many of these same features were cited by White et al.²⁰ in arguing that A. afarensis is more primitive than A. africanus. Features showing KNM-WT 17000 to be more primitive than A. africanus that were also used to distinguish the primitiveness of A. afarensis

Table 3 Tooth measurements of KNM-WT 16005 (mm)

	Mesiodistal	Buccolingual
Left P ₃	10.7	13.8
P ₄	(12.0)	(15.0)
M ₁	15.7	14.3
M ₂	(17.0)	16.7

are: a very flat, shallow palate; pronounced subnasal prognathism; compound temporal/nuchal crests; sagittal crest with emphasis on posterior fibres of the temporalis muscle; an extensively pneumatized squamous temporal, which in KNM-WT 17000 is 11.5 thick just above the supraglenoid gutter; small occipital relative to nuchal plane; pneumatization of lateral cranial base to produce strongly flared parietal mastoid angles; shallow and mediolaterally broad mandibular fossae; tympanics completely posterior to the postglenoid process. In KNM-WT 17000, the asterionic region is poorly preserved, but an asterionic notch was probably present, which is an additional feature also cited to demonstrate the primitiveness of A. afarensis.

Other primitive features found in KNM-WT 17000, but not known or much discussed for A. afarensis, are: very small cranial capacity; low posterior profile of the calvaria; nasals extended far above the frontomaxillary suture and well onto an uninflated glabella; low calvaria with receding frontal squama; and extremely convex inferolateral margins of the orbits such as found in some gorillas. Thus there are many features in which KNM-WT 17000 is more primitive than A. africanus and similar to A. afarensis yet KNM-WT 17000 is clearly a member of the A. boisei clade. Further, although the dating of the South African sites is admittedly still imprecise and populations of ancestral species may survive a speciation event, the time sequence of the fossils is becoming increasingly less supportive of the idea of an africanus-robustus-boisei lineage.

Finally, it is striking that many of the features of this cranium shared by A. afarensis are primitive and not found in A. robustus or later specimens of A. boisei. These primitive featuresshared by KNM-WT 17000 and A. afarensis are almost exclusively confined to the calvaria, despite the largely complete face of KNM-WT 17000 and the existence of several partial facial specimens at Hadar. However, not one individual adult specimen of A. afarensis preserves a facial skeleton attached to a calvaria. This observation raises two alternatives: first, that these features are primitive to the Hominidae and therefore not of great taxonomic value in determining relationships among hominids; second, that, Olson²⁶ has suggested, the specimens identified as

Received 7 April; accepted 2 July 1986.

- 1. Howell, F. C. in Evolution of African Mammals (eds Maglio, V. J. & Cooke, H. B. S.)
- 154-248 (Harvard, Cambridge, 1978).

 2. Coppens, Y. in Morphologie Evolutive—Morphogenese du Crane at Origine de l'Homme (ed. Sakka, M.) 155-168 (CRNS, Paris, 1981); Bull Mem. Soc. Anthrop. Paris 3, 273-284 (1983).
- 3. Tobias, P. V. A. Rev. Anthrop. 2, 311-334 (1973).
 4. Rak, Y. The Australopithecine Face, 1-169(Academic, New York, 1983); Am. J. phys. Anthrop. 66, 281-288 (1985).
- Boaz, N. T. in New Interpretations of Ape and Human Ancestry (eds Ciochon, R. L. & Corruccini, R. S.) 705-720 (Plenum, New York, 1983).
- Wclpoff, M. H. Palaeoanthropology 131-157 (Knopf, New York, 1980). Leakey, L. S. B. Nature 184, 491-493 (1959).

- Tobias, P. V. Olduvai Gorge Vol. 2 (Cambridge University Press, 1967). Robinson, J. T. in Evolution und Hominisation (ed. Kurth, G.) 120 (Fischer, Stuttgart, 1962); in Evolutionary Biology (eds Dobzhansky, T., Hecht, M. K. & Steere, W.) (Appleton-Century Crofts, New York, 1967).
- 10. Johanson, D. C. & White, T. D. Science 203, 321-330 (1979).

A. afarensis include two species, one of which gives rise directly to A. boisei. Whatever the final answer, these new specimens suggest that early hominid phylogeny has not yet been finally established and that it will prove to be more complex than has been stated.

We thank the Government of Kenya and the Governors of the National Museums of Kenya. This research is funded by the National Geographic Society, Washington, D.C., the Garland Foundation and the National Museums of Kenya, F.H.B. was funded for analyses by NSF grant BNS 8406737. We thank Bw. Kamoya Kimeu and his team for invaluable help. Many colleagues, but especially M. G. Leakey and P. Shipman, helped in various ways.

- Tobias, P. V. Palaeont. afr. 23, 1-17 (1980).
 Olson, T. R. in Aspects of Human Evolution (ed. Stringer, C. B.) 99-128 (Taylor & Francis, London, 1981).
- 13. Harris, J. M. & Brown, F. H. National Geographic Res. 1, 289-297 (1985)
- Brown, F. H., McDougall, I., Davies, T. & Maier, R. in Ancestors: the Hard Evidence (ed. Delson, E.) 82-90 (Liss, New York, 1985).
 Hillhouse, J. J., Cerling, T. E. & Brown F. H. J. geophys. Res. (in the press).
- Leakey, R. E. F., Mungai, J. M. & Walker, A. C. Am. J. phys. Anthrop. 35, 175-186 (1971).
 Kimbel, W. H., Johanson, D. C. & Coppens, Y. Am. J. phys. Anthrop. 57, 453-499 (1982).
 Dart, R. A. Am. J. phys. Anthrop. 6, 259-284 (1948).
 Dean, M. C. & Wood, B. A. Am. J. phys. Anthrop. 59, 157-174 (1982).

- White, T. D., Johanson, D. C. & Kimbel, W. H. S. Afr. J. Sci. 77, 445-470 (1981).
 Leakey, M. G. & Leakey, R. E. Koobi Fora Research Project, 100, 169 (Clarendon, Oxford,
- Skelton, R. R., McHenry, H. & Drawhorn, G. M. Curr. Anthrop. 27, 21-43 (1986).

- Leakey, L. S. B. & Leakey, M. D. Nature 202, 5-7 (1964).
 Arambourg, C. & Coppens, Y. C. r. Hebd. Séanc. Acad. Sci., Paris 265, 589-590 (1967).
 Robinson, J. T. Early Hominid Posture and Locomotion (University of Chicago Press, 1972).
- 26. Olson, T. R. in Ancestors: the Hard Evidence (ed. Delson, E.) 102-119 (Liss, New York,

LETTERS TO NATURE

Steep-spectrum radio lobes near the galactic centre

N. E. Kassim, T. N. LaRosa & W. C. Erickson

Astronomy Program, University of Maryland, College Park, Maryland 20742, USA

In a previous paper1 we reported the discovery of an extended steep-spectrum radio lobe located ~34 arc min north-east of the galactic centre (the northern galactic centre lobe). Based on the similarity of the observed properties of this object to the radio lobes observed in the nuclei of Seyfert galaxies2, we suggested that this source may be a manifestation of nuclear activity associated with the compact non-thermal source³ located at the galactic centre. However, no clear evidence for a second opposing lobe was evident from the 80-MHz observations. Here we report observations at 110.6 and 123.0 MHz which confirm the existence of a second steep-spectrum feature, first discovered by Yusef-Zadeh et al.4 at 160 MHz, which extends ~10 arc min to the south-east of the radio source Sagittarius-A. These new observations are in the only frequency range in which it is possible to view both of these features simultaneously and to display their morphology as a function of frequency. At lower frequencies the features are obscured by thermal absorption; at higher frequencies they blend into the background emission. Based on this unique perspective, we propose that these radio sources are related, and associated with activity at the galactic nucleus.

Our observations were made in April-May 1985 with the TPT telescope of the Clark Lake Radio Observatory⁵. This instrument is a T-shaped array of 720 conical-spiral antennas, measuring 3.0×1.8 km, operating in the range 15-125 MHz. The beamwidth in the direction of the galactic centre is 3.6×6.2 arc min at 110.6 MHz and 3.3×5.8 arc min at 123.0 MHz. The 110.6-MHz map is the sum of three nights' observations; two nights' observa-

Table 1 Observed properties of features located near the galactic centre

	110.6-MHz flux density (Jy)	Luminosity (erg s ⁻¹)	α
Northern lobe	65	2×10^{34}	≤-1.0
Jet feature	10	2×10^{33}	≤-0.7
Central compact source	- Marine	2×10^{34}	≈ -0.25

tions are summed at 123.0 MHz. Maps made from each night individually and maps made from data taken before and after transit are all consistent with each other. Observations of sources from the 3C and Culgoora catalogues were used for flux calibration and indicated that ionospheric refraction was not important. Flux densities have been referred to the absolute scale of Baars et al.6.

Figure 1 shows a superposition of the relevant portions of the Clark Lake 110.6- and 123.0-MHz maps on the 160-MHz Culgoora radioheliograph map of Yusef-Zadeh et al.4. The peak of the 160-MHz emission is located at (RA = 17 h 42 min 36.7 s, $dec. = -28^{\circ}58'17''$), which is coincident with the northeastern part of the non-thermal Sgr-A radio shell. The emission extending 10 arc min to the south-east of Sgr-A has been identified as a low-energy jet and is hereafter referred to as the jet feature. Our 123.0-MHz map is in excellent agreement with the Culgoora map and clearly confirms the existence of extended steep-spectrum emission in this region. However, both maps are still dominated by emission from Sgr-A.

At 110.6 MHz the emission from Sgr-A has weakened considerably relative to the emission from the steep-spectrum jet feature lying to the south-east. This is clearly illustrated by the portion of the 110.6-MHz map shown in Fig. 1. This result is partly due to the steep spectrum of the jet feature, and also to the turnover in the spectrum of Sgr-A. (Sgr-A is surrounded by a halo of ionized gas^{7,8} which causes absorption at low frequencies.)

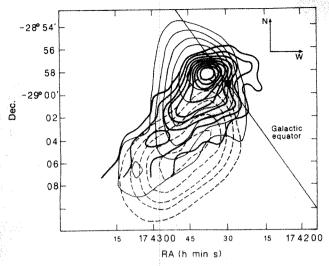


Fig. 1 Contour maps of the galactic centre jet feature. Thick lines, 160-MHz Culgoora map: beam-width, 1.9×1.9 arc min; first contour, 1.2 Jy per beam area; contour interval, 1.2 Jy per beam area. Thin lines, 123-MHz Clark Lake map: beam-width, 3.3×5.8 arc min; peak brightness temperature, 49,193 K; first contour, 19,120 K; contour interval, 5,461 K. Dashed lines, 110.6-MHz Clark Lake map: beam-width, 3.6×6.2 arc min; peak brightness temperature, 10,770 K; first contour, 2,700 K; contour interval, 1,795 K. The black dot indicates the position of the galactic centre (l=0,b=0).

Figures 2 and 3 show the complete 123.0- and 110.6-MHz maps. The three most prominent emission features on the 123.0-MHz map are the continuum arc (G0.16-0.15), the northern galactic centre lobe and Sgr-A. At 110.6 MHz the steep-spectrum jet feature has replaced Sgr-A as a prominent source in the field. The dashed lines on these maps correspond to regions of absorption produced by ionized gas along the line of sight¹.

The 110.6-MHz map (Fig. 3) is important because it reveals the similarities of the northern galactic centre lobe and the jet feature. Both of these objects are extended, steep-spectrum features which are seen only at low frequencies. Moreover, whereas the jet feature appears to be directly linked to the centre, the 110.6-MHz map indicates that the northern lobe extends towards Sgr-A and thus may also be physically connected to the centre. In fact, we would not expect to observe any connection at these frequencies because of the absorption caused by thermal gas in the region between the northern lobe and the centre. The absorption region observed at 110.6 and 80 MHz coincides with a peak in the 55- and 125-µm infrared emission. Unfortunately, the 160-MHz map does not extend far enough north to include the northern lobe.

Recent observations^{10,11} at 10 GHz have also revealed an apparently separate core-lobe system associated with the non-thermal portion of the continuum arc, G0.16-0.15. Evidence for these features is present on our 110.6-MHz maps ('arc lobes'); the observation of these features at low frequencies leaves no doubt as to their non-thermal nature.

Table 1 summarizes the observed properties of the northern galactic centre lobe, the jet feature and the central compact source. We have assumed standard synchrotron source theory. Accurate measurement of the spectral index (α) of the jet feature between 110.6 and 160 MHz is not possible because it depends crucially on the knowledge of the flux contribution from Sgr-A. Also, the spectrum of the jet is subject to significant free-free absorption. We have estimated an upper limit for the spectral index of the jet feature by comparison with higher-frequency maps where this object is not detected. The result of this estimate is $\alpha \le -0.7$, consistent with the estimate by Yusef-Zadeh et al.⁴ of $\alpha \le -0.85$. A new estimate of the spectral index of the northern radio lobe based on the 110.6-MHz map and higher-frequency

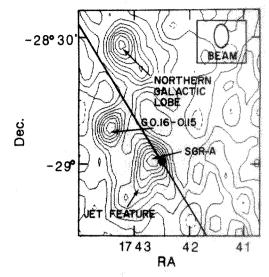


Fig. 2 Contour map at 123 MHz of the galactic centre region: beam-width, 3.3 × 5.8 arc min; peak brightness temperature, 54,600 K; first contour, 2,753 K; contour interval, 5,461 K. Black dot, galactic centre.

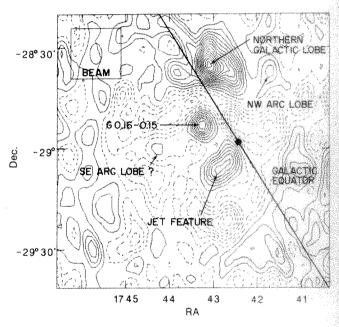


Fig. 3 Contour map at 110.6 MHz of the galactic centre region: field, 1.4° × 1.4°; beam-width, 3.6 × 6.2 arc min; peak brightness temperature, 26,994 K; first contour, 905 K; contour interval, 1,795 K. Black dot, galactic centre.

maps is consistent with the limit of $\alpha \le -1.0$ obtained previously.

We propose that the northern galactic centre lobe and the jet feature have been produced by similar processes associated with the galactic nucleus. In their geometry and other properties, these objects bear a strong resemblance to features observed in the nuclei of Seyfert and active galaxies^{2,12}. These similarities include the spatial scale of the lobes with respect to the central compact source, the fact that the luminosity of these lobes is similar to that of the central compact source, and the fact that the spectra of the lobes are much steeper than that of the central compact source. Similar radio features have been observed in several apparently normal spiral galaxies^{13,14}, substantiating the claim that Seyfert-like activity may be common among spiral galaxies^{15,16}. Asymmetry of these features with respect to Sgr-A

is not surprising. The asymmetrical geometry of these lobes is reminiscent of the 'dog leg' structures observed in several quasars17. These 'dog leg' structures are most probably produced by a collision of the radio lobe with an intergalactic cloud. Given the lower energy of the galactic features and the density of interstellar clouds near the galactic centre, bent radio lobe structures would be probable. Our observations are evidence for activity at the galactic centre driven by physical mechanisms which are similar 18, although scaled down, to those which operate in active galaxies and quasars.

This work was supported by NSF grant AST 8416179. We thank A. Szabo, B. J. Hamlet and M. J. Mahoney for help with the observations and reductions. T.N.L. thanks Professor Donat Wentzel for encouragement.

Received 23 April; accepted 9 May 1986.

- LaRosa, T. N. & Kassim, N. E. Astrophys. J. 299, L13-L17 (1985).
 Ulvestad, T. S. & Wilson, A. S. Astrophys. J. 285, 439-452 (1984).
- Lo, K. Y. et al. Nature 318, 124-126 (1985). Yusef-Zadeh, F., Morris, M., Slee, O. B. & Nelson, G. J. Astrophys. J. 300, L47-L50 (1986).
- Frickson, W. C., Mahoney, M. J. & Erb, K. Astrophys. J. Suppl. Ser. 50, 403-419 (1983).

 Baars, J. W. M., Genzel, R., Pauliny-Toth, I. I. K. & Witzel, A. Astr. Astrophys. 61, 99-106
- 7. Brezgunov, V. N., Dagkesamansky, R. D. & Udal'tsov, V. A. Astrophys. Lett. 9, 117-119
- Dulk, G. A. & Slee, O. B. Nature 248, 33-34 (1974).
- Dent, W. A. et al. in The Galactic Center (eds Reigler, G. R. & Blandford, R. D.) 33-41 (American Institute of Physics, New York, 1982)
- 10. Tsuboi, M., Inoue, M., Handa, T., Tabara, H. & Kato, T. Publs astr. Soc. Japan 37, 359-368.
- 11. Seiradakis, J. H., Lasenby, A. N., Yusef-Zadeh, F., Wielebinski, R. & Klein, U. Nature 317, 697-699 (1985).
- 12. Wilson, A. S. in Extragalactic Radio Astronomy (eds Heeschen, D. S. & Wade, C. M.) 179-188 (Reidel, Dordrecht, 1981).
- 13. Duric, N., Seaquist, E. R., Crane, P. C., Bignell, R. C. & Davis, L. E. Astrophys. J. 273, L11-L15 (1983).
- Hummel, E., van Gorkom, J. H. & Kotanyi, C. G. Astrophys. J. 267, L5-L9 (1983).
 Jones, D. L., Sramek, R. A. & Terzian, Y. Astrophys. J. 246, 28-37 (1981).
- 16. Keel, W. C. Astrophys. J. 269, 466-486 (1983).
- Stocke, J. T., Burns, J. O. & Christiansen, W. A. Astrophys. J. 299, 799-813 (1985)
- Begelman, M. C., Blandford, R. D. & Rees, M. J. Rev. mod. Phys. 56, 225-351 (1984).

An interstellar line coincident with the P(2,1)transition of hydronium (H₂O⁺)

J. M. Hollis*, E. B. Churchwell†, E. Herbst‡ & F. C. De Luciat

*Laboratory for Astronomy and Solar Physics, Code 684, NASA Goddard Space Flight Center, Greenbelt, Maryland 20771, USA † Astronomy Department, University of Wisconsin,

475 North Charter Street, Madison, Wisconsin 53706, USA ‡ Department of Physics, Duke University, Durham,

North Carolina 27706, USA

Gas-phase interstellar chemistry is thought to be dominated by ion-molecule reactions. Neutral molecular species abound in the dense interstellar clouds, but only seven molecular ions have been detected. Hydronium (H3O+) is predicted in all ion-molecule reactions¹⁻³ to be an abundant molecular ion, forming OH and H₂O by dissociative electron recombination reactions. Here we report the detection, towards the Orion-KL nebula, of a weak emission spectral line coincident in frequency with the P(2,1) rotation-inversion transition of H₃O⁺. Although we cannot be certain that this single-line detection is H₃O+, we evaluate this possibility with regard to its observed line parameters and, using theoretical chemical models, derive an Orion fractional abundance for H₂O (relative to H₂) of 10⁻⁵ and 10⁻⁶ in thermal and nonthermal cases, respectively. We also report 1-mm-wavelength observations towards Orion which yield new interstellar transitions of CH₃OH, ³⁴SO₂, H₂CS, SO, OCS, SiO and two unidentified lines at 307,313 and 304,374 MHz.

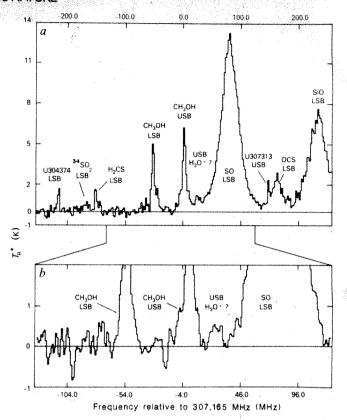


Fig. 1 a, Orion-KL line spectrum at 2 MHz resolution (see Table 1). The abscissa is USB frequency relative to 307,165 MHz, assuming a source $V_{\rm LSR}$ of ± 8.8 km s⁻¹. As this spectrum represents the alignment and averaging of data taken at centre frequencies of both 307,165 and 307,161 MHz, to de-correlate filters, only the USB features are displayed at the correct frequency; the LSB lines are smeared across two channel widths (4 MHz). These data represent 7.1 h of integration time. b, Smoothed version (Hanning smooth) of a portion of the Orion-KL line spectrum at 1 MHz resolution; abscissa as in a. The LSB lines are smeared across four channel widths (4 MHz). These data represent 7.3 h of integration time.

OH and H₂O are well-known and abundant constituents of interstellar clouds, but H₂O does not possess easily observable transitions from which abundances can be determined. In interstellar molecular sources, successful observations of interstellar H₃O⁺ would provide an indirect method of estimating H₂O abundances⁴. Several transitions of the rotation-inversion spectrum of H₃O⁺ have now been measured in the laboratory^{5,6} making possible an interstellar search for this ion. The P(2,1) transition is at a rest frequency of 307,192.41(5) MHz, and the P(3,K) transition with K=0, 1 and 2 lies between 360 and 400 GHz. The upper energy level of the P(2,1) transition is ~105 K above the ground state; this relatively low degree of excitation is seen in other molecular species in molecular clouds such as Orion and SgrB2. Towards the Orion-KL nebula we detected a weak emission feature, coincident in frequency with the P(2,1) transition of H_3O^+ , with line parameters ($T_R^* = 0.6 \text{ K}$, $\Delta V = 10 \text{ km s}^{-1}$, $V_{LSR} = 11 \text{ km s}^{-1}$), which would be consistent with a weak molecular species detected in the 'plateau' or 'doughnut' region of this source7,8.

Although this feature is by no means certain to be attributable to H₃O⁺, we have no other candidate for its identification, and, because of the importance of this species to interstellar chemistry, we are reporting our preliminary observations now and expect that we or others will confirm our present work with further observations of the P(2,1) and the higher-frequency P(3,K) transitions.

Table 1 Observed line parameters

Molecule				Orion-KL†				SgrB2‡				
	; •	Frequency (MHz) Band	Resol.	T _R * (K)	ΔV (km s ⁻¹)	$V_{LSR} \over (km s^{-1})$	Resol. (MHz)	T _R * (K)	$\frac{\Delta V}{(\text{km s}^{-1})}$	$\frac{V_{1.SR}}{(km s^{-1})}$		
U307313§	*****	307,313 (1)	USB	i	1.0(2)	4(1)	8.8 (10)					
H ₃ O ⁺ ?	P(2, 1)	307,192.41 (5)	USB	1	0.6(1)	9.6 (20)	11 (1)				and show a	
СН₁ОН	4,-4 ₀ A	307,165.94 (5)	USB	1	6.6(1)	6(1)	8.8 (10)	2	0.8(1)	17 (2)	53 (2)	
U304374	11 .0	304,374 (1)	LSB	2	1.6(2)	5 (2)	8 (2)					
34SO ₂	$3_{3,1}$ $-2_{2,0}$	304,332.1 (2)	LSB	2	0.7(2)	29 (2)	8 (2)					
H ₂ CS	91,9-81,8	304,305.97 (50)	LSB	2	2.0(2)	5(2)	8 (2)					
CH ₃ OH	$2_{1}-2_{0}$ A	304,208.35 (5)	LSB	1	7.2(3)	5 (1)	8(1)	2	0.5(1)	14(2)	51 (2)	
³² SO	8,-76	304,077.84 (10)	LSB	2	13 (1)	36 (2)	6(1)	2	0.6(1)	20 (4)	62 (2)	
ocs	25-24	303,993.24 (10)	LSB	2	3.3 (10)	7.8 (20)	5(2)					
SiO $v = 0$	7-6	303,926.96 (10)	LSB	2	8 (1)	32 (4)	6 (2)					

Line parameters T_R^* , antenna temperature; ΔV , line-width; V_{LSR} , velocity with respect to the local standard of rest.

The double-sideband observations were made on 12-16 March 1986 with the National Radio Astronomy Observatory (NRAO) 12-m radio telescope. The single-channel, cooled mixer receiver has a single-sideband receiver temperature of ~4,000 K. The sideband separation was 3,000 MHz with a spectrometer consisting of two 256-channel filter banks with 1-MHz and 2-MHz filters. The upper sideband (USB) contained the H₃O⁺ line frequency. Calibration by the chopper method was used to correct for telescope losses and atmospheric extinction. Atmospheric conditions were highly variable, although some stable conditions did occur during observations of Orion and SgrB2. During the stable periods, zenith opacities for Orion observations on 12, 14 and 15 March were 1.1, 1.1 and 0.3, respectively; for SgrB2 on 13, 15 and 16 March they were 0.5, 0.3 and 0.2, respectively. The half-power beam-width was ~21 arc s at 307 GHz. Data were taken while the beam position was switched by 1° in azimuth for SgrB2 and 0.5° for Orion-KL. The antenna temperatures are in terms of T_R* and have not been corrected for beam dilution; we estimate that our calibration scale is correct to within 20%.

Figure 1 shows the H₃O⁺ candidate line at 307,192 MHz at 2 MHz (a) and 1 MHz (b) resolution, along with two unidentified lines and newly detected transitions of several known interstellar species, all of which are reported with line parameters in Table 1. Figure 1 represents a total of more than 7 h of integration time at USB centre frequencies of 307,165 and 307,161 MHz (to de-correlate filters). Complementary integration for 5 h centred on 307,236 MHz showed similar results, and by observing how the spectral lines of the lower sideband (LSB) shifted with respect to the USB centre frequencies, we could identify the sideband of each spectral feature, and thus determine the line rest frequency to within the filter resolution. In all data sets for Orion-KL, the line at 307,192 MHz was evident at $\ge 3\sigma$. The data sets were then frequency-aligned for the USB and averaged, weighted by the integration time and the inverse of the square of the system temperature, to produce the $\geq 5\sigma$ feature shown in Fig. 2 (12 h of integration) at 1 MHz resolution. A similar alignment and averaging for the LSB showed that no LSB spectral feature could account for the USB line at 307,192 MHz. Thus, by these techniques, the reality of the spectral feature at 307,192 MHz was proved.

Assuming that the Orion-KL spectral feature at 307,192 MHz is H₃O⁺, its observed line parameters and calculated transition dipole moment of 1.44 D yield total column densities $N_{\rm T}({\rm H_3O}^+)$ of 7.7×10^{13} and 8.7×10^{13} cm⁻², in the optically thin thermal cases for excitation temperatures of 50 and 90 K, respectively. We point out that the line width may be underestimated due to the weak intensity of the feature, the possible confusion with the nearby CH₃OH line in the USB and the proximity of the SO line in the LSB. Assuming $N_T(H_2) = 3 \times 10^{23} \text{ cm}^{-2}$ for Orion10, a crude estimate of the volume density ratio $n(H_3O^+)/n(H_2) = 2.6 \times 10^{-10}$ and 2.9×10^{-10} can be made for the thermal cases at excitation temperatures of 50 and 90 K, respectively. We estimate a minimum H₂ density of ~106 cm⁻³ for thermalization of the transition to these excitation temperatures. If a density of 105 cm⁻³ characterizes the bulk of the H₃O⁺ emitting region, a far lower excitation temperature (~5 K) prevails for the two levels connected by the P(2,1) transition, although the population in the lower level of this transition is probably thermalized at the temperature of the gas. Under

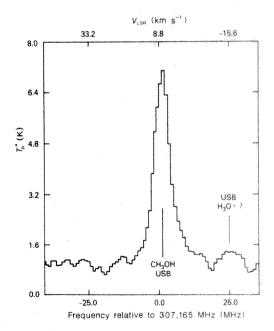


Fig. 2 Hanning smooth spectrum obtained from 12 h of integration towards the Orion-KL nebula with 1 MHz resolution. The lower abscissa is USB frequency relative to 307,165 MHz; the upper abscissa displays the USB velocity scale, assuming a $V_{\rm LSR}$ source velocity of +8.8 km s⁻¹ at a rest frequency of 307,165. The spectrum represents alignment and averaging (see text) of data taken at centre frequencies of 307,161, 307,165 and 307,236 MHz. The CH₃OH line in the USB is blended slightly with a weak H₂CS feature in the LSB for data taken at 307,236 MHz. The -5σ feature labelled H₃O⁺? was apparent in each individual data set at ≥3σ.

[†] Orion-KL J1950.0 position: (05 h 32 min 47 s, -05° 24' 21").

[‡] SgrB2 J1950.0 position: (17 h 44 min 11s, -28° 22′ 30″). § The 4_1-4_0 A transition of 13 CH₃OH is calculated to be 307,311.4 (20) MHz; laboratory measurements are pending.

these conditions, for the non-thermal case we obtain $n(H_3O^+)$ / $n(H_2) = 2.3 \times 10^{-9}$ and 2.8×10^{-9} for gas temperatures of 50 and 90 K, respectively. Our thermal and non-thermal sets of fractional abundances are in reasonable agreement with ion-molecule models, which yield 10^{-11} - 10^{-9} , depending on cloud age, gas density and elemental depletion2. We have assumed that the volume density ratio can be estimated by the column density ratio. This is not strictly true where fractional abundances change and line saturation effects occur along the line of sight. However, our order-of-magnitude estimate indicates that the spectral feature at 307,192 MHz is roughly consistent with H₃O⁺ abundances in present chemical models for Orion-like interstellar clouds.

The estimated fractional abundance of H₃O⁺ can be used to determine the fractional abundance of gas-phase H₂O by considering a limited set of ion-molecule reactions⁴. Assuming a rate coefficient of 6×10^{-6} cm³ s⁻¹ for the dissociative recombination reaction of H₃O⁺, a branching ratio of 0.5 to form H₂O+H (ref. 11), rate coefficients of $\sim 10^{-8}$ cm³ s⁻¹ for the destruction of H₂O by ion-molecule reactions¹², and a value of 0.1 for the ratio of the total abundance of reactive ions to the electron abundance, we obtain fractional abundances for H2O in Orion of 10^{-5} and 10^{-6} for the non-thermal and thermal cases, respectively.

We thank Mr John Payne, NRAO engineer, for providing a working 307-GHz receiver system on very short notice; Mr Ray

Lichtenhahn and Mr Calvin Sparks for assisting with the observations; and Dr Philip Jewell for advice concerning execution of the observations and publication of results. F. C. De L. and E. H. acknowledge the support of NASA grant NAGW-189. NRAO is operated by Associated Universities. Inc., under contract with NSF.

Note added in proof: Independent confirmation of our Orion-KL results was provided by H. A. Wootten (NRAO) and coworkers during 17-21 March 1986. Our laboratory measurements reveal a weak, unassigned (presumably high-excitation) line of CH₃OH at 307,193.27 (5) MHz, which we doubt could account for our Orion-KL line labelled 'H3O+?', due to linewidth, velocity and intensity arguments.

Received 24 March; accepted 16 May 1986.

- Herbst, E. & Klemperer, W. Astrophys. J. 185, 505-533 (1973).
 Leung, C. M., Herbst, E. & Huebner, W. F. Astrophys. J. Suppl. Ser. 56, 231-256 (1984).
 de Jong, T., Dalgarno, A. & Boland, W. Astr. Astrophys. 91, 68-84 (1980).

- de Jong, H., Darganio, A. & Bolano, H. Astrophys. J. 215, 503-510 (1977).
 Herbst, E., Green, S., Thaddeus, P. & Klemperer, W. Astrophys. J. 215, 503-510 (1977).
 Plummer, G. M., Herbst, E. & De Lucia, F. C. J. Chem. Phys. 83, 1428-1429 (1985).
 Bogey, M., Demuynck, C., Denis, M. & Destombes, J. L. Astr. Astrophys. 148, L11-L13
- Plambeck, R. L. et al. Astrophys. J. 259, 617-624 (1982). Vogel, S. N. et al. Astrophys. J. 283, 655-667 (1984).
- Botschwina, P., Rosmus, P., and Reinsch, E.-A. Chem. Phys. Lett. 102, 299-306 (1983).
 Lizzt, H. S. et al. Astrophys. J. 190, 557-564 (1974).
- Green, S. & Herbst, E. Astrophys. J. 229, 121-131 (1979).
- 12. Adams, N. G., Smith, D. & Clary, D. C. Astrophys. J. 296, L31-L34 (1985).

Impact-induced atmospheres and oceans on Earth and Venus

Takafumi Matsui* & Yutaka Abe

Geophysical Institute, Faculty of Science, University of Tokyo, Bunkyo-ku, Tokyo 113, Japan

High-velocity impacts of planetesimals onto a growing planet result in the impact-degassing of volatiles and the formation of an impact-induced atmosphere. Because of the blanketing effect of such an atmosphere, it is likely that the surface of the proto-Venus melted once the radius exceeded ~40% of the final radius. The final mass of H₂O in the impact-generated atmosphere, predicted to be $\sim 10^{21}$ kg on the basis of thermal evolution models of the growing proto-Venus, does not depend on the initial water content of the Venus-forming planetesimals and is almost identical to the present mass of the Earth's oceans. We show here that an impact-induced H₂O atmosphere of ~10²¹ kg mass probably formed on both Venus and Earth during accretion, but that whereas H₂O in the proto-atmosphere of the Earth could condense to form a hot (~600 K) ocean, such condensation probably did not occur on Venus.

Recent studies^{1,2} have suggested that an impact-induced atmosphere increases the surface temperature of the Earth to a stage where a magma ocean is possible, and that the total mass of H₂O in an impact-induced atmosphere clusters around 10²¹ kg, a value which is rather insensitive to variations in the input data. As the accretion of planetesimals is fundamental to the process of planetary formation, development of an impactgenerated atmosphere during accretion may have occurred on other terrestrial planets. In particular, the early evolution of Venus might be expected to be similar to that of the Earth, because the two planets are of similar size and mass and were formed at comparable distances from the Sun. Why then have Venus and Earth experienced different histories?

Assuming that Venus-forming planetesimals contained H₂O in amounts similar to those retained in Earth-forming planetesimals, we can calculate the evolution of an impactinduced H₂O atmosphere during accretion (see ref. 2 for details of the calculation). Figure 1 shows the atmospheric evolution during accretion for two Venus models. The accretion times, $\tau_{\rm acc}$, are assumed to be 1.6×10^7 yr, which is about one-third of $au_{\rm acc}$ of the standard Earth model. The degassing parameter and critical pressure for impact dehydration are 0.2 and 2.28× 10¹⁰ Pa, respectively. The solid and dash-dot curves represent the results of the standard model (initial water content of planetesimals $X_w = 0.1\%$) and higher water content model $(X_w = 1\%)$, respectively. As shown in Fig. 1, the final amount of H₂O in the atmosphere does not differ greatly between these two models and is $\sim 10^{21}$ kg. This amount does not vary significantly with changes in $X_{
m w}$ and $au_{
m acc}$ for $0.03 < X_{
m w}(\%) < 1$ and $10^6 < \tau_{\rm acc}(yr) < 10^8$ (ref. 2). This is because the solubility of water in silicate melt controls the amount of H₂O in the proto-atmosphere. Note that the final amount of H₂O in the atmosphere is almost identical to the amount presently found in the Earth's oceans (1.4×10²¹ kg). These are the same features which we found in our model for the Earth2. Therefore, we can reasonably consider that both planets originally had proto-atmospheres of similar mass, composed primarily of H2O. An initial mass of atmospheric water equal to the mass of the terrestrial oceans is also consistent with the present deuterium-to-hydrogen ratio on Venus³.

Given the apparent similarity of the initial atmospheric conditions on Venus and the Earth, it is interesting to study the divergence which subsequently took place in the development of the atmospheres of these two planets. The qualitative nature of the evolution of an impact-generated atmosphere can be inferred simply from its radiative equilibrium thermal structure. The main heat source of such a proto-atmosphere is the impact energy released during accretion. In this case, the atmosphere is heated from below, and thus its thermal structure is determined by the opacity of the atmosphere to infrared radiation (that is, by the blanketing effect). The solar flux supplants the impact energy flux as the main heat source of the atmosphere when its formation is complete, as the Safronov-type accretion rate assumed in this study² decreases rapidly as the final radius is

Present address: Department of Earth, Atmospheric, and Planetary Sciences, Massachusetts Institute of Technology, Cambridge, Massachusetts 02139, USA.

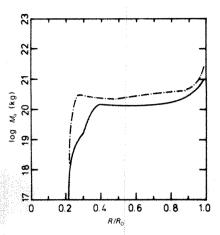


Fig. 1 Total mass M_a of the impact-generated H_2O atmosphere on Venus, plotted against normalized radius for the standard (solid curve) and higher water content (dash-dot curve) models. Note that the final mass of H_2O in the atmosphere is similar to the present mass of the Earth's oceans (10^{21} kg).

approached. When the atmosphere is heated primarily by solar radiation, its thermal structure is determined by the so-called greenhouse effect, which depends on the opacity of the atmosphere not only to long-wave (infrared) radiation, but also to short-wave (visible) radiation. This is because only the solar radiation that is able to penetrate the atmosphere can serve as a heat source. The difference between the blanketing effect and the greenhouse effect is small for a thin atmosphere, because most of the received solar radiation penetrates the atmosphere and heats it from below. For the case of a thick atmosphere, however, most of the solar radiation does not penetrate the atmosphere, as it is scattered and/or absorbed.

We can obtain the temperature profile of a plane parallel atmosphere in radiative equilibrium by solving the equations: $dF_u/d\tau = F_u - \pi B$, $df_u/dt = f_u - \omega (f_u + f_d)/2$, $dF_d/d\tau = -F_d + \pi B$, $df_d/dt = -f_d + \omega (f_u + f_d)/2$ and $F_u - F_d + f_u - f_d = F_0$, with the boundary conditions: $F_u = (1 - A)S_0/4 + F_0$, $f_u = AS_0/4$, $f_d = S_0/4$ and $F_d = 0$ at the top of the atmosphere ($\tau = 0$ and t=0), and $F_{\rm u}=\sigma T_{\rm s}^4$ and $f_{\rm u}=\mu f_{\rm d}$ at the base of the atmosphere $(\tau=\tau_{\rm s} \text{ and } t=t_{\rm s})$. Here, F and f are the long- and short-wave radiation fluxes, τ and t are the normal optical depths for the long- and short-wave radiation fluxes, B is the Planck function, ω is the albedo for single scattering, σ is the Stefan-Boltzmann constant, F_0 is the thermal energy flux given at the base of the atmosphere, S_0 is the solar flux, A is the planetary albedo, T_s is the temperature at the base of the atmosphere, and μ is the reflectivity of the short-wave radiation at the bottom of the atmosphere. The subscripts u and d denote upward and downward radiation, respectively. For a grey atmosphere, $\pi B = \sigma T^4$, where T is the temperature. To derive the above equations, we assumed local thermodynamic equilibrium for long-wave radiation and isotropic scattering for short-wave radiation, and we used a two-stream approximation. Assuming that $\lambda = \tau/t$ and ω is constant, the solutions are given by

$$\alpha T^4 = F_0 \frac{\tau + 1}{2} + \frac{S_0}{4} \frac{(\lambda + \alpha) + (\lambda - \alpha)\beta + (\alpha^2/\lambda - \lambda)(e^{-\alpha t} + \beta e^{\alpha t})}{(1 + \alpha) + (1 - \alpha)\beta}$$

$$\sigma T_s^4 = F_0 \frac{\tau_s + 2}{2} + \frac{S_0}{4} \frac{[(\lambda + \alpha) - (\lambda - \alpha) e^{-\alpha t_s}](1 - \beta_0 e^{\alpha t_s})}{(1 + \alpha) + (1 - \alpha)\beta}$$

where $\alpha = \sqrt{(1-\omega)}$, $\beta = \beta_0 e^{-2\alpha t}$, and $\beta_0 = [\mu(1+\alpha) - (1-\alpha)]/[(1+\alpha) - \mu(1-\alpha)]$.

Figure 2 shows the radiative equilibrium thermal structures of the proto-atmospheres of Venus and the Earth, as determined from the above equations. As mentioned previously, the radia-

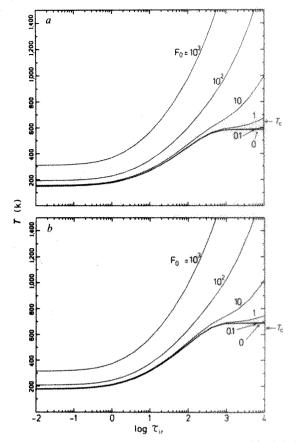


Fig. 2 The radiative equilibrium thermal structures of the proto- $\rm H_2O$ atmospheres for: a, the Earth, $S_0 = 960~\rm W~m^{-2}$; b, Venus, $S_0 = 1,830~\rm W~m^{-2}$. S_0 is the solar flux (we used a value 30% less than the present value), and F_0 is the energy flux released at the surface of a planet (in W m⁻²). $\tau_{\rm ir}$ is the optical depth of the atmosphere to infrared radiation. Note that with a decrease in F_0 the temperature at the base of the Earth's atmosphere becomes lower than the critical temperature T_c for H_2O to liquefy at a pressure of $\sim 100~\rm bar$.

tive equilibrium structure depends mainly on the ratio λ of the optical depths of infrared (long-wave) and visible (short-wave) radiation. Although it is difficult to estimate this ratio theoretically and/or experimentally, we may infer it from Pioneer-Venus data on the absorptional features of the venusian atmosphere*, where surface pressure is $\sim \frac{1}{4}$ or $\frac{1}{5}$ that of the proto- H_2O atmosphere. The planetary albedo and the net solar radiation flux f_a at the surface are given by $A = [(1-\alpha) + \beta_0(1+\alpha)\varepsilon^2]/[(1+\alpha) + \beta_0(1+\alpha)\varepsilon^2]$ $\beta_0(1-\alpha)\varepsilon^2$ and $f_s = \alpha S_0(1-\beta_0)\varepsilon/2[(1+\alpha)+(1-\alpha)\beta_0\varepsilon^2],$ where $\varepsilon = \exp(-\alpha t_s)$. Using the observed values of A (0.77), f_s/S_0 (0.005), S_0 (2,620 W m⁻²), T_s (750 K) and μ (0.1) for the present venusian atmosphere⁴, we can determine $\omega = 0.98$ and $\lambda = 31$ from the above equations (ω and λ are almost independent of μ). As the pressure effect on the absorption features of the atmosphere may not change significantly with wavelength, the ratio λ is expected to be insensitive to variations of pressure. The temperature effect on the absorptional features is also small, for temperature variations on the order of several hundred degrees. Therefore, we may consider $10 < \lambda < 100$ for the H_2O proto-atmosphere. In this respect, the following results are insensitive to this ratio. For both planets, the equilibrium thermal structure shifts to a lower level as the impact energy rate decreases. As the impact energy rate approaches zero (greenhouse case), the equilibrium thermal structure for the Earth falls below the vapour pressure, which means that the H₂O in the Earth's proto-atmosphere can condense to a liquid. The equilibrium thermal structure for Venus, however, remains higher than the vapour pressure. It is therefore possible that the H₂O

in the Earth's proto-atmosphere condensed to form oceans. while in the proto-venusian atmosphere it remained in gaseous form. Studies of the escape of H₂O from the proto-venusian atmosphere (see ref. 5) suggest that the H₂O in the protovenusian atmosphere may have disintegrated into hydrogen and oxygen through photodissociation, with the resulting H2 subsequently escaping through a hydrodynamic process⁵.

Figure 2 shows that the temperature of the first rain on Earth was ~600 K, and thus a hot proto-ocean may have resulted. The mean temperature of this ocean has been estimated from measurements of the oxygen isotope composition of metamorphosed sedimentary rock. According to Oskvarek and Perry⁶, the mean temperature of the early Archaean ocean may have been as high as 420 K. Our result is consistent with this observation. Sagan and Mullen noted that the surface temperature of the proto-Earth would have been too cold for water to be liquid if the atmosphere had the same composition as at present; they argued for the existence of a reduced atmosphere, which would lead to warmer conditions on the proto-Earth. Our model, in contrast, does not require such an ad hoc assumption. We speculate that the interactive evolution of the hot proto-atmosphere, proto-ocean and proto-crust may have played an important role in the origin of the continents on the Earth; this topic deserves further study.

We thank S. C. Solomon for comments and Jan Nattier-Barbaro for assistance in manuscript preparation. This study was partially supported by grants-in-aid for scientific research from the Ministry of Education of Japan (60540247 and 59390007) and, in the final stage of preparation at MIT, by NASA grant NSG-7297.

Received 6 December 1985; accepted 20 May 1986.

- 1. Abe, Y. & Matsui, T. J. geophys. Res. 90, C545-C559 (1985).
- Matsui, T. & Abe, Y. Nature 319, 303-305 (1986). Donahue, T. M. et al. Science 216, 630-633 (1982).
- Tomasko, M. G. et al. J. geophys. Res. 85, 8167-8186 (1980).
 Kasting, J. F. & Pollack, J. B. Icarus 53, 479-508 (1983).
- Oskvarek, J. D. & Perry, E. C. Jr Nature 259, 192-194 (1976). Sagan, C. & Mullen, G. Science 177, 52-56 (1972).

The quasi-crystalline phase in the Mg-Al-Zn system

T. Rajasekharan, D. Akhtar, R. Gopalan & K. Muraleedharan

Defence Metallurgical Research Laboratory, Hyderabad-500 258, India

Shechtman et al.1 have reported a phase in rapidly solidified Al86Mn14 alloy with long-range orientational order, but with icosahedral point-group symmetry, which is inconsistent with lattice translations. However, Pauling² has argued that the apparent icosahedral symmetry in Al86Mn14 alloy is due to directed multiple twinning of cubic crystals with a cube edge of 26.7 Å. We report here the powder X-ray diffraction study of a rapidly solidified Mg₃₂(Al, Zn)₄₉ alloy which shows 5-3-2 symmetry diffraction in transmission electron microscopy (TEM). Also reported is a study of rapidly solidified Mg2Al3 alloy. The advantage of these alloys is that B-Mg2Al3, which has nearly the same structure as proposed by Pauling for the rapidly quenched Al₈₆Mn₁₄, is an equilibrium phase. This is unlike the Al-Mn system, where, according to Pauling, the cubic phase occurs in a metastable and already twinned form. The present choice of alloy systems makes it possible to compare the X-ray diffraction patterns from the quasi-crystalline phase and a cubic phase with nearly the same structure as proposed by Pauling. We observe that the X-ray diffraction pattern of rapidly

Table 1 Analysis of the X-ray diffraction pattern (Fig. 1c) obtained from rapidly quenched Mg₂Al₃

						3 3 3 3	
(hkl)	d _{cal} (Å)	d _{obs} (Å)	I/I_0	(hkl)	d _{cal} (Å)	d _{obs} (Å)	I/I ₀
		1/	-7-0			()	- / -0
(001)	9.65			(031)	1.63		
(010)	4.95			(123)	1.62		
(002)	4.83			(006)	1.61		
(011)	4.40	4.42	2	(115)	1.60		
(012)	3.45			(032)	1.56		
(003)	3.22			(016)	1.53		
(110)	2.86			(124)	1.48	1.48	3
(111)	2.74	2.73	3	(033)	1.47		
(013)	2.70	2.66	3	(220)	1.43	1.43	8
(020)	2.47	2.47	100	(221)	1.41	1.42	4
(112)	2.46			(116)	1.40		
(004)	2.41			(007)	1.38		
(021)	2.40	2.40	78	(130)	1.37		
(022)	2.20	2.20	9	(222)	1.369		
(014)	2.16			(034)	1.361		
(113)	2.13	2.13	3	(131)	1.358		
(023)	1.96	2.00	3 1	(026)	1.348		
(005)	1.93			(125)	1.343		
(120)	1.87			(017)	1.328		
(114)	1.84			(132)	1.320		
(121)	1.83			(223)	1.306		
(015)	1.80			(133)	1.260		
(122)	1.74			(035)	1.254		
(024)	1.73			(117)	1.240		
(030)	1.65			(040)	1.237	1.239	2

Table.2 Analysis of the X-ray diffraction pattern (Fig. 1a) from rapidly quenched Mg₃₂(Al, Zn)₄₉ alloy

d(Å)	I/I_0	Icosahedral indices	Observed $d(100000)/d$	Theoretical $d(100000)/d$
4.23	5	(110001)	0.57	0.56
3.74	4	$(1110\bar{1}0)$	0.65	0.65
2.423	51	(100000)	1.00	1.00
2.292	100	(110000)	1.057	1.051
2.129	6	(561033)	1.138	1.136
2.032	23	(111101)	1.192	1.193
1.778	1	(220001)	1.363	1.358
1.428	19	(101000)	1.697	1.701
1.351	2	(210000)	1.793	1.792
1.224	4	(110010)	1.980	1.973
1.217	1	(200000)	1.991	2.000

solidified Mg32(Al, Zn)49 alloy is distinct from those of the equilibrium phases and that the pattern can be completely indexed to an icosahedral phase. We argue that the above observation is inconsistent with the proposal that the material consists of an aggregate of twinned cubic crystals. Therefore, the alternative is to invoke a quasi-crystalline lattice to explain the observed 5-3-2 symmetry diffraction in TEM.

Although selected area electron diffraction patterns (SADP) displaying 5-fold, 3-fold and 2-fold axes can be explained by multiple twinning of cubic crystals³, Shechtman et al. argued that their phase shows long-range orientational order with icosahedral point-group symmetry because the dark-field images taken from any reflection had the entire grain illuminated. Also, micro-diffraction from many different volume elements of a grain (each with an area of ~200 Å²) displayed all reflections in the SADPs. However, their contention in support of the absence of microtwinning, that the X-ray diffraction pattern of rapidly quenched Al₈₆Mn₁₄ alloy cannot be indexed to any Bravais lattice, has been re-examined by Pauling², after including the unindexed lines in a pattern obtained from Schechtman.

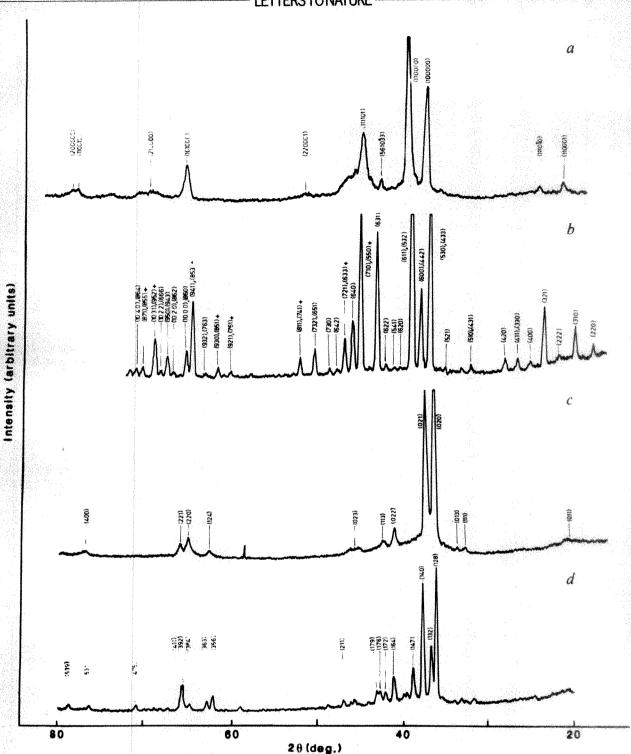


Fig. 1 X-ray diffraction pattern (CuK α radiation) from: a, rapidly quenched Mg₃₂(Al, Zn)₄₉, indexed to an icosahedral phase (see text); b, rapidly quenched Mg₃₂(Al, Zn)₄₉ after transformation (cI162, a=14.16 Å); c, rapidly quenched Mg₂Al₃ (hexagonal with a=5.73 Å, c=9.54 Å); and d, rapidly quenched Mg₂Al₃ after transformation (cF1192, a=28.28 Å).

Pauling re-indexed the entire pattern to a cubic cell with an edge of 26.7 Å. However, because the proposed cubic cell is large and intensity calculations have not been made, the accuracy of the indexing proposed by Pauling is highly dependent on the reliability of his model for the contents of the unit cell.

Pauling proposed a model in which a molten alloy of $Al_{86}Mn_{14}$, on sudden cooling, could form metastable cubic crystals of cube edge ~ 26.7 Å, with the unit cube containing $\sim 1,120$ atoms; and that these crystals would show ordered multiple growth such that 20 of them grow out from a central seed to

produce an aggregate with icosahedral symmetry. The arrangement of the atoms in the unit cell is similar to that in the unit cell of rare-gas hydrates. β -Mg₂Al₃, which is cubic with cube edge 28.24 Å and 1,192 atoms per cell, has essentially the same structure² as the metastable cubic phase.

In this context, the X-ray diffraction pattern from rapidly quenched Mg₃₂(Al, Zn)₄₉ alloy, which gives 5-3-2 symmetry diffraction patterns in TEM⁴, is of interest. We prepared the alloys Mg₃₂(Al, Zn)₄₉ (with Al and Zn in the ratio 1:2) and Mg₂Al₃ from the pure elements (better than 99.9% in all cases) by r.f. induction melting over a water-cooled copper hearth. The

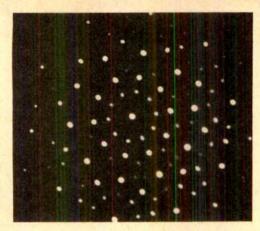


Fig. 2 Selected area diffraction pattern from a typical grain of rapidly solidified Mg32(Al, Zn)49 alloy displaying 5-fold symmetry.

alloys were re-melted in quartz nozzles and rapidly solidified into thin ribbons by ejecting onto a rotating copper wheel under argon cover. The quenched ribbons were thinned by electropolishing and were examined by TEM. X-ray diffraction patterns were obtained using a Siemens diffractometer with CuKa radiation.

The X-ray diffraction patterns from rapidly quenched Mg₃₂(Al, Zn)₄₉ and Mg₂Al₃ are shown in Figs 1a and c, respectively. Although there is an apparent similarity in these patterns, the latter could be indexed completely to a hexagonal unit cell with a = 5.73 Å, c = 9.54 Å (see Table 1), and its SADPs revealed no axis with 5-fold symmetry. In the case of rapidly quenched Mg₃₂(Al, Zn)₄₉ alloy, the TEM patterns showed 5-3-2 symmetry. The SADP along a 5-fold axis is shown in Fig. 2. The X-ray pattern in Fig. 1a could be completely indexed, following Bancel et al.5, using the 12 vectors pointing to the vertices of an icosahedron, which are generated by cyclic permutation of $(q_x, q_y, q_z) = (\pm 1, \pm \tau, 0)$. The six independent vectors chosen are $q_1 = (1, \tau, 0), q_2 = (1, -\tau, 0), q_3 = (0, 1, \tau), q_4 = (0, 1, -\tau), q_5 =$ $(\tau, 0, 1), q_6 = (-\tau, 0, 1),$ where τ is the golden mean, $(1+\sqrt{5})/2$. The observed d-spacings and the icosahedral indices are given in Table 2.

Differential scanning calorimetric (DSC) scans of asquenched Mg32(Al, Zn)49 and Mg2Al3 showed well-defined exotherms with peak temperatures of 613 and 568 K, respectively (Fig. 3). The ribbons were annealed at temperatures beyond the exotherms for 15 min in the DSC cell in argon atmosphere. The annealed specimens showed no axis with 5-fold symmetry in TEM.

X-ray diffraction patterns were obtained from the annealed specimens in identical conditions as for the as-quenched alloys. The patterns obtained from annealed Mg₃₂(Al, Zn)₄₉ and Mg₂Al₃ are shown in Fig. 1b and d, respectively. The former can be indexed to the equilibrium cubic phase (cI162, a = 14.16 Å; ref. 6) and the latter to β -Mg₂Al₃ (cF1192, a = 28.3 Å; ref. 7).

A comparison of the diffractograms in Fig. 1a, b, for the rapidly quenched and annealed Mg32(Al, Zn)49 alloy, respectively, suggests that if we were to assume that the 5-fold symmetry in TEM results from 20 cubic crystals with definite angular relationships in their orientations, the obvious choice for the cubic unit cell will be the c1162 type. The reason for this is that

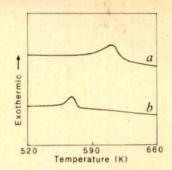


Fig. 3 DSC thermograms from rapidly quenched Mg₃₂(Al, Zn)₄₉ (a) and Mg2Al3 (b).

the major lines in Fig. 1b coincide with the lines in Fig. 1a. The rapidly quenched Mg32(Al, Zn)49 alloy shows a distinct transformation temperature in DSC. This transformation could be a crystal structure change or an irreversible change in which the cubic crystals lose their mutal angular relationships. However, only a crystal structure change can be expected to cause a substantial change in the X-ray powder diffraction patterns. The X-ray diffraction pattern in Fig. 1b shows many intense lines which are missing altogether in Fig. 1a. Therefore, the exotherm in the DSC thermogram does not correspond to a transformation in which the mutual angular relationships between the cubic crystals are destroyed. As most of the lines in Fig. 1a have d-spacings in common with those in Fig. 1b, the question of texture in the as-quenched ribbons also arises. However, a comparison of diffractograms obtained from the strips and a fine powder made from the strips ruled out texture in the as-quenched ribbons as a cause for there being relatively fewer lines in Fig. 1a. Note also that the diffraction pattern in Fig. 1a is not similar to that of β-Mg₂Al₃ in Fig. 1d.

Thus, the rapidly quenched Mg32(Al, Zn)49 alloy does not consist of aggregates of cubic crystals of either type, cI162 or cF1192. The X-ray pattern is completely indexable to an icosahedral phase. Hence, a quasi-crystalline lattice is necessary to explain the observed 5-3-2 symmetry diffraction in TEM.

Pauling (personal communication) has suggested that the pattern given in Fig. 1a can be indexed to a disordered NaCd2type structure with a = 27.82 Å (cF1120), and that on annealing there are changes in the structure such as to eliminate all or most of the randomness. However, it is not clear as to how, on annealing, the material transforms to a cI162-type structure rather than to an ordered form of NaCd2-type structure. The indexing of the pattern in Fig. 1a to a disordered NaCd2-type structure is not necessarily unique. One could also assign the pattern to a cI162-type phase with disorder in the unit cell, as the major lines in Fig. 1b coincide with the lines in Fig. 1a. However, there has been no report of a disordered Mg32(Al, Zn)49-type structure. The equilibrium Mg32(Al, Zn)49 phase has a unit cell in which spherical aggregates of atoms which basically have 5-3-2 symmetry are packed in bodycentred cubic lattice positions. The question of whether disorder in such a lattice would lead to a quasi-crystalline structure, yielding the X-ray diffraction pattern shown in Fig. 1a, becomes interesting.

We thank Professor P. Rama Rao for critical discussions and permission to publish this letter.

Received 21 January; accepted 16 May 1986.

Shechtman, D., Blech, I., Gratias, D. & Cahn, J. W. Phys. Rev. Lett. 53, 1951-1953 (1984).
 Pauling, L. Nature 317, 512-514 (1985).
 Field, R. D. & Fraser, H. L. Mater. Sci. Engng 68, L17-L21 (1984-85).

Ramachandra, Rao, P. & Sastry, G. V. S. Pramana - J. Phys. 25, L225-L230 (1985).
 Bancel, P. A., Heiney, P. A., Stephens, P. W., Goldman, A. I. & Horn, P. M. Phys. Rev. Lett. 54, 2422-2425 (1985).

Bergman, G., Waugh, J. L. T. & Pauling, L. Nature 169, 1056 (1952); Acta crystallogr. 10, 254 (1957).

Samson, S. Nature 295, 259-262 (1962).

High-resolution transmission electron microscopy of silicon re-growth at controlled elevated temperatures

R. Sinclair & M. A. Parker

Department of Materials Science and Engineering, Stanford University, Stanford, California 94305, USA

Direct observations of atomic surface rearrangements and dislocation reactions using high-resolution transmission electron microscope (TEM) techniques have been described for gold and for cadmium telluride1-6. A major disadvantage of these experiments has been that they rely on the heating effect of the imaging electron beam to raise the temperature of the sample so that thermally activated processes can be induced. This severely restricts the materials which can be studied and significantly reduces the control of the observer in bringing about changes of interest. We have previously suggested4 that many solids would be open to such investigation if an appropriate temperature range could be reached. Using a simple Arrhenius kinetic law, we estimated, for example, that silicon would need to be held at ~600 °C to make equivalent observations to those seen in CdTe. Recognizing the contemporary technological applications of silicon, such a step would be important in fundamental studies of device circuits. We report here that this type of imaging can indeed be performed successfully, without recourse to specialized instrumentation, and that new insights can be gained concerning defect production and phase transformations in this important material.

The experiment involved the observation of silicon re-growth in situ in a TEM at temperatures between 500 and 800 °C. A silicon thin film (300 nm) had been epitaxially deposited on a sapphire substrate and had undergone a dual ion-implant and annealing treatment. The implants have the effect of rendering the highly defective silicon crystal amorphous, while the annealing produces a virtually defect-free single-crystal film. We investigated this latter reaction (the amorphous to crystalline transformation) during solid-phase epitaxial re-growth.

Samples were made for TEM using a standard cross-sectioning technique⁸, which allowed high-resolution electron microscope (HREM) imaging in the standard [110] orientation. The electron microscope was a conventional Philips EM400 ST operating at 120 kV, with a resolution of ~0.32 nm. Heating was achieved with the standard, commercially available holder (model number PW 6592), in which an electrical feed-through heats a platinum pad on which was placed the 3-mm disk specimen. The temperature is measured by a thermocouple attached to the pad. Because of the high thermal conductivities of sapphire and silicon, the thermocouple reading should be

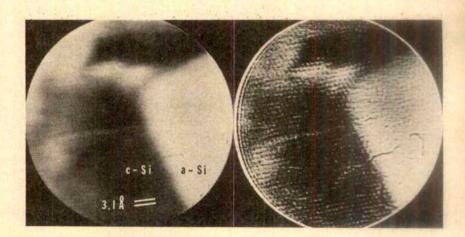
reasonably close to the actual specimen temperature. Care was taken to use reproducible imaging conditions so that any beamheating or other effects would give rise to a systematic error in the apparent temperature.

One of the most important experimental parameters for the HREM is the specimen orientation with respect to the imaging electron beam. As the present holder has only single-tilting capability, the external configuration must be used to facilitate orientation control. The surface normal of the silicon film is [100]. In a cross-section specimen, the thin film is easily seen as a line across the middle of the disk. When this line is oriented perpendicular to the holder rod, the tilt axis is then accurately the [100] crystal direction. Appropriate sectioning therefore allows attainment of the desired orientation. Axial crystal lattice images were produced using the transmitted and six diffracted beams. A Philips plumbicon image pick-up system (model number PW 6326/50), coupled to a standard video recorder and television monitor, was used to display and record the pictures. Subsequent image processing was carried out with a Quantex QX-9000 digital image processing and analaysis system; additional details are given elsewhere9. Starting from room temperature, it takes ~1 h for the image drift to stabilize sufficiently for reasonable HREM observations to be obtained at ~700 °C. The thermocouple reading can be maintained to within ±5 °C over several hours, and this is confirmed by the stability of the image itself. Controlled temperature changes can be effected, although a few minutes are required for re-stabilization.

Figure 1 shows a region of the crystalline/amorphous silicon interface. A photograph taken from continuous play-back of the video recording (Fig. 1a) is compared with the digitally enhanced image (Fig. 1b). The former image is of lower quality then conventional HREM images photographically recorded at room temperature; however, the processed image is adequate for standard image interpretation. Detailed studies of the kinetics of the crystallization process as a function of temperature yielded a variation and an activation energy consistent with those found by two alternative techniques, indicating that the same mechanism is operative 10. Our data show a small systematic displacement from the others which may arise either from an error of ~40 °C in the apparent temperature or from an influence of the TEM thin foil on the reaction rate.

Crystallization is observed to occur by the gradual advance of the crystalline/amorphous interface; there is no detectable crystal nucleation ahead of this interface. Faceting on low-index planes is common, particularly on {100} (which is the broad face of the epitaxial growth) and {111}. The latter give rise to protrusions, or recessions, of the growth front, as shown in Fig. 1. One peculiarity, which cannot be detected by bulk investigative techniques, is that occasionally the interface would advance over several atomic distances apparently instantaneously (that is, between two successive 1/30 s video frames). Thus, a large

Fig. 1 Comparison of video-recorded lattice images of the amorphous/crystalline silicon interface at 720 °C: a, 1-s exposure photograph during play-back of the video-tape; b, photograph of the image after digital filtering and eight-frame averaging.



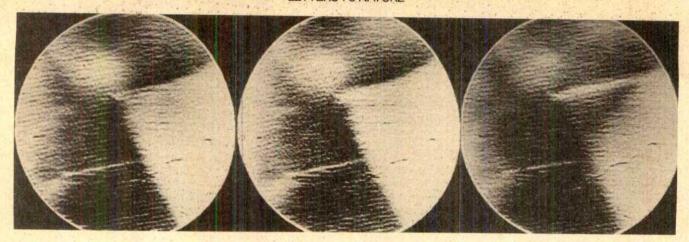


Fig. 2 Sequence of micrographs at 720 °C, taken 1 s apart, showing sudden crystallization of many atoms, advancing the crystalline/amorphous interface. Frame-by-frame analysis shows that the event occurs between two successive frames, 1/30 s apart.

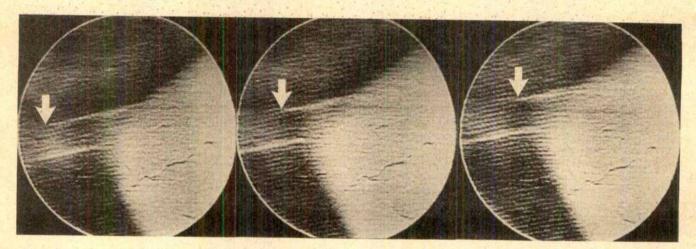


Fig. 3 Sequence of micrographs at 720 °C, taken 10 s apart, showing the gradual motion of a Shockley partial dislocation (arrowed) towards the amorphous/crystalline interface, annihilating a stacking fault in the process. This sequence is similar to that observed previously in CdTe (refs 5, 6).

number of atoms, in some cases >10⁴, extend the epitaxial crystal spontaneously. This suggests that under certain conditions the mechanism of crystallization occurs by something other than a simple atom-by-atom process, and that the silicon tetrahedral network can be created perfectly with much coordination of the atomic rearrangement. Such cooperative phenomena would be expected in a heterogeneous nucleation event. This behaviour is illustrated by the sequence shown in Fig. 2, from growth at a measured temperature of 720 °C.

Also unexpected was the observation that the interface sometimes regresses. This can be explained if we invoke the influence of interfacial stresses (arising from the volume change of the transformation), as well as the influence of interfacial surface energies for the differing crystallographic orientations, as playing some part in the behaviour. We speculate that these videorecordings of the regressions and advances of the interface are the first direct record, at near-atomic resolution, of the fluctuations expected from transition-state theory between a metastable and a stable phase. The presence of oxygen and aluminium (from the sapphire), as well as the thinness of this particular region, may also have some influence on the fluctuations.

Lattice imperfections can also be created at the interphase interface, which lends credence to the idea that significant stresses are present, particularly at 'corners' like that shown here. Shockley partial dislocations can be ejected, passing along a {111}-type slip plane and resulting in an intrinsic stacking fault. More complex dislocation reactions can occur which can be analysed in detail by Burgers circuits drawn around the

dislocation cores at various stages of the reaction. Although we observed several different events, the image quality was not sufficiently good for the analysis to be carried out with real certainty in all cases. However, this should not be a problem with the new generation of high-resolution TEMs now available. Figure 3 shows a sequence in which a Shockley partial is approaching the interface and recreating the perfect crystal, an observation identical to that made in cadmium telluride, described previously^{5,6}. One has the impression that the interface region is unstable, and that unusual events can occur at any instant. Furthermore, although stacking faults in many materials are thought to arise from accidents of growth, we see here that they are directly created by a dislocation mechanism.

We have been successful in obtaining lattice-resolution micrographs and continuous recordings at controlled elevated temperatures, using a conventional TEM and heating stage. We have studied crystallization and defect reactions in silicon at a temperature (~700 °C) similar to that referred to in our original predictions⁴ (that atomic rearrangements would occur in silicon at ~600 °C), and the phenomena are exactly analogous to those observed in CdTe using beam heating^{5,6}. Therefore, it is reasonable to conclude that atomic-level events of this type, including phase transformation processes, may be investigated in detail in many materials, at the appropriate temperature.

M.A.P. thanks IBM (SPD) for an IBM resident study fellowship, during which this work was carried out. R.S. thanks the HREM laboratory and Jesus College, Cambridge for hospitality while the article was written. Partial financial support was provided by the NSF-MRL program through the Center for Materials Research, Stanford University. We acknowledge R. E. Reedy and T. W. Sigmon for specimens and many helpful discussions.

Received 20 February; accepted 6 May 1986.

- 1. Hashimoto, H. et al. Jap. J. appl. Phys. 19, L1-L4 (1980).
- Bovin, J. O., Wallenberg, R. & Smith, D. J. Nature 317, 47-49 (1985).
 Iijima, S. Proc. Arizona State Univ. Centennial Symp. on High-Resolution Microscopy, Scottsdale, Arizona, preface (North-Holland, Amsterdam, 1985)
- 4. Sinclair, R., Yamashita, T. & Ponce, F. A. Nature 290, 386-388 (1981).

- Sinclair, R. et al. Nature 298, 127-131 (1982).
 Yamashita, T. & Sinclair, R. Mater. Res. Soc. Symp. Proc. 14, 295-299 (1983).
 Parker, M. A., Sinclair, R. & Sigmon, T. W. Appl. Phys. Lett. 47, 626-628 (1985).
- 8. Bravman, J. C. & Sinclair, R. J. Electron Microsc. Technol. 1, 53-61 (1985).
 9. Parker, M. A. & Sinclair, R. Proc. 43rd Meet. Electron Microsc. Soc. Am. 358-359 (ed. Bailey,
- G. W.) San Francisco Press (1985).
- 10. Parker, M. A., Sinclair, R. and Sigmon T. W. Mater. Res. Soc. Symp. Proc. (in the press).

A new type of host compound consisting of α -zirconium phosphate and an aminated cyclodextrin

Tsuyoshi Kijima* & Yoshihisa Matsui†

- * National Institute for Research in Inorganic Materials, Sakura-mura, Niihari-gun, Ibaraki, 305 Japan
- † Department of Agricultural Chemistry, Shimane University, Nishikawazu, Matsue, 690 Japan

Pillaring of layered compounds by polynuclear hydroxy metal cations or bulky organic species has been applied to the formation of microporous networks analogous to zeolites1.2. Similar types of compound may be obtained by the intercalation of host molecules such as cyclodextrins in layered parent hosts. Our previous work^{3,4} first demonstrated such a combined host compound, in which molecules of mono-(6-β-aminoethylamino-6-deoxy)-β-cyclodextrin (CDen) are intercalated as a bi-layer with their cavity axes perpendicular to the silicate layers of Cu(II)-montmorillonite. We have now prepared a complex of layered α -zirconium phosphate with CDen, in which the CDen molecules are arranged as a bi-layer but with their cavity axes parallel to the inorganic layers. The dextrin moiety of the present complex also appears to possess a zeolitic character.

Cyclodextrins contain a cylindrical cavity capable of including a variety of molecules, together with catalytically active hydroxyl groups. The cyclic dextrins and their derivatives therefore serve as micro-encapsulating agents for drugs or as models of enzymes⁵. Zirconium phosphate is an inorganic ion exchanger with a layered structure and acts as an intercalating agent for polar organic substances⁶. The crystalline phase with composition Zr(PO₄)₂·H₂O has an inter-layer spacing of 7.6 Å and is called α -zirconium phosphate (α -ZrP).

The α -ZrP sample was the same as that used previously⁷; the CDen was prepared as described in refs 3, 4. Crude CDen was purified by chromatography, using a carboxymethyl cellulose column with 0.1 M ammonium bicarbonate as an eluant, followed by repeated evaporation of the cluate in the presence of a small amount of ammonia. The phosphate sample was soaked in an aqueous solution containing varying amounts of CDen at 25 °C for 14 days, centrifuged, fully washed with water, and air-dried at 40 °C.

Figure 1 shows the X-ray diffraction patterns of the resulting solids. As a result of the addition of CDen, the peak at d = 7.6 Åattributable to the (002) reflection of α -ZrP decreased considerably in intensity, while a new diffraction peak (C(001)) appeared at d = 35.6 Å along with its higher-order counterparts. This indicates that the \alpha-ZrP phase is directly converted into its CDen complex with an inter-layer spacing of 35.6 Å. This con-

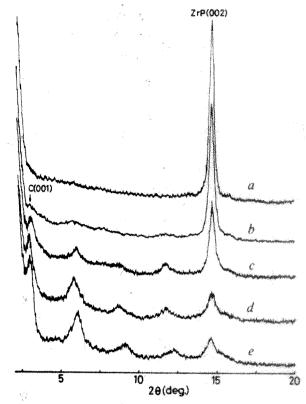


Fig. 1 X-ray diffraction patterns of α -zirconium phosphate (a) and its complexes with CDen (FeKa radiation). CDen addition levels (mmol g⁻¹): 0.43 (b), 1.3 (c), 2.3 (d) and 5.2 (e).

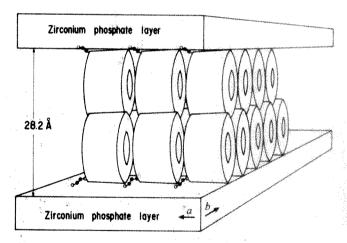


Fig. 2 Model proposed for the packing of CDen molecules in the inter-layer space of α -zirconium phosphate. Directions a and brefer to the axes of the α -ZrP unit cell (see Fig. 3).

version proceeded with increasing amounts of CDen until, at a level of 5.2 mmol CDen per g α -ZrP, the rate of conversion ξ amounted to 88%, according to a rough estimate based on the peak area of the (002) reflection for the residual phosphate phase. The amounts of CDen and water, x and y, per formula weight of α -ZrP for the solid obtained at this highest level of CDen addition (sample A) were determined to be 0.368 and

5.3 mol, respectively, by thermo-gravimetric analysis.

Similarly to basic amino acids, CDen is likely to be intercalated by α -ZrP in such a way that the inter-layer surface protons are replaced by the terminal NH₃⁺ cations. The thickness of the intercalated layer, Δ , for the resulting CDen-ZrP complex is estimated as 28.2 Å by subtracting 7.4 Å for the thickness of the inorganic layer from the observed inter-layer spacing. It is therefore reasonable to assume that CDen molecules, each 15.4 Å in

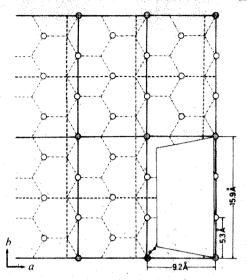


Fig. 3 An idealized relationship between the arrangements of the POH groups and CDen molecules in the inter-layer space of α -zirconium phosphate (projection on the a-b plane). The upward-pointing POH groups in the lower layer are represented by circles and the downward-pointing ones in the upper layer are located at the triple points of dash-dot lines. Each CDen molecule with its cavity axis parallel to the a axis anchors through the basic terminus to the POH site (shaded for the lower layer) and is placed in the rectangle surrounded by the solid (lower layer) or broken (upper layer) lines.

diameter and 8.0 Å in the thickness of the torus, are intercalated as a bi-layer with their cavity axes perpendicular or parallel to the phosphate layers. Assuming hexagonal close packing of CDen molecules in a plane perpendicular to their cavity axes, the effective area per molecule is evaluated as $2\sqrt{3} \times (15.4/2)^2$ or 205 Å². The effective area per POH site in α -ZrP is 24.3 Å² (ref. 7). Hence, the maximum values of x and Δ for the perpendicular arrangement can be calculated, respectively, as 2× 24.3/205 = 0.24 and as twice 11.8 Å, which is the sum of the thickness of the torus and the extended chain length of the aminoethylamino group, or 23.6 Å. These calculations are not consistent with the observed data. On the other hand, the parallel arrangement yields a maximum x value of $2 \times 24.3/(15.8 \times 8.0) =$ 0.40 and a minimum Δ value of 15.4(1+ $\sqrt{3/2}$) = 28.7 Å, in fairly close agreement with the observations. Thus, we propose the model shown in Fig. 2 as the probable arrangement of CDen molecules in the inter-layer space of α -ZrP. This model gives a ξ value for sample A of 0.368/0.40 = 92.0%, which is close to the value roughly estimated from the X-ray observations. It can also be assumed that sample A is a mixture of 92 mol% of a complex, $Zr(HPO_4)_2(CDen)_{0.4} \cdot 5.7H_2O_1$, and 8 mol% of α -ZrP.

Referring to the crystal structure of α -ZrP, the POH groups pointing up or down in each layer are located in a monoclinic cell with dimensions of 9.2 and 5.3 A along the a and b axes, respectively⁶, as shown in Fig. 3. Any two adjacent layers of ZrP are staggered in such a way that the downward-pointing POH groups in the upper layer are shifted by 3.07 Å along the a axis relative to the layer below. It is therefore conceivable that the first intercalated layer of CDen molecules, with their cavity axes parallel to the a axis of the a-ZrP crystal, anchors through the basic termini to every POH site, at 9.2-Å intervals, in every sixth row, 15.9 Å apart, along this axis in the ZrP layer below. The second intercalated layer is probably bonded in the same manner to the ZrP layer above, but is shifted by 7.7 and 8.0 A along the a and b axes, respectively, relative to the first layer. Thus, the parallel bi-layer model suggested above is also consistent with the geometrical arrangement of POH sites at the inorganic layer surface.

Depending on the size and ionic or molecular character of

the substrate, the cyclodextrins and their adducts are crystallized as empty molecules or as inclusion complexes, with channel or cage structures in which the cyclodextrin molecules are stacked like coins in a roll or arranged in a herring-bone pattern⁵. The channel structure is formed only as inclusion complexes with long-chain molecules such as poly-iodine. As the hydrate of β -cyclodextrin contains 7 water molecules within the cavity is probable that $0.4 \times 7/5.3 = 49\%$ of the water molecules in sample A are located in the cavity of the intercalated CDen molecules. According to thermo-gravimetric observations, this sample released 85 mol% of its water during heating to 120 °C, and the dehydrated solid re-adsorbed 92 mol% of the desorbed water by exposure to saturated water vapour at 25 °C, followed by air-drying under the same conditions as for sample A. These preliminary results and the above geometrical considerations suggest that the CDen molecules in one intercalated layer are arranged with their cavity axes parallel to the inter-layer surface, either in alignment to form empty channels, 6 Å in diameter, or, if displaced, with bottlenecks large enough to allow water molecules 2.65 Å in diameter to diffuse. Thus, the dextrin moiety of the CDen-ZrP may possess a zeolitic character, at least for small molecules such as water and hydrogen, although definite conclusions must await further work. Complexes of α -zirconium phosphate with CDen or other cyclodextrin derivatives may prove useful as solid supports in gas or liquid chromatography and as micro-encapsulating agents for various substances such as drugs.

Received 31 December 1985; accepted 15 May 1986.

- Pinnavaia, T. J. Science 220, 365-371 (1983)
- Ferragina, C., Massucci, M. A., Patrono, P., Ginestra, A. L. & Tomlinson, A. A. G. JCS Dalton Trans., 265-271 (1986).
- Kijima, T., Tanaka, J., Goto, M. & Matsui, Y. Nature 310, 45-47 (1984). Kijima, T., Kobayashi, M. & Matsui, Y. J. Inclusion Phenom. 2, 807-813 (1985). Saenger, W. Angew. Chem. 19, 344,362 (1980).
- 6. Alberti, G. & Constantino, U. in Intercalation Chemistry (eds Whittingham, M. S. & Jacobson, A. J.) Ch. 5 (Academic, New York, 1982):
- Kijima, T. Thermochim. Acta 59, 95-104 (1982). Kijima, T., Ueno, S. & Goto, M. JCS Dalton Trans., 2499-2503 (1982).
- Linder, K. & Saenger, W. Angew. Chem. 17, 694-695 (1978).

Plume versus lithospheric sources for melts at Ua Pou, Marquesas Islands

R. A. Duncan*‡, M. T. McCulloch*, H. G. Barsczus† & D. R. Nelson*

* Research School of Earth Sciences, The Australian National University, Canberra, ACT 2601, Australia

† ORSTOM, Centre de Papeete Tahiti, French Polynesia, and Géologique et Géophysique du CCNRS, USTL,

Montpellier, France

§ Permanent address: College of Oceanography, Oregon State University, Corvallis, Oregon 97331, USA

The remarkable distinction between the compositions of ocean island basalts (OIBs) and mid-ocean ridge basalts (MORBs) provides an important constraint on models of mantle composition and structure ¹⁻³. Previous studies of OIBs⁴⁻⁸, however, have emphasized regional isotopic variations, often relying on a small number of samples from many separate volcanoes. Although this type of sampling has now established the basic range of isotopic variations, with the notable exception of the Hawaiian Islands there is little information on either spatial or temporal variations within a single volcano. Here we report isotopic (Sr, Nd and Pb) and K-Ar age measurements for tholeiites, alkali basalts and differentiated rocks from the island of Ua Pou. In this island volcanism spanned the interval from 5.6 to 1.8 Myr, with the ratio of highly to moderately incompatible trace elements increasing

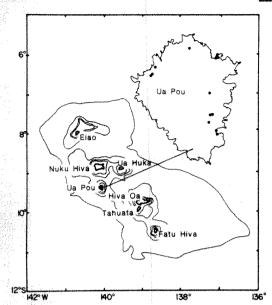


Fig. 1 Map of the Marquesas Islands, an age-progressive volcanic lineament in the south-central Pacific basin, showing the island of Ua Pou. Solid circles (on the enlarged map of the island) mark the location of samples (tholeiites, alkali basalts and differentiates) analysed in the present study.

with time; however, in contrast to Hawaii, ⁸⁷Sr/⁸⁶Sr and ²⁰⁷Pb/²⁰⁴Pb increased while ¹⁴³Nd/¹⁴⁴Nd decreased from the tholeitic to alkalic magmas. The total variation in isotopic composition within this single island is nearly as great as within the entire French Polynesian region^{8,11,12}, and argues against systematic geographical correlations¹³.

The island of Ua Pou, at 9°24′S, 140°04′W, is one of a chain of more than 20 volcanic islands and seamounts which constitute the Marquesas archipelago in the south-central Pacific Basin (Fig. 1). These volcanoes are linearly arrayed in a WNW-ESE direction, sub-parallel with other young intra-plate Pacific island chains. This characteristic geometry and the reported southeasterly progression in volcano ages^{14,15}, from 6.3 to 1.4 Myr, has linked Marquesan volcanism to a hotspot origin. The abyssal (>4,000 m) ocean floor on which these islands were constructed formed at the Galapagos Rise (ancestral East Pacific Rise) between 50 and 60 Myr (ref. 16).

Ua Pou hosts a particularly wide range of rock compositions, from tholeitic to alkalic basalts; the latter have undergone low-pressure fractionation towards trachytic and phonolitic rocks^{17,18}. Although tholeites are the main rock type in the Hawaiian islands¹⁹, they have not been reported elsewhere in the French Polynesian region; their occurrence in the initial stage of volcanism at Ua Pou suggests that tholeitic eruptions may occur throughout this region, but may be almost totally confined to submarine portions of the volcanoes.

We report here age determinations for rocks from Ua Pou. Previous age studies¹⁴ on other islands from the Marquesas chain have documented an age progression in volcanism from north-west to south-east at a rate of ~10.4 cm yr⁻¹ (ref. 9). From this regular age distribution along the lineament, the expected age range at Ua Pou is 4.0-2.7 Myr. Re-examination²⁰ of the published age data showed that at the islands of Nuku Hiva and Hiva Oa dated rocks defined two age groups separated by about the same timespan, 0.6 Myr. Furthermore, at each island the older group was predominantly olivine tholeitte while the younger group was alkali basalt. To investigate this apparent petrogenetic evolution at individual Marquesan volcanoes, additional sampling was undertaken by one of us (H.G.B.).

Ua Pou does not exhibit the central collapsed caldera commonly seen at other Marquesas Islands; instead, the island's

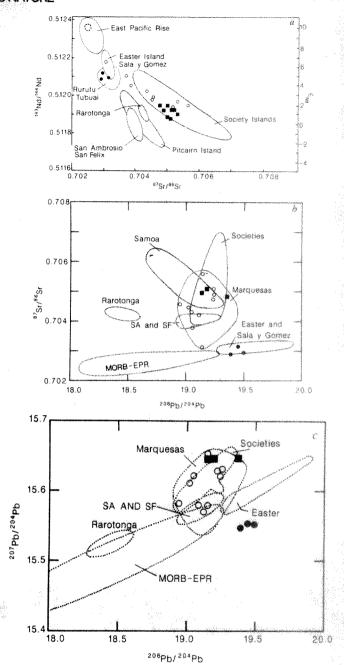


Fig. 2 Isotopic compositions of lavas from Ua Pou compared with those for other basaltic rocks from the south-central Pacific basin. a, 143 Nd/144 Nd versus 87 Sr/86 Sr; b, 87 Sr/86 Sr verus 206 Pb/204 Pb; c, 207 Pb/204 Pb versus 200 Pb/204 Pb. Fields of data are from ref. 25 for islands and East Pacific Rise, except Rurutu and Pitcairn Islands 30. Solid circles and squares are tholeities and alkali basalts, respectively, from Ua Pou. Open circles are other analysed samples from the Marquesas Islands 12. SA, San Ambrosio; SF, San Felix; EPR, East Pacific Rise.

centre is a complex zone of high-level intrusions of trachytic and phonolitic rocks which have obscured the early shield structure of the volcano. Shield lavas outcrop around the perimeter of the island, in stream valleys, in road cuts and along wave-cut cliffs. The samples analysed in this study are well distributed, coming from the northwestern, northern and eastern sides of the island (Fig. 1).

Initial studies¹⁸ of trace element compositions of tholeittes and alkali basalts collected from Ua Pou revealed striking differences in the inferred source compositions for the two groups. Rocks which plot as tholeittes in a standard alkalis versus silica diagram predate the alkali basalt assemblage. The

Table 1 Sr, Nd and Pb isotopic compositions and K-Ar ages for volcanic rocks from Ua Pou, Marquesas Islands

Samples	Rock type	K (%)	Rb (p.p.m.)	Sr (p.p.m.)	Sm (p.p.m.)	Nd (p.p.m.)	⁸⁷ Sr/ ⁸⁶ Sr	¹⁴³ Nd/ ¹⁴⁴ Nd	$\epsilon_{ m Nd}$	²⁰⁶ Pb/ ²⁰⁴ Pb	²⁰⁷ Pb/ ²⁰⁴ Pb	²⁰⁸ Pb/ ²⁰⁴ Pb	K-Ar age (Myr) ±1σ
UAP-011	Tholeiite	0.554	15	548	10.3	43.3	0.70289 ± 2	0.512070 ± 12	+4.6	19.50	15.54	39.15	4.46 ± 0.0
UAP-017	Tholeiite	0.204	3	434	10.0	40.3	0.70294 ± 4	0.512118 ± 16	+5.5	19.39	15.54	38.99	4.51 ± 0.1
UAP-024	Tholeiite	0.651	11	610	13.0	57.6	0.70318 ± 5	0.512084 ± 24	+4.8	19.45	15.55	39.01	5.61 ± 0.0
UAP-001	Alkali basalt	0.871	41	985	11.4	71.4	0.70500 ± 5	0.511944 ± 27	+2.1				2.75 ± 0.0
UAP-002	Alkali basalt	0.554	76	904	11.8	62.4	0.70497 ± 5						2.78 ± 0.0
UAP-003	Alkali basalt	0.855	40	972	11.3	61.5	0.70482 ± 5						2.70 ± 0.0
UAP-010	Alkali basalt	1.039	145	1,235	13.3	76.0	0.70509 ± 5	0.511867 ± 14	+0.6	19.18	15.65	39.31	2.70 ± 0.0
UAP-026	Alkali basalt	0.524	84	910	11.5	60.7	0.70497 ± 5	0.511876 ± 20	+0.8	19.14	15.64	39.20	2.88 ± 0.0
UAP-012	Tephrite	2.640	116	1,373	15.3	84.6	0.70515 ± 5	0.511918 ± 10	+1.6				2.24 ± 0.0
UAP-015	Hawaiite	2.643	241	1,358	7.9	48.6	0.70481 ± 5	0.511907 ± 12	+1.4	19.36	15.65	39.35	1.78 ± 0.0
UAP-025	Mugearite	4.276	72	1,282	13.0	52.2	0.70531 ± 6	0.511891 ± 25	+1.1				2.49 ± 0.0
UAP-004	Trachyte			•			0.70508 ± 5						
UAP-019	Phonolite	5.693	240	146	15.3	108.0	0.70497 ± 4	0.511917 ± 22	+1.6				2.42 ± 0.0
UAP-037	Phonolite	5.887	235	136	6.9	52.8	0.70474 ± 5						2.42 ± 0.0

 87 Sr/ 86 Sr and 143 Nd/ 144 Nd ratios are normalized to 86 Sr/ 88 Sr = 0.1194 and 146 Nd/ 142 Nd = 0.636151, K-Ar ages were calculated using the following decay and abundance constants: $\lambda_e = 0.581 \times 10^{-10} \text{ yr}^{-1}$; $\lambda_B = 4.963 \times 10^{-10} \text{ yr}^{-1}$; 40 K/K = 1.167 × 10⁻⁴ mol mol⁻¹ respectively. For the standard NBS 987, 87 Sr/ 86 Sr = 0.71023 and for BCR-1 143 Nd/ 144 Nd = 0.511833. Rb, Sr, Sm and Nd concentrations are from ref. 18.

tholeiitic phase of volcanism (5.6-4.5 Myr) is separated from the alkali basalt eruptions (2.9-2.7 Myr) and subsequent flows and intrusions of liquids evolved by high-level fractional crystallization (2.5-1.8 Myr). The entire age range of subaerial volcanism at Ua Pou is ~3.8 Myr (Table 1). The apparent 1.6-Myr hiatus between the tholeiitic and alkalic stages of volcanism could be the result of incomplete sampling and may be reduced by future geochronological studies on well-mapped sections. The progression from tholeiitic to alkalic volcanism at Ua Pou and its likelihood at the neighbouring islands of Nuku Hiva and Hiva Oa²⁰ is reminiscent of the volcanic evolution of the Hawaiian Islands¹⁹. In the Marquesas Islands, however, no very undersaturated, post-erosional eruptions have followed the alkali basalt stage. It is probable, therefore, that each of the Marquesas islands evolved through a common sequence. Initially, eruptions may have been a mixture of tholeiitic and alkalic compositions, as seen at Macdonald²¹ seamount at the southeastern end of the Austral Islands, and Loihi seamount²² in the Hawaiian Islands. Tholeiitic compositions dominated the early shield-building phase, which at Ua Pou barely reached sea level. This was followed by eruptions of alkali basalt and, later, highly evolved rocks. It is not yet known whether the change from tholeiites to alkali basalts occurred as a gradual transition or as a sharp compositional break after a significant hiatus in volcanic activity.

Major and trace element concentrations for Ua Pou rocks have been reported elsewhere 17,18. Liotard et al. 18 identified tholeiitic rocks at many of the Marquesas Islands and, in particular, quartz-normative tholeiites at Ua Pou, in addition to the earlier described alkali basalts. The tholeiites and alkali basalts cannot be related to one another by either variable partial melting from a common source or fractional crystallization from a parental melt, because of many clear differences in their trace element patterns. Both groups are enriched in light rare earth elements, relative to MORBs, but whereas the alkali basalts exhibit uniformly steep patterns, the tholeiltic samples show much flatter profiles between La and Sm. The tholeiite trace element patterns are similar in shape to those for Hawaiian tholeiites^{23,24}, with normalized La = normalized Ce, but abundances are higher in Ua Pou tholeiites. Tholeiites and alkali basalts at Ua Pou can also be distinguished by Zr/Nb (11.3 versus 4.8, average values, respectively), La/Nb (0.85 versus 0.98) and La/Ce (0.37 versus 0.51). In addition, on a spidergram diagram the tholeiites show significant depletions of Ba, Rb, Th, K and Sr relative to La.

To characterize further the two magma types present at Ua Pou, we have measured Sr, Nd and Pb isotopic compositions (Table 1). Previous isotopic studies of Marquesas Islands rocks^{11,12,25} have not recognized the importance of the tholeites,

nor have they examined the compositional variation with age at a single island. Our results are in excellent agreement with the isotopic analyses of alkali basalts from Ua Pou reported by Vidal et al.¹². The data were obtained using separation techniques and mass spectrometric analysis, as described in refs 26 (Sr and Nd) and 27 (Pb). Measured Sr, Nd and Pb isotopic ratios are generally within the analytical uncertainty of initial ratios because of the young age of the samples. Corrections to ⁸⁷Sr/⁸⁶Sr were applied only to the high Rb/Sr phonolite samples. Our results are plotted on three diagrams: ¹⁴³Nd/¹⁴⁴Nd against ⁸⁷Sr/⁸⁶Sr (Fig. 2a), ⁸⁷Sr/⁸⁶Sr against ²⁰⁶Pb/²⁰⁴Pb (Fig. 2b), and ²⁰⁷Pb/²⁰⁴Pb against ²⁰⁶Pb/²⁰⁴Pb (Fig. 2c).

Tholeiites are distinguishable from alkali basalts and differentiated rocks using each of the three isotopic systems. The strontium composition of the tholeiites is among the least radiogenic reported from oceanic islands, while the alkali basalt ⁸⁷Sr/⁸⁶Sr values fall in the middle of the range for other Marquesas and Society Islands^{8,11,12}. The corresponding 143 Nd/ 144 Nd values are also distinctive ($\varepsilon_{Nd} = 4.6-5.5$ for tholeiites verus 0.6-2.1 for alkali basalts) and, together with the Sr data, form an array parallel to the Society Islands compositions but oblique to the mantle array⁵⁻⁸. The extreme isotopic heterogeneity of the French Polynesian region has been noted, but at Ua Pou, as recognized for Nuku Hiva by Vidal et al. 12, nearly the entire range of variability exists on the scale of a single island. At Ua Pou the tholeiltic magmas have low 87Sr/86Sr ratios and moderate 143 Nd/144 Nd ratios, indicative of a mantle source with low time-integrated Rb/Sr and a (chondrite-normalized) Nd/Sm < 1. The later alkali basalt magmas have high 87Sr/86Sr and low 143Nd/144Nd, which would derive from a less depleted mantle source. This contrasts with the Hawaiian Islands volcanism, where the tholeiites have higher 87Sr/86Sr and lower $\varepsilon_{\mathrm{Nd}}$ values than the alkali basalts and post-erosional lavas^{9,10}.

The Pb compositions of the two magma types are equally distinct, as seen in the $^{207}\text{Pb}/^{204}\text{Pb}$ versus $^{206}\text{Pb}/^{204}\text{Pb}$ diagram (Fig. 2c). The tholeiites are most similar to rocks from Easter and Sala y Gomez Islands near the East Pacific Rise²⁵, whereas the alkali basalts lie in the field of other reported Pb isotopic analyses from the Society and Marquesas Islands^{12,25}. The Pb isotopic compositions of the Ua Pou tholeiites are not as extreme as those of rocks from Tubuai¹² (Austral Islands) which exhibit similar low $^{87}\text{Sr}/^{86}\text{Sr}$ and moderate ε_{Nd} . They are similar, however, to analysed rocks from Rimatara²⁸ and Rurutu²⁹, neighbouring volcanoes in the Austral Islands.

There has been much recent interest in the geographical distribution of isotopic compositions at oceanic islands, culminating in the Dupal anomaly proposal¹³, which postulates a region of higher ⁸⁷Sr/⁸⁶Sr, ²⁰⁷Pb/²⁰⁴Pb and ²⁰⁸Pb/²⁰⁴Pb, circling the globe at ~30° S. The new isotopic data for Ua Pou presented

here do not, however, support this view. The Marquesas Islands lie within the proposed Dupal anomaly belt, but only the alkali basalts have the appropriate radiogenic compositions. Apparently both Dupal and non-Dupal mantle reservoirs have been tapped at Ua Pou. The same sequence might also be seen at other French Polynesian islands, if the suspected early tholeite phase of volcanism could be sampled. Hence, the regional significance of the Dupal anomaly, at least in this area, is questionable (see also refs 8, 26, 30).

It is evident from trace element and isotopic compositions that the tholeiites and alkali basalts at Ua Pou cannot be related by variable degrees of partial melting or crystal fractionation of primary melts from a common mantle or lithospheric source. Thus at least two, and probably three distinct source endmember compositions have contributed to volcanism at this island. In addition, the alkali basalts postdate the tholeiites in a clear age progression implying that the chemically distinct sources were tapped at different times. This suggests that the sources are not ubiquitous and continuously available for melting, but are likely to be physically separate. We will consider two possibilities for the spatial distribution of these source components: first, partial melting of both the mantle plume and the overlying lithosphere, and second, melting of the plume alone. In the first case the lithospheric mantle and plume have differing isotopic compositions and are the sources for the tholeiitic and alkali basalts respectively; in the second, both the alkalic and tholeiitic melts are derived from the plume, implying an isotopically heterogeneous plume.

The lower oceanic lithosphere probably consists of an unmelted mix of enriched mantle blobs and depleted asthenosphere which could possess considerable isotopic heterogeneity $^{26,31-33}$ (Fig. 3a). Samples from the East Pacific Rise exhibit a rather small range of 87 Sr/ 86 Sr and $\varepsilon_{\rm Nd}$ compositions (Fig. 2a), but are quite variable in 206 Pb/ 204 Pb composition 25,33 (Fig. 2b). Variation in these MORB compositions can be explained by mixing melts from depleted upper mantle with those from a small proportion of enriched mantle of the Rurutu/Tubuai type (low 87 Sr/ 86 Sr, moderate $\varepsilon_{\rm Nd}$, high 206 Pb/ 204 Pb). Interestingly, rocks from Easter and Sala y Gomez Islands have compositions at the high- 206 Pb/ 204 Pb end of this trend 25 (Fig. 2b). Mantle upwelling in this region of the East Pacific Rise may be a major source for the enriched mantle blobs which became incorporated into the lower oceanic lithosphere by thickening of the plate during cooling away from the spreading centre.

At Ua Pou we propose that such heterogeneous oceanic lithosphere of 50-60 Myr age approached and crossed the Marquesas hotspot (Fig. 3a). Melts and heat from the mantle plume entered the lower lithosphere, where wall rock reached temperatures sufficient to melt. The plume and lithosphere melts could then mix to produce the magmas seen at the island. The trace element and isotopic compositions of the mixed magmas would vary depending on the degree of melting of each source and the proportions of melt contributed. At Ua Pou the isotopic composition of the early tholeiitic phase lies on a mixing line between MORB and Rurutu/Tubuai compositions, and reflects the proposed composition of the lower oceanic lithosphere beneath the island. Hence, in this model, melting of the lower lithosphere was significant and dominates the composition of tholeiitic magmas.

As the volcano migrated away from the hotspot, temperatures at the base of the lithosphere decreased. Smaller degrees of melting (of alkali basalt character) developed in the margin of the plume (Fig. 3a). These melts passed through the same column of oceanic lithosphere which had earlier yielded its low-temperature melting fraction; hence, the wall rock was much more refractory and less assimilation occurred at this stage, so that the alkali basalt compositions essentially reflect the isotopic composition of the plume. Contemporaneous with this phase of Ua Pou volcanism was tholeitic, shield-building volcanism at Hiva Oa, the next major volcano upstream, and perhaps the

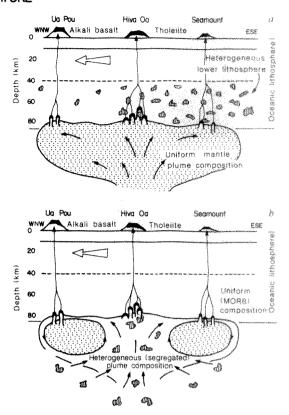


Fig. 3 Two models for the isotopically distinct magmas at Ua Pou. illustrated by vertical cross-sections along the line of the Marquesas Islands. Both models show volcanic activity at ~2.5 Myr, when alkali basalts erupted onto an older tholeiite shield at Ua Pou, concurrently with tholeiitic basalts at Hiva Oa and, possibly, with the initial seamount basalts beneath Fatu Hiva. a. Heterogeneous lower lithosphere. The plume (~400 km diameter) has a uniform, undepleted isotopic composition and is crossed by a Pacific plate composed of an upper section of uniform, MORB-like isotopic composition formed at the East Pacific Rise and an isotopically heterogeneous lower lithosphere accreted to the plate as it cooled away from the spreading ridge. Tholeiitic melts are formed over the centre of the plume as melts from the plume mix with melts from the lower-lithosphere wall rock. Alkali basalt melts erupt from the margin of the plume, where temperatures are cooler, and pass through previously heated lithosphere without significant contamination. b. Heterogeneous plume. The lithosphere has a uniform, MORB-like isotopic composition throughout and passes over a plume which has developed large-scale chemical heterogeneities by entraining depleted upper mantle material during its diapiric rise³⁴. The original plume material concentrates in a torus around the plume margin (shaded), while entrained material flows into the centre³⁵. Hence tholeiitic melts from the plume centre are MORB-like in isotopic character, whereas alkali basalt melts from the margin are more like the original plume. The lower lithosphere may melt but the isotopic differences in erupted magmas are controlled by heterogeneities in the plume.

seamount phase at Fatu Hiva, another 100 km to the south-east. From this model we would expect the same correlation of trace element and isotopic composition with time to emerge at other Marquesas islands.

An analogous model for the origin of Hawaiian tholeiitic and alkali basalts has been proposed by Chen and Frey. At Hawaii, however, there is an inverse correlation between 87 Sr/86 Sr and abundances of incompatible elements; that is, the tholeiitic phase is dominated by the composition of melts from the plume, whereas the alkali basalts are thought to reflect the composition of the lower lithosphere. This relationship is thought to result from small degrees of melting of the lower lithosphere and variable proportions of mixing with plume-derived melts. Although lithosphere melting occurs during the tholeiitic phase,

the volume of melts from the plume is sufficiently high that these determine the composition of Hawaiian tholeites. During the formation of alkali basalt melts, however, very small (<1%) degrees of melting of the wall rock produce high concentrations of trace elements which dominate the composition of smallvolume plume melts. Thus the isotopic composition of the Hawaiian alkali basalts reflects that of the lower lithosphere.

The source end-members for melting and magma mixing are different for the two island chains. At Ua Pou the enriched mantle, or plume composition, has 87 Sr/ 86 Sr > 0.7053 and ε_{Nd} < 0.5 and lies to the right of the Sr-Nd mantle array. This may be similar to, but possibly not so extreme as, the plume component for Society Islands alkali basalt magmas^{1,12}. The lower lithosphere beneath Hawaii, as reflected by the isotopic composition of the alkali basalts, does not appear to contain the Rurutu/Tubuai component seen in the Ua Pou tholeiites. This model therefore requires that the oceanic lithosphere of the Pacific plate has accreted mantle blobs of different isotopic character.

An alternative explanation for the isotopically distinct phases of tholeiitic and alkalic volcanism at Ua Pou is that heterogeneities occur within the plume or diapir itself. These heterogeneities may be either a consequence of initial heterogeneities in the plume source, or result from the incorporation of asthenospheric mantle material into the diapir during its ascent. Recent experimental and theoretical studies 34,35 have demonstrated that thermally activated diapirs will entrain a significant quantity of surrounding mantle material during their ascent. This is illustrated in Fig. 3b, where the central portion of the diapir consists of entrained depleted upper mantle (MORB-like plus mantle blobs), while the original plume material is contained in an outer torus. Tholeitic melts are generated over the centre of the plume while smaller-volume alkali basaltic melts form over the perimeter. If isotopic heterogeneities are distributed uniformly through the diapir, then isotopically distinct magmas could be formed by variable degrees of partial melting. Larger degrees of melting (tholeiite) would tend to homogenize the variable composition of the diapir, whereas smaller degrees of melting (alkali basalt) would emphasize the composition of incompatible-element rich segregations^{31,32}

We thank W. F. McDonough for technical assistance and thoughtful discussions, and W. M. White for data in advance of publication. We also thank Y. and J. Hituputoka and J.-L. and C. Candelot for their assistance during fieldwork on Ua Pou. R.A.D. acknowledges the support of NSF and H.G.B. the support of ORSTOM.

Received 17 October 1985; accepted 9 April 1986.

- 1. White, W. M. & Hofman, A. W. Nature 296, 821-825 (1982).
- Davies, G. F. Nature 290, 208-213 (1981). Ringwood, A. E. J. Geol. 90, 611-643 (1982).
- Basaltic Volcanism on the Terrestrial Planets (eds Kaula, W. M. et al.) 161-192 (Pergamon,
- New York, 1981).

 DePaolo, D. J. & Wasserburg, G. J. Geophys. Res. Lett. 3, 743-746 (1976).

 O'Nions, R. K., Hamilton, P. J. & Evensen, N. M. Earth planet. Sci. Lett. 34, 13-22 (1977).

- O'Nions, R. K., Hamilton, P. J. & Evensen, N. M. Earth planet. Sci. Lett. 34, 13-22 (1976).
 Richard, P., Shimizu, N. & Allègre, C. J. Earth planet. Sci. Lett. 31, 269-278 (1976).
 White, W. M. Geology 13, 115-118 (1985).
 Chen, C.-Y. & Frey, F. A. Nature 302, 785-789 (1983).
 Stille; P., Unruh, D. M. & Tatsumoto, M. Nature 304, 25-29 (1983).
 Duncan, R. & & Compston, W. Geology 4, 728-732 (1976).
 Vidal, Ph., Chauvel, C. & Brousse, R. Nature 307, 536-538 (1984).
 Hart, S. R. Nature 309, 753-757 (1984).

- Duncan, R. A. & McDougall, I. Earth planet. Sci. Lett. 21, 414-420 (1974).
 Brousse, R. & Bellon, H. C. r. hebd. Séanc. Acad. Sci., Paris 278, 827-830 (1974).
- 16. Epp, D. J. geophys. Res. 89, 11273-11286 (1984). 17. Bishop, A. C. & Woolley, A. R. Contr. Miner. Perol. 39, 309-326 (1973).
- 18. Liotard, J. M., Barsczus, H. G., Dupuy, C. & Dostal, J. Contr. Miner. Petrol. 92, 260-268
- 19. Macdonald, G. A. & Katsura, T. J. Petrol. 5, 82-133 (1964).

- Macdonaid, G. A. & Katsura, I. J. Fetrol. 5, 82-135 (1904).
 Barsczus, H. G. Notes Doc. (Géophys.) ORSTROMA Papeete 1981, 1-22 (1981).
 Barsczus, H. G & Liotard, J. M. C.r. hebd. Séanc. Acad. Sci., Paris 300, 915-918 (1985).
 Frey, F. A. & Clague, D. A. Earth planet. Sci. Lett. 66, 337-355 (1983).
 Leeman, W. P., Budahn, J. R., Gerlach, D. C., Smith, D. R. & Powell, B. N. Am. J. Sci. 2012, 124 (1982). 280A, 794-819 (1980).
- Wright, T. L. J. geophys. Res. 89, 3233-3252 (1984). White, W. M. EOS 66, 408 (1985).
- McDonough, W. F., McCulloch, M. T. & Sun, S.-S. Geochim. cosmochim. Acta 49, 2051-2068

- 27. Nelson, D. R., McCulloch, M. T. & Sun, S.-S. Geochim. cosmochim. Acta 50, 231-246 (1986). 28. Tatsumoto, M., Unruh, D. M., Stille, P. & Fujimaki, H. Proc. 27th int. Geol. Congr. 11, 485-501 (1984).
- Palacz, Z. & Saunders, A. D. Abstr. int. Volcanol. Congr. Feb., 194 (1986).
- McDonough, W. F. et al. Abstr. int. Volcanol. Congr. Feb., 180 (1986).
 Zindler, A., Staudigel, H. & Batiza, R. Earth planet. Sci. Lett. 70, 175-195 (1984).
- Staudigel, H. et al. Earth planet. Sci. Lett. 69, 13-29 (1984).
 Hamelin, B., Dupré, B. & Allègre, C. J. Earth planet. Sci. Lett. 67, 340-350 (1984).
- Griffiths, R. W. Earth planet. Sci. Lett. (submitted).
- 35. Griffiths, R. W. Phys. Earth planet. Inter. (submitted).

Geophysical evidence for the East Antarctic plate boundary in the Weddell Sea

Yngve Kristoffersen & Kristen Haugland

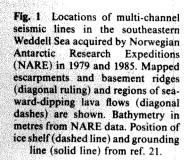
Seismological Observatory, University of Bergen, Allegt. 41, 5000 Bergen, Norway

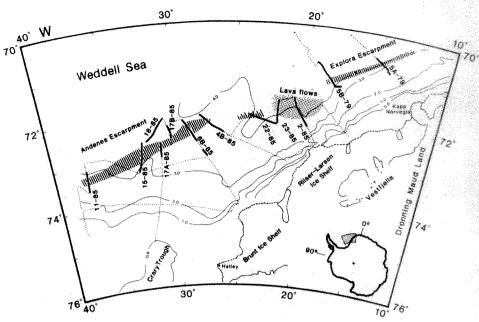
An improved Gondwanaland reconstruction compatible with geological and geophysical information from the surrounding oceans and continents seems to require microplates to solve the enigmatic pre-early-Mesozoic tectonic relation between West and East Antarctica1. New multi-channel seismic reflection data from the southeastern Weddell Sea acquired during the 1984-85 Norwegian Antarctic Research Expedition (NARE) have outlined a linear WSW-ENE-trending basement ridge buried below the continental slope over a distance of 700 km. This structural high truncates the trend of the large sedimentary basins below the Filchner and Ronne ice shelves and may continue to within a few hundred kilometres of the Antarctic Penninsula. We interpret the basement ridge as part of the East Antarctic plate boundary during the break-up of Gondwana. The morphology and structure of this boundary show greater apparent similarity to a rifted or obliquely rifted margin than to the sheared margin which is predicted by current reconstructions^{2,3}. A linear East Antarctic plate margin extending to the vicinity of the Antarctic Peninsula makes any post-rift microplate motion in the Weddell Embayment unlikely.

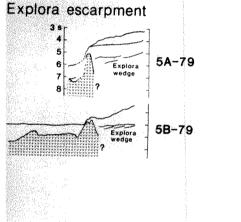
Major linear basement highs have been found below the lower continental slope of the southeastern Weddell Sea margin (Fig. 1). In the north-east, the Explora Escarpment⁴-is characterized by a well-defined 10-20-km-wide basement ridge of 1-2 km elevation with respect to hyperbolated acoustic basement on the seaward side (Fig. 2). On the landward side, a wedge of seawarddipping seismic reflectors, the Explora wedge, unconformably overlain by a 1-2-km-thick section of nearly flat-lying seismic sequences, abuts the ascarpment. Towards the south-west (20 °W), the Explora Escarpment becomes more subdued. The new NARE seismic data demonstrate that a major basement structure collinear with the Explora Escarpment extends at least 700 km farther towards the south-west, but also reveal considerable lateral variation in basement morphology (Figs 1, 2). Between 19 and 23° W a sharp, piece-wise-continuous reflector forms the upper boundary of a sequence of low-frequency seismic reflections whose landward termination is abrupt in some places and more diffuse in others (Fig. 3). We interpret these seismic reflection events as representing a region of seaward-dipping lava flows. We note that the top of this sequence is at a level comparable to the top of the escarpments to the north-east and west.

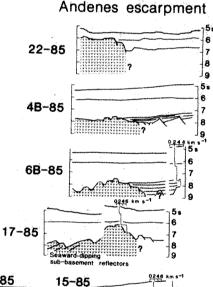
Further west, between 23 and 25° W, is a zone where acoustic basement forms a steep, landward-facing escarpment with downfaulted blocks of lava flows (?) at its base (Fig. 2, line 22-85). Here the escarpment appears to be offset from the landward boundary of the lava pile to the north-east.

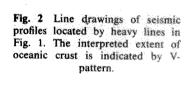
At 26° W, the WSW-trending collinear basement structure is a subdued, 15-30-km-wide ridge with a relief of ~600 m which increases westwards to >2,000 m at 32° W (Fig. 2). We name the basement structure between 23 and 38° W the Andenes

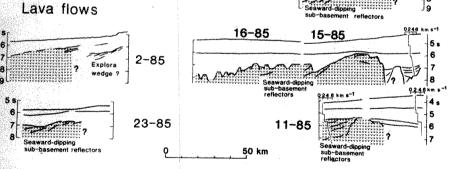












Escarpment after the expedition vessel Andenes of the Norwegian Coast Guard.

The Andenes and Explora Escarpments form a linear basement structure >1,000 km long which coincides with the transition between regions of contrasting reflection characteristics of the transition between terms of contrasting reflection characteristics of the transition between regions of contrasting reflection characteristics of the transition of the t

On the seaward side of the basement ridge is an uneven coustic basement with abundant diffraction hyperbolae, with trong similarity to the acoustic character of oceanic crust (Fig. 1, lines 5B-79, 16-85 and 17-85). There is also evidence of eaward-dipping, low-frequency, sub-basement reflectors leveloped seaward of the escarpments (Fig. 2, lines 11-85, 6-85, 17-85 and 23-85).

On the landward side, the Explora wedge of seaward-dipping and divergent reflectors constitutes the deepest seismic sequence landward of the Explora Escarpment, and acoustic basement is observed only on isolated highs⁴. However, west of 23° W, we can observe acoustic basement for >150 km landward of the Andenes Escarpment and interpret it as a series of tilted blocks, locally with internal reflectors. Another characteristic feature in this area is the distinct low-frequency acoustic character and undisturbed nature of the material $(v_p > 4.5 \text{ km s}^{-1})$ infilling topographic lows in acoustic basement (Fig. 2, lines 4B-85, 6B-85 and 15-85).

The magnetic signature associated with the Explora Escarpment is a positive magnetic anomaly, whereas the relationship along the Andenes Escarpment is more complex (Fig. 4). On

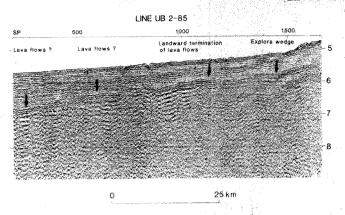


Fig. 3 Seismic reflectors interpreted as seaward-dipping lava flows. SP, shot-point.

the landward side of the escarpments, and paralleling the margin outside the Riiser-Larsen Ice Shelf, is a positive-negative pair of long-wavelength (<100 km) magnetic anomalies which extend southwestward towards the Filchner Ice Shelf and diverge with the trend of the basement ridge^{5,6}. To the south, short-wavelength, high-amplitude magnetic anomalies are associated with magnetic⁵ and acoustic⁷ basement of the east Antarctic craton exposed at the sea floor in a 50-70-km-wide swath along the barrier between Filchner Ice Shelf and Halley (30-37° W). In the northern part of the Soviet survey area (74° S), there is a conspicuous change in magnetic field character towards short-wavelength, high-amplitude, E-W-trending lineations collinear with the Andenes Escarpment. This strongly suggests that the tectonic grain represented by the escarpments may continue

towards the Antarctic Penninsula at least to 55° W.

To the north of the Andenes-Explora escarpments, lineated magnetic anomalies have been related to oceanic crust formed by seafloor spreading^{6,8}. Thus, the escarpments could represent an ancient Gondwana plate boundary in the Weddell Embayment, between oceanic crust to the north and crust of unknown origin to the south.

Gondwana reconstructions using current knowledge of magnetic anomalies in the South Atlantic and Indian Ocean predict large initial strike-slip motion along the Dronning Maud Land (DML) margin during the early opening^{2,3}. The lineated magnetic anomalies observed in the Weddell Sea are strong evidence of underlying oceanic crust formed at a spreading centre subparallel to the Explora escarpment^{6,8}. Thus the Andenes-Explora escarpments may have one or several modes of origin: (1) a fracture zone; (2) a rifted margin; (3) a sheared margin subsequently overprinted by rifting.

The morphological signature of a fracture zone in the oceanic crustal domain is most often a paired basement ridge and trough⁹, whereas a single ridge is most often observed at sheared continental margins^{10,11}. Also, in the latter environment, the ancient fracture zone location at the margin is associated with a precipitous increase in water depth from a shelf or plateau to abyssal depths.

Basement morphology and structure along the Explora Escarpment have affinities with those of a sheared continental margin (Fig. 2). However, the collinear region of lava flows between 18 and 23°W and the Andenes Escarpment shows stronger similarities to a rifted margin segment, the principal evidence being the seaward-dipping sub-basement reflectors to the north of the lava front (line 23-85) or escarpment (lines 16-85, 17-85), respectively. Wedges of seaward-dipping sub-

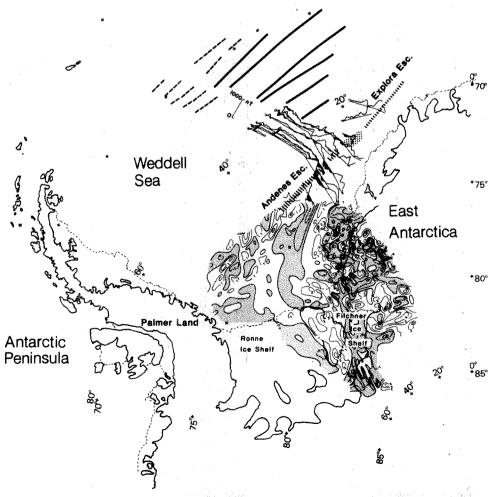


Fig. 4 Compilation of aeromagnetic data⁵ (areas of negative anomalies shaded) and marine magnetic data⁶, together with mapped magnetic lineations in the Weddell Embayment.

basement reflectors, often terminated on the landward side by an escarpment, have been observed along several rifted continental margins and are thought to be at or near the transition from continental to oceanic crust¹². Paralleling the Andenes and Explora escarpments at a distance of <300 km towards the south is the 130-km-long Vestfiella chain of nunataks, which experienced a regime of NW-SE tension during the early to middle Jurassic¹³⁻¹⁵. A 1-2-km-thick section of mostly tholeitic basalts was laid down in subaerial conditions. The volcanic pile is cut by many dykes of predominantly NE-SW strike, and by normal faults with no significant component of strike-slip. Also, basement depths landward of the escarpments (Fig. 2) require a thin crust from isostatic considerations. Thus, the evidence available favours an interpretation of the Andenes-Explora escarpments as structures of a rifted margin or possibly a plate boundary with oblique spreading rather than pure strike-slip. A sequence of events beginning with a large initial shear and subsequent overprint by rifting cannot be ruled out, but is considered less likely in view of the structural history of adjacent land areas, as well as the structural simplicity of the Andenes and Explora escarpments.

A major event in the evolution of the Weddell Embayment was mid-Jurassic crustal extension between the East Antarctic craton and the Pacific facing arc¹⁶, forming major north-south grabens below the Ronne and Filchner ice shelves^{5,17}. A Gondwana plate margin represented by the linear Andenes-Explora escarpments and their western continuation cuts across the early extensional tectonic trend (Fig. 4), indicating a post-mid-Jurassic change in the regional stress field.

A post-rift-phase Filchner microplate^{1,3} probably did not exist. The available multi-channel seismic data^{4,7} (Fig. 1) demonstrate that the sediments below the continental slope and shelf between 15 and 40° W are characterized by a total absence of fold and fault structures induced by post-rift basement tectonics. Also, preliminary results of a seismic survey by Polarstern¹⁸ along portions of a traverse from the East Antarctic craton to the Antarctic Peninsula, outside the Filchner and Ronne ice shelves. show the upper 1 s (two-way travel time) of sediments to be undisturbed except in an area within 150 km of the peninsula. Thus, the locus of any post-rift relative motion between the Antarctic Peninsula 19,20 and the East Antarctic craton is certainly west of 40° W and probably near the peninsula itself.

We thank Captain T. Myhre and the officers and crew of K/V Andenes, also G. Grikurov, I. Kadmina and R. Kurinin at VNIIOkeanologia, Leningrad, Karl Hinz at Bundesanstalt für Geowissenschaften und Rohstoffe, Hannover and colleagues at the Sixth Gondwana Symposium, Columbus, Ohio, for fruitful discussions. Publication 80 of the Norwegian Antarctic Research Expeditions (1984-85).

Received 21 January; accepted 7 May 1986.

- 1. Dalziel, I. W. D. & Elliot, D. Tectonics 1, 3-19 (1982).
- Norton, I. O. & Sclater, J. G. J. geophys. Res. 84, 6803-6830 (1979). Lawver, L. A., Sclater, J. G. & Meinke, L. Tectonophysics 114, 233-255 (1985).
- Hinz, K. & Krause, W. Geol. Jb. 23, 17-41 (1982).
- Masolov, V. N. in Geophysical Investigations in Antarctica, 16-28 (NIIGA, Leningrad, 1980; transl. from Russian)
- Barker, P. F. & Jahn, R. A. Geophys. J. R. astr. Soc. 63, 271-283 (1980).
- Barket, F. F. & Jami, R. A. Ocophys. J. R. astr. Soc. 63, 271–283 (1980).
 Haugland, K., Kristoffersen, Y. & Velde, A. Tectonophysics 114, 293–315 (1985).
 LaBrecque, J. L. & Barker, P. F. Nature 290, 489–492 (1981).
 Sandwell, D. T. J. geophys. Res. 89, 11401–11413 (1984).
 Rabinowitz, P. D. & LaBrecque, J. L. J. geophys. Res. 84, 5973–6002 (1979).

- Sibuet, J. G. & Mascle, J. J. geophys. Res. 83, 3401-3421 (1978).
 Mutter, J. C. Tectonophysics 114, 117-131 (1985).
- 13. Hjelle, A. & Winsnes, T. in Antarctic Geology and Geophysics 539-547 (Universitets forlaget,
- Furnes, H. & Mitchell, J. G. Norsk Polarinst. Skr. 169, 45-68 (1978).
 Spaeth, G. in Proc. 6th Gondwana Symp., Columbus, Ohio (American Geophysics Union,
- Elliot, D. in Antarctic Earth Science, 347-351 (Cambridge University Press, 1983)
- 7. Grikurov, G. et al. in Geophysical Investigations in Antarctica, 29-43 (NIIGA, Leningrad, 1980: trans, from Russian)
- 8. Miller, H. Lippmann, E. & Kallerhoff, W. Rep. Pol. Res. 19, 116-129 (1984)
- Rowley, P. D. et al. in Antarctic Earth Science 245-250 (Cambridge University Press, 1983). Meneilly, A. W., Harrison, S. M., Piercy, B. A. & Storey, B. C. in Proc. 6th Gondwana Symp
- (American Geophysical Union, in the press).

 1. Drewry, D. J. in Antarctica: Glaciological and Geophysical Folio 2 (Scott Polar Research Institute, Cambridge, 1983).

Capacity of purified Lyt-2⁺ T cells to mount primary proliferative and cytotoxic responses to Ia tumour cells

J. Sprent & Mary Schaefer

Department of Immunology, IMM4A, Scripps Clinic and Research Foundation, 10666 North Torrey Pines Road, La Jolla, California 92037, USA

Allogeneic gene products of the major histocompatibility complex. the HLA complex in man and the H-2 complex in mice, induce T lymphocytes to exert powerful mixed lymphocyte reactions (MLR) and cell-mediated lympholysis (CML). In mice, the subset of T cells carrying the L3T4 surface antigen but lacking the Lyt-2 antigen responds predominantly to H-2 class II (Ia) differences whereas the L3T4 Lyt-2 subset reacts to class I (K/I) differences^{1,2}. For primary responses the stimulus for MLR and CML appears to be controlled by Ia+ cells of the macrophage/dendritic cell lineages, for both L3T4+ and Lyt-2+ cells3-6. The finding that Ia+ cells are required for responses involving Lyt-2+ cells has been taken to imply that triggering of these cells is controlled by la-restricted L3T4⁺ cells^{7,8}. Lyt-2⁺ cells have thus come to be regarded as crippled cells which are heavily dependent on 'help' from other T cells⁹⁻¹¹. This well-entrenched view is challenged by evidence presented here that purified Lyt-2+ cells can give high primary responses to certain Ia tumour cells in vitro.

Recent studies from this laboratory showed that highly purified Lyt-2+ cells were able to mount high primary MLR and CML responses to class I but not class II H-2 differences in

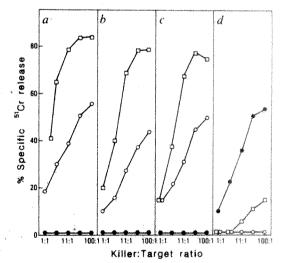


Fig. 1 Cytolytic activity of purified B6 (H-2b) Lyt-2 cells cultured for 4 days in vitro with P815 (H-2^d) tumour cells. Doses of 2×10^6 responder cells were cultured with lightly irradiated (1,500 rad) DBA/2 (H-2^d) spleen cells or with 0.5×10⁶ heavily irradiated (20,000 rad) P815 tumour cells in a volume of 2 ml in 24-well plates; as controls for specificity of lysis, DBA/2 T (J11d-treated LN) cells were cultured with B10 (H-2b) spleen cells. In experiment c, the purified Lyt-2+ cells were pretreated with anti-lab antibody plus C' before culture. After 4 days the cells pooled from several wells were counted and then cultured in varying numbers for 3 h at 37 °C with fixed numbers (10⁴) of ⁵¹Cr-labelled target cells, that is, P815 cells ([]), concanavalin A-stimulated B10.D2 (H-2^d) (()) or B10 (H-2b) () spleen cells; target cells were labelled with $300\,\mu\text{Ci}^{51}\text{Cr}$ per 4×10^6 cells at 37 °C for 1 h and then washed thoroughly. The per cent ^{51}Cr release from target cells was measured by standard techniques, taking release of isotope from detergent-treated cells as 100% release. Each data point represents the mean per cent specific 51Cr release of triplicate cultures; the data in a, b, and in c, d were obtained in two different experiments.

Table 1 Primary MLR of B6 T cells and purified B6 Lyt-2+ cells stimulated with H-2-incompatible spleen cells or P815 tumour cells

)	3 H-TdR incorporation (c.p.m. $\times 10^{3}$) with responders (2 $\times 10^{5}$)								
	No. of stimulators	B6 T (H-2 ^b)			В6	Lyt-2 ⁺ (H-	2 ^b)	No responders		
Stimulators	(×10 ⁵)	Day 3	Day 4	Day 5	Day 3	Day 4	Day 5	Day 3	Day 4	Day 5
B6 spleen	0.2	0.3	0.4	1.3	0.1	0.1	0.1	-		*****
$(H-2^{\rm b})$	1	0.6	1.1	7.6	0.1	0.1	0.1		-	
(11-2-)	5	2.3	6.7	17.8	0.3	0.7	0.7	0.2	0.3	0.5
DBA/2 spleen	0.2	15.9	34.1	51.8	18.8	44.5	25.5	-	-	
$(H-2^{\rm d})$	1	86.7	171.4	44.6	82.4	188.3	16.1			~~~
(11-2)	5	144.2	275.0	58.9	132.6	263.0	44.9	0.4	0.5	0.5
P815 (H-2 ^d)	0.2	28.0	62.7	14.4	38.8	66.7	11.5	0.4	0.5	0.2
	1	8.2	16.9	16.3	26.8	49.4	30.6	0.4	0.3	0.2
(TI-#)	5	4.3	3.6	3.8	3.3	3.6	4.4	2.3	2.7	2.1

T cells and T-cell subsets were purified from pooled lymph nodes (LN) of adult B6 mice as described elsewhere². To purify T cells, LN cells were pretreated at 37 °C for 1 h in vitro with an anti-B-cell monoclonal antibody (J11d) plus guinea pig serum as a source of complement (C'); the surviving cells (>98% Thy 1⁺) were then passed through Ficoll gradients to remove dead cells. To prepare Lyt-2⁺ cells, LN cells were first pretreated at 37 °C in vitro with a mixture of J11d and anti-L3T4 (GK1.5) antibodies plus C'. The surviving cells were then washed and allowed to adhere to anti-Lyt-2-coated dishes for 1 h at 4 °C. After gently washing non-adherent cells from the dishes, the adherent cells were eluted by vigorous pipetting. The adherent cells were >99% Lyt-2⁺ by FACS analysis and contained no detectable L3T4⁺ cells². For MLR, doses of 2×10⁵ B6 T or Lyt-2⁺ responder cells were cultured in flat-bottom microtitre plates with varying numbers of lightly irradiated (1,500 rad) normal B6 or DBA/2 spleen cells or with heavily irradiated (20,000 rad) in vitro-passaged P815 tumour cells in a final volume of 200 μl. Cells were cultured in RPMI 1640 medium supplemented with 10% fetal calf serum and standard additives²; IL-2 was not added to the cultures. Cultures were pulsed with 1 μCi tritiated thymidine (³H-TdR) 18 h before collection. The data show the mean levels of radioactivity in triplicate cultures. s.d., omitted for simplicity, were generally within 10-20% of the mean. Pretreatment of P815 cells with mitomycin C rather than irradiation led to comparable MLR with B6 Lyt-2⁺ cells.

vitro2; other workers have reported similar findings12. MLR to class I differences were not reduced by removing T cells from the stimulator population or by adding anti-L3T4 monoclonal antibody to the cultures^{2,12}; addition of anti-la monoclonal antibody caused only minimal inhibition of the response. Although these findings suggested that the response of Lyt-2+ cells could not be attributed to minor contamination of the cultures with L3T4⁺ cells, removal of Ia⁺ cells from the stimulator population (spleen cells) virtually abolished the response^{2,12}. At face value the simplest explanation of this finding is that the response of Lyt-2+ cells to alloreactive class I molecules requires co-recognition of class II (Ia) molecules. The problem with this notion is that, unless one invokes cryptic participation of L3T4+ cells, it is difficult to envisage how la molecules might control Lyt-2+ cell induction. In addition, one must account for the fact that certain Ia+ cells-small B lymphocytes—are non-stimulatory for unprimed Lyt-2+ cells⁶. An alternative possibility is that Ia+ cells with stimulatory function display a putative 'second signal' required by Lyt-2+ cells12,13 with the joint expression of Ia molecules and the second signal being largely coincidental. This raises the question of whether some Ia cells might be stimulatory for Lyt-2+ cells. Rammensee et al.14 have shown that Ia Lyt-2+ T cells have the capacity to 'veto' the induction of allogeneic Lyt-2+ cytolytic precursors, the veto function of T cells being attributed to the failure of these cells to express a requisite second signal. Since spleen cell suspensions depleted of Ia+ cells consist largely of T cells, the poor antigen-presenting cell function of Ia spleen cells thus does not preclude the possibility that a spectrum of cell types might act as antigen-presenting cells for Lyt-2+ cells, the notable exception being T cells. To assess this idea, we arbitrarily tested the antigen-presenting function of Ia tumour cells.

Although certain Ia tumours, such as the P815 mastocytoma, are known to elicit primary T-cell responses in vitro^{13,15}, it is unclear whether these responses require help from the L3T4⁺ T-cell subset. Table 1 compares the capacity of B6 (H-2^b) T cells and >99% purified B6 Lyt-2⁺ cells to mount primary MLR to DBA/2 (H-2^d) spleen stimulators (1,500 rad) or P815 (H-2^d) tumour stimulators (20,000 rad) in the absence of added interleukin-2 (IL-2); the P815 tumour, of DBA/2 origin, completely-lacks Ia molecules as assessed by fluorescence-activated cell sorter (FACS) analysis, but is strongly positive for class I

molecules (data not shown). B6 T and B6 Lyt-2+ cells both gave high responses to DBA/2 spleen. Peak responses occurred on day 4 and the responses decreased progressively as the dose of stimulators was lowered. With P815 stimulators, large doses of tumour cells (5×10⁵ per culture) elicited virtually no MLR. Low tumour doses (10⁴-10⁵), by contrast, elicited highly significant MLR. Responsiveness to the P815 tumour seemed to be restricted to Lyt-2+ cells because: (1) responses were appreciably higher with B6 Lyt-2+ cells than with unseparated B6 T cells (Table 1), (2) there was no response to the tumour using purified B6 L3T4+ cells (Table 2, expts a, b) (implying that the tumour cells remained Ia in culture), and (3) in marked contrast to anti-Lyt-2 monoclonal antibody, adding anti-L3T4 to the cultures failed to inhibit the response of B6 Lyt-2+ cells to the tumour (Table 2, expt a; the response to the bm1 and bm12 mutants controlled for the specificity of the blocking effects of anti-Lyt-2 and anti-L3T4 monoclonal antibodies, see Table 2 legend). Heat-killed P815 cells and P815 cells exposed to ultraviolet light were completely non-stimulatory, even when reconstituted with recombinant IL-1 (data not shown).

The response of B6 Lyt-2+ cells to the P815 tumour appeared to be specific for H-2 antigens, as the tumour failed to stimulate H-2-identical DBA/2 Lyt-2⁺ cells (Table 2, expt b) but did stimulate Lyt-2+ cells from another H-2b strain, C3H.SW (Table 2, expt a). Further evidence for antigen specificity was obtained by studying the capacity of the tumour to elicit CML activity In all three experiments performed, two of which are illustrated in Fig. 1, culturing B6 Lyt-2+ cells for 4 days with irradiated P815 cells in the absence of added IL-2 led to high levels of lysis against 51Cr-labelled P815 cells. With concanavalin A. stimulated spleen blast cells as targets, lysis was high on B10.D2 (H-2^d) targets but absent on B10 (H-2^b) targets, implying that lysis was directed to H-2^d determinants rather than to tumour specific antigens. The specific lytic activity of B6 Lyt-2+ cells cultured with P815 stimulators was only slightly lower than with cells cultured with DBA/2 spleen stimulators (compare Fig. 1c and b). Pretreating the B6 Lyt-2+ cells with anti-I-Ab antibody plus complement (C') to remove any residual la cells before culture failed to impair CML activity (Fig. 1c).

The above results indicate that Ia P815 tumour cells are able to stimulate purified allogeneic Lyt-2 cells to proliferate exten sively and differentiate into H-2-specific (presumably class I

Table 2 MLR of T-cell subsets to P815 (H-2^d) and L929 (H-2^k) tumour cells: failure of anti-L3T4 antibody to inhibit MLR of Lyt-2⁺ cells

				³ H-TdR incorporation (c.p.m.×10 ³) with responders				
Stimulators	No. of stimulators (×10 ⁵)	No. of responders (×10 ⁵)	Antibody added to cultures	B6 Lyt-2 ⁺ (bbbb)	C3H.SW Lyt-2 ⁺ (bbbb)	B6 L3T4 ⁺ (bbbb)	No responders	
Expt a						· · · · · · · ·	a series and a series of a	
B6 spl (bbbb)*	5	1		0.3	0.8	2.1		
	5	2	*****	0.8	1.2	3.1	· ·	
bml spl (bmlbbb)	5	1		74.5	57.4	6.3 3.8	- rypendy	
	5	1	Anti-L3T4	74.5	51.0		Anamaji.	
	5	ī	Anti-Lyt-2	2.7	2.7	vikóya	electronic	
	5	2		178.3	82.0	şmiyes.	Verificação	
bm12 spl (bbm12bb)	5	1	·	2.2	1.9	22.9	synalizes ²	
	5	1	Anti-L3T4		1.3	2.1	, militage and	
	5	i	Anti-Lyt-2		******	30.3	***************************************	
	5	2	7 Milling 1-2				-constitut	
P815 (dddd)	0.5	$\tilde{2}$		25.4	18.2	81.5	servers Service	
	0.5	2	Anti-L3T4	21.9	17.6	0.3	0.2	
	0.5	2	Anti-Lyt-2	0.8	0.6	MONEY.	elimen.	
		~	Anti-Lyt-2		0.0	imenaños.	in minister	
				B6	DBA/2	B6		
				Lyt-2 ⁺	Lyt-2+	L3T4+	No	
Expt b				(bbbb)	(dddd)	(bbbb)	responden	
	_				3	***		
B6 spl (bbbb)	5	2		1.1	29.0	4.2	0.1	
DBA/2 spl (dddd)	5	2		104.1	0.4	210.2	0.1	
P815 (dddd)	0.25	2		32.3	0.5	1.1	0.1	
	0.5	2	W/A	40.9	1.2	0.8	0.1	
	1	2		43.0	1.4	3.1	0.2	
				B6		W. F. W.	1000	
				Lyt-2 ⁺	CBA/Ca	16. V		
					Lyt-2 ⁺	No		
Expt c†				(bbbb)	(kkkk)	responders		
B6 spl (bbbb)	5	1		0.3	40.7			
CBA/Ca spl (kkkk)	5	1		0.2	20.7	0.1		
bml spl (bm1bbb)	0.2	i		55.5 2.2	0.7	0.3		
	5	1			0.8	0.3		
됐다면 하게 되었다.	5	1	Anti-L3T4	70.5	31.1	0.1		
	5	1		62.0		* protestania		
L929 (kkkk)	0.04	1	Anti-Lyt-2	3.2		-		
Section 1	0.2	1	******	5.5	0.6	0.5		
	0.2	1	A wai i z gótta	16.7	1.1	1.1		
	0.2		Anti-L3T4	24.8		**************************************		
	1	1	Anti-Lyt-2	2.2		integrapion.		
	5	1	-	22.4	1.7	1.7		
80.00	J	1		0.6	0.4	0.4		

Lyt-2⁺ cells were prepared as for Table 1. An analogous procedure was used to prepare L3T4⁺ cells; that is, pretreatment of LN cells with J11d+anti-Lyt-2 (3.168) antibodies+C⁺ followed by positive panning on dishes coated with anti-L3T4. The P815 mastocytoma and the L929-transformed fibroblast line were both totally I-A-negative by FACS analysis but were strongly positive for expression of class I molecules. As for P815, the L929 cells were passaged in vitro without feeder cells; the cells were exposed to 20,000 rad before use as stimulators. The amount of antibody added to the cultures was 2 µl of undiluted ascites fluid for anti-Lyt-2 and 2 µl of 1:10 diluted ascites fluid for anti-L3T4. As controls for the specificity of inhibition by anti-L3T4 and anti-Lyt-2, these antibodies were added to cultures in which MLR were directed solely to a class I H-2 difference (B6 Lyt-2⁺ cells responding to the H-2K-different B6.C-H-2^{bm1} (bm1) mutant) or to a class II H-2 difference (B6 L3T4⁺ cells responding to the I-A-different B6.C-H-2^{bm12} (bm12) mutant); as reported elsewhere² (confirmed in the table), anti-L3T4 selectively inhibits anti-class II MLR whereas anti-Lyt-2 selectively inhibits anti-class I MLR. MLR (mean of triplicate cultures) were measured on day 4 for each experiment shown.

specific) cytotoxic cells in the absence of exogenous IL-2 (although IL-2 production by a subset of Lyt- 2^+ T 'helper' cells' cannot be excluded). Similar findings were observed with the L929 (H- 2^k) Ia transformed fibroblast line (tested only for MLR) (Table 2, expt c). In the case of non-neoplastic cells, we have obtained preliminary evidence that Thy 1 Ia cells from normal bone marrow can stimulate primary MLR by allogeneic Lyt- 2^+ cells (unpublished data). Thus, the capacity to stimulate Lyt- 2^+ cells is apparently not a property unique to Ia tumour cells.

In contrast to these findings with Thy 1⁻ cells, studies with three Thy 1⁺ Lyt-2⁻ T-cell tumours have shown that, like normal T cells, these tumours cannot stimulate unprimed allogeneic Lyt-2⁺ cells in the absence of added IL-2 (unpublished data of

the authors); the reason for this is unclear. Interestingly, the ability of T cells to mediate veto function is largely restricted to activated Lyt-2⁺T-killer cells and is abolished by irradiation¹⁴. Hence, the poor stimulatory function of typical small T cells (for example, anti-Ia+C'-treated spleen) and Lyt-2⁻ T tumours is unlikely to reflect a veto effect. Moreover, we have seen no evidence of suppression when Lyt-2⁺ responders are exposed to a mixture of spleen stimulators supplemented with irradiated small T cells or T tumours. The most likely explanation for the poor stimulatory function of (non-cytotoxic) T cells is that these cells simply lack some requisite second signal required by Lyt-2⁺ cells.

Although the nature of the putative second signal provided by Thy 1 Ia H-2-different tumour cells is unknown, it is

^{*} Alleles of H-2 subregions, that is, H-2K, I-A, I-E, H-2D.

f Responder T cells in this experiment were pretreated with anti-I-Ab+C' before culture.

possible that such tumours are directly immunogenic for Lyt-2+ cells in vivo, involvement of L3T4+ cells responding to 'processed' tumour H-2 antigens being unnecessary for tumour rejection. In this respect, we now have preliminary evidence that the subcutaneous growth of P815 tumour cells in irradiated B6 mice can be prevented by mixing the injected tumour cells with unprimed purified B6 Lyt-2+ cells (unpublished data).

Received 6 January; accepted 22 April 1986.

- Swain, S. L. Immun. Rev. 74, 129-142 (1983).
 Sprent, J. & Schaefer, M. J. exp. Med. 162, 2068-2088 (1985).
 Shreffler, D. C. & David, C. Adv. Immun. 20, 125-195 (1975).
 Thomas, D. W., Yamashita, U. & Shevach, E. M. Immun. Rev. 35, 97-120 (1977).
 Pettinelli, C. B., Ahmann, G. B. & Shearer, G. M. J. Immun. 124, 1911-1920 (1980).
 Singer, A., Kruisbeek, A. M. & Andrysiak, P. M. J. Immun. 132, 2199-2209 (1984).

We thank J. Benedetto for growing the tumour cells, which were kindly made available by M. J. Bevan. This work was supported in part by NIH grants AI 21487, CA 38355, CA 25803 and CA 35048.

Note added in proof: We have recently found that one T cell tumour (EL4) does stimulate high primary MLR by allogenic Lvt-2+ cells.

- 7. Weinberger, O., Germain, R. N. & Burakoff, S. L. Nature 302, 429-431 (1983)

- Weinberger, O., Germain, R. N. & Burakoff, S. L. Nature 302, 429-431 (1983).
 Rock, K. L., Barnes, M. C., Germain, R. N. & Bernacerraf, B. J. Immun. 130, 457-462 (1983).
 Cantor, H. & Boyse, E. A. J. exp. Med. 141, 1390-1399 (1975).
 Bach, F. H. et al. Immun. Rev. 35, 76-96 (1977).
 Wagner, H. & Rollinghof, M. J. exp. Med. 148, 1523-1538 (1978).
 von Boehmer, H., Kisielow, P., Weiserson, W. & Haas, W. J. Immun. 133, 59-64 (1984).
 Lafferty, K. J., Andrus, L. & Prowse, T. Immun. Rev. 51, 279-314 (1980).
 Rammensee, H-G., Fink, P. J. & Bevan, M. J. J. Immun. 133, 2390-2396 (1984).

- 15. Romani, L. & Mage, M. G. Eur. J. Immun. 15, 1125-1130 (1985).

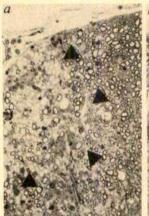
Increased levels of myelin basic protein transcripts gene in virus-induced demyelination

K. Kristensson*, K. V. Holmes†, C. S. Duchala†, N. K. Zeller‡, R. A. Lazzarini‡ & M. Dubois-Dalcq‡

- * Department of Pathology (Division of Neuropathology), Karolinska Institutet, Huddinge, Sweden
- † Department of Pathology, Uniformed Services University of the Health Sciences, Bethesda, Maryland 20814, USA
- Laboratory of Molecular Genetics, NINCDS, National Institutes of Health, Bethesda, Maryland 20892, USA

In multiple sclerosis, a demyelinating disease of young adults, there is a paucity of myelin repair in the central nervous system (CNS) which is necessary for the restoration of fast saltatory conduction in axons 1,2. Consequently, this relapsing disease often causes marked disability. In similar diseases of small rodents, however, remyelination can be quite extensive, as in the demyelinating disease caused by the A59 strain of mouse hepatitis virus (MHV-A59)3,4, a coronavirus of mice. To investigate when and where oligodendrocytes are first triggered to repair CNS myelin in such disease, we have used a complementary DNA probe specific for one major myelin protein gene, myelin basic protein (MBP), which hybridizes with the four forms of MBP messenger RNA in rodents5. Using Northern blot and in situ hybridization techniques, we previously found that MBP mRNA is first detected at about 5 days after birth, peaks at 18 days and progressively decreases to 25% of the peak levels in the adult5-7. We now report that in spinal cord sections of adult animals with active demyelination and inflammatory cells, in situ hybridization reveals a dramatic increase in probe binding to MBP-specific mRNA at 2-3 weeks after virus inoculation and before remyelination can be detected by morphological methods. This increase of MBP-specific mRNA is found at the edge of the demyelinating area and extends into surrounding areas of normal-appearing white matter. Thus, in situ hybridization with myelin-specific probes appears to be a useful method for detecting the timing, intensity and location of myelin protein gene reactivation preceding remyelination. This method could be used to elucidate whether such a reactivation occurs in multiple sclerosis brain tissue. Our results suggest that in mice, glial cells react to a demyelinating process with widespread MBP mRNA synthesis which may be triggered by a diffusible factor released in the demyelinated areas.

Earlier studies have shown that some MHV-A59 strains can cause chronic demyelination in mice and rats^{4,8-15}. For instance, a high incidence of demyelination occurs in C3H and C57 black mice3,4 after intracerebral inoculation of the prototype MHV-A59 strain16. The virus replicates preferentially in oligodendrocytes, destroying the cells in focal areas of the white matter during the first weeks of infection^{3,4,8-15}. Viral antigen persists in the cytoplasm of oligodendrocytes within the demyelinating



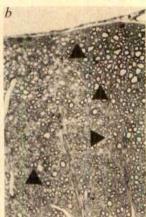


Fig. 1 Micrographs showing demyelinated (a) and remyelinated (b) areas (delineated by arrowheads) in the anterior column of mice at 4(a) and 10(b) weeks post-inoculation with MHV-A59. Active demyelination is seen at 4 weeks while thinly remyelinated axons are seen at 10 weeks. Animals were perfused with 4% glutaraldehyde in Sorensen phosphate buffer, and slices of various levels of the spinal cord were embedded in Epon. 1-µm-thick sections were stained with toluidine blue. ×200.

lesions for up to 4 weeks3. Untranslated viral genome may be present in other areas of the CNS and in other cell types1

In the present investigation, 4-week-old C57Bl/6J mice (obtained from Jackson Laboratories, Bar Harbor, Maine) were injected intracerebrally with 500-1,000 plaque-forming units of MHV-A59 (obtained from Dr L. S. Sturman, New York State Department of Health, Albany, New York). At 1, 2, 3, 4 and 8 weeks after injection, groups of three or four mice were perfused through the heart with periodate-lysine-formaldehyde18, and the brains and spinal cords of the perfused animals were then dissected. Transversely cut slices of various regions of the brain and spinal cord were prepared by freezing and cryosectioning for in situ hybridization as described in Fig. 2 legend. As a probe, we used a small cDNA clone, NZ-112, which encodes amino acids 60-93 of mouse MBP5. By adding 20-25 35S-labelled dATP residues to the 3' ends of the gel-purified DNA fragments using terminal deoxynucleotidyl transferase, a specific activity of 1-2×109 d.p.m. per μg DNA was obtained6,7. Other CNS tissue slices were embedded in paraffin for histological examination and immunocytochemistry. For histology, paraffin sections were stained with Luxol fast blue and cresyl violet or haematoxylin/eosin. For immunocytochemistry, paraffin sections were incubated with dilutions of mouse or goat anti-MBP antibodies and stained by the peroxidase-antiperoxidase method19. In addition, two or three mice at each time point were perfused and processed as described in Fig. 1 legend in order to analyse the details of the demyelinating and remyelinating process in semi-thin plastic sections.

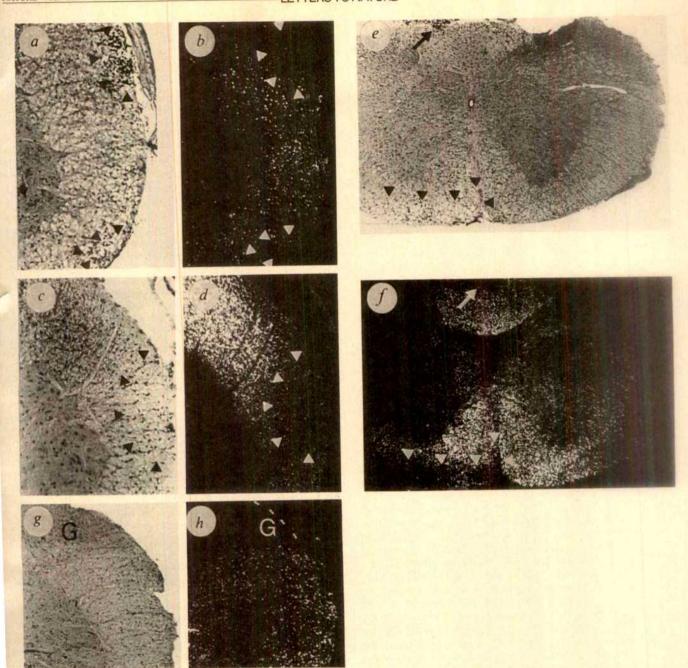


Fig. 2 Micrographs showing the location of MBP-specific transcripts in cervical spinal cords of virus-infected animals at 2(a,b), 3(c,d), 4(e,f) and 8(g,h) weeks post-inoculation. Bright-field views of histological stained sections are shown (a,c,e,g), together with corresponding dark-field cryostat sections after in situ hybridization (b,d,f,h). The number of grains observed in dark field is directly proportional to the amount of hybridization with the MBP probe and thus the number of MBP-specific transcripts. Note some hybridization of the MBP-specific probe in white matter at 2 weeks post-inoculation, with a decrease in labelling in the lesion containing inflammatory cells (delineated by arrowheads). In contrast, at 3 and 4 weeks, intense hybridization is seen in regions surrounding the lesions (delineated by arrowheads) which are devoid of label. Increased hybridization extends into the normal-looking white matter: in f, the left ventral column has a lesion (under arrowheads) but increased label is also seen in the right ventral column. The dorsal right column also has a small lesion (arrow) surrounded by increased label. At 8 weeks (g,h), there is still a slight increase in white matter labelling without the differential distribution (G, grey matter of subtantia gelatinosa) observed in the 3-4-week samples. $\times 200$.

Methods. For these in situ hybridization experiments, samples from the spinal cord were cryoprotected in 15% sucrose (RNase-free) before freezing in liquid nitrogen. Cryostat sections (10 μm thick) were cut and hybridized as described in detail previously⁷. Briefly, the sections were treated with 0.2 M HCl for 20 min, washed in phosphate-buffered saline, incubated with 1 μg ml⁻¹ proteinase K (Boehringer Mannheim) for 15 min at 37 °C, and then with the hybridization mixture without the probe for 2 h. The hybridization mixture was as follows: 50% formamide, 2×SSC, 1×Denhardt's solution, salmon sperm DNA (Sigma) at 450 μg ml⁻¹, Escherichia coli transfer RNA (Sigma) at 500 μg ml⁻¹, 200 μg ml⁻¹ poly(A) (Sigma), 40 nM oligonucleotide d(pT)₈ (Collaborative Research, Inc.). The probe, at a concentration of 100 μg ml⁻¹ and specific activity of 1×10⁷ d.p.m. ml⁻¹, together with the salmon sperm DNA and E. coli tRNA, was denatured for 3 min at 100 °C, quenched on ice for 3 min and mixed with the other constituents of the hybridization mixture with 40 mM dithiothreitol. The mixture was incubated for 15 min at 50 °C, denatured again and incubated at 50 °C for another 15 min. Each section was then incubated at 40 °C with 10 μl of the hybridization mixture in a sealed chamber overnight (about 16 h), washed in 0.1×SSC at 55 °C for 3 h, treated with 75% and 95% ethanol with 300 mM ammonium acetate and air-dried. The slides were dipped in a Kodak NTB-2 emulsion with 300 mM ammonium acetate and stored at 4 °C for 3 days before being developed using standard procedures. The sections were counterstained with cresyl violet before mounting in Permount.

The clinical and pathological features of the disease have been described elsewhere^{3,4}. Briefly, 5-7 days after infection, the mice developed signs of acute disease characterized by apathy, hunched posture, ruffled fur and tremor. Some mice exhibited paresis spontaneously whereas others showed more subtle motor deficits only during testing. During this acute episode, 70% of the mice died, but the remainder recovered from the disease. Signs of motor deficits were less obvious after 4 weeks. Histological examination of the brain and spinal cord at 7 days post-inoculation revealed scattered infiltrations of inflammatory cells. C3H mice, however, showed few perivascular infiltrates3. After 14-21 days, numerous focal lesions exhibited vacuolation and fragmentation of the myelin sheaths. Naked axons, necrotic cells and macrophages containing myelin debris were evident around the lesions. Mild perivascular infiltration with mononuclear inflammatory cells was also seen in these plaques of demyelination. Such demyelinating lesions were present in amost every section of the spinal cords examined and were situated in the central, lateral or posterior columns. Immunocytochemistry revealed a significant decrease in MBP in these lesions, the remaining stain being associated with meylin debris. After 4 weeks, the demyelinated foci were more prominent and most of the degenerated myelin had been phagocytosed (Fig. 1a). A few partially demyelinated axons with abnormally thin myelin sheath were scattered in the lesion at this time. Ten weeks after infection, remyelination was prominant and most axons in the previously demyelinated areas were surrounded by thinner than normal myelin sheaths (Fig. 1b). Immunostaining showed that MBP had reappeared in these areas and was associated with the newly formed myelin sheath. Invasion of the CNS by Schwann cells to remyelinate bare axons20-22 was not detected.

We next examined the cryostat sections of the spinal cord of animals at different stages of the disease after hybridization with the MBP-specific probe and autoradiography (Fig. 2). Since the sections were also stained with cresyl violet, we compared the distribution of the grains (corresponding to the amount of hybridization with the MBP cDNA probe) with the distribution of the lesions. In spinal cord of uninfected mice, more grains were seen in the white matter than in the grey matter, as expected from dot-blot hybridization studies of 1-month-old mice⁵ (Table 1). An unrelated probe (a cDNA of the non-structural phosphoprotein gene of vesicular stomatis virus²³) showed no significant hybridization to grey or white matter in either normal or infected animals. With the MBP-specific probe, however, a slight increase of labelling of the white matter was detected at 2 weeks (Fig. 2b), and fewer grains were seen in areas of white matter inflammation (Fig. 2a, b). At 3-4 weeks post-inoculation (Fig. 2c-f), the intensity of labelling had increased dramatically in some areas of the white matter. When the distribution of the grains in dark field was compared with the size and location of the lesion as seen after cresyl violet staining (Fig. 2a, c, e, g), it became clear that the foci with inflammation and tissue degeneration were devoid of labelling. However, a striking increase in the number of grains was present at the edge of the lesion as well as in the surrounding, normal-appearing white matter of the entire column (Fig. 2d) and even in the opposite column (Fig. 2f). Animals examined 8 weeks after inoculation had slightly higher levels of labelling in the white matter than had the normals (Table 1), but there were no clearly demarcated unlabelled areas such as those seen during the peak of demyelination (Fig. 2g, h).

The evidence presented here suggests that, during a demyelinating process caused by a virus in rodents^{3,4,8-15}, an increase in transcription of the gene coding for MBP, a major myelin protein, occurs early when demyelination is still progressing. Similarly, in CNS demyelinating lesions caused by cuprizone in rats, MBP can be detected by immunocytochemistry in oligodendrocytes before remyelintion²⁴. However, as MBP staining is also seen in macrophages containing myelin debris, it is difficult to distinguish between 'old' MBP and newly synthesized MBP in these lesions. In contrast, in situ hybridization with a MBP-specific probe has revealed an approximate 10-fold increase in the number of MBP transcripts in a widespread area surrounding the demyelinating lesions 3-4 weeks after inoculation (Table 1). In normal rodents only basal levels of MBPspecific RNA are expressed at this stage in development^{5,7}. Thus, in situ hybridization may be the method of choice for detecting the effects of a demyelinating process on myelin protein gene expression. At 2 months post-inoculation, the remyelinated areas showed only a slight increase in MBP mRNA in a diffuse area including the lesion. This suggests that myelin-forming cells have repopulated the demyelinated area and are completing the synthesis of MBP mRNA at that time. It also implies that, in the adult rodent CNS, a cell of the glial lineage may be capable of dividing and probably of migrating into the lesion to repair myelin^{25,27}. Transplantation studies have recently shown that myelinating cells can migrate significant distances in the CNS²⁸. Earlier electron microscope and autoradiographic studies have shown that the cells associated with remyelination after a viral

Table 1 Quantitation of MBP mRNA levels in spinal cord sections of MHV-A59-infected animals using in situ hybridization

Day post-inoculation	0	7	14	20	28	60
No. of mice	4	1	3	4	4	2
Degree of labelling	. +	*	++	++++	++++	++

The appearance of MBP mRNA was quantified by counting grains over the white matter using a scaled reticule and rates as follows: +, 2-3 times more grains over white than grey matter; ++, 3-6 times more grains over white than grey matter; ++++, 10 times more grains over white than grey matter.

disease are newly generated oligodendroglia¹¹. Moreover, recent studies on newborn rat optic nerve have demonstrated the existence of a progenitor cell which, after a number of mitoses, can differentiate into an oligodendrocyte²⁹. In the adult CNS, similar progenitor cells have been identified in the optic nerve and in the rat cerebral cortex²⁵⁻²⁷. Thus, it is now necessary to improve the resolution of our in situ hybridization method and combine this approach with the use of cell-specific markers in order to identify precisely the cell type responsible for remyelination in the CNS.

To our surprise, the increase in MBP gene transcription seemed to radiate from the edge of the plaque, far away into the surrounding normal white matter. This suggests that, in this virus-induced demyelinating disease in mice, a factor may be produced in the lesion which could diffuse into the normal white matter and trigger oligodendrocytes and/or their progenitor cells²⁹ to participate in myelin repair^{11,25-27}. One possibility is that such a factor is secreted by inflammatory cells in the lesion, since it has been shown that spleen cells in mice^{30,31} and T lymphocytes in humans³¹ produce factors which promote proliferation and maturation of astrocytes and oligodendrocytes in vitro. Moreover, interleukin-2 was recently shown to enhance MBP expression in cultured oligodendrocytes.

We thank Eileen Bauer and Ray Rusten for technical assistance and Judy Hertler for typing and editing the manuscript. This work was supported in part by USUHS grant R07403.

Received 18 February; accepted 14 May 1986.

- Perier, O. & Gregoire, A. Brain 88, 937-950 (1965).
 Raine, C. S. in Myelin 2nd edn (ed. Morell, P.) 259-310 (Plenum, New York, 1984).
 Woyciechowska, J. L. et al. J. exp. Path. 1, 295-306 (1984).
 Lavi, E., Gilden, D. H., Wroblewska, Z., Rorke, L. B. & Weiss, S. R. Neurology 34, 597-603
- 5. Zeller, N. K., Hunkeler, M. J., Campagnoni, A. T., Sprague, J. & Lazzarini, R. A. Proc. natn, Acad. Sci. U.S.A. 81, 18-22 (1984)
- 6. Zeller, N. K., Behar, T. N., Dubois-Dalcq, M. E. & Lazzarini, R. A. J. Neurosci. 5, 2955-2962 7. Kristensson, K., Zeller, N. K., Dubois-Dalcq, M. & Lazzarini, R. A. J. Histochem. Cytochem.
- 34, 467-473 (1986) 8. Weiner, L. P. Archs. Neurol. 28, 298-303 (1973).

- Lampert, P. W., Sims, J. K. & Kniazeff, A. J. Acta neuropath. 24, 76-85 (1973).
 Powell, H. C. & Lampert, P. W. Lab. Invest. 33, 440-445 (1975).
- 11. Herndon, R. M., Price, D. L. & Weiner, L. P. Science 195, 693-694 (1977)
- 12. Haspel, M. V., Lampert, P. W. & Oldstone, M. B. A. Proc. natn. Acad. Sci. U.S.A. 75, 4033-4063 (1978).
- Knobler, R. L., Haspel, M. V., Dubois-Dalcq, M., Lampert, P. W. & Oldstone, B. A. in Biochemistry and Biology of Coronaviruses (eds ter Meulen, V., Siddell, S. & Wege, H.) 341-348 (Plenum, New York, 1981).
 Knobler, R. L., Haspel, M. V., Dubois-Daleg, H., Lampert, P. W. & Oldstone, B. A.
- J. Neuroimmun. 1, 81-92 (1981).
- Wege, H., Koga, M., Wege, H. & ter Meulen. V. in Biochemistry and Biology of Coronaviruses (eds ter Meulen, V., Siddell, S. & Wege, H.) 327-340 (Plenum, New York, 1981).
 Styrman, L. S. & Holmes, K. V. Virology 77, 650-660 (1977).
 Sorensen, O. & Dales, J. Virology 56, 434-438 (1985).
 McLean, I. W. & Nakane, P. K. J. Histochem. Cytochem. 22, 1077-1083 (1974).
 Sternberger, N. H., del Cerro, C., Kies, M. W. & Herndon, R. M. J. Neuroimmun. 7, 355-363 (1994).

- (1985)
- 20. Ludwin, S. K. Adv. Neurol. 31, 123-168 (1981).
- 21. Itoyama, Y., Webster, H. deF., Richardson, E. P. & Trapp, B. D. Ann. Neurol. 14, 339-346 (1983).
- 22. Blakemore, W. F. Rec. Adv. Neuropath. 2, 53-81 (1982).
- Hudson, L. D., Condra, C. & Lazzarini, R. A. J. gen. Virol. (in the press).
- Ludwin, S. K. & Sternberger, N. Acta neuropath. 63, 240-249 (1984).
- ffrench-Constant, C. & Rafl, M. Nature 319, 499-502 (1986).
 Reyners, H., Gianfelici de Reyners, E. & Maisin, J.-R. J. Neurocytol. 11, 967-978 (1982).
- 27. Reyners, H., Gianfelici de Reyners, E., Regniers, L. & Maisin, J. R. J. Neurocytol. (in the
- Lachapelle, F. et al. Devl Neurosci. 6, 325-334 (1984).
 Raff, M. C., Miller, R. H. & Nobie, M. Nature 303, 390-396 (1983).
- 30. Fontana, A., Dubs, R., Merchant, R., Balsiger, S. & Grob, P. J. J. Neuroimmun. 2, 55-71
- A., Otz, U., De Weck, A. L. & Grob, P. J. J. Neuroimmun. 2, 73-81 (1981).
- 32. Merrill, J. E. et al. Science 224, 1428-1430 (1984)
- 33. Benveniste, E. N. & Merrili J. E. Nature 321, 610-613 (1986).

Tumour necrosis factor α stimulates resorption and inhibits synthesis of proteoglycan in cartilage

Strangeways Research Laboratory, Worts' Causeway, Cambridge CB1 4RN, UK

During inflammatory reactions, activated leukocytes are thought to produce a variety of small proteins (cytokines) that influence the behaviour of other cells (including other leukocytes). Of these substances, which include the interleukins, interferons and tumour necrosis factors (TNFs), interleukin-1 (IL-1) has been considered potentially a most important inflammatory mediator because of its wide range of effects (reviewed in refs 1, 2). In vivo it is pyrogenic and promotes the acute phase response; in vitro it activates lymphocytes3 and stimulates resorption of cartilage4 and bone^{5,6}. Cartilage resorption is a major feature of inflammatory diseases such as rheumatoid arthritis, and IL-1 is the only cytokine hitherto known to promote it. TNFs are characterized by their effects on tumours and cytotoxicity to transformed cells⁷⁻⁹, but share some actions with IL-1. I report here that recombinant human TNF α stimulates resorption and inhibits synthesis of proteoglycan in explants of cartilage. Its action is similar to and additive with IL-1, and it is a second macrophage-derived cytokine whose production in rheumatoid arthritis, or inflammation generally, could contribute to tissue destruction.

Two human TNFs have been isolated: TNF α (refs 8, 9) is a product of activated mononuclear phagocytes, TNF β (ref. 7) of activated lymphocytes. The proteins show about 50% homology in nucleotide sequence and compete for a common class of receptors on the cervical carcinoma line ME-180 (ref. 10). TNF α is probably identical with cachectin¹¹, a factor that suppresses production of lipoprotein lipase in cultured adipocytes, and may play a part in the development of cachexia during infection¹². IL-1 shows some biological similarity to TNF: it is cytotoxic to certain transformed cells¹³ and it suppresses production of lipoprotein lipase in adipocytes¹⁴. Furthermore, cachectin has recently been shown to stimulate production of prostaglandins and latent collagenase by human synovial and dermal fibroblasts in a manner similar to IL-115. In view of these findings, I have investigated the effect of $TNF\alpha$ on both the resorption and synthesis of proteoglycan by explants of cartilage.

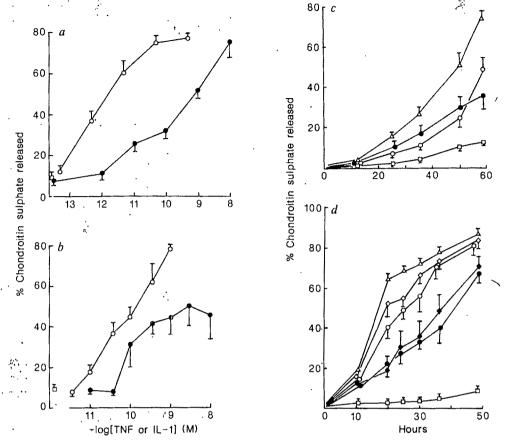
Chondroitin-sulphate-rich proteoglycan is an essential component of the matrix of cartilage since it enables the tissue to resist compression during load-bearing. Loss of proteoglycan, such as occurs in rheumatoid arthritis, osteoarthritis and other joint diseases, results in severe impairment of the function of cartilage. IL-1 is the only purified cytokine known to cause cartilage to degrade its proteoglycan4,16, and to inhibit resynthesis1

Figure 1a shows the amount of proteoglycan (measured as percentage of total chondroitin sulphate) released from porcine articular cartilage during 6 days of culture in the presence of human recombinant TNF α or pure porcine IL-1. The TNF α caused up to 75% of the proteoglycan to be released, although it was less potent than the IL-1, which was significantly active at a 20-fold lower dose (0.5 pM). Figure 1b shows a similar experiment carried out on cartilage from bovine nasal septum which was cultured for a shorter period (48 h): again, the IL-1 was more potent. The time dependence of the release of proteoglycan from bovine cartilage caused by sub-maximal concentrations of the two agents revealed that their effects were additive. Figure 1c shows that 50 pM IL-1 or 290 pM TNFα caused a similar rate of release, and that this was approximately doubled when the agents were combined. Maximal stimulation of cartilage by IL-1 caused more rapid release of proteoglycan than did TNF α (Fig. 1d): results for two concentrations of each cytokine demonstrate that responses were maximal. Supramaximal doses of the two agents in combination caused a rate of release that was considerably faster than that due to $TNF\alpha$ alone, but was not significantly greater than that seen with IL-1 alone. The failure of TNF α to augment the maximal response to IL-1 may be because the limit of the chondrocytes' ability to degrade their matrix in vitro was being approached.

The enzymatic mechanism by which the proteoglycan is degraded in cartilage is not understood. Normally, cartilage proteoglycans aggregate in a specific manner with hyaluronic acid, and it is thought that the large size of these aggregates causes them to be trapped in the matrix. Cartilage stimulated by IL-1 releases fragments of proteoglycan which, as judged by gel filtration, are smaller than normal proteoglycan monomers and are unable to aggregate with hyaluronic acid¹⁸. There is no evidence of degradation of their chondroitin sulphate chains. These changes suggest that degradation is by limited proteolysis of the protein core. The fragments of proteoglycan that were released by cartilage stimulated with TNF behaved similarly on gel filtration to those generated by stimulation with IL-1 (Fig. 2). The bulk of the fragments generated by stimulation with either agent emerged from a Sepharose 2B column at a region between the elution positions of intact proteoglycan and proteoglycan digested with papain (which consists largely of single-chain chondroitin sulphate peptides). Addition of hyaluronic acid to the proteoglycan fragments before chromatography caused little or no formation of aggregates. This suggested that the hyaluronate binding region was blocked or had been lost. When the proteolgycan fragments were chromatographed under dissociative conditions (4 M guanidine-HCl in the chromatographic buffer) the position of the main peak was unchanged. These experiments showed that chondrocytes activated by TNF or IL-1 caused a similar limited proteolysis of the proteoglycans.

In order to study the effect of TNF α on the synthesis of proteoglycan, cartilage was stimulated for 48 h, and 35SO₄ was added to the culture medium for the last 6 h. In this procedure the isotope becomes incorporated into newly synthesized sulphated glycosaminoglycan (mainly chondroitin sulphate). At the end of the experiment the medium and cartilage were digested with papain, and glycosaminoglycan was precipitated from the digests with cetylpyridinium chloride. The amount of radioactivity present in the precipitates was a measure of chondroitin sulphate (and, by inference, proteoglycan) synthesis. In experiments made with porcine articular (Fig. 3a) or bovine nasal septal (Fig. 3b) cartilages, TNF α caused a marked supFig. 1 Stimulation of release of proteoglycan from cartilage TNFα or IL-1. a, Porcine articular cartilage. The amount of chondroitin sulphate released was expressed as a percentage of the total (the content of the medium and tissue combined)21. Results are shown as means of quintuplicate cultures ± s.e.m. , TNF; \bigcirc , IL-1; \square , no addition. b, Bovine nasal septal cartilage. Symbols as for a. c, Time course for bovine cartilage disks cultured as in b with no addition (
), 50 pM IL-1 (O), 290 pM TNF (•), 50 pM IL-1 and 290 pM TNF in combination (A). Chondroitin sulphate released was measured at the indicated times and results are means ± s.e.m. of eight individual disk cultures. d, Time course for bovine cartilage discs cultured as in c, with no addition (□), 30 nM TNF (●), 90 nM TNF (♠), 1.5 nM IL-1 (O), 4.5 nM IL-1 (♦) and 90 nM TNF and 4.5 nM IL-1 in combination (\triangle).

Methods. a, Pieces of articular cartilage were removed from the metacarpal heads of freshly slaughtered young pigs. Pieces (~4 mg wet weight) were maintained for 48 h at 37 °C in CO₂/air 1:19 in culture medium [Dulbecco's modified. Eagle's medium (DMEM)] containing 5% normal bovine serum that had been heat-inactivated at 56 °C



for 30 min). Each was then transferred to a well of a 96-well multititre plate and incubated under the same conditions in 0.2 ml of culture medium, either with no addition, or with human TNF α or porcine IL-1 of pI 5. The medium was changed at 3 days and the culture was terminated after 6 days. Human TNF α was a recombinant protein expressed in Escherichia coli and purified as described previously^{7,22}. Porcine IL-1 was a natural leukocyte protein purified to homogeneity as described elsewhere¹⁶. The pI 5 form rather than the pI 8 form was used for these experiments. After culture the medium and cartilage were separated. The cartilage was digested completely with papain (see legend to Fig. 3). The chondroitin sulphate content of this digest and culture medium was estimated by use of the metachromatic dye, dimethylmethylene blue (Serva); whale chondroitin sulphate (Sigma) was used as a standard. b, Disks (2×1 mm) of cartilage were cut from the bovine nasal septa of freshly killed animals. Disks were precultured for 48 h and then stimulated for 48 h with TNF α or IL-1. The chondroitin sulphate content of medium samples and tissue digests was measured exactly as described for pig particular cartilage.

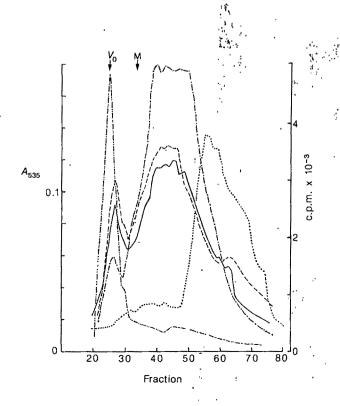


Fig. 2 Gel chromatography of proteoglycans released from stimulated cartilage. Samples of culture supernatants from stimulated bovine nasal cartilage were chromatographed on a column (930× 6.5 mm) of Sepharose 2B (Pharmacia) eluted with 0.5 M acetate buffer pH 5.8. Fractions (0.4 ml) were collected. Proteoglycan was detected as chondroitin sulphate by the dye dimethylmethylene blue (see Fig. 1) and is shown as A_{535} . — , Culture supernatant from bovine nasal cartilage cultured as in Fig. 1 in the presence of 5 nM TNF; ----, the same supernatant to which hyaluronic acid (2%) had been added before chromatography; ----, culture supernatant from cartilage stimulated with 0.5 nM porcine IL-1, and to which hyaluronic acid had been added before chromatography;, a papain digest of proteoglycan extracted from fresh cartilage by 4M guanidine-HCl. -.., proteoglycan (+2% hyaluronic acid) extracted by guanidine-HCl (4M) from unstimulated cartilage that had been biosynthetically labelled with 35SO4 for 24 h, measured as c.p.m. Arrows are: V_0 , void volume; M, elution position of 35SO4-labelled proteoglycan without addition of hyaluronic acid.

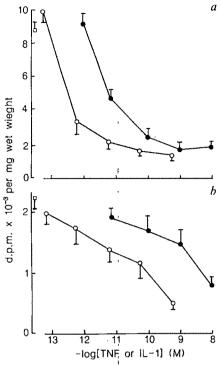


Fig. 3 Effects of TNFα or IL-1 on the incorporation of ³⁵SO₄ into glycosaminoglycans of cartilage. a, Porcine articular cartilage; b, Bovine nasal septal cartilage. Each assay point is the mean of five separate explants \pm s.e.m. \bullet , TNF α ; O, IL-1; \square , no addition. Methods. a, Pieces of pig articular cartilage were dissected, precultured and then stimulated either with TNF α or porcine IL-1 for 48 h exactly as described for Fig. 1, except that the culture medium (DMEM) contained 1% normal bovine serum (heat inactivated) during the stimulation period. For the last 6 h the medium was replaced with SO_4 -free culture medium (still containing $TNF\alpha$ or IL-1) to which was added 2.5 μ Ci ml⁻¹ of ³⁵SO₄ (25-40 Ci mg⁻¹; Amersham). After culture, the cartilage pieces were separated from the medium, briefly blotted to remove excess medium, and then weighted. Each piece was digested at 65 °C for 2 h.in 0.2 ml of 0.05 M sodium phosphate buffer pH 6.5 containing 1 mM EDTA, 2 mM N-acetylcysteine, 28 μg ml⁻¹ papain (Sigma Type III). Samples of medium (0.2 ml) were also digested with 0.1 ml of the papain solution under the same conditions. Chondroitin sulphate (0.1 ml of 2 mg ml⁻¹) was added to all the samples followed by 0.1 ml of cetylpyridinium chloride (10% w/v). Samples were centrifuged, the precipitates were washed twice in 3% cetylpyridinium chloride, then dissolved in 0.5 ml of formic acid and added to 5 ml of a scintillation mixture (Pico-fluor-30, Packard) and counted in a liquid scintillation counter. The radioactivity of the digests of tissue and medium were added together and the results expressed as d.p.m. per mg wet weight of cartilage. b, As for a except that disks of bovine nasal septal cartilage were used (see Fig. 1), and the culture medium contained 5% normal bovine serum throughout the experiment.

pression of proteoglycan production as judged the incorporation of ³⁵SO₄ into glycosaminoglycan, but was less potent than IL-1. The porcine IL-1 inhibited incorporation in porcine articular cartilage in the range 0.1-10 pM; TNF α was 20-fold less active. A similar differential was observed on the bovine cartilage. The lower potency of the human TNF α compared with porcine IL-1 may be due to species differences.

Taken together, the experiments demonstrate that TNF α has a similar action to IL-1 on chondrocytes. It causes them to degrade proteoglycan by limited proteolysis and inhibits their synthesis of new proteoglycan. Exposure of cartilage to either of these leukocyte products during inflammation could lead to loss of proteoglycan and impairment of function; furthermore, their effects may be additive.

Pigs¹⁶, like humans¹⁹, have two different IL-1 proteins: for these experiments the pI 5 IL-1 was used rather than the pI 8

form. The IL-1s are equipotent on cartilage16 and compete for the same receptors on porcine synovial fibroblasts: $TNF\alpha$ at 400 times excess over IL-1) did not compete for these receptors (T. A. Bird and J. S., in preparation). The augmentation of the effect of maximal doses of TNF α by IL-1 reported here is consistent with there being different receptors on chondrocytes for the two cytokines. Since they are apparently not homologous^{8,16}, IL-1 and $TNF\alpha$ would be expected to combine with different receptors. These considerations suggest that chondrocytes (and probably other connective tissue cells) could have two distinct types of receptor (one for IL-1 and one for TNF) whose interaction with ligand promotes resorption of matrix polymers while inhibiting their synthesis. Such a possibility could have important implications for the pharmacological control of inflammatory tissue destruction.

Following submission of this manuscript, Bertolini et al.20 have reported that human TNFs, like IL-1, stimulated Ca2+ release from fetal rat bones.

I thank Dr M. Palladino (Genentech) for supplying TNF, Dr C. A. Dinarello (Tufts University) for suggesting the experiments, Dr J. Tyler (Strangeways Laboratory) for doing the gel chromatography, Mrs V. Curry and Mrs J. Mason for technical help, and the Arthritis and Rheumatism Council for financial support.

Received 11 February: accepted 20 May 1986

- Dinarello, C. A. Rev. infect. Dis. 6, 51-95 (1984).
 Durum, S. K., Schmidt, J. A. & Oppenheim, J. J. A. Rev. Immun. 3, 263-287 (1985).
 Mizel, S. B. Immun. Rev. 63, 51-72 (1982).
- Saklatvala, J., Pilsworth, L. M. C., Sarsfield, S. J., Gavrilovic, J. & Heath, J. K. Biochem. J. 224, 461-466 (1984).
- Gowen, M., Wood, D. D., Ihrie, E. J., McGuire, M. K. B. & Russell, R. G. G. Nature 306, 378-380 (1983).
- Heath, J. K., Saklatvala, J., Meikle, M. C. Atkinson, S. J. & Reynolds, J. J. Calc. Tiss. Int. 37, 95-97 (1985).
- 7. Gray, P. W. et al. Nature 312, 712-724 (1984). 8. Pennica, D. et al. Nature 312, 724-728 (1984). 9. Wang, A. M. et al. Science 228, 149-154 (1985)
- Aggarwal, B. B., Eessalu, T. E. & Hass, P. E. Nature 318, 665-667 (1985).
 Beutler, B. et al. Nature 316, 552-554 (1985).
- 12. Beutler, B., Mahoney, J., Le Trang, N., Pekala, P. & Cerami, A. J. exp. Med. 161, 984-995 (1985).
- 13. Onozaki, K., Matsushima, K., Aggarwal, B. B. & Oppenheim, J. J. J. Immun. 135, 3962-3968
- Beutler, B. A. & Cerami, A. J. Immun. 135, 3969-3971 (1985).
- Beutier, B. A. & Cetanii, A. J. Immun. 123, 3799-3971 (1963).
 Dayer, J.-M., Beutler, B. A. & Cerami, A. J. exp. Med. 162, 2163-2168 (1985)
 Saklatvala, J., Sarsfield, S. J. & Townsend, Y. J. exp. Med. 162, 1208-1222 (1985).
 Tyler, J. A. Biochem. J. 227, 869-878 (1985).
 Tyler, J. A. Biochem. J. 225, 493-507 (1985).

- 19. March, C. J. et al. Nature 315, 641-647 (1985).
- Bertolini, D. R., Nedwin, G. E., Bringman, T. S., Smith, D. D. & Mundy, G. R. Nature 319, 516-518 (1986).
- Saklatvala, J. Biochem. J. 199, 705-714 (1981).
 Aggarwal, B. B. et al. J. biol. Chem. 260, 2345-2355 (1985).

Post-translational insertion of a fragment of the glucose transporter into microsomes requires phosphoanhydride bond cleavage

Mike Mueckler*‡ & Harvey F. Lodish*†

- * Whitehead Institute for Biomedical Research,
- Nine Cambridge Center, Cambridge, Massachusetts 02142, USA
- † Department of Biology, Massachusetts Institute of Technology,
- Cambridge, Massachusetts 02139, USA
- ‡ Present address: Department of Cell Biology and Physiology, Washington University School of Medicine, St Louis, Missouri 63110,

Most eukaryotic secretory and membrane proteins insert co-translationally into the membrane of the rough endoplasmic reticulum (RER), and are targeted there by one or more NH2-terminal or internal signal sequences (for reviews see refs 1, 2). However, little is known about the actual translocation and membrane integration processes. In particular, any energy requirements for targeting and integration have remained obscure because of the inability to uncouple the processes from concomitant protein synthesis. We recently showed that the human glucose transporter (GT), an integral membrane glycoprotein³, can insert post-translationally into dog pancreatic microsomes with low but demonstrable efficiency in vitro, and that a fragment corresponding to the NH2-terminal 340 amino acids and 8 of the 12 membrane-spanning α -helixes of GT (GT-N) can insert with significantly greater efficiency⁴. We report here that post-translational insertion of GT-N into pancreatic microsomes requires energy in the form of a phosphodiester bond, and suggest that co-translational insertion of proteins into the RER may also require energy independent of that used for polypeptide synthesis.

From experiments using in vitro translation and membrane translocation⁵⁻⁸, Walter and Blobel^{1,8} proposed the following sequence of events for the targeting of proteins for translocation across the RER membrane. Initiation of synthesis of a secretory polypeptide starts on a messenger RNA-ribosome complex free in the cytosol. The emergence of an N-terminal signal sequence from the large ribosomal subunit triggers the binding of cytosolic signal recognition particle (SRP) and arrest of polypeptide chain elongation. The complex then binds to the surface of the RER via a transient interaction between SRP and the membranebound SRP receptor⁹⁻¹¹ (docking protein¹²). Integral membrane proteins¹³⁻¹⁷ which may possess one or more^{4,13} N-terminal or internal signal sequences also utilize this targeting process, although specific arrest of polypeptide chain elongation by SRP does not always occur during translation in vitro4,14. Subsequent events in the translocation/integration process remain obscure. particularly whether the nascent chain traverses the membrane through an aqueous pore^{5,18} or directly through the fatty acyl core of the lipid bilayer19.

To investigate the energetics of membrane protein insertion, we used a recently developed in vitro assay in which efficient insertion into RER membranes of a fragment of the human glucose transporter, corresponding to the NH₂-terminal 340 amino acids (GT-N), is uncoupled from protein synthesis⁴.

RNA was transcribed from a SP65 plasmid construction encoding GT-N and used as a template for the synthesis of GT-N in a reticulocyte cell-free translation system. GT-N can insert post-translationally into dog pancreatic microsomes with a conformation resembling that of the corresponding region of the native membrane-bound protein⁴. Figure 1a shows that 50% of GT-N inserted into microsomes is added post-translationally, as monitored by the appearance of the 36,000 (36K) relative molecular mass (M_r) glycosylated form of the polypeptide (GT-N₁) (Fig. 1a, lane 2). Additionally, trypsin digestion of pancreatic microsomes generates the appropriate fragment containing the first six membrane-embedded helices of GT^{3,4} (Fig. 1b, lane 8). The addition of glucose (Fig. 1a, lane 3), hexokinase (lane 4) or glucose 6-phosphate (lane 6) alone had a negligible effect on post-translational insertion; in contrast, depletion of ATP by the addition of both glucose and hexokinase effectively abolished insertion (Fig. 1a, lane 5, Fig. 1b, lanes 3, 6). Because yeast hexokinase can use other purine nucleoside triphosphates as cofactors, although with less efficiency than when using ATP²⁰, we cannot conclude that the observed effect is due solely or directly to the depletion of ATP.

Figure 1b shows that post-translational insertion of GT-N in ATP-depleted extracts could be reconstituted by the addition of excess creatine phosphate. This is demonstrated by the appearance in pelleted microsomes of glycosylated GT-N after the microsomes have been washed in a neutral buffer (Fig. 1b, compare lane 4 with lanes 2 and 3). When the microsomes are washed in buffer at alkaline pH, peripherally associated membrane proteins as well as the vesicle contents are extracted, so that only integral membrane proteins sediment with the microsomes $^{21-23}$. By this criterion, insertion of GT-N into the lipid bilayer was restored after addition of excess creatine phosphate (Fig. 1b, compare lane 7 with lanes 5 and 6). This is also demonstrated by the generation of the glycosylated 22K NH₂-terminal fragment of GT^4 after the addition of excess creatine

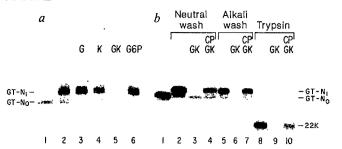


Fig. 1 Membrane insertion of GT-N is inhibited by depletion of nucleoside triphosphates. Synthesis of GT-N mRNA using SP6 RNA polymerase and synthesis of 35S-methionine-labelled GT-N in a reticulocyte cell-free system have been described previously4. Translation was allowed to proceed at 30 °C for 90 min (45 min after net protein synthesis was complete). a, After translation 1 mM cycloheximide was added, sufficient to inhibit incorporation of ⁵S-methionine into GT-N protein by >99% (data not shown). The translation mixture was divided into five 25-µl aliquots and then incubated at 30 °C for 10 min without any additions (lane 2). with 5 mM glucose (lane 3), 1.4 U of yeast hexokinase (lane 4), 5 mM glucose and 1.4 U of hexokinase (lane 5), or with 5 mM glucose 6-phosphate (lane 6). Dog pancreatic rough microsomes (3 equiv.²⁹) were then added and incubation was continued for) were then added and incubation was continued for 20 min. The microsomes were sedimented by centrifugation for 20 min in an Eppendorf microfuge, resuspended in 50 µl of 0.25 M STBS (0.25 M sucrose, 10 mM Tris-Cl pH 7.5, 150 mM NaCl), and re-sedimented. The membrane pellets were dissolved directly in sample buffer and analysed on a 12% polyacrylamide gel using the systems of Laemmli³⁰. Aliquots $(5 \, \mu l)$ of translation reaction to which microsomes were not added were analysed in lane 1; this is the 100% value used here and in subsequent figures to calculate per cent insertion. The gel was washed for 30 min in 10% trichloroacetic acid, 30% isopropanol, treated with Enlightening autoradiography enhancer (Dupont-NEN), dried and exposed to Kodak XAR-5 film for 1 h. b, After translation the reaction was adjusted to 1 mM cycloheximide and 50 µg ml⁻¹ of RNase A and then divided into 20-µl aliquots. Samples were incubated as described above with no additions (lanes 1, 2, 5, 8) or after addition of 5 mM glucose and 1.4 U of hexokinase (lanes 3, 4, 6, 7, 9, 10). Creatine phosphate (20 mM) was then added to some samples (lanes 4, 7, 10) followed by the addition of microsomes (3 equiv.²⁹ per 20-µl reaction; lanes 2-10). After 20 min incubation, the microsomes were sedimented as described above and washed in 0.25 M STBS (lanes 2-4 and 8-10) or 0.25 M STBS adjusted to pH 11.5 with NaOH (lanes 5-7), then analysed as described above. Aliquots (5 µl) of translation reaction to which microsomes were not added were analysed in lane 1. Abbreviations used are: G, 5 mM glucose; K, 1.4 U hexokinase; GK, glucose and hexokinase; CP, 20 mM creatine phosphate; G6P, 5 mM glucose 6-phosphate; GT-N₀, unglycosylated GT-N; GT-N₁, glycosylated GT-N.

phosphate followed by trypsin digestion of the microsomes (Fig. 1b, compare lane 10 with lanes 8 and 9).

After depletion of ATP under the conditions used in these experiments, variable amounts of unglycosylated GT-N sedimented with washed microsomes (Fig. 1a, lane 5; Fig. 1b, lane 3). Only a small fraction of this is due to nonspecific pelleting of GT-N in the absence of microsomes (data not shown). Thus, we do not know whether targeting of GT-N to microsomes is energy dependent.

Figure 2 shows that, after translation, removal of low- M_r components from the lysate by gel filtration inhibits post-translational insertion, as monitored by the appearance of glycosylated GT-N associated with the microsomes (Fig. 2, compare lanes 2 and 3). Addition of 1 mM Mg-ATP (Fig. 2, lane 4) or 10 mM Mg-ATP (Fig. 2, lane 5) to the lysate after gel filtration restored the appearance of glycosylated GT-N. The non-hydrolysable β , γ -methylene ATP analogue did not promote insertion of GT-N, and inhibited the residual insertion observed after gel filtration of the lysate (Fig. 2, compare lane 6 with lanes 2 and 3).

In this assay, ATP and GTP are equally effective in promoting insertion; UTP and CTP are less effective (data not shown).

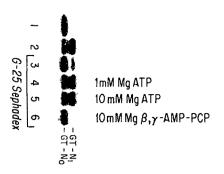


Fig. 2 ATP restores membrane insertion of GT-N in gel-filtered lysates. After synthesis of GT-N in a reticulocyte lysate, as described in Fig. 1 legend, the lysate (100 µl) was adjusted to 1 mM cyclohexamide and centrifuged through two successive 0.9 ml Sephadex G-25 columns equilibrated in column buffer (50 mM HEPES pH 7.5, 5% glycerol, 0.1 M KAc, 5 mM MgAc, 2 mM dithiothreitol, 1% bovine serum albumin, 1 mM TPCK and TLCK, 1 mM cycloheximide). The gel-filtered lysate was then treated with 50 μg ml⁻¹ RNase A for 10 min at 30 °C. Microsomes were then added (3 equiv.29) to 25-µl aliquots without any additions (lane 3) or with 1 mM MgAc-ATP (lane 4), 10 mM MgAc-ATP (lane 5) or 10 mM MgAc-AMP-PCP (lane 6) and incubated for an additional 30 min. The microsomes were sedimented by centrifugation in an Eppendorf microcentrifuge for 20 min, resuspended and washed in 0.25 mM sucrose, 50 mM Tris-Cl pH 7.5, 25 mM KAc, 5 mM MgAc, and analysed by polyacrylamide gel electrophoresis as described in Fig. 1 legend. Aliquots (5 µl) of lysate to which microsomes were not added were analysed in lane 1. A microsomal fraction added to 25 µl of unfiltered lysate was analysed in lane 2.

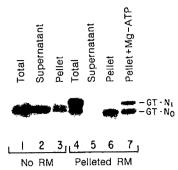


Fig. 3 Only GT-N associated with ribosomes acts as a substrate for membrane insertion. GT-N was synthesized in a reticulocyte lysate as described in Fig. 1 legend. The lysate was then adjusted to 1 mM cycloheximide and fractionated into a ribosomal pellet and a post-ribosomal supernatant by centrifugation for 30 min at 300,000 g in a Beckman TL-100.2 rotor. The ribosomal pellet was resuspended in a volume of column buffer (see Fig. 2 legend) equal to that of the original lysate. Rough microsomes (RM, 3 equiv.²⁹) were then added to aliquots of the unfractionated lysate, postribosomal supernatant and resuspended ribosomes. The sedimented microsomal fractions were then washed and analysed by polyacrylamide gel electrophoresis as described in Fig. 2 legend. Lane 1, 5 µl of unfractionated lysate; lane 2, 5 µl of post-ribosomal supernatant; lane 3, 5 µl of resuspended ribosomes; lane 4, microsomes from 25 µl of unfractionated lysate; lane 5, microsomes from 25 µl of post-ribosomal supernanant; lane 6, microsomes from 25 µl of resuspended ribosome fraction; lane 7, microsomes from 25 µl of resuspended ribosome fraction supplemented with 5 mM MgAc-ATP.

Because enzymes that catalyse the transfer of phosphate from one nucleotide to another (for example, nucleoside diphosphate kinase) may well be present in these crude extracts, and the removal of low- M_r components may not be quantitative, we do not know which nucleotide (or other high-energy phosphate compound) is the proximal source of energy.

Under the washing conditions used in this experiment (25 mM potassium acetate, 5 mM magnesium acetate), a considerable fraction of unglycosylated GT-N sedimented with the microsomes. Only a small fraction of the non-glycosylated GT-N was inserted, since most could be removed by alkali extraction (data not shown). Whether the alkali-labile fraction represents a genuine intermediate in membrane insertion, or simply an adventitious association of the unintegrated protein with the microsomes, is not known.

The GT-N mRNA used in these experiments lacks a termination codon, so that proper polypeptide chain termination and release of the completed polypeptide should not occur. Surprisingly, Fig. 3 shows that about 75% of GT-N synthesized was recovered in a post-ribosomal supernatant (compare lanes 2 and 3) and presumably represents completed and released polypeptides. The remaining 25% of GT-N sedimented with ribosomes and presumably is a completed peptidyl-transfer RNA-ribosome complex. Supporting this latter point is the observation that the yield of GT-N in the ribosomal fraction was reduced by at least 50% if the lysate was incubated with puromycin before sedimenting the ribosomes (data not shown). In this experiment about 25% of GT-N in the unfractionated lysate inserted post-translationally into the microsomes (Fig. 3, lane 4). The GT-N in the post-ribosomal supernatant did not insert (Fig. 3, lane 5). As monitored by the appearance of glycosylated GT-N, very little GT-N in the resuspended ribosomal pellet inserted in the absence of added ATP (Fig. 3, lane 6). Insertion was increased by including ATP in the buffer (Fig. 3, lane 7). Adding a ribosome fraction obtained from reticulocyte lysate not programmed with mRNA to the GT-N in the post-ribosomal supernatant did not reconstitute insertion, indicating that the lack of insertion of released GT-N was not due to the lack of

a soluble factor that sedimented with the ribosomes (data not shown). Thus, the behaviour of GT-N is unlike that of the intact GT, which can insert (with a lower efficiency) into microsomes as a completed polypeptide⁴.

One possible explanation for these observations is that glycosylation of GT-N does not occur in the absence of ATP, and that glycosylation is necessary for insertion. Several considerations argue against this interpretation. Insertion of other proteins into membranes both in vivo and in vitro does not require Asn-glycosylation (see, for example, ref. 24). In our system, glycosylation is unaffected by concentrations of tunicamycin in vast excess of that required to inhibit formation of GlcNAc-P-Pdolichol in vivo and in vitro (our unpublished observations), indicating that de novo synthesis of the dolichol-core oligosaccharide is not required. Furthermore, significant glycosylation of GT-N is observed in the absence of nucleoside sugars (which should not be present at significant levels after gel filtration of lysate or in the resuspended ribosomal fraction: see Figs 2, 3), indicating that elongation of GlcNAc-P-P-dolichol is not required in our system. Thus, sufficient preformed core oligosaccharide-dolichol donor must be be present in our microsomal preparation, and transfer of the core oligosaccharide from the dolichol donor to asparagine residues does not require a nucleotide cofactor²⁵.

Our observations suggest that targeting and/or insertion of GT-N into pancreatic microsomes is dependent on energy in the form of a nucleotide triphosphate cofactor. Whether this dependence involves known factors in the targeting process, or an as yet unknown factor or factors involved in translocation, remains to be determined. Since no ionophore tested (monensin, gramicidin, A23187) blocks insertion (not shown), we feel that hydrolysis of a phosphoanyhdride bond is not used to generate an electrochemical potential across the ER membrane which is in turn used to power translocation. In this respect, post-translational insertion into RER membranes is different from energy-dependent translocation across the bacterial²⁶ or mitochondrial²⁷ inner membrane and sim ilar to polypeptide import into chloroplasts²⁸. We speculate that co-translational insertion of

membrane and secretory proteins into or across the RER also requires energy in addition to that consumed in protein synthesis. This could involve an ATP- or GTP-driven translocase that is part of a transmembrane channel^{5,11} through which the nascent polypeptide moves.

This research was supported by NSF grant CDR8500003 and NIH grants AI 22347. M.M. was a postdoctoral fellow of the Damon Runyon-Walter Winchell Cancer Fund (DRG-711).

Received 10 February; accepted 25 April 1986.

- Walter, P., Gilmore, R. & Blobel, G. Cell 38, 5-8 (1984).
 Wickner, W. T. & Lodish, H. F. Science 230, 400-407 (1985).
 Mueckler, M. et al. Science 229, 941-945 (1985).

- Mueckler, M. & Lodish, H. F. Cell 44, 629-637 (1986).
 Bobel, G. & Dobberstein, B. J. Cell Biol, 67, 835-851 (1975)
- Walter, P., Ibrahimi, I. & Blobel, G. J. Cell Biol. 91, 545-550 (1981).
- Walter, P. & Blobel, G. J. Cell Biol. 91, 551-556 (1981). Walter, P. & Blobel, G. J. Cell Biol. 91, 557-561 (1981).
- Gilmore, R., Blobel, G. & Walter, P. J. Cell Biol. 95, 463-469 (1982).
 Gilmore, R., Walter, P. & Blobel, G. J. Cell Biol. 95, 463-469 (1982).

- Gilmore, R. & Blobel, G. Cell 35, 677-685 (1983).
 Meyer, D. I., Krause, E. & Dobberstein, B. Nature 297, 647-650 (1982).
- Friendlander, M. & Blobel, G. Nature 318, 338-343 (1985).
- 14. Anderson, D. J., Mostov, K. E. & Blobel, G. Proc. natn. Acad. Sci. U.S.A. 80, 7249-7253
- Anderson, D. J., Walter, P. & Blobel, G. J. Cell Biol. 93, 501-506 (1982).
 Rottier, P., Armstrong, J. & Meyer, D. I. J. biol. Chem. 260, 4648-4656 (1985).
 Spiess, M. & Lodish, H. F. Cell 44, 177-185 (1986).
 Gilmore, R. & Blobel, G. Cell 42, 497-505 (1985).

- Olmore, R. & Blobel, G. Cell 42, 497-303 (1983).
 Engelman, D. M. & Steitz, T. A. Cell 23, 411-422 (1981).
 Hohnadel, D. C. & Cooper, C. Eur. J. Biochem. 31, 180-185 (1972).
 Steck, T. L. & Yu, J. J. supramolec. Struct. 1, 220-232 (1973).
 Mostov, K. E., DeFoor, P., Fleischer, S. & Blobel, G. Nature 292, 87-88 (1981).
 Fujiki, Y., Fowler, S., Shio, H., Hubbard, A. & Lazarow, P. J. Cell Biol. 93, 103-110 (1982).
- Rothman, J. E., Katz, F. N. & Lodish, H. F. Cell 15, 1447-1454 (1978).
 Das, R. C. & Heath, E. C. Proc. natn. Acad. Sci. U.S.A. 77, 3811-3815 (1980).
- Bakker, E. P. & Randall, L. L. EMBO J. 3, 895-900 (1984)
- 27. Gasser, S., Daum, G. & Schatz, G. J. biol. Chem. 257, 13034-13041 (1982).
- Grossman, A., Bartlett, S. & Chua, N.-H. Nature 285, 625-628 (1980).
 Walter, P. & Blobel, G. Meth. Enzym. 96, 682-691 (1983).
- 30. Laemmli, U. K. Nature 227, 680-685 (1970).

Role of ion flux in the control of c-fos expression

James I. Morgan* & Tom Curran†

Departments of * Neurosciences and † Molecular Oncology, Roche Institute of Molecular Biology, Roche Research Center, Nutley, New Jersey 07110, USA

There has been much interest in the biochemical and biophysical processes that couple extracellular signals to alterations in gene expression. While many early events associated with the treatment of cells with growth factors have been described (for example, ion flux and protein phosphorylation^{1,2}), it has proved difficult to establish biochemical links to gene expression. Recently, the study of such genomic control signals has been facilitated by the demonstration that the c-fos proto-oncogene is rapidly and transiently induced by treatment of several cell types with polypeptide growth factors and other growth modulating substances³ one particular system it has been shown that nerve growth factor (NGF) causes a transient induction of c-fos in the phaeo-chromocytoma cell line PC12, within 15 min⁹⁻¹¹. Furthermore, the magnitude of this induction can be modulated with pharmacological agents such as peripheral-type benzodiazepines (BZDs)9. Thus, the study of c-fos expression in PC12 cells could yield valuable clues to the coupling mechanisms linking cell surface activation to genomic events. Here we demonstrate that c-fos is induced in PC12 cells either by receptor-ligand interaction or by agents or conditions that effect voltage-dependent calcium channels.

In the following experiments the synthesis of the c-fos protein has been monitored by immunoprecipitation after metabolic labelling with 35S-methionine. For quantitative analysis, immunoprecipitates from equivalent amounts of cell lysate, as

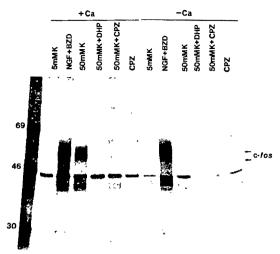


Fig. 1 Induction of c-fos protein by 50 mM potassium is calciumand calmodulin-dependent. PC12 cells were incubated in basal medium with the following additions: 5 mM potassium chloride (5 mM K), 200 ng ml⁻¹ NGF plus 100 μM benzodiazepine (7-3351) (NGF+BZD), 50 mM potassium chloride (50 mM K), 50 mM potassium chloride plus 15 µM dihydropyridine (nisoldipine, 1,4dihydro-2,6-dimethyl-4-(2-nitrophenyl)-3,5-pyridenedicarboxylate) (50 mM K+DHP), 50 mM potassium chloride plus 30 μ M chlorpromazine (50 mM K+CPZ) or 30 µM chlorpromazine (CPZ), in the presence (+Ca) or absence (-Ca) of 1.1 mM calcium chloride. The drugs chlorpromazine and nisoldipine were added to cultures 5 min before the other reagents. In the experiment shown, nisoldipine was used at a saturating concentration (15 μM), however, 50 nM nisoldipine also attenuated potassium-induced c-fos expression (data not shown). Incubation was continued for 30 min at 37 °C then 300 μCi ml⁻¹ ³⁵S-methionine (≈800 μCi mmol⁻¹; Amersham) was added for a further 15 min. Extracts were prepared and immunoprecipitated with fos-specific antibodies. The immunoprecipitation products from 107 c.p.m. of TCA-insoluble proteins were analysed by SDS-polyacrylamide gel electrophoresis (SDS-PAGE). Arrows indicate the position of the c-fos protein. The numbers on the left indicate the relative molecular masses $(M_r s)$ of the ¹⁴C-methylated marker proteins (Amersham). Methods. PC12 cells³³ were cultured in RPMI medium (Gibco) containing 10% horse serum, 5% calf serum and 4 mM Lglutamine. For experimentation, cells were seeded onto 35-mm Petri dishes (Falcon) and allowed to attach and proliferate for 48 h. Immediately before experimentation this medium was removed and replaced with 1 ml of incubation buffer (basal

medium) or 1 ml of Dulbecco-Vogt modified Eagle's medium (DMEM) lacking methionine. Basal medium comprised 20 mM HEPES, 146 mM NaCl, 4.2 mM KCl, 0.5 mM MgCl₂ and 0.2% D-glucose. Preparation of cell lysates, immunoprecipitation, SDS-PAGE and fluorography were as described previously^{6,34,35}. The fos-specific antibodies used were affinity-purified against a peptide predicted from the c-fos nucleotide sequence³⁴

measured by trichloroacetic acid (TCA)-insoluble radioactivity, were compared. Care was taken to ensure that the various treatments did not result in more than a 50% reduction of 35S-methionine incorporation as some inhibitors of protein synthesis can cause an accumulation of c-fos messenger RNA^{3,4,6}. Dose-response analyses were performed for all the agents used so as to obtain the maximal specific effect of each.

We demonstrated previously that NGF induces c-fos in PC12 cells and that this effect is enhanced in the presence of peripherally active BZDs9. Chronic depolarization of PC12 cells due to an increased extracellular potassium concentration has also been shown to influence neurite growth in a calciumdependent manner^{12,13} and to induce c-fos expression^{10,11} (Fig. 1). Thus, we asked whether NGF and elevated K⁺ induce c-fos via the same mechanism. Figure 1 shows that the superinduction of c-fos by NGF plus benzodiazepine is independent of extracellular calcium, as is NGF induction of c-fos (Fig. 2b).

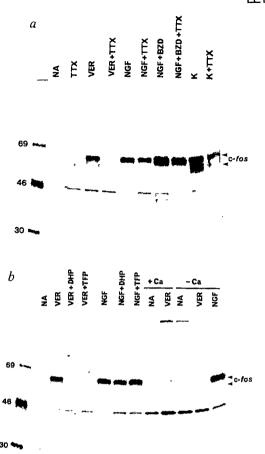


Fig. 2 Veratridine-mediated depolarization induces synthesis of c-fos protein. a, PC12 cells were incubated in methionine-free DMEM with the following additions: no addition (NA), 3 µM tetrodotoxin (TTX), 200 μM veratridine (VER), 200 μM veratridine plus 3 μ M TTX, 200 ng ml⁻¹ nerve growth factor (NGF), 200 ng ml⁻¹ NGF plus 3 μ M TTX, 200 ng ml⁻¹ NGF plus 100 μ M benzodiazepine (7-3351) (NGF+BZD), 200 ng ml⁻¹ NGF plus 100 µM benzodiazepine (7-3351) plus 3 µM TTX (NGF+ BZD+TTX), 50 mM potassium (K), or 50 mM potassium plus 3 μM TTX (K+TTX) for 30 min before labelling with methionine. b, PC12 cells were incubated in methionine-free DMEM containing: no additions (NA), 200 µM veratridine (VER), $200\,\mu M$ veratridine plus $15\,\mu M$ dihydropyridine (nisoldipine) (VER+DHP), 200 µM veratridine plus 15 µM trifluoperazine (VER+TFP), 200 ng ml⁻¹ NGF, 200 ng ml⁻¹ NGF+15 µM dihydropyridine (NGF+DHP), or 200 ng ml⁻¹ NGF plus 15 μM trifluoperazine (NGF+TFP); in basal medium with: no additions (NA), or 200 µM veratridine (VER) in the presence of 1.1 mM calcium chloride (+Ca); and in basal medium with no additions (NA), $200 \,\mu\text{M}$ veratridine (VER) or $200 \,\text{ng ml}^{-1}$ NGF in the absence of calcium (-Ca). ³⁵S-methionine labelling, preparation of cell lysates, immunoprecipitation and SDS-PAGE were as described in Fig. 1 legend. The numbers on the left indicate the Mrs of marker proteins. Arrows indicate the position of the c-fos protein. Tetrodotoxin, nisoldipine and trifluoperazine were added 5 min before incubation with the other agents.

In contrast, elevated potassium induces c-fos only when calcium is present in the extracellular environment (Fig. 1); this suggests that depolarizing concentrations of potassium induce c-fos by provoking an influx of calcium ions, presumably via voltage-dependent calcium channels. This interpretation is supported by the finding that the 1,4-dihydropyridine calcium channel antagonist nisoldipine (DHP)¹⁴ completely blocks potassium-induced c-fos expression (Fig. 1), consistent with the known ability of nisoldipine to block potassium-stimulated calcium uptake into PC12 cells¹⁵. In contrast, the induction of c-fos

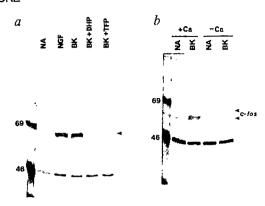


Fig. 3 Stimulation of c-fos expression by the calcium channel agonist BAY K 8644. a, PC12 cells were incubated in methionine-free DMEM containing: no additions (NA), 200 ng ml⁻¹ NGF, 300 nM BAY K 8644 (BK), 2.5 μM BAY K 8644 plus 15 μM dihydropyridine (nisoldipine) (BK+DHP) or 2.5 μM BAY K 8644 plus 15 μM trifluoperazine (BK+TFP). b, PC12 cells were incubated in basal medium with either no additions (NA) or 2.5 μM BAY K 8644 (BK) in the presence (+Ca) or absence (-Ca) of 1.1 mM calcium chloride. The numbers on the left indicate the M_rs of marker proteins. Arrows indicate the position of the c-fos protein. Nisoldipine and trifluoperazine were added (where indicated) 5 min before incubation with the other agents. BAY K 8644 (methyl 1,4-dihydro-2,6-dimethyl-3-nitro-4-(2-trifluoromethylphenyl)-pyridine-5-carboxylate) was synthesized by the research division of Hoffmann-La Roche Inc.

protein (NGF+DHP, Fig. 2b) and mRNA (data not shown) by NGF is insensitive to dihydropyridine treatment.

The depolarization-induced calcium influx (via the voltagedependent calcium channels) appears to elicit c-fos expression by an interaction with calmodulin since chlorpromazine (CPZ), a calmodulin antagonist¹⁶, blocks the action of elevated potassium (see Fig. 1, 50 mM K+CPZ). This notion was further corroborated using another calmodulin inhibitor, trifluoperazine (TFP)¹⁶, which also blocks K⁺-induced c-fos expression (data not shown). These agents did not reduce the level of c-fos after treatmenet with either NGF or 12-O-decanoylphorbolmyristic acetate (PMA) (data not shown). As PMA presumably acts via protein kinase C17, the lack of effect of either CPZ or TFP on this response suggests that the drugs are targeting calmodulin and not protein kinase C, their alternative site of action 18. The more specific calmodulin inhibitor W7 (N-(6-aminohexyl)-5chloro-1-naphthalenesulphonamide¹⁹) clearly veratridine-induced c-fos expression but did not affect NGF induction of c-fos (data not shown). Thus, the available evidence points to calmodulin having a role as a mediator in the coupling mechanism of one group of inducers. These observations emphasize further the mechanistic dichotomy between induction of c-fos by NGF and by elevated potassium.

An alternative method of depolarizing PC12 cells is to use the alkaloid veratridine which holds voltage-dependent sodium channels in their open state^{20,21}. Veratridine, like elevated potassium, provokes an induction of c-fos in a dose-dependent manner (Fig. 2a (VER), and data not shown). This action of veratridine is mediated by the well-characterized adult form of the voltage-dependent sodium channel as it is antagonized by tetrodotoxin (TTX)²² (see Fig. 2a). It has been reported that PC12 cells do not exhibit voltage-sensitive sodium currents in the absence of NGF²³. Thus, our data may have two interpretations. First, this may reflect a fundamental difference between the PC12 cells in various laboratories. Second, PC12 cells may contain a class of TTX-sensitive sodium channels that can be activated only by veratridine. We noted that tetrodotoxin blocks veratridine-induced c-fos expression and is much less effective at reducing the level of c-fos observed following treatment with NGF or other agents, thus precluding a nonspecific inhibition

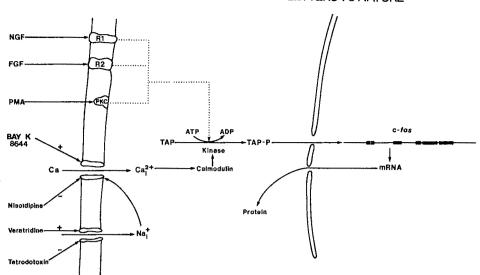


Fig. 4 Schematic representation of the molecular events involved in c-fos induction. The figure includes a summary of the data presented in Figs 2 and 3. The action of ion-channel agonists (+) and antagonists (-) is indicted.

(Fig. 2a). Veratridine stimulation of c-fos expression, like that of elevated potassium, is also calcium-dependent and is blocked by both nisoldipine and antagonists of calmodulin (Fig. 2b). Thus, depolarization of PC12 cells, either by abolishing the ion gradient for potassium or by specifically holding voltage-dependent sodium channels in their open state, results in c-fos induction. The second-messenger coupling mechanism is the same in both instances and seems to involve activation of voltage-dependent calcium channels with a subsequent interaction of calcium with the calmodulin system.

The next question to be addressed is whether the opening of calcium channels alone can lead to induction of c-fos. This proposition was tested using the calcium channel agonist BAY K 8644 (ref. 24), which stimulates calcium uptake in PC12 cells²⁵ and is a potent inducer of c-fos expression in these cells; at a concentration of 300 nM, it elicits the same response as 200 ng ml⁻¹ of NGF (see Fig. 3a). Stimulation of c-fos expression by BAY K 8644 occurs only in the presence of extracellular calcium (Fig. 3b) and is blocked by both nisoldipine and the calmodulin inhibitor trifluoperazine (Fig. 3a). Thus, the action of BAY K 8644 mimics that of extracellular potassium and veratridine treatment both qualitatively and quantitatively. It has been demonstrated recently that BAY K 8644 opens only a limited population of voltage-dependent calcium channels (the so-called long-term or L channels) in dorsal root ganglion neurones²⁶; this suggests that a very specific gated calcium signal is responsible for c-fos activation.

The data presented here demonstrate a close link between the biophysical processes involved in neuronal excitation and gene transcription. In particular, the results show that agents or conditions that modify the open time of voltage-dependent calcium channels can modulate expression of the fos protooncogene. Figure 4 depicts a model of the sequence of events that couple these agents to the transcriptional activation of c-fos. Depolarization of PC12 cells with elevated potassium or veratridine results in prolonged opening of voltage-dependent calcium channels, based on three lines of evidence. First, both of these agents require extracellular calcium to induce c-fos. Second, both veratridine- and potassium-induced c-fos expression are blocked by voltage-dependent calcium channel antagonists such as nisoldipine. Third, a known agonist for the voltage-dependent calcium channel, BAY K 8644, induces c-fos directly. Thus, while veratridine and potassium influence the movement of several ionic species across the plasma membrane, the opening of the calcium channel is the common denominator in the cascade of events that result in c-fos induction. Activation of the voltage-dependent calcium channel then leads to an influx of calcium ions. This supposition is based on the fact that veratridine, elevated potassium and BAY K 8644 all require extracellular calcium in order to induce c-fos. Thus, activation of the voltage-dependent calcium channel must lead to an increase in intracellular calcium to trigger c-fos induction.

All three agents activate calmodulin either as a direct effect of increased calcium levels or by some other indirect route. Calmodulin is implicated because both trifluoperazine and chlorpromazine block c-fos induction by veratridine and potassium. As induction by BAY K 8644 is also blocked by calmodulin inhibitors, calmodulin must be involved at a step subsequent to calcium channel activation. Following stimulation of calmodulin, we propose that there is a calmodulin- or calmodulin kinase-mediated modification of a transcription activating protein (TAP). This modified factor then acts, directly or indirectly, to stimulate c-fos transcription. Although the latter two steps are speculative there is some evidence to suggest that the c-fos gene has an enhancer element which can be activated in trans by inducible factors (ref. 27 and T.C., unpublished data). The existence of a similar agent for the haemoglobin gene has been demonstrated in nuclei of stimulated erythroid precursor cells²⁸. In addition, calmodulin has recently been implicated in the control of the prolactin gene²⁹.

Previously, prompted by observations of c-fos induction by polypeptide mitogens, a number of investigators suggested that c-fos plays a part in controlling cell cycle events. Since then it has been demonstrated that c-fos induction is not restricted to a particular phase of the cell cycle and is not necessarily associated with mitogenesis^{7,30,31}. Indeed, in some systems c-fos expression has been associated with cellular differentiation^{8,9,11,32}. Our own studies on PC12 cells led us to propose a more general role for c-fos in coupling early events associated with receptor occupation (such as phosphorylation, methylation and ion flux) to long-term changes in gene expression⁹. We have now confirmed and extended these data to include an independent biochemical pathway for c-fos induction that appears to be particularly prevalent in neuronal cells, and which involves a gated calcium signal. The induction of c-fos seems to be associated with, and is a genetic harbinger for, a change in state of many cell types. The change in state may be from quiescence to proliferation or from less to more differentiated for example. We suggest that the target genes for c-fos are different in the many and varied situations in which induction occurs. We have shown that agents that classically depolarize neurones lead to an induction of c-fos by a gated calcium signal. Thus, we propose that c-fos and its co-regulated genes are excellent candidate genes for coupling excitation of the neurone to long-term adaptive modifications of transcription.

We thank D. Alkon, P. Brehm, J. Connor, K. Magleby, M.

Montal, J. Reeves and D. Triggle for helpful discussions and suggestions; F. Margolis, E. P. Reddy and A. M. Skalka for critical reading of the manuscript; and K. Rubino for technical assistance.

Received 27 January; accepted 29 April 1986.

- Halegoua, S. & Patrick, J. Cell 22, 571-581 (1980).
 Rozengurt, E. & Heppel, G. A. Proc. natn. Acad. Sci. U.S.A. 72, 4492-4495 (1975).
 Greenberg, M. E. & Ziff, E. B. Nature 311, 433-438 (1984).
- Cochran, B. H. et al. Science 226, 1080-1082 (1984).
- Kruijer, W. et al. Nature 312, 711-716 (1984).
 Muller, R. et al. Nature 312, 716-720 (1984).
- Bravo, R. et al. EMBO J. 4, 1193-1197 (1985).
- 8. Muller, R. et al. Nature 314, 546-548 (1985).
- Curran, T. & Morgan, J. I. Science 229, 1265-1268 (1985).
- Kruijer, W., Schubert, D. & Verma, I. M. Proc. natn. Acad. Sci. U.S.A. 82, 7330-7334 (1985).
 Greenberg, M. E., Green, L. A. & Ziff, E. B. J. biol. Chem. 260, 14101-14110 (1985).
 Schubert, D. et al. Nature 273, 718-723 (1978).
 Traynor, A. & Schubert, D. Devi Brain Res. 14, 197-203 (1984).

- Kazda, S. et al. Arzneimittel Forsch. 30, 2144-2162 (1980).
 Toll, L. J. biol. Chem. 257, 13189-13192 (1982).
- 16. Prozialeck, W. C. & Weiss, B. J. Pharmac exp. Ther. 222, 509-516 (1982).
 17. Nishizuka, Y. Nature 308, 693-697 (1984).
- 18. Schatzman, R. C., Wise, B. C. & Kuo, J. F. Biochem. biophys. Res. Commun. 98, 669-676 (1981).
- Hidaka, H. & Tanaka, T. Meth. Enzym. 102, 185-194 (1983).
 Shanes, A. M. Pharmac. Rev. 10, 59-274 (1958).
 Narahashi, T. Physiol. Rev. 54, 813-889 (1974).

- Narahashi, T., Moore, J. W. & Scott, W. R. J. gen. Physiol. 47, 965-974 (1964).
 Dichter, M. A., Tischier, A. S. & Greene, L. A. Nature 268, 501-504 (1977).

- Schramm, M. et al. Nature 303, 535-537 (1983).

 Greenberg, D. A., Carpenter, C. L. & Cooper, E. C. J. Neurochem. 45, 990-993 (1985).

 Nowycky, M. C., Fox, A. P. & Tsien, R. W. Proc. natn. Acad. Sci. U.S.A. 82, 2178-2182 (1985).
- Nowycky, M. C., Pox, A. P. & Isien, R. W. Proc. nun. Actac. Sci. C.S.A. 22, 2178-217
 Treisman, R. Cell 42, 889-902 (1985).
 Bazett-Jones, D. P., Yeckel, M. & Gottesfeld, J. M. Nature 317, 824-828 (1985).
 White, B. A. J. biol. Chem. 260, 1213-1217 (1985).
 Hann, S. R., Thompson, C. B. & Eisenman, R. E. Nature 314, 366-369 (1985).

- 31. Thompson, C. B. et al. Nature 314, 363-366 (1985). 32. Muller, R. & Wagner, E. F. Nature 311, 438-442 (1984).
- 33. Greene, L. A. & Tischler, A. S. Proc. natn. Acad. Sci. U.S.A. 73, 2424-2428 (1976)
 34. Curran, T. et al. Molec. cell Biol. 5, 167-172 (1985).
- 35. Laemmli, U. K. Nature 227, 680-685 (1970).

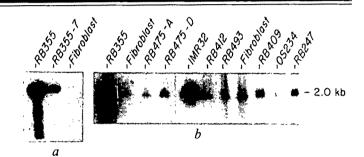
Tumour induction by the retinoblastoma mutation is independent of N-myc expression

Jeremy Squire*, Audrey D. Goddard*, Marc Cantont, Andrew Becker‡, Robert A. Phillips* & Brenda L. Galliet

Departments of * Medical Biophysics, † Ophthalmology and ‡ Medical Genetics, University of Toronto, and † The Hospital for Sick Children, 555 University Avenue, Toronto, Canada M5G 1X8

Retinoblastoma (RB) tumours form in the eyes of young children when homozygosity for a mutation at the Rb-1 locus develops in a somatic retinal cell^{1,2}. A similar shift to homozygosity for the RB mutation has been observed in osteogenic sarcoma (OS) tumours that commonly arise as second tumours in children who survive RB3. This observation suggests that the Rb-1 locus controls the expression of genes with oncogenic potential; a possible target is the oncogene N-myc, which is sometimes amplified and overexpressed in the neuroectodermal tumours neuroblastoma⁴⁻⁷ and RB⁵⁻⁸. However, N-myc is developmentally regulated in normal murine embryogenesis9, and an alternative possibility is that the expression of the gene in tumour cells reflects their embryonic origin and is unrelated to the RB mutation. We have therefore examined N-myc expression in various fetal, adult and tumour tissues, and report here that the gene is expressed in fetal but not in adult brain and retina and in near-diploid RB tumour samples at levels similar to those observed in normal fetal retina. Only RB tumours with genomic amplification of the N-myc gene exhibited increased levels of expression; and no N-myc transcripts were detected in osteogenic sarcomas initiated by mutations at the Rb-1 locus³. We therefore conclude that the expression of N-myc in RB tumours probably reflects the origin of the tumour from an embryonic tissue normally expressing the gene and is not directly associated with the mutation at the RB locus.

The Rb-1 locus may have a regulatory function like that of the diploid regulatory/suppressor genes postulated by Comings to control expression of other genes¹⁰. In the absence of the normal RB gene product, such target genes may lead to malignancy because they continue to be expressed at inappropriate levels. N-myc is a developmentally regulated proto-oncogene which is a candidate for regulation by a tumour suppressor gene like the RB gene. N-myc is normally expressed in the early stages of development in multiple differentiation pathways Differentiation of neuroblastoma¹¹ and teratocarcinoma cells⁹ in culture is accompanied by a decrease in the level of N-myc



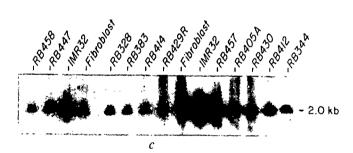


Fig. 1 Southern blot analyses of 17 RB tumours or cell lines and one osteogenic sarcoma cell line (OS234) probed with N-myc. DNA was extracted from 5×10^7 - 10^8 cultured cells or tumour cells or tumour material by the standard method of phenol and isoamyl alcohol extraction, followed by ethanol precipitation²⁴. DNAs (10 µg) were digested with EcoRI (Boehringer Mannheim) using conditions recommended by the supplier. Digested genomic DNA was separated by gel electrophoresis in 0.8% agarose, and blots were made onto nitrocellulose membrane²⁵. The recombinant plasmid pNB-1 (N-myc)⁵ was labelled with 32 P-dCTP by nick-translation²⁶ to a specific activity of 3×10^8 c.p.m. μ g⁻¹. Washing of filters after probing was carried out in either high-stringency conditions $(0.1 \times SSC, 0.2\% SDS, 65 ^{\circ}C)$ (a) or conditions of moderate stringency $(1 \times SSC, 0.1\% SDS, 65 ^{\circ}C)$ (b, c). The blots were reprobed with pESD14.1.1 (ref. 18) to control for the amount of DNA loaded per lane, and then transferred to the filter. The resultant ratios between the two signals were compared for all lanes except RB375A, RB475D, RB458 and RB447; the average ratio was Nmyc/ESD = 0.84:1.0, with a range of 0.21-2.00, indicative of no amplification. a, RB355-7 is a subclone of RB355. This filter was washed to show the relative copy numbers of N-myc. Fibroblast DNA was used as a diploid control. b, c, Several RB samples and one osteogenic sarcoma (OS234). IMR32 and RB355 are positive controls for N-myc-amplification; fibroblast DNA is a diploid control. DNA sources are as follows (1) Fresh tumour material: RB475-A and -D (from separate eyes of one patient), RB493, RB458, RB457 and RB328. (2) Tumour cell culture: OS234, RB383, RB429R, RB405-A, RB430, RB344 and IMR32. (3) RB tumour cell culture derived from xenografts: RB355, RB355-7, RB412, RB409, RB247, RB447 and RB414.

Table 1 Relative levels of N-myc genomic amplification and mRNA in nine RB tumours, fetal retina, two OS tumours and control cell lines

				Level of N- relative to	myc RNA relative to
Cells	Source	DM/HSR	DNA	β -tubulin	ESD
Y79-T	С	+	40×	69×*	4×
IMR32	C	+	20×	120×*	NT
RB355	MC	+	35×	13×*	NT
RB409	MC	-	1×	1.0×	1.0×
RB344	C	-	1×	1.2×	NT
RB247C	MC	-	1×	1.1×	NT
RG412	MC	-	1×	0.48×	NT
RB447	MC		1×	Present†	NT
RB430	С	_	1×	0.81×	NT
RB430	S	-	1×	NT	1.9×
RB517	S	-	1×	NT	1.9×
Fetal retina	S	NT	NT	0.32×	1.6×
Adult retina	S	NT	NT.	NT	< 0.05
Fetal brain	S	NT	NT	NT	0.27‡
Adult Brain	S	NT	NT	NT	< 0.05
OS108	M	-	1×	NT	< 0.05
OS234	M	+	1×	NT	< 0.05
HL60	C	+	NT	< 0.05	< 0.05
HeLa	С	-	NT	< 0.05	NT
Fibroblast	С	NT	1×	NT	NT

Tumour samples were obtained from three sources: S, surgical specimen; M, grow in nude mice; C, grown in vitro. Where there are two letters, the last letter indicates the source of tumour cells studied and the preceding letter indicates the culture history of the tumour cells; for example, MC indicates that the tumour was grown in xenografts in nude mice before passage to tissue culture. The presence of double minute (DM) or homogeneous staining regions (HSR) was tested on G-banded karyotype preparations. DNA copy number is given relative to single-copy fibroblast hybridization on Southern blots (Fig. 1). Relative levels of DNA and RNA were estimated by grain density using a BioRad 620 video densitometer and BioRad Model 3392A integrator. N-myc RNA levels were normalized with respect to β -tubulin¹⁷ or ESD¹⁸ signals. RB409 N-myc expression was assigned an arbitrary value of 1.0 as it was present on all Northern blots analysed. NT, not tested.

- * An approximation because the signal was beyond the linear response region of the film.
 - † Densitometry was not done on this blot.
 - ‡ Densitometry done using the longer exposure (see Fig. 2b).

expression, suggesting that regulatory mechanisms for N-myc are intact in these malignant cells. Genomic amplification of N-myc is restricted primarily to neuroectodermal tumours^{4,6-8,12,13}, and many correlate with poor clinical prognosis^{14,15}.

We studied genomic amplification of N-myc in 17 RB tumours (Fig. 1) and 2 OS cell lines derived from second primary malignancies in patients who had previously had RB (one OS tumour not shown). N-myc amplification was found in only one of 17 RB tumours, RB355¹², and in neither OS line despite cytological evidence of gene amplification. The known N-myc amplification in the neuroblastoma line IMR32⁵, and in the long-established RB line Y79 ^{7,16}, were used as positive controls. No rearrangements of N-myc were detected.

Nine RB tumours were examined for levels of N-myc expression using Northern blotting techniques. Seven RB tumours were studied after culture or xenografts, one directly from the surgical specimen (RB517) and one from both the surgical specimen and tissue culture (RB430). RB517 has a consitutional deletion at chromsome band 13q14. The presence of intact RNA on the Northern blots was determined by probing sequentially with N-myc and β -tubulin¹⁷ or concurrently with N-myc and a complementary DNA clone of the esterase D (ESD) gene¹⁸ (Fig. 2). ESD and β -tubulin are constitutively expressed¹⁹. All RB tumours expressed the expected major 4.0-kilobase (kb) transcript of the N-myc gene⁵. Fresh RB tumours expressed levels of the N-myc transcript comparable to those

in RB samples from cell lines or xenografts and fetal retina (Fig. 2; Table 1). RB430 was examined both as a fresh surgical specimen and after tissue culture for 3 years, and no change in N-myc expression was observed. Both RB tumours with genomic amplification, Y79 and RB355, and the neuroblastoma line IMR32, expressed N-myc at high levels. Expression of N-myc was not detected in HeLa cells or in the promyelocytic leukaemia cell line HL60. No N-myc signal was observed even when HL60 was overloaded in the Northern blot.

The cells of origin of RB have not yet been identified, but are probably the embryonic cells of the fetal retina²⁰. Therefore, we collected fetal retinas at weeks 6-10 of gestation, and pooled them for use as a source of RNA. We found that N-myc was expressed at equivalent levels in fetal retina, in the RB tumours without genomic amplification of N-myc, and in fresh RB tumours (Table 1). We suggest that the presence of N-myc messenger RNA in RB tumours is a consequence of the normal expression of this gene in the retinal precursor cells which transform into RB tumours. It is difficult to determine whether there is cellular heterogeneity in the specimens of fetal retina used since, morphologically, all of the cells in the retina have a similar appearance at this stage of development. The observation that the level of N-myc expression in fetal retina was equivalent to the level in pure populations of RB tumour cells is consistent with the conclusion that the fetal retinal specimen was not significantly contaminated with other cells. In fact, most retinal cells at this early developmental time may be potential precursors for RB tumour development. Alternatively, at this gestational stage all retinal cells, whether potential retinoblastoma precursors or not, may express N-myc transcripts. The lack of N-myc transcripts in adult retina indicates that N-myc expression is regulated during the differentation of the retina and that the terminally differentiated cells no longer express the gene. Loss of the normal alleles at the Rb-1 locus may prevent the normal differentiation of the fetal retinal cell involved in transformation, and thus N-myc expression may be maintained at embryonic levels of expression.

Fetal brain showed a low level of N-myc expression when the Northern blots were exposed more intensely (Fig. 2b). This low level is not surprising in view of the reported N-myc heterogeneity observed in fetal brain in early development²¹. On the Northern blot shown in Fig. 2, the adult brain sample was underloaded but did not give a signal for N-myc even in the more intense exposure, when control ESD transcripts were detectable (Fig. 2b). We conclude that N-myc expression is regulated during development of the brain, as has been shown in mouse brain²¹.

Patients with bilateral RB tumours are reported to have a predisposition to develop specific second malignancies, most commonly osteosarcomas, subsequent to and independent of the initial RB tumour²². Reduction to homozygosity in the region of the Rb-1 locus also occurs in osteogenic sarcoma, indicating that recessive mutations of this gene are involved in the induction of osteosarcoma and retinoblastoma³. OS234 and OS108 are second tumours from RB patients; OS108 has been shown to reduce to homozygosity at chromosome 13³. The critical test for an intimate relationship between N-myc and the Rb-1 mutation is the expression status of N-myc in the osteosarcomas of RB patients. Neither OS tumour studied was expressing N-myc (Fig. 2). Therefore, we conclude that Rb-1 mutations can lead to malignancy without the overexpression or deregulation of N-myc.

Two other groups have studied N-myc expression in RB tumours. Lee et al.⁸ compared N-myc RNA levels in RB tumours with those in one human fetal retina of undefined gestational age and in one bovine adult retina. They detected N-myc expression only in the tumours, and concluded that N-myc was abnormally highly expressed in RB tumours and suggested that this gene could be the regulatory target of the RB gene. Schwab et al.⁶ detected no N-myc expression in three cell lines derived

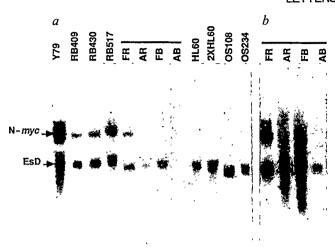


Fig. 2 Northern blot of two RB tumour cell lines (Y79, RB409), two fresh RB tumours (RB430, RB517), fetal (F) and adult (A) retina (R) and brain (B), two OS tumours (OS108 and OS234), and one promyelocytic leukaemia cell line (HL60). Total cellular RNA was prepared by guanidine thiocyanate-caesium chloride gradient centrifugation²⁷. Poly(A)⁺ RNA was obtained by oligo(dT)-cellulose chromatography. N-myc and pESD14.1.1 (ref. 18) were radiolabelled as described in Fig. 1 legend and simultaneously hybridized to GeneScreen membrane according to the method of Church and Gilbert 28 . ESD served as an internal control for the presence of intact mRNA. 25 μg of total RNA was loaded per lane, except for three lanes: 50 μg of total RNA for 2×HL-60; and 2 µg of poly(A)+RNA for fetal retina and for OS108. a, 22-h exposure at room temperature with no intensifier; b, 19-h exposure at -70 °C with an intensifier.

from RB surgical specimens, but several observations in our laboratory suggest that these lines may have originated from the non-RB component of the surgical specimen: two of the cell lines do not have any of the cytogenetic abnormalities characteristic of RB tumours²³, fail to stain with a monoclonal antibody that reacts positively with all other RB tumours and lines, and do not resemble RB tumours in suspension tissue culture.

The expression of N-myc RNA in normal fetal retina and in RB tumours suggests that N-myc is a normal product in developing retina. The RB cell lines that do develop genomic amplification of N-myc may gain proliferative advantage by means of the accompanying excessive expression of N-myc, a gene normally functioning in the cells from which RB tumours arise. It is possible that N-myc is not normally expressed in the bone cells in which homozygosity for the RB mutation leads to OS tumours. Consequently, no N-myc transcripts are observed in the OS tumours. We have clearly demonstrated equal levels of expression of N-myc in RB tumours and in normal fetal retina, and that N-myc is not expressed in the OS tumours induced by the RB mutation. Thus, expression of N-myc cannot be essential to the initiating malignant process in these tumours.

We acknowledge the help from Wendy Holmes, Joan Cocking and Joan Chin in culturing RB tumour cells, and thank Dr J. M. Bishop for the N-myc probe and Dr D. W. Cleveland for the β -tubulin probe. This work was supported by grants from the Hospital for Sick Children Foundation, the MRC of Canada, the National Cancer Institute of Canada and Fight-For-Sight Incorporated, New York. J.S. was supported by the Canadian National Institute for the Blind (Canada). A.D.G. is supported by MRC Studentship. B.L.G. is a Research Associate of the Ontario Cancer Treatment and Research Foundation.

Received 17 April; accepted 19 May 1986.

- 1. Cavence, W. K. et al. Nature 305, 779-784 (1983).
- Cavenee, W. K. et al. Science 228, 501-503 (1985).
- 3. Hansen, M. F. et al. Proc. natn. Acad. Sci. U.S.A. 82, 6216-6220 (1985).
- Kohl, N. E., Gee, C. E. & Alt, F. W. Science 226, 1335-1337 (1984). 5. Schwab, M. et al. Proc. natn. Acad. Sci. U.S.A. 81, 4940-3944 (1984).

- Schwab, M. et al. Nature 305, 245-248 (1983).
 Kohl, N. E. et al. Cell 35, 359-367 (1983).
- Lee, W.-H., Murphree, A. L. & Benedict, W. F. Nature 309, 458-460 (1984)
- Jakobovits, A., Schwab, M., Bishop, J. M. & Martin, G. R. Nature 318, 185-191 (1955-10. Comings, D. E. Proc. natn. Acad. Sci. U.S.A. 70, 3324-3328 (1973)
 Thiele, C. J., Reynolds, C. P. & Israel, M. A. Nature 313, 404-406 (1985)
 Sakai, K. et al. Cancer Genet. Cytogenet. 17, 95-112 (1985)
 Nau, M. M. et al. Nature 318, 69-73 (1985).

- Seeger, R. C. et al. New Engl. J. Med. 313, 1111-1116 (1985)
 Brodeur, G. M., Seeger, R. C., Schwab, M., Varmus, H. E. & Bishop, J. M. Science 124. 1121-1124 (1984). 16. Reid, T. W. et al. J. natn. Cancer Inst. 53, 347-360 (1974).
- Reid, I. W. et al. J. Italia. Cancer Inst. 55, 347-360 (1974).
 Cleveland, D. W., Pittenger, M. F. & Feramisco, J. R. et al. Nature 305, 738-740 (1974).
 Squire, J. et al. Proc. natn. Acad. Sci. U.S.A. (in the press).
 Varki, A., Muchmore, E. & Diaz, S. Proc. natn. Acad. Sci. U.S.A. 83, 882-8 6 (1976).
 Becker, L. E. & Hinton, D. Hum. Path. 6, 538-550 (1983).
 Zimmerman, K. A. et al. Nature 319, 780-783 (1986).

- 22. Abramson, D. H., Ellsworth, R. M., Kitchen, F. D. & Tung, G. Ophthalmology 91, 1351-1355 (1984).
- 23. Squire, J., Gallie, B. L. & Phillips, R. A. Hum. Genet. 70, 291-301 (1935)
 24. Maniatis, T., Fritsch, E. F. & Sambrook, J. Molecular Clonung. A Laboratory Manual (Co. 3) Spring Harbor Laboratory, New York, 1982).
 25. Southern, E. M. J. molec. Biool. 98, 503-517 (1975).

- Southern, E. W. J. Molec. Biol. 98, 303-317 (1973).
 Rigby, P. W. J., Dieckmann, M., Rhodes, C. & Berg, P. J. molec. Biol. 113, 227-251 (1973).
 Chirgwin, J. M., Pryzbyla, A. E., MacDonald, R. J. & Rutter, W. J. S. chemittry, 16, 5294-5299 (1979).
- 28. Church, G. M. & Gilbert, W. Proc. natn. Acad. Sci. U.S A. 81, 1991-1995 (1954)

Discrete cis-active genomic sequences dictate the pituitary cell type-specific expression of rat prolactin and growth hormone genes

Christian Nelson*†, E. Bryan Crenshaw III*†, Rodrigo Franco*†, Sérgio A. Lira*, Vivian R. Alberto, Ronald M. Evans‡§ & Michael G. Rosenfeld*§

* Eukaryotic Regulatory Biology Program, School of Medicine and † Department of Biology, University of California, San Diego, La Jolla, California 92093, USA

‡ Molecular Biology and Virology Laboratory, Salk Institute, La Jolla, California 92037, USA

§ Howard Hughes Medical Institute, 7984 Old Georgetown Road, Bethesda, Maryland 20814, USA

The anterior pituitary gland, which is derived from a common primordium originating in Rathke's pouch, contains phenotypically distinct cell types, each of which express discrete trophic hormones: adrenocorticotropic hormone (ACTH), thyroid-stimulating hormone (TSH), prolactin, growth hormone, and follicle stimulating hormone (FSH)/luteinizing hormone (LH) (reviewed in ref. 1). The structurally related prolactin and growth hormone genes, which are evolutionarily derived from a single primordial gene2, are expressed in discrete cell types-lactotrophs and somatotrophs, respectively—with their expression virtually limited to the pituitary gland1. The pituitary hormones exhibit a temporal pattern of developmental expression with rat growth hormone and prolactin characteristically being the last hormones expressed3-8. The reported co-expression of these two structurally related neuroendocrine genes within single cells prior to the appearance of mature lactotrophs, in a subpopulation of mature anterior pituitary cells, and in many pituitary adenomas 1,6-9 raises the possibility that the prolactin and growth hormone genes are developmentally controlled by a common factor(s). We now report the identification and characterization of nucleotide sequences in the 5'-flanking regions of the rat prolactin and growth hormone genes, respectively, which act in a position- and orientation-independent fashion to transfer cell-specific expression to heterologous genes. At least one putative trans-acting factor required for the growth hormone genomic sequence to exert its effects is apparently different from those modulating the corresponding enhancer element(s) of the prolactin gene because a pituitary 'lactotroph' cell line producing prolaction but not growth hormone selectively fails to express fusion genes containing the growth hormone enhancer sequence.

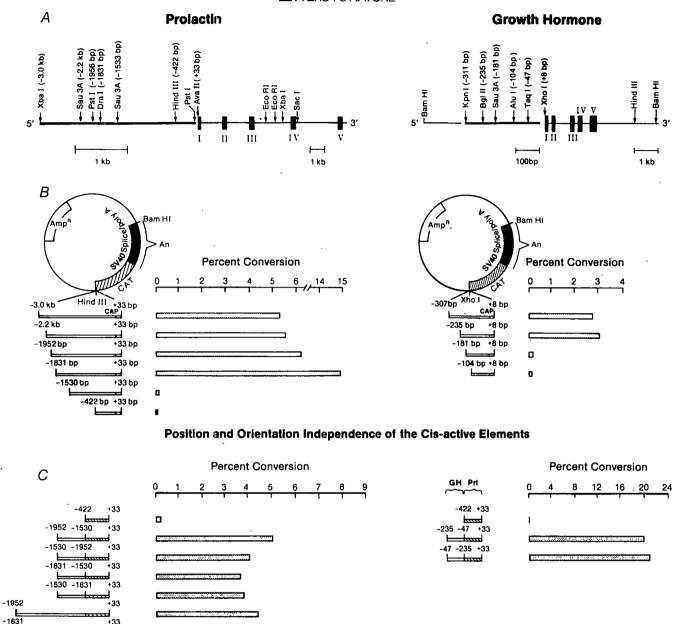


Fig. 1 Identification of cis-active region(s) in the 5' flanking prolactin and GH genomic sequences which confer cell-specific expression. A, Activity of rat prolactin genomic, CAT fusion constructions. The sites used for the constructions are listed on the map of the rat prolactin and growth hormone genes, based on previous reports. Fragments of the indicated sizes, each utilizing a common. 3' end (+33 for prolactin, +8 for growth hormone) were ligated into pSV2 CAT such that the promoter and CAP site were contributed by the prolactin or growth hormone genomic fragments. No viral enhancers were present in the final construction. B, Sites used for deletional analysis are indicated, and the diagrammed fusion genes were transfected into rat pituitary cell lines (GH4, G/C). Mapping the cis-active genomic sequences for each gene was accomplished using expression of a reporter gene, bacterial CAT¹⁵, in GH4 cell lines, assessed in cells harvested 48 h after transfection. Results are the average of duplicate determinations differing by <5% of 3-12 experiments in GH4, G/C, and GH3 cell lines. All data were significant (P <0.001). C, Position- and orientation-independence of the rat prolactin and GH genomic enhancer sequences. A 188-bp GH genomic sequence (-235 to -47) was placed in both orientations 5' to a gene containing the prolactin promoter fused to the CAT gene (the Prl-422 CAT construction) and used to transfect GH4, cells in three experiments of similar design. Prolactin genomic fragments (-1,831 to -1,532) and (-1,952 to -1,532) were fused in both orientations to the Prl-422 CAT construction. Transfections were performed in GH4 cells. In additional experiments, the -235 to -47 and -1,831 to -1,532 regions of the growth hormone and prolactin genes, respectively, were placed in both possible orientations 3' of the CAT transcription unit, located approximately 350 bp 3' of the poly(A) site in the Prl-422 CAT construction. Even in the inverted (3' to 5') orientation, these constructions

Methods. The fusion genes containing the GH fragments diagrammed above were constructed by converting the HindIII site in pSV2 CAT to an XhoI site and ligating GH 5' flanking fragments into the BamHI, XhoI sites of the vector. 5' GH sites were converted to BamHI sites following filling using T4 polymerase for the KpnI site, or ligating into the BamHI in the case of BgIII and SauIIIA's sites, using conventional techniques, and placing these fragments into PSV2 CAT, as diagrammed. In the case of the prl/CAT fusion genes, an AvaII site 33 nucleotides 3' to the CAP site was converted to a HindIII site and indicated 5' sites (XbaI, PstI, DraI, SauIIIA) were either converted to Bam HI sites using T4 polymerase-catalysed fill reactions where appropriate or ligated into the BamHI site (SauIIIA). The vector containing the HindIII to AvaII (-422 to +33) fragment of the prolactin gene fused to the CAT gene is referred to as Prl-422 CAT. In addition to the diagrammed constructions, a 5' flanking GH sequence extending -7 kb (using an EcoRI site) and an XhoI to BamHI fragment encompassing the entire coding portion and 2.7 kb of 3' flanking GH genomic sequences ligated in opposite orientation 5' to the Prl-422 CAT fusion gene were tested; these constructions did not exhibit enhancer function.

To ascertain the existence of genomic regions that determine pituitary-specific gene expression, fusion genes containing 3 kilobases (kb) or 235 base pairs (bp) of prolactin or growth hormone genomic 5'-flanking sequences, respectively, were fused to a reporter gene encoding bacterial chloramphenicol acetyltransferase (CAT) (Fig. 1) and introduced into a series of heterologous cell lines. As shown in Table 1, the fusion genes are expressed only in prolactin and growth hormone-producing pituitary cell lines (GH₄, G/C).

The growth hormone and prolactin cis-active elements responsible for cell-specific expression were characterized by generating a series of deletions extending from -3 kb to -172 bp in the 5' flanking prolactin genomic sequences (Fig. 1A) and from -2 kb to -104 bp of the 5' flanking growth hormone genomic sequences (Fig. 1A). In the case of the prolactin genomic sequences, enhanced expression of the CAT gene product was observed with sequences extending 1.83 kb 5' of the prolactin gene transcription initiation (CAP) site, and was virtually eliminated with deletion to -1.53 kb, although a small residual enhancement was observed with 5' flanking fragments as short as 172, but not 70, base pairs. In the case of growth hormone 5' flanking genomic sequences, maximally enhanced expression of the reporter gene was observed in constructions containing >235 base pairs of 5' flanking information, while deletion to -181 base pairs 5' of the CAP site virtually abolished expression of reporter function in these cells (Fig. 1B).

As shown in Fig. 1C, both prolactin and growth hormone genomic fragments extending from -1.95 or -1.83 to -1.53 kb and from -235 to -47, respectively, fused to a 422-bp prolactin gene promoter region resulted in marked stimulation of the expression of the fusion genes in the growth hormone-producing cells, irrespective of orientation or position. The prolactin or growth hormone cis-active elements enhanced reporter gene expression even when placed 3' of the reporter gene (Fig. 1G). Primer extension analysis confirmed correct CAP site usage in both the prolactin and growth hormone constructions (Fig. 2).

The prolactin and growth hormone cis-active sequences acted in a cell-specific manner independent of possible transcriptional restriction imposed by their respective promoters. Chimaeric genes containing either the prolactin genomic fragment from -1.83 kb to -1.53 kb or the growth hormone genomic fragment from -235 bp to -47 bp ligated to a herpes thymidine kinase (tk) promoter, CAT gene fusion resulted in no enhancement of gene expression in heterologous cell types, while expression of these chimaeric genes in GH₄ and G/C cell lines was markedly enhanced (Fig. 1C). The possibility that a restriction in tissuespecific expression was imposed by the prolactin promoter itself is unlikely because the prolactin promoter (-422 to +33) was efficiently expressed in fibroblasts and CV1 cells in the presence of the simian virus 40 (SV40) enhancer (Table 1). Despite the 2.5- to 3.5-fold increase in expression of constructions containing the -1.83 kb compared to -1.95 kb 5'-flanking prolactin genomic fragment (Fig. 1B), the presence of a biologically important suppressor or silencer sequence appears less likely because both the -1.95 to -1.53 and -1.83 to -1.53 kb fragments exerted comparable effects when inserted in front of the prolactin genomic promoter extending to -422 bp (Fig. 1C).

Based on these analyses, we conclude that a 298-bp sequence located approximately 1.85 kb upstream of the prolactin gene CAP site, and a 188-bp sequence located approximately 200 bp upstream of the growth hormone gene CAP site, act as enhancers in the GH cells and appear to be critical for the tissue-specific expression of these genes.

More detailed analyses were performed to identify the minimal sequences in the prolactin and growth hormone genes sufficient for enhancer function. As diagrammed in Fig. 3, a series of genomic fragments inserted in front of the prolactin promoter, CAT fusion gene (the -422 to +33 fragment, the plasmid referred to as Prl-422 CAT, Fig. 1) were tested for ability to confer enhanced expression of the reporter gene.

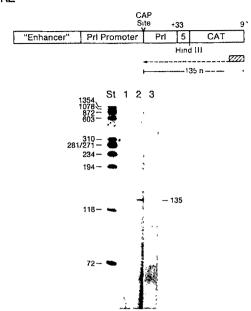
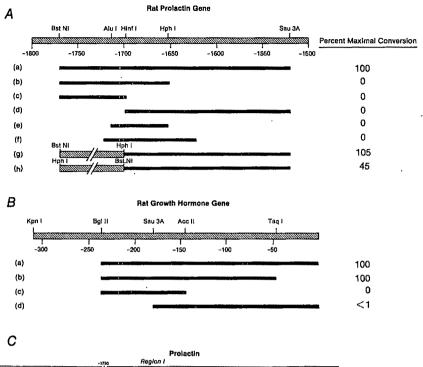


Fig. 2 Mapping the transcription initiation sites of the chimaeric genes containing the prolactin and growth hormone enhancer elements. Chimaeric genes containing the growth hormone or prolactin cis-active elements (-235 to -47 and -1,952 to -1532, respectively), fused to the Prl-422 CAT fusion gene, as described in Fig. 1C, were transfected into GC2 cells, and RNA was prepared and subjected to primer extension analysis, as described under methods. As diagrammed in A, for both constructions, the expected primer extension product was 135 nucleotides if the expected prolactin gene CAP site was utilized. B. The primer extension products using RNA from cells transfected with: lane 1, the prolactin -1,952 to -1,532, Prl-422 CAT fusion gene, from which the prolactin promoter region (-422 to -33) was removed. No CAT activity was detected in cells transfected with this construction; lane 2, the prolactin -1,952 to -1,532, Prl-422 CAT fusion gene; lane 3, the growth hormone -235 to -47, Prl-422 CAT fusion gene. Standards are the HaeIII digests of ΦX174 DNA. Autoradiograph shown was developed following a 7-day exposure

Methods. Total RNA was isolated from GC₂ cells 48 h following transfection with 10 µg plasmid DNA per plate, by homogenization in thiocyanate and pelleting through cesium chloride to remove DNA. A single-stranded primer of sequence 5' GTTCTTTAC-GATGCCATTGGGATATATCAACGG 3' complementary to nucleotides 29-61 of the CAT coding sequence, was labelled on the 5'-terminus to a specific activity of 10^9 c.p.m. μg^{-1} using T_4 polynucleotide kinase and $(\gamma^{-32}P]ATP$ (7,000 Ci mmol⁻¹. ICN). For each reaction, 50 µg total RNA and 3 ng labelled primer were heated to 70 °C in 12 µl RT buffer (50 mM Tris pH 8.0, 8 mM MgCl₂, 50 mM KCl, 40 mM dithiothreitol) and slowly cooled to 55 °C. The annealed primer and RNA were then precipitated with 0.3 M sodium acetate and 1 volume of isopropanol and resuspended in RT buffer. dATP, dCTP, dGTP and dTTP were added, to a final concentration of 1 mM each in a final volume of 20 µl. The reaction was initiated with 24 units of reverse transcriptase and allowed to proceed for 30 min at 42 °C. After phenol/chloroform extraction, the extension products were analysed on 8% denaturing polyacrylamide gels.

Deletion of 61 5' nucleotides of the 298-bp prolactin enhancer element (-1,831 to -1,769) resulted in no loss of activity (Fig. 3 (a)); however, dividing the region by cleavage at a *HinfI* site at nucleotide -1,698 resulted in virtually complete loss of activity of both of the resultant fragments (Fig. 3 (c), (d)), apparently splitting a critical site or separating two discrete sequences. To test the possibility that a critical site was split, regions extending both 5' and 3' of the *HinfI* site were tested. Neither a 50-bp sequence (-1,713 to -1,663), nor a 98-bp fragment (-1,722 to -1,625) exhibited any enhancer activity (Fig. 3 (e), (f)). Therefore, a fragment containing 106 nucleotides including the 5' sequences known to be sufficient for activity (-1,769 to -1,663) was tested. This region was entirely silent in GH cell lines (Fig.

Fig. 3 Mapping the 5' and 3' limits of the cis-active prolactin and growth hormone genomic sequences specifying cell-specific gene expression. A, A series of prolactin 5' genomic restriction fragments were preepared as diagrammed and placed 5' to the fusion gene Prl-422 CAT, containing the prolactin genomic sequences from -422 to +33 (shown in Fig. 1). These plasmids were used to transfect GH₄, G/C, and 235-1, as described in the legend to Fig. 1. The -1,769 to -1530fragment, which gave a 24±8% conversion in different experiments, represented 100% for the prolactin gene fragment series. Similar results were obtained in five experiments of similar design. The fragment -1,769 to -1,663 exhibited 0% of expression in five separate experiments (GH₄, G/C and 235-1 cell lines); but 15% maximal activity was observed in two separate experiments. B, Growth hormone genomid fragments were tested for their ability to direct CAT expression in GH₄ cells. The -235 to -47 fragment and the -235 to -146 fragment were fused to the prolactin -422 CAT fusion gene. The -235 to -47 fusion gene activity (5-12% conversion in separate experiments) represented maximal activity (100%). C, Sequences of the cellspecific enhancer elements of the rat prolactin and growth hormone genes. The boxed sequences indicate regions which are critical for activity based on deletion mapping in A. There appear to be two functionally separable regions in the prolactin enhancer (Region I and Region II). The growth hormone sequence is based on the data of Barta et al.²⁰. The prolactin genomic sequence was determined for the fragments used in these experiments using dideoxynucleotide, enzymatic sequencing methods²¹, and is in agreement with the recently published data of Maurer¹⁵ except for the identification of residue -1,667



Growth Hormone

as a T. Results shown are the average of three or four separate experiments.

Methods. Prl 5' flanking fragments from BstNI, SauIIIA (-1,769 to -1,530), BstNI, HinfI (-1,769 to -1,695), HinfI, SauIIIA (-1,697 to -1,530), AluI-HphI (-1,713 to -1,663 and BstNI, HphI (-1,769 to -1,663) were inserted into the plasmid Prl -422 CAT using the strategy described in the legend to Fig. 2. The 98-bp fragment extending from -1,722 to -1,625 was constructed by synthesis of two synthetic oligonucleotides using phosphoramidite chemistries (71-mers) corresponding to sense (-1,722 to -1,658) and antisense (-1,691 to -1,625), and including sequences generating a 5' XhoI site and 3' BamHI site, annealing, filling using the Klenow fragment of Escherichia coli polymerase, cleaving with XhoI and BamHI, and inserting into the Prl -422 CAT vector. The final construction involved placing the BstNI to HphI fragment (-1,769 to -1,663) ligated with XhoI linkers, in front of the construction containing the HinfI to SauIIIA fragment (-1,697 to -1,530). All plasmids were purified by two CsCl gradients prior to transfection, which was performed using GH₄, G/C, and 235-1 cell lines. Results are the average of duplicate determinations (50 μg protein, 10 h assays) in three separate experiments. The GH genomic constructions involved ligating an XhoI linker at the AccII site, and inserting the resultant Bg/II, XhoI fragment (-235 to -146) into the Prl -422 CAT construction. Other constructions are described for above.

3 (b)); however, in two experiments with GC₂ cells, approximately 15% of maximal activity was observed, perhaps reflecting altered levels of a required trans-acting factor(s) in some GH cell lines. Based on these data, it appeared possible that there were two separate regions required for prolactin gene enhancer function. This possibility was tested by the ligation in both possible orientations of the inactive 106 nucleotide fragment (-1.769 to -1.663), to the silent region 3' of the HinfI site (-1,697 to -1,530) (see Fig. 3 (g), (h)). Although in five separate experiments neither component fragment alone exhibited any activity, the chimaeric constructions were always active. The fusions in which the two fragments were in the same orientation exhibited 100% of maximal enhancer activity (Fig. 3 (g)), while the chimaeric construction in which the 106 nucleotide 5' fragment was placed in a 3' to 5' orientation exhibited approximately 45% of maximal enhancer activity (Fig. 3 (h)). Inspection of the fusion junctions revealed no fortuitous reconstitution of sequences around the HinfI or HphI sites in either construction.

These data indicate the presence of two discrete, separable sequences, both of which are required for full enhancer function, with no absolute constraints on the relative position or orientation of these two elements for their functional complementation.

Because an 89-bp growth hormone gene region extending from -235 to -146 was insufficient to produce any enhancement, there would appear to be >35 bp spanning the 5' and 3' boundaries of the growth hormone gene enhancer sequence (Fig. 3).

To test the possibility that different factor(s) confer activity characteristic of the respective enhancer elements, the prolactin and growth hormone genes were tested in a rat pituitary cell line (235-1) which produces prolactin but no detectable growth hormone 10. Although the prolactin enhancer is highly active in this cell line, the growth hormone enhancer fails to function even when fused to the prolactin gene promoter (Fig. 4), suggesting different trans-acting factors regulate the two enhancers despite the evolutionary relatedness of the two genes. A chimaeric construction containing the prolactin enhancer

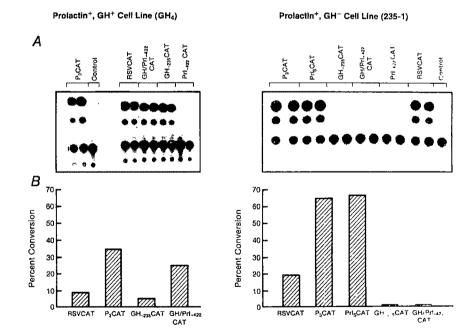
Table 1 Identification of cis-active regions in the 5' flanking sequences of the rat prolactin and growth hormone genes

				Per cent conversi	on
Cell	Species	Type	Prl-5'F	<i>GH</i> -5'F	RSV-EN
MCF7	Human	Mammary epithelium	$\bar{0}$	ō	18
208F	Rat	Fibroblast	ō	$ar{0}$	70
F9	Mouse	Embryonic	ō	$\bar{0}$	50
HIT	Hamster	Pancreatic (endocrine)	$\bar{0}$	$ar{0}$	19
MTC-CA	Rat	Thyroid 'C' cell (endocrine)	ō	Ō	6
JEDEDIAH	Rat	Pituitary (non-endocrine)	ō	Ō	28
GH₄	Rat	Pituitary (endocrine)	6	4	22
G/C	Rat	Pituitary (endocrine)	11	15	15

Fragments extending from -3 kb to +33 bp of the rat prolactin (PI) gene and from -235 to +8 bp of the rat growth hormone (GH) gene were fused to the HindIII site of the bacterial chloramphenicol acetyl transferase (CAT) gene¹⁵, as diagrammed in Fig. 1, such that the promoter and cap site were contributed by the inserted fragment (referred to as Prl 5'F and GH 5'F, respectively). These constructions, and a comparable construction containing the Rous sarcoma virus (RSV) promoter/enhancer [RSV-EN] were used for DNA mediated gene transfer using a series of cell lines, and the activity of expressed CAT enzyme was quantitated 48 h later; the per cent conversion of ¹⁴C-chloramphenicol to the acetylated form is presented. Results are the average of duplicate determinations differing by <5%, and the results were confirmed for each cell line in 3-15 separate experiments. The average expression \pm s.e.m. for the prolactin and growth hormone fusion genes was $18.2\% \pm 3.5\%$ and $4.3\% \pm 0.8\%$, respectively; results were significant at P < 0.001. In other experiments, RSV CAT recorded up to 45% conversion in MTC-CA cells while Prl 5'F and GH 5'F still gave undetectable signals. SV40 enhancer, promoter and Moloney leukaemia virus (MLV) enhancer, promoter, CAT fusions were also used as controls, confirming efficient transfection into the heterologous cell lines. Function of the prolactin promoter in heterologous cell lines was confirmed by demonstration of reproducibly efficient expression of chimaeric constructions containing SV40 enhancer, prolactin promoter (Prl-422, CAT, Fig. 1) in 208F fibroblasts and CV1 cells (6-8% and 25-30% conversion, respectively). A construction containing the MLV enhancer, prolactin promoter was also expressed in these cell lines. $\bar{0}$ = no detectable conversion above mock transfection.

Methods. Plasmids were constructed as described in the legend to Fig. 1, using a BglII-TaqI (-235 to +8 bp) fragment of the GH gene; and XbaI site (-3 kb) and AvaII sites (+33 bp) of the prolactin gene, and the BamHI and HindIII sites of the vector following appropriate site conversions using synthetic linkers by standard techniques. XhoI and HindIII linkers were added at the XbaI and AvaII sites, respectively, of the prolactin genomic fragment, and the fragment was ligated into the XhoI/HindIII sites of the modified vector pSV2 CAT¹⁵. The HindIII site of pSV2 CAT was converted to an XhoI site prior to the insertion of the GH fragments into the BamHI/XhoI sites. All transfections were performed using 10 μg ml⁻¹ of plasmid DNA and the calcium phosphate co-precipitation method¹⁶ or DEAE-dextran sulphate method¹⁷ 48 h prior to harvest. Chloramphenicol acetyl transferase activity was quantitated using 50 μg of protein extract and 10 h incubations, and subjected to chromatography as previously described¹⁵. The RSV, CAT plasmid construction used has been reported¹⁷. In the assay conditions used, there was a linear relationship between chloramphenicol acetylation and CAT activity. Each cell line was grown in serum-containing medium, and medium was changed 3 h prior to transfection.

Fig. 4 Evidence for discrete trans-acting factors mediating the prolactin and growth hormone enhancers. A rat pituitary cell line of lactotroph origin (235-1)¹⁰, which produces only prolactin was used to assess cell-specific action of the GH and Prl gene enhancer sequences. Plasmids analyzed were the GH (-235 to +8) CAT fusion (GH - 235 CAT), the RSV CAT fusion (RSV CAT), the Prl (-422 to +33) CAT fusion (Prl-422 CAT), and a GH (-235 to -47) fragment inserted into the Prl/CAT fusion gene (GH/Prl-422 CAT), the 3-kb prolactin CAT fusion (P3 CAT), and a fusion gene containing Prl -1,831 to -1,530 ligated to the Prl-422 CAT (Prls CAT), as diagrammed in Figs 1 and 2. A shows the autoradiograph of the CAT assay of the plasmids transfected into GH₄ cells (left) or 235-1 cells (right). B shows the per cent conversion for both cell lines in a different experiment. Results were confirmed in five separate experiments of similar design, using 50 µg protein, 10 h assays as previously described



(-1,831 to -1,530) fused 5' to the 235 bp growth hormone flanking region was analysed for expression in the 235-1 cell line and found to be fully active, indicating the growth hormone promoter region was competent for expression, and that failure to express the growth hormone gene in 235-1 cells reflects the apparent absence of a critical *trans*-acting factor.

Despite their reported co-expression during development⁸, the cell-specific expression of the growth hormone and prolactin genes appears to be controlled by structurally distinct, cis-active sequences under regulation of discrete trans-acting factors. The

location of the prolactin gene enhancer described in this manuscript corresponds to a reported pituitary-specific pattern of chromosomal DNase I hypersensitivity, approximately 1.8 kb upstream of the CAP site¹¹. Because the prolactin *cis*-active sequence contains two separable regions which can be placed in either orientation with respect to each other and continue to functionally complement, we suggest that two (or more) *trans*-acting factors are required for the prolactin gene enhancer function in lactotrophs. Exonuclease protection assays of the prolactin enhancer region following binding of extracts from

GH cells tentatively identify at least two distinct and specific protein binding regions coincident with those defined by the mapping analyses.

Although the enhancer sequence of the growth hormone gene contains a region (at -190 bp) which corresponds to the 'core' enhancer sequences identified in the immunoglobulin and several viral genes¹²⁻¹⁴, the growth hormone enhancer core sequence alone is insufficient for function because a region containing >40 bp on each side of this sequence exhibits no enhancer activity. Preliminary footprint analysis reveals that one region located 3' in the growth hormone gene enhancer specifically binds a factor in cells which express the gene (GH cells) but not in cells (235-1) in which the growth hormone enhancer fails to function.

Further understanding of the molecular basis for the selective activation or/and silencing of growth hormone or prolactin gene expression in the development of mature somatotrophs and lactotrophs will require analysis of the expression of transcription units containing heterologous promoters and the respective enhancer sequences in transgenic animals, and the identification and characterization of the cognate trans-acting factors.

We thank Charles Nelson for maintaining the cell culture requirements of the project, Drs John Porter and Michael Cronin for the 235-1 cell line, and Drs Patty Hinkle and Benita Katzenellenbogen for characterized cell lines. C.N., E.B.C. and R.F. are supported by training grants to the Department of

Biology, UCSD; S.L. is on leave of absence from the Universidade Federal de Pernambuco, Brazil. These studies were supported by grants from the US NIH and the McKnight Foundation.

Received 28 August 1985; accepted 24 April 1986.

- Frohman, L. A. in Endocrinology and Metabolism (eds Felig, I. P., Baxter, J. D., Broadas, A. D. & Frohman, L. A. 151-231 (McGraw-Hill, New York, 1981).
 Cooke, N. E., Coit, D., Weiner, R. I., Baxter, J. D. & Martial, J. A. J. biol. Chem. 256,
- 4007-4016 (1981).

- 4007-4016 (1981).

 3. Gash, D., Ahmad, N. & Schechter, J. Neuroendocrinology 34, 222-225 (1982).

 4. Khorram, O., Depalatis, L. R. & McCann, S. M. Endocrinology 115, 1698-1704 (1984).

 5. Oliver, C., Eskay, R. L. & Porter, J. C. Biol. Neonate 37, 145-152 (1980).

 6. Watanabe, Y. G., Daikoku, S., Devl Biol. 68, 557-567 (1979).

 7. Chtetlain, A., Dupuoy, J. P. & Dubois, M. P. Cell Tissue Res. 196, 409-427 (1979).

 8. Hoeffler, J. P., Bookfor, F. R. & Frawley, L. S. Endocrinology 117, 187-195 (1985).

 9. Bancroft, F. C. Functionally Differentiated Cell Lines 47-55 (Liss, New York, 1981).

 Permond M. I. Narral, D. P. Burcow, G. H. Newyer, W. P. & Botter, I. C. Astendor
- 10. Reymond, M. J., Nansel, D. D., Burrows, G. H., Neaves, W. B. & Porter, J. C. Acta endocr.
- Kriegler, M. & Botchan, M. Molec. Cell Biol. 3, 325-329 (1983).
- 13. DeVilliers, J. L., Olson, L., Tyndall, C. & Schaffner, W. Nucleic Acids Res. 10, 7965-7976 (1982).
- 14. Gluzman, Y. & Shenk, T. (eds) Enhancers and Eukaryotic Gene Expression (Cold Spring Harbor Laboratory, New York, 1983).

- Gorman, C. M., Moffat, L. F. & Howard, B. H. Molec. Cell Biol. 2, 1044-1051 (1982).
 Graham, F. L. & Van der Eb, A. J. Virology 52, 456-457 (1973).
 Gorman, C., Merlino, G. T., Willingham, M. C., Pastan, I. & Howard, B. Proc. natn. Acad. Sci. U.S.A. 79, 6777-6781 (1982).
- 18. Cooke, N. G. & Baxter, J. D. Nature 297, 603-606 (1982).
- Maurer, R. A. DNA 4, 1-9 (1984).
 Barta, A., Richards, R. I., Baxter, J. D. & Shine, J. Proc. natn. Acad. Sci. U.S.A. 78, 4862-4871
- 21. Sanger, F., Nicklen, S. & Coulson, A. R. Proc. natn. Acad. Sci. U.S.A. 74, 5463-5467 (1977).

Transcriptional interference and termination between duplicated α -globin gene constructs suggests a novel mechanism for gene regulation

N. J. Proudfoot

Sir William Dunn School of Pathology, University of Oxford, South Parks Road, Oxford OX1 3RE, UK

The interesting possibility that transcriptional interference can occur between eukaryotic genes was raised by studies on the avian leukosis retrovirus (ALV)1 which showed that deletion of the promoter in the 5' long terminal repeat (LTR) activates the 3' LTR promoter, linked to a downstream gene. These observations provide a molecular explanation for the fact that insertional oncogenesis by the ALV promoter is invariably associated with either a rearranged or deleted 5' LTR sequence2-4. This letter extends these findings to chromosomal RNA polymerase II genes by studying transcriptional interference between duplicated α globin gene constructions. I demonstrate that transcriptional interference causes substantial inhibition of the downstream α gene by transcription of the upstream α gene. Furthermore, this inhibition is alleviated by placing transcriptional termination signals between the two α genes. Because many eukaryotic genes may be arranged in tandem on a chromosome, these observations suggest that transcriptional termination is an important mechanism for preventing interference between adjacent genes. The selective use of termination signals may provide a novel way of regulating the activity of eukaryotic genes.

The HeLa cell transient expression procedure^{5,6} was used initially as a convenient system to study α -globin gene transcription. In this technique, the a genes are introduced into HeLa cells as part of an episomal plasmid that may be present at copy numbers as high as 10,000 or more per cell nucleus⁶. Figure 1a shows a diagram of the pSVod plasmid⁶ containing two human α -globin genes ($\alpha\alpha$ pSVod). The α genes are separated by about 700 base pairs (bp) and each one contains more than 300 bp of 5'-flanking sequences but only about 100 bp of 3'-flanking

sequence. Therefore, although the poly(A) sites of each α gene are intact, they are unlikely to contain possible 3'-flanking region termination signals. pSVod is a transient expression vector based on pBR322 containing the simian virus 40 (SV40) replication origin but not the enhancer sequence (72-bp repeat). The SV40 early and late promoters are also present in the SV40 origin (ori) region but will be largely inactive in pSVod, since the early promoter requires the enhancer^{7,8}, and the late promoter has its major initiation sites within the 72-bp repeat sequence, absent in pSVod9. Co-transfection of pSVod with another plasmid (SVpBR328Rβ1)¹⁰ containing both the SV40 large-T antigen and rabbit β -globin genes allows replication of SV40 origincontaining plasmids⁵ as well as providing a control to test for efficiency of transfection. The 5' α -globin gene has a 13-bp insert in its 5' noncoding sequence, called Tag, to allow the otherwise identical 5' termini of the two α -gene transcripts to be distinguished by the primer extension RNA mapping technique¹¹. Figure 1a also shows two constructs in which either the 5' α -gene or 3' α -gene promoter is deleted ($\Delta P \alpha \alpha$ and $\alpha \Delta P \alpha$).

Figure 1b shows the primer extension analysis on $\alpha\alpha$, $\Delta P\alpha\alpha$ and $\alpha \Delta P \alpha$ transfections. The relative efficiency of each transfection is indicated by the intensity of the 3'-end signal produced by S_1 nuclease mapping¹² of rabbit β -globin messenger RNA in turn produced by the co-transfected plasmid shown under each lane. RNA from cells transfected with $\alpha\alpha$ pSVod gives two extension products corresponding to the Tag-containing 5' α gene mRNA and normal 3' α -gene mRNA. The product bands are doublets, as is usually observed with primer extension, possibly reflecting partial extension onto the 5' CAP structure of the mRNA. Deletion of the promoter of the 5' α gene as shown by $\Delta P \alpha \alpha$ results in an approximately threefold increase in the 3' α -gene signal. Surprisingly, deletion of the promoter of the 3' α gene also results in an approximately threefold increase in the 5' α -gene signal as can be seen by comparing $\alpha\alpha$ and $\alpha\Delta P\alpha$. These data indicate that each α -gene promoter exerts an inhibitory effect on the other α -gene promoter. One possible cause of this inhibition could be through a competitive effect between the two α -gene promoters for possibly limiting factors. Alternatively, a transcriptional interference mechanism may be responsible for the observed modulation in mRNA levels.

b

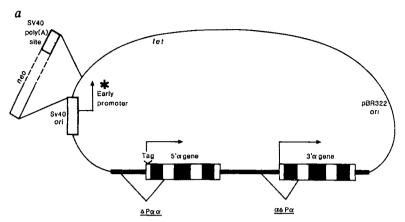
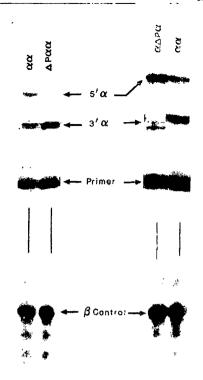


Fig. 1 a, Diagram of $\alpha\alpha$ pSVod (ref. 6). α Genes are depicted by a thick line for flanking sequences, open boxes for noncoding and intron sequences, solid boxes for exon sequences. The positions of the promoter deletions in $\Delta P\alpha\alpha$ and $\alpha\Delta P\alpha$ are indicated. \Box Denotes position and direction of promoter. * Indicates that the SV40 early promoter is only functional in pSVedneo. The pBR322 sequence is depicted by a thin line. Note that the sequence in pBR322 found to inhibit SV40 replication (between the pBR322 replication origin and tetracycline resistance gene (tet^r) gene) is deleted in pSVod. SV40 sequences are depicted by shaded boxes. The SV40 ori sequence in pSVod contains the replication origin but not the enhancer. As indicated, the neomycin resistance gene and SV40 poly(A) site¹⁷ were added to the plasmid. In addition, the SV40 origin region was expanded slightly to include the enhancer sequence as this is required for the early promoter^{7,8}. b, Primer extension RNA analysis¹¹ on cytoplasmic RNA purified from HeLa cells transiently transfected with $\alpha\alpha$ -; $\Delta P\alpha\alpha$ - and $\alpha\Delta P\alpha$ SVod, together with the co-transfection control plasmid SVpBR328R β 1 (ref. 10). 3'-End S₁ mapping 12 data on rabbit β -globin mRNA produced by SVpBR328R β 1 are shown beneath each lane.



Methods. DNA constructions: The Tag α promoter was constructed by ligating a 134-bp human α 1-globin gene HinfI fragment containing 112 bp of 5'-flanking sequence together with 22 bp of 5' noncoding sequence into the polylinker Sall site of pUC9²³ This Hinfl fragment contained all the sequence required for initiation of transcription of the α 1-globin gene promoter. Next, an 894-bp Hinfl-Pul fragment containing the rest of the α 1-globin gene was ligated into the BamHI site of pUC9, next to the previously used Sall site. This effectively results in expansion of the 5' noncoding Hinfl site of the α 1-globin gene by 13 nucleotides and thereby 'Tags' the 5' end of the α 1 gene²³. $\alpha\alpha$ -, $\Delta P \alpha \alpha$ - and $\alpha \Delta P \alpha p S V$ od were made by cutting α 1pSVod with Smal to remove the promoter region and exon 1 of α 1. Tag α pSVod was then made by ligating the same Smal fragment from Tag alpUC9 into the Sma-cut alpSVod vector. APapSVod was made by ligating alpSVod Sma vector back together without an insent fragment The second al gene as a 1.6-kb PstI fragment was then added to Tag or APalpSVod at a unique PstI site in the 3'-flanking sequence of the a gene to make ααpSVod and ΔΡααpSVod. Similarly, a ΔΡα1 gene fragment was added 3' to Tag α1pSVod to make αΔΡαpSVod. pSVedneo: The plasmid pSV2*neo containing the Tn5 neomycin phosphotransferase gene which contains the SV40 early promoter and poly(A) site flanking the neo gene has been described elsewhere HindIII-BamHI fragment containing the neo gene and the SV40 early poly(A) site from pSV2*neo was ligated into pSVed between the HindIII and BamHI sites pSVed is a variant on pSVod containing slightly more SV40 origin sequence to include the transcriptional enhancer²⁴. Various α-gene-containing pSVod plasmids were then converted into pSVedneo plasmids by exchanging the EcoRI-BamHI fragment in pSVod for the equivalent SV40 origin neo fragment in pSVedneo HeLa cell translent expression: Transfections were carried out as described previously^{6,24}. Briefly plasmid DNA was precipitated with calcium phosphate and added to subconfluent Petri dishes of HeLa cells. After 10-16 h, the medium was changed and the cells allowed to grow for another 48 h. The HeLa cells were collected, lysed in Nonidet P-40 detergent buffer, and the cytoplasmic and nuclear fractions separated by centrifugation through a sucrose cushion. Following incubation with proteinase K, cytoplasmic RNA was purified by phenol chloroform extraction and ethanol precipitation. RNA mapping: Primer extension11 DNA primer for α -globin mRNA 5'-end analysis was a single-strand HinfI-HaeIII fragment extending from the middle of the first exon to the middle of the 5'-noncoding region of the α 1-globin gene. This was obtained by filling in the HinfI end of the double-strand DNA with $[\alpha^{-3^2}P]$ dATP and fractionating on α denaturing 7 M urea 12% polyacrylamide gel. DNA primer (20 c.p.m., specific activity 3,000 Ci mmol⁻¹) and cytoplasmic RNA (~20 µg) were annealed in 10 µl of 10 mM PIPES pH 6.4, 0.4 M NaCl at 80 °C for 10 min and at 63 °C overnight. 50 µl of reverse transcriptase buffer (50 mM Tris pH 8.2, 10 mM duthiothicuol. 6 mM MgCl₂, 0.5 mM dATP, dCTP, dTTP and dGTP plus reverse transcriptase (5 U)) were added to hybridizations and incubated at 42 °C for 1 h. RNave (20 µg) was added to incubation and left a further 15 min at 42 °C. The reaction was phenol extracted, ethanol precipitated and fractionated by electrophoresis on 7 M urea polyacrylamide gels. S_1 mapping 12 : SVpBR328R β 1 was digested with EcoRI and the ends filled in with $[\alpha^{-32}P]$ dATP using standard procedures. This gives urea polyacytamine gets. 5₁ mapping: Syphologory i was digested with Ecoki and the ends filled in with [α-T-P]dAIP using standard procedures. This gives a rabbit β-globin mRNA S₁ probe labelled at an EcoRi site at the beginning of the last exon. The 3'-end signal for rabbit β-globin mRNA is approximately 200 nucleotides. The S₁ probe (-20 c.p.m., specific activity 3,000 Ci mmol⁻¹) was annealed to HeLa cell cytoplasmic RNAs (-20 μg) in 30 μl of 80% formanide, 0.04 M PIPES pH 6.8, 0.4 M NaCl, 0.1 mM EDTA by denaturation at 80 °C for 10 min, then 53 °C overnight. Ice-cold S₁ buffer (0.3 ml; 0.25 M NaCl, 0.0) M NaOAc pH 4.6, 2 mM ZnSO₄, 50 μg ml⁻¹ denatured sonicated carrier DNA) plus S₁ (3,000 U) was quickly added to each hybridization and incubated for 1 h at 30 °C. S_I reactions were ethanol precipitated and fractionated on denaturing, 7 M urea polyacrylamide gels.

To test which of these two explanations is correct, I investigated the effect of placing RNA polymerase II termination signals between the two α genes. Two termination signals have been identified and characterized for RNA polymerase II genes, one for the sea urchin H2A histone gene^{13,14} and the other for the mouse β -globin gene^{15,16}. However, in both cases, it was necessary to include fairly extensive regions of sequence including both the 3' end of the gene as well as 3'-flanking sequence, since neither terminator signal has vet been localized more precisely. Figure 2a demonstrates the various positions in which these terminators were placed with respect to the duplicated α -globin genes. First, the histone terminator was positioned either between $(\alpha T\alpha)$ or after $(\alpha \alpha T)$ the two α genes. As a control, a deleted form of the histone terminator which is known to have lost its termination activity¹³ was placed between the two α genes ($\alpha\Delta T\alpha$). Second, the mouse β termination sequences were placed in both orientations between the two α genes $(\alpha \vec{m} \beta \alpha \text{ and } \alpha \vec{m} \beta \alpha).$

Figure 2b shows the primer extension data obtained for this second set of $\alpha\alpha$ pSVod constructs. No co-transfection controls are shown for these experiments, since each primer extension experiment is internally controlled by the ratios of the Tag α and α bands. As indicated, $\alpha T\alpha$ caused an approximately threefold increase in the 3' α - as compared with the 5' α -gene signal while $\alpha\alpha T$ caused a similar threefold increase in the 5' α -gene signal. Thus, placing a terminator sequence between or after the duplicated α genes has a similar effect to deleting either of the two α -gene promoters. The control $\alpha\Delta T\alpha$ with a nonfunctional termination signal¹³ gave more equal ratios of 5' and 3' α signals, demonstrating that the 3:1 ratio for 5' α to 3' α in $\alpha T\alpha$ is caused by a termination process. In fact, the 5' α signal is routinely lower than the 3' α signal in $\alpha\alpha$ pSVod, possibly due to the Tag sequence which may reduce the efficiency of the α -gene promoter. Finally, $\alpha\vec{m}\beta\alpha$ gave threefold more 3' α signal

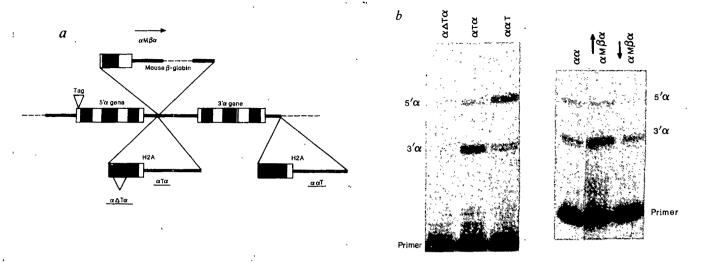


Fig. 2 a, Diagram showing positions of H2A histone and β -globin gene termination signals with respect to the two genes in $\alpha\alpha$ pSVod. The mouse β -globin terminator was placed in both orientations between the two α genes. The arrow denotes the normal direction of transcription on the β -globin gene. Key as for Fig. 1a. b, Primer extension RNA analysis on $\alpha\alpha$ pSVod terminator transfection as in Fig. 1.

Methods. DNA constructions: H2A histone terminator: A 0.9-kb TaqI fragment containing the 3' side of the sea urchin H2A histone gene together with nearly all of its 3'-flanking sequence was purified from a larger plasmid containing the whole gene (a generous gift from Professor M. Birnstiel, University of Zurich). This fragment has been shown to contain all of the necessary signals to elicit transcriptional termination (ref. 13). The histone H2A gene Taq fragment (T) was then added to either of the PatI sites flanking the 3' α 1-slobin gene $(\alpha T\alpha$ - and $\alpha\alpha$ TpSVod). Finally, α T α was cut with Sac I and PvuI to excise a region of the histone

fragment has been shown to contain all of the necessary signals to elicit transcriptional termination (ref. 13). The histone H2A gene Taq fragment (T) was then added to either of the PstI sites flanking the 3' α1-globin gene (αTα- and ααTpSVod). Finally, αTα was cut with SacI and PvuI to excise a region of the histone gene that is essential for transcriptional termination (ref. 13). Mouse β major globin terminator: An EcoRI-BgIII DNA fragment containing the whole mouse β-major globin gene plus extensive 3'-flanking sequence was subcloned into pSVed (ref. 24) between the EcoRI and HincII sites (amp gene): mβmajpSVed. A PstI fragment was then excised from mβmajpSVed which extended from the 3' end of intron 2 to the PstI site in pSVed 300 bp beyond the HincII site. This fragment contains the essential D, E and F fragments defined by Falck-Pedersen et al. 16 as well as 300 bp of pBR322 amp resistance gene sequence. The 2.0 kb PstI fragment was then ligated into the PstI site between the two α genes in ααpSVod in both orientations to form αmβα- and αmβαpSVod.

while $\alpha \tilde{m} \beta \alpha$ and $\alpha \alpha$ gave nearly equal levels of 5' and 3' α signal. These results confirm the data obtained for $\alpha T \alpha$ by demonstrating that a second terminator sequence, that from the mouse β -globin gene, behaves exactly as the histone terminator and, furthermore, that it is orientation specific. Taken together, these data argue that transcriptional interference does occur between the duplicated α genes, rather than a promoter competition effect. In fact, the data indicate that not only does the first α gene interfere with the second α gene, but also that the second α gene, presumably by transcription all around pSVod, in turn interferes with the first α gene. This would suggest that in $\alpha\alpha$ both α genes are subject to equal transcriptional interference. so that the two α gene signals are nearly equal. However, with $\alpha T \alpha$ the second α gene is released from interference but the first is not, resulting in a 1:3 ratio. Finally, with $\alpha\alpha T$, the first α gene, but not the second, is released from interference, giving a ratio of 3:1.

The present studies on the transcription of duplicated α genes in a transient expression assay demonstrate that a nearly threefold transcriptional interference effect occurs between the two adjacent α -globin genes. The observation that the 3'-positioned α gene inhibits the 5' α gene by transcription all the way around the plasmid suggests that transcriptional interference occurs over a distance of at least 3 kilobases (kb). In fact, this possibility is confirmed by the $\alpha m\beta \alpha pSVod$ constructs which effectively separate the two α -globin genes by 3 kb and yet clearly demonstrate a transcriptional interference effect between the two α globin genes (Fig. 2b). Clearly, the study of multiple genes in transient expression plasmids must take into account transcriptional interference as a possible cause of modulation in promoter efficiency. The molecular basis of this interference effect is probably due to RNA polymerase II molecules first transcribing the 5' gene and then reading on into the 3' gene. This effectively obscures the promoter of the 3' gene from independent initiation of transcription by other RNA polymerase II molecules. Transcriptional termination would thus alleviate this interference

effect. The observation that both the H2A and mouse β -globin terminator sequences prevent this interference effect is therefore strong confirmatory evidence that these sequences are transcriptional terminators.

The fact that I observe a threefold interference effect in transient expression may not reflect the true physiological levels of this phenomenon. In transient expression, as many as 10,000 copies of the plasmid are generated by replication. Thus, pSVod

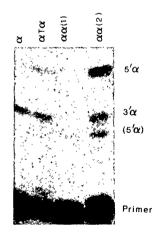


Fig. 3 Primer extension analysis on G418-resistant HeLa cell pools transfected with either $\alpha\alpha$ pSVedneo (two separate pools) or α T α pSVedneo. The α lane is a control experiment using RNA purified from the α -globin-producing cell line K562 (ref. 24).

Methods. The $\alpha\alpha$ - and α T α pSVedneo plasmids together with SVpBR328R β 1 as a source of large-T antigen were transfected onto HeLa cells as for Fig. 1. Following exposure to the calcium phosphate-DNA precipitates, the HeLa cells were incubated for 48 h and G418 (80 μ g⁻¹) was then added to the medium. After about 2 weeks of G418 selection, small, resistant colonies were obtained and allowed to grow to confluence. Primer extension assays were performed as for Fig. 1, but ~100 μ g of cytoplasmic RNA was used in each reaction to obtain detectable signals.

possesses an SV40 replication origin that is stimulated by large-T antigen⁵ produced by the RβSVpBR328 co-transfected plasmid. The high copy number of α -globin genes obtained in transfected HeLa cell nuclei may effectively be in excess of the endogenous RNA polymerase II. Transcriptional interference effects would thus be diminished. However, endogenous chromosomal RNA polymerase II genes are usually single copy, so that RNA polymerase II should be in excess. Interference between adjacent genes could therefore be much higher. To test this possibility, I transfected $\alpha\alpha$ pSVod and α T α pSVod plasmids containing the neomycin drug resistance gene (neo)17 as part of the SV40 early gene transcription unit (Fig. 1a and legend) into HeLa cells. Following conditions for selection with the antibiotic G418, pools of resistant HeLa cell clones that had stably integrated the neo gene-containing plasmids were obtained, one pool for α T α pSVod and two separate pools for $\alpha\alpha$ pSVod. In each case, the complexity of each pool was in excess of 100 independent clones. Therefore, any specific chromosomal position effects on one clone should be averaged out. Similarly, clones in which integration of the plasmid occurred either between or within the two α genes should not influence the average levels of α -globin mRNA expression by the whole pool.

Figure 3 shows the primer extension data for RNA purified from the three G418-resistant HeLa cell pools. High amounts of RNA were used in the reverse transcriptase reactions because the level of α mRNA was lower than in the transient expression experiments. As indicated, both $\alpha\alpha$ pSVod pools gave a strong 5' α signal relative to the 3' α signal. Indeed, for $\alpha\alpha(1)$, which overall gave rather low α mRNA signals, no 3' α signal was detected at all, while for $\alpha\alpha(2)$, the 3' α signal was 20-fold lower than the 5' α signal. A third $\alpha\alpha$ pSVod pool has recently been analysed and shows 5-fold less $3'\alpha$ signal than $5'\alpha$ (data not shown). In contrast, with $\alpha T \alpha$ both 5' and 3' α signals were nearly equivalent. Note that a band (5') was routinely observed below the 3' α signal. Indeed, this band was more noticeable when using the high amounts of RNA necessary to detect α mRNA signal with the transfected HeLa cell pools. This band clearly derives from the 5' α signal, since no such band is visible with the α control lane but is detectable in the 5' α signal shown for $\alpha\Delta P\alpha$ in Fig. 1b. Presumably, this is due to the different RNA secondary structure of the Tag-containing α mRNA. Taken together, these data demonstrate a 5-to-20-fold level of transcriptional interference between the duplicated α genes when placed in a chromosomal environment. This interference can be wholly alleviated by placing the histone terminator between the two α genes.

The demonstration of a threefold interference effect between duplicated α genes in episomal plasmids and the greater, effect in chromosomes, clearly underlines the essential role of transcriptional terminators in eukaryotic gene transcription. Although in these experiments I have intentionally placed the two α genes in close proximity (~700 bp apart), it is probable that interference can occur over greater distances, especially since many gene transcription units are longer than 100 kb^{18,19}.

Received 13 March; accepted 9 May 1986

- 1. Cullen, B. R., Lemedico, P. T. & Ju, G. Nature 307, 241-245 (1984)
- 2. Neel, B. G., Hayward, W. S., Robinson, H. L., Fang, J. & Astrin, S. M. Cell 23, 323-334
- Fung, Y. T., Fadly, A. M., Crittenden, L. B. & Kung, H. J. Proc. natn. Acad. Sci. U.S.A. 78, 3418-3422 (1981).
- 4. Varmus, H. E. & Swanstrom, R. in RNA Tumor Viruses 2nd edn, 369-512 (Cold Spring
- Harbor Laboratory, New York, 1982).

 Banerji, J., Rusconi, S. & Schaffner, W. Cell 27, 299-308 (1981).

 Mellon, P., Parker, V., Gluzman, Y. & Maniatis, T. Cell 27, 279-288 (1981).

 Benoist, C. & Chambon, P. Nature 290, 304 (1981).

- Fromm, M. & Berg, P. J. molec. appl. Genet. 111, 457 (1982). Ghosh, P. K., Reddy, V. B., Swinscoe, J., Lebowitz, P. & Weissman, S. M. J. molec. Biol. 126, 813 (1978).
- 10. Grosveld, G. C., de Boer, E., Shewmaker, C. K. & Flavell, R. A. Nature 295, 120-126 (1982).

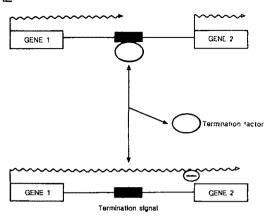


Fig. 4 Model for gene regulation by transcriptional interference.

The interesting possibility that the control of a gene could be partly mediated by transcriptional interference from an upstream gene is now a serious possibility. Figure 4 demonstrates a possible model for this type of control process. The model requires that a termination factor must recognize the termination signal to elicit transcriptional termination. Such an interaction would allow the downstream gene to operate free from upstream gene transcriptional interference. However, the absence or dissociation of the termination factor from the termination signal would allow upstream gene transcripts to read through the terminator to interfere with transcription of the downstream gene. So far, no such terminator factors have been identified for RNA polymerase II genes, although RNA polymerase I terminator factors have recently been identified²⁰. A possible variation on the model depicted in Fig. 4 could be that the factor recognizing the terminator sequence is an anti-termination factor, so that interference of the downstream gene would occur by anti-terminator factor binding rather than terminator factor release. Such terminator and anti-termination factors are well documented in prokaryotes, with the Escherichia coli termination factor rho and the bacteriophage λ N and Q antiterminators as classic examples²¹. It remains to be established whether or not equivalent termination factors are involved in the regulation of eukaryotic gene expression.

A number of my colleagues have contributed significantly to this project, Mike Johnson constructed the Tag α gene and did some preliminary experiments²³, Chris Norman constructed the H2A termination constructs, and Sarah Hargreaves carried out primer extension analysis on the $\alpha m \beta \alpha$ constructs. I also thank the members of my laboratory for many helpful discussions throughout these studies.

- 11. Proudfoot, N. J., Shander, M. H. M., Manley, J. L., Gefter, M. L. & Maniatis, T. Science 209, 1329-1336 (1980).
- 12. Weaver, R. F. & Weissmann, C. Nucleic Acids Res. 7, 1175-1193 (1979)
- 13. Johnson, M. R., Norman, C., Reeve, M. A., Scully, J. & Proudfoot, N. J. Molec. (ell Biol. (submitted).
- 14. Birchmeier, C., Schumperli, D., Sconzo, G. & Birnstiel, M. L. Proc. natn. Acad. Sci. U.S. 5 81, 1057-1061 (1984).
- 15. Citron, B., Falck-Pedersen, E., Salditt-Georgieff, M. & Darnell, J. E. Jr Nucleic Acids Res. 12, 8723-8732 (1984).
- 16. Faick-Pedersen, E., Logan, J., Shenk, T. & Darnell, J. E. Jr Cell 40, 897-905 (1985).
- 17. Southern, P. J. & Berg; P. J. molec. appl. Genet. 1, 327-341 (1982).
 18. Bender, W. et al. Science 221, 23-29 (1983).
- Toole, J. J. et al. Nature 312, 342-347 (1984).
- Grummt, I., Maier, U., Ohrlein, A., Hassouna, N. & Bachellerie, J.-P. Cell 43, 801-810 (1985).
 Rosenberg, M. & Court, D. A. Rev. Genet. 13, 319-353 (1979).
 Vicira, J. & Messing, J. Gene 19, 259-272 (1982).
 Johnson, M. R. thesis, Univ. Oxford (1984).

- 24. Proudfoot, N. J., Rutherford, T. R. & Partington, G. A. EMBO J. 3, 1533-1540 (1984).

Cloning of a major surface-antigen gene of *Trypanosoma cruzi* and identification of a nonapeptide repeat

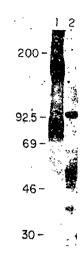
David S. Peterson, Ruth A. Wrightsman & Jerry E. Manning

Department of Molecular Biology and Biochemistry, University of California, Irvine, Irvine, California 92717, USA

The parasitic protozoan Trypanosoma cruzi can establish infection in humans and other vertebrate hosts through direct penetration of host cells by trypomastigotes transmitted by the insect vector¹. Although the molecular processes involved in trypomastigote interiorization of vertebrate cells are unknown, several studies suggest that surface glycoproteins are involved2-4. It is likely that the proteins involved are specific to the trypomastigote stage of the parasite, since only trypomastigotes found in both the insect vector and the vertebrate host bloodstream are capable of invading vertebrate cells. In contrast, the epimastigote stage, found exclusively in the vector, and the amastigote stage, an intracellular stage in the vertebrate host, cannot penetrate the cell directly. We have therefore concentrated our efforts on trypomastigote surface proteins and, along with others, have identified two trypomastigotespecific surface glycoproteins of relative molecular mass (M_r) 90,000 (90K) and 85,000 (85K)^{5,6}. Antibody neutralization experiments indicate that the 85K glycoprotein is necessary for efficient interiorization of trypomastigotes in mammalian cells. Here we describe the molecular cloning of a genomic DNA fragment that encodes antigenic determinants present in the 85K trypomastigote surface antigen. The polypeptide fragment encoded by the cloned DNA is recognized by serum from a T. cruzi-infected host and is inferred by DNA sequence analysis to contain a nonapeptide unit that is tandemly repeated five times. Also, the messenger complementary to the cloned DNA fragment is present only in the trypomastigote stage of the parasite.

We have previously reported that the major surface proteins of the trypomastigote stage can be isolated free of most cytosolic components by using iminobiotin-avidin interaction⁶. This preparation of iminobiotinylated surface proteins (IBSP) contains

Fig. 1 Immunoblot analysis of SDS-lysates of Peru strain trypomastigotes (lane 1) and Peru strain epimastigotes (lane 2) using anti-IBSP antibodies. Total cellular proteins were solubilized in Laemmli sample buffer¹⁵ at a concentration of 2×10^8 cells ml⁻¹. After being heated for 3 min, 25 µl of each lysate was added to each lane of a 10% polyacrylamide SDS gel. After electrophoresis the gel was electroblotted to nitrocellulose and processed as described previously⁶. The serum used to probe the filter was a 1:1,000 dilution of rabbit anti-IBSP serum. Detection of the rabbit antibody was with 125 Igoat-anti-rabbit IgG. Markers for calibration of the gel are ¹⁴C-methylated myosin (200,0000). phosphorylase-b (92,5000), bovine serum albumin (69,000), ovalbumin (46,000), carbonic anhydrase (30,000).

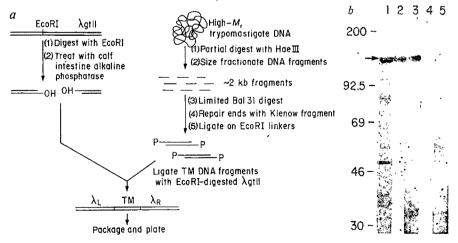


the major 85K and 90K glycoproteins as well as several minor surface polypeptides. Sera from rabbits immunized with the IBSP preparation recognized polypeptides of 90K, 85K and 76K in trypomastigotes, but not in epimastigotes, as determined by Western blot analysis (Fig. 1). In contrast, a 105K antigen was recognized in both forms of the parasite.

To obtain DNA fragments which encode a portion of the surface polypeptides, a recombinant DNA library was constructed in the expression vector λ gt11 (ref. 7) using fragments of Peru strain trypomastigote genomic DNA (Fig. 2a). Approximately 100,000 recombinant phage were screened with the anti-IBSP sera and 6 phage expressing T cruzi antigens were identified. One of these clones, Tcg-1, encoded a hybrid protein of M_r 132,000, which is approximately 16,000 daltons larger than β -galactosidase. In Western blots the fusion protein was recognized by the anti-IBSP sera as well as by sera from a mouse infected with T cruzi, thus indicating that the epitope(s) encoded in Tcg-1 is also recognized by the immune system of the infected host during an active T cruzi infection (Fig. 2b).

Since the anti-IBSP sera recognized several surface proteins, it was necessary to determine which surface protein was represented in the Tcg-1 fusion protein. BALB/c mice were immu-

Fig. 2 a, Construction and screening of a trypomastigote genomic DNA library. DNA of high Mr was isolated from culture-form trypomastigotes of the Peru strain, partially digested with endonuclease HaeIII, size fractionated by centrifugation on a 10-40% sucrose gradient and fragments with an average length of 2,000 bp were collected. After a 30 min digestion wih slow Bal31 nuclease, 5 µg DNA per unit of enzyme (International Biotechnologies Inc.), the resected DNA fragments were repaired with the Klenow fragment of Escherichia coli DNA polymerase I, and EcoRI linkers were added to the ends of the fragments to allow insertion into the single EcoRI site of λgt117. The recombinant molecules were packaged in vitro and plated on E. coli strain Y1090. Using 5-bromo-4-chloro-3-indolyl-α-D-galactopyranoside as an indicator, recombinant phage represented 85% of all plaques. Approxi-



mately 100,000 plaques were screened for antigen producers using a 1:500 dilution of rabbit anti-IBSP sera as described previously 16 except that 125 I-protein A was used to detect λ plaques recognized by the anti-IBSP sera. Six plaques produced positive signals upon successive rescreens with the anti-IBSP sera. b, Analysis and partial purification of the fused polypeptides encoded in Tcg-1. Tcg-1 hybrid protein and native β -galactosidase were partially purified as described by Hall et al. 18 . The proteins isolated from the induced lysogens were electrophoresed on a 10% polyacrylamide SDS gel at a concentration of 15 μ g protein per lane. After electrophoresis, lane 1 was stained with Coomassie blue and lanes 2-5 were electroblotted to nitrocellulose. In lane 1 the arrow denotes the position of the fusion protein at 132,000 M_r . Lanes 2 and 3 are Western blots of Tcg-1 fusion protein reacted with anti-IBSP sera (lane 2) and sera from a mouse infected with T cruzi (lane 3). Partially purified β -galactosidase from λ gt11 was Western blotted and reacted with anti-IBSP sera (lane 4) and T cruzi-infected mouse sera (lane 5).

1 2 3

92.5

69

46-

30~

Fig. 3 Identification of native proteins that share antigenic determinants with Tcg-1 fusion protein. Western blots of a trypomastigote lysate (lane 2) and epimastigote lysate (lane 3). Lane 1 shows a Western blot of a trypomastigote lysate probed with anti-IBSP sera at a 1:1000 dilution, Methods. Tcg-1 fusion protein (270 µg) was electrophoresed on a preparative 10% polyacrylamide SDS gel and electroblotted to nitrocellulose. Two strips of the extreme ends of the nitrocellulose blot were removed and probed with anti-IBSP sera to determine the precise location of the Tcg-1 fusion protein. The region of the nitrocellulose containing the fusion protein was excised and reacted with 5 ml of undiluted anti-IBSP sera plus 5 ml of blocking buffer as described previously8. After 10 washes in buffer containing 10 mM Tris pH 7.4, 0.9% saline, 0.05% Tween-20 and 0.01% gelatin, the bound antibody was eluted by incubation in 1.0 ml of 0.1 M glycine-HCl pH 2.6, 0.15 M NaCl and

immediately neutralized by addition of an equal volume of 1 M Tris-HCl pH 8.0. This antibody solution was used to probe the Western blots.

nized with a protein fraction enriched for Tcg-1 fusion protein. The mouse anti-Tcg-1 sera were absorbed against induced \(\lambda\) gt11 lysogens and used to probe lysates of trypomastigotes and epimastigotes on Western blots (not shown). While no polypeptides in the epimastigote lysate were recognized by the serum antibodies, two polypeptides of M_r 85,000 and 76,000 were recognized in the trypomastigote lysate. However, the intensities of the bands in the autoradiogram were weak, suggesting that a strong immune response was not elicited against the fusion protein. We used antibody selection⁸ to confirm the identity of the T. cruzi polypeptide encoded in Tcg-1. Tcg-1 fusion protein bound to nitrocellulose was used to affinity-purity antibodies from rabbit anti-IBSP sera. The affinity-purified antibodies recognized two polypeptides of 85K and 76K in Western blots of a trypomastigote lysate (Fig. 3). However, no polypeptides were detected in Western blots of epimastigote lysates. In a control experiment using native β -galactosidase under the same conditions as for antibody selection with Tcg-1 fusion protein, no polypeptides in either of the T. cruzi lysates were recognized. We conclude from these results that Tcg-1 contains DNA sequences that encode an epitope(s) present in the 85K and 76K polypeptides.

As shown in Fig. 1, both the 85K and 76K polypeptides are

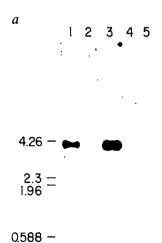
present in the trypomastigote but not epimastigote stage of the parasite. To determine whether the mRNA(s) which code for these polypeptides are also stage specific, the 500-base-pair (bp) T. cruzi DNA fragment in Tcg-1 was hybridized to a Northern blot containing poly(A)⁺ RNA and/or total cytoplasmic RNA extracted from trypomastigotes, epimastigotes and amastigotes. Hybridization was observed to a single mRNA band with an apparent molecular length of 3.8 kilobases (kb) only in trypomastigote RNA, thus confirming the stage specificity of these polypeptides (Fig. 4a).

The T. cruzi fragment in Tcg-1 was excised by cleavage with endonuclease EcoRI, re-cloned into the sequencing vector M13mp9 and sequenced by the Sanger dideoxy chain-termination method⁹. The DNA fragment encoding the surface antigen was 500 bp long, and contained a 27-bp repeat unit which occurred five times in tandem within the sequence (Fig. 4b). Degenerate repeats of 33 bp and 21 bp preceded and followed the five tandem repeats, respectively. Within the repeat unit, a single base change of $A \rightarrow G$ occurred once (nucleotide 223) and a $T \rightarrow C$ transition twice (nucleotides 189 and 215).

Since no protein sequence data are available for T. cruzi surface proteins, the amino-acid sequence encoded in the T. cruzi DNA fragment in Tcg-1 was deduced from the DNA sequence. The coding strand was determined by hybridization of poly(A)+ trypomastigote RNA to M13mp9 recombinants containing the two complementary DNA strands. A single open reading frame encoding 139 amino acids in frame with β galactosidase was observed. The predicted reading frame terminated with a TGA stop codon immediately followed by a second TGA codon 3 bp downstream. In this reading frame the $A \rightarrow G$ transition occurred in the second base of the code, resulting in a Glu → Gly amino-acid change. The T → C transition resulted in a third position change in Asp, but the amino acids remained unchanged. With regard to the two degenerate repeat units, the 33-bp unit was generated by the insertion of an additional Lys-Gly between amino acids 4 and 5 while the 21 bp partial repeat terminated prematurely at amino acid 7.

In summary, clone Tcg-1 encodes antigenic determinants present in the trypomastigote 85K surface antigen as well as a 76K protein. The relationship between the 85K and 76K proteins is unclear, but it is possible that the 76K protein represents either a precursor or breakdown product of the 85K surface protein. The observation that a 76K protein is not present in the IBSP preparation used in these studies and that the Tcg-1 DNA insert hybridizes to a single- M_r RNA argues in favour of one rather than two polypeptides being represented by the $T.\ cruzi$ DNA insert present in Tcg-1.

Fig. 4 a, Northern blot of poly(A)⁺ RNA from trypomastigotes (lane 1) and epimastigotes (lane 2), and total RNA from trypomastigotes (lane 3), epimastigotes (lane 4) and amastigotes (lane 5) hybridized to the 500-bp Tcg-1 insert DNA nick-translated with $[\alpha^{-32}P]$ dCTP to a specific activity of 2×10^8 c.p.m. per µg. Processing of the blot was as described previously¹⁷. b, Nucleotide sequence of the genomic DNA insert in Tcg-1. The sequence was determined by use of the dideoxy chain-termination method9 after subcloning the EcoRI fragment of Tcg-1 into M13mp9 in both directions 18. The reading frame is shown in phase with β -galactosidase and the TGA termination codons are



CAL THE CTC ACA THE CTA CTT TGG GGG GGA GGA GGG AGA CAG CGG CAA CGT GCC ACG TTC 6CG CLU PBE LEU THE PHE LEU LEU TRP GLY ARG ARG GLY ARG GLN ARG GLA AGA CAG ACA CAC AGA GGA 12C THR ASP VAL PBE LEU TYR ASN ARG PRO LEU SER VAL GLY GLU LEU LYS NET ILE LYS GLU CTT AGA GAT AGA AGA GGA AGC GGT GAA GAT GAA GAA AGA GAA 12C GTT GAA GAT AGA AGA AGA AGA GGA AGA GGA AGA GGA AGA GGA AGA AG

denoted by an asterisk (*). The repeat unit is indicated by the boxed regions and the partial repeat units are included in broken boxes. Códing strand preference was determined by hybridization of recombinant M13mp9 DNA with poly(A)⁺ trypomastigote RNA (data not shown).

One of the most interesting features of the Tcg-1 antigen is the presence of the tandem repeating regions; these are strikingly similar in architecture to tandem repeating regions in both the S-antigen and the circumsporozoite surface (CS) protein of Plasmodium¹⁰⁻¹⁴. As in the malarial proteins, the repeat unit is well conserved, with some base changes occurring in the third base of the codon, and thus no concomitant change occurring in the amino acid. Also, the repeat unit is rather small, with the more homogeneous core repeats being flanked by degenerate repeats. In addition, the repeat units are found in surface or secreted proteins whose synthesis is stage specific.

It would be of particular interest to determine the degree to which the repeat unit is conserved among different T. cruzi strains. It is known that the repeat units present in the CS protein of two strains of Plasmodium knowlesi12 and the repeat units present in the S-antigen of two strains of Plasmodium falciparum14 are totally divergent and share essentially no sequence homology. If this should be the case for the repeat unit in the 85K trypomastigote surface protein, the repeat unit might serve as a convenient means of identification of specific strains of the parasite by direct immunodiagnostic techniques.

We do not know what role the repeat unit may have in the biological function of the 85K surface protein, nor the function of the 85K protein in the life-cycle of the parasite. However, a more thorough knowledge of the conservation of the repeat among different T. cruzi isolates and the immunological properties of the repeat should elucidate its usefulness to the survival of the parasite in the host as well as its potential as a diagnostic antigen and/or a vaccine.

We thank J. Massey and B. Granger for technical assistance. This investigation was supported by NIH grant AII8873 and the UNDP/World Bank/WHO programme in tropical diseases.

Received 8 January: accepted 7 May 1986.

- 1. Brener, Z. A. Rev. Microbiol. 27, 347-383 (1973).
- Crane, M. J. & Dvorak, J. A. Molec biochem. Parasit. 5, 333-341 (1982). Zingales, B., Andrews, N. W., Kuwajima, U. Y. & Colli, W. Molec biochem. Parasit. 6. 111-124 (1982)
- 111-124 (1982).
 Katzin, A. M. & Colli, W. Biochem. biophys. Acta 727, 403-411 (1983).
 Andrews, N. W., Katzin, A. M. & Colli, W. Eur. J. Biochem. 140, 599-604 (1984).
 Beard, C. A., Wrightsman, R. A. & Manning, J. E. Molec. biochem. Parasit. 16, 199-212 (1985).
 Young, R. A. & Davis, R. W. Proc. natn. Acad. Sci. U.S.A. 80, 1194-1198 (1983).

- Hall, R. et al. Nature 311, 374-381 (1984). Sanger, F., Nicklen, S. & Coulson, A. R. Proc. natn. Acad. Sci. U.S.A. 74, 5463-5467 (1977). 10. Ozaki, L. J., Juec, P., Nussenzweig, R. S., Nussenzweig, V. & Godson, G. N. Cell 34, 815-822 (1983).
- Dame, J. B. et al. Science 225, 543-599 (1984).
 Sharma, S., Suec, P., Mitchell, G. H. & Godson, G. N. Science 224, 774-782 (1985).
- Coppel, R. L. et al. Nature 306, 751-756 (1983).
 Coloman, A. F. et al. Cell 40, 775-783 (1985).
- Laemmli, U. K. Nature 227, 680-685 (1970).
- Young, R. A. et al. Proc. natn. Acad. Sci. U.S.A. 82, 2583-2587 (1985). Levy, L. S. & Manning, J. E. Devl Biol. 85, 141-149 (1981).
- 18. Messing, J. & Vieira, J. Gene 14, 269-276 (1982).

Apparent eukaryotic origin of glutamine synthetase II from the bacterium Bradyrhizobium japonicum

Todd A. Carlson*† & Barry K. Chelm*‡

* Department of Energy Plant Research Laboratory, Departments of † Biochemistry and ‡ Microbiology and Public Health Michigan State University, East Lansing, Michigan 48824, USA

The Rhizobiaceae family of bacteria is characterized by the ability to form cortical hypertrophies on plants, and the ability to reisolate the bacteria from these galls or nodules1. This family includes the genera Rhizobium, Bradyrhizobium, Agrobacterium and Phyllobacterium. Another unique feature of these bacteria is that they contain two forms of the enzyme glutamine synthetase, termed GSI and GSII^{2,3}. GSI is typical of prokaryotic glutamine synthetases with respect to enzyme structure, the modulation of activity by post-translational modification, immunological crossreactivity, and amino-acid sequence^{2,4,5}. By contrast, GSII is distinct from all other known prokaryotic glutamine synthetases in structure and immunological reactivity, and is not known to be post-translationally modified. In these respects GSII is similar to eukaryotic glutamine synthetases. We have isolated and characterized the gene encoding GSII, which we term glnII, from Bradyrhizobium japonicum, the soybean symbiont. We show here that the amino-acid sequence of GSII, as inferred from the gene sequence, is highly homologous to plant glutamine synthetases, suggesting that this bacterial gene is of eukaryotic origin.

The GSII enzyme was purified as described in the Table 1 legend. This preparation was >95% pure as indicated by SDSpolyacrylamide gel electrophoresis. The amino-acid sequence of the amino terminus of GSII was determined by sequential Edman degradation and was used to design a mixed oligonucleotide probe with homology to the DNA which encodes the first six amino acids of GSII (Fig. 1a). An ambiguity at position 16 of the oligonucleotide was not included because two of the leucine codons, UUA and UUG, are infrequently utilized in B. japonicum. Two cosmids, pRjcos7-20 and pRJcos13-79, were isolated from a *B. japonicum* library constructed in the cloning vector pLAFRI^{7,8} by hybridization with radiolabelled oligonucleotide9,10. The region of hybridization in pRjcos7-20 was

Table 1 Purification of GSII					
Fraction	GSII activity (units)	Total protein (mg)	Specific activity (units mg ⁻¹)	Purification factor	Yield (%)
Extract Affi-Gel Blue DEAE HPLC fraction 17	149 39.1 9.92	48 0.89 0.12	3.10 43.9 82.7	(1) 14 27	(100) 26 6.7

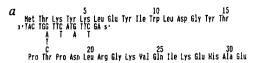
Bradyrhizobium japonicum USDA 110 was grown to mid-log phase in 2 litre of MBX medium⁵ with 10 mM glutamate. Cell extracts were prepared by the method of Tronick et al.4 using GS buffer (GSB is 10 mM imidazole-HCl pH 7.15 and 1.0 mM MnCl₂). GS activity is expressed in units of μ mol of γ -glutamylhydroxamate per min. as measured by the reverse transferase assay²³. Heat inactivation of GSII was carried out on undiluted extracts by incubation at 58 °C for 30 min. In the extract used for purification, GSII accounted for 88% of the total GS activity. All purification steps were done at 4 °C. The extract was diluted with GSB to a protein concentration of 1 mg ml⁻¹ and loaded on a 10 ml Affi-Gel Blue (Bio-Rad) column at a flow rate of 0.5 ml min⁻¹. The column was washed with 50 ml of GSB and eluted with a 50-ml linear gradient of 0-5 mM ATP in GSB. A broad peak of GS activity, including both GSI and GSII, eluted immediately upon the initiation of the ATP gradient. The fractions with the highest specific GS activity were combined and loaded onto a Bio-Rad Bio-Gel TSK DEAE-5-PW ion-exchange HPLC column (75×7.5 mm) equilibrated with GSB, at a flow rate of 1 ml min⁻¹. The column was eluted with a 40-ml linear gradient of 0-500 mM KCl in GSB. The first and second peaks of GS activity corresponded to GSII and GSI respectively. Fractions (1 ml) for sequence determination were desalted on a 10 ml Bio-Rad P-6 column and lyophylized.

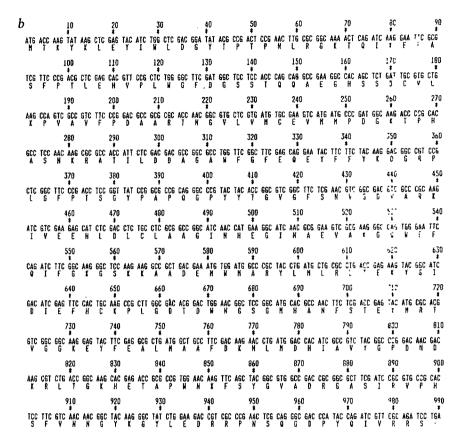
localized to 5.0 kilobase-pair (kbp) EcoRI, 1.0 kbp BglII and 2.1 kbp SalI fragments. These fragment sizes agree with those detected by hybridization to Southern transfers¹¹ of total genomic DNA restriction digests.

The 2.1-kbp SalI fragment with homology to the oligonucleotide probe was subcloned in both orientations in pBR322¹². The resulting plasmids, pBJ196A and pBJ196B, were tested for their ability to complement glutamine auxotrophy in Escherichia coli ET8051 [Δ (rha-glnA) hut C_K rbs nal^r]¹³. ET8051/pBJ196A grew well on defined medium plates with ammonia as the sole nitrogen source and yielded extracts with 0.82 units of GS activity per mg of protein. This GS activity was completely heat labile, a property specific to GSII, and co-sedimented with the GSII activity of B. japonicum in sucrose density gradient centrifugation. These data indicate that the entire glnII gene is located 2.1-kbp SalI fragment insert of pBJ196A. ET8051/pBJ196B, ET8051/pRjcos7-20 and the control strain ET8051/pBR322 gave no detectable growth on defined-medium

Fig. 1 a, The sequence of the amino terminus of GSII and the sequence of the mixed oligonucleotide hybridization probe used for gene identification. b, The complete DNA sequence of the coding region of glnII and the predicted amino-acid sequence of GSII.

Methods. Protein sequencing was performed on an Applied Biosystems Model 470A gas phase sequencer at the University of Michigan protein sequencing facility. Oligonucleotide probes were synthesized by the phosphoramidite method on an Applied Biosystems Model 380A synthesizer. Oligonucleotides were purified by denaturing 12% polyacrylamide gel electrophoresis²⁴. DNA was sequenced by the dideoxy-nucleotide chain termination method²⁵. Random fragments were generated by sonication²⁶ and subcloned into the SmaI site of M13-mp19²⁷. All regions were sequenced either on both strands or from three different fragments of the same strand. Plasmids were tested for their ability to complement glutamine auxotrophy in E. coli ET8051 on M9 defined-medium agar plates²⁸ with 0.2% glucose and 1 mM thiamine. GSI and GSII were separated by sucrose density gradient centrifugation as described previously⁵ except that the centrifugation was carried out at 50,000 r.p.m. for 3 h at 4°C.





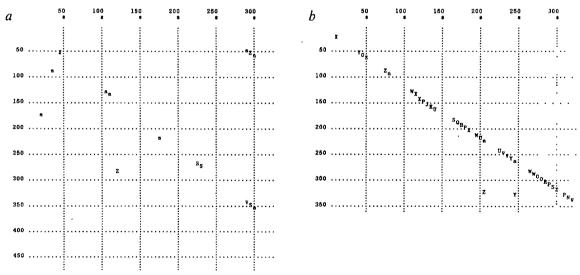


Fig. 2 Amino-acid homology matrices comparing B. japonicum GSII (x axis) to Anabaena 7120 (y axis, panel a) and Phaseolus vulgaris root GS (y axis, panel b). Homology matrices were plotted with the Pustel and Kafatos sequence analysis program¹⁷ using the following parameters: range = 11, scale factor = 0.75, minimum value = 47, compression = 5. Each letter represents a 2% extent of homology in that region of the matrix (A = 100-99%, B = 98-97% ... Z = 50-49%; a = 48-47%).

plates and produced no detectable glutamine synthetase activity. This indicates that the complementation observed with ET8051/pBJ196A was due to glnII expression from the tet promoter of the vector, in agreement with the gene orientation as indicated by sequence determination (see below).

In order to determine the precise location of the glnII gene, we sequenced the 2.1-kbp SalI fragment carried in pBJ196A.

The DNA sequence contains a single long open reading frame which encodes GSII (Fig. 1b). The relative molecular mass of the subunit of GSII, predicted by the complete amino-acid sequence, is 36,904, in good agreement with 36,000 as determined by SDS-polyacrylamide gel electrophoresis¹⁴. The amino terminus of GSII matches the protein sequencing data in 28 of 31 positions. The discrepancies at positions 24, 29 and 31 are

Table 2 Statistical significance of amino-acid sequence homologies between B. japonicum GSII and other glutamine synthetases

Glutamine synthetase source	% Identity to GSII	Similarity score	z yalue
Bradyrhizobium japonicum GSII	100	1719	208.4
Phaseolus vulgaris 16	43.8	663	77.3
Pisum sativum*	46.6	642	73.9
Medicago sativa ²¹	43.8	674	78.9
Nicotiana plumbaginifolia*	42.6	667	74.0
Anabaena 712013	24.4	114	8.83

All scores are from optimized alignments calculated with ktup = 1 and 1,000 randomized sequences using the RDF program of Lipman and Pearson¹⁸. The z value equals the similarity score minus the mean of the similarity scores with randomized sequences divided by the standard deviation of the randomized comparisons. A similarity score is considered significant if its z value is greater than 10 while z values less than 3 are not significant.

* G. Coruzzi, S. Tingey and B. Walker, personal communication.

presumably due to inaccuracies in the final cycles of the protein sequencing.

The comparisons of the B. japonicum GSII amino-acid sequence with the Anabaena 7120 GS15 and the Phaseolus vulgaris root GS16 sequences are shown as homology matrixes in Fig. 3. These matrixes were generated using the analysis program of Pustell and Kafatos¹⁷ with parameters set so that each letter within the matrix represents a match of 47%, or greater, over a span of 23 amino acids. It can be seen that GSII has only limited homology to the bacterial GS (Fig. 3a) but extensive homology to the plant GS (Fig. 3b).

GSII was compared with a variety of glutamine synthetases using the method of Lipman and Pearson 18 which optimizes the alignment between amino-acid sequences and quantitates the significance of the similarity (Table 2). Despite extensive homology among most prokaryotic glutamine synthetases, the homology between GSII and the typical bacterial glutamine synthetase of Anabaena 7120 is only marginally significant. In contrast, GSII has extensive homology with all eukaryotic glutamine synthetases that we have examined. Because all suggested cases of convergent evolution result in similarities of enzyme function without extensive sequence homology¹⁹, and because GSII is found only in the Rhizobiaceae³, we conclude that the B. japonicum glnII gene is the result of a eukaryote to prokaryote gene transfer event. We suggest that a plant served as the source of the progenitor glnII gene because of the plant pathogenic nature of the Rhizobiaceae.

The presence of the glnII gene in the Rhizobiaceae is the first evidence of gene transfer to symbiotic bacteria from the eukaryotic host. Another suggested example of eukaryote to prokaryote gene transfer, involving bacteriocuprein of Photobacterium leiognathi19, has recently come under dispute20

Although sequence homology suggests the origin of the glnII gene, questions pertaining to the mechanism, frequency or function of gene transfer between symbionts or pathogens cannot be directly addressed. Since plant GS genes are known to contain introns²¹, B. japonicum glnII had to evolve further by the loss of the introns, or the gene transfer must have occurred prior to the acquisition of introns in the plant genes. In addition, there is no obvious reason why the aquisition of a eukaryotic gene would confer a selective advantage on a plant symbiotic bacterium. GSII is not known to serve an essential function, acting only to provide extra ammonia assimilatory capacity during growth under nitrogen limited conditions²². Nevertheless, it appears that the ability to aquire genetic information from eukaryotes can be a source of genetic diversity in the evolution of bacteria.

We thank Tony Bleeker and Hans Kende for assistance in the HPLC analysis, Mike Shimei and Jan Watson for assistance in the oligonucleotide synthesis, Ron Davis for assistance in sequencing methods and analysis, and Benjamin Mifflin, Howard Goodman and Gloria Coruzzi for providing eukaryotic glutamine synthetase sequences before publication. This work was supported by the US Department of Energy Division of Biological Energy Research under contract DE-AC02-76ER01-1338 and by US Department of Agriculture grant 85-CRCR-1-1739. This is article 11983 from the Michigan Agricultural Experiment Station.

Received 18 February; accepted 9 May 1986.

- 1. Jordan, D. C. in Bergey's Manual of Systematic Bacteriology Vol. 1, 234-242 (ed. Drieg, N. R.) (Williams & Wilkins, Baltimore, 1984).
- Darrow, R. A. & Knotts, R. R. Biochem. biophys. Res. Commun. 78, 554-559 (1977). Fuchs, R. L. & Keister, D. L. J. Bact. 144, 641-648 (1980).

- Tronick, S. E. & Ketster, D. L. J. Bact. 144, 641-646 (1980).
 Tronick, S. R., Chardi, J. E. & Stadtman, E. R. J. Bact. 115, 858-868 (1973).
 Carlson, T. A., Guerinot, M. L. & Chelm, B. K. J. Bact. 162, 698-703 (1985).
 DeVries, G. E., Oosterwijk, E. & Kijne, J. W. Pl. Sci. Lett. 32, 333-341 (1983).
 Friedman, A. M., Long, S. R., Brown, S. E., Buikema, W. J. & Ausubel, F. M. Gene 18, 289-296 (1982)
- Adams, T. H., McClung, C. R. & Chelm, B. K. J. Bact. 159, 857-862 (1984).
 Whitehead, A. S., Goldberger, G., Woods, D. E., Markham, E. F. & Colten, H. R. Proc. natn. Acad. Sci. U.S.A. 80, 5387-5391 (1983).
- 10. Wood, W. I., Gitschier, J., Lasky, L. A. & Lawn, R. M. Proc. natn. Acad. Sci. U.S.A. 82, 1585-1588 (1985).
- Southern, E. M. J. molec. Biol. 98, 503-517 (1975).
- Bolivar, F. et al. Gene 2, 95-113 (1977).
 Fisher, R., Tuli, R. & Haselkorn, R. Proc. nain. Acad. Sci. U.S.A. 78, 3393-3397 (1981).
- Darrow, R. A. in Giutamine Synthetase: Metabolism, Enzymology and Regulation, 139-166 (eds Mora, J. & Palacios, R.) (Academic, New York, 1980).
- 15. Tumer, N. E., Robinson, S. J. & Haselkorn, R. Nature 306, 337-342 (1983).
- Gebhardt, C., Oliver, J., Forde, B. G., Saarelainen, R. & Miffin, B. EMBO J. (in the press).
 Pustell, J. & Kafatos, F. C. Nucleic Acids Res. 12, 643-655 (1984).
- Lipman, D. J. & Pearson, W. R. Science 227, 1435-1441 (1985).
 Bannister, J. V. & Parker, M. W. Proc. natn. Acad. Sci. U.S.A. 82, 149-152 (1985).
- Dunlap, P. V. & Steinman, H. M. J. Bact. 165, 393-398 (1986).
 Tischer, E., DasSarma, S. & Goodman, H. M. EMBO J. (in the press).
- Hischer, E., Dassama, S. & Goodman, H. M. EMBO J. (in the press).
 Darrow, R. A. et al. in Current Perspectives in Nitrogen Fixation, 182-185 (eds Gibson, H. H. & Newton, W. E.) (Australian Academy of Sciences, Canberra 1981).
 Bender, R. A. et al. J. Bact. 129, 1001-1009 (1977).
 Maxam, A. M. & Gilbert, W. Meth. Enzym. 65, 499-580 (1980).
 Sanger, F., Nicklen, S. & Coulson, A. R. Proc. natn. Acad. Sci. U.S.A. 74, 5463-5467 (1977).

- Deininger, P. L. Analyt. Biochem. 129, 216-223 (1983).
 Norrander, J., Kemp, T. & Messing, J. Gene 26, 101-106 (1983).
 Miller, J. H. Experiments in Molecular Genetics (Cold Spring Harbor Laboratory; New York, 1972).

Ultrafast carotenoid to pheophorbide energy transfer in a biomimetic model for antenna function in photosynthesis

Michael R. Wasielewski*, Paul A. Liddell†, Donna Barrett†, Thomas A. Moore† & Devens Gust†

- Chemistry Division, Argonne National Laboratory, Argonne, Illinois 60439, USA
- † Department of Chemistry, Arizona State University, Tempe, Arizona 85287, USA

Carotenoids serve as light-harvesting pigments and as photoprotective agents in photosynthetic organisms 1-9. Their role as antenna pigments involves absorption of photons in the blue-green spectral region followed by highly efficient singlet-singlet energy transfer to a neighbouring chlorophyll. The dependence of both the rate and mechanism of energy transfer on carotenoid-chlorophyll distance and orientation is unknown. Here, we have directly measured both the rate and efficiency of singlet energy transfer from a carotenoid covalently linked to pyropheophorbide a (PPheo a) in two model compounds, using picosecond transient absorption spectroscopy. In one model the π systems of the carotenoid and PPheo a possess a maximum edge-to-edge distance of 5 Å, while in the other model this distance is only 2 A. Energy transfer occurs from the carotenoid to PPheo a at the 2-A distance with a rate constant of $7\pm2\times10^{10}\,\text{s}^{-1}$ and $53\pm5\%\,$ efficiency, while energy transfer at the 5-Å distance occurs at a rate constant of $<3 \times 10^9 \, \text{s}^{-1}$ and with <5% efficiency. These results provide evidence that short distances and strong electronic interactions between carotenoids and chlorophylls are necessary to achieve the high energy transfer efficiencies observed in vivo.

The lifetimes of the lowest excited singlet state, S_1 of several carotenoids including β -carotene have been measured recently by transient absorption spectroscopy after direct excitation of the carotenoids with 4-ps pulses of 510-nm light¹⁰. That study showed that a combination of an unusually small radiative rate with an extremely fast rate of internal conversion results in carotenoid lifetimes that are of the order of 10 ps (for example, 8.4 ps for β -carotene). The short lifetimes of these states suggest that the rate of energy transfer from carotenoids to chlorophylls required to achieve very efficient energy transfer must be $>10^{11} \, \mathrm{s}^{-1}$. This requirement further implies that the electronic interaction between the carotenoid donor and the chlorophyll acceptor must be very strong¹¹⁻¹⁴.

The two model compounds that we studied (see below) differ in that the carotenoid moiety of compound (1) is linked to the

$$0 = C$$

$$0 = C$$

$$R' = -CH = CH_2, R' = -N$$

$$R' = -CCH_3$$

$$R' = -CCH_3$$

7-propionic acid side chain of the PPheo a via an amide bond, whereas in compound (2) the 2-vinyl group of methyl pyropheophorbide a has been replaced by a carboxylic acid which in turn has been linked to the same 4-aminophenyl carotenoid via an amide linkage. High-resolution ¹H-NMR spectroscopy of compounds (1) and (2) establishes that the time-averaged orientation of the carotenoid relative to the PPheo a in both (1) and (2) is such that the carotenoid is extended away from the macrocycle, rather than tightly folded back across the PPheo a. Thus, the maximum edge-to-edge distance between the carotenoid and PPheo a π system in (1) is \sim 5 Å, while that in (2) is \sim 2 Å. Moreover, in compound (2) the amide bond possesses a resonance structure which allows a degree of direct conjugation between the carotenoid and PPheo a π systems.

The rate and efficiency of energy transfer from the carotenoid to PPheo a in compounds (1) and (2) were determined directly by picosecond transient absorption spectroscopy. For this, solutions of compounds (1), (2) and carotenoid acetamide (3) (see below) were prepared in deoxygenated, spectral-grade toluene

and placed in cells with a 2-mm pathlength (A = 0.8). The optical absorption spectra of compounds (1) and (2) can be closely approximated as a simple superposition of the spectrum of compound (3) with that of the respective PPheo a derivative.

Figure 1 shows the transient absorption spectra of compounds (1)–(3) obtained at 0 ps relative to a 4-ps, 515-nm laser flash. In each case the carotenoid band is strongly bleached with a positive absorbance appearing near 560 nm. Similar spectral features have been observed previously for β -carotene and related carotenoids and are characteristic of carotenoid S_1 formation¹⁰.

Figure 2 shows the behaviour with time of the carotenoid

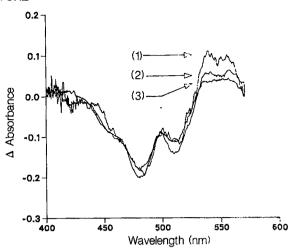


Fig. 1 Transient absorption spectra of the indicated compounds at 0 ps relative to a 4-ps, 25-µJ, 515-nm laser flash.

Methods. The 610-nm, 0.4-ps, 0.5-nJ output of a mode-locked Ar+-synchronously pumped R6G/DQOCI dye laser was amplified to 1.5 mJ using a four-stage R640 dye amplifier pumped by a frequency-doubled Nd-YAG laser operating at 10 Hz. The amplified laser pulse was split with a dichroic beam splitter. A 610-nm, 0.5-ps, 0.8-mJ pulse was focused into ethanol to generate a 5-µJ anti-Stokes Raman-shifted pulse at 515 nm. This pulse was amplified to 150 µJ using a two-stage coumarin-500 dye amplifier pumped by a frequency-tripled Nd-YAG laser. During amplification the 515-nm pulse broadened to 4 ps. The remaining 610-nm, 0.5-ps, 0.7-mJ pulse was used to generate a 0.5-ps whitelight continuum probe pulse. A 25-µJ, 515-nm pulse was used to excite a spot of 1 mm diameter on the sample cuvette. Absorbance measurements were made in a double-beam configuration which used optical multichannel detection. Delays between pump and probe pulses were achieved using an optical delay line. The absorbance of the carotenoid at 515 nm is ~7 times that of PPheo a in (1) and (2), and the carotenoid is therefore preferentially excited.

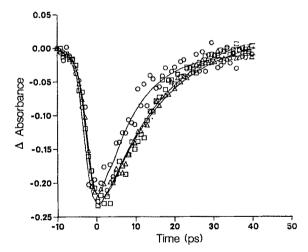


Fig. 2 Decay of the transient absorption at 480 nm of compounds (1) (\square), (2) (\bigcirc) and (3) (\triangle) following a 4-ps, 25- μ J, 515-nm laser flash. The solid curves are the best single exponential fits to the data.

absorbance changes at 480 nm. Each absorbance decays to zero with single exponential kinetics¹⁵, with $\tau = 15.9 \pm 0.8$, 7.6 ± 0.8 and 16.2 ± 0.8 -ps for compounds (1)-(3), respectively. Note that the time constant for recovery of the 480-nm bleach of the carotenoid in (1) is very similar to that of the carotenoid (3) alone, whereas the corresponding time constant for (2) is smaller than that of (3) by more than a factor of 2. From these results it is clear that the carotenoid S_1 population of (2) is depleted by an additional decay pathway that competes effectively with the intrinsic decay of the carotenoid S_1 state, whereas a similar competitive pathway in (1) is much less efficient.

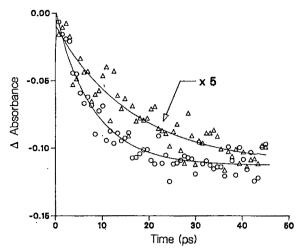


Fig. 3 Appearance of the transient bleach of compound (1) at 670 nm (\triangle) and of compound (2) at 675 nm (\bigcirc) following a 4-ps, 25-µJ, 515-nm laser flash: The absorbance change data for compound (1) are multiplied by 5 for comparison with those of compound (2). The solid curves are the best single exponential fits to the data.

Because the carotenoid does not absorb light at wavelengths >600 nm, this new decay pathway can be shown to be energy transfer to the attached PPheo a by examining the transient absorption changes of the PPheo a bands at 670 nm in (1) and at 675 nm in (2) after 515-nm excitation. Figure 3 shows the appearance kinetics of the bleach of these bands. The band at 675 nm in (2) bleaches with a 7.8 ± 0.8 -ps time constant whereas that of (1) bleaches with a 17.2 ± 0.8 -ps time constant. Also, the yield of S_1 of the PPheo a in (1) is much smaller than that of (2). The inverse of the time constant for the appearance of the PPheo a band bleach, which is the same as that for the recovery of the respective carotenoid bleach, is $k_{et} + k_{d}$, where k_{et} is the singlet-singlet energy transfer rate constant and k_d is the intrinsic carotenoid S_1 decay rate constant. Rate constant k_d is obtained from the S_1 decay of carotenoid (3). Thus, the rate of energy transfer for (2) is $7 \pm 2 \times 10^{10}$ s⁻¹, while that for (1) is $< 3 \times 10^9$ s⁻¹ based on the error limits of the measurements.

These results show that the carotenoid in compound (1) does not transfer energy efficiently to the PPheo a bonded to it. Better than 95% of the excited carotenoid molecules decay directly to ground state through their dominant radiationless pathways. On the other hand, the carotenoid in compound (2) transfers energy efficiently to the PPheo a. As no other decay mechanisms for S_1 are observed, the energy transfer efficiency is $k_{\rm et}/(k_{\rm et}+k_{\rm d})=$ $53 \pm 5\%$ for compound (2).

In conclusion, our results suggest that very strong electronic coupling between the π systems of a carotenoid donor and a chlorophyll derivative acceptor is necessary to achieve efficient singlet energy transfer rates. Strong electronic coupling between an energy donor and acceptor implies that terms involving orbital overlap must be included in the quantum mechanical description of the energy transfer mechanism¹¹⁻¹⁴. This in turn implies that in natural photosynthetic membranes where the coupling interaction is governed by the three-dimensional structure of the pigment-bearing proteins, the distances between donor and acceptor must approach van der Waals' contact. The successful characterization of singlet energy transfer in a welldefined model system augurs well for future direct measurement of energy transfer kinetics in natural photosynthetic antenna preparations.

This work was supported by the Division of Chemical Sciences, Office of Basic Energy Sciences of the US Department of Energy under contract W-31-109-ENG-38 (ANL) and the US Department of Energy and Saudia Arabian National Center for Science and Technology, grant no. DE-FG02-84CH10198 (to Arizona State University, ASU). ASU thanks the NSF (grant -----

CHE-8409644) for its contribution to the purchase of a high-field NMR spectrometer.

Received 24 March; accepted 22 April 1986.

- 1. Griffiths, M., Sistrom, W. R., Cohen-Bazire, G. & Stanier, R. Y. Nature 176, 1211-1214
- Cohen-Bazire, G. & Stanier, R. Y. Nature 181, 250-252 (1958).
- Wolff, Ch. & Witt, H. T. Z. Naturf, 24b, 1031-1037 (1969).

 Monger, T. G., Cogdell, R. J. & Parson, W. W. Biochim. biophys. Acta 449, 136-153 (1976).

 Goodwin, T. W. in Chemistry and Biochemistry of Plant Pigments Vol. 1 (ed. Goodwin,
- T. W.) 228 (Academic, London, 1976).
 Mathis, P., Butler, W. L. & Satoh, K. Photochem. Photobiol. 30, 603-614 (1979).
- Cogdell, R. J., Hipkins, M. F., MacDonald, W. & Truscott, T. G. Blochim. biophys. Acta 634, 191-202 (1981).
- van Grondelle, R., Kramer, H. J. M. & Rijgersberg, C. P. Biochim. biophys. Acta 682, 208-215 (1982).
- 208-213 (1982). Siefermann-Harms, D. Biochim. biophys. Acta 811, 325-355 (1985). Wasielewski, M. R. & Kispert, L. D. Chem. phys. Lett. (in the press).
- Razi Naqvi, K. Photochem. Photobiol. 31, 523-524 (1980).
- Dirks, G., Moore, A. L., Moore, T. A. & Gust, D. Photochem. Photobiol. 32, 277-280 (1980).
 Moore, A. L., Dirks, G., Gust, D. & Moore, T. A. Photochem. Photobiol. 32, 691-696 (1980).
- Bensasson, R. V. et al. Nature 290, 329-332 (1981).
 Grinvald, A. Analyt. Biochem. 75, 260-280 (1976).

Chloroplast gene organization deduced from complete sequence of liverwort Marchantia polymorpha chloroplast DNA

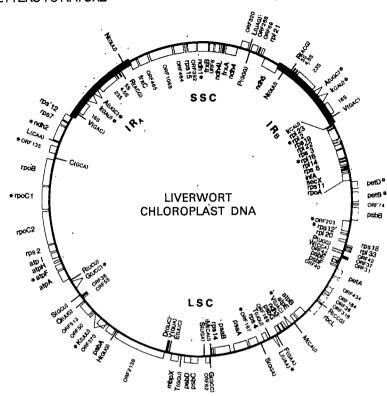
Kanji Ohyama*, Hideya Fukuzawa*, Takayuki Kohchi*, Hiromasa Shirai*‡, Tohru Sano*, Satoshi Sano*, Kazuhiko Umesono†, Yasuhiko Shiki†, Masayuki Takeuchi†, Zhen Chang†, Shin-ichi Aota†, Hachiro Inokuchi† & Haruo Ozeki†

* Research Center for Cell and Tissue Culture, Faculty of Agriculture, and † Department of Biophysics, Faculty of Science, Kyoto University, Kyoto 606, Japan

Chloroplasts contain their own autonomously replicating DNA genome. The majority of proteins present in the chloroplasts are encoded by nuclear DNA, but the rest are encoded by chloroplast DNA and synthesized by the chloroplast transcription-translation machinery 1-4. Although the nucleotide sequences of many chloroplast genes from various plant species have been determined, the entire gene organization of the chloroplast genome has not yet been elucidated for any species of plants. To improve our understanding of the chloroplast gene system, we have determined the complete sequence of the chloroplast DNA from a liverwort, Marchantia polymorpha, and deduced the gene organization. As reported here the liverwort chloroplast DNA contains 121,024 base pairs (bp), consisting of a set of large inverted repeats (IRA and IR_B, each of 10,058 bp) separated by a small single-copy region (SSC, 19,813 bp) and a large single-copy region (LSC, 81,095 bp). We detected 128 possible genes throughout the liverwort chloroplast genome, including coding sequences for four kinds of ribosomal RNAs, 32 species of transfer RNAs and 55 identified open reading frames (ORFs) for proteins, which are separated by short A+T-rich spacers (Fig. 1). Twenty genes (8 encoding tRNAs, 12 encoding proteins) contain introns in their coding sequences. These introns can be classified as belonging to either group I or group II, as described for mitochondria⁵. Interestingly, seven of the identified. ORFs show high homology to unidentified reading frames (URFs) found in human mitochondria^{6,7}.

The genes encoding the chloroplast rRNAs (16S, 23S, 4.5S and 5S rRNAs) were localized by Southern hybridization with specific rRNA probes⁸⁻¹⁰. DNA sequences also confirmed the presence of the rRNA operons in both inverted repeat regions. Genes encoding tRNAs were localized using the T ψ loop sequence (GTTCRA) and identified by constructing the familiar

Fig. 1 Gene organization of the chloroplast genome from a liverwort, Marchantia polymorpha. Thick lines indicate the inverted repeats (IRA and IRB). SSC and LSC indicate the small single-copy region and large single-copy region, respectively. Genes shown outside the map are transcribed anticlockwise, and those inside are transcribed clockwise. The tRNA genes are identified by the one-letter aminoacid code with their anticodons given in parentheses. Asterisks indicate genes having introns in their sequences. The genes for the 50S and 30S ribosomal proteins are shown as rpl and rps, respectively. atp, psa, psb and pet represent the genes for subunits of H⁺-ATPase, proteins in photosystem I, photosystem II, and cytochrome b_6/f complex, respectively. We tentatively designated chloroplast ORFs which exhibited homology to those found in human mitochondria, as ndh, ORFs which showed homology to 4Fe-4S proteins as frx, and inner membrane permease protein found in E. coli as mbp. infA and secX represent genes for initiation factor 1 and functionally unidentified protein expressed in E. coli, respectively. rbcL, the gene for the large subunit of ribulose bisphosphate carboxylase. rpoA, rpoB, rpoC1 and rpoC2 are the genes for RNA polymerase subunits. Ribosomal RNA operons are located in both IR regions (16S, 23S, 4.5S and 5S). Methods. For DNA sequencing, we first construct gene libraries from BamHI-, BglII-, PstI-, XhoI-, HindIII-, EcoRI-, BelI-, ClaI- and AluI-generated chloroplast DNA fragments using the plasmids pBR322, pKC7, pUC13, pUC18 and pUC19. These clones were used for DNA sequencing by the method of Maxam and Gilbert30, and the dideoxy chain termination procedure³¹. About 95% of the sequence of each clone was obtained from both



strands by the shotgun procedure³² and progressive deletion method³³, then the single-stranded region or ambiguities were resolved by the more directed enzymatic digestion method. We have sequenced both IR regions and found them to be identical. The data were compiled in computers using the program DNASIS (Hitachi SK Ltd.).

clover-leaf structure, except for tRNA^{Pro}_{GG} in which the aminoacyl stem structure is incomplete. We identified 37 tRNA genes encoding 32 species, including 5 duplicated ones in the inverted repeat regions. The accepting amino acids were deduced from their unmodified anticodons according to the standard codon table¹¹. The tRNAs encoded by the chloroplast genome are sufficient to read all codons, taking into account wobbling and modification in the anticodons¹² and assuming that no tRNA is imported from the cytoplasm¹³. An analysis of codon usage in the ORFs reveals a preference for A or U in the third position of the codons.

Significant open reading frames were identified using the universal codon table (AUG as the initiation codon; UAA, UAG and UGA as termination codons). The introns in the ORFs were predicted from the presence of the 5' consensus sequence (GUGYG) and 3' consensus secondary structures characteristic of group II introns found in fungal mitochondrial genes⁵. These significant ORFs were identified by computer search¹⁴ using the protein sequence database NBRF PIR Release 6.0. The genes identified on the chloroplast genome are summarized in Table 1.

Chloroplasts contain their own ribosomes (70S) which are active in protein synthesis. About one-third of the ribosomal proteins are encoded by the chloroplast genome and the remainder by the nuclear genome¹⁵. We identified genes encoding ribosomal proteins by comparing amino-acid sequences with homologous genes in Escherichia coli. Moreover, there are clusterings of S12-S7 and L23-L2-S19-L22-S3-L16-L14-S8-infA-secX-S11-rpoA genes in a similar order to the clusters that have been reported in the E. coli ribosomal protein operons, that is, the str operon (S12-S7-fus-tufA) and a large cluster of ribosomal protein genes consisting of three operons, S10 (S10-L3-L4-L23-L2-S19-L22-S3-L16-L29-S17)¹⁶-spc (L14-L24-L5-S14-S8-L6-L18-S5-L30-secY-secX)¹⁷-α and (S13-S11-S4-rpoA-L17)¹⁸, respectively; the genes found in chloroplast clusters are italicized. In contrast, the chloroplast genes rps2, rps4, rps14, rps15, rps18, rpl20, rpl21 and rpl33 were scattered throughout the

chloroplast genome¹⁹. We have reported previously that the coding sequence for the ribosomal protein S12 (*rps12*) is interrupted and located far apart on different DNA strands, suggesting the possibility of *trans*-splicing²⁰.

We also identified the genes rpoA and rpoB, which respectively encode the α - and β -subunits of E coli RNA polymerase. The coding region for the β' -subunit consists of two separate ORFs (rpoC1 and rpoC2, which correspond to the N-terminal and C-terminal halves of the β' -subunit, respectively), but this does not exclude the possibility of an intron lying between them (see Fig. 1). So far no gene has been detected corresponding to an E coli type of σ factor²¹.

The most important feature of chloroplasts is their role in photosynthesis. Complete sequence analysis of the liverwort chloroplast DNA has revealed that there are nine genes (psaA, psaB, psbA, psbB, psbC, psbD, psbE, psbF and psbG) in photosystems I and II. We also identified the genes encoding six of the nine subunits of H+-ATPase (atpA, atpB, atpE, atpF, atpH and atoI). In addition, we have identified and mapped three genes (petA, petB and petD) encoding proteins involved in the photoelectron transport system. The gene for the large subunit of a ribulose bisphosphate carboxylase (rbcL) is encoded by the chloroplast genome as expected, the small subunit being encoded by the nuclear genome. Our results revealed that the liverwort chloroplast genome is comparatively small (121,024 bp), nevertheless it possesses all the photosynthetic genes and others which have been reported previously in various plant species²², except the genes tufA (ref. 23) and rps16 (ref. 24). These results imply that the chloroplast genomes in plants from liverwort to higher plants, have basically the same gene composition.

We have described a number of ORFs which have not been reported or identified previously. Our computer analysis revealed seven ORFs (ndh1, ndh2, ndh3, ndh4, ndh4L, ndh5 and URF6) whose aminoacid sequences show significant homology (11.3-31.3% over their entire length, but much higher in specific

Table 1 Genes encoded by the chloroplast DNA from a liverwort, M. polymorpha

16S, 23S, 4.5S and 5S tRNA genes 37 tRNAs (see Fig. 1) RNA polymerase genes rpoA: homologous to E. coli α-subunit rpoB: homologous to E. coli β-subunit rpoC1*: homologous to E. coli β'-subunit rpoC2: homologous to E. coli β'-subunit Ribosomal protein genés and related genes

rRNA genes (IRA and IRB)

Others infA, secX

50S subunit

rpl23, rpl33

rpl2*, rpl14, rpl16*,

rpl20, rpl21, rpl22,

Genes for photosynthesis rbcL, large subunit of ribulose bisphosphate carboxylase. psaA, photosystėm I P700 chlorophyll a apoprotein psaB (same as above) psbA, photosystem II 32K protein psbB, photosystem II P680 chlorophyll a apoprotein psbC (same as above) psbD, photosystem II D2 protein psbE, cytochrome b₅₅₉ psbF (same as above) psbG, photosystem II G protein atpA, ATPase F₁ subunit α atpB, ATPase F_1 subunit β atpE, ATPase F_1 subunit ε atpF*, ATPase Fo subunit I atpH ATPase Fo subunit III atpl, ATPase Fo subunit IV petA, cytochrome f $petB^*$, cytochrome b_6 $petD^*$, subunit 4 of cytochrome b_6/f complex Genes predicted by amino-acid sequence homology ndh1*, homologous to mammalian mitochondrial URF1 ndh2*, URF2 (same as above) ndh3, URF3 (same as above) ndh4, URF4 (same as above) ndh4L, URF4L (same as above) ndh5, URF5 (same as above) URF6, homologous to Aspergillus nidulans mitochondrial URFC (human mitochondrial URF6) frxA, homologous to 4Fe-4S type ferredoxin frxB (same as above) frxC, homologous to 4Fe-4S protein found in R. capsulata mbpX, homologous to ATP-binding subunit of inner membrane permease in E. coli (malK) or Salmonella typhmurium (hisP)29

Abbreviations for genes are the same as in Fig. 1

* Indicates the presence of introns in the coding sequences.

30S subunit

rps18, rps19

rps2, rps3, rps4,

rps7, rps8, rps11, rps12*, rps14, rps15,

regions) to those of human mitochondrial genes (URFs)6. Six of the ORFs (URFs 1-5 and 4L) were identified as genes for components of the NADH dehydrogenase in human mitochondria⁷. There has been no previous report of the presence of these genes in the chloroplast genome. However, an NADH-plastoquinone-(PQ) oxidoreductase activity has been detected in the chloroplasts of Chlamydomonas reinhardii25, thus it is possible that these ORFs encode subunits of the NADH-PQ oxidoreductase. There are two cysteine-rich ORFs (frxA and frxB) in which the periodic appearance of cysteines is typical of that in 4Fe-4S ferredoxin²⁶, and an ORF (frxC) whose amino-acid sequence is highly homologous (44.3%) to that of the ORF in the photosynthetic gene cluster of *Rhodopseudomonas capsulata*²⁷. These findings imply that basic genes which encode components of the large subunit of ribulose biphosphate carboxylase photosystem I, H⁺-ATPase, the cytochrome b_6/f complex, photosystem II and NADH-PQ oxidoreductase, all reside on the chloroplast genome. These functionally related gene groups are to some extent clustered in the chloroplast genome (see Fig. 1).

Thus, the liverwort chloroplast genome contains genes encoding the transcription-translation system as well as genes for protein complexes involved in chloroplast photosynthesis.

However, it seems that no functionally active complex is formed without nuclear-encoded protein subunits. Strikingly, chloroplasts and mitochondria have been found to have genes with a common function, in particular, the genes encoding H⁺-ATPase; NADH dehydrogenase and the cytochrome complex²⁸. These observations can be interpreted as suggesting that chloroplasts and mitochondria arose from a common ancestor. Further detailed information obtained from the complete sequencing of liverwort chloroplast DNA will be published elsewhere (but liverwort chloroplast DNA sequence data are available on request).

Unidentified genes More than 28 ORFs

We thank Dr C. J. Leaver for critical reading of the manuscript, and Drs T. Maruyama and T. Ikemura for computer analysis. We also thank Drs Y. Uchida and Y. Yamano for their preparations of chloroplast DNA clones, and Y. Yamashita, T. Tanaka, S. Asano and M. Toda for their assistance in DNA sequencing. We appreciate the continued support and encouragement of Dr Yasuyuki Yamada, Director of the Research Center for Cell and Tissue Culture. Faculty of Agriculture, Kyoto University. This research was supported in part by a Grant-in-Aid for Special Research Projects from the Ministry of Education, Science and Culture of Japan, and in part by the Yamada Science Foundation (H.O.).

Received 19 May; accepted 25 June 1986.

1. Bogorad, L. Genetic Engineering Vol. 1 (eds. Setlow, K. & Hollaender, A.) 181-203 (Plenum,

New York, 1979). Whitfeld, P. R. & Bottomley, W. A. Rev. Pl. Physiol. 34, 279-310 (1983).

3. Palmer, J. D. A. Rev. Genet. 19, 325-354 (1985).

4. Herrmann, R. G. et al. in Structure and Function of Plant Genomes (eds Ciferri, O. & Dure, Herrmann, R. G. et al. in Structure and Function of Plant Genomes (eds Citerri, O. & L.) 143-153 (Plenum, New York, 1985).
 Michel, F. & Dujon, B. EMBO J. 2, 33-38 (1983).
 Anderson S. et al. Nature 290, 457-465 (1981).
 Chomyn, A. et al. Nature 314, 592-597 (1985).
 Ohyama, K. et al. Molec. gen. Genet. 189, 1-9 (1983).
 Yamano, Y., Ohyama, K. & Komano, T. Nucleic Acids Res. 12, 4621-4624 (1984).
 Yamano, Y. et al. FEBS Lett. 185, 203-207 (1985).
 Crick, F. et al. FEBS Lett. 185, 203-207 (1985).

Crick, F. H. C. Scient. Am. 245(4), 55-62 (1966).
 Crick, F. H. C. J. molec. Biol. 19, 548-555 (1966)

Ellis, R. J. A. Rev. Pl. Physiol. 32, 111-137 (1981).
 Wilbur, W. J. & Lipman, D. J. Proc. natn. Acad. Sci. U.S.A. 80, 726-730 (1983).

15. Dorne, A.-M., Lescure, A.-M. & Mache, R. Pl. molec. Biol. 3, 83-90 (1984).

Zurawski, G. & Zurawski, S. M. Nucleic Acids Res. 13, 4521-4526 (1985).
 Cerretti, D. P. et al. Nucleic Acids Res. 11, 2599-2616 (1983).

Bedwell, D. et al. Nucleic Acids Res. 13, 3891-3903 (1985).
 Umesono, K. et al. Nucleic Acids Res. 12, 9551-9565 (1984).

Fukuzawa, H. et al. FEBS Lett. 198, 11-15 (1986).
 Yura, T. et al. Proc. natn. Acad. Sci. U.S.A. 81, 6803-6807 (1984).
 Crouse, E. J., Schmitt, J. M. & Bohnert, H.-J. Pl. molec. Biol. Reptr. 3, 43-89 (1985).
 Montandon, P. E. & Stutz, E. Nucleic Acids Res. 11, 5877-5892 (1983).

Shinozaki, K. et al. Molec. gen. Genet. 202, 1-5 (1986).
 Bennoun, P. Proc. natn. Acad. Sci. U.S.A. 79, 4352-4356 (1982).

Yasunobu, K. T. & Tanaka, M. Meth. Enzym. 69, 228-238 (1980).

Hearst, J. E. et al. Cell 40, 219-220 (1985).
 Widger, W. R. et al. Proc. natn. Acad. Sci. U.S.A. 81, 674-678 (1984).
 Higgins, C. F. et al. EMBO J. 4, 1033-1040 (1985).
 Maxam, A. M. & Gilbert, W. Meth. Enzym. 65, 499-560 (1980).

Sanger, F., Wicklen, S. & Coulson, A. R. Proc. natn. Acad. Sci. U.S.A. 74, 5463-5467 (1977).

32. Messing, J., Crea, R. & Seeburg, P. H. Nucleic Acids Res. 9, 309-321 (1981).

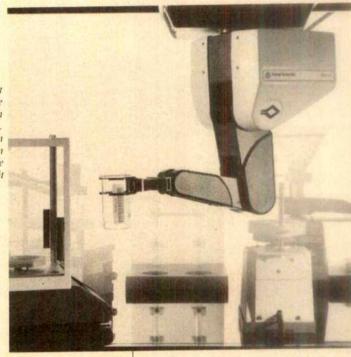
33. Yanisch-Perron, C., Vieira, J. & Messing, J. Gene 33, 103-119 (1985).

Tradition takes an unexpected turn

New equipment and methodology keep breaking old moulds. This week an all-purpose robot rides on the ceiling, mussels make tissue culture a sticky situation and a fungus fights the planthopper that feeds it.

A microdialysis probe that acts as an "exogenous blood vessel" could help monitor the activities of neurotransmitters and the effects of neurotoxins (Reader Service No. 100). The probe represents the combined efforts of Carnegie Medicine in Sweden and a research team at the Karolinska Institute, who sought to find a technique that could dynamically follow chemical events in living tissue. Using two concentric steel cannulas tipped with a dialysing membrane, the collaborators found that substances diffuse across the membrane when a physiological fluid enters through the inner cannula, flushes the inside of the membrane and exits through the outer cannula. Hence Carnegie's probe can recover endogenous substances without removing fluid and introduce exogenous substances without injecting liquid. Although the concept originated with studies of the brain, the company now supplies probes for different purposes and locations within the body. An

Fisher keeps its robot in suspense, but the Maxx-5 can work on solid ground as well. The robot runs on an IBM PC that can manage both the robot and the data it collects.



A simple solution for complex studies.

assortment of membranes is also available with molecular weight cut-offs between 5,000 and 50,000. Complete instrumentation for microdialysis includes the probe, a pump and a liquid switch, but Carnegie also manufactures tools for subsequent fraction analysis by liquid chromatography.

Low overhead

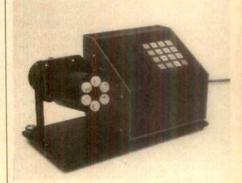
It weighs 30 lb. runs by computer and costs between \$30,000 and \$50,000 (US) and it won't get in the way (Reader Service No.101). Fisher's Maxx-5 robot can be mounted on laboratory ceilings or overhead frames using a motorized track that

can propel it along at a foot per second. The track, which also mounts on benchtops, adds a sixth dimension to Maxx-5's five-axis articulated arm. With adjustable grip strength, programmable arm speed and the aid of an IBM PC, the robot will dilute, mix, centrifuge, pipette, filter, concentrate and separate samples. Its fingers can hold beakers with up to 800 ml of solution. Maxx-5 also reads bar coding, so it can process samples according to individual labelling rather than by relying on station position. At this year's Pittsburgh Conference, the company said that Maxx-5 drew 570 inquiries. Fisher has a brochure entitled "Partners in Productivity" that describes the system in greater detail. The personal computer, software. linear track and numerous appliances are available as accessories.

Making the gradient

High reproducibility and convenience have rarely been the hallmarks of sucrose gradient generators. But a fresh approach from a professor at Canada's University of New Brunswick may turn gradient making around (Reader Service No. 102). According to inventor David Coombs. BioComp's model 105 will generate six identical sucrose gradients in 2.5 min without requiring any user supervision. Tubes that have been layered half and half with heavy and light sucrose are put in the instrument. It then tilts them to a predeter-

mined angle and rotates them for a pre-set time, at a pre-set speed. Different and pre-dictable gradient distributions result from different combinations of angle, time and speed. These parameters can be stored in the 105's non-volatile computer memory. Interchangeable holders will accommodate most tube sizes. At about \$1,900

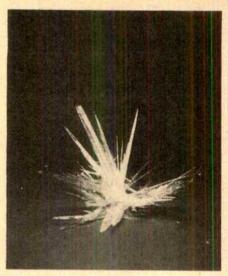


An innovation in reproducible gradients.

(US). Coombs says that the model is "more expensive, but less trouble" than traditional two-chamber devices.

Mussel power

The same adhesive that keeps the common blue mussel anchored to rocks and piers can now be used to attach cells and tissue to glass, plastic and even Teflon (Reader Service No. 103). Connecticut based BioPolymers Inc supplies the pro-



Skeletal imposters

THIS PRISTINE form belies its origin in oil and sediments far beneath the Earth's surface (Reader Service No. 104). The crystalline (18\(\beta\text{H}\))-olean-12-ene-3-one pictured is just one of the many substances that clutter petrochemical and geochemical analyses. In the search for oil in particular, reliable internal standards for analysis equipment are necessary to ensure the authentic identification of deposits. Recently, high purity "biomarkers" have emerged in the fossil fuel industry as dependable reference sources. These markers mimic the carbon skeletons of the organisms from which oil deposits are formed. By calibrating gas chromatography and mass spectrometry equipment with these synthetic markers, the distribution, history and progressive transformation into fossil fuel of the genuine organisms can be "unearthed".

tein, which it calls Cell-Tak, in 2 mg quantities of sterile aqueous solution for \$90 (US). The company claims Cell-Tak works rapidly with virtually any substrate: typically greater than 80 per cent of cells attach within 10 min of seeding, suggesting a diffusion-limited process. The adhesive does not alter cell morphology or doubling time and its effects appear to be independent of cell type. BioPolymers has already tested its product with anchorage-dependent cell lines such as vascular endothelium, as well as anchorageindependent lines such as U-937 human lymphoma. The company must shell, by hand, about 3 million mussels to extract 1 lb of Cell-Tak' adhesive. Thankfully, it takes only 50µl of Cell-Tak to coat a 35 ml Petri dish.

Instant access

The British Bureau of Hygiene and Tropical Diseases now provides several comprehensive current awareness services on AIDS and retroviruses (Reader Service No. 105). The bureau's update service publishes monthly an annotated bibliography of all the papers and articles on AIDS that the bureau has located, grouped by subject category. The update subscription rate is £80 (UK) or \$160 (US). Selected papers on AIDS and retroviruses also make it into one of the bureau's two abstract journals, and an AIDS newsletter has been established to cover the main AIDS news stories and commentaries on scientific developments. The BHTD recently made both the update and the abstract journals available for on-line searching through CAB International. These services are also on DataStar and BRS Information Technologies.

A free literature search from Radiometer Analytical can bring a wealth of experience as close as the telephone (Reader Service No. 106). Radiometer compiled selections from its applications library into a computer data base, organised by key words such as ion species or sample types. RADABASE now contains more than 1,500 references on Radiometer equipment use and misuse. The company supplies hard copies of the search for every request.

Small wonder

A cell disrupter for small samples uses minute glass beads and violent agitation to accomplish its ends (Reader Service No. 107). The Mini-BeadBeater, a recent release from Biospec Products in Oklahoma, uses a sealed polypropylene chamber within which 1 ml of beads will disrupt about 1 ml of sample in 1 to 3 min. Biospec



Small-scale destruction from Biospec

says that the collisions of the glass beads will crush even tough samples, like bone or microbial spores, without foaming or aerosol formation. The company thinks its system is safe for isolating enzymes and organelles or for extracting nucleic acids by phenol/chloroform procedures. In addition to applications with biological materials. Biospec recommends the Mini-BeadBeater for wet milling and emulsifying non-biologicals such as soil, paint pigments and pharmaceutical samples. With 15 disposable vials, two bead sizes optimized for eukaryotic or bacterial disruption and a 0.62 amp motor, the instrument sells for \$365 (US).

Beckman has tilted its latest spectrophotometry system towards the nucleic acid researcher, with a design that accommodates sample volumes of less than 50 µl (Reader Service No. 108). The company says its Micro-Leader package gives repeatable measurements and virtually full recovery that simplify purity analyses in DNA preparation. Beckman



Beckman's spectrophotometer is made for minute samples.

credits this performance to the microvolume cuvette and cell holder that it designed specifically for the Micro-Leader
system. With this cuvette samples are inserted and removed with a micropipette or
pasteur pipette. The full \$8,800 (US) system includes a DU-50 spectrophotometer
and a software applications module with
five procedures for purity assessment by
ratio methods. These programs, says
Beckman, reduce wavelength selection,
measurement and calculation to a few key
strokes.

Courses of action

Hands-on experience with sophisticated techniques can be a rarity for biology undergraduates, so a Purdue professor decided to pull together the materials and literature needed to teach them electrophoresis (Reader Service No. 109). Today the electrophoresis educational kits are marketed by Indiana-based Biostar Corp. Biostar adapted research procedures for use in student laboratories, and now even high schools are taking advantage of the opportunity — they comprise 25 per cent of sales. The kits are divided into three different levels of user experience and each provides the chemicals, equipment and manuals for about 16 students. Biostar considers its product a helpful boost into a biotechnology career.

Time for quick decisions: prices are about to go up on LC Resources' five-hour video primer for HPLC (Reader Service No. 110). The course, entitled "Getting Started in HPLC", covers the basic aspects of the chromatography method in five modules that can be purchased separately or as a \$1.795 (US) package. Pricing may limit the feasibility of the course to group training.

and LC Resources expects to raise its price to \$2,250 (US) in September. But the company guarantees the programme with complete "credit" (presumably not a refund) on returns within 30 days, and negotiates discounts for multiple orders. Video tapes come in 1/2-inch VHS and 3/4-inch U-Matic formats.

Savant's 10th anniversary catalogue gives a run-down of current training programmes in analytical, clinical and chemical instrumentation, along with three of the California company's latest additions (Reader Service No. 111). The new programmes include: training for inductively coupled plasma MS, enzyme immunoassays and gas chromatography analysis. The latter two programmes are authored by William Ulrich at Smith-Kline Beckman and Virginia Polytechnic's Harold McNair, respectively. Savant provides its training courses as slides or video tapes. The slide packages contain about 50 slides, a script and a cassette tape: the videos are available in VHS



Savant trains all types.

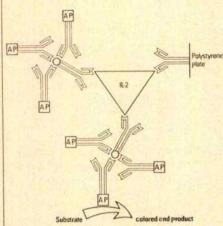
or Beta formats. Savant says the courses last about 45 minutes, and prices are listed in the catalogue.

The AIDS brigade

Earlier this summer. Du Pont announced the arrival of a radioimmunoassay that directly detects a structural core protein of the AIDS virus, HTLV-III (Reader Service No. 112). Du Pont says that its method is 25 to 200 times more sensitive than reverse transcriptase assaving and cuts cell culturing time down to as few as 3 days. The kit, which is at present available for research purposes only, measures viral activity as represented by the amount of p24, a core protein. According to the company it "virtually eliminates cross reactivity with other human cellular and viral proteins, and has been able to detect all human AIDS-associated retroviruses tested to date". Du Pont includes

recombinant human interleukin-2 in the kit to amplify cell growth in culture. Assays can be performed in less than a day. Du Pont charges S650 (US) for the kit, which contains enough material for 125 assays.

A scheme for detecting human interleukin-2 using monoclonal antibodies hit the market recently when Genzyme Corp in



The final step in Genzyme's analysis

Boston introduced its InterTest-2 kit (Reader Service No. 113). Taking less than 8 hours to complete, the ELISA-based technique is distributed for research use only and can detect IL-2 in serum, blood and other biolo-

gical fluids, says Genzyme. The company collaborated with a Boston group called Endogen to produce the kit, and expects the assay to speed IL-2 research into cancer and AIDS treatment. Genzyme sells InterTest-2 kits for \$395 (US) each, and each kit can perform up to 84 tests.

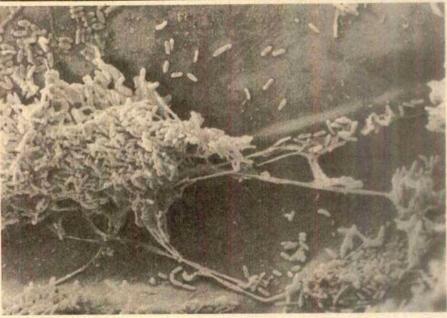
Dealing with DNA

Applied Biosystems keep experimenting with the chemistry for their DNA synthesizers, and they are now producing strands up to 175 bases long (Reader Service No. 114). AB's model 380B synthesizer is one of a family of machines capable of this sort of



New chemistry boosts Applied Biosystems synthesizer.

production. Using β-cyanoethyl phosphoramidite methods, the 380B routinely gener-



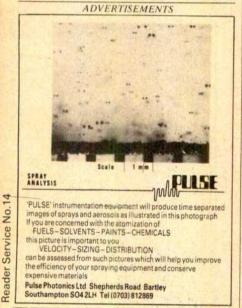
Spore wars

This seemingly sedate micrograph actually depicts a vicious attack by the green fungus Metarhizium anisopliae upon the brown planthopper Nilaparvata lugens (Reader Service No. 115). Three researchers at King's College, London and the Berkshire company Microbial Resources plan to make M. anisopliae even more adept at victimizing the planthopper, which causes serious losses to rice crops in China, Japan, Korea and India. The investigators want to exploit the

microbe's role as a natural pesticide. Using techniques for genetic recombination, such as somatic hybridization and traditional heterokaryon fusion, they hope to increase the fungus's effectiveness in the field. Already the team has isolated one recombinant that gives nearly twice the total spore production and over 1,000 times the ease of spore release of either parent. These improvements have so far been achieved without any adverse effects on M. anisopliae's growth rate.

ates 50- to 100-mers and quantities that range from primers and probes up to 10 mg for physical studies. Coupling yields vary between 98 and 100 per cent. according to AB. A single-column instrument costs \$45,000 (US) and a 5-column, \$49,500 (US). A menu-driven touchscreen control allows the user to operate standard synthesis cycles including automatic deprotection and cleavage), or develop new procedures.

Two new synthesizers from Biosearch in California have also been making their mark (Reader Service No. 116). The models 8650 and 8750 have one and four columns, respectively, and according to Biosearch have been producing DNA fragments up to 180 bases in length. An IBM PC/AT computer workstation manages the unit, stores sequence and protocol data and simplifies sequence entry and editing. Biosearch mentions that the computer can also be connected via a modem to libraries of DNA



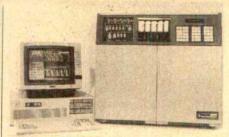


Eliminates evaporation loss and contamination. Easy to use — flush with gas mixture, seal, place at appropriate temperature. Stackable, see-through. Quantity discounts. billups-rothenberg, inc., pob 977, Del Mar, CA USA 92014. Call 619-755-3309 or contact your Flow Laboratories representative.

Reader Service No.12

Copies of articles from this publication are now available from the UMI Article Clearinghouse.

Mail to: University Microfilms International 300 North Zeeb Road, Box 91 Ann Arbor, MI 48106



Biosearch is joining the synthesizer league.

sequences and to software that could translate sequences into protein equivalents. The IBM will control up to eight of Biosearch's instruments, which cost \$42.900 and \$53.900 (US), depending on the number of columns, and use \$\beta\$-cyanoethyl phosphoramidite chemistry.

Proteins A and G

An alternative to protein A as an immunological reagent has come from Amersham in the form of protein G, a bacterial cell wall protein with a high affinity for the Fc region of a range of immunoglobulins (Reader Service No. 117). Amersham lists among protein G's advantages high affinity binding to IgGs from rat, goat and sheep and binding almost exclusive to IgG without crossreactions with other classes. The reagent, according to Amersham, also binds to a wider range of species IgG and subclasses than protein A. But the company suggests

Amersham's protein G may beat protein A

Ig	Bacterial Ig	Fc receptor type
	S.aureus	Group C and
		G streptococci
N. P. S. S. S. S.	(Protein A)	(Protein G)
Human IgG1		
Human IgG2	796	
Human IgG2		
Human IgG4		
Mouse IgG1	\boxtimes	×
Mouse IgG2a		
Mouse IgG2b		
Mouse IgG3		250
Rat IgG1	\boxtimes	[X]
Rat IgG2a		
Rat IgG2b		
Rat IgG2c		
Rabbit IgG		
Bovine IgG1		
Bovine IgG2		e levi
Sheep IgG1		
Sheep IgG2		
Goat IgG1	\boxtimes	
Goat IgG2		
Horse IgG(ab)	\boxtimes	
Horse IgG(c)	\boxtimes	
Horse IgG(T)		×

- No reaction
- Strong reaction

that ultimately its E-labelled protein G would best be viewed as a complement to protein A. As such, it could be particularly useful in blotting procedures to detect specific IgGs, in the study of antigenantibody interactions and for antibody screening where protein A fails to bind.

Two fusion vectors and a revised Sepharose gel put the punch into Pharmacia's system for the production, purification and characterization of protein A fusion protein conjugates (Reader Service No. 118). The company's fusion system uses the two vectors to induce high levels of expression of intracellular proteins (vector pRIT2T) and of proteins transported to the periplasmic space or secreted (pRIT5). According to Pharmacia, conjugates thus produced in prokaryotic expression systems can be purified in a single step owing to improved mechanical characteristics of IgG Sepharose 6 gel. The company points out that the repetitive structure of the protein A moiety may enhance the immune response, making conjugates well-suited for direct immunization. Immunological assays will also provide rapid detection due to the protein A tail.

Good references

A simple test for pipetters can provide reassurance when the instruments are accurate and warning when they go on the blink (Reader Service No. 119). Bel-Art Products supplies an accuracy test kit that determines whether pipettes from Gilson, Eppendorf, Oxford, Finn and other manufacturers still conform to those brands' specifications for precision. An adaptor slips into the pipetter tip, then a capillary is inserted in the adaptor's distal end. Next the pipetter plunger is depressed, the capillary immersed in water and the plunger slowly released. The liquid level in the capillary should be within 1.5 mm of Bel-Art's mark on the glass; otherwise, the pipetter is not performing within manufacturer's specifications. The \$87 (US) kit has two soft adaptors and six different sizes of glass inserts to adjust for volumes between I and 1,000 ul.

A set of nine mercury-filled thermometers may look ordinary but carry a hidden value: Brooklyn Thermometer Co's reference set has NBS traceable certification (Reader Service No. 120). The yellowback glass thermometers cover the temperature range between -36° and 761° F. Brooklyn guarantees fractional degree accuracy for one year and charges \$1,124 (US). The set comes with factory certificates and corrections for the five text points on each thermometer, as required by the American Society for Testing and Materials.

These notes are compiled by Karen Wright from information provided by the manufacturers. To obtain further details about these products, use the reader service card bound inside the journal. Prices quoted are sometimes nominal and apply only within the country indicated.

BOOKS RECEIVED

Mathematics

Differential Calculus. By A. AVEZ. Wiley:1986. Pp.179. Hbk ISBN 0-471-90873-8. Np.

I Want to be a Mathematician, an Automathography. By PAUL R. HALMOS. Springer-Verlag:1985. Pp.421. Hbk ISBN 0-387-96078-3/3-540-96078-3. \$41.50.

Introduction to Mathematical Control Theory, 2nd Edn. By S. BARNETT and R.G. CAMERON. Oxford University Press:1985. Pp. 404. Hbk ISBN 0-19-859640-5. £25.

Measures on Infinite Dimensional Spaces. Series in Pure Mathematics Vol.5. By Y. YAMASAKI. World Scientific Publishing: 1985. Pp. 256. Hbk ISBN 9971-978-52-0. £22.

Numerical Methods for CAD. Mathematics and CAD. Vol.1. By YVON GARDAN. Kogan Page, 1985. Pp. 165. Hbk ISBN 0-85038-817-1. £18.

Stochastic System Reliability Modeling. By SHUNJI OSAKI. World Scientific:1985. Pp.285. ISBN 9971-978-56-3. £23.90.

Turbulence and Diffusion in Stable Environments. The Institute of Mathematics and its Applications Conference Series, New Series No.4, J. C. R. HUNT (ed.), Clarendon Press: 1985. Pp.319. Hbk ISBN 0-19-853604-6. £32.

Physics

Acoustical Imaging, Vol.14. A.I. BERKHOUT, J. RIDDER, and I.F. VAN DER WAL (eds). Plenam: 1985, Pp.801, 11bk ISBN 0-806-42094-5, Np.

Advances in Atomic and Molecular Physics, Vol.21.
DAVID BATES and BENJAMIN BEDLERSON (eds). Academic:1985. Pp.382. 116k ISBN 0-12-003821-8, E85, 50, 899.

Advances in Nuclear Physics. Vol.16. J.W. NEGELL and ERICH VOGT (eds.). Plenum:1986. Pp.327. Hbk ISBN 0-306-41997-1, Np.

Antinucleon— and Nucleon-Nucleus Interactions. GEORGI: E. WALKER, CHARLES D. GOODS-MAN and CATHERINE OLMER (eds.). Plenum: 1985. Pp.504. Hbk ISBN 0-306-420888. Np.

Applied Superconductivity, Metallurgy and Physics of Titanium Alloys, Vol.1, Fundamentals, E.W. COLLINGS, Plenum: 1986, Pp.808, Ilbk ISBN 0-306-41690-5, Np.

The Concept of Physical Law. By NORMAN SWARTZ. Combridge University Press: 1985. Pp. 220. Hbk. ISBN 0-521-25838-3: £22.50, \$29.95.

A Course of Experiments with He-Ne Laser. By R. S. SIROHI. Wiley 1985. Pp. 108. Hbk. ISBN 0-470-20250-5-16.60.

Diffusion: Mass Transfer in Fluid Systems. By E.L. CUSSLER. Cambridge University Press: 1986. Pp. 525. Pbk ISBN 0-521-29846-6. £15. \$24.95.

Elements of Relativity Theory. By D.F. LAWDEN. Wiley: 1985. Pp. 108. Pbk ISBN 0-471-90852-5. Pbk

Equilibrium Capillary Surfaces. By ROBERT FINN. Springer-Verlag 1986. Pp.245. Hbk ISBN 3-540-96174-7. DM 158.

Finite Element Methods in Linear Ideal Magnetohydrodynamics. By RALF GRUBER and JACQUES RAPPAZ. Springer-Verlag:1985. Pp.180. ISBN 3-540-13398-4-0-387-13398-4. DM 110.

The Free-Lagrange Method. Lecture Notes in Physics, Vol.238. M.J. FRITTS, W.P. CROWLEY and H. TREASE (eds). Springer-Verlag:1985. Pp.313. Phk 18BN 3-540-15992-4. DM 45.

From SU(3) to Gravity. ERROL GOTSMAN and GERALD TAUBER (eds). Cambridge University Press:1986. Pp. 457. Hbk ISBN 0-521-30784-8. \$59.50.

Fundamentals of Hot Wire Anemometry. By CHARLES G. LOMAS. Cambridge University Press: 1986. Pp.211. ISBN 0-521-30340-0-135, \$52.50.

General System Theory. Cybernetics and Systems Series. By ANATOL RAPOPORT. Abacus Press: 1986. Pp.270. Hbk ISBN 0-85626-172-6. £24.50. \$34.50.

Geometric Aspects of the Einstein Equations and Integrable Systems. Lecture Notes in Physics, Vol.239. R. MARTINI (ed.). Springer-Verlag: 1985. Pp. 344. Pbk ISBN 3-540-16039-6. DM 45.

Infrared and Millimeter Waves, Vol.13, Millimeter Components and Techniques (Part IV), KENNETH J. BUTTON (cd.), Academic:1985, Pp.363, Hbk ISBN 0-12-147713-4, £75, \$85.

Infrared and Millimeter Waves. Vol.14, Millimeter Components and Techniques, Part V. KENNETH J. BUTTON. Academic:1985. Pp. 418. Hbk ISBN 0-12-147714-2. £87, \$99.

Magnetic Resonance Annual 1986. HERBERT Y. KRESSEL (cd.). Raven Press:1985. Pp.267. Hbk ISBN 0-88167-155-X. \$64.

Mossbauer Spectroscopy and its Applications. By T.E. CRANSHAW, B.W. DALE, G.O. LONG-WORTH and C.E. JOHNSON, Cambridge University Press; 1986. Pp. 119. Hbk ISBN 0-521-30482-2; pbk ISBN 0-521-31521-2. Hbk I20, \$29.95; pbk I7.95, \$12.95.

Multiple Photon Infrared Laser Photophysics and Photochemistry. By V.N. BAGRATASHVILI, V.S. LETOKHOV, A.A. MAKAROV and E.A. RYABOV. Harwood Academic Publishers:1985. Pp.512. Hbk ISBN 3-7186-0269-5, 865.

Nuclear Statistical Spectroscopy. By S.S.M. WONG. Oxford University Press: 1986. Pp. 241. ISBN 0-19-504004-X. £25.

On Growth and Form: Fractal and Non-Fractal Patterns in Physics. H. EUGENE STANLEY and NICOLE OSTROWKY (eds). Martinus Nijhoff: 1986. Pp.308. ISBN 90-247-3234-4. Np.

Optical Interferometry. By P. HARIHARAN. Academic:1986. Pp.303. Hbk. ISBN 0-12-325220-2. L49.50, \$58.

Permanent-Magnet and Brushless DC Motors. By T. KENJO and S. NAGAMORT. Oxford University Press:1986. Pp.194. ISBN 0-19-856217-9. Hbk £25: pbk £9.95.

Physics and Technology of Nuclear Materials. By IOAN URSU. Pergamon: 1985. Pp. 528. Hbk ISBN 0-08-032601-3, £45.50, \$59.50.

Principles and Methods of Nuclear Geophysics. By V.L.S. BHIMAŠANKARAM. N. VENKAT RAO. K. SRIRAMA MURTI and E.I. SAVENKO. Association of Exploration Geophysicists. Osmania University Campus, Hyderabad, 500 007. India:1985. Pp. 325. Hbk 850.

The Propagation of Radio Waves: The Theory of Radio Waves of Low Power in the Ionosphere and Magnetosphere. By K. G. BUDDEN. Cambridge University Press: 1985. Pp. 669. ISBN 0-521-25461-2. £60, \$89.50.

Quantum Electrodynamics of Strong Fields With an Introduction into Modern Relativistic Quantum Mechanics. By W. GREINER B. MÜLLER and J. RAFELSKI. Springer-Verlag: 1985. Pp. 594. Hbk. ISBN 3-540-13404-2. DM 140

Quantum Physics: Illusion or Reality? By ALISTAIR RAE. Cambridge University Press:1986. Pp.123. Hbk ISBN 0-521-26023-X, £17.50, \$29.95.

Quark Model and High Energy Collisions. By V.V. ANISOVICH. M.N. KOBRINSKY. J. NYIRI and YU M. SHABELSKI. World Scientific: 1985. Pp. 435. Hbk ISBN 9971-966-68-9. £29-80.

Radionuclide Imaging Techniques. By PETER F. SHARP. PHILIP P. DENDY and W. IAN KEYES. Academic:1985. Pp.271. Hbk ISBN 0-12-639020-7; pbk. ISBN 0-12-639021-5. Hbk £58, \$63.50; pbk £34.95, \$88.95.

Rate Equations in Semiconductor Electronics. By J.E. CARROLL. Cambridge University Press:1986. Pp. 177. Hbk ISBN 0-521-26533-9, 125, 339-50

Renormalization. By JOHN COLLINS. Cambridge University Press:1986. Pp.380. Pbk ISBN 0-521-31177-2, £13-95

Stability of Parallel Gas Flows. By B.K. SHIVA-MOGGI. Ellis Horwood/Wiley:1986. Pp.169. Hbk ISBN 0-7458-0001-7, £20.

Teaching Thermodynamics. JEFFREY D. LEWINS (ed.). Plenum:1985. Pp.517. Hbk ISBN 0-306-42207-7. Np.

Thin Films From Free Atoms and Particles. KENNETH J. KLABUNDE (ed.). Academic:1986. Pp.363. Hbk ISBN 0-12-410755-9. £51, 860.

VLSI Handbook, NORMAN G. EINSPRUCH (ed.) Academic:1985. Pp.902. ISBN 0-12-234100-7. \$125. £107.50.

Environmental Sciences

Atmospheric Chemistry and Physics of Air Pollution. By JOHN H. SEINFELD. Wiley 1986. Pp. 738. Hbk ISBN 0-471-82857-2. £61.35.

Epidemiology and Quantitation of Environmental Risk in Humans from Radiation and Other Agents. A. CASTELLANI (ed.). Nato ASI Series. Plenum: 1985. Pp. 584. iibk ISBN 0-306-42093-7. Np.

Industrial Hygiene Aspects of Plant Operations. Vol. 1, Process Flows. LESTER V. CRALLEY and LEWIS J. CRALLEY (eds). Collier Macmillan: 1985. Pp. 630. Hbk ISBN 0-02-949350-1. £70.

Industrial Hygiene Aspects of Plant Operations. Vol.3, Engineering Considerations in Equipment Selection, Layout and Building Design. LESTER V. CRALLEY, LEWIS J. CRALLEY and KNOWLTON J. CAPLAN (eds). Collier Macmillan: 1985. Pp. 785. Hbk ISBN 0-02-949370-6, £65.

Management of Toxic and Hazardous Wastes, H.G. BHATT, ROBERT M. SYKES and THOMAS L. SWEENEY (eds). Lewis Publishers, Michigan, US:1985. Pp.418. Hbk ISBN 0-87371-023-1_£43-95.

Marine Pollution. By R.B. CLARK. Oxford University Press:1986. Pp.215. Hbk 18BN 0-19-854183-X; pbk 1SBN 0-19-854182-1. Hbk £19.50; pbk £9.95.

Oil in the Sea: Inputs, Fates and Effects. OCF AN SCIENCES BOARD. National Academy of Sciences, Wiley:1985. Pp.601. ISBN 0-309-03479-3. £41.80.

Solid Waste Management: Selected Topics. MICHAEL J. SUESS (ed.). World Health Organization. Regional Office for Europe. Copenhagen: 1985. Pp. 210. Pbk 18BN 92-890-1023-1. SwFr. 15

Biological Sciences

*Atlas of Diseases of the Oral Mucosa. By J.J. PIND-BORG. Munksguard: 1985. Pp. 357. ISBN 87-16-09880-3. DKr. 500.

Butterfly and Caterpillar. By BARRIE WATTS. A&C Black: 1985. Pp. 25. ISBN 0-7136-2709-3, £3.95. Chirotteri Italiani. By DOMENICO SCARA-MELLA. Edagricole. Casella Postale 2202, 40139 Bologna, Italy: 1985. Pp. 124. Pbk ISBN 88-206-2517-2, Pbk L 12.

Chronological Phenomena in Plant Communities, R. NEUHÄUSL, H. DIERSCHKE and J.J. BARK-MAN (eds). Dr. W. Junk:1985. Pp. 270. ISBN 96-6193-515-6. Djl. 225. 875, £62.56.

A Colour Atlas of Virology. By JAN VERSTEEG. Wolfe Medical Publications, 3 Conway Street, London W1P 6HE, UK:1985, Pp.240, ISBN 0-7234-0808-4, £60.

Communication in the Chiroptera. By M. BROCK FENTON. Indiana University Press: 1985. Pp. 361-ISBN 0-253-31381-3. \$35.

Foundations of Parasitology, By GERALD D. SCHMIDT and LARRY S. ROBERTS. Blackwell Scientific: 1985. Pp. 775. Hbk. ISBN 0-8016-1385-6. 133-50.

Gastrointestinal Motility: The Integration of Physiological Mechanisms. By DAVID GRUNDY MTP Press:1985. Pp.183. ISBN 0-85200-894-5. £29-95.

The Genetics and History of Drosophila, Vol. 3d. M. ASHBURNER, H.L. CARSON and J.N. THOMPSON Jr. (cds), Academic:1985, Pp. 382, Hbk ISBN 0-12-064948-9, \$95.

Handbook of Marine Mammals. SAM H. RIDG-WAY and SirglCHARD HARRISON (eds). Academic: 1985. **?PF:362.** Hbk. ISBN 0-12-588503-2 564-50, E58-50.

Human Nature: Darwin's Views. By ALEXAN-DER ALLAND Jr. Columbia University Press; 1985. Pp. 242. 18BN 0-231-05898-5, \$25.

Introducing Immunology. By NORMAN STAINES, JONATHAN BROSTOFF and REITH JAMES, Gower: 1985, Pp. 59, Phk ISBN 0-906923-57-3, Phk FL 95.

Introduction to Bryology. By WILFRED B. SCHOFIELD, Macmillan, New York: 1985, Pp. 431, Hbk ISBN 0-02-949660-8, \$45

An Introduction to Ethology. By P.J.B. SLATER. Cambridge University Press;1985. Pp. 195. ISBN 0-52130266-8. Hbk £22.50, \$39,50; pbk £7.95, \$12.95.

Molecular Biology of Development, Vol. 1: Molecular Events. By A.A. NEYFAKH and M.Ya. TIMO-FEEVA. Plenum, USA/Nanka, USSR:1985, Pp.351. Hbk ISBN 0-306-413337. S95.

Mongoose Watch: A Family Observed. By ANNE RASE, John Murray 1985. Pp.298. ISBN 0-7195-1240-5-410-95.

Monoclonal Antibodies Against Bacteria, Vol. 1. ALBERTO J.L. MACARIO and EVERLY CONWAY DE MACARIO (eds). Academic:1985. Pp.320. ISBN 0-12-463001-4. \$45. £39.50.

Morphometrics in Evolutionary Biology. By F. BOOKSTEIN. B. CHERNOFF. R. ELDER. J. HUMPHRIES. G. SMITH and R. STRAUSS. The Academy of Natural Sciences of Philadelphia:1985. Pp.277. Hbk ISBN 0-910006-47-4; pbk ISBN 0-910006-48-2. Np.

Neurobiology: Molecular Biological Approaches to Understanding Neuronal Function and Development. PAUL O'LAGUE (ed.). Alan R. Liss:1985. Pp.212. Hbk ISBN 0-8451-2623-7. £52.

Nutrient Cycling in Tropical Forest Ecosystems. By CARL F. JORDAN. Wiley: 1985. Pp. 190. ISBN 0-471-90449-X. £13.95.

Pertussis Toxin. RONALD D. SEKURA, JOEL MOSS and MARTHA VAUGHAN (eds). Academic: 1985. Pp.255. Hbk ISBN 0-12-635480-4. \$34.50, £30:50.

Phospholipids in Nervous Tissues. By JOSEPH EICHBERG. Wiley:1985. Pp.386. ISBN 0-471-86430-7-f88-10.

The Platelets: Physiology and Pharmacology. GESINA L. LONGENECKER (ed.). Academic: 1985. Pp. 489, 15BN 0-12-455555-1. 865, £56.50.

Recognition and Regulation in Cell-Mediated Immunity. JAMES D. WATSON and JOHN MAR-BROOK (eds). Marel Dekker:1985. Pp. 480. ISBN 0-8247-7268-7. \$75.

Seed Ecology. By MICHAEL FENNER. Chapman & Hall:1985. Pp.151. ISBN 0-412-25930-3. Np.

Selected Topics from Neurochemistry. NEVILLE N. OSBORNE (ed.). Pergamon:1985. Pp. 534. ISBN 0-08-031994-7. £65, \$85.

Sensory Perception and Transduction in Aneural Organisms. GIULIANO COLOMBETTI, FRANCESCO LENCI and PILL-SOON SONG (eds). Plenum: 1985. Pp. 330. Hbk ISBN 0-306-42000-7. Np.

Sex and Repression in Savage Society, By BRONIS-LAW MALINOWSKI. University of Chicago Press: 1985, Pp.285. Pbk ISBN 0-226-50287-2. Pbk \$10.95.

The Thalamus. By EDWARD G. JONES. Plenum:1985. Pp. 935. ISBN 0-306-41856-8. Np.

Theories and Models in Cellular Transformation. L. SANTI and LUCIANO ZARDI (eds). Academic: 1985. Pp.179. ISBN 0-12-619080-1. \$25, £22.50.

The Tungara Frog. By MICHAEL J. RYAN. The University of Chicago Press:1985. Pp. 230. Hbk ISBN 0-226-73228-2; pbk ISBN 0-226-73229-0. Hbk £27.95; pbk £12.75.

Virus Structure and Assembly. SHERWOOD CASJENS (ed.). Jones and Bartlett, Boston:1985. Pp.295. Hbk ISBN 0-86720-044-8. Np.

The World's Whales: The Complete Illustrated Guide. By STANLEY M. MINASIAN, KENNETH C. BALCOMB III and LARRY FOSTER. W.W. Norton:1985. Pp.224. ISBN 0-89599-014-8. \$30, £25.

Psychology

Behaviour Analysis and Contemporary Psychology. C.F. LOWE, M. RICHELLE, D.E. BLACKMAN and C.M. BRADSHAW (eds). Lawrence Erlbaum Associates: 1985. Pp. 297. Hbk. ISBN 0-86377-025-8. F19 95

Current Issues in Clinical Psychology, Vol.2. ERIC KARAS (ed.). Plenum:1985, Pp.370, Hbk ISBN 0-306-42088-0, Np.

Epidemiology and Community Psychiatry: Psychiatry: The State of the Art, Vol.7. P. PICHOT, P. BERNER, R. WOLF and K. THAU (cds), Plentin: 1985, Pp.693, Hbk ISBN 0-306-41607-7. Np.

Evaluating Competencies: Forensic Assessments and Instruments. Perspectives in Law and Psychology, 7. By THOMAS GRISSO. Plenum: 1986. Pp. 404. Hbk ISBN 0-306-42126-7. Np.

The Handbook of Behavioral Group Therapy. DENNIS UPPER and STEVEN M. ROSS.

(cds), Plenum: 1985, Pp. 513, ISBN 0-306-41989-

0. Np. Health Psychology: A Psychobiological Perspective. By MICHAEL FEUERSTEIN, ELISE E. LABBE and ANDRZEJ R. KUCZMIERCZYK. Plenum: 1986. Pp. 511. Hbk ISBN 0-306-42037-6. Np.

History of Psychiatry, National Schools, Education and Transcultural Psychiatry, P. PICHOT et al. (eds.), Plenton: 1985, Pp. 744, ISBN 0-306-41608-5, Np.

Issues in Cognitive Modeling. By A.M. AIT-KEN-HEAD and J.M. SLACK. Lawrence Erlbaims: 1985, Pp. 349, ISBN 0-86377-030-4. Pbk 15, 95

The Nightmare: The Psychology and Biology of Terrifying Dreams. By ERNEST HARTMANN. Harper & Row 1986. Pp. 294. Hbk ISBN 0-465-05109-X.

The Psychoanalytic Movement. BY ERNEST GEL-LNER. Granada Publishing: 1985. Pp. 241, Pbk 1SBN 0-586-08436-3, £3.50.

Psycholinguistics. By ALAN GÁRNHAM. Methuen: 1985. Pp. 269. Pbk ISBN 0-416-36620-

Psychotherapeutic Change. An Alternative Approach to Meaning and Measurement. By ALVIN R. MAHRER. W.W. Norton:1986. Pp.208. Hbk ISBN 0-393-70007-0. £19.50, \$28.50.

Self-Psychology and the Humanities: Reflections on a New Psychoanalytic Approach. By HEINZ KOHUT. W.W. Norton: 1986. Pp. 290. Hbk ISBN 0-393-70000-3. £22, \$30.

Social Relationships and Cognitive Development. ROBERT A. HINDE. ANNE-NELLY PERRET-CLERMONT and JOAN STEVENSON-HINDE (eds). Oxford University Press: 1986. Pp., 384. Hhk ISBN 0-19-852157-3; pbk ISBN 0-19-852167-7. Hbk £37,50; pbk £19,50.

Surface Dyslexia: Neuropsychological and Cognitive Studies of Phonological Reading. K.E. PATTER-SON, R.C. MARSHALL and M. COLTHEART (eds). Lawrence Erlhaum Associates: 1985. Pp.544. 0-86377-026-6. Np.

Why Isn't Johnny Crying? Coping with Depression in Children. By DONALD'H. McKNEW Jr. LEON CYTRYN and HERBERT YAHRAES. Norton: 1986, Pp.187. Pbk ISBN 0-393-30240-7. £4.50. \$6.30.

General

Drinking Water Materials: Field Observations and Methods of Investigation. By D. SCHOENEN and H.F. SCHÖLER. Ellis Horwood;1985. Pp.195. Hbk ISBN 0-85312-929-0. £25.

Emile du Bois Reymond (1818–1986) — Anton Dohti (1840–1909). Briefwechsel. CHRISTIANE GROEBEN and KLAUS HIERHOLZER. Springer Verlag: 1985. Pp. 322. Pbk ISBN 3-540-15812-X. Np.

Evolving Hierarchical Systems. By STANLEY N. SALTHE. Columbia University Press: 1985. Pp. 343. ISBN 0-231-06016-5. \$30.

Fire. By JOHN W. LYONS. W.H. Freeman: 1985. Pp. 170. ISBN 0-7167-5010-4. £15.95.

Games Pets Play, or How Not to be Manipulated by Your Pet. By BRUCE FOGLE. Michael Joseph: 1986. Pp. 218. Hbk ISBN 0-7181-2674-2. £9.95.

The Harvey Lectures, 1983-1984. By RICHARD AXEL et al. Academic: 1985. Pp. 286. ISBN 0-12-312079-9. \$65, £56.50.

Hedges, Walls and Boundaries. By ROMOLA SHOWELL. Dryad Press Limited, London, UK: 1986. Pp.48. Hbk ISBN 0-8521-96245. £6.50.

How Nuclear Weapons Decisions are Made. SCILLA MCLEAN (ed.). Macmillan, in association with the Oxford Research Group:1986. Pp.264. Pbk ISBN 0-333-40583-8. £6.95.

Humanism and Anti-Humanism: Problems of Modern European Thought. By KATE SOPER. Http://doi.org/10.1009

Imposing Aid: Emergency Assistance to Refugees. By B.E. HARRELL-BOND: Oxford University Press:1985. Pp. 440. Pbk ISBN 0-19-261543-2. Hbk £15; pbk £2.50.

Influence of Modern Style of Life on Food Habits of Man. J.C. SOMOGYI and G. VARELA (eds). Karger: 1985. Pp.91. ISBN 3-8055-4152-X. DM 99, \$35.50.

An Introduction to Minimal Currents and Parametric Variational Problems. By ENRICO BOMBIERI. Harwood Academic Publishers:1985. Pp. 384. Pbk ISBN 3-7186-0299-7: \$25.

Islamic Metalwork in the Freer Gallery of Art. By ESIN ATIL, W.T. CHASE and PAUL JETT. Smithsonian Institution Press:1985. Pp.273. Pbk ISBN 0-87474-249-8. \$17.50.

Leviathan and the Air-Pump. Hobbes, Boyle and the Experimental Life. By STEVEN SHAPIN and SIMON SCHAFFER. Princeton University Press: 1986. Pp. 440. Hbk ISBN 0-691-08393-2. \$60.

The Management of Productivity and Technology in Manufacturing. PAUL R. KLEINDORFER (ed.). Plenum: 1985. Pp. 331. ISBN 0-306-42032-5. Np.

Mathematical Methods in Human Geography and Planning, By A.G. WILSON and R.J. BENNETT. Wiley:1985. Pp.411. Hbk ISBN 0-471-10521-X. £29.95.

Methodological and Statistical Advances in the Study of Individual Differences. CECIL R. REYNOLDS and VICTOR L. WILLSON (eds). Plenum: 1985. Pp. 472. Hbk ISBN 0-306-41962-9. Np.

The Mind Palace. By STEVE R. PECZENIK. Simon and Schuster:1985. Pp.335. Hbk ISBN 0-671-52433-X. \$16.95.

52433-X. 510.95.

The Origins of Logic: One to Two Years. By JONAS LANGER. Academic: 1985. Pp. 415. Hbk ISBN 0-12-436555-8. £65, \$75.

Pressures on the Countryside. By DERRICK GOLLAND. Dryad Press Limited, London, UK: 1986. Pp. 48. Hbk ISBN 0-8521-9625-3. £6.50.

Scientific Evidence for Dietary Targets in Europe. J.C. SOMOGYI and A. TRICHOPOULOU (eds). Karger:1986. Pp.162. Hbk ISBN 3-8055-4161-9. SwFr. 150, DM 180, \$64.

Selecta, 3 Vols. By DONALD C. SPENCER. Wiley:1985. Pp.1754 ISBN (Vol. 1) 9971-978-02-4. (Vol. 2) 9971-978-02-4. (Vol. 3) 9971-978-04-0. £154.

Sky with Ocean Joined. Proceedings of the Sesquicentennial Symposia U.S. Naval Observatory. STEVEN J. DICK and LEROY E. DOGGETT (eds). U.S. Naval Observatory:1983. Pp. 190. Pbk np.

Standard Potentials in Aqueous Solution. ALLENJ, BARD, ROGER PARSONS and JOSEPH JORDAN (eds). Dekker:1985. Pp.848. ISBN 0-8247-7291-1. \$29.95.

Star Wars: Suicide or Survival? By ALUN CHALFONT. Weidenfeld and Nicolson:1985. Pp.169. Hbk ISBN 0-297-78464-1. Np.

Stories for the Third Ear. By LEE WALLAS. W.W. Norton:1986. Pp.178. Hbk ISBN 0-393-70019-4. £11.95, \$16.95.

Structural Optimization. Vol.1, Optimality Criteria. M. SAVE and W. PRAGER (eds). Plenum: 1985. Pp.334. Hbk ISBN 0-306-41861-4. Np.

Successful Small Farming. By MALCOLM BLACKIE. Angus & Robertson: 1986. Pp. 176. ISBN 0-207-15248-9. Pbk £5.95.

Survey Design and Analysis. By F.R. JOLLIFFE. *Wiley:1986. Pp.178. Hbk ISBN 0-85312-599-6.* £28.50.

Time Resolution in Auditory Systems. AXEL MICHELSEN (ed.). Sprinter-Verlag 1985. Pp.242. ISBN 0-387-15637-2. DM 64.

Tourism: A Community Approach. By PETER E. MURPHY. Methuen:1985. Pp.200. ISBN 0-416-39790-5. £19.95.

Transmission Lines, Waveguides and Smith Charts. By RICHARD L. LIBOFF and G. CONRAD DALMAN. Macmillan:1985. Pp.269. ISBN 0-02-949540-7. £40.

Travel by Air. By MICHAEL POLLARD. Macmillan: 1986. Pp. 48. ISBN 0-333-40939-6. £4.95.

Travel by Water. By MICHAEL POLLARD. Macmillan: 1986. Pp. 48. ISBN 0-333-40940-X. £4.95.

Trees and Shrubs Cultivated in Ireland. By MARY FORREST. Boethius Press, for the Heritage Gardens Committee, Dublin:1985. Pbk ISBN 0-86314-116-1. IR £7.50, GB £6.80, \$9.00.

Underwater Photography and Television for Scientists. J.D. GEORGE, G.I. LYTHGOE and J.N. LYTHGOE (eds). Oxford University Press:1985. Pp.184. Hbk ISBN 0-19-854141-4. £32.50.

Vaccination Certificate Requirements and Health Advice for International Travel, 1986. World Health Organization, Geneva: 1985. Pp.81. Pbk ISBN 92-4-158011-9. SwFr 13.

Editorial Board

T. Bennett, Nottingham N.J.M. Birdsall, London

C.M. Bradshaw, Manchester G Rurnstock London

J.B. Caldwell London

B.A. Callingham. Cambridge

J.A.J.H. Critchley, Edinburgh

M. Maureen Dale, London

R.J. Flower, Bath

J.C. Foreman, London

A.R. Green, London M.C. Harris, Birmingham

G. Henderson, Cambridge

C.R. Hiley, Cambridge

R.G. Hill, Cambridge

J.R.S. Hoult, London

P.P.A. Humphrey, Ware

L.L. Iversen, Harlow

D.H. Jenkinson, London

P.G. Janner London

W.E. Lindup, Liverpool

D. Lodge, London

R. McBurney, Newcastle

J.C. McGrath, Glasgow

D.S. McQueen, Edinburgh

C.A. Marsden, Nottingham

R.J. Marshall, Newhouse

S.R. Nahorski, Leicester

D.A.A. Owen, Welwyn Garden City

M.E. Parsons, Welwyn

Priscilla J. Piper, Landon

British Journal of **Pharmacology**

Edited for the British Pharmacologic J F Mitchell (Chairman) G M Lees (Secretary)
Margaret Day (Press Editor)
C V Wedmore (Assistant Press Editor)

N.L. Poyser, Edinburgh

T.W. Robbins, Cambridge

M. Spedding, Edinburgh

T.L.B. Spriggs, Cardiff T.W. Stone, Landon

E. Szabadi, Manchester

D.A. Terrar, Oxford

D.R. Tomlinson, Nottingham

E.M. Vaughan Williams

R.M. Wadsworth, Glasgow

D.I. Wallis, Cardiff

D.F. Weetman, Sunderland T.J Williams, Harrow

G.N. Woodruff, Harlow

J.M. Young, Cambridge

Corresponding Editors

PR Arisms, Galveston USA

J. Axelrod. Bethesda USA

C. Bell, Melbourne, Australia

F.E. Bloom. La Jolia, USA

A.L.A. Boure, Clayton.

P.B. Dews, Boston, USA

T. Godfraind, Brussels, Beigium

L.I. Goldberg, Chicago. USA

S.Z. Langer, Pans, France

R.A. Lewis, Harvard, USA

E. Muscholl, Mainz, Germany

M. Otsuka, Tokyo, Japan

R.H. Roth, New Haven, USA:

M. Schachter, Alberta.

B. Uvnas, Stockholm Sweden

PA Van Zwieten

Amsterdam, Netherlands

G. Velo. Verona Italy

M.B.H. Youdim. Haifa Israel

- one of the top five most cited pharmacology journals in the world
- ☆ a vital source of relevant information for physiologists, immunologists, molecular biologists and biochemists, in addition to pharmacologists
- presents original papers submitted from all parts of the world
- ☆ includes a regularly up-dated, fully international list of forthcoming meetings
- ☆ supplements provide full coverage of the proceedings of the meetings of the British Pharmacological Society
- published in three volumes a year, each with an index

Subscription Order Form

- To: Richard Gedye, the British Journal of Pharmacology, Farndon Road, Market Harborough, Leicestershire LE16 9NR, UK
- Please enter my subscription to the British Journal of Pharmacology for TWO YEARS commencing with the current year @ £350.00 thereby avoiding any price increase
- Please enter my subscription to the British Journal of Pharmacology for ONE YEAR commencing with the current year @ £175.00
- l'enclose a cheque madé payable to Macmillan Journals for £*
- lauthorise you to charge my VISA*/ACCESS*/MASTERCARD* the

Credit card Account No

Expiry date

Strong School Control

All orders must be accompanied by cheque or credit card authorisation. delete as applicable

Subscription Information

ISSN 0007-0920

Frequency: Monthly - Two volumes per year

Language: English

Rates per year

UK & Eire: £175.00, USA/Canada: US\$410.00 (surface) US\$500.00 (airmail), Rest of World: £199.00 (surface) £279.00 (airmail)

Two Year Subscription

Save money and ensure an uninterrupted supply of the Journal - simply double the payment sent.

Please write in BLOCK CAPITALS

Name

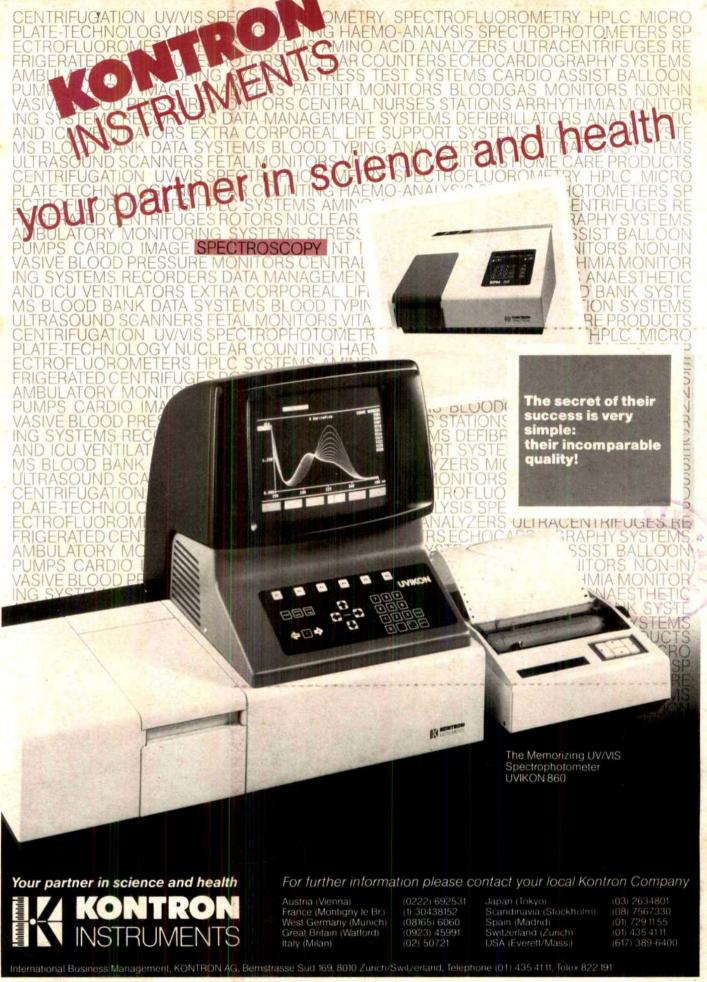
Address

Postal/Zip code

Date

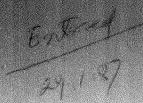
☐ Please send me a free sample copy of the **British Journal of Pharmacology**

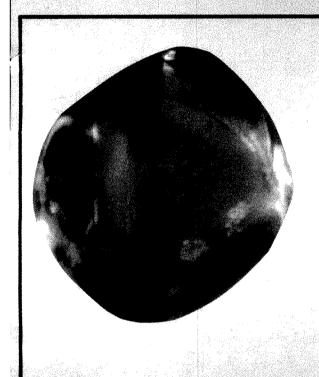
ACMILLAN PRESS

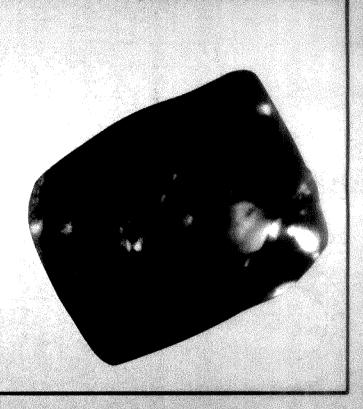


WEEKLY JOURNAL OF SCIENCE ust 1986 £1.90

Volume 322 No.6080 14-20 August 1986 £1.90

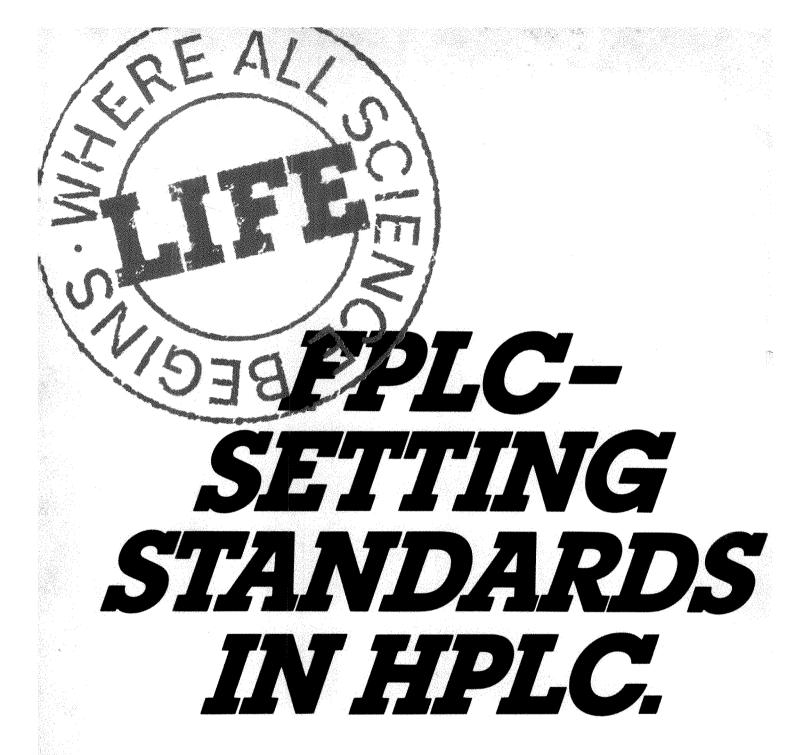






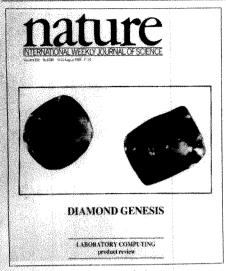
DIAMOND GENESIS

iastorationy completele



nature

NATURE VOL. 322 14 AUGUST 1986

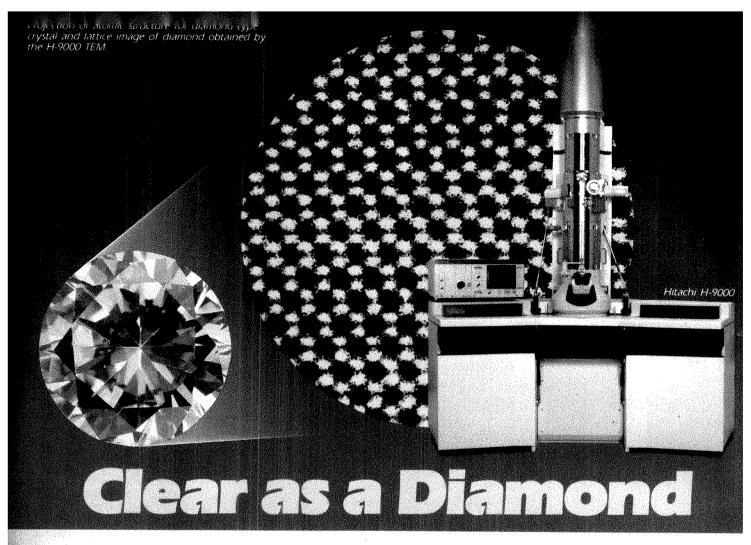


Pale-green clinopyroxene and deep-orange garnet crystals, found as tiny (~250 µm) inclusions in diamonds from the Premer mine, South Africa. These inclusions yield ages contemporaneous with the magmatism which brought the diamonds to the surface (see p.623), implying an origin for these diamonds which is related to their host magmas, and distinct from that of older olivine-bearing diamonds.

OPINION	*****
A tale of two companies	581
Nuclear regulation	
Deeper pork barrels	582
NEWS	************
NASA	
Japanese space plans go ahead	583
European Commission	
Israeli science	584
Strategic Defense Initiative	
Environmental pollution	585
Computer models	
Nuclear forecast	
Return of tamarins proves expensive	586
Seismic monitoring	
Ariane ride for Indian satellite	
Doing things the all-American way	587
Chernobyl accident	
Japan ready to participate	
Guatemala accused	-00
of political killings	588
Hubble space telescope	***
Weight problems	589
CORRESPONDENCE	ndeleneral congruences.
Sequencing human genome/	
Special relativity/science and faith	590
NEWS AND VIEWS	erenenen visconen
What happens on Cygnus X-3?	591
Where now with superstrings?	
Robert Walgate	592
Sulphur and volcanism on Io	
David A Crown & Ronald Greeley	593

Plant viruses: New threats to crops from changing farming practice Robert Coutts Hunting tropospheric OH ions	594	Bovine papillomavirus genome elicits skin tumours in transgenic mice M Lacey, S Alpert & D Hanahan	609
D Perner	595	LETTERS TO NATURE	
Japanese agricultural beginnings Gina L Barnes Invertebrate neurobiology:	595	Looking for cosmic strings A Vilenkin	613
Catching up with peptides Mark Tyrer Gene regulation: Fingers and DNA half-turns	596	Cooling flows in ellipticals and the nature of radio galaxies M C Begelman	614
Stephen C Harrison	597	Secular change in solar activity	
-SCIENTIFIC CORRESPONDENCE The stability of biological	CE-	derived from ancient varves and the sunspot index	
nomenclature: yeasts		C P Sonett & T J Trebisky	615
J A Barnett Microtubule assembly in the axon	599	Diurnal cycle of tropospheric OH T M Hard, C Y Chan, A A Mehrabzadeh.	
FSolomon	599	WHPan & RJO'Brien	617
Disease gene relationship seen A Ashworth, E A Shephard & I R Phillips Mankind's genetic bottleneck	599	Structure determination of a-CrPO ₄ from powder synchrotron X-ray data J P Attfield, A W Sleight & A K Cheetham	620
J S Jones & S Rouhani	599	AND THE RESERVE AND ADDRESS OF THE PROPERTY OF	
Transfer of radioiodide to milk and its inhibition P J Mountford, A J Coakley, I R Fleet, M Hamon & R B Heap	600	Formation of ultra-fine amorphous alloy particles by reduction in aqueous solution J van Wonterghem, S Mørup, C J W Koch, S W Charles & S Wells	622
BOOK REVIEWS	Minimum landar barrers	Latter-day origin of diamonds of	
The Lead Debate: The Environment,		eclogitic paragenesis S H Richardson	623
Toxicology and Child Health R Lansdowne and W Yule, eds Josef Eisinger Lindow Man: The Body in the Bog	601	Upper mantle oxygen fugacity recorded by spinel Iherzolites G S Mattioli & B J Wood	626
I M Stead, J B Bourke and D Brothwell, eds Theya Molleson Cloning Vectors: A Laboratory Manual	602	Crustal detachment during South Atlantic rifting and formation of Tucano-Gabon basin system N Ussami, G D Karner & M H P Bott	629
PH Pouwels, BE Enger-Valk and WJ Brammar, eds Tim Harris Modeling Nature. Episodes in the	603	Oldest primitive agriculture and vegetational environments in Japan TTsukada, S Sugita & Y Tsukada	632
History of Population Ecology by S E Kingsland John H Lawton		Olfactory dysfunction in humans with deficient guanine nucleotide-binding protein	
The Biochemistry and Physiology of Plant Disease by R N Goodman, Z Király		R S Weinstock, H N Wright, A M Spiegel, M A Levine & J A Moses	635
and K R Wood Richard Dixon	604	Synthesis of fast myosin induced	100
ARTICLES	W-J-1	by fast ectopic innervation of	
ANTICLES Aleutian terranes from		rat soleus muscle is restricted to the ectopic endplate region	
Nd isotopes R W Kay, J L Rubenstone		G Salviati, E Biasia & M Aloisi	637
& SM Kay	605	Contents continued 69	erkaf

Nature® (ISSN 0028-0836) is published weekly on Thursday, except the last week in December, by Macmillan Journals Ltd and includes the Annual Index (mailed in February). Annual subservoition for USA and Canada US \$240. USA and Canadian orders to: Nature, Subscription Dept, PO Box 1501, Neptune, NJ 07753, USA. Other orders to: Nature, Brunet Road, Basingstoke, Flana RO22 2XS, UK, Second class postage paid at New York, NY 10012 and additional mailing offices. Authorization to photocopy material for internal or personal use, or internal or open sonal use, or in



The Hitachi H-9000 300-kV TEM produces images with the stunning brilliance of a diamond.

The incredible penetration power and superb ultrahigh resolution of the Hitachi H-9000 300-kV transmission electron microscope has produced the world's first micrographs of the atomic structure of the diamond.

Dramatic Improvement Over Conventional 100-kV and 200-kV TEMs

Combining improved imaging resolution, a specimen penetration proportional to the electron velocity, an improved electron diffraction mode accuracy, and an improved spatial resolution for X-ray analysis, in which spread of beam penetration within a specimen is inversely proportional to the accelerating voltage, the Hitachi H-9000 TEM has produced stunningly clear micrographs of the diamond at the atomic level in remarkable detail.

This important achievement dramatically demonstrates the H-9000's ability to observe and analyze thicker specimens — a capability critical to the advancement of materials science, semiconductor technology, biomedical research, and other high-tech fields.

Compact Power

Based on Hitachi's extensive experience in million-volt microscopes, the H-9000 features a 10-stage acceleration system that provides ultrastable accelerating voltages of up to 300kV in an instrument of modest proportions. Enabling simple installation, use, and maintenance, the H-9000 easily fits in a normal-sized laboratory room, and operates just like a conventional 100-kV or 200-kV TEM.

Sophisticated Analytical Features

In addition to the conventional Be-window detector, a UTW detector may be mounted simultaneously, forming a dual EDX detection system. A special EELS using secondary aberration corrected three-dimensional focus spectrometry provides optimum analytical capability at 300kV. A TV monitor image intensifier system, SEM/STEM analytical applications, and a CBED fine probe add to the capabilities of the H-9000, one of the most powerful analytical microscopic systems available today.

Reader Service No.296



NISSEI SANGYO AMERICA, LTD. Tel: (415) 969-1100 NISSEI SANGYO CANADA, INC. Tel: (416) 675-5860 NISSEI SANGYO CO., LTD. England Tel: (0734) 66-4149 NISSEI SANGYO GmbH West Germany Tel: (0211) 450982—9 NISSEI SANGYO CO., LTD. Japan Tel: (03) 504-7111 HITACHI, LTD., INSTRUMENT DIVISION Japan Tel: (03) 214-3123

That important research article you've been looking for located instantly!



If you store your copies of Nature for future reference, then the annual index of subject and author is an essential part of your collection. These comprehensive annual indexes are available for all issues of Nature from 1971 to 1985.

Prices and address for orders are set out below.

Annual Subscription Pri	ices	
UK & Irish Republic		£104
USA & Canada		US\$240
Australia, NZ &		
S. Africa	Airspeed	£150
	Airmail	£190
Continental Europe	Airspeed	£125
India	Airspeed	£120
	Airmail	£190
Japan	Airspeed	Y90000
Rest of World	Surface	£120
	Airmail	£180
Orders (with remittance) to:	

USA & Canada

UK & Rest of World Nature Subscription Dept PO Box 1501 Circulation Dept Brunel Road Neptune NJ 07753 Basingstoke Hants RG212XS, UK Tel: 0256 29242 (The addresses of Nature's editorial offices are shown

facing the first editorial page)

Japanese subscription enquiries to: Japan Publications Trading Company Ltd. 2-1 Sarugaku-cho 1-chome Chiyoda-ku, Tokyo, Japan Tel: (03) 292 3755

Personal subscription rates: These are available in some countries to subscribers paying by personal cheque or credit card. Details from:
USA & Canada
UK & Europe

Nature Felicity Parker 65 Bleecker Street Nature 4 Little Essex Street London WC2R 3LF, UK New York NY 10012, USA Tel: (212) 477-9600 Tel: 01-836 6633

Back issues: UK, £2,50; USA & Canada, US\$6.00 (surface), US\$9.00 (air); Rest of World, £3.00 (surface), £4.00 (air)

Binders

Single binders: UK, £5.25; USA & Canada \$11.50; Rest of World, £7.75. Set of four: UK, £15.00; USA & Canada \$32.00; Rest of World, £22.00

Annual indexes (1971-1985) UK, £5.00 each; Rest of World, \$10.00

Nature First Issue Facsimile UK. £2.00; Rest of World (surface). \$3.00; (air) \$4.00

Nature in microform Write to University Microfilms International, 300 North Zeeb Road, Ann Arbor, MI 48106, USA

The	tight	junct	ion	does	not all	ow
lipi	d mol	ecules	to d	liffus	e from	ŧ
one	epith	elial c	ell t	o the	next	
~		**	-	* *		

G van Meer, B Gumbiner & K Simons

Synthetic peptides as nuclear localization signals

D S Goldfarb, J Gariépy, G Schoolnik & R D Kornberg

Loss of genes on chromosome 22 in tumorigenesis of human acoustic neuroma

B R Seizinger, R L Martuza & JF Gusella

Tissue-specific expression of the human tropomyosin gene involved in the generation of the trk oncogene FCReinach & ARMacLeod

Sequences similar to the I transposable element involved in I-R hybrid dysgenesis in D. melanogaster occur in other Drosophila species A Bucheton, M Simonelig, C Vaury & M Crozatier

Cryptic simplicity in DNA is a major source of genetic variation D Tautz, M Trick & G A Dover

Nuclear factor III, a novel sequencespecific DNA-binding protein from HeLa cells stimulating adenovirus **DNA** replication

G J M Pruijn, W van Driel & PC van der Vliet

Green light-mediated photomorphogenesis in a dinoflagellate resting cyst B J Binder & D M Anderson 659

The crystal structure of d (GGATGGGAG) forms an essential part of the binding site for transcription factor IIIA M McCall, T Brown.

WN Hunter & O Kennard

MATTERS ARISING

The mechanism of activation of porcine pepsinogen

HE Auer & DM Glick Reply: M N G James & A R Sielecki

PRODUCT REVIEW

The laboratory networking dilemma 665 W H Jennings The binary breakthrough

-MISCELLANY-**Books received**

-NATURE CLASSIFIED

Professional appointments -

Research posts — Studentships Fellowships — Conferences Courses — Seminars — Symposia:

Back Pages

Next week in Nature:

- How many Chernobyls?
- Selenium as atmospheric redox tracer

639

641

644

648

650

652

656

661

664

669

- Stereochemistry of water
- Antarctic melting over 60,000
- Permafrost formation
- Oldest oil in the world?
- Another bird for Enantiornithes
- Monitoring fission yeast growth
- Gene regulatory proteins
- Mechanism of c-myc oncogene

GUIDE TO AUTHORS

Authors should be aware of the diversity of Nature's readership and should strive to be as widely under-

Review articles should be accessable to the whole results ership. Most are commissioned, but unsolicited reviews are welcome (in which case prior consultation with the office is desirable).

Scientific articles are research reports whose consciusions are of general interest or which represent suffstantial advances of understanding. The text should not exceed 3.000 words and six displayed items (illgures plus tables). The article should include an italie heading of about 50 words.

Letters to Nature are ordinarily 1,000 words long with no more than four displayed items. The first paragraph (not exceeding 150 words) should say what the letter is about, why the study it reports was under taken and what the conclusions are

Matters arising are brief comments (up to 500 words) on articles and letters recently published in Nature The originator of a Matters Arising contribution should initially send his manuscript to the author of the original paper and both parties should, wherever possible, agree on what is to be submitted

Manuscripts may be submitted either to London or Washington. Manuscripts should be typed (double spacing) on one side of the paper only. Four copies are required, each accompanied by copies of lettered artwork. No title should exceed 80 characters in length. Reference lists, figure legends, etc. should be on separate sheets, all of which should be numbered. Abbreviations, symbols, units, etc. should be identified on one copy of the manuscript at their first

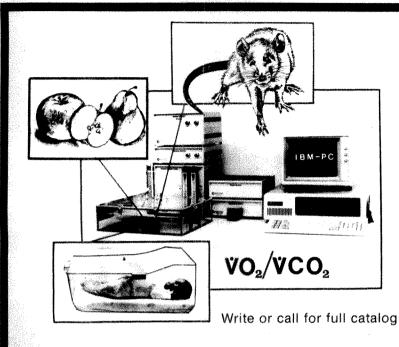
References should appear sequentially indicated by superscripts, in the text and should be abbreviated according to the World List of Scientific Periodicals, fourth edition (Butterworth 1963-65). The first and last page numbers of each reference should be effect. Reference to books should clearly indicate the pulslisher and the date and place of publication. Unpublished articles should not be formally referred to unless accepted or submitted for publication, but may be mentioned in the text.

Each piece of artwork should be clearly marked with the author's name and the figure number. Original artwork should be unlettered. Suggestions for cover illustrations are welcome. Original artwork (and one copy of the manuscript) will be returned when manuscripts cannot be published.

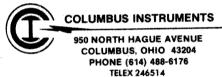
Important: Manuscripts or proofs sent by air courses should be declared as "manuscripts" and "value \$5" to prevent the imposition of Customs duty and Value Added Tax in the United Kingdom.

Requests for permission to reproduce material from Nature should be accompanied by a self-addressed (and, in the case of the United Kingdom and United States, stamped) envelope.

O₂ CONSUMPTION / CO₂ PRODUCTION "OXYMAX" COMPUTERIZED SYSTEMS



- ★ Utilized IBM-PC computer.
- ★ Prints and stores results on the disk in one minute intervals.
- ★ Monitors simultaneously 1 to 4 compartments (cages).
- ★ For animals, measures respiration rate and locomotor activity along with $\mathring{V}O_2/\mathring{V}CO_2$
- ★ Can easily be modified to suit variety of animal sizes.
- ★ High accuracy and stability. (better than 1%)
- ★ Twenty-four hours unattended operation.



Reader Service No.7

New New New New

Computer Graphics and Molecular Modeling

Edited by Mark Zoller, Cold Spring Harbor Laboratory; Robert Fletterick, University of California School of Medicine, San Francisco

COMPUTER GRAPHICS AND MOLECULAR MOD-ELING summarizes work presented at a December 1985 Cold Spring Harbor Laboratory Banbury Center meeting at which a diverse group of researchers addressed issues such as protein sequence homology, three-dimensional structure homology in proteins, molecular design of functional macromolecules, X-ray crystallography, hardware and software for displaying and analyzing three-dimensional macromolecules, and software for the analysis of the energetics and dynamics of proteins.

Molecular biologists, crystallographers, and computer specialists will find COMPUTER GRAPHICS AND MOLECULAR MODELING a useful collection of extended abstracts indicating directions for integrating the various approaches to the study of protein structure and function.

1986, 145 pp., illus., colorplates, appendix Paper \$29 ISBN 0-87969-193-X



Cold Spring Harbor Laboratory P.O. Box 100 Cold Spring Harbor, New York 11724

M-Sean

Mass Spectrometry Consultants and Analysts



Protein/ Carbohydrate Structure Analysis Service

World leaders in the application of new Mass Spectrometric techniques including High Field Fast Atom Bombardment to the solution of PROTEIN and CARBOHYDRATE research problems.

- Analysis of recombinant DNA protein and glycoprotein products.
- # Identification of post-translational modifications including sites of glycosylation.
- Protein sequence determination.
- **M** Confirmation of identity of synthetic peptides.
- Structure of oligosaccharides and glycoconjugates including identification and points of attachement of non-glycosyl substituents.

For information contact

M-Scan Ltd

Silwood Park, Sunninghill, Ascot, Berkshire SL5 7PZ England.

Tel: (0990) 27612/27072 Telex: 849337 (M SCAN)

M-Scaninc (U.S.)

P.O. Box 5368 Wilmington, Delaware 19808 Telephone: (302) 453 8151

Reader Service No.8

Reader Service No.34

nature

NATURE VOL. 322 J4 AUGUST 1986

A tale of two companies

The British government has made a muddle of its decision to prevent one electronics company from taking over another. It should pay more attention to what happens in the United States.

By an historical accident dating from the nineteenth century, Britain and the United States have in common not merely some usages of the same language, but also the existence of two public companies (corporations), one British and one American, that are called the General Electric Company. Both companies owe their origins to the demand, at the turn of this century, for machines for the generation, distribution and use of electric power. With the passage of time, both have become hugely successful and enormously diversified. Each, for example, has an interest in the manufacture of military aircraft, no doubt because the traditional manufacture of steam turbines for electricity generating sets provided a natural opening into the manufacture of jet engines. Inevitably, each has also an interest in consumer electronics.

The parallel between the British and the US companies has recently been even more striking; both have been seeking to grow by the acquisition of others. This is the spirit in which, earlier this year, GE of the United States merged with RCA Inc., itself a diversified conglomerate. It is also the spirit in which the British General Electric Company (GEC Ltd) had sought to merge with the smaller but still very substantial company called Plessey. The difference, between the United States and Britain, is that the British government has now used its anti-monopoly regulations to deny GEC the opportunity to pursue its commercial bid for Plessey.

Why should the British and US governments react so differently? Both governments are rightly concerned that companies should not become monopolists in their markets, charging their customers prices unrestrained by competition and serving the while as brakes on technical innovation. In the United States, the proposed acquisition of RCA by GE was formally studied by the US Department of Justice, which decided that the huge scale of the proposed merger was not in itself objectionable and that the fields in which the interests of GE and RCA most nearly coincide (defence and consumer electronics) are so competitively occupied by others that the merged company is unlikely to be a monopolist. In Britain, the proposed merger between GEC and Plessey was referred for consideration to the quasi-judicial Monopolies and Mergers Commission, which has the duty to consider the monopolistic risks of circumstances referred to it by the government, and whose conclusions may either be accepted (and then enforced) or, alternatively, may be rejected. On this occasion, the monopolies commission came out against the merger. The Secretary of State for Trade and Industry last week accepted this conclusion, the zeal with which his civil servants argued in the opposite direction when presenting their department's evidence to the commission notwithstanding.

Lessons

It will not be long before those concerned with this decision will be wishing they had behaved differently. The report of the monopolies commission, and the British government's ready acceptance of it, is a sign that people in Britain who should know better have not yet learned the lessons of the past few decades of industrial decline. The idea that GEC and Plessey should be merged is, ironically, itself a direct consequence of the policies of past and present governments towards telecommunications. Once upon a time, nearly two decades ago, the then nationalized telecommunications authority set about the development of digital electronic switching systems (called trendily "System X") by inviting manufacturers to belong to a joint "research committee" constituted so as to persuade them to help pay for the high cost of developing such a system by promising them a share of the business that would eventually result, both domestically and from export sales. In the event, that enterprise has been a cruel disappointment. Of the original group of manufacturers, only GEC and Plessey survive. System X compares reasonably well with other modern equipment, but has been much delayed and is unlikely to command the huge export markets once talked of.

Worse still, for the companies concerned, their once-cosy relationship with the monopoly customer for telecommunications equipment has been undermined by the decision, fully implemented only two years ago, that British Telecom should become a commercial company. Not surprisingly, this monopoly customer now says it does not wish to have to depend on the old ring of suppliers. Now it plans to order some switching gear from other than British companies.

Rationalization

Accordingly, it is generally agreed, even by the monopolies commission, that GEC and Plessey must do something to rationalize their interests in System X. Indeed, the proposal that one should buy the other appears to have arisen directly out of the abortive talks between them over the past few years. What the commission now suggests is either that one should sell its switching business to the other or that they should jointly set up a separate company to handle their combined interest in digital telecommunications. The commission's report (Cmnd 9867, HMSO £9.80) unfortunately says nothing of the obvious snags. Is either of the two companies likely permanently to opt out of a field of technical development of such manifest importance, and would it be in the British national interest if that could be arranged? Even the suggestion that these two independent companies should be forced into a joint venture under the banner of a third company has little to be said for it, given the well-known instability of shotgun marriages and the nearcertainty that both parties to such an enterprise intended merely to market a particular digital switching system would promptly (and sensibly) lose interest once a more attractive venture came along. If telecommunications were the only issue, the case for encouraging one company to buy the other would be irresistible.

So why should the argument have gone the other way? What seems most of all to have weighed with the monopolies commission, and eventually with the government, is the protest by the British Ministry of Defence that a merger of GEC and Plessey would give the combined company a virtual monopoly of the capacity to supply particular kinds of equipment, with the result that the ministry would not be able fully to implement its present policy of buying as much as possible of the defence equipment it needs only after companies working in the field have put in competitive tenders. But this argument is humbug.

The ministry is right to wish to buy its defence equipment as cheaply as possible, but is wrong to advance, for the purposes of a monopoly investigation, the argument that there have to be two potential British suppliers of everything it may choose to buy. The monopolies commission might just as sensibly have invited the defence ministry to follow British Telecom in listing overseas suppliers among those competing for its business.

This is the nub of the difficulty the British government has now created for itself. Although GEC is among the largest of British companies, it is tiny by the yardsticks of its direct competitors elsewhere, with annual sales roughly one sixth of the new combination of GE and RCA in the United States. Yet what the past few years have shown, specifically in the development of digital switching systems but generally, in electronics as a whole, is that the costs of launching new projects are invariably huge. Moreover, speed is of the essence; there are no prizes for being second. The point has probably now been reached at which only huge companies with long pockets can hope successfully to launch new projects that are technically interesting and likely to change the world in important and profitable ways. The sad history of System X shows the penalties of spending too little too late.

The British government, which for most of its spell in office has stuck to the principle that governments should not second-guess entrepreneurs, has on this occasion allowed itself to make industrial policy by default, by tamely accepting what the majority of the monopolies commission had to say (there is a dissenting minority report). The wisdom of this easy course will never be directly tested, for there may not now be a chance to tell what a slightly larger company than GEC might be able to accomplish by way of technical innovation. But there can be no doubt of its inequity; under British as distinct from US law, there is no way in which such decisions, however unfair they may be to shareholders of companies such as GEC, can be tested in the courts.

The moral in this sad tale is that all governments should take this opportunity to look again at their arrangements for regulating monopolies. In Britain, it is plainly an expensive luxury that companies are prevented from doing what makes economic sense for the sake of giving the defence procurement people the choice of several competitors for defence contracts; if that is what they believe they need, they should be prepared to throw the bidding open to all comers. In most European countries, there is an urgent need to ask how national legilation on monopolies can be squared with the general doctrine that trade flows freely across what used to be national frontiers. And to the extent that the United States now feels as much threatened by Japan as by the danger that its own companies might rig the domestic and overseas markets to their own advantage, there is a strong case for asking that the full rigours of the anti-trust legislation should be softened in the interests of the ultimate beneficiaries — those who buy the products of the new technology.

Nuclear regulation

The International Atomic Energy Agency has handled Chernobyl deftly. What next?

This is bound to be more than an unusually formative year for the International Atomic Energy Agency (IAEA) at Vienna; the next few weeks could tell just what the agency's future holds. This is the season at which the agency's board of governors holds its annual meeting, in recent years a more or less routine affair concerned with the difficulty of recruiting enough skilled inspectors to operate the safeguards system and with the constant anxiety about the budget (which amounted to \$87 million last year, modest for a UN agency). The difference this year is Chernobyl and its consequences, both immediate and for the future development of nuclear energy.

How has the agency, by instinct (and formal constitution) a sponsor of nuclear energy, handled the past few weeks? First, it has done well to ensure a reasonably regular and frequent flow of information about the damaged reactor at Chernobyl. After ten tense days from 26 April, pressure from the agency seems to have been instrumental to that end, while its constitution as an international agency appears to have made it acceptable to the Soviet authorities and other governments in Eastern Europe as a repository of information. More recently, the agency has done a valuable job in persuading member states to give some thought to the steps that need taking to keep each other alert to the risks of cross-border pollution by radioactive materials; in due course, these arrangements may have the force of a convention. Later this month, the agency hopes to go one important step further with the consultation that has been arranged at which the Soviet side says it will tell all about the accident at Chernobyl.

Sponsor of nuclear power though the agency may be, it plainly recognizes that its sponsorship will lead nowhere if ordinary people in its members states are left with the dark suspicion that each nuclear power station is potentially as much a source of catastrophe as was Chernobyl. That is the only sensible view to take. The agency's problem, in the years that lie ahead, will be to blend realism and optimism in a convincing way. That will be a formidable task.

Deeper pork barrels

Is the academic community in the United States too exercised by Congress's wayward ways?

For the past few years, the US Congress seems to have become an embarrassment to many in the academic community who are resentful of the notion that research funds should be distributed by congressional whim rather than by the more familiar techniques of judicious peer review and solemn committee discussion. Last year, Cornell University turned down the offer of a research grant it had not sought and in the process won the approval of those who believe that the award of money for research is a process far too serious to be left to the hunches of people whose only achievement is merely to have run successfully for public office. Most other recipients of these funds, which amount in total to rather more than \$10 million in any year, but probably less than \$50 million, have kept the money but have not advertised the fact. This year, in the rush to finish off the new tax bill and the budget for the financial year beginning in just six weeks, it is inevitable that many proposals for the support of specified research projects will finish up as amendments which are added almost surreptitiously to legislation making its way through the Congress for other purposes.

The US research community will do itself very little good if it takes too prim a view of these developments. Naturally, it would indeed be disastrous for the pattern of research in the United States if any but a small proportion of the funds available for research were to escape the standard system of scrutiny, or if the only means open to researchers for recruiting support for their work required, in the first instance, close personal acquaintance with an elected member of the Congress. But the sprinkling of research grants so far awarded from the pork barrel into which Congress from time to time dips hardly amounts to a substantial threat to the system as its stands. To the extent that most of the grants awarded in this informal way stem from the personal concern (however self-interested) of a congressman for a local academic institution, their frequency may even be regarded as a welcome sign that legislators are not as indifferent to the needs of the research community as they are sometimes said to be. Provided that the frequency of these grants does not get out of hand (in which case the spending agencies would no doubt decline to accept the instructions foisted upon them), there is a case for regarding them as a welcome way of bridging gaps in the orthodox system. Is not plurality still a benefit?

NASA

US space station heads for deep freeze

Washington

BUDGET pressures on the National Aeronautics and Space Administration (NASA), together with management changes recommended by the Rogers commission and astronauts' heightened concern about safety, are forcing a major rethink of the agency's plan to build a habitable space station by 1994. NASA Administrator James Fletcher has ordered a thorough re-evaluation of current plans to take account of questions raised both by astronauts and by members of Congress sceptical of the feasibility of the dual-keel design announced in April.

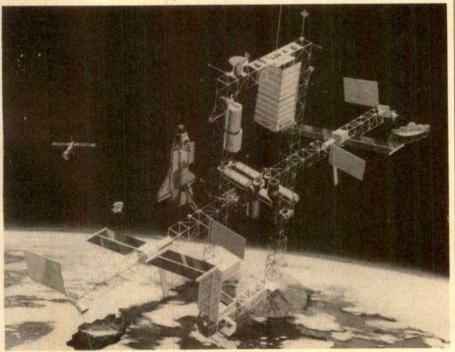
Worries about safety and feasibility have become enmired in a political row over NASA's plan to transfer development of the station's crew modules from Johnson Space Center in Texas to Marshall Space Flight Center in Alabama; much of the criticism of the present design has come from Johnson. The subcommittee in the House of Representatives that oversees NASA has directed the agency to delay implementation of Fletcher's proposals, and congressional representatives from Texas queued up in Congress last week to lambast the new management plan and to demand greater consultation.

The astronauts' primary concerns are that the current design includes no provision for an escape system and that construction will require too much extravehicular activity by astronauts. A simpler one-keel structure could, it is argued, be

built at less risk. Astronaut Gordon Fullerton, in a briefing paper for NASA officials, also said that morale on the space station programme is poor and that there is concern that NASA is misrepresenting what it can do to Congress. Fullerton called for development of a new heavy lift vehicle in conjunction with the Department of Defense that would be used to lift the core components on the space station. A radical reappraisal of the space station has also been called for by Senator Spark Matsunaga (Democrat, Hawaii), who favours separate government and commercial stations with different design objectives.

NASA officials say that although reviews of alternative construction plans are in progress, the basic dual-keel design formally proposed to Congress last April still stands. Provision of an escape module or a "safe haven", and a revised construction plan that would allow for earlier use of the space station, are among the options being studied. But Fletcher told Congress last week that the current design could be built only if a fourth shuttle orbiter to replace the Challenger is built. The administration should soon announce how a fourth shuttle would be paid for.

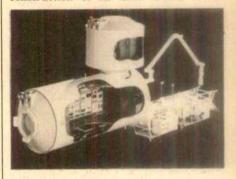
The extent of European participation in the space station is also still far from clear. The European Space Agency (ESA) is adamant that the permanently attached pressurized module for which preliminary design studies were agreed on 1 August



Japanese space plans go ahead

Tokyo

Despite uncertainties over the future of the US space station, Japan's Space Activities Commission has just released a report recommending continued "positive" participation. Over the past two fiscal years, Y5,500 million (\$36 million) has been allotted to the design of an experimental space module (above) to be attached to the space station, and the report recommends that construction of its main frame should



begin in 1989 with a view to launch in 1994.

The module will consist of a pressurized cabin ten metres long for use in experiments on new materials under gravity-free conditions, an exposed service platform equipped with a manipulator and a storage cabin. One or two astronauts will man the station and the report urges the government to begin training in earnest. The estimated cost of the module is Y350,000 million (\$2,300 million). David Swinbanks

will be used mainly for materials research, where profitable spin-off technologies are most likely to emerge. But a congressional committee that approves NASA's budget recently recommended that \$150 million of the \$410 million sought by the agency for space station development next year should be reserved until certain conditions had been met, among them that ESA's pressurized module will be restricted to life science research.

The 1 August agreement indicates that ESA will also conduct preliminary design work on a man-tended free-flying pressurized module that could dock on the space station, as well as a polar orbiting platform. In return, NASA has agreed that it will study the man-tended free-flyer module jointly with ESA. This is essentially a compromise to allow ESA to continue work on the free flyer, which it has favoured all along as its primary contribution but about which NASA is unenthusiastic. The interim agreement covers only preliminary design.

All concerned acknowledge that the NASA/ESA agreement has merely allowed work to continue and has not resolved fundamental differences of approach between the two sides.

Tim Beardsley

European Commission

Framework to be scaled down

Ambitious plans for a major expansion of European research and development are cut back by 30 per cent in the latest proposals from the European Commission. The European "framework programme" was to have cost in excess of



10,000 million ECU (over £15,000 million). But European research ministers, meeting in June, protested when they saw the budget was more than double the cost of research at present being sponsored by the Commission.

Commission officials had hoped for better progress on the Common Agricultural Policy (CAP), which absorbs more than two-thirds of total Commission spending in farmers' subsidies. If CAP had been trimmed, that could have left room for a larger research programme, now representing only 2 per cent of national research and development budgets. Instead, CAP has grown, the Commission budget has been pushed to its legal ceiling (1.4 per cent of member states' value added tax receipts), and smaller programmes have little chance of gaining extra funds.

Commission research, mostly performed in national, university or industrial laboratories, is strongest in energy (including nuclear fission safety research and fusion), the environment, information and communications technologies, biotechnology (particularly in relation to agricultural change and development), new materials, optical computing and technologies thought likely to revive old industries. Its objective is to unite European research groups on long-term projects and reduce duplication in national programmes. The framework programme is designed to set priorities for the next five years. Two years ago, when planning began, major expansion seemed both politically and financially possible. Now that CAP has eaten the cupboard bare, the Commission's research directorate must hope that increasing political interest in technological cooperation in Europe will generate support. There is plenty of competition, however, from independent projects such as Eureka aimed at stimulating Europe's hightechnology industries.

The new price-tag for the framework programme is 7,735 million ECU. The adjustments have been made to balance the differing national interests expressed at the last research council meeting: West Germany is reluctant to go into joint telecommunications research, where its principal company, Siemens, feels it has more to lose than to gain, while the British insist on continous programme assessment by outside experts.

Newer activities, such as information technology for the disabled, where the Commission has less experience, are also being cut back. A programme for research on "intelligent transport", involving advanced computers and communications in road vehicles has been cut because of strong overlap with a Eureka programme. New technologies for old industries are also out of favour. But energy research sees a slight increase in response to the

Chernobyl disaster. The whole of the Commission's nuclear fission research programme, much of it at the Commission's own Ispra laboratory in northern Italy, is now concerned with nuclear safety.

Will member states support the new proposals for the programme? Britain, whose technology minister Mr Geoffrey Pattie will be influential as he chairs the council of research ministers until the end of this year, believes there is room for an increase in total research spending, but not such a substantial one as the Commission is requesting, even in its revised budget. Commission officials certainly believe the larger member states, which pay most of the Commission's bills, are going to be reluctant, but will argue that everybody's long-term interests will be served by improving European cooperation in this area. Britain, however, with its reseach community in revolt at low levels of support at home, will be nervous about the impact of increased international spending on its national research budgets, a matter which is not entirely in Pattie's control. But with the Commission's final proposals now in the hands of national governments, real negotiation can begin.

Robert Walgate

Israeli science

Medical schools seek US students

Rehavot

US MEDICAL students at Tel Aviv University pay tuition fees of \$15,000 a year, a lot more than their Israeli counterparts, who pay only \$900 (a remarkably low sum decided on by the government). Yet there are far more US applicants for the programme in Tel Aviv than can be accepted. says Yehuda Bar-Shaul, rector of the university. That, he says, is because "the special English-language course at Tel Aviv is not like those of the dubious 'offshore universities' which many American students attend". The Tel Aviv institution has the status of a New York state medical school, and participants in the course who come from New York have more than 40 per cent of their tuition paid for by the state. Moreover, after graduation, the students do their residency in New York hospitals, "and the very best ones at that", the rector adds with pride.

Each year, Tel Aviv University's Sackler Medical School takes in some 60 students from the United States and about 80 from Israel. The US intake causes resentment among Israelis whose applications are rejected and who must therefore go to Italy or Rumania in order to study medicine, but, Ben-Shaul says, there is no justification for such resentment. "Even if this special programme were abolished", he declares, "we would not accept more local students because the 300 new doctors who graduate each year from the country's four medical schools are more than sufficient to meet Israel's needs."

The example set by Tel Aviv University over the past six years is to be copied by two other major institutions. A few weeks ago, the Haifa Technion decided in principle to begin a similar scheme at its own medical school. But Technion officials speak of fulfilling a Zionist mission, since most of those who would come to study in Haifa are likely to be Jews (as is the case in Tel Aviv). Officials readily admit that they also see the course as a potential source of income for the financially troubled Technion, which will be able to accept overseas students and their tuition fees without investing money in new facilities.

A similar scheme is on the agenda at the newly established Korat School of Veterinary Medicine of the Hebrew University. Its director, Professor Kalman Perk, expects an annual intake of 30 students, half Israeli and half foreign. But the programme will begin only in two years' time, after the opening of a veterinary hospital near the campus and after the first veterinary school class has graduated.

Unlike Tel Aviv University and Technion, overseas participants in the Hebrew University scheme will be expected, after the first year, to attend regular Hebrewlanguage classes.

Nechemia Meyers

Strategic Defense Initiative

Japan ready to participate

Tokyo

BUOYED by its landslide victory in the last Japanese election, the Nakasone administration is galloping to join the US Strategic Defense Initiative (SDI). The last barrier to participation, an all-party resolution banning the militarization of space, has been brushed aside and Japan is expected to decide to join the SDI research programme by the beginning of September. But there is less enthusiasm among those who will actually carry out the research.

In March last year, Mr Caspar Weinberger, US Secretary of Defense, formally invited Japan as well as other allies to participate in SDI. Since then, three Japanese delegations have been dispatched to the United States, the last of which, after its visit in April, strongly recommended participation on the grounds that SDI research would greatly benefit Japanese industry (see *Nature 321*, 5; 1986).

Since the July general election, two cabinet-level meetings on SDI have been held and several key decisions have been made. First, all patent rights to technology developed through SDI research will pass to the United States, although Japan will try to work out an agreement to ensure the return of technology to Japan. Without such a provision, the prime incentive for Japan's private industry to take part would be lost, as the main benefits for Japan are seen to lie in commercial spinoffs from SDI.

Second, although most research will be carried out by private enterprise, government agencies will be allowed to join the research effort, and secrecy will be maintained under the existing Secrets Protection Law. Finally, the six cabinet ministers, at their meeting last week, concluded that participation in the research phase of SDI would not violate a 1969 all-party Diet resolution banning military use of space. Defence-related issues usually provoke heated debate in Japan, and last week's cabinet decision would normally raise a storm. But opposition parties have remained remarkably silent on SDI following their crushing election defeat.

Dissent within Prime Minister Yasuhiro Nakasone's own Liberal Democratic Party (LDP) has also failed to materialize. Former Foreign Minister Shintaro Abe, a contender for the LDP leadership, is known to be cool towards SDI, but in his new post as chairman of the LDP executive council he no longer has a direct say in SDI and his successor at the Foreign Ministry, Tadashi Kuranari, is a close political ally of Nakasone. Nakasone himself has made no secret of his enthusiasm for SDI since he first discussed the issue with President Reagan last year, and a decision to go ahead would no doubt

strengthen the friendship between the US president and the Japanese prime minister.

Private industry's enthusiasm for SDI is more guarded. There are fears that it could merely end up being exploited, without enjoying the "fruits" of the research, and the decision to transfer patent rights to the United States will do little to allay such concern.

Although government research agencies

will also be able to participate in the SDI programme, there may be a lack of scientists willing to carry out the research. Nearly 5,000 Japanese scientists have signed petitions against SDI, including more than 1,600 at the national science research laboratories in Tsukuba, the very laboratories at which government SDI research is likely to be carried out. The scientists' chief concern seems to be that their research would be restricted as "military secrets", but they also fear an arms race in space and the increased dangers of nuclear war.

David Swinbanks

Environmental pollution

Pushing for a new clean-up law

Washington

AFTER languishing in legislative limbo, the US Comprehensive Environmental Response, Compensation and Liability Act, better known as the Superfund, is on the road to reauthorization. A conference committee last month completed the task of reconciling differences in new authorizing legislation already passed by the House of Representatives and the Senate.

Congress established Superfund in 1980 to clean up hazardous waste sites created before the passage of legislation regulat-



ing the dumping of such wastes. Superfund's first five-year authorizing legislation expired last October. The Environmental Protection Agency (EPA), responsible for Superfund clean-ups, has kept the programme going with residual funds and stop-gap appropriations from Congress. In the final version of the reauthorizing legislation, Superfund is authorized to receive \$9,000 million over the next five years, compared with \$1,600 million called for in the 1980 legislation.

One major obstacle to the implementation of Superfund is the issue of who will foot the bill for the clean-ups. The primary reason Congress failed to reauthorize Superfund when it expired last fall was an inability to come to terms with this issue. The Congress is in the process of working outa complete overhaul of the United States' tax code. So far, the issue of new

taxes to fund Superfund has not been taken up, and the issue is a divisive one. The petrochemical industry has claimed that paying the entire cost for clean-ups could be devastating for the industry's international competitiveness. One alternative is a value-added tax.

Under the new statutes, a timetable will be established for clean-ups to prod EPA to move more aggressively than it has in the past. Over the next four years, EPA will review some 23,000 potential Superfund sites around the country, with some 2,000 sites likely to be added to the 888 at present on EPA's National Priority List. Federal clean-up standards, absent from the original legislation, appear now, along with a provision that allows state standards to apply if they are more stringent.

Partly in response to the chemical plant disaster in Bhopal, India in 1984 (see Nature 312, 581; 1984), companies either using or creating toxic chemicals in manufacturing processes must inform local jurisdictions of their activities. This community "right-to-know" database could become a boon for epidemiologists if it is established as planned, providing information about environmental hazards. The new rules also require the Department of Health and Human Services to compile a toxicology profile on the commonest chemicals at Superfund clear-up sites.

Some critics of the new bill are concerned that issues of corporate liability have still not been adequately dealt with. Others say it does not go far enough to solving the problems caused by hazardous waste sites. A report by the Office of Technology Assessment (OTA) suggested that it would cost closer to \$100,000 million to clean up all the dump sites that could be eligible for Superfund action. OTA's Joel Hirschhorn says that for the first time funds will be available for developing new clean-up technologies, but otherwise sees no major improvement in the Superfund law. "It's one thing to throw money at a problem", says Hirschhorn, "and another to solve the problem."

Joseph Palca

Computer models

Cooperation on new molecules

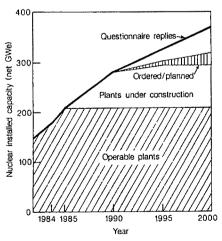
Washington

COMPUTER models are becoming increasingly popular for designing new molecules. But all such efforts face a fundamental problem: what parameters and potential-energy equations should be used in estimating the final energy state and geometry of a novel molecule? A recently formed consortium has set itself the ambitious task of supplying those parameters and equations. A successful outcome will mean model-builders will sleep easier, confident that their new creations will behave in nature the way they do on a computer screen.

The new three-year project is headed by Biosym Technologies, Inc., a company based in San Diego specializing in software for computer-assisted molecular design (CAMD). Each year, consortium members will contribute money and manpower: \$30,000 in cash support and six months of personnel time from a doctoral-level chemist. In return, consortium members have a say in the direction the

Nuclear forecast

AMID Chernobyl gloom, the Nuclear Energy Agency of the Organisation for Economic Cooperation and Development (OECD) is still presenting an optimistic picture of the growth of nuclear power worldwide. In 1985, there was a 19.2 per cent increase in nuclear electricity production, the largest increase since 1977. Twenty-one per cent of electricity generated in the OECD countries comes from nuclear power stations, ahead of hydro-



thermal and geothermal (20 per cent) and oil and gas (17 per cent) but behind coal (42 per cent). Forecasts to the end of the century shown in the graph were prepared from questionnaires returned by member countries. The highest forecast includes power stations not yet at the planning stage, where worries over safety may have their effect.

project takes, as well as gaining first access to the new database and any software tools that are developed. Companies participating in the consortium are Abbot Laboratories, Cray Research, E.I. du Pont de Nemours, Merck Sharp and Dohme Research Laboratories, Monsanto, Rohm & Haas and the Upjohn Company.

For certain classes of molecules, such as polypeptides and nucleic acids, these energy functions, known as force-field functions, have been fairly well approximated. The parameters are derived not only from bond energies, but from non-bonded molecular interactions as well. Peter Kollman, professor of pharmaceutical chemistry at the University of California, San Francisco, is the author of one widely used set of these functions. But Kollman says that, when looking beyond well-characterized classes of molecules, the applicability of the force-field functions becomes uncertain.

As an example, the van der Waals forcesbetween molecules in two classes of compounds may be similar, but the electrostatic charges may differ, forcing a model-builder to make assumptions about the best way to alter the force-field equations. The consortium hopes to develop a more generally applicable set of parameters and equations.

Biosym's chief scientific officer, Arnold Hagler, has also developed a well-known set of force-field equations. Hagler's plan is to use both empirical data gathered from existing literature and research done by consortium members, as well as quantum mechanics calculations, to develop a "second generation database of potential energy surfaces for organic, pharmacological and other biomolecules".

While most consortium members are also fierce competitors in the market-place, Upjohn's director of computational chemistry, Gerry Maggiora, explains that it will be to everyone's advantage to have a good set of potential energy functions. Upjohn is heavily involved in CAMD, one focus of which is developing inhibitors of renin for use as antihypertensive agents. As the three-dimensional structure of renin has not yet been worked out, Upjohn and others have turned to related compounds such as aspartyl proteinases to study molecules that will bind to renin's active site.

John Wendoloski of du Pont says companies should probably have put more money and effort into joint developments of force-field functions in the past. Although there is nearly uniform agreement that Biosym has undertaken a potentially useful task, there are those who doubt that a general set of force-field functions can be developed at present. Cyrus Levinthal of Columbia University, who is developing a special application computer with Brookhaven National Laboratory for computing interacting forces between molecules, says it is not clear whether sufficient empirical data exist to generate appropriate parameters. That sentiment is echoed by Kollman, as well as by John McAlister, director of research for Tripos Associates, another software company also working on the force-field problem. Even consortium members confess that hoping for a "second generation" database may be optimistic, but Abbot's Jonathan Greer says a better set of parameters than those currently available will be welcome. Joseph Palca

Return of tamarins proves expensive

Tokye

THE World Wildlife Fund has agreed to an unprecedented payment of about 10 million yen (\$65,000) to ensure that ten goldenheaded lion tamarins illegally imported to Japan three years ago return home to Brazil, according to the Japanese Foreign Ministry. Despite the acute embarrassment the illegal import of these rare primates has brought to Japan, the Japanese government is making no move to introduce legislation to prevent a repetition of such incidents, and has failed to provide funds for the safe return of the animals.

The weakness of Japan's laws has been quickly spotted by the yakuza, Japan's own mafia. Just a few weeks ago, they put a black tamarin on sale on the street outside a police station at Tokyo's Shinjuku station. Their sales point, capitalizing on media attention to the smuggling of endangered species, was that the tamarin had been brought in illegally from Brazil. No action was taken against them.

The lion tamarins, trade in which is banned under the Washington Convention on International Trade in Endangered Species, to which Japan is a signatory, were brought into Japan in 1983 with false import documents (see *Nature* 318, 200; 1985). The infringement was spotted by the World Wildlife Fund's TRAFFIC office. But, having got the monkeys past customs, the importers were free from prosecution as there is no domestic legislation to back up the terms of the convention.

Only constant lobbying by the World Wildlife Fund and international protests forced the government to take action. But it has no intention of paying the bill. According to the Foreign Ministry, the monkeys will be shipped to São Paulo Zoo in mid-September at a cost of 15 million yen, two-thirds of which will be paid by the World Wildlife Fund. The remaining one-third will come from the importer and keepers of the tamarins. David Swinbanks

Seismic monitoring

Station goes with a bang

THE Soviet-US seismic monitoring expedition to Karkaralinsk in Kazakhstan is essentially a confidence-building exercise aimed at showing it is possible to detect infringements of any future nuclear testban treaty, according to Oleg Stolyarov, a laboratory head from the Schmidt Institute of Earth Physics of the Soviet Academy of Sciences.

The expedition has been a unique cooperative venture that has allowed a team of US scientists to set up a seismic monitoring station in the Soviet Union. The Soviet side will reciprocate later and help to set up a station in Nevada. But the US government has not been involved: the



agreement is between the National Resources Defense Council, a private environmental group, and the Soviet Academy of Sciences (see *Nature* 321, 638; 1986).

Stolyarov, who has been acting as spokesman for the Soviet side, maintains that all the scientists on the expedition agree that seismic tremors can be monitored with sufficient accuracy to detect nuclear tests. The real purpose of the exercise, he maintains, is to convince the US authorities, who would prefer not to believe it.

Since the US participants do not have government backing, Stolyarov may have assumed that the government was hostile to the project. Other difficulties may have helped confirm this impression. As Co-Com regulations forbid the export of Western state-of-the-art technology to the Soviet bloc, the US equipment taken to Karkaralinsk was somewhat outmoded.

In the event, the Americans working at Karkaralinsk, a geological freak area where outcrops of bedrocks that are highly conductive to vibrations make it a natural seismic observation site, obtained excellent signals from nuclear blasts in Nevada.

Despite the political tensions generated by US reluctance to follow the Soviet example of declaring a nuclear moratorium, the two teams are said by Stolyarov to have "worked hard in a friendly way . . . brought together by a noble purpose".

Vera Rich

Ariane ride for Indian satellite

Bangalore

THE Ariane launch vehicle of the European Space Agency (ESA) will launch India's multi-purpose domestic satellite INSAT-1C in early 1988 according to an agreement signed between the Indian Space Department and Paris-based Arianespace. This agreement brings to an end uncertainty over the launching of INSAT-1C, originally planned for the space shuttle (see *Nature* 322, 198; 1986).

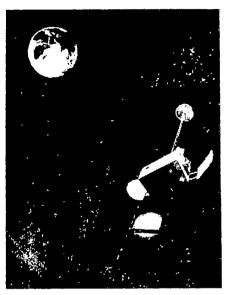
The INSAT spacecraft, described as the first civilian geostationary satellite to combine telecommunications, direct television broadcasting and meteorological observation tasks, are being built by the Ford Aerospace Communications Corporation (FACC) of Palo Alto, California, under a contract from the Indian Space Department.

With a launch weight of 1,180 kg, INSAT-1C is similar in configuration and performance to INSAT-1B, now in orbit. INSAT-1A, the first in the series, was launched in April 1982 but was switched off six months after its launch following a series of malfunctions. INSAT-1B went up in August 1983 and is running smoothly. All the spacecraft are designed for seven years active life in orbit. Successful launch of INSAT-1C will complete plans to have one operational satellite and one spare in orbit. INSAT-1D is expected to be launched in late 1988 or early 1989.

According to Professor U. R. Rao, secretary of the Indian Space Department, Arianespace offered the only competitive option after the shuttle failure had been followed by problems with the US conventional launcher, the Delta rocket. He said that the European launching system is as

good as the US system although it is a little costlier at US \$33 million. "But the French have gone out of their way to accommodate us", he said.

Frederic d'Allest, chairman of Arianespace, and Rao hailed the agreement as a



milestone in the long-standing and steadily growing cooperation in the field of space between India and Europe in general and France in particular. They are confident of further expansion of Indo-French cooperation in other areas such as remote sensing, satellite-aided search and rescue for the benefit of both countries.

Meanwhile, India is busy designing the second-generation INSAT spacecraft which will be built and launched in India. A liquid oxygen/liquid hydrogen launcher is being developed. Radhakrishna Rao

Doing things the all-American way

Washington

A BILL that would limit European and Japanese participation in the US Strategic Defense Initiative (SDI) has passed the Senate, and will be acted on by the House of Representatives this week. In a rare Saturday session, the Senate adopted an amendment, sponsored by Senator John Glenn (Democrat, Ohio), to the defence authorization bill that would prohibit the SDI office from signing contracts with foreign companies unless the Secretary of Defense certified that the work could not be performed in the United States. The amendment does not cover work subcontracted to companies outside the United States

In the House of Representatives, a similar amendment, sponsored by Representative Les AuCoin (Democrat, Oregon), would place a size limit of \$100,000 on SDI contracts with non-US companies. AuCoin's amendment does not permit ex-

ceptions. The House amendment is intended both to provide additional jobs for US workers and to prevent the Reagan administration from buying support for SDI from US allies with fat research contracts. It was impossible earlier this week to estimate the amendment's chances of success.

The Federation of American Scientists estimates that foreign SDI contracts at present amount to \$75 million. Although this represents only a small fraction of SDI's 1986 budget of \$3,050 million, some countries clearly hope for a much larger role in the project (see *Nature*, 322, 300; 1986).

The version of the defence authorisation bill passed by the Senate would limit spending on SDI to \$3,950 million, well below the administration's \$5,400 million budget request. That figure is likely to be trimmed even further in the House of Representatives' version.

Joseph Palca

Chernobyl accident

Reactor design not perfect

ACADEMICIAN Vitalii Legasov, a deputy director of the Kurchatov Nuclear Energy Institute, last week said that the design of the RBMK reactor was partially to blame for the Chernobyl disaster. The official Soviet viewpoint, embodied in a Politburo statement last month, was that human "irresponsibility" and "lack of labour discipline" was the cause. Workers at the power station, the Politburo said, had carried out unauthorized experiments on the Number 4 reactor, when it was undergoing a routine shutdown.

Although he did not disagree with the accident scenario, Legasov added some important details. In an interview for Japanese television, he said that the workers had not only carried out the "experiment" without the appropriate experts being present, they had also committed the "unbelievable" error of "keeping the emergency cooling system out of operation".

The experiment, he said, was intended to ascertain how long a power supply (for operating the reactor's own housekeeping functions) could be maintained after switching to the standby diesel generators. Such an experiment, he maintained, should have been carried out only with the reactor completely shut down and steam generation stopped. This account is compatible with the speculations of Western experts (see Nature 322, 399; 1986), that attempts to draw energy from the reactor in these conditions, well below the designed power range for the RBMK, produced steam voids within the cooling system, which caused power surges that

Guatemala accused of political killings

Washington

THE American Association for the Advancement of Science (AAAS) has submitted to President Vinicio Cerezo of Guatemala a grim catalogue of more than 200 political killings, "disappearances" and arbitrary detentions of Guatemalan academics and students between 1980 and 1985. Most are believed to have been killed with the approval or the tolerance of the military governments that ruled Guatemala between 1978 and last January.

The reports prepared by AAAS's commission scientific freedom and responsibility, urges President Cerezo, a civilian, to investigate the cases and to allow families to seek judicial redress. Most of the cases describe scientific and medical professionals who were shot or abducted by unidentified men. Estimates of the total number of political killings in Guatemala over the past 15 years range up to 100,000.

After AAAS presented a similar report to the new civilian government of Argen-

tina in 1984 detailing disappearances of 55 Argentinian scientists, the Argentine government requested forensic science assistance from AAAS to investigate the cases. Cerezo has pledged to foster greater respect for human rights and to reform the national police and security forces, but those in the military responsible for unlawful killings cannot be brought to justice until an amnesty declared by the outgoing military government is repealed. It is not clear whether Cerezo will be able or willing to repeal the amnesty.

Plans for an independent human rights commission on Guatemala with international representation have so far come to nothing, but the government has indicated that it may be willing to appoint a special ombudsman to investigate allegations of human rights abuses. In the meantime, one judge has been appointed to hear 1,400 writs of habeas corpus submitted by Grupo de Apoya Mutuo, a local human rights group.

could not be controlled by the slow-moving control rods of this type of reactor.

Where Legasov differs from the official Soviet viewpoint is in maintaining that not only were the "experimenting" workers at fault, but also the design team, who should have foreseen these events.

For some time, Legasov has been suggesting that the explanation of the Chernobyl disaster would be a complex one. Interviewed last month for the Soviet journal *New Times*, he described it as a "scarcely probable thing . . . a combination of several events, each of them scarcely probable either". The idea that the designers should be able to predict accidents is not entirely new to the Chernobyl coverage; interviewed by the Mos-

cow weekly Literaturnaya Gazeta in June, Academician Boris Semenov, deputy chairman of the State Committee for the Use of Atomic Energy, said that the safety systems at Chernobyl were sufficient to prevent any escape of radioactive material in even the worst scenario foreseen by the designers — clearly implying that some possibilities had been overlooked.

By placing the responsibility on the Chernobyl workers, the Politburo statement implicitly exonerated the RBMK design, which is one of the two basic types used in the current Soviet nuclear power programme. During the past few weeks, official statements have made it clear that there are no plans to phase out or close down RBMK-powered stations in the immediate future, although there have been some exhortations to the scientists to produce a "new, safer" generation of nuclear reactors as soon as possible. A need to express government confidence in the RBMK may well lie behind the appointment to the new post of All-Union Minister of Nuclear Energy of Nikolai Lukonin, formerly director of the RBMKpower stations at Leningrad (1976-83) and Ignalina, near Vilnius (1983-86). Behind the scenes, however, the government and party leadership may be less happy with the design. One of the four top officials dismissed in July as a result of the official inquiry into the accident was Ivan Emelyanov, who some 20 years ago was head of the design team that produced the RBMK. Retraining programmes for the staff of nuclear power stations, including computer simulation of accidents and emergencies, are being introduced, and the siting of some projected power-station is now said to be under review.

Japan's sunset export industry

Tokvo

THERE is nothing like an old solution for a new problem. For years, Japan's Ministry of International Trade and Industry (MITI) has been exhorting industry to export, export and export some more. Now the nation has a new problem: with the Japanese the longest-lived people in the world, there are soon going to be far too many old people. The MITI solution — export them!

Under the "Silver Columbia '92" plan, Japan's old-age pensioners will be able to set off to foreign lands where they can live in peace and comfort supported by an everrising yen. Life back home would be much harder, given the poor provision for pensions and the unwillingness of the government to take on any new financial commitments.

MITI foresees the establishment of

Japanese villages of around 1,000 people each, with construction beginning in 1990. Of course, a few problems remain. Next year, MITI and the Japan External Trade Organization will work out where the villages should be and ways of tackling language barriers and supplying Japanese food. Countries will be selected in the light of climate, law and order, medical services, housing and popular sentiment towards Japan.

Although the Japanese government would negotiate with the prospective host country, MITI wants the private sector to run the scheme. It is not yet clear how foreign governments will react. Will they see it as a welcome transfer of "intellectual property" or just another case of "dumping"? Could a trade develop? And would Japan be happy to import a few pensioners from elsewhere?

David Swinbanks

Vera Rich

Hubble space telescope

Every delay has a silver lining

Baltimore, Maryland

THAT the launch of the Hubble Space Telescope seems likely to be delayed until 1989 may yet turn out to be a blessing in disguise. Many project scientists believe that the three-year delay, caused by the Challenger space shuttle accident, will give time to make the telescope more



Riccardo Giaccon

effective – provided the National Aeronautics and Space Administration (NASA) can avoid making major cutbacks.

Samuel Keller, deputy associate administrator of NASA's Office of Space Science and Applications, says the agency hopes to avoid redundancies at the Space Telescope Science Institute (STSI) in Baltimore, but that a 10–20 per cent fall in staff numbers is likely, due to natural wastage. No new staff are being taken on. At Marshall Space Flight Center in Alabama, staff reductions have taken effect. As Keller points out, NASA has to comply with levels of funding and directives imposed by Congress.

The telescope's large size (43 ft) and weight (around 24,000 lb) mean that only the shuttle could put it into space. NASA recently announced that the shuttle will not fly before 1988, but Dr Riccardo Giacconi, director of STSI, believes it "still reasonable" to hope for launch during 1988. Giacconi thinks the telescope could be the third to the fifth payload in line once flights resume. The first will probably be military, and the second a tracking and data relay satellite to replace that lost with Challenger (one such satellite is now in operation for dual military and civilian use, but at least two are needed for safe control of the telescope).

Keeping the telescope waiting is not likely to cause problems. But the delay will necessarily mean large cost increases at Lockheed Missiles and Space Corporation in California, where about 150 people are testing the telescope. NASA has considered stopping work until close to launch, but it would still be necessary to keep an experienced engineering team together for pre-flight tests. Giacconi now thinks he has NASA's support for keeping the telescope accessible for testing until launch, but major reductions in the

Lockheed workforce are still likely.

There is clearly still much to do. The main controlling system, the space operations ground system, is installed in a basic form, but the final version will not be delivered by TRW Inc. until the end of the year because of development delays. In its present form, the system could not, for example, control the telescope so as to track moving targets such as planetary moons. Other systems, such as that which will calculate optimal timing of observations, are still in development. Some upgrading of hardware at STSI is also now thought to be necessary, but their cost, though counted in hundreds of thousands of dollars, is small compared with the software. All agree that it will be easier to complete installation and testing of complicated control systems with the instrument still on the ground.

Giacconi also wants to use the delayed deadline to allow institute astronomers to catch up on their own research and to foster a "more academic atmosphere". Although the official target for institute staff has always been that they would

Weight problems

IMPROVEMENTS to the shuttle recommended by the Rogers commission investigation of the Challenger accident will add weight and could impair the shuttle's ability to put the massive Hubble Space Telescope into a high enough orbit. Although the ideal height would be 360 nautical miles or more, even the unmodified shuttle is unlikely to manage 320 nautical miles.

At this height, atmospheric drag would gradually bring the telescope down: the plan was that a shuttle flight two years or so after launch would boost the telescope up to the desired 360 miles. (Some point out that if NASA by then has an operational orbiter transfer vehicle — at present still on the drawing board — the telescope may even be taken up to 400 nautical miles, where it would be stable indefinitely.) But if the modified shuttle is incapable of getting close to 320 nautical miles, there may be problems caused by orbital decay and atmospheric interference.

NASA officials Fred Wojtalik of Marshall and Frank Carr of Goddard Space Flight Center do not expect there will be problems, however. Keller, at NASA headquarters, points out that the weight of improvements to the shuttle has not yet been determined and thinks the rumoured figure of 12,000 lb may be pessimistic. The more modest weight increases he thinks likely would, he estimates, result in an orbit only 10–15 miles lower than that now planned.

spend 50 per cent of their time on research, in February the figure was still less than 25 per cent. Proposals for guest astronomers will not now be taken until March 1987 to take account of the launch delay.

Last June, the telescope successfully completed its first major test; a thermal vacuum test which used a simulated solar source to investigate heating effects, and other calibrated light sources for basic checks of the major instruments. Although many minor problems were found. none require extensive redesign or rebuilding. The test did, however, indicate that the telescope takes longer than expected to reach thermal equilibrium, necessary to avoid structural distortion. Among solutions being considered are extra insulating material and more solar cells to make more use of heating elements. The thermal vacuum test also included the first end-to-end test of the telescope's science operations and data analysis system.

Commands were successfully sent from STSI via Goddard through a simulated tracking and data relay satellite to the instrument itself. Although STSI sees the test as a major success, it is only a beginning. Just three of the main instruments were tested, and because of the incomplete control system and software incompatibilities with Lockheed, many of the commands had to be translated manually.

STSI has in the past been criticized for failure to control its budget. But Giaccom says that earlier antagonism between the institute and NASA has now disappeared, as "they recognize a competent group when they see one". Independent consultants agree that the institute has performed impressively in a task whose immensity was not fully realized at the outset. One example: software for the telescope is expected to be 1.5 million lines of code. 10 per cent of that thought necessary for the Strategic Defense Initiative.

Much of the work outside the basic control system has been done in-house at STSI, which is managed independently of NASA. STSI is particularly proud of its guidestar selection calalogue, which contains the coordinates of 40 million celestral sources to unprecedented accuracy. Giacconi claims that running a project at a single institute is often more cost-effective than use of external contractors, and criticizes NASA for wanting to contract out development of the telescope's embryonic data archiving system at a cost he estimates at \$20 million. Giacconi claims STSI can develop a basic but operable system for \$0.5 million, and unfavourably compares NASA's decision to the procurement style of the Department of Defense. But he believes STSI has proved itself and speculates that it will be in business in 20 years' time "for son of the Hubble Space Telescope". Tim Beardsley

CORRESPONDENCE:

Sequencing the human genome

SIR—The prospect of sequencing the entire human genome (Nature 322, 11; 1986) raises a number of questions, some answers to which we wish to suggest.

The first is "why?". After all, not only do we not have any idea what we would find in such an alphabetic morass, but we do not even know enough about genomic structure to know what to look for. The fact that such a bizarre project may be "technically feasible" is hardly a justification. It is as technically feasible to excavate the entire country of Kenya to a uniform depth of six metres for hominid fossils, or to determine the wiring diagram of all the synaptic connections in the human brain; but any biologists who proposed such projects would doubtless be obliged to carry them out in a padded laboratory. Similarly, sequencing the genome would be about as useful as translating the complete works of Shakespeare into cuneiform, but not quite as feasible, or as easy to interpret.

A better reason is that such a major endeavour would occupy every living molecular biologist, regardless of competency, for several years, thus solving the growing unemployment crisis. The social consequences of keeping molecular biologists off the streets, where they might develop into thugs, ruffians, land-fraud swindlers, or worse, are obvious. Alternative suggestions, such as obtaining a genetic map of humans using restriction fragment length polymorphisms, suffer in that they would employ clinicians and (far worse) population geneticists and anthropologists. Any sense of social responsibility dictates keeping these latter groups on the streets where they belong. Similarly, all attempts to limit the project to sequencing only a single small chromosome must be resisted, as this would not be sufficiently labour-intensive to employ enough molecular biologists.

Second, whose genome gets sequenced? As both X and Y chromosome sequences are required, women must be excluded from consideration. A haploid set is required as diploids often show an embarrassing amount of variation between homologues. The extraction of such a set will prove difficult, given the scarcity of recorded haploids in human history. As molecular biologists generally ignore any variability within a population, the individual whose haploid genome is chosen will provide the genetic benchmark against which deviants are determined. Much care must be taken in the selection of the exemplary individual to serve as this ultimate genetic role-model: it would be most embarrassing to throw out the first 500,000 kilobases and have to start resequencing a new individual if some character flaw is discovered late in the project.

However, the recent success of obtaining DNA from both an extinct species (Nature 312, 282; 1984) and a mummy (Nature 314, 644; 1985) suggests the possibility of using a venerable deceased human for a subject. This is quite in keeping with the spirit of the proposed sequencing project, as much of its justification involves the creation of new technologies. We would like therefore to be the first to suggest that the genome of the father of modern biology, Charles Darwin, be the one sequenced. We leave it to our English colleagues to arrange to have his remains exhumed from Westminster Abbey for the honour.

Unfortunately, it would hardly honour Darwin's memory, as the conceived sequencing project violates one of the most fundamental principles of modern biology: that species consist of variable populations of organisms. Alas, every dog has his day, and if the molecular vulgarians have theirs, "the" genome of "the" human will be sequenced, gel by acrylamide gel.

And what is to be done, finally, when this sequence is obtained? Perhaps the scientific community can enlist David Wolper to stage a worldwide tribute to the genome, culminating with every person on Earth symbolizing a nucleotide and joining hands to form all 22 autosomes and both sex chromosomes. It would be a fitting finale to a grand scientific project.

JAMES BRUCE WALSH

Department of Ecology and Evoulutionary Biology, University of Arizona, Tucson, Arizona 85721, USA

Jon Marks

Department of Genetics, University of California, Davis, Davis, California 95616, USA

Special relativity

SIR—Aspden¹, Psimopoulos and Theocharis2 discuss the need for a Michelson-Morley type test in space and raise interesting points about the effects of standing waves in rotating and translational motion of optical apparatus. Some time ago, I carried out a relevant investigation using a special standing-wave sensor manufactured by the General Electric Co.3. This photoelectric sensor incorporates a photomultiplier tube through which a laser beam can pass to be reflected back on itself by a mirror. This allows the device to scan translationally along the standing wave set up by the interference in the beam. The experiment shows that the spacing between nodes in the standing wave set up by two oppositely-directed light rays from the same laser source is a function of the orientation of the apparatus.

The forced optical condition assuring light speed isotropy as suggested by Aspden is not supported by the experiment, and initial indications are that the beam modulation pattern is attributable to the Earth's motion through space at cosmic speeds commensurate with those found from the isotropy assumption of 3K cosmic background radiation. In effect, it appears that in the standing-wave conditions, the waves move at different speeds in opposite directions relative to the apparatus and, as their frequencies are the same, they present different wavelengths in the two directions and so affect the nodal spacing.

A detailed report on the experiment is available prior to eventual formal publication. Meanwhile, it is of interest to note that the optical configuration resembles that of the Sagnac experiment, the basis of the ring laser gyro technology mentioned by Aspden, Psimopoulos and Theocharis. However, the sensor scans linearly along a section of the modulated beam in a nonrotating system, rather than being at rest, as in the gyro, and sensing effects of rota-

tion of the apparatus.

Clearly, this research will have interesting implications for the theory of relativity, as foreseen by your recent leading article4. It may also help us to resolve the large errors found in the global satellite positioning system. If present findings are sustained, it may not be necessary to extend the Michelson-Morley tests into outer space in order to obtain positive, as opposed to null, results in interferometric tests of linear motion.

E.W. SILVERTOOTH

Star Route, Box 166, Olga, Washington 98279, USA

1. Aspden, H. Nature 321, 734 (1986).

- Psimopoulos, M. & Theocharis, T. Nature, 321, 734 (1986). 3. Silvertooth, E.W. & Jacobs, S.F. Applied Optics 22, 1274
- 4. Maddox, J. Nature 316, 209 (1985).

Science and faith

SIR-In his review of John Barrow and Frank Tipler's The Anthropic Cosmological Principle (Nature 320, 315; 1986), William H. Press comments that the authors' end "... is nothing less than the fusion of matters of science with matters of individual faith and belief. It has taken us a long time to separate these matters, each to its own legitimate arena in human affairs. We should not lightly allow them to become once again jumbled

Although they are generally accepted, is it helpful to be given such delineations of "legitimate" arenas, which would seem to carry restrictive bias into the unfolding of human thought and experience? I personally find a segmented life no more attractive than a jumbled one.

RICHARD A. McCORKLE

RR1, Box 210, South Salem, New York 10590, USA

What happens on Cygnus X-3?

The notion that a periodic X-ray source may also be giving off streams of massive particles which are unknown from accelerator experiments is still, against the odds, alive.

OUTWARDLY, Cygnus X-3 is a run-of-the mill celestial source of X-rays, first recognized as such (in 1966) by early rocket observations which have since been amply confirmed by measurements from Earth satellites. One of the most striking features of the object is that it is a regularly periodic source of X rays with a period of 4.8 hours, which fits in well with the assumption that it is a binary star, one partner of which is a massive neutron star while the other is a less compact, more "normal", companion.

Cygnus X-3 is also distinguished by its intensity as a source of X rays. Indeed, the source is thought to be rather more than 10,000 parsecs distant from the Solar System, a substantial fraction of the diameter of the Galaxy. But this circumstance goes only to sharpen another puzzling feature of the properties of the object, that it is a source not merely or ordinary X rays but of X rays so energetic that they are properly known as gamma rays. Indeed, there have been suggestions (see, for example, A.M. Hillas, Nature 312, 50; 1984) that a few sources as powerful as Cygnus X-3 might be sufficient to account for the total content of cosmic rays in the Galaxy.

This leads to the most curious and unexpected feature of Cygnus X-3, the sketchy but intriguing suggestion that this very distant binary star may be the source of energetic particles whose nature is at present entirely unknown but which are nevertheless responsible for the production of mu-mesons (muons) at the surface of the Earth. The evidence is sketchy in the sense that it is urgently in need of independent verification, but it is also the kind of evidence that people cannot entirely set to one side.

Observations that suggest some connection between the X-ray star and the detection of cosmic rays at the surface of the Earth go back for several years. In 1983, for example, J. Lloyd-Evans and a group of colleagues at the University of Leeds (see Nature 305, 705; 1983) showed that there is a correlation between the detection of energetic cosmic-ray showers in the atmosphere of the Earth and the phase of the supposed binary source of X rays from Cygnus X-3. Whatever else may emerge about this strange object, two things are clear from the cosmic-ray observations: first, the object is a source of energetic cosmic rays that are detectable at the surface of the Earth; and, second, that the sheer production of energy in the form of energetic particles, say gamma-ray photons, must be very large.

The measurements that have raised new possibilities were undertaken with the equipment installed deep underground in recent years in the hope of detecting the predicted radioactive decay of the proton. An unavoidable complication of these measurements is the background flux of energetic muons, which explains why there have recently accumulated data on the occurrence near the surface of the Earth of muons energetic enough to penetrate at least through the overburden of rock to the subterranean detectors.

The first reports that something remarkable may be afoot appeared just over a year ago (M.L. Marshak et al., Phys. Rev. Lett. 54, 2079; 1985), and were based on measurements of background muons at the proton-decay detector operated jointly by the University of Minnesota and the Argonne National Laboratory. What Marshak and his colleagues claimed is that muons observed deep underground correlate significantly with the phase of the distant X-ray star in its binary orbit. Supporting evidence has been produced by G. Battistoni et al., based on measurements with the proton-decay equipment under Mont Blanc (Phys. Lett. 155B, 465; 1985).

For the past year, the bare bones of the mystery of Cygnus X-3 have been plain for all to see. If there is indeed a correlation between the phase of Cygnus X-3 and the time of detection of energetic cosmic-ray particles of some kind at the surface of the Earth, the implication is that the propagation of some influence over the 10,000 parsecs between the double source and the Solar System must be accomplished in such a way that phase information is not lost on the journey, which in turn implies that differences of travel time over 10,000 parsecs must be a small fraction of the orbital period, a few minutes perhaps.

Since these circumstances were first appreciated, there has been a gale of speculation about the means by which the influence of Cygnus X-3 might be propagated over these distances. First, the precision of the timing implies that the speed of propagation must be a very large proportion of the velocity of light, which in turn implies that if particles are the medium by which the message is transmitted, they cannot be massive-particles. Indeed, Marshak et al. last year gave good reasons why particles as massive as

neutrons would not meet the need, while particles as light as photons were similarly excluded on the grounds that there would have to be more of them than could possibly be consistent with other observations.

K. Ruddick (from the Minnesota group) now takes the argument further by pursuing the suggestion, originally made by Marshak et al., that the intermediary between Cygnus X-3 and the Solar System is a flux of particles that are electrically neutral (so as not to be smeared out by the intragalactic magnetic field), relatively small in mass (so as to preserve the synchroneity of the events) and previously unknown. Ruddick's account of the problem appears in Phys. Rev. Lett. 57, 531; 1986. The essence of his case is that light neutral particles are transmitted from Cygnus X-3 until they meet the rocks of the surface of the Earth, whereupon they are converted into other particles.

In principle, the argument is simple enough. Here is a set of data that cannot easily be explained in terms of existing theories, so why not invent a novel particle to account for what may be happening? The innovation in Ruddick's argument is that the primary novel particles (called "cygnets", which is natural enough given where they come from) do not interact directly with terrestrial nucleons to give the muons observed, but instead do so through the intermediary of a second unknown particle, necessarily more massive than the first. Ruddick argues that neither particle need have been observed in accelerator experiments.

The temptation to mock at the inven ion of a new particle of matter to solve each new problem in astrophysics should be firmly suppressed. By any yardstick, Cygnus X-3 is a remarkable object. Most of what people have written about it has been concerned with explaining how it may function as a source of very energetic X rays. Several models have been ad anced, most of which entail the impact of a particle beam from the neutron star on the more extended envelope of its larger companion. Until the likely spectral distribution of the energy produced by such a process is more exactly known, it will be hard to tell how strong is the case for extra particles. And, meanwhile, there is a great need that the original measurements should be repeated in such a way that people can tell more precisely how critical is the apparent synchroneity of phase. John Maddox

Particle physics

Where now with superstrings?

from Robert Walgate

LITTLE more than a year since superstring theory, the best attempt yet at a 'theory of everything', began to drag particle theorists into its net, superstrings are still "the only game in town" for the unification of forces, including gravity, in a quantum framework. So says Steven Weinberg (University of Texas), who with Abdus Salam and Sheldon Glashow developed the first modern unification of forces, 'electroweak' theory, that combines electromagnetism and the weak interaction. Weinberg gave the summary talk at a recent high-energy physics conference*, where it was clear that superstrings have become an important part of particle physics.

The basic idea underlying superstring theory is that the Universe is a world of many more dimensions than the four now apparent (the number ten is now usually favoured) inhabited by myriad, almost infinitesimal, elastic strings. These strings, sometimes looped, charged, spinning and vibrating, interact to pull the extra (usually six) dimensions into a tiny, closed structure full of gaps and holes that is left attached, almost like hair, to the remaining still-extended four dimensions, a process compactification. Particular arrangements of this stringy hair, such as a string winding once through a particular kind of six-dimensional hole, then lead to the particles we see.

But the theory has its problems. One of them is its uniqueness: the meeting showed that there are at least six candidate theories, all of which seem (so far) to be self-consistent and free of 'anomalies', the hidden quantum violations of charge and energy-momentum conservation that have dogged all other attempts at unification. According to Weinberg, John Schwartz, who with Michael Green launched the first more-or-less realistic anomaly-free string theory, said at the meeting that the number of candidate theories (which differ in the number of dimensions, the exact constitution and charges of the strings) could even increase, although it could decrease again if inconsistences are found in some versions.

Weinberg says the meeting was not perturbed by this development. All the versions of the theory may be the same in substance, each possibly being a different dynamical solution of a single underlying theory. This, according to one controversial view, could take the form of a string theory originally introduced many years ago as a model of the strong interactions: a bosonic string in 26-dimensional space-

*XXIII International Conference on High-Energy Physics, 16–23 July 1986, Berkeley, California.

time. Furthermore, another problem of non-uniqueness in superstring theory, the variety (thousands) of possible fourdimensional worlds it allows, is showing some signs of resolution. "The trouble with superstring theory, though this may not last, is that there don't seem to be any easy problems" says Weinberg. A theory should not be thrown away because it is difficult to use (the equations of hydrodynamics remain true even though it is almost impossible to calculate turbulent flow), but most difficult theories, including hydrodynamics, have certain key simple predictions through which they can be tested. But for superstrings "Schwartz said, and I agree, that there seem to be no decisive tests in sight". So superstrings remain with the theorists.

Weinberg points out that superstring theory has also disappointed early hopes of a natural solution of the 'cosmological constant problem', the question of how gravity behaves as if the vacuum is empty although in all unified field theories it is packed with a hornets' nest of forces and curvatures. Nevertheless the theory has had "many qualitative successes" and remains "a very beautiful theory, partly because of its logical rigidity".

Could there be experimental tests of the existence of strings? The phenomenology of the theories remains "murky", says Weinberg, precisely because of the number of ground-state 'worlds' which are still in practice indistinguishable. There may still be thousands of ground states to explore. One such exploration reported at the meeting requires a "great deal of mathematical virtuosity"; the resulting world' is "very encouraging, in that there are no problems like the proton decay being too fast, and the general pattern of quark and lepton masses looks vaguely reminiscent of the real world". But there are many 'worlds' yet to explore, each requiring its degree of virtuosity, and we may not be able to muster the labour to find the solution.

Although no projected experiments can bear directly on superstrings, there are nevertheless still some experiments of great interest that can be done. Next year should see the first experiments on the Fermilab Tevatron Collider, which will reach 2-TeV collision energies between protons and antiprotons, and the Stanford Linear Collider (SLC), which will be a 'factory' of Z's, the intermediate vector bosons that mediate the neutral part of the weak interaction. The prospect of these experiments, particularly those at the Tevatron, "loomed" over the conference,

says Weinberg. Although they are unlikely to reveal anything directly about superstrings, the SLC experiments should provide "exquisitely detailed" data on the decays of the Z", thus producing fine tests of the 'standard model', (the Weinberg-Salam electroweak theory plus quantum chromodynamics for the inter-quark force). Experiments, especially those with the Tevatron, "are going to settle the question of whether or not there is a vestige of supersymmetry at low energies".

This bears on string theory because superstrings are also supersymmetric, in that for every low-energy particle they create they also create a massive 'superpartner', a partner differing only in its higher mass, spin and quantum statistics. (Thus, if a particle obeys the Pauli exclusion principle, like the electron, its superpartner will not; and if a particle does not obey the exclusion principle, like the photon, its superpartner will do so.) Superpartners are useful in that they help explain why the weak interaction separates from the electromagnetic at energies of just a few hundred GeV, compared with the 1015 GeV or so at which electroweak forces separate from colour (the 'hierarchy problem'). However, superpartners only do the trick if their mass is sufficiently low. The Tevatron should see squarks, the superpartners of quarks, if their masses are less than 200-300 GeV, "a very plausible mass for them to have". If the Tevatron sees no superparticles, supersymmetry will lose its value in the hierarchy problem, and hence half its motivation. If the superpartners are found, on the other hand, we will know the masses and interactions of these long-dreamed-of particles, and "I can't even imagine what impact that's going to have on our models" says Weinberg. Superstring theory, however, could survive a non-discovery: the Calabi-Yau compactifications of the six extra dimensions were chosen, in part, to produce low-energy supersymmetry. It should be possible to find other classes of solution to the superstring equations that push the superpartner masses higher.

On other experimental issues, Weinberg is convinced by contributions at the meeting that there is a scientific "no-lose theorem" for results from the proposed superconducting supercollider (SSC), a 20-TeV collider now awaiting a decision on its construction from the US Department of Energy. Rigorous calculations in which space-time is approximated as a lattice (a common technique in modern quantum field theory) show that the SSC must reveal the origin of the symmetry breaking that divides electromagnetism from the weak interaction at low energies. This mechanism could either involve a vacuum full of a 'Higgs field', or a new superstrong 'technicolour' force that could lead to strong interactions between intermediate vector bosons. According to

this no-lose theorem, the Weinberg-Salam electroweak theory, which is a lowenergy approximation invoking the Higgs mechanism, must break down to some 'new physics' at an energy that depends on the mass of the lightest observable Higgs particle. If the Higgs mass is low (100 GeV), the breakdown does not appear until 1019 GeV where quantum gravity enters and new physics is certain. If the Higgs mass is only 10 times higher, new physics sets in "almost immediately". In either case, the corollorary for the SSC is that there will be something fundamental to observe: either Higgs at 100 GeV; or both Higgs and the new physics, possibly technicolour.

Solar neutrinos were also central to discussions at the meeting. The new 'resonance' mechanism explains the low incidence of solar neutrinos in Raymond Davis's electron neutrino detector at Homestake Mine, South Dakota in terms of a resonant, efficient conversion of solar electron neutrinos into higher-mass neutrino species in the Sun. This mechanism requires the neutrinos to have masses that turn out to be of exactly the order predicted by a wide class of unified field theories, according to Weinberg, who presented very general arguments that the mass of the heaviest neutrino should be around the square of the top quark mass divided by the grand unification scale (about 1015 GeV). This works out at around 10⁻³ eV. whereas the solar resonance model is tolerant of a range from 10⁻³ to 10⁻⁵ eV, depending on mixing angles between neutrino types. Weinberg argues, therefore, that a test of the resonance model is now "as important as anything else in particle physics". Several experiments are already at proposal stage. The best method would be to look for weak neutral current interactions of the solar neutrinos arriving at the Earth, Weinberg suggests, because all the incoming neutrinos would interact equally, the neutral current being 'democratic' in neutrino types.

If the Davis experiments, which measure charged-current interactions, are seeing few electron neutrinos because there are fewer of these particles produced in the solar core (perhaps because the temperature is lower than expected) then a neutral current experiment will see the same number. But if the threefold depression below predicted rates that Davis sees is caused by the conversion of two-thirds of the electron neutrinos to other neutrino types, then a neutral current experiment will see three times Davis's signal. Weinberg says that this experiment "may be our lucky break", the only indication of the grand unification of forces that comes down to us from 10¹⁵ GeV, now proton lifetimes seem too long to detect.

Robert Walgate is European Correspondent of Nature

Planetology

Sulphur and volcanism on Io

from David A. Crown and Ronald Greeley

SULPHUR on Io was suggested even before Voyager 1 and 2 flew by the jovian system in 1979^{1,2}, and although its existence is now generally accepted, its precise role remains controversial. The morphology of volcanic landforms argues for a surface formed by silicate volcanism, whereas spectral data indicate a surface dominated by sulphur (see ref. 3 for review). Lunine and Stevenson' recently presented a model for hot spots, regions of intense volcanism on the surface of Io, as lakes of molten sulphur.

Active volcanoes were observed on Io

into account the physics of convecting, boiling systems and the transport of vapour away from such systems. The authors suggest that the temperatures and thermal fluxes observed in the Loki Patera region of Io (see figure) are consistent with their model of a convecting sulphur lake and that the total thermal flux is consistent with the maximum that could be derived from a convecting silicate magma chamber. Their model also explains the distribution of thermal energy around Loki Patera observed during the Voyager missions and indicates that evaporation

constrains the maximum surface temperature of a sulphur lake under steady-state conditions.

Lunine and Stevenson's model provides the means to relate the surface heat detected by Earthbased infrared observations to changes in the temperature of a sulphur lake and variations in the output of silicate magma chambers in Io's crust. The authors estimate that if lake renewal or magma chamber lifetimes are limited to years, then changes in the thermal output in detected based observations at



Voyager I mosaic showing the eruption of Loki (lower left). Plumes emerge from a linear black fissure approximately 200 km long. The crescent-shaped large dark patch to the left of the fissure may be a lava lake with a section of solidified crust in its interior. Other vents are seen in the image as dark, nearly circular patches surrounded by lava flows and volcanic plains. The original mosaic was processed by A.S. McEwen (Arizona State University) and the US Geological Survey.

during the Voyager I and 2 missions and are attributed to the dissipation of tidal energy resulting from the configuration of Io's orbit in the jovian system'. McEwen et al.', using Voyager infrared interferometric spectrometer results and multispectral data, correlated dark calderas with areas of high heat flow. Recent experiments concerning the optical properties of sulphur are consistent with this correlation and indicate that molten sulphur on the surface of Io would be black as observed by Voyager instruments'.

Lunine and Stevenson explain the hot spots using a model for a convecting sulphur lake heated by an underlying silicate magma chamber. The model considers the physical and chemical processes in convective sulphur lakes, including the thermodynamic and transport properties of sulphur and the effects of some possible impurities. In addition, the model takes

infrared wavelengths are important to distinguish between: (1) high temperature (600 K) outbursts isolated from the Loki region (volcanic eruptions); (2) independent changes in warm or hot components in the Loki region (the warm component, the result of the latent heat released on condensation of evaporative sulphur in the atmosphere surrounding a sulphur lake, and the hot component caused by the heat released by convecting molten sulphur); and (3) changes in sulphur lake temperature and the corresponding evaporative sulphur flux. Consequently, Earth-based monitoring could provide important information about Io's thermal output and volcanic activity.

Lunine and Stevenson also consider the effects of impurities such as sodium polysulphides. If the base of a sulphur lake became enriched in sodium polysulphides, convection of this material might

occur and a liquid polysulphide melt could be exposed at the surface on evaporation of the overlying sulphur. Sodium polysulphide lakes or remnants of such lakes may occur in the Loki Patera region and elsewhere on Io and could be distinguished from convecting sulphur lakes using infrared observations at several wavelengths. Lunine and Stevenson suggest that such polysulphide lakes could be the source for the sodium-enriched material in the Io torus.

Although many assumptions are involved, Lunine and Stevenson's rigorous application of theory to both Earth-based and Voyager observations demonstrates the importance of continued monitoring of Io from Earth and is an example of the type and quality of work necessary to plan future observations effectively. In particular, the sulphur lake model can be

evaluated during the Galileo mission in I the 1990s. Lunine and Stevenson suggest that during the cruise phase of each orbit. thermal measurements, including those from the night side of Io, could be used to characterize and to detect variations in hot-spot activity.

- 1. Fanale, F.P., Johnson, T.V. & Matson, D.L. Science 186,
- 2. Wamsteker, W., Kroes, R.L. & Fountain, J.A. Icarus 23. 417 (1974).
- 3. Nash, D.B., Carr, M.H., Gradie, J., Hunten, D.M. & Yoder, C.F. in Satellites (eds Burns, J.A. & Mathews, M.S.) 629 (University of Arizona Press, Tucson, 1986).
- Lunine, J.I. & Stevenson, D.J., Icarus 64, 345 (1985).
- 5. Peale, S.J., Cassen, P. & Reynolds, R.T. Science 203, 892
- 6. McEwen, A.S., Matson, D.L. Johnson, T.V. & Soderblom.
- McEwell, A.J., Matsoli, D.L. Johnson, T. V. & Soderblom,
 L.A. J. geophys. Res. 90, 12345 (1985).
 Sasson, R., Wright, R., Arakawa, E.T. Khare, B.N. & Sagan, C. Icarus 64, 368 (1985).

David A. Crown and Ronald Greeley are in the Department of Geology, Arizona State University, Tempe, Arizona 85287, USA.

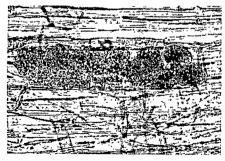
Plant viruses

New threats to crops from changing farming practices

from Robert Coutts

In the 25 years since it was first suggested that root-inhabiting fungi act as vectors of plant viruses', many such viruses have been identified and some characterized in detail (see ref. 2 for a recent review). The importance of these viruses as plant pathogens in the United Kingdom was largely ignored until recent changes in agricultural practice as well as the geographical proximity of the fungus-vectored viral agent of rhizomania, beet necrotic yellow-vein virus, renewed interest'. Will an increased awareness of the incidence of soil-borne viruses or further changes in agricultural practice result in the appearance of further 'new' viruses and their associated diseases?

Of immediate concern to farmers in the United Kingdom is the spread of barley yellow mosaic virus^{4,5} carried by zoospores of the primitive plasmodiophoromycyte Polymyxa graminis Ledingham, that affects winter barley. (Beet necrotic



Infected barley root cell full of resting spores (cystospori) of P. graminis, the vector of barley yellow mosaic virus. (Photograph courtesy of E.J.F. Roberts and K.G. Laing.)

yellow-vein virus is transmitted by another member of this group, P. betae Keskin.) The barley virus is widespread, causing variable reductions in grain yield, because farmers now grow winter malting barley as a profitable spring crop. Local soil conditions, such as low temperature and high humidity, are ideal for fungus transmission of the virus and the development of symptoms. As temperatures rise in the spring the symptoms of the disease fade but infected plants remain stunted.

After transmitting the virus to the plants, the zoospores develop into cystosori which are found in the roots and which can remain viable for extended periods (see figure). This feature of the fungal life-cycle ensures perpetuation of the fungus and virus in areas of intensive winter barley production. Recent reports of the incidence of more than one naturally occurring strain of the virus' suggests any inbred resistance may not be durable.

In the long term, biological control of Polymyxa with other rhizosphere-inhabiting microorganisms may be possible. For example, cystosori of P. betae can be parasitized and completely degraded by Trichoderma harzianum Rifai in vitro¹, offering hope for the control of rhizomania, the sugar-beet disease that causes havoc in Europe. This disease and the causal agent, beet necrotic yellow-vein virus, have recently been diagnosed in France, the Netherlands, Belgium and Luxembourg. Import of sugar-beet stecklings from Europe to the United Kingdom is now banned³.

P. graminis and P. betae can be differ-

entiated only by host specificity, and the spread and transmission of the beet and barley viruses described here appears similar. A recent survey8 failed to find the beet virus or the disease in the United Kingdom but does reveal the presence of a morphologically similar but serologically distinct virus8. This virus, or one very similar to it, had been isolated previously from beet plants in Norfolk displaying root-symptoms of the Barney patch disorder. The virus, provisionally named beet soil-borne virus, is also apparently transmitted by P. betae but its pathogenic effects, if any, are unknown. The catastrophic effects of rhizomania are well documented, with the sugar content of infected beets reduced to 10 per cent or less of that found in uninfected controls³.

Changes in horticultural practice have increased the incidence of another group of fungus-borne viruses whose appearance coincides with the increased growing of plants in soil-free environments, where plants are cultivated on solid-support matrices and fed with liquid nutrients. Nutrient-film growing is popular with growers for several reasons, such as its application to greenhouse crops, ease of maintenance, monitoring of nutrient supply, quality control and cost. But two outbreaks of disease in the last six years, lettuce big vein virus and necrotic spot virus in cucumber seem to be a direct result of nutrient-film growing.

The lettuce and cucumber viruses are transmitted by zoospores of the aquatic phycomycetes Olpidium brassicae and O. radicale, respectively. However dissimilar from the situation with the plasmodiophoraceous fungi, chemical control of phycomycete fungi and the diseases they transmit appears feasible — the two outbreaks of lettuce and cucumber viruses were successfully controlled by continuous application of a non-ionic liquid surfactant that killed the transmitting zoospores 9,10

It is unlikely that the viruses I have described in this article are new to the United Kingdom. It is more plausible that interactions between the viruses, vectors and hosts are now acting under the correct environmental conditions for infection to result.

- Teakle, D.S. Nature 188, 431 (1960).
- 2. Brunt, A.A. & Shikata, E. in The Rod-shaped Plant Viruses (ed. van Regenmortal, M.H.V.) (Plenum, New York, in the press).

 3. Dunning, R.A. Brit. Sugar Beet Rev. 52, 47 (1984).
- Adams, M.J. Rothamsted A. Rep. Part I 130 (1984). Hill, S.A. Plant Path. 29, 197 (1980).
- Ehlers, U. & Paul, H.-L. J. Phytopath. 115, 294 (1986).
 D'Ambra, V. & Mutto, S. J. Phytopath. 115, 61 (1986).
- Henry, C.M., Jones, R.A.C. & Coutts, R.H.A. Plant Path. (in the press).
- Tomlinson, J.A. & Faithfull, E.M. Ann. Appl. Biol. 93, 13
- 10. Tomlinson, J.A. & Thomas, B.J. Ann. Appl. Biol. 108, 71

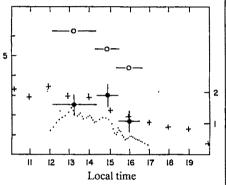
Robert Coutts is Lecturer in Plant Virology in the Department of Pure and Applied Biology, Imperial College, London SW72BB, UK.

Atmospheric chemistry

Hunting tropospheric OH ions

from D. Perner

Is the self-cleansing capacity of the troposphere still adequate to cope with the ever-increasing amounts of emitted gases? Or could unchecked anthropogenic emissions eventually make populated areas uninhabitable? To measure accurately concentrations of the free hydroxyl radical (OH), generally regarded as the main agent for direct oxidation and for removal of substances from the atmosphere, has been a major challenge14. The article by Hard and co-workers on page 617 of this issue' describes measurements obtained by a promising new spectroscopic technique which should allow a test of whether



Comparison of the diurnal variation of measured OH concentrations × 106 ml⁻¹ (left-hand scale) observed by optical absorption on 19 May 1983 at Deuselbach (black circles), and by laser-induced fluorescence⁵ on 18 June 1985 at Portland (crosses). Also shown are the O_3 photolysis frequency \times 10^{-5} s⁻¹ (right-hand scale; dotted line) and the calculated OH concentration (open circles), both for Deuselbach*.

our understanding of atmospheric photochemistry is consistent with measured OH concentrations.

It is only since the early 1970s that the central role of the OH free radical in the troposphere has become apparent. In 1969 Weinstock⁶ ascribed the strong variability of carbon monoxide in the troposphere to the action of OH radicals, but he could not identify their source. Two years later, Levy found that not all of the Sun's ultraviolet light, which produces excited oxygen atoms from ambient ozone, was filtered out by the stratosphere. Because this excited oxygen is the primary intermediate for OH formation, an appreciable source of OH therefore exists in the troposphere.

Although highly labile, OH does not react with any of the major atmospheric components, so it can exert its full oxidative power on trace gases such as methane, carbon monoxide and methyl chloride, which are eventually converted into carbon dioxide, water and other

stable products that are washed out of the atmosphere. This process has prevented trace compounds from building up in the atmosphere over the millenia. OH is important because it is regenerated in these oxidation processes: in the free atmosphere, typically up to five oxidation reactions are initiated by OH before it is scavenged. Despite this amplification of OH, fast chemical reactions keep its ambient concentration quite low, to about a few million molecules per millimetre in sunlit air. It is also commonly accepted that the concentrations at night are considerably below those in the daytime.

Several in situ techniques for measuring OH concentrations are presently in use. Radiolabelled products, such as ¹⁴CO, formed from ¹⁴CO by the OH reaction, can be measured with high-sensitivity or spectroscopic methods to probe the OH concentrations directly¹⁻³. Hard et al.⁵ apply laser-induced fluorescence at low pressure in a manner that excludes ambient light from the detector. In this way difficulties previously found using this technique are circumvented and the instrument can be converted easily for aircraft measure-

The midday OH concentrations found in Portland by Hard et al.5 can be compared with similar observations in Deuselbach by my own group obtained by longpath optical absorption (see figure). Whereas in Deuselbach the OH signal disappears at 1700 h, the OH in Portland

extends fairly late into the evening and, surprisingly, is found at night. The reason for this unexpected and interesting observation is unknown. Other types of data from Portland are not detailed enough to calculate a model of the OH distribution. In contrast, other types of data from Deuselbach predict much higher OH concentrations than are found experimentally there. Thus the theoretical description at Deuselbach cannot be applied.

I still believe that direct evidence for free tropospheric OH, preferably by spectroscopy, is needed. Simultaneous measurements of all species and parameters in the OH photochemical cycle. together with the OH measurements, are now a prerequisite to test our atmospheric theory. Investigations of various air masses should be made to represent the whole of the troposphere, and then we could distinguish between the importance of homogeneous gas-phase chemistry and heterogeneous processes taking place at the surface of aerosols or in droplets. Only then shall we learn whether the observed increase in concentration of climate-effective gases like methane is caused in part by a decline in atmospheric self-cleansing by OH.

- Davis, L.I. et al. J. geophys. Res. 90, 12833 (2003)
 Huebler, G., Perner, D., Platt. U. Tochasen, V. & Ehhalt, D. J. geophys. Res. 89, 1309 (1984)
 Rodgers, M.O., Bradshaw, J.D., Sandhofm, S.I., Kr.Sh., g. S. & Davis, D.D. J. geophys. Res. 90, 12849 (1985)
 Sheppard, I.C., Hardy, R.J., & Hopper, I. Manaett, J. 200 (1992)
- 5. Hard, T.M. et al. Nature 322, 617 (1986)
- Weinstock, B. Science 166, 224 (1969)
 Levy, H. Science 173, 141 (1971)
- 8. Perner, D. et al. J. atm Chem (submitted)

D. Perner is in the Department of Atmospheric Chemistry at the Max Planck Institute for Chemistry, Postfach 3060, D-6500 Mainz,

Archaeology

Japanese agricultural beginnings

from Gina L. Barnes

AGRICULTURE in the Japanese islands was long thought to begin with the importation of wet rice technology from the continent at around 300 BC, an event taken to mark the transition from a hunting and gathering economy in the postglacial Jomon period to a period of settled agricultural communities. But this traditional view has been thoroughly overturned in the past ten years with discovery of the remains of many cultivated plants — including rice from Jomon sites'. The recovery of buckwheat pollen from the Ubuka bog in southwestern Japan, reported on page 632 of this issue2, provides the strikingly early date of 6,600±75 years before present (BP) for buckwheat cultivation, paralleled only by the finds of beans and gourd at the Torihama site which are dated to 5,000-

3,500 BC. If these data become widely accepted, they may lead to a substantial revision of our ideas about the pattern of human settlement during this period

Models allowing flexibility in determining the role of plants in the different regional and temporal complexes of the Jomon period have already been developed^{3,4} and a major advance has been the correlation of population densities with forest and fishery zones'. This correlation indicates that the population occupying the southwestern evergreen oak-laurel forest at low density was less dependent on hunted animals - scarce in such a forest regime - and therefore more dependent on plant foods. The abundant floral remains at Torihama from the early Jomon period support this idea and

Akazawa believes this background accounts for the rapid spread of rice agriculture through western Japan once it was introduced from the continent towards the end of the Jomon period⁷. His corollary is that the populations of coastal northeastern Japan that had highly successful fishing economies resisted the introduction of rice technology.

The beginnings of plant cultivation in western Japan are based on the concept of the 'Laurilignosa culture' developed by Nakao (see ref. 8). The composition of the evergreen oak-laurel (Laurilignosa) forest that became established around 7,000 BC was part of a greater continental forest zone occupied by people practising 'slash and burn' agriculture. The extension of this economy into the Japanese portion of this forest zone is held by numerous Jomon archaeologists who have interpreted charred layers in excavation stratigraphy as the remains of burnedforest fields. Although slash and burn systems that include systematic fallowing cannot yet be distinguished stratigraphically from simple forest-clearing activities using fire, Tsukadas not only shows the sudden appearance of charcoal fragments in the Ubuka bog cores but he also provides palynological evidence for the crops being grown — in this case buckwheat.

Most evidence for Jomon cultivation has been in the form of macroremains or seeds (for example, see ref. 9). Methods of identifying cultivated plants from fossil pollen and plant phytoliths" have only recently been refined to the point of credibility, and palynological evidence is still viewed with scepticism by many Jomon archaeologists. Tsukada's method of filtering out large pollen grains in order to count the percentage occurrence of buckwheat is still unpublished, and his identifications of millet pollen remain tentative". Moreover, the method used by Japanese palynologists to identify rice pollen (see ref. 12) is not yet complete.

Nakamura's method combines transmission electron microscopy and phasecontrast microscopy, by which three groups of grass pollen are distinguished according to their surface morphologies. Nakamura states that this is at best a method for tentative identification, for although rice (Oryza) can be distinguished from pollen of the other types, it cannot be

distinguished from Agropyron (Graminae) and Arundinaria (Bambusoidae); both of which grow in similar ecological niches as Oryza.

Nevertheless, Nakamura and colleagues have identified rice pollen in Jomon sites dating to 1,200, 1,000 and 900 BC (for example, ref. 11). Japanese archaeologists are reluctant to accept these early dates, however, and still consider the appearance of rice-growing in Japan at around 400 BC on the basis of archaeological evidencé of field systems and rice

Clearly, research on the different crops and their cultivation systems in the Jomon period of Japan is extremely controver-

sial, with various disciplines offering differing forms of evidence and interpretations. The debates may lead to substantial revision of ideas on the Jomon, once thought to be a very stable and long period of foraging, and may reveal a number of adaptive strategies and mixed subsistence economies existing through time and space". These results are important not only for Japanese prehistory but also for understanding changing human-plant relationships throughout the world in the postglacial period.

Gina L. Barnes is in the Centre for Japanese and Korean Studies, University of Leiden, 2300 RA Leiden, Netherlands.

Invertebrate neurobiology

Catching up with peptides

from Mark Tyrer

Our knowledge of the structure of most bioactive peptides in invertebrates is too scanty to exploit the experimental advantages provided by their large, accessible central neurones. If we could use these advantages to the full, invertebrate neurones could provide model systems for testing at the cellular level some intriguing hypotheses about peptide function in the vertebrate central nervous system. Paradoxically, the small size of the invertebrate nervous system, which makes it so attractive for physiology, is an obstacle to isolating and sequencing native peptides. At a recent meeting* it was clear that many invertebrate peptides are now beginning to yield to developments in high-pressure liquid chromatography, amino-acid sequencing and recombinant DNA technology. These developments mean that the small amounts of nervous tissue available from invertebrates are becoming less of a problem and the distribution and function of some native peptides are now being studied in detail.

The structures of several invertebrate peptides have now been deduced, including the crustacean cardioactive peptide CCAP, a nonapeptide different from any previously described peptide in that it has two cysteine residues which are thought to form a disulphide bridge, producing a hairpin shape (J. Stangier, Bonn). A neuropeptide from the sea anemone Anthopleura and three new peptides from Aplysia have also been sequenced. Insect diuretic hormone has been partially sequenced and others, such as argininevasopressin-like insect diuretic hormone (AVP-DH); a moth pheromone-releasestimulating peptide; and a crustacean moult-inhibiting hormone, are on the way.

Invertebrate Peptides and Amines, Bordeaux, 16-18 April 1986, to be published in the seminar series of the Society for Experimental Biology.

The purification of prohormones for invertebrate peptides is particularly exciting. Because several peptides are com- ... monly cleaved from one prohormone, cleavage products may include, in addition to known peptides, some which have not yet been identified. The prohormones for locust AVP-DH, locust adipokinetic hormone, Aplysia pro-FMRF amide (Phe-Met-Arg-Phe-NH,, or Femerfamide) and snail ovulation hormone have been isolated. The amino-acid sequence of the FMRF-amide precursor (R. Scheller, Stanford University) has been obtained by recombinant DNA techniques. It contains multiple copies of FMRF amide, a single copy of Phe-Leu-Arg-Phe-NH, (FLRF amide) and three regions that have some amino acids in common with mammalian corticotrophin, melatonin-stimulating hormone and corticotrophin-like internal peptide.

Several peptides produce membrane changes in target cells in preparations such as the motor nerve net of the coelenterate Polyorchis (A.N. Spencer, Edmonton), and central neurones in Aplysia (Scheller) and Helix (G. Cottrell and N.W. Davis, St Andrews). In leg muscle cells in locusts and cockroaches, M. O'Shea (Geneva) demonstrated the value of invertebrate preparations for examining the interactions of peptides with other transmitters. All the neurones innervating the muscle have been identified and are accessible to intracellular recording and biochemical analysis. The classical transmitter L-glutamate and the peptide proctolin co-exist in the slow motor neurone to the coxal depressor muscle. Proctolin released from this neurone amplifies the twitch responses of the muscle to coreleased glutamate. At the same time proctolin causes a direct slow contraction of the coxal depressor muscle that seems

^{1.} Rowley-Conwy, P. World Archaeol. 16, 28 (1984).

Tsukada, M., Sugita, S. & Tsukada, Y. Nature 322, 632

^{3.} Nakao, S. Dorumen 13, 6 (1977).

Nishida, M. J. anthrop. Archaeol. 2, 305 (1983). Koyama, S. Senri ethnol. Stud. 2, 1 (1978). Akazawa, T. Senri ethnol. Stud. 9, 1 (1981).

Akazawa, T. Univ. Mus. Univ. Tokyo. Bull. 27, 73 (1986).

Tsukada, M. Kodansha Encyclopedia of Japan 5, 92: 7, 177

^{(1983).} Kotani, Y. Senri ethnol, Stud. 9, 201 (1981).

¹⁰ Crawford, G. Anthrop Pap. No. 73 (University of Michigan; 1983).

^{11.} Tsukada, M. in Windows on the Japanese Past: studies in archaeology (eds Pearson, R. et al.) (University of Michi-

^{12.} Nakamura, J. Quat. Res. 13, 187 (1974).

to result from release of intracellular calcium. Octopamine released from another motor neurone also amplifies glutamate-induced contractions in the extensor tibialis of the insect. It is probable that cyclic AMP is the second messenger for octopamine and that inositol phosphates mediate the action of proctolin.

Because it has been so difficult to purify invertebrate bioactive peptides many researchers have used antibodies directed against vertebrate peptides for immunohistochemistry on invertebrate systems. Immunoreactivity to vertebrate neuropeptides can provide useful anatomical information; it can also be used to purify a native peptide, either as an effective assay (H. Duve and A. Thorpe, Queen Mary College, London; J. Proux et al., Bordeaux) or as a useful ligand for immunoaffinity chromotagraphy (Proux et al.).

The importance of peptides for signalling in nervous systems is becoming increasingly apparent. Most neurones, both in invertebrates and vertebrates, probably contain peptides as well as classical neurotransmitters. Whereas classical transmitters are released at specialized synaptic junctions, exocytosis of granule-containing peptides often occurs at unspecialized regions of the plasmalemma. This was first recognized in the central nervous system of the earthworm (D. Golding, Newcastle) and is now widely seen if tannic acid (which appears to prevent immediate dispersion of the exocytosed granule) is used in fixing specimens for electron microscopy. Both Golding and J. Joosse (Amsterdam) suggested that peptide transmission is the more primitive method of signalling; classical synaptic transmission could be a specialized development to produce a highly efficient but more inflexible means of information transfer. Joosse argued further that peptides, because of their close relationship to the genome, can be viably altered by any change in the DNA and hence can easily alter their function. Thus, although they may be a less precise method of signalling than classical transmitters, peptides could be involved in adaptation of individuals or populations to changes in the environment.

Mark Tyrer is a Lecturer in the Department of Biochemistry and Applied Molecular Biology, UMIST, Manchester M60 1QD, UK.

Gene regulation

Fingers and DNA half-turns

from Stephen C. Harrison

AT first sight the DNA sequences from eukaryotic transcriptional control regions give an impression of overwhelming complexity. The precedent of prokaryotic control suggested simplification should come from structural analysis of the proteins that recognize these sequences; and indeed it seems that understanding of transcriptional regulation of 5S RNA genes in the toad Xenopus laevis has now reached this stage'. At least three protein factors are required for transcription of these genes by RNA polymerase III. One of them, transcription factor IIIA (TFIIIA), has in its amino-acid sequence an approximately 30-residue motif repeated nine times, probably corresponding to nine zinc-binding sites². In the 4 July issue of Cell, Rhodes and Klug³ point out a corresponding repeat in the sequence of DNA bound by TFIIIA and suggest that it has some unusual structural features. Moreover, they identify similar repeats of approximately 5 base pairs (bp) in control regions of other genes, including some transcribed by RNA polymerase II. The possibility that these DNA sequences have overall structural features important for recognition by transcription factors is also raised directly by the report of McCall et al. on page 661 of this issue⁴. They describe the crystal structure of a double-stranded nonadeoxynucleotide that corresponds to the tightest binding

part of the sequence recognized by TFIIIA and show that it has an A-type rather than a B-type conformation.

There are two multigene families for 5S RNA in Xenopus, differentially expressed in oocytes and in somatic cells, respectively'. A single molecule of TFIIIA binds to an approximately 50-bp control region in the middle of the genes, and this interaction is essential for the formation of a transcription complex that directs accurate initiation by RNA polymerase III^{5,6} The site has been defined by deletion mapping⁷, by DNase I protection and by binding interference from base methylation or phosphate ethylation8. TFIIIA also forms a 7S complex with the 5S transcript, and immature oocytes store a vast number of 5S RNA molecules in the form of this 1:1 complex⁹. Proteolytic cleavage of 7S particles divides the TFIIIA polypeptide, which has a relative molecular mass of 40,000 (40K), into two domains — a 30K amino-terminal domain with full binding activity and a 10K carboxy-terminal domain essential for transcriptional activation¹⁰. One amino-terminal domain binds to 50 bp of DNA, and Smith et al. 10 postulated a very extended structure for the protein. Miller et al.2 show that the complementary DNA-derived amino-acid sequence of the 30K domain has nine units of an approximately 30-residue, tandemly repeated motif. Each copy of the motif

contains two cysteine and two histidine residues in conserved positions. The 7S TFIIIA/5S RNA complex contains Zn, and TFIIIA requires this ion tor DNA binding. In proteins, Zn is generally tetrahedrally coordinated, often by cysteine or histidine side chains, and indeed Miller et al. find sufficent Zn in the 7S particles to propose that each 30-residue motil constitutes a Zn-binding 'finger'. The 30K, DNA-binding domain of TFIIIA thus appears to be a nine-finger repeated structure.

Sequence comparisons indicate the presence of similar motifs in other proteins that interact with DNA or RNA. These include the small RNA-binding protein encoded in the gag genes of retroviruses; the E1A gene-activating protein of adenoviruses; and the large-T antigens of papovaviruses. An even more extensive similarity has been found between TFIIIA and the product of the Drosophila developmental, regulatory Krüppel locus. Thus TFIIIA probably represents a class of structures, with a metal-binding site as a significant element of organization.

If TFIIIA contains a nine-finger repeat. is there a corresponding repeat in the 50bp intragenic control region to which it binds? Rhodes and Klug present evidence for such a repeat in the DNA itself. not obvious from casual inspection, but revealed by quantitative study of DNase I cleavage patterns and by mathematical analysis of the sequence. Cleavage of defined restriction fragments at different positions by DNase I is strikingly nonuniform, suggesting strong dependence of the cleavage rate on details of local DNA backbone conformation. DNase I binds across the minor groove, cutting each strand separately¹⁴. Activity may be influenced by the width of the minor groove or the orientation of phosphates A periodicity in the probability of DNase I cleavage along a given strand therefore probably reflects a periodicity in the DNA

Rhodes and Klug's Fourier analysis of DNase I cleavage patterns of the TFIIIA binding sequence shows a periodicity of about 5.7 nucleotides. The periodicity is characteristic of both strands, with a relative stagger of about 1, rather than 2 or 3 as generally observed for B-type DNA The smaller stagger suggests that base pairs are tilted, as in A-form DNA, so that phosphodiester bonds staggered by only one step lie nearly under each other across the minor groove14. Recognition of an Aform structure would of course be convenient for a protein that must bind specifically to RNA as well. Rhodes and Klug³ also observe an approximately 5.6base perodicity in the sequence of the TFIIIA binding site by focusing on the distribution of guanines. Fourier analysis confirms the significance of this repeat, which is not characteristic of randomly

selected nucleosome core DNA. The total of nine such repeats in the internal control region of the 5S RNA corresponds precisely to the nine putative binding fingers in TFIIIA, each of which would tend to make the same sort of contact with DNA.

The crystal structure of a 9-bp doublestranded deoxyribonucleotide with the sequence d(GGATGGGAG) representing base pairs 81-89 of the TFIIIA binding site, is reported in this issue. It supports the notion that the 11-bp repeat $(2 \times 5.7 \text{ in})$ the DNase I analysis or 2×5.6 in the sequence periodicity) and the 1-bp DNase I cleavage stagger observed by Rhodes and Klug3 do reflect an A-type conformation. The structure has been determined and refined at 3.0 Å resolution. It has a mean twist of 31.3°, corresponding to a loosely defined helical repeat of 11.5 bp, and an overall configuration rather close to the model derived from fibrediffraction studies of A' RNA15. The major groove in A-DNA is narrower and deeper than in B-DNA, but the structure determined by McCall et al.4 shows that there is room for a loop of polypeptide to fit — for example, the twisted β -ribbon suggested as a model for a single TFIIIA finger. McCall et al. propose that the GpG steps are the origin of the A-form structure for this fragment. In all structures with GpG/CpC observed to date, the five-membered ring of one guanine base lies stacked on the six-membered ring of its neighbour, an apparently favourable base-to-base overlap that is characteristic of A-form double helices.

The significant conformational plasticity of DNA gives rise to a caveat, however, which McCall et al. discuss. The A structure often occurs in crystals of oligonucleotides — perhaps more often than for the corresponding sequences in solution — and the relationship between solution and crystal conformations is not completely understood. In particular there are unknown influences of endeffects; of electrostatic interaction; and of solvent dielectric constant (the crystals studied by McCall et al. were prepared in 20 per cent methylpentanediol). Nonetheless, it is probably safe to assume that a structure found in a highly hydrated crystal will not differ drastically in free energy from whatever configuration dominates in solution and that the crystal structure represents an important component of any equilibrium distribution.

The significance of the half-turn repeat discovered in the internal control region of 5S RNA genes is enhanced by indication of similar repeats in other control elements. Rhodes and Klug' present evidence for a repeated motif of pairs of guanines within the split transfer-RNA gene promoter of various eukaryotes and within homologous positions of Alu sequences. They also observed that the so-called 21-bp repeats in Simian virus 40

(ref. 16), three tandem elements known to bind transcription factor Sp1 (ref. 17), have an effective 5 1/4-bp periodicity that is particularly striking when the positions of guanines are analysed. They propose that many factors directing transcription of transfer RNA genes by RNA polymerase III, as well as Sp1, which directs transcription by RNA polymerase II, contain TFIIIA-like fingers that interact with halfturn sequences of DNA.

The modular character of this proposed one-finger/one-half-turn correspondence is its most striking feature. Because there is good evidence that TFIIIA binds to one side of the DNA helix18, it is plausible that the fingers project alternately into the major groove on either side of the double helix. Evolutionary schemes can be constructed that would add modules and modify local binding affinities if such a linear relationship between protein modules and DNA half-turns indeed turns out to be true. The position of introns in the TFIIIA, most of which lie just between the putative fingers, is certainly consistent with these ideas19

Such an evolutionary history does not, however, imply that the repeat structures in TFIIIA bind independently. Indeed, analysis of binding to deletion mutants in the TFIIIA site, preferential proteolytic cleavage patterns and fragment-binding experiments all suggest that the aminoterminal part of TFIIIA, the 20K segment that corresponds to the first five repeats, binds as a unit^{7,10}. Moreover its binding is required for binding the next part of the protein (the remaining four repeats). The nine fingers might be grouped into two hands.

Several bacterial control proteins have a different but equally striking modular character. The recurring module is a 20residue helix-turn-helix elbow first identified in the cro repressor protein of bacteriophage lambda²¹ and in the catabolite activator protein of Escherichia coli²². This structure has so far always been found embedded in a larger DNA-binding domain (60-90) residues) of a dimeric or tetrameric protein. The 2-fold symmetry of the protein corresponds to an approximate 2-fold symmetry in the DNA sequence with which it interacts. Contacts to the DNA backbone, made by residues at various positions in the binding domain, position the helix-turn-helix module to interact with bases in the major groove. In most cases, the points of major-groove interaction by the two members of the dimer are one turn apart, although in at least one case, the interaction may be two turns apart²⁴. The repressor of bacteriophage 434, for which the crystal structure of a complex with operator is known. exhibits a specificity for B-form DNA23. The same seems to be true for other helixturn-helix-containing proteins. This sort of modularity found in the prokaryotic repressors and activators is different from that proposed for TFIIIA, most simply because it involves a nearly precise 2-fold symmetry rather than approximate translational symmetry, and structurally because it involves identical protein subunits associated as dimers rather than homologous units concatenated in a single polypeptide chain.

TFIIIA and many of the prokaryotic repressors and activators have one significant structural characteristic in common. One domain directs DNA binding, while a second mediates formation of functional complexes with other proteins. For example, cooperative binding of the lambda repressor at adjacent operator sites is brought about by interacting carboxyterminal domains25, and this interaction is also a model for loop-forming contacts between proteins bound at more distant sites26,27. The carboxy-terminal domain of TFIIIA is essential for correct transcriptional initiation, presumably because it binds to other components of the transcription complex.

There are hints of further structural classes for DNA-binding domains of sequence-specific transcription factors. The yeast GAL4 protein, which binds to upstream activating sequences, and the Simian virus 40 large-T antigen, which regulates transcription and stimulates DNA replication, may contain elements that are examples of such classes. The lesson of progress with TFIIIA is that structural characterization of such proteins and careful analysis of their binding sites can indeed make the apparent complexity of control sequences much less bewildering.

- 1. Brown, D.B. in The Harvey Lectures Ser. 76, 27 (Acad-
- emic, New York, 1982).

 2. Miller, J., McLachlan, A.D. & Klug, A. *EMBO J.* 4, 1609
- Rhodes, D. & Klug, A. Cell 46, 123 (1986).
- McCall, M. et al. Nature 322, 661 (1986).
 Engelke, D.R. et al. Cell 19, 717 (1980).
- Bogenhagen, D.F. et al. Cell 28, 413 (1982).
- Sakonju, S. et al. Cell 23, 665 (1981).
 Sakonju, S. & Brown, D.B. Cell 31, 395 (1982).
- 9. Picard. B. & Wegnez. M. Proc. natn. Acad. Sci. U.S.A. 76,
- Smith, D.R. et al. Cell 37, 645 (1984).
 Hanas, J.S. et al. J. biol. Chem. 258, 14120 (1983).
 Berg, J. Science 232, 485 (1986).
 Rosenber, V.B. et al. Nature 319, 336 (1986).

- Drew. H. & Travers. A. Cell 37, 491 (1984).
 Arnott, S. et al. J. molec. Biol. 81, 107 (1973).
- 16. Tooze, J. Molecular Biology of Tumor Viruses Part 2: DNA Tumor Viruses 2nd edn (Cold Spring Harbor
- Laboratory, New York, 1981).
 17. Dynan, W.S. & Tjian, R. Cell 32, 669 (1983).
 18. Rhodes, D. EMBO J. 4, 3473 (1985).
- Tso, J.Y. et al. Nucleic Acids Res. 14, 2187 (1986).
 Pabo, C. & Sauer, R. A. Rev. Biochem. 53, 293 (1984).
 Anderson, W.F. et al. Nature 290, 754 (1981).
 McKay, D.B. & Steitz, T.A Nature 290, 744 (1981).

- Anderson, J.E. et al. Nature 316, 596 (1985).
 Hendrickson, W. & Schleif, R. Proc. natn. Acad. Sci. U.S.A. 82, 3129 (1985).
 Johnson, A. et al. Proc. natn. Acad. Sci. U.S.A. 76, 5061
- 26. Dunn, T.M. et al. Proc. natn. Acad. Sci. U.S.A. 81, 5017
- 27. Hochschild, A. & Ptashne, M. Cell 44, 681 (1986).

Stephen C. Harrison is in the Department of Biochemistry and Molecular Biology at Harvard University, 7 Divinity Avenue, Cambridge, Massachusetts 02138, USA.

SCIENTIFIC CORRESPONDENCE-

The stability of biological nomenclature: veasts

SIR—The strictures of Erzinclioglu and Unwin on the inconvenient instability of zoological nomenclature (Nature 320, 687; 1986) apply equally to other kinds of organism, including the yeasts. For nontaxonomists, the rapidity with which yeast names change is farcical. For example, Zygosaccharomyces fermentati' was altered to Saccharomyces cerevisiae by Lodder and Kreger-van Rij in 1952, back to Zygosaccharomyces fermentati by Kudriavzev in 1954', to Saccharomyces montanus by Phaff, Miller and Shifrine in 19564, to Torulaspora manchurica in 1975 by van der Walt and Johannsens and finally (?) back again to Zvgosaccharomyces fermentati by von Arx and his colleagues in 1977. The same process continues even now. As part of a major work on yeast taxonomy, C.P. Kurtzman gave descriptions of thirty species of the genus Hansenula, which he then proceeded to abolish in a paper published the same years.

Part of the trouble comes from the romantic confusion of biological classification with evolutionary studies, exemplified by S. J. Gould's words":

"taxonomies are not neutral hat-racks for the pristine facts of nature. They are theories that create and reflect the deep structure of science and human culture.'

Too many taxonomists appear to subscribe to this kind of sentimental codswallop and seem quite unable to understand that instability of nomenclature seriously impairs the value of their work to biology as a whole. How many biologists who work with yeasts know that publications on Saccharomyces carlsbergensis, Saccharomyces uvarum, Saccharomyces cerevisiae or Saccharomyces logos might refer to the same yeast? At best, this is an inconvenience; at worst, it retards understanding of the biology of that yeast.

It would be perfectly practicable for there to be an international body, responsible for the nomenclature of each group of organisms, and briefed to give their names helpful stability.

J. A. BARNETT

School of Biological Sciences, University of East Anglia, Norwich NR47TJ, UK

- 1. Naganishi, H. J. Fermentation Stud. 6, 1-12 (1928).
- Lodder, J. & Kreger-van Rij, N. J.W. The Yeasts: a Taxo-nomic Study (North-Holland, Amsterdam, 1952).
- Kudriavzev, V.I. Sistematika Drozlizhei (Akademii Nauk, Moscow, 1954).
 Phatf, H.J., Miller, M.W. & Shitrine, M. Antonie van Lecu-
- wenhoek 22, 145-161 (1956). 5. van der Walt, J.P. & Johannsen, E. S. Afr. Council Sci. Ind.
- Res. Res. Rep. No. 325 (1975).
 6. von Arx, J.A., Rodrigues de Miranda, L., Smith, M. F. &
- Yarrow, D. The Genera of Yeasts and the Yeast-like Fungi (Centraalbureau voor Schimmelcultures, Baarn, 1977).
- Kurtzman, C.P. in *The Yeasts: a Taxonomic Study* (ed. Kreger-van Rij, N.J.W.) 165-213 (Elsevier, Amsterdam.
- 8. Kurtzman, C.P. Antonie van Leeuwenhoek 50, 209-217
- 9. Gould, S.J. Nature 313, 505-506 (1985).

Microtubule assembly in the axon

SIR-Bamburg et al. (Nature 321, 788; 1986) present a novel view of microtubule assembly in the axon. They show that axonal elongation can be inhibited by an application of microtubule depolymerizing drugs or taxol at the growth cone. The same concentrations of these drugs applied to the neurite or cell body have no effect on motility. The authors conclude that the drugs may act by inhibiting microtubule assembly at the distal tip of the axon. They also postulate that unassembled tubulin is transported along the axon to the growth cone, and there adds on to existing microtubules.

presented, the experimental measurements of axonal length with time are interpreted as a reflection of the extent of microtubule assembly. Such measurements of extent cannot be used to distinguish between effects of the drugs on the rate constants for assembly or disassembly. The microtubule-depolymerizing drugs could act by increasing the rate of disassembly at the tip. For this alternative explanation to hold, one must postulate only that microtubules at the growth cone, but not along the neurite, are in dynamic equilibrium with a pool of monomer. There is no need to require that a net assembly reaction occurs in this region. The drugs could have their effect by shifting the dynamic equilibrium towards monomer. The existence of such an equilibrium state is a feature of other models of microtubule control in axons. For example, if microtubules are transported in the assembled state, they must be disassembled at the end of the axon. Should such an equilibrium exist, sufficiently high concentrations of drug not only might inhibit neurite extension but also cause net retraction. That outcome is reported by Bamberg et al. Thus, these data do not demonstrate microtubule assembly at the ends of axons. More direct experiments are required to demonstrate this reaction. FRANK SOLOMON

Department of Biology, Massachusetts Institute of Technology, Cambridge. Massachusetts 02139, USA

Disease gene relationship seen

SIR-A recent article by Royer-Pokora et al. described the isolation of a gene that is abnormal in the X-linked form of the phagocytic disorder chronic granulomatous disease (X-CGD), which is thought to be due to a lesion in the NADPH-oxidase system of these cells'. An unusual b-type cytochrome³ and a flavoprotein have been proposed as candidates for the polypeptide encoded by the Z-CGD locus, but the nucleotide

sequence of the cDNA clones isolated by Royer-Pokora et al. predicted a polypeptide that showed no significant homology to known sequences in the GENBANK or protein databases The authors could not identify any potential haem-binding region in the primary structure of the X-CGD protein.

We have, however, found a region of the predicted X-CGD sequence that is similar to the haem-binding region of the cytochrome P-450 proteins, and in particular to cytochrome P-450 form PBel from rabbit liver5. The figure below illustrates the point, and identifies with an asterisk the cysteine thiolare ligand to the haem prosthetic group of the cytochrome.

X-CGD protein LCGPEALAET Cytochrome P-450 V C*V G E A L A R M form PBc1

The haem-binding region is highly conserved among cytochromes P-450, some of which have only a slight overall sequence similarity to one another. It is of interest that the two regions are located at equivalent positions in X-CGD and cytochrome P-450 (at about amino acid 435).

> ALAN ASHWORTH ELIZABETH A. SHEPHARD

Department of Biochemistry, University College London, London WCIE 6BT, UK

IAN R. PHILLIPS

Departments of Pharmaceutical Chemistry and Pharmacology. The School of Pharmacy, University of London, London WCIN 1AX.

- Royer-Pokora, B. et al. Nature 322, 32-38 (1986).
- Tauber, A.I., Borregaard, N., Simons, F. & Wright, J. Medicine 62, 286-309 (1983).
- Segal, A.W. et al. New Engl. J. Med. 308, 145-251 (1983)
 Markert, M., Glass, G.A., & Barbiot B.M. Prec. nath. Acad. Sci. U.S.A. 82, 3144-3148 (1985)
- 5. Leighton, J.K., DeBrunner-Vossbrinck, B. V. & Kemper, B. Biochemistry 23, 203-210 (1984).

Mankind's genetic bottleneck

SIR—Your correspondents question whether our interpretation of a small bottleneck in human evolution based on the patterns of distribution of β -globin haplotypes4 is correct and, if so, whether it is relevant to the origins of mankind. Our brief answer is that, although the modern distribution of these genes can in itself tell us rather little about where and how modern Homo sapiens originated, it is nevertheless the case that — given the assumptions of our very simple model and applying it only to β -globins -- passage through such a bottleneck is an inevitable implication of the present-day distribution of β -globin variants. We attempted to 'root' our evolutionary tree by reference to recent work on human fossils, which suggests that the most ancient H. sapiens are found in Africa. It is of course the case

that the geography of β -globin variants is in itself compatible with an African, an Asian or a dual origin of mankind, but the fossil record does seem to indicate an African birthplace for modern humans. As geneticists fallen amorig palaeontologists, we are not qualified to comment on the controversy as to the dating of African fossils, but have accepted the consensus view and used this (and not the β -globin tree) to suggest an African origin for mankind. Our deduction of a bottleneck at the origin of the rest of the world's human population is the simplest model consistent with the fossil data and the geography of the β -globins. Simplicity has forced us to make a number of assumptions.

One of these is that β -globin variants are selectively neutral. Nothing would delight us more than to learn that the possession of alternative haplotypes altered their carriers' ability to escape from sabretoothed tigers, but in the absence of evidence to the contrary we have accepted the view, implicit in most theories of molecular evolution, that natural selection does not act on noncoding sequences of DNA. As both your correspondents point out, this is not necessarily correct; and there certainly exist quite feasible modes of selection on noncoding variants by virtue of their linkage to strongly selected alleles such as that for sickle cell haemoglobin'. As there is simply no information on this possibility, we have, with Occam, chosen the more straightforward alternative. The model also includes the arbitrary; but simple, suggestion that the four commonest modern haplotypes were at equal frequencies in the ancestral African population. This assumption is not central to the existence of a bottleneck, but does influence its size. The frequencies in modern African populations pointed out by Giles and Ambrose could either reflect a conservation of their ancient values suggesting an even smaller bottleneck in the emergent population — or a change within Africa arising from genetic drift in small populations (which could be many times larger than our supposed bottleneck of emigrants).

Despite the widespread popularity among palaeontologists of models of a multiple origin of mankind (for example ref. 7 of Van Valen), theoretical population genetics suggests that any population's ability to undergo speciation is so limited that it is extremely unlikely that H. sapiens arose simultaneously in different parts of the world from different ancestors. For example, using a simple model of change by genetic drift, Sewall Wright showed in the 1940s that the probability of a chromosome rearrangement with a selective disadvantage to hybrids of 5% becoming established in a local population of 200 individuals is about 10 5 per generation. The chance of this happening simultaneously in two separate populations is about 10⁻¹⁰ per generation, which is extremely small, but may still be greater than the chance of simultaneous speciation in two separate populations. Van Valen's alternative suggestion — that of simultaneous global appearance of H. sapiens - implies extensive gene flow among its evolving populations, so extensive that both the ancestral H. erectus and the derived H. sapiens must be thought of as effectively sympatric. Sympatric speciation is itself difficult to accommodate into population genetics theory, and in Van Valen's scheme one is forced to explain the observed patterns of β -globin divergence by postulating long periods when large African and Eurasian populations of mankind were isolated from each other.

Our model, like many others, exists simply to show the evolutionary implications of an observed genetic structure. Its main point is to show that some of the demographic consequences of human gene frequency change are quite startling; startling enough, perhaps, to lead us to try to formulate a better model. A successful model would also, as we point out, have to explain why different genes seem to imply different demographic patterns during the spread of mankind.

> J.S. JONES S. ROUHANI

Department of Genetics and Biometry, University College London. London NWI 2HE, UK

- Giles, E. & Ambrose, S.H. Nature 322, 21 22 (1986).
- Van Valen, L. Nature 322, 412 (1986).
- Jones, J.S., & Rouhani, S. *Nature* 319, 449 486 (1986).
 Wainscoat, J.S. et al. *Nature* 319, 491 493 (1986).
- Antonarakis, S.E., et al. Proc. nam. Acud. Sci. U.S.A. 79. 137 [41 (1982)]
- 6. Wright, S. Genetics 28, 114 (1943).

Transfer of radioiodide to milk and its inhibition

SIR-Following the increased atmospheric levels of radioactivity resulting from the Chernobyl reactor accident, one of the main radiological concerns has been the entry of radioiodide into the human food chain through animal milk, and its subsequent uptake into the thyroid gland, as reported recently in your columns2

Current studies of transport mechanisms for various radionuclides in the mammary gland emphasize the rapidity with which blood-borne radioiodide can enter milk. The mammary gland of two goats was continuously infused for 15 min with 123 I (2.78 MBq; sodium iodide, AERE Harwell) through an indwelling polyvinyl chloride catheter placed in the external pudic (mammary) artery. Milk was completely removed by hand at 15 min intervals with oxytocin treatment (100 mUnits intravenously) and total radioactivity measured in a LKB Wallac 80000 gamma-sample counter. The total 123I activity secreted into the milk rose rapidly to a peak concentration just 30 min after the start of infusion followed by a slower

decrease. The fractional activity of 123I secreted in milk during a 2 h period was 1.0 and 1.5% of the infused activities.

The iodide concentrating activity of the mammary gland has long been recognized^{3,4}, and earlier work showed that the secretion of radioiodide into milk could be inhibited by competing anions such as perchlorate and thiocynate^{3,5}. We repeated the above experiment by infusing sodium perchlorate (100 mg) closearterially for 30 min before and during 123 I infusion. The total fractional 123I activity transferred into milk during 2 h was reduced by 60-66%.

Perchlorate has previously been found to be a more efficient inhibitor of radioiodide transfer into milk than thiocyanate, iodide or iodate³. Thiocyanate was not concentrated in rabbit milk3, but we are unaware of any data that quantifies perchlorate transfer into milk. This information is urgently needed before perchlorate administration could be considered as a means of protecting against the entry of radioiodide into the human food chain or into breast-fed infants after a reactor accident7. The use of perchlorate is not unprecedented since the compound has been used without deleterious effects in nuclear medicine to block, for example, the uptake of radionuclides into the maternal thyroid during diagnostic investigations. There is also a clear need to identify inhibitors which block mammary transport of other radionuclides, including fission products.

> P.J. MOUNTFORD A.J. COAKLEY

Department of Nuclear Medicine, Kent & Canterbury Hospital, Canterbury, Kent CT1 3NG, UK

> I.R. FLEET M. Hamon R.B. HEAP

AFRC Institute of Animal Physiology and Genetic Research, Babraham, Cambridge CB2 4AT, UK

- L. Fry. F.A., Clarke, R.H. & O'Riordan, M.C. Nature 321
- F.A. Canke, R.H. & O Rordan, M.C. Nature 321, 193-195 (1986).
 Hill, C.R., Adam, L., Anderson, W., Ott, R.J. & Sowby, F.D. Nature 321, 655-656 (1986).
- Brown-Grant, K. J. Physiol. Lond. 135, 644-654 (1957).
 Brown-Grant, K. Physiol. Rev. 41, 189-213 (1961).
- Lengemann, F.W. J. Dairy Sci. 56, 753-756 (1973).
 Hoffman, F.O. Hilli Phys. 35, 413-416 (1978).
- Lecliner, W., Huter, O., Daxenbichler, G. & Marth, C. Lanceti, 1326 (1986).
- Coakley, A.J. & Mountford, P.J. Br. Med. J. 291, 159-160

Scientific Correspondence

Scientific Correspondence is intended to provide a forum in which readers may raise points of a scientific character. They need not arise out of anything published in Nature, but those that do should not be highly technical comments on Articles or Letters (where the Matters Arising section remains appropriate).

Our daily lead

Josef Eisinger

The Lead Debate: The Environment, Toxicology and Child Health. Edited by R. Lansdowne and W. Yule. Croom Helm: 1986. Pp.276. Hbk £25, Pbk £14.95.

LEAD may be, with the exception of 1 smoke, the oldest man-made environmental toxin. The manifold benefits which the element has bestowed on civilization - from plumbing to pigments - have been paid for heavily in human lives. Lead mining and manufacturing have of course been known as dangerous occupations since ancient times, but it was not until 1656 that Samuel Stockhausen, the first genuine occupational physician, presented clear evidence that lead was responsible for the particular ills and short life span of men and women engaged in these occupations.

Lead disease was, however, by no means confined to these and other lead workers. Lead was used as a wine additive

for many centuries (it is a bacteriocide and has a sweet taste), and inadequately fired leadglazed cooking utensils in 18thcentury Germany, were just two of many causes of widespread non-occupational plumbism. In contrast, massive chronic exposures are, in our own times, rare, but ingestion and inhalation of low levels of lead in the environment has become inescapable for all. As a result, the body burden of lead in modern man exceeds that of prehistoric

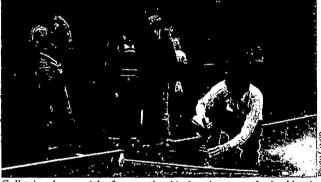
man by orders of magnitude. The leadsensitivity of different human enzyme systems varies greatly, however, so that the health effects of our lead environment are subtle, variable and often escape correct diagnosis. It is therefore not surprising that the toxicity of prevalent lead exposures presents a difficult problem and often provokes impassioined debates.

The Lead Debate is a multi-authored compendium of articles centered around the health effects of non-occupational lead exposure, particularly in children. It attempts to distil a vast amount of relevant information into a small volume, in order to make it accessible to a broad range of readers, including medical and social workers, environmental scientists and policy makers. The attempt is, except for some lapses noted below, successful.

The book is divided into three parts, of which the first deals adequately with the historical, chemical, geological and medical background of lead. Environmental lead disease is of course best controlled by limiting the amount of lead which industrial societies inject into air, water and | ZPP and PbB below that level, which is | lead, with particular emphasis on the

soil; and legislation which controls the amount of alkyl lead added to petrol represents a step in the right direction. The next line of defence against chronic exposure is clearly an effective screening programme for populations at risk, particularly for children, and the book includes a, regrettably, brief section on the methodology of measuring levels of lead in humans and in the environment.

The two screening methods which have been used more than any other are based on the concentration, in blood, of lead (PbB) and of zinc protoporphyrin (ZPP), respectively. The latter is a lead-induced, fluorescent metabolite which mimics the haem in haemoglobin during erythropoiesis and is most conveniently measured



Collecting dust particles from a school in London to test for lead levels.

by a dedicated, portable instrument called a haematofluorometer. Of these two assays, the ZPP assay is much cheaper, requires much less blood (generally a drop obtained by finger stick), provides an immediate result, and has a significantly higher correlation with the symptoms of chronic lead disease than PbB assays. For these reasons, the US Centers for Disease Control has recommended ZPP assays for the primary screening of children for lead poisoning and, incidentally, for iron deficiency anaemia. According to the Public Health Foundation, more than 700,000 such screening tests are performed by state health departments in the US each year; over 90 per cent of which use the ZPP haematofluorometer.

In light of this, it is strange that the chapter devoted to lead exposure measurements does not mention this instrument! It is even stranger that, despite its admitted advantages, the ZPP assay is "not recommended at blood lead levels of about '15 µg/dl". The reason given is that there is only a weak correlation between well within the range considered "normal" (< 25 µg/dl). Leaving aside the questionable relevance of this correlation, it is not clear why an efficient screening tool like the ZPP haematofluorometer should not be used to identify children with PbB levels above 15 µg/dl, for they have, without doubt, the greatest need for medical attention!

The second part of the book offers several well organized and informative chapters on the distribution and sources of lead exposure. Because they are written by only two authors, they avoid the unevenness of the earlier sections (where the references to primary sources are occasionally too sparse). Here one finds an account of, possibly, the most significant and elegant environmental lead study, in which the variation in the isotopic ratio (Pb206/Pb207) of the alkyl lead additives used in petrol was varied slowly over a period of six years. This variation was found to be closely linked to the isotopic ratio of airborne particulate lead as well as by the isotopic ratio of lead in the blood of subjects living in Turin and the surrounding countryside, where the experiment was

> conducted with the cooperation of Italian oil companies.

> This and similar studies in the US and UK have established that anthropogenic lead - principally from petrol combustion - is the most important component of lead pollution. Once it is injected into the air this lead finds its way into the human body, primarily by way of the food and water supply. Excessive concentrations in tap water have long haunted regions where lead pipes continue in use, as

for instance in Scotland. Reductions in the lead content of water have now been achieved by raising the pH of the water and buffering it with the aid of sodium hydroxide and inorganic phosphate additives.

In the UK and the US, the most serious cases of lead poisoning in children can be traced to lead-pica - the chewing of either peeling paint or of painted articles. prompted by the sweet taste of the lead ion (Pb2+). (The term pica is derived from the much maligned magpie, Pica pica.) The strategy for prevention is clear: removal of old paints and the use of nonlead paints for interior surfaces. What the book's authors fail to mention is that well-meaning government regulations are, because of their enormous cost, rarely enforced, so that effective screening programmes for young children again offer the best hope for finding and eliminating trouble spots and for providing needed medical attention.

The remainder of the The Lead Debate addresses the health effects of ingested

psychological development of children exposed to ordinary environmental lead levels. It opens, appropriately enough, with a discussion of the methodological difficulties of interpreting the numerous studies which attempt to identify the disease-exposure relationship. It is unfortunate that most of these studies use PbB as the only exposure index, although the most important study in America does include dentine lead as a cummulative index. The warning against equating correlations with causal relationships are well taken, and the critical commentary on the conclusions drawn from studies exploring lead-effects on intelligence and behaviour are particularly helpful. Although caution in the interpretation of low-level exposure data is clearly in order, there is no lack of evidence, from epidemiological studies and animal experiments, that massive and moderate exposure produces measurable neurobehavioural effects.

The enduring dilemma surrounding the lead debate is that the threshold of leadrelated disease continues to defy definition. This should surprise no one for it requires a quantitative determination of such multivariate parameters as intelligence, behaviour and learning. But supposing that such a threshold could be translated into an indicator of exposure (for example PbB or ZPP levels, vide supra) a second, even more difficult question faces policy makers; what is the fiscal value which society attaches to the elimination of marginal plumbism? In crasser terms, how much is the taxpayer willing to pay, in order to raise the average intelligence of the population by, say, 1 per-

It is unfortunate that these tricky issues are rarely touched upon in *The Lead Debate*. Usually, the authors prefer to remain on the safe technical level and to quote from general conclusions of governmental commission reports. A chapter on real and perceived risk of lead disease compared to other health insults which we are exposed to, together with estimates of their cost of abatement, would have been welcome (c.f. *New England Journal of Medicine* 1982:1392).

On the other hand, the contributors have collected a lot of extremely useful scientific information which will undoubtedly help to keep the continuing debate about plumbism on a firm scientific footing. They have succeeded in avoiding polemics, albeit at the cost of avoiding novel or controversial approaches. Nevertheless *The Lead Debate* is an important and useful interdisciplinary review of where we stand in our efforts to unravel the complexities of this ancient environmental hazard.

Dr Josef Eisinger is in the Department of Physiology and Biophysics at the Mount Sinai School of Medicine, 5th Avenue and 100th Street, New York, NY 10029, USA.

Visitors from the past

Theya Molleson

Lindow Man: The Body in the Bog. Edited by I.M. Stead, J.B. Bourke and Don Brothwell. British Museum Publications, London: 1986. Pp.208: £15.

The great interest that attaches to any bog body derives not simply from the rarity of such finds but also from the intrinsic nature of the body: it is almost a visitor from the past. Such bodies should tell us more of the life and character of the earlier people. To deduce the age and sex of a body is one thing; but to know something of his clothing and ornaments and to discover the ingredients of his last meal and, above all, to see his face is somehow to perceive the whole anima of his time. I don't think that we should be disappoin-

one of the most significant bog findings in Britain and the greatest challenge to archaeological conservation. Within days the police moved out, the hospital wanted the body removed and the conservationists were asked to take over. They were expected to prevent any deterioration of the body while allowing endless study, photography, sampling and dissection. And all they knew from previous experience was what *not* to do. By a conscientious and didactic approach it does seem that Lindow Man has been preserved for posterity.

The volume, Lindow Man, presents the progress reports of the wide range of exploratory studies — from identification of the surrounding peat and of the pollen, cereals and parasites in the stomach to interpretation of the context both geographic and cultural. Some papers are too clearly hurriedly written; others tend to be discursive for want of factual evidence. It is surprising how little appears to be known of our Celtic heritage.



Lindow Man has his back cleaned, taken from The Bog Man and the Archaeology of People (British Museum Publications, Pbk £5.95). In this book, Don Brothwell gives a briefer, less technical account of the Lindow project. Lindow Man is also on display at the British Museum in London, together with the results of the research programme, as part of the exhibition Archaeology in Britain which runs until 15 February 1987.

ted when our expectations are but inadequately realised. Lindow Man has been thoroughly studied but has yet to tell his full story and, not least, to declare his age.

Enormous credit must go to Rick Turner, the county archaeologist for Cheshire, where Lindow Man was discovered in 1984. He was able immediately to appreciate the archaeological potential that lay in just a fold of skin exposed in the section at the peat cutting. He even managed to convince all concerned that the correct procedure then was to delimit the area of the body, if body there was; to cut it out and crate it for removal to the local mortuary. At this stage the investigation was still a police matter, and not

Concepts of sacrificial ritual emanating from the bog finds in Europe have dominated the approach to the study of Lindow Man. Several workers have found it hard to view their data independently of these theories so that the final interpretation tends to be prejudiced. Yet the information as presented is open to other constructs than that of a ritual killing on the lines of the Danish Bog burials. And that is the advantage of the presentation of the independent studies in detail and in one volume. Readers can make up their own minds.

Theya Molleson is in the Department of Palaeoentology, British Museum (Natural History), London SW75BD, UK.

Dial a vector

Tim Harris

Cloning Vectors: A Laboratory Manual. Edited by P.H. Pouwels, B.E. Enger-Valk and W.J. Brammar. Elsvier:1985. Approximately 400 sheets in Loose-leaf binder. \$55, Dfl. 160.

LABORATORY manuals have become a popular means of disseminating the complicated protocols of modern molecular genetics, the best example being Molecular Cloning — A Laboratory Manual, referred to by some as the cloning bible, by Maniatis et al. Some of these manuals, like the above, combine theory with practice while others are simply sophisticated recipe books. Although described as a laboratory manual, Cloning Vectors is a directory of the vectors currently available for introducing genes into a variety of organisms. The vital statistics of some 300 vectors, both plasmid and phage in origin, are described by means of clear, singlepage diagrams. About one-third of the plasmids are those used for the most commonly employed cloning host — the gram negative bacterium E. coli. The remaining chapters cover vectors for gram positive bacteria (for example, Streptomyces), fungi (including yeast) and plant and animal cells.

The work is comprehensive, as up to date as might be expected in a fast-moving field, and the clarity and simplicity of the figures is impressive. Provided you know what you are looking for, the salient facts are easy to obtain. It is possible to use the summary tables at the end of each chapter to locate vectors with desired characteristics (one of the objectives of the book) but it's a pity little attempt was made to rank or distinguish commonly used vectors from more esoteric and not necessarily more useful ones. The loose-leaf format of the directory is designed so that annual updates can be included; some of the newer cosmid vectors for genome walking and vectors for insect cell expression can be expected*.

The lack of theoretical back up — the introductions to each chapter are only one or two pages — indicates that this book is not intended for the individual graduate or postdoctoral molecular biologist. Rather, like a telephone directory, it is a reference book that every genetic engineering lab will want access to, be it on their library, laboratory or office shelf.

*These are indeed included in the first update which will be available in September. Price \$20, Dfl. 60. Orders for the main manual plus three annual updates are entitled to the reduced price of \$97.75, Dfl. 287.

Tim Harris is Head of Molecular Biology at Celltech, 244-250 Bath Road, Slough, Berks SLI 4DY, UK.

Copies of articles from this publication are now available from the **UMI** Article Clearinghouse.

For more information about the Clearinghouse, please fill out and mail back the coupon below.

UMIIArticle Clearinghouse

Yes! I would like to know more about UMI Article Clearinghouse. I am interested in electronic ordering through the following

☐ DIALOG/Dialorder ☐ ITT Dialcom

☐ OnTyme

□ OCLC ILL Subsystem

☐ Other (please specify).

- ☐ I am interested in sending my order by
- Please send me your current catalog and user instructions for the system(s) I checked above.

Institution/Company____

_State___Zip__

Phone (___

Mail to: University Microfilms International 300 North Zeeb Road, Box 91 Ann Arbor, MI 48106

History isn't bunk

John H. Lawton

Modeling Nature. Episodes in the History of Population Ecology. By Sharon E. Kingsland. University of Chicago Press: 1985. Pp.267. \$27.50, £23.50.

As every schoolboy knows, Henry Ford thought that history was bunk, a view that is certainly common, if not universally held by many creative and successful scientists about their own subject. There is, after all, too much to read about what is happening today to care about what happened yesterday, still less about events 50 or more years ago. But a sense of perspective is no bad thing in any walk of life, and science is no exception, as Sharon Kingsland's book makes plain.

The book is a detailed history of the rise of population ecology from its early beginnings in the writings of Frederic Clements and Stephen Forbes (who in turn drew their inspiration from Charles Darwin, Herbert Spencer and so on, but historians have to stop going backwards somewhere), through Alfred Lotka, Raymond Pearl and Vito Volterra, and from there on a direct intellectual route via Georgii Gause to Evelyn Hutchinson, David Lack and Robert MacArthur. There were, of course, other contributors, some major some minor, but this pedigree is particularly clearly defined, and gives a good indication of the scope of the book, and the time-scale involved.

Reviewing books is often a chore, is usually educative, but is only infrequently a real pleasure. Modeling Nature unfolds like a good detective story, and is a delight to read for at least two reasons. It is a beautifully written, well-crafted account of a complex subject; although I thought I knew the roots to population ecology fairly well, I found that many of my ideas were either fuzzy or wrong. It is extremely useful to have the key intellectual advances so clearly laid out. Second, and probably more important, the book is about people as well as ideas. It was, after all, no lesser historian than Edward Gibbon who said that history is "little more than a register of the crimes, follies, and misfortunes of mankind"! One would hesitate to use quite these terms to describe the history of population biology. but the founding fathers were not modest angels. They were certainly clever, but they were also - in varying degrees opinionated, scheming and paranoid, as well as insightful, helpful and wise. And all of them were men, which in itself is an interesting comment on the sociology of science, although Kingsland does not open this particular can of worms.

Population ecology is currently in the throes of a series of intense and, at times, acrimonious debates. The arguments have several overlapping strands, including the role of density-dependent processes in population regulation, the importance of interspecific competition in structuring communities, the value of mathematics in ecology, and the proper way of doing science that would solve all these problems if only everybody would adopt the true way. Not one of these problems is new. All have been debated with just as much ferocity in the past, and what history shows is that the entrenched positions of the principal assailants have almost always proved to be misguided, irrelevant or wrong. History isn't bunk; it gives a sense of proportion.

Confronted with the realisation that we have been here before, sometimes more than once, it is easy to believe that population ecology has simply wandered round in aggressive circles, getting nowhere since Lotka published Elements of Physical Biology in 1925 and Volterra his famous letter to Nature a year later. Nothing could be further from the truth. Population and community ecology have made great strides over the past 60 years, despite the complexities of natural communities. From the fires of strong disagreement ultimately emerges the phoenix of scientific progress. But a better sense of history might reduce the sparks currently flying round population ecology, and help to generate less heat, more light and greater tolerance.

John H. Lawton is a Professor in the Department of Biology, University of York, Heslington, York YOI 5DD, UK.

Plants in distress

Richard Dixon

The Biochemistry and Physiology of Plant Disease. By Robert N. Goodman, Zoltán Király and K.R. Wood. *University of Missouri Press:1986. Pp.433.* \$45.

RESEARCH in plant pathology is now entering an exciting period. Pathologists are becoming increasingly aware of the potential of new molecular techniques, while plant biochemists and molecular biologists are showing corresponding interest in plant-pathogen interactions as important systems for studies of cellular recognition, metabolic integration and gene expression. Any new, comprehensive review of this field should be judged in terms of its success in presenting the bases (often multidisciplinary) of current concepts, and its exposition of new experimental approaches. My first impressions of The Biochemistry and Physiology of Plant Disease were of a magnum opus, among whose wealth of detail would surely be found the signposts to future research. A full reading of the book left me impressed by the scale of the authors' understanding, but somewhat disappointed by the book's lack of direction and its conclusions.

Most chapters consist of brief descriptions of the biochemistry or physiology of a particular aspect of the healthy plant (respiration, photosynthesis, cell walls and so on) followed by detailed analyses of the effects of infection under the separate headings of viruses, bacteria and fungi. Taken together, the introductory sections almost make up a basic plant bio-

chemistry text, good in some sections (particularly cell walls), but in others too condensed to be of much value to non-biochemists (for example, the glyoxylate cycle is presented with no mention of its role in metabolism). Although the conceptual aspects are presented critically and lucidly, there are a relatively large number of material inaccuracies, particularly in the introductory biochemical sections — tyrosine is not only found in the *Gramineae* (p.211), acetyl CoA units are certainly not condensed to yield malonyl CoA (p.212) and phenylalanine is not altered by hydrolases (p.226).

The organization of the material, based on physiological divisions rather than temporal sequences of events, has inevitably led to repetition of information under different headings, although this is less apparent in the sections on viruses. Such repetition in a long work is often no bad thing, but some important topics are never fully dealt with in one section and appear piecemeal throughout the book. The accounts of the *Agrobacterium* system, fungal and host elicitors, and induced host gene expression fall into this category.

The scope of the book is, of course, clear from its title, and the depth of treatment and excellence of the illustrations will no doubt ensure its success as a standard text for advanced students. I was, however, disappointed by the lack of attention to genetics, both classical and molecular (viral nucleic acid metabolism excluded), as it is from the application of recombinant DNA techniques that the most promising developments in plant pathology will probably arise. In this respect, I feel that the authors' honestlyconfessed lack of agreement in several areas, particularly the molecular basis of disease resistance, rather robs the book of an important component — that of informed prediction, even if based on personal prejudice. The search for avirulence, virulence and resistance genes is now a central effort in plant pathology, and more speculation in these areas, at the expense of repetition of correlative phenomena reviewed earlier in the book, would have increased the impact of the final "rounding-off" chapter on disease resistance. Likewise, the concluding sections to the individual chapters, each headed "Comparative Analysis of Disease Physiology", simply summarize rather than integrate the views of the individual authors.

Such problems apart, it is perhaps unfair to criticize the book too much for what it does not cover. It stands as a detailed source of information on physiological plant pathology, one which will certainly be widely read.

Baking and brewing in Egypt around 2400 BC, taken from the Open University study pack on Biotechnology (PS621, £119). Designed for those with no specialist knowledge, the pack consists of over 600 pages of text divided between eight books, including two volumes Laboratory to Marketplace which look at the impact of biotechnology on a number of key industries, a series of case studies and two books of supporting technical material. Although the modular pack is designed to be free-standing, there is an associated set of six video tapes (£115 each or £299 for the set). Available from Learning Materials Sales Office, The Open University, PO Box 188, Milton Keynes MK7 6DH, UK.

Richard Dixon is a Reader in the Department of Biochemistry, Royal Holloway and Bedford New College, University of London, Egham TW200EX, UK.

Aleutian terranes from Nd isotopes

R. W. Kay*†, J. L. Rubenstone‡ & S. Mahlburg Kay*

* Institute for the Study of the Continents (INSTOC), and † Department of Geological Sciences, Cornell University, Ithaca, New York 14853, USA ‡ Lamont-Doherty Geological Observatory, Palisades, New York 10964, USA

Nd isotope ratios substantiate the identification of oceanic crustal terranes within the continental crustal basement of the Aleutian island arc. The oceanic terranes are exposed in the westernmost Aleutians, but to the east, they are completely buried by isotopically distinct arc-volcanic rocks. Analogous oceanic terranes may be important components of the terrane collages that comprise the continents.

CONTINENTAL crust is a mosaic of structurally coherent terranes. Palaeomagnetic investigations have revealed that the terranes often originated within ocean basins, or at their margins, and travelled great distances before 'docking' at continental margins. The crust of the Aleutian island arc is analogous to that of many of these far-travelled terranes, and yet is simpler in structure, having not yet experienced the deformation and metamorphism which accompany terrane suturing. The Aleutian crustal building blocks are terranes themselves, and include oceanic crust, back-arc crust and subduction-related arc magmas. We show here that Nd isotope ratios are remarkably successful in identifying Aleutian terranes. We then define the lateral and vertical variations in Aleutian crustal architecture, and contrast a cross-section of oceanic (back-arc)-dominated crust in the western Aleutians with our previously documented¹ arc-magma-dominated crust in the eastern Aleutians.

Recent volcanic rocks

As a starting point, we note the isotopic homogeneity of Nd $(\varepsilon_{\rm Nd} = 7.30 \pm 1.25$; see Table 1 for definition) in a wide compositional spectrum of recent Aleutian volcanic rocks (see Figs 1, 2). This isotopic monotony contrasts with the distinctive chemical and mineralogical trends developed during the magmatic evolution of the volcanic rocks^{2,3}. Although there is no agreement as to how the Nd isotopic homogeneity was acquired⁴⁻⁸, for the present purpose it is more important to establish that the narrow range of ε_{Nd} that characterizes magmatically evolved Aleutian lavas was not acquired in the crust. To establish this we show that the same narrow range extends to minerals that have fractionated at depth from primitive (mantle-derived) magmas. For example, voluminous pyroclastic flows from Moffett volcano, Adak island, central Aleutians (Fig. 1), contain cumulate-textured xenoliths of mafic and ultramafic composition⁹. The xenoliths are mid-crustal crystalline wall rocks of dykes that carried the magmas to the surface. The xenoliths represent magma compositions ranging from olivine tholeiite (capable of precipitating Ni-rich ölivine, Cr-rich clinopyroxene and Cr-rich amphibole, the cumulate minerals of xenolith MM76-102)9 to andesite (capable of precipitating clinopyroxene, amphibole and plagioclase, the cumulate minerals of the least magnesian xenolith, MM76-10)9. Nd isotope ratios of three of these xenoliths and the host andesite are the same (Table 1); thus ϵ_{Nd} is independent of crustal-level fractionation processes, and is characteristic of mantle-derived arc magmas. 10 Be, a cosmogenic nuclide (half-life 1.5 Myr) which is present in young volcanic rocks of the arc, is also present in the most mafic of the xenoliths, MM76-102¹⁰ (the only Moffett xenolith analysed so far). From the standpoint of tectonics, an Aleutian cross-section would include these volcanic and plutonic rocks in the same terrane.

As a second example, ultramafic (olivine-clinopyroxene) xenoliths from Moffett's sister volcano Adagdak (see Fig. 1) are

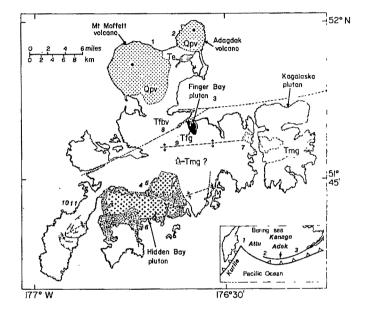


Fig. 1 Generalized geological map of Adak island⁴⁰, in the Central Aleutian island arc. For the Hidden Bay pluton, distribution of more silicic (>60% SiO₂, 'granodiorite') interior and less silicic (<60% SiO₂ 'diorite') exterior is after ref. 41. The plutons intrude the Finger Bay Volcanics (areas with no symbol on the map). Adak xenolith localities are Mt Moffett (51°58.01′ N, 176°43.55′ W, locality 1) and Mt Adagdak (51°58.78′ N, 176°37.36′ W, locality 2). These and numbers 3-11 refer to the location of samples listed in Table 1. The generalized inset map shows the locations of Attu, Kanaga and Adak islands and of the Komandorski back-arc basin (1), Amchitka Island (2) and Unalaska Island (3). Tooth marks indicate the trench segments that have associated active volcanoes.

ductilely deformed tectonites 9,11 . The $\varepsilon_{\rm Nd}$ values of one of these tectonites is +7.2 (Table 1), and it contains small amounts of ¹⁰Be (ref. 10). Thus, we infer that the tectonites are geochemically related to the magmas of the recent volcanoes. On a tectonic cross-section, we infer that the deformation (which by textural arguments occurred at high temperature) is recent, and thus represents an active tectonic feature of the arc. We have proposed^{1,11,12} that the rocks are early-stage cumulates of arc magmas that reside in the sub-arc asthenosphere, which extends to depths as shallow as the Moho under the present arc. Stated in tectonic language, the brittle-ductile transition has reached shallow (Moho) levels directly under the Aleutian arc (see Fig. 3a). Note that the ε_{Nd} values for recent Aleutian volcanic rocks are higher than those for many other arcs with older continental basement, and apparently these high values extend to the Kurile Arc, based on two analyses (Table 1) which are within the narrow range of the Aleutian values.

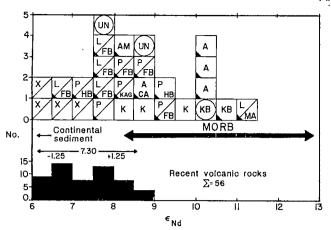


Fig. 2 Histogram of ε_{Nd} values of Aleutian volcanic and plutonic rocks^{18,24}, plotted relative to a BCR-1 ε_{Nd} value of -0.4 (ref. 7). \square , Adak: L, lava (FB, Finger Bay; MA, magnesian andesite); X, xenolith; P, pluton (KAG, Kagalaska; HB, Hidden Bay; FB, Finger Bay). K, Kanaga xenoliths; AM, Amchitka pluton; \square , Unalaska pluton; A, Attu (CA, calc-alkaline); KB, Kamchatka basin. L, LDGO; \square , literature. Recent volcanic rocks $6^{-8,14,15,24,42,43}$, mid-ocean-ridge basalts (MORB)^{30,31}, Unalaska pluton (Captains Bay, ref. 24) and Komandorski basin basalt are all from the literature. (Other analyses, including an independent analysis of the Komandorski basin basalt, are listed in Table 1.) Note the coincidence of: (1) Attu island lavas and Komandorski basin basalt; (2) Finger Bay lavas (early Tertiary) and 56 Recent volcanic rocks; (3) Adak xenoliths (from Moffett and Adagdak volcanoes) and Recent volcanic rocks plot between recent volcanic rocks and the Attu-Komandorski basin lavas. We interpret the rocks with intermediate ε_{Nd} as geochemical hybrids.

A singular lava

It has been known for some time that lavas of the Aleutian arc have variable Sr and Pb isotopic compositions 13,14 . The most isotopically extreme lava comes from a thick, magnesian andesite flow or sill at the base of Mt Moffett (Fig. 1). It has very non-radiogenic Sr and Pb (ref. 14) and very radiogenic Nd ($\varepsilon_{\rm Nd} = +11.3$ (ref. 15; see Table 1), a value which is at the high end of the mid-ocean-ridge basalt (MORB) range (Fig. 2)). This lava also differs in its trace element content from all other Aleutian lavas analysed so far 14. We infer that a region under the main volcanic arc, but at unknown depth, has MORB-like character. Some possibilities are: the subducted oceanic crust (but without isotopic or trace element contamination from hydrothermal alteration by sea water), the overlying asthenosphere, or even, as we will see, the crustal or mantle lithosphere.

Older magmatic rocks

The magmatic history of the Aleutian arc reaches back to the early Tertiary¹⁶⁻¹⁹. On Adak island, the early volcanic and volcaniclastic rock units, mapped as the Finger Bay Volcanics (Fig. 1), are cut by plutons of several ages. On the westernmost Aleutian Islands (Attu and the other Near Islands) and the Komandorski Islands there are no active volcanoes (plate motion up to ~5 Myr ago was nearly strike-slip)20, but there are excellent exposed sections of Tertiary volcanic rocks, cut by intrusives 18,21. Isotopic contrasts between the Tertiary lavas of Adak and Attu¹⁸ constitute our first indication that the Aleutian arc crust is not comprised entirely of arc magmas of the type that are erupting today. The early Tertiary (40Ar/39Ar crystallization ages >50 Myr¹⁸) Finger Bay volcanics from Adak have the same ε_{Nd} as recent Aleutian volcanic rocks (see Fig. 2). In contrast, the earliest volcanic rocks on Attu (probably 20-30 Myr in age)¹⁸ have higher ε_{Nd} (well within the range of mid-ocean-ridge or back-arc-basin basalt; see Fig. 2) than any magmatic rocks of any age in the arc (except, as always, the

Mg-andesite from Adak). However, not all Attu lavas have high $\varepsilon_{\rm Nd}$. A hornblende andesite representing the volumetrically minor, youngest (Miocene) volcanic rocks on Attu has ε_{Nd} that is in the range (within error) of values of recent volcanic rocks. These data from Attu can be explained either by evolution of magmas from high to low ε_{Nd} during the Tertiary, or by an origin of the earliest Attu magmas in a back-arc setting. A third alternative, origin at a mid-ocean ridge, is not consistent with recent syntheses of the plate kinematics of the North Pacific^{22,23}. The apparent invariance of ε_{Nd} with age over the same time period (30 Myr) on Adak and Unalaska^{18,24} (an eastern Aleutian island; see Fig. 1) argues against isotopic evolution of the arc from high to low ε_{Nd} (ref. 7). The similarity of the oldest Attu lavas and a Miocene back-arc lava from the Komandorski basin (Table 1), not only in ε_{Nd} but in Sr isotope ratio⁷ and a wide range of lithophile elements (in particular, the rare earths)¹⁸ supports our proposal that the Attu section represents lavas and interbedded cherts and turbidites from a back-arc basin analogous to the younger Komandorski basin. Subsequently, these 'basement' rocks were intruded by subduction-related dykes, and in places they are overlain by basaltic and andesitic lavas fed by the dykes, but this arc-related magmatism is minor in volume.

Some units of plutons that intrude the Finger Bay Volcanics on Adak (see Fig. 1) have $\varepsilon_{\rm Nd}$ values which are slightly higher than those of the highest- $\varepsilon_{\rm Nd}$ volcanic rocks (see Fig. 2). Within both the Hidden Bay and Finger Bay pluton it is the most mafic samples (the gabbros) that have these high $\varepsilon_{\rm Nd}$ values. McCulloch and Perfit's²⁴ analyses of an Unalaska pluton show the same trend. The variability within the plutons indicates a heterogenous source, or mixing of igneous rocks from more than one source. It is somewhat perplexing that the most mafic lavas do not show this tendency towards high $\varepsilon_{\rm Nd}$. We believe that this is the first indication that the volcanic and plutonic rocks are petrogenetically distinct. We tentatively identify the high- $\varepsilon_{\rm Nd}$ end-member as oceanic crust buried within the arc crust.

Crustal and mantle tectonites

A remote cluster of later Tertiary basaltic intrusives on the magmatically inactive southern part of Kanaga Island (~30 km west of Adak) has yielded mafic and ultramafic xenoliths which contrast strongly with those from Adak (discussed above). To the previously documented mineralogical contrasts²⁵⁻²⁹, most obviously the fact that they are amphibole-free, unlike their Adak counterparts, we now add a contrast in ε_{Nd} . Both mafic and ultramafic tectonites have higher ε_{Nd} than the Adak cumulate and tectonite xenoliths. The highest value ($\varepsilon_{Nd} = +9.6$) lies well outside the range of Aleutian lavas, and within the range of both mid-ocean-ridge and back-arc-basin basalts30,31. But the xenoliths are clearly not pieces of the subducted oceanic plate (from 100 km depth), for their mineralogy indicates equilibration at much shallower depths, within the spinel lherzolite stability field or shallower (for the plagioclase-bearing but garnet-free mafic granulites) We have proposed that the xenoliths originated as buried pieces of oceanic or back-arc lithosphere. They have been almost completely recrystallized and therefore retain few textural or mineralogical clues to their origin. They also appear to be hybrids: they are geochemically intermediate between arc and MORB types. Assimilation of some of this hybridized lithosphere by arc magmas may account for the unusually high ε_{Nd} of some of the plutons, noted above.

By analogy, this interpretation finds some support in a study of ophiolites. In the Troodos ophiolite³¹, a range of ε_{Nd} values can be interpreted as reflecting two-component mixing (although at a depth greater than that envisioned here) between a MORB-like ($\varepsilon_{Nd} \ge +8$) and a continental-crustal (ε_{Nd} negative) source. The Sr isotopic composition of the Troodos ophiolite rocks varies widely (87 Sr/ 86 Sr ranges from 0.70415 to 0.70705), and is independent of the Nd isotopic values. Much the same can be

Table 1 Isotopic results from the Aleutian arc								
Rock type	Locality* (ref.)	¹⁴³ Nd/ ¹⁴⁴ Nd (Laboratory)†	ε _{Nd} ‡	Nd (p.p.m.)	Sm (p.p.m.)	⁸⁷ Sr/ ⁸⁶ Sr†	Rb (p.p.m.)	Sr (p.p.m.)
Cumulate xenoliths, Moffett volcano,								
Adak								
MM76-102 olivine-clinopyroxene	1 (9)	0.512170 (14) (C)	6.31 ± 0.28	8.5	2.0	0.703119 (25)	4.91	246
MM-DK olivine-hornblende gabbro	1 (9)	0.512198 (21) (C)	6.86 ± 0.42	3.6	1.1	0.703270 (33)	3.20	469
MM76-10 hornblende gabbro	1 (9)	0.512165 (18) (C)	6.22 ± 0.35	8.36	1.95	0.703309 (33)	5.53	426
ADK54 host lava	1 (9)	0.512984 (17) (L)	6.20 ± 0.34	8.23	2.66	0.702998 (42)		745
Tectonized Xenoliths, Adagdak volcan	0,							
	2 (11)	0.512215 (16) (C)	7.19 ± 0.31	1.33	0.64	0.703355 (63)	0.103	31.3
ADAG81-DR clinopyroxenite	2(11)	0.312213 (10) (C)	7.19±0.31	1.33	0.04	0.705555 (05)	0.103	51.5
Arc lavas	(8)	0.512218 (15) (C)	7.24 ± 0.30	19.2	4.14	0.703130 (38)	34.7	596
B11/538 (Chirinkotan volcano)	-(§)	0.312218 (13) (C)	1.24 ± 0.30	19.2	4.14	0.703130 (36)	34.1	370
Kurile basalt	- (§)	0.512242 (10) (C)	7.74 ± 0.35	23.0	6.8	0.70287	34.3	518
116/81 (Bogdan Khmelnitskii	-(8)	0.512243 (18) (C)	7.74±0.33	23.0	0.0	0.70267	J-7.J	310
Volcano, Itirup)								
Kurile basalt	1 (14 15)	0.612044 (00) (1.)	11.3 ± 0.43	33.0	5.7	0.702795 (31)	16.4	1,780
ADK 53 Aleutian andesite	1 (14, 15)	0.513244 (22) (L)	11.3 ± 0.43	33.0	3.7	0.702793 (31)	10.4	1,760
Komandorski basin	T (20)	0.512210 (22) (7.)	106+044	14.1	4.65	0.70289 (3)	7.3	173
DSDP191 basalt	Inset (38)	0.513210 (22) (L)	10.6 ± 0.44	14.1	4.03	0.70289 (3)	7.3	173
Arc plutons	2 (20)	0.612144 (10) (1)	02:020	12	2.1	0.70202 (2)	18	728
FB53 gabbro	3 (39)	0.513144 (19) (L)	9.3 ± 0.38	13	3.1	0.70303 (3)	25	753
FB97 gabbro	3 (39)	0.513095 (19) (L)	8.4±0.38	17	3.8	0.70326 (7)	58	733 514
FB61 monzodiorite	3 (39)	0.513125 (21) (L)	8.9 ± 0.42	38	7.7	0.70336 (4)		
HB7-10 gabbro	4 (41)	0.513152 (20) (L)	9.4 ± 0.40	12.8	3.51	0.70305 (5)	28	735
HB7-16 diorite	5 (41)	0.513062 (22) (L)	7.7 ± 0.44	12.2	2.94	0.70323 (4)	19	1,140
HB5-137 granodiorite	6 (41)	0.513032 (22) (L)	7.1 ± 0.44	40.5		0.70328 (4)	23	601
K7-32A granodiorite	7 (41)	0.513089 (21) (L)	8.3 ± 0.42	10.7	2.36	0.70350 (4)	41	730
AM33 granodiorite, Amchitka	-(18)	0.513098 (23) (L)	8.4 ± 0.46	14.9	3.64	0.70330(3)	26	400
Arc Lavas								
Tertiary, Adak								
LB8-10A basalt	8 (18)	0.513015 (25) (L)	6.8 ± 0.50	9.8	2.79	0.70332 (3)	9.7	523
LB80-39 basalt	9 (18)	0.513053 (17) (L)	7.6 ± 0.52	35.1	8.35	0.70316 (3)	53	526
BW8-R30 basalt	10 (18)	0.513061 (27) (L)	7.7 ± 0.54	27.2	6.29	0.70296 (3)	15.4	1,010
BW8-R36 basalt	11 (18)	0.513052 (17) (L)	7.6 ± 0.34	14.6	3.81	0.70306 (4)	14.3	900
Tertiary, Attu	_							
SB80-1A basalt	-(18)	0.513199 (18) (L)	10.4 ± 0.36	10.1	3.22	0.70357 (3)	4.9	183
H09-25B basalt	- (18)	0.513203 (17) (L)	10.5 ± 0.34	6.6	2.25	0.70369 (3)	11	313
H09-14B basalt	-(18)	0.513186 (22) (L)	10.1 ± 0.44	13.4	3.75	0.70281 (4)	4.3	229
AT80-32 andesite	-(18)	0.513114 (23) (L)	8.7 ± 0.46	11.1	2.70	0.70306 (4)	11	468
Tectonized xenoliths, Kanaga Island								
KAN80-6-5 peridotite	-(27)	0.512339 (19) (C)	9.62 ± 0.37	1.42	0.69	0.706427 (38)	0.74	39.0
KAN80-6-69 wehrlite	-(26)	0.512272 (23) (C)	8.31 ± 0.45	3.09	0.972	0.703843 (40)	0.318	30.6
KAN80-6-27 2-pyroxene granulite	-(28)	0.512286 (23) (C)	8.58 ± 0.44	1.89	0.70	0.703329 (50)	0.27	308

^{*} Localities refer to Fig. 1.

said for the Samail ophiolite³⁰, but with much smaller ε_{Nd} variation, and for the Kanaga xenoliths and the older Attu volcanic rocks (Table 1).

Tectonic cross-sections

The brief (55 Myr)^{18,19} history of the Aleutian island arc records the juxtaposition of several geochemically distinct terranes: oceanic and back-arc lithosphere occurring either at the surface (Attu) or buried under younger arc magmas (Kanaga); continent-derived sediment, with $\varepsilon_{\rm Nd}$ values near zero⁷, retained within the arc crust or added to it by off-scraping or subcretion^{32,33}; and subduction-related magmas intruded along an arc axis which has migrated northward during the Tertiary (see Fig. 1). The proportion of these terranes varies along the arc: a western Aleutian cross-section (near Attu) will have a higher proportion of oceanic lithosphere than one through the central Aleutians (near Adak). Further east, along the Alaska Peninsula we expect additional terranes, including isotopically distinct older continental crust and exotic lithospheric fragments carried

from far to the south³⁴. Sediment draping the flanks of the arc contains a variable proportion of erupted and eroded arc material representing the exposed terranes.

Figure 3a is a tectonic cross-section of the central Aleutian arc¹, which applies more specifically to the Adak-Kanaga region. A second section (Fig. 3b), representing the Attu region (consistent with shallow, thrust-mechanism seismicity, Fig. 3c)^{35,36} looks quite different. Here, we postulate that structural thickening of the crust by nearly arc-parallel thrusting is necessary to elevate the back-arc oceanic crust now exposed at the surface. We find very little arc-related magmatism that could build the crust up from abyssal depth to sea level over the past 30 Myr.

Note, in Fig. 3a, that the oceanic or back-arc crustal section (and in particular the sediment associated with it) is completely recrystallized during arc-related deformation and heating. It has also been intruded by arc magmas (it was an arc magma that carried xenoliths of the section to the Earth's surface on Kanaga island). The arc magmas have variably contaminated the

[†] C, CIT; L, LDGO. Analytical procedures are described in refs 7 (CIT) and 15 (LDGO). Sr and Nd isotope analyses were performed in the same laboratory.

[†] $\varepsilon_{Nd} = [((^{143}Nd/^{144}Nd)_{sample (t)}/(^{143}Nd/^{144}Nd)_{bulk Earth (t)}) - 1] \times 10^4$. For all analyses, ε_{Nd} of BCR-1 standard was taken to be -0.4, measured $^{143}Nd/^{144}Nd$ values were: CIT, 0.511826; LDGO, 0.512645. Direct comparison of samples: DSDP191, CIT, +10.2; LDGO, +10.6. For both CIT and LDGO, $^{87}Sr/^{86}Sr$ was normalized to $^{86}Sr/^{88}Sr = 0.1194$.

[§] Quaternary lavas; A. Tsvetkov, personal communication.

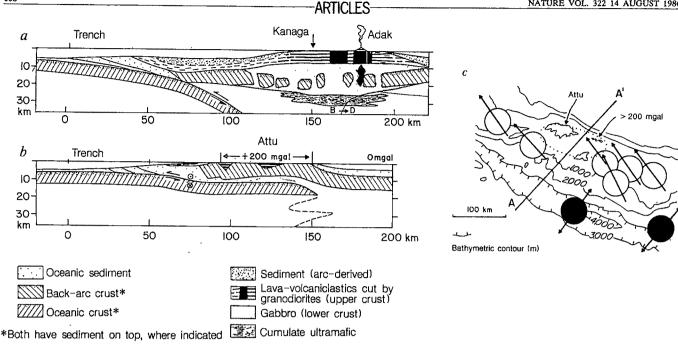


Fig. 3 a, b, Tectonic cross-sections of the central and western Aleutian arc (no vertical exaggeration). a, Section in the region of Adak and Kanaga (Fig. 1); near-surface tectonic features are after refs 44-46. Oceanic terranes are represented by symbols on the left, subduction-related terranes by those on the right. Geometry of lower-crustal terranes after ref. 1. Projected positions of Adak and Kanaga xenolith localities are shown, as is the present position of the brittle-ductile transition (B + D). Migration of the brittle-ductile transition away from the trench in the Tertiary is inferred from the deformation of mantle and lower crustal xenoliths from Kanaga island. b, Cross-section along A-A' in map c. Crustal imbrication is inferred from earthquake mechanisms, from the paucity of arc-related igneous rocks, and from the extensive sections of back-arc-related volcanic rocks exposed on the surface of the islands. c, Map view of Attu region, showing earthquake mechanisms 35,36 and extent of +200 mgal free-air gravity anomaly³⁷.

xenoliths (and the deep crust of the arc), yet not to the extent of erasing their Nd isotope signature. From textural studies, it appears that some mineralogical vestiges of a pre-contamination condition exist²⁶⁻²⁹.

How much crustal contamination of arc magmas by buried hydrothermally altered oceanic crust (including sediment) occurs? We may speculate that water makes melting relatively easy and that the buried oceanic crust should contribute disproportionately to the arc magma contamination. The constant $\varepsilon_{\mathrm{Nd}}$ (and ⁸⁷Sr/⁸⁶Sr) of the Moffett cumulate-textured xenoliths (see Table 1) is important in this context, for with contamination, $\varepsilon_{\rm Nd}$ and $^{87}{\rm Sr}/^{86}{\rm Sr}$ should be dependent on fractionation stage (as they apparently are for the plutons). Despite our published opinion to the contrary4,14, we suggest that the trapped oceanic crust may melt to yield the enigmatic, high-ε_{Nd} Mg-andesites, and may yield a high- ε_{Nd} component for Tertiary plutons.

In Fig. 3b, we correlate the shallow, thrust-mechanism earthquakes^{35,36} (Fig. 3c) with oblique intracrustal thrusting (parallel to the trench). We have indicated intracrustal thrusting at the interfaces between imbricated oceanic and back-arc crustal sections. These interfaces will act as strain guides, because of the presence of both water (hydrothermal alteration) and sediment. The interfaces are also the likely intrusion sites for the small amounts of arc-related intrusives. Shallow structural imbrication of oceanic and back-arc crust, (perhaps including oceanic plateaus) is consistent with a +200 mgal free-air gravity anomaly and the high gravity gradient in the region³⁷. Note that immediately west of Attu, the arc crust is very much thinner and deeper. In our interpretation, Attu represents a structural culmination of arc-parallel oblique thrusting.

Discussion

The identification of geochemically coherent terranes within the Aleutian arc lithosphere provides a rational and useful framework for consideration of the chemical controls on arc tectonics ('chemotectonics'). The creation of mixed terranes by erosion and magmatic assimilation should also be well described within this framework, as should the comparison of the Aleutians and other arcs. The structural response of various levels in the arc lithosphere to the stress regimes within a convergent plate margin will be controlled by water, and to a lesser degree by rock type within the arc crust. We note specifically the potential role of trapped hydrothermally altered oceanic crust at midcrustal levels and its potential role as a strain guide (see Fig. 3b). This makes plausible the coincidence of major geochemical and tectonic boundaries within the arc crust.

We thank G. J. Wasserburg for hospitality and access to the Lunatic Asylum, and A. Zindler for access to the LDGO isotope laboratory. H. Ngo assisted R.W.K. at CIT. Research support is from NSF (R.W.K., S.M.K., G.J.W., A. Zindler) and NASA (G.J.W.). This is INSTOC contribution 45.

Received 10 February; accepted 13 June 1986.

- 1. Kay, S. M. & Kay, R. W. Geology 13, 461-464 (1985).
- Kay, S. M., Kay, R. W. & Citron, G. P. J. geophys. Res. 87, 4051-4072 (1982).
 Kay, S. M. & Kay, R. W. Contr. Miner. Petrol. 90, 276-290 (1985).
- Kay, R. W. J. Geol. 88, 497-522 (1980).
 Perfit, M. R. & Kay, R. W. Geochim. cosmochim. Acta 50, 477-481 (1986).
- Morris, J. D. & Hart, S. R. Geochim. cosmochim. Acta 47, 2015-2030 (1983)
- VonDrach, V., Marsh, B. D. & Wasserburg, G. J. Contr. Miner. Petrol. 92, 13-34 (1986). White, W. H. & Patchett, J. Earth planet. Sci. Lett. 67, 167-185 (1984).
- Conrad, W. K. & Kay, R. W. J. Petrol. 25, 88-125 (1984).
- Tera, F. et al. Geochim. cosmochim. Acta (in the press).
- DeBari, S., Kay, S. M. & Kay, R. W. J. Geol. (in the press).
 Swanson, S., Kay, S. M., Brearley, M. & Scarfe, C. in Mantle Xenoliths (ed. Nixon, P. H.) (Wiley, New York, in the press).
 Kay, R. W., Sun, S.-S. & Lee-Hu, C.-N. Geochim. cosmochim. Acta 42, 263-273 (1978).
 Kay, R. W. J. Volcanol. geotherm. Res. 4, 117-132 (1978).
 Goldstein, S. thesis, Columbia Univ. (1985).

- Borsuk, A. M. & Tsvetkov, A. A. Int. Geol. Rev. 24, 317-327 (1982).
 Kay, R. W., Rubenstone, J. L. & Kay, S. M. Abstr. 27th int. geol. Congr. Vol. 3, 252 (Izdatelstvo Nauka, Moscow, 1984).
- Rubenstone, J. L. thesis, Cornell Univ. (1984).
 Scholl, D. W., Vallier, T. L. & Stevenson A. J. Geology 14, 43-47 (1986).
 Cox, A. & Engebretson, D. Nature 313, 472-474 (1985).
- 21. Gates, O., Powers, H. A. & Wilcox, R. E. Bull. U.S. geol. Surv. 1028U, 709-822 (1971).

- Engebretson, D., Cox, A. & Gordon, R. J. geophys. Res. 89, 10291-10310 (1984).
 Rea, D. & Duncan, R. A. Geology 14, 373-376 (1986).
 McCulloch, M. T. & Perfit, M. R. Earth planet. Sci. Lett. 56, 167-179 (1981).

- 25. DeLong, S. E., Hodges, F. N. & Arculus, R. J. J. Geol. 83, 721-736 (1975).
- 26. Johnston, L. thesis, Cornell Univ. (1983).27. Pope, R. thesis, Cornell Univ. (1983).
- 28. Kay, S. M., Johnston, L. & Kay, R. W. Geol. Soc. Am. Abstr. Progm. 15, 603 (1983). 29. Pope, R. S., Kay, S. M. & Kay, R. W. Eos 62, 1092 (1981).
- McCulloch, M. T., Gregory, R. T., Wasserburg, G. J. & Taylor, H. P. Earth planet. Sci. Lett. 46, 201-211 (1980).
- McCulloch, M. T. & Cameron, W. E. Geology 11, 727-731 (1983)
- 32. Karig, D. L. & Kay, R. W. Phil. Trans. R. Soc. A301, 233-251 (1981).
 33. Kay, R. W. Tectonophysics. 112, 1-15 (1985).
- 34. Stone, D. B. & Packer, D. R. Tectonophysics 37, 183-201 (1977).

- Cormier, V. Geol. Soc. Am. Bull. 86, 443-453 (1975).
 Newberry, J., LaClair, D. L. & Fujita, K. J. Geodyn. (in the press).
 - 37. Bowin, C., Warsi, W. & Milligan, J. Geol Soc. Am. Map Ser. MC-45 (1981) 38. Kay, R. W. & Hubbard, N. J. Earth planet. Sci. Lett. 38, 95-116 (1978)
- 39. Kay, S. M., Kay, R. W., Bruecker, H. K. & Rubenstone, M. L. Contr. Miner Petrol 82, 99-116 (1983).
- 40. Fraset, G. D. & Snyder, G. L. Bull. U.S. geol. Surv. 1028-M, 371-408 (1959)
- 41. Citron, G. thesis. Cornell Univ. (1980).
- 42. DeLong, S. E., Perfit, M. R., McCulloch, M. T. & Ach, J. J. Geol. 93, 609-618 (1985).
 43. Nye, C. & Reid, M. J. geophys. Res. (in the press).
- 44. Scholl, D. W., Vallier, T. L. & Stevenson, A. J. Am. Mem. Am. Ass. Petrol. Geol 34, 413-439
- Scholl, D. W., Vallier, T. L. & Stevenson, A. J. Geology 14, 43-47 (1986).
 Engdahl, E. R. & Billington, S. Bull seism. Soc. Am. 76, 77-93 (1986).

Bovine papillomavirus genome elicits skin tumours in transgenic mice

Mark Lacey, Susan Alpert & Douglas Hanahan

Cold Spring Harbor Laboratory, Cold Spring Harbor, New York 11724, USA

Transmission of the bovine papillomavirus-1 (BPV-1) genome through the mouse germ line results in the heritable formation of fibropapillomas of the skin, a tissue-specific phenotype analogous to that observed in natural BPV-1 infection of cattle. Oncogenesis is slow, with tumours first arising at 8-9 months of age, usually in areas prone to wounding. Extrachromosomal BPV-1 DNA is detected in all tumours, whereas normal tissues show only integrated DNA.

BOVINE papillomavirus 1 (BPV-1) is an icosahedral virus which infects cutaneous tissues of cattle and induces benign fibropapillomas with proliferative squamous epithelial and dermal fibroblast components^{1,2}. The BPV-1 genome is circular doublestranded DNA of ~8 kilobases (kb). The virus infects both dermal fibroblasts and epidermal epithelial cells, where the BPV-1 genome replicates as an autonomous plasmid, inducing proliferation of both cell types. Virus particles are produced only in terminally differentiated epidermal keratinocytes, where the BPV-1 DNA replicates to a very high copy number (about. 10,000 copies per cell). In contrast, the copy numbers range from 50 to 500 per cell in the proliferating dermal fibroblasts and in the squamous epithelial cells of the lower epidermis. BPV-1 shows a broad experimental host range; it has been shown to infect horses, hamsters and one inbred strain of mouse (C3H_eB). Infection of these heterologous species results in the development of fibroblastic tumours, generally at the site of infection/inoculation, but without the subsequent production of infectious virus particles.

The genetics of BPV-1 replication and transformation have been studied principally in cultured murine cells^{1,2}. BPV-1 replicates as a stable extrachromosomal element in a variety of cultured mouse fibroblasts, and is able to morphologically transform a cell line (C127) derived from a murine mammary tumour. as well as NIH 3T3 cells. The necessary cis- and trans-acting elements for both transformation and replication have been localized to a fragment which comprises 69% of the viral genome, given that the genetic assay is restricted to a few established cell lines.

In the present study we have sought to address the properties of the BVP-1 genome when transmitted through the mouse germ line, in order to assess the ability of BPV to replicate in and transform murine cells in the context of its stable presence in every cell of the animal.

Generation of transgenic mice

The bovine papillomavirus genome was injected into fertilized mouse embryos as a SalI-linearized plasmid clone, which is shown in Fig. 1. The plasmid (called pBPV1.69) carries a partial tandem duplication of the complete BPV-1 genome. This configuration was used for two reasons: first, to provide an

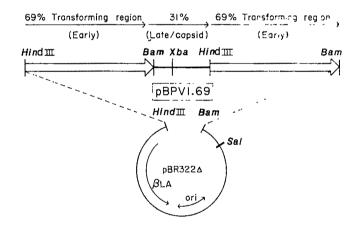


Fig. 1 Structure of the plasmid pBPV1.69. Two copies of the 69% transforming region (HindIII-Bam) of BPV-1 are separated by the 31% 'late' region, thereby generating a reiterated copy of the intact BPV-1 genome-a 100% fragment plus an additional copy of the 69% transforming region.

Methods. The plasmid pBV1.69 was linearized by digestion with Sall, purified by phenol and chloroform/isoamyl alcohol extraction, and ethanol precipitation. The concentration was adjusted to ~1,000 ng ml⁻¹ before injection into fertilized one-cell embryos, which were implanted into pseudopregnant female mice and allowed to develop. The embryos were derived from intercrosses of (C57BL/6J \times DBA/2J) F_1 hybrid mice, and thus were F_2 hybrids The one transgenic mouse (M120) which survived to sexual maturity was backcrossed to C57BL/6J females, and subsequent generations were either intercrossed to derive homozygotes, or backcrossed to C57BL/6J mice. The microinjections, embryo transfers and DNA analyses were performed essentially as described else-

uninterrupted colinear copy of the genome, as is encountered in its normal circular configuration; second, to examine the possibility that BPV-1 could excise and replicate as an extrachromosomal element. Experiments with integrated simian virus 40 (SV40) genomes have demonstrated that partial tandem duplications facilitate precise excision by homologous recombination in conditions permissive for SV40 replication³⁻⁵. A previous study showed that when circular BPV-1 DNA was injected into mouse embryos, the transgenic mice which arose carried only integrated forms (F. Costantini, personal communication), suggesting that early mouse embryos are nonpermissive for BPV-1 plasmid replication. Thus in the present study we intended to create transgenic mice carrying integrated BPV-1 DNA in the germ line, but with a topology that might allow excision and extrachromosomal replication in somatic tissues.

Two transgenic mice arose from embryos injected with the linearized pBPV1.69 plasmid. One mouse (116) was born with limb deformities and died ~36 h after birth, and will not be discussed further. The second mouse (120) carried about five copies of the BPV1.69 plasmid, integrated in a head-to-tail tandem array. This mouse developed normally, was fertile, and trasmitted the acquired DNA as a single insertion in a mendelian fashion. Homozygotes were derived from intercross mating of siblings. No abnormalities were observed in either heterozygotes or homozygotes during the early breeding analysis.

Development of cutaneous tumours

Transgenic mice harbouring the pBPV1.69 insertion are phenotypically normal during development and early adult life. However, skin tumours begin to appear as the mice grow older. Tumours are first apparent at about 8 months of age, arise in multiple locations on the body, and eventually develop in almost every transgenic mouse in this lineage. In addition to obvious protuberant growths, large areas of the skin become abnormal, with thickening, hardening, and marked hair loss. Small wartlike protrusions are often scattered throughout areas of the abnormal skin. Tumours are most frequent in the face and head area, and on the ends of the tails of heterozygous mice, which were clipped at 3 weeks of age for DNA analysis. The tumours are initially benign, but can become malignant and locally invasive, although they have not been found to metastasize to other tissues. No examples of primary tumours arising in internal organs have been observed. Occasionally, mice become severely affected, with most of the skin becoming grossly abnormal, and multiple protuberant tumours developing on the face, neck, mouth, body and tail. There have been no examples of nontransgenic mice developing skin tumours, even following extended cohabitation with affected transgenic mice, which suggests that infectious BPV-1 virus is not being produced. This conclusion is supported by immunohistochemical analyses of affected tissues using antisera that recognize the BPV-1 capsid proteins, which have failed to detect these virion components (P. Howley, personal communication). Representative examples of the skin tumours which arise in these transgenic mice are shown in ref. 20.

Tumour pathology

Various protuberant tumours and abnormal skin were analysed after formalin fixation, standard tissue sectioning, and histochemical staining with haematoxylin and eosin: four examples are shown in Fig. 2, together with normal skin. In all cases, the affected tissues contained proliferating dermal fibroblasts, in rather disorganized sworls of densely packed cells. The obvious proliferation and disorganization of the dermal layer is characteristic of all tumours examined, and is almost always the major component of affected tissues. This characteristic is similar to that observed in dermatofibromas and fibromatoses which arise in humans⁶.

There are two different histopathologies observed in the epidermis of the affected tissues. Abnormal skin shows a grossly thickened dermal layer and an atrophic epidermis, with significant loss and disorganization of hair follicles and glands. The epidermis is only a few cells thick. One can speculate that the thickened and disorganized dermis (or the transformed state of the dermal fibroblasts) may somehow be impaired in its ability to provide the proper stratum or the required nutrients and growth factors for normal epidermal cell growth. Abnormal skin

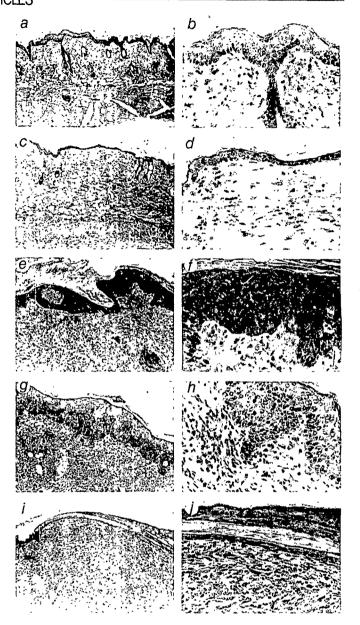


Fig. 2 Histological analysis of affected cutaneous tissue. In each case the tissue is shown at two magnifications, ×30 (left) and ×120 (right). a, b, Normal skin, with hair follicles and glands embedded in the dermis, and an epidermal layer of average size for body skin. c, d, Abnormal skin, showing hyperplasia of the dermal fibroblasts and thinning of the overlying epidermis, with loss of hair follicles and glands. e, f, Tumour at the tip of a tail, showing a disorganized and enlarged mass of dermal fibroblasts, and a hyperplastic epidermal layer. g, h, Facial tumour, with dermal fibroblast proliferation and thickening of the overlying epidermis. i., j, An anaplastic tumour, which arose on a hingleg, with multinucleated cells that are not readily identifiable as either dermal fibroblasts or epidermal epithelial cells. Tissues were excised and fixed in 10% formalin, after which they were embedded in paraffin, and thin sections taken. The sections were stained with haematoxylin and eosin in a standard histochemical process.

also shows scattered small wart-like protrusions, which appear to be focal proliferations of melanocytes characteristic of blue nevus⁶.

The second class of abnormality seen in the epidermis is associated with protuberant tumours, where the epidermis shows considerable hyperplasia. The layer of keratinocytes appears unusually thick, and the cell types may be disorganized as well. Although the extent of epidermal hyperplasia is significant, it is less than the degree of dermal fibroblast proliferation. This

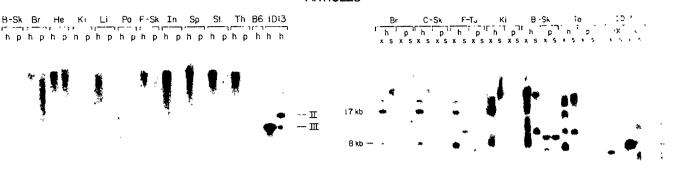


Fig. 3 BPV DNA in the tissues of a young mouse. Total DNA was isolated from a series of tissues, and fractionated into a high-M_r spooled portion (h) and a pellet fraction (p) composed of the low-M, DNA which did not spool. The DNAs were digested with SacI, which does not cut the pBPV1.69 plasmid. The DNAs were electrophoresed through a 0.5% agarose gel, transferred to nitrocellulose, and hybridized to a radiolabelled BPV plasmid. The tissues analysed are body skin (B-Sk), brain (Br), heart (He), kidney (Ki), liver (Li), pancreas (Pa), facial skin (F-Sk), small intestine (In), spleen (Sp), stomach (St) and thymus (Th). Additional tissues examined but not shown include testes, tail, body wall, lung and skeletal muscle. ID13 is a BPV-transformed C127 cell line containing ~400 copies of episomal BPV DNA. B6 is C57BL/6J DNA (from a normal mouse, which lacks BPV sequences). The positions of the relaxed circular and linear forms of extrachromosomal BPV are indicated (forms II and III, respectively). High-M, ID13 DNA (h) was digested with Xba (left- or Sac (right), to either linearize the resident BPV genome or leave it untouched.

is in contrast to naturally occurring fibropapillomas in cattle, where the dermal fibroblast and epidermal components are approximately equally represented. There are several possible explanations for this difference. One is that the penetrance of the BPV-1 oncogenes is different in two cell types, being more effective in the dermal fibroblasts than in the squamous epithelial cells; this assumes that the epithelial proliferation is a direct result of BPV-1 gene expression. A second possibility, however, is that the epidermal response is reactive to the dermal proliferation, and is not induced directly by a BVP-1-encoded function. Conversely, a third possibility is that BPV-1 gene expression in the epidermis is directing the fibroblast proliferation. The examination of these possibilities will require separate analysis of the two tissue layers.

BPV-1 genome in normal and tumour tissues

The structure and form of the BPV-1 genome has been examined in a variety of tissues in both young normal mice and in older tumour-bearing mice. In view of the possibility that BPV excises and replicates as an episome, the analysis was designed to detect free copies of the BPV genome. DNA from each tissue was separated into low- and high-relative molecular mass (M_r) fractions, which were then digested with restriction enzymes that cleave the BPV-1 genome either once (XbaI) or not at all (SacI). The SacI digestion should leave the pBPV1.69 plasmid in a fragment of very high M_r (>85 kb), composed of the head-to-tail tandem array (of about five copies) that was produced during integration after microinjection of the original embryo. In contrast, free copies of BPV-1 DNA should migrate on gels in the 8-kb range.

Figure 3 shows an example of a DNA blotting analysis of tissues in a young mouse, ~ 6 weeks old. No hybridizing bands were observed in the SacI digests of either high- or low- M_r fractions of any tissue. In comparison, the ID13 cell line, which is transformed by BPV DNA, shows 8-kb bands, demonstrating the presence of extrachromosomal DNA. This and similar analy-

Fig. 4 BPV DNA in a tumour-bearing mouse. Mouse 907 carried a facial tumour, a tail tumour growth and an area of affected skin, with substantial hair loss and dermal thickening. Tissues were collected, and DNAs extracted and analysed as described in Fig. 3 legend. The tissues analysed are brain (Br), facial tumour (F-Tu), cheek skin near the facial tumour (C-Sk), kidney (K1), abnormal body skin (B-Sk), and tail with tumour (Ta). Both spooled (h) and pellet (p) fractions were digested with either Xbal (X) or Sacl (S). Kidney DNA was applied to this analysis in a fourfold greater amount than the other tissues examined, to verify the lack of appreciable rearranged or extrachromosomal DNA in normal tissue. The positions of the three forms of extrachromosomal BPV-1 in ID13 cells are indicated by I (supercoiled), II (relaxed circular) and III (linear). Digestion with XbaI, which cuts once within the 31% fragment of BPV, should release the full-length 17-kb pBPV1.69 plasmid from the integrated concatenate, as well as linearize the 100% BPV circular form (7.9 kb) that would be released by homologous recombination across the reiteration in the plasmid. The 8-Kb band in the Xba digests of brain and cheek skin represents a rearranged copy of the input 17-kb BPV 1.69 plasmid that releases this fragment (the 100% BPV genome) from the integrated concatenate (data not shown), which was apparently produced by recombination between injected molecules during integration.

ses have shown that the BPV genome does not undergo detectable excision events in the tissues of young transgenic mice, including the skin, where tumours will arise in later life. When these same DNAs were digested with restriction enzymes that cleave the pBPV1.69 plasmid, an identical pattern was observed in every tissue; this pattern is consistent with the plasmid being present as a stable head-to-tail concatenate in high- M_r DNA (not shown).

In contrast, the analyses of mice bearing tumours revealed rearrangements in the BPV genome in all affected tissues. Figure 4 presents the analysis of one such mouse. The low M_c DNA fractions in a facial tumour, a tail tumour and abnormal skin all show free copies of BPV-1. Comparison with the unit-length BPV-1 genome maintained in cultured mouse C127 cells indicated that the episomes are predominantly full-length BPV, presumably arising from precise excision from the integrated DNA. Most of the extrachromosomal copies migrated as relaxed circular or linear DNAs (forms II and III, respectively). It is not clear whether this represents the authentic condition in the tumour cells, or rather results from the DNA isolation and Sacl digestion, which was performed to facilitate migration of high- M_r DNA in the agarose gel. Some DNAs showed additional bands which may represent the excision of the BPV/plasmid recombinant, which is also duplicated as a consequence of the head-to-tail integration observed in early embryos. The spooled high-M, fractions of the affected tissues also showed amplified BPV DNA. In skin, it seems that both free copies and in situ integrated copies contribute to the amplification. Again, normal tissues, incuding facial skin, show no amplified, rearranged or

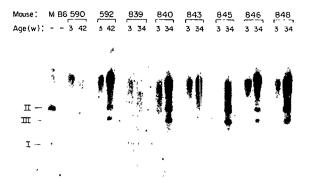


Fig. 5 Correlation between tumours and episomes. Tail DNAs were isolated from eight mice at both 3 weeks and 9-10 months old. Five of these mice (592, 840, 845, 846 and 848) had a tumour on the tip of the tail, while the other three appeared normal. The DNAs were digested with SacI and analysed as described for Figs 3, 4. The marker lane (M) contains DNA from the ID13 cell line, which contains episomal BPV: the supercoiled, relaxed circular and linear forms are indicated. B6 is C57BL/6J DNA, which does not contain BPV sequences.

free DNA. This was particularly apparent in the analysis of the kidney DNA, which was used at about a fourfold higher DNA concentration. Examination of the SacI digest revealed no extrachromosomal copies of the BPV-1 genome, and the XbaI digest was comparable to (although more intense than) brain or normal skin.

Analysis of a number of affected mice bearing protuberant tumours and abnormal skin has revealed a correspondence between the tumours and the presence of free copies of the BPV-1 genome in the DNAs of those tumours; a pertinent example is shown in Fig. 5, in which the tail DNAs of several mice are analysed. The tails were originally clipped at 3 weeks old, to assess transmission of the transgene. At approximately 10 months of age, an additional portion of the tail from each mouse was removed, and the DNAs were subjected to the blotting analysis described above. Five mice were seen to have free copies of the BPV-1 genome in their tail tissue at 10 months of age, while none had any detectable levels at 3 weeks. These five mice had tumour growth on the tips of their tails, while their siblings did not. As in the results shown in Fig. 4, again there was a correspondence between free copies of the BPV-1 genome and the presence of abnormal tissue.

Genetic aspects of tumour development

The characteristics of tumour formation suggest that these transgenic mice will be useful in the study of secondary events which participate in oncogenesis. The presence of the BPV oncogenes is apparently insufficient, in that the tumours arise after a long latency. Furthermore, tumours occur most frequently in areas prone to wounding. There is precedent for irritation and wounding as cofactors in a variety of cancers, including BPV-induced fibropapillomas in cows^{1,2}, crown gall tumours in plants⁷, and Rous sarcoma virus-induced sarcomas in chickens⁸, as well as in experimental animal models of tumour progression9-11.

Thus, the BPV-1 genome can be considered to be a genetic predisposition to the induction of fibropapillomas of the skin, one which requires additional events before oncogenesis occurs. One prospective event might be the transcriptional activation of a dormant BPV genome, as this has been observed both in studies of BPV-1 transformation of cultured cells12, and in oncogenesis induced through persistent papillomavirus infection of the Brazilian rat¹³. In addition, there is a high incidence of BPV-1-induced tumours in cows grazing on bracken fern, which is tumourigenic in laboratory animals, and which may be acting as a cofactor in this natural oncogenesis¹⁴. The ability of carcinogens15 or prospective cellular (growth) factors16 to complement the BPV oncogenes in tumour development can be assayed directly using these transgenic mice.

In a previous study (R. Palmiter and R. Brinster, personal communication), 15 lines of transgenic mice harbouring the BPV 69% transforming region were generated and maintained for 10 months. No abnormalities were observed in any of these lineages, which suggests that either the topology of the BPV1.69 plasmid or the presence of the 31% portion of the BPV genome is important for the phenotype described here. Consistent with this possibility is the observation of Sarver et al. 17 that the complete genome is more efficient at transforming C127 cells than is the 69% fragment, as well as the recent studies of Lusky and Botchan¹⁸, which demonstrated that the 31% region contains a cis-acting element that stimulates efficient BPV plasmid replication in cultured cells.

Thus, transgenic mice provide a new model in which to study the tissue specificity of BPV gene expression, the activities of the BPV oncogenes, and the genetic requirements of the BPV-1 genome in eliciting neoplasia—in particular, the implications that either the 31% region, extrachromosomal replication, or gene amplification could be important for oncogenesis. The present results also presage similar application of this approach to human papillomavirus genomes.

We thank Peter Howley for many helpful discussions, for advice and analyses on tumour pathology and for comments on the manuscript; Dan DiMaio for the gift of the pBPV1.69 plasmid and for discussions during the initiation of this project; Richard Palmiter for discussions and comments on the manuscript: Jean Roberts, Mike Ockler and Dave Green for artwork and photography; and Marilyn Goodwin for preparing the manuscript. The research was supported by a grant from Monsanto Company, as well as by funds from the National Foundation for Cancer Research and the Leukemia Society of America.

Received 1 May; accepted 18 June 1986.

- Lancaster, W. D. & Olson, C. Microbiol. Rev. 46, 191-207 (1982).
 Pfister, H. Rev. Physiol. Biochem. Pharmac. 99, 111-181 (1984).
 Botchan, M., Topp, W. & Sambrook, J. Cold Spring Harb. Symp. quant. Biol. 43, 709-719 (1982).

- Schaffner, W., Topp, W. & Botchan, M. Alfred Benzon Symp. 13, 191-203 (1979). Hanahan, D., Lane, D., Lipsich, L., Wigler, M. & Botchan, M. Cell 21, 127-139 (1980). Lever, W. F. & Schaumburg-Lever, G. Histopathology of the Skin (Lippincott, London, 1983).
- 7. Stachel, S. E., Messens, E., Van Montagu, M. & Zambryski, P. Nature 318, 624-629 (1985).
- Dolberg, D. S., Hollingsworth, R., Hertle, M. & Bissell, M. J. Science 230, 676-678 (1985). Pozharisski, K. M. Cancer Res. 3824-3830 (1975).
- Marks, F., Bertsch, S., Grimm, W. & Schweizer, J. Carcinogenesis Vol. 2 (eds Slaga, T. J., Sivak, A. & Boutwell, R. K.) 97-116 (Raven, New York, 1978)
- 11. Konstantinidis, O. A., Smulow, J. B. & Sonnenschein, C. Science 216, 1235-1237 (1982).

- Konstantiniais, O. A., Smulow, J. D. & Somienscient, C. Science 219, 1237-1237 (1762).
 Amtmann, E. & Sauer, G. Nature 296, 675-677 (1982).
 Amtmann, E., Volm, M. & Wayss, K. Nature 308, 291-292 (1984).
 Jarrett, W. F. H., McNeil, P. E., Grimshaw, W. T. R., Selman, I. E. & McIntyre, W. I. M. Nature 274, 215-217 (1978).
- Hecker, E., Fusenig, N. E., Kunz, W., Marks, F. & Theilmann, H. W. (eds) Co-Carcinogenesis and Biological Effects of Tumor Promoters (Raven, New York, 1982).
 Sporn, M. B. & Roberts, A. Nature 313, 745-747 (1985).
- Sarver, N., Bryne, J.-C. & Howley, P. M. Proc. natn. Acad. Sci. U.S.A. 79, 7147-7151 (1982). Lusky, M. & Botchan, M. Proc. natn. Acad. Sci. U.S.A. 83, 3609-3613 (1986).
- 19. Hogan, B., Costantini, F. & Lacy, L. Manipulating the Mouse Embryo-A Laboratory Manual (Cold Spring Harbor Laboratory, New York, 1986).
 20. Hanahan, D., Alpert, S. & Lacey, M. Alfred Benzon Symp. 24 (in the press).

Looking for cosmic strings

Alexander Vilenkin

Physics Department, Tufts University, Medford, Massachusetts 02155, USA

Cosmic strings predicted in some grand unified theories can produce double images of distant galaxies and quasars¹⁻³, and it has been argued that some of the known double quasars may be due to strings²⁻⁴. To test this hypothesis, one can look for other characteristic effects of strings in the vicinity of double quasars, such as a discontinuous change of the microwave background temperature across the string^{3,5}, lines of double galaxies², and images of galaxies with a sharp edge4. In most of the previous work on the gravitational effects of strings it was assumed either that the string is static or that both the string and its velocity are perpendicular to the line of sight. Here I show that in more general configurations the expressions for the angular separation of double images and for the temperature discontinuity $\delta T/T$ across the string are modified by trigonometric and relativistic factors. More importantly, the line connecting the double images is not, in general, perpendicular to the apparent direction of the string (contrary to what one would naively expect). Although the analysis presented here is rather elementary, the results may nevertheless be useful for interpreting the observations.

We first consider the situation in the rest frame of the string. The metric of a straight static string is a conical space^{1,3}. It is locally flat, but has an angle deficit

$$\delta = 8\pi G\mu \tag{1}$$

where G is the gravitational constant and μ is the mass per unit length of string. This space can be obtained from a euclidean space by cutting out a wedge of angular width δ and identifying the exposed surfaces. The existence of strings can be consistent with the isotropy of the cosmic microwave background only if $G\mu < 10^{-5}$, and we shall assume this to be the case. The angular separation of double images due to a string is given by^{2,3}

$$\delta\varphi_0 = l(d+l)^{-1}\delta\sin\theta\tag{2}$$

where d and l are the normal distances from the observer and from the quasar to the string and θ is the angle between the string and the line of sight.

Strings are expected to move at relativistic speeds, the mean square velocity (in units of c, the speed of light) being $\langle v^2 \rangle = 0.5$ (with respect to local co-moving frames). Because only transverse motion of strings is observable, we shall assume that \mathbf{v} is perpendicular to the direction of the string. To find the angular separation between the images in the observer's frame, let \mathbf{k} and \mathbf{k}' be the four-dimensional wave vectors of the light waves (with frequencies ω and ω') corresponding to the two images, and consider the invariant $\mathbf{k} \cdot \mathbf{k}' = \omega \omega' [1 - \cos{(\delta \varphi)}] \approx 0.5 \ \omega \omega' (\delta \varphi)^2$.

consider the invariant $\mathbf{k} \cdot \mathbf{k}' = \omega \omega' [1 - \cos{(\delta \varphi)}] \simeq 0.5 \omega \omega' (\delta \varphi)^2$. In the rest frame of the string, S_0 , the two frequencies are equal: $\omega = \omega' = \omega_0$. In the observer's frame, S_0 , ω and ω' are slightly different because of the difference in the directions of \mathbf{k} and \mathbf{k}' . However, the difference is of the order of $\delta \varphi$ and can be neglected to the lowest order in $G\mu$; thus, $\omega \delta \varphi = \omega_0 \delta \varphi_0$. The frequencies ω and ω_0 are related by $\omega = \gamma (1 - \mathbf{n} \cdot \mathbf{v}) \omega_0$, where \mathbf{n} is the direction from the observer to the quasar, \mathbf{v} is the velocity of the string (that is, the velocity of S_0 relative to S) and $\gamma = (1 - v^2)^{-1/2}$. Hence,

$$\delta \varphi = \gamma^{-1} (1 - \mathbf{n} \cdot \mathbf{v})^{-1} \delta \varphi_0 \tag{3}$$

Depending on the relative directions of **v** and **n**, the angular separation has a value in the range $\kappa^{1/2}\delta\varphi_0 < \delta\varphi < \kappa^{-1/2}\delta\varphi_0$, where $\kappa = (1-v)/(1+v)$. Note that long strings are expected

to be at large redshifts, and hence to have a tendency to move away from us. (Here and below, I ignore the complications introduced by space-time curvature.)

The temperature discontinuity across the string arises because the relative velocity of two objects in a conical space is double-valued⁵: the answer depends on which way one parallel-transports the velocities around the string. In the rest frame of the string, S_0 , the observer moves past the string with velocity $-\mathbf{v}$. If the observer is at rest with respect to the sources of radiation on one side of the string, then the velocity of the sources on the other side of the string is $-\mathbf{v}+\mathbf{u}_0$, where $\mathbf{u}_0=8\pi G\mu$ $\mathbf{v}\times\mathbf{s}$ and \mathbf{s} is a unit vector along the string. The corresponding velocity difference in the observer's frame S is $\mathbf{u}=\gamma\mathbf{u}_0$. (Here I have expanded \mathbf{u} to the lowest order in $G\mu$ and used the fact that $\mathbf{u}_0\cdot\mathbf{v}=0$.) The temperature discontinuity can be found from the Doppler formula, $\delta T/T=\mathbf{u}\cdot\mathbf{n}$, where \mathbf{n} is a unit vector along the line of sight; thus,

$$\delta T/T = 8\pi G\mu\gamma \mathbf{n} \cdot (\mathbf{v} \times \mathbf{s}) \tag{4}$$

This expression has been derived in a different way by Vachaspati⁶.

If a segment of rapidly moving string is not perpendicular to the line of sight, then the observer sees more distant parts of the string with a retardation, and the apparent direction of the string differs from its actual direction. For simplicity, I shall consider only the case when the velocity of the string is perpendicular to the line of sight. Consider a coordinate system with y-axis along the line of sight and z-axis along the velocity of the string, so that the orientation of the string is parallel to the x-y plane. The observer sees a projection of the string on the x-z plane. Two points of the string with x-coordinate difference Δx are seen with a relative time delay $\Delta t = \Delta x \cot \theta$; hence, the observed difference in z-coordinates is $\Delta z = v\Delta t = (v \cot \theta)\Delta x$. The angle χ between the apparent and the actual direction of the string can be found from

$$\tan \chi = v \cot \theta \tag{5}$$

If there is a double quasar due to this string, then the line connecting the two images is along the z-axis and is not, in general, perpendicular to the apparent direction of the string (which can be observed, for example, by detecting the microwave temperature discontinuity).

Equation (5) applies to a relatively short segment of string subtending a small angle from the position of the observer. If an infinite straight string moves past the observer, he sees its distant parts with a retardation, so that the string appears to him to be curved. In the rest frame of the string, S_0 , light rays received at the origin at time $t_0 = 0$ were emitted from the string at space-time points

$$x_0^{\mu} = \{-(a^2 + \sigma^2)^{1/2}, \mathbf{a} + \sigma \mathbf{s}\}$$
 (6)

Here, a is the normal vector from the origin to the string, $s \perp a$ is the unit vector along the string and σ is a parameter on the string (equal to the length along the string measured from the end of vector a). We introduce a coordinate system with x-axis parallel to the string and z-axis along the velocity of the string in the observer's frame, S, and assume that the origins of S_0 and S momentarily coincide at $t = t_0 = 0$. The coordinates of the emission events in frame S are found from equation (6) by a Lorentz transformation; the spatial components are given by $x = \sigma$, $y = a_y$, $z = \gamma [a_z - v(a^2 + \sigma^2)^{1/2}]$, where $a^2 = a_y^2 + a_z^2$. To represent the apparent shape of the string, this three-dimensional curve must be projected onto a plane. A central projection from the origin to the plane $y = a_y$ gives

$$z = \gamma v [a - (a^2 + x^2)^{1/2}] \tag{7}$$

where I have set $\alpha_z = va$, so that z(x=0) = 0. Hence, a rapidly

moving infinite straight string appears to have the shape of a

I thank J. R. Gott and T. Vachaspati for discussions. This work was supported in part by NSF.

Received 17 April; accepted 23 May 1986.

- 1. Vilenkin, A. Phys. Rev. D23, 852-857 (1981).
- Vilenkin, A. Astrophys. J. 282, L51-L53 (1984).
- Gott, J. R. Astrophys. J. 288, 422-427 (1985).
 Paczynski, B. Nature 319, 567-568 (1986).

- Vachaspati, T. Nucl. Phys. B. (in the press).

Cooling flows in ellipticals and the nature of radio galaxies

Mitchell C. Begelman

Joint Institute for Laboratory Astrophysics, University of Colorado and National Bureau of Standards, Boulder, Colorado 80309-0440, USA

One of the great puzzles in the study of active galaxies is the relationship between the properties of the nucleus and the largescale morphology of the host galaxy. Galaxies which produce extended radio sources but little optical, ultraviolet or X-ray emission are invariably giant ellipticals or cD galaxies, whereas spirals tend to host 'optically active' nuclei, such as Seyferts¹ and at least some quasars^{2,3}. Rees and co-workers⁴⁻⁶ have interpreted this difference in radiative efficiency as a manifestation of the accretion flow close to the central black hole. But why should the mode of accretion at several Schwarzschild radii depend on the large-scale morphology of the host galaxy? I argue here that the connection arises from the manner in which interstellar gas is fed into the nucleus.

According to the scheme proposed by Rees et al.4, radio galaxies possess tenuous 'ion tori' which produce little radiation at optical, ultraviolet and X-ray wavelengths, whereas quasars and Seyfert galaxies possess optically thick accretion flows which radiate copiously. The mode of accretion depends on the ratio \dot{m} of the accretion rate to the 'critical' accretion rate $L_{\rm F}/c^2$, where $L_{\rm E}$ is the Eddington limit and c is the speed of light. Given a viscosity parameter α (ref. 7), the flow is always a gas-pressure-supported 'ion torus' for $\dot{m} < 10^{-7} \alpha^2$ and is either a standard thin accretion disk ($\dot{m} < 10$) or a 'radiation torus' $(\dot{m} > 10)$ for $\dot{m} > 50\alpha^2$. For intermediate values of \dot{m} , however, the flow may assume one of two possible states: a thin disk or an ion torus. The flow pattern adopted probably depends on the manner in which gas is fed into the nucleus. In a spiral galaxy, the bulk of the interstellar medium resides in a disk, and it is plausible that a radiatively efficient flow pattern persists all the way to the black hole. Thus it seems natural that spiral galaxies should produce optically active galactic nuclei.

The situation is quite different for elliptical galaxies, which are permeated by a hot interstellar medium at a temperature close to the virial temperature of the galaxy⁸⁻¹⁰. X-ray measurements of this gas suggest that it is slowly cooling and settling into the potential well of the galaxy at a rate ranging from $\sim 1~M_{\odot}~\rm yr^{-1}$ for isolated ellipticals^{8,11,12} to $\sim 1,000~M_{\odot}~\rm yr^{-1}$ for the outer regions of central ellipticals in rich clusters^{13,14}. (M_{\odot} is the mass of the Sun.) Cooling flows are strongly thermally unstable to the formation of cool clumps, and it has been suggested that the formation of low-mass stars continuously removes mass from these flows at all radii15,16. Indeed, there are observational indications that the mass flux declines steadily towards the centre^{13,17}. In the limiting case, thermal instabilities could remove enough material at every radius so that the residual inflow of hot gas would remain subsonic, cooling on a timescale

comparable to or longer than the free-fall time in the galactic potential⁸. Matters are complicated somewhat if the flow passes through a sonic point^{18,19}. In principle, a cold supersonic flow could continue into the nucleus with the mass flux conserved; however, it is more likely that inhomogeneities in the flow, leading to shocks, would reheat some of the gas to a temperature comparable to the virial temperature, while most of the gas condenses into cold blobs which follow ballistic trajectories. Even a small amount of angular momentum will deflect these blobs from radial orbits; the high pressure in the ambient hot gas will compress them, reducing their collision cross-sections and making it likely that they, too, will form stars before they coalesce into an accretion disk at the galactic centre. As in the subsonic case, the characteristic cooling time of the hot gas will be comparable to or longer than the free-fall time.

Suppose there is a black hole at the centre of the galaxy, of mass $M_h = 10^9 \,\mathrm{M}_\odot \,M_\odot$ (that is, of mass M_\odot in units of $10^9 \,M_\odot$). The gravitational potential of the black hole begins to dominate the dynamics of the hot gas at a radius

$$R_{\rm h} \simeq GM_{\rm h} m_{\rm o}/kT \simeq 50 \ M_{\rm g} T_{\rm 7}^{-1} \ {\rm pc}$$
 (1)

where T_7 is the temperature of the gas in units of 10^7 K. If the cooling time of the hot gas at $R \ge R_h$ is comparable to or longer than the local free-fall time, then the density of hot gas at R_h , $n(R_h)$, satisfies

$$n(R_{\rm h}) \le 10 \ M_9^{-1} T_7^{3.1} \ {\rm cm}^{-3}$$
 (2)

where I have used a power-law approximation²⁰ for the cooling rate at $10^5 \text{ K} < T < 3 \times 10^7 \text{ K}$. The Bondi theory of spherical accretion21 then gives an upper limit to the black hole accretion rate (first pointed out by Nulsen et al.8):

$$\dot{M} \lesssim 2 M_9 T_7^{1.6} M_{\odot} \text{ yr}^{-1}$$
 (3a)

$$\dot{m} \leqslant T_7^{1.6} \tag{3b}$$

Equations (3a) and (3b) are valid whether or not additional cooling occurs at $R < R_h$.

In fact, the hot inflow is likely to become angular-momentumdominated before it reaches R_h . If the timescale for angular momentum transport reduces the inflow speed by a factor α , then the upper limits given in equations (3a) and (3b) will be reduced by a factor α^2 . As the cooling time is already of the order of the inflow time at $R \ge R_h$ (the definition of a cooling flow), one can show that the flow at $R \leq R_h$ will never be able to cool by line-cooling or bremsstrahlung, provided α does not decrease too rapidly with decreasing R (ref. 4). Under the assumptions made by Rees et al.⁴, the inner parts of the flow will form an ion torus if $\dot{m} < 50 \ \alpha_{\rm in}^2$, where $\alpha_{\rm in}$ is the value of α in the inner parts of the flow. This condition is satisfied if

$$T_7^{1.6} < 50(\alpha_{\rm in}/\alpha)^2$$
 (4)

Again, we conjecture that the highly compressed cold clumps will form stars before they are able to coalesce to form a nuclear disk; hence, only the hot gas participates in the angularmomentum-dominated accretion flow.

Equation (4) is probably satisfied in most elliptical galaxies; therefore, most active elliptical galaxies should possess radiatively inefficient ion tori, consistent with observations. As suggested by Sparke and Shu²², the development of large-scale collimated radio jets may be fostered by the presence of a hot interstellar medium in ellipticals, and suppressed by its absence in spirals. I therefore suggest that the large-scale morphology of the galaxy governs both the large-scale radio structure and the small-scale structure of the active nucleus.

Note that the upper limit on \dot{m} (Equation (3b)) depends only on the temperature of the cooling flow in the galactic potential and is independent of the mass of the hole. For a variety of plausible galactic potentials, $T^{1/2}$ would scale with the central stellar velocity dispersion (excluding the cusp surrounding the black hole), which in turn is correlated with the luminosity of the galaxy according to the Faber-Jackson relation²³. This chain of argument leads to a predicted correlation between \dot{m} and the luminosity of the host galaxy. In particular, equation (4) may be violated for the most luminous ellipticals. The inflow would become a radiatively efficient thin disk or radiation torus, and the resulting objects would be classified as luminous quasars. Besides residing in elliptical galaxies, these 'elliptical' quasars might be expected to differ from 'spiral' quasars in their radio properties. If we accept the view of Sparke and Shu²², the distant guasars which produce highly collimated luminous jets extending to several hundred kiloparsecs—such as 4C32.69 (refs 24, 25)—should be examples of this second class of quasars. There are additional indications from optical studies that radio-loud quasars tend to be associated with elliptical galaxies^{26,27} although these studies are far from definitive.

Certain classes of active ellipticals, notably BL Lac objects and N galaxies, might be considered optically active, yet are not excessively luminous. It is not clear whether these can be easily accommodated in the scheme outlined above. For BL Lac objects, a case can be made that we are viewing an ion torus pole-on. Alternatively, catastrophic Compton cooling resulting from pair production can sometimes collapse the inner regions of an ion torus, converting it to a radiatively efficient thin disk³⁰. Finally, emission lines from photoionized gas have been detected in the nuclei of many 'normal' radio galaxies, indicating that some ultraviolet or X-ray continuum is produced in these objects as well. This need not imply a high radiative efficiency of the central engine, as ion tori are expected to produce a certain amount of hard radiation. In fact, a modest radiative efficiency in X-rays may reduce the accretion rate below the value estimated above, by heating the inflowing gas^{28,29}

I thank Craig Sarazin, Marek Sikora and Janet Drew for helpful criticism. This research was funded in part by NSF grant AST83-51997 (Presidential Young Investigator Award), by NASA Astrophysical Theory Center grant NAGW-766, and by grants from Ball Aerospace Systems Division, Rockwell International Corporation and the Exxon Education Foundation.

Received 21 January; accepted 8 May 1986.

- 1. Adams, T. F. Astrophys. J. Suppl. Ser. 33, 19-34 (1977).
- Malkan, M. A., Margon, B. & Chanan, G. A. Astrophys. J. 280, 66-78 (1984)
 Hutchings, J. B., Crampton, D. & Campbell, B. Astrophys. J. 280, 41-50 (1984).
- Rees, M. J., Begelman, M. C., Blandford, R. D. & Phinney, E. S. Nature 295, 17-21 (1982). Begelman, M. C. in Astrophysics of Active Galaxies and Quasi-Stellar Objects (ed. Miller, J. S.) 411-452 (University Science Books, Mill Valley, 1985).
- Rees. M. J. A. Rep. Astr. Astrophys. 22, 471-506 (1984)
- Pringle, J. E. A. Rev. Astr. Astrophys. 19, 137-162 (1981).
- Nulsen, P. E. J., Stewart, G. C. & Fabian, A. C. Mon. Not. R. astr. Soc. 208, 185 195 (1984)
- Forman, W., Jones, C. & Tucker, W. Astrophys. J. 293, 102-119 (1985)
- Trinchieri, G. & Fabbiano, G. Astrophys. J. 296, 447-457 (1985). White, R. E. & Chevalier, R. A. Astrophys. J. 280, 561-568 (1984)
- 12. Sarazin, C. L. Proc. Green Bank Workshop Gaseous Galactic Haloes (National Radio
- Astronomy Observatory, in the press). 13. Fabian, A. C., Nulsen, P. E. J. & Canizares, C. R. Nature 310, 733-740 (1984)
- Sarazin, C. L. Rev. mod. Phys. 58, 1-115 (1986)
- Sarazin, C. L. Rev. mod. Phys. 58, 1-115 (1986).
 Fabian, A. C., Nulsen, P. E. J. & Canizares, C. R. Mon. Not. R. astr. Soc. 201, 933-938 (1982)
 Sarazin, C. L. & O'Connell, R. W. Astrophys. J. 268, 552-560 (1983).
 Fabian, A. C., Arnaud, K. A. & Thomas, P. A. Proc. IAU Symp. 117 (in the press).
 White, R. E. & Sarazin, C. L. Astrophys. J. Suppl. Ser. (submitted).
 White, R. E. & Sarazin, C. L. Astrophys. J. Suppl. Ser. (submitted).

- McKee, C. F. & Cowie, L. L. Astrophys. J. 215, 213-225 (1977).
 Bondi, H. Mon. Not R. astr. Soc. 112, 195-204 (1952).
 Sparke, L. S. & Shu, F. H. Astrophys. J. 241, L65-L68 (1980).
- Faber, S. M. & Jackson, R. E. Astrophys. J. 204, 668-683 (1976). Potash, R. A. & Wardle, J. F. C. Astrophys. J. 239, 42-49 (1980)
- Owen, F. N. & Puschell, J. J. Astr. J. 89, 932-957 (1984).
 Malkan, M. A. Astrophys. J. 287, 555-565 (1984).
- 27. Gehren, T., Fried, J., Wehinger, P. A. & Wyckoff, S. Astrophys. J. 278, 11-27 (1984) 28. Begelman, M. C., McKee, C. F. & Shields, G. A. Astrophys. J. 271, 70-88 (1983).
- Begelman, M. C. Astrophys. J. 297, 492-506 (1985).
- 30. Begelman, M. C., Sikora, M. & Rees, M. J. Astrophys. J. (submitted)

Secular change in solar activity derived from ancient varves and the sunspot index

C. P. Sonett* & T. J. Trebisky†

* Department of Planetary Sciences and Lunar and Planetary Laboratory, and † Steward Observatory, University of Arizona, Tucson, Arizona 85721, USA

The Hale solar period, $\tau_{H(1)} \approx 22 \text{ yr}$, and its second harmonic, $\tau_{H(2)} \simeq 11$ yr, which characterize the sunspot index and are thus hydromagnetic, are imprinted in certain varved rocks of Archaean1to late Precambrian2 age, but the varves record climate and thus are sensitive to solar insolation^{2,3}. We report here apparent collective behaviour of the two kinds of data. The 22yr/11-yr amplitude spectral density (ASD) ratio, β_i (i = 1) of the sunspot index (which is a measure of solar-cycle asymmetry), plotted together with β_i s from three ancient varve thickness sequences against the age for each β_i , results in a remarkably close fit to a decreasing exponential with time constant $\tau \approx 2$ Gyr. These varves and the sunspot index appear to link solar luminosity and the solar field, implying that a common forcing mechanism affects luminosity and the dynamo periods through the common decay time, τ .

Varve data comprise a sequence of thickness values of sediments or chemical layers indexed by integers hypothesized to correspond to solar years. The observation of ~11- and ~22-'year' periodicities lends strength to the hypothesis. (The lack of exact correspondence for all the data of this report is discussed below.) Data of the quality of the Elatina sequence² have been reported nowhere else; the Hamersely group has much more material but has not been fully surveyed for data pertaining to the solar problem. In view of the paucity and special qualities of these data, it cannot be guaranteed that further 'finds' will not alter the interpretation given here; nevertheless, we think it

important to report these very tentative findings for their potential role in solar physics. The four sources of data used to determine the β_i s and τ were: (1) the Weeli Wooli (Hamersely) banded iron formations¹ (2.5 Gyr BP); (2) the Wolongorang (McArthur basin) dolomitic varves⁴ (1.75 Gyr BP); (3) the Elatina sedimentary varves² (0.67 Gyr BP); and (4) the presentepoch sunspot index, representing a significant spread in ages. Errors in ages are uncertain, but are in all cases much smaller than the confidence spreads shown in Fig. 2. For Weeli Wooli (thin-section photographic transparency) and Wolongorang (thin section) the procedure for determining varve thicknesses was that used previously⁵ for the light bands in the Elatina sequence, namely, measurement of thickness using a long stagemicrometer with an optical shaft-encoder fed to a small computer for recording.

For computing spectra we generally used the preferred digital Fourier transform (DFT), supported on occasion by a maximum entropy method (MEM). The sunspot index spectrum (computed by DFT) is shown in Fig. 1a, b. In a the plot is linear-linear for clarity, whereas b is log-linear (and filtered) to enhance the small response near 22 yr. We used the prior knowledge of these periods to aid identification of the region in frequency space (unsmoothed for maximum resolution) where the Hale line and its second harmonic were expected. For Elatina those periods were previously determined to be ~12 and 24 yr (ref. 5), rather than the modern 11 and 22 yr from the sunspot index. For the more ancient Wolongorang varves the shift was greater, corresponding to periods of ~14.8 and 28.8 yr, respectively. (A correspondingly greater shift for Weeli Wooli is not apparent, but its does have a 23.3-yr period¹.) The 'solar' lines were further certified as the strongest present, and also as satisfying closely a 2:1 ratio of periods. For the final ASD estimates used to calculate β_i s, a simple 5-point boxcar averaging filter was used to smooth the spectra.

As the DFT estimates follow a χ^2 distribution, the β_1 s (being a ratio) follow an F distribution. Our next point, regarding degrees of freedom, is crucial to the estimation of the confidence

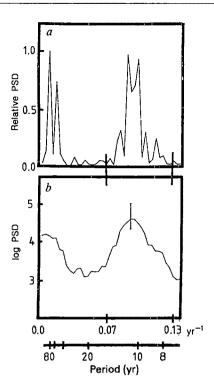


Fig. 1 Digital Fourier power spectral density (PSD) of the Wolf yearly averaged sunspot index. a, Unsmoothed 2-DOF relative amplitude, plotted against frequency (upper x-axis) and period; linear-linear plot. Plot b (log-linear) emphasizes minor 22-yr power by using a logarithmic ordinate. Error bar, 90% χ^2 confidence limit. This present-epoch case shows $\beta_1 \approx 0.1$.

intervals. Assuming that all four β_i s are independent, the filtering yields 10 degrees of freedom (DOF) per DFT datum and narrows the χ^2 confidence range considerably. But these data must be and are obviously correlated. The optimistic limit would be \sim 40-80 DOF per datum. For the 80% confidence level of the final F distributions, the sensitivity of the confidence range to changes in the number of DOF near 40 is small⁶, and the 80% ranges in Fig. 2 are reasonable. (In the indexing of β_i , i increases with age.)

Fig. 2 shows the least-squares fit of the β_i s to an exponential function. The fit is computed assuming equal relative weighting, as all confidence levels are equal. Although significant deficiencies exist in the Wolongorang data, it is remarkable that β_3 lies almost exactly on the least-squares line. (As it is only the ratios of ASDs which are required, common-mode sources of error, which are independent of frequency, are unimportant.) The secular trend in the β_i s and the time constant τ are most readily explained as being due to a relict magnetic field⁷—but only if it is accepted that somehow the varves are proxy field detectors and therefore equivalent to the sunspot index in detecting the hydromagnetic asymmetry found in that index.

The decay of an axially symmetric eddy current for an isotropic sphere of radius R, with homogeneous conductivity σ , has a time constant τ_s , given by

$$\tau_s = \mu_0 \sigma R^2 / \pi^2 s^2 \text{ (MKS)} \tag{1}$$

where $\mu_0 = 4\pi \times 10^{-7}$ H m⁻¹ is the permeability of free space and s is the multipole order. It is reasonable to take s=1, for a relict field must be of odd order to explain the sunspot sequence asymmetry. As τ_s varies inversely with s^2 , it seems unlikely that any higher-order multipole from the time of the Sun's formation is still significant. Cowling⁸ computed the value $\tau_s=5$ Gyr for a relict solar field using a homogeneous sphere of radius equal to half the solar radius and $\sigma=10^7$ S m⁻¹; the value of τ_s found here is in reasonable agreement. Estimation of τ_s is made more complex by the strong variation of conductivity with temperature

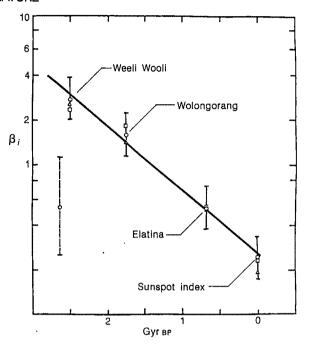


Fig. 2 Least-squares fit of the four values of β_i . The vertical errors are estimated from the F distribution function with 40 DOF. (As noted in the text, in this range of large DOF, F varies little.) Horizontal errors from geochronology and stratigraphy are unimportant compared with those of the β_i s and are not shown. \bigcirc , 5-datum filter; \square , 3-datum filter; \triangle , unfiltered. Solid line, semi-log fit $y = a \exp(-bt)$ with $b = 2 \text{ Gyr}^{-1}$; dashed line, confidence estimate for a single value of β with 10 DOF; that is, the worst possible case (independent or uncorrelated β_s).

(and therefore radius), and because the circulating currents are likely to occur where the conductivity gradient is largest; Cowling's conductivity varies with solar radius by nearly three orders of magnitude. Considering the paucity of data, we are not prepared to claim that a relict magnetic field must be responsible for the apparent joint 'bolometric'-hydromagnetic behaviour summarized in Fig. 2, but this is the best interpretation of the data available so far.

Although the Wolongorang data is of marginal quality, it covers a crucial time period (~1.75 Gyr BP); the short (54 data) sequence had to be subjectively selected from a longer sequence displaying distortion similar to the inclusions seen in the Weeli Wooli formation, possibly due to diagenesis. The dominant spectral peak positions for the Wolongorang varves may be artefacts of the short and distorted record, but the lines chosen are the strongest ones of the DFT and adhere closely to the 2:1 rule regarding harmonic periods. As both the Elatina and Wolongorang varves exhibit 'solar' lines displaced from the modern values, the periods increasing with age, perhaps something more may be indicated, such as a secular decrease in the convective zone thickness with age, in turn affecting the dynamo period. However, this must be regarded as conjecture until more data become available.

The major issue raised by these data is why luminosity and magnetic activity should appear to be linked, as shown in Fig. 2. The magnetic field is favoured as the basic variable only because it is the only solar parameter, except the core composition itself, that is capable of entering into a secular decay measured in Gyr. A relict field can explain the asymmetry in the sunspot sequence (or equivalently why both 22- and 11-yr periods are present), provided that the sunspot index varies with the energy in the field, that is, with B^2 . The sunspot index y(t) can be predicted by the equation

$$y(t) \simeq [\delta + \beta \cos(\omega_c t)]^2$$

= $\delta^2 (1 + \varepsilon^2 / 2) + 2\varepsilon^2 \cos(\omega_c t) + (\varepsilon^2 / 2) \cos(2\omega_c t)$ (2)

where β is the Hale-period amplitude in the sunspot index sequence, ω_c the Hale frequency, δ an offset (relict), $\varepsilon = \beta/\delta$, and the ratio of 22- to 11-yr amplitudes is $4\delta/\varepsilon$. A simpler model assumes that v(t) depends only on the magnitude of solar activity, but to explain the asymmetry requires complications beyond the scope of the present work. We cannot distinguish between a steady or secular value of δ and one which oscillates so slowly as to appear constant over the 282 yr of unbroken sunspot index record, but the latter option has difficulty in explaining the very long characteristic time, τ , shown in Fig. 2.

The sunspot asymmetry alone suggests a relatively small value of steady magnetic field strength; the inferred time constant, if attributed to magnetism, is consistent with its being the vestige of a much stronger pre-main-sequence field. Although a field of the magnitude inferred for the present epoch is dynamically unimportant now (except for the angular momentum problem¹⁰), it could explain the appearance of both the 11- and 22-yr activity periods. It also supports the general principle of an early Solar System magnetic field, either a compressed nebular remnant, a consequent of a nebular dynamo, or some combination of these¹¹. Although the results reported here suggest a role for magnetic fields in association with the protosolar condensation, a relict field offers no obvious explanation for the apparently coupled behaviour of insolation and solar activity. Furthermore, even a modest present-epoch relict field is inconsistent with the observed increase of angular velocity with depth

in the deep solar interior^{12,13}, a problem which is much more severe for the ancient Sun. Finally, the discussion here of periodicities bypasses consideration of statistically oriented (for example, strange attractor) models of solar activity, which may require consideration, although there appear to be difficulties with data quality14.

We are indebted to M. J. Jackson for the loan of a Wolongorang core thin section, to A. F. Trendal and R. Davy for their illumination of the systematics of the Weeli Wooli banded iron formation and the donation of a specimen, and to G. E. Williams for discussions of the subject of varves and for the loan of a Weeli Wooli thin section. This work was supported by the research program of the Atmospheric Sciences Division of NSF.

Received 30 January: accepted 8 May 1986.

- 1. Trendall, A. F. Econ. Geol. 68, 1089 (1973).
- Williams, G. E. Nature 291, 624-628 (1981).
 Sonett, C. P. & Williams, G. E. J. geophys. Res. 90, 12019-12026 (1985).
 Jackson, M. J. Geology 44, 301-326 (1985).

- 5. Williams, G. E. & C. P. Sonett Nature 318, 523-527 (1985).
 6. Abramowitz, M. & Stegun, I. A. (eds) Handbook of Mathematical Functions (Dover, New York, 1965). Sonett, C. P. Nature 306, 670-673 (1983).

- Soniet, C. P. Value Son, Not. R. astr. Soc. 105, 166-174 (1945).
 Sonett, C. P. Geophys. Res. Lett. 9, 1313-1316 (1982); 10, 491 (1983)
 Rosner, R. and Weiss, N. O. Nature 317, 790-792 (1985).
- Boyer, D. W. & Levy, E. H. Astrophys. J. 277, 848-861 (1984).
 Duvali, T. L. Jr & Harvey, J. W. Nature 310, 19-22 (1984).

- Duvall, T. L. Jr et al. Nature 310, 22–25 (1984).
 Gudzenko, L. I. & Chertoprud, V. E. Soviet Astron.-AJ, 8, 555 (1965).

Diurnal cycle of tropospheric OH

T. M. Hard, C. Y. Chan, A. A. Mehrabzadeh, W. H. Pan & R. J. O'Brien

Chemistry Department and Environmental Sciences Doctoral Program, Portland State University, Portland, Oregon 97207, USA

The hydroxyl free radical, OH, is sunlight's prime agent in maintaining the trace-gas composition of the Earth's troposphere, and at the same time serves as the catalyst responsible for many of the symptoms of urban and regional air pollution. We have used low-pressure fluorescence to measure the ambient concentration of this radical during two continuous 36-hour periods in early summer and late autumn, 1985. The summer and autumn maxima were 3×10^6 and 4×10^5 molecules cm⁻³ (10^{-13} and 2×10^{-14} relative to air), respectively. The observed concentrations lie within the rather large latitude of current estimates based on trace-gas lifetimes or atmospheric photochemical models.

In the global troposphere, reactions with OH are part of a cleansing process, countering natural and man-made inputs. In this contest, interest has centred on methane, the most abundant atmospheric hydrocarbon. Recent observations¹⁻³ imply a persistent imbalance between methane's sources and its removal by OH. Where anthropogenic emissions of other trace gases are concentrated, some of the intermediate products of the OHcatalysed cleansing process are known as urban smog, and some of the final products are known as acid rain. Moreover, because OH controls the atmospheric lifetimes and distributions of most trace gases, secular changes in the tropospheric OH concentration will modify the global thermal radiation budget and the total ozone column.

Direct local observation of tropospheric OH has been notoriously difficult, due to its high reactivity and low concentration. OH measurements have been sporadic, and reported concentrations have varied over a large range, with large measurement uncertainties⁴. Laser-excited fluorescence^{5,6} measurements have suffered from ambient light background, fluorescence of other species, photolytic production of OH by the laser, and

calibration uncertainties. The obstacles to fluorescence determination of OH are significantly lowered by expansion of the air sample to low pressure, in a procedure we have named FAGE (fluorescence assay with gas expansion)⁷. The chief obstacles to previous determinations of OH have been the solar background at the fluorescence wavelength, and production of OH by the laser itself through photolysis of ambient ozone in the sequence:

$$O_3 + h\nu \to O(^1D) + O_2$$
 (1)

$$O(^{1}D) + H_{2}O \rightarrow 2 OH$$
 (2)

Here $h\nu$ indicates the exciting laser radiation (which then detects the spurious OH during the same pulse) and O(¹D) is the first excited state of the oxygen atom. In FAGE, we draw ambient air through an orifice and down a tube to the excitation and detection zone at a pressure of ~5 torr. This pressure drop strongly discriminates against step (2) above and against Rayleigh and Mie scattering, the latter particularly a problem in polluted air. The contained environment excludes ambient light. The roughly 100-fold drop in OH concentration associated with the expansion is compensated by an approximately equal increase in the fluorescence yield due to reduced fluorescence quenching at the lower pressure. In addition, reduced quenching results in a longer fluorescence lifetime so that most of the fluorescence waveform is temporally separated from the instantaneously scattered pulse. Finally, the low-pressure transit down the tube to the detection zone allows reagents added at the inlet to react selectively with OH, so that the background signal may be accurately and continuously determined (chemical modulation of the signal).

The FAGE method and instrument have been described elsewhere⁷. To make the measurements reported here, we have substantially improved the sensitivity to ambient OH with a new YAG/dye laser (repetition rate increased from 6 to 30 Hz and 282-nm pulse energy increased from 0.1 to 1 mJ); by replacing the monochromators at f/4 (where f is the focal length) by 3-nm (FWHM) multi-layer dielectric filters at f/1.5; and by the use of two parallel air-sampling and fluorescence-detection channels, sharing one 0.5-m White cell. A flow of isobutane sufficient to remove 95% of the OH is injected alternately into the interior of each probe, giving a modulation cycle of 90 s duration. Thus, the signal and the background are measured simultaneously by the pair of probes. Figure 1 is a diagram of the FAGE sampling cell. This sampler was placed 2 m above the roof of our four-story building; the vacuum pump, laser and signal-processing electronics were in the laboratory immediately below.

Our initial goal in developing this technique has been to determine the diurnal concentration profile of OH in tropospheric air, to verify the behaviour projected by atmospheric models. Figure 2 shows the OH concentration observed during a 36-h experiment in Portland, Oregon, on 17-19 June 1985. The darker points are a 1-h moving average; the lighter points are at ±2 standard deviations, as dictated by the photon counting statistics of the total signal and background. (This uncertainty is twice the square root of the sum of the photon counts from the two probes.) Averaging of the raw data is necessary to reduce noise—a 1-h average results in negligible distortion of the true curve.

'The concentration scale in Fig. 2a is determined by the FAGE instrument's OH response, which was measured before and after the experiment, over the range of (intended) measurements. Full calibration of the response (Fig. 3) was carried out by surrounding the sampling probes with an ultraviolet-transparent teflonfilm bag, into which flowed a continuous air stream containing trace levels of nitric oxide (NO) and hydrocarbon (mesitylene). The bag was irradiated continuously with ultraviolet fluorescent lamps, and the hydrocarbon, NO and ozone concentrations were measured at the bag inlet and in the interior. A fan ensured that the bag operated as a well-mixed reactor with a residence time t_{res} , given by the ratio of its volume V to the total air flow rate F. The input flow was greater than that required by the NO. ozone, hydrocarbon and FAGE measurements, and excess air escaped from the bag through an outlet to the atmosphere. Once steady state has been achieved (as evidenced by unchanging concentrations), mass balance of the hydrocarbon (HC, which reacts only with OH) requires that $F[HC]_0 - k_{OH+HC}[OH] \times$ [HC]V - F[HC] = 0, where the subscript zero denotes the inlet concentration. Substituting for the bag residence time gives

$$[OH] = \frac{1}{k_{OH+HC}t_{res}} \left(\frac{[HC]_0}{[HC]} - 1 \right)$$
 (3)

For mesitylene, $k_{\rm OH^+HC}=6\times10^{-11}$ molecule⁻¹ cm³ s⁻¹ (ref. 8). The residence time was obtained from the response of [NO] or [HC] to a step change in [NO]₀ or [HC]₀ in the dark. The inlet-to-outlet ratio [HC]₀/[HC] was determined by gas chromatography with a variety of lamp intensities and inflow rates of NO, thereby producing a wide range of OH concentrations. This also produced values of the ratio [NO]/[O₃] respresentative of the entire span of NO photo-oxidation in 'classical' photochemical air pollution⁹⁻¹¹. This calibrator represents an eulerian approach to each point in the NO photo-oxidation sequence, in contrast to our previous calibration⁷, which employed a lagrangian sweep through the whole sequence. Both give similar results, and in our previous calibration the decay of two separate hydrocarbon species was monitored, each one giving the same value for the OH concentration.

The rather large scatter of the points in Fig. 3 is due in part to the fact that they were obtained over the course of about a week, with variations in laser energy and alignment with roof-top optics un-normalized. The central line in Fig. 3 is the linear-least-squares fit of the measured (hydrocarbon decay) OH concentrations to the FAGE signal.

The precision of the net OH signals in Fig. 2a is equivalent to an error in OH concentration of $\pm 4 \times 10^5$ cm⁻³ at 2 standard deviations (95% confidence, 1-h average). The accuracy of the concentrations in Fig. 2a is limited by the uncertainties in slope and intercept of the calibration in Fig. 3. The intercept uncer-

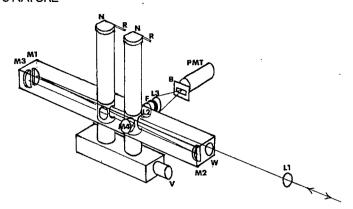


Fig. 1 Diagram of 2-channel FAGE sampler. N, nozzle, 1 mm i.d.; R, reagent/carrier inlet; V, vacuum connection; W, entrance/exit window for laser beam; L1, positive lens focused near W for enlarged beam at sample zone; M1, M2, M3, White-cell mirrors for 18 laser passes through sample; M4, concave mirror; L2, f/1.5 lens; F, filter, 4 nm FWHM at 309 nm; L3, f/2 lens; B, image mask; PMT, photomultiplier. For clarity, only one of the two detection trains is shown.

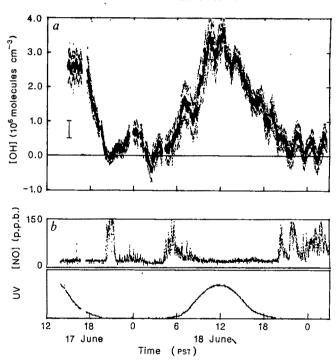


Fig. 2 a, Ambient OH concentration during 17-19 June 1985. The darker points represent a 1-h moving average; the lighter points are at ± 2 standard deviations, based on the photon-counting statistics of the signal and background. The vertical error bar represents the 1σ calibration uncertainty. b, Concurrent measurements of NO concentration (parts per 10^9) and relative ultraviolet intensity (UV) (250-400 nm).

tainty is an inescapable feature of all analytical methods. In Fig. 3, the upper and lower lines are drawn from the 1σ intercept uncertainties using the 1σ slope uncertainties. The vertical displacement of these lines gives the 1σ calibration uncertainty, which is $\sim 5 \times 10^5$ cm⁻³ for the concentration range occupied by the ambient data of Fig. 2. The total photon-counting uncertainty in the calibration is a function of the broad-band fluorescence level of the sampled air. This uncertainty (defined above) is shown as a horizontal error bar and is smaller than those in the hydrocarbon determination in this calibration, which are shown as vertical bars, based on error propagation through equation (3) and using a 2% uncertainty in the determination of the chromatographic peak heights. This calibration uncertainty can be improved in future measurements.

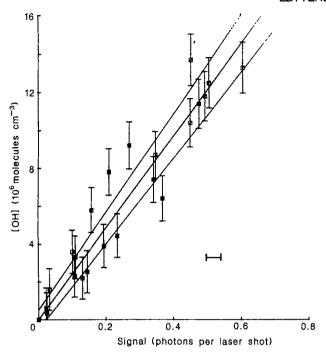


Fig. 3 FAGE calibration using OH-catalysed hydrocarbon consumption in a continuous-flow, ultraviolet-irradiated, Teflon-film bag. Vertical error bars are due to uncertainties in the measurement of hydrocarbon consumption. The horizontal error bar represents the (2σ) photon-counting statistics of the background and signal.

The detailed chemical composition of the air at our urban site is unknown, and its complexity precludes rigorous comparison with tropospheric chemical models. Nevertheless, the diurnal cycle exhibited on the relatively unpolluted day of 18 June (near the summer solstice) is similar to that predicted by clean-air photochemical models at ground level, 45° N latitude. Hydroxyl concentrations in clean air vary largely in response to diurnal variation in ultraviolet light intensity (Fig. 2b). Crutzen and Gidel¹² have calculated a July daytime average [OH] of 2×10^6 cm⁻³; Logan et al.¹³ predicted a diurnal cycle with a peak of $\sim 1.5 \times 10^6$ cm⁻³ at the lower light intensities and water vapour concentrations of the equinox. We used the mechanism and rate constants of ref. 13, with appropriate changes in ultraviolet light intensity and water vapour concentration, to find a maximum clean-air [OH] of 6×10^6 cm⁻³ summer solstice. Inclusion of our measured concentrations of NO, O₃, and H₂O reduces the calculated maximum OH concentration to 2×10^6 cm⁻³. No attempt is made here to include the non-methane hydrocarbon chemistry, which may alter the model predictions further. Graedel et al.14 predicted a peaksummer [OH] of 1.7×10⁶ cm⁻³ in an urban-air modelling study, and Calvert¹⁵ derived a value of ~2×10⁶ cm⁻¹ in an analysis of hydrocarbon consumption in the summer Los Angeles atmosphere. Our results are not inconsistent with global [OH] averages and distributions derived from the known sources and atmospheric distributions of CH₃CCl₃ (ref. 16) or ¹⁴CO (ref. 17).

Hydroxyl signals were detected during both nights, but were higher on the first. In contrast, [NO] was much higher on the second night (Fig. 2b). Although daytime photodissociation processes are thought to be the prime source of OH in both clean and polluted air, there are several mechanisms which could account for the presence of OH at night: (1) HO₂ is predicted to persist through the night in clean air at levels > 10⁶ molecules cm⁻³ (ref. 13), and mixing of such air with urban air containing NO could generate OH; (2) peroxynitrates serve as free-radical reservoirs which dissociate to generate OH precursors; (3) NO₃ can react with hydrocarbons or aldehydes to give other radicals. Although these sources may require the presence of NO to reduce precursor radicals (such as HO₂) to OH, NO also pro-

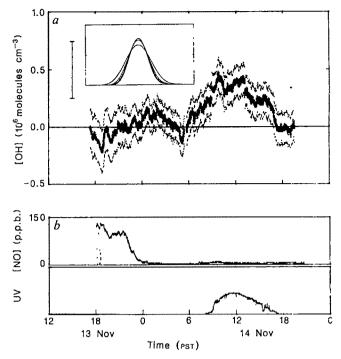


Fig. 4 Ambient [OH] (a) and related variables (b) during 13-14 November 1985. A 4-h averaging tme was used for [OH] because of its lower concentration and the higher background relative to the summer measurements; the relative ultraviolet intensity curve cannot be compared on an absolute basis with Fig. 2b; otherwise, as in Fig. 2. The inset shows the effect of several averaging intervals (1, 2, 4 h) on a diurnal [OH] profile generated by numerical integration of a clean-air mechanism.

vides a sink for OH, forming nitrous acid, which is stable in the dark. For a fixed precursor-free-radical source strength, nocturnal [OH] is expected to be inversely related to the NO concentration, consistent with the [OH] signals on the two nights.

Although the night-time OH signals exhibit adequate precision relative to photon-counting uncertainties, their magnitude lies within the calibration uncertainties of Fig. 3; thus, further nocturnal OH measurements are needed.

A second measurement was carried out on 13-14 November 1985, and the results are shown in Fig. 4. Due to lower signal level and higher background, a 4-h moving average is shown here—this will broaden the actual curve, as shown in the figure inset. Here it was necessary to shift the baseline by 2×10^5 cm ³ [OH] to compensate for an apparent negative offset. This offset was not present in the June data and, although of undetermined origin, it may be due to fluorescence of impurities in the modulating reagent. These data show a diurnal pattern similar to that of the summer data, but with a greatly reduced maximum concentration, presumed to be due in large part to reduced light intensity. The maximum concentration is again in agreement with clean-air chemical models, although this agreement may be fortuitous, given the actual composition of the urban air analysed.

The experiments reported here confirm the tropospheric presence of OH and its dependence on light intensity at concentrations in reasonable agreement with tropospheric chemical theory. The experiments do not yet explore the detailed photochemical mechanism that supports OH, which must be understood in order to predict the tropospheric effects of natural cycles and man-made pollution. Besides OH, a key species for this exploration is HO₂, which can also be determined by FAGE⁷. More rigorous comparison of these radical concentrations with clean-air atmospheric models can be achieved by refinement of the calibration of the FAGE instrument, its movement to sites truly representative of the clean troposphere, and the accumulation of data in different seasonal conditions. We

are combining the HO and HO2 procedures into a single instrument for the initiation of these experiments.

Supported by the NSF (grant ATM-85-05615) and by the U.S. Environmental Protection Agency (grant R811341).

Received 11 February; accepted 9 May 1986.

- 1. Khalil, M. A. K. & Rasmussen, R. A. Science 232, 56-57 (1986).
- Rinsland, C. P., Levine J. S. & Miles, T. Nature 318, 245-249 (1985). Stauffer, B., Fischer, G., Neftel, A. & Oeschger, H. Science 229, 1386-1388 (1985).
- Hewitt, C. N. & Harrison, R. N. Atmos. Envir. 19, 545-554 (1985).
- Wang, C. C. & Davis, L. I. Geophys, Res. Lett. 9, 98-100 (1981).
- Davis, D. D., Fischer, S. D. & Rodgers, M. O. Geophys. Res. Lett. 9, 101-104 (1982).
 Hard, T. M., O'Brien, R. J., Chan, C. Y. & Mehrabzadeh, A. A. Envir. Sci. Technol. 18,
- Atkinson, R., Darnall, K. R., Lloyd, A. C., Winer, A. M. & Pitts, J. N. Jr Adv. Photochem. 11, 375-487 (1979).
- Perry, R. A., Atkinson, R. & Pitts, J. N. Jr J. phys. Chem., Ithaca 81, 296-304 (1977).
 Finlayson-Pitts, B. J. & Pitts, J. N. Jr Angew. Chem. 14, 1-14 (1975).

- Niki, H., Daby, E. E. & Weinstock, H. Adv. Chem. Ser. 113, 16-42 (1972).
 Crutzen, P. J. & Gidel, L. T. J. geophys. Res. 88, 6641-6661 (1983).
 Logan, J. A., Prather, M. J., Wofsy, S. C. & McElroy, M. B. J. geophys. Res. 86, 7210-7254 (1981).
- 14. Graedel, T. E., Farrow, L. A. & Weber, T. A. Atmos. Envir. 10, 1095-1101 (1976).
- 15. Calvert, J. G. Envir. Sci. Technol. 10, 256-262 (1976).
- 16. Singh, H. B. Geophys. Res. Lett. 4, 453-456 (1977).
- 17. Volz, A., Ehhalt, D. H. & Derwent, R. G. J. geophys. Res. 86, 5163-5171 (1981).

Structure determination of α -CrPO₄ from powder synchrotron X-ray data

J. Paul Attfield*‡, A. W. Sleight* & A. K. Cheetham†

- * E. I. du Pont de Nemours and Company, Central Research and Development Department, Experimental Station, Wilmington, Delaware 19898, USA
- † Chemical Crystallography Laboratory, University of Oxford,
- 9 Parks Road, Oxford OX1 3PD, UK

Knowledge of the ordered atomic structures of crystalline materials is essential in many areas of science. Single-crystal X-ray diffraction is the technique most often used for both solving and refining crystal structures, but recently, powder diffraction methods have become increasingly important. Many structures have been successfully refined with powder data by using the Rietveld profile method1 to overcome the problem of overlapping Bragg peaks, but attempts to solve structures ab initio, which require a set of well-resolved Bragg intensities, have proved unsuccessful (with a few notable exceptions^{2,3}). However, a new generation of extremely high-resolution powder X-ray4 and neutron5 diffractometers now allows the ab initio determination of crystal structures from powder data (see ref. 6). As part of our study of the structural and magnetic properties of transition-metal phosphates^{7,8}, we present here the structure of \alpha-CrPO_4, solved from powder X-ray data obtained at the Brookhaven National Synchrotron Light Source, and confirmed by a Rietveld analysis of neutron data collected with the diffractometer Dla at the Institut Laue-Langevin, Grenoble.

Two isostructural modifications of $CrPO_4$ are known⁹. β -CrPO₄ is isostructural with CrVO₄¹⁰, and its atomic and spiral magnetic structure have recently been refined using low-temperature neutron data⁸. Above 1,175 °C, the light-green β phase transforms to the dark-blue α form, considered here. In order to compare the magnetic properties of the two polymorphs in detail, it is necessary to know the structure of α -CrPO₄, but neither this material, nor CrAsO₄¹¹, its only known isotype, has been prepared as single crystals. However, α-CrPO₄ is formed as a highly crystalline powder, making it a suitable candidate for study by high-resolution powder methods.

A polycrystalline sample of α-CrPO₄ was prepared by evaporating a solution containing equimolar quantitites of Cr(NO₃)₃·9H₂O (Fisher, certified) and (NH₄)₂HPO₄ (Fisher,

Table 1 Profile and structural parameters from the Rietveld analysis of the second synchrotron data set

Profile parameters

Half-width parameters (0.01°)*

U = 320(15),V = -115(6), Gaussian W = 12.7(5)

X = 4.2(3), Lorentzian Y = 0.46(6)

Zero-point $(0.01^{\circ}) = -1.50(2)$

Cell constants (Å) a = 10.40583(11),b = 12.89952(11), c = 6.29933(6)

Structural parameters†

Overall isotropic temperature factor = $0.57(8) \text{ Å}^2$ Fractional atomic coordinates in Imma (no. 74)

Atom	Symmetr postion	•	у	z
Cr(1)	4b	0.5000	0,5000	0.0000
Cr(2)	8g	0.2500	0.3659(3)	0.2500
	_		0.3650(3)N‡	
P(1)	4e	0.5000	0.2500	0.0801(13)
				0.0824(6)N
P(2)	8g	0.2500	0.5740(5)	0.2500
			0.5739(2)N	
O(1)	8i	0.3800(11)	0.2500	0.2275(17)
		0.3778(3)N		0.2267(4)N
O(2)	16j	0.3601(7)	0.4912(6)	0.2155(12)
		0.3613(2)N	0.4903(1)N	0.2146(3)N
O(3)	16j	0.2259(7)	0.6353(6)	0.0576(10)
		0.2234(1)N	0.6367(1)N	0.0553(2)N
, O(4)	8h	0.5000	0.3507(8)	-0.0468(16)
			0.3490(2)N	-0.0448(4)N
Bond distan				
Cr(1)-O(2)		1.994(8)	$P(1)-O(1) (\times 2)$	
Cr(1)-O(4		1.95(1)	$P(1)-O(4) (\times 2)$	
Cr(2)-O(1		2.02(1)	$P(2)-O(2) (\times 2)$	1.58(1)
Cr(2)-O(2)		1.99(1)	$P(2)-O(3) (\times 2)$	1.47(1)
Cr(2)-O(3	3) (×2)	1.95(1)		

^{*}The two full-width at half maximum (FWHM) functions are: $FWHM = (U \tan^2 \theta + V \tan \theta + W)^{1/2}$ $FWHM = X \tan \theta + Y/\cos \theta.$

certified A.C.S.) until a green, glassy residue remained, and then heating this residue at 1,400 °C for 20 min. Prolonged heating of α -CrPO₄ above 1,175 °C was found to cause decomposition, although the material seems to be stable at ambient temperatures. The composition was confirmed by atomic absorption analysis: observed %Cr = 35.40, %P = 18.27; calculated %Cr = 35.36, % P = 21.08. The X-ray powder pattern agreed with that reported for α -CrPO₄¹², and all the reflections could be indexed on a body-centred orthorhombic cell with a = 10.405 Å, b =12.898 Å, c = 6.297 Å. We also observed the reflection condition h, k = 2n, making Imma the highest-symmetry space group possible.

Synchrotron X-ray data were collected on the X13A beam-line at the Brookhaven NSLS. X-rays with a wavelength of 1.323 Å from a perfect Ge(111) crystal monochromator, diffracting in the horizontal plane, impinged upon a flat-plate sample, and the scattering in the vertical plane was measured using a perfect Ge(220) analyser crystal and detector. A full description of the diffractometer and its resolution will be given elsewhere (D. E. Cox, L. P. Carduso, J. B. Hastings & L. W. Finger, in preparation). The sample was mixed with an equal volume of amorphous silica to minimize preferred orientation effects, and the sample tray was oscillated by 1° around the θ -axis to further reduce these effects and to increase the number of crystallites sampled by the beam. Data were collected from 10.50 to 64.50° 2θ at 0.01° intervals, with a count time of 2 s per step. The incident beam intensity was $\sim 5 \times 10^9$ photons s⁻¹, with the storage ring operating at 2.4 GeV and 50 mA.

All of the sharp diffraction peaks observed could be indexed

[‡] Permanent address: Chemical Crystallography Laboratory, University of Oxford, Oxford OX1 3PD, UK.

[†] Refined coordinates from the neutron experiment at 25 K (marked N) are given for comparison.

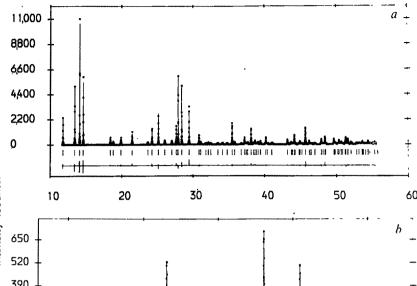


Fig. 1 Observed (points), calculated (bold line), and difference profiles for: a, the second synchrotron dataset ($\lambda = 1.323 \, \text{Å}$), and b, neutron data collected at 25 K ($\lambda = 1.95 \, \text{Å}$). Reflection positions are marked (short vertical lines).

25 50 75 100 125 2e (deg.)

on the unit cell of α-CrPO₄ in space group Imma, and integrated intensities were obtained for 68 well-resolved peaks. After multiplicity and Lorentz corrections, these were used to generate a Patterson map which yielded two heavy-atom positions (Cr(2) and P(2)). These were used to start phasing the data, and the remaining atoms were located using several Fourier maps, bearing in mind geometric considerations. During this process-we realized that only 12 formula units were present in the unit cell, instead of 16 as had been proposed¹². The resulting coordinates were used as the starting model for a Rietveld analysis of the entire profile. A modified version of the standard Rietveld/ Hewat^{1,13} program was used¹⁴, with peaks shapes described by a 'pseudo-Voigt' function¹⁵. This approximates the convolution of gaussian (instrumental resolution) and lorentzian (sample broadening) functions. However, variations in peak shape and poor counting statistics gave a relatively poor fit $(R_{WP} = 24.1\%)$, and did not improve the structural model $(R_{\text{NUC}} = 11.8\%)$; R_{WP} and R_{NUC} are defined in reference (1).

To obtain a better refinement of the structure, a second set of synchrotron data was collected from the same α -CrPO₄/silica mixture, placed in a glass capillary tube (1.0 mm radius) which was rotated around the θ -axis. This reduces preferred orientation effects more effectively than the rocking flat-plate method used above. The region around each Bragg peak position was counted for 4s per 0.01° step. The longer count time and an increased beam current of 100 mA gave better statistics on the diffraction intensities than those of the first data set. The data were corrected for capillary absorption and the above starting model was refined using the same Rietveld program. A significantly better fit was obtained ($R_{\rm WP}$ =16.9%) and the quality of the structure also improved ($R_{\rm NUC}$ =7.0%). The results of this refinement are given in Table 1, and the observed, calculated, and difference profiles are shown in Fig. 1a.

In addition, during our studies of the low-temperature magnetic properties of α -CrPO₄, a set of neutron data was collected using diffractometer D1a at the ILL, Grenoble. The scattering from a sample of pure α -CrPO₄, held in a vandium can in a cryostat at 25 K, was measured in the range 6-136° 2θ in 0.05°

steps at a mean neutron wavelength of 1.95Å. A Rietveld analysis of this data set, which contains no magnetic diffraction peaks, gave an excellent fit ($R_{\rm WP}=10.4\%$), as shown in Fig. 1b, confirming the structure and showing that there is no evidence for the symmetry of the structure being lower than Imma. The refined coordinates are given in Table 1 for comparison with the X-ray values; a fuller discussion and more details of these refinements will be presented in a future publication.

The structure of α -CrPO₄ consists of an infinite network of linked CrO₆ octahedra and PO₄ tetrahedra. Pairs of edge-sharing Cr(2)O₆ octahedra, interconnected by P(2)O₄ tetrahedra, form sheets in the b-c plane (Fig. 2). These are linked to each other

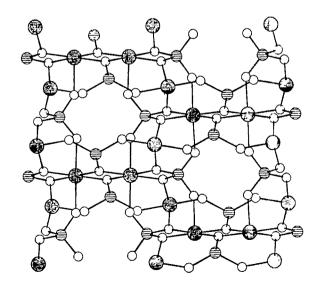


Fig. 2 View of the (100) plane of α -CrPO₄ (y horizontal, z vertical), showing the coordination of the bidentate phosphate groups to edge-sharing pairs of CrO₆ octahedra (Cr, large shaded circles, P, medium striped circles; O, small open circles).

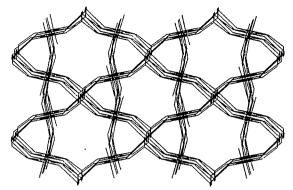


Fig. 3 Stick model of the structure of α -CrPO₄ close to (010), showing the channels parallel to b. x is near-horizontal and z is vertical.

by chains of alternating Cr(1)O₆ octahedra and P(1)O₄ tetrahedra running parallel to b, resulting in the formation of large channels in this direction (Fig. 3). An interesting feature of this structure is the sharing of a common edge between a P(2)O₄ tetrahedron and a Cr(2)O₆ octahedron, both of which are distorted, resulting in a short non-bonding Cr-P distance of 2.68(1) Å and an O-O contact of 2.33(2) Å. The bond distances given in Table 1 and the bond angles (which can be obtained from the authors) are similar to those in β-CrPO₄¹¹ and other chromium phosphates. Although the $3d^3$ electronic configuration of the Cr3+ ion favours regular octahedral coordination, the connectivity of this framework necessarily gives rise to distortions of the polyhedra.

The fact that neither α-CrPO₄ nor CrAsO₄ is thermally stable under the conditions of their formation implies that these compounds are metastable. The persistence of these materials at ambient temperatures may be due to the well-known kinetic

inertness of octahedral Cr3+ towards the dissociative ligand exchange that must accompany their decomposition. This also explains why no other trivalent metal phosphate, nor any other ABO₄ compound, has been found to adopt this structure. The cause of this instability is presumably the strained planar fourmembered ring resulting from the bidentate phosphate group. The intra-annular angles around Cr(2), P(2) and the two O(2)atoms are 72, 95 and 97° respectively, showing that all are highly distorted from their preferred geometries.

This work was made possible by the excellent instrumentation and software on the X13A beam-line at the National Synchrotron Light Sourse, Brookhaven National Laboratory, which is supported by the U.S. Department of Energy, Divisions of Materials Sciences and Chemical Sciences. In particular, we thank, Drs D. E. Cox (BN Laboratory) and L. W. Finger (Carnegie Institute) for their efforts in making this a highly valuable facility. The authors also wish to thank SERC for the provision of neutron facilities and a studentship for J.P.A., and Drs J. C. Calabrese, C. J. Eyermann, R. Fischer and R. L. Harlow for assistance with local computer programs.

Received 20 March: accepted 16 May 1986.

- 1. Rietveld, H. M. J. appl. Crystallogr. 2, 65-71 (1969)
- Berg, J.-E. & Werner, P.-E. Z. Kristallogr. 145, 310-320 (1977).
- Christensen, A. N., Lehmann, M. S. & Neilsen, M. Aust. J. Phys. 38, 497-505 (1985).
 Cox, D. E., Hastings, J. B., Thomlinson, W. & Prewitt, C. Nucl. Instrum. Meth. 208, 573-578
- 5. Johnson, M. W. & David, W. I. F. Rutherford-Appleton Lab. Rep. No. 85/112 (1985).
- Cheetham, A. K. et al. Nature 320, 46-48 (1986)
- Battle, P. D. et al. J. Phys. C15, 1919-1924 (1982).

 Attfield, J. P., Battle, P. D. & Cheetham, A. K. J. Solid St. Chem. 57, 357-361 (1985).
- Shafer, M. W. & Roy, R. J. Am. chem. Soc. 78, 1087-1089 (1956).
 Frazer, B. C. & Brown, P. J. Phys. Rev. 125, 1283-1291 (1962).
- 11. Ronis, M. M. C. r. hebd. Séanc. Acad. Sci., Paris 271C, 64-66 (1970).
- 12. Swanson, H. E. et al. Natn. Bur. Sids. (U.S.), 25, 2, 12 (1963)
- 13. Hewat, A. W. U.K. Atom Energy Auth. Res. Gr. Rep. No. RRL73/897 (1973).
- Cox, D. E. Acta crystallogr. A40, C369 (1984).
 Young, R. A. & Wiles, D. B. J. appl. Crystallogr. 15, 430-438 (1982).

Formation of ultra-fine amorphous alloy particles by reduction in aqueous solution

Jacques van Wonterghem*, Steen Mørup*, Christian J. W. Koch†, Stuart W. Charles‡ & Steven Wells‡

* Laboratory of Applied Physics II, Technical University of Denmark, DK-2800 Lyngby, Denmark

† Chemistry Department, Royal Veterinary and Agricultural University, DK-1871 Frederiksberg C, Denmark

‡ Department of Physics, University College of North Wales, Bangor LL57 2UW, UK

Amorphous alloys are normally prepared as thin ribbons or films by the liquid quench technique or by vapour deposition. Recently we have shown that ultra-fine amorphous Fe-C alloy particles can be prepared by thermal decomposition of Fe(CO), in an organic liquid; that is, by a chemical reaction. Here we report the preparation of small alloy particles by reduction of metal ions by KBH4 in aqueous solutions. Mössbauer and X-ray diffraction studies show that the particles are amorphous. The amorphous phase is formed because the chemical reaction takes place below the glass transition temperature and because boron atoms are present in the particles. The method may be used for the large-scale production of ultra-fine amorphous alloy particles, which may have applications in ferrofluids, magnetic memory systems and catalysis.

Reduction of metal ions in aqueous solutions by use of KBH₄ has been described elsewhere^{2,3}. Oppegard et al.³ found that reduction of solutions of FeSO₄ or mixtures of FeSO₄ and CoCl₂ by KBH₄ resulted in the formation of small magnetic particles. X-ray diffraction studies of the particles revealed the presence of diffuse lines corresponding to α -iron.

In the present study we have prepared similar material by adding drops of an aqueous solution of FeSO₄ and CoCl₂ with an Fe: Co molar ratio of 7:3 to an excess of 1 M KBH₄. The solutions were mixed by vigorous stirring and the black precipitate was washed in water and then in acetone. Mössbauer spectra were obtained using a constant-acceleration spectrometer with a source of ⁵⁷Co in rhodium. X-ray diffractographs were obtained with a powder diffractometer equipped with a diffracted-beam graphite monochromator. Magnetic measurements were made with a vibrating-sample magnetometer. The samples were studied before and after annealing at 725 K for 2 h in H₂.

Figure 1 shows room-temperature Mössbauer spectra of the sample. Before annealing, the spectrum exhibits very broad lines, indicating a distribution in magnetic hyperfine fields. The isomer shift relative to α -Fe is 0.19 mm s⁻¹ and the quadrupole

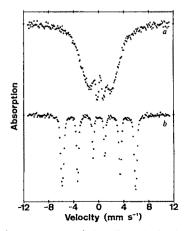


Fig. 1 Mössbauer spectra of the alloy obtained at room temperature: a, before annealing; b, after annealing at 725 K.

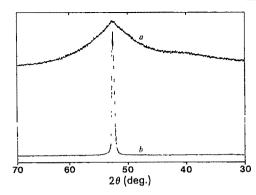


Fig. 2 X-ray diffractographs of the alloy: a, before annealing; b, after annealing at 725 K. The diffractographs were obtained using Co K, radiation.

shift is negligible. The average magnetic hyperfine field is ~18 T, which is considerably smaller than those of crystalline Fe-Co alloys. The magnetic hyperfine field is also smaller than those of amorphous (Fe_{1-x}Co_x)₈₀B₂₀ alloys produced by the liquid quench technique⁴, but is similar to those of amorphous Fe-B alloys with higher boron content.

After annealing, the Mössbauer lines are considerably sharper and the average magnetic hyperfine field increases to 36.5 T, whereas the isomer shift decreases to $\sim 0.03 \text{ mm s}^{-1}$. These parameters are close to those of a crystalline Fe-Co alloy with an Fe:Co ratio of 7:3 (ref. 6). Thus the Mössbauer results indicate that amorphous Fe-Co-B particles are formed during the preparation and that these particles crystallize during annealing at 725 K.

Further evidence for this conclusion is obtained from the X-ray diffraction studies (Fig. 2). Before annealing, the diffractograph shows only a very broad line, indicating the absence of crystalline phases⁷. After annealing, a sharp diffraction line is observed corresponding to a well-crystallized Fe-Co alloy.

Chemical analysis of the particles showed that the composition of the amorphous alloy is Fe₄₄Co₁₉B₃₇; that is, the ratio between iron and cobalt atoms is identical to that in the original aqueous solution. The relatively high boron content explains the low value of the magnetic hyperfine field.

The saturation magnetization of the amorphous Fe₄₄Co₁₉B₃₇ alloy is 89 J T⁻¹ kg⁻¹. After annealing it rises to 166 J T⁻¹ kg⁻¹ which is below the value of 240 J T⁻¹ kg⁻¹ for a pure crystalline Fe₇₀Co₃₀ alloy. The lower value is presumably due to the presence of boron in the alloy or in a separate phase. Infrared spectroscopy of the annealed samples indicated the presence of a boron oxide.

From the Mössbauer and X-ray diffraction spectra it can be concluded that the material formed by reduction of iron and cobalt ions in solution is an amorphous alloy which crystallizes during annealing at 725 K. We have also studied samples prepared from solutions with iron and nickel or with iron alone, and the Mössbauer and X-ray diffraction results for these samples are similar to those of the Fe-Co-B alloy particles. Chemical analysis yielded the compositions Fe₃₇Ni₂₈B₃₄ and Fe₆₂B₃₈, respectively. Electron microscopy of the samples revealed that the particle dimensions are in the range 10-100 nm, depending on the preparation conditions.

Because amorphous alloys are stable only below the glass transition temperature, Tg, a requirement for the formation of amorphous alloy particles by chemical methods is that the chemical reaction takes place below T_g . For pure iron, T_g is far below room temperature; therefore, one or more other elements must be present in order to stabilize the amorphous structure at room temperature. In the present particles, boron atoms from KHB₄ have entered into the alloy particles as a stabilizing element during the chemical reaction.

When amorphous alloys are prepared by the conventional liquid quench technique it is essential that the material is cooled

very rapidly from the melting temperature to a temperature below $T_{\rm g}$. This is because the alloys crystallize easily between these temperatures. Therefore, when using this technique, a composition close to the eutectic one facilitates the formation of an amorphous phase. However, when producing amorphous alloys by chemical methods at low temperature the only restriction is that the reaction take place at a temperature below $T_{\rm g}$. It is therefore likely that these chemical techniques may allow the formation of amorphous alloys with compositions which cannot easily be produced by the liquid quench technique.

Financial support from the Danish Technical Research Council is gratefully acknowledged.

Received 17 April; accepted 21 May 1986.

- 1. van Wonterghem, J., Mørup, S., Charles, S. W., Wells, S. & Villadsen, J. Phys. Rev Lett **55**, 410–413 (1985).

- Schlesinger, H. et al. J. Am. chem. Soc. 75, 215-219 (1953).
 Oppegard, A. L., Darnell, F. J. & Miller, H. C. J. appl. Phys. 32, 1848-1858 (1961).
 Dey, S., Deppe, P., Rosenberg, M., Luborsky, F. E. & Walter, J. L. J. appl. Phys. 52. 1805-1807 (1981).
- 5. Nakajimi, T., Nagami, I. & Ino, H. J. Mater. Sci. Lett. 5, 60-62 (1986).
- Johnson, C. E., Ridout, M. S. & Cranshaw, T. E. Proc. phys. Soc. 81, 1079-1090 (1963).
 Klug, H. P. & Alexander, L. E. X-ray Diffraction Procedures for Polycrystalline and Amorpho Materials, 2nd edn (Wiley, New York, 1974).

Latter-day origin of diamonds of eclogitic paragenesis

Stephen H. Richardson

Laboratoire de Geochimie et Cosmochimie, Institut de Physique du Globe de Paris, 4, place Jussieu. 75252 Paris Cedex 05, France

Syngenetic mineral inclusions in diamonds provide the best means of determining their origin. Among such inclusions, the peridotitic paragenesis of olivine, orthopyroxene and chrome-pyrope garnet is on average far more abundant than the eclogitic paragenesis of pyrope-almandine garnet and omphacitic clinopyroxene 1-3. Diamonds of peridotitic paragenesis from the ~100-Myr-old Kimberley and Finsch kimberlites in southern Africa were previously shown to have originated in 150-200-km-thick lithosphere beneath the Kaapvaal craton ~3,300 Myr ago^{4,5}. At a few localities, such as the Premier kimberlite in southern Africa and the Argyle lamproite in northwestern Australia, diamonds of eclogitic paragenesis predominate⁶⁻⁸, allowing recovery of sufficient material for complementary analysis, the results of which are reported here. Eclogitic garnet and clinopyroxene inclusions in Premier and Argyle diamonds yield Sm-Nd isochron ages of 1,150 and 1,580 Myr respectively, compared with host diatreme emplacement ages^{9,10} of 1,100-1,200 Myr. Eclogitic inclusion ages and precursor isotopic signatures indicate a second genetically distinct origin of diamonds, apparently related in time and space to kimberlite or lamproite magmatism.

The Premier kimberlite is located in the interior of the Archaean Kaapvaal craton and is the only Precambrian diatreme in southern Africa currently exploited for diamonds⁶. It has been difficult to determine the precise age of emplacement because of the altered nature of the kimberlite matrix material, thermal effects of a cross-cutting sill and absence of zircons for U-Pb analysis. Nevertheless, a phlogopite Rb-Sr age of ~1,250 Myr has been available for some time11, together with a minimum age of 1,100 Myr dictated by the cross-cutting sill¹². Then, following early work by Welke et al.¹³, Kramers⁹ obtained a model Pb age of ~1,200 Myr for presumed sulphide inclusions in Premier diamonds. More recently, two essentially identical Rb-Sr and Sm-Nd ages of 1,180±30 Myr have been obtained using diopside and garnet megacrysts14,15

The Argyle lamproite is located in the Proterozoic Halls Creek mobile zone adjacent to the Kimberley craton in northwestern

Table 1 Rb-Sr and Sm-Nd concentrations* and isotope ratios† for eclogitic garnet and clinopyroxene inclusions in diamonds‡ from the Argyle lamproite and Premier kimberlite

	Wt (mg)	Rb	Sr	⁸⁷ Rb/ ⁸⁶ Sr	⁸⁷ Sr/ ⁸⁶ Sr	⁸⁷ Sr/ ⁸⁶ Sr _i	Sm	Nd	¹⁴⁷ Sm/ ¹⁴⁴ Nd	¹⁴³ Nd/ ¹⁴⁴ Nd	143 Nd/144 Nd
Argyle§						•					
d.o.gar	4.61	0.003	15.85	0.0006	0.70588 (2)	0.70587	3.231	5.392	0.3623	0.514205 (16)	0.51045
p.o.gar	1.91	0.009	19.87	0.0013	0.70540(2)	0.70537	3.220	6.946	0.2803	0.513288 (17)	0.51038
p.g.cpx	0.22	0.381	427.8	0.0026	0.70589 (2)	0.70583	1.084	5.357	0.1224	0.511719 (79)	0.51045
Premier		1									
d.o.gar	2.56	0.004	1.74	0.0058	0.70270(3)	0.70260	0.8545	1.101	0.4696	0.515112 (49)	0.51156
p.o.gar	4.71	0.002	3.00	0.0023	0.70233 (2)	0.70229	0.7463	1.068	0.4226	0.514537 (27)	0.51134
p.g.cpx	1.86	0.167	103.6	0.0047	0.70225 (2)	0.70217	0.5721	2.044	0.1692	0.512840 (63)	0.51156

* Concentrations in p.p.m. (µg per g), after correction for minimum applicable blanks: Rb, 3 pg; Sr, 3 pg; Sm, 2 pg; Nd, 2 pg. Estimated analytical

uncertainties in concentrations (ignoring small-sample weighing errors) indicated by number of significant digits.

† Present-day ⁸⁷Sr/⁸⁶Sr and ¹⁴³Nd/¹⁴⁴Nd ratios normalized to 0.70800 and 0.51264 for standards E & A SrCO₃ and BCR-1, respectively. In-run precision given by errors $(2\sigma_{\text{mean}})$ corresponding to least significant digits. Initial ratios (denoted by subscript i) calculated for Argyle and Premier diamond crystallization ages of 1,580 and 1,150 Myr, respectively, using $\lambda_{\text{Rb}} = 1.42 \times 10^{-11} \text{ yr}^{-1}$ and $\lambda_{\text{Sm}} = 6.54 \times 10^{-12} \text{ yr}^{-1}$.

‡ Selected from -7+5 diamond sieve fraction (1.8-2.5 mm diameter) of general mine production.

§ Argyle composites: ~460 deep-orange garnets (d.o.gar) and 190 pale-orange garnets (p.o.gar) (avg. wt 10 μg); ~70 pale-green clinopyroxenes (p.g.cpx) (avg. wt 3 μg).

Premier composites: ~175 d.o.gar and 325 p.o.gar (avg. wt 15 μg); ~250 p.g.cpx (avg. wt 7 μg).

Australia, and is the first diamondiferous diatreme in the region to be brought into commercial production¹⁶. A preliminary phlogopite Rb-Sr age of 1.130 Myr for the magmatic phase of the intrusion¹⁰ is consistent with the geochronology of the host country rock succession, which has a maximum age of \sim 1,200 Myr (refs 16-18).

Premier diamond inclusion mineralogy, abundances and major element compositions are described in detail in ref. 6. The eclogitic assemblage of sulphides, orange garnet, pale-green clinopyroxene and rare kyanite and coesite comprises ~60% of inclusions, with the peridotitic assemblage of sulphides, olivine, orthopyroxené, minor purple garnet and chromite, and rare bright-emerald-green clinopyroxene accounting for the remainder⁶. Argyle diamond inclusion characteristics are outlined in refs 7 and 8. Here the eclogitic assemblage of orange garnet, pale-green clinopyroxene, sulphides, and minor kyanite, rutile and coesite is even more dominant, accounting for up to 90%

To study the age and origin of these assemblages, the most suitable radiogenic isotope systems are Sm-Nd, Rb-Sr and U-Th-Pb. Although sulphides, the most likely carriers of Pb (ref. 9), appear to be a major inclusion phase at Premier (and to a lesser extent at Argyle), they are difficult to characterize and cannot easily be assigned to either paragenesis^{6,8}. In contrast, the different garnets and clinopyroxenes, the major carrier phases of Nd and Sr, are relatively easily distinguished on the basis of colour, especially after they have been broken out of the host diamonds. This is important because small inclusion size, coupled with Nd concentrations of only a few p.p.m., necessitates the combining of cogenetic inclusions of a given phase⁴. Eclogitic garnets and clinopyroxenes selected for each composite sample in Table 1 were recovered from diamonds bearing monomineralic inclusions, except for scarce Argyle clinopyroxenes, most of which came from diamonds also containing garnets. Touching clinopyroxene and garnet inclusions, which at mantle temperatures would tend to equilibrate continuously with each other by interdiffusion, are rare and such specimens were excluded. Otherwise, Nd and Sr diffusion through intervening diamond is assumed to be negligible⁴. Eclogitic garnets were subdivided on the basis of colour into deep-orange and pale-orange fractions, a distinction which is more clearly developed at Argyle than at Premier. No convincing examples of a pale-orange garnet-clinopyroxene pair were found in available bimineralic-inclusion-bearing diamonds, indicating that pale-orange garnets probably did not coexist with a separate clinopyroxene phase, as also suggested by Sm/Nd partition relationships. Small-sample preparation tech-

niques and mass spectrometric facilities for determination of Sm, Nd, Rb and Sr concentrations and isotope ratios (Table 1) are the same as those used by Richardson et al.4 except for a new (1985) clean lab (belonging to S.R. Hart) and an improved Sr loading technique with higher ion yield19

Nd and Sr concentrations in Argyle inclusions are, on average, five times higher than those in their Premier counterparts, while Sm/Nd ratios are lower by a factor of 1.4 (Table 1). The Sm/Nd ratios, particulary those for garnet (0.5-0.8), are sufficient to produce substantial increases in the 143Nd/144Nd ratio on a timescale of 1,000 Myr, whereas the Rb/Sr ratios are all extremely low (0.0002-0.002), resulting in barely significant increases in 87 Sr/ 86 Sr ratio. Thus, 87 Sr/ 86 Sr ratios can be used to verify the cogeneticity of garnet and clinopyroxene inclusions from separate diamonds, which have been combined and paired

for the derivation of Sm-Nd isochron age relationships.

Present-day ¹⁴⁷Sm/¹⁴⁴Nd and ¹⁴³Nd/¹⁴⁴Nd ratios (Table 1) are plotted on a Sm-Nd isochron diagram in Fig. 1. The Argyle

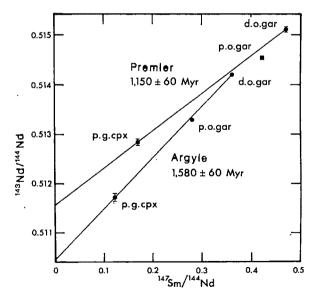


Fig. 1 Sm-Nd isochron diagram for eclogitic garnet and clinopyroxene inclusions in Argyle and Premier diamonds. Measurement errors $(2\sigma_{mean})$ are indicated except where smaller than the size of plotted points. Ages are for deep-orange garnetpale-green clinopyroxene pairs, using $\lambda_{Sm} = 6.54 \times 10^{-12} \, \text{yr}^{-1}$. Assigned errors are derived from the maximum and minimum slopes allowed by measurement errors.

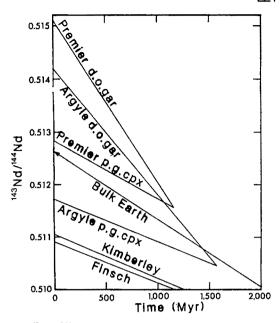


Fig. 2 ¹⁴³Nd/¹⁴⁴Nd evolution diagram, showing curves for eclogitic garnet and clinopyroxene inclusions in Argyle and Premier diamonds. Curves are constructed from measured ¹⁴³Nd/¹⁴⁴Nd and ¹⁴⁷Sm/¹⁴⁴Nd ratios and terminate at the times of diamond crystallization from Fig. 1. Curves for peridotitic garnet inclusions in Kimberley and Finsch diamonds and the bulk Earth curve are from Richardson et al.⁴ and references therein.

deep-orange garnet-clinopyroxene pair defines an age of 1,580 ± 60 Myr, with assigned error derived from the maximum and minimum slopes allowed by $2\sigma_{mean}$ measurement errors (Table 1). The Argyle pale-orange garnet with intermediate Sm/Nd ratio falls below and outside the analytical errors of this twopoint isochron. In addition, the initial 87Sr/86Sr ratios of the deep-orange garnet and clinopyroxene are within error of each other (0.7059), while that of the pale-orange garnet is slightly but significantly lower (0.7054). In analogous fashion, the Premier deep-orange garnet-clinopyroxene pair defines an age of 1,150 ± 60 Myr, with the pale-orange garnet again having an intermediate Sm/Nd ratio and lying below the two-point iso-chron. In this case, all three initial ⁸⁷Sr/⁸⁶Sr ratios are slightly but significantly different (d.o.gar: 0.7026; p.g.cpx: 0.7022; p.o.gar: 0.7023). However, the deep-orange garnet Sr concentration (1.7 p.p.m.) and amount (4 ng) were the lowest measured, and minor sample impurity may have affected the measurement. Thus, the clinopyroxene Sr isotope ratio is considered to be more representative.

The Argyle eclogitic diamond inclusion age of 1,580 Myr is ~450 Myr greater than the host lamproite emplacement age10 of 1,130 Myr, and closer to the ~1,800 Myr age of stabilization of the surrounding Halls Creek mobile zone¹⁶. Although this indicates that Argyle eclogitic diamonds are xenocrysts in the host lamproite, it does not preclude an original phenocrystal relationship with similar small-volume mantle magmatism ~450 Myr earlier and subsequent lithospheric storage. In contrast, the Premier eclogitic diamond inclusion age of 1,150± 60 Myr is within error of the preferred host kimberlite age^{14,15} of 1,180 ± 30 Myr, and in agreement with the sulphide inclusion Pb model age of ~1,200 Myr obtained by Kramers⁹. There is thus no resolvable time difference between Premier eclogitic diamond crystallization and host kimberlite emplacement. However, the aggregation state of nitrogen in Premier eclogitic diamonds³⁰ requires mantle storage for a finite time interval (~1-10 Myr at 1,270 °C, the crystallization temperature⁶; T. Evans and J. W. Harris, personal communication) before removal to the surface.

Further evidence relating to eclogitic diamond origin is pro-

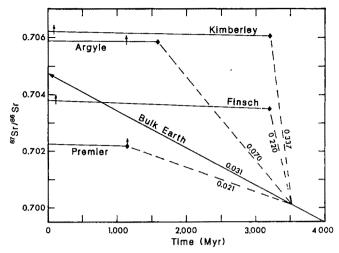


Fig. 3 87Sr/86Sr evolution diagram, showing curves for eclogitic garnet and clinopyroxene inclusions in Argyle and Premier diamonds. Curves are constructed from measured 87Sr/86Sr and 87Rb/86Sr ratios and terminate at the times of diamond crystalization (diamond symbols) from Fig. 1. Times of host diatreme emplacement are also indicated (vertical arrows). Garnet and clinopyroxene Rb/Sr ratios are so low that the corresponding evolution curves are virtually horizontal. Hypothetical precursor evolution curves (dashed) emanating from the bulk Earth at 3,500 Myr and corresponding time-integrated Rb/Sr ratios are shown for reference. Curves for peridotitic garnet inclusions in Kimberley and Finsch diamonds and the bulk Earth curve are from Richardson et al.14 and references therein.

vided by the initial Nd and Sr isotopic ratios of the inclusions at the time of their crystallization and encapsulation by diamond (Table 1). These are plotted in Nd and Sr isotope evolution diagrams (Figs 2, 3), for comparison with those of potential precursors. The Premier deep-orange garnet-clinopyroxene pair (and to a lesser extent the pale-orange garnet) has a substantially higher initial Nd isotopic ratio ($\varepsilon_{Nd} = +8$) and lower initial Sr isotopic ratio (0.70217) than those of the bulk Earth at 1,150 Myr. These are the isotopic characteristics of asthenospheric upper mantle such as that now giving rise to the most depleted (low time-integrated Nd/Sm and Rb/Sr) mid-ocean-ridge basalts (MORB). Similar, although less extreme, initial Sr and/or Nd isotopic ratios have previously been measured in Premier clinopyroxene inclusions^{13,9}, carbonatite¹³ and megacryst garnet and diopside¹⁵, although apparently not in kimberlite matrix material²⁰. In addition, the majority of Premier eclogiticinclusion-bearing diamonds have δ^{13} C values of -3 to -6 (ref. 21), consistent with a MORB-type mantle carbon source (see, for example, ref. 22) and within the relatively narrow range of -1 to -8 observed for peridotitic-inclusion-bearing diamonds worldwide23. In contrast, the Argyle deep-orange garnetclinopyroxene pair (and similar pale-orange garnet) has initial Nd and Sr isotopic ratios ($\varepsilon_{\rm Nd} = -3$; $^{87}{\rm Sr}/^{86}{\rm Sr}_{\rm i} = 0.7059$) respectively lower and higher than those of the bulk Earth at 1,580 Myr (Figs 2, 3). These isotopic characteristics are indicative of a mildly enriched (high time-integrated Nd/Sm and Rb/Sr) component (or mixture of depleted and highly enriched components) akin to that found in old subcontinental lithosphere²⁴ and manifest in young West Kimberley lamproites^{25,26}, although the initial ratios for the host Argyle lamproite itself have yet to be determined. Eclogitic-inclusion-bearing diamonds from Argyle have δ^{13} C values of -8 to -16 (E. M. Galimov, personal communication), clearly distinct from those at Premier but within the range of values (+2 to -25) for eclogitic-inclusion-bearing diamonds worldwide²³.

The asthenospheric isotopic signature and almost immediate removal to the surface of Premier eclogitic diamonds contrasts with the lithospheric Nd and Sr component, ¹³C depletion and significant lithospheric storage of their Argyle counterparts.

Evidently, eclogitic-inclusion-bearing diamonds do not have a unique age or precursor but appear to be related in time and space to kimberlite or lamproite magmatism. In addition, these latter-day diamonds of eclogitic paragenesis are distinct in origin from those of the dominant peridotitic paragenesis formed ~2,000 Myr earlier in residual yet highly enriched Archaean lithosphere⁴ (Figs 2, 3). Further study of eclogitic-inclusionbearing diamonds from Cretaceous eruptives such as Orapa, in the Archaean Limpopo mobile belt²⁷, and Monastery, where garnets with high-pressure phase chemistry have recently been described²⁸, should help to elucidate this distinction and constrain global models of diamond genesis²⁹.

De Beers Consolidated Mines is acknowledged for providing specimens and support for the analytical phase of this work; the initiative of J. B. Hawthorne, expert supervision of J. W. Harris and efforts of J. Scott, A. van Niekerk and V. Anderson are appreciated. Special thanks to S. R. Hart, K. Burrhus, L. Gulen and J. Alley at MIT, where S.R.H.'s isotope lab is funded by NSF grant EAR83-08809. Continuing support from C. J. Allègre at IPG is gratefully acknowledged.

Received 15 April; accepted 19 May 1986.

- Meyer, H. O. A. & Tsai, H.-M. Miner. Sci. Engng 8, 242-261 (1976).
 Yefimova, E. S. & Sobolev, N. V. Dokl. Akad. Nauk SSSR 237, 1475-1478 (1977).
- Hawthorne, J. B., Gurney, J. J. & Harris, J. W. Ext. Abstr. 12th int. miner. Ass. Meet. (Novosibirsk, 1978).

- Richardson, S. H., Gurney, J. J., Erlank, A. J. & Harris, J. W. Nature 310, 198-202 (1984).
 Boyd, F. R., Gurney, J. J. & Richardson, S. H. Nature 315, 387-389 (1985).
 Gurney, J.J., Harris, J. W., Rickard, R. S. & Moore, R. O. Trans. geol. Soc. S. Afr. (in the press).
 Hall, A. E. & Smith, C. B. in Kimberlite Occurrence and Origin: A Basis for Conceptual
- Models in Exploration (eds Glover, J. E. & Harris, P. G.) 167-212 (University of Western Australia, Nedlands, 1984). 8. Harris, J. W. & Collins, A. T. Ind. Diam. Rev. 45, 128-130 (1985).

- 9. Kramers, J. D. Earth planet. Sci. Lett. 42, 58-70 (1979).
 10. Skinner, E. M. W., Smith, C. B., Allsopp, H. L., Scott-Smith, B. H. & Dawson, J. B. Trans. geol. Soc. S. Afr. (in the press).
- 11. Barrett, D. R. & Allsopp, H. L. Extr. Abstr. 1st int. Kimberlite Conf. 23 (University of Cape

- Allsopp, H. L., Burger, A. J. & Van Zyl, C. Earth planet. Sci. Lett. 3, 161-166 (1967).
 Welke, H. J., Allsopp, H. L. & Harris, J. W. Nature 252, 35-37 (1974).
 Smith, C. B. thesis, Univ. Witwaterstand (1983).
 Jones, R. A. thesis, Univ. Leeds (1984).
 Arkinson, W. J., Hughes, F. E. & Smith, C. B. in Kimberlites I: Kimberlites and Related Rocks (ed. Kornprobst, J.) 195-224 (Elsevier, Amsterdam, 1984).
- Roffinger, V. M. thesis, Australian National Univ. (1967).
 Bund, K. A., Derrick, G. M., Needham, R. S. & Shaw, R. D. in Precambrian of the Southern Hemisphere (ed. Hunter, D. R.) 205-307 (Elsevier, Amsterdam, 1981).
- Birck, J. L. Chem. Geol. (in the press).
 Basu, A. R. & Tatsumoto, M. Contr. Miner. Petrol. 75, 43-54 (1980).
- Deines, P., Gurney, J. J. & Harris, J. W. Geochim. cosmochim. Acta 48, 325-342 (1984).
 Des Marais, D. J. & Moore, J. G. Earth planet. Sci. Lett. 69, 43-57 (1984).

- Galimov, E. M. Geochem. Int. 22, 118-142 (1985).
 Richardson, S. H., Erlank, A. J. & Hart, S. R. Earth planet. Sci. Lett. 75, 116-128 (1985).
- McCulloch, M. T., Jaques, A. L., Nelson, D. R. & Lewis, J. D. Nature 302, 400-403 (1983). 26. Fraser, K. J., Hawkesworth, C. J., Erlank, A. J., Mitchell, R. H. & Scott-Smith, B. H. Earth planet. Sci. Lett. 76, 57-70 (1985).
- 27. Gurney, J. J., Harris, J. W. & Rickard, R. S. in Kimberlites II: The Mantle and Crust-Mantle Ourney, J. J., Frants, J. W. & Kickard, R. S. In Kimbernies II; The Mantin Relationships (ed. Kornprobst, J.) 1-9 (Elsewier, Amsterdam, 1984).
 Moore, R. O. & Gurney, J. J. Nature 318, 533-555 (1985).
 Haggerty, S. E. Nature 320, 34-38 (1986).

- 30. Davies, G. Nature 290, 40-41 (1981)

Upper mantle oxygen fugacity recorded by spinel lherzolites

Glen S. Mattioli & Bernard J. Wood

Department of Geological Sciences, Northwestern University, Evanston, Illinois 60201, USA

The oxygen fugacities (f_{O},s) recorded by rocks from the Earth's upper mantle have been the subject of much recent study and controversy1-7. Discussion has been stimulated by reported differences of several orders of magnitude between measurements made by different methods (Fig. 1). Oxygen fugacity is an important parameter because, together with temperature, pressure and composition, f_{O} , controls the petrogenesis of mantle-derived magmas, affects the composition and speciation of mantle fluids, and is an initial input into geochemical models of the evolution of the Earth's crust, mantle and hydrosphere. Here we report the determination of the f_{O_2} recorded by upper mantle spinel-lherzolite xenoliths entrained in alkaline magmas. This was done by experimentally calibrating the activity of the Fe₃O₄ (magnetite) component in MgAl₂O₄-rich synthetic spinel and applying these data to calculate thermobarometric f_{O} , s for the three-phase assemblage olivine-orthopyroxene-spinel. Results for appropriate model xenolith compositions, corrected to 15 kbar total pressure⁸ and plotted in temperature- f_{O_2} space, fall at or above the synthetic quartz-fayalite-magnetite buffer (Fig. 3). In contrast to earlier studies^{2,3}, we conclude that the shallow upper mantle does not retain an f_{O_2} signature of equilibrium with the metallic core, and that gaseous species in the C-H-O system will be dominated by CO₂ and H₂O (refs 9, 10), rather than CH₄ and H₂.

The f_{O_2} recorded by mantle spinel may be determined from either thermobarometric⁵⁻⁷ or intrinsic¹⁻⁴ measurements. In the thermobarometric method, a heterogeneous equilibrium, such as

$$= 6 \text{ Fe}_2 \text{SiO}_4 \text{ (in olivine)} + \text{O}_2 \tag{1}$$

is used together with analysed compositions of the relevant mineral phases and experimentally calibrated activity-composition relationships to yield an estimate of the f_0 , at constant

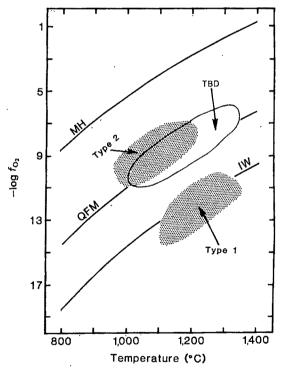


Fig. 1 Compilation of previous estimates of upper mantle f_{O_2} versus temperature at 1 atm total pressure. The stippled regions represent intrinsic measurements of type 2 spinel-lherzolite whole rocks and ilmenite separates⁴ ('Type 2'), and of type 1 spinel separates from spinel-lherzolite xenoliths²⁻⁴ ('Type 1'). The unshaded area ('TBD') represents thermobarometric data from ilmenite-bearing mantle nodules⁵, ilmenite-spinel intergrowths⁶ and terrestrial basalts7.

temperature and pressure⁵⁻⁷. In contrast, the intrinsic method is based on determination of single-phase, homogeneous defect equilibria¹¹. It is assumed that the concentration of defects (vacancies in the octahedral sublattice of the spinel phase, for example) is sufficient to buffer the f_{O_2} of a small volume of inert gas at the equilibrium value, which is measured using a zirconia solid electrolyte.

Figure 1 shows previous estimates of upper mantle f_{Ω} , together with the standard synthetic Fe-bearing buffers magnetitehaematite (MH), quartz-fayalite-magnetite (QFM) and ironwüstite (IW) at 1 atm total pressure. The oxygen fugacity estimates fall into two groups. First, thermobarometric estimates⁵⁻¹ for ilmenite-bearing mantle nodules and megacrysts, spinelilmenite intergrowths in nodules found in kimberlite, and Fe-Ti oxides in terrestrial basalts, all group within 1.5 log units of QFM. Second, intrinsic data, collected using a solid zirconia electrolyte technique, show a wide range of apparent f_{O_2} s. Early work on olivine phenocrysts from an oceanic tholeiite pillow¹ and the more recent data²⁻⁴ on spinel separates from type 1 lherzolite xenoliths (Cr-rich suite, Basaltic Volcanism Study Project¹²) are grouped near or below IW. This is up to four orders of magnitude more reducing than the f_{O_2} estimates calculated by thermobarometric methods on the same rocks. Intrinsic measurements of ilmenite separates and type 2 (Cr-poor suite) whole rocks, however, fall at or above QFM⁴. It is unclear why there is such a disparity between the intrinsic f_{O_2} s of type 1 and type 2 spinel lherzolites, as the spinels contain very similar amounts of Fe₃O₄. Intuitively, the similar mole fractions of Fe₃O₄ imply similar Fe₃O₄ activities and, from equilibrium (1), similar f_{O_2} s. In an effort to resolve the discrepancy, we present an experimentally calibrated data set for dilute magnetite activities on the pseudo-binary spinel join Fe₃O₄-MgAl₂O₄, at 800, 900 and 1,000 °C and 1 atm total pressure. This system approximates closely the compositions of spinels from the type 2 Iherzolite suite, and these data, when combined with published experiments on Cr-Al-Fe mixing in spinel¹³⁻¹⁵, may be used to calculate thermobarometric f_{O_2} s for most mantle-derived spinels.

Synthetic spinel solid solutions were prepared initially at 1400-1500 °C in air at 1 atm. Under these conditions, the spinels crystallize in the ternary system MgAl₂O₄-Fe₃O₄-γ-Fe_{8/3}O₄; that is, a small amount of defect spinel (maghemite) is present. Defect spinels were re-equilibrated in a variety of reducing conditions, such as in a 1.0% CO/Ar atmosphere or in a ${\rm CO/CO_2}$ gas mix with an $f_{\rm O_2}$ of 10^{-8} at 1,000 °C, and at 1,400 °C in an atmosphere with $f_{\rm O_2} = 10^{-4}$. Ammonium metavanadate titration was used to determine Fe(II)/Fe(III) ratios of selected products. The reducing environments yielded spinels with slightly different defect concentrations; nevertheless, these spinels (between 2 and 20 mol% Fe₃O₄) are essentially stoichiometric within the analytical uncertainty of ~2 mol%. In addition, the spinels were checked for crystallinity and homogeneity by X-ray diffraction, and optical and electron microscopy. Complete details of synthesis conditions, analysis methods, and defect-molar volume relations will be presented elsewhere³¹.

Magnetite activity was measured by mixing haematite with the spinel solid solutions and determining f_{O_2} as controlled by the equilibrium:

$$4 \text{ Fe}_3\text{O}_4 \text{ (in spinel)} + \text{O}_2 = 6 \text{ Fe}_2\text{O}_3 \text{ (in haematite)}$$
 (2)

We employed an yttria-stabilized-zirconia solid-electrolyte oxygen sensor to measure the shift in f_{O_2} relative to the MH buffer. At constant temperature and known Fe₃O₄ and Fe₂O₃ concentrations in the spinel and orthorhombic phases, respectively, the magnetite activity was given directly by the e.m.f. of the zirconia cell relative to a gas of known f_{O_2} . Al₂O₃ solubility in the haematite phase was modelled using published data¹⁶. At fixed Fe₃O₄ mole fraction, spinels synthesized under oxidized and various reduced conditions yielded the same Fe₃O₄ activity. This implies that the amount of γ -Fe_{8/3}O₄ component in the spinel phase must closely approximate the equilibrium concentration at the temperature and f_{0} , of the experiment. Equilibrium was demonstrated by in situ addition or subtraction of oxygen from the sample (coulometric titration) and verification that the e.m.f. was affected by these perturbations. The sample usually approached equilibrium fairly quickly after perturbation, so that the variation in e.m.f. with time became negligible within an

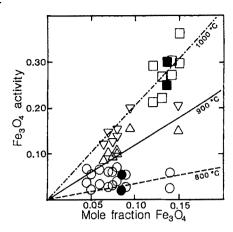


Fig. 2 Experimentally calibrated activity data for the Fe_3O_4 component in the spinel phase, plotted against the mole fraction of Fe_3O_4 component in MgAl₂O₄-rich synthetic spinel at 800, 900 and 1,000 °C (circles, triangles and squares, respectively) and 1 atm total pressure. Open symbols represent approach to equilibrium from high and low f_{O_2} with spinels synthesized in reducing conditions; shaded symbols are for runs with spinels synthesized in air. The size of the symbols reflects the approximate cumulative experimental uncertainty.

hour at 900 °C. X-ray diffractograms were obtained for all run products, to ensure that both phases were present and to determine the final spinel and haematite compositions.

Figure 2 shows the results of our activity measurements, as a plot of the reversed magnetite activities against the final spinel phase composition, determined using X-ray diffraction. We include experiments with spinel solid solutions made in the various reduced conditions as well as two runs with spinels made in air. The size of the symbols represents the approximate cumulative uncertainty for each reversal bracket. At each composition, the pair of symbols represents approach to equilibrium from high (lower symbol) and low (upper symbol) f_{O} . Note that our experiments are in the composition and temperature range appropriate for Cr-free mantle spinels. Our observation of increasing magnetite activity with increasing temperature at constant composition is probably due to changes in the equilibrium ordering state of the mixed spinels relative to the pure magnetite standard state¹⁷. This behaviour persists across the entire Fe₃O₄-MgAl₂O₄ join at 900 and 1,000 °C. We have used approximate linear (Henry's law) fits to the dilute magnetite activites (Fig. 2) in order to estimate upper mantle f_{O_2} . The fit lines are calculated from the equation

$$A_{\text{Fe}_3\text{O}_4} = (\alpha + \beta T) X_{\text{Fe}_3\text{O}_4} \tag{3}$$

where $X_{\text{Fe}_3\text{O}_4}$ and $A_{\text{Fe}_3\text{O}_4}$ are the mole fraction and activity of magnetite in spinel, $\alpha = -6.5 \pm 0.5$, $\beta = 8.5 \pm 0.5 \times 10^{-3}$, and T is temperature in °C.

Upper mantle f_{O_2} recorded by spinel-lherzolite xenoliths, the three-phase assemblage spinelcontain orthopyroxene-olivine, may now be calculated thermobarometrically from equilibrium (1). Fe₃O₄ activity was taken from equation (3), with Fe₂SiO₄ and FeSiO₃ activities and standard-state data from the literature^{18,19,32}. The Mg number $(Mg^{2+}/(Mg^{2+}+Fe^{2+}))$ of the silicate phases was fixed at 0.90, and the spinel phase composition was varied between 0.01 and 0.10 mole fraction Fe₃O₄ component. The latter range corresponds to the approximate limits observed by electron microprobe, wet chemistry and Mössbauer spectroscopy for spinel in mantle-derived spinel-lherzolite xenoliths. Figure 2 shows the results of these calculations as a temperature-log $f_{\rm O_2}$ plot at 15 kbar total pressure. Pressure-corrected Fe buffers are also included for reference. The f_{O_2} s shown in Fig. 3 were calculated at 15 kbar pressure using a ternary-spinel molar volume

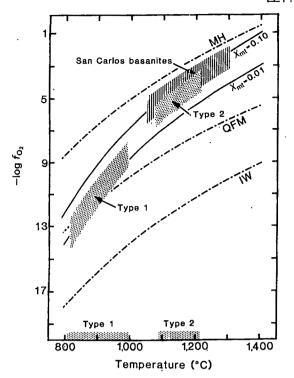


Fig. 3 Thermobarometric spinel data at 15 kbar total pressure. Solid lines are the loci of $(\log f_{O_2}, T)$ data calculated from equilibrium (1) for magnetite mole fractions ($X_{\rm mt}$) of 0.01 and 0.10 in the Cr-free spinel. Magnetite activity was calculated using equation (3). The stippled regions refer to type 1 and type 2 spinels, with the former casé including a correction for Cr substitution. Temperature ranges (shown on the abscissa) are taken from the literature²³. The lined region is the f_{O_2} -T range for the San Carlos basanites²⁵. Note the more reduced f_{O_2} s for type 1 xenoliths, and the considerable overlap in $f_{\rm O_2}$ of type 2 xenoliths with the San Carlos basanites.

model^{8,31} and published data for orthopyroxene²⁰ and olivine²¹, neglecting the small expansivities and compressibilities of the phases. The effect of Cr substitution in the spinel phase was estimated using published phase equilibrium data^{13,14} and the formalism of Sack¹⁵. This approach suggests a slight lowering (<1 log unit) of $f_{\rm O_2}$ relative to the Cr-free system if the spinel contains 25 mol% ${\rm Cr^{3+}}$ as ${\rm FeCr_2O_4}$. Preliminary ${\rm Fe_3O_4}$ activity experiments on Cr-bearing synthetic spinels confirm that f_{O_2} is not reduced significantly relative to the Cr-free system.

Received 27 January; accepted 21 May 1986

- 1. Sato, M. Mem. geol. Soc. Am. 135, 289-307 (1972).
- Arculus, R. J. & Delano, J. W. Nature 288, 72-74 (1980).
 Arculus, R. J. & Delano, J. W. Geochim. cosmochim. Acta 45, 899-913 (1981).
- Arculus, R. J., Dawson, J. B., Mitchell, R. H., Gust, D. A. & Holmes, R. D. Contr. Miner. Petrol. 85, 85-94 (1984).

- Eggler, D. H. Geophys. Res. Lett. 10, 365-368 (1983).
 Haggerty, S. E. & Tomkins, L. A. Nature 303, 295-300 (1983).
 Haggerty, S. E. Geophys. Res. Lett. 5, 443-446 (1978).
 Mattioli, G. S. & Wood, B. I. Geol. Soc. Am. Abstr. Progm. 17, 655 (1985).
- Mattoll, G. S. & Wood, B. L. Geol. Soc. Am. Abstr. Frogm. 17, 633 (1985).
 French, B. M. Rev. Geophys. 4, 223-253 (1966).
 Eggler, D. H. & Baker, D. R. in High-Pressure Research in Geophysics (eds Akimoto, S. & Manghnani, M.) 237-250 (Center for Academic Publications, Tokyo, 1982).
 Dieckmann, R. Ber. Bunsenges. phys. Chem. 86, 112-118 (1982).
 Basaltic Volcanism Study Project Basaltic Volcanism on the Terrestrial Planets (Pergamon, Namy Volcal, 1981).
- New York, 1981).
 13. Webb, S. A. C. & Wood, B. J. Contr. Miner. Petrol. 92, 471-480 (1986).
- 14. Oka, Y., Steinke, P. & Chatterjee, N. D. Contr. Miner. Petrol, 87, 196-204 (1985).

The observed composition and temperature range for natural spinels in spinel therzolites is shown in Fig. 3 (stippled areas), and gives f_{O} , s which range from slightly below QFM to approximately two orders of magnitude more oxidized. The type 1 (Cr-rich) suite is certainly more reduced than the type 2 (Crpoor) suite; however, our estimates for upper-mantle f_{O_2} are all near or above QFM, in general agreement with previous thermobarometric data⁵⁻⁷, and in sharp contrast to the intrinsic data for spinel separates from type 1 xenoliths (Fig. 1)²⁻⁴. Extremely low Fe₃O₄ concentrations $(X_{\text{Fe}_3\text{O}_4} \approx 10^{-4})$ in the spinel phase would be necessary to stabilize spinel-orthopyroxene-olivine assemblages at an f_{O_2} near IW. However, published analyses $^{22-24}$ do not in general report such vanishingly small magnetite contents; most spinels from spinel-lherzolite xenoliths contain $X_{\text{Fe}_{2}O_{4}} \ge 0.01$. The discrepancy between intrinsic and thermobarometric results must be due to errors in some spinel analyses or to carbon interference in some intrinsic measurements; pressure effects on the latter can be discounted^{8,31}. Experiments are now under way to investigate this discrepancy.

Figure 3 also shows the approximate \bar{f}_{O_2} range for the San Carlos basanites²⁵, corrected to the appropriate temperature and 15 kbar pressure²⁶⁻²⁸. Note the general agreement between the $f_{\rm O_2}$ recorded by type 2 xenoliths and that calculated for the San Carlos basanitic magmas, in which examples of both xenolith suites are entrained. The f_{O_2} data support the conclusion of Frey and Prinz²⁵, based on trace-element abundance patterns of xenoliths from San Carlos and elsewhere, and of Menzies²⁹, based on Sr and Nd isotopic abundances of xenoliths relative to their host magmas, that type 2 xenoliths are cognate, and thus genetically related to the basanites which entrain them, although not necessarily of the same generation. We find no evidence to support the suggestion² that partial melting in the Earth's shallow upper mantle results in a melt-residua system with an f_{O_2} near the IW buffer. This eliminates the need for extensive H_2 loss during magma ascent to explain the observed f_{O_2} s at or above QFM for alkaline and basaltic extrusives⁷.

Our results show that the f_{O_2} accompanying upper mantle processes is not uniform, and may vary from slightly below to approximately two orders of magnitude more oxidized than OFM at 15 kbar total pressure. Our data do not preclude the possibility that low- f_{O_2} zones occur at greater depth or that the mantle was more reduced in Archaean times than at present³⁰. In the spinel-lherzolite facies, however, f_{O_2} s are close to QFM and gaseous species are dominated by CO₂ and H₂O (refs 9, 10), rather than CH₄ and H₂.

We thank Dr Ian Carmichael for performing the wet chemical analyses of our synthetic spinels, and Dr R. J. Arculus for helpful comments on the manuscript. This research was supported by NSF grants EAR-821502 and EAR-8409666.

- 15. Sack, R.O. Contr. Miner. Petrol. 79, 169-186 (1982).
- 16. Muna, A. Am. J. Sci. 256, 413-422 (1958).
- Muna, A. Am. J. Sci. 256, 415-422 (1988).
 Mattioli, G. S. & Wood, B. J. Proc. 14th Conf. Miner. Soc. (in the press).
 Wood, B. J. & Kleppa, O. J. Geochim. cosmochim. Acta 45, 529-534 (1981).
 Bohlen, S. R., Essene, E. J. & Boettcher, A. L. Earth planet. Sci. Lett. 47, 1-10 (1980).
 Newton, R. C. & Wood, B. J. Am. Miner. 65, 733-745 (1980).
 Fisher, G. W. & Medaris, L. G. Jr Am. Miner. 54, 741-753 (1969).
- Basu, A. R. & MacGregor, I. D. Geochim. cosmochim. Acta 39, 937-945 (1975).
 Sachtleben, Th. & Seck, H. A. Contr. Miner. Petrol. 78, 157-165 (1981).

- Fujii, T. & Scarfe, C. M. Contr. Miner. Petrol. 80, 297-306 (1982). Frey, F. A. & Prinz, M. Earth planet. Sci. Lett. 38, 129-176 (1978).
- Sack, R. O., Carmichael, I. S. E., Rivers, M. & Ghiorso, M. S. Contr. Miner. Petrol. 75, 369-376 (1980).
- 27. Kilinc, A., Carmichael, I. S. E., Rivers, M. L. & Sach, R. O. Contr. Miner. Petrol. 83, 136-140
- 28. Mo, X., Carmichael, I. S. E., Rivers, M. & Stebbins, J. Mineralog. Mag. 45, 237-245 (1982).
- 29. Menzies, M. A. in Continental Basalts and Mantle Xenoliths (eds Hawkesworth, C. J. & Norry, M. J.) 92-110 (Shiva, Nantwich, 1983).
- Arculus, R. J. A. Rev. Earth planet. Sci. 13, 75-95 (1985).
 Mattioli, G. S., Wood, B. J. & Carmichael, I. S. E. Am. Miner. (submitted).
- 32. Myers, J. & Eugster, H. P. Contr. Miner. Petrol. 82, 75-90 (1983)

Crustal detachment during South Atlantic rifting and formation of Tucano-Gabon basin system

Naomi Ussami, Garry D. Karner & Martin H. P. Bott

Department of Geological Sciences, University of Durham, South Road, Durham DH1 3LE, UK

A series of major sedimentary basins of Mesozoic to Tertiary age are associated with the Brazilian continental margin between 8° and 14° S (Fig. 1). This passive continental margin formed when Africa and South America split apart with the initiation of seafloor spreading in the Aptian/Albian3. The offshore basins which border the continental margins on both sides of the Atlantic show evidence of both rifting and crustal attenuation before break-up and thermal subsidence after it. In contrast, a combined stratigraphical and gravity study of the Brazilian onshore basins, which are separated from the offshore basins by a northward-widening strip of Precambrian, suggests that up to 7 km of non-marine sediments were deposited during the rifting stage of the South Atlantic, with no apparent extension of the lower crust beneath these basins and no subsequent thermal subsidence. A mechanism for the linked development of these onshore and offshore basins is proposed here along the lines suggested by Wernicke^{4,5}, in which upper crustal extension in the onshore region is connected to, and balanced against, deeper lithospheric extension beneath the incipient passive margin by intracrustal detachments.

As shown in Fig. 1, the basins adjacent to the Brazilian margin are the coastal Sergipe-Alagoas Basin, and the less well known

offshore Jacuipe Basin which initially adjoined the complementary Gabon Basin on the opposite continental margin. The Brazilian onshore basins extend northward from Reconcavo and include the Tucano and Jatobá 'aborted rift' basins⁶. These are separated from the coast by a triangular Precambrian block.

The Bouguer anomaly map (Fig. 2a) of this section of the Brazilian coast shows that all the basins are characterized by large-amplitude local negative gravity anomalies, indicating thick, low-density sediment infills. The maximum thickness of 7-8 km of sediments in the Tucano Basin produces a local gravity effect of -100 mgal amplitude. Gravity modelling of the Tucano Basin, using sediment densities obtained from density logs of commercial wells, suggests that the observed sediments adequately account for the observed gravity anomaly (Fig. 2b). There is no indication from flanking positive anomalies of significant upwarping of the underlying Moho immediately beneath the basin. In contrast, modelling of the Jacuipe Basin, which has a maximum sediment thickness of $\sim 3-4$ km (ref. 8), suggests that considerable crustal thinning and Moho upwarp has occurred beneath this offshore basin (Fig. 2b).

The Tucano Basin thus gives no evidence of local isostatic compensation, suggesting that it has been formed by uppercrustal extension without complementary extension of the underlying rigid lower crust and uppermost mantle. The lack of local Moho topography as determined by the gravity studies suggests that the lithosphere had a large flexural rigidity at the time of basin formation, and that it has remained high since. Assuming that lithospheric flexure can be modelled as a thin elastic plate overlying a weak fluid substratum, an effective elastic plate thickness of 50-80 km produces a compensating gravity effect of only 10 mgal associated with a regional Moho uplift of ~2 km with a wavelength of 1,000 km (Fig. 2c). This

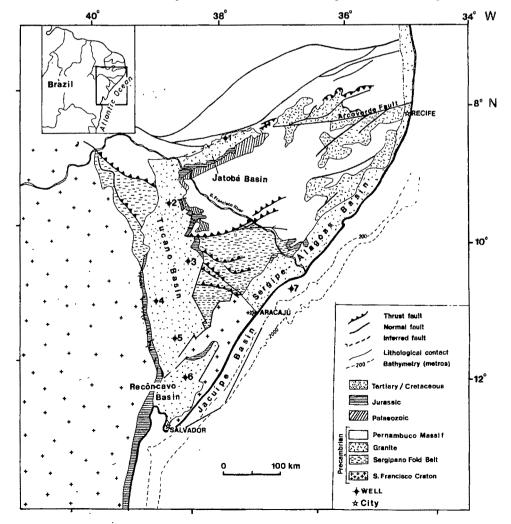


Fig. 1 Geological map of northeastern Brazil (conical projection), modified from ref. 1 to show the Mesozoic to Tertiary sedimentary basins. The onshore Jatobá, Tucano and Recôncavo basins cut across the NW-SE-trending Sergipano fold belt, which extends into Gabon and Angola as the Ndjolé Series². 1-7, Location of wells used in this study.

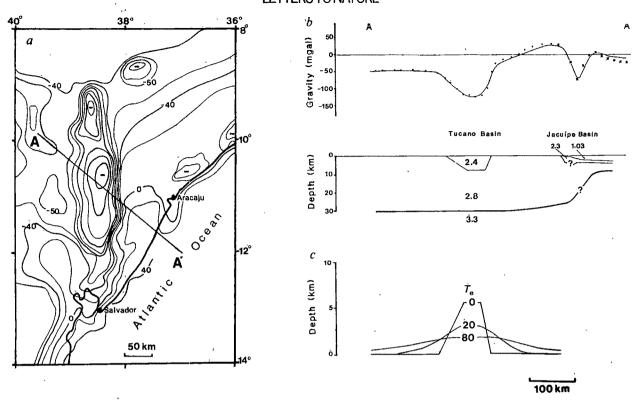


Fig. 2 a, Bouguer anomaly map of northeastern Brazil approximately coinciding with Fig. 1, using Bouguer density of 2.67 g cm⁻³ and referenced to IG\$N71. Contour interval is 20 mgal. Source: Petrobras and DNPM/Brazil. b, Interpretation of a gravity anomaly profile across the Tucano and Jacuípe basins (A-A' in a), based on the Bouguer anomalies (points) and free-air marine anomalies (crosses). The curve is the gravity anomaly profile calculated from the crustal model shown below, in which average densities from commercial wells are shown in g cm⁻³. In the absence of deep seismic data, the depth to the Moho beneath the craton has been assumed to be 30 km. c, Upwelling of the Moho produced by the Tucano Basin upper-crustal mass deficiency, plotted as a function of the effective elastic thickness T_e of the lithosphere.

Moho topography consistent with gravity observations suggests T_e is between 50 and 80 km.

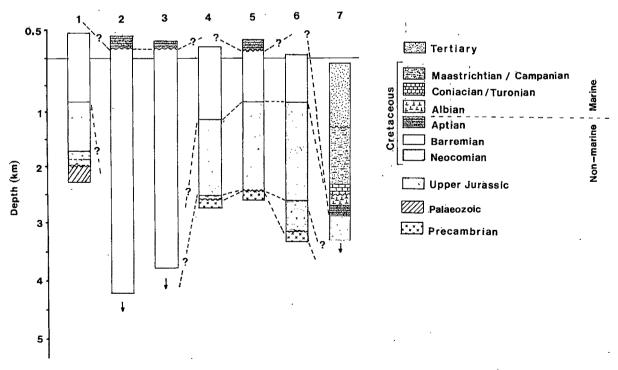


Fig. 3 Simplified stratigraphy of the Jatobá, Tucano, Recôncavo⁹ and Sergipe-Alagoas¹⁰ basins, based on well data provided by Petrobras (Fig. 1). The Upper Jurassic and Neocomian in all basins consist of non-marine shales and sandstones with intercalations of arkose and siltstone. Non-marine sandstones and siltstones of great thickness dominate the onshore basins in the Barremian, and post-rift marine sediments are found only in the Sergipe-Alagoas Basin (well 7).

long-wavelength gravity effect would contribute to the regional anomaly, and the local basin would appear to be uncompensated. Furthermore, the existence of a large rigidity at the time of basin formation implies that the rifting responsible for the Tucano and Jatobá basins was not associated with any significant modification of the thermal structure of the lithosphere immediately below.

Although gravity is useful in defining the present structure of the basins and their isostatic state, it cannot describe their temporal development. However, the stratigraphic evidence obtained mainly from deep wells in the basins is potentially a sensitive indicator of the history of basin subsidence, and thus a further pointer towards the mechanism of formation.

Figure 3 shows the subsidence history and stratigraphy of the Recôncavo, Tucano, Jatobá9 and Sergipe-Alagoas10 basins. Rift subsidence affected all the basins during the period from Upper Jurassic to Neocomian. A total of 5 and 7 km of non-marine Upper Jurassic to Barremian rift sediments were deposited in the onshore Jatobá and Tucano basins, respectively, over a period of ~24 Myr and there is no evidence of any further significant subsidence. The offshore Sergipe-Alagoas and Gabon^{11,12} basins display 3-4 km of non-marine sediments deposited during the rifting stage. In the Sergipe-Alagoas Basin, rift sedimentation terminated in the Barremian, when it was at a maximum in the onshore basins. The initiation of thermal subsidence within the Sergipe-Alagoas and Gabon basins was marked by a major Aptian/Albian marine transgression¹³ which was approximately contemporaneous with the onset of seafloor spreading, and coincident with the abrupt termination of sedimentation and subsidence within the onshore basins. Following non-marine rift sedimentation in the Sergipe-Alagoas and Gabon basins. 3-4 km of post-rift marine sediments were deposited in response to the thermal subsidence of the margin. Thus, there is an intimate relationship between the differing tectonic histories of the onshore basins (Recôncavo, Jatobá, Tucano) and offshore basins (Sergipe-Alagoas, Gabon, Jacuípe), and the inception of the Atlantic seafloor spreading. The lack of thermal subsidence in the onshore basins confirms the inference from the gravity anomalies that their extension was confined to the upper crust during rifting.

According to the mechanism of McKenzie¹⁴ for the formation of sedimentary basins by uniform lithospheric extension, and more recent modifications^{15,16}, rapid rift-stage subsidence is followed by much slower thermal subsidence, with a time constant between 50 and 150 Myr. The simple McKenzie model fails to explain this coupled system of offshore and onshore basins

We suggest that all the basins were formed by lithospheric extension during the rifting phase of Atlantic break-up. Upper crustal extension affected both the onshore and offshore basins, but the extension at deeper lithospheric levels, including the lower crust, was concentrated beneath the offshore basins, as evidenced by the degree of thermal subsidence. In order to permit such coupled differential stretching of the lithosphere, the offshore and onshore regions must have been connected by a low-angle crustal detachment surface.

The potential importance of the crustal detachment in controlling basin formation is strengthened by the evolutionary link between onshore and offshore basins. Whereas all of the basins were initiated at the same time, the cessation of rifting terminated onshore basin development at about the same time as the offshore basins entered into the thermal subsidence phase. The detachment has allowed the transfer of extension between the upper crust and the deeper part of the lithosphere during the rifting stage (Fig. 4b). The origin of the onshore Brazilian basins and the Sergipe-Alagoas and Gabon basins conforms to the 'simple shear model' of Wernicke^{4,5}, in which the non-uniform extension of the crust is balanced by lower crustal and subcrustal lithospheric extension across a detachment surface. Figure 4b shows a schematic but balanced cross-section sum-

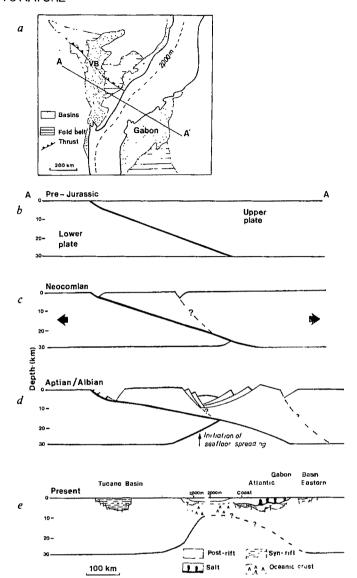


Fig. 4 Suggested history of evolution of the Tucano-Gabon basin system: a, Map showing the line of section (A-A') on a pre-drift reconstruction of Brazil and west Africa; VB, Vaza Barris fault. b, The postulated contact between the African plate (upper plate) and the São Francisco craton (lower plate) is shown as a preexisting thrust fault cutting through the crust and possibly the lower lithosphere, c. Upper Jurassic-Lower Cretaceous extensional regime allows the upper crust to extend and the basal contact to detach, with complementary extension of the lower part of the lithosphere beneath the incipient marginal basins. The collapse of the hanging wall formed the Tucano basin. d, Initiation of seafloor spreading, showing the pronounced thinning of the lithosphere beneath the offshore basins and the asymmetrical position of the split. e, Drifting stage, with thermal subsidence of the offshore basins only. Crustal section based on gravity (Tucano and Jacuípe basins), well¹¹ and seismic data¹² (Gabon Basin). The depth of the Moho under the Gabon Basin is only suggested.

marizing the development history of the Brazilian and African basins using the Wernicke model. The upper plate represents the detached thrust block of the Sergipano fold belt and the African craton; the lower plate represents the Brazilian São Francisco craton.

The Tucano and Recôncavo basins cut across the Upper Proterozoic Sergipano fold belt (Fig. 4a), which extends into Gabon and Angola in western Africa². It is possible that the basal thrust plane of this fold belt has been reactivated as an intracrustal detachment during the Mesozoic extension to form the Jatobá and Tucano basins, while synchronous extension and

rifting was taking place further east, with maximum subsidence affecting the Gabon Basin. The final rupture leading to seafloor spreading took place closer to the present Brazilian margin, where only a small thickness of rift sediments had accumulated in the Jacuípe Basin. The exact break-up position is a complicated function of the changing rheological properties of the extending crust and mantle, the evolving lithospheric temperature structure, and any pre-existing crustal fabric 17,18

In plan view, the upper plate has rotated anticlockwise relative to South America^{19,20}, resulting in the observed distribution of basins around its boundaries. In addition to extension leading to basin formation, complementary compression should be induced along the northeastern border of the block. Such compression may be expressed by the major Harmonia and Itapecuru thrust faults along the northeastern segments of the Arcoverde fault²¹ (Fig. 1).

The formation of the entire Jatobá-Tucano-Gabon basin system in the Lower Cretaceous was controlled by a detachment surface. This detachment allowed the onshore Jatobá and Tucano basins to form by brittle failure of the upper crust in extension, without substantial alteration of the thermal structure of the lithosphere beneath the basins, and it has also acted as a mechanical and temporal link between the onshore basins and the continental margins off Brazil and Africa, thereby allowing balancing of lithospheric extension.

We thank John Dewey and Webster Mohriak for helpful discussions and Petrobras for providing the gravity and well data of the Jatobá and Tucano basins. This work was supported by grants from FAPESP (82/0573-0), CNPq (200348-82), Overseas Research Student Award to N.U. and the Durham University Research Foundation of the Society of Fellows to G.D.K.

Received 18 February; accepted 19 May 1986.

- Schobbenhaus, C., Campos, D. A., Derze, G. R. & Asmus, H. E. Geological Map of Brazil, scale 1:2,500,000 (Departamento Nacional da Produção Mineral, Brasilia, 1984).
- Allard, G. O. & Hurst, V. J. Science 163, 528-532 (1969).
 Rabinowitz, P. D. & LaBrecque, J. J. geophys. Res. 84, 5973-6002 (1979).
 Wernicke, B. Nature 291, 645-647 (1981).
 Wernicke, B. Can. J. Earth. Sci. 22, 108-125 (1985).

- 6. Nairn, A. E. M. & Stehli, F. G. (eds) in The Ocean Basins and Margins. The South Atlantic, 1-20 (Plenum, New York, 1973).
- 7. Rabinowitz, P. D. & Cochran, J. R. Free-Air Gravity Anomalies of the Continental Margin of Brazil (American Association of Petroleum Geologists, Tulsa, 1978).

 8. Kumar, N., Leyden, R., Carvalho, J. & Francisconi, O. Sediment Isopach Map of the Brazilian
- Continental Margin (AAPG, Tulsa, 1979).

 9. Viana, C. F., Gama, E. G. Jr, Simões, I. A., Moura, J. A., Fonseca, J. R. & Alves, R. J.
- Bolm téc. Petrobrás 14, 157-192 (1971).
- Asmus, H. E. & Ponte, F. C. in The Ocean Basins and Margins. The South Atlantic (eds Nairn, A. E. M. & Stehli, F. G.) 87-133 (Plenum, New York, 1973). 11. Brink, A. H. Bull. Am. Ass. petrol. Geol. 58, 216-235 (1974).
 12. Driver, E. S. & Pardo, G. The Geology of Continental Margins (eds Burk, C. A. & Drake,
- C. L.) 293-295 (Springer, New York, 1974). Reyment, R. A. & Tait, E. A. Phil. Trans. R. Soc. B264, 55-95 (1972).

- Keyment, K. A. & tait, E. A. Fill. 17ans. R. Soc. B204, 35-95 (1972).
 McKenzie, D. Earth planet. Sci. Lett. 40, 25-32 (1978).
 Royden, L. & Keen, C. Earth planet. Sci. Lett. 51, 343-361 (1980).
 Watts, A., Karner, G. D. & Steckler, M. S. Phil. Trans. R. Soc. A305, 249-281 (1982).
 England, P. J. geophys. Res. 88, 1145-1152 (1983).
 Sawyer, D. S. J. geophys. Res. 90, 3021-3025 (1985).

- Cohen, C. R. Bull. Am. Ass. petrol. Geol. 69, 65-76 (1985).
 Szatmari, P., Milani, E., Lana, M., Conceição, J. & Lobo, A. Oil Gas J. 76, 107-113 (1985).
- 21. Santos, E. J. Minerac. Metall. 313, 35-40 (1971).

Oldest primitive agriculture and vegetational environments in Japan

Matsuo Tsukada, Shinya Sugita & Yorko Tsukada

Quaternary Ecology Laboratory AK-60, Department of Botany, University of Washington, Seattle, Washington 98195, USA

In Japan, shifting agriculture as part of a hunting and gathering strategy was generally thought to have started during the Middle Jomon period (5,000-4,000 BP)¹⁻⁴. We present here evidence of primitive agricultural activities at least 1,600 years earlier than this date. At the Ubuka bog on the coast of the Sea of Japan in southwestern Honshu (34°29' N, 131°35' E, 390 m altitude) buckwheat cultivation dates back to as early as 6,600 BP in the Early Jomon period (7,000-5,000 BP). The warm-temperate climatic regime in that period supported the growth of Podocarpus, Cyclobalanopsis, Ilex crenata/I. serrata and Viscum album var. coloratum. Slash-and-burn agriculture was intensified ~2,000 BP and rice cultivation was introduced ~1,500 BP.

The evidence that slash-and-burn agriculture in the Japanese Archipelago began as part of a generalized subsistence system during the Middle Jomon period is: (1) the abundant occurrence of stone mortars and pestles and chipped stone axes; (2) the establishment of large, permanent villages; and (3) the occurrence of functionally diverse pottery associated with a plant diet1-4. However, there has been no direct evidence of agricultural activities, with the exception of nine Phaseolus aureus legumes and nine Lagenaria leucantha seeds at the Torihama shell mound site³ of the Early Jomon period (Fig. 1).

Fagopyrum esculentum (buckwheat), Setaria italica (foxtail millet), Echinochloa crus-galli var. frumentaceum (Chinese barnyard grass), Panicum miliaceum (Chinese millet) and Oryza sativa (rice) are all native to the Asiatic mainland⁵⁻¹⁰. These crop plants cannot survive in the moist forested landscape of Japan, unless they are protected by humans, and no pollen grains or seeds of these species have been found in Japanese Pleistocene sediments which have been extensively studied. The

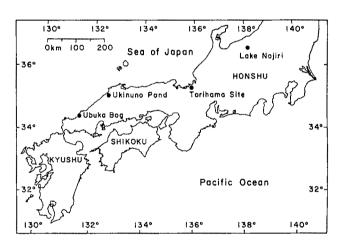


Fig. 1 Index map of sites mentioned in the text.

presence of macroscopic and pollen remains of these plants in Japanese sediments therefore indicates that people were growing them at the time of their deposition¹⁰. Buckwheat, whose pollen can be identified to the species level^{11,12}, is an excellent index species to assess past agricultural activities.

Fossil buckwheat pollen grains were first found in sediments of Lake Nojiri (36°50' N, 138°14' E, 654 m altitude), dated between 1,500 BP and the present¹¹. In these sediments, the pollen of herbaceous taxa, for example Chenopodiaceae and Liguliflorae, and *Pinus densiflora*, a lowland "pioneer" pine species, begin to increase in frequency immediately after the first occurrence of buckwheat pollen, indicating that shifting agriculture intensified ~1,500 years ago^{10,12}. Some species of these herbaceous taxa can become weeds in agricultural and deserted lands.

Since this first discovery, fossil buckwheat pollen grains have been found at various archaeological sites of the Late Jomon period (4,000-3,000 BP)¹³⁻¹⁵ and a single, carbonized fragment of buckwheat seed has been found on a house floor of the Early Jomon period in southern Hokkaido¹⁶. However, archaeological

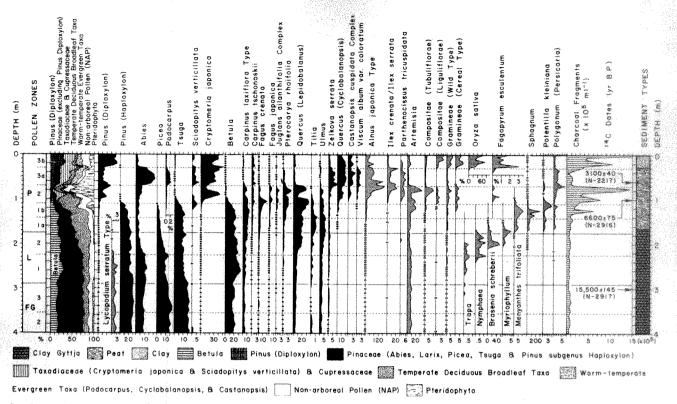


Fig. 2 A pollen diagram of the Ubuka bog, southwestern Japan. Analysis was made at 5-cm intervals from the surface to the 270-cm level, and at 10-cm intervals below the 270-cm level. Percentages are based on the pollen sum (>1,000 grains per level) of upland arboreal taxa, and those listed in the summary diagram (left column) are based on the sum of pollen and spores of terrestrial plants. Dots indicate values of less than 0.2% for Lycopodium and Tilia, 0.3% for Carpinus latifolia type, Juglans, Pterocarya, Viscum, Compositae (Liguliflorae), Myriophyllum, Potentilla, and Persicaria, 0.5% for Abies, Picea, Tsuga, Zelkova, Menyanthes, and Compositae (Tubliflorae), 1.0% for Pinus, Cryptomeria, Betula, Fagus, Quercus, Carpinus laxiflora type, Gramineae and Ilex, and 5% for Alnus.

sites are often disturbed by past occupations, making it impossible to reconstruct the history of fossil pollen and seeds precisely, and one seed is not a conclusive demonstration that buckwheat cultivation was practised at a particular site. In contrast to this, bog and lake sediments are well stratified and can provide a reliable picture of buckwheat history.

We have now found definitive evidence of primitive agriculture at the Ubuka bog shown in Fig. 1 (1,000 m N-S ×1250 m E-W). During the full- and late-glacial period the basin was a lake, characterized by gyttja sediments with cladoceran remains, but it was gradually obliterated by sediment accumulation between ~13,000 and 8,500 BP. All dates are based on three ¹⁴C datings [3,100±90 BP at 60 cm (Nippon Isotope Association sample number N-2217), 6.600±75 BP at 100 cm (N-2916), and 15,500±175 BP at 300 cm (N-2917)] and the correlation with dated pollen zonal boundaries in southwestern Japan. A well-ordered succession from shallow-lake aquatic plants (Trapa, Nymphaea tetragona, Brasenia schreberii, Myriophyllum and Menyanthes trifoliata) to bog plants (Sphagnum, Potentilla kleiniana and Persicaria) is evidence of this change (Fig. 2).

About 7,700 years ago, or soon after the bog was formed, the forest surrounding the basin was disturbed. This is indicated by a sudden increase in the deposition of charcoal fragments of woody plants at this time. These fragments are large in size but make up only 1.1% of the total (Fig. 3). Grass pollen grains found in these strata have not been identified at the species level but many are $>41~\mu m$ (Fig. 2), suggesting that cereal plants $^{17-20}$ may have been under cultivation in the Early Jomon period. No grass pollen $>35~\mu m$ occurred in sediments accumulated before $\sim 7,500~\rm Bp$.

The deposition of charcoal fragments increased further $\sim 6,600$ BP. Some of these fragments are 150-400 μm (Fig. 3), indicating that forest fires occurred nearby. Buckwheat pollen

grains were found in abundance $(75.8 \pm 61.7 \text{ cm}^{-3})$ in sediments dated $\sim 6,600-4,500 \text{ BP}$. Herbaceous 'pioneers', for example Artemisia and other Compositae, are also conspicuous during this period and pine (mostly *P. densiflora*) reaches a frequency of 28% total pollen. It is unlikely that buckwheat was cultivated on the Ubuka bog at this time because no peat disturbance was observed and Alnus japonica and Ilex crenata/I. serrata actively invaded the bog during this period (Fig. 2).

Even after a considerable search of the Ubuka sediments. neither buckwheat nor cereal pollen were found in the sediments deposited between ~4,500-2,000 BP, approximately corresponding to pollen zone P-3a time21 (Fig. 2), probably because agricultural activities were moved to sites at a distance from the bog. Temperate conifers (Abies firma and Cryptomeria japonica) increased in frequency immediately after agricultural activities ceased. Carbon fragments became smaller and the Kolmogorov-Smirnov two-sample test²² shows that, at the 0.01 significance level, their frequency curve is identical to those of distant fires recorded at the 230-cm level (~12,400 BP) and other late- and full-glacial levels not shown in Fig. 3. Heavy charcoal and buckwheat pollen should have not been carried from the distant sites to the bog during the P-3a zone. However, a relatively high frequency of Diploxylon pine pollen during this period indicates that human groups still continued to disturb the forests distant from the bog (Fig. 2).

The primitive agricultural activities approximately correspond to the Japanese Hypsithermal interval, or pollen zone P-2 time $(7,000-4,000 \text{ BP})^{21,23}$. By $\sim 7,000 \text{ BP}$, populations of many cool-temperate species, for example spruce (*Picea*), basswood (*Tilia*) and birch (*Betula*), declined in frequency or disappeared completely from the Ubuka area. A rapid decline of beech (*Fagus*) and oak (*Quercus*) pollen $\sim 6,600 \text{ BP}$ suggests that forest fires may have killed many trees around the Ubuka bog and that

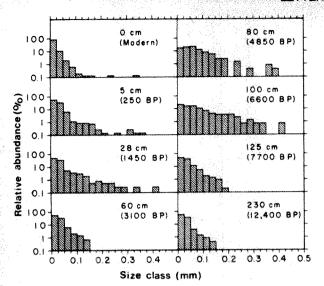


Fig. 3 Frequency curves of charcoal fragments at selected levels of the Ubuka core. N (total number fragments counted) = 224 at level 230 cm; 621 at 125 cm; 261 at 100 cm; 245 at 80 cm; 294 at 60 cm; 357 at 28 cm; 797 at 5 cm; 1,593 at 0 cm. Approximate dates, calculated from three radiocarbon dates (Fig. 2) and dated pollen zonal boundaries^{21,28}, are given in brackets.

after these disturbances Pteridophyta (which includes bracken) characterized the Early Jomon landscape. Also common were warm-temperate species such as Podocarpus (which can grow in areas above the 2 °C January isotherm24) and Cyclobalanopsis (cyclic cup oak, a subgenus of Quercus).

Cryptomeria japonica, a temperate moisture-loving species which requires at least 1,600 mm of annual precipitation^{25,26} began to increase at the beginning of pollen zone P-2 time. Both this species and Sciadopitys verticillata declined temporarily ~5,000-4,000 BP as a result of forest disturbances. Ilex pollen is unusually high (6-20% of total tree pollen) during this period. Pollen of this entomorphilous genus would not be found in such abundance unless the swamp species, either Ilex crenata, I. serrata, or both, had invaded the bog 7,000 BP. A more important finding is that Japanese mistletoe (Viscum album var. coloratum) arrived at this area ~7,500 BP and has continued to grow up to the present day. Although the climatic factors under which this species can grow and reproduce sexually have not been studied (as has been done for the European species²⁷), its presence together with Podocarpus suggests a warm winter climate.

About 2,000 years ago, buckwheat was again cultivated near the bog; people have continued to grow it here until the present day. The buckwheat pollen frequency for the past 2,000 years is much higher than that observed during the first period of cultivation. Large charcoal fragments are also observed at all analytical levels deposited during this period. The fragments $>150 \mu m$ are 16.9% at level 100 cm (\sim 6,600 BP), 9.4% at 80 cm (4,850 BP), 3.6% at 28 cm (1,450 BP), 1.8% at 5 cm (250 BP) and 0.4% at 0 cm (Fig. 3). The frequency for the upper levels is low because small charcoal fragments were carried from distant agricultural areas to the bog and further fragmented by farming activities on the paddy field. These facts suggest that much more intensified slash-and-burn agriculture has been practised in the area for the past 2,000 years.

Although the clay sediments above the 28-cm level were disturbed by rice cultivation on the bog, pollen succession of upland plants here is almost identical to that established at the nearby Ukinuno Pond site28 about 127 km northeast of Ubuka (Fig. 1). At Ubuka, however, buckwheat pollen was found in an undisturbed peat layer, indicating that intensified shifting agriculture began slightly before the disturbance of the bog caused by wetland rice cultivation. By interpolating the sedimentation rate between the modern level and the level radiocarbon-dated at 3,100 ± 90 yrs, the date of the first rice pollen can be estimated at about 1,500 BP. This is within the period when rice agricultural practice was intensified along the coast of the Sea of Japan in southwestern and central Honshu²⁸.

These intensified agricultural activities almost completely

destroyed the temperate Abies and Cryptomeria forests at the Ubuka area. Red pine increased further and currently comprises ~40% of total tree pollen. Among the herbaceous pollen, an increase of Liguliflorae is also conspicuous; its abundance level is higher than that observed during the earlier agricultural episode. Since rice cultivation was practised on the bog, plants such as Ilex and Alnus have sharply declined in abundance

The presence of fossil buckwheat pollen grains and the sudden increase of charcoal fragments at the Ubuka basin ~6,600 radiocarbon years ago provide evidence of agricultural activities in Japan at least 1,600 years earlier than the previously inferred date. Buckwheat was introduced from central China, which is considered to be the probable centre of buckwheat cultivation⁵⁻⁹. The coast of the Sea of Japan in southwestern Japan, directly facing mainland Asia, is a likely place for shifting agriculture to have begun. Further extensive studies along this line, with detailed pollen and charcoal analyses, are needed to clarify the existence of earlier agriculture and its migration routes both in East Asia and within the Japanese Archipelago.

Received 19 March 1985; accepted 30 April 1986.

- 1. Ezaka, T. The Origin of Japanese Culture (Kodansha, Tokyo, 1967).*
- Fujimori, E. The Jomon Culture (Gakuseisha, Tokyo, 1970) Sasaki, K. Before Rice Agriculture (Nippon Hoso Kyokai, Tokyo, 1971).*
- Sasaki, K. in Rice and Iron: Foundation of Various Regal Powers (eds. Amino, Y., Ohbayashi, T., Takatori, M., Tanikawa, K., Tsuboi, H., Miyata, N. & Mori, K.) 56-130 (Shogakukan,
- Vaviloy, N. I. The Origin, Variation, Immunity and Breeding of Cultivated Plants (Ronald, New York, 1951).
- Bailey, L. H. Hortus Third (MacMillan, New York, 1976).
- Shiotani, I. The History of Cultivated Plants (Hosei Univ. Press, Tokyo, 1977). Hoshikawa, K. The Origin and Spread of Cultivated Plants (Ninomiya-shoten, Tokyo, 1978).
- Nakao, S. Cultivated Plants and the Origin of Agriculture (Iwanami-shoten, Tokyo, 1966).*
- Tsukada, M. Bot. Mag., Tokyo 80, 323-336 (1967).*
 Ananova, Y. N. Dokl. (Proc.) Acad. Sci. U.S.S.R. 128, 165-167 (1959)
- Tsukada, M. Bot. Mag., Tokyo 79, 179-184 (1966).*
 Miyoshi, N. & Usui, Y. in Palynological Studies on the Origin and Migration of Rice Agriculture (ed. Nakamura, J.) 30-35 (Kochi University, Kochi, 1977).*
 Yamanaka, M. Ecol. Rev., Tohoku Univ. 19, 113-121 (1979).
- Nakamura, J. Proc. 4th Int. Palynol. Conf. Lucknow, 3, 238-247 (1981).
 Crawford, G. W., Hurley, W. M. & Yoshizaki, M. Asian Perspectives 19, 145-155 (1976).
 Firbas, F. Z. Bot. 31, 447-478 (1937).
- Beug, H.-J. Leitfaden der Pollenbestimmung (Fischer, Stuttgart, 1961).
- Tsukada, M. Pollen Spores 6, 393-462 (1964). Nakamura, J. Daiyonki-kenkyu (Quat. Res.) 13, 187-193 (1974).*
- Tsukada, M. in Vegetation of Japan VII. Kanto (ed. Miyawaki, A.) 78-103 (Shibundo Tokyo, 1986).*
- Campbell, R. C. Statistics for Biologists (Cambridge University Press, 1974).
- Tsukada, M. Jap. J. Ecol. 32, 113-118 (1982).
 Tsukada, M. in Encyclopedia of Japan 7, 177-179 (Kodansha, New York, 1983).
- Tsukada, M. Am. J. Bot. 54, 821-831 (1967). Tsukada, M. Quat. Res. 26, 135-152 (1986).
- Iversen, J. Geol. Foren. Forhandl. 66, 463-483 (1944)
- Tsukada, M. in Windows on Japanese Past: Studies in Archaeology and Prehistory (ed. Pearson, R. J.) 11-56 (University of Michigan, Press, Ann Arbor, 1986). * In Japanese.

Olfactory dysfunction in humans with deficient guanine nucleotide-binding protein

Ruth S. Weinstock*, Herbert N. Wright*, Allen M. Spiegel†, Michael A. Levine‡ & Arnold M. Moses§

* Departments of Medicine and Otolaryngology, Clinical Olfactory Research Center, State University of New York Health Science Center, Syracuse, New York 13210, USA

† Molecular Pathophysiology Section, National Institute of Arthritis, Diabetes, Digestive and Kidney Diseases, National Institutes of Health, Bethesda, Maryland 20892, USA

Department of Medicine, Johns Hopkins University School of Medicine, Baltimore, Maryland 21205, USA

Veterans Administration Medical Center, Syracuse, New York 13210, USA

The guanine nucleotide-binding stimulatory protein (G,) couples hormone-receptor interaction to the activation of adenylate cyclase and the generation of cyclic AMP (see ref. 1 for a review). Studies using frog neuroepithelium indicate that the sense of smell is mediated by a G,-adenylate cyclase system2, and this prompted us to test olfaction in the only known model of G, deficiency in the animal kingdom, G_s-deficient (type 1a) pseudohypo-parathyroidism (PHP), which occurs in humans³⁻⁸. Such patients are resistant to the cAMP-mediated actions of several hormones9. (Although Henkin10 has reported disturbances in the sense of smell in six patients with PHP, currently available biochemical measurements such as the cAMP response to parathyroid hormone (PTH) and determination of G, activity were not reported and olfactory

testing was limited.) In the present study, we found that all Gsdeficient patients had impaired olfaction when compared with PHP patients who had normal G, activity (type 1b PHP, in which patients are resistant only to the action of PTH in the kidney). This is the first evidence of human olfactory impairment which can be related to G. deficiency and suggests that G.-deficient PHP patients may be resistant to cAMP-mediated actions in other non-endocrine systems.

We tested olfaction in five patients with type 1a PHP, who typically express variable resistance to the cAMP-mediated actions of several hormones^{3,9,11-13} and in seven patients with type 1b PHP, who are not resistant to the action of other hormones whose activities are mediated via cAMP9. Informed consent was obtained. The diagnosis of PHP was based on the information shown in Table 1. All PHP patients had hypocalcaemia with elevated PTH levels at the time of diagnosis, normal renal function, and all required therapy with calcium and vitamin D. Nine of the 12 patients were infused with 250 U of parathyroid extract and had markedly impaired urinary cAMP responses. All five type 1a PHP patients had deficient erythrocyte G_s activity and features of Albright's osteodystrophy. All were resistant to thyroid stimulating hormone (TSH) with elevated basal or thyrotropin releasing hormone-stimulated TSH levels, and all require treatment with thyroid hormone (Ta) for hypothyroidism. These five patients all had negative titres of anti-thyroid antibodies, suggesting that such patients are demonstrating thyroid resistance to TSH for reasons other than autoimmune thyroid disease. At the time of olfaction testing, all PHP patients were being treated with calcium and vitamin D and all the type 1a patients were also receiving supplements of thyroid hormone. This is important because several endocrine deficiencies, including hypothyroidism, have been reported to be associated with olfactory dysfunction¹⁴. Serum calcium, phosphorus,

Table 1 Pretreatment characteristics of patients with pseudohypoparathyroidism

Patient no.	Age (yr)	Sex	Untreated serum calcium (mg dl ⁻¹ ; low limit of normal = 8.4)	Untreated serum phosphorus (mg dl ⁻¹ ; upper limit of normal = 4.8)	Serum PTH when hypocalcaemic†	Peak urinary cAMP response to PTH (nmol per mg Cr; normal 90-315)	G, activity (% of normal; normal > 75%)
Type 1a PH	P patients						
1	37	F	7.2*	4.8*	Elevated	ND	55
2	26	F	8.0	4.9	Elevated	8.80	66
3	30	F	8.2	4.6	Elevated	. ND	48
4	36	F	6.6	4.3	Elevated	4.25	51
5	20	F	6.0	7.1	Elevated	7.0 °	51
Type 1b PH	P patients						
6	60	F	5.5	3.3	Elevated	4.16	87
7	47	F	6.3	ND	Elevated	15.83	85
8	30	F	6.4	4.7	Elevated	5.07	78
9	31	F	6.8	5.6	Elevated	4.08	ND; normal
							phenotype, sister of patient 8
10	38	F	7.2*	4.3*	Elevated		ND; normal phenorype
11	38	F	6.8	4.4	Elevated	ND	78
12	22	M	8.4*	5.1*	Elevated	6.0	88

Erythrocyte G_s activity was determined as previously reported^{5,8}. Blood was anticoagulated with acid citrate dextrose and erythrocyte membranes were prepared within 48 h of collection. Erythrocyte membranes were prepared by hypotonic lysis in 5 mM sodium phosphate (pH 8.0) at 0 °C and stored at -70 °C. G. activity was extracted from erythrocyte membranes in detergent and assayed by addition to CYC membranes. Membranes from the CYC clone (94-15-1) of \$49 mouse lymphoma cells, genetically deficient in G_s activity ¹⁶, were prepared as described previously ¹⁷. Erythrocyte membrane pellets were prepared by centrifugation and solubilized in buffer A (2.0 mg protein ml -1, 10 mM Tris-HCl pH 7.5, 10 mM MgCl₂, 0.1 mM EDTA, 1 mM dithiotreitol, 0.2% (w/v) Lubrol PX) and incubated at 4 °C for 60 min with frequent vortexing. The membrane suspensions were then centrifuged for 3 min at 50,000g and the supernatant solutions (membrane extract) collected and retained at 0-4 °C for immediate assay of G, activity. CYC membranes (200 µg) and soluble erythrocyte membranes (10 µg) were incubated for 20 min at 30 °C in 80 µl of buffer B containing 30 mM Tris-HCl (pH 7.5), 10 mM MgCl₂, 1 mM dithiothreitol, 20 µM cAMP, 5 mM creatine phosphate, 3.3 IU of creatine phosphokinase, 100 µM ATP, isoprenaline (10 µM) and guanosine 5'-O-(3-thiotriphosphate (GTP-y-S; 100 µM). After the 20-min incubation, 20 µl of buffer B containing [a⁻²³P]ATP (0.1 Ci mmol⁻¹) was added and incubation continued for a further 20 min at 30 °C. cAMP was isolated and determined by the method of Salomon et al. Expitrocyte extracts alone did not show measurable adenylate cyclase activity. Adenylate cyclase activity of CYC membranes in response to isoprenaline/GTP-y-8 (1.0-1.5 pmol cAMP per tube) was subtracted from the activity of combined erythrocyte extract and CYC membranes to obtain the increment due to addition of erythrocyte G activity. Results of assays are expressed in relation to the activity of a standard membrane preparation consisting of pooled erythrocytes from four normal persons and represent the mean of three determinations. ND, not done.

Values obtained when the patient was receiving treatment with calcium and vitamin D.

† Serum PTH determinations were performed by four different research or reference laboratories. ‡ Plasma cAMP=25 pmol ml⁻¹ (normal > 150).

Table 2 Serum values at the time of olfaction testing

Patient no.		$(mg dl^{-1});$ normal = 8.4)	Phosphorus (mg dl ⁻¹ ; upper limit of normal = 4.8	T_4 ($\mu g dl^{-1}$; lower limit of normal = 5)	TSH (µl ml ⁻³ ; upper limit of normal = 6)
Type 1a PHP pa	tients				
1	9	0.0	3.6	4.5	1.6
2	9	0.0	4.0	7.4	7.8
3	8	3.8	3.4	7.7	3.8
4	· 9	0.8	4.3	8.6	3.3
5	9	0.6	4.0	9.3	< 0.1
Type 1b PHP	patients				
6		3,4	4.3	9.2	3.4
7	. 9	0.2	3.7	5.1	5.2
8	8	3.0	4.0	5.8	3.5
9	9	0.2	3.6	6.4	5.3
10	. 7	1.2	4.3	7.1	13.1*
11		.4	3.9	5.2	1.8
12		3.4	5.1	6.4	2.6

All G_s-deficient patients were receiving therapy with calcium, vitamin D and thyroid hormone. All PHP patients with normal G_s activity were receiving therapy with calcium and vitamin D.

Anti-thyroid antibodies present.

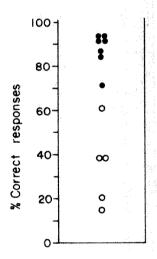


Fig. 1 Results of olfaction testing in patients with type 1a PHP (open circles) and patients with type 1b PHP (closed circles). Methods. Each patient was evaluated by asking them to identify repeatedly 10 common odorants presented at concentrations found to be representative of their counterparts in nature, which frequently are odorant mixtures rather than single pure chemicals: 3.6015 M ammonia (ammonia), 0.0622 M trans-cinnamaldehyde (cinnamon), 0.0130 M anethole (licorice), 0.3990 L-carvone (mint), 0.0244 M napthalene (mothballs), 0.0121 M D-limonene (orange), 1.0467 M phenethyl alcohol (rose), 0.7425 M isopropyl alcohol (rubbing alcohol), 0.0273 M vanillin (vanilla), and 4.3714 M acetic acid (vinegar)15. The diluent was odourless propylene glycol. The odorants were successively presented with the sniff-bottle technique randomly for each subject in blocks of 10, with the constraint that when moving continuously from one block to the next, no one odorant followed itself. The subjects were informed of the odorants which were to be presented and could use any sniffing strategy they desired, but were encouraged to make their identification decision after about two sniffs. It has been shown that a single natural sniff is usually sufficient for optimum odorant perception, and that additional sniffs are probably only confirmatory¹⁹. The results are expressed as the percentage of 100 odorant presenta-

T4. TSH and PTH values at the time of testing are shown in Table 2. No patients had upper respiratory infections or other active nasal problems that could influence their sense of smell.

Olfaction was evaluated by a quantitative test which required patients to identify 10 common odours that were repeatedly presented in a random fashion15. Figure 1 shows the results. All five type 1a PHP patients demonstrated impaired olfaction compared with the seven type 1b PHP patients. One of the latter group had quantitative olfactory dysfunction when compared with normal subjects, but even this patient scored much better on olfactory testing than any of the type la patients.

Received 20 February; accepted 7 May 1986.

Levine, M. A. et al. Am. J. Med. 74, 545-556 (1983).

Our study shows that G, deficiency is associated with decreased olfactory ability and provides the first evidence of a mechanism involving G_s-adenylate cyclase in human olfaction. It further demonstrates that PHP, a disease traditionally thought to be characterized by endocrine dysfunction, may involve other organ systems in which specific effects are mediated via cAMP.

tions (10 for each odorant) identified correctly

This research was supported by grants RR-229 and RR-35 from the General Clinical Research Centers Program of the Division of Research Resources, NINCDS Program Project Grant NS 19568, the Molecular Pathophysiology Section, NIADDK, NIH, Bethesda, and VA research funds.

10. Henkin, R. I. J. clin. Endocr. Metab. 28, 624-628 (1968)

^{1.} Spiegel, A. M., Gierschik, P., Levine, M. A. & Downs, R. W. Jr New Engl. J. Med. 312, 26-33 (1985).

Pace, U., Hanski, E., Salomon, Y. & Lancet, D. Nature 316, 255-258 (1985).

Spiegel, A. M. et al. Am. J. Physiol. 243, E37-E42 (1982)

Farfel, Z., Brickman, A. S., Kaslow, H. R., Brother, V. M. & Bourne, H. R. New Engl. J. Med. 303, 237-242 (1980).

Levine, M. A. et al. Biochem. biophys. Res. Commun. 94, 1319-1324 (1980)

Farfel, Z., et al. Proc. natn. Acad. Sci. U.S.A. 78, 3098-3102 (1981).

Spiegel, A. M. & Downs, R. W. Jr. Endocr. Rev. 2, 275-305 (1981). Levine, M. A., Eil, C., Downs, R. W. Jr & Spiegel, A. M. J. clin. Invest. 72, 316-324 (1983).

Hernkin, R. I. J. Cum. Endocr. Metab. 28, 024-028 (1990).
 Marx, S. J., Hershman, J. M. & Aurbach, G. G. J. clin. Endocr. Metab. 33, 822-828 (1971).
 Werder, E. A. et al. Pediat. Res. 9, 12-16 (1975).
 Wolfsdorf, J. I. et al. Acta endocr. Copenh. 88, 321-328 (1978).
 McConnell, R. J., Menendez, C. E., Smith, F. R., Henkin, R. I. & Rivlin, R. S. Am. J. Med. 59, 354-364 (1975)

Wright, H. N. Archs Otolar. (in the press)

Ross, E. M., Howlett, A. C., Ferguson, K. M. & Gilman, A. G. J. biol. Chem. 253, 6401-6412 (1978).

Nielsen, T. B., Ladd, P. M., Preston, S. J. & Rodbell, M. Biochim. biophys. Acta 629, 143-155

Y., Lonzos, C. & Rodbell, M. Analyt. Biochem. 58, 541-548 (1974). 19. Laing, D. G. Perception 12, 99-117 (1983).

Synthesis of fast myosin induced by fast ectopic innervation of rat soleus muscle is restricted to the ectopic endplate region

G. Salviati*†, E. Biasia† & M. Aloisi†

* Centro di Studio per la Biologia e Fisiopatologia Muscolare del CNR and † Istituto di Patologia Generale dell'Universita' di Padova, via Loredan 16, 35131 Padova, Italy

Skeletal muscle fibres, long multinucleated cells, arise by fusion of mononucleated myoblasts to form a myotube that matures into the adult fibre. The two major types of mature fibre, fast and slow fibres, differ physiologically in their rate of isotonic shortening1. At the molecular level these type-specific physiological properties are ascribed to different isoforms of myosin, a major protein involved in shortening^{2,3}. Differentiation of fast and slow fibres seems to be under the control of motoneurones4, and mature fibres are innervated by only one motoneurone. When rat soleus muscle (SOL, a slow muscle) is dually innervated with a fast nerve, it acquires some properties of a fast muscle, that is, low sensitivity to caffeine and high glycogen content5. We report here that in dually innervated soleus muscle the foreign fast nerve induces synthesis of fast isoforms of myosin, but only in the segment of the muscle fibre that is close to the foreign endplate. The localized influence of the nerve endplates suggest that factors controlling the phenotypic expression of the muscle fibre have a short range

The nerve of the fast extensor digitorum longus (EDL) muscle of male Wistar rats (each weighing 160 g) was transposed and inserted with the aid of a glass capillary under the fascia of the soleus muscle, in the proximal third of the muscle. Care was taken not to damage the muscle fibres underneath. After 3 weeks, the SOL was temporarily denervated by crushing and freezing its motor nerve with clamps that had been immersed in liquid nitrogen. This procedure enables the soleus muscle fibres to be innervated rapidly (as early as 3 days after nerve crushing⁶) by the fast nerve, which forms new endplates that are functionally normal and remain active for long periods, perhaps indefinitely Also, after 2 weeks the normal nerve re-establishes contacts with the target fibres at the orginal neuromuscular junctions7. We studied the dually innervated SOL either 3 or 14 months after surgery, electrically stimulating the muscles via the nerve to be certain that both normal and foreign nerves could induce contraction. All operated muscles (n = 10) contracted on stimulation of either nerve. We dissected the operated soleus muscle, and, as a control, the contralateral muscle, and mounted them on a wooden stick, then chemically skinned the fibres to extract soluble sarcoplasmic proteins that would interfere with the identification of myosin light chains and regulatory proteins in the gels8.

To identify dually innervated fibres, we treated bundles of muscle fibres with a skinning solution (170 mM K-propionate, 2.5 mM Mg propionate, 2.5 mM ATP, 5 mM EGTA, 10 mM imidazole-propionate, pH 7.0) containing bungarotoxin labelled with fluorescein isothiocyanate, a reagent that binds to the acetylcholine receptors. In both control and experimental muscle fibres, a-bungarotoxin was localized exclusively at the endplates. We dissected single fibres and examined them by fluorescence microscopy to identify those with two endplates. These were found in the proximal end (1-2 mm from tendon insertion, ectopic endplate) and in the middle region of the muscle fibre (5-6 mm from the ectopic endplate) where endplates are normally localized. We solubilized fibres in SDS-containing solution and analysed myofibrillar protein isoforms by SDS-gel electrophoresis on a discontinuous

Table 1 Localization of fast MHC isoforms in single soleus fibres bearing two separate endplates

			Proximal end Ectopic endplate	2	Original endplate	Distal end
Segment	no.		1			
				nonths oper	rated	
Fibre no.	1	F	4	+++	+++	+++
	2	F	++	777	-	***
	2	S	++	+++	+++	+++
	3	F	+	5 f t		**************************************
	,	s	++	+++	+++	+++
	4	F	+			4 (12)
	•	ŝ	++	+++	+++	+++
	5	F	+		same).	più (A)
	_	S	++	+++	+++	444
	6	F	+	, -	HORE	***
		S	++	+++	+++	444
	7	F	+	attace.	neeri	sine ()
		S	++	+++	+++	+++
			Faurtaan	.manthe an	fintania	
Fibre no.	1	F	++	-months op +	CI ALCU	ataba.
r tore no.	1	S	+	++	+++	4.4
	2	F	+	****		Landy.
	-	S	++	+++	+++	+++
	3	F	++	+		***
		S	+	++	+++	+++
	4	F	++	apain.	Majori;	weeks.
		S	+	+++	+++	+++
	5	F	++		7990	- A
		S	+	+++	+++	+++
	6	F	++	+	diagn.	nilge
		S	+	++	+++	+++
	7	F	++	-	THEFT	
		S	+	++	+++	+++
	8	F	++	****	amov	****
	_	S	+	+++	+++	+++
	9	F	++	+	buller.	-
		S	+	++	+++	+++
	10	F	+		men.	
		S	++	+++	4-4-4	4++
	11	F S	++	++		
,	12	F	++	-	+++	+++
	12	S	+	+++	nga nga nga	+++
1	13	F	++	TTT	all	T T T
		Š	+	+++	+++	+++
1	14	F	++	+	* * *	
•	•	S	+	++	+++	++4
1	15	F	++	+		**************************************
		S	+	++	+++	+++
1	16	F.	+	Aven.	96947	- August 1
		S	++	+++	+++	-
1	17	F	++		Mou	game.
		S	+	+++	+++	+++
1	8	F	++	****	-myg-	
		S	+	+++	+++	+++

Single muscle fibres, showing two separate endplates after abungarotoxin labelling, were isolated from 3-months (4 muscles) or 14-months (6 muscles) operated soleus muscles. Each fibre was cut into four segments (each 2 mm long starting from the proximal end). Fast (F) and slow (S) myosin heavy chains were separated by 5% SDS-gel electrophoresis and stained with silver. (+) indicates the amount of fast and slow MHC in each fibre segment. Fibre segments were 2 mm long.

system9 as described previously8,10.

The presence of two separate endplates in the same fibre may not be an absolute criterion for dual (fast and slow) innervation. It has been reported that in some instances branches of the same foreign motor nerve form separated endplates on the same muscle fibre when the original nerve was cut and prevented from reinnervating the muscle¹¹. Furthermore, many denervated

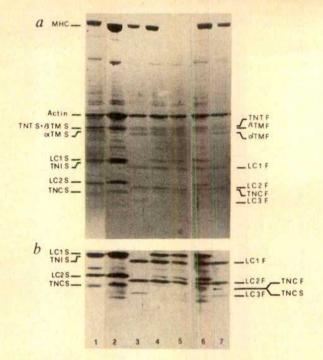


Fig. 1 Pattern of myofibrillar proteins of single fibres from operated soleus muscle. SDS-gel electrophoresis on 10-20% polyacrylamide linear gradient of chemically skinned single-fibre proteins. Lanes 1, 2, control slow fibres from SOL muscle; 3, 7, control fast fibres from EDL muscle; 4-6, dually-innervated soleus fibres identified by fluorescent α-bungarotoxin labelling (see text). In lane 5, MHC material is missing because of a cracking in the gel. After electrophoresis the gel was stained with Coomassie Brilliant Blue (panel a), destained and stained with silver (panel b); in b only the region of MLC is shown. F, fast; S, slow; MHC, myosin heavy chain; LC, myosin light chain; TNT, TNI, TNC, troponin T, I or C; TM, tropomyosin.

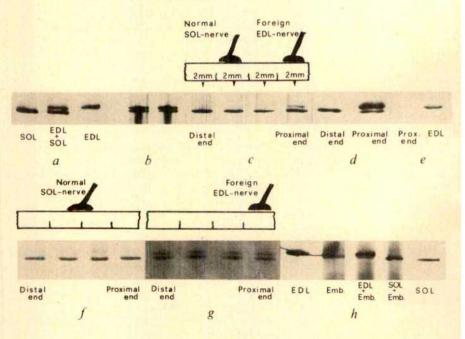
endplates of muscle cross-innervated by a foreign nerve at a distant location continue to bind normal amounts of α -bungarotoxin for more than 4 months¹². However, at later stages (30-40 weeks) after denervation of the original nerve, a decreased acetylcholine sensitivity has been demonstrated in non-reinnervated original endplates⁷. Most of our fibres were analysed 14 months after the operation and no differences were found in the intensity of α -bungarotoxin fluorescence between ectopic and original endplates. This result and the fact that operated soleus muscles contracted to electrical stimulation of either normal or foreign nerve suggest, although do not prove, that most of the original endplates were reinnervated by the normal nerve⁷. The possibility still exists that not all the fibres studied were in fact dually innervated.

Fast and slow myosin light chains (MLC), tropomyosin (TM) and troponin (TN) showed different apparent relative molecular mass (Fig. 1; lanes 3, 7 and 1, 2, respectively). Fourteen months after surgery, all experimental soleus fibres (n = 13) contained

both fast and slow isoforms of MLC, TM and TN (Fig. 1; lanes 4-6), indicating that the foreign fast nerve could activate synthesis of fast isoforms of MLC and the regulatory proteins. Fast and slow rat myosin heavy chains (MHC) can be identified by an electrophoretic gel system that requires very little protein (ref. 13; Fig. 2a), making it possible to study the composition of MHC in single fibres. In all experimental fibres (n = 13), we found both fast and slow MHC (Fig. 2b), although the relative proportion of the two isomyosins varied. Furthermore, the additional protein band which appeared in experimental fibres was selectively immunostained by a monoclonal antibody specific for adult fast MHC (Fig. 2e). These findings indicate that a fast nerve implanted onto a normally innervated slow fibre modify the 'trophic' effect of the slow nerve, activating genes encoding fast myosin.

Our results, however, raise another question: whether the effect of the fast nerve was exerted on the entire fibre or only near the fast endplate. To answer this question, we cut experi-

Fig. 2 Expression of fast myosin heavy chains by single fibres from operated soleus muscle. MHC (~50 ng protein) were separated by SDSgel electrophoresis on 5% polyacrylamide gel and stained with silver, a. Control muscles: b. total protein of two dually innervated fibres (see Fig. 1); c, dually innervated fibre 3 months after surgery-4 fibre segments of the same length (2 mm) were cut as shown by the upper scheme and separately electrophoresed; d, dually innervated fibre 14 months after surgery-the fibre was cut into two halves about 4 mm long, that were separately electrophoresed; e, dually innervated fibre cut as in d and EDL control fibre after blotting²³ and immunostaining with anti-rat fast MHC monoclonal antibody (24D5); f, contralateral, control, soleus muscle fibre-four segments (2 mm long) were cut and processed as c; g, fibre (10 mm long) from 14months operated soleus. This fibre, after fluorescent a-bungarotoxin labelling, showed only the foreign endplate at the proximal end-MHC were analysed in four segments as shown in c; h, rat embryonic MHC does not co-migrate with adult fast and slow MHC. Embryonic myosin was purified from 12 days rat fetus hind limb muscles according to ref. 24.



mental fibres into four segments (2 mm long) from the proximal end, where the fast endplate was located. Although fast MHC are found in all fibres 3 or 14 months after surgery (Fig. 2C-D; Table 1), they are detected almost exclusively in the segment of fibre that bears the fast endplate and no fast MHC is ever detected in the segment containing the slow endplate or that located more distally. Only the proximal segment of six 14month dually innervated fibres is stained by histochemical myofibrillar ATPase reaction, after precincubation at pH 10.4, that is, after inhibition of slow myosin ATPase activity (data not shown). Normal soleus fibres contained only slow MHC, even in the segment corresponding to the proximal end (Fig. 2f). By contrast, a fibre from a single 14-month operated soleus muscle, in which only the foreign endplate at the proximal end was demonstrated by the α -bungarotoxin labelling, contained both fast and slow MHC, but the relative amounts of the two isoforms were constant throughout the entire fibre length (Fig. 2g).

We conclude that this fibre is a slow fibre 'cross-innervated' by the fast nerve that undergoes a partial slow-to-fast transformation, in agreement with previous results14. The possibility that the additional band seen in experimental fibres could have been contributed by synthesis of embryonic myosin induced by denervation was excluded because the heavy chains of purified rat embryonic myosin show an electrophoretic mobility intermediate between those of heavy chains of adult fast and slow myosin, and closer to that of slow MHC (Fig. 2, lane 4) and, therefore, it cannot co-migrate with the additional band. These findings demonstrate that the phenotypic expression of myosin isoforms may differ along the length of these single muscle fibres and suggest that this localization is related to the presence of a specific neural input. Clearly this trophic influence may only be exerted over a rather short distance from the endplate.

It is not known what is the message transmitted from nerve to muscle, nor which mediators in the muscle cell activate gene expression. Electrical activity may be the main message transmitted by a nerve^{5,16}, but there may be certain chemical factors (trophic factors)^{17,18}, some of which appear to control specific electrical characteristics of the muscle surface membrane¹⁹. The pattern of electrical activity seems important because the trains of action potentials propagate all along the fibre and could induce formation of mediators that control in a coordinated manner the activation of either 'fast' or 'slow' genes in all nuclei of the fibre. Moreover, direct stimulation by short highfrequency bursts of impulses (fast pattern of stimulation) is more effective than more prolonged trains of low-frequency impulses (slow pattern) in restoring normal membrane properties after denervation²⁰. But the pattern of electrical activity cannot fully explain why the expression of fast genes is restricted to the region around the endplate.

Nonetheless, the localized synthesis of fast myosin in a slow fibre indicates that only a few nuclei are affected by the fast endplate, and that specific chemical mediators must be formed in the muscle cell, but near the endplate. A preferential localization of a muscle membrane antigen (5.1.H11) near the nucleus responsible for its production has been reported in muscle heterokaryons in vitro²¹. On the other hand, 'mosaic' skeletal muscle fibres from mouse chimaeras show no spatial phenotypic heterogeneity related to genotypically distinct myonuclei2 These findings are not inconsistent with our results, because in mosaic fibres genotypically distinct myonuclei are randomly distributed, whereas in our experimental model it is the cytoplasmic mediator(s) which have a limited range of activity.

We thank Professor F. Clementi (Department of Pharmacology, University of Milan) for the gift of fluorescein isothiocyanate-labelled α -bungarotoxin; Professor S. Schiaffino for the monoclonal antibody; and Dr D. Parry for help in the immunostaining experiment and a critical review of the manuscript. We also thank Drs I. Mussini and V. Benvenuti for design of surgical procedures, and Drs L. P. Rowland, S. Di Mauro

and A. Miranda (Department of Neurology, Columbia University, New York) for helpful discussion. Supported by institutional funds from the Consiglio Nazionale delle Ricerche and by a grant from the Ministero della Pubblica Istruzione.

Received 10 February; accepted 22 May 1986

- Close, R. I. Physiol. Rev. 52, 129-197 (1972)
- Barany, M. J. gen. Physiol. **50**, 197-218 (1967). Dhoot, G. K. & Perry, S. V. Nature **278**, 714-718 (1979). Buller, A. J., Eccles, J. C. & Eccles, R. M. J. Physiol., Lond. **150**, 417-439 (1960).
- Gutmann, E. & Hanzlikova, V. Physiol. Bohem. 16, 244-250 (1967) Lomo, T. & Slater, C. R. J. Physiol. Lond. 275, 391-402 (1978).
- Frank, E., Jansen, J. K. S., Lomo, T. & Westgaard, R. H. J. Physiol., Lond. 247, 725-743 (1975).
- Salviati, G., Betto, R. & Danieli-Betto, D. Biochem. J. 207, 261-272 (1982) Laemmli, U. K. Nature 227, 680-685 (1970).
- Salviati, G., Betto, R., Danieli-Betto, D. & Zeviani, M. Biuchem. J. 224, 215-225 (1984).
- Kuffler, D. P., Thompson, W. & Jansen, J. K. S. Proc. R. Soc. B208, 189-222 (1980) Frank, E., Gautvik, K. & Sommerschild, H. Acta Physiol., Scand. 95, 66-76 (1976).
- Carraro, U. & Catani, C. Biochem. biophys. Res. Commun. 116, 793-802 (1983).
 Gauthier, G. F., Burke, R. E., Lowey, S. & Hobbs, A. W. J. Cell Biol. 97, 756-771 (1983).
- Salmons, S. & Sreter, F. A. Nature 263, 30-34 (1976). Pette, D. & Schnez, U. FEBS Lett. 83, 128-130 (1977).
- 17. Guth, L. Physiol. Rev. 48, 645-687 (1968).
- Gutmann, E. A. Rev. Physiol. 38, 177-216 (1976).
- 19. McArdle, J. J. Prog. Neurobiol. 21, 135-198 (1983)
- Lomo, T. & Westgaard, R. H. J. Physiol., Lond. 252, 603-626 (1975).
- 21. Pavlath, G. K. & Blau, H. M. J. Cell Biol. 102, 124-130 (1986)
- Frair, P. M. & Peterson, A. C. Expl. Cell Res. 145, 167-178 (1983).
 Towbin, H., Staehelin, T. & Gordon, J. Proc. natn. Acad. Sci. U.S.A. 76, 4350-4354 (1879).
- 24. Szent-Gyorgyi, A. G. J. biol. Chem. 192, 361-369 (1951).

The tight junction does not allow lipid molecules to diffuse from one epithelial cell to the next

Gerrit van Meer, Barry Gumbiner* & Kai Simons

European Molecular Biology Laboratory, Postfach 10.2209, D-6900 Heidelberg, FRG

The tight junction (zonula occludens) links epithelial cells into a monolayer by forming a continuous belt of sealing contacts around the apex of each cell. They appear in thin sections as if they were 'fusions' between the apposed plasma membranes' and in freezefracture replicas as patterns of complementary strands and furrows2. These images have led to the proposal that the core of the tight junction is formed by a hexagonal cylinder of lipids^{3,4}. In this model, the cytoplasmic leaflet of the apical and basolateral plasma membrane domains would be continuous, whereas the exoplasmic leaflets of the two plasma membrane domains of the same cell would be separated at the tight junction and are instead predicted to be continuous between the plasma membranes of neighbouring cells. We demonstrate here that this prediction does not hold true. An endogenous glycolipid (Forssman antigen), present in the exoplasmic leaflet of the apical membrane of MDCK strain II cells 5,6, is unable to pass to MDCK strain I cells (which lack this glycolipid) under conditions where these cells are connected by tight junctions. In addition, fluorescent lipids which have been fused into the plasma membrane^{7,8} of one MDCK cell do not diffuse to neighbouring cells while the tight junctions between the cells are intact.

To test whether lipids can diffuse from one epithelial cell to another through continuous exoplasmic leaflets of their apical plasma membranes, we studied the behaviour of endogenous glycolipids. Strain II MDCK cells, a subline of the MDCK cell line9, possess a series of glycolipids, the globo series, which are not found in MDCK strain I cells, a different MDCK subline "" Forssman antigen, one glycolipid of this series [GalNAc(α)-3)GalNAc(β 1-3)Gal(α 1-4)Gal(β 1-4)Glc(β 1-1)Cer], constitutes 21% of the total neutral glycosphingolipids of MDCK strain II cells⁵. When a monolayer of these cells was labelled

Present address: Department of Pharmacology, School of Medicine, University of California

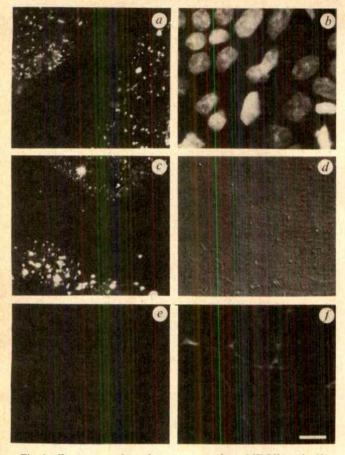
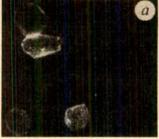


Fig. 1 Forssman antigen does not move from MDCK strain II cells to MDCK strain I cells during 96 h of co-culture. a, A mixed monolayer of MDCK strain I and strain II cells on nitrocellulose filters was fixed with 3% formaldehyde and incubated on the apical surface with monoclonal IgGs against Forssman antigen. Clustering of the fluorescent anti-Forssman antibodies in Fig. 1a is prevented if unfixed cells are incubated with the antibody at 0 °C and postfixed before addition of the second antibody (C. M. B. Butor and J. Davoust, unpublished results). As a second antibody we used rhodamine anti-mouse IgG. b, The same field of cells after staining the DNA in the nuclei by Hoechst dye 33258. c, A mixed monolayer grown on a glass coverslip stained apically against Forssman antigen as described for a. d, Nomarski optics micrograph of the field shown in c. e, Parallel monolayers on coverslips were incubated on the apical surface with a monoclonal antibody against uvomorulin, a lateral membrane marker in these cells1 As a second antibody we used rhodamine anti-mouse IgG. f. Staining with the anti-uvomorulin antibody after opening of the junctions by incubation with 2 mM EGTA for 5 min at 37 °C (ref. 10). Scale bar, 10 µm.

from the apical side with a monoclonal antibody against Forssman antigen, apical staining was observed (see also Fig. 4 of ref. 5). This glycolipid was therefore present in the exoplasmic leaflet of the apical plasma membrane. We co-cultured MDCK strain II cells with MDCK strain I cells which do not express Forssman antigen. The presence of intact tight junctions between the two cell types was demonstrated by adding a monoclonal antibody which recognizes uvomorulin, a protein present on the lateral membrane of MDCK cells10, and showing that it did not label the lateral membrane unless the tight junctions had been opened by treatment with 2 mM EGTA for 5 min at 37 °C before fixation (Fig. 1). Therefore, tight junctions were present between strain I and II cells grown together on nitrocellulose filters or glass slides. Staining with 33B12, a monoclonal IgG2c against Forssman antigen¹¹, demonstrated Forssman antigen on the apical surface of about 50% of the cells in the mixed monolayer under both growth conditions. The boundary between stained and unstained cells was sharp. Thus, the endogenous glycolipid



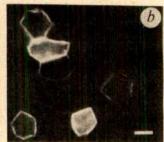


Fig. 2 The fluorescent phospholipid N-rhodamine phosphatidylethanolamine (N-Rh-PE) does not diffuse to neighbouring cells in a monolayer of MDCK strain I cells grown on nitrocellulose filters. N-Rh-PE, a water-insoluble lipid¹², was fused into the apical plasma membrane^{7,8} using unilamellar liposomes containing the fluorescent lipid equally distributed over both bilayer leaflets16 The cells were infected with 4 plaque-forming units per cell of influenza N virus and infection allowed to proceed for 4 h at 37 °C. The liposomes were prepared by reverse-phase evaporation 19 from egg phosphatidylcholine, egg phosphatidylethanolamine, cholesterol, ganglioside $G_{\rm D1a}$ and N-Rh-PE (25:25:50:5:1, mol/mol). 20 nmol total lipid was added in 500 µl of serum-free medium to a monolayer of 3 × 106 cells. After 30 min at 0 °C, fusion was initiated by treatment with a serum-free medium buffered at pH 5.0 by 20 mM succinate, at 37 °C for 60 s. The cells were then returned to pH 7.4 medium and put on ice. Treatment of the cell surface with trypsin, necessary to cleave the haemagglutinin to its fusogenic form^{7,8}, was omitted because in strain I MDCK cells the haemagglutinin is cleaved spontaneously by a secreted protease (G.vanM., unpublished observations). Electrical resistance before infection was $6 \pm 2 \times 10^3 \,\Omega$ cm² (n = 3), and after the complete procedure it was $1.2 \pm 0.2 \times 10^3 \Omega \text{ cm}^2$ (n = 6). The microscope, equipped with a water immersion objective, was focused at the apical surface of the living cells (a) or halfway down the lateral surface (b), after liposome-cell fusion. Scale bar, 10 μm.

could not pass from MDCK strain II cells to the apical surface of neighbouring MDCK strain I cells over a period of 96 h of co-culture at 37 °C.

As an alternative approach, we fused 7.8 fluorescent lipids into the apical plasma membrane of 50% or less of MDCK cells in a confluent monolayer and used a fluorescence microscope to observe whether the fluorescent lipid would move to non-fluorescent neighbour cells. For this, the fluorescent lipids dioleoyl N-rhodamine phosphatidylethanolamine (N-Rh-PE) or octadecyl rhodamine B (R18), which do not spontaneously exchange through the aqueous phase 12,13, were incorporated into liposomes. These liposomes were then added at 0 °C to the apical surface of MDCK cells infected with influenza virus. They were bound to the viral haemagglutinin glycoprotein expressed on the apical surface of these cells by including a haemagglutinin receptor into the liposomal membrane, the GDIa ganglioside. Fusion was induced by a short treatment (60 s) at low pH (5.0) and 37 °C7.8, after which the medium was readjusted to pH 7.4 and 0 °C. Lipid insertion was limited to a fraction of the cells in the epithelial monolayer by infecting the cells with a low multiplicity of influenza virus; in this way, only part of the cells in the monolayer became infected. Only the infected cells subsequently bound and fused liposomes.

MDCK strain I cells were selected for one set of experiments because they develop monolayers possessing a high electrical resistance (>2,000 Ω cm²) when grown on a permeable support¹⁴, and this resistance can be used to assay the intactness of the tight junctions during the experiment¹⁰,¹⁵. The fluorescent phospholipid N-Rh-PE was fused into the apical plasma membrane of about 50% of the MDCK strain I cells in a confluent monolayer (Fig. 2). Fusion was evident from the fact that the fluorescent phospholipid reached the basolateral surface (Fig. 2b). This process will be demonstrated and discussed in more detail elsewhere¹⁶. Fusion was also assayed by the hydrolysis of liposomal cholesterol oleate by a cellular enzyme⁶. The

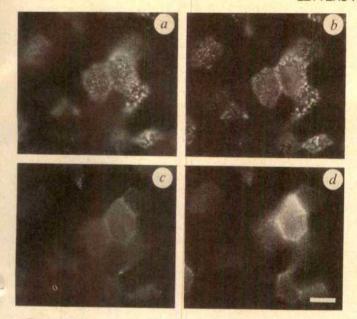


Fig. 3 The fluorescent lipid probe octadecyl rhodamine B (R18) does not pass from cell to cell in a monolayer of MDCK strain II cells on nitrocellulose filters. R18, a positively charged rhodamine lipid unable to exchange spontaneously between membranes13 was fused into the apical plasma membrane as in Fig. 2 with the following differences. At 5 h after infection with 4 plaque-forming units per cell of influenza N virus, the cell monolayer was treated with trypsin as described elsewhere 7.8. Large unilamellar liposomes were prepared by octyl β -D-glucoside dialysis from the same lipids as used in Fig. 2 but containing 1 mol % R18 instead of N-Rh-PE. The microscope was focused from the apical surface (a) down the lateral surface (b-d). The contorted orthogonal morphology of the columnar MDCK cells on nitrocellulose filters is clearly visible. Scale bar, 10 µm.

electrical resistance of the monolayer was $1,200 \pm 160 \,\Omega$ cm² (n=6) after the experiment, indicating that the tight junctions between the cells were essentially intact. In comparison, the electrical resistance across an intact polarized monolayer of strain II MDCK cells without virus infection was 160 Ω cm². Under these circumstances, no spreading of the fluorescent phospholipid to the adjacent non-infected cells was observed. Bright and dark cells remained juxtaposed in the cell monolayer for hours.

Similar experiments were performed on low-resistance MDCK strain II cells using another lipid probe (Fig. 3). The fluorescent lipid R18 was fused into the apical plasma membrane. R18 differs from N-Rh-PE in that it carries one positive charge at neutral pH. As a criterion for intactness of the tight junction, the impermeability of the tight junction to antibodies was monitored as described above. The antibody rrl against the lateral protein uvomorulin¹⁰ was unable to label its antigen throughout the experiment. Like N-Rh-PE, R18 remained confined to the cells into which it had been fused (Fig. 3a-d). No spreading from bright to dark cells was observed for hours at 0 °C.

We have presented evidence that three different types of lipids present in the apical plasma membrane domain are unable to diffuse into the apical membrane of adjacent cells. Dragsten et al.17 earlier observed that after partitioning water-soluble fluorescent probes into a monolayer of epithelial cells and bleaching one cell completely, no fluorescence returned into this black cell from the surrounding bright cells. In our experiments we used endogenous glycolipids and water-insoluble probes introduced by fusion, which we know are present in the outer leaflet of the apical membrane. We avoided the potentially damaging effects of photobleaching by observing mixed populations of cells containing and lacking the lipid studied. Finally, we also demonstrated that the tight junctions between relevant

cells were intact according to two criteria, both the transepithelial electrical resistance and the impermeability of the cell monolayer to antibodies. Moreover, we have tested the behaviour of the lipids at both 37 °C and 0 °C. Our observations argue against a continuity between the external leaflets of the apical plasma membrane in adjacent epithelial cells. The results are thus difficult to reconcile with the hexagonal lipid model of tight junction structure where the outer leaflets of the plasma membranes of neighbouring cells are fused3,4. It seems more likely that proteins which are part of the tight junction structure 10,18 bring the plasma membranes of adjacent cells very close together but do not induce a partial fusion. This would also be more consistent with the fact that the tight junction, as a barrier to ion diffusion between cells, displays ion selectivity

We thank Thomas Gabran and Hilkka Virta for technical assistance, Annie Steiner and Anne Walter for typing the manuscript, Arnoud Sonnenberg (Netherlands Cancer Institute, Amsterdam) for the monoclonal anti-Forssman and Jean Davoust, Stephen Fuller, Henrik Garoff and Wieland Huttner for critically reading the manuscript and for helpful suggestions.

Received 27 March; accepted 9 May 1986.

- Farquhar, M. G. & Palade, G. E. J. Cell Biol. 17, 375-412 (1963). Goodenough, D. A. & Revel, J. P. J. Cell Biol. 45, 272-290 (1970).
- Kachar, B. & Reese, T. S. Nature 296, 464-466 (1982).
 Pinto da Silva, P. & Kachar, B. Cell 28, 441-450 (1982)

- Hanson, G. C., Simons, K. & van Meer, G. EMBO J. S., 483-489 (1986).
 Nichols, G. E., Lovejoy, J. C., Borgman, C. A. & Young, W. W. Jr J. Cell Biol. 101, 64a (1985).
 van Meer, G. & Simons, K. J. Cell Biol. 97, 1365-1374 (1983).
 van Meer, G., Davoust, J. & Simons, K. Biochemistry 24, 3593-3602 (1985).
 Balcarova-Ständer, J., Pfeifler, S. E., Fuller, S. D. & Simons, K. EMBO J. 3, 2687-2694 (1984).
 Gumbiner, B. & Simons, K. J. Cell Biol. 102, 457-468 (1986).
 Sonnenberg, A. et al. J. Immun. (in the press).
 Struck, D. K. Heckster, D. & Passers, P. E. Biochemistry 20, 1000 (1986).

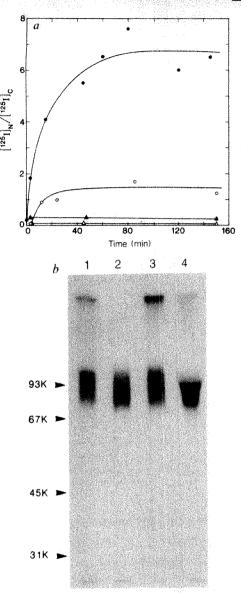
- Struck, D. K., Hoekstra, D. & Pagano, R. E. Biochemistry 20, 4093-4099 (1981).
 Hoekstra, D., de Boer, T., Klappe, K. & Wilschut, J. Biochemistry 23, 5675-5681 (1984).
 Fuller, S., von Bonsdorff, C.-H. & Simons, K. Cell 38, 65-77 (1984).
 Cereijido, M., Robbins, E. S., Dolan, W. J., Rotunno, C. A. & Sabatini, D. D. J. Cell Biol. 77, 83, 880 (1972). 77, 853-880 (1978).
- van Meer, G. & Simons, K. EMBO J. 5, 1455-1464 (1986).
- Dragsten, P. R., Blumenthal, R. & Handler, J. S. Nature 294, 718-722 (1981).
 Stevenson, B. R. & Goodenough, D. A. J. Cell Biol. 98, 1209-1221 (1984).
 Szoka, F. Jr & Papahadjopoulos, D. Proc. natn. Acad. Sci. U.S.A. 75, 4194-4198 (1978).

Synthetic peptides as nuclear localization signals

David S. Goldfarb*, Jean Gariépy†, Gary Schoolnik† & Roger D. Kornberg*

Departments of * Cell Biology and † Medical Microbiology, Stanford University School of Medicine, Stanford, California 943-5, USA

The nuclear envelope defines a compartment boundary which is penetrated by pores that mediate a remarkable transport process. Precursor RNAs are retained in the nucleus, while processed messenger RNA1, transfer RNA2 and ribosomal subunits3 are transported to the cytoplasm. Proteins destined for the nucleus become localized soon after synthesis and again following mitosis, while cytoplasmic proteins are excluded4. The process is highly specific: a single base change in vertebrate initiator tRNA Met (tRNA_i^{Met}) reduces the rate of export 20-fold⁵; a point mutation within the simian virus 40 (SV40) large-T antigen, converting Lys 128 to Thr (ref. 6) or Asn (ref. 7), prevents import. Lys 128 lies within a short 'signal' sequence which, when fused to large non-nuclear proteins, causes their accumulation in nuclei6-Regions of other eukaryotic proteins also seem to contain nuclear localization signals, although a single consensus sequence has not emerged9-13. We report here that a synthetic peptide containing 10 residues of large-T antigen sequence serves as a nuclear localization signal when cross-linked to bovine serum albumin (BSA) or immunoglobulin G (IgG) and microinjected in Xenopus oocytes. Substitution of Thr at the position of Lys 128 in this peptide



toethanol, 50 mM Tris-HCl pH 6.8, boiled and centrifuged. Supernatants (5,000 c.p.m.) were analysed by electrophoresis in a SDS-10% polyacrylamide gel²¹ and autoradiography. Methods. Peptides were prepared using a Beckman 990B synthesizer as described previously^{22,23}. Crude peptides in 0.1% aqueous trifluoroacetic acid were purified by HPLC on a C18 Ultrasphere ODS reverse-phase column (Altex; 250×10 mm i.d.). The composition and concentration of purified peptides were verified by amino-acid analysis. Peptides were cross-linked to proteins (BSA, Pentex Fraction V, Miles Scientific, or mouse monoclonal antibody My1, directed against Dictyostelium discoideum myosin²⁴) as follows. Protein (10 mg in 2 ml of PBS²⁵) was treated with m-maleimidobenzoyl-N-hydroxysuccinimide ester (Pierce; 5 mg in 0.5 ml of dimethylformamide) for 1 h at 20 °C. Modified protein was purified by filtration through Sephadex G-25 in 0.1 M sodium phosphate, pH 6.0. Peptide solution (5 mg ml⁻¹ in 0.1 M sodium phosphate, pH 6.0) was added dropwise and allowed to react for 1 h at 20 °C. Peptide-linked protein was purified by filtration through Sephadex G-25 in 0.1 M NH₄HCO₃. Numbers of peptides per molecule of BSA, determined by SDS-gel electrophoresis (and by amino-acid analysis) were: P(Lys), 5-22 (7.2 ± 4.5); P(Thr), 7-21 (11.5 \pm 6.7); P(H2B), 13-25. Peptide-linked proteins were labelled by treatment with 125 I-sodium iodide and Enzymobeads (BioRad), filtered through Sephadex G-25 in PBS²⁶, and concentrated with the use of Centricon-30 filters (Amicon). Specific activities ranged from 1,500 to 2,500 c.p.m. ng⁻¹. Labelled proteins were microinjected with bevelled glass needles (10-20 µm o.d.)

Fig. 1 a, Nuclear accumulation of peptide-linked BSA.

P(Lys)-BSA; \bigcirc , P(Thr)-BSA; \blacktriangle , P(H2B)-BSA; \triangle , BSA. Each point represents a mean of determinations on 6-10 oocytes, injected with ~5 ng of ¹²⁵I-protein per oocyte. Incubations were at 18 °C, except for the point for P(Lys)-BSA at zero time, which was taken at 0 °C. The ratio of nuclear to cytoplasmic ¹²⁵I-protein concentration, ¹²⁵I-N/[¹²⁵I]C, was calculated from the expression (% c.p.m. nuclear/12)/(% c.p.m. cytoplasmic/88), assuming that the nucleus contains 12% of the accessible aqueous volume of an oocyte ¹⁶. b, Stability of ¹²⁵I-P(Lys)-BSA following microinjection in oocytes and incubation for 12 h at 18 °C. Intact oocytes (lane 1), starting ¹²⁵I-P(Lys)-BSA (lane 2), oocyte nuclei (lane 3) and oocyte cytoplasm (lane 4) were dispersed in 10% SDS, 100 mM β -mercap-

renders it six- to sevenfold less effective. The uptake of peptidelinked BSA is saturable, and the rate is diminished by co-injection of free peptide. These findings are indicative of a receptor-mediated uptake process. With the use of anti-peptide antibodies, a family of proteins is revealed in nuclear but not cytoplasmic extracts of human lymphocytes which contain large-T antigen-like sequences.

Deletion analyses from either end of a large-T antigen sequence incorporated in fusion proteins have defined two minimal segments required for nuclear localization, with a region of overlap containing Lys 128 (ref. 8). The signal peptide synthesized for use in the present study, designated P(Lys), spanned these minimal segments (Table 1). P(Thr) contained the substitution of Thr for Lys 128 (ref. 6). A third peptide, P(H2B), contained residues 1-17 of Xenopus histone H2B (ref. 14), but presumably no nuclear localization signal, as assessed by microinjection experiments⁴ with residues 1-58 and genetic studies of the corresponding region of yeast histone H2B (R. Moreland and L. Hereford, personal communication). All three peptides included carboxy-terminal tyrosine and cysteine residues, for radioiodination and chemical cross-linking, respectively. Cross-linking was accomplished with a sulphydryl-toamino group reagent, and gave 10-20 peptides per molecule of BSA (see Fig. 1 legend).

On injection of SV40 DNA in Xenopus oocytes, large-T antigen accumulates in the nucleus, showing that a large-T antigen signal sequence is recognized by the *Xenopus* nuclear uptake apparatus¹⁵. We find that P(Lys)-BSA, bearing large-T antigen signal peptides, also accumulates, reaching a six to sevenfold higher concentration in the nucleus than in the cytoplasm (Fig. 1a). By contrast, P(Thr)-BSA only equilibrates between nucleus and cytoplasm, and both P(H2B)-BSA and unmodified BSA (see also ref. 16) are virtually excluded from the nucleus (Fig. 1a). Similar results were obtained with P(Lys)- and P(Thr)-IgG (data not shown). Entry of P(Lys)-BSA into nuclei, as opposed to binding at the surface, was confirmed by fluore-scein-labelling and epi-fluorescence microscopy of frozen thin

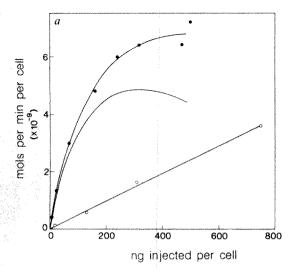
along the line dividing the animal and vegetal hemispheres towards the centre of stage 5 or 6 Xenopus oocytes, maintained in modified Barth's saline at 18 °C as described elsewhere²⁶. Following incubation, oocytes were suspended in 20% trichloroacetic acid on ice and dissected with forceps¹⁶. ¹²⁵I in nucleus and cytoplasm was

determined with an LKB 1260 Multigamma II counter. Protein concentrations were determined as described by Bradford²⁷.

Table 1 Synthetic peptides used in this work



Bars above the sequence of P(Lys) indicate minimal segments required for nuclear localization of SV40 large-T antigen⁸. Carboxy-terminal tyrosine and cysteine residues were added for radioiodination and chemical cross-linking, respectively.



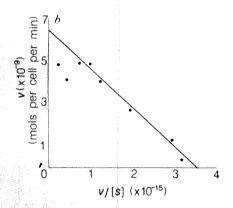


Fig. 2 a, Initial rate of nuclear accumulation of P(Lys)-BSA as a function of amount injected. ♠, P(Lys)-BSA; ○, BSA. Each initial rate was determined from measurements on at least two groups of six to eight oocytes, injected with ¹²⁵I-P(Lys)-BSA or ¹²⁵I-BSA, incubated for 10-45 min at 25 °C, and processed as for Fig. 1. The central curve (no data points) represents the difference between the two experimentally determined curves. b, Eadie-Hofstee plot of data from a. Reaction velocites (v) were derived from the initial rate data for P(Lys)-BSA by subtraction of values from the curve for BSA. Concentrations ([S]) of P(Lys)-BSA in oocytes were calculated as described for Table 2.

sections (data not shown). P(Lys)-BSA isolated from nuclei was indistinguishable in size from starting material (Fig. 1b) and therefore had not entered as proteolytic fragments. We conclude that the attachment of signal peptides to the surface of proteins too large to enter the nucleus by diffusion is sufficient to effect their nuclear localization, and moreover, that the process is signal-sequence-specific, with no simple dependence on amino-acid composition (for example, on net positive charge^{17,18}).

The nuclear accumulation of P(Lys)-BSA showed saturation kinetics (Fig. 2a), when corrected for entry into the nucleus by diffusion 19 , which became appreciable when large amounts of material were injected. (Rates of entry by diffusion were determined with unmodified BSA, and may represent slight overestimates for P(Lys)-BSA, which is expected to enter more slowly due to its larger size.) An Eadie-Hofstee plot was linear (Fig. 2b), with intercepts corresponding to a $K_{\rm M}$ of 1.8×10^{-6} M and $V_{\rm max}$ of 6.4×10^{9} molecules per cell per min. (Rates of nuclear accumulation varied, depending on the batch of oocytes and extent of iodination of the protein, so the values of $K_{\rm M}$ and $V_{\rm max}$ should be regarded as approximate.) Deviations from linearity at the two highest values of substrate concentration probably reflect the inaccuracy of the correction for diffusion.

The peptide-linked proteins used in this work differ from natural substrates for nuclear transport in possessing multiple signal sequences, and the question arises of whether a single peptide would be effective. We investigated this question by co-injecting P(Lys)-BSA with excess free peptide (Table 2).

Table 2 Effect of free peptide on nuclear accumulation of peptidelinked BSA

Free peptide	Expt 1	Expt 2
None	23.6 ± 8.2	27.1 ± 11.1
P(Lys)	10.9 ± 3.4	11.3 ± 4.1
•	(0.01 < P < 0.02)	(0.02 < P < 0.05)
P(Thr)	19.0 ± 4.4	19.0 ± 6.9
	(0.02 < P < 0.05)	(0.05 < P < 0.1)
P(H2B)	-	25.1 ± 8.7
		(0.2 < P < 0.5)

Approximately 5 ng of 125 I-P(Lys)-BSA (6×10^{-5} nmol) was injected alone or with the free peptide (0.5 nmol) indicated in 16-18 oocytes. Approximate concentrations of P(Lys)-BSA and free peptide in an oocyte were 1×10^{-7} and 0.9×10^{-3} M, respectively, based on an accessible aqueous volume of $0.5\,\mu$ l (one-third) 16 of a total volume of $1.5\,\mu$ l) plus an average volume injected of 60 nl. Following incubation for 40 min at $18\,^{\circ}$ C, 125 I in nucleus and cytoplasm were determined as in Fig. 1. Data are expressed as the per cent of the total counts found in the nucleus. The probability (P) that added peptide did not affect uptake was determined with a two-tailed t-test.

Nuclear accumulation of the peptide-linked protein was markedly reduced by free P(Lys) and to a lesser extent by P(Thr). Only the rate and not the final extent of nuclear accumulation was affected (data not shown). Co-injection of P(H2B) caused no significant reduction in rate, arguing against indirect effects of the peptide preparations. We conclude that free peptide interacts specifically with a component of the nuclear transport apparatus, although the affinity of the interaction is low, as 1 mM peptide is required for $\sim 50\%$ inhibition of transport. The difference between the micromolar $K_{\rm M}$ for P(Lys)-BSA and the much lower affinity for free peptide may reflect a multivalent interaction of the peptide-linked protein (see ref. 18), but further work is needed to explain the discrepancy.

The saturation kinetics and effect of free peptide on nuclear transport are indicative of a limiting component of the uptake apparatus. This component may be a receptor for the signal peptide or it may interact with a receptor-signal peptide complex. The receptor may be diffusible, as in the case of 'signal recognition particle' in the synthesis of membrane and secreted proteins²⁰, or it may reside in the nuclear pore complex. Signal peptide may interact not only with this receptor but also with factors inside the nucleus. Thus, the apparent capacity of P(Thr)-linked proteins to enter but not accumulate in the nucleus may be explained either by their altered interaction with the receptor or by their lack of retention (for example, through binding) in the nucleus. Further modifications of the signal peptide sequence and kinetic analyses may help to distinguish between these possibilities.

A nuclear uptake receptor would presumably be general, recognizing signal sequences not only in large-T antigen but also in other nuclear proteins. We have used anti-signal peptide antibodies to investigate the occurrence of large-T-like sequences in other proteins. Antisera against P(Lys) reacted strongly with several nuclear proteins from human lymphocytes (Fig. 3). This strong reaction was abolished by pre-incubation of antisera with P(Lys) (two weakly reacting components at relative molecular mass $(M_{\rm r}) \sim 45,000~(45{\rm K})$ and 65K persisted). There was only a weak reaction with a small number of cytoplasmic proteins, and these appeared to correspond with nuclear proteins, which may have leaked from nuclei during isolation. These data are indicative of a family of proteins bearing homologous nuclear localization signals and sharing a common receptor. Conceivably, all nuclear proteins share the same receptor, whose



Fig. 3 Reaction of antiserum against P(Lys) with proteins from human lymphocytes. A SDS-10% polyacrylamide gel of cytoplasmic (lanes 1, 4) and nuclear (lanes 2, 3) extracts is shown before (lanes 3,4, stained with Coomassie blue) and after (lanes 1, 2) immunoblotting. M_r of markers from the top of the gel, are 200 K, 97.4 K, 68 K, 43 K, 25.7 K, 18.4 K.

Methods. MICH cells (an Epstein-Barr virus-immortalized human B-lymphocyte line, from Dr P. Parham, Stanford University) were grown in RPMI-1640 supplemented with 10% fetal bovine serum. Cells (6×108) were washed with cold phosphate-buffered saline and lysed by suspension in 14 ml of 0.34 M sucrose, 10 mM Tris-HCl pH 7.8, 2 mM MgCl₂, 1 mM CaCl₂, 0.2% NonidetP-40, 10 mM β-mercaptoethanol, 0.5 mM phenylmethysulphonyl fluoride (PMSF). One ml of the lysate was centrifuged (Eppendorf) for 5 min, and the supernatant was retained as cytoplasmic extract. To the remaining lysate was added 14 ml of buffer B (2 M sucrose, 10 mM Tris-HCl pH 7.8, 5 mM MgCl₂, 10 mM β-mercaptoethanol, 0.5 mM PMSF), and the mixture was layered over 3 ml of buffer B and centrifuged for 50 min at 25,000 r.p.m. in a Beckman SW41 rotor. The pellet was suspended in 3 ml of 50 mM Tris-HCl pH 7.8, 0.1 M NaCl, 10 mM β-mercaptoethanol, 0.5 mM PMSF, and 2 ml of 2.5 M KCl was added to give nuclear extract. The cytoplasmic and nuclear extracts were centrifuged for 30 min at 50,000 r.p.m. in a Beckman TL-100 ultracentrifuge. Aliquots (30 µg of protein) of the supernatants were fractionated in polyacrylamide gels and electroblotted onto a nitrocellulose filter, and the filter was washed in 0.9% NaCl, 10 mM Na-phosphate, 0.05% Tween-20 pH 7.4 and incubated for 1 h with anti-P(Lys) antiserum (1:500 dilution). Antibody bound to the filter was detected with the Vectastain ABC horseradish peroxidase system as described by the manufacturer (Vector). Anti-P(Lys) antiserum was obtained from rabbits 10 days after a second injection with 200 µg of P(Lys)-thyroglobulin (prepared as for Fig. 1 with bovine thyroglobulin type 1 (Sigma), injected first with Freund's complete adjuvant and 14 days later with incomplete adjuvant).

specificity is broader than that of the anti-peptide antibodies used here. Alternatively, there may be additional receptors for other classes of nuclear protein bearing different signal

We thank Dr Peter Sargent for access to his Xenopus colony, Dr Peter Parham for monoclonal anti-myosin antibody, and Alan Sachs for discussion. This research was supported by NIH grants GM-30387 to R.D.K. and AI-21912 to G.S. (fellow of John A. Hartford Foundation). D.S.G. was a postdoctoral fellow of the American Cancer Society. J.G. is a postdoctoral fellow of the MRC of Canada.

Received 17 March; accepted 15 May 1986.

- Wickens, M. P. & Gurdon, J. B. J. molec. Biol. 163, 1-26 (1983)
- Welton, D. A., DeRobertis, E. M. & Cortese, R. Nature 284, 143-148 (1980).
 Warner, J. R., Tushinski, R. J. & Wejksnora, P. J. in Ribosomes: Structure, Function and Genetics (eds Chambiss, G. et al.) 889-902 (University Park Press, Baltimore, 1980).
- 4. Bonner, W. M. in The Cell Nucleus Vol. 6C (ed. Busch, H.) 97-148 (Academic, New York,
- Zasloff, M. Proc. natn. Acad. Sci. U.S.A. 80, 6436-6440 (1983). Kalderon, D., Richardson, W. D., Markham, A. F. & Smith, A. E. Nature 311, 33-38 (1984). Lanford, R. E. & Butel, J. S. Cell 37, 801-813 (1984).

- Kalderon, D., Roberts, B. L., Richardson, W. D. & Smith, A. E. Cell 39, 499-509 (1984).
 Dingwall, C., Sharnick, S. V. & Laskey, R. A. Cell 30, 449-458 (1982).
 Silver, P. A., Keegan, L. P. & Ptashne, M. Proc. natn. Acad. Sci. U.S.A. 81, 5951-5955 (1984).
 Hall, M. N., Hereford, L. & Hershowitz, I. Cell 36, 1057-1065 (1984).
- Moreland, R. B., Nam, H. G., Hereford, L. M. & Fried, H. M. Proc. natn. Acad. Sci. U.S.A. 82, 6561-6565 (1985).
- Davey, J., Dimmock, N. J. & Colman A. Cell 40, 667-675 (1985).
 Van Helden, P., Strickland, W. N., Brand, W. F. & Von Holst, C. Biochim. biophys. Acta 533, 278-281 (1978).

- 533, 278-281 (1978).
 Michaeli, T. & Prives, C. Molec. cell. Biol. 5, 2019-2028 (1985).
 Bonner, W. M. J. Cell Biol. 64, 421-430 (1975).
 Smith, A. E. et al. Proc. R. Soc. B226, 43-58 (1985).
 Richardson, W. D., Roberts, B. L. & Smith, A. E. Cell 44, 77-85 (1980).
 Paine, P. L., Moore, J. R. & Horowitz, S. D. Nature 254, 104-114 (1975).
 Wickner, W. T. & Lodish, H. F. Science 230, 400-407 (1985).
 Laemmli, V. K. Nature 227, 680-685 (1970).
 Erickson, B. W. & Merrified, R. B. in The Proteins Vol. 2, 3rd edn (eds Neurath, H., Hill, R. L. & Boeda, C.-L.) 257-493 (Academic, New York, 1976).
 Watts, T. H., Garièpy, J., Schoolnik, G. K. & McConnell, H. M. Proc. natn. Acad. Sci. U.S.A. 82, 5480-5484 (1985).
 Peltz, G., Spudich, J. A. & Parham, P. J. Cell Biol. 100, 1016, 1023 (1085).
- C.S.A. 84, 3480-3484 (1983).
 Peltz, G., Spudich, J. A. & Parham, P. J. Cell Biol. 100, 1016-1023 (1985).
 Dulbecco, R. & Vogt, M. J. exp. Med. 99, 167 (1954).
 Gurdon, J. B. J. Embryol. exp. Morph. 36, 523-540 (1976).
 Bradford, M. Analyt. Biochem. 72, 248-254 (1976).

Loss of genes on chromosome 22 in tumorigenesis of human acoustic neuroma

Bernd R. Seizinger*, Robert L. Martuza† & James F. Gusella*

* Neurogenetics Laboratory, Massachusetts General Hospital and Department of Genetics, Harvard Medical School, Boston, Massachusetts 02114, USA

† Department of Surgery, Neurosurgery Service, Massachusetts General Hospital and Harvard Medical School, Boston, Massachusetts 02114, USA

The application of recombinant DNA techniques has identified two fundamental mechanisms of tumorigenesis in man. The first involves a qualitative or quantitative change in an oncogene (see ref. 1 for review). In the second, discovered in embryonal tumours, a primary mutation occurs which is recessive at the cellular level to the normal allele. The growth of a tumour ensues only after a secondary change, such as chromosome loss or mitotic recombination, eliminates the normal allele, thereby unmasking the altered allele2-7. Because its effect is recessive, the primary mutation may also occur and be transmitted in the germ line, resulting in a familial pattern for the disease. In familial cases, independent bilateral tumours are common, since the tumours result from a single event-loss of the normal genes-which can occur in any cell. This contrasts with non-familial (sporadic) cases where solitary tumours result from the infrequent occurrence of two rare events within the same cell²⁻⁷. By a molecular genetic approach we have now shown that acoustic neuroma, one of the most common tumours of the human nervous system8, is specifically associated with loss of genes on human chromosome 22 and may result from the mechanism of tumorigenesis discovered in embryonal tumours. This finding might provide a clue to the chromosomal location of the defective gene in bilateral acoustic neurofibromatosis, an autosomal dominant disorder with the hallmark of bilateral acoustic neuromas 9-12. In view of the frequent occurrence of meningiomas in patients with bilateral acoustic neurofibromatosis and the association of meningioma with loss of chromosome 22 previously reported in cytogenetic studies 13-15, we suggest that a common event underlies tumorigenesis in acoustic neuroma and meningioma.

Table 1 Loss of heterozygosity on chromosome 22 in acoustic neuromas											
Marker Enzyme	SIS Hin3	D22\$1 Bg/11	IGLC EcoRI	NGFB Bglli	Taql	Hin III	I Msp1	Taql	HRAS1 Taq1	D11S17 Msp1	D11S17 Bglil
Chr	. 22	22	22	1	1	4	4	10	11	11	11
Patient											
ANI	12	12	-	-	****		_			12	
AN2	12	12	12	-			_		12	12	12
AN3		2			12	12	1000	***	**	12 12	12
AN4 AN5		1		***	12	12	-	***	12	12	\$ 65 min
AN6		12		_	-	-	12		12	12	12
AN7	1			12	_	_		-	12	14-140	12
AN8		- - - 2 - - 2	-sken	12	-				12		1 ft - 1
AN9			***	12		12		·			
ANI0	12			wee	-	mark.	12	-	week		
ANII	-	2	where		***	12	Acres		12		12
AN12		7	1	12	12			Augus.	***		<u> </u>
ANI3	2	-		***	12	12	12	1.2	etden. stilden		***
AN14 AN15	1464	12	12	_	***			12	12		
ANIS ANIS		12	1.2	_		12			12		m,
AN17		12	44	***	12	-		***	12		12
AN18		12	***			12		,	-		12
AN19		_					-	-		week	pow.
AN20			***	wee-	****	12		12	NAME:		12
AN21	-	.12	12	12	-	12		12	12	material distribution for a single medical distribution and	
	****	*****	n	D. 4.0.4	D.1206 D			r 13.001	03	633	25.04.27.470
Marker Enzyme	INS Sact	KRAS2 Taq1	D13S1 Mspl				14S1 G. coRI Ms		C3 Hin111	C3 Sac1	D21S17 8gH1
Chr	11	12	13	13	13	•	14 1'		19	19	21
	* *	120	1.7	1.0	1.5					K.9	***
Patient											
ANI	12	-	12	12			12 1		_	,,,,,,	12
AN2 AN3	12	12	12 12	12	***		12 1: - 1:		1000		12
AN4	12		12	1.2	***	-	- 1		need.	12	12
AN5		-	12	_	12		- 1		***	544	12
AN6	12	12	12	12		aine	-		12	Name .	12
AN7		12		12	-	_	12 1	2	viger	rate	~
AN8		desir		-			12 1		***	12	,
AN9				-	-		12	12	~	***	12
AN10		-		12	12				****	4000	
ANII		***			12		12 - 12 -			-miles Antonio	12
AN12 AN13				12	12		12 -		whe	And a	See
ANIA ANIA		12		12	12		12 -		***	12	12
AN15		2.4		12	1.2		- 1		12	12	3.85
AN16						-				***	Algorithm (
AN17							12 1	2 12	***	12	wen
AN18				12		***	_		and a	wire	400a
AN19		4					12 -				12
AN20		12		سيد عداد					ene.	12	12
AN21		**		12	12	12	12 -	- 12	· ·	12	12

Chr, chromosome. Tumour and normal DNA from acoustic neuroma patients was digested with the indicated restriction enzymes, fractionated by agarose gel electrophoresis, transferred to nylon membranes, and hybridized to probes for the indicated loci as described in Fig. 1. In addition to the three chromosome 22 probes are the probes from other chromosomes were used: N8C6 (NGFB)^{21,22}, G8 and R7 (D4S10)^{23,24}, G9 (D4S35)²⁵, Dry5-1 (D10S1)²⁶, pEl6.6 (HRAS1)²⁷, pHINS321 (INS)²⁸, pJ19.4 (D11S17)²⁶, p640 (KRAS2)²⁷, p7F12 (D13S1)²⁹, p1E8 (D13S4)²⁹, pHUB8 (D13S5)³⁰ pHU26 (D13S7)³⁰, pAW101 (D14S1)³⁵, C-H800 (GH)³², B74 (D18S3)²⁶, pC3 (C3)³³ and pGSH8 (D21S17)³⁴. These probes are known to reveal RFLPs in human genomic DNA digested with the indicated restriction enzymes. The phenotype observed in the tumour DNA is shown for every case where the blood DNA displayed heterozygosity: '12' indicates heterozygosity (even though different pairs of alleles may be present for certain multi-allele markers), '1' indicates continued presence of the larger allelic restriction fragment and loss of the smaller allelic fragment relative to normal tissue DNA, and '2' indicates continued presence of the smaller allelic restriction fragment and loss of the larger fragment. Where the normal DNA was tested but was uninformative because it did not display heterozygosity a '-' has been entered to simplify consideration of the data. The absence of an entry indicates that a marker was not tested or did not give a readable result for that particular patient.

Acoustic neuroma (also called vestibular schwannoma or acoustic neurinoma) derives from Schwann cells enveloping the vestibular branch of the vestibulocochlear nerve¹⁶. The majority of acoustic neuromas occur as solitary non-inherited unilateral tumours. By contrast, bilateral tumours are the hallmark of the familial cases of acoustic neuroma that characterize central or 'bilateral acoustic' neurofibromatosis⁹⁻¹². The differences in presentation of sporadic and familial cases of acoustic neuroma are reminiscent of retinoblastoma and Wilms' tumour, two cancers for which loss of a particular chromosomal region (13q and 11p respectively) has been implicated in tumour development²⁻⁷.

We therefore used polymorphic DNA markers to search for similar loss of particular chromosome regions in acoustic neuroma. DNA was isolated from primary acoustic neuromas and corresponding leukocytes from 21 patients (5 male, 16 female). The frequency of both meningiomas and acoustic neuromas in bilateral acoustic neurofibromatosis, and the loss of chromosome 22 previously reported in cytogenetic investigations of meningioma¹³⁻¹⁵ prompted us to focus our initial efforts on DNA markers for chromosome 22. We typed genomic DNA with three polymorphic chromosome 22 markers: SIS, the platelet derived growth factor locus homologous to the sis oncogene mapping to 22q12.3-13.1; D22SI, an anonymous DNA locus detected by probe pMS3-18 mapping to 22pter-q13; and IGLC, the λ immunoglobulin constant region at 22q11. The results of this analysis are presented in Table 1.

Sixteen patients were heterozygous in their normal tissue for at least one of the three polymorphic DNA markers and were consequently informative for determining whether loss of

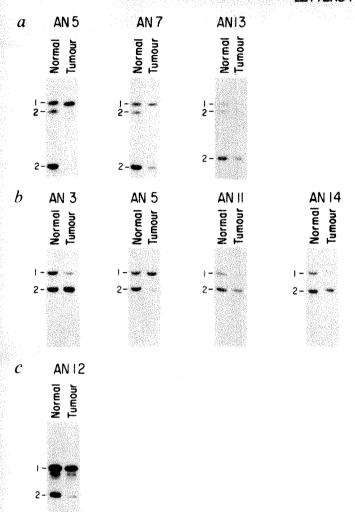


Fig. 1 Loss of constitutional heterozygosity of loci on human chromosome 22 in acoustic neuromas. Patient designations are shown above the autoradiograms. Numbers on the left indicate the observed alleles, with '1' and '2' referring to the larger and smaller allelic restriction fragments respectively. Southern blots were hybridized²² to ³²P-labelled DNA probes for the following loci on chromosome 22: a, Psis.1 (Oncor) (SIS oncogene); b, pMS3-18 (D22S1); c, HuAC2 (IGLC). Psis.1 reveals a RFLP with fragments of 21 kilobases (kb) ('1'-allele), and 14.5 and 6.5 kb ('2'-allele) in HindIII-digested human genomic DNA^{35,36}. pMS3-18 probe detects a RFLP in BglII-digested human DNA, with fragments of 9.5 kb ('1'-allele) and 6.5 kb ('2'-allele)³⁷. The HuλC2 probe reveals a multi-allele RFLP represented by fragments of 8 kb, 13 kb, 18 kb and 23 kb in EcoRI-digested human genomic DNA²⁶. To simplify the nomenclature, the higher relative molecular mass allele is called the '1'-allele, whereas the lower relative molecular mass allele is termed the '2'-allele in each case. Methods. High relative molecular mass DNA was isolated from surgical tumour specimens and corresponding normal tissue (peripheral leukocytes). The tumour specimens which had been immediately frozen on dry ice after operation, were rapidly washed, rinsed and suspended overnight at 37 °C in a TNE-SDS-proteinase K solution (10 mM Tris, pH 8.0; 100 mM NaCl; 1 mM EDTA, 1% SDS; 200 μg ml⁻¹ proteinase K). Nuclei from peripheral leukocytes were isolated by gently homogenizing peripheral venous blood in a solution containing 0.64 M sucrose, 20 mM Tris, 10 mM MgCl₂, 5% (v/v) Triton X-100 pH 7.6 at 4 °C. The isolated nuclei were subsequently incubated overnight at 37 °C in the TNE-SDSproteinase K-solution. DNA from tumour and leukocyte tissue samples was purified by phenol and chloroform extraction²³. Approximately 5 μ g of DNA was digested to completion with the restriction enzymes HindIII, BglII or EcoRI (New England Biolabs). The resulting DNA fragments were fractionated by agarose gel electrophoresis and transferred to nylon membrane

constitutional heterozygosity had occurred in their respective tumour tissue. Seven of the 16 informative cases (44%) showed loss or marked reduction in the intensity of one of the two alleles in their tumour tissue (Table 1). These cases are displayed in Fig. 1. When analysed by densitometry, the hybridization signals corresponding to the deleted allele were estimated to be diminished by 60% (patient AN3), 86% (AN5), 75% (AN7), 73% (AN11), 75% (AN12), >90% (AN13) and 78% (AN14), respectively. The remaining hybridization signals in the tumour DNAs might be due to contaminating non-tumour cells (vascular or connective tissue) which may be present in primary surgical specimens. Alternately, the acoustic neuromas might consist of a mosaic of cells with normal karyotype, and cells with monosomy for chromosome 22.

To distinguish among the different mitotic mechanisms that might have produced this loss of heterozygosity, the hybridization signals from Fig. 1 were compared with those obtained when the same filters were rehybridized with several probes for loci on other chromosomes. The results obtained are presented in Table 2. The ratio of the copy number of chromosome 22 between tumour and normal tissue was approximately 1:2 in all seven cases. This is indicative of 'true' loss of one copy of the chromosome 22 locus, rather than mitotic recombination, loss and reduplication, or gene conversion. Furthermore, patient AN5 was constitutionally heterozygous for two of the three chromosome 22 loci tested. Heterozygosity was lost at both loci in the corresponding tumour tissue, suggesting loss of the entire chromosome rather than a small partial deletion. None of these acoustic neuromas showed mitoses or other aggressive features upon pathological examination; neither did hemizygosity for chromosome 22 show any striking correlation with the patient's age, sex, tumour size or clinical course.

Loss of genes on chromosome 22 was not restricted to unilateral sporadic cases of acoustic neuromas, but was also observed in a tumour from patient AN14 who had bilateral acoustic neuromas. By analogy to inherited cases of retinoblastoma and Wilms' tumour, the defect in bilateral acoustic neurofibromatosis could map to chromosome 22. Tumours from patients AN10 and AN18, two cases of bilateral acoustic neurofibromatosis, did not show loss of heterozygosity for chromosome 22 markers. It should be noted, however, that alternative mitotic or mutational events leading to expression of a recessive disease gene could occur in either sporadic or familial cases without apparent loss of heterozygosity for the available DNA markers. For example, neither a new mutation, a gene conversion, nor a mitotic recombination with a breakpoint distal to the three markers would be recognized. It is conceivable that one or more of these three mechanisms have occurred in the nine tumours for which heterozygosity of the chromosome 22 markers was maintained.

The chromosomal specificity of the loss of heterozygosity in acoustic neuromas was investigated with several polymorphic DNA markers for 11 other chromosomes (Table 1). In each case where constitutional heterozygosity was observed, heterozygosity was also maintained in the corresponding tumour tissue. Thus, acoustic neuromas exhibit a remarkable genome stability, with chromosomal losses being highly specific to chromosome 22. The data in Table 1 also provide assurance that the differences between tumour and normal DNA on chromosome 22 did not arise from simply mispairing of the samples or unreliability

Table 2 Quantitative densitometry of probe hybridization for acoustic neuromas losing heterozygosity on chromosome 22

		Chromosome 22		
Patient	Tissue	Control chromosome	Tumour Normal	
AN3	Acoustic neuroma	0.58	0.50	
	Leukocytes	1.17		
AN5	Acoustic neuroma	0.14	0.42	
	Leukocytes	0.33		
AN7	Acoustic neuroma	0.71	0.52	
	Leukocytes	1.35		
AN11	Acoustic neuroma	0.08	0.50	
	Leukocytes	0.16		
AN12	Acoustic neuroma	1.48	0.43	
	Leukocytes	3.46		
AN13	Acoustic neuroma	0.09	0.63	
	Leukocytes	0.14		
AN14	Acoustic neuroma	0.09	0.51	
	Leukocytes	0.17		

Densitometry of autoradiograms is subject to a number of variables. Therefore, to determine whether loss of one allele for chromosome 22 was associated with duplication of the remaining allele, it was necessary to control for these variations by normalizing the data for chromosome 22 probes to that obtained from the same blots using probes for other chromosomes. Southern blots which had been hybridized to probes for chromosome 22 (Fig. 1) were freed of these probes in distilled water for 2 h at 65 °C and rehybridized with probes for loci on other chromosomes ('Control chromosomes'): (1) D4S10 on chromosome 4p for AN7 and AN13; (2) D21S17 on chromosome 21q for AN3, AN5, AN11 and AN14; and (3) D13S5 on chromosome 13q for AN12. Heterozygosity for RFLPs of these markers frequently provided clear confirmation that they were not deleted in the tumor DNA. The autoradiograms from all hybridizations were analysed by scanning densitometry with an LKB Ultrascan XL. The peak areas corresponding to each hybridization signal were calculated by electronic integration. In order to determine that the approach of normalizing the hybridization signals yielded reliable results, we first compared hybridization signals for pairs of markers from other chromosomes (selected from the markers used in Table 1) for which heterozygosity in the tumours was maintained. These invariably gave constant ratios for tumour and normal DNA. We then determined whether any chromosome 22 alleles had been duplicated in the tumours by normalizing hybridization signals specific to chromosome 22 relative to hybridization signals for control chromosome probes in the same sample, and then obtaining a ratio of the normalized values for each tumour/normal tissue pair.

of the applied techniques. Indeed, all data in Table 1 with probes detecting restriction fragment length polymorphisms (RFLPs) in HindIII, BgIII and EcoRI digested DNA were obtained by rehybridizing the respective Southern blot filters already used for studies on chromosome 22.

The finding that acoustic neuromas specifically lose genes on chromosome 22 has several major implications. It extends the concept that specific somatic loss of constitutional heterozygosity can be a mechanism of tumorigenesis by demonstrating that it can operate in neural crest-derived tumours of the adult nervous system. It suggests that a similar mechanism is involved in development and growth of acoustic neuromas and meningiomas since the latter are also associated with loss of chromosome 2213-15 and both tumours occur frequently in bilateral acoustic neurofibromatosis⁹⁻¹². Of particular interest, this result may lead to the chromosomal localization of the defect causing bilateral acoustic neurofibromatosis, a serious genetic disorder that can lead to deafness or other neurological morbidity or mortality within the first few decades of life⁹⁻¹². Retinoblastoma and Wilms' tumour have become models for the concept that chromosomal mechanisms may serve to unmask recessive mutant alleles by elimination of the wild-type gene²⁻⁷. Unilateral occurrence of acoustic neuromas in sporadic cases, and bilateral tumour formation as the hallmark of the inherited form (bilateral acoustic neurofibromatosis) agree well with this model. Thus, genes on chromosome 22 may play a part in acoustic neuroma analogous to that of genes on chromosomes 11 and 13 in Wilms tumour and retinoblastoma, respectively. This would suggest that chromosome 22 contains a gene important for the development of acoustic neuromas that is transmitted in its defective form in bilateral acoustic neurofibromatosis.

The region of 11p associated with Wilms' tumour has more recently been tied to rhabdomyosarcoma and hepatoblastoma All three of these rare embryonal cancers cluster in the Beckwith-Wiedemann syndrome¹⁷. Similarly, the region of 13q implicated in retinoblastoma has now been associated with osteosarcoma¹⁸. The human genome may contain a limited number of such loci whose defective alleles predispose to tumour formation in particular tissues. The striking frequency of clinical association of acoustic neuromas and meningiomas in bilateral acoustic neurofibromatosis 9-12 and the observation that meningioma tissue can be adjacent to or within acoustic neuroma tissue 19,20 suggests that the selective loss of genes on chromosome 22 in both tumours is not pure coincidence but reflects a common mechanism of tumorigenesis.

We thank Dr R. Ojemann and the Massachusetts General Hospital neurosurgical staff for their assistance in providing specimens, Dr S. de la Monte for assistance in pathological interpretation, and K. Dashner and K. Riley for technical assistance. We thank the following scientists for providing DNA probes: Drs A. Ullrich, J. Habener, T. Dryja, G. Bell, C. Shih, R. Weinberg, R. White, H. Goodman, J. L. Mandel, G. Fey, G. Stewart and P. Leder. B.R.S. is supported by a fellowship from the National Neurofibromatosis Foundation, and R.L.M. is recipient of an NINCDS Teacher-Investigator Career Development Award (NS00654). J.F.G. is a Searle Scholar of the Chicago Community Trust. Funds for this research were provided by NIH grants NS22224 and NS20025, and by the McKnight Foundation.

Received 20 February; accepted 30 April 1986.

- Bishop, J. M. A. Rev. Biochem. 52, 301-354 (1983).
- Koufos, A. et al. Nature 309, 170-172 (1984)
- Orkin, S. H., Goldman, D. S. & Sallan, S. E. Nature 309, 172-174 (1984). Reeve, A. E. et al. Nature 309, 174-176 (1984).
- Fearon, E. R., Vogelstein, B. & Feinberg, A. P. Nature 309, 176-178 (1984). Cavenee, W. K. et al. Nature 305, 779-784 (1983).
- Dryja, T. P. et al. New Engl. J. Med. 310, 550-553 (1984).
- Schoenberg, B. S., Christine, B. W. & Whisnant, J. P. Am. J. Epidemiol. 104, 499-510 (1976). Eldridge, R. Adv. Neurol. 29, 57-65 (1981).
- Martuza, R. L. & Ojemann, R. G. Neurosurgery 10, 1-12 (1982).
 Kanter, W. R., Eldridge, R., Fabricant, R., Allen, J. C. & Koerber, T. Neurology 30, 851-859
- 12. Huson, S. M. & Thrush, D. C. Q. Jl Med. 218, 213-224 (1985).

- Zang, K. D. Cancer Genet. Cytogenet. 6, 249-274 (1982).
 Mark, J. Adv. Cancer Res. 124, 165-222 (1977).
 Zankl, H. & Zang, K. D. Cancer Genet. Cytogenet. 1, 351-356 (1980).
 Rubenstein, L. J. Tumors of the Central Nervous System (Armed Forces Institute of Pathology, Washington, DC, 1972). Koufos, A. et al. Nature 316, 330-334 (1985).
- Hansen, M. F. et al. Proc. natn. Acad. Sci. U.S.A. 82, 6216-6220 (1985).
 Davidoff, L. M. & Martin, J. J. Neurosurg. 12, 375-384 (1955).

- Gardner, W. J. & Turner, O. Archs. Neurol. Psychiat. 41, 76-99 (1940).
 Breakefield, X. O. et al. Proc. natn. Acad. Sci. U.S.A. 81, 4213-4216 (1984).
- Darby, J. K. et al. Am. J. hum. Genet. 37, 52-59 (1985).
 Gusella, J. F. et al. Nature 306, 234-238 (1983).
- Gusella, J. F. et al. Nature 318, 75-78 (1985).
 Gusella, J. F. J. clin. Invest. (in the press).
- Willard, H., Scolnick, M. H., Pearson, P. L. & Mandel, J. L. Cytogenet. cell. Genet. 48, 360-489 (1985)
- Barker, D. et al. Molec. biol. Med. 1, 199-206 (1983).
 Bell, G. I., Horita, S. & Karam, J. H. Diabetes 33, 176-183 (1984).
- Cavenee, W., Leach, R., Mohandas, T., Pearson, P. & White, R. Am. J. hum. Genet. 36, 10-24 (1984).
- 30. Dryja, T., Rapaport, J. M., Weichselbaum, R. & Bruns, G. A. P. Hum. Genet. 65, 320-324
- Wyman, A. R. & White, R. L. Proc. natn. Acad. Sci. U.S.A. 77, 6754-6758 (1980)
- Chakravarti, A., Phillips III, J. A., Mellits, K. H., Buetow, K. H. & Seeburg, P. H. Proc. natn. Acad. Sci. U.S.A. 81, 6085-6089 (1984).
- Davies, K. et al. J. med. Genet. 20, 259-263 (1983).
- 34. Stewart, G. D., Harris, P., Galt, J. & Ferguson-Smith, M. A. Nucleic Acids Res. 13, 4125-4132
- 35. Barker, D. & White, R. Cytogenet, cell. Genet. 37, 250 (1984).
- 36. Julier, C. et al. Cytogenet. cell Genet. 40, 664 (1985). 37. Barker, D., Schafer, M. & White, R. Cell 36, 131-138 (1984).

Tissue-specific expression of the human tropomyosin gene involved in the generation of the *trk* oncogene

Fernando C. Reinach* & Alexander R. MacLeod

Ludwig Institute for Cancer Research, MRC Centre, Hills Road, Cambridge CB2 2QH, UK

* Present address: Departmento Bioquimica, Instituto Quimica, Universidade de Sao Paulo, Caixa Postal 20.780, CEP 01489, Sao Paulo SP, Brazil.

The trk oncogene is a human transforming gene generated by the fusion of tropomyosin gene sequences to a truncated tyrosine kinase receptor gene1. We have now characterized the normal tropomyosin gene from which the trk oncogene is derived. At least two different transcripts are expressed by this gene using a tissue-specific alternative messenger RNA splicing mechanism: a 2.5-kilobase (kb) mRNA encoding a 248-amino-acid tropomyosin in human fibroblasts and a 1.3-kb mRNA encoding a 285-amino-acid tropomyosin in human skeletal muscle. The rearrangement which generates the trk oncogene preserves most of the tropomyosincoding sequences of the normal gene, including exons alternatively spliced in muscle and non-muscle tissue. We therefore expect the trk oncogene to show a tissue-specific pattern of transforming activity. Correct expression of the trk oncogene can occur only in non-muscle tissues. In muscle tissue the oncogene would almost certainly be inactive, as splicing according to the alternative muscle pattern aborts synthesis of the tryosine kinase domain.

We have described an RNA-copy pseudogene hTM_{nm} -1 which defines a 2.5-kb-mRNA encoding a 248-amino-acid tropomyosin in human fibroblasts². The pseudogene hTM_{nm} -1 is colinear with the 2.5-kb fibroblast mRNA and very closely related but not identical in sequence to it. Similarly, the tropomyosin-coding sequences of trk were found to be very closely related but not identical to hTM_{nm} -1 (ref. 1). This suggests that the RNA-copy pseudogene hTM_{nm} -1, the 2.5-kb fibroblast mRNA and the tropomyosin-coding sequences of trk all originate from a common tropomyosin gene which we will call the hTM_{nm} structural gene. This is confirmed by DNA sequence analysis of complementary DNA clones of the 2.5-kb mRNA (not shown) which demonstrates that the tropomyosin-coding sequences of trk are identical to those of the 2.5-kb mRNA.

Tropomyosin genes have been shown to express structurally distinct protein isoforms by a tissue-specific alternative mRNA splicing mechanism³⁻⁶. We have therefore examined the expression of the hTM_{nm} structural gene in different tissues by hybridization of hTM_{nm} -1 to blots of human fibroblast and muscle RNA (Fig. 1). The 2.5-kb mRNA characterized pre-

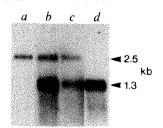
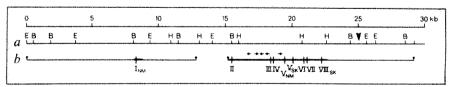


Fig. 1 Northern blot analysis of human non-muscle and muscle RNA. Poly (A)-containing RNA (0.5 μ g) from cultured MRC-5 fibroblasts (lane a), adult heart muscle (lane b), fetal skeletal muscle (lane c) and adult skeletal (leg) muscle (lane d) was denatured with formaldehyde, subjected to electrophoresis and blotted onto nitrocellulose⁹. The filter was probed with M29, a probe derived² from the coding region of hTM_{nm} -1. Hybridization was carried out under stringent conditions (50% formamide, 42 °C) followed by washing in 0.2×SSC at 67 °C. The human fibroblast and adult skeletal muscle tracks were exposed to film for 24 h, the other tracks for 96 h. Sizes of the mRNAs were determined by comparison with known mRNA standards.

viously is found in the fibroblast, heart and fetal muscle RNA samples. In all the muscle preparations an additional 1.3-kb mRNA is apparent which cross-hybridizes with hTM_{nm} -1 under stringent conditions. This transcript is particularly abundant in adult skeletal muscle, in which the 2.5-kb fibroblast mRNA is undetectable. Clones containing the complete coding sequence of the 1.3-kb muscle mRNA were isolated from a library of human skeletal muscle cDNA using hTM_{nm} -1 as a probe (Fig. 2). The deduced protein sequence of this mRNA is 285 amino acids long (numbering from the initiator methionine) and is very closely related to the protein sequence of rabbit skeletal muscle α -tropomyosin⁷.

Comparison with the tropomyosin-coding sequences of trk reveals a very striking homology (Fig. 2). The two mRNAs encode distinct N-terminal protein sequences; that of the 1.3-kb mRNA is characteristic of a 284-amino-acid skeletal muscle tropomyosin while the N-terminal protein sequence of trk is characteristic of a 247-amino-acid cytoskeletal tropomyosin. However, the nucleotide sequences encoding amino acids 80-188 and 214-257 of the 1.3-kb muscle mRNA are identical to sequences found in trk and the 2.5-kb fibroblast mRNA. These two regions of sequence identity are interrupted by a short region of non-identity encoding amino acids 189-213 of the muscle tropomyosin. This pattern of regions of nucleotide sequence identity interrupted by regions of nucleotide sequence non-identity is characteristic of transcripts derived from a common structural gene by alternative mRNA splicing.

Fig. 2 Restriction map of a region of the hTM_{nm} structural gene. Probes derived from the pseudogene hTM_{nm}^{-1} were used to screen libraries of human fibroblast DNA. These libraries were constructed as described elsewhere² using partial digestion with Sau3A, HindIII or BgIII to generate the 15-20-kb DNA



fragments suitable for insertion into $\lambda 1059$ (ref. 12) or $\lambda 2001$ (ref. 13). Both clones were isolated from the partial BgIII library. a, Restriction enzyme mapping was carried out with BamHI (B), HindIII (H) and EcoRI (R). b, Positions of exons containing tropomyosin-encoding sequences. Although the clones do not overlap, a single BamHI fragment spanning the 2.5-kb gap was found in Southern blots of BamHI-digested human fibroblast DNA using single-copy probes from the isolates. The large arrow indicates the approximate point of divergence of the trk map from the normal hTM_{nm} gene; trk contains the BamHI site on the left of the arrow but does not contain the EcoRI sites on the right side of the arrow¹. The small arrows indicate the position and orientations of the Alu repeat sequences located by DNA sequencing. The thick lines indicate the regions sequenced, and the vertical bars indicate the positions of the exons within this sequence. Exons containing the trk and 2.5-kb fibroblast mRNA sequences were located by comparison of the DNA sequence with that of hTM_{nm}^{-1} . Exons containing other tropomyosin-coding sequences were identified by comparing three phase protein translations of the DNA sequence with all known tropomyosin sequences¹⁴ using the program DIAGON¹⁵. The trk sequence varies from the normal gene sequence at two positions (337 and 456), one of which (337) leads to a Lys \rightarrow Glu amino-acid replacement. Where it is possible to make the comparison, the 1.3-kb muscle mRNA sequence is identical, base for base, with the normal gene sequence.

1 3 6 796 1.3 ATM GGATTCCATTTGGGTCAGCCTGGCTGGTCCCCAAGGCATTAGGATGGGGGAGCAAAAAGCAACTTATGTATTTTCTTECACCOCCACCCC 7.3 4896 AAATTAAAATGTTAAGCTGCTGGAAAAAAAA

Fig. 3 Cloning and sequence analysis of the 1.3-kb skeletal muscle RNA transcript. A cDNA library of human skeletal muscle RNA in Agt10 was generated using procedures described in detail elsewhere^{6,10}. This was screened with the hTM_{nm}-1 and positive clones were taken for further analysis, subcloned into M13 mp18 and sequenced by the processive degradation procedure¹¹. This yielded the complete coding sequence of the 1.3-kb muscle mRNA (1.3 ATM) together with 57 bases of the 5'untranslated sequence and the complete 3'untranslated sequence. The deduced protein sequence is numbered by homology to rabbit skeletal muscle α -tropomyosin⁷. The sequence is shown compared with that of trk1. The coding sequences of trk are shown only where they differ from those of the 1.3-kb muscle mRNA.

This hypothesis is confirmed by analysis of genomic clones containing hTM_{nm} structural gene sequences. Two genomic clones, isolated by hybridization to $hTM_{nm^{-1}}$, were characterized by restriction enzyme mapping (Fig. 3) and DNA sequence analysis (not shown). Nine exons were found in the 7,900 bases sequenced, 8 of them, from exon II to exon VIIIsk, forming a single contiguous sequence. The regions of mRNA sequence encoded by these exons are shown in Fig. 2. As expected, the boundaries of the regions of sequence identity correspond to splice junctions defining exon boundaries (Fig. 2). The regions of identical sequence shared by the 1.3-kb muscle mRNA, 2.5-kb fibroblast mRNA and trk oncogene are found in exons II, III, IV, VI and VII. The two different sequences encoding amino acids 189-213 are found in two adjacent exons, one (exon V_{nm}) found in the trk and 2.5-kb fibroblast mRNA, the other (exon V_{sk}) found in the 1.3-kb muscle mRNA. The unique N-terminal sequences of trk and the 2.5-kb fibroblast mRNA are found in exon I_{nm}. The exons encoding the unique N-terminal sequences of the 1.3-kb muscle mRNA are not found in either of these genomic clones and are presumed to lie a considerable distance upstream of exon Inm. Similarly, exon VIIIsk, encoding the unique C-terminal 27 amino acids of the 1.3-kb muscle mRNA,

is found immediately downstream from the common exon VII sequence, although exon VIII_{nm}, encoding the unique C-terminal sequence of the 2.5-kb fibroblast mRNA, has not been found in these genomic clones and is presumed to lie far downstream

Our analyis indicates that the 1.3-kb muscle mRNA, 2.5-kb fibroblast mRNA and tropomyosin-coding sequences of trk are all derived from hTM_{nm} structural gene sequences. The 2.5-kb fibroblast mRNA and the 1.3-kb muscle mRNA are expressed by the normal hTM_{nm} structural gene using a tissue-specific alternative mRNA splicing mechanism. The trk oncogene is a recombinant of the hTM_{nm} structural gene with a tyrosine kinase receptor gene. Comparison of the genomic restriction map of trk with that of the normal hTM_{nm} gene indicates that the rearrangement has occurred downstream from exon VIII_{sk} (ref. 1 and M. Barbacid, personal communication). Thus, the oncogene preserves most of the tropomyosin sequences of the normal hTM_{nm} gene, including exons spliced alternatively in muscle and non-muscle tissue. Therefore, we expect that expression of the trk oncogene will be subject to the same alternative mRNA splicing rules which govern expression of the normal tropomyosin gene. The exons used in the trk transcript

exan UTT turosine kinase exon UIIIsk turosine kinase

Fig. 4 Splicing according to a non-muscle pattern (top) with fusion of exon VII to the tyrosine kinase produces the correct frame of protein translation. Splicing according to a muscle pattern (bottom) with fusion of exon VIII_{sk} to the tyrosine kinase changes the frame of translation and results in the appearance of an in-frame stop codon only five nucleotides downstream from the splice junction (arrowhead).

are those found in the 2.5-kb fibroblast mRNA except that exon VII is joined to tyrosine kinase sequences to generate the transforming protein (Fig. 4).

How would trk behave if it were expressed in muscle tissue using the exons found in the 1.3-kb muscle mRNA? Certainly the tropomyosin sequence expressed by trk would be fundamentally altered. In particular, we would expect exon VII to be joined to exon VIIIsk, as it would be in the normal muscle tropomyosin, rather than directly to the tyrosine kinase sequence. Subsequent joining of exon VIIIsk to the tyrosine kinase sequence could occur but this would change the reading frame of the trk sequence and abort the synthesis of the tyrosine kinase domain (Fig. 4). Therefore, we expect that trk will show a tissue-specific pattern of transforming activity, being active only in tissues which also express the non-muscle tropomyosin. This arises as a direct consequence of the alternative mRNA splicing mechanism which governs expression of the normal hTM_{nm} structural gene.

We thank Drs G. Modi and F. Walsh for providing samples of human muscle RNA, Mrs S. Hamilton for preparation of the typescript, and M. Barbacid and collegues for communicating their results before publication. This work was supported in part by a travel grant to F.C.R. from CNPg (20.0694/84), Brazil.

Received 10 March: accepted 13 June 1986.

- Martin-Zanca, D., Hughes, S. H. & Barbacid, M. Nature 319, 743-748 (1986).

 MacLeod, A. R. & Talbot, K. J. molec. Biol. 167, 523-537 (1983).

 Karlik, C. C., Mahaffey, J. W., Coutu, M. D. & Fyrberg, E. A. Cell 37, 469-481 (1984).

 Basi, G. S., Boardman, M. & Storti, R. V. Molec. cell. Biol. 4, 2828-2836 (1984).
- Ruiz-Opazo, N., Weinberger, J. & Nadal-Ginard, B. Nature 315, 67-70 (1985). MacLeod, A. R. et al. Proc. natn. Acad. Sci. U.S.A. 82, 7835-7839 (1985).

- Stone, D. & Smillie, L. B. *J. biol. Chem.* **253**, 1137-1148 (1978). Lewis, W. G., Coté, G. P., Mak, A. S. & Smillie, L. B. *FEBS Lett.* **156**, 269-273 (1983).
- Scheller, R. H. et al. Cell 28, 707-719 (1982).
- MacLeod, A. R. Nucleic Acids Res. 9, 2675-2689 (1981).
- Henikoff, S. Gene 28, 351-359 (1984).
- Karn, J., Brenner, S., Barnett, L. & Cesarini, G. Proc. natn. Acad. Sci. U.S.A. 71, 5172-5176
- Karn, J., Matthes, H. W. D., Gait, M. J. & Brenner, S. Gene 32, 217-234 (1984). Sanders, C. & Smillie, L. B. J. biol. Chem. 260, 7264-7275 (1985).
- 15. Staden, R. Nucl. Acids. Res. 10, 2951-2961 (1982).

Sequences similar to the I transposable element involved in I-R hybrid dysgenesis in D. melanogaster occur in other Drosophila species

Alain Bucheton, Martine Simonelig, Chantal Vaury & Michèle Crozatier

Laboratoire de Génétique, Unité Associée au CNRS 360, Université de Clermont-Ferrand II, BP 45, 63170 Aubière, France

The I factor is a transposable element controlling the I-R system of hybrid dysgenesis in Drosophila melanogaster. This phenomenon occurs when males from the inducer class of strains are crossed with females from the reactive class of strains1. Inducer strains contain complete 5.4-kilobase (kb) I factors, reactive strains do not^{2,3}. Incomplete I elements are present in peri-centromeric regions of both categories of strains2. The 5.4-kb I factors are genetically active in stimulating hybrid dysgenesis and can transpose, whereas incomplete I elements seem to be genetically inactive and transpose rarely. The results of in situ hybridization and Southern transfer experiments indicate that most incomplete I elements are at constant locations in all D. melanogaster populations, suggesting that they were present in the genome before the spread of this species throughout the world. To investigate the evolutionary origin of the I factor, we have studied various Drosophila species for the presence of sequences homologous to it. We find that such sequences are widespread. Moreover, elements that are very similar to complete and active I factors occur in the species most closely related to D. melanogaster.

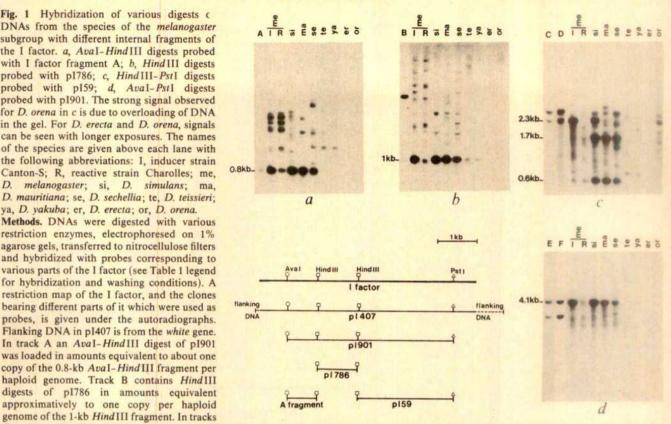
Species of the genus Drosophila have been assigned to several subgenera, the largest of which are the Sophophora and the Drosophila. D. melanogaster is a species of the subgenus Sophophora, which is divided into four groups, obscura, saltans, willistoni and melanogaster, the last one being divided in various subgroups⁴. We have studied some species of the subgenera Sophophora, Drosophila and Dorsilopha for the presence of I homologues. The results (Table 1) show that such sequences are not restricted to D. melanogaster. We have found that, except for D. takahashii, the DNAs of all the species studied in the melanogaster group show homology to the I factor. Sequences homologous with I seem to be much less frequent outside this group, for homology has been detected in only one species among eight tested in the other groups of the subgenus Sophophora and one among five in the other two subgenera. Sequences homologous to the I factor also occur in much more distant species such as Scaptomyza pallida, which belongs to another genus.

Within the melanogaster subgroup, the homology with the I factor is strongest in D. simulans, D. mauritiana and D. sechellia, weaker in D. teissieri and D. yakuba, and weaker still in D. erecta and D. orena. This correlates very well with the phylogenetic relationships between these species⁵.

Experiments were carried out to investigate the structure of the elements present in these species and to try to determine whether they are similar to the complete I factors of the inducer strains of D. melanogaster. Bucheton et al.2 have shown that restriction fragments from within the I factor are more abundant in DNA from inducer strains than from reactive strains. This is particularly true for the 2.3-kb Hind III-PstI internal fragment of I (see Fig. 1). Therefore, we used clone p159, which contains this fragment, to probe HindIII-PstI digests of genomic DNA from stocks of various species of the melanogaster subgroup.

Figure 1c shows that, as reported previously, the inducer strains of D. melanogaster contain several copies of the 2.3-kb fragment per haploid genome whereas the reactive strains do not contain it. This provides a simple means of distinguishing between reactive and inducer strains in Southern blot experiments. There is no 2.3-kb fragment hybridizing to this probe in DNA from D. erecta, D. orena, D. yakuba and D. teissieri, but the DNA from D. simulans gives a similar pattern to that obtained with the inducer strains of D. melanogaster. Indeed, this species gives a 2.3-kb fragment which hybridizes strongly to the probe as well as two smaller fragments of 1.7 and 0.6 kb. Experiments which are not reported here indicate that these smaller fragments result from the presence, in some elements, of an additional Hind III restriction site within the Hind III-PstI fragment. Very similar results are obtained with D. mauritiana and D. sechellia and in both cases many I elements have this additional Hind III restriction site.

Fig. 1 Hybridization of various digests c DNAs from the species of the melanogaster subgroup with different internal fragments of the I factor. a, AvaI-HindIII digests probed with I factor fragment A; b, Hind III digests probed with p1786; c, Hind III-Pst1 digests probed with p159; d, Ava1-Pst1 digests probed with pI901. The strong signal observed for D. orena in c is due to overloading of DNA in the gel. For D. erecta and D. orena, signals can be seen with longer exposures. The names of the species are given above each lane with the following abbreviations: I, inducer strain Canton-S; R, reactive strain Charolles; me, D. melanogaster; si, D. simulans; ma, D. mauritiana; se, D. sechellia; te, D. teissieri; ya, D. yakuba; er, D. erecta; or, D. orena. Methods. DNAs were digested with various restriction enzymes, electrophoresed on 1% agarose gels, transferred to nitrocellulose filters and hybridized with probes corresponding to various parts of the I factor (see Table 1 legend for hybridization and washing conditions). A restriction map of the I factor, and the clones bearing different parts of it which were used as probes, is given under the autoradiographs. Flanking DNA in pI407 is from the white gene. In track A an AvaI-HindIII digest of pI901 was loaded in amounts equivalent to about one copy of the 0.8-kb AvaI-Hind III fragment per haploid genome. Track B contains Hind III



C and D a HindIII-PstI digest of clone pI59 was loaded in amounts equivalent, respectively, to about one and five copies of the 2.3-kb Hind III-Pst1 fragment. Tracks E and F contain AvaI-Pst1 digests of p1901 in amounts equivalent respectively, to one and five copies per haploid genome of the 4.1-kb Ava I-Pst I fragment.

In other experiments, the same genomic DNAs were digested with AvaI and HindIII, and probed with the 0.8-kb fragment A of the I factor which had been gel purified from clone pI901 (Fig. 1a), or with Hind III and probed with clone p1786 which contains the 1-kb Hind III internal fragment of the I factor (Fig. 1b). Both of these internal fragments are present in several copies in reactive and inducer strains of D. melanogaster as well as in D. simulans, D. mauritiana and D. sechellia, but not in the other species.

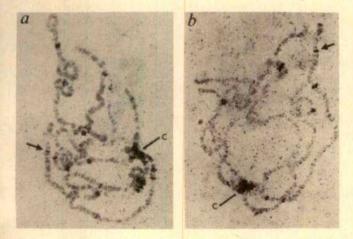


Fig. 2 Location of I factor sequences on D. simulans (a) and D. mauritiana (b). 3H-labelled pI407 was hybridized to chromosome squashes as described previously2. In each case C shows hybridization to the chromocentre. The arrow indicates region 3C, which contains the white locus. Hybridization in this region is thought to be caused by the white sequences carried by clone p1407 (see Fig. 1).

In the last Southern blot experiment, the DNAs were digested with AvaI and PstI and hybridized with clone p1901. This digestion produces a large 4.1-kb internal fragment (see Fig. 1). The results shown in Fig. 1d suggest that this large fragment is present in several copies only in the inducer strains of D. melanogaster and in the sibling species D. simulans, D. mauritiana and D. sechellia, indicating that several I homologues in these species contain most of the sequence of the complete I factor.

We have studied the distribution of I elements in the genomes of D. simulans and D. mauritiana by in situ hybridization to salivary gland chromosomes of the larvae. The results (Fig. 2) indicate that, as for the inducer strains of D. melanogaster, these sequences are present in both the peri-centromeric regions and chromosome arms of these species.

All the above results indicate that the stocks of D. simulans, D. mauritiana and D. sechellia used in these experiments differ from reactive strains of D. melanogaster and look more like the inducer strains. The sequences found in these species which are homologous to the I factor are strikingly similar to the functional I factors found in the inducer strains.

The survey of various Drosophila species reported in Table 1 indicates that I elements are an old component of the genomes and were probably present before the radiation of the melanogaster group. Many results suggest that in D. melanogaster the complete I factor appeared in natural populations in the 1930s or 1940s^{6,7}. One hypothesis advanced to explain the relationships between incomplete I elements and complete I factors is that incomplete I elements could be the result of mutational inactivation of an old transposable element, and that the complete I factor could have been formed by reactivation of some of these incomplete and defective I elements, perhaps by recombination2. Such a reactivation could have occurred in one of the four species bearing potentially active I factors-D. melanogaster, D. simulans, D. mauritiana or D. sechellia-but

Table 1 Distribution of I homologues among the subgenera Sophophora. Drosophila and Dorsilopha

Subgenus	Species group	Subgroup	Species	Homology to I factor DNA
Drosophila			virilis	****
			funebris	
			immigrans	_
			fraburu	***
Sophophora	willistoni		willistoni	
		*	nebulosa	
	saltans		prosaltans	
			sturtevanti	. +
	obscura		obscura	ema
			ambigua	m/m
			guanche	
			bifasciata	
	melanogaster	melanogaster	melanogaster	+++
			simulans	+++
			mauritiana	+++
			sechellia	+++
			teissieri	++
			yakuba	++
			erecta	+
			orena	+
		eugracilis	eugracilis	+
		takahashii	takahashii	***
		montium	burlaï	++
			bocqueti	+
			davidi	+
			serrata	+
		,	malagassya	++
\$- 1			vulcana	+
			kikkawaï	+
			tsakasi	+
			bakoue	+
	ananassae		ananassae	++
			malerkotliana	+
Dorsilopha			busckii	+

DNA from various Drosophila species was prepared from adult flies and digested with restriction enzymes. The fragments were electrophoresed on agarose gels, transferred to nitrocellulose filters 14 and hybridized with clones bearing various parts of the I factor, usually p1901 and p1407 (see Fig. 1), and labelled with 32 by nick translation. to a specific activity of 3-10×10. d.p.m. per µg. Hybridization conditions were 1×Denhardt's solution (0.02% Ficell, 0.02% polyvinylpyrrolidone, 0.02% bovine serum albumin), 4×SSC, 50% formamide for at least 16 h at 37 °C. The filters were washed for 2 h in 2 × SSC, 0.1% SDS at room temperature and then for a further 2 h in 1×SSC, 0.1% SDS at 37 °C. The number of plus signs indicates the intensity of the signal observed on the autoradiographs. Most of the stocks were kindly provided by the Laboratoire de Génétique Evolutive of the CNRS at Gif-sur-Yvette (France).

it is unlikely that this occurred independently four times in each of the four species. It is more likely that the functional I factor formed only once in one species, and was then transmitted to the other three species. This could happen by horizontal transfer via an unknown vector. Another possibility resides in the fact that certain of these species can mate. The hybrids are usually sterile, but one can imagine that in such crosses some DNA sequence could be transmitted from one species to another as the result of very rare events such as polyspermy. However, the present data suggest strongly that the complete I factor was present in the ancestral species of D. melanogaster, D. simulans, D. mauritiana and D. sechellia and has been lost in D. melanogaster when this species diverged from the other three, possibly by drift. Then it could have re-invaded the D. melanogaster genome in the 1930s either by reactivation of defective I elements or by horizontal transfer from D. simulans.

The interspecific distribution of I elements is quite different from that of sequences homologous to the P factor, which is the transposable element involved in the P-M system of hybrid dysgenesis^{8,9}. Indeed, P homologues do not occur in the close relatives of D. melanogaster10 but are common in the obscura,

willistoni and saltans groups 11-13. This suggests that the two systems of hybrid dysgenesis have evolved in very different ways.

We thank Alain Pélisson for the in situ hybridization experiments shown in Fig. 2, J. C. Bregliano and D. Finnegan for criticisms of the manuscript, and J. David and D. Anxolabehere for discussions and for providing most of the stocks used in these experiments. This work has been financed by CNRS, grants UA 360 and ATP 8304, the Association pour la Recherche contre le Cancer, INSERM and Fondation pour la Recherche Médicale Française.

Received 24 March; accepted 21 May 1986.

- 1. Bregliano, J. C. & Kidwell, M. G. in Mobile Genetic Elements (ed. Shapiro, J.) 363-410 (Academic, New York, 1983).
- Bucheton, A., Paro, R., Sang, H. M., Pélisson, A. & Finnegan, D. J. Cell 38, 153-163 (1984). 3. Finnegan, D. J. & Fawcett, D. H. in Oxford Surveys on Eucaryotic Genes Vol. 3 (Oxford
- University Press, in the press). 4. Throckmorton, L. H. in Handbook of Genetics Vol. 3 (ed. King, R. C.) 421-469 (Plenum,
- New York, 1975).
- Lemeunier, F., David, J., Tsacas, L. & Ashburner, M. in The Genetics and Biology of Drosophila Vol. 3e (eds Ashburner, M., Carson, H. L. & Thompson, J. N.) (Academic, London, in the press).
- 6. Kidwell, M. G. Proc. natn. Acad. Sci. U.S.A. 80, 1655-1659 (1983)
- Kidwell, M. G., Frydryk, T. & Novy, J. B. Drosoph. Inf. Serv. 59, 63-69 (1983). Engels, W. R., A. Rev. Genet. 17, 315-344 (1983). O'Hare, K. Trends Genet. 1, 250-254 (1985).

- Brookfield, J. F. Y., Montgomery, E. & Langley, C. H. Nature 310, 330-332 (1984).
 Daniels, S. B., Strausbaugh, L. D., Ehrman, L. & Armstrong, R. Proc. natn. Acad. Sci. U.S.A. 81, 6794-6797 (1984).
- Anxolabehere, D., Nouaud, D. & Périquet, G. Genet. Select. Evol. 17, 579-584 (1985)
- Lansman, R. A., Stacey, S. N., Grigliatti, T. A. & Brock, H. W. Nature 318, 561-563 (1985).
 Southern, E. M. J. molec. Biol. 98, 503-517 (1975).
- 15. Rigby, P. W., Dieckmann, M., Rhodes, C. & Berg, P. J. J. molec. Biol. 113, 237-251 (1977).

Cryptic simplicity in DNA is a major source of genetic variation

Diethard Tautz*, Martin Trick* & Gabriel A. Dover†

Department of Genetics, University of Cambridge, Cambridge CB2 3EH, UK

DNA regions which are composed of a single or relatively few short sequence motifs usually in tandem ('pure simple sequences') have been reported in the genomes of diverse species (for reviews see refs 1-4), and have been implicated in a range of functions including gene regulation (for reviews see refs 5-7), signals for gene conversion and recombination8-10, and the replication of telomeres¹¹. They are thought to accumulate by DNA slippage¹²⁻¹⁶ and mispairing during replication and recombination or extension of single-strand ends^{2,4,10,11}. In order to systematize the range of DNA simplicity and the genetic nature of the regions that are simple, we have undertaken an extensive computer search of the DNA sequence library of the European Molecular Biology Laboratory (EMBL)¹⁷. We show here that nearly all possible simple motifs occur 5-10 times more frequently than equivalent random motifs. Furthermore, a new computer algorithm reveals the widespread occurrence of significantly high levels of a new type of 'cryptic simplicity' in both coding and noncoding DNA. Cryptically simple regions are biased in nucleotide composition and consist of scrambled arrangements of repetitive motifs which differ within and between species. The universal existence of DNA simplicity from monotonous arrays of single motifs to variable permutations of relatively short-lived motifs suggests that ubiquitous slippage-like mechanisms are a major source of genetic variation in all regions of the genome, not predictable by the classical mutation process.

To assess the frequencies and types of simple sequence motifs, we made a systematic survey of published sequences¹⁷ using

^{*} Present addresses: Max-Planck-Institut für Entwicklungsbiologie, Spemannstrasse 35/11, D-7400 Tübingen, FRG (D.T.); Plant Breeding Institute, Maris Lane, Cambridge CB2 2LQ,

[†] To whom correspondence should be addressed

Table 1 Number of matches with simple sequence probes found in the EMBL library of DNA sequences (a) and in different groups of organisms (b)

, Matches wi	th mononucleoti	de motifs				M	latches with sim	ple dinucleotid	e motifs	
	AA/TT	GG,	/CC			AT/AT	GC/GC	GT	/AC	GA/TC
13/15	196	43	3		13/15	26	4		11	43
14/15	74		3		14/15	6	vertex.	:	22	26
15/15	36	1	2		15/15	1	eserci.	1	12	16
1777					•	M	latches with ran-	dom dinucleoti	de motifs	
					13/15	22.3	7.3	2	1.5	7.5
					14/15	2.5	0.3	-		0.3
					15/15	0.3	***************************************			minimin.
782 . i.s										
Matches w	th simple trinucl								and the second second	and time time or three being to
	AAT/ATT	AAC/GTT	AAG/CTT	ATG/CAT	TAG/CTA	CCT/AGG	CCA/TGG	CGA/TCG	GCA/TGC	CCG/CG(
	ATA/TAT	ACA/TGT	AGA/TCT	TGA/TCA	AGT/ACT	CTC/GAG	CAC/CTG	GAC/GTC	CAG/CTG	CGC/GCI
	TAA/TTA	CAA/TTG	GAA/TTC	GAT/ATC	GTA/TAC	TCC/GGA	ACC/GGT	ACG/CGT	AGC/GCT	GCC/GG/
13/15	80	30	49	25	12	59	43	10	64	49
14/15	17	5	13	7	1	26	5	2	17	11
15/15	8	2	3	2	AMAZONE	4	1	1	4	4
Matches wi	th random trinue	cleotide motifs								
13/15	19.0	7.8	11.5	1.0	1.0	9.0	4.5	2.5	1.0	11.0
14/15	1.5	0.3	0.8		********	0.5	0.3	enterpoli	-	1.3
151/5					evelore.	****		anterior	water	- Services

b, No. of matches per 100 kb

		Mononucleotide motifs	Dinucleotide motifs	Trinucleotide motifs
Vertebrates	13/15	18.1	11.0	23.7
645 kb	14/15	6.5	6.7	7.3
	15/15	3.7	3.6	2.0
Non-vertebrates	13/15	26.7	7.5	29.2
240 kb	14/15	11.7	2.1	6.3
	15/15	4.2	0.8	2.9
Plants & algae	13/15	11.4	5.7	31.4
35 kb	14/15	8.5	5.7	5.7
	15/15	2.8	5.7	2.8
Chloroplasts	13/15	26.6	6.6	10.0
30 kb	14/15	3.3		- manuscri
	15/15	, uppersons		-memory
Mitochondria	13/15	10.0	7.0	30.0
100 kb	14/15	2.0	Workers	4.0
	15/15		-	Shadeni
Viruses	13/15	5.5	1.8	18.9
550 kb	14/15	0.9	0.7	5.3
	15/15	0.5	0.4	1.5
Prokaryotes	13/15	1.3	1.3	11.9
320 kb	14/15	0.3	Alamenter	1.9
	15/15	-		waterfor-
Phages	13/15	1.2	manufa.	7.1
170 kb	14/15	****		0.6
	15/15		-00-mar	- etantio
Matches with random	probes			
Whole library	13/15		1.9	3.2
2,090 kb	14/15		0.1	0.2
	15/15		0.0	

a, The library was searched using the MATCH program³⁵ on the Cambridge IBM 3081 computer. We used 15-nucleotide (nt)-long probe sequences with matches of 13 out of 15 nt (13/15), 14 out of 15 nt (14/15) and complete matches (15/15). The actual number of matches found with each of the simple sequence probes is shown. For matching sequences longer than 15 base pairs, only one match is recorded. All possible combinations of one, two and three nucleotides were tested. In the case of the trinucleotide repeats, only one of the three possible permutations (which are indicated in the headline) was tested. The results from the runs with complementary strands and the runs with RNA probes (U instead of T) were merged. Matches with yeast mitochondrial sequences were excluded from this search because of their unusual nucleotide composition (80-90% AT). Matches due to duplicate entries of the same sequences in the library were also excluded. Testing with randomized probes was done at least four times for each nucleotide combination (two for each strand) and the values given are averages. Standard deviations are in the order of 3 for the 13/15 matches and 1 for the 14/15 matches. b, The values represent the number of matches found per 100 kb in each organism group and are therefore directly comparable. For the calculation of the proportional representation of each group of organisms, yeast mitochondrial sequences were excluded, but duplicate entries could not be excluded. It is thought, however, that this leads to an insignificant error.

two criteria. The first was to scan for direct sequence homologies to 15-nucleotide-long probes, each consisting of an array of one of all possible mono-, di- and trinucleotide motifs. Three different stringencies of homology were recorded: 13 out of 15, 14 out of 15 and 15 out of 15 bases matched. In test runs using random sequence motifs of balanced nucleotide composition, we found an average of four matches with 13/15 in the whole library (~2,100 kilobases; kb) and none with either 14/15 or 15/15. Thus, a 13/15 match could be considered as being at the borderline of significance. Controls consisted of randomized probes with equivalent nucleotide compositions.

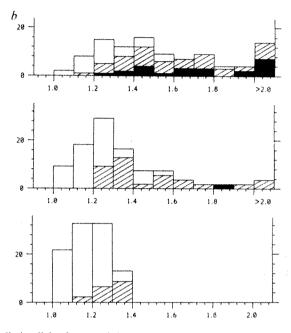
The results (Table 1; see legend for details of the tests) indicate that nearly all simple sequence motifs are considerably more

frequent than their randomized counterparts (Table 1a). The only notable exceptions are the AT/AT and GC/GC motifs. With respect to the latter, there is a known suppression of CG dinucleotides in eukaryotic nuclear DNA¹⁸. However, the level of suppression probably cannot account for the insignificant representation of this motif in simple dinucleotide repeats. Furthermore, the trinucleotide repeats composed of C and G (column CCG/CGG in Table 1a) are fairly frequent and fit into the overall frequency pattern of other trinucleotide repeats. Although it is possible that tandem arrays of GC/GC motifs are suppressed because of their potential to form Z-DNA⁵, GT/AC repeats can form the same structures and seem not to be particularly suppressed. In general, it does not seem as if



No of tetranucleotide matches: 3 (x4)= 1

Fig. 1 a, The computer algorithm. The program counts how often the oligonucleotide motif which starts to the right of each nucleotide is repeated in its direct neighbourhood. A range of parameters (motif length and window length) were tested on randomized sequences. Our actual motif and window lengths were chosen as a balance between reducing background noise and optimizing the match signal. We chose tri- and tetranucleotide motifs and a window of ±32 nucleotides. In a random sequence consisting of 25% of each nucleotide, one would expect 1 match with a trinucleotide and 1/4 match with a tetranucleotide within 64 nt. Therefore, the number of tetranucleotide matches detected are multiplied by four in the program. The final score for the respective nucleotide is then the sum from both match comparisons. This is demonstrated for the T at position 39 in the figure. The rightward trinucleotide motif from this T is TAT and the tetranucleotide motif is TATG. It is indicated which region around these is searched and where the matches were found. For six trinucleotide and three tetranucleotide matches a final score of 18 is calculated and assigned to the T at position 39. The program would then go onto the next nucleotide and repeat the cycle. Hence, each nucleotide is assigned a simplicity score. The figure also demonstrates the inbuilt correction system which eliminates double scorings due to overlapping matches. For the motif TATAT at position 43. only one match with TAT is recorded. Furthermore, the program obviates edge effects by not assigning scores to the first 32 nucleotides and the last 35 nucleotides of a sequence. The overall simplicity factor for a given sequence is calculated by summing all scores and dividing the sum by the number of nucleotides in the sequence. The relative simplicity factor is then obtained by dividing this overall simplicity factor by the overall simplicity factor obtained from 10 or 100 randomized sequences with the same nucleotide composition and a length of 10,000 nt each. Thus, the relative simplicity factor would be expected to be close to 1.0 for a sequence with no simplicity and higher for sequences with simple regions. Using 10 different



runs of randomized sequences, we can calculate a standard deviation for the overall simplicity factors of the runs and use it to assess the significance of the simplicity factor of the natural sequence. Typical results from this comparison give a significance (P < 0.01) for relative simplicity factors larger than 1.1 to 1.2. The program was written in Fortran 77 and run on the Cambridge IBM 3081 computer. b, Comparison of the frequency of simplicity factor classes between eukaryotes and prokaryotes. The histograms show the percentage of each class of simplicity factors found in sequences from eukaryotes (upper), eukaryotic cDNAs (middle) and prokaryotes (lower). All tested sequences were larger than 1 kb and were taken randomly from the EMBL library of DNA sequences (release 5). For eukaryotes, 98 different sequences were tested, 52 for eukaryotic cDNAs and 46 for prokaryotic sequences. The hatched parts of the bars represent the fraction of those sequences which contain at least one region of high simplicity. The criterion for this was that in the graphical display of the simplicity profile, at least one peak had to be higher than the line which indicates the highest peak from any of the randomized sequences of equivalent composition (the broken reference line, in Fig. 2). The filled parts of the bars represent the fraction of those sequences which contained a pure simple sequence. The criterion for this was that the sequence had to contain an uninterrupted pure simple sequence at least 15 nt long. Stretches of this length (or longer) would be expected to be detectable by direct hybridization experiments.

particular types of sequences (for example, polypurinic sequences¹⁹) are over- or under-represented.

Table 1b shows the average number of matches per 100 kb within the different species groups. The results clearly indicate that simple sequence matches are most frequent in eukaryotic nuclear genomes and very rare in prokaryotes. Chloroplasts, mitochondria and eukaryotic viruses occupy a somewhat intermediate position in this table.

In order to detect accumulations of direct oligonucleotide repeats which need not have a regular spacing (cryptic simplicity), we devised a computer program to search for such regions: Fig. 1a outlines how it works. A sequence is given an overall 'simplicity factor', which is a measure of the combined frequencies of naturally occurring, directly repeated motifs in the sequence (see Fig. 1 legend for details of the algorithm). The profile of simplicity of a given region can be displayed graphically. In addition, the program calculates a 'relative simplicity factor', which is the ratio of the simplicity factor of a test sequence to the mean simplicity factor calculated from 10 or 100 randomized sequences each consisting of 10 kb of equivalent nucleotide composition. Standard deviations were found to be very small under these conditions. The relative simplicity factor is expected to be close to 1.0 for a sequence with no cryptic simplicity, while relative simplicity factors above 1.1-1.2 are significant (P < 0.01) under our test conditions (see Fig. 1 legend).

We have tested a few hundred natural sequences with the program and found that most of them have a relative simplicity factor which is clearly higher than 1.0. As with the previous method of analysis, there is a clear difference between eukaryotic and prokaryotic sequences. The simplicity factors of the latter are clustered within a range of 1.0-1.4 (Fig. 1b, bottom), and the eukaryotic sequences are spread more evenly within a range of up to 2.0 and occasionally higher (Fig. 1b, top). Complementary DNA sequences show a somewhat intermediate position (Fig. 1b, middle), as do viral sequences (not shown). In the case of the cDNA sequences, the high simplicity regions are not only confined to the 5' or 3' untranslated regions, but can be found within the coding regions themselves (see also Fig. 2). Most of the eukaryotic sequences tested have high simplicity factors even if they do not have long arrays of pure simple sequence motifs (Fig. 1b). This implies that cryptic simplicity (the frequent occurrence of several directly repeated short motifs in close proximity) is widespread and an important component of eukaryotic genomes.

Sophisticated comparative statistics have recently been described for measuring the significance of the occurrence of repetitive motifs and other non-random properties of DNA

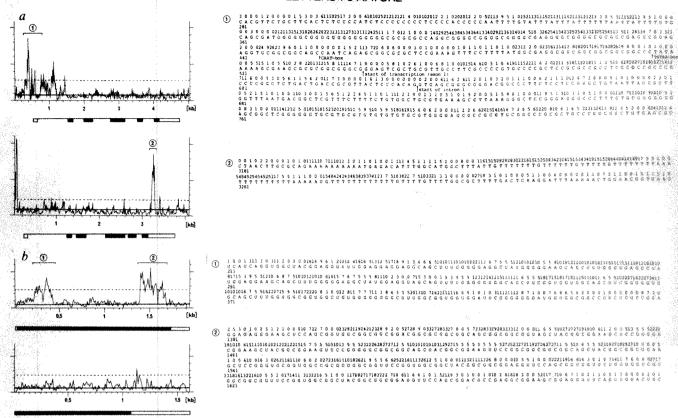


Fig. 2 Examples of high simplicity regions in eukaryotic genes. The figure shows the distribution of simple sequence regions across the genes. For this purpose, the scores from the simplicity factor calculations (averaged in 10-nt steps) are displayed in a graph above the appropriate positions in the sequence. The structure of the genes is displayed beneath the graphs. The thin line shows the length of the transcription unit, the open boxes are nontranslated parts of the mRNA and the filled boxes are the coding regions. The continuous horizontal line in the graphs is the level of the mean overall simplicity factor of 10 randomized sequences of similar composition to the test sequence. The broken line in the graphs shows the level of the highest peak in any one of the randomized sequences. Only peaks above this line are considered as high simplicity regions. Some of these were numbered and the corresponding sequences are shown to the right of the graph together with the simplicity scores found for each nucleotide. a, Upper part, chicken cytoplasmic actin gene (ref. 36, accession number in the EMBL library: X00182); lower part, rat cytoplasmic actin gene (ref. 37, accession no. V01217). b, Upper part, mouse keratin gene (cDNA) (ref. 24, accession no. V00830); lower part, human keratin gene (cDNA), the 5' end of the gene is not sequenced (ref. 38, accession no. V01516).

organization in defined sequences^{20,21}. It is satisfying that both these and our methods reveal that many (probably most) coding and noncoding sequences show significantly high numbers of short repetitive motifs, in a seemingly limitless number of permutations.

To determine whether new motifs are continually being generated on an evolutionary timescale, equivalent DNA regions were compared between species; Fig. 2 shows some characteristic examples. In the chicken cytoplasmic actin gene (Fig. 2a), a large region of simplicity composed of various different motifs stretches from a point upstream of the start of transcription and into most of the first intron. The same region in the rat gene has a far lower simplicity, even though it is also G+C-rich. Instead, there is a new high simplicity region in the 3' noncoding part of the messenger RNA which is based on oligo(T) stretches interspersed with Gs. It is unlikely that this arose by a recent integration of a retrotransposon²², because the sequences flanking it are partly conserved between chicken, rat and human and might actually be of functional significance²³. The large peak in front of the rat gene is also due to an oligo(T) stretch.

Figure 2b shows cryptic simple sequences in the coding sequences of the rat keratin gene. There are two glycine-rich regions which are highly divergent between the keratin genes, while the body of the gene, which our analysis indicates is not simple, is fairly strongly conserved, even between different types of intermediate filaments²⁴. The human keratin gene is much less simple in the equivalent regions (only part of the human gene sequence is known).

It has been noted previously that some regions of mammalian 28S ribosomal RNA genes are highly divergent in close species comparisons²⁵. Detailed examination of the distribution of cryptic simplicity in mouse and rat 28S rDNA shows that they coincide exactly and in very great detail with the regions of divergence in the two genes as depicted by standard dot matrices (Fig. 3). The regions in question are known to be insertions (when compared with other eukaryotic rRNA genes), probably originating by slippage-like mechanisms and not by the drift of point mutations in neutral sequences that were once shared by all species.

Our results show that there is a significantly frequent occurrence of nearly all possible short simple sequence motifs in natural DNA sequences in both coding and noncoding regions of eukaryotic genomes. There must be a mechanism active throughout most of the genome which can create simplicity, and which acts largely independently of the actual sequences involved. It is reasonable to assume that this mechanism is slippage. It is known that short oligonucleotide motifs can slip easily against each other⁷, for this is a very efficient way to produce simple sequence DNA in vitro 14,15. From direct comparisons of closely related natural DNA sequences, it is clear that slippage can also occur in vivo between short direct repeats, leading to deletions or expansions of the motifs involved (for examples see refs 4, 10, 12, 13, 16, 26-28).

The apparent under-representation of simplicity in prokaryotes is probably not due to the absence of such mechanisms, but merely to the more economical use of DNA in these

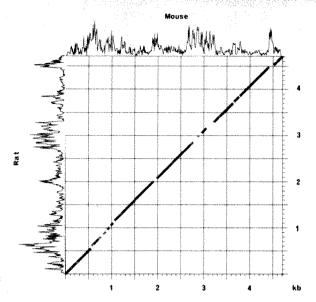


Fig. 3 Comparison of the genes for the 28S ribosomal RNA from mouse to rat. The figure shows a standard dot matrix plot between mouse³⁹ and rat⁴⁰ 28S rRNA genes. Match stringency was 20 nt perfect match. The plot is superimposed with the simplicity profiles of these genes, with the mouse gene on the upper axis and the rat on the left axis.

organisms, for they have low amounts of noncoding spacer DNA. Interestingly, prokaryotes also have a more frequent occurrence of simple trinucleotide motifs (compare Table 1), possibly due to their tolerance by the triplet code.

Two broad categories of simplicity can be distinguished—pure simple sequence regions and regions of less regularity but with a clear bias in nucleotide composition (compare Fig. 2). Ohno has suggested that the latter regions, where they occur within genes, might be the remnants of the former, which gradually diverged with the accumulation of point mutations²⁹. However, it is inconceivable that random point mutations within a simple sequence could by itself lead to the observed biases in nucleotide composition and to scrambling of new and old motifs. The observations can be more easily explained in terms of an interaction between point mutations and continual slippage.

The turnover of simple motifs could make some contribution to the observed differences in codon usage between genes and species, and in the potential of chromatin to undergo conformational changes and bind to regulatory proteins associated with gene transcription. Furthermore, it seems unlikely that substantial amounts of complex 'single-copy' DNA exist which are diverging in a clock-like manner, given that most DNA is subject to one or other turnover mechanism^{30,41}.

Mechanisms of continuous gain and loss of DNA variants by unequal crossing over and gene conversion can lead to the homogenization (molecular drive) of any given variant in a sexual population^{30-33,41}. No large-scale homogenization is occurring by gain and loss due to slippage because our survey shows that the unit of slippage can occasionally be out of phase with pre-existing motifs. Thus, any homogenization is continually being obliterated by the generation and combinatorial reshuffling of short and short-lived motifs differing in sequence and length. The effects on the overall genetic composition of a population and any interaction with selection are probably complex^{4,30,34,41}. It appears that the genetic material acquires its new forms more as a consequence of novel combinations between simple units than by the point-by-point substitutions of one base by another in a passive DNA molecule.

Received 10 March; accepted 21 May 1986.

- Tautz, D. & Renz, M. Nucleic Acids Res. 12, 4127-4138 (1984). Greaves, D. R. & Patient, R. K. EMBO J. 4, 2617-2626 (1985).
- Dover, G. A. & Tautz, D. Phil. Trans. R. Soc. 312, 275-290 (1986). Wang, A. J. H. et al. Nature 282, 680-686 (1979).
- Weintraub, H. & Groudine, M. Science 193, 348-856 (1976). Hentschel, C. C. Nature 295, 714-716 (1982).
- Shen, S. H., Slighton, J. L. & Smithies, O. Cell 26, 191-203 (1981).

- Goodman, M. Bioessays 3, 9-14 (1985).

 Jeffreys, A. J., Wilson, V. & Thein, S. L. Nature 314, 67-72 (1985).

 Blackburn, E. & Szostak, J. A. Rev. Biochem. 53, 163-152 (1984).

 Drake, J. W., Glickman, B. W. & Ripley, L. S. Am. Scient. 71, 621-630 (1983).
- Streisinger, G. et al. Cold Spring Harb. Symp. quant. Biol. 31, 77-84 (1966). Wells, R. D., Ohtsuka, E. & Khorana, H. G. J. molec. Biol. 14, 221-240 (1965).
- Morgan, A. R. et al. Biochemistry 13, 1596-1603 (1974).
- 16. Efstratiadis, A. et al. Cell 21, 653-668 (1980).
- Cameron, G. et al. EMBL Sequence Data Library Release 4 (1985).
- Bird, A. P. Nucleic Acids Res. 8, 1499-1504 (1980).
 Straus, N. A. & Birnboim, H. C. Biochim. biophys. Acta 454, 419-428 (1976).
- Karlin, S. & Ghandour, G. Proc. natn. Acad. Sci. U.S.A. 5800-5804 (1985). Karlin, S., Ghandour, G. & Foulser, D. E. Molec. Biol. Evol. 2, 35-45 (1985).
- Rogers, J. Nature 305, 101-102 (1983). Yaffe, D. et al. Nucleic Acids Res. 13, 3723-3737 (1985).
- Steinert, P. M. et al. Nature 302, 794-800 (1983)
- Hassouna, N., Michot, B. & Bachellerie, J. P. Nucleic Acids Res. 12, 3563-3583 (1984)
- Moore, G. P. Trends biochem. Sci. 8, 411-414 (1983).
- Jones, W. C. & Kafatos, F. C. J. molec. Evol. 19, 87-103 (1982). Brown, S. D. M. & Piechaczyk, M. J. molec. Biol. 165, 249-256 (1983)
- Ohno, S. & Epplen, J. T. Proc. natn. Acad. Sci. U.S.A. 80, 3391-3395 (1983). Dover, G. A. Nature 299, 1121-119 (1982).
- Coen, E. S., Thoday, J. M. & Dover, G. A. Nature 295, 564-568 (1982). Strachan, T., Webb, D. A. & Dover, G. A. EMBO J. 4, 1701-1708 (1985).
- Dover, G. A. & Flavell, R. B. Cell 38, 623-624 (1984)
- Ohta, T. & Dover, G. A. Genetics 108, 501-528 (1984). Kneale, G. G. & Kennard, O. Biochem. Soc. Trans. 12, 1011-1014 (1984).
- Kost, T. A. et al. Nucleic Acids Res. 11, 8287-8301 (1983) Nudel, U. et al. Nucleic Acids Res. 11, 1759-1771 (1983).
- Hanukoglu, I. & Fuchs, E. Cell 33, 915-924 (1983). Hadjiolov, A. A. et al. Nucleic Acids Res. 12, 3677-3583 (1984).
- Chan, Y. L., Olvera, J. & Wool, I. G. Nucleic Acids Res. 11, 7819-7831 (1983).
- 41. Dover. G. A. Trends Genet. 2, 159-165 (1986).

Nuclear factor III, a novel sequence-specific DNA-binding protein from HeLa cells stimulating adenovirus DNA replication

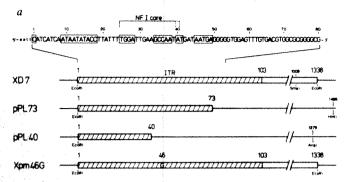
Ger J. M. Pruijn, Wim van Driel & Peter C. van der Vliet

Laboratory for Physiological Chemistry, State University of Utrecht, Vondellaan 24 a, 3521 GG Utrecht, The Netherlands

Dissection and reconstitution of the adenovirus DNA replication machinery has led to the discovery of two HeLa nuclear proteins which are required in conjunction with three viral proteins 1-4. One of these, nuclear factor I (NF-I), recognizes an internal region of the origin between nucleotides 25 and 40 (refs 4-8) and by binding to one side of the helix stimulates the initiation reaction up to 30-fold. NFI-binding sites have been observed upstream of several cellular genes, such as chicken lysozyme^{9,10}, human IgM¹¹ and human c-myc12, and coincide in most cases with DNase I hypersensitive regions. Here we report the identification of a novel DNA-binding protein from HeLa nuclei, designated NF-III, that recognizes a sequence in the adenovirus origin very close to the NFI-binding site, between nucleotides 36 and 54. This sequence includes the partially conserved nucleotides TATGATAATGAG. NF-III stimulates DNA replication four- to sixfold by increasing the initiation efficiency. Potential cellular binding sites include promoter elements of the histone H2B gene, the human interferon β gene, the human and mouse immunoglobulin V_{κ} and $V_{\rm H}$ genes and the mammal/chicken/Xenopus laevis U1 and U2 small nuclear RNA genes. Furthermore, a subset of the herpes simplex virus immediate early promoter specific TAATGARAT elements is homologous with the adenovirus 2 (Ad-2) NFIII-binding site.

Replication of adenovirus DNA in human cells occurs by a protein-priming mechanism in which a precursor to the viral terminal protein (pTP) becomes covalently bound to the first nucleotide, a dCMP residue. The 3'-OH group of dCMP in this

^{1.} Hamada, H., Petrino, M. G. & Kakunaga, T. Proc. natn. Acad. Sci. U.S.A. 79, 6465-6469



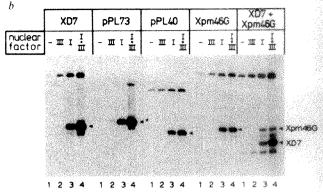
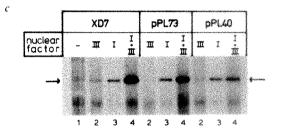


Fig. 1 Template-dependent stimulation of adenovirus DNA replication in vitro by NF-III. a, DNA sequence of part of the Ad-2 ITR containing the origin region and structure of the mutants. The C at position 1 is the left terminal nucleotide of the Ad-2 ITR (top strand). Sequences conserved between the various human adenovirus serotypes are boxed. The core of the NFI binding site extends from position 25 to 39 or 40 as indicated. The adenovirus inserts in the plasmids are indicated by bars, ITR sequences by hatched bars. Relevant restriction sites are marked. b, In vitro replication of fragments containing terminal Ad-2 DNA sequences. Appropriate plasmid digests were incubated with purified viral replication proteins under the conditions described below, in the absence of nuclear proteins (lane 1) or in the presence of NF-III (lane 2), NF-I (lane 3) or a combination of both proteins (lane 4). The reaction products were separated by agarose gel electrophoresis in the presence of 0.1% SDS followed by autoradiography. As a consequence of the protein priming mechanism, newly replicated DNA fragments are covalently coupled to the precursor to the terminal protein (pTP) leading to a shift in mobility. Replicated fragments are indicated by arrowheads. c, Initiation of adenovirus DNA replication stimulated by NF-III. A



digest of XD7, pPL73 or pPL40 was incubated as described in b, but in the presence of $[\alpha^{-32}P]dCTP$ as the only nucleotide triphosphate. The products were analysed for the formation of the pTP-dCMP initiation product by SDS-polyacrylamide gel electrophoresis and autoradiography. The arrow indicates the position of pTP-dCMP.

Methods. The constructions of XD7 (ref. 28), pPL73 (ref. 17), pPL40 (ref. 7), and Xpm46G (ref. 8) have been described. XD7 was digested with EcoRI, pPL73 with EcoRI and HinfI, pPL40 with EcoRI and AvaI and Xpm46G with EcoRI, while for the replication of a mixture of XD7 and Xpm46G, XD7 was also digested with SmaI. DNA replication assays were performed in a final volume of 15 μ l containing 25 mM Hepes-KOH (pH 7.5), 4 mM MgCl₂, 0.4 mM DTT, 1.7 mM ATP, 5 mM creatine phosphate, 5 μ g ml⁻¹ creatine kinase, 17 μ M each of dATP, dGTP and dTTP, 2 μ M [α -²P]dCTP (25 Ci mmol⁻¹), 2 mU pTP-adenovirus DNA polymerase complex, 1.25 µg adenovirus DNA-binding protein, 1 µl HeLa cytosol, 0.6 mM aphidicolin, 30 ng XD7 or 14 ng pPL73 or 22 ng pPL40 or 30 ng Xpm46G or 15 ng XD7 and 15 ng Xpm46G and 1 μl NF-I or NF-III when indicated. The amounts of plasmid DNA were chosen to obtain identical concentrations of origin fragments. Reaction mixtures were incubated for 60 min at 37 °C. When assaying initiation dATP, dGTP and dTTP were omitted. The purification of pTP-DNA polymerase. DNA-binding protein of cytosol and NF-I has been described. For NF-I hydroxylapatite fractions were used. NF-III was purified as follows. Nuclei from 10 HeLa cells were isolated and washed three times with 25 mM Tris-HCl (pH 7.5), 10% sucrose, 1 mM phenylmethylsulphonyl fluoride (PMSF) and 20 µg ml⁻¹ L-1-tosylamide-2-phenyl-ethylchloromethyl ketone (TPCK). The nuclei were suspended in the same buffer containing 1 mM EDTA and 1 mM dithiothreitol (DTT). Nuclear proteins were extracted by addition of 5 M NaCl to 0.3 M final concentration and slow stirring at 0 °C for 30 min. Cellular debris was removed by successive centrifugations at 12,000 g for 20 min and 105,000 g for 40 min. The final supernatant was adjusted to 0.2 M NaCl by addition of buffer A (25 mM Tris-HCl (pH7.5), 1 mM EDTA, 1 mM DTT, 1 mM PMSF, 20 µg ml⁻¹ TPCK, 20% glycerol) and applied to a DEAE-cellulose column equilibrated with buffer A containing 0.2 M NaCl. The flow-through was dialysed against buffer B (25 mM Tris-HCl pH 7.5), 1 mM EDTA, 1 mM DTT, 1 mM PMSF, 20 µg ml⁻¹ TPCK, 20% glycerol, 10% sucrose, 0.01% Nonidet P40) containing 0.03 M NaCl and applied to a second DEAE-cellulose column equilibrated with buffer B containing 0.03 M NaCl. The column was washed with buffer B-0.03 M NaCl and eluted with a linear gradient of 0.03-0.3 M NaCl in buffer B. The peak of NF-III activity was present in the first wash fractions following the flow-through. These fractions were applied to a phosphocellulose column equilibrated with buffer B-0.03 M NaCl. Bound material was eluted with a linear gradient of 0.03-1 M NaCl in buffer B. NF-III activity eluted at 0.15 M NaCl. NF-III-containing fractions were combined, adjusted to 0.05 M NaCl by addition of buffer B and applied to a denatured DNA-cellulose column equilibrated with buffer B-0.05 M NaCl Bound material was eluted with a linear gradient of 0.05-1 M NaCl in buffer B. NF-III activity eluted at 0.24 M NaCl. All purification steps were performed on ice or at 4°C. Throughout the purification, NF-III activity was monitored by its ability to stimulate the replication of the origin containing 6146 and 5641 bp XhoI B and C fragments, respectively, obtained from the Ad-5 DNA-TP complex 14.

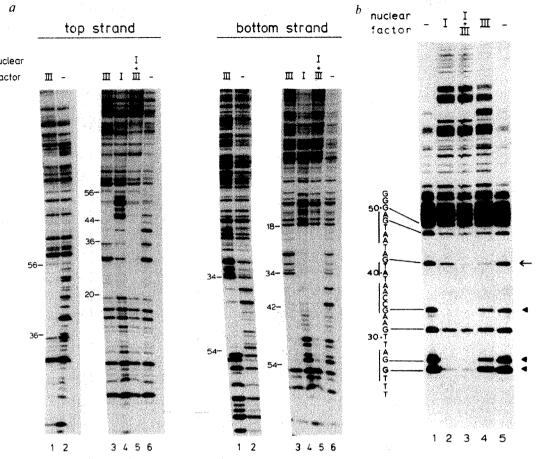
pTP-dCMP complex serves as a primer for further polymerization by a strand displacement mechanism (for reviews, see refs 1, 2, 13). Both initiation and elongation can be accomplished in vitro using five purified proteins. Three of these are encoded by the virus: the single-strand DNA-binding protein (DBP). DNA polymerase (pol) and pTP. The remaining proteins, NF-I and-II, are purified from HeLa nuclei3,4. Previously we observed that sera from patients suffering from various autoimmune diseases inhibit adenovirus DNA replication in vitro 14. This inhibition was only observed when crude HeLa nuclear extracts were used, but not in the presence of purified NF-I. As NF-II was not required in the assay, this suggested the existence of additional HeLa proteins required for optimal replication. Therefore, we searched directly for such proteins using a replication assay containing DBP, pTP, pol and NF-I. HeLa nuclei were extracted with 0.3 M NaCl and the extract was fractionated on DEAEcellulose. Screening of the column fractions revealed the presence of a new protein that stimulated replication four- to sixfold. This protein, NF-III, eluted at 30 mM NaCl whereas NF-I eluted at 80 mM NaCl. NF-III was further purified by phosphocellulose and denatured DNA cellulose chromatography. The

stimulatory activity of NF-III was sensitive to 0.1 mM N-ethylmaleimide and was 90% inactivated by heat treatment for 15 min at 50 °C.

To determine whether specific regions of the Ad-2 inverted terminal repeat (ITR) were required for stimulation by NF-III we used plasmid DNA containing either the wild-type origin (XD7) or several mutant origins. Origin-containing plasmid DNA can replicate in vitro provided that the DNA is linearized at the origin ^{15,16}. Protein-primed replication is visualized by a shift in electrophoretic mobility of the origin fragment caused by covalent binding of the pTP to the synthesized DNA. The plasmids pPL73 and pPL40 contain the terminal 73 and 40 base pairs (bp) of the Ad-2 ITR, respectively (Fig. 1a). Xpm46G is a derivative of XD7 with an $^{\Lambda}_{-} \rightarrow ^{C}_{G}$ transition at position 46.

Replication of all these mutants was stimulated by NF-I similar to wild type (Fig. 1b) in accordance with previous results 7.8.17. However, only wild-type XD7 and pPL73 were stimulated by NF-III, whereas pPL40 and Xpm46G were not. Similar results were obtained when the initiation reaction (pTP-dCMP synthesis) was studied (Fig. 1c). This indicates that NF-III, like NF-I, exerts its effect on the level of initiation. But

Localization of the NF-III binding site in the Ad-2 ITR. a, DNase I footprint analysis of NF-III- and NF-Ibinding sites in the Ad-2 ITR. The figure shows autoradio- nuclear graphic exposures of 10% polyacrylamide sequencing gels used to analyse the partial DNase I digests of end-labelled Ad-2 origincontaining DNA fragments. Lanes 2 and 6 show control DNase digestion patterns in the absence of nuclear protein fractions. Lanes 1 and 3 show the DNase cleavage pattern in the presence of NF-III. The remaining lanes show the DNase digestion patterns in the presence of NFI (lane 4) or both NFI and NFIII (lane 5). Numbers, positions in the Ad-2 ITR as in Fig. 1a, which were determined using Gtracks and specific restriction fragments as markers. b, Methylation protection analysis of NF-III and NF-I binding sites in the Ad-2 ITR. Autoradiographic exposure of a 10% polyacrylamide sequencing gel used to analyse the partially methylated endlabelled Ad2 origin containing DNA fragments after cleavage by piperidine treatment. Lanes 1 and 5 show control methylation patterns in the absence of nuclear protein fractions. Lanes 2 and 4 show pattern



obtained in the presence of NF-I and NF-III, respectively, while lane 3 shows the methylation pattern obtained in the presence of both NF-I and NF-III. The sequence at the left of the autoradiogram shows part of the Ad-2 ITR (top strand) and indicates the position of primary methylation sites. The G-residue protected by NF-III is indicated with an arrow, while residues protected by NF-I are indicated by arrowheads.

Methods. The footprint and methylation protection probes were constructed as follows: To the single-stranded M13 clones MXE-1 and MXE-4, 5' end-labelled synthetic oligonucleotides were hybridized. MXE-1 (ref. 8) and MXE-4 contain the top strand and the bottom strand of the EcoRI fragment of XD7, respectively. For top strand analyses the oligonucleotide was complementary to a M13 sequence in MXE-4 ranging from position -21 to -5 relative to position 1 of the Ad-2 insert. For bottom strand analyses the oligonucleotide was complementary to the Ad-2 sequence in MXE-1 ranging from position 65 to 81 of the Ad-2 insert. After hybridization the oligonucleotide primers were elongated with Klenow DNA polymerase giving the double-stranded constructs containing the Ad2 origin, 5' end-labelled at either the top (position -21) or the bottom strand (position 81). These constructs were incubated with 15 μl NF-III (denatured DNA-cellulose fraction, see legend to Fig. 1) and/or 10 μl NF-I (hydroxyl apatite fraction) in a total volume of 75 μl containing 25 mM Hepes-NaOH (pH 7.5), 1 mM DTT, 0.5 mM MgCl₂, 50 mM NaCl, 50 ng pBR322, and 5 μg bovine serum albumin for 60 min at 0 °C. For DNase I footprints 5 μl 50 mM MgCl₂ and 0.1 U DNase I were added. Digestion was allowed for 90 s at 24 °C and stopped by addition of 4 μl 0.2 M EDTA, 10% SDS. For methylation protection analyses 200 μl sodium acetate, 50 mM, 1 M β-mercaptoethanol. After ethanol precipitation the DNA was dissolved in 100 μl 1 M piperidine, incubated at 90 °C for 30 min and analysed as described above.

stimulation by NF-III is dependent on the presence of sequences between 40 and 73, outside the recognition sequence of NF-I. Furthermore, a point mutation at position 46, located in a highly conserved pentanucleotide sequence ⁴⁵AATGA⁴⁹, completely prevents stimulation by NF-III. This suggests that NF-III acts by binding to sequences between 40 and 73 including ⁴⁵AATGA⁴⁹. Specific binding to origin fragments could indeed be demonstrated using a nitrocellulose-filter binding assay or an exonuclease III protection assay (data not shown).

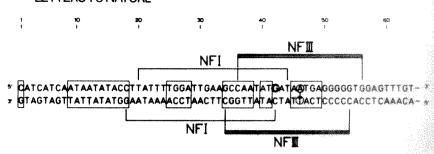
To identify the sequences involved in binding, we determined the region of the Ad-2 ITR that is protected against DNase I by footprint analysis. The Ad-2 origin containing region of the single-stranded M13 clones MXE-1 and MXE-4 were converted to double-stranded DNA by hybridization to 5' end-labelled synthetic oligonucleotides and elongation of these oligonucleotides using Klenow DNA polymerase. These constructs were partially digested with DNase I in the presence or the absence of NF-III (Fig. 2a, lanes 1, 2). NF-III protected the region between positions 36 and 56 of the top strand and the region between positions 34 and 54 of the bottom strand. Figure 2a also shows that the NF-III footprint partially overlaps the NF-I footprint (Fig. 2a, lanes 3, 4) and that mixtures of NF-I and NF-III protected the combined regions (Fig. 2a, lane 5). This

indicates that NF-I and NF-III can simultaneously bind to their recognition sequence and do not exclude each other.

Methylation protection experiments were performed to analyse possible contact points between NF-I and NF-III and their recognition sequence (Fig. 2b). NF-I protected G-residues at positions 26, 27 and 34 in the top strand from methylation by dimethylsulphate, whereas NF-III protected only the G-residue at position 42. Surprisingly, the conserved G-residue at position 48 was not a contact point. As guanosines are methylated at the N⁷ position located in the major groove this suggests that, like NF-I, NF-III binds at least in part in the major groove of the DNA helix. Mixtures of NF-III and NF-I protected all four G-residues (Fig. 2b, lane 3) confirming that NF-I and NF-III can simultaneously bind to their recognition sequence.

The results are summarized in Fig. 3. The DNase I footprint of NF-III partially overlaps both the NF-I footprint and the NF-I core recognition sequence (Fig. 1a). This close spacing of the two proteins is remarkable. Using extensive contact point analysis we have recently shown that NF-I binds to one side of the helix (E. de Vries et al., in preparation). The presence of a contact point between NF-III and a G-residue at position 42, only 6 bp removed from a contact point between NF-I and a G-residue at position 36, suggests that NF-III could bind at

Fig. 3 NF-III binding site in the adenovirus-2 origin. Highly conserved nucleotides within the terminal part of the Ad-2 ITR are boxed. Large brackets indicate the regions of both strands that are protected against DNase I digestion by either NF-I or NF-III. Circles, the G-residue protected against methylation by NF-III binding and the AT base pair essential for NF-III stimulation of replication.



least in part at the opposite side of the double helix compared to NF-I. At present we do not know whether the two proteins interact physically at their binding site. So far, we have not observed protein-protein interactions in solution between NF-I and NF-III during purification, comparable to, for example, the pTP-pol complex

The region protected by NF-III contains in its centre the sequence ³⁹TATGATAATGAG⁵⁰, much of which is conserved among the human and simian adenoviruses. A computer search reveals several homologous sequences in cellular DNA. A striking similarity was found with a promoter element of histone H2B genes, the H2B-specific homology block GTATGCAAATGAG, located close to the TATA box¹⁹. Several conserved promoter elements of other genes display similar homologous sequences. These genes include the human and mouse immunoglobulin V_{κ} and $V_{\rm H}$ genes²⁰ (consensus ATGCAAATNA, ~100 nucleotides upstream of the start of the coding region), the human interferon β (ATGTAAATGA, about 100 nucleotides upstream of the transcription start site) and the mammal/chicken/Xenopus laevis U1 and U2 snRNA genes^{22,23} (consensus PyATGPyAPuATG located 250-220 nucleotides upstream from the 5' terminus of mature RNA). Furthermore, some TAATGARAT elements of the herpes simplex virus immediate early promoters²⁴ are highly homologous with the Ad-2 NF-III-binding site (consensus PuPyGNTAATGAPuATNC). It would be interesting to see whether NF-III binds to any of these regulatory elements.

The requirement for a functional NF-I site for adenovirus DNA replication in vivo has been established^{25,26}, but the role of NF-III is unclear. Plasmids containing either nucleotides 1-45 or 1-67 are reported to be fully active in replication in vivo^{25,26}. Interestingly, replication-competent Ad-4 DNA which lacks a functional NF-I site²⁷ binds NF-III efficiently in filter binding assays (G.J.M.P., A.M.A.A. Kavelaars, and P.C. van der V., unpublished observations). Recently, we were informed that a protein with similar properties to NF-III has been found by P. J. Rosenfeld and T. J. Kelly (personal communication).

Since submission of this manuscript, in collaboration with Drs G. Tebb, D. Bohmann and I. W. Mattaj (EMBL, Heidelberg) we have shown by footprint analysis that NF-III binds well to the Xenopus laevis U2 upstream conserved sequence (-269 to -259). This sequence is required for efficient transcription of U2 snRNA genes (D. Bohmann, T. Dale, G. Tebb, H. R. Schöler, I. W. Mattaj & W. Keller, in preparation) suggesting that NF-III can function both in DNA replication and transcription.

We thank Drs E. de Vries, P. A. J. Leegwater and R. T. Hay for providing mutants. This work was supported in part by The Netherlands Foundation for Chemical Research and The Netherlands Organization for the Advancement of Pure Research.

Received 28 April; accepted 5 June 1986.

- Challberg, M. D. & Kelly, T. J. A. Rev. Biochem. 51, 907-934 (1982).
 Sussenbach, J. S. & Van der Vliet, P. C. Curr. Top. Microbiol. Immun. 109, 53-73 (1983).
 Nagata, K., Guggenheimer, R. A. Enomoto, T., Lichy, J. H. & Hurwitz, J. Proc. natn. Acad. Sci. U.S.A. 79, 6438-6442 (1982).
- 4. Nagata, K., Guggenheimer, R. A. & Hurwitz, J. Proc. natn. Acad. Sci. U.S.A. 80, 4266-4270
- Rawlins, D. R., Rosenfeld, P. J., Wides, R. J., Challberg, M. D. & Kelly, T. J. Cell 37, 309-319 (1984).
- 6. Guggenheimer, R. A., Stillman, B. W., Nagata, K., Tamanoi, F. & Hurwitz, J. Proc. natn. Acad. Sci. U.S.A. 81, 3069-3073 (1984).

- Leegwater, P. A. J., Van Driel, W. & Van der Vliet, P. C. EMBO J. 4, 1518-1521 (1985).
 De Vries, E., Van Driel, W., Tromp, M., Van Boom, J. H. & Van der Vliet, P. C. Nuclea Acids Res. 13, 4935-4952 (1985).
- Borgmeyer, U., Nowock, J. & Sippel, A. E. Nucleic Acids Res. 12, 4295-4311 119843.
- owock, J., Borgmeyer, U., Püschel, A. W., Rupp, R. A. W. & Sippel, A. E. Nucleic Acids Res. 13, 2045-2061 (1985).
- 11. Hennighausen, L. et al. Nature 314, 289-292 (1985).
- 12. Siebenlist, U., Hennighausen, L., Battey, J. & Leder, P. Cell 37, 381-391 (1984).
- Stevenins, O., Freimgnauser, E., Dancy, J. & Electric St. Stillman, B. W. Cell 35, 7-9 (1983).
 Pruijn, G. J. M., Kusters, H. G., Gmelig Meyling, F. H. J. & Van der Viket, P. C. Eur. J. Biochem. 154, 363-370 (1986).
- Tamanoi, F. & Stillman, B. W. Proc. natn. Acad. Sci. U.S.A. 79, 2221-2225 (1982).
 Van Bergen, B. G. M., Van der Ley, P. A., Van Driel, W., Van Mansfeld, A. D. M. & Vander Vliet, P. C. Nucleic Acids Res. 11, 1975-1989 (1983).
 Leegwater, P. A. J., Van der Vliet, P. C., Rupp, R. A. W., Nowock, J. & Sippel, A. E. EMBG.
- J. 5, 381-386 (1986).
- Enomoto, T., Lichy, J. H., Ikeda, J.-E. & Hurwitz, J. Proc. nam. Acad. Sci. U.S.A. 78, 6779-6783 (1981).
 Harvey, R. P., Robins, A. J. & Wells, J. R. E. Nucleic Acids Res. 10, 7851-7863 (1982).
- 20. Falkner, F. G. & Zachau, H. G. Nature 310, 71-74 (1984).
- Fujita, T., Ohno, S., Yasumitsu, H. & Taniguchi, T. Cell 41, 489-496 (1985). Krol, A., Lund, E. & Dahlberg, J. E. EMBO J. 4, 1529-1535 (1985).
- Ciliberto, G., Buckland, R., Cortese, R. & Philipson, L. EMBO J. 4, 1537-1543 (1985).
 Whitton, J. L. & Clements, J. B. Nucleic Acids Res. 12, 2061-2079 (1984).

- 25. Hay, R. T. EMBO J. 4, 421-426 (1985). 26. Wang, K. & Pearson, G. D. Nucleic Acids Res. 13, 5173-5187 (1985) 27. Hay, R. T. J. molec. Biol. 186, 129-136 (1985)
- Pearson, G. D. et al. Gene 23, 293-305 (1983)
- 29. Rijnders, A. W. M., Van Bergen, B. G. M., Van der Vliet, P. C. & Sussenbach, J. S. Nucleic Acids Res. 11, 8777-8789 (1983).
- Tsernoglou, D., Tucker, A. D. & Van der Vliet, P. C. J. molec. Biol. 172, 233-239 (1988)
- Van der Vliet, P. C., Van Dam, D. & Kwant, M. M. FEBS Lett. 171, 5-8 (1984)
- 32. Challberg, M. D. & Kelly, T. J. Proc. natn. Acad. Sci. U.S.A. 76, 655-659 (1979)

Green light-mediated photomorphogenesis in a dinoflagellate resting cyst

Brian J. Binder & Donald M. Anderson

Department of Biology, Woods Hole Oceanographic Institution, Woods Hole, Massachusetts 02543, USA

Developmental responses to light are well known and ubiquitous among higher plants1, but examples of such responses among the algae are less common. Those responses which have been reported in this group are generally photoperiodic or require prolonged light exposures; most involve macrophytes2. We now report a non-photosynthetic, low-threshold, photomorphogenic response in a unicellular alga, the dinoflagellate Scrippsiella trochoidea (Stein) Loeblich. In contrast to the reported behaviour of most other dinoflagellate species, resting cysts of S. trochoidea require light to germinate. This requirement is satisfied to a large extent by low photon fluences delivered in exposures as short as I second. Green light is most effective in eliciting the response. Given the importance of dinoflagellates as primary producers in many aquatic ecosystems and the potential role of resting cysts in controlling the dynamics of natural dinoflagellate populations, the present observations are of obvious ecological significance. The primitive phylogenetic standing of dinoflagellates³, and the relative rarity of green light-mediated photomorphogenic responses in eukaryotes generally 4,5, suggest that this phenomenon may also hold considerable evolutionary and photophysiological interest.

Temperature has been almost universally cited as the environmental factor exerting primary control over germination in dinoflagellate resting cysts^{6,7}. When considered, light conditions have generally been found to exert little effect on cyst germination 8-11

In the two studies to date which have demonstrated a light effect, germination was delayed but not prevented by darkness^{12,13}. Preliminary studies with *S. trochoidea* have confirmed that temperature is important in controlling germination in cysts of this species, but have also demonstrated that germination may be significantly reduced in the absence of light¹⁴. The present study was undertaken to elucidate the influence of light on germination in cysts of *S. trochoidea*.

Scrippsiella trochoidea is a small photosynthetic marine dinoflagellate of widespread neritic distribution. Cysts for the present study were produced in axenic clonal cultures (clone SA10, from Perch Pond, Falmouth, Massachusetts) under a 14:10 h daily light: dark (L:D) cycle at 18 °C¹⁴. Within a week of the appearance of cysts, the cultures were enriched with inorganic nutrients at f/2 levels¹⁵ and placed in darkness at 3 or 18 °C. Every precaution was taken to insure that no further light reached these cultures. Sampling and manipulations, when necessary, were carried out in total darkness.

Under these strictly dark conditions, cysts stored at 18 °C failed to germinate over the 120 days of the experiment, although conditions should otherwise have been optimal for excystment (Fig. 1). Exposure of these cysts to the standard 14:10 h L:D cycle (\sim 650 μ mol photons m⁻² s⁻¹), at the same temperature,

resulted in rapid germination.

An upward shift in temperature commonly results in rapid and complete germination of dinoflagellate cysts which have been stored at low temperature (Fig. 1)^{6,7}. In the present case, however, no germination occurred among cysts so treated if they were deprived of all light (Fig. 2). In contrast, cysts exposed to as little as 2 min of light germinated rapidly and only slightly less successfully (though significantly so) than those exposed to the same level of illumination for 14 h daily (P < 0.001). The response to 60 min of light was indistinguishable from that in the 2-min treatment.

The relationship between total 'white light' photon fluence and germination underscores the sensitivity of S. trochoidea cysts to low levels of light (Fig. 3). A 50% response (based on a maximum achieved germination frequency of 60%) occurs in these cysts at approximately 0.2 μ mol m⁻² photon fluence. This photon fluence corresponds to an exposure time at standard culturing irradiances (see above) of far less than 1 s.

The germination response appears to be dependent upon photon fluence (μ mol m⁻²), rather than fluence rate (μ mol m⁻² s⁻¹) or exposure time separately. Thus, equivalent germination is elicited by equal photon fluences, whether applied over 10 or 1,000 s (Fig. 4).

These results clearly demonstrate that light is required for germination in S. trochoidea cysts. Furthermore, the fact that a low-irradiance exposure lasting 1s is sufficient to stimulate germination raises the possibility that previous studies with dinoflagellate cysts (including our own), designed primarily with longer-term light effects in mind, may have been unable to distinguish between such a low threshold response and true

'dark' germination.

The response by S. trochoidea cysts to the same photon fluence (0.12 \(\mu\text{mol m}^{-2}\)) at different wavelengths is shown in Fig. 4. Germination is maximal in the 550-nm (yellow-green) band, with wavelengths above 620 nm being ineffective at this fluence level. The response drops more slowly on the low side of 550 nm, and is still apparent in the blue (450 nm) band. There was no evidence of modification of the 550-nm band response by subsequent exposure to red or far-red light (650 ± 20 nm or 750 ± 20 nm) at equivalent fluence levels (data not shown). The relatively low germination frequency among all the wavelength-band treatments is consistent with the low response achieved in the white-light controls of this experiment (Fig. 4) and therefore cannot be taken to indicate a low response to monochromatic light generally. The cause of the reduced germination in this experiment is not known, but the pattern of response to different wavelength bands was confirmed by preliminary experiments

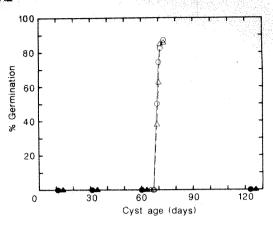


Fig. 1 Germination of S. trochoidea cysts placed in the dark at 3 °C (♠) or 18 °C (♠) starting at age 7 days. On day 65, some cysts from both the 3 °C and 18 °C dark storage (○, △, respectively) were placed under a continuing 14:10 h L:D cycle at 18 °C.

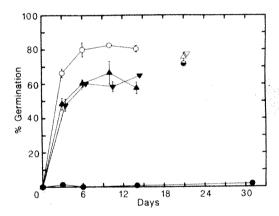


Fig. 2 Time course of germination by cysts (stored at 3 °C in the dark) on transfer to 18 °C and exposure to a continuing 14:10 h L:D cycle (\bigcirc), to 60 min of light only (\blacktriangledown), to 2 min of light (\blacktriangle), and to no light (\spadesuit). On day 14, cysts from the three latter treatments were exposed to the continuing 14:10 h L:D cycle and assessed 6 days later (\triangledown , \triangle , \Longrightarrow , respectively); means ± 1 s.e. (n = 2).

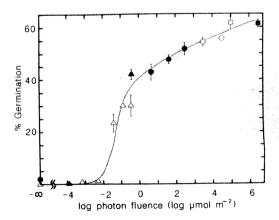


Fig. 3 Effect of 'white light' photon fluence $(\mu \text{mol m}^{-2})$ on germination frequency. Incandescent source, except \square and \blacksquare (which are taken from Fig. 2), illuminated with a cool white fluorescent source. Photon fluence is the product of exposure time and fluence rate [measured for photosynthetically active wavelengths only $(400 \text{ nm} < \lambda < 700 \text{ nm})$ with a scalar irradiance meter (Biospherical Instruments, Inc.) and adjusted, as necessary, with neutral density filters]. Exposure times are \triangle , 1 s; \triangle , 5 s; \bigcirc , 12 s; \square , \bigcirc , 120 s; \blacksquare , 3,600 s; means \pm 1 s.e. (n=3), except n=6 for \square and \blacksquare). Line drawn by eye.

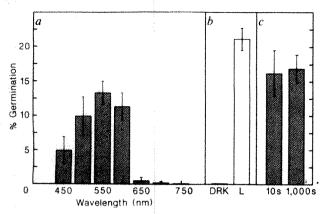


Fig. 4 Germination response of S. trochoidea cysts to wavelength. a, Bars show the frequency of germination achieved in cysts exposed to equal photon fluences ($\sim 0.12 \,\mu\text{mol m}^{-2}$) in seven different wavelength bands. Incandescent source, in combination with wide-band interference filters (40 nm half-power bandwidth, blocking outside of band better than 0.1% between low ultraviolet and 1,000 nm; Ditric Optics Inc.). Exposure time was 10 s in all cases; fluence rate was adjusted with neutral density filters and by varying source voltage; means ± 1 s.e. (n = 3); bar width represents half-power bandwidth, on wavelength scale shown. b. Open bar is the 'white light' control; unfiltered incandescent source, 4.2 umol m^{-2} (corresponding to $\sim 0.5 \, \mu \text{mol m}^{-2}$ in the $550 \pm 20 \, \text{nm}$ band). DRK bar, the dark control. c, Germination response to approximately equivalent photon fluences ($\sim 1 \, \mu \text{mol m}^{-2}$, $\lambda = 550 \pm 20 \, \text{nm}$) administered over 10 s or 1,000 s, as indicated.

which, however, involved less complete coverage of the spectrum.

Overall, our data indicate that the response to light in S. trochoidea cysts is not photosynthetic. This conclusion is based on the low photon fluence requirement of the response and its relative sensitivity to green light as compared with blue or red. The conclusion is further supported by the inability of darkstored S. trochoidea cysts to photosynthesize immediately after their transfer to light¹⁴.

Other non-photosynthetic responses to light which have been reported in dinoflagellates include phototaxis 16-18 and growth inhibition by far-red exposures 19. Generally, green wavelengths are not active in these phenomena; the photoreceptor systems responsible are therefore probably different from that involved in the light-triggered germination of S. trochoidea cysts.

Among algal resting stages generally, germination of cyanobacterial akinetes²⁰⁻²² and diatom resting spores^{23,24} has been widely found to be light-dependent. In contrast to the present case, the response in akinetes is maximal in the red wavelengths and generally requires extended exposures (hours to days) and high photon fluences^{21,25}. Similarly, diatom resting spores are responsive only to relatively high fluence rates²³. In neither of these cases can photosynthetic involvement be confidently discounted.

The extent to which the unique light requirement described here could control the germination of S. trochoidea cysts in the natural system depends on several factors, including the optical properties of overlying waters (note that coastal waters generally transmit maximally in the green band), the extent to which reciprocity in the response holds (that is, the maximum time over which 'photon counting' can occur), and the influence of cyst age and environmental parameters on the response itself. Preliminary calculations, based on conservative assumptions about these factors (including a maximum photon counting time of 1,000 s), indicate that in average coastal waters of moderate depth (~40-80 m) significant germination will occur, although the germination frequency ultimately achieved could be light limited14. On the other hand, in particularly deep or turbid waters, light could be sufficiently attenuated to prevent germination completely. Furthermore, the burial of cysts in the sediment

would probably result in prohibitively low light levels regardless of the depth of the overlying water column. In these latter cases, resuspension from the sediment surface and/or advection to shallower depths would presumably be required before significant germination could occur.

Although the ecological consequences of light-triggered germination in S. trochoidea cannot be fully appraised without further information on the physiology of the response, it is clear that light can no longer be ignored in considerations of the behaviour of dinoflagellate cysts in the natural system.

This work was supported in part by NSF grants OCE-8208739 and OCE-8400292 and by the Coastal Research Center and the Education Programme at the Woods Hole Oceanographic Institution. Contribution No. 6167 from the Woods Hole Oceanographic Institution.

Received 17 March; accepted 9 May 1986.

- 1. Shropshire, W. Jr & Mohr, H. (eds) Encyclopedia of Plant Physiology, new Ser. Vol. 184, B
- (Springer, Berlin, 1983).
 Dring, M. J. & Luning, K. in Encyclopedia of Plant Physiology, new Ser. Vol. 16B (eds. Shropshire, W. Jr & Mohr, H.) 545-568 (Springer, Berlin, 1983).
- Dodge, J. D. Br. phycol. J. 18, 335-356 (1983).
 Klein, R. M. Pl. Physiol. 63, 114-116 (1979).
- Tanada, T. Physiol. Pl. 58, 475-478 (1983)
- 6. Dale, B. in Surpival Strategies of the Alege (ed. Fryxell, G. A.) 69-136 (Cambridge University Press, 1983).
- 7. Pfiester, L. A. & Anderson, D. M. in The Biology of Dinoflagellates (ed. Taylor, F. J. R.) (Blackwell Scientific, Oxford, in the press). Huber, G. & Nipkow, F. Flora 116, 114-215 (1923). Anderson, D. M. & Wall, D. J. Phycol. 14, 224-234 (1978).

- Krupa, D. Ekol. pol. 29, 545-570 (1981).
 Hall, S. thesis, Univ. Alaska (1982).

- Endo, T. & Nagata, H. Bull. Plankt. Soc. Japan 31, 23-33 (1984).
 Anderson, D. M., Taylor, C. D. & Armbrust, E. V. Limnol. Oceanogr. (submitted).
- Binder, B. J. thesis. Massachusetts Inst. Technol. Woods Hole Oceanographic Institute WHOI-86-9 (1986).
- Guillard, R. R. L. & Ryther, J. H. Can. J. Microbiol. 8, 229-239 (1962).
- Halldal, P. Physiol. Pl. 11, 118-153 (1958).
 Hand, W. G., Forward, R. B. & Davenport, D. Biol. Bull. 133, 150-165 (1967).
- Forward, R. B. Jr Planta 92, 248-258 (1970).
 Lipps, M. J. J. Phycol. 9, 237-242 (1973).
- Yamamoto, Y. J. gen. appl. Microbiol. 22, 311-323 (1976). Braune, W. Arch. Microbiol. 122, 289-295 (1979).
- 22. Chauvat, F., Corre, B., Herdman, M. & Joset-Espardellier, F. Arch. Microbiol. 133, 44-49
- 23. Hollibaugh, J. T., Siebert, D. L. R. & Thomas, W. H. J. Phycol. 17, 1-9 (1981).
- 24. Hargraves, P. E. & French, F. W. in Survival Strategies of the Algae (ed. Frysel), G. A.) -68 (Cambridge University Press, 1983).
- 25. Reddy, P. M. & Talpasayi, E. R. S. Biochemie Physiologie Pflanzen 176, 165-107 (1981).

The crystal structure of d(GGATGGGAG) forms an essential part of the binding site for transcription factor IIIA

Maxine McCall, Tom Brown*, William N. Hunter & Olga Kennard

University Chemical Laboratory, Lensfield Road, Cambridge CB2 1EW, UK

Most genes in higher organisms are activated by the binding of proteins called transcription factors. One such protein, transcription factor IIIA (TFIIIA) from the frog, activates the gene for 58 RNA by binding to the region of the gene between nucleotides 45 and 97. This binding site has been defined by a variety of blochemical studies, including base-deletion experiments and DNase I footprinting1. The protein also binds to the gene product: in immature frogs it is stored as a complex with 5S RNA. From the observation that TFIIIA can bind to either double-helical DNA or RNA, and from their own measurements, Rhodes and Klug have proposed that the DNA-binding site for TFIIIA has an RNA-like structure. Here we present the crystal structure analysis of a part of the DNA-binding site (nucleotides 81-89 of the gene)

^{*} Present address: Department of Chemistry, University of Edinburgh, Edinburgh 1849 347, 136

which forms a particularly strong interaction with the protein, and show that it has a conformation similar to the A' form of doublehelical RNA.

Miller et al.3 have shown recently that the amino-acid sequence of TFIIIA contains multiple repeats of a 30-residue unit which they called a 'finger'. There are nine such fingers in the 344-residue TFIIIA, each of which contains the sequence Cys...Cys.... His.. His and is thought to complex a zinc ion. Finger sequences have now been found in at least four other DNA-binding proteins from higher organisms^{2,4-6}, suggesting that this structural unit is of primary importance in many cell processes. It is not known definitively how much DNA each finger covers but assuming that there is one TFIIIA protein bound per 50 base pairs (bp) of DNA7, each finger would have to recognize about 5.5 bp, or one-half of a double-helical turn. Indeed. Rhodes and Klug2 have recently provided evidence for a structural repeat of 5.7 bp in the TFIIIA binding site, to match the required amount of DNA per finger. At the suggestion of Dr A. Klug we have investigated the three-dimensional structure of part of the gene for 5S RNA by single-crystal X-ray diffraction methods. Nucleotides 81-89 of the gene were chosen because, as shown by methylation interference8, methylation protection9 and base deletion experiments 10,11, this stretch of DNA is more important for the binding of TFIIIA than any other part. The base sequence of our selected molecule, and its relation to the length of DNA covered by TFIIIA, are shown in Fig. 1.

The two strands d(GGATGGGAG) and d(CTCCCATCC) were synthesized by the triester method¹² and purified separately. They were then mixed in equimolar proportions, as calculated from their respective ultraviolet absorbances at 260 nm, to form a double helix of relative molecular mass 5,500. Crystals were grown by vapour diffusion against 6-20% 2-methyl-2,4pentanediol (MPD) from a mixture which initially contained 0.2 mM DNA, 12 mM magnesium acetate, 12 mM sodium cacodylate (pH 6.5) and 0.8 mM spermine HCl. The crystals grew as tetragonal rods to a size of $0.5 \times 0.18 \times 0.18 \text{ mm}^3$ during 5 months at room temperature, and were stabilized by diffusion to 60% MPD. Precession photographs show that the space group is P4₁ or P4₃, with cell dimensions a = b = 45.29 Å, c = 24.73 Å. The unit cell contains eight strands, with one double helix of 9 bp in the asymmetric unit. A total of 1,786 reflections were measured between 25.0 and 2.7 Å on a diffractometer. These were corrected for the Lorentz factor, polarization and absorption effects, and then symmetry-equivalent reflections were averaged. Of the 1,459 unique reflections obtained, slightly fewer than 50% in the range 3.0-2.7 Å have intensities $I > \sigma(I)$. Thus, the resolution is approximately 3.0 Å.

The unit cell dimensions suggested that our crystal structure might be nearly isomorphous with those of d(CCGG) and d(GGCCGGCC), both of which crystallize in the related space group P4₃2₁2 with 4 bp in the asymmetric unit^{13,14}. Hence, the starting coordinates for the 9-bp double helix in P43 were taken from our previously published model for poly(dG).poly(dC)¹⁵ and imposed on the coordinates of two d(CCGG) molecules in space group P4₃2₁2, with an appropriate shift in the origin. The model was refined against the X-ray data, first as a rigid body16 and then as a set of individual atoms connected by distance restraints17. Each atom in a base, sugar or phosphate group was assigned a temperature factor of 36, 41 or 46 Å², respectively, based on an overall temperature factor 18 for the crystal of 40 Å² These were not refined further due to the limited number of observations. Many electron density maps were calculated to follow the progress of the refinement. No solvent molecules were included in the phasing model because the resolution was relatively low. After 80 cycles of refinement, the agreement, or 'R-factor', between measured and calculated structure factors for all 1,032 zero-sigma data in the range 10.0-3.0 Å is 33%. The R-factor for the same phasing model, but with the X-ray data weighted according to their observed standard deviations, is 18%. Further efforts to test the correctness of our structure

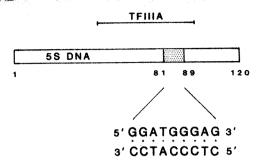


Fig. 1 A one-dimensional representation of the 120-bp codingregion for 5S RNA which shows the position of nucleotides 81-89 and the binding site for TFIIIA⁷. The numbering scheme used places the start of transcription at nucleotide 1.

solution are described in the legend to Fig. 2.

The double helix formed by d(GGATGGGAG) and its complementary strand d(CTCCCATCC) is shown in Figs 2 and 3. The identity of the bases cannot be assigned with certainty at 3 Å resolution, as the contribution of the bases to the calculated X-ray intensities does not change very much when the molecule is turned upside-down, by rotating it about its central axis of approximate 2-fold symmetry. Nevertheless, the positions of the sugar-phosphate chains, which give the overall shape of the structure, are defined clearly by the electron density and, in either orientation of the molecule, these positions refine to closely similar fractional coordinates. Figure 2 shows a view of the molecule looking into the minor groove. This groove is shallow, but not flat, and its width (as measured by the distance between phosphorus atoms) varies from 15.7 Å near the bottom of Fig. 2 to 14.3 Å near the top. By way of comparison 19, for example, fibre A-DNA has a minor-groove width of 17.0 Å, and fibre B-DNA, 11.7 Å.

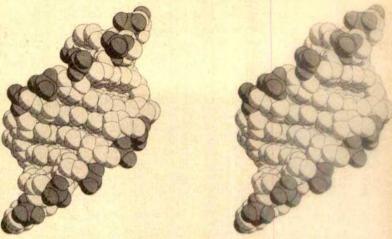
Figure 3 shows a view of the molecule looking into the major groove. This groove is both deep and wide, the mean separation of phosphorus atoms being 14.8 Å (s.d. 0.1 Å). In the model for fibre A-DNA, the major groove width is 8.2 Å, and in the model for B-DNA, 17.0 Å. Along each strand, the distances between adjacent phosphates vary considerably about a mean of 5.9 (0.6) Å. Thus, the structure seen here is clearly distinct from models of DNA which are shown in textbooks.

The ways in which the base-pairs stack on each other are described directly by the parameters 'slide' and 'roll'20. Slide is the distance by which the base pairs slip over each other in the direction of their long axes: in this structure the mean slide is 1.5 (0.7) Å. Roll, the angle by which adjacent base pairs open to the minor groove, averages 5 (13)°. The orientation of the base pairs can also be described in terms of parameters calculated relative to an imaginary helix axis. In our structure, the mean twist of base pairs with respect to this axis is 31.3 (9)°, yielding a loosely defined helical repeat of 11.5 bp. Other global parameters are the rise per residue of 3.0 (0.3) Å, a base-pair tilt of +10 (6)° and a displacement of base pairs from the central axis by 4.2 (0.3) Å. These averaged values are very close to those of the uniform model derived from the A' X-ray diffraction intensities of fibrous RNA^{21,22}. The model for A'-RNA has a helical repeat of 12.0 bp, a rise per residue of 3.0 Å, a base-pair tilt of +10° and a displacement of 4.5 Å.

Although some of the results from nuclear magnetic resonance experiments on DNA fragments in solution have been interpreted as being due to B-form structures, it is doubtful whether the technique can distinguish between the various global conformations of DNA such as 'A' and 'B'²³. However, as in the case of proteins, the three-dimensional structure of a DNA molecule in a highly hydrated crystal might indeed be the viable model for its stable conformation in vivo.

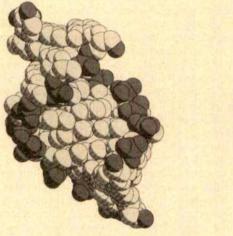
The results of our X-ray diffraction studies therefore agree with the proposal of Rhodes and Klug² that the DNA-binding

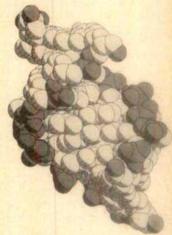
Fig. 2 Stereoscopic view the of structure of d(GGATGGGAG) and its complement d(CTCCCATCC), looking into the minor groove. Atoms P, C, N and O are represented by spheres of radii 1.9, 1.6, 1.5 and 1.4 Å, respectively; phosphate groups are shaded. In this view, the predominantly purine strand is on the left, with base G₈₁ at bottom. It is possible that the double helix packs in the crystal in a statistical fashion, using two orientations which are related to one another by a rotation of 180° about a line through the central base pair and perpendicular to the page. To assess the relative occupancies of these two possible orientations, the structure was refined independently in both settings. After 40 cycles in either case, the R-factor between measured and calculated structure factors (not weighted for noise) for all zero-sigma data to 3 Å was 33% for the model shown here, and 36% for the other orientation. Thus, it is not possible at present to determine which of the two orientations is preferred, but the



one shown here agrees marginally better with the data. In both orientations, the cytosine base nearest to the crystallographic 4-fold screw axis (C₈₉ or C₈₁) is poorly defined in the electron density. As a check, we also analysed the structure using a real-space search program²⁸, choosing as models the coordinates of fibre B-DNA, fibre A-DNA¹⁹ and, as a control, those of the refined crystal structure. Searches were carried out in both P4₁ and P4₃. At low resolution, in the range 25-10 Å, the best solution for the B-model yields an R-factor of 40%, while both the A-model and the crystal coordinates yield a much lower 30%. At moderate resolution, in the range 10-5 Å, the best solution for the A-DNA fibre model yields 50% in both P4₁ and P4₃, whereas the refined crystal coordinates yield 22% in P4₃, but 52% in P4₁. These results confirmed the choice of space group as P4₃, and further showed that the crystal X-ray structure is distinct from either the A or B forms of DNA found in pulled fibres^{19,29-32}.

Fig. 3 Stereoscopic view of the structure showing the major groove (centre) and parts of the minor groove (top left and bottom right); the purine strand is on the right, with base G₈₁ at bottom. Based on methylation protection and nuclease digestion data, Fairall et al.9 have proposed a model for TFIIIA binding to 5S DNA in which the protein lies on one side of the double helix with its 'fingers' inserted every half-turn into the major groove. The fingers of the protein are hypothesized to fold as a twisted β -sheet³. Clearly, there is plenty of room for a twisted β -sheet to fit into the major groove shown in this figure. The ability of proteins to fit into the major groove of A-form double helices has been emphasized recently by Arnott³³. A further consequence of their model is that the protein residues between adjacent fingers would span the minor groove of the DNA, a distance which in our crystal structure is 15 Å. There is an invariant tyrosine or phenylalanine in these regions of the protein; this residue could lie in van der Waals contact with the exposed sugar rings of the minor groove,





just as the terminal base pairs of DNA helices stack on the sugar residues of symmetry-related DNA molecules in this and many other structures 13-15,26. Huber and Wool 34 have studied the complex of TFIIIA with 5S RNA in solution. From their observation that the protein covers approximately the same region of bases in the RNA as in the DNA, they have also proposed that the DNA could have an RNA-like structure, at least when it is bound to the protein.

site of TFIIIA has an RNA-like structure, at least for nucleotides 81-89 in the crystal. What can be said about the conformation of this DNA in solution? Rhodes and Klug2 have used Fourier methods on nuclease digestion data to show that the entire TFIIIA-binding site has an underlying structural repeat of 5.7 bp, or 11.4 bp in two repeats. Our 9-bp molecule is not long enough to show the characteristic variation in structure which accompanies this repeat. However, the local pattern of nuclease digestion for nucleotides 81-89 in solution2 may be of interest. The enzyme DNase I does not cut well on either strand between nucleotides 82 and 83 (GpA = TpC), 84 and 85 (TpG = CpA), or 86 and 87 (GpG=CpC). These steps, in our best-refined model, are those which have extremes of local conformation such that they would be resistant to DNase I cleavage24. The GpA step has a large positive roll of 27°, compared with a mean for the structure of 5°; the TpG step a very low twist of 16°, compared with a mean of 31°; and the GpG step has a high roll 17° and a high slide of 2.6 Å, compared with a mean of 1.5 Å.

Accompanying the periodicity in structure of the TFIIIAbinding site is a periodicity in sequence²: short runs of guanine bases occur once every 5.6 bp. It seems likely that the preferred geometry of base stacking at the GpG step is the origin of an RNA-like structure for this region of DNA. Steps of the type GpG/CpC have now been observed in eight single-crystal X-ray structures: d(\(^1\)CCGG()\(^1\)3, d(GGCCGGCC)\(^1\)4, d(GGGCCCCC)\(^2\)5, d(GGGCCCCC)\(^2\)5, d(GGGATCCC) (U. Heinemann, unpublished results), d(GGTATACC)\(^2\)6 and d(GGATGGGAG). In all of these, the five-membered ring of one guanine base lies above the six-membered ring of its neighbour. Such a local base-to-base overlap is characteristic of all A-form double helices: the sideways slippage of base pairs generates a double helix with a large hole in the centre when viewed from above\(^{15,20}\).

Many other important DNA control regions are known to contain repeats of GpG². One example is the DNA-binding site for transcription factor Sp1, which contains repeats of the sequence GGGCGG²⁷. The structure of such control regions should resemble that shown here and in the other crystals mentioned.

We thank Dr A. Klug for suggesting the project, Drs B. Luisi

and M. F. Perutz for help with data collection, and especially Drs H. R. Drew and D. Rhodes for encouragement and advice. The work was supported by an MRC Program Grant (to O.K.).

Received 12 May; accepted 2 June 1986

- Brown, D. D. Harvey Lect. 76, 27-44 (1982). Rhodes, D. & Klug, A. Cell 46, 123-132 (1986)
- Miller, J., McLachlan, A. D. & Klug, A. EMBO J. 4, 1609-1614 (1985). Rosenberg, U. B. et al. Nature 319, 336-339 (1986).
- Vincent, A., Colot, H. V. & Rosbach, M. J. molec. Biol. 186, 149-166 (1985).
- Hartshorne, T. A., Blumberg, H. & Young, E. T. Nature 320, 283-287 (1986). Rhodes, D. EMBO J. 4, 3473-3482 (1985).
- Sakonju, S. & Brown, D. D. Cell 31, 395-405 (1982).

- Fairall, L., Rhodes, D. & Klug, A. Cell (submitted).
 Sakonju, S., Bogenhagen, D. F. & Brown, D. D. Cell 19, 13-25 (1980).
 Bodenhagen, D. F., Sakonju, S. & Brown, D. D. Cell 19, 27-35 (1980).
- 12. Gait, M. J., Matthes, H. W. D., Singh, M., Sproat, B. S. & Titmus, R. C. Nucleic Acids Res. 10, 6243-6254 (1982)
- 13. Conner, B. N., Yoon, C., Dickerson, J. L. & Dickerson, R. E. J. molec. Biol. 174, 663-695
- 14. Wang, A. H.-J., Fujii, S., van Boom, J. H. & Rich, A. Proc. natn. Acad. Sci. U.S.A. 79, 3968-3972 (1982).

- 15. McCall, M. J., Brown, T. & Kennard, O. J. molec. Biol. 183, 385-396 (1985).
- 16. Sussman, J. L., Holbrook, S. R., Church, G. M. & Kim, S. H. Acta crystallage. A33, 800-804 (1977)
- 17. Hendrickson, W. A. & Konnert, J. H. in Biomolecular Structure, Conformation, Function and Evolution Vol. 1 (ed. Srinivasan, R.) 43-57 (Pergamon, Oxford, 1981). Wilson, A. J. C. Nature 150, 152 (1942).
- MISOH, S. & Hukins, D. W. L. Biochem. biophys. Res. Commun. 47, 1504-1509 (1972).
 Calladine, C. R. & Drew, H. R. J. molec. Biol. 178, 773-782 (1984).
- 21. Arnott, S., Hukins, D. W. L. & Dover, S. D. Biochem. biophys. Res. Commun. 48, 1392-1399
- 22. Arnott, S., Hukins, D. W. L., Dover, S. D., Fuller, W. & Hodgson, A. R. J. molec. Biol. 81, 107-122 (1973)
- 23. Nilsson, L., Clore, G. M., Gronenborn, A. M., Brünger, A. T. & Karplus, M. J. molec. Biol. 188, 455-475 (1986).
- 24. Drew. H. R. & Travers. A. A. Cell 37, 491-502 (1984).
- Haran, T. thesis, Weizmann Inst. (1986)
- 26. Shakked, Z. et al. J. molec. Biol. 166, 183-201 (1983)
- Kadonaga, J. T., Jones, K. A. & Tjian, R. Trends biochem. Sci. 11, 20-23 (1986).
- Rabinovich, D. & Shakked, Z. Acta crystallogr. A40, 195-200 (1984).
 Watson, J. D. & Crick, F. H. C. Nature 171, 737-738 (1953).
 Franklin, R. E. & Gosling, R. G. Acta crystallogr. 6, 673-677 (1953).
 Langridge, R. et al. J. molec. Biol. 2, 38-64 (1960).

- 32. Fuller, W., Wilkins, M. H. F., Wilson, H. R. & Hamilton, L. D. J. molec. Biol. 12, 60-80 (1965).
 33. Arnott, S. Nature 320, 313 (1986).
- 34. Huber, P. W. & Wool, I. G. Proc. natn. Acad. Sci. U.S.A. 83, 1593-1597 (1986).

MATTERS ARISING

The mechanism of activation of porcine pepsinogen

IN a recent paper we studied the early events in the activation of porcine pepsinogen using fluorescence-detected stopped flow kinetics1. We characterized two first-order decays when working with both native pepsinogen and a covalent conjugate between the fluorescent moiety 6-(ptoluidinyl)-naphthalene-2-sulphonyl- and pepsinogen1. This result was demonstrated to be consistent with a model in which concurrent first-order transformations are undergone by two species of zymogen which are related by an ionization-dependent equilibration between them. (A sequential model was ruled out by an analysis of the data.) We hypothesized that the two species initiate two concurrent pathways of activation. Subsequently, James and Sielecki, in an extrapolation from their new crystallographic structure of porcine pepsinogen, also proposed two alternative pathways for activation². They did not explicitly suggest, however, that the two paths are followed simultaneously under a given set of conditions. It will be noted that their proposal bears a close resemblance to the model we had already worked out' based on the kinetic analysis described above. Most recently we have demonstrated that the pH-dependent segregation of pepsinogen molecules between alternative pathways persists at least through the process which exposes the active site³. This was shown by following the kinetics of binding of a fluorescent analogue of pepstatin to pepsinogen upon acidification. It was again observed that there are two firstorder processes consistent with the concurrent reaction model described above.

The crystal structure of pepsinogen reported by James and Sielecki² permits a much clearer understanding of the origins of the changes in intrinsic fluorescence that we obtained1. They noted that the environment of at least four tyrosyl residues must be perturbed upon release of Lys 36P (residues 1P-44P comprise the activation peptide) from its electrostatic interaction with the carboxylates of the catalytically-active residues Asp 32 and Asp 215. The fluorescence changes that we observed occur on the millisecond time scale, and are followed by no further change for several seconds¹. This strongly suggests that very soon after acidification the activation peptide is released from its initial position in which it blocks the catalytic site².

The distinguishing conformational features of the two molecular species of acidified pepsinogen, which form a Bronsted acid-base conjugate pair, remain to be identified. Further studies by us, as well as results obtained by crystallographic analysis, may provide a means to this end.

H. E. AUER

International Minerals & Chemical Corp., 1810 Frontage Road, Northbrook, Illinois 60062, USA

D. M. GLICK

Department of Biochemistry, Medical College of Wisconsin, Milwaukee, Wisconsin 53226, USA

- 1. Auer, H. E. & Glick, D. M. Biochemistry 23, 2735-2739
- James, M. N. G. & Sielecki, A. R. Nature 319, 33-38 (1986).
 Glick, D. M., Auer, H. E., Rich, D. H., Kawai, M. & Kamath, A. Biochemistry 25, 1858-1864 (1986).

JAMES AND SIELECKI REPLY-Acid activation of porcine pepsinogen has long been known to involve conformational changes^{1,2} that can be reversed by rapidly returning the pH of the solution to neutrality. Conformational changes on a time scale of 5 ms-2 s have also been detected by stopped flow fluorescence kinetics.3 Analysis of these data suggests that there are two concurrent activation pathways for pepsinogen. Exposure of the active site of the enzyme occurs on roughly the same time scale (1-2 s). The kinetic

data for the binding of a fluorescent pepstatin analogue are also interpretable in a two concurrent pathway model.4

The crystal structure of porcine pepsinogen has shown that the pepsin active site is fully formed in the zymogen but that it is blocked competitively by the specific folding of the activation peptide (Leu1P-Leu44P). This blocking takes place in a manner different from that expected for productive substrate binding. The two alternative steps in the proposed activation pathway⁵ are concerned only with repositioning the activation peptide so that the scissile bond (Leu16P-Ile17P) can approach the catalytic aspartates. This cleavage step has a relatively longer halftime of ~28 s (ref. 6). Unfortunately, a static crystal structure cannot provide definitive data on dynamic events that are occurring at millisecond or second time scales. However, the three-dimensional structure allows us to propose the two alternative pathways for productive binding of the scissile peptide bond of pepsinogen in the unimolecular cleavage reaction. Whether our alternative binding modes are associated with relatively rapid fluorescence changes and the concurrent pathways so deduced remains to be seen.

We thank Drs Auer and Glick for the opportunity to read their manuscript⁴ prior to publication.

> MICHAEL N. G. JAMES Anita R. Sielecki

Medical Research Council of Canada Group in Protein Structure and Function.

Department of Biochemistry, University of Alberta, Edmonton, Canada T6G 2HY

- Perlmann, G. E. J. molec. Biol. 6, 452-463 (1963). McPhie, P. J. biol. Chem. 247, 4277-4281 (1972). Auer, H. E. & Glick, D. M. Biochemistry 23, 2735-2739
- Glick, D. M., Auer, H. E., Rich, D. H., Kawai, M. & Kamath, A. Biochemistry 25, 1858-1864 (1986). 5. James, M. N. G. & Sielecki, A. R. Nature 319, 33-38 (1986).
- 6. Al-Janabi, J., Hartsuck, J. A. & Tang, J. J. biol. Chem. 247, 4628-4632 (1972).

The laboratory networking dilemma

from W.H. Jennings

Computer networking in the research laboratory is still a rarity. But growing demands for shared resources may prompt laboratories to make the connection . . . the question is when and how.

WITH the advent of microcomputers, data acquisition and control became dominated by systems dedicated to or embedded within the research instrument. The constraints of real-time operation and the limited computational capacity of these systems favours the transfer of raw data files to another machine for computationally intensive processing. While most scientists are familiar with this sort of transfer, local area networks that make the various computers within a department accessible to all department staff are still uncommon. Yet many research laboratories could benefit enormously from systems that distribute data to the computer most appropriate for a particular computational task.

Presently, moving data between machines is often accomplished by media transfer using magnetic tape or some form of disk, the difficulties of media transfer have encouraged the development of file transfer techniques that use serial transmission to transport data, often via telephone lines. Although vendors have been dragging their feet in devising common file format and transfer protocols for larger machines, several reasonably documented protocols exist for personal computers, and some of these have been adapted to large machines. There is then the potential for any computer-based laboratory instrument to transfer data to a departmental host machine or even some remote computer.

But realizing this potential at a level truly useful to laboratory scientists requires networking technology, and this technology is in flux. Herein lies the first element of the dilemma: when is it appropriate for a laboratory to implement a computer network?

Choosing the moment

Unfortunately, very few laboratories have the luxury of implementing a network de novo because of the computer-based instruments and/or the relatively expensive departmental computers they may have already accumulated. Interconnecting a variety of vendors' products, some of which may be obsolete, can pose problems. And of the many network products now available, there is probably no one product that is appropriate for all laboratory applications.

Nonetheless, rather straightforward means are available to remedy most of these complications, even though in some cases the solutions may be only marginally adequate. Networks are intrinsically expandable and extensible and their future value may be far more important than present economic or productivity gains. Current network standards offer both physical connectivity with fairly long lifetimes and protocols that, being software,

cannot be upgraded with a network interface can gain network access through terminal concentrators, which accept RS-232 serial transmissions and perform the necessary hardware and software functions to interface to the network. This access is limited in functionality and

Computer networks at work

Du Pont Experimental Station Wilmington, Delaware

Upjohn pharmaceutical R&D complex Kalamazoo, Michigan

General Motors research facility Warren, Michigan An Ethernet system connects 40 buildings over 150 acres

A network comprised of 5 km of cable is tied to seven systems in separate facilities

Over 300 IBM and DEC microcomputers are linked by a minicomputer intermediary

can be upgraded. There is then no compelling argument here to wait for further developments.

In fact, the decision to implement a laboratory network does not depend so much on issues of technology as on the commitment of laboratory personnel and funding. Even though its tangible portions may be limited to cables and connectors, a network requires considerable management and support, and in most labs these functions must be provided by existing personnel. Because the majority of networks are implemented at the departmental level rather than in top administrative or corporate echelons, the laboratories that will share the network usually have to dip into their own financial and personnel resources to sustain it.

The department that has decided to commit itself to networking confronts the second element of the dilemma: how can a laboratory network its computer resources? A variety of consultants and manufacturers provide technology support for networking projects, but the development of in-house expertise is desirable for both implementation and subsequent operations management.

Casting the net

The volume and characteristics of the data handled within a laboratory will determine a rough lower limit for network capacity. Generous margins should be added to allow expansion. Where very high data volume is required, a limited local network with a gateway to other networks can be a worthwhile option.

"Dumb" terminals and instruments that

speed: however, it is adequate for the majority of these devices.

The nearly ubiquitous personal computer can be connected either directly through an interface card or indirectly through a terminal concentrator. Terminal emulation software disguises the personal computer so that it appears to a remote computer as one of a variety of popular terminals. The networked PC can thus perform interactive file manipulation and execute programs on the remote system. Most emulation software provides for file transfer to or from the remote as well

Techniques for access and sharing of files and programs throughout a network are being extensively tested on advanced networks of more than 1,000 nodes. Meanwhile the next generation of computer systems, the personal workstation, is beginning to appear in the research laboratory. This device has a large memory, high resolution graphics and computational power exceeding that of some minicomputers. Most are sold with a network interface and AT&T's operating system UNIX, which already contains many networking functions.

The goal of networking is to make efficient use of computer resources, providing access to any level of computational power that the user might require without the bother of juggling cables, connections or conversions. For any laboratory ready to commit modest resources, this goal is already in sight.

William Jennings is at the National Institutes of Health, Room 108, Building 2, Bethesda, Maryland 20892, USA.

The binary breakthrough

From data acquisition to manuscript submission, computers aid research every step of the way and the computers often jump in where their owners may fear to tread.

WITTIN weeks, California-based Intelli-Genetics will be releasing molecular biology software that the company says can perform over 50 analyses of peptide and nucleic acid structure, both primary and secondary (Reader Service No. 100). The

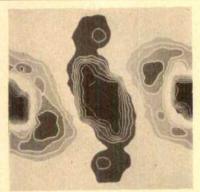


PC/GENE is based on published methods.

PC/GENE microcomputer package will search for specified sequences, predict helix distortion and hairpins, find probable coding regions and simulate restriction digestions. Capable of drawing over 20 different types of plots, PC/GENE runs on IBM PCs and compatibles with graphic cards. IntelliGenetics' commercial price is \$3.500 (US); academic institutions can purchase the package for \$2.500 (US) and BIONET subscribers gain access to PC/GENE at no additional cost. Programs allow file transmission between PC/GENE and BIONET, the company's mainframe timesharing system.

Two software packages for protein analysis and restriction mapping are among DNASTAR's offerings for molecular biologists (Reader Service No. 101). The company says its protein programs calculate plots of secondary structure and hydrophilicity by two different methods, and can determine optimal DNA probes, titration curves, isoelectric points and molecular weights. DNA-STAR asks about \$3,000 (US) for that package. The \$990 (US) R-MAP program derives circular or linear restriction maps from enzyme digestion data by way of an algorithm that the company claims is unique. Both products run on IBM PCs and compatibles.

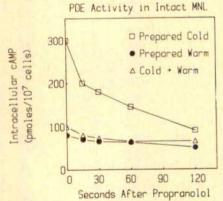
Chemical Design Ltd thinks its latest addition to the Chem-X molecular modelling family will make traditional laboratory notebooks obsolete (Reader Service No. 102). Chem DBS-1 is a database software module that also automatically records the results of Chem-X calculations and accompanying comments. Energy



A Chem-X energy analysis map for histamine. values, significantly positive or negative map volumes and user-defined geometries can be stored in DBS-1, in addition to structural information on several hundred molecules. "Pages" containing records of Chem-X calculations such as molecular fitting and spatial analyses can be located later by page number, date of entry, type of calculation and molecular name. Chemical Design's turnkey system Micro-GRAF-4, which starts at \$95,000 (US). incorporates Chem-X software for DEC MicroVAX II. DBS-1 will be demonstrated at September's ACS meeting in Anaheim.

Graphic detail

Plotting presentable graphs is the aim of software from Academic Press called Graph-PAD (Reader Service No. 103). Using an IBM PC with graphics capabilities and a Hewlett-Packard plotter or compatible equipment, the program can



Academic Press's program can graph multiple

plot bars, data points or curves from any of 10 available equations. Graph-PAD accepts data typed into a spreadsheet or contained in external files. The program can also digitize existing graphs via a plotter pen. Data manipulation features include calculations of average replicate values.

error bars, linear regressions and logarithmic transformations. Academic Press says no computer experience is necessary to be able to create graphs in less than 10 minutes and offers a \$5 (US) demonstration disk to make its point. The com lete diskette and its 98-page manual cost \$340 (US).

Janssen's life sciences division now offers a novel interpretation of numerical tabular data in the form of SpectraMap (Reader Service No. 104). Unlike bar. line or pie chart graphs, Janssen's program elucidates the ratios generated from problems involving many parameters. SpectraMap uses factor analysis and advanced computer graphics to arrive at a display complex enough to require instructions for interpretation. The company says its profiles can be applicable to studies in disciplines ranging from biophysics to epidemiology. Janssen provides the service on a piecemeal basis starting at £150 (UK) per graph. Alternatively. licensing of SpectraMap's PC version for £2,535 (UK) can be arranged for regular

Mathematical equations are unruly entities in the word-processing world. But recently a Massachusetts company, Technical Support Software, began marketing

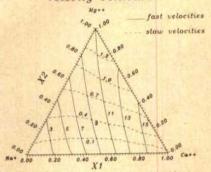


EXACT puts mathematics in the picture.

typesetting software that enables scientific and mathematical expressions to be incorporated into standard word-processing text and printed on garden-variety printers (Reader Service No. 105). Called EXACT, the program loads into RAM before the word processor and performs split-screen editing within the context of the target document. The editing mode displays characters exactly as they will appear in the printed document, automatically re-scaling radicals, braces, brackets, parentheses and boxes. EXACT's vocabulary includes 20 different fonts and over 1,000 symbols and characters. TSS guarantees its program on any word processor and sells a demo disk at \$5 (US); the real thing cost \$475 (US).

The chore of visualizing relationships amongst large data volumes is simplified with GRAPHER. Golden Software Inc's answer to plotting (Reader Service No. 106). With five types of regression curves, four types of error bars and graphs includ-

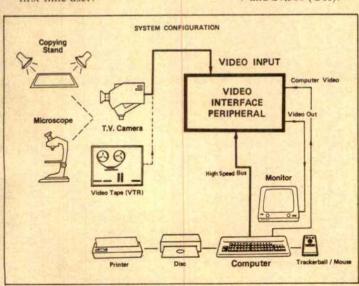
ing linear-linear, linear-log and triangular, GRAPHER can unveil the implications obscured by sheer numbers. It will Velocity Contours



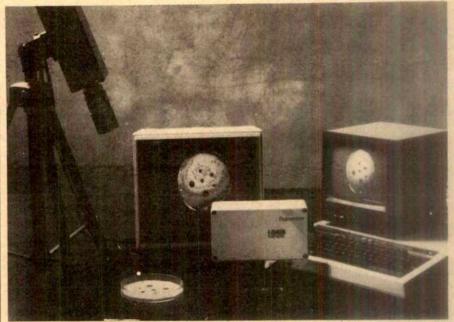
Complex relationships come to light with GRAPHER.

generate grid lines and any number of data scales or data lines can be combined on one graph. The \$199 (US) program's worksheet loads from keyboard or external data files; it will annotate graphs with text. Golden says GRAPHER runs on IBM PCs and compatibles with several kinds of graphics adaptors. A \$10 (US) demonstration disk can be supplied upon request.

A personal software series for chemists comes from ECS Chemical Systems in the UK (Reader Service No. 107). From CHEMTALK, a £1,000 (UK) program, to CHEMBASE, the series' modelling component. ECS's software aids in the storage, retrieval and display of chemical information. A hand-held mouse can select commands, draw structures or assemble reactions. The graphics-based word processor CHEMTEXT accepts transfers from CHEMBASE, while CHEMHOST and CHEMTALK link mainframe databases to the PC software. ECS expects its system to accelerate research formerly harnessed with the tedium of producing polished reports by hand. The IBM-compatible software boasts 500 different help screens for the first-time user.



Slight Systems has designed its image analyser to accept many different video sources and give standard video output. The Video Interface Peripheral can also be used as a video event recorder. The system employs a high order of noise reduction, and a phase lock circuit synchronizes the VIP to the incoming video.



In this FrameStore configuration, the right monitor shows a monochrome digitized image and the left displays the image with false colour generated by Data Harvest software.

Worth 1,000 words?

A menu-driven image analysis system from Sight Systems uses two video frame stores with 512×512 resolution for image storage (Reader Service No. 108). The grey and binary framestores of the company's Video Interface Peripheral (VIP) work in tandem at video rate; the menu that occupies one quarter of the screen provides a space for text and headings for routines or measuring processes. Sight Systems' analyser also achieves fast thresholding, according to the company. providing an image that is simpler to understand than unembellished images. The computer can read or write to any pixel in the binary store, grey store or menu area at any time. Because the VIP can analyse images live with no adverse affects, pseudo-real time analysis is possible, says Sight Systems. The company sells VIP in configurations costing between £2,000 and £4,500 (UK).

Data Harvest has pulled the price of its FrameStore analyser down to £395 (UK) (Reader Service No. 109). The company says its economy-line system can distinguish up to 64 discrete levels of image intensity and provide resolution of 192 × 256 pixels. A microcomputer allows manipulation, processing or transfer of digitized data. Because outlines can be identified through contrast enhancement. FrameStore can make area measurements/ratios calculations by pixel count. The analyser accepts video signals from sources such as video cameras, cassette recorders and disks and can be purchased separately or as part of a complete video

A desktop X-ray microanalysis system has been introduced as an "economic



Link Systems backs up the QX200 with full support services.

alternative" by Link Systems in High Wycombe (Reader Service No. 110). The company says its model QX200 offers display capabilities ranging from on-screen peak seek to labelling and KLM identification, and stores data via 3.5-inch floppy drives. Extensive data acquisition and manipulation capabilities are part of the OX200 package, as well as spectrum processing. A mouse is optional to simplify operating procedures, and the £24,000 (UK) system includes a bidirectional printer/plotter. Link says that in addition to the quantitative X-ray microanalysis program included with the package, an extended range of application software is available.

Designs for data

Computer analysis without computer expertise is the promise of Macmillan software's ASYSTANT package (Reader Service No. 111). The new software, says Macmillan, puts advanced application functions in a menu-driven format for ease of use. The company's basic \$495 (US) package performs integrated data reduction and analysis with high-resolution colour graphics; an \$895 (US) version

ADVERTISEMENTS



Reader Service No.12

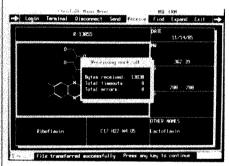


Reader Service No.50

called ASYSTANT+ adds data acquisition capabilities to the basic software. Macmillan's programs are designed for IBM personal computers.

A PC program from Laboratory Technologies Corp builds a bridge between the company's LABTECH NOTEBOOK data acquisition software and standard PC/MS-DOS applications programs (Reader Service No. 112). LABTECH Real Time Access, a \$195 (US) option for the \$895 (US) acquisition package, moves data samples from NOTEBOOK directly into spreadsheet, statistical data analysis, data base management and display programs. Hence the numbers generated by an external process and acquired by NOTEBOOK could appear in real time. continuously updated, on a Lotus 1-2-3 worksheet.

Nearly a decade of experience in chemical database management has given rise to MACCS-II, an integrated and customizable information system from Molecular Design (Reader Service No. 113). The company claims that the advantage of its latest system lies in its potential to be



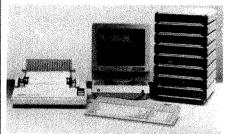
MACCS-Hallows custom design of help menus.

tailored to particular circumstances in particular laboratories. With a flexible program sequence language, MACCS-II simplifies operations and automation. Information such as test results, statistical analyses and graphic output from laboratory instruments can all be accessed via MACCS-II, and pooled in hard copy reports.

Life for LIMS

Tips on improving the performance and security of laboratory information management systems (LIMS) abound in a technical bulletin from Beckman (Reader Service No. 114). The bulletin uses Beckman's recent revision of its own CALS LabManager product to illustrate measures that can simplify organization and protect data copies. By dividing active samples from completed samples within the database. Beckman reports, the company was able to improve search time for many retrievals and create back-up versions of the completed base. Such insurance against disk drive failures provides the rationale for Beckman's Lab-Manager Safegard as well, an optional configuration that automatically maintains mirror images of active sample files on a separate disk.

In designing its LIMS, Trivector Systems tried to develop a network microcomputer approach rather than build the



A turnkey service is available for TRINET system around a centralized super-minicomputer (Reader Service No. 115). The result: TRINET, an information manager that Trivector hopes will provide both modest beginnings and considerable potential for expansion. At the heart of the system, a dedicated information manager with ports for up to 16 stations coordinates data management, whilst the stations are engaged in manual input, enquiries, program development and data transfer or collection. A database management package with its own screen and report generation programs makes LIMS design quick and easy, according to Trivector, which asks £15,000 (UK) and up for TRINET.

Guides to programs

A brochure detailing Fisher's toxic substance database shows full-colour examples of the program's display (Reader Service No. 116). These glimpses of ChemPro give a fair idea of the software's functioning, which gives information on any of 4,100 hazardous chemicals most frequently found in research laboratories, according to the company. Fisher kept the program's format uncomplicated so that substances could be located quickly in an emergency, and there are special keys for fires, spills and poisonings. ChemPro runs on an IBM AT.

The scientific software and educational programmes marketed by Autoscribe Ltd are reviewed in the company's latest catalogue (Reader Service No. 117). Autoscribe offers software such as Molecular Presentation Graphics for chemical structure drawing and Datalyst for chemical databases. Educational programmes are available on various media. The company hopes to expand both its education and software ranges shortly.

These notes are compiled by Karen Wright from information provided by the manufacturers. To obtain further details about these products, use the reader service card bound inside the journal. Prices quoted are sometimes nominal and apply only within the country indicated.

Astronomy

Astrophotography for the Amateur. By MICHAEL COVINGTON. Cambridge University Press:1985. Pp. 168. Hbk ISBN 0-521-25391-8. £15, \$24.95.

Astrophysics of Active Galaxies and Quasi-Stellar Objects. By J.S. MILLER. Oxford University Press:1985. Pp.519. Hbk ISBN 0-19-8557-17-5. £37.50.

Beyond the Black Hole: Stephen Hawking's Universe. By JOHN BOSLOUGH. Fontanal Collins: 1986. Pp. 127. Pbk ISBN 0-00-636652-X. £2.50.

Birth and Evolution of Massive Stars and Stellar Groups. W. BOLAND and H. VAN WOERDEN (eds). D. Reidel: 1985. Pp. 377. Hbk ISBN 90-277-2135-1. Dfl. 150, £41.75, \$59.

Early History of Cosmic Ray Studies: Personal Reminiscences with Old Photographs. YATARO SEKIDO and HARRY ELLIOT (eds). D. Reidel: 1985. Pp. 444. Hbk ISBN 90-277-2083-5. Dfl. 250, £69-25, \$89.

Mass Loss from Red Giants. MARK MORRIS and BEN ZUCKERMAN (eds). Reidel:1985. Pp.320. ISBN 90-277-2075-4. Dfl.135, \$49.

The Planet Sun (enlarged 1985 edition). By TASSOS A. KAROUSATOS. Laboratory of Magneto-Optical Research, 43 Levidou Street, GR-145 63. Kifissia, Athens, Greece:1985. Pbk np.

Supernovae. By PAUL and LESLEY MURDIN. Cambridge University Press:1985. Pp.185. Hbk ISBN 0-521-30038-X. £12.95, \$24.95.

Physics

Advanced Fracture Mechanics. By MELVIN F. KANNINEN and CARL H. POPELAR. Oxford University Press: 1985. Pp. 563. ISBN 0-19-503532-1. £40.

Amorphous Solids and the Liquid State, NORMAN H. MARCH, ROBERT A. STREET and MARIO TOSI (eds). Plenum:1985. Pp.339. Hbk ISBN 0-306-110475-8.

Cryogenic Systems, 2nd Edn. By RANDALL F. BARRON. Oxford University Press: 1985. Pp. 507. ISBN 0-19-503567-4. f60.

Desorption Induced by Electronic Transitions. W. BRENIG and D. MANZEL (eds). Springer-Verlag: 1985. Pp.291. ISBN 3-540-15593-7/0-387-15593-7.

Dynamical Phenomena at Surfaces, Interfaces and Superlattices. F. NIZZOLI, K.H. RIEDER and R.F. WILLIS (eds). Springer-Verlag:1985. Pp.329. ISBN 3-540-15505-8/0-387-15505-8. DM 89.

Elements of Modern Optical Design. By DONALD C. O'SHEA. Wiley: 1985. Pp. 402. Hbk ISBN 0-471-07796-8. £40.85.

Foundations of Quantum Mechanics II. By G. LUDWIG. Springer-Verlag: 1985. Pp. 416. Hbk ISBN 3-540-13009-8. DM 228.

Fundamental Interactions in Low-Energy Systems. P. DALPIAZ, G. FIORENTINI and G. TORELLI (eds). Plenum:1985. Pp.501. ISBN 0-306-42002-3.

Fourier Techniques and Applications, JOHN F. PRICE (ed.). Plenum:1985. Pp.231. Hbk ISBN 0-306-42100-3. Np.

Introduction to Concepts and Theories in Physical Science (2nd Edn.). By GERALD HOLTON, revised and with new material by STEPHEN G. BRUSH. Princeton University Press:1985. Pbk ISBN 0-691-08284.2 \$10.05

Molecular Electromagnetism. By A. HINCHLIFFE and R.W. MUNN. Wiley:1985. Pp.252. Pbk ISBN 0-471-90721-9. Pbk £9.95.

Applied Biological Sciences

Advances in Cancer Research, Vol.45. Academic: 1985. Pp.324. Hbk ISBN 0-12-006645-9. £48, \$55.

Advances in Human Genetics, Vol.15. H. HARRIS and K. HIRSCHHORN (eds). *Plenum:1986. Pp.299. Hbk ISBN 0-306-42155-0. Np.*

Advances in Veterinary Science and Comparative Medicine, Vol.30. CHARLES E. CORNELIUS and CHARLES F. SIMPSON (eds). Academic:1985. Pp.339. Hbk ISBN 0-12-039299-1. £52, \$59.50.

Advances in Pain Research and Therapy. Vol.9, Proceedings of the Fourth World Congress on Pain. HOWARD L. FIELDS, RONALD DUBNER and FERNANDO CERVERO (eds). Raven Press:1985. Pp.951. Hbk ISBN 0-88167-121-5. \$153.

Animal Behaviour and Its Applications. By DEREK V. ELLIS. Lewis Publishers: 1985. Pp. 329. Hbk ISBN 0.87371-020.7-627-55

Aortitis: Clinical, Pathological and Radiographic Aspects, ADAM LANDE, YAHYA M. BERKMEN and HUGH A. McALLISTER, Jr (eds). Raven 1085 Pp. 288 Hist. IERN 0.88167, Ltd. V. S. 3.50.

1985. Pp. 288. Hbk ISBN 0-88167-141-X. 563.50. Atlas of Cancer in Scotland 1975-1980: Incidence and Epidemiological Perspective. I. KEMP, P. BOYLE, M. SMANS and C. MUIR (eds). IARC Scientific Publications, Lyons:1985. Pp. 282. Hbk ISBN 928-321172-3. £35.

The Autoimmune Disease, NOEL R. ROSE and IAN R. MACKAY (eds). Academic:1986. Pp.727. Hbk ISBN 0-12-596920-1. £75, \$85.

Bacteria and Complement. Current Topics in Microbiology and Immunology, Vol.121. MICHAEL LOOS (ed.). Springer-Verlag:1985. Pp.191. Hbk ISBN 3-540-15877-4. Np.

Biological Effects and Dosimetry of Static and ELF Electromagnetic Fields. M. GRANDOLFO, S.M. MICHAELSON and A. RINDI (eds). *Plenum:1985*. *Pp.697. Hbk ISBN 0-306-41923-8. Np.*

Biology of Sewage Treatment and Water Pollution Control. By K. MUDRACK and S. KUNST. Ellis Horwood: 1986. Pp. 193. Hbk ISBN 0-85312-912-6. £27.50.

Biorhythms and Epilepsy. A. MARTINS DA SILVA, C.D. BINNIE and H. MEINARDI (eds). Raven:1985. Pp.254. Hbk ISBN. 0-88167-124-X.

Capnography in the Operating Room, an Introductory Directory. By W. SAMUEL MAY Jr. JAMES E. HEAVNER, DOROTHY McWHORTER and GABOR RACZ. Raven Press:1985. Pp.64. Pbk ISBN 0-88167-128-2. \$14.00.

Cell Culture and Somatic Cell Genetics of Plants. Vol.2, Cell Growth, Nutrition, Cytodifferentiation and Cryopreservation. INDRA K. VASIL (ed.). Academic:1985. Pp.330. Hbk ISBN 0-12-715002-1. £42 50 849 50

Cell Membranes and Cancer, T. GALEOTTI, A. CITTADINI, G. NERI, S. PAPA and L.A. SMETS (eds). Elsevier:1985. Pp. 446. Hbk ISBN 0-444-80723-3. Dfl. 230, \$85, 25.

Chemotherapy of Parasitic Diseases. WILLIAM C. CAMPBELL and ROBERT S. SHAW (eds). Plenum:1986. Pp.655. Hbk ISBN 0-306-42029-5. Np.

Congenital Adrenal Hyperplasia. MARIA I. NEW (ed.). New York Academy of Sciences:1985. Pp.290. ISBN 0-89766-311-X. Np.

Contact Allergy Predictive Tests in Guinea Pigs. Current Problems in Dermatology, Vol.14. K.E. ANDERSEN and H.I. MAIBACH (eds). Karger: 1985. Pp.300. Hbk ISBN 3-8055-4053-1. SFr. 162, DM 194, £50.70, \$69.00.

Contemporary Issues in Pesticide Toxicology and Pharmacology. By JUDITH K. MARQUIS. Karger: 1986. Pp.108. Hbk ISBN 3-8055-4215-1. SFr. 89, DM 107-677-90, \$38

Control of Animal Cell Proliferation, Vol.1. ALTON L. BOYNTON and HYAM L. LEFFERT (eds). Academic:1985. Pp.557. Hbk ISBN 0-12-123061-9.£60.50, \$68.50.

Control of Pig Reproduction II. Proceedings of the Second International Conference on Pig Production Held at Columbia Missouri, USA. G.R. FOXCROFT. D.J.A. COLE and BARBARA J. WEIR (eds). Journal of Reproduction and Fertility: 1985. Pp. 266. Hbk ISBN 0-906545-10-2, \$63.

Deep Dyslexia. MAX COLTHEART et al. (eds). Routhledge & Kegan Paul: 1986. Pp. 444. Pbk ISBN 0-7102-0834-0. Pbk F8 95.

Dietary Fiber and Obesity. Current Topics in Nutrition and Disease, Vol.14. Alan R. Liss:1985. Pp. 126. Hbk ISBN 0-8451-1613-4. £17.

Ear, Nose and Throat Disorders in Children. By JOHN E. BORDLEY, PATRICK E. BROOK-HOUSER and GABRIEL FREDERICK TUCKER, Jr. Raven:1985. Pp.456. Hbk ISBN 0-89004-324-8. \$52.50.

Economic Aspects of Biotechnology. Cambridge Studies in Biotechnology. By ANDREW J. HACK-ING. Cambridge University Press: 1986. Pp. 306. Hbk ISBN 0-521-25893-6. \$39.50.

Epidemiology of Leukaemia and Lymphoma, M.F. GREAVES and L.C. CHAN (eds). *Pergamon: 1985. Pp.163. Hbk ISBN 0-08-032002-3. £19, \$25.*

Equine Surgery and Medicine, Vol.1. JOHN HICK-MAN (ed.). Academic:1985. Pp. 398. Hbk ISBN 0-12-347221-0. £69.50. \$80.

Evaluation of Cyclamate for Carcinogenicity. Commission on Life Sciences, National Research Council. National Academy Press, Washington, US:1985. Pp. 196. Pbk ISBN 0-309-03546-5. Pbk Fl4 50.

Forest Ecosystems: Concepts and Management, By RICHARD H. WARING and WILLIAM H. SCHLESINGER. Academic:1985. Pp. 340. Hbk ISBN 0-12-735440-9. £39.50, \$45.

Gaba and Mood Disorders: Experimental and Clinical Research. L.E.R.S Monograph Series, Vol.4. G. BARTHOLINI, K.G. LLOYD and P.L. MORSELLI. Raven Press:1986. Pp.240. Hbk ISBN 0-88167-129-0. \$32.50.

Gene Manipulations in Fungi. J. W. BENNETT and LINDA L. LASURE (eds). Academic 1986. Pp.558-Hbk ISBN 0-12-088640-5. £65, \$75.

Genetic Approaches to Microbial Pathogenicity. Current Topics in Microbiology and Immunology, Vol.118. W. GOEBEL (ed.). Springer-Verlag:1985. Pp.283. Hbk ISBN 3-540-15597-X. DM 160.

Genetic Basis of Biochemical Mechanisms of Plant Disease. JAMES V. GROTH and WILLIAM R. BUSHNELL (eds). The American Phytopathological Society Press:1985 Pp.157. Phk ISBN 0-89054-068-3. 524

Genetic Perspectives in Biology and Medicine. EDWARD D. GARBER (ed.). The University of Chicago Press: 1986. Pp. 500. Hbk 1SBN 0-226-287215-5; pbk ISBN 0-226-28216-3. Hbk £25.50; pbk £10.25.

Genetics, Cell Differentiation and Cancer. Bristol-Myers Cancer Symposia, Vol.7, PAUL A. MARKS (ed.). Academic:1985. Pp.209. Hbk ISBN 0-12-473060-4.£22.50, \$25.

Genetics and the Law III. AUBREY MILUNSKY and GEORGE J. ANNAS (eds). Ptenum: 1985. Pp.514. Hbk ISBN 0-306-41983-1. Np.

Genetics in Clinical Oncology. R.S.K. CHAGANTI and JAMES L. GERMAN (eds). Oxford University Press:1985, Pp.280. Hbk ISBN 0-19-503609-3. £35.

Hormonally Responsive Tumours. VINCENT P. HOLLANDER (ed.). Academic:1985. Pp. 558. Hbk ISBN 0-12-352560-8. £59, \$68.

Humour Therapy in Cancer, Psychosomatic Diseases, Mental Disorders, Crime, Interpersonal and Sexual Relationships. By BRANKO BOKUN. Via Books, 26 Chelsea Square, London SW3. UK:1986. Pp.221. Pbk ISBN 0-9510525-0-0. £5.00.

Hyperalimentation: A Guide for Clinicians. MITCH-ELL V. KAMINSKI Ir. (ed.) Dekker:1985. Pp.744. Hbk ISBN 0-8247-7375-6. 895 (US and Canada), \$114 (other countries).

Implantation of the Human Embryo. R.G. EDWARDS. JEAN M. PURDY and P.C. STEP-TOE (eds). Academic:1985. Pp. 459. Hbk ISBN 0-12-232455-2. £52, \$59.50.

Interrelationship Among Aging, Cancer and Differentiation. The Jerusalem Symposia on Quantum Chemistry and Biochemistry, Vol.18, BERNARD PULLMAN, PAUL O.P. TS'O and EDMUND L. SCHNEIDER (eds). D. Reidel: 1985 Pp.345. Hbk ISBN 90-277-2117-3. Dfl 145, £40.25, \$57.

Large-Scale Mammalian Cell Culture. JOSEPH FEDER and WILLIAM R. TOLBERT (eds). Academic:1985. Pp.159. Hbk. ISBN 0-12-250430-3. £22.50, \$25.

The Limbic System: Functional Organization and Clinical Disorders. BENJAMIN K. DOANE and KENNETH F. LIVINGSTON (eds). Roven Press: 1985. Pp.365. Hbk ISBN 0-88167-134-7-364-50.

Mathematical Physics. By ROBERT GEROCH. The University of Chicago Press: 1986. Pp.351. 4164. ISBN 0-226-28861-7. £25.50.

Mechanism of Menstrual Bleeding, D.T. BAIRD and E.A. MICHIE (eds). Raven:1985. Pp.276. Hbk. ISBN 0-88167-094-4, \$43.50.

Medicinal Chemistry Research in India. By HAR-KISHAN SINGH, A.S. CHAWLA and V.K. KAPOOR. National Information Centre for Drugs and Pharmaceuticals, Lucknow, India:1985. Pp.184. ISBN 81-85042-00-4. §35.

Medicinal Plants in Tropical West Africa. By B.E.P. OLIVER-BEVER. Cambridge University Press: 1986. Pp.375. Hbk ISBN 0-521-26815-X. £40, \$75.

Methods for Nutritional Assessment of Fats. JOYCE BEARE-ROGERS (ed.). American Oil Chemists Society: 1985. Pp.255. Hbk ISBN 0-935315-11-X. \$50.

Methods in Porphyrin Photosensitization. Advances in Experimental Medicine and Biology, Vol. 193. DAVID KESSEL (ed). Plenum:1985. Pp.352. Hbk ISBN 0-306-42210-7. Np.

Migraine: Clinical and Research Advances. Fifth International Migraine Symposium, London 1984. F. CLIFFORD ROSE (ed.). Karger: 1985. Pp. 280. Hbk 15BN 3-8055-4039-6. SFr. 175, DM 210, £54.70, \$74.50.

Migraine (new edn.). By OLIVER SACKS. Duckworth: 1986. Pp.270. Hbk ISBN 0-7156-2087-8.

Models for Biomedical Research: A New Perspective. Commission on Life Sciences, National Research Council. National Academy Press:1985. Pp.180. Pbk ISBN 0-309-03538-4. £19.60

Molecular Biology and Biotechnology. J.M. WALKER and E.B. GINGOLD (eds). Royal Society of Chemistry: 1986. Pp.340. Pbk ISBN 0-85186-985-8. Pbk ISSN 0-85186-985-8.

Molecular Dynamics and Protein Structure, JAN HERMANS (ed.). University of North Carolina Printing Dept.: 1985. Pp. 195. Pbk. \$10.

Monoclonal Antibodies Against Bacteria, Vol.II. ALBERTO J.L. MACARIO and EVERLY CON-WAY de MACARIO (eds). Academic:1986. Pp.,335. Hbk ISBN 0-12-463002-2. £42. \$49.

New Directions for Biosciences Research in Agriculture: High Reward Opportunities. National Academy Press:1985. Pp.122. Pbk ISBN 0-309-03542-2. £10.55.

Non-Hodgkin's Lymphomas: New Techniques and Treatments. Fourth Cancer Research Workshop, Grenoble 1984. J.J. SOTTO, C. VROUSOS, M.F. SOTTO and F. VINCENT (eds). Karger:1985. Pp.232. Hbk ISBN 3-8055-4064-7. SFr 162, DM 194, £50.70, \$69.

Nutrition in Cancer and Trauma Sepsis. F. BOZZETTI and R. DIONIGI (eds). Karger:1985. Pp.203. Pbk ISBN 3-8055-3959-2. Pbk DM 88, 831-50.

Papillomaviruses, Molecular and Clinical Aspects. PETER M. HOWLEY and THOMAS R. BROKER (eds). Alan R. Liss:1986. Pp. 598. Hbk ISBN 0-8451-2651-2631-8. F72

Parmacokinetics of Cardiovascular, Central Nervous System and Antimicrobial Drugs. Royal Society of Chemistry, London:1985. Pp.462. Hbk ISBN 0-85186-937-8, \$71, £39.

The Pathologist and the Environment. DANTE G. SCARPELLI, JOHN E. CRAIGHEAD and NATHAN KAUFMAN (eds). William & Wilkins: 1985. Pp.239. ISBN 0-683-07516-0. £47.50.

Pathology of Unusual Malignant Cutaneous Tumours. MARK R. WICK (ed.). Dekker:1985. Pp. 440. Hbk ISBN 0-8247-7377-2. (USA & Canada) \$69.75, (other countries) \$83.50.

Pedigree Analysis and Human Genetics. By ELIZA-BETH A. THOMPSON. The John Hopkins University Press:1986. Pp.213. Hbk ISBN 0-8018-2790-6. £28.50.

The Peptides: Analysis, Synthesis, Biology. Vol.7, Conformation in Biology and Drug Design. VICTOR J. HRUBY (ed.). Academic: 1985. Pp. 495. Hbk ISBN 0-12-304207-0. £85.50 \$99.

Pocket Atlas of Cranial Magnetic Resonance Imaging. By VICTOR M. HAUGHTON and DAVID L. DANIELS. Raven:1986. Pp.61. Pbk ISBN 0-88167-171-1. Pbk \$14.

Population Genetics in Forestry: Proceedings, Göttingham 1984. Lecture Notes in Biomathematics, 60. H.R. GREGORIUS (ed.) Springer-Verlag:1985. Pp. 287. Pbk ISBN 3-540-15980-0. DM 43.

Positron Emission Tomography and Autoradiography: Principles and Applications for the Brain and Heart. MICHAEL E. PHELPS et al. (eds). Raven: 1985. Pp. 690. ISBN 0-88167-118-5. \$98.50

Progress in Clinical Biochemistry and Medicine. Vol.2, Oncogenes and Human Cancer, Blood Groups in Cancer, Copper and Inflammation, Human Insulin. (Contributions by) T.L.J. BOEHM, U. DEUSCHLE, W.J. KUHNS, R. OBERMEIER, F.J. PRIMUS, U. WESER and M. ZOLTOBROCKI. Springer-Verlag:1985. Pp.163. Hbk ISBN 3-540-15567-8. DM 84.

Progress in Nucleic Acid Research and Molecular Biology, Vol.32. WALDO E. COHN and KIVIE MOLDAVE (eds). Academic:1985. Pp.340. Hbk ISBN 0-12-540032-2. £43.50, \$49.50.

Prostanoids: Pharmacological, Physiological and Clinical Relevance. By P.K. MOORE. Cambridge University Press:1985. Pp.263. Hbk ISBN 0-521-26081-7; pbk ISBN 0-521-27827-9. Hbk £32.50, \$54.50; pbk £12.50, \$19.95.

Protective Effect of BCG in Experimental Tuberculosis. By D.W. SMITH. Karger: 1985. Pp. 97. ISBN 3-8055-4089-2. DM 107, \$38, £22.

The Role of the Registry in Cancer Control. D.M. PARKIN, G. WAGNER and C.S. MUIR (eds). International Agency for Research on Cancer:1985. Pp.155. ISBN 92-832-1166-9. £10.

Serotonin and Microcirculation. Progress in Applied Microcirculation, Vol.10. R.S. RENEMAN and A. BOLLINGER (eds). Karger: 1986. Pp. 92. Hbk ISBN 3-8055-4163-5. SwFr. 66, DM 79, £20, 70, \$28.25.

Survey of Drug Research in Immunologic Disease. Vol.6. Noncondensed Aromatic Derivatives. By V. ST. GEORGIEV. Karger: 1985. Pp. 586. ISBN 3-8055-3962-2. DM 588, \$208.75.

Synthetic Peptides as Antigens, CIBA FOUNDA-TION SYMPOSIUM 119. Wiley:1986. Pp.307. ISBN 0-471-99838-9, £27.50,

Testicular Cancer. Progress in Clinical and Biological Research, Vol.203. SAAD KHOURY, RENE KUSS. GERALD P. MURPHY, CHRISTIAN CHATELAIN and JAMES P. KARR (eds). Alan R. Liss:1985. Pp. 774. Hbk ISBN 0-8451-5053-7. 175.

Textbook of Adverse Drug Reactions, 3rd Edn. D.M. DAVIES (ed.). Oxford University Press:1986. Pp.814. Hbk ISBN 0-19-261479-7, £75.

The Thorax, Part A. Lung Biology in Health and Disease, Vol.29. CHARIS ROUSSOS and PETER T. MACKLEM (eds). Dekker:1985. Pp.1.616. Part A. Hbk ISBN 0-8247-7299-7. Part B, Hbk ISBN 0-8247-7300-4. £252 (sold only as a set).

TNM-Atlas: Illustrated Guide to the TNM/pTNM-Classification of Malignant Tumour, 2nd Edn. International Union Against Cancer. B. SPIESSL, P. HERMANEK, O. SCHEIBE and G. WAGNER (eds). Springer-Verlag:1985. Pp.269. Pbk ISBN 3-540-13443-3. DM 30.

Transformation Assay of Established Cell Lines: Mechanisms and Application. Proceedings of a Workshop organized by IARC in Collaboration With the US National Cancer Institute and the US Environmental Protection Agency held in Lyon, 15-17 February 1984. T. KAKUNAGA and H. YAMASAKI (eds). International Agency for Research on Cancer, Lyons:1985. Pp.225. Hbk ISBN 92-832-1167-7 Nn.

Trauma of the Middle Ear: Clinical Findings, Postmortem Observations and Results of Experimental Studies, By M. STROHM. Karger: 1986. Pp. 254. Hbk ISBN 3-8055-4087-6. SwFr 174, DM 208, £54.40, \$74.25.

Trends in Autonomic Pharmacology, Vol.3. STAN-LEY KAISNER (ed.). Taylor & Francis:1985. Pp.366. Hbk ISBN 0-85066-327-X. £45.

Tropical Disease Research, Seventh Programme Report (1 January 1983–31 December 1984. UNDP/ WORLD BANK/WHO. World Health Organization: 1985. Pp. 272. Pbk ISBN 92-4-156085-1. SFr 45

Archaeology

Evolutionary Case Histories from the Fossil Record. Special Papers in Palaeontology, No.33. J.C.W. COPE and P.W. SKELTON (eds). The Palaeontological Association, London, UK:1985. Pp.202. Pbk ISBN 0038-6804. £30.

L'Environnement au Temps de la Prehistoire. By J. RENAULT-MISKOVSKY. Masson:1985. Pp.184. Pbk ISBN 2-225-80536-9. F 160.

Preserving Field Records: Archival Techniques for Archaeologists and Anthropologists. By MARY-ANNE KENWORTHY, ELEANOR M. KING, MARY ELIZABETH RUWELL and TRUDY VAN HOUTEN. The University Museum, University of Pennsylvania:1985. Pp.102. Pbk ISBN 0-934718-72-5. Np.

Quaternary Evolution of the Great Lakes. P.F. KARROW and P.E. CALKIN (eds). Geological Association of Canada:1985. Pp.258. Hbk ISBN 919216-29-3. \$42 (Canadian).

General

Advances in Heat Transfer. JAMES P. HART-NETT and THOMAS F. IRVINE Jr (eds). Academic:1985. Pp.360. Hbk ISBN 0-12-020017-1. \$79.00

Atti della Società Toscana di Scienza Naturali Residente in Pisa, Serie A (1984). Grafiche Pacini Editore:1985. Pp.264. Pbk np.

Atti della Società Toscana de Scienza Naturali Residente in Pisa, Serie B (1984). Grafiche Pacini Editore: 1985. Pbk np.

Concert Hall Acoustics. By Y. ANDO. Springer-Verlag: 1985. Pp. 151. Hbk ISBN 3-540-13505-7. DM

The Countryside in Winter. By BRIAN JACK-MAN. Hutchinson:1985. Pp.160. Hbk ISBN 0-09-161810-X. £12.95.

Dynamical Systems: A Differential Geometric Approach to Symmetry and Reduction. By GIU-SEPPE MARMO et al. Wiley:1985. Pp. 377. ISBN 0-471-90339-6. £36.95.

Economic and Medicinal Plant Research, Vol. 1. H. WAGNER, HIROSHI HIKINO and NORMAN R. FARNSWORTH (eds). Academic:1985. Pp.285. Pbk ISBN 0-12-730062-7. £60.50, \$69.50.

Energy and Ecology. By DAVID M. GATES. Sinauer Associates, Inc., Sunderland, Massachusetts: 1985. Pp.377. Hbk ISBN 0-87893-230-5; pbk ISBN 0-87893-231-3. Hbk £37.50; pbk £23.50.

Explosive Remnants of War: Mitigating the Effects. ARTHUR H. WESTING (ed.). Taylor and Francis:1985. Pp.143. Hbk ISBN 0-85066-303-2. \$25.00, £14.00.

Frantz Fanon and the Psychology of Oppression. By HUSSEIN ABDILAHI BULHAM. Plenum:1985. Pp.299. Hbk ISBN 0-306-41950-5. Np.

Here the People Rule: Selected Essays. By ED-WARD C. BANFIELD. Plenum:1985. Pp.348. ISBN 0-306-41969-6. Np.

An Introduction to Twistor Theory. By S.A. HUG-GETT and K.P. TOD. Cambridge University Press:1985. Pp.145. ISBN 0-521-30879-8. Hbk £20, \$39.50; pbk £6.95, \$13.95.

Katahdin: A Guide to Baxter State Park and Katahdin. By STEPHEN CLARK. Thorndike Press, PO Box 157, Thorndike, Maine 04986, USA:1985. Pp.211. ISBN 0-89621-092-8. Pbk \$8.95.

The Living House. By GEORGE ORDISH. Bodley Head: 1985. Pp. 256. ISBN 0-370-30499-3. £12.95.

Metamorphic Reactions: Kinetics, Textures and Deformation. A.B. THOMPSON and D.C. RUBIE (eds). Springer-Verlag:1985. Pp.291. ISBN 0-387-96077-5. DM 154.

Multiple Time Scales, JEREMIAH U. BRACK-BILL and BRUCE I. COHEN (eds). Academic:1985. Pp. 442. ISBN 0-12-123420-7, \$75, £65.

Plain Pictures of Plain Doctoring, By JOHN D. STOECKLE and GEORGE ABBOTT WHITE. MIT Press:1985. Pp.250. ISBN 0-262-19236-5. \$19.95.

Quaternary Science Reviews, Vol 3, D.Q. BOWEN (ed.). Pergamon Press:1985. Hbk ISBN 0-08-032760-5. \$96.00, £60.00.

Scientometric Indicators. By T. BRAUN, W. GLÄNZEL and A. SCHUBERT. World Scientific:1985. Pp. 424. ISBN 9971-966-69-7. £29.60.

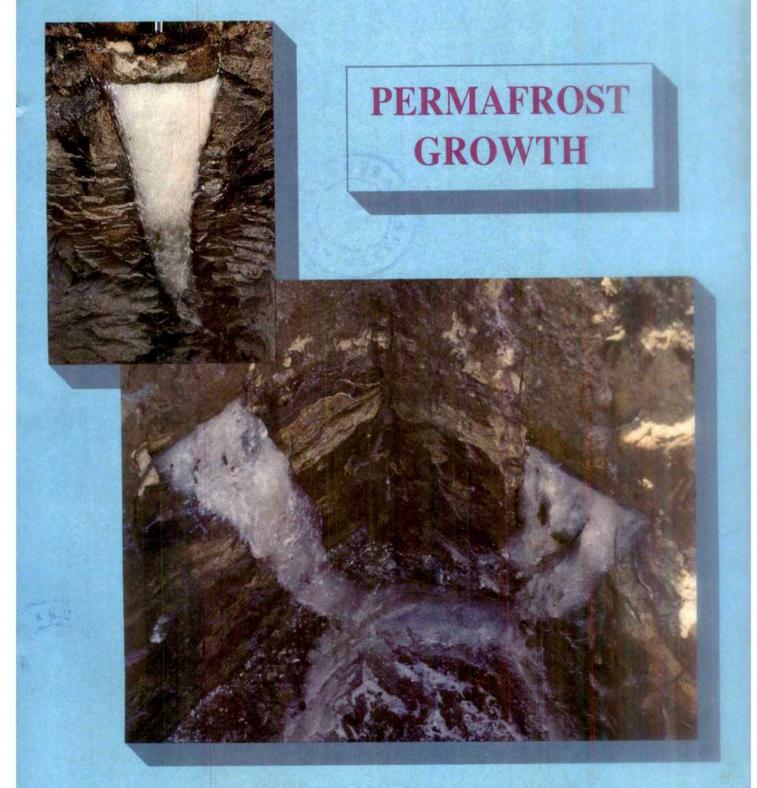
Surnames and Genetic Structure. By G.W. LAS-KER. Cambridge University Press:1985. Pp.148. Hbk. ISBN 0-521-30285-4. £15.00, \$24.95.

The Toxic Time Bomb. By SAM ZIFF. Thorsons Publishers, Wellingborough, Northamptonshire:1985. Pp.171. Pbk ISBN 0-7225-1232-5. £2.99.

Voyage of the Iceberg: The Story of the Iceberg that Sank the Titanic. By RICHARD BROWN. Bodley Head: 1985. Pp. 160. ISBN 0-370-30628-7. £9.95.

10 atule International Weekly Journal of Science

Volume 322 No.6081 21-27 August 1986 £1.90



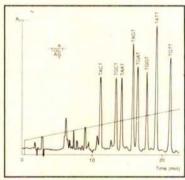


No other medium combines such high selectivity with such versatility. MinoRPC is unparalleled. It is optimised to give you fast, high resolution results.

To ensure high reproducibility, we have developed a special synthesis. You can always rely on MinoRPC to be the same every time we make it; every time you use it. And for that extra efficiency and reproducibility, you can work at elevated temperatures, carefully controlled by the Pharmacia high performance Column Heater.

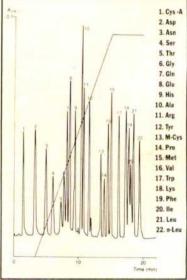
MinoRPC reflects the high standard you've come to expect from Pharmacia. Our contribution to high performance liquid chromatography has already brought success to thousands of chromatographers.

Share the success. Contact your local Pharmacia representative for more information on columns prepacked with MinoRPC.

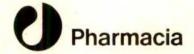


SEPARATION OF OLIGONUCLEOTIDE: "WOBBLE SEQUENCES."

MinoRPC IS PART OF THE FPLC SYSTEM, TODAY'S MOST VERSATILE AND BIOCOM-PATIBLE CHROMATOGRAPHY PROGRAM FOR THE FAST SEPARATION OF BIOMOLECULES

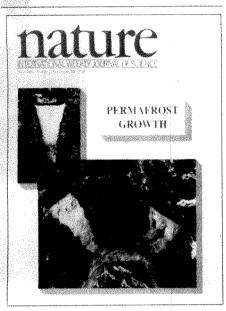


ANALYSIS OF PTH-DERIVATIZED AMINO ACIDS



nature

NATURE VOL. 322 21 AUGUST 1986



Sections of ice-wedges from the permafrost of the Canadian subarctic. As is discussed on pages 724 to 727, these palaeoclimatic indicators have been used to reveal the behaviour of the permafrost following deforestation during the Holocene. See also News and Views p.683.

-OPINION

01 11 11 01 1	
Can there be an end to spying?	671
Chernobyl made plainer	672
NEWS	
Official Chernobyl report	673
Environmental research	
Rocket launchers	674
US space policy	
More open UK research?	675
Creation science	676
Price—Anderson Act Change of priorities in French scier	
Israel's water	677
Fossil bird shakes evolutionary hy	
Weapons potential	678
Computers thriving from NSF co	ffers
CORRESPONDENC	Έ
Falkland penguins/Turkish visas/	Lake
Malawi/Paranevehology/Nice tree	

NEWS AND VIEWS

What is the scientific literature? 681
Bacterial-plant conjugation:
A bizarre vegetal bestiality
Conrad Lichtenstein 682

Permafrost and ice-wedge	
growth	
Peter Worsley	683
Complement-like cytotoxicity?	
Kenneth B M Reid	684
Membrane biophysics: Surface	
conduction of protons	
MJSelwyn	685
Neutron stars in Nanjing	
Virginia Trimble	686
The ins and outs of antigen	
processing and presentation	
Ronald N Germain	687
-SCIENTIFIC CORRESPONDENCE	E
Radionuclide deposition from	
the Chernobyl cloud	

will there be? S Islam

How many reactor accidents

FR Smith &

M J Clark

& K Lindgren

In ruminant thyroids after
nuclear releases
IR Falconer
Fault striations slip from sight?
C A Boulter

-BOOK REVIEWS

The Nemesis Affair: A Story of the Death of Dinosaurs and the Ways of Science by D M Raup 693 Colin Patterson Science in the Provinces: Scientific Communities and Provincial Leadership in France, 1860 - 1930 by MJ Nye Robert Fox The Stones of Britain by R Muir DV Ager **Blackbirds of the Americas** by G Orians 695 Frances C James World Resources 1986: World Resources Institute and International Institute for Environment and Development Lynton K Caldwell The Vital Force: A Study of Bioenergetics by F M Harold 696 Owen T G Jones

REVIEW ARTICLE

Gene regulation by proteins acting nearby and at a distance M Ptashne

ARTICLES

Melting history of Antarctica	during
the past 60,000 years	
L D Labeyrie, J J Pichon,	
M Labracherie, P Ippolito.	
J Duprat & J C Duplessy	70

Generation of single-stranded
T-DNA transfer from Agrobacterium tumefaciens to plant cells
S E Stachel, B Timmerman
& P Zambryski
706

-LETTERS TO NATURE

Binary pulsar with a very small mass function R J Dewey, C M Maguire, L A Rawley, G H Stokes

690

692

692

& J H Taylor 712
New millisecond pulsar

in a binary system
D J Segelstein, L A Rawley,
D R Stinebring, A S Fruchter
& J H Taylor

Repulsive regularities of water structure in ices and crystalline hydrates HF1Savage & 11 Finney

GA Cutter & TM Church

HFJ Savage & JL Finney 717

Selenium in western

Atlantic precipitation

720

722

724

727

730

711

Correlations between stream sulphate and regional SO, emissions R A Smith & R B Alexander

Dating ice-wedge growth in subarctic peatlands following deforestation S Payette, L Gauthier & I Grenier

Hydrocarbon shows and petroleum source rocks in sediments as old as 1.7×10° years M J Jackson, T G Powell, R E Summons & 1 P Sweet

Amino acid epimerization in planktonic foraminifera suggests slow sedimentation rates for Alpha Ridge, Arctic Ocean S A Macko & A E Aksu

Thermal and mechanical constraints on the lithosphere beneath the Marquesas swell K M Fischer, M A McNutt

K M Fischer, M A McNut & L Shure

Contents continued overleaf

Nature* (ISSN 0028-0836) is published weekly on Thursday, except the last week in December, by Macmillan Journals Ltd and includes the Annual Index (mailed in February). Annual subscription for USA and Canada US \$240. USA and Canadian orders to: Nature, Subscription Dept. PO Box 1501. Neptune. NJ 07753, USA. Other orders to Nature. Brunel Road, Basingstoke. Hants RG21 2XS, UK. Second class postage paid at New York, NY 10012 and additional mailing offices. Authorization to photocopy material for internal or personal use, or internal or internal or personal use, or internal or internal or personal use, or internal or in

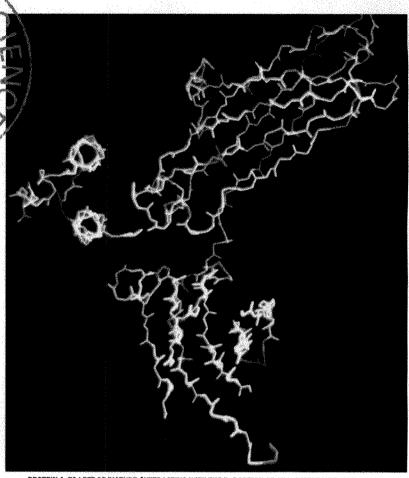
WHY WOULD ANYBODY **WANTAN** ANTIBODY?

For a wide variety of reasons: Today, monoclonal antibodies can be used as aids to purification. diagnostic reagents, cell surface probes... the list grows for these most versatile of molecules. As a group, they represent one of the

most purified proteins in the world today.

Protein A-Sepharose® CL-4B provides the almost universal chromatographic method to purify monoclonal antibodies, a fact that is comforting after the inevitable investment in time necessary to produce them. It is fortunate that, for such a diverse representative or, should you require it, group of molecules, they are relatively easy ask for further information. In addition to to purify.

As soon as Pharmacia recognised the importance of Protein A specificity for antibodies, we utilised it in an affinity chromatography matrix; using our knowledge to give you success with confidence.



PROTEIN A, TO LEFT OF PICTURE, INTERACTING WITH THE Fc PORTION OF AN IEG MOLECULE, THE HINGE REGION IS CLEARLY VISIBLE. THREE DIMENSIONAL COMPUTER MODEL DERIVED USING FRODO SOFTWARE (T. ALWYN JONES) AND BASED ON X-RAY CRYSTALLOGRAPHY DATA (J. DEISENHOFER, BIOCHEMISTRY 20, 1981, 2361-2370) SUPPLIED BY THE PROTEIN DATA BANK.

Confidence in a product attested by thousands of researchers. Confidence in a product that comes from the biggest manufacturer of affinity chromatography media in the world.

To order, contact your Pharmacia product information, we have a comprehensive Reference List which we would be pleased to send you.

ORDERING INFORMATION	CODE NO.	PACK	FORM SUPPLIED
PROTEIN A-SEPHAROSE® CL-4B	17-0780-01	1.5 g/5 ml	FREEZE DRIED
PROTEIN A-SEPHAROSE* CL-4B	17-0963-03	25 mi	PRESWOLLEN



That important research article you've been looking for located instantly!



If you store your copies of Nature for future reference, then the annual index of subject and author is an essential part of your collection. These comprehensive annual indexes are available for all issues of Nature from 1971 to 1985.

Prices and address for orders are set out below.

		•
Annual Subscription Pr UK & Irish Republic	ices	£104
USA & Canada		US\$240
Australia, NZ &		
S. Africa	Airspeed	£150
	Airmail	£190
Continental Europe	Airspeed	£125
India	Airspeed	£120
	Airmail	£190
Japan	Airspeed	Y9(KR))
Rest of World	Surface	£120
	Airmail	£180
Orders (with remittance	e) to:	
USA & Canada	UK & Rest of	World
Nature	Nature	
Subscription Dept	Circulation D	ept
PO Box 1501	Brunel Road	
Neptune	Basingstoke	
NJ07753	Hants RG212	XS UK
USA	Tel: 0256 2924	
(The addresses of Natu		
facing the first editorial		
		į
Japanese subscription e		_
Japan Publications Trac		1
2-4 Sarugaku-cho l-cho	me	1

Chiyoda-ku, Tokyo, Japan Tel. (03) 292 3755 Personal subscription rates: These are available in some countries to subscribers paying by personal cheque or credit card. Details from: USA & Canada UK & Europe

Felicity Parker 65 Bleecker Street Nature 4 Little Essex Street London WC2R 3LF, UK Tel: 01-8366633 New York NY 10012, USA Tel: (212) 477-9600

Back issues: UK, £2.50; USA & Canada, US\$6.00 (surface), US\$9.00 (air); Rest of World, £3.00 surface), £4.00 (air)

Binders

Single binders: UK, £5.25: USA & Canada \$11.50; Rest of World, £7.75. Set of four: UK, £15.00: USA & Canada \$32.00; Rest of World, £22.00

Annual indexes (1971-1985) UK, £5,00 each; Rest of World, \$10,00

Nature First Issue Facsimile

UK, £2.00; Rest of World (surface), \$3.00; (air) \$4.00

Nature in microform

Write to University Microfilms International, 300 North Zeeb Road, Ann Arbor, MI 48106, USA

An enantiornithine bird from the Lower Cretaceous of Queensland, Australia R E Molnar

Oxytocin induces morphological plasticity in the adult hypo-

thalamo-neurohypophysial system DT Theodosis, C Montagnese, F Rodriguez, J-D Vincent

& D A Poulain

Serine esterase in cytolytic T lymphocytes

M S Pasternack. CR Verret, MA Liu & HN Eisen

Interferon response sequence potentiates activity of an enhancer in the promoter region of a mouse H-2 gene

A Israel, A Kimura, A Fournier, M Fellous & P Kourilsky

& JM Thornton

Continuous and discontinuous protein antigenic determinants D J Barlow, M S Edwards

Expression of a transfected human c-mvc oncogene inhibits differentiation of a mouse erythroleukaemia cell line

E Dmitrovsky, W M Kuehl, G F Hollis, I R Kirsch, TPBender & SSegal

DNA loops induced by cooperative binding of λ repressor J Griffith, A Hochschild & M Ptashne 750

Length growth in fission yeast cells measured by two novel techniques JW May & JM Mitchison 752

Propulsion of organelles isolated from Acanthamoeba along actin filaments by myosin-I

R J Adams & TD Pollard

Lateral proton conduction at lipid-water interfaces and its implications for the chemiosmotic-coupling hypothesis M Prats, J Teissie

& J-F Tocanne

MISCELLANY 100 years ago 686

NATURE CLASSIFIED

Professional appointments -Research posts — Studentships — Fellowships — Conferences Courses — Seminars — Symposia:

Back Pages

Next week in Nature:

- Fractal growth processes
- Galactic chemistry
- Microwaves and quasar lenses
- Ozone decrease in Antarctica
- Etna's plume

736

738

740

743

747

748

754

756

- Cretaceous/Tertiary boundary in Australia and New Zealand
- Bone nitrogen isotope ratios
- Sewage beneficial to lakes
- Breeders' rights
- Phenylketonuria mutation
- Functional Na channels from cloned DNA

GUIDE TO AUTHORS

Authors should be aware of the diversity of Nature's readership and should strive to be as widely under stood as possible

Review articles should be accessible to the whole readership. Most are commissioned, but unsolicited reviews are welcome (in which case prior consultation with the office is desirable).

Scientific articles are research reports whose conclussions are of general interest or which represent substantial advances of understanding. The text should not exceed 3.000 words and six displayed items (file gures olus tables). The article should include an italic heading of about 50 words.

Letters to Nature are ordinarily 1,000 words long with no more than four displayed items. The first page graph (not exceeding 150 words) should say what the letter is about, why the study it reports was undertaken and what the conclusions are

Matters arising are brief comments (up to 500 words) on articles and letters recently published in Nature. The originator of a Matters Arising contribution should initially send his manuscript to the author of the original paper and both parties should, wherever possible, agree on what is to be submitted

Manuscripts may be submitted either to London or Washington, Manuscripts should be typed (dead)le spacing) on one side of the paper only. Four copies are required, each accompanied by copies of lettered artwork. No title should exceed 80 characters in length. Reference lists, figure legends, etc. should be on separate sheets, all of which should be numbered Abbreviations, symbols, units, etc. should be identified on one copy of the manuscript at their first appearance.

References should appear sequentially indicated by superscripts, in the text and should be abbreviated according to the World List of Scientific Periodicals fourth edition (Butterworth 1963-65). The first and last page numbers of each reference should be eited. Reference to books should clearly indicate the publisher and the date and place of publication. Unpulslished articles should not be formally referred to unless accepted or submitted for publication, but may be mentioned in the text

Each piece of artwork should be clearly marked with the author's name and the figure number. Original artwork should be unlettered. Suggestions for cover illustrations are welcome. Original artwork tand one conv of the manuscript) will be returned when manusscripts cannot be published.

Important: Manuscripts or proofs sent by air courses should be declared as "manuscripts" and "value \$5" 30 prevent the imposition of Customs duty and Value Added Tax in the United Kingdom.

Requests for permission to reproduce material tradition Nature should be accompanied by a self-addresself tund, in the case of the United Kingdom and United States, stamped) envelope,

Why YOU should become a personal subscriber to Nature in 1986

There will never be a better opportunity than now to take advantage of our personal subscription scheme.... offering direct delivery to your home or to vour place of work at HALF PRICE!

Consider the convenience of having your own personal copy delivered each week carrying crucial research results, news and job opportunities in your specific field HOT OFF THE PRESS! When Nature is such a vital ingredient in your scientific career a subscription is a very small investment to make – in fact the cost works out at less than your daily newspaper.



All you need to do to subscribe is fill in the form below and send it with your personal payment FREEPOST to our offices in Basingstoke. You'll receive your first copy within four to six weeks of your order and thereafter weekly for a year. We *quarantee* that when we invite you to renew your subscription it will be at the lowest rate available.

Orde	er Form
------	---------

	Orde	i FOIIII
Return to: Circulation	Manager, FREEPOST Macmillan	Journals Ltd., Houndmills, Basingstoke, Hants, RG21 2X
☐ YES, please ente Nature at £52	r my personal subscription to	
☐ Lenclose my cheque ☐ Please charge my c	e for £52 made payable to Nature redit card account:	Name
Access Diners Club	☐ American Express ☐ Barclaycard	Address
Account No.	Expiry Date	
Signature		
Diamon allow 1 - 6 massker for	delivery of first issue. This after applies to l.k.	rocidents anh _averseas subscription rates in allable from alone address

nature

NATURE VOL. 322 21 AUGUST 1986

671

Can there be an end to spying?

Public espionage, a prolific source of scandal this year, is a serious cause of international friction, a restraint on good relations and even a perversion of national civility. Can it be restrained?

Spies and the public agencies employing them seem to be half way through another bad year. In the United States, a rash of prosecutions of ex-servicemen and ex-agents has made plain the uncomfortable if unsurprising truth that, in a market economy, even loyalty has a price. There has been particular chagrin in the United States at the revelation, unconvincingly disputed, that even the Israeli government has spent resources (from the US military aid budget?) keeping tabs on the government which is its own chief political and economic supporter. The United States has also found itself alternatively able to boast of a harvest of counter-intelligence information gathered from defectors and then embarrassed by the discovery that defectors can defect back again. This painful double and even triple dealing, unfamiliar in the United States, is well-known in Western Europe, where 1986 (so far) has seen yet another eastern intelligence network unmasked in West Germany, the usual crop of expulsions of Soviet diplomats from western capitals (followed by retaliatory expulsions from Moscow) and a general reinforcement of the sense that secrets are no longer safe, whatever they may be. Spies, and their employers, must be asking whether their game is still worth playing.

The issue is further sharpened by the latest twist in the long saga of double-espionage in Britain, a matter of public record since the defection of two Foreign Office officials to the Soviet Union in the 1950s, in circumstances suggesting a tip-off from a sympathizer in counter-intelligence. Who might that have been? The first candidate to come to light was Mr Kim Philby, off and on employed as a British spy, who was recognized (after his disappearance to Moscow in the 1960s) to have been a Soviet agent as well. A second is Sir Anthony Blunt, himself a one-time member of British intelligence, afterwards curator of the Royal family's art collection, who was discovered to have recruited Philby as a double agent and who was stripped of his knighthood a short while before his death. A third is Sir Christopher Hollis, who was for several years the head of one half of the British intelligence network, that called MI5, and who is now (after his death) accused of having been another double agent. One result is yet another bout of speculation about the motives of those who become spies, the supposedly special motives of those who become double spies and the efficiency of the services which employ them.

Moles

The latest most bizarre development concerns Hollis and related matters. In 1981, the British prime minister, Mrs Margaret Thatcher, said that the accusations that he was a double agent had been considered and that they could not be sustained. But, last week, lawyers representing the British government before an Australian court which is being asked to restrain publication of a book by a British ex-agent, said they were prepared to acknowledge, for the purposes of that hearing only, the truth of the allegations against Hollis. (The British courts have already given the government an injunction preventing two British newspapers from serializing the disputed book and even from reporting its allegations.) The strategem will have the effect of concentrating the court's deliberations on the claim that publica-

tion would be a breach of confidentiality, but it is bound to sound like a version of that confusing lawyers' doublespeak typified by the defence of a person against a murder charge which asserts that the defendant acted out of self-defence and was, in any case, elsewhere at the time.

Whatever happens in the Australian courts, the British government is bound to find itself under further pressure to tell more when the British Parliament reassembles in October. The position that the validity of the allegations is irrelevant to the trial is legitimate enough, but it will be interesting to see whether the British government's lawyers can persuade an Australian court that a breach of its contractual relationship with an exemployee can damage the Australian national interest. Meanwhile, the government's critics might usefully use the interval to clarify their complaint: is it the narrow complaint that the government (retrospectively) is incompetent in having allowed its intelligence services to be riddled with double agents or that, these days, there should be more intelligent ways of conducting these affairs?

Vanity

Double agents, whatever their motives, are an inescapable part of the spy business. Those who doubt that should read an account of the mismanagement of the British Special Operations Executive (SOE), a secret organization set up in Germanoccupied France in 1940, which has been contributed to Intelligence Quarterly (a London-based newsletter) by one James Rusbridger, himself an ex-agent. SOE and its doings has become part of the mock-heroic folklore of British exploits during the Second World War. The chief objective was to help organize indigenous resistance to the occupation, but SOE was put together hurriedly, amateurishly and in a way that guaranteed that German intelligence would know what was afoot. One especially damaging double agent, according to Rusbridger, was a Frenchman called Dericourt who was from September 1942 both SOE's Paris agent for the transport of people into and out of France and a regular confidant of the German counterintelligence agencies. When members of the SOE network were being arrested by the score (usually to be executed), how was Dericourt allowed to carry on? Rusbridger's arresting explanation is that his immediate boss in London, parachuted into France with a radio operator to discover what had gone wrong with the network's security, was warned by Dericourt that he would be arrested at a planned rendezvous and so sent his operator to the assignment and to a predictable death. The guilf engendered ensured safe conduct for the French double agent in the damaging months that followed.

What this unheroic tale shows is that all kinds of venality can contribute to the recruitment of agents and double agents and to their survival. But that does not explain the rash of double agents with which the professional intelligence services have been afflicted in the past half-century. Why have so many talented people chosen this tortured and, for some, disastrous way of earning a living? Part of the explanation is that given by Mr Andrew Sinclair earlier this year (see William Cooper's review in *Nature* 322, 317; 1986); now-unfashionable intellectual

coteries (in this case, the Cambridge-based "society of the apostles") may engender that blend of vanity and arrogance that tempts people to believe they can mould the course of history by the secret exercise of their own wits. But in reality it is a shabby business, not merely damaging for those concerned when they are found out and for those whom they betray meanwhile, but for the conduct of normal relations between intellectual communities throughout the world.

The ubiquity of the spy has become an abomination. In many parts of the world, scientists and other intellectuals are habitually supposed to be potential agents when they travel abroad—and may be suspected of potential treason when they return. Who knows how much of the present fragmentation between East and West of the science enterprise derives from the brooding suspicion of the intelligence agencies, vulnerable though they are themselves to infiltration, of the movement of people from one place to another?

That is merely one of the reasons why the time has come to put intelligence-gathering on a proper footing. Another, perhaps even more urgent, is that the repeated discovery of espionage networks in different places is a constant source of sourness in international relations. That intelligence services from time to time embark deliberately on subversive and even criminal activities, and must otherwise operate in some degree outside the normal rules of public accountability, is especially offensive. That many advanced societies must now put up with the indignity of self-imposed self-surveillance by telephone tapping and other such means is another part of the price that everybody pays for the dubious luxury of sustaining espionage. What can possibly be done to restrain not so much the curiosity of governments about what others do (which is legitimate), but the means by which they seek to satisfy that curiosity?

The best hope of progress must be technical, based on the use of electronic means of monitoring and analysing other people's electronic messages. This is the chief function of the National Security Agency in the United States and the General Communications Headquarters (GCHQ) in Britain, which in principle offer a means of learning about the military capabilities of other governments without requiring that people elsewhere should be actively disloyal. Is it entirely out of court that the major espionage governments should agree among themselves to rely on devices such as these wherever possible? (The fact that even organizations such as GCHQ may be penetrated by spies, as has been spectacularly demonstrated in Britain, is probably not nearly as relevant as it seems; those with secrets to hide should be able to guess which are at risk from listening posts and should plan accordingly.) Economic and political secrets, also common objectives of intelligence agencies, are less easily accessible to electronic surveillance, but are much more often within reach of an intelligent reading of other people's newspapers than the intelligence community would like to think. The underlying fallacy of much of what the intelligence services get up to is the assumption that each marginal element of information is almost priceless. Especially when the price already being paid includes a large element of self-imposed illiberality, this cannot be the case

But an agreement to restrain mutual curiosity, even if it were a formal convention, would hardly be sufficient by itself. Why not go further, and amend the Vienna Convention that regulates the use made of diplomatic missions in such a way as to deprive diplomats found guilty of espionage of the immunity from prosecution which they enjoy at present? There would be obvious difficulties is getting governments to agree that their nationals should be tried under other national laws, which vary enormously both in what they require as evidence and in penalties they impose, but it should not be beyond the wit of well-intended people to develop a system of international criminal law to meet the need for an effective stick to beat the spies. The carrot, of course, is the benefit of the civility that would follow for the rest of us.

Chernobyl made plain

This is what the Soviet Union should say next week about the Chernobyl accident, and why.

NEXT week, there will be a gathering in Vienna, under the auspices of the International Atomic Energy Agency, to discuss the report prepared by the Soviet Union on the reasons for the accident at the Chernobyl reactor at the end of April. Only the sketchiest information about the Soviet document is as yet available (see opposite), and is certainly not sufficient in itself to satisfy legitimate curiosity elsewhere about the accident and its consequences. The chances are that even the full report will not do that: most official statements hurriedly put together leave unanswered questions that are best dealt with in the kinds of technical discussions arranged for next week, and in which the Soviet Union has agreed to take part. So far, so good.

That there is a legitimate curiosity in what happened at Chernobyl may seem to many in the Soviet Union to beg the question of the right by which people elsewhere inquire into strictly domestic matters, such as the arrangements for generating electricity. The simple answer, that the Chernobyl accident polluted the territory of other nations, is only part of the reason why some kind of explanation must be forthcoming, and by itself only requires from the Soviet Union an estimate of the amount and composition of the radioactivity released, an attempt to agree on estimates of the damage that may have been done with those affected and, if appropriate, an undertaking that there would be negotiations about compensation. Nothing has been heard, as vet, about formal demands for compensation, which would have to be raised through diplomatic channels by the governments believing themselves to have been injured, not at technical meetings such as that planned for next week. Meanwhile, the Soviet Union has implicitly acknowledged a wider legitimate interest in Chernobyl by its agreement to appear in Vienna.

A second explanation, but equally insufficient, for the Soviet decision to say more than the bare minimum is the need to head off future trouble with now-nervous neighbours. Long before the accident, there were protests about the siting of reactors near the borders between France and Belgium and between Czechoslovakia and Austria. So far, there has been relatively little complaint about Soviet reactor policy from the countries most at risk, those of the Warsaw Pact in Eastern Europe, but that may require special explanation. It is common prudence to take whatever steps are possible to anticipate and counter such anxieties. But the Soviet Union has gone further by agreeing to participate at Vienna and by doing some homework in advance.

What else can the world legitimately ask of the Soviet Union? Because even the Chernobyl accident might have been worse, people elsewhere have a right to be assured that the management of these complicated machines is conducted with the zealous regard for worked-out procedures which is the nuclear industry's standard boast on its own behalf. As things are shaping up, the Soviet Union plainly intends to meet this demand indirectly, by using an account of how laid-down procedures were not followed to suggest that the same need never happen again. But such an account will not suffice. Inevitably, and properly, questions will be raised at Vienna about the arrangements now in place for regulating the use of nuclear reactors. By what means are matters like this decided? Who are the people concerned? These will be painful questions for the Soviet Union to answer, but they cannot easily be ducked. Beyond them are the even larger issues in which external curiosity is legitimate: what can be gleaned over the years about the effects of radiation on people exposed to excessive doses of it? And what, in any case, is being done to safeguard or even monitor those at risk? There is no requirement in international law that one country must account to others for its care of its own people, but these exceptional circumstances require concessions even in that direction.

Official Chernobyl report

Timetable for a reactor disaster begins to emerge

THE Soviet report on the Chernobyl reactor accident, distributed to the Vienna delegations to the International Atomic Energy Agency last week, is said by those who have read it to be strong on details of the reactor design but thin on details of how the accident happened. But the sequence of events leading to the accident. and more details of the "unauthorized experiment" said to have been under way on 25-26 April, have emerged.

For the first time since the accident, there are suggestions in the Soviet document that the RBMK reactor design is not fault-free. Thus the report suggests that existing reactors of this type should be modified by means of longer control rods, 2.4 per cent uranium enrichment (now 2.0 per cent) and extra reactor sensors even if these measures "degrade the economics" of the reactor type.

The report is intended as the basis for a discussion of the accident to be held at Vienna next week. The confusion attending its appearance stems from what appears to have been a Soviet requirement that the agency itself should distribute the report to national delegations only, but allowing national delegations to deal with the document (382 pages of Russian text) as they see fit.

Other information about the content of the report has appeared in Sweden and from the Atomic Industrial Forum of the United States which on Monday this week released a brief summary of the sequence of events leading to the accident. The forum said that "at first glance... the report appears to be complete and frank".

According to a report in the Japanese newspapers Asahi Shimbun, the "experiment" was intended to determine the amount of energy that might be recovered from a spinning electrical generating set and the coupled steam turbine after the steam input had been disconnected. According to this account, more than one assessment of this kind was planned, using the generating set at Chernobyl called Number 7 and for this reason, the reactor providing steam for the generator was not shut down. However, the system that would have caused the reactor to shut down of its own accord was disabled.

One of the difficulties in reconstructing the course of events at Chernobyl reactor Number 4 appears to have been that the data-recording system used for monitoring normal operations had been switched to the monitoring of the electrical test. with the result that capacity for the recording of reactor data had been preempted. As a consequence, the sequence of events has had to be inferred from a mathematical model of the reactor.

The sequence of events began roughly 24 hours before the first release of radioactivity, at 01:00 local time on 25 April. when steps were taken to reduce the operating power of the reactor. Twelve hours later, at 13.05, the Number 7 turbine generator was disconnected from the system, but its electrical output switched to turbine Number 8. These are two generating sets handling the thermal outputs of the damaged reactor, Number 4 out of four completed reactors at the site.

The rate at which the speed of the Number 7 generating set would have declined would have been determined by the magnitude of the external electrical load. The emergency cooling system was disabled at 14.00 on 25 April, but the report says that the control room explicitly instructed that the reactor should continue

When instabilities appeared, two extra pumps were added to the water-cooling circuit some three and seven minutes respectively after 01.00 on 26 April, but the Soviet document says that the reactivity of the reactor had reached the point, at 01.22, at which the reactor should immediately have been shut down. In the event, the reports say, the operators persisted with their experiments on the turbines, including the closing of the stop control valve of turbine Number 8 four seconds after 01.23 on 26 April.

Within half a minute, the accounts continue, the reactor began to generate more power, and the operatives sought to close it down by means of the control rods. But in the event, the full entry of the rods was prevented by an explosion. A witness is reported as saying that he heard two loud explosions at that time and saw a fireball

scattering sparks on the roof.

The Soviet report outlines a series of errors in safety procedures of which the reactor staff were guilty, including the disablement of all but six or eight of the control rods with which the reactor is equipped, and the disablement of the power control system that would normally maintain the power output near that for which the machine was designed. The result is that control of the reactor would have been more difficult. The decision to disable the automatic shut-down system for the reactor would have made it necessary to use manual procedures for controlling the power output in case of an emer-

One of the puzzling features of the report is the statement that, after the explosions, the temperature of the uranium fuel increased to between 1,600 and 1,800 °C, hot enough to volatilize some fission products but not enough to vapourize the refractory components of the fuel. But that step could be the one that apparently led to the further release of radioactivity on 29 April.

Environmental research

Making the most of Chernobyl

BRITISH scientists are hoping that a £1 million package of research projects can be put together to seize the scientific opportunities presented by the Chernobyl nuclear accident. Radionuclides were released into the atmosphere on a scale that would never be contemplated experimentally, giving a unique chance to study their pathways in the environment.

An expert committee organized by the Natural Environment Research Council, the Coordinating Group on Environmental Radioactivity, hopes to include researchers from government departments, the universities, the Central Electricity Generating Board, British Nuclear Fuels and the Meteorological Office in an integrated programme. Much of the information gained would be of direct benefit for it would aid understanding of the consequences of other accidental releases of radioactive material.

Studies carried out so far already reveal a few surprises. Radionuclides are much "stickier" than expected; once deposited on vegetation they are not quickly washed into the soil. Thunderstorms, triggered as warm, moist air containing the plume of fall-out, prove to be particularly effective in washing radionuclides out of the atmosphere (see p.690 of this issue). These topics will be studied further: others needing attention are the overall pattern of deposition, which is highly heterogenous; the storage of radionuclides in snow and their release on melting; and whether the radionuclide pulse will confuse other studies on radionuclides in the environment.

Any programme would best be integrated with an overall European effort. Already attempts are under way for collaboration within the European Economic Community and it is possible that some money might be found from the European Commission. Otherwise national programmes will have to be tied together and funds for the British part must come from other programmes - there is little chance of extra money being granted in present political circumstances. Alun Anderson

Rocket launchers

Japan enters the space race

AFTER the successful launch of the H-I rocket last week, Japan's rocket experts are bursting with confidence. For now nothing seems to stand in the way of Japan entering the commercial satellite launching business in the 1990's — nothing, except perhaps a small group of tuna fishermen.

The two-stage H-I rocket blasted off from the National Space Development Agency (NASDA)'s space centre on Tanegashima island southwest of Kyushu at 5.45 am on 13 August. About 4 minutes later, the domestically-built cryogenic second-stage engine burst into life boosting the launcher into an eliptical orbit 1,500 km above the Pacific. Coasting over South America about 50 minutes later, the second-stage reignited for a brief 20-second burn that transfered the launcher to a circular orbit before release of first the Experimental Geodetic later named (Hydrangea), and then the Japan Amateur Satellite-1, christened "Fuji" (Wisteria).

News that radiowaves from Fuji had been received in Chile was greeted with shouts of "banzai" at the headquarters of the Japan Amateur Radio League whose members have invested 5 years and 120 million ven (£0.5 million) in building Japan's first ham radio satellite. It is only to be hoped that Japan's 720,000 ham enthusiasts do not overtax the little 50 kg satellite. Takeshi Saito, the league's amateur satellite committee chairman remembers with embarassment an incident three years ago when Japanese hams jammed the frequency band for communication with the US space shuttle Columbia and then vented their frustration by trading abuses such as "bakayaro!" - meaning "you idiot"

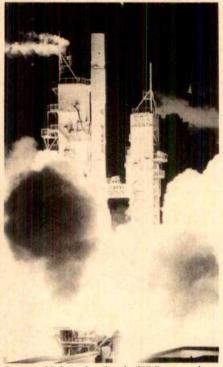
Equipped with 10 channels for analog communications and four for digital, Fuji comes over the Japanese archipelago six times a day permitting communications for about 10 minutes each time. A digital relay allows storage of messages which can be retransmitted on the other side of the Earth.

Ajisai, a 2-m diameter mirror ball to be used for triangulation surveys was also successfully put into orbit alongside Fuji. But the real hero of the day was the H-I rocket itself.

The LE5 second-stage cryogenic engine developed by NASDA at a cost of 44 billion yen (£192 million) performed flawlessly, as did the Japanese-built inertial guidance system. And in a spectacular finale five hours into orbit, the LE5 released a burst of liquid hydrogen fuel over the eastern United States, prompting reports of UFOs and exploding

satellites. This is the first time the US has found itself downrange of a nation with cryogenic launchers, and may be an omen of things to come.

Japan can now forge ahead with development of the bigger H-II which is scheduled for completion in 1991 and will be entirely made in Japan. The stage will then be set for Japan to enter the commercial market for satellite launchers. But will NASDA be able to increase launch frequency at its Tanegashima



Last week's launch utilized a US first stage but a Japanese cryogenic second stage.

Space Centre to meet the demands of foreign users?

The waters off Tanegashima teem with tuna, and under an agreement with the local fishing cooperative NASDA can only launch rockets during 90 days of the year, 45 days in summer and 45 in winter. This effectively limits NASDA to two launches a year, and for "compensation" NASDA annually pays the fishermen 600 million yen (£2.6 million). This is over and above the 1,300 million yen reputedly paid to the fishermen when the launch site was first built.

The only inconvenience to fishermen is that during the launch a 300 km² area of ocean extending about 30 km downrange of the launch site is closed to shipping. But fishing cooperatives in Japan, like other rural groups loyal to the ruling Liberal Democratic Party, have considerable political power. And if NASDA wishes to increase launch frequency in the 1990s, the local fishermen will have the final say.

David Swinbanks

US space policy

No business for new shuttle

Washington

PRESIDENT Reagan last week ended months of uncertainty over the future of the US space programme by telling the National Aeronautics and Space Administration (NASA) to build another space shuttle orbiter to replace Challenger, thus restoring the size of the shuttle fleet to four. Reagan also signalled a major policy turnaround by saying that NASA would not in future be allowed to compete with the private sector to launch commercial satellites on the shuttle, but would instead concentrate on military and research payloads. The announcement marks the end of the policy of trying to make the shuttle commercially viable.

Senior administration officials have for some months been divided over how a replacement shuttle would be paid for, and last week's announcement from the White House did little to clarify where the required \$2,800 million will be found. The White House plans to ask Congress for \$2,350 million in extra budget authority for NASA over the next 5 years, using in part "unspent funds" from other government agencies. But it is unclear to what extent NASA's other programmes will be affected. Some additional belt-tightening at the agency seems a possibility, although Reagan renewed his commitment to build a space station.

The replacement shuttle will incorporate several improvements to the existing models. New brakes, engines and computer systems were mentioned, as well as other possible safety improvements recommended by the Rogers commission into the *Challenger* accident. The new orbiter is not expected to be completed until 1991.

Of the 44 commercial satellites NASA is already contracted to launch aboard the shuttle, only 16 will be launched by NASA before 1992. The remainder may be shifted back to commercial unmanned launch vehicles. But because it has been US policy to rely on the space shuttle as the nation's main launch system, US aerospace manufacturers have been unwilling to get into the private launching business, and even if there is now a scramble to manufacture new commercial launchers - which some doubt - many of the payloads that might have flown on the shuttle seem destined to be launched by foreign commercial services. Besides the French Ariane rockets, which are booked up for the next several years, both China and Japan have embryonic launching services that may take a significant proportion of the backlog of satellites now waiting to be launched. **Tim Beardsley** UK research

Call for more open councils

REFORM of Britain's research councils is called for in a new report from a body representing more than two-thirds of university teaching and research staff. The Association of University Teachers (AUT) wants to see more open research councils among a host of other changes it claims are necessary to deal with the "crisis" in university research.

The crisis is attributed to the breakdown of the dual-funding system. Although the universities carry out more than half of all basic research in the United Kindgom, the budget supplied through the University Grants Committee (UGC) (to maintain "well-founded" laboratories) and the five research councils (to support research projects) has declined in real terms while the costs of research are rising rapidly. Increasing numbers of researchers are joining the brain drain; libraries have had to cut back book purchases by 40 per cent since the 1970s; the student/staff ratio has deteriorated; and an increasing percentage of researchers face an uncertain life on short-term contracts.

The fight put up by UGC and the research councils to try to remedy matters seems not to have impressed AUT. UGC's new policy of trying to assess the quality of research carried out at different university departments and to concentrate scarce resources at those rated highly is seen as exacerbating the effects of the cuts and is "emphatically rejected". Selectivity, the report says, favours those areas in which short-term returns can be easily identified while university research should be of the "fundamental kind" from which "major breakthroughs rather than marginal advances result". The effect of selectivity may undermine university autonomy and create a hierarchy of universities.

The five research councils come in for some criticism. Their "success. . . in predicting growth areas in research has not been great", the report says. The councils are appointed by the Secretary of State but AUT believe they should be more directly representative of scientists. Nominations to the councils and their committees should be by learned societies and regular open meetings held to discuss priorities in research funding. Particular difficulties now arise because not all research proposals rated "alpha" (to be funded "at all costs") by peer review can now be funded. In that sense the report says "peer review has broken down" and personal views may be substituted. Safeguards to ensure that committee members do not receive preferential treatment, and full explanations of all decisions, including the reasons for choices between applicants, given publicly, are called for.

The Advisory Board for the Research

Councils (ABRC) could also be made more open, the report says. Each year, in its advice to government, the board has protested more strongly about the parlous condition of the universities. But the government shows little sign of listening. To add clout the report suggests that Parliament be given the right to discuss the advice of ABRC and to cross-question it. Whether this could be done without changing ABRC's status is not yet clear.

An additional body is needed as a national forum to discuss research and development policy. The National Economic Development Council, an organization with representation from government, industry and unions, would be suitable.

British industry is seen as needing encouragement to commission research in the universities: there is evidence that foreign industrial investment in British universities exceeds that of British companies. Changes in tax-exemption rules and the establishment of a fund to help small firms sponsor university research are possible solutions.

Alun Anderson

Creation science

Nobel laureates go into battle

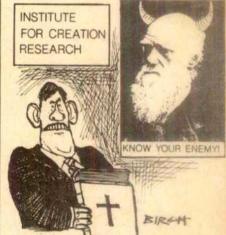
Washington

SEVENTY-TWO US Nobel laureates have signed a brief filed with the Supreme Court this week urging the court to declare unconstitutional a Louisiana law requiring balanced treatment of evolution and creation in state schools. According to organizers of the brief, this is the largest group of Nobel laureates ever to sign a single document.

The Supreme Court agreed in May to hear arguments on the constitutionality of the Lousiana statute. In 1982, a federal district court struck down a similar Arkansas law because definitions in the law made it clear that creation science was directly derived from descriptions of creation in the Bible. The Louisiana statute removed the specific definitions of what creation science is, leaving only the tautology that creation science means "the scientific evidences [sic] for creation". The Nobel laureates' brief sets out to show that the Louisiana statute originally included language similar to the Arkansas statute. but lawmakers altered it after the Arkansas decision. The brief further attacks the law for singling out evolution as a theory. rather than emphasizing the uniformly tentative nature of science and argues that by creating a distinction between scientific



Murray Gell-Mann, one of the laureates leading the fight against the "forces of darkness".



fact and evolutionary theory, the statute implicitly tells schoolchildren that "while most of what they learn in science class is 'proven scientific fact', evolution is not".

Murray Gell-Mann, who won the Nobel prize for physics in 1969, says it is not just biological science that has come under attack from creationists. Gell-Mann feels the Lousiana act represents a "grave danger to the Republic," one that will result in a decreased ability of schoolchildren to deal with scientific issues. Francisco Ayala, director of the Institute of Ecology at the University of California at Davis and a member of the National Academy of Sciences committee on science and creationism, agrees that nothing less than the "survival of rationality in this country's schools" is at stake. The Academy is preparing its own brief. Duana Gish, vicepresident of the Institute for Creation Research (ICR), says his organization has not taken a position on the Supreme Court

The Supreme Court will hear oral arguments in the case sometime late this year or early next. Frank Press, president of the National Academy of Sciences says the debate should not be taken lightly. According to Gell-Mann, it is the "old struggle of science against the forces of darkness".

Joseph Palca

Price-Anderson Act

Regulatory bill goes critical

Washington

AFTER months of hearings, meetings in smoke-filled rooms and political threats and counter-threats, Congress appears ready to extend the Price-Anderson Act. Due to expire next year, Price-Anderson establishes limits on the financial liability of commercial nuclear power plant owners in the event of an accident. With four different versions of the legislation currently floating around Congress, there still must be a lot of horse trading before a bill is passed. What finally emerges will go a long way towards determining the future of nuclear power in the United States.

The Price-Anderson Act, enacted into law in 1957, offered government indemnification to protect the fledgling nuclear power industry from financial losses resulting from a power plant accident. In its original form, Price-Anderson required utilities to insure themselves to the maximum amount commercially available then \$60 million — and the government to provide indemnification for an additional \$500 million. In 1975, Congress modified the act, making utilities liable up to a fixed limit for claims not covered by their insurance. A \$5 million "retroactive premium" can be levied against utilities for each of their plants in the event of an accident. A key feature of the scheme is its "no-fault" provisions. Utilities will be liable collectively, regardless of which of them is at fault in an accident.

Today, with 101 operating plants and \$160 million in commercial insurance available, the total compensation to vic-

tims of a nuclear accident is \$665 million. The only real test of Price-Anderson was the accident at Three Mile Island, all claims related to which were settled out of the utility's commercial insurance cover.

A recent report* by the General Accounting Office (GAO) estimates that a \$665 million liability limit would be sufficient to settle claims related to a catastrophic accident for only 4 per cent of existing reactors. Even staunch supporters of Price-Anderson admit that the \$665 million figure is now unrealistically low. What the industry dreaded is that a new version of Price-Anderson would remove liability caps. But unlimited liability, vigorously supported by environmental groups, was shot down earlier this month when its principal congressional proponent, Senator Robert Stafford (Republican, Vermont) agreed to accept a realtively high, but fixed, limit on liability.

Current versions of the bills extending Price-Anderson vary widely in their liability limits. At one end of the spectrum, a bill sponsored by Representative Morris Udall (Democrat, Arizona) calls for retroactive premium payments of up to \$63million per reactor per accident, limiting payments in a single year to \$10 million. The Udall bill also requires utilities to carry a minimum of \$200 million worth of insurance for each reactor, bringing the total liability limit for an accident to \$6,563 million. According to GAO calculations, this limit would be adequate to give full compensation for a catastrophic accident at 95 per cent of power plants. At the other end of the spectrum, a bill reported from the Senate Committee on Energy and Natural Resources calls for a single payment, maximum \$20 million, per reactor per accident, for a total liability limit of \$2,180 million. GAO concludes that 64 per cent of reactors would be covered by this limit. The current prevailing view is that a cap in the region of \$5,400 will emerge in the final bill.

Industry reaction to the proposed changes in Price-Anderson is curiously mixed. Although industry may be forced to accept liability limits higher than it would like, the nuclear lobby appears to have prevailed on many aspects of its agenda. Environmental groups had sought changes in the law that would allow utilities to sue for recovery of their retroactive premiums from a negligent plant operator where an accident occurred. Keike Kehoe, director of the nuclear accountability and insurance project at the Environmental Policy Institute, says this would bring financial accountability to the industry, encouraging high safety standards to avoid huge financial losses. The industry position is likely to prevail.

Environmental groups are bitterly disappointed by the direction renewals are taking. Kehoe points out that in a 1983 report to Congress the Nuclear Regulatory Commission recommended shifting the full costs of a catastrophic nuclear accident to utilities, a position it has since backed away from. But Kehoe believes without unlimited liability, victims of a nuclear power plant accident may never receive fair compensation. Kehoe says the industry can provide \$10 million per year for as long as it takes to settle all claims. She points out that the industry is already committed to spending around \$5 million a year in insurance for each plant.

One contentious provision of proposed Price—Anderson extensions that could ultimately torpedo the bill's chances is indemnification of the government's own nuclear activities. Under current law, non-defence government nuclear activities have a \$500 million limit on liability. In some versions of the new legislation these liability limits would be removed entirely, both for nuclear plant activities and for nuclear waste activities.

If Price-Anderson is allowed to expire, all currently licensed nuclear plants would continue to be covered under existing law, meaning that liability would only rise slowly from its current \$665 million level as plants under construction come on-line. But without an extension to Price-Anderson, the next generation of power plants will face the prospect of unlimited liability. The industry says that means they simply would never be built.

Joseph Palca

Change of priorities in French science

SUPPORT for basic research in France will be little changed next year, in real terms, from 1985, the last full year of the previous socialist administration, according to unofficial figures published by the newspaper Le Monde. But direct government aid for industrial research will be cut.

The level of support comes nowhere near that foreseen in the three-year research plan for which the French National Assembly voted last December. That would have given by 1987 some 8 per cent real growth in research budgets, and 2,800 new posts for scientists and technicians. The Le Monde report foresees just 280 new research posts and 500 technicians, engineers and administrators are to be sacked or not replaced.

The special funds of the ministry of research (spent directly in industry or government and university laboratories, rather than through research councils on applied topics) will also fall from FF1,200 million (£120 million) in 1985 to FF750

million in 1987. The new government is apparently not convinced that ministry research judgements, at least on the previous scale, are better than industry's own. ANVAR, the government agency promoting research in small and medium-sized industries, including the thousands of companies making up France's agro-food sector, can also expect to lose 30 per cent of its funds.

Senior government advisers appointed by the previous administration and still in post, do not think the new government has abandoned industry, however. They expect new tax breaks on research and development budgets to be announced. But many doubt whether such fiscal incentives will do much to change the present extreme concentration of French industrial research in a few major companies, or to treat the basic French malaise: poor links between academics and industry caused by traditional divisions in the education system.

*Nuclear Regulation: Financial Consequences of a Nuclear Power Plant Accident (General Accounting Office, Washington DC GAO/RCFD-86-193BR). Israel's water

Down to the very last drop

Rehovot

DESPITE having the most comprehensive water-planning system in the world and a plethora of internationally recognized water experts, Israel is now suffering the worst water shortage in its history. Government officials blame three years of drought, but most scientists blame the officials.

Dr Gerald Stanhill, an agricultural meteorologist at the Ministry of Agriculture's Volcani Centre, says that, statistically, the past three years were not exceptionally dry. Indeed, they fell well within the rainfall values to be expected from the pattern of the past 55 years. Over that period, annual rainfall within the geographical boundaries of Mandatory Palestine (the area controlled by Israel today) averaged eight cubic kilometres, with a standard deviation of 25 per cent. Perhaps, as the cloud seeders claim, seeding operations have somewhat increased rainfall since the late 1960s. However, the statistics certainly show that rainfall has not declined.

"Israel's water crisis is like its money crisis. It has simply drawn more out of its account than has gone into it", Stanhill says. He welcomes the government's decision to cut back water consumption by 10 per cent this year, although he thinks that what is needed is a policy to build up and maintain a national water reserve at a level equal to three years' consumption.

Dr Joseph Shalheveth, acting director of the Volcani Centre and chief scientist at the Ministry of Agriculture, is less alarmed by developments than other scientists. In his view, "the situation is tight but not impossible". If next winter is also dry, however, drastic cutbacks will be required, as they were, he points out, in California seven years ago. In that case, Israel, for some years a net exporter of agricultural products, would become an importer.

Meanwhile, Volcani scientists who are largely responsible for the exceptionally efficient use of water in Israel's agriculture, are looking for new ways of getting more dollars out of every drop. They have successfully introduced mangoes, avocados, spices, medicinal plants and new varieties of flowers. But each has only a limited export market, and all of them together cannot possibly replace waterhungry cotton, now the main cash crop of Israeli farmers.

Nevertheless, cotton acreage is being reduced this year, as an emergency measure by one-third, and some water experts — who point out that it has been grown at a loss in recent seasons — say it should be eliminated completely, even if this clashes with the Zionist dream and

drives thousands of farmers off the land.

Agriculturalists and their supporters are unwilling to write off cotton, pointing out that flowers, export earnings from which went up this year from \$74 million to \$104 million, were cultivated at a loss for some time and have now bounced back.

Advocates of cotton point out that it can be irrigated with sewage water, but this could be potentially dangerous, says Weizmann Institute Professor Mordeckai Magaritz and Daniel Ronen of the Israel Hydrological Service. Irrigation with treated sewage introduces undesirable amounts of pollutants into the soil, and unless comprehensive preventive measures are taken, into the aquifer as well. Magaritz and Ronen would therefore limit the irrigation of cotton with treated sewage to areas such as the semi-arid Negev, where there is practically no danger of polluting important aquifers.

Nechemia Meyers

Fossil bird shakes evolutionary hypotheses

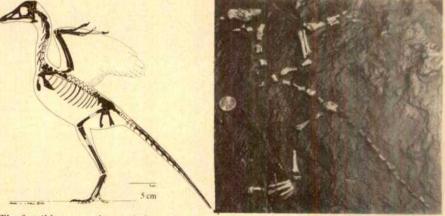
Washington

Fossil, remains claimed to be of two crowsized birds 75 million years older than Archaeopteryx have been found in the 225-million-year old Dockum Formation near Post, Texas. Sankar Chatterjee, a palaeontologist at Texas Tech University, who found the fossils, says they have advanced avian features that place them closer to the ancestor of modern birds than Archaeopteryx and make them possible direct ancestors.

Chatterjee intends to assign the find to a new genus, Protoavis. Among the features that Chatterjee claims identify Protoavis as a bird are elongated forelimbs, temporal fossae confluent with the eye socket, a definite furcula (wishbone), and a plate-like sternum (breastbone) with a small keel. The quadrate is also said to be typically avian. Other avian features are a cnemial crest on the tibia and flight-muscle attachment sites on the humerus. No feather impressions have been found, but Chatterjee claims to see quill nodes on the ulna and hand bones and he believes that Protoavis could fly. Protoavis also has reptilian features: four teeth in the forward part of its jaw, a tail and clawed fingers.

Protoavis seems certain to reopen a longrunning controversy on the evolution of birds, in particular whether the common ancestor of birds and dinosaurs was itself a dinosaur. Protoavis, from the late Triassic, appears at the time of the earliest dinosaurs, and if the identification is upheld it seems likely that it will be used to argue against the view of John Ostrom of Yale University that birds are descended from the dinosaurs. It also tends to confirm what many palaeontologists have long suspected, that Archaeopteryx is not on the direct line to modern birds. It is in some ways more reptilian than Protoavis, and the period between the late Jurassic Archaeopteryx and the worldwide radiation of birds in the Cretaceous has to some seemed suspiciously brief.

Chatterjee's research has for the past six years been supported by the National Geographic Society, which publicized the find last week. The work has yet to be published in a peer-reviewed journal, but two independent palaeontologists (including Ostrom) who have examined Protoavis agree it should probably be classified as a bird. Ostrom stresses, however, that the remains are very fragmentary, and while agreeing with Chatterjee's tentative classification says the case is not finally proven. But Ostrom disagrees with Chatterjee in not seeing even indirect evidence of feathers, saying the bones where quill nodes might be seen are badly preserved, nor does he consider the forelimbs especially elongated. Tim Beardsley



The fossil bones and an artist's reconstruction showing the recovered fossils (dark bones) of the putative Protoavis "bird".

Weapons potential

Defence lobby eyes antimatter

THE US Air Force appears to be taking seriously a report from the Rand Corporation that antimatter might be used as a component of weapons systems. Antimatter packs a tremendous punch, equivalent to some 44 tons of TNT per milligram, when it annihilates with ordinary matter, but until particle physicists began to make and handle antimatter (particularly antiprotons) routinely, any thought of using the material was mere science fiction. But the report, commissioned from Rand, a non-profit US think-tank, by the US Air Force in 1983 and released last year, claims that problems facing the use of antimatter in rocket motors for reversing direction in Earth orbit, beam weapons and the pumping of X-ray lasers could be resolved within five years. Sufficient amounts of antimatter to be militarily "interesting" — some 10 mg a year could be produced within another 15 years if the US government were prepared to spend between \$5,000 and 15,000 million on a development programme.

Basic research on antiproton trapping is already under way at laboratories such as the European Organization for Nuclear Research (CERN) near Geneva. The report says that interaction with basic science could push a military programme forward: "Our position is that the critical experimental work... is so rich with interest and so widespread in the area it intersects that researchers outside existing defense research (as well as those in it) should find it stimulating and an opportunity for creative invention". This interest leads to Rand's "reasonably confident prediction" that five years of research would resolve whether military applications are possible.

But could antimatter, currently produced in only miniscule amounts (some 10^{11} antiprotons per day, or 10^{-8} – 10^{-7} mg per year at CERN, for example) really be collected and used? According to Rand, the production and storage problems will be difficult and complex, and "there can be no confident assertion" that they will be solved. Many handling issues might be solved in experiments on normal matter (such as negative hydrogen ions that simulate the mass and charge of antiprotons) and others with present antiproton production technologies. Antiprotons could be held in static or dynamic electromagnetic traps (for example, Penning traps); at special sites in normal matter (for example in liquid helium bubbles); as spinpolarized antihydrogen; or as condensed antihydrogen in a cryogenic enclosure.

Antimatter has already been stored in minute quantities, and an experiment approved at CERN by a collaboration led by a Los Alamos group could lead to the storage of 10¹¹ antiprotons per cubic centimetre. The main aim of this experiment is the collection and cooling of single antiprotons to measure their weight (do they fall upwards?), but the funding for this part of the experiment has not yet been raised. The rest of the experiment involves antiproton accumulation in a Penning bulk ion storage trap. The experiment has nothing to do with Rand's proposals, a spokesman points out.

Production of sufficient antiprotons to be useful, and the energy costs involved, may be the hardest problem facing weapons designers. Produced by colliding a proton beam to a target, at most one antiproton is collected per 100 incident protons, and this at the highest beam energy in use for the purpose (120 GeV at the Fermi National Accelerator Laboratory near Chicago). Taking into account the energy efficiency of accelerators, and assuming a "difficult near-term improvement" in antiproton collection technology, some 4 GW of external power would be needed to produce the militarily useful amounts of 10 mg of antiprotons a year, the report estimates. This is a huge and expensive power consumption but the gaseous diffusion plants for the separation of uranium isotopes once used in the manufacture of nuclear weapons consumed 6 GW. With the same parameters, antimatter production costs would reach \$133 million per mg. "Some applications" could easily accommodate such costs, the report says.

Antimatter could be used for propulsion, power generation, beam weapons and "classified additional special weapons roles". In propulsion, for example, the annihilation of antihydrogen with hydrogen could produce effective exhaust velocities of 10 km s⁻¹ to a major fraction of the speed of light. Propulsion missions otherwise more or less impossible because of weight of fuel (such as Earth orbit reversal), would become feasible if antimatter were used.

In power generation, antimatter could be used for orbital prime power "for engagement". Antimatter could also help in the design of lightweight beam weapon systems, be used as beams for "hard kills", or help produce the very short energy pulses required in pumping X-ray lasers.

Understanding antimatter would be a "prudent" goal for the US Air Force and worth an investment of \$1 million on basic research as a preliminary study, and if that went well another \$100 million spent on a phase-A (pre-prototype production factory) study. The Air Force appears to have taken this recommendation seriously, and a research programme has begun.

Robert Walgate

Computers thriving from NSF coffers

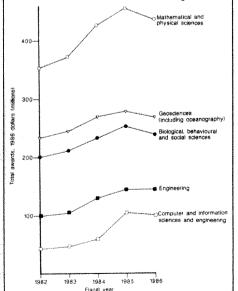
Washington

The total value of research awards by the National Science Foundation (NSF) has increased substantially over the past four years, although some subjects have done much better than others (see below). The graph shows total awards made by each of the foundation's research directorates in constant dollars; retroactive adjustments have been made as necessary to take account of changes in jurisdiction, so that categories are consistent. Average award size by each directorate also increased over the same period.

All directorates' awards increased between 1982 and 1986, but a fall between 1985 and 1986 is evident, caused in part by the effect of Gramm—Rudman budget cuts in the current fiscal year. Much the largest increase was for computer and information sciences and engineering (129 per cent after inflation over the four years). This largely reflects NSF's establishment of five supercomputer centres. The other increases were 45.3 per cent for engineering, 23 per cent for mathematics and physical sciences, 14.4 per cent for geosciences and 21 per cent for biological and social sciences.

The administration proposed an increase again in 1987 for NSF, but Congress may yet baulk at the idea (see *Nature* 322,

487; 1986). NSF's budget proposal for 1988, now ready to go the Office of Management and Budget, will, according to director Erich Bloch, be "highly responsive" to the call of the Packard report ear-



lier this year (*Nature* 321, 372; 1986) for NSF to administer a \$10,000 million 10-year programme to improve university research facilities.

Tim Beardsley

Penguin deaths questioned

SIR-Reports that the penguins in the Falkland Islands are dying on a large scale and that this may be due to competition for food from fishermen or marine pollution¹² seem premature. I happened to be watching birds at sea off the Falklands during the season of the recent rockhopper penguin (Eudyptes chrysocome) mortality in both 1985 and 1986.

Most of the Falkland seabirds appear to benefit greatly from the activities of the fishermen, following their boats in hundreds of thousands to feed on the spilt fish and offal from deep-water species that would not otherwise be available to them. and their populations are obviously flourishing

The penguins are usually difficult to see at sea, but although they frequent the same area along the edge of the continental shelf they do not normally appear to follow the fishing fleets, either because, being unable to fly, they have difficulty in keeping up, or because they appear to feed in roughly equal proportions upon plankton and smaller squid of the genus Teuthowenia' which the fishermen do not appear to catch yet, taking larger fish and squid of the genera Illex and Loligo instead

The main difference between the two years in fact appeared to be that the southern summer of 1986 was unusually hot in the South Atlantic, with the result that among other things there was an influx of warm-water seabirds from the north, and the spring fires intended to remove the dead grass in the Falklands escaped control and burnt in the peat for months over areas of up to 6,000 acres, which one would have thought ought to be of much more concern to local naturalists. More penguins fed inshore than in 1985, possibly because the warm weather affected the growth or accessibility of their food at sea in the way that occurs when the warm current El Niño extends southwards off Peru in the Pacific5.

A few dozen penguin bodies were seen both at sea and on the beaches, with more reported at the breeding colonies, but the number was not large by other standards' for a population estimated at five million breeding birds7.

The main cause for concern appears to be that the huge breeding population on Campbell Island, formerly the largest in the South Pacific and possibly the world. has already been declining on a much larger scale for over forty years, though fortunately this appears to be offset by an increase on the islands off Tierra del Fuego (G.S. Clark et al. in preparation.).

Thus it would appear that the numbers of southern seabirds as well as those breeding in Britain' have been fluctuating for longer and on a larger scale than there have been local overfishing and pollution problems.

W.R.P. BOURNE

3 Contlaw Place. Milltimber, Aberdeen ABI 0DS, UK

- Lyster, S. Falkland Island Fdn. Newsl. 5, 2-4 (1986).
- Nature 322, 4 (1986).
- Croxall, J.P., Prince, P.A., Baird, A. & Ward, P. J. Zool, Lond. (A) 266, 485-496 (1985). Beddington, J.R., Brault, S. & Gulland, J. The Eisheries
- around the Falklands (HED/IUCN Marine Resources Assessment Group. Centre for Environmental Technology Imperial College, London). Schreiber, R.W. & Schreiber, E.A. Science 225, 713-716.
- Bourne, W.R.P. in Marine Pollution (ed. Johnston, R. 403-502 (Academic London, 1976).
- Croxall, J.P., McInnes, S.J. & Prince, P.A. *ICBP Tech Publ.* **2**, 271–291 (1984).
- Moors, P.J. Polur Rec. 23, 69-73 (1986).
 Bourne, W.R.P. in Enjoying Ornithology (ed. Hickling, R.) 226-231 (Poyser, Calton, 1985).

Turkey maligned

Sir-Nechemia Meyers (Nature 321, 801; 1986) claims that visas had been denied by the Turkish Foreign Office to Israeli scientists seeking to take part in the Subcommission on Triassic Stratigraphy's field workshop (of whose organizing committee we are members) in Western Turkey between 14 and 23 July 1986. It seems, however, that Meyers was not particularly well-informed, for Dr Mordeckai Magaritz of the Weizmann Institute, to whom a visa had allegedly been denied, had left Israel before a visa could be issued to him. It was subsequently requested that his visa be sent to him in Milan, Italy, where he was attending the meeting on the Permian and Permo-Triassic boundary in western Tethys held in Brescia, Italy, between 4 and 12 July. The Turkish Foreign Office obliged him, thanks to the timely intervention of Dr Remzi Akkök, but Magaritz then claimed that it was too late for him, although it was certainly not too late to attend the meeting in Turkey. Two other Israeli scientists, Dr Baruch Derin and Dr Tuvia Weissbrod, not only obtained their visas, but also attended the Turkish field workshop. One thus wonders whether there really was any difficulty associated with the visa that prevented Magaritz from coming to Turkey.

Turkey is indeed cautious about issuing visas to foreigners for scientific work and visits. The reason for this is a long history of scientific plunder, first made famous by Heinrich Schliemann, mainly in such

fields as archaeology, epigraphy and mineralogy, to which this country has been subjected. This has harmed not only Turkey but also science itself. No particular nation has therefore been immune to close scrutiny in this regard by the Turkish Foreign Office and there is no reason why Israelis should be an exception.

AYMON BAUD

Musée de Géologie, Lausanne, Switzerland

JEAN MARCOUX

Université Paris VII. Laboratoire de Tectonique, 2 Place Jussieu. Paris, France

A.M.C. ŞENGÖR

İ.T.Ü. Maden Fakültesi. Jeoloji Bölümü, Teşvikiye, İstanbul, Turkey

African lakes

SIR-You published a year ago (Nature 315, 19; 1985) an article by Barel et al. entitled "Destruction of fisheries in African lakes".

Since then, a number of articles and reports have been published suggesting that Malawi plans to introduce the clupeid fish Stolothrissa tanganicae and Limnothrissa miodon (Kapenta or Ndagaa), which occur naturally in Lake Tanganyika, into Lake Malawi (formerly Lake

The government of Malawi therefore wishes to make it clear that it has no current plans, nor has it had any plans in the past, to introduce any exotic fish species into Lake Malawi.

Although the Malawi government wishes to maximize the sustainable fish yield from all its waters, it does not contemplate achieving this by resorting to the hasty introduction of exotics.

The views of the Malawi government on the subject of introducing clupeid planktivores into Lake Malawi are as follows:

- (1) There is at present insufficient knowledge of the chemistry, primary and secondary productivity, energy budget or trophic interactions of Lake Malawi to allow reliable predictions to be made about the outcome of any introduction.
- (2) Without such information, no introduction of any kind is justifiable.
- (3) If scientific studies suggest that the introduction of exotic clupeids could substantially increase the annual fish yield from Lake Malawi on a sustainable basis, without threatening the extinction of the lake's endemic fishes. Malawi would recommend the convening of multinational meetings, to include representatives of the three countries surrounding Lake Malawi and prominent fisheries scientists and biologists, to discuss and debate the issue before any action was taken.

G.M. NONGWA (Acting Chief Fisheries Officer)

Ministry of Forestry and Natural Resources, Fisheries Headquarters, PO Box 593, Lilongwe, Malawi

Investigating the paranormal

SIR—In his Commentary on "Investigating the Paranormal" (Nature 320, 119: 1986) David Marks raises important issues about the problems of studying claims in areas where strong beliefs may be involved. With regard to parapsychology, however, his analysis (and that of many others quoted by him) appears to suffer from a lack of knowledge of the more process-oriented, systematic research that characterizes much present-day parapsychology. He claims that parapsychology is functioning without any theoretical bases. without any idea of what variables are relevant, in such a way that "every new investigator must start afresh, as though he or she is the first worker in the field". Yet much research in parapsychology explores the effect of experimental manipulations, as independent variables, upon measures of psi scoring as dependent variables. To appreciate this, one must be familiar with the details of original research reports. There are areas of research with partial replicability, that cannot yet be dismissed as "abortive leads"; current research does attempt to build upon them, as is evident from reading the introductory and discussion sections of research reports.

In his surveying of the value of the experimental research, Marks has relied upon two surveys of portions of that work, one by Akers' and one by Hyman². Both surveys conclude that parapsychological studies have many methodological flaws. I agree that much of the work has been flawed, but there has been considerable debate about the extent of such flaws. Marks, for instance, has ignored a fortypage response to Hyman's article by Honorton³ which appeared in the same journal issue. The debate over specifics continues, and doubtless will for some time

As Marks notes in his article, both John Beloff and I acknowledge that there has never been a perfect parapsychological experiment. What he does not explain, however, is that we argue that in areas studying extremely complex systems, as in the social sciences, it may be impossible to design, conduct and report a "perfect" study. In my article⁴, I list several groups of counterhypotheses to any given study which, by their very nature, are difficult if not impossible to falsify, such as experimenter fraud or improper description of procedure. Rather, I argued, it is better to evaluate parapsychology by focusing on groups of studies that appear to find consistent relationships between a measure of psychic functioning and some other variable; that such studies would provide more relevant evidence than studies merely finding simple deviations from baseline. I did not advocate examining "groups of studies which, although individually flawed reveal the undeniable presence of psi", nor did I advocate considering badly controlled experiments. As near as I can tell, Marks and I would agree that science progresses in its understanding by exploring functional relationships rather than merely documenting anomaly.

Lest I be misconstrued, certainly I agree that much of what has been done in parapsychology leaves something to be desired. Mistakes have been made, strong claims have been made by enthusiastic advocates, and theory construction has often been vague. Marks makes many good points about how advocates can be misled. But it is a mistake to assume that all who are willing to adopt the working hypothesis that there are new means of exchange between organism and environment are committed to a metaphysical belief system of some sort. If we are to improve our understanding of the phenomena explored by parapsychology, it will probably be through a more integrative approach, with more thorough evaluation of past work and better design of new research. An important component of such an integrative parapsychology would be the development of far more effective models for the strategies by which observers throughout the continuum of advocacy can be deceived by themselves and others about the nature of what they observe, perhaps along lines currently being developed by this writer's.

ROBERT L. MORRIS

2 Strathalmond Green, Edinburgh EH48AQ, UK

- Akers, C. in Advances in Parapsychological Research Vol. 4 (ed. Krippner, S.) 112–164 (McFarland, Jefferson, North Carolina, 1984).
- 2. Hyman. R. J. Parapsychol. 49, 3-49 (1985)
- Honorton, C. J. Parapsychol. 49, 51-91 (1985).
 Morris, R.L. J. Am. Soc. psychical Res. 74, 425-443 (1980).
- Morris, R.L. in Foundations of Parapsychology (eds. Edge. H., Morris, R., Palmer, J., & Rush, J.) 70–110 (Routledge & Kegan Paul, London, 1986).

SIR—I should like to expose Marks's misleading simplification in the section of his paper on the paranormal headed "Coincidences".

Marks refers to Arthur Koestler and L.E. Rhine as publishing cases easily subsumed under the heading of coincidence. However, Koestler, for all his services to psychical research, did not investigate cases and neither, strictly speaking, did Rhine, who simply scanned for recurring features in reports that correspondents sent her. With the exception of one of Rhine's cases, those published by her and Koestler may indeed be interpreted as "simple coincidences". Other cases cannot be so readily explained.

The Society for Psychical Research gave attention to possibilities of coincidence from its earliest studies of apparitions in the late nineteenth century. This explanation may be appropriate for many ex-

periences that laymen attribute to a paranormal process. They sometimes claim that a dream or hallucination of a fairly ordinary type has a paranormal link with a contemporaneous or future event that corresponds in a general way with the dream or hallucination. However, the events concerned in other cases are not ordinary, recurring ones, but unique events. A man dies only once in his lifetime, and if another person at a distance becomes aware of unusual details in his manner of dying at the time it occurs, something more than coincidence must be in play.

Consider the case of Mrs Agnes Paquet, who had a vision of her brother falling overboard when his foot got caught in a tow-rope on a tugboat (almost) at the time the brother actually drowned in this manner. Her vision included details of her @ brother's clothing, such as that his pants legs were rolled up so that, as he went overboard, she could "see" their white lining. She was approximately 50 miles away when she had her vision of the accident to which it corresponded. She told her husband about her vision before learning of her brother's death by telegram. and he corroborated this. The event was unique and so was the perception⁶.

Students of paranormal phenomena, from Dr Johnson in the eighteenth century⁷ to Henri Bergson in the twentieth, have emphasized that when details of unique events are correctly communicated over long distances without the normal sensory channels we should not dismiss such experiences as coincidences.

Many cases, perhaps hundreds, like Mrs Paquet's have been published. Why should we not continue to study them?

IAN STEVENSON

Department of Behavioral Medicine and Psychiatry,

Box 152, Medical Center, University of Virginia, Charlottesville, Virginia 22908, USA

- 1. Marks, D.F. Nature 320, 119-124 (1986).
- Koestler, A. The Roots of Coincidence (Hutchinson, London, 1972).
- 3. Rhine, L.E. J. Parapsychol. 15, 164-191 (1951)
- Gurney, E., Myers, F.W.H. & Podmore, F. Phantasms of the Living (Trübner, London, 1986).
- Sidgwick, H. & Committee Proc. Soc. psychical Res. 10, 25–422 (1894).
- Sidgwick, E.M. Proc. Soc. psychical Res. 7, 30–99 (1981).
 Boswell, J. The Life of Samuel Johnson 246 (Modern Library, New York, 1931).
- 8. Bergson, H. Proc. Soc. psychical Res. 26, 462-479 (1913).

Trouble on the farm

Sir—"Cheap and nasty trees" (leading article *Nature* **322**, 195; 1986) are the backbone of Scandinavian forestry. To suggest that they are not good enough for Britain is a striking example of how widespread is that British malaise responsible for so many of our current problems.

E. NICHOLL

Llangunville, Llanrothal, Monmouth, NP5 3QL, UK

What is the scientific literature?

Professional people have won a poor reputation for their skill at communicating with each other. The complaint may unfortunately be justified.

By what test are the scientific journals counted as literature? The bare minimum of an answer is that they are collectively referred to in this way by their contributors. Collectively, they also have the quality of permanence; they sit on library shelves for decades on end, and are referred to with reverence by those who contribute to later issues. So much is the bread and butter, or at least the bread and water, of scholarship; there are few complaints at the value of the accumulation of journals as the means by which the record of discovery may be reconstructed. But the same cannot be said of the value of the scientific literature as a means by which information is conveyed between people unable to communicate directly, by dialogue. Why should the general admiration of the way that discoveries roll off the laboratory benches coincide with a general belief that the scientific literature is impenetrable, often to its users?

There are some obvious excuses that do not deserve the dignity of being called explanations. Thus, some hold that the process of discovery inevitably splinters previously coherent fields of study, giving sub-fields an existence and a language of their own and creating barriers over which the practitioners no longer wish to jump. Others say that the content of science steadily becomes conceptually more difficult than can be handled by language as it is, which is a way of saying that the problem is not the fault of professional scientists but of other unspecified professionals. Still others protest that there would be no difficulty if only journals and their editors were more generous with the space they allow to the practitioners who are the creators of this growing volume of literature. All three defences are implausible.

That seems to be a legitimate inference from the opinions of regular readers of the journals, even journals such as this which aim to cater for readers with a variety of interests, both in particular but different fields of research and in more general matters. It is sobering how often those who kindly answer questionnaires about this weekly partial diet of science reply with the opinion that it must all be worthy, but that there are only a few parts of it that they could hope, and even wish, to understand. That there are conceptual difficulties that many people do not have the time to surmount is forgiveable. It is even proper that people working in some chosen field should choose to stay there, at least | for the time being. Why should everybody be required to be a generalist? But the sheer clumsiness of the scientific literature is a needless impediment not merely to wider understanding but even to the understanding of those at whom a specialized paper may be directed.

Although the common faults are not easily categorized (and people are forever inventing more), the general drift of error is generally understood even by the transgressors. There is, for example, a disinclination to believe that rules of grammar are particularly relevant to the understanding of scientific prose, whatever their significance in other connections. To judge from the literature as a whole, scientists care less for the accuracy with which the number of a pronoun agrees with that of its noun than they do for the numerical data they report, which is strange to say the least. It is also strange that people who fuss endlessly about the quality of reproduction of a diagram can so fecklessly scatter a word such as "only" in a sentence, forgetting that it belongs only where it most properly qualifies its antecedent.

To judge from much of what is published, most contributors must hope that inventiveness will see them (and others) through. Stringing long lists of words together was the strategem of the 1970s (as in "language-inventing-capability" or "DNA-binding-protein-sequence-homology"). The strategem serves no useful purpose because, until the string of words is so familiar within a sub-discipline that it can be represented simply by initials, it remains for the reader to unpackage the concatenation each time he comes across it. To how many is RFLP for "restrictionfragment-length-polymorphism" (or is it FLRP for "fragment-length-restrictionpolymorphism"?) a concept to hold in one's head as clearly as that of, say, "rabbit"? Even so some journals have now gone so far as to grade the length of the hyphens by which the words are separated in such a string, as if it were always possible to tell which pairs of consecutive words are the more closely related.

Meanwhile, new forms of inventiveness have already begun to appear. Ribose is a sugar which, when combined appropriately with a purine or pyrimidine phosphate, will make a nucleotide; everybody knows that. So why not coin the verb "to ribosylate"? There can be no objection. But what is the object of this ribosylation? ATP, or GTP, or something quite diffe-

rent? No problem. The statement suggests the solution. Why not "ATP-ribosylate", in whatever tense may be appropriate? The difficulty that unfamiliarity may often impede the understanding of even those who know what is intended will surely melt away in time, as the whole world takes the trouble to learn this special language?

The difficulty of the literature derives in part from the neglect of many common rules and the accompanying invention of others which are thought preferable. perhaps because they are better suited to the circumstances. But there are faults of a more structural character. The conventions of the research business, for example, require that authors' delight in what they have accomplished should be restricted to the use of conventional phrases, among which "for the first time" is unaccountably one. The result is that an author is prevented from giving an account of why his or her paper is important (which would help towards its understanding) but is allowed baldly to state that an observation has been made for "the first time in a closed vessel under water . . . ". Similarly, the convention that a person describing the results of a series of biochemical experiments should give such a full account of the details that a novice starting from scratch could repeat the work unaided is a pleasing concession to the need that work should be reproducible, but no substitute for an intelligent variation on some phrase such as "we followed so-and-so's method with this difference . . . ". Yet nobody seems to care that readers must each time unpackage each account of an experiment in the literature before they can properly understand its novelty.

Thus the underlying fault with the scientific literature is its intricacy, its requirement of readers that they should not merely read and understand, but read. pull to pieces and then put together again in ways they understand. Given the requirement, the process is plainly more prone to ambiguity than the ordinary person would think credible. And there is nothing in the demands of specialization. or in those made by editors on authors, to suggest that the characteristics of the scientific literature that give it a bad name are externally imposed. This, it seems, is what people want. But is not much of the rest of scholarship much the same? Of John Maddox

Bacterial-plant conjugation

A bizarre vegetal bestiality

from Conrad Lichtenstein

AGROBACTERIUM tumefaciens, a soil bacterium that transfers genetic material to plants, causes crown gall disease where the infected tissue divides rapidly to produce a tumour. Although much is now understood about this process, the mechanism by which the exchange of genetic information takes place remains mysterious. In a series of elegant experiments described on page 706 of this issue'. Stachel, Timmerman and Zambryski provide evidence that this mechanism is similar to that of bacterial conjugation. involving the unidirectional transfer of a single-stranded plasmid DNA sequence from bacterial to plant cells.

Virulent strains of Agrobacterium contain large (about 200 kilobase) tumourinducing (Ti) plasmids which have evolved an ingenious strategy for survival (see ref.2). When these strains infect wounded plants, a discrete portion of the Tiplasmid, the T-DNA, is transferred to and integrated within the nuclear genome of infected cells. The T-DNA encodes various genes which, by virtue of the possession of appropriate eukaryotic regulatory signals, are transcribed and translated in the plant tissue to produce novel enzymes. One enzyme (encoded by the tmr gene) directs the synthesis of a cytokinin (ribosylzeatin) and another two enzymes (encoded by tms1 and tms2. respectively) direct the synthesis of an auxin (indole acetic acid). It is the synthesis of these plant hormones at elevated levels that results in proliferation of plant cells to produce a callus or gall. Because the biochemical pathway for this synthesis is unusual, the normal plant mechanisms for regulation of phytohormone biosynthesis are evaded. Also encoded within the T-DNA are enzyme(s) that direct the synthesis of amino-acid derivatives collectively called opines; Ti-plasmids are classified according to the type of opine they specify, for example, nopaline or octopine. Once the plant is infected, the tumour (no longer requiring A. tumefaciens) continues to grow, releasing opines to the environment. These opines can be the sole carbon and nitrogen source for growth by agrobacteria that contain the relevant Ti-plasmid. Moreover, they act as molecular aphrodisiacs to derepress Ti-plasmid-encoded genes for conjugal transfer of the plasmid to avirulent agrobacteria in addition to derepressing the genes for opine catabolism.

How is the T-DNA element transferred to plant cells? Genetic analysis reveals three components required for this process: first, two genes, chvA and chvB, located on the agrobacterial chromosome, express products required for the initial binding or attachment of agrobacteria to plant cells'. Second, the T-DNA within the Ti-plasmid is flanked by cis-essential 25-base pair (bp) near-perfect direct repeats, the left and right borders (LB and RB, respectively). The T-DNA often terminates within (RB) or internal to (LB) the borders. Deletion of Ti-plasmid DNA encompassing RB (but not LB) prevents T-DNA transfer. Working on the nopaline Ti-plasmid. Wang et al.4 demon-

Plant cell Agrobacterium cell Cytoplasm (7) T-DNA Bacterial chromosome integration genome Bacteria can grow on octopine Octopine enters and conjugate with bacteria protien Vir nuclear (1) Gene products **‡**@ for attachment Sic **-**(⊕) 8 T-DNA genes expresse <u></u>₹€ 6 T-strand made Ti Plasmid Vir B ③ Vir A protein transports or activates AS AS inducer Vic A enters bacterial (1) octopine (A) AS + vir G \odot cell protein activate B,C,D,E,F,G

Schematic diagram of bacterial-plant conjugation.

strated that the 25-bp RB alone is sufficient to promote T-DNA transfer, but is only fully functional in one orientation (that normally found in the Ti-plasmid). This was the first clue that T-DNA transfer has a polarity, suggesting similarities to bacterial conjugation (see ref.5 for review). Third, the Ti-plasmid contains a large region (about 40 kilobases), the virulence (vir) region, encoding transacting functions required to promote T-DNA transfer; vir DNA itself is never integrated into the plane genome'. (These processes are shown in the figure.)

The realization that T-DNA itself encodes no trans-acting functions required for its own transfer has led to the exploitation of the Ti-plasmid as a vector to produce transgenic plants: a dominant drug-resistance marker plus other genes of interest replace the usual T-DNA genes. The transformed plant tissue can then be regenerated into a normal plant6.

Stachel et al.' performed a detailed genetic analysis of the vir region of an octopine Ti-plasmid. They constructed a transposon mutagen where the transposase is replaced by a promoterless lacZ gene encoding β -galactosidase. By supplying transposase in trans this transposon will insert randomly into a target DNA sequence. Insertion into an operon/ cistron will result in gene inactivation and also produce, in one orientation, a transcriptional/translational fusion to lacZ, so allowing analysis of gene regulation and direction of transcription by assaying for β -galactosidase activity. Using this tool, Stachel et al. show that the vir region contains six distinct operons, vir A, B, C, D, Eand G, involved in T-DNA transfer. Although virA and virG are transcribed constituitively, the other operons are expressed only when agrobacteria are cultured with metabolically active plant cells*.

Signal molecules present in Nicotiana tabacum (tobacco) exudates have been purified and identified as the phenolic compounds acetosyringone (AS) and α -hydroxy-acetosyringone (OH-AS)^{9,16}. These molecules, which fully induce vir expression, are produced by various plant cells at levels limiting for maximal vir expression. However, wounded plant tissue (the very tissue susceptible to infection) produces AS and OH-AS in greater amounts10. Thus, Agrobacterium has evolved to respond to compounds specifically representative of plants susceptible to transformation.

What other components are required for regulation of the vir regulon? The virA and virG loci are both needed for ASinduction of vir. Because this induction is highly attenuated and totally absent in virA and virG mutant cells, respectively, Stachel and Zambryski" speculate that virA encodes a membrane-associated sensory function that transmits the presence of the phenolic signal into the bacterium; this step leads to the activation of the virG protein which positively regulates vir transcription. Interestingly, virG expression is both constitutive and plant-inducible and produces two distinct differentially regulated transcripts: the constituitive transcript is shorter than the induced transcript and lacks sequences required for efficient translation. This feature is reminiscent of the PRE- and PRM-driven transcripts of the CI gene of bacteriophage lambda11

DNA sequence analysis also suggest that the virG locus encodes a 267-aminoacid protein with significant similarity to the ompR gene product of Escherichia coh^{v} . The ompR gene is needed for activation of expression of the outer membrane porins, encoded by ompC and ompF, and required for response to osmotic pressure. Quite how the virG protein activates transcription of the inducible vir loci is not yet clear. It could bind to operator sequences to allow RNA polymerase holoenzyme to initiate transcription. But virG appears to be expressed at a significant level, unusual for an activator, and maximal induction of the vir loci takes 12-18 hours. Alternatively the virG protein could replace the normal vegetative sigma factor in the holoenzyme complex specifically to transcribe the vir loci. Those loci, which are exclusively induced by AS, lack the -35 bp consensus sequence in the promoter yet have other hexanucleotide DNA sequences common around this region, which might function as cis-acting regulatory elements for vir induction13. Further mysteries remain with regard to vir regulation: although virG is absolutely required for expression of the other inducible loci, AS alone is partially able to induce virG transcription even when the virG protein is non-functional".

What is the mechanism of T-DNA transfer from agrobacteria to plant cells that results from vir activation? Initially it was thought that before transfer the T-DNA excises from the Ti-plasmid to form a double-stranded circular DNA molecule joined precisely within one border sequence repeat (by recombination between the two borders)14. However, this genetic evidence was circumstantial. In the report in this issue', Stachel et al. provide direct biochemical evidence that AS specifically induces the production of a linear, single-stranded, T-DNA molecule designated the T-strand; such strands are detected by Southern blot analysis of total DNA prepared from induced agrobacteria and are sensitive to different single-strand specific nucleases. These molecules correspond to the bottom strand of the Ti plasmid such that its 5' and 3' ends map to RB and LB, respectively, matching the genetic polarity of the border repeats. T-strand formation is probably associated with DNA synthesis as AS induction also yields molecular changes to

T-DNA sequences in the Ti plasmid — a strand-specific nick associated with the 25bp border repeats, and Ti-plasmids whose internal T-regions show partial singlestranded and/or triple-stranded character (presumably replicative intermediates). The border nicks probably direct sitespecific recombination to yield the doublestranded T-DNA circle molecule observed at low frequency after induction14.

This evidence suggests the following analogy to bacterial conjugation: after induction of the vir regulon by AS, a nick is made within the RB. New data (S.E. Stachel, personal communication) indicate that the function responsible for this nick (and T-strand formation) is encoded by the upstream cistron of virD. The virD gene is also necessary for the generation of T-DNA circle molecules¹⁸. Rolling-circle DNA replication is then initiated, and in conjunction with a helicase activity, extrudes the T-strand in the 5' to 3' direction. The LB nick signals termination of transfer and, when deleted, results in termination further along. The polar function of RB within the large Ti-plasmid indicates that in the wrong orientation transfer initiates in the other direction and is unlikely to traverse the entire Ti-plasmid to reach the T-DNA (analogous to an interrupted mating); in smaller plasmids the RB is fully functional in both orientations16. Can transfer initiate from the LB too? Probably, but recent evidence from octopine Ti plasmids indicates that RB is used more efficiently.

Many questions remain to be answered. How is the T-DNA transported from Agrobacterium to the plant nucleus? Where is the complementary strand to the T-strand made and what primes its synthesis? How does T-DNA integrate into the nuclear genome? Clearly, further exciting discoveries lie ahead in the understanding of the Agrobacterium-plant-cell interaction

- Stachel, E.E., timmerman, B. & Zambevski, F. Nature 322, 706 (1986)
- Gheysen, G., Dhaese, P., Van Montagu, M. & Schell, J. in Genetic Flux in Plants (eds Hohn. B. & Dennis, E.S.) 11
- CSpringer, Wein, 1985).

 Douglas, C.J., Standoni, R.J., Rubin, R.A. & Nester, E.W. J. Bact. 161, 850 (1985).

 Wang, K., Herrera-Estrella, L., Van Montagu, M. &
- Zambryski, P.C. Cell 38, 455 (1984). Willetts, N. & Wilkins, B. Microbiol, Pry. 48, 74 (1984).
- Lichtenstein, C. & Draper, J. in DNA Closing Vist. II (ed.)
- Glover, D.M.) Ch. 4 (TR.L. Oxford, 1985).
- Stachel, S.E., An. G., Flores, C. & Nester, E.W. EMBO, J. 4, 891 (1985).
- Stachel, S.E. & Nester, E.W. EMBO J. 5, 1145 (1986)
- Stachel, S.E., Nester, E.W. & Zambryski, P.C. Proc. natn. Acad. Sci. U.S.A. 83, 379 (1986).
 Stachel, S.E., Messens, E., Van Montagu, M. & Zambryski, P.C. Nature 318, 624 (1986).
- Stachel, S.E. & Zumbryski, P.C. Cell.46, 325 (1986) 12. Ebert, P., Stachel, S.E., Winans, S.C. & Nester, E.W.
- Das, A. et al. Nucleic Acids Res. 14, 1335 (1986).
 Koukolikova-Nicola, Z., Shillito, R.D. & Hohn, B.
- Nature 313, 191 (1985).
- Alt-Moerbe, J., Rak, B. & Schröder, J. EMBO J. 5, 1129
- Rubin, R.A. Molec. gen. Genet. 202, 312. (1986). Peroka, E.G., Hellmiss, R. & Ream, W. EMBO / 5, 1137

Conrad Lichtenstein is in the Centre for Biotechnology, Imperial College of Science and Technology, London SW7 2AZ, UK.

Palaeoclimate

Permafrost and ice-wedge growth

from Peter Worsley

PERMAFROST, any natural material that contains a thermal state of 0°C or less for two or more years, underlies one fifth of the terrestrial surface of the Earth. Its formation is a direct function of climate; its boundaries are determined by a mean annual air temperature of 0 to -1°C. There are few precise data on permafrost establishment, so the study reported in this issue (Peyette, S. et al. Nature 322, 724; 1986), demonstrating that the removal of a forest cover, which normally promotes snow accumulation and hence protection from deep freezing, appears to be the key factor causing permafrost growth, is a significant confirmation of the sensitive environmental thresholds governing the onset of permafrost.

Permafrost is generally divided into three types - continuous, discontinuous or alpine - depending on its relative extent in the subsurface. Alpine permafrost is restricted to high mountains and plateaux outside the main polar-centric belt where altitudinal cooling replicates the severe subarctic. In the Northern Hemisphere the continuous/discontinuous permafrost areas form two concentric zones with boundaries frequently transverse to latitude because of permafrost sensibility to land-mass configuration. The transition between continuous and discontinuous zones corresponds roughly with a mean annual air temperature of -6 to -8° C.

Cracking of permafrost arises as a consequence of rapid cooling during winter in conjunction with ground temperatures in the −15 to −20°C range. Once initiated. the repeated annual cooling induces cracking of the frozen ground at the same location; successive events over several years, together with attendant infilling of the cracks with blown snow and hoar frost. leads to the slow growth of ice wedges. linear ground-ice bodies with V-shaped cross-profiles. Active growth of ice wedges has until recently been considered to be an exclusive property of continuous permafrost and, although ice wedges in discontinuous permafrost were known. climates associated with the arctic and I they were regarded as being dormant



Medium-sized ice wedges on an actively eroding coast in Banks Island, Canada (72°N, 130°W) in continuous permafrost (mean annual air temperature is about –15°C).

because of a climatic amelioration. Hence the wedges were thought to be relics from a former, more severe, climatic regime that could sustain continuous permafrost in the subsurface. The reappraisal of this view by Peyette et al., leading to the conclusion that active ice wedges do occur within discontinuous permafrost, was prompted by the study of T.D. Hamilton et al. (Arctic Alp. Res 15, 157; 1983) who, as a result of trench excavation during design of the trans-Alaskan pipeline. demonstrated ice-wedge growth in a mean annual temperature close to -3.5°C. The vegetation cover in the study of Hamilton et al. was similar to that which prevails in the interior subarctic boreal forest of Quebec.

Pevette et al. studied a site near Clearwater Lake in subarctic Quebec which has a mean annual air temperature of -5°C and extensive discontinuous permafrost. The association of ice wedges and peat allows radiocarbon isotope-dated, palaeoecological reconstructions of vegetation history, the latter being the key to their demonstration that ice-wedge initiation was a consequence of the removal of tree cover. The relationships between ice-wedge width and distance from the contemporary forest border uncovered by Peyette et al. are an elegant proof of the diachronous nature of ice-wedge initiation. Without the progressive retreat of the forest border no growth would have occurred, which emphasizes the need for caution in the deduction of climatic significance from such structures. But the host materials are highly organic and a low preservation potential is likely if the permafrost should degrade in the future.

Wedge-shaped sedimentary structures

in the geological record are usually considered to be casts arising from the melt of ice wedges. Such melting can be caused by regional climatic change or local factors such as thermal erosion of the ice by melt water during the summer. They are very valuable indicators of the former presence of permafrost and thus important aids to palaeoclimatic reconstruction. Climatic parameters derived from ice-wedge casts are usually based on the assumption that ice-wedge growth signifies continuous permafrost and therefore mean annual temperature of at least -6°C. No active

ice wedges have yet been found that originate in non-organic sediments within a zone of discontinuous permafrost. But in the light of the findings of Peyette et al. and Hamilton et al., a cautious re-assessment of the climatic values that control ice-wedge initiation and subsequent growth is necessary: factors such as rates and degree of cooling of the upper permafrost must now be considered.

Peter Worsley is in the Department of Geography, University of Nottingham, Nottingham NG72RD, UK.

Immune system

Complement-like cytotoxicity?

from Kenneth B.M. Reid

BOTH cytotoxic T cells and natural killer cells have cytoplasmic granules containing the protein perforin, which appears to have an analogous function to that of serum complement component C9 in the lysis of target cells12. Activation and regulation of the complement system is quite well understood but little is known about the system that controls perforin activity. Efficient and controlled lysis of target cells by the complement system involves six serine proteases3. It might be expected that natural killer and cytotoxic T cells contain a complex complement-like regulatory system and recent studies at the protein and complementary DNA levels, one of which appears on page 740 of this issue', indicate that this is the case as there appear to be at least two serine proteases involved in cytotoxic T-cell activity.

Pasternack et al. find that a serine protease is involved in the antigen-specific lysis of target cells by mouse cytotoxic T cells (and certain helper T cells). The principal protease identified is composed of two, probably identical, disulphide-linked subunits of approximate relative molecular mass (M_i) 32,000 (32K). Inhibition of this protease by diisopropyl-phosphorofluoridate and its limited trypsin-like activity indicate that it belongs to the serine protease family. The enzyme appears to be associated with the membranes of the perforin-containing cytoplasmic granules and its release is specifically triggered by the interaction of cytotoxic T cells with target cells.

Studies at the cDNA level by the isolation of clones specific for cytotoxic T cells predict protein sequences for three molecules having the characteristic features of the classical serine proteases, that is, a chain of $M_r \approx 25 \text{K}$ containing the highly conserved residues, such as those at the active catalytic site, His, Asp and Ser. Brunet et al. reported the isolation by subtractive hybridization of a mouse cDNA clone (CTLA-1) specific for cytotoxic T

cells but not helper T cells or B cells. The sequence predicts a leader peptide of up to 20 amino acids followed by a sequence of 227 residues resembling a serine protease beginning with the characteristic Ile-Ile-Gly-Gly amino-terminal sequence.

An identical cDNA sequence has been identified by Lobe et al." who first found two genes encoding serine proteases that appeared to be specifically expressed in activated cytotoxic T cells, just before the cytotoxic reaction. But on screening cDNA libraries using the genomic probes, coding sequences for only one of the proposed proteases (CCP1) could be isolated. In another study the cDNA encoding a serine protease-like sequence different to that seen for CTLA-1/CCP1 clones, was isolated from a mouse cytotoxic T-cell cDNA library' using an RNA hybridization competition procedure. The sequence of this clone predicted an aminoterminal sequence of 14 amino acids (which seems likely to be part of an activation peptide rather than a leader sequence) followed by 232 amino acids of serine protease-like sequence. The molecule identified (HF) was found in all cytotoxic T-cell clones, nude mice spleen cells and rat natural killer cells examined but not in control tissues and cell lines.

The derived amino-acid sequences for the two serine protease-like molecules CTLA-1/CCP1 (refs 5,6) and HF (ref. 7), show 40 and 35 per cent homology with rat mast cell protease II, an intracellular serine protease found in the granules of atypical mast cells8. Human factor D (refs 9,10), the first enzyme involved in the activation of the alternative pathway of complement, shows 36 per cent homology with the rat mast cell protease" and appears to be the most closely related of the complement serine proteases to the mouse cytotoxic T-cell-specific proteases. The presence of an Asp residue in the position determining the substrate specificity of the HF protease indicates that, like

factor D and the other complement enzymes, it would have a preference for lysyl or arginyl bonds. This is consistent with the observation of Pasternak et al.4 that the protease they describe has a limited trypsin-like activity.

The presence of Ala in the equivalent position in the other cytotoxic T-cellspecific protease, CTLA-1/CCP1, makes this likely to be more similar to the rat mast cell protease II in its activity. The CTLA1/CCP1 protease further resembles the mast cell protease in that it has Phe, rather than the highly conserved Cvs seen in all other serine proteases, at the position four residues on the amino-terminal side of the serine at the active site, and this could affect the substrate binding pocket. Also, the presence of an uneven number of Cys residues in the derived amino-acid sequence for the CTLA-1 and CCP1 sequences (and perhaps HF) implies that the Cys at position 74 has a free sulphydryl group, or is linked by a disulphide bond to another chain, as it has no homologous counterpart in all other known serine protease sequences. It is possible that the disulphide bond in the dimer observed by Pasternack et al.4 involves this Cvs residue. This would certainly be a novel observation and could be a feature of cytotoxic T-cell-specific serine proteases.

Thus it is possible that the CTLA-1/ CCP1 and HF clones encode two of several distinct serine proteases in a lytic pathway common to natural killer and cytotoxic T cells. Cytotoxic T cells perhaps follow a classical antigen-mediated pathway whereas natural killer cells may use an alternative pathway not involving the T-cell receptor, with both pathways culminating in a common lytic process. If there is close homology between the lytic processes of these two cell types and that of the serum complement system then proteins homologous with the complement components C3, C4 and C5 may be found acting as substrates for these recently identified serine proteases, thus allowing generation of complex proteases similar to C4b2a3b and C3bBb3b that are involved in the generation of C5b in the serum complement system.

- Podack, E.R., Young, I.D. & Cohen, Z.A. Proc. natn. Acad. Sci. U.S.A. 82, 8629 (1986).
- Henkart, P.A., Millard, P.J., Reynolds, C.W. & Henkart, M.P. J. exp. Med. 160, 75 (1984). 3. Reid, K.B.M. & Porter, R.R. A. Rev. Biochem. 50, 433
- Pasternack, M.S., Verret, C.R., Liu, M.A. & Eisen, H.N. Nature 322, 740 (1986).
- Brunet, J.-F. et al. Nature 322, 268 (1986)
- Lobe, C.G., Finlay, B.B., Paranchych, W., Paetkau, V.H. & Bleackley, R.C. Science 232, 858 (1986).
 Gershenfeld, H.K. & Weissman, I.L. Science 232, 854
- Woodbury, R.G., Katunuma, N., Kobayashi, K., Titani, K. & Neurath, H. *Biochemistry* 17, 811 (1978).
- Johnson, D.M.A., Gagnon, J. & Reid, K.B.M. FEBS Lett. 166, 347 (1984).
- Niemann, M.A., Bhown, A.S., Bennett, J.C. & Volanakis, J.E. Biochemistry 23, 2482 (1984).

Kenneth B.M. Reid is in the MRC Immunochemistry Unit, University of Oxford, Oxford OXI 3QU, UK.

Membrane biophysics

Surface conduction of protons

from M.J. Selwyn

In an elegant series of experiments on phospholipid monolayers, Prats, Teissié and Tocanne, on page 756 of this issue, report that protons move much more rapidly in a thin layer (less than 0.5 nm thick) at the interface between the lipid and aqueous phases than through the thickness of the aqueous phase (a few millimetres). This model system provides experimental evidence for a reactionfacilitating function of membranes and is particularly interesting in relation to chemiosmotic coupling by protons. The result also has implications for the study of reactions at non-biological interfaces, such as catalysis by immobilized enzymes.

The Langmuir trough technique, used since 1917 for measuring the surface pressure and the cross-sectional area of the constituent molecules of monolayers is that they can measure this parameter for any phospholipid without the perturbations caused by an added probe group.

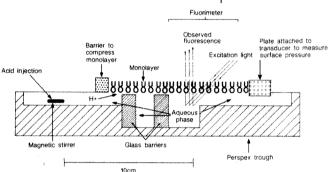
They find that reporter-group signals change more rapidly than the pH of the aqueous phase and that there is both a pH gradient along the surface of the membrane and a steep pH gradient from the interface through a thin layer (measured by the linked fluorescein, estimated to be 1.0 ± 0.5 nm into the aqueous phase) to the bulk aqueous phase. Thus, fast diffusion along the interface and slower diffusion into the bulk aqueous phase compete for interfacial protons. Fast diffusion disappears if the lipids are not sufficiently tightly packed in the monolaver. which suggests some structural requirement. But increasing the ionic strength with NaCl or thiocvanate does not alter

> the rates of diffusion². which indicates that 'structured' water is not involved. In contrast, increasing the concentration of K'phosphate in the buffer increases trapping of the protons by the aqueous phase much that conduction along the interface

> cannot be detected' Although it is now generally agreed that electron transfer and synthesis oxidative and photosynthetic phosphorylations are coupled by the flow of protons. quantitative some data do not

with P. Mitchell's original concept' that the protons equilibrate with the bulk aqueous phases and others exclude the alternative hypothesis of R.J.P. Williams in which the protons are confined to the membrane. Since then there have been a plethora^{6,7} of hypotheses suggesting semilocalized proton coupling in which the resistance to transfer of protons to the bulk phase is neither infinite (as in Williams hypothesis) nor zero (as in Mitchell's).

The main points of contention are whether there are structural barriers to proton flow to and from the bulk aqueous phases; whether there are specific channels between the proton-linked enzymes: and the extent of localization of the protons, ranging from the whole surface of each vesicle membrane down to units comprised of single sets of the proton-



Diagrammatic longitudinal section of a Langmuir trough modified for injection of acid and measurement of fluorescence changes at and near the surface (from refs 1-3). Fluorescence is detected both in the monolayer and in the aqueous phase just below it. Thus, depending on whether the fluorescein pH indicator is attached to the lipids in the monolayer or free in solution the fluorimeter responds to the pH at the interface or to the pH of the bulk aqueous phase, respectively. Controls are provided by pH measurements at the same position in the bulk aqueous phase without the monolayer or the glass barriers. The shorter time-constant for pH change when the monolayer is present demonstrates rapid conduction of protons at the interface.

spread on a water surface, is adapted by Prats et al. so that they can inject acid at one end of the trough and, further along, measure changes in the aqueous pH and signals from chemical groups attached to the monolayer (reporter groups) which have a readily measurable property that responds to changes in the local environment (see figure). In previous experiments^{2,3} they found the pH close to the lipid-water interface by changes in the fluorescence of fluorescein that is covalently linked to phosphatidylethanolamine. In their new work1 they use americium electrodes to measure changes in the surface potential of the lipid monolayer and thus the state of ionization of the lipid headgroups. This ionization depends on the pH precisely at the interface and one advantage for Prats et al. linked enzymes. Calculations suggest that even in the aqueous phase the movement of protons should be so rapid that without special barriers the protons have rapid access to the whole surface of the membrane and to the bulk aqueous phases. But the results of Prats et al. indicate that proton movement away from a phospholipid membrane is not rapid, even in the absence of special barriers, and so steady-state fluxes of protons between sources and sinks on the membrane surfaces and to the internal and external aqueous phases should be considered.

On this basis the bulk-phase pH and membrane potential are not equal to the local values either for the reductionoxidation enzymes or for the ATPase, but there is no definite distinction between localized and delocalized coupling. An analogy can be made with a spring or fountain where a collector placed close to the source can collect water at a higher potential energy than that in the surrounding pool. Unless diffusion of protons across the surface of the membrane is infinitely fast then there will be a progressive tendency for proton-linked enzymes to be more tightly coupled and more isolated from the bulk phases the closer they are on the membrane surface. With this type of situation, depending on conditions, the system may tend either towards localized or delocalized behaviour, and indeed Beard and Dilley8 recently showed such a change by storing thylakoids in high rather than low ionicstrength medium.

Adam and Delbrück" proposed that intracellular membranes enhance reactions rates by constraining diffusion to two dimensions on the surface of the membrane. This hypothesis has been criticized10, partly on the grounds that a great reduction in diffusion rate at the surface offsets much of the advantage. But the rapid movement of protons at the membrane surface may affect the rate of many reactions and maintain uniformity of cytoplasmic pH. Although monolayer experiments are a very simple model, they should also stimulate investigation of other ions and non-biological surfaces.

- 1. Prats, M., Teissić, J. & Tocanne, J.-F. Nature 322, 756
- Teissié, J., Prats, M., Soucaille, P. & Tocanne, J.F. Proc. nam. Acad. Sci. U.S.A. 82, 3217 (1985). Prats. M., Tocanne, J.-F. & Tetssie, J. Eur. J. Biochem.

- 149, 663 (1985). Mitchell, P. Biol. Rev. 41, 445 (1966). Williams, R.J.P. Biochim. biophys. Acta 505, 1 (1978). Westerhoff, H.V., Melandri, B.A., Venturoli, G., Azzone, G.F. & Kell, D.B. Biochim, biophys. Acta 768, 257 (1984). Ferguson, S.J. *Biochim. biophys. Acta* **811**, 47 (1985).
- Beard, W.A. & Dilley, R.A. FEBS Lett. 201, 57 (1986). Adam, G. & Delbrück, M. in Structural Chemistry and Molecular Biology (eds Rich. A. & Davidson, N.) 198
- (Freeman, New York, 1968) 10. McCloskey, M.A. & Poo. M. J. Cell Biol. 102, 88 (1986).

M.J. Selwyn is in the School of Biological Sciences at the University of East Anglia, Norwich NR47TJ, UK.

Astronomy

Neutron stars in Nanjing

from Virginia Trimble

NEUTRON stars form in supernova explosions, manifest themselves as radio pulsars or X-ray binaries, and fade away as their rotation slows, their magnetic fields decay away and their energy supplies are used up. This basic framework has been accepted for nearly 15 years, so that one might wonder whether there was anything left for a conference on the origin and evolution of neutron stars* to discuss.

But several fundamental questions (and a host of minor ones) remain. Are there other ways of making neutron stars? And, perhaps most important, when and how do they acquire, then lose, the strong dipole magnetic fields and rapid rotation that permit pulsar emission and provide signatures of neutron-star presence in X-ray sources? Unsurprisingly some possible answers are emerging from studies of two very rare classes of pulsars — those with rotation periods less than 10 ms and those with compact (white dwarf or second neutron star) binary companions. The classes overlap in that two of the three known millisecond pulsars are among the seven known binary ones. Two papers by Joseph H. Taylor and colleagues on pages 712 and 714 of this issue^{1,2} report the most recent additions to each group. More can be expected, for they probably make up about 10 per cent of all galactic pulsars, according to Taylor (Princeton University) and Ramesh Narayan (University of Arizona), and are currently under-represented in catalogues only because their intrinsic faintness and rapid pulsation makes detection difficult.

What are the binary and millisecond pulsars telling us? First, they provide the firmest evidence so far for neutron-star formation not from the collapse of the core of a massive star, but rather from collapse of a roughly solar mass white dwarf driven above the Chandrasekhar (maximum stable) mass by accretion from a companion³.

This mechanism, originally invoked to account for young-looking neutron stars with 1012 Gauss magnetic fields among old, low-mass X-ray binaries, seems to be the only way to explain the combination of young neutron star (1011 Gauss surface field) and old system (wide, circular orbit) that characterizes the binary pulsar 0820+ 02 (ref. 4). A recent detection of the companion' strengthens the explanation. The other star is a hot white dwarf, which must have ceased transferring material to its companion about 107 years ago, the elapsed time being just right for the white

*IAU Symposium No. 125 was held in Nanjing, China, 26–30 May 1986.

dwarf to cool to its present temperature and for the neutron star to have reached is present field and rotation period (0.865 s).

Initially strong fields and rapid rotation are expected simply from conservation of magnetic flux and angular momentum as stellar cores collapse to neutron stars. Statistics of pulsar periods, period changes, and associations with supernova remnants tell us, however, that only about 20 per cent are born with the largest possible values of both field and angular velocity. Stanford E. Woosley (University of California, Santa Cruz) suggested that some neutron stars might be born as slow rotators from progenitor stars larger than 10 solar masses, because core convection during carbon and silicon burning could transport angular momentum outward. Lower masses without such convection would give rise to rapid rotators.

The alternative of low initial surface field must also sometimes occur, for instance in LMC X-4, whose massive companion requires the neutron star to be young. Given the 69-ms rotation period, the accretion that fuels observed X-ray emission can only occur with a surface field less than 3×10^{10} Gauss, according to Nicholas E. White (Darmstadt). If, when



100 years ago

The August Perseids

THE shower of Perseids has been a fairly conspicuous one this year notwithstanding the somewhat unfavourable circumstances attending the display. On the nights of August 9, 10, and 11 the nearly-full moon was visible during the greater part of the time available for observation, and robbed the phenomenon of its chief prominence during the evening hours. Those, however, who continued to watch the heavens until after the moon set on the early morning of the 11th must have been rewarded by a tolerably rich exhibition of meteors. The number observable by one person fell little short of 100 per hour, and this rate compared with similar observations in past years proves the late display to have fully maintained its decided character. Numerically this shower of Perseids cannot be placed in the same category as the brilliant meteoric storms of November 13, 1866, and November 27, 1872 and 1885, but it must be remembered that the August shower is one which returns annually, and apparently without much variation in its leading features.

From Nature 34, 372; 19 August 1886.

or how such initially low fields grow to typical values of 10¹² Gauss is not certain, though mechanisms have been suggested.

In any case, pulsars then live on their rotational (and, perhaps, magnetic) energy until dropping below detectability at periods of a few seconds and affective fields of 1011 Gauss, preventing the study of later phases. One catch is that only the dipole part of the field perpendicular to the rotation axis is measured, so that one could not rule out the field aligning or evolving to higher multipoles rather than decaying in the 10°-10' years over which pulsars fade away. The binary pulsars have opened a new window for observation of senile neutron stars. As the companion evolves and expands, gas transferred to the neutron star spins it back up to an equilibrium rotation period, depending somewhat on orbit parameters and field strength, but typically a few milliseconds. Later, when the companion itself has become compact or unbound and ceased to interfere, we see a recycled pulsar with rapid rotation and low field.

One might expect the magnetic field strength to continue to drop. Apparently it does not'. All three millisecond pulsars have fields very close to 5×10^8 Gauss. according to Taylor. This includes the binary 0655+64, whose white dwarf companion' has been cooling for several billion years since it stopped spinning up the neutron star. Corroborative evidence for stalling of field decay at 108-109 Gauss comes from models for quasi-periodic oscillations in old (low mass) X-ray binaries*, although so many different kinds of correlations of the frequencies of these oscillations with X-ray intensity and colour temperature have now been seen that the connection with any one model has become very tenuous according to Guenther Hasinger (Max Plank Institute, Munich).

Apparently, then, we can add to the basic framework mentioned above an alternative mechanism (accretion-driven white dwarf collapse) and alternative evolutionary histories for rotation and surface magnetic field more complex than simple monotonic decay with time.

Other neat, new things that were reported at Nanjing included a report from Andrew Lyne (Jodrell Bank) of the largest glitch ever, $\Delta P/P = 4 \times 10^{-6}$, which occurred in January or February 1986 in PSR 0355+534 (P=0.156 s). The recovery has also been unprecendentedly rapid ($\vec{P} = -52 \times 10^{-24} \,\text{s}^{-1}$). One might or might not want to tie this up with the suggestion by Charles Alcock (MIT) that post-glitch behaviour is a possible test to distinguish true neutron stars from interlopers made of strange quark matter. Claire Flanagan (SAAO) described a new glitch in the Vela pulsar almost as large $(\Delta P/P = 10^{-6}).$

Jiehao Huang (Nanjing University)

advocated dividing pulsars into two roughly equally numerous groups that emit at polar caps and at their speed-oflight cylinders respectively; and Tan Lu (Nanjing University) had statistical evidence that the fading of pulsar radio luminosities may not be monotonic with time.

Patrizia Caraveo and Giovanni Bignami (Milan) have added another late-1985 EXOSAT point to the curve of period as a function of time for the 60 s pulsation of Geminga. The object is still slowing down and now shows two harmonics as well as the fundamental. Caraveo and Bignami have not, however, been able to get additional optical images to test the possibility of large proper motion. Zhenru Wang (Nanjing University) suggested several new possible identifications between Chinese guest stars and young neutron stars and supernova remnants (including Geminga!).

W. David Arnett (Chicago) has found a new instability following core collapse in massive stars that may advect enough energy and momentum outward to cause envelope ejection and a supernova explosion. The most recent round of neutronstar cooling calculations requires pion condensation, strange quark matter or some other non-standard physics to prevent the Vela pular from emitting more thermal X rays than the observed upper limit, according to Ken'ichi Nomoto (Tokyo) and Sachiko Tsuruta (Montana State University). These are just a few of the facts presented at Nanjing, which it is hoped will form the raw materials for a new synthesis

- Dewey, R.J. et al. Nature 322, 712 (1986)
- Segelstein, D.J. et al. Nature 322, 714 (1986)
- Whelan, J.A.J. & Iben, I. Astrophys. J. 186, 1907 (1973).
- van den Heuvel, E.P.J. & Taum, R.E. Nature 309, 235
- Kulkarni, S. Astrophys. J. Lett. 306, L85 (1986).
- Blandford, R.D., Applegate, J.H. & Hernquist, L. Mon. Not. R. astr. Soc. 204, 1025 (1983).
 Bhattacharia, D. & Srinivasam, G. Curr. Sci. 55, 327 (1986).
- Alpar, M.A. & Shaham, J. Nature 316, 239 (1985) Romani, R. & Trimble, V. Nature 318, 230 (1985).

Virginia Trimble is at the University of California, Irvine, California 92717 and is in the Astronomy Program, University of Maryland, Mary-

Immunology

The ins and outs of antigen processing and presentation

from Ronald N. Germain

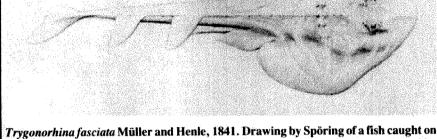
THE striking differences in antigen reactivity shown by T and B lymphocyte subpopulations has been the primary research interest of many members of a whole generation of immunologists. The expectation that elucidation of the structure of the T-cell receptor would, by itself, reveal the how and why of the differences has proved false1. Therefore, increasing attention has been paid to understanding the form of antigen actually involved in the T-cell recognition process. The studies of Townsend and his collaborators²⁻⁴, culminating in a recent paper', provide a major advance in our understanding of the form of antigen seen by T cells and provide an intellectually and physiologically satisfying explanation for several poorly understood immunological phenomena.

Although very similar gene segments and DNA rearrangement events are involved in generating the receptors used by T and B cells, the functional specificity of these two cell types differs markedly. B cells express surface membrane versions of serum immunoglobin molecules that directly bind soluble antigens of diverse chemical composition. In contrast, T cells use a recently characterized heterodimer to co-recognize particular combinations of protein antigen and class I or class II major histocompatibility complex (MHC)encoded molecules on the surface membrane of other cells⁷.

As early as 1958, Gell and Benacerrafs pointed out that antibodies tend to be specific for native protein molecules, whereas cell-mediated (now known to be T-cell-mediated) responses such as delaved-type hypersensitivity are stimulated by determinants preserved after protein denaturation. Pioneering work by Ziegler and Unanue' demonstrated that antigen presentation to class II MHC-restricted T cells is an active time-dependent process involving an acidified intracellular compartment whose function is sensitive to drugs such as chloroquine. These results suggested that the antigen seen by T cells is not intact, but rather degraded or denatured intracellularly before exposure on the surface of the antigen-presenting cells10. Shimonkevitz et al.11 direct evidence in support of this hypothesis by showing that proteins enzymatically degraded in vitro could be presented by metabolically inactive cells bearing the proper class II molecules.

Thus, physiological priming of class III restricted T cells to degraded forms of antigen accounts for the presence of secondary T-cell responses to protein antigens denatured in vitro and for the success many have had using protein fragments or synthetic peptides as stimuli for T cells originally generated by immunization with intact proteins. Both indirect and direct methods have now revealed that at

Pictures from the *Endeavour* voyage of 1768



Trygonorhina fasciata Müller and Henle, 1841. Drawing by Sporing of a fish caught on 29 April 1770 at Sting Ray Bay (later Botany Bay), Australia. T. fasciata was based by Müller and Henle partly on this drawing, but also on another specimen in alcohol at the Paris museum. From Catalogue of the Natural History Drawings commissioned by Joseph Banks on the Endeavour Voyage 1768–1771 Part 3: Zoology, recently published by the Bulletin of the British Museum (Natural History). (Historical series vol. 13; London, 1986.) This catalogue lists all the drawings of animals from James Cook's voyage on the Endeavour that were made by artists employed by Joseph Banks. Most of the drawings were kept in Banks' home until his death in 1820 and then transferred to the Museum. This catalogue attempts to record comprehensively the surviving animal drawings from the voyage of the Endeavour, and examines and discusses the history of the drawings as well as providing notes on the artists, none of whom survived the voyage.

least some of these minimal antigens interact physically with class II molecules in the absence of the T-cell receptor, providing an understandable picture of how simultaneous recognition of the two is achieved.

This view of antigen presentation to class II-restricted T cells diverges markedly from the present view of antigen recognition by class I-restricted T lymphocytes, especially cytotoxic T lymphocytes (CTL). These cells seem specific for integral cell-membrane molecules such as viral envelope glycoproteins, allogeneic MHC molecules, or minor histocompatibility antigens that have been assumed (without any experimental evidence) to be uncharacterized membrane proteins. Immunologists presumed that these intact membrane proteins interacted directly with class I MHC molecules on the cell surface. However, such a marked difference between class I and class II antigen interaction became less and less likely as accumulating data showed striking similarities between the relationship of both class I and class II molecular structures to T-cell recognition¹³, and the use of the same Vand V_n gene segments by the receptors of class I- and class II-restricted T cells.

Experiments

The experiments of Townsend et al. 5 now reveal that these differences are more imagined than real, and that similar (though not necessarily identical) forms of antigen participate in recognition by all MHC-restricted T cells. The new findings

come from work on the specificity of both human and murine CTL generated by immunization with the influenza virus. Early studies' demonstrated many CTL clones that recognized specificities shared by distinct serotypes of this virus. The viral protein accounting for this cross-reactivity was, unexpectedly, the nucleo-protein and not the membrane-expressed haemagglutinin molecule. Confirmation of these results was obtained using L cells co-transfected with the proper class I gene and the nucleoprotein gene. These cells were recognized appropriately by the cross-reactive CTL clones'.

Given that interaction of CTL receptors with target cells occurs at the outer surface of the cell membrane, how can a molecule that does not appear on the membrane serve as a target antigen? This conundrum was partially solved by the demonstration that transfectants expressing truncated forms of the nucleoprotein molecule could serve as adequate CTL targets4. Finally, the experiments described in their most recent paper? show that, just as synthetic peptides could be used to stimulate class II-restricted T cells, target cells exposed in vitro to short synthetic peptides corresponding to certain regions of the nucleoprotein molecule could be recognized by nucleoprotein-specific CTL. The active peptides, as would be expected, correspond to regions of nucleoprotein sequence of the immunizing strain of virus that differ from the sequence of nucleoprotein of a strain of virus incapable of sensitizing cells for recognition by these particular CTL clones. Thus, it appeared unnecessary for the intact nucleoprotein mysteriously to reach the cell surface. Instead, some fragmented or degraded form probably serves as the antigen after travelling to the membrane by a mechanism independent of the normal intracellular sorting process acting on the intact nucleoprotein.

Similarities

Thus, we now have a satisfying similarity in the general nature of antigen recognized by both class I- and class IIrestricted T cells. The new data on CTL recognition also provide an explanation for the repeated failure of investigators to generate antibodies to minor histocompatibility antigens. Rather than constituting a family of intrinsic cell-membrane molecules, these antigens are more likely to represent processed fragments of cytoplasmic or nuclear proteins that normally never reach the membrane in an intact state, just as with influenza nucleoprotein. Even if antibodies were raised in response to the very small amount of such fragments that probably are present on the cell surface, they are not likely to be detected in binding or cytotoxcity assays.

The studies on influenza-specific CTL support the emerging view that antigen processing is not a specialized function of a small subset of class II-bearing, bone marrow-derived cells, but rather the reflection of a more fundamental set of intracellular activitites occurring in virtually all cells. An early hint that this might be the case came from experiments showing that fibroblasts made to express class II antigens by DNA-mediated gene transfer could also present various protein antigens to T cells, and that this function is susceptible to the same inhibitors that interfere with processing by haemato-poietic-presenting cells¹³. The demonstration by Townsend et al.5 that class Irestricted T cells are specific for antigen fragments suggests that most, if not all, cells have some capacity for antigen processing, because class I molecules are widely distributed on various somatic cell types, and CTL recognize virally infected or minor histocompatibility antigenbearing cells of diverse tissue origin.

Is the same intracellular pathway used for processing those antigens taken up from the external environment of the cell and those synthesized endogenously? Do both classes of MHC molecules interact with or present the same processed antigens? Recently published work by Morrison et al. "suggests the answer to both of these questions may be 'no'. These investigators find that influenza haemagglutinin sythesized endogenously can not be recognized by class II-restricted, haemagglutinin-specific T-cell clones, but provide an adequate target for class I-restricted cells. Conversely, the class I-restricted

clones ignore class II-bearing cells that had taken up haemagglutinin protein from the culture medium, which are excellent stimulators of class II-restricted lymphocytes. Furthermore, only the class IIdependent antigen presentation is sensitive to the drug chloroquine. Thus, there may be at least two distinct mechanisms for the production of immunogenic protein fragments, and there may be different pathways of intracellular transport for class I and class II molecules that determine the nature of the antigens with which they are recognized.

Model

possible

plasmic

A speculative scheme of antigen processing and presentation to T cells that takes into account these new data, the demonstration of binding between antigenic peptides and MHC molecules¹², and the recent intriguing report by Cresswell¹⁵ on the presence of class II molecules within the endocytic pathway, is given in the figure.

For exogenous protein antigens, the universally distributed endosomal recycling pathway¹⁶ is considered to have the central role, accounting for the ability of diverse cells to carry out antigen processing. Intact proteins enter the cell by either (fortuitous) binding to molecules engaged in receptor-mediated endocytosis, or as a result of pinocytosis. As the endosomes acidify during their intracellular passage,

this change itself, or the activation of acidpH-dependent, cathepsin-like proteases leads to the denaturation and-or fragmentation of the original protein molecules. A subset of the resultant peptides, perhaps already associated with class II MHC products, is transported to the cell surface in vesicles bringing molecules such as discharged transferrin receptors back to the membrane. The remaining peptides may go to the lysosomal compartment for complete degradation.

For endogenous proteins, processing may occur in a region of the transitional Golgi specialized for dealing with improperly folded proteins synthesized by the cell. Denatured or fragmented molecules in this compartment may escape sorting into secondary lysosomes, and be transported to the cell membrane along or together with class I molecules.

In both cases, selection of peptides for surface expression presumably depends on structural features that either enhance binding to MHC molecules or other potential carrier proteins cycling to the cell membrane, or that reduce the potential for transport to lysosomes. The α helical state that is hypothesized to be an important feature of immunogenic segments of a protein molecule may be critical in this regard^{17 18}. Once it is on the cell membrane, the antigen fragment would be available for recognition by the T.cell in conjunction with the appropriate MHC molecule.

Why did such complex schemes of antigen processing and presentation evolve? It has been suggested that antigen denaturation or fragmentation is necessary to create molecules with increased lipophilicity, thereby stabilizing interaction with the plasma membrane and increasing the effective local concentration of antigen in the environment of the MHC molecules. In addition, if direct binding of antigen to MHC molecules is essential for T-cell recognition, then proteins that in their native state are much larger than MHC molecules may need to be fragmentated to be effective immunogens.

What is particularly apparent in this emerging story is that phenomena considered to be primarily of immunological interest turn out to involve processes of substantial general importance to cell biology. Elucidation of the intracellular events involved in antigen processing will have broad import for our understanding of the traffic patterns followed by proteins within cells. The contributions of Townsend et al. remove a major conceptual stumbling block to research in this area and progress should now occur at an accelerating rate. It is also clear that this new picture of antigen recognition by CTL has important implications for the rational design of synthetic vaccines.

Finally, one should not forget the original question — what does the T cell see? With a solution of the crystal structure of HLA close at hand, the capacity to identify the minimal antigenic peptide recognized by a specific T cell together with this class I MHC n lecule may provide the means to create a physical picture of the antigen-MHC at lecular complex bound by the T-cell receptor.

illustration shows a schematic view of the several R (He pathways followed by antigen and MHC-encoded (H) B molecules in an antigen-presenting cell. E Endogenous antigens, such as viral ٥ Ď GOLGglycoproteins or nuc-ENDOSOME leoprotein, are syn-♦ ٥ LOW pH thesized in the endo-reticulum LYSOSOME and transported to the Golgi where they B are shown in an Ð intact and partially 0 degraded from. The peptide representing the immunogen then reaches the cell surface either 1) already G. ⅆⅎ associated with class (H-2, HLA-R CLASS II MHC (la) **EXOGENOUS ANTIGEN ENDOGENOUS ANTIGEN** A,B,C) molecules also exiting from ■ - PRESENTED R - PRESENTED 4 the Golgi in exoo - DEGRADED → - DEGRADED CLASS I MHC (H-2,HLA) cvtic vesicles (Path-

way A, top left), or 2) alone (Pathway C, bottom left), following which the peptide associates with class I molecules already on the cell membrane. For exogenous antigens presented in the context of class II molecules, intact antigen enters the cell by means of endocytic vesicles. As these acidify and partial proteolysis occurs, the immunogenic peptides are associated either 1) with class II molecules recycling from the cell surface in the same endosomes (Pathway B, upper right); 2) with newly synthesized class II molecules from the Golgi (Pathway E, centre); or 3) with class II molecules on the membrane, following transport of the peptide to the cell surface in exocytic vesicles (Pathway D, lower right). In all cases, other peptides are shown here as being transported directly into lysosomes for complete degradation, never reaching the membranes, and hence are unavailable to serve as immunogens.

Robertson, M. Nature 317, 768 (1985).

Townsend, A.R.M. & McMichael, A 1 Prog. Allerg. 36 10 (1985). Townsend, A.R.M., McMichael, A.J.

Huddleston, J.A. & Brownlee, G. G. Cell 39, 13 (1984) Townsend, A.R.M., Gotch, F.M. & Davey, J. Cell 42, 457

Townsend, A.R.M. et al. Cell 44, 959 (1986)

Kronenberg, M., Siu, G., Hood, L. F. & Sha tro N. 3. Rev. Immun. 4, 529 (198).

Schwartz, R.H. A. Rev. Immun 3, 23 + 1985)

Gell, P.G.H. & Benacerraf, B. Immunology = 54 (1979) Ziegler, H.K. & Unanue, F.R. Proc. natn. Vead. Sci. U.S.A. 79, 175 (1982).

Benacerraf, B. J. Immun. 120 1809 (1978)

Shimonkevitz, R., Kappler, J. Marrack, P. & Grey, H. J. exp. Med. 158, 303 (1983).

Schwartz, R.H. Natur 317.

- 13. Germain, R.N. & Wlissen, a (1986).
- Morrison, I. A., Luka Jer, A., J. Braciale, T.G. J. p. Med. 163. J
 Cresswell, P. Proc. natn. Acad. Sci. U
- (1985). Willingham, M.C. & Pastan, 1 Cell 21 7/1980
- Pincus, M.R., Gerewitz, F., Schwartz, R. H. & ... a. H.A. Proc. nam. Acad. Sci. U.S.A. 80, 3297 (1985). DeLisi, C. & Berzofsky, J.A. Proc. nam. Acad. Sci.
- U.S.A. 82, 7048 (1985).

Ronald N. Germain is in the Laboratory of Immunology, National Institutes of Health, Bethesda, Maryland 20892, USA.

Radionuclide deposition from the Chernobyl cloud

SIR—The accident at the Chernobyl nuclear power station in the Soviet Union created a cloud of radioactivity that affected a surprisingly large area of Europe. This letter concentrates on the main passage of this cloud over the United Kingdom and presents some results of preliminary investigations into the collected data on radioactivity levels in the air, in rain water, on grass and in milk, and attempts to link the time variations of these levels to meteorological conditions. In particular, we report that high levels measured on grass are linked to heavy rainfalls associated with thunderstorms embedded in the radioactive cloud.

The accident is believed to have begun at 01:23 local time on Saturday 26 April (20:23 GMT on Friday 25 April) and to have ended on the following Wednesday or Thursday. By the Monday, countries throughout Europe had been alerted and possible trajectories of the plume were being estimated, based on standard meteorological data. In many cases, analyses and forecasts from numerical weather prediction models were being used. Trajectories calculated at the Meteorological Office early in the week indicated a possible risk to the United Kingdom, and this possibility was strengthened when, on Wednesday, enhanced radiation levels were reported in northern Italy, indicating a first arrival in the United Kingdom on Friday 2 May.

Since then, more thorough analyses of the cloud movement have been carried out at the Meteorological Office and at many other centres throughout Europe, and Fig. 1 shows the most probable path of the cloud that affected the United Kingdom. This part of the cloud appeared to leave Chernobyl at ~12.00 GMT on 26 April, ~16 h after the start of the accident. The cloud moved rather slowly within the lower layers of the atmosphere towards the Baltic, and then on the Monday a finger moved more quickly southwestwards over Poland, Czechoslovakia, Austria and the Alpine area, as a result of a growing zone of high pressure running across the Low Countries from south-west to north-west and a depression over the Adriatic. When this high moved away on Thursday towards the north-west, the cloud turned forthwestwards over France towards the United Kingdom.

The requency of environmental montoring at a number of stations was inerce ed, and the National Radiological Protection Board acted as a focal point for collating and interpreting these data¹². Reports of elevated radiation levels in southern England were received before midday on Friday 2 May, and by late evening the cloud had reached the north

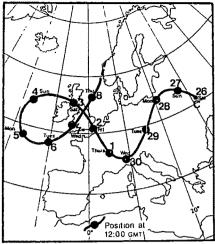


Fig. 1 Estimated path of the Chernobyl radioactive cloud which ultimately crossed the British Isles (26 April to 8 May 1986).

of England. The peak levels of γemitting radionuclides in the cloud were in the ranges shown in Table 1, and air concentrations in this range were observed later in Scotland and other parts of the British Isles, during the period 3-5 May. From this monitoring data and the data collected at the Meteorological Office we can derive a picture of the passage of the cloud, and Fig. 2a,b shows its position at 03:00 and 18:00 GMT on Saturday, 3 May. The cloud had entered Britain across the Kent-Sussex coast at ~05:00 GMT on the Friday morning, and moved northwards, until by the end of the day most of Britain was covered except for Cornwall, Devon, the western extremities of Wales and north-west Scotland. Generally, Friday was dry 'nd sunny, the air being of continental origin, although a few showers were experienced in the Solway and Clyde areas late in the day.

On Saturday some old thunderstorms moving up from France were revitalized as colder air aloft was advected over the warm continental air, owing to a rapidly deepening low-pressure area to the southwest of the country. These storms first affected the south-east in the early hours, and then moved over East Anglia and out into the North Sea. New storms developed rapidly in the morning over central England. These moved slowly northwards to Cumbria and south-west Scotland, feeding off the warm air in the lowest kilo-

metre of the atmosphere containing radionuclides from Chernobyl, and causing the cloud to shrink in area. By early Sunday morning the cloud was affecting Scotland alone, and by 09:00 GMT it had been swept westwards from the Outer Hebrides, only to return, at much lower concentrations, the following Wednesday and Thursday, having been swept right around the large low to the west. There is some evidence for a separate small part of the cloud having affected the United Kingdom on Sunday, when it seems the winds turned towards the south-east for a couple of hours, allowing a remnant from France to move northwards along the extreme east coast onto the far north of Scotland, where local rain gave high levels of radioactivity.

Radionuclides washed out by the rain produced elevated y-ray backgrounds of up to 0.6 uSv h⁻¹ (about three times the normal level) in areas where it rained heavily, and this rain-out effect could be observed directly by measuring deposition densities on grass, as has been reported'. The effect was reflected more directly in concentrations in rain water (Table 1), which varied from 10 to 1×10^4 Bq I⁻¹ for ¹³¹I. The highest levels were those reported from Scotland², which were very close to the derived emergency reference level (DERL) for ¹³⁴I in drinking water³. The DERLs are based on an effective dose equivalent of 5 mSv or an organ dose of 50 mSv, which ever is the more restrictive, corresponding to the annual dose limits recommended by the International Commission on Radiological Protection for exposure of the public over a few years. The levels in rain water were followed by elevated levels in foodstuffs such as vegetables and cows' milk, but levels of "I in these foodstuffs did not exceed DERLs in any part of the country. The incorporation of radionuclides into animal tissues has been monitored by the Ministry of Agriculture, Fisheries and Food, which has issued data on meat, milk, vegetables and other foodstuffs5.

It is possible to use food monitoring data to infer deposition in areas of the country that could not be directly monitored, and match this with data on rainfall from the Meteorological Office. For example, subsequent monitoring of

Table 1 Ranges of peak air and rain-water concentrations of radionuclides observed in the British Isles during 2–5 May 1986

Radionuclide	Air concentrations (Bq m ⁻³)	Rain-water concentrations (Bq l ⁻¹)
131 <u>T</u>	1–10	10-10,000
¹³² Te- ¹³² I	1–10	10-10,000
¹⁰³ Ru	0.5–5	20-2,000
¹⁰⁶ Ru	0.3–3	10-1,000
¹³⁴ Cs	0.3-3	10-1,000
¹³⁷ Cs	0.5–5	20-2,000
140Ba-140La	0.3-3	10-1,000

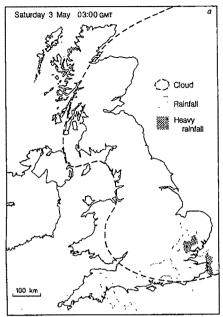




Fig 2 Chernobyl cloud and associated rainfall on 3 May 1986.

levels of 191 in cows' milk2 and sheep's milk from the south-east, East Anglia and the Midlands confirm that some wet deposition occurred in parts of southern England during the early hours of Saturday, 3 May (see Fig. 2), although the rainfall was not so prolonged as that observed later in parts of north Wales. north-west England and Scotland.

F.B. SMITH

The Meteorological Office. Bracknell RG122SZ, UK

M.J. CLARK

National Radiological Protection Board. Chilton, Didcot OX11 0RQ, UK

- 1. Fty, F.A., Clarke, R.H. & O'Riordan, M.C. Nature 321, 193-95 (1986).
 2. Levels of Radioactivity in the UK from the Accident at
- Chernobyl (HMSO, London 1986). NRPB DL10 (HMSO, London 1986).
- International Commission on Radrological Protection, Ann. ICRP 14 (2), (1984).
- Ministry of Agriculture, Fisheries and Food Press Release, 30 May (1986).

How many reactor accidents will there be?

SIR—The designers of nuclear reactors claim that the chance of a reactor accident should be less than one in 10° per reactor year. The US Rasmussen report and the German safety study found that there is a fifty-fifty chance that such accidents could occur every 23,000 and 10,000 reactor-years respectively. Two or three serious accidents suggest the standard has not been met in practice, and that the method of 'technical risk assessment' used to calculate such probabilities must be replaced by risk assessments which use data from operating experience.

At the end of 1985, according to the IAEA data file', there were 374 reactors in operation in the world with a total operating experience of 3,831 years. We assume that until the end of May 1986, the cumulative operating experience had been 4,000 years. There had been two major accidents - Three Mile Island and Chernobyl — during this operational period.

We do not count the Windscale of 1957 because it was a military reactor. We think that the reactor designers would claim that the safety systems of early reactors were not as good as the present ones. The British reactor designers were under pressure at that time. Military commitment to build several plutonium producing reactors came at a time when the civilian nuclear programme was emerging. The nuclear industry was expanding so quickly that there was an acute shortage of experienced scientists and engineers.

We assume that the accidents are a Poisson process with intensity r. The probability of finding two accidents in an interval of length T = 4,000 reactor-years is then Poisson distributed:

$$P(2, rT) = r^2 T^2 e^{-rT}/2$$
 (1)

If we want this to be a probability density, we have to normalize it. The normalization being:

$$N(T) = \int_{-\infty}^{\infty} dr P(2, rT) = 1/T$$
 (2)

The density is then

$$P_r = r^2 T^3 e^{-rT}/2 (3)$$

The numerical value of P_r is not a probability. However, we can think of P.dr as the element of probability — for example, the probability that r lies between r_1 (0.0004) and r, (0.006) is obtained by integrating equation (3) between r_1 and r_2 and is found to be 0.21. This indicates that the probability that one significant accident will occur between 1,667 and 2,500 reactor years is 21%.

Another way of dealing with this density is to take into consideration that the

probability of the occurrence of at least one accident in a Poisson process of intensity r in a time interval t is

$$P(1,rt) = 1 - e^{-n} \tag{4}$$

Since r is unknown, we have to integrate equation (4) overall r with the 'empirical' density P as a weighting factor, that is:

$$P(1,t) = \int_{0}^{\infty} dr (1 - e^{-rt}) r^{2} T^{3} e^{-rt}/2$$

= 1 - (1 + t/T)⁻³ (5)

Equation (5) gives the probability of having at least one accident during the next t years. The probability that a reactor accident could happen during the next decade ($t = 374 \text{ reactors} \times 10 \text{ years} =$ 3.740 reactor-years) is 86%.

There is no circularity in the arguments used above. There must be some input data in any model. Our input is two accidents in 4,000 reactor years. Of course, we know that two accidents are not 'representative'. With 374 reactors in operation. we would naively expect one accident every 5.4 years. But our model assigns a 70% probability that one accident could happen in the next 5.4 years, not a certainty. Similarly the probability of having one accident every two decades is more than 95%.

It is true that events with high probability need not necessarily materialize. But how can we reconcile these findings with the claims of the reactor designers that the chance of a reactor accident should be less than 10 " per reactor-year? The reactor designers calculate such probabilities with

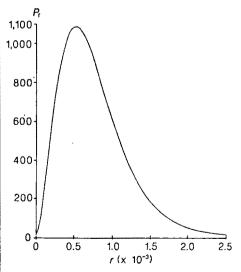


Fig. 1 P_c gives the likelihood of a significant accident given the total operating experience of 4,000 reactor-years and two significant accidents. The number of significant accidents per reactor year is measured by r. The probability that this number lies between r_1 and r_2 accidents per reactor year is given by the area under the curve between r_1 and r_2 , that is, by integrating equation (1) between r_i and r_{ij} .

the help of a decision tree. The likelihood of the failure of a reactor component or safety system is assessed and its consequences on other components or subsystems are estimated. These results in their turn are inputs for a chain of calculations leading to probabilistic risk assessment used by the reactor designers. Since the number of vulnerable components is rather high, this procedure cannot be rigorous. Our view is that this method should be replaced by risk assessment using the observed data.

We thank Professor K.E. Eriksson of Göteborg and Dr K. Hildenbrand of Bonn for helpful discussion and correspon-

S. ISLAM

International Study Group on Self-organization Bohlweg 44, 3300 Braunschweig, FRG

K. LINDGREN

Physical Resource Theory Group, Chalmers University of Technology, University of Göteborg, 41296 Göteborg, Sweden

- Reactor Sufety Study (Nuclear Regulatory Commission, Washington DC, 1975).
- Die deutsche Risikostudie (Federal Ministry of Research and Technology, Bonn, 1979).
 IAEA Bull. 28(1), 71 (1986).

¹³¹I in ruminant thyroids after nuclear releases

SIR—The substantial yield of 131 I from nuclear fission, its energetic β and γ emission and its concentration in the thyroid gland have led to the recognition of this nuclide as a significant nuclear hazard¹⁻³. In the late 1950s the Medical Research Council funded a study of 131 I accumulation in the thyroid glands of sheep from fallout arising from nuclear weapons tests. This study was in progress during the accident at Windscale in October 1957 and during the Northern Hemisphere weapons testing of October-December 1958 in which 29 (17 Soviet and 12 American) weapons were detonated. British weapons at that time were detonated in the Southern Hemisphere, having little effect on fallout in the United Kingdom².

It was therefore of interest to measure 131 I accumulation in sheep thyroid glands following pasture contamination with fallout from the Chernobyl reactor, to obtain a comparison with the earlier measurements. Thyroid glands were collected from fatstock from 20 May to 17 June. At this time sheep were at pasture and hence directly ingesting any nuclides on the grass. Because of the late spring, fat cattle were generally not at pasture at the time of maximum contamination, on 2 May'.

Figure 1 shows thyroid ¹³¹I radioactivity from sheep grazing in Scotland during the autumn of 1958' and in East Anglia during

the spring of 1986. It can be seen that thyroid radioactivity following the Chernobyl accident was marginally higher than that resulting from the nuclear weapons testing during the autmun of 1958. By contrast, the highest sheep thyroid "I measured in the maximum deposition area near Windscale 31 days after the reactor accident was 7.4×10⁴ Bq g⁻¹, 300 times higher than the radioactivity measured after Chernobyl. In the sheep thyroid glands recently measured, the radioactivity had a half-life on storage of 8.05 days, showing that ¹³¹I alone was present. Comparison of radioactivities on different dates of collection showed a biological half-life of about 6 days.

Cattle thyroid glands are less useful than those of sheep for monitoring fallout, because of the widespread practice of feeding beef cattle indoors on stored fodder for much of the year. Thyroid 131 I in stall-fed sheep following a period of radioactive fallout from nuclear weapons testing by the United States showed only 0.7% of the radioactivity in grazing sheep4; a limited number of human thyroids also showed ~ 1% of the radioactivity of sheep4. Five cattle thyroids collected recently in East Anglia showed a mean of 0.97 ± 0.13 Bq g⁻¹, compared with $99\pm5 \,\mathrm{Bg}\,\mathrm{g}^{-1}$ for sheep killed the same day. One other cow, however, had 61.7 Bq g 131 I, which must have resulted from grazing on contaminated pasture.

Data already published showed human thyroid radioactivities after Chernobyl of 2-33 Bq, the highest concentration being ~7 Bq g⁻¹, in a child, while adults showed a maximum radioactivity of 1.7 Bq g⁻¹. Sheep thyroid radioactivity on the same date measured 243 \pm 48 Bq g⁻¹ (n=15), with a range of 39-703 Bq g

¹³¹I from a reactor accident is capable of contaminating pasture for a considerable distance downwind. Most human inges-

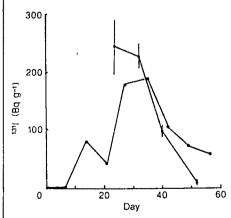


Fig. 1 Sheep thyroid radioactivity following the reactor accident at Chernobyl (1) and the nuclear weapons testing of the autumn of 1958 (•). Day 0 has been taken as the day of the Chernobyl accident (26 April 1986), or the peak of nuclear weapons testing (3 November 1958). ¹³I activity is given in Bq g⁻¹ wet weight of gland (± standard error of mean).

tion of tal derived from fallout comes through milk, as the mammary gland effectively concentrates dietary iodine into milk". To minimize the human ingestion of ¹⁴I, a reasonable precaution would be to feed dairy cattle stored fodder while pastures are measurably contaminated.

I thank Mr Martin Collins for collection of the thyroid glands and the University Pathology Department for the use of their γ-counter.

IAN R. FALCONER

Department of Biochemistry, University of Cambridge, Tennis Court Road. Cambridge CB2 1QW, UK

- Van Middlesworth, L. Science 123, 982 (1956).
- Marston, H.R. Aust, J. biol. Sci. 11, 382 (1958).
- Maycock, G. & Vennart, J. Nature 182, 1545-1547
- 4. Robertson, H.A. & Falconer, I.R. Nature 184, 1699-1703 (1959).
- Hill, C.R., Adam, J., Anderson, W., Ott, R.J. & Sowby, F.D. Nature 321, 655-656 (1986).
- 6. Robertson, H.A. & Falconer, I.R. J. Endocr. 22, 133-

Fault striations slip from sight?

SIR—Communication of ideas begins with agreement on the meaning of terms. Unfortunately, in discussions on mesofaults and their surface textures, terms are endowed with different meanings with alarming ease thus giving rise to considerable confusion. A glaring example is the term 'slickenside'.

Linear structures on fault planes (grooves or fibrous grains) represent the orientation of the relative displacement between adjacent fault blocks. Recently many techniques have been developed to determine from slip orientation data the attitude and relative magnitudes of the principal stresses responsible for the deformation. Such data are of paramount importance in the study of neotectonics relating recent plate motions to deformation within continents. The problem is that some authors12 use slickenside to refer to planar structures whereas others² use it to describe a lineation.

Etymologically slickenside smooth plane, which is how it was first defined in 1822. Surely this should remain as the agreed meaning. The associated linear structures are best termed striations; qualifying words, such as fibre and scratch, are adequate to distinguish accretionary crystal growths from abrasion structures4.

CLIVE A. BOULTER

Department of Geology, University of Nottingham, University Park, Nottingham NG72RD, UK

- Fleuty, M.J. Geol. Mag. 112, 319-322 (1975).
- Dennis, J.G. Am. Ass. Petrol. Geol. Mem. No.7 (1967).
 Peltzer, G., Tapponnier, P., Zhang Zhitao & Xu Zhi Qin. Nature 317, 500-505 (1985).
- Sporli, K.B. & Anderson, H.J. N.Z. J. Geol. Geophys. 23, 155-166 (1980).

Star on the make?

Colin Patterson

The Nemesis Affair: A Story of the Death of Dinosaurs and the Ways of Science. By David M. Raup. Norton: 1986. Pp. 220. \$15.95, £12.

"I HAVE never seen Francis Crick in a modest mood" is one way to start a book; "This is the story of an emerging scientific theory about the extinction of dinosaurs and other prehistoric life forms" is another. With the first sentence of *The Double Helix* we know just where we are—the academician is out of school, the bag is open and the cat is flying, together with whatever else was in there. The opening of *The Nemesis Affair* does not set the scene so plainly. Is the academician in or out of school, and if in, what class are we with?

Of course it is unfair to compare David Raup's book with Watson's, but Raup is used to the ways of science and knows they are not paved with fairness. It is not often that a leading professional tells the tale while still close to the events — Raup calls it "a view from the trenches" - and the Watson/Raup comparison does bring out aspects of the ways of science. For one thing, the pace is killing today: there was a gap of 15 years between the events Watson wrote of and his book, whereas Raup hits the streets only two years after the birth of Nemesis, the name given in Nature of 19 April 1984 to a possible companion star to the Sun, producing periodic comet showers and mass extinc-

Nemesis was born as one of several possible causes for a possible series of events. In February 1984 (Proceedings of the National Academy of Sciences, 81, 801-805), Raup and Jack Sepkoski published a statistical analysis of Sepkoski's data on the first and last appearance of each marine family in the fossil record. They concluded that extinction is non-random, with a 26 Myr periodicity; one of their eight bestfitting mass extinctions is at the Cretaceous/Tertiary boundary, hot property since 1980 because of the iridium spike which may imply extraterrestrial impact. Six weeks after the Raup and Sepkoski paper in PNAS came the 19th April Nature containing an editorial by John Maddox, a "News and Views" piece by Tony Hallam, and a block of five papers, all bearing on extraterrestrial causes of periodic mass extinction. (Turning back to Nature in 1953, the Watson and Crick paper didn't merit mention in "News and Views", which then read rather like the Court Circular.) Maddox's editorial commented (Raup calls it "mild wrist slapping") on the practice of distributing preprints, which in this case resulted in the possibility of the *Nature* papers appearing *before* the Raup and Sepkoski data they purported to explain. John Maddox saw this as "a kind of nonsense", but at least it is nonsense with a limit. The pace can get no hotter once the hound and hare coincide.

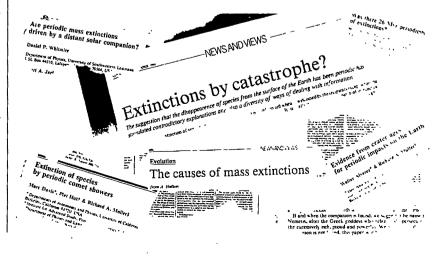
Since 1984, it is hard to pick up a journal in the fields of geology and evolutionary biology which doesn't contain a paper, review or meeting report touching on mass extinctions. DNA was slower to get up steam, but once it got going it was unstoppable, and we all know what has been achieved. Can we expect a similar profoundly important research programme from Nemesis et al? I think not, and Raup gives no real sign that he thinks otherwise. He ends his book with some comments on the pecking order from "hard" to "soft" science, placing molecular biology at the hard end and palaeontology (his own field) at the soft. We can see now that Watson and Crick's achievement was to begin to move parts of biology from the historical (soft) towards the physical (hard) end of the spectrum to put some determinism among the contingency. Periodicity in mass extinctions, and extraterrestrial explanations for it, might seem to promise the same for parts of palaeontology. But, so far, the controversies over periodicity and the less general question of extraterrestrial impact as the cause behind particular extinctions exemplify the field of sociology (which Raup puts right at the bottom of the pecking order) as much as hard science. Recalling Raup's "view from the trenches", those involved seem first instinctively to have either volunteered for the neocatastrophist revolutionary force

rallied to the flag of Lyellian uniformitarianism, and then started looking around for ammunition. (The latest skirmish in *Nature* was "Matters Arising" in May this year (321, 533-536).)

Raup has some level-headed comment on the prevalence of prejudice and preconception in his chapter on "Belief Systems in Science", but ultimately the Raup and Sepkoski periodicity thesis (and so the possibility of Nemesis) rests on the quality of Sepkoski's taxonomic data. That is where I believe the thesis is weakest, but the attack will necessarily be slow and piecemeal. The Double Helix was a success story, whereas Raup's book may turn out to be (as he acknowledges) just the happier half of a chronicle of failure. If so, he may find a benefit in avoiding "saganization", the word he coins for the (unmerited) fall in professional esteem that accompanies the rise in visibility of any scientist taken up by the

Like The Double Helix, Raup's book can be read at a sitting. What gripped the reader in Watson's story was the personalities, the emotions, the indiscretions. Perhaps because he is still so close to the events and to the people, Raup has left all that out; his colleagues or opponents are characterised as no more than "brilliant", "prominent" or "hardworking". No one will take offence at the book, but the lack of emotion or indiscretion means that the narrative and the writing have to do a lot of work. On the whole, they stand up to the strain; the pace of the narrative picks up in the second half of the book once the scene has been set, and the writing is good popularization, though occasionally slipping a bit too far down market. The first words of "what is known as the Upper Eocene" or "what are called the Middle and Upper Jurassic" are no sop to anyone, and the sentence that Raup and I (unfairly) begin with does not set the true tone of the book.

Colin Patterson is a vertebrate palaeontologist at the British Museum (Natural History), London SW75BD, UK.



When they stayed away from Paris

Robert Fox

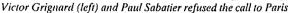
Science in the Provinces: Scientific Communities and Provincial Leadership in France, 1860-1930. By Mary Jo Nye, *University of California Press*, 1986. Pp. 328. \$39.95, £33.95.

OVER the past decade, the community and institutions of French science in the nineteenth and early twentieth centuries have been subjected to an unprecedented onslaught by historians. Oddly, the trail has been blazed by scholars working in Britain and North America, and it is they above all who have fashioned the developing consensus to which Mary Jo Nye's book makes a notable contribution. In the new orthodoxy, two points have emerged strongly. The first is that in the half century or so before the First World War the majority of French savants abandoned their traditional preoccupation with abstraction and pure knowledge and became increasingly concerned, even besotted, with the applications of science. The second is that the scientific life of the provinces deserves to be treated quite as seriously as that of the capital and that it is quite misleading (though understandably convenient) to equate an assessment of Parisian science with that of French science as a whole.

Both of these points are developed to good effect in Science in the Provinces. The book is structured around a series of studies of the science faculties of Nancy. Grenoble, Toulouse, Lyons and Bordeaux, and it uses those studies to display the faculties as seats of scientific vitality and institutional innovation, with local industrial, agricultural and commercial interests often serving as a source of problems and a spur to action. Strikingly, Nye's faculties all lie in a crescent sweeping from the Gironde, through the Midi and up into Lorraine. Here, it seems the provincial tradition in science developed with special vigour: certainly, it would be hard to think of professors in the faculties of the centre or the north-west of France at Clermont-Ferrand, Poitiers or Rennes, for example - who would bear comparison with the undisputed "stars" who sustain Nye's case for each of her five

By digressing liberally on the work of individuals, rather than attempting a comprehensive prosopography. Nye allows the content of the science she treats to come to the foreground, where it belongs. Not all the science has stood the test of time, to be sure: René Blondlot's false discovery of a new radiation — N-rays — in 1903 is a case in point. But by the time





Victor Grignard (of Lyons and then Nancy) and Paul Sabatier (of Toulouse) shared the Nobel prize for chemistry in 1912, the provincial faculties of science had to be taken seriously, the more so as certain professors (including Grignard and Sabatier) ostentatiously refused the call to a Parisian chair. Their resistance was understandable: good facilities, local adulation and a sense of contributing to the regional economy were the rewards on offer and, for about 20 years from 1900, they sufficed to reduce the flow of talent to the capital. In the longer run, however, what seems to have been the natural order of things reasserted itself. By the 1930s, the provincial faculties had become once again the poor relations of a cripplingly impoverished university system, and even Grignard had lost his old assertiveness and hope that the imbalance between Paris



and the provinces might be removed.

Nye's discussion of Grignard adds poignancy to the story of a valiant but doomed campaign for diversity. It is a story well worth telling and with some bearing on present educational debates not only in France but also in Britain. It suggests, at least to a reader of gloomy disposition, that although centres of excellence can be fashioned on the margins of the traditional academic world, they are instrinsically fragile creations condemned to a thorny path and, in all probability, an ephemeral existence.

Robert Fox is British Academy Reader in the Humanities at the University of Lancaster, Lancaster LAI 4YG. From September, he will be Director of the Centre de Recherche en Histoire des Sciences et de l'Industrie at the Cité des Sciences et de l'Industrie, 75930 Paris Cedex 19, France.

Stones in the service of society

D.V. Ager

The Stones of Britain: Landscapes and Monuments, Quarries and Cathedrals. By Richard Muir. *Michael Joseph: 1968. Pp.288. £15.95.*

When we were in the United States and our daughter was only one year old, she greatly impressed the locals by referring to the erratic blocks of the glaciated Mid-West as "rocks" rather than "stones". That came of growing up in a geological family. Geologists do not study "stones" unless they be of the "precious" or "semi-precious" variety. The only other exception is building "stones", which are the main subject of Richard Muir's book.

Muir is a geographer and tells us right at the beginning that he is not writing about geology because "geology is a technical Skara Brae in the Orkneys. I have a theory

subject". So this is a book for the architect and the aesthete rather than the scientist. It is a book about man in Britain using the rocks beneath his feet, first for implements, then for monuments and finally for buildings.

The first part deals with "stone" in the landscape. This Muir divides into three: "Hard Rock Landscapes", which means chiefly the granites of Cornwall and the Ordovician volcanics of the Lake District; "Sandstone Scenery", which curiously includes the brick-making clay-pits; and "Landscapes of Limestone", which includes the chalk but hardly the flints which that lithology contains.

Flints come into their own in the next part of the book, on the use of stone by prehistoric communities. Here are accounts of stone tools (which, it is worth recalling, served man for nearly 99 per cent of his history and of which there is a particularly good record in Britain), cave dwellings (somewhat inappropriately) and then the first stone huts, starting with Skara Brae in the Orkneys. I have a theory

that the oldest buildings in Europe — in the Orkneys and in Malta – are still there simply because of the ease with which the local stone could be worked so that it was not worth the trouble of pulling the huts down again to build more up-to-date residences. Muir then moves on to burial chambers and stone monuments. He makes some rather doubtful remarks about Stonehenge but does not mention the unlikely theory (albeit sanctified in the Geological Museum) that the "blue stones" were brought from Wales by ice rather than by human muscle.

The third and most interesting part of the book deals with what the author calls "The Rise and Fall of Building Stone" in the great mediaeval cathedrals and castles. The biggest problem was the cost of transport before the coming of canals and railways, when the movement of heavy materials was largely restricted to natural waterways. The local stone was mostly Jurassic limestone or Devonian sandstone, though other local rocks were obviously used when convenient. Muir describes quarrying methods, and the mason's art in relation to changing architectural styles, and relates economic and social history to the remarkable phenomenon of great stone buildings which only ended (as I see it) with gunpowder, Ann Boleyn and the Reformation.

There is much less in the book about domestic architecture, the triumph of which was surely the cottages and walls of the Cotswolds with the "sunlight" in their local Middle Jurassic limestones, and even less on post-mediaeval building in stone. The use of Permian Magnesian Limestone in the Houses of Parliament is mentioned, though not the disastrous effects of the acid London atmosphere in turning them into Epsom Salts!

Muir talks disparagingly of brick (also apparently a form of "stone"), but does not, in my view, say enough about the uppermost Jurassic Portland Stone which Wren used to rebuild church and state in London after the great fire of 1666 and which then spread throughout southern Britain as the pale face of bureaucracy. Thus, characteristically, it is used in Swansea for the Guildhall, whilst the prison is built more prosaically of the local Pennant Sandstone. Banks, on the other hand, seem to depend on the Aberdeen granites to give them a proper air of dependability, while Cornish granites provide our hardwearing kerb-stones.

For its intended audience this is a fascinating book, well-written and easy to read. Personally, I would have liked to have had also a simpler guide, little more than: "Salisbury Cathedral — Chilmark Stone" and then where Chilmark is and the geological age of its building stone.

Derek Ager is Research Professor in the Department of Geology, University College of Swansea, Swansea, SA2 8PP, UK.

Fascinating family

Frances C. James

Blackbirds of the Americas. By Gordon Orians. *University of Washington Press:* 1985. Pp.163. \$24.95, £18.

When American ornithologists use the term "blackbird", they mean a member of the subfamily Icterinae, a group confined to the Western Hemisphere. Among the 94 species are not only the familiar red-winged blackbird, the brown-headed cowbird and the common grackle, whose immense roosts are a nuisance to farmers, but also many colourful species of New World orioles and meadowlarks, and the tropical oropendolas and caciques. The lineage is as diverse in social behaviour and breeding biology as it is in physical appearance and distribution.

Gordon Orians' fascination with blackbirds has taken him from Canada to Argentina, from marshes to deserts, from savannas to tropical forests. In this attractive volume, he introduces American blackbirds to the layman, the birdwatcher who has mastered the field guide and wants to learn more. His informal writing style, in combination with the many striking drawings by Tony Angell, makes the book seem friendly, even though it is densely packed with information. And the comparative approach, a la David Lack, leads to new perspectives on the subject matter.

In an attempt to touch more generally on what evolutionary biologists do. Orians describes his own experiments and those of others. He discusses applications of optimal foraging theory and kin selection theory to interpretations of behavioural data, and confesses that the work was not designed to test these constructs but merely to use them to organize information. Here both the strengths and weaknesses of a controversial area of biology are revealed. The sceptical layman may well decide that biologists are still a long way from the goal of understanding mechanisms of adaptation

The book is dressy, rich in detail and vet easy to read. References and appendices are included for the reader who wants to go further. Orians has fully achieved his objectives, perhaps even more than he intended.

Frances C. James is a Professor with Department of Biological Science, The Florida State University, Tallahassee, Florida 32306 U.S.A.

For the future

Lynton K. Caldwell

World Resources 1986: An Assessment of the Resource Base that Supports the Global Economy. World Resources Institute and International Institute for Environment and Development. Basic Books/Harper & Row:1986. Pp.353. Hbk \$32.95, £22.95; pbk \$16.95, £11.95.

This reference source is the first volume of a projected annual series. Aspects of ten resource-environment topics are reviewed, with data tables for each of them and also for selected materials, minerals and basic economic indicators. Subsequent volumes will cover other aspects of the subject and a new one, on biogeochemical cycles, is planned for 1987.

Among the topics covered are population; human settlements; food and agriculture; forests and rangelands; wild-life and habitat; energy; freshwater; oceans and coasts; atmosphere and climate; and policies and institutions. The editors acknowledge the difficulty of organizing a volume in which all the material is interrelated, but while some division by topic was unavoidable and artificial the reader is assisted by a detailed table of contents, an index and frequent cross-referencing.

A further difficulty in compiling a book such as this is the frequent inadequacy of

the information available. The editors found "gaping holes in basic knowledge", and the prospects for closing these gaps are often diminished by lack of reliable indicative criteria and of comparability of the data. One of the main objectives of the World Resources series is to help remedy these deficiencies, and to provide assessments of the global resource base that can be relied upon in the formulation of national and international policies for resources and environment.

World Resources 1986 is an impressive compilation, well-designed for ready reference. Some minor textual errors are inevitable in a production of this kind, out I found no misleading errors of substance. It is not, however, the only source of information on world resources and environment. Since 1984 the Worldwatch Institute, under the direction of Lester R. Brown, has published an annual State of the World report - but although the two publications deal with many of the same issues they are complementary rather than competitive. Both are predicated on the proposition that the world environment is rapidly deteriorating under human mismanagment, but can be saved if timely action is taken. Both avoid the "gloom and doom" approach to the predicament of mankind. In 1984 the World Resources Institute sponsored The Global Possible Conference, principal papers from which were published in 1985 by Yale University Press. Similarly, the Worldwatch volume is advocacy for an

ecologically sustainable society which its editors and authors believe to be possible.

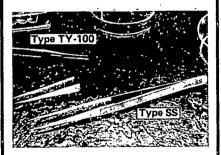
Having emphasized the virtues of these reports. I should point out what they do not offer. They do not provide a comprehensive survey of scholarly and scientific research on the topics covered (nor should this be expected). And, although they are policy-orientated. I believe that few social scientists would regard their views on such matters as adequate or indeed as realistic.

World Resources 1986 is largely a straightforward and factual account. I have no quarrel with the conclusions reached in the treatment of policies and institutions, but the report as a whole does not address the question of the human will to achieve the "global possible". Neither. unfortunately, have social and behavioural scientists seriously addressed this question, although some have begun to ask it. The "global probable" would have more to do with values, assumptions, ideologies and behavioural patterns than with ecosystems or energy production. An assessment of human prospects for realizing the possible could be very useful in developing strategies for a sustainable

Lynton K. Caldwell is Arthur F. Bentley Professor of Political Science Emeritus, Advanced Studies in Science, Technology, and Public Policy, Indiana University, Bloomington, Indiana 47405, USA.

NEW CERAMICS PRECISION: FUNA-TWEEZERS =





"FUNA-TWEEZERS" can eliminate all demerits of stainless or plastic tweezers. The stainless stems of Type SS and the Derlin stems with glass reinforcing agent of Type TY-100 give appropriate elasticity.

These show excellent features such as high anti-corrosiveness, heat insulation, high flame resistance, etc. These are also free from plastic deformation, metallic contamination and magnetization, etc.

These tweezers are contributing to the industries and research such as Biotechnology, Electronics, etc.

FUNAKOSHI PHARMACEUTICAL CO., LTD. Science Business Div. Research Material Sect. 2-3 Surugadai, Kanda, Chiyoda-ku, Tokyo, Japan Telephone: Tokyo 03-293-2352

Telefax : 81-3-295-5545 Telex : J28469 FUNA

Energy for life

Owen T.G. Jones

The Vital Force: A Study of Bioenergetics. By Franklin M. Harold. W.H. Freeman: 1986. Pp.577. Hbk \$37.95.£19.95.

BIOENERGETICS attempts to explain how cells generate useful energy and how this conserved energy is used in the enormous range of activities that can be defined as work. As these activities include the capacity to respond to changes in the environment, to move, to grow and to reproduce. it is apparent that a comprehensive account of bioenergetics could encompass much of biochemistry and cell biology. Dr Franklin Harold has accepted the challenge in The Vital Force. He not only covers well the expected topics of oxidative phosphorylation, photophosphorylation, ion transport, active transport processes and muscle contraction, but also includes the motility of bacterial and animal cells and the involvement of ion fluxes in the transduction of signals from the cell membrane to the cytosol and the nucleus.

It is, of course, ambitious of one author to range over topics which are so extensive and which are developing rapidly, but his attention to the bioenergetic aspects of these complex events permits him to disentangle common properties of apparently disparate processes. The significance of protein phosphorylation in regulating cellular activities and the everincreasing evidence of the importance of changes in the concentration of intracellular Ca²⁺ and other ions in cell division and differentiation support Harold's wide-ranging coverage.

The book opens with a comprehensible and simplified account of the thermodynamics necessary to understand problems of bioenergetics. The author adopts the view that the major disputes of the chemiosmotic wars are now settled and that energy conservation is by mechanisms closely related to those proposed by Peter Mitchell. He does, however, give an account of the background to these disputes - such as whether energy coupling arose from protons extruded into the bulk phase or from protons localised within the anhydrous phase of the membrane - and also explains why there have been such a range of values for the ratio of protons translocated during electron flow to ATP produced. In following his explanations. the reader will gain an understanding of the thermodynamics of ion movement and ATP synthesis and why it is important. From this clear account, the reader will also learn what a proton-motive Q cycle is. why it is necessary for a satisfactory formulation of the chemiosmotic hypothesis, and the relative merits of redox loops

and conformational pumps as mechanisms to transport protons.

The author is particularly familiar with the energetic problems of microorganisms and he writes on these with authority. Bacteria can face alarming problems of maintaining osmotic pressure and cytoplasmic pH near neutrality whilst growing at a pH2 or pH11 or in salt concentrations around 5M. Their strategies for coping with life at these extremes are not fully understood, but Harold does show how much information of very general significance can come from the study of relatively obscure organisms. Halobacteria. for example, have the simplest of proton pumps and the determination of its structure has been a great stimulus to thought. One minor criticism is that Harold's description of the reaction centre of photosynthetic bacteria does not include an account of its crystal structure which has so elegantly confirmed the arrangement of pigments and electron transport carriers which he describes. These had been predicted by bioenergeticists from their more usual techniques of measurement of flash-induced spectroscopic changes during the generation of light-driven transmembrane electric field. Such structural studies on complex protein assemblies are at last starting to answer some of the important questions about fundamental mechanisms in energy conservation.

The Vital Force is a substantial volume. in size and content. It will be a useful reference book for the specialist and will provide a good initiation for the more general reader. In the area of accepted bioenergetics its coverage is comprehensive and authoritative. On the topics Harold is now claiming for bioenergetics - the cytoskeleton, the generation of intracellular signals and morphogenesis he brings to our attention much important and exciting work. The measurement of the movement of Ca²⁻ ions is likely to provide as much employment for biochemists and cell biologists in the future as has the measurement of proton movements in the past.

Owen T.G. Jones is Professor of Biochemistry, Medical School, University of Bristol, Bristol BS8 1TD, UK.

New Editions

- Energy and the Atmosphere, 2nd Edn, by I.M. Campbell (Wiley; hbk \$57, £34,95; pbk \$22,25, £13,50).
- State of the World 1986, by Lester Brown et al., Worldwatch Institute, (Norton: pbk \$10.50, £7.50).
- Techniques in Bioproductivity and Photosynthesis, 2nd Edn, edited by J. Coombs et al. (Pergamon; hbk £24.50, \$32; pbk £12.75, \$17).
- The Periodic Table of the Elements (2nd Edn), by R.J. Puddephatt and P.K. Monaghan (Oxford UP: hbk £15, \$27.50; pbk £6.95, \$10.95).

Gene regulation by proteins acting nearby and at a distance

Mark Ptashne

Department of Biochemistry and Molecular Biology, Harvard University, 7 Divinity Avenue, Cambridge, Massachusetts 02138, USA

Transcription of genes can be controlled by regulatory proteins that bind to sites on the DNA either nearby or at a considerable distance. Recent experiments suggest a unified view of these apparently disparate types of gene regulation.

THERE are many examples in prokaryotes and eukaryotes of the following phenomenon: a protein bound at a specific DNA site influences the transcription of a gene hundreds or even thousands of base pairs away. For example, in eukaryotes, proteins bound at a site called an enhancer can turn on transcription of a distant gene. Regulatory proteins thus influence the activity of another protein (RNA polymerase) at a distance—how is this possible? Those who would tentatively throw all such examples into one basket and search for a common mechanism (and I am one) divide into distinct camps: the twisters; sliders, oozers and loopers.

My purpose is to review selectively recent experiments that support the loopers and to varying degrees weigh against the first three camps. The discussion unfolds within the context of our firm understanding of how one class of regulators, exemplified by the λ -phage repressor, recognizes DNA and turns transcription on or off. In that case proteins bind to adjacent sites on helical DNA and regulate transcription by touching one another, a matter I explain more fully below. The loopers imagine that proteins bound at widely separated sites act in the same way, contacting each other, with the intervening DNA looping or bending to allow the protein-protein interaction. According to this idea, it is the interaction between DNA-bound proteins, not the looping per se, that regulates gene expression.

In the course of this article I shall first consider the evidence for looping and then define and argue against the contrasting mechanisms. I shall consider experiments involving both gene transcription and site-specific recombination. The latter phenomenon (at certain stages) requires that proteins acting at separated sites on the same DNA molecule communicate with each other, and mechanisms for how that interaction occurs have been critically tested.

The case for looping

The first indication of looping came from studies of gene regulation in Escherichia coli. Adhya and co-workers^{1,2} showed that two operators separated by some 90 base pairs are required for efficient repression of the gal operon and suggested, as one possible mechanism, interaction between Gal repressors bound at these operators. Schleif and co-workers³ similarly discovered that complete repression of the araBAD operon depends upon an operator site to which the regulatory protein AraC binds, located some 200 base pairs upstream of the transcription start site. They deduced that the AraC protein bound to the upstream operator interacts with another protein bound near the transcriptional start site, the intervening DNA looping to allow the interaction. This conclusion followed from the remarkable observation that efficient repression was maintained when an integral number of helical turns of DNA was added or deleted between the operator and the gene, but not when the spacing was varied by half-integral numbers of turns. They reasoned that proteins separated by the relatively short distance of a few

hundred base pairs can interact by simple looping only if located on the same side of the helix; introduction of half-integral turns would place the proteins on opposite sides of the helix and the energy required both to bend and twist the DNA would be prohibitive. Schleif and colleagues^{4,5} have since presented additional evidence consistent with the idea of DNA looping.

The ideas discussed above have recently been extended to the case of a mammalian virus, in particular the early gene promoter of simian virus 40 (SV40). This promoter contains three adjacent sets of sequences that influence transcription: the 'TATA' region near the transcription start site; a middle segment of 60 base pairs called the 21-base-pair repeats; and further upstream the enhancer, covering some 150 base pairs. Efficient transcription evidently requires that proteins bind to each of these segments. Takahashi et al.6 report that the insertion of 5 or 15 base pairs between the enhancer and the middle segment decreases transcription in vivo more drastically than does insertion of 10 or 21 base pairs. Similar results have been found for insertions between the middle segment and TATA. The former result is particularly striking because the enhancer functions even when re-positioned hundreds of base pairs from the middle segment. A simple interpretation of these experiments is that proteins bound to the enhancer contact other proteins bound to the middle segment and that these in turn contact a protein bound at TATA. When the enhancer is re-positioned at a distance (and perhaps in the normal position as well) the DNA presumably loops to allow the interaction to take place.

Our most direct demonstrations of interaction between adjacent DNA-bound proteins and between separated proteins with concomitant DNA looping come from studies of the λ -phage repressor. Figure 1 and its legend summarizes several aspects of the structure and activities of this protein. Briefly, the repressor, which can activate as well as repress transcription. normally binds to two adjacent sites on the λ chromosome. A repressor dimer bound at the stronger of the two sites helps a second dimer bind to the weaker site. This cooperative binding, which depends upon contact between the proteins, increases the affinity of the weaker site some 10-fold. The repressor at the weaker site then directly contacts RNA polymerase and helps it to bind and begin transcription of the adjacent gene. At each operator site, repressor is bound along one face of the helix (for a review see ref. 7).

Thus, interacting λ repressors normally lie adjacent to each other on the DNA; our recent experiments show that they also interact when separated. Hochschild and I⁸ used the technique of 'DNase footprinting' to show that λ repressor binds cooperatively to operator sites separated by approximately integral numbers of turns (five, six and now seven). Just as when the sites are in their normal positions, binding to the strong site increases binding to the weak site some 10-fold. In contrast, cooperative binding to operators separated by, for example, 6.5 turns was observed only if a four-base gap was introduced into

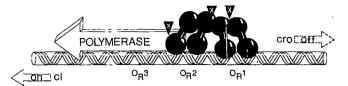


Fig. 1 Action of λ repressor. The λ repressor is both a negative and a positive regulator of gene expression. When bound to the right operator on the phage chromosome (O_R) , the repressor shuts off (rightward) transcription of a gene required for lytic growth (cro) and, simultaneously, activates (leftward) transcription of its own gene (cI). Repressor bound to the strong site O_R1 helps another repressor bind to the weaker adjacent site $O_R 2$ and this arrangement activates expression of the repressor gene as follows: the repressor at $O_{\rm p}2$ contacts polymerase and thereby helps it bind and begin transcription at the adjacent leftward promoter. At the same time rightward transcription is repressed because the bound repressors prevent polymerase from binding to the rightward promoter. Three protein-protein interactions are indicated by 'X' in the figure: each repressor dimer, the DNA-binding species, is held together primarily by contacts between carboxyl domains; interactions between carboxyl domains are also responsible for cooperative repressor binding to adjacent operator sites, but it is an amino domain of the repressor dimer at $O_R 2$ that contacts polymerase at the adjacent promoter. If the concentration of repressor increases transiently, site O_R 3 becomes occupied by a third repressor dimer and transcription of the repressor gene is turned off. (See ref. 7)

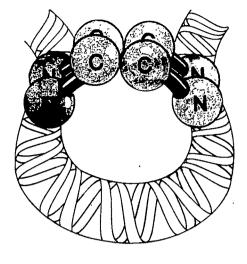


Fig. 2 λ repressors bound to two operator sites separated by seven helical turns. Although the precise points of contact between the dimers seem different from those indicated in Fig. 1, we suspect that either flexibility of the protein or some modification in the path of the DNA allows similar interactions in both cases⁸.

one of the DNA strands between the sites. This alteration presumably increases the torsional flexibility of the DNA and facilitates twisting, so that the proteins can be apposed. Whether the operator sites are adjacent or separated, cooperative binding of λ repressor depends upon the carboxyl domain of the protein, which does not contact DNA. These and other results suggest that λ repressors bind cooperatively to separated operator sites just as they do to adjacent sites, the DNA in between bending smoothly to accommodate the interaction as indicated in Fig 2.

The idea that cooperative binding of λ repressor to separated sites induces a smooth bend in the DNA plausibly accounts for the following observation: as repressor binds, the DNA between the sites becomes alternately hypersensitive and resistant to DNase, the interval separating these recurring hypersensitive and resistant sites being five base pairs. We imagine that in the DNA between the bound repressors, the minor groove (the site recognized by DNase) is expanded along the outside surface of the loop and compressed along the inside surface (see Fig. 2), thereby periodically changing the DNase sensitivity. The pattern of DNase sensitivity resembles that observed with DNA wrapped around a protein⁹⁻¹¹ or in a nucleosome¹², but as confirmed by the electron microscopy experiments I describe below, the looped DNA in between the sites is not in contact with repressor. Perhaps the DNase-hypersensitive sites found near active genes in eukaryotic chromosomes¹³ are regions of distorted DNA structure caused by looping.

In collaboration with J. Griffith, we have now used electron microscopy to provide direct visual evidence for DNA looping induced by λ repressor binding¹⁴. The pictures show λ repressors bound to DNA fragments bearing two λ operators separated by 5 helical turns, measuring from the centres of the sites. The repressors are evidently in contact, the DNA in between looped out. The looped structures are not seen if the spacing between the operator sites is 4.5 or 5.5 helical turns. The results reinforce our conclusion that the bound repressors interact only if the operators are positioned so that the repressors are on the same side of the helix, a finding consistent with the assumption that the energy needed to twist DNA one-half turn (and thereby align repressors fixed to opposite sides of the helix) is prohibited.

Cooperative binding of λ repressors to separated sites, with concomitant DNA looping, requires no special DNA sequences

(as far as we know) and is readily observed on linear DNA under roughly physiological conditions using purified repressor and DNA. The repressor is not specially designed for looping because, as noted above, the operator sites are immediately adjacent on the ordinary λ chromosome. We do not yet know how increased separation between the sites (beyond seven turns) will affect the reaction, nor do we yet know whether supercoiling the DNA, or adding nonspecific DNA-binding proteins (for example, the HU protein of E. coli, or histones) will facilitate or hinder the reaction. Unpublished experiments (A. Hochschild and M.P., in preparation) show that the cooperative binding to separated sites observed in vitro can also be detected in vivo using appropriately designed DNA molecules.

New cases of gene regulation at a distance in bacteria are now coming to light^{15,16}. Even the Lac repressor, long thought to be a paradigm of single-site binding, can bind cooperatively to separated sites and there is some evidence that this binding may be physiologically important (J. Gralla, B. Muller-Hill, personal communications; see also ref. 17). Although there are cases involving the non-cooperative binding of regulatory proteins (for example the λ Cro protein) they may prove to be the exceptions. I have argued elsewhere that cooperative DNA binding of regulatory proteins is a useful strategy for increasing the specificity of DNA-protein interactions and for constructing sensitive genetic switches⁷. In some cases the protein binding sites are adjacent (as is ordinarily the case in λ and SV40) and in other cases they are separated, DNA looping allowing the same interactions as when the proteins are adjacent. Perhaps we have here another example of a common motif: viruses use their DNA more economically than do cells.

I now consider alternative models designed to explain action at a distance. Various experimental results, all consistent with looping, argue against the alternative models.

Twisting

One version of this model would have regulatory proteins bind directly to some altered form of DNA, for example left handed or single stranded; another version imagines that the regulatory protein has an enzymatic activity that alters DNA conformation, for example by unwinding it. Gene activation would then be a

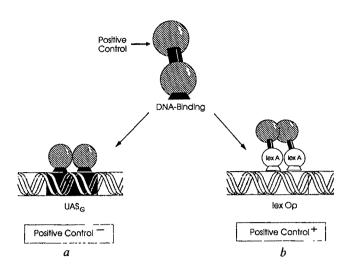


Fig. 3 Separation of the DNA-binding and positive control functions in a eukaryotic transcriptional regulator. The top line imagines the yeast activator GAL4 as consisting of two domains, the amino domain which recognizes sequences in the galactose upstream activating sequence (UAS_G) and the carboxyl domain which, when bound to DNA through the amino domain, contacts another protein to mediate positive control. In a, the carboxyl domain has been removed; this fragment recognizes UAS_G but fails to activate transcription. In b, the DNA-binding domain has been replaced with that of the bacterial protein LexA. This protein activates transcription in yeast if a lexA operator is positioned near the start site of a gene. The proteins are shown as binding to DNA as dimers but we are not certain this is correct^{25,26}.

consequence of conformation changes propagated through the DNA which allow other proteins to bind and begin transcription. The following considerations argue against these views.

A large number of known or suspected DNA-binding regulatory proteins have been isolated from both prokaryotes and eukaryotes and there is good reason to believe that all recognize ordinary helical DNA. For one class of these proteins, exemplifted by λ repressor, the structure of the protein-DNA complex is known. Each of these proteins bears protruding α -helices that fit into the DNA major groove and make sequence-specific contacts with functional groups exposed along the edges of base pairs. As expected, these proteins do not greatly alter the structure of DNA upon binding (see ref. 18, for example). Other transcriptional regulators probably recognize specific DNA sequences using probes other than α -helices (see, for example, ref. 19) but there is no hint that these proteins recognize greatly altered forms of DNA. The known regulatory proteins recognize their sites in linear DNA with binding constants that approach those that describe the well-characterized Lac or λ repressoroperator interactions. Were these proteins to recognize some greatly altered DNA structure, this result would not have been

One specific suggestion, namely that enhancer sequences are recognized as a form of left-handed DNA called Z-DNA²⁰, now appears to be incorrect. Mutational analyses of enhancers fail to confirm the simple prediction that alternating purines and pyrimidines, the likeliest Z-forming sequences, are required for enhancer function²¹. The presumed correlation between active genes and Z-DNA in *Drosophila*, suggested by experiments with antibodies, has been demonstrated to be an artefact of sample preparation²².

If a transcriptional regulator does not change DNA structure, how does it activate transcription? For the case of λ repressor we know the answer: one surface of repressor contacts DNA and another contacts RNA polymerase and activates gene

expression. An important argument supporting this picture was the isolation of mutant λ repressors (called pc for positive control) that bind DNA normally but that fail to activate transcription²³. The changed amino acids in these mutants are found on that surface of repressor that had been predicted, on independent grounds, to approach most closely the adjacent RNA polymerase. The properties of these mutants thus show that although DNA binding of repressor is necessary for gene activation, it is not sufficient; an additional site, presumably a site of contact with polymerase, is also required.

We have extended these ideas to a eukaryotic case, showing that the DNA-binding and gene activation functions of a yeast transcriptional regulator can be separated. The protein we study, GAL4, activates transcription of the GAL genes in the presence of galactose. The protein binds to sequences in a control element called the UAS_G (the galactose upstream activating sequence) and activates transcription at sites about 250 base pairs away in wild-type strains and as far as 750 base pairs away in modified strains²⁴.

Figure 3 shows the properties of two fragments of GAL4, one of which (a) bears the GAL4 DNA-binding function and the other of which (b) bears the activation function. Protein fragment a, consisting solely of the first 98 amino acids of GAL4, binds the GAL4 recognition sites as assayed in vitro and in vivo but fails to activate transcription. A hybrid molecule bearing the amino-terminal portion of GAL4 fused to β -galactosidase has similar properties. These GAL4 derivatives, lacking aminoacid sequences from the carboxyl end of the molecule, are formally equivalent to the pc mutants of λ repressor²⁵. Protein b, bearing the carboxyl 800 amino acids of GAL4 attached to a DNA-binding domain of the bacterial repressor LexA, acts as a positive regulator in yeast in the absence of the ordinary GAL4 recognition sequences. The hybrid protein binds to lexA operators but not to UASG and its activity as a positive regulator requires that a lexA operator be positioned near the transcription start site of the gene²⁶.

These experiments argue that, for GAL4 as for λ repressor, the role of DNA binding is to position the protein on the DNA so that it can use some other activity to stimulate transcription. Although there is no indication that GAL4 itself can twist DNA, none of these experiments excludes the possibility that GAL4 helps some other protein to bind adjacent to UAS $_G$ and that that protein activates transcription by untwisting (or twisting) DNA. However, the following experiment, performed with a mammalian virus, argues against this possibility.

Plon and Wang²⁷ have designed an incisive experiment that topologically separates the DNA site recognized by a regulatory protein (or proteins) from a gene without destroying gene activation. They constructed a 'tailed circle' (see Fig. 4) in which the regulatory sequence (the SV40 enhancer) forms a hairpin protruding from an otherwise intact circular DNA molecule that includes a gene (human β -globin). The strong result is that, when this construct is introduced into cells, transcription of the gene is enhancer dependent, as it is when gene and enhancer are disposed on ordinary DNA molecules. Thus, twisting of the enhancer cannot be responsible for gene activation, because twisting the protruding enhancer could have no effect on the topology of the gene.

Sliding

In this model a protein recognizes a specific site on DNA and then moves (slides, tracks) along the DNA to another specific sequence where, perhaps by interacting with another protein, it initiates transcription. Another version of essentially the same idea imagines that the regulatory protein remains bound at the original site and the DNA is threaded past or through the bound protein until the second critical site is encountered. (I am restricting the discussion to cases involving communication between two specific DNA sites. Where one specific and one nonspecific

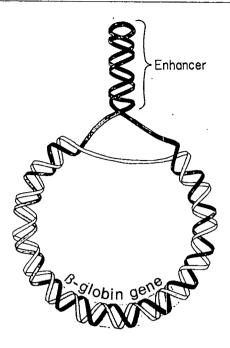


Fig. 4 The 'tailed circle' consists of an enhancer linked to, but topologically separated from, a gene. One of the DNA strands of this plasmid bears two copies of an SV40 enhancer sequence, one copy inverted with respect to the other. This extra region protrudes from the circle and self-pairs to form a functional enhancer. The main body of the circle contains the β -globin gene, transcription of which is increased by the enhancer. Twisting of the enhancer has no effect on the winding of the strands on the main body of the circle; nevertheless, the enhancer efficiently increases β -globin transcription²⁷.

site are involved, for example in the action of type I restriction enzymes, sliding may operate²⁸.)

No experiment involving transcriptional regulation, to my knowledge, directly argues against the sliders. But the strongest presumed example of bona fide sliding has been convincingly reinterpreted in the light of recent experiments. The cases in point involve two examples of site-specific recombination in bacteria. Both illustrate a remarkable common property of various site-specific recombination systems: two sites separated by many thousands of base pairs recombine only if the two sites are in a specified orientation; if one of the sites is inverted with respect to the other no recombination is observed. How does a protein bound at one site 'sense' the orientation of another which is 50,000 base pairs away? Tracking seemed a reasonable explanation and this mechanism could explain other experimental findings²⁹.

Craigie and Mizuuchi³⁰ have now eliminated tracking as a mechanism for site-specific recombination involving the ends of the bacteriophage Mu. This recombination reaction proceeds in vitro at high efficiency with purified proteins and ATP. Craigie and Mizuuchi³⁰ show that two Mu sites not on the same DNA molecule can nevertheless recombine if they are part of separate molecules that are intertwined (Fig. 5); in this case a protein could not track from one site to the other. These findings are consistent with tests of the tracking model involving the bacterial transposon Tn3, in which Benjamin et al.³¹ used electron microscopy, as well as other techniques, to analyse products of recombination in vitro. They found a distribution of structures inconsistent with the tracking model.

Boocock et al.³² have also described experiments which strongly support the idea that the ends of Tn3 find themselves by looping, and they have described a plausible model, which I shall not review here, that explains the orientation dependence

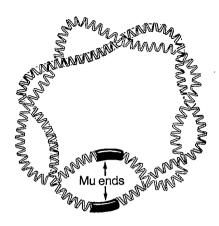


Fig. 5 Two intertwined DNA circles show that recombination is possible without tracking. Each line represents a double-stranded DNA molecule and each bears a Mu phage end. These sites efficiently recombine in vitro under the direction of site-specific recombination proteins. Because the sites are on separate molecules, it is impossible to travel from one to the other by tracking³⁰.

of the reaction. These findings help to unify our understanding of site-specific recombination; in another case, that involving the ends of the λ prophage, it is already well accepted that the sites find each other by looping^{33,34}.

Oozing

The simplest form of this model is that the binding of a regulatory protein to its operator helps binding of another protein to adjacent sequences, which in turn helps another to bind next to it, and so on, until a procession of proteins has oozed out from the control sequence to the gene where transcription is initiated. This idea as applied to transcription cannot be discounted entirely, and indeed some oozing around the control sequence or around the transcription start site seems a possibility (see, for example, the line-up of proteins in Fig. 1). But it seems implausible to imagine such an effect working over thousands of base pairs. The idea under consideration here should not be confused with nonspecific wrapping of DNA around histone-like proteins.

Oozing is not important for site-specific recombination. Experiments performed *in vitro* show that for the case involving the ends of Tn3, the amount of protein sufficient to catalyse the reaction is insufficient to cover the DNA between the sites³⁵.

Generalizations

If the thrust of these arguments is correct, we have the outlines of a unified view of gene regulation. In its simplest form this view would make two statements. First, regulatory proteins recognize specific sequences in DNA using structures that are complementary to the ordinary helix. The α -helix that protrudes from the surface of λ repressor and explores functional groups exposed in the major groove of DNA is an example of such a structure. Second, DNA-bound regulatory proteins influence transcription by excluding binding of other proteins (for example by competing with polymerase for an essential site) or, more generally, by touching another DNA-bound protein. In the λ case, for example, one DNA-bound repressor helps another to bind, and the latter in turn helps polymerase to bind and begin transcription, and these cooperative effects are mediated by protein-protein interactions. The point I have explicitly argued in this review is that these descriptions hold whether the interacting proteins are adjacent on DNA or whether they are separated—in the latter case the DNA in between the separated sites loops out to allow the protein-protein interactions.

Should looping prove to be a general phenomenon in gene regulation at a distance, it is not difficult to imagine how various forms of positive and negative control might be effected. For example, a protein bound to a distal site might help another protein bind to a proximal site and the latter might then directly activate or repress a gene. Alternatively, a bound activator protein might be constrained and rendered inactive by interaction with another protein bound at a distal site. Proteins binding within the loop might break it, thereby relieving the negative or positive effect of the interaction. Proteins bound to the same DNA sites might have quite different effects on gene regulation depending upon the nature of their interaction with other proteins. Our problem is no longer to invent a possible mechanism; rather, it is to see how far one operative idea, looping, will

I thank students and colleagues at Harvard; also Ben Lewin, Howard Nash and Bob Schleif for helpful comments and Carol Morita for the figures. This work has been supported in part by NIH grant GM22526 to M.P.

- 1. Irani, M. H., Orosz, L. & Adhya, S. Cell 32, 783-788 (1983).
- Majumdar, A. & Sankar, A. Poc. natn. Acad. Sci. U.S.A. 81, 6100-6104 (1984).
 Dunn, T., Hahn, S., Ogden, S. & Schleif, R. Proc. natn. Acad. Sci. U.S.A. 81, 5017-5020 (1984).
 Hahn, S., Hendrickson, W. & Schleif, R. J. molec. Biol. 188, 355-367 (1986).
- Martin, K., Huo, L. & Schleif, R. Proc. nain. Acad. Sci. U.S.A. 83, 3654-3658 (1986).
 Takahashi, K. et al. Nature 319, 121-126 (1985).
- 7. Ptashne, M. A Genetic Switch (Cell & Blackwell Scientific Press, Cambridge & Palo Alto,

- Hochschild, A. H. & Ptashne, M. Cell 44, 681-687 (1986).
 Kirkegaard, K. & Wang, J. C. Cell 721-729 (1981).
 Morrison, A. & Cozzarelli, N. R. Proc. natn. Acad. Sci. U.S.A. 78, 1416-1420 (1981).
- Sawadogo, M. & Roeder, R. Cell 43, 165-175 (1985).
 Noll, M. J. molec. Biol. 116, 49-71, (1977).
- Noll, M. J. molec. Biol. 116, 49-71, (1977).
 Wu, C., Bingham, P. M., Livak, K. J., Holmgren, R. & Elgin, S. C. R. Cell 16, 797-806 (1979).
 Griffith, J., Hochschild, A. & Ptashne, M. Nature 322, 750-752 (1986).
 Dandanell, G. & Herman, K. EMBO J. 4, 3333-3338 (1985).
 Reitzer, L. J. & Magasanik, B. Cell 45, 785-792 (1986).

- Mossing, M. & Record, T. Science (in the press).
 Anderson, J., Ptashne, M. & Harrison, S. Nature 316, 596-601 (1985).
- 19. Miller, J., McLachlan, A. D. & Klug, A. EMBO J. 4, 1609 (1985)

- Nordheim, A. & Rich, A. Nature 303, 674-679 (1983).
 Zenke, M. et al. EMBO J. 5, 387-397 (1986).
 Stollar, D. CRC crit. Rev. Biochem. 20, 1-36 (1986).
- Hochschild, A., Irwin, N. & Ptashne, M. Cell 32, 319-325 (1983)
 Giniger, E., Varnum, S. M. & Ptashne, M. Cell 40, 767-774 (1980).
- Genger, E., Varidin, S. M. & Peasing, M. Science 131, 699-704 (1986).
 Keegan, L., Gill, G. & Ptashne, M. Science 231, 699-704 (1986).
 Brent, R. & Ptashne, M. Cell 43, 729-736 (1985).
 Plon, S. & Wang, J. Cell 45, 575-580 (1986).

- 28. Yuan, R. A. Rev. Biochem. 50, 285-315 (1981). 29. Krasnow, M. A. & Cozzarelli, N. R. Cell 32, 1313-1324 (1983).
- Craigie, R. & Mizuuchi, K. Cell 45, 793-800 (1986).
 Benjamin, H. W., Matzuk, M. M., Krasnow, M. A. & Cozzarelli, N. R. Cell 40, 147-158
- 32. Boocock, M. R., Brown, J. L., Sherratt, D. J. Biochem. Soc. Trans. 14, 214-216 (1986)

- Mizuuchi, K., Gellert, M., Weisberg, R. A. & Nash, H. J. molec. Biol. 141, 485-494 (1980).
 Spengler, S. J., Schasiak, A. & Cozzarelli, N. R. Cell 42, 325-334 (1985).
 Krasnow, M. A., Matzuk, M. M., Dungan, J. M., Benjamin, H. W. & Cozzarelli, N. R. in Mechanisms of DNA Replication & Recombination (ed. Cozzarelli, N. R.) 637-659 (Liss, New York, 1983).

ARTICLES

Melting history of Antarctica during the past 60,000 years

L. D. Labeyrie, J. J. Pichon, M. Labracherie, P. Ippolito, J. Duprat[†] & J. C. Duplessy^{*}

* Centre des Faibles Radioactivités, Laboratoire Mixte CNRS/CEA, Domaine du CNRS, 91190 Gif-sur-Yvette, France † Département de Géologie et Océanographie, L. A. 197, Université de Bordeaux 1, Avenue des Facultés, 33405 Talence, France

Marked changes in the surface-water hydrology of the Southern Ocean during the past 60 kyr are revealed by a detailed comparison of the oxygen isotopic composition of planktonic and benthic foraminifera from sediment cores and the surface-water temperature estimated by a transfer function derived from the distribution of diatoms in the same sediments. From 35 to 17 kyr BP, the Southern Ocean polar front was covered by a melt-water lid containing a significant contribution from melting icebergs, calved from Antarctic ice shelves. These icebergs may have originated from a succession of surges of the ice shelves.

THE melting history of Antarctica during the most recent climatic cycle is a challenging problem which has an important bearing on global climatic models¹, on the formation of bottom and intermediate water, and consequently on the CO2 content of the atmosphere². One open question is the possibility of large surges of part of the Western Antarctic ice sheet3. Such abrupt events should be detectable using the oxygen isotopic composition of fossil planktonic foraminifera or other epipelagic organisms, because Antarctic ice, due to its conditions of accumulation, is depleted by 35-50% in δ^{18} O compared to mean ocean water. However, as the foraminiferal isotopic ratio is a function of both the temperature and the isotopic composition of the surrounding water, we must estimate the water temperature independently. Imbrie and Kipp4 have shown that surface-water temperature may be accurately estimated by transfer functions based on quantitative micropalaeontological analyses. Using a transfer function derived from Southern Ocean diatoms⁵, we may estimate independently the two components of the oxygen

isotopic record of the epipelagic foraminifera. The oxygen isotopic ratio of the benthic foraminifera analysed at the same levels in sediment cores gives the fraction of the sea-water isotopic changes which affects the whole water column, this being connected with the evolution of the continental ice sheets. We may thus estimate the local surface-water isotopic changes. We present here the results of such a study, carried out on two sediment cores from the southern Indian Ocean which cover the period including isotopic stages 3 and 2 of the last glacial (ref. 6), and the following deglaciation.

¹⁸O results and chronology

The cores MD73026 (44°59' S, 53°17' E) and MD84527 (43°49' S, 51°19' E) are located in the high-productivity belt north of the Crozet Plateau. Their position within the polar front system⁷, the major boundary between subtropical and Antarctic surface waters, makes them ideal for a study of hydrographic changes in the Southern Ocean. The high sedimentation rate

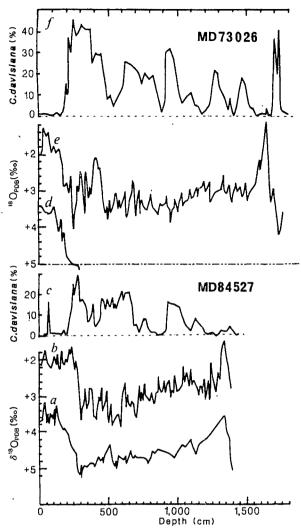


Fig. 1 a-c, Records from core MD84527 (43°49.3′ S, 51°19.1′ E; 3,262 m depth). a, δ^{18} O (in parts per 10³, relative to the PDB standard) (δ^{18} O = [($R_{carbonate}/R_{standard})$ - 1]×10³, where R = { 18 O/ 16 O}) of the benthic foraminifera Cibicides wuellerstorfi, plotted against depth in the core (corrected by +0.64% to take into account the specific fractionation⁴⁸). b, δ^{18} O_{PDB} for the planktonic foraminifera Neogloboquadrina pachyderma l.c. c, In the same core, relative amount of the radiolarian species Cycladophora davisiana. d-f, Records from core MD73026 (44°59′ S, 53°17′ E; 3,429 m depth). d, δ^{18} O_{PDB} of the benthic foraminifera Nonion sp., corrected by +0.4% for specific fractionation. e, δ^{18} O_{PDB} for N. pachyderma l.c. f, In the same core, relative amount of C. davisiana.

 $(>8~{\rm cm~kyr^{-1}})$ has provided a highly detailed record of the most recent climatic cycle. We have analysed in these cores the oxygen isotopic ratio of the epipelagic foraminiferal species Neogloboquadrina pachyderma left-coiled and, wherever possible, the benthic species Melonis barleanum and Cibicides wuellerstorfi. We have also analysed the foraminiferal δ^{13} C and the diatom δ^{18} O values, the diatom, foraminiferal and radiolarian specific abundances, and the abundance of ice-rafted detrital grains (L.D.L. et al., in preparation). Figure 1 shows the relative abundance of the radiolarian species Cycladophora davisiana, a good stratigraphic marker in the Southern Ocean^{8,9}, together with the foraminiferal δ^{18} O values, as a function of depth in the cores. These records are similar to the published records of nearby cores MD73025¹⁰⁻¹² and RC11-120⁸, if we take into account the varying sedimentation rates.

We have referred the records of MD84527 and MD73026 to the SPECMAP time scale¹³, based on RC11-120, to allow a

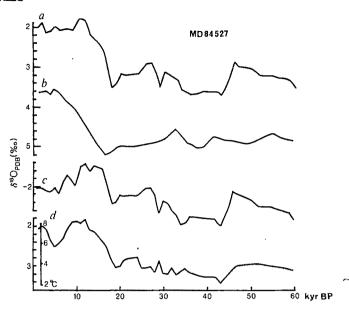


Fig. 2 Records from core MD84527, plotted against time. a, Planktonic isotopic record; b, benthic isotopic record; c, local isotopic changes (δ^{18} O (planktonic) – δ^{18} O (benthic)), expressed on the same timescale. A correction factor of +0.4% has been added to all the values in the period 0-9 kyr BP to correct for the effect of bottom-water temperature change (see text). d, Surfacewater temperature change at the location of the core. To allow direct comparison with the other records, the isotopic effect of these temperature changes is plotted on the δ^{18} O scale of N. pachyderma, using the calibration of Table 1.

better comparison between them and with other records. This has been done by adjusting, at each depth level in the three cores, the foraminiferal $\delta^{18}O$ and $\delta^{13}C$ values, and the relative abundance of *C. davisiana*. The accuracy of the correlation is better than 1 kyr during deglaciation, but only 3-5 kyr for isotopic stages 2 and 3. This is not critical for the present study.

The benthic foraminiferal record of core MD73026 covers' only the period from 0 to 18 kyr BP. However, whereas the North Atlantic Ocean experienced significant deep-water temperature changes during the most recent glacial period¹⁴, the isotopic records of benthic foraminifera during the most recent climatic cycle are congruent in the Indian and Pacific Oceans¹¹. We have therefore used the δ^{18} O record of *C. wuellerstorfi* in core MD84527 as a reference for core MD73026. The resulting foraminiferal δ^{18} O records of cores MD84527 and MD73026 are plotted against age in Figs 2 and 3.

The surface-water isotopic signal

Significant differences in the isotopic records of the planktonic and benthic foraminifera are evident in both cores. Note in particular the earlier (by 2-3 kyr) decrease in the isotopic ratio of the planktonic foraminifera during deglaciation (17-10 kyr BP), and the anomalously low isotopic ratio of these foraminifera before and during the glacial maximum (35-17 kyr BP). Such differences also exist in the nearby core MD73025¹⁵. The sediments in these three cores are not obviously disturbed, and they contain normal records of the other stratigraphical indexes (benthic foraminifera δ^{18} O, radiolarian species *C. davisiana* and diatom species *Eucampia antarctica*). The effects of bioturbation on the isotopic records have been recently quantified by ¹⁴C dating of the same monospecific samples used for isotopic analyses¹⁶; we conclude that bioturbation cannot explain the observed isotopic anomalies.

The differences in the isotopic records between surface (planktonic) and deep (benthic) foraminifera must be explained by

Table 1 Data used for calculations of oxygen isotopic fractionation between N. pachyderma and water

Sample	Lat.	Long.	S (%)	$\delta^{18} {\rm O}_{ m water}$	T (°C)	$\delta^{18}O_{pachy}$
MD73026	44°59′ S	53°17′ E	34.40	+0.3	+8.5	2.00
V2786	66°36′ N	01°07' E	35.15	+0.55	+6	2.60
V2838	69°23′ N	04°24′ W	35.1	+0.5	+6	2.93
K11	71°47′ N	01°36′ E	35.1	+0.5	+5	2.94
V2760	72°11′ N	08°35′ W	35.05	+0.45	+5	2.84
HU7541	62°39' N	53°52' W	34.5	+0.1	+5	3.00
HU7542	62°39′ N	53°54′ W	34.5	+0.1	+5	2.58
MD80304	51°04' S	67°44' E	33.80	-0.15	+3.5	2.91
MD84551	55°00' S	73°16′ E	33.90	-0.15	+1.5	3.15
CH7707	66°36' N	10°30′ W	34.9	+0.4	+1	3.68
MD82424	54°05′ S	00°21′ W	33.93	-0.15	+1	3.59
M269-965	60°54′ S	57°06′ W	33.60	-0.15	-0.25	3.9

 $8^{18}{\rm O_{PDB}}$ of the planktonic foraminifera N. pachyderma sen. in samples extracted from core tops, and a single sediment trap sample (M269-965)⁴⁵. The temperatures (T) and salinities (S) are the mean summer values extracted from atlases^{46,47} for 80-100 m water depth at the sample locations. The water $8^{18}{\rm O}$ values are calculated from the salinities²³.

differences in the evolution of the surface and deep waters in the Southern Ocean during the past 60 kyr. Both the temperature and the isotopic composition of the waters may be involved. and these must be estimated independently. Duplessy et al. 10 have used the benthic record of MD73025 as a reference for global sea-water isotopic changes during the accumulation and melting of the continental ice sheets. More recent results14 indicate that of the 1.6% total isotopic difference between the last glacial maximum and the Holocene in that core, 0.4% has to be attributed to a 1.5 °C warming of the deep Indian Ocean water at ~9 kyr BP, when the present mode of formation of the North Atlantic Deep Water developed. Accordingly, we adopt the benthic foraminiferal record of core MD84527 for the past 60 kyr as a reference for the isotopic record for mean ocean water, after correcting by +0.4% all isotopic values from the period 0-9 kyr BP. By subtracting the corrected benthic signal from the N. pachyderma records of MD84527 and MD73026, we obtain the 'local' isotopic records for the planktonic foraminifera (Figs 2c, 3c).

These records integrate the effect of the surface-water temperature change on the isotopic fractionation during carbonate precipitation. The first step in estimating this effect is to reconstruct the temperature changes during the past 60 kyr at the location of the cores. This has been done using a transfer function derived by multivariate correlation⁴ between the diatom specific abundance in Holocene core tops from the Southern Ocean and the present surface-water temperature at the location of the cores⁵. The summer (February) surface temperature is calculated by this method with an accuracy of ± 1.1 °C.

The temperature records obtained by this method (Figs 2d, 3d) show two interesting features. First, the increase in surfacewater temperature preceded by $\sim 2-3$ kyr the changes in isotopic ratio of the benthic foraminifera, which marks the initiation of the Northern Hemisphere deglaciation. This confirms the results of Hays et al.¹⁷, who have shown that the temperature maximum in the Southern Ocean core RC11-120 was near 9.4 kyr BP, that is, leading by ~ 2 kyr the Northern Hemisphere Holocene optimum. Secondly, the summer temperature was fairly stable in core MD84527 (between +2 and +4.5 °C) throughout the period 17-60 kyr BP. This means that the Antarctic polar front remained at the latitude of this core throughout this period. The temperature record of MD73026 is presently available only until 35 kyr BP, thus limiting the quantitative interpretation of the isotopic anomaly in that core.

The temperature dependence of the oxygen isotopic fractionation during carbonate precipitation in *N. pachyderma* was obtained by comparing *N. pachyderma* isotopic analyses from 12 Holocene core tops with the present summer water temperature at the location of these cores (Table 1). The depth

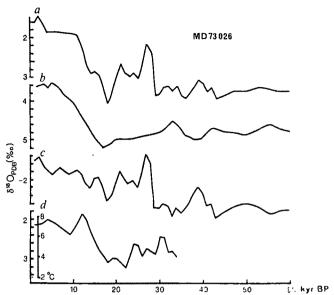


Fig. 3 8¹⁸O_{PDB} of the foraminifera in core MD73026, plotted against time. a, Planktonic foraminifera N. pachyderma 1 c.; b, benthic record of core MD84527; c, local isotopic changes for core MD73026 (as for Fig. 2c); d, summer surface-water temperature changes at the location of the core (as for Fig. 2d).

habitat of this species in low-productivity areas is in the 80-100 m range¹⁸, of the same order or slightly deeper than that of the diatoms¹⁹. In the higher-productivity area of the North Pacific, *N. pachyderma* 1.c. occupy the entire surface mixed layer²⁰. Regression analysis over the temperature range -1 to +9 °C yields $\delta^{18}O_{pachy} - \delta^{18}O_{water} = 3.84 - 0.25 T$ with 1σ errors of 0.12 in the constant and 0.03 in the slope. These results are in agreement with the estimate of Shackleton²¹ for benthic foraminifera living in this temperature range. Using the relationship obtained for *N. pachyderma*, we may now calculate the isotopic changes which would have been due solely to the changes in water temperature. The corresponding $\delta^{18}O$ scales are reported beside the temperature scales in Figs 2d and 3d.

The variations of the surface-water δ^{18} O have been calculated by correcting the local isotopic records of the planktonic foraminifera (Figs 2c, 3c) for the effect of temperature changes. These estimates of the net surface-water isotopic changes are shown in Fig. 4a, b. Although there is some variability, the general trend in the signal corresponds to a negative shift in the surface-water isotopic ratio for the entire glacial period compared to the present. Several shifts of large amplitude (1%) occur between 17 and 30-35 kyr BP; these are particularly evident in core MD73026 (Fig. 4a).

Low- δ^{18} O water from melting icebergs

Several mechanisms may be invoked to explain the decrease in the surface-water isotopic ratio. There is today a 0.4% negative gradient in the surface-water isotopic ratio from north to south through the Antarctic polar front^{23,24}. The subtropical water is enriched in ¹⁸O by evaporation (+0.2% relative to standard mean ocean water, SMOW), and surface Antarctic water is depleted by excess precipitation (-0.2%). Studies in progress using global climatic models with isotopic tracers indicate that neither this isotopic gradient, nor the precipitation over the Southern Ocean. could have increased significantly during the most recent glacial (J. Jouzel, in preparation). We have therefore to look for a source of water with a much lower isotopic ratio than that of the rain and snow which today fall over the Southern Ocean Melting sea ice is of no effect, because there is very little isotopic fractionation during freezing of sea water²⁵. On the other hand, melting icebergs could be of significant influence; their isotopic ratio, depending on the source of ice within Antarctica, he-

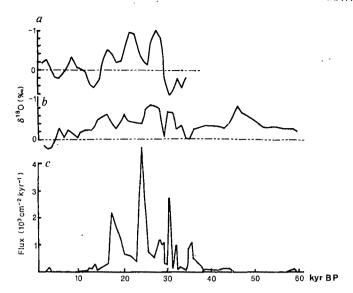


Fig. 4 a, b, Net surface-water isotopic variations for cores MD73026 (a) and MD84527 (b), obtained by subtraction of the surface-temperature signal from the local isotopic changes. c, Absolute fluxes of glacial detrital quartz grains in core MD84527.

between -35 and -55% (ref. 25). To date, however, such an input of iceberg melt water has been measured only along the Filchner Ice Shelf, in the Weddell Sea²⁵. To explain the isotopic anomalies, we must therefore consider periods of major increase in the production and melting of icebergs during the last glacial.

The first piece of evidence in support of this hypothesis is the distribution of ice-rafted detritus (IRD). The relationship between glaciation and the abundance of IRD in the sediments of the Southern Ocean is well known^{9,26-28}. Keany et al.²⁸ have connected the north-south shifts in IRD deposition to the northsouth shifts in the iceberg melting zone. Although a large part of the IRD deposited between the Scotia Sea and Kerguelen Islands consists of tholeitic glass shards transported by sea ice and icebergs from the South Sandwich Islands^{26,27}, quartz and chlorite probably originate only from the old continental crust of Antarctica. Their incorporation in icebergs could have been facilitated by the extension of the grounded ice shelves over the continental margins. To test for a possible increase in the amount of IRD transport by Antarctic icebergs, we have estimated the fluxes of quartz grains during the last glacial in core MD84527. We sub-sampled known sediment volumes, and counted all the quartz grains in the size fraction larger than 63 µm, thereby excluding wind-transported detritals. As shown in Fig. 4c, the quartz flux increases dramatically during the period from 17 to 35 kyr BP, that is, at the time of the major isotopic anomaly in both cores. Small differences in the relative depths of the IRD maxima and isotopic anomalies may be explained by several factors. The sampling for isotopic and IRD studies was done on separate occasions, at different levels in the core. Furthermore, the wet density of the IRD is much higher than for foraminifera and diatoms, thus allowing for differential settling of a few centimetres within the water-rich upper sediment before compaction. The earlier isotopic anomaly (at ~50 kyr BP) recorded in core MD84527 but not in the planktonic record of core MD73026 (Figs 2a, 3a) does not correspond to any significant increase in detrital quartz.

Other observations may help to explain the surface hydrography during these periods. Cooke and Hays⁹ have remarked that during the last glacial maximum (broadly defined as the *C. davisiana* zone b), IRD fluxes were large in both the Atlantic and south-west Indian sectors of the Southern Ocean. Before this time (*C. davisiana* zones c-d, ~40-60 kyr BP), the area of large IRD fluxes was limited to the Atlantic sector, a result

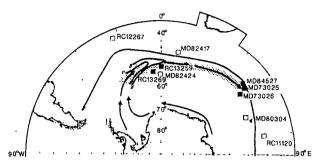


Fig. 5 Distribution of the surface-water isotopic anomaly at 18-20 kyr BP. ■, Cores containing the anomaly in the planktonic foraminifera or diatom records²²; □, cores with normal isotopic records; →, estimated trajectory of the icebergs extrapolated from present trajectories⁴⁹; —, position of the polar front at 18 kyr BP. The shading indicates regions of high loadings at 18 kyr BP for factor 2 of Burckle's diatom factorial analysis, which is mostly composed of E. antarctica, and indicates surface-water low salinity from melting sea-ice and icebergs.

which agrees with our quartz flux study. However, for both these periods, and in the different sectors, there was a significant increase in the relative amount of C. davisiana. In its present habitat in the Okhotsk Sea, this species is associated with specific hydrographic conditions, namely a surface water lid of less saline water with a strong temperature minimum near its base, and the formation in winter of sea ice which melts in the summer²⁹. Morley and Hays²⁹ have proposed this hydrological situation as a modern analogue for the periods of high abundance of this radiolarian, and specifically for the last glacial in the Southern Ocean. The diatom Eucampia antarctica is abundant today around the Antarctic peninsula. Burckle³⁰ associates this species with neritic and/or low-salinity waters (melting sea ice and icebergs). The surface-water conditions favourable for its development are thus the same as those for C. davisiana. Burckle³⁰ interprets the distribution of E. antarctica in the sediment of the last glacial maximum around Antarctica as indicating an extension of a low-salinity belt south of the polar front. In our set of cores, there is also a good correlation between the relative abundance of C. davisiana (Fig. 1), several species of diatoms (E. antarctica and Thalassiosira antarctica) and the isotopic anomalies²². Figure 5 shows the distribution of the E. antarctica factor of Burckle³⁰, together with the cores with and without the isotopic anomaly, at ~18 kyr BP. This distribution corresponds to the high IRD fluxes at that period9. We interpret this data to be an indication of the trajectory of melting sea-ice and icebergs from the Weddell Sea south of the polar front, along the circumpolar drift. With this hypothesis, the lack of detrital quartz and other IRD in the south-west Indian sector during the surface-water isotopic anomalies of the 40-60 kyr BP period would indicate that most of the icebergs melted faster at that time, within the Atlantic sector. Cooke and Hays consider that sea ice was more restricted at ~50 kyr than at 18 kyr BP, thus allowing faster melting: We do not have data to substantiate this argument, and therefore will not discuss this early part of the last glacial.

The magnitude of the ice flux from Antarctica necessary to give the 1% isotopic anomaly may be estimated from Fig. 5. Assuming that the ice isotopic ratio was -40%, the water mixed-layer thickness during periods of melt-water input was 60 m, and the surface covered by the melt water was 2×10^6 km² (30° W to 60° E, by 4° latitude), we need 10,000 km³ of melt water from Antarctic ice. This number should be compared with the present-day volume of 2,000 km³ melt water produced annually from melting Antarctic ice (refs 31, 32). It is not possible, therefore, to attribute the isotopic anomalies recorded during the last glacial to a regular calving, at the present rate, of icebergs from the ice shelves.

A much larger accumulation rate of the Antarctic ice sheet during the last glacial is most unlikely. The ice flow models developed to explain the data from the Dome C33 and Vostok34 ice cores imply a smaller ice accumulation rate during the last glacial. This is confirmed by the higher ¹⁰Be specific activity observed in the Vostok ice core at that time35. The higher gas content of the Bird ice core during the last glacial maximum also indicates a lower altitude of ice formation in the central part of the West Antarctic ice sheet³⁶. There are conflicting land-based geological observations suggesting that the ice sheet could have had a larger extension and was also thicker at the periphery during the last glacial³⁷. It is thus possible that during at least part of the last glacial, accumulation rates were significantly larger than today around the periphery of Antarctica, but not in the more central parts. Taking into account the estimated volume of the total Antarctic ice sheet during the glacial period of 3.67×10⁷ km³ (ref. 38), an erosion rate of ~10⁴ km³ yr⁻¹ could not be sustained for several kyr without being recorded in the Dome C and Vostok cores. The constraints are not so strong for the West Antarctic ice sheet. The lower altitude of ice accumulation during the glacial³⁶ could be interpreted as being due to a greater erosion rate than at present. Additional contributions from icebergs from the coastal ice sheets of the Antarctic Peninsula and the South Shetland and South Orkney Islands³⁹ are probable, but not quantifiable. Moreover, due to their proximity to the evaporation zones, these small ice caps probably had oxygen isotopic ratios similar to that of normal precipitation and therefore had a minor effect on the observed isotopic anomaly.

These arguments lead us to conclude that erosion of the Antarctic ice sheet could not have produced the volume of icebergs necessary to induce the observed isotopic anomalies as a more-or-less permanent regime during the last glacial. However, the detailed record of core MD73026 (Fig. 4a) does indicate that the ice output was irregular, with three well-defined peaks, one approximately every 6 kyr. We do not have a sufficiently precise chronology to estimate the duration of each melt-water event. The chronostratigraphy used in Fig. 3 is defined by a small number of references to the SPECMAP timescale (18, 21, 29, 35, 43 and 57 kyr BP, for isotopic stages 2 and 3), with the sedimentation rate taken as constant within each interval. However, Cooke and co-workers^{26,40} have demonstrated that the peaks of high IRD coincide with periods of high productivity of several species of radiolarians, and, indeed, our cores also have high accumulation rates of radiolarians which correlate with the high IRD and the melt-water events. Icebergs. due to their large size both above and below sea level, create small 'island effects' while drifting under the mixed influence of wind and currents. Reaching the area of high winds and rough seas (45-50° S), they will contribute to the vertical mixing, and hence increase the primary productivity. Neshyba41 has pointed out the importance of the iceberg-induced upwellings in the Weddell Sea. On the other hand, productivity is much smaller under a semi-permanent sea-ice cover⁸. It is therefore probable that sedimentation rate (both detrital and biogenic) was significantly higher during the melt-water events than it was between them. A duration of 1 kyr for each melt-water event, separated by 5 kyr of re-equilibration of the ice profile, is compatible both with the observed isotopic effects and with the present rate of ice accumulation. If similar phenomena were occurring at other places around Antarctica (especially east of the Ross Sea), each of the events would have had to be proportionately shorter to keep within the hypothetical constraint of a constant mean ice accumulation rate of 2,000 km³ yr⁻¹.

We therefore propose that the isotopic anomalies we observe record a succession of pulse-like surge events. Denton and Hughes³⁷ have stressed the importance for marine-based ice sheets of the removal of material by ice streams ('downdraw'). This mechanism feeds most of the present ice shelves in Antarctica. A large extension of the peripheral floating ice shelf around

Antarctica during the last glacial could have dramatically increased the volume of ice eroded by downdraw around the margins of the Antarctic ice sheet. Such a system would be semi-oscillatory, as ice streams would remove ice much more quickly than it could be replenished from the main body of the ice sheet. Within a few hundred years, all of the ice available at the head of the ice shelf would be removed, thus draining the coastal glaciers and ice streams. They will be reactivated only after a sufficient part of the ice sheet becomes once again marine-based. Similar models, with changes of smaller amplitude, have been discussed with respect to the present evolution of western Antarctica^{42,43}.

Denton and Hughes³⁷ have also stressed the teleconnections between Northern and Southern Hemisphere marine-based ice sheets. Their floating periphery is very sensitive to destabilization by sea-level changes. Moreover, each of the isotopic anomalies would represent an increase of several metres in global sea level, at the time when the boreal ice sheet was near its maximum extension. This may have helped to destabilize the marine-based ice sheets of the Northern Hemisphere, thus providing the amount of melting necessary to explain the high sea-level stands known around 25-30 kyr BP⁴⁴. A precise mapping of the net surface-water isotopic composition over the different oceans during the 17-30 kyr BP period, using a methodology similar to that presented here, should help to solve that problem.

Conclusions

Our results give new insight into the dynamics of the Antarctic ice sheet during the last glacial period. It is generally accepted that the Antarctic ice sheet had characteristics similar to those seen today³⁸, with a lower accumulation rate³⁴ and a surface temperature which responded in phase with global sea-level changes^{33,34}. We have demonstrated that the interactions between sea level, sea surface temperature around Antarctica, and the erosion rate of the Antarctic ice sheet may be more complicated. There is a definite indication that the Southern Ocean led by 2 kyr the North Atlantic warming and Northern Hemisphere deglaciation. A more important result of our study is that there have been several periods during the last glacial of large isotopic anomalies in the surface waters of the Antarctic polar front, particularly between 35 and 17 kyr BP. These anomalies are due to a large input of melt water during periods when the periphery of the Antarctic ice sheet was rapidly eroded. We propose that these events occurred during maximum extension of the marine-based ice sheets, and were due to the rapid erosion of the periphery of the Antarctic ice sheet by ice streams, flowing towards the ice shelves. When most of the ice available for feeding the coastal ice streams had been eroded, the ice shelves were destroyed, and iceberg calving decreased dramatically, until a new equilibrium ice-sheet profile was attained.

This work was supported by Programme National d'Etude de la Dynamique du Climat, Mission Scientifique des Terres Australes et Antarctiques Françaises, Centre National de la Recherche Scientifique, Commissariat à l'Energie Atomique, Université de Bordeaux 1 and Institut Géologique du Bassin d'Aquitaine. Sediment samples came from the Centre des Faibles Radioactivités and the Lamont-Doherty Geological Observatory core collections (the latter is supported by NSF). We acknowledge support from J. Antignac, H. Leclaire and B. Le Coat for the isotopic analyses, L. Burckle, J. Jouzel, C. Lorius, J. Moyes and J. L. Turon for useful discussions, M. Fontugne as chief scientist of the cruise APSARA 2, and captains, officers, and crews of M.S. Marion Dufresne for their work during the different cruises in the Southern Ocean. Drs S. Calvert, J. Hays and N. Shackleton reviewed and improved the manuscript. C. F. R. contribution 782.

Received 1 April; accepted 19 June 1986.

- 1. CLIMAP Science 191, 1131-1137 (1976).
- 2. Knox, F. & McElroy, M. E. J. Geophys. Res. 89, 4629-4637 (1984).

- 3. Hollin, J. T. J. Glaciol 4, 173-175 (1962).
- Imbrie, J. & Kipp, N. J. in The Late Cenozoic Ages (ed. Turekian, K. K.) 71-79 (Yale University Press, New Haven, 1971).
- 5. Pichon, J. J., Labracherie, M. & Labeyrie, L. D. Palaeogeogr. Palaeoclimatol. Palaeoecol. (submitted).
- Emiliani, C. J. Geol. 74, 109-124 (1966).
- Gordon, A. I. in Antarctic Oceanology 1 (Antarctic Research Series Vol. 15) (ed. Reid, J. L.) 169-203 (American Geophysical Union, Washington, 1971).
- J. D., Lozano, J. A., Shackleton, N. & Irving, G. Mem. Geol. Soc. Am. 145, 337-372
- Cooke, D. W. & Hays, J. D. Proc. 3rd Symp. Antarct. Geol. Geophys. (ed. Craddock, C.) 1017-1025 (University of Wisconsin Press, Madison, 1982).
 Duplessy, J. C., Moyes, J. & Pujol, C. Nature 286, 279-482 (1980).
- Labeyrie, L. D. & Duplessy, J. C. Palaeogeogr. Palaeoclimat., Palaeoecol. 58, 217-240 (1985).
 Caulet, J. P. Bull. Soc. Géol. Fr. 24, 555-562 (1982).
- Imbrie, J. et al. in Milankovitch and Climate (eds Berger, A. L., Imbrie, J., Hays, J., Kukla, G. & Saltzman, B.) 269-306 (Reidel, New York, 1984).
- Duplessy, J. C., Labeyrie, L. D., & Shackleton, N. J. Eos 66, 292 (1985).
 Labeyrie, L. D., Juillet, A. & Duplessy, J. C. in Proc. 7th Diatom Symp. 1982 (ed. Cramer, J.) 477-491 (Gantner, Vaduz, 1984).
 Duplessy, J. C. et al. Nature 320, 350-352 (1986).
- 17. Hays, J. D., Imbrie, J. & Shackleton, N. J. Science 194, 1121-1132 (1976).

- rays, J. D., Intoric, J. & Shackleton, N. J. Science 194, 1121-1132 (1976).
 Kellog, T. B., Duplessy, J. C. & Shackleton, N. J. Boreas 7, 61-71 (1978).
 Reynolds, L. A. & Thunell, R. C. Micropaleontology 32, 1-18 (1986).
 MacIsaac, J. J., Dugdale, R. C., Barber, R. T., Blasco, D. & Packard, T. T. Deep Sea Res. 32, 503-529 (1985).
- 21. Shackleton, N. J. in Variations du Climat au Cours du Pleistocene, 203-209 (Centre National de la Recherche Scientifique, Gif, 1974).
- Labeyrie, L. D. et al. Geol. Soc. Am. Abstr. Progm. 17, 637 (1985).
 Craig, H. & Gordon, L. in Stable Isotopes in Oceanographic Studies and Paleotemperatures. 9-131 (Consiglio Nazionale delle Richerche, Pisa, 1965).

- 24. Duplessy, J. C. C. R. hebd. Séanc. Acad. Sci., Paris 271, 1075-1078 (1970)
- Duplessy, J. C. C. R. Reda. Seant. Acad. Sci., Parts 271, 1075-1078 (1970). Weiss, R. F., Ostlund, H. G. & Craig, H. Deep Sea Res. 26A, 1093-1120 (1979). Cooke, D. W. Ihesis, Columbia Univ. (1978). Smith, D. G., Ledbetter, M. T. & Cieselski, P. F. Mar. Geol. 53, 291-312 (1983).

- Keany, J., Ledbetter, M., Watkins, N. & Huang, T. C. Geol. Soc. Am. Bull. 87, 873-882 (1976).
 Morley, J. J. & Hays, J. Earth planet. Sci. Lett. 66, 63-72 (1983).
 Burckle, L. H. Mar. Micropaleont. 9, 241-261 (1984).
- 31. Jacobs, S. S., Gordon, A. L. & Amos, A. F. Nature 277, 469-471 (1979)
- Orlheim, O. U.S. Dep. Energy Rep. No. DOE/EV/602351, 210-215 (1984).
 Lorius, C., Merlivat, L., Jouzel, J. & Pourchet, M. Nature 280, 644-648 (1979).
 Lorius, C. et al. Nature 316, 591-596 (1985).
- 35. Yiou, F., Raisbeck, G. M., Bourles, D., Lorius, C. & Barkov, N. I. Nature 316, 616-617 (1985).
- Raynaud, D. & Whillans, I. M. Ann. Glaciol. 3, 269-273 (1982).
- 37. Denton, G. H. & Hughes, T. J. Quat. Res. 20, 125-144 (1983).
 38. Hughes, T. J. et al. in The Last Great Ice Sheets (eds Denton, G. H. & Hughes, T. J.)
- 263-317 (Wiley, New York, 1981). 39. Sugden, D. E. & Clapperton, C. M. Quat. Res. 7, 268-282 (1977).
- 40. Burkle, L. H. & Cooke, D. W. Micropaleontology 29, 6-10 (1983). 41. Neshiba. S. Nature 267, 507-508 (1977).
- Weertman, J. Nature 260, 284-286 (1976)
- 43. Thomas, R. H. Nature 259, 180-183 (1976). 44. Chappell, J. Search 14, 99-101 (1983).
- Wefer, G. et al. Nature 299, 145-147 (1982).
- Henry, G. et al. Indiane 239, 143-141 (1982).
 Dietrich, G. Atlas of the Hydrography of the Northern North Atlantic Ocean (Conseil International pour l'Exploration de la Mer, Charlottenlund Slot, 1969).
 Wyrtki, K. Oceanographic Atlas of the International Indian Ocean Expedition (National
- Science Foundation, Washington, 1971).
 48. Duplessy, J. C. et al. Quat. Res. 21, 225-243 (1984).
- Tchernia, P. & Jeannin, P. F. Quelques Aspects de la Circulation Océanique Antarctique Révélés par l'Observation de la Dérive d'Icebergs (Centre National d'Etudes Spatiales,

Generation of single-stranded T-DNA molecules during the initial stages of T-DNA transfer from Agrobacterium tumefaciens to plant cells

Scott E. Stachel', Benedikt Timmerman & Patricia Zambryski'

Laboratorium voor Genetica, Rijksuniversiteit Gent, B-9000 Gent, Belgium

Activation of the T-DNA transfer process of Agrobacterium by the plant signal molecule acetosyringone generates a single-stranded, unipolar, linear T-DNA molecule (T-strand)—a potential conjugative intermediate in the transfer of the T-DNA to plant cells. Acetosyringone induction also leads to S_1 nuclease-sensitive sites at the Ti plasmid T-DNA borders, and other molecular changes associated with the Ti plasmid T-DNA sequences, which may correspond to specific steps of T-strand synthesis.

DURING the genetic transformation of plant cells by the soil pathogen Agrobacterium tumefaciens (reviewed in ref. 1), a specific segment of DNA, the T-DNA, is recognized in and mobilized from the large (>200 kilobase pairs; kbp) Ti plasmid of the bacterium, transferred across the cell walls of the bacterium and plant cell, and integrated as an unaltered fragment into the plant nuclear genome. Analysis of the transfer process has focused on what defines the T-DNA; the genetic requirements for transfer other than the T-DNA; and the mechanism of transfer.

In the Ti plasmid the T-DNA is bounded by essentially identical 25-base pair (bp) direct repeats²⁻⁵. These sequences define the T-DNA, for any DNA, and only DNA, located between T-DNA borders is efficiently transferred and integrated⁶⁻⁹. The T-DNA transfer process is directed by the products of the Ti plasmid virulence (vir) and chromosomal virulence (chv) loci (reviewed in refs 10, 11). Whereas chv

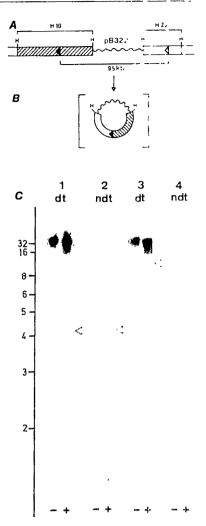
* Present address: Institute of Cancer Research and Howard Hughes Medical Institute, College of Physicians and Surgeons, Colombia University, New York 10032, USA (S.E.S.); Division of Molecular Plant Biology, Hilgard Hall, University of California, Berkeley, California 94720, USA (P.Z.).

expression is constitutive, vir expression is tightly regulated 12,13, and its activation initiates the transfer process. This activation is mediated by specific phenolic compounds present in the exudates of wounded and actively metabolizing plant cells. One such compound is dimethoxyphenol)¹⁴. acetosyringone (AS; 4-acetyl-2,6-

Genetic analyses of the 25-bp sequences have indicated that they are polar in function^{15,16}. While deletion of the left border repeat has no significant effect on pathogenicity¹⁷, deletion of the right repeat totally abolishes it^{15,16,18}. Furthermore, when the orientation of the right border is reversed with regard to its natural orientation on the Ti plasmid, the efficient transfer and/or integration of the T-DNA sequences is greatly attenuated. These results indicate that T-DNA transfer may occur in a rightward to leftward fashion, determined by the orientation of the 25-bp border repeats, and suggest that transfer might be via a conjugative mechanism¹⁵.

Here we use hybridization techniques to directly identify and characterize novel structures associated with the T-DNA and its border sequences in Agrobacterium following induction of vir gene expression with AS. A variation of the Southern blotting transfer procedure is used to distinguish between single-stranded (ss) and double-stranded (ds) DNA molecules present in total Fig. 1 Hybridization analysis of total DNA prepared from AS-induced Agrobacterium. A, T-DNA region of the pGV3850 Ti plasmid⁶. The interior portion of the T-DNA of pTiC58 has been replaced with PBR322 (wavy line). HindIII fragments 10 (hatched) and 23 (white) from pTiC58 carrying the right and left 25-bp T-DNA border sequences respectively (black arrows); H, HindIII restriction site. B, Structure of the 9.5-kbp ds T-DNA circle molecule isolated after transformation of E. coli with undigested total DNA from AS-induced pGV3850 Agrobacteria. C, Southern blot hybridization analyses of Agrobacterium DNA. Total DNA prepared from ininduced (-) and AS-induced (+) 3850 agrobacteria was analysed by hybridization against nick-translated ³²P-labelled pBR322 probe. Lane 1, denatured transfer (dt) of untreated DNA; lane 2, non-denatured transfer (ndt) of untreated DNA; lane 3, denatured transfer of total DNA digested with S₁ nuclease; lane 4, non-denatured transfer of S₁-treated DNA. Scaling on left is in kbp. Arrows indicate novel signals observed in the AS-induced lanes. Note that all of these novel signals are also observed, albeit at a lower level, with DNA prepared from Agrobacterium co-cultivated with Nicotiana tabacum protoplast cells (data not shown).

Methods. An overnight culture of 3850 Agrobacteria grown in YEB liquid medium was resuspended in MSSP medium¹⁴ at $0.05 A_{600}$ units ml⁻¹ and grown at $28 \,^{\circ}$ C with high aeration. After 5 h of preincubation growth, acetosyringone (Janssen) was added to half of the MSSP culture at 100 µM, a concentration that is non-limiting for induction of the Ti-plasmid vir genes¹⁴. The uninduced and AS-induced cultures were grown for another 12-18 h and a parallel culture of the virB:: lac strain A348(pSM30) (refs 10, 14) was used to monitor vir induction; under these conditions the cultures undergo two to three doublings, and >100-fold increases in β -galactosidase activity are observed in A348(pSM30). The bacteria were collected by centrifugation and total DNA prepared as described previously³³. Briefly, the pellet from 5 ml of cells is lysed in 200 µl TE (50 mM Tris, 20 mM Na₂-EDTA, pH 8.0), 100 µl 5% sodium sarkosyl and 100 µl pronase (10 mg ml⁻¹) for 45 min at 37 °C. The lysate is then vortexed for 15 s (light-shear), extracted twice with phenol and twice with chloroform, and the DNA recovered by EtOH precipitation. E. coli was transformed with uninduced and AS-induced DNA as described previously¹⁹, and the AS-induced preparation was determined to give transformants carrying the ds T-DNA circle molecule diagrammed in B. Aliquots (1 µg) of total Agrobacterium DNA (either untreated or S1-digested) were then electrophoresed in 0.9% TBE agarose gels containing 0.5 µg ml⁻¹ EtBr, transferred to nitrocellulose in 10×SSC, and analysed by Southern blot filter hybridization. Two different transfer condtions have been used, denatured and non-denatured. For denatured transfer, the agarose gel is soaked in denaturing solution for 60 min followed by neutralizing solution for 60 min before capillary blotting. For non-denatured transfer, the gel is soaked in H₂O for 10 min, then 10×SSC for 10 min, before blotting. For the S₁ nuclease digestions, 1 μg total DNA in 200 μl S₁ digestion buffer was incubated with 50 U S₁ nuclease (Boehringer Mannheim) for 30 min at 20 °C. The reaction is terminated by adding 20 µl 10×S₁ termination buffer, followed by phenol extraction and EtOH precipitation. Unless otherwise specified, all buffers and conditions used here and in Figs 2-5 are according to Maniatis et al.34.



DNA prepared from these cells. Evidence is presented for (1) free ss T-DNA molecules (T-strands) whose polarity corresponds to that of the T-DNA borders; (2) ss endonucleases ensitive structures associated with the Ti plasmid T-DNA borders (S₁ border sites); and (3) molecular alterations associated with the internal sequences of the Ti plasmid T-region (T-region structures). We discuss the potential role of each of these AS-induced T-DNA homologous molecules in the transfer of the T-DNA to the plant cell.

Free T-DNAs in AS-induced cells

For these studies we used Agrobacterium carrying Ti plasmid pGV3850 (ref. 6). pGV3850 has been derived from the nopaline C58 Ti plasmid, and the structure of its minimal T-DNA region is shown in Fig. 1A. Strain 3850 has been used previously to isolate and identify a 9.5 kbp ds T-DNA circle molecule (Fig. 1B) following transformation of Escherichia coli with total DNA prepared from plant¹⁹ or AS-induced Agrobacteria¹⁴; this T-DNA circle has been proposed as a candidate for the T-DNA molecule that is transferred to the plant cell. Our initial experiments aimed to identify the presence of this molecule directly in Agrobacterium.

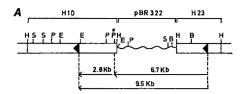
Total DNA was prepared from AS-induced cells and found to produce ds T-DNA circles in *E. coli*; this AS-induced DNA, along with total DNA prepared from uninduced cells, was fractionated by agarose gel electrophoresis and transferred to a nitrocellulose filter following gel denaturation (normal Southern transfer procedure, see below). Two T-DNA homologous signals are observed in Fig. 1*C*, lane 1. Since the DNA is undigested, the upper signal represents Ti-linked T-DNA sequences, while

the lower signal represents free T-DNA sequences. This novel signal is specific to the AS-induced DNA, and thus corresponds to a Ti-independent T-DNA molecule whose synthesis is the result of the AS-induced activation of the pGV3850 vir loci.

The free T-DNA signal does not migrate as a 9.5-kbp ds DNA molecule (supercoiled, relaxed-circular or linear), but instead migrates at a size corresponding to a ds linear molecule of 4.4 kbp. Thus, by hybridization we find no evidence for ds T-DNA circles in AS-induced bacteria. This result is not totally unexpected because the frequency of recovery of these molecules in E. coli is low. We obtain on average 50 ds circle transformants per µg AS-induced DNA (at a transformation efficiency of 10 transformants per µg supercoiled pBR322 plasmid DNA). Since 1 μg of total Agrobacterium DNA contains ~1.7 ng of pGV3850 T-DNA¹⁹, at most only one in every 100 AS-induced cells harbours a ds T-DNA circle. That these molecules are not detected by hybridization indicates that the transformation results are representative of their actual concentration in the AS-induced DNA. We discuss below a model for how ds circle molecules might be generated at a low frequency as a result of AS induction (Fig. 6).

Free T-DNAs are single stranded

Since the size of the AS-induced free T-DNA molecule is about half that of the T-region of pGV3850 (Fig. 1A), it may be a single-strand copy of the pGV3850 T-DNA. The following experiments demonstrate that the free T-DNA molecule has properties characteristic of ss DNA. Evidence is also given for other novel T-DNA-homologous molecules present in the AS-induced bacteria; in contrast to the free T-DNA, these structures



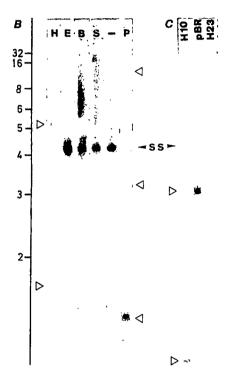
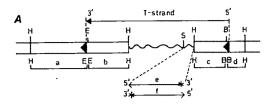


Fig. 2 Restriction endonuclease treatment of AS-induced DNA. A, Restriction map of the T-DNA region of pGV3850. Black arrows, T-DNA border sequences; the 9.5-kb arrow designates the ss T-DNA molecule, and the 2.8-kb and 6.7-kb arrows correspond to the ss fragments that would be produced by PstI cleavage of the ss T-DNA molecule at the PstI* site. B, Aliquots (1 µg) of ASinduced DNA were digested to completion with five restriction endonucleases, fractionated on 0.9% agarose, transferred under non-denaturing conditions to nitrocellulose, and analysed by hybridization against HindIII fragment 10/pBR322 probe. H, HindIII; E. EcoRI; B. BamHI; S. SalI; P. PstI; -, undigested; ss, free T-DNA molecule; open arrows, unexpected fragments produced by HindIII or PstI digestion of the AS-induced DNA. C, Three equivalent non-denatured transfers of PstI-digested ASinduced DNA were hybridized against HindIII fragment 10 probe (H10); pBR322 probe (pBR); and HindIII fragment 23 probe (H23). Scaling is different from that in B, such that the signals marked with triangles correspond to ss DNA molecules of ~6.6 and 2.8 kb, respectively. Note that different preparations of ASinduced DNA were used in the experiments of B and C. The \sim 9.2-kbp signal observed in the PstI digest in B is not observed in C; this difference may reflect the detection of different levels of AS-induced events in the two preparations.

are still linked to the Ti plasmid, as they are only detected after enzymatic digestion.

Transfer assay for ss T-DNAs. DNA binds to nitrocellulose only if it is single-stranded²⁰ or associated with protein²¹. In the Southern blotting technique, ds DNA fragments fractionated in an agarose gel must be denatured before being transferred to nitrocellulose²⁰. Thus, ss (and protein-associated) DNA molecules can be easily distinguished from ds molecules by comparing their transfer to nitrocellulose from agarose gels treated with or without NaOH before transfer. Figure 1C, lanes 1 and 2, show the denatured and non-denatured transfers of



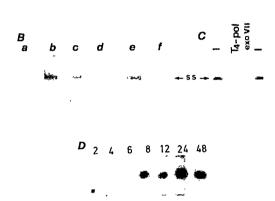


Fig. 3 Molecular characterization of ss T-DNA molecules. A, Six probes used to analyse the sequence content and strandedness of the ss T-DNA molecule. B, BcII; E, EcoRI; H, HindIII. The EcoRI site of probes a and b falls 55 bases inside the left T-DNA border, and the BcII site of probes c and d falls 42 bases inside the right border.

Methods. Fragments a, b, c and d were gel-purified twice and labelled by nick translation. Probes e and f are 3'-end-labelled probes where the position of the label is marked by an asterisk, and correspond to the upper and lower strands of the pGV3850 T-DNA, respectively. For probe e, pBR322 was digested with HindIII, 3'-end-labelled at the HindIII site by Klenow fill-in, recut with SalI, and the resultant 622-bp HindIII/SalI fragment was gel-purified. For probe f, the order of the restriction digests was reversed to give a 622-bp Sall/HindIII fragment, 3'-end-labelled at the SalI site. The polarity of the ss T-DNA molecule, or T-strand, is shown at the top of the figure. B, Sequence content and strandedness of the ss T-DNA. Six equivalent strips of a non-denatured transfer of undigested AS-induced DNA hybridized against the six probes shown in A. ss, Single-stranded T-DNA signal. C, Exonuclease sensitivity of the ss T-DNA. The non-denatured transfer of untreated (-), T4 polymerase-digested (T4-pol), and exonuclease VII-digested (ExoVII) AS-induced DNA was hybridized against nick-translated pBR322 probe. For exonuclease digestion, 1-µg aliquots of AS-induced DNA were incubated with 2.5 U T4 polymerase (Anglian Biotechnology Ltd) or 1.1 U exonuclease VII (Gibco-BRL), respectively, for 30 min at 37 °C. Each reaction was carried out in 15 µl in the enzyme buffer recommended by the manufacturer. Note that under identical conditions these treatments have no effect on M13 ss circular phage DNA; also, the ss T-DNA is fully degraded after 90 min digestion with T4 polymerase (data not shown). D, Kinetics of synthesis of the ss T-DNA molecule. A 50-ml culture of pGV3850 Agrobacteria pregrown for 5 h was then induced with AS at 100 μM. At 2, 4, 6, 8, 12, 24 and 48 h after the start of induction, 5-ml aliquots were removed, frozen at -70 °C, and total DNA was then prepared. These DNA samples were fractionated on agarose and transferred to nitrocellulose without gel denaturation, and the amount of ss T-DNA molecules present in the AS-induced cells for each time point was assessed by hybridization against nick-translated pBR322 probe. Note that by EtBR staining the amount of DNA in the 24-h lane was about double that for the other lanes.

uninduced and AS-induced total DNA. Of the two T-DNA-homologous signals present in the AS-induced DNA sample, only the lower signal, which represents the free T-DNA molecule, transfers without gel denaturation (Fig. 1C, lane 2). This free T-DNA must be ss DNA because the AS-induced total DNA has been fully deproteinated during its preparation (Fig. 1

legend) and RNase digestion of the DNA before hybridization analysis does not affect the ss signal (data not shown).

Nuclease sensitivity of ss T-DNAs. S_1 nuclease is a ss-specific endonuclease²². In Fig. 1C, the denatured (lane 3) and non-denatured (lane 4) transfers of S_1 nuclease-digested samples of uninduced and AS-induced total DNA demonstrate that the free T-DNA molecule is fully degraded by S_1 nuclease. Interestingly, S_1 treatment also appears to release the T-region from the AS-induced T1 plasmid. A novel T-DNA homologous signal is observed in the S_1 -treated AS-induced sample in the denatured transfer (Fig. 1C, lane 3), and this signal corresponds to a ds molecule, which migrates as a linear fragment of 9.5 kbp, the precise size of the pGV3850 T-DNA from its left to right T-DNA borders (Fig. 1A). Thus, AS induction also results in a Ti plasmid whose T-DNA borders are sensitive to cleavage by S_1 nuclease (see Figs 4 and 5).

The activity of type II restriction endonucleases is limited primarily to duplex DNA. Aliquots of AS-induced DNA were digested to completion with BamHI, EcoRI, HindIII, PstI and SalI (each of these enzymes cleaves within the T-DNA region of pGV3850; Fig. 2A), and hybridized to the HindIII fragment 10/pBR probe following non-denatured transfer (Fig. 2B). Because the ss signal is present in all the digests (except for PstI), the free T-DNA is generally resistant to restriction digestion.

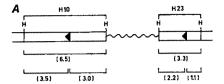
The HindIII and PstI results are more complex. The ss signal is weak in the HindIII lane and absent in the PstI lane; also, several novel signals are observed in these lanes. Several restriction enzymes have been shown to restrict ss DNA²³, and the sensitivity of the free T-DNA to HindIII and PstI may be an example of this effect. Interestingly, fragments both smaller and larger than the ss T-DNA molecule are produced by HindIII and PstI digestion (Fig. 2B). While the smaller fragments can be cleavage products of the ss T-DNA, the larger fragments must be derived from a large molecule, presumably the AS-induced Ti plasmid. Thus, AS induction also results in a Ti plasmid molecule whose T-region carries ss sequences (see Fig. 5).

Characterization of ss T-DNAs

ss T-DNAs are full-length and unipolar. Six identical strips of a non-denatured transfer of undigested AS-induced DNA were hybridized separately with the six probes labelled a to f in Fig. 3A. Probes a and d correspond to pGV3850 sequences just outside the left and right T-DNA border repeats; probes b and c correspond to T-region sequences just within these repeats; and probes e and f correspond to the upper and lower strands of the pGV3850 T-DNA region, respectively. Figure 3b shows that the ss T-DNA molecule hybridizes only to probes b, c and e. Thus, it is composed only of sequences located internal to the T-DNA borders, and which correspond to the lower strand of the pGV3850 T-region. We designate this unipolar ss T-DNA molecule as the T-strand.

T-strands are linear. The T-strand is sensitive to both exonuclease VII $(3' \rightarrow 5')$ and $5' \rightarrow 3'$ activities specific for ss DNA²⁴ and T4 polymerase $(3' \rightarrow 5')$ exonuclease that accepts both ss and ds DNA as substrate (Fig. 3C). Thus, the T-strand, as isolated, must be a linear ss DNA molecule whose 3' terminus (and perhaps also 5' terminus) is available to exonuclease digestion.

The PstI cleavage products of the T-strand indicate that its 5' and 3' ends map to the right and left T-DNA borders, respectively. Two fragments of ~3.3 and 1.4 kbp (~ss lengths 6.7 and 2.8 kbp) are detected. The 6.6-kbp fragment is homologous to pBR322 and HindIII fragment 23, while the 2.8-kbp fragment is homologous only to HindIIII fragment 10 (Fig. 2C). Cleavage of a circular T-strand molecule at any (or all) of its three PstI sites would yield fragments of different sizes and sequence content from those observed. The simplest explanation for the results of Fig. 2C is that the T-strand is a linear ss molecule, cleaved by PstI principally at its middle PstI site (just within



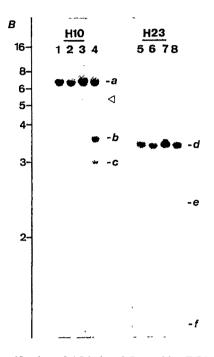


Fig. 4 Identification of AS-induced S₁-sensitive T-DNA border structures. A. HindIII fragments produced by ds cleavages of the pGV3850 T-DNA borders. Fragments b and c result from cleavage of the left border repeat carried by HindIII fragment 10 (a). Fragments e and f result from cleavage of the right T-DNA border carried by HindIII fragment 23 (d). Fragment sizes are in kbp. Black arrows, T-DNA border sequences; H, HindIII. B, Uninduced and AS-induced DNA was digested with HindIII, and half of each sample was treated further with S1 nuclease. The four samples were analysed on two denatured transfers hybridized against nick-translated HindIII fragment 10 (lanes 1-4) or HindIII fragment 23 probe (lanes 5-8). Lanes 1, 5, uninduced DNA; lanes 2, 6, uninduced DNA plus S₁ treatment; lanes 3, 7, AS-induced DNA; lanes 4, 8, AS-induced DNA plus S₁ treatment. a-f refer to the fragments shown in A. The open arrow indicates a novel S_1 -sensitive fragment of ~ 5.2 kbp. Scaling is in kbp. Note that the low level of the border cleavage fragments (b, c, e, f) seen in the absence of S₁ treatment (lane 3, and lane 7 after long exposure) may reflect mechanical breakage of the AS-induced S₁-sensitive border structures during sample preparation.

the right end of its *HindIII* fragment 10 sequences), to produce a 6.7-kbp 5' and a 2.8-kbp 3' fragment.

T-strand synthesis is limited. Using a probe homologus to both strands of the T-DNA, the intensity of the T-strand signal is ~5-10-fold less than the Ti-plasmid T-region signal (Fig. 1C, lane 1; also Fig. 5). As the T-strand corresponds to one strand of the T-region, and the copy number of the Ti plasmid is about two (and assuming no specific loss of T-strands during DNA preparation), we estimate that on average each AS-induced cell carries 0.4-0.8 T-strand molecules. As T-DNA homologous molecules are not found in the culture medium (data not shown), this low copy number is probably not due to export of the T-strand. Figure 3D demonstrates that the relative amount of T-strands begins to plateau within 8 h after the start of AS induction, and shows only a doubling during an additional 40 hours of induction. Thus, T-strand synthesis is a limited process.

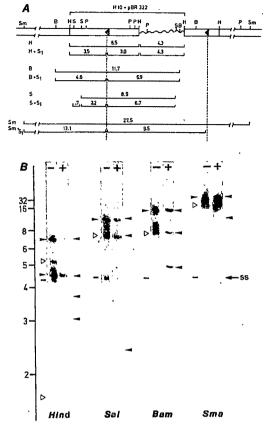


Fig. 5 Hybridization analysis of T-region intermediate structures. A, Restriction map of the left portion of the pGV3850 T-DNA region and border cleavage fragments predicted to arise after S1 treatment of AS-induced DNA. Sizes are given in kbp. B, BamHI; H. HindIII; P, Pst1; S, SalI; Sm, SmaI; S1, S1 nuclease. The black arrows and dotted lines indicate the positions of the T-DNA borders. B, Denatured transfers of HindIII, BamHI, SalI and Small digests of AS-induced DNA treated (+) and untreated (-) with S₁ nuclease were hybridized against nick-translated HindIII fragment 10/pBR322 probe (A). Scaling on left is in kbp. The single-stranded T-strand is indicated by ss and the bar adjacent to the digests. Solid arrows indicate the expected fragments before and after S₁ treatment and correspond in size to the fragments shown in A. The open arrows indicate unexpected AS-induced fragments which correspond to novel T-DNA homologous structures linked to pGV3850. Note that other unexpected signals are observed when the filter is reprobed with HindIII fragment 23 sequences, and that all of the unexpected fragments are specific to AS-induced DNA and have been observed with DNA prepared from at least two independent AS-induced bacterial cultures (data not shown).

AS-induced alterations of the Ti plasmid

Since the T-strand must be produced from the Ti-plasmid T-region, several molecular reactions involving these sequences should occur in bacterial cells that are actively carrying out different steps of T-strand synthesis, or other early steps of T-DNA transfer. To gain insight into these reactions, the novel T-DNA homologous hybridization signals that result from fragmentation of the AS-induced Ti plasmid with restriction enzymes and S₁ nuclease are characterized below. These data provide evidence for specific reactions associated with the Ti-plasmid T-DNA border repeats and with the internal sequences of the T-region.

 S_1 -sensitive T-DNA border sites. Figure 4 demonstrates that AS induction leads to the generation of Ti-plasmid T-DNA border structures which are sensitive to cleavage by S_1 nuclease. Uninduced and AS-induced DNA was restricted with *HindIII*, half of each sample was treated further with S_1 nuclease, and the

fragments homologous to the left and right border regions of pGV3850 were detected by hybridization. The AS-induced DNA lanes contain novel signals whose sizes correspond exactly to the fragments that would be produced by ds cleavages at the left and right T-DNA border sequences of pGV3850 (Fig. 4A), and the intensities of these signals are greatly increased by S_1 digestion of the DNA. We designate these S_1 -sensitive structures S_1 border sites.

The relative intensities of the signals which correspond to the S_1 border cleavage fragments show that ~30% of the left T-DNA borders and ~10% of the right T-DNA borders of the ASinduced Ti plasmid population are S₁-sensitive. Thus, the generation of S, border sites is a frequent event. Furthermore, since a 9.5-kbp ds T-DNA fragment is produced by S, digestion of AS-induced DNA that is unrestricted (Fig. 1C, lane 3), or restricted with SmaI (which does not cleave within the pGV3850 T-region (Fig. 5)), S₁ border sites can simultaneosly occur at both the right and left border repeats on a single Ti plasmid. We note that incubation of the uncut AS-induced DNA at 65 °C does not result in the release of the 9.5-kbp T-DNA fragment from the AS-induced Ti plasmid (data not shown); that is, the S₁ border site does not correspond to a ds staggered cleavage of the T-DNA border sequence. Other experiments have shown that the S₁-sensitive structure corresponds to an AS-induced ss endonucleolytic cleavage in the bottom strand of the 25-bp border sequence (K. Wang and M. Van Montagu, in preparation); S₁ is known to cleave opposite such structures^{26,27}.

Other AS-induced T-region structures. Figure 5 demonstrates that other novel Ti-plasmid-linked T-region structures are also present in the AS-induced cell population. Three different classes of T-DNA-homologous signals are observed when AS-induced DNA is digested with various restriction enzymes and S_1 nuclease (Fig. 5B): those that correspond to the ss T-DNA molecule (black bars, $-S_1$ lanes); those that correspond to the predicted border cleavage fragments (Fig. 5A) produced by S_1 digestion of the AS-induced S_1 border sites (solid arrows, $+S_1$ lanes); and those that correspond to novel unexpected fragments (open triangles) derived from pGV3850 Ti plasmids whose internal T-region sequences have been altered as a result of AS induction.

For example, the 5.2-kbp fragment present in the -S₁ HindIII sample (Fig. 5B; also Figs 2B and 4B) is S_1 -sensitive, binds to nitrocellulose, specifically hybridizes to HindIII fragment 10 (and not to pBR322 or HindIII fragment 23; data not shown), and is ~ 1.3 kbp smaller than HindIII fragment 10 (Fig. 5A). Thus, this novel HindIII fragment must be partially singlestranded and derived from an AS-induced Ti plasmid whose T-region is partially single-stranded or associated with ss T-DNA sequences, as in a D-loop structure. More perplexing fragments are also detected: the ~15-kbp S₁-insensitive SmaI signal corresponds to a ds DNA fragment which is ~12 kbp smaller than the Smal fragment that covers the T-region of the uninduced Ti plasmid; also, in the -S₁ BamHI and SalI lanes, signals are observed whose sizes correspond to the S₁ cleavage fragments of these digests (Fig. 5A) which are internal, but not external, to the left T-DNA border. While the present data do not allow the precise identification of the T-region structure(s) to which these unexpected fragments correspond, they illustrate the complexity of the molecular reactions associated with the Ti-plasmid T-DNA sequences which occur in AS-induced Agrobacteria.

Discussion

Agrobacterium tumefaciens transfers its Ti-plasmid T-DNA to plant cells, and this process is activated by the induction of the Ti-plasmid virulence genes with the plant phenolic compound AS. We show that AS induction results in the generation of several novel T-DNA homologous molecules in Agrobacterium: a linear ss molecule, the T-strand, which corresponds to the lower strand of the Ti-plasmid T-region; and Ti-plasmid molecules whose T-DNA border repeats are sensitive to cleavage

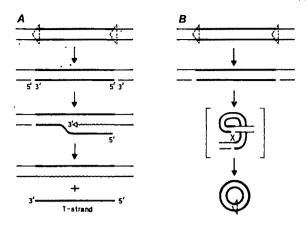


Fig. 6 Proposed reactions associated with the Ti-plasmid Tregion in AS-induced cells. A, Model for the generation of the T-strand; B, model for the generation of a ds T-DNA circle molecule. Thick lines represent T-region sequences, thin lines represent adjoining Ti-plasmid sequences external to the 25-bp T-DNA border repeats, indicated by the dashed triangles, as breaks in the bottom strand of the border repeats correspond to Siborder sites, and the wavy line corresponds to a newly synthesized bottom strand of the T-region. This model implies that ss molecules are not generated leftward of the left T-DNA border; while we have not observed such molecules, they might not have been detected if they are heterogeneous in length.

by S₁ nuclease (S₁ border sites), and whose internal sequences have been altered (T-region structures). The specific properties of these AS-induced molecules allows the formulation of mechanistic models for the generation of the T-strand, and for its potential transfer to the plant cell.

Figure 6A presents a model for the generation of the T-strand molecule. First, ss endonucleolytic cleavages occur within the left and right T-DNA border sequences on the Ti plasmid. These cleavages correspond to S₁ border sites and provide free 3' OH groups from which DNA synthesis can be primed. Second, using the top strand of the T-region as template, DNA synthesis initiates at the right border cleavage site, and proceeds unidirectionally across the T-region. This synthesis displaces the bottom strand of the T-region and produces a transitory triple-stranded structure which may correspond to one of the AS-induced Tregion structures that we have detected. Third, DNA synthesis terminates when it encounters the left border cleavage site, and the displaced bottom strand is released from the Ti plasmid, as the free T-strand ss molecule. Alternatively, a $5' \rightarrow 3'$ helicase activity unwinds the T-region of the nicked Ti plasmid to free the T-strand molecule and produce a Ti plasmid whose T-region is momentarily ss prior to replacement strand synthesis. Since we observe at most one T-strand molecule per AS-induced cell. T-strand production must be tightly regulated.

The sequences internal to the T-DNA of the wild-type Ti plasmid encode genes whose expression in the transformed plant cell result in the tumorous phenotype, crown gall¹, and when the orientation of the right border on the Ti plasmid is flipped (by in vitro manipulation), phenotypically transformed plant cells are not obtained 15,16. The model of Fig. 6A explains this functional polarity of the right T-DNA border; that is, the T-strand corresponds to the bottom strand of the T-region and must be generated in a right-to-left (5' to 3') direction. Thus, if the orientation of the right border is reversed in the Ti plasmid, ss molecules will be generated away from (rightward of) the T-DNA tumour genes. This model may also explain how the ds T-DNA circle molecules, recovered in E. coli transformed with AS-induced DNA, are generated at a low frequency in response to AS induction. Since nicked DNA stimulates recombination events²⁸, the S₁ border sites could promote pairing and recombination between the T-DNA border repeats of the AS-induced Ti plasmid (Fig. 6B).

Assuming that the T-strand is the transfer intermediate, we can speculate on the mechanism of its transfer. This mechanism might share features with known bacterial processes which mediate the transfer of specific DNA molecules between bacteria, such as phage infection or conjugation. An important distinction between these two processes is that only phage infection involves the synthesis of many copies of the molecule destined for transfer. Since the T-strand is present at about one copy per ASinduced cell, it is unlikely that it is transferred to the plant cell as an infectious phage particle.

In bacterial conjugation, one strand of a ds donor molecule is transferred as a linear ss molecule from the donor to recipient cell²⁹. This process is initiated by nicking one strand of the donor molecule at a specific site (designated oriT, origin of transfer)³⁰, and the strand destined for transfer is unwound in a $5' \rightarrow 3'$ direction. Concomitant to unwinding, the unwound strand is mobilized to the recipient cell, and this transfer is accompanied by DNA synthesis on the donor molecule to replace the mobilized strand. The T-DNA homologous molecules that we have described correspond to the structures which would be predicted to occur if T-DNA transfer occurs through a conjugative mechanism. The S₁ border sites are analogous to nicked oriT sites, the T-strand is analogous to the linear ss DNA molecule transferred during bacterial conjugation, and the internal T-region structures are analogous to the replacement strand synthesis intermediates of the donor molecule. Furthermore, bacterial conjugation requires direct contact between donor and recipient cells11, and the same requirement is observed for the T-DNA transfer process¹².

If the T-strand is transferred by conjugation to the plant cell. it is still not known how it ultimately finds its way into the plant cell nucleus and becomes integrated into the nuclear genome. While the deproteinized T-strand that we have described is a naked linear molecule, presumably it is transferred as a complex that carries proteins which in part mediate the post-transfer events. These proteins, as well as the proteins involved in the generation and transfer of the T-strand, are probably encoded by the plant-inducible Ti-plasmid vir loci10

We thank Marc Van Montagu for his encouragement and suggestions for the exonuclease studies, Kan Wang for helpful discussion, Jeff Schell for support, and Martine De Cock, Karel Spruyt and Albert Verstraete for preparation of this manuscript and figures. This work was supported by grants from the 'ASLK-Kankerfonds', the 'Fonds voor Geneeskundig Wetenschappelijk Onderzoek' (FGWO 3.001.82), and the Services of the Prime Minister (OOA 12.0561.84) (to Jeff Schell and Marc Van Montagu),

Note added in proof: The nondenatured transfer assay for singlestranded DNAs has also been recently described by Reile, H. T., Michel, B. and Ehrlich, S. D. Proc. natn Acad. Sci. U.S.A. 83, 2541-2545 (1986).

Received 24 April; accepted 19 June 1986.

- Gheysen, G., Dhaese, P., Van Montagu, M. & Schell, J. in Advances in Plant Gene Research Vol. 2 (eds Hohn, B. & Dennis, E. S.) 11-47 (Springer, Vienna, 1985).
- 2. Zambryski, P., Depicker, A., Kruger, K. & Goodman, H. J. molec. appl. Genet 1, 361-373
- 3. Yadav, N. S., Vanderleyden, J., Bennett, D. R., Barnes, W. M. & Chilton, M. D. Pro. Ca. Acad. Sci. U.S.A. 79, 6322-6326 (1982).

- Acad. Sct. U.S.A. 79, 6322-6326 (1982).

 Simpson, R. B. et al. Cell 29, 1005-1014 (1982).

 Holsters, M. et al. Molec. gen. Genet. 190, 35-41 (1983).

 Zambryski, P. et al. EMBO J. 2, 2143-2150 (1983).

 de Framond, A. J., Barton, K. A. & Chilton, M.-D. Bio/technology 1, 262-159 1983.
- 8. Bevan, M. Nucleic Acids Res. 12, 8177-8721 (1984).

- An, G., Watson, B. D., Stachel, S., Gordon, M. P. & Nester, E. W. EMBO J 4, 2 7-284 (1985)
 Stachel, S. E. & Nester, E. W. EMBO J. 5, 1445-1454 (1986).
 Douglas, C. J., Staneloni, R. J., Rubin, R. A. & Nester, E. W. J. Bact. 161, 850-860 1985. 12. Stachel, S. E., Nester, E. W. & Zambryski, P. C. Proc. natn. Acad. Sci. U.S A 83, 779 353
- 13. Stachel, S. E. & Zambryski, P. Cell (in the press).
- Stachel, S. E., Messens, E., Van Montagu, M. & Zambryski, P. Nature 318, 624-629 (1985)
 Wang, K., Herrera-Estrella, L., Van Montagu, M. & Zambryski, P. Cell 38, 455-462 (1984)
 Peralta, E. G. & Ream, L. W. Proc. natn. Acad. Sci. U.S.A. 82, 5112-5116 (1985)
- 17. Joos, H. et al. Cell 32, 1057-1067 (1983).

- Shaw, C. H., Watson, M. D., Carter, G. H. & Shaw, C. H. Nucleic Acids Res. 12, 6031-6041 (1984).
- Koukoliková-Nicola, Z. et al. Nature 313, 191-196 (1985).
 Southern, E. M. J. molec. Biol. 98, 503-518 (1975).
- 21. Bourgeois, S. Meth. Enzym. 21, 491-500 (1971). Voet, V. Eur. J. Biochem. 33, 192-200 (1973)
- 23. Nishigaki, K., Kaneko, Y., Wakuda, H., Husimi, Y. & Tanaka, T. Nucleic Acids Res. 13, 5747-5760 (1985)
- 24. Huang, W. M. & Lehman, I. R. J. biol. Chem. 247, 3139-3146 (1972).
- Chase, J. W. & Richardson, C. C. J. biol. Chem. 249, 4545-4561 (1974).
 Lilley, D. M. J. Nucleic Acids Res. 9, 1271-1289 (1981).

- Panayotatos, N. & Wells, R. D. Nature 289, 466-470 (1981).
 Dressler, D. & Potter, H. A. Rev. Biochem. 51, 727-761 (1982).
 Willetts, N. & Wilkins, B. Microbiol. Rev. 48, 24-41 (1984).
- Thompson, R., Taylor, L., Kelly, K., Everett, R. & Willetts, N. EMBO J. 3, 1175–1180 (1984).
 Manning, P. A. & Achtman, M. in Bacterial Outer Membranes (ed. Inouyc, M.) 409-447
- (Wiley, New York, 1979).32. Douglas, C. J., Halperin, W. & Nester, E. W. J. Bact. 152, 1265-1275 (1982).
- Dhaese, P., De Greve, H., Decraemer, H., Schell, J. & Van Montagu, M. Nucleic Acids Res. 7, 1837-1849 (1979).
- 34. Maniatis, T., Fritsch, E. F. & Sambrook, J. Molecular Cloning, a Laboratory Manual (Cold Spring Harbor Laboratories, New York, 1982).

ERS TO NATURE

Binary pulsar with a very small mass function

R. J. Dewey*, C. M. Maguire†, L. A. Rawley†, G. H. Stokes† & J. H. Taylor†

* Center for Radiophysics and Space Research, Cornell University, Ithaca, New York, 14853, USA † Joseph Henry Laboratories and Physics Department, Princeton University, Princeton, New Jersey 08544, USA

Much of the interesting physics concerning neutron stars and their evolution depends for its experimental foundation on observations of the rotation rates of pulsars. To continue recent efforts of our group in this area 1-3, we began a series of pulse-arrival-time observations of ~70 pulsars in January 1985. Most of the pulsars in this study were discovered in the Princeton/NRAO pulsar survey of the preceding two years^{4,5}. Soon after we began these observations it became clear that PSR2303+46 was a binary pulsar2; it is now evident that PSR1831-00 is also a member of a binary system, the seventh such radio pulsar known. It moves in an orbit with a period of 1.81 days, a small eccentricity, and an unusually small mass function of 0.90012 M_{\odot} (where M_{\odot} is the mass of the Sun). With a period P = 0.521 s and period derivative $\dot{P} \leq 10^{-17}$ s s-1, PSR1831-00, like the other known binary pulsars, has a relatively weak magnetic field. We discuss the features of this system that provide clues to its evolutionary history and outline possible models for its formation.

Most of our observations were made with the 92-m transit telescope at Green Bank, West Virginia, at a frequency of 390 MHz. The data acquisition system has been described by Stokes et al.5. Briefly, a dual-channel parametric up-converter amplifies two orthogonal linear polarizations and provides a system noise temperature of 50 K at high galactic latitudes. In the direction of PSR1831-00 (galactic coordinates $l = 30.8^{\circ}$, b =3.7°) the system temperature is 180 K, equivalent to a flux density of ~150 Jy. In each polarization an 8-MHz pass-band is divided into 32 sub-channels, each 250 kHz wide; the signals are detected, summed in a de-disperser, and then integrated for two minutes in a signal averager synchronized to the apparent pulsar period. For each pulsar, the resulting profiles are cross-correlated with a standard profile for that pulsar. This procedure determines phase offsets which, when added to reference times near the centre of the integrations, yield effective pulse arrival

For PSR1831-00, one to ten arrival times were obtained in this way on each of 19 days in January, February, April, July and November 1985, and February 1986. The number of observations obtainable on a single day is limited by the small hour-angle range through which the 92-m telescope can track (~20 min at the celestial equator), and this in turn limits the accuracy with which one can measure a pulsar's apparent period on a given day. Neverthless, for virtually all non-binary pulsars it is possible to fit data obtained over two or three days to a single barycentric period and to count pulses unambiguously

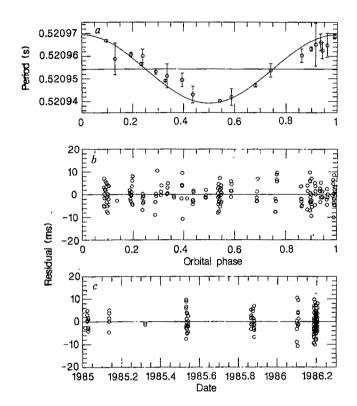


Fig. 1 Pulsar period as a function of orbital phase (a), and arrival-time residuals as function of both orbital phase (b) and date (c). The sinusoid superimposed on the measured periods in a corresponds to the orbital parameters listed in Table 1.

from day to day. The data for PSR1831-00 were not amenable to such treatment; it was rarely possible to fit data taken one or two days apart to a single period. However, the day-to-day period changes were small (a few parts in 10⁵) and only marginally significant, making the binary nature of this pulsar hard to recognize.

These difficulties were compounded by the weakness of the pulsar's signal (2-5 mJy) and its variability. We did not detect the pulsar in a number of our attempts to observe it, and there is some evidence that it has become weaker in the past year. The variability may be due to refractive interstellar scintillation. Our failures to detect the pulsar show no correlation with orbital phase, so there is no evidence that eclipses are involved.

Redoubled observational efforts in February 1986 showed that the data were consistent with a nearly circular orbit having a 1.81-day period and a maximum radial velocity of ±8.7 km s We were still not able, however, to connect pulsar phases unambiguously between observing days. Consequently, during March 1986 we observed PSR1831-00 at 430 MHz with the Arecibo 305-m telescope. The data acquisition scheme is described in ref. 6. The pulsar is close to the southern declination limit of the Arecibo antenna and can therefore be observed for only 50 min each day; however, the improvement in tracking time over that available at Green Bank allowed us to connect pulsar phases between observations made on 10, 12, 13, 14 and 16 March. An orbital solution obtained using the method described by Manchester and Taylor⁷ was good enough to allow unambiguous phase connection to all of the earlier Green Bank data. The resulting global solution for pulsar and orbital parameters is presented in Table 1, and the orbital velocity curve

Table 1 Parameters of the PSR1831-00 system						
Right ascension (1950.0)	$\alpha = 18 \text{ h } 31 \text{ min } 43.23 \pm 0.08 \text{ s}$					
Declination (1950.0)	$\delta = -00^{\circ} \ 13' \ 13.5 \pm 1.8''$					
Pulsar period	P = 0.5209543084(3)s					
Period derivative	$P = (0.2 \pm 1.6) \times 10^{-17} \text{ s s}^{-1}$					
Dispersion measure	$DM = 94 \pm 6 \text{ cm}^{-3} \text{ pc}$					
Projected semi-major axis	$a_1 \sin i = 0.7227 \pm 0.0010$ light s					
Eccentricity	e < 0.005					
Orbital period	$P_b = 156478.9 \pm 0.4 \text{ s}$					
Time of periastron	$T_0 = 2,446,460.3411 \pm 0.0011 \text{ JD}$					
Assumed longitude of periastron	$\omega = 0.0^{\circ}$					

and post-fit arrival-time residuals are shown in Fig. 1. We note that our measured period derivative, although effectively an upper limit, already places PSR1831-00 among the dozen pulsars with the smallest slow-down rates, as can be seen in Fig. 2. A small rate of spin-up is also consistent with our data—and would be most interesting if confirmed—but is not yet required. At present only an upper limit is available for the orbital eccentricity. If it is as small as the eccentricities of the PSRs 0655+64, 1855+09 and 1953+29, it will be impossible to measure because the ratio $(a_1 \sin i)/P$ for PSR1831-00 is so small. $(a_1 \text{ is the orbital semi-major axis; } i$ is the angle between the plane of the orbit and the plane of the sky.)

The orbital period and semi-major axis determine the mass function:

$$f(m_1, m_2) = \frac{(m_2 \sin i)^3}{(m_1 + m_2)^2} = \frac{4\pi^2}{G} \frac{(a_1 \sin i)^3}{P_b^2} = 0.000123 \ M_{\odot}$$

where m_1 and m_2 are the masses of the pulsar and companion, respectively. As shown in Fig. 3, this constraint implies a very small companion mass, $\sim 0.05-0.15~M_{\odot}$, unless cos *i* is implausibly close to 1.

As can be seen in Table 2, the 1831-00 system is similar in many respects to the other known binary pulsars. Like the other binaries, the pulsar has an unusually small spin-down rate and an unusually small inferred magnetic field, $B=3.2\times10^{19}\,(P\dot{P})^{1/2}<8\times10^{10}\,\mathrm{G}$. All seven binary pulsars lie between the 'spin-up line' and the 'death line'^{3,8} in the $P-\dot{P}$ diagram, as shown in Fig. 2. Taylor and Stinebring' note that the known binary pulsars and the millisecond pulsar 1937+21 show a correlation between magnetic field and distance |z| from the galactic plane, a pattern into which PSR1831-00 fits nicely (see Table 2). Although this relation may be partly due to selection effects—searches for millisecond pulsars (expected to have small magnetic fields) have tended to concentrate at low latitudes—it may also provide information about how binary

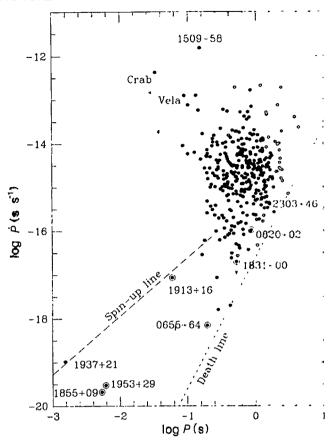


Fig. 2 Distribution of periods and period derivatives for 353 pulsars. The seven known binary pulsars, indicated by circles around the dots, have unusually small period derivatives and hence relatively weak magnetic fields.

and millisecond pulsars are formed, and may be related to the correlation between magnetic field and velocity first noted by Anderson and Lyne¹⁰. This correlation does not, however, follow simply from models of binary pulsar formation such as those outlined by van den Heuvel⁸.

What makes the 1831–00 system atypical, and its evolutionary history somewhat difficult to understand, is its relatively tight orbit (component separation $\sim 6~R_{\odot}$, where R_{\odot} is the radius of the Sun) and extremely small mass function. Models for the formation of binary pulsars⁸ suggest that during evolution a low-mass companion will spiral away from a neutron-star primary, leaving a final system with a wide orbit similar to those of PSRs 1953+29 and 0820+02. Nevertheless, a number of features of the evolution of the 1831–00 system may be inferred from its orbital parameters and the pulsar's period and spindown rate.

The pulsar's small magnetic field suggests that it is relatively old ($\ge 3 \times 10^7$ yr, assuming a magnetic field decay time of 10° yr and a magnetic field of 10^{12} G at birth¹¹). As the system presently

Table 2 Parameters of binary and millisecond pulsars										
PSR	P (ms)	log Þ	log <i>B</i> (G)	z (pc)	$a_1 \sin i$ (R_{\odot})	P _b (days)	e	$f(m_1, m_2) \\ (M_{\odot})$	Likely m;	
1937 + 21	1.6	19.0	8.6	20		-		_		
1855 + 09	5.4	-19.7	8.5	20	4.0	12.33	0.00002	0.0052	0.2-0.4	
1953 + 29	6.1	-19.5	8.6	20	13.6	117.35	0.0003	0.0027	0.2-0.4	
0655+64	195.6	-18.2	10.0	120	1.8	1.03	< 0.00005	0.0712	0.7-1.3	
1913 + 16	59.0	-17.1	10.3	190	1.0	0.32	0.6171	0.1322	1.4	
1831 - 00	520.9	<-17.0	<10.9	190	0.3	1.81	< 0.005	0.00012	0.06-0.13	
0820+02	864.9	-16.0	11.5	280	70.0	1.232.40	0.0119	0.0030	0.2-0.4	
2303 + 46	1,066.4	-15.4	11.8	480	14.1	12.34	0.6584	0.2463	1.2-2.5	

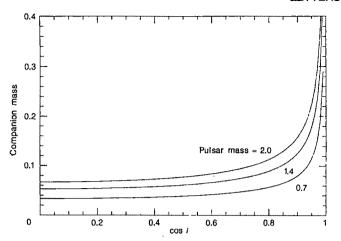


Fig. 3 Mass of the companion of PSR1831-00, plotted as a function of cos i and assuming three different values for the mass of the pulsar. All masses are in units of M_{\odot} .

lies ~200 pc above the galactic plane, such an age implies a velocity of ≤10 km s⁻¹, substantially smaller than that of the average pulsar. A shorter magnetic field decay time or smaller initial magnetic field would allow a larger velocity. The position of the pulsar in the $P-\dot{P}$ diagram (Fig. 3) allows, but does not require, that the pulsar has been spun up by accretion from its companion.

The system's circular orbit is compatible with the companion having undergone mass loss after the pulsar was created. If this is the case, the pulsar may have been formed by the accretioninduced collapse of a white dwarf, which would explain the system's low apparent velocity. However, it is also possible that no mass transfer has occurred since the formation of the neutron star in a supernova explosion, and that tidal forces have circularized the orbit. If the companion has a substantial convective envelope, such forces may be able to do this quite effectively¹².

For cos $i \le 0.95$ the companion mass is too small for the companion to be the white-dwarf or helium-core remnant of a star that has evolved off the main sequence in the age of the universe. If the companion is the remnant of an evolved star which underwent mass loss, that mass loss must have occurred before the end of the star's hydrogen burning, and before a sizeable compact core could develop.

This evidence points to two alternative evolutionary models, one involving mass transfer after (or during) the formation of the neutron star, and one in which no mass transfer has occurred. In both models the neutron star is formed from the primary of the original main-sequence system. In the former case, because the companion must have overflowed its Roche lobe before leaving the main sequence, the orbit after the collapse of the primary must have been quite small. This suggests that the progenitor system passed through a contact phase during the primary's evolution. During this phase the secondary may have accreted a significant amount of matter, but this is not required. Once the secondary overflowed its Roche lobe, the system may have appeared as a cataclysmic variable or low-mass X-ray binary and during this stage a white dwarf might be pushed over the Chandrasekhar limit. The compact primary's motion must have acted to eject the envelope of the secondary, a process which appears to be possible, given suitable conditions¹³. If the pulsar was formed by accretion-induced collapse, the most likely pre-neutron-star candidates are an O-Ne-Mg white dwarf whose progenitor was a fairly massive ($\geq 8 M_{\odot}$) star, or a very old CO white dwarf14

In the alternative model, the companion is a normal low-mass star which has evolved very little since the formation of the pulsar in a supernova explosion. In order for the system to have remained bound, the primary must have had a mass of \sim 3 M_{\odot} when it exploded, unless very limiting assumptions are made

about asymmetries in the supernova explosion. This again requires a contact phase during the evolution of the primary, in this case, one in which the companion accreted very little matter. The explosion of any helium star massive enough to have formed a neutron star would have induced a substantial (≥0.5) eccentricity in the system's orbit, so this model is viable only if tidal forces could have circularized the orbit within the lifetime of the pulsar.

We are grateful to T. H. Hankins, D. R. Stinebring and K. Turner for allowing us to use the Arecibo telescope during part of their scheduled time, and to J. M. Cordes and A. Wolszczan for help with some of the observations. We thank the staffs of the National Radio Astronomy Observatory and the National Astronomy and Ionosphere Center for assistance with the observations and NSF for financial support. R.J.D. thanks E. E. Salpeter for informative discussions on the evolution of low-mass stars.

Received 18 April: accepted 13 June 1986.

- Davis, M. M., Taylor, J. H., Weisberg, J. M. & Backer, D. C. Nature 315, 547-550 (1985).
 Stokes, G. H., Taylor, J. H. & Dewey, R. J. Astrophys. J. 294, L21-L24 (1985).
 Rawley, L. A., Taylor, J. H. & Davis, M. M. Nature 319, 383-384 (1986).
 Dewey, R. J., Taylor, J. H., Weisberg, J. M. & Stokes, G. H. Astrophys. J. 294, L25-L29 (1985).

- 6. Stokes, G. H., Taylor, J. H., Weisberg, J. M. & Dewey, R. J. Nature 317, 787–788 (1985). 6. Segelstein, D. J., Rawley, L. A., Stinebring, D. R., Fruchter, A. S. & Taylor, J. H. Nature
- 7. Manchester, R. N. & Taylor, J. H. Pulsars (Freeman, San Francisco, 1977).
- van den Heuvel, E. P. J. J. Astrophys. Astr. 5, 209-233 (1984)
- Taylor, J. H. & Stinebring, D. R. A. Rev. Astr. Astrophys. (in the press).
 Anderson, B. & Lyne, A. G. Nature 303, 597-599 (1983).
- Lyne, A. G., Manchester, R. N. & Taylor, J. H. Mon. Not. R. astr. Soc. 213, 613-639 (1985).
 Lecar, M., Wheeler, J. C. & McKee, C. F. Astrophys. J. 205, 556-562 (1976).
- 13. Tamm, R. E., Bodenheimer, P. & Ostriker, J. P. Astrophys. J. 222, 269-280 (1978).
- 14. Trimble, V. J. Astrophys. Astr. 5, 389-402 (1984).

New millisecond pulsar in a binary system

D. J. Segelstein, L. A. Rawley, D. R. Stinebring, A. S. Fruchter & J. H. Taylor

Joseph Henry Laboratories and Physics Department, Princeton University, Princeton, New Jersey 08544, USA

Recent observations^{1,2} at the Arecibo Observatory have resulted in the discovery of PSR1855+09, a pulsar with period P =5.362 ms, moving in a nearly circular orbit of period 12.3 days. The pulsar is only the third one known with P < 10 ms, and the sixth known radio pulsar in a binary system. (Discovery of a seventh binary pulsar is announced in an accompanying paper3.) Three of the seven binaries are among the fastest five of more than 400 pulsars—a fact that provides strong support for the conclusion that fast pulsars are 'recycled' neutron stars, spun up during a phase of mass accretion from an evolving companion star. The pulsar has a small dispersion measure (13.3 cm⁻³ pc), suggesting a distance of only ~350 pc. The proximity of this pulsar and its location within 25 pc of the galactic plane argue that millisecond pulsars form a significant fraction ($\sim 10\%$) of the pulsar population, leaving many detectable ones undiscovered^{4,5}. Its signal is strong enough to permit pulse-arrival-time measurements with single-day uncertainties of <3 \(\mu s\). Timing observations already suggest that PSR1855+09, like the 1.5-ms pulsar PSR1937+21, will prove to be a natural clock of extremely high stability⁶. The existence of a second pulsar with extremely small timing uncertainties will greatly aid the search for background gravitational waves using millisecond pulsars as detectors.

Observations leading to the discovery of PSR1855+09 were part of a survey specifically designed to detect fast pulsars¹. The Arecibo 305-m telescope was used at a frequency of 430 MHz, where a 30-m line feed provides a sensitivity of up to 19 K Jy⁻¹

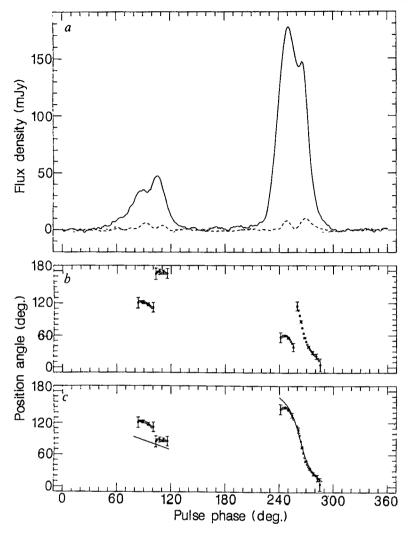


Fig. 1 Total intensity and polarization profiles for PSR1855+09. a. Total intensity (solid line), linear polarization (dashed line) and circular polarization (dotted line) for a synchronous average of ~560,000 pulses. There are 256 samples across the pulse (20.9 µs per sample), dispersion smearing was 40 µs across a 1 MHz bandwidth and the post-detection time constant was 50 µs. The total intensity data are shown at full resolution, whereas the linear and circular polarization data have been boxcarsmoothed over four time samples. b, Position angle of the linear polarization, plotted wherever the linear polarization was >3.0 times the r.m.s. (root mean square) noise. Representative error bars are ±1.0 the r.m.s. error in the position angle. c, Position angle, with two segments shifted by 90°, plotted together with a representative fit to a Radhakrishnan and Cooke¹⁵ model ($\alpha = 30^{\circ}$, $\beta = 25.5^{\circ}$. $\theta_0 = 91^{\circ} \text{ and } \phi_0 = 263^{\circ}).$

in each sense of circular polarization and a half-power beamwidth of 10'. At zenith angle 10° and galactic background temperature 150 K, parameters typical of the region of sky surveyed, the flux density equivalent to the total system noise was \sim 17 Jy.

During the survey we observed a grid of 14,452 beam areas, with 9' spacing between points, for 39 s each. A filter-bank spectrometer provided 16 adjacent channels of 60 kHz width for each circular polarization. Detected power from the two polarizations was summed for each channel, and the sixteen resulting signals were smoothed with a time constant of 400 μ s, sampled every 300 μ s, digitized to 3-bit precision, and stored on magnetic tape for later analysis. Further details of the searching procedure are contained in ref. 1. The survey observation in the direction of PSR1855+09 was made in October 1984, and confirming observations followed in July and November 1985. By mid-December it was clear that a new millisecond pulsar had been found, and that its period was changing significantly on a timescale of several days. The pulsar's mean flux density at 430 MHz is ~10 mJy.

Starting on 20 December 1985, we have made timing measurements of the new pulsar with equipment and techniques similar to those used to observe PSR1953+29 7 . The Arecibo telescope was used for these observations, usually at 1,400 MHz, with a $2\times32\times250$ kHz filter bank. Because interstellar scintillation causes the signal strength to vary widely (with a decorrelation bandwidth of \sim 8 MHz, a timescale of \sim 40 min, and a peak-tomean flux density ratio approaching 10), we choose an exact observing frequency, somewhere in the range 1,360-1,440 MHz, at the time of each observation. A 32-channel signal averager samples the total-power signals 256 times per pulsar period and records 32 integrated pulse profiles every two minutes. Up to

45 such observations can be made on a given day. Cross-correlation of the observed profiles with a standard profile produces a set of phase delays which are corrected for dispersion, averaged and added to a reference time near the midpoint of the integration to yield an effective pulse arrival time. Based on the variance of dispersion-corrected phase delays, the uncertainties in arrival times for 2-min integrations are between 2 and 15 μs, depending on signal strength. The total-intensity pulse profile is shown in Fig. 1a, together with the linear and circular polarization.

A 15-min observation made with the Very Large Array (VLA) on 28 February 1986, using two 50-MHz bandwidths centred at 1,464.9 MHz and 1,514.9 MHz, found an average pulsar flux density of 1.5 mJy, and provided a position measurement in the FK4 coordinate system of $\alpha(1950) = 18 \text{ h}$ 55 min 13.681 \pm 0.009 s, $\delta(1950) = +09^{\circ}$ 39' 12.80 \pm 0.15". Because the product of the decorrelation bandwidth and the peak-to-mean flux ratio is as large as our total bandwidth, the measured flux over a 15-min period is subject to large statistical fluctuations. Our estimated flux density, therefore, is accurate only to about a factor of two. For these observations we used the radio source 1821 + 07 as a phase calibrator; its position was assumed to be $\alpha(1950) = 18 \text{ h}$ 21 min 41.655 s, $\delta(1950) = +10^{\circ}$ 42' 43.90".

The timing data were analysed using a procedure similar to that described by Rawley et al.⁷. We first determined the best-tit Solar System barycentric period for each available 20-min interval of data. These periods were used to carry out a least-squares solution for the pulsar period in its own rest frame, P, the binary orbital period, P_b , the projected semi-major axis, $a_1 \sin i$ (where i is the angle between the plane of the orbit and the plane of the sky), and a time of passage through the

ascending node. The sinusoidal velocity curve determined from these parameters is superimposed on a plot of the barycentric period measurements at the top of Fig. 2.

Unambiguous pulse numbers could then be assigned to the 1,073 pulse arrival times obtained between 20 December 1985 and 24 May 1986. A least-squares fit yielded the pulsar parameters and orbital elements listed in Table 1. Figure 2 shows

Table 1 Parameters of the PSR1855+09 system

Right ascension (1950.0) $\alpha = 18 \text{ h} 55 \text{ min } 13.6834 \pm 0.0006 \text{ s}$ Declination (1950.0) $\delta = \pm 09^{\circ} 39' 13.278 \pm 0.009''$ $P = 5.362,100,452.39 \pm 0.03 \text{ ps}$ Pulsar period $\dot{P} = (2.1 \pm 0.5) \times 10^{-20} \text{ s s}^{-1}$ Period derivative $DM = 13.2943 \pm 0.0002 \text{ cm}^{-3} \text{ pc}$ Dispersion measure $a_1 \sin i = 9.2307850 \pm 0.0000004$ light s Projected semi-major axis $e = (21.27 \pm 0.08) \times 10^{\circ}$ Eccentricity Orbital period $P_b = 1,065,067.593 \pm 0.004 s$ Longitude of periastron $\omega = 277.10210 \pm 0.33^{\circ}$ $T_0 = 2,446,433.3026117 \pm 0.0114 \text{ JD}$ Time of periastron

post-fit residuals for this solution, plotted as a function of both data and orbit phase. The timing position shown in Table 1 is based on the coordinate system of the PEP740-R ephemeris (J. F. Chandler *et al.*, personal communication). Positions obtained from this ephemeris must be rotated by $\sim 0.4''$ before they can be compared with FK4 coordinates^{8,9}. After this is done, the discrepancy between the VLA and timing positions is about two standard deviations—probably not significant.

The very small period derivative (\dot{P}) observed for PSR1855+09 implies a surface magnetic field strength of $\sim 3 \times 10^8$ G—very close to the values obtained for the other two millisecond radio pulsars^{6,7}, and consistent with binary spin-up models for their evolution (refs 10, 11 and references therein). A small \dot{P} also suggests that the rotational stability of this pulsar, like that of PSR1937+21, is probably very high⁶. This conjecture is supported by the fact that after averaging our timing data to give a single equivalent arrival time for each of the 21 observing days, we obtain a post-fit weighted r.m.s. residual of only 2.6 μ s. Future comparison of timing residuals of PSR1855+09 with those of PSR1937+21 may be able to distinguish effects external to the Solar System (such as a cosmic background of gravitational radiation⁶) from inaccuracies in the Earth's ephemeris or in the realization of atomic time.

Because of the extremely small eccentricity of the orbit of PSR1855+09, relativistic effects will not be readily detectable in its timing data. General relativistic advance of periastron should occur at a rate of $\sim 15''$ yr⁻¹, but with present accuracies it will require a century or more to detect. Some further conclusions concerning statistics of the population of binary radio pulsars are discussed in ref. 3.

On 7 and 18 January 1986 we made phase-resolved polarization observations of the new pulsar at 1,400 MHz, using a procedure similar to that described by Stinebring¹². The mean polarization of this pulsar at 1,400 MHz reaches a maximum of ~10% circular (near the peak of the main pulse) and 10% linear (on the trailing edge). The circular polarization changes sign at the centre of the main pulse and the linear polarization goes to zero between the components of the main pulse and interpulse, indicating the presence of orthogonally polarized radiation^{13,14}.

The position-angle swing of the linear polarization of many pulsars is consistent with a simple model first put forward by Radhakrishnan and Cooke¹⁵, in which the position angle at a particular rotational phase is determined by the projection of the local magnetic field direction onto a plane perpendicular to the line of sight. Assuming a purely dipolar magnetic field structure, the position angle χ is given by 16

$$\tan(\chi - \chi_0) = \frac{\sin \alpha \sin(\phi - \phi_0)}{\cos \alpha \sin \beta - \sin \alpha \cos \beta \cos(\theta - \theta_0)}$$

where α is the angle between the rotational axis and the magnetic dipole axis, β is the angle between the rotational axis and the

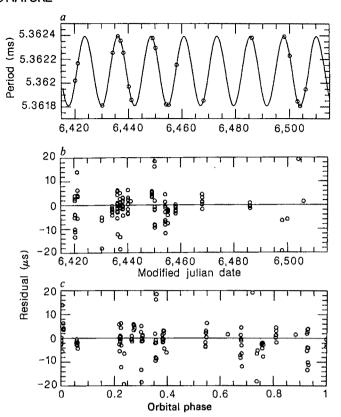


Fig. 2 Summary of PSR1855+09 timing data, 20 December 1985 to 16 March 1986. a, Sinusoidal fit to pulse period measurements (circles) on 21 different days. For the sake of clarity only one period measurement per day is plotted. b, c, Residuals from fit (Table 1) to pulse arrival times, plotted against time in b and orbital phase (fraction of an orbit since periastron passage) in c. Each circle corresponds to 10 min of observing time. No attempt is made to distinguish among data of widely varying quality.

line of sight, and ϕ is the azimuth of the line of sight relative to the projection of the magnetic axis onto the equatorial plane. The angles ϕ_0 and χ_0 are physically uninteresting, as the origin of pulse phase and position angle are arbitrary.

A fit of this equation to the position-angle data is shown in Fig. 1c, where the position angle has been shifted by 90° on the trailing half of the interpulse and the leading half of the main pulse, assuming that this radiation is in an orthogonal polarization state. A least-squares fit for α and β was performed after fixing $\phi_0 = 263^\circ$ and $\chi_0 = 91^\circ$ because of the obvious symmetry point at the centre of the main pulse. Over the range $10^\circ \le \alpha \le 90^\circ$ we find good fits to the main-pulse position-angle sweep for an intercept angle $\alpha - \beta = q\alpha$, where q varies smoothly from 0.2 at $\alpha = 10^\circ$ to 0.1 at $\alpha = 90^\circ$. Although the fit shown is not very good in the interpulse region, the position-angle swing does match the slope of the interpulse data fairly well. Any fit with $\beta > \alpha$ can be ruled out because the observed position-angle gradient has the same sign across the interpulse and the main pulse.

The position angle data are consistent with an interpulse produced at either the same magnetic pole as the main pulse or at the opposite magnetic pole¹⁷. The symmetry of the mainpulse and interpulse morphology, as well as the indication that corresponding components of the main pulse and interpulse are in the same polarization mode, lead us to favour a one-pole model similar to that proposed by Narayan and Vivekanand¹⁸ for PSR0950+08. Their model, in which α is relatively small and we cut across both edges of a hollow cone twice, is in good qualitative agreement with the polarization and pulse morphology data for this pulsar. Such a model is made more likely by the evidence that pulsar beams are elongated in the direction

of latitude and that this elongation is more marked for shorterperiod pulsars¹⁹. The deviation of the interpulse position angle from the simple model considered here may arise from a departure from dipolar magnetic field geometry, magnetospheric propagation effects²⁰, or interpulse emission from a much higher altitude than for the main pulse²¹.

The discovery of a third millisecond pulsar so nearby indicates that millisecond pulsars, although difficult to find, are not rare objects in the pulsar population. As their presumed progenitors—the low-mass X-ray binary systems—are rare, millisecond pulsars may be observable for much longer than the 108-yr lifetimes of the X-ray systems. This, in turn, implies that pulsar magnetic fields may not decay below a level of $\sim 5 \times 10^8$ G within a Hubble time, an idea discussed in detail by other authors^{5,11}. Independent evidence that millisecond pulsars are very old and long-lived comes from the detection of cool white dwarf companions for PSR0655+64 and PSR0820+02 by Kulkarni²², and for the millisecond pulsar reported here by Wright and Loh²³

We thank the staff of the Arecibo Observatory, and in particular A. Wolszczan, for help with the observations and the U.S. National Science Foundation for financial support. We would also like to thank J. H. van Gorkom for providing observing time and technical assistance at the VLA.

Received 18 April: accepted 13 June 1986.

- 1. Segelstein, D. J. thesis, Princeton Univ. (1986).
- Segelstein, D. J., Taylor, J. H., Rawley, L. A., Stinebring, D. R.: Wolszczan, A. IAU Circ. No. 4262 (1986).
- 3. Dewey, R. J., Maguire, C. M., Rawley, L. A., Stokes, G. H. & Taylor, J. H. Nature 322, 712-714 (1986).
- Stokes, G. H., Segelstein, D. J., Taylor, J. H. & Dewey, R. J. Astrophys. J. (submitted).
- Bhattacharya, D. & Srinivasan, G. Curr. Sci. 55, 327-330 (1986).
 Davis, M. M., Taylor, J. H., Weisberg, J. M. & Backer, D. C. Nature 315, 547-550 (1985).
- Rawley, L. A., Taylor, J. H. & Davis, M. M. Nature 319, 383-384 (1986).
 Bartel, N. et al. Astr. J. 90, 318-325 (1985).
- Backer, D. C., Fomalont, E. B., Goss, W. M., Taylor, J. H. & Weisberg, J. M. Astr. J. 90, 2275-2280 (1985).
- 10. van den Heuvel, E. P. J. J. Astrophys. Astr. 5, 209-233 (1984).
- van den Heuvel, E. P. J., van Paradijs, J. & Taam, R. E. Nature 322, 153-155 (1986).
 Stinebring, D. R. Nature 302, 690-692 (1983).
- Backer, D. C. & Rankin, J. M. Astrophys. J. Suppl. Ser. 42, 143-173 (1980).
 Stinebring, D. R., Cordes, J. M., Weisberg, J. M., Rankin, J. M. & Boriakoff, V. Astrophys.
- J. Suppl. Ser. 55, 247-277 (1984).
 Radhakrishnan, V. & Cooke, D. J. Astrophys. Lett. 3, 225-229 (1969).
- Radnakrishnan, V. & Cooke, D. J. Astrophys. Lett. 3, 225-229 (1969).
 Manchester, R. N. & Taylor, J. H. Pulsars, 218 (Freeman, San Francisco, 1977).
 Hankins, T. H. & Cordes, J. M. Astrophys. J. 249, 241-253 (1981).
 Narayan, R. & Vivekanand, M. Astrophys. J. 274, 771-775 (1983).
 Narayan, R. & Vivekanand, M. Astr. Astrophys. 122, 45-53 (1983).

- Barnard, J. Astrophys. J. (in the press)
- Gil, J. Astrophys. J. 299, 154-160 (1985).
 Kulkarni, S. R. Astrophys. J. 306, L85-L89 (1986).
- Wright, G. A. & Loh, E. D. Nature (in the press).

Repulsive regularities of water structure in ices and crystalline hydrates

Hugh F. J. Savage* & John L. Finney†

- * Center for Chemical Physics, National Bureau of Standards, Gaithersburg, Maryland 20899, USA
- † Department of Crystallography, Birkbeck College, University of London, Malet Street, London WC1E 7HX, UK

Hydrogen-bonded structures display wide ranges of the various angles (such as O-H···O) and distances (such at H···O) used to describe their intermolecular geometry. For example, O···O distances are found to vary between ~2.5 and 3.2 Å, and the hydrogen bond angles normally vary between 120 and 180°. Although correlations between distances and angles may be found (for example, between H...O distance and O-H...O angle), these geometrical characteristics are generally too 'soft' to be used as stereochemical restraints in, for example, refining the solvent structure in protein crystals. Moreover, although many potential functions exist for describing water-water interactions, none of them is totally satisfactory in reproducing experimental results, even for pure water1. We present here the initial results of an analysis of water structures in high-resolution neutron crystal structures² which is much more successful in rationalizing the stereochemistry of water interactions. Rather than considering the structures in terms of weak, orientation-dependent attractions, a concentration on the repulsive interactions leads to a set of very much stronger stereochemical constraints, which not only rationalize the structures but appear largely to control the orientational correlations in aqueous systems. Looked at this way, water network structures in crystal hydrates and, we suspect, in the liquid itself, become for the first time comprehensible. The approach provides a much firmer base from which to build realistic potential functions to model and simulate solvent structures.

A significant number of atomic-resolution neutron diffraction studies are now available in which the hydrogen (deuterium) atoms can also be located. Figure 1a shows a well-known plot relating to small hydrate crystals3; we see that as the H···O distance of hydrogen bond increases, the mean O-H···O bond angle tends to decrease. However, there is a large scatter in the H-bond geometries about the regression line that can be drawn: some short H-bonds are very bent, while some long ones tend to be very straight. A similar spread of values appears (Fig. 1b) when we restrict ourselves to the H-bond geometries of water molecules in a variety of crystal hydrates (containing between 1 and 18 water molecules per asymmetric unit) and ice polymorphs analysed by high-resolution (≤1.0 Å) neutron diffraction. Rather than draw a regression line as in Fig. 1a, however, we draw a limiting line below which configurations are notwithin experimental error—observed. There is thus apparently an excluded region. This limiting line represents the extreme limits of H-bond bending, which can be thought of as

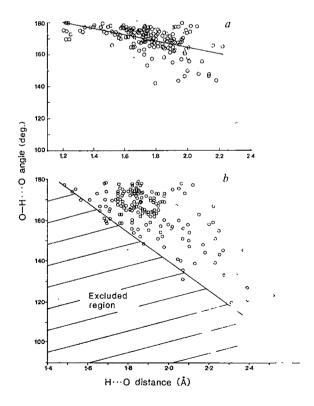


Fig. 1 Plots of O-H...O angle versus H...O distance: a, for H-bonds in small neutron structures (redrawn from ref. 3); b, for water H-bond geometries found in high-resolution neutron hydrate structures, showing the effect of repulsive restraint RR1 (see Fig. 2a) (see ref. 2 for full list of structures and source references).

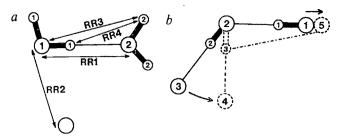
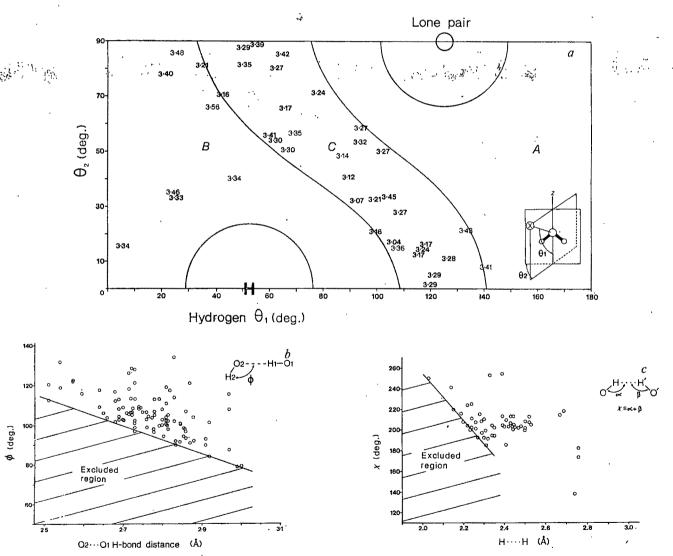


Fig. 2 a, Schematic diagram of the four proposed repulsive restraints: RR1, O···O repulsion of H-bond; RR2, O···O non-bonded repulsions; RR3, H2···O1 oxygen-remote-neighbour-hydrogen non-bonded interaction; RR4, H···H non-bonded repulsion. b, Schematic diagram of how the operation of RR3 relates an increase in H-bond distance to a decrease in O···O··O H-bond angle. If we start with a tetrahedral conformation of O1···O2···O3 with H-bond lengths of 2.76 Å, then on moving O3 to O4 (assuming H-bond linearity), the H3···O1 distance becomes less than the acceptable minimum contact of ~3.0 Å, and to relieve this strain, the O2···O1 H-bond must lengthen (O1 moves to O5), to retain a minimum H3···O1 contact of ~3.0 Å.

characterizing the limits of the O···O repulsions of the water hydrogen-bonded neighbours. We label this 'repulsive restraint' RR1 which is illustrated, together with three other repulsive restraints, in Fig. 2a.

The second repulsive restraint, RR2, describes the significant anisotropy of $O\cdots O$ non-H-bonded contacts, which range from 3.1 to 3.6 Å. Figure 3a shows the minimum $O\cdots O$ next-nearest-neighbour contacts observed in water molecules with respect to the two orientational angles defined in Fig. 3a inset, and can be discussed in terms of three regions. In the 'lone pair' region, A, there are no contacts ≤ 3.5 Å. In the hydrogen-bonding region, B, the minimum contact distance is ~ 3.3 Å, whereas between the lone pairs and hydrogens (region C) a minimum separation of ~ 3.1 Å is observed. These data can be rationalized to a first approximation if we tentatively assign to the three separate regions around the water molecule the following van der Waals' radii: 1.7-1.8 Å in the lone-pair region, 1.6-1.7 Å between the hydrogens, and 1.5-1.6 Å between the lone pairs and the hydrogens.

The third restraint, RR3, relates to the $H2\cdots O1$ remote neighbours (Fig. 2a) and appears to be the key to water molecule



 Γ_{3} . 3 a, $\theta_{1}-\theta_{2}$ orientational angle plot for the non-bonded O···O, C contacts around four-coordinated water molecules in the neutron structures examined. Bold numbers are water-oxygen contact distances (in Å) to oxygens; lighter numbers to carbons. θ_{1} and θ_{2} are the angles of approach of the contact, as defined in the inset. The significance of regions A, B and C to RR2 is discussed in the text. b, Plot of H2—O2···O1 angle (ϕ) versus O2···O1 H-bond distance, showing the effect of repulsive restraint RR3, relating to H2···O1 contacts (see Fig. 2a). In this part of the analysis, the O—H covalent bonds were standardized to 0.8 Å, to enable the approximate centre of the electron density of the hydrogens to be represented. This distance, the numerical value of which is not critical, was chosen on the basis of results from high-resolution X-ray structure analyses. 7 and deformation studies 8-10. c, Plot of the sum (χ) of the O—H···H angles subtended at the hydrogens (see inset) versus the H···H contact distance, showing the effect of repulsive restraint RR4 (see Fig. 2a).

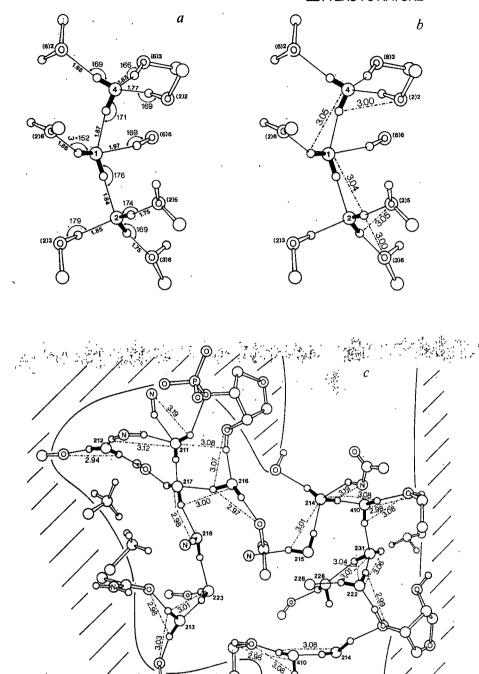


Fig. a, b,Hydrogen-bond networks in a local region of α -cyclodextrin, showing a, the range of Hbond distances (in A) and particularly H-bond angles (in degrees); and b, an explanation of the orientations on the basis of minimum oxygen-remote-hydrogen (H2···O1) contacts (shown in Å) of ~3.0 Å (effect of RR3). c, H2···O1 contacts (in Å) around water molecules in vitamin B₁₂ co-enzyme hydrate, shown in projection.

orientations. Figure 4a shows a region in α -cyclodextrin⁴. The hydrogen-bond distances and angles vary widely within the range shown in Fig. 1. Using the regression line as a target geometry, we would expect the H-bond angle ω (152°) to be greater, as a largely rotational motion of water 1 could be made without significantly affecting the near-linear O1—H···O2 angle. However, experimentally, this does not happen. Figure 4b shows the same region, but with the relevant remote-neighbour $H2 \cdots O1$ distances given, and immediately we may understand the situation: no remote-neighbour $H \cdots O$ distances are found which are ≤ 3.0 Å. Viewed in this way, an attempt to increase ω would begin to compromise the presumably repulsive interaction with the oxygen of water 4.

Figure 4c shows the $H2\cdots O1$ minimum contacts between water molecules in the crystal hydrate of co-enzyme B_{12} (ref. 5

and J.L.F., P. F. Lindley, H.F.J.S. and P. A. Timmins, in preparation), and the same pattern is apparent. These minimum contacts appear to 'fix' the mutual orientations of the water molecules at the expense of distortions of the H-bond geometries. In Fig. 3b, the H2—O2···O1 angle is plotted against the O2···O1 H-bond distance. As in Fig. 1, rather than draw a regression line to represent the mean values, a line representing the minimum values of the H2···O1 contacts (H2···O1 limiting curve) is drawn to give another section through what is presumably an excluded volume of the total configurational space.

The fourth constraint, RR4, relates to the $H \cdots H$ repulsions and Fig. 3c shows a plot of the water $H \cdots H$ repulsive contacts as a function of the angle χ (defined as the sum of the two angles subtended at the hydrogens, see Fig. 3c inset). The shortest water $H \cdots H$ contacts are ~ 2.1 Å and occur when the

O-H groups are arranged more nearly 'head-on': the majority are between 2.3 and 2.4 Å. Again, an excluded region can be specified.

Using these regularities, we can now understand more clearly some structural tendencies shared by ices and hydrates. For example, there are two ways of obtaining a more compact water structure than in ice Ih: by decreasing some of the O···O··O H-bond angles and/or by forming interpenetrating H-bond lattices (for example, at high pressures). By the former method, some of the O···O H-bond distances must increase in order to maintain the minimum H2···O1 contacts (Fig. 2b). These contacts appear to play a dominant role in determining the immediate local water structure. For example, acceptor waters, which form very short H-bonds (down to ~2.5 Å), tend towards a trigonal planar coordination, in order to maintain the H2...O1 minimum contacts of ~3.0 Å (ref. 2). Where longer H-bonds of 2.8-3.2 Å occur, significant distortions from the expected tetrahedral structure are allowed. Thus, in water structures in which the number and strength of the H-bonds are maximized (shorter H-bonds), the H2. O1 minimum contacts tend to enforce a tetrahedral-like structure (for example, in the ice polymorphs).

The exact nature of these interactions is not clear in all cases; however, we can make some proposals which may assist in developing better potential functions for simulation calculations. RR2 can be considered in terms of an angular-dependent van der Waals' radius which is, not surprisingly, larger around the lone-pairs region. The RR3 and RR4 interactions may be understood in terms of assigning a variable, angular-dependent van der Waals' radius to the polar water-hydrogens. Values of ~1.5 Å in the H—O direction and ≤1.0 Å in the O—H direction may be appropriate. This type of model is consistent with the known asphericity of the electron cloud around hydrogens attached to polar groups^{6,7}. More exact values may be obtained from more detailed analyses of the interactions between electron clouds of neighbouring water molecules (for example, by performing detailed high-level quantum mechanical calculations).

In the absence of a full physical explanation of the nature of these interactions, the very clear pattern of excluded regions, with no known significant violations, gives us confidence in using these minimum values as strict constraints in interpreting water organization in crystals (for example, during protein refinement). The 'hardness' of these excluded regions makes them far more reliable than the softer, more indefinite bondangle and bond-length restraints which have been used until now and which, as shown in Fig. 4a, b, can lead to incorrect structures.

The repulsive restraints discussed here can also be used to improve potential functions widely used in computer simulations of aqueous systems. A reasonable model for the nonbonded intermolecular structure will have to take into account the asymmetric character of both the oxygens and the hydrogens; that this has not been done may account for the difficulty in obtaining a satisfactory agreement with experiment¹. We are pursuing the incorporation of repulsive restraints in water potentials for the simulation of liquid water and other chemically and biologically important aqueous systems.

Received 11 April; accepted 7 May 1986.

1. Finney, J. L., Quinn, J. E. & Baum, J. O. in Water Science Reviews Vol. 1 (ed. Franks, F.)

33-170 (Cambridge University Press, 1985).

2. Savage, H. F. J. in Water Science Reviews Vol. 2 (ed. Franks, F.) (Cambridge University

3. Olovsson, I. & Jönsson, P. G. in The Hydrogen Bond Vol. 2 (eds Schuster, P., Zündel, G. Solvisson, I. a. Johnson, F. G. III. In Produced Both Vol. 2 (ed. Schicker, F., Edudel, G. a. & Sandorfy, C.) 1931 (North-Holland, Amsterdam, 1976).
 Klar, B., Hingerty, B. & Saenger, W. Acta crystallogr. B36, 1154-1165 (1980).
 Savage, H. F. J. Biophys. J. (in the press).
 Hamilton, W. C. & Ibers, J. A. Hydrogen Bonding in Solids (Benjamin, New York, 1968).

7. Bacon, G. E. Neutron Diffraction 355 (Clarendon, Oxford, 1975).
8. Savariaulf, J. M. & Lehmann, M. S. J. Am. Chem. Soc. 102, 1298-1303 (1980).
9. Dam, J., Harkema, S. & Feil, D. Acta crystallogr. B39, 760-768 (1983).

10. Hermansson, K. & Thomas, J. O. Acta crystallogr. C39, 930-936 (1983).

Selenium in western Atlantic precipitation

Gregory A. Cutter* & Thomas M. Church†

* Department of Oceanography, Old Dominion University, Norfolk, Virginia 23508, USA † College of Marine Studies, University of Delaware, Newark, Delaware 19711, USA

The trace element composition of precipitation (rain and snow) provides a way of monitoring anthropogenic and natural emissions to the atmosphere; the subsequent deposition of such emissions (for example, as acid precipitation) can have important effects on aquatic ecosystems. In this regard, the mobilization of selenium by fossil fuel combustion1 and selenium's toxicity2 provide compelling reasons to examine this element's atmospheric transport and removal. Furthermore, recent investigations suggest that atmospheric deposition is an important selenium input to oceanic surface waters^{3,4}. Here we examine data on the concentration and oxidation state of selenium in precipitation over coastal and midocean regions of the western Atlantic Ocean. The results indicate that fossil fuel combustion enriches selenium in wet depositional fluxes to western Atlantic surface waters, and that selenium's oxidation state in precipitation may be a sensitive oxidationreduction (redox) tracer.

Selenium is removed from the atmosphere by processes such as wet deposition, through its association with sub-micrometre aerosols⁵ and the efficient scavenging of these small particles during precipitation events⁶. As a Group VI element, selenium can exist in four oxidation states (-II, selenide; 0, elemental selenium; IV, selenite; VI, selenate). Selenium is thought to be naturally emitted to the atmosphere as volatile dimethyl selenide⁷; selenium dioxide [Se(IV)] or elemental selenium may be released during fossil fuel combustion⁸. In rainwater samples from Japan⁹ and coastal California¹⁰, selenite is the major selenium species; rain and snow in urban Belgium contain variable quantities of both selenite and selenate¹¹. Further studies of selenium's chemical speciation in precipitation may help to identify the sources of atmospheric selenium; elucidate the equilibrium state and kinetics of atmospheric redox reactions, and quantify the contribution of atmospheric deposition to the oceanic selenium cycle.

Precipitation samples were obtained at Lewes, Delaware and High Point, Bermuda, from August 1983 to January 1984 using automated Aerochem Metrics precipitation samplers¹². Rain water was placed in acid-cleaned borosilicate bottles, acidified to pH2 (with HCl), and refrigerated to minimize biological growth. Determinations of selenite selenate, and selenide+ elemental selenium were made using the procedures described in refs 3, 10 and 13; sulphate, sodium and pH were determined using the methods in refs 14 and 15. To evaluate possible artefacts arising from sample collection, two precipitation events were sampled using three different collection devices; the concentration and speciation of selenium from all three systems were within 10% of each other. In addition, artefacts from sample storage appeared to be minimal, as no selenium speciation changes were detected between rain water analysed within hours of collection and that analysed one month later. Thus, the data presented below are assumed to be representative of atmospheric processes and not procedural aberrations.

The sampling site at Lewes receives precipitation which is fairly representative of northeastern United States air masses¹⁶ and winter storm fronts often pass over Bermuda from North America after 1-2-day transit times¹⁷. Thus, the rain water concentration and speciation of selenium collected at these locations may reflect the combined effects of source strengths (marine and continental), and processes which occur during atmospheric transport and deposition. Figure 1a is a plot of total selenium concentration versus sodium at Lewes and Bermuda. The

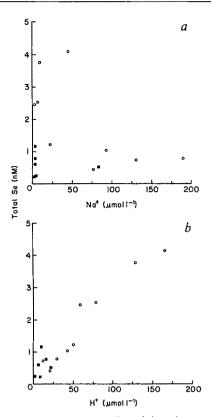


Fig. 1 Total selenium versus sodium (a) and protons (b) in precipitation samples collected at Lewes, Delaware (○) and Bermuda (■). Values for total selenium are based on triplicate determinations, with the procedural precision (expressed as relative standard deviation) not exceeding 3%. The correlation coefficient (r) for a linear regression fit of the total selenium/proton data is 0.9589 (n = 15).

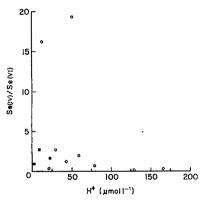


Fig. 2 The ratio of selenite to selenate [Se(IV)/Se(VI)] versus protons in Lewes, Delaware (○) and Bermuda (■) precipitation samples. Determinations of selenite and selenate were made in triplicate, and the procedural precision (expressed as relative standard deviation) did not exceed 7%.

apparent lack of correlation between selenium and sodium indicates that processes generating sea-salt aerosols do not contribute selenium to precipitation. However, there appear to be two distinct groups of precipitation events, those with low selenium-high sodium (marine origin) and those with high selenium-low sodium (non-marine). The low selenium-concentration background is in accord with the presence of uniform concentrations of aerosol selenium in the global marine atmosphere⁵. In contrast, Fig. 1b shows a strong correlation between total selenium and protons. A similar correlation is found between total selenium and excess (non-sea-salt) sulphate (r=0.9505, n=15). Previous studies of western Atlantic precipitation have attributed increased acidity and excess sulphate to

anthropogenic emissions from North America^{16,18} The data shown in Fig. 1b suggest that fossil fuel combustion in North America also contributes selenium to western Atlantic precipitation.

In Fig. 2, the ratio of selenite to selenate in precipitation is plotted against proton concentration. During this study, selenide + elemental selenium was detected in only one sample (Lewes; 28% of the total selenium). Furthermore, with the exception of two samples from Lewes, the range of selenite/selenate values at both sites is small $[Se(IV)/(Se(VI) = 1.26 \pm 0.95,$ n = 10]. The two samples with the highest selenite/selenate ratios came from storms travelling in northerly directions, placing the coal-fired Indian River Station power plant 30 km upwind of the rain sampler. Thus, a local anthropogenic input may account for the enrichment of selenite in these two events. For the remaining samples, the source-type (that is, natural or anthropogenic) cannot be identified on the basis of oxidation state in Fig. 2. If the oxidation states of atmospheric selenium inputs are correctly assigned (as above), then the rates of redox reactions during transport and deposition must be sufficiently rapid to obscure discrete oxidation state signals.

If the results in Fig. 2 are generally indicative of oxidation-reduction equilibrium, then the apparent redox intensity of precipitation, pE (where $pE = -\log [e^-]$), can be estimated using the equation: $SeO_4^{2-} + 3H^+ + 2e^- = HSeO_3^- + H_2O$; $E^0 = 1.075$ V. The pE of 11.50 ± 1.01 (n = 10) calculated in this manner is close to values for the nitrate-nitrogen dioxide and peroxide-oxygen couples reported elsewhere¹⁹. However, more data are needed on the speciation of selenium, as well as other redox couples, in precipitation, to determine more accurately the oxidation intensity of corresponding air masses.

The volume-weighted average selenium concentration (that is, the total selenium normalized to rainfall amount) at Bermuda is <20% of that at Lewes (Table 1). However, the washout

Table 1 Selenium in western Atlantic precipitation						
Volume-weighted average total selenium (pmol cm	3)					
Bermuda	0.38					
Lewes	2.20					
Average rainfall (cm yr ⁻¹)						
Bermuda	150					
Lewes	90					
Average total selenium in air (pmol m ⁻³)						
Bermuda ²⁰	2.4					
Coastal Thode Island ⁵	11.8					
Washout ratio (volwtd avg./air conc.)						
Bermuda	2,000					
Lewes (using Rhode Island air conc.)	2,365					
Wet depositional flux (pmol cm ⁻² yr ⁻¹)						
Bermuda	57					
Lewes	190					
Average upwelling flux, central Atlantic*						
$(pmol cm^{-2} yr^{-1})$	264					
*						

^{*} Assumes total sub-surface $Se = 0.66 \text{ nmol } 1^{-1}$ (ref. 23); average upwelling rate = 400 cm yr⁻¹ (ref. 24).

ratios (volume-weighted average concentration in precipitation divided by concentration in air) at the two sites are equally large, suggesting that removal by wet deposition predominates. The wet depositional flux of selenium at Bermuda (Table 1) is similar to the average total deposition estimated from aerosol measurements (38 pmol cm⁻² yr⁻¹) by other workers²⁰ for the same site. Although no independent data are available, the calculated wet depositional flux at Lewes (Table 1) falls between the values estimated by Ross²¹ for remote continental (75 pmol cm⁻² yr⁻¹) and "urban" (840 pmol cm⁻² yr⁻¹) wet deposition. In spite of the large reduction in selenium flux between the coastal United States and Bermuda, this atmospheric input to the central Atlantic is still significant (22% of that due to vertical upwelling; see Table 1). These flux data

support the hypothesis by Measures et al.4 that atmospheric deposition elevates surface-water selenium concentrations in the western Atlantic. Furthermore, selenite is enriched in precipitation over the western Atlantic relative to sub-surface waters (average sub-surface selenite/selenate = 0.09, ref. 21). As a result, inputs of selenite and selenate through wet deposition and upwelling have different effects on parameters such as surface-water residence times for these two species³.

The selenium speciation data obtained for wet deposition suggest that the element may act as a useful tracer of oxidationreduction equilibrium and kinetics. More thorough sample collection and analysis efforts will be required to verify the extent of this equilibrium. In addition, the sequential sampling of

Received 24 February; accepted 8 May 1986.

- Bertine, K. K. & Goldberg, E. D. Science 173, 233-235 (1971).
- Shamberger, R. J. The Biochemistry of Selenium, 185 (Plenum, New York, 1983).
 Cutter, G. A. & Bruland, K. W. Limnol. Oceanogr. 29, 1179-1192 (1984).
- Measures, C. I., Grant, B., Khadem, M., Lee, D. S. & Edmond, J. M. Earth planet. Sci. Lett. 71, 1-12 (1984).

- Mosher, B. W. & Duce, R. A. J. geophys. Res. 88, 6761-6768 (1983).
 Jickells, T. D., Knap, A. H. & Church, T. M. J. geophys. Res. 89, 1423-1428 (1984).
 Jiang, S., Robberecht, H. & Adams, F. Almos. Envir. 17, 111-114 (1983).
 Andren, A. W., Klein, D. J. & Talmi, Y. Envir. Sci. Technol. 9, 856-858 (1975).
 Suzuki, Y., Sugimura, Y. & Miyake, Y. J. met. Soc. Japan 59, 405-409 (1981).
 Cutter, G. A. Analyt. chim. Acta 98, 59-66 (1978).
- 11. Robberecht, H. & Van Grieken, R. in Trace Substances in Environmental Health Vol. 14 (ed. Hemphill, D. D.) (University of Missouri, Columbia, 1980).

individual storm events at the coast and at multiple sites across the Atlantic should yield data on the kinetics of oxidationreduction reactions affecting selenium. The chemical similarity between selenium and sulphur increase the interest of such studies. The equilibrium between sulphur dioxide and sulphuric acid is affected by the atmosphere's redox intensity (pE). The rate at which this equilibrium is reached controls the long-range atmospheric transport of sulphur, the deposition of sulphuric acid, and thus affects acid precipitation²².

This is a contribution to the WATOX program, supported by a grant from the NOAA Air Resources Laboratory. We thank J. Scudlark for sample collection and L. Cutter for sample analysis.

- 12. Tramontano, M., Scudlark, J. S. & Church, T. M. Environ. Sci. Technol. (submitted).
- 13. Cutter G. A. Analyt. chim. Acta 149, 391-394 (1983).
- Cauter, G. A. Andry. Chank. Acta 149, 391-394 (1993).
 Galloway, J. N., Crosby, B. J. Ir. & Likens, G. E. Linnol. Oceanogr. 24, 1161-1165 (1979).
 Galloway, J. N. & Likens, G. E. Tellus 30, 71-82 (1978).
 Church, T. M., Galloway, J. N., Jickells, T. D. & Knap, A. H. J. geophys. Res. 87, 11013-11018
- 17. Miller, J. M. & Harris, J. M. Atmos. Envir. 19, 409-414 (1985).
- Jickells, T. D., Knap, A. H., Church, T. M. & Galloway, J. N. Nature 297, 55-57 (1982).
 Morgan, J. J. in Atmospheric Chemistry (ed. Goldberg, E. D.) (Springer, New York, 1982).
 Duce, R. A. et al. in Marine Pollutant Transfer (eds Windom, H. L. & Duce, R. A.) (Lexington
- Books, Lexington, 1976). 21. Ross, H. B. Tellus 37, 78-90 (1985).
- Rohde, H., Crutzen, P. & Vanderpol, A. Tellus 33, 132-141 (1981).
 Measures, C. I. & Burton, J. D. Earth planet. Sci. Lett. 46, 385-396 (1980).
- 24. Broecker, W. S. & Peng, T. H. Tracers in the Sea (Eldigio, New York, 1982).

Correlations between stream sulphate and regional SO₂ emissions

Richard A. Smith & Richard B. Alexander

United States Geological Survey, Reston, Virginia 22092, USA

The relationship between atmospheric SO₂ emissions and stream and lake acidification has been difficult to quantify, largely because of the limitations of sulphur deposition measurements. Precipitation sulphate (SO₄) records are mostly <5 yr in length¹ and do not account for dry sulphur deposition2. Moreover, a variable fraction of wet- and dry-deposited sulphur is retained in soils and vegetation and does not contribute to the acidity of aquatic systems^{3,4}. We have compared annual SO₂ emissions for the eastern United States from 1967 to 1980 with stream SO₄ measurements from fifteen predominantly undeveloped watersheds (Figs 1, 2). We find that the two forms of sulphur are strongly correlated on a regional basis and that streams in the southeastern United States (SE) receive a smaller fraction (on average, 16%, compared with 24%) of regional sulphur emissions than do streams in the northeastern United States (NE). In addition to providing direct empirical evidence of a relationship between sulphur emissions and aquatic chemistry, these results suggest that there are significant regional differences in the fraction of deposited sulphur retained in basin soils and vegetation.

The stream SO₄ data (Table 1) are from monitoring stations in the USGS Hydrologic Benchmark Network⁵. Five stations were used to estimate average annual SO₄ yield in the NE, and 10 stations were used in the SE (Fig. 1). Stream SO₄ at these stations is believed to be largely of atmospheric origin^{6,7}. The SO₄ yield for each year from 1967 to 1980 was estimated as the product of the annual discharge-weighted mean SO₄ concentration and mean basin runoff for the 14-yr period. The regional SO₄ yield was estimated as the average of the individual basin yields.

Regional SO₂ emission densities were based on state-level data from two recent sources^{8,9} which used alternative methods of estimating emissions. Regressions against stream sulphate were conducted separately for the two sets of emission data in order to determine the sensitivity of results to the choice of methods. Husar's 'production-driven' estimates are based on

records of the sulphur content and distribution of produced fuels, whereas those from Gschwandtner et al.9 are 'consumption-driven' and are based on fuel consumption records. Emission estimates from Hidy et al. 10 for southeastern Ontario were added to both data sets in calculating NE emission densities and represent ~17% of the regional total. Trends in state-level SO₂ emissions^{8,9} and stream SO₄ concentrations (Table 1) were nearly homogeneous in direction (decreasing in the NE and increasing in the SE) within the defined regions during the study period. Varying the size of the defined regions through the addition or deletion of states near the regional boundaries has relatively little effect on regional emission densities, which, like stream yields, are expressed as areal averages (g m⁻² yr⁻¹).

Regressions of stream SO₄ yield against SO₂ emission density give slope values ranging from 0.14 to 0.25 for various combinations of region and source of emission data (Fig. 2). The results are similar for the two sets of emission data and suggest that,

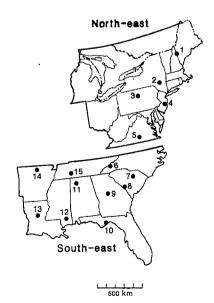


Fig. 1 Locations of stream sampling stations in the northeastern and southeastern United States. The numbered stations are identified in Table 1.

Table 1 Stream SO₄ data and wet SO₄ deposition estimates for Benchmark stream monitoring sites in the eastern United States

Station	Basin area (km²)	Mean discharge (m ³ s ⁻¹)	Avg. stream SO ₄ concentration (µeq l ⁻¹)	SO ₄ trend ⁷	Mean SO_4^* yield, Y $(g m^{-2} yr^{-1})$	Wet SO ₄ * deposition ¹³ , D (g m ⁻² yr ⁻¹)	Y/D
North-east region (NE)							
1. Wild River at Gilead, Maine	180	4.56	102.7	-	1.31	0.86	1.51
2. Esopus Creek at Shandaken, New	,						
York	154	3.79	162.1	_	1.95	1.16	1.68
3. McDonalds Branch in Lebanon							
State Forest, New Jersey	6	0.06	154.6	-	0.75	1.08	0.69
4. Young Woman's Creek near							104
Renovo, Pennsylvania	120	2.04	164.0	_	1.44	1.16	1.24
5. Holiday Creek near Andersonville,	20		(0.6		0.24	1.00	0.24
Virginia	22	0.23	60.6	-	0.34	1.00	0.34
South-east region (SE)							
6. Cataloochee Creek near							
Cataloochee, North Carolina	127	3.17	25.6	+	0.35	1.09	0.32
7. Scape Ore Swamp near Bishopville,							
South Carolina	249	2.77	63.0	+	0.36	0.89	0.40
8. Upper Three Runs near New	·						
Ellenton, South Carolina	225	3.11	21.7	+	0.14	0.88	0.16
9. Falling Creek near Juliette, Georgia	187	1.50	101.1	0	0.44	0.81	0.55
Sopchoppy River near Sopchoppy,							
Florida	264	4.44	94.4	+	0.90	0.91	0.99
11. Sipsey Fork near Grayson, Alabama	233	4.41	85.7	+	0.81	0.95	0.85
12. Cypress Creek near Janice,					0.40	0.80	0.75
Mississippi	135	2.72	44.4	+	0.49	0.73	0.67
13. Big Creek at Pollock, Louisiana	132	1.47	47.4	+	0.29	0.68	0.42
14. North Sylamore Creek near Fifty	150	1 10	110.1	,	0.47	0.00	0.52
Six, Arkansas	150	1.19	119.1	+	0.47	0.89	0.53
15. Buffalo River near Flat Woods,	1 157	21.24	04.2		0.85	1.16	0.74
Tennessee	1,157	21.34	84.2	_	0.85	1.10	0.74

^{*} Expressed as sulphur.

an average, streams transport $\sim 20\%$ of sulphur emissions in the eastern United States. However, an analysis of covariance¹¹ indicates that, for both sets of emission data, a regression model with a single intercept but regionally separate slope estimates is preferable to other models. Slope estimates for both data sets show significantly higher values for the NE region than for the SE (an average of 24%, compared with 16%). All four regression lines pass close to the origin, a result which supports the assumption that stream SO₄ at these sites is largely of atmospheric origin and comes primarily from sources within the region.

origin and comes primarily from sources within the region.

Johnson et al.¹² have suggested that streams in the southeastern United States might be expected to transport a smaller fraction of deposited sulphur than northeastern streams, on the basis of experiments showing greater sulphur retention in soils typical of the SE. Southeastern soils are predominantly ultisols, which contain subsurface clay horizons with high SO₄-adsorption capacities¹². The hypothesis of greater SO₄ retention in the SE is strongly supported by the regional differences in regression slopes observed in this study, together with SO₄

deposition measurements¹³ for the regions. Comparison of stream SO_4 yields with wet SO_4 deposition estimates (Table 1) gives significantly larger ratios of yield to deposition (Y/D) in the NE. Ratios for the SE are all <1.0, whereas those for the NE are mostly >1.0. The sulphur-adsorbing properties of basin soils are thought to be an important factor controlling the acidification of surface waters because mobility of sulphate in soils is required for the transport of hydrogen ions (as well as base cations) through basin soils to streams^{3,14}.

The regression results and yield-to-deposition ratios presented above can be used to calculate approximate sulphur budgets for the NE and SE (Table 2). Regression slopes for the two regions indicate that 16% of the sulphur emitted in the SE (24% in the NE) is transported by streams, and that the remaining 84% (76% in the NE) is either retained in basin soils and vegetation or is deposited outside the region. If dry deposition is assumed to be equal to wet deposition 15, then median basin retention of SO₄ is 35% of emissions in the NE and 59% of emissions in the SE. Basin retention is considerably smaller,

Table 2 Estimated sulphur budgets for the northeastern and southeastern United States (1980)

		Regional	estimates	
]	NE	SI	3
Budget component	Quantity (g m ⁻² yr ⁻¹)	Per cent of emissions	Quantity (g m ⁻² yr ⁻¹)	Per cent of emissions
SO ₂ emissions	3.7	100	2.4	100
Atmospheric transport out of the region	1.5	41	0.6	25
Total deposition	2.2	- 59	1.8	75
Basin retention	1.3	35	1.4	59
Stream transport	0.9	24	0.4	16

Total deposition is calculated as twice the measured¹³ wet deposition, atmospheric transport of sulphur from the region as the difference between SO₂ emissions and total deposition, and basin retention as the difference between stream SO₄ transport and total deposition.

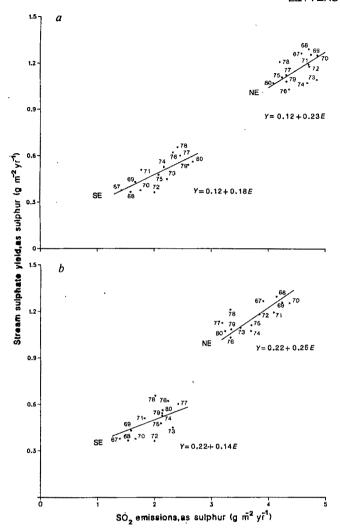


Fig. 2 Average stream yield (Y) of SO₄ at USGS Benchmark stations in the eastern United States, plotted against regional SO₂ emission density (E) for the years 1967-80 (shaded numbers). Plots are presented for two recent sets of emission estimates^{8,9}, based on alternative methods of estimating the sulphur content of combusted fuels (a, production-driven emissions⁸; b, consumptiondriven emissions⁹). Both emissions and stream yield of sulphur decreased in the NE but increased in the SE during the 1967-80 period. Analyses of covariance for both sets of emission estimates result in a two-slope, one-intercept model with smaller slopes for the SE than for the NE. All slopes are significant at $\alpha = 0.01$. Intercepts are not significantly different from zero at $\alpha = 0.05$.

however, for certain of the NE basins with non-ultisolic soils. Average retention for Maine, New York and Pennsylvania, for example, is only 14%. Assuming that dry and wet deposition are equal, atmospheric transport from the region is 41% in the NE and 25% in the SE. These estimates of extra-regional transport bracket a previously reported estimate 16 (30%) for sulphur transport from eastern North America, thus supporting the earlier estimate.

There has been continuing uncertainty concerning the quantitative reltionship between atmospheric SO₂ emissions and sulphur deposition in North America and, to a lesser extent, in Europe^{15,17}. This uncertainty stems from the shortage of longterm deposition records on which to base correlative studies as well as from problems with the measurement of dry deposition. The relationship between SO₂ emissions and aquatic transport of SO₄ has remained even less clear because of a shortage of empirical data on the retention of wet- and dry-deposited

sulphur in a variety of soil types⁶. The results described here indicate that an approximately linear (and nearly proportional) relationship exists between SO₂ emissions and stream transport of atmospheric sulphur in the eastern United States. These results appear to demonstrate the response of stream SO₄ to both increases and decreases in emissions over a wide range of emission densities. There is evidence that the slope of the relation between SO₂ emissions and stream SO₄ is somewhat smaller in the SE due to greater basin retention of SO₄. Greater SO₄ retention may initially serve to reduce the acidifying effects of SO₄ deposition in the SE, but gradual accumulation of SO₄ in soils may lead to increased stream transport of SO₄ in the future. Additional variability in the effects of acid deposition can be expected to result from differences in the ability of basins to neutralize acids by supplying base cations^{6,19}. Budgets for the environmental fate of atmospheric SO₂ emissions, including basin retention of SO₄, could be further refined by reliable measurements of dry deposition.

We thank J. Turk, G. Oehlert and A. Johnson for helpful discussions, and O. Bricker, H. Lins and J. Pickering for reviewing the manuscript.

Received 24 February: accepted 9 May 1986.

- 1. Stensland, G. J., Whelpdale, D. M. & Oehlert, G. in Acid Deposition: Long-Term Trends, 128-199 (National Academy Press, Washington, 1986).

 2. Hicks, B. B. (ed.) Deposition Both Wet and Dry Vol. 4 (Butterworth, Boston, 1984).

 3. Reuss, J. O. & Johnson, D. W. J. environ. Qual. 14, 26-31 (1985).

- Rebuss, J. O. & Johnson, D. W. J. environ. Qual. 14, 26-31 (1983).
 National Research Council Acid Deposition: Processes of Lake Acidification (National Academy Press, Washington, 1984).
 Cobb, E. D. & Biesecker, J. E. U.S. geol. Surv. Circ. No. 460-D (1971).
 Kramer, J. R. et al. in Acid Deposition: Long-Term Trends, 231-299 (Washington Academy
- Press, Washington, 1986).
- Smith, R. A. & Alexander, R. B. U.S. geol. Surn. Circ. No. 910 (1983).
 Husar, R. B. in Acid Deposition: Long-Term Trends, 48-92 (National Academy Press, Washington, 1986).
- Gschwandtner, G., Gschwandtner, K. C. & Eldridge, K. Historical Emissions of Sulfur and Nitrogen Oxides in the U.S. from 1900-1980 (EPA 600/7-85-009a) (Environmental Protection Agency, Washington, 1985).
- 10. Hidy, G. M., Henry, R. C., Hansen, D. A., Ganesan, K. & Collins, J. J. Air Pollut. Control. Ass. 34, 333-345 (1984).
- Kleinbaum, D. G. & Kupper, L. L. Applied Regression Analysis and Other Multivariable Methods (Wadsworth, Belmont, 1978).
 Johnson, D. W., Horabeck, J. W., Kelly, J. M., Swank, W. T. & Todd, D. E. in Atmospheric
- Sulfur Deposition: Environmnetal Impact and Health Effects (eds Shriner, D. S., Richmond, C. R. & Lindberg, S. E.) 507-520 (Ann Arbor Science, 1980).
- Gibson, J. H. & Baker, C. V. 1980-81 Wet-Deposition Measurements (National Atmospheric Deposition Program, Colorado State University, Ft. Collins, 1982).
 Cosby, B. J., Hornberger, G. M., Galloway, J. N. & Wright, R. F. Wat. Resour. Res. 21,
- 51-63 (1985).
- 15. National Research Council Acid Deposition: Atmospheric Processes in Eastern North America (National Academy Press, Washington, 1983). Galloway, J. N. & Whelpdale, D. M. Atmos. Envir. 14, 409-417 (1980).

- Eliassen, A. & Saltbones, J. Almos. Envir. 17, 1457-1473 (1983).
 Oppenheimer, M., Epstein, C. B. & Yuhnke, R. E. Science 229, 859-862 (1985).
 Driscoll, C. T. & Likens, G. E. Tellus 34, 283-292 (1982).

Dating ice-wedge growth in subarctic peatlands following deforestation

Serge Payette, Line Gauthier & Ivan Grenier

Centre d'études mordiques, Université Laval, Québec, Canada G1K 7P4

Ice wedges are one of the most prominent periglacial features in the zone of continuous permafrost, and constitute significant climatic and palaeoclimatic markers 1-4. Active ice wedges are found in areas with a mean annual air temperature below -6 °C (ref. 5), although recent data⁶ suggest that they can form at -3.5 °C. Most of the reports⁷⁻⁹ dealing with ice wedges have referred to Arctic and Antarctic conditions, whereas subarctic ice wedges from glaciated areas are poorly known. Ice-wedge inception and spatial development as orthogonal and polygonal nets were inferred generally from theoretical analysis 10,11 and sparse detailed field work 7,8. Because ice wedges occur also in subarctic permafrost

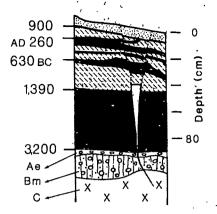


Fig. 1 Stratigraphy of a peat section from outside the studied quadrangle, showing the relationship between radiocarbon-dated wood layers and ice-wedge growth. The formation of this 8-cm-wide ice began sometime after AD 900 (extrapolated from radiocarbon-dated growth curve) when spruce (black) and Sphagnum (hatched) cushions, always intermingled with spruce branches and leaves, were replaced by a snow-free lichen-Dicranum cover (dotted), The layer from 3,200 to 1,390 BC is made of intermingled spruce and Sphagnum. From 3,200 BC to AD 900, this site was snow-protected because of continuous spruce-Sphagnum growth. Ae, Bm and C at the bottom of the peat profile refer to pedogenetic horizons.

peatlands^{12–15}, the combined use of macrofossil peat stratigraphy and radiocarbon dating may yield useful information concerning their development. Here we present the first account of such a framework, derived from the analysis of marginal ice wedges developed in the eastern Canadian Subarctic. We show that the inception and spatial development of epigenetic ice wedges in some subarctic peatlands occurs after the natural removal of coniferous vegetation, which induces snow-free conditions, permafrost aggradation and, ultimately, deep frost cracking. We have dated ice wedges indirectly, using combined curves of rates of spruce removal and ice-wedge growth.

In North America, subarctic ice wedges are found mostly in peat plateaus and palsa bogs¹²⁻¹⁴. Their presence is generally inferred from the polygonal network which dissects the extensive, windswept lichen-heath vegetation occurring above the fossil peat. A closer look at the upper peat stratigraphy where epigenetic ice wedges develop reveals in most cases a charcoal horizon or a non-charred wood layer indicative of the former presence of coniferous vegetation. As long as the coniferous vegetation was able to maintain itself on the peatland, buffered thermal conditions prevailed in the peat substrate because of snow insulation. Removal of the coniferous cover induces snowdrift conditions and creates snow-free sites that change the overall thermal regime, favouring deeper cold penetration into the peat substrate. This close relationship between coniferous vegetation, snow conditions and thermal characteristics of substrates forms the basis of our hypothesis, which states that ice wedges found in many subarctic peatlands in eastern Canada, where continental deglaciation occurred during early to mid-Holocene times^{16,17}, were formed sometime after site defores-

A small insular Sphagnum bog in the Clearwater Lake area, subarctic Québec ($56^{\circ}30'$ N, $75^{\circ}30'$ W; mean annual air temperature ≈ -5 °C), has been used to test the hypothesis. The peat stratigraphy of the bog (Fig. 1) shows a cyclic alternation of Sphagnum and spruce (Picea mariana (Mill.) BSP.) which persisted for several thousand years 18; cessation of cyclic replacement occurred during the past 2,000 years, particularly in the most exposed sites where a lichen-Dicranum-heath vegetation now covers the fossil peat. Ice wedges develop in these sites and form an irregular polygonal pattern at the surface. The

measurement of 26 polygonal cells separating individual icewedge lineaments has indicated an average dimension of 7×9 m, although many polygons were incompletely formed. We have studied in detail ice wedges developed under a lichen-Dicranumheath cover in a representative section of the selected peatland. Within a 1,444-m² quadrangle (38×38 m), the ice wedges were mapped and measured (Fig. 2). Correlation between ice-wedge yertical length and width was established by direct observation in manually excavated peat sections. Ice wedges were distinguished from frost cracks, also filled with ice but confined to the active layer, by a detailed study of their melting pattern during summer 1982. The surface topography of the quadrangle was determined with an electronic level (GDD Instrumentation Inc.); and the thickness of the peat deposit (ranging from 85 to 260 cm) was evaluated by coring at several sites. The coniferous cover of low krummholz (stunted spruces) has been mapped, and the uppermost fossil-wood layer laying immediately under the lichen-Dicranum-heath cover was radiocarbon dated at nine different sites within the quadrangle (Fig. 2). The ¹⁴C dates were calibrated to calendar dendroyears¹⁹, to determine regression rates of coniferous vegetation and ice-wedge age (Fig. 3).

Frost cracks were particularly extensive in the study area in March-April 1982 and 1983. In 1982, the cracks were 36 ± 6 cm long, (n=133), and the depths of the active layer in July, August and September were, respectively, 29 ± 2 cm (n=29), 40 ± 5 cm (n=113) and 42 ± 4 cm (n=42). In 1983, the frost cracks were slightly longer, 39 ± 6 cm (n=52). Their spatial pattern was irregular, sometimes linear or arcuate, but rarely polygonal (Fig. 2).

Ice wedges were found at 49 ± 6 cm (n = 153) from the peatland surface; that is, at the present maximum depth of the active layer. The wedges were made of white foliated ice including vertically oriented air bubbles and occasionally peat (Fig. 4a). The width of the ice wedges ranged from 0.1 to 48 cm, and was

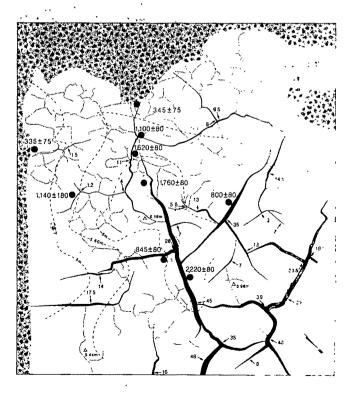


Fig. 2 Distribution of ice wedges (black) and frost cracks (dotted lines) on lichen ground cover surrounded by spruce krummholz (grey pattern). Numbered arrows denote maximum ice-wedge widths (cm). Dashed lines, contours of the peatland surface in m above lake level; open triangles, bench marks; large dots, ¹⁴C dates.

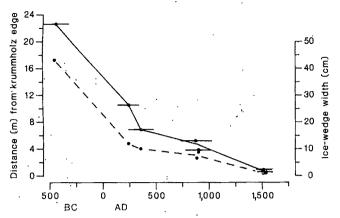


Fig. 3 Regression of coniferous vegetation (solid line), based on position of radiocarbon-dated fossil wood layers (calibrated to calendar years) relative to present krummholz edge. Horizontal bars indicate the 2σ (95% confidence) intervals for the calibrated ¹⁴C dates. The curve of ice-wedge width versus time (broken line) is similar to the conifer regression curve, which gives a reliable method for ice-wedge dating in subarctic peatland ecosystems.

highly correlated (r = 0.95) with vertical length (maximum icewedge length 190 cm). The ice wedges were slightly arcuate, especially at the bottom tip. Loose ice crystals (depth hoar?) were predominant at the bottom tip of large ice wedges. The basic spatial pattern consisted of individual lineaments of variable length and width, orientated in all directions. Most icewedge lineaments are independent features that converge occasionally in a semi-orthogonal pattern. Their horizontal growth always stops at the intersection of a nearby ice wedge, so that the longest ice wedges are those that do not merge into one another (Fig. 2). An extensive oblique layer of foliated ice formed within the mineral substrate was also observed at the intersection of two ice wedges, at a site where the peat deposit is shallower (Fig. 4b). This ice shows a structure similar to that of the wedges, an indication that its presence is associated with ice-wedge formation. Some very short but relatively wide ice

wedges have also developed, which supports the idea that horizontal growth stops when two ice wedges meet. Only two closed ice-wedge polygons were observed; they were characterized by relatively large lineaments compared to those found elsewhere.

Before ~500 BC, the peatland was entirely covered by coniferous vegetation (based on radiocarbon dating of the uppermost wood layers). Along the NE-SW direction, where two independent ice-wedge lineaments have developed in similar environments (Fig. 2), spruce regression began earlier at the higher site, and progressed radially at different rates towards the modern krummholz edges (Fig. 3). A highly significant correlation (r = 0.98) was found between ice-wedge width and distance in metres from the modern krummholz edge; thus, the curve of maximum ice-wedge width measured near the radiocarbon-dated sites shows a pattern similar to the spruce regression curve (Fig. 3). This suggests a direct relationship between deforestation and ice-wedge inception; the age of an ice wedge is therefore very close to the age of deforestation. However, two radiocarbon dates were excluded from the analysis. The 14 C date of $845 \pm$ 80 yr BP obtained from a sample close to the oldest deforested site (Fig. 2) may appear to contradict the radial pattern of spruce regression. But this date came from a charcoal sample associated with a palaeo-Indian camp fire located, probably for convenience, on the open lichen ground. All the fragments of three small boulders thought to have surrounded this fire were also recovered from the peat deposit, just above a 25-cm-wide ice wedge. This suggests that the fire was ignited from wood of nearby provenance, probably at the edge of the 850 yr BP spruce cover. Additionally, it indicates that ice-wedge activity has caused boulder burial along the thermal cracks. The 14C date of 800 ± 80 yr BP appears to be anomalous according to position along the ice-wedge lineament; this may be related to the uncertain position of the sample, associated with problems of surface disturbance during peat excavation. All of the radiocarbon dates (except 845±80 yr BP) confirm the radial pattern in spruce regression: from the highest site, at an altitude > 6.0 m above the Clearwater Lake level, to the modern krummholz edges, generally at an altitude <5.0 m, spruce regression has progressed radially but at different rates according to site exposure (Fig.



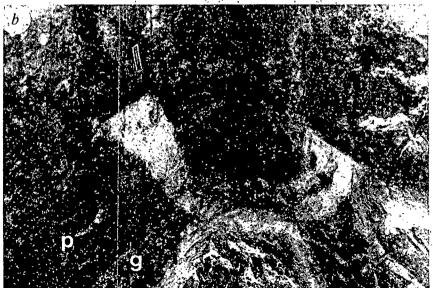


Fig. 4 a, Section of a 48-cm-wide ice wedge (ruler, 15 cm); ice-wedge vertical length, 190 cm. In March 1983, the left part of this ice wedge was opened by a thermal crack ~0.10-0.15 mm wide and 220 cm long. b, Intersection of two ice wedges, showing an extensive oblique layer of foliated ice formed within the gravelly substrate (g). The peat layer (p) is ~1 m thick.

3). The radiocarbon dates of the uppermost wood layers correspond therefore to maximum ages of ice wedges, assuming that they began to develop immediately after the removal of coniferous vegetation. Note that ice wedges do not open each winter, particularly in such marginal permafrost areas, given that in Arctic sites only 40% of the ice-wedge population is active each year⁷. In April 1983, for example, only a few ice wedges were active, although conditions for thermal contraction were particularly favourable. One 48-cm-wide ice wedge was opened by a crack $\sim 0.10-0.15$ mm wide and at least 220 cm deep (Fig. 4a); the crack was located not at the centre, but rather along one side of the ice wedge, as has frequently been observed in the study area.

The inception and spatial development of ice wedges in the subarctic requires particular microclimatic conditions that simulate the Arctic environment, where ice wedges occur extensively in mineral lowlands. These conditions are usually found in ombrotrophic peatlands, with Sphagnum peat as an insulating blanket. In general, ombrotrophication appears to be the necessary step for permafrost aggradation in subarctic peat-lands^{12,14}, occurring some time before the microclimatic condi-, occurring some time before the microclimatic conditions for ice-wedge formation are met. In northern Canada. permafrost invasion in peatland is associated with a change in drainage conditions which is emphasized in peat stratigraphy by a shift towards ombrophilous (Spagnum, Picea, Ericacaea) species^{12,14}. Although regional conditions may vary² development of epigenic ice wedges coincides generally with treeless, somewhat dried, raised peatlands characterized by a very low peat growth rate; spruce removal and expansion of windswept lichen cover seem to be the ultimate prerequisites for such a development, at least in the snowier eastern Canadian Subarctic. Subsequent ice-wedge development at these sites appears to be a slow and irregular process. Mean annual icewedge growth rates measured in this study vary from a maximum of 0.18 mm yr⁻¹ to a minimum of 0.04 mm yr⁻¹ (Fig. 3), a very low figure compared to modern Arctic and Antarctic ice-wedge growth rates^{7,9}. The average dimensions of these subarctic polygons are very small compared to Arctic polygons, which range from 15 to 40 m (ref. 3). Because these ice wedges have formed in a climatically marginal environment, they developed slowly, allowing us to follow the changing spatial arrangement with time. Their horizontal growth towards polygon formation did not show any defined order in time, as proposed elsewhere¹¹; in fact, the spatial growth of individual ice wedges, based on their distribution today (Fig. 2), suggests that the different segments of an ice-wedge polygon may vary in age. Whether this time-sequence in polygon formation is the rule remains to be substantiated. Our data indicate that subarctic ice-wedge expansion is a palaeocological event closely tied to local vegetation development. Thus, the onset of ice-wedge development in the subarctic may have been directly controlled by Holocene deforestation, a long-term, time-transgressive ecological process operating at the microscale. It implies that subarctic ice wedges could have responded directly to climate forcing only when the habitat development had reached a critical threshold emphasized by deforestation. That is why the palaeoclimatic significance of subarctic ice wedges should be interpreted cautiously.

We thank Professor J. Ross Mackay (University of British Columbia) for discussion and for very useful suggestions on an earlier draft. This study has been financially supported by the Ministère de l'Éducation of Québec (FCAR Program) and the Natural Sciences and Engineering Research Council of Canada (NSERC).

Received 11 February; accepted 16 May 1986.

Washburn, A. K. Geocryology (Wiley, New York, 1980).

- 5. Péwé, T. L. Proc. 1st int. Permafrost Conf., 76-81 (National Academy of Science-National Research Council of Canada, Washington DC, 1966).
- Hamilton, T. D., Ager, T. A. & Robinson, S. W. Arct. alp. Res. 15, 157-168 (1983)
 Mackay, J. R. Can. J. Earth Sci. 11, 1366-1383 (1974).
- Mackay, J. R. Can. J. Earth Sci. 12, 1668-1674 (1975).
- 9. Black, R. F. Proc. 2nd int. Permafrost Conf., 193-203 (National Academy of Science-National Research Council of Canada, Washington DC, 1973).
- Lachenbruch, A. Proc. 1st int. Permafrost Conf., 63-71 (National Academy of Science National Research Council of Canada, Washington DC, 1966).
- Dostovalov, B. N. & Popov, A. I. Proc. 1st int. Permafrost Conf., 102-105 (National Academy of Science-National Research Council of Canada, Washington DC, 1966)
- Zoltai, S. C. & Tarnocai, C. Can. J. Earth Sci. 12, 28-43 (1975).
 Dredge, L. A. Geol, Surv. Pap. Can. 79-1C, 27-30 (1979).
- Couillard, L. & Payette, S. Can. J. Bot. 63, 1104-1121 (1985).
- Dionne, J. C. Géogr. phys. Quat. 37, 127-146 (1983).
 Allard, M. & Seguin, M. K. Géogr. phys. Quat. 39, 13-24 (1985)
- 17. Richard, P. J. H., Larouche, A. & Bouchard, M. A. Géogr. phys. Quat. 36, 63-90 (1982)
- 18. Payette, S. Ecology (submitted).
- Klein, J., Lerman, J. C., Damon, P. E. & Ralph, E. K. Radiocarbon 24, 103 150 (1982)
 Ovenden, L. Boreas 11, 209-224 (1982).

Hydrocarbon shows and petroleum source rocks in sediments as old as 1.7×10^9 years

M. J. Jackson, T. G. Powell, R. E. Summons & I. P. Sweet

Division of Continental Geology, Bureau of Mineral Resources, Geology and Geophysics, GPO Box 378, Canberra, ACT 2601, Australia

We report the discovery of indigenous 'live' oil in ~1.4-Gyr-old rocks in the McArthur Basin of northern Australia. Previously reported occurrences of indigenous Precambrian oil are <1 Gyr old¹⁻⁵. Potential petroleum source rocks in the McArthur Basin range in age from 1.4 to 1.7 Gyr and were deposited in marine and lacustrine environments. In parts of the basin they have been buried sufficiently deeply to have generated hydrocarbons. They span the period corresponding to the appearance of eukaryotic organisms, and because of their low degree of thermal alteration, they provide a valuable resource for the study of primitive biota through their hydrocarbon biomarkers. The hydrocarbon composition of the oil is consistent with a derivation from organic matter of prokaryotic origin. These results show that exploration of previously ignored mid-Proterozoic sediments may lead to the discovery of new reserves of oil.

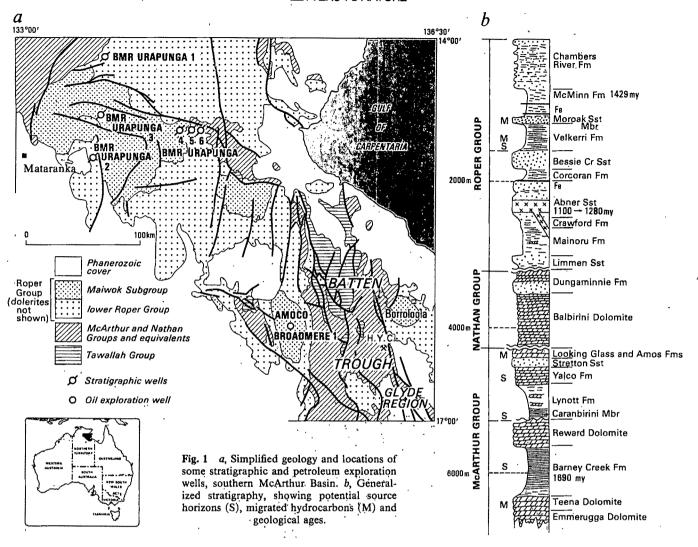
Despite the occurrence of commercial Proterozoic oil and gas fields in the Soviet Union, Oman and China^{1.5}, rocks of this age are not generally considered to be likely sources of petroleum⁶. The McArthur Basin (Fig. 1a) contains an unmetamorphosed, structurally simple sedimentary sequence. A sequence of stromatolitic and evaporitic carbonates with interbedded shales (McArthur and Nathan groups) is overlain unconformably by quartz arenites and interbedded shales (Roper Group)⁷. The sequence ranges in age from 1,690.23 Myr for the Barney Creek Formation8 of the McArthur Group to 1.429 ± 31 Myr for the McMinn Formation of the Roper Group (Fig. 1b). The presence of extensive unmetamorphosed carbonaceous shales, widespread microbial remains 10-15 and reports of bitumen and gas in the McArthur Group¹⁶ prompted an investigation of the hydrocarbon potential of the basin.

Organic-rich sediments, at various stages of hydrocarbon generation (maturation) have been found at five different stratigraphic levels (Fig. 1b, Table 1). McArthur Group sediments were deposited in lacustrine and perhaps very shallow marginal marine environments in fault-bounded grabens'. The thick organic-rich shales of the Barney Creek Formation are intimately interbedded with talus breccias and sabkha-like evaporite cycles, indicating deposition in arid climates in shallow playas or nearshore lagoonal complexes¹⁷. The Yalco Formation contains thin (1-4 m) organic-rich shales (Table 1, Fig. 1b) within a series of

^{1.} Jahn, A. Problems of the Periglacial Zone (Polish Scientific, Warsaw, 1975).

Black, R. F. Quat. Res. 6, 3-26 (1976).

French, H. M. The Periglacial Environment (Longman, London, 1976).



variable cherty, stromatolitic carbonates and minor sandstones deposited in ephemeral lakes in a dominantly humid climate¹⁸. The Roper Group, in contrast, comprises a laterally extensive sequence of well-sorted quartz arenites and grey shales deposited in marine conditions. Depositional environments range from inner shelf for the arenites to low-energy, deeper marine environments for the organic-rich sediments of the Velkerri Formation (Table 1).

Oil bubbled from thin laminae of siltstone enclosed in black mudstone of the Velkerri Formation at a depth of 345.4 to 346.5 m in the BMR Urapunga no. 4 stratigraphic hole (Fig. 1). Preliminary GCMS (gas chromatography/mass spectrometry) analyses of the oil and marginally mature source rocks in the McArthur Basin show a preponderance of hydrocarbons derived

from organic matter of prokaryotic origin (see Fig. 2). Analyses of the C₁₂₊ hydrocarbon fraction from the oil revealed a mixture dominated by n-alkanes of low relative molecular mass without odd-over-even predominance, 1- and 2-methylalkanes, ω-cyclohexyl alkanes and a series of unresolved mixtures, possibly of monomethylalkane isomers. The last may be similar to those found in Upper Proterozoic oils from Oman¹⁹. Only a trace of pristane was detected, and sterane and hopane biomarkers were absent. In contrast, less mature Velkerri sediments contained low amounts of pristane, phytane, hopanes and steranes. Lowmaturity sediments from the Barney Creek Formation contained abundant pristane, phytane, extended acyclic isoprenoids, hopanes and traces of steranes.

These results demonstrate for the first time the presence of

I/II

Organic C Hydrocarbons‡ Potential† Kerogen§ (kg tonne⁻¹) (H/C)(mg per g org. C) Organic type^{||} Formation (maturity)* ·(%) II/III McMinn (Immature) 0.7-2.9 2.3-14.6 0.76 - 1.01Velkerri (Mature) 1.7-7.2 8.4-33.3 30-110 II 3.8-33.0 3.5 - 330.92 - 1.20II Yalco (Immature) 0.8 - 5.4Caranbirini (Overmature) 0.2 - 3.4<0.32 Barney Creek <20 I/II

2.5-71.3

1.3-39.6

0-0.85

Table 1 Summary of source-rock characteristics of black shales, McArthur Basin

(Immature)

(Overmature)

(Mature)

0.6 - 10.4

0.8-7.6

0.2 - 3.2

12-87

<6

^{*} Maturity level where sampled.

[†] Total pyrolysis yield from Rock Eval analysis²³.

[‡] Soluble hydrocarbons expressed as mg per g organic carbon²⁴.

[§] From elemental analysis of isolated kerogens. Interpreted organic matter type, after ref. 25.

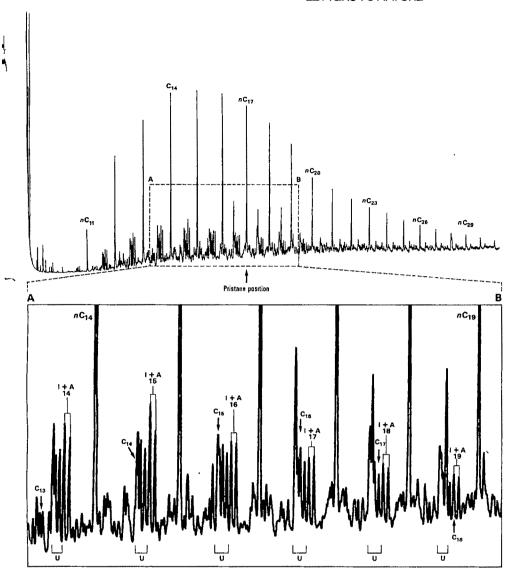


Fig. 2 Saturate fraction gas chromatogram from BMR Urapunga no. 4 oil, showing compound classes identified by GCMS. ${}_{n}C_{11}$ - ${}_{n}C_{29}$, *n*-alkanes, I+A(14)-I+A(19), C_{14} - C_{19} iso- and anteisoalkanes; C13-C18, C₁₃-C₁₈ ω-alkylcyclohexanes; U, unidentified methyl alkanes.

'live' oil and petroleum source rocks in 1,400-1,670-Myr-old sediments, and record the oldest unequivocally indigenous hydrocarbon biomarkers so far identified. They significantly change our estimate of the volume of sediments that may contain petroleum in Australia and elsewhere. Although the oil and sediments contain hydrocarbons which imply prokaryotic precursors, in general, they are not significantly different from many Phanerozoic samples, emphasizing the importance of the contribution of prokaryotic organic matter to source rocks of all ages²⁰ Subtle compositional differences in the contents of acyclic and cyclic biomarkers between the Velkerri Formation (marine) and the Barney Creek Formation (lacustrine) illustrate that environmental differences are reflected in the composition of sedimentary organic matter, even in the Proterozoic. In all the McArthur sediments, the extremely low abundance of steranes (biomarkers for eukaryotic organisms²¹) compared with hopanes, supports the concept of the rise of the eukaryotes in the latest Proterozoic (that is, after 1,400 Myr)²². However, this evidence remains equivocal until environmental influences on organic matter composition in these sediments can be determined.

We thank C. Boreham and Z. Horvath for analyses and M. R. Walter and P. J. Cook for helpful discussion. This paper is published with permission of the director of the Bureau of Mineral Resources, Geology and Geophysics. The Australian National Energy Research, Development and Demonstration Program supported this work.

Received 13 December 1985; accepted 2 June 1986.

- 1. Meverhoff, A. A. Mem. Am. Ass. Petrol. Geol. 30, 225-252 (1980).
- Meyerhoff, A. A. Dist. Lect. Ser. (Petrol. Explor. Soc. Aust.) (August 1982).
- 3. Murray, G. E., Kaczov, M. J. & McArthur, R. E. Bull. Am. Ass. Petrol. Geol. 64, 383-390
- 4. Petrov, A. A., Mokshantsev, K. B., Fradkin, G. S. & Barykin, S. F. Petrol. Geol. 18, 384-390
- Scott, R. W. Wld Oil 189, 55-61 (1979).
- 6. Hobson, G. D. & Tiratsoo, E. N. Introduction to Petroleum Geology, 2nd edn (Gulf, Houston,
- 7. Jackson, M. J., Muir, M. D. & Plumb, K. A. Bull. Bur. Miner. Resour. Geol. Geophys. Aust (in the press).

 8. Page, R. W. Econ. Geol. 76, 648-658 (1981).
- Kralik, M. Precambr. Res. 18, 157-170 (1982)
- 10. Muir, M. D. Origins Life 5, 143-173 (1974).
 11. Muir, M. D. Alcheringa 1, 143-158 (1976).
- 12. Oehler, J. H. Alcheringa 1, 315-349 (1977).
- Oehler, D. Z. Alcheringa 2, 269-309 (1978).
- Peat, C. J., Muir, M. D., Plumb, K. A., McKirdy, D. M. & Norvick, M. J. Bur Miner. Resour. J. Aust. Geol. Geophys. 3, 1-17 (1978).
- Muir, M. D. Bot. J. Linn. Soc 86, 1-18 (1983).
 Muir, M. D., Armstrong, K. J. & Jackson, M. J. Bur. Miner. Resour. J. Aust. Geol. Georhys. 5, 301-304 (1980).
- 17. Logan, R. G. & Williams, N. 7th Aust. Geol. Conv. Abstr. 12, 339 (Geological Society of Australia, 1984).

 18. Muir, M. D., Lock, D. & von der Borch, C. C. Spec. Publs Soc. econ. Paleont Miner 28,
- 51-67 (1980).

 19. Klomp, U. C. Abstr. 12th int. Meet. org. Geochem., (Julich, European Association of Organic
- Geochemists, 1985).
- 20. Ourisson, G., Albrecht, P. & Rohmer, M. Scient. Am. 251(2), 34-41 (1984)

- Rohmer, M., Bouvier, P. & Ourisson, G. Proc. nam. Acad. Sci. U.S.A. 76, 847-851 (1973)
 Schopf, J. W. Precambr. Res. 5, 143-173 (1977).
 Espitalie, J., Madec, M., Tissot, B., Meening, J. J. & Leplat, P. Offshore Tech. Conf.. Prep. 9, 3, 439-444 (1977).
- 24. Powell, T. G. Geol. Surv. Pap. Can. 78-12 (1978).
- Tissot, B., Durand, B., Espitalie, J. & Combaz, A. Bull. Am. Ass. Petrol. Geol. 58, 499 506 (1974).

Amino acid epimerization in planktonic foraminifera suggests slow sedimentation rates for Alpha Ridge, Arctic Ocean

S. A. Macko & A. E. Aksu

Department of Earth Sciences, Memorial University of Newfoundland, St John's, Newfoundland, Canada A1B 3X5

Interpretations of the palaeoclimatic and palaeooceanographic histories of the Arctic Ocean^{1,2} have been hampered by conflicting chronologies obtained using different dating methods. Magnetostratigraphic and micropalaeontological data¹⁻⁴ have suggested a sedimentation rate of ~1 mm kyr⁻¹, whereas the rate indicated by amino acid epimerization analyses on foraminifera⁵ is an order of magnitude higher. To establish a firm chronology for cores from the Alpha Ridge, Arctic Ocean, and to help resolve the controversy between the ages assigned by different dating methods, we have carried out detailed amino acid epimerization analyses on planktonic foraminifera Neogloboquadrina pachyderma sinistral from a long gravity core. Assuming that the temperature in the Arctic Ocean did not exceed 3 °C during the past 1 Myr, the alloisoleucine/isoleucine (alle/Ile) ratios obtained from this core suggest a sedimentation rate of ~1 mm kyr⁻¹, supporting previous magnetostratigraphic and micropalaeontological studies.

This study was primarily based on amino acid epimerization analyses on planktonic foraminifera extracted from core CESAR 83-102 (85°38' N, 111°07.1' W), raised from a depth of 1,495 m on the Alpha Ridge, Arctic Ocean (Fig. 1). The core includes down-core sequences of sediments typical of previously studied Arctic Ocean cores (Fig. 2). Three lithostratigraphic units (K-M) identified in this core are fully discussed elsewhere⁶, and are briefly described here: lithological unit M is a partially bioturbated, foraminifera-rich, yellowish sandy to silty mud, with up to three pink-white carbonate hardground layers. Unit L consists of foraminifera-poor, light brown sandy-silty mud, and unit K is a partially bioturbated, dark brown silty-sandy mud with variable numbers of foraminifera. High-resolution seismic profiles show smooth, flat-lying reflectors over the core site⁷. Detailed examination of X-radiographs shows the absence of internal sedimentary structures usually associated with resedimentation. The presence of widespread bioturbational sedimentary structures suggests that the sediments recovered in this core represent pelagic or hemipelagic deposition. The magnetostratigraphic data from this core² indicate that the boundary between the Brunhes and Matuyama magnetochrons lies in unit K at ~87 cm depth. This boundary is generally accepted to occur at 0.73 Myr (ref. 9).

Amino acid epimerization reaction rates are species-dependent^{10,11}; therefore, only monospecific samples of N. pachyderma sinistral were used for the analyses. This taxon, however, shows large morphological variations and includes several morphotypes, such as N. polusi and N. cryophila, that are considered by some^{4,12} to be separate species. Therefore, only the fourchambered quadrate forms of N. pachyderma sinistral were used for the amino acid analyses. Twenty-seven levels were analysed in CESAR 83-102, each sample comprising a 1-cm-thick slice of the core. Despite much greater sensitivity in detection level for the amino acid technique, enabling smaller samples to be analysed, larger sample sizes were used to reduce potential laboratory contamination and to ensure sample integrity and homogeneity. About 1,000 specimens (~10 mg) were handpicked from each sample; foraminiferal shells were ultrasonically cleaned in distilled water three times and each sample was rinsed with distilled water twice. Samples were sealed under nitrogen with a stoichiometrically related excess of hydrochloric acid to yield final solutions of 6 M HCl, which were then hydrolysed for 24 h at 100 °C. Portions of the hydrolysate were

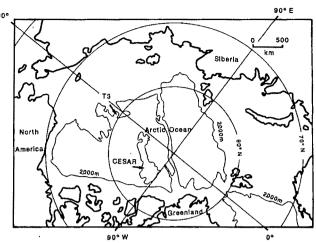


Fig. 1 Map of the Arctic Ocean showing the locations of the CESAR and T-3 ice camps.

analysed by stepwise isocratic elution with baseline separation of the alloisoleucine/isoleucine pair, fluorescence detection and peak integration on an ion-exchange HPLC (high-pressure liquid chromatograph) with a detection limit of ~ 10 pM (ref. 13). Triplicate analyses show that the reproducibility is ± 0.025 in the alle/Ile value. For chronostratigraphic calibration, alle/Ile was determined on two additional samples of N. pachyderma sinistral, extracted from well-dated ash layers 2 and 3 of the North Atlantic cores K708-1 and K708-7, respectively. Results of these analyses as well as an interlaboratory sample of Saxidomus sp. (ILC-A) are presented in Table 1. This

Table 1 Ratio of alle/Ile in *N. pachyderma* sinistral from Arctic Ocean core 83-102 and Atlantic Ocean cores K708-1 and K708-7, corresponding to volcanic ash layers 2 and 3 respectively¹⁴

Core	Depth (cm)	aIle/Ile	Core	Depth (cm)	aIle/Ile
83-102	0-1	0.034	83-102	31-32	0.253
83-102	1-2	0.041	83-102	38-39	0.235
83-102	3-4	0.075	83-102	39-40	0.288
83-102	4-5	0.091	82-102	42-43	0.223
83-102	5-6	0.110	83-102	44-45	0.220
83-102	7-8	0.085	83-102	81-82	0.280
83-102	9-10	0.119	83-102	82-83	0.267
83-102	13-14	0.204	83-102	84~85	0.287
83-102	14-15	0.193	83-102	87-88	0.322
83-102	15-16	0.140	83-102	89-90	0.318
83-102	18-19	0.209	83-102	90-91	0.287
83-102	19-20	0.214	83-102	91-92	0.275
83-102	22-23	0.229	K708-1	390	0.102
83-102	24-25	0.242	K708-7	810	0.236
83-102	27-28	0.224	ILC-A		0.167

ILC-A, interlaboratory calibration standard Saxidomus sp. 15.

standard is reported for comparison as recommended by Wehmiller¹⁵.

The plot of alle/Ile in N. pachyderma from CESAR 83-102 against depth reveals two regions of linearity (Fig. 3). The upper 13 samples show a constant increase in alle/Ile to \sim 23 cm depth in the core, and this data set displays a highly significant correlation ($r^2 = 0.83$; Pearson r, 0.01 level). The second zone extends from \sim 23 to 93 cm depth. Linear regression over this region shows a significant correlation (0.05 level), with an r^2 value of 0.31. Sediments between 47 and 81 cm depth in the core were barren of foraminifera (Fig. 2). The alle/Ile value at the intersection of these two regions is 0.229, and is comparable to that observed elsewhere 10,16,17 . The exact nature of the change in slope between these two regions is not fully understood. A variation in protein content (free versus bound) or the presence of more than one type of protein with different resistance to

Ŋ

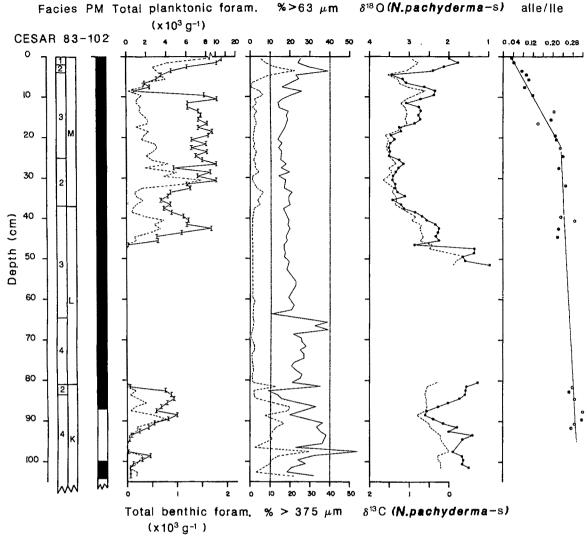


Fig. 2 Averaged amino acid epimerization data plotted against depth, together with lithofacies⁶, palaeomagnetic timescale², foraminiferal, grain size and stable isotope data⁸. Facies: 1, clayey mud; 2, carbonate hardgrounds; 3, silty mud; 4, sandy mud; units K-M are explained in text. Dashed lines refer to lower axes.

degradation or associated rates of epimerization may be the cause¹⁶.

It has been demonstrated that the epimerization reaction of isoleucine

L-isoleucine
$$\xrightarrow{k_{\text{lle}}}$$
 D-alloisoleucine (1)

obeys first-order reaction kinetics¹⁷⁻¹⁹. The reaction rate constants k_{Ile} and k_{alle} are temperature-dependent and are governed by the Arrhenius equation:

$$k_{\text{Ile}} = A e^{(-E_a/RT)} \tag{2}$$

where A is the species-dependent Arrhenius frequency factor¹¹, E_a the genus-dependent activation energy¹⁷⁻¹⁹, R the gas constant and T the temperature (K). The rate constants for the North Atlantic core samples can then be calculated using a solution to the differential rate expression²⁰:

$$\ln \left\{ \frac{1 + \frac{\text{aIle}}{\text{Ile}}}{1 - K' \frac{\text{aIle}}{\text{Ile}}} \right\}_{t} - \ln \left\{ \frac{1 + \frac{\text{aIle}}{\text{Ile}}}{\frac{1 - K' \text{aIle}}{\text{Ile}}} \right\}_{t=0} = (1 + K') k_{\text{Ile}} t \quad (3)$$

where $K' = k_{\text{alle}} = 1/K_{\text{eq}}$, the inverse of alle/IIe at equilibrium, and t is the time. Although alloisoleucine may be present in

living foraminifera and isoleucine may generate alloisoleucine during acid hydrolysis, these contributions (t = 0 term in (3)) are negligible^{21,22}.

The value for K_{eq} is ~1.3-1.4 (refs 17, 20, 22). Taking this value to be 1.4 (refs 20-22), with ages for ash layers 2 and 3 of 65,000 and 340,000 yr BP (ref. 14), respectively, the forward rate constants for epimerization in these two samples are calculated to be 1.551×10^{-6} and 6.803×10^{-7} yr⁻¹, respectively, using measured alle/Ile values (Table 1). An additional rate constant of 1.545×10^{-6} yr⁻¹ is calculated using published data⁵ from the same core, K708-7 (alle/Ile = 0.078, age = 50,000 yr BP, depth = 140 cm). Ages calculated using first-order reversible kinetics of epimerization in marine fossils are found to be optimal for samples with aIle/Ile ≤ 0.25 (refs 16, 20-23); because the value in ash layer 3 is near this limit, the alle/Ile and derived rate constant for this sample are not used for further calculations. The Arrhenius frequency factor ($\log A$) is calculated to be 15.70 using the average of the remaining two rate constants and assuming an activation energy of 113.4 kJ mol⁻¹, which was calculated from a bulk foraminiferal sample¹⁷. This value is nearly identical to the value of 15.77 calculated²⁰ from a North Atlantic core. From these calculations, the relationship between forward epimerization rate constant and temperature for N. pachyderma can be expressed as:

$$\log k_{\text{He}} \, \text{yr}^{-1} = 15.70 - 5.939 / T \tag{4}$$

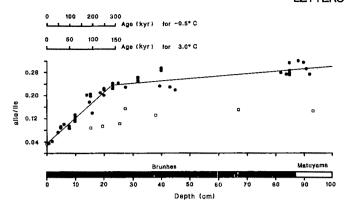


Fig. 3 Epimerization of isoleucine in N. pachyderma sinistral versus depth in core 83-102. Age scale discussed in text, palaeomagnetic scale from ref. 2. \square , from ref. 5, re-plotted based on the Brunhes/Matuyama boundary as the reference point.

Present-day Arctic water temperatures vary from −0.5 °C in the Canada Basin and the Alpha Ridge bottom waters to a maximum in the water column not exceeding +3 °C (ref. 24). First-order epimerization rate constants based on the above temperature range are 8.194×10^{-7} and 1.548×10^{-6} for -0.5 and 3 °C, respectively. Relative ages of sediment can then be calculated using equation (2) (Fig. 3). For example, the sample at 20 cm depth, with an alle/Ile of 0.214 (average of 3 analyses) yields ages of 256,100 and 135,600 yr BP for the maximum- and minimum-temperature rate constants. These ages give sedimentation rates of 0.8-1.5 mm kyr⁻¹ for the Alpha Ridge region of the Arctic Ocean.

This deposition rate is consistent with previous magneto-stratigraphic and biostratigraphic studies 1-4,8,12,24-26, but conflicts strongly with the conclusions of the recent amino acid epimerization study⁵ of the Arctic Ocean core T3-67-11. These authors⁵ have argued that a significant portion of the foraminifera analysed from their core were reworked, and that the alle/Ile measured on the deepest sample (260 cm) was closest to the in situ ratio in this core. Consequently, their age estimate, using calculations similar to those presented here, was based solely on this sample. The rate constant derivation for their estimate was based on benthic foraminifera C. lobatulus. There is no evidence for significant reworking of fauna in studied CESAR cores^{2,6,8}. Palynological data² from a long CESAR core show several first-appearance and last-appearance data of dinoflagellate and pollen and spore taxa in the appropriate sequence, generally supporting little reworking of fauna and flora. It has been demonstrated 6.24 that there is a strongly correlatable downcore sequence of 13 lithological units in >500 cores collected from the Arctic Ocean. Several studies have indicated that there are also correlatable faunal and floral abundance and assemblage variations associated with the lithostratigraphic units2-The paleomagnetic data from several cores from the Arctic Ocean have shown the presence of normal and reversed polarity chrons that are correlated with known magnetic timescales 1,2,25,26. Core T3-67-11, studied by Sejrup et al.5, shows litho-, bio- and magnetostratigraphic variations similar to other cores from the Arctic Ocean^{1,4}. Therefore, the assumption that most foraminifera from core T3-67-11 are reworked may not be warranted.

The foraminifera analysed from core T3-67-11 (ref. 5) show a down-core increase in alle/Ile to a depth of 120 cm. This trend is similar to that observed in CESAR core 83-102 (Fig. 3). The reason for the difference in the slopes of the two data sets is not clear. A variation of this magnitude requires a decrease of \sim 3-5 °C in the average temperature of epimerization for T3 with respect to CESAR sites. Assuming that foraminifera recovered from this core were not reworked and that the average bottom water temperature was -0.5 °C, the alle/Ile values reported by Sejrup et al.⁵ yield respective sedimentation rates of ~ 1.9 and 2.6 mm kyr⁻¹ for samples from 33 and 35 cm depth in T3-67-11. These rates are only slightly higher than the value of 1.6 mm kyr⁻¹ predicted by the palaeomagnetic data from this core¹. We recognize that a single sedimentation rate for the entire Arctic Ocean is unlikely. Based on the above calculations. the sedimentation rates in the Canada Basin (T3) are slightly higher than those calculated for the Alpha Ridge (CESAR); however, these rates are 10-15 times slower than that suggested by Sejrup et al.5.

The amino acid data presented in this paper independently demonstrate a slow sedimentation rate (~1 mm kyr⁻¹) for the Alpha Ridge region of the Arctic Ocean, supporting previous magneto- and biostratigraphic timescales. Through detailed multidisciplinary investigations, the chronology of the Arctic Ocean sediments is believed to have been resolved. A reliable chronology is an important prerequisite in studying the palaeoclimatic and palaeooceanographic histories of the Arctic Ocean and its role in Northern Hemisphere glacial/interglacial cycles.

We thank M. J. Keen and H. R. Jackson of the Bedford Institute of Oceanography for making the CESAR 83-102 samples available and K. Pulchan for assistance in laboratory measurements. This study was supported by the Natural Sciences and Engineering Research Council of Canada. Acknowledgement is made to the donors of The Petroleum Research Fund, administered by the American Chemical Society, for partial support. W. F. Ruddiman provided North Atlantic samples from cores K708-1 and K708-7 and J. F. Wehmiller supplied the interlaboratory standard ILC-A. We thank J. F. Wehmiller, J. A. Welhan, D. J. W. Piper and C. Pereira for critical comments.

Received 10 February; accepted 2 May 1986.

- 1. Hunkins, K., Be, A. W. H., Opdyke, N. D. & Mathieu, G. The Late Cenozoic Glacial Ages (ed. Turekian, K. K.) 215-237 (Yale University Press, 1971). Aksu, A. E. & Mudie, P. J. Nature 318, 280-283 (1985).
- Clark, D. L. Bull. geol. Soc. Am. 82, 3313-3323 (1971).
 Herman, Y. Marine Geology and Oceanography of the Arctic Seas (ed. Herman, Y.) 283-348
- (Springer, Berlin, 1974).

 5. Sejrup, H. P., Miller, G. H., Brigham-Grette, J., Lovlie, R. & Hopkins, D. Nature 310, 772-775 (1984).
- Mudie, P. J. & Blasco, S. M. Geol. Surv. Pap. Can. 84-22, 59-99 (1985).
- Jackson, H. R. Geol. Surv. Pap. Can. 84-22, 19-23 (1985).
 Aksu, A. E. Geol. Surv. Pap. Can. 84-22, 115-124 (1985).
- Harland, W. B. et al. A Geologic Time Scale (Cambridge University Press, 1982). 10. King, K. & Neville, C. Science 195, 1333-1335 (1977).

- King, K. & Neville, C. Science 195, 1333-1335 (1977).
 Miller, G. H., Sejrup, H. P., Mangerud, J. & Anderson, B. G. Boreas 12, 107-124 (1983).
 Herman, Y. Palaeogeogr. Palaeoclimatol. Palaeoecol. 6, 251-276 (1969).
 Hare, P. E., St. John, P. A. & Engel, M. H. Chemistry and Biochemistry of Amino Acids (ed. Barnett, G. C.) 415-425 (Chapman and Hall, London, 1984).
 Ruddiman, W. F. & McIntyre, A. Soc. Am. Mem. 145, 111-146 (1976).
 Wehmiller, J. F. Quat. Res. 22, 109-120 (1984).
 Schroeder, R. A. & Bada, J. L. Earth Sci. Rev. 12, 347-391 (1976).
 Park, J. & Schroeder, B. A. Mottowitzenskoften 53, 71, 70 (1975).

- Schroeder, R. A. & Bada, J. L. Earth Sci. Rev. 14, 347-391 (1976).
 Bada, J. L. & Schroeder, R. A. Naturwissenschaften 62, 71-79 (1975).
 Miller, G. H. & Hare, P. E. Biogeochemistry of Amino Acids (eds Hare, P. E., Hoering, T. C. & King, K.) 415-444 (New York, 1980).
 Mitterer, R. M. Geology 2, 425-428 (1975).
 Bada, J. L. & Schroeder, R. A. Earth planet. Sci. Lett. 15, 1-11 (1972).

- 21. Bada, J. L. & Mann, E. H. Earth Sci. Rev. 16, 21-55 (1980).
- Wehmiller, J. F. & Hare, P. E. Science 173, 907-911 (1971).
 King, K. & Hare, P. E. Yb Carnegie Instn. Wash. 71, 596-598 (1972).
- Coachman, K. L. & Aagaard, K. Marine Geology and Oceanography of the Arctic Seas (ed. Herman, Y.) 1-72 (Springer, Berlin, 1974).
- 25. Clark, D. L., Whitman, R. R., Morgan, K. A. & Mackey, S. D. Geol. Soc. Am. spec. Pap. 181 (1980).
- Steuerwald, B. A., Clark, D. L. & Andrew, J. T. Earth planet. Sci. Lett. 5, 79-85 (1968).
 Clark, D. L. Bull. geol. Soc. Am. 81, 3129-3134 (1970).

Thermal and mechanical constraints on the lithosphere beneath the Marquesas swell

Karen M. Fischer*†, Marcia K. McNutt* & Loren Shure†

* Department of Earth, Atmospheric and Planetary Sciences, Massachusetts Institute of Technology, Cambridge, Massachusetts 02139, USA † Woods Hole Oceanographic Institution, Woods Hole, Massachusetts 02543, USA

The Marquesas Islands, like most active or recently active hotspot chains, lie on anomalously shallow sea floor, and their subsidence history points to a fundamentally thermal origin for the swell¹, as do heat flow and subsidence data for the swells beneath Bermuda² and Hawaii³.⁴. Here we apply a new linear filtering technique to geoid height and depth anomaly data over the Marquesas, to constrain the depth to the high-temperature, low-density material responsible for elevating the swell. We determine an isostatic compensation depth of $45\pm5\,\mathrm{km}$ for the swell, and best-fitting values for lithospheric flexural rigidity and island load density of $5\times10^{22}\,\mathrm{N}$ m and 2,700 kg m $^{-3}$, respectively. The swell's shallow compensation depth and low flexural rigidity call for anomalously high temperatures within the lithosphere 5,6 .

Crough and Jarrard¹ have computed an isostatic root depth of 30 ± 40 km for the Marquesas swell using a geoid height-depth anomaly transfer function. Their result suggests anomalously high temperatures well into the lithosphere, as isostatic compensation depth provides a fairly direct estimate of the depth to the thermal anomaly². Their study is compatible with the low flexural rigidity of 4×10^{22} N m for the Marquesas derived by Cazenave et al.⁷, given that the thickness of the elastic plate supporting intraplate volcanoes has been shown to be thermally

controlled. However, the transfer function method, and other current techniques for estimating swell compensation depth, use assumed values for swell height and width taken from geoid or depth anomaly data. In the Marquesas, the overlap in wavelength between the isostatically compensated swell and the mechanically supported islands makes it difficult to obtain estimates of swell height that are unbiased by island-related topography.

In the present study we apply a new method for estimating swell compensation depth to updated depth anomaly and geoid height maps over the Marquesas. The technique, described more fully in ref. 9, does not require initial estimates of swell amplitude or wavelength, nor does it require that the swell and islands be separated in the spectral domain.

The two primary data sets discussed here are seafloor depth anomalies and geoid height anomalies computed between 160 and 125° W, and 5 and 30° S, an area loosely covering French Polynesia. As we are interested only in hotspot signatures, we attempt to remove from the data all effects of non-hotspot-related processes.

Bathymetry at 5' intervals from the Synbaps data set¹⁰ were averaged to a new spacing of 15' and then corrected for sound velocity variations with a quadratic fit to the Matthews tables¹¹ (L. Wixom, personal communication). The effect of sediment loading was removed according to the empirical relation given in ref. 12, using sediment thicknesses measured from ref. 13. Finally, we accounted for thermal subsidence due to the cooling of the oceanic lithosphere using the depth-age relationship for the North Pacific from ref. 14. Seafloor ages were inferred from the isochron locations of refs 1, 15 and H. W. Menard (unpublished data), and the fracture zone identifications of ref. 16. We estimate the maximum errors in the depth anomaly map for the Marquesas (Fig. 1a) to be less than the 250-m contour interval.

Geoid height data are from the GEOS-3 and Seasat altimeter missions as compiled in ref. 17, at a 15' spacing. Components of the field with wavelengths >4,000 km were eliminated by subtracting the observed field up to degree 10 using the Gem-9

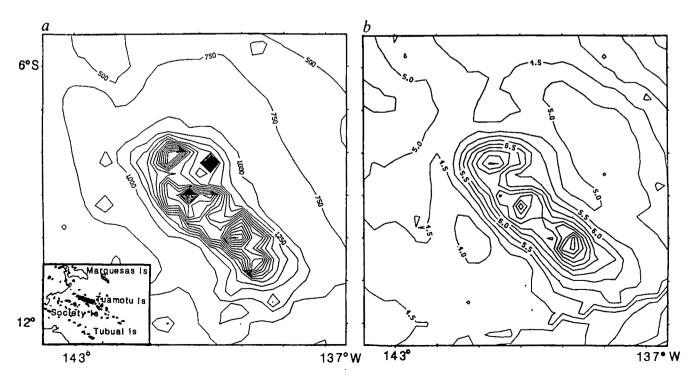


Fig. 1 Maps of reduced depth (a) and geoid (b) anomaly over the Marquesas Islands. a, Contour interval 250 m. The inset shows the major bathymetric features in the area of French Polynesia between 160 and 125° W, and 5 and 30° S (after ref. 1). The single contour in the inset is at 5 km depth. b, Contour interval 0.5 m. Note the flexural moat signatures to the north-east and south-west of the islands.

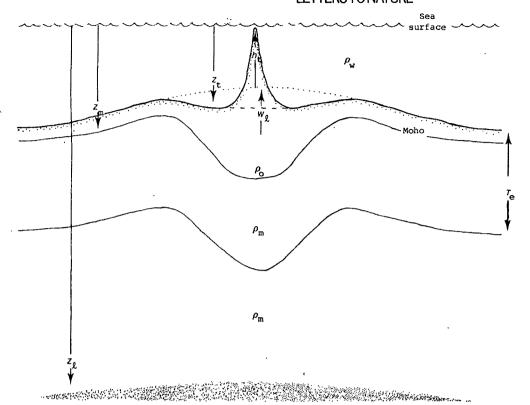


Fig. 2 Schematic cross-section of a swell (from ref. 9). The densities of sea water, volcanic rock and the mantle are $\rho_{\rm w}$, $\rho_{\rm 0}$ and $\rho_{\rm m}$, respectively. The height of the surface load is $h_{\rm t}$, superimposed on the height of the swell, $w_{\rm l}$. Average depth to the sea floor, Moho and swell compensation (shaded, density $\rho_{\rm l}$) are $z_{\rm l}$, $z_{\rm m}$ and $z_{\rm l}$, respectively. $T_{\rm e}$ is the thickness of the elastic plate.

coefficients¹⁸ for the spherical harmonic expansion of the Earth's geoid, and the data were then corrected for the decrease in geoid height due to thermal cooling with age using the geoid heightage relationship of ref. 19 and the North Pacific thermal parameters of ref. 14. At this point the residual geoid showed a long-wavelength NE-SW trend over the Marquesas, in addition to the swell and island signatures. This feature was removed by subtracting the best-fitting plane (in the least-squares sense) from the data between 144 and 136.5° W, and 5 and 12.5° S, leaving the residual geoid shown in Fig. 1b.

Our method for estimating the compensation depth of intraplate swells, explained in more detail in ref. 10, assumes an elastically compensated island topography, h_i , superimposed on a swell with amplitude w_i above normal seafloor depth, due to a sub-plate load with thickness h_i at an average depth z_i , which is the effective compensation depth of the swell (Fig. 2). The observables are the total age-corrected geoid anomaly, N_i , and the total age- and sediment-corrected depth anomaly, $h = h_i + w_i$. If we were to make the false assumption that the observed geoid is due only to the compensation of the observed topography at the Moho by elastic flexure of the oceanic crust, we would predict a geoid anomaly \hat{N}_i , which we define as

$$\hat{N}(k_{x}, k_{y}) = \frac{G(\rho_{0} - \rho_{w})}{gk} \left\{ e^{-2\pi k z_{t}} - \frac{e^{-2\pi k z_{m}}}{1 + k^{4}\alpha} \right\} (H_{t} + W_{1})$$

$$= F_{1}(k) \cdot H(k_{x}, k_{y})$$
(1)

where $\alpha = (2\pi)^4 D/((\rho_{\rm m} - \rho_0)g); \ D = ET_{\rm o}^3/12(1-\nu^2);$ Young's modulus $E = 8 \times 10^{10} \ {\rm N \ m^{-2}}; \ T_{\rm c}$ is the elastic plate thickness; Poisson's ratio $\nu = 0.25; \ k_x$ and k_y are the horizontal wavenumbers; $k = (k_x^2 + k_y^2)^{1/2}; \ \rho_0, \ \rho_{\rm w}$ and $\rho_{\rm m}$ are the densities of volcanic rock, water and mantle, respectively; G is the gravitational constant; g is the acceleration due to gravity; z_i is the average depth of topography; $z_{\rm m}$ is the average depth of the Moho; and upper-case letters are the Fourier transforms of their lower-case counterparts.

By subtracting \hat{N} from the observable N, we obtain a form of reduced geoid anomaly, N_R , which in turn enables us to infer

the swell topography, W_1 :

$$W_{1}(k_{x}, k_{y}) = gk/G \left\{ \left(\frac{\rho_{0} - \rho_{w}}{1 + k^{4}\alpha} + (\rho_{m} - \rho_{0}) \right) e^{-2\pi k z_{m}} - ((\rho_{m} - \rho_{w}) + (\rho_{m} - \rho_{0})k^{4}\alpha) e^{-2\pi k z_{1}} \right\}^{-1} N_{R}(k_{x}, k_{y})$$

$$= F_{2}(k, z_{1}) \cdot N_{R}(k_{x}, k_{y})$$
(2)

The filter F_2 corrects for the compensation falsely assumed in \hat{N} and N_R , and provides an estimate of swell amplitude independent of island topography.

Our method, then, is to assign values for D, ρ_0 , ρ_m , z_t and z_m , the geophysical parameters in the filter F_1 which describe the geoid signature due to plate flexure. We apply the filter F_1 to observed depth anomaly data to obtain N, and then we subtract N from the total observed geoid N, which gives us N_R . We then assume a value of z_1 , apply the filter F_2 to N_R , and obtain an estimate of the swell topography. The best-fitting z_1 values are those which generate profiles of predicted swell topography that match the swell outline seen in the total observed topography. We then test a given value of z_1 in two dimensions by subtracting the predicted swell topography from the observed depth anomalies. The remaining topography should show only the volcanic islands and the signature of their flexural compensation.

Values of z_1 between 25 and 55 km were tested in 5-km increments, along with many values of ρ_0 and D. Load densities between 2,500 and 2,800 kg m⁻³ were considered to be reasonable^{20,21}, although the chemistry of the Marquesas²² suggests that values in the upper end of this range are the most plausible. Values of flexural rigidity were varied from the low value of 2×10^{22} N m suggested by McNutt and Menard²⁰ for the Cook and Tuamoto islands, up to 10^{23} N m. In all cases ρ_m was set to 3,300 kg m⁻³, z_m to 11 km and z_t to 6 km.

The parameter values that produce the best fit to the observed swell (Fig. 3a) and yield a residual topography with clear island signatures (Fig. 4) are $z_1 = 45 \pm 5$ km, $D = 5 \times 10^{22}$ N m and $\rho_0 =$

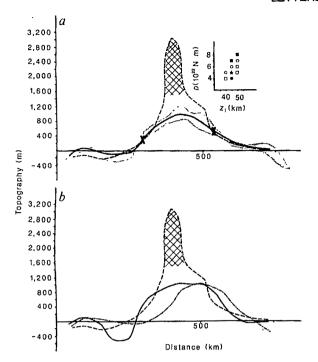


Fig. 3 a, Profiles of observed topography (dashed line) and swell predicted by $z_1 = 45$ km, $D = 5 \times 10^{22}$ N m and $\rho_0 = 2,700$ kg m⁻³ (solid line). The cross-hatched peak gives an example of a typical island feature superimposed on the swell, and the shading indicates the profiles of the envelope of plausible parameter values, shown in the inset ($\rho_0 = : \oplus$, 2,800; \square , 2,700; \bigcirc , 2,600; \boxtimes , 2,500 kg m⁻³; \bigstar , best-fitting parameters). The positions of the flexural moats seen in the observed geoid are shown by crosses (see also Fig. 4). Note that the observed topography here and in b has been shifted downwards by a constant value of 500 m. b, Profiles of two models whose predicted swells do not fit the observed swell topography (dashed line) as well as do the models in a. Solid line, $z_1 = 50$, $D = 5 \times 10^{22}$ N m, $\rho_0 = 2,600$ kg m⁻³; dash-dot line, $z_1 = 40$ km, $D = 5 \times 10^{22}$ N m, $\rho_0 = 2,700$ kg m⁻³.

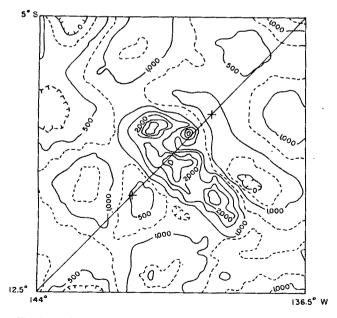


Fig. 4 Residual topography over the Marquesas Islands produced by the preferred values, $z_1 = 45$ km, $D = 5 \times 10^{22}$ N m and $\rho_0 = 2,700$ kg m⁻³. Note the signatures of the volcanic islands and their flexural compensation. The diagonal line shows the locations of the profiles in Fig. 3, and the crosses correspond to the moat positions seen in the observed geoid. Solid contours are at 500-m intervals, dashed contours at 250-m intervals.

2,700 kg m⁻³. The diagonal line in Fig. 4 indicates the location of the profiles in Fig. 3. The only assumption made in fitting predicted swell profiles to observed topography is that off-centre, shorter-wavelength features, such as the dotted area in Fig. 3a, are mechanically compensated islands. Given the ambiguity in separating island and swell contributions near the crest of the swell, preference was given to those models which best matched the flanks of the observed topography, plus or minus a constant value. The approximate locations of the flexural moats were obtained from the observed geoid (Fig. 1b), and allowance was made for their signature in fitting the predicted swell to observed topography profiles. Bathymetric highs corresponding to island locations, a clear flexural moat and an absence of broad highs or lows corresponding to the swell were the features sought for in the residual topography maps.

Surrounding the preferred model is an envelope of parameter values which produce less adequate fits to the swell profile (shown in the shaded area in Fig. 3a) and similar residual topography patterns. The range of acceptable flexural rigidity values within this envelope (shown in Fig. 3a inset) represents the error bars on the best-fitting flexural rigidity value of 5×10^{22} N m, and is largely constrained by the 15' spacing of the data values. An examination of the parameter envelope suggests that for a given surface load density, an increase in compensation depth may be roughly balanced by an increase in flexural rigidity. Alternatively, increasing z_1 or D offsets a decrease in ρ_0 . For instance, for the value of $\rho_0 = 2,800$ kg m⁻³ used by Cazenave et al.⁷ and our preferred compensation depth of 45 km, we obtain their flexural rigidity of 4×10^{22} N m. For comparison, Fig. 3b shows two models which lie outside the envelope of best-fitting parameters.

We also checked the fit of predicted swell heights to observed topography for profiles to the north-west and south-east of those shown in Fig. 3. Over the islands to the north we obtain an identical range of best-fitting parameters. To the south, however, models with deeper compensation depths and larger flexural rigidities are called for both by swell profiles and by the apparent widening of the island moat seen in Fig. 4. Given the younger ages of the islands in this area²³, heat from a lithospheric source would have had less time to elevate lithospheric isotherms conductively, resulting in a thicker apparent lithosphere than is observed in the north.

A compensation depth of 45 km certainly suggests the presence of anomalously buoyant material within the lithosphere. If we equate the geoid anomaly due to an infinitesimally thin layer at z_1 =45 km with the geoid anomaly due to a uniform column of low-density material⁹, the upper boundary of the low-density mass extends well into the upper half of the lithosphere, perhaps to within several kilometres of the surface, depending on the assumed thickness of the column. The actual depth distribution of the low-density material is, however, notably non-unique, and so we look to thermal modelling to shed some light on the significance of z_1 . Some of the Marquesas swell signature may be due to chemically defined low-density material, but as subsidence data¹ and low flexural rigidities suggest that thermal anomalies probably dominate, here we will address only possible thermal models.

Timescales associated with pure conduction are too long to explain the Marquesas swell. Assuming a lithospheric thickness of 70 km, ~20 Myr (at least twice the age of the oldest Marquesas volcanism²³) is required for a thermal anomaly to propagate from the base of the lithosphere to at least 45 km depth. Furthermore, if the base of the conducting region is allowed to migrate upwards as the lithosphere warms, the excess mantle heat flux must be at least four times normal in order to obtain plate thinning rates consistent with the age of the Marquesas²⁴.

Thermal structures produced by simple models of large-scale convection beneath the lithosphere are also incapable of explaining the shallow compensation depth. Calculations involving convection of a constant-viscosity material beneath a conducting

lithosphere of normal thickness (70 km) produce apparent compensation below the base of the plate²⁵, too deep to explain the observed value of 45 km, and decreases in the thickness of the conducting layer will not sufficiently diminish the calculated compensation depths25. However, Robinson et al26 suggest that convection within certain non-uniform viscosity structures may produce thermal anomalies below 70 km depth which merely mimic compensation at depths shallower than the conducting lid thickness. More complex viscosity models may produce an apparent compensation depth at 45 km without the necessity of invoking a thinner conducting lid beneath the Marquesas.

Alternatively, Fleitout et al.27 have proposed that if one accounts for both the temperature and pressure dependence of viscosity, a mantle heat source is liable to create convective instabilities which will erode the base of the lithosphere. This process may continue until the anomalously warm material encounters an abrupt decrease in lithospheric density, such as at the base of the basalt-depleted zone at ~40 km depth²⁸. According to this model, the 45-km compensation indicates that the lithosphere beneath the Marquesas Islands has been thinned to the maximum possible extent.

Using a linear filtering technique which requires a minimum of assumptions about swell height and wavelength9 we obtain a compensation depth for the Marquesas swell of 45 ± 5 km, a density of 2,700 kg m⁻³ for the volcanic islands, and a flexural rigidity of 5×10^{22} Nm for the lithosphere. While our flexural rigidity value is comparable to that of Cazenave et al.7, our compensation depth is somewhat deeper and more tightly constrained than the results of Crough and Jarrard¹. These low values for compensation depth and flexural rigidity call for anomalously high temperatures within the lithosphere and can be used to constrain models for the formation of hotspot swells.

We thank Jim Marsh for providing the geoid data, Linda Meinke for assistance with preparing the geoid and bathymetry databases, and Barry Parsons, Steve Daly, Luce Fleitout and Beth Robinson for helpful comments. H. W. Menard provided previously unpublished isochron identifications. This project was funded by NSF OCE-8409157 and ONR N00014-82-C-0019. Woods Hole contribution 6089.

Received 2 December 1985; accepted 30 April 1986.

- Crough, S. T. & Jarrard, R. D. J. geophys. Res. 86, 11763-11771 (1981).
 Detrick, R. S., Von Herzen, R. P., Parsons, B., Sandwell, D. & Dougherty, M. J. geophys. Res. 91, 3701-3723 (1986).
- 3. Detrick, R. S., Von Herzen, R. P., Crough, S. T., Epp, D. & Fehn, U. Nature 292, 142-143
- 4. Von Herzen, R. P., Detrick, R. S., Crough, S. T., Epp, D. & Fehn, U. J. geophys. Res. 87, 6711-6723 (1982).

 5. Menard, H. W. & McNutt, M. K. J. geophys. Res. 87, 8570-8580 (1982).

 6. McNutt, M. K. J. geophys. Res. 89, 11180-11194 (1984).

- 7. Cazenave, A., Lago, B., Dominh, K. & Lambeck, K. Geophys. J. R. astr. Soc. 63, 233-252
- 8. Watts, A. B., Bodline, J. & Steckler, M. J. geophys. Res. 85, 6369-6376 (1980).
- McNutt, M. & Shure, L. J. geophys. Res. (in the press).
 Van Wykhouse, R., SYNBAPS (Synthetic Bathymetric Prefiling Systems), Tech. Rep. TR-233 (Naval Oceanographic Office, Washington, D.C., 1973).
- 11. Matthews, D. J. Tables of the Velocity of Sound in Pure Water and Sea Water (HMSO, London, 1939).
- Le Douran, S. & Parsons, B. J. geophys. Res. 87, 4715-4722 (1982).
 Ludwig, W. J. & Houtz, R. E. Isopach Map of Sediments in the Pacific Ocean Basin and Marginal Sea Basins (American Association of Petroleum Geologists, Tulsa, 1979).

- Parsons, B. & Sclater, J. G. J. geophys. Res. 82, 802-827 (1977).
 Sclater, J. G., Parsons, B. & Jaupart, C. J. geophys. Res. 86, 11535-11552 (1981).
 Mammerickx, J., Smith, S., Taylor, I. & Chase, T. Topography of the South Pacific (Scripps
- Institute of Oceanography, La Jolla, 1975).

 17. Marsh, J. G., Brenner, A. C., Becklett, B. D. & Martin, T. V. J. geophys. Res. 91, 3501-3506
- 18. Lerch, F. J., Klosko, S. M., Laubscher, R. E. & Wagner, C. A. J. geophys. Res. 84, 3897-3916 (1979).

- Parsons, B. & Richter, F. M. Earth planet. Sci. Lett. 51, 440-450 (1980).
 McNutt, M. K. & Menard, H. W. J. geophys. Res. 83, 1206-1212 (1978).
 Lambeck, K. Geophys. J. R. astr. Soc. 67, 91-114 (1981).
 Barsczus, H. G. & Liotard, J.-M. Cr. hebd. Séanc. Acad. Sci., Paris 299, 61-64 (1984).
- Duncan, R. A. & MacDougall, I. Earth planet. Sci. Lett. 21, 414-420 (1974).
 Spohn, T. & Schubert, G. Tectonophysics 94, 67-90 (1983).
 Parsons, B. & Daly, S. J. geophys. Res. 88, 1129-1144 (1983).

- Robinson, E. M., Parsons, B. & Daly, S. Earth planet. Sci. Lett. (submitted).
 Fleitout, L., Yuen, D. & Froidevaux, C. Annls Geophysicae (submitted).
 Oxburgh, E. R. & Parmentier, E. M. J. geol. Soc. Lond. 133, 343-355 (1977).

An enantiornithine bird from the Lower Cretaceous of Queensland, Australia

R. E. Molnar

Queensland Museum, Queensland Cultural Centre, South Brisbane. Queensland 4101, Australia

Current classification of birds recognizes four subclasses: the Archaeornithes, the Enantiornithes, the Odontornithes and the Neornithes. Three of these subclasses were proposed during the nineteenth century, but the Enantiornithes was proposed only five years ago, based on material from the Lecho Formation (Maastrichtian) of Salta Province in Argentina¹. Further material from Asia (Mongolia) and North America (Mexico) has been referred to the Enantiornithes², all of it from the Campanian. Now, in addition, a small tibiotarsus found in the Lower Cretaceous (Albian) of Queensland not only represents the first bony material of Mesozoic birds from Australia, but is also the first reported occurrence of an enantiornithine bird in the Lower Cretaceous.

The unique structure of the distal articulation of the enantiornithine tibiotarsus, with a transversely elongate medial condyle and a markedly narrower lateral condyle, identifies this tibiotarsus as enantiornithine. The specimen (QM F12992) was recovered from a limestone flag of the marine Toolebuc Formation. It was found on Warra Station, on the east side of the Hamilton River, near Hamilton Hotel, west Oueensland, Further details of the stratigraphy and locality are given elsewhere³. The tibiotarsus was one of several small tetrapod elements recovered by acetic acid solution of the limestone and inspection of the residue. It was associated with plentiful small teleost remains as well as remains of other fish, turtles, ichthyosaurs and a pterosaur3.

The tibiotarsus indicates a bird the size of the European blackbird Turdus merula, or the American robin Turdus migratorius, and shows distinctions from the Salta enantiornithine material which render it desirable to erect a new genus

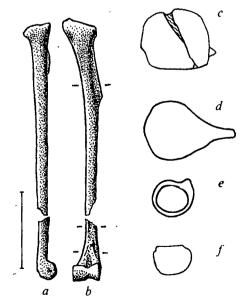


Fig. 1 The tibiotarsus (QM F12992) of Nanantius eos, gen. et sp. nov., in medial aspect (a) and anterior aspect (b). c, The head in proximal aspect; d, e, f, cross-sections of the shaft (with the extent of the internal cavity indicated only in e) at the three levels marked in b. Scale bar, 1 cm.

and species for this oldest-known enantiornithine. Hitherto, the only trace of birds from the Australian Mesozoic has been feathers found at Koonwarra, Victoria (Albian)⁴⁻⁶. These feathers are all small, about 2 cm long⁴⁻⁶ and hence are consistent, at least, with a bird about the size of that represented by the Hamilton tibiotarsus. Other previously reported bird material⁷ from the Australian Mesozoic seems to be dinosaurian.

The enantiornithine tibiotarsus is unique in the narrow intercondylar sulcus and unequal development of the distal condyles¹. The medial condyle is elongate while the lateral condyle is narrow, about half the length of the medial. No theropod dinosaur tibiotarsus (or astragalus) shows this: the condyles are more nearly equally developed, as in birds other than enantiornithines¹. The theropod tibia is distinguished by a short but prominent tibial crest. The Hamilton tibiotarsus has condyles and an intercondylar sulcus like those of the enantiornithines and lacks the tibial crest. Ornithischian dinosaurs have neither a tibiotarsus nor an ascending process of the astragalus, both found in the Hamilton tibiotarsus.

Those pterosaurs with a tibiotarsus have more evenly developed distal condyles which are more pulley-like in form⁸. The pterosaur astragalus has a distinct posterior groove⁹, and the epicondyles are offset in that a line drawn between them is inclined, not perpendicular, to the long axis of the element⁸. The tibia and fibula are fused in pterosaurs⁹. The unequal development of the distal condyles, epicondyles that are not offset, a separate tibia and fibula and the absence of a posterior groove indicate that this tibiotarsus is not derived from a pterosaur. These features indicate that it pertains to an enantior-nithine, and hence to a bird.

Class Aves Subclass Enantiornithes Family?*

* No families have yet been formally proposed for the Enantiornithes; however, in view of the treatise on this group by C. A. Walker (manuscript in preparation) it would be inappropriate to propose families here.

Nanantius, gen. nov.

Type species: Nanantius eos sp. nov.

Type specimen: QM F12992, an isolated left tibiotarsus (Fig. 1).

Locality: North-east paddock of Warra Station, Queensland. Stratigraphy: Toolebuc Formation.

Age: Albian. 10

Diagnosis: A small enantiornithine, smaller than the smallest known from Salta and about the size of Alexornis antecedens, tibiotarsus more slender than any from Salta and similar in proportions to that of Alexornis, fibular crest relatively longer and stronger (Fig. 1d) than in the tibiotarsi from Salta, distinct ascending process of astragalus, marked depression anterior to fibular crest proximally, medial condyle more nearly cylindrical than in any other described enantiornithine.

Etymology: The generic name derives from the Greek $\nu\alpha\nu\sigma\varsigma$, dwarf, and $\dot{E}\nu$ - $\alpha\nu\hat{\tau}i\sigma\varsigma$, opposite, used here in reference to the subclass Enantiornithes. The specific name derives from the Greek $\dot{\eta}\dot{\omega}\varsigma$, dawn, in reference to the earlier occurrence of this specimen than those of other enantiornithine taxa.

The tibiotarsus is preserved in two portions not sharing a contact, one 27 mm long, comprising the proximal two-thirds of the element, and the other, 9 mm long, the distal part. The entire tibiotarsus was probably no more than 40 mm in length. Comparison with the tibiotarsi from Salta clearly indicates that both pieces pertain to a single element. The subrectangular proximal articular face is lengthened transversely (Fig. 1c). The head is expanded, and overhangs anteriorly. The long, low fibular crest extends well down the shaft (Fig. 1b): proximally it merges with the head, leaving a marked concavity just below

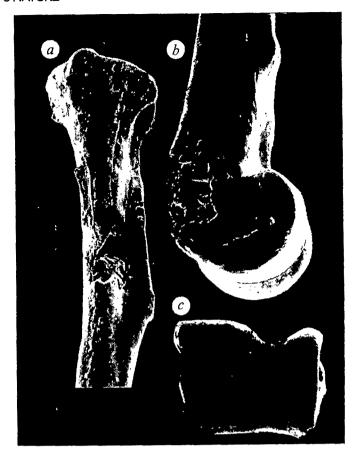


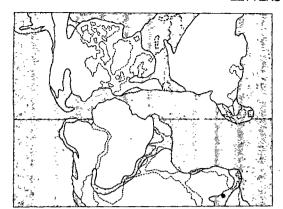
Fig. 2 The tibiotarsus of *Nanantius eos* (QM F12992). a, Proximal portion in anterior view; b, distal condyles in medial view; c, in distal view. Not to scale.

the head and anterior to the crest (Fig. 2a). A much lower crest lies on the anterior side of the shaft, presumably a part of the anterior cnemial crest (Fig. 1a). The lateral cnemial crest is absent (as in the Salta tibiotarsi).

A low crest lies at the medial edge of the anterior face of the shaft, just distal to the break (Fig. 1e). The distal portion of the tibia is fused to the astragalus, leaving no discernible joint (Fig. 2b). The long axis of the astragalar portion is nearly perpendicular to the long axis of the tibial shaft. The medial condyle is elongate and cylindrical in form, whilst the lateral condyle is narrower and with an articular surface formed like the basal part of a cone (Fig. 2c). The groove between the condyles is deeply V-shaped. The ascending process is broad and shallowly concave (Fig. 1f), with a low projection marking its apex. Breakage reveals that the shaft was hollow throughout, with thin walls (Fig. 1e).

The slender construction of the tibiotarsus may be related to the small size of this bone. However, the form of the medial condyle and distinctness of the astragalar ascending process may not be. The latter character is probably plesiomorphic for birds, in view of the evidence for their descent from small theropod dinosaurs, and hence to be expected in an early member of the class.

The unique and recognizable structure of the enantiornithine tibiotarsus clearly apparent here indicates reference of this tibiotarsus to the Enantiornithes. This tibiotarsus differs from the enantiornithine tibiotarsi from Salta in having a narrower and relatively longer anterior cnemial crest and an elongate, rather than approximately square, proximal articular face. The Salta tibiotarsi have medial condyles that constrict slightly towards their medial terminations, while that of Nanantius does not. Nanantius also shows the fibular crest extending proximal



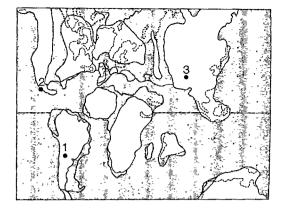


Fig. 3 Distribution of enantiornithines. Lower Cretaceous occurrences (left): Queensland, Nanantius. Upper Cretaceous occurrences (right): 1, Salta, Enantiornis and unnamed taxa; 2, Baja California, Alexornis; 3, Mongolia, Gobipteryx.

to the head and the astragalar ascending process, neither of which is apparent on the Salta material. The only preserved tibia of Gobipteryx minuta is very incomplete and from a hatching specimen11, and hence cannot be satisfactorily compared with that of Nanantius. Only the proximal portion of the tibiotarsus of Alexornis antecedens is preserved¹², and this agrees in both size and proportions with that of Nanantius. However, the proximal part of the shaft in Alexornis is straight, whilst in Nanantius it curves medially (as is found in the Salta tibiotarsi). As in Alexornis, the fibular crest extends all the way up the shaft to the head, and the anterior and posterior faces of the crest are concave in section. The proximal internal articular surface is swollen, as in Alexornis, but shows a distinct posterior overhang lacking in that genus. Both cnemial crests are found in Alexornis, but only the anterior in Nanantius. Thus, Nanantius eos can be distinguished from the other enantiornithines known from comparable material, and this, together with its greater age, lends confidence to the conjecture that it may also be distinct from Gobipteryx.

Enantiornithines are known from the Maastrichtian of Argentina (Enantiornis leali and four other as yet undescribed taxa¹), the Campanian of Mexico (Alexornis antecedens¹²), the Campanian of Mongolia (Gobipteryx minuta¹¹) and the Albian of Australia. The reported occurrence of enantiornithine birds on four continents (Fig. 3), and ranging from the late early Cretaceous throughout the late Cretaceous, indicates that these birds were probably more widespread in the late Mesozoic than has hitherto been recognized. In addition, it emphasizes the widespread distribution of birds as a whole in the Lower Cretaceous, and provides another example of a bird in this period.

This discovery also suggests a link between the Australian Cretaceous vertebrate fauna and that of South America. Such a link has been suggested previously from the occurrence of allosaurid dinosaurs^{13,14} and similar ceratodontid lungfish¹⁵ on the two continents.

Much assistance has been provided in the study of this specimen by Drs N. Fraser, K. Campbell, P. H. V. Rich and R. Wild, and especially by Mr C. A. Walker, through whose courtesy I was able to examine undescribed material from Salta, Argentina. Mrs M. Norrie and Mr S. M. Van Dyck assisted in the collection and development of this material. Financial support of field work was provided by the Australian Research Grants Scheme.

Received 27 March; accepted 16 May 1986.

- 1. Walker, C. A. Nature 292, 51-53 (1981).
- Martin, L. D. in Perspectives in Ornithology, 291-338 (Cambridge University Press, 1983).
- 3. Molnar, R. E. & Thulborn, R. A. Nature 288, 361-363 (1980)
- Talent, J. A., Duncan, P. M. & Handby, P. L. The Emu 66, 81-86 (1966).
- 5. Waldman, M. Condor 72, 377 (1970).
- 6. Rich, P. V. Proc. 16th int. orn. Congr. 53-65 (Australian Academy of Science, 1976).

- Elzanowski, A. Acta palaeont. pol. 28, 75-92 (1983).
 Galton, P. M. Palaeont. Z. 54, 331-342 (1980): Pls. 2M & 20.
 Padian K. Postilla 189, 1-44 (1983).
- 10. Senior, B. R., Mond, A. & Harrison, P. L. Bull. Bur. Miner. Resour. Geol. Geophys. Aust. 167, 1-102 (1978).
- 11. Elzanowski, A. Nature 264, 51-53 (1976): Palaeont, pol 42, 147-179 (1981).
- Brodkovski, A. Naline 204, 51-35 (1767); Function poi 42, 141-177 (1971).
 Brodkovi, P. Smithson. Contr. Paleobiol. 27, 67-83 (1976).
 Molnar, R. E., Flannery, T. F. & Rich, T. H. Alcheringa 5, 141-146 (1981); J. Paleont. 69, 1513-1515 (1985).
- 14. Bonaparte, J. F. Science 205, 1377-1379 (1979).
- 15. Kemp, A. & Molnar, R. E. J. Paleont. 55, 211-217 (1981).

Oxytocin induces morphological plasticity in the adult hypothalamo-neurohypophysial system

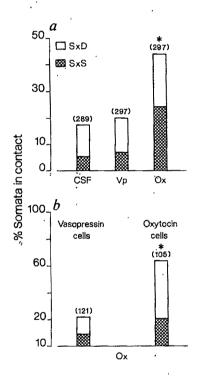
Dionysia T. Theodosis, Catherine Montagnese, Floreal Rodriguez, Jean-Didier Vincent & Dominique A. Poulain

INSERM, U176, Unité de Recherches de Neurobiologie des Comportements, Rue Camille St Saëns, Bordeaux, F33077 Cedex, France

The hypothalamo-neurohypophysial system offers a unique example in the adult mammalian central nervous system (CNS) of a functional and structural plasticity related to a physiological state. During lactation, oxytocin neurones evolve a synchronized electrical activation which permits pulsatile hormone release at milk ejection1. At the same time, in the supraoptic (SON) and paraventricular nuclei, glial coverage of neurones diminishes, so that large portions of their surface membrane become directly juxtaposed; synaptic remodelling also associates pairs of neurones through the formation of common presynaptic terminals²⁻⁵. These structural changes, reversible after weaning4, affect exclusively oxytocinergic neurones⁵ and could facilitate their synchronized electrical activity. As several observations suggest that oxytocin itself is released centrally6-8, we have examined the effect of prolonged intracerebroventricular infusions of oxytocin on the structure of the SON of non-lactating animals. We report here that the peptide indeed engenders the structural reorganization characteristic of the oxytocin system when it is physiologically activated. Similar infusion of vasopressin has no effect. Our observations thus demonstrate that a central neuropeptide can induce anatomical changes in the adult CNS, and suggest that oxytocin can regulate its own release by contributing to the dramatic restructuring of the nuclei containing the neurones responsible for its secretion.

Our experiments were performed on primiparous Wistar rats from our colony 1 month after weaning their first litter. The

Fig. 1 Electron micrographs of oxytocinergic neurones in the supraoptic nucleus (SON) of rats given an intracerebroventricular infusion of oxytocin for 8 days. In a, the surface membranes of two soma profiles are seen to be in extensive apposition, that is, they are not separated by any neuropile or glial element (small arrows). Only a portion of the 15-µm-long apposition is shown in this micrograph. The oxytocinergic nature of the somata is revealed by colloidal gold particles (10 nm) over their secretory granules (see also insets), after immunostaining with a rabbit anti-oxytocin serum and immunoglobulin-coupled colloidal gold. In b, a presynaptic terminal (asterisk) synapses (between arrowheads) onto two adjacent soma profiles that are also juxtaposed (ap, attachment plaque bridging the apposed surface membranes). Colloidal gold particles (5 nm) over secretory granules in their cytoplasm identify the somata as oxytocinergic (see also inset). Scale bars, 0.5 µm; insets, 0.1 µm.



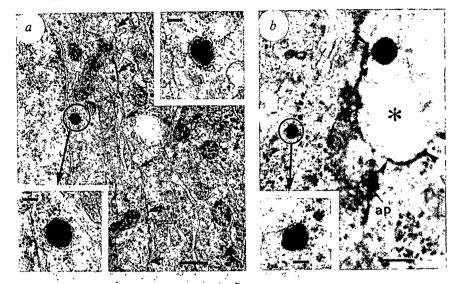


Fig. 2 a, Percentage of neurosecretory soma profiles showing neuronal appositions in the SON of rats after chronic (8 days) intracerebroventricular infusion of artificial cerebrospinal fluid (CSF), vasopressin (Vp) or oxytocin (Ox). This analysis was carried out without immunocytochemical identification of the neurones. Following infusion of oxytocin, nearly half of all the observed neurosecretory soma profiles were directly apposed to adjacent somata (S×S) or dendrites (S×D). b, Percentage of oxytocinergic and putative vasopressinergic soma profiles, identified immunocytochemically using anti-oxytocin serum, involved in S×S and S×D contacts in the SON of rats given intracerebroventricular infusions of oxytocin. In both histograms, numbers in parentheses represent the total number of soma profiles examined in each group. * P < 0.001, χ^2 analysis on raw data.

Methods. Two different quantitative analyses were carried out by two separate investigators, unaware of the experimental conditions. In the first (a), the analysis was performed on electron micrographs of neurosecretory soma profiles selected by a random sampling procedure (for further details see ref. 2); for each group, each composed of 5 animals, 128 micrographs were examined. In the second analysis (b), counting was performed directly at the electron microscope. In order to examine in detail larger areas of tissue surrounding each neurosecretory soma profile, all tissue falling within the whole surface of randomly chosen grid squares covering the whole frontal span of the SON was examined⁵. Four sections, each cut from different anterior-posterior levels of the SON of each of four animals that had been infused with oxytocin, were examined; the sections had been immunostained with a rabbit anti-oxytocin serum (preabsorbed with vasopressin adsorbed to CNBr-activated Sephadex beads) and immunoglobulin-coupled colloidal gold (a postembedding immunocytochemical procedure described fully elsewhere⁵). The same parameters were noted in each analysis: (1) total number of neurosecretory soma profiles; in the case of the immunostained SON, the peptide content of the somata was also noted (see Fig. 1); (2) number of soma profiles in juxtaposition to an adjacent soma or dendritic profile; (3) number of dendritic contacts per soma profile; and (4) number of 'double' synapses making contact with two neurosecretory soma or dendritic profiles simultaneously.

animals were deeply anaesthetized with sodium pentobarbital (50 mg per kg), and a cannula, connected to an Alzed miniosmotic pump (Scientific Marketing), delivering fluid at a rate of 0.5 µl h⁻¹, was inserted stereotaxically into the third ventricle. The pump was then left under the skin of the back at the level of the shoulders. The pumps contained synthetic oxytocin or vasopressin (Peninsula, 2 µg ml⁻¹ dissolved in artificial cerebrospinal fluid (CSF)), or artificial CSF alone. Eight days later, the animals were anaesthetized and perfused intracardially with heparinized saline followed by fixative (4% paraformaldehyde and 2.5% glutaraldehyde in 0.1 M sodium phosphate buffer). The brains were removed and 100-µm coronal slices were cut on a vibratome. The position of the cannula was verified on these sections. Each pump was emptied and the remaining fluid volume measured. The concentration of oxytocin and vasopressin remaining at the end of each infusion was measured by radioimmunoassay9. The biological activity of the remaining oxytocin was also tested by its potency to induce an increase in intrammamary pressure in mammary glands of lactating rats. Once it was ascertained that the cannula had been correctly

placed, and that the pumps had functioned properly, blocks containing the SON were dissected from the vibratome slices and processed further for electron microscopy (see ref. 5).

In the SON of animals infused with artificial CSF or vasopressin, as in nuclei from unstimulated animals (hydrated male^{2,10,11}, virgin female^{2,4} or post-weaned rats⁴), most neurosecretory soma profiles were separated from other neuronal profiles by glial or neuropile elements. On the other hand, in the SON of rats infused with oxytocin, glial coverage diminished markedly and close to 45% of all neurosecretory soma profiles were directly juxtaposed to adjacent soma or dendritic profiles (Figs. 1a, 2a). Moreover, the number of neuronal contacts more than doubled in this group, from 0.2 to 0.7 soma or dendritic contacts per soma profile. Concurrently, many of the same neurones (13%) were bridged by the same presynaptic terminal ('double' synapses; Fig. 1b), a type of synapse rarely seen in the nuclei of untreated animals $(<5\%^{2-4,11})$ or of animals infused with vasopressin or CSF (6%). In order to identify the neurones, a separate analysis was carried out on sections of the SON that had been immunostained for

oxytocin (Fig. 1a,b), using a post-embedding immunocytochemical procedure described in detail elsewhere⁵. This revealed that most of the soma profiles showing surface membrane appositions and sharing the same synapse after oxytocin infusion were oxytocinergic (Figs 1, 2b).

Our experiments demonstrate that a sustained elevated level of oxytocin in the third ventricle leads to morphological changes in the SON which are identical in nature and extent to those that occur under physiological^{2,4,5,11} or experimental^{10,11} conditions when the oxytocinergic system is activated. Our observations strongly suggest, therefore, that oxytocin does indeed take part in the restructuring of the hypothalamo-neurohypophysial system. Moreover, since infusion of the structurally similar neuropeptide vasopressin had no effect, it seems that oxytocin is specifically responsible for the anatomical changes.

Under normal conditions, oxytocin is present in the CSF¹² but its origin remains unclear. It may be released from oxytocincontaining neurones located in many areas of the CNS¹³. In particular, recent observations have described a local, calciumdependent release of this peptide from the magnocellular nuclei^{6,7}, and oxytocinergic terminals that are in contact with oxytocin cell bodies and dendrites have been noted in the SON8. Unlike the blood-brain interface, there is no barrier to the diffusion of oxytocin between the third ventricle and neighbouring cerebral structures¹². Our intracerebroventricular infusions of oxytocin would thus mimic an enhanced central release of oxytocin. The question then arises as to how a centrally circulating neuropeptide can induce anatomical changes in a particular

region of the CNS. Central oxytocin has been shown to increase the electrical activity of oxytocin neurones¹⁴ and the anatomical changes could be a consequence of such an activation. This possibility is supported by the observation that restructuring of the nuclei occurs under other situations, such as parturition³ and chronic dehydration^{10,11}, which also enhance the overall activity of oxytocinergic neurones¹. It is also possible, however, that oxytocin itself is the signal, acting on the surface membranes of oxytocin neurones, their synapses, or surrounding glia by an unknown mechanism.

The anti-oxytocin serum was generously provided by Dr A. Burlet. We also thank Mme A. Bonhomme for technical assistance and Mr S. Senon for photographic work.

Received 14 April; accepted 12 June 1986.

- 1. Poulain, D. A. & Wakerley, J. B. Neuroscience 7, 773-808 (1982).
- Theodosis, D. T., Poulain, D. A. & Vincent, J. D. Neuroscience 6, 919-929 (1981). Hatton, G. I. & Tweedle, C. D. Brain Res. Bull. 8, 197-204 (1982).
- Theodosis, D. T. & Poulain, D. A. Neuroscience 11, 183-193 (1984).
 Theodosis, D. T., Chapman, D. B., Montagnese, C., Poulain, D. A. & Morris, J. F., Neuroscience 17, 661-678 (1986).
 Moos, F. et al. J. Endocr. 102, 63-72 (1984).
- Mason, W. T., Hatton, G. I., Ho, Y. W., Chapman, C. & Robinson, I. C. A. F. Neuroendo-crinology 42, 311-322 (1986).
- 8. Theodosis, D. T. Nature 313, 682-684 (1985).
- Cazalis, M., Dayanithi, G. & Nordman, J. J. J. Physiol., Lond. 369, 45-60 (1985).
 Tweedle, C. D. & Hatton, G. I. Brain Res. 309, 373-376 (1984).
- Chapman, D. B., Theodosis, D. T., Montagnese, C., Poulain, D. A. & Morris, J. F. Neuroscience 17, 679-686 (1986).
- 12. Robinson, I. C. A. F. Prog. Brain Res. 60, 129-145 (1983).

 13. Softoniew, M. V. in Handbook Chemical Neuroanatomy Vol. 4, Pt 1 (eds Bjorklund, A. & Hokfelt, T.) 93-165 (Elsevier, Amsterdam, 1985).
 14. Freund-Mercier, M. J. & Richard, P. J. Physiol., Lond. 352, 447-466 (1984).

Serine esterase in cytolytic T lymphocytes

Mark S. Pasternack*†‡, C. Reynold Verret*, Margaret A. Liu*† & Herman N. Eisen*

* Center for Cancer Research and Department of Biology, Massachusetts Institute of Technology, Cambridge, Massachusetts 02139, USA

Children's and ‡ Medical Services, Massachusetts General Hospital, Boston, Massachusetts 02114, USA and Departments of Medicine and Pediatrics, Harvard Medical School, Boston, Massachusetts 02115, USA

The mechanisms that enable cytotoxic T lymphocytes (Tc cells) to destroy target cells are only vaguely understood. However, recent studies have identified in T_c cells¹ and natural killer cells² cytoplasmic granules that contain perforin, a cytolytic protein that resembles the ninth component of complement (C9)3. Antigenspecific lysis of target cells, traditionally ascribed solely to T_c cells, has now also been demonstrated in some T-helper cell (Th cell) lines, referred to here as T helper-killer or T_{h/c} cells⁴⁻⁶. We recently found a novel serine esterase that is present at greatly elevated levels in cloned murine Tc cell lines and one Th/c cell line, but not in two non-cytolytic Th cell lines7. These findings suggest that the serine esterase is involved in cytolytic activity and that a variety of effector cells share a common cytolytic mechanism. To explore the role of the serine esterase in this process, we have been studying additional properties of the enzyme in murine T cells. We show here that (1) it is a membrane-associated, disulphidelinked dimer, (2) it has trypsin-like properties but is not a general protease, (3) in density gradient centrifugation it sediments with perforin, (4) it is secreted by Tc cells during their cytolytic attack on target cells, and (5) antiserum to Tc-cell serine esterase reacts with the enzyme in $T_{h/c}$ cells.

The serine esterase was isolated from T_c clone G4 cells as described in Fig. 1 legend, and the isolated protein was analysed by SDS-polyacrylamide gel electrophoresis (PAGE) under reducing and nonreducing conditions. Under both conditions the same complex was observed, but their apparent relative molecular mass (M_r) differed by a factor of about two (31,000-34,000 reduced and 55,000-60,000 nonreduced). Exactly the same difference in M_r was seen under these conditions when the enzyme was visualized by subjecting unfractionated cell lysates to affinity labelling with ³H-diisopropylphosphofluoridate (3H-DFP)7 and autoradiography (data not shown). It appears, therefore, that the enzyme is a disulphide-linked dimer. Whether its evident microheterogeneity reflects variable glycosylation or the presence of a few distinct but related ³H-DFPreactive serine esterases is not clear.

To determine whether all of the disulphide-linked subunits have DFP-reactive sites, the enzyme was examined under reducing conditions by two-dimensional PAGE (using non-equilibrium pH gradient electrophoresis (NEPHGE) in the first dimension)^{8,9}, visualizing the protein in some gels by silver stain¹⁰ (Fig. 1c) and in others by affinity labelling with ³H-DFP (Fig. 1d). In both cases, the appearance of the reduced protein was the same: a predominant component of $M_r \sim 31,000$ located close to the basic edge of the pH gradient with some heterogeneity evident in the form of a trail of slightly less basic protein of slightly higher M_r (32,000-34,000) (Fig. 1c, d). A single component, like that of Fig. 1c and d, was also seen following very brief NEPHGE electrophoresis (800 Vh. data not shown), indicating that another, more basic subunit had not been overlooked. Because the appearance of the reduced and nonreduced enzyme was the same when visualized by silver stain and ³H-DFP, both subunits in each dimer must be labelled by DFP, and have the same or very similar net positive charge; they are thus very similar and possibly identical.

To facilitate comparison of serine esterase in diverse clones of cytotoxic cells, rabbit antisera were raised against the purified enzyme (Fig. 1). The antisera immunoprecipitated only one ³Hlabelled component from ³H-DFP-treated lysates of G4 cells (data not shown) and they also reacted with the unlabelled lysates of cytolytic T cells by Western blotting (Fig. 2). In both assays the reactive material evidently corresponded to the serine esterase, as it was indistinguishable in M_r and appearance from the ³H-DFP affinity-labelled and silver-stained enzyme seen in Fig. 1 a, Purification of serine esterase from a clone of T_c cells, monitored by enzyme activity (absorbance at 412 nm) and by SDS-PAGE (insert), using silver impregnation to visualize protein. Insert: Lane A, the eluate from a lentil-lectin column (see Methods below) loaded on the lysine-Sepharose column; B-N, fractions from the lysine-Sepharose column; B, fraction 4; C, fraction 7; D, fraction 10; E, fraction 13; F, fraction 16; G, fraction 19; H, fraction 22; I, fraction 25; J, fraction 28; K, fraction 31; L, fraction 34; M, fraction 37; N, fraction 40; O, M, markers (×10⁻³). b-d, Some physical properties of the T-cell serine esterase. b, SDS-PAGE of purified esterase (pooled fractions 25-40, a) stained by silver impregnation. M, M, markers (top to bottom ×10⁻³): 90, 67, 45, 31 and 17. NR, nonreduced; R, reduced. c, Two-dimensional electrophoresis under reducing conditions of 5 μ g of purified serine esterase. The first dimension was non-equilibrium pH gradient electrophoresis (NEPHGE) and the second dimension was SDS-PAGE; protein was visualized by silver impregnation. d, Two-dimensional electrophoresis as in c of an Nonidet P-40 (NP40) extract of T_c cells (clone G4) labelled with 3 H-DFP. The DFP-rective protein was visualized by autoradiography of the slab gel.

Methods. $a_1 = 2 \times 10^9$ cells of T_c clone G4 (BALB.B anti-D^d, ref. 19) were suspended in lysis buffer (135 mM NaCl, 10 mM HEPES pH7.4, 3.5 mM MgCl₂) at ~10⁸ cells ml⁻¹ and disrupted by nitrogen cavitation (300 p.s.i. 15 min, 4 °C). Nuclei and whole cells were pelleted by centrifugation at 300g, 5 min. A wash of the pellet with lysis buffer was added to the post-nuclear supernatant, which was centrifuged at 100,000g for 1 h at 4 °C. The resulting supernatant (which had <1% of the initial esterase activity) was discarded and the pelleted membranes were suspended in 150 mM NaCl, 10 mM Na phosphate pH 7.4, 0.5% NP40 and 0.02% NaN3 (PBS/NP40) and loaded onto a lentil-lectin Sepharose column (Pharmacia) equilibrated in PBS/NP40 and washed with additional buffer. Approximately 60% of the activity was not retained and treatment of the pass-through with ³H-DFP revealed a single sharply defined band of M_r 31,000 on SDS-PAGE (not shown). The remaining 40% of estaerase activity, retained on the lentil-lectin column, was recovered by elution with 0.5 M α -methyl mannoside (α -MM) in PBS/NP40. After dialysing this eluate against 15 mM Tris-HCl pH 8.1, 0.02% NaN3, it was loaded (a, insert) onto a 5-ml lysyl-Sepharose column (Pharmacia) previously equilibrated with 15 mM Tris-HCl pH 8.1, 0.5% NP40, 0.02% NaN3 (TNA) and washed with this buffer. The column was monitored by assaying 1 µl of each fraction (~1.0 ml) for esterase activity, using benzyloxycarbonyl lysyl thioester (BLT) (Calbiochem) as described previously⁷. No esterase activity was detected in the pass-through. A NaCl gradient (0-500 mM in TNA) eluted the activity as a single peak, as shown, with the peak height at about 250 mM NaCl. For some preparations the column was equilibrated and washed with 1% octylglucoside in 15 mM Tris-HCl pH 8.1, before applying the NaCl gradient. Aliquots (20 µl) of fractions from the lysyl-Sepharose column were analysed under reducing conditions by electrophoresis in a 10% acrylamide gel in the presence of 0.1% SDS²⁰. After fixation of the slab gel in 50% methanol-10% acetic acid, the proteins were visualized by silver impregnation 25-40 were pooled. The serine esterase activity in the pool usually represented ~20% of the total initial activity and ~70% of the activity added to the lysine-Sepharose column. b, Purified esterase (~2.5 µg) was heated to 100 °C for 3 min in sample buffer not containing (NR) or containing (R) 5% 2-mercaptoethanol and analysed by electrophoresis in a 10% polyacrylamide gel in the presence of 0.1% SDS²⁰. Silver impregnation was performed as described elsewhere ¹⁰. c, Purified esterase (~5 µg) was dissolved in 25 µl of isoelectric focusing sample buffer containing 5% 2-mercaptoethanol, applied to a 4% polyacrylamide gel (2.5 mm × 12.5 mm) and electrophoresed under non-equilibrium conditions^{8,9} for 1,400 Vh. The gel was get (2.5 mm) and electrophoresed under non-equinorium conditions for 1,400 vn. The get was incubated with SDS sample buffer containing 5% 2-mercaptoethanol and layered on a 10% polyacrylamide slab gel and run in the presence of 0.1% SDS²⁰. Silver impregnation was performed as described elsewhere of d. An extract of 3×10° G4 cells in PBS containing 0.5% NP40 was treated with 10⁻⁵ M³H-DFP for 30 min at 37 °C and prepared for electrophoresis as described elsewhere. NEPHGE (1,300 Vh) and SDS-PAGE were performed as for b. The gel was impregnated with Autofluor (National Diagnostics, Somerville, New Jersey), dried and exposed for 8 days at -70 °C using XAR-5 film (Eastman Kodak).

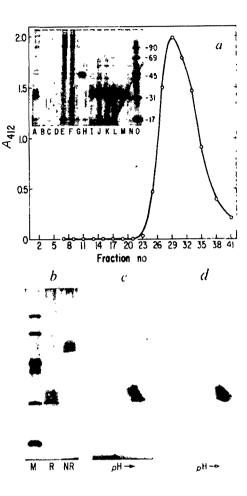




Fig. 2 Western blot analysis of cloned T_c , T_h and $T_{h/c}$ cell lines. Lane 1, purified scrine esterase (Fig. 1); lane 2, T_h cells (clone TDH-1); lane 3, $T_{h/c}$ cells (clone 5.5); lane 4, T_h cells (clone D10), lane 5, T_c cells (clone 2C); lane 6, normal thymocytes; lane 7, Con-A-activated thymocytes, lane 8, T_c cells (clone G4). M_r markers at the left are bovine serum albumin (67,000), ovalbumin (45,000), carbonic anhydrase (31,000).

Methods. Antiserum to the serine esterase was raised by injecting rabbits with $\sim 100 \,\mu g$ of purified enzyme (Fig. 1) in complete Freund's adjuvant and boosting them twice at 1-2-month intervals with the same amount of the enzyme in incomplete adjuvant. Cell extracts were prepared by washing cells several times in PBS and incubating them in 0.5% PBS/NP40 at 0 °C for 30 min with frequent vortexing. SDS was added to 0.1% and incubation was continued for another 15 min. After centrifuging the lysates at 8,000g for 10 min, supernatants (1-4 × 10⁶ cell-equivalents) were subjected to electrophoreis in SDS-10% polyacrylamide gels. Proteins were transferred electrophoretically from gels to nitrocellulose or Zeta-bind filters (A.M.F. Cuno) and, to reduce nonspecific binding in subsequent steps, the filters were incubated (1 h, room temperature) in 5% low-fat milk (Carnation) in PBS or in a 1:5 dilution of fetal calf serum in TBS (155 mM NaCl, 10 mM Tris-Cl pH 7.5) (TBS-FCS). The filters were then incubated for at least 3 h in anti-serine esterase antiserum diluted 250-fold in PBS-low fat milk or TBS-FCS, washed copiously with 0.05% Tween 80 in TBS, and finally treated sequentially with biotinylated anti-rabbit globulin and an avidin complex with biotinylated horseradish peroxidase, as described previously21 was developed with 4-chloro-1-naphthol and hydrogen peroxide as described elsewhere21. Clone TDH-1 is an L3T4⁺, 2,4,6 trinitrophenyl + H-2^d-specific clone of BALB/c origin; clone 5.5 is an L3T4+, ovalbumin+I-Ed-specific clone of BALB/c origin4; D10 is a conalbumin +1-specific clone of AKR origin⁵; clone 2C is BALB.B anti-L^{d'} (ref. 22); activated thymocytes were generated as described previously^{7,11}; G4 is described in Fig. 1 legend.

other gels (Fig. 1 and ref. 7). The Western blots (Fig. 2) showed the enzyme to be present at a high level in three cytolytic cell lines (two T_c and one $T_{h/c}$ cell line: 2C, G4 and 5.5, respectively) but to be undetectable in two non-cytolytic (T_h) cell lines (TDH-1 and D10). The antisera also detected the esterase in Western blots of murine thymocytes, providing these cells had been previously stimulated for 4 days in culture by concanavalin A (Con-A, Fig. 2, lanes 6, 7); these conditions induce the

expression of both cytotoxic¹¹ and serine esterase activity⁷. The antiserum to the enzyme from the T_c G4 cells reacted with enzyme in all of the other T_c clones tested and also in a $T_{h/c}$ -cell line. The slight variations in M_r values in different T-cell lines, and in the Con-A-activated thymocytes, suggest that there may be several related T-cell serine esterases or that a single enzyme is modified differently (for example, by glycosylation) in different T-cell lines.

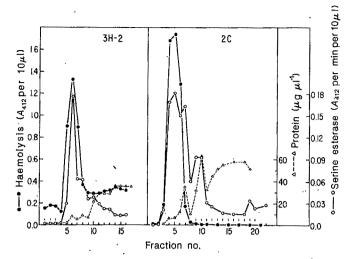


Fig. 3 Percoll-gradient fractionation of two cloned T_o-cell lines. a, Clone 3H2; b, clone 2C.

Methods. 5×108 3H2 cells (BALB.B anti-Dd, Lyt-2+, ree ref. 23) and 2.5×108 2C (ref. 22) cells were washed twice in Hank's balanced salt solution and once in 'relaxation' buffer (100 mM KCl, 3 mM NaCl, 3.5 mM MgCl₂, 1.25 mM EGTA, 1 mM ATP, 10 mM PIPES pH 6.8)²⁴. The cells were resuspended in relaxation buffer and lysed by nitrogen cavitation at 350 p.s.i. for 30 min. Nuclei and debris were removed by centrifugation at ~1,000 g for 5 min, and the supernatant was applied to a discontinuous gradient of Percoll in relaxation buffer (4 ml 90% Percoll, 2 ml 60%, 3.5 ml 39%) and subjected to centrifugation at 20,000 r.p.m. in a Beckman SW27 rotor for 30 min. Fractions containing ~0.8 ml were collected from the bottom of the tube with a peristaltic pump. Assay for haemolytic activity: The assay is a modification of Masson and Tschopp's procedure¹². Sheep erythrocytes were washed in HEPES buffered saline (HBS: 155 mM NaCl, 10 mM HEPES pH 7.3) and suspended at ~3×108 cells ml-1 in HBS containing 5 mM CaCl₂. Diluted or undiluted fractions (10 µl) were added to 100 µl of a sheep erythrocyte suspension. After 15 min at 37 °C, 1 ml of PBS containing 1 mM EGTA was added and the mixture was centrifuged at 1,500g for 5 min. Haemoglobin released in the supernatant was determined from the absorbance at 412 nM. Esterase activity was determined from plots of A_{412} against time. Protein was quantitated with the BCA protein assay reagent (Pierce) using bovine serum albumin standard. Percoll was removed after colour development by centrifugation at 8,000g for 5 min. Background due to Percoll and relaxation buffer was negligible.

All nine T_c cell lines tested showed markedly elevated enzyme levels: for example, $50\text{--}200\,\mathrm{U}$ per 10^6 cells⁷, corresponding at the upper limit to 1 μg trypsin-equivalents per 10^6 cells⁷. The enzyme level was also elevated in two $T_{h/c}$ -cell lines (clones 5.5 and 18) but not in four non-cytolytic T_h -cell lines (O_3 , O_5 (ref. 7), D10 and TDH-1). Although the presence of elevated serine esterase thus seems to correlate with cytolytic activity, many more murine T-cell lines, especially T_h and $T_{h/c}$ lines, will have to be examined to determine how consistently the correlation holds up.

The cytolytic protein perforin has been identified in cytoplasmic granules of human and mouse natural killer cells and mouse T_c -cell lines^{1,2}. By virtue of their high density, the granules can be separated from other cell lysate components and their isolation can be monitored by their lysis of sheep red blood cells. As Fig. 3 shows, the haemolytic and serine esterase activities sedimented together in T_c -cell lysates in dense fractions near the bottom of the Percoll gradient. This apparent association of the serine esterase with the cytolytic granules is supported by a recent analysis of M_r values of the reduced and nonreduced proteins isolated from the dense granules of a murine T_c -cell line¹² (compare our Fig. 1b with Fig. 2c in ref. 12) and by our unpublished observations that the ³H-DFP affinity-labelled pro-

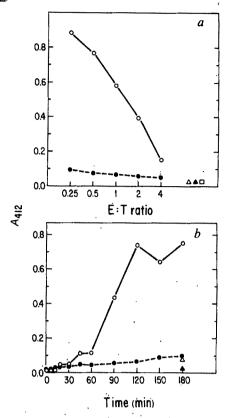


Fig. 4 Serine esterase secretion is triggered by cytolytic attack of T_c cells on specific target cells. a, Influence of the ratio of effector (T_c) cells to target cells (E:T ratio). b, Time course of serine esterase secretion. \bigcirc , Cells of T_c clone G4 (anti- D^d) incubated with P815 $(H-2^d)$ target cells; \blacksquare , G4 cells incubated EL-4 $(H-2^b)$ cells; \triangle , G4 cells incubated alone; \square , EL4 incubated alone.

Methods. G4 cells¹⁹ were collected, washed, resuspended at 5×10^5 cells ml⁻¹ in complete medium containing 20 U ml⁻¹ recombinant interleukin-2 and distributed into flat-bottomed microtitre wells (Costar 3596) at 105 cells per well. G4 cells readily attached to the plastic surface. After overnight incubation, the wells were gently aspirated and filled with cold KB1 medium (complete medium supplemented with bovine serum albumin (Boehringer Mannheim) at 1 mg ml⁻¹ in place of fetal calf serum). After several minutes on ice, the wells were aspirated again and to them were added (in triplicate) 100 µl medium alone or 100 µl medium containing varying numbers of P815 or EL-4 cells which had been washed two or three times in KBI medium and resuspended in KB1 at the designated concentration. The plates were incubated at 37,°C for 3 h in a or for the time noted in b. Samples (50 µl) were removed from replicate wells and pooled. Esterase activity in 10 µl of the pooled supernatants was measured as described elsewhere⁷. In a, E:T ratios were based on the nominal number of T_c cells seeded before the assay. Recovery experiments showed that no cell proliferation had occurred during overnight culture (data not shown). In b, the E:T ratio was held constant at 0.5 and plates were centrifuged briefly (500 r.p.m., 45 s) at 4 °C before initiation of the 37 °C incubation. The use of adherent T_c cells facilitated the detection and measurement of secreted esterase.

tein is present in the dense fractions that possess haemolytic activity (Fig. 3). Taken together, these findings strongly suggest that in murine T_c cells the serine esterase is present in the dense cytotoxic granules that contain perforin.

The serine esterase was previously shown⁷ to be blocked by DFP and phenylmethylsulphonyl fluoride, typical inhibitors of serine proteases. It is also blocked by aprotinin (data not shown), another typical inhibitor of trypsin-like serine proteases. However, the serine esterase did not cleave ¹²⁵I-casein (data not shown), suggesting that it may have restricted proteolytic specificity, as is characteristic of regulatory proteases¹³ (for

example, in some of the sequentially acting components of the complement 'cascade'). Whether the substrate for the serine esterase is perforin, or another component of the perforincontaining granules, or perhaps a surface protein of Tc or target cells remains to be be determined.

T_c cells normally lyse only cells whose surface antigens they recognize, not neighbouring cells that lack these antigens, suggesting that target cell lysis by T_c cells is not due to secretion of a diffusible cytotoxic molecule. However, when clone G4 cells were incubated with target cells, serine esterase activity appeared in the extracellular medium (Fig. 4). The enzyme released during lysis of the target cells remained in the supernatant after low-speed centrifugation (300 g, 5 min), sufficient to sediment intact cells, but was almost entirely (95%) sedimented following centrifugation at 100,000 g for 1 h. Under the latter conditions the purified enzyme (Fig. 1) is not sedimented, and thus the released enzyme was probably still largely associated with granule membranes or with another granule component, perhaps a proteoglycan^{14,15}. Enzyme release clearly accompanied the cytolytic attack on H-2d antigen-bearing target cells (P815), since it was not observed (Fig. 4) in various controls, for example, G4 cells alone or G4 cells incubated with cells possessing the wrong H-2 haplotype (EL-4 cells, H-2^b).

The amount of enzyme secreted varied with the ratio of effector (T_c) cells to target cells (E:T ratio). With an excess of target cells (low E:T ratio) the amount secreted was high, probably because under these conditions almost every T_c cell was likely to be interacting with a target cell; with a scarcity of target cells (high E:T ratios) the amount secreted was low, probably because under these conditions many Tc cells were not engaged with target cells (Fig. 4a).

The time course of secretion is shown in Fig. 4b. About twothirds of the amount present initially in the T_c cells was released. Whether enzyme biosynthesis keeps pace with secretion, or whether secretion results in sufficient depletion to reduce cytolytic activity ('killer cell exhaustion') are among the many issues that remain to be investigated. Target cell-triggered secretion of γ -interferon¹⁶ and interleukin-2 (ref. 17) from T_c cells has been observed previously. Comparison of the slow rate of secretion of γ -interferon¹⁸ with the far more rapid rate for the serine esterase suggests that the encounter of T_c with target cells induces the T_c cells to synthesize and then secrete γ interferon, whereas the same stimulus triggers the T_c cells to release their preformed serine esterase, contained in the cytolytic granules. Thus, in addition to their cytolytic effects the release of this enzyme and perhaps additional granule components by T_c and T_{h/c} cells might contribute to the slowly evolving local tissue injury known as delayed-type hypersensitivity.

We thank the following for providing cloned T-cell lines that have not yet been described in publications: David M. Kranz for T_{h/c} clone 18, Edward B. Reilly for T_c clone 3H2, and George Sigal for T_h clone TDH-1. We also thank Charles Janeway and John Tite for $T_{h/c}$ clone 5.5 and T_h clone D10, Robert D. Rosenberg and James Marcum for valuable discussions and purified casein, and Ann Hicks for preparation of this manuscript. This work was supported by research grants (CA-15472 and CA-28900) and a Cancer Center Core Grant (CA-14051) from the National Cancer Institute, NIH. C.R.V. is the recipient of a Massachusetts Institute of Technology Minority Fellowship Award and M.A.L. is the recipient of a Physician-Scientist Award frim the NIH.

Received 4 February; accepted 22 May 1986.

7. Pasternack, M. S. & Eisen, H. N. Nature 314, 743-745 (1985).
8. O'Farrell, P. Z., Goodman, H. M. & O'Farrell, P. H. Cell 12, 1133-1142 (1977).

Jones, P. P. in Selected Methods in Cellular Immunology (eds Mishell, B B. & Shiigi, S. M.) 398-440 (Freeman, San Francisco, 1980).

10. Morrissey, J. H. Analyt. Biochem. 117, 307-310 (1981).

Irle, C., Piquet, P. F. & Vassalli, P. J. exp. Med. 148, 32-45 (1978).
 Masson, D. & Tschopp, J. J. biol. Chem. 260, 9069-9072 (1985).

Neurath, H. Fedn Proc. 44, 2907-2913 (1985).
 Schmidt, R. E. et al. Nature 318, 289-291 (1985).

- MacDermott, R. P. et al. J. exp. Med. 162, 1771-1787 (1985).
 Klein, J. R., Raulet, D. H., Pasternack, M. S. & Bevan, M. J. J. exp. Med. 155, 1198-1203
- Andrus, L., Granelli-Piperno, A. A. & Reich, E. J. exp. Med. 159, 647-652 (1984).
 Klein, J. R., Pasternack, M. S. & Bevan, M. J. Immun. 134, 2456-2461 (1985).
- Pasternack, M. S., Sitkovsky, M. V. & Eisen, H. N. J. Immun. 131, 2477-2483 (1983).
 Laemmli, U. K. Nature new Biol. 227, 680-684 (1970).

- Huynh, T. V., Young, R. A. & Davis, R. W. in DNA Cloning Techniques: A Practical Approach (ed. Glover, D.) 49-78 (IRL Press, Oxford, 1985).
 Kranz, D. M., Sherman, D. H., Sitkovsky, M. V., Pasternack, M. S. & Eisen, H. N. Proc. natn. Acad. Sci. U.S.A. 81, 573-577 (1984).
- Reilly, E. B., Kranz, D. M., Tonegawa, S. & Eisen, H. N. Nature 321, 878-880 (1986).
 Borregaard, N., Heiple, J. M., Simons, E. R. & Clarke, R. A. J. Cell Biol 97, 52-61 (1983).

Interferon response sequence potentiates activity of an enhancer in the promoter region of a mouse H-2 gene

Alain Israel, Akinori Kimura, Agnès Fournier*, Marc Fellous* & Philippe Kourilsky

Unité de Biologie Moléculaire du Gène, U277 INSERM, UA 535 CNRS and * Unité d'Immunogénétique Humaine, U276 INSERM, Institut Pasteur, 25 rue du Dr Roux, 75724 Paris Cedex 15, France

The expression of class I transplantation antigens encoded in the major histocompatibility complex (H-2 in mouse, HLA in man) can be induced by α -, β - and γ -interferons¹⁻⁵. Both transcriptional and post-transcriptional mechanisms have been postulated. Recently, a common sequence has been found in the promoter region of several human genes responsive to IFN- α (ref. 6). The promoters of $H-2K^b$ and several other mouse class I genes contain a similar interferon response sequence⁷. We show here, in a transient assay, that the $H-2K^b$ promoter can be induced by all three types of interferon and that the interferon response sequence is necessary for induction to occur. However, the response sequence is active only when associated with a functional enhancer sequence which we have recently identified in the promoter of $H-2K^b$ and other class I genes⁷. The combination of these two sequences can render a heterologous promoter responsive to interferon, irrespective of its orientation relative to the cap site.

We have previously noted the presence of an interferon response sequence (IRS) in the promoter of several H-2 class I genes⁷. In $H-2K^b$ and $H-2L^d$, the IRS overlaps with an enhancer⁷. To establish the role of IRS in the stimulation of class I gene expression by interferon (IFN), we have used a hybrid gene in which the bacterial chloramphenicol acetyltransferase (CAT) gene is fused to the $H-2K^b$ promoter⁸. This construct, called pH2CAT, has been transfected into mouse 3T6 cells. At 16-18 hours after transfection, the cells were treated, or not treated, with mouse type I IFN (100 U ml⁻¹) for 24 hours and CAT activity was assayed. In the same conditions, we confirmed by Northern blotting analysis that transcription of endogenous class I genes is stimulated two- to threefold by type I IFN (not shown). Results in Fig. 1a show that, in this transient assay, CAT activity is increased by IFN treatment. We then tested 5' deletion mutants of pH2CAT and found that dl393, which carries the IRS, responds to IFN, while dl122 and dl61, which do not have the IRS, are not stimulated (Fig. 1a). Similarly, the thymidine kinase (TK) and simian virus (SV40) early promoters in the constructs pTKCAT⁷ and pSV2CAT⁹ respectively were not stimulated (not shown). We analysed the

^{1.} Podack, E. R. & Konigsberg, P. J. J. exp. Med. 160, 695-710 (1984).

^{2.} Henkart, P. A., Millard, P. J., Reynolds, C. W. & Henkart, M. P. J. exp. Med. 160, 75-93 (1984).
3. Podack, E. R., Young, J. D. & Cohn, Z. A. Proc. natn. Acad. Sci. U.S.A. 82, 8629-8633 (1985).

Tite, J. P. & Janeway, C. A. Eur. J. Immun. 14, 878-886 (1984).
 Tite, J. P., Powell, M. B. & Ruddle, N. H. J. Immun. 135, 25-33 (1985).
 Nakamura, M., Ross, D. T., Briner, T. J. & Gefter, M. L. J. Immun. 136, 44-47 (1986).

Fig. 1 a, Effect of type I IFN treatment on the activity of pH2CAT and 5' deletion mutants. A (-193 to -159) and B (-76 to -66) indicate the enhancer regions of the $H-2K^b$ promoter. I indicates the IFN response sequence (IRS:-165 to -137) which is closely homologous to the consensus sequence described by Friedman and Stark (see Table 1A). SE, stimulation effect. b, Effect of IFN treatment on the level of mRNA induced by pH2CAT and its 5' deletion mutants. Odd-numbered lanes: without IFN; even-numbered lanes: with IFN. Lanes 1, 2, dl122; lanes 3, 4, dl393; lanes 5, 6, pH2CAT; lane M, markers are pBR322 cut with HpaII and labelled with the Klenow enzyme. The sizes of the specific initiation (SI) and upstream initiation (UI) protected fragments are 283 and 344 nucleotides respectively.

Methods. a, Details of the construction of the plasmids and analysis of the enhancer activity have been described before⁷. Duplicate cultures of 3T6 cells (3×10^5) cells per 5-cm dish) were treated for 16-18 h with 0.5 ml of a 1.0-ml calcium phosphate co-precipitate containing 10 µg of plasmid DNA. The cells were then rinsed once and re-fed with fresh Dulbecco's modified Eagle's medium with 10% fetal calf serum with or without 100 U ml⁻¹ of type I IFN. Mouse type I IFN was a purified preparation (a mixture of IFN- α and - β) given by Drs I. Gresser and M. Tovey (specific activity 2.4×10^7 U mg⁻¹) and used in all experiments. A cytoplasmic extract was prepared 24 h later and CAT activity measured⁷. The protein concentration in the extract was measured with the BioRad protein assay. The ratio of the specific CAT activity (CAT activity/protein concentration) of cells treated with IFN to that of non-treated cells is shown as the stimulation effect (SE). The basal (unstimulated) levels of CAT activity were: 0.45, 1.45, 0.16 and 0.05 units per mg protein for pH2CAT, dl393, dl122 and dl61 respectively (1 unit represents 1 nanomol of chloramphenicol acetylated per h at 37 °C). These values are the results of both the deletions in the promoter and variable levels of upstream initiation. Experiments were performed at least five times and the average was obtained. Variations in stimulation effect between individual experiments never exceeded 20%. b, The steady-state level of CAT mRNA was measured by S, mapping analysis. The probe was a uniformly labelled EcoRI-HincII 600-bp fragment derived from dl61 and cloned in M13mp9; this fragment contains part of CAT gene, 75 bp of the K^b promoter (-63 to +12) and part of vector DNA. Using this probe, both SI and UI could be detected⁷. Total RNA was extracted 40 h after transfection from cells treated as described for a. To correct for variations in the efficiency of transfection, we included the plasmid pCH110¹⁹ in the transfection mixture and measured the β -galactosidase activity as described previously⁷. An average of 30 µg of RNA was hybridized with the probe for 16 h at 42 °C. Details for the probe, normalization of the quantity of RNA and S₁ mapping procedure have been described previously⁷.

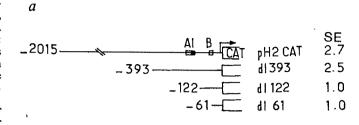
RNA transcripts by quantitative S_1 mapping experiments, with similar conclusions (Fig. 1b). It is important to note that transcription in pH2CAT and dl393 is stimulated from the authentic cap site of the $H-2K^b$ gene. However, nonspecific initiation from upstream site(s)⁷ located in the vector is also stimulated (Fig. 1b), as if the IRS would act as, or in conjunction with, an

Table 1 Stimulation by cloned human IFNs of $H-2K^b$ -derived constructs transfected into HeLa cells

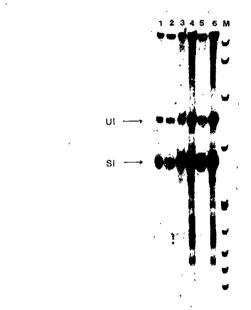
	α	β	γ	A*	IRS*	в*
dl393	1.9	1.8	2.5	+	+	+
dl122	1.0	1.0	1.0			+
Dde-cII	2.8	3.1	3.9	+	+	
Dde-Hf	1.0	1.0	1.0	+		

HeLa cells were transfected as described for 3T6 cells (see Fig. 1 legend). IFN- α , - β or - γ were used at 200 units per ml of medium. The values given indicate the stimulation effect due to IFN and are the average of three experiments. The basal CAT values were similar to those obtained with 3T6 cells. Recombinant human IFN- α , - β and - γ have been produced by CHO cells transfected with the corresponding complementary DNAs, and purified by affinity chromatography 16-18. Their specific activities were respectively 2×10^8 U mg⁻¹, 5×10^8 U mg⁻¹ and 4×10^8 U mg⁻¹.

*These columns indicate the presence or absence in the construct of enhancer A, interferon response sequence (IRS) and enhancer B, respectively.



b



enhancer sequence. This observation prompted us to examine more closely the functional relationship between the IRS and the $H-2K^b$ enhancers.

We showed previously that two sequences derived from the $H-2K^b$ promoter, shown as A and B in Fig. 2a, display an enhancer-like activity when studied in the pconaCAT system⁷. Various fragments cloned in this vector were assayed for stimulation by IFN as described above and the results are shown in Fig. 2a. Stimulation is observed with the Sau3A-Sau3A fragment (which contains A, B and IRS) in both orientations, with the DdeI-HincII fragment (which contains A and IRS) but not with DdeI-HinfI (containing A alone) or HinfI-Sau3A (containing IRS and B). We conclude that both enhancer A and IRS are necessary for inducibility, and that they can act in both orientations on a heterologous promoter. Thus, IRS increases the activity of enhancer A upon IFN treatment. Not all enhancers can act jointly with IRS: enhancer B does not, nor does the SV40 enhancer which we cloned upstream of the HinfI-Sau3A fragment (Fig. 2a).

The Q10 gene¹⁰, which maps in the Qa region and is expressed specifically in the liver, also contains an IRS and an enhancer A-like sequence⁷. However, no stimulation by IFN can be observed with either the HinfI-HinfI (which contains the enhancer A-like sequence) or the HpaII-HaeIII (A-like sequence+IRS) fragment of the Q10 promoter cloned in pconaCAT (Fig. 2b). Both Q10 IRS and enhancer A-like sequence display some nucleotide differences from their homologues in $H-2K^b$ (Table 2A), and could thus be inactive. In fact, the Q10 enhancer

Table 2	Converse of the emberson	A IDC region in the verticue	constructs described in the text
ranie z	Sequence of the enhancer	A-IKS region in the various	constructs described in the text

	SV40 ENHANCER	CONSENSUS IRS	RESPONSE TO IFN
Α	CAGGTGTGGAAAGTCCCCAGGCT TTCN	CNACCTCNGCAGTTTCTCTTCT-CT	22.0
I.	CAGGGGTGGGGAAGCCCAGGGCTGGGGATTCC	CCATCTCCACAGTTTCACTTCTGCA	+
II.		.A.GGG.TCC.ATTGAGAAAC	
III.	AC.AT.C.TCCGGCGTAGAA.CC	*********	-
IV.	AC	т	-
В	ENHANCER A	Q10 IRS	
ī.	CAGGGCTGGGGATTCCCAAGCTCCGGATCTCC	CCATCTCCCCAGTTTCACTTCTGCT	+
II.	AC		-
III.	G.TAGG.GCTGA.GA		-
IV.	TCA .A .ACACC .GAAAAGGTTGT .A		
A r	: pH2CAT, pdl393, Sau3A-Sau3AconaC	CAT, Dd-cliconaCAT	
	: Dde-HfconaCAT	•	
III	: Hf-Sau3AconaCAT		
IV	: HpaII-Hae(Q10)conaCAT		
B	: Qlo CAT dll67xHf-Hf(Kb), Dde-Hf	(K ^b), Hf-Hf (L ^d)	
II	: Q10 CAT d1167xHf-Hf (Q10)		
III	: Q10 CAT d1375		
TV	: Q10 CAT d1167		

Part of the SV40 enhancer surrounding the core sequence¹⁵ and the consensus IRS⁶ are shown on the first line. Enhancer A of K^b is underlined in AI. The equivalent sequence and the IRS in the Q10 gene are underlined in BI. Lines II, III and IV show the nucleotides differing from line I in the different constructs indicated below. The + sign indicates positive response to IFN, while - denotes no effect (detailed in Figs 1-3).

A-like sequence is at least five times less active than the corresponding sequence of the K^b or L^d genes when assayed in 3T6 cells⁷. We constructed a hybrid Q10-CAT gene and derived two internal deletion mutants, pQ10CAT dl375 and dl167 (Fig. 3). We then built hybrid promoters by cloning enhancer A of the K^b , L^d or Q10 genes into pQ10CAT dl167 (Fig. 3). Neither deletion mutants respond to IFN, but the K^b and L^d sequences restore the responsiveness of the promoter to IFN treatment while Q10 enhancer A-like sequence does not (Fig. 3). In constructs which display IFN induction, specific as well as non-specific initiation is stimulated (confirmed by quantitative S_1

mapping analysis, data not shown), similar to results with the K^b promoter (Fig. 1b). Therefore, the IRS of the Q10 gene is potentially active, that is, it can also increase the activity of an enhancer A from K^b or L^d .

Some of these experiments have been repeated with a highly purified mouse IFN- γ preparation (kindly provided by Dr J. Wietzerbin), showing that the IRS sequence also responds to IFN- γ (data not shown). However, since the observed stimulations with mouse type I as well as IFN- γ were only two-to threefold, and since the type I IFN preparation which we used had not been purified to homogeneity, we wished to confirm

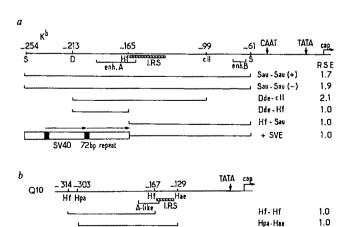


Fig. 2 a, Map of the promoter of $H-2K^b$ and various subfragments cloned in pconaCAT. S, Sau3A; D, DdeI; cII, HincII; Hf, HinfI; SVE, SV40 enhancer; Hpa, HpaII; Hae, HaeIII. RSE, relative stimulation effect. Orientation is indicated by arrows and the 'core sequence' by filled boxes. b, Map of Q10 promoter and subfragments cloned in pconaCAT.

Methods. Various fragments were cloned at the BamHI site (-102) of pconaCAT, in which the CAT gene is driven by the conalbumin promoter (-102 to +62)7, using BamHI linkers, except for the DdeI-HinfI fragment which was cloned by successive addition of HindIII and BamHI linkers. Further details for construction of pconaCAT and cloning of these subfragments are given in ref. 7. The 72-base-pair (bp) repeats of SV40 were derived from pSV23-2AgptΔLR (T. Kadesch, personal communication) as a 200-bp BamHI fragment (coordinates 273 to 95 in ref. 20) and cloned at the 5' BamHI site of the (HinfI-Sau3A) conaCAT construct. Transfection and enzyme assays were performed as described in Fig. 1a legend. Stimulation effect by IFN treatment for each plasmid is indicated as the relative stimulation effect (RSE), being compared with that for the pconaCAT construct, which does not respond significantly to IFN. The basal levels of CAT activity in a were 0.97, 0.45, 0.90, 2.2, 0.38 and 8.5 units per mg of protein for the Sau-Sau(+), Sau-Sau(-), Dde-cII, Dde-Hf, Hf-Sau and +SVE constructs, respectively. In b, the basal level of CAT activity was 0.38 units per mg protein for the two constructs.

Fig. 3 Map of the promoter of the Q10 gene and the Q10-CAT hybrid genes. Xba, XbaI; Bam, BamHI; HdIII, HindIII; (Hf), HinfI-HinfI fragment; (Dd), DdeI-HinfI fragment; IV, sequence identified in ref. 7 which corresponds to enhancer A for K^b or L^d , and to the enhancer A-like sequence for Q10. BL indicates the basal level relative to pQ10CAT dl167. The basal CAT activity of this construct was 0.2 units per mg protein.

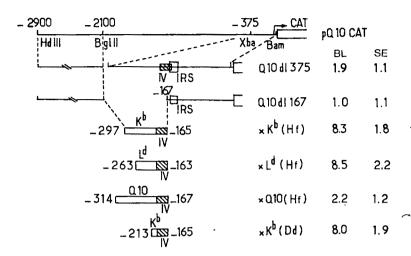
Methods. A HindIII-BamHI fragment (-2,839 to +14) of the Q10 gene (gene 8 in the cosmid library of Steinmetz et al.21) was isolated from cosmid 36.2 and cloned with HindIII linkers into pC α CAT²² between HindIII sites. This construct, named pQ10CAT, was linearized at the unique XbaI site and treated with Bal31 followed by digestion with BglII, treatment with Klenow polymerase and re-circularization, to construct internal deletion mutants (pQ10CAT dl375 and pQ10CAT dl167). The deletion end points were determined by sequencing analysis. A HinfI fragment which contains enhancer A of the $H-2K^b$ gene or its equivalent region in the $H-2L^d$ or Q10 gene as well as a DdeI-HinfI fragment derived from the $H-2K^b$ promoter (K^b (Dd); see Fig. 2a) were cloned in pO10CAT dl167 at the unique BglII site (-167) using successive addition of HindIII and BamHI linkers (to conserve the sequence of enhancer A 3' to the HinfI site except at one position, see Table 2). These fragments have been shown to have an enhancer activity when assayed in the pconaCAT vector system. A HinfI-HinfI fragment derived from the Q10 promoter has an enhancer activity about five times less than the K^b or L^d derived fragments \tilde{j} . The stimulation effect (SE) of IFN treatment was determined as described in Fig. 1a legend.

our results with recombinant IFN. Mouse recombinant IFN were not easily available to us. We therefore turned to human recombinant IFN. Since H-2 class I genes transfected into human cells can be regulated by human interferons¹¹, we decided to analyse the regulation of the $H-2K^b$ promoter in human HeLa cells, in response to recombinant human IFN- α , - β or - γ . Results in Table 1, obtained with the dl122, dl393, Dde-Hf and Dde-cII constructs, are similar to those obtained in 3T6 cells with mouse IFN, and demonstrate that all three IFNs stimulate the $H-2K^b$ promoter in a similar fashion. This strongly suggests that although the receptors for IFN- β and IFN- γ have been shown to be distinct¹², the final target on the $H-2K^b$ promoter is the same.

Our experiments with mouse type I IFN demonstrate that the IRS potentiates the action of a functional enhancer in the presence of IFN. This process is specific in the sense that the enhancer A needs to be functional, and that not all enhancers can be made responsive, as illustrated by enhancer B and the SV40 enhancer. The sequence arrangements of enhancer A and IRS in the various constructs described above are shown in Table 2. Interestingly, three mismatches in the enhancer A sequence (Table 2, compare AI and AIV, also BI and BII) are enough to abolish inducibility. Besides, as can be seen in Table 2 (compare AI and BI), enhancer A and IRS can be separated by several nucleotides and still respond to IFN. This suggests that the specific requirement for enhancer A may not be of topological nature. However, we cannot rule out the possibility that the SV40 and B enhancers could be potentiated at an appropriate distance. We have not shown that sequences located in the -137 to -99 region of $H-2K^b$ are irrelevant to IFN inducibility, but they are not conserved in the various IFN inducible genes⁶ and we did not find that they have any significant role in class I gene expression'.

This functional cooperation between an enhancer sequence and a second regulatory element is reminiscent of the response of the human metallothionin IIA (MTIIA) gene to heavy metals¹³. In the present case, the results could be interpreted in terms of a cooperative interaction between putative trans-acting factors binding to enhancer A and IRS.

Our results confirm that regulation of class I gene expression



by IFN- α , $-\beta$ and $-\gamma$ is, at least partly, transcriptional. We do not exclude additional post-transcriptional mechanisms, considering the relatively low degrees of induction observed and the findings of Yoshie et al.¹⁴ that an integrated truncated HLA gene, lacking the promoter region, still responds to IFN. Finally, it should be noted that, in the human MTIIA gene and in H-2and HLA class II genes, the IRS is located much further upstream from the cap site than in class I genes⁶. No homology with the class I enhancer A can be found in its vicinity. The mechanism by which these genes are regulated may then differ from class I genes. In this respect, it is noteworthy that maximum induction of the MTIIA gene requires 100 times more IFN-α than class I genes⁶.

We thank Drs I. Gresser and M. Tovey for the gift of type I IFN, Dr J. Wietzerbin for purified mouse IFN-γ, Dr D. Novick and Professor M. Revel for human IFN- α , - β , - γ , and Dr M. Steinmetz for making available to us the cosmid clone carrying the O10 gene. A.K. was a recipient of an IARC (WHO) fellowship, then a Foundation pour la Recherche Médicale Française fellowship.

Received 23 December 1985; accepted 23 June 1986.

- 1. Lindahl, P., Leary, P. & Gresser, I. Proc. natn. Acad. Sci. U.S.A. 70, 2785-2789 (1973).

- Burrone, O. R. & Milstein, C. EMBO J. 1, 345-349 (1982).
 Wallach, D., Fellous, M. & Revel, M. Nature 299, 833-836 (1982).
 Fellous, M. et al. Proc. natn. Acad. Sci. U.S.A. 79, 3082-3086 (1982).
 Rosa, F., Berissi, H., Weissenbach, J., Maroteaux, L., Fellous, M. & Revel, M. EMBO J. 2, 239-243 (1983). 6. Friedman, R. L. & Stark, G. R. Nature 314, 637-639 (1985).
- 7. Kimura, A., Israel, A., Le Bail, O. & Kourilsky, P. Cell 44, 261-272 (1986).
 8. Daniel-Vedele, F., Israel, A., Bénicourt, C. & Kourilsky, P. Immunogenetics 21, 601-611
- Gorman, C. M., Moffat, L. F. & Howard, B. H. Molec, cell. Biol. 2, 1044-1051 (1982).
- Devlin, J. J., Lew, A. M., Flavell, R. A. & Coligan, J. E. EMBO J. 4, 369-374 (1985).
 Rosa, F., Hatat, D., Abadie, A. & Fellous, M. Ann. Inst. Pasteur, Immun. 136, 103-119 (1985).

- Rosa, F., Hatat, D., Abadie, A. & Fellous, M. Ann. Inst. Pasteur, Immun. 136, 103-119 (1985).
 Branca, A. A. & Baglioni, C. Nature 294, 768-770 (1981).
 Haslinger, A., Heguy, A., Deitman, T., Cooke, T. & Karin, M. (in preparation).
 Yoshie, O. et al. Proc. natn. Acad. Sci. U.S.A. 81, 649-653 (1984).
 Weiher, H., König, M. & Gruss, P. Science 219, 626-631 (1983).
 Novick, D., Eshhar, Z. & Rubinstein, M. J. Immun. 129, 2244-2247 (1982).
 Chernajovsky, Y. et al. DNA 3, 297-308 (1984).
 Novick, D., Eshhar, Z., Fisher, D. G., Friedlander, J. & Rubinstein, M. EMBO J. 2, 1527-1520 (1982). 1527-1530 (1983).
- 19. Hall, C., Jacob, E., Ringold, G. & Lee, F. J. molec. appl. Genet. 2, 101-109 (1983).
- Fromm, M. & Berg, P. J. molec. appl. Genet. 1, 457-481 (1982).
 Steinmetz, M., Winoto, A., Minard, K. & Hood, L. Cell 28, 489-498 (1982).
- 22. Herbomel, P., Bourachot, B. & Yaniv, M. Cell 39, 653-662 (1984).

Continuous and discontinuous protein antigenic determinants

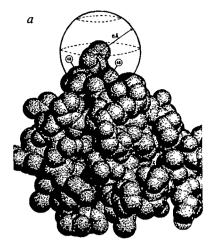
D. J. Barlow, M. S. Edwards & J. M. Thornton

Laboratory of Molecular Biology, Department of Crystallography, Birkbeck College, University of London, Malet Street, London WC1E 7HX, UK

Protein antigenic determinants have been classified as continuous or discontinuous 1,2. The continuous determinants are composed of residues which are local in the polypeptide sequence, while discontinuous determinants consist of residues from different parts of the sequence, brought together by the folding of the protein to its native structure. Searches made for protein determinants using peptide fragments which compete with protein-antibody complex formation, or peptides that can be used to raise antibodies which crossreact with the native protein, are limited to the simulation of continuous determinants. However, recent experiments^{2,3} suggest that most determinants are discontinuous. We now show, by consideration of protein surfaces, that if the recognition zone between a protein and antibody has the same dimensions as those found for the lysozyme-antibody complex⁴, none of the protein's surface will be 'continuous'. We suggest that all determinants are discontinuous to some extent, and that crossreacting peptides mimic only the 'primary' interaction site. In addition, we show that the parts of a protein's surface which are most continuous fall predominantly in the loops and/or protruding regions. This explains why quantities such as hydrophilicity⁵, accessibility⁶, mobility⁷ and protrusion⁸ can be used to predict which parts of a polypeptide provide the 'best' antigenic peptides.

The surface of a globular protein, as defined by X-ray crystallographic coordinates, is very complex and convoluted. However, visual inspection of any structure shows that most residues on the surface have neighbouring residues that are distant in the sequence. To quantify this observation, we have used the atomic coordinates available from the protein databank9 to search for 'continuous patches' on the surface of a protein. The method used (see Fig. 1a) involves centering a sphere of radius (r) on each surface atom in the protein, and calculating the proportion (F) of the other surface atoms enclosed by the sphere which belong to residues local in the amino-acid sequence. If a sphere encloses only local surface atoms, then we have identified a continuous patch. Surface atoms are defined as those with contact areas (calculated by the method of Lee and Richards¹⁰) >2Å²; local surface atoms are those belonging to residues in the sequence $i - n \rightarrow i + n$, where i is the residue containing the surface atom at the origin of a sphere, and n is an integer in the range 1-10.

When the percentage of surface atoms which lie at the centre of a continuous patch is plotted as a function of sphere radius, we obtain the surface 'continuo-grams' shown in Fig. 1b. Four separate plots are presented to show how the results depend on the definition for a local surface atom. These graphs are averaged over three proteins (myoglobin, trypsin and lysozyme), but the individual plots are essentially identical. Note that as the size of the sampling sphere increases, the percentage of the surface which is continuous decreases rapidly, until at a radius of ~10 Å virtually all of the surface is discontinuous, that is, there is no region of 20 Å diameter which contains only atoms from residues local in the amino-acid sequence. This relates directly to the observations made for the lysozyme-antibody complex, where the recognition zone is estimated to be 20 × 25 Å, and is discontinuous4. Note however, that this is a monoclonal antibody and has a reasonable affinity for its antigen; the association constant, K_A , is in the range $2-4\times10^7$ mol⁻¹ (R. Poljak, personal communication). Other antibodies that bind more weakly to their antigens may have smaller combining sites, which might there-



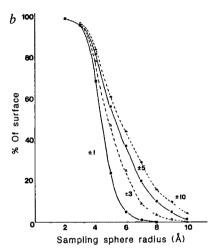


Fig. 1 a, Illustration of the method used to calculate the percentage of 'continuous surface' for a protein. The figure shows part of a space-filling model of lysozyme. A sampling sphere of radius 6 Å is centred on one of the surface atoms in the molecule: CG2 of Thr 47. The sphere encloses the atom centres of six other surface atoms, all of which are considered here as local surface atoms. since they belong to residues in the sequence 44-50. Two of the local surface atoms are labelled by residue number. Because all of the atoms enclosed by the sphere belong to local amino-acid residues, CG2 of Thr 47 is considered as the centre of a surface 'continuous patch'. b, Surface 'continuo-grams', showing the percentage of surface atoms which lie at the centre of a continuous patch as a function of sampling sphere radius. The four curves are obtained using different definitions for a local surface atom. (Specifically, these are atoms which belong to residues $i-1 \rightarrow i+1$, $i-3 \rightarrow i+3$, $i-5 \rightarrow i+5$, $i-10 \rightarrow i+10$, where i is the residue containing the surface atom at the origin of the sampling sphere.) Note that since the calculations (described in a and in the text) consider only atoms whose centres are enclosed by a sampling sphere, these curves represent conservative estimates of the percentage of continuous surface. If the intrusion of any fraction of an atom into the sampling sphere is considered, all of the curves will be shifted to the left.

fore be continuous. As we demonstrate below, however, this is not likely to be the case.

A low-affinity antibody, with $K_A = 10^4 \,\mathrm{mol}^{-1}$, will have a standard free energy of binding of $-6 \,\mathrm{kcal}\,\mathrm{mol}^{-1}$ (ref. 11). Assuming, therefore, that each Å² of the protein surface buried during association contributes 20 cal (ref. 12) to the binding energy, the buried area will be ~300 Å². Using sampling spheres of various sizes centred on each of the surface atoms in lysozyme, we calculate that this amount of the protein's surface area would typically involve a patch of ~8 Å radius. As shown in Fig. 1b, <10% of the surface patches of this size are continuous. Thus,

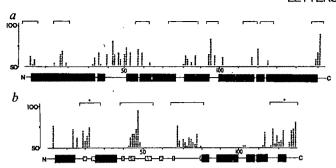


Fig. 2 Variation in $\langle F \rangle$ along the sequence of myoglobin (a) and lysozyme (b). (F) values for residues are plotted along the ordinate and the sequences of each protein along the abscissa. The locations of secondary structures in the proteins are shown below the corresponding plot; helices are represented by solid bars, \(\beta\)-strands by stippled bars and loop/turn regions by single lines. The locations of antigenic peptides¹³⁻¹⁵ are indicated above each plot; those labelled in b by • are discontinuous.

binding sites even for low-affinity antibodies are unlikely to involve only local amino-acid residues. We conclude that heptapeptides which cross react with protein antibodies mimic only part of the recognition area. Similarly, anti-peptide antibodies which recognize native protein will be limited to surface patches dominated by a short peptide, where interference from non-local residues is minimal.

On this basis, therefore, it would be reasonable to expect that the parts of a protein that are 'most continuous', should provide the best antigenic peptides. As Fig. 2 shows, this is indeed the case; the two plots illustrate the variation in $\langle F \rangle$ along the sequences of myoglobin and lysozyme, where $\langle F \rangle$ represents the mean value of F for all surface atoms in a residue, calculated using a sampling sphere radius of 10 Å (residues which do not contain surface atoms are assigned a value of $\langle F \rangle = 0$). The 'most continuous' patches in each protein are those where the residues have $\langle F \rangle > 50\%$. Note that there is a strong correlation between these regions and the location of antigenic peptides¹³⁻¹⁵.

An analysis of the surface compositions of 12 proteins shows that $\sim 50\%$ of all loop residues have $\langle F \rangle$ values > 50% (Fig. 3). The corresponding figures for helix and sheet residues are only 23% and 16%, respectively. As would be expected, therefore, most of the residues which form the most continuous regions lie in loops which protrude from the surface of the protein. Some are also found in helices, but none are found in the central strands of a β -sheet (where residues which are distant in the sequence will always be in close proximity).

These results provide a satisfying rationale, taken together with the necessity for antibody accessibilty⁶ or protrusion⁸, to explain which regions of a protein provide the 'best' antigenic peptides.

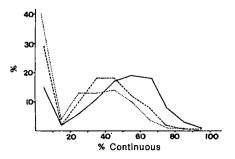


Fig. 3 The distribution of $\langle F \rangle$ values for residues in loop (helix (---) and β -strand (\cdots) regions. % Indicates the frequency of residues with an $\langle F \rangle$ value (% continuous) in a given

We thank the SERC for financial support. M.S.E. holds a CASE studentship in collaboration with Dr Peter Murray-Rust

Received 25 April; accepted 4 June 1986.

- 1. Atassi, M. Z. Immunochemistry 12, 423-438 (1975).
- Atassi, M. Z. Immunochemistry 12, 423-438 (1975).
 Benjamin, D. C. et al. A. Rev. Immun. 2, 67-101 (1984).
 Regenmortel, M. H. U. Hybridonia Technology in Agriculture and Veterinary Research (eds Stern, N. J. & Cramble, H. R.) Ch. 3 (Rowman & Allanheld, New Jersey, 1984).
 Amit, A. G., Mariuzza, R. A., Philips, S. E. V. & Poljak, R. J. Nature 313, 156-158 (1985).
 Hopp, T. P. & Woods, K. R. Proc. natn. Acad. Sci. U.S.A. 78, 3824-3828 (1981).
 Novotny, J. et al. Proc. natn. Acad. Sci. U.S.A. 83, 226-230 (1986).
 Westof, E. et al. Nature 311, 123-126 (1984).

- Thornton, J. M., Edwards, M. S., Taylor, W. R. & Barlow, D. J. EMBO J. 5, 409-413 (1986).
 Bernstein, F. C. et al. J. molec. Biol. 112, 535-542 (1977).
- 10. Lee, B. & Richards, F. M. J. molec. Biol. 55, 379-400 (1971).
- 11. Schulz, G. E. & Schirmer, R. H. Principles of Protein Structure Ch. 3 (Springer, New York,
- Richards, F. A. Rev. Biophys. Bioengng 6, 151-176 (1977).
 Atassi, M. Z. Eur. J. Biochem. 145, 1-20 (1985).
- 14. Ibrahimi, I. M., Eder, J., Prager, E. M., Wilson, A. C. & Arnon, R. Molec. Immun. 17, 37-46
- 15. Takagaki, Y., Hirayama, A., Fujio, H. & Amano, T. Biochemistry 19, 2498-2505 (1980).

Expression of a transfected human c-mvc oncogene inhibits differentiation of a mouse erythroleukaemia cell line

Ethan Dmitrovsky*, W. Michael Kuehl*, Gregory F. Hollis*, Ilan R. Kirsch*, Timothy P. Bender* & Shoshana Segal*†

* NCI-Navy Medical Oncology Branch, National Cancer Institute, and † Department of Medicine, Uniformed Services University of the Health Sciences, National Navy Medical Center, Bethesda, Maryland 20814-2015, USA

The Friend-virus-derived mouse erythroleukaemia (MEL) cell lines represent transformed early erythroid precursors that can be induced to differentiate into more mature erythroid cells by a variety of agents including dimethyl sulphoxide (DMSO)2. There is a latent period of 12 hours after inducer is added, when 80-90% of the cells become irreversibly committed to the differentiation programme, undergoing several rounds of cell division before permanently ceasing to replicate^{3,4}. After DMSO induction, a biphasic decline in steady-state levels of c-myc^{5,6} and c-myb⁶ messenger RNAs occurs. Following the initial decrease in c-myc mRNA expression, the subsequent increase occurs in, and is restricted to, the G₁ phase of the cell cycle⁷. We sought to determine whether the down-regulation is a necessary step in chemically induced differentiation. Experiments reported here indicate that expression in MEL cells of a transfected human c-myc gene inhibits the terminal differentiation process.

To study the relationship between the down-regulation of the c-myc mRNA and cellular differentiation, a plasmid (PL¹hmcneo^r) containing the pSV2neo and the human c-myc genes was transfected into MEL cells (line 745). The stable G418-resistant transfectants (Fig. 1) were induced with DMSO to determine their differentiation potential. Strikingly, all transfectants which expressed the exogenous human c-myc gene failed to develop a red pellet or a positive reaction with benzidine after 7 days of induction. This inhibition of differentiation is not a transfection artefact. The parental MEL cells were subcloned after undergoing a sham transfection without selection, and all 24 subclones examined differentiated after 7 days of DMSO induction. In addition, transfectant T57, which expressed only the neomycin resistance gene, differentiated normally after induction. Introduction of another selection marker, the APRT (adenine phosphoribosyltransferase) gene, also does not interfere with induced differentiation of MEL cells8.

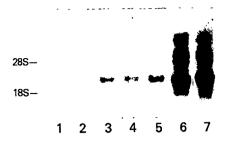


Fig. 1 RNA expression of the exogenous human c-myc in stable MEL transfectants. The inducible murine Friend-virus-derived1 erythroleukaemia cell line 745 (a gift from Dr J. Bilello) was transfected by a modified 16 calcium phosphate technique 17 with PL¹hmeneo' (a gift from Dr W. Lee). This plasmid is a derivative of the pCV108 vector¹8. It contains a 5.8-kb XhoI/EcoRI genomic human c-myc fragment (including all three c-myc exons) fused at the XhoI site of the first exon to a portion of the U3 and R of the Moloney murine leukaemia LTR. Total cellular RNA was prepared from the uninduced MEL parent and stable transfectants using the guanidine thiocyanate method previously described19. Total cellular RNA (10 µg per lane) was loaded, electrophoresed on a 1% agarose formaldehyde gel and blotted²⁰. The nitrocellulose filter was hybridized to a ³²P-dCTP nick-translated human c-myc 1.5-kb Cla1/EcoRI third exon probe overnight at 42 °C in a 10% dextran sulphate, 5×SSC, 40% formamide solution. After hybridization, the filter was washed for 1 hour at 60 °C with 0.1×SSC, 0.1% SDS and analysed by autoradiography using Kodak XRP.5 film and an overnight exposure with an intensifying screen. The five transfectants were obtained from three independent transfection experiments. The numbered lanes show the 745 MEL parent (lane 1), T57 (lane 2) T61 (lane 3), T62 (lane 4), T60 (lane 5), T56 (lane 6) and T55 (lane 7).

Two transfectants were selected for further studies to better define the effect of exogenous human c-myc expression on DMSO induction: T56, which expressed high levels of human c-myc mRNA, and T57 (Fig. 1). Both T56 and T57 were cloned by limiting dilution. Since the usual induction procedure (designated stationary phase induction) is limited by the 3-4 days taken for MEL cells to reach stationary growth^{2,3}, we modified this procedure to continue the induction longer. MEL cells were fed with enough medium (with or without DMSO) each day to maintain logarithmically growing cells at approximately the same density (designated logarithmic phase induction). Exponentially growing cells of clone 56 and 57 were seeded in medium without (control) or with (induced) DMSO. As shown (Fig. 2), clone 57, like the parental MEL cells, accumulated benzidine-positive cells to a maximum level of 90%. In contrast, cells from clone 56 were benzidine unreactive and the cell pellet remained white even after 14 days of induction. Another assay for terminal differentiation is clonability. Following DMSO induction, clone 57 rapidly lost its ability to generate subclones, while clone 56 showed no decrease in clonability after 14 days.

Steady-state levels of α -globin, c-myb and β -actin mRNAs, as well as exogenous human c-myc mRNA, were determined by Northern blots of total RNA prepared from clones 56 and 57 with or without DMSO (Fig. 3). The expression of β -actin was similar for the two clones, and remained essentially constant for control or induced cultures. Expression of exogenous human c-myc was stringently assayed so that the endogenous c-myc mRNA was not detected. As shown (Fig. 3), clone 56 expressed relatively high levels of two human c-myc mRNA species (approximately 2.3 and 2.1 kilobases (kb) in size). It is possible that transcription of these two mRNA species is initiated at the long terminal repeat (LTR) and P2 c-myc promoters, respectively. Notably, the expression of human c-myc mRNA decreased 6 hours after DMSO was added, and then declined more gradually during the next 10 days.

Using an α -globin cDNA probe, clone 57 expressed a basal level of α -globin mRNA which increased substantially during

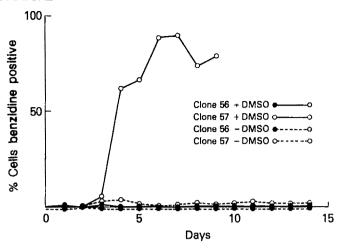


Fig. 2 Accumulation of benzidine-stained cells of clones 56 and 57 for uninduced and 'logarithmic-phase' induced cultures. Logarithmically growing cells of these clones were seeded at a density of 5×10^5 per ml on day -1 and split to 10^5 per ml one day later (day 0) in Joklik's modified medium supplemented with 75 µg ml⁻¹ of G418 (Geneticin, Gibco) and 10% fetal calf serum with or without 1.5% DMSO (Sigma). Each day half of the cells were removed from culture, harvested by centrifugation, washed twice with phosphate-buffered saline (PBS), and then stained for haemoglobin using the acid benzidine stain as previously described3. The remaining cells were replenished with an equal volume of fresh Joklik's modified medium containing G418 and 10% fetal calf serum, with or without 1.5% DMSO as indicated. For both the induced and uninduced cultures, 200 cells were daily assessed for benzidine reactivity and the percentage of benzidinepositive cells are provided for the indicated time points. The cell pellet of clone 57 became red approximately one day before the majority of individual benzidine-positive cells were seen.

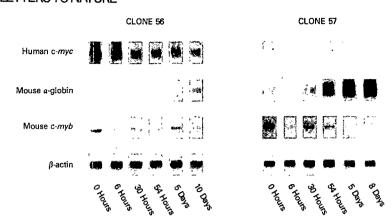
DMSO induction. This increase in α -globin mRNA expression was comparable in kinetics and magnitude to that observed with the parental 745 MEL line under stationary-phase induction conditions^{5,6}. In marked contrast, clone 56 expressed substantially lower basal levels of α -globin mRNA, which increased minimally after 10 days of induction. We do not know if this reflects low levels of expression in all cells or selective expression in a subpopulation of cells.

Changes in the expression of c-myb mRNA provide another marker for DMSO response. As expected, for clone 57 the changes in c-myb were indistinguishable from those previously observed for parental MEL cells (Fig. 3). For clone 56, the basal c-myb mRNA level was lower than for clone 57. This level of mRNA decreased within 6 hours after induction. Unlike the parental cells or clone 57, the level of c-myb mRNA stayed relatively constant during the remainder of the induction period.

To compare changes in expression of endogenous c-myc mRNA in the transfected cells, we used an S₁ nuclease protection assay to ensure that the endogenous mouse c-myc could be distinguished from the exogenous human c-myc expressed in clone 56 (Fig. 4). Despite the presence of high levels of exogenous c-myc mRNA, the endogenous c-myc mRNA continues to be expressed and the initial transient decline occurs although the second decline does not even after 10 days of induction.

The six parameters used to assess the response of clones 56 and 57 to DMSO induction were: cell pellet colour and benzidine staining of single cells; endogenous α -globin, c-myc and c-myb mRNA levels; and cell cloning efficiencies. These experiments clearly indicate a failure of clone 56 to differentiate normally, unlike clone 57 or the parental MEL cells. This inhibition occurs in five transfectants that expressed various levels of exogenous human c-myc mRNA (Fig. 1)¹⁰. These results are consistent with evidence from the avian myoblast cell culture system where myoblasts infected with retrovirus and expressing high levels of

Fig. 3 Expression of human c-myc, α -globin, c-myb and β-actin mRNAs in clones 56 and 57 during logarithmicphase induction by DMSO. Logarithmically growing cells of clones 56 and 57 were seeded, grown and harvested as described in Fig. 2. However, after washing in PBS, the removed cells were resuspended in guanidine thiocyanate for total cellular RNA analysis. Total RNA (10 µg) was applied to each lane, electrophoresed on a 1% agarose/formaldehyde gel and blotted²⁰. The obtained nitrocellulose filters were hybridized as described in Fig. 1 to the following probes: a, 1.5-kb ClaI/EcoRI third exon and 3' flanking human c-myc probe; b, 3-kb SstI fragment representing a murine α -globin cDNA prepared from a plasmid provided by Dr Y. Nishioka; c, 582 base pairs (bp) Smal/EcoRI murine c-myb cDNA fragment²¹; d, 1.9-kb BamHI fragment representing approximately full-length cDNA for human β -actin provided by Dr L. Kedes. The hybridized filters were then washed at 54 °C



as described in Fig. 1 except for filters hybridized to the ClaI/EcoRI human c-myc which were washed at 62 °C. Autoradiographs were obtained after exposure to XRP.5 film and an intensifying screen. Steady-state levels of the indicated mRNAs remained relatively constant for uninduced cultures. Densitometric analysis of Southern blots demonstrated 36 copies of the human c-myc gene integrated in the genome of clone 56 whereas clone 57 does not contain an intact human c-myc gene (data not shown).

v-myc protein fail to differentiate into myotubes¹¹. Recently, similar findings were reported in a thymidine kinase—MEL cell line where transfection of a simian virus 40—driven c-myc inhibits erythroleukaemic differentiation¹². Experiments to determine whether other oncogenes can substitute for this inhibitory effect are under way.

Some tumours can be induced to differentiate in culture. In many of these cases, the expression of the c-myc and c-myb oncogenes decreases during differentiation^{5,6,13-15}. Two patterns of decline have been observed. The first is a gradual disappearance of c-myc or c-myb mRNAs following induction of differentiation, as seen in the HL60¹³, WEHI3B¹⁴, and F9 cell lines¹⁵. The second is a biphasic decline in steady-state levels of c-myc^{5,6} and c-myb⁶ mRNA as seen in MEL cells. In general, malignant cells appear 'frozen' in a particular state of differentiation. Since qualitative or quantitative changes in oncogene expression are implicated as a cause of malignant transformation, it is possible that the apparent block in differentiation of tumour cells is due to abnormal oncogene expression. Our results suggest that c-myc expression plays a central role in determining whether a cell remains in a continuous cycle of growth and proliferation or enters a differentiation pathway.

We thank William Lee for use of the PL¹hmcneo^r plasmid,

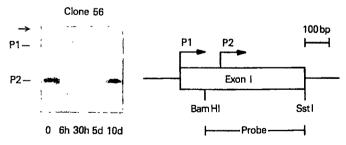


Fig. 4 Expression of endogenous c-myc mRNA determined by S₁-nuclease protection with clone 56 total cellular RNA obtained during logarithmic-phase induction (from the experiment described in Fig. 3). The single-stranded S₁ probe was prepared by primer extension of an M13 clone containing the 400-bp BamHI/SstI fragment derived from exon I of a genomic murine c-myc clone (obtained from Dr J. Battey). The probe was hybridized overnight at 55 °C to 10 µg of RNA using the previously described method²². After digestion with S₁-nuclease, the fragments were fractionated on an 8 M urea-5% polyacrylamide gel. The time points are hours (h) or days (d) after initiation of DMSO induction. The arrow indicates the position of the undigested probe. P1 and P2 represent promoters 1 and 2 of murine c-myc gene9.

James Battey for helpful discussions, and Virginia Bertness and Laura Minna for technical assistance.

Received 31 March; accepted 16 May 1986.

- 1. Friend, C., Scher, W., Holland, J. G. & Sato, T. Proc. natn. Acad. Sci. U.S.A. 68, 378-382
- Marks, P. A. & Rifkind, R. A. A. Rev. Biochem. 47, 419-448 (1978).

- Marks, P. A. & Kilkind, R. A. A. Rev. Biochem. 41, 415-446 (1976).
 Fibach, E., Reuben, R. C., Rifkind, R. A. & Marks, P. A. Cancer Res. 37, 440-444 (1977).
 Gusella, J., Geller, R., Clarke, B., Weeks, V. & Housman, D. Cell 9, 221-229 (1976).
 Lachman, H. M. & Skoultchi, A. I. Nature 310, 592-594 (1984).
 Kirsch, I. R., Bertness, V., Silver, J. & Hollis, G. F. J. cell. Biochem. (in the press).
- Lachman, H. M., Hatton, K. S., Skoultchi, A. I. & Schildkraut, C. L. Proc. natn. Acad. Sci. U.S.A. 82, 5323-5327 (1985).
- Charnay, P. et al. Cell 38, 251-263 (1984).
- Yang, J. Q. et al. Curr. Topics Microbiol. Immun. 113, 146-153 (1984).
 Dmitrovsky, E. et al. Curr. Topics Microbiol. Immun. (in the press).
 Falcone, G., Tato, F. & Alema, S. Proc. natn. Acad. Sci. U.S.A. 82, 426-430 (1985).
 Coppola, J. A. & Cole, M. D. Nature 320, 760-763 (1986).

- Westin, E. H. et al. Proc. natn. Acad. Sci. U.S.A. 79, 2490-2494 (1982).
 Gonda, T. J. & Metcalf, D. Nature 310, 249-251 (1984).
- 15. Campisi, J., Gray, H. E., Pardee, A. B., Dean, M. & Sonenshein, G. E. Cell 36, 241-247 (1984). 16. Davis, L., Dibner, M. & Battey, J. Methods in Molecular Biology (Elsevier, Amsterdam,

- Graham, F. L. & Van der Eb, A. J. Virology 52, 456-467 (1973).
 Lau, Y.-F. & Kan, Y. W. Proc. natn. Acad. Sci. U.S.A. 80, 5225-5229 (1983).
 Chirgwin, J. M., Przybyla, A. E., MacDonald, R. J. & Rutter, W. J. Biochemistry 18,
- Southern, E. M. J. molec. Biol. 98, 503-517 (1975).
 Bender, T. P. & Kuehl, W. M. Proc. natn. Acad. Sci. U.S.A. 83, 3204-3208 (1986).
- 22. Battey, J. et al. Cell 34, 779-787 (1983).

DNA loops induced by cooperative binding of λ repressor

Jack Griffith, Ann Hochschild* & Mark Ptashne*

Lineberger Cancer Research Center, University of North Carolina Medical School, Chapel Hill, North Carolina 27514, USA * Department of Biochemistry and Molecular Biology, Harvard University, 7 Divinity Avenue, Cambridge, Massachussetts 02138, USA

It has been shown by Hochschild and Ptashne¹ that λ repressors bind cooperatively to operator sites separated by five or six turns of the helix. Cooperative binding is not observed if the sites are separated by a nonintegral number of turns, unless a four-nucleotide gap is introduced into one of the strands between the two sites. These and other facts suggested that repressors at the separated sites touch each other, the DNA bending smoothly so as to accommodate the protein-protein interaction. Here we use electron microscopy to visualize the predicted protein-DNA complexes.

Figure 1 shows the DNA molecules used in our experiments as well as the anticipated protein-DNA complexes. Fragments I and III bear two operator sites separated by five helical turns,

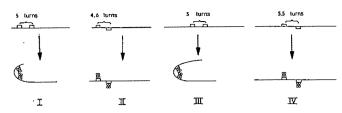


Fig. 1 DNA molecules used and expected shapes of complexes formed with λ repressor. The centre-to-centre distances separating the operator sites are given in helical turns and the molecules are drawn approximately to scale. DNA sequences spanning the two operator sites for each of these molecules are as previously described.

Table 1	Electron	microscopic	count of	DNA	fragments

DNA fragment	No. straight	No. bent	% Bent
1. I	36	8	19
2. I	50	32	39
3. II	213	0	0
4. II	37	0	0
5. II	32	0	0
6. II	46	1	2
7. III	113	9	7
8. III	67	7	9
9. IV	106	0	0
10. ÌV	86	0	0
11. IV	38	0	0

Each line represents a separate experiment. The repressor concentration in the first four experiments was one half that of the other experi-

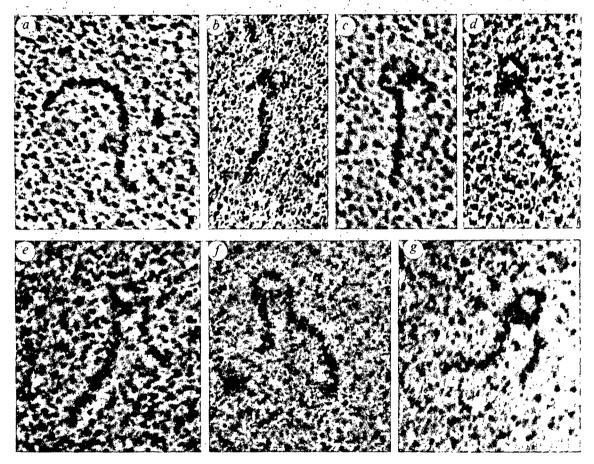


Fig. 2 Visualization of λ repressor bound to DNA fragments shown in Fig. 1. Purified λ repressor is shown bound to DNA fragments I (b-d), III (e-g) and II (a), as visualized by electron microscopy. In these experiments, 300-400 base-pair fragments containing repressor binding sites (20 ng ml⁻¹) were incubated with purified repressor (2 or 4 μg ml⁻¹) in a buffer containing 10 mM Tris-HCl, pH 7.0; 25 mM MgCl₂; 10 mM CaCl₂; 1 mM EDTA and 200 mM KCl. Supertwisted pBR322 DNA was included at 2 μg ml⁻¹ to reduce nonspecific protein binding. Following 20-min incubations at 37°, the complexes were fixed by the addition of HEPES buffer to 20 mM and formaldehyde to 1% for 5 min at 20°, followed by the addition of glutaraldehyde to 0.6% for an additional 5 min. The samples were directly mounted onto thin carbon films, washed with water and ethanol rinses, air dried and rotary shadowcast with tungsten as previously described¹⁰. Shadowcasting was done in a fully cryopumped system at a vacuum of 2×10⁻⁷ torr. The micrographs were taken with a Phillips EM400 instrument operated at 20 kv. Bar equals 0.1 μm.

assuming 10.5 base pairs per turn and measuring from the central base pair. The disposition of the two sites with respect to the ends of the molecule are different in the two cases and the protein-DNA complexes were expected to be distinguishable under the electron microscope. Fragments II and IV bear operator sites separated by 4.6 and 5.5 turns respectively and in this case we expected to see no looped DNA structures upon addition of repressor. In each case the two sites were those used previously¹. One is the wild-type site 0_R1 and the other a mutant

derivative $0_R 1^m$ that binds repressor sixfold more weakly than its wild-type parent. Experiments using DNase I to measure equilibrium binding show that repressor binds cooperatively to the separated sites on molecules I and III but non-cooperatively to the sites on molecules II and IV¹.

Figure 2 shows representative electron micrographs of protein-DNA complexes using three of our four DNA fragments. These samples were prepared by incubating repressor and DNA in conditions like those used to measure cooperative binding

using the DNase footprinting assay1. The samples were then fixed and shadowed with tungsten (see legend to Fig. 2). At the magnification required to visualize the short DNA fragments. two or more fragments were seldom found in the same field. Nonetheless it was not difficult to count and examine a statistically significant number of molecules for each sample. The DNA fragments were scored visually in the electron microscope as being either straight or bent with a small protein complex on the inside of the bend. Those that were scored as bent were photographed and subsequently examined to confirm this classification. Table 1 summarizes the distributions of molecules

Many examples of DNA fragment I were found in which the DNA was bent into a J shape with protein bound on the inside of the bend. (Fig. 2b-d; Table 1, lines 1 and 2). The loop between the bound repressors measured 15±5 nm, corresponding to 50 ± 15 base pairs. The location of the loop along the length of the 300-base-pair fragment and the length of the short arm (25 ± 5) base pairs) were consistent with the complex drawn in Fig. 1.

In contrast, only one in the 238 molecules of DNA fragment II examined appeared bent when repressor was complexed with this fragment (Fig. 2a; Table 1, lines 4-6). Repressor concentrations tenfold higher than those needed to produce looped structures with fragments I and III also failed to produce such structures (data not shown).

DNA fragments III and IV were prepared in Cambridge and sent to Chapel Hill labelled in code. Numerous bent complexes were found with one DNA sample (Fig. 2 e-g; Table 1, lines 7 and 8) but none with the other (Table 1, lines 9-11). As expected the former proved to be fragment III; the latter fragment IV. Note that the size of the loop observed with fragment III is similar to that observed with fragment I but that the shorter of the two arms emerging from the complex is approximately four times longer. This result is as predicted (see Fig. 1).

For all four fragments examined, it was common to observe what appeared to be a repressor on the DNA at one or the other binding site (see for example Fig. 2a). In most cases, the repressor appeared to be bound to the side of the DNA. As expected¹, there is no indication that the binding of a repressor to a single operator site bends the DNA. Very few fragments were found with two repressors bound, however, even though this was expected with fragments II and IV. It is possible that the fixation steps used here may have released many singly bound repressors from the DNA.

Several examples have now been reported of apparent protein-protein interactions "at a distance" that regulate gene expression²⁻⁸. Some if not all of these cases presumably involve formation of DNA loops^{2,3,9}. The electron micrographs described here provide the first direct visualization of loops formed when proteins bind cooperatively to separated sites on the DNA.

This research was supported in part by NIH grants GM31819 to J.G. and GM22526 to M.P., A.H. was supported in part by NIH Genetics Training grant GM07620 to the Department of Cellular and Developmental Biology, Harvard University.

Received 23 May; accepted 6 June 1986.

- Hochschild, A. & Ptashne, M. Cell 44, 681-687 (1986).
- Dunn, T., Hahn, S., Ogden, S. & Schleif, R. Proc. natn. Acad. Sci. U.S.A. 81, 5017-5020 (1984). Majumdar, A. & Adhya, S. Proc. natn. Acad. Sci. U.S.A. 81, 6100-6104 (1984).
- Dandaneli, G. & Herman, K. EMBO J. 4, 3333-3338 (1985). Takahashi, K. et al. Nature 319, 121-126 (1985).
- Brent, R. & Ptashne, M. Cell 43, 729-736 (1985).
- Keegan, L., Gill, G. & Ptashne, M. Science 231, 699-704 (1986). Riddihough, G. & Pelham, H. R. B. EMBO J. (in the press).
- Ptashne, M. A Genetic Switch (Cell, Palo Alto & Blackwell, Cambridge 1986).
- 10. Griffith, J. & Christiansen, C. A. Rev. Biophys. Bioengng. 7, 19-37 (1978).

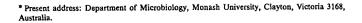
Length growth in fission yeast cells measured by two novel techniques

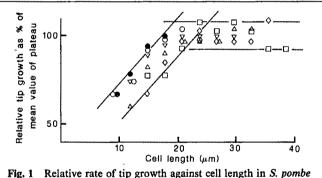
J. W. May* & J. M. Mitchison

Department of Zoology, University of Edinburgh, West Mains Road, Edinburgh EH9 3JT, UK

Time-lapse films have shown that cells of the fission yeast Schizosaccharomyces pombe exhibit a sharp increase in the rate of length growth at one stage of the cell cycle and that the same periodic increase in growth rate, a cell-cycle event, occurs in a cell-cycle mutant after the DNA division cycle has been blocked1. The continued periodicity of cell-cycle events after such a block has been shown in other systems^{2,3} and has intriguing implications for cell-cycle control models. We have therefore developed two new methods for measuring the rate of length growth which are equivalent to pulse labelling. The results confirm the evidence from films and also show that the rate of growth reaches a plateau after the blocked cells have achieved a critical size.

Time-lapse films are the most direct way of measuring cell growth, but analysis accurate enough for rate determinations is very time-consuming. In addition, some cell cycle mutants only grow under mounting conditions that prevent good optical resolution1. Our methods made use of the fact that Bandeiraea simplicifolia lectin (BSL) binds to the cell wall of S. pombe⁴. They also took account of the need to measure cell size as well as rate of growth, since the point where the rate changes in wild-type cells is size-related1. In our initial experiments with wild-type cells, an overall coating of BSL coupled to fluorescein isothiocyanate (FITC) was applied. The cells were then washed





cdc 2.33 at increasing times after shift-up to the restrictive temperature. Cells were grown up overnight at 28 °C in a minimal medium EMM3 (ref. 9) + 0.5% yeast extract + 0.1 µg ml⁻¹ biotin (this extra biotin was to guard against binding by traces of avidin). The medium was adjusted to pH 6.0 to promote lectin binding. The culture $(1.2 \times 10^6 \text{ cells ml}^{-1})$ was shifted to 36.5 °C at time zero. Samples were taken at 1 h (\bullet), 2 h (\bigcirc), 2.5 h (∇), 3 h (\triangle), 3.5 h (♦) and 4 h (□). Each sample was treated as follows: 1 min in biotinylated BSL (type BS 1) at 5 µg ml⁻¹; washed once; 1 min in avidin conjugated with Texas Red at 1.3 $\mu g \, ml^{-1}$ plus avidin at 5 μg ml⁻¹; washed twice; suspended in conditioned medium and incubated, one part (experimental) at 36.5 °C for 30 min and the other part (control) at 0 °C; then tip coating put on by 1 min in BSL-FITC at 2 µg ml⁻¹; washed once and preserved with formalin at 1%. Washing was done by centrifugation in a small bench centrifuge for 30 s at 13,400g. All reagents were from Sigma. Analysis was done in a FACS IV (Becton Dickinson) on 25,000 cells. The results were grouped for red fluorescence (length) and the peak value found for the green fluorescence (tip growth). There was appreciable penetration of the green lectin into the areas coated by the first red lectin. This was allowed for by taking the peak value of the green fluorescence in the control above (where there had been no tip growth) and subtracting this from the peak value of the experimental sample. The red fluorescence has been converted into cell length by taking the results from an earlier experiment in which cell length was measured against time after shift-up.

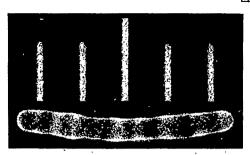
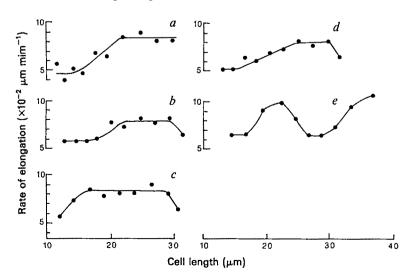


Fig. 2 A cell of S. pombe cdc 2.33 growing at both ends and coated alternately with lectin with FITC and lectin without FITC; a 'double-ended tiger-tail'. The coating procedure was as for Fig. 3 except that the intervals between coatings was 40 min. Scale divisions at 10-μm intervals.

and left to grow for 30 min (20% of the generation time). During this time, new uncoated wall was generated at the ends of the cell, as *S. pombe* grows by tip extension. At the end of the period, the new wall was coated with the same lectin but coupled with Texas Red through a biotin-avidin link. Under fluorescence microscopy, the cells were green with red tips. There was an intermediate yellow zone between body and tips due to overlap between the two lectins, and a mixing of old and new wall material at the growing tip.

Most of the experiments were done with a temperature-sensitive mutant of S. pombe cdc 2.33 (ref. 5). When the culture was shifted to the restrictive temperature (36.5 °C), mitosis was blocked but the cells continued to grow for several generation times and became very elongated. The coating procedure described above was used on cells of cdc 2.33 except that the sequence was reversed, with Texas Red being used as the body coating and FITC as the tip coating. This was done on samples taken every 30 min from 1 h after shift for 4 h. The samples were then analysed in a fluorescence-activated cell sorter (FACS) which measured each cell for red fluorescence (cell length minus tips) and green fluorescence (tip growth). The grouped results in Fig. 1 show that, as would be expected, the later samples had more large cells and fewer small cells. They also show that, irrespective of sampling time, the rate of tip growth increased with cell length up to a limiting length of about 20 µm. Thereafter the rate plateaued. These results are quite consistent with the rate changes observed in the time-lapse films since sharp steps in rate in individual cells would be spread out to give a slower rise in cell populations. What is missing is an initial rate plateau in the smallest cells before the rise. It proved impossible, however, to obtain reliable measurements of green fluorescence in these cells because they were contaminated by a subpopulation of small non-growing cells.



The second method used a coating procedure similar to the first one except that no fluorochrome was conjugated to the avidin. The important difference was that the procedure was continued for 6 h with alternate treatments every 30 min with lectin plus FITC and with lectin without a fluorochrome. The cells were photographed with a fluorescence microscope at the end of the experiment. They showed a pattern of bands (we call them 'tiger-tails') which define the history of length growth of each cell (Fig. 2). Analysis was by a ruler rather than a FACS. Growth appeared to be unaffected by the coating procedures, as we used short centrifugation times and worked in a warm room at 36 °C to avoid releasing the mutant block. Pulse times below 30 min were impracticable because the overlap mentioned above reduced contrast between the bands.

Cells which were small initially grew at one end and those which were large grew at both ends. The critical length was 11.5 µm at 1 h after shift-up. Double-enders were difficult to analyse, partly because many of them had a different number of bands at each end (see, for example, Fig. 2). Figure 3 therefore shows some representative graphs of the growth rate of singleenders. Of 32 cells analysed, 14 showed stepwise rises in rate (Fig. 3a,b). The mid-point of the step was at a mean of 18.3 µm (s.d. 2.36) and the mean increase in rate at the step was $\times 1.48$. This is in good accord with the results from films where the equivalent values were 19.4 µm and ×1.33. Other cells reached a plateau either with a very early step (Fig. 3c) or with a prolonged one (Fig. 3d). Taking these cells together with those with well-defined steps, 20 cells reached a plateau in rate at a mean length of 19.4 μ m (s.d. 3.1). This is very similar to the results in Fig. 1 from the FACS analysis. Nevertheless, there was a substantial minority of cells (14 out of 32) which did not fit these patterns and an extreme, though rare, example is shown in Fig. 3e. This variability in pattern (also found in the film results) is real and very probably greater in blocked mutants than in normal cells, but our results do emphasize the fact that analyses of whole populations can conceal what individual cells do. A final point about Fig. 3 is that three out of the five graphs show a fall in rate at the end, in contrast to Fig. 1. This is because the experiments were continued for 7 h, 2.5 h longer than in Fig. 1, and blocked mutants show a fall-off in rate after prolonged periods.

In conclusion, these two methods confirm the results from films¹ but by very different methods. The FACS analysis has also established a plateau in rate with longer cells. This was not previously known for cell length but has been shown for enzyme potential⁶ and for the rate of synthesis of protein⁷ and ribosomal RNAd⁸. We believe that the methods should have wider application in other cells which have rigid cell walls and defined growing points.

This work was supported by the SERC and the Cancer

Fig. 3 Representative patterns for rate of tip growth against cell length in individual cells of S. pombe cdc 2.33 for 7 h after shift-up. Cell growth, medium and shift-up were as for Fig. 1. Cells were taken at 1 h after shift-up; treated for 1 min in biotinylated BSL at 5 μg ml⁻¹; washed once; 1 min in avidin at 5 μg ml⁻¹; washed twice; resuspended in conditioned medium and incubated at 36.5 °C for 30 min; then treated for 1 min in BSL-FITC at 2 μg ml⁻¹; washed once; incubated for 30 min and the BSL-biotin-avidin coating repeated. The cycle of alternate avidin-biotin and FITC coatings was repeated every 30 min until 7 h after shift-up. The cells were finally fixed in 1% formalin and photographed in a Zeiss Photomicroscope I with a ×40 objective and the exciting wavelength for FITC. The band positions were measured on photographic enlargements.

Research Campaign. We thank Drs J. Creanor, P. A. Fantes and R. A. Gray and Mr A. B. Sanderson for assistance in some experiments and for helpful discussions.

Received 21 April: accepted 4 June 1986.

- Mitchison, J. M. & Nurse, P. J. Cell Sci. 75, 357-376 (1985).
 Yoneda, M., Ikeda, M. & Washitani, S. Deul Growth Differentiation 20, 329-336 (1978).
 Newport, J. W. & Kirschner, M. W. Cell 37, 731-742 (1984).
 Horisberger, M., Vonlanthen, M. & Rosset, J. Archs Mikrobiol. 119, 107-111 (1978).
- Nurse, P., Thuriaux, P. & Nasmyth, K. Molec gen. Genet. 146, 167-178 (1976). Benitez, T., Nurse, P. & Mitchison, J. M. J. Cell Sci. 46, 399-431 (1980).
- Creanor, J. & Mitchison, J. M. J. Cell Sci. 69, 199-210 (1984).
- 8. Elliott, S. G. Molec, gen. Genet. 192, 212-217 (1983). 9. Creanor, J. & Mitchison, J. M. J. Cell Sci. 58, 263-285 (1982).

Propulsion of organelles isolated from Acanthamoeba along actin filaments by myosin-I

Richard J. Adams & Thomas D. Pollard

Department of Cell Biology and Anatomy, Johns Hopkins University School of Medicine, 725 North Wolfe Street, Baltimore, Maryland 21205, USA

Eukaryotic cells are dependent on their ability to translocate membraneous elements about the cytoplasm. In many cells long translocations of organelles are associated with microtubules 1-3 In other cases, such as the rapid cytoplasmic streaming in some algae, organelles appear to be propelled along actin filaments⁴. It has been assumed, but not proven, that myosin produces these movements. We have tested vesicles from another eukaryotic cell for their ability to move on the exposed actin bundles of Nitella⁵ as an indiction that actin-based organelle movements may be a general property of cells. We found that organelles from Acanthamoeba castellanii can move along Nitella actin filaments. Here, we report two different experiments indicating that the singleheaded non-polymerizable myosin isozyme myosin-I (ref. 6) is responsible for this organelle motility. First, monoclonal antibodies to myosin-I inhibit movement, but antibodies that inhibit double-headed myosin-II do not. Second, ~20% of the myosin-I in homogenates co-migrates with motile vesicles during Percoll density-gradient ultracentrifugation. This is the first indication of a role for myosin-I within the cell and supports the suggestion of Albanesi et al.7 that myosin-I moves vesicles in this way.

We saw directed motion of vesicles and aggregates of vesicles from Acanthamoeba on the substrate of Nitella actin bundles (Fig. 1). Movements were in the same direction as those of endogeneous algal organelles but substantially slower (Fig. 2b),

the average rates of movement being $0.24 \pm 0.11 \,\mu\text{m s}^{-1}$ (mean \pm s.d., n = 50) compared with $\ge 40 \,\mu\text{m} \text{ s}^{-1}$ for endogeneous movements8. The distribution of rates of movement for Acanthamoeba vesicles was wide (Fig. 2b) and varied from batch to batch. The vesicles in some preparations were never seen to move; the cause of this variation is unknown. Further, in any one extract, not all of the vesicles that settle onto the substrate were seen to move. We could follow moving vesicles for tens or hundreds of micrometres; the data in Fig. 2 represent the average rate measured over a distance of 20-140 µm. Rates of motion were relatively constant over these distances without the saltations or interruptions characteristic of oganelle movements within live cells. Most of the movements that ceased in the field of view appeared to result either from damage in the substrate or from steric interference. We are confident that the movements of Acanthamoeba vesicles is independent of those of Nitella organelles for several reasons: no endogeneous organelles are seen to move with this speed and all that show any signs of movement are lost from the preparation soon after dissection. (Experiments were not performed on dissected Nitella preparations while endogeneous organelles were still moving.) To check this, two preparations of dissected Nitella were incubated in 5 mM N-ethylmaleimide for 5 min to inhibit the activity of the endogeneous myosin species⁹. After treatment with 7 mM dithiothrietol to neutralize the N-ethylmaleimide, no endogeneous organelles moved but organelles in Acanthamoeba extracts moved normally. The enzyme responsible for their motion would, therefore, appear to be associated with the vesicles themselves.

Acanthamoeba contains two distinct species of myosin^{6,10,11} which are candidates for the motor driving of these vesicles along the actin bundles of the Nitella cortex. The two species differ, both physically and enzymatically: myosin-I is enzymatically highly active⁶ but, unlike Acanthamoeba myosin-II and other known myosins, it consists of only one heavy chain which lacks the long α -helical tail required for polymerization into thick filaments^{6,7}. Like most other myosins, myosin-II has two heads and a tail and can form bipolar filaments.

We used monoclonal antibodies to show that myosin-I but not myosin-II is required for organelle movements along actin filaments. Antibody M1.5 inhibits stochiometrically the actinactivated ATPase of myosin-I (ref. 12) and antibodies M2.3, M2.10 and M2.26 all stoichiometrically inhibit the actin-activated ATPase of purified myosin-II as well as the contraction of actin gels in crude cytoplasmic extracts¹³. These four antibodies react with the heavy chains of either myosin-I (M1.5) or myosin-II (M2.3, M2.10 and M2.26) among the various proteins in cellular extracts^{12,14}. M1.5 and other monoclonal antibodies to myosin-I also bind to nuclear proteins¹². In blind experiments antibody M1.5 completely stopped all organelle movement on

Tab	le 1 Antibody inhibition of move	ements	•
Experimental preparation	Antigen	Antibody: myosin ratio	Presence of movement
Untreated extract Untreated extract on substrate pretreated with			+ ;
5 mM N-ethylmaleimide then dithiothreitol			+
Extract treated with antibodies*:			· -
M2.3	Myosin-II	10:1	+
M2.10	Myosin-II	20:1	+
M2.26	Myosin-II	20:1	+
M1.5	Myosin-I	20:1	
		2:1†	+/-
		0.2:1	+
		0.02:1	+
Alice‡	Chicken muscle myosin	- Auto-	+

^{*} Results of blind experiments in which the experimenter did not know the treatment of the organelle preparations.

[†] Results of two sets of blind experiments carried out at this ratio of antibody to antigen showed inhibition in one but not the other experiment.

[‡] Monoclonal antibody raised against chicken muscle myosin; does not cross-react with Acanthamoeba myosins.

Fig. 1 a. Organelles (arrows) moving on a substrate of Nitella actin bundles, photographed at 15-s intervals. The image-processing procedure (see below) causes the image of the organelles to change from frame to frame. Photographs prepared from moving organelles recorded on videotape. Scale bar, 10 µm. Actin bundles oriented horizontally. b, Phagocytic vesicles rendered visible by feeding the cells fluorescent beads before homogenization. Fluorescent organelles (arrows) are seen against the autofluorescence of the Nitella chloroplasts. Photographs taken at 30-s intervals from an unprocessed video-recording. Scale bar, 10 µm. Actin bundles oriented horizontally.

Methods. Acanthamoeba castellanii were grown in liquid culture as described previously6. Organelles were prepared freshly each day starting from approximately 0.2 g wet weight of compacted cells, washed three times in 50 mM NaCl. The cells were resuspended in 1 ml of homogenization buffer (60 mM potassium glutamate, 2 mM EGTA, 2 mM MgCl₂, 10 mM imidazole pH 6.4, 0.1 mM benzamidine, 1 mM phenylmethylsulphonyl fluoride and 4 mM ATP) and disrupted by eight strokes with a tight-fitting pestle in a 7-ml Dounce homogenizer. The homogenate was cleared of unbroken cells and large particles with a 5-s spin at 10,000 g in a bench-top Eppendorf centrifuge. The resulting supernatant was used for all the experiments. In some experiments cells were preprared with fluorescent phagocytic vesicles. Washed cells were incubated, with occasional mixing, for 15 min at room temperature in a dense suspension of rhodaminelabelled polyacrolein beads in 50 mM NaCl. (Beads of $\sim 0.5 \,\mu m$ diameter were prepared by

the method of Margel et al.²³). Labelled cells were further washed three times in cold saline and processed as before. Nitella was dissected as described by Sheetz and Spudich' in a buffer of 20 mM KCl, 4 mM EGTA, 4 mM MgCl₂, 10 mM sucrose, 5 mM imidazole pH 7.0 and 2 mM ATP. The suspension of organelles was mixed 1:1 with homogenization buffer containing 0.2 M sucrose and added to a region of exposed Nitella ectoplasm with a microcapillary. Motion of organelles on Nitella was observed on an upright Zeiss microscope with a ×40 water-immersion, phase-contrast objective. At this magnification movements were too slow to be discerned by eye but became obvious when speeded up by time-lapse video microscopy. The microscope was fitted with Dage-MIT Newvicon video camera, the output of which was passed through a Quantex digital image processor (DS 30) and Colorado Video analogue video processor (604) before being recorded at 1/18 real-time on a National Panasonic (NV 8030) time-lapse video recorder. Detection of movement of small vesicles on the complex substrate was difficult, so the following image-processing regime was used to selectively enhance moving particles. The image processor continuously subtracted an image of the non-moving Nitella background from the incoming picture. Thus, only differences between the two images are seen, that is, objects that moved. This technique is complicated because the Nitella substrate distorts to some extent during the experiment (~20 min). To overcome this, the background image was itself slowly averaged using a rolling average, with the incoming image, that replaces the stored image every 128 frames. It is necessary to ensure that the rate of averaging is slower than the rate of detection of the differences (the rate of recording on the video recorder). The contrast of the difference image from the digital processor was further enhanced with the Colorado Video analog processor.

Nitella actin bundles, whereas antibody inhibitors of myosin-II (M2.3, M2.10 and M2.26) had no obvious effect on organelle movements (Fig. 2a). The average rate of movement was $0.23 \pm 0.09 \,\mu\text{m s}^{-1}$ (mean $\pm \text{s.d.}$, n=12) in the presence of myosin-II antibodies. A ratio of M1.5 antigen binding sites (this antibody is an immunoglobulin M) to estimated myosin-I content of the extract (1.3 μ mol per kg of wet cells⁶) of 20:1 reproducibly inhibited motion whereas a ratio of 2:1 inhibited motion in one but not a second of two sets of experiments. Ratios of 0.2:1 or 0.02:1 did not inhibit movement (Table 1). These experiments provide evidence that the movement of the organelles is driven by the smaller myosin species, myosin-I. The rate of motion of these organelles is ~10 times higher than that recently reported for plastic beads coated with myosin-I on a Nitella preparation⁷.

The composition of the homogenate used for these experiments is highly heterogeneous so we do not yet know which organelles are moving. But by pre-labelling phagocytic vesicles of the cells with fluorescent beads we could show that these were among the organelles that move in our experiments (Fig. 1b). This could be a subset of the total moving population.

We used cell fractionation to test whether myosin-I is physically associated with the motile vesicles (Fig. 3). When the crude extracts used in the motility experiments were centrifuged on a Percoll gradient, organelles sedimented into the density gradient and were separated from the soluble components at the top of the tube. Organelles that came to equilibrium at a density of 1.08-1.13 g ml⁻¹ were motile on *Nitella* actin bundles. This fraction was also greatly enriched in myosin-I relative to myosin-II, which remains essentially in the supernatant. Approximately 20% of the myosin-I in the extract sedimented with these motile organelles. Tests with specific monoclonal antibodies¹⁰ showed that both myosin-IA and -IB are associated with organelles. Therefore, there is a stable interaction of myosin-IA and -IB with organelles that persists through centrifugation, is insensitive to ATP and is competent to move organelles along actin bundles.

These experiments show that an actomyosin system can provide the force for some membrane movements within the cell, as has been speculated based on experiments with myosin-coated beads⁵⁻⁷. The heterogeneity of the organelles in our preparation and the fact that we used a cell-free system do not

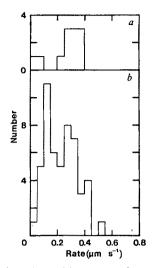


Fig. 2 Distribution of velocities of Acanthamoeba vesicles on a Nitella actin bundle substrate. a, Movement of 12 organelles in the presence of antibodies to myosin-II; b, accumulated results from 50 organelles measured in control preparations.

Methods. The net speed of movement for a vesicle was measured from the replay of a videotape recording of an experiment. The positions at the beginning and end of a timed motion were marked on the video monitor. The screen coordinates of these two points were read using a Colorado Video analyser (321) and the corresponding displacement calculated with account being made of lateral distortions introduced by the video camera. Speeds were recorded for displacements of 20-140 µm.

yet permit us to identify directly the nature or role of these movements in the cell. Immunofluorescent localization of myosin-I in the cell^{12,15} reveals a cortical concentration which suggests an involvement of myosin-I-powered movements in endocytosis or surface movements in addition to organelle movements. Such processes may be important in other cells since myosin-I has now been indentified in Dictyostelium¹⁶ and a

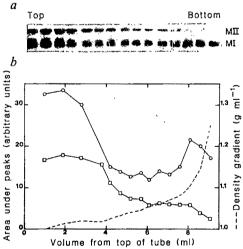


Fig. 3 Acanthamoeba cytoplasmic extract (0.5 ml) was layered onto 9.0 ml of 1.08 g ml^{-1} Percoll in homogenization buffer and centrifuged at 27,000 r.p.m. in a Beckman Ti 50 rotor for 15 min. The gradient was unloaded from the bottom of the tube; the densities of Percoll in the collected fractions was determined from refractive indices. Aliquots of these fractions were electrophoresed on 7.5% gels²⁴, transferred to nitrocellulose²⁵ and radioimmunologically stained with antibodies to myosin-I and -II (a). The autoradiogram shown in a was scanned using a soft-scanning laser densitometer to show the distribution of the antigens in the fractions collected from the gradient. MI, myosin-I; MII, myosin-II. b. Relative areas scanned under the peaks of myosin-I and -II were plotted for each fraction through the gradient. Circles, myosin-I; squares, myosin-II.

similar ATPase has been identified as the link between the actin filaments and the membrane in microvilli¹⁷. Previous results which suggested a possible role for actin filaments in organelle movements in other cell types^{1,18-22} may also be mediated by proteins like myosin-I.

This work was supported by NIH research grants GM 26338 and GM 26132 (to T.D.P.) and a Postdoctoral Fellowship from the Muscular Dystrophy Association (to R.J.A.).

Received 10 March: accepted 2 June 1986.

- Schliwa, M. Cell Muscle Motil. 5, 1-82 (1984).
- Schnapp, B. J., Vale, R. D., Sheetz, M. P. & Reese, T. S. Cell 40, 455-462 (1985). Allen, R. D. et al. J. Cell Biol. 100, 1736-1752 (1985). Kachar, B. Science 227, 1355-1357 (1985).

- Acatal, B. P. & Spudich, J. A. Nature 303, 31-35 (1983).
 Pollard, T. D. & Korn, E. D. J. biol. Chem. 248, 4682-4690 (1973).
 Albanesi, J. P. et al. J. biol. Chem. 260, 8649-8652 (1985).
- Kamiya, N. & Kuroda, K. Bot. Mag. 69, 544-554 (1956).
- Chen, J. C. W. & Kamiya, N. Cell Struct. Funct. 1, 1-9 (1975).
 Maruta, H. & Korn, E. D. J. biol. Chem. 252, 6501-6509 (1977)
- Maruta, H. & Korn, E. D. J. biol. Chem. 282, 6501-6509 (1977).
 Pollard, T. D., Stafford, W. F. & Porter, M. E. J. biol. Chem. 253, 4798-4808 (1978).
 Hagen, S. C., Kiehart, D. P., Kaiser, D. A. & Pollard, T. D. J. Cell Biol. (in the press).
 Kiehart, D. P. & Pollard, T. D. J. Cell Biol. 99, 1024-1033 (1984).
 Kiehart, D. P., Kaiser, D. & Pollard, T. P. J. Cell Biol. 99, 1002-1014 (1984).

- 15. Gadasi, H. & Korn, E. D. Nature 286, 452-456 (1980).
- 16. Cote, G. P., Albanesi, J. P., Ueno, T., Hammer, J. A. & Korn, E. D. J. biol. Chem. 260, 4543-4546 (1985).
- 17. Collins, J. H. & Borysenko, C. W. J. biol. Chem. 259, 14128-14135 (1984).
- Edds, K. T. J. Cell Biol. 66, 145-155 (1975).

- Bradley, T. J. & Satir, P. J. supramolec Struct. 12, 165-175 (1979).
 Isenberg, G., Schubert, P. & Kreutzberg, G. W. Brain Res. 194, 588-593 (1980).
 Goldberg, D. J., Harris, D. A., Lubit, B. W. & Schwartz, J. H. Proc. natn. Acad. Sci. U.S.A. 77, 7448-7452 (1980).
- Brady, S. T. Lasek, R. J., Allen, R. D., Yin, H. L. & Stossel, T. P. Nature 310, 56-58 (1984). Margel, S., Beitler, U. & Ofarim, M. J. Cell Sci. 56, 157-175 (1982). Laemmli, U. K. Nature 229, 680-685 (1970).

- Towbin, H., Staehlin, T. & Gordon, J. Proc. natn. Acad. Sci. U.S.A. 76, 4350-4354 (1979).

Lateral proton conduction at lipid-water interfaces and its implications for the chemiosmotic-coupling hypothesis

Michel Prats, Justin Teissié & Jean-François Tocanne*

Centre de Recherche de Biochimie et de Génétique Cellulaires du CNRS, 118 Route de Narbonne, 31062 Toulouse Cédex, France

The driving force in energy-transducing membranes is now recognized to be linked to a flux of protons between membrane-bound donors and acceptors. The question of whether the proton pathway is delocalized within the two bulk aqueous phases on each side of the membrane (delocalized chemiosmotic theory1), or is localized at its surface (semi-localized hypothesis2) still remains open to discussion^{3,4}. Using an original fluorescence monolayer technique, we have recently been able to provide direct experimental evidence that a phospholipid-water interface can act as an efficient proton conductor^{5,6}. This observation strongly supports the semi-localized hypothesis². In the present study, comparisons between surface potential and fluorescence measurements in monolayers provide additional evidence of a facilitated proton conduction along phospholipid-water interfaces. They suggest the existence of an induced steep surface pH gradient from a more acidic surface towards the bulk. They also show that lateral proton transfer along the surface of a biological membrane would alter the surface potential of that membrane.

The surface potential ΔV which is measured for lipids in monolayers is known to originate primarily from the polar headgroups and to depend on their ionization state⁷. Therefore, since the lipid is the probe itself, this technique affords an elegant way of observing the lateral movements of protons and of

^{*} To whom correspondence should be addressed.

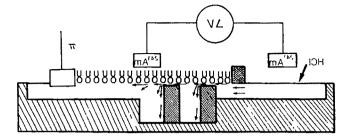


Fig. 1 Schematic drawing of the experimental set-up. The monolayer experiments were carried out with the same trough and using the same experimental conditions as previously described for fluorescence experiments^{5,6}. The trough comprised one 'injection' and one 'observation' compartment separated by two glass barriers. Continuity of the subphase occurred via a very thin water layer, about 1 mm in depth, between the water surface and the top of the barriers. π was measured by means of a platinum plate connected to a force transducer of our own manufacture. Surface potential was measured by two americium electrodes¹¹. One (reference) was located above the lipid-free region of the 'injection' compartment. The other (measurement) faced the lipid film. The 'standard' conditions^{5,6} we used were: the 'measurement' electrode was centred at a distance of 4.3 cm from the first glass barrier; the area of the monolayer in direct contact with the acidic subphase in the 'injection' compartment was 12.6 cm²; protons (150 µl 3 M HCl) were injected under stirring (Teflon bar, 90 r.p.m.). 'Standard' conditions of subphase (1 mM phosphate, pH 6.8) and film surface pressure (25 mN m⁻¹) were used. Arrows indicate the various diffusion pathways of protons which can move along the lipid/water interface and which can also diffuse through the bulk of the water phase by a combination of diffusion and convection movements.

determining to what extent the polar headgroups are involved in the proton conduction process.

Three phospholipids were examined: phosphatidy-lethanolamine (PE) from Escherichia coli (Sigma), phosphatidylserine (PS) from bovine brain (Sigma) and dilauroylphosphatidylglycerol (PG) of synthetic origin⁸. As shown in Fig. 1, the trough, the method for generating the flux of protons and the experimental conditions used were identical to those previously described for the fluorescence experiments^{5,6}.

Typical ΔV recordings with time are shown in Fig. 2. Less than 3 min after proton injection, a large increase in ΔV was observed for each lipid. A positive change in ΔV is expected if protons concentrate at the lipid-water interface⁷. From these curves, two parameters were determined: (1) $TH_{\Delta V}^{+}$, the time which is necessary to detect a change in the surface potential and which relies on the rate of proton transfer along the lipid/water interface^{5,6}, (2) $\Delta \Delta V$, the change in surface potential which, like the change in surface fluorescence ΔF (refs 5, 6), accounts for the variation in proton concentration at the interface. $TH_{\Delta V}^{+}$ and $\Delta \Delta V$ values measured for each lipid are shown in Table 1.

Fluorescence investigation of proton conduction by phosphatidylserine and phosphatidylglycerol was carried out exactly as previously described for phosphatidylethanolamine^{5,6}. 'Standard' conditions of subphase (1 mM phosphate, pH 6.8) and

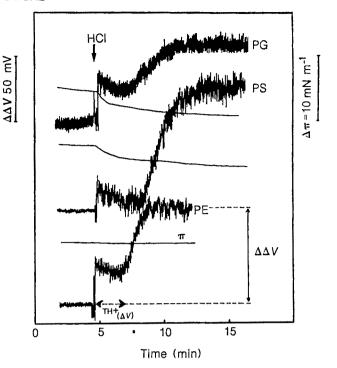


Fig. 2 Kinetics of the surface potential and surface pressure changes after an acid jump. Phosphatidylglycerol (PG), phosphatidylserine (PS) and phosphatidylethanolamine (PE) were spread at a surface pressure of 25 mN m⁻¹ by stepwise deposition of the lipids onto the subphase. The left part of the curves refers to the surface potential which was initially measured after spreading the lipids on the 1 mM phosphate subphase at pH 6.8. Addition of HCl gave rise to an immediate drop of the pH from 6.8 to 2.2 in the 'injection' compartment. This resulted in a rise of the surface potential due to polarization of the 'reference' electrode. Control experiments carried out in the absence of film showed that this rise in ΔV rapidly vanished with time. After about 5 min, the ΔV returned to its initial value. Changes in ΔV resulting from proton translocation along the various lipid monolayers were therefore determined from the surface potential measured before the addition of HCl, which can be considered as a 'reference' potential. $TH_{\Delta V}^+$ is the delay between H⁺ injection and the beginning of the change in ΔV . $\Delta \Delta V$ is the change in surface potential which is measured at equilibrium, when a plateau is again observed. The thin continuous curves are the recorder traces of the surface pressure π .

surface pressure (25 mMm^{-1}) were used. The TH_F^+ and ΔF values which were measured for the two lipids are shown in Table 1, together with those already reported for PE^{5,6}. As expected, the two techniques lead to similar TH^+ (around 2 min) for each lipid. From these values, PS would be a less efficient proton translocator than PE or PG, which exhibit the same behaviour.

translocator than PE or PG, which exhibit the same behaviour. The change in 'interfacial' pH which originates from proton conduction cannot be determined directly from the ΔF or $\Delta \Delta V$ values of Table 1. Nevertheless, and as a first approximation, this change in 'interfacial' pH can be related to the change in subphase pH for which the same ΔF and $\Delta \Delta V$ values would

Table 1 Changes in surface potential, surface fluorescence and pH for various phospholipids								
Phospholipids		Surface	potential			Fluores	сепсе	
• •	$TH_{\Delta V}^{+}(s)$	$\Delta\Delta V (mV)$	pΗ	ΔpH^*	$TH_F^+(s)$	$\Delta F(\%)$	pH	$\Delta p H^*$
PE	140 ± 20	61 ± 10	2.6 ± 0.2	4.2 ± 0.2	120 ± 5†	$78 \pm 18 \dagger$	5.0 ± 0.8	1.8 ± 0.3
PG	130 ± 10	40 ± 20	3.1 ± 0.4	3.7 ± 0.4	120 ± 10	65 ± 5	5.5 ± 0.2	1.3 ± 0.3
PS	170 ± 15	75 ± 25	3.7 ± 0.5	3.1 ± 0.5	160 ± 5	41 ± 6	6.0 ± 0.2	0.8 ± 0.3

 TH^+ , changes in surface potential $\Delta\Delta V$ and in surface fluorescence ΔF and measured equivalent bulk-phase pH and ΔpH values for films of phosphatidylethanolamine (PE), phosphatidylgycerol (PG) and phosphatidylserine (PS) (average of three to seven determinations)

^{*} ΔpH is defined as the difference between the initial subphase pH (6.8) and the measured equivalent bulk-phase pH.

[†] From ref. 5.

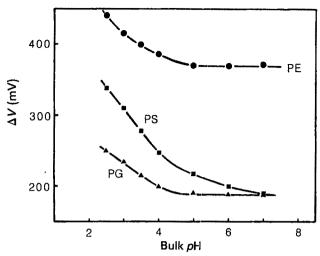


Fig. 3 Surface potential versus subphase pH titration curves. Phosphatidylethanolamine (PE), phosphatidylserine (PS) and phosphatidylglycerol (PG) were spread at a constant molecular area of 0.54nm², 0.66 nm² and 0.56 nm² respectively by stepwise deposition of the lipids onto various 1 mM phosphate subphases at the desired pH. For each lipid, these molecular areas correspond to a film surface pressure of 25 mN m⁻¹ at pH 6.8. Data presented are the average of five determinations.

be measured at equilibrium in surface fluorescence and surface potential against subphase pH titration curves, by reference to the initial subphase pH of 6.8. In the following, the change in 'interfacial' pH approximated in this way will be referred to as the 'equivalent bulk-phase' ΔpH .

Surface potential/subphase pH titration curves of PE, PS and PG are shown in Fig. 3. The apparent pK measured for our fluorescent pH indicator fluorescein thiocarbamide phosphatidylethanolamine (F-PE) in the presence of PG and PS (titration curves not shown) was not significantly different from that already determined for PE5.

The 'equivalent bulk-phase' pH and ΔpH values determined are shown in Table 1. For each lipid, these values indicate a monolayer in contact with an interfacial water phase more acidic than the bulk water phase. The equivalent bulk-phase ΔpH values found by fluorescence were always lower than those obtained through surface potential measurements, by about 2.5 pH units. Both approaches lead to the same decreasing order of proton conduction efficiency PE > PG > PS. This order agrees with the observed increase in TH⁺. Furthermore, control experiments showed that the aqueous phase which was sucked from underneath the lipid film (about 2-3 mm from the surface), just after protons were detected by fluorescence or ΔV measurements, was still at the initial pH of 6.8.

For each lipid, the observed differences in 'equivalent bulkphase' ΔpH can be accounted for by a steep pH gradient between a more acidic interface plane and the bulk of the water phase, as proposed in Fig. 4 for PE. Indeed, the surface potential senses the ionic conditions that prevail in the interface plane, where the polar headgroups are located. Fluorescein when attached to PE does not penetrate the lipid film but remains in solution in the water phase, hanging perpendicular to the interface plane⁵. The ionizable groups of this chromophore are difficult to locate accurately. From calculations based on molecular models, fluorescein should probe a thin layer of the interphase water, at a distance between 0.5 and 1.5 mm from the interface plane. A linear extrapolation of these ΔpH values over increasing distances into the bulk aqueous phase leads to the conclusion that the equivalent bulk-phase ΔpH would again be zero at a distance of about 1-3 nm from the interface plane.

Three main conclusions are to be drawn from this study. First, our fluorescence and ΔV data provide experimental evidence that proton conduction facilitated by phospholipids could occur

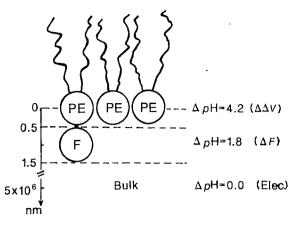


Fig. 4 Diagrammatic representation of the 'interfacial' pH gradient which is postulated to exist in the vicinity of a protonconducting lipid film. The indicated ΔpH values refer to the 'equivalent bulk-phase' ΔpH determined in Table 1 for phosphatidylethanolamine (PE) from the corresponding surface potential and surface fluorescence data. 4.2 is the ΔpH value sensed by ΔV measurements, in the interface plane. 1.8 is the ΔpH value monitored by the fluorescent pH indicator fluorescein thiocarbamide phosphatidylethanolamine (F-PE) which probes the interphase between 0.5 and 1.5 nm from the interface plane. A ΔpH of 0 shows that the pH measured by means of a pH electrode for a few millilitres of the subphase sucked up at a distance of about 5 mm from the water surface, just underneath the ΔV 'measurement' electrode and after an increase in ΔV due to proton conduction had been observed, kept the initial value of 6.8.

at the surface of energy-transducing membranes. This provides strong support for the semi-localized chemiosmotic hypothesis². Second, in our experimental conditions, large increases in surface potential were observed for each lipid tested. This means that in the case of a localized proton pathway, changes in the surface potential of energy-transducing membranes are expected. This could have consequences for certain membrane functions⁹. Third, the comparison between fluorescence and ΔV data strongly suggests that proton conduction is accompanied by a steep pH gradient from the membrane surface towards the bulk aqueous phase, the highest proton concentration being found in the interface plane. This means that protons are picked up and transported in this interface plane, where the polar headgroups of the lipids are located. In addition, the observed differences between each lipid in TH^+ and ΔpH values (Table 1) indicate that proton conduction depends on the nature of the lipid polar headgroups, as has been postulated^{5,6,10}.

It is finally worth emphasizing that the occurrence of such an interfacial pH gradient at the surface of an energy-transducing membrane might imply that the transmembrane bulk-to-bulk water phase ΔpH which is usually measured for the determination of the protonmotive force Δp , actually does not account for the real number of protons which are exchanged in the course of energy transduction.

We thank Professor Winterton for re-reading the manuscript.

Received 25 February; accepted 4 June 1986.

- Boyer, P. D., Chance, B., Ernster, L., Mitchell, P., Racker, E. & Slater, E. A. Rev. Biochem. 46, 955-1026 (1977).
- Kell, D. B. Biochim. biophys. Acta 549, 55-99 (1979).
 Ferguson, S. J. Biochim. biophys. Acta 811, 47-95 (1985).
 Haraux, F. Physiol. vég. 23, 397-410 (1985).
- 5. Teissié, J., Prats, M., Soucaille, P. & Tocanne, J. F. Proc. natn. Acad. Sci. U.S.A. 82, 3217-3221
- Frats, M., Tocanne, J. F. & Teissié, J. Eur. J. Biochem. 149, 663-668 (1985).
 Lakhdar-Ghazal, F., Tichadou, J. L. & Tocanne, J. F. Eur. J. Biochem. 134, 531-537 (1983).
 Tocanne, J. F., Verheij, H. M., op den Kemp, J. A. F. & van Deenen, L. L. M. Chem. Phys.
- Wojtczak, L. & Nalecz, M. J. Eur. J. Biochem. 94, 99-107 (1979).
 Haines, T. H. Proc. natn. Acad. Sci. U.S.A. 80, 160-164 (1983).
- 11. Sacré, M. M., El Mashak, E. M. & Tocanne, J. F. Chem. Phys. Lipids 20, 305-318 (1977).



As simple and friendly as soft gel chromatography. Powerful and productive as HPLC. Now uniquely combined into one totally new and radically different system. ULTRO-CHROM GTi. To separate, purify, quantitate and recover proteins, peptides, nucleic acids and even carbohydrates. With biological activity that can reach 100%. And in runs that only take minutes.

From pump heads to fraction collector, GTi means glass, titanium and inactive polymers. Giving you biocompatibility for complex protein mixtures. Replacing stainless steel at every liquid interface. Securing protection against buffers. Against corrosion by halide ions. Against denaturization by organic solvents. But with all the performance of a truly advanced and highly proven HPLC pump.

Meeting all your needs for multidimensional separation. Beginning with GFC. Switching columns for Ion Exchange, and then again for Hydrophobic Interaction Chromatography. Getting you higher resolution and increased purity all the way. With rapid analysis of sample complexity, continuously progressive purification and successful isolation of your important biomolecules. Completing separation strategies in hours instead of days. Solving particular problems with the most appropriate chromatography. Even reversed phase including microbore and fast LC. On just one system with unlimited potential. Giving you the most versatile chromatography in the world. Already being used by hundreds of biochemists. Getting them more results. Much faster. Much simpler. More reliably. One word says it all. GTi. You'll find it solving problems faster and better than any other separation system available. Get in touch with LKB. You're in for a winner.



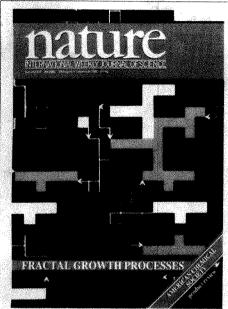
Reader Service No.40

LKB-Produkter AB, Box 305, S-161 26 Bromma, Sweden. Tel. +46(8)98 00 40, telex 10492

Antwerp (03) 218 93 35 · Athens-Middle East +30 (1) 894 73 96 · Copenhagen (01) 29 50 44 · Hongkong (852) 5-555555 London (01) 657 88 22 · Lucerne (041) 57 44 57 · Madras (044) 45 28 74 · Moscow (095) 255-6984 · Munich (089) 85 830 Paris (01) 64.46.36.36 · Rome (06) 39 90 33 · Stockholm (08) 98 00 40 · Tokyo (03) 293-5141 · Turku (021) 678 111 Vienna +43 (222) 92 16 07 · Washington (301) 963 3200 · Zoetermeer (079) 31 92 01 Over 60 qualified representatives throughout the world.

nature

NATURE VOL. 322 28 AUGUST 1986



Computer simulation of particle aggregation of the type which forms colloids and aerosols such as soot or smoke. Means of classifying and modelling such non-equilibrium growth processes are reviewed on page 789

OPINION	mentura di sanggara
Economic revolution postponed	
for now	759
EPA discovers radon	760
NEWS	
Research donations	761
European agriculture	762
Japanese space science	
Drama of human perversity	763
Private money for AIDS research	
Space station UK universities	764
US defence	765
Chernobyl accident	700
Japanese mega-prizes announced	
CORRESPONDENCE	
Miracles/Who was Buckminster Fuller?/Spain/Risk/Genetic screening/Pesticides/etc.	766
NEWS AND VIEWS-	Marie Colombia (Sandrala de Ca
New ways with	
interatomic forces	769
Neurochemistry: Lessons from	Mark Control
large molecules	
William S Agnew	770
Hungry komatiites and	
indigestible zircons GREdwards&EGNisbet	771
O IV LUMBIUS OF L'O INISUEI	771

No.	***************************************
New mechanism of antibody diversity revealed	
Frederick W Alt	772
How great white sharks,	114
sabre-toothed cats	
and soldiers kill	
Jared M Diamond	774
Anthropology: The	
longest human record	ger Park Ster
John E Yellen	774
Parallel channels and redundant	
mechanisms in visual cortex	
N V Swindale	775
Fish with toothed spines	
MJBenton	775
Asymmetric epoxidation gives	
organic chemists a hand	
Martin Bryce	776
New views of the red cell network	
Velia M Fowler	777
Glaciology: Frozen news on	
hot events	
Claus Hammer	778
-SCIENTIFIC CORRESPOND	TNIOT
Chernobyl fallout on Ioannina, G	геесе
N G Alexandropoulos,	
T Alexandropolou,	
D Anagnostopoulos, E Evangelo	
KT Kotsis & I Theodoridou	779
The Origins of the Earth's Oceans	
JS Roth	779
Frequency of dizygotic twinning DE Atkinson	mon
	780
How to abbreviate recombinant go	enes 780
R C King A system of nomenclature for	/00
murine homoeo boxes	
P Gruss & M Kessel	780
T OT USS CE IVI IX COSCI	700
BOOK REVIEWS	
Diamond Dealers and Feather	. [
Merchants: Tales from the Science	es
by 1 M Klotz	
Walter Gratzer	781
Laboratory Animal Husbandry	
by M W Fox	
Marian Stamp Dawkins	782
Transform Coding of Images	
by R J Clarke	1
Peter Hawkes	
The World of Science	
and the Rule of Law	
by J Ziman, P Sieghart	and the second
and J Humphrey	
John Maddox	783
American Archaeology Past and F	uture
by D J Meltzer, D D Fowler	
and J.A. Sabloff, eds	1.50
Warwick Bray	784

COMMENTARY-	
Breeder's rights and patenting life forms	
	785
Fractal growth processes	789
	de established (1980)
The Cretaceous/Tertiary boundary in the Gosau Basin, Austria	
A J Gratz, R Lahodynsky, M Becke	
H J Mauritsch, G Eder, F Grass, F Rögl, H Stradner & R Surenian	794
Tight linkage between a splicing mutation and a specific DNA haplotype in phenylketonuria A G DiLella, J Marvit,	
	799
the microwave background, and 1146+111B,C	
	804
background radiation near the double quasar 1146+111B,C	
A A Stark, M Dragovan, R W Wilson & J R Gott III	805
The chemical evolution of the Galaxy G Gilmore & R F G Wyse	806
Nimbus 7 satellite measurements	era et ar arjadeka
ozone decrease	
M R Schoeberl, R D McPeters.	
white the property of the second seco	808
Are Antarctic ozone variations a manifestation of dynamics or chemistry?	
K-K Tung, M K W Ko. J M Rodriguez & N D Sze	811
The state of the s	
High-resolution lattice imaging reveals a 'phase transition' in	
High-resolution lattice imaging reveals a 'phase transition' in Cu/NiPd multilayers CS Baxter & WM Stobbs	814
reveals a 'phase transition' in Cu/NiPd multilayers CS Baxter & WM Stobbs New method for the measurement of osmium isotopes applied to a	814
reveals a 'phase transition' in Cu/NiPd multilayers CS Baxter & WM Stobbs New method for the measurement	814
	and patenting life forms J-P Berland & R Lewontin REVIEW ARTICLE Fractal growth processes L M Sander ARTICLES The Cretaceous/Tertiary boundary in the Gosau Basin, Austria A Preisinger, E Zobetz. A J Gratz, R Lahodynsky, M Becke H J Mauritsch, G Eder, F Grass, F Rögl, H Stradner & R Surenian Tight linkage between a splicing mutation and a specific DNA haplotype in phenylketomuria A G DiLella, J Marvit, A S Lidsky, F Güttler, S L C Woo LETTERS TO NATURE Effect of gravitational lenses on the microwave background, and 1146+111B,C J P Ostriker & E T Vishniac Observations of the cosmic background radiation near the double quasar 1146+111B,C A A Stark, M Dragovan, R W Wilson & J R Gott III The chemical evolution of the Galaxy G Gilmore & R F G Wyse Nimbus 7 satellite measurements of the springtime Antarctic ozone decrease R S Stolarski, A J Krueger, M R Schoeberl, R D McPeters, P A Newman & J C Alpert Are Antarctic ozone variations a manifestation of dynamics or chemistry? K-K Tung, M K W Ko,

Nature* (ISSN 0028-0836) is published weekly on Thursday, except the last week in December, by Maemilian Journals Ltd and includes the Anjural Index (mailed in February). Annual subscription for USA and Canada US \$240, USA and Canada in orders to: Nature. Subscription Dept. PO Box 1501, Neptune. NJ 07753. USA. Other orders to Nature. Branel Road. Basingsteke, Harns 8722 2XS, UK. Second class postage paid at New York. NY 10012 and additional mailing offices. Authorization to photocopy material for internal or personal use, or internal or internal or internal or internal or internal or internal or internal or internal or internal or internal or internal internal internal internal or internal internal internal internal internal internal internal internal internal internal internal internal internal internal internal internal internal internal inter

CUSTOM SYNTHETIZED DNA AT EXTREMELY LOW PRICES

Prices (USD) per purified oligomer up to the length of 35:

				Basic fee	Per base
0.05	A260 un	its (~ 1	.5 μg)	8 5	5.50
0.2	A260 un	its (~ 6	μ g)	125	7.50
1	A 260 un	it (~30	μ g)	170	10.00

SPECIAL OFFER: FREE OLIGONUCLEOTIDES

FOR EVERY FIVE OLIGOMERS YOU BUY
YOU GET ONE ADDITIONAL OLIGOMER FOR FREE

WHY BUY MORE THAN YOU ACTUALLY NEED?

1 μg OF OLIGONUCLEOTIDE IS SUFFICIENT FOR:

- 10 oligonucleotide-directed mutagenisis experiments.
- 100 hybridization and gene synthesis experiments.
- 1000 dideoxy sequencing experiments.
- More than 1000 cloning experiments.

EVALUATE YOUR ACTUAL NEEDS BEFORE ORDERING!

FOR PRICE LIST AND PRODUCT INFORMATION, CONTACT:

SYN-TEK AB

Box 1010 S-901 20 Umeå, SWEDEN Phone +46-90-13 24 10 Telefax +46-90-12 32 05 Telex 54920 syntek s SYN-TEK CORP.

P.O. Box 50068 Palo Alto, CALIFORNIA 94303 Phone 415-494-8690 Telefax 415-494-0762



SUBSCRIPTION SERVICE

Your mailing label contains your unique subscriber identification number



To ensure prompt service, please quote this number whenever you speak or write to us about your subscription

HELP US TO HELP YOU

100		
Ammuni Cultura function of		140000
Annual Subscription P	rices	and the same of
UK & Irish Republic		£1(14
USA & Canada		US\$240
Australia. NZ &		
S. Africa	Airspeed	£150
	Airmail	£190.
Continental Europe	Airspeed	£125
India	Airspeed	£120 l
	Airmail	£190
Japan	Airspeed	Y90000
Rest of World	Surface	£120
7 17 17 17 17 17 17 17 17 17 17 17 17 17	Airmail	£180 l
		EIMI
Orders (with remittance		I
USA & Canada	UK & Rest o	f World
Nature	Nature	1
Subscription Dept	Circulation	Dent
PO Box 1501	Brunel Road	
Neptune	Basingstoke	·
NJ07753	Hants RG21	200 110
USA	Tel: 0256 29	
	101.0230 29.	
(The addresses of Natu	re semioriai om	ces are shown
facing the first editorial Japanese subscription of		
Japan Publications Tra 2-1 Sarugaku-cho 1-che Chiyoda-ku, Tokyo, Ja Tel: (03) 292 3755	me	ld
Personal subscription r	ator Thornard	milable in
some countries to subsc	ribor rosida k	vanaoie in
cheque or credit card. [Theis paying by	personai [
USA & Canada		1
Nature	UK & Europ	
65 Bleecker Street	Felicity Park	er
New York	Nature	
	4 Little Essex	
NY 10012, USA	London WC:	
Tel: (212) 477-9600	Tel: 01-8366	
Back issues: UK, £2,50;	USA & Canada	11556 00
(surface), US\$9,00 (air	Rest of World	£3.00
surface), £4.00 (air)	THE MEN OF THE MINE.	
Binders		I
omaers		
Single binders: UK, £5.	25: USA & Cana	da \$11.50:
Rest of World, £7.75. S	et of four: UK, £)	15.00: USA
x Canada \$3.2.(0); Rest	of World, £22;00	
Annual indexes (1971-19	985)	I
UK, £5.00 each; Rest of	World \$10.00	1
		I
Nature First Issue Facsi	mue	
JK. £2:00; Rest of Worl	d (surface), \$3 (X)	: (air) \$4.00
3. A		3

Nature in microform

Write to University Microfilms International, 300

North Zeeb Road, Ann Arbor, MI 48106, USA

in the plume of Etna volcano	
R Lefèvre, A Gaudichet	
& M A Billon-Galland	817
Sewage sludge as an activity	
filter for groundwater-fed lakes W Davison	930
	820
Climatic influence on the isotopic composition of bone nitrogen	
THE Heaton, JC Vogel,	
G von la Chevallerie	
& G Collett	822
Functions of the ON and OFF	74
channels of the visual system P H Schiller, J H Sandell	
& JHR Maunsell	824
Expression of functional sodium channels from cloned cDNA	
M Noda, T Ikeda, H Suzuki,	
H Takeshima, T Takahashi,	
M Kuno & S Numa	826
Analysis of T-cell subsets in	
rejection of K" mutant skin allografts differing at class I MHC	
A S Rosenberg, T Mizuochi	
& A Singer	829
Structural/functional similarity	
between proteins involved in	
complement- and cytotoxic T-lymphocyte-mediated cytolysis	
J Tschopp, D Masson	
& K K Stanley	831
Probing the phagolysosomal	PROPERTY OF THE PARTY OF THE PA
environment of human	
macrophages with a Ca ^{3*} -responsive operon	
fusion in Yersinia pestis	
C Pollack, S C Straley	
& M S Klempner	834
Diversity of murine gamma genes	
and expression in fetal and adult T lymphocytes	
J S Heilig & S Tonegawa	836
A novel $V_{_{\rm H}}$ to $V_{_{\rm H}}DJ_{_{\rm H}}$ joining	***************************************
mechanism in heavy-chain-	
negative (null) pre-B cells	
results in heavy-chain production M Reth. P Gehrmann.	
E.Petrac & P.Wiese	840
Recombination between an expressed	
and indicate of the captessed	ı

and a germline variable gene in a Ly 1 B-cell lymphoma R'Kleinfield, R R Hardy. D Tarlinton, J Dangl, L A Herzenberg & M Weigert 843 Distinct factors bind to apparently

homologous sequences in

J Weinberger, D Baltimore

the immunoglobulin

& P A Sharp

heavy-chain enhancer

Deregulated expression of c-myc by murine erythroleukaemia cells prevents differentiation EV Prochownik & J Kukowska

NAN

PRODUCT REVIEW

Vibrational CD of biopolymers T A Keiderling ACS in Anaheim

251 XXX

NATURE CLASSIFIED

Professional appointments -Research posts — Studentships — Fellowships — Conferences Courses — Seminars — Semposia:

Back Pages

Next week in Nature:

- Cosmic strings
- Organic grains in Halley
- Saturn's new satellites
- North Sea mantle mapped
- New Zealand and South American bats related
- An aquatic cuckoo
- Crayfish electric synapse
- Tumour necrosis factor action
- Chernobyl after Vienna

GUIDE TO AUTHORS

Authors should be aware of the diversity of Nature - readership and should strive to be as widely understood as possible

Review articles should be accessable to the whole readership Most are commissioned, but unsufficited reviews are weigh (in which case prior consultation with the office is destrable).

Scientific articles are research reports whose conclusions are sill general interest or which represent substantial advances of understanding. The text should not exceed 3 000 words and say displayed items (figures plus tables). The article should include an italic heading of about 50 words.

Letters to Nature are ordinarily (188) words long with no market than four displayed items. The first paragraph (not exceeding 150 words) should say what the letter is about, why the study it reports was undertaken and what the conclusions are

Matters arising are brief comments (up to 500) words (on articles and letters recently published in Nature. The originator of a Matters Arising contribution should initially send his manuscript to the author of the original paper and both parties should, wherever possible, agree on what is to be submitted.

Manuscripts may be submitted either to London or Washing ton. Manuscripts should be typed (double spacing) on one sale of the paper only. Four copies are required, each accompanied by copies of lettered artwork. No title shand exceed shipharacters in length. Reference fists, figure legends, etc. shand by on separate sheets, all of which should be numbered. Abbreviations, symbols, units, etc. should be identified on one cope of the manuscript at their first appearance

References should appear sequentially indicated by super-scripts, in the text and should be abbreviated according to like World List of Scientific Periodicals, fourth edition (Bistlerworth 1963-65). The first and last page numbers of each reference should be cited. Reference to books should clearly indicate the publisher and the date and place of publication. Combisshed articles should not be formally referred to indess accepted of submitted for publication, but may be mentioned in the text

Each piece of artwork should be clearly marked with the author's name and the figure number. Original artwork should be unlettered. Suggestions for over illustrations are welcome Original artwork (and one copy of the manuscript) will be returned when manuscripts caused be published.

Important: Manuscripts of proofs sent by an courser should be declared as "manuscripts" and value 35 to present the imposition of Customs day and Value Added Fax in the United Kingdom

846

EXPLORING THE HU

THE EIGHTH INTERNATIONAL NATURE BOSTON, SEPTEN

Be in Boston in September with your colleagues and the publishers of NATURE, The International Weekly Journal of Science, for an update on some of the central issues in molecular biology for 1986 and beyond. Join us in *Exploring the Human Genome* as a distinguished panel of speakers share their research and outline their varying approaches to the concept of human gene therapy.

Human gene therapy is coming close to reality. An explosion of information on the human genome is flowing from the introduction of new methods. The mystery is being removed from such structures as the ends of chromosomes and the "junk" DNA that lies between genes. Ever more genes are mapped ever more precisely on to human chromosomes. Even where a gene cannot be directly mapped, its location can now be identified; great ingenuity is going into proceeding from a location to an exact site. In this way the defective genes of, for example, muscular dystrophy and cystic fibrosis will soon be identified. Knowledge of the mutations that underlie diseases, including cancer, is greatly increasing our understanding of the diseases and leading to new diagnostic techniques.

New products on view

In conjuction with the conference, there will be an exhibition of the latest scientific products and services offered by leading research labs, pharmaceutical firms, publishers and many others. Representatives will be on hand to discuss their products and to answer your questions.

Conference puts you in the heart of historic Boston

The conference setting is the The Boston Park Plaza and Towers, overlooking the picturesque Boston Common and Public Garden. You'll be just a short walk from Beacon Hill, the Theatre District, Government Center, and Copley Place. In minutes, you can be at colorful Quincy Market, the historic waterfront, and the Freedom Trail. This convenient location will offer you many opportunities for relaxation during your free time.

Day 1 — Gene Mapping

Where Are We Now?

Victor McKusick, Johns Hopkins University

Somatic Cell Genetics

Frank H. Ruddle, Yale University

In Situ Hybridization

Mary Harper, National Institutes of Health

Restriction Fragment Length Polymorphisms
David Botstein, Massachusetts Institute of
Technology

Round Table: Bridging the Resolution Gap

Francis Collins, University of Michigan Charles Cantor, Columbia University Peter Goodfellow, Imperial Cancer Research Fund

The Limits of Genetics

Richard C. Lewontin, Harvard University

Poster Sessions

If you would like to have your poster considered for inclusion in the conference, please send a working title and a brief synopsis to:

Posters Editor

Nature Publishing Company 65 Bleecker Street New York, NY 10012



How to register:

Mail the registration form to: Nature Conference, Nature Publishing Company, 65 East Bleecker Street, New York, NY 10012 If the form has already been taken, write to the above address or call: (212) 477-9600.

Registration fees:

Full 3-day registration: \$195.

Student registration: \$75 (student status must be confirmed in writing). Your registration could be tax-deductible.

Hotel Reservations:

Nature has reserved a limited number of rooms at special rates for conference attendees. If you will require a hotel room, please contact the hotel directly:

The Boston Park Plaza & Towers

Park Plaza at Arlington Street, Boston, Massachusetts 02117, (800) 225-2008, Continental U.S., (800) 462-2022, Massachusetts only Telex: 940107

Ask for special Nature conference rates: Single, \$98; Double, \$120

Travel

To obtain air tickets at special conference rates, contact Aaron Krumbein or David Chan at Consolidated Tours, 250 West 57th Street, New York, NY 10019, 1-800-228-0877. In NY State, 212-586-5230.

nature

NATURE VOL. 322 28 AUGUST 1986

759

Economic revolution postponed for now

Governments have been succeeding in hiding from the consequences of industrial change. When will they begin to prepare for what lies ahead?

Opp things are happening to the world's economy, with the oddest consequences, one of which is that economists, the practitioners of the "dismal science", are now more dismal than usual. The familiar shrugging of the shoulders by which they disclaim the accuracy of their predictions is now often accompanied by protestations that they no longer understand the basis on which predictions should be made. Critics should be charitable. The conundrums which now abound betoken structural changes in the economic pattern of the world whose full effects are far from being realized.

The symptoms of impending change are striking. Here are a few. Earlier this year, it was widely expected that the dramatic decrease by about two-thirds of the international price of oil would have the effect of stimulating the economy of the industrialized West; now, after half a year, it seems more likely that economic activity will decline, which is one of the reasons why the New York Federal Reserve board, the US central bank, last week reduced the general level of interest rates to 5.5 per cent. During the same period, the value of the US dollar on the foreign exchanges has fallen, against some currencies by as much as a quarter, but there is no sign as yet that the US trade deficit, obdurately stuck above \$100,000 million a year, will be abated in the near future.

Meanwhile, the huge amount of debt run-up by the developing countries of the world with the commercial banks of the West remains substantially unchanged; after three years of fear that defaults might bring the whole house of cards crashing down, there has evolved a network of arrangements by which the debts persist (interest continues to be paid) but not even the banking community knows when, if ever, the principal will be repaid. Nevertheless, the stock markets of the world have just sustained a year-long bull market, bidding up the value of industrial stocks and shares to unprecedented levels. The proportions of people out of work in advanced societies are also unprecedented, as are the low prices of the commodities (not only oil) by which the developing countries of the world must hope to earn a living. What can be going on?

Paradox

The most sensible reading of these paradoxical events is that they mark the emergence of structural change in the pattern of economic activity on a scale that financial institutions can contemplate only in disbelief. The case of economic relations between the United States and Japan is a familiar pointer to what is happening. These years, the trade surplus of Japan amounts to roughly half of the deficit of the United States, but the effects of this imbalance are concealed by the willingness of Japanese to spend their surplus on investment in the United States, where steadily increasing proportions of industrial and commercial assets are owned by foreigners. The result is that the dollar has not depreciated against the yen by nearly as much as it would have done in normal circumstances. Japan does not seem as rich as it really is, while the true poverty of the United States is temporarily concealed. Both governments appear to benefit from these arrangements; Japan would no more welcome a more rapid increase of personal prosperity than the United States would enjoy a reduction of living standards. But this trend can be concealed only for a time.

Much the same is true of the strategems by which governments are seeking to conceal from themselves the patterns of impending economic change. Both in the United States and Western Europe (but also in Japan), governments spend substantial proportions of their domestic revenues on the support of agriculture, for example. In the United States, the cost will exceed \$30,000 million in the year ahead, something like a sixth of last year's budget deficit and rather more in 1987 if the US Congress manages to keep the total budget within the limits of the Gramm-Rudman Act.

The European Community's Common Agricultural Policy has the same effect. For the governments concerned, it seems preferable to sustain high-cost food production at levels the market cannot absorb (both by direct subsidy and by devices such as the artificial restraint of farm productivity such as the nonsensical European decision two weeks ago to ban the use of animal hormones — see page 762). The losers are not merely taxpayers but countries elsewhere in the world, chiefly developing countries, that might look for a more prosperous future in the development of trade in food.

Hiding

Once-prosperous governments are also bent on concealing from themselves the consequences of both the shift from manufacturing to service industries, under way for the past thirty years, and the shift, within manufacturing, from the products of heavy industry (such as steel) to those of light precision industry (such as electronics). Part of the motivation for this unwillingness to face reality is the sheer discomfort of rapid change, but there is also an underlying fear that countries such as Britain that used to be successful at heavy engineering are ill-equipped with the skills needed for survival in what has become the modern world. One glaring sign of the general fearfulness is the attempt now being made, by an alliance of European and North American electronics manufacturers and music publishers, to persuade Japanese electronics manufacturers to withold from the market the digital audio-recording equipment they are bursting to sell. If this scheme succeeds, where will protectionism end? Persistently high unemployment, made socially just acceptable by welfare schemes (as it should be), is a mark of the mismatch between the pattern of supply and demand.

This state of affairs cannot persist indefinitely. Water will sooner or later find its own level. But the readjustment, when it comes, could be catastrophic. What will happen, for example, in the slow-moving industrial communities when it turns out that the industrial equities whose prices have been bid up over the past several months by financial institutions buying financial assets with the intention of paying the huge impending cost of people's pensions turn out to be much less valuable than now? In this period of change suspended, the more far-sighted governments should be preparing themselves for what lies ahead, chiefly by investing in the intellectual skills that will be required. For most of them, unfortunately, propping up the past is the easier choice.

EPA discovers radon

The US Environmental Protection Agency risks stirring up a hornet's nest over radon.

It is a great shame that even the natural life is not entirely free from hazard, but that appears to be the case. For centuries, no doubt millenia, people and proto-people have been dying prematurely of natural causes - catastrophes, infections, climatic fluctuations and starvation, for example. Much of what passes for modern civilization is a marvellous defence against hazards such as these. Housing, by keeping people warm and dry, helps powerfully in this sense, which it is why it is one of life's little ironies that housing has also emerged, in the past few decades only, as a hazard in its own right. For houses, especially when they are of mineral construction such as stone, are also either a source of radon, the radioactive rare gas whose atoms are inescapably intermediates in the radioactive decay of the uranium and thorium series, or traps for it. One consequence is that all creatures on the surface of the Earth take in radon with every breath they breathe. Another is that those who live in houses may be exposed to extra amounts of radon generated from the construction materials. A third is that, in fashionable regard for energy conservation, houses are now less well ventilated and thus more efficient traps for radon.

The ubiquity of radon has been known for almost as long as radioactivity itself, the best part of a century. Only in comparatively recent decades, with better measurement techniques and accompanying conceptual refinements, has it become apparent that radon exposure must be, for most people, a greater source of biological hazard than other natural sources of radiation. The 1984 report of the UN Scientific Committee on the Effects of Atomic Radiation (UNSCEAR) gives a good synoptic account of the problem. The hazards of this exposure, chiefly the risk of usually fatal lung cancer, have been estimated from records of the incidence of lung cancer in people occupationally exposed to radon in, for example, uranium mines (see, for example, Evans et al. Nature 290, 98; 1981). In very round numbers, the radon contributes more than a half of the average effective dose equivalent of about 2.0 mSv a year which people acquire on account of exposure to natural sources of radiation. The dose due to cosmic rays is roughly 0.30 mSv a year, varying with latitude and

Most public authorities appear to have awakened only late in the day to the importance of radon as a natural hazard, but the US Environmental Potection Agency (EPA) has been later than most. It seems now to be embarking on a crusade against radon pollution with a zeal and innocence that suggest it may have heard of radon only recently. In Washington two weeks ago, James A. Barnes, deputy administrator of EPA, acknowledged that "radon is a serious public health problem" and that "virtually no one" recognized it as such eighteen months ago. He added somewhat regretfully that radon, being a natural hazard, "does not lend itself to traditional regulatory solutions".

Precautions

What EPA has done so far is to publish two helpful booklets, one for members of the public explaining what the problem is and the other for householders and/or their builders suggesting what might be done about it (sealing off ground beneath houses, better ventilation and so on). There is also a modest programme of survey and demonstration, in conjunction with the states (especially Florida, Pennsylvania, New Jersey and New York), and the promise of more action in the future.

How to give radon the attention it deserves without creating panic? Part of the difficulty is that the two isotopes, ²²⁰Rn (commonly called thoron) and ²²²Rn, with half-lives of 55 seconds and 3.8 days respectively, are ubiquitous only in the sense that small concentrations are found in the atmosphere everywhere; on the basis of the total content of radon in the atmosphere (which,

measured in bequerels, is merely an order of magnitude less than that released from the Chernobyl reactor in April), the activity at ground-level should range from 1 to 100 Bq m⁻³, depending on the weather. But there are huge variations from one place to another, depending on such things as the upward flux of radon from the soil in the immediate locality, the flux from buildings and volcanic regions and even that artificially released into the atmosphere by drilling holes through granitic rocks in the pursuit of petroleum or of geothermal steam.

This is why the radon problem is a haunting problem. While the average effect of atmospheric radon on people living in the United States may be small, enough people are probably subjected to enough radiation dose for the personal consequences to be significant. Mr Barnes said that there may be 8 million people whose involuntary risk of death from lung (and other) cancer caused by radon and its decay products is comparable with that smoking from a pack of cigarettes each day, a lifetime chance of, say, less than one in six.

Costs

Mr Barnes' problem (and other people's) is that there is no way of telling what will be the financial consequences of avoidance. The retro-construction of buildings is not cheap, especially when the few people competent to do the work know that there is a panic on. So, in a roundabout way, the radon question raises a more general and difficult conundrum: by what means does a civilized community strike a balance between precaution and cost in the pursuit of an environment free from a natural risk? Can the community afford the cost of being as free from avoidable risk as it would like to be?

In due course, no doubt, in the special circumstances of the United States, the market may help solve Mr Barnes' problem. Realtors may be required to quote measurments of radon doses when they offer houses for sale, and may find that higher doses mean cheaper prices; that exceptional dwelling will be significantly if stochastically hazardous, people will for the first time find themselves picking and choosing where to live on grounds of radiation exposure.

Two particular considerations complicate EPA's problem: houses built in the 1950s in western states with US funds from materials salvaged from the tailings of uranium mines and subsequently found to leak radon were dealt with stringently at government expense, while the more recent recognition that radon concentrations in the so-called Reading triangle reaching north from Pennsylvania affect millions of people, on whose behalf such stringent standards will not be as readily applied.

Buildings accentuate the natural patchiness of radon distribution. The materials of which they are constructed are a source of radon, while the fact that they are of necessity enclosed allows them to become storage reservoirs for radon from the subsoil. The concentration of radon in the atmosphere of a room will be determined by competition between the rate at which the radon accumulates from external sources, abated by its natural decay, and ventilation in the sense of the rate at which air is exchanged with less contaminated air from outside.

The consequence is that radon radiation doses to the tissues of the human lung vary enormously with location and circumstances. The mean dose (arithmetical, geometrical or some other) will reflect regional characteristics, but the doses to which individuals are exposed will more often be very much greater than very much smaller (which is to say that the distribution is skewed). EPA's problem is that of helping individuals especially at risk to identify themselves, and perhaps to protect themselves, without alarming others. That, no doubt, is why the agency sounds so much like a newcomer to the scene. But it must also face the more enduring and, in the long run, more daunting task of knowing what to say to people whose radiation exposure is about average for where they live, but who know (perhaps by reading journals such as this) that their norm is higher than that of others.

Research donations

Tax bill provides fewer breaks for US education

Washington

CHEERS rang out late Saturday night 17 August in a room crowded with lobbyists, journalists and legislators, as a House of Representatives and Senate conference committee reached an agreement on a major overhaul of US tax law. The agreement came only after weeks of give and take among conferees, watched and prodded by a dizzying array of lobbyists, as they struggled to find a bill acceptable to both houses of Congress. The new law has the White House's blessing, and final passage is expected when legislators return from their summer recess.

The new tax law will mean significant changes for all sectors of the economy. The number of tax brackets for individual taxpayers will be reduced to two, with a maximum rate of 28 per cent, down from the current 50 per cent. For corporations, the top rate drops from 46 to 34 per cent. The bill is not intended to raise or lower total revenues generated by taxes. Instead, it is an attempt at a more equitable system, with narrower loopholes and fewer breaks for special interest groups. The tax burden will fall more heavily on businesses under the new law, although lowered rates for individuals will be offset by the loss of certain allowances.

Few segments of the economy emerged as clear-cut winners or losers, but one selfdeclared loser is higher education. Thomas Head, senior federal relations officer for the Association of American Universities (AAU), says education took a beating on nearly every item on its tax agenda. Head feels the biggest blow is the way gifts of appreciated property are treated. Under current law, the entire value of a donated gift can be deducted from taxable income. In the new law, the amount the gift has appreciated is used in calculating a special "alternative minimum" tax that is usually applied to wealthier taxpayers — those most likely to make sizeable donations. The cost of giving appreciated property is therefore much increased. Sheldon Steinbach, general counsel for the American Council on Education, says that 40 per cent of gifts over \$5,000 to universities and colleges come in the form of appreciated property.

Gifts from smaller donors are also likely to decrease because of a change in the reporting requirements for charitable contributions. Taxpayers are offered a choice between taking a standard deduction and itemizing their expenses: under the new law, only itemizers may claim a deduction for their charitable contributions. Only 20

per cent of tax payers are expected to itemize their deductions under the new law. Also limiting donations will be the lowered tax rates, as tax savings from contributions will be proportionately lower.

Gifts to charitable institutions, including those that support scientific research, will also decrease markedly under the new law. Dr Lawrence Lindsey of Harvard University has used an econo-



metric model to predict that total charitable donations in fiscal year 1988 would have been between \$72,000 million and \$75,000 million. But with the new rules total donations will fall by about 14 per cent, and donations by the wealthiest taxpayers by about 36 per cent, or \$1,000 million. The drop in charitable contributions that will be brought about by the inability of nonitemizers to deduct contributions is estimated at \$6,000 million, and that due to the overall drop in tax rates at \$4,000 million. Some charities are planning major fund-raising campaigns this year to take advantage of the existing law before it is superceded.

Major private research universities expect to be hurt by restrictions on access to the tax-free bond market. Tax-free bonds generally have lower interest rates than taxable ones, making them a cheaper way to borrow money. The new law places a \$150 million cap per institution on these bonds. Says David Morse, director of federal relations at the University of Pennsylvania, as many as twenty large universities will be shut out of the tax-free bond market. Smaller private colleges will be unaffected.

Universities are also dismayed by the change in tax status for scholarships and fellowships given to students. In the past, these funds have not been subject to income tax, but the new law makes any funds not applied directly to tuition or re-

quired equipment taxable. AAU's Head points out that since gifts are not taxable, students whose families can afford to give them money for their education would pay no taxes, but a poorer student on a scholarship could face a tax liability.

Another potentially expensive change for universities and colleges is the treatment of pension plans, says Head. These must be shown to apply equally to all university employees. Head says that most plans tend to be more favourable to faculty, and universities may have to cut back on faculty benefits to make plans equitable. In any case proving that plans are equitable will be a drain on university resources.

Not all the news for universities is bad. A new 20 per cent tax credit for industry support of basic research performed at universities and tax-exempt, independent research institutes appears in the new tax law. Dr. Melvin Eggers, Chancellor of the Syracuse University and vice-chairman of the Coalition for the Advancement of Industrial Technology (CAIT), an ad hoc group backing the new tax credit, says it will encourage closer cooperation between company and university researchers, speeding up commercialization of research efforts. According to CAFF's estimates, the new credit could bring as much as \$475 million in new research investments at universities. This is a relatively small amount compared to the estimated \$50,000 million industry spends annually on research and development, but supporters believe it is a step in the right direction. The credit will be available through 1988

Despite criticism that has been levelled against it in the past (see Nature 310, 615; 1984), the existing research and development tax credit is preserved in the new tax bill through 1988, although the rate drops from 25 to 20 per cent. Robert Lawrence. a senior fellow at the Brookings Institution, says that in real terms the credit only amounts to about 6 per cent because of the way it is calculated — the credit applies to spending above the previous three years average. Only 65 per cent of money spent in supporting university-based research figures in the credit calculations. While some have called for eliminating the research and development tax credit. Lawrence thinks the government must give industry even stronger incentives to encourage more spending on research

The new tax law's chances for passage when Congress returns are good, but some changes may still occur. The rationale for the tax reforms was to deemphasize taxation as a driving force behind business decisions. But taxes are bound to remain an important consideration for corporate decisions, and whole legions of tax lawyers will be kept busy figuring out just what the new realities are.

Joseph Palca & Tim Beardsley

European agriculture

Politics before scientific advice

Last week's decision by the British agriculture minister to ban the use of growth-promoting hormones in cattle, following a European Commission directive to that effect, has drawn attention to an extraordinary incident last October. Then, the European Commissioner for Agriculture, Mr Frans Andriessen, suddenly suspended his scientific committee just four days before it was to prepare its final advice on the use of the hormones.

The committee, chaired by Professor G. E. Lamming of the Department of Physiology and Environmental Studies at the University of Nottingham, had reported in 1983 that the use of natural hormones such as oestradiol, progesterone, and testoterone in the form of implants in the ear of an animal was harmless to final consumers of the meat, even to pre-pubescent children, potentially the most sensitive group. Last year the committee, containing 22 senior European endocrinologists and toxicologists, was putting the final touches to its report on 'zenobiotics', or artificial hormones, such as zeronol and trenbolone when Commissioner Andriessen gave the order to stop. This effectively gagged the scientists as they are forbidden to reveal the results of their five-year study without the permission of the Commission; but it is widely believed that they would have given zenobiotics the same clean bill of health, provided use were controlled and monitored, as that gained by natural hormones. Just two months later, Andriessen successfully steered through the Council of Ministers a directive banning all agricultural use of hormones.

The British government, facing less public opposition to hormone use than its continental partners, voted against the ban in the Council of Ministers. But, faced with a possible loss of European markets if Britain failed to ban hormones, it now has little choice but to implement the directive. According to the Ministry of Agriculture. Fisheries and Food (MAFF). British meat exports to Europe are worth some £400 million annually. The use of hormones (to make the 50 per cent of British beef which comes from castrated cattle grow faster and produce leaner meat) probably adds only £40 million to meat values, MAFF estimates. Nevertheless Britain is pursuing its action in the European Court challenging the legality of the vote on the directive last December.

Lamming says he "does not want to get involved in politics", and is bound by contract to say nothing about his committee's report on the zenobiotics, but he is clearly disturbed at the possible consequences of the blanket ban on hormone growth promoters now in place in Europe. He believes that the ban could make the situation

more, rather than less, dangerous. Hormones in open use, are supplied from slow-release implants in the ear, a part of the animal not used for meat and where the implant can easily be detected. The implants diffuse small amount of hormones through the body of the animal; a pre-pubescent girl having 100 times more testosterone in her body than she could receive from a normal diet of hormone-treated meat; or a pre-pubescent boy 300 times the oestradiol he might receive from the same source. With the hormones banned, unscrupulous farmers will bury

the implants deep in the muscle tissue of the animals, probably in the most expensive cuts where inspectors are least likely to disturb a carcass, so certain slices of meat could contain far above average levels of hormone.

Lamming and his committee are, to say the least, put out by the Commission's decision. "We've done five years' work, collected voluminous data, and can't publish". Lamming for one will not be joining an ad hoc European committee again. But the major issue, which has risen again and again in Europe, is the preparedness of European ministers, who after all backed Andriessen's directive, to go ahead without listening to effective scientific advice.

Robert Walgate

Japanese space science

Joint project for solar maximum

Tokve

Japan's space programme may be tiny compared with that of the United States but its size is not preventing it offering a little hospitality to others. The Institute of Space and Astronautical Science (ISAS) has invited US researchers to place a soft X-ray telescope aboard their solar observation satellite scheduled for launch at the start of the next solar maximum in 1991.

The Japanese High Energy Solar Physics (HESP) mission follows ISAS's Hinotori satellite and the US Solar Maximum Mission that observed solar flares during the last solar maximum in 1981–82. The new ISAS solar satellite, Solar A, will be placed in low-Earth orbit where the US soft X-ray telescope and a Japanese hard X-ray telescope will be trained on the Sun.

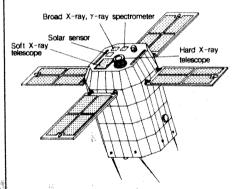
Designed to give high spatial and time resolution, both telescopes will allow second-by-second image analysis of solar flares as they grow and die. The hard X rays will reveal the hottest (greater than 30 million kelvin) kernel of flares during their flash phase, whereas the soft X rays will provide images of the cooler pre- and post-flash phases. If there is room for them, spectrometers will also be carried aboard the satellite.

According to the director of ISAS. Professor Minoru Oda. US participation in HESP will be funded through NASA's Explorer programme. An announcement of opportunity was made by NASA last March and official selection of the US team is expected this month.

Difficulties in setting up the joint project occurred, according to Oda, because of differences in approach between the United States and Japan. Whereas ISAS scientists gradually develop, refine and polish a project, and obtain final budget approval once a fairly concrete plan has emerged. NASA starts with a concrete plan and budget and solicits proposals. Other problems arose over the designation of the problems arose over the designation.

nation of principal investigators. But eventually, says Oda, a *tamamushi* agreement was reached (the *tamamushi* is an iridescent beetle whose colour changes according to the angle you look at it).

The satellite is expected to be about 2 m long and 1 m wide with three-axis stabilization to point the long axis towards the Sun. Weighing about 400 kg it will be launched to an altitude of 550–600 km by a



US and Japanese X-ray telescopes will share the new satellite.

Mu-3S-II rocket from the Kagoshima Space Centre during the August-September 1991 launch window. Apart from the US telescope, the total budget for the mission, which awaits final approval by Japan's Ministry of Finance, is expected to be about 4,000 million yen (£17 million), a mere fraction of the cost of launching a comparable satellite in the United States.

The cheapness of ISAS missions is easy to explain. ISAS scientists design, test, launch, monitor and sometimes even build their satellites and rockets, and although work is farmed out to private companies such as Nissan and NEC, there is no principal contractor. Final liability thus rests with ISAS, which substantially reduces the costs. Such an approach also has the advantage of great flexibility, but as Oda points out, it leaves precious little time for science.

David Swinbanks

Chernobyl report

Drama of human perversity

Vienna

The world's nuclear engineers gathered to hear the Soviet account of the Chernobyl accident on 26 April do not yet know whether they are at a wake for nuclear power or at a launching ceremony for a new generation of safe reactors. Nervously, they have crossed their fingers and praised the Soviets for their frankness.

The head of the Soviet delegation, Academician V.A. Lugasov, won over many critics with a gripping five-hour presentation of the authentic accident report, including personal asides hinting at disagreements on technical matters among Soviet officials. The highlight of the presentation was a video film, made under obviously hazardous conditions, showing the huge scale of the damage caused by the explosion of the No.4 reactor, with its contiguous neighbour miraculously undamaged. As in films of the Titanic at the bottom of the Atlantic, four of the eight reactor cooling pumps picked out through the gloom by a flickering spotlight seem as pristine as when they left the factory.

By Lugasov's account, the causes of the accident were not so much human error as human perversity. Plant operators in a hurry to complete a test of the reactor turbine's capacity to span a few seconds interruption of power supply, itself "poorly" designed, dealt with successive danger signals by disabling the safety systems meant to deal with them. In resignation, Lugasov said that when the RMBK-1000 reactor was designed 20 years ago, people had thought that human beings would be more reliable than automatic safety systems. Now he was not so sure.

The Soviet delegation has nevertheless acknowledged several technical defects of the reactor, whose merits are said to include simplicity and low cost. Lugasov pointed in particular to the disadvantage that, as excess steam forms in the water-cooled fuel channels, the reactivity of the reactor increases and also the complexity of the control system required to keep the power output stable.

Other RMBK reactors operating in the Soviet Union will be modified by 1987, chiefly by increasing the fuel enrichment from 2.0 to 2.4 per cent, with an estimated loss of 10 per cent of power output. Thereafter, there will be more radical modifications not yet decided.

The future of the Chernobyl site is much less clear. Two of the four reactors completed at Chernobyl have been decontaminated, but cannot yet be brought back into action for lack of housing for the operating staff now that the towns of Pripyat and Chernobyl are uninhabitable. Decisions remain to be made about reactor No.3 and the two other reactors whose

construction was under way at the time of the accident.

Lugasov's statement has also cleared up some of the questions that have been puzzling the West since the end of April. Thus, he said, there was no undue delay before the plant operators told Moscow of the accident, which meant that a team of specialists could be despatched to Kiev by 8 p.m. on 26 April. But the plant operators subsequently transmitted misleading information about the state of the reactor, the effect of which was to underplay the damage to the reactor and the release of radioactivity.

Lugasov also stoutly defended the decision not to evacuate 49,000 people from Pripyat until 11 a.m. on 27 April, more than 30 hours after the accident. "Strange as it may seem", he said, there was no significant contamination until 9 p.m. on 26 April, when it was judged safer to keep people indoors overnight.

The second wave of radioactivity after a week's delay was explained this week by the heating of the damaged reactor core to an estimated 2,000°C because of the thermal insulation of the clay and sand which, with other materials, had by then been dumped on top of it. More could not be added for fear of making the reactor foundation collapse, but there seems to have been no danger of a fuel meltdown.

John Maddox

Private money for AIDS research

Washington

THE US Public Health Service (PHS) wants to encourage private sector involvement in its efforts to find a vaccine to prevent acquired immune deficiency syndrome (AIDS). To that end, PHS spelled out in the 23 August Federal Register a more formal framework for collaborative efforts between the government and private institutions. The hope is that such collaborations will speed up the search for an AIDS vaccine, but some wonder whether the government has a sufficiently succulent "carrot" to encourage industry to play along.

Under the framework, PHS will not provide any financial assistance to its collaborators. Instead, it will offer knowhow from its component agencies - the Alcohol, Drug Abuse and Mental Health Administration, the Centers for Disease Control, the Food and Drug Administration (FDA) and the National Institutes of Health (NIH). This assistance could include patent licences, research results, facilities, animal models and animal testing, and help in formulating clinical protocols and clinical trials. PHS is interested in finding collaborators who will be involved in all steps in vaccine development, from basic molecular biology to clinical trials to marketing and commercial production. Companies unable or unwilling to participate in such a large scale project are encouraged to find others in the private sector to join with them in collaborating with the government.

PHS identifies two basic approaches to vaccine development that it wants to pursue. One is the development of a synthetic vaccine, generating viral antigens from whole virus, or using recombinant DNA techniques, chemical synthesis or anti-idiotype antibodies. The other is development of a live, genetically altered viral vector or attenuated vaccine. PHS will also consider other approaches, such as passive immunization, if they show promise.

A special committee established by the assistant secretary for health of the Department of Health and Human Services will make final decisions on collaboration following a review by the applicable PHS agency. PHS decisions will be based on an applicant's experience and ability to achieve its stated goals.

In the past, some companies have been reluctant to enter into collaborations with the government for fear that their proprietary research could be made public under the Freedom of Information Act. Lowell Harmison, science adviser for PHS, says companies will be protected from unwarranted disclosures as far as the law allows. but otherwise will have to give careful thought to how they word their applications. George Galasso, assistant director for extramural research at NIH, does not think these caveats will be sufficient. Companies that really have a promising vaccine approach "will go it alone", leaving the "also-rans" to seek government help.

Galasso also wonders whether formal collaborations with the government will speed the development of a vaccine. Scientist-to-scientist relationships have worked well so far, says Galasso, and will continue to be available when the need arises. Dino Dina, director of virology for Chiron Corporation, says having FDA help in developing acceptable standards for animal trials and initial clinical trials would be useful. But he feels a more efficient approach would be to make such information available to all comers.

Dina also worries that previous offers of "collaboration" from the government have turned out to be more take than give. But Harmison says the PHS plan is a fresh approach to cooperative arrangements. He hopes that the offer of government facilities and expertise will encourage companies with interesting ideas about vaccine development to pursue them.

Joseph Palca

Space station

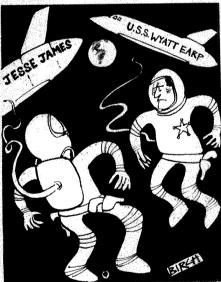
Taming the last lawless frontier

Washington

ALTHOUGH it will be several years before astronauts are working together in a multinational space station, it is not too soon for Congress to start considering legal questions that might arise, according to the Office of Technology Assessment (OTA).

Some US laws, Congress's research office notes in a recent background paper*, do not make much sense in space. The US Uniform Commercial Code, for example, with its definitions of personal property and real estate, and what is movable and what immovable, could not be applied "without serious uncertainty". The wisdom of applying the Buy-America Act is similarly unclear. And OTA notes it might be "inappropriate" to apply the Fair Labour Standards Act, with its stipulated 8-hour maximum working day.

More seriously, the application of intellectual property, product liability and export laws in a space station is likely to be important for commercial companies working on the space station. Although the 1967 Outer Space Treaty established some basic principles governing countries' responsibilities and liabilities in space, it leaves many questions unanswered. OTA recommends that Congress start thinking



immediately about how far US federal and state law can be applied in space, and how disputes might be resolved.

How to determine the jurisdiction of different countries over different parts of a multinational space station is seen by OTA as central. Both Europe and Japan are expected to contribute habitable modules; although the simplest thing from the US point of view would be to have everything under US law, this "may be politically unacceptable to other space station partners". OTA notes.

Patent law is likely to be especially diffi-

cult to sort out in space. There is already a variety of opinions on how far US patent law can be applied, and attempts in Congress to clarify the situation have not been very successful. Real disputes are likely to arise, since there are important differences in patent laws between nations.

In the case of criminal law, the question on enforceability also arises. So far crews have been highly disciplined and engaged in specific tasks. But as more people start to live and work in space there may be disputes. On space shuttle missions, the

commander has broad authority to enforce discipline. But if a British astronaut were to assault an American astronaut in the British portion of a space station, US laws could not be enforced without a prior agreement.

One way of avoiding complicated legal entanglements, according to OTA, would be for participating countries to enter in to "pre-launch agreements" modelled on the "status of force agreements" between members of the North Atlantic Treaty Organization which clarify legal questions about forces stationed in different countries.

Tim Beardsley

*Space Stations and the Law: Selected Legal Issues. Office of Technology Assessment Background Paper, 1986.

UK universities

Government yields just a little

THE British government now seems willing to provide the extra money needed to prevent university closures — provided, that is, universities agree to reform and to their performance being monitored.

The news represents a victory for those who believe the only way to persuade the government to invest more heavily in the universities is by showing a quiet willingness to make improvements (or by being submissive, as cynics have it). Beginning in 1981, financial cuts have brought several universities to their knees: at least four are thought likely to have to close during 1987 if help is not forthcoming. The political embarrassment that this could generate in an election year, plus the new willingness of the universities to accept reform and monitoring seems, according to reports from the Department of Education and Science, to have persuaded the Secretary of State, Mr Kenneth Baker, to take out his chequebook, if not actually to sign the cheque.

Some of the changes the universities may have to accept are contained in the report on "Academic Standards in Universities" just released from the Committee of Vice Chancellors and Principals. Perhaps its most radical suggestion, for British academics at least, is that students should help appraise courses and lecturers. A host of other course evaluation measures are suggested: the number of applicants, the qualifications of entrants, degree results, percentage of drop-outs and so on. The report also seeks to lay down codes of conduct for external examiners, who will ensure that degrees awarded in similar subjects are comparable in standard in different universities; for postgraduate training and research; and for an appeals procedure for postgraduates who fail to be awarded degrees. The latter codes are intended to help deal with the embarrassingly high drop-out and failure rates among post-graduate students. The responsibilities of a doctoral supervisor

are made explicit for the first time and it is recommended that a statement to establish clear mutual expectations between student and supervisor always be drawn up.

The other issues on which the government wants to see progress are financial management, the creation of performance indicators so that whole universities might be appraised, and the rationalization of university departments that are judged too small or too weak. University performance indicators were set out in the Jarrat report last year; they include, among other things, the success of graduates in obtaining employment; publications by staff and citations; patents, inventions, and consultancies; prizes; and papers given at conferences (see *Nature* 314, 393; 1986).

The University Grants Committee has already set in motion an assessment of individual departments' research quality which seems set to lead to the closure of those judged inefficient. This has proved controversial; not only because of the uncertainties involved in assessment (see Nature 322, 219; 1986), but because small departments are emerging as the prime candidates for closure. While many will acknowledge this makes sense in areas where a critical mass of researchers is required to maintain expensive laboratory facilities, it may be a different story when it comes to subjects like the history and philosophy of science. There is a strong argument that the present situation, with sixty or so staff scattered over 25 universities, is the best way to allow many scientists to absorb some history and philosophy of science: to say that it should be concentrated in a few places is to denv its general relevance. Similar arguments over the rationalization of departments of philosophy are now provoking public debate and it is too soon to say whether philosophy will be seen as just a discipline for specialists. Alun Anderson US defence

Congress takes a moderate line

Washington

GROWING impatience with President Reagan's arms control policies has prompted the House of Representatives to take actions on its own. Before leaving for its summer recess, the Democrat-controlled House passed a decidedly "doveish" defence authorization bill and the Republican-controlled Senate also showed signs that it is ready for a more moderate buildup of US military capabilities.

Both houses of Congress have now completed work on versions of the defence authorization bill. Neither house went along with the administration request for \$320,300 million for the Pentagon: the House authorized \$286,000 million, while the Senate agreed to \$295,000 million.

The issue of chemical weapons has proven particulary divisive for Congress. The House agreed by just one vote to delay procurement of binary nerve-gas weapons until 1 October 1987. The Senate continued a string of close votes on chemical weapons and a measure that would have deleted funds for the Bigeye bomb, a new binary nerve-gas bomb that has failed many of its developmental tests, was defeated by one vote.

Although President Reagan has indicated that he no longer intends to abide by the terms of SALT II, the strategic arms treaty negotiated in 1979 but never ratified by Senate, opposition to that decision has been fairly strong in Congress. The House adopted a measure that would force the President to abide by SALT II by prohibiting funds to be spent on any weapons system that would be in violation of the treaty. The Senate would only go as far as requesting a Pentagon report on the consequences of violating the terms of SALT II and other strategic arms control

Spending on research on a space defence system was cut in half by the House, but authorized for the full \$278 million requested by the administration in the Senate. The Senate bill also includes \$28.5 million to begin procurement of a space defence system. Both houses made deep cuts in the administrations request for funding for the Strategic Defense Initiative.

The Pentagon officially runs out of money at the end of next month. Even if Congress cannot reach a compromise on the two authorization bills, similar language on weapons reduction schemes is included in appropriations bills working their way through Congress. One way or another, there is sure to be a shoot out on arms control before the Pentagon gets any more money. Joseph Palca Chernobyl accident

Fallout pattern puzzles Poles

"Hotspots" of radioactive fallout from Chernobyl are puzzling Polish scientists, Dr Zbigniew Jaworoski of the Central Radiological Protection Institute in Warsaw told a Japanese reporter. Mr Fumihiko Yoshida, of the Asahi Shimbun recently. The Japanese media have been particularly successful in elucidating details of the Chernobyl disaster and its aftermath - presumably the governments involved respect their unique positions as the only victims of a nuclear bombing. It was on Japanese television that Dr Valerii Legasov, deputy director of the Kurchatov Nuclear Energy Institute of the Soviet Academy of Sciences, revealed that almost all the safety circuits at the Chernobyl power station had been disabled during the unauthorized experiments that led to the disaster.

Dr Jaworowski, who is a leading adviser to the United Nations on nuclear fall-out, is recorded as saying that the hotspots. which measure several tens to several hundred metres across, exhibit levels of radio-activity some ten times higher than the surrounding area. The spots are roughly circular in shape and, in the immediate post-Chernobyl period, it appears their outline could be mapped by field observers with geiger counters. Analysis shows that ruthenium (an element whose name, ironically, derives from the Latin designation for Ukraine) is the major radioactive material in the hotspots, although there are a few in which lanthanum or barium isotopes predominate. Although most common in north-east Poland, they could be observed all over the country. Dr Jaworoski reportedly

Details of the level of radioactivity of the hot-spots have not been given, but similar ruthenium particles deposited in Sweden have registered levels of 1,000 -10,000 becquerels per particle.

The Polish scientists, Yoshida reported. have no idea why the hot-spots are so widely distributed, nor why they consist predominantly of ruthenium. An apparently similar phenomenon in the Mahileu rayon of the Byelorrusian SSR (well away from the total exclusion zone) has been attributed to a freak rain-shower, but, as the "self-help" advice issued by underground Solidarity makes clear, the one thing the Poles were longing for in the immediate aftermath of the disaster was rain which would, they hoped, wash away the air-borne hazard. Dr F.B. Smith, an expert on air-borne pollution from the UK Meteorological Office at Bracknell, suggests that the radioactive material was deposited by dew, which is sensitive to the temperature differences generated by soil-type and land use. Vera Rich

Japanese mega-prizes announced

ONE of science's newest - and biggest prizes has gone to Professor G. Evelyn Hutchinson of Yale University and Professor Nicole M. LeDouarin of the Institut d'Embryologie, Nogent-sur-Marne.

Each will receive the Kyoto Prize medal and Y45 million (\$300,000) at a ceremony to be held in Japan in November.

The prize was set up last year by Kazuo Inamori, founder of Kyocera Corporation, Japan's most famous and fastest-growing hightechnology ceramics company. In just twenty-five years Kyocera has "by the grace of God" grown to produce annual pre-tax profits of Y53 thousand million. That has made it possible to endow the Inamori Foundation with Y20,000 million to provide for the award of an annual prize.

The aim of the prize is to en- Prizewinners LeDouarin and Hutchinson - each with courage balance between scien- \$300,000 to spend tific and technological development on the one hand and psychological and emotional maturity on the other: equilibrium between the "ying and the yang, the light and the dark" is sought.

Many would say that equilibrium has

been achieved by Professor Hutchinson who is known both as an essavist and a scientist. He did much to establish ecology as a science and was the first to develop the concept of the ecological niche. Born in England in 1903, Professor Hutchinson is now an emeritus professor and still writing and researching.



Professor LeDouarin, born in 1930, is known for the work that led to the creation of quail-chicken chimaeras. The distinctive properties of the tissues of the two animals make it possible to follow previously-unobservable events in development.

Belief in miracles

Sig-With regard to R.J. Berry's question "What to believe about miracles" (Nature 322, 321, 1986), I think it more interesting, and more of a scientific question, to ask how one can understand and explain belief in miracles. Belief in miracles is a widespread and very influential psychological phenomenon, underpinning value systems and cosmologies that have shaped the history of the world. The events called "miracles" may or may not have occurred in the form in which they are described. but their existence as a phenomenon of social fact is very real. This deserves serious investigation.

The main problem with most miracles is the ambiguity of testimony. Often they were reported long after the event, at second-hand; even if the reports are firsthand and attested to "by thousands", it is usually one person who wrote the description. So the data are usually shaky.

There are therefore, a variety of possible hypotheses. One is that the event occurred, and that it was due to divine intervention in some form. A second is that the event did not happen at all, that nothing remotely like the event occurred, but that people at a subsequent date constructed mythical events and actions surrounding charismatic figures. This is a virtually universal psychological phenomenon, and indeed there are certain common myths that existed long before their adoption by Christians - the virgin birth, and the death and resurrection of the God, for example, and many religions whose origins are in floodplains have Noah-like heroes in their mythology.

A third hypothesis is that something happened, but there was inadequate information about it, and the ambiguities are resolved in a way that provides both consistency and charisma - such psychological processes are demonstrated for every first-year student in social psychology in laboratory classes.

These explanations do not deny the possibility of miracles, but they do bring into question Berry's distinction between domains of faith and domains of science by asking what parameters of miracles are scientifically interesting. Indeed, Berry's point about reductionism is an important one, and something that the newer sciences and social sciences have been plagued with. Setting limits to one's science is a way of achieving rigour, by defining what is possible for investigation given the methodological resources available. But such rigour becomes rigor mortis if the limits set are those of one's actual and present methodological constraints, not those of some potential and future, more sophisticated methodology. Developments in psychology have frequently depended on researchers going "off limits"

and defining a problem as interesting some time before the methods existed to study it; undoubtedly this is true of all sciences. Berry argues that it is reductionist to say, in effect, that because we cannot study them (given present techniques). miracles are impossible; he is, I would argue, equally reductionist in saying that it is not possible to investigate miracles using scientific measures. It depends which science one applies to the problem. HELEN WEINREICH HASTE

University of Bath, School of Humanities and Social Sciences, Claverton Down, Bath BA2 7AY, UK

What's in a name?

Sir-That (novel carbon cluster C,) which we call Buckminsterfullerene has excited considerable interest while the name we have chosen has stimulated comment². Although many have approved of this name, there have also been criticisms that it is too long (one should consider the IUPAC name), that it is clumsy (which is irrelevant), that nobody has heard of Buckminster Fuller (the name thus has educational value) or that an injustice has been done to almost everyone who has played with symmetrical objects from Plato and Archimedes to Stanley Matthews (the professional footballer).

The molecule we believe we have discovered consists of a sheet network of carbon atoms linked to form a highly resilient hollow sphere. The names of Plato and Archimedes are linked with the regular and semi-regular solids, an association, by the way, which may not be totally justified. The earliest hollow association I have found is in the work of Leonardo da Vinci3.

Buckminster Fuller showed that a hollow, light, strong structure could be constructed out of a network of struts using the known principle of Euler that, for closure, 12 pentagonal configurations must be dispersed among the hexagonal ones. The spherical structures such as the Montreal Expo '67 dome, the Epcot Dome and numerous radomes are constructed to take advantage of the lightness, strength (the strains are evenly distributed) and of course the internal cavity. that such a geodesic dome affords. C, is a geodesic carbon atom network with a very strong inert structure and a large central cavity that can trap other atoms. These three major properties are important for this molecule's behaviour and have direct analogues in the success of Buckminster Fuller's geodesic structures, factors that are not inherent in other names. C₁₀₀ Buckminsterfullerene itself is only one

member of a set of structures (C₁₄-C₈₀) that appear to be closed and, although they must have 12 pentagonal configurations, do not have to have t-icosahedral symmetry. Buckminster Fuller also considered such structures.

H. W. Kroto

School of Chemistry and Molecular Sciences. University of Sussex, Falmer, Brighton BN1 9QJ, UK

Kroto, H.W., Heath, J.R., O'Brien, S.C., Curl. R.F. & Smalley, R.E. *Nature* 318, 162 (1985).
 Stewart, P.J. *Nature* 319, 444 (1986).

- Fra Lucia Pacioli *De Divina Proportione* Ambrosiana. Milan; Diagrams by Leonardo da Vinci.
- Buckminster Fuller, R. *Inventions* (St Martins Press, New York, 1983).

Spanish universities

SIR-In two recent issues of Nature (319, 710 and 322, 198; 1986) Juan A. Subirana and Pedro Puigdomenech have pointed out the danger of "inbreeding" in the Spanish universities, as a consequence of the new recruiting system for academic posts. That this danger is becoming fact is demonstrated by the first examinations carried out under the new system.

In most cases, the process of appointment seems to have been a mere formality, the final decision being taken before the examination. Nearly all those obtaining posts were the so-called "official candidates", who were proposed and supported by the university departments before the vacancy was publicly announced. Such candidates began with at least two out of the five votes of the selection committee, those of the members of the department concerned. Other applicants, even those with scientific qualifications superior to those of the official candidates, were often eliminated on the basis of subjective arguments. Work carried out at foreign institutions was undervalued, while some foreign candidates were eliminated by questions such as "What are the idiosyncracies of local students?".

In those circumstances, it is unlikely that many Spanish graduate students and postdoctoral fellows now working in foreign scientific institutions will ever get positions at Spanish institutions. This will not encourage the return of such people to Spain. As a logical consequence, the standard of scientific research in Spain (already much lower than in other Western European countries) will not be raised in the future. This is a serious deficiency in a law that otherwise has many positive features and that was intended to improve the general level of Spanish research. It is a matter of great urgency to reform this system by a new or additional policy.

JAVIER NAVAL

Chimie des Protéines. Institut de Recherches sur le Cancer, BP 8, 94802 Villejuif, France

Law and genetic testing

SIR-Bains observes that genetic screening may have attendant legal ramifications. This has certainly been demonstrated in the United States.

The expanding ability of medical science to predict and detect defects before birth may have important applications in clinical medicine. Genetic counselling and prenatal testing may potentially provide valuable information to patients planning families about the likelihood of various defects in their offspring. The development of various genetic screening techniques, at least in the United States, has further spawned the birth of various classes of lawsuits. "Wrongful pregnancy" actions refer to cases where the parents of a child file a claim for the monetary and emotional damages suffered as the result of giving birth to a healthy, albeit unwanted, child2. The action may arise where a child's conception was due to the alleged negligent performing of a sterilization procedure. "Wrongful birth" suits are those instituted by parents claiming that they would have avoided conception or terminated the pregnancy had they been advised of the risks of birth defects in their offspring'. "Wrongful life" cases are instituted by the infant and allege that, as the result of the negligence of the defendent health-care provider, birth has occurred. The infant is claiming essentially that the defendant has wrongfully deprived the parents of information, which would have resulted in the child not being born.

The three classes of lawsuits are thus different. Wrongful pregnancy cases typically involve a healthy, although unwanted, child, whereas wrongful birth actions normally involve planned children who are born deformed. Both actions are normally brought by parents. However, the wrongful life action is brought by the infant. Allegations in recent, selected lawsuits have involved the failure to diagnose Down's syndrome during pregnancy', failure to diagnose rubella suffered by the mother during pregnancy resulting in the birth of a rubella baby with severe congenital defects³, failure correctly to type and record maternal blood and the later birth of a child with erythroblastosis fatalis', the "wrongful birth" of children suffering from fetal hydantoin syndrome associated with the mother's use of dilantin during pregnancy', negligent performing of a vasectomy and the negligent performing of tubal ligation'.

With the increased knowledge in the field of genetic screening, there has been a concomitant recognition by various courts that the appropriate standard of professional care may require the use of available, pertinent prenatal tests and genetic counselling, particularly for patients at high risk of having children with birth defects. Perhaps it may be helpful to seek definitive legislative guidance concerning the vexing legal questions potentially raised by genetic screening.

LEO UZYCH

103 Canterbury Drive. Wallingford, Pennsylvania, USA

- Bains, W. Nature 322, 20 (1986).
 Continental Cas. Co. v. Empire Cas. Co., 713 P.2d 384
- Blake v. Cruz, 698 P.2d 315 (Idaho 1984).
- Harbeson v. Parke-Davis, Inc., 656 P.2d 483 (1983) James G. v. Caserta, 332 S.E.2d 872 (W.Va. 1985).
- 6. Garrison v. Foy, 486 N.E.2d 5 (Ind. App. 3 Dist. 1985).

Models of man

SIR-In the context of the diversion of psychological research funds to cognitive science and computing projects, the argument below must be considered:

There are two flaws in computational models of man: (1) in human beings there can be no certainty what the programs are; (2) in human beings the database is unknown and different for every person. It therefore follows that computational models, being quite unlike the human case, are doomed to failure.

PAUL KLINE

Department of Psychology. Washington Singer Laboratories, University of Exeter, Exeter EX4 4QG, UK

Help for Africa

SIR-Michael Spencer's letter (Nature 322, 10; 1986) prompted me to read again your leading article "Who will pity Africa?" (Nature 321, 548; 1986). Pity and political posturing seldom assist the objective assessment of any problem, least of all the vast and complicated set of problems that afflict Africa today. Spencer highlights some of the external political and economic pressures, whereas your leading article, like the United Nations' statement of early June, drew attention to the contributions to the chaos made by some of the African governments themselves. All these have to be taken into account, and much else besides, not least the vastness and heterogeneity of Africa itself - some 45 separate states and ecological conditions ranging from complete desert to tropical rain-forest, with montane and temperate regions besides.

You call for "a political clearing-house for good ideas that have already contributed to the improvement of Africa's conditions on a small scale... which... could be spread more widely". I hope your call will be heeded, but I would suggest that the emphasis should be not so much on good ideas as on good projects that have proved themselves over a reasonable period of time.

As Spencer says, there has been no

shortage of good ideas, but some of these have proved to be disastrous. They range from simple wells in arid regions which have attracted so many people and their animals that the surrounding land has been destroyed, to multi-million dollar irrigation and farming projects that have impoverished the local farmers and their land

Most of Africa never was and never will be "a Garden of Eden" - the ecology is not like that - but there are instances, past and present, where sensible efforts, with or without outside help, have led to real improvements in the lives of ordinary people. We need to hear more about these, and less about who is to blame for the present troubles.

RONALD KEAY

38 Birch Grove, Cobham. Surrey, KT112HR, UK

Darwin's yellow rain

SIR-In the light of the continuing controversy over yellow rain, it might interest your readers to know that Charles Darwin observed and reported a case of yellow rain. The report was quoted in the 18 July 1863 issue of the Gardeners' Chronicle and Agricultural Gazette¹. The letter from Darwin reads in part:

A very slight shower, lasting hardly more than a minute, fell here this morning (July 2) about 10 o'clock. My wife gathering some flowers immediately afterwards noticed that the drops of water appeared yellowish. and that the white roses were all spotted and stained. I did not hear of this circumstance till the evening; I then looked at several roses and Syringas and found them much stained in spots. Between the petals of the double white roses there were still drops of the dirty water: and this when put under the microscope showed numerous brown spherical bodies, 1/1000 of an inch in diameter, and covered with short, conical transparent spines.

Darwin goes on to describe additional small particles "only just visible with a quarter-inch object glass". The author of the article, designated only as M.J.B., reports examining rose petals forwarded by Darwin, and observing "multitudes of irregular bodies so minute as to present the Brownian molecular motion". M.J.B. concludes that "it is quite astonishing what a multitude of bodies are carried about by the wind in the form of dust"

Indeed, it is equally astonishing that we should still be arguing about yellow rain 125 years later.

BRUCE E. FLEURY

Science and Engineering Division, Howard-Tilton Memorial Library, Tulane University, New Orleans, Louisiana 70118, USA

 Gdnrs' Chron. No. 29, 18 July, p.675 (1863): reprinted in The Collected Papers of Charles Darwin Vol. 2 (ed. Barrett, P.H.) 81-82 (University of Chicago Press, 1977)

Science and faith

Sir.—In seeking to refute the beliefs and arguments of creationists, J. Richard Wakefield (*Nature* 320, 392; 1986) makes four unjustified generalizations to which I must object as a Christian and as a scientist

My first point deals with the limits to science. Wakefield states categorically that nothing is potentially beyond science. This is questionable. The scientific method is empirical and depends on testing one's hypotheses against what happens in the real world. Its conclusions ("scientific laws") are inductive and provisional, and they remain open to revision in the light of new and more comprehensive experience. Scientific knowledge is still partial and incomplete, and many things lie beyond its boundaries. The day may come when science can satisfactorily describe, predict and explain every phenomenon in the cosmos that can be subjected to scientific analysis; but the possibility that the universal set of real phenomena extends far beyond the finite subset of scientifically verifiable phenomena will remain and cannot be disproved by science. How can science ever illuminate what lies behind the beauty of form, of poetry, of music, of humour, and of human emotion? Humans are physical, rational, intuitive, emotional, personal, cultural, social, moral and spiritual beings. Science is only one of the forms of knowledge available to us; we are familiar with different kinds of knowledge in art, in love, in politics and in religion. Science is not served by making exaggerated claims on its behalf, any more than is creation-

My second objection is to Wakefield's view of faith, which he defines as "belief without evidence". St Paul, however, taught that "faith gives substance to our hopes", faith is "the proving (or test) of things not seen" (Hebrews 11.1; New English Bible, Revised Standard Version emphases mine). In the classical tradition of Christian experience and understanding, faith is trust that leads to action; and the outcome of living by faith, in the testimony of countless Christians, amply substantiates and justifies it. As science generally considers it good practice to test hypotheses before discarding them as invalid, I suggest that Wakefield and those who sympathize with his views subject mainstream scriptural Christian faith to the same test before they totally discount

Third, according to Wakefield, "we all know that science accepts nothing on faith". Science can provide us with statements about degrees of probability and correlation. To speak of the provisional and ever-cautious statements of science as if they were eternal proclamations of certainty and causality is to distort the truth.

As D.H. Koobs points out (*Nature* 319, 172; 1986), to assert today that the Universe and its life forms occurred spontaneously remains "clearly a matter of faith".

Finally, Wakefield claims that "creationists do their best to twist, lie, fabricate, misrepresent all they can of reality to deceive their followers and the lay public". While this may be true of some creationists. I cannot believe it is true of all. It is possible to hold a creationist view of the origin of life and the Universe with sincerity and intellectual integrity. And in the interests of scientific objectivity, it must be pointed out that scientists, too. have sometimes distorted the truth: let us remember Burt's obsessional prejudices about race and IQ which he dishonestly presented as if they were real experimental findings.

VALERIE VENTURA

21 Mountsfield Court, Hither Green Lane, London SE13 6RR, UK

Risk analysis

S_{IR}—S.O. Funtowicz and J.R. Ravetz (*Nature* 321, 644; 1986) are, of course, correct in writing that society must recognize that large improbable accidents can and will happen, whether they be collisions of Boeing 747 aircraft over Wembley Stadium during a Cup Final, or the failure of a nuclear power plant.

Their rejection of probabilistic risk analysis (PRA), however, is factually incorrect. It was not used in either of the two examples he cites — Three Mile Island or Chernobyl. In 1977, the US Nuclear Regulatory Commission instructed its staff not to use PRAs in the licensing procedures. As a result, nobody calculated for a Babcock-Wilcox reactor until the afternoon of 28 March 1979. If they had. the weakness of the operating procedure would have been quickly recognized and the accident at Three Mile Island avoided. In spite of numerous reports and discussions, both official and unofficial, nobody in the West has seen a PRA for Chernobyl. I do not believe that a complete one exists.

It is the procedure of thinking carefully about accidents, using logically plausible scenarios, that is our best and possibly our only defence against these scenarios occurring. This is what a PRA accomplishes.

Some responsible, competent person must have thought through the problem enough to derive a number with its uncertainty. Whether Funtowicz and Ravetz believe the number is comparatively irrelevant. But they should not discourage the procedure itself, which is almost the only procedure that we have.

RICHARD WILSON

Department of Physics. Harvard University. Cambridge, Massachusetts 02138, USA

Pesticide regulation

SIR—I appreciated Kenneth Mellanby's letter in *Nature* (321, 465; 1986) about my objection (*Nature* 320, 391; 1986) to a sentence in Lord Ashby's review of John Sheail's book (*Nature* 318, 21; 1985).

I have admired the British method of pesticide regulation, and Sheail performed a good service by describing the collaboration there between industry and government.

I certainly did not intend to imply that it was Mellanby's British colleagues who resorted to "such unscientific methods as deliberately distorting or omitting all the data that refuted their (anti-DDT) allegations". Instead I had in mind only the work of several notorious US scientists, especially some employees of our federal Fish and Wildlife Service and a few in the California Department of Fish and Game. Their statements were frequently published, without competent peer review, in magazines such as Science. BioScience. Scientific American and various "bird" journals. Specific refutations of their allegations have been published elsewhere by many concerned US scientists. but were ignored by the US Environmental Protection Agency (EPA).

EPA joined the attack, and sought to direct a worldwide condemnation of agrichemicals and chemicals used to alleviate insect-borne disease outbreaks, via its Toxic Substances Control Act (TSCA). In response, British Science Attaché Alan Smith was applauded by over 600 specialists at a meeting called by EPA to discuss the act when he stated: "This draft is like the jabberwocky of Lewis Carroll the language of chemistry mixes uneasily with the language of metaphysics and the overlay of legal jargon makes the whole incomprehensible." After calling it an "absurd piece of gobbledegook", Smith suggested that EPA should "not presume to legislate for the Universe and the whole human race" and that "there is a limit to the number of times even the greatest country in the world can afford to appear ridiculous in international affairs" (Science 196, 1182-83; 1977).

Although DDT is no longer used in the United States, false claims about it continue to be repeated. The reasons are varied, but are well-known. The same sort of campaign that succeeded in banning DDT has more recently been directed against 2,4,5-T, malathion. DES and many other useful chemicals of very slight hazard to man or the environment. Unless the scientific community actively exposes such false statements as have been made in journals and indicates disapproval of those who deliberately make them, the human race faces a very bleak future.

J. GORDON EDWARDS

San Jose State University, San, Jose, California 95192, USA

New ways with interatomic forces

Attempts to calculate the properties of real materials from those of their constituents have never been outstandingly successful. New, but still empirical, techniques may help.

Since the year dot, or thereabouts, all kinds of people have been calculating the properties of matter of various kinds by making assumptions they know to be inadequate about the forces between constituent particles. The process continues, and discontent with the assumptions is, if anything, made more explicit by the availability of computers and the associated computer codes that will allow the treatment of systems large enough to be considered "realistic". But supply tends to grow to meet demand, and the invention of novel schemes for representing interatomic forces is now also flourishing. One such is a way of representing long-range interatomic forces developed by a group based at the University of Trieste (F. Ercolessi, E. Tosatti and M. Parrinello) and applied to the structure of the surface of gold crystals (Phys. Rev. Lett. 57, 719;

The problem of calculating ab initio the properties of a material is indeed intractable. Even that model of the ideal gas in which the atoms are perfectly elastic solid spheres is useful only for as long as the spheres are not so large, relative to their container (again assumed perfectly elastic) that geometrical effects make them clump together in some sense. More realistically, the forces between pairs of atoms in, say, a monatomic gas are better represented by a distance-dependent mutual potential energy leading to forces that are repulsive at short distances (reflecting the solidity of atoms) which may be offset by attractive forces at greater distances. Van der Waals is the name to conjure with; physically, what happens is that random intra-atomic fluctuations giving individual atoms an electrical dipole moment will tend to synchronize with the instantaneous dipole moments of interacting atoms, dragging the two together, which is why gases whose constituents are either polar or highly polarizable molecules depart most conspicuously from the perfect gas laws.

Mischievously, real substances are more cussed than these simple examples allow. Even in gases, three and multibody forces are bound to be relevant, and properties may depend not only on the positions of atoms or molecules instantaneously, but on their velocities as well. A further complication, especially when the average inter-particle distance is small, is that there may be literally no limit to the distance over which inter-particle forces

exert themselves because of cooperative effects in which the miscroscopic interactions have the effects of enforcing long-range order, when a material behaves as if the range of the physical force between a particle and the environment of which it is a part is literally infinite.

So what happens in, for example, a metal, which may be taken, for the sake of argument, to be a lattice of positively charged ions embedded in a sea of negative electricity? Simple calculations based on the assumption that the ions interact with each other by some defined interionic potential energy will not wash, because the electron sea is of necessity a long-range system whose collective properties and, in partucular, energy may not be simply expressed by the distance between the members of an arbitrarily chosen pair of atoms.

Ideally, people wishing to calculate the binding energy of a metal should proceed differently: first, make an assumption about the geometry of the ion lattice, then calculate the allowable quantum states of electrons, finally allow that the electron distribution will seek a lower level of energy in which ionic charges are more completely shielded from each other (which is where the Thomas-Fermi and other selfconsistent field calculations come into their own). The results are reasonable enough, although not especially persuasive, for one thing because nobody is confident of being able to adapt the selfconsistent calculations to the real case in which the ions of the ion-lattice are in motion, as they must be.

That is why there is such ample room for more empirical ways of tackling the problem by the invention of novel ways of describing the forces between ions in, say, a metallic crystal. The obvious difficulty is that the bulk properties of metals do not provide a sufficiently stringent test of possible refinements of assumed interatomic force laws, all of which must have certain general properties in common. But distortions at the surfaces of metallic crystals to the regular distribution of ions in the bulk may be an opportunity for verification, which is where Ercolessi and his colleagues begin, with the surface structure of metallic gold.

Like many other solid lattices, but more markedly, the surface of a metallic gold crystal is not a simple projection onto a crystallographic surface of the structure of the crystal lattice in bulk. Instead, the atoms of this structure, whose unit cell is face-centred cubic, appear on simple crystallographic surfaces — such as (001) — to be arranged in stripes, five rows of atoms wide within which atoms are arranged on a triangular rather than a square pattern. This has been shown experimentally by, for example, low-angle electron diffraction.

Ercolessi et al. apply to this structure a force-law they have developed in other connections, one that allows not only for pair-wise forces between atoms (including other than pairs of nearest neighbours) but for a generalized glue-like force which has the effect of making it energetically adventageous, in a system such as a metallic crystal, that the coordination number should be increased. Their two-body force is conventional enough, implying repulsion at short distances, a minimum energy at about 0.27 nm and attractive forces at greater distances. The glue force is harder to visualize, but represents a kind of tradeoff between high coordination number and proximity between pairs of atoms.

The outcome is remarkably suggestive even though it leaves much to be desired. By a suitable choice of the empirical constants in the force laws, five-row stripes of atoms can indeed be made to appear on the simple surfaces of gold crystals. The obvious snag is that there seems very little hope of being able to calculate either the pair-wise forces or those that represent the glue from what might be called first principles. Even so, especially because of the importance of, for example, the surface structure of semiconducting materials such as silicon, there is every prospect that this new technique of calculation will quickly become fashionable. It may even become a fashion that will last.

The situation in the calculation of the properties of metals, in other words, may soon not be very different from that in the calculation of the properties of gases half a century ago. Then it was that people were aware of the complexity of the pair-wise interatomic force as well as of the need to pay some attention to three and multibody forces. The force-laws were for the most part empirical, but it is remarkable how useful they proved to be. Nobody will weep if there is a period, perhaps a long one, during which the calculation of the properties of metals is as much a matter of finding, through trial and error, which methods work and which do not.

John Maddox

Neurochemistry

Lessons from large molecules

from William S. Agnew

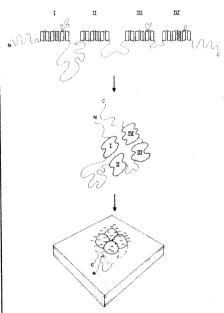
THE nervous impulse is one example of a major, easily observable physiological phenomenon that results from the action of a particular type of protein molecule, in this case the voltage-sensitive sodium channel. The nature of the smallest molecular unit that constitutes a functional sodium channel is, therefore, of considerable interest. In the most recent work from the laboratory of S. Numa, reported by M. Noda and co-workers on page 826 of this issue (ref. 1, see also refs 2,3), the authors use molecular cloning techniques to provide convincing evidence that the minimum molecular element constituting a sodium channel is a large, heavily glycosylated polypeptide of relative molecular mass 260,000-295,000 (260-295K). This finding helps to constrain models for ionic permeation and voltage-dependent gating mechanisms, and has probably resolved the question of the obligatory role of the small peptides found in preparations of brain and muscle channels.

The origin of this question lies in studies in which sodium channels have been isolated, mainly from three tissue sources: eel electroplax4.5, mammalian muscle6 and brain7. Common to all three preparations are the 260-295K glycopeptides. Brain channels include two smaller glycopeptides, 36 and 33K, the former linked to the larger peptides by disulphide bridges. There is at least one peptide of 39K in muscle, although no small peptides have been found in the electroplax protein.

Each of these preparations, including the single-peptide electroplax protein, has been successfully reconstituted in biochemical and biophysical studies8-10 Because of the similarities of the large peptides, these findings appear to argue against a mechanistic role for the smaller subunits. Nevertheless, evidence from subunit-dissociation studies led Catterall and co-workers to conclude that they are involved in neurotoxin binding", suggesting that they are essential in channel activity in vivo, perhaps for activity or for expression at the cell surface.

The three recent reports from Numa's laboratory1-3 cast the whole constellation of questions about sodium-channel structure and function in a new light. In the first of these2 the authors cloned and sequenced the 8-kilobase complementary DNA that encodes the large peptide of electroplax. The deduced amino-acid sequence is consistent with previous compositional studies and provides an intuitively satisfying indication that the 208K polypeptide portion of the glycopeptide probably folds into a tetrameric structure.

But messenger RNA transcribed from this DNA apparently does not yield functional channels when microinjected into frog oocytes, possibly because of failure of post-translational modifications. Thus, in a second study'. Numa's group cloned the large subunit of the brain channel, only to discover that in this tissue not one, but at least three species of channel are expressed, closely related both to one another



Sodium channel amino-acid sequences suggest that a tetrameric bracelet of domains (I-IV) contain most glycosylation sites and predicted membrane-spanning a-helices. Negative surface charges derive from sialic acids and a possible cytoplasmic domain could act as a substrate for protein kinases or mediate interactions with other proteins.

and to the electroplax protein. These findings at least briefly raised the spectre that there could be as many as six smaller peptide constituents: identifying which are associated with and required for the activity of each large peptide might have demanded an entire new round of detective work before mutagenesis studies could begin.

In the study reported in this issue, the authors prepared messenger RNA by in vitro transcription of each of the three variant brain clones. When the RNA from one of these, rtII, is microinjected into frog oocytes, comparatively large voltageregulated sodium currents appear after 3-5 days of incubation. These currents are tetrodotoxin-sensitive, sodium selective and exhibit voltage activation and inactivation. Activation- and inactivationgating parameters are within the range expected for conventional sodium channels. Expression is not enhanced by ad-

dition of low molecular mass poly(A)' messenger RNA from brain, consistent with earlier fractionation studies. The possibility that the protein has combined with endogenous small peptides still needs to be tested directly, but seems unlikely because oocyte sodium channels are markedly different from those produced by RNA injection.

Thus, at least one of the brain-derived large peptides is sufficient to form a traditional, voltage-responsive sodium channel. In turn, because of the similarities in the sequences and the biophysical and pharmacological properties of sodium channels from different tissues, many of the structures of greatest initial interest (such as the ion pore, voltage-sensing elements, sites of interaction with neurotoxins and anaesthetics) are probably all specified within the large polypeptides. The use of single-channel recording techniques, together with genetically altered channels or with chemically modified reconstituted molecules, should help in the analysis of these essential proteins.

What, then, are some of general structural features of sodium channels that are emerging? First, within the amino-acid sequences of all of the peptides there are four very similar stretches, perhaps reflecting replication of a primordial gene (see figure). These regions (I-IV), each of about 30K, contain all the sequences predicted to form membrane-spanning a-helices. Among these are intriguing periodic sequences in which two hydrophobic residues are followed by an arginine or lysine residue for 4-8 cycles. inviting speculation about gating mechanisms^{13.1} . The intervening sequences. together with the carboxy and amino termini, are polar and not expected to span the membrane. The homologous repeats can be compared with the subunits of the pentameric acetylcholine receptor. suggesting pseudo-subunits on a string which may form a tetramerically ordered bracelet structure (see figure).

The repeat domains are very closely conserved between the electroplax and brain channels, whereas the intervening

Noda, M. et al. Nature 322, 826 (1986).

Noda, M. et al. Nature 312, 121 (1984). Noda, M. et al. Nature 320, 188 (1986).

Miller, J.A., Agnew, W.S., & Levinson, S.R. Biochemi-stry 22, 462 (1983).

Norman, R.I., Schmid, A., Lombet, A., Barhanin, J & Lazdunski, M. Proc, natn. Acad. Sci. U.S.A. 80, 4164

Barchi, R.L. J. Neurochem. 40, 1377 (1983).

Hartshorne, R.P., Messner, D.J., Coppersmith, J.C. & Catterall, W.A. J. biol. Chem. 257, 13888 (1982). Weigele, J & Barchi, R.L. Proc. nam. Acad. Sci. U.S.A.

^{79. 3651 (1982).} Talvenheimo, J.A., Tamkunn, M.M. & Catterall, W.A. J.

biol. Chem. 257, 11868 (1982).
Rosenberg, R.L., Tomiko, S.A. & Agnew, W.S. Proc. nain. Acad. Sci. U.S.A. 81, 1239; 5594 (1984).

Messner, D.J. & Catterall, W.A. J. biol. Chem. 261, 211

Sumikawa, K., Parker, I. & Miledi, R. Proc. nam. Acad. Sci. U.S.A. 81, 7994 (1984). Guy, H.R. & Seetharamulu, P. Proc. natn. Acad. Sci.

U.S.A. 83, 508 (1986).

^{14.} Catterall, W.A. Trends Neurosci. 91, 7 (1986).

and tail sequences are far more divergent, suggesting that the highly conserved biophysical and pharmacological properties can be accounted for largely by domains within the repeat segments. Interestingly, the brain proteins have a large (19–20K) sequence between repeats I and II, containing several consensus phosphorylation sites, that is not present in the electroplax protein. This domain could be involved in modulation, in interactions with smaller subunits or in cytoskeletal attachment. It probably does not participate directly in the 'activity cycle'. In addition, all the peptides are heavily glycosylated; in the electroplax protein sialic acids contribute up to 120 negative charges to the extracellular surface although there may be less in brain and muscle proteins. The new work suggests that for this second ion-channel

prototype the striking departure from the multi-subunit design of the acetylcholine receptor may be more apparent than real.

Also worth mentioning is the discovery of a family of sodium-channel proteins in brain. Some of these may be specific for particular neurones, and some neurones may exhibit multiple species of channel; some channels may be associated with glial cells. If there are banks of genes for ionic channels, their expression in specific cells at appropriate topographical locations must involve regulatory mechanisms that influence and perhaps even respond to the flow of electrical information in neurones and neuronal networks.

William S. Agnew is in the Department of Physiology at Yale University School of Medicine, New Haven, Connecticut 06510, USA.

Archaean geology

Hungry komatiites and indigestible zircons

from G.R. Edwards and E.G. Nisbet

THERE has been much recent academic interest in the rocks hosting the Kambalda nickel deposit in Western Australia. This is presumably not because salaries are so low that research workers are hoping to find a new mine, but rather because these rocks are forcing a reassessment of one of the most important dating methods in old rocks and are causing us to think again about the processes that occurred when hot lavas erupted through and onto the continental crust 2,700 million years ago'.

At Kambalda, nickel sulphide ores are closely associated with komatiites, lavas with high magnesium contents that generally occur in rocks older than 2.5×10^9 years. The high Mg content implies that komatiites were very hot (up to 1,650°C) when they erupted. Interest in the Kambalda rocks has concerned the age of the komatiites as well as the way in which the sulphide deposits were formed. The debate began when an array of Sm-Nd isotope data from Kambalda was interpreted as evidence that the Kambalda lavas are 3.2×10" years old. Another group interpreted the same data as the result of mixing of material derived from a depleted mantle source with either an undepleted mantle source or material from the lower continental crust'. This group went on to show that Pb-Pb isotopes defined an age of 2.73×10" years, and that Pb isotopes in the rocks may be dominated by the effects of contamination with crustal or surfacederived material.

Compston et al. now provide additional evidence from zircons that not only supports the $2.7 \times 10^{\circ}$ -year estimates but also provides further evidence for crustal contamination. Zircons separated from basalts at Kambalda and analysed for U, Th and Pb isotopes using the SHRIMP ion microprobe have distinct cores with minimum ages ranging from greater than 3,400 to 3,100 million years and surrounded by mantles of younger zircon.

The old zircons are thought to be xenocrysts, partly because there were also zircon mantles and whole zircons with ages less than 2,700 million years in the sample, but also because the zircons are rich in U and Th, suggesting crystallization from felsic magma or recrystallization in felsic rock rather than crystallization from basalt. Mantling of the structural cores of the complex zircons seems to have occurred in two steps: (1) metamorphic recrystallization of the zircons while in their parent rock about 3.1×10° years ago, probably under granulite conditions; and (2) new growth around the metamorphically mantled zircon cores after their inclusion in the mafic-ultramafic magma. From their analysis of younger zircons, Compston et al. suggest the age of extrusion of the lavas is $\leq 2.669 \pm 11$ million years.

What is the ultimate source of the zircons? They are soluble in high-Mg basaltic magmas and would be unlikely to survive a long journey to the surface unless protected by enclosure in small xenoliths. It is also unlikely that new zircons or zircon mantles will grow in zirconium-undersaturated high-Mg basaltic magmas. Nevertheless, zircons are notoriously resistant to melting, so they may survive these processes virtually unscathed and l

the mantles may thus represent an attempt at solid-state re-equilibration by zircons derived from the continental crust. Alternatively, some of the zircons may have been locally derived by assimilation of some of the zircon-bearing interflow sediments. The weight of the isotope evidence thus suggests that there was some contamination of the Mg-rich magmas at Kambalda. Contamination is greatest when heat transfer to the country rock is most rapid, as is the case during turbulent flow in hot, low-viscosity komatiitic magma*.

Ascending hot komatiitic magmas could have thermally eroded the wall rocks of conduits to become contaminated: on eruption, komatiites could have eroded underlying strata. Trace-element evidence⁵ implies that komatiite at Kambalda was contaminated by thermal erosion and assimilation of a mixture of sediment and tholeiites, whereas the high-Mg basalts at Kambalda are the result of up to 25 per cent contamination of komatilte, at depth, by material similar to upper continental crust. As for the nickel sulphide deposits — the reason why so many geologists descended on Kambalda in the first place — Groves et al. concluded from field evidence that thermal erosion occurred, but only where concentrations of sulphide liquid (which has a high thermal conductivitiy) were present at the base of lava channels. Some of this sulphide liquid may have formed from initial thermal erosion of sediments.

What can we learn from all this? The first lesson is that Sm-Nd data from komatiite rocks must be treated with great caution. On the other hand, zircons are extremly interesting if one has an ion microprobe. More generally, the controversy may help to elucidate the mechanisms of komatiite eruption and also the history of the continental crust, which has been sampled by the erupting liquids. Thus some zircon-containing lavas may be useful geochemical probes of the ancient lower continental crust. But some komatiites (especially the most magnesian) may be little contaminated. Perhaps they erupted through conduits that split slightly older komatiite dykes and were erupted on top of komatiite flows. Other komatiitic basalts may be the highly contaminated end-products of the eruption of originally highly magnesian liquids. And as for the nickel deposits, perhaps erosional effects under komatiites are a sign of a nearby sulphide pool.

- Compston, W. et al. Earth planet Sci. Lett. 76, 299; 1986) Claoue-Long, J.C. Nature 307, 697 (1985). Chauvel, C. et al. Earth planet. Sci. Lett. 74, 315 (1985). Huppert, H.E. & Sparks, R.S.J. Earth planet. Sci. Lett. 74, 274, 1985. 371 (1985).

 5. Arndt, N.T. & Jenner, G.A. Chem. Geol. (in the press).
- 6. Groves, D.I. et al. Nature 319, 136 (1986)

G.R. Edwards and E.G. Nisbet are in the Department of Geological Sciences, University of Saskatchewan, Saskatoon S7N 0W0, Canada.

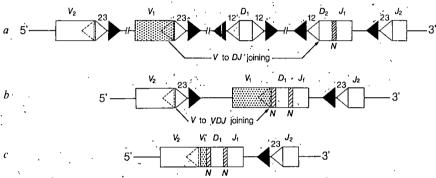
Antibody diversity

New mechanism revealed

from Frederick W. Alt

THE production of a functional antibody molecule requires the rearrangement of separate gene segments within the germ line of B lymphocytes. Three different segments are rearranged to produce the antigen-binding variable region of the antibody heavy chain. It was thought that no further rearrangements of completely assembled variable-region genes can occur, but two groups^{1,2} report on pages 840 and 843 of this issue that permanent cell lines of the B-cell lineage can exchange most of the body of a rearranged heavy chain variable-region segment with that of an upstream, germ-line variable region gene segment. This novel rearrangement has implications for the effiquences containing 23-bp spacers, D segments are flanked on both sides by 12-bp spacers, and $V_{\rm H}$ segments are flanked downstream by recognition sequences with 23-bp spacers (see figure).

In accord with the 12/23 rule, assembly of the $V_{11}DJ_{11}$ gene occurs by joining of D and J_{11} segments followed by joining of a V_{11} segment to the pre-existing DJ_{11} complex. A consequence of the 12/23 rule is that a pre-formed DJ_{11} rearrangement can be replaced by joining an upstream D to a downstream J_{11} but a $V_{11}DJ_{11}$ rearrangement, once formed, cannot be replaced by joining events to downstream J_{11} segments because direct V_{11} to J_{11} joining is prohibited by the 12/23 rule and all intervening D



a. Scheme for the chromosome after a $DJ_{\rm H}$ join. Recognition heptamers are indicated by open triangles and nonamers by closed triangles; 12- and 23-bp spacers are indicated. The heptamer within the V segment is represented by a dashed triangle. b, A $V_{\rm H}$ to $DJ_{\rm H}$ join; intervening D segments (and 12-bp spacers) are deleted; added N segments are indicated. c, A $V_{\rm H}$ to $V_{\rm H}DJ_{\rm H}$ join; in this case the final assembled V gene consists of the body of $V_{\rm H}2$, a small segment of $V_{\rm H}1$, a 5' N region; a D segment, a 3' N region, and a $J_{\rm H}$ segment. Sizes of the segments not drawn to scale.

ciency of B-cell differentiation and establishes a new mechanism for generating the antibody diversity essential for a competent immune system.

The three germ-line DNA elements of the variable (V) region of an immunoglobulin heavy chain: variable (\dot{V}_{11}) , diversity (D) and joining (J_{tt}) segments, are found on the same chromosome. In the mouse four $J_{\rm II}$ segments are followed immediately upstream by about 12 D segments that are in turn followed at an unknown upstream distance by 200 or more $V_{\rm H}$ segments³. Recombination between these elements is mediated by conserved recognition sequences that consist of a palindromic heptamer (related to the sequence CACTGTG) and an AT-rich nonamer separated by a spacer of either 12 or 23 base pairs (bp). Joining appears to occur only between elements flanked respectively by recognition sequences having spacers of 12 and 23 bp (the 12/23 rule)4.5. This requirement restricts the possible rearrangments as J_{11} segments are flanked upstream by recognition sesegments (12-bp recognition sequences are deleted during $V_{II}DJ_{II}$ assembly).

The novel V_{11} to $V_{12}DJ_{11}$ rearrangment described by Reth et al. and by Kleinfield et al.2 in this issue occurs by a recombination mechanism similar to that used for normal V-gene assembly but uses a recognition heptamer (TACTGTG) found in the 3'-region of most V_{II} genes' (see figure). Notably, this heptamer is identical to that within the recognition sequence flanking the 5' border of most D segments so that although the heptamer 5' of the D segment is deleted after V_{ii} to DJ_{ii} joining. an identical heptamer within the $V_{\rm II}$ gene is now present. The $V_{\rm II}$ gene sequence does not contain an obvious nonamer so the complete upstream recognition sequence is not replaced. However the structure of the V_{11} to $V_{11}DJ_{11}$ recombinants suggests that the internal heptamer mediates site-specific joining, rather than conversion or homologous recombination

Site-specific immunoglobulin-gene recombination mediated by an isolated

heptamer has been shown previously in the light chain? ". In addition, although the TAC and TGT codons of the heptamer encode a conserved Tyr and Cys found in most V-gene segments, Kleinfield et al. note little third-base variation within these residues in V_{11} gene segments, which they believe suggests conservation of the sequence itself. This is perhaps surprising in the light of recent evidence that immunoglobulin recombinase accepts wide sequence variation within the heptamer, at least when it is associated with a nonamer. But Reth et al. indicate that V_0 to $V_{\rm H}DJ_{\rm H}$ joining occurs frequently even though direct $V_{\rm H}$ to $J_{\rm H}$ joining does not occur, perhaps suggesting that the nonamer restricts recombination in the context of the 12/23 rule. Clearly more remains to be learned about the role of recognition sequences.

Assembly of the elements in the V-region gene is not precise and bases can be lost and/or added at the joining point (N regions). The V_{11} - DJ_{11} joint region of the antibody molecule is involved in antigen contact; thus, junctional diversification provides antibody diversity. The studies indicate that V_{11} to $V_{11}DJ_{11}$ joining may allow additional diversification of this important region; sequences left attached from the first V-region provide an additional N-like region (see figure).

Junctional diversification mechanisms have another important consequence for differentiating B lymphocytes. The reading frame of the heavy-chain messenger RNA is determined by the start site for translation at the 5' end of the V_{ii} . Because of random insertion and deletion of bases and the triplet reading frame, approximately 2 out of 3 $V_{II}DJ_{II}$ joins link the V in a different translation reading frame from the J. Such rearrangments are 'aberrant'; they produce heavy-chain mRNA that cannot be translated into a complete heavy-chain protein. Given the inaccuracy of the joining process, in spite of the opportunity for rearrangment on both chromosomes, nearly 50 per cent of differentiating B cells should join both heavychain alleles out of frame'. Previously. such cells were thought to lost from the differentiation pathway, because aberrant $V_{\rm R}DJ_{\rm H}$ joints could not be salvaged. However. Reth et al. demonstrate that permanent pre-B lines that have formed two aberrant $V_{II}DJ_{II}$ rearrangements can rescue the heavy-chain production by $V_{\rm H}$ to $V_{\rm B}DJ_{\rm H}$ recombination. Because of the same imprecise recombination this secondary join can provide a productive reading frame and could make this phase of B-cell differentiation nearly 100 per cent efficient.

The production of complete heavy chains is restricted to a single allele in B cells. Such allelic exclusion appears to result from cessation of V_{11} to DJ_{11} rearrangement when the initial V_{11} to DJ_{11} join

is productive. In the event studied by Kleinfield et al.², the V_{ii} of a productive $V_{11}DJ_{11}$ rearrangement is exchanged with an upstream V_{μ} segment to produce a novel productive rearrangment, indicating that the recombinase is still active in cells with a productive $V_{II}DJ_{II}$. This finding may, at first glance, seem inconsistent with an allelic exclusion mechanism regulating V_{ii} to DJ_{ii} rearrangement. However, current evidence suggests that joining is prevented in cells with a productive $V_{\rm H}DJ_{\rm H}$ rearrangement by limiting access of the recombinase to $V_{\rm H}$ gene segments rather than by turning off recombinase activity'. Recombinase is thought to lose access because transcription of germ-line V_{ii} segments stops in cells that produce complete heavy chains".

Notably, the described V_{II} to $V_{II}DJ_{II}$ recombinations seem to involve proximal $V_{\rm tr}$ segments and it has been shown that the activity of the heavy-chain enhancer in the J_{ii} to \tilde{D}_{ii} intron allows transcription of the proximal unrearranged V_{ij} segment¹²; perhaps by providing access to recombinase. Because allelic exclusion appears to occur in nearly 100 per cent of normal B cells, it seems that V_{ii} to $V_{ii}DJ_{ii}$ joining does not frequently activate expression of both heavy-chain alleles.

 $V_{\rm n}$ to $V_{\rm n}DJ_{\rm n}$ joining may also prevent bias in the development of the heavychain V-region repertoire. Differentiating B cells use the V_{II} segments nearest the J_{II} elements at high frequency to form $V_{11}DJ_{11}$ rearrangements', which limits the spontaneously generated heavy-chain repertoire. But the repertoire of mature peripheral B cells appears to involve all V segments equally. How this occurs is not known, although cellular selection mechanisms have been implicated. Kleinfield et al. suggest that V_{tt} to $V_{tt}DJ_{tt}$ joining may be a means of successively replacing rearranged 3' V segments with more 5' V segments. However, if replacement involves nearest neighbours, as suggested from the data of Reth et al., it is difficult to imagine successive recombination events between hundreds of V genes playing a major role in the process. Final understanding awaits further elucidation of the mechanism and frequency of this process.

- Reth, M., Gehrmann, P., Petrac, E. & Wiese, P. Nature 322, 840 (1986).
- Kleinfield, R. et al. Nature 322, 843 (1986).
 Alt. F.W. et al. Immun. Rev. 89, 5 (1986).
- Early, P. et al. Cell 19, 981 (1980).
- Sakano, H. et al. Nature 286, 676 (1980).
- Early, P. et al. Molec, cell. Biol. 2, 829 (1982). Seidman, J. & Leder, P. Nature 286, 779 (1980).
- Durdik, J., Moore, M.N. & Selsing, E. Nature 307, 749
- Siminovitch, K.A. et al. Nature 316, 260 (1985)
- Yancopoulos, G.D. et al. Cell 44, 251 (1986). Yancopoulos, G.D. & Alt, F.W. Cell 40, 271 (1985).
- Wang, X.-F & Calame, K. (ell 43, 659 (1985)
 Dildrop, R. et al. Eur. J. Immun. 15, 1154 (1985).

Frederick W. Alt is in the Department of Biochemistry and Molecular Biophysics at the College of Physicians and Surgeons, Columbia University, New York, New York 10032, USA.

Animal behaviour

How great white sharks, sabretoothed cats and soldiers kill

from Jared M. Diamond

PREDATORS that attack large prey enformidable dowed with defensive weapons face a dilemma. If the victim is not incapacitated by the first blow and the predator must continue to engage the victim in order to kill it, the predator itself risks injury. For example, lions are occasionally crippled or killed by zebra, giraffe or rhinoceros prey. Recent studies suggest that two quite different large predators - the great white shark12 and the extinct sabre-toothed cats3 — independently evolved the same solution to this dilemma.

Adult great white sharks (Carcharodon carcharias), the largest living marine fish capable of preying on vertebrates, often feed on seals, whales and other sharks. Common victims in Californian waters are elephant seals, which have formidable teeth combined with a maximum size exceeding that of the shark. The seal is more agile than the shark and is therefore most efficiently hunted by surprise. Timothy Tricas and John McCosker^{1,2} reconstructed the shark's strategy from observations of attacks; scars on seals that got away; and underwater observations (while protected within steel cages) of sharks approaching bait. Bite scars on surviving seals indicate a single massive bite on the l

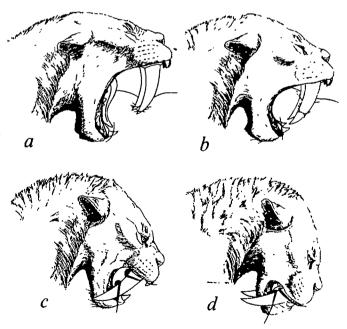
underside of the body. Apparently a shark cruising underwater sees above it the silhouette of a seal basking at the surface, rises undetected towards the seal from behind and below, quickly bites out a large chunk of the seal (the entire biting takes only 1 second), and rapidly retreats to avoid injury. The shark then waits for the seal to go into shock or to haemorrhage before closing in to complete the kill and to feed.

This reconstructed sequence helps one to understand what happens to human victims of great white sharks. Most survivors never saw the shark that attacked them: they merely

felt themselves lifted into the air and then dropped after suffering a single haemorrhaging bite. Victims usually die from loss of blood, not of limbs or vital organs

A similar strategy appears to have been practised on land by extinct sabre-toothed cats of the genera Smilodon and Homotherium³. These lion-sized predators take their name from their very long upper canines (exposed tooth up to 15 cm long in Smilodon). How these weapons were used to kill has been in dispute. The prevalent view until recently was that the upper canines were used to stab or slash the victim while the lower jaw was merely drawn down out of the way. However, closer examination casts doubt on the usefulness of the blunt sabres for stabbing and slashing: they are round-tipped, oval rather than knife-like in cross-section, and barely clear the lower jaw.

Our most detailed information about the preferred prev of sabre-tooths comes from a probable den, Friesenhahn Cave in Texas, where remains of adult plus very small juvenile Homotherium co-occur with scores of baby mammoths, presumably killed by the adult cats and dragged to the den to feed the kittens. Even a baby mammoth could hardly have been killed by the cat at a single blow. Yet it would



How Smilodon used its peculiar anatomy to rip a large piece of flesh out of its prey. Propping its mandible on the prey (a), the cat used its powerful head-depressing muscles to drive in the upper canines (b), rotate the head until the jaws closed (c, d) and pull out a fold of flesh. (Drawing by Mark Hallett. From ret. 3 courtess of the Los Angeles County Museum of Natural History.)

have been suicidal for the cat to continue to grip the baby, as the mother would then have time to crush or impale the cat.

A solution to this dilemma is suggested by William Akersten's anatomical studies3 of remains of Smilodon trapped in the famous La Brea tar pits of Los Angeles. Muscle scars on Smilodon bones show that the muscles for closing the jaws were not especially strong but that the muscles to depress the head by rotating it downwards around the joint with the first neck vertebra were massive (see figures). The chin was flanged, and the jaws opened to the enormous gape angle of 95° to permit the same clearance between the long upper and lower canines as does the 65° gape of modern cats. Akersten suggests the following sequence. A cat ambushes a baby mammoth straying from its mother and uses its powerful fore-limbs to pull down the baby, exposing the abdomen. The cat opens its jaws wide, catches a large fold of flesh between the upper and lower



Cranium and mandible of Smilodon.

canines, wedges the lower jaw firmly against the prey by the chin flanges, and then completes the bite by the head-depressing muscles. It then flees from the approaching mother mammoth and waits for the baby to haemorrhage, die, and be abandoned by its mother.

Yet one more predator has independently evolved a similar solution to the problem posed by a formidable victim. The most dangerous prey of all is an armed man, routinely hunted only by other armed men. Inexperienced soldiers aim for the head or heart, but these small targets are easily missed. "Always aim for the stomach when you shoot" was the advice of an experienced African bush fighter — "it is just as good, because no man can live long after his intestines have been shot away". Nor could an elephant seal or baby mammoth.

- Tricas, T.C. & McCosker, J.E. Proc. Calif. Acad. Sci. 43, 221 (1984).
- McCosker, J.E. Calif, Acad. Sci. Mem. no. 9, 123 (1985).
 Akersten, W.A. Los Ang. County Mus. nat. Hist. Contr.
- Sei, no. 356 (1985).
 Bosman, H.C. in The Collected Works of Herman Charles Bosman 64 (Ball, Johannesburg, 1981).

Jared M. Diamond is Professor of Physiology at the University of California Medical School, Los Angeles, California 90024, USA.

Anthropology

The longest human record

from John E. Yellen

THE recent conference* to honour J. Desmond Clark for his contributions to African pre-history provided a unique opportunity to review current ideas about the archaeological record of this continent. African palaeoanthropology is most clearly distinguished by its quest for the first uniquely hominid antecedent: the earliest known hominid fossils derive from the Eastern Rift Valley in Kenya. Evidence for the first million years of cultural development, in the form of stone tools, butchered animal remains and possibly the controlled use of fire, are also limited to the African continent. The first modern humans, Homo sapiens sapiens, were widely distributed in Africa well before their appearance in Europe and the near East and the development of complex societies, in relative independence from those in other parts of the Old World.

Excavations this past summer near Ishango, eastern Zaire, produced stone artefacts associated with faunal remains that are just over two million years old (Jack Harris, University of Wisconsin; Noel Boaz, Virginia Museum of Natural History). In conjunction with stone-tool assemblages from Ethiopia of about the same age, systematic lithic modification must have appeared more than two million years ago. Unfortunately, these artefacts cannot be assigned to specific species.

Arguments were presented that *Homo habilis* was capable of speech (Dean Falk, University of Puerto Rico; Philip Tobias, University of the Witwatersrand). This species had a larger brain than australopithecine forms with prominent enlargement of Broca's and Wernicke's areas, both associated with language in modern humans. These advances appeared at about the same time as the first stone tools.

Whereas most palaeoanthropologists agree that by the mid-Pleistocene Homo erectus had controlled use of fire, there has been no evidence for earlier occurrences. Because charcoal decomposes in tropical environments, African evidence is extremely difficult to obtain. Recently discovered patches of reddened earth in East African sites dates between 1.5 and 1.7 million years ago and which are associated with cultural remains were suggested to indicate much earlier human use of fire (Desmond Clark, University of California; Jack Harris, University of Wisconsin). But palaeomagnetic and thermouminescent analyses failed to provide unequivocal evidence of sediment heating.

*The Longest Record: The Human Career in Africa. Berkeley. California. 12 - 16 April 1986.

The question of early hominid hunting reflects on cognitive ability and social organization. Although animal bones with stone-tool cutmarks provide evidence of carcass use by humans earlier than 1.5 million years ago, it is uncertain whether these remains were acquired by hunting or by scavenging from carnivore kills. If hominids were primarily scavengers, they would be left with the less-choice body parts, which would be reflected in the skeletal elements recovered and the way they were treated to remove remaining scraps of meat. Using such criteria, faunal remains from both Olduvai and Koobi Fora can be interpreted to indicate hunting as cutmarks appear on the primary meat-bearing bones of small bovids which would be unlikely to survive the attention of large carnivores (Henry Bunn, University of Wisconsin).

Also at issue was a large sample of excavated cattle and sheep bones from the Neolithic site of Ngamuriak in southern Kenya. In this butchered assemblage the larger and smaller species are processed differently and a similar pattern is evident in early hominid material (Fiona Marshall, University of California). On the other hand, analysis of the Olduvai Bed I fauna shows 13 cases of overlapping stonetool and carnivore tooth marks. In eight of these the tool mark overtides that made by tooth, indicating human scavenging (Pat Shipman, Johns Hopkins University).

Recent work on the eastern margin of the Kalahari Desert shows a pattern of increasing complexity and hierarchical organization which, in effect, set the stage for the emergence of the Zimbabwe culture (James Denbow, National Museum of Botswana. The Venda, who are among the lineal descendents of Zimbabwe people, use variation in motifs on compound walls to denote status. Direct counterparts exist in Zimbabwe period stone-walled structures and, by application of Venda data, it has been possible to reconstruct a five-level hierarchy which extended from heads of individual households to the divine national leader (Thomas Huffman, University of the Witwatersrand). Because the gradual evolution of this system can be traced through time it is highly unlikely that the final structure was a direct results of outside stimulus (trade with Indian Ocean powers) but more probably derived from indigenous roots.

John E. Yellen is in the Anthropology Program at the National Science Foundation, 1800 G Street NW, Washington DC 20550, USA.

Neurophysiology

Parallel channels and redundant mechanisms in visual cortex

from N.V. Swindale

ALL too rarely, pharmacologists come up with a drug that interferes selectively with a particular pathway or a single welldefined function of the nervous system. Ideally the drug should be easily administered, specific and reversible, but such combinations are not often achieved. One molecule that does seem to satisfy these criteria is the glutamic acid analogue 2-amino-4-phosphonobutyric acid (APB) which has been studied by P.H. Schiller and collaborators and whose latest work is reported on page 824 of this issue¹. APB blocks the function of a class of retinal ganglion cells, and it is hoped that it will help to determine to what extent the visual system functions as an integrated whole or whether its differrent components are capable of some degree of independent function.

The pathway from retina to brain is divided into parallel channels, each selective for different attributes of the image, such as light intensity, colour and spatial frequency. Each channel consists of neurones of two types, ON and OFF, the former responding only to light levels that are greater than the local average in the image and the latter responding (by an increase in firing rate) to levels that are less than the local average. Thus, ON channels carry information about bright spots or areas in the image and OFF channels do the reverse. This division of labour, which resembles that of the pushpull output stage of an amplifier probably has more than one advantage: it allows cells to have low levels of activity when the retina is in darkness or uniformly illuminated, reducing metabolic requirements, and it effectively doubles the dynamic range over which neurones can signal information about light levels in the retinal image.

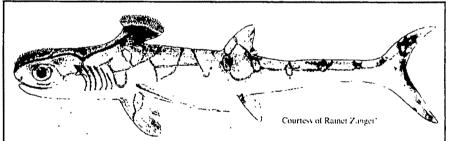
The separation between ON and OFF pathways occurs at the synapse between the rod and cone photoreceptors and bipolar cells, the earliest stage in the visual pathway. All photoreceptor cells hyperpolarize in response to light, but the bipolar cells to which they are connected are of two types: ON bipolars that depolarize when the photoreceptor to which they are connected hyperpolarizes, and OFF bipolars that hyperpolarize when the photoreceptor hyperpolarizes. If APB is applied to the retina it hyperpolarizes the ON bipolars, silencing cells post-synaptic to them². The action of APB appears to be the same in retinas from all species of vertebrate, and is specific to all classes of ON channel.

One of the first observations made with the drug' was that it did not abolish the antagonistic centre-surround organization of either retinal cells or lateral geniculate nucleus cells to which the retina projects. This means that the inhibitory actions involved in generating the surround must occur entirely within the OFF pathway. The same is probably true for the ON pathway. ON and OFF channels thus remain separate in the retina and the lateral geniculate nucleus, and the pathways do not converge until the inputs reach the visual cortex.

The ability to disable half of the visual system in this way raises obvious questions. Can each half function on its own and, if so, how well? Because an edge normally has both light and dark components, it might be thought that the detection of edges and their orientation (a function of the visual cortex) will depend on the proper functioning of both ON and OFF channels. Blocking the ON channels by applying APB to the retina might be expected to interfere seriously with vision. But it appears that, although APB does have some deleterious effects, they are much less than had been supposed.

The carefully controlled experiments on awake monkeys reported in this issue show that, when treated with APB, the animal cannot detect a light coming on. although it can still detect the onset of a dark spot. Perhaps more relevant is that many visual functions are relatively unimpaired by APB. For example, the report shows that monkeys treated with the drug have qualitatively normal stereopsis when tested with random-dot stereograms and can detect apparent motion in randomdot kinematograms. Both these tasks are normally regarded as rather severe tests of visual performance. Other studies show that cortical neurones in APB-treated animals, although lacking in ON responses, still possess orientation and direction selectivity.

Although interactions between ON and OFF channels are not necessary for the generation of many neuronal-response properties, they do not prove that such interactions do not occur, or that they have no important functional role. A really careful comparison of the properties of cortical cells between normal and APB treated animals has vet to be carried out, and strong interactions between ON and OFF inputs to the cortex are known to exist (see, for example, ref.4). It seems



New discoveries of some remarkable Lower Carboniferous fish1-5 show that they had vast toothed spines apparently suspended directly above their heads. Stethacanthus, a 1-m-long shark, now known from nearly complete specimens from Scotland and Montana¹⁻³, had a remarkable spine shaped like a shaving brush just behind its head. The spine stands nearly vertical and is topped by dozens of small teeth. It is clearly an unwieldly structure and must have had an important function. The spine was present in both males and females, and Zangerl' suggests that it was used to scare off potential predators: Stethacanthus had a patch of teeth on top of its head as well and, when partially buried in the mud, the two toothed areas would have mimicked a vast gaping mouth, as if of some giant predator. The figure illustrates the possible appearance of the fish3.

A second stethancanthid, Falcatus⁴, is a small shark up to 14.5 cm long and has a long, shelf-like spine extending from roots deep in the muscles of the 'shoulder' region to run over the head, like a sunshade. The spine is in two parts, the fixed base and the horizontal portion which slots on to it, and is present only in sexually mature males. Lund' suggests that male Falcatus sharks aggregated before the breeding season for display-courtship rituals. The third complete Stethacanthid shark, Damocles', is also small (up to 20 cm long) and differs from Falcatus in having a simpler spine with many sharp teeth. Michael J. Benton

- Wood, S. Nature 297, 574 (1982).
- Lund, R. Géobios 17, 281 (1984). Zangerl, R. J. vertebr, Paleontol. 4, 372 (1984).
- Lund, R. J. vertebr. Paleontol. 5, 1 (1985).
 Lund, R. J. vertebr. Paleontol. 6, 12 (1986).

Michael J. Benton is in the Department of Geology, The Queen's University of Belfast, Belfast BT7 INN, Northern Ireland.

very likely that in many cases these interactions must be involved in generating orientation selectivity (for example, in cells that are believed to receive inputs from only a single ON centre and a single OFF centre cell, side by side).

Other recent results support the idea that orientation selectivity is produced by more than one mechanism, and in more than one location in the visual cortex. Inactivation of the A layers of the lateral geniculate nucleus (a major source of visual input to the cortex) abolishes all responses in the middle layers of the cortex, but leaves orientation selectivity in the upper cortical layers unimpaired. Conversely, inactivating the upper cortical layers by cooling leaves orientation selectivity in the middle layers of the cortex intact⁶. It had previously been thought that orientation selectivity in the upper layers was merely a passive reflection of the orientation selectivity of their inputs from the middle layers of the cortex but these results^{5,6} mean this cannot be entirely true.

The idea that many cortical properties are generated redundantly, by interactions both within and between different parallel afferent pathways to the cortex, in

different cortical layers and perhaps by different mechanisms, has several attractions. Redundancy of mechanism would render the brain less sensitive to pathological or experimental damage to particular subdivisions in the nervous system. Inadequacies in any one mechanism might be compensated for by some corresponding advantage in another. More than one type of processing algorithm is needed to account for other aspects of visual performance, such as stereopsis7, and perhaps it is easier to evolve several relatively crude neural mechanisms that work in parallel to achieve a particular goal than to evolve just one especially effective one. Single elegant solutions to particular problems may not exist in the brain: quantity, rather than quality, of mechanism is what counts.

- Schiller, P.H., Sandell, J.H. & Maunsell, J.H.R. Nature 322, 824 (1986).
- Slaughter, M.M. & Miller, R.F. Science 211, 183 (1981). Schiller, P.H. Nature 297, 580 (1982).
- Hammond, P. & Mackay, D.M. Expl. Brain Res. 49, 453 (1983)
- Malpeli, J. J. Neurophysiol. 49, 595 (1983).
- Baker, F.H. & Malipeli, J. Expl. Brain Res. 29, 433 (1977). Mitchison, G. Nature 304, 123 (1983).

N.V. Swindale is in the Department of Psychology at Dalhousie University, Halifax B3H 4J1, Canada.

Chiral chemistry

Asymmetric epoxidation gives organic chemists a hand

from Martin Bryce

THE asymmetric epoxidation of allvlic alcohols is one of the most innovative reactions introduced into organic chemistry in modern times1. The tremendous potential of this reaction was recognized soon after its discovery six years ago by Sharpless and Katsuki². However, as the target molecules for organic chemists become ever more complex, several years' work may be needed to complete intricate, multistep syntheses, and it is only within the context of such challenging synthetic chemistry that the true value of a new reaction can be seen. Recently, Sharpless and colleagues have made an important improvement in the reaction conditions3, and it is now clear that the Sharpless époxidation has come of age as a practical method for the introduction of chirality into a wide range of organic molecules.

To understand the significance of this reaction we must be aware that the organic molecules of life are chiral (that is, like right and left hands, the molecules are mirror images of each other) but they are not identical because they are non-superimposable. From the most primitive to the most highly developed organisms, the life processes at the molecular level depend critically on this chirality. A molecule which on further substitution can become chiral is termed prochiral. A chiral reagent will distinguish between the faces of a symmetrical, prochiral structure giving rise to unequal amounts of chiral products, whereas an achiral reagent will show no selectivity. For example, reduction of a prochiral amino-acid precursor (see figure: structure 1) by an achiral reagent such as hydrogen can occur with equal probability from each of the two faces of the C=N bond, giving rise to a 50:50 mixture of the two chiral forms of the amino acid (structure 2); there will be no selectivity. These chiral products are termed (S) and (R) enantiomeric forms. However, the two faces of prochiral molecule (structure 1) are not the same to a chiral reagent, such as an enzyme, which will attack one side to the virtual exclusion of the other. Indeed, for the most part, enzymes produce only the amino acids having the (2)-(S) configuration (see figure).

Organic chemists strive to develop highly efficient methods of synthesizing pure enantiomers of organic compounds,

both for academic interest and for commercial application, for example in the fields of pharmaceuticals and pesticides where, frequently only one enantiomer of a compound is biologically active. Thus, asymmetric hydrogenation using chiral catalysts has become a well-established laboratory procedure over the past decade4. Until recently, however, the counterpart of this reaction, asymmetric oxidation, has met with little success.

The answer has proved to be the Sharpless reaction, which is based on both organic and inorganic stereochemistry

and uses reagents that are either commercially available or easy to prepare. The reaction, which involves treatment of an allylic alcohol (see figure: structure 3) with a mixture of titanium tetra-isopropoxide, t-butyl hydroperoxide and diethyltartarate (DET) (structure 4) to give an epoxy alcohol (5), can be controlled, with (5a) or (5b) forming in more than 95 per cent enantiomeric excess. Thus, remarkably, the reaction approaches the stereoselectivity of an enzyme system and even surpasses most enzymes in the variety of substrates (groups R, R' and R" in structure 3) that will react. In a recent improvement³, the addition of molecular sieves to the reaction mixture enables as little as 5 moles per cent of titanium tartrate complex to be used to ensure high enantioselectivity of the epoxidation.

Sharpless considers that the titanium metal catalyst serves to organize the epoxidizing agent (t-butyl hydroperoxide). the chiral-inducing agent (diethyl tartrate) and the substrate (the allylic alcohol) into such geometry that reaction at one face of the double bond is greatly preferable to reaction at the other face. In the key step, the epoxide oxygen is always delivered to the same face of the olefin for reaction involving a specific tartrate isomer (structure 4a or 4b). If the allylic alcohol (structure 3) is represented by the stereochemical model (6), the oxygen is delivered from the bottom face using L(+) DET and the top face using D(-) DET, to give chiral epoxy alcohols (5a) and (5b), respectively.

The ability of epoxy alcohols to retain chirality while undergoing a wide range of subsequent transformations has enabled the Sharpless epoxidation to be incorporated into numerous multistep syntheses of chiral compounds (see ref. 1 for a recent review). For example, Mori's synthesis of structure 9, the sex pheromone of the beetle Hylecoetus dermestoides (a pest of European hardwood and softwood trees) starts from prochiral allylic alcohol (structure 7). This alcohol was transformed by the Sharpless reaction into epoxy alcohol (8) which contains the required stereochemistry for elaboration into the desired chiral product (9) (see figure: scheme 1).

A class of pharmaceuticals where improved synthetic routes incorporating the Sharpless oxidation have been described are leukotrienes, important in various inflammatory diseases. A new synthesis of leukotriene A (structure 12) involves, as a key step, formation of chiral epoxide (11) from prochiral allylic alcohol (10) (see figure: scheme 2).

The Sharpless epoxidation procedure also provides easy access to rare monosaccharides which are important structural components of certain natural products and are also valuable synthetic intermediates. For example, epoxy alcohol (structure 13) can be converted into hexose derivative (14) which is a component of the antibiotic olivomycin A.

These examples show how important asymmetric epoxidation reactions can be for those who wish to make chiral molecules with high enantiomeric purity by simple and reliable procedures.

- Pfenninger, A., Sviahesis 89 (1986)
 Katsuki, J. & Sharpless, K.B. J., Am. Chem. Soc., 102, 5974 (1980).
- Sharpless, K.B. & Hanson R.M. J. Org. Chem. 51, 1922
- Mosher, H.S. & Morrison, J.D. Science 221, 1013 (1983).
- Sharpless, K.B., Woodward, S.S. & Finn, M.G. Pure Appl. Chem. 55, 1823 (1983)

Martin Bryce is a Lecturer in Organic Chemistry at Durham University, Durham DH13LE, UK.

Cytoskeleton

New views of the red cell network

from Velia M. Fowler

THE elaborate schemes of the molecular anatomy of the erythrocyte membrane skeleton that have evolved over the years' are based almost exclusively on studies of the properties and associations of purified proteins in vitro. Attempts to analyse the structure of the membrane skeleton in situ have been impeded by the enormous density of the components, particularly spectrin, in the plane of the membrane. Several groups'h, most recently Steck and his colleagues, have succeeded in artificially spreading out the spectrin network without (apparently) disrupting the linkages holding it together. Far from being ". . . an anastomosing framework woven by a myopic fisherman", the membrane skeleton is organized as a strikingly regular lattice in the plane of the membrane.

Five to seven long, thin filaments (about 180 nm long), whose morphology corresponds to purified spectrin tetramers, are attached by their ends to junctions comprised of short, stubby actin filaments (33-37 nm long), thus generating a series of polygons, mostly hexagons, in which the sides are spectrin molecules and the vertices actin filaments (see figure)6.7. The latter appear thicker than normal actin filaments, implying that additional proteins are associated with them (see below). There is even a glob near the middle of the spectrin tetramers that is in the right place to be the ankyrin-band 3 membrane attachment site for spectrin". What is so satisfying about these negatively stained images of the spread membrane skeleton is that they are completely consistent with the models inferred from work with purified proteins.

The surface area of the spread membrane skeleton is calculated to be about 9-10 times that of the unspread membrane, indicating that the fully extended spectrin molecules (about 180 nm) are around three times longer than necessary to span the distance between adjacent actin filaments in the unperturbed membrane (about 60 nm)". It is an interesting question whether the spectrin tetramers in the unperturbed membrane are actually folded or coiled into a conformation with a more compact structure, or whether they are simply looped passively from one actin filament to the next so as to accommodate the surface area of the lipid bilayer itself. This distinction could have implications for the molecular mechanism of ervthrocyte shape transformations and for the viscoelastic properties of the erythrocyte

One source of support for the second

model is the observation that images of the spread membrane skeleton of reticulocytes are practically indistinguishable from those of the mature cell with respect to the essentially hexagonal pattern of the lattice (S.-C. Liu and J. Palek, personal communication), although the surface area is about three times greater in the one than in the other .

Thus, it seems that the reduction in membrane surface that accompanies maturation takes place without major changes in the organization of the membrane skeleton. Because analogues to spectrin, ankyrin and protein 41 arc present on the plasma membranes of nonerythroid cells', it will be interesting to



Negatively stained preparation of the spread crythrocyte membrane skeleton (from ref. 4)

see if the organization of the membrane skeletons in these cells uses similar principles to achieve local changes in membrane area during some cell movements.

Complexes that evidently represent isolated lattice vertices and that consist of about six spectrin 'legs' extending from a body containing a short actin filament have recently been isolated contain protein 41, which promotes complex formation, and protein 49, which is thought to be bound to actin (see refs 2-4). Tropomyosin may also be associated with the junctional complexes in situ, as this protein is present on the membrane in sufficient quantity to satisfy the binding capacity of the actin

A dimeric calmodulin-binding protein of relative molecular mass (M) 97,000 103,000 has just been discovered in the membrane skelton. It is also thought to be associated with the junctional complexes. as there are about the right number (30,000 copies) per cell, that is I dimer per filament of 16 actin monomers. But it is not yet known with which of the proteins in the membrane skeleton it is associated Immunolocalization of these various proteins in the membrane skeleton will be necessary to ascertain whether they are indeed associated with the junctional complexes that form the vertices of the spectrin lattice.

Why should the molecular substructure of the junctions in the erythrocyte membrane skeleton be so complex? An attachment site for about six spectrins would need only a small actin filament containing six actin monomers, along with six molecules of protein 4.1. However, a junctional complex composed only of spectrin, protein 4.1 and actin would not be self-limiting because of the propensity of actin to polymerize into long filaments under physiological conditions.

Restriction of actin-filament length by the accessory proteins mentioned above (alone or in combination) could serve to regulate the number of spectrin molecules attached to the junctions and thus specify the surprisingly regular lattice structure of the network. Some slippage in filament length regulation could easily account for variation in numbers of spectrin molecules attached to the junctions 3-7.

An apparent paradox is that although the stoichiometry of spectrin-protein 4.1 binding to actin filaments in vitro is equimolar, there are only about six spectrin molecules attached to any one of the 13- to 15-monomer-long actin filaments⁵⁻⁷: Because tropomyosin binds in the two grooves of the actin-filament helix without restricting filament length¹³, and protein 4.9 bundles actin filaments in vitro¹⁵, we still have no explanation for the actinfilament length restriction that is observed in situ.

In addition to ensuring the correct assembly of the membrane skeleton, it is conceivable that changes in the structure of the junctional complexes mediate the calcium- and ATP-dependent discocyte

- Lux, S.E. Nature 281, 426 (1979).
 Cohen, C.M. Semin. Hemat. 20, 141 (1983).
- Bennett, V. A. Rev. Biochem. 54, 273 (1985).
 Marchesi, V.T. A. Rev. Cell Biol. 1, 531 (1985).
- Beaven, G.H. et al. Eur. J. Cell Biol. 36, 299 (1985). Byers, T.J. & Branton, D. Proc. natn. Acad. Sci. U.S.A.
- Shen, B.W., Josephs, R. & Steck, T.L. J. Cell Biol. 102, 997 (1986).
- Tilney, L.G. & Detmers, P. J. Cell Biol. 66, 508 (1975).
- Stokke, B.T., Mikkelsen, A. & Elgsaeter, A. Biophys. J. 39, 319 (1986). 10. Waugh, R. & Evans, E.A. Biophys. J. 26, 115 (1979).
- 11. Shattil, S.J. & Cooper, R.A. J. Lab. clin. Med. 79, 215
- 12. Matsuzaki, F., Sutoh, K. & Ikai, A. Eur. J. Cell Biol. 39,
- 13. Fowler, V.M. & Bennett, V. J. biol. Chem. 259, 5978
- (1984). Gardner, K. & Bennett, V. J. biol. Chem. 261, 1339
- 15. Siegel, D.L. & Branton, D. J. Cell Biol. 100, 775 (1985).
- Cohen, C.M. & Foley, S.F. J. biol Chem. (in the press). Ling, E. & Sapirstein, V. Biochem. biophys. Res. Com-
- mun. 120, 291 (1984). 18. Raval, P.J. & Allan, E. Biochem. J. 232, 43 (1985).
- 19. Palfrey, H.C. & Waseem, A. J. biol. Chem. 260, 16021
- 20. Horne, W.C., Leto, T.L. & Marchesi, V.T. J. biol. Chem. 260, 9073 (1985).
- Eder, P.S., Soong, C.-J. & Tao, M. Biochemistry 25, 1764
- 22. Correas, E., Leto, T.L., Speicher, D.W. & Marchesi, V.T. J. biol. Chem. 261, 3310 (1986).

-echinocyte shape transformations of erythrocytes. A calcium- and calmodulindependent protein kinase activity has just been identified in erythrocyte membranes which phosphorylates both protein 4.1 and an M. 100,000 doublet of polypeptides in the membrane skeleton¹⁶, which could well represent the M, 97,000/103,000 calmodulin-binding dimer¹⁴. Protein 4.1, as well as protein 4.9 and the same(?)' M. 100,000 doublet are also phosphorylated by a recently identified protein kinase C activity in the erythrocyte 16-20. In addition. proteins 4.1 and 4.9 are phosphorylated by a cyclic AMP-dependent kinase, but at different sites from those phosporylated by protein kinase C211

A recent observation by Tao and coworkers21 provides evidence that these phosphorylations influence the organization of the membrane skeleton. The affinity of protein 4.1 binding to spectrin in vitro is reduced by about fivefold on phosphorylation of protein 4.1 (but not spectrin) by a purified cyclic AMP-independent kinase from red cells21. It is also suggestive that the cyclic AMP phosphorylation site on protein 4.1 has just been found to reside in a spectrin-binding domain of M, 8,000 (ref. 22). Undoubtedly, these observations are only a taste of things to come, and many of the protein associations in the erythrocyte membrane skeleton may prove to be dynamically regulated in response to physiological signals in vivo.

Velia M. Fowler is in the Department of Anatomy and Cellular Biology, Harvard Medical School, Boston, Massachusetts 02115, USA

Glaciology

Frozen news on hot events

from Claus Hammer

ICE CORES from Antarctica and Greenland provide information on the number and dates of violent volcanic eruptions and their contributions to the upper atmospheric composition of trace substances. Intérpretations of the ice-core records, particularly deductions about the influence of local eruptive activity and the varying meteorological and climatological conditions during trace-substance transfer from the volcano to the ice sheets, are difficult, partly because the techniques used in various studies have not been coordinated. A recent article by R.J. Delmas et al. (J. geophys. Res. 90, 12; 1986) concludes that the techniques used to detect volcanic signals in ice cores are all in essential agreement. Although the visible fine-ash (tephra) layers observed in antarctic ice cores must be considered separately from other data, the conclusion of Delmas et al., that the sulphuric acid record in the cores reveals remote and violent eruptions, remains unchanged.

Delmas et al. analyse ice cores from various sites in Antarctica, both from coastal regions of high precipitation and central sites that show very low annual accumulation. They look at acidity, electrical conductivity of melted ice samples and ionic composition during the past 200 years. The lack of historic data on eruptions in the Antarctic area limits the analysis, but the authors are able to conclude that local volcanic activity in the Antarctic contributes only little to the ice-core chemistry. The fallout of fine ash is only significant close to local volcanoes (some 200 km) and the SO, and/or HCl from such eruptions is apparently washed out before reaching the more central parts of Antarctica, where the volcanic acid signal is particularly clear. (This conclusion does not, of course, cover violent or substantial regional activity.) Thus the major increases in sulphuric acid concentration of the central Antarctic ice is caused by remote volcanic eruptions. Transportation of the volcanic products occurred mainly via the stratosphere, although some arrived via the upper troposphere: NH, neutralization is virtually absent. Transfer from the site of eruption to the ice sheet during glacial times has yet to be quantitatively assessed.

The conclusions of Delmas et al. provide a global perspective and agree with the results obtained from the Greenland Ice Sheet (see, for example, Hammer, C.U., Clausen, H.B. & Dansgaard, W. Nature 288, 230; 1980). The Antarctic ice cores provide information on past volcanic eruptions south of 20° N, whereas Greenland registers eruptions north of 20° S, so data series from the two ice sheets offer global coverage and overlapping information.

To establish a detailed and well-dated ice-eruption record; to estimate from the chemistry of the cores the influence on atmospheric composition; and to identify the geographical sites or zones of the eruptions are formidable tasks which will require not only a good deal of optimism but also new and faster techniques for analysing the details of the chemical composition of the several thousand-metre-long ice cores. More data from the smaller ice caps, for example in the Canadian arctic, are needed.

Claus Hammer is at the Geophysical Institute, University of Copenhagen, Haraldsgade 6, 2200 Copenhagen N. Denmark.

SCIENTIFIC CORRESPONDENCE

Table 1 Radioisotopes identified from air filters

Chernobyl fallout on Ioannina, Greece

SIR-We have measured the y-ray spectrum of the fallout from the Chernobyl nuclear reactor accident at Ioannina, located in northwestern Greece, nearly 1,500 km south-west of Chernobyl. We have examined air filters collected every 24 h since 29 April to monitor the yradiation activity, using an intrinsic germanium high-resolution detector, shielded to reduce background. The fallout probably reached Ioannina between 1 and 2 May, and the activity peaked on 5 May. After that we noticed a reduction of the air contamination, mainly due to local

Figure 1 shows a typical γ-ray spectrum from one of our filters, the activity of which was measured three times at monthly intervals to estimate the halflives of the radionuclides present. From a number of spectra, 14 different nuclides were identified by their energy spectra and half-lives and 9 additional peaks in the spectral region between 50 and 800 KeV remain unidentified.

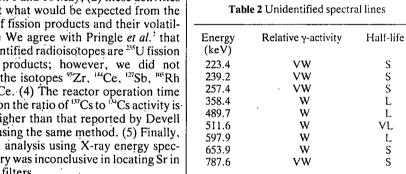
In Table 1 the activity of each of the most prominent radioisotopes is characterized as very strong (VS), strong (S), weak (W) or very weak (VW), and the respective half-life as very long (VL), long (L) or short (S). The ¹³¹I activity is defined 'strong' and its half-life as 'long'. Table 1 also lists the masses of fission decay products generated in the reactor'. Table-2 lists the energies of the unidentified lines.

From our air-filter measurements we conclude that: (1) the relative activities for the most prominent isotopes remained unchanged during most of the period

•			•
Isotope	Relative γ-activity	Half-life	Mass of fission products (mg MW ¹ day ¹)
⁹⁵ Nb	vw	VL	0.33
⁹⁹ Mo	W	S	107.0
¹⁰³ Ru	VS	VL	
	ι		65.4
¹⁰⁶ Ru	W	VL	
^{129m} Te	VW	VL	
			15.7
¹³² Te	S .	S	
131 I	S	L	5.86
132 _I	S	S	
¹³⁴ Cs	S	VL	
¹³⁶ Cs	VW	, L	90.4
¹³⁷ Cs	S ·	, VL	
¹⁴⁰ Ba	W	L	38.6
¹⁴⁰ La	W	S	39.8
¹⁴¹ Ce	VW	VL	86.0

between I and 10 May; (2) these activities are not what would be expected from the mass of fission products and their volatility. (3) We agree with Pringle et al.2 that the identified radioisotopes are 235U fission decay products; however, we did not locate the isotopes 95Zr, 144Ce, 127Sb, 1018Rh and ¹¹³Ce. (4) The reactor operation time based on the ratio of 137Cs to 134Cs activity is 15% higher than that reported by Devell et al.' using the same method. (5) Finally, a trace analysis using X-ray energy spectrometry was inconclusive in locating Sr in our air filters.

The extreme conditions in the reactor core after the accident make it hard to know in what chemical compounds the radioisotopes appear in the radioactive cloud. Unfortunatly, information about core conditions before and during the accident is not yet available to us, and therefore we cannot verify our assumption



that the surprisingly high proportion of non-volatile nuclides (such as "Ru) and the absence of volatile nuclides reflect the chemical compound which hosted the nuclides at the time of release to the atmosphere.

N.G. ALEXANDROPOULOS T. ALEXANDROPOULOU D. Anagnostopoulos E. Evangi lou K.T. Kotsis I. Theodoridou

Department of Physics. University of Joannina, 453 32 Ioannina, Greece

- 1. Farmer, F.R. (ed). Nuclear Reactor Safety (Academic, New
- 2. Pringle, D.M., Vermeer, W.J. & Allen, K.W. Nature 321,
- 3. Devell, L. et al. Nature 321, 192-193 (1986).

Counts per channe 200 600

Fig. 1. A typical complex γ-ray spectrum obtained with an intrinsic Ge detector from an air filter.

The origins of the Earth's oceans

Six—Several mechanisms have been proposed for the origin of the Earth's oceans. such as the degassing of crustal rocks over geological time and the formation of impact produced atmosphere, including water, by accretion of planetesimals2 early during the Earth's formation. The available evidence suggests that sizeable oceans were present early in the Earth's history3 and that the early Solar System

was fractionated, with nickel-iron and carbonaceous chondrites largely contained in the volume on the sunward side of Mars's orbit, and gases (hydrogen, helium, methane, water) and some carbonaceous chondrites in the volume from Jupiter's orbit outward.

Present theories on the origin of the oceans fail to account for the fact that Venus, a planet very similar to Earth in size and composition, has no surface water and only small amounts of atmospheric water. This could be explained by assuming that, early in its history, Earth collided with an ice moon approximately 900 to 950 miles in diameter, which could have furnished all the water presently on Earth. This collision, obviously a rare event, would have provided for rapid cooling of the Earth's crust, prevention of a runaway greenhouse effect by the absorption of most atmopsheric CO₂, and rapid evolution of life. This theory is also in accord with the fractionated nature of the early Solar System.

JAY S. ROTH

Department of Molecular and Cell Biology. University of Connecticut, Storrs, Connecticut 06268, USA

- Weinaupt, J.G. Exploration of the Oceans, (Macmillan, New York, 1979).
- Matsui, T. & Abe, Y. Nature 319, 303-305 (1986). Cogley, J.G. & Henderson-Sellers, A. Rev. Geophys. space Phys. 22, 131-175 (1984).
- 4. Walker, J.C.G. in The Early History of the Earth (ed. Windley, B.F.) 357 (Wiley, New York, 1976).

Frequency of dizygotic twinning

SIR—From the assumption that ovulation with intercourse leads to a live birth with probability 1/4 for each egg, double ovulation may be expected to lead to dizygotic twin births with probability 1/16. From that realtionship, J. Diamond (Nature 320, 488; 1986) suggested that an observed frequency of 4.9% dizygotic twin births among the Yoruba implies a double ovulation frequency of 16 times 4.9, or 78%.

M. Sipser (Nature 321, 570; 1986) pointed out that this suggestion is incorrect. On the simplest set of assumptions, double ovulation will lead to no birth in 1/16 of cases, to a single birth in 5/16 of cases, and to dizygotic twins in 1/16 of cases. From those relative frequencies, Sipser asserted that an observed frequency of 4.9% dizygotic twin births implies a double ovulation frequency of 7 times 4.9 or 34%.

In fact the relationship between the frequencies of double ovulation and of dizygotic twin births cannot be expressed by a constant factor. When the frequency of double ovulation is extremely low, the single births that result from double ovulation can be ignored, and the observed frequency of dizygotic twin births must be multiplied by 4 to obtain the frequency of double ovulation (single births=1/4 of single ovulations; dizygotic twin births= 1/16 of double ovulations). When the frequency of double ovulations is high, the single births that result from double ovulations must be taken into account, and the factor rises. In the extreme case, if the probability of double ovualtion were 1.0, by of the births would be dizygotic twins; the factor would be 7. Sipser's comment is valid only for this case, which is of no biological significance for any known human population.

The general expression to be used is F=T/(pT+p-T), where T is the fraction of dizygotic twin births, p is the probability per egg of a live birth, and \vec{F} is the fraction of double ovulation. When p is assumed to be 0.25, this becomes F=4T/(1-3T).

In any real case, the factor [4/(1-3T)] is much closer to 4 than to 7. For the dizygotic twinning frequencies that occur in the human populations tabulated in Diamond's article (0.22% to 4.9%) the appropriate factors are between 4.03 and 4.7. In the Yoruba population the frequency of dizygotic twin births was 4.9%, and the estimated frequency of double ovulation, if $P = \frac{1}{4}$, is 23%.

DANIEL E. ATKINSON

Department of Chemistry and Biochemistry, University of California, Los Angeles, California 90024, USA

How to abbreviate recombinant genes

SIR-We are all aware that recombinant DNA technologies have generated tremendous progress and spawned a literature that seems to grow exponentially. Unfortunately a custom is developing of using the abbreviation rDNA to refer to the hybrid molecules formed by uniting two or more heterologous DNA molecules; this leads to confusion, since rDNA has long been used to refer to ribosomal DNA. The abbreviation rRNA and r proteins are also in common use with r again meaning ribosomal.

To avoid confusion. I suggest the use of rt for recombinant and that editors of journals start insisting on a differentiation between rDNA and rtDNA and rRNA and rtRNA.

ROBERT C. KING

Northwestern University, Evanston. Illinois 60201, USA

A system of nomenclature for murine homoeo boxes

SIR—There is at present a considerable degree of confusion amongst workers on mammalian homoeo boxes because each group has tended to select a different system of nomenclature. It is now very difficult to follow the literature appropriately. To help avoid this confusion we would like to offer the following system.

A unifying nomenclature for murine homeo boxes should consider the chromosomal location and the number of boxes on a chromosome. Clusters of boxes should preferably be numbered consecutively and in the direction of transcription. The two known clusters are probably transcribed in one orientation only and do not contain additional boxes. Thus, at least these two would be numbered consecutively from the 5' to the 3' end of the cluster. The nomenclature should further allow a logical naming of newly discovered

We suggest the new prefix 'Mox', followed by two numbers: the first one giving the chromosomal location, the second identifying an individual box on the respective chromosome. This procedure leads to the following nomenclature for a selection of published murine homeo boxes:

Proposed name	Original designation	Chromo- some	Ref.
Mox 1.1	Mo-en.1	1	1
Mox 6.1	m6	6	2
Mox 6.2	m5	6	3 3
Mox 6.3	m2	6	3
Mox 6.4	HBT-1, MH3.		
-	Hox 1.3.	6	4.5
Mox 6.5	Mo 10, Hox 1.4.	6	6
Mox 6.6		6	
Mox 11.1	Hox 2.4	11	7
Mox 11.2	Hox 2.3	11	7
Mox 11.3	Hox 2.2	11	7
Mox 11.4	Hox 2.1, H24.1,		
	Mul '	11	7-9
Mox 15.1	Hox 3, m31	15	10,11

For new isolates, we suggest the following, assuming that the description of these boxes will include the information on chromosomal location and occurrence of clusters. In this case, we propose the term 'Mox', followed by the chromosome number, a period and the lowest unused number on the respective chromosome for the most 5' box of a new cluster.

After a box has been designated in this way, the name should be kept unchanged even if new information reveals a violation of the consecutivity rule. Non-mapped isolates (from cDNAs, for example) have to obtain a preliminary designation.

PETER GRUSS MICHAEL KESSEL

Zentrum für Molekulare Biologie, Universität Heidelberg, Im Neuenheimer Feld 282, Postfach 10,6249. D-6900 Heidelberg 1, FRG

- Joyner, A.L. et al. Cell 43, 29-37 (1985). Colberg-Poley, A.M. et al. Nature 314, 713-718 (1985).
- Colberg-Poley, A.M. et al., Cell 43, 39-45 (1985). Wolgemuth, D.J. et al. EMBO J. 5, 1229-1235 (1986).
- Duboule, D. et. al. EMBO J. (in the press). McGinnis, W. et al. Cell 38, 675-680 (1984).
- Hart, C.P. et al. Cell 43, 9-18 (1985).
 Hauser, C.A. et al. Cell 43, 19-28 (1985).
- 9. Jackson, L.J. et al. Nature 317, 745-748 (1984). 10. Awgulewitsch, A. et al. Nature 320, 328-335 (1985).
- 11. Breier, G. et al. EMBO J. (in the press).

A litany of folly

Walter Gratzer

Diamond Dealers and Feather Merchants: Tales from the Sciences. By Irving M. Klotz. *Birkhäuser:1986. Pp.120.* \$24.95.

"As to the opinion which explains the putrefaction of animal substances by the presence of microscopic animalcula, it may be compared to that of a child who would explain the rapidity of the Rhine's current by attributing it to the violent movement of the numerous mill wheels at Mainz." The view is that of Justus von Liebig (echoed some time later by, I think, James Thurber, who held that wind is caused by trees waving their branches), and the child in question is Pasteur. Or try this: "Recently I pointed out that deficiencies in fundamental chemical knowledge and the lack of a good liberal education characteristic of many professors is responsible for the current decline in chemical research . . . If anyone thinks my concerns are exaggerated, he should read, if he can stomach it, a recent monograph of a Mr van't Hoff, entitled The Arrangement of Atoms in Space, a book swollen with infantile foolishness." That egg was laid by the great Hermann Kolbe, the first man to synthesize a organic compound, acetic acid, from its elements. In Diamond Dealers and Feather Merchants. Professor Klotz has assembled a wonderful collection of such philippics in his exploration of how these thunderous gaffes come to be perpetrated — hostages heedlessly offered to fortune by those best placed to know better.

Perhaps success, like power, tends to corrupt; Ambrose Bierce in *The Devil's Dictionary*, ever a sound guide to human nature, encapsulates the matter thus: "Intolerance is natural and logical, for in

"Klotz suggests that the strange passions that cloud the judgement and take the reason prisoner can express themselves as much in credulity as in obduracy."

every dissenting opinion lies an assumption of superior wisdom." The uninhibited ferocity and vindictiveness with which academic vendettas were publicly conducted belong of course to a bygone age of polemic. The heavy, snarling sarcasm, the pseudonymous lampoon on the rival's work, have given way to a little discreet disparagement in the intimacy of the grant committee; but the results are similar and it is probably an inalienable part of the scientific process. Max Planck said that radical scientific innovations do not prevail by overcoming prejudice, but rather through the eventual demise of their

opponents, to make way for a new generation of scientists whose prejudices have not yet hardened.

Klotz suggests that the strange passions that cloud the judgement and take the reason prisoner can express themselves as much in credulity as in obduracy. Chauvinism and political engagement play a part in two spectacular scientific debacles that he chronicles with relish, but not without compassion: N-rays were named after the city of Nancy by the respected French physicist, Blondlot, Klotz surmises that Blondlot's formative years would have been darkened by the defeat and disintegration of the Second Empire and the loss of much of Lorraine, which brought the German border almost to Nancy. This must have inflamed the rivalry, already intense, between French and German science. In addition, Blondlot was probably still grieving at the turn of the century that the discovery of X-rays had eluded him.

N-rays were an electromagnetic radiation emitted from electric discharges and many other sources, such as hot metals. They were taken up with fervour by French physicists, chemists and indeed biologists, for it soon emerged that nerves, muscles and even enzymes were abundant emitters. By 1904 the ratio of papers in the Comptes Rendus on N-rays to those on X-rays was 53:3. The outside world was more cautious and the end came when the great American spectroscopist, farceur and eccentric, R.W. Wood (the man who trained his cat to clear the cobwebs from the 40-foot optical path of his spectrograph), visited Blondlot's laboratory to observe the measurement of wavelengths in the N-ray spectrum, dispersed by an aluminium prism. The room being dark, Wood adroitly trousered the prism, with no detriment to the process of data collection. Wood spared no feelings when he subsequently described the events in Nature. J.A. Le Bel expressed what many French scientists must have felt: "What a spectacle for French science that one of its distinguished savants determines the position of lines in the spectrum while the prism sits in the pocket of his American colleague."

it is probably an inalienable part of the scientific process. Max Planck said that radical scientific innovations do not prevail by overcoming prejudice, but rather through the eventual demise of their Klotz seeks a parallel between the N-ray affair and the curious mirage, half a century later, of polywater — an associated form of water reported by the Russian surface physicist. Boris Derja-

guin, to form in fine silica capıllaries -- for here too political prejudice may have exerted a baleful influence. J.D. Bernal. who was preoccupied at this time with the structure of water, must, so Klotz believes, have badly wanted Soviet science to come up trumps. (He continued, for instance, to support Lysenko long after the truth had come out in all its squalor.) Bernal did in the event jump off the polywater bandwagon before that vehicle careered over the precipice, taking many reputations with it. Joel Hildebrand, the Methuselah of physical chemistry who published his last paper at the age of a hundred, seemed in no doubt from the outset. "Water and silica." he wrote, "have been in intimate contact in vast amounts for millions of years; it is hard to understand why any ordinary water should be left." Another physical chemist. R.E. Davis, put it succinctly "We must conclude that all polywater is polycrap and that the American scientists have been wasting their time studying the subiect". In retrospect it seems that most of these scientists could have believed in polywater only because they wanted

"Chauvinism and political engagement play a part in two spectacular scientific debacles that Klotz chronicles with relish, but not without compassion."

polywater to exist. Derjaguin accepted earlier than many that he had been wrong, and emerged with dignity from the reeking shambles.

Klotz concludes with some examples of credulity and ignorance to make your toes curl. Thus: "From experience with non-science college students. I know that the majority predict that if a silver dollar and a silver dime are simultaneously dropped from the top of the Sears Tower the former will hit the ground first. An even larger fraction when asked whether a two-inch line or a one-inch line has more points will vote in favour of the former: the remainder exercise their democratic privilege of not voting. The general public would overwhelmingly endorse [this] view." I understand the flat-Earthers are still among us, satellite pictures notwithstanding: common sense lives.

Professor Klotz's name is familiar to all protein chemists, and generations of science students were brought up on his celebrated textbook of chemical thermodynamics. He now reveals himself as a writer of wit, wisdom and originality in a different genre. This admirable little book will give much pleasure.

Walter Gratzer is in the Medical Research Council's Cell Biophysics Unit, King's College London (KQC), 26–29 Drury Lane, London WC2B 5RL, UK.

Looking beyond creature comforts

Marian Stamp Dawkins

Laboratory Animal Husbandry: Ethology, Welfare and Experimental Variables. By Michael W. Fox. State University of New York Press: 1986. Pp.267. Hbk \$39.50; pbk \$9.95.

I MUST confess that most books on animal welfare give me a sinking feeling even before I read them. I have a prejudice, no doubt grossly exaggerated and unrelated to the real world, that there are only two types of book about this subject. The first treats animals in a mystic, reverential way and castigates humans for interfering in the natural balance of things and, sometimes, for having anything to do with animals at all. The other goes to the opposite extreme and talks mostly about sq cm of cage size and the regular collection of faeces. There seems to be little in between: it is as if one has either to be poetical in one's attitude to animals or adopt the earthiest sort of banality about the size of their cages or the cleanliness of their drinking water.

The sinking feeling occurred when I first looked at Laboratory Animal Husbandry by Michael W. Fox. However, despite its title, the book certainly does not fall into either of the usual categories. On the contrary, it is innovative in several important ways.

First, it documents recent evidence about the effects that totally unexpected factors may have on animal health and well-being. It is perhaps not surprising that noise, ventilation and ambient temperature can have significant effects on the health of animals and their susceptibility to disease. But it is probably less well known that the exact age of weaning and the amount of handling from a human being can affect, among other things, plasma cortiscosterone, prolactin and growth hormone levels. The behavioural and physiological changes that have been found can in turn affect not only the animals' own well-being but the results of experiments on, say, drugs. Some of these unexpected factors may radically alter the conclusions about how effective a treat-

A second, related point that Fox makes concerns an animal's social environment. It should be obvious, but it clearly is not to judge from current practice, that an animal's welfare cannot be safeguarded simply by concentrating on the bare necessities of food and water or even on the physical environment of its cage. Many animals are highly social. They interact, both positively and negatively, with other members of their species; it should not be BOOK REVIEWS





Improved conditions for animals could benefit humans too

surprising, therefore, that disturbances in their social lives can significantly affect their behaviour and health. Fox argues that our understanding of human ailments is far from complete and it is often impossible to pinpoint why one person becomes ill when another does not. If we are attempting to use animals as models of puzzling human diseases, he argues, we will continue to be ignorant unless we also begin to consider the complexity of the factors, including social ones, that affect the development of diseases in animals.

He concludes that there is a double imperative on us to imprové the welfare of laboratory animals. One is for the animals themselves: if we use them we should look after their welfare better than we do now by taking into account the range of factors, both physical and social, that can affect them. The other is for humans: if we want good scientific results, we should be more careful about the conditions in which we keep animals. There follows a useful chapter giving practical suggestions as to how laboratory animal husbandry could be improved for the benefit of both human and non-human animals. Another chapter contains a review of the main findings on pain and suffering in research animals.

One particularly appealing feature of the book is that the discussion of animal rights is kept to the last chapter. This means that even if you disagree with Fox on this issue or lose sympathy with the "land ethic" or "One Medicine", the rest of the book with its more down-to-earth reviews and suggestions, loses none of its value. The ethical issues are discussed but they do not intrude, so that the book can potentially appeal to, and be profitably read by, people with very divergent attitudes to animals.

The common thread is a concern for the welfare of animals in laboratories. Fox's contribution is to bring common-sense and research findings to bear on the problem of how we might improve it. He points to the arbitrariness of the present guidelines and laws as to how animals should be kept (the fact that recommended cage sizes for dogs, cats and primates in Britain are double those suggested by the American authorities, for instance). And his insistence that we should take more notice of the social needs and interactions of animals, and not just think in terms of their physical comfort, is a message that cannot be broadcast too loudly or too frequently.

Marian Stamp Dawkins is Fellow in Biological Sciences at Somerville College, Oxford OX2 6HD, UK. She is also author of Animal Suffering: the Science of Animal Welfare (Chapman & Hall, 1980).

Economical images

Peter Hawkes

Transform Coding of Images. By R.J. Clarke. Academic: 1985. Pp.432. Hbk. \$69.50, £60.50; Pbk. \$34.95, £31.

From the point of view of a computer, an image is a voluminous and cumbersome object. The human eye and brain can handle a continuous-tone picture effortlessly and almost instantaneously; for a computer, the image must be broken into small zones, each of which corresponds to a number representing the grey-level. There are typically 256 of the latter, and the number of image-elements or "pixels" can easily reach a million. For these values the computer already has 8 megabits to cope with, but if the image is coloured rather than black-and-white this must be multiplied by three. Worse still, although we may regard such an image as a 1024 × 1024 matrix, each element of which is an (eight-bit) number representing the greylevel of the corresponding pixel, in image processing we are also interested in statistical properties. If the image is represented by an N \times N matrix (N = 1024 in our example), then the matrix corresponding to such statistics will be $N^2 \times N^2$.

Everyday images contain much redundant information — uniform or slowly varying areas for example - and it is natural to ask whether a typical image could not be represented in the computer in a more economical way. This question has long preoccupied the image processing community and, although not quite so pressing with the advent of parallel and special-purpose computers, it will surely always be important for archival purposes. Various ways of coding images that occupy less memory space have been explored, and Roger Clarke's book is a detailed introductory account of one of these ways, notably the use of transforms, of which the Fourier is the best known.

The underlying idea is simple. Fourier transforms tell us what weight is associated in some signal with the corresponding frequency. We can therefore expect that if we suppress frequencies with very low weights, and reconstruct the signal from the remainder, the result will differ only slightly from the original. Converting this qualitative notion into quantitative terms is not so simple: how low must a weight be to be regarded as very low and hence negligible? How slight must the difference between original and reconstruction be to be acceptable? Is the Fourier transform a good choice and if not, which is the best transform to use? It is these and related questions that Clarke sets out to answer. He does so in eight chapters, plus an introduction, in which he examines image statistics, suitable orthogonal transforms, quantization, practical coding, the human visual response, fast transforms, errors and noise and, finally, rate distortion theory and coding. Seven appendices are concerned with specific mathematical points.

How successful he is depends on the sophistication of the reader. Everything is spelt out in detail: the laboriously gentle introduction of a matrix product at the beginning of the chapter on orthogonal transforms is a glaring example. Any physicist who has followed a course on quantum mechanics, not to say applied mathematics, will be exasperated by this, as will many electrical engineers, especially those with any familiarity with coding. Conversely, many readers will appreciate the detailed and careful definition of the many matrices that arise in image coding, and will be grateful for the frequent numerical examples that add flesh to the bare mathematical bones.

It must be said too that Clarke's is a leisurely style: "At the outset, it is worth clarifying one matter concerning the application of the theory...", he observes; and he likes telling us that "it is a truism nowadays to say" and that "it is no exaggeration to say that...". His discursiveness seems at odds with the aim of transform coding! Nevertheless, he has written a clear, readable and easy introduction to his subject, and those of us with images to code will often turn to his book to see what he has to say about some specific problem.

Peter Hawkes is Directeur de Recherche at the Laboratoire d'Optique Electronique du CNRS, BP 4347, F-31055, Toulouse Cedex, France.

Catalogue of inequities

John Maddox

The World of Science and the Rule of Law. By John Ziman, Paul Sieghart and John Humphrey. Oxford University Press: 1986. Pp. 343. £19.50, \$37.

This is not so much a book about the world of science and the rule of law as about what are called, in the United States, human rights — conflicts between personal liberty and the interests of the state. John Ziman, Paul Sieghart and J. H. Humphrey are, respectively, distinguished physicists, lawyers and biologists whose interests have repeatedly strayed beyond the narrow boundaries of their professions. Their failure, in this book, to do much more to describe a haunting problem is not their fault, but a measure of its difficulty.

The book has its origins in a pamphlet published more than ten years ago by the British organization called the Council for Science and Society, an unpaid and sometimes unprofessional Office of Technology Assessment. The starting point is the observation that the complaints of scientists that their professional freedom is too often administratively constrained is often at odds with the way in which most formal constitutions formally guarantee the freedom of the individual to do what he pleases.

Given the signature of the agreements on European security at Helsinki in 1979, the book cannot but in part be an account of the lamentable record of what has happened since. But little has changed. People who work in states where freedom of communication is guaranteed by the laws still discover that their letters are opened, sometimes to be confiscated, and their telephones disconnected. People whose governments are supposedly bound by the rule that employment should be open to all still find themselves denied the chance to work at what they do best when they give offence; the case of the Jewish refusniks in the Soviet Union is familiar, and necessarily a large part of the litany of oppression making up this book. Indeed, the Eastern bloc gets a real drubbing.

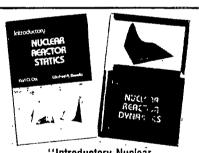
The authors might have made more of the way in which many western European States have been compelled by the European Convention on Human Rights to do the decent thing, against their first inclinations. Maybe there is more freedom now than, say, in the eighteenth century, even though the continuing deficiency of what is on offer remains just as offensive now as then. So the authors are right to ask why performance should so often fall short of promise. Why? A discussion of this point

would have been rewarding.

The truth is that the human failing of believing well and behaving badly applies to governments as well. Let us hope they may improve. How might the professional community urge them on? After what is a moving catalogue of unjustice, the authors have next to nothing to offer by way of remedy. They approve of the way that two successive presidents of the Royal Society have "spoken out", but have surprisingly little to say about the need for the outspoken to contain their protests within the other fellow's law. UNESCO's statements on the status of scientific workers are approvingly reprinted as an appendix, but the authors seem to share the general conviction that the source of all the words has no act to perform: ICSU is a better bet. Weisskopf's dilemma, that an illiberal society ostracized into exclusion can only become even more illiberal, is described but not resolved. And nowhere in this flat peroration is there a clear explanation, for the benefit perhaps of the young and cynical. of why it is that, if the law has a built-in momentum sweeping illiberality out of the way, then surely science must work the same magic but more powerfully. But is that not the only way in which it will come

John Maddox is editor of Nature

NEW TITLES BY ANS



"Introductory Nuclear . Reactor Statics" by Karl O. Ott Winfred A. Bezella

Recommended as an undergraduate or graduate textbook. Valuable source book for reactor analysis and design.

"Introductory Nuclear Reactor Dynamics" by Karl O. Ott Robert J. Neuhold

Examines fundamental principles of Nuclear Dynamics. Companior volume to Nuclear Reactor Statics, published in 1983.



For additional information write

American Nuclear Society 555 North Kensington Avenue La Grange Park, IL 60525 USA

Reader Service No.7

Plenum: The Practical Source

MICRODOMAINS IN POLYMER SOLUTIONS

edited by Paul Dubin

Brings together current research and experimental studies on concentrated solutions in both synthetic and natural polymer systems.

Volume 30 in Polymer Science and Technology.

0-306-42110-0/proceedings 472 pp./ill./1985 \$75.00 (\$90.00 outside US & Canada)

Forthcomina

MULTINUCLEAR NMR

edited by Joan Mason

Covers the entire NMR Periodic Table from a chemical and biochemical standpoint. It can be used as a handbook of first resort by the professional or as an advanced textbook for students in chemistry or biochemistry.

0-306-42153-4/approx. 750 pp./ill.

THE JOURNAL OF SCIENTIFIC COMPUTING

Editor-in-Chief: Steven A. Orszag

This new journal serves as a forum for state-of-the-art developments in scientific computing over broad interdisciplinary grounds. The key goals of the journal are to stimulate the development and dissemination of ideas related to large-scale scientific computing and to foster increased communication between university researchers and the designers of computer hardware and software.

Volume 1, 1986 (2 issues) Institutional rate: \$50.00 in US/\$56.00 elsewhere Personal rate: \$25.00 in US/\$29.00 elsewhere Volume 2, 1987 (4 issues) Institutional rate: \$95.00 in US/\$107.00 elsewhere Personal rate: \$35.00 in US/\$41.00 elsewhere

CHEMISTRY BY COMPUTER An Overview of the Applications of Computers in Chemistry by Stephen Wilson

In this broad survey, Dr. Wilson covers the methods used by the computational chemist, including quantum chemistry, molecular mechanics, collision theory, chemical kinetics, organic synthesis, Monte Carlo simulation, and molecular dynamics.

0-306-42152-6/224 pp. + index/ill. 1986/\$37.50 (\$45.00 outside US & Canada)

Plenum Publishing Corporation 233 Spring Street New York, N.Y. 10013-1578 In the United Kingdom: 88/90 Middlesex Street London E1 7EZ, England

Fifty years on

Warwick Bray

American Archaeology Past and Future: A Celebration of the Society for American Archaeology 1935-1985. Edited by David J. Meltzer, Don D. Fowler and Jeremy A. Sabloff. Smithsonian Institution Press: 1986. Pp.479. Hbk \$35, £35; pbk \$19.95, £19.75.

On 28 December 1934 the Society for American Archaeology came into existence. The following year the initial volume of American Antiquity appeared and the first annual meeting of the SAA was held (with 8 papers and 75 participants). American Antiquity has since become the leading journal in its field, and many people would argue that the SAA meeting is the major conference of the archaeological year. The present volume is a celebration of the society's 50th birthday — an appropriate age for looking back to the past, taking stock of the present and trying to set the younger generation on the right path for the future.

The 17 contributions are by North American practitioners belonging to the older and middle generations, but representing a range of differing archaeological theologies. They are neither complacent nor self-congratulatory. Cumulatively, the book adds up to a lively, and conspicuously well written, critique of the strengths and weaknesses of archaeology in North America. By sheer weight of numbers, the Americans have played a dominant role in changing the theoretical basis of archaeology (in the non-Communist world, at least), so this study is of more than parochial importance.

The editors divide the volume into three sections. The first looks backwards: it includes a personal reminiscence by Jesse Jennings, and historical surveys of the development of field techniques, the rise of the conservation ethic and the changing employment of the concept of culture. Bruce Trigger examines archaeology as a social phenomenon which reflects the changing interests and prejudices of the society that sponsors and pays for it (as an example, he notes how today's explanatory models reflect "current anxieties in middle-class American society about unchecked population growth, environmental destruction and the depletion of nonrenewable resources"). In similar vein. Don Fowler observes that the roots of the majority of Americans do not lie in the Indian past and, in consequence, there is no strong impulse to identify with and conserve that past. Each generation, it seems, gets the archaeology it deserves.

The middle section of the book consists of state-of-the-art surveys of three major problems: the nature of hunter-gatherer

societies, the origins of food production, and the evolution of civilized states and empires. These papers, though good of their kind, do not treat the issues historically and therefore seriously interrupt the continuity of the book. The main theme returns in the final section on current trends and future prospects (the role of mathematics and formal methods, problems of cultural resource management, how to reconstruct the symbolic and cognitive values of extinct communities, and an evaluation of our long-term intellectual options).

Sections One and Three should be compulsory reading for any one, not only Americanists, interested in the historical development and present health of the discipline. As the editors point out, in 1935 American archaeology was remarkably uniform, with generally agreed goals (historical reconstruction, above all) and universally accepted research methods. That is not true today, and one of the book's many virtues is that the polemics of recent years are not merely described, but also evaluated from a longterm historical perspective. One of the faults of recent Messiahs and their followers is a reluctance to read anything more than 10 years old, and it is good to see Donald Grayson demonstrating that "middle range research" — though not under that jargon title — goes back to the days of the controversy over eoliths, and to read Jennings's casual comment that he had "discovered, studied and discarded" (my italics) the philosophers of science long before Hempel was so uncritically taken up by the New Archaeology. Some scholars, including some of the most innovative, are traditionalists by considered conviction, not through ignorance or lack of imagination.

Without naming names or reopening old wounds, one can recognize from the data in this volume a fairly standard cycle of events. A new movement emerges (generally based on ideas developed in another discipline, and often just as these are beginning to go out of fashion on their home ground), is accepted uncritically by its devotees, fails to deliver the promised goods, gradually loses its adherents and is in turn replaced by another "new wave". The historical view presented in this volume demonstrates that, in the long run, the good (and there is always some) is retained and adopted into the mainstream of archaeology, and the sillinesses - like puberty spots — fade away with maturity. If archaeology is not to stagnate, this kind of intellectual ferment is vital to the wellbeing of the subject. Like most of the contributors, I look forward to the future with a guarded optimism.

Warwick Bray is Reader in Latin American Archaeology at the Institute of Archaeology, University of London, 31-34 Gordon Square, London WCIHOPY, UK.

Breeders' rights and patenting life forms

from Jean-Pierre Berland and Richard Lewontin

Academic freedom and scientific advance could be the casualties if the patenting of microorganisms becomes the norm.

WITH the advent of genetic engineering, I biologists have suddenly become acutely conscious that plants and animals can be factors in the production of consumer goods: like machines, they are commodities, sold for profit to manufacturers. This development has raised a host of issues about property rights in living organisms, the patenting of life forms and other questions that arise when commodities are produced for profit.

The excitement over genetic engineering may, however, obscure the fact that plants and animals have been factors of production of consumer goods for a very long time. The production of seeds and of animal breeding stocks for sale to farmers by seed companies and breeders have long ago raised the legal and economic issues of life forms as private property, used by manufacturing firms to appropriate profit. Moreover, research devoted to the production of new varieties or to methods of plant and animal breeding has always been, at least in part, influenced by the drive to increase the profits of breeders and seed companies. An analysis of the economic forces in the seed industry, as they have operated in the past and at present, may provide us with a framework for understanding future questions raised by newer biotechnologies.

Seed business

Seeds are a special kind of factor of production because, at least potentially, they are reproduced in the production process itself. Thus, in principle, a farmer could produce his own seed by withdrawing a small portion of his crop from the market. The problem for the seed company is to convince the farmer not to do this, but to buy this factor of production each year, just as he does fertilizer and herbicide.

There are two pathways open to the seed producer. The first is to achieve economies of scale, that is, to produce seed of the appropriate quality cheaper than can the farmer himself. As we will show, the profits from economies of scale are, in general, quite small. The second is to reap monopoly profits by creating seeds that are consumed in the production process; by providing objects that are not really seed in the biological sense that they are self-reproducing.

This is the secret of the hybrid method of breeding, which makes it impossible for

the farmer to hold back some of his crop as seed for the next year and which forces him to return each time to the seed company. Such monopoly profits can be very high. The search for them has had a strong influence on the direction of breeding research and on the drafting of laws and regulations governing seed production and sales in North America and Europe for 60 years.

It is our purpose here to provide a sketch of the economic analysis of the seed industry and to show how the attempt to maximize profits in the seed industry has influenced breeding and its organization. We will then discuss briefly the consequences of breeders' rights and the essential contradiction involved in patenting life forms.

Property rights

Any bag of seeds has two characteristics that must be distinguished carefully. The first set of characteristics, that the seeds should be weed-free, sized to fit mechanical planters, free from seed transmitted diseases, that they should germinate consistently to reach the proper plant density and that they should be available when needed in convenient forms at a reasonable price, are all traits that are a function of the technical process of seed production and marketing; they contribute to the profits of the seed producer under the heading of economies of scale. The second set pertains to the variety itself, its adaptation to the environment, its earliness, disease resistance, stress tolerance, yield, taste, processing qualities, nutritive value and so on. These characteristics are the result of the breeder's work, whether public or private. They are embodied in the genetic framework of the variety, are of a strategic nature and have an immense value. Marquis wheat, for instance, because of its earliness and disease resistance, made it possible to expand vastly the wheat-belt in the northern United States and Canada.

Yet, breeders find themselves in dire difficulties, for they have no property rights in the result of their labour. Farmers, no matter how much they benefit from the breeder's work, will pay only for the services of the seed producer, but not willingly for the work of the breeder. This is why breeding has had to be publicly financed until varieties - the result of breeding research and the invention that | pean system of protection:- the *catalogue*,

stems from it - become saleable commodities.

Historically, this has been done in two different ways. In Europe, governments have undertaken regulatory activities for a very long time and, more recently, this long-standing administrative protection has been reinforced by a legal system of plant breeders' rights. In the United States since the mid-1930s, the same goals have been achieved in the production of F hybrids, as is the case with corn. We will describe the historical origins of the system of breeders' rights and analyse its anticipated consequences before we turn to the biological solution sought by US plant breeders in the 1910s and 1920s

Breeders' rights

Breeders' rights have existed in Europe for more than 50 years, thanks to seed trade regulations, although the final convention forming the Union pour la Pro ection des Obtentions Végétales (UPOV) was not signed until 1961 and not ratified by national legislation until 1970 To understand how these rights were finally developed, we have to go back to the beginning of the twentieth century.

The first attempt to create a system of protection was to extend the patent system to new varieties, but patent lawyers rejected this solution on the ground that one of the basic requirements of patent law cannot be satisfied with biological material. Specifically, even full disclosure of the breeding work would not make it possible for anyone to reproduce the variety. Accordingly in France, breeders had to find more imaginative solutions, which resulted in a series of decrees, beginning in 1922, requiring that (1) seeds be sold under their proper variety name, labelled by variety and producer; (2) the breeder of the variety becomes the owner of the variety name, which is registered; and (3) only seeds of registered varieties can be offered for sale. Therefore, the breeder owns the variety.

In 1928, an "identity and purity" service was set up within the French ministry of agriculture to check the identity of the genetic material offered for sale and to control the purity of the seeds, thus establishing a de facto protection of breeders'

These are the two pillars of the Euro-

originally called the register, and (borrowed from the Dutch) certification, to protect farmers from poor plants. Fields are inspected, tests are run and plants are sold with a certification tag attached to the bag. If the tags are numbered and mention the name of the variety and of the producer of the plant, and if the records are kept, the breeder knows exactly the quantities of his variety sold.

When the catalogue and certification coexist, breeders are protected and de facto property rights to plant varieties are created without the intervention of legislation (see ref. 1). Only in the 1970s did European countries adopt legislation on plant breeders' rights giving this regulatory procedure a legal basis. But no such system can provide a mechanism to set the price of a breeder's work, nor is there a market mechanism that can establish one. This problem had to be solved by a regulatory mechanism to decide what the breeder's royalty should be.

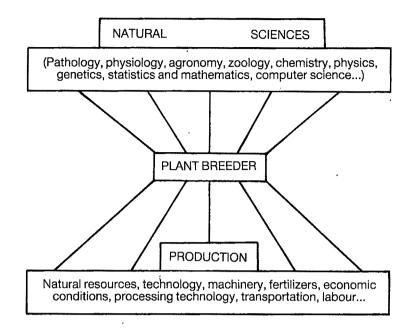
For clarity, we shall assume that the two functions of breeding on the one hand and of commercial seed production on the other are separate. We might suppose that, under the regulatory system of protection (or a breeders' rights system), the breeder can collect his royalties. The seed company can then add the royalty to its costs to set the price of the commercial seed, so that the cost of the breeding work would be paid for by the farmer.

This is not the case, however. Why would a rational farmer pay a second time for something he has already bought and still possesses in the form of his seed crop? The harvested grain has to be processed into seed; the farmer has the choice of doing it himself or buying the seed from a commercial seed company. Whether he chooses one or the other hinges on the importance of the economies of scale in seed processing.

Cleaning and sorting the harvested grain to get rid of foreign matter and of weed seeds, coating the seed with fungicides and insecticides and storing and keeping it in good condition until the next growing seson, after checking that it germinates, are simple and cheap operations; in France, they represent about 30 per cent of the value of the harvested seed. The sorting and cleaning equipment is cheap, easy to operate and readily available from country elevator operators at off-season times and prices. If necessary, machinery can be purchased and used cooperatively.

All this means that the profitability of the seed companies is low. Requiring them to pay for the breeding work is, for many, the last straw. In Britain, for example, a number of small seed companies went under after the breeders' rights law was passed. In France, where commercial seed is generally produced by cooperatives on behalf of their members, this

The strategic position of plant breeding



operation is often in the red.

To further illustrate this point, in 1985 the French government made it illegal for seed companies to process farmers' grain into seed. Why had seed companies apparently been undermining their own market? Because they were thus able to keep for themselves the benefit of economies of scale when processing farmers' seed, whereas they had to pay the breeder his royalty for every bushel of commercial seed they sold. Breeders and breeding companies sought to close this loophole and succeeded.

In the United States, the law allows farmers to use the harvested crop to provide seed for the next generation and even to sell it (although advertising is forbidden). This law is ambiguous on the question whether farmers may collectively use equipment to process their grain into seed, or have it processed for a fee, or trade the seeds of various varieties within a clearing house to avoid having to grow, harvest and process small quantities of each cultivar. It is likely that strong pressure will be exerted in the future by breeders and private seed companies to prohibit such operations, as the example of France demonstrates.

From this analysis, it can be seen that it does not make sense for a business enterprise to seek to integrate breeding and seed production: one loses what the other gains. (There is a striking difference with hybrids.) But breeding is a strategic activity that benefits the entire society. Should the cost be met by taxpayers or by a small group of enterprises, the small seed companies? And if the second, what steps can be taken to ensure that seed producers' profits will be sufficient to sustain such a

crucial activity? Especially now that breeding autogamous plants is less and less of a craft, and has become a specialized and capital-intensive operation, assurance is not easily arrived at.

As well as the hybrids, there is another significant exception to the qualitative conclusion of this analysis — the case of the occasional crops, such as soya beans, where the economies of scale in seed preparations can be very great. Because of the supposed fragility of the soya bean seed, it is said to be difficult for farmers to reproduce their own seed from the harvested crop. The question why mechanization research at agricultural experimental stations has not devoted more attention to harvesting techniques that would be less damaging to soya bean germ apart, soya bean is idiosyncratically closer to the category of monopoly profit seed production (see below) than to that of the small-grain cereals.

Changing rules

When no breeders' rights are in force, a public breeder will replace a variety only if he has developed a clearly better material. If a variety is widely used for years on end, so much the better. His fame, and that of his experiment station will be increased, and the farming community will lobby for increased appropriations when it becomes necessary.

For a private breeder, the problem is quite different. He has first to make his company profitable, which requires that there should be a commodity for sale. The strongest sales pitch is to offer "new" varieties. In other words, a private breeder has a vested interest in reducing as far as possible the lifetime of his varieties, to-

wards the ideal that farmers should adopt new varieties every year.

It is not therefore surprising that the statistics presented to the US Congress in 1980 have been described as "impressive". The same source says that ". . . three to six times more varieties of wheat, soybeans, and cotton were produced in the decade after the passage of the 1970 Act than in the preceding decade . . . This is probably a case in which the patent system actually achieves the intended goal of increasing research investment.

No seed company will advertise a nonproprietary item. Product differentiation through the creation and sale of proprietary varieties is essential if it is to remain competitive. The increase in the number of varieties offered for sale after the Breeder's Rights Act was passed in the United States is, for these reasons, not an adequate measure of the breeding effort aimed at increasing the agronomic value of the genetic material because, meanwhile, the objective of the breeders has shifted from that of increasing farm productivity to that of giving sales arguments to the marketing departments of the seed

Most breeders recognize that varieties offered by private companies are very similar. The argument that the number of varieties offered for sale has been multiplied, implicitly suggesting that it could be an index of the actual breeding work, is tantamount to measuring a temperature first with a Celsius thermometer, then with a Farhrenheit thermometer, and concluding that the temperature has approximately doubled. What the figures show is that breeders' rights increase oligopolistic non-price competition, but they leave unsettled how, and what sort of agronomic progress flows from the new rules of the game and whether it is more or less efficient than the alternative of publicly funded breeding work.

We would add at this stage that to contrast "market" and "public" breeding work is simplistic and inappropriate. The expensive, risky, time-consuming and unattributable task of developing new breeding techniques is carried out by the "public sector" with the intention that they should become the general property of all seed companies. At this point, private breeders step in to add small touches that can be made proprietary at small expense.

The structure that replaces a totally public breeding system is thus one of division of labour between public research, which does the non-proprietary work, and private breeders, who endeavour to use the work of public breeders in their own breeding programmes and proprietary commercial varieties. Far from disappearing into oblivion, public research will remain active, but will have to give up the production of commercial varieties. The

process of adjustment may be long and arduous, especially for the older public breeders who may cling to their ideal of serving the farmer, whereas they have now first to serve the seed industry, hoping that the "invisible hand" will accomplish what they used to do consciously. The United States and France, where it is a quasi-official policy that public research should keep out of commercial varieties, clearly illustrate the division of tasks created by a breeders' rights system.

Biological implications

It took four years for a committee of experts to elaborate the statute of UPOV (the Union for the Protection of Plant Invention). One of the stumbling blocks was the definition of the object of the convention⁴:

The word variety . . . applies to any cultivar, clone, line, strain hybrid susceptible to be grown and satisfying the dispositions of paragraphs (c) and (d) of Article 6. These paragraphs state that a new variety must be sufficiently homogenous and stable.

In fact, as UPOV itself recognizes, a variety is almost impossible to define⁵ "... the word 'variety' which is currently used does not have a commonly accepted precise definition". Since the very object of the convention is without a biological definition, we will not use the word "variety", which refers to a common sense notion and may confuse the issue, but instead use a meaningless term, varitrick, which is legally defined.

A new varitrick must be distinct from others. It has to be homogenous — the plants belonging to the same varitrick must look alike - and it has to be stable a varitrick should remain identical or almost identical over time. While these are the minimum criteria of patentability, they are also nothing other than a description of the steps of the method of breeding widely used for self-pollinated plants or to produce inbreds. Breeders artifically cross homozygous plants which display desirable qualities and then breed a series of generations, sorting out the plants which display the qualities of both parents, until they get a homozygous plant which, by definition, is a new (distinct) homogenous and stable varitrick. We thus have the principles of distinctiveness, homogeneity and stability (D-H-S) which are the basic principles for protection of breeders' rights all over the world.

In essence reliance on D-H-S as a criterion for a varitrick to be the property of a breeder outlaws other methods of breeding. The biological object, the variety, with its immense potential of variation, adaptation and evolution, is reduced to a varitrick, a much narrower legal object. For the sake of establishing property rights, plant breeders' imagination has to time, energy, and money have to be expended in fixing small anatomical differences (sometimes sensitive to the environment) in order to comply with the legal definition.

Let us again stress the self-contradiction of the system: if a varitrick is stable, the harvested grain is genetically identical with the seed and there is no need for an integrated seed industry. Breeders cannot make a living out of their work if they do not squeeze it out of the seed producer. If the variety is unstable and if the breeder/ seed producer knows how to control this instability and to maintain the basic agronomic characteristics of his variety (by F. hybrids, for example), only then will the farmer be ready to pay dearly for the breeders' services and be compelled to pay for the expenses of research and development.

Hybrids and monopoly

Barton, in his review of breeders' rights raises the science-fiction possibility that "DNA engineering will be applied to make the second generation of a seed artificially sterile . . ." and concludes that such an 'innate patent system' could pose enormous social costs in a concentrated industry. This forecast is to the point but at least 60 years behind the times. The F, generation of hybrid maize, if not biologically sterile, is economically unusable as seed, producing anywhere from 20 per cent to 40 per cent less than the F hybrid. For all practical purposes, such a loss of yield amounts to biological sterility.

In good maize areas, the use of F, seeds instead of commercial hybrids will cause a loss of 45 bushels per acre if a potential yield is 150 bushels per acre. The maximum price per bushel that an economically rational farmer will be willing to pay for his hybrid seed corn is theoretically equal to the loss per acre (45 times the price of maize per bushel) multiplied by the area sown with a bushel of seed corn (about 4 acres), which is the equivalent of 180 bushels of maize.

Even at present low grain prices, a bushel of hybrid seed corn is thus a potential gold mine, although seed companies do not, in fact, realize the maximum price. With grain selling at about \$3.00 per bushel, the maximum price of hybrid seed would be approximately \$450 per bushel, while the price, if the farmer could produce his own non-hybrid seed, would be a little over \$3.00. The actual price charged by seed companies for hybrid seed is about \$70 per bushel.

In the case of F, hybrids, monopoly profits are possible because the farmer is no longer the principal competitor of his supplier, and the regular game of interenterprise competition is re-established. Market structure then determines the profitability of the seed industry. If entry into be channelled into this narrow definition: I the market is easy and barriers to entry low, competition and particularly price competition will be intense, with the result that margins and profits will be low. On the other hand, if a seed company achieves a monopolistic position, it will charge much more. Research and development play the same role as expenditure on sales promotion and, under modern economic conditions, are in reality key elements in the strategy by which enterprises build barriers to entry through this sales effort.

Not only do the marketing staff and sales personnel need new products or varieties to launch their sales campaigns, but the creation of new varieties depends on the past investment in research and development. A breeding program may take anything up to 10 years to yield a commercial variety. Seed maize companies devote 3 to 5 per cent of their total income to breeding activities. This may not seem a very impressive figure when compared to sales expenses (20 per cent or more of total income) but for any newcomer, it is a formidable obstacle: one would have to invest money for years, perhaps in vain, before getting any return on one's investment. Since the time horizon of entrepreneurs is short, oligopolistic market structures are very stable over

Because hybrids expand the physical market for seed to the total acreage sown and because they make it possible entirely to disconnect seed prices from actual costs of production, they open up enormous opportunities for profit for private enterprise. In the last 15 years, most of the vegetable crops have become hybrid, but the great breakthrough that private (and, in many cases, public breeders as well) are pursuing is the production of hybrid seed for wheat, barley and soya beans.

Insofar as the breeders' hope is to repeat the success achieved with maize, however, they are likely to be disappointed. Success, of course, means profits. The claims that hybrid maize increased yields by a large proportion are totally unsubstantiated. Moreover, it can be shown that the margin of the seed industry in the sale of a variety of seed depends on the multiplication rate (the ratio of the quantity harvested to the quantity sown) of the variety⁷. The higher the rate, the higher the potential profits. But wheat, barley and soya beans have multiplication rates which are one tenth or less of that of maize. This explains why the only other grain crops so far to have gone hybrid are sorghum, millet and sunflower, the multiplication rates of which are at least equal to that of maize. The multiplication rate, the key to profits, has little to do with hybrid vigour, the biological phenomenon that allegedly justifies hybrid breeding schemes.

For wheat and barley, chemical inducing tillering is likely to increase the multiplication rate and therefore solve the seed companies' problem to some degree. If this is the case, the circle will be closed; the world seed industry has, in the past decade, passed into the control of powerful petrochemical and pharmaceutical corporations.

Conclusions

What we have described can be conveniently summarized in a set of concepts that provides a general framework for understanding some of the debates about biotechnology and property.

The specific factor of production implied in any biological process of production is genetic information. A wheat variety is a form of genetic information that makes it possible to make a better or more efficient use of the available resources, natural or technical. A strain of microorganisms used for the production of antibiotics is genetic information that makes it possible efficiently to use a substrate under precise conditions of pressure, temperature, acidity and so on.

Production in the economic sense involves a biological reproduction, which entails the production of genetic information in successive generations which can be identical, statistically similar or different to various degrees. For autogamous plants, barring mutations, the genetic information is identical. For a strain of microorganisms, mutations may occur during production, but the chance that they affect the useful part of the genome are negligible and, if they do, they can be selected against occasionally to keep their frequency low. For animals, the extent to which the useful genetic information is transmitted from parents to offspring depends upon the heritability of the character under consideration. In the case of openlypollinated varieties of plants, both the gene frequency and random disorder are preserved; for production purposes, the offspring are similar to their parents only on the average.

Thus, except for hybrid varieties, production implies a diffusion of genetic information which is available to anybody and which becomes a public good. Street corner sellers of tomatoes, beans and potatoes transfer, gratis, the genetic information built into the commodity sold. The case of microorganisms is different; the commodity sold is not the living thing but

its product once it has been killed. Between the fermenters and the pill or injection, there may be several complicated steps; the customer is not, in any case, a direct competitor of his supplier. Nevertheless, the genetic information circulates easily; the folklore of the pharmaceutical industry is full of stories of visitors carefully wiping their noses and sending back the tissues to their own laboratories. The essential point is that the good concerned, genetic information, is difficult to control exclusively and tends to circulate freely.

Those who have been promoting breeders' rights in Europe, in the United States and in the rest of the world, particulary in the developing countries, as well as those who seek to patent other forms of life, have not paid attention to the innate contradiction in what they do.

Limiting the use of a good available in limitless quantities at no cost will not be socially useful, will limit the full use of biological potential only to what is patentable, will erect barriers to entry in branches of production where competition is necessary and wil limit the free exchange of information between scientists so crucial to science. It would be unfortunate if the patenting system were surreptitiously extended to microorganisms. One may wonder what would have happened if the "Petition of Candle Merchants and Associated Industries against the Unfair Competition of the Sun", with its request that all openings of houses and buildings be covered, had been taken seriously. Frederic Bastiat's witty essay deriding the anti-free traders of his time applies exactly to the present situation.

Part of this work was financed by the Science-Technologie-Societe Research Programme of CNRS. □

Jean-Pierre Berlan is at INRA-CEDEC, Université d'Aix-Marseille II, Marseille, France and Richard Lewontin is at the Museum of Comparative Zoology, Harvard University, Boston, USA.

- Actes des Conferences Internationales pour la Protection des Obtentions Vegetales 1957-72. (Proces-Verbal Résume des Déliberations de la Première Session de la Conférence ciable par le Secrétaire de la Conférence. M. ladwière, Paris 7-11 Mai 1975, page 24 (UPOV, Genève, 1974).
- . Barton, J. Science 216, 1071-1075 (1982).
- Testimony of representative of National Science Foundation in. U.S. Congress, House of Representatives, Committee on Agriculture Hearings before the Subcommittee on Department Investigations, Oversight, and Research, 96th Congress, First and Second Session, "Plant Variety Protection act amendment" (US Government Printing Office, 1980).
- Convention International pour la Protection des Obtentions Végetales, Actes des Conférences Internationales, p. 133-134, (UPOV, Geneva, 1972).
- (UPOV, Geneva, 1972).
 5. UPOV, Informations Génerales, Genève, 1975, p.7
- Barton, J. "The International Breeders' Rights System."
 Berlan, J.P., L'industrie des Sémences, Economie et Politique, Economie Rurale, 158: 18-28, 1983.

Fractal growth processes

Leonard M. Sander

Physics Department, University of Michigan, Ann Arbor, Michigan 48109, USA

The methods of fractal geometry allow the classification of non-equilibrium growth processes according to their scaling properties. This classification and computer simulations give insight into a great variety of complex structures.

ALMOST every theoretical tool of the condensed-matter scientist uses the assumption that the system considered is of high symmetry and is in equilibrium. These assumptions have led to enormous progress; however, to much, if not most, of the natural world such tools cannot be applied. Many systems that we would like to understand are very far indeed from perfectly ordered symmetry and are not even in local equilibrium. Perhaps the most extreme example is disorderly irreversible growth. We mean by this the sort of process which is very familiar in the formation of dust, soot, colloids, cell colonies and many other examples; roughly speaking, things often stick together and do not become unstuck. For example, a particle of soot grows by adding bits of carbon and coagulating with other particles in a random way. A possible result is shown in Fig. 1. We are thinking about cases which are, in some sense, as far from equilibrium as possible, and which have no obvious order.

It is remarkable that the introduction of simplified models has led to quite a good understanding of the morphology of such growth, despite the inapplicability of our usual modes of thinking. Here I will discuss this progress, drawing examples mostly from subjects which have traditionally interested physicists and chemists. However, disorderly growth is ubiquitous in the world around us, and is certainly not limited to inanimate matter. For example, some of the ideas which I will discuss, such as anomalous scaling in kinetic processes, will be useful to biologists. The purpose of the review is to introduce ideas from the area which may be of general use.

The key to our recent progress is the recognition that the most 'interesting' non-equilibrium structures (say, from a visual point of view) are not merely amorphous blobs; they still have a symmetry, despite their random growth habit, albeit a different one than they might have had, had they grown near equilibrium. For example, consider the soot of Fig. 1, or the electrolytic deposit of zinc shown in Fig. 2. Many people will be familiar with branched deposits such as this, and with similar looking objects which form on automobile windshields on cold mornings. In all these cases the structure is disordered, but it is not random. A manifestation of this is that each section of the picture contains holes in the structure comparable in size with that of the section itself. This can only occur if there are longrange correlations in the pattern; particles 'know' about each other over distances far in excess of the range of the forces between them. A truly random pattern, such as that of salt scattered on a table top, shows no such scaling of holes, and correlations are of short range only.

Studies of fractal growth have focused on two questions: how can we characterize and quantify the hidden order in complex patterns of this type, and when and how do such correlations arise? The answer to the first question is now relatively clear, and lies in an application of the fractal geometry of Mandelbrot¹. The next section gives a brief review of relevant aspects of this subject. The second question has received a partial answer in the formulation and analysis of models suitable for computer



Fig. 1 Electron micrograph of soot. (Supplied by G. Smith, General Motors.)

simulation, which will also be reviewed. For more extensive treatments see refs 2-4.

Fractals and scale invariance

In pure mathematics, it has long been common to study certain 'pathological' geometric shapes that elude ordinary notions such as those of length and area. Figure 3 shows a famous example, which has, in some sense, infinite length, but zero area. It falls between our usual 'notions of line and solid. Mandelbrot¹ systematized and organized mathematical ideas concerning such objects due to Hausdorff, Besicovitch and others. But, more importantly, he pointed out that such patterns share a central property with complex natural objects such as trees, coastlines, patterns of stars and (as was later discovered) the non-equilibrium growths of Figs 1 and 2. This property is a symmetry which may be called scale invariance. These objects are invariant under a transformation which replaces a small part by a bigger part, that is, under a change in scale of the picture. Scale-invariant structures are called fractals.

There are a number of related properties which follow from the assumption of scale invariance. Consider, for example, the

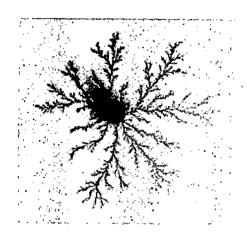


Fig. 2 Zinc electrodeposit produced in a thin cell under conditions of low ZnSO₄ concentration (0.01 mol l⁻¹). The outer electrode (not shown) is in the form of a ring 6.3 cm in radius. (Supplied by D. Grier, University of Michigan.)

density correlation function c(r), of a fractal. This is defined as the average density of the object at distance r from a point on the object, and is a measure of the average environment of a particle. Clearly, c(r) must reflect the scale invariance. It is easy to show that the only way that c may vary is as a power law in r; any other function would have an intrinsic scale. It is convenient to write c in the following form:

$$c(r) = kr^{-(d-D)} \tag{1}$$

Here, k is a constant, and the exponent is written in terms of the dimension of space, d, and a new quantity, D, the fractal dimension. The reason for this terminology will become evident in a moment. As the objects we are dealing with are tenuous, c(r) is a decreasing function of r: the average density decreases as the object becomes larger. Now consider how the total mass of the object, M, scales with the mean radius, R. We can estimate this by multiplying a typical density, from above, by the volume:

$$M(R) = KR^{D-d}R^d = KR^D \tag{2}$$

Here, K is another constant. We can now see why D is called a dimension. For an ordinary curve, D=1: twice the length gives twice the mass. For a disk, D=2. For simple objects D coincides with the usual notion of dimension. But in the cases we are discussing D is not an integer; it has been measured to be ~ 1.7 for the deposit in Fig. 2, and is 1.26 for the fractal of Fig. 3.

This anomalous scaling with radius, measured by D, is a very useful means of characterization because the fractal dimension is a 'robust' quantity. Like the famous scaling exponents of phase-transition physics, it has to do with long-range properties, indeed, with the relationship between properties at different scales. Thus we can expect it to be universal in the sense that it should be independent of the details of the interactions between the objects which stick together during the growth, of their detailed composition, and so forth. But, as we will see, the mechanism of growth does affect D.

Growth models

How might one visualize the growth of an object such as the electrolytic deposit in Fig. 2? As we are interested in long-range properties we can ignore the complications of electrochemistry and simply imagine that ions wander randomly in solution (in many cases the electric field is screened out so that this is a good approximation) and stick to the deposit when they happen to get near it.

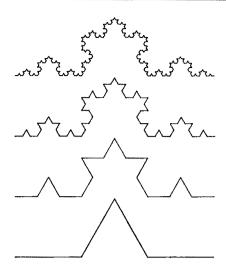


Fig. 3 Four stages in the growth of an exact fractal, the Koch curve. This and many other examples are discussed in ref. 1. The fractal dimension may be deduced by thinking of each picture as a part of the picture above, with a change of scale. For each scale change by three, we need four such parts. Thus, according to equation (2), $D = \log 4/\log 3 = 1.26$.

To make a computer model which is a literal translation of this process we start with a centre. Then we liberate a diffusing particle, a 'random walker', and let it wander freely until it is within a fixed distance of the centre, where it sticks. Then we liberate another particle and let it walk until it sticks to the centre or the first particle, and so on. We may, for our purposes here, idealize the process of formation as being completely irreversible: we ignore the possibility that the particles rearrange after sticking to find a more energetically favourable location. This is the diffusion-limited aggregation (DLA) model of Witten and Sander^{5,6}. The application of DLA to electrodeposition is due to Brady and Ball⁷ and Matsushita et al.⁸.

Figure 4 shows the result of an extensive simulation according to the DLA rules; its resemblance to Fig. 2 is evident. Measurements of DLA clusters have shown them to scale according to the relations quoted above, with D=1.7 for d=2, and D=2.4 for d=3. Note that the structure is tenuous and open because holes are formed and not filled up. Filling up the holes would require wandering down one of the channels in the cluster without getting stuck on the sides; a random walker cannot do this.

There are several features of the DLA model which should be mentioned. Although it is simple to describe, no progress has been made towards 'solving' it. That is, although we suspect, on the basis of simulations, that DLA clusters are fractals, we cannot prove it. And we have no method of calculating D (or any other property): we must measure it. There are several reasons for this (I will mention a rather technical one below), the primary one being that DLA presents us with a situation in which our experience in equilibrium systems doesn't seem to help. Note that D, along with other scaling properties, arises in a non-trivial way from the kinetics of growth: there is no simple geometric argument with which to predict them.

The DLA model can be generalized in various ways, for example, to describe deposition on a surface rather than a point. A more profound generalization is to use the model to describe systems which apparently have nothing to do with particle aggregation, but which share the same universal properties. We may see how one is led to do this by observing 5,10 that the probability, u, of finding a random walker at some point on its way to the aggregate has the following well-known properties: the flux of walkers; v, is proportional to the gradient of u, and, because walkers are absorbed only on the aggregate, this flux

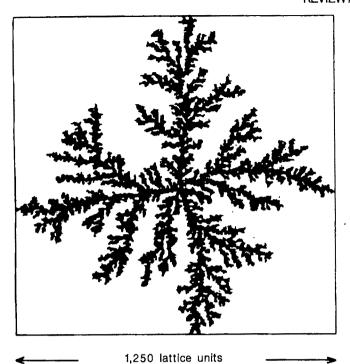


Fig. 4 A large DLA cluster (~50,000 particles) grown on a square lattice. Note the resemblance to Fig. 2, and the beginning of distortion towards a dendritic outline, as discussed in the text. (Supplied by P. Meakin, Dupont.)

has no divergence:

$$\mathbf{v} \propto \nabla u \tag{3}$$

$$\nabla \cdot \mathbf{v} = \nabla^2 u = 0 \tag{4}$$

As walkers are not allowed to escape from the aggregate, we set u = 0 on the surface. The growth of the aggregate is given by the flux at its surface, that is, by ∇u .

As Niemeyer et al.10 pointed out, a set of equations of identical form govern dielectric breakdown of a solid if we ignore many short-range details. As we are looking for universal features, making such simple, indeed, crude approximations is justified. If we think of u as the electrostatic potential in a solid about to be destroyed by a discharge, its negative gradient is, of course, the electric field. But u then obeys the Laplace equation of electrostatics, which is of the same form as the steady-state diffusion equation, equation (4), above. The breakdown channel will grow in a way determined by the electric field, that is, the gradient of u, on its surface. If the growth rate is linear in the field, we expect to have exactly the same situation as in DLA, and indeed, direct solutions of the equations, as well as measurements of photographs of real discharges, give the same fractal dimension as DLA. Non-linear breakdowns (lightning in the atmosphere is probably an example) give rise to patterns with different values of D.

Paterson¹¹ noticed an even more remarkable manifestation of the wide applicability of the model. When a fluid flows under conditions of large friction, inertial effects are negligible and the flow rate can be taken to be proportional to the hydrostatic force, that is, to the gradient of the pressure: this is known as D'Arcy's law. The situation is commonly realized in the laboratory by letting fluid flow between thinly spaced plates, a so-called Hele-Shaw cell. In nature, the flow of crude oil through the porous rock in which it is found is an example of quite serious interest. Suppose we try to force such flow by blowing a bubble of air or another low-viscosity substance into the cell (or by pumping water into an oil field—a scheme known as enhanced recovery). It has long been known that the air will not uniformly displace the fluid; instead it will break up into a complex

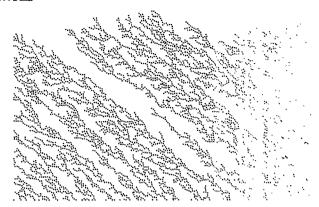


Fig. 5 Columnar microstructure in ballistic aggregation. Particles stick to the substrate and to each other after raining onto the structure in parallel trajectories at an angle to the vertical somewhat smaller than that of the columns. The fluctuations of the upper surface scale with the height for small height, and with the total width for large height. (Simulation performed by P. Ramanlal, University of Michigan.)

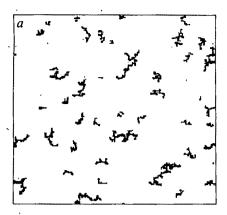
structure with many arms¹², which are called 'viscous fingers'. This phenomenon has an obvious detrimental effect on enhanced recovery.

Paterson's¹¹ speculation was that the pattern of the viscous fingering would scale like DLA. His reasoning was as above: the pressure in an incompressible fluid obeys equation (4), with u now standing for pressure, because fluid, like particles, is conserved. D'Arcy's law is of the same form as equation (3). Once more, many details have been ignored. In particular, the role of surface tension in this and similar situations will be discussed below.

The reasoning has been verified most directly by Chen and Wilkinson¹³, who introduced discrete randomness into a Hele-Shaw cell—the effect should be that of the random arrivals of Wilkinson¹³ particles. Their patterns look almost exactly like Figs 2 and 4. Another experiment, by Nittmann et al.14, used the clever trick of eliminating surface effects by taking for the two fluids water and an aqueous polymer solution; the fluids are miscible but mix slowly. Once more the pattern of fingering resembled the simulations. There seems to be a source of randomness in this experiment, probably arising from the non-newtonian flow characteristics of the polymer solution; such shear thinning could amplify noise. Even more startling is the experiment of Ben-Jacob et al. 15, who used a smooth Hele-Shaw cell, and one with a periodic pattern, with newtonian fluids. In some conditions they observed DLA-like scaling without an evident source of randomness, and without discrete 'particles'.

Experts will notice that equations (3) and (4) are of the same form (except for surface effects) as the description of solidification when the limiting factor in growth is diffusion of latent heat away from the surface of the growing crystallite. Why, then, does a snowflake (unlike the crystalline deposit of Fig. 2) not look like DLA, but is instead dominated by the crystal symmetry? I will return to this aspect of growth in the final section.

If particle aggregation doesn't need particles, what does it need? More generally, we can ask what different types of model give rise to scaling objects. For example, it is often the case that aggregates are formed by adding particles with a long mean free path, for example, in the formation of thin films by vapour-phase deposition¹⁶. In this case we may assume that the paths of the particles are straight lines. This model has become known as ballistic aggregation, and it has a number of very curious features. It is now known that the deposit itself is not a tenuous object but achieves a constant density^{17,18}. (In contrast, diffusion-limited growth on a surface⁹ yields an open deposit whose average density decreases with height.) It is of great interest to understand the upper surface of the film, which is a



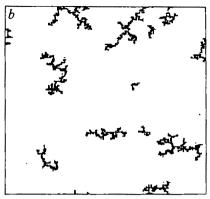


Fig. 6 Two stages in the formation of cluster-cluster aggregates: a, t=3,669; b, t=17,409. Note the resemblance of the clusters in b to the soot particle of Fig. 1. (Supplied by P. Meakin, Dupont.)

model of a random rough surface. It has been shown numerically¹⁹ that for normal incidence of the depositing particles this surface also has scaling properties: for example, the fluctuation of the height scales with a non-integral power of the height, for small height. This surface is probably not an ordinary fractal curve, like Fig. 2, but is probably an example of a self-affine fractal^{1,20}. 'Self-affine' means that the scaling in two different directions (width and height in this example) is different.

For non-normal incidence another effect appears, which is well-known in thin-film technology¹⁶. This is the columnar microstructure: the film spontaneously forms as a set of nearly parallel columns as it grows (see Fig. 5). The beginnings of a theory of this effect exist²¹, but it is not known what; if any, relationship these giant fluctuations have with the scaling fluctuations at normal incidence.

The simplest aggregation process of all was introduced into mathematical biology by Eden²². This is a model for the growth of a cell colony: a cluster is grown by adding particles at random to perimeter sites. Once again the object is compact, but the surface has interesting scaling properties which seem to be the same as for ballistic aggregates with normal incidence²³. Scaling is ubiquitous, and tends to have common features despite widely different details of growth.

We still have not described how soot forms. The structure of Fig. 1 is far more open than a DLA cluster: its fractal dimension is ~ 1.8 (DLA in three dimensions has D = 2.4). Extensive measurements of soot²⁴, colloids²⁵ and other similar objects leads one to suspect that a different class of clusters is involved. In fact, we have omitted a central feature of the formation process of clusters which can coagulate, namely the aggregation of clusters with each other^{26,27}. Figure 6 shows two stages of a simulation of this process in two dimensions. We start with a vapour of freely moving particles which stick together whenever they come into contact, and then allow the clusters to continue to move with, perhaps, a smaller diffusion constant. The large fractals which are eventually formed have D = 1.4. The corresponding simulations in three dimensions give D = 1.8 and yield the open structure of real colloids and aerosols. At each stage of the process almost all of the clusters are of roughly the same size.

The open structure and low fractal dimension which characterize cluster-cluster aggregation are relatively easy to understand. It is difficult for a random-walking particle to penetrate a significant fraction of the radius of a growing cluster for particle aggregation; it is even more difficult for an aggregate of comparable size to do so. Thus, as aggregation proceeds, open, fluffy structures are produced.

One variant of this model which is worth mentioning is reaction-limited (chemically limited) aggregation²⁸. In many cases, because of the details of the growth process, the sticking is inefficient, and many attempts are required to form a new cluster. In the limit of a very large number of attempts, the fractal dimension increases from 1.8 to ~2. Reaction-limited aggregation was probably discovered experimentally²⁹, before the simulations were done. Later experiments³⁰ have carefully

controlled the growth conditions and shown both growth mechanisms, and both types of geometry, in the same system for different growth rates. The encoding of kinetics in the scaling in a form independent of details should be a powerful tool for identifying growth mechanisms.

Attempts at theory

There is no general theory of irreversible growth. The descriptions given in the previous section must be regarded as a kind of phenomenology, albeit a useful one. We can point to situations in which there is scaling, but we are compelled to do experiments, either in the laboratory or on the computer to calculate anything. We do have a few analytical results, but they give only partial information.

The best understood type of aggregation is the cluster-cluster process. Suppose we assume, as stated above, that the dominant cluster-cluster collision is between clusters of similar mass. If we make the masses strictly equal we have a hierarchical model³¹. It is easy to believe then that we do have a fractal: agglomerating parts in this way is exactly how the artificial fractal of Fig. 2 was made. (Note that particle aggregation is not hierarchical, but it seems to be fractal nonetheless.) The specification of the size distribution of clusters in the vapour, and the verification of the hierarchical assumption, have been the objects of detailed studies³² which have shown that, indeed, the most common collision is between clusters of nearly equal mass. Some of these investigations use the techniques of colloid chemistry, in particular the Schmoluchowski kinetic equations, as well as computer simulations.

There remains the problem of finding the geometry of the clusters formed. Some progress has been made here because of a detail which allows one of the favourite tricks of the theoretical physicist to be applied. The real difficulty in visualizing the process is excluded volume, that is, the tendency of clusters to get in each other's way because they can attach to each other only on the outside. If they could attach anywhere it would be much simpler to sort out what is going on. It is quite obvious that excluded volume problems become less serious in high spatial dimensions: there are more ways into a three-dimensional cluster than into a two-dimensional one. Often, in equilibrium studies, it is found that for sufficiently large dimension of space, d, excluded volume is no problem at all: essentially any part of a cluster is accessible from outside. The dimension at which this starts to happen is called the upper critical dimension.

Above the upper critical dimension, calculations are simple, anomalous scaling is independent of d, and there exist methods (for equilibrium problems) which allow us to extrapolate to the physical world of d=3. For cluster-cluster processes, this is exactly what happens³³. The fractal dimension, D, for a cluster-cluster aggregate cannot grow above ~ 3.4 and it attains this value at about d=7. This is rather far from the real world, of course, and no one has yet figured out how to extrapolate.

The situation for particle aggregation is very different. Suppose that the entire cluster were to become accessible to added particles for a large enough value of d. Then the mass in the

interior would grow without adding to the volume. The cluster would quickly become so dense that it would no longer be accessible. Thus, there is no upper critical dimension for DLA. In fact, careful considerations of this sort can be turned into a bound³³ on D:

$$d-1 \le D \le d \tag{5}$$

The fractal dimension is never independent of the spatial dimension, and the standard technique cannot be applied.

Some progress has been made in the study of particle aggregation by exploiting the similarity of the process to the famous 'snowflake' problem, that is, the study of dendritic crystallization³⁴. We can see, for example, why tenuous structures are likely to arise in DLA and not in ballistic aggregation by noting that in the DLA case we have a growth instability of exactly the same form as the well-known Mullins-Sekerka35 instability of crystal growth. The reasoning^{5,35} goes as follows: suppose we start with a smooth aggregate and ask why it grows sharp tips. If we start with a tiny bump on the surface it will be magnified into a tip by the fact that the bump will grow faster than the rest of the surface: it will catch random walkers more efficiently than the flat portions of the surface, and certainly much more efficiently than the holes in the aggregate. The analogous dielectric breakdown case will make this even clearer: recall that the growth rate of any point on the surface of the structure is proportional to the electric field there. Sharp tips have large electric fields (the lightning rod effect). They grow ever sharper and dominate the growth. In the viscous fingering problem the same instability arises because it is easy for viscous fluid to flow away from a growing tip. It is even possible to specify a relationship between D and the characteristic opening angle of the tips³⁶ by using the mathematical theory of lightning rods. Unfortunately, no one knows how to calculate these angles. In fact, recent work indicates that there is an array of sharp tips on the surface of the fractal DLA cluster whose distribution is itself fractal37

For ballistic aggregates or for the Eden model there is no growth instability: it is easy to see that a bump on the surface neither grows or shrinks, but just adds a uniform skin, and tips do not grow. The bulk of the material remains compact.

Fractals and snowflakes

In the last section we noted the usefulness of the analogy of DLA with the kind of solidification most familiar (at least to those in cold climates) in the formation of snowflakes, that is, branched (dendritic) crystals. But particle aggregates do not look like snowflakes. To be precise, in a typical dendrite, a growing tip forms by the Mullins-Sekerka instability but then stabilizes. It retains its shape and continues in a definite direction, although it may spawn side-branches as it grows. In DLA (and in, for example, the zinc deposit of Fig. 2) the tips repeatedly split and wander.

- Mandelbrot, B. The Fractal Geometry of Nature (Freeman, San Francisco, 1982).
- Family, F. & Landau, D. (eds) Kinetics of Aggregation and Gelation (North-Holland, New York, 1984).
- 3. Pynn, R. & Skjeltorp, A. (eds) Scaling Phenomena in Disordered Systems (Plenum, New Fynn, R. & Skjeltorp, A. (eds) Scaling Prenomena in Disorderea Systems (Plenum, 1 York, 1985).
 Stanley, H. & Ostrowsky, N. (eds) On Growth and Form (Nijhoff, The Hague, 1985).
 Witten, T. & Sander, L. Phys. Rev. Lett. 47, 1400-1403 (1981).
 Witten, T. & Sander, L. Phys. Rev. B 27 5686-5697 (1983).
 Brady, R. & Ball, R. Nature 309, 225-229 (1984).

- Matsushita, M., Sano, M. Hayakawa, Y., Honjo, H. & Sawada, Y. Phys. Rev. Lett. 53, 286-289 (1984).
- 9. Meakin, P. Phys. Rev. A 27, 2616-2623 (1983).
- Niemeyer, L., Pietronero, L. & Wiesmann, H. Phys. Rev. Lett. 52, 1033-1036 (1984).
 Paterson, L. Phys. Rev. Lett. 52, 1621-1624 (1984).
 Saffman, P. & Taylor, G. Proc. R. Soc. A245, 312-329 (1958).

- 13. Chen, J. & Wilkinson, D. Phys. Rev. Lett. 55, 1892-1895 (1985)
- Nittman, J., Daccord, G. & Stanley, H. Nature 314, 141-144 (1985).
 Ben-Jacob, E. et al. Phys. Rev. Lett. 55, 1315-1318 (1985).
- Leamy, H., Gilmer, G. & Dirks, A. in Current Topics in Materials Science Vol. 6 (ed. Kaldis, E.) (North-Holland, New York, 1980).

- 17. Bensimon, D., Shraiman, B. & Liang, S. Phys. Lett. 102A, 238-240 (1984).
 18. Meakin, P. Phys. Rev. B 28, 5221-5224 (1983).
 19. Family, F. & Viscek, T. J. Phys. A 18, L75-L81 (1985).
 20. Voss, R., in Scaling Phenomena in Disordered Systems (eds Pynn, R. & Skjeltorp, A.) 1-11 (Plenum, New York, 1985).
- 21. Ramanial, P. & Sander, L. Phys. Rev. Lett. 54, 1828-1831 (1985).
- 22. Peters, H. P., Stauffer, D., Holters, H. P. & Loewenich, K. Z. Phys. B34, 399-408 (1979).

There are three obvious differences between DLA clusters and dendritic crystals: DLA has essentially zero surface tension, it has a significant source of noise in the discrete arrivals of the particles, and it has (at least in some versions of the model) no analogue of crystal anisotropy. Sorting out how these affect the process is a subject of current controversy and great intrinsic interest.

Surface effects can be added in various ways to DLA simulations^{5,38,39}; the result is to thicken the branches of the aggregate, but the scaling is unaffected for large sizes. Nor do surface effects, by themselves, make the equations of crystallization give rise to snowflakes^{40,41}. Instead, something unexpected happens: a growing tip with surface tension does not stabilize, but undergoes repeated splittings, which are caused by the surface tension itself. This is because surface tension slows the growth of sharply curved surfaces and the end of the tip is the most sharply curved. In order to make real dendrites, anisotropy arising from the crystal structure must be introduced. The relationship of anisotropy to tip-splitting was verified experimentally¹⁵ using fluid flow in a Hele-Shaw cell with a lattice of grooves.

How does this relate to DLA? It is common to do DLA simulations on a lattice (for convenience). Will the same thing happen here as in the noise-free case; that is, will stable tips form because of lattice anisotropy? It seems that the answer is yes^{42,43}: sufficiently large clusters on a lattice have the outline of a crystallite, with tip splitting only on a small scale. But why, without surface tension, do we ever get tip splitting? This is because noise due to the discreteness of the arriving particles can split the tips. This can be verified in various ways, for example, by experiments and calculations which vary the noise¹³ at fixed anisotropy. In cases where tip splitting is mainly due to surface tension rather than noise, will we get an object which scales? The answer to this question is not yet clear, but there are indications^{15,44} that there is scaling, and that it is close to that of DLA.

These considerations are of more than technical interest, because they show how small effects (such as anisotropy) can make qualitative changes in growth habit. A series of recent experiments^{45,46} have shown, for example, how changes in growth conditions, such as an increase in voltage in electrodeposition, can change a fractal pattern like Fig. 2 into an ordered dendritic crystal by increasing the effective anisotropy. This is a fascinating example of the competition between scaling symmetry and ordinary spatial symmetry.

This work was supported in part by NSF grant DMR 85-05474. I thank M. Sander and R. Merlin for comments on the manuscript, P. Meakin, G. Smith, D. Grier and P. Ramanlal for illustrations.

Note added in proof: There have been two interesting recent attempts 47,48 to explicate the competition between anisotropy and noise.

- 23. Racz. Z. & Plischke, M. Phys. Rev. A31, 985-993 (1985).
- Racz, Z. & Pischke, M. Phys. Rev. A31, 985-993 (1983).
 Richter, R., Sander, L. & Cheng, Z. J. Coll. Interf. Sci. 100, 203-209 (1984).
 Weitz, D. & Oliveria, M. Phys. Rev. Lett. 52, 1433-1436 (1984).
 Meakin, P. Phys. Rev. Lett. 51, 1119-1122 (1983).
 Kolb, M., Botet, R. & Jullien, R. Phys. Rev. Lett. 51, 1123-1126 (1983).
 Jullien, R. & Kolb, M. J. Phys. A 17, L639-L643 (1984).

- Schaefer, D., Martin, J. Wiltzius, P. & Cannell, D. Phys. Rev. Lett. 52, 2371-2374
- 30. Weitz, D., Huang, J., Lin, M. & Sung, J. Phys. Rev. Lett. 54, 1416-1419 (1985)
- Botet, R. Jullien, R. & Kolb, M. J. Phys. A 17, L75-L79 (1984).
 Botet, R. & Jullien, R. J. Phys. A 17, 2517-2530 (1984).
- 33. Ball, R. & Witten, T. J. statist. Phys. 36, 863-866 (1984) 34. Langer, J. Rev. mod. Phys. 52, 1-28 (1980).

- Mullins, W. & Sekerka, R. J. appl. Phys. 34, 323-329 (1963).
 Turkevich, L. & Scher, H. Phys. Rev. Lett. 55, 1026-1031 (1985).
 Halsey, T., Meakin, P. & Procaccia, I. Phys. Rev. Lett. 56, 854-857 (1986).
 Kadanoff, L. J. statist. Phys. 39, 267-283 (1985).
- 39. Viscek, T. Phys. Rev. Lett. 53, 2281-2284 (1984)
- Srower, R., Kessler, D., Koplik, J. & Levine, H. Phys. Rev. A29, 1335-1342 (1984)
 Brower, R., Kessler, D., Koplik, J. & Levine, H. Phys. Rev. A29, 1335-1342 (1984)
 Ben-Jacob, E., Goldenfeld, N., Langer, J. & Schon, G. Phys. Rev. A29, 330-340 (1984)
 Ball, R. & Brady, R. J. Phys. A 18, L809-L813 (1985).
 Ball, R., Brady, R., Rossi, G. & Thompson, B. Phys. Rev. Lett. 55, 1406-1409 (1985).

- Sander, L., Ramanial, P. & Ben-Jacob, E. Phys. Rev. A32, 3160-3163 (1985).
 Grier, D., Ben-Jacob, E., Clarke, R. & Sander, L. Phys. Rev. Lett. 56, 1264-1267 (1986).
- Sawada, Y., Doughtery, A. & Gollub, J. Phys. Rev. Lett. 56, 1260-1263 (1986).
 Kertesz, J. & Vicsek, T. J. Phys. A 19, L257-L262 (1986).
- 48. Nittmann, J. & Stanley, H. E. Nature 321, 663-668 (1986).

The Cretaceous/Tertiary boundary in the Gosau Basin, Austria

A. Preisinger*, E. Zobetz*, A. J. Gratz*#, R. Lahodynsky*, M. Becke*, H. J. Mauritsch*, G. Eder*, F. Grass*, F. Rögl", H. Stradner* & R. Surenian*

* Institut für Mineralogie, Kristallographie und Strukturchemie, Technische Universität Wien, Getreidemarkt 9, A-1060 Vienna, Austria
† Institut für Geologie, Universität Wien, A-1010 Vienna, Austria
‡ Institut für Geophysik, Montanuniversität Leoben, A-8700 Leoben, Austria
§ Atominstitut der Österreichischen Universitäten, A-1020 Vienna, Austria

Naturhistorisches Museum, Burgring 7, A1014 Vienna, Austria
¶ Geologische Bundesanstalt, Rasumofskyg. 23, A-1031 Vienna, Austria

The Cretaceous/Tertiary boundary has been identified in the Gosau beds (Elendgraben) near Salzburg, Austria. The undisturbed 2-mm thick boundary clay in the palaeomagnetic G^- zone differs from the surrounding sediments in having significant colour, no biogenic calcite and different contents of rare-earth and siderophile elements, carbon and magnetic minerals. The clay also contains shocked quartz and plagioclase particles, and indicates a dramatic change in sedimentation caused by a short-lived event.

THE discovery of an iridium anomaly at the Cretaceous/Tertiary (K/T) boundary has prompted a worldwide search for complete boundary sections. In Austria, prospective areas were examined for undisturbed boundary layers marking the event at the end of the Cretaceous period. To date, among several sections visited, only the Elendgraben in the Gosau Basin has been found to contain a complete sequence of sediments 18.

We present here a brief but thorough study of the outstanding exposure at Gosau. The combination of geochemical, geomagnetic, mineralogical, palaeontological and sedimentological analyses provides a coherent and surprisingly precise picture of the events which took place at the K/T boundary. A more detailed presentation will appear elsewhere (A.P. et al., in preparation).

Methods

In the course of detailed mapping of the Upper Gosau formation, hundreds of spot samples were collected and their fossil contents (nannoflora and microfauna) examined; this allowed the position of the boundary to be accurately located. In addition, 187 oriented rock cores were drilled for magnetostratigraphic studies. All core samples were thermally cleaned at 300 °C (and some cores at 360 °C) for rock magnetic analyses. The carrier minerals of the remanence are magnetite and/or titanomagnetite, as well as haematite. The mineral composition

Grain-size analyses of the sediments were performed with a sedigraph; chemical element analyses were carried out by X-ray fluorescence. For trace element analyses, neutron activation was performed at the Atominstitut der Österreichischen Universitäten, Vienna.

Site description

In the Elendgraben, near Gosau, which is a steep creek on the western slope of the Hornspitz-Höhbühel ridge (13°28′20″ E; 47°33′23″ N), flyschoid sediments of the Zwieselalm strata are exposed at an altitude of 1235 m (Fig. 1). The outcrop contains a >30-m thick sequence of southeastward-dipping sediments (dip angle 40°; dip azimuth 140°). The flyschoid sediments consist of alternating sandstones, siltstones, limestones, marly limestones and marls, which are partly turbiditic and partly hemipelagic. The sequence of these sediments indicates sedimentation in a deep-sea environment above the calcium carbonate compensation depth (CCD)². As shown by palaeocurrent patterns, the transported material, mostly metamorphic grains, was moving from south-east to north-west³.

The remarkably well preserved K/T boundary layers lie in a 16.7-m section of the palaeomagnetic reversed G⁻ zone (chron 29-R), 12.0 m above the magnetic polarity zone F₃⁺ (top of chron

^{**} Present address: Department of Earth and Space Sciences, University of California, Los Angeles, California 90024, USA.

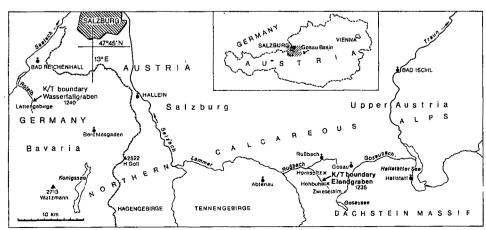


Fig. 1 Geographical position of the K/T boundary in the Elendgraben (Gosau Basin), south-east of Salzburg.

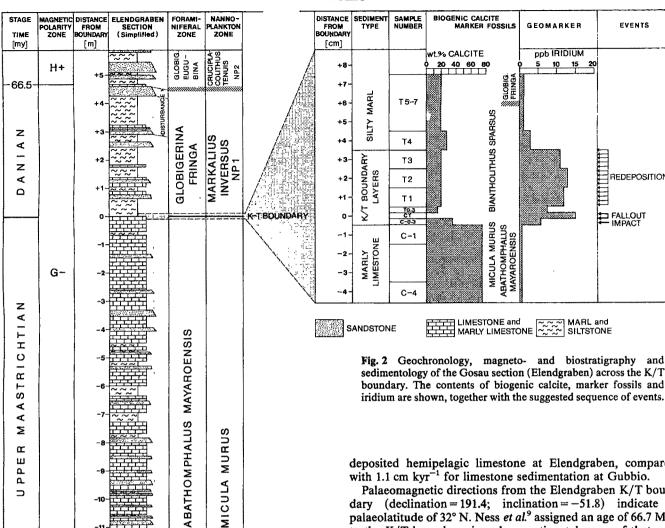
was determined by means of X-ray diffraction, microprobe analysis, optical methods and electron microscopy. The samples were decalcified by decomposition with dilute acetic acid (10%), and the carbon contents determined by microanalyses.

EVENTS

REDEPOSITION

67.0

F3+



30-N) and 4.7 m below the H⁺ (base of chron 29-N), as shown in Fig. 2. Figure 3 shows a comparison of the sediment thickness of the G-zone at Gosau (16.7 m) with those of other K/T boundary sites—such as Caravaca, Spain (16.8 m), DSDP site 524, South Atlantic (13.9 m), Stevns Klint, Denmark (8.8 m) and Gubbio, Italy (5.2 m)—which have approximately constant ratios of G⁻ (Tertiary) to G⁻ (Cretaceous)⁴⁻⁷. The overall thickness of the G zone depends on the type of sedimentation, specifically, the extent to which biogenic calcite is diluted by turbidites and/or continuously deposited terrigenous materials. The lowest sedimentation rates are found in pelagic deep-sea sediments, where the highest biogenic sedimentation rates are combined with the smallest amounts of terrigenous dilution (for example, the Gubbio G⁻ zone is only 5.2-m thick and contains 95% CaCO₃). The much greater thickness of the G⁻ zone at the Elendgraben section (Gosau) results from turbiditic and hemipelagic sedimentation. Discontinuously deposited turbidites account for ~48% of the thickness of these sediments (8.1 m); the remaining 8.6 m is taken up by hemipelagic limestone sediments containing 62% calcite (5.3 m biogenic calcite and 3.3 m terrigenic material); thus, the total amount of terrigenous material (bulk density $\approx 2.55 \text{ g cm}^{-3}$) deposited within the G zone is 8,400 kg m⁻²

The duration of the G⁻ zone is 470 kyr (ref. 8): this yields a mean sedimentation rate of 1.83 cm kyr⁻¹ for the continuously

deposited hemipelagic limestone at Elendgraben, compared with 1.1 cm kyr⁻¹ for limestone sedimentation at Gubbio.

Palaeomagnetic directions from the Elendgraben K/T boundary (declination = 191.4; inclination = -51.8) indicate a palaeolatitude of 32° N. Ness et al.9 assigned an age of 66.7 Myr to the K/T boundary; in palaeocontinental maps of that age, the Gosau Basin is shown lying within the Tethys, which at that time had open connections with an east-west circulation system 10,11 .

Biostratigraphy

Two major fossil groups showing characteristic changes at the K/T boundary were studied in detail: the calcareous nannofossils and the planktonic foraminifera (Fig. 2). In the former group, the uppermost Maastrichtian assemblage contains the marker fossil Micula murus. In the marly limestone below the K/T boundary layers (samples C-1 to C-30), the nannofossils are partly recrystallized and poorly preserved; however, in the 3 mm of grey marl (C-0.3) of the K/T boundary layers underlying the light-brown K/T boundary clay (CT), they are well preserved. The K/T boundary clay itself is practically devoid of nannofossils, although some chamber fillings of foraminifera of uncertain origin are found. The foraminiferal microfauna below the K/T boundary layers belongs to the Abathomphalus mayaroensis zone. In the few centimetres above the K/T boundary clay, some reworked Maastrichtian foraminifera were found. Reworking of nannofossils from Cretaceous to Tertiary is also demonstrated by the presence of both Maastrichtian and Campanian coccoliths, such as Aspidolithus parcus.

Two centimetres above the K/T boundary clay, there is a sharp increase (by a factor of at least 10) in the frequency of the spherical calcareous shells of the dinoflagellate Thoracosphaera operculata, which is rather rare in the Upper Maastrichtian and becomes the dominant nannoplankton species in the K/T boundary layers. Perhaps the cells of Thoracosphaera operculata had better survival chances in case of a strong reduction of photosynthesis than many other unicellular species and also

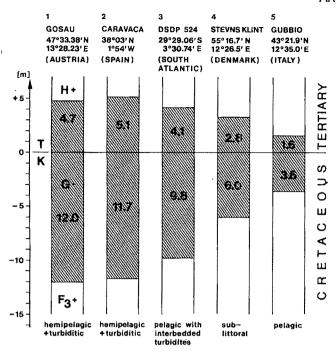


Fig. 3 Comparisons of the magnetic polarity zone G⁻ (chron 29-R) at different sites (Austria, Spain, South Atlantic, Denmark and Italy), with different types of marine deposits. The numbers above and below the K/T level indicate sediment thickness within that chron in Tertiary and Cretaceous, respectively.

had the ability to form close protective globular cysts. Biantholithus sparsus, the first Danian marker among the nannofossils (zone NP 1), is found immediately above the K/T boundary clay.

The first specimens of Globigerina fringa were discovered ~6 cm above the K/T boundary clay. In the Elendgraben outcrop, the lowest occurrences of the nannofossils Cruciplacolithus primus, C. tenuis (marking the base of the NP2 zone) and Globigerina eugubina lie very close to the change from the G⁻ to the H⁺ palaeomagnetic chron. There is strong agreement in biostratigraphical data between the Elendgraben section and equivalent sediments ~46 km away, in the Lattengebirge, Upper Bayaria¹².

Deep-sea sediments

The deep-sea sediments across the K/T boundary at the Elendgraben consist of marly limestone, K/T boundary layers and silty marl (Fig. 2), and do not contain turbidites.

The marly limestone (C-30 to C-1; thickness 30 cm) underlying the K/T boundary layers is consolidated and compact; it consists of 77% biogenic calcite (nannofossils and foraminifera), diluted by 23% non-biogenic components (quartz, feldspars consisting predominantly of oligoclase, mica, 14-Å-chlorite, smectite, illite and mixed-layer clays), the terrigenous sediments having the grain-size distribution: 3% sand, 30% silt and 67% clay. The Ir content is <0.5 p.p.b., the magnetic fraction is <0.02% and the organic carbon level is $\sim 0.1\%$.

The K/T boundary layers (C-0.3 to T3) comprise $\sim 4 \text{ cm}$ of unconsolidated and porous material. The boundary layers comprise (from base to top) 3 mm of grey marl (C-0.3), 2 mm of light-brown K/T boundary clay (CT), 3 mm of grey marl (T0.3) and another 30 mm of grey marl (T1 to T3). The mean composition of layers T1 to T3 is 20% biogenic calcite, diluted by 80% non-biogenic components (quartz, feldspars, mica, 14-Å-chlorite, smectite, illite, mixed-layer clays and kaolinite) with mean grain-size fractions: 8% sand, 54% silt and 38% clay.

The 2 mm of light-brown boundary clay (CT) has a very different chemistry and mineralogy from the rest of the sediments

(see below); notably, it contains no biogenic calcite, and displays characteristic changes in the contents of certain trace elements ('geomarkers'), which reveal an event in Earth history by a marked increase or decrease in their quantity. Because of the worldwide presence of a significant iridium peak, the middle level of this thin layer (CT) is defined as the level of the Cretaceous/Tertiary (K/T) boundary. All distances given here are referred to this level.

The silty marl (T4 to T17) above the K/T boundary layers is 13 cm thick and friable. The content of biogenic calcite lies between 20 and 27%. The non-biogenic components have nearly the same mineral composition as the Cretaceous marly limestone but coarser grain sizes.

The grain size distributions show a mean size of quartz grains of $\sim 8 \mu m$ for the Cretaceous marly limestone, and $\geq 20 \mu m$ for the Tertiary marls and silty marls.

Chemistry and mineralogy

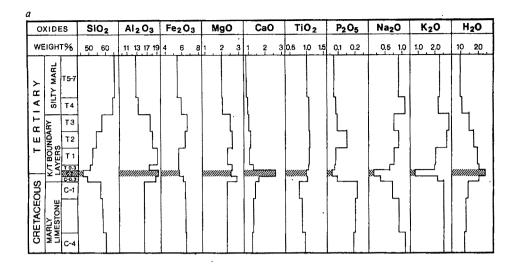
We have used a combination of X-ray fluorescence, X-ray diffraction and microprobe analysis to determine the chemical contents and mineral compositions and abundances in decalcified samples. Some trace elements were analysed by neutron activation. Figure 4 shows the results of the chemical analyses of oxides and trace elements in samples C-4, C-1, C-0.3, CT, T0.3, T1, T2, T3, T4 and T5-7 across the K/T boundary, as well as information regarding their contents of transported quartz, expandable clays, kaolinite, magnetic fraction, elemental and organic carbon.

The samples of the Cretaceous marly limestone (C-4 and C-1) and the Tertiary silty marl (T5-7) are of similar composition. In contrast to these, however, is the dramatically different composition of the K/T boundary layers (C-0.3 to T3), especially the boundary clay (CT) with its extraordinary chemical and mineral composition. The 2-mm boundary clay (CT) contains no biogenic calcite (Fig. 2); a minimum of quartz, plagioclase, mica and 14-Å-chlorite; a minimum of SiO₂, Na₂O and K₂O; relatively high amounts of kaolinite and expandable clays with high water content (Ca-smectite and mixed-layer clays); and peak values of magnetic minerals, such as exsolved ilmenite (FeTiO₃) in magnetite (Fe₃O₄), formerly titanomagnetite. The weight percentages of the authigenically formed minerals (kaolinite, Ca-smectite and mixed-layer clays) total ~94%, which, like the Ir content of 14.5 p.p.b. (parts per 10°), is a peak value. The high Ir content of the boundary clay (CT) was shown to be related to the titanium mineral and not to the magnetite. A marked increase of carbon, as determined by microanalyses, is also apparent in the K/T boundary layers.

The bulk of the 2-mm-thick boundary clay (CT) is comprised of fallout material (mainly glass and its derivates, and shocked and deformed minerals). The succeeding sequence of K/T boundary layers (T0.3 to T3) also contains reworked, transported and redeposited material, indicating different sedimentation processes.

The >20- μ m fractions of decalcified marl and clay (C -0.3 and CT) were examined for the presence of shocked particles (Fig. 5), using a polarizing microscope equipped with a universal stage, and also by means of X-ray diffraction and transmission electron microscopy (TEM). X-ray analysis shows that 70% of the fraction is quartz, the remainder consisting of feldspar and kaolinite. Whereas the quartz in the underlying Maastrichtian (C-1 and C-4) is a fine groundmass with <10% of 10- μ m clasts (undeformed to slightly deformed), the quartz of the samples C-0.3 and CT is clearly shocked. Shocked quartz was first reported at the K/T boundary in Montana¹³.

In the shocked quartz of the Elendgraben, shock features include lamellae indexed to $\{10\overline{1}3\}$, $\{10\overline{1}1\}$, $\{10\overline{1}2\}$, $\{0001\}$, $\{11\overline{2}2\}$ and $\{11\overline{2}1\}$, planar cleavages shown to be microfaults in laboratory shock specimens, symplectic material, and widespread vitrification¹⁴. Eighty-two of more than 100 grains in sample C-0.3 were identified as quartz, showing the following



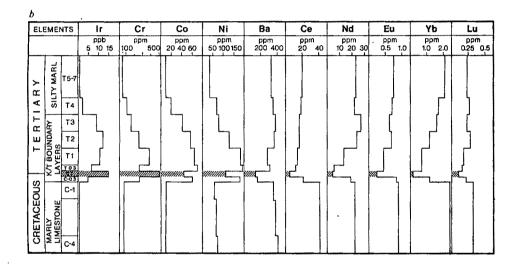
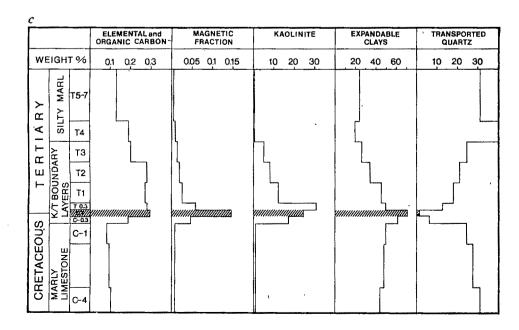
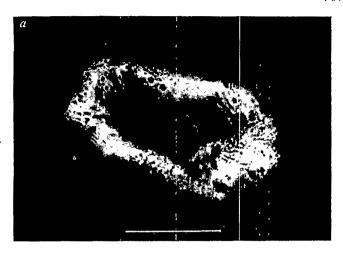


Fig. 4 Analyses of samples across the K/T boundary (Elendgraben), after decalcification. a, Distribution of major-element oxides; b, contents of trace elements (geomarkers); c, biogenic and non-biogenic material. Shaded area, K/T boundary clay (CT).





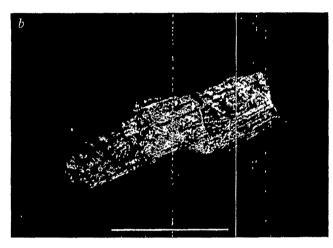


Fig. 5 Photomicrographs of minerals deformed by the K/T boundary event (Elendgraben). a, Shocked quartz grain (sample C-0.3) with lamellae; b, shocked plagioclase grain (sample C-0.3), with numerous planar features. Scale bars, $10 \mu m$.

features: 8 grains contain shock lamellae; 40 grains contain microfault sets: 26 grains contain isolated microfaults, decorated (partially annealed) microfaults, and/or planar edges; 3 grains are largely vitrified, symplectic, or melted; 3 grains show only internal fracturing; and 2 grains show no distinct signs of shock. All grains show mild to extreme undulatory extinction. These results are confirmed by TEM, which showed an enormous quantity of amorphous material; microcrystallites distributed in amorphous material; consistently planar grain edges, usually decorated with glass; planar glassy areas; and no or few dislocations. It appears that essentially all quartz grains examined are shocked and broken along shock microfaults. Furthermore, material too fine or too coarse for the survey shows a similar distribution of effects, so that the majority of 20-µm quartz—that is, approximately half of the 11% quartz from sample C-0.3—is shocked to varying degrees (Fig. 5a).

Feldspar grains show similar effects (Fig. 5b), including planar features and edges, undulatory extinction, and widespread glass in TEM. Phyllosilicates, however, have none of the distinctive shock kink bands. Material from the boundary clay (CT) is similarly shocked, but contains conglomerates of shocked grains, more rounded grains, and recrystallized material with relict microfaults and lamellae. This material was shocked and then annealed and deposited. Also, large, euhedral, twinned calcite crystals are found.

The presence of shocked particles in sediments, in connection with the mass extinction of foraminifera and nannoplankton is considered to be evidence for an extraordinary event. Furthermore, the enrichment of geomarkers such as Ir, Cr, Co and Ni, and the depletion of geomarkers such as Ba and the rare-earth elements (Fig. 4), indicate that the event marking the K/T boundary could be caused by an impact of an asteroid of nearly chondritic composition, as suggested previously^{15,16}. The mass of such an asteroid can be estimated from the total amount of excess Ir deposited in the K/T boundary layers. Such a calculation¹⁷ yields a diameter of >8 km, which is in agreement with data in ref. 1. The shocked quartz and plagioclase, the rock fragments, the Ca-smectite, the twinned calcite crystals, the excess of Mg and Ca ions in the K/T boundary layers, and the global distribution of a large amount of chondritic material indicate that the event was initiated in the ocean. The amount of the crater material that was ejected into the atmosphere after the impact and distributed across the globe can be calculated from the fallout and its derivatives (kaolinite, mixed-layer clays and Ca-smectite), plus the amounts of reworked and redeposited

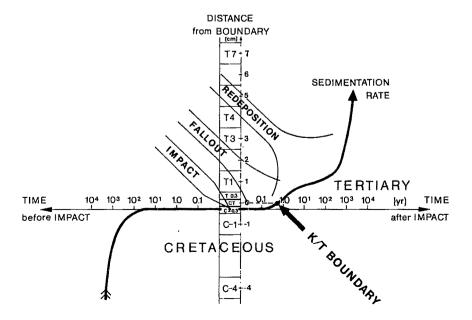


Fig. 6 Time structure of the event at the end of the Cretaceous period: sediment thickness (linear scale) is plotted against time before and after impact (logarithmic scale). Periods of impact, fallout and redeposition are indicated, as is the K/T boundary (defined by the Ir peak).

material¹⁷. This amount deposited as a compact sediment layer across the globe corresponds to a thickness of ~9 mm.

Conclusions

The distribution of the geomarkers and the mineral components (Figs 2, 4) in the K/T boundary layers (C-0.3 to T3) suggests that there was a short period of 'fallout', followed by a redeposition of the fallout material over a longer period of time. On the basis of the analyses given here, Eder and Preisinger¹⁷ have concluded that the time required for the deposition of the K/T boundary layers was much shorter than for any other layers in the sequence. As shown in Fig. 6, where sediment thickness is plotted on a linear and time on a logarithmic scale, the impact itself (t=0) occurred within layer C-0.3 and is not identical with the K/T boundary indicated within layer CT. This is consistent with the idea that the material ejected into the atmos-

Received 10 February; accepted 19 June 1986.

- Alvarez, L. W., Alvarez, W., Asaro, F. & Michel, H. V. Science 208, 1095-1108 (1980).
 Faupl, P. Mitt. Ges. geol. Bergb. Öst. 25, 81-110 (1978).
 Lahodynsky, R. Verh. geol. Bundesanst., Wien, 109-110 (1979).
 Smit, J. Spec. Pap. geol. Soc. Am. 190, 329-352 (1982).
 Hsü, K. J., McKenzie, J. A. & He, Q. H. Spec. Pap. geol. Soc. Am. 190, 317-328 (1982).
 Mörner, N.-A. J. Geol. 90, 564-573 (1982).
- Roggenthen, W. M. & Napoleone, G. Geol. Soc. Am. Bull. 88, 378-382 (1977).
- La Breque, J. L., Kent, D. V. & Cande, S. C. Geology 5, 330-335 (1977). Ness, G., Levi, S. & Couch, R. Rev. Geophys. 18, 753-770 (1980).

phere returned to the Earth over a period of time, which would explain why the Ir peak is not synchronous with the impact.

The combination of the analytical results and the time-structure analysis of the K/T event suggest that, 66.7 Myr ago, an impact of an asteroid took place, producing a worldwide geochemical and mineralogical anomaly within a very short stretch of time and causing conditions for mass extinctions of large quantities of biota.

We thank Doz. Dr G. Kurat and Dr F Brandstätter (Museum for Natural History, Wien) for microprobe analyses, Dr P. Pongratz (Institute for Applied Physics of the Technical University, Wien) for transmission electron microscopy, Dr J. Zak (Microanalytical Laboratory of the University, Wien) for carbon microanalyses, the Research Center Seibersdorf, Austria, for radiation time and the Fonds zur Förderung der wissenschaftlichen Forschung in Österreich (FWF) for financing part of the nannoplankton research (project no. 2659).

- Smith, A. G., Hurley, A. H. & Briden, J. C. in Phanerozoic Palaecontinental World Maps (Cambridge University Press, 1981).
 Haq, B. U. Oceanol. Acta 71-82 (1981).
 Herm, D., von Hillebrandt, A. & Perch-Nielsen, K. Geologica bav. 82, 319-344 (1981).
 Bohor, B. F., Fodrd, E. E., Modreski, P. J. & Triplehorn, D. M. Lunar planet. Sci. 15, 74-75

- 14. Gratz, A. J. J. Noncryst. Solids 67, 543-558 (1984).
- Smit, J. & Ten Kate, W. G. H. Z. Crettac Res. 3, 307-332 (1982).
 Hsü, K. J. Patterns of Change in Earth Evolution, 63-74 (Springer, Berlin, 1984)
- 17. Eder, G. & Preisinger, A. Naturwissenschaften (in the press).
 18. Stradner, H. et al. Terra Cognita 5, 247 (1985).

Tight linkage between a splicing mutation and a specific DNA haplotype in phenylketonuria

Anthony G. DiLella*, Joshua Marvit*, Alan S. Lidsky*, Flemming Güttler* & Savio L. C. Woo*

* Howard Hughes Medical Institute, Department of Cell Biology and Institute of Molecular Genetics, Baylor College of Medicine, One Baylor Plaza, Houston, Texas 77030, USA † John F. Kennedy Institutiet, Gl. Landevej 7, DK-2600 Glostrup, Denmark

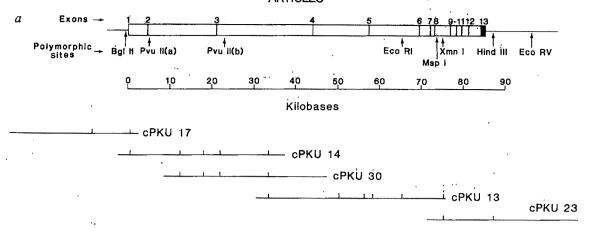
The first phenylketonuria mutation identified in the human phenylalanine hydroxylase gene is a single base substitution (GT→AT) in the canonical 5'-splice donor site of intron 12. Direct hybridization analysis using specific oligonucleotide probes demonstrates that the mutation is tightly associated with a specific restriction fragment-length polymorphism haplotype among mutant alleles. The splicing mutation is the most prevalent phenylketonuria allele among Caucasians, and the results suggest the possibility of detecting carriers of the genetic trait who have no family history of phenylketonuria.

CLASSICAL phenylketonuria (PKU) is an autosomal recessive human genetic disorder caused by a deficiency of hepatic phenylalanine hydroxylase (PAH, phenylalanine 4-monooxygenase, EC1.14.16.1). In the normal human liver, PAH catalyses the rate-limiting step in the hydroxylation of phenylalanine to tyrosine. The reduction in PAH activity causes an accumulation of serum phenylalanine, resulting in hyperphenylalaninaemia and abnormalities in the metabolism of many compounds derived from the aromatic amino acid. PKU is the most common inborn error in amino-acid metabolism. Its incidence among Caucasians ranges from 1:4,500 in Ireland to 1:16,000 in Switzerland, with an average incidence of about 1:8,000 in the United States. The mutant gene frequency is such that 1 in 50 Caucasians is a carrier of the disease trait. Without early detection of PKU, followed by rigid implementation of a restricted diet low in phenylalanine during the first decade of life, affected

children develop severe mental retardation (for reviews see ref.

Although neonatal screening for PKU is routinely carried out in Western countries, there has been no conventional means of identifying affected fetuses. We used a full-length human PAH complementary DNA clone⁴ to identify and map eight restriction fragment-length polymorphisms (RFLPs) at the human PAH locus⁵⁻⁷. These RFLPs segregate in a mendelian manner and concordantly with the mutant alleles in PKU kindreds. The frequency of the RFLPs in the PAH gene is such that the observed heterozygosity in the general population is about 87% (ref. 8). Thus, prenatal diagnosis can be performed in most PKU families by RFLP analsis9. However, the analysis is limited in that it can only be used in families with a history of PKU.

We recently used RFLPs to identify 12 haplotypes of normal and PKU alleles in the Danish population, and observed a h



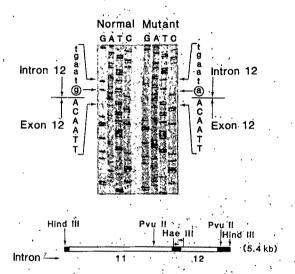


Fig. 1 Identification of a PKU splicing mutation. a, Physical map of the mutant gene. The maps of five overlapping cosmid clones (cPKU 17, cPKU 14, cPKU 30, cPKU 13 and cPKU 23) were used to characterize the mutant gene. The subcloned EcoRI fragments containing exon sequences were used for Sanger dideoxynucleotide sequence analysis as described previously for the normal PAH gene? The detailed structure of the mutant gene in the 5' to 3' orientation and the location of RFLP sites are also shown. The cosmid library construction and gene characterization were carried out as described previously. b, Sequence analysis of the 5'-donor splice site of exon 12. The 114-base-pair (bp) HaeIII fragment (bottom) containing 90 bp of exon 12 and 24 bp of the downstream intron was inserted into the SmaI site of M13mp18¹⁹ and sequenced in both directions (arrows) by the dideoxynucleotide chain-termination method 18. A comparison of the normal and mutant sequence at the intron/exon border illustrates the single base substitution.

strong association among distinct RFLP haplotypes and PKU alleles. A close association has been observed previously between RFLP haplotypes of the β -globin locus and specific β -thalassaemia mutations in different ethnic populations (for review see ref. 10). Whether such tight association between RFLP haplotypes and specific mutations exists in PKU due to linkage disequilibrium can be verified only by molecular analysis of the mutant genes. Having established the molecular structure and RFLP haplotype linkage map of the PAH gene⁷, this important issue can be addressed by cloning and characterizing the mutant PAH alleles of the prevalent RFLP haplotypes.

Isolation and sequencing of a mutant PAH gene

RFLP haplotypes for both PKU and normal PAH genes have been determined for 33 informative Danish PKU families. About 75% of the normal and 90% of the mutant PAH genes are confined to four common RFLP haplotypes (Table 1; haplotypes 1, 2, 3 and 4). Thirty-eight percent of the mutant alleles have a single haplotype (haplotype 3) that is relatively rare among the normal gene pool (3%). A cosmid genomic

DNA library was thus constructed from leukocyte DNA isolated from a PKU individual who is homozygous for haplotype 3. The library was screened with a full-length human PAH cDNA probe⁴ and several corresponding genomic clones were isolated (Fig. 1a). To identify the mutation causing PKU, exoncontaining regions of the gene were subcloned into the vector M13mp18 for sequence analysis. The mutant gene sequence is identical to that of the normal PAH gene reported previously⁷ except for a silent nucleotide substitution ($A \rightarrow G$) in the third base of codon 232 ($G\ln$)⁴⁻⁷, and a G to A transition at the 5' splice donor site of intron 12, altering the obligatory G-T donor dinucleotide to A-T (Fig. 1b). Gene transfer and expression experiments demonstrated that this mutation results in abnormal processing of PAH mesenger RNA and loss of PAH activity (J.M. et al., unpublished results).

Design and testing of probes

Figure 2b shows the nucleotide sequence at the mutation site in the gene; this did not result in any alteration in restriction recognition sequence from the normal PAH gene. Since a single base-pair mismatch is sufficient to destabilize duplex structures

Table 1 RFLP haplotype distribution of the PAH alleles in Denmark

	Normal	alleles	Mutant alleles		
Haplotypes	Number*	%	Number*	%	
1	23	34.8	12	18.2	
2	3	4.6	13	19.7	
3	2	3.0	25	37.9	
4	21	31.8	9	13.6	
5	7	10.6	0	0	
6	0	0	2	3.0	
7	7	10.6	1	1.5	
8	1	1.5	0	0	
9	0	0	1	1.5	
10	1	1.5	0	0	
11	1	1.5	1	1.5	
12	0	0	2	3.0	

* Number of alleles observed in a total of 66 chromosomes analysed. All tested families were Caucasian and had no history of consanguinity. Clinical criteria of the probands as affected PKU individuals and parents as heterozygotes in the families have been reported previously¹⁵.

in DNA hybrids^{11,12}, oligonucleotide probes can be used to distinguish between normal and mutant alleles in the human genome. Thus, we synthesized a normal-specific probe (21-mer) which is complementary to the sense-strand of the normal gene (Fig. 2b) and forms a C-A mismatch at the mutation site with the mutant gene. For the mutant-specific probe, a 21-mer of the sense-strand sequence was synthesized. At the mutation site this probe forms a C-A mismatch with the normal gene sequence (Fig. 2b).

The fidelity of the two oligonucleotide probes in detecting the respective sequences was then tested using the normal and mutant genomic DNA clones. Due to the high A+T contents of the normal and mutant probes (76% and 81%, respectively), we used the base-composition-independent oligonucleotide hybridization method^{13,14} to analyse the point mutation. *PvuII* digestion of the 12-kilobase (kb) *EcoRI* fragment isolated from both the normal (N) and mutant (M) gene clones generated a 2-kb fragment containing the entire exon 12 plus flanking intronic sequences. Under the hybridization conditions used, the normal probe hybridized only to the 2-kb *PvuII* fragment of the normal gene (Fig. 2a, middle panel), and the mutant probe hybridized specifically to the mutant gene (Fig. 2a, right panel).

Mendelian segregation of PAH alleles

Using the appropriate hybridization conditions described in Fig. 2 legend, the synthetic oligonucleotide probes were used to identify the mutant alleles in genomic DNA and to analyse their segregation in PKU kindreds. The first family analysed was the one from which the mutant allele had been isolated and characterized. In this family, both parents contain a mutant haplotype 3 gene which hybridized to the mutant probe (Fig. 3a, lanes 1, 2), suggesting that both mutant alleles in this family may contain the same mutation. Since this disorder is autosomal recessive in nature, both parents are obligate carriers of the PKU trait and both must also contain a normal gene. In this case, both normal alleles in the two parents corresponded to haplotype 4, and both hybridized to the normal probe as expected (Fig. 3a, lanes 7, 8). There are two affected individuals in this family; both are homozygous for the mutant haplotype 3 alleles which hybridized strongly to the mutant probe (Fig. 3a, lanes 3, 4), but not to the normal probe (Fig. 3a, lanes 9, 10).

The results confirm that both mutant alleles in this family contain the same mutation. An unaffected sibling in this family is homozygous for the normal haplotype 4 alleles which hybridized to the normal probe (Fig. 3a, lane 11) but not to the mutant

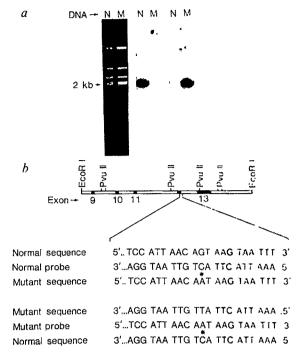


Fig. 2 Oligonucleotide specificity for the detection of the PKU mutation in cloned DNA by direct-gel hybridization. a, The 12-kb EcoRI fragment containing exons 9 to 13 was isolated from normal (N) (ref. 7) and mutant (M) cosmid clones and inserted into plasmid pBR322. PvuII plus EcoRI digests of the recombinant clones were electrophoresed on 1% agarose gels, stained with ethidium bromide (left panel), and processed for direct-gel hybridization as described previously11. Dried gels were hybridized to oligonucleotide probes specific for normal (middle panel) and mutant (right panel) cloned PAH genomic DNA sequences. Exon 12 plus flanking intronic sequences are contained in a 2-kb Prull fragment. The gels were overexposed intentionally in order to demonstrate the differential hybridization signals generated by the two oligonucleotide probes. b, Oligonucleotide probes used to detect the normal and mutant 5'-donor splice site of exon 12. The asterisks denote the C-A mismatch between the normal probe and mutant gene sequence, and the mutant probe and normal gene sequence.

Methods. Oligonucleotides were synthesized by an automated (SYSTEC, Inc.) solid-phase phosphite triester method. High specific activity probes (1010 c.p.m. µg-1) were generated by the primer extension method¹². The normal probe was synthesized on a 21-base template (5'-TCCATTAACAGTAAGTAATTT-3') by hybridized 9-base primer (3'-TTCATTAAA-5'), while the mutant probe was synthesized by extension of a 9-base primer (5'-TCCAT-TAAC) hybridized to a 21-base template (3'-AGGTAATTGTTATTCATTAAA-5'). Dried gels were hybridized overnight at 37 °C in 6×NET (0.9 M NaCl, 6 mM EDTA, 0.5% SDS and 0.09 M Tris, pH 7.5) containing 0.2 mg of salmon sperm DNA and 2×106 c.p.m. of probe per ml of hybridization solution¹⁴. The gel membranes were then washed twice at 0 °C for 30 min in TMA (3 M tetramethylammonium chloride (Aldrich), · 2 mM EDTA and 50 mM Tris pH 8.0), once each at 23 °C (30 min) and 60 °C (7 min) in TMA containing 0.2% SDS, and at 23 °C for 30 min in TMA¹⁴. The gel strips were then autoradiographed between two Quanta III intensifier screens (Dupont) at -80 °C.

probe (Fig. 3a, lane 5). As expected, a second unaffected sibling in this family who is heterozygous for mutant haplotype 3 and normal haplotype 4 alleles hybridized to both the mutant and normal probes (Fig. 3a; lanes 6 and 12, respectively). Thus the oligonucleotide hybridization analysis not only was able to detect the specific mutation in genomic DNA, but also demonstrated concordant segregation of the normal and mutant alleles in this PKU family.

To verify that the mutation is not a constitutive part of the normal haplotype 3 allele, we analysed a PKU family possessing

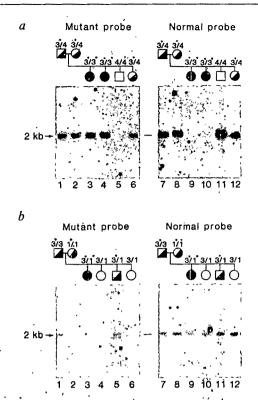


Fig. 3 Oligonucleotide hybridization analysis of two Danish PKU families. In both families, the probes used for lanes 1-5 and lanes 7-12 were the mutant and normal oligonucleotides, respectively. Squares, male; circles, female; open symbols, normal haplotype; solid symbols, mutant haplotype; a, Lanes 1 and 7, father; lanes 2 and 8, mother; lanes 3, 4, 9, 10, two affected children; lanes 5, 6, 11, 12, two unaffected children, b, lanes 1 and 7, father; lanes 2 and 8, mother; lanes 3 and 9, proband; lanes 4-6 and 10-12, three unaffected siblings. DNA was isolated from leukocytes of family members, digested with PvuII and analysed by dried-gel hybridization as described in Fig. 2 legend. The segregation of the PKU alleles (*) and the appropriate RFLP haplotypes are shown at the top of each autoradiograph.

both normal and mutant haplotype 3 alleles. The father in this family, who is homozygous for haplotype 3 but an obligate carrier of the PKU trait, possesses a mutant haplotype 3 allele which hybridized to the mutant probe (Fig. 3b, lane 1) and a normal haplotype 3 allele which hybridized to the normal probe (Fig. 3b, lane'7). The results demonstrated conclusively that the splicing mutation is not a constitutive part of the normal haplotype 3 alleles per se. In contrast, the mother possesés normal and mutant haplotype 1 PAH alleles. The mutant probe did not hybridize to DNA isolated from this individual (Fig. 3b, lane 2), while the normal probe did (Fig. 3b, lane 8). The data indicate that the PKU mutation associated with the haplotype 1 allele in this family is not the same as that identified in the mutant haplotype 3 allele. The proband in this family, having inherited a mutant haplotype 3 allele from the father and a mutant haplotype I allele from the mother, hybridized to both the mutant and normal probes (Fig. 3b, lanes 3, 9). This individual apparently contains two different mutant alleles and is thus a compound heterozygote.

Carrier detection by oligonucleotide analysis

Our hybridization analysis of the above family also illustrated the feasibility of using the mutant probe to detect carriers of the PKU trait. There are three phenotypically normal siblings in addition to the proband in that family. Since both parents are haplotype homozygotes (1/1 and 3/3), all offspring are haplotype heterozygotes (1/3) and the RFLP haplotype analysis is therefore totally non-informative. The observed 'normal'

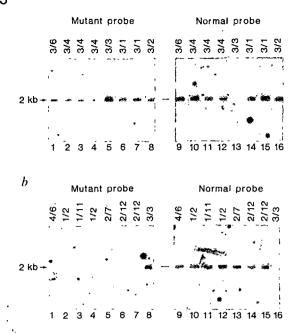


Fig. 4 Oligonucleotide hybridization analysis of Danish PKU individuals of defined RFLP haplotypes. DNA was isolated from leukocytes of PKU individuals and analysed using mutant (lanes 1-8) and normal (lanes 9-16) oligonucleotide probes as described in Fig. 2 legend. a, Haplotype 3 genotypes; b, non-haplotype 3 genotypes. The previously characterized RFLP haplotypes are shown at the top of each lane.

phenotypes in the unaffected siblings can result from three genotypes: normal haplotype 3/normal haplotype 1; mutant haplotype 3/normal haplotype 1; and mutant haplotype 1/normal haplotype 3. These genotypes can be partially distinguished by direct analysis of the splicing mutation site within the gene. DNA from one of the siblings hybridized to the mutant oligonucleotide (Fig. 3b, lane 5), suggesting that this individual has inherited the mutant haplotype 3 allele from his father and the normal halplotype 1 allele (Fig. 3b, lane 11) from his mother, and must therefore be a carrier of the PKU trait. In the absence of information for the haplotype 1 mutant gene sequence, the carrier status of the other two siblings cannot yet be fully determined. Nevertheless, the possibility that they have also inherited the mutant haplotype 3 allele from their father is excluded by the negative hybridization data obtained with the mutant oligonucleotide probe (Fig. 3b, lanes 4, 6).

Mutation frequency and haplotype association

We next determined the frequency of the splicing mutation and the degree of its association with haplotype 3 in the Danish population. RFLP haplotype analysis of 33 informative PKU families (66 normal and 66 mutant PAH chromosomes) provided a repertoire of mutant alleles for such an analysis (Table 1). Genomic DNA samples isolated from all PKU individuals containing a mutant haplotype 3 allele hybridized to the mutant probe (Fig. 4a, lanes 1-8). One PKU individual possesses two copies of the mutant haplotype 3 allele, and his DNA hybridized more strongly to the mutant probe (Fig. 4a, lane 5). The results suggested that all mutant haplotype 3 alleles in Denmark contain the same mutation in the PAH gene.

Although the homozygous haplotype 3 patient showed no hybridization with the normal probe as expected (Fig. 4a, lane 13), the normal probe did hybridize to all mutant alleles in the remaining individuals who possess non-haplotype 3 chromosomes (Fig. 4a, lanes 9-12, 14-16). Another group of PKU individuals possessing various non-haplotype 3 mutant alleles were also analysed. DNA isolated from these individuals did not hybridize to the mutant probe (Fig. 4b, lanes 1-7), while

Table 2 Association of splicing mutation with mutant haplotype 3 alleles in Denmark

	Mutant analy		Normal probe analysis*			
Haplotypes	Normal	PKU	Normal	PKU		
1	0/5	0/10	5/5	10/10		
2	ND	0/12	ND	12/12		
3	0/2	23/23	2/2	0/23		
4	0/6	0/8	6/6	8/8		
5	0/1	0	1/1	0		
6	Ó	0/2	Ö	2/2		
7	0/2	0/1	2/2	1/1		
8	0/1	Ô	1/1	0		
9	Ó	0/1	0	1/1		
10	0/1	0	1/1	Ô		
11	ND	0/1	ND	1/1		
12	0	0/2	0	2/2		

ND, not determined due to lack of DNA samples.

strong hybridization signals were obtained with the normal probe (lanes 9-15). As controls in these experiments, we included DNA isolated from a homozygous haplotype 3 PKU individual: this hybridized to the mutant probe (Fig. 4b, lane 8) but not to the normal probe (lane 16). Our experiments strongly suggest that the mutations in all non-haplotype 3 alleles are distinct from the G-T to A-T transition mutation present in the mutant haplotype 3 allele.

Table 2 summarizes the population genetic data. A total of 91% (60 out of 66) of the available PKU chromosomes and 27% (18/66) of the available normal chromosomes were analysed with the mutant and normal oligonucleotide probes. All mutant haplotype 3 alleles hybridized with the mutant probe and none hybridized with the normal probe (Table 2). The remaining mutant alleles of other haplotypes and all of the normal alleles hybridized specifically with the normal probe. The results demonstrate unambiguously that the splicing mutation is specifically associated with the mutant haplotype 3 alleles, and the association is both inclusive and exclusive.

Discussion

Although PKU appears to be a heterogeneous disorder at the clinical level, controversy has persisted over whether this heterogeneity results from multiple mutations in the PAH gene varying in their degree of severity (for review see ref. 15). We recently reported that the cause of the disease must be heterogeneous because PAH mRNA was detected in some, but not all, PKU liver biopsy specimens¹⁶. Liver-specific expression of the PAH gene in man and the general lack of hepatic tissues of sufficient quantity and quality has precluded study of the molecular basis of PKU at the mRNA and protein levels. Having recently established the normal PAH gene structure, however, PKU mutations can be identified at the genomic DNA level by characterization of the mutant genes.

Extensive RFLP halplotype analysis of the PAH locus in the

Danish population provided the theoretical basis for selection of mutant alleles for molecular characterization. It is interesting that 90% of the PKU genes in the Danish population are confined to four common haplotypes. We have reported here the molecular cloning of a mutant PAH gene associated with haplotype 3, which comprises 38% of all mutant alleles in the Danish population. Sequence analysis of this gene demonstrated a single base substitution at the 5' splice donor site of intron 12. Expression studies using the mutant sequence has demonstrated that the mutation causes aberrant RNA splicing by skipping exon 12 in the mature mRNA, and the mRNA is translated into a truncated protein product that is unstable in the cell (J.M. et al. unpublished results). DNA hybridization analysis using an oligonucleotide probe specific for the genetic lesion demonstrated an absolute association of this mutation with the mutant haplotype 3 alleles in the Danish population. The results strongly suggest that the G-T to A-T mutation occurred relatively recently on a normal haplotype 3 gene and spread in the Danish population by a founder effect. In addition, the specific mutation is not present in mutant alleles of other haplotypes, providing unambiguous evidence that there are multiple and distinct mutations in the PAH gene which are reponsible for PKU.

Since PKU frequency among Caucasians is the highest in Ireland and progressively less prevalent throughout northern and southern Europe, it has been proposed that the PKU allele is of Celtic origin and spread to various European populations¹⁷ Using the mutant-specific probe to analyse DNA samples of PKU kindreds from various European countries, we have obtained preliminary evidence that the splice donor site mutation of intron 12 is also present in England, Ireland, Scotland, Switzerland and Italy (data not shown). In those families that are informative for RFLP haplotype analysis, the association between the specific mutation and RFLP haplotype 3 is also preserved in these populations. Thus, the data suggest the spread of a single mutant haplotype 3 chromosome in the Caucasian race by founder effect.

The future characterization of PKU mutations arising on the other prevalent haplotypes (haplotypes 1, 2 and 4) will clarify whether PKU is caused by a limited number of mutations that spread throughout the Caucasian race or whether multiple PKU mutations arose independently in various population backgrounds. Such a study will provide insight into the evolution and molecular origin of mutations in the PAH gene which cause PKU. If such studies confirm our hypothesis regarding the linkage of specific mutations and RFLP haplotypes in the PAH locus, it should be possible to design a cassette of oligonucleotide probes to detect 90% of the mutation chromosomes in the Caucasian population and provide a potential molecular means for PKU carrier detection in individuals with no family history of PKU.

We thank Ms Kelly Brayton for technical assistance, Mr David Nunn for the synthesis of specific oligonucleotides, and Ms Kelly Porter for typing the manuscript. This work was partially supported by NIH grant HD-17711 to S.L.C.W., who is also an Investigator of the Howard Hughes Medical Institute. A.G.D. is the recipient of NIH postdoctoral fellowship HD-06495.

Received 19 May; accepted 23 June 1986.

^{*} Number of hybridizing alleles/number of genes analysed.

^{1.} Scriver, C. R. & Rosenberg, L. E. (eds) in Amino Acid Metabolism and Its Disorders 290-337

⁽Saunders, Philadelphia, 1973).
Scriver, C. R. & Clow, C. L. New Engl. J. Med. 303, 1336-1343 (1980).
Scriver, C. R. & Clow, C. L. A. Rev. Genet. 14, 179-202 (1980).
Kwok, S. C. M., Ledley, F. D., DiLella, A. G., Robson, K. J. H. & Woo, S. L. C. Biochemistry

<sup>24, 556-561 (1985).

5.</sup> Woo, S. L. C., Lidsky, A. S., Güttler, F., Chandra, T. & Robson, K. J. H. Nature 366, 151-155 (1983).

^{6.} Lidsky, A. S. et al. Am. J. hum. Genet. 37, 619-634 (1985).

^{7.} DiLella, A. G., Kwok, S. C. M., Ledley, F. D., Marvit, J. & Woo, S. L. C. Biochemistry 25, 743-749 (1986).

^{8.} Chakraborty, R. et al. Proc. natn. Acad. Sci. U.S.A. (in the press).

Chakraborty, R. et al. Proc. natn. Acad. Sci. U.S.A. (in the press).
 Lidsky, A. S., Güttler, F. & Woo, S. L. C. Lancet 1, 549-551 (1985).
 Orkin, S. H. & Kazazian, H. H. A. Rev. of Genet. 18, 131-172 (1984).
 Kidd, V. J., Wallace, R. B., Itakura, K. & Woo, S. L. C. Nature 304, 230-234 (1983).
 Studencki, A. B. & Wallace, R. B. DNA 3, 7-15 (1984).
 Wood, W. I., Gitschier, J., Lasky, L. A. & Lawn, R. M. Proc. natn. Acad. Sci. U.S.A. 82, 1505 (1984). 1585-1588 (1985).

^{14.} DiLella, A. G. & Woo, S. L. C. Meth. Enzym. (in the press).

Güttler, F. Acta paediat., Stockh. Suppl. 280, 7-80 (1980).

DiLella, A. G., Ledley, F. D., Rey, F., Munnich, A. & Woo, S. L. C. Lancet 1, 160-161 (1985).
 Woolf, L. I. J. Ir. med. Ass. 69, 398-401 (1976).

Sanger, F., Nicklen, S. & Coulson, A. R. Proc. natn. Acad. Sci. U.S.A. 74, 5463-5467 (1977).
 Messing, J. Meth. Enzym. 101, 20-78 (1983).

^{20.} DiLella, A. G. and Woo, S. L. C. Meth. Enzym. (in the press).

Effect of gravitational lenses on the microwave background, and 1146+111B,C

Jeremiah P. Ostriker* & Ethan T. Vishniac†

* Princeton University Observatory, Princeton, New Jersey 08544, USA † Astronomy Department, University of Texas, Austin, Texas 78712, USA

We suggest a simple check of the proposal by Turner et al. that the pair of quasars 1146+111B,C are, in fact, two images of the same object lensed by an intervening object. If the lens is a cluster, either of normal galaxies or of dark matter, the microwave background seen through the cluster will be distorted by the Zeldovich-Sunyaev effect at the 10⁻³ level.

A new and exceptional candidate for an astronomical gravitational lens system has been found by Turner et al.1. Two quasars separated on the sky by 157 arcs have very similar spectra and redshifts agreeing to within 100 km s⁻¹. If confirmed by further observations, this would be by far the largest angular splitting observed. Galaxies in clusters will typically produce a splitting of ~3 arcs (ref. 2), not far from the average of the six known systems, which is 4 arc s. As the splitting angle is proportional to $(v_{\parallel}/c)^2$, where v_{\parallel} is the internal one-component velocity dispersion and c is the velocity of light, clusters of galaxies can produce far larger splittings. In fact, on this basis Paczynski³ proposed that the 1146+111B,C pair might be such a lens system before the recent observations.

This system, if it is a gravitational lens, may have been produced by a massive black hole⁴ or by a cosmic string⁵, but it is worth exploring the more conventional possibility that it arises from an intervening cluster of matter. We now show that, if a cluster has acted as a gravitational lens, it is essentially guaranteed that it will also produce an observable Zeldovich-Sunyaev effect. The new lens system corresponds to a very large and detectable effect. This is not surprising, as typical clusters can produce a nearly detectable effect, and this lens system would require an unusual cluster.

Turner et al.² showed that, under normal circumstances, the production of a double image requires a projected mass distribution (on the plane of the sky) greater than Σ_c , where for a universe with density parameter $\Omega_0 = 1$

$$\Sigma_{c} = \frac{cH_0}{8\pi G} \frac{x^2(y^{1/2} - 1)}{(y^{1/2} - x^{1/2})(x^{1/2} - 1)}$$
(1)

where $y = 1 + z_Q$ and $x = 1 + z_L$ are the redshifts of the quasar and the lens, respectively, $H_0 = 100h \text{ km s}^{-1} \text{ Mpc}^{-1}$ is the Hubble constant, and G is the universal gravitational constant. This surface density is of order 1 g cm^{-2} , and thus the optical depth to electron scattering (τ_{es}) is likely to be significant for all gravitational lens systems. If the ratio of baryonic mass to total mass is f_b , and the matter in the lens has normal composition, and is ionized, then

$$\tau_{\rm es,c} = 0.35 f_{\rm b} h \Sigma_{\rm c} \tag{2}$$

so that, if $\Sigma > \Sigma_c$, then $\tau_{\rm es} > \tau_{\rm es,c} \simeq 1$. The angular splitting $(\Delta \theta)$ for an isothermal distribution of mass is, for the chosen cosmology²,

$$\Delta\theta = (v_{\parallel}/c)^2 8\pi \frac{y^{1/2} - x^{1/2}}{x^{1/2}(v^{1/2} - 1)}$$
 (3)

For an isothermal sphere with gas in equilibrium with the same distribution as the gravitating mass, $v_{\parallel}^2 = C_s^2$, where c_s is the speed of sound, we will take as a general result that

$$c_{\rm s}^2 \equiv \beta v_{\parallel}^2 \tag{4}$$

Finally, the Zeldovich-Sunyaev effect for temperature fluctuations in the microwave background can be written as

$$\Delta T/T = -2.2 \times 10^3 c_{\rm s}^2 / c^2 \tau_{\rm es} \tag{5}$$

in the long-wavelength limit.

Combining equations (1)-(5) we obtain

$$|\Delta T/T| \ge |(\Delta T/T)c| = 1.78 f_b \beta \Delta \theta h g(x, y)$$
 (6)

where

$$g(x, y) = \frac{x^{5/2}(y^{1/2} - 1)^2}{(y^{1/2} - x^{1/2})^2(x^{1/2} - 1)}$$

For the case at hand, y = 2.01. The minimal value of g(x, y) occurs, for a fixed quasar position y, at $x = [y^{1/2} + 3/4 - ((4y^{1/2} +$ $(3)^2 - 40y^{1/2})^{1/2}/4$. In this case this is x = 1.20, which gives a value of g(x, y) = 27.8. Therefore, for the system 1146 + 111B,C where $\Delta\theta = 157$ arcs, we find

$$|\Delta T/T| \ge 0.038\beta f_{\rm b}h\tag{7}$$

From light-element nucleosynthesis, the fraction of the critical density contributed by baryons, $\Omega_b \approx 0.03 \ h^{-2}$ (ref. 6), so that if $f_b = \Omega_b$, then $|\Delta T/T| = 1.2 \times 10^{-3} \beta/h^{-2}$, which should definitely be detectable. For the more likely value of x = 1.5, the numerical coefficient is larger by a factor of ~ 1.77 .

This calculation has assumed that the cluster has the shape of an isothermal sphere. Is this a fair assumption? The relationship between the angular splitting and the surface density of material is relatively insensitive to the shape of the cluster. However, if the cluster is elongated towards the observer, then the integrated electron pressure is no longer simply related to the angular splitting. This is the significance of the factor β in our calculation. Assuming we are observing lensing due to a prolate spheroid pointed at us with an axis ratio <1, then β is roughly proportional to the value of the axis ratio. For an average lens system we can be confident that this will not greatly lower our estimate of the induced temperature distortion. For the particular case of 1146+111B,C we have no basis on which to constrain the axis ratio.

Suppose that the region has, for some reason, excluded gas, or that the gas has been kept cold, or that f_b is in fact quite small. In this case, there will be no electrons in the intracluster gas and therefore no Zeldovich-Sunyaev effect. There will still be an effect on the microwave background due to the mass concentration. This is due to purely gravitational effects on the background photons as they traverse the lens system. This effect is approximately given by $|\Delta T/T| = (\Delta \theta)^2$ (see ref. 7), which in this case gives a temperature distortion of $\sim 6 \times 10^{-7}$. This is smaller than present limits on detectability.

We see that an unusual cluster of a normal type would produce a large effect. Even if the cluster were made of dark matter without galaxies, but contained baryons in a normal ratio, the effect would be undiminished. In the unlikely event that the cluster were devoid of hot gas or of some very unusual shape so that the normal effect were absent, there would still be an effect not far below our present ability to look for temperature distortions. These results suggest that the microwave background at the lens system 1146+111B,C, and any other lens candidates with large separations, necessarily provide us with an independent way of confirming their status as gravitational lenses.

We thank Edwin L. Turner for helpful comments. This work was supported by NSF grant AST-8451736 and NASA grant NAGW-765.

Received 4 April; accepted 2 May 1986.

- 1. Turner, E. L. et al. Nature 321, 142-144 (1986).
- Turner, E. L., Ostriker, J. P. & Gott, J. R. Astrophys. J. 284, 1-22 (1984).
 Paczyński, B. Nature 319, 567-568 (1986).
 Paczyński, B. Nature 321, 419-420 (1986).

- Gott, J. R. Astrophys. J. 288, 422-427 (1985).
 Yang, J., Turner, M. S. & Steigman, G., Schram, D. N. & Olive, K. A. Astrophys. J. 281, 493-511 (1984).
- 7. Rees, M. J. & Sciama, D. W. Nature 217, 511-516 (1968).

Observations of the cosmic background radiation near the double quasar 1146 + 111B,C

Antony A. Stark, Mark Dragovan, Robert W. Wilson & J. Richard Gott III

AT&T Bell Laboratories, Holmdel, New Jersey 07733, USA Princeton University Observatory, Princeton, New Jersey 08544, USA

Paczynski¹ and Turner et al.² have suggested that the extraordinary double quasar 1146+111B,C found by Hazard et al.3 is a possible gravitational lens. The hypothetic lensing object is unknown. If the lensing object is a cluster of galaxies4 or a cosmic string5,6, it may cause observable effects in the cosmic background radiation. At millimetre wavelengths, a cluster would be expected to cause a reduction in the temperature of the background in the vicinity of the cluster as the result of the Zeldovich-Sunyaev effect. The area of sky on one side of a cosmic string would have a different radiation temperature from that on the other side. If either of these expected signatures were seen in the cosmic background, it would be strong evidence in favour of that hypothesis. We have searched for microwave background inhomogeneities near 1146+ 111B,C. An east-west strip of sky, 16 arc min long and centred on the point between the quasars, was observed with a beam of diameter 105 arcs at 3 mm wavelength. Our observations show only noise with an r.m.s. noise level of 0.0010 K. These observations set limits on the properties of the lensing object if it is a cosmic string or a cluster of galaxies, and we do not confirm either hypothesis.

Observations were made for 4-h periods on each of seven nights in March and April 1986, using the 7-m-diameter antenna at AT&T Bell Laboratories, Crawford Hill. At 100 GHz, this antenna has a beam efficiency of 0.92 and a beam size of 105 arc s (full width at half maximum). The receiver is a superconductorinsulator-superconductor (SIS) mixer followed by an FET (field-effect transistor) amplifier with 512 MHz bandwidth. Double-sideband receiver temperatures were typically 90 K, and the total system temperature including atmospheric corrections was 180-300 K. The receiver gain and noise were measured every half hour by chopping between a liquid-nitrogen-cooled absorber and a room-temperature absorber. The sky temperature was measured by chopping between the sky and the liquid nitrogen absorber, which allows a calculation of the atmospheric opacity.

The observing method was a beam-switched drift scan, as described by Radford et al.7. As the source moved across the sky, the antenna was driven to a position ahead of the source and then held stationary with respect to the Earth. The observed strip would then drift through the beam. To eliminate the effect of gain fluctuations, the receiver was chopped at a frequency of 15 Hz between the primary beam and a reference position at 30 arc min greater azimuth, so that the observed value of a point on the strip is the difference in antenna temperature between that point and the reference position. The time series that resulted from each drift scan was binned at intervals corresponding to 1 arc min on the sky, slightly larger than half a beam-width. Many drift scans were averaged to yield the plot in Fig. 1. The reference positions changed as the source moved across the sky, because of field rotation. The chopping was done with a rotating blade at the Cassegrain focus8. Before each night's observations the system was checked by drift-scan observations of calibration sources with known millimetre-wave fluxes.

The results are shown in Fig. 1. Here, all the drift-scans have been averaged. None of the data have been discarded. Figure 1 shows corrected antenna temperature as a function of position along the strip. The zero-point of the temperature scale has been arbitrarily set so that the average value along the strip is zero;

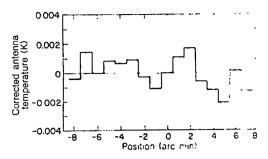


Fig. 1 Corrected antenna temperature at 100 GHz as a fail of the of position along a constant declination strip passing by tween the quasars 1146+111B,C. The 0 arc min position s 11 " 46 min 06 s, $\delta_{1950} = 11^{\circ}$ 05' 28". West is to the left, east to the right

therefore, the data do not show possible different as between the strip and the reference positions. However, a step or a stepe in the brightness as a function of position along the strip would appear in the plot.

These data seem to be random. The r.m.s make level is 0.0010 K. If the lensing object is an isothermal chatter there is a predicted⁴ Zeldovich-Sunyaev dip of $\Delta T = 7.003 \text{ is }^{-10}$: centred on the 0 arc min position in Fig. 1, where 9 is geometrical factor of order unity, f is a factor of order g at that measures the fraction of the mass in the for: of ion and gas $(f \equiv M_{\text{ionized}}/[0.03 \ M_{\text{virtal}}];$ for the Coma cluste $f = 10^{\circ} \text{ nd}$ $h \equiv H_0/100 \text{ km s}^{-1} \text{ Mpc}^{-1},$ where H_0 is the Hubble cone for -10° the lensing object is a stright cosmic string there is a produced step of $\Delta T \approx 0.002 \text{ K} \text{ v}_s/c$ of either sign where v_s is the schools of the presumably relativistic string perpendicular to its length and to our line of sight. The step could be located anywhere from position -3 to +3 arc min, because the stong might be anywhere between the quasars. It would be or adenee 5. ~2 beam-widths because the position angle of the samp is reast likely to be 63°, that is, perpendicular to the line between the quasars. Both a cluster and a string would be expected to a leaf several of the independently measured points on our spilits strip, so the statistical significance of our non-detection is grower than the noise in any single point. The data are consistent with a limit of $\beta fh^{-2} \le 0.3$ for the cluster. The hypothetical cluster would then have to be relatively poor in ionized gan the feature $M_{
m ionized}/M_{
m virial}$ would be one third of the Coma cluster v. Hz The data are also consistent with a limit of $v_i \in 0$ between is the speed of light) for the case of a string. A string would no expected⁵ to have $v_s = 0.5$ c, so our measurment does not also out the string hypothesis, but this measurement or istrains the properties of the string. For example, the apparent projected angle, x, between the string and the normal to the line between the quasars is given by $^6 \tan(\chi) = (v_s/c) \tan(\alpha)$, where α is the angle between the string and the plane of the sky

The data are, of course, also consistent with the negative hypothesis that B and C are two different quasars that coincidentally have very similar spectra, and that there is no lens a, all At the 3σ level of statistical significance, there is no effect on scales of ≥105 arcs at a level of 10° of the cosmic background radiation.

We thank R. E. Miller for the SIS junction used in the reciver, and W. H. Bent for contributions to instrumentation on the 7-m antenna.

Received 14 April: accepted 10 June 1986

- Paczynski, B. Nature 319, 567-568 (1986).
- Turner, E. L. et al. Nature 321, 142-144 (1986)
- 3. Hazard, C., Arp, H. & Morton, D. C. Nature 202, 271-277, 1877 4. Ostriker, J. P. & Vishniac, E. T. Nature 322, 804 (1908)
- Gott, J. R. Astrophys. J. 288, 422-427 (1985)
 Gott, J. R. Nature (submitted).

- Radford, S. J. E. et al. Astrophys. J. 300, 159-166 (1975)
 Goldsmith, P. F. Bell System Tech. J. 56, 1483 (1977)

The chemical evolution of the Galaxy

Gerard Gilmore* & Rosemary F. G. Wyse†

* Institute of Astronomy, Madingley Road, Cambridge CB3 0HA, UK † Space Telescope Science Institute, Baltimore, Maryland 21218, USA

The distribution of enriched material in the stars and gas of our Galaxy contains information pertaining to the chemical evolution of the Milky Way from its formation epoch to the present, providing general constraints on theories of galaxy formation. Detailed studies of the metallicities of well-defined samples of long-lived G-dwarf stars in the solar neighbourhood have ruled out the 'simple closed-box' model of galactic chemical evolution-too few very metal-poor stars are observed 1-3. The weakest assumption inherent in this model is that the galactic disk formed and evolved as a closed system. Allowing accretion of gas, either metal-enriched or primordial (the latter requiring a particular dependence of star formation on gas density), can yield an improved fit to the observations³. However, secondary infall from the galactic extreme spheroid provides only a slight alleviation of this 'G-dwarf problem'4. Here we show that consideration of the chemical properties of the thick-disk population of the Galaxy^{5,6} results in a selfconsistent model for galactic chemical evolution.

Motivation for the closed-box model for the galactic disk came from the proposal⁷ that the formation of the spheroid of the Galaxy, and the collapse of residual gas to a thin disk, was extremely rapid, having been largely completed in a free-fall time. However, recent evidence from in situ observations of a stellar component of the Galaxy with kinematics and metallicity distribution intermediate between those of the extreme spheroid and thin disk^{5,6,8-11} has shown that this picture of Galaxy formation and evolution is oversimplified. Here we investigate the metal-enrichment history of an evolutionary sequence in which a short-lived phase of rapid star formation forms the extended, metal-poor, pressure-supported extreme spheroid, with the thick disk forming subsequently before a final equilibrium state is attained, the centrifugally supported thin disk forming over a long timescale once the Galaxy potential is unperturbed and steady^{6,12,13}

The transition between extreme spheroid and thick disk can be investigated using the two-zone model⁴. Thus, we assume that gas is removed from the spheroid star formation process at a rate which is a constant multiple, denoted by c, of the star formation rate. This may be expected if the gas is heated by supernova explosions, and within the context of the modified simple model has the same effect as a lowered nucleosynthetic yield4. We keep the remaining major assumptions of the simple model; namely, that the stars enrich the gas instantaneously and that the system is well mixed and chemically homogeneous. The parameters in the model have standard values: solar neighbourhood yield¹⁴ and stellar initial mass function¹⁵, with a lock-up fraction of gas into stars of 0.6-0.8 (ref. 16). For the extreme spheroid, we also keep the assumption of zero initial metallicity, in keeping with the most recent derivation of the metallicity distribution of extremely metal-poor spheroid stars¹⁷

The theoretical cumulative metallicity distribution, whose form in the adopted model is independent of the unknown star formation rate, may be compared with observations to solve for the value of the constant c. We have used the metal-poor galactic globular clusters to define the observed extremespheroid metallicity distribution (Fig. 1a). This distribution is in excellent agreement with that derived by Sandage 10 for his

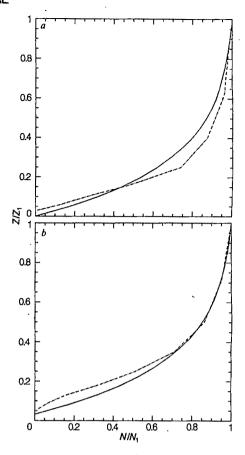


Fig. 1 Comparison of observed (dashed lines) and predicted (solid lines) cumulative metallicity distributions for the extreme spheroid⁸ (a) and thick disk^{6,10,11} (b). Plots show the total number, N, of tracers with metallicity $\leq Z$, normalized to the maximum abundance, Z_1 . In a, the observed distribution⁸ is defined by the metal-poor ([Fe/H] < -0.8) galactic globular clusters; the model shown model has c = 10. In b, the observed log metallicity distribution has been approximated by a truncated gaussian ($\pm 2\sigma$), with mean [Fe/H] = -0.6, σ = 0.3; the model shown has c = 1.

J1

large, kinematically defined sample of subdwarf stars. Norris11 has shown that this distribution represents the true metallicity structure of the extreme spheroid, independent of the detailed selection criterion for the sample. For the adopted stellar nucleosynthesis parameters, these data are fit well by removal of gas from the star-forming process at a rate ~5-20 times the spheroid star formation rate (see refs 4, 18, 19). The uncertainty in c results from the possible range of the lock-up fraction in the extreme spheroid, and from the observational spread; the use of the cumulative metallicity distribution forces a smooth distribution through the observations. These values of c yield an average metallicity of the residual gas of $[Fe/H] = -1.4 \pm 0.2$. (As the gas removed from the spheroid star-forming process is, as usual, assumed to be well mixed and enriched with stellar ejecta with a time-independent, solar distribution of elements, the time-averaged metallicity is most meaningful.) This metallicity is in excellent agrement with the metal-poor tail of the thick-disk stars^{6,9,11}, but is much too metal-poor for the thin-disk stars—showing explicitly that an initial enrichment due to rapid infall from the extreme spheroid cannot alone provide a resolution of the thin-disk G-dwarf problem⁴.

In the present model, the residual gas after spheroid star formation ceases is treated as simply providing the proto-thick disk with a non-zero initial metallicity, equal to the mean gas enrichment found above. This treatment is consistent with the high star formation rate suggested by the extreme-spheroid kinematics and the rapid removal of all gas from the spheroid

star-formation process in the present model (c = 5-20). As the thick-disk metallicity distribution overlaps that of the extreme spheroid at the metal-poor end, and that of the thin disk at the metal-rich end, one must be careful to ensure minimal intercomponent contaminations. The thick disk may be defined in three ways, the first by a volume sample in situ above the galactic plane, where it is expected to dominate⁶, the second kinematically10, and the third by a combination of spectroscopic and kinematic data11. These three determinations are in good agreement, so that the adopted metallicity structure is not sensitive to a specific criterion. Additionally, the most recent analogous determinations of the thin-disk metallicity structure^{6,10,20} show that there is no difficulty in isolating the thick- and thin-disk parameters with sufficient precision for the present problem.

Figure 1b shows the cumulative metallicity distribution for thick-disk stars^{6,10,11}. The best-fitting theoretical curves have net outflow parameter c = 1-2, and a corresponding mean value of the metallicity of the ejecta from thick to thin disks of [Fe/H] = -0.6 ± 0.1 . This level of pre-enrichment agrees well with the metallicity determined for the oldest, most metal-poor Gdwarfs^{3,6}. Hence, inclusion of the thick disk in this simple model resolves the G-dwarf problem for thin-disk stars in the solar neighbourhood.

Pre-enrichment of the thin disk was recognized previously3,16 as a resolution by itself to the G-dwarf problem. For the present model, detailed calculations show that the cumulative metallicity distribution for thin-disk stars limits any infall of un-enriched material following the prompt enrichment by the thick-disk ejecta to a rate of <0.2 times the star formation rate, assuming constant relative rates, as may be expected14. This is in agreement with limits on present-day high-velocity infall²¹. Constraints on our model from other quantitites, such as the age-metallicity relation and the age-velocity dispersion relation for long-lived thin-disk stars, are weak, as the two recent calibrations of these relations 12,20 are in significant disagreeement. The apparently extremely-high-metallicity K-giants found in the direction of the galactic centre²² are difficult to understand if they are members of the extreme-spheroid population, unless the gas which formed the central regions of the spheroid was decoupled from the rest, but their spatial frequency and velocity dispersion are, in fact, compatible with their being disk stars.

The ratio of the mass of the second zone (thick plus thin disks), to the mass of the first zone (extreme spheroid) is approximately c/α , where α is the lock-up fraction in the first zone. Adopting a value of 0.8 for α , we then predict a present-day mass ratio, between the extreme spheroid and thick and thin disks together, of ~1:15. The thick- to thin-disk transition as modelled here predicts a further decomposition of masses to -1:3:12 for the ratios extreme spheroid:thick disk:thin disk. The later infall of primordial material, expected in most theories of galaxy formation and suggested by the thin disk metallicity distribution, will modify these ratios somewhat.

The global parameters of the Galaxy, which are required to estimate luminosities to compare with these predictions, are as

vet ill-determined. In particular, neither the radial scale-lengths nor axial ratios of any of the three major components of the Galaxy have been measured unambiguously. The most reliable technique available assumes that our Galaxy is extremely similar to other well-studied Sbc disk galaxies²³. This gives a decomposition of our Galaxy into extreme spheroid, thick disk and old thin disk²³, which implies a value of 1:11 for the ratio of the J-band luminosity of the extreme spheroid to that of the sum of the disks. Assuming similar mass-to-light ratios (~6), as for SO to Sbc galaxies in the B-band²⁴, yields good agreement with the value predicted above. The further decomposition into extreme spheroid:thick disk:old thin disk yields luminosity ratios 1:0.2:11, suggesting a less massive thick-disk component than predicted here. (Note that the young thin disk has negligible mass compared to the old thin disk.) However, these observational estimates for the thick disk are highly uncertain, being based in part on an extrapolation²³ of star counts in a single field to determine the global parameters. Indeed, Sandage¹⁰ finds the galactic thick disk to have a local normalization higher by a factor of $\sim 3-5$ than the earlier determination²³; this new value yields adequate agreement with the present model. By comparison, in NGC891, thought to be extremely similar to our Galaxy, the thick disk and extreme spheroid are of comparable mass²³. Even the r^{1/4} extreme-spheroid component in our Galaxy is poorly constrained by available data, two recent analyses differing by a factor of 3.45 in the luminosity of this component^{23,25}. Improved determinations of both the metallicity and spatial-structural parameters will only be available once the major statistical surveys underway by ourselves and others are completed.

The chronological sequence of formation of the three components proposed here may be tested by study of their detailed elemental and isotopic abundances²⁶. The transitions between components are likely to occur on timescales long compared with the lifetimes of the massive stars which explode as type II supernovae, but of the order of the lifetimes of the stars that produce carbon, nitrogen and type I supernovae. The available data on the variation of oxygen (from massive stars) and iron (from intermediate-mass stars) in stars over a range of metallicities spanning extreme-spheroid to thin-disk^{27,28} show a feature near $[Fe/H] \approx -1$, the transition metallicity between the extreme spheroid and thick disk. More exact location of this feature will allow us to estimate the duration of the formation of the extreme spheroid.

Although a full analysis of the chemical evolution of the Galaxy involves too many parameters for an analytical understanding, we believe that the simple model presented here offers new insight into the formation and evolution of the Galaxy. The galactic thick disk has a significant influence on the chemical evolution of the other components of the Milky Way.

We thank NATO for a travel grant (490/84) to aid collaborative research, the American Astronomical Society for grants (to R.F.G.W.) from the Small Research Grants Program, and Jim Truran for helpful comments.

Received 10 April; accepted 20 June 1986.

- van den Bergh, S. Astr. J. 67, 486-490 (1962).
- Schmidt, M. Astrophys. J. 137, 758-769 (1963).

- Schmidt, M. Astrophys. J. 137, 758-769 (1963).
 Pagel, B. E. J. & Patchett, B. E. Mon. Not. R. astr. Soc. 172, 13-40 (1975).
 Hartwick, F. D. A. Astrophys. J. 209, 418-423 (1976).
 Gilmore, G. & Reid, I. N. Mon. Not. R. astr. Soc. 202, 1025-1047 (1983).
 Gilmore, G. & Wyse, R. F. G. Astr. J. 90, 2015-2026 (1985).
 Eggen, O. J., Lynden-Bell, D. & Sandage, A. R. Astrophys. J. 136, 748-766 (1962).
 Zinn, R. Astrophys. J. 293, 424-444 (1985).
 Norris, J., Bessel, M. S. & Pickles, A. J. Astrophys. J. Suppl. Ser. 58, 463-492 (1985).
 Sandage, A. R. in Selfage Regulations (Ad. Bartinia A. Tori, M. S. M. 603-492 (1985).
- Sandage, A. R. in Stellar Populations (eds Renzini, A., Tosi, M. & Norman, C.) (Cambridge University Press, in the press).
- University Press, in the press).

 11. Norris, J. Astrophys. J. Suppl. Ser. (in the press).

 12. Jones, B. J. T. & Wyse, R. F. G. Astr. Astrophys. 120, 165-180 (1983).

 13. Gilmore, G. Mon. Not. R. astr. Soc. 207, 223-240 (1984).

 14. Twarog, B. A. Astrophys. J. 242, 242-259 (1980).

- Scalo, J. Fundam. Cosmic. Phys. (in the press).
 Tinsley, B. M. Fundam. Cosmic Phys. 5, 287-342 (1980).
 Beers, T. C., Preston, G. W. & Shectman, S. A. Astrophys. J. (in the press).
 Hartwick, F. D. A. Memorie Soc. astr. ital. 54, 51-64 (1983).
- Fall, S. M. in The Milky Way Galaxy (eds van Woerden, H., Allen, R. J. & Butler, W) 603-610 (Reidel, Dordrecht, 1985).
- Carlberg, R. G., Dawson, P. C., Hsu, T. & VandenBerg, D. A. Astrophys. J 294, 674-681 (1985).
- Mirabel, I. F. & Morras, R. Astrophys. J. 279, 86-92 (1984).
 Whitford, A. E. & Rich, R. M. Astrophys. J. 274, 723-732 (1983).

- Van der Kruit, P. C. Astr. Astrophys. 140, 470-475 (1984).
 Van der Kruit, P. C. Astr. Astrophys. 140, 470-475 (1984).
 Faber, S. M. & Gallagher, I. S. A. Rev. Astr. Astrophys. 17, 135-187 (1979).
 de Vaucouleurs, G. & Pence, W. Astr. J. 83, 1163-1173 (1978).
 Truran, J. in Stellar Populations (eds Renzini, A., Tosi, M. & Norman, C.) (Cambridge University Processing the new parts). University Press, in the press).

 27. Sneden, C., Lambert, D. L. & Whitaker, R. W. Astrophys. J. 234, 964-972 (1979)
- 28. Clegg, R. E. S., Lambert, D. L. & Tomkin, J. Astrophys. J. 250, 262-275 (1981).

Nimbus 7 satellite measurements of the springtime Antarctic ozone decrease

R. S. Stolarski, A. J. Krueger, M. R. Schoeberl, R. D. McPeters, P. A. Newman & J. C. Alpert*

NASA/Goddard Space Flight Center, Laboratory for Atmospheres, Greenbelt, Maryland 20771, USA

Farman et al. have reported a rapid decrease, since their measurements started in 1957, of the total column amount of ozone in late winter and early spring over the Halley Bay station in Antarctica (76° S, 27° W). The decrease was most pronounced in October, early spring in the Southern Hemisphere. They attributed the decrease to the increase in stratospheric chlorine due to chlorofluorocarbon release, and proposed that the unique conditions of extreme cold and low sunlight in the Antarctic winter and spring enhanced the effect. We report measurements from the Solar Backscatter Ultraviolet (SBUV) instrument and the Total Ozone Mapping Spectrometer (TOMS) aboard the Nimbus 7 satellite, a Sun-synchronous polar-orbiting satellite which passes any given point on the dayside near local noon. These provide global measurements of ozone from November 1978 to the present which confirm the reported decline of total ozone and show the phenomenon to be regional in extent. The decrease occurs during September as the Sun rises, reaching a minimum in mid-October. Seven years (1979-1985) of October monthly means show a 40% decrease in the ozone minimum and a 20% decrease in the surrounding ozone maximum.

The SBUV is a nadir-viewing instrument which obtains total ozone from measurements of the backscattered solar ultraviolet radiation in the wavelength range 310-340 nm (refs 2, 3). Measurements in the 250-310 nm range by the SBUV instrument provide information on the distribution of ozone with altitude. The TOMS instrument is designed to measure the spatial distribution of total ozone by scanning across the track of the satellite to obtain data between successive satellite orbital tracks. Both instruments make total ozone determinations using a differential absorption method which tends to cancel effects of neutral absorbers or scatters. Thus, stratospheric aerosol, such as polar stratospheric clouds (PSC), produce only second-order errors in retrievals. Errors due to wavelength-dependent scattering exist at large solar zenith angles⁴; however, PSCs are most common in winter, and vanish as the stratosphere warms in the spring^{5,6}, the time of the maximum decrease in ozone. Instrumental interference from PSCs, therefore, cannot account for the large observed ozone decrease.

One of the major advantages of the TOMS instrument is its ability to map total ozone over the entire globe on a daily basis. Figure 1 shows a daily sequence of total ozone observations for October 1984. The low total ozone over Halley Bay (indicated by an asterisk in Fig. 1) is part of a larger, elliptically shaped minimum region extending out to $\sim 60-70^{\circ}$ S. This region, which rotates about the pole with an irregular period of $\sim 7-10$ days, is bounded by a steep gradient where total ozone increases to values exceeding 300 Dobson units (1 DU = 10^{-3} atm cm). At $50-60^{\circ}$ S total ozone reaches a maximum, which exhibits larger variability due to travelling planetary waves. The polar minimum and mid-latitude maximum in total ozone are features of the normal, long-term climatology of the Southern Hemisphere⁷.

The 12 panels in Fig. 1 show 12 consecutive days, from 11 to 22 October 1984. This is the time period for which the lowest values are generally recorded. Each panel is centred about the South Pole and includes data out to 45° latitude. On 11 October, Fig. 1 shows that the minimum in total ozone is relatively symmetrical about the pole and the maximum in total ozone is

located in the lower right, between ~ 90 and 180° E. On succeeding days the total ozone maximum region rotates clockwise, while the minimum region elongates and begins to co-rotate with the maximum. On 16 and 17 October the maximum region has reached the lower left-hand corner, between 180 and 270° E, where it seems to dissipate and subsequently reappear in the upper right-hand corner. From there it continues to move around the pole but does not pass over Halley Bay. By 20 October the ozone distribution has returned approximately to the original situation on 11 October, giving a rotation period at this time of 9 days. The next 2 days are near repeats of 12 and 13 October.

Total ozone is proportional to the pressure-weighted integral of the ozone mixing ratio, and fluctuations in the amount of total ozone may indicate a relative increase in altitude of the mixing ratio distribution, a chemical loss in the lower stratosphere, advection of ozone into a region from other locations, or all of the above. Comparisons of National Meteorological Center (NMC) 50-mbar temperatures and TOMS total ozone reveals a high degree of spatial correlation on all of the days that have been examined. This correlation can be understood as resulting from the adiabatic ascent and descent of air as it moves around the vortex. Air which descends tends to increase total ozone while warming adiabatically. The reverse occurs when air ascends

The isobars at middle latitudes in the lower stratosphere are generally not parallel to the isotherms. As the isobars approximate the streamlines for air parcel motion, air parcels will experience large temperature excursions (20-30 K) as they circulate through the polar vortex. These excursions could play an important role in the chemistry of the air parcels and should not be neglected in model simulations. We have also noted that the streamlines pass through the edges of both the high and low total ozone regions. This suggests that the observed decrease in both the total ozone maxima and minima result from the year-to-year decrease in the mixing ratio of the group of parcels moving between the two regions. Thus, the total ozone maxima and minima decreases do not necessarily involve separate processes.

Evidence that the long-term total ozone decrease observed at Halley Bay is not unique to Halley Bay is shown in Table 1,

Table 1 Zonal mean, local minimum and local maximum total ozone values (DU) for October at 70-80° S latitude

Year	Zonal mean	Local minimum	Local maximum
1970	306	240	484
1971	334	249	482
1972	337	237	539
1979	333	235	515
1980	270	212	467
1981	266	206	422
1982	283	186	494
1983	245	166	479
1984	240	162	446

Data from Nimbus 4 BUV (1970-72) and Nimbus 7 SBUV (1979-84).

which lists the zonal mean, local minimum and local maximum total ozone values for 70-80° S latitude, for October 1970-72 from BUV and October 1979-84 from SBUV. Data from the Nimbus 4 BUV instrument, the predecessor to SBUV, were fairly complete for the 1970-72 period; in later years, coverage of the Antarctic by BUV was reduced. The BUV ozone data have been re-processed with the algorithm used for SBUV and with compatible instrument characterization functions, making it reasonable to compare the BUV total ozone with the SBUV total ozone. Antarctic total ozone in 1979 appears comparable to that observed in the early 1970s, indicating that most of the total ozone decrease has occurred since 1979, in agreement with the Halley Bay observations.

^{*} Present address NOAA/NMC, Camp Springs, Maryland 20233, USA.

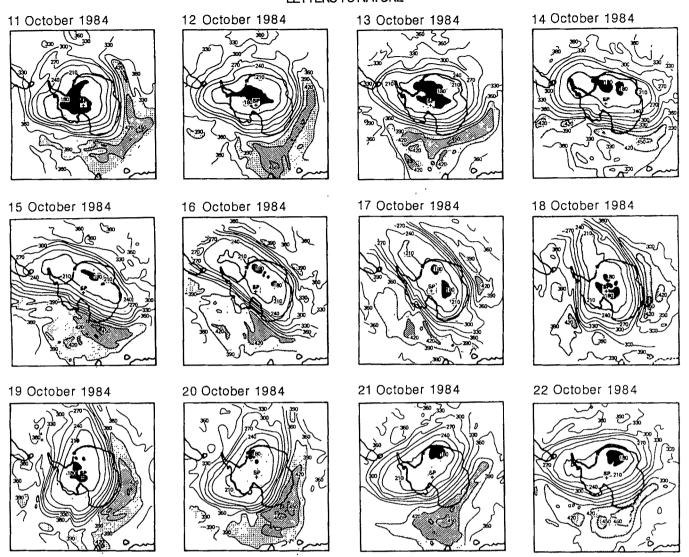


Fig. 1 Twelve-day sequence (11-22 October 1984) of TOMS measurements of total ozone content. The data are shown in south-polar projections, with the pole indicated by a cross (SP) and Halley Bay shown by an asterisk. Contours are every 30 Dobson units (1 DU = 10^{-3} atm cm). The region shown extends to ~45° latitude and the Greenwich meridian is towards the top of each diagram. Shaded regions indicate total ozone values <180 and 210 DU and >390 and 420 DU.

The nature of the decrease is shown more clearly in Fig. 2, which shows October monthly mean TOMS total ozone maps for the Southern Hemisphere in each of the seven years from 1979 to 1985. Table 2 lists the October monthly means over

Table 2 October mean ozone column over three Antarctic stations, along with the minimum and maximum values of the monthly mean (all in DU)

				•	
Year	Halley Bay (76° S, 27° W)	Syowa (69° S, 39° E)	Amundsen-Scott (90° S)	TOMS minimum	TOMS maximum
1979	273 ± 19	367 ± 47	266±25	259	458
1980	232 ± 11	276 ± 22	218±9	215	433
1981	244 ± 12	312 ± 30	223 ± 9	219	449
1982	221 ± 12	240 ± 49	220 ± 22	205	432
1983	199±13	239 ± 32	182±8	178	414
1984	190 ± 8	245 ± 24	187 ± 14	181	404
1985		•	•	152	351

Data from Nimbus 7 TOMS. Stated ranges are 1σ variances of the daily values from the monthly mean for each location.

three stations (Halley Bay, Syowa and Amundsen-Scott), as well as the minimum and maximum values of the monthly mean. The monthly mean values in the minimum region decrease from 259 DU in 1979 to 152 DU in 1985. The total ozone values for Halley Bay agree closely with those reported by Farman et al.¹.

We have also examined four years (1979-82) of NMC 50-mbar temperature data. The interannual variations in temperature were similar to the total ozone variations, but no conclusive trend could be determined from such a short data set.

The phase of the maximum in the October monthly mean total ozone at $\sim 60^{\circ}$ S latitude (Fig. 2) shifts from year to year, ranging from ~ 90 to 180° E. In 1979 the maximum monthly mean total ozone value exceeds 450 DU. By 1985 the maximum is barely > 350 DU, a decrease of > 20% in seven years. There also seems to be a biennial modulation of the decrease in both the maximum and minimum. A quasi-biennial oscillation in total ozone has been observed previously, but with a magnitude of only $\sim 6-8$ DU (refs 8, 9).

The data given by Farman et al.¹ for Halley Bay showed total ozone amounts at the end of the polar night in 1984 which were a few tens of per cent lower than those at the start of the polar night. The ozone algorithms for both TOMS and SBUV have been carefully scrutinized for their behaviour at high solar zenith angles and return accurate results for zenith angles up to 85° (ref. 3 and P. K. Bhartia, personal communication). We thus have observations back through the month of September for the latitude of Halley Bay (76° S). The results show values of total ozone as this region leaves polar night which are very close to those observed entering the polar night. This result is also in

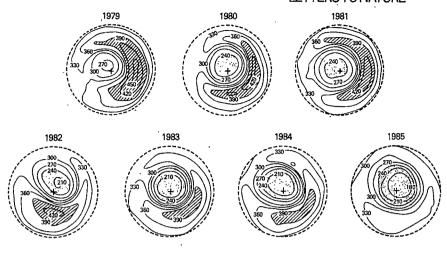
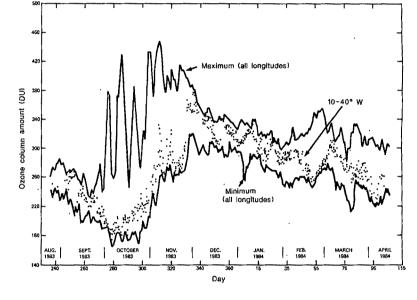


Fig. 2 Six-year sequence of October monthly means of total ozone. South polar projections, with the pole indicated by a cross and 30°S latitude by a dashed circle. The Greenwich meridian is towards the top of each panel. Contours are every 30 DU. The shaded regions indicate monthly mean total ozone amounts of <240 DU and >390 DU.

Fig. 3 Nimbus 7 SBUV data for total ozone content between latitudes 74°S and 78°S for September 1983 to April 1984. Dots, data within 15° longitude of Halley Bay (10-40° W). Solid lines, maximum and minimum values found around the entire latitude circle.



agreement with the observations of total ozone made at Syowa station (69° S) in 1982¹⁰. However, there is some indication from lunar Dobson and ozone-sonde measurements at Syowa that total ozone increases slowly until winter solstice, then decreases again until sunrise, with a more rapid decrease thereafter¹⁰.

Throughout the month of September and the first week in October, a rapid decline is observed in total ozone by both SBUV and TOMS, until the previously mentioned low values are obtained. Figure 3 shows this pattern in data from the SBUV instrument for late August 1983 to April 1984. The data points are the satellite data that are centred within $\pm 2^{\circ}$ latitude and $\pm 15^{\circ}$ longitude of Halley Bay. The solid lines are the maximum and minimum of values reported at all longitudes within the latitude band 74-78° S. Throughout October and November, the data over Halley Bay are consistently near the minimum values for all longitudes for this and other years. The decline in the minimum value of ozone column extends from late August to early October at a rate of ~0.6% per day. At longitudes on the other side of the pole from Halley Bay (near the total ozone maximum), the total ozone amount is more variable.

Near the end of November the low values have disappeared completely and the minimum curve attains its largest values. The jump in total ozone occurs several weeks after the final warming in the Southern Hemisphere, and marks the switch from winter to summer circulation. A similar process occurs in the Northern Hemisphere, but usually only three months after the winter solstice rather than five months, as seen here^{11,12}. Throughout the Antarctic summer the ozone column decreases again, and the Halley Bay values oscillate between the maximum

and minimum curves as lower stratospheric travelling waves pass over the station.

Our data place significant constraints on possible mechanisms for explaining the decrease. The deep minimum, or hole, follows the polar vortex, and its position is well correlated with the temperature minimum in the lower stratosphere. There also appears to be a smaller but significant decrease (~20%) in the total ozone maximum surrounding the polar region over the seven years studied. The decrease in the total ozone maximum is related to the decrease in the total ozone minimum, in that the streamlines indicate that air in the maximum region has passed through the periphery of the low-temperature region which is associated with the total ozone minimum.

An important constraint placed on theoretical models by these data is that the decrease in total ozone near the pole appears to take place largely in September, during twilight, not in the polar night. The maximum rate of decrease in total ozone occurs after most of the polar region is sunlit, and in 1983 was $\sim 0.6\%$ per day, extended over 40-50 days.

Any explanation of the total ozone change must be consistent with the year-to-year changes in the polar vortex, as well as with the rate of decrease through September. Various ideas have been proposed, involving combinations of chlorine chemistry, heterogeneous chemistry taking place in polar stratospheric clouds, bromine chemistry and dynamical elevation of the polar stratosphere^{1,13-15}.

We estimate that in order for chlorine chemistry at 1983 concentrations to cause the 0.6% per day decline in September, virtually all of the chlorine must be in its active state, that is,

Cl and ClO, with little or no interference from NO_x. Therefore, any proposed chlorine mechanism must be able to remove most of the chlorine from both the HCl and ClONO2 reservoirs and to tie up NO_{xx} probably as HNO₃. Such a mechanism could involve the cold temperatures and/or polar stratospheric clouds that form within the polar vortex⁶.

Any conclusions concerning the implications of the observed Antarctic decreases in total ozone for predictions of the effects of chlorine from chlorofluorocarbons must await a proven mechanism and continued observations to verify the persistence of the phenomenon. Only then will we be able to evaluate clearly the relative roles of chemistry, radiation and dynamics in contributing to the observed decrease.

We thank the Nimbus 7 ozone processing team (A. Fleig, chairman) for making available TOMS data from October 1983, 1984 and 1985; the Real-Time TOMS Project for data for a few days in October of 1985 before regularly scheduled processing; Reggie Galimore for image processing which helped make the data readily available for visual examination; S. Solomon, S. Wofsy and N. D. Sze for discussing and making available preprints of their papers: S. Chandra for useful discussions: and Lori Winter and Roberta Duffy for typing the many versions of this manuscript.

Received 8 April; accepted 1 July 1986.

- Farman, J. C., Gardiner, B. G. & Shanklin, J. D. Nature 315, 207-210 (1985).
 Heath, D. F., Krueger, A. J., Roeder, H. A. & Henderson, B. D. Opt. Engng 14, 323-330
- 3. Klenk, K. F. et al. J. appl. Met. 21, 1672-1684 (1982).
- Dave, J. V. J. atmos. Sci. 35, 889-911 (1978).
 Iwasaka, Y. et al. Middle Atmosphere Program Handbook, Vol. 18 (ed. Kato, S.) 450-452 (SCOSTEP Secretariat, Urbana, 1985).
- 6. McCormick, M. P., Steele, H. M., Hamill, P., Chu, W. P. & Swissler, T. J. J. atmos. Sci. 39, 1387-1397 (1982).
- 7. Sticksel. P. R. Mon. Weath. Rev. 98, 787-788 (1970)
- 8. Hasebe, F. in Dynamics of the Middle Atmosphere (eds Holton, J. R. & Matsuno, T.) 445-464
- (Terra Scientific, Tokyo, 1984).

 9. Hilsenrath, E. & Schlesinger, B. M. J. geophys. Res. 86, 12087-12096 (1981).
- 10. Chubachi, S. in Atmospheric Ozone (eds Zerefos, C. S. & Ghazi, A.) (Reidel, Dordrecht,
- Miller, A. J., Finger, F. G. & Gelman, M. E. NASA tech. Memo. No. TMX-2109 (Washington, DC, 1970).
- 12. Rood, R. B. Pure appl. Geophys. 121, 1049-1064 (1983).
- Solomon, S., Garcia, R. R., Rowland, F. S. & Wuebbles, D. J. Nature 321, 755-758 (1986).
 McElroy, M. B., Salawitch, R. J., Wofsy, S. C. & Logan, J. A. Nature 321, 759-762 (1986).
- 15. Tung, K. K., Ko, M. K. W., Rodriguez, J. M. & Sze, N. D. Nature 322, 811 (1986).

Are Antarctic ozone variations a manifestation of dynamics or chemistry?

Ka-Kit Tung*, Malcolm K. W. Ko†, José M. Rodriguez† & Nien Dak Sze†

* Massachusetts Institute of Technology, Cambridge, Massachusetts 02139, and Clarkson University, Potsdam, New York 13767, USA

† Atmospheric and Environmental Research, Inc., Cambridge, Massachusetts 02139, USA

Observations¹⁻³ reveal a large seasonal decrease in the column density of ozone during Antarctic early spring, followed by a rapid increase after October beyond its pre-spring value. Given the unique circumstances that exist in the Antarctic environmentrelatively stable circumpolar vortex, cold air temperature achieved during polar night, and the increase in absorption of solar radiation by ozone as the Sun returns—we surmise the existence of a reverse circulation cell with rising motion in the polar lower stratosphere. The upwelling brings ozone-poor air from below 100 mbar to the stratosphere, possibly contributing to the observed ozone decline in early spring. At the same time, the Antarctic stratosphere might contain a very low concentration (<0.1 p.p.b.v. (parts per 10⁹ by volume) of NO_x(NO+NO₂), a condition that could favour a greatly enhanced catalytic removal of O₃ by halogen species^{2,4,5}.

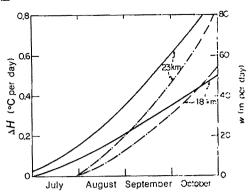


Fig. 1 Calculated heating rate (ΔH) from O₃ absorption over a 24-h period, as a function of time, for 69° S (--) and 76° S (- · - · -) at different altitudes. The heating rates are calculated from the local O₃ concentration using the parameterization of Strobel³¹. The time variation mainly reflects the seasonal changes in the number of sunlit hours. The observed O₃ profile from Syowa Station in July is adopted as the initial condition. For this calculation, horizontal transport and photochemical removal are ignored. The O3 profile is updated in time by accounting for the effect of the upward advection w by equation (4). The right-hand scale indicates the approximate value of \vec{w} , assuming that $\Gamma = 10 \,^{\circ}\text{C km}^{-1}$.

We argue that heterogeneous processes and formation of OCIO by the reaction BrO + ClO → OClO + Br before and after the polar night might help to suppress the NO_x levels during the early spring period. However, the dilution of the concentrations of the chlorine species by the upwelling may reduce the effectiveness of the photochemical removal of O3.

The zonal mean transport in the lower stratosphere normally takes the form of a two-cell diabatic circulation, with rising motion in the tropics and subsidence near both poles⁶⁻¹⁰. For a species such as O₃, whose source is in the stratosphere, upward transport tends to reduce its column abundance, as tropospheric air with low O₃ mixing ratio is brought up to the stratosphere. Poleward and downward transport in the subsiding branches tends to increase its abundance at high latitudes. This situation is further accentuated in winter by the downward branch of the one-cell circulation that exists above 25 km (refs 11, 12). The latitudinal distribution of the column abundance of O₃ does not, however, have north-south symmetry 13,14, as the spring maximum in the Southern Hemisphere is located closer to the Equator than in the north.

The winter polar vortex that encircles Antarctica is less disturbed than its counterpart in the Northern Hemisphere because of the weaker stationary planetary wave perturbations forced by large-scale continental elevations and land-sea contrasts. Although the vortex may shift in position and deform in shape in response to wave perturbations, its integrity (as defined in ref. 15) is usually maintained until its breakdown in early November. It therefore appears that irreversible wave-induced transports16 do not effectively reach Antarctica during this period.

During the polar winter in the Southern Hemisphere, dynamical transport of heat into the circumpolar vortex is weak. Local temperatures in the Antarctic lower stratosphere have time to adjust so that cooling, C(T), approximately balances diabatic heating, H, to reach low values 17, approaching the radiative equilibrium temperature T_e (refs 18, 19), with $H - C(T_e) = 0$. The situation changes abruptly when the Sun returns. Absorption of solar radiation by O3 causes H to increase rapidly as the number of sunlit hours increases. However, radiative cooling to space, which is temperature-sensitive, remains close to the low value achieved during the polar night. The temperature evolution is constrained by the prognostic zonal momentum and energy equations through the thermal wind relationship and mass continuity equation. Thus, local temperature can adjust

only on a longer dynamical timescale, due to 'dynamical inertia' ^{18,20}. In the absence of wave transports, the dynamical timescale is found²⁰ to be related to the newtonian cooling timescale of about 1-2 months for the Antarctic lower stratosphere²¹. The radiative imbalance temporarily leads to a positive net heating,

$$O = H - C \approx \Delta H > 0 \tag{1}$$

where ΔH is the incremental increase in heating due to absorption of solar radiation.

The above increase in net heating may be balanced by an increase in local air temperature (T), or by a vertical ascent of the heated air mass or both. This follows from the zonal-mean thermodynamics equation, which is, neglecting wave transports,

$$\bar{Q} = \frac{\partial}{\partial t} \, \bar{T} + \Gamma \bar{w} \tag{2}$$

where $\Gamma = (\partial \bar{T}/\partial z) + 9.8$ °C km⁻¹ is the static stability parameter, the overbar denotes the zonal mean and \bar{w} is the residual mean vertical velocity. Because of the 'dynamical inertia', the net heating should lead mainly to an upward circulation with vertical velocity

$$\bar{w} \simeq \bar{Q}/\Gamma$$
 (3)

during early spring. The upward branch of this reverse circulation in the lower stratosphere occurs in the vortex where $\bar{T} < T_c$, while the downward branch occurs at the edge of the polar vortex where $\bar{T} > T_c$. As upwelling (subsidence) lowers (raises) the column density of O_3 , it follows from the above arguments that, during the Antarctic spring, cold (warm) temperature should be correlated with O_3 minimum (maximum) at the altitude where O_3 concentration is largest. This is consistent with observation³. In the northern polar stratosphere, winter temperatures are maintained by dynamical transport, leading to values ~20-30 °C warmer than the temperature that prevails over the southern winter pole. Radiative cooling thus tends to exceed heating in Arctic winter, resulting in a downward diabatic circulation, as evidenced by the movement of stratospheric aerosols²².

To estimate the effect of upwelling on O_3 , we use a simple model based on the zonal-mean equation for the O_3 mixing ratio \bar{f} ,

$$\frac{\partial \vec{f}}{\partial t} + \vec{v} \frac{\partial \vec{f}}{\partial y} + \vec{w} \frac{\partial \vec{f}}{\partial z} = 0 \tag{4}$$

where the effect of irreversible mixing and photochemical reactions are neglected. As the residual mean meridional velocity (\bar{v}) is small near the pole, the effect of horizontal transport is also neglected. Figure 1 shows the calculated heating rate, ΔH , due to the absorption of solar radiation by ozone alone. The vertical advective velocity is calculated using equations (3) and (1), as described in Fig. 1 legend. Figure 2a, b shows a comparison of our calculated column densities of O_3 with observations at Syowa Station for 1982 (ref. 1) and with those at the latitude of Halley Bay for 1983 (ref. 3). The calculated rate of decline in September and October appears to be consistent with the observed zonal mean values³, but is smaller than the minimum over all longitudes.

An assessment of the photochemical contribution is hampered by the lack of kinetic data. The following discussion should be viewed as an assessment of the requirements on photochemistry for it to explain the observed O₃ behaviour. McElroy et al.⁴ have proposed that catalysis of O₃ recombination involving the bromine-chlorine cycle²³ may be important in Antarctic early spring:

$$Br + O_3 \rightarrow BrO + O_2$$

$$Cl + O_3 \rightarrow ClO + O$$

$$ClO + BrO \rightarrow Cl + Br + O_2$$

$$2O_3 \rightarrow 3O_2$$
(5)

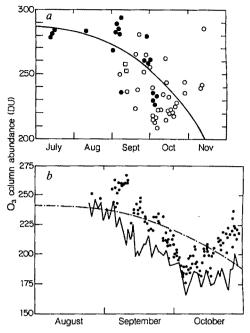


Fig. 2 a, Calculated column abundance (in Dobson units; 1 DU = 10^{-3} atm cm) of O_3 at 69° S (curve), compared with observations for the Syowa Station¹. The O_3 profile is calculated as described in Fig. 1 legend. The O_3 advected out of the top of the vortex (at ~ 30 km) is assumed to be swept away by horizontal motion and will not contribute to the column content. The data are from Dobson instrument by direct Sun (\bigcirc), by cloudy zenith (\square) and by Moon (\bigcirc). b, Calculated column abundance of O_3 at 76° S ($-\cdot-\cdot$) compared with observations from the Total Ozone Mapping Spectrometer (TOMS)³. The computation procedure is as stated in a, except that solar insolation is calculated for 76° S and the initial O_3 profile is adjusted to give an initial value of 240 DU for the column content. The data from TOMS³ comprise the minimum observed values for all longitudes between 74° S and 78° S (solid line) and observations at Halley Bay (dots).

In order for reaction (5) to provide a decrease of 0.5% per day in the column abundance of O_3 , the 24-h-averaged abundances of ClO and BrO at ~18 km must be ~0.4 p.p.b.v. and 20 p.p.t.v. (parts per 10^{12} by volume), respectively.

Results of our two-dimensional model¹¹ indicate a total chlorine (ClY) mixing ratio of 2.6 p.p.b.v. in the upper stratosphere and 1.5 p.p.b.v. at 18 km, of which 30% is in the form of ClO_x (ClNO₃+Cl+ClO+OClO+2×Cl₂+HOCl). If the observed decrease in O₃ were to be explained by photochemistry alone, ClO would have to be the major ClO_x species in early spring. The daytime abundances of the species Cl, ClO and CINO₃ are primarily determined by the equilibrium between production of ClO by photolysis of ClNO3 and rapid re-formation of CINO3, with equilibrium achieved within 1-2 h of daylight²⁴. To maintain the high ClO concentration, we must consider processes which both convert ClNO₃ to ClO_v (Cl+ClO+ OCIO+2×Cl₂+HOCl) and maintain sufficiently low NO_x to inhibit re-formation of ClNO₃. It is also important to consider the initial conditions of chlorine and nitrogen species in late autumn when the polar vortex is established before entering polar night.

Figure 3 summarizes the possible chemical mechanisms controlling chlorine and nitrogen species from Antarctic late autumn to early spring. Net conversion of NO_x to N_2O_5 occurs in the late autumn due to the rapidly decreasing photolysis rates of N_2O_5 with increasing solar zenith angles and shorter days. As the NO_x decreases, the daytime ClO increases, until the ClO and NO_x concentrations are comparable. From that point on, all ClO and NO_x will be sequestered in ClNO₃ within 1-2 h of darkness. Under these conditions, we calculate daytime concentrations of ClO of 0.07 p.p.b.v. at 18 km during late autumn

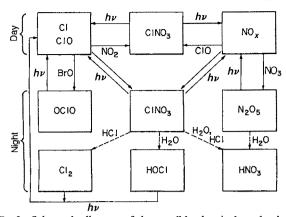


Fig. 3 Schematic diagram of the possible chemical mechanisms controlling nitrogen and chlorine species from late autumn to early spring in Antarctica. Species in the upper ('day') and lower ('night') portions are formed primarily during the day and night, respectively. Dashed lines: reactions proceeding through both homo- and heterogeneous channels. We note that although HOCl and HNO3 are produced primarily during the day for mid-latitude conditions, such production is negligible for high-latitude late autumn to early spring, due to the low abundances of OH and HO2.

and early spring, corresponding to a 24-h-averaged ClO of 0.02 p.p.b.v.

Further net conversion of NO_x to N₂O₅ is possible only if there is another night-time sink for ClO to prevent formation of CINO₃. Bromine chemistry may provide such a mechanism through the reaction²⁵

$$BrO+ClO \rightarrow Br+OClO$$
 (6)

The measured rate constant²⁵ implies a ClO time constant of 1 h for a BrO mixing ratio of 20 p.p.t.v. Conversion of ClO to OCIO by reaction (6) will dominate over CINO3 formation if the abundance of NO_x is <0.1 p.p.b.v., again facilitating the conversion of NO₂ to N₂O₅ at night and correspondingly increasing the equilibrium concentration of ClO during the day by a factor of 3. Reaction (6) effectively removes all ClO at night, restricting the effect of reaction (5) to daytime only.

Photolysis of N₂O₅ would constitute an important source of NO_x within 1 week after emergence from polar night, thus re-forming ClNO₃ at the expense of ClO. Concentrations of N₂O₅ may be kept low by assuming the heterogeneous reaction²⁶

$$N_2O_5 + H_2O (aerosol) \rightarrow 2 HNO_3$$
 (7)

with an equivalent first-order rate of $10^{-6}\,\mathrm{s}^{-1}$ near 18 km. This rate implies values of 10^{-2} for γ , the probability of reaction per collision with an aerosol surface, if we assume the background aerosol concentrations of ref. 27. The required value of γ could be reduced by more than a factor of 10 if we adopt the enhanced aerosol abundances for periods of high volcanic activity or the existence of polar stratospheric clouds²⁸.

Other heterogeneous processes have been proposed to convert CINO₃ to CIO_y and maintain low NO_x concentration. We find that the reactions^{4,5,32}

$$CINO_3 + H_2O (aerosol) \rightarrow HOCl + HNO_3$$
 (8)

$$ClNO_3 + HCl (aerosol) \rightarrow Cl_2 + HNO_3$$
 (9)

could achieve substantial conversion of ClNO₃ if an equivalent first-order rate of 10⁻⁶ s⁻¹ is assumed, leading to daytime ClO abundances in August of 0.5 p.p.b.v. and 1 p.p.b.v. with reactions (8) and (9), respectively. Higher rates are needed if reactions (8) and (9) are to counteract the production of NO_x by photolysis of HNO₃ a month after emergence from polar night⁴. In our proposed model upwelling may become important at this time, lowering the concentrations of ClY as well as O3, and reducing the importance of photochemistry. The extent of photochemical depletion during the first month will, however help determine

the magnitude of the subsequent October minimum and possibly contribute to the interannual trend.

The above discussion pertains to seasonal variations of Antarctic ozone and does not address the observed interannual trend of decreasing October minimum values since 1979 (refs 2, 3) While theories based on chemistry mostly attribute the secular trend to increases in stratospheric chlorine^{2,4,5}, enhanced upwelling over recent years may also play a part. Aerosol loading of the Antarctic stratosphere has increased by almost an order of magnitude in recent years²⁹, due probably to a series of major volcanic eruptions since 1979. Absorption of solar radiation by aerosol particles³⁰ would increase ΔH . During the polar night, increased cooling in the 10-50 mbar region from the higher aerosol loading could lead to a more negative vertical temperature gradient and a smaller Γ . Equation (3) then implies a stronger upwelling when the Sun returns. Our present calculation does not incorporate these additional factors and presents only a baseline model for a 'clean' atmosphere, designed to demonstrate the seasonal trend.

The proposed mechanisms (dynamical and chemical) have different implications for the susceptibility of stratospheric O₃ to atmospheric perturbations, and may manifest themselves in different ways and at different times in spring. The chemical mechanism may be dominant during the initial decline after the return of the Sun, when the strength of upwelling is still weak. Thereafter, however, the CIY concentrations may be reduced by the upwelling, effectively diminishing the catalytic removal of O₃. Future measurements should be aimed at evaluating the relative importance of the two separate processes.

The radiative-dynamical mechanism we have described should be reflected in the temporal and spatial behaviour of many long-lived species and stratospheric aerosol. As a result of the existence of the reverse circulation, we may expect to see increasing abundances of 'upward-diffusing' species (such as chloro-fluorocarbons, N2O and CH4) and decreasing concentrations of 'downward-diffusing' species (HNO3, HCl, stratospheric aerosol) during early spring in the Antarctic lower stratosphere. Simultaneous observations of these trace gases and aerosols will be useful. Observations of the vertical temperature gradient will determine values for Γ , providing better estimates of \bar{w} from ΔH .

The chemical mechanisms require concentrations of ~0.5-1 p.p.b.v. for CIO and 20 p.p.t.v. for BrO. Levels of OCIO comparable to those of daytime ClO could be obtained at night starting in late autumn, if sufficient BrO is present. The OClO is photolysed within minutes after sunrise, with a correspondingly rapid increase in ClO. Observations of the diurnal variation of both ClO and OClO will yield indirect evidence of the magnitude of the BrO abundance. Measurements of NO2 in the lower stratosphere are also needed. The technology for measuring these species is presently available and should be used.

This research has been supported by NASA grants NAGW-798 to MIT and NAGW-4080 to AER. K.-K.T. acknowledges support from the John Simon Guggenheim Foundation during his sabbatical year. Work at AER is also supported by the Fluorocarbon Program Panel of the Chemical Manufacturers Association. We thank M. McIntyre, M. Prather and A. Tuck for comments, S. Chubachi for reprints, and M. McElroy, S. Solomon and R. Stolarski for providing us with their results before publication.

Received 7 March: accepted 12 June 1986.

- 1. Chubachi, S. in Proc. Quadrenn. Ozone Symp. (eds Zerefos, C S & Chazi, A) (Reidel,
- Dordrecht, 1985). 2. Farman, J. C., Gardina, B. G. & Shanklin, J. D. Nature 315, 207-210 (1985)
- Stolarski, R. S. et al. Nature 322, 808 (1986).
 McElroy, M. B., Salawitch, R. J., Wofsy, S. C. & Logan, J. A. Nature 321, 759-761 (1986)
- Solomon, S., Garcia, R. R., Rowland, F. S. & Wuebbles, D. J. Nature 321, 755-758 (1986)
 Brewer, A. W. Q. Jl R. met. Soc. 75, 351-363 (1949).
- Dobson, G. M. B. Proc. R. Soc. A235, 187-192 (1956).
 Murgatroyd, R. J. & Singleton, F. Q. Jl R. met. Soc. 87, 125-135 (1961).
- Dunkerton, T. J. atmos. Sci. 35, 2325-2333 (1978).
 Tung, K. K. J. atmos. Sci. 39, 2230-2355 (1982).

- 11. Ko, M. K. W., Tung, K. K., Weisenstein, D. K. & Sze, N. D. J. geophys. Res. 90, 2313-2329 (1985).
- 12. Solomon, S., Garcia, R. R. & Stordal, F. J. geophys. Res. 90, 12981-12990 (1985).

- Dütsch, H. U. Pure appl. Geophys. 116, 511-529 (1978).
 Bütsch, H. U. Pure appl. Geophys. 116, 511-529 (1978).
 Bowman, K. P. & Krueger, A. J. J. geophys. Res. 90, 7967-7976 (1985).
 McIntyre, M. E. J. met. Soc. Japan 60, 37-65 (1982).
 McIntyre, M. E. & Palmer, T. N. Nature 3205, 593 (1983).
 Murgatroyd, R. J. in The Global Circulation of the Atmosphere (ed. Corky, G. A.) (Royal Meteoclopics). Society, Locales, 1969). Meteorological Society, London, 1969).
- 18. Fels, S. B., Mahlman, J. D., Schwarzkopf, M. D. & Sinclair, R. W. J. atmos. Sci. 37, 2265-2297 (1980).
- 19. Wehrbein, W. M. & Leovy, C. B. J. atmos. Sci. 39, 1532-1544 (1982).
- WMO/NASA, Atmospheric Ozone: Assessment of our Understanding of the Process Controlling its Present Distribution and Changes (in the press).
- Kiehl, J. T. & Solomon, S. J. atmos. Sci. (in the press).
 Kent, G. S., Trepte, C. R., Farrukh, U. O. & McCormick, M. P. J. atmos. Sci. 42, 1536-1551 (1985). 23. Yung, Y. L., Pinto, J. P., Watson, R. T. & Sanders, S. P. J. atmos. Sci. 37, 339-353 (1980).

- Ko, M. K. W. & Sze, N. D. J. geophys. Res. 89, 11619-11632 (1984).
 Clyne, M. A. A. & Watson, R. T. JCS Faraday Trans. 1, 73, 1169 (1977).
- Wofsy, S. C. J. geophys. Res. 83, 364-378 (1978).
- Turco, R., Hamill, P., Toon, O. B., Whitten, R. C. & Kiang, S. S. J. atmos. Sci. 36, 699 (1979).
 McCormick, M. P., Steele, H. M., Hamill, P., Chu, W. P. & Swissler, T. J. J. atmos. Sci. 39,
- 1387-1397 (1982).
- 29. Hoffman, D. J. & Rosen, J. M. Geophys. Res. Lett. 12, 13-16 (1985).
- Mugnai, A., Fiocco, G. & Grams, G. Q. Jl R. met. Soc. 104, 783-796 (1978)
 Strobel, D. F. J. geophys. Res. 83, 6225-6230 (1978).
- Rowland, F. S., Sato, H., Ichwaja, H., Elliott, S. M. J. Phys. Chem. 90, 1985-1988 (1986).

High-resolution lattice imaging reveals a 'phase transition' in Cu/NiPd multilayers

C. S. Baxter & W. M. Stobbs

Department of Metallurgy and Materials Science, University of Cambridge, Pembroke Street, Cambridge CB2 3QZ, UK

Considerable interest has been generated in metal multilayers by the discovery of anomalous variations in their physical properties as a function of layer thickness. Of particular interest is the 'supermodulus effect', observed for several multilayer systems at modulation wavelengths of 1.6-3.0 nm, in which an elastic modulus can increase by up to 400% (ref. 1). Various explanations for this effect have been suggested, and as part of an investigation aimed at clarifying the role of coherency strains in multilayer properties we are studying the behaviour of Cu/NiPd multilayers. We have developed transmission electron microscopy (TEM) techniques which allow the structural characterization of these materials, including the measurement of both the extent of interlayer mixing and the lattice plane spacings. Here we present some of our results in the latter category and discuss data which indicate that a novel form of 'phase transition' occurs as the modulation wavelength is decreased.

Metal multilayers typically consist of ~1,000 alternating layers of two metals or alloys, with modulation wavelengths (defined as the combined thickness of adjacent layers of each material) in the range 1.0-6.0 nm. Explanations which have been put forward for wavelength-dependent multilayer property changes range from theories based on critical Fermi surface/Brillouin zone interactions to arguments that consider the consequences of interlayer stress relaxation by the generation of misfit dislocations. The development of Fermi surface theories is hindered by the fact that the precise form of multilayer Fermi surfaces is not known, but as a first approximation these can be taken as equivalent to those of the corresponding homogeneous alloys. For example, it has been shown² that the peaks in modulus of both Ag/Pd and Cu/Ni multilayers occur at modulation wavelengths for which the additional Brillouin zones introduced by the modulations make tangential contact with the alloy Fermi surfaces. Any theoretical approach necessitates the selection of appropriate structural models to represent the multilayers, so we have had to develop new TEM techniques allowing better structural characterization of a multilayer than is possible by X-ray methods. The Cu/NiPd multilayer system has the added advantage in this context that the difference



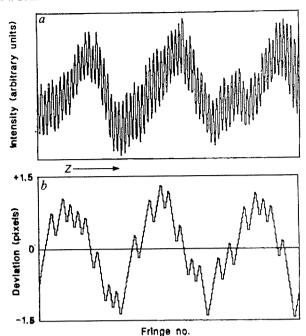
Non-axial lattice image of a Cu/NiPd multilayer taken on the Cambridge HREM operated at 500 kV. Scale bar, 2 nm.

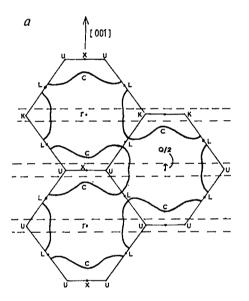
between the bulk lattice parameters of the layers (and hence the resulting coherency strains) can be altered systematically by varying the Ni: Pd ratio. Our observations indicate that interfacial dislocations do not play a critical role in the behaviour of the Cu/NiPd system at or near critical wavelengths, and this result is discussed elsewhere³.

The multilayers we have used were deposited by Somekh using a magnetron sputter deposition system⁴. Although we have examined films grown with both [001] and [111] epitaxial orientations, the results we report here are for [001]-oriented films only.

A fundamental part of our structural studies has been an attempt to locate the atomic positions as accurately as possible using high-resolution electron microscopy (HREM). Obtaining analysable high-resolution images of a modulated structure, even when thin enough to be treated as a weak-phase object, requires better resolution than is needed for the measurement of lattice spacings in either layer alone. This is because the modulated spacing variations are associated primarily with the high-frequency Fourier coefficients. Simulations for idealized specimens (that is, those exhibiting no variations in phase caused by, for example, local thickness changes) indicate that the lattice plane spacing variations should be detectable in axial lattice images, although the fringe positions would be too sensitive a function of defocus to be analysed reliably. In fact, despite sufficient resolution for accurate imaging of the spacings concerned in uniform specimens, in practice the variation cannot be detected⁵—presumably because when working near the limit of the transfer function the sensitivity of the image to inevitable local phase changes is accentuated. We have overcome this problem by using non-axial rather than axial illumination conditions, which increases the accuracy to which lattice spacings can be measured⁶; a typical image of a 4.4-nm modulationwavelength Cu/NiPd multilayer is shown in Fig. 1. Images of this type now contain modulated fringe spacings, as revealed by the measurements shown in Fig. 2b, obtained from the fringe intensity profile shown in Fig. 2a. Our analysis of these profiles has allowed us to determine the lattice strains of multilayers with relatively large modulation wavelengths and lattice mismatch⁷, but for specimens for which either the lattice mismatch is small or, more frustratingly, the wavelength is low (including the anomalous range near 2.0 nm), the modulation cannot be detected above the random noise in the fringe measurements. However, in these cases it is still possible to gain significant structural information by measuring the average lattice spacings in directions parallel and perpendicular to the layer normal $(\bar{d}(002))$ and $\bar{d}(020)$ respectively). The lattice mismatch between the layers in our multilayers is accommodated by coherency strains, and conventional elasticity theory can be used as a first approximation to predict the expected values of these average spacings, which will not generally be the same. The relative values of $\bar{d}(002)$ and $\bar{d}(020)$ can be measured from lattice images with a high degree of accuracy ($\sim \pm 0.2\%$), and when this is done for a relatively long-wavelength (4.4 nm) Cu/NiPd multilayer we find that the measured difference in the two spacings has the same sense and size $(\bar{d}(020) \ 1\%$ bigger than $\bar{d}(002))$ as

Fig. 2 a, Intensity profile of lattice fringes from a Cu/NiPd multilayer as used for measuring fringe positions. b, Deviations from line of least-squares fit of fringe positions measured from a; the mean fringe spacing is 6.6 pixels. To show the modulation clearly, these data have been presented as the deviation of each successive fringe position from the line of least-squares fit through the fringe positions: in this format, the maximum spacing is associated with the maximum positive gradient and the minimum spacing with the maximum negative gradient. As with any high-resolution imaging, care is needed in the interpretation of these measurements and the measured fringe spacings cannot be directly related to the lattice spacings in the multilayer. Instead, the spacings measured from a focal series of images were compared with spacings in images simulated using multilayer models with different interlayer strains. These models were based on composition profiles determined by a Fresnel method^{5,7}. For the image series including the example shown in Fig. 2, the best match between the simulated and measured spacing variations (9% in Fig. 2b) was found for a model with a 6% variation in lattice plane spacing. The fit with a value of 6% is less than would have been expected for a nominal misfit of 3.5% (as for Cu/Ni_{0.5}Pd_{0.5}), but the reduced value is presumably explained by surface relaxation in the TEM specimen⁸.





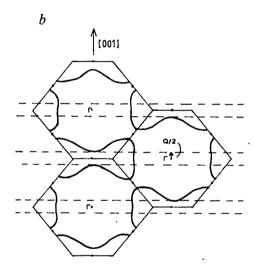


Fig. 3 a, Possible Fermi surface of Cu/NiPd drawn in the periodic zone scheme (based on Fermi surface of CuNi (ref. 9) and with I, X, L, K and U used conventionally to indicate high-symmetry points of the Brillouin zone). The zone boundary introduced by a 1.6-nm wavelength modulation along [001] (wave-vector (1) are also shown. No points of tangential contact occur, but contact could occur at C with a shorterwavelength modulation, b, Possible Fermi surface of Cu/NiPd with a tetragonal distortion of the unit cell such that the mean (002) lattice spacing is increased by 10%. The zone boundaries corresponding to the 1.6-nm modulation now make contact with the Fermi surface.

predicted by our linear elasticity calculations. However, at the shorter wavelength of 1.6 nm, $\tilde{d}(002)$ is 2.5% greater than d(020), and this cannot be accounted for using conventional elasticity theory. We are convinced that this result reflects a genuine wavelength-dependent change in the structure of the specimens rather than an electron-optical imaging artefact, because both differences were found to be consistently measureable to an accuracy far greater than the random errors involved for a range of specimen thickness, objective defocus and illumination conditions. Furthermore, surface relaxations, although undoubtedly important⁸, could not provide an explanation for this phenomenon: such effects are most marked when the specimen thickness is comparable to the wavelength, but the anomalous spacings are found in short-wavelength multilayers where the specimen thickness is at least 10 times the wavelength. We therefore conclude that an anomalous change has occurred in the structure of the shorter-wavelength multilayer, which can be thought of as a transformation to a novel tetragonal 'phase'. The transformation is difficult to model because of uncertainties in the electronic structure, but a consistent qualitative interpretation can be obtained by examining the consequences of the observed structural distortion on possible Fermi surface/Brillouin zone interactions. As a starting point, we have taken the Fermi surface of a Cu/NiPd multilayer as being approximately equivalent to that of a homogeneous CuNi alloy: this is shown in Fig. 3a for an undistorted cubic unit cell, together with the Brillouin zone introduced by a 1.6-nm modulation along [001]. No points of critical contact occur at this wavelength, but contact would occur at the points marked 'C' for shorter-wavelength (longer-wave-vector) modulations. However, critical contact is obtained at a wavelength of 1.6 nm if a tetragonal distortion of the crystal structure is introduced such that the dimensions of the Fermi surface remain approximately constant with respect to the origin but the lattice dimension along [001] is increased by $\sim 10\%$ (see Fig. 3b). The distortion required for contact is more than twice the observed change in the mean spacings (~4%), but both the substitution of Pd for Ni and the presence of the lower band gaps introduced by the modulation will raise the Fermi energy, while the Fermi surface would be expected to be increasingly distorted towards the Brillouin zone boundary as the modulation wavelength is decreased towards the value at which critical contact can occur by a 'transformation' of structure. This argument is clearly grossly oversimplified and a full calculation of any accuracy would be very difficult, but it is apparent that the trends indicated are in the observed direction.

This picture has several consequences: for example, while the transformation would be first-order thermodynamically, given

the associated changes in volume, precursory effects would be expected which should be reflected in progressive changes in physical properties on either side of the critical wavelength (as are, in fact, generally observed). A transformation-induced mechanism for the changes in physical properties of otherwise isostructural metal multilayers could thus have general significance. It is not clear whether the transformation we have observed occurs in one or both components of the multilayer, but it might be possible to design a system for which both layers exhibit transformations at different wavelengths. Any correlated anomalies in the physical properties, if observed, would be useful in testing the ideas outlined.

Whatever the precise mechanism for the 'transformation', our data demonstrate a fundamental change in the structure of Cu/NiPd multilayers as a function of the modulation wavelength. Experiments are in hand to correlate the wavelength dependence of the structural and physical anomalies of this system.

Received 8 April; accepted 25 June 1986.

- Henein, G. E. & Hilliard, J. E. J. appl. Phys. 54, 728-733 (1983).
 Pickett, W. E., J. Phys. F12, 2195-2204 (1982).
 Baxter, C. S. & Stobbs, W. M. Pap. 44th a. Meet. Electron Microsc. Soc. Am. (San Francisco
- Somekh, R. E. & Baxter, C. S. J. Cryst. Growth (submitted).
 Baxter, C. S. & Stobbs, W. M. EMAG 85, 387-390 (Institute of Physics Conf. Ser. No. 78,
- 6. Hall, D. J., Self, P. G. & Stobbs, W. M. J. Microsc. 130, 215-224 (1983).
- Baxter, C. S. Thesis, Univ. Cambridge (1986).
 Treacy, M. M. J., Gibson, J. M. & Howie, A. Phil. Mag. A51, 389-417 (1985).
- 9. Gordon, B. E. A., Temmerman, W. M. & Gyorffy, B. L. J. Phys. F11, 821-857 (1981).

New method for the measurement of osmium isotopes applied to a New Zealand Cretaceous/Tertiary boundary shale

Frederick E. Lichte*, Shane M. Wilson†, Robert R. Brooks†, Roger D. Reeves†, Jiri Holzbecher‡ & Douglas E. Ryan‡

- * US Geological Survey, Federal Center, Denver, Colorado 80225, USA
- † Department of Chemistry and Biochemistry, Massey University, Palmerston North, New Zealand
- ‡ Trace Analysis Research Centre, Dalhousie University, Halifax, Nova Scotia, Canada B3H 4J1

The determination of osmium content and isotopic abundances in geological materials has received increasing attention in recent years following the proposal of Alvarez et al. 1 that mass extinctions at the end of the Cretaceous period were caused by the impact of a large (~10 km) meteorite which left anomalously high iridium levels as a geochemical signature in the boundary shales. Here we report a new and simple method for measuring osmium in geological materials, involving fusion of the sample with sodium peroxide, distillation of the osmium as the tetroxide using perchloric acid, extraction into chloroform, and absorption of the chloroform extract onto graphite powder before instrumental neutron activation analysis. In a variant of this technique, the chloroform extract is back-extracted into an aqueous phase and the osmium isotopes are determined by plasma-source mass spectrometry (ICPMS). We have used this method on the Woodside Creek (New Zealand) Cretaceous/Tertiary boundary clay and have obtained the first osmium content (60 ng g^{-1}) for this material. The $^{187}Os/^{186}Os$ ratio is 1.12 ± 0.16 , showing a typical non-crustal signature. This combined distillation-extraction-ICPMS method will prove to be useful for measuring osmium isotopes in other geological materials.

Although ~50 Cretaceous/Tertiary (K/T) boundary sites with anomalous iridium levels have now been discovered2, only one of these, at Woodside Creek, New Zealand, is on land in the Southern Hemisphere and is therefore of some importance for an interpretation of the events which occurred at the end of the Cretaceous. The geochemistry of the Woodside Creek occurrence has been reported by Brooks et al.3, who found 153 ng g⁻¹ iridium (carbonate-free basis) in the basal layer of the 8-mmthick boundary shale, together with an integrated iridium deposition of 187 ng cm⁻²

Most of the original work on the K/T boundary in different parts of the world involved the use of iridium as a marker. particularly as this element is easier to determine by neutron activation analysis (NAA) than are the other platinum metals. Osmium, which has a similar abundance to iridium, serves almost equally well as an indicator of extraterrestrial (or mantle) material, but has a sensitivity ~30 times poorer than that of iridium when determined by neutron activation. The isotopic ratio 187Os/186Os is also of use in explaining the nature of geochemical signatures, as meteorites (and mantle material) typically have ratios near 1.0 (ref. 4), whereas crustal material averages ~ 10.0 (refs 5, 6).

The recent development of ICPMS for determining isotopic abundances⁷ has opened up exciting new possibilities for determining these isotopes in geological materials. We have therefore developed a technique of removing osmium from rocks by distillation, followed by ICPMS or instrumental NAA (INAA) determinations. This procedure has been applied to the measurement of osmium isotopes in the Woodside Creek K/T boundary shale, as described below.

Samples of the basal 2-mm layer of the boundary shale (0.5 g) were fused with 5 g of sodium peroxide at 650 °C for 2 min. After cooling, the melt was transferred to a 50-ml flask together with 20 ml of 70% perchloric acid, and distillation was carried out into a receiver initially containing 2 ml of the same acid. After 8 ml of mixture had been recovered, distillation was terminated and the distillate was shaken for 5 min with 10 ml of chloroform. The extract was used either for INAA or for ICPMS determinations. For the former purpose the extract was mixed with 10 ml of a 1:1 chloroform/ethanol reagent containing 0.5% thiourea acidified with perchloric acid (2% v/v), and the combined mixture was absorbed and evaporated drop by drop on 1 g of high-purity graphite powder. The powder was analysed for osmium by INAA using a Slowpoke reactor with a flux of 5×10^{11} n cm⁻² s⁻¹. The irradiation time was 16 h and counting was performed for 16 h or longer using a Ge(Li) detector or LEPD (low-energy particle detector) after a decay period of 7

For the ICPMS determinations the chloroform extract was back-extracted into 2 ml of an aqueous phase containing 1% thiourea and 0.5 M sulphuric acid. The spectrometer was a Sciex Elan ICP-MS instrument with a glass frit nebulizer⁸ which

Table 1 Osmium, iridium and gold concentrations (ng g⁻¹) and osmium isotopic ratios in meteorites and Cretaceous/Tertiary boundary shales

	Woodside Creek†	Allende chondrite	Stevns Klint	All chondrites
Au	59³‡	137 ⁹ , 145 ¹⁰	·7 ¹¹	
Ir	127 ³ ‡	$745^{12}, 785^{10}$	4611	*******
Os	60*	720*, 759 ¹² , 828 ¹⁰	6011	
Os/Au	1.12*	4.96*	8.5711	
Ir/Au	2.15^{3}	5.13 ^{7,10}	6.5711	
187Os/186Os	1.12*	0.91*	1.655	1.114

Superscript numbers are references.

This work.

† Woodside Creek CaCO3 is 17%, not 7% as quoted in ref. 3.

‡ Values from which the CaCO3-free concentrations of ref. 3 were derived.

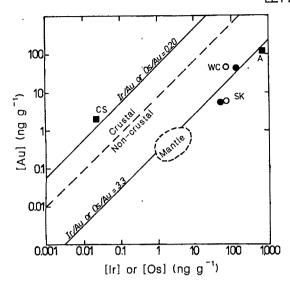


Fig. 1 Plots of gold versus iridium (•) or osmium (O) in crustal, meteoritic and K/T boundary material (, both Ir and Os). CS, mean for Canadian Shield⁷; SK, Stevns Klint⁸; WC, Woodside Creek (this work); A, Allende carbonaceous chondrite (this work).

increased nebulization efficiency to 90%, compared with 1-3% for conventional nebulizers. Each sample was analysed 10 times with a total integration time of 15 min at a nebulization rate of 30 μ l min⁻¹. Standard deviations (2 σ) were calculated automatically by the on-board computer. Other instrumental conditions were: r.f. power 1,150 W, nebulizer gas flow rate 0.7 litre min⁻¹, plasma gas 13 litre min⁻¹, sheath gas 1.0 litre min⁻¹, plasma sampling distance 22 mm from the load coil. The instrument was calibrated using an osmium standard dissolved in thiourea and sulphuric acid to match the sample solutions. The normalized instrument response was verified against the Allende meteorite standard, which has documented isotopic abundances. A reagent blank showed no detectable blank for any osmium

Table 1 lists the data for total iridium and osmium and for the ¹⁸⁷Os/¹⁸⁶Os isotopic ratios. The osmium data are the first reported for the New Zealand material. Our data for the Allende carbonaceous chondrite and other data for K/T boundary material from Stevns Klint, Denmark, are also given.

Experiments with samples spiked with known amounts of osmium indicated a recovery of 93% in the distillation-extraction procedure. After allowing for this factor, we obtain a total osmium content of 720 ng g⁻¹ (by INAA) for the Allende specimen, which is close to the values of 745 ng g⁻¹ (ref. 9) and 828 ng g⁻¹ (ref. 10) reported by other workers. Our value of 60 ng g⁻¹ for osmium in the Woodside Creek basal layer is identical to that found by Kyte et al. 11 for Stevns Klint, and is in line with the observation of Brooks et al.3 that the New Zealand and Danish K/T shales have similar chemical compositions (apart from the higher CaCO₃ content of the latter).

Palme et al. 12 have pointed out that the Ir/Au ratio in geological materials is a reliable geochemical signature by which to separate crustal and non-crustal samples. As the osmium and iridium concentrations in chondrites are almost identical (~700 ng g⁻¹), the Os/Au ratio should be an equally reliable marker for non-crustal materials. Figure 1 shows a plot of gold versus iridium or osmium for the New Zealand and Danish boundary shales, as well as for the Allende meteorite and for crustal material represented by mean values for the Canadian Shield12. The data clearly indicate a non-crustal source for the New Zealand material, and because the values lie well outside the field for mantle material, an extraterrestrial source is indicated.

Our value of 1.12 ± 0.16 (2 σ) for the ¹⁸⁷Os/¹⁸⁶Os isotopic ratio is the same as that reported by Luck and Allègre⁴ for the mean of 10 chondrites (1.11±0.01), suggesting an extraterrestrial source for the osmium. It is true that the ratio is also typical of mantle material but this question has already been dealt with above (see also Fig. 1) and we prefer to propose a probable extraterrestrial origin for the osmium. Certainly the findings clearly negate any arguments that the osmium is of crustal origin. Using our value of 10.4% for the extraterrestrial component of the New Zealand boundary shale3, we can calculate that correction for terrigenous osmium would lower our ratio from 1.12 to 1.10. This is still extremely close to the ratio for chondrites and gives the best evidence so far for the non-crustal origin of the osmium (and by inference also probably the iridium) in the Woodside Creek material.

It is suggested that our combined distillation-extraction-ICPMS procedure will have a continuing use for the determination of osmium isotopic ratios in a wide variety of geological materials. In the application reported here, measurements were made on solutions containing only ~0.15 ng ml⁻¹ of the two osmium isotopes (that is, ~5 ng total osmium), and our combined procedure should prove to be an acceptable alternative to the chemical separation-mass spectrometric ion probe method now in use.

Received 31 December 1985; accepted 30 May 1986.

- Alvarez, L. W., Alvarez, W., Asaro, F. & Michel, H. V. Science 208, 1095-1108 (1980). Alvarez, W., Alvarez, L. W., Asaro, F. & Michel, H. V. Spec. Pap. geol. Soc. Am. 190, 305-315
- Brooks, R. R. et al. Science 226, 539-542 (1984). Luck, J. M. & Allègre, C. J. Nature 302, 130-132 (1983)
- Luck, J. M. & Turekian, K. K. Science 222, 613-615 (1983). Palmer, M. R. & Turekian, K. K. Nature 319, 216-220 (1986).
- Date, A. R. & Gray, A. L. Analyt. Lond. 108, 159-165 (1983). Layman, L. R. & Lichte, F. E. Analyt. Chem. 54, 638-642 (1982).
- Takahashi, H., Janssens, M. J., Morgan, J. W. & Anders, E. Geochim. cosmochim. Acta 42, 97-106 (1978)
- 10. Kallemeyn, G. W. & Wasson, J. T. Geochim. cosmochim. Acta 45, 1217-1230 (1981).
- 11. Kyte, F. T., Zhou, Z. & Wasson, J. T. Nature 288, 651-656 (1980).
 12. Palme, H., Janssens, M. J., Takahashi, H., Anders, E. & Hertogen, J. Geochim. cosmochim Acta 42, 313-325 (1978).

Silicate microspherules intercepted in the plume of Etna volcano

R. Lefèvre*, A. Gaudichet*† & M. A. Billon-Galland†

* Laboratoire de Microscopie Analytique Appliquée aux Sciences de la Terre, Université Paris XII, 94010 Créteil, France † Laboratoire d'Etude des Particules Inhalées, 44, rue Charles Mourau, 75013 Paris, France

A possible volcanic origin has been suggested for the micrometresized spherules that have been discovered in polar snows or icecores¹⁻³, and in the stratosphere^{6,7}. However, although such particles, especially when black and magnetic, have been identified among the tephra deposits of some volcanoes^{3,8-12}, their volcanic emission has never been directly observed. Here we describe microspherules intercepted in the plume of Mount Etna, Sicily, during moderate recurring volcanic activity. Their study, using analytical transmission and scanning electron microscopy (ATEM and ASEM) demonstrates the simultaneous presence in the plume of glassy silicate microspherules of various chemical compositions (47-98% SiO₂).

Particles were collected in September 1984 and August 1985 on a Nuclepore membrane (porosity 0.4 µm) by bulk filtration of the aerosol flux emitted by a summit crater of Mount Etna (Bocca Nuova, elevation 3,340 m above sea level). A volume of 2-3 m³ of diluted volcanic plume was filtered at a flow rate of 1 m³ h⁻¹. The sampling head was placed inside the crater at the end of a 6-m-long flexible fishing rod, 2 m beneath and 2 m away from the crater rim. Because the wind blowing onto the crater was weak or moderate during sampling, only rising

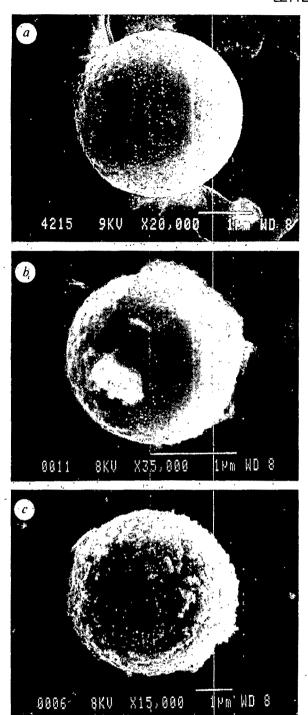


Fig. 1 Scanning electron micrographs of three typical microspherules intercepted in the permanent plume of Mount Etna volcano and washed with filtered distilled water (JEOL JSM 840 electron microscope; accelerating voltage, 8 kV; scale bar, 1 μm). a, Smooth and clean microspherule showing small punctuations; b, Microspherule coated with microparticles, among them a probable feldspar crystal. c, Granular microspherule.

aerosols were collected and these showed no evidence of contamination by wind-blown tephras from the external flanks of the volcano.

The Nucleopore membrane, which has been covered with a carbon layer before sampling, received a second carbon layer after particle collection. The collected particles, trapped between the two carbon layers, were then transferred onto gold grids for analysis by ATEM^{13,14}. This transfer was performed by chloroform dissolution of the membrane under moderate aspir-

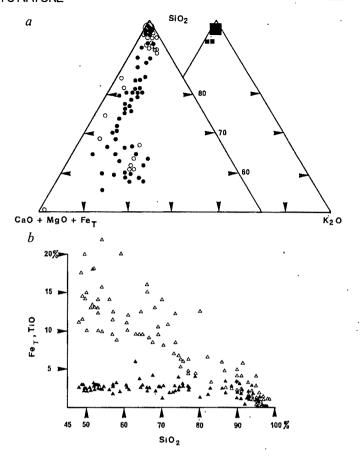


Fig. 2 a, Chemical compositions plotted in an SiO₂ versus K₂O and CaO+MgO+Fe_T diagram of 54 glassy microspherules intercepted in September 1984 (●) and 36 in August 1985 (○), compared with 17 shards of volcanic glass intercepted in September 1984 (■), in the plume of Mount Etna. These diagrams show the variation of the compositions of microspherules and the hypersiliceous composition of shards. b, Relationship between SiO₂ content and Fe_T (△) or TiO₂ (▲) of 90 microspherules. Note the Fe_T decrease linked with the SiO₂ increase. Titanium remains almost constant, except for the most SiO₂-enriched spherules.

ation. For analysis by ASEM the membrane was not dissolved and was placed directly on the specimen holder.

Among the collected particles, non-silicate species (such as sulphates and oxides) are predominant. The silicates consist of crystals (such as feldspars), shards of silicate glass¹⁵ and microspherules. The diameter of the microspherules ranges from 0.1 to 5 μ m and is <2 μ m for 85% of them. The concentration of microspherules was estimated to be $3\times10^6\,\mathrm{m}^{-3}$ in September 1984 and $7\times10^6\,\mathrm{m}^{-3}$ in August 1985. Their external morphology is either smooth and clean (Fig. 1a), coated with fine grains or crystals (Fig. 1b), or granular (Fig. 1c). Electron microdifraction demonstrates the glassy structure for the smallest spherules (0.5 µm in diameter). The individual quantitative chemical composition of the microspherules was obtained by X-ray energydispersive spectrometry using the peak ratio method and taking Si as an internal reference element 16. This is valid if the particles can be considered to be thin layers (<2 µm). The results are highly variable, even within a given sample. In particular, the SiO₂ content ranges from 47 to 98%, that is, from values typical of Etnean lavas (but with a noticeable K-enrichment) to values corresponding to nearly pure silica (Table 1 and Fig. 2). No correlation is observed between morphology, size and composition.

Assuming that each microspherule has a mean diameter of 1.4 µm and a mean density of 2.75 g cm⁻³ (between 2.85 for basalt and 2.26 for tridymite), the 10⁶ microspherules we have

encountered per m³ of filtered air have a total mass $\sim 4 \times 10^{-3}$ mg. The SO₂ discharge from Mount Etna averages $\sim 4 \times 10^3$ tonne day⁻¹, with a mean SO₂ concentration in the plume ^{17,18} of ~ 10 mg m⁻³. The discharge of microspherules can then be roughly estimated at 1.6 tonne day⁻¹.

The genesis of such microspherules and their surprisingly variable chemical composition within the same sample of diluted volcanic plume need to be explained. Some possible hypotheses are discussed below (Fig. 3):

- (1) Contamination of the volcanic plume by industrial fly-ash seems to be excluded: the concentration of fly-ash samples in the same conditions at the periphery of the volcano and the limit of its sedimentary basement (Village of Maletto, elevation 975 m) is a $\sim 10^4$ m³, much lower than the concentration of glassy microspherules in the Mount Etna plume. Moreover, the chemical composition of industrial fly-ash is not commonly hypersiliceous 19,20 , in contrast to a large proportion of our volcanic microspherules. A volcanic origin of these particles is therefore likely.
- (2) The spheroid shape of the particles may be explained by two physical processes of emission: lava fountaining and/or phreato-magnetic eruptions. (a) Spheroidal droplets of glass are produced by highly fluid lava fountaining, as for example in Hawaii^{11,12,21,22}. Intense degassing of fluid lavas allows the dispersal of a spray of liquid magma droplets, which are then rapidly cooled to form simple glass spheres²³. The same mechanism has been proposed for the glass spheres discovered in Apollo 15 and 17 lunar samples²¹. However, the analysis of both terrestrial and lunar spheres has shown that their composition is constant. Therefore, although the mechanism of lava fountaining could be responsible for the presence of microspherules in the Etna plume, it does not explain the chemical variation. (b)Spheroidal-shaped particles have been observed²⁴ by SEM in the debris collected after experimental explosions, simulating phreato-magmatic eruptions produced by the reaction of water with a melted mixture of $Al_2O_3 + Fe$. These particles are very similar to hydrovolcanic ash²⁵. A phreato-magmatic process may thus explain the shape of our microspherules, but cannot account for their variable composition. (c) Whatever the genesis of microspherules (lava fountaining or phreato-magmatic explosions), the stagnation in the air-plume column between magma surface and crater rim of microspherules emitted by magmas of various compositions following one another in the pipe, is not compatible with the monotonous chemistry of the Etnean basaltic lavas produced by lateral eruptions^{26,27} (Table 1). However, note that siliceous xenoliths derived from the sedimentary substratum of Mount Etna have been described in the pyroclastic

products of Mount Rossi and Mount Silvestri eruptions (1669 and 1892), on the southern flank of the volcano²⁸. The mechanism of generation and extraction of this material, in microspherical form, from such partially assimilated xenoliths is difficult to imagine.

- (3) Incipient liquid immiscibility has also been suggested²⁹ to explain the presence of SiO₂-rich spherules (in the micrometre size range) found in the products of the experimental alteration of Etnean basaltic glass by hot water in a Soxhlet apparatus. If such microspherical domains were present in the magma, they would be emitted in the plume directly after solidification at the surface. Such an explanation seems implausible in the present circumstances.
- (4) Pre-existent microspherules could be extracted from weathered tephra deposits falling onto the magma surface before explosive or phreato-magmatic eruptions. The same microspherules found in the weathered tephra deposits on the inner flanks of the crater could be mobilized by the ascending gaseous flux which forms the permanent plume of the Mount Etna volcano. This hypothesis appears to be unlikely, as such structures have not been described in weathered volcanic tephra.
- (5) Volcanic water emission by the Mount Etna plume has been evaluated 18 at $\sim 1.4-2\times 10^5$ tonne day $^{-1}$. This water is mostly meteoric in origin. During its circulation through the volcanic edifice, it would become heated and enriched in silica and ionic salts. At the magma/atmospheric interface, the water is released as vapour, and we may consider that dissolved silica-rich products could then be condensed as microspherules with varying chemical composition.
- (6) Some experiments³⁰ emphasize the role of sulphur reacting with many of the common rock-forming silicates over wide temperature and pressure ranges to produce sulphides, oxides and pure silica. Depending on the amount of SO₂ discharge from Mount Etna^{17,18}, the sulphurization may be an important and suitable process for the generation of SiO₂-enriched microspherules and, depending on the speed of transport, may explain the observed compositional spectrum.
- (7) Combustion of volcanic gases at the magma/atmosphere interface may be responsible for an increase in temperature, causing differential fusion of the solid silicates present in the magma, followed by a quenching of microspherules of various compositions. This mechanism is invoked to explain the fly-ash formation in coal-burning power-station furnaces: their morphology is acquired during cooling of the non-combustible mineral content of the coal, melted at temperatures >1,500 °C, while being carried along with the gaseous combustion products 31,32

Table 1 Typical chemical compositions (oxide weight) of small volcanic glass shards (A to C) and microspherules intercepted in September 1984 (D to H) and August 1985 (I to M) in the permanent plume of Mount Etna, compared with the mean bulk composition of recent lavas and tephras (N)^{26,27}

	Shares of volcanic glass (September 1984)		Glassy microspherules (September 1984)			Glassy microspherules (August 1985)				Etna lavas				
	A	В	C	D	Е	F	G	Н	I	J	K	L	М	N
SiO ₂	93.8	93.3	95.2	96.3	82.7	71.6	64.5	49.3	95.3	86.6	70	60.6	49.8	47.8
Al_2O_3	2.4	3.1	3	2.2	3.9	5.1	9.5	14.3	0.3	1.7	11.7	11.3	14.2	17.3
FeO _T	1.1	0.9	0.3	0	3.4	10.9	12.5	11.4	0.7	2,4	13.7	11.8	10.2	10.8
MgO	0	0	0	1	0.4	0	0.7	2.1	0	0	0	2.1	2.3	5.2
CaO	0	0.3	0.1	0.1	1.7	4	2.6	8.2	0.1	0.9	0.2	5	6.7	10.4
Na ₂ O	0.9	0.8	0	0	0	0	0	0	0	0	0	0	0.7	4
K ₂ Ö	1.5	1.4	1	0	5	5.7	7.2	11.8	2.5	5.2	3.1	6.5	13.3	1.7
TiO,	0	0	0.1	0	2.5	2.3	2.7	2.5	0.7	2.9	1.1	2.3	2.4	1.7
MnÕ	0	0	0	0.2	0	0	0	0	0	0	0	0.1	0	
Total	99.7	99.8	99.7	.99.8	99.6	99.6	99.7	99.6	99.6	99.7	99.8	99.7	99.6	99.1

The volcanic glass shards are always hypersiliceous; the microspherules vary from a typical Etna composition (with K-enrichment) to hypersiliceous composition (the Na-depletion is probably an artefact). Analyses were performed by ATEM (JEOL 100C fitted with an energy-dispersive x-ray spectrometer EDAX 711).

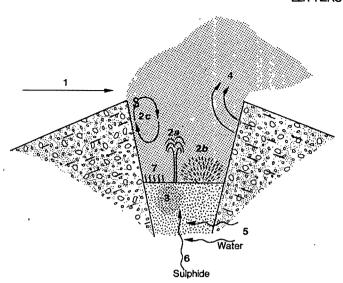


Fig. 3 Illustration of the hypotheses proposed in the text to explain the genesis and variable chemical composition of microspherules intercepted in the permanent plume of Mount Etna. (1), Contamination by industrial fly-ash; (2a) lava fountains; (2b) phreato-magmatic explosions; (2c) stagnation in the crater of different generations of microspherules emitted by successive magmas; (3) extraction of microspherules from SiO2-enriched domains in the magma (incipient liquid immiscibility). (4) extraction of pre-existent microspherules from weathered tephras; (5) dissolution by meteoric water, followed by water-emission and condensation of silica-rich products; (6) interaction between sulphur and silicates and/or magma to produce sulphides, oxides and silica; (7) combustion of volcanic gases and quenching of magmatic silicates; S, sampling location.

In the present state of our study, the more plausible hypotheses seem to be (2a), (5), (6) and (7) or a combination of these: the dissolving properties of water for silica at high temperatures and sulphurization of silicates are probably involved to produce SiO₂-enriched microspherules; the lava fountains^{33,34} and similar phenomena involving gas emissions occur at Etna and, finally, the surprising morphological analogies between Etnean glassy microspherules and industrial fly-ash generated in power plant furnaces suggest similar thermal conditions.

This work was supported by the Centre National de la Recherche Scientifique, Paris: Associated Unity 717, Physico-Chemistry and Geochemistry of the Atmosphere and Programme Interdisciplinaire de Recherches sur la Prévision et la Surveillance des Eruptions Volcaniques. We thank Professor D. Velde, Dr P. Allard and Dr K. H. Wohletz for stimulating discussions.

Received 27 January, accepted 15 May 1986.

- Fredriksson, K. & Martin, L. R. Geochim, cosmochim, Acta 27, 245-248 (1963),
- Wright, F. W. & Langway, C. C. J. geophys. Res. 68, 19, 5575-5587 (1963). Hodge, P. W. & Wright, F. W. J. geophys. Res. 69, 12, 2449-2454 (1964).
- Hodge, P. W., Wright, F. W. & Langway, C. C. J. geophys. Res. 69, 2919-2931 (1964). King, E. A. & Wagstaff, J. Antarct. J. U.S. 15, 78-79 (1980). MacKinnon, I. D. R. et al. J. geophys. Res. 87, A413-A421 (1982).
- 7. Clanton, U. S. et al. Cosmic Dust Catalog, Vol. 3, 1 (Lyndon B. Johnson Space Center,
- Wright, F. W. & Hodge, P. W. Ann N.Y. Acad. Sci. 119, 1, 1-361 (1964).
 Wright, F. W. & Hodge, P. W. J. geophys. Res. 70, 16, 3889-3898 (1965).
 Heiken, G. & Wohletz, K. Volcanic Ash, University of California Press, Berkeley (1985).
- 11. Heiken, G. & Lofgren, G. Bull. geol. Soc. Amer. 82, 1045-1050 (1971).
- Baker, G. Miner. Mag. 36, 1012-1023 (1967).
- Sébastien, P., Gaudichet, A. et al. J. microsc. spectrosc. Electron. 5, 83-97 (1980).
 Gaudichet, A. J. Phys. C2 45, Suppl. 2, 789-792 (1984).
 Lefèvre, R. et al. Cr. hebd. Séanc Acad. Sci., Paris 301, 1433-1438 (1985).
 Cliff, G. & Lorimer, G. W. J. Microsc. 103, 203-207 (1975).

- 17. Buat-Ménard, P. & Arnold, M. Geophys. Res. Lett. 5, 4, 245-248 (1978). 18. Faivre-Pierret, R. et al. Bull. volc. 43, 473-485 (1980).
- Roy, W. R. et al. Illinois State Geol. Surv. Environ. Geol. Not. 96, 1-69 (1981).
 Roymaden, A. R. & Shibaoka, M. Atmos. Envir. 16, 9, 2191-2206 (1982).
- Reid, A. M. et al. Eos 54, 606-607 (1973).
 Heiken, G. H. et al. Geochim. cosmochim. Acta 38, 1703-1718 (1977).

- Heiken, G. H. & McKay, D. S. Proc. 8th Lunar Sci. Conf. 3243-3255 (1977).
 Wohletz, K. M. & McQueen, R. G. Geology 12, 591-594 (1984).

- Wohletz, K. M. J. Volcan, geotherm. Res. 17, 31-63 (1933). Cristofolini, R. & Romano, R. Mem. Soc. geol. It. 23, 99-115 (1982). Clocchiatti, R. et al. Bull PIRPSEV, CNRS, Paris 104, 1-8 (1985).
- Clocchiatti, R. & Metrich, N. Bull. PIRPSEV, CNRS, Paris 92, 1-13 (1984). Trichet, J. & Sella, C. Cr. hebd Seanc. Acad. Sci., Paris 267, 1084-1086 (1968).
- Kullerud, G. & Yoder, H. S. Jr Yb Carnegie Instn Wash. 63, 218-222 (1964).
 Deuser, W. G. et al. Nature 305, 210-218 (1983).
- Hulett, L. D. Jr et al. Science 210, 1356-1358 (1980).
 McGetchin, T. R. & Head, J. W. Science 180, 68-70 (1973). 34. McGetchin, T. R. et al. J. geophys. Res. 79, 3257-3272 (1974).

Sewage sludge as an acidity filter for groundwater-fed lakes

W. Davison

Freshwater Biological Association, The Ferry House, Ambleside LA22 OLP, UK

The acidification of lakes by acid rain has increased awareness of the problems associated with acid waters¹, and has stimulated work on self-neutralization mechanisms² and liming strategies³. However, some very acid lakes, particularly those which have been newly formed by the widespread extraction of coal, mineral ores and sand and gravel, owe their acidity to another source. If pyrite is present, as it often is, its exposure to air induces microbially mediated oxidation, resulting in the production of sulphuric acid4. The waters of the lakes then resemble dilute acid, typically with pH < 3, with an impoverished flora and fauna. Neutralizing such waters with lime ameliorates the situation, but only temporarily because further supply of acidic groundwater inexorably lowers the pH. Here I report the use of a combined treatment of lime and sewage sludge, which has produced a self-regulating system, capable of maintaining a stable pH. The organic material which is spread over the bottom of the lake acts as a chemical filter, removing acidic sulphate as it enters, and converting it to neutral sulphide.

The use of sewage sludge for lake reclamation was tested in a pilot scheme. British Industrial Sand Ltd provided a small $(3.6 \times 10^4 \text{ m}^2)$ lake, Blue Lagoon, which had been formed by excavating sand below the water table at their Leziate site, near King's Lynn, Norfolk, England. It had no inflows, negligible catchment, a maximum depth of 4.5 m and a mean depth of 1.5 m. Over the past 10 years, during which time it had remained undisturbed, its waters had been consistently acid $(pH \sim 3)$. Analysis showed that the major acid components were H₂SO₄, 0.35 mM, Al₂(SO₄)₃, 0.11 mM and Fe(OH)SO₄, 0.05 mM.

On 3 April 1984, 477 m³ of activated sewage sludge containing 4.2% solids was pumped into the lake through a pipeline which was moved in an arc to cover approximately one quarter of the lake area. On 30 April 1984, 16.98 tonnes of calcium hydrated lime, equivalent to 15.3 tonnes of calcium hydroxide, were added through a submerged pipe to the deepest point.

Within days the sewage sludge settled out to leave clear water. The pH quickly rose to ~ 10 on adding the lime, after which, as carbon dioxide was supplied from the atmosphere, the solubility of calcium carbonate became the controlling factor and the pH stabilized between 7 and 8. To assess the pH without the effects of supply and removal of carbon dioxide by respiration and photosynthesis, it was also recorded after bubbling the sample with air for ≥30 min (Fig. 1). After two years the lake was still neutral.

Many factors may affect the pH, including the residence time of the water and further dissolution of precipitated calcium carbonate. The real test of the scheme is whether, first, sulphate is reduced and removed as sulphide, and, second, the rate of removal of sulphate is sufficient to cope with the further supply of acid from groundwater.

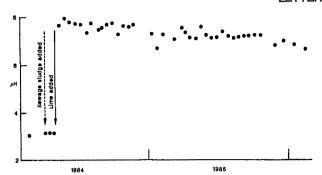


Fig. 1 Air-equilibrated pH of the surface waters of Blue Lagoon, plotted against time. The neutralization reactions involved are: $H_2SO_4 + Ca(OH)_2 = CaSO_4 + 2H_2O$; $AI_2(SO_4)_3 + 3Ca(OH)_2 = 2AI(OH)_3 + 3CaSO_4$; $Fe(OH)SO_4 + Ca(OH)_2 = Fe(OH)_3 + CaSO_4$.

On 27 August 1985, four cores of sediment and overlying water were collected from the deepest site using a Jenkin corer⁵. Analysis of two of the sediment cores revealed contents of organic carbon (11-20%) and acid volatile sulphide (1.2-18 mg per g dry weight) which were higher than would be normally expected for a very productive lake⁶. Evidently, appreciable quantities of sulphate had been reduced.

To quantify the rate and extent of sulphate reduction, two sealed sediment-water cores were incubated in the dark, initially at 17 °C, and then, after replenishing the sulphate-depleted water, at lower temperatures. Analysis of sulphate in the overlying water showed that sulphate was being removed at a rapid rate (Fig. 2), 835 mg m⁻² day⁻¹ at 17 °C and 278 mg m⁻² day⁻¹ at 10 and 4 °C. Knowing the original sulphate concentration of the lake water (\sim 125 mg l⁻¹), and assuming it is the same in the groundwater, one can calculate the minimum water residence time required for the reduction of sulphate to sulphide in the sediment to be able to cope with additional supply of acid from the groundwater. At the rate of consumption for 17 °C the minimum residence time is 6 months; at the lower temperatures it is 1.5 yr. As the mean annual temperature will be within this range, the residence time must exceed 1 yr if the chemical filter is to keep pace with the input of acid. There is evidence to show that at the outset of our study the residence time of Blue Lagoon was ~1 yr, but that it has since progressively increased to several years, presumably due to organic matter clogging the pores of the sand. If reduction of sulphate occurs as efficiently in the lake as in the laboratory experiment, this mechanism alone will prevent re-acidification. When these incubation results are applied to the whole lake, they are equivalent to an annual base production of 0.7-2.1 mequiv. 1⁻¹, which agrees with the figure of 1 mequiv. 1⁻¹ for hypolimnetic water².

So far only the consumption of freshly entering sulphate has been considered, but there is also sulphate already present within the water. Its associated acid was neutralized by the initial lime, so there is no requirement for this sulphate to be consumed to maintain neutrality. The concentration of sulphate, normalized with respect to sodium to compensate for evaporation and dilution effects, is highly variable, but did undoubtedly decline over a 2-yr period (Fig. 3). This indicates that removal of sulphate from the sediment was more than balancing further supply.

If the only supply of organic matter were from sewage sludge, the sediment's capacity for sulphate reduction would soon be exhausted. However, liming and the nutrients associated with the sludge stimulated high biological productivity, so that within a few months of treatment, algal populations were typical of a eutrophic pond. Thus, additional carbon, originating as atmospheric CO₂, is continually supplied to the lake and eventually accumulates as organic-rich sediment. Photosynthesis is effectively used, through artificially induced eutrophication, to combat acidification.

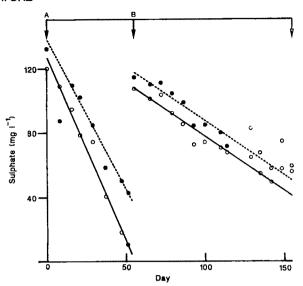


Fig. 2 Sulphate concentrations in the waters overlying the sediment of two sealed cores incubated in the dark. Initially (A-B) they were maintained at 17 °C, after which (at point B) the overlying waters were exchanged, under anoxic conditions, with water from the lake that had been deoxygenated using an Ar-CO₂ gas mixture to leave the pH unaltered. One core (O) was then incubated at 10 °C and the other (●) at 4 °C.

This scheme of permanent neutralization will be most effective when applied to large lakes with flat bottoms and deep water. Deep water (>5 m) prevents disturbance of the organic-rich sediment by wind-induced water movements, and flat bottoms help to ensure that the covering is uniform. Reduction of sulphate occurs readily in a sediment overlain by oxygenated water, but it proceeds with greater efficiency if the overlying waters become anoxic, a situation encouraged by depths >5 m. Covering the sediment with reducing organic material cuts off an important supply of oxygen to the groundwater. This limitation of oxygen, which will decrease the rate of production of acid from pyrite, will be more effective, the greater the area of the lake.

Unfortunately, the only experimental site available, Blue Lagoon, is smaller and shallower than ideally required, according to the above criteria. It is not surprising, then, that the pH appears to be slowly declining (Fig. 1), indicating that the lake may return to an acidic state. However, sulphate has been consumed by the sewage sludge and photosynthesis will continue the process, so the new equilibrium pH which will event-

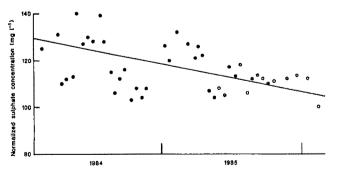


Fig. 3 Concentration of sulphate in Blue Lagoon, normalized with respect to the concentration of sodium. Normalized SO_4^{2-} concentration = $[SO_4^{2-}]_t \times [Na^+]_{in}/[Na^+]_t$, where the subscripts 'in' indicates initial concentration, and t the concentration at time t. Acidity removal is accomplished by the reduction of sulphate and ferric iron by organic material, and their precipitation as ferrous sulphide: $SO_4^{2-} + 2H^+ + Fe(OH)_3(s) + 9/4$ $CH_2O = FeS(s) + 9/4$ $CO_2 + 19/4$ H_2O .

ually be established will be higher than the original value. Thus, the feasibility of using organic material as a chemical filter for acidity has been established. The effectiveness of the scheme will vary from lake to lake, depending on the relative fluxes of acid and base. For lakes of appropriate morphology this scheme offers the possibility of permanent neutralization from one initial treatment.

One of the main features of this scheme is the use of organic matter to provide a chemical filter to neutralize the supply of acid from groundwater. Lakes affected by atmospheric acidification are not usually supplied with acid groundwater, except perhaps those in a peat terrain. However, introducing organic carbon, by adding sewage sludge or by adding nutrients to stimulate primary productivity, may still effectively combat acidification. Even in acidic conditions⁸, the decomposition of organic material will introduce base². The level of base production measured in this and other studies², ~ 1 mequiv. 1^{-1} yr⁻¹. is large compared with the acidity of rainwater, which at pH 4 is 0.1 mequiv. 1⁻¹. Evidently, by artificially inducing eutrophication, sufficient base can be produced to neutralize acidification from atmospheric sources. Further work is urgently needed to test such schemes and to compare them with liming strategies.

I thank BIS Ltd for sponsoring this work and many BIS and FBA staff for their enthusiastic involvement.

Received 7 April; accepted 11 June 1986.

- Mason, J. & Seip, H. M. Ambio 14, 45-51 (1985).
 Cook, R. B., Kelly, C. A., Schindler, D. W. & Turner, M. A. Limnol. Oceanogr. 31, 134-148 (1986).
- Fraser, J. E. & Brit, D. L. Preprint, General Research Corporation, McLean, Virginia (1982).
- Stumm, W. & Morgan, J. J. Aquatic Chemistry (Wiley, New York, 1981). Mortimer, C. H. Limnol Oceanogr. 16, 387-404 (1971).
- Northick, G. I. Zamine, Vectoring, 1971.
 Davison, W., Lishman, J. P. & Hilton, J. Geochim. cosmochim. Acta 49, 1615-1620 (1985).
 Kelly, C. A. & Rudd, J. W. M. Biogeochemistry 1, 63-77 (1984).
 Herlihy, A. T. & Mills, A. L. Appl. envir. Microbiol 49, 179-186 (1985).

Climatic influence on the isotopic composition of bone nitrogen

Tim H. E. Heaton, John C. Vogel, Gertrud von la Chevallerie & Gill Collett

Natural Isotopes Division, National Physical Research Laboratory, CSIR, Pretoria, South Africa

The 13C/12C isotope ratios in animal and human bone can be used as indicators of diet, more recently it was shown that the ¹⁵N/¹⁴N ratios of animals and humans are similarly determined by the food they eat³⁻⁵. Specifically, the stable carbon isotope composition reflects the proportion of C₃ and C₄ plants at the base of the food chain^{1,2}, while both ¹⁵N and ¹³C reveal the difference between a marine and terrestrial diet in modern as well as archaeological contexts⁵⁻⁷. Here we present data for human and animal bones from southern Africa which only partly conform to previously recognized patterns for 15N/14N ratios. Prehistoric human bones from a particular coastal region of South Africa show 15N/14N ratios consistent with the marine and terrestrial diets indicated by the 13C/12C ratios, but bones of both prehistoric humans and modern wild animals from a larger part of the subcontinent show variations in 15N/14N ratios which cannot be ascribed to known variations in diet. It appears that, in some environments, nitrogen isotope studies must also take into account the possible influence of the climate.

Collagen or gelatine was isolated from the bones of protohistoric and prehistoric human skeletons and modern wild herbivorous animals from a variety of climatic/vegetational habitats in South Africa and Namibia (Fig. 1). Isotopic ratios were determined on N2 and CO2 produced by combustion of the

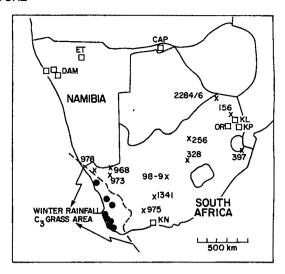


Fig. 1 Locations from which bone samples were obtained. •. Human skeletons from sites 0-60 km from the south-west coast. x, Human skeletons from sites 60-500 km from the coast, laboratory sample numbers are shown.

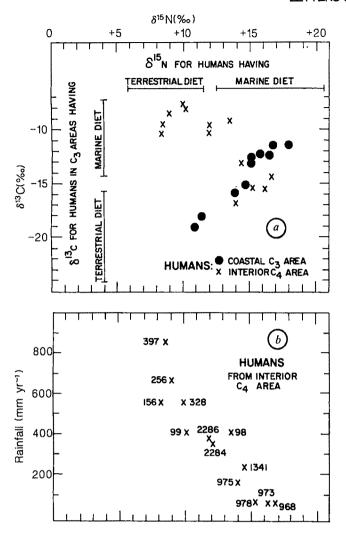
, Herbivorous terrestrial animals from game reserves as indicated (CAP=Caprivi; DAM= Damaraland; ET = Etosha; KL = Klaserie; KN = Knysna; KP = Kruger Park; OR = Origstad dam).

isolates⁸, and on N₂ produced by the Kjeldahl digestion-lithium hypobromite method⁹. The ratios are reported in the usual δ^{15} N and δ¹³C notation versus atmospheric N₂ and PDB carbonate standards, respectively. In all cases the N content of the samples ranged between 14% and 17%, within 10% of the expected value for protein. We therefore do not expect a noticeable postmortem shift in the isotopic values10

The isotopic data indicated by the solid circles in Fig. 2a are for human bones from sites in the southwestern part of South Africa, an area with winter rainfall in which C₃ grasses (and other C₃ plants) predominate¹¹. Sealy and van der Merwe¹². presenting carbon isotope data for a set of samples from the same region, suggest that in this C_3 area a higher $\delta^{13}C$ value in the skeletons reflects a higher marine/terrestrial food ratio in the prehistoric human diet. Data for human bones from other parts of the world indicate that a larger proportion of marine food in the diet should also be reflected by higher δ^{15} N values⁶. The solid circles in Fig. 2a in fact show a close correlation of increasing $\delta^{15}N$ with increasing $\delta^{13}C$, and it appears that in this region the nitrogen isotope data for human skeletons independently confirm the marine/terrestrial dietary interpretation of the carbon isotopes.

Human skeletons from a large area in the interior of South Africa (crosses in Fig. 2a) have $\delta^{15}N$ values similar to those of skeletons from the south-west coast, extending into the range of $\delta^{15}N$ for a marine diet. The samples from the interior, however, were from sites 60 to 500 km from the nearest coast and, whilst some of the nomadic people may have spent part of their life at the coast, these distances imply that terrestrial rather than marine food would have formed the major component of their diet. The unexpected range of $\delta^{15}N$ values for bones of humans from the interior is moreover also displayed by bones of herbivores feeding exclusively on terrestrial plants. Thus bones of a single herbivorous species, the African Elephant, have $\delta^{15}N$ values from +2.6 to +14.6%—a range which is wider than that previously reported for terrestrial herbivores, and which extends into the range of marine 'herbivores' (Fig. 2c).

Human bones from the interior and all the animal bones were from areas in which C₄ grasses grow among C₃ shrubs and trees. The range in δ^{13} C for the human (Fig. 2a) and animal bones¹



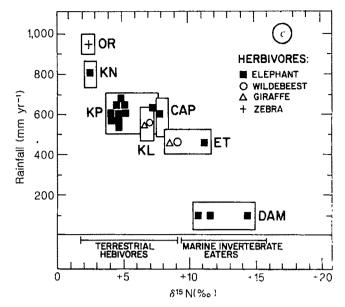


Fig. 2 Nitrogen isotope ratios of human and animal bones, $\delta^{1^4}N$ (in per mil) = {[($^{15}N/^{14}N$)_{sample}/($^{15}N/^{14}N$)_{standard}] - 1) × 10³; the standard is atmospheric N_2 . a, Nitrogen and carbon isotope ratios of humans (symbols as in Fig. 1) compared with the suggested range of isotopic compositions for humans having terrestrial and marine diets⁶. b, Nitrogen isotope ratios of humans from the interior vs. the mean annual rainfall of the collection site (numbers as in Fig. 1). c, Nitrogen isotope ratios of terrestrial herbivores versus the general range of mean annual rainfall for the collection area (letters refer to game reserves listed in Fig. 1). The horizontal bars show the published range of isotopic compositions for bones of terrestrial herbivores and marine invertebrate eaters for comparison5.

in these areas reflects the different 13C/12C ratios for C4 and C3 plants and the variation in grazing versus browsing in the diet. There is no evidence, however, for a related effect on the nitrogen isotopes: C_4 and C_3 plants have similar $\delta^{15}N$ values¹³, and grazers (wildebeest) and browsers (giraffe) from the same area, whilst having very different δ^{13} C values¹, have very similar δ^{15} N values (Fig. 2c). Published analyses for the δ^{15} N values of modern nitrogen-fixing and non-fixing plants differ, on average, by only 2 to 3%13; it therefore appears that the range in bone $\delta^{15}N$ values also cannot be explained in terms of different proportions of leguminous and non-leguminous plants in the diet.

We suggest that the wide range in $\delta^{15}N$ for human and animal bones in southern Africa reflects the very wide range of climatic habitats. In Fig. 2b and 2c the δ^{15} N values of the humans from the interior and of the herbivores are plotted against the mean annual rainfall for the sites from which the bones were collected. Bearing in mind the fact that some of the humans and animals are migratory (elephants moving between Etosha and Damaraland, for example), it nevertheless appears that there is a definite tendency for increasing 15N with increasing aridity. Thus the animal or human bones with $\delta^{15}N$ values higher than +10% or +13% respectively, falling into the range of a 'marine diet' isotopic signature, are from areas receiving less than about 400 mm of rain per year (Fig. 2b, c).

The increase in nitrogen isotope fractionation that is observed in the bones of humans and particular species of ungulates living in arid environments must take place somewhere along the food chain. It occurs either in the plants growing under hot xeric

conditions or in the animals themselves. Measurements on C₃ and C₄ plants from a variety of habitats in southern Africa thus far show no obvious relationship of $\delta^{15}N$ with rainfall or photosynthetic pathway. The higher $\delta^{15}N$ values of animals in arid areas are therefore more likely to be linked with the nitrogen metabolism in the body of the animal itself.

The data presented here indicate that the interpretation of the nitrogen isotope ratios of bones in terms of diet may be more complicated than previous studies suggest, and that the influence of climate also needs to be taken into account. 15N/14N ratios may in fact prove to be a useful tool for studying past climatic variations, especially in areas where large changes in precipitation have occurred.

We thank S. Braine, Möwe Bay, R. Thwaites, Saasveld and A. Hall-Martin, Skukuza, for supplying some of the elephant bone samples, and Siep Talma for supervising mass spectrometric analyses in the laboratory.

Received 31 December 1985; accepted 22 May 1986.

- 1. Vogel, J. C. S. Afr. J. Sci. 74, 298-301 (1978).
- Vogel, J. C. & van der Merwe, N. J. Am. Antiq. 42, 238-242 (1977)

- Vogel, J. C. & van der Merwe, N. J. Am. Antig. 42, 238-242 (1977)
 DeNiro, M. J. & Epstein, S. Geochim. cosmochim. Acta 45, 341-351 (1941)
 Minagawa, M. & Wada, E. Geochim. cosmochim. Acta 48, 1135-1140 (1984)
 Schoeninger, M. J. & DeNiro, M. J. Geochim. cosmochim. Acta 48, 625 639 (1984)
 Schoeninger, M. J., DeNiro, M. J. & Tauber, H. Science 220, 1381-1383 (1982)
 Tauber, H. Nature 292, 332-333 (1981)
 Schiegl, W. E. & Vogel, J. C. Earth planet. Sci. Lett. 7, 307-313 (1970)
 Heaton, T. H. E. & Collett, G. M. CSIR Res. Rep. 624 (1985)
 DeNiro, M. J. Mattre 317, 806, 809 (1985)

- DeNiro, M. J. Nature 317, 806-809 (1985).
 Vogel, J. C., Fuls, A. & Ellis, R. P. S. Afr. J. Sci. 74, 209-215 (1978)
 Sealy, J. C. & van der Merwe, N. J. Nature 315, 138-140 (1985).
- 13. DeNiro, M. J. & Hastorf, C. A. Geochim. cosmochim. Acta 49, 97-115 (1985)

Functions of the ON and OFF channels of the visual system

Peter H. Schiller, Julie H. Sandell & John H. R. Maunsell

Whitaker College, Massachusetts Institute of Technology, Cambridge, Massachusetts 02139, USA

In the mammalian eye, the ON-centre and OFF-centre retinal ganglion cells form two major pathways projecting to central visual structures from the retina. These two pathways originate at the bipolar cell level: one class of bipolar cells becomes hyperpolarized in response to light, as do all photoreceptor cells, and the other class becomes depolarized on exposure to light, thereby inverting the receptor signal. It has recently become possible to examine the functional role of the ON-pathway in vision by selectively blocking it at the bipolar cell level using the glutamate neurotransmitter analogue 2-amino-4-phosphonobutyrate (APB)1. APB application to monkey, cat and rabbit retinas abolishes ON responses in retinal ganglion cells, the lateral geniculate nucleus and the visual cortex but has no effect on the centre-surround antagonism of OFF cells or the orientation and direction selectivities in the cortex²⁻⁵. These and related findings⁶⁻¹¹ suggest that the ON and OFF pathways remain largely separate through the lateral geniculate nucleus and that in the cortex, contrary to some hypotheses, they are not directly involved in mechanisms giving rise to orientation and direction selectivities. We have examined the roles of the ON and OFF channels in vision in rhesus monkeys trained to do visual detection and discrimination tasks. We report here that the ON channel is reversibly blocked by injection of APB into the vitreous. Detection of light increment but not of light decrement is severely impaired, and there is a pronounced loss in contrast sensitivity. The perception of shape, colour, flicker, movement and stereo images is only mildly impaired, but longer times are required for their discrimination. Our results suggest that two reasons that the mammalian visual system has both ON and OFF channels is to yield equal sensitivity and rapid information transfer for both incremental and decremental light stimuli and to facilitate high contrast sensitivity.

Six monkeys were anaesthetized with halothane and given more than 50 vitreal injections by sterile procedures. The volume of APB used was 75 µl (4-20 mM APB in sterile saline) to yield estimated concentrations of 100-500 µM in the eye. The effects of such injections were assessed in separate experiments with the electroretinogram, since our previous studies had shown that when the ON channel is blocked as determined by single-cell recordings in the lateral geniculate nucleus, the b-wave of the electroretinogram is eliminated 12. Although there is some variability in the exact time-course of APB action with the intravitreal injection method, we found that a single injection was usually effective within 1 h and lasted 3-8 h. With the concentrations used in this study, recovery was complete by the following day. In all cases only one eye was injected and the other was patched.

Monkeys were deprived of water and rewarded with apple juice. Their eye movements were monitored with the scleral search coil technique, and they were rewarded for correctly making saccades to visual stimuli presented on a colour monitor. A PDP 11/73 computer was used to drive the monitor, control the experiment and record and store the eye movement and performance data. All trials began with the appearance of a small central spot. In the detection paradigm, after the animal had made saccades to this spot and maintained fixation on it for 400-800 ms, a target stimulus appeared at one of several randomly chosen locations, and the animal's task was to make saccades to it; the stimulus remained on until it was foveated.

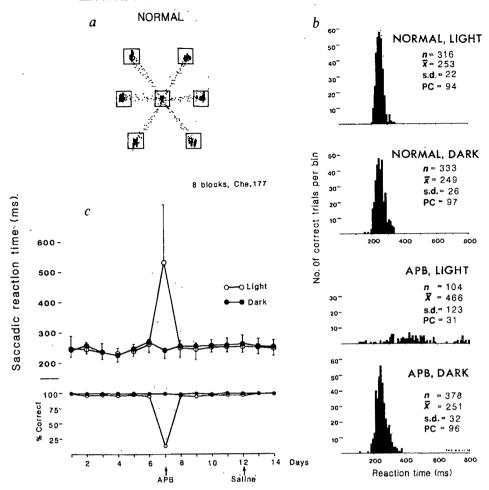
Trials on which saccades were made to locations other than the target were aborted. When the saccade brought the fovea to within 2° of the target centre, it was judged by the programme to be successful and the animal was rewarded with a drop of apple juice. This paradigm, which permits accurate placement of stimuli on selected portions of the retina, is learned rapidly and performed accurately. Trials can be run in close succession without fatigue (with inter-trial intervals of 2–3 s), and monkeys regularly perform 1,500–2,000 trials per day. This permits relatively speedy generation of psychophysical functions. Figure 1a shows eye movement data collected for 48 successive errorless trials in which a target appeared 8 times at each of 6 target locations, showing the normal animal's characteristic, disciplined performance.

To test the hypothesis that the ON channel contributes predominantly to the detection of stimuli seen by virtue of light increment while the OFF channel contributes to the detection of light decrement, we trained monkeys to make saccades to targets which were either lighter than or darker than the background. Figure 1b shows the distribution of saccadic latencies on a set of light and dark stimuli in the normal and APB-injected monkey. One to six hours after APB administration (75 µl of 8 mM APB), there was a pronounced deficit in the detection of light incremental stimuli, accompanied by a large increase and spread in saccadic latencies. Performance on light decremental stimuli was unaffected. Figure 1c shows the monkey's performance over 14 successive days on this task, plotting the saccadic reaction times and the per cent correct performance on one set of light and dark stimuli. The APB was injected on day 7 during this sequence, showing the selective impairment for stimuli brighter than background, and also showing that saline injection of the same volume on day 12 did not affect the animal's performance. Similar effects were obtained using a range of target stimuli measuring 17-220 cd m⁻². We also obtained thresholds for the detection of light stimuli in dark-adapted animals: when the ON channel was blocked, detection thresholds were raised by 1.5-2.0 log units, suggesting that APB has a dramatic effect on the eye's rod system.

We examined several other perceptual functions for which we used discrimination rather than detection tasks. The paradigm was quite similar to that used for the detection of light increment and decrement, but instead of one target, several stimuli appeared after the central spot was fixated. One of these stimuli was different from the rest and the animal's task was to make saccades to this target. The physical characteristics of the stimuli could be varied systematically and were presented in randomized sequences. These tests assessed thresholds for the detection of colour stimuli of different degrees of saturation, the maximal temporal rate of flicker discrimination, minimal stereoscopic depth perception using random-dot stereograms, grating acuity, movement perception using random dot displays and the discrimination of gratings having different orientations. Only mild deficits were found on these tasks when the ON channel was blocked with APB. On all of the tasks, however, there was a consistent increase in the latency to performance, averaging 50 ms.

We also examined the contrast sensitivity of animals following APB administration and found considerable impairment using a variety of contrast sensitivity tests. Figure 2 shows the results from one of these. Monkeys were shown six stimuli, five of which were checkerboards while one was a homogeneous stimulus of the same flux. The animal was trained to make saccades to this homogeneous stimulus. Checkerboards of six different spatial frequencies were used, all at the same contrast, randomized over successive trials within a single block. Different contrasts were used in successive blocks. The stimuli appeared at equally spaced locations around the fixation spot at a distance of 8°. The results show a significant loss in contrast sensitivity, particularly at optimal spatial frequencies, as seen in both the per cent correct and the reaction time data. In other tests a

Fig. 1 a, An x-y frame showing traces of saccades made from a central fixation point to a target presented randomly at one of six positions. Targets are 8° eccentric and are squares subtending 1° of visual angle; data from 48 successive trials are shown. Boxes represent spatial limits set for correct acquisition. b, Distribution of saccadic latencies and per cent correct performance before and after APB injection (75 µl of 8 mM) to light incremental and light decremental stimuli. Base illumination set at 121 cd m⁻². The light stimuli measured 186 and the dark 59 cd m⁻². n, Number of trials per histogram; x, mean; s.d., standard deviation. PC, per cent correct. c, Saccadic reaction times and per cent correct performance on 14 successive days for incremental (circles) and decremental (disks) stimuli. APB (75 µl of 8 mM) was injected on day 7 and saline (75 µl) on day 12. Vertical bars show standard deviations, upward for incremental and downward for decremental stimuli.



two-alternative forced-choice staircase procedure was used in which sinusoidal gratings had to be discriminated from homogeneous stimuli; injections of 450 µM APB resulted in a loss of foveal contrast sensitivity of up to 25%.

These results suggest two possible reasons for the existence of both an ON and an OFF channel in the mammalian visual system. One is to provide a means for transmitting information about both light increment and light decrement with an excitatory process to the central nervous system. Since the maintained activity of retinal ganglion cells is relatively low, the information conveyed by a decrease in activity (for example, the effect of

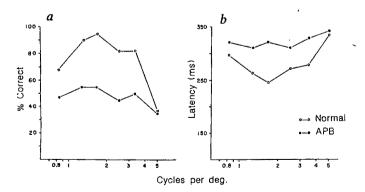


Fig. 2 Per cent correct (a) and mean saccadic latencies (b) on a discrimination task requiring an animal to make saccades to a homogeneous stimulus paired with a set of five checkerboard stimuli; sets were of different spatial frequencies but of the same contrast. Background illumination was 25 cd m⁻², the homogeneous stimulus was 68 cd m⁻² and the high- and lowcontrast checkerboards were 88 and 48 cd m⁻², respectively. Each point is based on 60 trials.

light increment on OFF cells) is difficult to utilize effectively by central visual system neurones, particularly since their maintained activity is even lower than that of retinal ganglion cells. Having both an ON and an OFF channel therefore makes possible efficient information transfer for either sign of contrast change. This is necessary because of the high premium that exists on the speed of information processing in the animal kingdom, both for appetitive and for avoidance behaviours. The second reason for the existence of the ON and OFF channels is to provide increased contrast sensitivity, probably as a result of some form of push-pull interaction between the ON and OFF channels at higher levels in the visual system. High contrast sensitivity is undoubtedly a most desirable attribute for optimal visual function. Neither of these considerations identifies a unique solution to a biological problem. Rapid information transfer and high contrast sensitivity could probably also be accomplished by having a single channel with a rather high maintained discharge throughout the visual system. Such a solution, however, would probably require an unacceptably high rate of metabolic activity.

This research was supported by NIH grant EY00676, NSF grant BNS-8310399 and NRSA grant F32 NS06971-02. We thank David Wilson for his help in training the animals.

Received 28 February; accepted 20 May 1986.

- Slaughter, M. M. & Miller, R. F. Science 211, 182-184 (1981).
- Schiller, P. H. Nature 297, 580-583 (1982). Horton, J. C. & Sherk, H. J. Neurosci. 4, 374-380 (1984).
- Sherk, H. & Horton, J. C. J. Neurosci. 4, 381-393 (1984)
- Knapp, A. G. & Mistler, L. A. J. Neurophysiol. 50, 1236-1245 (1983). Conway, J. L. & Schiller, P. H. J. Neurophysiol. 50, 1330-1342 (1983).
- LeVay, S. & McConnel, S. K. Nature 300, 350-351 (1982). Norton, T. T., Rager, G. & Kretz, R. Brain Res. 327, 319-323 (1985).
- Raczkowski, D. & Fitzpatrick, D. Neurosci. Abstr. 68(9), 227 (1985).
 Stryker, M. P. & Zahs, K. R. J. Neurosci. 3, 1943-1951 (1983).
- Waessle, H., Boycut, B. B. & Illing, R. B. Proc. R Soc. B212, 177-195 (1981).
 Knapp, A. G. & Schiller, P. H. Vision Res. 24, 1841-1846 (1984).

Expression of functional sodium channels from cloned cDNA

Masaharu Noda, Takayuki Ikeda, Harukazu Suzuki, Hiroshi Takeshima, Tomoyuki Takahashi*, Motoy Kuno* & Shosaku Numa

Departments of Medical Chemistry and Molecular Genetics and * Physiology, Kyoto University Faculty of Medicine, Kyoto 606, Japan

The voltage-gated sodium channel is a transmembrane protein essential for the generation of action potentials in excitable cells1. It has been reported that sodium channels purified from the electric organ of the electric eel, Electrophorus electricus^{2,3}, and from chick cardiac muscle⁴ consist of a single polypeptide of relative molecular mass $(M_r) \sim 260,000$, whereas those purified from rat brain⁵ and from rat^{6,7} and rabbit skeletal muscle⁷ contain, in addition to the large polypeptide, one or two smaller polypeptides of M, 33,000-43,000. The primary structures of the Electrophorus sodium channel⁸ and two distinct sodium channel large polypeptides⁹ (designated as sodium channels I and II) from rat brain have been elucidated by cloning and sequencing the complementary DNAs. The purified sodium channel preparations from *Electrophorus* electroplax¹⁰ and from mammalian muscle^{11,12} and brain¹³⁻¹⁵, when reconstituted into lipid vesicles or planar lipid bilayers, exhibit some functional activities. The successful reconstitution with the Electrophorus preparation would imply that the large polypeptide alone is sufficient to form functional sodium channels. However, studies with the rat brain preparation suggest that the smaller polypeptide of M_r 36,000 is also required for the integrity of the saxitoxin (STX) or tetrodotoxin (TTX) binding site of the sodium channel¹⁶. Here we report that the messenger RNAs generated by transcription of the cloned cDNAs encoding the rat brain sodium channel large polypeptides, when injected into Xenopus oocytes, can direct the formation of functional sodium channels.

Recombinant plasmids that carry the bacteriophage SP6 promoter^{17,18}, linked to the entire protein-coding region of the cDNA for rat sodium channel I (pRI-4 with the 33-nucleotide insertion⁹ or pRI-3 without the insertion) or sodium channel II (pRII-2), were constructed (Fig. 2). Plasmid transcription in vitro by SP6 polymerase generated mRNAs specific for the respective sodium channel large polypeptides (Fig. 1). The estimated sizes of the mRNAs agree with those expected from the structure of the plasmids, except that smaller RNA species were contained in the preparations derived from pRI-3 and pRI-4.

Xenopus oocytes that had been injected with the sodium channel II-specific mRNA derived from pRII-2 and then incubated for 3-6 days showed a transient inward current when the holding membrane potential was shifted from -100 mV to -10 mV under voltage clamp. Following application of TTX (0.3 µM), the inward current was progressively diminished and disappeared within a few minutes (Fig. 3a). Similarly, STX (0.3 µM) blocked the inward current completely. The effects of both the toxins were reversible. In Ringer's solution, the maximum inward currents induced by the sodium channel IIspecific mRNA ranged up to 26 µA, being much larger than those observed in oocytes injected with poly(A)+ RNA from rat brain (up to 1.5 µA) (see also refs 19, 20). On the other hand, oocvtes injected with the sodium channel I-specific mRNA showed only a small response; the mRNA derived from pRI-3 evoked maximum inward currents up to ~50 nA, which were TTX-sensitive, whereas the mRNA derived from pRI-4 induced no detectable currents. Because of the low signal-to-noise ratio for the response evoked by the sodium channel I-specific mRNAs, we restricted our further analysis to the current induced

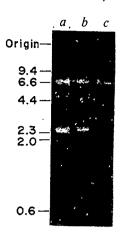


Fig. 1 Electrophoretic analysis of the mRNAs synthesized in vitro using pRI-3 (a), pRI-4 (b) or pRII-2 (c) as template. Samples of the mRNAs (5 μ g in a, b; 1.3 μ g in c) were denatured with 1 M glyoxal and 50% dimethyl sulphoxide³³ and electrophoresed on a 1.5% agarose gel in 10 mM sodium phosphate buffer (pH 7.0). RNA was visualized by staining with ethidium bromide. The size markers used were the HindIII cleavage products of phage λ DNA (sizes in kilobases). The estimated size of the largest mRNA species on each lane agrees with the expected size (~6.7, ~6.7 and ~6.5 kilobases, respectively, in a, b and c).

by the sodium channel II-specific mRNA and compared its properties with those of the current induced by poly(A)⁺ RNA from rat brain.

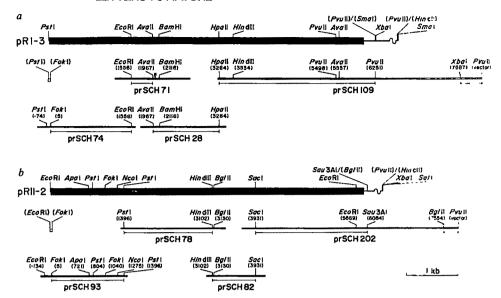
Figure 3b shows an example of the dose-response curves for TTX obtained from oocytes injected with the sodium channel II-specific mRNA. The apparent dissociation constant for TTX (K_{TTX}) ranged from 10 nM to 14 nM. This was comparable to the K_{TTX} value (6-7 nM) obtained for the sodium channels produced in oocytes injected with rat brain poly(A)⁺ RNA; the latter value is similar to that reported previously (9-10 nM)^{19,20}.

When the external Na+ concentration was lowered by replacement with tetraethylammonium, tetramethylammonium or sucrose, the TTX-sensitive inward current was reduced in a dose-dependent manner, being virtually abolished at ~3 mM Na⁺ (Fig. 4a). The fast Na⁺ current observed in the injected oocytes differed clearly from the persistent Na⁺ current which can be induced in native oocytes only by prolonged depolarization and is blocked by TTX only at a dose of ~0.5 mM (refs 21, 22). The fast Na⁺ current was not detected in non-injected oocytes. Figure 4b exemplifies current recordings in Ringer's solution that were made when the oocyte membrane potential was stepped from -100 mV to various levels between -51 mV and +59 mV. In these records, the TTX-insensitive components were subtracted. The peak current-voltage (I-V) relationship obtained by this procedure is shown in Fig. 4c. The maximum current occurred in a range of -12 to +2 mV. This range was similar to that observed for the Na+ current measured in oocytes injected with rat brain poly(A)+ RNA (-8 to 0 mV) (see also refs 19, 20). From the internal Na+ concentration measured in Xenopus oocytes^{23,24}, the reversal potential of the Na⁺ current would be expected to be 40-66 mV. However, the inward current was not reversed at potential levels up to 80 mV. A decrease in the external Na⁺ concentration from 118 mM to 80 mM reduced the inward current, but again failed to reverse the current. A significant permeation of Ca2+ through the TTX-sensitive channel was unlikely because the inward current was not affected by replacement of external Ca²⁺ with equimolar Mn²⁺ or by an increased Ca2+ concentration (20 mM). The TTX-sensitive inward current observed in oocytes injected with rat brain poly(A)+ RNA was also unaffected by Ca2+-free saline, in

Fig. 2 Construction of recombinant plasmids used for expression of rat sodium channel I (pRI-3) (a) and sodium channel II (pRII-2) (b). Only relevant restriction endonuclease sites are shown and identified by numbers indicating the 5'terminal nucleotide generated by cleavage (for nucleotide numbers, see ref. 9); endonuclease sites that no longer exist in pRI-3 or pRII-2 and those corresponding to the ends of the synthetic linkers (indicated by narrow open boxes) are parenthesized. Protein-coding regions are represented by solid boxes, 5'- and 3'-noncoding regions and vector sequences immediately following the poly(dA) · poly(dT) tract by solid lines, and poly(dA) poly(dT) tracts by wavy lines. The cDNA clones used for the construction are indicated by thick lines, and their fragments constituting pRI-3 or pRII-2 by bars underneath. The 33-nucleotide insertion in prSCH71 is shown by an inverted triangle. A scale of 1 kilobase pair (kb) is given.

Methods. The pSP64 (ref. 18) recom-

binants carrying the cDNA for rat brain sodium channel I with (pRI-4) or without



the 33-nucleotide insertion (pRI-3) were constructed as follows. To delete the ATG triplet composed of nucleotides –8 to –6 in the 5'-noncoding region, the synthetic oligonucleotide linker' was prepared using an automatic DNA synthesizer (Applied Biosystems). The ~19-kb FokI(5)/FokI (on vector DNA) fragment from prSCH74 was ligated with the synthetic linker and cleaved with FcoRI. The ~16-kb fragment formed was isolated and cleaved with FxI. The resulting PstI/EcoRI fragment and the ~2.7-kb EcoRI/PstI fragment from pUC18 (ref. 30) were ligated to yield pURI-1. The PstI(~74)/EcoRI(1,556) fragment from prSCH74, the EcoRI(1,556)/AvaII(1,957) fragment from prSCH71, the AvaII(1,967)/BamHI(2,116) and BamHI(2,116)/HpaII(3,264) fragments from prSCH28. The HpaII(3,264)/HindIII(3,534) fragment from prSCH109 and the ~3.0-kb HindIIII/PstI fragment from pSFG5 (ref. 18) were ligated to yield pSRI-A, which was used to construct pRI-3; for the construction of pRI-4, the EcoRI(1,556)/BamHI(2,116) fragment from prSCH71, instead of the EcoRI(1,556)/AvaII(1,967) fragment from prSCH71 and the AvaII(1,967)/BamHI(2,116) fragment from prSCH28, was used to yield pSRI-B. The PvuIII(5,498)/PvuIII(6,251) fragment of 1,945 (or 1,978) base pairs (bp) from pSRI-A (or pSRI-B), the HindIII (3,534)/AvaII(5,557) fragment from prSCH109, the 703-bp AvaIII/XbaI (on vector DNA) fragment from pURI-2 and the ~3.0-kb XbaI/EcoRI fragment from pURI-3 and the ~3.0-kb XbaI/EcoRI fragment from pURI-4 (or pURI-B), the ~0.4-kb XbaI (7,887)/PvuII (on vector DNA) fragment from pURI-1, the 4,671-bp (or 4,704-bp) EcoRI/XbaI fragment from pURI-4 (or pURI-B), the ~0.4-kb XbaI (7,887)/PvuII (on vector DNA) for rat brain sodium channel II (pRII-2) was constructed as follows. The synthetic oligonucleotide linkert was prepared to delete the ATG triplet composed of nucleotides ~8 to ~6 in the 5'-noncoding region. The FokI(5)/FokI(1,040) fragment from prSCH39 was ligated with the synthetic linker and cleaved with PstI. The ~0.8-kb fragment from prSCH39, the HindIII(3,102

Fig. 3 Effect of TTX on depolarization-activated whole-cell inward currents in Xenopus oocytes injected with the sodium channel II-specific mRNA. a, Time course. The inward currents were elicited by a 50-ms pulse stepped from -100 mV to -10 mV. The five records (from bottom to top) were obtained before and 15 s, 20 s, 35 s and 70 s after superfusion with 0.3 µM TTX, respectively. The response obtained 10 min after washing the TTX solution was 88% of that observed before TTX application. Transient capacitative currents were roughly compensated by a network with three adjustable time constants. b, Dose-response curve obtained from another oocyte. The peak inward current evoked by a step from -100 mV to -10 mV, relative to that observed before TTX application, is plotted against the logarithm of TTX concentration. Each point was obtained 3 min after exposure to a new dose of TTX. The measurements were made in the direction of increasing TTX concentration. The record obtained with ~1 µM TTX was subtracted from the control and those obtained with other doses of TTX. The curve represents the dose-response relation expected from a K_{TTX} of 14 nM (indicated by a horizontal bar) according to the equation $y = (1 + T/K_{TTX})^{-1}$, where T is the TTX concentration.

Methods. Total RNA was extracted from the whole brain of male Wistar rats (~200 g body weight) by the phenol method³⁴, and poly(A)⁺ RNA was isolated by oligo(dT)-cellulose chromatography³⁵. Fractionation of poly(A)^{*} RNA by sucrose gradient centrifugation³⁵ was performed as follows. Poly(A)⁺ RNA (100 μg per tube) was centrifuged in linear sucrose gradients (15-30%, w/v) in a Beckman SW-41 rotor at 40,000 r.p.m. for 16h at 4 °C and 25 fractions were collected from each gradient. The fractions sedimenting more slowly than 28S ribosomal RNA and the remaining fractions were each pooled, extracted with phenol/chloroform, precipitated with ethanol and dissolved in water. Xenopus laevus oocytes were injected with the following RNA preparations separately or in combination: sodium channel I-specific mRNA with or without the 33-nucleotuse insertion (1.0 μg μl⁻¹), the sodium channel II-specific mRNA (0.2 μg μl⁻¹), poly(A)⁺ RNA (1.0 μg μl⁻¹), the slow-sedimenting fraction (<28 S) of poly(A)⁺ RNA (1.6 μg μl⁻¹). The average volume injected was ~50 nl per oocyte. The injected oocytes were incubated at 19 °C for 3-6 days in modified Barth's medium³⁷ containing gentamicin (0.1 mg ml⁻¹) and mycostatin (15 μg ml⁻¹). The follicular cell layer was removed^{26,38} from oocytes prior to electrophysiological measurements. Whole-cell currents were recorded with a two-microelectrode voltage clamp et 20+2 °C in Ringer's solution of the following composition (in mM) unless otherwise specified: NaCl, 115; KCl, 2.5; CaCl₂, 1.8; HEPES (pH 7.4), 5 (containing 2 75 mM Na⁺). The voltage recording electrode was filled with 3 M KCl. The current electrode was filled with a solution of (in mM): CsF, 250; CsCl, 250; EGTA, 50; HEPES (pH 7.4), 10.

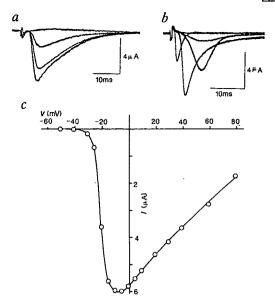


Fig. 4 Properties of depolarization-activated whole-cell inward currents in oocytes injected with the sodium channel II-specific mRNA. a, Effects of changes in external Na⁺ concentration replaced by tetraethylammonium ions. The inward currents were elicited by a 50-ms pulse stepped from -100 mV to -10 mV. The four records (from bottom to top) were obtained at external Na+ concentrations of 118 mM, 80 mM, 41 mM and 2.75 mM, respectively. Each response was recorded 3 min after exposure to a new Na+ level. Transient capacitative currents were roughly compensated by a network with three adjustable time constants. b, Sample records of currents evoked by a voltage step from -100 mV to -51 mV, -25 mV, -21 mV, -6 mV and +59 mV in Ringer's solution. TTX-insensitive currents were subtracted. c, Peak current-voltage relationship by step depolarizations from a holding potential of -100 mV in Ringer's solution. Data from the same oocvte as in b.

agreement with a recent report²⁵. It is possible that, because of the presence of microvilli and indentations on the oocyte surface and the resultant large membrane capacitance²³, the entire plasma membrane is not adequately clamped during the generation of the fast inward current26.

The TTX-sensitive fast current induced by the sodium channel II-specific mRNA showed inactivation following a depolarizing prepulse in a time- and voltage-dependent manner. In view of the large membrane capacitance, the steady-state inactivation was measured with a test pulse to 0 mV following a long (2 s) prepulse stepped from -100 mV to different potential levels (-95 to -10 mV). The potential at which activation of the inward current was 50% (ref. 27) ranged from -61 mV to -57 mV. This range was comparable to that observed for the Na+ current exhibited by oocytes injected with rat brain poly(A)⁺ RNA (-56 to -50 mV) (see also ref. 25).

Our results indicate that the mRNAs derived from the cDNAs encoding the rat brain sodium channel large polypeptides can direct the formation of functional sodium channels in Xenopus oocytes, although the magnitude of the current induced by the sodium channel I-specific mRNA is small. The functional properties of the sodium channels resulting from injection of the sodium channel II-specific mRNA are comparable to those of the sodium channels produced in oocytes injected with poly(A)+ RNA from rat brain. These findings suggest that the sodium channel large polypeptide alone is sufficient to exhibit the function of this channel. The possibility that Xenopus oocytes themselves contain equivalents to the sodium channel small polypeptides, which may associate with the large polypeptide to form functional sodium channels, cannot be excluded. In this context, we observed that a slowly sedimenting fraction (<28S) of rat brain poly(A)⁺ RNA (presumably containing the mRNAs encoding the sodium channel small polypeptides), when injected into oocytes in combination with the sodium channel II-specific mRNA (or the sodium channel I-specific mRNA with or without the 33-nucleotide insertion⁹), did not enhance the TTX-sensitive response. We also observed that a fast-sedimenting fraction (≥28S) of rat brain poly(A)+ RNA alone, in contrast with the slowly sedimenting fraction, induced TTX-sensitive inward currents (up to $1.0~\mu A$) in oocytes, in general agreement with previous reports^{28,29}. The small TTXsensitive response observed in oocytes injected with the sodium channel I-specific mRNA may be due to inefficient synthesis, modification or transport of the channel protein or to the intrinsic properties of this particular sodium channel.

This investigation was supported in part by research grants from the Ministry of Education, Science and Culture and the Science and Technology Agency of Japan, the Mitsubishi Foundation and the Japanese Foundation of Metabolism and Diseases.

Received 21 April; accepted 6 June 1986.

- 1. Hille, B. Ionic Channels of Excitable Membranes (Sinauer Associates Inc., Sunderland, Massachusetts, 1984).
- 2. Agnew, W. S., Levinson, S. R., Brabson, J. S. & Raftery, M. A. Proc. natn. Acad. Sci. U.S.A. 75, 2606-2610 (1978).
 3. Miller, J. A., Agnew, W. S. & Levinson, S. R. Biochemistry 22, 462-470 (1983).

- Mesner, J. R., Egitev, W. Eur. J. Biochem. 141, 651-660 (1984).
 Mesner, D. J. & Catterall, W. A. J. biol. Chem. 260, 10597-10604 (1985).
 Barchi, R. L. J. Neurochem. 40, 1377-1385 (1983).
- Barchi, R. L., Tanaka, J. C. & Furman, R. E. J. cell. Biochem. 26, 135-146 (1984). Noda, M. et al. Nature 312, 121-127 (1984).
- Noda, M. et al. Nature 326, 188-192 (1986).
 Rosenberg, R. L., Tomiko, S. A. & Agnew, W. S. Proc. natn. Acad. Sci. U.S.A. 81, 1239-1243 (1984)
- 11. Tanaka, J. C., Eccleston, J. F. & Barchi, R. L. J. biol. Chem. 258, 7519-7526 (1983).
- Kraner, S. D., Tanaka, J. C. & Barchi, R. L. J. biol. Chem. 260, 6341-6347 (1985).
 Hanke, W., Boheim, G., Barhanin, J., Pauron, D. & Lazdunski, M. EMBO J. 3, 509-515
- 14. Hartshorne, R. P., Keller, B. U., Talvenheimo, J. A., Catterall, W. A. & Montal, M. Proc.
- natn. Acad. Sci. U.S.A. 82, 240-244 (1985). Feller, D. J., Talvenheimo, J. A. & Catterall, W. A. J. biol. Chem. 260, 11542-11547 (1985).
- 16. Messner, D. J. & Catterall, W. A. J. biol. Chem. 261, 211-215 (1986).

- 17. Green, M. R., Maniatis, T. & Melton, D. A. Cell 32, 681-694 (1983).

- Melton, D. A. et al. Nucleic Acids Res. 12, 7035-7056 (1984).
 Gundersen, C. B., Miledi, R. & Parker, I. Proc. R. Soc. B220, 131-140 (1983).
 Gundersen, C. B., Miledi, R. & Parker, I. Nature 308, 421-424 (1984).
 Baud, C., Kado, R. T. & Marcher, K. Proc. natn. Acad. Sci. U.S.A. 79, 3188-3192 (1982).
- Baud, C. & Kado, R. T. J. Physiol, Lond. 356, 275-289 (1984).
 Kusano, K., Miledi, R. & Stinnakre, J. J. Physiol, Lond. 328, 143-170 (1982).
- Barish, M. E. J. Physiol., Lond. 342, 309-325 (1983). Leonard, J., Snutch, T., Lubbert, H., Davidson, N. & Lester, H. A. Biophys. J. 49, 386a (1986).
- Methfessel, C. et al. Pflügers Arch. ges. Physiol. (in the press).
 Hodgkin, A. L. & Huxley, A. F. J. Physiol, Lond. 117, 500-544 (1952).
 Sumikawa, K., Parker, I. & Miledi, R. Proc. natn. Acad. Sci. U.S.A. 81, 7994-7998 (1984).
 Hirono, C. et al. Brain Res. 359, 57-64 (1985).
- Yanisch-Perron, C., Vieira, J. & Messing, J. Gene 33, 103-119 (1985). Messing, J. Meth. Enzym. 101, 20-78 (1983).
- Konarska, M. M., Padgett, R. A. & Sharp, P. A. Cell 38, 731-736 (1984).
- McMaster, G. K. & Carmichael, G. G. Proc. natn. Acad. Sci. U.S.A. 74, 4835-4838 (1977).
 Miledi, R. & Sumikawa, K. Biomed. Res. 3, 390-399 (1982).
 Aviv, H. & Leder, P. Proc. natn. Acad. Sci. U.S.A. 69, 1408-1412 (1972).
 Houghton, M. et al. Nucleic Acids Res. 8, 1913-1931 (1980).

- 37. Gurdon, J. B. The Control of Gene Expression in Animal Development (Clarendon, Oxford,
- 38. Sakmann, B. et al. Nature 318, 538-543 (1985).

Analysis of T-cell subsets in rejection of K^b mutant skin allografts differing at class I MHC

Amy S. Rosenberg, Toshiaki Mizuochi & Alfred Singer

Immunology Branch, National Cancer Institute, National Institutes of Health, Bethesda, Maryland 20892, USA

The T-cell subpopulations which initiate and mediate tissue allograft rejection remain controversial1-5. In the present study we attempted to identify the phenotype and function of the T-cell subset(s) primarily responsible for the rejection of skin allografts differing at a single class I locus in the major histocompatibility complex (MHC). We found that the rejection rates by B6 mice $(H-2^b)$ of four different class I mutant (K^{bm}) skin allografts form a distinct hierarchy. This hierarchy correlates strikingly and uniquely with the relative precursor frequencies of Lyt2+ interleukin-2-secreting T-helper cells reactive against the various K^{bm} mutants. To investigate the role of Lyt2+ T cells in the rejection of class I-disparate skin allografts directly, H-2b nude mice were engrafted with Kbm skin allografts and then reconstituted with L3T4⁺ or Lyt2⁺ T-cell subpopulations from syngeneic H-2^b mice. Lyt2+ T cells were observed to be both necessary and sufficient for the rejection of class I-disparate K^{bm} skin allografts, whereas L3T4+ T cells were neither necessary nor sufficient. These results identify the Lyt2+ interleukin-2-secreting T-cell subset as the critical cell type determining the rejection rate of class I-disparate K^{bm} skin allografts.

Because the cellular mechanisms involved in allograft rejection are likely to be diverse and dependent upon the antigenic disparity expressed by the graft, we limited our present study to the rejection of skin allografts expressing isolated class I MHC disparities. We chose to investigate the rejection of skin allografts from K^b mutant mice^{6,7} by normal B6 mice because (1) each K^b mutant strain in theory differs from wild-type B6 mice only in the expression of a mutant H-2Kb molecule; (2) each Kbm class I molecule is well characterized biochemically8; (3) the various K^{bm} mutations alter the K^{b} molecule differently so that they are of varying antigenicity9,10. In the first set of experiments, female B6 mice were engrafted with female bm1, bm3, bm6 or bm10 skin allografts. Each graft was scored daily until rejection or day 150. As can be seen in Fig. 1, the rejection rates form a distinct hierarchy, in which bm1 skin allografts are rejected most rapidly, with a median survival time (MST) of 16 days; bm3 and bm10 skin allografts are rejected less rapidly (MST = 22 days) and bm6 skin allografts are rejected least rapidly, the majority of bm6 skin allografts being retained over the 150 days they were followed. A second bm6 skin allograft on mice that failed to reject their initial bm6 graft was also not rejected (data not shown). Nevertheless, the Kbm6 molecule is not itself defective in triggering skin allograft rejection since bm6 skin allografts are rapidly rejected by control bm1 hosts (MST=17 days) which, unlike normal B6 hosts, can react against both mutant and wild-type epitopes on the Kbm6 molecule.

We hoped to identify the function and phenotype of the T-cell subset(s) primarily responsible for the observed hierarchy of B6 anti- K^{bm} rejection rates by assessing *in vitro* the precursor frequencies of the various K^{bm} -reactive T-cell subpopulations present in the spleens of normal B6 host animals. We assessed two distinct T-cell functions: (1) cytolytic activity as assayed by the ability to specifically lyse 51 Cr-labelled target cells following stimulation with spleen cells from each K^{b} mutant strain, and (2) helper activity mediated by interleukin-2 (IL-2) and assayed by the ability to secrete IL-2 in response to stimulation with mutant spleen cells 11 . Fractionated L3T4 $^{+}$ or Lyt2 $^{+}$ T-cell sub-

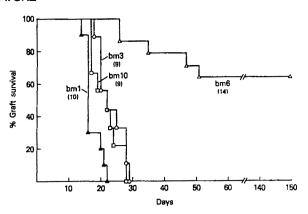


Fig. 1 Rejection of K^{bm} skin allografts by B6 mice. Female B6 mice were engrafted with a tail-skin allograft from female bml (Δ) , bm3 (\bigcirc) , bm6 (\triangle) or bm10 (\square) mice using an adaptation of the method of Billingham and Medawar²⁹. Grafts were scored daily until rejection or day 150. Numbers in parentheses indicate the number of mice in each group. Control B6 grafts were not rejected.

populations were obtained from the spleens of normal B6 mice by pretreatment with either anti-Lyt2.2 or anti-L3T4 monoclonal antibody and complement. The average precursor frequency determinations from several limiting dilution experiments are shown in Table 1, together with the skin graft rejection rates determined from Fig. 1. The precursor frequencies of anti-Kbm L3T4⁺ cytolytic T lymphocytes (T_c) are not given in Table 1 because none were detected¹². In contrast, anti-K^{bm} L3T4⁺ IL-2-secreting helper (T_h) cells were detected, consistent with previous observations that L3T4+ T cells recognize class I alloantigens in the context of self-Ia determinants and function as IL-2-secreting T_h cells but not as T_c effectors in class I allospecific responses ¹³⁻¹⁵. It can be seen in Table 1 that bm1-reactive T cells were the most frequent of any of the anti-K^{bm} specificities examined, regardless of the function or phenotype of the T-cell subset assessed. This result is consistent with the observation that bml skin allografts were the most rapidly rejected, but is unhelpful in identifying the T-cell subset(s) primarily responsible for determining allograft rejection rate. It can also be seen in Table 1 that the precursor frequencies of anti-bm6 cells were approximately equal to the precursor frequencies of anti-bm3 and anti-bm10 cells in both unseparated and L3T4* Th-cell populations, as well as in both unseparated and Lyt2+ T_c populations. These results are markedly discordant with the slow and variable rejection of bm6 versus bm3 or bm10 skin allografts, and suggest that none of these T-cell subsets is the one primarily responsible for determining the rejection rate of class I-disparate K^{bm} skin allografts. However, most interestingly, it can be seen in Table 1 that the relative precursor frequencies of Kbm-reactive T cells in the Lyt2+ IL-2-secreting Th-cell subset correlate perfectly with the rates at which skin allografts from these various mutant strains are rejected. Most B6 mice fail to reject bm6 skin allografts and B6 spleen-cell populations contain few, if any, T cells that secrete IL-2 in response to bm6 stimulator cells. The K^{bm6} molecule effectively triggers Lyt2* T cells from H-2Kk mice to secrete IL-216, so that the failure to detect significant numbers of bm6-reactive Lyt2⁺ IL-2 secreting T cells in B6 mice reflects their low frequency and is not the result of a unique defect in the ability of the K^{bm6} molecule to trigger Lyt2+ T cells to secrete IL-2. These data imply that the number of specifically reactive IL-2-secreting Lyt2+ T cells is the limiting and critical determinant of the rate at which rejection of K^{bm} skin allografts can occur and suggest that Lyt2 T cells in general, and IL-2-secreting Lyt2+ T cells in particular, are required for such allografts to be rejected at all.

To examine the role of Lyt2⁺ T cells in the rejection of class I-disparate K^{bm} skin allografts directly, we made use of an experimental model in which isolated T-cell subpopulations can

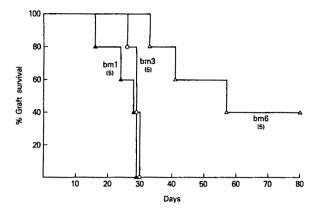


Fig. 2 Rejection of K^{bm} skin allografts by reconstituted B10 nude mice. Female B10 nude mice were engrafted on day 0 with tail-skin allografts from female bml (\triangle), bm3 (O) or bm6 (\triangle) mice. On day 1, each mouse was injected intravenously with 50×10^6 untreated spleen cells from unprimed B6 female mice. Grafts were scored daily until rejection or day 80. Numbers in parentheses indicate the number of mice in each group. MST in days were as follows: bml = 28, bm3 = 29, bm6 = 57. Control B6 grafts were not rejected.

be assessed for their ability to mediate skin allograft rejection after transfer into T-cell-deficient nu/nu mice¹⁷, H-2^b nude mice were engrafted with skin allografts on day 0, reconstituted with 50×10⁶ H-2^b spleen cells or spleen cell subpopulations on day 1, and then examined daily for the status of their skin grafts. To ascertain that skin graft rejection in this experimental model depended upon the adoptive transfer of immunocompetent T cells, we engrafted B10 nude mice with B10.BR (H-2k) skin and reconstituted them with 50×10⁶ spleen cells from either normal or T-cell-deficient, nude B10 mice. The H-2k skin allografts were rapidly and completely rejected by nude mice reconstituted with normal B10 spleen cells (MST=14 days) but were not rejected by any of the nude mice reconstituted with T-celldeficient, nude B10 spleen cells (MST>33 days). To determine if the mechanisms of skin graft rejection in this experimental model reflect those operative in normal mice, we engrafted B10 nude mice with bm1, bm3 or bm6 skin allografts and reconstituted them with normal B6 spleen cells (Fig. 2). Precisely the same hierarchy of rejection rates was observed as had been seen in normal mice, namely bm1>bm3 » bm6, suggesting that similar rejection mechanisms are involved (Fig. 2). Finally, to identify the phenotype of the T cells able to effect the rejection of class I-disparate Kbm allografts, we engrafted B10 nude mice with bml skin allografts and then reconstituted them with 50× 10⁶ untreated normal B6 spleen cells or 50×10⁶ normal B6

spleen cells that had been depleted either of Lyt2+ cells or of L3T4⁺ cells (Fig. 3). The depletion procedures were >99% effective as shown by immunofluorescence and flow microfluorometry (data not shown). The results (Fig. 3) demonstrated that the isolated Lyt2+ T-cell population was both necessary and sufficient to reject bm1 skin allografts. Interestingly, nude mice reconstituted with the isolated Lyt2+ T-cell population rejected bm1 skin allografts more rapidly (MST = 10 days) than did nude mice reconstituted with unfractionated T-cell populations containing both Lyt2⁺ and L3T4⁺ T cells (MST = 22 days), indicating that L3T4⁺ T cells do not synergize with Lyt2⁺ T cells to effect the rejection of bm1 skin allografts and that they might conceivably interfere with the rejection. Finally, nude mice reconstituted with the isolated L3T4⁺ T-cell population were incapable of rejecting bm1 skin allografts (MST >60 days) (Fig. 3), although they were immunocompetent as indicated by their rapid rejection of control class II-disparate skin grafts (data not shown).

The present study provides strong support for the role of Lyt2⁺ T cells in general, and IL-2-secreting Lyt2⁺ T cells in particular, in skin allograft rejection. It significantly extends earlier observations¹⁸⁻²² by demonstrating that Lyt2⁺ T cells are not only able to mediate allograft rejection but are the predominant T cells in the rejection of class I-disparate K^{bm} skin allografts. Interestingly, the presence in B6 mice of both K^{bm}-

Table 1 Rejection rates of Kbm skin allografts and precursor frequencies of Kbm-reactive T cell subsets

			Precursor frequencies ($\times 10^3$) of K^{bm} -specific T cells in unprimed B6 spleen-cell populations							
Strain Graft surv		Graft survival	IL-2	e-secreting T ce	llst	Cytolytic T cells‡				
Responder	Target	MST (days)*	Unseparated	L3T4 ⁺	Lyt2 ⁺	Unseparated	Lyt2 ⁺			
В6	bm1	16	1/16	1/44	1/24	1/3	1/0.6			
B6	bm3	22	1/61	1/136	1/73	1/6	1/5			
B 6	bm10	22	1/53	1/45	1/93	1/23	1/6			
B6	bm5	>150	1/59	1/67	<1/1,000	1/6	1/4			

^{*} Obtained from Fig. 1.

[†] Summary of seven experiments. Each limiting-dilution titration consisted of 6-8 experimental points, representing 24-48 replicate cultures. Individual 0.2-ml cultures contained graded numbers of untreated or fractionated responder spleen-cell populations, 5×10^5 2,000R-irradiated stimulator spleen cells and 0.01% (v/v) ascites of 7D4 monoclonal antibody²⁵, specific for the murine IL-2 receptor. The addition of monoclonal anti-IL-2 receptor antibody to the response cultures significantly improves the accuracy of IL-2 production measurements by blocking the consumption of IL-2 during the culture period without interfering with either the production of IL-2 or its subsequent measurement¹¹. After 5 days of culture at 37 °C and 5% CO₂, 0.1 ml of supernatant was collected from each well and assayed for their ability to maintain the proliferation of 4×10^3 indicator HT-2 cells²⁶. Individual cultures were considered positive if the ³H-thymidine incorporation by HT-2 cells in response to their supernatant was more than 3 s.d. above that stimulated by medium alone. Minimal estimates of the frequencies of T_h cells were calculated by analysis of the Poisson distribution relationship between the percentage of negative cultures per group and the number of responding cells²⁷. The T-cell fractionation procedures using monoclonal anti-L3T4 and anti-Lyt2 antibodies are described in Fig. 3 legend.

[‡] Summary of two experiments. Each limiting-dilution titration consisted of 6-8 experimental points, representing 24-48 replicate cultures. Individual 0.2-ml cultures contained graded numbers of untreated or fractionated responder spleen-cell populations, 5×10^5 2,000R-irradiated stimulator spleen cells, and 12.5% supernatant from concanavalin A-induced spleen-cell cultures²⁸, to which α -methyl mannoside had been added. After 7 days of culture at 37 °C and 7.5% CO₂, 4×10^3 51Cr-labelled concanavalin A-induced spleen blast cells were added to each culture as target cells in a 4-h 51Cr-release assay. Cultures were considered positive if their 51Cr release was 3 s.d. above spontaneous release. Minimal estimates of the frequencies of T_c precursors were calculated as previously described²⁷. The T-cell fractionation procedures are described in Fig. 3 legend.

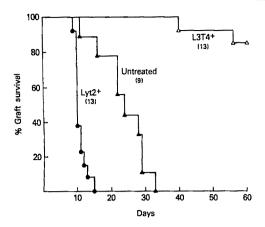


Fig. 3 Ability of isolated T-cell subpopulations to reject bm1 skin allografts. Female B10 nude mice were engrafted on day 0 with tail-skin allografts from female bm1 mice. On day 1, the mice were injected intravenously with 50×10⁶ B6 spleen cells which: were untreated and so contained both L3T4⁺ and Lyt2⁺ T-cell subpopulations (A); had been pretreated with anti-Lyt2.2 monoclonal antibody+complement and so contained only the L3T4+ T-cell subset (Δ); had been pretreated with anti-L3T4 monoclonal antibody+complement and so only contained the Lyt2+ T-cell subset (). Numbers in parentheses indicate the number of mice in each group. Grafts were scored daily until rejection or day 60. MST in days of bm1 skin allografts on B10 nude mice reconstituted with various T-cell populations were as follows: Lyt2+ T cells = 10; unfractionated T cells = 22; L3T4+ T cells > 60.

Methods, Anti-L3T4 monoclonal antibody was a culture supernatant of the hybridoma cell line GK1.5 (ref. 30) provided by Dr Frank Fitch. Anti-Lyt2.2 monoclonal antibody was a culture supernatant of the hybridoma cell line 83-12-5 provided by Dr Jeffrey Bluestone. Depletion of L3T4+ T cells or Lyt2+ cells was accomplished by incubating spleen cells at a density of 107 cells ml-1 with anti-L3T4 (1:2 dilution of culture supernatant) or anti-Lyt2.2 monoclonal antibody (1:5 dilution of culture supernatant) for 30 min on ice. Cells were then pelleted, resuspended and incubated with complement for 40 min at 37 °C. Treated cells were washed three times before injection into experimental animals or before addition to experimental cultures. Efficacy of each treatment (>99%) was confirmed by immunofluorescence and flow microfluorometry. Spleen cells from each group of engrafted and adoptively reconstituted nude mice were assessed 30 days after reconstitution by immunofluorescence and flow microfluometry for numbers of L3T4⁺ and Lyt2⁺ T cells. Spleens from bm1 engrafted nude mice reconstituted 30 days previously with L3T4⁺ T-cell populations contained <1% Lyt2⁺ T cells, whereas spleens from bm1 engrafted nude mice reconstituted 30 days previously with Lyt2+ T-cell populations contained <1% L3T4⁺ cells.

reactive L3T4+ Th and Lyt2+ Tc is not predictive of whether or not Kbm skin is rejected, even though these two T-cell subpopulations collaborate effectively in vitro to generate Kbm-specific Tc responses^{13,15,23}. Since class I-reactive L3T4⁺ T_h cells recognize a composite determinant composed of class I+class II MHC molecules 13-15, the deficient expression of class I MHC on class II-bearing skin epidermal cells²⁴ provides a plausible explanation for the failure of these T_h cells to participate in the rejection of Kbm allografts. Thus, class I-reactive L3T4+ Th cells may never encounter a class (I+II) antigenic complex on individual cells within a skin allograft.

In conclusion, the present study makes three points regarding the rejection of class Î-disparate Kbm skin allografts by wild-type H-2^b mice: first, Lyt2⁺ T cells are the only T cells required to effect the rejection of class I-disparate K^{bm} skin allografts; second, while Lyt2⁺ T_c effectors may contribute importantly to the rejection of K^{bm} skin allografts, it is the number of IL-2secreting, Kbm-reactive T cells within the Lyt2+ T-cell subpopulation that is limiting and that determines the rates at which K^{bm} skin grafts are rejected; and third, potential collaborations

between anti- K^{bm} L3T4⁺ T_h cells and Lyt2⁺ T_c precursors do not have a prominent role in the rejection of K^{bm} skin allografts

We thank Dr Jeffrey Bluestone for helpful discussions and Drs Ronald Gress, Richard Hodes, Susan McCarthy, David Sachs and Dinah Singer for critical readings of the manuscript

Received 13 March; accepted 8 May 1986.

- 1. Loveland, B. E., Hogarth, P. M., Ceredig, R. H. & McKenzie, I & C. J. exp. Med. 153 1044-1057 (1981).
- LeFrancois, L. & Bevan, M. J. J. exp. Med. 159, 57-67 (1934)
- 3. Hall, B. M. & Dorsch, S. E. Immun. Rev. 77, 31-59 (1984)
 4. Lafferty, K. J. & Simeonovic, C. J. Transplantn Proc 16, 92 930 (1984)
- Steinmuller, D. Transplantation 40, 229-233 (1985)
- 6. Melvold, R. W. & Kohn, H. I. Immunogenetics 3, 185-191 (1976)
- Kohn, H. I. et al. Immunogenetics 77, 279-294 (1978)
 Nairn, R., Yamaga, K. & Nathenson, S. G. A. Rev. Genet 14, 241 27 (1980)
 Melief, C. J. M., Schwartz, R. S., Kohn, H. I. & Melvold, R. W. Immun. genetics 2, 137-148
- Mellef, C. J. M., de Waal, L. P., van der Meulen, M. Y., Melveld, R. W. & Kobe, H. J. exp. Med. 151, 993-1013 (1980).
 Mizuochi, T., Ono, S., Malek, T. R. & Singer, A. J. exp. Med. 163, 603 619 (1986).
- Golding, H. & Singer, A. J. Immun. 135, 1610-1615 (1985)
 Singer, A., Kruisbeek, A. M. & Andrysiak, P. M. J. Immun. 132, 2193-2269 (1984)
- 14. Golding, H. & Singer, A. J. Immun. 133, 597-605 (1984)
- Mizuochi, T. et al. J. exp. Med. 162, 427-433 (1985)
 Mizuochi, T. et al. J. Immun. (in the press).
- 17. Lynch, D. H., Welland, D. J., Rosenberg, S. A. & Hodes, R. J. Transplantation in the press
- 18. Engers, H. D., Galsebrook, A. L. & Sorenson, G. D. J. etp. Med. 156, 1250-1255 (1982). Engers, H. D., Sorenson, G. S., Geronimo, T., Horvath, C. & Brunner, K. J. J. Coman. 129, 1292-1298 (1982).
- Hodgkin, P. D., Agostino, M. & Lafferty, K. J. Transplin Proc. 17, 1644-1645-1975
 Warren, H. S., Prouse, S. J., Agostino, M. & Lafferty, K. J. Iransplin Proc. 16, 954-954-954
 Sprent, J., Schaefer, M., Lo, D. & Korngold, R. J. exp. Med. 163, 993-1011 (1986)

- 23. Weinberger, O., Germain, R. N. & Burakoff, S. J. Nature 302, 429 431 11983.
- 24. Caughman, S. W. et al. Proc. natn. Acad. Sci. U.S.A. (in the press)
- Malek, T. R., Robb, R. J. & Shevach, E. M. Proc. natn. Acad Sci. U.S.A. 83, 5694-5693-1983.
 Watson, J. J. exp. Med. 150, 1510-1519 (1979).
 Taswell, C. J. Immun. 126, 1614-1619 (1981).
- 28. Kruisbeek, A. M., Zystra, I. J. & Krose, T. J. M. J. Immun 125, 995 11 02 (1953) 29. Billingham, R. E. & Medawar, P. B. J. exp. Biol. 28, 385 401 (1951)
- 30. Dialynas, D. P. et al. Immun, Rev. 74, 29-56 (1983)

Structural/functional similarity between proteins involved in complement- and cytotoxic T-lymphocyte-mediated cytolysis

Jürg Tschopp*, Danièle Masson* & Keith K. Stanley?

* Institute of Biochemistry, University of Lausanne, CH-1066 Epalinges, Switzerland † EMBL, Meyerhofstrasse 1, Postfach 10.2209, D-6900 Heidelberg, FRG

Cytolysis mediated by complement or cytolytic lymphocytes results in the formation of morphology similar lesions in the target membrane¹⁻⁶. These lesions, formed by the polymerization of C9 or perforin respectively, contribute the major killing action by causing osmotic lysis of the target cell. Following the suggestion of Mayer7 that the mechanisms of humoral and cell-mediated cytotoxicity might be related, studies into the morphology of the membrane lesions formed⁸⁻¹³, and the proteins responsible for causing the lesions^{9,14,15}, have shown several similarities. While the lesion caused by natural and T-killer cells is a little larger than that caused by complement, its overall shape is similar and in both cases the cylindrical pore is formed by polymerization of a monomeric subunit, C9 (relative molecular mass, $M_r = 71,000$) for complement⁹, and perforin $(M_r = 66,000)$ for cell-mediated cytotoxicity^{14,15}. C9 has an absolute requirement for a receptor in the target membrane formed by the earlier membrane attack complex components, C5b, C6, C7 and C8 (ref. 8). For perforin. polymerization in a target membrane requires no receptor, specificity being derived from the specific recognition between killer and target cell. Both proteins can be made to polymerize in vitro by the addition of divalent cations (Zn²⁺ for C9 (ref. 16) and Ca²⁺ for perforin^{10,12,13}) and the resultant complexes closely resemble their physiological counterparts. Antibodies raised

against lymphocyte-killed targets have also been shown to cross-react with complement proteins 17,18,33, but the antigenically related proteins were not determined in these studies. We show here using purified proteins that perforin, C9 and complexes involving C7 and C8 share a common antigenic determinant which is probably involved in polymerization.

During the expression screening of a human cDNA library in pEX (ref. 19) it was noted that one clone, which did not contain C9 sequences, reacted strongly with a polyclonal antibody of high specificity to C9 (clone C9.1 in ref. 19). When the antibody affiinity purified on this fusion protein was tested in Western blots of purified proteins it was found that it bound strongly to mouse perforin. This fusion protein was therefore used to boost rabbits initially injected with mouse perforin.

Figure 1 shows the Western blot analysis using this particular antiserum named C9.1 (Fig. 1a). Not only were purified perforin and C9 immunostained, but a single band appeared with the same apparent M_r as perforin when whole cytoplasmic cytotoxic T-lymphocyte (CTL) granules were analysed. The antiserum did not react with bovine serum albumin or other serum proteins; however, in half of the experiments, C7 was also detected (data not shown).

When a panel of monoclonal antibodies raised against human monomeric C9 was tested, none reacted with mouse perforin, but one monoclonal antibody (BC5), originally described as binding only to epitopes present on poly C9 (ref. 19), did cross-react. This neoantigen-specific antibody binds to a nonconsecutive epitope, and thus binds only weakly to C9 separated in the presence of SDS and transferred to nitrocellulose. In contrast, dot-blot analysis, which presumably conserves this epitope, can be used for its analysis (Fig. 1b). Less than 160 pg of poly-C9 can be immonostained using this antibody, whereas C5b-6, C7, C8 and monomeric C9 do not stain. In contrast, when the late components are first mixed to form the respective complex and then applied to the nitrocellulose, C5b-7, C5b-8, C5b-9 (comprising poly C9) and poly-C9 are all stained. These complexes must therefore exhibit a common epitote not present on the individual precursor proteins.

The amino-acid sequence of C9^{19,20} contains two cysteine-rich regions¹⁹ which show sequence and predicted structural homology²¹ to the low-density lipoprotein (LDL) receptor and urokinase. The function of these regions is unknown, but one hypothesis is that these regions form compact globular domains involved in the polymerization of C9. We therefore postulated that if mouse perforin and human C9 shared a common domain, it was most likely to be found in one of these conserved regions, since both molecules polymerize in a similar manner.

Two peptides were synthesized corresponding to amino acids 74-86 (peptide A) and 101-111 (peptide B) of C9, that is, the segment with high homology to the LDL receptor (Fig. 2). Antibodies raised against the peptides coupled to ovalbumin were tested for their reactivity to C9 and perforin. Both antipeptide A and anti-peptide B immunostained human C9 and mouse perforin (Fig. 3). Perforin staining was considerably weaker, especially when immunoblotting was performed using anti-peptide A. These results suggest that the amino-acid sequence of perforin must be slightly different, especially in segment 74-86 of C9. This second segment also shows a lower degree of homology to the LDL receptor than does the segment corresponding to peptide B. In addition to C9, anti-peptide B bound to $C8\alpha$ (ref. 22), to C7, and weakly to C6. Anti-peptide A also reacted with $C8\alpha$, C7 and C6, although binding to C7 was extremely weak. Other proteins tested, such as bovine serum albumin, were not stained at all with anti-peptide B²² and anti-peptide A (Fig. 3). Binding could also be inhibited by addition of the corresponding peptide. This was true for antibody binding to C9 (Fig. 3), $C8\alpha$ (ref. 22), C7, C6 and perforin (data not shown).

To exclude the possibility that the binding of the anti-peptide entibodies to these proteins was a chance event, the Dayhoff

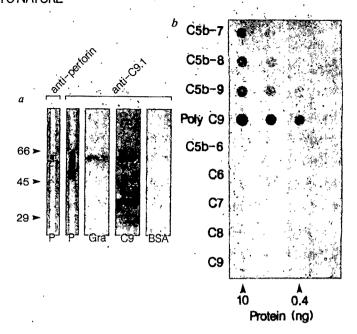


Fig. 1 a, Cross-reactivity of C9 with perforin. Perforin (P), granules (Gra), C9 and bovine serum albumin (BSA) were separated under reducing conditions on a 10% polyacrylamide²⁷ gel in the presence of SDS (SDS-PAGE) and transferred to nitrocellulose²⁸. As a control, perforin was incubated with a specific rabbit anti-perforin antiserum under the same conditions (left panel). b, Dot-blot analysis of complexes of the late components of complement using monoclonal antibody BC5 as a probe.

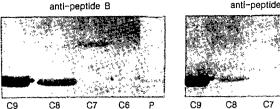
Methods. a, The nitrocellulose membrane was incubated for 2 h in a buffer containing 20 mM Tris-HCl pH 8.4, 150 mM NaCl, 5 mM EDTA, 1% gelatin and 0.1% BSA. Anti-C9.1 antiserum was then added at a 1:100 dilution in the same buffer. The blot was developed with protein-A-peroxidase conjugate using 4-chloro-1-naphthol and H₂O₂ as substrates. Perforin and granules were isolated from the mouse CTL line B6.1 as described elsewhere 12,14. Antibody C9.1 was raised in rabbits by injection of 20 µg purified mouse perforin in Freund's complete adjuvant into popliteal lymph nodes of rabbits followed by three boosts with 20 µg of perforin administered intradermally. Fusion protein from clone C9.1 (ref. 19) was then injected intradermally three times at intervals of 3 weeks and the animal bled 11 days after the final injection. b, Complement proteins C5b-6, C7, C8 and C9 were prepared according to standard procedures²⁹. 10 ng, 2 ng, 0.4 ng, 80 pg of the proteins were adsorbed to nitrocellulose using the dot-blot microfiltration apparatus (BioRad). The different complexes were formed by mixing the respective proteins C5b-6 (1 µg), C7 (0.5 µg), C8 (0.6 µg) and C9 (1.3 µg) in 100 µl Tris-buffered saline (TBS, 10 mM Tris-HCl pH 7.4 containing 150 mM NaCl), incubating them at 20 °C for 15 min (in the case of the C5b-9 complex, incubation temperature was 37 °C). Poly-C9 was formed by incubating 10 µg C9 in 10 µl TBS containing 10⁻⁴ M ZnCl₂ for 2 h at 37 °C. The protein mixtures were diluted to the appropriate concentration and then applied onto the nitrocellulose membrane. Immunostaining was performed as described in a, using a 1/500 dilution of the monoclonal antibody.

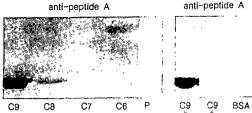
EDAEDDCGND FQCSTGRCIKMRLRCNGDNDCGDFSDEDDCESE PPKTCSQDEFRCHDGKCISRQFVCDSDRDCLDGSDEASCPVL

Fig. 2 Comparison of the homology regions of C9 and the LDL receptor^{19,24}. The peptides synthesized are indicated in the boxed area.

Methods. Peptides were synthesized according to a modified Merrifield method³⁰, using (fluoroenylmethoxycarbonyl) protected amino acids (Bachem). A semiautomatic peptide syntesizer (Labortec) was used for the synthesis. Peptides were purified on a preparative Mono Q column (Pharmacia, FPLC system).

Fig. 3 Western blot analysis of C6, C7, C8, C9 and perforin (P). Samples of 3 μ g of C6 (M_r 115,000), C7 (M_r 110,000), C8 (C8 α , M_r 68,000, C8 β , M_r 65,000, C8 γ , M_r 15,000), C9 (M_r 71,000) and perforin (M_r 66,000) were separated under reducing conditions by SDS-PAGE and transferred to nitrocellulose²⁸. Antipeptide A antiserum and anti-peptide B antisera were added at a 1:100 dilution. Binding of the antibodies was revealed using protein-Aperoxidase conjugates (1:1,000 dilution,





Sigma). The specificity of anti-peptide A antiserum is shown in the right panel: nitrocellulose-bound C9 was incubated with the antiserum in the presence and absence of 100 μ M peptide A. Blotted BSA incubated with anti-peptide A is shown as an additional control. Antisera to the peptides were raised by injecting 200 μ g of peptides coupled to ovalbumin with bis-diazobenzidine³¹ in complete Freund's adjuvant on day 0. The animals were boosted with the same quantity of peptide in incomplete Freund's adjuvant on days 14 and 28 and were bled on day 35.

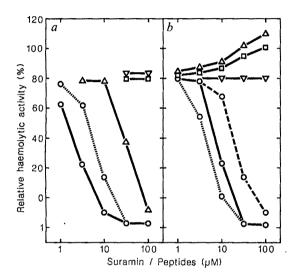


Fig. 4 Effect of peptides and suramin on C7, C8, C9, CTL granule and perforin haemolytic activity. a, Inhibition of perforin (dashed line) and granule activity (solid lines) by peptide A (\square), peptide B (\triangle), a peptide (CDDDPPEIPHAT, ∇) derived from the sequence of the interleukin-2 receptor³² and suramin (\bigcirc) (Bayer, Wupperthal). b, Inhibition of C7 (dashed line), C8 (dotted line) and C9 activity (solid line) with the agents detailed in a.

Methods. Granules (100 µl) isolated from the CTL line B6.1 (ref. 12) or purified perforin¹⁴ were adjusted to a concentration lysing 80% of the sheep red blood cells, and mixed with the peptides/suramin and 300 μ l sheep erythrocytes (1.5 × 10⁷ cells per ml) in a solution containing 10 mM Veronal buffer pH 7.4, 142 mM NaCl, 0.1% gelatin, 1 mM Ca²⁺ and 0.15 mM Mg²⁺ (GVB). The mixture was incubated for 15 min at 37 °C, the erythrocytes spun down at 1,500 r.p.m. for 5 min, and the degree of haemolysis measured by determining the haemoglobin release at 412 nm in a Gilford spectrophotometer. The haemolytic activity was calculated as Z number ¹³. The decrease in the Z number was then transformed into relative haemolytic activity. b, C9 haemolytic test9 was performed by diluting C9 to a concentration causing 80% lysis of the erythrocytes (usually 1-2 ng ml⁻¹). C9, inhibitors and erythrocytes bearing complement components C1-C8 on their surface (1.5× 10⁷ cells per ml) were then mixed in a total volume of 400 µl GVB and incubated for 30 min at 37 °C. The degree of lysis was determined as outlined above. C8 activity²² was carried out by incubating erythrocytes having C1 to C7 bound $(1.5 \times 10^7 \text{ cells per ml})$ with inhibitors and 0.1 µg ml⁻¹ C8 for 15 min at 37 °C in 400 µl GVB. The cells were washed twice in GVB and resuspended in 400 μl GVB containing 1 μg ml⁻¹ C9. Incubation was continued for 30 min at 37 °C and the degree of haemoglobin release determined. C7 activity was determined accordingly with C1-C6 bearing erythrocytes. The inhibitors were added with C7 (0.1 µg ml⁻¹) and after washing, excess of C8 and C9 was added. C6 activity could not be determined, since erythrocytes carrying C1-C5b lose C6 binding activity instantaneously.

protein sequence data bank was scrutinized for the presence of one of the sequences corresponding to the C9-derived peptides. Using the MATCH routine of the Protein Identification Resource²³, we searched for proteins having 6 out of the 11-13 amino acids of peptide A or peptide B in common on the assumption that 6 amino acids are sufficient for an antigenic site. Seven proteins (including the LDL receptor) fulfilled this criterion for peptide B and 15 proteins for peptide A. However, only C9 showed up in both searches, indicating the low probability that a random protein could be detected by the two antipeptide antibodies.

The above results thus suggest that C6, C7, C8 α , C9 and perforin all contain structures homologous to the aminoterminal cysteine-rich region of the LDL receptor. In the LDL receptor, this region binds to the LDL apoprotein B²⁴ in a manner inhibited by two negatively charged molecules, suramin²⁵ and heparin²⁶, suggesting an electrostatic interaction with its ligand. Since a similar interaction within the C9 molecule might account for its polymerization, we tested suramin and the peptides A and B for a direct effect on cytolysis. Figure 4 shows that both C9 and perforin activity were completely abrogated at concentrations above 30 μ M and 10 μ M suramin, respectively. A twofold higher concentration was required for the suppression of perforin activity when perforin was present in CTL granules. C7 and C8 activity were suppressed over a similar range of concentrations.

When the peptides themselves were tested for their inhibitory action, peptide B was found to inhibit granule-mediated cytolysis at concentrations above $100~\mu\text{M}$, but C9 activity was unexpectedly enhanced. At $100~\mu\text{M}$ peptide concentration, C9 activity was augmented 1.3-fold. The same enhancing effect on C9 activity was observed when peptide A was tested, although this peptide did not affect granule or perforin activity (Fig. 4). As a control, a peptide derived from the interleukin-2 receptor showed no effect at all.

We have shown that C9 and perforin contain one or more similar antigenic determinants which cross-react with antibodies raised against intact proteins and synthetic peptides. One of these similar antigenic regions is located in the segment of C9 bearing homology to the LDL receptor. The ability of suramin to inhibit cytolytic activity of C9 suggests that the negatively charged region of the LDL receptor homology region is involved in C9 polymerization. Peptide B, which encompasses this negatively charged region, has opposite effects on perforin and C9 activity. This is particularly interesting because C5b8 complexes, which are essential components in a target membrane for C9 activity, also contain a determinant antigenically related to peptide B. It is possible therefore that the potentiation of C9 activity in the presence of peptide B is also a reflection of the catalytic activity of C5b8.

We thank Dr H. Haymerle and Dr E. Mollnes for antisera, E. Burnier, R. Etges and Z. Freiwald for help in preparing the manuscript, and Ch. Estrade and S. Schäfer for technical assistance. J.T. is supported by a grant of the Swiss NSF.

Received 25 February; accepted 22 April 1986.

- Bhakdi, S. & Tranum-Jensen, J. Biochim. biophys. Acta 737, 343-372 (1983). Lachmann, P. J. & Thompson, R. A. J. exp. Med. 131, 643-652 (1970). Müller-Eberhard, H. J. A. Rev. Biochem. 44, 697-723 (1975). Lachmann, P. J. Nature 305, 473 (1983).

- Podack, E. R. Immun. Today 6, 21-27 (1985).
- Dourmashkin, R. R., Deteix, P., Simon, C. B. & Henkart, P. Clin. exp. Immun. 42, 554-559
- Mayer, M. M. J. Immun. 119, 1195-1202 (1977).
 Tschopp, J., Müller-Eberhard, H. J. & Podack, E. R. Nature 298, 534-538 (1982).
- Podack, E. R. & Tschopp, J. Proc. natn. Acad. Sci. U.S.A. 79, 574-578 (1982).
 Henkart, P. A., Millard, P. J., Reynolds, C. W. & Henkart, M. P. J. exp. Med. 160, 75-91

- (1984).
 11. Dennert, G. & Podack, E. R. J. exp. Med. 157, 1483-1495 (1983).
 12. Masson, D., Corthésy, P., Nabholz, M. & Tschopp, J. EMBO J. 4, 2533-2538 (1985).
 13. Podack, E. R. & Königsberg, P. J. J. exp. Med. 160, 695-710 (1984).
 14. Masson, D. & Tschopp, J. J. biol. Chem. 260, 9096-9072 (1985).
 15. Podack, E. R., Young, J. D. & Cohn, Z. A. Pròc. natn. Acad. Sci. U.S.A. 82, 8629-8633 (1985).
 16. Tschopp, J. J. biol. Chem. 259, 10569-10573 (1984).
 25. Sunders, L. S. & Miller Eberger, H. L. J. Lewing, 122, 2371, 2378 (1075).
- 17. Sundsmo, J. S. & Müller-Eberhard, H. J. J. Immun. 122, 2371-2378 (1975).
 18. Ward, R. H. R. & Lachmann, P. J. Immunology 56, 179-188 (1985).
- 19. Stanley, K. K., Kocher, H. P., Luzio, J. P., Jackson, P. & Tschopp, J. EMBO J. 4, 375-382
- 20. DiScipio, R. G. et al. Proc. natn. Acad. Sci. U.S.A. 81, 7298-7302 (1984).
- Stanley, K. K., Page, M., Campbell, A. K. & Luzio, J. P. Molec. Immun. (in the press).
 Stanley, K. K., Page, M., Campbell, A. K. & Luzio, J. P. Molec. Immun. (in the press).
 Tschopp, J. & Mollnes, T. E. Proc. nath. Acad. Sci. U.S.A. 83, 4223-4227 (1986).
 George, D. G., Barker, W. C. & Hunt, L. T. Nucleic Acids Res. 14, 11-15 (1986).
 Südhof, T. C., Goldstein, J. L., Brown, M. S. & Russel, D. W. Science 228, 815-822 (1985).
- 25. Schneider, W. J., Beisiegel, U., Goldstein, J. L. & Brown, M. S. J. biol. Chem. 257, 2664-2673
- Goldstein, J. L., Basu, S. K., Brunschede, G. Y. & Brown, M. S. Cell 7, 85-95 (1976).
- Lämmli, U. K. Natúre 227, 680-685 (1970).
- Towbin, H., Staehelin, T. & Gordon, J. Proc. natn. Acad. Sci. U.S.A. 76, 4350-4358 (1979).
- Podack, E. R. & Tschopp, J. Molec. Immun. 21, 589-603 (1984).
 Atherton, E., Gait, M. J., Sheppard, R. C. & Williams, B. J. Bioorg. Chem. 8, 351-370 (1979).
- Bassiri, R. M., Dyorak, J. & Utiger, R. D. in Methods of Hormone Radiu Jaffe, B. M. & Behrman, H. R.) 46-47 (Academic, New York, 1979). e Radioimmunoassay (eds
- Cosman, D. et al. Nature 312, 768-771 (1984).
- 33. Zalman et al. Bioscience rep. 5, 1093-1095 (1985).

Probing the phagolysosomal environment of human macrophages with a Ca²⁺-responsive operon fusion in Yersinia pestis

Charles Pollack*, Susan C. Straley† & Mark S. Klempner*‡

* Department of Medicine, Tufts University School of Medicine, New England Medical Center, Boston, Massachusetts 02111, USA † Department of Medical Microbiology and Immunology, Albert B. Chandler Medical Center, University of Kentucky, Lexington, Kentucky 40536, USA

Several microorganisms, including Yersinia sp., Salmonella sp., Brucella sp., Mycobacterium sp. and Leishmania sp., have successfully adapted to grow within macrophage phagolysosomes. Infections caused by these intracellular pathogens are among the most difficult to treat. As part of an antimicrobial strategy directed at modifying the phagolysosomal environment to the disadvantage of these important pathogens, we are defining the ambient conditions within the organism-containing phagolysosome. To probe this environment, we have used Yersinia pestis, whose expression of several virulence attributes is highly dependent on the Ca2 concentration in its growth environment. We first genetically engineered a strain of Y. pestis which responds to a low-calcium environment by transcription of inserted structural genes of the Escherichia coli lac operon. Using this mutant organism as a relevant biological probe, we demonstrate here that the calcium concentration in Y. pestis-containing phagolysosomes is sufficiently low to permit virulence gene expression; this resolves the question of where Y. pestis might express its Ca2+-regulated genes in vivo.

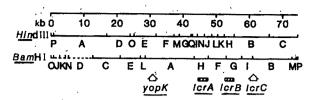


Fig. 1 Location of the mutation used in the present study within the physical map of pCD1. The site of the insertion mutation (yopK) is indicated for the BamHI and HindIII restriction maps of pCD1. Also shown are the locations of low-Ca2+-response (lcr) genes necessary for the growth requirement for Ca²⁺ at 37 °C and for high expression of the V antigen. Broken lines indicate sections where the restriction fragment order is uncertain.

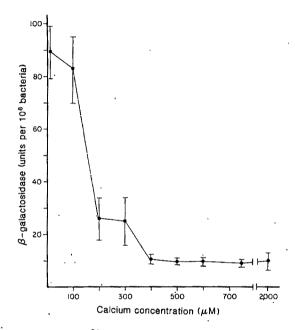


Fig. 2 Effect of Ca^{2+} on β -galactosidase production by Y. pestis KIM6 (pCD1:: Mu dI1-31): The enzyme activity is expressed as a function of the number of bacteria, as determined by counting in a Petroff-Hausser chamber under a microscope. One unit of β -galactosidase activity is equal to 10 μ mol of p-nitrophenyl cleaved from the substrate p-nitrophenyl-D-galactopyranoside, per min, measured over a 12-h period. Each point represents the mean ±s.e.m. of 4-11 separate experiments, each run in duplicate. Methods. Y. pestis KIM6 (pCD1:: Mu dI1-31), which had been maintained at 26 °C, was grown at 37 °C in heart infusion broth supplemented with 0.2% xylose, 2 mM MgCl₂ pH 7.0, at the indicated free Ca²⁺ concentration. The free Ca²⁺ concentration of solutions was calculated from the contaminating Ca²⁺, measured with a Ca²⁺-sensitive electrode (model F2112, Radiometer, Inc., Copenhagen, Denmark), and the amount of Ca2+ added. After 8 h exponential growth, the bacteria were lysed with SDS/chloroform and β -galactosidase production was measured at pH 8.0 according to the method of Conchie et al.12.

Y. pestis, the bacterium which causes plague, is a facultative intracellular organism which grows and multiplies in phagolysosomes within macrophages of the mammalian reticuloendothelial system¹. At least five virulence determinants have been identified for Y: pestis²; one of the most important of these is the response to low Ca²⁺, which is manifested as two coordinately expressed properties: the requirement for millimolar Ca2+ for growth at 37 °C and the ability to synthesize a set of virulenceassociated proteins, including the plague virulence antigens V and W (Vwa⁺ or Lcr⁺ phenotype)^{3,4}. While the precise functions of these proteins are unknown, mutational loss of the ability to express them results in loss of virulence. For example, the mouse

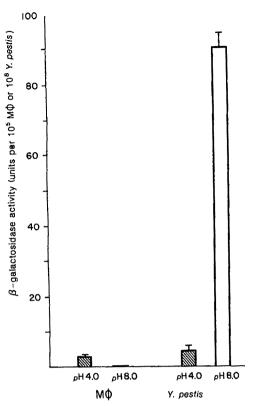


Fig. 3 Effect of pH on β-galactosidase activity of human macrophages and Y. pestis KIM6 (pCD1::Mu dI1-31).

Methods. Y. pestis KIM6 (pCD1::Mu dI1-31) was grown in the presence of 1.0 μM Ca²⁺, as described in Fig. 2 legend. Human mononuclear cells were isolated from heparinized peripheral blood from healthy volunteers and cultured for 24 h in RPMI 1640 tissue culture medium supplemented with 10% fetal calf serum (FCS)¹³. All cells were lysed with SDS/chloroform, as described by Miller¹⁴, and β-galactosidase activity was measured as described by Conchie et al. ¹² at pH 4.0 or pH 8.0. β-galactosidase activity is expressed in units (see Fig. 2).

LD₅₀ (50% lethal dose) for subcutaneously or intravenously injected Lcr+ Y. pestis is less than 10 bacteria, but >107 bacteria for Lcr Y. pestis. At 37 °C the expression of V and W antigens by Y. pestis is closely controlled by the calcium concentration in the growth environment, that is, the coordinated induction of these virulence proteins occurs only when the ambient calcium concentration is in the submillimolar range, well below the extracellular calcium concentration of the human host. Therefore, in order to express V and W antigens and remain virulent, Y. pestis must inhabit an intracellular environment with a low toncentration. The unusual sensitivity of this organism to ambient calcium provides an opportunity to gain information about the phagolysosomal Ca²⁺ concentration. As precise measurement of V and W antigens is cumbersome, we have exploited an insertion mutant of the pCD1 plasmid which encodes the low-Ca2+ response, Y. pestis KIM6 [pCD1:: Mu dI1(Ap lac)::Tn9-31], hereafter called Y. pestis KIM6 (pCD1:: Mu dI1-31)5.

This mutant contains an insertion of the transposing operon fusion bacteriophage Mu dI1(Ap lac)⁶ that eliminates expression of YopK, an outer membrane protein necessary for virulence of Y. pestis⁵ (Fig. 1). The insertion does not affect the expression of V antigen or the growth requirement for Ca^{2+} at 37 °C (ref. 5). The insertion was stabilized against additional transposition or induction of phage functions by the presence of Tn9 in the Mu B gene⁵. Mu dI1(Ap lac) contains the structural genes of the E. coli lac operon, which are expressed as a result of readthrough from the yopK promoter. Y. pestis normally is lac^- ; accordingly, expression of the lacZ gene product, β -galac-

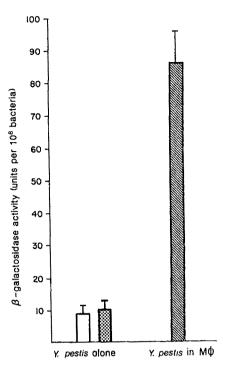


Fig. 4 β -Galactosidase production by extracellular Y. pestis recovered from dishes either without (open bar) or with (stippled bar) macrophages compared with β -galactosidase production by macrophage-associated Y. pestis (hatched bar). β -Galactosidase activity was assayed at pH 8.0 and is expressed as in Fig. 2. Results are the mean \pm s.e.m. of five separate experiments each run in duplicate.

Methods. Y. pestis KIM6 (pCD1:: Mu dI1-31), which had been grown at 37 °C in supplemented heart infusion broth containing 2.0 mM Ca2+ (ref. 1), were washed and resuspended in Hank's balanced salts solution (HBSS) containing 1.0 mM Ca2+ Mg²⁺ and 10% FCS, pH 7.4. The bacterial suspension (10⁸ organisms) was added to Petri dishes in the absence or presence of a monolayer of human macrophages. The macrophage monolayers had been cultured at 37 °C in a humidified atmosphere of 95% air/5% CO₂ in RPMI-1640 medium plus 10% FCS for 24 h, and then washed with HBSS (as above) before addition of the bacterial suspension. In those dishes containing macrophages, the final ratio of bacteria to macrophages was ~10:1. After 8 h of incubation at 37 °C, extracellular Y. pestis were recovered by decanting the dishes, and the organisms were counted in a Petroff-Hausser chamber. The dishes with a macrophage monolayer were gently washed with prewarmed (37 °C) HBSS (1.0 mM Ca+, pH 7.4), leaving behind adherent macrophages containing intracellular and tightly attached Y. pestis. The cells were dislodged with a rubber policeman, counted in a haemocytometer and using an electronic particle counter (Coulter), and macrophage-associated Y. pestis were counted using the fluorescent acridine orange staining procedure of Bertalanffy et al.15.

tosidase, provides a measure of the transcription of yopK. Even though yopK is distant from the lcr genes (Fig. 1) and the V gene (S.C.S., unpublished), it shows the same pattern of expression as V antigen in yersiniae grown under different conditions⁵

Figure 2 shows that the synthesis of β -galactosidase by Y. pestis KIM6 (pCD1::Mu dI1-31) is strictly controlled by the environmental calcium concentration. When grown at calcium concentrations between 400 and 2,000 μ M, a condition in which Lcr⁺ Y. pestis expresses V and W antigens only weakly, β -galactosidase production was suppressed. In growth media with a calcium concentration of 200-300 μ M, there was a small increase in β -galactosidase production. In contrast, ambient calcium concentrations between 1 and 100 μ M induced maximal expression of β -galactosidase.

As our goal was to use bacterial β -galactosidase activity as an indicator of the phagolysosomal calcium concentration, it was important to distinguish between the B-galactosidase activity of the macrophage and that of Y. pestis; we therefore examined the pH optima for expression of macrophage and mutant Y. pestis β -galactosidase activity (Fig. 3). β -Galactosidase from disrupted macrophages was almost undetectable at pH 8.0, but fully active at pH 4.0. In contrast, β -galactosidase produced by the mutant Y. pestis grown in a low-calcium (1.0 µM) environment was highly active at pH 8.0; at pH 4.0, less than 10% of the microbial β -galactosidase activity was

Figure 4 compares β -galactosidase activity of extracellular mutant Y. pestis with that of organisms contained within human macrophages. In media containing 1 mM calcium, extracellular Y. pestis which had never been exposed to the macrophages produced little β -galactosidase. Similarly, extracellular Y. pestis recovered from the supernatant of dishes containing infected macrophages also produced little β -galactosidase. In contrast, the mutant Y. pestis contained within the human macrophages produced large quantities of β -galactosidase.

These studies, in which we used a genetically engineered intracellular pathogen to elucidate the environmental conditions in which it grows and multiplies in vivo, demonstrate that the intraphagolysosomal calcium concentration surrounding Y. pestis is sufficiently low to promote expression of calcium-sensitive virulence genes. We hypothesize that those genes encoding V antigen and outer membrane proteins are expressed during intraphagolysosomal growth of this pathogen; this was not expected, because it has been assumed that the Y. pestiscontaining phagolysosome contains millimolar levels of free Ca²⁺ (ref. 1). Based on our data (Fig. 2), we predict that the intraphagolysosomal calcium concentration is <100 µM. This is a surprising result in view of recent descriptions of ATP-dependent Ca²⁺ translocating pumps located in the plasma membrane of macrophages⁸ and neutrophils⁹ as well as a similar Ca²⁺ uptake pump in neutrophil lysosomes¹⁰. If the portion of the phagocyte plasma membrane which formed the phagocytic vacuole contained Ca2+ pumping activity and fused with lysosomes containing a similar Ca2+ pump, both of these ion translocating pumps would tend to raise the calcium concentration within this compartment. The consequences to intracellular Y. pestis would be the inability to express certain virulence genes and the organism would then be eradicated. It remains to be determined whether the calcium concentration is generally low in this intracellular compartment or whether Y. pestis, like Toxoplasma gondii11, can modify its ambient growth environment to its own advantage.

We thank Robert Gelfand for technical assistance and Ms Debra Becky and Ms Carol McClarey for preparation of the manuscript. These studies were supported by NIH grants AI16732 and AI21017.

Received 19 March; accepted 7 May 1986.

- 1. Straley, S. C. & Harmon, P. A. Infect. Immunity 45, 655-659 (1984).
- 2. Brubaker, R. R. in Microbiology-1979, 168-171 (American Society of Microbiology, Washington, D.C., 1979).
- Brubaker, R. R. Rev. Infect. Dis. 5 (Suppl. 4, 748-758 (1983).
 Goguen, J. D., Yother, J. & Straley, S. C. J. Bact. 160, 842-848 (1984).

- Straley, S. C. & Bowmer, W. S. Infect. Immunity (in the press).
 Casadaban, M. J. & Cohen, S. N. Proc. natn. Acad. Sci. U.S.A. 76, 4530-4533 (1979).
 Horst, J., Kluge, F., Beyreuther, K. & Gerok, W. Proc. natn. Acad. Sci. U.S.A. 72, 3531-3535
- Lew, P. D. & Stossel, T. P. J. biol. Chem. 255, 5841-5846 (1980).
 Lagast, H., Lew, P. D. & Waldvogel, F. A. J. clin. Invest. 73, 107-115 (1984).
 Klempner, M. S. J. clin. Invest. 76, 303-310 (1985).
 Sibley, L. D., Weidner, E. & Krahenbuhl, J. L. Nature 315, 416-419 (1985).

- Conchie, J., Findley, J. & Levvy, G. A. Biochem. J. 71, 318-325 (1959).
 Klempner, M. S., Cendron, M. & Wyler, D. J. J. infect. Dis. 148, 377-384 (1983).
- 14. Miller, J. H. Experiments in Molecular Genetics 355 (Cold Spring Harbor Laboratory, New
- 15. Bertalanffy, L. V., Masin, M. & Masin, F. Cancer 11, 873-887 (1958).

Diversity of murine gamma genes and expression in fetal and adult T lymphocytes

Joseph S. Heilig & Susumu Tonegawa

Center for Cancer Research and Department of Biology, Massachusetts Institute of Technology, Cambridge, Massachusetts 02139, USA

The search for the genes encoding the T-cell receptor α and β chains revealed a third gene, Ty (ref. 1), which shares with the $T\alpha$ (refs 2-7) and $T\beta$ (refs 8-15) genes a number of structural features, including somatic rearrangement during T-cell development. Ty gene expression appears to be unnecessary in some mature T cells^{16,17} and is at its greatest in fetal thymocytes^{18,19} encouraging speculation that $T\gamma$ has a role in T-cell development and may be involved in the recognition of polymorphic major histocompatibility complex (MHC) products during thymic education^{20,21}. One argument against the participation of $T\gamma$ in such a process has been its apparently limited diversity, due to the small number of gene segments available for rearrangement^{1,22}. We here describe the identification of additional Ty V-gene segments and demonstrate that they can be rearranged to previously identified J- and C-gene segments and are expressed in fetal thymocytes. In addition we describe a variety of patterns of Ty mRNA processing which may be significant for Ty gene regulation.

Previous studies^{1,22} identified three cross-hybridizing mouse V_{γ} -gene segments, V_1 , V_2 and V_3 , and three sets of crosshybridizing J_{γ} - and C_{γ} -gene segments, J_1 - C_1 , J_2 - C_2 and J_3 - C_3 (see ref. 23 for nomenclature). Recently Iwamoto and coworkers²⁴ have reported a fourth set of J and C segments, J_4 - C_4 , which does not cross-hybridize with the other three (see Fig. 3). Although none of these germline gene segments have (with possible exception of C_3) obvious structural defects only the V_2 - J_2 - C_2 combination has been found as a complete rearranged gene^{1,16}. However, the existence of additional germline V_{γ} -gene segments, which do not cross-hybridize to the first three \dot{V} -gene segments and are also rearranged in T cells, is suggested by two observations. First, many T-cell clones and splenic and peripheral T cells carry, in addition to a joined V_2 - J_2 - C_2 gene, an EcoRI DNA fragment containing a rearranged J_1 - C_1 segment^{1,16,17,22}. Second, fetal thymocytes seem to contain more transcripts hybridizing to a C_{γ} -probe which detects C_1 , C_2 and C_3 sequences than to a V_2 -probe which detects V_1 , V_2 and V_3 sequences18.

To confirm this suspicion we constructed a cDNA library from fetal thymocytes and isolated cDNA clones which hybridize to a C_{γ} -probe but not to a V_{γ} -probe. Sequence analysis of one of these clones (FT2) revealed a new V_{γ} -gene segment (V_4) which shares 50% amino acid sequence homology with V_2 and is rearranged to the J_1 - C_1 gene segment (Fig. 1). As is often the case with $T\gamma$ -gene transcripts^{1,16,23,25} the V_4 - J_1 joint in FT2 results in a frame shift such that a translation product would terminate in the J region. Another clone, FT6, contains part of the sequence of another V_{γ} -gene segment (V_5) which is also rearranged to J_1 - C_1 (Fig. 1). Although the complete sequence of V_5 was not contained in this clone, sufficient sequence was obtained to distinguish it from other V-gene segments. The V_5 - J_1 joint in FT6 would also result in premature termination of translation. Nevertheless these new V_{γ} -gene segments indicate

the potential of additional variability in the γ -gene family. Figure 2 shows the result of a Southern blot analysis²⁶ in which DNA from a variety of T-cell clones and a 17-day-old fetal thymocyte population was analysed using C_2 -, V_2 -, V_4 and V_5 -probes in panels a, b, c and d, respectively. The C_2 probe detects C_1 , C_2 and C_3 ; the V_2 -probe V_1 , V_2 and V_3 . The characteristic pattern of double rearrangement with C_2 and

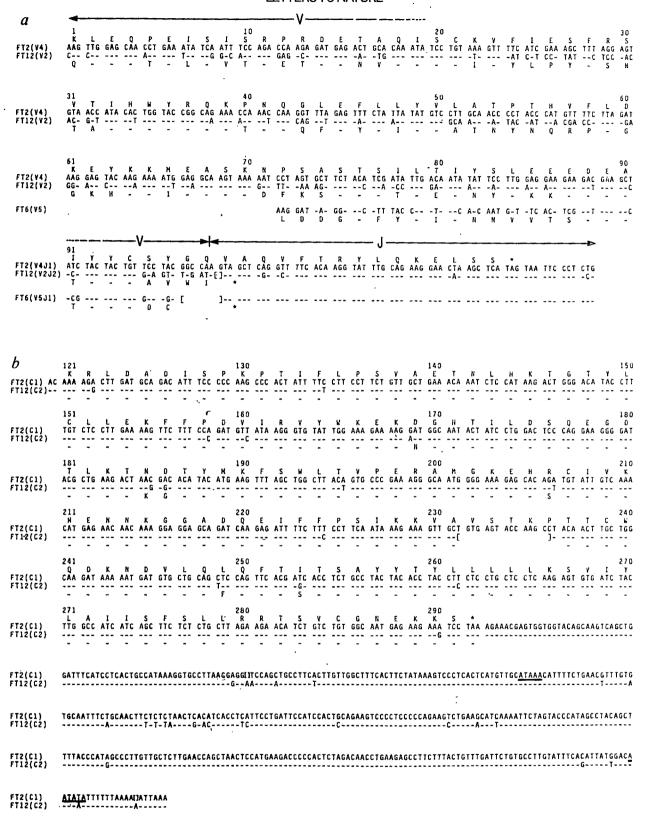


Fig. 1 The nucleotide sequences of $T\gamma$ -cDNA clones. a, the V- and J-region sequences of three cDNA clones. FT2 (V_4 - J_1 - C_1), FT12 (V_2 - J_2 - C_2) and FT6 (V_5 - J_1 - C_1). b, C_1 sequence, determined by analysing clone FT2, compared with C_2 sequence from FT12. The predicted amino acid sequences are indicated by the single-letter code. Dashes indicate sequence identity to that of FT2; parentheses enclose gaps necessary to align the sequences. The underlined regions in b indicate polyadenylation signals.

Methods. Pregnant BALB/cByJ mice at day 17 of gestation were killed and the fetuses removed. Thymuses of 82 fetuses were pooled and disrupted by gentle homogenization in a ground-glass tissue grinder. The thymocytes were collected and washed twice in cold phosphate buffered saline (PBS) and RNA was prepared by the guanidinium/CscI method³⁴. Poly(A)⁺ RNA was isolated³⁵ and used as a template for cDNA synthesis³⁶ and the resulting double-stranded DNA was cloned into λ gt10 by standard procedures³⁷. All sequences were determined by the method of Maxam and Gilbert³⁸.

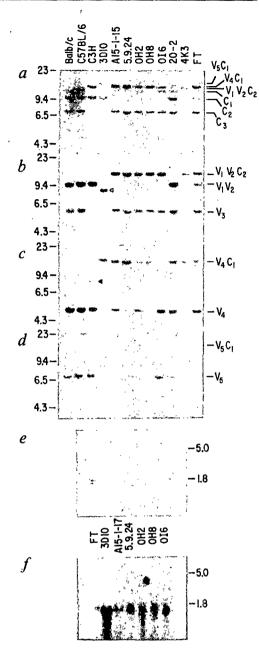


Fig. 2 Southern²⁶ and Northern³⁹ blot analyses of T-cell lines and fetal thymocytes. Panels a-d show Southern blot data while panels e and f show Northern blot data. In the Southern blots, BALB/c, C57BL/6 and C3H indicate kidney DNA of the designated strains; FT, DNA or RNA from 17-day-old BALB/c fetal thymocytes; 3D10, a KLH-specific suppressor T-cell line from C3H⁴⁰; A15-1-17, an alloreactive anti-I-A^k cytolytic T-cell line from A.TH⁴¹; 5-9-24, an I-A^d- ovalbumin-specific cytolytic/helper T-cell line from BALB/c (gift of B. Jones and C. Janeway); OH-2 and OH-8, Db- H-Y-specific cytolytic T-cell lines from C57B/6 (gift of O. Kanagawa); OI-6, an I-Ab H-Y- specific helper T-cell line from C57BL/6 (gift of O. Kanagawa); 20.2, an anti-H-2^b alloreactive helper T-cells line from BALB/c¹⁶; 4K3, an anti-L^d alloreactive cytolytic T-cell line from BALB.K²³. The unrearranged and rearranged gene segments are identified on the right hand side of panels a-d. The arrow in b indicates a V_2 -cross-hybridizing band rearranged to unidentified sequence; probably an example of V_1 - J_4 - C_4 rearrangement (see Fig. 3 and ref. 24). The arrow in c indicates a V₄ crosshybridizing band which may indicate partial digestion of the C3H kidney DNA.

Methods. In the Southern blot analysis, DNA samples were digested with EcoRI. Approximately 2 μ g of each sample was electrophoresed in a 0.8% agarose gel, transferred to nitrocellulose and hybridized by standard procedures⁴². For the Northern blot analysis, RNA was prepared by the guanidinium/CsCl method³⁴ and approximately 12 μ g of each sample was electrophoresed, transferred to nitrocellulose and hybridized as previously described^{17,39,42}. Probes used are: (a), the DNA encoding nearly the entire C_2 region depicted in Fig. 1b (detects C_1 , C_2 and C_3); b, f, the region encoding the first 100 amino acids of V_2 (Fig. 1a) (detects V_1 , V_2 and V_3); c, e, the region encoding the first 78 amino acids of V_4 (Fig. 1a); d, V_5 as described below. C_2 , V_2 and V_4 probes were labelled by nick translation⁴³. Filters hybridized with these probes were washed in 0.4 × SSC/0.1% SDS at 65 °C. The V_5 probe was prepared and used as follows. A synthetic oligonucleotide corresponding to the 76 nucleotides of V_5 (Fig. 1a) was prepared and purified as described⁴⁴. A sesquidecamer complementary to the 3' end of this sequence (5' GCAGGCACAGTAGTA 3') was also synthesized. The probe was radiolabelled by a modification of the primer extension method⁴⁵. Hybridization was carried out at 55 °C. Filters were washed in $2 \times SSC/0.1\%$ SDS at 55 °C and exposed to film.

 C_1 previously reported^{1,16} can be seen in most of these cells. In 20-2 however only C_1 rearrangement has occurred and in OI-6 only C_2 rearrangement. In cells containing a rearranged C_1 segment, the V₄ segment always rearranged to the same EcoRI fragment (Fig. 2a, c). The same correlation applies to C_2 - and V_2 -segments (Fig. 2a, b). By contrast, despite its rearrangement to the J_1 - C_1 segment in the 17-day-old thymocytes, as evidenced by the Southern blots (Fig. 2a, d) and the isolation of the FT6 cDNA clone (Fig. 1), V_5 is not rearranged in any of the T-cell clones studied. Instead, V_5 is present only in those T-cell clones that retain at least one copy of unrearranged V_4 - and C_1 segments, suggesting that rearrangement of V_4 to J_1 - C_1 results in deletion of V_5 . When these DNA samples are hybridized with a probe detecting a part of the C_4 gene, rearrangement is seen only in 3D10 DNA (data not shown, but apparently the same band as the one indicated by the arrow in Fig. 2b) which suggests that the $V_1J_4C_4$ rearrangement reported by Iwamoto and coworkers²⁴ is not very frequent among T-cell clones. The most probable organization of the various γ -gene segments, on the basis of all available data, is shown in Fig. 3.

The level of RNA containing V_2 - or V_4 -sequences was examined in 17-day-old fetal thymocytes as well as in a variety

of T-cell clones (Fig. 2e, f). All cells examined contained V_2 RNA. By contrast only fetal thymocytes contained V_4 RNA. Further analysis by cDNA cloning and sequencing revealed that most of the y RNA in 17-day-old fetal thymocytes, whether of the V_2 - J_2 - C_2 , V_4 - J_1 - C_1 or V_5 - J_1 - C_1 type, is apparently nonfunctional because of out-of-frame V-J junctions. Of eight cDNA clones sequenced which contain a rearranged V_2 -, V_4 - or V_5 segment, all had out-of-frame V-J junctions (see Fig. 1a, clones FT2, FT12 and FT6). Furthermore, many of these cDNA clones use splice sites other than those used in generating normal γ mRNA. Thus, as shown in Fig. 4, clone FT11 uses a splice acceptor in what is normally the V_2 coding region, clone FT6 employs a splice acceptor in what is normally the J_1 - C_1 intron and clone FT5 uses the same acceptor and a splice donor also in the J_1 - C_1 intron. In addition, clone FT10 presumably resulted from transcription initiating upstream of an unrearranged J2gene segment and clone FT13 uses an alternate polyadenylation site.

This study has added two V_{γ} - gene segments, V_4 and V_5 , to the previously recognized sets of three V- and four J-C-gene segments. We now have evidence for rearrangement and expression at the RNA level of at least three types of $T\gamma$ genes,

Fig. 3 The arrangement of the γ genes, inferred from all available data. The orientation of the three gene clusters with respect to one another has not yet been determined. The broken line indicates the J_4 - C_4 cluster described elsewhere²⁴.

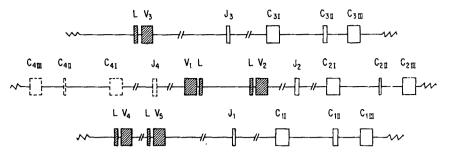
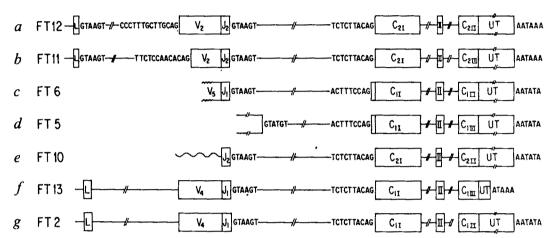


Fig. 4 Alternate splice patterns of y-gene transcripts. Several types of mRNA generated by use of different splice signals are shown schematically. The boxed regions indicate exons and are labelled when the identity is known. The leader region is indicated by L; the first, second and third exons of the C regions by I, II and III respectively; the untranslated regions by UT. Straight lines represent introns and are flanked by the nucleo-



tide sequences of the splice signals. Only the sequences of relevant splice signals are indicated. In clone FT10 the wavy line indicates chromosomal sequence 5' of I2. The nucleotide sequence to the right of the UT region is the polyadenylation signal⁴⁶ presumed to be used by that clone. The normal splice patterns are depicted by clones FT12 and FT2. In clone FT6 the novel splice acceptor is 13 nucleotides upstream of the C_{11} exon. In clone FT5 a splice donor in the J_1C_1 intron 248 nucleotides 5' of C_{11} is used, as the acceptor described for clone FT6. The polyadenylation signals are underlined in Fig. 1b. We sequenced ten cDNA clones, two examples each of types a, b and g and one each of c, d, e and f. In each of the eight cDNA clones containing a V-J junction (FT5 and FT10 do not) the sequence at the V-J junction was different and resulted in frame shift. Splice signals were deduced by comparison to the consensus sequences suggested in ref. 47.

 V_2 - J_2 - C_2 , V_4 - J_1 - C_1 and V_5 - J_1 - C_1 . Within each type there exists sequence variability in the V-J junction (this study and refs 16, 17, 23), indicating that the structural diversity of the Tγ-gene products is not as limited as previously thought. Additional Ty-gene segments may exist which do not hybridize with the available γ probes. In humans, at least two C_{γ} - and six V_{γ} -gene segments have been identified 27,28. The expanded T_{γ} -gene diversity and the structural similarity of this gene to the T_{α} and T_{β} genes support the idea that the role of the Ty gene is in the recognition of polymorphic determinants on target cells. RNA transcripts detected by a C_2 or V_2 probe accumulate in the fetal thymocyte population, which is relatively rich in immature T cells, and are barely detectable in the resting T-cell population obtained from adult lymph nodes 18,19 , suggesting that the $V_2J_2C_2$ gene product is involved in the early development of T cells, perhaps in the interaction with the polymophic MHC determinants presented to immature T cells by thymic epithelial cells^{29,30}. The present finding that V_4 - J_1 - C_1 and V_5 - J_1 - C_1 transcripts are present in fetal thymocytes but not in a variety of T-cell clones supports this hypothesis. However, the fourth $T\gamma$ gene, V_1 - J_4 - C_4 , does not appear to be used abundantly in 17 day-old fetal thymocytes preferentially because it is not represented in our cDNA library, as shown by the fact that all clones hybridizing to a V_2 - probe also hybridize to a C_1 probe $(V_2 \text{ and } V_1 \text{ cross hybridize}).$

The present study shows that most of the Ty RNA present in 17-day-old fetal thymocytes is defective due to out-of-frame V-J joining and abnormal splicing. Examples of out-of-frame joining and abnormal splicing of T-cell-receptor genes have been reported^{4,17,25}. However, the strong bias in favour of presumably nonfunctional mRNA for Ty is striking. Since it is difficult to imagine that in-frame V-J joining is specifically suppressed, the high incidence of out-of-frame cDNA may reflect an aspect of regulation of $T\gamma$ -gene expression. It is possible that the γ protein is required only during an early phase of T-cell development and its continued presence is detrimental to the cell. If so, T cells will be more tolerant to continued transcription of an out-of-frame T_γ gene than an in-frame gene. The implication of this view is that the 17-day-old fetal thymocyte population is dominated by immature T cells that have already passed through the stage in which the Ty gene plays a critical role. Alternatively, the functional expression of the T, gene is restricted to a small fraction of thymocytes destined to become a subset of T-cells as yet unidentified. The significance of the high incidence of apparently abnormal RNA splicing is unclear but may also reflect the need to eliminate in-frame Ty gene products once the cell has passed a critical stage in development. Precedents exist in the literature for the role of alternative splicing in the inactivation of a gene function during viral and cellular development³¹⁻³³

We thank R. Garman, D. Raulet and Y. Takagaki for helpful advice, J. McMaster, H. Siegel and D. Wilson for technical assistance, H. N. Eisen, M. Iwashima, C. Janeway, B. Jones, O. Kanagawa, D. Kranz, M. Pierres, E. Reilly and T. Tada for the T cell lines used in this study and W. A. Gilbert for assistance in preparation of Fig. 1, N. Hopkins for comments on the manuscript and Elly Basel for preparing the manuscript. This work was supported by NIH grants CA28900 and AII7879 to S.T. and P30-CA14051-14 (a core grant to P. Sharp).

Note added in proof: After submission of this paper other groups have reported the identification and sequencing of additional V_{γ} -gene segments: V_4 in refs 48, 49; V_4 , V_5 , V_6 in ref. 50

Received 30 April; accepted 6 June 1986.

- Saito, H. et al. Nature 309, 757-762 (1984).
- Saito, H. et al. Nature 312, 36-39 (1984).
 Chien, Y-h. et al. Nature 312, 31-35 (1984).
- Arden, B., Klotz, J. L., Siu, G. & Hood, L. E. Nature 316, 783-787 (1985)
- 5. Hayday, A. C. et al. Nature 316, 828-832 (1985).

- Winoto, A., Mjolsness, S. & Hood, L. Nature 316, 832-836 (1985).
 Yoshikai, Y. et al. Nature 316, 837-840 (1985).

- Yanagi, Y. et al. Nature 308, 145-149 (1984). Hedrick, S. M., Cohen, D. I., Niclsen, E. A. & Davis, M. M. Nature 308, 149-153 (1984). 10. Hedrick, S. M., Nielsen, E. A., Kavaler, J., Cohen, D I. & Davis, M. M. Nature 308,
- 11. Chien, Y-h., Gascoigne, N., Kavaler, J., Lee, N. E. & Davis, M. M. Nature 309, 322-326 (1984).
- Siu, G. et al. Cell 37, 393-401 (1984).

153-158 (1984).

- Mallissen, M. et al. Cell 37, 1101-1110 (1984).
 Gascoigne, N., Chien, Y-h., Becker, D., Kavaler, J. & Davis, M. M. Nature 310, 387-391
- (1984). 15. Siu, G. et al. Nature 311, 344-350 (1984).

- Siu, G. et al. Nature 313, 344-350 (1984).
 Kranz, D. M. et al. Nature 313, 752-755 (1985).
 Heilig, J. S. et al. Nature 317, 68-70 (1985).
 Raulet, D. H., Garman, R. D., Satto, H. & Tonegawa, S. Nature 314, 103-107 (1985).
 Snodgrass, H. R., Dembic, Z., Steinmetz, M. & vonBoehmer, H. Nature 315, 232-233 (1985).
- Zinkernagel, R. M. Immun. Rev. Rev. 42, 224-270 (1978).
 Bevan, M. J. & Fink, P. J. Immun. Rev. 42, 3-19 (1978).
 Hayday, A. C. et al. Cell 40, 259-269 (1985).

- Reilly, E. B., Kranz, D. M., Tonegawa, S. & Eisen, H. N. Nature 321, 878-880 (1986).
 Iwamoto, A. et al. J. exp. Med. 163, 1203-1212 (1986).
 Dialynas, D. P. et al. Proc. natn. Acad. Sci. U.S.A. 83, 2619-2623 (1986)
 Southern, E. J. molec. Biol. 98, 503-517 (1975).

- 27. Lefranc, M.-P. & Rabbitts, T. H. Nature 316, 464-466 (1985).
- Ouetermous, T. et al. Science 231, 252-255 (1986)
- 29. Jenkinson, E. J., Franchi, L., Kingston, R. & Owen, J. J. T. Eur. J. Immun. 12, 583-587 (1982).

- Lo, D. & Sprent, J. Nature 319, 672-675 (1986).
 Sharp, P. A. in The Aderoviruses (ed. Ginsberg, H. S.) 173-204 (Plenum, New York, 1984).
 Laski, F. A., Rio, D. C. & Rubin, G. M. Cell 44, 7-19 (1986).
 Rio, D. C., Laski, F. A. & Rubin, G. M. Cell 44, 21-32.28 (1986).

- 34. Chirgwin, J. M., Przybyla, A. E., Macdonald, R. J. & Rutter, W. J. Biochemistry 18, 5294-5299
- 35. Aviv, H. & Leder, P. Proc. natn. Acad. Sci. U.S.A. 69, 1408-1412 (1972).
- 36. Gubler, U. & Hoffman, B. J. Gene 25, 263-269 (1983).
 37. Huynh, T. V., Young, R. A. & Davis, R. W. in DNA Cloning: A Practical Approach (ed.
- Glover, D.) 49-78 (IRL, Oxford, 1984). 38. Maxam, A. & Gilbert, W. Meth Enzym. 65, 499-560 (1980)
- Thomas, P. S. Proc. natn. Acad. Sci. U.S.A. 77, 5201-5205 (1980).
 Nakauchi, H., Ohno, I., Kim, M., Okumura, K. & Tada, T. J. Immun. 132, 88-94 (1984).
- 41. Pierres, A., Schmitt-Verhulst, A. M., Bufesne, M., Golstein, P. & Pierres, M. Scand. J. Immun. 15, 619-625 (1982).
- Maniatis, T, Fritsch, E. F. & Sambrook, J Molecular Cloning: A Laboratory Manual (Cold Spring Harbor Laboratory, New York).
 Rigby, P. W. J., Dieckmann, M., Rhodes, C. & Berg, P. J. mol. Biol. 113, 237-256 (1977).
- Reilly, E. B., Reilly, R. M., Breyer, R. M., Saver, R. T. & Eisen, H. N. J. Immun. 133, 471-475 (1984).

- 4/1-4/5 (1984).

 45. Studencki, A. B. & Wallace, R. B. DNA 3, 7-15 (1984).

 46. Proudfoot, N. J. & Brownlee, G. G. Nature 263, 211-214 (1976).

 47. Breathnach, R. & Chambon, P. A. Rev. Biochem. 50, 349-383 (1981).

 48. Traunecker, A. et al FMBO J. 5, 1584-1594 (1986).
- Rupp, F., Frech, G., Hengartner, H., Zinkernagel, R. M. & Joho, R. Nature 321, 876-878
- 30. Garman, R., Doherty, P. J. & Raulet, D. H. Cell 45, 733-742 (1986).

A novel $V_{\rm H}$ to $V_{\rm H}DJ_{\rm H}$ joining mechanism in heavy-chain-negative (null) pre-B cells results in heavy-chain production

Michael Reth, Peter Gehrmann, Eva Petrac & Petra Wiese

Institute for Genetics, University of Cologne, Weyertal 121, D-5000 Köln 41, FRG

During B-cell development, the $V_{\rm rf}$ genes of immunoglobulin heavy (H) chains are assembled from three different germline components: the variable (V_H) segment, the diversity (D) segment and the joining (J_H) segment^{1,2}. The joining between two segments involves the recognition of conserved nonamer-heptamer sequences bordering each segment, double-stranded cuts at the heptamersegment border, and the re-ligation of the two segment ends which have frequently been modified by the deletion and addition of nucleotides³⁻⁶. The flexibility of the joint increases $V_H DJ_H$ variability. However, it also results in many pre-B cells which do not produce immunoglobulin H chains and have non-functional $V_{\rm H}DJ_{\rm H}$ complexes carrying the $V_{\rm H}$ and $J_{\rm H}$ coding sequences in different reading frames? We show here that such 'null cells' are not dead-end products of the B-cell developmental pathway but can perform a novel V_H to $V_H DJ_H$ joining using a 5' V_H segment to replace the $V_{
m H}$ sequence of the $V_{
m H}DJ_{
m H}^-$ complex. This process can result in the generation of a $V_H DJ_H^+$ complex and the subsequent expression of an immunoglobulin heavy chain.

In the past we have studied the order and control of immunoglobulin gene rearrangements in the Abelson pre-B-cell line 300-19 (refs 8-11) derived from the bone marrow of an outbreed NIH/Swiss mouse¹². 300-19 cells which originally carry a DJ_H3 complex on each J_H allele⁸ undergo D to J_H and and $V_{\rm H}$ to $DJ_{\rm H}$ assembly while growing in culture. Approximately 30% of the V_H to DJ_H joints of 300-19 place the V_H and $J_{\rm H}$ coding sequence in the same reading frame thus resulting in the production of a μ -chain⁹, the first H chain class expressed in pre-B cells. Many of the 300-19 subclones, however, contain $V_{\rm H}DJ_{\rm H}^{-}$ complexes and fail to produce a μ -chain. To study the fate of such null cells, we analysed P17 and Pa2-5, two isolates of 300-19 carrying unproductive $V_H DJ_H$ complexes.

Aberrant V_H to DJ_H joints had obviously occurred on both $J_{\rm H}$ alleles of P17 because we could not detect any μ -chains nor 5' D sequences in P17 (data not shown). Indeed, all 5' D sequences are generally deleted during the V_H to DJ_H joint of a $J_{\rm H}$ allele³. To our surprise, P17 became more and more μ -

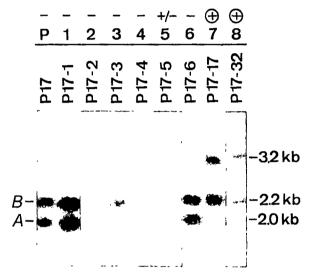


Fig. 1 $J_{\rm H}$ rearrangement in subclones of P17. The two parental $V_{\rm H}DJ_{\rm H}$ alleles of P17 are labelled A and B. Approximately 10 μ g of genomic DNA of the different subclones was digested with EcoRI, electrophoresed through 1% agarose, blotted onto nitrocellulose and assayed for hybridization to a 32 P-lablled $J_{\rm H}$ probe as described previously 3,8 . μ Production in the subclones was determined by Western blotting (see Fig. 2) and is indicated by + or -.

positive over a 3-4 week culture period. After 4 weeks of culture we subcloned P17 by limiting dilution and analysed μ production and J_H rearrangement of isolated subclones. Of 55 P17 subclones analysed, 8 (15%) were found strongly μ -positive in a Western dot assay (data not shown). On a Southern blot the two $V_H DJ_H^-$ alleles of P17 (A and B) are visible as J_H -positive EcoRI fragments of 2 and 2.2 kilobases (kb) respectively (Fig. 1, lane P). In the μ -positive subclones P17-17 and P17-32, the 2-kb EcoRI fragment of the P17-A allele had undergone rearrangement and appeared in a new J_H-positive EcoRI fragment of 3.2 kb (Fig. 1, lanes 7, 8). Three of the six randomly picked subclones had deleted the 2-kb EcoRI fragment (Fig. 1, lanes 2-4). Another of these subclones (P17-5) with weak μ expression (data not shown) showed a faint band of 3.2 kb (Fig. 1, lane 5), suggesting that part of the P17-5 culture was undergoing the same rearrangement event as that occcurring in P17-17 and P17-32. The 2.2-kb EcoRI fragment of the P17-B allele stayed unchanged in all P17 subclones. Thus only the $V_H DJ_H$ complex of the \tilde{A} allele of P17 had undergone genetic alterations. These were either its complete deletion or a further rearrangement correlated with μ production.

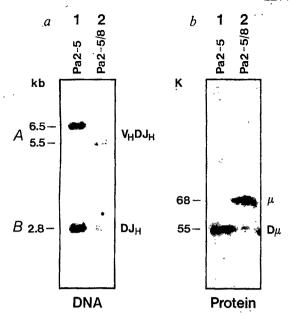
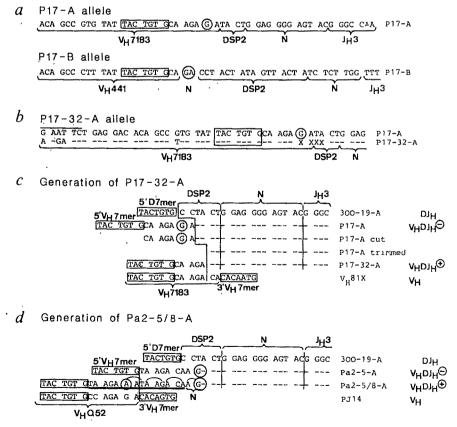


Fig. 2 $J_{\rm H}$ rearrangement and μ production in subclones Pa2-5 and Pa2-5/8. a, Approximately 10 $\mu{\rm g}$ of genomic DNA was double digested with $Bam{\rm HI}$ and $Eco{\rm RI}$ and probed for hybridization with a $J_{\rm H}$ pobe as described previously 3,8 . The position of the two $J_{\rm H}$ alleles is indicated by A and B. b, Intracellular protein of 10^7 cells of each subclone was fractionated by electrophoresis through 10% polyacrylamide gels and electrotransferred to nitrocellulose. Bound μ protein was detected by $^{125}{\rm I}$ -labelled antibodies as described previously 3 .

Fig. 3 Nucleotide sequence of $V_{\rm H}$ to $DJ_{\rm H}$ and $V_{\rm H}$ to $V_{\rm H}DJ_{\rm H}$ rearrangements in 300-19 subclones. The heptamer recognition sequence is boxed. Sequences derived from VH, D, N and $J_{
m H}$ 3 are labelled accordingly. The $V_{
m H}$ sequences are given the names of their respective Vh family as described by Brodeur and Riblet 13,14. Circled nucleotides mark the position where the V_H and DJ_H reading frames are not matched (out of phase). a, Sequence of the two $V_HDJ_H^$ alleles (A and B) of P17. b, Comparison of the P17-32-A sequence with that of P17-A. The P17-A sequence is given and the identity of the P17-32-A sequence is indicated by a dash. Nucleotide deletions in the P17-32-A sequence are indicated by crosses. An internal EcoRI site in the $V_{\rm H}$ sequence of P17-A is overlined, indicating the position up to which both sequences could be compared. c, Generation of P17-32. The sequence of the 300-19 $DJ_{\rm H}3$ A allele8 is given in the first line and the remaining $D-N-J_H3$ sequence in the V_HDJ_H3 complexes is indicated by dashes. All $V_{\rm H}$ sequences are shown up to the border of the internal $V_{\rm H}$ heptamer. The $V_{\rm H}$ sequence of P17-32-A is compared with that of $V_{\rm H}81{\rm X}$ (ref. 41) a germline $V_{\rm H}$ element of the $V_{\rm H}7183$ family. d, Generation of Pa2-5/8. V_H-D-N-J_H3 sequences are presented as described above. The partial duplication of the seven terminal VH nucleotides is underlined. The reading frame of the $V_{\rm H}$ and $J_{\rm H}$ coding sequence at the $V_{\rm H}$ to $V_{\rm H}DJ_{\rm H}$ joint is indicated above the sequence. The $V_{\rm H}$ sequence of Pa2-5/8 is compared with that of PJ14 (ref. 4), a germline V_H segment of the VhQ52 family.

Rearrangement of a $V_H DJ_H$ complex was also seen in Pa2-5, another isolate of the 300-19 culture. Pa2-5 carried an aberrant $V_{\rm H}$ to $DJ_{\rm H}$ rearrangement on the A allele and a parental (300-19) DJ_{H} 3 complex on the B allele. The DJ_{H} 3-B allele is expressed in Pa2-5 as well as in 300-19 (ref. 8) and gives rise to a short $D\mu$ -chain of relative molecular mass, 55,000 (55K; Fig. 2b, lane 1). After 2 weeks of culture, we subcloned Pa2-5 and randomly chose 12 subclones to analyse their $J_{\rm H}$ rearrangements and μ production. One of these subclones, Pa2-5/8, expresses both μ and $D\mu$ -chains (Fig. 2b, lane 2). The presence of the $D\mu$ -chain suggested that the μ expression of Pa2-5/8 did not result from a regular V_H to DJ_H3 rearrangement on the B allele but rather from an alteration of the $V_{\rm H}DJ_{\rm H}^-$ A allele. A Southern blot analysis confirmed this interpretation (Fig. 2a). The 2.8-kb BamHI/EcoRI fragment of the DJH B allele was present in both lines while the 6.5-kb fragment of the Pa2-5 A allele was rearranged to a $J_{\rm H}$ -positive fragment of 5.5 kb in Pa2-5/8 (Fig. 2a, lanes 1, 2). Reprobing the Southern blot with V_{H^-} specific probes demonstrated that the $V_H DJ_H$ complexes of both Pa2-5 and Pa2-5/8 contained a $V_{\rm H}Q$ 52 element (data not shown). Because we have characterized and mapped most V_HQ52 elements used by 300-19 cells⁹, we could identify the rearranged $V_{\rm H}$ elements of Pa2-5 and Pa2-5/8 as being the two most 3' situated V_H segments of the VhQ52 family (for definition of $V_{\rm H}$ families see refs 13-15). This suggested that the $V_{\rm H}Q52$ sequence in the $V_{\rm H}DJ_{\rm H}^-$ complex of Pa2-5 was replaced in Pa2-5/8 by a neighbouring $V_{\rm H}$ segment.

To further characterize the unexpected rearrangement in the P17 and Pa2-5 culture, we cloned the $V_{\rm H}DJ_{\rm H}^-$ alleles of P17 and Pa2-5 as well as the newly generated productive rearrangement of P17-32 and Pa2-5/8. The sequence of the P17 $J_{\rm H}$ alleles (Fig. 3a) confirmed that both had assembled a $V_{\rm H}DJ_{\rm H}$ complex by joining either a $V_{\rm H}7182$ (allele A) or a $V_{\rm H}441$ element (allele B) to the previously sequenced $DJ_{\rm H}3$ complexes of $300 \cdot 19^8$.



Methods. All $V_{\rm H}DJ_{\rm H}$ alleles were cloned as $J_{\rm H}$ -positive EcoRI fragments in either CH16A or CH35⁴². Restriction fragments carrying the respective rearrangement were subcloned into pUC-19 and sequenced according to Maxam and Gilbert⁴³. The Vh family of the rearranged $V_{\rm H}$ segments was determined by a comparison of their amino-acid sequence to a representative collection of $V_{\rm H}$ sequences¹⁵ and by a blotting analysis using $V_{\rm H}$ -specific pobes⁴¹.

Both $V_H DJ_H$ alleles of P17 carry the V_H and J_H coding sequences in different reading frames (see circled nucleotides in Fig. 3a), thus explaining the absence of μ production in P17. A similar out of phase joint has also occurred in the V_H to DJ_H rearrangement of Pa2-5 (Fig. 3d). The rearranged A allele of P17-32 carries a V_HDJ_H complex which obviously was derived from the $V_H DJ_H^-$ complex of P17-A because both complexes contain identical $D-N-J_H$ 3 sequences (Fig. 3b, c). The $V_HDJ_H^+$ complex of P17-32-A also contains a V_H7183 segment whose determined sequence (see legend to Fig. 3b), however, differs from that of P17-A by an exchange of four nucleotides and a deletion of four nucleotides at the V_{H} -D border (Fig. 3b).

How can the new $V_H DJ_H$ complex of P17-32-A have been generated from that of P17-A? Although alternative explanations exist¹⁶, we suggest that the P17-32-A V_HDJ_H complex results from a V_H to $V_H DJ_H$ joining event. The V_H sequence of P17-A as well as that of most $V_{\rm H}$ elements contains the conserved heptamer TACTGTG seven nucleotides away from the 3' end (boxed in Fig. 3). As also noted by others¹⁷, the sequence of this internal V_H heptamer is identical to that of 5' D heptamers (see Fig. 3c). Therefore, like a DJ_H complex, a V_HDJ_H complex carries a 5' heptamer and thus could be partner in the joining to a new $V_{\rm H}$ segment. Figure 3c depicts the proposed steps in such a $V_{\rm H}$ to $V_{\rm H}DJ_{\rm H}$ joining to generate P17-32-A. The joining would start with a precise cut in P17-A at the very end of the internal V_H heptamer, followed by the terminal deletion of seven V_H and two D'nucleotides and the addition of a new 5'-located $V_{\rm H}$ 7183 element to the remaining $D-N-J_{\rm H}$ 3 sequences. In Pa2-5/8 the $V_{\rm H}$ to $V_{\rm H}DJ_{\rm H}$ joint obviously occurred without any nucleotide deletion or addition (Fig. 3d, see vertical line between the heptamers), resulting in a $V_{\rm H}DJ_{\rm H}^{-1}$ complex with a partial duplication of the last seven $V_{\rm H}$ nucleotides (underlined in Fig. 3d). Both the $V_{\rm H}$ to $V_{\rm H}DJ_{\rm H}$ joints described brought the $V_{\rm H}$ and $J_{\rm H}$ coding sequence back into the same reading frame and thus allowed μ expression.

The consensus recognition sequence consists of a conserved heptamer and nonamer separated by a spacer of either 12 or 23 base pairs and joining normally occurs only between segments flanked by recognition sequences of different spacer length $(12/23 \text{ joining rule})^{1,4}$. The V_H to $V_H DJ_H$ joining seems to violate this rule because it employs an isolated heptamer in the $V_{\rm H}$ sequence of the $V_H DJ_H$ complex. Joining events involving an isolated heptamer, however, also occur at the mouse and human κ locus and seem to be a possible variation of the rearranging process $^{18-20}$. The $V_{\rm H}$ replacement of Pa2-5/8 seems to involve two neighbouring $V_{\rm H}$ segments and the same may be true for P17-32 where the $V_{\rm H}$ to $V_{\rm H}DJ_{\rm H}$ joint did not result in the deletion of many V_H 7183 germline segments (data not shown). The use of neighbouring V_H segments in the V_H to $V_H DJ_H$ joint may be connected with the local activation of $V_{\rm H}$ germline transcripts on a V_HDJ_H allele, and stresses the known correlation between

Received 31 March; accepted 21 May 1986.

- 1. Tonegawa, S. Nature 302, 575-581 (1983).
- Yancopoulos, G. D. & Alt, F. W. A. Rev. Immun. 4, 339-368 (1986).
 Alt, F. W. et al. EMBO J. 3, 1209-1219 (1984).

- Sakano, H., Maki, R., Kurosawa, Y., Roeder, W. & Tonegawa, S. Nature 286, 676-683 (1980).
 Alt, F. W. & Baltimore, D. Proc. natn. Acad. Sci. U.S.A. 79, 4118-4122 (1982).
 Steinmetz, M., Altenburger, W. & Zachau, H. G. Nucleic Acids Res. 8, 709-1720 (1980).
- 7. Hagiya, M. et al. Proc. natn. Acad. Sci. U.S.A. 83, 145-149 (1986).
- Reth, M. G. & Alt, F. W. Nature 312, 418-423 (1984).
 Reth, M. G., Jackson, S. & Alt, F. W. EMBO J. (in the press).
 Reth, M. G., Ammirati, P., Jackson, S. & Alt, F. Nature 317, 353-355 (1985).
- 11. Alt, F. W., Blackwell, T. K., DePinho, R. A., Reth, M. G. & Yancopoulos, G. D. Immun. Rev. 89, 5-20 (1986).

- Rev. 89, 5-20 (1986).

 22. Rosenberg, N. & Baltimore, D. J. exp. Med. 143, 1453-1463 (1976).

 13. Brodeur, P. & Riblet, R. Eur. J. Immun. 14, 922-930 (1984).

 14. Brodeur, P. & Riblet, R. UCLA Symp. molec. cell. Biol. new Ser. 18, 445 (1984).

 15. Dildrop, R. Immun. Today 5, 85-86 (1984).

 16. Krawinkel, U., Zoebelein, G., Brüggemann, M., Radbruch, A. & Rajewsky, K. Proc. natn. Acad. Sci U.S.A. 80, 4997-5001 (1983).

 17. Early, P., Nottenburg, C., Weissman, I. & Hood, L. Molec. cell. Biol. 2, 829-831 (1982).

 18. Hochtl, J. & Zachau, H. G. Nature 302, 260-263 (1983).

- 19. Moore, M. W., Durdik, J., Persiani, D. M. & Selsing, E. Proc. natn. Acad. Sci. U.S.A. 82, 6211-6215 (1985).
- Siminovitch, K. A., Bakhski, A., Goldman, P. & Korsmeyer, S. J. Nature 316, 260-263 (1985).

transcription and rearrangement at the immunoglobulin loci²¹⁻²⁶. Wang and Calame²⁷ have described the transcription of a normally silent V_H germline segment in B cells which carry a $V_{\rm H}DJ_{\rm H}$ complex 16 kb downstream from this $V_{\rm H}$ segment. The upstream $V_{\rm H}$ transcription is thought to be activated once the $V_{\rm H}$ to $DJ_{\rm H}$ joint has placed the immunoglobulin H gene enhancer element close to the 5'-located $V_{\rm H}$ segment. The local action of the H gene enhancer ²⁸⁻³⁰ may also be an explanation for the local activation of the V_H to $V_H DJ_H$ joint. Thus our studies support the idea of a dual function of the H gene enhancer, namely to provide transcriptional as well as recombinational enhancement^{2,31}

By completely replacing one $V_{\rm H}$ sequence by another (see P17-32), a $V_{\rm H}$ to $V_{\rm H}DJ_{\rm H}$ joint may generate a $V_{\rm H}DJ_{\rm H}$ sequence indistinguishable from that derived from a V_H to DJ_H joint. Thus the importance and frequency of V_H to V_HDJ_H joints during B-cell development cannot easily be evaluated from an analysis of published $V_H DJ_H$ sequences³². In the two subclones analysed, however, $V_{\rm H}$ to $V_{\rm H}DJ_{\rm H}$ joining seems to occur with a frequency similar to that of V_H to DJ_H rearrangements in the 300-19 culture⁹. Furthermore, the internal $V_{\rm H}$ heptamer which mediates the $V_{\rm H}$ to $V_{\rm H}DJ_{\rm H}$ joint is highly conserved in most mouse and human $V_{\rm H}$ segments³². Specifically, the heptamer is found in V_H segments of all mouse Vh families except those of Vh J606, the most 5' located Vh family 14 . Most of the V segments of other gene loci $^{33-35}$ (those of the immunoglobulin light chains or T-cell receptor chains) do not carry an internal V heptamer with the interesting exception of the T-cell receptor γ-chain where the heptamer has been found in all mouse and human

 V_{γ} segments sequenced³⁶⁻³⁸.

The strong conservation of the internal $V_{\rm H}$ heptamer suggests that V_H to $V_H DJ_H$ joining is important for the generation of functional $V_H DJ_H$ complexes at the V_H locus. Indeed, a V_H to $DJ_{\rm H}$ joint can occur only once on a $J_{\rm H}$ allele because all germline D segments which are mediating the V_H to J_H joint are deleted during the joining process³. Statistically, two out of three $V_{\rm H}$ to $DJ_{\rm H}$ joints place the $V_{\rm H}$ and $J_{\rm H}$ coding sequences in different reading frames, generating up to 50% of null pre-B cells with aberrant $V_{\rm H}DJ_{\rm H}$ complexes on both $J_{\rm H}$ alleles. The $V_{\rm H}$ to $V_{\rm H}DJ_{\rm H}$ joining mechanism may have specifically evolved to rescue these null pre-B cells. $V_{\rm H}$ replacements could occur repeatedly on a $J_{\rm H}$ allele, increasing its chance of generating a productive $V_{\rm H}DJ_{\rm H}$ complex which leads to the expression of a μ -chain. V segments of other V-gene loci (see above) may not need a V replacement mechanism because they have the possibility of multiple V to J joints^{39,40}. The consequences of the $V_{\rm H}$ to $V_{\rm H}DJ_{\rm H}$ joining mechanism for allelic exclusion, VH usage and generation of diversity in developing B cells are being investigated.

We thank Lise Leclercq and Klaus Rajewsky for critical reading of this manuscript. This work was supported by BMFT grant BCI-0365/2, Project 12.

```
21. Kemp, D. J., Harris, A. W., Cory, S. & Adams, J. M. Proc. natn. Acad. Sci. U.S.A. 77,
```

- Kemp, D. J., Harris, A. W., Cory, S. & Adams, J. M. Proc. nam. Acad. Sci. U.S.A. 11, 2876-2880 (1980).
 Yan Ness, B. G. et al. Cell 27, 593-602 (1981).
 Picard, D. & Schaffner, W. EMBO J. 3, 3031-3039 (1984).
 Yancopoulos, G. D. & Alt, F. W. Cell 40, 271-281 (1985).
 Blackwell, T. K., Yancopoulos, G. D. & Alt, F. W. UCLA Symp. molec. cell. Biol., new Ser. 12, 21069. 19, 537 (1984).
- Siu, G. et al. Nature 311, 344-350 (1984).
- Wang, X. F. & Calame, K. Cell 43, 659-665 (1985).
 Gillies, S. D., Morrison, S. L., Oi, V. T. & Tonegawa, S. Cell 33, 717-728 (1983).
 Banerji, J., Olson, L. & Schafiner, W. Cell 33, 729-740 (1983).
 Neuberger, M. S. EMBO J. 2, 1373-1378 (1983).

- Yancopoulos, G. D., Blackwell, T. K., Suh, H., Hood, L. & Alt, F. W. Cell 44, 251-259 (1986). Kabat, E. A., Wu, T. T., Bilofsky, H., Reid-Miller, M. & Perry, H.(eds) Sequences of Proteins
- of Biological Interest No. 80-2008 (NIH, Bethesda, 1983). 33. Barth, R. K. et al. Nature 316, 518-523 (1985).
- 34. Arden, B., Klotz, J., Siu, G. & Hood, L. Nature 316, 518-523 (1985). 35. Becker, D. et al. Nature 317, 430-434 (1985).
- 36. Kṛanz, D. M. et al. Nature 313, 752-755 (1985). 37. Hayday, A. C. et al. Cell 40, 259-269 (1985).

- Lefranc, M. P., Forster, A. & Rabbitts, T. H. Nature 319, 420-422 (1986).
 Lewis, S., Rosenberg, N., Alt, F. & Baltimore, D. Cell 30, 807-816 (1982).
 Feddersen, R. M. & Van Ness, B. G. Proc. natn. Acad. Sci. U.S.A. 82, 4793-4797 (1985).
- 41. Yancopoulos, G. D. et al. Nature 311, 727-733 (1984). 42. De Wet et al. J. Virol. 33, 401-410 (1980).
- 43. Maxam, A. & Gilbert, W. Meth, Enzym, 65, 419-460 (1980).

Recombination between an expressed immunoglobulin heavy-chain gene and a germline variable gene segment in a Ly 1⁺ B-cell lymphoma

Robert Kleinfield*, Richard R. Hardy†, David Tarlinton†, Jeffery Dangl†, Leonard A. Herzenberg† & Martin Weigert*

* Institute for Cancer Research, Philadelphia, Pennsylvania 19111, USA † Department of Genetics, Stanford University, Stanford, California 94305, USA

The early stages of murine B-cell differentiation are characterized by a series of immunoglobulin gene rearrangements which are required for the assembly of heavy(H)- and light(L)-chain variable regions from germline gene segments. Rearrangement at the heavychain locus is initiated first and consists of the joining of a diversity $(D_{
m H})$ gene segment to a joining $(J_{
m H})$ gene segment. This forms a $DJ_{\rm H}$ intermediate to which a variable $(V_{\rm H})$ gene segment is subsequently added. Light-chain gene rearrangement follows and consists of the joining of a V_L gene segment to a J_L gene segment: once a productive light-chain gene has been formed the cell initiates synthesis of surface immunoglobulin M (sIgM) receptors (reviewed in ref. 1). These receptors are clonally distributed and may undergo further diversification either by somatic mutation^{2,3} or possibly by continued recombinational events⁴. Such recombinational events have been detected in the Ly 1+ B-cell lymphoma NFS-5, which has been shown to rearrange both λ and H-chain genes subsequent to the formation of sIgM $(\mu\kappa)$ molecules⁵. Here we have analysed a rearrangement of the productive allele of NFS-5 and found that it is due to a novel recombination event between V_H genes which results in the replacement of most or all of the coding sequence of the initial $V_{\rm H}Q52$ rearrangement by a germline $V_{\rm H}7183$ gene. Embedded in the $V_{\rm H}$ coding sequence close to the site of the cross-over is the sequence 5' TACTGTG 3', which is identical to the signal heptamer found 5' of many $D_{\rm H}$ gene segments⁶. This embedded heptamer is conserved in over 70% of known $V_{\rm H}$ genes⁷⁻¹⁷. We suggest that this heptamer mediates $V_{
m H}$ gene replacement and may play an important part in the development of the antibody repertoire.

The Ly 1⁺ B-cell lymphoma NFS-5 was generated by inoculating a newborn NFS/N mouse with ecotropic murine leukaemia virus (Cas 2SM)¹⁸. Recent studies have indicated that this lymphoma is capable of expressing a number of distinct surface immunoglobulin phenotypes during growth in vitro⁵. Analysis of primary cultures of NFS-5 on the fluorescence-activated cell sorter (FACS) shows a $\mu^-\kappa^-$ population from which $\mu^+\kappa^-$ cells spontaneously arise. Kappa light-chain synthesis can be induced by treatment with the B-cell mitogen lipopolysaccharide (LPS), to give a $\mu^+ \kappa^+$ population. Continued growth of these κ expressing cells in LPS results in the appearance of a small population, comprising 1-5% of the culture, expressing λ light chains. These λ -expressing cells generally have a $\mu^+\lambda^+$ surface phenotype, however $\mu^+\kappa^+\lambda^+$ co-expressors have also been detected. Hardy et al. have cloned a series of cell lines representing each of the various phenotypic forms of NFS-5 (ref. 5). These cloned lines have been designated as follows: 5.3 ($\mu^+ \kappa^-$), 5.4κ $(\mu^+\kappa^+)$, $5.4\kappa\lambda$ $(\mu^+\kappa^+\lambda^+)$ and 5.4λ $(\mu^+\lambda^+)$. The two λ expressing lines, 5.4κλ and 5.4λ, which represent progeny derived from a single expanded population of 5.4k, contain immunoglobulin gene rearrangements not present in either the parental lymphoma or the $\mu^+\kappa^+$ precursor, 5.4 κ . Thus, although all lines contain shared rearrangements on both κ alleles, lines differ in the organization of both the λ and H-chain genes. Distinct rearrangements at the λ locus are found in 5.4 $\kappa\lambda$ and

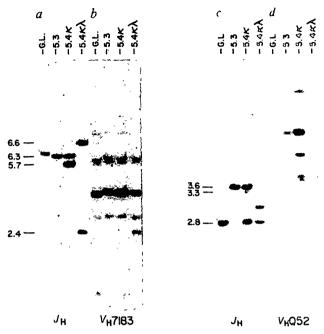


Fig. 1 Context of immunoglobulin variable (V_H) and joining (J_H) gene segments in NFS-5-derived cell lines. Approximately 10 µg of genomic DNA was digested with either EcoRI (a, b) or Hindl! (c, d), fractionated on 0.8% agarose gels and transferred to nitrocellulose filters²⁷; duplicate blots were assayed for hybridization to the ³²P-labelled $J_{\rm H}$ probe, pJ11 $(a,c)^{28}$, and to either a $V_{\rm H}7183$ (b) or $V_{\rm H}Q52$ (d)²⁹ gene probe. After hybridization, blots were first washed at low stringency (3×SSC, 68 °C) and then at high stringency (0.2×SSC, 68 °C). The cell lines assayed include: 5.3 $(\mu^+\kappa^-)$, 5.4 κ $(\mu^+\kappa^+)$ and 5.4 $\kappa\lambda$ $(\mu^+\kappa^+\lambda^*)$. G.L., germline DNA from a NFS/N×NZB RI line homozygous for the NFS/N heavy-chain locus. The J_H region probe, pJ11, consists of a 2.0-kb BamHI/EcoRI fragment containing the J_H3 and J_H4 gene segments subcloned into pBR322; the V_HQ52 probe (pV_HQ52NHhal) consists of a 0.3-kb HhaI fragment subcloned into the Smal site of puC12; the V_H7183 probe (pV_HSAPC-15) derives from a 0.9-kb EcoRI/HaeIII restriction fragment subcloned into the EcoRI/SmaI site of puc12. The 4.1-kb fragment seen in all lanes of c and d is due to plasmid contamination. Sizes (in kb) of restriction fragments hybridizing to both VH and JH probes are given on the left of the autoradiographs. The 3.3-kb fragment in c represents a nonproductive $V_{\rm H}DJ_{\rm H}2$ rearrangement (see text, and data not shown). The light hybridization of this band is thought to be due to a HindIII site between the JH3 and JH4 gene segments which cuts the pJ11-hybridizable region into two fragments of 2.8 and 3.3 kb; the 3.3-kb fragment contains the variable region and 400 bases of sequence hyridizable to pJ11.

5.4 λ ; whereas 5.4 $\kappa\lambda$ contains a $V_{\lambda}1J_{\lambda}1$ gene, 5.4 λ has a rearranged $V_{\lambda}2J_{\lambda}2$ gene⁵. As these rearrangements are not evident in either the parental lymphoma or 5.4 κ , λ light-chain gene recombination has occurred during growth in vitro. In addition, these λ -expressing lines are unusual in that they contain H-chain gene rearrangements not present in the $\mu^{+}\kappa^{-}$ precursor, 5.4 κ . As both H-chain alleles in 5.4 κ consist of complete $V_{\rm H}DJ_{\rm H}$ variable regions, these 'secondary' H-chain gene rearrangements have been investigated further.

DNA of high relative molecular mass (M_r) from NFS-5.3, 5.4 κ and 5.4 κ λ was digested with either EcoRI or HindIII and analysed by Southern blot hybridization using the J_H -region probe, pJ11 (Fig. 1a, c). Both H-chain alleles of 5.4 κ are rearranged and detected in HindIII digests as 3.6-kilobase (kb) and 3.3-kb restriction fragments (Fig. 1c). Restriction fragments of identical size are detected using a V_HQ52 gene probe (Fig. 1d), suggesting that these rearrangements consist of complete V_HDJ_H joins which utilize V_H genes belonging to the V_HQ52 gene family. This conclusion is supported by Northern

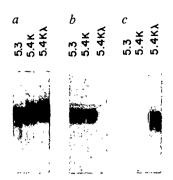


Fig. 2 Northern blot analysis of total RNA from NFS-5-derived cell lines using C_{μ} (a), $V_{\rm H}$ Q52 (b) and $V_{\rm H}$ 7183 (c) gene probes. Total cellular RNA was prepared from homogenized cells lysed in 6 M urea/3 M LiCl, extracted with phenol/chloroform and ethanol-precipitated³⁰. Approximately 10 μ g of RNA from each cell line was electrophoresed through a 1.5% agarose/formal-dehyde gel³¹, transferred to nitrocellulose and hybridized with nick-translated ³²P-labelled probe in 50% formamide, 5×SSC, 1×Denhardt's, 20 mM NaHPO₄ pH6.5, 10% dextran sulphate at 42 °C (ref. 32). Blots were initially washed at low stringency (2×SSC, 0.1% SDS, 52 °C), followed by high-stringency washes (0.1×SSC, 0.1% SDS, 52 °C). Transcript sizes correspond to those expected for mature μ mRNA.

blot analysis which indicates that 5.4κ synthesizes a mature transcript that hybridizes to both C_{μ} (Fig. 2a) and $V_{\rm H}Q52$ (Fig. 2b) gene probes. This transcript appears to be encoded by the 3.6-kb HindIII restriction fragment, as the $\mu^+\kappa^-$ cell line, 5.3, which has retained this restriction fragment but deleted the 3.3-kb fragment (Fig. 1c), nevertheless continues to produce both mature μ messenger RNA (Fig. 2a) and protein¹⁸. We conclude that the 3.6-kb HindIII fragment contains the productive H-chain allele. This allele is rearranged to $J_{\rm H}4$ because the 5.3 cell line, which is haploid at the J_H locus (see Fig. 1a, c), has deleted the 2.8-kb germline-encoded HindIII fragment; this deletion is diagnostic of rearrangements to $J_{\rm H}4$ (Fig. 1c). The 3.3-kb HindIII fragment contains a J_H2-rearranged H-chain allele, as determined both by hybridization using J_{H} -specific probes and detailed restriction mapping of the cloned allele (R.K., unpublished data). This allele appears to be nonproductive as $J_{\rm H}2$ -containing transcripts cannot be detected in 5.4 κ RNA (data not shown).

Continued rearrangement of both the productive and nonproductive H-chain alleles is evident in $5.4\kappa\lambda$. The relationship between these alleles has been determined by Southern blot analysis using $J_{\rm H}1-J_{\rm H}2$ and $J_{\rm H}3-J_{\rm H}4$ -specific probes (data not shown). Rearrangement of the nonproductive allele results in a

change in the HindIII fragment size, from 3.3 to 2.8 kb (Fig. 1c). The 2.8-kb $J_{\rm H}$ -hybridizable fragment is also detected using the $V_{\rm H}O52$ probe (Fig. 1d), indicating that this allele still contains a complete V_HQ52DJ_H rearrangement. Accompanying this rearrangement, germline genes in both the $V_{\rm H}Q52$ (Fig. 1d) and $V_{\rm H}$ 7183 (Fig. 1b) gene families have been deleted suggesting an event occurring over many kilobases of DNA extending from the $J_{\rm H}$ region to the germline $V_{\rm H}$ locus. Rearrangement of the productive allele in 5.4kh is accompanied by a change in the HindIII fragment from 3.6 to 3.0 kb (Fig. 1c), and a change in the EcoRI fragment from 6.3 to 2.4 kb (Fig. 1a). As shown in Fig. 1d, the 3.0-kb fragment does not hybridize to the $V_{\rm H}Q52$ gene probe, despite its derivation from the 3.6-kb $V_{\rm H}Q52$ containing variable region (see above). Rather, as shown in the EcoRI digests, the productive allele of 5.4κλ, contained on a 2.4-kb fragment (Fig. 1a), hybridizes to a $V_{\rm H}7183$ gene probe. Thus, secondary rearrangement of the productive allele results in replacement of the initial $V_{\rm H}Q52$ gene by a $V_{\rm H}7183$ gene. Northern blot analysis of total RNA from 5.4kh indicates that this replacement is accompanied by a change in V_H RNA expression from $V_{\rm H}Q52$ to $V_{\rm H}7183$ (Fig. 2c).

To gain insight into the mechanism of this $V_{\rm H}$ gene replacement, we have sequenced the expressed variable regions of 5.4κ and 5.4κλ using RNA primer extension techniques¹⁹. Analysis of 5.4 κ yields a single $V_{\rm H}Q52DJ_{\rm H}4$ sequence (Fig. 3), indicating that the remaining V_HQ52 rearrangement (the 5.7-kb EcoRIfragment in Fig. 1) in this cell line does not accumulate RNA to any significant extent and is therefore nonproductive at the phenotypic level. Analysis of the H-chain mRNA in 5.4κλ similarly yields a single $V_{\rm H}7183DJ_{\rm H}4$ sequence. No $V_{\rm H}Q52$ transcript is detected in these cells by Northern analysis (Fig. 2b), indicating that the remaining $V_{\rm H}Q52$ rearrangement (the 6.6-kb EcoRI fragment) is not expressed. As the productive $V_{\rm H}$ 7183 rearrangement in 5.4 $\kappa\lambda$ derives from a $V_{\rm H}$ Q52 rearrangement, V_H gene replacement has occurred during propagation in vitro. This conclusion is supported by sequence identity of the N, $D_{\rm H}$ and $J_{\rm H}$ segments expressed in 5.4 κ and 5.4 $\kappa\lambda$. The N sequences are of particular interest as they are created de novo during the V-D recombinational process. Identity of N sequences confirms the common origin of these alleles (see Fig. 3). The variable gene segments of these alleles, however, show marked differences in sequence. Comparison of the 5.4k sequence with a representative germline $V_{\rm H}Q52$ sequence (M141; ref. 16) confirms that this gene is a member of the $V_{\rm H}Q52$ gene family. A similar comparison of the 5.4κλ sequence with a representative germline $V_{\rm H}7183$ sequence ($V_{\rm H}E4.30$; ref. 15) establishes that the productive allele of 5.4kh is derived from a member of the $V_{\rm H}7183$ gene family. Recombination, therefore, results in replacement of most or all of the coding sequence of

Fig. 3 Nucleotide sequence comparison between the expressed alleles of 5.4κ and $5.4\kappa\lambda$. Sequence homologies are shown and reference $V_{\rm H}Q52$ (MOPC 141)¹⁶ and $V_{\rm H}7183$ ($V_{\rm H}E4.15$)¹⁵ germline sequences are given to indicate $V_{\rm H}$ gene family relationships (>80% sequence homology)³⁰. Because of identity in the terminal three bases of the $V_{\rm H}$ segments, the exact site of the recombination cannot be determined precisely; however, four bases 5' of the $V_{\rm H}D_{\rm H}$ junction, a single germline-encoded base difference between 5.4κ (cytosine) and $5.4\kappa\lambda$ (adenine) indicates the 5' boundary of the recombination. Base sequences identical to the recombination signals found 5' of many D elements (5'TACTGTG 3')¹⁷ are boxed.

MOPC 141	ATC AGC AAG GAC AAC TCC AAG AGC CAA GTT TTC TTA AAA ATG AAC AGT CTC			
5.4K	ATC AGC AAG GAC AAC TCC AAG AGC CAA GTT TTC TTA AAA ATG AAC AGT CTC			
5.4 κλ V _H E4.15	ATC TCC GAA TAC AAT GCC AAG AAC ACC CTG TAC CTG CAA ATG AGC AGT CTG ATC TCC AGA GAC AAT GCC AAG AAC ACC CTG TAC CTG CAA ATG AGC AGT CTG			
VH -N-+ - D502				
MOPC 141	CAA ACT GAT GAC ACA GCC AGG TAC TAC TGT GCC AGA			
5.4K	CAA ACT GAT GAC ACA GCC ATG TAC TAC TGT GCC AGA CAT MAC TAT GGTIGAC			
5.4κλ	AGG TOT GAG GAC ACA GCC TTG TAT TAC TGT GCA AGA CAT AAC TAT GGT GAC			
V _H E4 . 15	AGG TOT GAG GAC ACA GCC TTG TAT TAC TGT GCA AGA			
, J _M 4 →				
5.4K	TAC TAT GCT ATG GAC TAC TGG GGT CAA GGA ACC TCA GTC ACC GTC TCC TCA			
5.4KX	TAC TAT GCT ATG GAC TAC TGG GGT CAA GGA ACC TCA GTC ACC GTC TCC TCA			

Methods. Sequences were obtained using RNA primer extension techniques according to Shlomchik et al.¹⁹. Briefly, total cellular RNA was extracted in guanidinium isothiocyanate³³, and poly(A)⁺ RNA was selected on oligo-(dT)-cellulose columns³². Synthesis of complementary DNA was primed with 50 ng of the 5'-end-labelled oligonucleotide (5'GCAGGAGAGGAGGGGGGA 3') homologous to μ constant-region exon 1. Labelled primer was annealed to 80-120 μ g of poly(A)⁺ RNA, and reverse transcription carried out in 100 mM Tris(8.3), 140 mM KCl, 10 mM MgCl₂, 0.5 mM dNTP₅, 10 mM dithiothreitol, 120 U RNasin, 40 U reverse transcriptase for 2 h at 42 °C. The cDNA was obtained by fractionation on a 5% polyacrylamide/7M urea gel for 2-3 h at 30 V cm⁻¹. Gel slices were chopped and eluted overnight at 37 °C in 0.5 M NH₄Ac, 1 mM EDTA. Full-length cDNA was ethanol-precipitated and washed extensively before sequencing by modified chemical degradations, as described by Rubin and Schmid³⁴ and Bencini et al.³⁵.

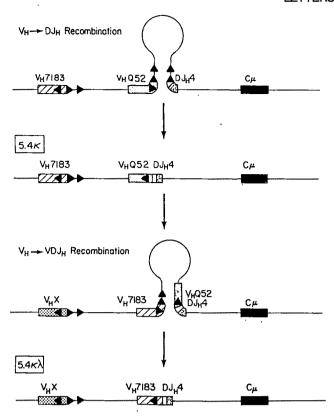


Fig. 4 Model of the $V_{\rm H}$ gene recombinations leading to the formation of the expressed H-chain allele of 5.4κλ. Heptameric and nanomeric signal sequences are indicated by black arrows, and component gene segments are indicated by patterned overlays. Both N and D_{SP2} sequences are depicted together in the figure as an open box. Top panel shows the initial V_HQ52 to DJ_H4 recombination, involving interaction of signal sequences found 3' of the $V_{\rm H}Q52$ gene with those 5' of the $DJ_{\rm H}4$ complex to form a hypothetical stem-loop structure. Excision at the base of the stem and fusion of $V_{\rm H}Q52$ gene to $DJ_{\rm H}4$ completes the formation of the intact variable region of 5.4k. Subsequent recombination between an upstream germline $V_{\rm H}7183$ gene segment and the productive $V_{\rm H}$ Q52 rearrangement is postulated to occur via interaction of the heptameric and nonameric signal sequences 3' of the V_H7183 gene with the embedded heptamer of the rearranged $V_{\rm H}$ Q52 gene, resulting in the replacement of the $V_{\rm H}$ Q52 coding region by a $V_{\rm H}$ 7183 gene segment. This recombination is precise, and does not result in the addition or deletion of bases: the 5' portion of the newly formed variable region is contributed by the incoming V_H 7183 gene, whereas the 3' portion, consisting of N, $D_{\rm SP2}$ and $J_{\rm H}4$ sequences, has been retained from the recombinations which initially formed the allele.

the resident $V_{\rm H}$ Q52 gene with that of the incoming $V_{\rm H}$ 7183 gene. This recombination has occurred so as to maintain a continuous open reading frame. Because of the identity of the 3'-terminal three bases of the germline $V_{\rm H}$ gene segments (both gene families use an AGA for this codon), the precise 3' point of the recombination cannot be identified. However, a single germline-encoded base difference between 5.4κ and $5.4\kappa\lambda$ delineates the 5' boundary of the recombination four bases 5' to the V-D junction.

A number of mechanisms such as gene conversion⁴ and homologous recombination²⁰ may be invoked to explain this $V_{\rm H}$ gene replacement. We consider yet a third model of $V_{\rm H^-}V_{\rm H}$ recombination by a mechanism analogous to V_{H} - D_{H} recombination. Embedded in the V_H coding region, close to the site of the recombination, is the sequence 5' TACTGTG 3'21, which is identical to the signal heptamer found 5' of many $D_{\rm H}$ gene segments¹⁷. We suggest that this heptamer functions as a pairing element in mediating V_{H} - V_{H} recombination (see Fig. 4). Here

a $V_{\rm H}$ O52 gene is paired by its 3' signal sequences to the signal sequences found 5' of DJ_H4 ; shown as a stem-loop structure. Endonucleolytic cleavage at the base of the stem, and fusion of the $V_{\rm H}Q52$ gene segment to this $DJ_{\rm H}4$ intermediate results in the formation of the productive allele found in 5.4k. Further rearrangement of this allele is postulated to occur by an interaction between the embedded heptamer of the $V_{\rm H}Q52$ gene and the signal sequences 3' of one of the germline $V_{\rm H}7183$ genes still present on the chromosome. This results in the replacement of the $V_{\rm H}Q52$ gene by a $V_{\rm H}7183$ gene to give the productive allele found in $5.4\kappa\lambda$.

Although conventional immunoglobulin gene recombination is correlated with the presence of both heptameric and nonameric signal sequences, recombination at isolated heptamers has also been reported. A precedent for heptamer-mediated recombination has been obtained at the k locus, where rearrangements of both V_{κ} and J_{κ} gene segments to an isolated heptamer in the J_{κ} - C_{κ} intron have been reported^{20,22}. Moreover, in many λ-producing plasmacytomas and hybridomas, deletion of the C_{κ} gene segment is mediated by a recombinational event between this intron heptamer and heptamer-nonamer sequences located 3' of the C_{κ} locus (such C_{κ} deletion has not, however, been observed in $5.4\kappa\lambda$)^{23,24}. It has been suggested that such a deletion may be an important preamble to λ gene recombination²³, implying that these heptamer-mediated recombinations may have biologically important consequences.

Yancopoulos et al.15 and Perlmutter et al.25 have recently described the preferential usage of $V_{\rm H}$ genes from the J-most proximal V_H gene family early in fetal development. This preference is not evident in the adult repertoire where the $V_{\rm H}$ gene families appear to be used at frequencies reflecting the relative complexity of each gene family²⁶. We suggest that V_H gene replacement mediated by the embedded heptamer may represent one mechanism leading to the random V_H usage observed in the adult repertoire. Indeed, the strong conservation of this heptameric sequence within the FR3 region where it encodes Tyr and Cys residues at positions 91 and 92 supports this hypothesis: over 70% of $V_{\rm H}$ genes which have been examined, including all functional members of the J-proximal $V_{\rm H}$ families (for example, $V_{\rm H}7183$, $V_{\rm H}Q52$ and $V_{\rm H}S107)^{7-17}$, have been found to contain this heptameric sequence. Thus, conservation is evident not only at the amino-acid sequence level, but also at the nucleotide level where little, if any, third base degeneracy is observed at both the Tyr and Cys codons. Such a high degree of conservation, even among highly diverged $V_{\rm H}$ gene families, suggests that this heptameric sequence has an important role in the somatic diversification of the antibody repertoire.

We thank G. Lennon and M. Shapiro for useful discussions, J. Brill Dashoff for expert technical assistance and M. Shlomchik for sequencing reagents. This work was supported in part by NIH grants GM-20964-13, CA-04681 and HD01287. R.R.H. was supported by the American Cancer Society, California Division (Fellowship S-12-84).

Received 6 May; accepted 28 May 1986.

1. Yancopoulos, G. & Alt, F. W. A. Rev. Immun. 4, 339-368 (1986).

Weigert, M., Cesari, I. M., Yonkovich, S. J. & Cohn, M. Nature 228, 1045-1047 (1970). McKean, D. et al. Proc. natn. Acad. Sci. U.S.A. 81, 3180-3184 (1984).

Dildrop, R., Brüggemann, M., Radbruch, A., Rajewski, R. & Beyreuther, K. EMBO J. 5, 635-640 (1982).

Hardy, R. R. et al. Proc. natn. Acad. Sci. U.S.A. 83, 1438-1442 (1986).
 Kurosawa, Y. & Tonegawa, S. J. exp. Med. 155, 201-218 (1982).
 Bothwell, A. L. et al. Cell 24, 625-637 (1981).

Sonwell, A. L. et al. Cet 24, 023-037 (1981).
 Crews, S., Griffin, J., Huang, H., Calame, K. & Hood, L. Cell 25, 59-66 (1981).
 Givol, D. et al. Nature 292, 426-430 (1981).
 Kaartinen, M., Griffiths, G. M., Martham, A. F. & Milstein C. Nature 304, 320-324 (1981).
 Loh, D. Y., Bothwell, A. L. M., White-Scharff, M. E., Imanishi-Kari, T. & Baltimore, D. College, 1982, 1982.

Cell 33, 85-93 (1983).
12. Near, R. I. et al. Proc. natn. Acad. Sci. U.S.A. 81, 2167-2171 (1984).

Kear, L. et al. Free name. Actas. Sci. Sci., 2
 Sims, J. et al. Science 216, 309-311 (1982).
 Kaartinen, M. et al. J. Immun. 130, 937-945 (1983)

Yancopoulos, G. D. et al. Nature 311, 727-733 (1984).
 Sakano, H., Maki, R., Kurosawa, Y., Roeder, W. & Tonegawa, S. Nature 286, 676-683 (1980).

Early, P., Huang, H., Davis, M., Calame, K. & Hood, L. Cell 19, 981-992 (1980).
 Davidson, W. F. et al. J. Immun. 133, 744-753 (1984).

- 19. Shlomchik, M. J. et al. J. exp. Med. (in the press).
- Seidman, J. G. & Leder, P. Nature 286, 779-783 (1980).
 Early, P., Nottenburg, C., Weissman, I. & Hood, L. Molec. cell. Biol. 2, 829-836 (1982).
 Kelley, D. E. et al. Molec. cell Biol. 5, 1660-1675 (1985).
 Durdik, J., Moore, M. W. & Selsing, E. Nature 307, 749-752 (1984).

- Siminovitch, K. A., Bakhski, A., Goldman, P. & Korsmeyer, S. J. Nature 316, 260-262 (1985). Perlmutter, R. M., Kearney, J. F., Chang, A. P. & Hood, L. E. Science 227, 1597-1600 (1985). Dildrop, R., Krawinkel, V., Winter, E. & Rajewsky, K. Eur. J. Immun. 15, 1154-1156 (1985).

- Dullop, R., Rawlinker, V., Willet, E. & Rajewsky, R. Eur. J. Immun. 15, 1134-1136 (1953).
 Southern, E. M. J. molec. Biol. 98, 503-517 (1975).
 Marcu, K. B., Banerji, J., Penncavage, N. A., Long, R. & Arnheim, N. Cell 22, 187-196 (1980).
 Brodeur, P., Riblet, R. Eur. J. Immun. 14, 922-930 (1984).
 Auffray, C. & Rougeau, F. Eur. J. Biochem. 107, 303-314 (1980).
 Thiele, C. J., Reynolds, C. P. & Israel, M. A. Nature 313, 404-406 (1985).

- 32. Maniatis, T., Fritsch, E. F. & Sambrook, J. Molecular Cloning: A Laboratory Manual (Cold Spring Harbor Laboratory, New York, 1982).
- Chirgwin, J., Przybyla, A., MacDonald, R. & Rutter, W. Biochemistry 18, 5294-5299 (1979).
 Rubin, C. & Schmid, C. Nucleic Acids Res. 8, 4613-4619 (1980).
- 35. Bencini, D., O'Donovan, G. & Wild, J. Biotechniques 4 (January/February 1984).

Distinct factors bind to apparently homolgous sequences in the immunoglobulin heavy-chain enhancer

Judah Weinberger*†§, David Baltimore†‡ & Phillip A. Sharp*†

* Center for Cancer Research and † Department of Biology, Massachusetts Institute of Technology, Cambridge, Massachusetts 02139, USA ‡ Whitehead Institute for Biomedical Research, Cambridge, Massachusetts 02142, USA

The intron separating the variable- and constant-region exons of the rearranged immunoglobulin heavy-chain locus contains a lymphocyte-specific transcriptional enhancer^{1,2}. The enhancer is a member of a class of cis-acting, tissue-specific, transcriptional control elements which are characterized by orientation-independent and relatively position-independent function^{1,2}. In vivo analysis of the position of DNA-binding factors, by assessing the availability of specific bases to chemical modification, has identified four sequence clusters within the heavy-chain enhancer, denoted E1 to E4 (refs 3, 4). These sites are protected (that is, occupied) only in B lymphocytes. A consensus sequence relationship (consensus CAGGTGGC) between these four sites was suggested where three of the sites conformed to the consensus in seven of eight positions while the other was homologus in six of eight positions. We proposed that a single trans-acting factor might recognize all four sites^{3,4}. Using an assay involving gel electrophoresis of DNA-protein complexes⁵⁻⁸ to detect sequence-specific DNA binding factors that recognize these related motifs, we have now identified a mouse B-cell nuclear factor (NF-µE1) which binds specifically to one such motif within the mouse heavy-chain gene enhancer. This factor binds poorly, if at all, to the other related motifs, and other factors have been identified which interact preferentially with some of these latter motifs. Dimethyl sulphate interference experiments suggest that the NF-µE1 factor is in contact with at least the guanine residues in the sequence GATGGCCGATC. This factor seems to be present in both lymphoid and non-lymphoid cell lines.

First, we searched for enhancer-binding factors for these sequence clusters in nuclear extracts from B-cell lines. For this we used a gel electrophoresis DNA-binding assay⁵⁻⁸ in which DNA-protein complexes are resolved by their slower mobility in a low-ionic-strength polyacrylamide gel. A 221-base pair (bp) HinfI fragment containing all in vivo identified binding sites was subcloned into the SmaI site of the pUC-13 vector (Fig. 1). The HindIII-PoulI fragment containing the E1 site and a segment of the polylinker (henceforth denoted as the E1 probe)

§ Permanent address: Department of Medicine, Harvard Medical School, Cardiovascular Division, Brigham and Women's Hospital, Boston, Massachusetts 02115, USA

was 3'-end-labelled and then incubated with increasing amounts of nuclear extract derived from a mouse B-cell lymphoma line. WEHI-231. The duplex alternating copolymer poly(dIdC) poly(dI-dC) was included in the binding reaction to suppress the effect of sequence-nonspecific binding of proteins. A distinct band, a putative protein-DNA complex, with a slower electrophoretic mobility than the free fragment, was observed (Fig. 2a). At higher concentrations of input nuclear extract, additional distinct species with even further retarded mobilities were noted. Competition experiments showed that these species resulted from non-sequence-specific complex formation (data not shown). To test the sequence-specific nature of the major complex, we examined the ability of DNA fragments containing the E1 sequence or other sequences to compete for factor binding to the E1 probe. Two restriction fragments were derived from the mouse immunoglobulin heavy-chain enhancer region. The 400-bp XbaI-PstI fragment (µ400), which contains E1 sequences (Fig. 1), efficiently competed with radiolabelled E1 probe for binding (Fig. 2b). A 300-bp PstI-EcoRI fragment (μ300) containing the balance of the enhancer (Fig. 1), including a partial E2 site and complete E3 and E4 sequences, was, however, unable to compete for NF-µE1 binding of the test fragment. Molar ratios of competitor DNA to probe DNA of 20-50 did not reduce the level of specific binding. Thus, there is no high-affinity NF-µE1-binding site in the µ300 fragment.

The µ300 fragment is recognized by two distinct factors which generate distinct mobility complexes in the gel shift assay8,9. One of these, IgNF-A, recognizes an octamer motif, ATTTGCAT, conserved between the mouse immunoglobulin heavy- and light-chain promoters, as well as the heavy-chain enhancer⁸. Another sequence-specific factor binds to a 70-bp AluI fragment containing E39. A possible way in which the four binding sites occupied in vivo might result from binding of a single factor, and yet without DNA containing the E3 site competing for binding to the E1 site, would be if binding to the E3 site was of lower affinity. To assess this possibility, a 5'-endlabelled E3 probe, the 70-bp AluI frgment, was incubated in WEHI-231 nuclear extract together with either μ400, containing the E1 site, or µ300, containing the balance of the known in vivo binding sites. Figure 2b shows that binding to the E3 probe was not efficiently competed for by excess E1 binding sites while the same binding was efficiently competed for by homologous sequences in the µ300 fragment. Titrations of low molar ratios of µ400 and µ300 fragments compete for E1 and E3 probe

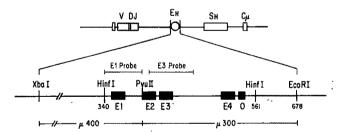
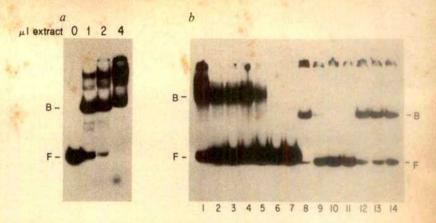


Fig. 1 Scheme of probes and competitor fragments used. The immunoglobulin heavy-chain locus is shown with the intron containing the enhancer (open circle) and the μ switch region (S_H, open bar) separating the rearranged V-D-J (variable-diversityjoining) exons and C_{μ} , the constant-region μ -chain gene. The enhancer is located in a 678-bp XbaI-EcoRI fragment with the indicated restriction sites. E1-E4 and O refer to sequences that are protected from chemical modification in intact B cells³ or in their nuclei4. The HinfI fragment, containing all the indicated sites, was blunted and subcloned into the Sma I site of pUC-13. The E1 probe was derived by cutting the resulting plasmid with HindIII, in the polylinker, and PvuII. The E3 probe is the 70-bp AluI fragment spanning the indicated region. A PstI site used for deriving two fragments indicated on the lowest line, µ400 and µ300, is located 6 bp downstream of the PvuII recognition site.

Fig. 2 Binding of a nuclear factor to E1 and competition analysis. a, Binding in WEHI-231 nuclear extract. The E1 probe was incubated with nuclear extract as described below. The bound protein-DNA complex and free DNA fragment were resolved on a polyacrylamide gel. The free fragment is labelled F, and a bound complex, B, b, Competition analysis of binding to E1 and E3. Lanes 1-7, binding reactions using 1 ng of a $[5'-\alpha^{-32}P]$ -end-labelled 70-bp E3 probe. Lane 1, a control reaction in the absence of additional competitor DNA; Lanes 2-4, binding reactions carried out in the presence of 25, 75 or 150 ng, respectively, of the μ 400 fragment (Fig. 1). Lanes 5-7, binding reactions carried out in the presence of 25, 75 and 150 ng of the µ300 fragment. Lanes 8-14, binding reactions using 1 ng of a radiolabelled



65-bp E1 probe. Lane 8, a control reaction carried out in the absence of additional competitor DNA. Lanes 9-11, binding reactions carried out in the presence of 25, 75 and 150 ng, respectively, of the μ400 fragment. Lanes 12-14, binding reactions carried out in the presence of 25,

75 and 150 ng, respectively, of the µ300 fragment.

Methods. The E1 probe was excised as described for Fig. 1, end labelled with $[\alpha^{-32}P]$ dATP and the large fragment of Eschrichia coli DNA polymerase I, and isolated by polyacrylamide gel electrophoresis. The ^{32}P -labelled fragment (\sim 0.5 ng, 10,000 c.p.m.) was incubated with the nuclear extract 14 of a murine B-cell lymphoma, WEHI-231. Binding reactions (10 μ l) contained 10 mM Tris-HCl (pH 7.5), 50 mM NaCl, 1 mM dithiotreitol, 1 mM EDTA, 5% glycerol, 1,600 ng poly(dI-dC) poly(dI-dC), and the indicated amounts of nuclear extract. After incubation at room temperature for 10 min, the complexes were resolved on a 4% polyacrylamide gel (acrylamide: bisacrylamide weight ratio of 29:1) in 45 mM Tris-borate, 1 mM EDTA pH 8.0 buffer. The gel was dried and autoradiographed.

binding with the expected quantitation (data not shown). Thus, NF-µE1 and NF-µE3° represent distinct factors with high affinity for distinct cognate sequences. Similar competition experiments using the human immunoglobulin heavy-chain enhancer¹⁰ demonstrate the existence of NF-µE1- and NF-µE3°-binding sites in this fragment. No binding activity specific for E4 or E2 sequences has been detected; however, all the probes

used to date have been derived from fragments that were cut at the PstI site, which may interfere with binding.

To elucidate the critical contact points for the binding of NF-µE1 protein, DNA methylation interference analysis was performed11. Dimethylsulphate (DMS) methylates the N-7 position of guanine which extends into the major groove of the B-helix12. The E1 probe was partially methylated with DMS, a binding reaction was performed with the WEHI-231 nuclear extract, and bands of the free fragment and the protein-DNA complex were resolved as described in Fig. 2. Fragments recovered from these bands were cleaved at methylated guanine residues with piperidine and the cleavage products were displayed on denaturing sequencing gels. Positions at which methylation of guanine residues interferes with factor binding should not be cleaved in fragments recovered from the DNA-protein complex band. Comparison of the cleavage pattern of radioactive fragments from the two bands revealed several discrete sites on both strands of the E1 probe where methylation interfered with binding (Fig. 3). These data suggest that the binding site of the factor must include contacts with the guanine residues in the sequence GATGGCCG. The identified interfering guanine residues are precisely the residues protected against DMS methylation in vivo3. Delineation of contact residues for NF-µE1 binding underscores a lack of significant homology with other putative enhancer-binding sites. In particular, the sequences identified for E3 binding^{3,4}, TGTGGCAAG, differ from the E1-binding site by four of eight bases. Furthermore, the above methylation pattern of the E1 site suggests a recognition sequence that only partially overlaps the consensus homology previously deduced by comparison of the four in vivo binding

When nuclear extracts from a panel of pre-B cells, B cells, plasma cells, T cells and various non-lymphoid cells were assessed for the level of NF-µE1 activity (Fig. 4), all were found to contain an activity that generated a band with the E1 probe which co-migrated with the NF-µE1 band from WEHI-231 cells. Some cell lines showed evidence that minor species migrated more rapidly than the NF-µE1 band. These complexes may represent degradation products of NF-µE1 because repeated freezing and thawing of some nuclear extracts increased the levels. Competition experiments and methylation interference analysis performed in various non-lymphoid nuclear extracts revealed sequence specificity identical to that described above for B-cell nuclear extracts (data not shown).

The biological function of NF-µE1 and its biochemical mode

Fig. 3 Methylation interference analysis of binding to E1. The E1 probe was uniquely radiolabelled at the HindIII site in the polylinker (5' to Hinfl site of the enhancer, see Fig. 1) by the large fragment of E. coli DNA polymerase I (a) or by polynucleotide kinase (b). F and B refer, respectively, to DNA recovered from the free and bound species, the products of the binding reaction. A+G chemical cleavage ladders¹² of the E1 probe were co-electrophoresed to map the binding domain.

Methods. The probe (5 ng, 105 c.p.m.) was methylated with DMS for 8 min at 20 °C12 After ethanol precipitation, a 30-µl binding reaction was carried out using the methylated probe, 6 µl of WEHI-231 nuclear extract and 3,600 µg of poly(dI-dC) poly(dI-dC). The remain-3,600 µg of of the reaction conditions were as described in the Fig. 2a legend. The products of the reaction were resolved as in the Fig. 2a legend. After autoradiography to visualize the various species, DNA was eluted from the free



and bound fragments, and cleaved with 1 M piperidine in 100 µl at 90 °C for 30 min¹². After overnight lyophilization, the products were analysed by separation in an 8% polyacrylamide gel (19:1) in the presence of 8 M urea followed by autoradiography at -70 °C with an intensifying screen. Essentially the entire probe is displayed in this figure and the only interference sites detected are those indicated.

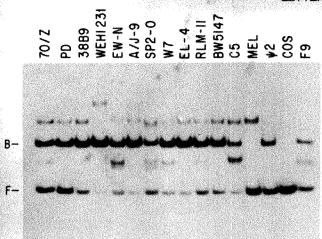


Fig. 4 Analysis of distribution of E1-binding activity in various cell types. Nuclear extracts were prepared 14 from murine or human pre-B-cell lines (70/Z, PD, 38B9), B-cell lines (WEHI-231, EW-N), a myeloma (W7), T-cell lines (EL-4, RLM-11, BW-5147), a primitive B-cell progenitor cell line¹ (C5, a derivative of Ba/F₃, a line like those described in ref. 15), an erythroid line (MEL), a fibroblast line (Ψ2), simian virus 40-transformed African green monkey kidney cell line (COS), and an embryonal cell line (F9). Binding reactions were carried out with the E1 probe as described in Fig. 2 legend. The results of the reaction were analysed by electrophoresis on native polyacrylamide gels. Autoradiography of the dried gels was performed at -70 °C with intensifying screens. Longer exposures of the autoradiogram reveal detectable levels of a species co-migrating with B, the bound complex, in MEL and COS cells.

of action are unknown. The evolutionary conservation of an E1-binding site between mouse and human immunoglobulin genes suggests an important biological function. Deletions of sequences containing the E1 site have been shown to produce severalfold reduction in the transcriptional stimulation activity of the immunoglobulin enhancer element in B cells^{2,13}. The E1 element may be a transcriptional control element, with either constitutive or lymphocyte-restricted transcriptional activation. Perhaps the most direct evidence for the involvement of binding to the E1 site is the previous in vivo methylation protection analysis. A factor is bound to the E1 site in situ which forms contacts with identical guanine residues to those found with the solubilized NF-µE1 factor³. This suggests that NF-µE1 is bound to the E1 site in B lymphocytes.

In the above studies, NF-µE1 binding in vivo was found only in cells of the B lineage. In vitro, however, factors with identical binding specificity are present in extracts from cells of nonlymphocytic lineage. Although similar binding specificities are defined, the proteins found in the various cell types may differ in important aspects that would not be detected by this assay. An obvious explanation for these apparently inconsistent observations is that the immunoglobulin enhancer is in an inactive conformation in non-B cells and thus inaccessible for binding by NF-µE1. The ubiquitous expression of an NF-µE1 activity suggests that this factor is probably important for expression of genes in non-lymphocytic cells. It is possible, for example, that NF-µE1 binding has completely different consequences in cells of different developmental lineages or stages or in different genomic contexts, including cis-dominant transcriptional suppression. These possibilities are being investigated.

Several sites (µE2, µE3 and µE4) with limited sequence homology to the E1-binding site have been identified within the immunoglobulin heavy-chain enhancer. It has been suggested that these four sites bind a common factor. Evidence presented here, in fact, suggests that this is not the case. NF-µE1 clearly does not bind to the µE3 or µE4 sites; conversely, a different factor, NF-µE3, binds with high affinity to E3 but does not bind El to a significant degree9. Thus, the immunoglobulin heavychain enhancer element must be recognized by at least three and probably more different factors. How the combination of these factors sum to a cell-type-specific enhancer is a fascinating problem.

We thank Dr L. Staudt for nuclear extracts from various cell lines, Dr A. Hayday for a plasmid containing the human heavychain enhancer, Drs J. LeBowitz and H. Singh for helpful discussions and a critical reading of the manuscript and M. Siafaca for preparation of the manuscript. J.W. acknowledges support from NIH Clinical Investigator Award HL01633. This work was supported by grants from NIH (CA38660 and GM32467), NSF (DCB8502718) and partially from NCI Cancer Center Support (Core) (CA14051) to P.A.S. and by a grant from the American Cancer Society (IM-355Q) to D.B.

Received 31 March: accepted 6 June 1986.

- Banerii, T., Olson, L. & Schaffner, W. Cell 33, 729-740 (1983)
- Gillies, S. D., Morrison, S. L., Oi, V. T. & Tonegawa, S. Cell 33, 717-728 (1983).

 Ephrussi, A., Church, G. M., Tonegawa, S. & Gilbert, W. Science 227, 134-140 (1985).

 Church, G. M., Ephrussi, A., Gilbert, W. & Tonegawa, S. Nature 313, 798-801 (1985).

- Fried, M. & Crothers, D. M. Nucleic Acids Res. 9, 6505-6525 (1981).
 Garner, M. M. & Rezvin, A. Nucleic Acids Res. 9, 3047-3060 (1981).
 Carthew, R. W., Chodosh, L. A. & Sharp, P. A. Cell 43, 439-448 (1985).
 Singh, H., Sen, R., Baltimore, D. & Sharp, P. A. Nature 319, 154-158 (1986).
- Sen, R. & Baltimore, D. Cell (in the press).
- Hayday, A. C. et al. Nature 307, 334-340 (1984).
- riayuay, A. C. et al. Ivature 2013 534-340 (1754). Sienbenlist, U. & Gilbert, W. Proc. natn. Acad. Sci. U.S.A. 77, 122-126 (1980) Maxam, A. & Gilbert, W. Meth. Enzym. 65, 499-525 (1980).
- Grosschedl, R., Constantini, F. & Baltimore, D. Banbury Rep. 20, 187-196 (1985).
- Dignam, J. D., Lebovitz, R. M. & Roder, R. G. Nucleic Acids Res. 11, 1475-1489 (1983).
 Palcios, R. & Steinmetz, M. Cell 41, 727-734 (1985).

Deregulated expression of c-myc by murine erythroleukaemia cells prevents differentiation

E. V. Prochownik & J. Kukowska

Department of Pediatrics and the Committee on Cellular and Molecular Biology, C. S. Mott Children's Hospital, University of Michigan School of Medicine, Ann Arbor, Michigan 48109, USA

Friend murine erythroleukaemia (F-MEL) cells are a permanent line of primitive erythroid precursors originally derived from the spleens of mice infected with the Friend strain of murine leukaemia virus1. F-MEL cells differentiate in vitro in response to various chemical inducers^{1,2}. Concomitantly with induction, a biphasic regulation of c-myc oncogene transcripts is observed3. Within one hour of the addition of dimethyl sulphoxide (DMSO) or hypoxanthine (Hyp), the levels of c-myc transcripts fall dramatically and remain virtually undetectable for the next few hours. Between 8 and 24 hours after induction, c-myc transcripts return to preinduction levels and then decline again between 3 and 5 days as most of the cells undergo terminal differentiation. To explore the potential relationship between c-myc expression and F-MEL terminal differentiation, we have investigated here whether reversing the early fluctuations in c-myc transcript levels affects the ability of F-MEL cells to differentiate. We therefore constructed an amplifiable plasmid vector containing a full-length mouse c-myc complementary DNA and introduced it stably into recipient F-MEL cells. The exogenous c-myc sequences are transcribed in F-MEL cells and the transcript levels do not change significantly in response to inducing agents. The net result is continued c-myc expression following DMSO or Hyp induction and a complete or partial inhibition of F-MEL differentiation.

Figure 1 shows the plasmid used for transfections. The backbone of this vector has been derived from pSV₂neo, in which bacterial neomycin resistance (neo) sequences have been replaced with a full-length murine c-myc cDNA clone. The simian virus 40 (SV40) early splice and poly(A) sites of pSV₂neo have been retained. Downstream of myc and in the opposite transcriptional orientation, we have introduced an expressible

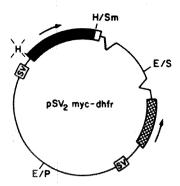


Fig. 1 Structure of an amplifiable mouse c-myc expression vector. SV, SV40 promoters; dark box, mouse myc cDNA sequences; light box, neo 3'untranslated region sequence; cross-hatched boxes, dhfr sequences SV40 splice junctions; H, HindIII; Sm, SmaI; E, EcoRI; S, SaII; P, PstI. Methods. All plasmids were purified by the alkaline lysis method plasmid pSV₂neo (ref. 28) was digested with HindIII and Smal to remove neo sequences and then treated with the large fragment of DNA polymerase I. A 1.5-kilobase (kb) HindIII fragment containing the entire coding region of a mouse c-myc cDNA was excised from the plasmid pMc-myc 54 (ref. 29), treated with the large fragment of DNA polymerase and ligated into the pSV₂neo-derived vector. The resultant plasmid, with c-myc sequences under the control of the SV40 early promoter, was treated with EcoRI and the large fragment of DNA polymerase. Into this site we cloned a 2.8-kb Pst1-Sal1 fragment from the plasmid pFR400 (ref. 4) after treating the fragment with T4 DNA polymerase and the large fragment of DNA polymerase to render it blunt-ended. This fragment contains the SV40 early promoter, a mutant dhfr cDNA and splice-polyadenylation sites derived from the gene encoding hepatitis-B virus surface antigen.

full-length cDNA encoding a mutant form of dihydrofolate reductase (dhfr) which facilitates a selective amplification of plasmid sequences in the presence of high concentrations of the antimetabolite methotrexate (MTX)⁴. We linearized pSV₂mycdhfr along with a selectable plasmid marker encoding neomycin resistance. The two plasmids were introduced by electroporation at a 10:1 molar ratio into recipient F-MEL-745 cells. We selected six clones which demonstrated resistance to both neomycin and MTX. Of these, three expressed the exogenously introduced c-myc sequences (not shown).

We first examined the levels of endogenous and exogenous c-myc transcripts in response to DMSO using an S₁ nuclease protection assay (Fig. 2). Transfected F-MEL cells were first removed from MTX-containing medium for 3-5 days, then washed and cultured in Dulbecco's minimal essential medium (DMEM) containing 1.5% DMSO for varying periods of time. Total RNAs were extracted and used in the S₁ protection assay. The results confirmed the previously reported changes in endogenous c-myc transcripts which occur after DMSO addition³. The behaviour of exogenous, pSV₂myc-dhfr-derived c-myc transcripts was quite different. Following the addition of DMSO. c-myc transcript levels declined by no more than 50%, remaining easily detectable even when endogenous transcripts were not. The net effect was therefore a partial reversal of the early DMSO-induced decline in c-myc transcript levels. Of particular interest was the failure of endogenous transcripts in transfected cells to decline significantly by day 5, suggesting that the cells still retained proliferative potential.

The experiments described above indicated that it was possible to reverse at least partially the inhibitory effects of DMSO on c-myc transcript levels. We therefore next investigated whether this reversal had any inhibitory effect on the differentiation capacity of F-MEL cells in response to two structurally unrelated inducers of differentiation. F-MEL cells were cultured for varying times in 1.5% DMSO or 5 mM Hyp. The extent of differentiation was monitored daily by determining the fraction of cells that stained with benzidine⁵. The results (Fig. 3) showed that in each of the three clones tested, the extent of benzidine positivity was significantly reduced in relation to non-transfected F-MEL-745 cells or to clones of F-MEL cells which had been

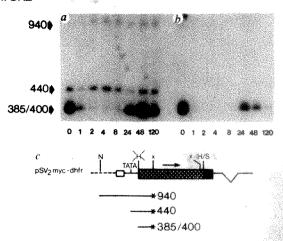


Fig. 2 Levels of mouse c-myc transcripts in F-MEL clone 13 (a) or 745 (b) following the addition of DMSO. The dark arrows indicate the 940-nucleotide reannealed input probe, the 440-nucleotide S₁-protected fragment representing pSV₂myc-dhfr-derived exogenous transcripts and the two unresolved 400- and 385-nucleotide fragments representing endogenous myc transcripts³⁰. Numbers below each lane indicate the length of time (in hours) that cells were incubated in the presence of DMSO. c, The S₁ probe was a 940-nucleotide long Nde1-XhoI fragment, derived from pSV₂ myc-dhfr and end-labelled at the XhoI site.

Methods. F-MEL cells (clone 745) were grown in DMEM supplemented with 10% fetal calf serum (FCS), 100 U ml penicillin, 100 µg ml tomycin and 2 mM glutamine (Gibco). Transfections were performed by electroporation as described previously 31,32 in 1 ml of phosphate-buffered saline containing $1-2\times10^7$ cells ml $^{-1}$, 20 μg of linearized SV₂myc-dhfr and 2 μg of linearized pSV₂neo DNA. Immediately after electroporation, cells were kept on ice for 10 min and then replated in a series of 6-well dishes in fresh DMEM containing dialysed FCS. Two days later, the antibiotic G418 (Gibco) was added to a final concentration of 1 mg ml 1. After 2 weeks, G418-resistant clones were replated in fresh medium containing 0.25 µM MTX (Lederle) plus dialysed FCS. Surviving cells from each well were cloned by limiting dilution in 96-well microtitre dishes. In this way, we insured that each clone originated from an independent transfection event. MTX-resistant clones were expanded with continuous growth in 0.25 uM MTX. Clone 8, 15 and 21 cells were each derived from single-cell isolates of 745 cells stably transfected with pSV2myc-dhfr and pSV2neo. For S₁ nuclease studies, clones were grown for 3-5 days in the absence of MIX. DMSO was added for the times indicated and total cellular RNAs were extracted by the guanidine hydrochloride method³³. Aliquots (10 µg) of each RNA were hybridized with an end-labelled 940-nucleotide Ndel-Xhol ragment derived from pSV₂myc-dhfr $(c)^{34}$. This probe was labelled with polynucleotide kinase and $(\gamma^{-32}P]ATP$ (Amersham) to a specific activity of $\sim 10^7$ d.p.m. μg^{-1} . Hybridization reactions contained 10^5 d.p.m. of probe and $10 \mu g$ of RNA in a total volume of $10 \mu l$ of hybridization solution (80%). formamide, 300 mM NaCl, 40 mM PIPES pH 6.4, 1 mM EDTA). Reactions were placed at 85 °C for 5 min followed by a 16-h incubation at 51 °C, then treated with 300 U of S₁ nuclease (Sigma) at 37 °C for 1 h, precipitated with isopropanol and subjected to analysis on a 1.8% agarose gel.

transfected with a derivative of the plasmid shown in Fig. 1 in which myc sequences were not included or were reversed. Control F-MEL cells demonstrated 85-95% benzidine positivity after 5 days of induction whereas pSV₂myc-dhfr clones showed 10-50% staining.

Transfected clones also failed to accumulate β^{major} -globin messenger RNA as determined by Northern blot analysis of cellular RNAs (not shown). Furthermore, unlike control F-MEL cells, all three transfected clones continued to proliferate after they had been incubated for 7 days in medium containing 1.5% DMSO (not shown). We conclude from these studies that the perturbations of myc expression seen in these clones are associated with the preservation of features normally associated with the uncommitted, non-terminally differentiated state.

The inability of clone 21 cells to differentiate as well as clones 8 and 15 might have been related to levels of exogenous c-myc transcripts. Indeed, we found that these levels are two to three-fold lower in clone 21 cells than in the other clones (not shown). To address this aspect more directly, we grew cells from clone 21 in increasing concentrations of MTX. At each stage, cells were tested for their ability to differentiate in response to DMSO. RNAs were also extracted and the ratios of exogenous to

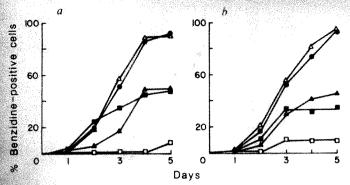


Fig. 3 Benzidine staining of F-MEL clones in response to dimethyl sulphoxide (DMSO) (a) or hypoxanthine (Hyp) (b). Equivalent numbers of cells from each of the indicated clones were cultured in the presence of 1.5% DMSO or 5 mM Hyp. At the times indicated, aliquots of cells were removed and stained with benzidine as described previously⁵. Clones 8 (**m**), 15 (**m**) and 21 (A) were each derived from single-cell clones of F-MEL clones which had been transfected with pSV₂myc-dhfr. Clone 101 (△) was derived from a transfection with the above plasmid minus the mouse c-myc sequences. Clone 745 cells () were the non-transfected parental line used for all transfection studies. Each point represents the average of three to five independent experiments.

endogenous transcripts examined. As shown in Fig. 4, benzidine staining of clone 21 cells was progressively inhibited as the concentration of MTX was raised. Exogenous c-myc transcript levels were also increased, indicating an amplification of plasmid sequences. These observations demonstrated that, at least in the case examined, progressive refractoriness to DMSO induction could be correlated with levels of exogenous mye transcripts.

The highly conserved nature of cellular oncogenes suggests that they are intimately associated with growth and/or differentiation processes. Indirect evidence in support of this comes from studies of both fresh and cultured tumour cells where aberrancies such as c-onc gene amplification, rearrangement and overexpression have been reported⁶⁻¹¹. Changes in the levels of transcripts of otherwise normal c-onc genes have been shown to accompany the normal differentiation and mitotic process both in vitro and in vivo 12-15

c-myc is a short-lived nuclear protein possessing DNAbinding properties 16 and is structurally related to the adenovirus E1A gene product which acts to trans-activate other viral genes. Indeed, c-myc itself can enhance transcription of a chimaeric gene containing the 5'-flanking region of the Drosophila hsp70 heat shock protein gene¹⁸. Together with the findings of c-myc transcript modulation during differentiation^{3,6}, these attributes make the c-myc gene product an ideal candidate to control developmental events, presumably by positively or negatively influencing the transcription of other cellular genes 19. This in turn might exert effects on proliferation since, in the case of F-MEL cells, proliferation and terminal differentiation have been shown to be intimately related²⁰.

Received 14 April; accepted 21 May 1986.

- Marks, P. O. & Rifkind, R. A. A. Rev. Biochem. 47, 419-448 (1978).
- 2. Friend, C., Scher, W., Holland, J. G. & Sato, T. Proc. natn. Acad. Sci. U.S.A. 68, 378-382
- 3. Lachman, H. M. & Skoultchi, A. I. Nature 310, 592-594 (1984).

- Lachman, H. M. & Skouten, A. I. Nature 319, 372-394.
 Simonsen, C. C. & Levinson, A. D. Proc. natn. Acad. Sci. U.S.A. 80, 2495-2499 (1983).
 Orkin, S. H., Harosi, F. I. & Leder, P. Proc. natn. Acad. Sci. U.S.A. 72, 98-102 (1975).
 Collins, S. & Groudine, M. Nature 298, 679-681 (1982).
 Nepveu, A., Fahrlander, P. D., Yang, J.-Q. & Marcu, K. B. Nature 319, 440-443 (1985).
 Brodeur, G. M., Seeger, R. C., Schwab, M., Varmus, H. E. & Bishop, J. M. Science 224, 1121-1124 (1984)
- Rechavi, G., Givol, D. & Canaani, E. Nature 300, 607-611 (1982).
- Heisterkamp, N. et al. Nature 306, 239-242 (1983).
 Leder, P. et al. Science 222, 765-771 (1983).

- Muller, R., Curran, T., Muller, D. & Guilbert, L. Nature 314, 546-548 (1985).
 Gonda, T. J. & Metcalf, D. Nature 310, 249-251 (1984).
 Siamon, D. J. & Cline, M. J. Proc. natn. Acad. Sci. U.S.A. 81, 7141-7145 (1984).
 Greenberg, M. E. & Ziff, E. B. Nature 311, 433-438 (1984).
 Persson, H. & Leder, P. Science 225, 718-721 (1984).

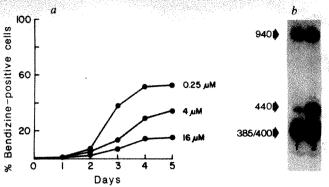


Fig. 4 The degree of F-MEL differentiation is related to the level of exogenous c-myc expression. Clone 21 cells were initially grown in 0.25 µM MTX. To amplify pSV2myc-dhfr sequences, MTX concentrations were increased fourfold for 14-day intervals. At the end of the incubation period, MTX was removed for 3-5 days to allow for recovery of viable cells. Cells were then induced with 1.5% DMSO to monitor benzidine staining (a) or were subjected to the next round of MTX selection. b, After growth in the indicated concentrations of MTX, cellular RNAs were extracted and the levels of exogenous and endogenous c-myc transcripts were determined as described for Fig. 2. The concentrations of MTX in which clone 21 cells were grown was either 0.25 µM (lane 1) or 16 µM

The aberrant expression of several c-onc genes can stimulate or inhibit differentiation in several in vitro systems²¹⁻²³. We are currently investigating the role of other c-onc genes in the differentiation of F-MEL cells. A more difficult problem will be that of the possible role of Friend virus complex genes in complementing the action of c-myc in this system.

c-myc transcripts originating from the SV40 promoter were less responsive to inducing agents than were endogenous c-myc transcripts. This is not surprising because the exogenous c-myc sequences are under the control of a foreign promoter, and the c-mye transcription unit has been substantially altered so as to contain a modification of the 5'-untranslated region and to lack first intron sequences. Both regions have been implicated in contributing to the considerable instability of normal myc mRNA²⁴. We also note that even high-level overexpression of the exogenous c-myc sequences did not affect the levels of endogenous transcripts. This result is consistent with previous observations regarding c-myc overexpression in NIH/3T3 and F-MEL cells^{25,26}.

After submission of this manuscript, Coppola and Cole reported findings similar to ours²⁶, in addition to demonstrating that some of the events leading to commitment have already occurred in c-mvc-transfected cells.

This work was suported by grants from NIH, the Children's Leukemia Foundation of Michigan, the University of Michigan Cancer Research Institute and Strokes Against Cancer. We thank M. Imperiale for pSV₂neo, K. Marcu for pMc-myc 54 and F. Collins for use of electroporation facilities.

- 17. Ralston, R. & Bishop, J. M. Nature 306, 803-806 (1983).

- Raiston, R. & Bishop, J. M. Nature 306, 805-806 (1983).
 Kingston, R. E., Baldwin, A. S. & Sharp, P. A. Nature 312, 280-282 (1984).
 Kingston, R. E., Baldwin, A. S. & Sharp, P. A. Cell 41, 3-5 (1985).
 Gusella, J., Geller, R., Clarke, B., Weeks, V. & Housman, D. Cell 9, 221-229 (1976).
 Falcone, G., Tato, F. & Alema, S. Proc. natn. Acad. Sci. U.S.A. 82, 426-430 (1985).
 Noda, M. et al. Nature 318, 73-75 (1985).

- Waneck, G. L., Keyes, L. & Rosenberg, N. Cell 44, 337-344 (1986).
 Piechaczyk, M., Yang, J.-Q., Blanchard, J.-M., Jenteur, P. & Marcu, K. B. Cell 42, 589-597
- Keath, E. J., Caimi, P. G. & Cole, M. D. Cell 39, 339-348 (1984).
- Coppola, J. A. & Cole, M. D. Nature 320, 760-763 (1986).
 Maniatis, T., Fritsch, E. F. & Sambrook, J. in Molecular Cloning: A Laboratory Manual
- (Cold Spring Harbor Laboratory, New York, 1982).

 28. Southern, P. J. & Berg, P. J. Molec. appl. Genet. 1, 327-341 (1982).

 29. Stanton, L. W., Fahrlander, P. D., Tesser, P. M. & Marcu, K. B. Nature 310, 423-425 (1984).

 30. Battey, J. et al. Cell 34, 779-787 (1983).
- Potter, H., Weir, L. & Leder, P. Proc. natn. Acad. Sci. U.S.A. 81, 7161-7165 (1984).
 Prochownik, E. V. Nature 316, 845-848 (1985).
- 33. Prochownik, E. V. & Orkin, S. H. J. biol. Chem. 295, 15386-15392 (1984).
- 34. Favaloro, J., Treisman, R. & Kamen, R. Meth. Enzym. 65, 718 (1980).

Vibrational CD of biopolymers

from T.A. Keiderling

Circular dichroism measurements in the infrared provide new insight into polypeptide structure and promise more detailed analyses of protein secondary structure.

CIRCULAR dichroism (CD), the differential absorption (ΔA) of left- and rightcircularly polarized light, has become a fundamental tool in the analysis of solution-phase protein and nucleic acid secondary structure. The method, however, has several limitations. Ordinarily studied in the ultraviolet (UV), electronic CD can access only a few excited states of the typical organic molecule. And frequently these transitions, largely dominated by π -excitations of aromatics and carbonyls, give featureless, overlapping spectral bands whose CD tends to interfere.

On the other hand, the vibrational transitions observed in the infrared (IR) region of the spectrum are typically much better resolved and more straightforward to assign and interpret than electronic transitions. Extensive spectroscopic studies have demonstrated that some aspects of vibrational spectra are characteristic of expected biomolecular structures. But sensitivity to molecular conformation is marginal.

Coupling IR and CD

Vibrational circular dichroism (VCD) combines the details of IR data with the conformational sensitivity and two-signed clarity of CD. Thus, the variety of possible spectral transitions increases dramatically, and such transitions can originate in any bond of the molecule. The great potential of VCD lies in its ability to probe discrete structural components of a molecule, vielding spectra that are unique and very strongly influenced by conformation. Thus VCD studies complement and extend the structural insights provided by the wealth of CD and vibrational spectroscopy data already available.

VCD spectra are measured on an infrared spectrometer (conventional or FTIR) that has been modified to produce and detect modulated circularly polarized light'. A wire grid polarizer creates linearly polarized light, which is subsequently oscillated between left and right circularity by means of a CaF, or ZnSe photoelastic modulator. If the sample is optically active, its VCD will in turn modulate the intensity of the incident light beam at the modulator frequency. Fast, highsensitivity IR detectors, such as Hg(Cd)-Te or InSb, are necessary to detect the modulated intensity. The signal is extracted with lock-in amplifiers and computer signal averaging.

With this apparatus, we routinely achieve a sensitivity of $\Delta A/A$ about [0]

and a range to about 900 cm. However, extension to approximately 600 cm⁻¹ and $\Delta A/A$ of 5×10^{-6} is possible. While these capabilities for the VCD of small molecules have been available for some time. only in the last two years have applications to biopolymers developed234. Part of this lag can be attributed to the difficulty of studying aqueous biological systems in the infrared. For such studies, VCD must be obtained on very thin, concentrated, deuterium-exchanged samples in D₂O held between two CaF, windows separated by a Teflon spacer. Even then, only the amide I band (C=O stretch) can be studied with present instrumentation. In non-aqueous environments, we can also study amide A (NH stretch) and II (CNH deformation) bands^{2,3,4}

Biopolymer applications

Figure 1 shows the amide I VCD and absorption spectra for three basic structural types of poly-t-lysine: random coil (rc), anti-parallel B-sheet and right-handed α -helix. Both the α -helical and rc amide I bands exhibit VCD couplets at about 1.650 cm 1, but they are of opposite sense. The β -sheet form has two negative VCD bands correlating to two absorption maxima near 1,620 and 1,680 cm

In comparison to near-UV CD findings. the re VCD results have a surprisingly large magnitude and are quite similar to the amide I VCD of left-handed α-helix previously reported14. This data has recently been interpreted as added evidence for substantial local order in the otherwise random coil". The re amide I VCD also resembles that of the poly-t-proline extended helix, which indicates the type of local structure present.

Poly-1-tyrosine in dimethylsulphoxide

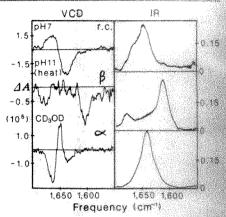


Fig. 1. Poly-t-lysine VCD and absorption spectra in the amide I region at pH 7.3 (random coil), pH 11.5 after heating (antiparalle) p sheet) and in a 96-to-4 ratio of CD OD to D.O. (right-handed α-helix). ΔA in units of 10

gives similar re spectra . Here the amide A band can be used to distinguish the respectrum from that of a left-handed or helix. Whereas interference from aros matic side chains makes electronic CD inconclusive as to secondary structure, the resolution afforded by vibrational spectra makes such analysis possible

The VCD data set for poly-t-lysine is analogous to that used initially for characterizing protein secondary structure in electronic CD. While our present data base is insufficient to make a significant impact upon such characterizations, we have obtained globular protein VCD that reflects the qualitative patterns shown in Fig. 1. For example, the amide I VCD of myoglobin and α-chymotrypsin at neutral pH demonstrate this qualitative resemblance (Fig. 2). The predominantly α-helical myoglobin clearly shows a triple-peaked VCD of the same sign pat-

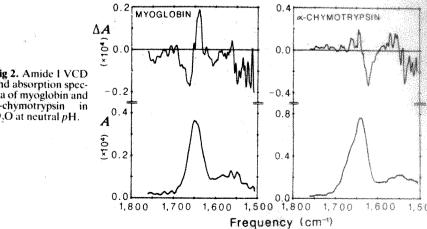


Fig 2. Amide I VCD and absorption spectra of myoglobin and α-chymotrypsin D.O at neutral pH.

tern, though of smaller magnitude, as the α-helical spectrum in Fig. 1. The αchymotrypsin, having a high β -sheet component, has a negative band at about 1,630 cm⁻¹ that parallels the high pH poly-L-lysine results. This qualitative success suggests a role for VCD in protein stereochemical studies if improved signal-tonoise ratios and VCD for other amide bands can be obtained.

But VCD's ultimate utility in protein secondary structure analysis depends in part on its sensitivity to polymer length and end effects, which has yet to be determined. In this regard, we have made studies of β -sheet-forming^{8,9} and 3_{in} helical forming oligopeptides. In particular, for the latter studies, we measured the VCD of the amide A, I and II bands of aminoisobutyric acid oligopeptides as a function of length to determine when the characteristic 3₁₀-helical VCD developed. For all three bands the characteristic magnitudes of $\Delta A/A$ are fully developed at the hexamer, which corresponds to almost two turns (three H-bonds) of an ideal 3₁₀helix. In fact the spectra evidence the same qualitative VCD as early as the tetramer, which can only form a single turn. Such results imply a dominance of relatively local interactions in VCD that is not seen in electronic CD. Thus from vibrational CD, a new level of structural insight may evolve.

Biological VCD applications are likely to focus next on the simultaneous empirical analysis of vacuum UV, near-UV and IR CD data for a series of proteins. 12 Developments with FTIR-based spectrometers should also permit better signal averaging and improved resolution.1 Finally, polarized interferometers or new modulator designs should bring the VCD of lower energy modes within range, disclosing folded biopolymer structure in even greater detail.

Tim Keiderling is at the Department of Chemistry, University of Illinois at Chicago, PO Box 4348, Chicago, Illinois 60680, USA.

- Keiderling, T.A. Appl. Spectrosc. Rev. 17, 189-226
- 2. Singh, R.D. & Keiderling, T.A. Biopolymers 20, 237-240 (1981)
- 3. Lal. B.B. & Nafie. L.A. Biopolymers 21, 2161-2180
- 4. Sen. A.C. & Keiderling, T.A. Biopolymers 23, 1519-1532 (1984)
- 5. Yasui, S.C. & Keiderling, T.A. J. Amer, Chem. Soc. 108. 5576-5581 (1986) 6. Paterlini, M.G., Freedman, T.B. & Nafie, L.A. Biopoly-
- mers (in the press).
- 7. Yasui, S.C. & Keiderling, T.A. Biopolymers 25, 5-15 8. Narayanan, U., Keiderling, T.A., Bonora, G.M. &

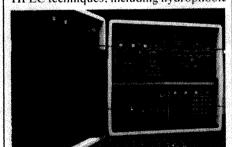
- Narayanan. U., Keiderling, T.A., Bonora, G.M. & Toniolo, C. Biopolymers 24, 1257–1263 (1985).
 Narayanan, U., Keiderling, T.A., Bonora, G.M. & Toniolo, C. J. Amer. Chem. Soc. 108, 2431–2437 (1986).
 Yasui, S.C., Keiderling, T.A., Bonora, G.M. & Toniolo, C. Biopolymers 25, 79–89 (1986).
 Yasui, S.C., Keiderling, T.A., Formaggio, F., Bonora, G.M. & Toniolo, C. J. Amer. Chem. Soc. 108, 4988–4993 (1986).
- (1986). 12. Hennessey, J.P. & Johnson, W.C. Biopolymers 20, 1085-1004/1981)
- 13. Lipp. E.D. & Nafie. L.A. Biopolymers 24, 799-812 (1985).
- 14. Dignam, M.J. & Buker, M.D. Appl. Spectr. 35, 186-193

ACS in Anaheim

Next week over 200 exhibitors at the American Chemical Society's West Coast meeting will be ushering in autumn with labware, instrumentation and schemes for automation.

An infrared detector built specifically for capillary gas chromatography will put in an appearance at Hewlett-Packard's stand (Reader Service No. 100). The HP 5965A system, which starts at \$47,000 (US), consists of a detection module and an HP IRD ChemStation that can combine data from both GC/FTIR and GC/MS for compound identifications. The ChemStation can also integrate library search results and rank probable internal diameters based on hit quality and common matches. Hewlett-Packard, showing in booths 141 through 147 (odd) at ACS, says the IR detector takes up less than 8 inches of bench space. The company thinks its dedicated instrument will have a heightened sensitivity for capillary GC eluents, allowing, for example, detection of 5 ng isobutyl methacrylate at a signal-to-noise ratio of 20 to 1.

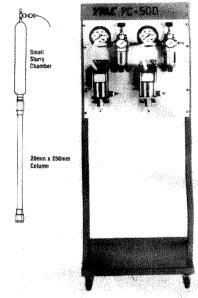
Combining non-metallic components with a novel detector array, Dionex has developed an HPLC system aimed at life sciences applications (Reader Service No. 101). The Series 4000i BioLC package has a quaternary pump that, Dionex says, can accommodate the "entire range" of HPLC techniques, including hydrophobic



The 4000i can store up to 10 programs.

interaction and ion pairing. The metalfree pump provides pressures up to 4.000 p.s.i. and flow rates from 100 µl per minute to 10 ml per min. The 4000i detectors can spot even non-chromophoric organic and inorganic ions at sub-p.p.m. levels, according to Dionex, with a pulsed amperometric detector and suppressors to reduce background and increase sensitivity. The whole assemblage will be on display in booth 717.

For chromatographers who prefer to pack their own columns, YMC Inc has two compact slurry packing systems that, the company says, can be 10 to 15 per cent more efficient than dry or tap packing methods (Reader Service No. 102). The PC-50D uses two air-actuated pressure amplifier pumps, which generate solvent flows up to 290 ml per min at pressures up



YMC packs two cohimns simultaneously

to 6,000 p.s.i., to pack LC columns with internal diameters from 4.6 mm to 20 mm. The larger PC-100D is capable of packing columns with internal diameters from 4.6 mm to 100 mm, with a larger pump to deliver solvent at 1.25 I per min at pressures up to 9,000 p.s.i. and a smaller one with the same specifications as those used in the PC-50D. YMC, at booth 705 in Anaheim, will have more information on its systems, which sell for \$3,200 (US) for the PC-50D and \$7.800 (US) for the PC-100D.

Automation links

Radiometer will have its new TitraLab wet chemistry analysis system at booth 305 in Anaheim (Reader Service No. 103). The company's programmable system automates titration procedures for both single and batch samples, switching automatically between multiple reagents, electrodes and titration procedures. Communicating via a CRT screen. TitraLab displays the titration curve during analysis and offers on-screen guidance with a HELP key. Its memory stores up to 60 user-defined methods. Radiometer's design features several different configurations for different applications to supplement the standard video titrator, triburette station and sample handler.

Software to boost the analytical prowess of Perkin-Elmer's model 7700 computer is now available for a variety of applications (Reader Service No. 104). The company claims it has written over one million lines of code to build a software selection that

spans all of its analytical instrumentation. The Perkin-Elmer Solvent Optimization System, for example, creates a multicoloured triangular graph representing the resolution of different solvent combinations. The company sells its menudriven software for prices ranging from \$400 (US) to \$3,000 (US), or in some cases as part of the hardware packages. PerkinElmer will be in a string of booths between 115 and 220 by the telephones in the Anaheim convention centre.

Three instrument couplers for laboratories undergoing automation are the subject of a new brochure from Beckman (Reader Service No. 105). Two of Beckman's Digimetry couplers, the MK5-4CV and the MK6, convert analogue signal outputs from chromatographs into digital format. Of the two, Beckman says, the

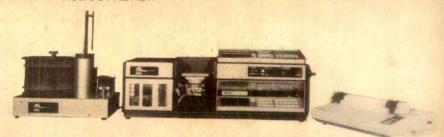


Beckman expands upon Diginetry couplers. MK5-4CV is more accurate and has onboard circuitry to validate the operational performance of each interface. The third Digimetry model, the MK5S, can collect data from as many as eight instruments with RS-232 output ports at a time. In Anaheim, Beckman will be at booths 335 through 339 (odd) to distribute further information.

Thermoanalytical determinations can now benefit from computer-aided in-



Mettler's menu-driven GraphWare system.



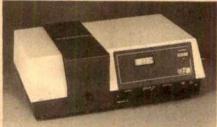
From halfway around the world, ARL's atomic absorption spectrometer has arrived

sights, owing to new software from Mettler (Reader Service No. 106). With TA70 GraphWare, up to four thermoanalytical curves can be depicted simultaneously, either superimposed or segregated each in its own window. Mettler designed the package for use with its TA3000 thermal analysis system and an IBM PC. The company, at booth 602 in the convention hall, will have more to say about TA70 GraphWare.

Scanning the spectrum

A joint effort that spanned an ocean produced the 902 atomic absorption spectrometer from Applied Research Laboratories (Reader Service No. 107). Australiabased GBC Scientific Equipment, in conjunction with ARL, engineered an AA system that is guaranteed to precision of 0.5 per cent RSD on 5 p.p.m. of Cu with an absorbance of 0.7. ARL/GBC also claims that the 902's background correction system makes the instrument "the fastest system optimized for graphite furnace signals." The AA spectrometer can be found at booth 519 at ACS. A complete doublebeam system with built-in data handling, software and a printer costs about \$17,000 (US).

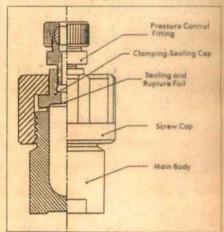
A British-made single beam spectrophotometer has just arrived on the market



AlphaSpec: filling a gap in the UK market? following an agreement between Camspec and EDT Research (Reader Service No. 108). The AlphaSpec range, priced between £1,500 and £2,530 (UK), is EDT's attempt to fill the gap Camspec identified for a low-cost single-beam instrument on the British market. Five AlphaSpec models are presently available, with visual or UV/vis ranges and digital or analogue readouts. EDT signed an original equipment manufacturer agreement with Camspec early this month for the AlphaSpec line, which will be distributed by the EDT group company Courtcloud, Courtcloud dealers and EDT itself.

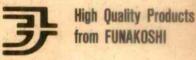
Catalogue chronicle

Berghof/America, striving to be Teflon's titan, has a 16-page new products cata-



Berghoff America unveils its Teflon line.

ADVERTISEMENT



Recombinant Mouse-Interferon-8

This is purified from E, coli carrying mouse IFN- β gene of mouse L-cell, using affinity chromatographies described by

S. Matsuda, et al. (to be published in J. Interferon Res).

Purity: higher than 99% by SDS-PAGE.



Blue-Cotton (Mutagen Adsorbent)

This is able to adsorb mutagens containing quite low concentration in aqueous solutions, especially those having more than three fused aromatics.

The adsorbed mutagens are easilly eluted by ammonia-methanol solution.
Blue-cotton is applied to Urine

Blue-cotton is applied to Urine, Feces, Foods, River Water, etc.

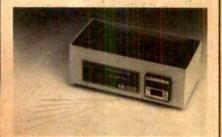
FUNAKOSHI PHARMACEUTICAL CO., LTD. Science Business Div. Research Material Sect. 2-3 Surugadai, Kanda, Chiyoda-ku, Tokyo, Japan

Telephone : Tokyo 03-293-2352 Telefax : 81-3-295-5545 Telex : J28489 FUNA

LIMUTESTER



(gelation-capillary method)



Precise Detection of Endotoxins

This LIMUTESTER detects Endotoxins promortly, applying to gelation reaction of LAL and a glass capillary.

The LIMUTESTER is simple, economical and usable anywhere, especially needs no endotoxin-free laboratory glass

LIMUTESTER INCUBATOR is available.

FUNAKOSHI PHARMACEUTICAL CO., LTD. Science Business Div. Research Material Sect.

Telephone: Tokyo 03-293-2352 Telefax 81-3-295-5545 : 128489 FUNA Telex

Reader Service No.16

Reader Service No.12

2-3 Surugadai, Kanda, Chiyoda-ku, Tokyo, Japan

Versatile Tissue Culture Incubator Modular Incubator Chamber (the Cell Sphere™) for all tissue cultures, aerobic or anaerobic. Low Cost

Eliminates evaporation loss and contamination. Easy to use - flush with gas mixture, seal, place at appropriate temperature. Stackable, see-through. Quantity discounts. billups-rothenberg, inc., pob 977, Del Mar, CA USA 92014. Call 619-755-3309 or contact your Flow Laboratories representative.

Medwire Div.

stocks a wide variety

TEFLON COATED*

Platinum alloys, stainless steel. silver, multistrand and single strand available for prompt shipment. Write for descriptive brochure and price lists



Medwire Div.

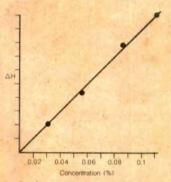
123 So. Columbus Ave. Mt. Vernon, N.Y. 10553 914-664-5300

Reg TM of E I. Dupont

Reader Service No.49

logue that outlines its latest laboratory equipment (Reader Service No. 109). Large volume high pressure autoclaves. Teflon-encased stainless-steel stir shafts. flexible corrugated tubing up to 150 feet long and pressure digestion heating blocks are just a few of the areas that incorporate PTFE, FEP, PFA and other fluorocarbon resins. Berghof will be showing its equipment at booth 428 in Anaheim.

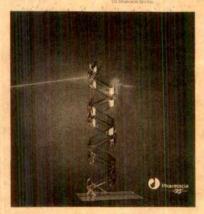
The Bioanalyzer brochure from Provesta details the theory and practice of its enzyme-electrode instrument (Reader Service No. 110). The Bioanalyzer,



A typical standard curve for the Bioanalyzer. according to Provesta, can determine the concentration of specific biochemicals or organic chemicals in complex mixtures at levels between 10 and 10 M. Using an oxygen electrode tipped with an oxidase in a gel matrix, the instrument works by measuring the decrease in oxygen at the electrode when the oxidase catalyses a reaction between oxygen and the biochemical being analysed. Information on Wednesday's Bioanalyzer workshop will be on hand at Provesta's ACS booth 726.

Pharmacia's catalogue reviews the company's recent arrivals for the molecular biologist (Reader Service No. 111). What isn't on exhibit at the biotech group's ACS booth 304 will surely be listed among the catalogue's pages. It describes many of the products Pharmacia has advanced during

Molecular **Biologicals**



Pharmacia tells all in its new catalogue.

the past year, including its DNA/RNA modifying enzymes, prokaryotic and eukaryotic vectors. DNA synthesizer and linkers for protein engineering.

For the life scientist

Right near the convention hall entrance. Orion Research in booths 702 and 704 will be touting the EA 940 pH/ISE meter with its unusual ability for expansion (Reader Service No. 112). Orion says the meter alone can be programmed to measure ions for which electrode and direct calibration procedures do not exist, or to measure samples with unknown concentrations and different sample types without calibration. But by adding the company's 960 autochemistry module, the meter can also be upgraded to a system capable of performing analyses ranging from endpoint titrations to incremental techniques. The



Three keys control most EA940 functions.

EA940 sells for \$1,995 in the United States.

Ohaus will debut its high-capacity toploading balance at ACS in booths 735 and



New heights in weights for Ohaus balances. 739 (Reader Service No. 113). The Galaxy 8000 weighs up to 8,000 g and reads to 0.1g; its taring range is also 0 to 8,000 g. The G8000's 7 × 9-inch weighing pan reflects its high capacity function. Ohaus also equipped its unit for RS-232 bidirectional data output and sample weight display in grams, pounds, troy or avoirdupois ounces, carats or pennyweights. Taring and calibration, says Ohaus, are accomplished with the touch of a button. The G8000 lists at \$1,150 (US).

These notes are compiled by Karen Wright from information provided by the manufacturers. To obtain further details about these products, use the reader service card bound inside the journal. Prices auoted are sometimes nominal and apply only within the country indicated.

CONVENIENT-INFORMATIVE-TIMELY-PROVOCATIVE

FOUR DYNAMITE REASONS WHY YOU SHOULD SUBSCRIBE TO BIO/TECHNOLOGY NOW . . .

You'll save time. Because you don't have time to read every journal in the field, BIO/TECHNOLOGY is written and edited to give you all the information you need in ONE convenient source. BIO/TECH-NOLOGY is the only journal to give you news. Features. Original research. Product evaluations. Industrial applications. Job openings. Book and product reviews. And more. If it's important to your work, you'll find it between the covers of BIO/TECHNOLOGY.

You'll learn new ways to improve your on-the-job skills and run a more successful operation. Each month BIO/TECH-NOLOGY gives you the scoop on invaluable start-up information...the latest instrumentation...marketing breakthroughs...funding sources...new technologies... patents and licences...profiles on how others are avoiding the pitfalls and reaping the rewards. In fact, just one practical tip from BIO/-TECHNOLOGY can be worth many times the cost of your subscription.



You'll be up-to-date on all major industry developments. With correspondents all over the world, BIO/TECHNOLOGY delivers the inside story on who's doing what, where You'll get the latest word on changing government regulations and tax law, and how they affect your work.

Plus you'll read original research papers by bench scientists, engineers, and biologists that will help keep you in the forefront of every new discovery worth knowing about.

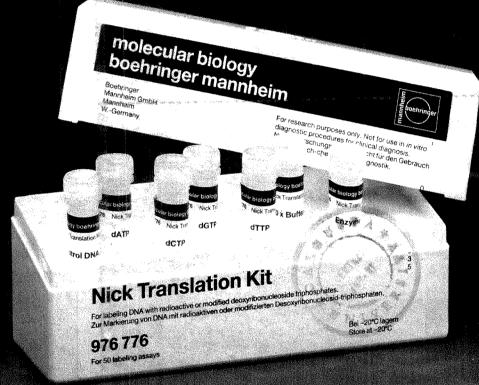
You'll get new ideas you can put to use immediately.BIO/TECHNOLOGY lets you rub elbows with eminent scientists, tour new facilities and learn how new processes work in every field from genetic engineering to molecular biology. Each month, BIO/TECHNOLOGY helps spark ideas for your own research, for new industrial applications and for getting along in the increasingly competitive financial arena.

If you're not already subscribing to BIO/TECHNOLOGY, don't delay the moment any longer - return the coupon below and we will send you twelve issues. You risk nothing. If for any reason BIO/TECHNOLOGY doesn't live up to your highest expectations, just let us know and you'll receive a full refund on all unmailed copies. Remember too, that your subscription may be tax deductible.

TO START RECEIVING YOUR SUBSCRIPTION, FILL OUT THE COUPON BELOW AND RETURN WITH PAYMENT TO:

U.S.A.: BIO/TECHNOLOGY Subscription Order Dept., P.O. Box 1543 Neptune, New Jersey 07754-1543 U.S.A. To speed up your subscription in the U.S.A., call toll free 1-4	Brunel Road, Houndmi	pt., Macmillan Journals, Ltd. ; ills, Basingstoke England
☐ YES! Please send me one year of ☐ BIO/TECHNOLOGY (12 issues). I understand that I may cancel my subscription at any time and receive a full refund on all unmailed issues. ☐ U.S.A\$59.00* ☐ Australia-A\$130** ☐ U.K£70** ☐ Elsewhere-U.S.\$112** ☐ Japan Publications Trading Company Ltd 2-1 Sarugaku-cho 1-chome ☐ Chiyoda-ku, Tokyo, Japan Tel: (03) 292 3755	☐ My payment is enclosed at the price checked. ☐ Please charge my credit card account: ☐ American Express ☐ Mastercard Card No.: ☐ Signature: Name: Company: Address: City/State/Postal Code:	
Chiyoda-ku, Tokyo, Japan Tel: (03) 292 3755 Note: 'Represents 24% off Basic Subscription Price of U.S. \$78.00 MAN other prices quoted are "Air Speed"	City/State/Postal Code:	7211

Nick Translation Kit from Boehringer Mannheim



the time & money saving alternative

Nick translation kit, Cat. No. 976776 contains all reagents ready for use for 50 labeling reactions

Get the detailed protocol from your local representative or



Boehringer Mannheim GmbH Biochemica P.O. Box 310120 D-6800 Mannheim W. Germany Reader Service No.1